15th - 19th September 2019
Florence Italy

BOOK of ABSTRACTS

12th European Congress of Chemical Engineering
ECCE 12

5th European Congress of Applied Biotechnology
ECAB 5

BRIDGING SCIENCE WITH TECHNOLOGY

A Renaissance in Chemical Engineering

www.ecce12-ecab5.org

Venue:
Florence, Italy
Fortezza da Basso
Piazza Adua, 1, 50123 Firenze (Italy)

Date:
From September 15 to September 19, 2019

Organized by:
AIDIC SERVIZI SRL
Via Giuseppe Colombo 81A, 20133 Milano (Italy)
Website: www.aidic.it
Email: aidic_accounting@aidic.it
Tel: +39 02 70608276
Fax: +39 02 70639402

Contacts:
Email: ecce12_ecab5@aidic.it
Tel: +39-02-70608276
Website: http://www.ecce12-ecab5.org/

Organizer

Promoters

GOLD SPONSOR

STUDENT PROGRAMME SPONSOR

CONTENT

Disclaimer

The Publisher

In order to make this volume available as economically and as rapidly as possible the typescript has been reproduced in its original form. This method unfortunately has its typographical limitations but it is hoped that they in no way distract the reader.

ISBN :978-88-95608-75-4
DOI :10.3303/BOA1901

PREFACE

The Event is organized by AIDIC, the Italian Association of Chemical Engineering, under the auspices of the European Federation of Chemical Engineering (EFCE), as well as of the European Society of Biochemical Engineering Science (ESBES).

EFCE scientific congresses and symposia are the heart of its activities. The first EFCE European Congress was held in 1997 in Florence, organized also at that time by AIDIC; and it marked the start of a grand journey of growth. The European Congress of Chemical Engineering has now become a biennial and world-famous event, attended by scientists, researchers, teachers, students, industry professionals, owners, contractors and suppliers from all the continents, who can interact, share, debate, collaborate and inspire one another, bringing chemical engineering expertise on an unprecedented scale to a single location.

A few years ago ESBES joined EFCE for the organization of the European Congress, thereby widening their scope and their field of application. ESBES contribution to the topics of the Florence 2019 Congress is particularly relevant, due to the importance that biotechnology is taking and will take in research, society and industry.

The joint Congresses ECCE12 (the 12th European Congress of Chemical Engineering) and ECAB 5 (the 5th European Congress of Applied Biotechnology) and the associated events stand under the common theme of

Bridging Science with Technology : a Renaissance in Science

The scientific content of both the congresses ECCE12 and ECAB 5 is set under the governance of EFCE and ESBES Working Parties and Sections.
The conferences cover a wide range of research themes under the umbrella of Chemical Engineering and Applied Biotechnology. The topics treated by WPs and Sections are all those ones typical of Chemical Engineering and Applied Biotechnologies, from the classical ones, like process simulation and reactor design, to the most current ones, like nanotechnologies, bio-fuels, bio-catalysts, food and water, that represent the challenges of the future and are of interest to everybody.

MAIN TOPICS

ECCE12

1 SUSTAINABLE PROCESSES
2 PARTICLE TECHNOLOGY
3 PRODUCTION , PROPERTIES AND TECHNOLOGY OF NEW MATERIALS
4 NANOTECHNOLOGY
5 SEPARATION TECHNOLOGY AND HEAT & MASS TRANSFER
6 THERMODYNAMICS AND INTERFACIAL PHENOMENA
7 FLUID MECHANICS AND TRANSPORT PHENOMENA
8 MULTIPHASE SYSTEMS
9 MEMBRANE ENGINEERING : Energy from salinity gradients, Hybrid artificial organs
10 INDUSTRIAL ELECTROCHEMISTRY
11 PROCESS SYSTEM ENGINEERING
12 CHEMICAL REACTION ENGINEERING
13 BIOMASS
14 FOOD ENGINEERING
15 ENERGY AND CHEMICAL ENGINEERING
16 ENVIRONMENT, SAFETY & QUALITY
17 QUALITY ASSURANCE, CONTROL & MANAGEMENT SYSTEMS
18 KNOWLEDGE, EDUCATION & TRAINING

ECAB5

ADVANCED AND INNOVATIVE TECHNOLOGY IN INDUSTRIAL
19 BIO-PRODUCTION, BIO-SEPARATION, AND BIO-DETECTION (BIOSENSORS)
BIOENERGY, BIOFUELS&RENEWABLES, BIORESOURCES,
20 BIOREFINERY AND BIOMATERIALS (BIO-ACTIVE COMPOUNDS, BIOFUELS, FINE CHEMICALS)
21 BIOCATALYSIS (FUTURE MICROBES AND ENZYMES)
22 NOVEL PROCESSING (E.G. MICROBIAL FUEL CELLS), DOWNSTREAM PROCESSING
23 FROM SMALL TO LARGE (NANO-BIOTECHNOLOGY, SCALE-UP/SCALE DOWN, LARGE-SCALE PRODUCTION)
24 SYSTEMS BIOTECHNOLOGY AND METABOLIC ENGINEERING
25 PROTEIN AND ENZYME STABILITY
26 ENVIRONMENTAL BIOTECHNOLOGY
27 BIOFILMS IN INDUSTRY AND BIOMEDICINE
28 CHEMICAL PRODUCT DESIGN AND BIOPRODUCTS
29 BIOECONOMY
30 BIOREACTOR PERFORMANCE
31 DOWNSTREAM PROCESSING
32 FOOD BIOPROCESSES
33 MICROALGAE BIOENGENEERING
34 MODELLING, MONITORING, MEASUREMENT & CONTROL
35 REGENERATIVE MEDICINE MANUFACTURING

The scientific programme of ECCE12-ECAB5 features more than 1200 Lecture and Poster presentations, including 6 plenary lectures and 8 keynote lectures by outstanding Researchers.
This Book of Abstracts consists of a summary of the topics treated and listed in the Congresses.

The Organizers

AUTHOR Index

ABSTRACT Index

PLENARY

KEYNOTE

SUSTAINABLE PROCESSES

PARTICLE TECHNOLOGY

NANOTECHNOLOGY

THERMODYNAMICS AND INTERFACIAL PHENOMENA

FLUID MECHANICS AND TRANSPORT PHENOMENA

MEMBRANE ENGINEERING

PROCESS SYSTEM ENGINEERING

CHEMICAL REACTION ENGINEERING

FOOD ENGINEERING

ENVIRONMENT, SAFETY & QUALITY

KNOWLEDGE, EDUCATION & TRAINING

ECAB5

SYMPOSIUM 1

SYMPOSIUM 2

SYMPOSIUM 3

ADREM

CoPro Project

Workshop on Crystallization

"Perspectives for CO2 Utilization"

Flavio Manenti

Politecnico di Milano l.

CO2 is dramatically impacting our life: climate change and consequent social-economic problems are identified as Grand Challenges of current century. Main agencies identified that 87% of anthropogenic CO2 emissions are due to combustion of fossil fuels and it is estimated that overall average anthropogenic carbon emissions were 30 Gt/y in last years. The technological problem with anthropogenic CO2 is not only inherent in the molecule chemistry but also in the form of exhausts: these are gases released into atmosphere at low pressure, in large amounts, where CO2 is mixed with H2O, N2 and other combustion products. As a consequence, it realizes to be difficult and costly to process such exhausts; CO2 sequestration by chemical-physical washing and subsequent disposal in remote storages still remains a challenging and questionable technique. In the last two decades, a large portion of the scientific and engineering community has faced the problem from upstream, therefore focusing on mitigation of CO2 impacts by reducing its production (i.e. renewable energies); on the other hand, the problem can be faced from downstream also by implementing utilization processes of produced CO2. Use of exhausted or atmospheric CO2 for direct methanol production (by CO2 hydrogenation), as proposed by Olah, represents an example of downstream approach to the problem and, according to post-Horizon2020 directives of European Community, CO2 utilization seems to be a faster track with respect to other routes to tackle CO2 emissions and the plenary contribution will mainly focus on existing and promising processes for bulk reusing of produced CO2 providing CO2-free perspectives for main chemical synthesis.

An Initiative on Safety Across the Chemical Engineering Curriculum

H. Scott Fogler

doctor honoris causa 2016, Universitat Rovira i Virgili, Tarragona, Spain Ame & Catherine Vennema Professor of Chemical Engineering,

and the Arthur F. Thurnau Professor

The University of Michigan

Ann Arbor, Michigan 48109-2136

Sometimes chemical process safety is taught in a separate safety course within the chemical engineering curriculum, and sometimes it is taught only in the senior year as a part of the process design course. The purpose of this initiative is to provide faculty and students with real case studies and resources so that process safety can be more effectively and easily learned throughout the curriculum and become an integral part of chemical engineering culture.

To achieve this culture, safety modules have been developed to be used as homework problems in every core chemical engineering lecture course (http://umich.edu/~safeche/). Each module consists of viewing a Chemical Safety Board Video, filling out an analysis of the accident, doing a course specific calculation, assigning the NFPA symbols and filling out a Bow Tie Diagram for the accident. For example, in the chemical reaction engineering course, the T2 laboratories accident and the ExxonMobil Refinery Fire are examples presented and analyzed.In addition to the core lecture courses, six video snippets (2-5 minutes each) on Laboratory Safety are included on the website.

In addition to the modules, tutorials are given on such things as the NFPA diamond, the Bow Tie Diagram, the Fire Triangle, the Process Safety Triangle and A Safety Analysis of the Incident. The solutions to the homework problems are also given on the website, but instructors will have to email the author to receive the password to enter the solutions. The website is free and accessible to all.

Challenges in modelling of biocatalytic reactions

Jürgen Pleiss

Institute of Biochemistry and Technical Biochemistry, University of Stuttgart, Germany

Enzymes are promising catalysts for a wide range of biocatalytic processes. Because protein engineers still lack a deep molecular understanding of biocatalytic systems, finding the optimal biocatalyst is time consuming, and trial-and-error strategies are widely used.

A more directed rational design strategy responds to three challenges. Although enzyme-substrate interactions are successfully modelled by molecular simulation and experimental data are successfully modelled by macroscopic ODE based models of enzyme kinetics, both modelling methods are separated by many orders of length and time scales. Therefore, the major challenge is to bridge the gap between molecular and kinetic modelling. The second challenge is a holistic model, which includes reaction conditions. Kinetic models describe the reaction medium by adjustable parameters and can therefore become complex. In contrast, molecular simulation allows for the reliable prediction of thermophysical properties of mixtures from first principles. The third challenge is data management. Due to high-throughput experimentation techniques for biocatalytic experiments, enzyme data is rapidly growing, complex, and unstructured. Making big biodata accessible to data mining and modelling is widely seen as a major bottleneck to the digitalization of industrial biotechnology, and rules for data management such as the FAIR data principles or the STRENDA recommendations are increasingly accepted by the scientific community.

Advancing Chemical Development through Process Intensification, Automation, and Machine Learning.

Klavs F. Jensen

Department of Chemical Engineering Massachusetts Institute of Technology 77 Massachusetts Avenue Cambridge MA 02139

Process intensification via continuous operation combined with automated optimization and screening techniques offer opportunities for faster development and more efficient manufacture of diverse chemical products. This presentation starts with advances in process intensification and green chemistry achieved through micro-reaction technology and continuous multistep synthesis (flow chemistry). Case studies include individual intensified reaction units as well as on-demand synthesis of common pharmaceuticals in a plug-and-play, manually reconfigurable, refrigerator-sized manufacturing platform. Next, advances in automated screening and optimization of chemical reactions are highlighted as methods to accelerate translation of laboratory discoveries to manufacturing. Examples include optimization of thermal- and photo-chemical reactions in 15 microliter droplets with respect to continuous process conditions
(temperature, time, concentrations…) and discrete process choices (catalysts, solvents, bases …). Finally, machine learning of chemical information is applied to computer aided chemical synthesis - the planning of reaction paths to a given molecular target from purchasable starting materials. With expert user input, the synthesis plans are converted into recipes that are executed by an automated modular continuous flow platform configured by a robotic arm, which sets up the required unit operations. Examples of automatic continuous syntheses of pharmaceutical compounds and libraries illustrate the promise of this combined approach of machine learning, reaction engineering, and robotics.

Chemical recycling of complex plastics

Marinke Wijngaard

MD TNO Circular Economy & Environment

There are too many plastics that we currently burn and do not make the most of. This can be prevented by keeping plastics in the value chain as long as possible, and thus reducing the use of fossil oil for plastic production. TNO achieves this by designing plastics that can be used for longer and which can be easier maintained an recycled and to develop chemical recycling technologies for complex plastics.

Although more simple plastics can be easily mechanically recycled, this is not possible for more complex plastics. For these complex plastics often chemical recycling need to be applied. TNO has broad experience in reclaiming polymers through chemical recycling technologies. In this lecture Marinke shares experience on gasification, pyrolysis and dissolution of plastics.

"Separation challenges in the quest for sustainability"

Immaculada Ortiz

University of Cantabria, Chemical & Biomolecular Engineering
Spain

Needs for separating mixtures are pervasive in many industrial sectors. In past decades the importance escalated with the emergence of new industries in biotechnology and high-performance materials. However, Separation Processes account for 40-70% of both the capital and operating costs in the process industries and are responsible for 10-15% of the world's total energy consumption. This is due in part because of the ubiquity of chemicals in the modern world and in part due to the fact that more than 80% of the energy associated with chemical separations is used in distillation and similar processes such as evaporation that rely on phase changes. Therefore, progress substitution of conventional separation methods by more efficient alternatives is challenging for a more sustainable development.

The drivers for new and more efficient separation alternatives are, i) design of high performance materials (functionalized membranes and nano-structured materials) capable of overcoming equilibrium constraints and increasing the separation selectivity at the same time that keep the productivity target, ii) progressive use of low energy driving forces such as magnetic fields targeting solutes with magnetic properties and, iii) advanced decision-making tools that integrate predictive modeling of separation units and materials function to provide the optimum process configuration that maximizes the profit and the protection of the environment and natural resources.

The Rational Purification of Proteins: Proteomics, Expert Systems, Modelling, Process Conditions and Optimization

J.A. Asenjo and B.A. Andrews

Centre for Biotechnology and Bioengineering, CeBiB, University of Chile
Beauchef 851, Santiago, Chile,
**Corresponding author: juasenjo@ing.uchile.cl*

Highlights

- Selection of optimal chromatographic sequence based on proteomic data of product and contaminants.
- Mathematical modelling of chromatography for accurate simulation including affinity.
- Optimization of chromatography process conditions including "peak cutting".

1. Introduction

Over the past years we have developed a Computer Based Expert System based on Proteomic Data of Proteins for the rational selection of optimal protein purification sequences [1], as well as Mathematical Models that simulate and allow optimization of chromatographic protein purification processes. These systems consider more "generic" purification procedures such as ion-exchange, hydrophobic interaction (HIC) and gel filtration chromatography, but also affinity chromatography both using salt and pH gradients in the selection of chromatographic processes and in the mathematical modelling and simulation of chromatographic performance.

2. Methodology

The chosen methodology was implemented in a computer- based Expert System. Two algorithms were developed, the first algorithm was used to select the most efficient purification method to separate a protein from its contaminants based on the physicochemical properties of the protein product and the protein contaminants and the second algorithm was used to predict the number and concentration of contaminants after each separation as well as protein product purity. Once the type of chromatography is chosen, optimization of the operating conditions is essential. For this two different mathematical models have been used [2]. These were the Plate Model and the more fundamentally based Rate Model. Operational conditions and the peak fraction collection is selected using a cost function of the production process which considers yield, purity, concentration, and process time that are obtained from simulations. This analysis allows optimization of process conditions [3].

3. Results and discussion

The theory developed for ion-exchange, HIC chromatography and affinity separations will be analyzed in this presentation. This is a unique contribution that allows investigation of chromatographic protein purification in a holistic approach that includes ion-exchange, HIC, gel filtration and affinity separations [4, 5, 6]. The methodology and experimental data required to

carry out such optimization will be analyzed and shown. This analysis that considers a first principles approach to rational protein purification will be presented and discussed.

The first step consists of the selection of the optimal chromatographic sequence of operations (2-3, usually) based on the proteomic data of the protein product and the contaminants. The second step consists of detailed and accurate mathematical modelling and rigorous simulation using experimental data of each chromatographic step including parameter estimation, gradient elution, pH and flow rate. Procedures have been carried out at low and high protein concentrations such as those used in process oriented situations [3].

A mathematical function was built that includes parameters to optimize protein production as well as the effects of chromatography performance such as yield, purity, concentration and the time needed to accomplish the separation. Operational conditions in all Chromatographic processes can be selected using this model [3, 7]. This mathematical function was successfully used for the selection of the operational conditions as well as the fraction of the product to be collected (peak cutting).

Finally, the present interest in carrying out protein separation and purification in a continuous process will be analysed and discussed.

4. Conclusions

We have developed a method to select the optimal chromatographic sequence of operations for protein purification based on detailed proteomic data of the protein product and its contaminants. We have also developed accurate mathematical models for the simulation of the chromatographic steps. A detailed procedure was developed that includes all chromatographic parameters to optimize protein production performance including purity, yield, concentration and operational time. This is a holistic approach for rational protein purification [7].

References

[1] Asenjo, J.A. and Andrews, B.A. Is there a Rational Method to Purify Proteins? : From Expert Systems to Proteomics. J.of Molecular Recognition. 2004;17: 236-247.

[2] Asenjo, J.A. and Andrews, B.A. Protein Purification using Chromatography: Selection of Type, Modelling, and Optimization of Operating Conditions. J. of Molecular Recognition. 2009;22: 65-76.

[3] Orellana, C.A., Shene, C. and Asenjo, J.A. Mathematical Modelling of Elution Curves for a Protein Mixture in Ion Exchange Chromatography Applied to High Protein Concentration. Biotechnol. Bioeng., 2009;104: 572-581.

[4] Sandoval, G., Shene, C., Andrews, B.A. and Asenjo, J.A. Extension of the Selection of Protein Chromatography and the Rate Model to Affinity Chromatography. J. of Molecular Recognition, 2010;23: 609-617.

[5] Sandoval, G., Andrews, B. and Asenjo, J.A. Elution relationships to model affinity chromatography using a general rate model. J.of Molecular Recognition, 2012;25: 571-579.

[6] Mejía-Manzano, L.A., Sandoval, G, Lienqueo, M.E., Moisset, P., Rito-Palomares, M., Asenjo, J.A. Simulation of mono-PEGylated lysozyme separation in Heparin Affinity Chromatography using a General Rate Model. J. Chem. Technol. Biotechnol., 2018; 93: 1980-1987.

[7] Asenjo, J.A. and Andrews, B.A. The Rational Purification of Proteins: Proteomics, Expert Systems, Modelling, Process Conditions and Optimization. 18th International Biotechnology Symposium, Montreal, Canada, 12-17 August, 2018.

Optimal design of supply chains for carbon capture, storage, and utilisation

Federico d'Amore, Fabrizio Bezzo*

CAPE-Lab - Computer-Aided Process Engineering Laboratory, Department of Industrial Engineering, University of Padova, via Marzolo 9, 35131 Padova PD (Italy).

**Corresponding author: fabrizio.bezzo@unipd.it*

Highlights

- Optimisation of a European carbon capture, transport, and storage network
- Aspects of societal risk and social acceptance can be included in the model
- Mechanisms for costs share and cooperation can foster implementation
- Challenges for carbon capture and utilisation are critically discussed

1. Introduction

The global anthropogenic emissions of greenhouse gasses (GHGs) experienced an exponential increase compared to pre-industrial levels and, among these, CO_2 is the most abundant, with an overall emission that raised globally from 2 Gt/year in 1850 to over 35 Gt/year in 2010 [1]. Carbon capture and storage (CCS), and utilisation (CCUS) has been highlighted as one of the most promising options to decarbonise the energy sector, which still heavily relies on fossil fuel-fed facilities. When dealing with the strategic design of a European CCS infrastructure, it clearly emerges the necessity of employing quantitative mathematical tools to treat the combinatorial complexity of such large scale networks, in particular, mixed integer linear programming (MILP) for supply chain (SC) optimisation [2]. Addressing the problem of the design and optimisation of a CCS SC in the context of Europe, including the possibility to include carbon conversion and utilisation pathways, while considering uncertainty and consequent risk, aspects of societal risk and social acceptance from the public, along with the assessment of financial schemes for cooperation between stakeholders, are still major challenges for fostering an effective implementation of such a complex system.

2. Methods

The base case deterministic framework has been developed according to a MILP model that describes Europe in terms of emissions from large-stationary sources (i.e., coal and gas power plants). Regarding the capture facilities, either post-combustion, pre-combustion, or oxy-fuel combustion have been included as possible options, whereas both pipelines and ships have been described in techno-economic terms as potential transport means [3]. Then, a risk assessment has been incorporated within the modelling framework, accounting for the societal risk generated by a potential leakage in the transport system (quantified according to the seriousness of the hazard), coupled with the choice of installing risk mitigation options (e.g., concrete slabs, deep burying, marker tape, surveillance) [4]. The societal response to CCS have been further analysed through the concept of social acceptance, described through the amount of risk perceived by a population inhabiting within the region where an infrastructure is planned. The social response has been modelled as proportional to the project size, to the amount of population, and to the differential

behaviour of the different European countries [5]. Furthermore, a set of constraints has been employed to balance the spread of installation and operation costs between countries, with the aim of fostering economic costs share and cooperation policies between different players. Finally, the effect of some utilisation pathways have been assessed in terms of economic and environmental benefits.

3. Results and discussion

The CCS models were optimised using the GAMS CPLEX solver on a 32GB RAM computer. Results from the deterministic framework demonstrated the good European potential for carbon sequestration and gave some indications on the total cost for CO_2 capture, transport and sequestration. Capture costs were found to be the major contribution to total cost, while transport and sequestration costs were never higher than 10% of the investment required to set in motion and operate the whole network. The overall costs for a deterministic European CCS SC were estimated in the range of 27-38 €/t of CO_2. The societal risk-constrained optimisation demonstrated the possibility to design a safe transport infrastructure with minor additional costs. Indeed, mitigation actions never represented more than 11% of total cost for installing and operating the transport network. However, no feasible solution could be found for a carbon reduction target higher than 50%, because of the unacceptable level of societal risk. When maximising social acceptance from the public (through minimising risk perception of CCS), results led to a massive exploitation of offshore sequestration solutions with a (possibly unacceptable) a total costs of about 50.88 €/t of sequestered, i.e. +34% with respect to the economic optimum, due to a more complex network configuration characterised by high transport (+434%) and sequestration (+853%) costs. A multi-objective optimisation analysis, however, allowed identifying a possible intermediate solution between the two conflicting objectives (i.e., economics against acceptance), capable of limiting risk perception, without excessively compromising the economic performance of the network. Regarding the model including costs share mechanisms between European countries, results showed that the additional European investment for cooperation (max. +2.6% with respect to a non-cooperative network) should not constitute a barrier towards the installation and operation of such more effective network designs. Finally, a preliminary analysis on CCUS indicated that some CO_2 utilisation pathways for the production of chemicals (e.g., PPP, MeOH) can have a positive effect in decreasing costs of the overall supply chain.

4. Conclusions

In this work it has been developed a time-dependent, multi-echelon, spatially-explicit, large-scale, European digital optimisation tool, aiming at the strategic high-level definition of a CCS SC. These models will provide valuable insights into the optimal economic deployment of CCS technologies at a noteworthy scale that was never investigated before, and will be able to steer relevant research and policy into addressing correctly the problem of global warming through CCS.

References

[1] IPCC, Climate Change-Synthesis Report, Geneva, 2014.
[2] M. Bui, et al., Energy Environ. Sci. 11 (2018) 1062-1176.
[3] F. d'Amore, F. Bezzo, Int. J. Greenh. Gas Control 65 (2017) 99-116.
[4] F. d'Amore, P. Mocellin, C. Vianello, G. Maschio, F. Bezzo, Appl. Energy 223 (2018) 401-415.
[5] F. Karimi, A. Toikka, Int. J. Greenh. Gas Control 70 (2018) 193-201.

CO_2 Hydrogenation to Methanol Using Cu/ZSM-5 Extrudates in a Cold DBD Plasma.

Maxwell Quezada[1], Federico Azzolina-Jury[2], Isabelle Polaert[1], Alain Ledoux[1], Christian Fernandez[2]

1 Normandie Univ, UNIROUEN, INSA Rouen, LSPC, Laboratoire de Sécurité des Procédés Chimiques 76000 Rouen, France

2 Normandie Univ, ENSICAEN, UNICAEN, CNRS, LCS, Laboratoire de Catalyse et Spectrochimie, 14000 Caen, France

**Corresponding authors: Isabelle.polaert@insa-rouen.fr; Federico.azzolina-jury@ensicaen.fr*

Highlights

- Preparation and optimization of Cu-ZSM-5 and Cu-Al_2O_3 extrudates catalysts
- Complete characterization of porous extrudates catalysts
- DBD Plasma-assisted low temperature methanol production from CO_2 hydrogenation
- Efficiency comparison between plasma and conventional catalysis in the CH_3OH production

1. Introduction

Carbon dioxide is one of the main greenhouse gases (after water vapor) and also an abundant source of C1. CO_2 is a non-toxic, non-corrosive, nonflammable molecule [1] and very stable thermodynamically, requiring thus large amounts of energy for its dissociation. CO_2 is produced from almost all combustion processes causing an increase in the world average temperature. To prevent its release into the atmosphere, one of the existing technologies is the capture and storage of CO_2 in underground reservoirs [2], but this does not benefit from this potential carbon source. A more valuable technology could be the chemical recovery of this captured CO_2 by its valorization into hydrocarbons, more specifically its chemical transformation into methanol.

CO_2 hydrogenation to methanol is accompanied by the reverse water-gas-shift (RWGS) reaction, which produces CO. These reactions have been well studied in the literature and two main problems have been detected: the important amounts of energy required for breaking the CO_2 bonds, and catalysts needing fairly high temperatures for activating the CO_2 molecule, both situations favoring the undesired RWGS reaction.

To address these problems, we propose a new catalytic process using copper catalysts synthetized on various supports and used in a cold DBD plasma reactor. This original technique allows to work at atmospheric or under moderate pressure and favoring methanol production.

2. Methods

We have first developed our own catalyst Cu/NaZSM-5 and compared it to Cu/Al_2O_3. These catalysts are in the form of cylindrical extrudes of 5 mm x 3 mm, aiming to deliver results closer to

industrial exploitation. In the literature, little research has been done on the use of the sodium form of the ZSM-5 to produce methanol [3]. A green template-free process to synthesize NaZSM-5 is used in this work. All corresponding characterization analyses have been conducted for the supports (N_2 physisorption, pyridine adsorption and XRD) and for the catalysts as well (N_2 physisorption, pyridine adsorption, H_2 chemisorption, CO adsorption, ICP, TPR and XRD).
Second, we have performed experiments using a non-thermal plasma reactor, which is able to activate the CO_2 molecule at room temperature and atmospheric pressure, increasing the CO_2 dissociation rate in gas phase and the methanol yield over catalysts. All experiments were performed with a molar ratio of H_2/CO_2 = 3 using argon as a vector gas to increase the dissociation rate of CO_2, inside of a dielectric barrier discharge reactor using Cu/Al_2O_3 and Cu/NaZSM-5 as catalysts, in parallel with a classic fixed-bed configuration in order to compare their catalytic performances in terms of methanol production.

3. Results and conclusions

Catalysts extrudates were successfully prepared, and their preparation was optimized. It was observed that there is an ideal range for the HNO_3/boehmite molar ratio (between 19 and 37) where reducibility and dispersion of the copper present on the catalyst were improved when compared to the acid-free catalysts. Also, the addition of HNO_3 improves the strength of the Lewis' acidic sites at temperatures higher than 200 °C, which are the usual reaction temperatures for the conventional fixed bed reactors.

First results have been obtained showing that methanol is produced when using both Cu/Al_2O_3 and Cu/ZSM-5 catalysts under cold DBD plasma at atmospheric pressure. The plasma assisted catalytic tests were evidenced to be more efficient than the conventional ones and a clear improvement was observed in terms of methanol yield and CO_2 conversion. A schema of the reactor is shown below:

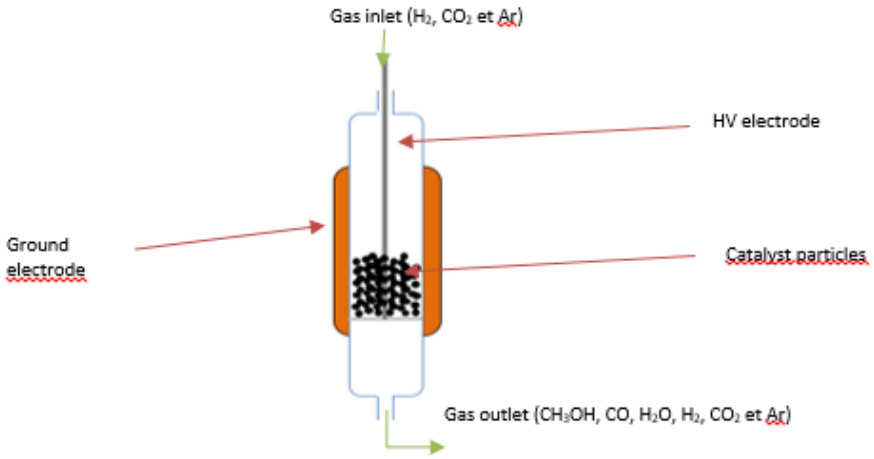

Figure 1. Cold plasma DBD reactor used for CO_2 hydrogenation into methanol.

References

[1] S. G. Jadhav, P. D. Vaidya, B. M. Bhanage, and J. B. Joshi, Chem. Eng. Res. Des., 92, 11, 2557–2567, 2014.
[2] M. Ha-Duong, M. Gaultier, and B. de Guillebon, Energy Procedia, 4, 6263–6272, 2011.
[3] C. Sriakkarin, W. Umchoo, W. Donphai, Y. Poo-arporn, and M. Chareonpanich, Catal. Today, 314,114-121, 2018.

Climate change mitigation: A techno-economic assessment of the formic acid production by electrochemical reduction of CO_2

Marta Rumayor*, Antonio Dominguez-Ramos, Angel Irabien

University of Cantabria, Department of Chemical and Biomolecular Engineering,

Av. Los Castros s/n, Santander, Spain

**Corresponding author: marta.rumayor@unican.es*

Highlights

- Formic acid production by electro-reduction of CO_2 was techno-economically assessed.
- The conventional fabrication process was used as a benchmark.
- Several sensitivity analyses evaluated the profitability of the CO_2 utilization plant.
- Results showed the benefits of the electrification of the chemical industry with FA.

1. Introduction

Turning the European Union (EU) into a resource-efficient, green, and competitive low-carbon economy is the key priority to meet the EU long-term goals by 2050 against climate change. The efforts require cutting-edge technological innovations to reduce our traditional fossil-dependent processes in order to curb the greenhouse gas emissions and the current consumption of natural resources in an economic way. This paper presents a techno-economical and resource saving assessment of an alternative based on the carbon dioxide (CO_2) utilization for the production of formic acid (FA) by electrochemical reduction (ER). The economic feasibility analysis of the plant includes the calculation of key performance indicators (KPIs) as the net present value (NPV) and the benefit/cost ratio (B/C). Several sensitivity analyses will evaluate the profitability of the CO_2 utilization plant for the production of FA by CO_2 ER. The study can help at pushing further the necessary developments towards a successful implementation of the CO_2 ER technology for the production of FA on a large scale.

2. Methods

A mathematical model built by the authors in a previous work [1] is used in the present study to obtain the life cycle inventory (LCI) of a hypothetical ER of CO_2 plan that produces 12,000 ton of FA per year. The system boundaries include the utilization plant itself (Figure 1) involving three main units: i) the ER of CO_2 in the ER cell, ii) the distillation of the azeotropic mixture FA/water to the desired purity (85% wt.), and iii) the compression of by-products H_2 and O_2 to the liquid forms. The ER process is included in the model as a black box unit. It was modelled using three sets of parameters that create the corresponding three scenarios: (i) an ideal scenario that represents the

minimum consumption of electricity and maximum Faradaic Efficiency, FE (100%); (ii) a baseline scenario that uses the current performance parameters obtained within our research group of the authors [2]; and (iii) an optimistic scenario that assumes a long-lasting cathode lifetime (capable to decrease the impact that the consumable cost has in the total cost of production) which is expected in a medium-term term. The conventional route of FA production by hydrolysis of methyl formate is used as the benchmark. Costs involved in the process are estimated using a bottom-up approach [3]. The KPIs of capital (CAPEX), operational expenditures (OPEX), net present value (NPV) and the benefit/cost ratio (B/C) are used to evaluate the economic feasibility of the plant. The reference cost of production is calculated and compared with the current FA market price c.a. 650 €·ton^{-1}. Sensitivity analyses are completed to account for uncertainty in the main variables that influence the process performance and the impacts on techno-economic results.

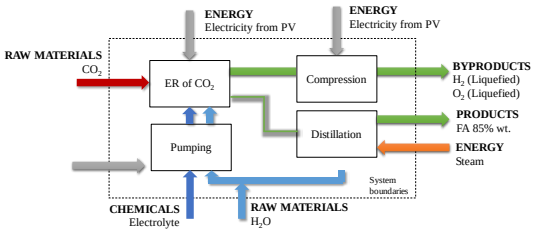

Figure 1. System boundaries

3. Results and discussion

The results display the specific techno-economic parameters such as the cathode lifetime, the CO_2 price, the price of electricity, the market price of FA as well as the break-even production of FA that will become the ER of CO_2 plant profitable while contributing to decreasing the CO_2 emissions and the resource depletion. It is demonstrated that under a CO_2 market price of 100 €·kg^{-1}, the break-even electricity market price could be between 23.5 €·MWh^{-1} and 29.9 €·MWh^{-1}; these values are in agreement with the perspective of the European levelised cost of electricity of large-scale PV electricity. The results obtained have shown that the electrification of the production plants of commodities, as FA, through renewables is needed for their future competitiveness.

4. Conclusions

This study has shown the potential of the ER of CO_2 route in the framework of climate change abatement objectives while contributing to a decrease of resources depletion. FA is shown here as an example of the benefits of the electrification of the chemical industry. The results obtained indicate that ER of CO_2 route could be profitable in a mid-term horizon under proper technological developments.

References

[1] M. Rumayor, A. Dominguez-Ramos, A. Irabien, Applied Sciences 8 (2018) 914.
[2] A. Del Castillo, M. Alvarez-Guerra, J. Solla-Gullón, A. Sáez, V. Montiel, A. Irabien, Journal of CO2 Utilization. 18 (2017) 222–228.
[3] G. Towler, R. Sinnott, Chemical Engineering Design, Principles, practice, and economics of plant design, 2013.

Enhancing palladium promotion of indium oxide for CO_2-based methanol production through synthetic control.

Matthias S. Frei[1], Cecilia Mondelli[1], Klara S. Kley[1], Begoña Puértolas[1], Rodrigo García-Muelas[2], Núria López[2], Olga V. Safonova[3], Joseph A. Stewart[4], Daniel Curulla Ferré[4] and Javier Pérez-Ramírez[1]*

1 ETH Zürich, 8093 Zürich, Switzerland; 2 Institute of Chemical Research of Catalonia (ICIQ), 43007 Tarragona, Spain; 3 Paul Scherrer Institute, 5232 Villigen, Switzerland; 4 Total Research & Technology Feluy, 7181 Seneffe, Belgium

**Corresponding author: jpr@chem.ethz.ch*

Highlights

- Controlled coprecipitation embeds Pd in the lattice leading to low-nuclearity clusters.
- The superiority of this Pd speciation is elucidated by theoretical and empirical methods.
- Record methanol productivity is sustained for 500 h.
- The benefits of nanoscale design for a sustainable large-scale process are demonstrated.

1. Introduction

Metal promotion is broadly applied to enhance the performance of heterogeneous catalysts to fulfil industrial requirements. Still, generating and quantifying the effect of the promoter speciation that exclusively introduces the desired property and ensures proximity to the active site and durability is very challenging. Recently, In_2O_3 was discovered as a highly selective and stable catalyst with the potential to realize green methanol production from CO_2 at a commercial scale [1]. Activity boosting with the H_2-splitter palladium led to partial success since Pd nanoparticles mediate the parasitic reverse water-gas shift (RWGS) reaction, reducing selectivity, and sinter or alloy with indium, limiting metal utilization and robustness. Herein we introduce a coprecipitation method leading to low-nuclearity Pd clusters anchored to the active site that curtail these limitations.

2. Methods

In_2O_3 and Pd(0.1-10 wt.%)-In_2O_3 catalysts were prepared by precipitation, and coprecipitation or dry impregnation, respectively, followed by calcination. They were characterized by inductively coupled plasma optical emission spectroscopy, N_2 sorption, X-ray diffraction, thermal techniques, electron microscopy, and X-ray photoelectron and absorption spectroscopy. CO_2 hydrogenation to methanol was conducted in a continuous-flow fixed-bed reactor setup at 473-653 K, 5 MPa, H_2/CO_2 = 1.8-5.7, and weight hourly space velocity = 24,000-48,000 $cm^3_{STP}\ h^{-1}\ g_{cat}^{-1}$. Pd speciation and reaction energetics were studied by Density Functional Theory (DFT).

3. Results and discussion

Pd-promoted In_2O_3 featuring palladium atomically dispersed in the oxide matrix was generated by coprecipitation and was benchmarked with dry impregnated systems comprising Pd clusters deposited onto the oxide. The first exhibited a stable activity enhancement compared to bulk In_2O_3

solely directed to methanol synthesis, while the second displayed a decaying improvement of both methanol and CO formation (**Figure 1**, left). Based on structural, spectroscopy, and microscopy (**Figure 1**, middle) analyses, Pd formed clusters of very low nuclearity attached to the lattice in the coprecipitated sample, whereas aggregated to form defined nanoparticles in the impregnated material. DFT calculations indicated that Pd atoms embedded into the oxide structure serve as effective anchoring sites for the noble metal atoms accommodated onto the surface hindering excessive agglomeration, which provides a molecular-level explanation to the profoundly diverse time-on-stream behaviors of the two catalysts. According to thermal characterization, theoretical simulations, and kinetic data, these Pd clusters do not significantly increase the number of active vacancies but impart an improved H_2-dissociation capability without enhancing the RWGS reaction (**Figure 1**, right), leading to a sustained record productivity (0.96 g_{MeOH}^{-1} h^{-1} g_{cat}^{-1} after 500 h on stream). In contrast, Pd nanoparticles supply activated hydrogen that fosters vacancy and methanol formation on In_2O_3 but also convert CO_2 into CO on their own surface.

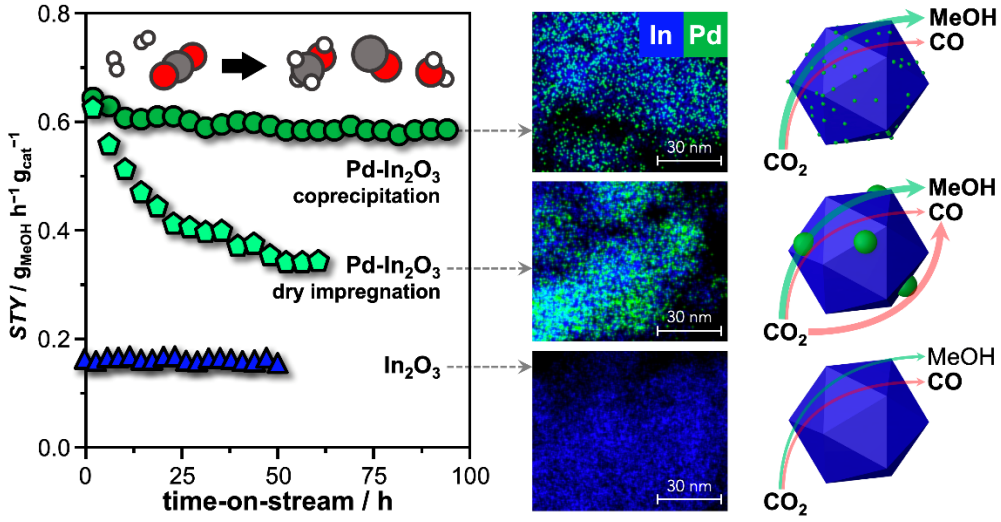

Figure 1. Methanol space time yield (*STY*) *versus* time-on stream over Pd(0.75 wt.%)-In_2O_3 catalysts and pure In_2O_3 during CO_2 hydrogenation at 553 K, 5 MPa, and H_2/CO_2 = 4 (left). EDX maps of In and Pd (middle) and representation of the distinct promotional effect of Pd (right) for the same catalysts after equilibration.

4. Conclusions

Controlled coprecipitation enables a fine tuning of the Pd speciation, generating small Pd clusters strongly bound to the oxide that offer a highly effective use of the noble metal and are robust, granting a sustained unparalleled methanol productivity. This permits to operate the catalyst at reduced temperature, with hydrogen-lean feeds, and in the presence of greater amounts of water, implying strong economic and ecologic benefits for a perspective CO_2-based methanol synthesis process.

Reference

[1] Martin, O., Martín, A.J., Mondelli, C., Mitchell, S., Segawa, T.F., Hauert, R., Drouilly, C., Curulla-Ferré, D., and Pérez-Ramírez, J. Angew. Chem., Int. Ed. 55 (2016) 6261–6265.

Sorption enhanced dimethyl ether synthesis for high carbon efficiencies

Jasper van Kampen[1,2], Jurriaan Boon[1,2], Jaap Vente[1], Martin van Sint Annaland[2]

1 Sustainable Process Technology, ECN/TNO, Petten, The Netherlands;
2 Chemical Process Intensification, TU/e, Eindhoven, The Netherlands

**Corresponding author: jasper.vankampen@tno.nl*

Highlights

- SEDMES: direct synthesis of DME from syngas and CO_2 by in situ H_2O adsorption.
- The dynamic cycle model adequately describes the SEDMES experimental results.
- The working capacity can be tuned by the adsorption and regeneration conditions.
- Cyclic stability confirmed for more than 100 cycles.

1. Introduction

Utilisation of CO_2 is expected to play a crucial role to enable sustainable industrial production of carbon-based products, the large-scale storage and transport of renewable energy, and the production of renewable fuels. An important criterion for the value chain for converting the available CO_2, e.g. from biogenic origin, is a high carbon efficiency [1]. Very high carbon efficiencies have indeed been demonstrated for the conversion of synthesis gas and CO_2 to DME (clean alternative fuel and platform chemical) by sorption enhanced DME synthesis (SEDMES) [2, 3], in which water is removed in situ by the use of a solid adsorbent. The concept is based on Le Chatelier's principle stating that reactant conversion to products in an equilibrium limited reaction is increased by selectively removing reaction products. Experimental proof-of-principle has shown increased DME yield, improved selectivity towards DME over methanol and reduced CO_2 content in the product [2, 4]. This contribution will present an elaborate model study on the cyclic SEDMES process, which is conducted in parallel to an experimental research line. The combination of theory and experiments in a fundamental way is crucial for a proper understanding of this type of process.

2. Methods

Both a 1D dynamic cycle model was developed and verified using Matlab, and transient experiments in a packed-bed reactor were performed for various stoichiometric feed compositions and inert N_2, Ar. Commercial copper/zinc oxide/alumina catalyst and commercial zeolite A steam adsorbent (mixed in different ratios) were used experimentally. Adsorption was conducted at 250-300 °C, 25-40 bar(a) and with different feed gas compositions. Regeneration was done by switching to dry gas, depressurisation and eventual heating to 400 °C. Analysis was done by a combination of mass spectrometry and GC.

3. Results and discussion

The results of a representative breakthrough experiment of sorption enhanced DME synthesis are shown in Figure 1. Pre-breakthrough of steam, DME and unconverted CO are the primary products. After steam breakthrough the concentration of DME drops, accompanied with the breakthrough of

CO_2 and methanol indicating saturation of the adsorbent. As can be seen in Figure 1 the dynamic cycle model, using reaction kinetics and a water adsorption isotherm from literature, adequately describes the experimental results. An elaborate model study, supported by experimental work, shows an operating window for the SEDMES process. For example, Figure 2 shows a process trade-off between carbon selectivity and productivity for various space velocities. The working capacity is a key parameter for optimizing the SEDMES process. Improving this capacity can be done by optimizing the reactive adsorption conditions, such as the space velocity, and by optimizing the inherent regeneration procedure.

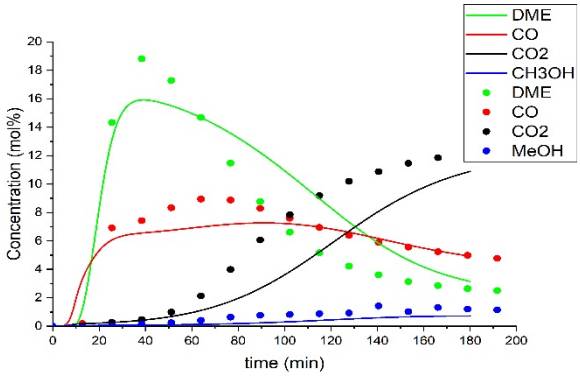

Figure 1. Breakthrough experiment (points) and model prediction (lines) at 40 bar(a), 275 °C, feed H_2:CO:CO_2 = 8:1:2 (regeneration to 400 °C)

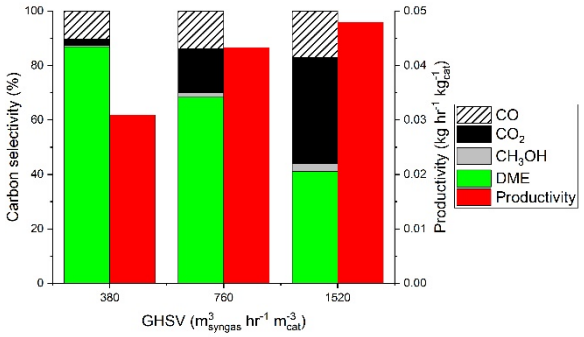

Figure 2. Model carbon selectivity vs. productivity for GHSV of 380, 760 and 1520 hr^{-1} at 30 bar(a), 275 °C, feed H_2:CO:CO_2 = 8:1:2 (regeneration to 400 °C).

In parallel to the dynamic SEDMES cycle model development, different commercial catalysts and steam adsorbents are tested and prove to be promising for further development of the process to industrial relevant conditions. Experimental campaigns, more than 100 cycles without observed degradation, support the model study indicating high carbon efficiency to DME and reduced CO_2 content in the product for a typical SEDMES operating window. The testing focuses on obtaining relevant data as input for validation and tuning of the SEDMES model, which in turn is used for the scale-up of the SEDMES process towards full cycle validation with continuous DME production.

4. Conclusions

The SEDMES process is a promising process intensification, easily achieving 70% single-pass DME carbon yield and minimal CO_2 by-product formation for a three reactor column system. This increased single-pass conversion requires less downstream separation, and smaller recycle streams especially for a CO_2-rich feed. Within EU Horizon 2020 project Fledged, further optimization of the SEDMES process is pursued by experimental and modelling studies.

Acknowledgement

This project has received funding from the European Union's Horizon 2020 research and innovation programme under grant agreement No 727600.

References

[1] SAPEA, Novel carbon capture and utilisation technologies: research and climate aspects, Berlin, 2018.
[2] J. Boon, F.P.F. van Berkel, H.A.J. van Dijk, J.F. Vente, 5th TMFB International Conference, Aachen, 2017.
[3] I. Iliuta, M.C. Iliuta, F. Larachi, Chem. Eng. Sci. 66 (2011) 2241–2251.
[4] J. van Kampen, J. Boon, F.P.F. van Berkel, H.A.J. van Dijk, J.F. Vente, M. van Sint Annaland, 25th International Symposium on Chemical Reaction Engineering, Florence, 2018.

Catalytic carbonation reaction coupled with pervaporation for the production of diethyl carbonate from ethanol and CO_2

Marie Décultot*, Alain Ledoux, Marie-Christine Fournier-Salaün, Lionel Estel

Normandie Univ, INSA Rouen, UNIROUEN, Laboratoire de Sécurité des Procédés Chimiques LSPC EA 4704, 76000 Rouen, France
**Corresponding author: marie.decultot@insa-rouen.fr*

Highlights

- Synthesis of DEC from ethanol and CO_2 is promising concerning the environmental aspect.
- This study highlights the use of pervaporation to dehydrate the reaction mixture.
- A circulation loop is used to remove continuously water molecules.

1. Introduction

Because of its low toxicity and high biodegradability, diethyl carbonate (DEC) has many potential applications like fuel additive, solvent or monomer. Nowadays it is produced mainly by phosgenation of ethanol, which uses toxic and harmful chemicals [1]. Several new synthesis are developing but the most interesting one concerning the environmental aspect and the sequestration of CO_2 is the carboxylation of ethanol with CO_2 represented in figure 1 [2]. However, yields obtained in the literature for this reaction are still low whatever the catalyst used because of the unfavourable thermodynamics of the reaction [3]. To improve this yield, we can move the equilibrium toward the formation of the diethyl carbonate by removing water molecules produced during the reaction. Our work is focused on the utilisation of a physical way to dehydrate: the pervaporation. This method, which uses a hydrophilic membrane to dehydrate the reaction mixture, is slightly studied in the literature [4].

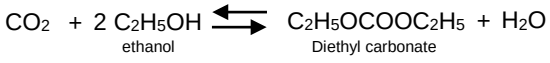

Figure 1. Ethanol carbonation with CO_2

2. Methods

A 100 mL batch reactor was used to study the reaction of carboxylation of ethanol with CO_2 with cerium oxide (CeO_2) as catalyst. A membrane cell with a membrane PERVAP 4100 purchased from DeltaMem were used to study the dehydration of the solution. The permeate side pressure is maintained at 2 mbar with a vacuum vane pump and the permeate is condensed in two cold traps immersed

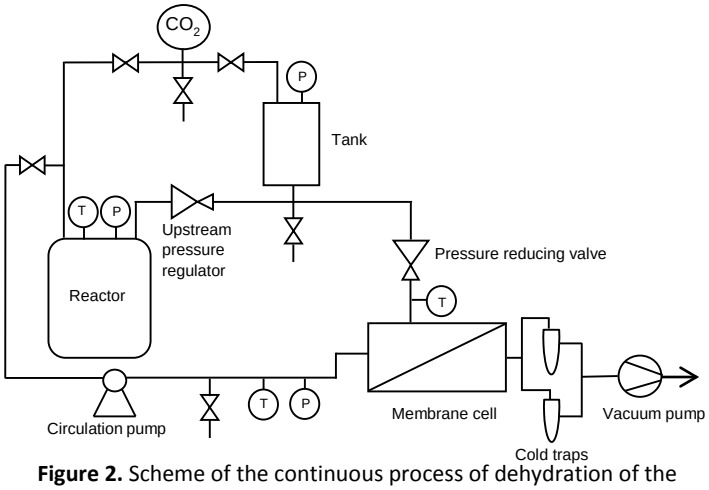

Figure 2. Scheme of the continuous process of dehydration of the reaction mixture of the carbonation of ethanol

in liquid nitrogen. The whole process used to study the dehydration of the reaction mixture in continuous is described in figure 2. As the reaction occurs at high pressure (between 20-50 bar), we used pressure reducing valves to ensure that the pressure on the membrane stays below 4 bar.

3. Results and discussion

A parametric study of the reaction was performed in the reactor to develop a kinetic model. Temperatures from 95 to 125 °C, pressures from 10 to 60 bar and different compositions of water or DEC were tested. The thermodynamic equilibrium was defined based on these experiments. Different mechanisms like Langmuir-Hinshelwood or Eley Rideal were used to develop the kinetic models. The dehydration on the membrane PERVAP 4100 of different solutions was performed. We studied the influence of temperature, pressure and composition in the retentate on the selectivities and fluxes of the membrane. Figure 3 represents an example of the results obtained on the influence of the temperature on the reaction (left) and on the dehydration of an ethanol-water solution (right).

We performed a parametric study on the whole process (figure 2) to optimize the parameters of the continuous dehydration. With this parametric study we can work with a larger range of composition because the amount of DEC is continuously increasing while the amount of water is decreasing. Results obtained are slightly different from the results obtained from the study of the two equipments separately because of the circulation loop. Indeed, temperature and pressure change all along the loop to respect the equipment characteristics and the volume of the solution in the reactor is lower because of the volume of solution in the loop.

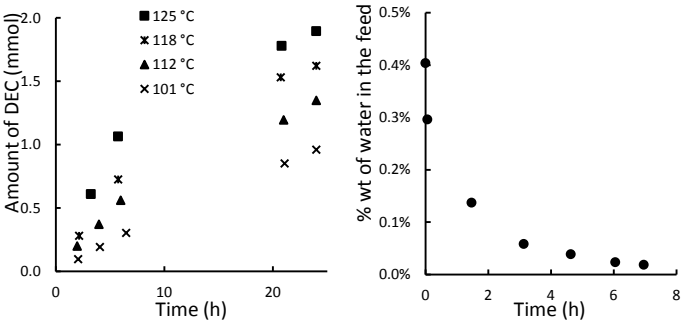

Figure 3. Left: production of DEC during reaction at different temperatures. Right: dehydration of 80 mL of an ethanol-water solution with 0.40% wt of water

4. Conclusions

This innovative work using pervaporation to dehydrate the reaction mixture of carboxylation of ethanol gives promising results. The circulation loop leads us to test the dehydration of the reaction mixture continuously. Temperatures, pressures and loop flow rate are the most important parameters to improve the performances and obtain better yields in DEC.

References

[1] K. Shukla, V.C. Srivastava, RSC Adv. 6 (2016) 32624–32645.

[2] J.G.M.-S. Monteiro, O. de Q.F. Araújo, J.L. de Medeiros, Clean Technol. Environ. Policy 11 (2009) 209–214.

[3] E. Leino, P. Mäki-Arvela, K. Eränen, M. Tenho, D.Y. Murzin, T. Salmi, J.-P. Mikkola, Chem. Eng. J. 176–177 (2011) 124–133.

[4] A. Dibenedetto, M. Aresta, A. Angelini, J. Ethiraj, B.M. Aresta, Chem. – Eur. J. 18 (2012) 10324–10334.

Maximising carbon efficiency through steam separation enhancement: carbon recycling into carbon monoxide, methane, methanol, DME

Jasper van Kampen[1], Jurriaan Boon[1]

1 ECN part of TNO, Westerduinweg 3, Petten, The Netherlands

**Corresponding author: jurriaan.boon@tno.nl*

Highlights

- Development of steam separation enhanced processes for utilisation of CO_2.
- Development of sorption-enhanced synthesis of CO, DME, and CH_4.
- Development of membrane-assisted methanol and DME.
- Steam separation enhancement key to maximising carbon efficiency CCU process.

1. Introduction

The capture and utilisation of CO_2 (CCU) presents important opportunities for industry in support of climate change objectives, circularity, the large-scale storage of renewable electricity, and emerging CO_2 capture processes [1]. While the relevant products in a CCU scheme can be rather conventional, such as carbon monoxide, methane, methanol, and DME – an optimised CCU value chain requires breakthrough innovation in (among others) the catalytic conversion steps involved in their production. Here, we propose the development and scale-up of steam separation enhanced processes for the utilisation of CO_2.

Conversion of CO_2 with H_2 involves the production of H_2O by-product, and reactions are generally equilibrium limited. By the principle of Le Chatelier, the in situ extraction of H_2O from the reaction mixture will result in a shift of the equilibrium to the product side and enhance the conversion [2]. Figure 1 shows the increase in product concentration for several reactions under representative conditions. Additionally, the reduction in steam partial pressure may improve catalyst performance.

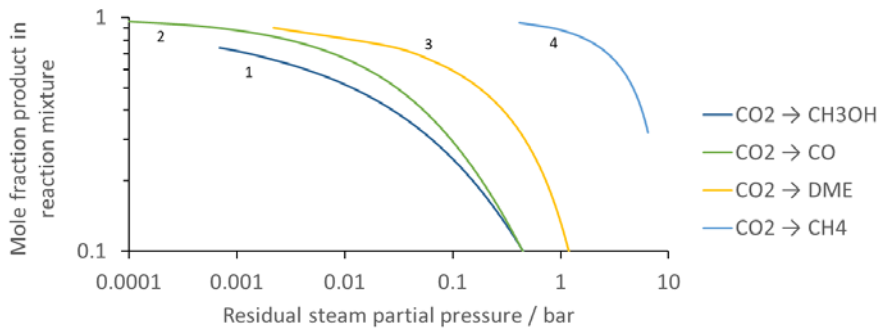

Figure 1. Molar fraction of product for stoichiometric H_2/CO_2 feed for the production of (1) methanol at 250 °C, 30 bar; (2) CO at 300 °C, 10 bar; (3) DME at 275 °C, 30 bar; (4) CH_4 at 300 °C, 10 bar.

Use of high-temperature steam adsorbents and steam permselective membranes will be shown to increase the carbon efficiency by intensification of the production of CO, CH_4, methanol, and DME.

2. Methods

CO, DME, and CH_4 have been produced in fixed bed temperature and pressure swing adsorption processes involving commercial catalysts and LTA zeolites. Methanol and DME are being investigated using ceramic-based membranes. In parallel, 1-D reactor models were developed in order to facilitate data interpretation, reactor design, and process scale-up.

3. Results and discussion

A combined approach of experimental scale-up and model development has been proven successful in the development and scale-up of steam separation enhanced processes. The processes mentioned above will be highlighted from the perspective of maximising the carbon efficiency of the CCU scheme. Exemplary results include (I) CH_4 synthesis by operating conventional methanation and sorption-enhanced methanation in series to allow for a remaining unconverted hydrogen concentration of < 0.1 mol% (Figure 2a), and (II) DME synthesis with an increased single-pass conversion and reduced CO2 content in the product for all syngas compositions and especially for H_2/CO_2 feed (Figure 2b).

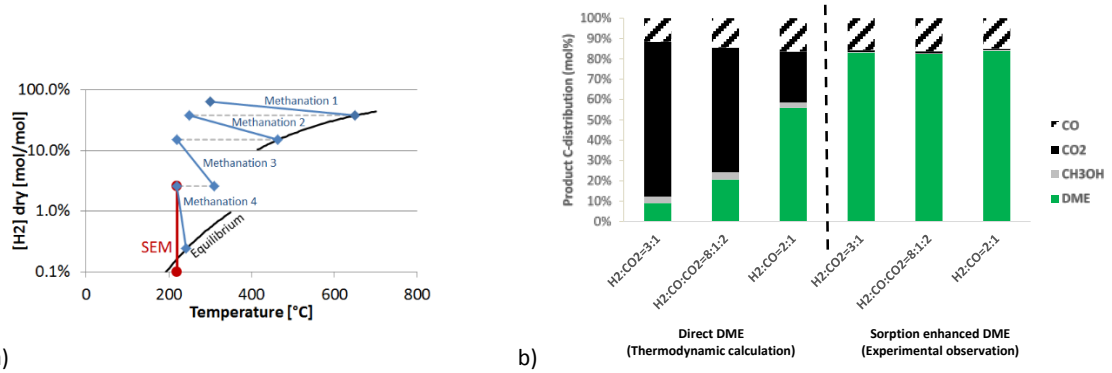

Figure 2. (a) 3 methanation reactors supplemented by sorption-enhanced methanation reach the unconverted H_2 specification of < 0.1 mol% (b) experimentally obtained increase in carbon selectivity to DME in sorption-enhanced DME synthesis relative to thermodynamic equilibrium for three different stoichiometric feed compositions at 275 °C, 40 bar.

It will be shown that crucial aspects in general for reactive steam permeation are the hydrothermal stability of the membranes and their permselectivity, whereas high temperature working capacities and heat management are crucial aspects for reactive steam adsorption. The peculiarities of the highlighted processes will however also demonstrate more specific learnings by, and necessity of, a strong interaction between experimental scale-up and reactor modelling.

4. Conclusions

Steam separation enhanced processes production of CO, CH_4, methanol, and DME have been demonstrated to improve the conversion and the carbon efficiency in the context of CCU.

References

[1] Schlögl, R., et al. (2018). Novel carbon capture and utilisation technologies: Research and climate aspects. SAPEA, Berlin. DOI: 10.26356/CARBONCAPTURE

[2] Van Kampen, J., et al. (2019). Steam separation enhanced reactions: Review and outlook. *To be submitted*.

Electric Steam Reforming – Reduction of CO_2-Emissions by Integration of Renewable Energy into the Steam Reformer

Peter Mølgaard Mortensen, Kasper Emil Larsen, Charlotte Stub Nielsen, Kim Aasberg-Petersen*

Haldor Topsøe A/S, Haldor Topsøes Allé 1, DK-2800 Lyngby, Denmark

**Corresponding author: kap@topsoe.com*

Highlights

- Electrically driven steam reformer
- Significant reduction of CO_2-emissions
- Highly compact

Through the last 20 years, a continuously increasing focus has been on how to limit the human impact on pollution, where especially CO_2-emission has been linked to a global impact on the climate. In parallel, sustainable electricity has made a significant technology leap and sustainable electricity production by wind and sun has become economically feasible. This development is an encouragement to rethink already existing technologies used in the chemical industry.

Many bulk chemicals, including for example methanol, acetic acid, and ammonia, are today produced in a process with multiple steps. Often the first step is steam reforming of natural gas to produce hydrogen or synthesis gas (a mixture with mainly hydrogen and carbon monoxide) followed by the actual synthesis and purification. A key process to produce synthesis gas is steam methane reforming (SMR). This is a strongly endothermic process requiring considerable fuel combustion to reach the desired exit temperature and methane conversion. According to some sources, SMR may account for nearly 3% of global CO_2 emissions. Hence, there is a considerable incentive to modify the technology to reduce the climate impact.

Several initiatives have improved the efficiency in synthesis gas based chemical plants in recent years. These include the use of bayonet type steam reformers, heat exchange reformers, and the use of electrically driven utilities. All of these improve the efficiency thus reducing the CO_2-emissions. However, the extensive use of fuel combustion for the SMR remains. This work presents a novel approach by which electricity is integrated into the steam reformer almost eliminating the need for fuel combustion.

The development of a compact electrically heated steam reformer integrating electricity into the catalyst will be described. Proof of concept experiments will be presented along with CFD and reactor analysis to demonstrate the performance of the technology.

Process development studies have been carried out in parallel to the experimental activities. These studies have been performed for production of hydrogen and carbon monoxide and for various

chemicals. Both natural gas and bio-derived feedstock have been considered. As an example, for a hydrogen plant the electric reformer offers a solution which:

- Uses up to 35% less natural gas compared to a tubular reformer.
- Has up 95% less CO_2 emissions compared to a tubular reformer based hydrogen plant.
- Is significantly more compact in size.

An economical analysis indicates that the electric reformer could be cost competitive to the more classical routes for chemicals production. The actual transition for when the electric reformer would be cheaper than the more traditional fired steam reformer depends on the prices of electricity and feedstock. The use of electricity is in most case more than 70% lower compared to alkaline electrolysis.

The presentation will describe the development of the electric reformer with selected experimental results. The potential of replacing the fired steam reformer with an electric steam reformer will be presented based on process economical calculations in comparison with state of the art technologies. Finally, the perspectives of the new technology as a means to reduce human climate impact will be discussed.

Scenario analysis of carbon capture, utilization (particularly producing methane and methanol) and storage (CCUS) systems

Grazia Leonzio[1], David Bogle[2], Edwin Zondervan[3], Pier Ugo Foscolo[1]

1Department of Industrial and Information Engineering and Economics, University of L'Aquila, L'Aquila, Italy; 2 Centre for Process Systems Engineering, Department of Chemical Engineering, University College London, London, UK; 3 Laboratory of Process Systems Engineering, Department of Production Engineering, Universität Bremen, Bremen, Germany

**Corresponding author: grazia.leonzio@graduate.univaq.it*

Highlights

- Exploring new proposed model for the carbon capture utilization and storage supply chain.
- Optimal layouts for carbon supply chains in Germany and Italy
- Product revenues and incentives strongly influence the supply chain design.

1. Introduction

A carbon dioxide economy has been proposed, characterized by the use of renewable energies as the basis for a circular economy. Atmospheric carbon dioxide reduction can be achieved by storage or by utilization: through production of methanol, methane and a range of other products [1]. Leonzio et al. [2, 3] developed a CCUS supply chain model including options of storage and utilization. The model has been developed for Germany including methanol, concrete, wheat, lignin, polyurethane, calcium carbonate, urea and also for Italy where methane is produced. In paper we evaluated the effects of a carbon tax, economic incentives and revenue on the system outputs of supply chains in Germany and Italy.

2. Methods

The mathematical model was used to determine optimal volumes of captured CO_2 and products [2, 3] and CO_2 sources they should be taken from. The objective function is the sum of total costs less the revenues, carbon tax and economic incentives. The mixed integer linear programming models are solved in AIMMS software.

3. Results and discussion

A local sensitivity analysis was carried out for the CCUS supply chain in Italy considering three levels of carbon tax (20 euro/ton, 40 euro/ton and 80 euro/ton) and economic incentives (240 euro/MWh, 270 euro/MWh and 300 euro/MWh). The minimum target for CO_2 reduction is 77 Mton/year; CO2 that is not captured is released into the atmosphere. Results (Table 1) show that system source locations change with tax rates and economic incentives. Also the total value and methane production are affected: at low, average and high level of these parameters the total values are respectively 12.8 billion euro/year, -2.43 billion euro/year and -70.7 billion euro/year, while methane production is 22.5 Mton/year, 22.5 Mton/year and 101.8 Mton/year. For high values

of tax and economic incentives at optimal profit all possible CO_2 is captured and sent to the utilization section. Results for changing only carbon tax show that only the total value is affected, while system topology (CO_2 source locations) and methane production are constant.

Carbon tax/ Economic incentives	To utilization (methane production)						To storage		
	Low values		Average values			High values	Low values	Average values	High values
CO_2 source	Puglia	Sicily	Sicily	Veneto	Sardinia	All regions	Lombardy	Lombardy	-
Capture technology	MEA	MEA	MEA	MEA	MEA	MEA	PSA	MEA	-
CO_2 captured (Mton/year)	61.8	0.024	37.4	20.3	4.17	279	15.2	15.2	-

Table 1. Results of sensitivity analysis for CCUS supply chain in Italy with Malossa San Bartolomeo as storage site

Similar results are found for the CCUS supply chain producing only methanol in Germany (Table 2). The minimum target for CO_2 reduction is 160 Mton/year and CO_2 not captured is released into the atmosphere. The total value is 16.3 billion euro/year, -30 billion euro/year and -0.197 trillion euro/year respectively for the low, average and high level of the parameters, while methanol production is respectively 203 Mton/year, 968 Mton/year and 968 Mton/year. A sensitivity analysis was again performed: results show that when changing the price of methanol the total value is changed with system topology.

Carbon tax/ Economic incentives	To utilization (methanol production)			To storage		
	Low values	Average values	High values	Low values	Average value	High values
CO_2 source	Dusseldorf	All regions	All regions	Magdeburg	-	-
Capture technology	MEA	MEA	MEA	MEA	-	-
CO_2 captured (Mton/year)	140	665	665	20.3	-	-

Table 2. Results of sensitivity analysis for CCUS supply chain producing only methanol in Germany

For a CCUS supply chain producing different products in Germany it was found carbon tax and revenues lead to a full possible capture of CO_2 and all CO_2 is sent to utilization. For increased carbon tax only the total value is increased. Changing the sales prices of products according to market value causes predicted values for lignin and wheat production change.

4. Conclusions

For the cases studied in this work carbon tax affects only the total value while changing economic incentives and product revenues also changes the system topology. Model optimization is a useful decision support tool for CCUS investment decisions.

References

[1] J. Patricioa, A. Angelis-Dimakisb, A. Castillo-Castillo, Y. Kalmykovaa, L. Rosadoa, Region prioritization for the development of carbon capture and utilization technologies, Journal of CO2 Utilization 17 (2017) 50–59. [2] G. Leonzio, P.U. Foscolo, E. Zondervan, An outlook towards 2030: optimization and design of a CCUS supply chain in Germany. CCE (under review) [3] G. Leonzio, P.U. Foscolo, E. Zondervan, Under what conditions CCUS supply chain is feasible? The case of Italy, C.E.R.D., Under review.

VOC Removal by Absorption in Silicone Oil and Biological Regeneration of the Oil in A TPPB: Pilot Scale Trials

Margaux Lhuissier[1], Annabelle Couvert[1,*], Abdeltif Amrane[1], Abdoulaye Kane [2], Jean-Luc Audic[1]

1 Univ Rennes, Ecole Nationale Supérieure de Chimie de Rennes, CNRS, ISCR-UMR 6226, F-35000 Rennes, France

2 UniLaSalle-Ecole des Métiers de l'Environnement, Campus de Ker Lann, 35170 Rennes, France

**Corresponding author: annabelle.couvert@ensc-rennes.fr*

Highlights

- VOC of different hydrophobicities were correctly removed by absorption in PDMS
- PDMS regeneration in a pilot-scale TPPB in a continuous mode was efficient for the studied loads
- After several cycles of PDMS regeneration in the process, absorption performances were preserved

1. Introduction

Volatile Organic Compounds (VOC) have harmful effects on both environment, through their global warming contribution, and human health. Several kinds of treatments are possible to remove VOC from air, including adsorption, thermal and catalytic oxidations, absorption and biological processes such as biofilters. Adsorption and oxidation can be very expensive and energy-consuming technologies for large flow rates with low concentrations in VOC, whereas biological processes present low operating costs and are adapted to the treatment of large VOC flow rates at low concentrations; but these latter are mainly suitable for water-soluble compounds removal [1]. For hydrophobic VOC, absorption in a non-aqueous phase (NAP) is possible [2]. Nevertheless, this NAP must be regenerated to reduce the operating cost of the installation. Regeneration methods, such as classic distillation or stripping at high temperature and low pressure can be applied, but they are energy-consuming. Performing a biological regeneration in a Two-Phase Partitioning Bioreactor (TPPB), a multiphasic bioreactor containing microorganisms able to degrade the absorbed VOC [3] would be much cheaper and more eco-friendly. The process studied in this work consists of the combination of VOC absorption in a packed column and biological regeneration of the liquid absorbent (NAP) followed by a separation device insuring a good separation between water, oil and sludge. Th**rough** an industrial partnership, the combined process was tested on a realistic application for the treatment of ~~a~~ complex mixture of different VOC at varying inlet concentrations.

2. Methods

The inlet gas consisted of a mixture of molecules of different chemical natures: alkanes, esters, alcohols, ketones and monoaromatic compounds. The NAP used was silicone oil,

(Polydimethylsiloxane, PDMS), having a viscosity of 20 mPa.s. The pilot unit included a column (diameter 0.15 m, height 1.3 m) packed with a random packing (IMTP), a bioreactor loaded with waste water plant activated sludge (total volume of 1.25 m^3, with 25% v/v of PDMS), a conical settler and a centrifuge (16,000 rpm). The total VOC concentration was measured at the inlet and the outlet of the column owing to a PID (Photo-Ionization Detector, IonScience). The overall pilot unit ran 8 hours a day and 4 days a week.

3. Results and discussion

Figure 1 shows the inlet (red squares) and outlet (blue diamonds) total VOC concentrations of the packed column during 160h of operation. Even if the inlet concentration varied between 5 and 450 mg.m-3 in total carbon (TC) with an average of 150 mg.m-3 TC, the outlet concentration stayed most of the time below 50 mg.m-3 TC, showing the performance of the process. After more than 150h of use, given that the total residence time of PDMS (both for absorption and regeneration) is about 15h, PDMS was biologically regenerated 10 times in the process. Looking at steady VOC removal performances, the studied process was efficient for PDMS biological regeneration. Further trials will be investigated in order to know if each VOC is well degraded and operating parameters will be optimized to improve the VOC removal yields.

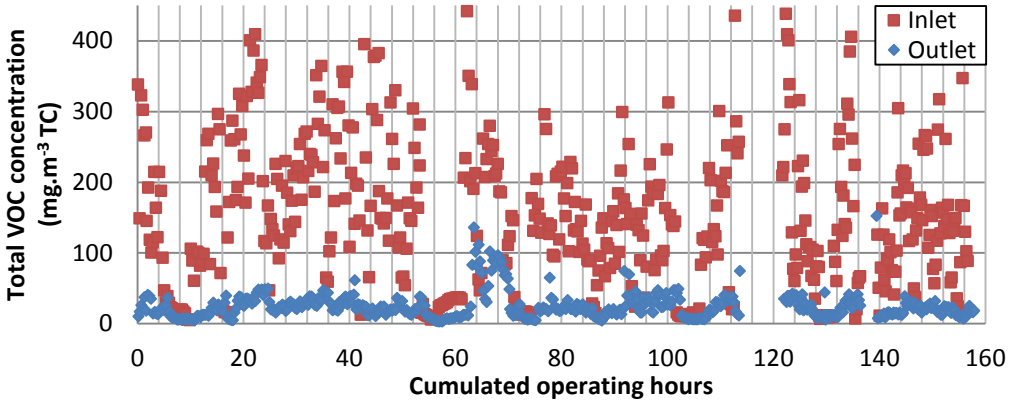

Figure 1. Total VOC concentration at the inlet and the outlet of packed column

4. Conclusions

The combination of VOC absorption in a packed column and PDMS regeneration in a TPPB showed that the early results are satisfactory towards VOC removal. Absorption performances were preserved after several cycles of PDMS regeneration and proved that biological regeneration is suitable to recycle NAP.

References

[1] P. Le Cloirec, *Techniques de l'Ingénieur*, vol. G1, n° 835, p. 1‑10, 2004.

[2] F. Heymes, P. Manno-Demoustier, F. Charbit, J. L. Fanlo, et P. Moulin, *Chemical Engineering Journal*, vol. 115, n° 3, p. 225‑231, janv. 2006.

[3] M. Guillerm, A. Couvert, A. Amrane, E. Norrant, A. Breton, et É. Dumont, *Chinese Journal of Chemical Engineering*, 2017.

Anaerobic Co-Digestion of Industrial Wastewater with Municipal Sludge.

Maggie Chetty[1], Jeremiah Adedeji[2]

[1,2] *Department of Chemical Engineering, Durban University of Technology, Steve Biko Campus, Durban , South Africa*

**Corresponding author: chettym@dut.ac.za*

Highlights

- AcoD of sewage sludge and industrial wastewater increase biomethane yield.
- COD reduction for both sludge and wastewaters was observed.

1. Introduction

The depletion and environmental impact of conventional fuel in form of greenhouse gases has led to the systemic shift on its dependence for generation of energy into alternative means known as renewable energy. In contrast, food industries are said to utilize large volumes of water daily in their production processes which in turn leads to increase wastewater generation [1]. The characteristics of these wastewater make them a potential source for generation of renewable energy when appropriate technology is applied [2].

This study is geared towards the use of industrial wastewater as co-substrate for digestion of sewage sludge (SS) while optimizing the process parameters to maximize biomethane production and minimize organic pollutants.

2. Methods

Anaerobic co-digestion (AcoD) techniques were employed in this study. The substrates considered were municipal SS, sugar wastewater (SW) and dairy wastewater (DW), while anaerobic digested sludge from the municipal treatment plant was used as the inoculum. Characterization of the substrates were done following the standard procedure for wastewater by APHA [3] for total solid (TS), volatile solid (VS), chemical oxygen demand (COD), mineral nutrients and volatile fatty acids (VFAs) in duplicate.

In order to achieve a good dilution, the ratio of wastewater to sludge used was 3:2 base on volume while the inoculum to substrate (ISR) ratios were varied at 1:2, 1:1 and 2:1. The digestion process was run at 25 and 35^{o}C and as semi-batch so as to accommodate for weekly analysis of the digestion assays for pH, solids and COD.

Gas analyses were carried out every 2 – 3 days to determine the composition of the biogas produced using gas chromatography. Bioreactors with a working volume of 5L were used for the digestion process. Two sets of bioreactors contain varying organic loading were set up in duplicate with a control.

3. Results and discussion

Characterization result indicate that the industrial wastewaters have high COD, VS and substantial minerals for improve microbial activity. The pH, VS, COD and ammonium content of SW were 6.30, 75.6 (%TS), 1778mgL^{-1}, 0.59 and 0.39, respectively while that of DW was 9.10, 86.4 (%TS), 3012.5mgL^{-1}, 0.38 and 0.71 respectively.

Figure 1 shows the preliminary yield of biomethane on a daily basis from each assay. The results reveal that the maximum production was obtained within the first 20 days of the digestion process and that the sugar wastewater has the highest methane content of 73% as compared to 70% for the dairy and 65% for sludge.

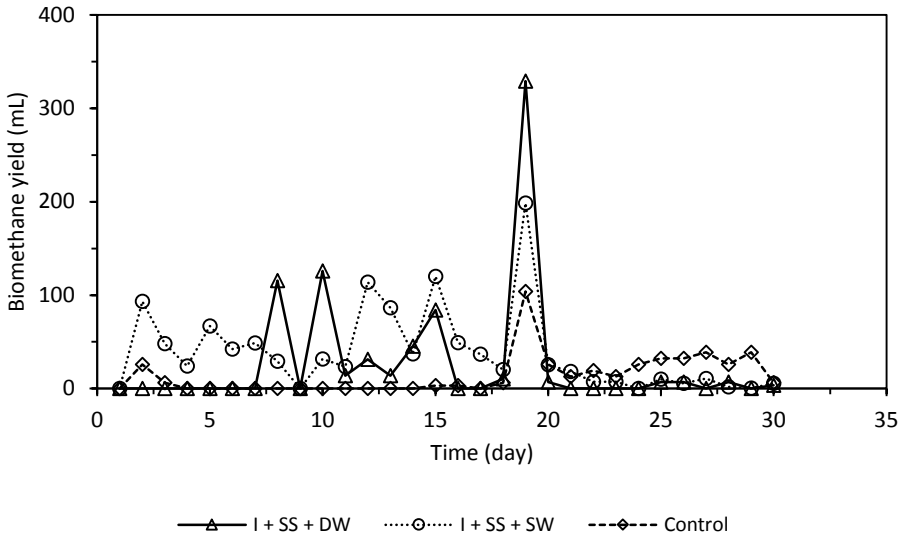

Figure 1. Daily biomethane yield at 35°C.

4. Conclusions

Preliminary analysis indicated that sugar wastewater co-digestion was more efficient for biomethane production as compared to dairy wastewater. Likewise, results show that co-digestion of sewage sludge helps in the reduction of VS and COD content. COD reduction was observed for both wastewaters and sewage sludge.

References

[1] Y.Y. Liu, R.J. Haynes, Origin, Nature, and Treatment of Effluents From Dairy and Meat Processing Factories and the Effects of Their Irrigation on the Quality of Agricultural Soils, Critical Reviews in Environmental Science and Technology 41 (2011) 1531-1599.

[2] J. Mata-Alvarez, J. Dosta, M.S. Romero-Güiza, X. Fonoll, M. Peces, S. Astals, A critical review on anaerobic co-digestion achievements between 2010 and 2013, Renewable and Sustainable Energy Reviews 36 (2014) 412-427.

[3] A.P.H.A. APHA, Water Environment Federation (APHA-AWWA-WEF). 2005, Standard Methods for the Examination of Water and Wastewater, 21st ed. Alexandria, Virginia: Water Environment Federation (2005).

Recovery of Phosphorus from Sewage Sludge and Subsequent Purification Using Reactive Extraction.

Zaheer Ahmed Shariff, Laurent Fraikin, Angélique Léonard, Andreas Pfennig

Department of Chemical Engineering, University of Liège, Belgium

**Corresponding author: za.shariff@uliege.be*

Highlights

- Development of new process for the recovery of phosphorus from partially or fully dried sludge
- Removal of heavy metals during purification by reactive extraction
- Solid-liquid equilibrium modelling in MATLAB for process optimization

1. Introduction

Phosphorous (P) is an essential element for life and has a limited availability in nature. Mineral P is mainly produced from phosphate rock, which was classified by the European Commission as a critical raw material in 2014. As a result, significant research has been directed towards finding economical ways of recycling P from waste streams which otherwise would be lost to landfills. The Phos4You (P4Y) project, funded under the Interreg North-West Europe Program, is aiming at improving the recovery potential of P from municipal wastewater and sludge, which could substitute for about 26% of mineral P demand in NWE.

In the framework of the P4Y project 6 different technologies for recycling of P will be demonstrated on pilot-plant scale. The university of Liège is developing one of the processes to be demonstrated which is called the PULSE (Phosphorus ULiège Sludge Extraction) process to recover P from fully or partially dried sewage sludge. The PULSE process is a modification of the PASCH process developed at RWTH Aachen to extract P from ashes obtained by incineration of sewage sludge [1]. Acidic extraction (leaching) of sludge or ashes is one of the most common method used for recovering P, however one big challenge is that the acidic leaching also results in dissolution of detrimental metals. Therefore, the removal of metals or purification of leach liquor is required before proceeding to the final step where final P products can be obtained either as salts of calcium or magnesium (struvite) by precipitation or as phosphoric acid.

2. Methods

At ULiège, the recovery of P from partially or fully dried sludge is carried out using acidic leaching. The process is optimized by systematic variation and combinations of different acids, pH, concentration of oxidizing agent, and drying levels. For the purification of the leach liquor, two approaches are tested using reactive extraction: extraction of metals from the leach liquor and extraction of P itself while leaving behind the metals in the aqueous phase. For this purpose, different extractants have been selected based on their extraction mechanism and tested for extraction efficiency. Further, different diluents were tested in order to find the best option in terms

of efficiency of extraction and toxicity, which are compared to at least one bio-diluent such as bio-diesel. Finally, depending on the extraction approach used above, the final product of the PULSE process can either be obtained as phosphate salt or phosphoric acid.

In the first part of the research, the experiments for determining the best process options for each of the unit operation of the PULSE process are conducted at lab-scale applying the cascaded option-tree methodology [2] for guiding through the process development. A solid-liquid equilibrium speciation model developed in MATLAB is used for optimizing process parameters for leaching, extraction, and precipitation.

3. Results and discussion

The leaching of P from dried sludge mainly depends on the pH of the leaching solution, while the type of acid used has little to no influence. The degree of drying and the drying temperature also affect the leaching of P. For the removal of metals, different extractant and combinations were tested. The extraction of metals strongly depends on the type of extraction mechanism, pH of the aqueous phase and also the metal complexes that exist in the aqueous phase. The code written in MATLAB simulates the pH and complexes existing at the corresponding pH. This information is further used to optimize the process conditions.

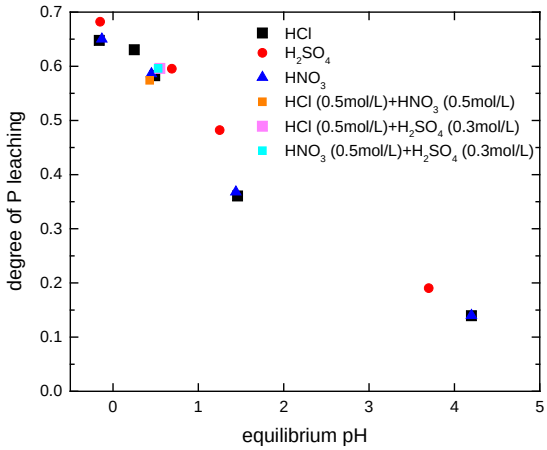

Figure 1. degree of P leaching from fully dried sludge with different acids

4. Conclusions

Drying results in ease of handling and storing of sludge, reduces the consumption of acid required for leaching and also filtration of solids after leaching is much easier. The leaching of P from undigested sewage sludge is optimal at a very low pH < 1. At this pH other metals and heavy metals are also leached, which have to be removed before producing the final P product. In the PULSE process metals are removed by using reactive extraction and finally salts of calcium phosphate are precipitated.

References

[1] Doetsch, P., Pinnekamp, J., Montag, D., Rath, W., Grömping, M., 2010. Rückgewinnung von Pflanzennährstoffen, insbesondere Phosphor aus der Asche von Klärschlamm. Institut für Siedlungswasserwirtschaft, RWTH Aachen, Aachen.

[2] Bednarz, A., Rüngeler, B., Pfennig, A., 2014. Use of Cascaded Option Trees in Chemical-Engineering Process Development. Chem. Ing. Tech. 86, 611-620.

Bioprocess development using municipal solid waste for the production of crude enzymes and fumaric acid in electrochemical bioreactor

Chrysanthi Pateraki[1,*], Eleni Derveni[1], Melissanthi Gkatzogia[1], Korneel Rabaey[2], Apostolis Koutinas[1]

1 Agricultural University of Athens, Iera Odos 75, Athens, Greece

2 Ghent University, Coupure Links 653, B-9000 Ghent, Belgium

**Corresponding author: paterakichr@aua.gr*

Highlights

- Municipal solid waste
- Biorefinery
- Fumaric acid production
- *Candida blankii*

1. Introduction

Valorisation of renewable resources is nowadays crucial for the production of bio-based products (chemicals, polymers and fuels) through fermentation. The biodegradable fraction of municipal solid waste (MSW) represents a potential low-cost feedstock for the production of bio-based products. Waste composition varies greatly across the world, depending on the level of socio-economic development. Bio-based fumaric acid production is mainly conducted with fungal fermentation on solid or liquid cultures. There are many challenges on fungal fermentations (like oxygen transfer, pellet generation etc) that could be faced by utilising yeasts. The aim of this work is the valorisation of biowaste fraction of MSW, for the production of fumaric acid. The sugar fraction was hydrolysed with crude enzymes that were previously produced by solid state fermentation using a fungus, *Aspergillus awamori*. The resulting hydrolysate was used as a nutrient supplement that contained assimilable sugars, free amino nitrogen (FAN) and inorganic phosphorus (IP). Bioconversion of sugars to fumaric acid was carried out using *Candida blankii*, a natural fumaric acid yeast strain. Fed-batch fermentations were conducted with the MSW hydrolysates in order to optimise the final fumaric acid production, yield and productivity. Separation of fumaric acid and electrocatalytic conversion of fumaric acid to succinic acid was achieved with membrane electrolysis, a novel electrochemical extraction technique in which electrodes are present in the fermentation broth to drive (bio)electrochemical reactions while utilising the electro-motive force to transport charged acid salts from a cathode across an anion exchange membrane (AEM or CEM) into a low volume, acidic anode solution.

2. Methods

The organic fraction of municipal solid waste (OFMSW) contained food waste and yard waste from selected households. Solid state fermentations were carried out with the fungal strain *Aspergillus awamori* at different initial moisture contents (50, 55, 60, 65 and 70%). OFMSW hydrolysates were

produced by mixing varying quantities of OFMSW with the enzyme-rich suspension. OFMSW hydrolysis was conducted at 55 °C with 100 g/L final solid concentration. Value added products were extracted from the raw material using hexane for lipid fraction, ultrafiltration with 3 kDa membrane for protein fraction and treatment with acidified ethanol for pectins. The remaining solids were hydrolysed utilising extracted crude enzyme consortia that were previously produced by solid state fermentation (SSF) using *A. awamori*. The hydrolysate was finally used as a substrate for fumaric acid production through microbial fermentation by *Candida blankii*. Fumaric acid was further converted to succinic acid in the fermented broth using an electrochemical bioreactor.

3. Results and discussion

OFMSW has been used as the sole substrate for the production of crude enzyme consortia via solid state fermentation of *Aspergillus awamori*. Glucoamylase, cellulase, cellobiase, invertase, phytase and protease enzyme activities were determined in order to select the optimal initial moisture content of 55%. Extraction of lipids, proteins and pectins was evaluated using untreated or enzymatically treated OFMSW and material balances were estimated in order to identify the optimal refining scheme. The OFMSW carbohydrates were enzymatically hydrolysed and the sugar-rich hydrolysate was used for fumaric acid production via fermentation with the yeast strain *Candida blankii*. Fumaric acid production exceeded 40 g/L and electrocatalysis was applied for its conversion and separation of succinic acid with a conversion yield of 80 %.

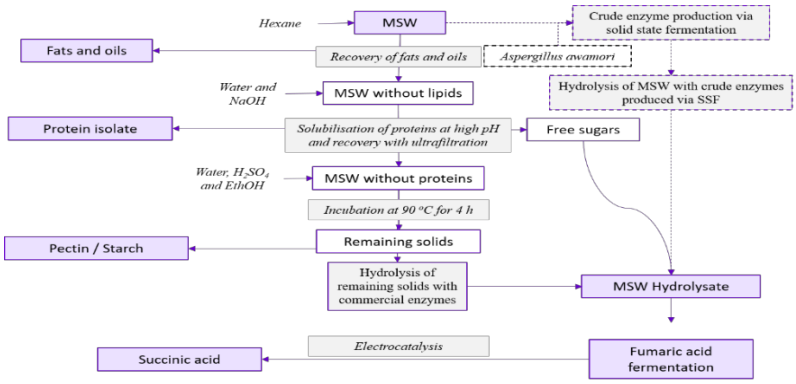

Figure 1. Biorefinery development of MSW

4. Conclusions

OFMSW was used for the production of crude enzyme consortia and fumaric acid. Value added co-products were recovered from OFMSW hydrolysate. Electrocatalytic conversion of fumaric acid to succinic acid was achieved via an electrochemical bioreactor.

Acknowledgments

Received funding by the Bio Based Industries Joint Undertaking under the European Union's Horizon 2020 research and innovation programme, grant agreement No 745828, entitled "Chemical building blocks from versatile MSW biorefinery" (Acronym: PERCAL).

Decentralized plastic waste recycling through pyrolysis – a feasibility study

Johan M. Ahlström[1], Ivar Petersson[1], Andreas Svensson[1], Simon Harvey[1], Stavros Papadokonstantakis[1*]

1 Chalmers University of Technology, 412 96 Gothenburg, Sweden

**Corresponding author: stavros.papadokonstantakis@chalmers.se*

Highlights

- Decentralized recycling of plastic waste.
- Process modeling and techno-economic assessment
- Pyrolysis of pure and mixed plastic fractions

1. Introduction

Plastic materials play a major role in society but pose certain challenges. Accumulation in nature has adverse effects on wildlife, and most plastics are currently produced from fossil resources which contradicts the demands on climate change mitigation stated by the UN. Today, a large part of plastic waste is incinerated or landfilled [1]. Legislators are raising the bar for recycling rates, with the EU setting a target of 50 % recycling of plastic packages by 2025 [2]. While mechanical recycling of plastics is efficient, it requires high feed purity and cannot be repeated indefinitely as the material degrades slightly over each cycle.

Meanwhile, thermo-chemical processes like pyrolysis and gasification can decompose plastics into their basic monomers, with lower requirements on feed purity. Pyrolysis of mixed plastics to obtain pyrolysis oil is well researched and companies are presently trying to commercialize the process [3, 4]. However, the potential for pyrolysis of pure plastic streams requires further research. Through pyrolysis, polymers like polystyrene (PS) and poly methyl methacrylate (PMMA) can be cracked into their monomers and repolymerized, allowing a less complex process design [5, 6]. The profitability of such a process will depend on how it is designed, as well as the scale of the plant.

The purpose of this study is to investigate the economic incentives for decentralized recycling of plastic waste, both in pure and mixed plastic fractions. There is a contradiction between achieving the economic benefits of a large process and transport associated costs relating to the corresponding geographical area from where the plastic feedstock is gathered. It is therefore of interest to investigate how a pyrolysis process can be designed to handle different types of plastic waste efficiently, and how large the plant would have to be to achieve economic feasibility. This study uses the Gothenburg region as a reference regarding waste flows, to assess the economic feasibility of implementing different pyrolysis-based processes.

2. Methodology

A literature study is conducted to estimate the quantity of plastics available in the region, and its composition with respect to different polymers. The mass and energy balance of the potential pyrolysis processes are attained through process modeling using process flow sheeting software

Aspen Plus. Knowledge of the product stream composition from different polymers are attained through published literature on experimental studies on pyrolysis of polymers. The most promising polymer feeds are chosen based on the availability of polymer and the benefit of pyrolyzing it separately, i.e. polymers that generate a product with a high share of valuable chemicals. The pyrolysis reactor mass and energy balance are calculated explicitly to mimic published results. Downstream process equipment required to separate and/or refine the products into saleable fractions are rigorously modelled.

The concept of constructing a flexible process which can use different pure plastic streams as well as mixed plastic streams is compared to processes handling a single type of plastic. Capital investment cost is estimated applying the Taylor method [7] as well as using the cost estimation tool in Aspen plus to get a larger span of the capital investment cost. Along with the feedstock and operational costs, the product revenue and economic performance is estimated for each process.

The economic performance depends on the recycling efficiency of the process. There is a tradeoff between product purity and capital costs; recovering more of the products and increasing purity generates more revenue but also requires more process steps and/or larger separation equipment. At a certain point, raising the recycling efficiency starts to have a negative impact on the overall economic performance. After optimizing the plant design, the size of the plant is varied to find the smallest size that is economically feasible, compared to the current waste handling system. The minimum size of the process is then compared to the size of available waste flows in the Gothenburg region, to assess the feasibility of implementation.

3. Results

Based on issues related to current waste treatment and potential value of the pyrolysis products, two types of pure plastic fractions have been identified as particularly interesting, Polystyrene for production of styrene and Polyvinylchloride (PVC) for production of HCl and alkanes or propene, depending on reactor temperature. These are compared to a mixed plastic fraction for production of ethylene.

References

[1] Plastics-the facts 2018: An analysis of European plastics production, demand and waste data. Available at https://www.plasticseurope.org/en/resources/publications/619-plastics-facts-2018.

[2] Council Directive (EU) 2018/852 of 30 May 2018 amending Directive 94/62/EC on packaging and packaging waste, art. 5.

[3] Lopez G, Artetxe M, Amutio M, Alvarez J, Bilbao J, Olazar M. Recent advances in the gasification of waste plastics. A critical overview. Renewable and Sustainable Energy Reviews, 82(September 2017):576–596, 2018.

[4] The RT7000 [Internet]. Swindon: Recycling Technologies; 2018 [Retrieved: 2019-02-13]. Available at: https://recyclingtechnologies.co.uk/technology/the-rt7000/.

[5] Achilias DS, Kanellopoulou I, Megalokonomos P, Antonakou E, Lappas AA. Chemical recycling of polystyrene by pyrolysis: Potential use of the liquid product for the reproduction of polymer. Macromolecular Materials and Engineering, 292(8):923–934, 2007.

[6] Kikuchi Y, Hirao M, Ookubo T, Sasaki A. Design of recycling system for poly(methyl methacrylate) (PMMA). Part 1: Recycling scenario analysis. International Journal of Life Cycle Assessment, 19(1):120–129, 2014.

[7] TAYLOR, J. H. The ‘process step scoring’method for making quick capital estimates. Engineering and Process Economics, 1977, 2.4: 259-267.

Design and Conception of a Membrane Pilot Plant for the In-Situ Treatment of Bioleaching Solutions.

Roland Haseneder[1], Arite Werner[2]

1 TU-Bergakademie Freiberg, Institute of Thermal-, Environmental-, and Recourses´ Process Engineering Leipziger Strasse 28, 09599 Freiberg, Germany; 2 Helmholtz Institute Freiberg for Resource Technology, Chemnitzer Str. 40, 09599 Freiberg, Germany

**Corresponding author: roland.haseneder@tun.tu-freiberg.de*

Highlights

- Enhancing of sustainability by a new ore extraction downstream method
- In-situ treatment of leaching solutions by selective membrane technology.
- Presentation of a Membrane pilot plant located at an underground mine site.

1. Introduction

Regarding the advancement of the industrialized world, the demand of strategic elements for the production of high tech products is rising steadily. Furthermore, the worldwide deposits of high-grade ores are going to be depleted within the next decades. The acceptance for new mining activities in the industrialized countries is very low. Consequently, there are two possibilities: First to enhance the processing of low-grade ores, overburden and waste material from former mining activities. Second to use new mining technologies which are more environmental friendly due to the combination of direct winning of solubilized product stream and in-situ down-stream-processing. Biohydrometallurgy is technically and economically employed for the treatment of ore material with depleted metal content as well as increasing complexity (1-3) which finally leads to a more sustainable technology of winning valuable metals.

A testing site for in-situ bioleaching was established in an underground mine to recover indium and germanium from a zinc sulfide ore vein. The downstream processing of the resulting pregnant leaching solution (PLS) is also realized as in-situ application by means of a membrane pilot plant, which was exclusively designed for this special application (4).

2. Methods

In-situ bioleaching is performed at the research and training underground mine ‘‘Reiche Zeche’’ of the Technical University Bergakademie Freiberg. The ore vein is embedded in gneiss as host rock and its main constituents are galena (PbS), sphalerite (ZnS), pyrite (FeS2), arsenopyrite (FeAsS) and chalcopyrite (CuFeS2). Indium is naturally enriched in sphalerite due to geochemical reasons (5).

The PLS is characterized by high concentrations of the main metal ions zinc, iron and copper. On the contrary indium and germanium are less concentrated by several orders of magnitude. The in-

situ bioleaching site has been extensively characterized by geoelectric and seismic measurements to determine the spatial dimension of the ore vein.

The nanofiltration (NF) experiments for the technical design of the membrane pilot plant were performed in cross-flow mode with flat-sheet membrane NF99HF (Alfa Laval) using a synthetic leaching solution (Zn, Fe, Cu, Cd, Pb, In, Ge) to guarantee experimental conditions which are close to the real application.

3. Results and discussion

When performing lab scale NF experiments in continuous cross-flow mode within a pH range between 2 and 8, the separating behavior of Zn, In and Cu is nearly identical and the retention rate is above 70 %. In contrast, germanium shows a significantly lower retention rate in the pH range under review. The high retention of In, Zn, Cu and Fe indicate a positive membrane charge due to electrostatic repulsion between the positively charged metal cations and the membrane charge (6).

Based on the experimental investigations of about 4 years, a membrane pilot plant including a microfiltration and NF stage was designed and constructed for the in-situ treatment of the PLS at the first level of the research mine (-147m). Regarding the extreme environmental conditions in terms of high humidity, the design and choice of construction material was of special concern. Furthermore, due to the compact design of the membrane pilot plant there is only little space required, which is especially suitable for underground mines.

4. Conclusions

Within the scope of current research an in-situ bioleaching testing site has been installed at the research and training mine Reiche Zeche of the Technical University Bergakademie Freiberg including an in-situ treatment of the PLS by using membrane technology. The bioleaching aims to win indium and germanium from a sulfidic ore vein. Lab-scale NF experiments in cross-flow mode showed that the leaching solution is successfully concentrated without a loss of separation performance. The membrane pilot plant was finally designed and constructed based on experimental results with the continuous cross-flow membrane unit.

By using membrane technology in the underground mine PLS is efficiently treated regarding pre-concentration of the valuable metal ions as well as reducing the total amount of process water.

References

[1] F. Anjum, M. Shahid, A. Akcil, Hydrometallurgy 117/118 (2012) 1 – 12.
[2] C. I. Brierley, J. A. Brierley, Appl. Microbiol. Biotechnol. 97 (2013) 7543 – 7552.
[3] A. Schippers, W. Sand, Appl. Environ. Microbiol. 65 (1) (1999) 319 – 321.
[4] A. Werner, R. Haseneder, J.-U. Repke, Chemie Ingenieur Technik 91 (2019) 1-7
[5] R. Schlueter, H. Mischo, in Proc. of 2015 SME Annual Meeting and Conference, Curran Associates Inc., Red Hook, NY (2015) 299.
[6] A. Werner et al., Chem.Bio.Eng. Reviews 5 (2018) 1-13

Optimization of Simultaneous Microwave-Ultrasound Assisted Extraction of Bioactive Compounds from Bark

Leyre Sillero[1]*, Raquel Prado[2], Jalel Labidi[1]

1 University of the Basque Country UPV/EHU, Department of Chemical and Environmental Engineering, Biorefinery Processes Research Group, Plaza Europa 1, 20018 Donostia-San Sebastian, Spain; 2 Imperial College London, Chemistry Department, Exhibition Road SW7 2AZ, London, UK

**Corresponding author: leyre.sillero@ehu.eus*

Highlights

- Pine bark was used as source for extraction of biomolecules.
- Potential use of simultaneous microwave-ultrasound assisted extraction (SMUAE) was demonstrated.
- Conditions for the optimum extractions were determined.

1. Introduction

Trees, which are constituted by wood and bark, are a very used natural source where bark is considered as waste. Taking into account that bark is about 9-15% of the total value of the tree [1] it could be consider as available cheap feedstock for biorefinery. Bark is a heterogeneous material and contain large number of bioactive compounds. These compounds could be applied in wide range of applications from bio-based material to pharmaceutical and chemicals.

The selection of an optimum extraction technique acquires a considerable importance due to the low amount of bioactive compounds present in tree barks. The most widely used technique is the solvent conventional extraction which require a huge amount of solvents, time and energy consumption. In order to improve the sustainability of the extraction process alternative extraction techniques are being investigated. Microwave assisted extraction (MAE) and ultrasound assisted (UAE) extraction are two of the most investigated options. They are considered as “Green techniques” because they permit the reduction of extraction time, volume of solvent and energy consumption leading to a higher extraction efficiency [2].

In this work, a simultaneous microwave-ultrasound assisted extraction (SMUAE) was studied and compared with the results obtained with a conventional extraction using pine bark (*Larix Decidua*). For that purpose, the optimization of the extraction yield was carried out varying the different parameters.

2. Methods

Larix Decidua bark was used with a particle size below 0.5 x 0.5 mm. The SMUAE was carried out in an ultrasound-microwave instrument (HIELSCHER UIP500hdT-MILESTONE flexiWAVE) using ethanol/water (50/50 (v/v)) mixture as solvent. Ten grams of dried bark were placed in a 500 mL borosilicate glass with a solid/liquid ratio of 1:10 (w/v). Before the extraction, the extracts were filtrated, and the yield of the extraction was calculated gravimetrically. The extraction yield was

studied changing different parameters values (reaction time (minutes), power of microwave (W) and power of ultrasound (W)).

3. Results and discussion

The preliminary results of SMUAE yield of pine (*Larix Decidua*) bark extracts are shown in a figure 1. The results of three different experiments are represented. The first experiment correspond to 5 minutes reaction, 300 W of microwave power and 100 W of ultrasound power, which match with the optimum point obtained by Luo for the extraction of phenolic compounds from walnut flour [3]. The second experiment correspond to the lower reaction time and the lower microwave and ultrasound power (1 min, 100 W and 50 W), and the third one corresponds to an intermediate between experiments 1 and 2 (5 minutes, 200 W for microwave and 100 W for ultrasound).

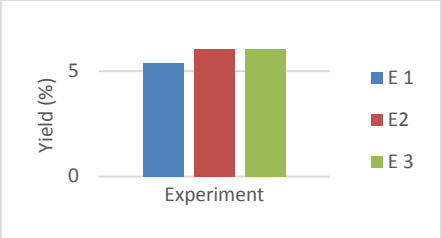

Figure 1. Extraction yield of the three experiments for the extraction of pine bark.

The highest extraction yield was obtained for the third experiment with a very close value to the obtained in the second experiment (6.06 % and 6.05 % respectively). The lowest value was obtained for the experiment with the highest power used in microwave and ultrasound with a value of 5.37%.

4. Conclusions

The lowest extraction yield could be explained by the degradation of the compounds due to the application of an excessive power. The comparison of the result of the first and third experiments confirm the possibility of that degradation. Further work is ongoing to optimize the extractions conditions.

References

[1] C. Leite, H. Pereira, Front. Mater. 3:63 (2017) 1–19.
[2] T. Belwal, S. M. Ezzat, L. Rastrelli, I. D. Bhatt, M. Daglia, Al. Baldi, H. P. Devkota, I. E. Orhan, J. K. Patra, G. Das, C. Anandharamakrishnan, L. Gomez-Gomez, S. F. Nabavi, S. M. Nabavi, A. G. Atanasov, Trac-Trend. Anal. Chem. 100 (2018) 82-102
[3] Y. Luo, W. Wu, D. Chen, Y. Lin, Y. Ma, C. Chen, S. Zhao, Pharm. Biol. 55 (2017) 1999-2004.

Microwave assisted synthesis of levulinic acid using organic acids as green catalysts

Kinana Aliko, Naomi Adjaklo, Bilaal Ahmed, Paul D Topham, Eirini Theodosiou

Aston Institute of Materials Research, School of Engineering and Applied Science, Aston University, B4 7ET Birmingham, UK

**Corresponding author: Alikok@aston.ac.uk*

Highlights

- Lignocellulosic biomass is a viable feedstock for the sustainable production of levulinic acid.
- Organic acids combined with microwave technology show great promise as a fast and environmentally friendly levulinic acid production route.
- Using maleic acid, in the presence of aluminium phosphate catalyst, can yield up to 45% levulinic acid from biomass waste.

1. Introduction

The chemical industry is moving away from petroleum-based products and focuses on the production and processing of 'green' chemical building blocks. Levulinic acid is amongst these 'platform chemicals' that can be developed in a sustainable way from bio-based sources. It acts as a precursor to a plethora of products, including pesticides, pharmaceuticals, solvents, cosmetics and food additives [1]. The global levulinic acid demand is predicted to reach 3,820 tonnes by 2020, which is a 30% increase since 2013, generating 19.65 million USD revenue.

Until now, the commonest commercial process to produce levulinic acid from agricultural residues depends mainly on a two-stage mineral acids catalysed reaction [1-3], which generates harmful environmental waste. The development, therefore, of a green catalyst for the above reaction remains key to the improved production of levulinic acid.

In this work, we detail the development of an environmentally friendly levulinic acid production route from very cheap and renewable feedstocks, such as barley straw, olive cake, beer waste, tomato peel, spent tea leaves and potato peel. Our process relies on the use of organic acids as catalyst substitutes for the mineral ones. These acids are less corrosive to the equipment, decrease the formation of humin (the major by-product of the reaction pathway) and can be degraded to nontoxic molecules [4, 5]. Our thermo-chemical method uses microwave heating, which compared to traditional heating methods, reduces reaction time and enhances the reaction rate.

2. Methods

Seven organic acids were employed in this study, namely: maleic; acetic; oxalic; malonic; tartaric; formic; and, citric. Dried samples of various biomass waste feedstocks were treated with each of these acids in the presence of different catalysts. The reactions were carried out in a laboratory microwave unit (CEM Discover S-Class, CEM Corporation, USA). The liquid phase was analysed by ^{1}H NMR to identify the composition of the reaction mixture, and HPLC to quantify the yield of levulinic

acid. Design-Expert Ver.11 was used for Response Surface Methodology (RSM) analysis, based on the following variables: temperature; time; biomass to acid ratio; amount of catalyst; and, acid concentration.

3. Results and discussion

Initial experiments using $AlCl_3$ as a catalyst, indicated that of all the acids tested, maleic acid produces the highest yield of levulinic acid (35.7%; see Fig. 1). RSM optimization showed that temperature (T) and acid concentration (A) were the most significant factors, and levulinic acid yields increased to 42% (Fig. 2). Numerical optimization predicted the optimum yield of levulinic acid to reach 50% using the following reaction variables: 180 °C; 0.1 g catalyst; 38 min reaction time; 2 M acid concentration; and, 22 g/ml biomass to acid ratio. The effect of different catalysts (namely: aluminium phosphate, zeolite Y, aluminum chloride and aluminium sulfate) on the final yield was also investigated. Aluminium phosphate proved to be the best option, resulting in levulinic acid yields of up to 45%.

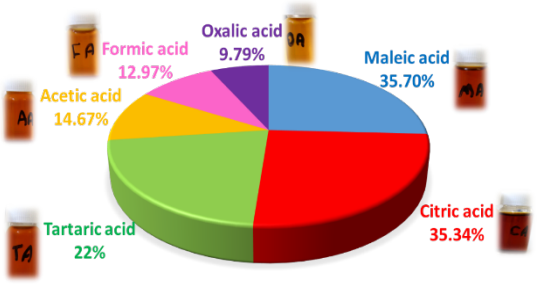

Figure 1. Levulinic acid production from barley straw using different organic acids and $AlCl_3$ as a catalyst.

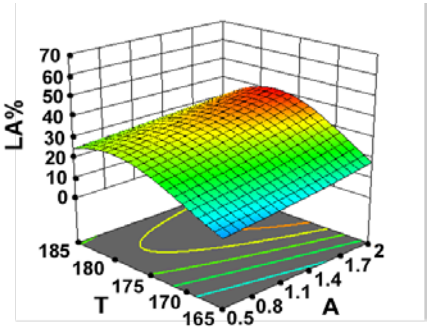

Figure 2. 3D surface plots of the effect of 2-way interaction variables on the yield of levulinic acid. Key: T (temperature, °C); and, A (acid concentration, M).

4. Conclusions

A green route using organic acids, with help of a Lewis acid, can be a viable option in the sustainable production of levulinic acid from inexpensive lignocellulosic biomass feedstocks. The additional use of microwave heating not only speeds up the reaction time, but is also a more environmentally friendly alternative to processes involving mineral acids.

References

[1] O. Adeeyo, O.M. Oresegun, T.E. Oladimeji, AJER . 4 (2015) 14-19.
[2] H. Heeres, L. Janssen, B. Girisuta, Chem. Eng. Res. Des. 84 (2006) 339-349.
[3] D.W. Rackemann, W.O. Doherty, Int. Sugar. J. 115 (2013) 28-34.
[4] J. Ahlkvist, Formic and Levulinic Acid from Cellulose via Heterogeneous Catalysis, Umeå Universitet, 2014.
[5] J. Shen, C.E. Wyman, AIChE J. 58 (2012) 236-246.

Photocatalytic Oxidation in a Rotor-Stator Spinning Disk Reactor: Improving Process Sustainability

Arnab Chaudhuri[1], Parimala Shivaprasad[1, 2], Koen Kuijpers[1], Emma Anna Carolina Emanuelsson[2], Timothy Noël[1], John van der Schaaf[1]*

[1] *Deparment of Chemical Engineering, TU Eindhoven, 5612 AZ, Eindhoven, Netherlands*

[2] *Department of Chemical Engineering, University of Bath, BA2 7AY, Bath, United Kingdom*

**Corresponding author: J.Vanderschaaf@tue.nl*

Highlights

- Photocatalytic Oxidation of L-methionine was investigated with a RS-SDR
- High conversions were obtained with short residence times indicating possibilities for improvements in process sustainability
- Results were compared to conventional reactor systems

1. Introduction

In recent years, process intensification (PI) has been a promising pathway to achieve sustainable chemical production [1]. The rotor-stator spinning disc reactor (rs-SDR) is one such PI reactor were high shear force on the feed due to velocity gradients between the rotor and the stator result in high rates of mass and heat transfer [2]. This leads to rs-SDR being a particularly interesting reactor for photochemical applications where photon transfer and mass transfer of the activated species are often limited (e.g. for high concentration). In this study, we demonstrate the potential of a photo-rs-SDR for applications towards photochemical reactions. A challenging reaction where additional gas-liquid mass transfer limitations are observed has been selected for this study [3].

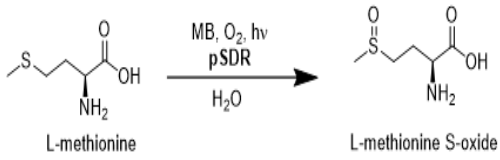

Figure 1: Reaction scheme

2. Methods

The oxidation of L-methionine with methylene blue as the catalyst (Fig.1) was chosen as the model reaction for this proof of concept study. The rs-SDR was illuminated using a solar light simulator (AM1.5G), to ensure no light limitations. The reaction was carried out by co-feeding the reaction solution and oxygen at the bottom of the reactor; samples were collected after a single pass and the reaction conversion was measured using HPLC. The schematic is illustrated in Fig 2.

3. Results and discussion

A few of the results obtained are presented in this abstract. As illustrated in Fig 3, the reaction conversion (residence times between 24—28 seconds) increased with increasing rotation speed

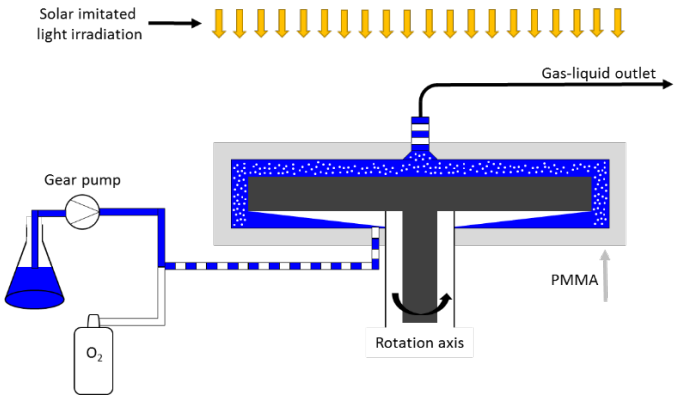

Figure 2: Schematic representation of the reactor set-up

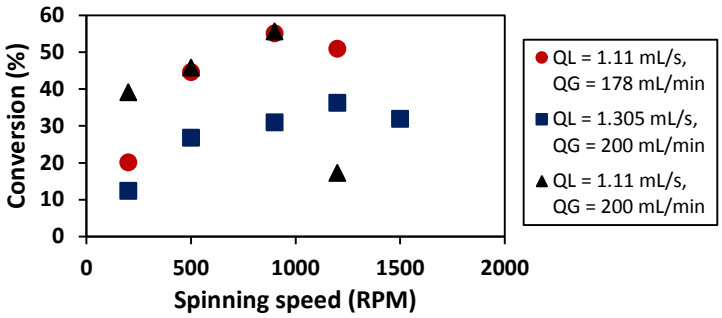

Figure 3: Effect of spinning speed and gas-liquid flowrate on reaction conversion

up to 900 RPM. A maximum conversion of 55% was observed at 900 RPM for an optimum gas-liquid flowrate. Such high conversions within 24 seconds of residence time indicate that productivity of photochemical reactions can be significantly improved. Larger phase separations were observed at higher RPMs which caused inefficient mixing, leading to lower conversions.

The effect of rotation speed, gas-liquid flowrate and catalyst concentration on the reaction conversion have also been investigated under both the solar limit simulator and more limiting conditions. Additionally, the results were compared to two conventional reactors which are currently used in photochemistry: batch and microflow.

4. Conclusions

To the best of the authors' knowledge, this is the first study of a successful synergistic reaction system using photochemistry and the rs-SDR. We are currently investigating the potential of the photo rs-SDR for targeted applications in pharmaceuticals and the fine chemical industries to further illustrate how process intensification can lead to improvements in sustainability.

References

[1] Vlachos, D.G. and S. Caratzoulas, Chemical Engineering Science **2010**, 18-29.

[2] Meeuwse, M., J. van der Schaaf, and J.C. Schouten, AIChE Journal **2012**, p. 247-255.

[3]Emmanuel, N., Mendoza, et. al., Organic Process Research & Development, **2017**, p. 1435-1438.

Modelling of a hydrogen production from solar and wind under Aspen Plus

Lokmane Abdelouahed*, Mohamad Zaher, Andres Martinez, Bechara Taouk, Lionel Estel

Normandie Univ, INSA Rouen Normandie, UNIROUEN, Laboratoire de Sécurité des Procédés Chimiques, LSPC EA-4704, 76000 Rouen, France

** Corresponding author: lokmane.abdelouahed@insa-rouen.fr*

Highlights

- Hydrogen production from solar and wind.
- Coupling solar and wind energy under Aspen Plus.

1. Introduction

Renewable energy sources continue to increase their share of installed capacity worldwide. This increase is pushed by the commitment to avert the risks that conventional non-renewable sources pose to health, geopolitics, the economy and the environment. According to the IEA, the renewable energy sources represents 13.4 % of the total world total primary energy supply (oil 31.8 %, natural gas 21.6 %, Nuclear 4.9 %, coal 28.1%) [1]. On the other hand, solar photovoltaic and wind energy supply has grown of an average annual growth rate of 45 % and respectively 24 % between 1990 and 2015 respectively [1]. Hydrogen is one of these carriers that has attracted much support from across many countries across the world. In fact, it has the potential to become one of the main energy carriers of the future as it can be easily produced using renewable energy, stored using commercially available technologies and used throughout the entire energy system [2] [3]. Hydrogen is considered today a very promising form of energy carrier by its ability to serve a buffer between renewable sources and the different forms of energy demand. Water electrolysis is considered one of the most mature and clean method to produced hydrogen. Renewable energy sources continue to increase their share of installed capacity worldwide. This increase is pushed by the commitment to avert the risks that conventional non-renewable sources pose to health, geopolitics, the economy and the environment. According to the IEA, the renewable energy sources represents 13.4 % of the total world total primary energy supply (oil 31.8 %, natural gas 21.6 %, Nuclear 4.9 %, coal 28.1%) [1]. On the other hand, solar photovoltaic and wind energy supply has grown of an average annual growth rate of 45 % and respectively 24 % between 1990 and 2015 respectively [1]. Hydrogen is one of these carriers that has attracted much support from across many countries across the world. In fact, it has the potential to become one of the main energy carriers of the future as it can be easily produced using renewable energy, stored using commercially available technologies and used throughout the entire energy system [2] [3]. Hydrogen is considered today a very promising form of energy carrier by its ability to serve a buffer between renewable sources and the different forms of energy demand. Water electrolysis is considered one of the most mature and clean method to produced hydrogen.

2. Methods

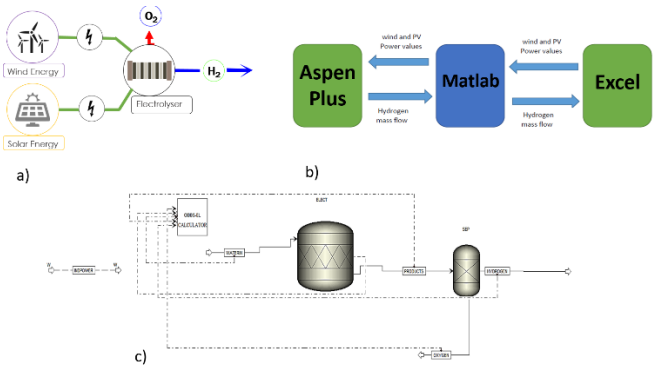

Figure 1: a) Global pilot scheme, b) Coupling Aspen Plus, Excel and Matlab and c) Modeling under Aspen Plus.

The objective of this work is to build a simulation model under Aspen Plus to estimate the hydrogen production from the electrolysis process using wind and solar energy as input power (Fig 1.a). This model will take into account the availability of solar and wind energy for different geographical locations and different PV and wind turbine technologies. The water electrolysis process is modeled in ASPEN PLUS and coupled with the renewable energy models thanks to Matlab and excel interaction. In the case study, the overall model shows a good performance and a high sensitivity to renewable energy availability.

3. Results and discussion

The water electrolysis process powered by renewable energy has been simulated in ASPEN PLUS. A case study in 2 geographical locations has been done to test the model. As a first validation, the results show a very good performance in reflecting the renewable energy availability between different locations and environmental conditions.

4. Conclusions

This work aims to create a techno-economic model and investment decision support tool that can technically and financially optimize the production and the commercialization of renewable hydrogen. The electrolysis simulation model can be enhanced by taking into account the over voltage and the faradic efficiency in an actual elecrtolyser. This will result in more power needed to obtain the same yield of hydrogen in the case of an ideal electrolyser.

References

[1] IEA, "Renewables Information," IEA publishing, Paris, 2017.

[2] [Online]. Available: http://www.nweurope.eu/media/3517/gencomm-smart-h2-positon-paper-march-2018.pdf.

[3] K. Mazloomi and C. Gomes, "Hydrogen as an energy carrier: Prospects and challenges," Renewable and Sustainable Energy Reviews, vol. 16, p. 3024–3033, 2012.

DR. JENNIFER HASSELBERG[*], DR. PETER KREIS[*], DR. FRANK STENGER[*], DR. CORINNA HECHT[*], PROF. ROBERT FRANKE[**], DR. MARCO HAUMANN[***], MARKUS SCHÖRNER[***], PROF. ANDERS RIISAGER[****], JAKOB MAXIMILIAN MARINKOVIC[****], MORTEN LOGEMANN[*****], NANETTE ZAHRTMANN[******]

[*]Evonik Technology & Infrastructure GmbH, Process Technology & Engineering, Marl, Germany, [**]Prof. Robert Franke, Evonik Performance Materials GmbH, Marl, Germany [***]Friedrich-Alexander-Universität Erlangen-Nürnberg (FAU), Germany, [****]Technical University of Denmark, Lyngby, Denmark, [*****] RWTH Aachen University, Aachen, Germany, [******]LiqTech Intl., Ballerup, Denmark

ROMEO – A MAJOR STEP TOWARD INDUSTRIAL MEMBRANE REACTOR APPLICATION FOR HYDROFORMYLATION

Introduction

The hydroformylation is one of the most prominent industrially applied reactions. More than 10 million tons of chemical products rely on this homogeneously catalyzed reaction step every year; thus, a permanent improvement of the hydroformylation process is of utmost interest for many chemical companies like Evonik. Especially, it is the researcher´s and company´s aspiration to find a heterogeneous-like catalyst. The improvement done within Evonik followed several approaches in the past including optimization of process technology as well as optimizing the catalytic system. Most of these developments were achieved by public funded projects together with experts from academia.

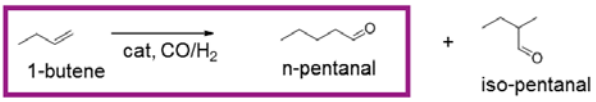

Fig. 1. Hydroformylation reaction formula

Experimental

This presentation gives an overview of the most relevant results of the currently running EU funded project ROMEO (Reactor Optimization by Membrane Enhanced Operation).

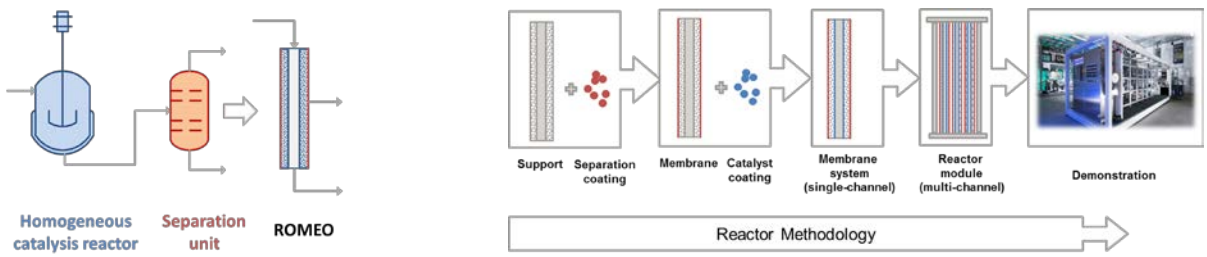

Fig. 2. 2-in-1 reactor principle (left) and reactor methodology (right)

The project aims at the combination of a catalytic reaction with the separation step on a single support structure. This combination in an innovative “2-in-1” reactor opens the possibility to omit or at least significantly downsize the separation units. In case of catalytic processes that are performed close to the chemical equilibrium the constant removal of one reaction partner from the reaction enhances the efficiency.

Results and discussion

The catalytic system contains of a ceramic support combined with a membrane coating and an impregnated hydroformylation catalyst. In order to evaluate the relevant long-term stability of such a catalytic system, a modular demonstration plant with a switchable reactor system was manufactured. With this modular design it is possible to compare the performance of a single monolith reactor with a multi-monolith reactor module. To operate the reactor with a technical industrial feed, a start-up procedure, an *insitu* catalyst impregnation and a catalyst recovery technology were developed.

The presentation will show relevant long-term experimental results as well as some sensibility studies of the membrane reactor modelling.

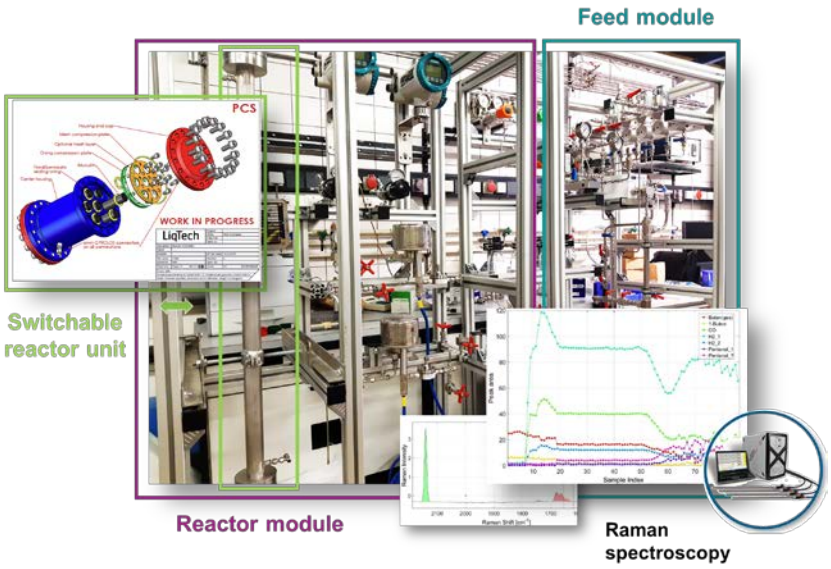

Fig. 3. Modular demonstration plant for long-term hydroformylation operation

Conclusions

Membrane optimization in terms of mechanical stability and material selectivity is still a challenge of the project but long-term demonstration already shows a significant economic benefit compared to the benchmark process concerning catalyst costs. The implementation of a pilot reactor to the benchmark process will be the next step to evaluate the technology in a bypass stream.

Acknowledgment
ROMEO has received funding from the European Union’s Horizon 2020 research and innovation program (grant agreement No 680395).

The Power-to-Liquid Concept: A Novel process for the production of (Poly-) Oxymethylene Dimethyl Ether (OME)

Franz Mantei[1,2], Lara Theiss[1], Mohamed Ouda[1], Dr. Achim Schaadt[1]

1 Fraunhofer Institute for Solar Energy Systems ISE, Heidenhofstraße 2, 79110 Freiburg, Germany
2 Chair of Chemical & Process Engineering, TU Berlin, Fraunhoferstraße 33-36, 10587 Berlin, Germany

**Corresponding author: franz.mantei@ise.fraunhofer.de*

Highlights

- A sustainable and efficient production of OME
- Overall Process energy efficiency of > 55 % starting from H_2 and CO_2
- Yield of > 45 % OME starting from H_2 and CO_2

1. Introduction

OME have interesting thermophysical and chemical properties which make them suitable for different applications as CO_2 absorption, solvent, in direct oxidation fuel cells (DOFC) and as diesel fuel blend or alternative. [1-3] OME have a relatively high energy density and are environmental benign which adds to their advantages as a fuel or chemical/solvent candidate. Especially OME_n with the chain length of n = 3-5 show fuel properties close to diesel fuel. Due to their high molecular bound oxygen content and missing C-C bounds, already low blends to diesel fuel can reduce soot emission considerably which enables a reduction for NO_x emissions. [4]

However studies regarding their applications and potential use as alternative fuel are extensive; a sustainable, economical, scalable and efficient industrial process for the production of OME_{3-5} is still not realized. In this work a simple and efficient OME synthesis process will be introduced. The aim is to reduce the number of process units and to increase the process energy efficiency and total yield of OME_{3-5} while considering scalability and economic feasibility. [5] The novel process addressed in this work comprises two steps, namely: (1) the oxidative dehydrogenation of MeOH towards Formaldehyde (FA) and OME_1 in a single reactor unit. (2) This mixture can subsequently be converted to OME_{3-5} at mild conditions. A major challenge for the OME processes is the water management, since it is produced as a side product of the reactions starting from MeOH. Its separation using thermal separation units is a complex challenge due to the formation of several azeotropes, reactions and miscibility gaps, thus some research is done investigating alternative separation tehnologies using membranes, adsorption or extraction. [6, 7]

2. Methods

In order to evaluate the potential of the investigated process based on the oxidative dehydrogenation of MeOH to produce OME, the process was simulated using commercial process simulation software. Different process units were experimentally validated to ensure realistic behavior of the applied models. To increase the process energy efficiency, heat integration was conducted for the whole process covering the MeOH synthesis based on H_2 and CO_2 and the subsequent OME synthesis. To compare this process with alternative OME synthesis processes,

key performance indicators (KPIs) were evaluated. Finally preliminary production cost estimation was conducted identifying the economic advantage of the investigated process.

3. Results and discussion

The production capacity of 35 kt OME per annum starting from H_2 and CO_2 to MeOH and further oxidative dehydrogenation to FA and OME_1, water separation and finally OME_n synthesis, is introduced. A scheme of the process is shown in Figure 1. The KPIs show great potential for the process in terms of process energy efficiency > 55% and yield of OME_n > 45% with estimated costs of > 1000 US$/$t_{OME}$. The costs are mainly influenced by the scale of the process and the costs for renewable H_2 which can be reduced in regions with lower costs for renewable electricity.

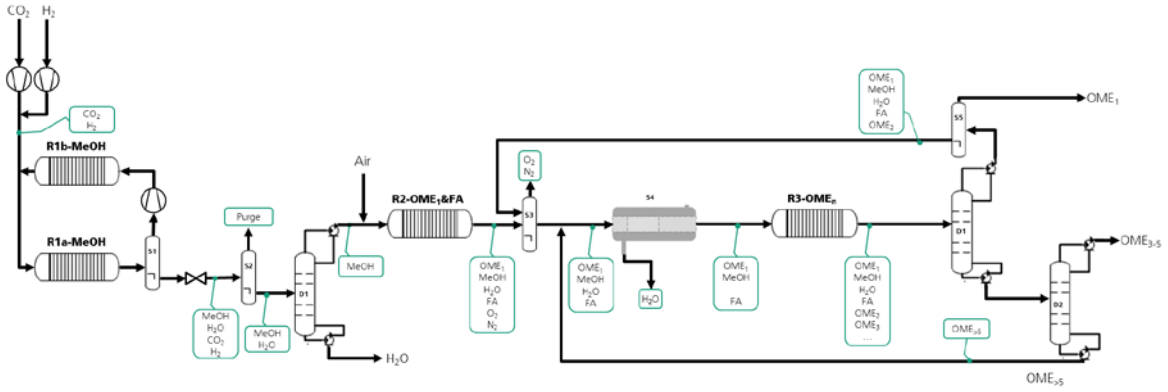

Figure 1 Scheme for the production of OME_n via oxidative dehydrogenation of MeOH starting from H_2 and CO_2

4. Conclusions

OME show promising properties for different applications. However, a sustainable, economical, scalable and efficient industrial process for the production of OME_{3-5} is still not realized. A novel process for a sustainable and efficient production of OME at high yield > 45% and high process energy efficiency > 55% with production costs of ca. 1000 US$/$t_{OME}$ was introduced. This cost is rather high for fuel applications but is promising for the chemicals and solvent market. The process steps are being validated in lab- and mini-plant scale and should be scaled up to several kt/a to validate the industrial application. In conclusion, the introduced process with the discussed KPIs offers a sustainable and economically feasible solution for the production of OME.

References

[1] Schappals, Breug-Nissen, Langenbach, Burger, Hasse, *Journal of Chemical & Engineering Data*, **2017**, DOI: 10.1021/acs.jced.7b00718

[2] Ouda, Mantei, Hesterwerth, Bargiacchi, Klein, White, *Reaction Chemistry & Engineering*, **2018**, DOI: 10.1039/C8RE00100F

[3] Gaukel, Pélerin, Härtl, Wachtmeister, Burger, Maus, Jacob, *37. Internationales Wiener Motorensymposium*, **2016**, 193–223

[4] Iannuzzi, Barro, Boulouchos, Burger, *Fuel*, **2017**, DOI: 10.1016/j.fuel.2017.04.089

[5] Schmitz, Breitkreuz, Ströfer, Burger, *Chemical Engineering Transactions*, **2018**, DOI: 10.3303/CET1869036

[6] Schmitz, Breitkreuz, Ströfer, Burger, Hasse, *Chemical Engineering and Processing - Process Intensification*, **2018**, DOI: 10.1016/j.cep.2018.06.012

[7] Schmitz, Breitkreuz, Ströfer, Burger, Hasse, *Journal of Membrane Science*, **2018**, DOI: 10.1016/j.memsci.2018.07.053

Process designs for converting biobased propylene glycol to acrylic acid via lactic acid and allyl alcohol

M.M. Buitelaar[1,*], E. van Daatselaar[1], D.G. van Teijlingen[1], R.J. De Sousa Ribeiro[1], H.I. Stokvis[1], J.D. Wendt[1], H. van den Berg[1], J.-P. Lange[1,2]

1 University of Twente, Sustainable Process Technology, P.O. Box 217, 7500 AE Enschede, Netherlands;
2 Shell Technology Center, Grasweg 31, 1031 HW Amsterdam, Netherlands

**Corresponding author: m.m.buitelaar@student.utwente.nl*

Highlights

- Techno-economical evaluation per route shows that reaction section is critical part
- Comparison between two processes to conclude which is inherently favored
- Separation section is remarkably similar for both processes
- Economic evaluation shows need for 50% drop in PG price for an economically viable process

1. Introduction

The price of Propylene Glycol (PG) is expected to drop dramatically with the increasing use of biomass as feedstock, since it is a byproduct of sugar hydrogenolysis [1, 2]. This could make PG a promising raw material to be upgraded to Acrylic Acid (AcrA). Two process designs for the conversion of PG to AcrA are proposed, either by oxidation of PG to lactic acid (LA) and dehydration to AcrA or by dehydration of PG to allyl alcohol (AA) and oxidation to AcrA [3] . A conceptual design for both routes was proposed, followed by a techno-economical evaluation on a basic engineering level. Both processes were evaluated individually on heat integration, sustainability, CAPEX and OPEX. The minimum PG price to reach economic break-even for the two routes was compared for a capacity of 150 kta for glacial acrylic acid (>99.5 % purity) from a 50/50 mol% water/PG feed.

2. Methods

Douglas methodology is followed - with different levels of detail, based on hierarchy of decision. During the process, several options are evaluated and the best alternative is chosen based on theoretical analysis and simulated results[4]. Consequently, a Process Flow Diagram is developed and evaluated using Aspen Plus V10 software. An improved heat integration system is suggested for both processes using pinch analysis. Finally, an economic analysis is performed to calculate the CAPEX and OPEX related to the process.

3. Results and discussion

Both flowsheet designs start with two reactors without a separation and recycle in between. Due to limited information of all the reactions, the same overall reaction yield for both processes is assumed in the paper. Despite the various by-products, the separation section for both processes is remarkably similar. Water removal is the key function of the first separation unit which in both processes is a liquid-liquid extractor. For the LA route, DIPE was found to be the most optimal solvent, whereas for the AA route octanol was found to be the most suitable, based on energy consumption and solvent recovery. Further purification is performed by (vacuum) distillation. AcrA recovery for the LA route and AA route are 99.7% and 99.1%, respectively, showing only minor differences in the separation.

Significant differences can be found in the heat integration. A high-temperature oxidation reaction (325 °C) in AA route provides valuable energy and covers almost all the hot utilities needed. The liquid phase oxidation in the LA route results in availability of energy at 80 °C, which is too low for steam generation and needs cooling by an external utility. Evaporation of the product stream in the LA route is expected to give polymerization issues. A novel spray evaporator unit was proposed to solve this problem by inducing instantaneous evaporation of both LA and water. This is however an expensive and high energy consuming unit.

Both processes will profit tremendously by reducing the required amount of water dilution. Table 1 shows the water usage per ton product for both routes. Less water present in the system reduces the volume of operation units, lowering the CAPEX and OPEX significantly. The difference in solvent loss (Table 1) between the two routes is mainly the result of a difference in the thermodynamic modelling of the extraction.

For both routes, the reactor section is a major cost contributor accounting roughly 50% of the investment. However, since the reactor design suffers from a lack of information, this cost factor is highly uncertain. Advances in the reaction section, such as higher catalytic performance, might lead to a significant reduction of the total investment. The largest difference between the routes is in the use of an air separation unit for the LA route, whereas the AA route uses air. This leads to a preliminary estimate of the total investment of 203 M$ for the LA route and 170 M$ for the AA route. Raw materials are by far the largest costs for operation in both routes. The AA route benefits from lower costs for utilities, since heat can be integrated better and the LA route uses a spray evaporator, which is a large energy consumer. In the end the necessary break-even price of PG on a preliminary basis for the LA and AA route is 940 $/ton PG and 1070 $/ton PG, respectively. With the current uncertainty margins of ± 30% in all economic calculations, a conclusion concerning a more attractive process would be premature.

Table 1. Important comparison parameters for both designs.

Description	LA route	AA route
Acrylic Acid recovery (%)	99.7	99.1
Heat integrated (MW)	55	89
Hot Utility (MW)	4	13
Cold Utility (MW)	141	52
Water usage (ton water/ton product)	5.1	3.9
E-factor (kg waste/kg product)	1.1	1.0
Solvent losses (kg/ton product)	139	23

4. Conclusions

The constructed processes show similarities regarding the flowsheet, proposed unit operations, CAPEX and sustainability. Liquid-Liquid extraction is used in both processes as the main separation unit due to the presence of large amounts of water. The reaction section design suffers from a lack of information but forms a critical difference between the two routes. The break-even feedstock price of PG is quite similar for both routes at this point. Further investigations should show which process is more feasible. Producing AcrA via high temperature dehydration and subsequent high temperature oxidation is shown to be inherently favoured, due to the opportunity to integrate the reaction heat available at high temperature. To conclude, the price of PG has to drop dramatically to replace the conventional production of acrylic acid with one of the routes proposed here.

References

1. Ruppert, A.M., K. Weinberg, and R. Palkovits, *Hydrogenolysis Goes Bio: From Carbohydrates and Sugar Alcohols to Platform Chemicals.* Angewandte Chemie International Edition, 2012. **51**(11): p. 2564-2601.
2. Lahr, D.G. and B.H. Shanks, *Effect of sulfur and temperature on ruthenium-catalyzed glycerol hydrogenolysis to glycols.* Journal of Catalysis, 2005. **232**(2): p. 386-394.
3. Pramod, C.V., et al., *Bio-based acrylic acid from sugar via propylene glycol and allyl alcohol.* Catalysis Science & Technology, 2018. **8**(1): p. 289-296.
4. Perkins, J.D., *Conceptual design of chemical processes J. M. Douglas, McGraw-Hill, New York, 1988. pp. xviii + 601, . ISBN 0-07-017762-7.* Journal of Chemical Technology & Biotechnology, 1989. **46**(3): p. 249-249.

Chlorine-free oxidation of starch and its derivatives using alkaline hydrogen peroxide and water-soluble iron- and manganese-based catalysts

Homer Genuino[1], Tim Meinds[1], Marcel Staal[2], Jelle Brinksma[2], Thomas Wielema[2], Francesco Picchioni[1], Peter Deuss[1], Wesley Brown[3], Hero Heeres[1,*]

1 Department of Chemical Engineering, Engineering and Technology institute Groningen (ENTEG), University of Groningen, Groningen, The Netherlands; 2 Avebe Foxhol, Foxhol, The Netherlands ; 3 Stratingh Institute for Chemistry, University of Groningen, Groningen, The Netherlands

**Corresponding author: h.j.heeres@rug.nl*

Highlights

- H_2O_2 combined with iron or manganese complex is an efficient system for starch oxidation
- Interplay between catalyst stability and applied process parameters dictates efficiency
- *In situ* Raman spectroscopic technique is developed to monitor catalyst stability
- Studies on model compounds provide insights into the mechanism of starch oxidation

1. Introduction

Oxidation is an attractive strategy to effectively reduce the high-molecular weight of native starch and improve its stability for various applications in paper and textile industries. Sodium hypochlorite (NaOCl) is a common oxidizing agent due to its efficiency in lowering the viscosity as well as introducing carbonyl/carboxyl functionality in the polysaccharide structure (**Figure 1, left**). However, it is highly desired to replace NaOCl with more environmentally-benign alternatives. In this work, H_2O_2 is used instead, in combination with iron (III) tetrasulfonatophthalocyanine (FePcS) or manganese (IV) 1,4,7-trimethyl-1,4,7-triazacyclononane (tmtacn) as the catalyst (**Figure 1, right**).

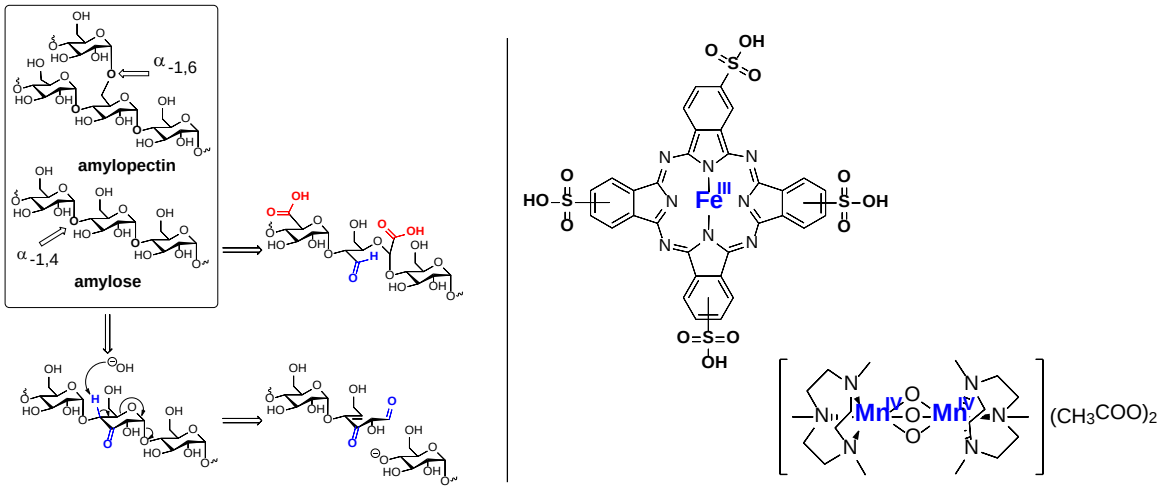

Figure 1. Catalytic oxidation of hydroxyl groups to carbonyl and carboxyl groups, and subsequent cleavage of the glycosidic bonds (left). Structure of iron and manganese complexes as catalysts used in this present work (right).

2. Methods

Typically, potato starch slurry in water (39 wt.%) was prepared and heated to the desired temperature. The pH was adjusted to 10 or 11 using NaOH. The catalyst was subsequently added, followed by H_2O_2. The influence of process parameters (i.e., time, temperature, oxidant, and catalyst and starch concentrations) for reactions carried out in both batch and continuous-flow set-ups on yield, viscosity, and degree of substitution (DS) was investigated. Yields were calculated based on the dry weight of product. Moisture content and urea viscosity were determined using a moisture analyzer and a rapid visco-analyzer, respectively. The carboxyl and carbonyl contents were determined by IR spectroscopy and by titration. Product properties were further characterized using various techniques including PXRD, SEM, FTIR, 2-D NMR HSQC, GPC, HPLC, and ESI-MS.

3. Results and discussion

At optimum batch conditions for the H_2O_2-FePcS system, a product yield of 91% was obtained with substantial degree of substitution (DS_{CO}=0.41, DS_{COOH}=0.014), combined with degradation to lower molecular weight (197 mPa·s) (**Table 1**). However, high [H_2O_2] and temperature promoted the degradation of the FePcS catalyst (by *in situ* Raman spectroscopy). For the H_2O_2-Mn(tntacn) system, starch oxidation was a clear function of time and showed a linear dependency with respect to carboxyl group formation, whereas an exponential decay was found for starch degradation. H_2O_2 and catalyst concentrations of 2 wt.% and 20 ppm, respectively, were already sufficient to significantly reduce the viscosity of starch samples within benchmark specifications (144 mPa·s with DS_{COOH}=0.04). For both catalytic systems, the morphology and structure of the starch remained unchanged after oxidation. A clear shift of the cumulative weight fraction to lower regimes was also obtained (by GPC), consistent with the observed extent of depolymerization and formation of water-soluble oxidized compounds. Studies on model compounds (i.e., glucose, fructose, maltose, cellulobiose, beta-cyclodextrin, inulin, amylose, and amylopectin) provided insights into structure-property relationships as well as the mechanism of oxidation and depolymerization.

Table 1. Catalytic oxidation of native potato starch with FePcS and H_2O_2 at 50 °C and pH 10 in batch.

Entry	FePcS (µM)	H_2O_2 (M)	time (min)[a]	Urea viscosity (mPa·s)	DS_{COOH} (mol mol^{-1})	DS_{CO} (mol mol^{-1})	Yield (wt.%)[b]
1	331	0.2	135-80-72	3692	0.004	0.15	97.4
2	331	0.4	112-90-90	1360	0.011	0.22	95.2
3	166	0.4	180-120-120	1690	0.010	0.33	95.0
4	166	1.0	180-120-120	197	0.014	0.41	90.7
5[c]	166	1.0	180-120-120	198	0.012	0.40	91.0

[a] H_2O_2 added in one or three steps dropwise with a concentration distribution of 30-35-35%.

[b] Weight of isolated oxidized starch divided by the initial weight of starch on a dry basis (total wt. 100 g).

[c] Upscale experiment of entry 4 with five moles (1000 g) of potato starch.

4. Conclusions

Environmentally-friendly oxidant, H_2O_2, in combination with low loadings of water-soluble Fe- and Mn-based catalysts are highly effective in the oxidation of abundant starch and starch derivatives. Some deactivation of FePcS was observed using *in situ* Raman spectroscopy depending on reaction conditions. These systems provide a promising alternative to hypochlorite (NaOCl) starch oxidation.

A Combination of Bio- and Chemo-Conversion of the Hemicellulose Xylan to Xylitol

Mick Miro Ayubi[1], Susanne Steudler[2], Anett Werner[2], Thomas Walther[2], Rüdiger Lange[1], Gerd Hilpmann[1]

1 Chair of Chemical Engineering and Process Plants, Institute of Process Engineering and Environ-mental Technology, Technische Universität Dresden, 01062 Dresden, Germany; 2 Chair of Bioprocess Engineering, Institute of Natural Materials Technology, Technische Universität Dresden, 01062 Dresden, Germany

**Gerd Hilpmann: gerd.hilpmann@tu-dresden.de*

Highlights

- Enzymatic hydrolytic hydrogenation of xylan to xylitol is possibel
- A hybrid one pot process achieved over 70% xylitol yield

1. Introduction

Lignocellulosic biomass consisting of the fractions cellulose, hemicellulose and lignin is a promising sustainable basis for a future biorefinery. They are many applications for cellulose for example in the pulp and paper industry. For an efficient operating of a future lignocellulosic biorefinery it's essential to include the fractions lignin and hemicellulose. Hydrolysis is a key step in this process. The focus of this work is the simultaneous use of chemical and biological catalysts and the combination of their advantages in one reactor for the conversion of xylan (beechwood) to xylitol. This involves the discussion of a classical one-pot and a new two-step process.

2. Methods

The experiments were carried out in a stainless steel batch reactor (Parr Inst.) with an inner volume of 300–600 ml. The analysis was performed by an HPLC (Smartline®, Knauer GmbH) unit. Hydrolysis was done by using commercially available enzymes. The subsequent refinement of the hydrolysis products was realized with the aid of a Ru/C catalyst.

3. Results and discussion

The classical one-pot process was carried out at a temperature of 60 °C, 20 bar hydrogen pressure and a stirring speed of 1000 rpm. The process realized under the before mentioned conditions achieved a xylitol yield below 20% after 8 hours. This is very low compared to the existing industrial process using Raney-Nickel.

The two-step process is composed of the following steps: 1. step hydrolysis followed by the 2. Step hydrogenation. The hydrolysis (1) is carried out at 250 rpm (low shear-stress), 50 °C and atmospheric pressure for 24 hours reaction time. After the hydrolysis phase the subsequent hydrogenation (2) was carried out at process conditions of 10 bar hydrogen pressure, 140 °C, stirring of 750 rpm under use of gas-entrainment and a reaction time of 4 hours. Comparably mild reaction parameters were chosen to maintain the enzyme activity for as long as possible under hydrogenation conditions. During the hydrolysis, with different enzyme loadings, a xylan conversion of around 70% was achieved. In the subsequent hydrogenation, the xylan conversion increases by approximately 10%. Control experiments show that under these conditions no xylan hydrolysis without enzymes takes place. After the second process stage, a xylitol yield of over 70% is achieved.

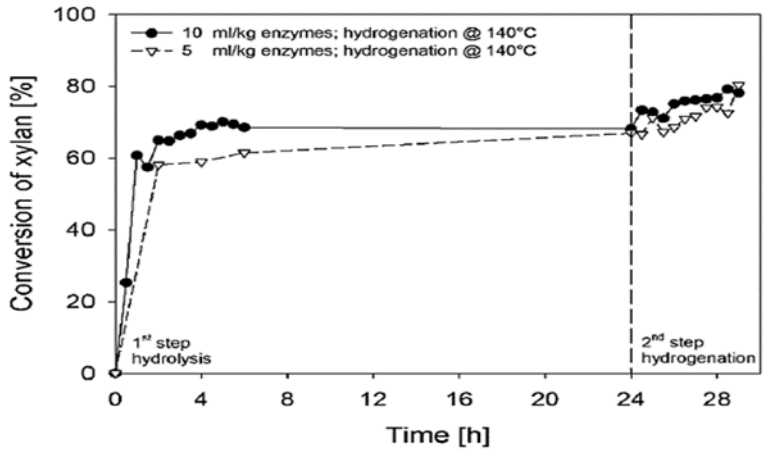

Figure 1. Fig. 1 xylan (1 wt%) conversion via two-step process with different enzyme loadings (250 rpm, 50 °C, atmospheric) during the 1st step 24 h and hydrogenation at 140 °C during 2nd step 4 h at 10 bar H_2 in the presence of 3 g/kg Ru catalyst (5 wt% Ru on act. C) [1]

4. Conclusions

The experiments show that enzymatic hydrolytic hydrogenation of xylan to xylitol is possible at low (60 °C) temperatures. The xylitol yield can be considerably increased by the application of a suitable reactor operating mode as a two-step process.

Acknowledgement: The presented results are part of the European project “CrossCat”. The authors thank the EU for funding supported by EFRE Program (ERA-IB) of Sächsisches Staatsministerium für Wissenschaft und Kunst (SMWK,Grant No. 100271549).

References

[1] Hilpmann, G., Steudler, S., Ayubi, M.M., Pospiech, A., Walther, T., Bley, T. Lange, R.: Combining Chemical and Biological Catalysis for the Conversion of Hemicelluloses: Hydrolytic Hydrogenation of Xylan to Xylitol. Catal Lett (2019),149:69-76. https://doi.org/10.1007/s10562-018-2598-7

Simulation of conductivity increase in closed papermaking circuits

Patrick Huber[1], Stéphanie Prasse[1], Eric Fourest [1]

1 Centre Technique du Paper, CS90251 38044 Grenoble cedex 9

**Corresponding author: Patrick.Huber@webctp.com*

Highlights

- Chemical process simulation could predict conductivity in a recycled tissue mill.
- Conductivity sources are raw material, chemicals, water and anaerobic activity
- Inhibiting microbial anaerobic activity may reduce conductivity two-fold.
- Water management strategies must be evaluated by a thorough simulation study

1. Introduction

Reduction of fresh water usage in papermills has some consequences on process water quality. In particular, organic and inorganic dissolved and colloidal substances build-up can cause operating difficulties. Increase of organic dissolved and colloidal substances have an impact on drainage, chemical additives, microbial activities and deposits. Solutions exist to limit their disturbing effects such as separation of water loops, counter-current washing or recycling bio-treated effluents. On the other hand, inorganic dissolved species may become the limiting factor for further circuit closure as they interfere with charged polymeric additives [1]. We present a chemical process simulation approach to predict salinity increase in process water. This will help determining acceptable conductivity limit for paper production and adequate water management strategies.

2. Methods

First, conductivity sources throughout the circuits are identified. Four types of sources are considered (i) raw materials, (ii) fresh water, (iii) chemicals and (iv) anaerobic activity.

For pure chemicals, dedicated sources are available in the chemical process simulation (for instance: caustic soda, sodium bisulfite, etc.). For charged polymers, their specific contribution to conductivity is firstly determined by plotting a dilution curve. Then corresponding sources of counter ions are implemented (Na^+ for anionic polymers and Cl^- for cationic polymers).

The process simulation (Fig.1, left) determines the conductivity by resolving chemical equilibria together with biochemical equilibria resulting from anaerobic activity [2], [3]. Chemical speciation is used to calculate the corresponding conductivity.

3. Results and discussion

The conductivity calculated from the simulated ionic distribution fitted the measured conductivity profile quite well (Fig.1, right). The simulation made it possible to estimate the relative contribution of each conductivity source. In the tested tissue mill case, all sources contributed significantly to conductivity. Raw material released various ions. Fresh water was a significant

source of ions as well. Chemicals were a significant source of conductivity as producing wet-strength grades requires alkaline conditions for broke repulping. In closed circuits conditions, anaerobic activity may cause important conductivity rise. The simulation showed that inhibiting anaerobic activity could reduce conductivity two-fold, as it is coupled to the other sources and effects, e.g. dissolution of calcium carbonate filler from the raw material due to produced organic acids.

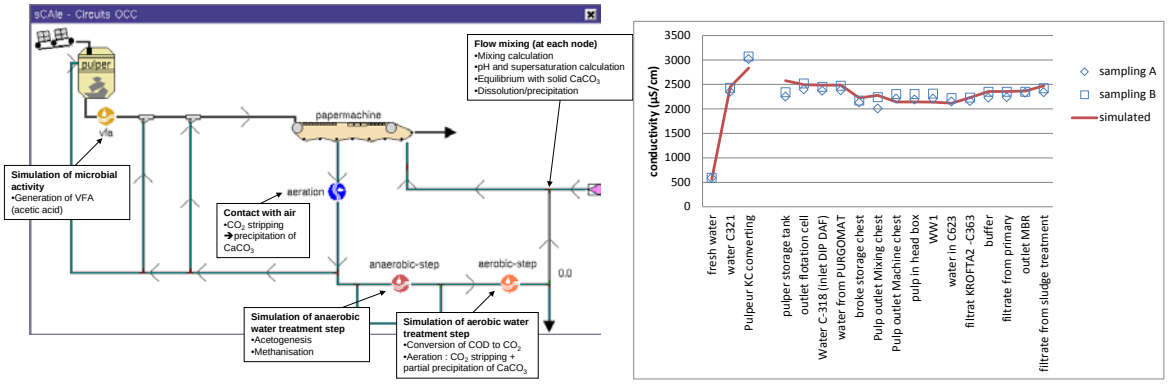

Figure 1. Simplified view of the process simulation with chemical modules (left) and prediction of conductivity throughout the process (right).

4. Conclusions

Results have shown that the relative contribution of each conductivity source is very mill-dependent. Therefore the strategy to help reducing conductivity rise in closed circuits conditions will be specific to each situation. This depends on produced grade, fresh water quality, initial water consumption, chemicals used and water management strategy.

The simulation can now be used to test various wastewater recycling scenarios. One promising option is to reduce fresh water consumption by recycling bio-treated effluent back to the process. This makes use of the waste water treatment plant as a kidney for organic material, but also deconcentrates the circuits in calcium as calcium carbonate is precipitated in the aerobic treatment. This has potential to help papermills limiting ionic species build-up when reducing their water footprint.

References

[1] R. Ordóñez, D. Hermosilla, E. de la Fuente, et Á. Blanco, I&ECR, 48(23):10247‑10252, 2009.
[2] P. Huber, S. Nivelon, P. Ottenio, et P. Nortier, I&ECR, 52(1):421‑429, 2013.
[3] P. Huber, P. Ottenio, S. Nivelon, C. Neyret, E. Fourest, et A. Burnet, « Chemical process simulations for the pulp and paper industry: towards reduced water footprint », in 6th EuCheMS Congress, Sevilla, 2016.

Electrochemical reduction of CO_2 paired with Cl_2 production.

Amanda Cristina Garcia*, Roman Latsuzbaia, Elena Pérez-Gallent, Susan Turk, Anca Anastasopol, Erwin Giling, Earl Goetheer.

Department of Sustainable Process and Energy Systems, TNO, Leeghwaterstraat 44, 2628 CA Delft, The Netherlands

**amanda.garcia@tno.nl*

Highlights

- Electrochemical carbon dioxide reduction.
- Electrochemical chlorine production.
- Paired electrolysis.
- Sustainable energy.

1. Introduction

Organic electrosynthesis is a potentially cost-effective, scalable and green method of synthesizing organic products using renewable electricity. In most cases, however, the chemistry that occurs at the counter electrode yields a waste product, which holds little economic value. To overcome this issue, paired electrolysis seems promising since it forms useful products at both electrodes. The electrochemical reduction of CO_2 has become one of the most interesting topics because of the worldwide interest in its conversion into valuable chemicals and fuels. The use of CO_2 as a C1 feedstock for the formation of more valuable chemicals offers the use of an easy, available and renewable carbon source, which is non-toxic and abundant.
On the other side, chlorine (Cl), the second most abundant halogen, is incorporated in about 70% of all manufactured chemical products. Nevertheless, some of the chlorine frequently combines with hydrogen, becoming hydrogen chloride (HCl) – a corrosive and hazardous waste material. In this context, pairing electro-oxidation of chloride with electro-reduction of CO_2 offers the possibility to make valuable chemicals on both electrodes.

2. Methods

Electrochemical measurements were carried out with an Autolab potentiostat connected to an H-type two compartment electrochemistry cell, which were separated by a Nafion 117 membrane. The anodic compartment was fed with 0.1 M HCl while the cathodic compartment was fed with 0.5 M $KHCO_3$ saturated with CO_2 gas. Platinum wire (Φ = 11 cm^2) , Au wire (Φ = 6.44 cm^2) and Ag/AgCl were used as working, counter and reference electrodes, respectively. Before electrolysis, cyclic voltammograms were performed for each reaction in a single cell. After matching the current density obtained for each single reaction, electrolysis was performed in galvanostatic mode during 1.5 hour. In order to compare the results with a more realistic system, electrochemical measurements were also carried out in a micro flow cell purchased from ElectroCell with two different compartments separated by a anionic exchange membrane (Nafion). The working electrode (WE) was a platinum plate (Alfa Aesar, 99.9%) with a surface area of 10 cm^2 and the counter electrode (CE) was a gold foil with a surface area of 10 cm^2. The anolyte and the catholyte were both recirculated through the electrochemical cell with a flow rate of 25 L/h. In both cell, the

cathodic compartment was connected to the gas chromatograph (Interscience) (GC) in order to identify gaseous products, while the anodic compartment was connected to a filter containing 1.0 M NaOH in order to collect the gas chlorine (Cl_2) produced. The concentration of Cl_2 was analyzed by using UV-vis.

3. Results and discussion

Based on the cyclic voltammograms (Figure 1) obtained for each single reaction, we found that a current density of 8 mA cm^{-2} matches for both electrochemical CO_2 reduction and Cl^- oxidation. The following discussion is based on the results obtained by using flow cell setup. Electrolysis electrolysis was performed by applying the corresponding current during 1.5 h. The cell voltage measured during electrolysis was 4.3 V *vs.* Ag/AgCl, which was stable from the beginning to the end of measurements. The anode potential (Pt – Cl_2 production) was 1.85 V *vs.* Ag/AgCl while the measured cathode potential (Au – CO_2 reduction)) was -2.5 V vs. Ag/AgCl (not showed).

During the simultaneous redox reaction, hydrogen and carbon monoxide were detected by GC as gaseous products from CO_2 reduction on Au electrode. The data are showed in Figure 2. According to the results, higher concentration of CO was obtained in the beginning of the reaction (3200 ppm) and it decreases to around 500 ppm over time, however the concentration of hydrogen increases. According to Surendranath et al.[1] it happens because of gold electrode deactivates during reaction due to the adsorption of metal impurities on the surface of the electrode leading to a decrease in product formation. Aliquots of NaOH solution, used to capture the Cl_2 produced at the anode was analyzed before and at the end of the electrolyses. The measured concentration of Cl_2 found was 930 mg / L.

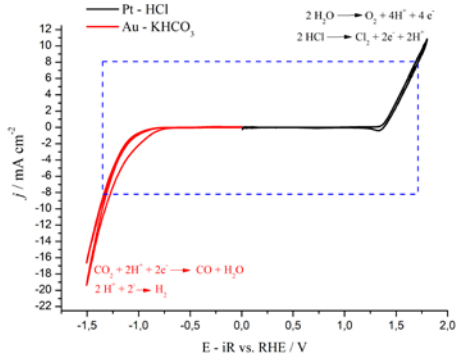

Figure 1. Cyclic voltammograms obtained at 10 mV s^{-1} for electrochemical CO_2 reduction (red line) and Cl^- oxidation (black line) on Au and Pt, respectively.

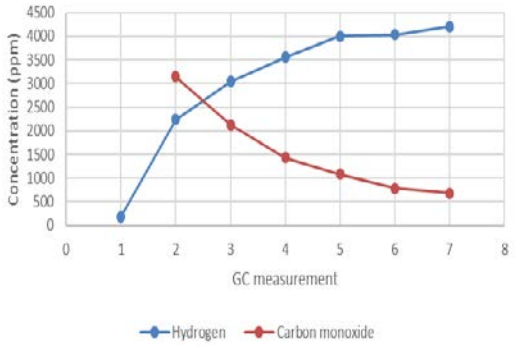

Figure 2. Concentration of CO and H_2 measured during electrochemical reduction of CO_2 on gold electrode paired with Cl_2 production.

4. Conclusions

Despite the low concentration of CO produced during the CO_2 electro-reduction reaction, our results proved the principle of the paired electrolysis of CO_2 reduction and Cl_2 production. New tests will be done in order to optimize the system, moreover this is a technology which can be applied not only for production of CO but also to other CO_2 electro-reduction products, such as ethylene, formic acid, ethanol and etc.

References

[1] Wuttig, A.; Surendranath, Y., Impurity Ion Complexation Enhances Carbon Dioxide Reduction Catalysis. ACS Catalysis 2015, 5 (7), 4479-4484.

Life Cycle Assessment of the replacement of hexane by ethanol in the soybean oil extraction Process

Simone Miyoshi[2,*], Erich Potrich[1], Felipe Furlan[2]; Raquel Giordano[1,2], Antonio Cruz[1,2]; Roberto Giordano[1,2]

1 Chemical Engineering Graduate Program, Federal University of São Carlos, UFSCar, Via Washington Luiz, km 235, São Carlos, São Paulo 13565-905, Brazil.
2 Chemical Engineering Department, Federal University of São Carlos, UFSCar, Via Washington Luiz, km 235, São Carlos, São Paulo 13565-905, Brazil.

[*] Corresponding Author. Email: simone.miyoshi@ufscar.br

Highlights

- Life cycle assessment of the extraction was performed with ethanol as solvent.
- Carbon footprint of bioethanol-extracted soybean oil is smaller than hexane-extracted.
- Bioelectricity may be co-product of the ethanol-soybean oil plant.

1. Introduction

The replacement of non-renewable solvents in industrial process will contribute to the consolidation of the low-C economy. In 2015, Brazil signed the Paris agreement and committed to reduce 37% of greenhouse gases emissions, based on 2005, until 2025. Other commitment was to reach 45% of renewable energy sources on the Brazilian energy grid and to promote clean technologies in the industrial sector. Brazil is the second larger producer of soybean, responsible for 35.38% of the worldwide production in 2015. According to [1], the 2020 soybean production forecast is 114.7 million metric tons and 10 million of tons of soybean oil. Although hexane is the conventional solvent used for soybean oil extraction the extraction of oilseeds with ethanol is a sustainable and technically feasible alternative [2,3,4]. Both anhydrous ethanol and hydrous ethanol (1G bioethanol from sugarcane) can be used for seed oil extraction. Besides, in order to contemplate a future biorefinery integration, vapor and electricity demands may be supplied in a cogeneration system using sugarcane bagasse. This work aims to simulate these oil extraction process, and to quantify the environmental impacts of this solvent replacement through LCA.

2. Methods

The process was simulated in the equation-oriented Environment for Modelling Simulation and Optimization (EMSO). The process consists of a cracker, conditioner, flaker, expander, extractor, desolventizer, toaster, evaporator, degumming, deacidified and solvent recovery section. Four scenarios assessed, using the solvents hexane, hydrous ethanol, anhydrous ethanol recovered by glycerol extractive distillation, and anhydrous ethanol recovered by mono ethylene glycol (MEG) extractive distillation. The solid fraction from the extraction proceed to the desolventizer-toster in

order to remove the solvent from the meal. The liquid fraction is carried to an evaporator and then to a solvent recovery section. Hexane is recovered in a set of evaporators and a stripping column. Hydrous ethanol is recovered through distillation. The anhydrous ethanol is recovered by extractive distillation using either MEG or glycerol. In order to proceed with LCA, an inventory of raw-materials, emissions and products was done. GWP gases emissions for each process were calculated, within a birth to gate scope (including the harvest in the field for soybean and sugarcane) and considering energetic allocation to the multiple products.

3. Results and discussion

Ethanol requires a higher solvent-soybean ratio when compared to hexane. So, the energy demands for the first alternative is higher. On the other hand, in a biorefinery concept, more bagasse will have to be burnt, and so more surplus bioelectricity may be sold to the grid. LCA shows that GWP emission in the whole ethanolic process of extraction are slightly higher, due to the higher vapor and cooling water demands. However, since more bioelectricity is produced, the GWP related to soybean oil with ethanol extraction is lower than the one with hexane extraction.

4. Conclusions

A life cycle assessment of the extraction of soybean oil with ethanol was performed, and compared to the conventional hexane extraction. The GWP emission related to the soybean oil extracted with ethanol was lower than the one with hexane. Boeletricity and vapor generated play an important role in this process. Further studies could contemplate the integration with ethanolic biodiesel processes.

References

[1] Abiove – Brazilian Association of Vegetal Oil Industries, 2016. Biodiesel: long term opportunities and challenges (in Portuguese).http://www.abiove.org.br/site/_FILES/Portugues/07102016-131231-07_10_2016_n-_cenario_para_o_biodiesel_em_2030(2).pdf (accessed 26 March 2019).

[2] Ferreira, M. C., Bessa, L. C., Abreu, C. R., Meirelles, A. J., Batista, E. A., 2018. Liquid-liquid equilibrium of systems containing triolein+(fatty acid/partial acylglycerols/ester)+ ethanol: Experimental data and UNIFAC modeling. Phase Equilib.(476), 186-192. https://doi.org/10.1016/j.fluid.2018.07.030

[3] Sawada, M.M., 2014. Effects of different alcoholic extraction conditions on soybean oil yield, fatty acid composition and protein solubility of defatted meal. Food Res. Int. 62, 662-670. https://doi.org/10.1016/j.foodres.2014.04.039.

[4] Toda, T.A., Sawada, M.M., Rodrigues, C.E., 2016. Kinetics of soybean oil extraction using ethanol as solvent: Experimental data and modeling. Food Bioprod. Process. 98, 1-10. https://doi.org/10.1016/j.fbp.2015.12.003

ECCE12
The 12th EUROPEAN CONGRESS OF CHEMICAL ENGINEERING
Florence 15-19 September 2019

The Application, Required Investments and Operational Costs of Geological CO_2 Sequestration: a Case Study.

Pedro Junior Zucatelli[1], Daniel da Cunha Ribeiro[1], Marielce de Cássia Ribeiro Tosta[1], Gisele de Lorena Diniz Chaves[1], Ana Paula Meneguelo[1]

1 Federal University of Espirito Santo, BR 101 Norte, São Mateus, Espirito Santo, Brazil. Tel: 5527-3312-1590.

**Corresponding author: ana.meneguelo@ufes.br*

Highlights

- Environment.
- Geological Storage.
- Operational costs.
- Global warming..

1. Introduction

Human actions, such as the burning of fossil fuels, the use of aerosols, and biomass combustion, liberate greenhouse gases (GHG) into the atmosphere [1]. The most abundantly released gases and therefore the most responsible for the greenhouse effect are N_2O, CH_4 and CO_2. In particular, CO_2 causes global warming and consequently climate changes.

Carbon sequestration through the Capture, Transport and Geological Storage of CO_2 (CCS technology) is an important alternative for reducing emissions [2] and stabilizing the atmospheric concentration of GHGs from a sustainable development perspective. The geological storage of CO_2 can be safely performed in three types of reservoirs: depleted oil and gas reservoirs, saline aquifers and coal layers. In depleted oil and gas reservoir after the beginning of CO_2 injection, the reservoir pressure increases and an increase of the oil production. However, when the geological storage is in saline aquifers the competitive differential between companies and industries will be based on providing services and manufacture of products with low carbon emissions. However, the main obstacle for CCS implementation in Brazil and in the other countries is the high financial cost [3].

This paper presents the CO_2 storage in a saline aquifer and oil and gas reservoir based on scenarios for the application of CCS projects, investments and operating costs.

2. Methods

The amount of recoverable oil by CO_2 injection varies as a function of the oil displacement mechanism and the characteristics of the field. The maximum amount of oil that can be recovered can be calculated using Equation as follows [4]. The extra percentage of recoverable oil due to CO_2 injection (%EXTRA) is an estimated value based on the API gravity of the oil. Probabilistic studies and simulations were performed by the IEA GHG to determine %EXTRA and was used in this study.

3. Results and discussion

To give an example of the estimated financial profitability resulting from CCS projects applied for CO_2 injection, the historical average of the Brent oil price [5] was designed between the years 2005 and 2018 (Figure 1). In this case study considers the Roncador field (original oil in place is 9.7 billion barrels). For the purpose of comparison, the extra recoverable oil percentages as a result of CO_2 injection were estimated to be 1.3%, 5.3% and 9.3%. From the analysis presented it can be observed that CCS projects yield variable amounts of gross revenue. This variation is directly linked, among other factors, to variations in oil prices and recoverable oil percentages.

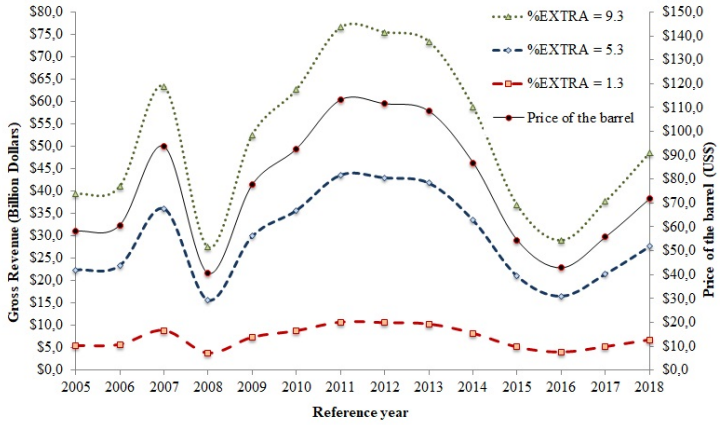

Figure 1 Variation of the average price of the Brent oil barrel and the gross revenue resulting from CCS projects.

The CO_2 storage potential in saline aquifers was analyzed: the Paraná Basin, Solimões Basin and the Santos Basin. These basins have, respectively, CO_2 storage potentials equal to 462 000, 252 000 and 148 000 MtCO2.

4. Conclusions

Using mathematical models, it can be concluded that the Roncador field presents higher gross revenue when the amount of extra oil that can be retrieved is 9.3% (US$ 48.55 billions approximately in 2018). Additional calculations show that the Paraná saline aquifer has the highest gross revenue (US$ 6.90 trillions in 2018) when compared to the Solimões (US$ 3.76 trillions approximately in 2018) and Santos saline aquifers (US$ 2.21 trillions approximately in 2018) if a CCS project were to be employed.

References [Calibri 10]

[1] X. Li, N. Wei, Y. Liu, Z. Fang, R.T. Dahowski, C.L. Davidson. CO2 point emission and geological storage capacity in China. Energy Proc.1 (2009) 2793-2800.

[2] Qiao, X. and Li, G. 2014. Factors influencing the safety of CO2 geological storage in deep saline aquifers. Environmental Engineering and Management Journal 13: 2917-2928.

[3] G.M. Jannuzzi M.K. Pop. Development, cooperation and transfer of low carbon energy technologies. In: Climate change in Brazil: economic, social and regulatory aspects. Brasília: IPEA (2011) 157.

[4] C. Hendriks, W. Graus, F. Van Bergen. Global Carbon Dioxide Storage Potential And Costs. Report nº EEP – 02001, ECOFYS. Utrecht, Netherlands (2004).

[5] Investing. Commodities. Accessed August 21, 2018. https://goo.gl/JM5ihY.

ECCE12
The 12th EUROPEAN CONGRESS OF CHEMICAL ENGINEERING
Florence 15-19 September 2019

Reuse of coke oven and flue gases into methanol: a techno-economic assessment.

Jean-François Portha[1], Wilmar Uribe-Soto[1], Jean-Marc Commenge[1], Laurent Falk[1]

[1] *Université de Lorraine, Laboratoire Réactions et Génie des Procédés, UMR 7274, 1 rue Grandville, BP 20451, 54001 Nancy Cedex, France.*

**Corresponding author: jean-francois.portha@univ-lorraine.fr*

Highlights

- Methanol synthesis process is simulated using a computer aided design software.
- A techno-economic assessment is performed to evaluate the process viability.
- A preliminary carbon balance is performed.

1. Introduction

The iron and steel industry is one of the main energy intensive industrial sectors in the world. The associated CO_2 emissions are then very large representing, in 2006, 30% of the 7.2 Gt of direct CO_2 industrial emissions [1]. To mitigate these Greenhouse Gases (GHG) emissions, the development of Carbon Capture and Utilization (CCU) processes to reuse wasted gases is a crucial point to succeed in the energetic transition. These gases can be converted into Added Value Products (AVP). Various studies [2] have shown that methanol is a serious candidate as an AVP because it represents an interesting intermediate in chemical industry and offers the possibility to recycle a large quantity of carbon. Moreover, the methanol synthesis process from syngas is available at a commercial stage.

Three main off-gases are generated in the steelwork sector: the Blast Furnace Gas (BFG), the Basic Oxygen Furnace Gas (BOFG) and the Coke Oven Gas (COG). These gases, produced transiently, are classically used for energy integration in the steel mills or even burnt in flares without any profit. The development of transient processes able to convert these gases could be an interesting solution. This work focuses on the thermochemical reuse of COG that can be produced either in a steelwork or in an isolated coking plant. Interesting ways of COG reuse could be considered such as hydrogen recovery, syngas production or chemical looping [3]. Different process structures are investigated and assessed to produce methanol by COG conversion and by CO_2 reuse from flue gases.

2. Methods

COG contains mainly H_2 and CH_4 leading to two main case studies considered in this work to produce almost pure H_2: (i) the direct recovery of H_2 in the COG, and (ii) the reforming of CH_4 contained in the COG into H_2. Besides, the required quantity of CO_2 is extracted from flue gases to be hydrogenated into methanol. Both solutions are modelled, simulated and assessed from economic, energetic and environmental point of view. The process structure is divided into four main building block: H_2 separation, CO_2 capture, COG reforming and methanol conversion/purification. For each block, the available technologies are compared based on

heuristic criteria [1,4]. Then, the selected technologies are modeled considering some hypothesis and simulated on a Computer Aided Design (CAD) software (Aspen Hysys) enabling to determine mass flow rates, utility needs and the equipment size. A pinch analysis is performed to improve the heat integration among the different process units. The *levelized cost of methanol* is then calculated using a factorial method. A preliminary carbon footprint analysis was also performed in order to evaluate the potential savings in terms of GHG. The main calculated criteria was the *avoided* CO_2 which corresponds to the CO_2 that is not emitted in the atmosphere with respect to a reference system (methanol from natural gas) of methanol production and takes into account the quantity of CO_2 entering in the reuse process.

3. Results and discussion

The *levelized cost of methanol* is equal to 228 €/ton (+/- 30 %) for the case study (i) and to 268 €/ton (+/- 30 %) for the case study (ii). At current conditions (fossil fuels price, methanol price on the market and level of carbon tax), the cost of methanol from COG is slightly higher than the one produced from fossil fuels. Nevertheless, for a price of Natural Gas (NG) of approximately 3 €/GJ, the methanol production cost of the fossil fuels route will be comparable to the one of the reuse route. Concerning the *avoided* CO_2 criterion, the results obtained for case study (ii) are in good agreement with those obtained in the literature [5].

4. Conclusions

Two process structures describing the reuse of COG and flue gases into methanol are studied. The techno-economic evaluation has enabled to evaluate the CAPEX, the OPEX and finally the *levelized cost of methanol*. This cost is slightly higher than the current production cost of methanol from NG. Nevertheless, the evolution of the NG price on the market together with the evolution of the carbon price may offer some interesting perspectives.

References

[1] A.A. Ramirez-Santos, C. Castel, E. Favre, A review of gas separation technologies within emission reduction programs in the iron and steel sector: current application and development perspectives, Separation and Purification Technology 194 (2018) 425-442.

[2] G.A. Olah, A. Goeppert, G.K. Surya Prakash, Chemical recycling of carbon dioxide to methanol and dimethyl ether: from greenhouse gas to renewable, environmentally carbon neutral fuels and synthetic hydrocarbons, J. Org. Chem.,74 (2009) 487–498.

[3] J.M. Bermudez, A. Arenillas, R. Luque, J.A. Menéndez, An overview of novel technologies to valorise coke oven gas surplus, Fuel Processing Technology, 110 (2013) 150-159.

[4] W. Uribe-Soto, J.-F. Portha, J.-M. Commenge, L. Falk, A review of thermochemical processes and technologies to use steelworks off-gases, Renewable and Sustainable Energy Reviews, 74 (2017) 809-823.

[5] M. Pérez-Fortes, J. C. Schöneberger, A. Boulamanti, E. Tzimas, Methanol synthesis using captured CO_2 as raw material: Techno-economic and environmental assessment, Applied Energy, 161 (2016) 718-732.

Sub- and Supercritical Hydrothermal Processing ror PET Waste Recycling.

Maja Čolnik, Željko Knez, Mojca Škerget*

University of Maribor, Faculty of Chemistry and Chemical Engineering, Laboratory for Separation Processes and Product Design, Smetanova 17, SI-2000 Maribor, Slovenia,

**Corresponding author: mojca.skerget@um.si*

Highlights

- The chemical degradation of PET in sub- and supercritical water.
- Complete depolymerization of PET at short reaction times.
- High yield of monomer TPA.

1. Introduction

Polyethylene terephthalate (PET) is a semi crystalline polymer derived from terephthalic acid (TPA) and ethylene glycol (EG). It has excellent tensile and impact strength, chemical resistance and appropriate thermal stability. Because of the low price it is suitable for wide use. Typical PET products are mainly foils, different plastic bottles, glazing panes, advertising, synthetic fibres [1,2]. Natural decomposition of PET waste is very slow, however, the amount of waste of this material dramatically increases every day on a global scale and consequently, recovery and recycling of PET waste seem to be the best alternatives to minimize its hazards [2]. PET waste can be recycled with four main methods namely, primary (re-extrusion), secondary (mechanical), tertiary (chemical) and quaternary (energy recovery) recycling. Chemical recycling is the most desirable process because the polymer is converted into its monomers (raw materials), which can be used for reuse [3]. Hydrothermal degradation of polymers e.g. PET with sub- and supercritical water is an attractive method for chemical degradation of waste plastics into a wide range of useful products, without expensive and often harmful organic solvents. Furthermore, sub-and supercritical water has a great advantage in use such as: short reaction times, use without catalysts, high yield of monomers and simple after treatment technology [4]. In this study, hydrothermal degradation of PET with sub- and supercritical water has been investigated.

2. Methods

The hydrolysis reaction of PET was carried out in a high pressure and high temperature batch reactor at different temperatures from 250 °C to 400 °C, for reaction time from 1 to 30 min and water/PET waste ratio 10/1. The certain amount of colourless post-consumer PET bottles and water was placed into the batch reactor. The batch reactor was several times flushed with N_2 to avoid oxidation. The initial pressure of N_2 was 20 bar. In addition, the batch reactor was heated to desired temperature and then maintained at the certain temperature for selected reaction time. When the hydrothermal reaction was completed, the reactor was immediately cooled down, the reaction products were collected and analysed. The main degradation products (TPA, EG) and secondary products were determined by HPLC and FT-IR analysis.

3. Results and discussion

PET waste treated in sub- and supercritical water at 250, 300, 350 and 400 °C and at reaction time 1, 10 and 30 min completely decomposed in each case. The experimental results showed that with increasing temperature and reaction time up to 300 °C and 10 min, the yield of TPA increased and then it started to decrease, or it remained the same. The highest yield of TPA has been identified at subcritical conditions, namely at 300 °C and at reaction time 10 min, and it was 96 %. The yield of TPA decreased at supercritical conditions, which can be a consequence of formation of higher amounts of secondary products (benzoic acid, 1,4-dioxane). The purity of precipitated TPA was also analyzed and it was very high (95 %).

4. Conclusions

PET waste was successfully decomposed to main products TPA and EG in sub- and supercritical water. The high yield and purify of monomer TPA were achieved under mild conditions. It was concluded that sub- and supercritical water is an excellent reaction medium for chemical recycling (decomposition) of synthetic polymers.

References

[1] K. Dutta, R. K. Soni, Polym. Sci. Ser. B 55 (2013) 430-452.
[2] A.M. Al-Sabagh, F.Z. Yehia, Gh. Eshaq, A.M. Rabie, A.E. ElMetwally, Egypt. J. Pet. 25 (2016) 53-64.
[3] T. Helmer Pedersen T, F. Conti, Waste Manag. 68 (2017) 24-31.
[4] R. Zhang, J. Bi, Fuel Process. Technol. 85 (2004), 1249-1258.

Reactive Extraction and Solvent Regeneration for Efficient Biobased Byproduct Isolation.

Daniela Painer[1], Susanne Lux, Matthäus Siebenhofer

1 Graz University of Technology, Institute of Chemical Engineering and Environmental Technology

**Corresponding author: d.painer@tugraz.at*

Highlights

- Reactive extraction is perfectly suited for recovery of dilute carboxylic acids.
- Reactive distillation shows high potential for efficient solvent regeneration.
- High yields of methyl esters were achieved in reactive distillation with catalysis.
- Homogeneous catalyst circulation between extraction and distillation is feasible.

1. Introduction

In the biorefinery, downstream processing is often faced with dilute multicomponent mixtures with high tendency to azeotrope formation. In pulping for example, a wastewater is produced, which contains carboxylic acids, mainly acetic acid and formic acid. For a 200 000 t a^{-1} pulp production capacity Sjöström [1] calculated the formation of carboxylic acid and hydroxycarboxylic acid with 75 500 t a^{-1}. Depending on the process, the volatile carboxylic acids are evaporated from the black liquor with the water before the black liquor is incinerated. Due to environmental reasons the carboxylic acids need to be removed from the wastewater. By isolating the pure acids wastewater treatment could contribute to process economics. State of the art process for the recovery of carboxylic acids from aqueous streams is reactive extraction with several distillation steps (e.g. entrainer distillation, vacuum distillation), necessary for solvent regeneration. The aim of this project is to simplify downstream processing for the economic recovery of carboxylic acids from pulping.

2. Methods

Process concept: Reactive extraction is well investigated and perfectly suited for acid recovery from aqueous effluents. For solvent regeneration, reactive distillation is investigated to improve separation performance in distillation. Therefore, the carboxylic acids are esterified with methanol to produce low boiling methyl esters. The esters are continuously separated in the distillate, which forces the reaction equilibrium composition in the solvent to complete conversion. The regenerated solvent with the reaction water is cycled back to the extraction step, where the reaction water is transferred to the raffinate.

Reactive extraction: Liquid-liquid equilibrium experiments were performed for single acid and multi acid aqueous mixtures with Cyanex®923 as reactive extractant (70 w% in *n*-undecane) at 25 °C. The influence of a strong acid (4-dodecylbenzenesulfonic acid) in the solvent phase on the equilibria was quantified.

Reactive distillation: Solvent regeneration was investigated in batch reactive distillation experiments with different acid concentrations and molar ratios of methanol to acid. To increase the reaction rates, strong acidic catalysts were admixed. For catalysis, Amberlite IR-120, a heterogeneous catalyst, and the homogeneous catalyst 4-dodecylbenzenesulfonic acid were studied.

3. Results and discussion

Reactive extraction: The reactive extractant Cyanex®923 showed good extraction efficiencies in single and multi-acid mixtures. In single-acid experiments, formic acid and acetic acid were extracted in a similar extent while for a multi-acid mixture, formic acid was preferably extracted to the solvent phase. This occurs due to the tendency of Cyanex®923 to adduct formation with stronger acids. This behavior was also observed when 4-dodecylbenzenesulfonic acid was admixed to the solvent phase. In this case, Cyanex®923 formed the adducts with the strongest acid, limiting the extraction efficiencies of formic acid and acetic acid. However, at low acid concentration like in wastewater from pulping, enough reactive extractant is available in the solvent phase for adduct formation with all acids. [2]

Reactive distillation: High solvent regeneration efficiency is essential for appropriate extraction efficiency. Uncatalyzed batch reactive distillation experiments showed already high yields of methyl formate transfer to the distillate of 95 %. Acetic acid reacted too slow for appropriate solvent regeneration. The low rate of acetic acid esterification was the main reason for admixing 4-dodecylbenzenesulfonic acid to the solvent phase for catalysis. The yield of methyl acetate increased from 19 % for uncatalyzed to 88 % for catalyzed experiments with an amount of 5 w% 4-dodecylbenzenesulfonic acid in the solvent phase. [2] The heterogeneous catalyst Amberlite IR-120 increased the reaction rate to a similar extent. The main advantage of heterogeneous catalysis is, that catalyst separation from the solvent is not necessary as it is fixed in the distillation column. However, a temperature limitation has to be considered.

In homogeneous catalysis, the drawback is the catalyst separation step. To avoid an additional process step, the influence of the catalyst in the solvent phase during extraction was investigated. As already mentioned the reactive extractant Cyanex®923 prefers adduct formation with strong acids, loss of catalyst to the aqueous phase can be neglected. The limited extraction efficiency can be circumvented by increased phase ratio of the solvent to the raffinate phase. Because of the partition characteristic of the system carboxylic acid/Cyanex 923 based solvent/water, which is a Langmuir-type liquid-liquid equilibrium, low acid concentration in the aqueous phase does not suffer from admixture of 4-dodecylbenzenesulfonic acid.

4. Conclusions

Reactive separation shows high potential for efficient downstream processing of aqueous multicomponent mixtures. Combination of reactive extraction and reactive distillation for solvent regeneration offers the opportunity of economic isolation of acetic acid and formic acid from waste effluents by transferring them into their methyl esters.

References

[1] E. Sjöström, Tappi 60 (1977) 151-154
[2] D. Painer, S. Lux, M., C. Almer, S. Daniel, Siebenhofer, Sep. Sci. Technol. 53 (2018) 1957-1965

Electroreduction of CO_2 to formate using carbon-supported Bi nanoparticles in Gas Diffusion Electrodes in a continuous mode

Guillermo Díaz-Sainz[1*], Manuel Alvarez-Guerra[1], José Solla-Gullón[2], Leticia García-Cruz[2], Vicente Montiel[2] and Angel Irabien[1]

[1]University of Cantabria, Dep. Chemical and Biomolecular Engineering, ETSIIT, Avda. de los Castros s/n, 39005, Santander, Spain; [2]Institute of Electrochemistry, University of Alicante, Apdo. 99, E-03080, Alicante, Spain

**Corresponding author: diazsg@unican.es*

Highlights

- Formate was obtained in a continuous mode with a single pass in a filter-press reactor.
- Bi-GDEs were able to work at a current density up to 300 mA cm^{-2}.
- At a 200 mA cm^{-2}, 4 g L^{-1} of formate was obtained with a high faradaic efficiency (80%).
- Concentrations of formate of up to 18 g L^{-1} were obtained.

1. Introduction

Electrochemical reduction of CO_2 is being considered as an interesting option to store energy from intermittent renewable sources in the form of chemical valued-added products. Among all the different valued-added products, formate is an attractive product used for several industrial applications and particularly, it has been highlighted as a promising fuel for low-temperature fuel cells and as renewable hydrogen carrier [1].

Our previous research on using Catalyst Coated Membrane Electrodes (CCMEs) using tin nanoparticles as catalyst [2] achieved formate concentration up to 19.2 g L^{-1} with a faradaic efficiency (FE) of 50%, a rate of 1.15 mmol m^{-2} s^{-1} and an energy consumption of 244 kWh $kmol^{-1}$ of formate in the output stream of the electrochemical reactor. These results could be improved using Bi as a catalyst material in the cathode according to the growing number of promising results that point to the possibility of electroreducing CO_2 to formate at lower potentials than other metals [3]. This communication is focused on the development of Gas Diffusion Electrodes using carbon-supported Bi nanoparticles (Bi-GDEs), operating in a continuous mode in a filter-press reactor.

2. Methods

Bi-GDEs were prepared by depositing carbon-supported Bi nanoparticles over a Toray carbon paper, used as a carbonaceous support. In the filter-press cell, Bi-GDEs were used as the working electrode and a Dimensionally Stable Anode was used as the counter electrode, whereas an aqueous solution of KCl+$KHCO_3$ and KOH is used as catholyte and anolyte respectively. A cation exchange membrane (Nafion 117®) divides the cathodic and anodic compartments in the cell. The concentration of formate is analyzed by ion chromatograph (Dionex IC 1100).

3. Results and discussion

Working with a electrocatalyst load of 0.75 mg cm^{-2} and electrode area of 10 cm^2, different experiments were carried out at different current densities and electrolyte flow/area ratios for continuous electroreduction of CO_2 to formate in the filter-press type cell, with only one pass of the electrolyte through the cell.

Working at a current density of 300 mA cm^{-2} and electrolyte flow/area ratio of 0.57 mL min^{-1} cm^{-2}, a formate concentration of 5.2 g L^{-1} with a FE, rate and energy consumption of 70%, 11 mmol m^{-2} s^{-1} and 410 kWh per kmol of formate, respectively, were achieved. Decreasing the current density from 300 mA cm^{-2} to 200 mA cm^{-2}, keeping the same value of electrolyte flow/area ratio, the formate concentration decreased to 4 g L^{-1} with a FE and rate around 80% and 8.3 mmol m^{-2} s^{-1}.

Subsequently, the influence of electrolyte flow/area ratio was analyzed in order to obtain a formate product as concentrated as possible, as can be shown in Figure 1.

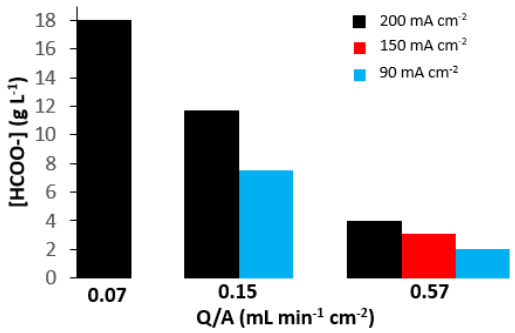

Figure 1. Formate concentration as a function of the current density and electrolyte flow/area ratio.

These results confirm that Bi-GDEs allow working in a continuous electrochemical reactor with higher current densities values compared with recent contributions in literature.

4. Conclusions

It is important to remark that these results were obtained working at higher current densities than previous studies reported in the literature, and they were also obtained in a continuous mode with only one pass of the catholyte through the filter press cell. These conditions are mandatory to remark the feasibility of the continuous electroreduction process using Bi/C-NPS in Bi-GDEs.,

References

[1] A. Irabien, M. Alvarez-Guerra, J. Albo, A. Domínguez-Ramos, Electrochemical Conversion of CO_2 to Value-Added Products, in: Carlos A. Martínez-Huitle, Manuel A. Rodrigo (Ed.), Electrochem, Water Wastewater Treat., Elsevier, 2018: pp. 29-59.

[2] G. Díaz-Sainz, M. Alvarez-Guerra, J. Solla-Gullón, L. García-Cruz, V. Montiel, A. Irabien, Catalyst coated membrane electrodes for the gas phase CO_2 electroreduction to formate, Catal. Today 2018, Article in press.

[3] C.W. Lee, J.S. Hong, K.D. Yang, K. Jin, J.H. Lee, H.Y. Ahn, H. Seo, N.E. Sung, K.T. Nam, Selective Electrochemical Production of Formate from Carbon Dioxide with Bismuth-Based Catalysts in an Aqueous Electrolyte, ACS Catal. 8 (2018) 931-937.

ECCE12
The 12th EUROPEAN CONGRESS OF CHEMICAL ENGINEERING
Florence 15-19 September 2019

Electrochemical Production, Downstream Processing and On-Site Application of Hydrogen Peroxide

Carsten Cremers, Jan Meier, Dusan Boskovic, Angelika Eberhardt, Alexander Mendl, Giancarlo Piscopo, Stefan Loebbecke[1]

[1] *Fraunhofer Institute for Chemical Technology ICT, 76327 Pfinztal, Germany*

**Corresponding author: Stefan.loebbecke@ict.fraunhofer.de*

Highlights

- Green electrochemical synthesis of hydrogen peroxide
- Purification and concentration of H_2O_2 by means of membrane distillation units
- Process analysis for monitoring H_2O_2 concentration
- On-site production and forward integration of H_2O_2 streams into subsequent reaction processes (here: selective oxidations)

1. Introduction

Today, in many countries the percentage of produced electricity that is obtained from renewable sources is significantly rising. This energy transition has led to the generation of low-carbon electricity, which opens up new pathways for the design of current-driven (›power-to-X‹) chemical processes.

Hydrogen peroxide H_2O_2 is considered one of the most versatile and powerful chemical oxidants for a wide range of chemical reactions. It is environmentally friendly, selective and also highly active for various oxidation processes including chemical production, paper and pulp bleaching, waste water treatment or disinfection processes. Today, hydrogen peroxide is mainly produced in world-scale production facilities consuming not only huge quantities of energy and organic solvents but also generating substantial quantities of waste. Moreover, large scale production processes of hydrogen peroxide require significant logistical resources concerning transport, storage and safety. Many users of smaller and medium quantities, however, would prefer to avoid the complicated logistics and storage, and to produce H_2O_2 themselves as required at their own location, using simpler methods.

2. Methods

We have developed a demonstration process for the decentralized electrochemical production of hydrogen peroxide and its continuous supply to a downstream chemical process. The key element of the here presented small-scale process is an on-site and on-demand production concept for H_2O_2 to avoid the transport, storage and handling of huge amounts of highly concentrated hydrogen peroxide.

3. Results and discussion

The demonstration process enables the continuous, electrochemical production of H_2O_2 in the aqueous reaction system through the cathodic partial reduction of atmospheric oxygen. Key issues were the development of suitable electrocatalysts and the design of the electrochemical reactor including the up-scaling of appropriate gas diffusion electrodes.

The synthesis is conducted in acidic electrolytes which are later separated in the process. Continuous processing techniques, some of which use micro-structured process components, have been developed for the subsequent purification and separation of the produced H_2O_2 from the electrolyte, and for the reuse of the electrolyte in the electrochemical process. The produced hydrogen peroxide can be directly connected to subsequent chemical processes where H_2O_2 solutions are required. As a consequence, the downstream processing of the electrochemical synthesis includes also a concentration step, where beforehand purified H_2O_2 is concentrated to the single-digit percentage range as it is typically required in fine chemical oxidation processes. Both separation units are based on membrane distillation. Raman spectroscopic process analysis allows tracking of the hydrogen peroxide concentration almost in real-time along the entire process chain (synthesis, separation, concentration, and hand-over to subsequent process).

The forward integration of the pre-treated H_2O_2 stream has been demonstrated using the example of a selective oxidation reaction being applied for the desulfurization of fuels. Through the parallel development of suitable oxidation catalysts, full conversion and fast desulfurization rates were demonstrated using low-concentrated (e.g. 3%) H_2O_2 solutions.

4. Conclusions

The application potential of decentralized, small-scale units for the continuous on-site production of H_2O_2, which can ideally be operated with 100% sustainable electricity, goes far beyond classical chemical synthesis processes. There is an increasing demand for environmentally-friendly oxidation and bleaching processes in numerous other sectors, such as medical and hygiene technology, food technology, agriculture, water treatment and the textile and cleaning industry.

A new heterogeneous organocatalyst for Knoevenagel Reaction process intensified by microwaves

Lilivet UBIERA [1], Isabelle POLAERT [1], Chandrashekhar RODE [2], Sanjay JADHAV [2], Dominique SEGUIN[1]

1 Normandie University, INSA Rouen, LSPC, Laboratoire de Sécurité des Procédés Chimiques, EA 4704 - INSA Rouen, Avenue de l'Université – Saint-Étienne-du-Rouvray cedex 76801 France
2 Chemical Engineering and Process Development Division, CSIR-National Chemical Laboratory, Dr. Homi Bhabha Road, Pashan, Pune 411008, India

**Corresponding author: E-mail address: Isabelle.polaert@insa-rouen.fr*
Tel: (33)-2-32-95-66-68 Fax: (33)-2-32-95-66-96

Highlights

- Heterogeneus organocatalyst under microwave heating
- Comparison between conventional and microwave heating for knoevenagel reaction
- Reuse of organocatalyst

1. Introduction

Sustainability in chemical synthesis is one of the main objectives nowadays, meant to be addressed by maximizing the industry production efficiency and minimizing the environmental costs. In order to develop an eco-friendlier relationship with our planet, the society has created new legislations which encourage the design of organic reactions using greener strategies such as the combination of microwave heating with effective, low cost and reusable catalysts.

One powerful and commonly used reaction for the formation of carbon-carbon bonds is the Knoevenagel condensation, an addition of a carbanion to an electrophilic carbonyl group in the presence of a weak base. Several reaction methodologies have been reported so far in literature and the interest is mainly focused on the development of environmentally and economically friendly reaction protocols. In this work, the Knoevenagel reaction was tested using 1,4-diabycyclo [2.2.2] octane (DABCO) an organic molecular catalyst (organocatalyst) which is attractive due to its easy reproducibility and low cost.

Various experimental conditions have been tested in order to obtain a greener protocol. The major drawback found was the difficulty to recycle the organocatalyst used due to its inherent instability and miscibility with solvents (2). To facilitate the reuse of the catalyst, the immobilization of DABCO over the mesoporous silica MCM-41 was done. To the best of our knowledge this was done for the first time in literature.

In this investigation, the objective was not only limited to a cleaner protocol but also extended to energy efficiency. The latter was achieved by coupling the process with microwave heating which resulted in a significant reduction in reaction time, precise control of temperature and hence better

energy efficient. The combination of these techniques promise to be an interesting way to intensify Knoevenagel condensation based processes.

2. Methods

The knoevenagel condensation using 4-chlorobenzaldehyde and malononitrile as reagents to obtain 4-chlorobenzilidene malononitrile as a product, was done using organocatalysts as DABCO and DABCO supported on mesoporous silica-MCM 41, allowing to have a homogenous and heterogeneous medium of reaction. The reaction was tested both in microwave and classical heating. For the identification and quantification of reagents and products a GC-FID (Gas Chromatography-Flame Ionization Detection) is used. The given results are used to calculate the reaction yield in time.

3. Results and discussion

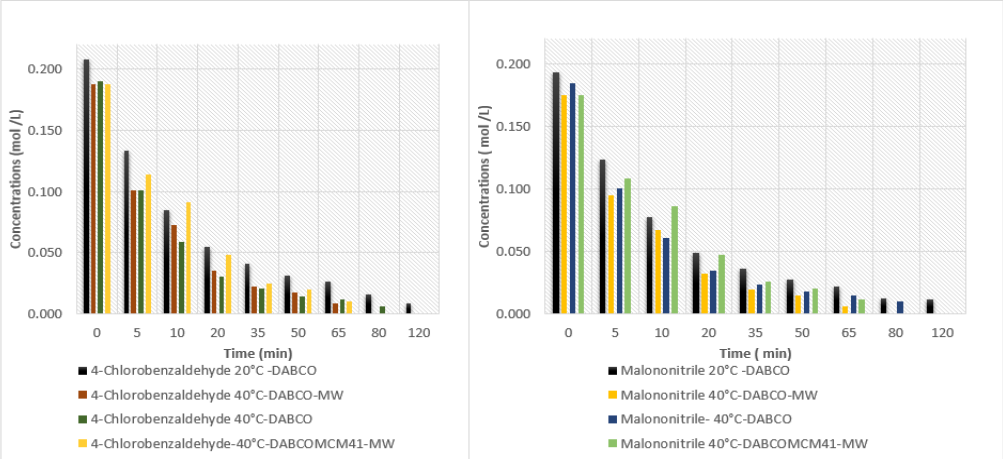

Graphic 1. Reagent's Concentration evolution with time for different operational conditions (Malononitrile = 0,20 mol/L 4-Chlorobenzaldehyde=0,20 mol/L DABCO= 0,00217 mol/L Agitation = 8 Pressure: 1 atm) *MW= Microwave heating

This supported catalyst was tested under the conditions same as its homogenous analogue (DABCO), resulting in the same efficiency in addition to the fact that it could be recovered from the reaction mixture and reused without any significant loss of activity. Microwave heating was also compared to classical one.

4. Conclusions

A new heterogeneously supported DABCO catalyst has been developed for improving the Knoevenagel reactions. It allows easy recovery of the catalyst and its reuse, without any significant loss of activity which is a great improvement towards more sustainable processes. The combination of this type of catalysts with microwave heating is also promising by reduction of reaction time and cost, and by using a non-toxic and environmentally friendly reaction protocol.

References

[1] Bandala,et al. (2009). Optimized Methodologies in Asymmetric Organic Synthesis Applying Microwaves. J. Mex.Chem.Soc., 53(3), 147-154.
[2] Shaikh, I. R. (2014). Organocatalysis: Key Trends in Green Synthetic Chemistry, Challenges, Scope towards Heterogenization, and Importance from Research and Industrial Point of View. Journal of Catalysis(402860).

doi:10.1155/2014/402860

Maximizing the use of regenerated Gas Oil Hydrotreating (HDT) catalyst for re-utilization in Kero HDT & Naphtha HDT units

Nilesh Chandak[1], Adel Hamadi, Menwa Dakhan, Ashjan Alkatheeri, Abraham George, Stephane Morin and Mikael Berthod

ADNOC Refining, Research Centre Division, P.O. Box: 3593, Abu Dhabi, U.A.E.

**Corresponding author[1] , Email: nchandak@adnoc.ae*

Highlights

- Applied research work for the refinery process optimization
- Experimental data from pilot plant to calculate reaction kinetics, analyze aromatics & H consumption
- Study Impact of the changes on catalyst activity, product yield & product quality
- sustainability objectives to reduce waste generation, recycle and reuse of spent catalyst

1. Introduction

Gas Oil (GO) hydrotreater in the ADNOC refinery is designed to process Heavy Gas Oil (HGO) and Light Gas Oil (LGO) coming from crude/condensate units and produce Gas Oil with total sulphur ≤ 10 ppmw. During turnaround, GO hydrotreating (GO HDT) catalyst was unloaded from this unit after serving one cycle of 4 years. On other hand, at the time of catalyst selection it was envisaged that this catalyst can be used for two cycles. So this catalyst still having useful life leftover was considered for reuse in other hydrotreaters viz. Naphtha HDT and Kerosene HDT units in the refinery. Naphtha HDT unit is processing Whole Naphtha (WN) coming from Crude Distillation Unit (CDU) to produce max 0.5 ppm sulfur content of Heavy Naphtha (HN) which is the feed stock of Catalytic Reforming (CR) unit. Kerosene HDT unit is processing Kero or light gas oil to produce Kero with less than 10 ppm sulphur. Hence pilot plant study was undertaken to evaluate the reuse of catalyst for the second cycle to process WN and Kero, to produce on spec product, to evaluate regenerated GO HDT catalyst, Estimate the H2 Consumption, Analyze product PONA at higher WABT & Assess the performance of catalysts at higher nitrogen content more than 10 ppm wt.

2. Methods

Hydrotreating experiments were carried out according to refinery unit test conditions, with reference feed stock Whole Naphtha & raw Kerosene and were processed using a GO HDT regenerated catalyst in a pilot reactor at fixed operating conditions, as listed below Table # 01. The pilot plant test started with LHSV 4 hr^{-1} at 275 ˚C and on specs product for Nitrogen were achieved but sulphur was at 1.3 ppm. Hence WABT was increased to 280 ˚C temperature to achieve product target sulphur content below 0.5 ppm. Test points were created for increased throughput upto to 5 hr^{-1} for NHDT. For Kero HDT, test points were also varied for pressure, temperature & LHSV.

3. Results and discussion

Whole Naphtha has low nitrogen content but the performance of the catalyst was tested at high nitrogen content in the feed (>10 ppm) because GO HDT catalyst has higher HDS activity than HDN activity and it was observed that this GO HDT catalyst is capable to handle feeds having the higher nitrogen range. Hydrogen partial pressure was reduced from 25.5 kg/cm^2 to 23.7 kg/cm^2 and there was no noticeable change in catalyst performance.

Table 1. Test operating conditions

Test	FEED	Pressure	LHSV	H2/HC	Temp	Sulfur in Product	N in Product
Nº		(kg/cm^2)	(h^{-1})	(Nm^3/m^3)	(°C)	(ppm)	ppm
1 - 7	Naphtha	25.5 to 23.7	4 to 5	44	275 to 320	1.2 to < 0.5	<0.3
8	Naphtha (10 ppm N)	23.7	4.5	44	280	< 0.5	<0.3
9-11	Kero	44.24 to 40.26	2 to 2.5	305	275 to 280	3.8 to 1.4 (Mercapan S)	-

For kerosene HDT, pilot plant test was started at LHSV 2 hr^1 at 275˚C and product specs were observed within acceptable range. The mercaptan sulphur in the product was reported around 3 ppm (on specs) for the first test point, then temperature was increased to 280 ˚C to compare the results with current operation of Kero HDT unit. Also at higher LHSV of 2.5 hr^{-1}, on spec Kero with <10 ppm mercaptan sulphur was achieved. Furthermore, hydrogen partial pressure was reduced from 44.24 kg/cm^2 to 40.26 kg/cm^2 and there was no noticeable change in mercaptan sulphur.

Hydrogen consumption has been estimated to 14.67 Nm3/m3 Kero HDT & 2.63 Nm^3/m^3 for Naphtha HDT, by performing a material balance for the selected test points at stable operating conditions accompanied by a series of analysis.

4. Conclusions

Based on the pilot plant test, it was concluded that the GO HDT catalyst is suitable to re-utilize to process whole naphtha and kero to produce on spec product. As per the results from the variable test points, both units can operate satisfactorily at higher LHSV and at lower hydrogen partial pressure without any impact in the product quality. For Naphtha HDT Unit, there is no tendency of aromatic saturation at higher temperature i.e. 320 ˚C. Hence there is no effect on feed selectivity for downstream reforming unit. Also it was observed that this catalyst is capable of handling higher nitrogen content i.e. 13.3 ppm in Naphtha feed. Taking into consideration the lower SOR temperature for Naphtha HDT unit at 280 ˚C and for Kero HDT unit at 295 ˚C, expected cycle length will be more than 4 years.

References

[1] M. Marafi, A. Stanislaus, Resources, Conservation and Recycling, 53 (2008) 1–26
[2] P Laveille,, A Riva, A Salameh, P Dufresne, S Morin, M Berthod, https://doi.org/10.2516/ogst/2018053
[3] R. Iwamoto, H. Koshika, N. Takahashi, K. Inamura, Japan Petroleum Institute, 48 (2005) 319-323
[4] I Guibard, S.Kressmann, V.Harle, www.eurecat.in/Technical_Doc/A_fresh_performance_2.pdf.
[5] J. Ancheyta, P. Morales, G. Betancourt, G. Marroquín, J. Muñoz, Energy Fuels, 18(4) (2004) 1001–1004
[6] N Chandak, A George, A Chaudhry, S Khalifa, S Morin, Cat Today, Volume 305, 1 May 2018, Pages 82-91
[7] R Venkatesh; M Bhaskar; S Sakthivel; N Selvaraju ; M Velan, Pet Sci Tech, 28:93–102, 2010

ECCE12
The 12th EUROPEAN CONGRESS OF CHEMICAL ENGINEERING
Florence 15-19 September 2019

Life Cycle Assessment of a Biomass-to-Liquids process

Caretta Antonio[1]*, Bua Letizia[1]

[1] Eni spa / Renewable Energy & Environmental R&D via Giacomo Fauser 4, 28100 Novara, Italy
*Corresponding author: antonio.caretta@eni.com

Highlights

- LCA of Biomass-to-Liquids (BTL) process
- Environmental impact assessment of biomass-derived fuel
- Comparison of LCA results to RED and to REDII
- Bio-fuels sustainability

1. Introduction

Reducing the environmental impact of technologies, processes and products is nowadays an important scientific challenge. In particular, the substitution of fossil fuel with biomass-derived fuels helps towards reaching this goal.
The scope of this work is to assess the environmental impact of the Biomass-to-Liquids (BTL) diesel. The Biomass-to-Liquids process (BTL) is a thermo-catalytic pathway to transform biomass to liquid fuels, in particular to middle distillates including diesel cuts.
The main steps of this technology include thermal gasification of biomass, followed by syngas clean up, Fischer-Tropsch synthesis and hydrocarbon isomerization to produce suitable synthetic fuels [1], [2].
The environmental impact of biomass-derived fuels has been calculated following the LCA methodology reported by the Renewable Energy Directive. The result must be compared to the limits imposed by RED (2009/28/EU) [3] and by the most recent RED II (2018/2001/EU) [4].
This study confirmed that the environmental impact (in term of Global Warming Potential, GWP) of BTL diesel is lower than the one of fossil diesel and respects the emission reduction suggested both in RED and in RED II framework.

2. Methods

The methodology followed is the LCA (Life Cycle Assessment) based on the International Organization for Standardization standard procedures (ISO 14040 – ISO 14044 series) [5], [6]. The tool used for evaluation is the software GaBi (property of the company Thinkstep).
The Life Cycle Inventory (LCI) for the LCA come from the BTL model simulation, developed internally during a project related to biofuel production. It is worth to noting that the LCA results are strictly affected by site characteristics and scenario definition.
In *Goal&Scope* definition, the Functional Unit (FU) is defined as 1 MJ of produced diesel and the System Boundaries are extended from raw biomass to bio-fuels products (diesel, naphtha). Starting from the available input data, a *Life Cycle Inventory* (LCI) has been built up and a model for the system has been defined and inserted in the software GaBi for simulation. The results have been expressed in terms of Global Warming Potential (GWP) using a 100-years timeframe according to CML2001–Apr.2013 method [8]. These results give the *Impact Assessment* related to the BTL

process. Each one of the three LCA phases (Goal&Scope, LCI and Impact Assessment) is subject to interpretation for results improvement.

3. Results and discussion

This LCA study describes a competitive path to produce fuels via BTL process. The assessment has been applied to different species of biomass in input. Each kind of biomass causes a different environmental impact. These differences could be related to cultivation procedures, water and fertilizers consumption. Usually, considering the RED, the cultivation phase (CO_2 capture by the biomass) balances the use phase of the fuel. In present study both phases are considered separately, in order to perform a sensitivity analysis related to the biomass.
The comparison between the environmental impact of BTL-diesel and of conventional fossil fuel defined by the RED and the REDII points out the environmental advantages by using BTL-fuels in the direction of reducing global greenhouse gas emissions.

4. Conclusions

The environmental impact of BTL-diesel is biomass dependent. In many cases analyzed it is plenty lower than the impact due to fossil fuel reference both as reported in RED and in REDII datasets and it respects the reduction of GHG higher than 60% as requested in RED (plant in operation after 6th October 2015) and than 65% as reported in REDII (plant in operation after 1st January 2021).

References

[1] Perego C., Bianchi D., Bua L., Biomass catalytic conversion to fuel and energy, La chimica e l'industria, Marzo 2010; 90-97.
[2] Zennaro R., Ricci M., Bua L., Querci C., Carnelli L., d'Arminio Monforte A., Syngas: The Basis of Fischer-Tropsch (Book Chapter), February 2013
[3] DIRECTIVE (EU) 2009/28 OF THE EUROPEAN PARLIAMENT AND OF THE COUNCIL of 23 April 2009 on the promotion of the use of energy from renewable sources and amending and subsequently repealing Directives 2001/77/EU and 2003/30/EU
[4] DIRECTIVE (EU) 2018/2001 OF THE EUROPEAN PARLIAMENT AND OF THE COUNCIL of 11 December 2018 on the promotion of the use of energy from renewable sources
[5] SO 14040: Environmental Management_Life Cycle Assessment_ Principals and Framework; International Organization for Standardization: Geneva, Switzerland, 2006a.
[6] ISO 14044: Environmental Management_Life Cycle Assessment_ Requirements and Guidelines; International Organization for Standardization: Geneva, Switzerland, 2006b.
[7] GaBi Software, ThinkStep: http://www.gabi-software.com/software/gabi-software/
[8] CML2001-Apr.2013: http://cml.leiden.edu/software/data-cmlia.html

Supercritical CO_2 impregnation of cotton gauze with bioactive compounds from *Olea europea* leaves

Lourdes Casas Cardoso, María Teresa Fernández Ponce, Cristina Cejudo Bastante, Casimiro Mantell Serrano, Clara Pereyra López, Enrique Martínez de la Ossa.

Chemical Engineering and Food Technology Department, Wine and Agrifood Research Institute (IVAGRO), University of Cadiz, Cádiz, Spain.

**Corresponding author: lourdes.casas@uca.es*

Highlights

- The extract from *Olea europea* leaf showed antioxidant and antidiabetic capacity.
- Loaded cotton gauze with olive extract was produced by SSI.
- Applying 100 bar and 55 °C favored olive extract impregnation in cotton gauze.

1. Introduction

Food processing generates a substantial volume of solid organic by-products, which are usually used for composting or even discarded in open areas, thus causing potentially environmental problems. The valorization of food industry waste may include several options including extraction and impregnation of bioactive compounds for utilization in the food, cosmetic and pharmaceutical industries.

Supercritical solvent impregnation (SSI), is an efficient and environmentally friendly technique, that is used to the deposition/incorporation of active agents into polymeric matrices. The impregnation of active molecules occurs as a consequence of the interaction balance between the active substance, the matrix and the supercritical phase, which results in an adsorption or a physicochemical attachment of molecules to the polymeric matrix. Furthermore, some of SSI's advantages are that processes run at moderate temperatures, thus avoiding degradation of thermolabile compounds, and solvent free products can be obtained from the complete desorption of CO_2 gas during the depressurization step.

SSI can be used to develop functional gauze textiles loaded with antioxidant, antimicrobial, anti-inflammatory or antidiabetic agents in order to produce functional textiles with potential applications for instance, in the pharmaceutical field. The main objective of this work was to study the SSI of bioactive leaves extract into cotton gauze. The potential biologically activity of extracts prepared from *Olea europea* leaves were evaluated.

2. Methods

Firstly, an extract from *Olea europea* leaf was obtained by Enhanced Solvent Extraction (Thar Technologies, model SF1000) using CO_2+ethanol (1:1 v/v) at 200 bar and 80 ºC, a flow rate of 10 g/min and during 2 h. Results were analyzed according to the global yield, antioxidant activity determined by 2,2-diphenyl-1-picrylhydrazyl assay [1] and inhibition of α-glucosidase evaluated by p-nitrophenyl-a-D-glucopyranoside [2].

Afterwards, the extract was used as active substance in the supercritical impregnation of cotton gauzes using an equipment supplied by Thar Technologies (Pittsburgh, PA, USA, model SF500). The influence of the operating conditions such as pressure (100-400 bar) and temperature (35-55 ºC) were studied.

3. Results and discussion

The use of ethanol as co-solvent in the enhanced solvent extraction of active compounds from *Olea europea* leaf favored the obtaining of high global yields (12.27 %). The antioxidant activity index of the *Olea europea* leaf extract labels it as "moderate antioxidant" following the Scherer et al. classification [1]. On the other hand, the pharmaceutical potential of olive extract was evaluated by the α-glucosidase inhibition assay as a determination of the antidiabetic capacity. This extract exhibited a total inhibition against α-glucosidase at 130 ppm.

The results from the experiments carried out at different pressures (100-400 bar) and temperatures (35-55 °C) on the SSI process are displayed in **Fig. 1**. It can be seen that extract was efficiently impregnated into cotton gauze. The best result was obtained at 100 bar and 55 ºC.

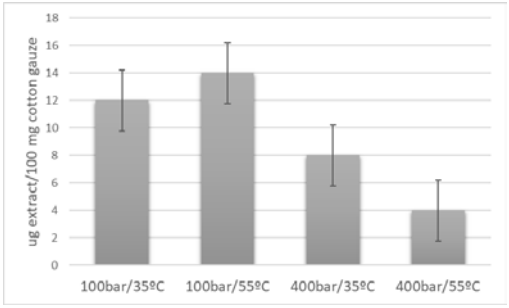

Figure 1. Load of cotton fabrics processed at the different pressures and temperatures.

The impregnation efficiency is governed by the partition coefficient defined as the ratio of equilibrium concentration of the active substance between the polymer matrix and the supercritical phase. In this case, a low solubility of active compounds at 100 bar and 55 ºC favored the impregnation of *Olea europea* leaf extract due to a higher affinity for the polymer matrix.

4. Conclusions

The use of ethanol as co-solvent favored the obtaining of high global yields and the recovery of antioxidant compounds. The extract exhibited a total inhibition against α-glucosidase with 130 ppm.

SSI process has demonstrated to be a promising alternative for the production of active cotton fabrics. Actually, cotton gauze with a high content in antioxidant and antidiabetic were produced in this study. This is a technology that presents an outstanding potential in pharmaceutical applications.

References

[1] R. Scherer, H.T. Godoy, Food Chem. 112 (2009) 654-658.
[2] Y.Li, S.Wen, B. Prasad Kota, G. Peng, G, Qian Li, J. Yamahara, B. Roufogalis. J. of Ethnopharmacology. 99 (2005) 239-244.

ECCE12
The 12th EUROPEAN CONGRESS OF CHEMICAL ENGINEERING
Florence 15-19 September 2019

Data intensive based tool for supporting circular economy in agri-food process.

Jean-Pierre Belaud[1], Nancy Prioux[2], Claire Vialle[2] et Caroline Sablayrolles[2]

[1] *Laboratoire de Génie Chimique, Université de Toulouse, CNRS, Toulouse, France;*
[2] *Laboratoire de Chimie Agro-industrielle, Université de Toulouse, INRA, Toulouse, France;*
**Corresponding author: jeanpierre.belaud@ensiacet.fr*

Highlights

- To support circular economy with agri-food waste valorization.
- To propose a life cycle thinking based approach for selecting biomass and process.
- To take benefit from public and scientific data.

Each year, agriculture generates 700 million tonnes of waste in Europe and with the increase of the world population this number increases. This augmentation of the waste production creates an increase of its environmental impacts. However, a part of this agricultural waste consists in lignocellulosic by-products which can be transformed into bio-energy, biomolecules or biomaterials. A solution to reduce the agricultural waste is to transform these lignocellulosic by-products thanks to sustainable process operations. The assessment of the sustainability is now integrated to more and more agrifood process. The sustainable development for the agricultural by-product valorization must be economically efficient, socially fair and environmentally sustainable like every sustainable development. A new business model appeared recently -the circular economy and industrial ecology- to lead a more sustainable development [1]. It contributes to reconcile the environmental, economic and social aspects of sustainability. Our application to contribute at this reconciliation is the creation of an approach to help for the choice between different biomasses and industrial paths. The tool created from this approach allows to compare six different biomasses (rice straw, bagasse, corn stover, sugarcane straw, wheat straw and spruce chips) and their associated processes.

To help the reconciliation, it is possible to use the Life Cycle Thinking (LCT), which considers the full life cycle of the agriculture supply chain. This thinking is used in the Life Cycle Assessment (LCA) method to evaluate the potential environmental impact of a product or service over its entire life cycle. A lot of articles are published to compare different waste management systems under a LCA. The data can be obtained by two ways: directly, by on-site measurement, or indirectly – from different data bases. Generally, the data for the foreground system are obtained directly and for the background system indirectly. There are more and more scientific articles published describing agricultural by-product valorization processes and operations. These articles are a high added value data source for the foreground system. As the on-site measurements are expensive and time-consuming, in this way the scientific articles allows the LCA researcher to save time and money. Yet, prospecting a huge quantity of unstructured data is difficult and cannot be done without some degree of automation. The utilization of the Big Data tools can be relevant to structure knowledge into formal representations for exploitation by computers. The main goal of this work is to develop a data intensive approach and the associate tool to supporting the decision in the context of circular economy in the domain of the agri-food industry. The three objectives set of this goal are (1) to benefit from a large quantity of data for a same process thanks to all the experiments carried out

by the researchers all around the world (2) to avoid experiments which are time consuming and expensive (3) to place the LCA upstream in a preliminary eco-design approach in order to select agriculture supply chain or to fix trends.

The approach proposed in this paper is based on big data tools, sustainability engineering and life cycle thinking for supporting decisions on agricultural by-product valorization dedicated to engineers, academics, managers and policy decision makers. The approach is divided into five steps - It is always possible to return to the previous stage to complete the data or to add details:

1. Definition of the goal and scope of the study
2. The extraction of relevant information from heterogeneous data sources (from big data)
3. Life cycle inventory
4. Indicators calculation (from Life Cycle Impact Assessments, “green chemical” metrics and economic indicators calculations)
5. Ranking the results and analysis (from data visualization)

To validate the approach, a tool is created with VBA-Excel. This tool allows to extract the process data, to make the LCI thanks to the EcoInvent v3 database, to calculate the environmental and economic impacts and then to visualize the results for the comparison of lignocellulosic biomass pretreatment processes. The bioconversion of lignocellulosic biomass is a promising method for the production of bio-energy, biomolecules or biomaterials. This bioconversion involves the enzymatic hydrolysis of the biomass to release glucose. Biomass pretreatment is essential, to decrease crystallinity, increase the specific surface area and porosity, and separate the major constituents.

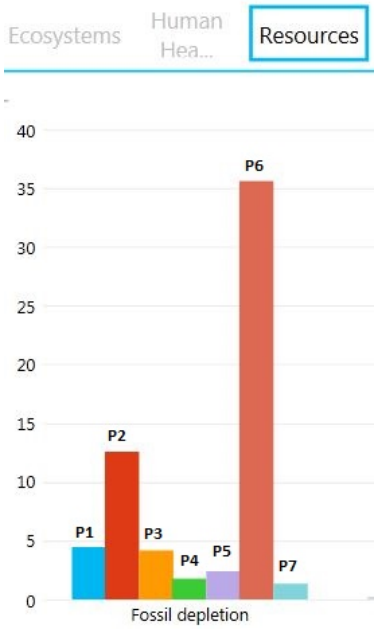

Corn stover illustrates the approach (picture beside). 7 processes involving different technologies are under study. Their sequence of unit operations are of 3 kinds: only mechanical operations (P7), mechanical and physico-chemical operations with press and separation (P3, P4, P5, P6), and mechanical, physico-chemical operations with press, separation and extrusion (P1, P2). LCA impact indicator “Fossil depletion” from ReCiPe 2008 end-point is shown. The approach should enable researchers, and other users, to identify the “best” process for a specific biomass. That could be improved by enhancing ranking procedures and including scaling (to address industry needs). The interactive visualization also allows the approach user to move in different levels of the results. Furthermore, in the tool created, the environmental indicators from LCA could be combined with economic indicators, providing a more general overview of the various processes and technologies regarding to sustainability management.

References

[1] JP Belaud, C Adoue, C Sablayrolles, C Vialle, A Chorro, Decision making approach for industrial ecology: layout and commercialization of an industrial park, Chemical Engineering Transactions 57, 1561-1566, 2017.

CO_2 reduction utilizing perovskites as photocatalysts in a versatile 3D printed microreactor

Jose A. Santamaría Cordero1[1,2], Leslie W. Pineda[2,3], Marisol Ledezma[2,3], J. Esteban Durán[1,2]

1 School of Chemical Engineering; 2 Electrochemical and Chemical Energy Recearch Center (CELEQ); 3 School of Chemistry, University of Costa Rica, San José, 11501, Costa Rica

**esteban.duranherrera@ucr.ac.cr*

Highlights

- Several perovskites were synthetized; $Cs_3Bi_2I_9$ (1.94 eV) was chosen for evaluation
- A maximum CO yield of 163.87 µmol/g_{cat}·h was obtained
- Highest CO_2 reduction was obtained at 42.5 µL/min and 150 mW/cm^2

1. Introduction

In recent years, research activities in the field of CO_2 reuse to produce synthetic fuels have been greatly stimulated by the growing concern about the effect of CO_2 emissions on global warming and fossil fuel dependency issues. A particularly emerging and promising technology for this process is perovskite-based heterogeneous photocatalysis. Perovskite oxides are promising photocatalysts due to their high catalytic activity, good stability, long charge diffusion lengths, and compositional flexibility that allows precise bandgap and band edge tuning. Furthermore, once an efficient catalyst is developed, the next step is to incorporate it in photoreactors capable of commercially produce the synthetic solar fuels. Multiple designs have been proposed and tested; however, limitations due to diffusional processes (mass transfer) and proper distribution of incident radiation on the reactor, hinder the efficient performance of the photocatalytic system. In this sense, microreactors have emerged as an excellent technological alternative to minimize these inconveniences and maximize the production of solar fuels. In this work, several perovskites were synthetized, characterized and $Cs_3Bi_2I_9$ photocatalytic activity was evaluated using a homemade 3D-printed photo-microreactor.

2. Methods

Perovskites such as $Cs_4CuX_2Cl_{12}$ with X: Bi, La, Al, Fe, Cr; $Cs_3X_2Cl_9$ with X: Sb, Bi, La, Al, Fe; $Cs_4SnX_2Cl_{12}$ with X: Sb, La, Al, Fe, Cr; $Cs_3Bi_2I_9$ and $Cs_3Sb_2I_9$ were synthetized. Band gap calculations were performed using UV-Vis Diffuse Reflectance measurements through Kubelka-Munk (K-M) model and Tauc's plot. Furthermore, some of them were characterized by means of SEM/EDX, ICP, XRD, Stylus Profilometry and Quantum Yield. The microreactor was designed to fit inside a Micronit™ chip holder and in a way that different catalyst-coated glass slides could be easily loaded and tested in the same reactor (see Fig. 1). It was printed using HIPS with a reactor chamber of 25.9 mm x 25.9 mm x 0.5 mm. Synthetized perovskites were coated in glass slides by drop casting and spin coating. A solar simulator (Oriel™ LCS-100) was used as radiation source. 99.99 % CO_2 was bubbled in a NaOH solution and then pumped into the reactor using a syringe pump. The samples at the outlet of the reactor were analyzed by GC-TCD (Shimadzu 2014) with a 30 m Carboxen® 1010 column.

3. Results and discussion

Calculations for direct and indirect band gap through Tauc's plot showed results varying from 1.07 eV to 3.36 eV, indicating promising activities in the visible spectrum for some of the synthetized perovskites. Within the synthetized perovskites, $Cs_3Bi_2I_9$ was chosen for evaluating its photocatalytic activity. CO_2 measurements in the liquid phase at the inlet and outlet of the reactor showed up to 67 % conversion, suggesting that CO_2 was being consumed. Furthermore, the presence of CO, a known product of CO_2 photoreduction, was detected in the product samples, thus leading to believe the photocatalytic reduction of CO_2 with the $Cs_3Bi_2I_9$ was achieved. The effects of operating parameters such as liquid flowrate and light intensity were then evaluated. CO was quantified obtaining concentrations from 1.07 mmol/L up to 6.15 mmol/L and yields from 89.71 µmol/g_{cat}·h up to 163.87 µmol/g_{cat}·h. These results are comparable to methanol yields obtained by Cheng et. Al [1] (111 µmol/g_{cat}·h) and Cheng et. al [2] (454.6 µmol/g_{cat}·h) in UV-microreactors using TiO_2 as catalyst. Analyzing the effect of liquid flowrate (see Fig. 2), the gas-phase concentration of CO at the outlet of the reactor increases as flowrate decreases, as a consequence of higher residence times. However, the amount of CO generated per gram of catalyst per hour (yield) shows a peak value at middle flowrate, due to mass transfer improvement in the reactor. Also, experiments performed using different light intensities showed that yield and CO concentration increase with higher light intensity; this due to the generation of more electron-hole pairs which enhances the reaction rate.

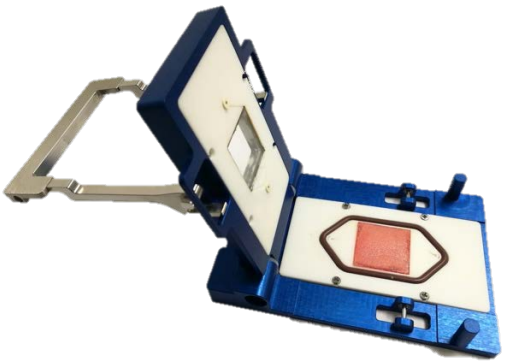

Figure 1. Microreactor

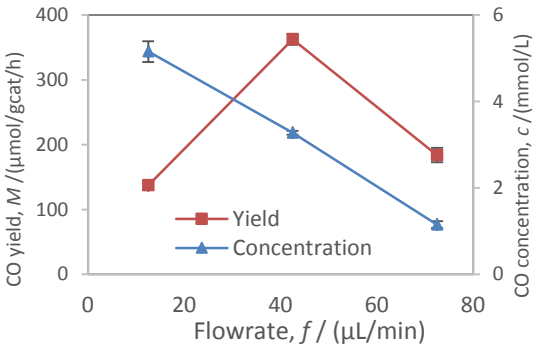

Figure 2. Effect of liquid flowrate on CO yield and concentration in gas phase.

4. Conclusions

Synthetized perovskites showed promising band gap values in the visible region; $Cs_3Bi_2I_9$ (1.94 eV) was chosen to evaluate its photocatalytic reduction of CO_2 in a planar 3D printed microreactor. CO_2 conversions of up to 67 % were determined and CO was identified as a product of the reaction. A maximum CO yield of 163.87 µmol/g_{cat}·h was measured and the effects of liquid flowrate and light intensity were analyzed, determining that maximum yield is achieved at 42.5 µL/min and 150 mW/cm^2.

References

[1] X. Cheng, X. Zhu, R. Chen, Q. Liao, X. He, S. Li, L. Li, Int J Hydrogen Energ 41 (2016) 2457–2465.
[2] X. Cheng, R. Chen, X. Zhu, Q. Liao, L. An, D. Ye, X. He, S. Li, L. Li, Energy 120 (2017) 276–282.

Nanofiltration for Arsenic Removal from natural contaminated groundwaters in Calabria Region (Italy)

A. Figoli[1], I. Fuoco[2], C. Apollaro[2], R. Mancuso[3], G. Desiderio[4], R. De Rosa[2], B. Gabriele[3], A.Criscuoli[1]

*[1]Institute on Membrane Technology (ITM-CNR), I-87036 Rende (CS) Italy; [2]Dept. of Biology, Ecology and Earth Sciences (DIBEST), University of Calabria, I-87036 Rende (CS) Italy; [3]LISOC Group, Department of Chemistry and Chemical Technologies, University of Calabria, I-87036 Rende (CS) Italy; [4]DeltaE, University of Calabria, I-87036 Rende (CS) Italy. *Corresponding author: a.figoli@itm.cnr.it*

Highlights

- Arsenic removal by Nanofiltration
- Membrane application for water purification
- Arsenic contaminated groundwater purification

1. Introduction

Arsenic is a toxic inorganic pollutant for both the environment and human health. The removal of arsenic is one of most problematic targets of hydrogeochemical research (Bhattacharya et al. 2002). The WHO drinking water guideline for As has been set to 10 µg/L and it has been adopted by many countries as a drinking water standard (WHO, 2001). For reaching this new value, several separation techniques have been studied. Membrane technology is one of these and pressure driven operation as nanofiltration (NF) and reverse osmosis (RO), often applied on synthetic solutions, have been already proved to accomplish the arsenic value below the drinking water standard (Figoli et al., 2016; Ahmad et al. 2017). In this study, NF has been applied for treating As contaminated groundwaters, coming from an area located in the Sila Massif (Calabria, Italy). Sila Massif represents the major morphostructural high of the Ionian margin of north-eastern Calabria and fall in the northern sector of the Calabrian Peloritan Arc (CPA). The water samples collected, labeled GW1, GW2, GW3, have interacted with the Calabride Complex formed by Hercynian and pre-Hercynian gneiss, granite and phyllite, which underwent intense weathering processes (Van Dijk et al., 2002). The performance (water flux and arsenic rejection) of the membranes has been evaluated too.

2. Methods

The three water samples (GW1, GW2, GW3) differ by the arsenic concentration, which is about 60, 120 and 430 ppb, respectively. The As is present mainly in the pentavalent form (As(V)). NF experiments were performed by using a laboratory pilot unit (SEPA CF). Four types of membrane modules commercialized by GE Osmonics, named HL (Polyamide), DK (proprietary thin-film) and CK (cellulose acetate) and by Microdyn Nadir, named NP030P (Polyethersulfone), were used. The samples, before and after membrane treatment, were analyzed, determining the major elements HPLC (Dionex ICS 1100). The total arsenic was evaluated by ICP-MS, Perkin Elmer/SCIEX, Elan DRCe.

3. Results and discussion

In Figure 1, it is reported the water flux plotted versus the trans-membrane pressure (TMP) variation, for the GW2 sample (feed stream). All the investigated membranes show a linear increase of water flux at higher TMP. In particular, only the NF membrane Type HL shows much higher water flux compared to the other ones, which could be explained by the polymeric nature of the material

as well as by its higher pore-size. The same results have obtained also for the other GW samples containing a lower and higher concentration of As(V).

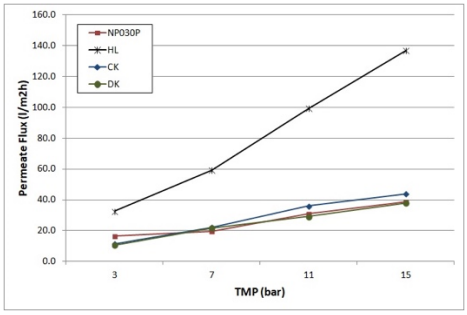

Figure 1. Effect of TMP on permeate flux for GW2 contaminated As(V) sample.

In Figure 2, it is reported the As(V) rejection and the arsenic concentration detected in the permeate (purified water) after the membrane treatment of GW2 contaminated As (V) sample.

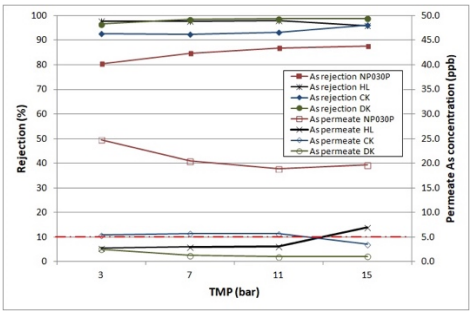

Figure 2: Effect of TMP on rejection (%) and permeate arsenic concentration for GW2 contaminated As(V) sample

The results show that all the investigated NF membra-nes, except the NP030P, reject the As(V) and that the As(V) concentration in the purified permeate water is below the WHO drinking water limit value of 10 µg/L.

4. Conclusions

The results clearly report that NF can be considered a valid technique for arsenic removal in the natural water, producing a permeate (purified water) with the As(V) concentrations within the allowed WHO limits for most of the membrane investigated.

5. Acknowlegment

The work has been supported by the project “AsSe” n. CUP: J28I17000030006, cofunded by Fondo FESR POR Calabria FESR FSE 2014-2020-Azione 1.2.2.

References

Bhattacharya, P., Frisbie, S.H., Smith, E., Naidu, R., Jacks, G., Sarkar B. 2002. Arsenic in the Environment: A Global Perspective. In: B.Sarkar (Ed.) *Handbook of Heavy Metals in the Environment*, Marcell Dekker Inc., New York, pp. 147-215.

Figoli, A., Hoinkis, J., Bundschuh, J. 2016. Membrane Technology for Water Treatment, Removal of toxic trace elements with emphasis on arsenic, fluoride and uranium, CRC Press, Taylor and Francis Group, ISBN978-1-315-73523-8.

WHO, Guideline for drinking-water quality: Arsenic in drinking water. Fact Sheet No. 210. Geneva. Switzerland, World Health Organization (2001).

ECCE12
The 12th EUROPEAN CONGRESS OF CHEMICAL ENGINEERING
Florence 15-19 September 2019

Simplified dual kinetics model for the extraction of high value-added components from coffee bean's silverskin.

Andrea Galeazzi[1], Giulia Bozzano[1], Flavio Manenti[1], Luisella Verotta[2], Rita Nasti[2], Stefania Marzorati[2]

1 Politecnico di Milano, DCMIC, p.zza L. Da Vinci, 32, Milano, Italy; 2 Università degli Studi di Milano, DESP, Via Celoria 2, Milano, Italy

**Corresponding author: f.manenti@polimi.it*

Highlights

- Supercritical carbon dioxide extraction from micronized silverskin matrices
- Extraction simplified model
- Experimental data

1. Introduction

Extraction of oils and other valuable components from wasted biomass, such as roasted coffee silverskin, offers the possibility to recover and create value in a sustainable way. Supercritical CO_2 is one of the most environmentally friendly extraction methods available, especially compared to traditional solvent techniques which are toxic and dangerous. By applying a proper mathematical approach to describe the extraction of natural products from silverskin, it is possible to predict the system behavior in different operative conditions. This enables to develop a reasonable design of experiment and to envisage a possible scale-up in industrial plants by also maximizing the output and minimizing wastes.

For doing so, a simplified mathematical model is proposed describing the supercritical carbon dioxide extraction of high value-added components from roasted coffee bean's silverskin. It is based on that first introduced by Sovová [1] in 1994 and later used in a myriad of cases [2]. Having an empirical approach in defining the mass transfer coefficient between the two phases, these models offer a simple solution, which is analytical, as well as good fitting of data. Through experimental data derived from silverskin extraction, the characteristic parameters of the model have been deduced. Such parameters allow to predict the behavior of the system in different operative conditions and optimize the system.

2. Methods

Experiments are carried out in a 100ml stainless steel vessel which can house approximately 40g of non-compressed micronized silverskin powder. Supercritical CO_2 is pumped at desired pressure by a compressor and flows inside the column from the bottom to the top. The solute extracted is collected in pre-weighted glass vials positioned after a small collection chamber at the exit of the vessel. At desired times the vial is substituted, the solute extracted is measured with a laboratory scale and data are collected. In the adopted model, the desorption of solutes is modeled with two different steps. At first, solute present on the outside of the solid matrix is extracted and later, when that solute is depleted, the extraction proceeds towards the solute present inside the solid. Solubility is the driving force that describes the mass transfer when solute is readily available and

in direct contact with the fluid, on the other hand diffusivity is responsible for the extraction of solute stranded inside the solid matrix.

Original Sovová's model considers also a third transient step. To further simplify the model, Patel [3] proposed to remove this transition period and consider the two principal stages only. It is assumed that an axial solvent flows, at a constant superficial velocity, through a fixed bed of cylindrical shape. The solvent is pure at the entrance. The temperature and pressure are kept constant throughout the fixed bed and the total time of extraction. Additionally, the bed is considered homogeneous in terms of solute distribution as well as particle size. The model also assumes pseudo-steady state with plug flow and neglects the accumulation of the solute in the fluid phase. It considers the solute solubility in the solvent and mass transfer coefficient both in solvent and in solid phases.

To verify the experimental data a non-linear regression is applied, the dimensionless parameters are calculated having the foresight of separating all the operative changing parameters like interstitial velocity or initial mass of solid from the constant ones.

3. Results and discussion

Preliminary results show a good fitting of the experimental data, although at the actual state the model suffers severely from the changing in CO_2 flowrate. In facts, the model right now describes quite good different operative conditions like changes in temperature as well as void factor (by reducing the initial solid in the vessel) but only if the fluid flowrate remains constant.

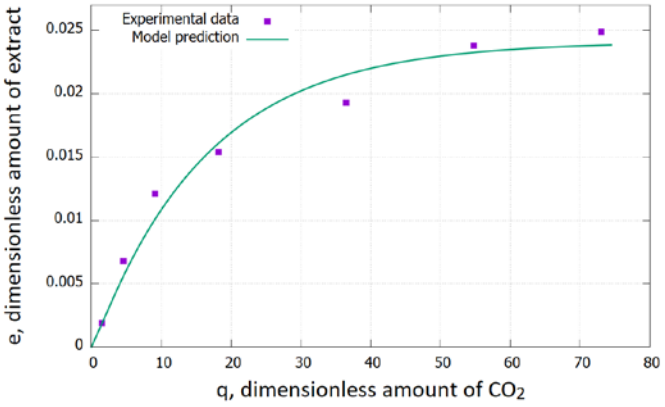

Figure 1. Example of model comparison for 300bar,330K and 4 hours extraction.

4. Conclusions

This model has a good potential but only if it would be possible to apply it to different ranges of flowrates. This problem might be caused by the changing in the mass transfer rates due to the changing in mass flow rate. It is evident that it is necessary to apply some more constraints and a mass transfer theory to further separate the variable parameters from the constant ones. Doing so might enhance the regression of the adjustable parameters making this model suitable to proceed to a possible design of experiment as well as optimization of operative conditions and possibly a scale-up.

References

[1] H. Sovová, Chemical Engineering Science, pp. 409-414, 1994.
[2] R.N. Patel, S. Bandyopadhyay, A. Ganesh, Energy Conversion and Management, pp. 652-657, 2011.
[3] J.M. Del Valle & J.C. De La Fuente, Critical Reviews in Food Science and Nutrition, pp. 131-160, 2006.

Scaling the Biobased chemistry, is decentralised production the future?

Ir. Thomas Ladrak, Zeton b.v., Enschede, the Netherlands;

The recommended approach for scaling biofuel and biochemical technology follows a similar stage gate process to that used in traditional Chemical Process Industry (CPI) processes. But the processing of biomass leads to some subtle differences, and unique challenges, that need to be considered. The typical scaling factors for bioenergy and biofuels processes are an order of magnitude lower, or more conservative, than is the case for an equivalent CPI process. This is as a direct result of the inherent challenges with biomass processing, and the fact that there is little published data, and a lack of experience in general, related to the scale up of advanced biofuels and biochemical processes.

One of the pitfalls of working with biomass projects is scaling up too fast. Often the step from lab-scale to pilot scale is taken with both scaling up significantly the process volume and shifting from batch to continuous processing. Pilot plants provide the first window into continuous processing and often incorporate unreacted feed or product recycles. This often leads to unforeseen challenges, in some cases even jeopardizing the projects. Scaling up from a smaller pilot to a demonstration plant, before working out the commercial scale process, is therefore the norm.

But is scaling up to the traditional world scale production a necessity? The availability of feedstock is often place specific, transport of raw materials reduces the efficiency of the overall processes. Often it is much more interesting to perform the first process steps decentralized, in small, flexible and in some cases even transportable installations. Produce there where the feedstock is! So demonstration scale can even become commercial scale.

Study of the addition of different ashes to cement: reactivity and resistance

Juan D. Alonso[1], Jimena C. Díaz[1], Andres M. Segura[1], Yuby Cruz[1], Ximena Gaviria[2], Idoia Estiati[3], Juan F. Saldarriaga[1]

1 Department of Civil and Environmental Engineering, Universidad de los Andes, Carrera 1Este #19A-40, Bogotá, Colombia; 2 Program of Industrial Engineering, Universidad de Medellín, Carrera 87 #30-65, Medellín, Colombia; 3 Department of Chemical Engineering, University of the Basque Country, B. Sarriena s/n, Leioa, Spain

**Corresponding author: jf.saldarriaga@uniandes.edu.co, juanfelorza@gmail.com*

Highlights

- The mixtures evaluated show similar behavior to the target
- The BIT-cement mixture presents better resistance after 90 days of curing
- Fly ash from hazardous waste can be used as a replacement for cement

1. Introduction

The world annual production of fly ash is estimated at around 780 million tons per year and has been used successfully in the cement industry for more than 50 years, mainly as a mineral additive in Portland cement concrete and also as a component of mixed cement[1]. They are composed mainly of amorphous silica and alumina [2] with a favorable diameter and size that improves workability and makes this material suitable, even, for the production of geopolymers [2]. Fly ash can be used partially as a substitute for Portland cement or applied as an addition to concrete in the batch plant [3,4]. The use of biomass ash and coal-biomass mixtures in cement has also been widely investigated [5,6]. In this work, the reactivity of hazardous waste, bituminous coal and sugar cane ash as supplementary cement materials was evaluated.

2. Methods

For this work, ash from incineration processes (hazardous waste, sugarcane and bituminous coal) was used. Each one of these ashes was used in different proportions in the mixture with cement. For the case of bituminous coal (BIT) and sugarcane (CAN), a 30% replacement ratio was used. In the case of the ashes of hazardous waste these were previously treated by means of washes (CITA). Both the treated and the untreated ashes were used in replacements. For the treated ashes two ratios of 5% and 3% were used. While for the untreated ashes a ratio of 10% was used. For this, the reactivity of the ashes in cement monoliths was analysed, focusing on thermogravimetric tests as a characterization technique to determine the present phases and compression resistance tests. The ashes were characterized by DRX and FRX, finding low content of SiO_2 and Al_2O_3 in the hazardous waste ashes, while in the coal and sugarcane ashes high contents of these oxides were found. The monoliths were prepared according to ASTM C-305, using a 0.5 water/lime ratio. The hydration process was stopped with acetone at the ages of 1, 3, 7, 14, 28, 56 and 90 days.

3. Results and discussion

After 90 days of curing, it was found that the mixtures presented similar resistance data with white respite, highlighting the 3 and 5% RPL and the bituminous coal mixtures. Similarly, the 10% -RPS mixture has a load very similar to white. It is advisable to perform metal leaching analysis, in order to evaluate possible environmental impacts that may occur in its application as a substitute for cement. Table 1 shows the average of the three failures made to each of the samples on each of the days evaluated. A very good behavior of the mixtures is observed from day 3 of curing of the monoliths.

Table 1. Analysis of the resistance of the different replacements

Day	Sample	Average Load (kgf)
90	UHW(10%)	844
	THW(5%)	1055
	THW(3%)	1094
	BIT	1205
	CANA	884
	WHITE	789

In table 1, it can be seen that on day 1 only the sugar cane has a good resistance compared to the white, but as the curing time progresses, all the mixes present good behavior. In Figure 1, the reactivity of these ashes can be corroborated, in which in the temperature curve between 50 and 200 ºC, the formation of very marked peaks that are related to different types of C-S-H gels are observed.

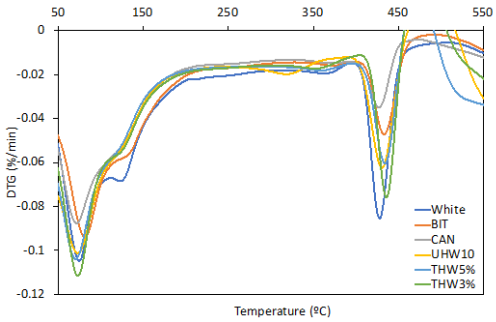

Figure 1. Total mass lost for a given temperature interval (DTG) for different combinations of ash at 90 days of curing.

4. Conclusions

It is observed that the mixtures evaluated have a good resistance and reactivity behavior after 90 days of curing, the DTG curves show the same crystal formations as the white. Likewise, the resistance of all the evaluated monoliths is very similar or even better than those of the target.

References

[1] P. Duan, C. Yan, W. Zhou, Ceramics International 42 (2016) 3504–3517.
[2] M. Toniolo, A. Boccaccini, Ceramics International 43 (2017) 14545–14551.
[3] F. Faleschini, M. Z anini, K. Brunelli, C. Pellegrino, Materials & Design 85 (2015) 687–694.
[4] R. Siddique, Materials & Design 32 (2011) 1501–1507.
[5] R. Rajamma, R. Ball, L. Tarelho, G. Allen, J. Labrincha, V. Ferreira, J. Hazard. Mater. 172 (2009) 1049–1060.
[6] M. Madurwar, R. Ralegaonkar, S. Mandavgane, Construction and Building Materials 38 (2013) 872–878.

ECCE12
The 12th EUROPEAN CONGRESS OF CHEMICAL ENGINEERING
Florence 15-19 September 2019

Investigation of the Contact Behaviour of Cylindrical Composite Particles For DEM-CFD Simulation of Fluidized Bed.

Philipp Grohn[1*], Tobias Oesau[2], Stefan Heinrich[2], Sergiy Antonyuk[1]

1 Institute of Particle Process Engineering, Technische Universität Kaiserslautern, Gottlieb-Daimler-Straße, 67663 Kaiserslautern, Germany; 2 Institute of Solids Process Engineering and Particle Technology, Hamburg University of Technology, Denickestraße 15, 21073 Hamburg, Germany

**Corresponding author: philipp.grohn@mv.uni-kl.de*

Highlights

- Compression tests of cylindrical particles
- Measurement of particle-wall sliding friction
- Magnetic Particle Tracking (MPT)
- For the used particles the stiffness is independent of the number of impact

1. Introduction

In many processes of particle technology, cylindrical particles produced by extrusion or press agglomeration are used and further processed in various production steps e.g. spheronization, fluidization, drying and coating. In order to control and optimize these processes the particle dynamics can be predicted with numerical simulation. The frequently used methods are computational fluid dynamics (CFD), the discrete element method (DEM) or the coupling of both methods (CFD-DEM). There are numerous CFD-DEM studies reported in the literature predicting spherical particles in complex processes, however, only few studies of fluidization processes with cylindrical particles can be found [1–3]. For cylindrical particles, there is a lack of understanding of how particle shape influences the particle contact behaviour during different loading scenarios. Especially for the exact calculation of the particle interactions in DEM, it is essential to describe the particle contact behaviour with a compatible contact model. The modelling of contact behaviour with DEM poses a number of challenges: the shape construction, the contact detection and the contact force calculation for different deformation behaviours [4,5].

2. Methods

In this work, the influence of loading direction (contact geometry) and deformation behaviour (from elastic to plastic) on force-displacement behaviour during compression and shearing of cylindrical particles is investigated. The compression tests are performed with a Texture Analyser®. For the measurement of particle-wall sliding friction, a self-developed setup at the TU Kaiserslautern is used. During the measurement of tangential force, the particles are fixed to a flat holder and moved over a defined wall surface at a constant normal load. In addition, experiments in a fluid bed rotor processor equipped with a Magnetic Particle Tracking (MPT) system are conducted in order to visualize and quantify the real particle behaviour [6–9]. In Figure 1, the function of the MPT system is shown. The anisotropic magnetoresistive (AMR) sensors detect the magnetic field lines of the

magnetic marker particles and allows the analysis of the movement and rotation behaviour of the marker particles.

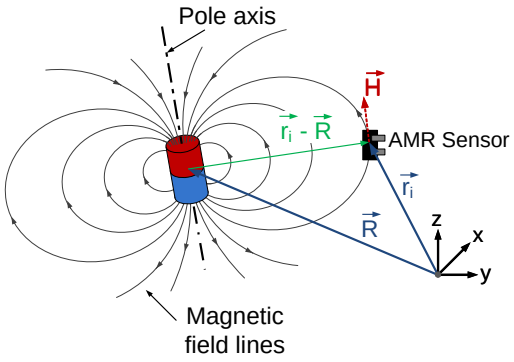

Figure 1. Functioning of the Magnetic Particle Tracking (MPT) system

3. Results and discussion

The intention of these investigations is the experimental calibration of contact models, which can be applied for numerical DEM studies of fluidization processes with cylindrical particles. Cyclic loading tests for different loading positions of the particles show that the stiffness is independent of the number of impacts. For the used particles sizes, different loading positions do not lead to significant differences in stiffness. The behaviour of different particle shape models with the multi-sphere approach is also performed and compared with experimental results.

4. Conclusions

With the conducted compression tests and measurement of particle-wall sliding friction it is now possible to calibrate a contact model, which can be used for DEM studies, in particular for a CFD-DEM simulation of a fluid bed rotor processor.

1. References

[1] T. Oschmann, J. Hold, H. Kruggel-Emden, Numerical investigation of mixing and orientation of non-spherical particles in a model type fluidized bed, Powder Technology 258 (2014) 304–323. https://doi.org/10.1016/j.powtec.2014.03.046.

[2] H. Kruggel-Emden, K. Vollmari, Flow-regime transitions in fluidized beds of non-spherical particles, Particuology 29 (2016) 1–15. https://doi.org/10.1016/j.partic.2016.01.004.

[3] H. Ma, L. Xu, Y. Zhao, CFD-DEM simulation of fluidization of rod-like particles in a fluidized bed, Powder Technology 314 (2017) 355–366. https://doi.org/10.1016/j.powtec.2016.12.008.

[4] S. Antonyuk, S. Heinrich, J. Tomas, N.G. Deen, M.S. van Buijtenen, J.A.M. Kuipers, Energy absorption during compression and impact of dry elastic-plastic spherical granules, Granular Matter 12 (2010) 15–47. https://doi.org/10.1007/s10035-009-0161-3.

[5] S. Antonyuk, S. Palis, S. Heinrich, Breakage behaviour of agglomerates and crystals by static loading and impact, Powder Technology 206 (2011) 88–98. https://doi.org/10.1016/j.powtec.2010.02.025.

[6] G. Mohs, O. Gryczka, S. Heinrich, L. Mörl, Magnetic monitoring of a single particle in a prismatic spouted bed, Chemical Engineering Science 64 (2009) 4811–4825. https://doi.org/10.1016/j.ces.2009.08.025.

[7] J. Neuwirth, Charakterisierung und Diskrete-Partikel-Modellierung des Strömungs- und Dispersionsverhaltens im Rotorgranulator, 1st ed., Cuvillier Verlag, Göttingen, 2017.

[8] J. Neuwirth, S. Antonyuk, S. Heinrich, M. Jacob, CFD–DEM study and direct measurement of the granular flow in a rotor granulator, Chemical Engineering Science 86 (2013) 151–163. https://doi.org/10.1016/j.ces.2012.07.005.

[9] Buist K.A., Novel experimental techniques for granular flow. Dissertation, Eindhoven, 2016.

Numerical Investigation of the Shear-Induced Hetero-Aggregation of Oppositely Charged Particles.

Graziano Frungieri[1], Matthäus Bäbler[2], Marco Vanni[1]

[1] *Dept of Applied Science and Technology, Politecnico di Torino, Corso Duca degli Abruzzi 24, Torino;*

[2] *Dept of Chemical Engineering and Technology, KTH Royal Institute of Technology, Teknikringen 42, Stockholm, Sweden*

**Corresponding author: graziano.frungieri@polito.it*

Highlights

- Modelling of hetero-aggregation by a Monte Carlo – Discrete Element Method.
- Size stabilization by hetero-aggregation.

1. Introduction

Over the last decades much research has been devoted to the study of the aggregation of identical particles (homo-aggregation), but little is known about hetero-aggregation, i.e. the aggregation occurring in systems in which dispersed particles differ in one or more characteristics. The present work aims to simulate the shear-induced aggregation process occurring in a dilute suspension where particles with opposite surface charges are dispersed.

2. Methods

We studied the shear-induced aggregation process occurring in aqueous dilute suspensions of spherical polystyrene particles, with 500 nm radius. Particles bearing opposite surface charges with low surface potentials (±40 mV) and surrounded by a thin electrical double layer (10 nm) are considered. A relatively mild shear rate is assumed to act on the suspension (10 s^{-1}). For this set of

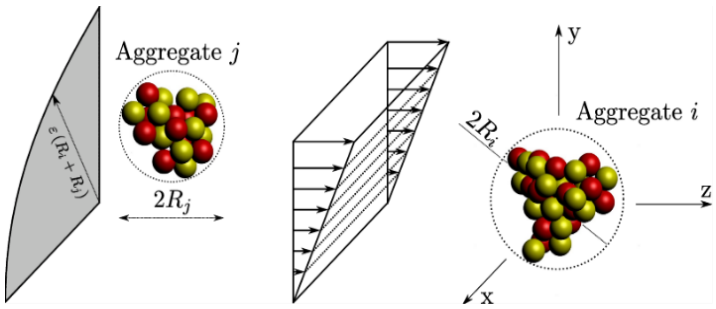

Figure 1. Typical initial setup of an aggregation event in shear flow. The DEM tracks the trajectory of each primary particles

parameters, only aggregation between unlike particles can occur. In dilute conditions, it is reasonable to reduce the aggregation dynamics to a sequence of binary aggregation events i.e., events which involve two aggregates at a time. Based on this assumption, we developed a mixed stochastic-deterministic method built on a combination of a Monte Carlo (MC) algorithm and a Discrete Element Method (DEM), built in the framework of Stokesian Dynamics. Based on the flow

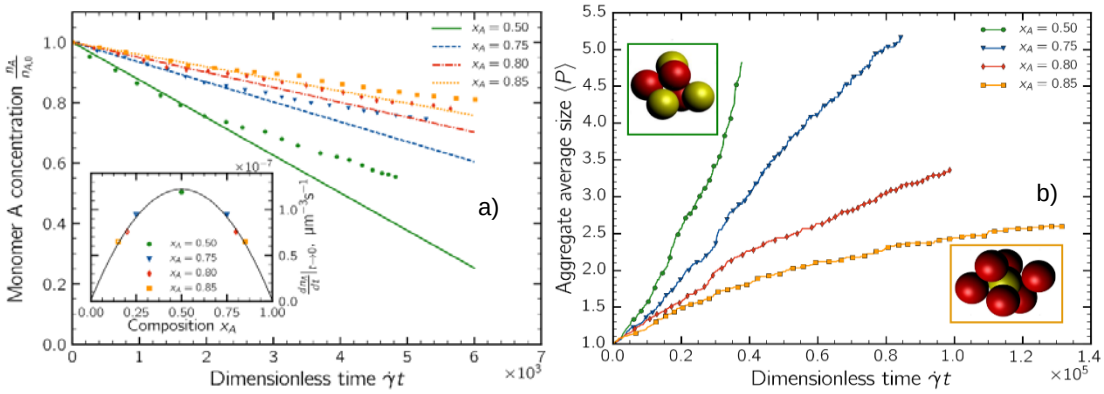

Figure 2. Aggregation kinetics for four different values of the population composition, expressed in terms of number fraction of cationic particles x_A. a) Temporal trend of the concentration of cationic particles. The inset report the dimer formation rate. b) Temporal trend of the aggregate average size, in terms of number of constituent primary particles. The insets show two small sample aggregates (red particles are the majority particles)

and population statistics, the MC is used to sample a statistically expected sequence of encounter events, whereas the DEM is used to simulate in detail each aggregation event [1]. Figure 1 represents the typical initial setup of a DEM simulation.

3. Results and discussion

Simulations were performed to ascertain the effect of the suspension composition, in terms of relative concentration of cationic (A) and anionic (B) particles, on both aggregation kinetics and aggregate morphology. Figure 2a reports the temporal trend of the concentration of cationic primary particles in the early stage of the process; as apparent the rate of disappearance is strongly affected by the population composition: when cationic and anionic particles are present in an equal amount (x_A=0.5) the aggregation is fast. As the composition parameter increases, the aggregation rate slows down. This effect is made more apparent in the inset of Figure 2a, where the rate of dimer formation is plotted together with the theoretical expected one. The late stage dynamics is also remarkably affected by the population composition. Figure 2b reports the aggregate average size as a function of time. In the symmetric system, the growth dynamics shows a self-accelerating behavior, with aggregates that soon reach large size. As the population is enriched in majority particles, the aggregation slows down and for concentration around 85% the aggregation rate progressively reduces in time, until a size stabilization takes place. Stable aggregates with a core-shell structure appear; such aggregates are seen to be formed by a core, in which the particles of the two classes are both present and by an external shell fully covered by majority particles, which provide a shielding effect against further growth.

4. Conclusions

The hetero-aggregation of oppositely charged particles is studied in the present work. Results reveal that in such systems a size stabilization effect should be expected when a large concentration disproportion between the two classes of particle is present.

References

[1] G. Frungieri, M. Vanni, Can. J. Chem. Eng. J. 95 (2017) 1768-1780.

ECCE12
The 12th EUROPEAN CONGRESS OF CHEMICAL ENGINEERING
Florence 15-19 September 2019

Controlled Manipulation of Size and Shape of Needle-like Compounds Using Wet-Milling

Ashwin Kumar Rajagopalan[1], Stefan Bötschi[1], Manfred Morari[2], Marco Mazzotti[1*]

1 Institute of Process Engineering, ETH Zurich , 8092 Zurich, Switzerland; 2 Department of Electrical and Systems Engineering, University of Pennsylvania, Philadelphia 19104, United States

**Corresponding author: marco.mazzotti@ipe.mavt.ethz.ch*

Highlights

- Manipulation of size and shape of needle-like compounds using wet-mill as actuator.
- Model-based operating policy is unable to guide arbitrary seed populations to targets.
- Incorporation of feedback action is key for robust performance of milling stage.

1. Introduction

In a crystallization process, the particle size and shape influences various downstream operations. The majority of the crystallization literature deals with manipulation of only the size of the crystals. Thanks to the recent advances in particle size and shape monitoring techniques, particles can be better characterized using multiple dimensions [1]. Even though the available literature on feedback control with the aim to manipulate particle size and shape is limited, model-based and model-free feedback controllers have been proposed recently using temperature as a control actuator [2,3].

For needle-like compounds that exhibit small changes in the shape by using only temperature as an actuator, milling can be a suitable alternative. In this work, several operating and control strategies are proposed, all of them using an *ex situ* wet mill as the control actuator, with the aim to guide various seed populations to different targets in the size and shape plane.

2. Methods

One model-based operating policy and several feedback control strategies were designed and tested in a lab-scale experimental setup. The setup consisted of an *ex situ* stereoscopic imaging device (for particle size and shape characterization), the μ-DISCO [1], an *ex situ* rotor-stator wet mill, and a control computer where the image analysis routines for the imaging device and the control strategies were implemented. The model-based operating strategy utilized a two-dimensional population balance model that describes the breakage phenomenon in the mill [4]. The proposed operating policy and control strategies were put to test using two model compounds, namely β L-glutamic acid (BLGA) and γ D-mannitol (GDM).

3. Results and discussion

Two different seed populations of BLGA and one seed population of GDM were milled to reach three different target average lengths in the particle size and shape plane. For the model-based

operating policy, it was observed that the multidimensional breakage model was unable to predict the rotor speed that would enable reaching the desired targets for arbitrary batches of seed populations. These experiments highlighted the importance of introducing feedback action to overcome unmodeled phenomena and to counteract process disturbances.

Different feedback control strategies using online observations of the evolution of the average dimensions of the populations subjected to milling were designed and applied. These control strategies applied multiple consecutive milling stages with varying rotor speeds, which enabled reaching the targets robustly and irrespective of the seed population and model compound used (see Figure 1).

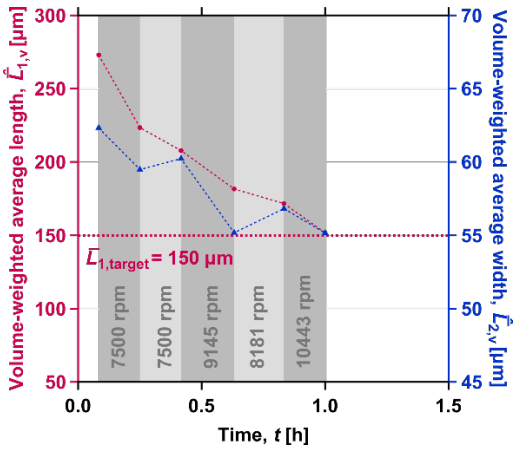

Figure 1. Time-resolved evolution of the measured volume-weighted average dimensions of BLGA seeds with a target average length of 150 µm. The shaded gray region indicates the milling stage with the corresponding rotor speeds.

4. Conclusions

Different operating and control strategies were exploited to manipulate the size and shape of needle-like particles using a wet mill as a control actuator. The control strategies that incorporated feedback action led to robust operation of the milling. Thus, the milling stage is ready to be integrated into complex processes, including crystal growth and fines removal by dissolution, to effectively manipulate the size and shape of needle-like compounds.

References

[1] Rajagopalan, A. K.; Schneeberger, J.; Salvatori, F.; Bötschi, S.; Ochsenbein, D. R.; Oswald, M. R.; Pollefeys, M.; Mazzotti, M. A Comprehensive Shape Analysis Pipeline for Stereoscopic Measurements of Particulate Populations in Suspension. *Powder Technol.* **2017**, *321*, 479–493.

[2] Eisenschmidt, H.; Bajcinca, N.; Sundmacher, K. Optimal Control of Crystal Shapes in Batch Crystallization Experiments by Growth-Dissolution Cycles. *Cryst. Growth Des.* **2016**, *16*, 3297–3306.

[3] Bötschi, S.; Rajagopalan, A. K.; Morari, M.; Mazzotti, M. Feedback Control for the Size and Shape Evolution of Needle-like Crystals in Suspension. I. Concepts and Simulation Studies. *Cryst. Growth Des.* **2018**, *18*, 4470–4483.

[4] Salvatori, F.; Mazzotti, M. Experimental Characterization and Mathematical Modeling of Breakage of Needle-like Crystals in a Continuous Rotor-Stator Wet Mill. *Cryst. Growth Des.* **2018**, *18*, 5957–5972.

Acknowledgements: The authors are thankful to the Swiss National Science Foundation for their financial support (Project Number 155971).

DEM simulation of breakage under compressive force using a particle replacement model

Vahid Hassanzadeh[1,*], Christopher Wensrich[2], Roberto Moreno-Atanasio[3]

1, 3 Chemical Engineering Department, School of Engineering, The University of Newcastle, Australia;
2 Mechanical Engineering Department, School of Engineering, The University of Newcastle, Australia
**Corresponding author: vahid.hassanzadeh@uon.edu.au*

Highlights

- A Particle Replacement Model was employed to simulate breakage using DEM.
- The effects of initial overlap during replacement on the system were studied.
- Relaxation factor was used to justify high contact force of particles after breakage.

1. Introduction

Comminution processes are the most expensive particle processing operations in terms of energy consumption as most of the energy is dissipated in the form of sound and plastic deformation. Therefore, this type of processes presents an important opportunity for optimization and improvement [1-3].

After introducing Discrete Element Method (DEM) by Cundall and Strack [4] many researchers took advantage of this simulation technique to study size reduction processes [5-9]. The Particle Replacement Model (PRM) has been proved to be one of the most successful models to simulate particle breakage in DEM simulations [9]. In this model, a broken spherical particle is replaced by a progeny of smaller particles instantaneously [5, 9]. PRM requires to specify the maximum stress at which the particle breaks and a breakage distribution function to determine the smaller progeny particles that are replacing the original particle.

During the replacement process, the progeny particles are required to have an initial overlap. This initial overlap causes high contact forces between the particles. Therefore, a relaxation factor has been used in the previous studies to damp the high elastic force artificially created during the replacement process [5]. In this research work, the effects of the relaxation factor on the single particle and particle bed breakage simulations were studied.

2. Methods

An in-house DEM code was developed in Fortran 77 programming language. The Hertz contact force model and equations of motions in both translational and rotational directions were used. Also, damping force models were employed to simulate the energy dissipation in particle contacts.

To simulate the breakage process the particle replacement model was implemented. When the value of the contact force exceeds a specified value, the particle is substituted by its progeny which is determined by the breakage function. The equation developed by Austin and Luckie (1972) was used to calculate the progeny particle size distribution [10]. In order to study the effect of the relaxation factor in the range between 0.05 and 1.00 two types of systems made of particles of 10

mm in diameter were considered: a single particle and a bed of 100 particles. In order to simulate the bed compression test, particles were randomly positioned within a cylinder of 5 cm in diameter. Then, a piston was moved downwards to compress the particle bed until achieving a maximum value of 450 N. An illustration of the simulations is shown in Fig. 1.

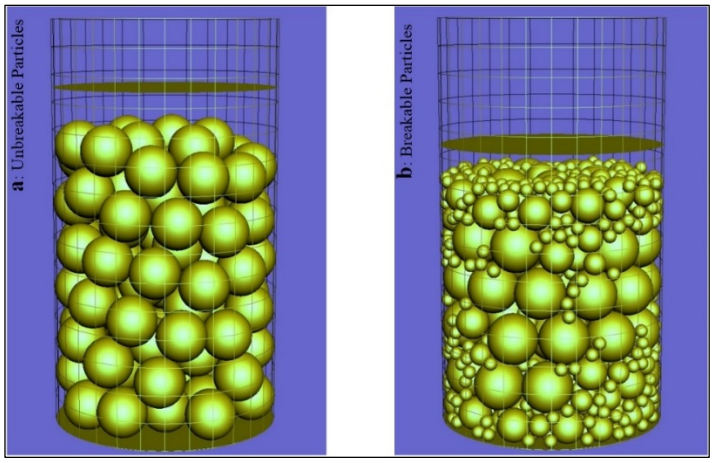

Fig. 1 Simulations of unbreakable and breakable particles after applying 450 N force on the particle bed

3. Results and discussion

In the single particle system, the kinetic energy of the progeny particles exhibited a maximum as a function of time. This maximum value and the rate at which the kinetic energy decayed after the maximum was achieved, increased by increasing the relaxation factor. This could be as a result of large energy dissipations during contacts of high-velocity particles.

For the particle bed simulations, the number of broken particles fluctuated with the relaxation factor. However, the curves of the contact force on the piston as a function of time for different values of the relaxation factor were close to each other and the elapsed times for reaching to 450 N were almost the same.

4. Conclusions

The relaxation factor used in the particle replacement model affects the simulation results considerably. However, it seems that because of the complexity of interactions between particles in a compacted bed, the influence of the factor on the results of the breakage process is not easily predictable. Therefore, it is recommended to find the optimum value of the relaxation factor by comparing the movements of the progeny particles after the breakage in the DEM simulations with the ones in the single particle breakage test. Then, the factor can be tuned finely according to the obtained particle size distribution of experimental data for the particle bed breakage tests.

References

1. Dahlstrom, D.A. and W.P. Kam, *Potential energy savings in comminution by two-stage classification.* International Journal of Mineral Processing, 1988. **22**(1-4): p. 239-250.
2. Napier-Munn, T., *Comminution Energy and How to Reduce it.* JKMRC (UQ) and CEEC, 2012.
3. Napier-Munn, T., *Is progress in energy-efficient comminution doomed?* Minerals Engineering, 2014. **73**: p. 1-6.
4. Cundall, P.A. and O.D.L. Strack, *A Discrete Numerical-Model for Granular Assemblies.* Geotechnique, 1979. **29**(1): p. 47-65.
5. Cleary, P.W., *Recent advances in dem modelling of tumbling mills.* Minerals Engineering, 2001. **14**(10): p. 1295-1319.

6. Potyondy, D.O. and P.A. Cundall, *A bonded-particle model for rock.* International Journal of Rock Mechanics and Mining Sciences, 2004. **41**(8): p. 1329-1364.
7. Metzger, M.J. and B.J. Glasser, *Numerical investigation of the breakage of bonded agglomerates during impact.* Powder Technology, 2012. **217**: p. 304-314.
8. Datta, A. and R.K. Rajamani, *A direct approach of modeling batch grinding in ball mills using population balance principles and impact energy distribution.* International Journal of Mineral Processing, 2002. **64**(4): p. 181-200.
9. Jiménez-Herrera, N., G.K.P. Barrios, and L.M. Tavares, *Comparison of breakage models in DEM in simulating impact on particle beds.* Advanced Powder Technology, 2018. **29**(3): p. 692-706.
10. Austin, L.G. and P.T. Luckie, *The estimation of non-normalized breakage distribution parameters from batch grinding tests.* Powder Technology, 1972. **5**(5): p. 267-271.

ECCE12
The 12th EUROPEAN CONGRESS OF CHEMICAL ENGINEERING
Florence 15-19 September 2019

Analysis of the Microstructure of Particles Obtained by Evaporating Acoustically Levitated Single Droplets Using X-Ray Computed Tomography.

Hassan Abdullahi [1], Thomas Vetter[1*], Christopher L. Burcham[2]

[1] School of Chemical Engineering and Analytical Science, University of Manchester, Manchester, UK;
[2] Eli Lilly & Company, Indianapolis, IN, USA
*Corresponding author: thomas.vetter@Manchester.ac.uk

Highlights

- *Drying of acoustically levitated droplets is investigated.*
- Characterization of the microstructure of the formed particles through X-ray tomography.
- Drying conditions and particle microstructures have been mapped against each other.

1. Introduction

The flowability and tabletability of powders is an important consideration in the manufacturing of pharmaceutical products. These properties can be successfully tuned by crystallising particles of a desired morphology, or, more flexibly, by engineering the microstructure of the individual particles in a spray drying process it can be tuned by altering the formulation and process conditions [1][2]. Therefore, spray drying offers a unique opportunity to design tailor made particles in a single step process involving simultaneous droplet drying and particle formation. However, carrying out an in-depth investigation of particle morphology and microstructure directly on the scale of a typical spray dryer (that contains millions of droplets at any time) is infeasible. Instead, single droplet studies are often used to understand how drying conditions affect the microstructure of the resulting dried particles [3][4].

2. Methods

In the present work, an acoustic levitation approach is used to suspend single droplets in an atmosphere of controlled relative saturation and temperature (Figure 1). Through a camera and automated image analysis, we study the droplet drying dynamics, as well as the macroscopic morphology of the resulting particle. We have further applied Raman spectroscopy and scanning electron microscopy to study the solid state form, as well as the surface characteristics. By applying X-ray computed tomography, we have elucidated the internal microstructure of the formed particles and have uncovered a fascinating variety of structures, depending on the mixture dried (we have investigated combinations of different solutes, solvents, and polymers acting as excipients), as well as the processing conditions (temperature and relative saturation of nitrogen used as drying gas). The results can be correlated with formulation and process conditions to produce drying maps for different systems.

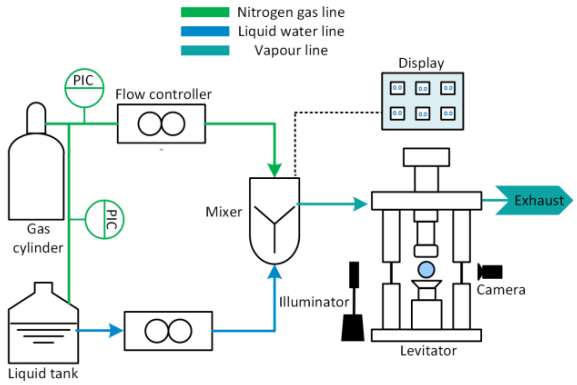

Figure 1: Suspension of a droplet in a controlled atmosphere using an acoustic levitator.

3. Results and discussion

The droplet drying history during evaporation is shown in Figure 2a for an aqueous formulation of mannitol (4.5 wt%) and PVP (0.9 wt%). In the first drying stage, the diameter of the droplet decreases as solvent is evaporated from the droplet surface. In the second drying stage, a shell forms and evaporation occurs through interstices in the shell. The evaporation rate hence reduces significantly due to the added resistance of the crust. When presented as a plot of normalised squared diameter D^2/D_o^2 against time, the two drying regimes can be clearly identified. We have performed such characterisation for a variety of process conditions and the particles obtained can be subsequently analysed to provide useful information on particle properties such as size, shape, porosity, roughness and crystal structure. Figure 2b and 2c shows exemplary images of particles obtained using SEM and micro X-ray computed tomography. By investigating the droplet drying dynamics and resulting particle microstructure, for a variety of mixtures and operating conditions enables us to gain deep insight into the process behaviour and the properties of the resulting particles.

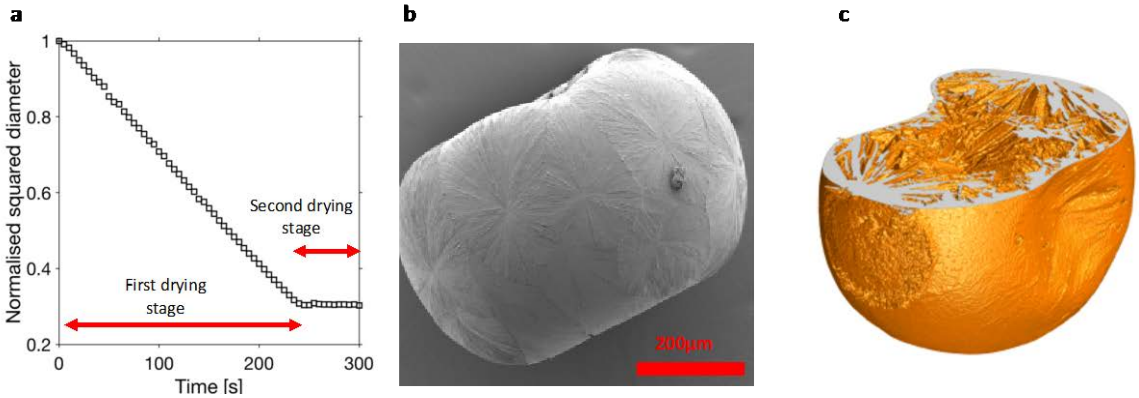

Figure 2: **a)** Droplet drying history and particle obtained from drying an aqueous formulation containing 0.9%w/w polymer, 4.5%w/w mannitol at 60C and 0% relative humidity **b)** SEM image **c)** cut-away surface from micro X-ray tomography.

References

[1] Carver, K. M., & Snyder, R. C. (2012). Ind. Eng. Chem. Res, *51*(48), 15720.

[2] Mönckedieck, M., Kamplade, J., Fakner, P., Urbanetz, N. A. (2017). *Drying Technology*, *35*(15), 1843.

[3] Osman, A., Goehring, L., Patti, A., Stitt, H., & Shokri, N. (2017). Ind. Eng. Chem. Res, *56*(37), 10506.

[4] Sugiyama, Y., Larsen, R. J., Kim, J., & Weitz, D. A. (2006). Polymer Suspensions, (8), 6024.

ECCE12
The 12th EUROPEAN CONGRESS OF CHEMICAL ENGINEERING
Florence 15-19 September 2019

Simulation of the mechanical and electrical behavior of lithium-ion battery electrodes

Clara Sangrós[1], Carsten Schilde[1], Astrid Pistoor, Arno Kwade[1]

[1] *Institute for Particle Technology, TU Braunschweig (Germany)*

**Corresponding author: c.sangros@tu-braunschweig.de*

Highlights

- Discrete element method (DEM) simulations can represent particulate electrodes
- Simulations give insight into structure-process-property relationships
- Electrical conductivity based on the electrode structure via an implemented algorithm

1. Introduction

Lithium-ion batteries are widely gaining popularity as electrochemical power sources, becoming also remarkably successful in the electric power vehicle market. Batteries are composed of electrodes which consist of porous composite materials coated on a substrate. To date, several investigations have clearly confirmed the impact of electrode microstructure on performance metrics such as energy and power densities, cycling stability, cell life and battery safety [1,2].

Bearing in mind the particulate nature of such electrodes, this work proposes a discrete element method (DEM) simulation approach to describe both the behavior of the particles and the binder along the calendering manufacturing step. Additionally, a post-processing tool is implemented to determine the electrical conductivity based on the DEM-generated structures and their connectivity. This electrode property is of considerable importance and ultimately controls the performance of the battery. However, an electrode structure which enables a proper electrical conductivity might hinder the ionic conductivity at the same time. As a consequence, finding optimal electrode architectures that offset competing tradeoffs can be challenging and thus, there is a clear need to fully comprehend the influence of electrode microstructure on cell performance.

2. Methods

Within this project, Li $[Ni_{1/3}\ Mn_{1/3}\ Co_{1/3}]O_2$ (NMC) cathodes were investigated. The discrete element method (DEM) was chosen as a valid simulation approach to represent particulate electrodes. Details on the numerical method can be found in [3]. In general lines, an elasto-plastic contact model was combined with a bond model to reproduce the mechanical response of NMC cathodes by taking into consideration the stiffness of the particles and the binder. The method to simulate the electrical conductivity was based on the connectivity of the numerical structures. To this aim, a pathfinding algorithm was implemented to design an equivalent circuit that can subsequently assess the overall network electrical resistance. Simulations were combined with experiments to calibrate and validate the outcomes. In particular, indentation measurements on

single NMC particles were carried out to parametrize the DEM contact model as shown in [3]. The specific electrical conductivity was measured according to [4].

3. Results and discussion

The calendering manufacturing process was investigated within this work via DEM simulations and real experiments. Once they were validated, the simulations could predict the elastic recovery of the cathode structure, a key aspect that cannot be experimentally determined to date. Figure 1 shows the evolution of the porosity under four different maximum calendering stresses. The elastic recovery of the electrodes, which was proved to depend on the calendering degree, ranged from 10.25 % up to almost 17 %.

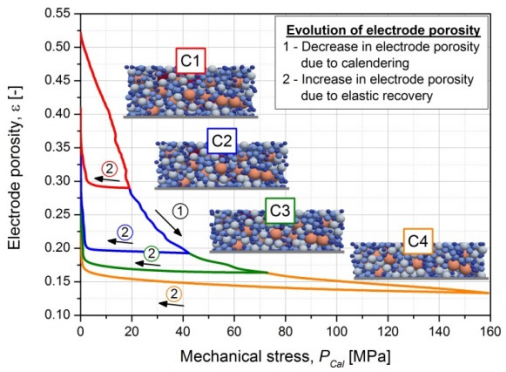

Figure 1. Evolution of the electrode porosity along the calendering process

Electrons move through the electrode particle assembly overcoming electrical resistances. Bearing this in mind, the implemented algorithm was used to identify the electrical pathways within the calendered cathodes. By considering particles as nodes and direct or bond contacts as lines, the structure could be converted into a resistance network. The overall resistance could be resolved afterwards by using Kirchhoff´s circuit laws, which allow to solve complex circuits defining a set of equations for the current and voltage. Results proved that the method could reproduce the experimental trend suitably. Furthermore, it was possible to successfully apply the method to other electrode configurations, which is of great importance in view of improving electrode design for a wide range of applications.

4. Conclusions

Within this work, lithium-ion battery cathodes were simulated to investigate their behavior during the calendering process and assess their specific electrical conductivity. By combining the numerical approach with experiments, the proposed simulation method can give insight into the overall electrode structural, mechanical and transport properties in view of predicting and designing improved materials.

References

[1] A.Kwade, W.Haselrieder, R.Leithoff, A.Modlinger, F.Dietrich, K.Droeder, Nat Energy 3 (2018) 290–300.
[2] H.Bockholt, M.Indrikova, A.Netz, F.Golks, A.Kwade, Journal of Power Sources 325 (2016) 140–151.
[3] C.Sangrós Giménez, C.Schilde, B.Finke, L.Froboese, A.Kwade, Powder Technology (2019) *submitted*.
[4] L.Froboese, P.Titscher, W.Haselrieder, A.Kwade, Materials Characterization 133 (2017) 102–111.

ECCE12
The 12th EUROPEAN CONGRESS OF CHEMICAL ENGINEERING
Florence 15-19 September 2019

Experimental and numerical analyses by DEM of the range of a probe in a granular medium

Julien Lehuen[1,2*], Jean-Yves Delenne[1], Abdelkrim Sadoudi[1], Denis Cassan[1], Agnès Duri[1] and Thierry Ruiz[2]

1 UMR IATE 1208 CIRAD/INRA/Montpellier SupAgro/Université Montpellier – 2 Place Pierre Viala, 34060 Montpellier cedex 5, France. ; 2 UMR QualiSud 95, CIRAD/Université Montpellier – 15 avenue Charles Flahault, 34093, Montpellier cedex 5, France

**Corresponding author: julien.lehuen@supagro.fr*

Highlights

- There is vertical stratification within a granular medium located in a reactor.
- The range of force imposed by the blade is all the lower when the speed is high.
- DEM simulations give the structural rearrangement which occurs during trials.
- Spatiotemporal correlations of particle motions observed by PIV could be explained by DEM.

1. Introduction

The study of stress transmission and motion typologies in a powder bed under low shear condition constitutes a challenging issue to achieve a monitoring of processes which involve particle mobility like kneading or agglomeration process [1]. This work deals with the ability of a probe to ensure the particle mobilities in a granular bed disposed in the tank of a reactor. An original experiment is developed (i) to allow the visualization of the behavior of particles in the neighborhood of an intruder (*i.e.* a horizontal flat blade design) in ascendant vertical motion, and (ii) to measure the drag force applied to the intruder during its extraction from an ensiled granular medium. In order to identify the force propagation in a granular ensiled medium, experiments and Discrete Element Method (DEM) simulations [2] are compared to investigate the propagation of the force imposed by the blade at different dimensionless speeds.

2. Methods

Experimental device. The granular medium is a population of glass beads of 1-2 mm diameter with a small span value. The experimental set-up consists of an open glass cell container (51x100x160 mm) made of transparent glass walls. The filling is provided by a funnel and the flow rate is modulated by the output diameter. A flat and rectangular steel probe is especially designed to fit into the glass container. It is screwed on a rod that is linked to a load cell of a texture analyzer (TA.XT2, Table Micro System), which is used as a force sensor. The probe is then removed from the granular packing. The drag force is measured and the velocity field is analyzed by PIV analysis. The visualization of the particle mobilities during the ascendant vertical motion of the probe is carried out using a high-speed camera and then, analyzed by Particle Image Velocimetry (PIV).

Numerical simulation. In order to reproduce the experimental conditions, a code using both the DEM and the coarse-graining method is developed to calculate the force network, the stress fields

and the solid fraction of the granular medium. It allows us to explore all the contacts network between the particles by the calculus of (i) normal and tangential forces, (ii) moment, (iii) mobility of each particle.

3. Results and discussion

Force measurements and PIV technique allow to identify different types of particle motions (compaction, loading and rupture of the chain forces, lateral collapsing, avalanches, etc.) as well as the mechanical state of the granular bed. These behaviors are confirmed by DEM simulations which indicate the evolution of the compactness and the lifetime of intergranular contacts. Fluctuations of stress are identified and depend on the dimensionless blade speed [3]. This result can be explained by successive loading and rupture cycles of horizontal force chains taking place above the blade, leading to fluctuations of the vertical stress. The analysis of spatiotemporal correlations of the velocity fields reveals the existence of a dihedral-shape assembly of grains which constitutes a permanent disturbance zone above the blade during its vertical rise whatever the blade speed. The range of the blade could be defined by a characteristic length links to the development of mobility gradients. A specific study of the velocity gradient generated above the blade is carried out for the different blade speeds.

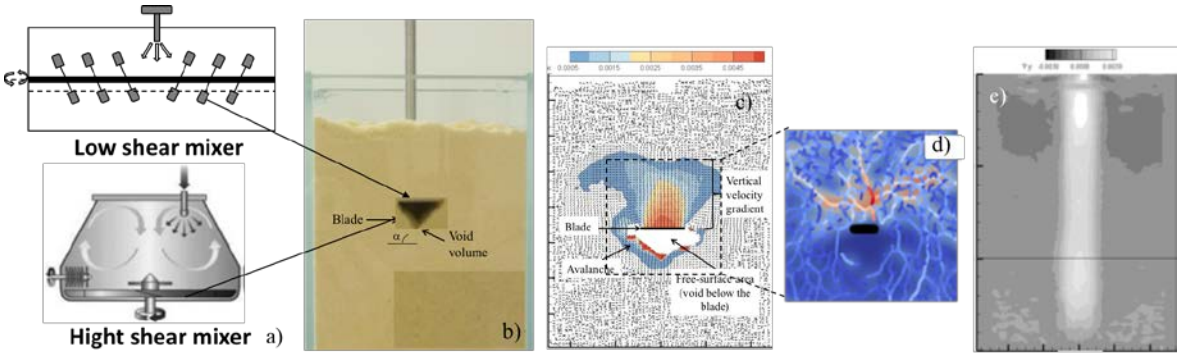

Figure 1. From reactors (a) to the experimental device (b) to identify particle mobilities by PIV (c) and DEM simulations (d) focused around the blade and the active and passive zones of mobilities in the granular medium (e).

4. Conclusions

Experimental observations coupled with DEM simulation allow to access to the phenomenon at the reactor and particle scales. The analysis of the local force network and the microstructure of the granular medium allows to define characteristic length and time. These parameters could be then used to optimize process control that involves particle mobilities induced by a mechanical input.

References

[1] S.L. Conway, A. Lekhal, J.G. Khinast, B.J. Glasser, Granular flow and segregation in a four-bladed mixer, Chemical Engineering Science 60 (2005) 7091-7107.

[2] G.R. Chandratilleke, K.J. Dong, Y.S. Shen, DEM study of the effect of blade-support spokes on mixing performance in a ribbon mixer, Powder Technology 326 (2018) 123–136.

[3] Y. Ding, N. Gravish, D.I. Goldman, Drag Induced Lift in Granular Media, Physical Review Letters 106 (2011) 028001.

ECCE12
The 12th EUROPEAN CONGRESS OF CHEMICAL ENGINEERING
Florence 15-19 September 2019

Multi-scale characterization of precipitated silica in terms of vacuum insulation panels

Manuel Meier[1], Sebastian Sonnick[2], Ermek Asylbekov[1], Mira Klinge[1], Matthias Rädle[2], Hermann Nirschl[1]

1 Karlsruhe Institute of Technology, Institute for Mechanical Process Engineering and Mechanics, Karlsruhe, Germany
2 Mannheim University of Applied Sciences, Institute of Process Control and Innovative Energy Conversion, Mannheim, Germany

Corresponding author: manuel.meier@kit.edu

Highlights

- Multi-scale characterization of precipitated silica using SAXS, AUC and REM
- Analysis of aggregate structure using pore size determination techniques
- Determination of fractal dimensions, sediment structure as well as porosity
- Correlation of the measurement data with mathematical models

1. Introduction

Ensuring the cold chain is a prerequisite for maintaining product quality in a global market. The requirements for insulation material are accordingly clearly defined: high insulation effect at low weight, high transport stability and low production costs. A material that meets all the requirements is foamed polystyrene. In terms of sustainability, oil free materials have been under investigation for their use as insulation material for some time now. However, in many cases, alternative materials are overpriced in production or delivery costs. Previous studies showed, that precipitated silica is an interesting alternative to conventional insulation materials. In addition to low production costs, precipitated silica has low bulk density, low flammability and good biodegradability. On market, there are a lot of materials available for a wide range of industrial applications. Nevertheless, most of these materials are developed in the respect of their effect on product but not in particle characteristics. This investigation takes into account both nanoscopic properties such as primary particle and aggregate size, their fractal dimension and the size distribution within the aggregate, as well as mesoscopic properties of the pellets.

2. Methods

This work deals with the metrological description of precipitated silica by a multi-scale characterization. Measurements by means of small angle X-ray scattering (SAXS) and electron microscopy allow a statement to be made about the basic structure levels of an aggregate: fractal dimension of surface, primary particle size, fractal dimension of mass and the aggregate size. To combine information about the aggregate with information about the sediment structure itself, porosimetry and centrifugation techniques were used.

3. Results and discussion

The obtained results allow a realistic aggregate computation and building of a sediment structure of precipitated silica by DEM simulations (see Figure 1). The computation based on a fundamental consideration of the structure of aggregates by diffusion-limited aggregation (DLA) made by Forrest and Witten [1] and Witten and Sander [2, 3]. Assumptions for the modelling of the compactness of the individual aggregates were examined under consideration of geometric and scatter-based approaches.

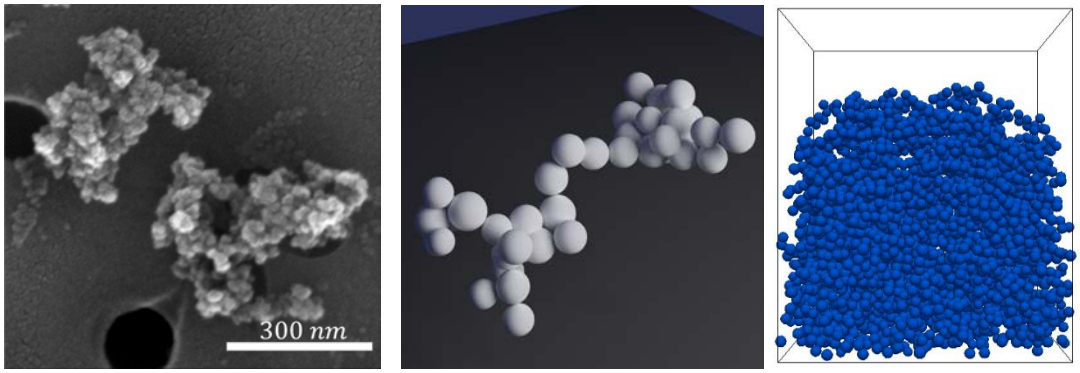

Figure 1. TEM image, aggregate computation and sediment structure of a precipitated silica.

4. Conclusions

In this study we performed a multi-scale characterization of several precipitated silica including small-angle X-ray scattering (SAXS), analytical (ultra-) centrifugation as well electron microscopy and pore size characterization techniques. The correlation of the obtained measurement data with mathematical models allow a statement to be made about the aggregate structure. Pore size characterization techniques using mercury and nitrogen provided information on the porous structure of the aggregates with respect to the pore inlet diameter and the pore diameter itself. The knowledge gained here allows us to gain a deeper understanding of the structure and description of fractal aggregates of precipitated silica.

References

[1] S.R. Forrest, J. T. A. Witten, Long-range correlations in smoke-particle aggregates, Journal of Physics A: Mathematical and General, 12 (1979) L109.
[2] T.A. Witten, L.M. Sander, Diffusion-Limited Aggregation, a Kinetic Critical Phenomenon, Physical Review Letters, 47 (1981) 1400-1403.
[3] T.A. Witten, L.M. Sander, Diffusion-limited aggregation, Physical Review B, 27 (1983) 5686-5697.

ECCE12
The 12th EUROPEAN CONGRESS OF CHEMICAL ENGINEERING
Florence 15-19 September 2019

Synthesis and Characterization of $CaCO_3$ Nanoparticles by Sol-gel Citrate Method: Effect of Citric Acid Concentration

Merve Şener, Çağla Gül Güldiken, Hasan Ferdi Gerçel

Department of Chemical Engineering, Eskişehir Technical University, Eskişehir 26555, Turkey

**Corresponding author: hfgercel@eskisehir.edu.tr*

Highlights

- Cost-effective and eco-friendly $CaCO_3$ nanoparticle synthesis process was developed.
- Calcination temperature was decreased using a sol-gel citrate method.
- Effect of citric acid concentration on particle size and morphology were investigated.

1. Introduction

$CaCO_3$, one of the most abundant minerals in nature, is used in wide range of engineering applications. $CaCO_3$ nanoparticles can be utilized as reinforcing agents in polymer matrix nanocomposites to enhance the mechanical properties and reduce cost [1, 2]. In the present study, $CaCO_3$ nanoparticles were synthesized via a sol-gel citrate method. Citric acid (CA) was used an organic additive in the $CaCO_3$ nanoparticle synthesis to achieve a homogeneous size distribution and smaller sized $CaCO_3$ particles. CA is non-toxic and non-carcinogenic contrary to the hydrazine-based additives which are commonly used for the same purposes. The chemical structures and morphologies of the synthesized nanoparticles were analyzed by Fourier transform infrared spectroscopy (FTIR) and scanning electron microscopy (SEM), respectively.

2. Methods

1 M aqueous solutions of $Ca(NO_3)_2.4H_2O$, as the precursor, were prepared. CA was added to the solution at weight ratios of 0.25 and 1.5 based on the weight of $Ca(NO_3)_2$ and heated to 70°C under constant stirring. Chemical reaction between the precursor and CA was conducted at 70°C for 24 hours. The resulting homogenous solution, obtained from the hydration reaction, was dried at 125°C for 24 hours. The porous and quite swelled product were grinded and then calcined at 600°C for 5 hours. Finally, the calcinated samples were washed several times with deionized water by ultrasonic mixing, centrifuged and dried at 105°C for 12 hours. The synthesized nanoparticles named $CaCO_3$_0.25CA and $CaCO_3$_1.5 CA.

The chemical structure of the synthesized nanoparticles was characterized in KBr disks by using a Perkin Elmer Frontier FTIR spectrometer between 400 and 4000 cm^{-1}. The morphology and particle size of the samples were investigated by using a scanning electron microscope (Carl Zeiss/Supra 40VP) at an accelerating voltage of 15 kV. All the samples were dried and sputter coated with Au/Pd prior to SEM analyses.

3. Results and discussion

Based on the FTIR spectra of the $CaCO_3$_0.25CA and $CaCO_3$_1.5 CA nanoparticles, shown in Figure 1, the wide band at 3645 cm^{-1} arises from the stretching mode of hydroxyl groups of $Ca(OH)_2$. The weak peak at 2885 cm^{-1} are assigned to the long alkyl chains of CA. The strong peak observed at

1428 cm^{-1} corresponds to the C=O stretching vibrations. The sharp peaks at 875 and 712 cm^{-1} indicates the existence of carbonate group. The FTIR spectra of both nanoparticles, which are differing in CA concentration, are consistent. This result shows that increasing CA concentration does not damage the chemical structure of the synthesized nanoparticles [1-3].

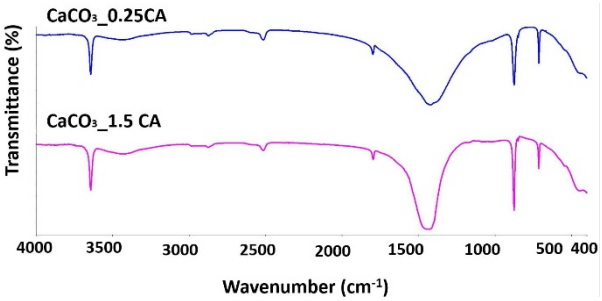

Figure 1. FTIR Spectra in Different CA Concentrations

SEM micrographs of the $CaCO_3$_0.25CA and $CaCO_3$_1.5 CA nanoparticles at 20kX magnification are presented in Figure 1(a, b). It is clearly seen that the particle size decreases with the increasing CA concentration. However, the decrement in particle size leads to aggregation of nanoparticles.

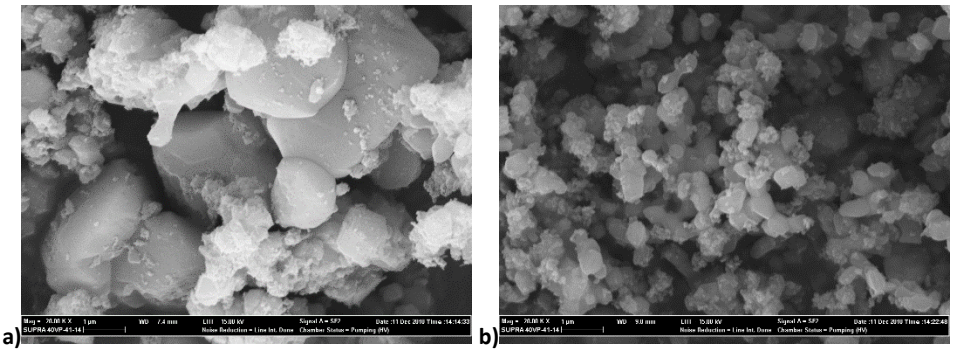

Figure 2. SEM micrographs of the (a) $CaCO_3$_0.25CA (b) $CaCO_3$_1.5 CA nanoparticles at 20kX magnification

4. Conclusions

The chemical structure of the nanoparticles has not been harmed by the addition of CA up to a mass ratio of 1.25 to the precursor. The upper limit for CA mass ratio in synthesis process can be determined in further studies. Based on the result that the particle size decreases with increasing CA concentration during the synthesis process, it can be deduced that nanoparticles with desired sizes can be synthesized by changing the CA concentration. In future studies, different surfactants can be used in the synthesis process to prevent nanoparticle agglomeration due to the particle size decrement.

References

[1] D. Uzunoğlu, A. Özer, IJARSET 2(3) (2018) 245-253.
[2] A. Barhoum, G. Van Assche, A. S. H. Makhlouf, H. Terryn, K. Baert, M.P. Delplancke, H. Rahier, Cryst. Growth. Des. 15(2) (2015) 573-580.
[3] Ghiasi, A. Malekzadeh , Cryst. Res. Technol. 47 (2012) 4 471 – 478.

ECCE12
The 12th EUROPEAN CONGRESS OF CHEMICAL ENGINEERING
Florence 15-19 September 2019

Experimental and numerical study of a radial multi-zone vortex chamber spray dryer

Thomas Tourneur[1], Axel de Broqueville[1], Anton Sweere[2], Albert Poortinga[2], Anton Wemmers[3], Umair Jamil Ur Rahman[4], Artur Pozarlik[4], Juray De Wilde[1,5*]

1. Université Catholique de Louvain, Material & Process Engineering, Louvain-la-Neuve, Belgium
2. FrieslandCampina Research, Wageningen, The Netherlands
3. Energieonderzoek Centrum Nederland, Petten, The Netherlands
4. University of Twente, Laboratory of Thermal Engineering, Enschede, The Netherlands
5. Institute for Sustainable Process Technology, Amersfoort, The Netherlands
**Corresponding author : juray.dewilde@uclouvain.be*

Highlights

- High-G spray drying intensification
- New radial multi-zone vortex chamber design
- Experimental and numerical study of the flow pattern and drying behavior
- Distinct temperature separation and short particle residence time in the hot zone allows efficient 2-step drying using hot (350°C) air without burning produced milk powder

1. Introduction

Vortex chambers introduce process gas via tangential inlet slots over the entire length of the cylindrical vortex chamber and evacuate the gas via a chimney in one of the end plates of the vortex chamber. A strong rotational flow is generated, allowing high-G operation. The latter intensifies interfacial mass, heat and momentum transfer by easily one order of magnitude and also facilitates the use of fine particles [1]. In previous studies, application to particle drying [2,3] and fine particle coating [4] was demonstrated. Applications taking advantage of the very short gas-solids contact time and combining high-G intensified gas-solids contact, gas-solids separation and solids segregation were also studied [5].

In the present work, a specific design called the radial multi-zone dryer (RMD) [6] is experimentally and numerically studied. Application to spray drying is focused on, characterized by dilute operation and very strong rotational flows. Two distinct temperature zones are created without physical barrier, a radially central zone where hot air with a temperature up to 350°C is injected and a peripheral zone where air at a temperature of around 100°C is injected through the vortex chambers (Figure 1). The proposed multi-zone operation allows significant process intensification while preventing degradation of the product. Liquid droplets are injected in the hot central zone, co- or counter-current with the hot air. Fast initial drying is achieved in this zone while burning the product is prevented by rapid evacuation of the produced particles to the colder periphery under the action of the centrifugal force generated by the vortex chamber(s). Typical residence time of the particles in the hot zone can be limited to a few milliseconds. Drying is continued in the colder periphery where high-G operation intensifies interfacial mass, heat and momentum transfer and ensures efficient gas-solids separation.

2. Methods

The experimental set-up that was used is flexible and allows studying various multi-zone concepts, varying the dimension/design of the different zones and the type of spray nozzle. Extension

chambers allowing to minimize air consumption and to optimize gas-solids separation can be added. Tests were carried out with total air flow rates of maximum 1000 Nm³/h, liquid flow rates of up to 6 g/s and hot air temperatures of maximum 350°C. Both hollow-cone and full-cone nozzles were tested. Three types of experiments were carried out: (i) in the absence of liquid injection, (ii) injecting water, and (iii) injecting milk. The axial and radial temperature profiles in the device were measured by means of 16 thermocouples. Comparison of the profiles in the three types of experiments and visual observations allowed gaining understanding in the complex flow pattern of the gas and droplets and the extent of evaporation in specific regions. Deposition of powder on the walls and in the gas and solids outlets was also carefully analyzed. Protection of the nozzle from fouling required a new protective sleeve design. To gain further insight in the flow pattern, CFD simulations were carried out, adopting the RANS-approach and a coarse-grained discrete particle model to track the motion of the droplets. Evaporation was accounted for and the behavior of droplets of different size studied.

3. Results and discussion

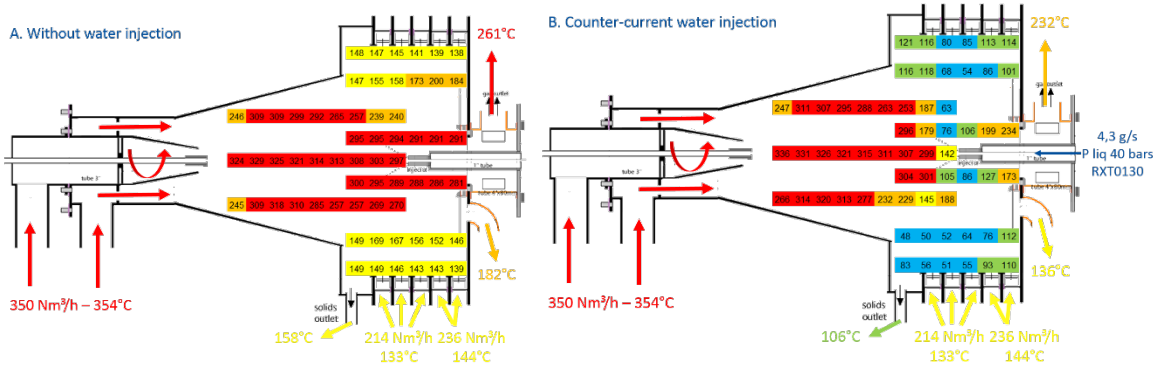

Figure 1. Measured temperature profiles in a radial multi-zone vortex chamber spray dryer with and without water injection.

The droplet/particle trajectories could be tracked by comparing detailed temperature measurements in the absence and presence of water injection (Figure 1) and by means of the CFD simulations. With a counter-current configuration (Figure 1), an S-shaped particle trajectory was observed. Radial multi-zone operation and mastering the axial motion of the gas and droplets/particles and the related residence times in the different zones remains challenging. Fouling also needs to be addressed. Promising results were obtained with an optimized radial multi-zone dryer design with a full cone nozzle and high-quality powder could be produced. Distinct separation of the two temperature zones was confirmed and could be maintained in the presence of droplets/particles (Figure 1), allowing efficient 2-step drying of the powder. A counter-current configuration (Figure 1) was found to be more efficient than a co-current configuration. Protection of the nozzle tip from fouling required a new protective sleeve design.

4. Conclusions

Experimental studies and CFD simulations of spray drying in a radial multi-zone spray dryer show that the technology is feasible and promising for intensified two-step drying. Efficient separation of a hot central zone and cold periphery and an extremely short residence time of the droplets/particles in the central hot zone can be achieved. As a result, using 350°C hot air, high-quality milk powder could be produced. A full cone nozzle was shown to be more efficient and stable than a hollow cone nozzle, especially with counter-current injection of hot air.

References

[1] Axel de Broqueville, Juray De Wilde, Numerical investigation of gas-solid heat transfer in rotating fluidized beds in a static geometry, In Chemical Engineering Science, Volume 64, Issue 6, 2009, Pages 1232-1248, ISSN 0009-2509.
[2] Eliaers, Philippe ; De Wilde, Juray. Drying of Biomass Particles: Experimental Study and Comparison of the Performance of a Conventional Fluidized Bed and a Rotating Fluidized Bed in a Static Geometry. In: Drying Technology, Vol. 31, no.2, p. 236-245 (2013)
[3] Philippe Eliaers, Jnyana Ranjan Pati, Subhajit Dutta, Juray De Wilde, Modeling and simulation of biomass drying in vortex chambers, In Chemical Engineering Science, Volume 123, 2015, Pages 648-664, ISSN 0009-2509,
[4] Philippe Eliaers, Axel de Broqueville, Albert Poortinga, Tom van Hengstum, Juray De Wilde, High-G, low-temperature coating of cohesive particles in a vortex chamber, In Powder Technology, Volume 258, 2014, Pages 242-251, ISSN 0032-5910
[5] Juray De Wilde, George Richards, Sofiane Benyahia, Qualitative numerical study of simultaneous high-G-intensified gas–solids contact, separation and segregation in a bi-disperse rotating fluidized bed in a vortex chamber, Advanced Powder Technology, Volume 27, Issue 4, July 2016, Pages 1453-1463, ISSN 0921-8831
[6] Axel de Broqueville, Juray De Wilde, Thomas Tourneur, Device for treating particles in a rotating fluidized bed, WO/2018/203745, November 2018

ECCE12
The 12th EUROPEAN CONGRESS OF CHEMICAL ENGINEERING
Florence 15-19 September 2019

Spray drying of alumina powders – impact of process parameters and powder properties upon final product

Antoine Marie[1], Mallorie Tourbin[2], Anne-Charlotte Robisson[1], Carine Ablitzer[1], Christine Frances[2]

1 CEA, DEN, DEC, Cadarache 13108 St Paul les Durance, FRANCE ; 2 Laboratoire de Génie Chimique INP – ENSIACET, 31400 Toulouse, FRANCE

**Corresponding author: antoine.marie@cea.fr*

Highlights

- Alumina spray drying was studied under different process conditions
- The spray drying gas temperature impacts the proportion of fines in the product
- The initial powder size distribution has an effect on the spray-dried agglomerates
- Ultrasonic nozzle technology allows producing strong alumina agglomerates

1. Introduction

Spray drying is a quite usual process in powder industry for the production of pharmaceutics, food or ceramics [1]. Concerning ceramic powders, alumina powders for instance can be dried by spraying in order to provide better flow properties [2]. The physical properties of spray-dried product (size distribution, agglomerate shape) depend on several parameters, in particular spray drying conditions (gas temperature or suspension flow rate [3]) and the properties of the initial suspension (particle size distribution, solid content, …). The spray dryer nozzle geometry also may affect the product properties. If bifluid nozzle has been widely used [2] [4], ultrasonic nozzle was less commonly mentioned [5]. The purpose of this study is to evaluate the influence of these main parameters and of the nozzle technology used on the spray-dried powders.

2. Methods

In order to study the aforementioned parameters, several suspensions of alumina were prepared, using 3 different powders supplied by Baikowski (CR6, CR15 and GE15) having different initial specific surface area (respectively 6, 15 and 14 $m^2.g^{-1}$) and different median size (respectively 0.5, 0.4 and 8 µm). Several tests were performed with a Büchi Mini Spray Dryer B290, using a bifluid or an ultrasonic nozzle under various operational conditions, varying parameters such as gas temperature, suspension concentration or suspension flow rate. Nozzles mainly differ in the technology used to form the spray: in case of bifluid it is formed by shear forces resulting of contact between liquid and high-speed air flow; with ultrasonic nozzle, by vibration induced by high frequency sonication.

Characterizations were led, pairing size distribution analysis (by laser diffraction) and Scanning Electronic Microscope (SEM) pictures to get the morphology of the dried agglomerates. The device used to evaluate the agglomerate size distribution (Malvern MS3000) was also used to investigate the de-agglomeration and re-agglomeration behavior of the spray-dried powders by changing the air flow pressure used to disperse the particles.

3. Results and discussion

The spheroidization of the particles by agglomeration generated by the spray drying technology was observed by comparing SEM pictures before and after the spray drying process. Size distribution analysis points out the impact of spray-drying on granulometry: the operation tends towards narrowing the size distribution of the powder.

Some results, showing the influence of several parameters: process temperature, suspension concentration and suspension flow rate using a bifluid nozzle on the CR6 particle size distribution, are illustrated on figure 1. If the two last parameters do not seem to have a huge influence upon granulometry, temperature appears to affect the proportion of fine particles (submicronic ones).

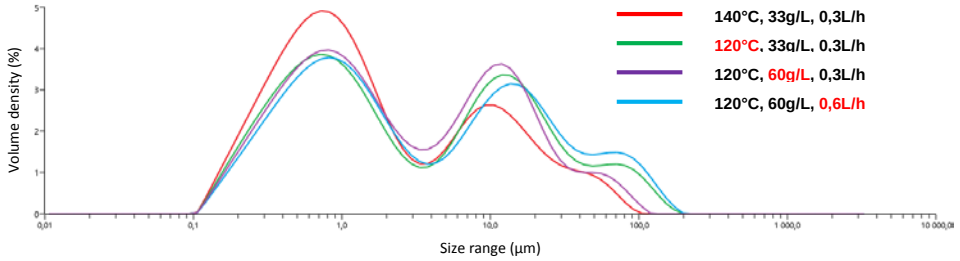

Figure 1. Size distribution curves depending on some process parameters

It was also found out that initial size distribution has an impact on powder behavior during spray drying since powder GE15, which has a higher median size than the two other powders, was not agglomerated but only dried during the experiments. Indeed, no significant change in morphology before and after spray drying was noticed using the bifluid nozzle for this powder. On the contrary, the ultrasonic nozzle allows GE15 powder to form spherical agglomerates, which let think that this technology is less sensitive to the initial characteristics of the powders.

The de-agglomeration tests performed under air flow pressure variations using the Malvern MS3000 dispersing system show that the agglomerates were more or less strong depending on the initial powders and process conditions. Indeed, some spray-dried powders with the bifluid nozzle tend to de-agglomerate increasing the air pressure while nearly no changes were observed with agglomerated powders produced using the ultrasonic nozzle. The ability of re-agglomeration of powders was also investigated in wet conditions.

4. Conclusions

The impact of some spray drying process parameters such as temperature or suspension flow rate, as well as suspension parameters like alumina concentration or powder initial granulometry, was studied. It appears that temperature has an influence on the proportion of fine particles (and consequently the size distribution) more distinctly than the other process parameters using a bifluid geometry in the spray-drying process. Runs were also performed using a recent nozzle technology (ultrasonic system) showing promising results, especially when an initial coarse powder, not easily agglomerated with a conventional bifluid system is used. More robust alumina agglomerates, not easily dispersed in air flow, were then obtained using the ultrasonic nozzle. The ability of the spray-dried powder to de-agglomeration or re-agglomeration phenomena is also discussed in this work.

References

[1] F. Gomez and K. Saleh, « Mise en œuvre des poudres - Séchage par atomisation. Procédé », p. 19, 2012.

[2] P. Ramavath et al., « Flow properties of spray dried alumina granules using powder flow analysis technique », *Adv. Powder Technol.*, vol. 24, n° 3, p. 667‑673, may 2013.

[3] O. Ozdikicierler et al., « The effects of spray drying process parameters on the characteristic process indices and rheological powder properties of microencapsulated plant (Gypsophila) extract powder », *Powder Technol.*, vol. 253, p. 474‑480, febr. 2014.

[4] S. Poozesh et al, « Assessment of predictive models for characterizing the atomization process in a spray dryer's bi-fluid nozzle », *Chem. Eng. Sci.*, vol. 180, p. 42‑51, apr. 2018.

[5] R. Rajan and A. B. Pandit, « Correlations to predict droplet size in ultrasonic atomisation », *Ultrasonics*, vol. 39, n° 4, p. 235‑255, june 2001.

Spray Drying Encapsulation of Geraniol Essential Oil using different wall materials

Duarte MJ[1] and Bittencout E[2]

[1] *University of Campinas (UNICAMP), School of Chemical Engineering, Laboratory of Optimization, Design, and advanced Control (LOPCA), Campinas, SP, Brazil* [2] *Technological Aeronautics Institute (ITA), Physics Department, São José dos Campos, SP, Brazil*
[1]Corresponding author: mduarte@ipafarma.com.br

Highlights
- Arabic Gum is an efficiency polymeric material to encapsulated Geraniol.
- The system has up to 15 days stability in environmental conditions.
- This system has great potential for use in crop protection and pollinators' attraction.

Introduction

Geraniol (GRL) is an acyclic monoterpene alcohol ($C_{10}H_{18}O$) derived from essential oils plants and showed several uses, such as pharmo-therapeutics (antitumor), preservative (bactericide), odorizing (for food and cleaning products), attraction agent to pollinators insects and repellent of a large number of insects considered as pests in agriculture [1-4]. However, GRL does not draw the interest from agro-industry when it is used "*in natura*" due to its short activity time since it is easily volatilizing or degrades by its high sensitivity to light, temperature and humidity [4,5]. One strategy to preserve unstable materials is the encapsulation. In this system essential oil is surrounded by a mono or multilayer coating layers that are able to preserves or control the release into the environment [6]. As example, the micro or nano carrier systems can be produced from different polymeric matrices such as Maltodextrin (ML) and Arabic Gum (AG) as well as by different encapsulation techniques (spray drying, fluidized bed, coacervation, extrusion and molecular inclusion). The atomization technique, also known as "Spray Drying" demonstrated efficacy in the studies with essential oils, besides its low cost [7-9]. The spray-drying process combines fluid colloidal materials in an emulsion (hydrophobic substance and polymer matrix in solution or suspension) converting them to dried particulates by the action of heated air in a drying chamber. In this study ML and AG were used in different proportions to produce the polymeric wall in the encapsulation process of GRL using spray drying technique as an alternative to protect the GRL when exposed to field conditions. In this way, this study open perspectives for the use of encapsulated GRL in crop protection as well as attractive for pollinators.

Methods

Three different formulations were prepared with GRL and polymeric materials wall. Each blend had 200 g as the final mass following these compositions (% w/w): A1 (30% ML, 10% GRL, 60% water); A2 (30% AG, 10% GRL, 60% water); A3 (15% ML, 15% AG, 60% water). Each sample was emulsified by ultraturrax (IKA T-18 ultra turrax emulsifier) at 17,000 rpm for 5 min (200 mL). Each emulsion had an aliquot diluted in deionized water at 1:1000 (v:v) at the 10, 20 and 30 minute intervals and

zeta potential was analyzed in triplicate using Zetasizer (Nano-ZS 90 Malvern Instruments). The zeta potential demonstrates that the stability of the emulsion along the drying period in Spray Dryer process. Spray dryer was setup using air inlet temperature 95 °C ± 5 °C; compressed air pressure 5 bar; compressed air inlet flow 40 L/min; blower flow 3.9 m³/min; liquid flow rate 0.5 L/h. The dried material obtained in the atomization was collected from the Spray Dryer and storage to characterization studies.

Capsules characterization - Encapsulation efficiency: The encapsulation efficiency of GRL was determined by the quantification of GRL loaded and unloaded using gas chromatography (GC). Capsule morphology: size, shape, influence of the matrix in capsule parameters were determined by scanning electron microscopy (SEM). Oil stability/release profiles: each capsule preparation was kept in a stability chamber (30 °C and 65 % humidity). The samples were kept in the chamber along 15 days and in the periods of 1, 7 and 15 days the materials were submitted to moisture analysis (% - using thermogravimetry at 80 °C) and oil content inside and outside the capsule (by gas chromatography) and morphology. (by SEM).

Results and discussion

To prepare A1 samples we have been used only ML as material to form the wall. After mixing all components and emulsifying them by Turrax, the water and ML formed an unbalanced system. As consequence, the ML concentration was increased to 40% and the matrix continued with heterogeneous aspect. The same behavior was described by Reineccius [10] where maltodextrin when used as an emulsifier providing an unstable film formation. In this way, due these results, the sample A1 was not considered in this study. However, for samples A2 and A3 were stable by visual analysis and for this reason they were considered in the next steps. In this context, the zeta potential was measured with 30 minutes, and the samples A2 and A3 presented stable values (A2 = 38 ± 2 mV; A3= 36 ± 3 mV). In addition, we have been observed that the zeta potential was also stable in acid pH (pH ~ 4) [11]. The SEM analysis showed that both samples presented spherical shape (**Figure 1**). The stability results showed that for A2 and A3 at t_{1day}, t_{7days} and t_{15days} a low decreasing in the internal volume of the capsules. This effect can be explained by the substitution of the geraniol present inside the capsule along the incubation time (15 days) in water in the stability chamber conditions (**Table 1**).

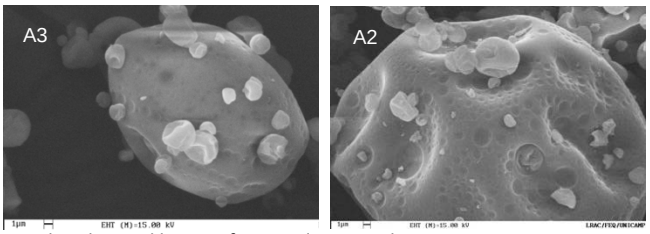

Figure 1. Morphology of the capsules obtained by SEM for samples A2 and A3.

Table 1. Results obtained for A2 and A3 samples:GRL assay (surface and inside capsules) and H_2O assay during the stability studies. Both results behaviors have correlation analyzed by Person in Microsof Excel® software.

Sample	Time (days)	GRL Assay inside (% w/w)	GRL Assay surface (%w/w)	H_2O assay (%w/w)	Person Correlation (H_2O and GRL assay)
A2 - AG	t_1	22.40	> 1%	5	-0.80
	t_7	21.06	> 1%	12	-0.80
	t_{15}	14.35	> 1%	18	-0.80
A3 - ML + AG	t_1	16.70	> 1%	11	-0.91
	t_7	14.30	> 1%	14	-0.91
	t_{15}	10.25	> 1%	21	-0.91

Also, the release of GRL from the capsules as described in **Table 1** can be explained by the two mechanisms: i) release of GRL by diffusion and ii) the degradation of GRL in/out the capsule. Another point is that there was an inverse relation between the increasing in the water inside and the decreasing in GRL inside the capsules. In addition, it is observed a strong linear correlation between these two variables that was determined by the analysis of the Person coefficient. These results were probably observed due the porosity increasing in the capsules and also to the exposure of GRL to oxygen that converts Geraniol ($C_{10}H_{18}O$) to Geranial and consecutively Geranioic acid ($C_{10}H_{16}O_2$).

Conclusion

The results showed that GRL and GA (as material wall) and its association with ML showed good results to produce capsules using Spray Drying technique. The characterization of both samples (A2 and A3) showed that the encapsulation efficiency remained in discrete decreasing in the first week (7 days) reaching approximately less than 50% of the total after 15 days. These results indicate that the encapsulation of Geraniol in both wall materials is able to preserve it for at least two weeks, therefore, a largest period comparing to GRL *in natura*. The results open perspectives for the use of GRL encapsulated in crop protection in field studies conditions.

References

1. Bakkali, F.; Averbeck, S.; Averbeck, D.; Idaomar, M. Biological effects of essential oils – a review. Food and Chemical Toxicology. Ed. 46, 446 – 475, **2008**.
2. Charbonneau, L.R; Hillier, N.K; Rogers, R.E.L; Williams, G.R; Shustler, D. Effects of *Nosema apis*, *N. ceranae*, and coinfections on honey bee (*Apis mellifera*) learning and memory. Scientific Reports. doi:10.1038/srep22626, **2016**.
3. Nerio, L.S.; Verbel, J.O.; Stashenko, E. Repellent activity of Essentials oils: a reveiw. Bioresource Technology. Ed. 101, 372-378, **2010**.
4. Malerbo, D.T.; Nogueira, C.R.H.; Couto, L.A. Honey Bee Attractants and Pollination in Sweet Orange, *Citrus sinensis* (L.) Osbeck, Var. Pera-Rio J. Venom. Anim. Toxins incl. Trop. Dis. 10 (2), 144-153, **2004**.
5. Oliveira, J.L.; Campos, E.V.R.C.; Anderson E.S.; Pereira, L.; Silva, C.C.L.; Pasquoto, T.; Lima, R.; Smaniotto, G.; Polanczyk, R.A.; Fraceto, L.F. Geraniol Encapsulated in Chitosan/Gum Arabic Nanoparticles: A Promising System for Pest Management in Sustainable Agriculture. *Journal of Agricultural and Food Chemistry 66* (21), 5325-5334.DOI: 10.1021/acs.jafc.8b00331, **2018.**
6. Bauer, K.; Garbe, D. Common Fragrance and Flavor Materials. Preparation, Properties and Uses. VCH Verlagsgesellschaft, Weinheim, p. 213, **1985**.
7. Augustin, M.A. Microencapsulation of food ingredients. Food Australia, 53 (6), 220-223, **2001**.
8. Re, M.I. Microencapsulation by Spray Drying. Drying Technology, 16 (6), 1195-1236, **1998**.
9. Roserberg, M.; Kopelman, I.J.; Talmon, Y. Factors affecting Retention in Spray-Drying Microencapsulation in volatile materials. Journal of Agriculture Food and Chemistry, 38, 1288-1294, **1990**.
10. Reineccius, G.A. Carbohydrates for Flavor Encapsulation. Food Techonology, 46(3), 144-149, **1991**.
11. Randall, R.C.; Phillips, G.O.; Williams, P.A. Fractionation and characterization of gum from Acacia Senegal. Food Hydrocolloids, 3 (1), 65-75, **1989**.
12. Ducel, V.; Richard, J.; Saulnier, P.; Popineau, Y.; Boury, F. Evidence and characterization of complex coacervates containing plant proteins: application to the microencapsulation of oil

droplets. Colloids and Surfaces A-Physicochemical and Engineering Aspects, 232 (2- 3), 239-247, **2004**.

Effect of Organo-Modified α–Sepiolite Content on Thermal and Mechanical Properties of Poly(ethylene oxide) Composite Films.

Çağla Gül Güldiken, Hasan Ferdi Gerçel

Department of Chemical Engineering, Eskişehir Technical University, Eskişehir 26555, Turkey

**Corresponding author: hfgercel@eskisehir.edu.tr*

Highlights

- α-Sepiolite is modified with poly(ethylene glycol) through hydrogen bonding interactions.
- Thermal stability of the composite is improved with modified α-sepiolite.
- Tensile properties are enhanced by modified clay addition to the structure.

1. Introduction

The incorporation of inorganic additives into a polymer matrix can improve the properties such as thermal stability, mechanical strength, ion exchange abilities, and solvent resistance [1,2]. Recently, clays have become increasingly popular as inorganic fillers in the field of organic-inorganic hybrid materials due to their superior properties such as their high surface area for polymer–filler interactions, small particle size, lightweight and low cost. In the present study, organo-modification of α-sepiolite, a natural clay, was performed using poly(ethylene glycol) (PEG) to improve the compatibility of the inorganic phase with the organic matrix. The modified α-sepiolite was introduced in the poly(ethylene oxide) (PEO) matrix to develop a composite film. The effect of modified clay additive on the mechanical and thermal properties was studied by comparing with the neat PEO film.

2. Methods

α-Sepiolite (Eskisehir/Turkey) was dried at 105°C for 24 hours and then ground into powder. PEG (Mw=950–1050) and α-sepiolite (1:1, wt/wt)) were added to water-ethanol (99.8%) (1:2, v/v) solution and ultrasonicated for 30 minutes. The resulting mixture was stirred overnight. Finally, the solution was poured into a petri dish, dried at 105°C for 24 hours and ground into powder. The obtained organo-modified clay was named PEG_α-Sepiolite. PEG_α-Sepiolite was distributed homogeneously in ethanol by ultrasonic mixing. PEO (Mw=40000) was dissolved in water (10%, w/v) under constant stirring at 70°C for 24 hours. The resulting transparent and viscous PEO solution was transferred into a beaker and the previously prepared PEG_α-Sepiolite/ethanol mixture was added gradually under ultrasonic mixing. The obtained PEO solution with 1% PEG_α-Sepiolite additive was casted onto a flat glass substrate (20 cm x 20 cm) and dried at 50°C for 24 hours. The resultant semi-transparent film named PEO/PEG_α-Sepiolite composite film. Neat PEO film was prepared following the same film preparation procedure except for the PEG_α-Sepiolite addition for comparison purposes and named PEO_control film. FTIR spectra of neat and PEG_α-Sepiolite samples were recorded as KBr pellets using a Frontier spectrometer (Perkin Elmer). Thermogravimetric analysis (TGA) of the film samples was performed using a STA6000

thermogravimetric analyzer (Perkin Elmer) with a heating rate of 10°C/min, under flowing nitrogen at a rate of 50 mL/min. The mechanical tests of the films were carried out using an Instron Mechanical Testing Machine 5581 test system following ASTM D882 method.

3. Results and discussion

FTIR spectra of the natural α-sepiolite and PEG_α-Sepiolite are presented in Figure 1. The shoulder, observed at 3690 cm^{-1} in the FTIR spectrum of neat α-sepiolite, is assigned to the -OH stretching vibrations of Mg-OH constituent of α-sepiolite and shifted to 3685 cm^{-1} with PEG modification. The wide band at 3570 cm^{-1}, indicating the -OH stretching vibration of bound water, shifted to 3566 cm^{-1} with PEG modification. The weak bands, observed at 1211 and 1018 cm^{-1} in the FTIR spectrum of neat α-sepiolite, corresponding to the stretching of Si–O in the Si–O–Si groups [3] disappeared after organo-modification with PEG. A new peak, indicating C-H stretching, was formed at 2932 cm^{-1} after the organo-modification. These differences may be resulting from the formation of new hydrogen bonding interactions between surface hydroxyl groups of α-sepiolite and PEG molecules, indicating the compatibility of α-sepiolite with PEG. Based on the TGA thermograms of the PEO_control and PEO/PEG_α-Sepiolite composite films, shown in Figure 2, both films represent a single-step thermal degradation behavior and the decomposition temperature increases from 355°C to 370°C with α-sepiolite incorporation. Tensile strength was increased from 12 MPa to 18 MPa and Young's modulus increased from 240 MPa to 360 MPa by α-sepiolite addition to the structure.

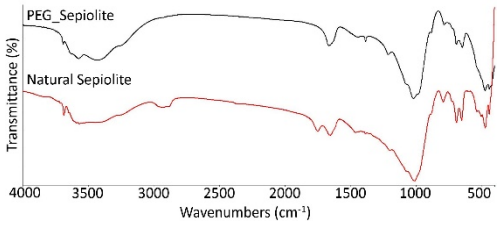

Figure 1. FTIR spectra of the natural α-sepiolite and PEG_α-Sepiolite.

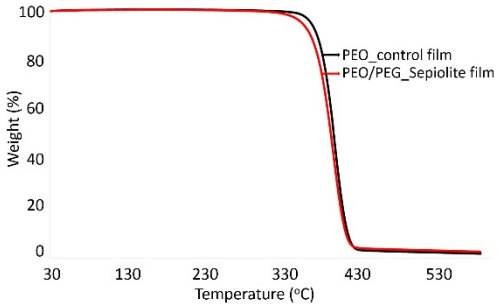

Figure 2. TGA thermograms of the PEO_control and PEO/PEG_α-Sepiolite composite films.

4. Conclusions

Based on the newly formed, disappeared, and shifted frequencies in the FTIR spectra after the modification process, it can be concluded that the organo-modification was achieved. α-Sepiolite, distributed at 1% by weight in the polymer matrix, has improved the thermal stability and mechanical strength of the resulting composite material. Considering the biocompatibility characteristic of PEO and α-sepiolite, potential use of the developed composite film in biomedical fields such as drug release and tissue engineering can be investigated in further studies.

Acknowledgements
This research was supported by Eskisehir Technical University Scientific Research Projects Committee. (Project No: 1709F507)

References

[1] Ş. Uğur, Ö. Yargi, A. Elaissari, Ö. Pekcan, Macromol. Symp. 281 (2009) 168–173

[2] H. M. Wilhelm, M. R. Sierakowski, G. P. Souza, F. Wypych, Carbohydrate Polymers. 52 (2003) 101-110.
[3] M. Alkan, G. Tekin, H. Namli, Microporous and Mesoporous Materials. 84 (2005) 75-83.

ECCE12
The 12th EUROPEAN CONGRESS OF CHEMICAL ENGINEERING
Florence 15-19 September 2019

Morphology and size control of calcium carbonate particles through carbonation route in a packed bed reactor.

Freddy Liendo[1,*], Fabio A. Deorsola[1], Samir Bensaid[1]

1 Department of Applied Science and Technology, Politecnico di Torino, Italy

**Corresponding author: Freddy.liendo@polito.it*

Highlights

- Size and shape of $CaCO_3$ particles were controlled by varying operating conditions.
- Stable calcite particles were synthesized by employed a packed bed reactor.
- High pH values avoid the agglomeration and growth phenomena.

1. Introduction

Nowadays, there are serious environmental issues due to the Green House Gas emissions. The cement, iron and steel production can be included among the most polluting industries. Thus, there is an important need of recovering of CO_2 from combustion gases of these industries, which in turn can be used to obtain added value products. Calcium Carbonate Nanoparticles (CCnP) are widely synthesized via carbonation route (1) and have a large gamma of applications, since their characteristics, such as size and morphology are easily tunable through the synthesis method. They are widely used as filler material and, because of their porosity, non toxicity and biocompatibility, they are also used in the biomedical and food industry (2). In this study, an alternative carbonation method to synthesize calcium carbonate particles and control their size and morphology by varying the operating conditions is reported.

2. Methods

$CaCO_3$ particles were synthesized through carbonation (pure CO_2) of a CaO slurry. A Packed Bed Reactor, with a monolith as structured packing, was employed for this study in a setup illustrated in Figure 1. The synthesis was carried out at constant gas and liquid flowrate and stirring. The CO_2 flux was stopped once the pH was less than 10.5, value at which, according to the carbonate equilibria, the CO_3^{2-} formation is not favoured, thus reducing the CCnP saturation. Two zones are individuated: *i*) the crystallization one in the PBR, whence the CO_2 and the calcium solution get in contact and the precipitation takes place and *ii*) the stabilization one in the feed tank, where the pH is maintained high enough to provide a stable environment to the CCnP, since under alkaline conditions growth and agglomeration phenomena of the CCnP are not favoured (1). Then, once the process was finished, the synthesized particles were filtered by vacuum (pore size=0.45 µm) and repeatedly washed with deionized water to eliminate ion excess. By last, the $CaCO_3$ powder was dried at 60 °C overnight and finally their size, morphology and crystal phase were characterized.

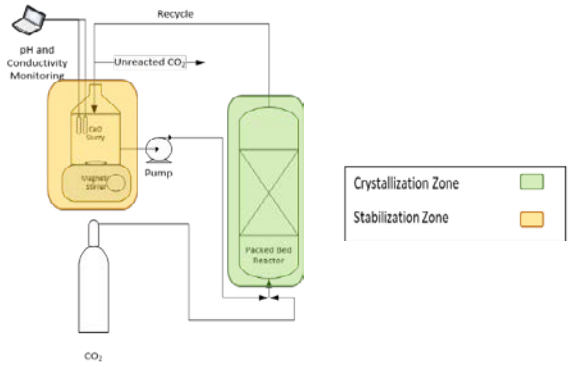

Figure 1. Packed bed reactor experimental setup.

3. Results and discussion

The operating conditions had an important effect on the properties of these particles. Cubic particles were obtained in the most of cases, in which the pH was maintained constant enough during the entire synthesis. The initial CaO concentration had an interesting effect on the particle size. Even if high CaO concentrations mean higher supersaturation levels, and then smaller particles would be obtained. At the beginning of the process, high saturation levels were present, but it led to higher synthesis times, and once the primary particles were formed, growth and agglomeration phenomena were prevalent, since they are favored by particle size and ion concentration respectively. Low liquid and CO_2 flowrates also led to elevated synthesis times, hence larger particles were synthesized. The flow regime, instead, affected the CO_2 absorption, controlling thus, the nucleation and growth rate. Higher liquid and gas flowrates led to smaller particles preparation, since they provide a more effective micromixing leading to a higher nucleation rate. In the cases where the CO_2 flowrate was too high (higher than 550 mL/min) and the pH suffered a progressive change during the synthesis, agglomerates were although formed. Consequently, this had an effect on the morphology of these particles, since hollow and particles with a wide PSD were obtained. Therefore, particles with mean particle size less than 200 nm were synthesized at optimal operating conditions, starting from a CaO slurry 0.015 M and liquid and gas flowrates equal to 300 and 400 mL/min respectively.

4. Conclusions

The size and morphology of calcite particles have been controlled in a carbonation precipitation for the CO_2 conversion. The shape of this particles reflects upon the operating conditions of the synthesis. The pH during the synthesis played a fundamental role, it controlled the agglomeration and growth phenomena. Hence, it had an important effect over the morphology and size. Higher pH values led to cubic calcite nanoparticles. Smaller particles were synthesized by employing higher liquid and gas flowrates, while low flowrates led to larger and agglomerated particles.

References

[1] Nano-CaCO3synthesis by jet flow. Eda Ulkeryildiz, Sevgi Kilic, Ekrem Ozdemir. 2016, Colloids and Surfaces A: Physicochemical and Engineering Aspects, p. 34-40.

[2] Formation of nanoparticles and nanostructures-an industrial perspective on CaCO3, cement, and polymers. Rieger, J., Kellermeier, M., Nicoleau, L. 2014, Angewandte Chemie - International Edition, p. 12380-12396.

Towards the quantitative prediction of precipitation of nanoparticulate pharmaceutical compounds

Tobias Schikarski[1]& Holger Trzenschiok[1], Andreas Güldenpfennig[1], Lukas Pflug[2], Marc Avila[3], Wolfgang Peukert[1*]

1 Institute of Particle Technology, Friedrich-Alexander Universität Erlangen-Nürnberg; 2 Chair of Applied Mathematics, Friedrich-Alexander Universität Erlangen-Nürnberg; 3 Center of Applied Space Technology and Microgravity, Universität Bremen

**Corresponding author: wolfgang.peukert@fau.de*

Highlights

- Precipitated nanoparticles of Ibuprofen down to 25nm
- Precise simulations of precipitation of Ibuprofen in a T-mixer
- Trend of particle size and shape of PSD are well captured for all Re in simulations

1. Introduction

It is estimated that more than 40% of new drug candidates fall into the Biopharmaceutic Class II and IV characterized by the low solubility of the active pharmaceutical ingredient (API), which results in low bioavailability **[1]**. Manufacturing drug particles in the nanometer range have been found to be a promising method to enhance the dissolution rate and, thus, the bioavailability. In particular, below 50nm the dissolution rate begins to drastically increase compared to the coarse-grained powder in the micrometer range. In doing so, precipitation of API nanoparticles attracted the attention in recent years due to the simple process condition, the easy scale-up as well as the low energy costs involved **[1,2]**. Still, the most challenging task remains on gaining suspensions stable with respect to the particle size distribution and crystallinity at defined process condition **[1,2]**. Numerical modeling of precipitation has been proven to be a useful tool to understand the interaction of the underlying processes for inorganic compounds. However, the transfer to organic compounds, e.g. API's, haven't led to great success so far, primarily due to the influence of the organic stabilizers usually applied. A recently in our group developed stabilization method closes this gap, provides insights into the underlying processes during precipitation of organic nanoparticles and allows to predict the resulting particle size distribution for well-stabilized nanoparticles.

2. Methods

A simple T-mixer is used to mix an alkaline aqueous ibuprofen solution with an acidic aqueous Zirconium chloride solution and to trigger the precipitation of Ibuprofen while Zr-ions stabilize the formed particles. The Villermaux-Dushmann reaction is conducted to quantify the mixing efficiency experimentally. The numerical approach consists of direct numerical flow simulations of the mixing process solving the Navier-Stokes and the convection-diffusion equation. A parameter-free approach is here applied which does not require any turbulence modeling. To describe particle formation, the nucleation and diffusion-limited growth is described by the population

balance equation along Lagrangian trajectories. Details on the mixing and precipitation experiments as well as on the flow simulations can be found in **[3,4]**.

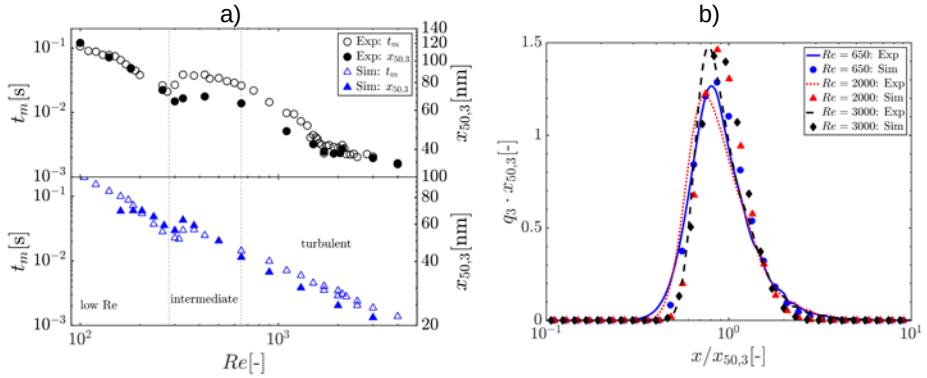

Figure 1. (a) Experimentally measured and computationally estimated mixing time t_m (left y-axis) and median particle size $x_{50,3}$ (right y-axis) as a function of Reynolds number Re. (b) Comparison of normalized particle size distributions at particular Re.

3. Results and discussion

The supersaturation is the thermodynamic driving force of the precipitation, which is here determined by the rate the two fluids are brought in contact with each other. Thus, the primary particle formation steps nucleation and growth are mixing controlled under the assumption of fast chemical reactions. This prevailing view is substantiated in Fig. 1a), which depicts a nearly perfect alignment of the experimentally determined mixing efficiency with the median particle size $x_{50,3}$ as Re increases. To properly simulate the precipitation, the mixing needs to be accurately captured at first, which was achieved in excellent qualitative agreement to experiments in our recent study **[4].** Subsequently, the particle formation induced by the inherent mixing history along each Lagrangian trajectory is simulated resulting in a finally accumulated PSD. With this approach, we are able to predict qualitatively the median particle size over the entire Re-regime considered without any modeling, see Fig. 1a). Note that only known physicochemical constants of Ibuprofen have been incorporated (particle density, molecular weight, diffusion coefficient). The only unknown parameter is the experimentally hardly accessible interfacial energy, which is determined by a model-based approach. The thus determined fixed, single value for all calculated PSD's is in the typical order of known organic substances. Remarkably, the shape of the particle size distributions is very well captured by the simulations in particular at high Re, see Fig 1b).

4. Conclusions

Modeling of precipitation, in particular, of organic nanoparticles is challenging. Our results demonstrate considerable progress and provide the potential for broader applications in future. In the talk, we will outline in detail the applied approach. In particular, we will focus on the interaction of mixing and supersaturation build-up, the prediction of PSDs and scale-up to very high Reynolds numbers and explain the role of the interfacial energy for predictive numerical modeling and simulation.

References

[1] A. A. Thorat, S.V. Dalvi, Chem. Eng. J. 181 (2012) 1-34.
[2] S. M. D'Addio, R.K. Prud'homme, Adv. Drug. Deliv. Rev. 63 (2011) 417-426.
[3] H. Trzenschiok, M. Distaso, W. Peukert. Chem. Eng. J. 361 (2019) 429-438.
[4] T. Schikarski, H. Trzenschiok, W. Peukert, M. Avila, Reac. Chem. Eng. (2019)

Rheological study of binary mixtures of powders using interparticular forces

Martin Giraud[1,2], Guillaume Bernard-Granger[2], Cendrine Gatumel[1], Stéphane Vaudez[2], Henri Berthiaux[1]

1 Centre RAPSODEE UMR CNRS 5302, IMT Mines Albi; 2 CEA-Marcoule, DEN/MAR/DMRC/SFMA

**Corresponding author: martin.giraud@mines-albi.fr*

This study has been carried out in order to improve the understanding of the mechanisms that occur during powder mixing operations, which are commonly used in many industrial processes. Up to now, the link between physicochemical and morphological properties of the powders and its flowability is still unclear. Likewise, for a mixture of several powders of different particle properties, the influence of the mass fraction of each powder within the mixture on its resulting rheology is not clearly established.

For this study, alumina (Al2O3), zircon (ZrO2) and yttrium oxide (Y2O3) powders of different grades have been selected in order to get a relevant range of size and shape for the study. The mixtures are prepared in a Turbula® mixer and the flowability of each blends has been assessed by Jenike shear cell yield locus measurements, performed with a powder rheometer.

A model linking the flowability of the mixtures to their composition and the morphological properties of each powder has been investigated using a population dependent Bond number which has been developed in previous studies [1]. This dimensionless number corresponds to the ratio between adhesive interparticular forces and the weight of the particles within the powder. It is then linked to the overall cohesion of the powder bed (Figure 1). The population dependent Bond number is assessed by fine characterization of each powder in terms of size distribution, surface roughness, specific surface area, surface energy and true density.

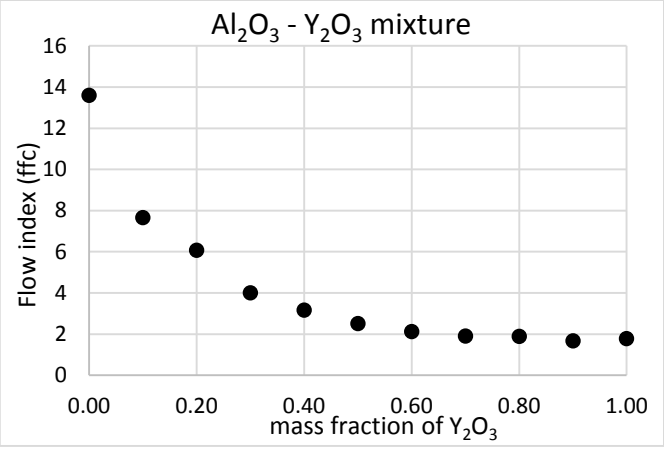

Figure 1 : Evolution of the flow index regarding the formulation of binary mixtures of alumina and yttrium oxide powders

[1]M. Capece, K. R. Silva, D. Sunkara, J. Strong, and P. Gao, "On the relationship of inter-particle cohesiveness and bulk powder behavior: Flowability of pharmaceutical powders," Int. J. Pharm., vol. 511, no. 1, pp. 178–189, Sep. 2016.

ECCE12
The 12th EUROPEAN CONGRESS OF CHEMICAL ENGINEERING
Florence 15-19 September 2019

Defluidization behaviour due to sintering of industrial reactive powders

Domenico Macri[1*], Paola Lettieri[1]

[1]Department of Chemical Engineering, University College London, London WC1E 7JE, UK

*Corresponding author: domenico.macri@ucl.ac.uk

Highlights

- The defluidization behaviour of mixtures of coke and titanium ores were studied
- Early stages of sintering process were experimentally simulated
- Sintered materials were analyzed by optical, chemical and mechanical tests

1. Introduction

Fluidized bed reactors are used in a wide range of industrial chemical processes and they are particularly useful in high temperature systems thanks to their ability to provide high heat transfer rates and rapid solids mixing which lead to isothermal and more controllable conditions. Their applications spread the environmental, chemical, energy and process industries. For example, they are a key technology in the petroleum industry, catalytic chemicals synthesis processes, combustion and gasification of solid fuels (coal, wastes and biomass), metals productions and many more.
Operations below incipient fluidizing conditions in combustion-type operations can lead to particles aggregation and sintering which change the characteristics of the bed and could cause bed defluidization with consequential unscheduled process downtime and additional costs.
However, the details of the physical processes under such conditions are still not well understood. Despite the countless researches that have been done so far, such processes still disclose unrevealed features and challenge the researchers worldwide.
The objective of this work is to assess the influence of operative conditions on the fluidization behaviour of mixtures of petroleum coke and different titanium ores industrial reactive powders.
The fluidization behaviour of several mixtures have been studied at process temperatures ranging from ambient up to 950 °C in a specially designed heated fluid-bed reactor, where the early stages of the sintering process were experimentally simulated.

2. Methods

In order to tackle the problem of assessing the defluidization behaviour of powders at operative conditions, the early stages of the sintering process were experimentally simulated in the fluidization rig for the mixtures of coke, rutile and slag by blowing air into the fluidized bed for a certain time [1]. The effects of high temperature and air flowrate were investigated systematically in different fluidization regimes. Fundamental fluidization tests were also carried out on the spent systems (i.e. after combustion and cooled down to ambient conditions) and compared to the fresh ones. The reactor was then emptied and the aggregates collected for further off-line examinations: mechanical properties evaluation by means of a vibrated plate friability test, optical and chemical composition assessment by SEM/EDX analysis.
Fundamental fluidization tests were also performed using the unique X-ray Imaging technique available at UCL, which enabled to visualize the internal flow pattern inside the metallic reactor and to obtain quantitative information. Simultaneous measurements of local temperatures and

pressure drop across the bed were carried out in order to detect possible aggregation and sintering phenomena.

3. Results and discussion

The tests showed that combination of operative conditions and coke characteristics have a significant role on the formation of the aggregates and on their properties. In particular, the mechanical strength of the aggregates was found to be strongly dependent on the coke particles size and the operating fluidizing regime: they appeared more friable with when larger coke particles size and low air flowrates were employed. The SEM/EDX analysis permitted the inspections of the bridges among particles and the assessment of the chemical composition of the sintered material. The results suggested that only particles of rutile and slag were involved in the formation of the sintered bridge (with a particular enrichment of Al-Si phase in the bond) and no relevant bonding structures involving coke particles were found.

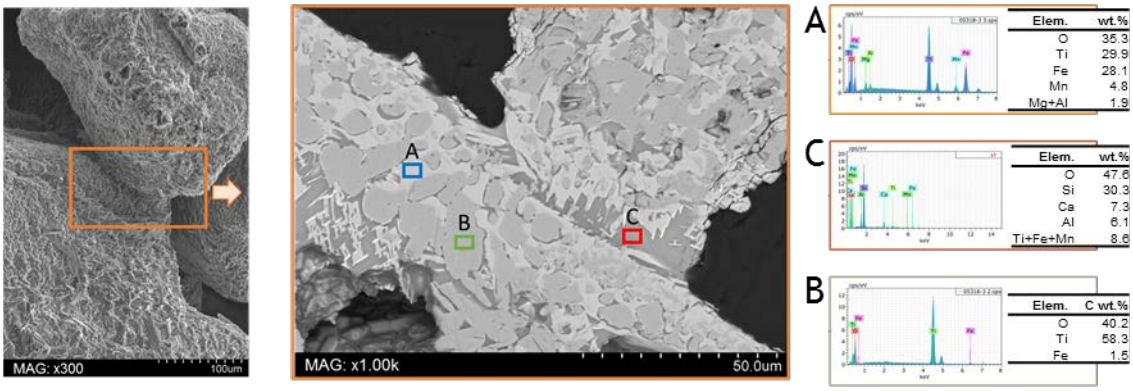

Figure 1. Example of SEM image and EDX spectrum on a sintered bridge

4. Conclusions

Inspections of the fluidization performance of different mixtures of titanium ores and coke showed that a number of factors are responsible for the onset of defluidization due to particles aggregation, such as rutile's nature, coke particles size, operative fluidization regime, etc.

The basis for a fundamental understanding of the investigated industrial process has been delivered by successfully reproducing and controlling the early stage stages of the sintering processes in a small pilot scale fluidized bed at temperature far below the real operative one. Moreover, a clear relationship between the characteristics of the final aggregates and the operative conditions was found.

References

[1] D. Macri, Study of defluidization behaviour of industrial reactive particles, Doctorate Thesis, UCL (University Coll. London).

Particules Surface Formulation Effects on Powder Rheology.

Shirin Enferad[1,2], Claire Gaiani[2], Jeremy Petit[2], Jennifer Burgain[2], Véronique Falk[3], Philippe Marchal[3], Sergiy Antonyuk[4], Fabian Krull[4], Sébastien Kiesgen de Richter[1], Mathieu Jenny[1]

1 Université de Lorraine, LEMTA UMR 7563, Nancy, France; 2 Université de Lorraine, LIBio, F-54000 Nancy, France; 3 Université de Lorraine, CNRS, LRGP, F-54000 Nancy, France; 4 Institute of Particle Process Engineering, Technische Universität Kaiserslautern, Kaiserslautern, Germany

**Corresponding author: shirin.enferad@univ-lorraine.fr*

Highlights

- Hydrophilic and hydrophobic formulation did not alter particle shape and size.
- Lactose-coated glass beads showed a surface roughness incensement.
- The hydrophilic glass bead showed highest, lactose coated bead lowest flowability.

1. Introduction

The study and comparison of formulated powders are a great interest as it can suggest solutions to improve the transport of real powders. The flowability of glass beads was largely investigated in previous studies [1-2]. The dependency of powders flowability to the moisture [3] and formulation [4] is known phenomenon. In fact, particle–particle interactions determine the macroscopic behavior of the powder. Powder flowability is expected to decrease due to liquid bridge formation between two particles dependently to the humidity [5]. Moisture sensitivity depends on hydrophilic and hydrophobic treatments. Furthermore, the friction between particles in granular materials is known to influence particles flowability [6]. By modifying the roughness of the surface, lactose coating may modify friction between particles. The surface roughness is comparable to the one of the particles obtained by lactose agglomeration (having a lactose core) but the Young modulus of particle core influence the collision effect during the flow. Therefore, aforementioned treatments may influence the interactions between particles, consequently powder flowability.
In this study, links between powder surface modification and rheology are investigated. For this purpose, glass beads with 100 µm mean size are employed. In order to study the influence of surface composition, various surface treatments leading to hydrophilic, hydrophobic and lactose-coating are performed on glass beads. Moreover, in order to investigate the influence of powder core composition, agglomerated lactose powders presenting similar mean particle size are also produced by high-shear wet granulation and characterized. Finally, the flowability of powders are studied and compared by performing tests with a FT4 powder rheometer (Freeman Technology) [7]. Furthermore, the TA Instruments AR 2000 Advanced Rheometer is in use to obtain the flow curves of powders. At the final, obtained results from both apparatuses will be compared to make links between the apparent viscosity of the powder depending on its formulation and the flowability measurements provided by FT4 rheometer.

2. Methods

The particle size distributions are determined by laser granulometry with a Mastersizer 3000 supplied with an Aero S dry dispersion unit. FT4 powder rheometer is used in order to study

powders flowability. In this paper, stability and rotational shear cell tests are performed on the powders. Stability test intends to evaluate powder flowability in a low-stress environment, whereas the rotational shear cell test is devoted to analysis of powder flow properties in high-stress conditions. Moreover, TA Instruments AR 2000 Advanced Rheometer is implemented with the objective of studying the rheology of powders. A cylindrical Couette geometry with a vane is used to insure that the powder does not slip on the inner cylinder walls. The angular velocity of the vane is imposed and the corresponding torque is measured by the rheometer. The torque time evolution monitoring ensures that a steady-state flow is established for each value of the rotational speed. Thus, the relation between the shear stress and the shear rate in permanent regime can be determined.

3. Results and discussion

Fig 1 shows the evolution of shear stress recorded at variable decreasing normal stress from 7 to 3 kPa for each sample. At the beginning of each test 9 kPa of pre-shear stress applied by FT4 in order to reach the critically consolidate state. In general, the higher the curve on the diagram, the poorer the flow properties [8]; therefore, according to this criterion, investigated powders can be ranked according to their flowability in shear stress conditions: hydrophilic glass beads ≈ control glass beads > hydrophobic glass beads> lactose-coated glass beads> agglomerated lactose powders.

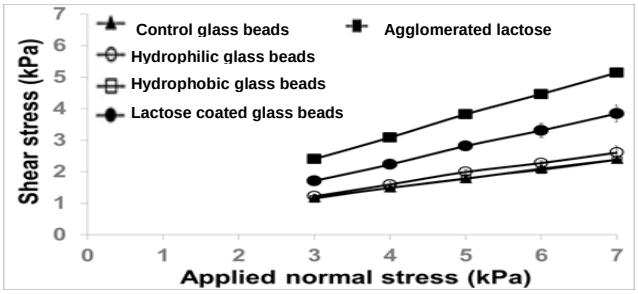

Figure 1. Evolution of shear stress with applied normal stress after pre-shear at 9 kPa applied on 100 µm powder samples. Error bars represent st -andard errors; some were not visible as their size was inferior to the marker size.

4. Conclusions

The size distribution measurement of particles after formulation evidenced that agglomerated lactose powders and lactose coated glass beads presented similar mean particle size but a wider size distribution than the rest of powders. Based on shear cell test of FT4 rheometer, hydrophilic and lactose coated glass beads were more and less flowable powders, respectively. The result of TA Instruments AR 2000 Advanced Rheometer (which is in progress) will be compared with the FT4 results. Besides, the microscale properties of powders will be studied by single particle impact and nanoindentation tests to determine the influence of the surface modification on the deformation and adhesion properties of particles. Also, links between flowability, rheometry and microscale properties of particle-particle interactions will be analyzed. Concerning nanoindentation tests low inter-particle friction and low elasticity expected to lead to good flowability.

References

[1] N. Gaudel, S. Kiesgen de Richter, N. Louvet, M. Jenny and S. Skali-Lami, Physical Review E, 94(2016), 032904.
[2] E.Y. Wornyoh, V.K. Jasti, and C.F Higgs, Journal of Tribology, 129(2007), 438-449.
[3] A. M. Stoklosa, R. A. Lipasek, L.S. Taylor and L. J. Mauer, Food Research International, 49(2012), 783-791.
[4] J. Yang, A. Sliva, A. Banerjee, R. N. Dave and R. Pfeffer, Powder Technology, 158(2005), 21-33.
[5] E. Teunou, and J.J. Fitzpatrick, Journal of Food Engineering, 42(1999), 109-116.
[6] F. Da Cruz., S. Emam, M. Prochnow, J.N. Roux, and F. Chevoir, Physical Review E, 72(2005), 021309.
[7] Jenike, A.W. Storage and flow of solids, Bullet, Salt Lake City, Utah, (1964), 123.
[8] R. Freeman, Particulate systems analysis. Harrogate, 2003.

Crystal engineering strategies to ensure the quality of particulate products for the food and pharmaceutical industries

Elena Simone[1*]

1 School of Food Science and Nutrition, University of Leeds, Leeds, United Kingdom

**Corresponding author: e.simone@leeds.ac.uk*

Highlights

- Crystal shape and polymorphism of lactose and ortho-aminobenzoic acid were tailored with combinations of solvents and structurally related additives.
- Temperature cycling was used to manipulate crystal shape of succinic acid without affecting its purity.
- Process analytical technology for online monitoring and control of crystallization.

1. Introduction

Crystallization is an important unit operation used in the pharmaceutical, agrochemical and food industries. Crystal size, shape and lattice structure (polymorphism) have a profound effect on the properties of the final particulate product as well as on the efficiency of the downstream operations (filtration, washing, drying, tableting etc.). Crystals can be engineered by opportune choice of crystallization conditions. Here, examples of how these processing conditions can affect crystal polymorphism, purity and size/shape distributions are presented [1-3]. The implementation of process analytical technology (PAT) tools during the development stage of APIs has largely helped in better understanding and optimizing crystallization processes. Specific instrumentation can be used to monitor on-line, in situ, crystal size and shape (focused beam reflectance measurement, FBRM, particle vision and measurement, PVM), polymorphism (Raman, spectroscopy) and liquid phase composition (Attenuated total reflectance, ATR, UV/VIS) [3]. Furthermore, feedback control strategies based on PAT tools signal can be implemented to specifically tailor the characteristics of the produced crystals. This work shows few examples of application of PAT tools for the study and control of crystallization processes.

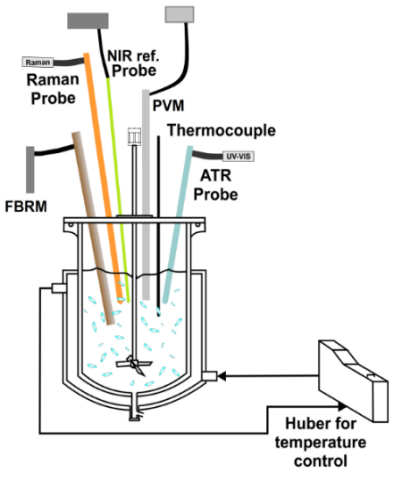

Figure 1. Schematic of the rig used for the experiments.

2. Methods

Three examples of crystal engineering strategies to control crystal polymorphism and shape are shown here. Cooling crystallization experiments were carried out at 400 mL scale in a jacketed vessel equipped with temperature control. Ortho-aminobenzoic acid (OABA), lactose and succinic acid were used as model compounds for the experiments. The shape and polymorphism of OABA were tailored via crystallization in

different solvent mixtures (water and isopropyl alcohol, IPA) and with the addition of a structurally related additive (benzoic acid, BA). Lactose polymorphism and size distribution were controlled via crystallization in water/acetone mixtures. Finally, succinic acid was crystallized from water and its crystal shape was controlled via applying heating (dissolution) and cooling (growth) cycles. The array of PAT tools shown in Figure 1 was used to monitor experiments online, while offline microscopy, X-ray and laser diffraction as well as chromatography were used to measure size, shape, purity and crystal polymorphism of the obtained crystals after filtration and drying.

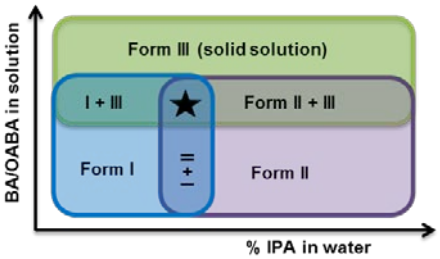

Figure 2. Polymorphic control of OABA.

3. Results and discussion

3.1 Polymorphic control using solvents and additives

Figure 2 shows the results obtained for the polymorphic control of OABA. Increasing the amount of IPA in water induced the formation of the metastable form II while high water concentrations favoured the nucleation of stable form I [2]. Introducing BA generated nucleation of the metastable form III regardless of the solvent used. BA was found to be easily incorporated in form II and III of OABA, generating solid solutions. Lactose crystallization was instead performed in solvent mixtures at different ratios of acetone and water. High concentrations of acetone determined faster nucleation and growth rate but poor control of polymorphism, with β-lactose crystals nucleating together with the desired α-monohydrate form. In water only the α-monohydrate form was obtained but with slow growth kinetic, leading to poor recovery yields [1].

3.2 Shape control using temperature cycling

Temperature cycling was used to modify the morphology of succinic acid crystals in water, exploiting the different rates of growth and dissolution for each specific facet (Figure 3). The shape of crystals moved from plate-like, with a dominant (100) face, to diamond-like. Because of the different facet-specific kinetics of growth and dissolution it was possible to completely eliminate the (100) facet in favour of the growth of the (110), (011), (-110) and (01-1) facets. This strategy allowed shaped manipulation without the introduction of additives of impurities [3].

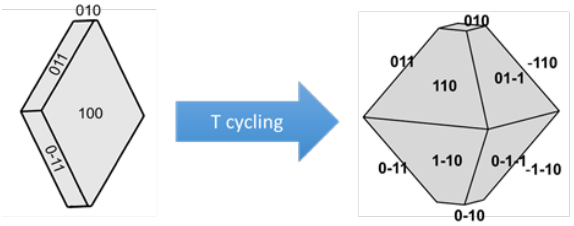

Figure 3. Shape control of succinic acid.

4. Conclusions

In this work different examples of crystal engineering approaches for the design of crystallization processes and their online monitoring and control are illustrated. Crystal properties could be fine-tuned by selecting opportune operating conditions.

References

[1] Simone, E., Tyler, A.I.I., Kuah, D., Bao, X., Ries, M.E., Baker, D. (2019) Org. Process Res. Dev., 23, 220-233.

[2] Simone, E., Steele, G., Nagy, Z. K. (2015) CryEngComm, 17, 9370-9379.

[3] Simone, E., Klapwijk, A.R., Wilson, C.C., Nagy, Z.K. (2017) Cryst. Growth Des., 17 (4), 1695–1706.

ECCE12
The 12th EUROPEAN CONGRESS OF CHEMICAL ENGINEERING
Florence 15-19 September 2019

Obtaining the True Process Value of the Fragmentation Kinetic Function (FKF) For The Breakage of Silica Flocs in Taylor Couette Flow Via Population Balance Simulation.

Y.K. Leong[1], P.I. Au, J.S. Liu, Y. Wang

1 Department of Chemical Engineering, The University of Western Australia, Crawley, Australia 6009

**Corresponding author: yeekwong.leong@uwa.edu.au*

Highlights

- A method for determining experimental FKF data presented
- Computed and experimental PSD matched.
- FKF data cannot be determined experimentally.
- FKF values very large for small flocs.

1. Introduction

The breakage or fragmentation kinetic function (FKF) of a given father size floc breaking to form two specific daughter size flocs cannot be measured experimentally. Indirectly it can be determined from the FKF model used to solve the population balance equation for floc fragmentation subjected to meeting two conditions: i) the computed and experimental particle size distribution function (PSDF) matched at all fragmentation time and ii) the PSDF data at zero fragmentation time was the input in the computation[1]. The fragmentation of compact polyelectrolyte-bridged silica flocs in a narrow gap concentric cylinder flow cell was investigated in the laminar Taylor vortex flow regime at Taylor number of 26000. A past study showed that the FKF values are smaller for large flocs as they tend to migrate to the low shear region[1]. Monodispersed SiO_2 particles of 0.34 μm were coated with a low Mw cationic PEI and then bridged with a high Mw anionic polyacrylamide flocculant.

2. Methods

This dimensionless PBE expressed in log-form given by[2]:

$$\frac{\partial N(\tau,10^{X})}{\partial \ddot{A}} = t_{scale} k_{F_{max}} v_{max} \int_{X_r = X \oplus X_{min}}^{X_{max}} K_F(10^{X_r},10^{X}) N(\ddot{A},10^{X_r}) 10^{X_r} \log_e 10 \, dX_r - \frac{1}{2} N(\ddot{A},10^{X}) t_{scale} k_{F_{max}} v_{max} \int_{X_p = X_{min}}^{X \leftrightarrow X_{min}} K_F(10^{X},10^{X_p}) 10^{X_p} \log_e 10 \, dX_p . \quad (1)$$

Is solved directly after being converted to ordinary differential equation by MOL. $X \equiv \log_{10} V$, $V = v/v_{max}$, $N = (v_{max})^2 n/m_F$, $K_F = k_F/k_{Fmax}$, $\tau = t/t_{scale}$ and $dV = \log_e 10 \times 10^X dX$. The experimental time scale t_{scale} must be used in the computation so that the simulated and experimental results are

$$S = 0.001 + 0.05e^{-0.8(5+\frac{Log[10^{X_r}]}{Log10})^2} + 7(1 - Tanh[1.13\left(5.45 + \frac{Log[10^{X_r}]}{Log10}\right)]$$

comparable.[1]The FKF used for 200rpm is:

$$K_F(10^{X_r},10^{X_p}) = \frac{S}{S_{max}}\exp[\sigma(10^{X_r})^g](10^{X_p} - 10^{X_{minin}})^h(10^{X_r} - 10^{X_p} - 10^{X_{minin}})^h / (\exp[\sigma]\left(10^{X_r - Log_{10}2} - 10^{X_{minin}}\right)^{2h}),$$

.

Continuous particle size distribution (PSDF) data at zero fragmentation time was the input in the computation to solve Eqn 1 to obtain temporal PSD data.

3. Results and discussion

The discrete and continuous PSD for fragmentation in Taylor Couette flow at 200 rpm are shown in Figure 1(a) PSDF in (b).

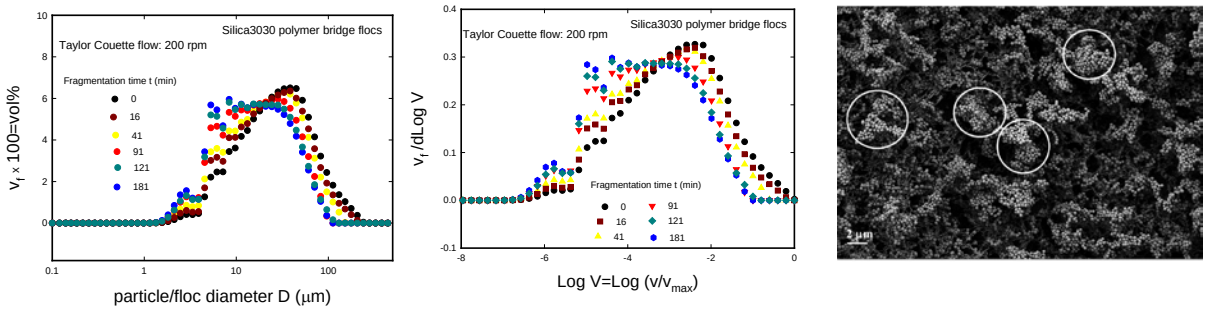

Figure 1. Temporal a) PSD and b) PSDF during fragmentation, and c) compact fragmented silica flocs.

The comparison between computed and experimental PSDF is shown in Figure 2 for dimensionless time τ a) 0 and 1, b) 0.24 and c) 0.68. The agreement are considered good. This means the the FKF data used in computation and some of which are shown in Figure 3 represents the experimental values.

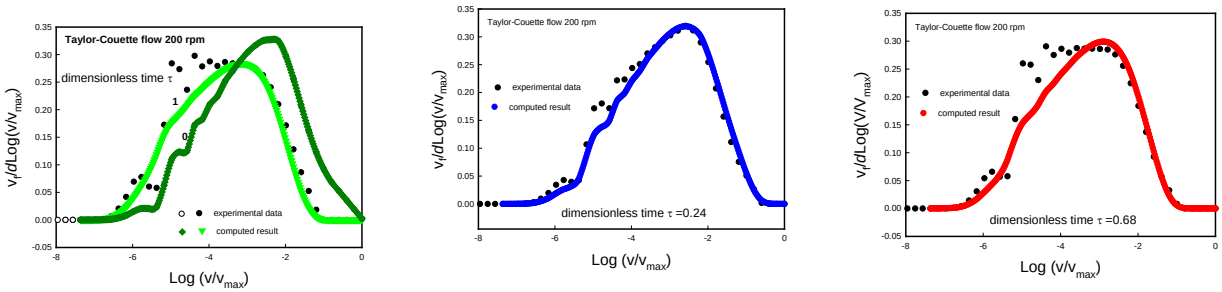

Figure 2. Computed and Experimental temporal PSDF comparison are various fragmentation time.

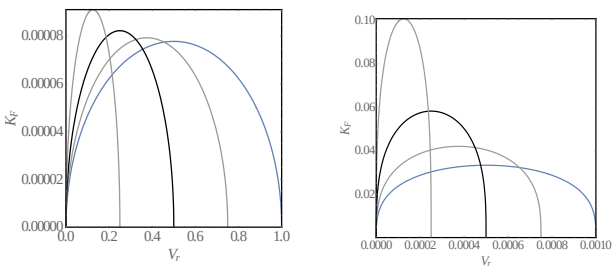

Figure 3. FKF data used in the PBE represent the true process values.

4. Conclusions

Computed and experimental PSDF matched at all fragmentation time. The FKF data used thus represent the true process value.

References

[1] P.I. Au, J.S. Liu, W. Zhang, S.B. Sun, Y.K. Leong, *Colloids Surf. A*. 52 (2018) 48-58.
[2] Y.L.Yeow, J.L. Liow, Y.K. Leong, *AIChE J*. 58 (2012) 3043-3053.

ECCE12
The 12th EUROPEAN CONGRESS OF CHEMICAL ENGINEERING
Florence 15-19 September 2019

Shape modification of needle crystals using polymer additives and temperature cycling

Wei li[1], Brahim Benyahia[1], Chris Rielly[1]

1 Department of Chemical Engineering, Loughborough University, Loughborough, Leics, LE11 3TU, UK
**e-mail: w.li@lboro.ac.uk*

Highlights

- Additives combined with temperature cycling helps to produce more equant shape crystals
- Optimized closed-loop temperature cycling can eliminate fines and agglomerates
- Polymer additives affect growth on specific crystal faces
- Seeded and mill-aided processes can further improve aspect ratio of needle crystals

1. Introduction

Crystal products which have a needle-like morphology tend not to compress well into tablets, and hence more equant shaped crystals are preferred for the secondary manufacturing process. Lovastatin has been studied in this work and is an active pharmaceutical ingredient widely used for the treatment of hypercholesterolemia. However, it forms needle-like crystals and is notorious for its poor processability and difficult formulation. High aspect ratio needle crystals often have poor processability for the filtration washing and drying stages [1]. Needle crystals are often brittle, and breakage results in fines and dust in the working environment. In the current work, lovastatin cooling crystallizations were conducted using polymer additives, namely polypropylene glycol (PPG-4000), coupled with temperature cycling profile using a direct nucleation control (DNC) approach [2], to improve the aspect ratio. This high-molecular-weight, high-boiling point polymer additive can block specific fast-growing crystal surfaces through a hydrogen bonding effect [3]. Hence, they modify the morphology, by inhibiting unwanted elongated growth in the length of the crystal and provide a selectively preference for growth on the short sides.

2. Methods

2.1 Materials:

Lovastatin, ethyl acetate, polypropylene glycol (PPG)

2.2 Equipment:

400ml crystallizer, process analytical tools were used to measure the particle counts, particle length, temperature and concentration profile.

2.3 Process:

- Cooling crystallization from saturation temperatures of 35°C to 10°C in the absence and presence of polymer additives was investigated
- DNC approach was applied to produce size and shape modification, using continuously heating and cooling cycles effectively by indirectly control growth and dissolution mechanisms

- Combination of polymer additives and temperature cycling effect were studied
- Different startup and nucleation conditions were studied, including classical seed addition and wet-mill facilitated nucleation

3. Results and discussion

Fig 1 shows PAT data and PVM images for batch cooling crystallizations. The *in situ* PVM images indicated that the aspect ratio was not improved much for crystallizations with linear cooling profiles (Fig 1b) and varying amounts of PPG, although the nucleation time and nucleation rate were suppressed with increasing mass of polymer additives. The particle counts, concentration and temperature time histories showed that an improved DNC method with PPG additives can shorten the isolation temperature cycle time (Fig 1c & e) and reduce the aspect ratio of the crystals. With an optimised temperature cycle process, agglomeration was not observed and fines were removed by dissolution. Furthermore, wet-mill-aided and seeded DNC can be applied for further shape modification of lovastatin crystals (Fig 1d & f).

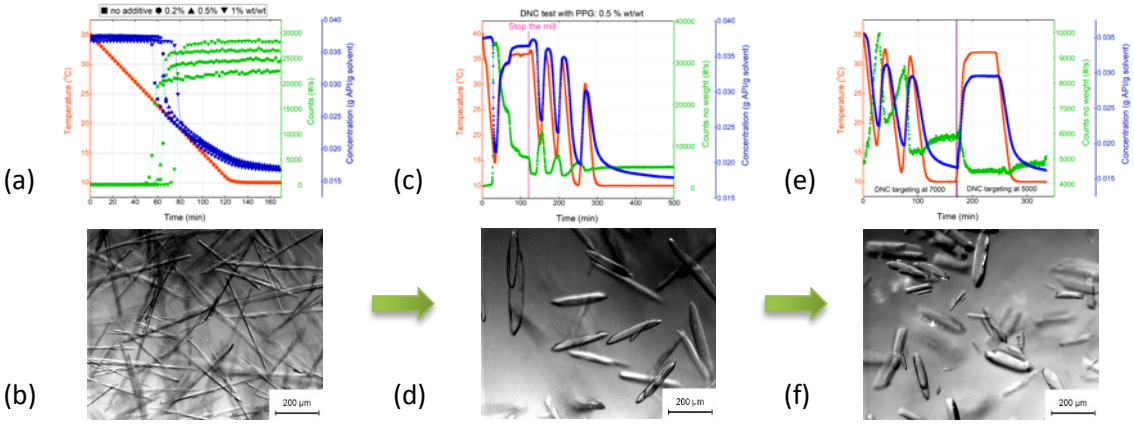

Figure 1. FBRM counts/s — temperature — and concentration — against time profiles and in situ PVM images captured of the final crystals for: (a) and (b) Linear cooling crystallization of lovastatin/ethyl acetate system; (c) and (d) Lovastatin/ethyl acetate/PPG-4000 system with mill-aided DNC T cycling crystallization; (e) and (f) Lovastatin/ethyl acetate/PPG-4000 system with seeded DNC T cycling crystallization

4. Conclusions

Additions of a polymer additive PPG-4000 on the linear cooling crystallization of lovastatin in an ethyl acetate solvent were investigated, resulting in a delay in the start of nucleation with increasing concentration of additives. Application of an optimized DNC approach (with and without polymer additives) was compared with a benchmark cooling crystallization. The aspect ratio was more significantly improved using a combination of temperature cycling from DNC and the presence of the polymer additive. The crystal size and shape distribution can be further improved by different seeding approaches.

References

[1] M.A. Lovette, M.F. Doherty, Cryst. Growth Des. 13 (2013) 3341–3352.
[2] M.R. Abu Bakar, Z.K. Nagy, A.N. Saleemi, C.D. Rielly, Cryst. Growth Des. 9 (2009) 1378–1384.
[3] T. Vetter, M. Mazzotti, J. Brozio, Cryst. Growth Des. 11 (2011) 3813–3821.

Relating crystalline properties with the bulk and surface chemistry of quercetin and its hydrate forms using molecular and synthonic modelling

Panayiotis Klitou[1*], Ian Rosbottom[2], Elena Simone[1*]

1 School of Food Science and Nutrition, University of Leeds, Leeds, U.K.; 2 School of Chemical and Process Engineering, University of Leeds, Leeds, U.K.

fspkl@leeds.ac.uk, e.simone@leeds.ac.uk

Highlights

- Water molecules satisfy hydrogen-bonding in hydrate structures
- Hydrate structures can pack more efficiently
- Hydrate structures can have different physiochemical properties

1. Introduction

Quercetin is a naturally occurring flavonoid which is ubiquitous in the human diet. It is found in many fruits and vegetables and it is known to be an antitumor agent and to exhibit antiallergic, anti-inflammatory and antioxidant activity. [1] Due to the wide range of health benefits, this compound finds use in nutraceuticals and food supplements. [1] Quercetin can exist as an anhydrous, monohydrate and dihydrate crystal form. Usually hydrates exhibit different physiochemical properties, like solubility, stability, morphology and surface chemistry. [2] Understanding these properties and selecting the most appropriate crystal form in terms of thermodynamic and kinetic stability is of critical importance for several industrial applications.

Molecular modelling is an inexpensive and quick way to gain insight into the link between crystal structure and powder properties. This can be achieved by calculating the strength, directivity and dispersive nature of the intermolecular interactions (synthons) within the crystal structure. [3]

In this work, synthonic modelling is used to explore three different hydrated crystalline structures of quercetin: the anhydrous, monohydrate and dihydrate forms, for which the bulk intrinsic and surface extrinsic synthons were examined. The role of water molecules within the three hydrated structures was studied to understand how water affects the packing and conformation energetics of quercetin crystals. This knowledge can then be used to predict physiochemical properties such as stability, and to better understand the mechanisms of nucleation and growth during the crystallization process. Furthermore, the attachment energy model is utilized here to predict the crystal morphology of each form, and by the characterisation of the surface extrinsic synthons, to explore the surface chemistry and predict surface properties such as polarity. [4]

2. Methods

The Habit 98 software (developed in house at the University of Leeds) was used for the calculation of the pairwise intermolecular interaction strengths and lattice energy. [3] This was achieved by summing all the interactions between a central molecule and all the other molecules within a sphere of fixed radius of 30Å around the central molecule. The intermolecular interactions were

calculated using the Momany force-field. [3] All visualization of molecular and crystal packing were carried out in Mercury CSD Version 3.10.

3. Results and discussion

By analyzing the bulk chemistry of quercetin anhydrous, it was found that all key synthons are polar interactions, involving hydrogen bonds and permanent dipole-dipole interactions, while in the monohydrate and dihydrate structures the synthon contributing more to the lattice energy is a non-polar π-π stacking interaction. The hydrogen bonding interactions in the two hydrates are satisfied partly (monohydrate) or exclusively (dihydrate) by interaction with the water molecules.

A conformational analysis was performed and revealed that the quercetin molecules within the anhydrous structure are organized in a less planar arrangement, thus being unable to pack as efficiently and resulting in a lower unit cell density. The quercetin molecules in the monohydrate and dihydrate structures are arranged in a more planar way, due to the fact that quercetin hydrogen bonding is satisfied by the presence of water molecules. Therefore, the presence of water allow quercetin molecules to pack more closely and form the strong π-π stacking interactions, which result in higher unit cell density and greater stability, agreeing with experimental solubility data. [1]

Finally, the attachment energy model was used to predict the growth rate of each face in the three structures and to identify the surface extrinsic synthons contributing to the growth of each facet. The extrinsic synthons were characterised and the surface chemistry of the different faces in each structure was studied, predicting different properties such as face polarity. The attachment energy model was further used to predict the morphology of the structures, illustrated in Figure 1.

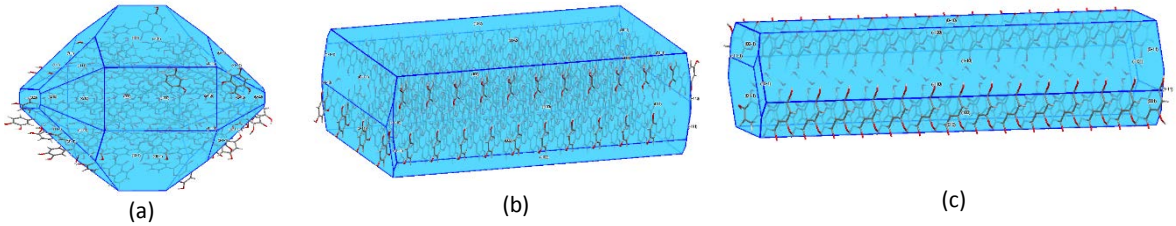

Figure 1. Morphological predictions of quercetin anhydrous (a), monohydrate (b), and dihydrate (c)

4. Conclusions

The presented modelling results show how the presence of water molecules in the quercetin hydrate structures impacts on the type and strength of intermolecular interactions within the crystal, affecting the conformation and packing of the quercetin molecules in each structure. This results in differences in physiochemical properties, such as stability, morphology and surface chemistry. This work shows how synthonic modelling can be used as a predicting tool to better understand the relationship between crystal properties and product quality, leading to a more efficient product formulation and faster development.

References

[1] K. Srinivas, J.W. King, L.R. Howard, J.K. Monrad, J. Food Eng. 100 (2010) 208–218.
[2] A.M. Healy, Z.A. Worku, D. Kumar, A.M. Madi, Adv. Drug Deliv. Rev. 117 (2017) 25–46.
[3] I. Rosbottom, K.J. Roberts, in: K.J. Roberts, R. Docherty, R. Tamura (Eds.), Springer Netherlands, Dordrecht, 2017, pp. 109–131.
[4] P. Hartman, J. Cryst. Growth 49 (1980) 166–170.

ECCE12
The 12th EUROPEAN CONGRESS OF CHEMICAL ENGINEERING
Florence 15-19 September 2019

Influence of fluid dynamics conditions on Pb-hematite nanoparticles mass transfer coefficient in Rushton equipped stirred tank reactor

Giorgio Vilardi[1*], Marco Stoller[1], Nicola Verdone[1], Luca Di Palma[1]

1 Dept. of Chemical Engineering Materials Environment, Sapienza University of Rome, via Eudossiana 18, Rome, 00184

**Corresponding author: giorgio.vilardi@uniroma1.it*

Highlights

- A CFD model was successfully applied to predict the mass transfer coefficients
- A notable Lead sorption capacity of 38 mg/g has been obtained by nano-hematite
- The coefficients of Sh correlation from predicted and regressed k_L were in agreement

1. Introduction

Only recently it has been recognized that various properties of iron (hydro)oxide, such as structure and stability besides the reactivity, might vary as a function of the mean particle's size [1]. In particular, the structure of hematite, α-Fe_2O_3, when it is of maximum particle's size of 40 nm, becomes similar to that of goethite, α-FeOOH [1]. It has already been demonstrated that when the hematite nanoparticles mean size is close to 40 nm, the surface characteristics of the minerals are similar to those of goethite for approximately 60% [1]. These characteristics are suitable in heavy metals separation processes from wastewater streams, by means of sorption phenomenon. In this work, hematite nanoparticles (nHP) have been synthetized using a Spinning Disk Reactor, according to a previous study [2] and have been employed in a Rushton equipped agitated vessel for the removal of Pb cations in aqueous solution. The kinetics of the process has been evaluated and modelled according to a film-diffusion mass transfer model and the influence on mass transfer coefficient of impeller Reynolds number (Re_I) and clearance (C) were evaluated.

2. Methods

The nHP were synthetized according to a previous work [2]. The particles were characterized by a unimodal size distribution and a mean size of 46 ± 1.8 nm and a pH of zero charge of 8.3. The particles were used for the removal of Pb (50 mg/L) at a concentration of 2 g/L (the optimal concentration and pH were found according to preliminary tests) and a pH higher than the pH of zero charge (pH=9.5) to maintain the particle's surface negatively charged and to favour the sorption of Pb. From equilibrium tests (25°C) using Pb solutions (10-100 mg/L) it has been observed that the Langmuir model was the most suitable one (compared with Freundlich and SIPS) to describe the experimental trend. The regressed isothermal parameter values were b, equilibrium constant, equal to 0.22 L/mg and q_{max}, maximum sorption capacity, equal to 38 mg/g (data not showed). The Re_I was varied in the range 1.4-3.5x10^4, to maintain full turbulent conditions, by varying the impeller rotational velocity (500-1250 rpm). The dimension of the tank diameter, T (m), was 0.123 m, whereas the liquid height, H (m) was fixed equal to T. The impeller diameter, D_i (m), was fixed equal to 0.33T, whereas C was varied as 0.15T, 0.25T, 0.33T and 0.4T (data not showed).

The number of baffles was 4 and their dimension was 0.1T. The tests were conducted with two identical reactors, and at selected time steps, the same liquid aliquot was withdrawn from the two reactors. The former was used to re-fill the first reactor, to keep its volume constant and to avoid the variation of the hydrodynamic field, whereas the second one was used for the analysis. The residual Pb concentration was measured by a Flame Absorption Spectroscopy instrument (Agilent). The kinetic experiments were interpreted according to a mass transfer model reported in a previous work, where also the fluid dynamic model (RANS + k-ε model) of the stirred tank has been described [2]. The regressed liquid film mass transfer coefficient, k_L (m/s), and the simulated ones (obtained from CFD simulations) were used to evaluate the empirical coefficients of the experimental relation between Sherwood, Reynolds and Schmidt numbers, as reported below:

$$Sh = \frac{d_p k_L}{D_{Pb}} = \left[2 + \alpha Re_p{}^c Sc^d\right] \quad (1)$$

$$Re_p = \frac{\varepsilon^{1/3} d_p^{4/3}}{\upsilon} \quad (2)$$

$$Sc = \frac{D_{Pb}}{\upsilon} \quad (3)$$

where ε (W/kg) is the specific power per unit of mass dispersed in the vessel, D_{Pb} (m^2/s) is the Pb bulk diffusion coefficient and ν (m^2/s) is the kinematic viscosity of the solution.

3. Results and discussion

The increase of impeller rotational velocity, i.e. Re_I and turbulence, favored the mass transfer phenomenon and led to a reduction of required residence time in the agitated vessel to reach the asymptote (Figure 1a). The empirical correlation among Sh, Re and Sc numbers was employed as model to fit both predicted and regressed k_L values and the obtained empirical coefficients (α, c and d) were quite similar, considering the accordance among the k_L values (Figure 1b)

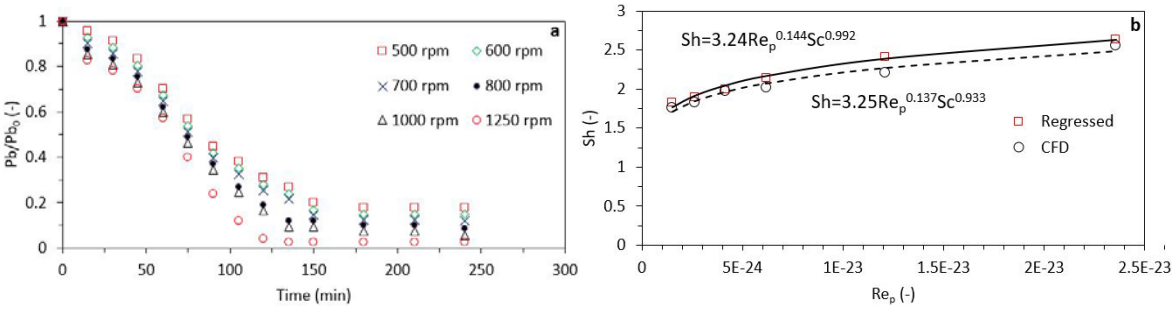

Figure 1. Pb sorption kinetics at different impeller rotational velocities (a) and Sh correlation obtained from CFD predicted and regressed k_L values..

4. Conclusions

The k_L obtained from CFD simulations were close to that obtained from data regression, as well as the empirical coefficients of Sh correlation with Re and Sc numbers. The nanohematite particles were able to sorb a considerable amount of Pb cations in alkaline environment and the process may be intensified by an accurate selection of impeller rotational velocity and reactor geometry.

References

[1] L. E. Barton, K. E. Grant, T. Kosel, A. N. Quicksall, P. A. Maurice, Env. Sci. Tech. 45 (2011) 3231-3237.

[2] G. Vilardi, M. Stoller, L. Di Palma, N. Verdone, Chem. Eng. Trans. 74 (2019) 101-106.

Effect of reactant molar ratio on the hierarchical morphology of a novel mesoporous silica

Layla Hosseini[1,*], Roberto Moreno-Atanasio[1], Frances, Neville[2]

1 Chemical Engineering Department, School of Engineering; 2 Chemistry Department, School of Life Sciences

The University of Newcastle, Australia

**Corresponding author: Layla.hosseini@uon.edu.au*

Highlights

- Using MTMS in the synthesis of mesoporous silica produced a novel material (MS-Asym)
- Increasing the silica to template relative molar ratio gave a hierarchical morphology
- All members of the MS-Asym sfamily possess a similar porous structure with the same pore size

1. Introduction

Porous materials and specially mesoporous silica particles are commonly used in a number of different applications such as petroleum refining, detergents, medicinal applications and separations [1]. MSP are very promising as they are cheap to synthesize and their surface properties can be tuned to suit specific functionalities [2]. The effect of employing the asymmetric methyltrimethoxysilane (MTMS) as the only silica source on the synthesis of mesoporous silica particles has been scrutinised for the first time in our previous work [3]. The resultant synthesis was a novel MSP, which we named MS-Asym. In the current study, we have focused on analyzing the MS-Asym particle's morphology, characteristic sizes and crystallinity, when increasing the silica to template relative molar ratio.

2. Methods

The novel mesoporous silica, MS-Asym, was synthesised using a triblock copolymer, Pluronic P123 ($EO_{20}PO_{70}EO_{20}$) in a highly acidic media, and trimethoxy(methyl)silane (MTMS, Sigma-Aldrich) as a new silica source via a sol gel method [3, 4].

To study the morphology transformation of the samples seven different experiments were conducted. The pH and the amount of Pluronic were kept constant in all the tests. The amount of MTMS was increased to reach the desired MTMS/Pluronic P123 molar ratio from 59 to 590. The produced samples were labelled MS-Asym-1 to MS-Asym-10 according to the relative molar ratio of silica/template. As a result, the silica source concentration increased from 0.3 mol/L to 2.24 mol/L, and the concentration of the template decreased from 0.53×10^{-2} mol/L to 0.38×10^{-2} mol/L.

The products were characterised using SEM to study the external morphology, TEM to investigate the internal structure and ATR-FTIR spectroscopy to confirm the conformation of the bonds. A Malvern Mastersizer was also employed to measure the particle size by laser diffraction.

3. Results and discussion

In the first three samples (MS-Asym-1, MS-Asym-2 and MS-Asym-3), the solid products were not discrete and they formed a structure with the characteristics of continuous solids [3]. However, according to the SEM results shown in Figure 1, MS-Asym-2 and MS-Asym-3 included many tiny spherical particles that were packed together. MS-Asym-4, MS-Asym-6, MS-Asym-8 and MS-Asym-10 were quite similar in shape, and consisted of spherical and rod-like individual particles, completely different from the first three samples.

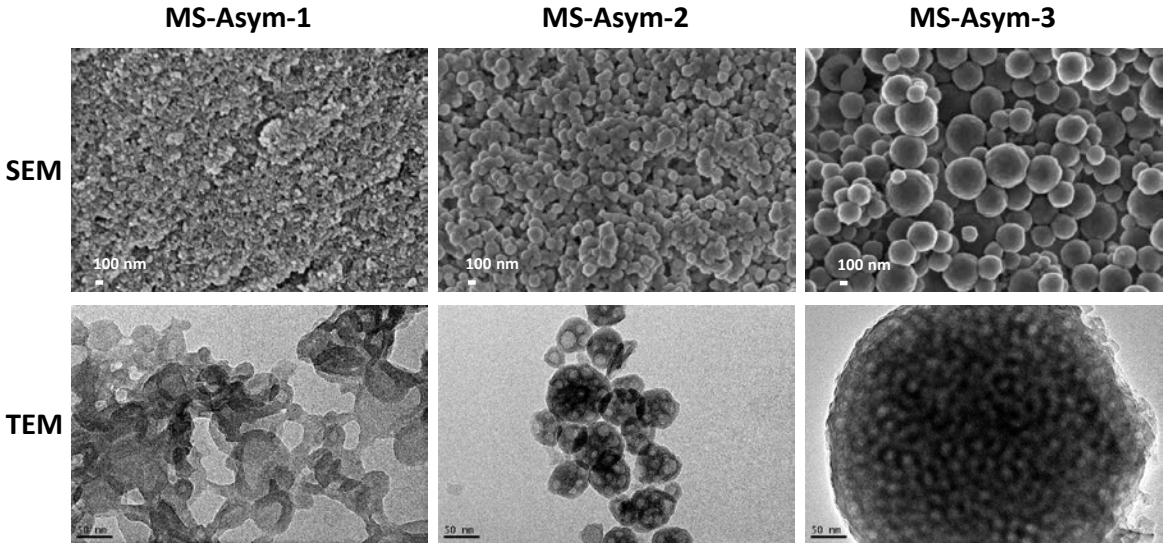

Figure 1 SEM and TEM results of MS-Asym-1, MS-Asym-2 and MS-Asym-3

From the size measurements of these samples demonstrated in Figure 2, it could be suggested that the outer diameter of the particles was mostly controlled by varying the concentration of the silica source. The higher the concentration of MTMS, the larger the characteristic sizes of the produced particles were, which is in accordance with what Neville et al. (2016) observed in the synthesis of nonporous PEI-MTMS particles [5].

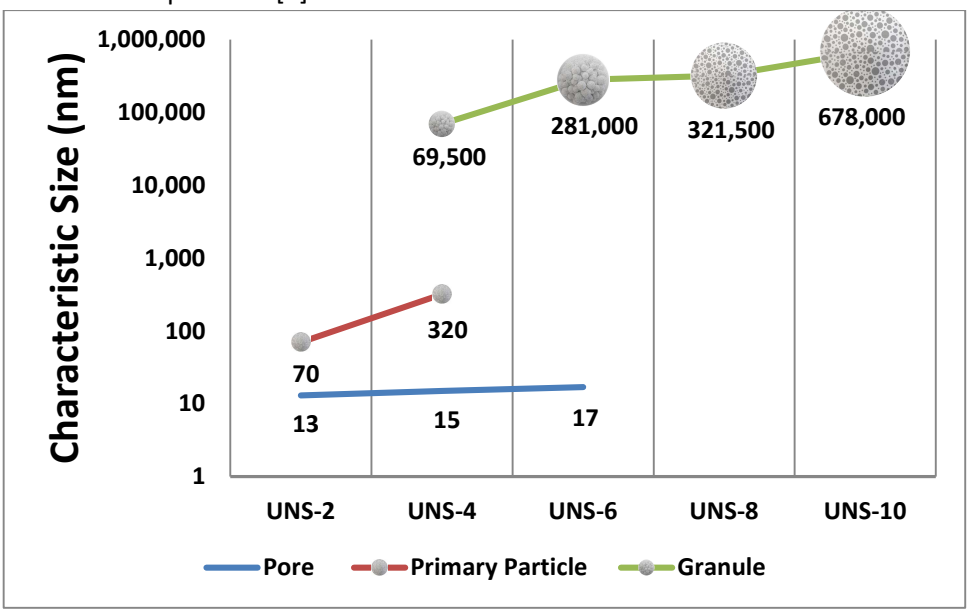

Figure 2 Comparison of the characteristic sizes of the samples

On the other hand, the pore size of all these samples obtained from their TEM images, proposes that all the porous samples from MS-Asym-2 to MS-Asym-6 have a similar pore size range. This similarity could be attributed to their similar process conditions such as pH and temperature as well as the employment of the same template in their fabrication. By further increasing the amount of MTMS and decreasing the concentration of Pluronic, MS-Asym-8 and MS-Asym-10 were produced, which were much less porous than the previous members of the family. MS-Asym-6, MS-Asym-8 and MS-Asym-10 also presented crystallinity, which did not appear in the other samples.

4. Conclusions

Altering the amount of MTMS resulted in a combined change in both MTMS and Pluronic concentration. By considering SEM and TEM results of the samples, a distinct pattern was identified as described in the results section. This study also found that the combined effect of MTMS and P123 concentrations played a crucial role in controlling the particle morphology of MS-Asym mesoporous material. With the increase in the MTMS concentration and decrease in the P123 concentration, the morphology of the spherical-like MS-Asym particles changed from aggregated nanoparticles to micrometre size granules.

The new developed porous silica family offers the possibility to be processed in a shorter time, which is beneficial in commercial applications since it undergoes a faster reaction and makes the project more feasible. It is also large and inert and its density covers a range which is lower than that of water density in MS-Asym-6. These characteristics could open up new horizons to enquire into different novel applications.

References

[1. Aquino, C. and T. Maschmeyer, *A New Family of Mesoporous Oxides-Synthesis, Characterisation and Applications of TUD-1*. 2009: Elsevier Science: Oxford.

2. Nandiyanto, A.B.D., et al., *Mesopore-free hollow silica particles with controllable diameter and shell thickness via additive-free synthesis.* Langmuir, 2012. **28**(23): p. 8616-8624.

3. Hosseini, L., R. Moreno-Atanasio, and F. Neville, *Synthesis of hollow silica nanoparticle aggregates from asymmetric methyltrimethoxysilane using a modified SBA-15 method.* Langmuir, 2019.

4. Zhao, D., et al., *Triblock copolymer syntheses of mesoporous silica with periodic 50 to 300 angstrom pores.* science, 1998. **279**(5350): p. 548-552.

5. Neville, F., L. Dixon, and E.D. Hyde, *A comparative study of hydrophobic silica particle synthesis.* Advanced Powder Technology, 2016. **27**(6): p. 2317-2323.

Precipitation of cobalt salts for recovery in leachates

N. Djoudi[1]*, M. Le Page Mostefa[1], H. Muhr[1]

[1]*Laboratoire Réactions et Génie des Procédés (LRGP) UMR 7274 CNRS,*

Université de Lorraine, 1 rue Grandville BP20451, 54001 NANCY,FRANCE

**Corresponding author: neila.djoudi@univ-lorraine.fr*

Highlights

- 99.8% of cobalt recovery from batteries leachate by precipitation
- Impact of temperature on cobalt precipitation kinetic
- Impact of temperature on particle size distribution
- Optimum precipitation conditions for cobalt recovery

1. Introduction

Fifty metals are considered strategic for industry and essential for global economic and geopolitical issues [1]. It is certain that, due to the communication development, information technologies, and electrical vehicles, demand for strategic metals will become more and more important counting cobalt. Indeed, this metal is present in all the technologies that are becoming essential for the energy and the digital transition. According to the European Commission, cobalt has been recognized as a critical raw material [2]. That is why, it is more important than ever to develop cobalt recovery processes for the coming years. Our current research work focuses on cobalt recovery from Li-ion batteries, by precipitation. After a bibliographical and simulation study, the precipitating agent chosen was the hydroxide ion. Simulation's result allows to determine cobalt precipitation conditions for a recovery of 99.8%. Experimentally, several operating parameters were varied on a solution containing only cobalt (II), results show the high impact of temperature on cobalt hydroxide precipitation kinetic and on particles size distribution.

2. Methods

To perform cobalt (II) precipitation with hydroxide ion: $Co^{2+} + 2\ OH^- = Co(OH)_{2\ (s)}$, the following reactants were used:

- Sodium hydroxide solution: NaOH (1 $mol.L^{-1}$, VWR Chemicals),
- Cobalt (II) sulfate heptahydrate solution: $CoSO_4,7H_2O$ (0.131 $mol.L^{-1}$, Fisher).

The experimental set-up is composed of:

- a double-jacketed reactor of one liter, a thermostatic bath (Julabo F32-EH),
- pH meter (Mettler Toledo)
- Büchner filtration system with 0.45 or 0.22 µm porosity,
- Laser diffraction particle size analyzer (Hydro MS 2000 Malvern)

Experiments were performed at different temperatures: 25°C, 56°C and 60°C. To precipitate 0.0131 mol of Co^{2+}, 0.0262 mol of OH^- are needed, which corresponds to a volume of 26.2 mL of soda (1 $mol.L^{-1}$). The thermostatic bath regulates the experimental media at the desired temperature. After that, all soda volume is rapidly introduced into the cobalt solution. Every 10 minutes, during 3 hours, pH is measured and a sample of the solution is taken for ICP analyses. These analyses allow to determine the cobalt concentration as a function of time and thereby cobalt hydroxide precipitation kinetic. Concerning particle size analyses, samples are analyzed in the same day.

3. Results and discussion

3.1 Temperature impact on particle size distribution

Particles size distributions show that the particle size decreased when the temperature increased. It is due to the larger Gibbs free energy; this energy is highly dependent on solution temperature. The increasing temperature (>50°C) lead to a more important supersaturation and thus to a large number of small particles [3]. Consequently, the median diameter is around 25 µm at 25 °C, d_{50}= 14 µm at 56 °C, and d_{50}= 12 µm at 60°C. According to different research studies [3], the kinetic energy of particles gets higher with increasing temperature, which allow to obtain a better precipitation efficiency [3].

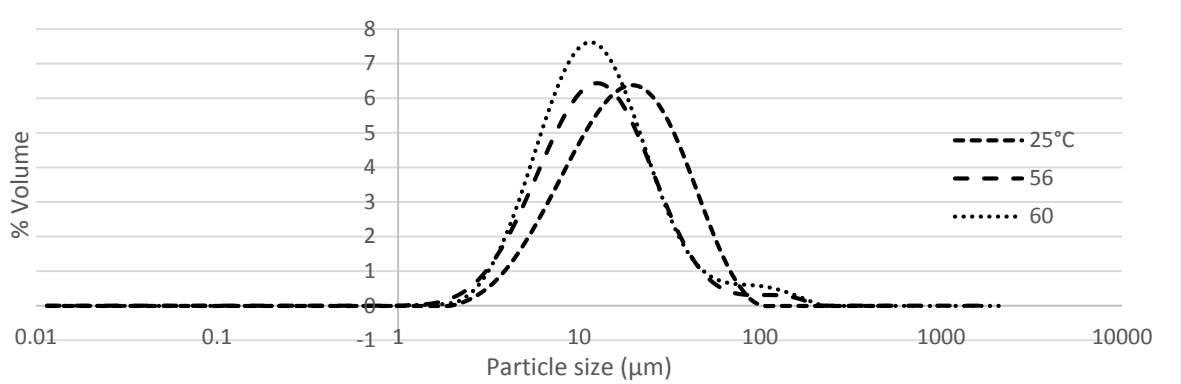

Figure 1. Particle size distribution in function of temperature.

3.2 Temperature impact on cobalt precipitation kinetic:

Temperature impact on Cobalt recovery were investigated at 25°C and 50°C (Figure 2). It appears that, at 25°C, the highest yield of cobalt recovery is obtained. Indeed, at t=28 minutes, 99. 98% of cobalt is in $Co(OH)_2$ form. In comparison, at 50°C, at t= 8 minutes, 99. 73% of cobalt has precipitated. Also, it can be seen a little dercrease of cobalt yield (0.8%) during time. It can be explained by $Co(OH)_2$ oxidation into $Co(OH)_3$ by oxygen from the air.

First of all, at 25°C, under a very high supersaturation effect, cobalt precipitates as $Co(OH)_2$ and reaches in a few minutes more than 99.9% precipitation. Its stabilization is between 16 and 30 minutes. This nearly stabilization amounts to the dissolution of α-$Co(OH)_2$ polymorph and its precipitation in its most stable form β-$Co(OH)_2$. Indeed, Cobalt hydroxides are known to crystallize in two polymorphic forms α and β. The pink colored ß-$Co(OH)_2$ is the most stable polymorph, with a brucite-like structure [4]. This crystallographic form doesn't have intercalated species, unlike the

alpha form. Indeed, the blue-green α-$Co(OH)_2$ is hydrotalcite-like structure, this ionic lamellar structure contains inorganic anions (e.g., NO_3^-, CO_3^{2-}, Cl^-…) and water molecules comprised in $Co(OH)_{2-x}$ monolayers charged positively. Experimentally, α-$Co(OH)_2$ appears first, then dissolves, to allow β-$Co(OH)_2$ precipitation. When this transformation process begins, a concentration plateau that lies between the solubilities of the two forms appears. Which can be explained by the growth of the thermodynamically stable phase β-$Co(OH)_2$, compensated by the less stable phase α-$Co(OH)_2$ dissolution. In addition, it is observed that this plateau is absent at 50°C, which means that α-$Co(OH)_2$ appears and disappears very quickly. Its transformation into β-$Co(OH)_2$ occurs in less than 8 minutes. Thus, temperature accelerates the process of phase transformation.

On the other hand, at 25°C, from 36 minutes onwards, cobalt concentration decreases slowly. This is explained by the gradual transformation of $Co(OH)_2$ into $Co(OH)_3$. In comparison to 50°C, where oxidation occurs more quickly, from 8 minutes and more significantly. Thus, temperature accelerates phases transition from α-$Co(OH)_2$ to β-$Co(OH)_2$. However, this transition occurs without improving cobalt recovery in solution, especially since the oxidation reaction is accelerated at high temperatures. Therefore, it will be more interesting to work at room temperature, in order to obtain a precipitation rate higher than 99.9% within a few minutes. After that, filter immediately afterwards in order to maintain the same precipitation rate.

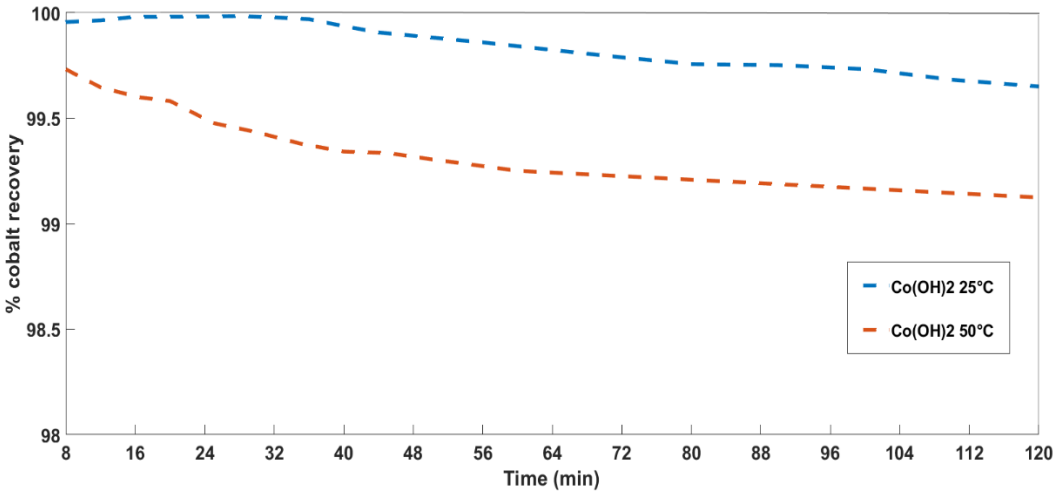

Figure 2: Cobalt recovery in function of time at 25°C and 50°C

Conclusions

This study allows to highlight temperature impact on cobalt hydroxide precipitation kinetic in one hand and to determine optimum precipitation condition in other hand. It was found that temperature increase accelerates phase transition of α-$Co(OH)_2$ into β-$Co(OH)_2$ and the oxidation reaction of $Co(OH)_2$ to $Co(OH)_3$. It has been demonstrated that cobalt recovery is optimal at 25°C with a yield of 99.98%. Therefore, it will be necessary to study synthetic solutions of battery

leachate, containing other metals, such as copper, nickel and manganese and to optimize the operating conditions for cobalt recovery, with high efficiency and good purity.

References

[1] Deloitte Sustainability, British Geological Survey, Bureau de Recherches Géologiques et Minières, Netherlands Organisation for Applied Scientific Research, Study on the review of the list of critical raw materials final report, Publications Office of the European Union, Luxembourg, 2017.

[2] J.H. Huang, C. Kargl-Simard, M. Oliazadeh, A.M. Alfantazi, Hydrometallurgy.75 (2004) 77-90

[3] GP.Bharat, VP.Dipak, SK.Sanjay, BP.Aniruddha. Chem Eng. (2012) 946–989

[4] Z. Liu, R. Ma, M. Osada, K. Takada, T. Sasaki, J. Am. Chem. Soc. 2005, 127 (40), 13869–13874. DOI: https://doi.org/ 10.1021/ja0523338

Stabilization of goethite suspensions using Zirconium(IV) salts and its application to an imaging-free bi-dimensional size analysis

M. Distaso[1,2], M. Uttinger[1,2], J. Walter[1,2], C. Lübbert[1,2], T. Thajudeen[1,2], W. Peukert[1,2]

1 Institute of Particle Technology, FAU Erlangen-Nuremberg, Cauerstraße 4, 91058 Erlangen, Germany;

2 Center for Functional Particle Systems, FAU Erlangen-Nuremberg, Haberstraße 9a, 91058 Erlangen, Germany

**Corresponding author: monica.distaso@fau.de*

Highlights

- Goethite particles are stabilized using Zr(IV) salts.
- The suspensions were further processed and a fine and coarse fractions of particles were separated.
- Size analysis was carried out by combining sedimentation- and gas-phase analysis.
- The results match the size distribution obtained from image analysis.

1. Introduction

Goethite (α-FeOOH) is a technologically relevant material, widely used as adsorbent in waste water treatment, as precursor for magnetic drives and as a yellow pigment.[1,2,3] Goethite typically comprise particles with acicular shape, often entangled in macroscopic agglomerates with limited dispersibility and only short time stabilization against agglomeration. The colloidal stability of suspensions is an important pre-requisite to ensure that the properties of the individual particles are extended to their ensembles in liquid phase. To achieve colloidal stability of goethite particles we consider for the first time the use of aqueous solution of Zr(IV) salts as stabilizers and we carry out a comparison with the already known $AlCl_3 \cdot 6H_2O$.

2. Methods

Sedimentation analysis by Analytical Centrifugation (AC) and Ultracentrifugation (AUC) supported by ξ-potential measurements, time resolved UV-Vis spectroscopy and FTIR spectroscopy is used thoroughly to ascertain the stability of the suspensions.

[1] R.M. Cornell, U. Schwertmann, The iron oxides: Structure, properties, reactions, occurrences, and uses, 2nd, completely rev. and extended ed. ed., Wiley-VCH, Weinheim, 2003.
[2] E. R. Encina, M. Distaso, R. N. Klupp Taylor, W. Peukert "Synthesis of Goethite alpha-FeOOH Particles by Air Oxidation of Ferrous Hydroxide Fe(OH)2 Suspensions: Insight on the Formation Mechanism" *Cryst. Growth Des.* **2015**, *15*, 194.
[3] A. Güldenpfennig, M. Distaso, R. N. Klupp Taylor, W. Peukert "Modelling the two-dimensional growth and oriented attachment of goethite nanorods synthesized via oxidation of aqueous ferrous hydroxide slurries" *Chem. Eng. J.* **2018**, *347*, 798.

3. Results and discussion

The colloidal stabilization enabled the separation between the fine and coarse fractions that constitute the particles ensemble. The fine fraction showed a ξ-potential > 50 mV and was found to be stable for more than 70 h at 25 °C. In a previous study, some of us demonstrated that the combination of two analytical techniques, namely AUC and scanning mobility particle size analysis (SMPS), enables an accurate characterization of the length and width of gold and ZnO nanorods.[4] This approach was applied to stabilized goethite particles suspensions, whereby a bi-dimensional size analysis was carried out showing excellent agreement with the results obtained by Scanning Electron Microscopy (SEM) analysis.

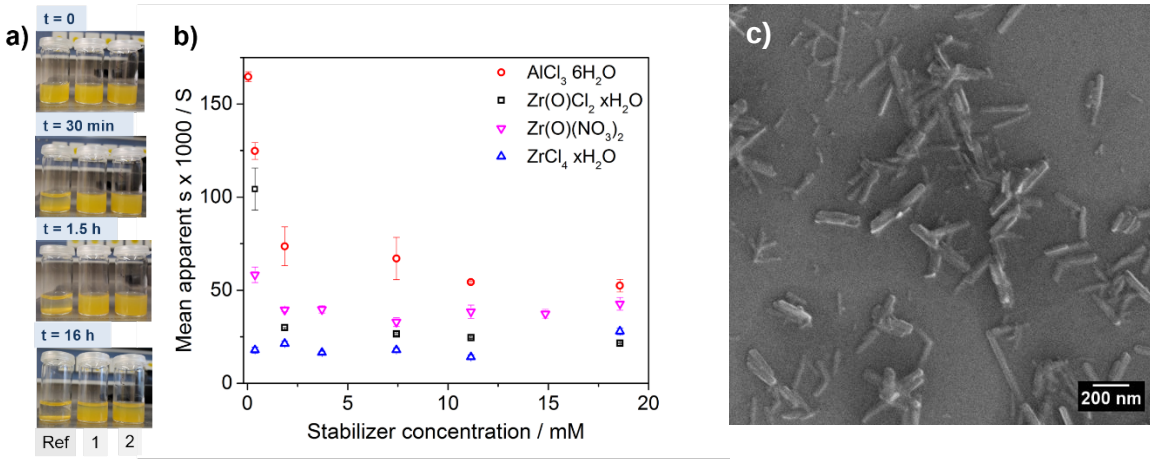

Figure 1. a) Digital micrographs of goethite suspensions in water and Zr stabilized suspensions with Zr(IV) concentration 3.71 mM (1) and 15 mM (2) at different time intervals; b) comparison between $AlCl_3 \cdot 6H_2O$ and Zr salts with different counter ions. [α-FeOOH] = 3.71 mM in all cases. Rods with mean width and length of (25 ± 8) nm and (135 ± 55) nm, respectively, were analyzed; c) SEM analysis of stabilized goethite particles.

4. Conclusions

Excellent colloidal stability of goethite particles with acicular shape was achieved using Zr(IV) salts as stabilizers. The suspensions could be further processed and a bi-dimensional size analysis was carried out by AUC and SMPS to assess the size distribution of the sample, without counting the particles from SEM images.

References

[1] R.M. Cornell, U. Schwertmann, The iron oxides: Structure, properties, reactions, occurrences, and uses, 2nd, completely rev. and extended ed. ed., Wiley-VCH, Weinheim, 2003.

[2] E. R. Encina, M. Distaso, R. N. Klupp Taylor, W. Peukert "Synthesis of Goethite alpha-FeOOH Particles by Air Oxidation of Ferrous Hydroxide Fe(OH)2 Suspensions: Insight on the Formation Mechanism" *Cryst. Growth Des.* **2015**, *15*, 194.

[3] A. Güldenpfennig, M. Distaso, R. N. Klupp Taylor, W. Peukert "Modelling the two-dimensional growth and oriented attachment of goethite nanorods synthesized via oxidation of aqueous ferrous hydroxide slurries" *Chem. Eng. J.* **2018**, *347*, 798.

[4] T. Thajudeen, J. Walter, R. Srikantharajah, C. Lübbert, W. Peukert "Determination of the length and diameter of nanorods by a combination of analytical ultracentrifugation and scanning mobility particle sizer" *Nanoscale Horizons* **2017**, *2*, 253.

Phase inversion temperature of polymeric surfactant-based emulsions for the formation of nanoemulsions

Martin Meulders, André Barrizzelli Murino, Véronique Sadtler, Cécile Nouvel*

LRGP Laboratoire Réactions et Génie des Procédés, UMR CNRS-Université de Lorraine 7274, Nancy F-54000, France

** cecile.nouvel@univ-lorraine.fr*

Highlights

- Nanoemulsions were obtained with polymeric surfactants through PIT process
- Cycling the process decreases the droplets sizes and narrows the size distribution
- PIT process heavily depends on the copolymer architecture to achieve nanoemulsions

1. Introduction

Nanoemulsions are remarkable for their high specific area and kinetic stability among others. They have many pharmaceutical or cosmetic applications for their high performances in drug delivery [1] and are often required as an intermediate for the formulation of nanocapsules [2]. Nevertheless, their making requires high mechanical energy input through traditional emulsification methods also called “high energy methods” [3]. Therefore, low-energy methods such as Phase Inversion Temperature (PIT) can be cost-effective alternatives for the production of nanoemulsions [4]. The principle of the PIT relies on the ability of a temperature-sensitive surfactant to shift its overall affinity from the aqueous phase of the emulsion [5] to the hydrophobic one with increasing temperature. Examples of PIT are reported with small commercially available surfactants but almost never for polymeric surfactants [6]. In this work, we have studied the PIT process on a dodecane/water system using various polystyrene-b-poly(oligo(ethylene glycol) methyl ether methacrylate) (PS-b-POEGMA) as surfactants. The influence of different process parameters was investigated to evaluate the potential of such surfactants to produce nanoemulsions.

2. Methods

A two-step synthetic pathway using the Atom Transfer Radical Polymerisation was adapted from the literature [6, 7] to synthesize PS-b-POEGMA copolymers with various molecular weights and POEGMA/PS weight ratios. The copolymers were solubilized at 8 wt% in aqueous solution, which was mixed with dodecane (80 v/v% water and 20 v/v% dodecane) and then used in the PIT process, monitored both by viscosimetry and conductimetry. Emulsification was carried out under a constant temperature rise at 0.5°C/min and under gentle stirring in a rheometer with a helical ribbon, equipped with conductivity and temperature probes (figure 1 a) as set up before in our laboratory [8]. Once the emulsion was inversed, highlighted by a dramatic conductimetry drop and viscosity increase, the system was rapidly cooled with an ice bath and the droplet size distribution was measured by laser granulometry. The procedure was cycled several times.

3. Results and discussion

The synthesis of the PS-b-POEGMA surfactants allowed us to design the molecular weight of each block, resulting in copolymers with various POEGMA/PS weight ratios (from 10 to 17) and total molecular weights ranging from 17 500 to 34 000 g/mol with a reasonable dispersity. The influence of the surfactant concentration, the number of cycles and the surfactant design on the PIT process was studied and compared to small surfactants (Brij30 and various Igepals). The conductivity dropped to zero because of the transition from a conductive oil-in-water emulsion to a water-in-oil emulsion (figure 1 b). Simultaneously, the viscosity increased rapidly due to the switchover from an aqueous continuous phase which was 80% of the emulsion volume to a more viscous oily continuous phase that only represented 20% of the system's volume. The local maximums for conductivity and viscosity can be attributed to a transitional bicontinuous phase. Submicron emulsion could be produced with the polymeric surfactant through the PIT process. Cycling the procedure significantly facilitated the phase inversion resulting in lower droplet sizes (down to 150 nm). The shortest copolymers were the most efficient to achieve nanoemulsions (smaller droplet sizes and fewer PIT cycles) which was attributed to their faster diffusion at the water-oil interface.

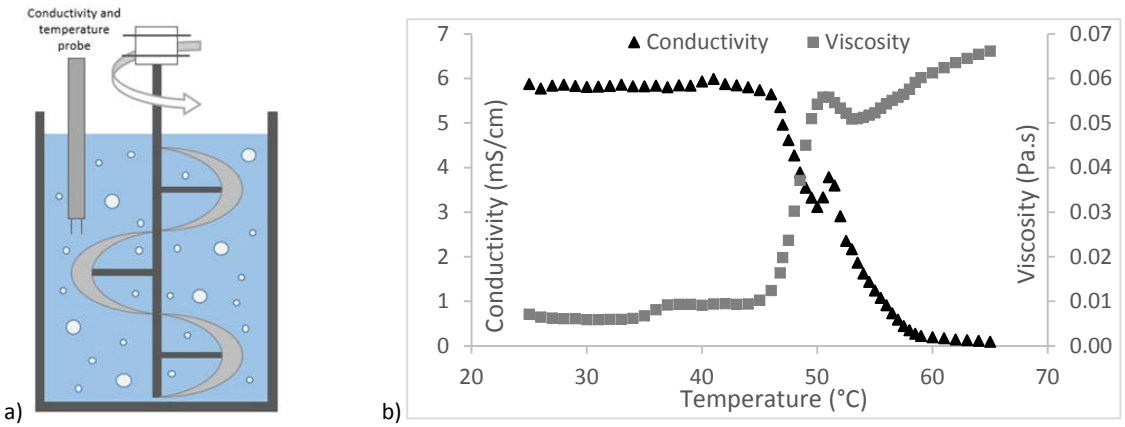

Figure 1. Conductivity and viscosity monitoring of the PIT a) Experimental setup b) Example of results with dodecane/water system using one PS-b-POEGMA surfactant (Mw = 17 500 g/mol, D=1.4).

4. Conclusions

This work has paved the way to the use of polymeric surfactants to produce nanoemulsions through the PIT process. The design of the copolymer (molecular weight, hydrophilic/hydrophobic ratio) has shown to be a crucial parameter to control the performances of the PIT process.

References

[1] S. Yuvraj, G.M. Jaya, R. Kavit, A.K. Farooq, C. Mohini, K.J. Nitin, C. Manish, J. Control Release 252 (2017) 28-49

[2] L.M. Forero, J. Babin, A. Durand, J-L Six, C. Nouvel, Colloids and Surfaces A, 486 (2015) 60–68; N. Anton, J.P. Benoit, P. Saulnier. J. Control Release 128 (2008) 185-199

[3] M. Jaiswal, R. Dudhe, P.K. Sharma, Biotech. 5 (2015) 1273-1277

[4] M.I. Guerra-Rosas, J. Morales-Castro, L.A. Ochoa-Martinez, L. Salvia-Trujillo L, O. Martin-Belloso, Food Hydrocoll. 52 (2016) 438– 446

[5] C. Solans, I. Solé, Curr. Opin. Colloid Interface Sci. 17 (2012) 246–254.

[6] Y. Sasaki, N. Konishi, M. Kasuya, M. Kohri, T. Taniguchi, K. Kishikawa, Colloids Surf. Physicochem. Eng. Asp. 482 (2015) 68–78

[7] W. Jakubowski, K. Min, K. Matyjaszewski, Macromolecules 39 (2006) 39-45

[8] J. Allouche, E. Tyrode, V. Sadtler, L. Choplin, J.L Salager, Langmuir 20(6) (2004) 2134-2140

Design And Development of an Innovative Aerosol Generation Setup for Simulating the Inhalation Exposure to Ambient $PM_{2.5}$.

Sina Taghvaee[1], Amirhosein Mousavi[1], Mohammad H. Sowlat[1], Constantinos Sioutas*[,1]

[1]*University of Southern California, Department of Civil and Environmental Engineering, Los Angeles, California, USA*

**Corresponding author: sioutas@usc.edu*

Highlights

- A new method was developed to generate aerosols that are representative of ambient PM.
- Re-aerosolizing the aqueous extracted filters recovered water soluble portions of PM.
- The VACES/aerosol-into liquid collector tandem was able to recover all components of PM.

1. Introduction

Several detrimental health impacts are documented as a result of exposure to ambient particulate matters (PM). While toxicological studies are in need of real-world ambient PM for inhalation exposure assessments, the commercially available aerosols are not good representatives of ambient PM, due to its complex chemical composition. Furthermore, the ambient PM concentrations are not at levels causing acute adverse health consequences. Therefore, the main purpose of this study was to develop an innovative method for generating physically and chemically stable aerosols that are well representative of ambient particulate matters (PM) and can further be used for health exposure studies.

2. Methods

In this research, the ambient PM samples were collected on filters (20 × 25 cm, 3.0 µm pore size, PALL Life Sciences, USA) by the means of a high-volume sampler; followed by aqueous extraction of filters in ultrapure Milli-Q water. In addition to these aqueous extracted slurries, the versatile aerosol concentration enrichment system (VACES)/aerosol-into-liquid tandem technology was employed to capture ambient particles directly into the Milli-Q water. Subsequently, we re-aerosolized the aqueous PM solutions from both methods using commercially available HOPE nebulizers (Model 11310, B&B Medical Technologies, USA). Afterward, the size distribution of nebulized aerosols were investigated under various compressed air pressures of the nebulizer, and dilution air flow rate, using a scanning mobility particle sizer (SMPS 3936, TSI Inc., USA) in conjunction with a condensation particle counter (CPC 3022A, TSI Inc., USA). In addition, the re-aerosolized PM were collected on filters for further chemical analysis. In this regard, the collected PM samples (both ambient and re-aerosolized) were analyzed for their chemical compositions including elemental and organic carbon (EC/OC), water soluble organic carbon (WSOC), polycyclic aromatic hydrocarbons (PAHs), metals and trace elements, and inorganic ions.

3. Results and discussion

Our finding revealed that the water soluble constituents of ambient PM (e.g., water-soluble organic matter, and water-soluble inorganic ions) can be recovered effectively by re-aerosolizing the aqueous extracted filters. However, this protocol was deficient in reconstructing EC, PAHs, and some of the redox-active metals and trace elements as important insoluble components of ambient PM. On the other hand, employing the VACES/aerosol-into-liquid tandem technology for collecting ambient PM directly into ultrapure water enabled us to effectively recover all components (i.e., water soluble, and water insoluble) of ambient PM. For instance as presented in Figure 1, there were great agreement between chemical compositions of ambient $PM_{2.5}$ (collected on VACES) versus re-aerosolized $PM_{2.5}$ (from the direct capturing of PM into the ultrapure water by the means of VACES/aerosol-into-liquid tandem technology).

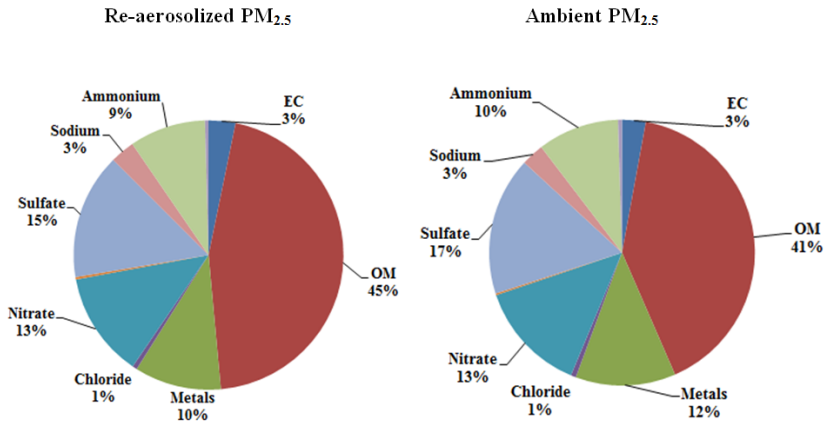

Figure 1. Chemical composition of re-aerosolized versus ambient $PM_{2.5}$

4. Conclusions

Our finding corroborate the superiority of implementing VACES/aerosol-into liquid tandem technology for producing PM solutions; followed by re-aerosolization procedure to generate stable aerosols that are fully representative of ambient PM in terms of physical and chemical compositions. Therefore, this protocol can be implemented to simulate the inhalation exposure to real world ambient PM. .

References

[1] S. Kim, M. Chang, D. Kim, C. Sioutas, Inhal. Toxicol. 12 (2000), 121–137.

[2] S. Kim, P.A. Jaques, M. Chang, T. Barone, C. Xiong, S.K. Friedlander, C. Sioutas, J. Aerosol Sci. 32 (2001), 1299–1314.

[3] D. Wang, P. Pakbin, A. Saffari, M.M. Shafer, J.J. Shauer, C. Sioutas, 2013. Aerosol Sci. Technol. 47 (2013), 1226–1238.

A Novel Closure Method for Pbes Based on Gram-Charlier Densities.

Grzegorz Tyl[1*], Jerzy Bałdyga[1], Mounir Bouaifi[2]

1 Faculty of Chemical and Process Engineering, Warsaw University of Technology, ul. Waryńskiego 1, 00-645 Warsaw, Poland

2 Centre de Recherche et d'Innovation de Lyon, Solvay, 85 Avenue des Frères Perret, BP 62, 69192 Saint-Fons Cedex,France

** grzegorz.tyl.dokt@pw.edu.pl*

Highlights

- A novel closure method for the nonlinear moment-transformed Population Balance Equations has been proposed and applied.
- Gram-Charlier type A densities allow to access the full distribution during simulation.
- The introduced method has been employed to solve PBE for Ostwald ripening problems.

1. Introduction

Population balance equations (PBE) are widely used to predict evolution of the particulate systems. To decrease computation time and incorporate PBE into CFD software one can use methods of moments and represent distributions with averaged values. When, however, nonlinear terms are present in PBE, a closure procedure is required. This is often done by using quadrature methods, which precisely approximate polynomial terms. In other cases an error of approximation can be significant. There is also no simple way to calculate pointwise values.

In this work a new method of closure, based on Gram-Charlier type A expansion [1] with GNT transformation [2], is presented. It allows to robustly retrieve a full distribution in each time step of the simulation and close the nonlinear terms of PBE.

2. Gram-Charlier densities

One of the approaches to retrieve a full probability density function (PDF) from its statistical parameters is an expansion of the searched PDF about another PDF with common mean and variance. A type A Gram–Charlier expansion is made about normal distribution density:

$$f(x) = \phi\left(x, \mu, \sigma\right)\left(1 + \sum_{s=1}^{N} a_S H_S\left(\frac{x-\mu}{\sigma}\right)\right) \tag{1}$$

where $\phi\left(x, \mu, \sigma\right)$ stands for the normal probability density function with a mean value μ and standard deviation σ, a_S are the moment dependent parameters and $H_s\left(x\right)$ are Hermite polynomials of order s. The series in Eq. (1) have to be truncated depending on the number of moments available and required precision. To obtain $f(x)$, being a positive function that integrates to unity, a squared transformation and scaling are applied ([2], [3]). The function given below can be used to execute further integration in nonlinear terms of PB:

$$f(x) = \frac{\phi\left(x, \mu, \sigma\right)}{w}\left(1 + \sum_{s=1}^{N} a_S H_S\left(\frac{x-\mu}{\sigma}\right)\right)^2 \tag{2}$$

$$w = \int_{-\infty}^{\infty} \left(1 + \sum_{s=1}^{N} a_s H_s\left(\frac{x-\mu}{\sigma}\right)\right)^2 \phi\left(x,\mu,\sigma\right) dx = 1 + \sum_{s=1}^{N} a_s^2 s! \tag{3}$$

3. Application to population balance

As a test case for the introduced closure method a simulation of the Ostwald ripening (OR) process has been chosen. Modeling with PBE of the size dependent dissolution, requires calculation of the pointwise values of the PDF. The moment-transformed PBE for OR reads:

$$\frac{dm_k}{dt} = k \int_{x_{\min}}^{\infty} x^{k-1} G\left(x\right) f\left(x\right) dx + x_{\min}^k G\left(x_{\min}\right) f\left(x_{\min}\right) \tag{4}$$

where m_k denotes k-th moment of the PDF, $G(x)$ is a size dependent growth rate such that particles smaller than x_{min} disappear and larger grow ([4], [5]):

$$G\left(x\right) = \frac{\alpha}{x}\left(\frac{1}{x^*} - \frac{1}{x}\right) \tag{5}$$

where x denotes the particle size, $x^* = x_{min}$ and α is proportional to the diffusion coefficient.

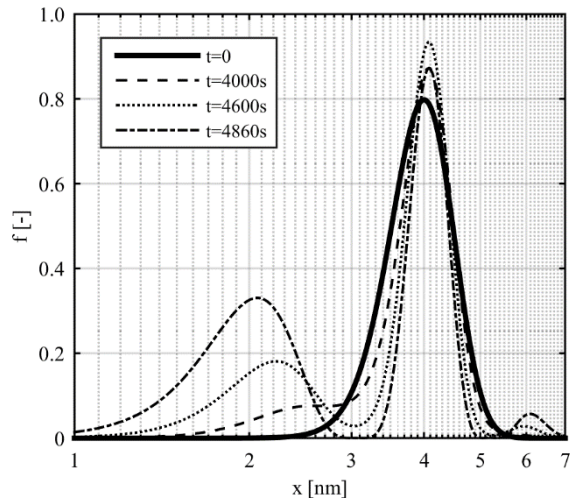

Figure 1. Time evolution of the particle size distribution ($n_0=10^{23}$, $\mu_0=4nm$, $\sigma_0=0.5nm$, $x_{min}=0.5nm$, $\alpha=10^{-30}$, $x^*=4nm$)

4. Discussion and conclusions

A time evolution of the normalized particle size distribution is presented in Figure 1. As one can see dissolution of particles smaller than 4nm results in creation of transient multimodal distributions. Results of simulations agree, at least qualitatively, with experimenal data.
A closure method is robust and can be used ragardless of the type of system simulated, including non-polynomial source terms and application of pointwise values of PDF if necessary.

The authors gratefully acknowledge the financial support from Solvay, France.

References

[1] E.B. Del Brio, J. Perote, Insur Math Econ. 51 (2012) 531-537.
[2] A.R. Gallant, D.W. Nychka, Econometrica. 55 (1987) 363–390.
[3] A.R. Gallant, G. Tauchen, Econometrica. 57 (1989) 1091–1120.
[4] I.M. Lifshitz, V.V. Slyozov, J. Phys. Chem. Solids. 19 (1961) 35-50.
[5] C. Wagner, Zeitschrift für Elektrochemie. 65 (1961) 581-591.

ECCE12
The 12th EUROPEAN CONGRESS OF CHEMICAL ENGINEERING
Florence 15-19 September 2019

Microwave processing of hydrocolloid membranes made with agro-industrial orange waste

Helbert Antonio Portugal Ochoa [1, *], Luis Felipe Miranda Zanardi [1]

1 San Agustin National University, Arequipa, Peru

**Corresponding author: helbertportugal@gmail.com*

Highlights

- Microwaves.
- Orange waste.
- Hydrocolloid membranes.

1. Introduction

The application of microwaves in the processing of different materials has a great potential because the dipolar polarization mechanism associated with it speeds up the heating and also different chemical reactions [1]. On the other hand, the agro-industrial residues of orange have in their composition mainly pectin, cellulose, hemicellulose and lignin [2], which can be used instead of being treated as waste.

2. Methods

Different solutions containing glycerin, pectin and orange waste, according to a mixture design, were homogenized and subjected to microwave radiation (2.45 GHz) for 2 minutes. After the radiation treatment, semi-rigid membranes were obtained, which were evaluated by tensile test (ASTM D638-14). In addition, the molecular structure of both the solutions and the resulting membranes were evaluated using FTIR infrared spectroscopy.

3. Results and discussion

Through infrared spectroscopy, important changes were observed in the hydroxyl group band after exposure to radiation. The presence of glycerin in high concentrations favored the formation of intermolecular hydrogen bonds, which was evidenced in low energy OH bands. On the other hand, the presence of high concentrations of pectin or lignocellulosic residues meant high energy bands, which implied that few intermolecular forces were generated due to the presence of branches in the polymer chains, mainly in the residues. In the mechanical evaluation, the tensile strength and the nominal strain at break were obtained as responses. The strength was greater in the presence of pectin and lower when the proportions of citrus or glycerin residues increased, this because the glycerin tends to increase the intermolecular spaces and weakens the polymer-polymer forces. The strain was more dependent on the presence of residues than glycerin. The higher the residue concentration, the lower the deformation. These results are explained by the weak interaction between glycerin and polymer chains with branches.

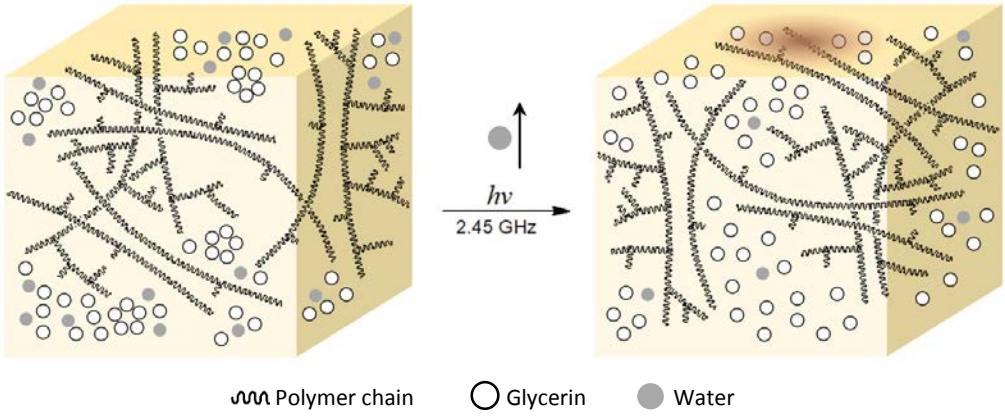

Figure 1. Effect of microwave radiation in mixtures of glycerin and orange waste.

4. Conclusions

Microwave processing of solutions containing pectin, glycerin and orange waste generates hydrocolloid membranes with acceptable mechanical properties because the radiation improves intermolecular forces.

References

[1] P. Lidström, J. Tierney, B. Wathey, J. Westman, Tetrahedron 57 (2001) 9225-9283.
[2] G. Aravantinos, V. Oreopoulou, C. Tzia, C.D. Thomopoulos, LWT 27 (1994) 468-471.

Novel bio-based polybenzoxazine/epoxy materials for self-healing and/or shape memory applications

Aleš Ručigaj, Rok Ambrožič, Matjaž Krajnc

University of Ljubljana, Faculty of Chemistry and Chemical Technology, Večna pot 113, 1000 Ljubljana, Slovenia

**Corresponding author: Ales.Rucigaj@fkkt.uni-lj.si*

Highlights

- Bio-based polybenzoxazine/epoxy (co)polymers were targeted designed.
- The DSC study showed several overlapping curing mechanisms.
- The prepared advanced materials showed self-healing and/or shape-memory potential.

1. Introduction

The growing demand for advanced materials synthesis along with the negative impact of classic petrol-based products on the environment forced both academic and industrial researchers to find new development pathways towards bio-based materials production. Preparation of polybenzoxazines, which are a newly developed class of thermosetting material with excellent thermal and mechanical properties, may be considered as a promising way to unlock different renewable resources, such as natural phenols and amines, and enable preparation of novel smart materials. In this context, unique benzoxazine monomers with designed properties of the final material, such as self-healing and/or shape memory ability, were synthesized from naturally occurring chemicals. To enhanced chain mobility, which should have a beneficial effect on self-healing and shape memory properties, bio-based epoxy resins were introduced and thermally copolymerized with benzoxazine monomers to form a final copolymeric network.

2. Methods

Chemical structure and thermal behavior of newly synthesized benzoxazine monomers were characterized by ^{1}H and ^{13}C NMR technique and DSC analysis, respectively. Once benzoxazine-epoxy (co)polymeric networks were formed by thermally induced ring-opening polymerization, mechanical properties of resulting material were investigated by DMA measurements. Final smart material shape memory and/or self-healing behaviors were quality and quantity studied by visual examinations and by performing DMA cycles and tensile stress tests, respectively.

3. Results and discussion

Initially, novel benzoxazine monomers were synthesized from bio-based phenols (resorcinol, diphenolic acid and cardanol) and amines (octadecylamine and series of polyether diamines), according to the standard procedure. Once benzoxazine monomers were fully characterized, thermal cross-linking and/or (co)polymerization with commercially available bio-based epoxy resin (resorcinol diglycidyl ether) took place. Recently published studies show excellent epoxy-

benzoxazine compatibility through ether linking copolymerization and formation of 3-dimensional structure. The DSC study of the cross-linking process indicates various curing mechanisms, such as thermally stimulated benzoxazine ring-opening, benzoxazine homopolymerization, benzoxazine catalysed epoxy ring-opening and epoxy-benzoxazine copolymerization, might occur. Moreover, by introducing epoxy resin into the polybenzoxazine network, higher chain flexibility, favourable for self-healing and shape memory ability, was formed. Therefore, all tested materials possessed thermally assisted shape memory (Figure 1), at least to a certain extent. In addition, final material properties can be target designed by suitable selection of raw materials. For instance, chemicals rich with aliphatic chains (from cardanol, octadecylamine and polyether diamines) resulted in higher chain flexibility, while chemicals rich with aromatic rings (from resorcinol, diphenolic acid) gave more rigid structure.

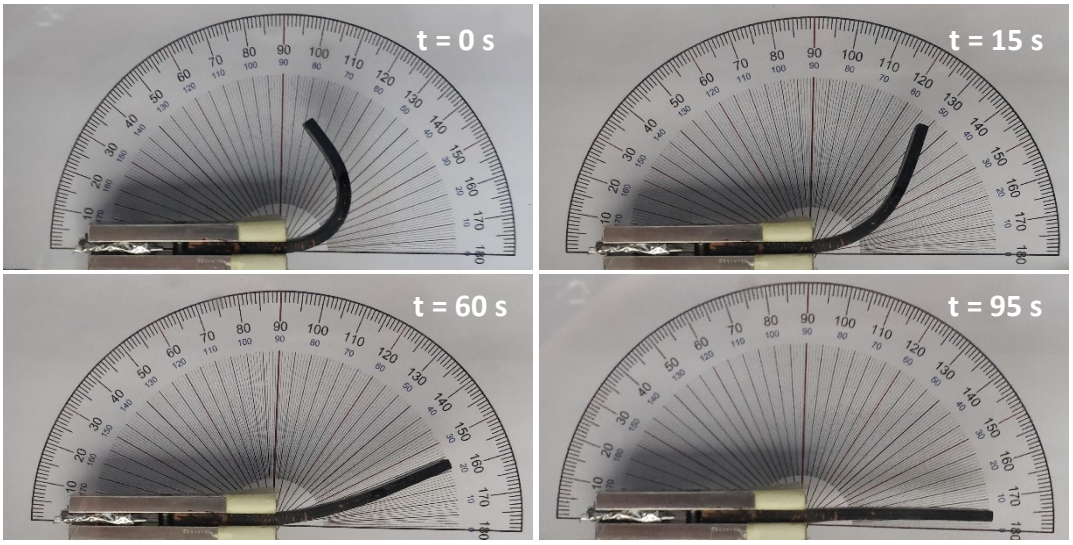

Figure 1. Thermally assisted shape memory effect of benzoxazine/epoxy copolymer based on resorcinol and octadecylamine.

Furthermore, self-healing ability of polybenzoxazines was accomplished by incorporation of additional site groups (COOH) capable of an extra intermolecular and intramolecular hydrogen bonding formation, which enables connection and reconnection between several bonding sections, leading to self-healing effect.

4. Conclusions

Bio-based polybenzoxazine/epoxy (co)polymers, as promising building blocks for advanced materials, were targeted designed, depending on selected starting chemicals. Such an approach represents significant applicative potential, since materials with shape memory, self-healing or even both effects (SMASH) can be optionally prepared.

References

[1] M. Arslan, B. Kiskan, Y. Yagci, Macromolecules 48(5) (2015) 1329-1334.
[2] Y.F. Liu, J.B. Huang, X.H. Su, M. Han, H. Li, M.T. Run, H.Z. Song, Y.G. Wu, React Funct. Polym. 102 (2016) 62-69.
[3] X.F. Luo, P.T. Mather, Acs Macro Lett. 2(2) (2013) 152-156.
[4] S. Rimdusit, M. Lohwerathama, K. Hemvichian, P. Kasemsiri, I. Dueramae, Smart Mater. Struct. 22(7) (2013) 12.

ECCE12
The 12th EUROPEAN CONGRESS OF CHEMICAL ENGINEERING
Florence 15-19 September 2019

Incorporation of paper sludge in clay mixtures used for fired-clay bricks manufacturing: understanding the bleaching phenomena issue observed on industrial products

Noémie Courtois[1,2], Isabelle Pochard[2], Jean-Yves Hihn[2], Laurent Tourneret[1]

1 Wienerberger, Laboratoire Central R&D, 25770 Franois, France; 2 Institut UTINAM, UMR6213CNRS, 25000 Besançon, France

**Corresponding author: noemie.courtois@wienerberger.com*

Highlights

- Brick manufacturing recycles paper mill sludge produced by waste water treatment.
- Drying and thermal insulation brick properties are improved by PS incorporation.
- PS can be degraded over time by bacterial decomposition process.
- Degradation produce intermediate compounds responsible for bleaching of products.

1. Introduction

Paper manufacturing produces large amounts of sludge residue, which is the final product of their waste water treatment process. Incorporation in clay brick formulation is one of the recycling alternatives for these wastes. Using paper sludge (PS) in bricks manufacturing [1] has two major advantages: due to the hydrophilic effect of vegetal fibers present in sludge, the drying is optimized and porosity is created by the fibers combustion during firing process. However, the organic matter present in PS, particularly cellulosic fibers, can be degraded over time by bacterial decomposition. This can lead to problematic phenomena on brick products like surface bleaching.

2. Methods

Paper sludges used in brick manufacturing are produced by several paper mills, which leads to various properties and compositions. In order to investigate which PS parameters are responsible for surface bleaching, four PS with different compositions, namely PS-1 to PS-4, were studied. The PS composition, principally fiber and calcium hydroxide contents, were determined by loss-on-ignition measured at 400°C and 1050°C respectively. Then, five mixtures were studied: a pure clay mixture used as reference (MR-0) and four mixtures obtained by incorporating the four different PS (MR-PS1 to MR-PS4) in the clay mixture in 88:12 mass clay:paper proportions. The drying property was characterized by the diffusivity coefficient of the ceramic samples, representing the drying speed of the products. This coefficient was determined by measuring the mass and dimensions of the samples in wet state, during drying and in dried state. Porosity of the fired products was evaluated by determining the rate of water absorption by the samples after water immersion for 2h under vacuum at 500mmHg. The surface of the samples (with bleaching problematic or not) were analyzed by IR-ATR spectroscopy between 2000cm^{-1} and 400 cm^{-1}.

3. Results and discussion

PS-2 has the highest fiber content and the lowest calcium hydroxide content, while PS-3 and PS-4 have the lowest fiber content and high calcium hydroxide content. PS-1 is intermediate (Fig 1). The analysis of the clay/PS mixtures shows that MR-PS2 and MR-PS4 have a particularly low diffusivity coefficient ($1.8.10^{-9}$ against 2.10^{-9} m²/s). The porosity is significantly greater when PS is incorporated in clay phases (increase of 4 to 7% between reference mixture and MR-PS mixtures). MR-PS1 presents the greater porosity while the three other MR-PS blends have a similar porosity at 21-22%.

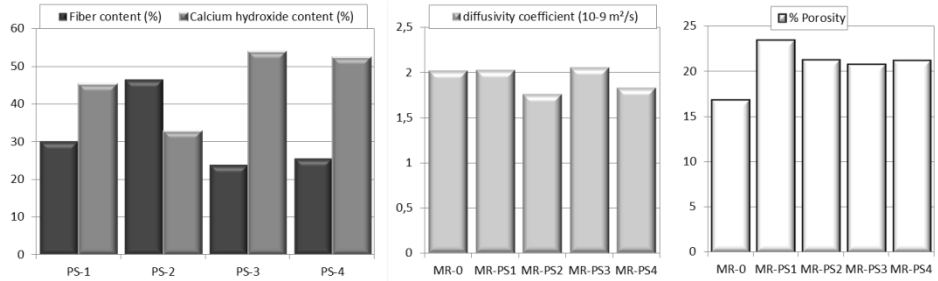

Figure 1. Compositions of the four paper sludges analyzed and properties of the five clay/PS mixtures.

A bleaching is observed on the MR-PS-2 and MR-PS-4 surfaces after drying (not shown). The FT-IR-ATR spectroscopy analysis reveals peaks at 1440 and 1560 cm^{-1} and a small one at 1300cm^{-1} (Fig 2). These vibration modes are absent on the other samples and thus, are characteristic of the compounds responsible for the bleaching.

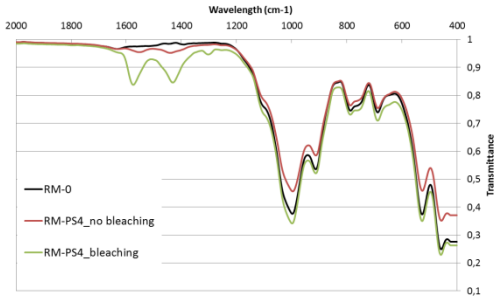

Figure 2. IR-ATR analyses of MR-0 and MR-PS4 with or without bleaching.

These characteristic peaks can be assigned to symmetric C-O stretching vibration, antisymmetric C-O stretching vibrations and symmetric methyl bending vibration of acetate anion respectively [2]. This means that bleaching at brick surfaces is due to the presence of organic compounds with carboxylate anion, like acetate salt. These organic compounds are formed during the bacterial anaerobic degradation of the cellulosic content of the PS [3].

4. Conclusions

The incorporation of PS in fired-clay brick formulation has several benefits. It also can lead to problematic phenomena like surface bleaching. This phenomenon is due to the presence of organic molecules in PS produced by cellulose degradation.

References

[1] V.Mymrim. Applied Clay Science, 2015, 107, 28-35.
[2] R.Frost, A.Musumeci. Spectrochimica acta Part A, 2007, 67 (3-4), 649-661.
[3] T.Meyer, E.Edwards. Water Research, 2014, 65, 321-349.

NETmix Technology for the continuous production of Pickering emulsions of hydroxyapatite nanoparticles

Andreia Ribeiro[1,2], Yaidelin A. Manrique[3], Isabel C.F.R. Ferreira[2], Maria F. Barreiro[2,3], José C.B. Lopes[1*], Madalena M. Dias[1]

1 Laboratory of Separation and Reaction Engineering – Laboratory of Catalysis and Materials (LSRE-LCM), Faculdade de Engenharia, Universidade do Porto, Portugal; 2 Centro de Investigação de Montanha (CIMO), Instituto Politécnico de Bragança, Portugal; 3 Laboratory of Separation and Reaction Engineering – Laboratory of Catalysis and Materials (LSRE-LCM), Instituto Politécnico de Bragança, Portugal

**Corresponding author: lopes@fe.up.pt*

Highlights

- Nanometric hydroxyapatite (n-HAp) was used to stabilize Pickering emulsions.
- Stable Pickering emulsions (PE) were successfully prepared in batch mode.
- NETmix technology allows the production of PE in continuous mode.

1. Introduction

Mixtures of two immiscible liquids – emulsions – are commonly used, and play an important role in several product's formulations. Examples include food, pharmaceuticals and personal care products [1]. Traditionally, their stabilization is achieved by one, or more, chemical emulsifiers, but it's can have limited use due thermodynamic instabilities, and due health problems because start to be associated with allergic reactions and carcinogenicity [1,2].

Pickering emulsions (PE) arise as an alternative to traditional emulsions and are receiving significant attention at industrial and academic level. In fact, the solid particles are able to be positioned in the oil-water interface forming a thicker barrier, acting as an emulsion stabilizers [3]. The "surfactant-free" character made PE more suitable for various applications, particularly in food area [1,3].

Hydroxyapatite (HAp) has been described as a suitable Pickering stabilizer, it tends to stabilize O/W emulsions due to its hydrophilicity [4,5]. Nowadays, previous works are focused in the production of PE using bath processes [1,2]. Aiming at achieving a more feasible industrial process, in this work, the NETmix technology is used for the first time to produce PE in continuous mode with high reproducibility. The NETmix was developed at the Associate Laboratory LSRE-LCM, it consists in a network of static mixing chambers interconnected by transport channels (Figure 1 A and B) [6].

2. Materials and Methods

To produce green PE**,** sunflower oil and water containing dispersed n-HAp were used as oil and aqueous phases, respectively. Two process were performed: *i*) batch mode (Figure 1 C): the mixing system was comprised by a high-speed homogenizing device Miccra D-9, a thermostatic bath and a peristaltic pump, the sunflower oil was injected into n-HAp aqueous phase; and *ii*) continuous mode (Figure B): in this process, both phases are feed into NETmix in a pre-mixed mode, with the total flow rate adjusted according to the desired Reynolds number (Re).

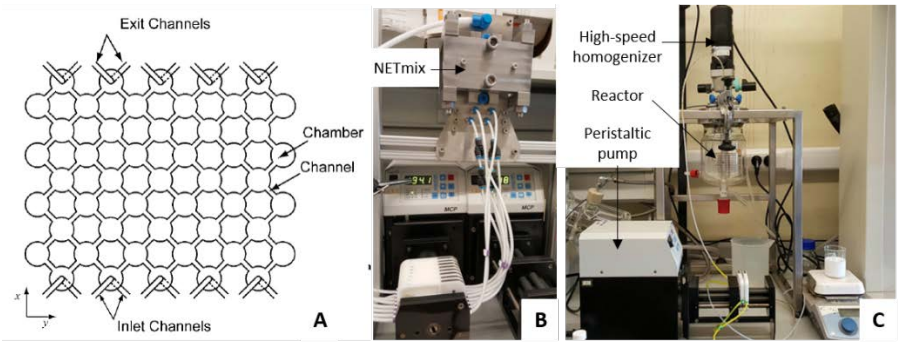

Figure 1. NETmix schematic representation (A). Experimental setup: NETmix (B) and batch (C).

3. Results and discussion

The PE were produced considering the relevant parameters affecting their stability, namely solids content and oil-water ratio. For both, batch and continuous (NETmix), a stable emulsion was achieved with 20-80 as the oil-water ratio and 5 %wt. of n-Hap. In batch mode, the average diameter of the oil droplets ranged between 10-25 µm (Figure 2 A). By cryo-SEM analysis was observed PE droplets with n-HAp layer around oil core (Figure 2 B), the EDS analysis (data not shown) confirmed the presence of these materials. This PE was stable for more than 8 weeks.

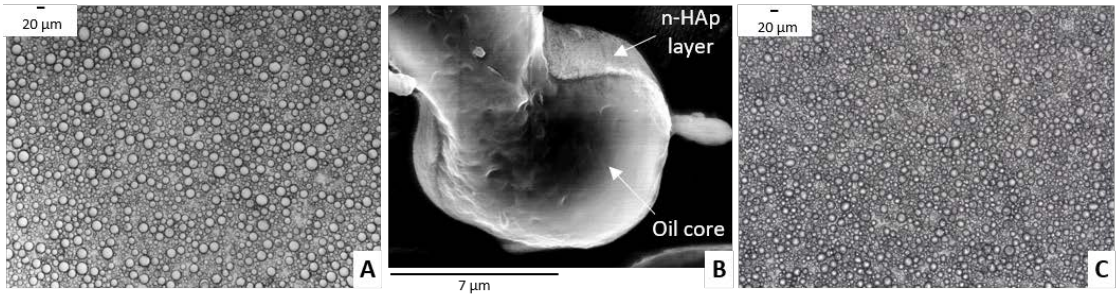

Figure 2. PE images: (A)- optical and (B) – cryo-SEM obtained by batch mode, and (C) – optical obtained using NETmix.

Regarding the production in continuous mode, preliminary results indicate that it is feasible to use the NETmix technology to produce PE. The achieved results are quite promising for Re ~500, the formed PE have average diameters of 5-7 µm (Figure 2 C) being smaller than obtained in batch mode.

4. Conclusions

Stable PE were produced using n-HAp as stabilizers with size distributions ranged between 10 to 25 µm (batch mode) and 5 to 7 µm (continuous mode). Moreover, the NETmix reactor can enable the production of these emulsions at pilot/industrial scale.

References

[1] X Li, J. Zhu, Y. Pan, R. Meng, B. Zhang, H. Chen, Food Hydrocolloids 90 (2019) 19-27.
[2] Y. Yang, Z. Fang, X. Chen, W. Zhang, Y. Xie, Y. Chen, W. Yuan, Front Pharmacol 8 (2017) 287.
[3] C. Berton-Carabin, K. Schroen, Annu Rev Food Sci Technol 6 (2015) 263-297.
[4] M. Zhang, A. Wang, J. Li, Y. Song, R. He, Mater. Sci. Eng. C, 70 (2017) 396-404.
[5] S. Fujii, M. Okada, T. Nishimura, H. Maeda, T. Sugimoto, H. Hamasaki, Y. Nakamura, J. Colloid Interface Sci. 374 (2012) 1-8.
[6] P.E. Laranjeira, A.A. Martins, J.C.B.Lopes, M.M.Dias, AIChem J. 55 (2009) 2226-2243.

Characterization of coccoliths from *Emiliania huxleyi* cultivations

Ulrich Teipel[1,3], Makrina A. Chairopoulou[1], Clara Pereyra[2],

1 TH Nürnberg Georg Simon Ohm, Faculty of Process Engineering, FPR, Wassertorstrasse 10, 90489 Nuremberg Germany; 2 Universidad of Cádiz, Departamento de Ingeniería Quimíca y Technología de Alimentos, Facultad de Ciencias, Avda. República Saharaui s/n, 11510 Ruerto Real, Spain; 3 Ulm University, Institute of Chemical Engineering, Albert-Einstein-Allee 11, 89081 Ulm

**Corresponding author: makrina.chairopoulou@th-nuernberg.de*

Highlights

- Characterization of biogenic particles.
- Wetting properties of coccoliths.
- Size estimations of oblate particles.

1. Introduction

The marine alga *Emiliania huxleyi*, one of the many species of the Coccolithophorida family was cultivated in this study with the intention to produce coccolith particles [1]. Coccolithophores are an extend group of calcifying unicellular algae found in the photic zone of oceans, best known for their ability to produce micron-sized calcareous platelets called coccoliths. Assumed to be responsible for half the existing global amount of calcium carbonate [2] their role in stabilizing the carbonate cycle is considered important as are also the data that have been retrieved from fossil particles for past climate conditions. Depending upon environmental availability, the algae are known to embed various elements in the particles' structure resulting to slight different chemical compositions which enables reconstruction of past temperatures [3]. Coccoliths are composed of radially oriented calcite crystals and organic matter and are the focus of this study. As they are biologically produced it is impossible to reconstruct them synthetically and remain therefore a unique structure of calcium carbonate. The particles are here characterized and efforts are being made to cover a literature gap surrounding their properties.

2. Methods

After recovering intact coccoliths from fresh cultivations the material was characterized chemically (ICP-OES), while particular attention was placed on its surface chemistry (Zeta Potential, FTIR). The above results aided a better understanding of the material's wetting behavior, estimated with the liquid penetration method and the Owens Wendt Rabel Kaelble (OWRK) model [4]. The surface free energy of the material was compared with synthetically $CaCO_3$, chalk and comminuted oyster shells, three broadly used calcium carbonate sources. Further the particular form of coccoliths, resembling that of an oblate disc, helped compare commonly used particle size estimation techniques and evaluate their applicability for non-spherical particle systems.

3. Results and discussion

The surface free energy (SFE) of coccoliths was found to be similar to that of the comminuted oyster shells, with values of 27.6 and 26.03 $mN \cdot m^{-1}$ respectively. The highest SFE was noted for the synthetically produced $CaCO_3$ at 34.7 $mN \cdot m^{-1}$ while chalk showed the lowest value at 16.4 $mN \cdot m^{-1}$. Based on the OWRK model, coccoliths showed the highest polar part of their SFE. In contrast to that the synthetically produced $CaCO_3$ showed the lowest polar part. These findings are particular valuable in all processes where the material comes into contact with a fluid.

In the second part of this study the influence of oblate shaped particles on size measuring techniques was reviewed. By comparing results obtained from an analytical (LUMsizer) and a differential (DCS) centrifuge and a laser diffraction spectrometer (LDS) with microscopic image size evaluations (LM), it was found that LDS results at better representing the true size of the particles.

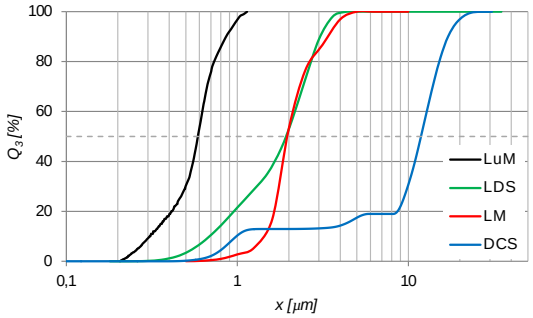

Figure 1. Particle size distribution (Q_3) measured by different techniques for coccoliths.

Figure 1 shows four cumulative distributions measured for coccoliths. The particles are depicted finer with the analytical centrifuge ($x_{50,LUM}$ = 0.79 µm; LumiSizer). The median of the LDS (Helos KR; Sympatec) and LM (Axiotech 100 HD camera; Zeiss) methods was estimated at 1.92 µm and 1.9 µm respectively. As seen from the figure above, the two curves seem to deviate mostly in the finer region with LDS depicting particles finer than they probably are. Continuing with the differential centrifugal sedimentation (CPS) the media was estimated at $x_{50,CPS}$ = 11.87 µm.

4. Conclusions

Through the liquid penetration method, the surface free energy of four calcium carbonate materials could be estimated. The differences in the polar components can be attributed to the presence of organic materials, confirmed also through FTIR analysis, that can stabilize the surface by neutralizing the surface charge.

Considering the particular shape of coccoliths and observing the results presented in **Figure 1** it was concluded that laser diffraction analysis best suited the requirements of the system and represented the distribution of the particles. By comparing the four methods for different shaped particles it could be eliminated that the measuring deviations displayed a measuring inaccuracy.

References

[1] N. Krumov, Green biosynthesis of Nanoparticles: Mechanisms and Applications, Berforts Information Press Ltd., UK, 2013
[2] C. de Vargas, Evolution of primary producers in the sea, first ed., Elsevier Inc., China, 2007
[3] H. M. Stoll, Geochemistry, Geophysics, Geosystems, Tech. Brief, Volume 2, (2001)
[4] U. Teipel, I. Mikonsaari, Part. Part. Syst. Charact. 21 (2004) pp. 255–260

ECCE12
The 12th EUROPEAN CONGRESS OF CHEMICAL ENGINEERING
Florence 15-19 September 2019

Removal of pharmaceuticals with supported ionic liquids

Márcia C. Neves*, Maria Santos, Beatriz Rocha, Guilherme Lobo-Sousa, Sandra C. Bernardo, Luciana Rocha, Hugo Almeida, Mara Freire

Department of Chemistry and CICECO-Aveiro Institute of Materials, University of Aveiro, 3810-193 Aveiro, Portugal

mcneves@ua.pt

Highlights

- Supported Ionic Liquids are efficient adsorbents for pharmaceuticals.
- Sodium diclofenac, ketoprofen, naproxen and acetylsalicylic acid undergo different adsorption processes onto SILs.
- Different ionic structures as counter ions in SILs lead to different adsorption processes.

1. Introduction

The presence of organic pollutants has been shown to have potentially adverse effects on man and the environment. Mainly due to their large worldwide consumption, active pharmaceutical ingredients (APIs) were already found in a wide variety of environmental aqueous samples, in concentrations ranging from ng/L to µg/L. This is due to the inability of current technologies used in sewage treatment plant (STPs) and wastewater treatment plants (WWTPs) to remove such compounds, thus leading to serious environmental and public health concerns after long-term exposures. Therefore, the treatment of water contaminated with these compounds is extremely important.

Ionic liquids (ILs) have a great potential to remove biomolecules from aqueous solutions [1], including pharmaceuticals [2]. Despite the many advantages associated to ILs, their immobilization in materials would overcome some leaching problems. ILs can be immobilized on solid supports by the covalent bonding of the cation, resulting in functionalized materials: supported ionic liquids (SILs). Based on the high potential of SILs in separation/removal techniques and on the health and environmental concerns that we aim to overwhelm, silica based SILs will be investigated to develop an efficient approach to remove pharmaceuticals from aqueous solutions.

2. Methods

SILs were obtained as described in the literature [3]. Silica gel 60 was used as supported for SILs synthesis, namely SilPrMImCl, SilPrNEt$_3$Cl, SilPrNBu$_3$Cl SilPrN(C$_8$)$_3$Cl, SilPrNMe$_2$BuCl (Figure 1). Five additional SILs were prepared from SilPrMImCl by anion exchange with the correspondent sodium salts, namely SilPrMImSCN, SilPrMImN(CN)$_2$, SilPrMImTos, SilPrMImMale and SilPrMImNTf$_2$.

3. Results and discussion

Adsorption kinetics and adsorption isotherms were performed for sodium diclofenac, ketoprofen, naproxen and acetylsalicylic acid with the synthetized SILs. The supported ionic liquid SilPrMImCl

showed to be the most efficient material for the adsorption of sodium diclofenac, ketoprofen and naproxen, being the removal efficiency 91, 51 and 59%, respectively. For sodium diclofenac, the obtained adsorption equilibrium data are well described by the Langmuir or the Freundlich isotherm models, being dependent on the imidazolium supported materials counter ion. A maximum equilibrium concentration of sodium diclofenac in the solid phase of 240 $mg.g^{-1}$ of adsorbent was obtained with SilPrMImCl. Regarding the ketoprofen and naproxen the obtained adsorption equilibrium data are best described by the Langmuir-Freundlich (or Sips) isotherm model and a maximum equilibrium concentration for these pharmaceuticals of 88 and 41 mgg^{-1} was obtained with SilPrMImCl.

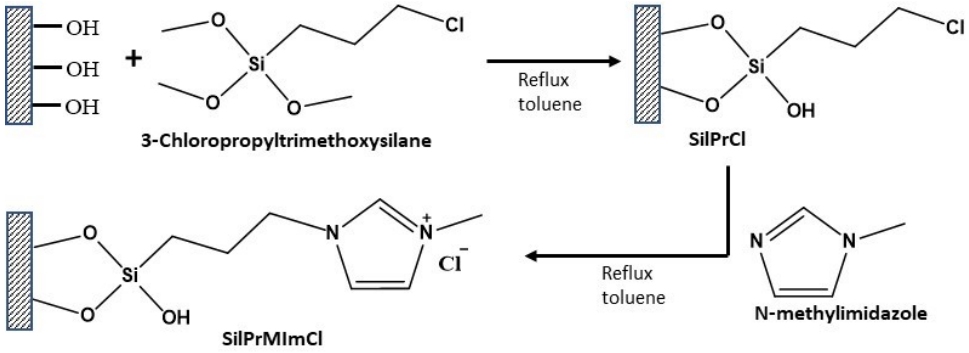

Figure 1- Synthetic route for SilPrMImCl.

In the case of acetylsalicylic acid, the equilibrium concentration of adsorbate in the solid phase decreases in the following sequence of SILs: $SilPrNMe_2BuCl$ > $SilPrNBu_3Cl$ > $SilPrN(C8)_3Cl$. The obtained adsorption equilibrium data are best described by the Langmuir model with a maximum equilibrium concentration of adsorbate in the solid phase of 220 mg of drug per gram of $SilPrNMe_2BuCl$.

4. Conclusions

The synthetized SILs are efficient adsorbents for pharmaceuticals. However, the adsorption mechanisms and maximum equilibrium concentrations depend on the SILs chemical structure and on the drug.

Acknowledgments

This work was developed within the scope of the project CICECO-Aveiro Institute of Materials, FCT Ref. UID/CTM/50011/2019, financed by national funds through the FCT/MCTES. This work is funded by national funds (OE), through FCT – Fundação para a Ciência e a Tecnologia , I.P., in the scope of the framework contract foreseen in the numbers 4, 5 and 6 of the article 23, of the Decree-Law 57/2016, of August 29, changed by Law 57/2017, of July 19. M.C. Neves acknowledge the Individual Scientific Employment Stimulus CEECIND/00383/2017.

References

[1] S.P.M. Ventura, F.A. e Silva, M. V. Quental, D. Mondal, M.G. Freire, J.A.P. Coutinho, Chem. Rev., 117 (2017) 6984–7052.
[2] H.F.D. Almeida, I.M. Marrucho, M.G. Freire, , ACS Sustain. Chem. Eng., 5 (2017) 2428–2436.
[3] H. Qiu, S. Jiang, X. Liu, J. Chromatogr. A, 1103 (2006) 265–270.

Investigation on the Limiting Oxygen Index of bitumen-organoclay nanocomposites

Miriam Cappello, Giovanni Polacco and Sara Filippi*

Dipartimento di Ingegneria Civile e Industriale, Università di Pisa, Largo Lucio Lazzarino 2, 56122 Pisa, Italy

**Corresponding author: sara.filippi@unipi.it*

Highlights

- Two clays were used to obtain exfoliated or intercalated bitumen nanocomposites
- A reduction of the limiting oxygen index LOI was observed on bitumen mixtures
- TGA analysis showed strong variations in the decomposition kinetic of the bitumen
- Organoclays significantly interact with the binder, modifying its colloidal structure

1. Introduction

Bitumen is a complex mixture of hydrocarbons that are quite flammable and tend to produce smoke and poisonous gases while burning. This is an important aspect in the case of fire events in highway tunnels. Organoclays are well-known fire retardants in the polymer field and have been recently introduced in bituminous binders. The effect of native and organo-modified clays on the fire resistance has been evaluated [1–4], but the chemical-physical interaction mechanism between bitumen and clay has not been investigated yet. Therefore, the main object of this study is to provide a first insight in this direction. For this reason, two organoclays with different degree of interaction with a base bitumen were used in order to obtain both exfoliated and intercalated nanocomposites. The blends were characterized by WAXD, Brookfield viscosity, LOI test and TGA analysis.

2. Methods

The two clays were Cloisite 20A and Cloisite 30B (referred as 20A and 30B) from Southern Clay Products and derive from a sodium montmorillonite by treatment with dimethyl-dihydrogenated-tallow ammonium chloride (20A), and methyl-tallow-bis-2-hydroxyethyl ammonium chloride (30B). Bitumen is a 50/70 penetration grade base bitumen, referred as B, kindly furnished by Eni. Bitumen-clay mixtures were prepared with a high shear mixer Silverson L5T at 4000 rpm, 140 °C for 30 minutes. Wide angle X-ray diffraction (WAXD) was made in reflection mode by a Siemens D500 Krystalloflex 810 apparatus, with a wavelength of 0.1542 nm at a scan rate of 2.0 °/min. Viscosity was measured at 135 °C by a Brookfield viscometer. Thermo-Gravimetric Analysis (TGA) was performed in air using a Q500 by TA Instruments. The LOI test was performed by LOI-Smoke-230, from Dynisco & Alpha Technologies, USA.

3. Results and discussion

From WAXD, after mixing with bitumen, 20A has an intercalated structure with interlayer distance of 4.3 nm and 30B has a prevailingly exfoliated structure (Fig. 1). In the case of polymer nanocomposites, clay exfoliation means high interaction between the matrix and the filler, good

interfacial adhesion, increased viscosity. Moreover, exfoliation improves the flame retardant properties of the materials because the delaminated platelets produce a labyrinth path to oxygen diffusion, thus decreasing the combustion kinetic. Surprisingly, the B/30B mixtures, which have a dominating exfoliated structure, did not show a significant viscosity increasing (Table 1). On the contrary, B/20A mixtures, which have an intercalated structure, showed a high increase in the binder viscosity. Both clays decrease the LOI value (Table 1) and this effect is more pronounced with clay 20A. The TGA derivative weight curves as a function of temperature are reported in Figure 2 for B, B/20A-4 and B/30B-4. The TGA spectra are significantly altered with respect to base bitumen even in the presence of small clay quantities. Moreover, there seems to be a direct correlation between LOI and the weight loss path of the binders.

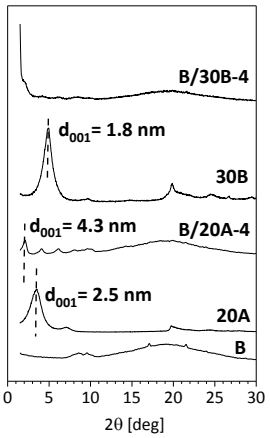

Figure 1. WAXD of B, 20A, 30B, B/20A-4 and B/30B-4.

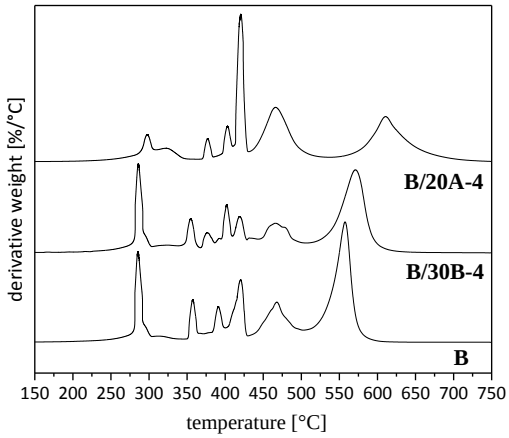

Figure 2. TGA derivative weight curves as a function of temperature for B, B/30A-4 and B/20A-4

Table 1 – LOI, viscosity and TGA data for the binary mixes.

Blend	Clay content (wt %)	LOI	Viscosity (135 °C, cP)
B	0	28	450
B/20A-2	2	26	608
B/20A-4	4	25	2304
B/20A-8	8	22	17000
B/30B-2	2	28	471
B/30B-4	4	29	542
B/30B-8	8	24	850

4. Conclusions

The organoclays significantly interact with the binder, thus modifying its colloidal structure. This effect prevails on the above-mentioned labyrinth-effect related to the presence of exfoliated or intercalated platelets in the bitumen matrix.

References

[1] P.M. Visakh Yoshihiko Arao, Flame Retardant Polymer Blends, Composites and Nanocomposites, Springer International Publishing, Switzerland, 2015

[2] C.A. Wilkie, Morgan AB. Fire retardancy of polymeric materials, second ed., CRC Press, USA, 2010.

[3] A. Bonati, F. Merusi, G. Polacco, S. Filippi, F. Giuliani, Constr. Build. Mat. 37 (2012) 660-668.

[4] A. Bonati, F. Merusi, G. Bochicchio, B. Tessadri, G. Polacco,S. Filippi, et al. Constr. Build. Mat. 47 (2013) 990-1000.

ECCE12
The 12th EUROPEAN CONGRESS OF CHEMICAL ENGINEERING
Florence 15-19 September 2019

Synthesis, electronic polarizability and optical basicity of a novel zinc phospho-tellurite glass

L. Boroica[1], B. A. Sava[1], M. Elisa[2], R.C. Stefan[2], I. C. Vasiliu[2], S. M. Iordache[2], A. C. Galca[3], V. Kuncser[4]

[1]*National Institute for Laser, Plasma and Radiation Physics, 409 Atomistilor Str, 077125 Magurele, Romania*
[2]*National Institute of R & D for Optoelectronics, INOE 2000, 409 Atomistilor Str., 077125, Magurele, Romania*
[3]*National Institute of Materials Physics, 405 A bis Atomistilor Str, 077125 Magurele, Romania*

[4]*National Institute of Materials Physics, 405 A bis Atomistilor Str, 077125 Department of Magnetism and Superconductivity, Magurele, Romania*

**Corresponding author:* boroica_lucica@yahoo.com

Highlights

- A novel zinc phospho-tellurite glass was synthesized for applications in photonic field
- Optical band gap was graphically determined based on optical absorption property
- Metallization criterion in dependency on different physical properties was evaluated
- Electronic polarizability was investigated in correlation with optical basicity

1. Introduction

The present work is focused on the investigation of optical properties, electronic polarizability, optical basicity and other physical features of a novel zinc phospho-tellurite glass, as good candidate for photonic devices. Based on the refractive index and optical band gap, molar refractivity and polarizability have been calculated that, in turn, is decisive for optical basicity [1, 2].

2. Methods

The vitreous material prepared in this work belongs to the 45ZnO $10Al_2O_3$ $40P_2O_5$ $5TeO_2$ system (code Te-5, taking into account the amount of TeO_2 in mol. %) being characterised by a chemical stable composition. The glass has been prepared by a non-conventional wet route of processing the starting reagents followed by melting-stirring and annealing of the glass [3, 4]. In order to prepare a glass having a high optical homogeneity, the melt batch was mechanically stirred aiming to reduce the gaseous inclusions and grooves embedded in the bulk samples. The density of the glass was experimentally determined by hydrostatic method [1, 2], absorption coefficients was plotted based on experimentally optical transmission spectroscopy [1, 2]. The refractive index was measured at λ_D = 589 nm (yellow doubled D line of sodium) by means of the Pulfrich refractometer. Mott and Davis relationship was applied to graphically determine the optical band gap, E_g and, subsequently, polarizability, metallization criterion and optical basicity have been calculated [1, 2]. Other physical properties, such as molar volume, oxygen packaging density, reflexion loss and optical transmission have been calculated [1, 2].

3. Results and discussion

In the Table 1, Te-5 glass properties are presented: glass density (ρ_{glass}), average molecular mass (M_{av}), molar volume (V_M), oxygen packaging density (OPD), refractive index measured at 589 nm (n_D), refractive index measured from dispersion graph (n_{DD}), molar refractivity (R_m), electronic polarizability (α_m), reflection loss (R_L), optical transmission (T) (see Fig.1, absorption coefficient). Table 2 presents: refractive index-based non-bridging oxygen atoms polarizability ($\alpha_{O_2^-}(n)$), band gap-based non-bridging oxygen atoms polarizability ($\alpha_{O_2^-}(nE_g)$), optical band gap (E_g) (Fig.2), refractive index-bazed metallization criterion (M(n)), band gap-based metallization criterion (M(E_g)), Duffy optical basicity (Λ_D), refractive index based-polarizability-based optical basicity ($\Lambda(\alpha_{O_2^-}(n))$, band gap based-polarizability-based optical basicity ($\Lambda(\alpha_{O_2^-}(E_g))$ and Pauling optical basicity (Λ_P).

Table 1. Te-5 glass properties: ρ_{glas}, V_M, OPD, M_{av}, n_D, n_{DD}, R_m, α_m, R_L, T

ρ_{glass} g/cm^3	V_M cm^3/mol	OPD O atom/l$_{glass}$	M_{av} g/mol	n_D	n_{DD}	R_m cm^3/mol	α_m cm^3/mol	R_L	T
2,936	37,95	75	111,45	1,54616	1,54	12,02	$4.75 \cdot 10^{-24}$	0,046	0,912

Table 2. Te-5 glass properties: $\alpha_{O_2^-}(n)$, $\alpha_{O_2^-}(n)$, M (n), M (E_g), Λ_D, $\Lambda(\alpha_{O_2^-}(n)$, $\Lambda(\alpha_{O_2^-}(E_g)$, Λ_P

$\alpha_{O_2^-}(n)$ cm^3/mol	$\alpha_{O_2^-}(E_g)$	M(n)	M(E_g)	Λ_D	$\Lambda(\alpha_{O_2^-}(n)$	$\Lambda(\alpha_{O_2^-}(E_g)$	Λ_P
1.59	1.59	0,6832	0,6832	0,702	0,62	0,62	0,4617

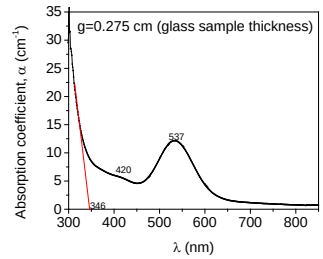

Fig.1. Optical absorption of Te-5 glass versus wavelength

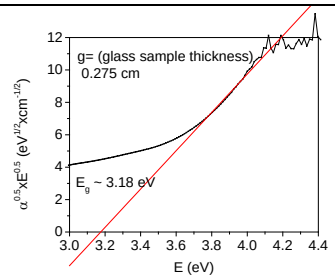

Fig. 2. Graphical determination of E_g for Te-5 glass

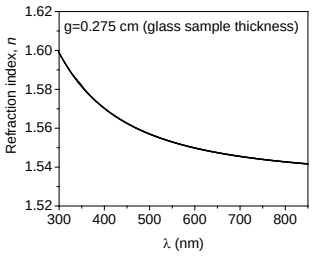

Fig.3. Refractive index dependence on wavelength for Te-5 glass

4. Conclusions

(i) Refractive index measured by Pulfrich refractometer is in a good accordance with the refractive index value determined from dispersion graph; (ii) the metallization criterion reveals an intermediate electrical conductivity vitreous material; (iii) Duffy optical basicity is relative close to refractive index-based polarizability- based optical basicity and to band gap-based polarizability-based optical basicity, respectively, but higher than Pauling optical basicity; (iv) based on optical basicity values it is worth to conclude that Te-5 oxide composition exhibits a relative high tendency to form a vitreous network structure.

References

[1] M. K. Halimah, M. F. Faznny, M. N. Azlan, H. A. A. Sidek, Results Phys. 7 (2017) 581–589.
[2] S. H. Elazoumi, H. A.A. Sidek, et.al., Results Phys. 8 (2018) 16–25.
[3] B. A. Sava, L. Boroica,, M. Elisa, O. Shikimaka, D. Grabco, M. Popa, Z. Barbos, R. Iordanescu, A. M. Niculescu, V. Kuncser, A. C. Galca, M. Eftimie & R. C. C. Monteiro, Ceram. Intern. 44 (6) (2018) 6016–6025.
[4] R. Iordanescu, M. Elisa, C. Vasiliu, B. A. Sava, L. Boroica, M. Valeanu, V. Kuncser, A. Volceanov, M. Eftimie, A. Melinescu, A. Beldiceanu, J. Non-Cryst. Solids 465 (2017) 55-58.

Acknowledgements: This work was supported by grants of the Romanian Ministery of Research and Innovation, CCCDI-UEFISCDI, projects PN-III-P1-1.2-PCCDI-2017-0871/47PCCDI/2018, PN-III-P1-1.2-PCCDI2017-0619/ 42PCCDI/2018, and PN 2019 LAPLAS VI, PN 2019 OPTRONICA VI and PN 2019 TEXMAV.

ECCE12
The 12th EUROPEAN CONGRESS OF CHEMICAL ENGINEERING
Florence 15-19 September 2019

Fixed-bed reactors from metal-foam pellets: experiments and CFD models

Gregor D. Wehinger[1], Ginu George[1], Stan T. Kolaczkowski[2],

Didier Beton[3], Leonhard Schmalhorst[3], and Lars Torkuhl[3]

1 Chemical and Electrochemical Process Engineering, Clausthal University of Technology; 2 Chemical Engineering, University of Bath, 3 Alantum Europe GmbH

**Corresponding author: wehinger@icvt.tu-clausthal.de*

Highlights

- Comprehensive and validated modeling approach for porous pellet fixed-beds.
- Synthetic bed generation gives realistic bed structure also for porous pellets.
- Porous resistance approach shows good results for pressure drop in full fixed beds.
- Explorative heat transfer study reveals promising characteristics of porous pellet beds.

1. Introduction

During the last two decades, a certain interest has arisen to apply open-cell solid foams as structured catalyst support. Kolaczkowski et al. compared pellets made from metal foams, see Figure 1, with monolith-foam structures in terms of pressure drop and heat transfer performance [1]. In the manufacturing process, different pellet shapes can be realized. The foam pellets showed advantages, especially due to their mixing behavior. However, a systematic investigation of the potentials and weaknesses of open-cell foam pellets applied in fixed-bed reactors is missing up to date.

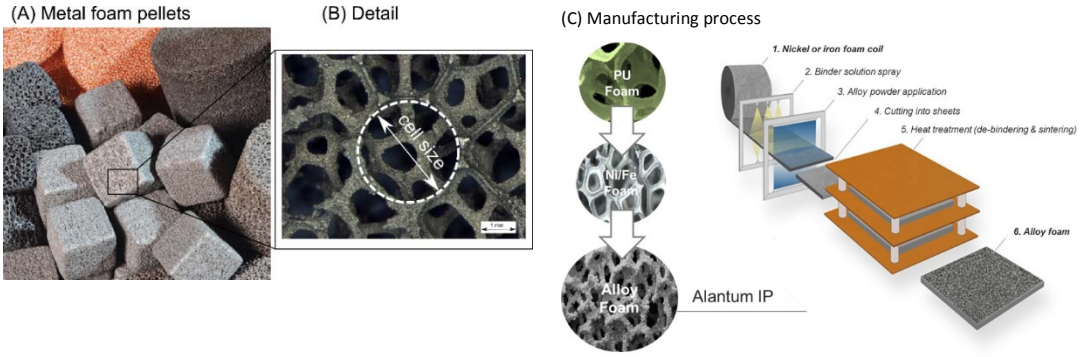

Figure 1: (A) Metal foam pellets with (B) details. (C) Manufacturing process of alloy metal foams.

2. Methods

In this contribution, the established particle-resolved CFD model [2] is transferred to fixed-bed reactors made of open-cell metal foams. The randomly oriented pellets forming the packed bed are captured geometrically. However, instead of resolving the inner structure of the foam, a pseudo-

homogeneous porous CFD-model is applied in order to describe the transport phenomena inside the porous foam pellets. Therefore, a pressure-drop [3] and an effective thermal conductivity correlation [4] are implemented into the model. The interstitial void is described with CFD and coupled with the porous pellet phase. Surface-to-surface radiation is included in the heat transfer simulations. The synthetic generation of fixed beds of foam pellets is validated against experimental x-ray computed tomography (µCT) data. This step is important, since the CFD results are highly sensitive to the underlying bed structure.

3. Results and discussion

In Figure 2, a comparison between µCT scanned structure and a synthetically generated bed is shown. There is an excellent agreement between simulation and experiments. In Figure 2 (D), the specific pressure drop over superficial velocity is illustrated for fixed-bed reactor made of porous cubes and porous cylinders. The agreement is reasonable between experimental data and the CFD simulations, which shows the accuracy of the model. The cubes show a larger pressure drop than the cylinders. Consequently, different pellet shapes are currently explored in terms of radial porosity distribution, pressure drop, and radial heat transfer characteristics.

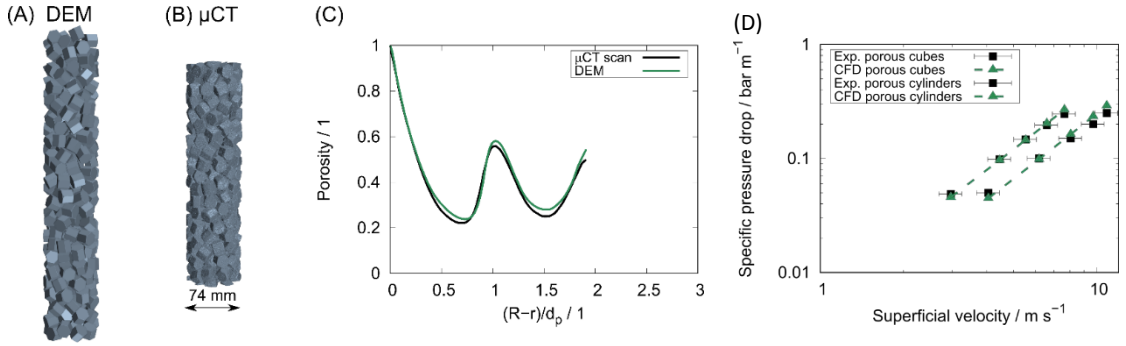

Figure 2. Bed structure in a 74 mm diameter tube with 16x15 mm hexagons. (A) DEM bed, (B) µCT scan, (C) radial porosity over normalized distance from wall. (D) Pressure drop: experiments vs. CFD for porous cubes (10 mm) and porous cylinders (15 mm).

4. Conclusions

We have shown that the synthetic bed-generation method developed in previous works can be applied also for porous pellets. This detailed CFD model was validated against µCT data of the bed structure and pressure drop over a packed bed. This numerical workflow allows the exploration of various novel pellet shapes, since it is independent of geometrical data. In the future, chemical reactions will be included to extend the model to catalytic fixed-bed reactors.

References

[1] Kolaczkowski, S. T., Awdry, S., Smith, T., Thomas, D., Torkuhl, L., & Kolvenbach, R. (2016). Catal. Today, 273, 221-233.
[2] Wehinger, G. D., Eppinger, T., & Kraume, M. (2015). Chem. Ing. Tech., 87(6), 734-745.
[3] Lacroix, M., Nguyen, P., Schweich, D., Huu, C. P., Savin-Poncet, S., & Edouard, D. (2007). Chem. Eng. Sci., 62(12), 3259-3267.
[4] Zhao, C. Y., Lu, T. J., Hodson, H. P., & Jackson, J. D. (2004). Mater. Sci. Eng., A, 367(1-2), 123-131.

ECCE12
The 12th EUROPEAN CONGRESS OF CHEMICAL ENGINEERING
Florence 15-19 September 2019

Chemically enhanced bitumen and road pavements of the future

Pilar Cabanillas[1*], María González[2], Vicente Pérez[2], Carlos Prieto[1], Juana Frontela[1]

[1] CEPSA Research Centre. Avda. Puntocom 1, 28805. Alcalá de Henares (Spain)

[2] CEPSA Comercial Petróleo. Ctra. Daganzo km 5.5. 28806. Alcalá de Henares (Spain)

*pilar.cabanillas@cepsa.com

Highlights

- A new generation of improved bituminous binders for paving solutions is being developed.
- Sustainability by developing long lasting materials with outstanding performance.
- Chemical modification of the base bitumen with additives is key to the project.

1. Introduction

The world is growing at a fast pace, a fact with great impact on the use of transport infrastructures and its weathering: more vehicles, heavy transports, roads with poor maintenance, climate change, etc.

Long-lasting pavements are currently a need for the higher demands of society, for the emerging economies where sustainability is a key factor to guarantee continuous growth. During the last decade, environmental aspects such as “life cycle inventory” or “carbon footprint” have gained importance and they have become familiar concepts to both the industry and the society. Therefore, improving durability of structures has become a goal for the paving industry [1, 2, 3].

In this work two strategies towards increasing sustainability of pavements have been studied, both of them focused in the bituminous binder. First, increasing the pavement durability by tuning the composition of bitumen in order to minimize the impact of aging processes and maximize the service life of pavements. Second, incorporating additives from either natural renewable sources or waste materials from other industries with the ability of restoring the damage resulting from aging phenomena (rejuvenating) or preventing it.

2. Methods

A set of model bitumen with different chemical compositions was produced using two different industrial processes (straight run and mild oxidation process) both at pilot and industrial scale. The materials obtained were fully analyzed according the current European Standard (EN 12591) and its chemical composition was determined by Iatroscan analysis (SARA).The materials were aged using two standardized aging methods: Rolling Thin Film Oven Test (which mimics the aging experienced by the binder during preparation of the asphalt mix) and Pressure Aging Vessel (mimicking aging after 10-20 years’ service life). Dynamic shear and bending beam rheological measurements (DSR and BBR respectively) of the materials at different aging stages were used to determine the binder with best performance when aged (and therefore highest durability). Also

Iatroscan analysis was performed in order to determine the chemical structure of the aged bitumen showing the best performance.

The highest performance binder was further chemically modified with additives from renewable sources with antioxidant or rejuvenator effect in order to yield a family of novel binders with improved lifespan and a novel eco dimension. These binders were also fully characterized, aged and rheologically tested in order to characterize its performance and suitability as paving grade binders.

3. Results and discussion

In this work it has been observed that the chemical parameter colloidal instability index of bitumen (defined as the ratio between the asphaltene + saturates and aromatics+resins fractions) is related with the performance if the material in in terms of fatigue (see figure 1). Tuning the manufacturing processes and the origin of the crude oil raw material makes possible obtaining high durability binders. Once the best performance bitumen is selected, its performance during service life was further improved by incorporating vegetal rejuvenators and antioxidants.

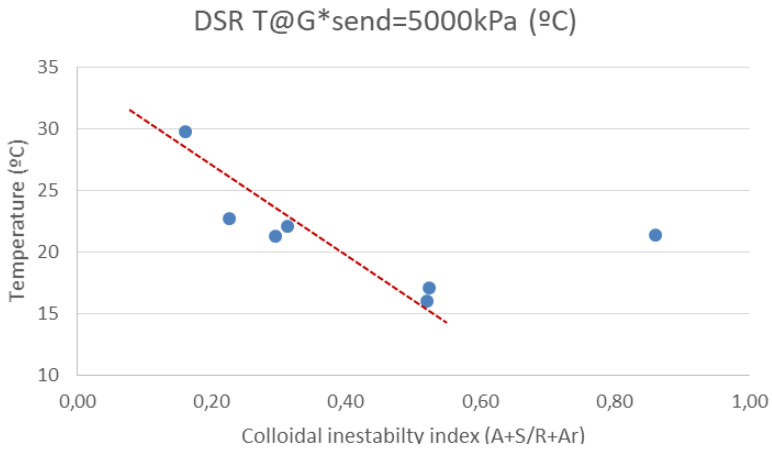

Figure 1. Dependence of fatigue resistance of bitumen on colloidal instability index

4. Conclusions

Improved durability bitumen materials have been manufactured on the basis of physical-chemical parameters. Different types of chemical additives from renewable sources have been assessed in order to improve the long term performance of the asphalt binder.

References

[1] Lu, X.; Talon, Y.; Redelius, P. (2008). 4th Eurasphalt Eurobitume Congress.
[2] Cortes, C.; Perez, A.; Fermoso, J.; Costa, A.; Guisado, F.; Esquena, J.; Potti, J.J.. (2010). V Jornada Nacional de ASEFMA, Madrid (Spain)
[3] Apeagyei, A. K. (2011). Construction and Building Materials 25(1), pp. 47–53.

Evaluation of synthesized castor oil-based bio-binders for automotive composite materials production

Ntsako Chauke-Khosa[1], Diakanua Nkazi[2], Hembe Mukaya[3] [Calibri 12]

School of Chemical and Metallurgical Engineering, University of the Witwatersrand,

Private Bag X3, P O Wits 2050, South Africa

**Corresponding author: E-mail: Ntsako.chauke@students.wits.ac.za, Tel: +2783 260 6581*

Abstract

The development of polymers in various industries has been deteriorating due to the depletion in fossil fuels and environmental concerns such as the effect of greenhouse gases, global warming and increasing population. However, vegetable oils have emerged as a worthy replacement for fossil fuels. The need to use non-edible oils is recommended for industrial processes to reduce the dependency on edible oils and hence increasing food security. This investigation uses an affordable process to develop bio-binders for composite materials using non-edible oil produced from castor seed. The oil was first extracted from the castor seeds, purified and then process to yield castor oil-based bio-binders using Epoxidation method. The Epoxidation catalyst was synthesized from of tungstic acid and hydrogen peroxide at 50 - 60 °C. The Epoxidation process temperature varied between 60 and100 °C while varying the catalyst loading and the reaction time. The epoxidized castor oil showed 70% binder yield with 1H NMR spectra showing peaks of an epoxy group at 3.0 – 3.2 ppm; and the epoxy peak was also observed using FTIR at 830 cm-1.

All in One - Advanced technologies for complex low-cost microfluidic devices in glass, silicon and quartz

Klaus Kadel[1], Alexander Schilling[1], Jing Becker[2], Claas Müller[2]

1 Affiliation and address Little Things Factory, D-56479 Elsoff, GERMANY;
2 Microfabrication Center, IMTEK, Department of Microsystem Engineering,
University of Freiburg, Georges-Koehler-Allee 103, D-79110 Freiburg, GERMANY
**Corresponding author: k.kadel@ltf-gmbh.de*

Highlights

- Multi level laser etching in glass silicon and quartz [Calibri 10].
- 3-D shaped nozzles with six levels in the bottom and the top layer
- Hermetically sealed electrical connectors through the glass

1. Introduction

The controlled generation of liquid micro droplets with uniform characteristics will be one of the future key technologies in research and in industrial production. The Little Things Factory covers the whole portfolio to set up new functionalities for microfluidic systems in glass and we describe recent innovations in this field.

We will show, what are state of the art manufacturing methods to make chips out of glass or quartz with different levels and different types of structures in one setup. Figure 1 shows an example of such a multilevel structure, with grids of posts and cavities, mixing structures and additional structures for detection.

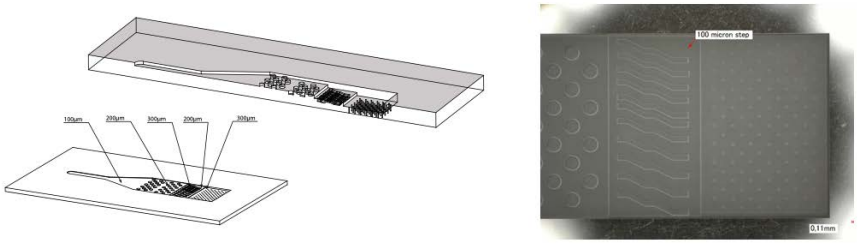

Fig. 1: Multilevel structure with five different levels and various types of structures realized in glass

2. Advanced methods of droplet generation

Figure 2 shows a prototype of the flow focusing chip (FFC). This chip was designed to modify the droplet diameter over the flow ratio and to create swarms of droplets. The FFC consists of a droplet generator combined with a reaction zone. The droplet generator of this chip consists of two 3-D laser etched nozzles, and the microchannels inside the inlet and outlet nozzles have been etched to different levels into the bottom as well as the top glass layer. In this work, six different levels have been applied to define the inlet and outlet nozzle structures in the bottom and the top glass layer.

3. Results and discussion

For a flow rate of 1,6µl/min the pressure loss in the central line was measured to 3.3bar, for the lines for the sheath flow to 2.6bar. The droplet size measured for different mixing ratios can be seen in figure 2. We will present how the droplet size can be modified by changing the flow rate in the central line or for the sheath flow and what happens when changing from Toluene to Cyclohexane.

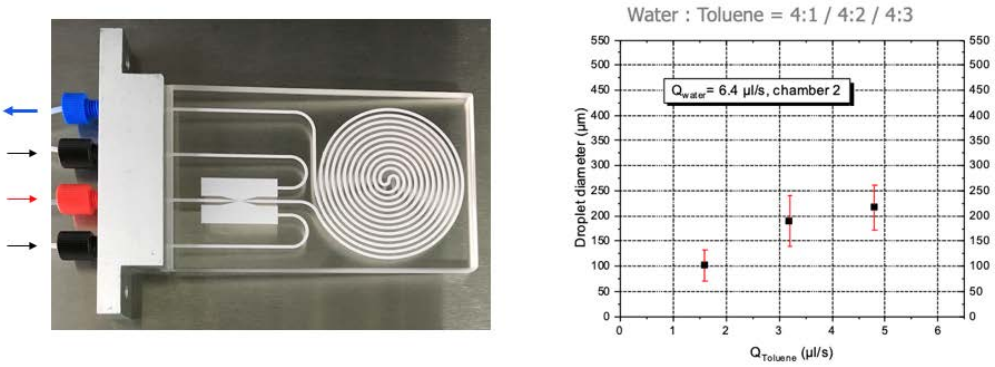

Fig. 2: Flow focusing chip with a droplet generator on the left and the reaction zone on the right. The right picture shows the measured droplet size for different mixing ratios of Toluene and Water

Through Glass Vias (TGV)

We will introduce new possibilities to combine microfluidics with hermetically sealed electrical connectors for various applications that needs electrodes in contact with fluids or electrodes isolated from fluids. The connectors are made of highly conductive silicon to have hermetically sealed feed troughs with a conductivity in the range of 0.01 to 0.02 Ωcm. Figure 3 show possible layouts (left side) and an example how to integrate such a TGV into a fluidic application. So, one can use the two orders of magnitude higher thermal conductivity of silicon compared to that to glass to have different temperatures on the chip, or one can heat or cool a fluid or run the chip on different temperature levels.

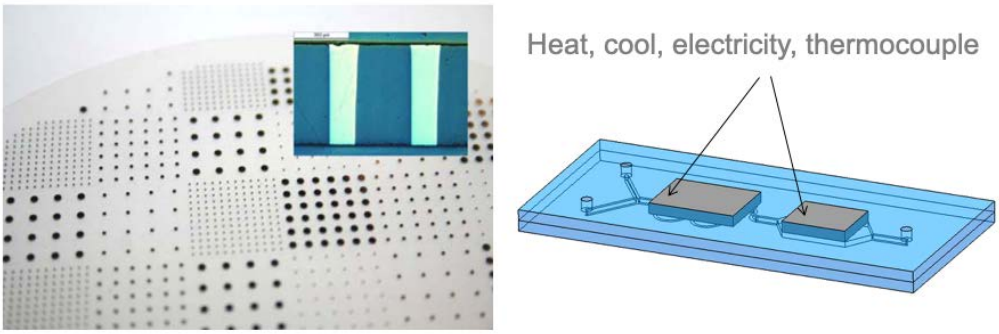

Fig. 3: TGV in glass and cross section (above) and integration in a fluid chip (below)

The conductive silicon could be in contact with the fluid, or not, just ending close to a channel or besides, so the silicon is isolated by a layer of glass to use the electric field. Possible applications may be the steering of fluids, catching cells, electrophoresis or electro kinetic actions. So, integrating a TGV in a fluidic device gives access to digital microfluidics.

Formation of $BiFeO_3$ and $LaPO_4$ nanoparticles during heat treatment of hydroxides co-precipitated in an impinging jets microreactor

O.V.Proskurina[1,2], R.S. Abiev[2,3*], M.O. Enikeeva[2], A.A. Sirotkin[2], V.V.Gusarov[1]

1 Ioffe Institute, Politekhnicheskaya st. 26, 194021, Saint Petersburg, Russia;
2 St. Petersburg State Institute of Technology, Moskovskii pr.26, 190013, Saint Petersburg, Russia;
3 Institute of Silicate Chemistry of RAS, Makarova emb. 2, 199034, Saint Petersburg, Russia;
**Corresponding author: abiev.rufat@gmail.com*

Highlights

- $BiFeO_3$ nanoparticles were obtained using an impinging jets microreactor.
- The synthesized $BiFeO_3$ particles about 20 nm in size are single-crystal.
- $BiFeO_3$ nanoparticles obtained without impurities of other phases.
- $LaPO_4$ nanoparticles were obtained using an impinging jets microreactor.

1. Introduction

Synthesis of nanocrystalline $BiFeO_3$ without admixtures of other compounds is a great challenge. It is hindered by the fact that reducing the number of impurity phases $Bi_{25}FeO_{39}$ and/or $Bi_2Fe_4O_9$ requires, as a rule, an increase in temperature and/or duration of heat treatment of the initial reagents, which leads to the growth of particles of the target product. In recent years, the impinging jets method has begun to attract attention as a tool for nanoscale particles synthesis [1-4]. It was shown [4] that the use of the impinging jets microreactor can significantly lower the synthesis temperature and reduce the crystallite size of the $CoFe_2O_4$ nanopowder. This fact was associated with a high rate of energy dissipation in the collision volume of impinging jets resulting in perfect mixing of reagents, which is a characteristic of this method.

The objective of this work was to study the possibility and conditions of using the method of impinging jets for co-precipitation of hydroxides to obtain single-phase powders based on nanocrystalline $BiFeO_3$ and $LaPO_4$.

2. Methods

A homemade glass microreactor with nozzles of 0.55 mm and 0.65 mm inner diameter was used. A mixture of $Bi(NO_3)_3{\cdot}5H_2O$ and $Fe(NO_3)_3{\cdot}9H_2O$ water solutions in HNO_3 was prepared as a first liquid. The second liquid was KOH water solution. Two jets of the liquids with velocities of 17.5 m/s and 12.5 m/s correspondingly were collided in the reactor. Co-precipitation products were then heat treated in air at 420°C-600°C within 15 minutes. X-ray diffraction, scanning (SEM) and transmission (TEM) electron microscopy, energy dispersive X-ray spectroscopy (EDS), Mössbauer spectroscopy and IR spectroscopy were used for characterization of co-precipitated and heat treated products.

3. Results and discussion

The Bi:Fe atomic ratio in the initial sample and in the samples after heat treatment according to EDS data remains at the same level Bi:Fe = (52 ± 2):(48 ± 2). After heat treatment at 420°C, reflections characteristic of bismuth orthoferrite appear on the diffraction pattern. The tendency described above is also maintained during heat treatment of co-precipitated hydroxides at temperatures of 440 and 600°C. Nanocrystalls of $LaPO_4$ having rhabdofan structure and sizes of 2-3 nm have been formed by use of the impinging jets microreactor (without additional heat treatment).

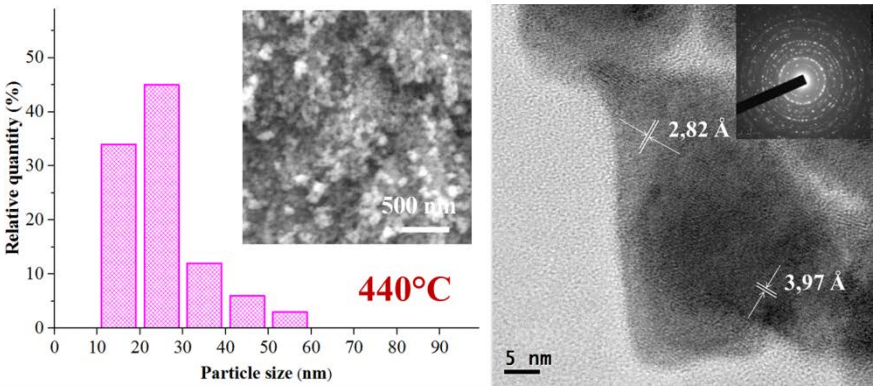

Figure 1. Left: size distribution of BiFeO3 particles obtained by heat treatment at 440°C.The inset shows SEM micrograph. Right: TEM micrograph of the particles. The inset shows selected area electron diffraction pattern

4. Conclusions

By heat treatment of hydroxides co-precipitated in an impinging jets microreactor, nanocrystalline bismuth orthoferrite was synthesized. It was shown that the formation of $BiFeO_3$ nanoparticles without admixtures of other phases with a narrow crystal size distribution and an average crystal size of about 20 nm is possible after heat treatment at 420-440°C of hydroxides co-precipitated in an impinging jets microreactor. The nanoparticles of $BiFeO_3$ obtained under these conditions were single-crystal. It was shown that the sizes of the formed bismuth orthoferrite nanocrystals were consistent with the sizes of the nanoparticles that can be formed in microvortices having a minimum Kolmogorov scale that are formed during the collision of the jets of reagent solutions in the microreactor.

Using the microreactor approach, a suspension of $LaPO_4$ nanoparticles with the structure of rhabdofan was obtained, which turned into a sol after some time, and then into a thixotropic gel. The size of $LaPO_4$ nanocrystalls in the gel according to X-ray diffraction data was 2-3 nm.

The authors acknowledge the partial financial support of this work in the form of RFBR grant 18-29-12119.

References

[1] B.K. Johnson, R.K. Prud'homme, AIChE J. 49 (2003) 2264-2282.
[2] J. Han, Z. Zhu, H. Qian, A.R. Wohl, C.J. Beaman, T.R. Hoye, C.W. Macosko, J. of Pharm. Sci. 101 (2012) 4018-4023.
[3] D.V. Ravi Kumar, B.L.V. Prasad, A.A. Kulkarni, Ind. Eng. Chem. Res. 52 (2013) 17376-17382.
[4] R.S. Abiev, O.V. Almyasheva, S.G. Izotova, V.V. Gusarov, J. Chem. Tech. App. 1 (2017) 7-13.

Comparison of crystal growth kinetics of Piracetam, Fenofibrate, Acetaminophen, Phenylbutazone, Risperidone and Carbamazepine in methanol

Rodrigo Soto[1*], Vivek Verma[1], B. Kieran Hodnett[1] and Åke C. Rasmuson[1,2]

1 Synthesis and Solid State Pharmaceutical Centre (SSPC), Bernal Institute, Department of Chemical and Environmental Science, University of Limerick. Limerick V94 T9PX, Ireland; 2 Department of Chemical Engineering and Technology, KTH Royal Institute of Technology, SE-100 44 Stockholm, Sweden

**Corresponding author: rodrigo.soto@ul.ie*

Highlights

- Crystal growth kinetics of six different API's in methanol have been studied.
- Experimental desupersaturation data is modeled using empirical and mechanistic equations.
- Solid-liquid interfacial energies and mean diffusion distances have been estimated.
- The relevance of bulk diffusion study suggests surface integration as the limiting-step.

1. Introduction

Crystallization is the bottleneck unit operation in the separation of solids in the pharmaceutical industry and it can be envisaged as a two-step process: nucleation and crystal growth. Both steps contribute to the final particle size distribution of the crystallization outcome but are insufficiently understood. The nature of the solute-solvent intra and intermolecular interactions influences both nucleation and growth. It is hence expectable that molecules with a relative ease of nucleation in a given solvent will also show a growth facility. Very often, however, nucleation experiments do not allow for separating the effects of the steps of new particles formation from those of pure growth because the nucleation outcome can only be evaluated when the solids have grown to a certain size [1]. The process of crystal growth comprises the diffusion of molecules from the bulk phase to the crystal surface and their subsequent integration into the crystals lattice. There are several mechanisms that can describe the surface integration step, e.g. the Burton Cabrera Frank (BCF) or screw dislocations mechanism, and Birth and Spread (B+S) or two-dimensional nucleation mechanism [2]. Additionally, empirical power law equations are useful because they can be applied in a wider range of supersaturations. This study focuses the growth of six different active pharmaceutical ingredients (APIs) in the same solvent aiming to shed light to some fundamental physicochemical aspects influencing the crystal growth kinetics.

2. Methods

Isothermal seeded desupersaturation experiments in methanol were carried out in the range of temperature 288-303 K and supersaturations below 1.32, for Acetaminophen (AAP), Carbamazepine (CBMZ), Piracetam (PCM), Fenofifrate (FF), Phenylbutazone (PBZ) and Risperidone

(RIS). The seed size was 100-180 µm and the stirring speed 250 rpm. The crystallizer (Easymax402, Mettler Toledo) was equipped with an *in-situ* IR probe (ReactIR15) to monitor the liquid concentration at any time and a FBRM probe (Particle track G400) to track the number of counts and their size distribution. After growth experiments, the crystals were harvested, dried and characterized by PXRD, SEM and in a particle size and shape analyzer (G3 morphology).

3. Results and discussion

The crystallographic habit of all the API studied is similar except for PBZ where a needle shape-like habit is distinguished. Experimental desupersaturation data was modeled using power law equations (Fig.1a), BCF and B+S theories. The fitting of power law equation was remarkably good and the involved parameters suggested that the growth is mainly surface integration controlled for the studied API's within the explored experimental conditions. The BCF model provided faintly better fitting than the B+S one being therefore more likely this mechanism to govern. At the same supersaturation and temperature (Fig.1b) the crystal growth rates decreased in the order PCM>FF>AAP> PBZ>RIS>CBMZ. From the B+S model, the estimated solid-liquid interfacial energies (γ_{sl}) and mean surface diffusion distances ranged 0.82-1.55 mJ/m^2 and $6.66\cdot10^{-9}$-$6.52\cdot10^{-8}$ m, respectively. γ_{sl} values are comparable to those determined by nucleation experiments [3] but do not follow the relative growth order mentioned, suggesting that there are more factors at play. Interesting and coherent correlations between growth rates, solubility, molecular volume, mass transfer coefficients and crystal lattice energies have been found, which allows for rationalizing the crystal growth kinetic behavior observed.

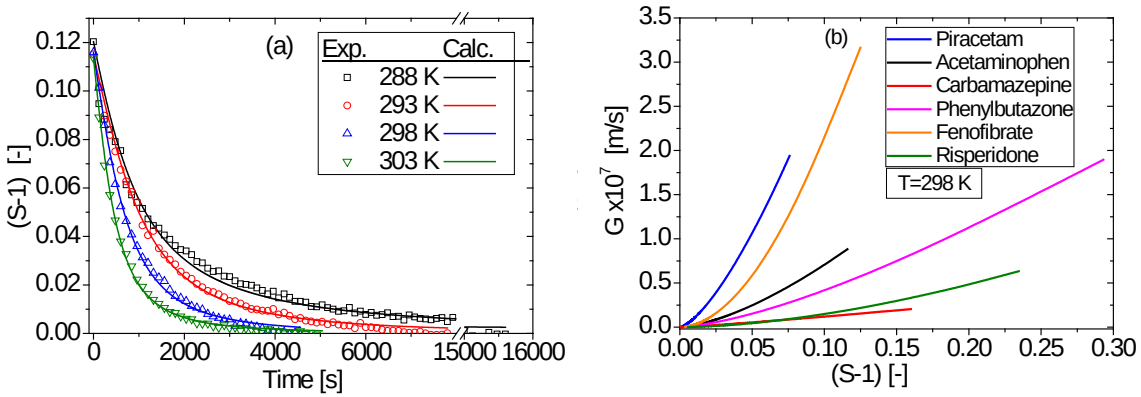

Figure 1. (a) Example of the fitting provided by power law equation for AAP experiments at different temperatures. (b) Comparison of growth rates obtained at 298 K for the different API studied.

4. Conclusions

The power law equation and the BCF model provided the best fit to the experimental desupersaturation data for the six API's studied in methanol. The crystal growth rates decreased in the order PCM>FF>AAP>PBZ>RIS>CBMZ, which can be correlated to fundamental physicochemical properties as solubility, mass transfer coefficients, molecular volume and crystal lattice energies.

References

[1] W. Du, A. J. Cruz-Cabeza, S. Woutersen, R. J. Davey, and Q. Yin, Chem. Sci., 6; 6 (2015) 3515–3524.

[2] A. Mersmann, Crystallization technology handbook. 2nd ed., Marcel Dekker, New York, 2001.

[3] V. Verma, J. Zeglinski, S. Hudson, P. Davern, and B. K. Hodnett, Cryst. Growth Des., 18; 11 (2018), 7158–7172.

ECCE12
The 12th EUROPEAN CONGRESS OF CHEMICAL ENGINEERING
Florence 15-19 September 2019

Charge-based agglomeration of submicron particles with potential for selective separation in grinding processes

Christoph Peppersack[1], Arno Kwade[1] and Sandra Breitung-Faes[1]

1Institute for Particle Technology, Technical University of Braunschweig, Braunschweig, GER

**Corresponding author: c.peppersack@tu-bs.de*

Highlights

- Top-down synthesis of submicron suspension with high quality standards
- Selective agglomeration in binary particle mixtures
- Separation of wear particles from wet grinding processes

1. Introduction

Within the top-down synthesis in stirred media mills, wear (abrasion) of the mill components, primarily the grinding media, is a major challenge in terms of lowering the product quality. A direct mechanical separation of the wear particles during/after the grinding process cannot be accomplished easily, as these usually have particle sizes similar to the product components.
The (hetero)agglomeration of submicron particle suspensions, induced by electrostatic particle-particle interactions, is a known process in literature. On the contrary, a selective agglomeration of certain components from a mixture of different materials has not been studied extensively yet. In this context, the principle of electrostatically induced agglomeration of submicron particles was investigated in a first step using zirconium dioxide suspensions as an exemplary wear component, since it is one of the most frequently used grinding media material. This study compares different agglomeration mechanisms with regard to their agglomerate size, strength as well as the yield of agglomerated particles. Subsequently, selective agglomeration of zirconium dioxide particles in a binary mixture with either an organic or inorganic material was evaluated. Here, this will be briefly described in its feasibility for anthraquinone as the organic material example.

2. Methods

For the data shown here, anthraquinone (product component, ρ = 1.31 g/cm^3) and zirconium dioxide (wear component, ρ = 5,68 g/cm^3) were chosen as materials. Using a stirred media mill (PML 2, Bühler AG), these substances were first ground in water to a defined particle size ($x_{50,3}$ = 0,3 µm for anthraquinone, $x_{50,3}$ = 0,3 µm for zirconium dioxide). To induce selective agglomeration of zirconium dioxide particles, the anthrachinone suspension was first mixed with a certain amount of agglomeration additive. Subsequently, the zirconium dioxide suspension was added in order to imitate the generation of wear. The final suspension had a mass concentration of anthraquinone equal to 4 %-w/w and of zirconium dioxide equal to 0.2 %-w/w. To analyse the success of selective agglomeration, samples of the suspensions were centrifuged for 5 minutes at different RCF values. Then, a defined volume was taken from the supernatants, which was first dried at 110 °C and then burnt out in a muffle furnace at 600 °C to decompose the organic material. After each heating step, samples were gravimetrically analysed in order to obtain both the loss of anthraquinone (product) and the loss of zirconium dioxide due to centrifugation.

3. Results and discussion

Figure 1. shows the percentage losses of anthraquinone (product) and zirconium dioxide in the supernatant obtained by centrifugation due to different RCF values with and without agglomeration additive. If the curves without additive are considered first, it can be seen that the zirconium dioxide particles can only be separated by higher centrifugal forces in larger quantities. However, this is associated with an undesired product loss, since anthraquinone particles are also centrifuged with the corresponding centrifugal forces. This effect would be enhanced if the centrifugal forces were increased or the centrifugation time extended.
In comparison, the curves with agglomeration additive show that a considerably higher proportion of zirconium dioxide could be separated from the suspension at significantly lower centrifugal forces (approx. 50 %-w/w at RCF = 380). This also ensures that almost the entire product material remains in the suspension because the centrifugal forces are too low to cause sedimentation of the anthraquinone particles. For this reason, it can be assumed from the results that the addition of the agglomeration ingredient resulted in selective agglomeration of the zirconium dioxide particles. This assumption can be supported by particle size analyses and SEM/EDX images (not shown).

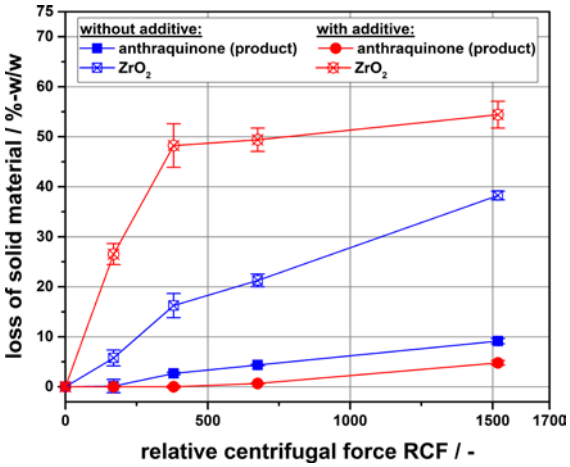

Figure 1. Gravimetrical analysis of selective agglomeration / separation

4. Conclusions

A promising method to selectively agglomerating the wear components is presented. It was shown that zirconium dioxide particles could be separated out of binary mixture with anthraquinone. Multiple variables in order to increase the yield of agglomeration are currently under investigation. The attained knowledge about an efficient, selective agglomeration can be used to remove the wear components from the product suspension in a suitable separation process. Hereby, this ensures that wear-free, submicron suspensions can be produced using a top-down process.

References

[1] S. Breitung-Faes and A. Kwade, A.Powder Technology, 212(3), 383-389, 2011.
[2] F. Flach et al., Advanced Powder Technology, 27(6), 2507-2519, 2016
[3] F. Flach, S. Breitung-Faes and A. Kwade, Colloids and Surfaces A: Physicochem. Eng. Aspects, 522, 140-151, 2017.
[4] W. Lin et al., (2006), Langmuir, 22, 1038-1047, 2006.

Scalable production of nanostructure materials via atomic layer deposition: a way to reduce the demand for scarce materials

J.Ruud van Ommen[1]

1 Delft University of Technology, Chemical Engineering dept., TU Delft Process Technology Institute, Delft, the Netherlands

**Corresponding author: j.r.vanommen@tudelft.nl*

Highlights

- Applying nanostructured materials can strongly reduce the use of scarce elements.
- Atomic layer deposition is a scalable process to make nanostructured materials.
- Several examples of the use of atomic layer deposition will be shown.

1. Introduction

Nanoscience holds the promise to deliver a plethora of solutions for several grand challenges, such as abundant sustainable energy, clean drinking water and personalized pharmaceuticals. However, many of such solutions never find practical implementation, since they require scarce materials or involve poorly scalable production processes. A marriage between chemical engineering and nanoscience – scalable nanotechnology – can tackle these problems: it is possible to make scalable processes, while strongly reducing the demand for scarce materials. In some cases, novel nanostructured materials can make the use of critical elements even superfluous. Atomic Layer Deposition (ALD) is a versatile and scalable technology for making such nanostructured materials.

2. Methods

We typically take a dry, powder-form substrate that we want to treat with ALD (nanoparticles, micron-sized particles, graphene platelets, …) [1] and load some grams of it into a glass column (typical sizes are 2.5 cm diameter, 50 cm high). The powder is fluidized in an upward nitrogen flow with a superficial gas velocity of typically about 5 cm/s. We deploy ALD by alternatingly adding the two required precursors to the nitrogen flow, e.g. trimethylaluminum and water for alumina, or trimethyl(methylcyclopentadienyl)platinum(IV) (IV) and oxygen for platina, while maintaining intermediate periods without precursor for purging. The alternating addition of the two precursors is repeated until the desired film thickness or cluster size has been reached.

3. Results and discussion

In heterogeneous catalysis, noble metal clusters on ceramic or carbon supports are widely used. Ideally speaking, all metal clusters have the same size, tailored for the targeted reaction. In practice, this is impossible to reach with the production techniques the catalyst industry currently uses, such as wet impregnation and spray-drying. Using ALD, it is much better possible to create a much narrower size distribution of noble-metal clusters [2] (see Fig. 1.a). This can be used to make either

catalysts with a much higher activity or a much lower noble metal loading. Either way leads to a strong reduction in the use of noble metals.

In thin film solar cells, currently often scarce materials such as indium and gallium are used. Here, using ALD alternative routes are possible than not just minimize the use of such scarce elements, but enable a completely different approach by using abundant elements such as copper, zinc and tin [3]. Another alternative might be to move to completely different technology, and apply quantum dot films that are stabilized using ALD overcoating for high-end PV applications [4].

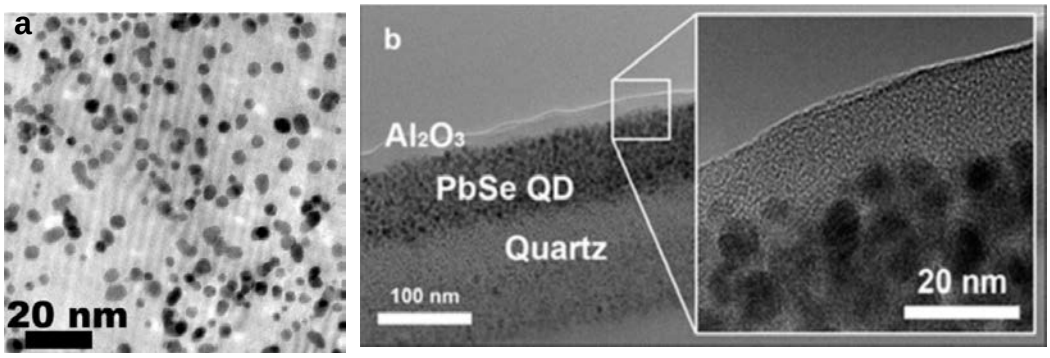

Figure 1. (a) TEM image of platinum nanoclusters deposited on graphene using ALD [2]; (b) Cross-sectional TEM image of a quantum film, in which a protecting alumina overcoating made by ALD is visible [4].

A third sector where materials scarcity plays an important role is the production of Li-ion batteries. The most pressing need for the Li-ion industry to move forward is a strong reduction of the amount of cobalt that is required [5]. Using atomic layer deposition, we can make more stable cathode materials, reducing the amount of cobalt required. However, this will need large amounts of powders to be coated. Most likely the batch-wise operation of fluidized beds is less suitable to achieve this: our continuous pneumatic transport reactor [6] will be a more attractive option for such a large-scale process.

4. Conclusions

Atomic layer deposition (ALD) can be used to provide powdered substrates with a thin film or with nanoclusters of the required materials. The high degree of control makes ALD perfectly suited to produced nanostructured materials that can be applied to strongly reduce the use of critical materials; the scalability of the method makes a smooth translation to industrial practice feasible.

References

[1] Van Bui, H., Grillo, F., & Van Ommen, J. R. 2017, Chemical Communications, 53(1), 45-71.

[2] Grillo, F., Van Bui, H., Moulijn, J. A., Kreutzer, M. T., & Van Ommen, J. R. 2017, The journal of physical chemistry letters, 8(5), 975-983.

[3] Sinha, S., Nandi, D. K., Kim, S. H., & Heo, J. 2018, Solar Energy Materials and Solar Cells, 176, 49-68.

[4] Valdesueiro, D., Prabhu, M. K., Guerra-Nunez, C., Sandeep, C. S., Kinge, S., Siebbeles, L. D., de Smet, L.C., Meesters, G.M., Kreutzer, M.T., Houtepen, A.J. & van Ommen, J. R. 2016, The Journal of Physical Chemistry C, 120(8), 4266-4275.

[5] Jaffe, S. 2017, Joule, 1(2), 225-228.

[6] van Ommen, J. R., Kooijman, D., Niet, M. D., Talebi, M., & Goulas, A. 2015, Journal of Vacuum Science & Technology A: Vacuum, Surfaces, and Films, 33(2), 021513.

Van Bui, H., Grillo, F., & Van Ommen, J. R. (2017). Atomic and molecular layer deposition: off the beaten track. *Chemical Communications*, *53*(1), 45-71.

Grillo, F., Van Bui, H., Moulijn, J. A., Kreutzer, M. T., & Van Ommen, J. R. (2017). Understanding and controlling the aggregative growth of platinum nanoparticles in atomic layer deposition: An avenue to size selection. *The journal of physical chemistry letters*, *8*(5), 975-983.

Sinha, S., Nandi, D. K., Kim, S. H., & Heo, J. (2018). Atomic-layer-deposited buffer layers for thin film solar cells using earth-abundant absorber materials: A review. *Solar Energy Materials and Solar Cells*, *176*, 49-68.

Valdesueiro, D., Prabhu, M. K., Guerra-Nunez, C., Sandeep, C. S., Kinge, S., Siebbeles, L. D., ... & van Ommen, J. R. (2016). Deposition mechanism of aluminum oxide on quantum dot films at atmospheric pressure and room temperature. *The Journal of Physical Chemistry C*, *120*(8), 4266-4275.

Jaffe, S. (2017). Vulnerable links in the lithium-ion battery supply chain. *Joule*, *1*(2), 225-228.

van Ommen, J. R., Kooijman, D., Niet, M. D., Talebi, M., & Goulas, A. (2015). Continuous production of nanostructured particles using spatial atomic layer deposition. *Journal of Vacuum Science & Technology A: Vacuum, Surfaces, and Films*, *33*(2), 021513.

Synthesis of eco-friendly amino acid biosurfactants and characterization of interfacial properties for cosmetics and household products

JongChoo Lim, SeonHui Jo, DaNan Yea

Department of Chemical and Biochemical Engineering, Dongguk University-Seoul, Korea

**JongChoo Lim: jongchoo@dongguk.edu*

Highlights

- Amino acid biosurfactants were prepared from readily biodegradable coconut oil.
- Newly synthesized biosurfactants possess superior interfacial properties.
- Synthesized biosurfactants are nontoxic, non-irritating, mild, and biodegradable.

1. Introduction

Currently, most of the surfactants widely used in various areas of industrial applications are prepared from petroleum base. These synthetic chemical surfactants have been known to be non-biodegradable, irritating, not mild and also detrimental to aquatic organisms. Strict environmental restrictions and rising recognition for the requirement to preserve the environment have leaded to growing attention in biosurfactants as a potential substitute to petroleum based surfactants. Biosurfactants have been known to possess merits over petroleum based surfactants in uniqueness, variety, selectivity, convenience of production, mildness and high efficiency even at harsh operation conditions such as high temperature and extreme high or low pH. Amino acid based biosurfactants are frequently used in detergents, household products, cosmetics, pharmaceuticals, personal care products, food ingredients, and so on due to their extremely low toxicity and excellent biodegradability [1]. In this work, 2 types of anionic amino acid based biosurfactants such as potassium cocoyl glycinate CGK and sodium cocoyl glycinate CGN were synthesized using nontoxic and readily biodegradable coconut oil derived from natural resources.

2. Methods

The structure of the resulting products was elucidated by FT-IR, ^{1}H NMR, and ^{13}C NMR spectroscopies and environmental compatibility such as biodegradability and acute oral toxicity was evaluated. The interfacial characteristics of the synthesized surfactant including surface tension, critical micelle concentration, interfacial tension, wetting property, emulsification activity, viscosity and foam property have been examined. Biodegradability, acute dermal irritation, acute eye irritation and acute oral toxicity have been measured for the newly synthesized surfactants in order to investigate environmental compatibility for cosmetics application. Detergency tests were also carried out with synthesized amino acid biosurfactants to examine the possible uses in detergent application.

3. Results and discussion

The measurement results of interfacial properties for the newly synthesized biosurfactants indicated that the prepared surfactants have excellent interfacial properties. Detergency test has been performed with newly synthesized surfactants by using an agitation/mixing type detergency tester at room temperature. The results suggested that the newly synthesized surfactants show moderately good detergency. Acute oral toxicity (LD_{50}) measurement showed that newly synthesized surfactants are very mild compared with conventional nonionic and anionic surfactants used in detergent and cosmetic formulations such as polyoxyethylene (9) lauryl ether (PLA) and dodecylbenzene sulfonic acid (LAS). The primary biodegradability of newly synthesized surfactants has been found to be greater than 95%, suggesting that newly synthesized surfactants are acceptable for cosmetic and detergent applications. Both acute dermal irritation and acute eye irritation tests revealed that surfactants are mild. In particular, the prescription test in shampoo formulation prepared with synthesized biosurfactants indicated better sensory feeling and excellent foaming ability compared with conventional surfactants used such as silicon. The patch test also indicated no irritation during 48 hours, indicating potential applicability in cosmetic and household products.

4. Conclusions

In this study, 2 types of anionic amino acid based biosurfactants such as CGK and CGN were synthesized using coconut oil and the structure identification of the CGK and CGN was carried out by FT-IR, ^{1}H NMR, and ^{13}C NMR spectroscopies. The interfacial properties of CGK and CGN surfactant systems have been evaluated such as CMC, static and dynamic surface tensions, emulsification activity, wetting property and foam property. The results suggested that both CGK and CGN surfactant systems possess superior interfacial properties. Washing test carried out with a Terg-o-tometer indicated relatively good detergency when comparing with surfactants employed in detergent formulation. Acute oral toxicity evaluation indicated that both CGK and CGN surfactants are nontoxic compared with PLA and LAS. Both acute dermal irritation and acute eye irritation tests showed that both CGK and CGN surfactants are non-irritating and very mild and the primary biodegradability of CGK and CGN evaluated using an activated sludge test KSM 2714 has been found to be 99% in both surfactants. In particular, CGK surfactant can be considered as a strong candidate for the potential applicability in detergent products formulation since CGK surfactant is very effective in lowering interfacial free energy, nontoxic, non-irritating, mild, and readily biodegradable.

References

[1] S. Vijayakumar, V. Saravanan. Res. J. Microbiol. 10 (2015) 181-192.

Acknowledgement

This work was supported by "the Technology Innovation Program“(10063387, Development of aryl phenol surfactants and paint additives for the replacement of nonyl phenol) funded by the Ministry of Trade, Industry & Energy, Korea.

Rheology and Draining Properties of Model Dry Powders in a Hopper: Effect of the Vibrations and Opening Geometry.

Arthur Pascot[1]*, Sébastien Kiesgen De Richter[1], Salaheddine Skali-Lami[1]

1 Laboratoire d'Energétique et de Mécanique Théorique et Appliquée, University of Lorraine, UMR 7563
**Corresponding author : arthur.pascot@univ-lorraine.fr*

Highlights

- Vibrations change the structure and rheology of the flow in a silo
- Vibrations prevent arches but tend to decrease the flowrate of the silo
- A law can be drawn between flow rate, geometry and vibrations parameters

This study is conducted in the framework of the "PowderReg" project, funded by the European programme Interreg VA GR within the priority axis 4 "Strengthen the competitiveness and the attractiveness of the Grande Région / Großregion".

1. Introduction

Granular materials are encountered in many fields, be it in Nature (sand castles, lava flows, avalanches…) or in industry (cosmetic powders, cereals, concrete flows…). Understanding the behaviour and flow properties (localization, jamming, aging…) of those materials is a major issue in rheology and fluids mechanic, mainly due to the complexity and multiscale aspect of the flow. Their comprehension is however important in order to optimize systems involving granular flows, such as hopper discharge.

2. Methods

The present work focus on the flow of dry powders in a quasi-2D silo (the depth allow only one layer of particle) when external vibrations are applied. The powders used are mainly spherical glass beads with a diameter around 1 mm. Numerical simulations using DEM [1] (Fig. 1.1) and experiments (Fig. 1.2) were performed in order to study the impact on the flow of the silo opening geometry and vibrations parameters.

For the geometry, various opening sizes between 4.5 to 18 particle diameters were tested, with opening angles ranging from 0 to 60°. For the vibrations, different amplitudes (10-5000 µm) and frequencies (15-600 Hz) were tested.

Experimentally, a scale follow the mass drained (measure of the flowrate) while the flow is recorded with a camera in order to determine the velocity fields (by PIV [2]) and the particle trajectories (by tracking) around the opening.

3. Results and discussion

We focus in particular on the effect of the vibrations on the flowrate, jamming properties (formation and destruction of arches) and local rheology of the flow. We show that, while vibrations

can prevent arches formation, they also tend to decrease the flowrate. Therefore, we also propose an adimensional law linking the flowrate and the different parameters including vibrations properties, based on the Beverloo law [3]. The goal being, in the framework of the “PowderReg” project, to size a 3D silo alimenting with different powders a full scale demonstrator of an industrial chain.

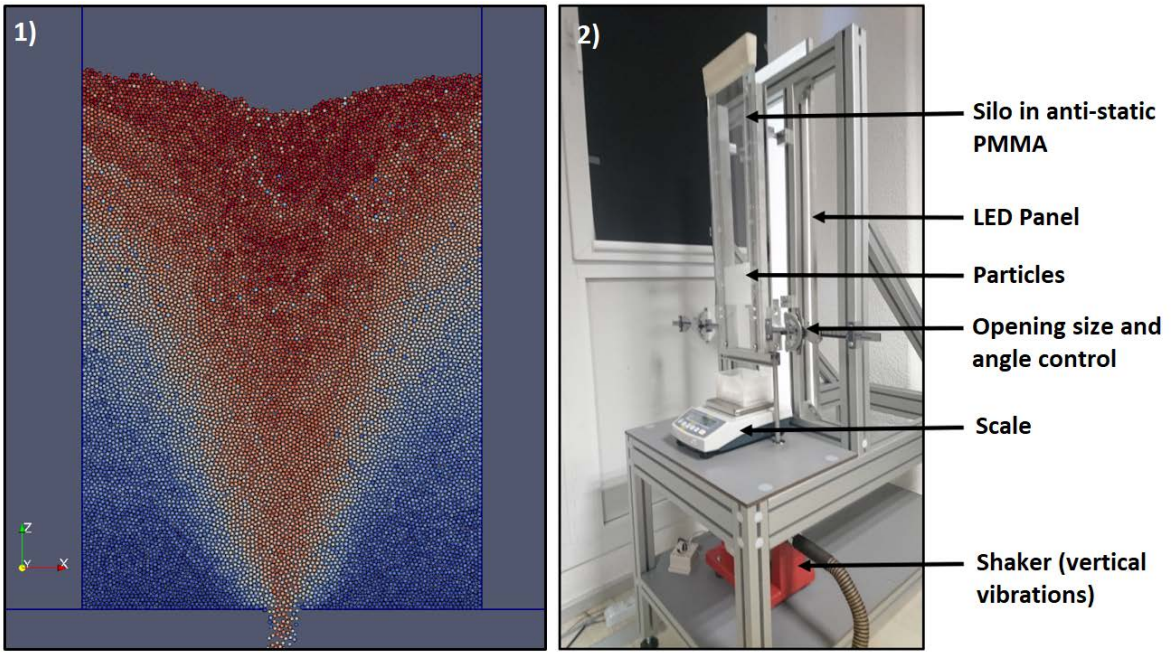

Figure 1. (1) Numerical simulation of the particle flow in the hopper and (2) Experimental setup.

References

[1] Peter A. Cundall, and Otto DL Strack. "A discrete numerical model for granular assemblies". Geotechnique 29.1 (1979): 47-65.

[2] D.A. Steingart and J.W. Evans. "Measurements of granular flows in two-dimensional hoppers by particle image velocimetry. Part I: experimental method and results". Chemical Engineering Science, 2005, vol. 60, no 4, p. 1043-1051.

[3] W. Beverloo, H. Leniger, and J. Van de Velde. "The flow of granular solids through orifices". Chemical engineering science, 1961, vol. 15, no 3-4, p. 260-269.

ECCE12
The 12th EUROPEAN CONGRESS OF CHEMICAL ENGINEERING
Florence 15-19 September 2019

Facile Synthesis of GO-Exfoliation/Goethite Functional Material and It Application in the Adsorption Of Cu(II).

Sidi Zhu[1]

1 School of Chemical Engineering, Nanjing University of Science and Technology, Nanjing 210094, Jiangsu, China.

**Corresponding author: sdzhu@njust.edu.cn*

Highlights

- GO-exfoliation/goethite functional material was first reported.
- The new material has higher adsorption capacity for Cu(II) than goethite.
- It can be used in a wide range of pH from 4 to 9.
- It is harmless to environment and has a good application foreground.

1. Introduction

It is widely recognized that Cu(II) has harmful effects on the environment and human health. The removal of Cu(II) from wastewater has become a hot issue in the world. The methods of removing Cu(II) have adsorption[1], ion exchange[2], chemical precipitation[3], etc. Among them, adsorption is a fast and relatively cost-effective technology for water treatment[4]. This work aims to prepare a new adsorption material to effectively remove Cu(II) from aqueous solution.

2. Methods

In this research, graphene oxide (GO)/goethite functional material was synthesized through a facile method. It consisted of the following steps. (1) The Hummers method was used for the preparation of GO-exfoliation[5]. (2) Goethite was prepared using a method based on the report of Atkinson[6]. (3) The functional material was synthesized via the ultrasonic method in aqueous solution with GO-exfoliation and goethite as precursors.

Adsorption experiments: the adsorption of Cu(II) onto the material was analyzed vs. temperature, adsorption time, pH values, as well as the associated adsorption isotherms. Then XRD, BET and TEM were used to explore the characteristics of the material.

3. Results and discussion

The results showed that GO has high surface areas and abundant oxygen-containing function groups. It can be used as an adsorbent in water treatment but difficult to be separated from water due to its hydrophilicity. The degree of GO-exfoliation was important for the adsorption capacity. The active functional material made it easier to be separated from water. The analytical results showed that the material has excellent adsorption efficiency than GO and goethite alone. The proportion of GO and goethite also played a key role for its adsorption capacity. This adsorption processes were rapid as occurred within the first 10 minutes and reached equilibrium in about 30 minutes. Adsorbent with a high removal capacity was important in the performance

of adsorbing Cu(II). The calculated adsorption capacity was 125.47mg/g for Cu(II), which decreased with increasing adsorption time. The material had good adsorption capacity in a wide range of pH from 4 to 9. Pseudo-second-order adsorption kinetic and Langmuir adsorption isotherm were applied to study Cu(II) adsorption process[7]. The main adsorption process is chemical adsorption. So the functional material would be useful for the purpose of environmental protection in design.

4. Conclusions

The results prove that the new material possesses high potential for the removal of Cu(II) in wastewater. GO, using as a kind of two-dimensional support, plays a key role to help the material to remove Cu(II). In addition, GO can be readily obtained from cheap natural graphite in large scale. As precursors are environment-friendly, it can practically usable for Cu(II) separation from water.

References

[1] X.L. Wu, L. Wang, C.L. Chen, A.W. Xu, X.K. Wang, J. Mater. Chem, 21 (2011) 17353.
[2] J. Kim, M.M. Benjamin, Water Res, 38 (2004) 2053-2062.
[3] M. Bilici Baskan, A. Pala, Desalination, 254 (2010) 42-48.
[4] S. Wang, Z.H. Zhu, A. Coomes, F. Haghseresht, G.Q. Lu, J Colloid Interface Sci, 284 (2005) 440-446.
[5] W.S.H. Jr, R.E. Offeman, J. Am. Chem. Soc, 80 (1958) 1339.
[6] R.J. Atkinson, A.M. Posner, J.P. Quirk, J. Inorg. Nucl. Chem, 30 (1968) 2371-2374.
[7] B. Hu, H. Luo, Appl. Surf. Sci, 257 (2010) 769-775.

ECCE12
The 12th EUROPEAN CONGRESS OF CHEMICAL ENGINEERING
Florence 15-19 September 2019

Particle Size Control of Recovered $Mg(OH)_2$ in Concentrated Brine Discharged from Sea Salt Manufacturing Process

Akira Kubo[1], Toshiyuki Sato[1], Masakazu Matsumoto[1], Toshihiko Hiaki[1*]

1 Department of Applied Molecular Chemistry, Nihon University, 1-2-1, Izumi-cho, Narashino, Chiba 275-8575 Japan

**Corresponding author: hiaki.toshihiko@nihon-u.ac.jp*

Highlights

- A morphology of $Mg(OH)_2$ is affected to stirring rate.
- A crystallinity is expected to change by stirring rate.
- The amount of $Mg(OH)_2$ depends on reaction time.

1. Introduction

Concentrated brine discharged from sea salt manufacturing process in Japan contains of value metal resources. The brine after recovering potassium chloride by cooling crystallization gives removed potassium bittern(RPB) as by-product. A part of RPB has been wasting to be hard to recover their resources, however, it is concerned with environment load. Combining their recovery increasing and to decrease environmental load are required, then Mg^{2+} is focus on as a representative resource. When Mg^{2+} is obtained from concentrated brine by reactive crystallization, $Mg(OH)_2$ would be produced to add a precipitator as primary product. However, the method gives a task to be slow on dry and filter process due to small crystal size of $Mg(OH)_2$. There have been many studies to increase a crystal size. For example, they are suggested kinds and addition method of precipitator. Otherwise, main cause of secondary nucleation in industrial equipment occurs from the stirring, there are hardly suggestion by the study to be controlled the crystal size.

The purpose of this study is to grow a $Mg(OH)_2$ crystals by the stirring conditions. For reagent, $MgCl_2 \cdot 6H_2O$ and $Ca(OH)_2$ were used by material and precipitator. Both reaction times and stirring condition are operation factors.

2. Methods

2.1 Material and operation

$Mg(OH)_2$ was precipitated by adding 6.0 mmol $Ca(OH)_2$ powder to 300 ml for 0.5 M $MgCl_2$ solution. The precipitate was filtered and washed third with 3 ml distilled water, dried at 60 ℃for 24 hours. The product was identified by X-Ray Diffraction (XRD) and a morphology was observed by Scanning Electron Microscope (SEM). The XRD pattern of $Mg(OH)_2$ is based on the JCPDS No. 07-0239.

2.2 Reaction time and stirring rate

Mixer (SM-101, AS ONE Co.) is equipped with 3-blades propeller (d = 55 mm). The reaction time was considered at 301 rpm from 60 min to 300 min, the precipitates were identified at constant time. The stirring rate was considered at 180 min from 301 rpm to 496 rpm. Their products were

compared with SEM images and XRD patterns.

3. Results and discussion

Fig. 1-(A) shows the XRD patterns of a precipitates to be altered reaction time. When the reaction time was 60 min, the characteristic peak of $Ca(OH)_2$ at $2\theta = 32°$ is detected. However, when reaction time was more than 120 min, the peak of $Ca(OH)_2$ could disappear. The peaks intensity of $Mg(OH)_2$ gradually increased as diminishing peaks intensity of $Ca(OH)_2$, the amount of $Mg(OH)_2$ is expected to increase.

Fig. 1-(B) shows the XRD patterns of a precipitates to be altered stirring rate. Pay attention at $2\theta = 38°$, the intensity of $Mg(OH)_2$ was stronger as slowing the stirring rate. This phenomenon is considered that decrease of the stirring rate is hard to occur the contact nucleation, then the crystal size is expected to grow. Otherwise, Fig.2 indicated the SEM images at their conditions. From the Fig.2-(a) and (b), the aggregation of primary particle was observed a ellipse-like morphology for secondary particle, however, Fig. 2-(c) cannot check a primary particle. A gap in secondary particle by distorted shape of primary particle is expected to decrease the crystallinity. Consequently, to be the slower stirring rate may facilitate the crystallinity and size of $Mg(OH)_2$.

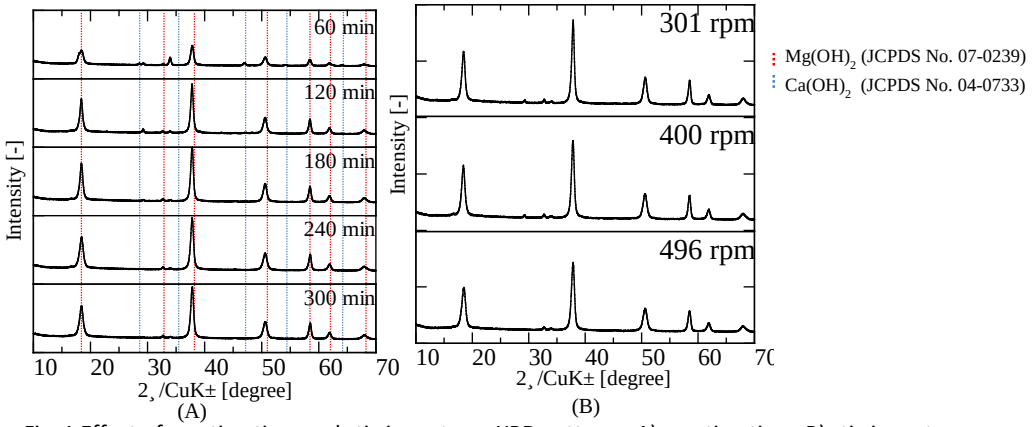

Fig. 1 Effect of reaction time and stirring rate on XRD patterns, A) reaction time, B) stirring rate

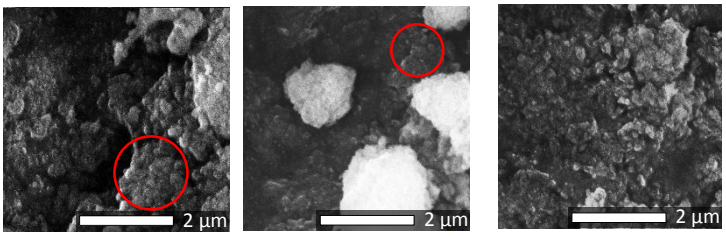

(a) **(b)** **(c)**

Fig. 2 Morphology of the products by changing the stirring rate, (a) 301 rpm, (b) 400 rpm, and (c) 496 rpm

4. Conclusions

This study was carried out to increase a crystal size of $Mg(OH)_2$ by reactive crystallization. The stirring rate and reaction time is considered to affect for the crystal size, their precipitates are identified and observed by XRD and SEM. From the XRD patterns, the amount of $Mg(OH)_2$ and crystal size were changed by operation conditions. From the SEM images, the crystallinity and the crystal size of $Mg(OH)_2$ are expected to increase at the slower stirring rate condition.

Acknowledgement

This research was supported by the Salt Science Research Foundation（No.18A5）, Japan.

Porous Magnetic Cross-Linked Enzyme Aggregates (Pm-Cleas) of Porcine Pancreas Lipase as Biocatalysts For Hydrolysis of Tributyrin.

José Renato Guimarães[1], Raquel de Lima Camargo Giordano[1], Roberto Fernandez-Lafuente[2], Paulo Waldir Tardioli[1*]

[1] *Graduate Program in Chemical Engineering, Department of Chemical Engineering, Federal University of São Carlos, São Carlos, Brazil*

[2] *Departmento de Biocatálisis, ICP-CSIC, Campus UAM-CSIC Madrid, Spain*

**Corresponding author: pwtardioli@ufscar.br*

Highlights

- Porous magnetic CLEAs (pm-CLEAs) of porcine pancreas lipase (PPL).
- High effectiveness factor and high thermal and operational stabilities.
- Easy recovery using external magnetic field and good reusability.

1. Introduction

Cross-linked enzyme aggregates (CLEAs) is an immobilization technique that does not require solid support, allows the use of semi-purified enzymes, and the biocatalyst has higher volumetric activity [1,2]. However, they present some problems, such as low mechanical resistance, difficulty of recovering and intraparticle diffusion limitations [2,3]. In this context, this work evaluated some strategies in the preparation of CLEAs of porcine pancreas lipase (PPL) to reduce these problems, such as: modification of the PPL surface with hydrophobic aldehyde, co-aggregation with protein feeders (soy protein (SP) and bovine serum albumin (BSA)), use of silica magnetic nanoparticles functionalized with amino groups (SMNPs) to aid the CLEA separation, and the use of starch as a pore forming agent.

2. Methods

The PPL surface was modified with dodecyl aldehyde (DDA) at a PPL:DDA mass ratio of 1:1 for 3 h at 25°C and pH 10 (100 mM sodium carbonate buffer) under 150 rpm stirring. After, sodium borohydride (1 mg/mL solution) was added to the solution and the reaction proceeded for 0.5 h. The modified enzyme was dialyzed at 4°C for 16 h. The aggregation/precipitation step was carried out by adding 3 mL of ethanol to 1 mL of modified PPL solution (5 mg/mL) prepared in 5 mM sodium phosphate buffer pH 7.0, containing 7.5 mg of BSA (or SP), 7.5 mg of SMNPs, and starch (0.8% w/v). The reaction proceeded for 0.5 h at 4°C under 150 rpm stirring. Glutaraldehyde was added to the suspension (5 μmoles of glutaraldehyde/mg total protein) and the cross-linking reaction proceeded for 15 h at 4°C under 150 rpm stirring. The precipitate was recovered by magnetic separation, washed, and resuspended in 3 mL of 5 mM sodium phosphate buffer pH 7.0. α-amylase (100 μL) was added in order to wash away the starch by hydrolysis at 25°C for 2 h. Porous magnetic CLEA of PPL (pm-CLEA) was physically and morphologically characterized, and applied in the hydrolysis of tributyrin at 40 °C, pH 8.0 for 4 h under 500 rpm stirring [4].

3. Results and discussion

The experimental strategies adopted in this work produced pm-CLEAs of PPL with immobilization yield (IY) around 100% and recovered activities (RA) between 67 and 81% for pm-BSA-CLEA and pm-SP-CLEA, respectively, suggesting that the proteins fedeers and nanoparticles reduced mass transfer problems in the CLEA supramolecular structure [4].

The highest activities for free PPL (32.2 ± 0.65 U/mg protein) and pm-SP-CLEA of PPL (24.13 ± 0.35 U/mg protein) were obtained at pH 8.0, while for pm-BSA-CLEA of PPL (19.14 ± 0.13 U/mg protein) was at pH 9.0. The pm-CLEAs of PPL were more thermally stable than the free enzyme, exhibiting maximum activity at 50°C, with pm-BSA-CLEA achieving 20% catalytic retention at 70 °C. The free PPL showed maximum activity under 500 rpm stirring, while the activities of the immobilized enzyme increased continuously within the range evaluated (250 to 1250 rpm). The pm-SP-CLEA and pm-BSA-CLEA exhibited high stability at 40 °C and pH 8.0, retaining approximately 50 and 80% of activity, respectively, after 10 h of incubation, while free PPL was inactivated after 2 h. These results suggest that pm-CLEAs have a fraction of PPL molecules more cross-linked to the nanoparticles, where stabilization effects should be higher due to the higher rigidity of this material compared to a protein, resulting in improved thermal stability to the immobilized enzyme.

The morphological characterization of pm-SP-CLEAs and pm-BSA-CLEAs using scanning electron microscopy (SEM) showed the presence of non-uniform and porous in the structure of the cross-linked PPL due to the hydrolysis of the starch molecules by the α-amylase, which could explain the high effectiveness factor (around $\eta = 0{,}65$), mainly for pm-CLEA of PPL prepared in presence of SP and SMNPs.

The hydrolysis profiles of tributyrin as a function of the time showed that the free enzyme rapidly loosed its catalytic activity, reaching yields of 36 and 52% for free PPL and pm-SP-CLEA, respectively. After five 4 h-batches, the hydrolysis yield of tributyrin decreased only 7% (from 52% to 45%), confirming the high mechanical and operational stability of pm-SP-CLEA.

4. Conclusions

Porous magnetic CLEAs co-aggregated with soy protein and magnetic nanoparticles showed good catalytic properties and performance/reusability in the hydrolysis of tributyrin. The strategies used in this work allowed reducing problems of low mechanical and operational resistance, improvements in intraparticle mass transport, and ease of recovery and reuse of the biocatalyst.

Reference

[1] Cao, L.; Rantwijk, F.; Sheldon, R.A. Cross-Linked enzyme aggregates: A simple and effective method for the immobilization of *Penicillin Acylase*. Org. Lett. 2000, 2, 1361–1364.

[2] Garcia-Galan, C.; Berenguer-Murcia, Á.; Fernandez-Lafuente, R.; Rodrigues, R.C. Potential of diferente enzyme immobilization strategies to improve enzyme performance. Adv. Synth. Catal. 2011, 353, 2885–2904.

[3] Cui, J. D.; Jia, S. R. Optimization protocols and improved strategies of cross-linked enzyme aggregates technology: Current development and future challenges. Crit. Rev. Biotechnol. 2015, 35, 15–28.

[4] Guimarães, J.R.; Giordano, R.L.C.; Fernandez-Lafuente, R.; Tardioli, P.W. Evaluation of strategies to produce highly porous cross-linked aggregates of porcine pancreas lipase with magnetic properties. Molecules, 2018, 23, 2993.

Porosity Control of Thin Film Prepared by Electrophoretic Deposition from Titania Nanoparticle Suspension.

Yasushige Mori*, Katsumi Tsuchiya, Yusuke Yagita

Department of Chemical Engineering and Materials Science, Doshisha University, Kyotanabe 610-0321, Japan

**Corresponding author: ymori@mail.doshisha.ac.jp*

Highlights

- The titania particle size can be controlled by milling condition.
- The porosity of the particle film prepared by EPD increased with used particle size.
- The film prepared from small-sized particles collapsed easily during drying process.
- The proposed force balance model could explain these conflicting phenomena.

1. Introduction

The particle film fabricated by depositing titania nanoparticles (NPs) is widely utilized for novel functional materials, such as the electrode of solar cells and lithium ion batteries, and water purification as photocatalysis. The major processes of making the particle film are the screen printing method, the spin coating method, the dip-coating method, and the electrophoretic deposition method (EPD) [1]. EPD has many superior features compared with other methods where the homogeneous films can be obtained on any forms of substrates, and easy control of the film thickness is achieved by adjusting the applied current and time. When the titania particle films are applied to use for the novel functional materials, the internal structure of the films is one of the key parameters to improve their abilities. However, the experimental conditions of EPD to control the internal structure of the film have not been discussed enough, although several studies have been pointed out to improve the performance of solar cells. In this paper, the effect of the titania particles size used for EPD on the internal structure, especially the porosity, of the film was reported.

2. Methods

The commercially available spherical P-25 NPs (Evonik) was used as the titania NPs for EPD. P-25 particle powder was dispersed into dehydrated-ethanol with acetylacetone by using the milling apparatus (HFM02, Ashizawa Finetech) with alumina beads. The particle size in the sample suspension was controlled by milling operation conditions. All the EPD experiments were carried out under DC constant current maintained by a potentiostat (AMEL 7050). The EPD electrodes were staged on a polyvinyl chloride plate with a 10-mm round hole and the distance between electrodes was 15 mm. The film thickness was measured with a surface profile meter (DEKTAK 150, Veeco). The weight of the deposited NPs was determined by the colorimetric method. The porosity of the thin film of particle deposition was calculated from the measured weight and thickness of film with the density of titania.

3. Results and discussion

When milling period increased, the particle size decreased, and then the mobility of particles during EPD and the electro conductivity of the suspension increased slightly. We found that the denser packed particle films were obtained by using the suspension with smaller-sized particles, and the local porosity of the film was increased with film thickness, as shown in Figure 1.

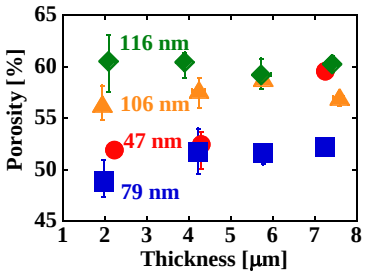

Figure 1. Effect of particle size on porosity of particle layer deposited by EPD.

Those phenomena could be explained that the new surface of titania particles was created due to break the aggregated particles during milling procedure, and then the surface charge density of titania particles and the counter ions in the medium increased as decreasing particle size. However, the total charge of individual particles increased with particle size, because the particle surface area increased more comparing with decreasing the surface charge density when particle size increased. This could be concluded that larger size particles with high total charge were repulsed strongly each other, and the porosity of the film prepared from those particles increased comparing with the case using small size particles, as a result. Therefore, changing the particle size is one of the effective methods to control the internal structure of the titania particle film fabricated by EPD.

However, the particle film prepared from smaller sized particles collapsed easily during drying process after EPD operation, in spite of the dense packed film. We proposed the force balance model for this phenomenon using van der Waals (F_v) and electrostatic (F_r) interactions between particles with the Coulomb force (F_E) from the electric field. The surface distance between particles was calculated, where the attraction forces (F_v + F_E) and the repulsion force (F_r) were balanced, and also determined its balanced force strength. In the case of small-sized particles, the surface distance was short, that means particles were packed closely. And the force strength at the force balanced point was weaker comparing with the case of large sized particles, that is particle adhesion force was weak. This calculation could explain the dependencies of the porosity of particle-deposited layer and the collapsed phenomenon at drying process on particle size of suspension.

4. Conclusions

In this study, the preparation of thin films of titania NPs by applying EPD from ethanol suspensions of different particle size led to the following findings: the porosity of deposition layer increased with particle size, but the strength of the deposition layer prepared from larger-sized particles was stronger than the case using smaller-sized particles. The proposed force balance model could explain those findings.

References

[1] Y. Mori, Y. Nobuzane, K. Nishimura, K. Yamada, K. Tsuchiya, Chem. Eng. Trans. 57 (2017) 1507–1512.

ECCE12
The 12th EUROPEAN CONGRESS OF CHEMICAL ENGINEERING
Florence 15-19 September 2019

Stability of polyurethane adhesives and rigid foams produced with industrial biomass by-products

Lukas Jasiunas*, Linas Miknius

Department of Organic Chemistry, Kaunas University of Technology, Kaunas, Lithuania

**Corresponding author: lukas.jasiunas@ktu.edu*

Highlights

- Polyurethane products were synthesized at significant levels of renewable content
- Comparable physical properties to commercial analogues were achieved
- Biopolyol blending shows promise at lowering isocyanate demands
- The products will be evaluated in terms of their stability, flammability and fire toxicity

1. Introduction

Multiple hydroxyl functional group containing compounds, commonly known as polyols, are currently produced from fossil resources, food competing or virgin feedstocks. Representing a significant portion of the polyol-isocyanate system in polyurethane production, their synthesis has to improve in order for humanity to advance into a more sustainable production of value added polymers. Previously produced renewable biopolyols are studied in the production of polyurethane wood adhesives and rigid foams [1].

Sugar beet pulp (residue from sugar production), hemp stalk hurds (residue from cannabidiol and hemp fibre production) and digested sewage sludge (waste water treatment residue) are the studied biomass feedstocks. The three represent by-products of well-established and upcoming industries. Crude glycerol (biodiesel production residue) is incorporated directly as the renewable low cost solvent for the liquefaction process. Finally, commercially available isocyanates are used as the second major component in the polyurethane product synthesis.

2. Methods

A two-step thermochemical liquefaction process, carried out at mild temperatures (110-170 C) and atmospheric pressure, was chosen to investigate the cumulative effects offered by homogeneous base and acid catalysis in batch biomass liquefaction. The stability of the produced wood adhesives (renewable content of 82-87%) and rigid foams (renewable content of 28-39 %) will be assessed in terms of thermal degradation (DTG, TGA-FTIR), fire properties and fire toxicity (Micro Combustion Calorimetry, Cone Calorimetry and Steady-State Tube Furnace), chemical resistance (water uptake and dimensional stability) and biodegradability (via soil burial tests).

3. Results and discussion

The objective of this work is to study the possibility of producing polyurethane products of high renewable content suitable for commercial applications by incorporating locally available biomass by-products. Furthermore, the effect of initial feedstock moisture (ranging from dry to as received) and particle size (from <0.2 mm to 0.5-1 mm fractions), parameters not studied extensively in previous research, are analysed in order to contribute to the knowledge base of direct and industry-friendly polyurethane synthesis. Finally, biopolyol blending is studied as an alternative mode of improving product properties at low isocyanate levels.

The novel findings on such product performance will aid in determining their feasibility. Thermal stability and pyrolytic-oxidative decomposition analyses will add clarity to how such composites compare in terms of fire safety and toxicity with their fossil-derived analogues. Finally, biodegradation adds yet another aspect to how sustainable future materials will have to be handled.

4. Conclusions

Polyurethane wood adhesives and rigid filler foams were successfully synthesized including various amounts of biopolyols. The products show comparable mechanical properties to their commercial counterparts. Meanwhile, the utilisation of biopolyol blending may have significant industrial benefits due to lower isocyanate demands. The products will also be evaluated in terms of their thermal and bio-stability, flammability and fire toxicity.

References

[1] Jasiūnas, L., Skvorčinskienė, R. and Miknius, L., 2018. Wet and Coarse: The Robustness of Two-Stage Crude Glycerol Mediated Solvothermal Liquefaction of Residual Biomass. *Waste and Biomass Valorization*, pp.1-11.

Co-precipitation of fluorescein with extracts of mango leaves by supercritical antisolvent process.

First Name Lastname[1], … First Name Lastname[2][Calibri 12]

1 Department of Chemical Engineering and Food Technology, Faculty of Sciences, University of Cadiz, International Excellence Agrifood Campus (CeiA3), Campus Universitario Río San Pedro, 11510, Puerto Real (Cadiz), Spain.

**Corresponding author: diego.valor@uca.es*

Highlights

- Enhanced solvent extraction was used to extract antioxidant compounds from mango leaves.
- Supercritical antisolvent process was an efficient method to obtain co-precipitated extract with fluorescein.
- Temperature, pressure and CO_2 flow rate had remarkable effects on particle formation.

1. Introduction

The use of polyphenols from natural resources as fruits, vegetables and nutraceuticals is increasing due to beneficial health effects. In fact, polyphenols possess diverse biological activities as antioxidant, antimicrobial, antidiabetic and anti-inflammatory properties [1]. Otherwise, fluorescein is a fluorescent organic substance which has important optical properties in solution. This characteristic allows it to be used as a marker [2] with interesting active ingredients to be able to track the substance in the organism. In the study reported here, the SAS technique (Supercritical Antisolvent process) optimization was carried out to obtain the co-precipitation of mango leaves extract and fluorescein microparticles. Organic solution containing the solute of interest is sprayed through a nozzle to generate drops of solution into a vessel containing CO_2 at supercritical conditions. During mixing, $scCO_2$ is quickly dissolved in the organic solution, causing the precipitation of solutes by antisolvent effect. Afterwards, scCO2 efficiently extracts the organic solvent, allowing to obtain completely solvent-free products.

2. Methods

2.1. Preparation of mango leaves extract

The extraction of antioxidant compounds of mango leaves was performed by enhanced solvent extraction. The ethanolic extract was obtained using the best conditions of pressure, temperature, CO_2 flow rate and solvent flow rate from previous studies [3]. The extract was obtained at 200 bar and 80 °C with 50% CO_2 – 50% Ethanol:50% water ratio.

2.2. Particle co-precipitation with the SAS process

The SAS technique was used to co-precipitate microparticles of mango extract and fluorescein. A pilot plant built by Thar Technologies® (SAS200) was employed for this purpose. A factorial of mixed levels desing ($3*2^2$ + 2 central points) was used to determinate the effect of pressure, temperature and CO_2 flow rate on the co-precipitation of mango leaves extract and fluorescein microparticles. The response variable used as control was the particle size. The conditions of the factorial desing were: temperatures of 35 and 55 °C; pressures of 150 and 200 bar; and CO_2 flow rates of 10, 20 and 30 g/min. In all the experiments, the concentration of the extract and fluorescein was 24 mg/ml and 6 mg/ml respectively.

3. Results and discussion

Most of the experiments in this work led to the successful co-precipitation of mango leaves extract and fluorescein together. The obtained particles from the extract were spherical, while fluorescein particles were precipitated with an irregular morphology, as show in Figure 1. In general, an increase in the values of the studied parameters led to an increase in the amount of precipitate in the tests performed.

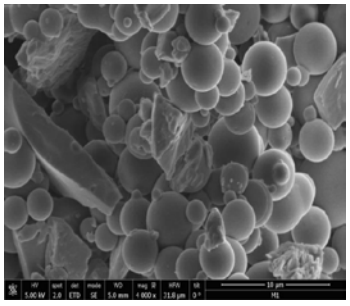

Figure 1. SEM Image of mango leaves extract with fluorescein microparticles

In reference to particle size distribution, it has been observed that the particle size of mango extract tended to decrease when pressure was decreased from 200 bar to 150 bar, obtaining particle diameters in the range of microns. In all cases, an increase in temperature led to a decline in both particle size. A decrease in CO_2 flow rate led to a smaller particle size in the case of fluorescein, but it happens in the opposite way to the mango leaves extract particles.

4. Conclusions

Microparticles of fluorescein with mango leaves extract have been obtained by a SAS process. Parameters that have a marked effect on particle size and size distribution have been evaluated in order to obtain the smallest particles possible. The experiments were successful in most cases. Higher temperature and lower pressure are recommended to obtain smaller particle size.

References

[1] H. Kim, J.Y. Moon, H. Kim, D.S. Lee, M. Cho, H.K. Choi, Y.S. Kim, A. Mosaddik, S.K. Cho, Food Chem. 121 (2010), 429-436.

[2] A. Clemente, R. Jiménez, M. Mar Encabo, M. Lobera, F. Balas, J. Santamaria, Journal of Hazardous Materials. 363 (2019), 358-365.

[3] M. Guamán-Balcázar, A. Montes, C. Pereyra, E. Martínez de la Ossa, J. Supercrit. Fluids. 128 (2017), 218-226.

ECCE12
The 12th EUROPEAN CONGRESS OF CHEMICAL ENGINEERING
Florence 15-19 September 2019

Electrochemical dissolution behavior of WC-Co in different electrolytes during micro wire-electrochemical machining

Abhijeet Sethi[1], Biswesh Ranjan Acharya[2], Partha Saha[3]*

1,2,3 Department of Mechanical Engineering, Indian Institute of Technology Kharagpur, West Bengal - 721302, India

**Corresponding author: psaha@mech.iitkgp.ernet.in*

Highlights

- Micro tool fabrication by micro wire-electro chemical machining process
- Study of electrochemical dissolution behavior of WC-Co in aqueous electrolytes
- Potentiodynamic polarization analysis through linear sweep voltammetry

1. Introduction

Micro tools, due to their versatility in creating profiles like micro holes, micro channels, micro gears, micro nozzles, micro grooves etc., have become the cornerstone of the micromachining industry [1]. The high hardness and the superior properties like high toughness and high rigidity of tungsten carbide cobalt alloy (WC-Co) have established it as an ideal material to be used as micro tools [2]. Electrochemical machining (ECM) easily dissolves hard metals with advantages like negligible tool wear, no machining force, no thermally induced stress, excellent surface quality and low roughness [1]. One of the most important factors in any electrochemical process is the selection of suitable electrolyte for successive electrochemical dissolution of work material. Therefore, attempts have been made in this study to investigate the performance of different electrolytes to find out their suitability in successive anodic dissolution of WC-Co using a cylindrical WC-Co rod of 510 µm initial diameter for fabricating micro tools, which are required for subsequent micro machining operations.

2. Methods

The electrolytes under this investigation were alkaline aqueous potassium hydroxide (KOH), neutral aqueous potassium nitrate (KNO_3) and acidic aqueous perchloric acid ($HClO_4$). To study the electrochemical dissolution behaviour of WC-Co in the above electrolytes, experiments were conducted by two processes: one is micro wire-electrochemical machining (WECM) and the other one is linear sweep voltammetry (LSV). The experiments in case of micro WECM process were conducted at three levels of a parameter keeping other parameters constant. Among the input parameters only electrolyte concentration and applied voltage were varied, one at a time. The electrolyte concentrations taken into consideration were 0.05 M, 0.15 M and 0.25 M and applied voltage 5 V, 10 V and 15 V for low, mid and high level respectively. The product oriented analysis like material removal rate (MRR) and average surface roughness (Ra) of the machined surface obtained through micro-WECM process were carried out. Furthermore, the electro chemical behaviour of WC-Co in three different electrolytes has been analysed by obtaining polarization curves from linear sweep voltammetry (LSV) where the voltage is varied from -1 V to 1 V at a rate of 0.05 V/s.

3. Results and discussion

As WC-Co is metal matrix composite of a hard phase (WC) enclosed in a binder phase (Co) its electrochemical dissolution needs to be homogenous for greater dissolution efficiency [3]. During the micro tool fabrication process through micro WECM, large amount of sludge is generated on the WC-Co alloy surface whose energy dispersive spectroscopy (EDS) study reveals the presence of tungsten, cobalt and oxygen. From figure 1 it can be found that the MRR in the alkaline electrolyte KOH is very poor, a higher MRR is obtained in case of neutral solution of KNO_3 at all levels, however, the MRR in case of $HClO_4$ is even higher in comparison to KNO_3. Figure 2 shows the comparison of average surface roughness of the machined surface. In case of neutral KNO_3 electrolyte the Ra values are found to be 0.469 µm,0.358 µm and 0.383 µm at low, mid and high level of parameters, respectively, which are lower in comparison to alkali and acidic electrolytes. The potentiodynamic polarisation curves (figure 3) obtained from linear sweep voltammetry show passivation in case of KOH electrolyte and the current density is very low in comparison to neutral and acidic electrolytes. In case of both KNO_3 and $HClO_4$, WC-Co alloy shows active dissolution and maximum current density is obtained in case of $HClO_4$, which confirms the higher MRR obtained in case of micro wire-ECM.

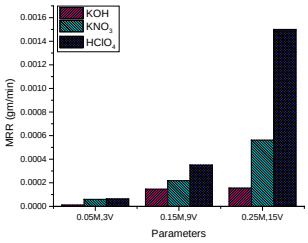

Figure 1. Relationship between material removal rate (MRR) and the level of process parameters for KOH, KNO_3 and $HClO_4$ electrolyte

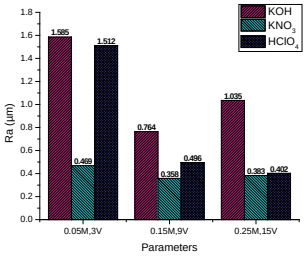

Figure 2. Relationship between material removal rate (MRR) and the level of process parameters for KOH, KNO_3 and $HClO_4$ electrolyte

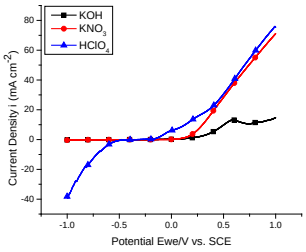

Figure 3. Linear sweep voltammetry (LSV) for WC-Co alloy in different electrolytes

4. Conclusions

The acidic electrolyte $HClO_4$ produces a higher MRR in comparison to both alkali KOH and neutral KNO_3 electrolytes at all levels of parameters. However, neutral electrolyte KNO_3 shows homogeneous dissolution of both WC and Co as the average surface roughness (Ra) values are found to be 0.469 µm, 0.358 µm and 0.383 µm at low, mid and high level of parameters, respectively, which are lower in comparison to alkali and acidic electrolytes. The potentiodynamic polarisation curves obtained from linear sweep voltammetry show better current density as evident for $HClO_4$ in comparison to KOH and KNO_3, which confirms the higher MRR obtained in micro WECM.

References

[1] Bhattacharyya, B., Electrochemical micromachining for nanofabrication, MEMS and nanotechnology. William Andrew, 2015.

[2] Bozzini B, De Gaudenzi GP, Fanigliul A, & Mele C, Electrochemical oxidation of WC in acidic sulphate solution. Corrosion science, 46.2 (2004) 453-469.
[3] Schubert, N., Schneider, M., Michaelis, A., Manko, M., & Lohrengel, M. M., Electrochemical machining of tungsten carbide. Journal of Solid State Electrochemistry, 22.3 (2018) 859-868.

ECCE12
The 12th EUROPEAN CONGRESS OF CHEMICAL ENGINEERING
Florence 15-19 September 2019

Control of Shell and Particle Porosity in Fluidized Bed Layering Granulation

Andreas Bück[1], Christoph Neugebauer[2], Carsten Seidel[2], Robert Dürr[3], Achim Kienle[2,3]

1 Institute of Particle Technology, Friedrich-Alexander University, 91058 Erlangen, Germany

2 Automation and Modeling, Otto von Guericke University, 39106 Magdeburg, Germany

3 Max Planck Institute for Dynamics of Complex Technical Systems, 39106 Magdeburg, Germany

**Corresponding author: andreas.bueck@fau.de*

Highlights

- steady-state operation of continues Fluidzed Bed Layering Granulation
- robust formation of tailor-made particle properties
- model-based process control with multiple input multiple output controller

1. Introduction

An important class of particle formulation processes is the fluidized bed layering granulation (FBLG). It is widely applied in processing industries to gain high-quality granules. In brief, a solid containing liquid is sprayed onto a bed of fluidized particles. Since the fluidization medium is a heated gas, the liquid phase of the injection evaporates while the solid remains on the particles surface inducing a layer-wise particle growth. On the large scale FBLGs are operated continuously. This allows the formulation of particles with uniform characteristics under steady state conditions.

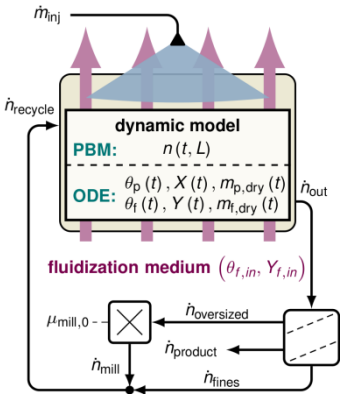

Figure 1. Structure of the dynamic model as presented in [4].

It is well known from previous studies that particle properties depend on the process conditions. For instance, Rieck et al. [1] showed by means of experiments that the thermal conditions of the FBLG process determine the porosity of the particle shell and, in consequence, the apparent particle porosity and density. As Litster and Ennis [2] pointed out, most of the other particle properties, e.g. particle strength, flowability, and dissolution behavior depend on the shell or apparent particle porosity and particle size. Therefore, constant thermal conditions are essential for the production of tailor-made particles. As was shown by Neugebauer et al. [3], the application of feedback controllers is promising to improve the performance of particulate processes. Scope of the present contribution is the development and validation of a multiple input multiple output MIMO control strategy which is capable to control both, particle size and porosity.

2. Methods

The present contribution is based on the dynamic model of FBLG presented in Neugebauer et al. [4]. The model consists, as depicted in Figure 1, of two bi-directional coupled sub-models: The first, a population balance model, represents the growth of the particles; the second considers the

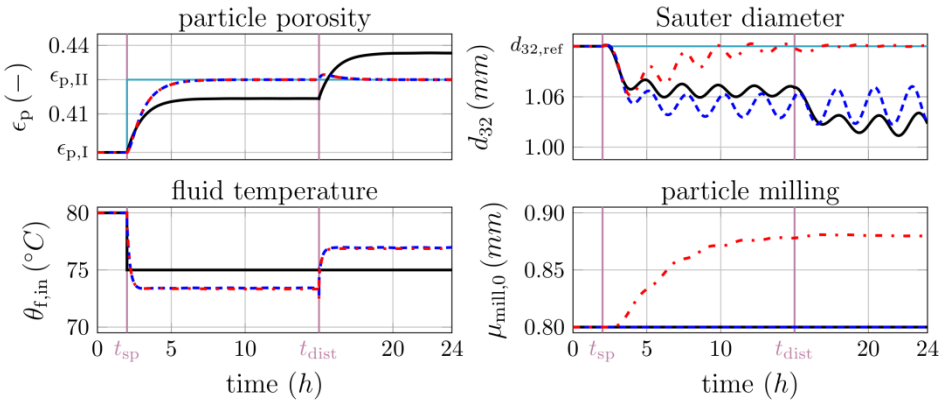

Figure 2. Simulation results according to different configurations: open-loop (black solid line), SISO (blue dashed), and MIMO control strategy (red dash-dotted).

thermal conditions within the granulation process. In the present contribution, the dynamic model is extended to account for (a) the dynamics of the temperature $\theta_{f,in}$ due to the heating and (b) the influence of particle porosity ε_p on the breakage behavior during milling. Afterwards, the resulting model is linearized in the vicinity of a given reference point. By means of the root-locus method two decentralized PI controllers are designed. The first controls ε_p by adjusting $\theta_{f,in}$, the second stabilizes the particle size distribution – here the Sauter diameter d_{32} is used as a representative - by actuating the mill $\mu_{mill,0}$.

3. Results and discussion

To study the influence of different operating parameters on the process dynamics and product properties the following scenario is defined: at t_{sp} = 2 h the set-point of ε_p is increased, whereas a process disturbance, in specific an increase of $Y_{f,in}$, appears at t_{dist} = 15 h. The corresponding simulation results are presented in Figure 2. As indicted by the open-loop results, the manipulation of $\theta_{f,in}$ and $Y_{f,in}$ induce variations of ε_p. However, a proper adjustment of ε_p is challenging as it depends significantly on both parameters. This issue can be overcome, as illustrated by the simulation results, by the application of the first controller: By actuating $\theta_{f,in}$ the particle porosity ε_p can be driven to its new reference value. In addition, the process disturbance at t_{dist} = 15 h can be rejected. On the contrary, a change of ε_p results in variations of the breakage behavior of particles. In consequence, as monitored by d_{32}, self-sustained oscillations of the particles size distribution can occur. As those highly undesired oscillations provoke variations of bed mass and mass flows they might result in a process break-down. To stabilize the particle size distribution, the control strategy is extended by the second controller. Referring to the simulation results presented in Figure 2, the application of the overall control strategy guarantees both, a stable process regime as well as constant product properties.

Acknowledgments The financial support of DFG (Deutsche Forschungsgemeinschaft) within the priority program SPP 1679 is gratefully acknowledged.

References

[1] C. Rieck et al., Powder Technology, 272 (2015), 120 – 131.
[2] J. Litster, B. Ennis, The Science and Engineering of Granulation Processes, 2004.
[3] C. Neugebauer et al., Powder Technology, in press, DOI: 10.1016/j.powtec.2019.05.030
[4] C. Neugebauer et al., Processes, 6 (2018), 235.

Novel Polymer Gel Electrolytes for Efficient Photo-Electrochemical Applications

Ji-Eun Lee, Bo-Sung Kang, Ji-Hyeon Lee, Moon-Sung Kang*

Department of Green Chemical Engineering, Sangmyung University, 31, Sangmyeongdae-gil, Dongnam-gu, Cheonan, Chungnam 31066, Republic of Korea

**Corresponding author: solar@smu.ac.kr*

Highlights

- Novel polymer gel electrolytes (PGEs) are prepared and characterized
- The PGEs are used for successful application to various photo-electrochemical applications
- The PGEs showed the merit of easy cell fabrication as well as high ion conductivity
- Durability of the photo-electrochemical cells is largely enhanced by employing the PGEs

1. Introduction

Polymer gel electrolytes (PGEs) have been widely investigated and utilized in various electrochemical applications such as lithium secondary batteries and dye-sensitized solar cells (DSCs) because they possess moderate ion conductivity and high physical stability [1,2]. They have also been developed for the application to electrochromic devices (ECDs). Recently, ECDs have been attracting much attention owing to their use as a smart window. A smart window or a smart glass can effectively control the light transmission properties for the purpose of proper lighting or heating etc. The PGEs as one of the key components of the ECDs can dominate the major characteristics of transmittance and colored time etc. Especially, the ion conductivity and volatility of the PGEs should be optimized for the fabrication of efficient and durable ECDs. In addition, efficient injection process of highly viscous PGEs during the fabrication of large area ECDs should also be considered. In this work, therefore, we have developed the PGEs which can be easily loaded as a film and then in-situ polymerized through UV irradiation. Moreover, we have developed and characterized novel PGEs consisting of ionic liquid and thermo-responsive polymer. We expect that the PGEs could also be applied to various photo-electrochemical devices such as DSCs for the efficient energy harvesting from solar irradiation.

2. Methods

Various solvents including sulfolane, propylene carbonate (PC), diethyl carbonate (DEC), ethylene carbonate (EC), γ-butyrolactone (GBL), dimethylformamide (DMF), N-methyl pyrrolidone (NMP), dimethyl sulfoxide (DMSO), and dimethylacetamide (DMAc) were used for preparing the PGEs. Several acrylate monomers and polyethers were employed for the formation of the interpenetrating polymer network (semi-IPN) in the PGEs. The ionic conductivity was measured using a 4-point probe cell connected to an impedance analyzer. The PGEs were also employed for

the fabrication of ECDs and DSCs and their photo-electrochemical performances were systematically investigated.

3. Results and discussion

In this work, the optimal composition of the PGEs has been systematically investigated. For example, we have evaluated the effect of a solvent on the optical density of an ECD cell as shown in Figure 1. The optical density of an ECD is shown to largely affected by solvent properties such as donor number, dielectric constant and, viscosity. Through several analytical investigations, we could determine the optimal composition of the PGEs. The more detailed results will be presented at the conference.

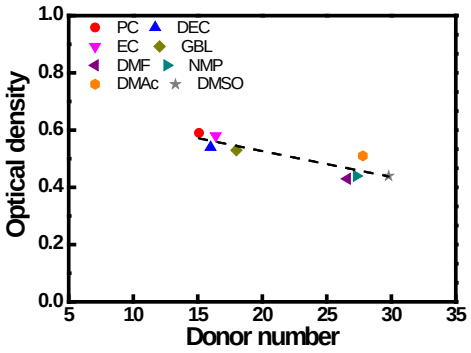

Figure 1. Relationship between solvent property (donor number) and optical density of ECD.

4. Conclusions

In this work, we have prepared novel PGEs for the successful application to various photo-electrochemical applications such as ECDs and DSCs. The prepared PGEs showed the merit of easy cell fabrication as well as high ion conductivity. In addition, the durability of the photo-electrochemical cells was shown to be largely enhanced by employing the PGEs.

This work was financially supported by the Environmental Industry Advancement Technology Development Project of Korea Environmental Industry & Technology (KEITI) funded by Korea Ministry of Environment (MOE) (No. 2017000140002/ RE201702218).

References

[1] F. Bella, E.D. Ozzello, A. Sacco, S. Bianco, R. Bongiovanni, Int. J. Hydrog. Energy 39 (2014) 3036-3045.
[2] H. Ben youcef, O. Garcia-Calvo, N. Lago, S. Devaraj, M. Armand, Electrochim. Acta 220 (2016) 587-594.

Properties of liquid marbles stabilized by stearate microparticles for microreactors

Shoma Tanaka[1], Hiroaki Okano[2], Nobuyuki Matsuda[2], Kazumitsu Naoe[1*], and Masanao Imai[3]

1 Dept. of Materials Sci. & Chem. Eng., Faculty of Advanced Eng., National Institute of Technology, Nara College, Yamato-Koriyama, Nara 639-1080, Japan; 2 Research Division, Taihei Chemical Industrial Co. Ltd., Ikaruga, Nara 636-0104, Japan; 3 Graduate School of Bioresource Sci., Nihon University, Fujisawa, Kanagawa 252-0880, Japan

**Corresponding author: naoe@chem.nara-k.ac.jp*

Highlights

- The height of liquid marbles increased and reached a constant value as the core liquid volume increased.
- Drying rate of liquid marble was dependent upon the core liquid solution in the liquid marble.
- Surfaces of the liquid marbles were not fully coated with the microparticles.

1. Introduction

Liquid marble is a non-stick drop coated with micro- or nano-scale particles demonstrating extremely low friction when rolling on solid substrates. Liquid marbles can be obtained easily by rolling water drops on a solid substrate covered with hydrophobic powder layer or by mixing a hydrophobic powder in water [1]. Liquid marbles have great potential in a wide range of applications such as water quality testing and micro bioreactor etc. [2, 3]. Stearates, salts of stearic acid included in animal fat, have insolubility in water and no toxicity, and are used in thickener as a food additive and an anti-adherent for the manufacture of medical tablets. In this study, preparation of liquid marbles (LMs) using stearate microparticles (SMs) and their properties for microreactors are investigated.

2. Methods

For preparation of LMs we used calcium SMs. It has peaks at 5 µm and 100 µm in the size distribution. Aqueous solutions were dropped by syringe onto a substrate surface covered with a layer of calcium SMs. Slight tilting of the covered substrate surface caused the drop to roll and become coated with calcium SMs. The height and drying rate of prepared LMs were measured. The weight of LMs was recorded with time by electronic balance in a low temperature & humidity test chamber at 35˚C and 40 % (RH) of humidity. The drying rate of the LMs was calculated from the weight data. The initial surface of LMs was observed by optical microscopy.

3. Results and discussion

At small core liquid volumes of the LMs they were spherical, but as the volume increased it changed to a puddle shape. The heights of LMs at various core liquid volumes are shown in Fig. 1. As the liquid volume increased, the height of LM increased and reached a constant value (H_{max}). The drying rates of LMs containing each core solution calculated from the weight data are shown

in Fig. 2. The drying rate of LMs was dependent upon the core liquid solution of LMs. The obtained drying curves of LMs were similar with general drying curves of wetted powders. Drying rate of liquid marble was dependent upon the core liquid solution in the liquid marble. The drying rate of the LMs prepared with 0.1 M $MgCl_2$ aqueous solution is the lowest.

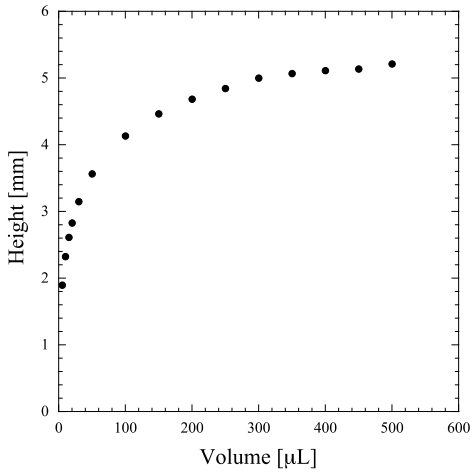

Fig. 1 Relationship between core liquid volume and height observed from side in the preparation of liquid marble.

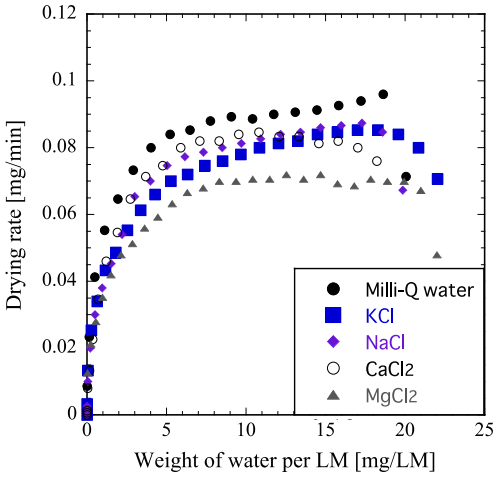

Fig. 2 Relationship between drying rate of LM and weight of core liquid per LM. Salt conc. = 0.1 M.

Fig. 3 shows a microscopic image of the surface of LMs prepared with $MgCl_2$ aqueous solution before drying. The initial surfaces of the LMs were not fully coated with SMs, indicating that gas or vapor can be transported through the surface of LMs.

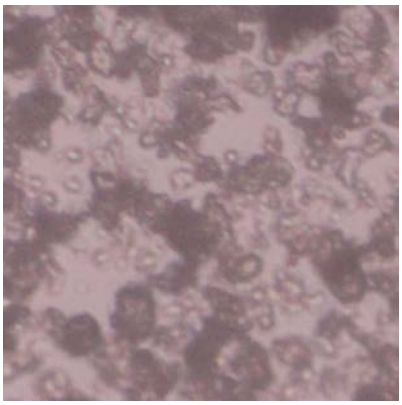

Fig. 3 Microscopic image of surface of SMs LMs prepared with 0.1 M $MgCl_2$ aqueous solution.

4. Conclusions

Preparation of LMs using SMs and their properties for microreactors were investigated. At small core liquid volumes of the LMs they were spherical, but as the volume increased it changed to a puddle shape. The heights of LMs at various core liquid as the liquid volume increased, the height of LM increased and reached a constant value (H_{max}). The drying rate of LMs was dependent upon the core liquid solution of LMs. The initial surfaces of the LMs were not fully coated with calcium SMs, indicating that gas or vapor can be transported from surface of LMs.

References

[1] Aussillous, P. and Quere, D. Nature, 411, 924-927 (2001)
[2] Junfei, T. et al., Chem. Eng. J., 165, 348-353 (2010)
[3] Vadivelu, R. K. et al., Sci. Rep., 7, 12388 (2017)

Preparation of UV-curable biodegradable functionalized polyesters

T. Cernadas[1], F. M. M. Gonçalves[1], P. Alves[1], Sónia P. Miguel[2], I. J. Correia[1,2], P. Ferreira[1]
1 CIEPQPF, Department of Chemical Engineering, University of Coimbra, Portugal; 2 CICS-UBI, University of Beira Interior, Covilhã, Portugal

**Corresponding author: pferreira@eq.uc.pt*

Highlights

- Photocrosslinkable biodegradable copolymers were developed based on unsaturated polyesters;
- Photocrosslinking was achieved with a UV exposure time of 2.5 minutes;
- Flexible materials at room and physiological temperatures were obtained;
- According to the obtained results, the materials are suitable for biomedical applications.

1. Introduction

Traditional methods of wound closure are suturing and stapling, but they are associated with pain, wound infection and low aesthetic results. As a result of these shortcomings, medical tissue adhesives are considered an attractive alternative since, besides wound closure, they can accomplish other tasks, such as haemostasis and the ability of sealing air leakages [1,2]. The most used surgical glues nowadays are the fibrin based adhesives [3] and cyanoacrylates [4]. Fibrin based adhesives present several problems, e.g. immunogenicity and risk of blood transmission diseases such as HIV and BSE [3]. Cyanoacrylates have been reported to degrade in aqueous media to produce formaldehyde, which causes inflammation and has got carcinogenicity potential [5]. Other options are now being considered, and among them, photopolymerizable/photocrosslinkable adhesives are the most promising.

The study and development of new biocompatible materials to be applied as UV-curable adhesives is extremely important to grant the preparation of matrices with controlled properties (such as mechanical, biological and thermal) with a fast curing rate when in contact with living tissues. Unsaturated polyesters (UP) present some interesting characteristics to be used in this application due to their inherent biodegradability (ester linkages), potential biocompatibility and to its internal carbon-carbon double bonds that allow them to be photopolymerized forming crosslinked networks [6].

2. Methods

Photocrosslinkable biodegradable copolymers were developed based on unsaturated polyesters (prepared from PEG modified with fumaric acid) and lactic acid oligomers (oligoLA) functionalized with 2-isocyanatoethyl methacrylate (IEMA® by BASF).

During this work, three stoichiometric proportions between the UPs and oligoLA were tested, which, after the addition of a biocompatible photoinitiator (Irgacure® 2959 by CIBA), allowed to obtain flexible, resistant and uniform matrices after 2 minutes and 30 seconds of UV irradiation. The prepared materials were then further characterized, by water sorption capacity evaluation,

determination of gel content, dynamic contact angles measurements, hydrolytic degradation in vitro, as well as thermal characterization (TGA and DMTA). ATR-FTIR and 1H NMR analyses were performed to allow a follow-up of the synthesis, functionalization and photocrosslinking reactions. Finally, their biocompatibility using human dermal fibroblasts (hFib) and antibacterial activity when incubated with Escherichia Coli and Staphylococcus Aureus were evaluated in vitro.

3. Results and discussion

ATR-FTIR and 1H NMR analyses allowed to confirm the reaction between the OH groups of PEG with the COOH of fumaric acid. Also, the bands and peaks correspondent to the C=C bonds were detected in both spectra proving the chemical functionalization of the materials.

Dynamic contact angles determination showed that incorporation of unsaturated polyester leads to more hydrophilic matrices.

It has been found that the rate of degradation of the matrices is closely related to the crosslinking degree and the swelling capacity. In other words, more hydrophilic materials with a lower gel content tended to degrade more rapidly, as did the adhesive composed mainly of UP.

Thermal analysis indicated that the films are stable at physiologic and room temperature. Despite the increase in Tg after curing, this fact does not compromise the film's flexibility since its value remains lower than physiological and room temperatures.

In cell viability studies, the results obtained were satisfactory for two of the three developed adhesives, with cell viability values of around 100% even after 7 days of incubation. The exception was the adhesive containing the highest amount of the oligomer functionalized, which, in turn, recorded values of 50% at the end of the same incubation period. Also, antibacterial activity in the presence of Escherichia Coli and Staphylococcus Aureus was assessed, and inhibition halos were visualized around the materials, allowing to conclude that they present antibacterial activity.

4. Conclusions

The adhesives resulting from the copolymerization of UP and oligoLA functionalized have been shown to be resistant, flexible and with adequate viscosity before a possible application and thermally stable, with very satisfactory crosslinking times.

Considering the obtained results, it is possible to affirm that the UV-curing surgical adhesives developed in this work may come to take a prominent place in the bioadhesive market.

References

[1] Y. Ikada, H. Tsuji, Macromol. Rapid Commun, 21 (2000) 117-132.
[2] M. Mehdizadeh, J. Yang, Macromolecular Bioscience, 13 (2013) 271-288.
[3] P. Ferreira, J. F. J. Coelho, J. F. Almeida, M. H. Gil, in Reza Fazel-Rezai (Ed.), Photocrosslinkable Polymers for Biomedical Applications, Biomedical Engineering - Frontiers and Challenges, InTech, 2011, pp. 55-74.
[4] A. P. Duarte, J. F. Coelho, J. C. Bordado, M. T. Cidade, M. H. Gil, Progress in Polymer Science, 37 (2012) 1031-1050.
[5] A. S. Karikari, W. F. Edwards, J. B. Mecham, T. E. Long, Networks, Biomacromolecules, 6 (2005) 2866-2874.
[6] K. Guo, C. C. Chu, Biomaterials, 28(22) (2007) 3284–3294.

Influence of process and formulation parameters for the encapsulation of ibuprofen by the co-spray drying process

Lucas Ruffel[1], Fabien Brouillet[2], Jérémy Soulié[2], Christine Frances[1], Mallorie Tourbin[1]

1 Laboratoire de Génie Chimique, Université de Toulouse, CNRS, Toulouse, France;
2 CIRIMAT, Université de Toulouse, CNRS, Toulouse, France

**Corresponding author: lucas.ruffel@ensiacet.fr*

Highlights

- Co-spray drying process is used as an encapsulation tool.
- Operating parameters affect the loading of mesoporous silica nanoparticles.
- Ibuprofen is present in different states and location is revealed.

1. Introduction

Nanosystems for biomedical applications present a great interest as therapeutic tools for the controlled release of active substances [1]. In this context, Mesoporous Silica Nanoparticles (MSN) are relevant drug carriers due to their biocompatibility [2] and high specific surface. Several processes may be used for drug loading [3]. Spray drying, currently used in the industry to dry a product, has a good potential for encapsulation [4], [5]. In this work, ibuprofen (poorly water-soluble molecule) is loaded inside the MSN by co-spray drying. Some properties after loading and their end-used properties can be modified depending on formulation parameters (Ibu/Si weight ratio (R=Ibu:Si), silica concentration, solvent) and process parameters (suspension flow rate, drying gas temperature, drying time, dispersion conditions, spray mesh size).

2. Methods

MSN with controlled properties (pore and particle diameter) were first synthesized with a semi-continuous sol-gel process. Then, the drug loading was performed using the Nano Spray Dryer B-90 (Büchi) [6]. An ultrasonic processor was used to facilitate the drug dissolution and the MSN dispersion. Several characterization techniques allowed improving the knowledge of the properties of the MSN and of the final carriers. Microscopic techniques (TEM, SEM) reveal the aspect of the material. The use of physico-chemical characterizations gives access to many information about the final product: DLS (MSN diameter), SAXS (porous organization), N_2 adsorption (specific area, pore diameter). The combination of different solid-state (SS) techniques informs about the physical state and the drug-silica interactions (TGA, XRD, SS NMR). Complementary and multi-scale characterization techniques permit a real understanding of the parameters influence on loaded-particles properties.

3. Results and discussion

As an example, the results for the influence of the Ibu:Si weight ratio are presented here. The presence of crystalline ibuprofen on dried powder from R=40:60 to 100:0 was shown with XRD patterns and confirmed by TGA (which quantifies the amount of crystalline and amorphous solid). SS NMR revealed information about its mobility (solid or liquid-like) and its interaction with silica

according to the Ibu:Si ratio. SEM and TEM observations suggested a conservation of the MSN matrix, but the MSN agglomerates did not have the same shape according to the Ibu:Si ratio, and the crystals shown by XRD seemed to be outside of the pores at R=75:25 (Figure 1). The pore and crystal sizes confirmed the impossibility for crystalline ibuprofen to be inside the pores [7]. SAXS and N_2 adsorption gave a decreasing trend of peak intensities (SAXS), surface area, pore volume and pore diameter (N_2 adsorption) as the Ibu:Si ratio increased, suggesting a loading of the active substance inside the pores of the MSN.

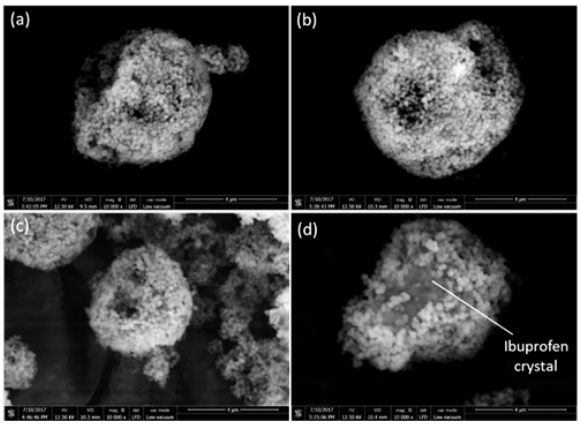

Figure 1. SEM images (x10k) of agglomerates with different R: 0:100 (a), 25:75 (b), 50:50 (c), 75:25 (d)

Sample (R=Ibu:Si)	Specific area ($m^2.g^{-1}$)	Pore volume ($cm^3.g^{-1}$)	Pore diameter (nm)
MSN	777	0.727	3.08
20:80	477	0.357	2.19
35:65	80	0.098	2.19

Table 1. Structural information determined by Nitrogen Adsorption

The combination of all these characterization techniques indicates links between the ibuprofen location (in or out of the pores) and its physical state (crystalline, amorphous, liquid-like). The other operating parameters had also an effect on the size of the particles and the ibuprofen loading.

4. Conclusions

The plentiful techniques permit to reveal that the drug is loaded firstly in the pores, and has been found in different states which are related to the localization inside the system (inside or outside the pores of the MSN). The Ibu:Si ratio influences drastically the agglomerate structure and the physical state of the substance. Afterwards, the effect of the parameters on the end-used properties like drug release kinetic will also be studied.

References

[1] A. Z. Wilczewska, K. Niemirowicz, K. H. Markiewicz, H. Car, Pharm. Rep. 64 (5) (2012) 1020-1037.
[2] M. Vallet-Regí, M. Colilla, I. Izquierdo-Barba, M. Manzano, Molecules. 23 (1) (2017) 47, 1-19.
[3] T. Numpilai, S. Muenmee, T. Witoon, Mater. Sci. Eng. C 59 (2016) 43-52.
[4] M. Fatnassi, C. Tourné-Péteilh, T. Mineva, J.-M. Devoisselle, P. Gaveau, F. Fayon, B. Alonso, Phys. Chem. Chem. Phys. 14 (35) (2012) 12285-12294.
[5] S.-C. Shen, W. K. Ng, L. Chia, J. Hu, R. B. H. Tan, In. J. Pharm. 410 (1-2) (2011) 188-195.
[6] K. Schmid, C. Arpagaus, W. Friess, Pharm. Dev. Technol. 16 (4) (2011) 287-294.
[7] T. Azaïs, C. Tourné-Péteilh, F. Aussenac, N. Baccile, C. Coelho, J.-M. Devoisselle, F. Babonneau, Chem. Mater. 18 (26) (2006) 6382-6390.

ECCE12
The 12th EUROPEAN CONGRESS OF CHEMICAL ENGINEERING
Florence 15-19 September 2019

A conceptual design of Cr(VI)-free anti-corrosion solutions for aerospace applications

Bhavya Goyal[1], Gabriela Hadiwinoto[1], Kleopatra Papamichou[1], Yuyang Tian[1], Zerui Zhang[1*], Pieter Swinkels[1]

1 Delft University of Technology, Faculty of Applied Science, Van der Maasweg 9, 2629 HZ, Delft, The Netherlands

**Corresponding author: Z.Zhang-9@tudelft.nl*

Highlights

- Chromium free anti-corrosive coating for the aerospace industry
- Rare earth metals as corrosion inhibitors and silyl ester as a healing agent

1. Introduction

The high standards of the Aerospace Industry often push the limits of science and one of those times is the protection of aircraft against corrosion. Currently, the coating of an aircraft is made by hand-spraying and the paint itself contains hazardous compounds, with Chromium (VI) to be the most infamous one. This process is not only harmful to the environment but creates major health issues to the painters and raises a lot of concerns. Chromium (VI) salts are very effective and provide a "self-healing" active corrosion inhibition to aluminium substrates. This carcinogenic and toxic compound is banned in the EU and is only permitted in situations where there are no good alternatives, such as in aircraft corrosion prevention. This work provides two Cr-free conceptual designs as the anti-corrosive solutions to be used in the aerospace industry. The two concepts try to mimic the two properties of Chromium (VI) in a safe way: corrosion inhibition and self-healing.

2. Methods

The Delft Design Map (DDM) was systematically followed to frame and organize the designs [1]. Design requirements were identified by translating the needs of stakeholders and the design specifications are generated and evaluated using House of Quality (HoQ) to determine the important features of the final product which were the basis of our design concepts. The corresponding manufacturing process is partially proposed and assessed via safety, health, environment, economic, technology and social (SHEETS) analysis.

3. Results and discussion

The first conceptual design concept proposes the use of rare earth metals as corrosion-inhibitors which work by creating effective protective barriers. Cerium salts, with which researchers have been experimenting for years, oxidize only once and the protective layer they create is not permanent [2]. Long-term protection, therefore, requires the continuous release of these inhibitors. For these, the proposed idea is borrowed from the biomedical community and includes the encapsulation and controlled release of the corrosion inhibitor by macroporous silica particles [3].

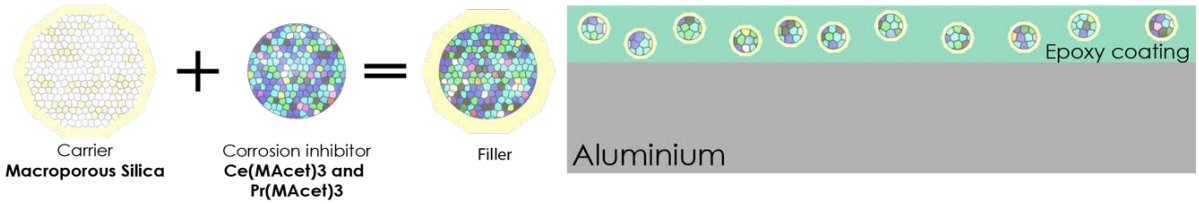

Figure 1. Corrosion inhibitors carried by macroporous silica.

The second conceptual design concept is oriented in the direction of actively protecting the surface of the aircraft against any kind of damage, by the use of "self-healing" materials. The idea is to prevent corrosion that is caused by cracks on the coating of the aircraft, by automatic repair of these cracks. The repair of these cracks can be promoted by silyl ester as a healing agent that can form an adhered-to-the-metal hydrophobic barrier system [4]. Relatively similar to the first concept, the self-healing agent is protected in microcapsules until the moment of action [4].

The preliminary analysis of the two designs shows promising results and a lot of margin for completion. This work can be seen as a thoughtful exploration of the alternatives to the problem of Chromium (VI).

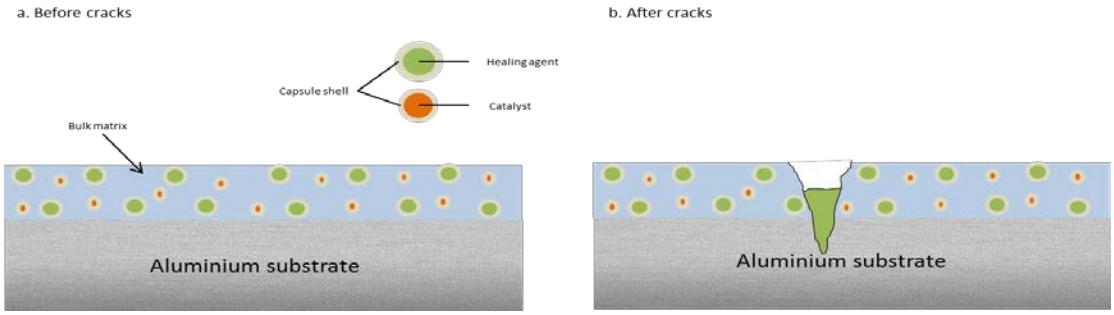

Figure 2. Capsule-based self-healing coating

4. Conclusions

The conceptual designs exhibit possibilities of providing adequate anti-corrosive properties without compromising the structural integrity of an aircraft. In terms of application and maintenance, they facilitate an easier and less hazardous process. However, the thickness of such a coating can exceed acceptable limits and add extra weight, creating issues with the aerospace industry. Therefore, it is proposed to focus on more research in order to combine the two concepts and eliminate their disadvantages.

References

[1] J. Harmsen, A. B. de Haan, P. L. Swinkels, Product and Process Design: Driving Innovation. Walter de Gruyter GmbH & Co KG, 2018.

[2] R. Catubig, A. E. Hughes, I. S. Cole, B. R. W. Hinton, and M. Forsyth, “The use of cerium and praseodymium mercaptoacetate as thiol-containing inhibitors for AA2024-T3,” *Corros. Sci.*, vol. 81, pp. 45–53, Apr. 2014.

[3] J. M. Falcón, F. F. Batista, and I. V. Aoki, “Encapsulation of dodecylamine corrosion inhibitor on silica nanoparticles,” *Electrochim. Acta*, vol. 124, pp. 109–118, 2014.

[4] S. J. García *et al.*, “Self-healing anticorrosive organic coating based on an encapsulated water reactive silyl ester: Synthesis and proof of concept,” *Prog. Org. Coatings*, vol. 70, no. 2–3, pp. 142–149, Feb. 2011.

ECCE12
The 12th EUROPEAN CONGRESS OF CHEMICAL ENGINEERING
Florence 15-19 September 2019

Selftuning adaptive control for convective drying of particulate solids

Robert Dürr[1,*], Carsten Seidel[2], Christoph Neugebauer[2], Andreas Bück[3]

1 MPI for Dynamics of Complex Technical Systems, Sandtorstraße 1, D-39106 Magdeburg, Germany;

2 Otto von Guericke University, Universitätsplatz 2, D-39106 Magdeburg, Germany;

3 Friedrich Alexander University, Cauerstraße 4, D-91058 Erlangen, Germany;

**Corresponding author: duerr@mpi-magdeburg.mpg.de*

Highlights

- Convective drying of particulate solids
- Model-based controller design
- Automatic adaption of controller parameters
- Guaranteed product quality under varying drying conditions

1. Introduction

Drying, the removal of a liquid from a solid material represents one of the most important operations in the chemical, pharmaceutical and food industries. Besides mechanical liquid removal, thermal drying is extensively applied: Here, a moist solid is heated resulting in subsequent phase change of the liquid into vapor and removal of the vapor from the solid. Thermal dryers are usually categorized by the respective method of heat supply, e.g. contact dryers and convective dryers. Considering the latter, characteristic evaporation rates depend on the moisture content as seen in Fig. 1. Within the second drying phase evaporation rates result from an complex interplay of thermal and moisture fields in the particle [1]. This coupling can be described by the concept of normalized drying curves. Given experimental data, such a curve can be fitted and used for further model-based control design and process intensification. However, such an appropriately designed controller may not be able to keep the desired quality of the product, e.g. moisture content of the dried solid, in presence of external influences like seasonal or local variations in the properties wet solid. Such deviations come along with unforeseen variations of the drying kinetics, i.e. shape variations of the normalized drying curve, and manifest for example in over-/underdrying of the product as well as on-set of unwanted reactions. As an alternative to robust control design techniques which use a fixed controller in order to cope with the described variations [2], adaptive controllers employing online-tuning can be applied to guarantee the desired product specifications [3].

2. Methods

Within this contribution convective conveyor belt drying of baker's yeast is considered which can be described by a set of nonlinear ordinary differential equations [2]. To cope with variations in the drying conditions a self-tuning adaptive controller is applied. Its basic structure is seen in Fig. 1: An approximate simple model of the process is identified online from process measurements via recursive least-squares estimation. The simplified model is used for adaption of the parameters of

the controller which is applied to the complex process . This procedure is also known as adaptive pole-placement.

3. Results and discussion

The selftuning regulator's performance is validated in a parametric study for several scenarios, including uncertainty of the shape of the normalized drying curve as well as disturbances of the solids and gas inlet temperature. The adaptive controller is applied to the nonlinear process and compared to the performance of a nominal PI-controller with fixed tuning parameters. The simulation results in Fig. 1 indicate that the latter is outperformed by the adaptive controller.

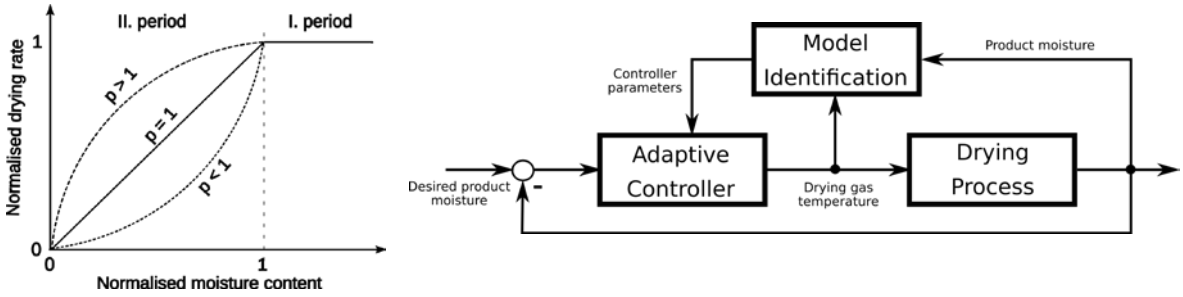

Figure 1. Normalized drying curve (left) and applied adaptive controller structure (right)

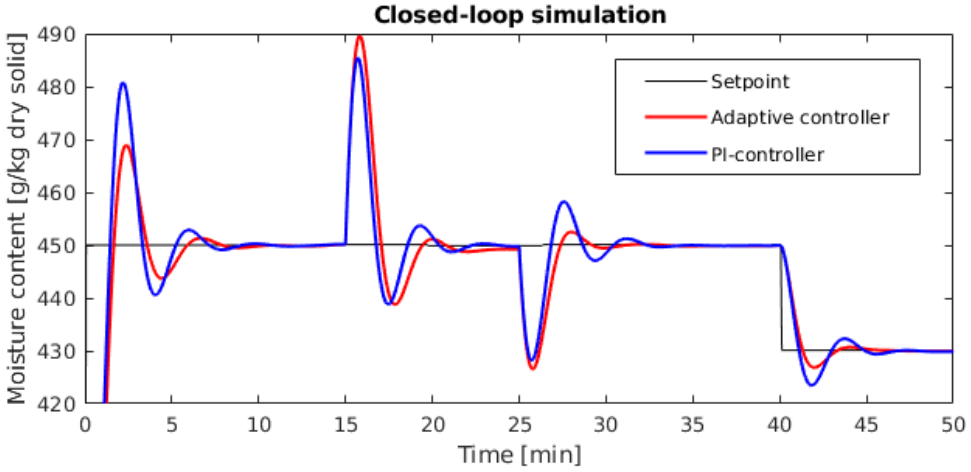

Figure 2. Simulation results adaptive controller and PI-controller for non-nominal process conditions: Disturbance in the gas inlet moisture content (t>15min) and solids inlets moisture content (t>25min)

4. Conclusions

The presented results indicate that the presented self-tuning controller represents a suitable method for control of convective drying processes under unforeseen changes in the material's drying characteristics.

References

1. van Meel, D., Chem. Eng. Sci. 9 (1958) 36-44.
2. Bück, A., Seidel, C., Dürr, R., Neugebauer, C., J. Proc. Contr. 69 (2018) 86-96.
3. K.J. Åström, B. Wittenmark, Adaptive Control, 2008.

ECCE12
The 12th EUROPEAN CONGRESS OF CHEMICAL ENGINEERING
Florence 15-19 September 2019

Synthesis and characterization of thermoplastic polyamide elastomers based on PA 1212

Jie Jiang[1], Zhenhao Xi*[2], Ling Zhao[3]

1 State Key Laboratory of Chemical Engineering, East China University of Science and Technology, Shanghai, China;

2 State Key Laboratory of Chemical Engineering, East China University of Science and Technology, Shanghai, China;

3 State Key Laboratory of Chemical Engineering, East China University of Science and Technology, Shanghai, China;

**Corresponding author: zhhxi@ecust.edu.cn*

Highlights

- Long chain polyamide as hard segment and amino-terminated polyether as soft segment.
- The thermoplastic elastomer is lightweight.
- Microphase separation of the copolymer is observed.
- The thermoplastic elastomer can be used as permanent antistatic agent.

1. Introduction

Thermoplastic polyamide elastomers (TPAEs) are block copolymers with hard blocks consisting of polyamide segments, and the soft blocks consisting of polyether segments usually including poly(ethylene glycol) (PEG), poly(propylene glycol) (PPG) or poly(tetramethylene glycol) (PTMG)[1,2,3]. The hard and soft segment are linked with ester group where thermodynamic incompatibility between the two segments results in a microphase separated morphology[4].

2. Methods

Thermoplastic polyamide elastomer was synthesized using PA1212 oligomer (Average molecular weight is from 1000 to 5000) and Jeffamine@ED2003 (or Jeffamine@D2000) via a "two-step" melt polycondensation. The TPAEs were characterized by FT-IR, ^{1}H-NMR, WAXD, DSC, DMA, TGA. Meanwhile, the inherent viscosity, density, rheology and dielectric properties of the TPAEs were determined.

3. Results and discussion

The hard and soft segment are linked with amide group (Figure 1a). The Jeffamine@ED2003 crystal melting peaks are observed within 0-40 ^{o}C which are lower than the reported T_m (43 ^{o}C) (Figure 1c). Two distinct glass transitions of TPAEs have been observed (Figure 1d). This result is attributed to the Jeffamine crystallization being confined by the PA1212 hard domains during cooling, a typical characteristic of microphase separation in elastomeric copolymers. The volume resistivity of the TPAEs decreases as increasing frequency and the values are between 10^5 and 10^{12} Ohms·cm (Figure 1e). The density of the synthesized TPAEs is 1.01-1.06 g·cm^3.

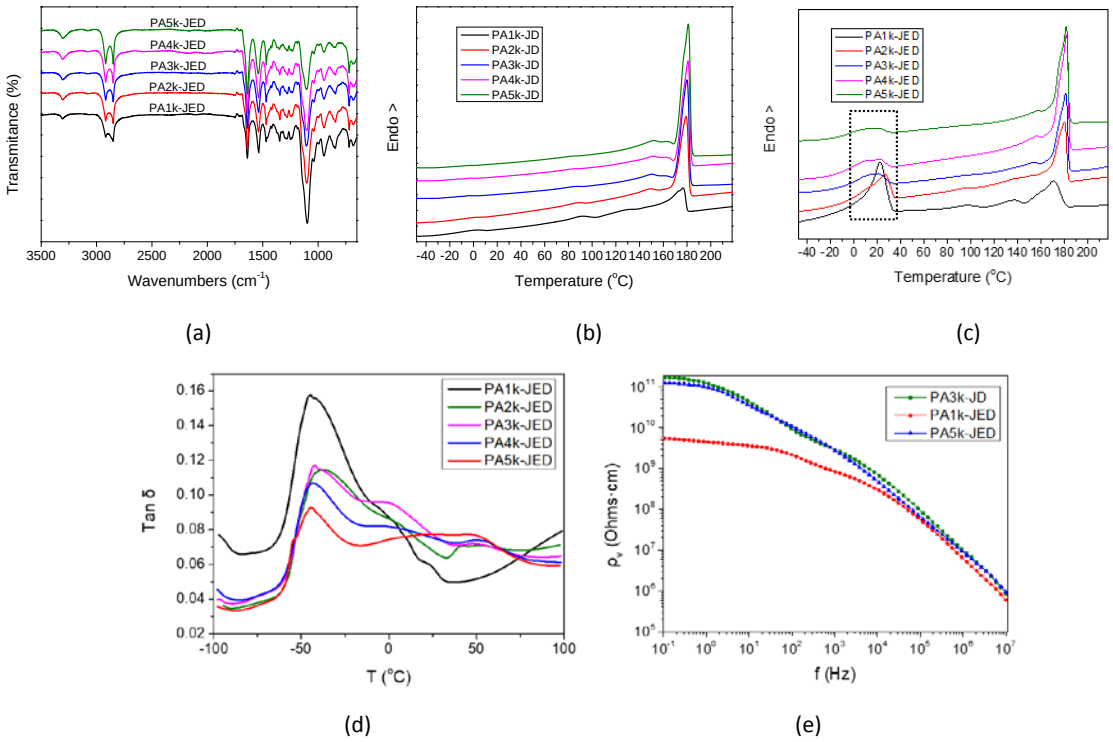

Figure 1. (a) FT-IR spectra of PA1212-co-Jeffamine@ED2003; (b) DSC thermographs of PA1212-co-Jeffamine@D2000; (c) DSC thermographs of PA1212-co-Jeffamine@ED2003; (d) DMA results of PA1212-co-Jeffamine@ED2003; (e)Dielectric properties of TPAEs

4. Conclusions

The hard and soft segment are linked with amide group rather than ester group, resulting in good resistance to hydrolysis and organic solvent. The typical characteristic of microphase separation is observed. The density of the synthesized TPAEs is 1.01-1.06 g·cm^3. The TPAEs can be used as permanent antistatic agent.

References

[1] Malet F L G.. Wiley-VCH Verlag GmbH & Co. KGaA, 2006.
[2] Boulares A, Tessier M, Marechal E. Polymer, 2000, 41(10): 3561-3580.
[3] Huo L, Dong C X. Advanced Materials Research, 2012, 512: 2127-2130.
[4] Yuan R, Fan S, Wu D, et al. Polymer Chemistry, 2018, 9(11): 1327-1336.

ECCE12
The 12th EUROPEAN CONGRESS OF CHEMICAL ENGINEERING
Florence 15-19 September 2019

Correlation of Powder Performance on Rotary Tablet Presses and Standardized Methods for Flowability

Maren Zimmermann, Kalaiarasi Sathiyaseelan, Markus Thommes

TU Dortmund, Laboratory of Solids Process Engineering, Emil-Figge-Str. 68, 44227 Dortmund, Germany

**Corresponding author: maren.zimmermann@tu-dortmund.de*

Highlights

- A quantitative classification of flowability is possible with a ring shear cell.
- The ff_c value correlates with the flow rate through a feed frame.
- Mass flow through a funnel does not predict powder performance on rotary tablet presses.

1. Introduction

In tablet manufacturing powder flow is frequently the rate limiting step as it directly influences several product quality attributes [1]. An insufficient powder flow may cause variations in tablet weight and dose which have to be minimized due to high quality requirements according to legal binding guidelines (e.g. European Pharmacopeia) [2]. Most rotary tablet presses contains feed frames consisting of rotating paddles in order to overcome challenges in powder flow. For the measurement of powder flowability various methods are known which are standardized to ensure comparability. These measurement procedures are used to qualitatively rank powder flowability and rather investigate the performance of powder in tablet manufacturing [3]. The aim of this study is the investigation of the correlation between flow behavior in a rotary tablet press and standardized measurement procedures for the evaluation of powder flowability.

2. Methods

Powder flow experiments were conducted on a feed frame (Fill-O-Matic, Fette Compacting, Schwarzenbek, Germany). The flow rate was measured on an external scale (MSA20201S-000-D0, Sartorius, Göttingen, Germany) (Figure 1). A ring-shear cell (RST-01, Dr.-Ing. D. Schulze Schüttgutmesstechnik, Wolfenbüttel, Germany) with a predefined shear stress (σ = 1000 Pa) was used to determine powder flowability. Flowability was also specified via the tap density (Tap density tester TD1, Sotax, Aesch, Switzerland), the angle of repose and the flow rate through a funnel (Powder flow tester PF1, Sotax, Aesch, Switzerland).

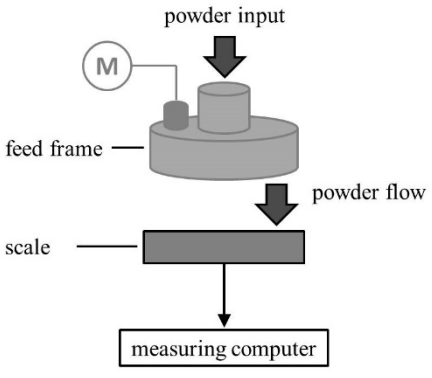

Figure 1. Schematic of the experimental set-up to determine the flow rate through a feed frame

Three powders were chosen as model substances due to their different flowability. Lactose monohydrate (GranuLac 200, Meggle Pharma, Wasserburg, Germany) is the most cohesive

powder. Microcrystalline cellulose (Emcocel 90M, JRS Pharma, Rosenberg, Germany) and dicalcium phosphate anhydrate (DI-CAFOS A150, Chemische Fabrik Budenheim, Budenheim, Germany) show a higher powder flow.

3. Results and Discussion

The results of the measurements with the ring shear cell (ff_c) are in the expected order: Di-Cafos A150 offers a high flowability due to a high and regular particle size (d_{50}=181 µm). GranuLac 200 is a cohesive powder (d_{50}=37 µm) and it consequently features low flowability. A similar order is found by determining powder flowability via the angle of repose α and the Hausner Ratio (HR). Contrary, the results of the mass flow through a funnel do not meet the expectations. The mass flow of Emcocel 90M is the smallest one, although the powder is less cohesive than GranuLac 200. This method should represent powder flow best, as it considers particle-related as well as dynamic process related factors [2]. By determining the powder flow rate through a feed frame of a rotary tablet press the same expected order can be measured as with the ring shear cell.

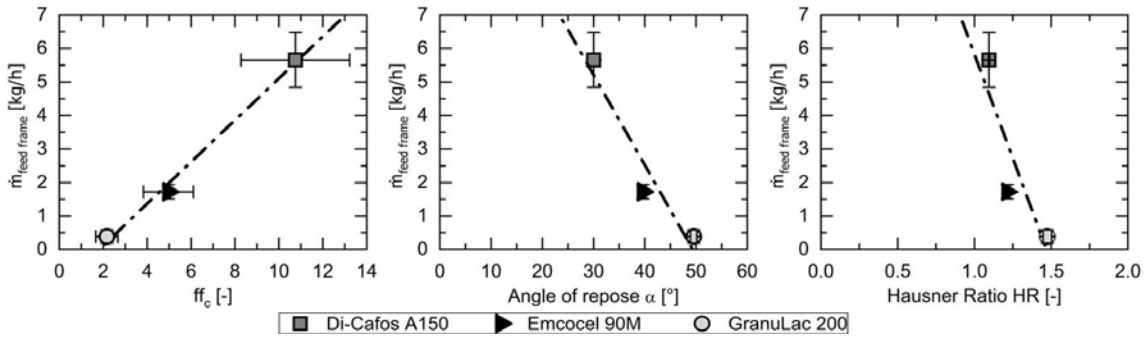

Figure 2. Correlation between powder flow rate through a feed frame (mean ± s, n = 10) and flowability index ff_c (mean ± s, n = 3), angle of repose α (mean ± s, n = 6) and Hausner Ratio (mean ± s, n = 6) of three model substances.

Correlation between mass flow rate through a rotary tablet press feed frame and values for flowability determined by standardized methods was proven (Figure 2). The characteristic coefficient of flowability ff_c is linearly dependent of the powder flow rate through the feed frame (coefficient of determination R^2 = 0.9938). Analyzing the angle of repose and the Hausner Ratio this correlation could not clearly be identified.

4. Conclusions

Powder flow rate through the feed frame of a rotary tablet press was investigated in order to determine a correlation with standardized methods. In comparison with the analyzed measurement methods the characteristic coefficient of flowability ff_c shows correlation with the mass flow from the feed frame best. Determining powder flowability by measuring the flow rate through an orifice even resulted in a different order.

References

[1] X. Xie, V.M. Puri, Part. Sci. Technol., 24 (2006) 411–426.
[2] European Pharmacopoeia Commission, European Pharmacopoeia, EDQM, Strasbourg (2019).
[3] A. Zettler, et al., J. Pharm. Innov., 11 (2016) 189-199.

ECCE12
The 12th EUROPEAN CONGRESS OF CHEMICAL ENGINEERING
Florence 15-19 September 2019

Poly(2-hydroxyethyl methacrylate) cryogels as the entrapment cell carriers for high-cell-density bioproduction

Na Xu[1], Meng Chen[1], Shaochuan Shen[1], Wei Zhang[2], Yunling Gao[1], Junxian Yun[1]

[1]*State Key Laboratory Breeding Base of Green Chemistry Synthesis Technology, College of Mechanical Engineering, Zhejiang University of Technology, Hangzhou 310032, China*

[2]*Institute of Process Equipment and Control Engineering, College of Mechanical Engineering, Zhejiang University of Technology, Hangzhou 310032, China*

**Corresponding author: yunjx@zjut.edu.cn*

Highlights

- PHEMA cryogels were prepared *via* cryopolymerization
- PHEMA cryogels were used as the cell entrapment carriers during *L. paracasei* fermentation
- Higher cell concentration using cryogels was observed than that without cryogels
- Dried cell concentration of 5.32 $g \cdot L^{-1}$ was achieved

1. Introduction

The bioproduction of high-value organic acids like phenyllactic acid (PLA) *via* microbial fermentation or biotransformation has received increasing attentions in biological and biotechnology fields in recent years. [1-4] During these processes, the culture of cells at high-cell-density to increase the total biomass concentration in the broth is of great important to the yield, the conversion rate and the productivity. In this work, the poly(2-hydroxyethyl methacrylate) (pHEMA) cryogels were prepared by cryo-polymerization under freezing conditions. The obtained cryogels were used the cell entrapment carriers during *L. paracasei* fermentation towards the production of PLA. The morphology and the cell concentration during the fermentation process were investigated experimentally.

2. Methods

Monolithic pHEMA cryogels were prepared by cryo-polymerization. Typically, the reactive solution containing HEMA (11.6%, w/w) and poly(ethylene glycol) diacrylate (PEGDA, 3.5%, w/w) initiated by TEMED and APS (both with the mass ratio of 4% to the total mass of HEMA and PEGDA) was poured into glass columns with inner diameter of 4-6 mm and height of 100 mm. Free radical cryo-polymerization was conducted under freezing condition for 48 h to get the cryogel.

The cryogels were cut into pieces with height of about 3-5 mm and used as the cell carriers. *L. paracasei* 16C3 strain was cultured in MRS medium with and without cryogel pieces and the cell mass was measured at given time intervals. The pore morphology of the cryogel was investigated by scanning electron microscope (SEM, S-4700, Hitachi, Japan). The samples were cut from the

middle of the sample columns, directly dehydrated using an ethanol-water solution (10-30-50-70-80-90-99.5%), dried at critical point, coated with gold and then observed by SEM.

3. Results and discussion

The results showed that pHEMA cryogels have supermacropores with the sizes from several to 200 μm. These pores provided enough void space for the growth, entrapment and deposition of microbial cells during fermentation processes. The cryogel carriers permit more surfaces for the attachment and deposition of cells and also contributed to the reduction of the substrate inhibition during cell growth. The cell concentrations by using these cryogels as the carriers were higher than those without cryogels for the growth of *L. paracasei* 16C3 strain in MRS medium. The maximum cell concentration of about 5.32 $g \cdot L^{-1}$ in the fermentation broth was achieved, as shown in Figure 1(a), indicating that the cryogels could be used as potential and interesting cell carriers for high-cell-density fermentation and bioconversion.

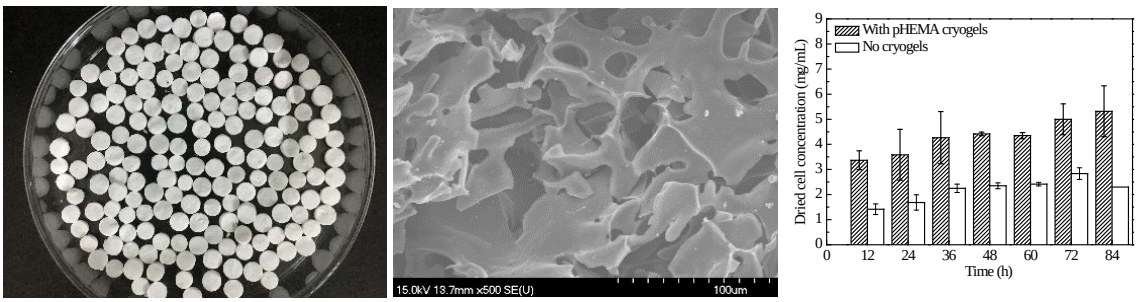

(a) (b) (c)

Figure 1. (a) Morphology of pHEMA cryogel carriers, (b) microstructure within the cryogels an (c) cell concentrations with and without cryogels during the fermentation of *L. paracasei* 16C3 in MRS broth for the production of PLA.

4. Conclusions

PHEMA cryogels were interesting cell entrapment carriers and can be used for the high-cell-density culture of microbial strains like *L. paracasei* 16C3 for the production of bio-based organic acids. The concentration of cells using cryogels as the cell carriers can be increased to twice the biomass in traditional fermentation without cryogels.

References

[1] J.T. Guan, C.F. Han, Y.X. Guan, S.H. Zhang, J.X. Yun, S.J. Yao, Chin. J. Chem. Eng., 27 (2019) 418−425.

[2] J.T. Guan, Y.X. Guan, J.X. Yun, S.J. Yao, J. Chromatogr. A, 1554 (2018) 92−100.

[3] N. Xu, J.T. Guan, S.H. Zhang, J.X. Yun, Y.X. Guan, S.J. Yao, J. Chem. Eng. Chin. Univ. 33 (2019). (In Chinese)

[4] W.M. Mu, S.H. Yu, L.J. Zhu, T. Zhang, B. Jiang, Appl. Microbiol. Biotechnol. 95 (2012) 1155−1163.

Acknowledgments

The authors gratefully acknowledge the financial supports partially by the National Natural Science Foundation of China (Nos. 21576240, 21777143, 21106132) and the Zhejiang Provincial Natural Science Foundation of China (Nos. LY14B060005, LZ14B060001).

ECCE12
The 12th EUROPEAN CONGRESS OF CHEMICAL ENGINEERING
Florence 15-19 September 2019

Tailoring hydroxyapatite powder properties for 3D printing based on selective laser melting or sintering

Pedro Navarrete-Segado[1, 2*], David Grossin[2], Mallorie Tourbin[1], Christine Frances[1]

1 Laboratoire de Génie Chimique, Université de Toulouse, CNRS, Toulouse, France ;

2 CIRIMAT, Université de Toulouse, CNRS, Toulouse, France

**Corresponding author: pedrojesus.navarretesegado@ensiacet.fr*

Highlights

- The hydrodynamic parameters mainly impact agglomerates size distribution.
- Pure HAP can be produced ensuring relevant physicochemical conditions.
- An absorbing additive such as graphite may be used to increase HAP powder absorptance.

1. Introduction

The selective laser melting/sintering (SLS/M) as promising additive manufacturing (AM) technique allows the shaping of bioceramic parts as patient matched tissue engineering materials. These parts must have complex structures and ideal properties, like bioactivity and biocompatibility to ensure a good osseointegration/osseoincorporation of the implants, as well as good mechanical and chemical resistance. However, a deeper study of ceramic feedstock properties to achieve a better laser-material interaction during the shaping of the parts is essential to obtain an accurate control of the porosity, interconnected pores and to avoid the formation of cracks. For that, the production of nano-structured agglomerates is required in order to increase the surface and thus the reactivity required for effective sintering while keeping suitable flowability and dispersing properties. [1] Besides, ceramic powders absorptance at Nd-YAG laser wavelength (1.06µm) is not enough to produce a suitable heat/matter exchange between the particles to trigger the material densification. Improving the laser radiation absorption by means of use of absorbing additives is also of particular interest. [2, 3]

In this communication, we discuss the relationship between the hydroxyapatite (HAP) powder properties and the synthesis process parameters. Optimal purity, aggregate size distribution, and morphology of powder have been tailored in order to improve the laser-material interaction during 3D printing process of ceramic parts. Moreover, the influence of a commercial graphite (TIMREX KS44) as absorbing additive in the absorptance of HAP powder at Nd-YAG laser wavelength has been studied.

2. Methods

A scale-up of the HAP synthesis process was realized from a 1L reactor to a reactor of 4L. The precipitation of hydroxyapatite results from the reaction at a high temperature of phosphoric acid and calcium nitrate in an aqueous ammonia medium:

$$10Ca(NO_3)_2,4H_2O + 6(NH_4)_2HPO_4 + 8(NH_4)OH \rightarrow Ca_{10}(PO_4)_6(OH)_2 + 20NH_4NO_3 + 6H_2O$$

A double-jacketed cylindrical glass vessel, and three glass containers for the reactants (calcium nitrate, phosphoric acid and ammonia) compose the lab-scale apparatus. Initially a given volume of an aqueous solution of calcium nitrate is put into the reactor, then raised at the desired temperature for the synthesis. During a first period of the synthesis process, only ammonia is fed in order to increase the pH of the solution inside the reactor. Then during a second period, in which the synthesis itself is performed, the three solutions are continuously fed. At the end of the synthesis, the feeding of the reactants and of the ammonia solution is stopped but the system is maintained under stirring at high temperature during a maturation phase. Finally the reactor is drained, the particles are washed, during the suspension filtering itself done by suction through a Buchner funnel using a filter paper. The filtration cake is then freeze dried and calcined at 1000°C during 10 hours into an oven. This final step allows the drying of the crystallized HAP and the removal of any remaining impurity. For analysis purposes, samples are collected all along the process, as slurries to allow particle size distribution measurement, or as dried or calcined powders, to characterize the HAP purity.

Analysis of powder microstructural, chemical and physical properties was done by X-ray diffraction, FTIR, morphometer and SEM. The influence of the graphite (TIMREX KS44) as absorbing additive is studied by preparing different mixtures with the synthesized HAP and a mass of graphite in the range of 0% and 2.5% by mechanical mixing and measuring the absorptance at Nd-YAG laser wavelength.

3. Results and discussion

The effect of the stirring rate applied and the reactants flow rates was studied by analyzing the product recovered at the end of the synthesis process using different rates and different synthesis durations. The results showed that both parameters are closely related with the aggregate size distribution of the final product. A rather high stirring rate is needed to properly mix the reactants and get a product with a narrow size distribution around a few microns. The whole duration of the synthesis can be adjusted without affecting the product chemical purity ensuring a relevant pH regulation. A value of absorptance higher than 40% was observed from the mixture containing a proportion of 0.75% of graphite mass onwards showing promising results.

4. Conclusions

Stoichiometric HAP synthesis was studied varying physico-chemical and hydrodynamical conditions and analyzing their effect both on agglomerates size distribution and product chemical composition. The change in the absorption by graphite mixing was also analysed. A small proportion of graphite in the mixture is enough to obtain an absorption value close to the one observed in metal powders often used in SLS/M and it is expected to be higher enough for the use of the ceramic composite powder in AM technologies.

References

[1] Monmaturapoj, N. Journal of Metals, Materials and Minerals 18 (2017).
[2] Nikolay K., Yurii V., Rapid Prototyping Journal 6 (2000) 155-61.
[3] Ferrage, L., Bertrand, G., Lenormand, P. et al. J Aust Ceram Soc (2017) 53: 11.

Synthesis and characterization of pitch from pyrolysed fuel oil (PFO)

Chul Wee Lee[1,2*], Seunghyun Ko[1,2], Jong-Eun Choi[1,2], Ji Sun Im[1,2], Young-Pyo Jeon[1,2]

[1] *Carbon Resources Institute, Carbon Industry Frontier Research Center, KRICT, Republic of Korea*

[2] *Adv. Materials and Chemical Engineering, University of Science and Technology, Republic of Korea*

**Corresponding author: chulwee@krict.re.kr*

Highlights

- Pitch was synthesized as a function of temperature in the range of 390-410°C.
- Pitch was identified by XRD, TGA, MALDI-TOF, EA, softening point analysis.
- Pitch showed enhanced stacking height (Lc), and C/H indicating graphitic structure.
- To control the softening point of pitch, a modified thermal treatment was studied.

1. Introduction

Petroleum residues can be used as a feedstock to prepare pitch which is one of a main precursors for the production of carbon materials [1]. The pitch characteristic is an important factor because the properties of carbon materials can be determined by the chemical and physical characteristics of pitch, which are classified as mesophase contents, solubility by organic solvents, softening point, chemical compositions, and molecular weight distribution (MWD) [2] etc. Previously, air-blowing is a simple and effective way to increase the softening point [3]. In this work, PFO based pitch was prepared by thermal reaction in the range of 390-410°C as a function of time, and the basic chemical/physical properties were characterized. Based on the results of MWD, a chemical reaction was suggested the changes of each molecular weight fraction during the thermal reaction. And also oxidative thermal treatment of pitch with O_2/N_2 mixture gas was investigated as an efficient way to increase softening point of pitch without loss of pitch yield. It is expected that using gas with a higher O_2 concentration than air would be a better effective way to increase softening point because a higher O_2 concentration could enable the condensation reaction to progress at lower gas flow rate, suppressing the volatilization of light components that can minimize the pitch yield.

2. Methods

PFO (Yeochun NCC Co., Korea) was used as a feedstock. 7,7,8,8-tetracyanoquinodimethane (TCNQ) was used as a matrix for MALDI-TOF analysis. The pitch synthesis reaction was conducted with a 1L scale batch type autoclave with the following procedure (1) 500g PFO was placed in the reactor, (2) 200cc/min of N_2 was injected for 30min, (3) the reactor was heated and the detailed reaction conditions and summarized in Table 1 In order to modify pitch properties, O_2 and/or N_2 containing gas was blown into the reactor with a flow rate of 0.5L/min at 360°C for 5hours. Treated pitch was identified by EA (Thermo Scientific FLASH EA-2000), XRD (Rigaku Ultima IV), softening point (DP-70, Mettler Toledo), MALDI-TOF (with Autoflex MALDITOF mass spectrometer).

3. Results and discussion

Table 1. Experimental conditions for synthesizing pitch from PFO

Sample	Reaction conditions					
	T (°C)	t (h)	P (P)	N_2 flow (cc/min)	Pitch yield (%)	Volatile mass (%)
P-390	390	1	1	100	28.9	67.5
P-400	400	1	1	100	26.5	68.3
P-410	410	1	1	100	25.4	69.2

The pitch synthesis reaction was considered with MWD variation relative to the area fractions as shown in Figure 1 [4]. Low boiling point components were emitted due to the volatilization during the thermal reaction or converted to the high molecular weight area fraction by means of condensation and polymerization reaction. The softening point increased linearly with vac. distillation time, as shown in Figure 2, the softening point was further increased with increasing flow rate reaching at 282°C. Heat treatment of PFO under inter condition at 360oC for 5h produced a pitch with a softening point of 130°C and a yield of 34.0%. In order to suppress the loss of pitch yield, O_2 concentration was increased rather than rather than increasing the flow rate of reaction mixture gas. When the O_2 concentration was increased to 35%, the softening point increased to 249°C [5].

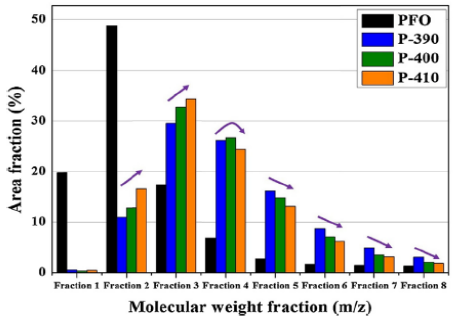

Figure 1. Diagram of the molecular weight fraction divided by the pseudo-component.

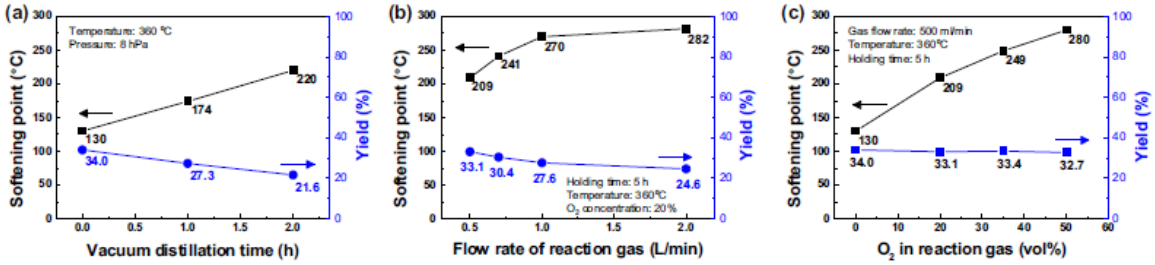

Figure 2. Softening point and yield variation of pitches prepared by thermal treatment as a function of (a) vacuum distillation time, (b) flow rate of reaction gas and (c) O_2 concentration of reaction gas.

4. Conclusions

(1) The empirical pitch synthesis reaction from PFO was carried out to reveal the physical and chemical properties of the feedstock and produced pitch. (2) The treatment was highly effective at increasing the softening point while maintaining high pitch yield by oxidative thermal condensation and suppressing volatilization of light components.

References

[1] I. Mochida, Y. Korai, C.-H. Ku, F. Watanabe, Y. Sakai, Carbon 38 (2000) 305- 328.
[2] J. G. Kim, J. H. Kim, B.-J. Song, Y.-P. Jeon, C.W. Lee, Y.-S. Lee, J.S. Im, Fuel 167 (2016) 25-30.
[3] J.J. Fernandez, A. Figueiras, M. Granda, J. Bermejo, R. Menendez, Carbon 33 (1995) 295-307.
[4] Jong Gu Kim, Ji Hong Kim, Byung-Jin Song, Chul Wee Lee, Ji Sun Im, J. Ind. Eng. Chem. 36 (2016) 297-293
[5] Seunghyun Ko, Jong-Eun Choi, Chul Wee Lee, Young-Pyo Jeon, J. Ind. Eng. Chem. 54 (2017) 252-261.

ECCE12
The 12th EUROPEAN CONGRESS OF CHEMICAL ENGINEERING
Florence 15-19 September 2019

Experimental and analytical study of heat transfers in granular media

Viet Dung NGUYEN, Christophe MARIE

Laboratoire des Eco-PRocédés, Optimisation et Aide à la Décision, EPROAD EA 4669,

IUT de l'Aisne, 48 rue d'Ostende, Saint Quentin 02100, France

**Corresponding author: christophe.marie@u-picardie.fr*

Highlights

- Thermal transfers in granular media
- Experimental data
- Analytical study

1. Introduction

Granular media are generally biphasic or triphasic, with a solid phase and a gaseous or/and liquid phase, and are characterized by their porosity. Particle size, shape, distribution, and pore size are parameters that characterize the microstructure of a granular medium and have a consequent impact on fluid flow, fluidization behavior or mechanism of heat transfers... The present paper aims at presenting an experimental and analytical study of heat transfers in granular medium which have an important impact for many industrial processes as well as powder metallurgy, chemical reactors, food technology, thermal insulation or even simply storing particles in a silo after drying. However, few studies in the literature are interested in the understanding of heat transfers across contact area between particles or particle/wall (conductance). In this research, we firstly present an experimental campaign. Then, an analytical approach is proposed by using the iterative procedure of energy balance. Finally, the experimental data coupled with the analytical results is used to identify the thermal conductance.

2. Method

The experimental setup, as shown schematically in figure 1, consisted of a column of 11 steel spheres of same diameter of 20 mm arranged vertically in a insulated tube. The first sphere is heated at 50°C and the temperature evolution of other spheres are measured.

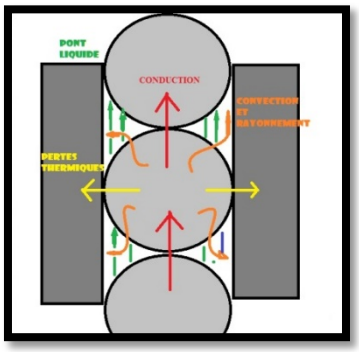

In the literature, the models for calculating the thermal conductivity of condensed or loose granular media have been developing for a few decades now. Most of the models proposed are generally simple models of the type series, parallel, or combination of the two, which do not take into account the constriction of thermal

flux lines. We have therefore developed a theoretical model for calculating the thermal conductivity of a stack of identical spherical particles by their diameter and composition. The principle of this model is the determination of the evolutions of the apparent thermal conductance according to the power and the heating time, and the stabilization of the transfer regime. This assessment, based on the obtaining of an analytical solution that binds thermal and mechanical behavior over time, allowed us to make comparisons between analytical and experimental measures.

3. Results

The following results present the comparison between experimental and analytical temperatures propagating through a pile of 5 heated spheres (among 11) under mechanical stress.

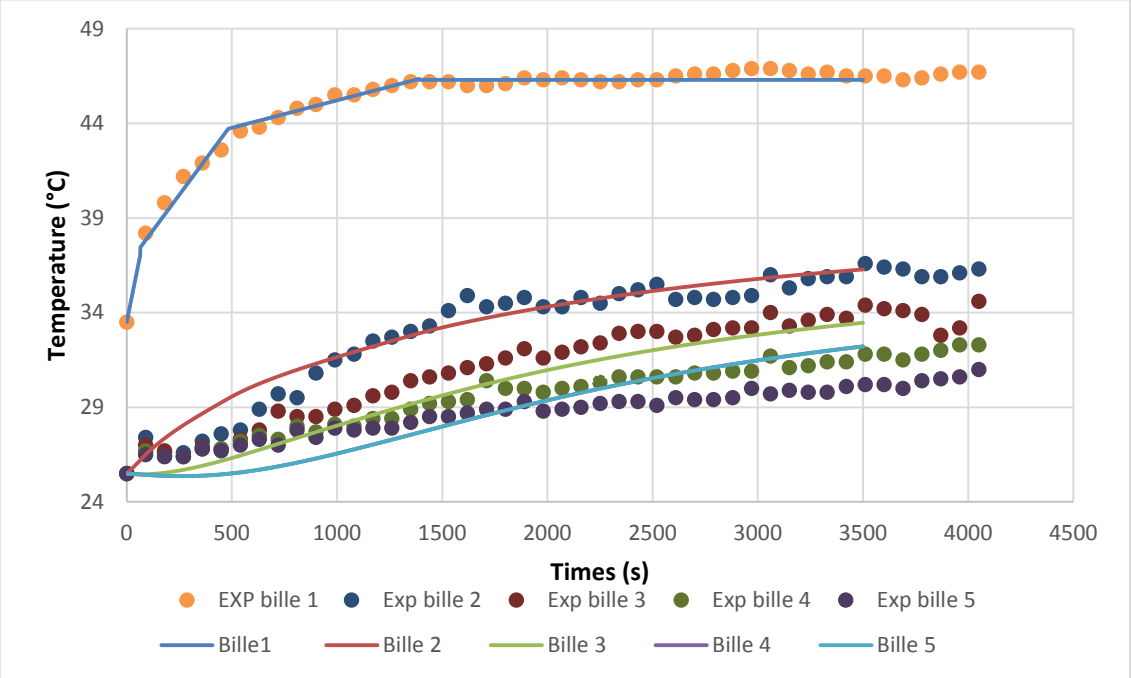

Figure 1. Experimental and numerical comparison of the temperature increase of a pile of spheres under mechanical stress

The graph shows that the numerical curves of spheres 4 and 5 (far from heat source) are confusing. The numerical curves of spheres 1, 2 and 3 are quite distinct, and are nearly superimposed with their experimental counterparts. While the experimental variations are clearly visible in the graph, the analytical variations are less and less precise and confirm the existence of a limit to the numerical model. However, these first results are promising, and will be completed by a Discrete Elements Method (DEM) comparison.

References

[1] Heat transfer in a granular media modeled by a coupled DEM-finite difference method: application to fluidized bed processes, VD Nguyen, K Benhabib, C Marie, P Coorevits, Procedia Engineering 42, 824-832, 2012

[2] Discrete modeling of granular flow with thermal transfer: application to the discharge of silos, VD Nguyen, C Cogné, M Guessasma, E Bellenger, J Fortin, Applied Thermal Engineering 29 (8-9), 1846-1853, 2009.

Impact of the Degree of Polymerization and Amino Group Addition on the Emulsifying Properties of Polyglycerol Esters.

Ana María Díaz Lasprilla [1*], Gustavo Emilio Ramírez Caballero [1,2*]

[1]Grupo de Investigación en Polímeros. [2]Centro de Investigaciones en Catálisis (@CICATUIS), all at Parque Tecnológico de Guatiguará (PTG), km 2 vía El Refugio, Universidad Industrial de Santander, Piedecuesta (Santander), 681011, Colombia.

*Corresponding author: ana2188238@correo.uis.edu.co, gusramca@uis.edu.co.

Highlights

- Microwave radiation shortens the reaction time for the etherification of glycerol to polyglycerols.
- New emulsifiers based in polyglycerol were synthesized.
  It is possible to produce emulsifiers with different functional properties by varying characteristics such as degree of polymerization and electric charge.

1. Introduction

The conversion to valued-added chemicals of the glycerol co-produced in the growing biodiesel industry is nowadays a focus of global research and a topic of great industrial importance. Among different approaches, the glycerol polymerization emerges as a promising alternative, leading to the formation of Polyglycerol (PG). Moreover, polyglycerol has been used as raw material for the production of polyglycerol esters, which are widely used as emulsifiers in different industries [1].

The properties of the emulsifiers and their particular applications depend on their structure. In the case of polyglycerol esters, it is possible to produce emulsifiers with different functional properties by varying characteristics such as the degree of esterification [2]. However, those properties are not only determined by the hydrophobic tail but also by the hydrophilic head features, for instance, the size or degree of polymerization and the electric charge.

In this work, we synthesized new emulsifiers based in PG and also analyzed the effects of degree of polymerization of polyglycerol and the cationic charge by Lysine amino acid addition on the emulsifying properties of polyglycerol esters The degree of polymerization leads to the synthesis of polymers with a variation of molecular weights and pendant hydroxyl groups. Meanwhile, the positive charge gives to the polymers the ability to absorb on negatively charged substrates to produce an antistatic and hydrophobic effect which is useful for a range of applications such as softeners and anti-static additives in textiles and, bitumen emulsifiers due to their compatibility with a range of aggregates [3].

2. Methods

Microwave radiation was used as the heat source in the synthesis of polyglycerol esters to reduce the reaction times compared to conventional thermal heating [4]. In order to form polyglycerol with different degrees of polymerization, the reaction was first carried out up to the gel point, i.e., an infinite polymer network first appears and the polymerization system loses its fluidity drastically.

After the termination of the gel point time, a polyglycerol sample was collected every 30 percent of the previously determined gel point. Polyglycerols with different degree of polymerization were characterized by Fourier transform infrared spectroscopy (FTIR) to confirm their chemical structure, the hydroxyl numbers were calculated according to ASTM D 4274-11 Test Method A, and molecular weight distributions were obtained using High-Performance Liquid Chromatography (HPLC) measurements.

Polyglycerol esters were synthesized using a proposed strategy of prepolymers complexes addition. Those complexes consist of glycerol esterified with (i) oleic acid and (ii) Lysine. This strategy was followed to guarantee the successful esterification of PG with each of these components. Infrared measurements confirmed the chemical structure of the synthesized complexes and their esterification reactions with PG. The hydrophilic-lipophilic balance (HLB) values of the emulsifiers from polyglycerol esters were calculated. Microscopy techniques studied the type of the resulting emulsion. The rheology, surface, and interfacial properties were also evaluated. The stability of emulsions, one of the more critical factor to be considered in the emulsion technology, was investigated and discussed at different concentrations of emulsifier and water-oil ratios (WOR) of emulsions. To measure emulsion stability, we used the half-life period.

3. Results and discussion

Polyglycerols with different degree of polymerization were synthesized. FTIR Results showed that functional groups presented in the reaction polymerization products are the same as polyglycerol functional groups identified in previous research studies [5]. Multimodal weight distributions were observed for all samples, and the number-average molecular weights and weight-average molecular weights showed an increase with the reaction time while the number of hydroxyl groups exhibited an expected decrease due to the progress of the polymerization. The esterification of polyglycerol with oleic acid and Lysine, through the proposed strategy of the addition of complexes, was corroborated by FTIR spectroscopy with the appearance of the bands associated with ester bonds. The hydrophilic properties of the emulsifiers increased with the molecular weight of polyglycerol. The degree of polymerization and the presence of the amino group in the modification of the PG determined the final characteristics of the type of emulsion, varying from the formation of W / O emulsions to O / W emulsions. The emulsions presented good stability that was examined using palm oil as the oil phase and distilled water as the aqueous phase.

4. Conclusions

The current study took advantage of the heating by microwave radiation in shortening the reaction time required for polymerization of glycerol. New emulsifiers were obtained from polyglycerol esters with fatty acid and amino acid. It was found that the structure of Polyglycerol ester emulsifiers could be tailored to stabilize different emulsion systems. The degree of polymerization and the amino group addition to polyglycerol esters influence the emulsifying Properties. Therefore, emulsifying properties of synthesized polyglycerol esters can be easily adjusted for target applications, this being of great interest for the industry of emulsion based products.

References

[1] Szelag, H; Sadecka, E; Pawlowicz; Kuziemska, A. Emulsifiers from renewable materials: an eco-friendly synthesis and properties. Polish Journal of Chemical Technology 15(2), pp. 128-135, 2013.

[2] Shikhlaliev, Kh.S.; Stolpovskaya, N.V.; Krysin, M.Yu.; Zorina, A.V.; Lyapun, D.V.; Zubkov, F.I.; Yankina, K.I. Production and emulsifying effect of polyglycerol and fatty acid esters with varying degrees of esterification. J. Am. Oil. Chem. Soc., 93, pp. 1429-1440, 2016.

[3] Kume, G; Gallotti, M; Nunes, G. Review on Anionic/Cationic Surfactant Mixtures. Journal of Surfactants and Detergents. Vol 11 (1),pp. 1-11

[4] Bookong, P ; Ruchirawat, S; Boonyarattanakalin, S. Optimization of microwave-assisted etherification of glycerol to polyglycerols by sodium carbonate as catalyst, Chemical Engineering Journal, Vol 275, pp. 253-261, 2015.

[5] Ardila-Suarez C, Rojas-Avellaneda D, Ramirez-Caballero, Effect of Temperature and Catalyst Concentration on Polyglycerol during Synthesis, International Journal of Polymer Science, vol. 2015, Article ID 910249, 8 pages, 2015.

ECCE12
The 12th EUROPEAN CONGRESS OF CHEMICAL ENGINEERING
Florence 15-19 September 2019

Segregation Modeling in the Course of rapid gravity Flow of particulate Solids on a vibrated rough Chute

Viktor Dolgunin[1]*, Andrei Kudi[1], Oleg Ivanov[1], Alexander Tarakanov[1], Vasilii Pronin[1]

1 106 Sovetskaya street, Tambov state technical university, Tambov, 392000, Russia

**Corresponding author: dolgunin-vn@yandex.ru*

Highlights

- One experimental kinetic constant needs to model segregation on size-density.
- The less vibration frequency the greater interdiffusion-induced migration.
- Segregation on size dominates in the area of high solid fraction plateau.

1. Introduction

Earlier [1] the profiles of velocity, fraction of the void volume and test particle distribution in rapid gravity flows of granular materials on a vibrated rough chute were investigated experimentally. In the present paper the profiles of test particle distribution in the flow of binary granular mixtures consisting of particles differing in size and density are calculated analytically. The earlier obtained profiles [1] of velocity and fraction of the void volume are used for the mathematical modeling. As a result the vibration influence of high and low vibration frequencies on segregation dynamics and basic segregation mechanisms in rapid gravity flows of particulate solids are studied analytically.

2. Methods

The mathematical modeling was carried out on the basis of a general equation of segregation dynamics [2, 3]. In the case of the steady state of two-dimensional rapid shear flow this equation takes into account the fluxes of test particles caused by convection in the shear direction *x*, quasidiffusion mixing, interdiffusion-induced separation (migration) and segregation in transversal direction *y*. The general equation of segregation dynamics with the above mentioned fluxes describes the distribution of test particles $c(x,y,t)$ in the following way

$$\frac{\partial(c\rho_b)}{\partial t} = -\frac{\partial(uc\rho_b)}{\partial x} + \frac{\partial}{\partial y}\left[\rho_b\left(D_{dif}\frac{\partial c}{\partial y} - cD_m\frac{\partial \ln s}{\partial y} - K_S c\Delta M\right)\right], \quad (1)$$

where t - time, $u(y)$ – mean velocity towards shear direction x, s – mean distance between particles, ρ_b – bulk density, ΔM – driving force of segregation (total excess moment of forces of friction, gravity and impact moments, acting on a test particle), D_{dif}, D_m, K_S – coefficients of quasidiffusion mixing, migration and segregation respectively.

The kinetic characteristics D_{dif}, D_m, ΔM are calculated analytically as functions of shear rate, void volume fraction, concentration of particles $c(x,y,t)$ and their physical and mechanical properties [3]. Only the segregation coefficient K_S is determined experimentally as the velocity of a test particle towards *y*-direction per unit driving force of segregation ΔM [2, 3]. It was found out [2] the segregation coefficient has properties which characterize K_S as the kinetic constant for wide range of flow parameters and particle characteristics. Boundary conditions for eq. (1) are formulated as the flux absence of particles through the bed boundaries (free surface and bed bottom). During the mathematical modeling the general equation of segregation dynamics (1) with the boundary conditions had been integrated numerically.

3. Results and discussion

Figs. 1 and 2 show the experimental and calculated distributions of large and light particles as well as the profiles of fraction of the void volume. The adequacy of the experimental and analytical results creates conditions for analysis of physical separation mechanisms.

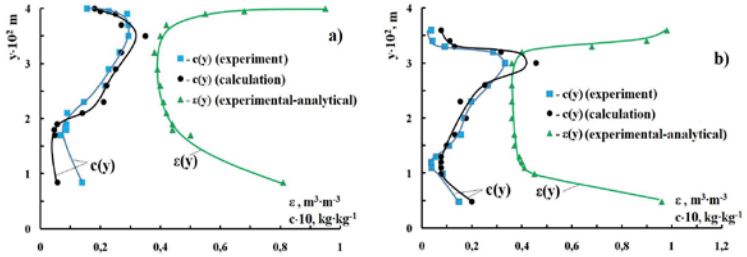

Fig. 1 Profiles of fraction of the void volume μ(y) and concentration of large particles c(y) in rapid gravity flow of binary mixture of glass beads (fractions +3.0-3.5 and +5-5.5 mm) on a vibrated rough chute (α=28.5°, a_v=2g) at vibration frequencies: a) – 15 Hz, b) – 50 Hz,

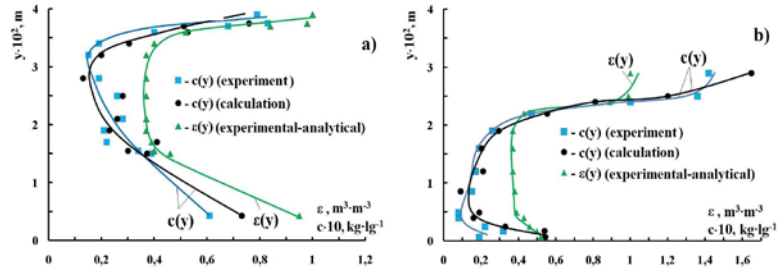

Fig. 2 Profiles of fraction of the void volume μ(y) and concentration of light particles c(y) in rapid gravity flow of particles differing in density (fraction +5-5.5 mm of glass beads and silica gel) on a vibrated rough chute (α=27°, a_v=2g) at vibration frequencies: a) – 15 Hz, b) – 50 Hz,

The combined analysis of distributions of the test particles and profiles of fraction of the void volume on the basis of the kinetics of separation fluxes in eq. (1) leads to the following conclusions. The segregation mechanism of separation dominates for particles differing in size and density when the relatively wide plateau of low values of void volume fraction is formed in the central part of the bed because of vibration of high frequency (Figs. 1-b and 2-b). Under such conditions $\partial ns/\partial y \approx 0$ and segregation of particles differing in size is most pronounced (Fig. 1-b). In the thin upper part of the bed of particles differing in density (Fig. 2-b) the effect of separation is enhanced by the coincidence of directions of segregation and migration.

On the contrary the migration mechanism of separation prevails when the relatively high gradients of the void volume fraction are formed in the most part of the bed volume under the action of low-frequency vibration (Figs. 1-a and 2-a). Under such conditions $\partial ns/\partial y >> 0$ and migration of particles differing in density is most pronounced (Fig. 2-a).

4. Conclusions

In order to study basic separation mechanisms of particles differing in size and density during rapid gravity flow on a vibrated rough chute mathematical modeling was used. It was found out that low-frequency vibration intensifies interdiffusion-induced separation (migration) and high-frequency vibration forms flow conditions conducive to segregation.

References

[1] V.N. Dolgunin, A.N. Kudi. A.A. Ukolov, M.A. Tuev, Chem. Eng. Research and Design 122 (2017) 22–32.

[2] V.N. Dolgunin, A.A. Ukolov, O.O. Ivanov, Theor. Found. of Chem. Eng. 40(4) (2006) 393-404.

[3] V.N. Dolgunin, A.A. Ukolov, O.O. Ivanov, Theor. Found. of Chem. Eng. 43(2) (2009) 187–196.

ECCE12
The 12th EUROPEAN CONGRESS OF CHEMICAL ENGINEERING
Florence 15-19 September 2019

Investigation of Metastable Zones and Induction Times in Glycine Crystallisation across Three Different Antisolvents

John McGinty[1,2], Lennart A. I. Ramakers[1], Wolfgang Beckmann[3], Guillaume Levilain[3], Mei Lee[4], Helen Wheatcroft[5], Ian Houson[1], Jan Sefcik[1,2,*]

1 Future Manufacturing Research Hub in Continuous Manufacturing and Advanced Crystallisation, University of Strathclyde, Glasgow, UK; 2 Department of Chemical and Process Engineering, University of Strathclyde, Glasgow, UK; 3 Bayer AG, Research & Development, Pharmaceuticals, Material Science, 42096 Wuppertal, Germany; 4 Product Development and Supply, GlaxoSmithKline, Stevenage, Hertfordshire SG1 2NY, UK; 5 PT&D, AstraZeneca Macclesfield, Macclesfield, SK10 2NA, UK.

**Corresponding author: jan.sefcik@strath.ac.uk*

Highlights

- Compared three different antisolvents for glycine crystallisation
- Measured solubilities, metastable zone widths and induction times across metastable zones for all antisolvents
- Assessed effect of rapid antisolvent addition vs continuous mixing on induction times

1. Introduction

There has been a significant amount of research on metastable zone width (MSZW) and induction times for cooling crystallisation, while relatively little has been done for antisolvent crystallisation. Experimental data on effects that different antisolvents and antisolvent addition strategies have on nucleation behavior in antisolvent crystallisation is very limited and our understanding of these effects is sparse. In literature there has been no direct comparison of the effects of different antisolvents on induction times and only a single publication directly assesses the MSZW for different antisolvents [1]. Furthermore, only a single publication was found which investigates both induction times and MSZW for the same antisolvent crystallisation system [2]. With regards to mixing effects only a single publication was found which uses a continuous static mixer when measuring induction times for antisolvent crystallisation [3]. In this work we measured solubilities and MSZWs in the antisolvent crystallisation of glycine using methanol, ethanol and DMF as antisolvents. We then investigated induction times across the metastable zone for these antisolvents. In order to investigate the effects of mixing, induction times were measured either with rapid antisolvent addition or using a continuous static mixer.

2. Methods

Solubilities were measured by equilibration of solids with solvent mixtures under agitation and gravimetric determination of equilibrated liquid phase compositions. The MSZW were assessed under isothermal conditions by adding the antisolvent at constant flow-rate via a syringe pump to an agitated undersaturated aqueous glycine solution in an 8 ml vial. The point at which the solution became turbid was taken as the metastable limit. The MSZW was determined by measuring a series

of metastable limits starting from different initial compositions. The induction times were measured by preparing supersaturated solutions by mixing an antisolvent with an undersaturated aqueous glycine solution, either by rapid antisolvent addition or using a continuous static mixer. Induction times were recorded under agitated isothermal conditions in 8ml vials. The static mixer had a 1/8 inch internal diameter.

3. Results and discussion

Figure 1A shows the comparison of induction times within MSZs for the three different antisolvents using batch rapid antisolvent addition. For these antisolvents, there was a little difference between induction times at similar supersaturations. At lower supersaturations induction times were very long as expected. However, at higher supersaturations induction times were relatively short, similar among different antisolvents and only weakly dependent on supersaturation. This indicates that crystal growth and secondary nucleation may become rate limiting factors in observed induction times as supersaturation increases. Investigation of mixing effects showed that using continuous mixing with the ethanol antisolvent decreased the induction times by up to one order of magnitude compared to batch rapid antisolvent addition while using continuous mixing with the methanol antisolvent increased the induction times by up to two orders of magnitude (Figure 1B).

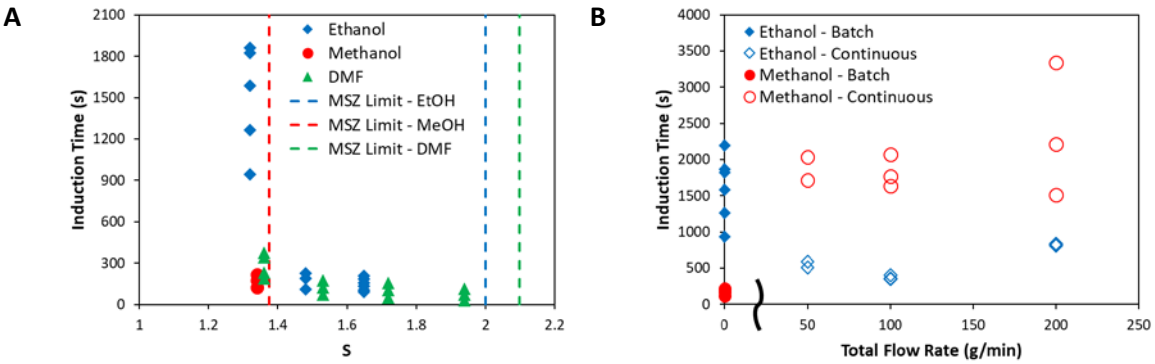

Figure 1. A) Induction time measurements for different antisolvents in batch rapid antisolvent addition. B) Comparison between batch rapid antisolvent addition and continuous static mixing (total flow rate = 0 is batch).

4. Conclusions

Well defined induction times were measured across MSZs which shows that primary nucleation is present at much lower supersaturations than those identified in conventional metastable zone width measurements. At higher supersaturations other factors become rate limiting, including crystal growth and secondary nucleation, which may need to be considered when interpreting induction time data in terms of primary nucleation kinetics as is commonly done in the literature. Induction times are strongly dependent on the mode of mixing (batch rapid antisolvent addition vs continuous mixing) which shows that appropriate mixing strategies are crucial for rational development of robust scalable antisolvent crystallisation processes.

References

[1] K. Sangwal, E. Mielniczek-Brzóska, Cryst. Res. Technol. 2017, 52, 1600361.
[2] C. T.Ó'Ciardhá, P. J. Frawley, N. A. Mitchell, Journal of Crystal Growth. 2011, 328, 50-57.
[3] S. K. Poornachary et al., Cryst. Growth Des. 2016, 16, 749-758.

ECCE12
The 12th EUROPEAN CONGRESS OF CHEMICAL ENGINEERING
Florence 15-19 September 2019

Impact of Partial Solid Miscibility on Impurity Rejection during Crystallisation

Stephanie J. Urwin,[1] Stephanie Yerdelen,[1] Ian Houson,[1] Guillaume Levilain,[2] Ivan Marziano,[3] Jeremy Merritt[4] and Joop H. ter Horst[1*]

[1]EPSRC Centre for Innovative Manufacturing in Continuous Manufacturing and Crystallisation, University of Strathclyde, Glasgow, G1 1RD, UK. [2]Bayer AG, Forschungszentrum Aprath, 42096 Wuppertal, Germany. [3]Pfizer Worldwide Research and Development, Sandwich, CT13 9NJ, UK. [4]Eli Lilly and Company, Small Molecule Design and Development, Lilly Technology Center North, Indianapolis, IN 46221, USA.

stephanie.urwin@strath.ac.uk

Highlights

- Workflow approach to distinguish between different mechanisms of impurity incorporation
- Impurity rejection during crystallization studied in three pharmaceutical systems
- Incorporation into the crystal lattice is experimentally observed using X-ray diffraction

1. Introduction

Crystallization is a purification technique used across the pharmaceutical sciences and industries. Ideally, the solid product is composed of one single target compound with all other chemical entities remaining in the liquid phase for disposal. In reality, however, this can be difficult to achieve. Due to strict control of impurities in pharmaceutical products, even a small miscibility can be a cause for serious concern.

Unwanted compounds, such as structurally similar organic impurities, have many mechanisms to end up in the isolated solid product. Particularly difficult to overcome is solid-phase miscibility of target compound and impurity, which results in impurity incorporation into the crystal lattice and very little impurity rejection. Here we present a workflow development approach to rapidly identify the mechanism of impurity incorporation, and demonstrate one case of significant solid miscibility.

2. Methods

Small scale cooling crystallizations were designed and carried out using the Technobis Crystal16 and Crystalline systems. The resulting solid material was analyzed using multiple physical characterization methods. Crystal purity was measured using an Agilent 1100 HPLC, and using this data the distribution and selectivity coefficients were calculated. The melting temperature of solid materials were determined using differential scanning calorimetry on a Netzsch DSC214 Polyma, enabling binary phase diagrams and Tamman plots to be constructed. Plate powder X-ray diffraction patterns of recrystallized samples were collected using a Bruker AXS D8 Advance II diffractometer, and the unit cell dimensions determined using Pawley refinement methods.

3. Results and discussion

A series of cooling crystallizations of paracetamol in the presence acetanilide and metacetamol revealed the two structurally similar impurities have different rejection/incorporation behavior.

Especially for metacetamol the crystallization does not result in a sufficiently improved solid product purity. The experimental distribution coefficients for these crystallizations was found to vary with increasing the amounts of impurity ($K_{metacetamol}$ = 0.05 to 0.41, $K_{acetanilide}$ = 0.06 to 0.12), and the same trend was observed in the experimental selectivity coefficients.

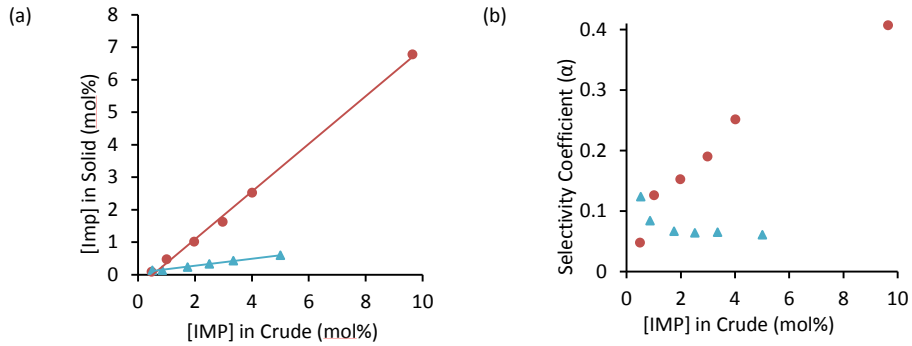

Figure 1. (a) Purification efficiency of crystallizations as measured by HPLC. Grey dashed line indicates no purification. Metacetamol (circles) linear regression y = 0.735x - 0.386, R^2 = 0.998. Acetanilide (triangles) linear regression y = 0.107x - 0.060, R^2 = 0.996. (b) The amount of impurity incorporation affects the selectivity coefficient of the crystallisations.

Investigating further, it was found that metacetamol incorporates into the paracetamol crystal lattice in significant amounts. X-ray powder diffraction revealed this incorporation modifies the crystal unit cell, with an elongation of one vertex and increase in cell volume thought to accommodate the intruding impurity molecule. The construction of Tamman plots for each binary system indicated a partial solid miscibility between paracetamol and metacetamol of 6.7 ± 2.1 %, further supporting the incorporation of the latter into the API crystal lattice.

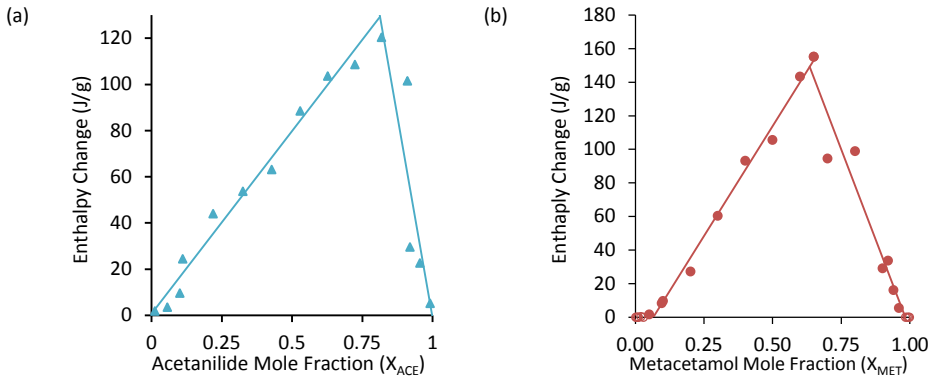

Figure 1. Tamman triangle plots. (a) Paracetamol-acetanilide. LHS regression y = 158.2x + 0.7, R^2 = 0.979, x-axis intercept = 0.002 ± 0.020. RHS regression y = -699.1x + 697.9, R^2 = 0.780, x-axis intercept = 0.981 ± 0.025. (b) Paracetamol-metacetamol. LHS regression y = 261.8x – 17.1, R^2 = 0.992, x-axis intercept = 0.067 ± 0.021. RHS regression y = -429.1x + 421.7, R^2 = 0.923, x-axis intercept = 0.972 ± 0.037.

This methodology has been formulated into a workflow and applied to two other systems; fenofibrate and mefenamic acid. These specific pharmaceutically relevant molecules have impurities which are difficult to remove using cooling crystallization techniques.

4. Conclusions

By utilizing physical characterization techniques, the mechanism of impurity incorporation during a cooling crystallization is determined. The specific incorporation of metacetamol into the paracetamol crystal lattice is due to partial solid miscibility, and so this impurity very difficult to remove by cooling crystallization.

ECCE12
The 12th EUROPEAN CONGRESS OF CHEMICAL ENGINEERING
Florence 15-19 September 2019

Particle comminution in stirred media mill and high-shear impeller – modelling and experimental approach

Norbert Wiatr[1], Radosław Krzosa[1], Radosław Adamek[2], Wojciech Orciuch[1*], Łukasz Makowski[1]

1 Faculty of Chemical and Process Engineering, Warsaw University of Technology, Warsaw, Poland; 2 ICHEMAD-Profarb, Gliwice, Poland

**Corresponding author: Wojciech.Orciuch@pw.edu.pl*

Highlights

- Particle comminution in stirred media mill and high-sheer impellers
- Influence of geometry and process parameters on the ultra-fine grinding process

1. Introduction

Size reduction process is crucial in many branches of the industry. It is commonly used in pharmaceutical, paint, cement, pyrotechnical industries and many others. Important problem is choosing the right parameters which will allow to optimize the cost of such an operation [1, 2].

In this work authors consider de-agglomeration and breakage process in two characteristic systems. The first device is a tank mixer equipped with a high-shear impeller. This type of agitators is usually high-speed and occur in the form of discs with protrusions to break up solid particles. The second device is stirred media mill that is one of the apparatus designed for ultra-fine grinding. The basic parameters describing the mixing process are: the amount of energy that is supplied into the fluid in a time unit by the mixer, mixing time, shear stresses, solids concentration and energy dissipation rate. The intensity of mixing, the speed of circulation and the presence of dead zones are also important in description of the mixing process. In stirred media mill the suspension mass flow, milling media size and material and mill geometry needs to also be considered. The set of these parameters allows to analyze the mixing process in terms of product quality and process economy [3, 4, 5]. Computational fluid dynamics is a convenient and fast tool for determining the influence of process parameters and system geometry on the considered process. It could reduce the cost of process optimization by reducing the number of experiments.

2. Methods

The systems geometries were created using SolidWorks software. Next for computational simulations the Ansys Fluent 19 software was used. To obtain detailed information of the hydrodynamics generated by the rotating element the multiple reference frame (MRF) approach was used. Turbulent flow k-ε and VOF models were used. It was checked that the results of the computations were not sensitive to a further increase of the number of computational cells. The SIMPLE method was used for the pressure-velocity coupling and the second-order discretization schemes were used for all variables to minimize numerical diffusion effects. The computations were regarded as satisfactorily converged when the total normalized residuals were smaller than 10^{-6}.

In breakage experiments silica (SiO_2) or titanium oxide (TiO_2) particles suspended in water were used. The particle sizes distributions during process time were determined using Beckman&Coulter LS 13320 device.

3. Results and discussion

In this work we consider the influence of rotational speed, mass flow of suspension and mixing time on the dispersion and comminution processes. Additionally, in the case of a tank mixer, changes in the shape of the impeller were considered, while in the case of the mill the number and shape of the holes in the rotating discs were tested. In all cases global parameters of the system were determined as mixing power, mixing time, effective pumping number. Simulations for both studied systems were validated by comparison with experimental data obtaining a good agreement. Example of such simulation results is shown on fig. 1.

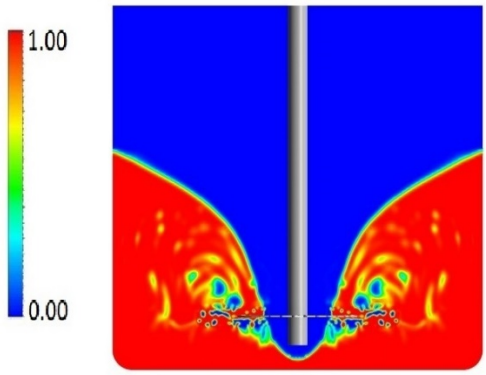

Figure 1. Volume fraction of suspension in tank mixer N=1000 rpm

4. Conclusions

Numerical simulations and experiments were carried out in order to gain influence of process parameters on comminution in two systems. Studying characteristic quantities as the power number or mixing time showed that the grinding process can be controlled by influence of the volume of the region of effective dissipation rate and particles residence time in this region. The obtained results help to predict better comminution conditions which may be useful especially when increasing the scale of process.

References

[1] J. Zhang, S. Xu, W. Li, High shear mixers: A review of typical applications and studies on power draw flow pattern, energy dissipation and transfer properties, Chem. Eng. Proc. 57– 58 (2012) 25– 41.

[2] Bałdyga J., Orciuch W., Makowski Ł., Malik K., Özcan-Taşkin G., Eagles W. and Padron G., “Dispersion of nanoparticle clusters in a rotor-stator mixer”, Industrial & Engineering Chemistry Research 47 (2005) 3652-3663.

[3] J. Ramírez-Muñoz, G. Martínez-de-Jesús, A. Soria, A. Alonso, L.G. Torres, Assessment of the effective viscous dissipation for deagglomeration processes induced by a high shear impeller in a stirred tank, Advanced Powder Technology 27 (2016) 1885–1897.

[4] D. Eskin, O. Zhupanska, R. Hamey, B. Moudgil, B. Scarlett, Microhydrodynamics of stirred media milling, Powder Technology 156 (2005) 95-102.

[5] S. Breitung-Faes, A. Kwade, Prediction of energy effective grinding conditions, Minerals Engineering 43–44 (2013) 36–43.

ECCE12
The 12th EUROPEAN CONGRESS OF CHEMICAL ENGINEERING
Florence 15-19 September 2019

Granular vertical bladed mixer: flow patterns and homogenization

Martin Kozakovic[1*], David Kramolis[1], Tereza Travnickova[2], Petr Stanovsky[2], Martin Kohout[3], Jaromir Havlica[1,2]

1 University of Jan Evangelista Purkyne in Usti nad Labem, Ceske mladeze 8, 400 96 Usti nad Labem, Czech Republic, 2 Institute of Chemical Process Fundamentals Czech Academy of Sciences, Rozvojova 2/135, 165 02 Prague, Czech Republic; 3 University of Chemistry and Technology Prague, Technicka 5, 166 28 Prague, Czech Republic

**Corresponding author: martin.kozakovic@gmail.com*

Highlights

- Formation of primary and secondary flow patterns was analyzed
- Description of the primary and secondary flows influence on the homogenization process
- Determination of the best working conditions for homogenization process

1. Introduction

This contribution is focused on mixing dynamics and homogenization process during mixing of the dry granular material. Inasmuch as a granular flow is a very complex problem, it is still intensively researched. Our motivation is to interpret the complex behavior of the granular flow and to describe the connection between dynamics of primary and secondary granular flows and the homogenization process during the convection mixing mechanism. The results presented here are the continuation of our previous publishing activities[1-3], which were particularly focused on the description of the secondary flow formation during the mixing process.

2. Methods

This contribution deals with numerical simulations and experimental measurements of the granular mixing process in a vertical cylindrical mixer with two opposed flat blades with a 45° rake angle. The mixing process was performed for 42212 monodisperse colored spherical glass particles with 2 mm diameter and three limit initial packing configurations: tangential (side-by-side), axial (bottom-up) and radial (inside-outside). The blade rotational speed was changed from 0.1 rpm to 960 rpm. Each of simulated processes was performed for 80 stirrer revolutions. The simulation was conducted using open-source code LIGGGHTS with implemented Discrete Element Method (DEM). The experiments consisted of a borosilicate cylindrical glass vessel and bottom part was made from polyamide. The whole mixing process was recorded by color high-speed camera Redlake MotionPro X-3 with 50mm (Nikon f/1.2) lens to obtain sharp images even for higher rotational speed (with resolution 1280x1024 in speed range 30-1040 fps and exposure 722ns) [3].

3. Results and discussion

In order to better understand the behavior of the mixing process and what aspects affect the resulting process of homogenization, individual particles were tracked, force chains were visualized and also discrete quantities, such as velocity or concentrations, were transformed into Eulerian 1D,

2D and 3D fields. An important part was also the evaluation of mixing indexes, displacement characteristics and variation of the interface surface between particles of different colors during mixing process.

Especially in the first stage of the mixing process, the dominant mechanism is convection. The homogenization process takes place, when the phase interface between different types of particles significantly increases. In order to increase the interface, it is necessary for particles to move in the normal direction with respect to the interface and at the same time their mutual normal velocity has to be of different magnitude. Using different initial configurations and different blades rotational speeds, the relationship between the orientation of the phase interface and velocities of individual particles was determined. It was also described the influence of primary and secondary flows on the homogenization process. Fig. 1 presents an evolution of concentration fields for blades rotational speed 150 rpm and two different initial packing configurations (tangential and radial). For a tangential initial configuration (Fig 1a), it is possible to monitor the effect of primary flows (tangential velocity) on the homogenization process. On the other hand, Fig 1b illustrates the importance of secondary flows for mixing process especially for initial packing configuration with phase interface oriented in the tangential direction to the primary flow.

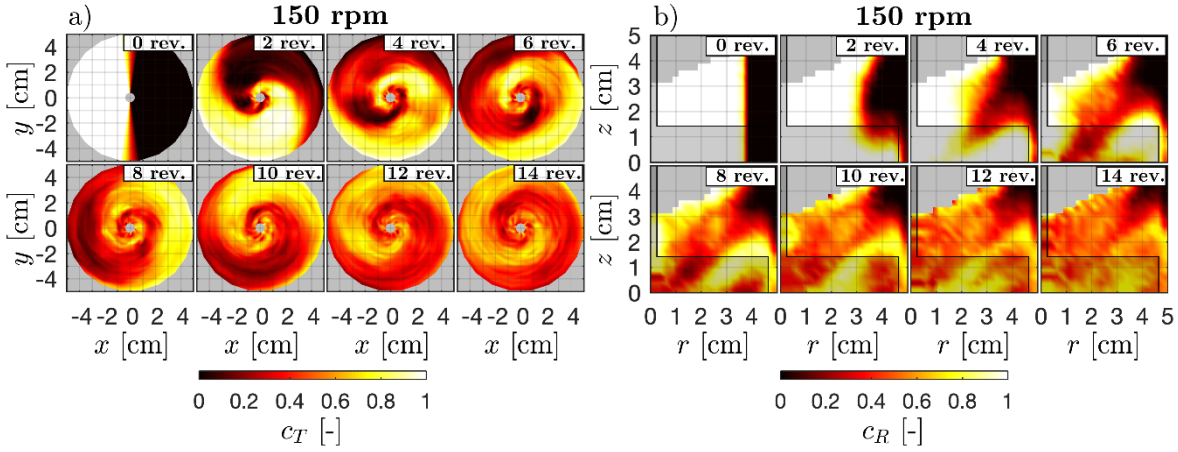

Figure 1. 2D concentration patterns for a) side-by-side and b) inside-outside initial packing. The stirrer is semi-transparent. The blades rotational speed is 150 rpm.

4. Conclusions

The mixing process of granular material in a vertical mixer with two opposed flat blades for different blades rotational speeds and initial configurations was studied by numerical simulations and experimentally. Results from simulations and experiments describe the mixing process in the same way with significant agreement in observations. This study shows the influence of both primary and secondary flows on the homogenization process. Based on these results, ideal working conditions were determined for investigated mixing process.

References

[1] J. Havlica, K. Jirounkova, T. Travnickova, M. Kohout, Powder Technol. 280 (2015), 180–190.
[2] T. Barczi, T. Travnickova, J. Havlica, M. Kohout, Chem. Eng. Technol. 38 (2015), 1195–1202
[3] J. Havlica, K. Jirounkova, T. Travnickova, P. Stanovsky, P. Petrus, M. Kohout, Powder Technol. 334 (2019), 79–88.

Acknowledgements: This research was supported by the grant UJEP-SGS-2018-53-002-2.

ECCE12
The 12th EUROPEAN CONGRESS OF CHEMICAL ENGINEERING
Florence 15-19 September 2019

Single crystals of metal-organic coordination complexes by using CO_2 as antisolvent

Margarethe Roskosz*[1], Sabine Kareth[1], Bert Mallick[2], Marcus Petermann[1]

1 Chair of Particle Technology, Ruhr University Bochum, Universitaetsstrasse 150, 44801 Bochum, Germany;

2 Inorganic Chemistry II, Ruhr University Bochum, Universitaetsstrasse 150, 44801 Bochum, Germany

**Corresponding author: roskosz@fvt.rub.de*

Highlights

- Gas antisolvent crystallization of metal-organic coordination complexes.
- Tunable crystal sizes and suitable crystals for single crystal X-ray diffractometry.
- Reduction of crystallization time compared to conventional methods.

1. Introduction

In pharmaceutical and fine chemicals industries, crystallization methods are well-established for the production of solid products. The driving force in crystal formation is supersaturation. Conventional techniques such as cooling or evaporative methods are not always suitable for producing fine and pure particles. Crystallization with compressed gases or supercritical fluids seems to be a promising alternative technique. One version of this technique is the gas antisolvent process (GAS). In this method, a gas is added to a solution, loaded with the desirable substance. The solvent power of the conventional solvent decreases, while a rapid volume expansion occurs. Supersaturation triggers off the precipitation of particles. [1-2]

Research on this method was focussing on precipitation of small and uniform crystals, modifying particle properties. We would like to introduce the GAS crystallization as a possible method for producing crystals large and clear enough for single crystal X-ray diffractometry. This analytical technique provides detailed information about the internal lattice of crystalline substances and is most commonly used for identification of crystal structures. The chosen class of metal-organic coordination complexes is a quite new one, in which direct structural solutions on the molecular level are important to reveal the chemical structure obtained. [3]

2. Methods

The gas antisolvent crystallization was tested on various metal-organic coordination complexes similar to the copper complex. These results are presented as example.

Complex synthesis. 0.1 g of copper(II) acetate and the organic linker, diethyl cyanomalonate, were dissolved in a 1:2 metal:ligand molar ratio in 70 ml chloroform and stirred for 24 h at room temperature. The metal-organic coordination complex was obtained as a precipitate in powder form, that was filtered and vacuum dried for 12 h.

Gas antisolvent crystallization. For the crystallization CO_2 was used as an antisolvent. The experiments were carried out in a high-pressure view cell loaded with a solution of the metal-organic coordination complex in a chosen solvent. A crystallization time of 2 h, a pressure of 100 bar and a temperature of 40 °C were set. After the specified time, the autoclave was purged for 30 min with CO_2. The precipitate was obtained as crystals. [4]

3. Results and discussion

The GAS crystallization was performed with three different starting concentrations, but same temperature and pressure profile. The products of the antisolvent crystallization were obtained as green crystals. With decreasing the initial concentration, a decreasing average size and an increase in uniformity of the crystals can be observed. Most of the crystals were obtained with a minimum size of 50-200 µm, sufficient for single crystal X-ray diffractometry (figure 1).

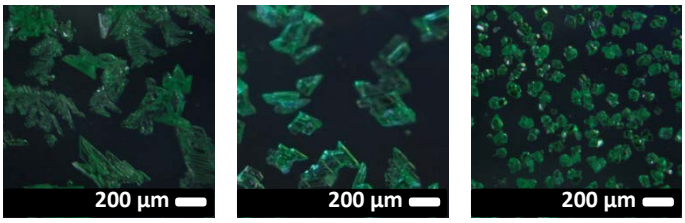

Figure 1. Microscopic images of crystals from GAS crystallization from different starting concentrations; A: 15 mg/ml; B: 7.5 mg/ml; C: 5 mg/ml.

The data sets from the X-ray analysis showed that the structure of the copper complex, obtained from the antisolvent crystallization, is a one-dimensional coordination polymer (figure 2). For comparison, the same copper complex was also crystallized by evaporating the solvent at room temperature. Crystals were obtained after days to weeks, depending on the concentration and the chosen solvent. Those data sets from the X-ray analysis showed the same one-dimensional coordination polymer, like from the GAS crystallization.

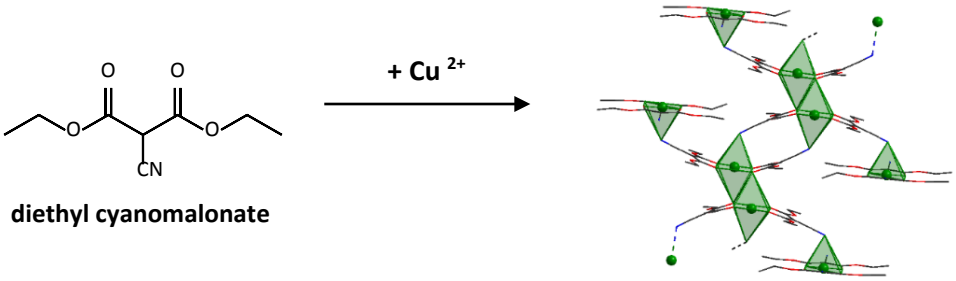

diethyl cyanomalonate

Figure 2. Formation route of the copper complex build of diethyl cyanomalonate and copper(II) acetate. Molecular crystal structure obtained from single crystal X-ray data sets. (copper: green; oxygen: red; nitrogen: blue; carbon: black)

4. Conclusions

The use of CO_2 as an antisolvent opens up new possibilities for the crystallization of metal-organic coordination complexes next to other solids. It was possible to get X-ray suitable single crystals from different starting concentrations. Compared to the conventional method, these crystals were obtained just in a few hours, instead of days or weeks. In this case no structural differences have been determined. Compared to the evaporation crystallization, this method would be a possible alternative to conventional crystallization methods.

References

[1] P.M. Gallagher, ACS Symp. Ser. 406 (1989) 334-35.
[2] J. Jung, M. Perrut, J. of Supercritical Fluids 20 (2001) 179–219.
[3] L. Li, CrystEngComm 15 (2013) 4094-4098.
[4] M. Roskosz, International Symposium on Supercritical Fluids (2018).

Supercritical Precipitation of PHB as a Potential Carrier for Antioxidant Delivery

Facundo Mattea*[1,2], Valentina Sosa[3], Matías Dalmasso[3], Javier Galfioni[3], Joaquín Orejas[3]

1 *Universidad Nacional de Córdoba. Facultad de Ciencias Químicas. Dpto. de Química Orgánica. Cba., Arg.; 2 Instituto de Investigación y Desarrollo en Ingeniería de Procesos y Química Aplicada, IPQA, CONICET. Cba., Arg.;3 Universidad Nacional de Río Cuarto, Facultad de Ingeniería, Dpto. de Tecnología Química.*

*corresponding author: fmattea@gmail.com

Highlights

- PHB, a biodegradable polymer was precipitated by supercritical fluid technology.
- Solvent selection is essential for the precipitation and future antioxidant inclusion
- Antioxidants were extracted and concentrated from green tea

1. Introduction

Supercritical antisolvent process (SAS) is widely being used to micronize pharmaceutical and nutraceutical compounds. The advantage of SAS over other conventional processes is that thermal degradation is avoided in the active compounds as the operating temperature is near to room temperature. Therefore, the micronization of thermally labile compounds such as antioxidants or colorants has been widely studied by SAS with carbon dioxide as antisolvent [1]. Also, by the coprecipitation of biodegradable polymers and active compounds it is possible to produce formulations with controlled release of the active compound prolonging its effect over time. The selection of the solvent is essential in this process, it must meet the solubility requirements for both the active compound, the polymer or carrier, and be miscible or form a single phase with the antisolvent fluid. On this study, two different solvents were used for an ultrasound assisted extraction of catechins and antioxidants from green tea, and to study the precipitation of a biodegradable polymer, namely Polyhydroxybutyrate (PHB) by means of the supercritical antisolvent process.

2. Methods

In the antioxidant extraction, 5.0 gr of green tea was extracted with 300 mL of the selected solvent assisted by ultrasound in an ultrasonic bath (Testlab TB04) for 30 minutes at 160 W. The total polyphenol content was quantified by the Folin-Ciocalteu. A scheme of the antisolvent precipitation process can be observed in Figure 1. In a typical experiment the whole process is filled with carbon dioxide and stabilized at the desired pressure and temperature and CO2 flowrate, then 250 mL of solution containing the polymer or active compounds is pumped into the precipitation unit, afterwards the solution inlet is stopped, and a certain amount of CO2 is introduced to remove any remaining solvent from the formed particles. The formed particles are retained by a metallic frit placed inside the precipitation unit.

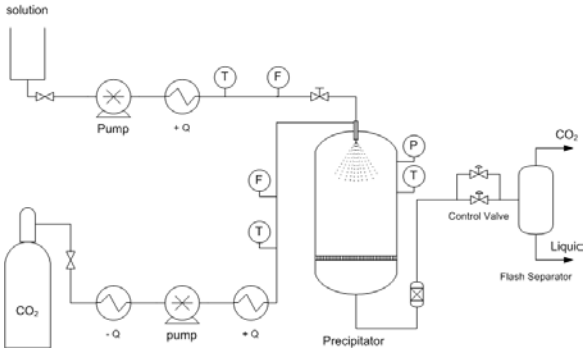

Figure 1. Antisolvent precipitation process scheme.

3. Results and discussion

The total amount of extracted polyphenols expressed as mg of polyphenol per gram of green tea was 3.02 for DCM and 126.06 for 1,3-dioxolane. The solubility of catechins in DCM is very low compared to other typical solvents like ethanol or water, however PHB has no appreciable solubility in those typical solvents. The precipitation of PHB from DCM solutions rendered particles with a mean size of 1.42 µm with a needle shape by using a pressure of 120 bar, temperature of 40°C, CO2 flow of 4Kg/h, solution flow of 1-2 mL/min and PHB concentration of 0.5 g/L. For the precipitation from 1,3-dioxolane similar operation conditions were used and concentrations of PHB ranging from 0.26 g/L to 0.75 g/L, obtaining particles with a mean size of 1.95 µm.

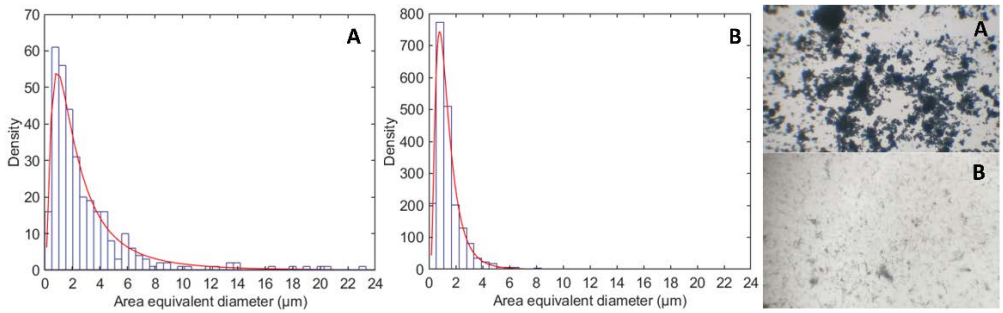

Figure 2. A) commercial PHB size distribution and morphology (left), B) particles of PHB obtained by supercritical antisolvent process from DCM solutions.

PHB microparticles obtained from SAS with DCM had a mean particle size of 1.42 µm with a variance of 0.94 µm, with represent a 53.2 % reduction on the mean size and 90.6 % reduction on the variance, compared from the commercial powder which has a mean size 3.04 µm of with a variance of 9.97 µm.

4. Conclusions

Both DCM and 1,3-dioxolane are suitable solvent for the precipitation of PHB with the CO2 antisolvent process. DCM is not as good as 1,3-dioxolane for the extraction of catechins and the later may be preferred for the coprecipitation and formation of antioxidant sustained delivery compound based on PHB.

References

[1] V. Prosapio, L. De Mrco, E. reverchon, The J. of Superc. Fluids. 138 (2018) 247-258.

ECCE12
The 12th EUROPEAN CONGRESS OF CHEMICAL ENGINEERING
Florence 15-19 September 2019

Modelling Antisolvent Impact on Active Pharmaceutical Ingredient Batch Crystallization

Marko Trampuž[1], Dušan Teslić[2], Blaž Likozar[1]

1 Dept. of Catalysis and Chemical Reaction Engineering, National Institute of Chemistry, Hajdrihova 19, 1001 Ljubljana, Slovenia; 2 Sandoz Development Centre Slovenia, Lek d.d., Kolodvorska 27, 1234 Mengeš, Slovenia

**Corresponding author: marko.trampuz@ki.si*

Highlights

- Batch crystallization of fesoterodine fumarate active pharmaceutical ingredient
- Mathematical model of the process was developed, optimized and validated
- Larger, but more agglomerated particles are formed by increasing antisolvent amount
- Solubility decreases and crystallization kinetic rates increase with antisolvent amount

1. Introduction

Crystallization of active pharmaceutical ingredients (API) is one of the most important separation and purification operations in pharmaceutical industry. However, it is also one of the most complex ones, due to various thermodynamic, transport, and kinetic phenomena taking place in a heterogeneous system [1-2]. Fesoterodine fumarate is an API used to treat overactive bladder. High temperature-dependent solubility, high secondary nucleation rate, and slow crystal growth rate have been acknowledged for fesoterodine fumarate crystallization from 2-butanone in our previous work [3]. The present work examines the impact of antisolvent cyclohexane on the various properties of cooling batch crystallization of fesoterodine fumarate in 2-butanone.

2. Methods

The experimental part of the work was performed in a 2 L batch reactor. It consisted of in-line attenuated-total reflectance Fourier-transform infrared spectroscopy (ATR-FTIR) calibration of fesoterodine fumarate solutions in two different solvent compositions (2-butanone with 5 wt. % cyclohexane and 2-butanone with 10 wt. % cyclohexane). Equilibrium solubility between -10 and 40 °C in both compositions was determined by ATR-FTIR. A specified number of cooling crystallization and dissolution experiments in both solvent mixtures under various operating conditions were performed for estimation of kinetic parameters of crystallization and dissolution, as well as model validation. Experiments were monitored by ATR-FTIR and final products were analyzed by microscopic, thermal, and X-ray techniques.

In-house mechanistic mathematical model of the crystallization process based on population balance equation methodology was developed. Equilibrium solubility, mass and energy transfer resistances, and kinetic equations for nucleation, crystal growth, crystal dissolution, and crystal agglomeration were incorporated into the model. Values of unknown kinetic parameters were estimated via nonlinear regression of simulated and experimental quantitative results.

3. Results and discussion

Increase in the amount of antisolvent in the mixture from 0 to 10 wt. % resulted in decrease in fesoterodine fumarate solubility in the studied temperature range (Figure 1). This stems from the fact that fesoterodine fumarate is a polar solute, while cyclohexane is a very nonpolar solvent. Due to similar physical properties of 2-butanone and cyclohexane, no major difference in convective solid-liquid mass transfer coefficient, average turbulent energy dissipation rate, and overall heat transfer coefficient were calculated for different solvent mixtures. Kinetic rates of secondary nucleation, crystal growth, crystal dissolution, and crystal agglomeration all increased. Mass transport limitations on crystal growth and crystal dissolution kinetics were shown to be negligible under the used operating conditions. This indicates that the amount of antisolvent influences these two processes due to different rates of various mechanisms on crystal surface, such as integration of molecules into the crystal lattice. Overall, the increased rate of crystal agglomeration has a prevailing effect on final particle size distribution and particle morphology, which may be important for further pharmaceutical operations.

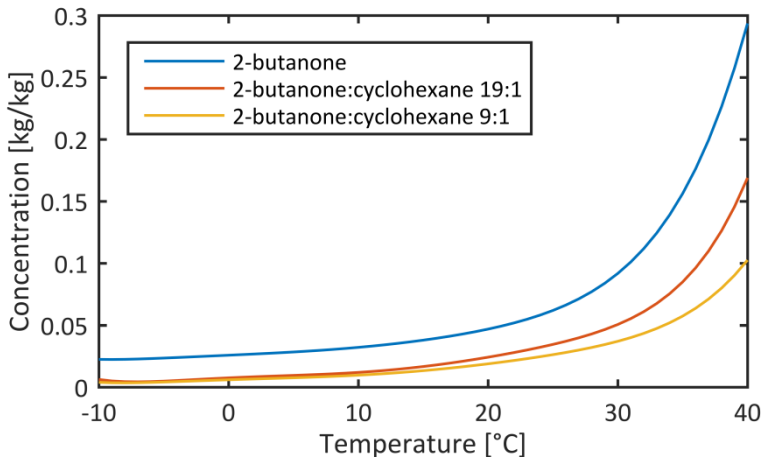

Figure 1. Solubility curves of fesoterodine fumarate in 2-butanone, 2-butanone with 5 wt. % cyclohexane, and 2-butanone with 10 wt. % cyclohexane, represented by sixth degree polynomials.

4. Conclusions

The impact of antisolvent cyclohexane on fesoterodine fumarate batch crystallization in 2-butanone was evaluated by combined experimental-modelling approach. Major influence on thermodynamic and kinetic properties of the system was observed and taken into account for model simulations. The present work thus shows a comprehensive mechanistic approach to take into account various possible ways how solvent composition may impact a crystallization process. It also presents further possibilities for model-based process optimization and intensification by tuning the amount of antisolvent and values of other operating variables.

References

[1] A.S. Myerson, Handbook of Industrial Crystallization, second ed., Butterworth-Heinemann, 2001.
[2] H.-H. Tung, E.L. Paul, M. Midler, J.A. McCauley, Crystallization of Organic Compounds: An Industrial perspective, first ed., Wiley, 2009.
[3] M. Trampuž, D. Teslić, B. Likozar, Chem. Eng. Sci. 201 (2019) 97-111.

ECCE12
The 12th EUROPEAN CONGRESS OF CHEMICAL ENGINEERING
Florence 15-19 September 2019

3D-structuring of highly filled nanoparticle-reinforced epoxy composites by vibration-controlled nozzle

Lisa Windisch[1], Benedikt Finke[1], Carsten Schilde[1]

[1] *Institute for Particle Technology, TU Braunschweig, Volkmaroder Str. 5, 38104 Braunschweig, Germany*

**Corresponding author: l.windisch@tu-bs.de*

Highlights

- Composite materials with particulate contents up to 90 wt% can be achieved.
- Material combinations and powder layering can generate functionally graded components
- Composite samples can further be adapted locally by microdosing of fine powders with high resolutions and accuracies.

1. Introduction

Composite materials are the fundament for a wide variety of applications in areas such as aerospace, shipbuilding, or electromobility. Compared to pure materials, they make it possible to increase the efficiency of structures significantly. Additionally, by using nanomaterials, especially nanoparticles, product properties can be further improved, or even new properties can be achieved. Through 3D-structuring of components, properties can be adapted even more individually and locally, resulting in a wide variety of design possibilities. Especially when dealing with fine powders, precise and high-resolution dosing of materials remains a major challenge in research and development. Microdosing is relevant, for example, in the pharmaceutical industry for exact dosing of smallest amounts of active substances or in additive manufacturing processes for varying the properties of the powder bed.

2. Methods

Nanoparticles (CNTs, Carbon Black and AluC) as well as the intermixture of epoxy resin HexFlow RTM6 (Hexcel Corporation) and the corresponding diamine based hardener were dissolved in MEK using an ultrasonic dispersing device at 40 °C for 30 – 120 min with particulate contents of 1-5 wt% in the suspension. The stability of these suspensions against reagglomeration was characterized via transmission measurements using the Turbiscan Lab (Quantachrome, 25 °C) and particle size analysis via laser diffraction method (Nanophox, Sympatec). Subsequently, the solvent phase was evaporated for 90 min in a lab kiln at 50 °C. The remaining suspensions with solids content between 10 wt% and 90 wt% were grinded in a steel mortar. The composite powder was further processed by hot press molding at a temperature of 150 °C and a specific molding pressure of approx. 6 kN/cm^2 for 180 min. The unmolded composite cubes were polished for further characterization, e.g. measurement of the electrical (four-point measurement) and mechanical (nanoindentation with Berkovich tip; Triboindenter, Hysitron) properties or visual analysis by scanning electron microscopy (Helios G4 CX, FEI). The 3D-structuring was carried out using a self-constructed setup for piezo-controlled microdosing of fine powders. The experimental

setup and the dosing behaviour were evaluated using model particles (boehmite, γ-AlOOH), whereby the influence of various particle properties such as surface roughness and bulk properties (e.g. flow properties) was investigated.

3. Results and discussion

The resultant mechanical, thermal and electrical properties show a distinct enhancement with increasing particulate content. By mixing and layering of powder based composite materials, tailor made functionally gradients like shown in Fig. 1 (left) have been generated. With CNT fillings maximal electric conductivities of 838 S/m at a content of 60 wt% have been achieved. Deviations can be seen in the peripheral areas of the specimens, caused by air inclusions in the composite structure due to the production process. Stabilization of the particulate material in the solvent matrix by additives showed a huge impact on the homogeneity of the samples. Specimen properties have further been adapted by local deposition of fine powder quantities. By varying dosing parameters like sonication energy, pulsation time and inner nozzle diameter a strong correlation between particle interactions and dosing behaviour was found. Powder quantities of down to 50 µg ($V_{Powder\ heap}$ = 0.5 x 0.5 x 0.2 mm = 0.05 mm³) were deposited with high accuracy (Fig.1, right).

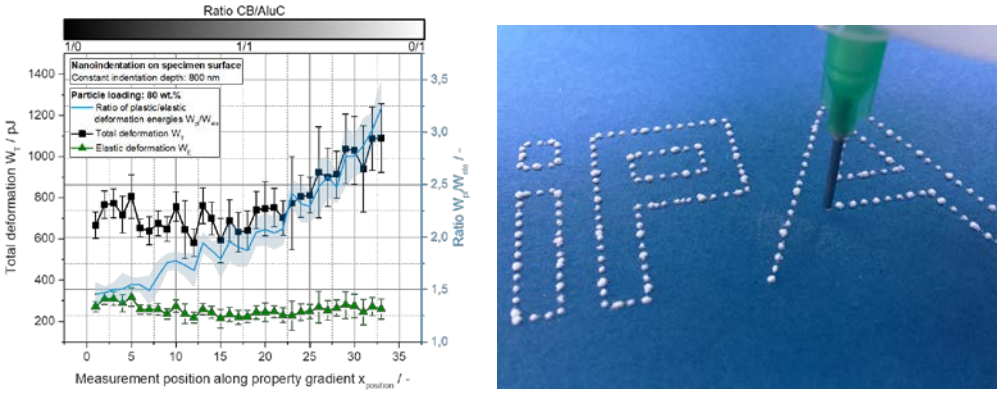

Figure 1. Property profile of a graded specimen with a CB and AluC content of 80 wt% (left) and micrometer ranged powder heaps deposited by vibration-controlled nozzle (right).

4. Conclusions

In this process high particulate loadings between 10 wt% to 90 wt% are realized. High loadings of filler materials have a great potential for an extraordinary modification and enhancement of epoxy resins and other polymers regarding thermal, electrical and mechanical properties and even though the processing is difficult, they are relevant for new design and construction concepts [1]. The resulting properties are investigated for various particle types, stabilization and loadings. By powder layering, functionally graded components have been generated. The gradient shows up as a clear profile in the measured values. An experimental setup for 3D-structuring of materials was successfully established and correlations between the dosing behaviour and the particle properties have been revealed, making it possible to produce tailor made components with individual properties.

References

[1] C. Schilde et al., Composites Science and Technology 117 (2015) 183–190.

ECCE12
The 12th EUROPEAN CONGRESS OF CHEMICAL ENGINEERING
Florence 15-19 September 2019

Rheological Spectra of New Cellulosic Ionogels with Cholinium Lysinate

M. Mar Villar-Chavero, Juan C. Domínguez, M. Virginia Alonso, Mercedes Oliet, Francisco Rodriguez

Chemical Engineering and Materials Department. Complutense University of Madrid. Av. Complutense S/N. 28040, Madrid, Spain.

**Corresponding author: mdm.villar@ucm.es*

Highlights

- Formulated cellulosic ionogels formulated were physical weak well-structured gels.
- Elastic behavior was dominant rheological behavior of the ionogels.
- The ionogel with 2% of cellulose exhibited the highest rheological properties.

1. Introduction

Cholinium amino acid ionic liquids (ChAAILs) are a type of ionic liquid (IL) classified as a third generation IL or bionic liquid (BIL) [1]. ChAAILs are composed of a cholinium cation and an amino acid anion (e.g. glycine, serine, lysine, etc.). The interest in these ILs is due to they are substantially harmlessness, biodegradable, and non-toxic [2]. In recent years, the applications of ChAAILs have gone beyond the field of biomass pretreatment. Thus, ChAAILs has been proposed to use in CO_2 capture, as lubricants, or in drug delivery formulations [2]. In this work, the use of ChAAILs for the development of gels, called ionogels, is proposed for their use in medical/pharmaceutical industry. Ionogels are composed of an IL and a continuous phase (CF). The interactions between IL and the CF can be physical or chemical, i.e. reversible and irreversible, respectively [3]. Cellulose can be used as CF for the development of ionogels due to its renewability, biodegradability, non-toxic and biocompatibility [4]. This work studies the influence of the amount of cellulose on the rheological spectra of reversible ionogels formulated with the ChAAIL cholinium lysinate (ChLys).

2. Methods

The ionogels were formulated by dissolution of microcrystalline cellulose in ChLys, both previously dried for 12 h in a vacuum oven at 40 °C. The dissolution process was conducted under magnetic stirring at 100 °C under N_2 atmosphere. The percentages of cellulose added for each ionogel were 0.5, 1, 1.5 and 2 wt. %. The dissolution time was determined by acquiring different aliquots every 30 min and visualizing them under a Carl Zeiss Axio Scope A1 microscope equipped with a Zeiss AxioCam ICc1. When the cellulose was dissolved completely, solutions are poured into a steel mold covered with PET film at room temperature up to gelation.

The rheological characterization was carried out in an Ares rheometer (TA Instruments). Dynamic frequency sweep tests from 0.01 to 50 Hz were conducted at 25 °C, with a strain of 0.01% (within the lineal viscoelastic region).

3. Results and discussion

The rheological spectra of the formulated cellulosic ionogels belonged to *plateau* region. The storage modulus (G') was higher than the loss modulus (G''), therefore the dominant behaviour was elastic in the studied range for all ionogels (Figure 1). The ratio G'/G'', or tan δ, for 1 Hz was ranged between 4.7 and 7.8, indicating that ionogels were physical weak well-structured gels.

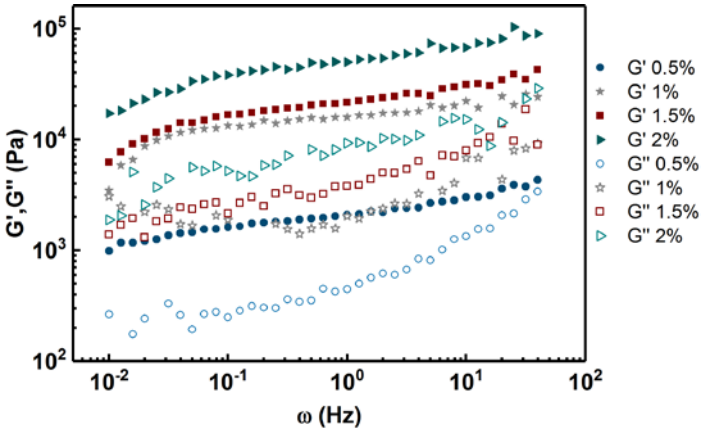

Figure 1. Rheological spectra of the cellulosic ionogels formulated.

The rheological behaviour of the ionogels was changed by the cellulose concentration (Figure 1). The elastic moduli increased as the load cellulose was increased; for 1 Hz, G' for 2% was nearly twenty-fold higher than that 0.5% of cellulose. However, this increase was less pronounced in the case of the loss moduli. Similar results and behaviours have been found for other polysaccharide-based ionogels, such as agarose or guar gum [5-6]. The ionogel strengths (G_0), defined as the measure of the elastic energy stored in the unit volume of network, were 2133, 16179, 22051, and 51586 Pa for 0.5, 1, 1.5 and 2%, respectively. For these reasons, the cellulose had an influence on the rheological properties of the ionogels.

4. Conclusions

The cellulosic ionogels were formulated successfully and can be classified as physical weak well-structured gels according to the obtained rheological spectra. The dissolved cellulose had a significant influence on the rheological properties, being the ionogel with 2% of cellulose the ionogel with the most solid-like behaviour.

Acknowledgments

The authors are grateful to “Ministerio de Ciencia, Innovación y Universidades” of Spain for financial support of project CTQ2017-88623-R.

References

[1] K.S. Egorova, E.G. Gordeev, V.P. Ananikov, Chem. Rev. 117(10) (2017) 7132-7189.
[2] A. Tarannum, J.R. Rao, N.N. Fathima, J. Phys. Chem. B 122(3) (2018) 1145-1151.
[3] P.C. Marr, A.C. Marr, Green Chem. 18(1) (2016) 105-128.
[4] D. Trache, M.H. Hussin, C.T.H. Chuin, S. Sabar, M.R.N. Fazita, O.F.A. Taiwo, T.M. Hassan, M.K.M. Haafiz, Int. J. Biol. Macromol. 93 (2016) 789-804.
[5] T.J. Trivedi, D. Srivastava, R.D. Rogers, A. Kumar, Green Chem. 14(10) (2012) 2831-2839.
[6] L. Verger, S. Corre, R. Poirot, G. Quintard, E. Fleury, A. Charlot, Carbohydr. Polym. 102 (2014) 932-940.

ECCE12
The 12th EUROPEAN CONGRESS OF CHEMICAL ENGINEERING
Florence 15-19 September 2019

Scalable production of silicate glass flakes via compression in the liquid phase

Julian Esper[1], Alexander Strobel[1,2], Stefan Romeis[1], Wolfgang Peukert[1,2]*

[1]Institute of Particle Technology, Friedrich-Alexander Universität Erlangen-Nürnberg; [2] Interdisciplinary Center for Functional Particle Systems (FPS), Friedrich-Alexander Universität Erlangen-Nürnberg

*Corresponding author: wolfgang.peukert@fau.de

Highlights

- Production of silica-based glass flakes in the liquid phase
- Characterization of process parameter influence on Feret diameter and flake thickness
- Influence of glass composition on brittle-ductile transition particle size

1. Introduction

Comminution is a frequently applied, scalable and versatile unit operation of chemical process engineering and particle technology [1-3]. Comminution processes are applied for a wide range of materials including minerals, ceramics, foods, drugs and waste. The acting stressing mechanisms are usually divided into one-sided impact or two-sided compression. In stirred media mills, particle stressing and size reduction takes place between colliding grinding beads, i.e. by compression. In general, comminution processes can be described by the 'process function' and the 'material function' [4-6]. The 'process function' links process parameters such as grinding bead size or stirrer tip speed to the actual stressing conditions in the mill. The 'material function' describes the reaction of a material to the stressing conditions. Clearly, both functions are widely distributed, are so far often unknown but can be determined by recent progress based on stressing of mechanically well-characterized model particles [4-6]. Typically irregular shaped particles with a rather wide size distribution are obtained from comminution. Whereas crystalline materials have been extensively studied there is only a very limited amount of information on wet comminution of amorphous materials with complex chemical composition. In this study, we characterize the stressing behavior and deformation of silica-based glasses with different chemical compositions in a stirred media mill and analyze characteristic dimensional parameters via SEM image analysis.

2. Methods

Commercially available soda lime glass (Carl Roth, Germany) and borosilicate glass (Schott, Germany) were used for all experiments. The as-received bulk materials were pre-crushed with pestle and mortar and classified to a size ≤ 250 µm prior to wet grinding. All wet grinding experiments were conducted in a stirred media mill PE075 (Netzsch, Germany). The grinding parameters were varied in terms of stirring speed and process time as well as grinding bead size to determine the possible influence of the process parameters on the final product particle size. All shape-anisotropic particles were characterized in means of the Feret diameter and average flake thickness via SEM image analysis. Furthermore, true powder density and mass-specific surface area were determined via helium pycnometry and nitrogen adsorption measurements, respectively. These results were used to

determine the Sauter diameter and the theoretical Feret diameter for comparison with experimental values from single particle micromanipulation experiments.

3. Results and discussion

All experiments show that the process can be divided into two distinct steps. The first step comprises the size reduction where irregularly shaped feed particles are crushed in between agitated milling beads until a certain particle size, also known as the brittle-to-ductile transition particle size, is reached. In the second step, the compression and deformation of the glass particles takes place without further fracture. The main size reduction can be observed during the first processing hour whereas plastic deformation is the predominant mechanism afterwards. This can be seen in Fig. 1 where the average flake thickness is shown for different stirring speeds and processing times. The average transferred energy E_{50} per collision determined according to Strobel et al. was 0.48 µJ (v_{tip} 4.87 m s^{-1}) which indicates that the energy transferred in one collision is sufficient to plastically deform a glass fragment into a plate-like particle [5]. The stirrer tip speed seems to exhibit only a minor influence on the average lateral dimensions of the flakes. However, it shows a significant influence on the average flake thickness. The average flake thickness decreases with longer processing times and converges at around 185 nm.

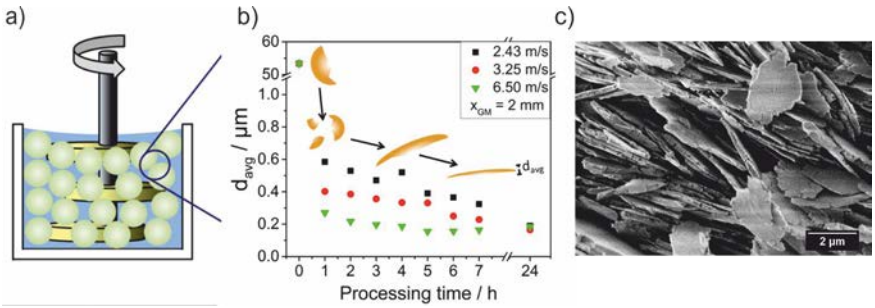

Figure 1. (a) Schematic of a stirred media mill and (b) flake thickness evolution of soda lime glass flakes for different process times and stirring speeds and (c) SEM side view of obtained glass flakes.

4. Conclusions

A facile and fully scalable method to produce amorphous silica-based glass flakes w presented. The influence and effects of stirring speed, process time and bead size is systematically examined and depicted. Our experiments show, that size reduction occurs only during the first hour of grinding while a plastic deformation of the glass fragments is the predominant mechanism in the following hours of process time. These remarkable results are unique because wet grinding is used here as a novel method for well-controlled particle shape formation. The Feret diameter and thickness distributions for all glasses as determined via SEM image analysis and the corresponding size distributions are found to be quite narrow.

References

[1] A. Kwade, Powder Technology 105 (1999) 14-20.
[2] F. Müller, R. F. Polke, Powder Technology 105 (1999) 2-13.
[3] O. Orumwense, E. Forssberg, Min. Processing and Extractive Metallurgy Review 11 (1992) 107-127.
[4] W. Peukert, Adv. In Chem. Eng. 46 (2015) 1-81.
[5] A. Strobel, W. Peukert, Chem. Eng. Res. & Design (2018) 859-869.
[6] A. Strobel, W. Peukert, Powder Technology 305 (2017) 652-661.

ECCE12
The 12th EUROPEAN CONGRESS OF CHEMICAL ENGINEERING
Florence 15-19 September 2019

Selecting concentrated seawater in salt manufacturing process for $CaMg(CO_3)_2$ production by CO_2 fine bubble injection

Masakazu Matsumoto[1*], Yoshinari Wada[1], Yuko Tsuchiya[1],
Koji Masaoka[1,2], Toshihiko Hiaki[1]

1 College of Industrial Technology, Nihon University, 1-2-1 Izumi-cho Narashino, Japan

2 Research Institute of Salt and Sea Water Science, The salt Industry Center, 4-13-20 Sakawa, Odawara, Japan

**Corresponding author: matsumoto.masakazu@nihon-u.ac.jp*

Highlights

- Fine bubble injection into the removed K brine is well suited for dolomite production.
- Production of dolomite accelerates with an increase in Ca and Mg concentrations.
- High CO_2 flow rate accelerates the crystallization of dolomite with higher Mg/Ca ratio.

1. Introduction

In the Japanese salt manufacturing process as one of the utilization system of seawater resources, the electrodialysis (ED) brine is obtained after concentrating seawater through an electric dialysis membrane. Thereafter, the concentrated brine is prepared by secondary concentration of ED brine using the evaporation operation up to the crystallization point of NaCl. Finally, NaCl is manufactured by evaporative crystallization from the concentrated brine, and then the removed K brine that separated KCl by cooling crystallization is obtained. In order to streamline the salt manufacturing process, a novel recovery and upgrading method for calcium (Ca) and magnesium (Mg) from the discharge concentrated seawater of salt manufactory is indispensable. In this study, we used the minute gas-liquid interfaces around CO_2 fine bubbles as new reaction fields where the crystal nucleation proceeds dominantly and selected the suitable concentrated seawater for synthesizing the dolomite ($CaMg(CO_3)_2$) with a high Mg/Ca ratio. Three concentrated seawater as ED brine, concentrated brine, and removed K brine coming from salt manufacture discharge each have a different concentration product of Ca^{2+} and Mg^{2+} ($[Ca^{2+}][Mg^{2+}]$). In this paper, we report the effects of $[Ca^{2+}][Mg^{2+}]$ as one of operational index and F_{CO2} on the reactive crystallization of $CaMg(CO_3)_2$.

2. Experimental

2.1 Concentrated seawater The ED brine, concentrated brine, and removed K brine coming from salt manufacture discharge in Japan was used. The major ion components of each concentrated seawater are shown in **Table 1**. The concentration ratio of Mg^{2+} for Ca^{2+} in the ED brine, concentrated brine, and removed K brine was approximately equal to 3.

Table 1 Concentrations of each concentrated seawater

Concentration [mol/*l*]	ED brine	Brine	Removed K brine
$[Ca^{2+}]$	0.031	0.062	0.67
$[Mg^{2+}]$	0.083	0.18	2.1
$[Na^{+}]$	2.6	4.0	0.84
$[Cl^{-}]$	2.9	4.6	7.0

2.2 Experimental apparatus The semi-batch type crystallization apparatus consists a gas flow controller, a pH/EC meter, a self-supporting bubble generator, a crystallization vessel, and a thermostatic bath. CO_2 fine bubbles with an average bubble diameter (d_{bbl}) of 40 µm were generated using a self-supporting bubble generator by the shear of the impeller and a negative

pressure owing to high-rotation [1], with the rotation rate maintained at 1500 min^{-1} and the CO_2 flow rate (F_{CO2}) controlled in the range of 5.96 – 23.8 mmol/(*l*·min).

2.3 Experimental procedure CO_2 fine bubbles with d_{bbl} of 40 µm were continuously supplied to 300 m*l* of ED brine, concentrated brine, or removed K brine in a crystallization vessel and the reactive crystallization of $CaMg(CO_3)_2$ was performed. The reaction temperature was maintained constant at 298 K using a thermostatic bath, and the reaction time (t_r) was controlled within 60 min. The solution pH during reactive crystallization was monitored and constantly adjusted to 6.8 by adding 4.0 mol/*l*-NaOH aqueous solution. The selectivity of solid products was identified by the peak area ratio from XRD and the Mg/Ca ratio of $CaMg(CO_3)_2$ was estimated from the amount of peak shift between calcite $CaCO_3$ (2θ = 29.4°) and $CaMg(CO_3)_2$ (2θ = 30.7°) [1,2].

3. Results and discussion

The relationships between $[Ca^{2+}][Mg^{2+}]$ and the production rates of aragonite $CaCO_3$ ($r_{aragonite}$) and $CaMg(CO_3)_2$ ($r_{dolomite}$) or the rate of increase in the Mg/Ca ratio of $CaMg(CO_3)_2$ ($r_{Mg/Ca}$) as a function of F_{CO2} are shown in **Figure 1**. At a ln $[Ca^{2+}][Mg^{2+}]$ of -6, aragonite $CaCO_3$ and $CaMg(CO_3)_2$ were obtained irrespective F_{CO2}. $r_{dolomite}$ and $r_{Mg/Ca}$ increased with an increase of $[Ca^{2+}][Mg^{2+}]$ in the concentrated seawater, and the dependence of $[Ca^{2+}][Mg^{2+}]$ on $r_{dolomite}$ and $r_{Mg/Ca}$ was increased with an increase in F_{CO2}. Consequently, when the removed K brine with a high $[Ca^{2+}][Mg^{2+}]$ was used, the increase in F_{CO2} is effective for the high-yield crystallization of $CaMg(CO_3)_2$ with higher Mg/Ca ratio.

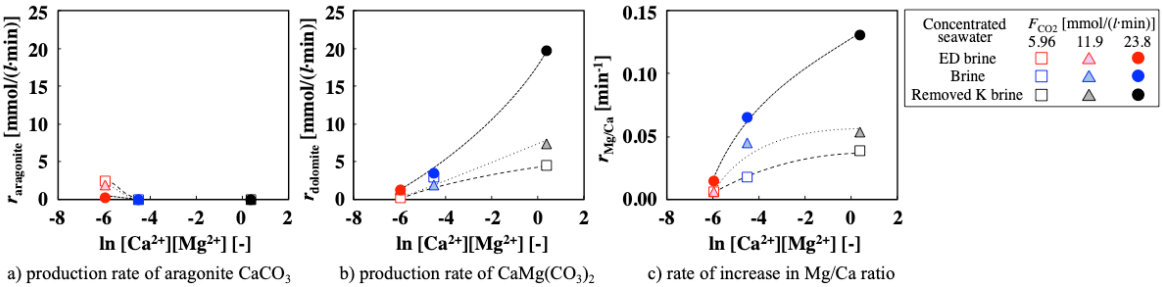

Figure 1. Relationships between $[Ca^{2+}][Mg^{2+}]$ and $r_{aragonite}$, $r_{dolomite}$, or $r_{Mg/Ca}$ at various F_{CO2} values.

4. Conclusions

In order to select the concentrated seawater in salt manufacturing process in Japan for the production of $CaMg(CO_3)_2$ with a high Mg/Ca ratio, CO_2 fine bubbles were supplied into the three concentrated seawater discharged from salt manufacturing process and $CaMg(CO_3)_2$ was crystallized. In the case where the removed K brine with a high $[Ca^{2+}][Mg^{2+}]$ was selected at greater F_{CO2}, $CaMg(CO_3)_2$ with higher Mg/Ca ratio can be produced by the reactive crystallization with briefer period.

Acknowledgments

This work was financially supported by the Salt Science Research Foundation (Nos. 17A3, 18A3), Japan. We also acknowledge the Naikai Salt Industry Co., Ltd. for provision of Bittern.

References

[1] Y. Tsuchiya, Y. Wada, T. Hiaki, K. Onoe, M. Matsumoto, J. Cryst. Growth 469 (2016) 36–41.

[2] T. Oomiri, Y. Kitano, Geochem. j. 21 (1987) 59–65.

ECCE12
The 12th EUROPEAN CONGRESS OF CHEMICAL ENGINEERING
Florence 15-19 September 2019

Pebax®2533 and Graphene Oxide-Based materials for Carbon Capture Membranes

*Riccardo Casadei[1], Marco Giacinti Baschetti[1], Myung Jin Yoo[2], Ho Bum Park[2]

1: Department of Civil, Chemical, Environmental and Material Engineering (DICAM) – University of Bologna, Via Terracini 28, 40131 Bologna, Italy ;

2: Department of Energy Engineering, Hanyang University, Seoul 133-791, Republic of Korea

**Corresponding author: riccardo.casadei11@unibo.it*

Highlights

- Flawless dispersion of GO in Pebax®2533 with concentration of 0,02 to 1 wt%
- Study of permeation trend caused by GO addition in Pebax®2533
- Comparison of permeation performances improvements of Pebax®2533 by addition of GO, PGO and PEAGO in low concentration (0,02 wt%)

1. Introduction

In this work, Pebax®2533 (figure 1a) and Its GO-based nanocomposites have been studied to check the CO_2 and N_2 permeation performances of these materials for carbon capture applications [1][2]. As nano-fillers, Graphene Oxide (GO), Graphene Oxide functionalized with Polyetheramine (PEAGO) [3] and Porous Graphene Oxide (PGO) [6] have been employed (Figure 1b, c, d respectively).

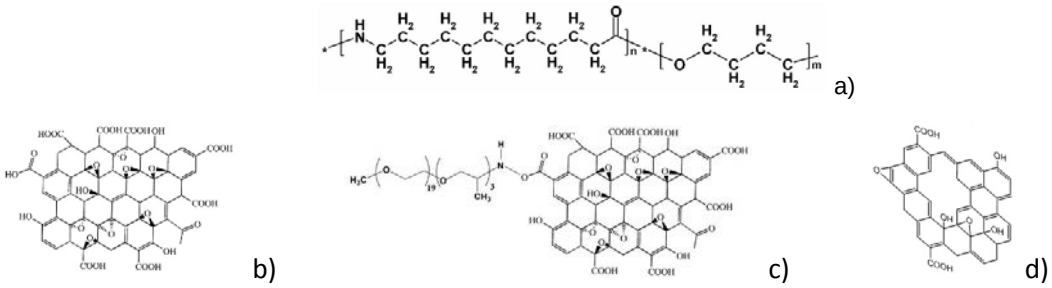

Figure 1: Structure of the materials used: a) Pebax®2533, b) GO, c) PEAGO and d) PGO

2. Methods

For the dispersion of GO in Pebax®2533, a double-solvent solution has been achieved: water dispersion of GO was dropped in a Pebax®2533 - ethanol solution in order to reach concentration GO/Polymer of 0,02 to 1 wt%, leading to smooth and totally homogeneous membranes. Same mixing procedure have been used for PEAGO and PGO, but in these cases only 0,02 wt% loaded composites were homogeneous and reasonable to test.

All membranes have been obtained by pouring some polymer solution, or polymer + filler dispersion, in a PTFE petri, to then let the solvent slowly evaporate at room temperature

CO_2 and N_2 permeation test on the different materials have been carried out by using a single-gas static permeometer. All permeation tests have been conducted at 35 °C. with an upstream pressure

of 1 bar. The permeability was measured by monitoring the pressure increase in the calibrated permeate site, which was in vacuum condition at the beginning of each test.

3. Results and discussion

Permeation results are reported in Figure 3 and table 1; the data in the figure in particular reports the effect of loading of separation performance on Pebax + GO matrix and showed that adding GO over 0,02 wt% decrease the CO_2 permeability while has no effect on CO_2/N_2 selectivity. At 0.02% loading on the other hand a slight increase in permeability was observed which became higher when other types of GO were considered. Porous GO in particular resulted the best material tested with a permeability increase in the order of 10% with respect to pure Pebax2533. As the increase in permeability did not caused any loss in selectivity, the addition og GO based nanofiller generally improved the separation performance of the original polymer.

4.

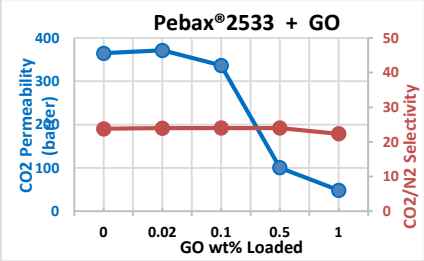

Figure 3 Pebax-GO permeability as a function of loading

Table 1 CO2 ppermeability and CO2/N2 selectivity of the different materials testedin the present work

Sample Name	wt% loaded	P CO2 (barrer)	Ideal α CO2/N2
Pebax2533 Pristine	0,00	364,62	23,80
Pebax2533 + GO	0,02	371,39	24,00
Pebax2533 + PEAGO	0,02	380,44	24,19
Pebax2533 + PGO	0,02	397,35	23,75

Conclusions

In this work, It has been shown that mixing ethanol solution of Pebax®2533 with water dispersion of graphene oxide leads to a very homogeneous system and membranes.

It has been also determined that low concentration (0,02 wt%) of nano-fillers used in Pebax®2533 increase CO2 permeability (1%, 5% and 10% increase respectively achieved with GO, PEAGO and PGO) without any loss of selectivity thus slightly improving the separation performance of the composite membranes with respect to the initial polymer.

Acknowledgements: This work has been performed in the framework of the European Project H2020 NANOMEMC² "NanoMaterials Enhanced Membranes for Carbon Capture", funded by the Innovation and Networks Executive Agency (INEA) Grant Agreement Number: 727734

References

[1] D.Y.C. Leung, G. Caramanna, M.M. Maroto-Valer, An overview of current status of carbon dioxide capture and storage technologies, Renew. Sustain. Energy Rev. 39 (2014) 426–443.

[2] I. Sreedhar, R. Vaidhiswaran, B.M. Kamani, A. Venugopal, Process and engineering trends in membrane based carbon capture, Renew. Sustain. Energy Rev. 68 (2017) 659–684.

[3] M.J. Yoo, H.W. Kim, B.M. Yoo, H.B. Park, Highly soluble polyetheramine-functionalized graphene oxide and reduced graphene oxide both in aqueous and non-aqueous solvents, Carbon N. Y. 75 (2014) 149–160.

[4] [6]C. Yu, B. Zhang, F. Yan, J. Zhao, J. Li, L. Li, Engineering nano-porous graphene oxide by hydroxyl radicals, Carbon N. Y. 105 (2019) 291–296.

ECCE12
The 12th EUROPEAN CONGRESS OF CHEMICAL ENGINEERING
Florence 15-19 September 2019

Mixing Studies Relating to Process Development for New Generation Automotive Coating Formulations

H. Yu[1,2], S. Tsochataridou[2], K. Parsons[1], K. Wojtas[2], C. D. Rielly[2], Gül Özcan-Taskin[2]

[1] MacDermid Enthone Industrial Solutions, Wantage, Oxon, OX12 7BZ, UK; [2] Loughborough University, Department of Chemical Engineering, Loughborough, LE11 3TU, Leicestershire, UK

*Corresponding author: herrick.yu@macdermidenthone.com

Highlights

- Sawtooth and 45°PBT impellers were studied to characterise their blending performance over the turbulent and transitional regimes at two scales of operation.
- Numerical modelling results under selected conditions could be validated with data.
- Experiments performed using liquids that simulate the physical properties of coating formulations have led to the development of a process for the manufacture of high performance automotive coatings.

1. Introduction

A formulation can require the introduction of several additives in different forms into a liquid and hence single and multiphase mixing processes (dispersion of agglomerates of solids or immiscible liquid droplets) are performed during manufacture. It is desirable to use the same equipment throughout the process or even for different products. In this study, the blending performance of a sawtooth impeller, which is typically used for dispersion processes, was investigated in comparison to that of the mixed flow pitched blade turbine (PBT). Blending performance of different types of sawtooth impellers has not been studied as widely as the PBT [1]. The study has been performed in support of process development for a new formulation coating for automotive applications. Simulant liquids were chosen to replicate the viscosity of the additives used in the new formulation coating allowing a range of Reynolds numbers to be covered at different scales of operation.

2. Experimental

Experiments were conducted using two tanks of a diameter of T= 0.13 and 0.30 m, equipped with 4 equally spaced wall baffles. The liquid height was equal to the tank diameter (H = T). Either a sawtooth impeller, R500, (SPXFlow) or a 6-blade 45° pitched blade turbine (PBT) was used. These were of a diameter of around half the tank diameter. Water and glycerol solutions of a viscosity range of 0.001 to 1.2 Pa s were used as simulant liquids to replicate the properties of the formulation and added liquids, some of which are of hazardous nature. Physical property differences taken into consideration[2] when preparing tracers. Power input was calculated from the measured torque value using torquemeters. Flow pattern observations and mixing time measurements were performed from the colourisation/decolourisation method by adding $Na_2S_2O_3$ into the aqueous mixtures in the presence of starch-iodine solution.

Under selected conditions numerical simulations were performed with STAR CCM+ 13.02 using the, moving reference frame approach.

3. Results and discussions

Power numbers obtained from numerical simulations were in agreement with those determined experimentally for both impellers with a higher value of the characteristic power number for the PBT compared to the sawtooth impeller as expected (Figure 1). These could be used to calculate the power input over a range of conditions.

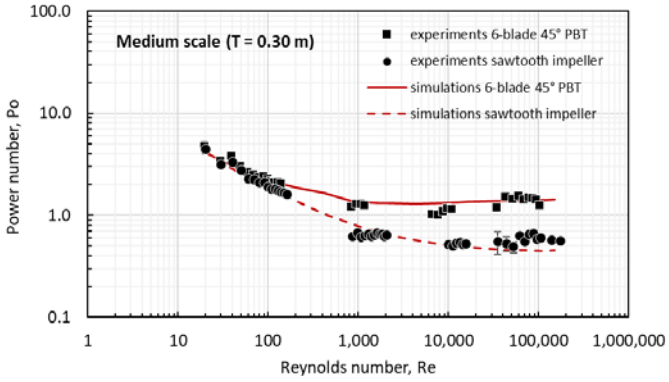

Figure 1: Characteristic power curves, T= 0.30 m

Results from blending experiments have shown that the dimensionless mixing time (Nθ) is inversely proportional to the Reynolds number with higher Nθ values for the sawtooth impeller (Figure 2). When mixing time results are compared on the basis of volumetric power input, the performance of both impellers appeared to be a comparable.

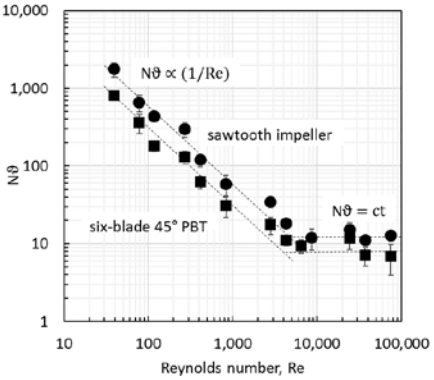

Figure 2: Dimensionless mixing time over a range of Re, T= 0.30 m

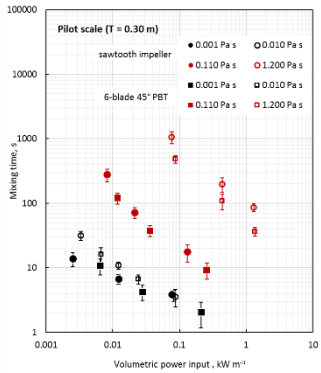

Figure 3: Mixing times at ct P/V (red are data in transitional regime)

Trends were similar in the smaller T= 0.13 m tank.

4. Conclusions

Power and flow characteristics of sawtooth impellers were studied over a range of Reynolds numbers using simulant liquids that replicate the viscosity during the manufacture of a new formulation automotive coating at two scales of operation. Numerical simulations performed under selected conditions showed good agreement in predicting the power input and hence can be used for different designs. Mixing times compared on the basis of constant volumetric power input were found to be comparable for the two impellers. Further work is underway in a larger scale tank.

Acknowledgements The authors gratefully acknowledge the InnovateUK project nb132726 and contribution in kind by SPX Flow.

References

[1] Grenville, R.K. (1992) PhD thesis, Cranfield Inst of Tech.

[2] Jones P.N.; Özcan- Taşkin, G. N. (2005) Chem. Eng and Tech. Vol 28, 8, p: 908- 914. DOI 10.1002/ceat.200500012

ENCAPSULATION OF DOCETAXEL WITH ELASTIN LIKE RECOMBINAMERS BY SUPERCRITICAL CO_2 FOR ADVANCED ANTICANCER APPLICATIONS

R. Vallejo Vicente [1,2], J. González-Valdivieso [2], M. Santos García [2], S. Rodríguez-Rojo [1], F. J. Arias Vallejo [2], M.J. Cocero Alonso [1].

[1] *BioEcoUVa, Research Institute on Bioeconomy, High Pressure Proces Group, University of Valladolid, Department of Chemical Engineering and Environmental Technology, C/Doctor Mergelina s/n, 47011 Valladolid, Spain.*

[2] *BIOFORGE Research Group, University of Valladolid, CIBER-BBN, LUCIA Building, Paseo Belén 19, 47011 Valladolid, Spain*

**Corresponding author: reinal.vv@gmail.com*

Highlights

- Set-up of the SAS process with ELRs was done reaching high process yields.
- Physico-chemical characterization shows particle size of 40 nm in aqueous solution.
- Drug delivery profiles were found to fit to the equation of Peppas-Sahlin.
- Breast cancer cells were more affected and showed diminished cell viability.

1. Introduction

The controlled release of drugs from biodegradable polymer nanoparticles is having a great medical impact in a wide range of therapeutic areas. Elastin Like Recombinamers (ELRs) [1] whose sequence is inspired in natural elastin and consist in repeats of the sequence (VPGXG)n, where X can be any amino acid except proline, are unique in this field thanks to their recombinant nature. ELR sequence can be altered by adding specific functionalities such as cell adhesion domains and their natural capacity of self-assembly and their stimuli responsiveness allow intelligent processes [2]. The encapsulation of Docetaxel (DTX) has been the subject of study by many researchers, implementing long and complex methods, which also involve the use of toxic organic solvents and post-processes. Therefore, a very powerful idea would be to coat the DTX avoiding toxic organic solvents and in one-step process. In this work, Supercritical AntiSolvent (SAS) [3] technique has been proposed to co-precipitate both compounds, due to, it serves as a completely clean separation agent since it uses mild temperatures in the process that do not harm the product, it is a non-flammable, non-corrosive, non-toxic, non-carcinogenic element, has a large selective capacity and does not generate waste [4].

2. Methods

Nanoparticles of DTX coated with ELRs, (EI)2 and (EI)2RGD, were obtained by Supercritical Antisolvent technology (SAS) studying process parameters to achieve the best operational conditions. The proportions of both compounds were determined by NMR. The morphology of the dry particles from SAS process was study by Scanning Electron Microscopy (SEM). Furthermore, Surface charge of the particles (ζ-Potential) and particle size in aqueous solution were measured by Dynamic light scattering (DLS) using a Zetasizer Nano ZS at 37°C and neutral pH. Particle morphology and amphiphilic behavior of the particles in aqueous media, was observed by TEM at neutral pH

and at room temperature. Drug delivery experiment was performed in triplicate using dialysis method at 37ºC under sink conditions and determined by UV-vis spectrometer and fitted with mathematical models. After characterization of nanoparticles, the effect of ELR-based nanoparticles was measured *in vitro* in endothelial (HUVEC) and breast cancer (MDA-MB-231) cells.

3. Results and discussion

The setting-up of the SAS pilot plant were performed with (EI)2 biopolymer and DMSO as a solvent, using a new coaxial nozzle designed in this work to get the best operational conditions. Results achieved with this conditions shows a drastic reduction in the solvent residues and a high process yield. The particles analyzed by SEM did not present a remarkable aggregation and has a smooth surface with many small particles stuck to them that provides a wide particle size distribution. Microparticles of (EI)2+DTX and (EI)2RGD+DTX obtained after the process can be disaggregate in aqueous solution forming a nanoparticulate delivery system keeping the drug inside with PDI below 0.2 and with ζ-Potential of around -30 mV, which clearly indicates that is monodisperse and stable in time. This results were confirmed by TEM where same size and behavior were found. Drug release study of the (EI)2+DTX particles shows a clear delay in the delivery of the DTX and the Peppas-Sahlin equation used to fit the profiles shows that the process is governed by the Fickian diffusion mechanism. In the cellular assays carried out, it has been proven that thanks to the incorporation of the RGD sequence in the ELR, the treated breast cancer cells were more affected and showed a lower cellular viability than cells treated with free DTX. This effect was not seen in HUVEC cells, which could be explained by the fact that cancerous cells have enhanced ability to internalize due to their enhanced metabolic rate and higher expression of integrins.

4. Conclusions

In this work, we have been able to set up the operational conditions in the Supercritical Antisolvent pilot plant with CO_2 to make both microparticles of Elastin Like Recombinamers and co-precipitated Docetaxel-ELRs in one step process. Microparticles after the SAS process are able to disaggregate in aqueous media forming stable nanoparticles with low PDI which shows a controlled DTX release profile following Fick diffusion mechanisms. In addition, we may emphasize that it has been possible to increase the solubility of this highly hydrophobic anti-tumoral drug in aqueous solution by 5 orders of magnitude. Moreover, in the cellular assays carried out, it has been proven that thanks to the incorporation of the RGD sequence in the ELR, the treated breast cancer cells were more affected and cell proliferation was completely abolished, therefore, the strategy developed in this work opens the way to new systems of controlled release, more precise than non-selective chemotherapeutic drugs and with a very promising potential.

References

[1] M. Santos, S.S.-D., J. Gonzalez-Valdivieso, R. Vallejo, A. Girotti, P. Cuadrado, F. J., Arias, Current Medicinal Chemistry, 25 (2018).

[2] J.C. Rodríguez-Cabello, FJ. Arias, M. Alonso and A. Girotti, Advanced Drug Delivery Reviews 97, (2016) 85-100

[3] A. Natolino, C. Da Porto, S. Rodriguez-Rojo, T. Moreno, M.J. Cocero. The Journal of Supercritical Fluids, 118 (2016) 54-63.

[4] M.J. Cocero, A. Martín, F. Mattea, S. Varona, The Journal of Supercritical Fluids,47 (2009) 546-555

ECCE12
The 12th EUROPEAN CONGRESS OF CHEMICAL ENGINEERING
Florence 15-19 September 2019

Multidimensional classification of quantum dots: Investigation of flock properties during selective agglomeration for process design

Christina Menter[1], Doris Segets[2]

[1] Institute of Particle Technology (LFG), Friedrich-Alexander-University Erlangen Nürnberg (FAU), Germany;

[2] Process Technology for Electrochemical Functional Materials and Center for Nanointegration Duisburg-Essen (CENIDE), University Duisburg-Essen (UDE), Germany

*Corresponding author: doris.segets@uni-due.de

1. Introduction

Quantum confined semiconductor nanoparticles (quantum dots, QDs) are highly interesting materials due to their unique electronic and optical properties and are used for various applications, such as dye sensitized solar cells and light-emitting devices. Within the relevant size range of a few nanometers, QDs exhibit pronounced and unique structure-property relationships. Hence, a narrow particle size distribution (PSD) becomes one of the most important factors to tailor product performance. **Size selective agglomeration** has already been proven to be an efficient post processing strategy for ZnS QDs [1,2]. It is based on the titration of a poor liquid into an already existing stable dispersion, which leads to a reduction of the particles' steric stabilization. Therefore, larger ZnS particles with larger van der Waals attraction flocculate first while smaller structures stay dispersed as primary particles. Finally, the flocculates have to be separated from the continuous phase. While on lab scale, the formed flocks of several 100 nm can be easily separated by centrifugation from the fine fraction that stays as primary particles in the supernatant, for larger scale preparation using continuous processes, new concepts are urgently needed. Herein, the objective was to develop a filtration process to achieve continuous flock removal by two alternating filtration units without affecting the separation efficiency governed by the microprocesses. Noteworthy, this is the first time that a scalable classification strategy for such small entities below 10 nm is reported. Key to reach this ambitious goal is to know how the properties of the flocks can be controlled and how stable the generated flocks are against shear forces.

2. Methods

For the synthesis of 3-mercapto-1,2-propanediol capped ZnS QDs a method of Nanda et al. was applied[3]. Via analytical centrifugation (AC) the sedimentation profiles of the flocculated dispersions were recorded to determine the sedimentation equivalent diameter distribution of the flocks. AC measurements were performed with a LUMiSizer LS 651 (LUM GmbH, Berlin, Germany). Absorbance spectra of ZnS QDs were recorded using a SPECORD Plus UV/Vis spectrophotometer (Analytik Jena AG, Germany) with quartz glass cuvettes of 0.2 mm optical path length. Absorbance measurements were analyzed with respect to their volume PSDs by means of a previously published and carefully validated deconvolution algorithm [4].

3. Results and discussion

In Figure 1 the classification procedure is summarized. After the flocculation of larger particles by the addition of a poor liquid to a stable ZnS dispersion, the complete separation of the flocks from the dispersed particles is fundamental. Entering of flocks to the fines would lead to a significant degradation of the classification result. Since separation by centrifugation is restricted to lab scale, our objective was to develop a filtration process for the separation of larger quantities. Continuous operation can then be achieved by using alternating filtration units.

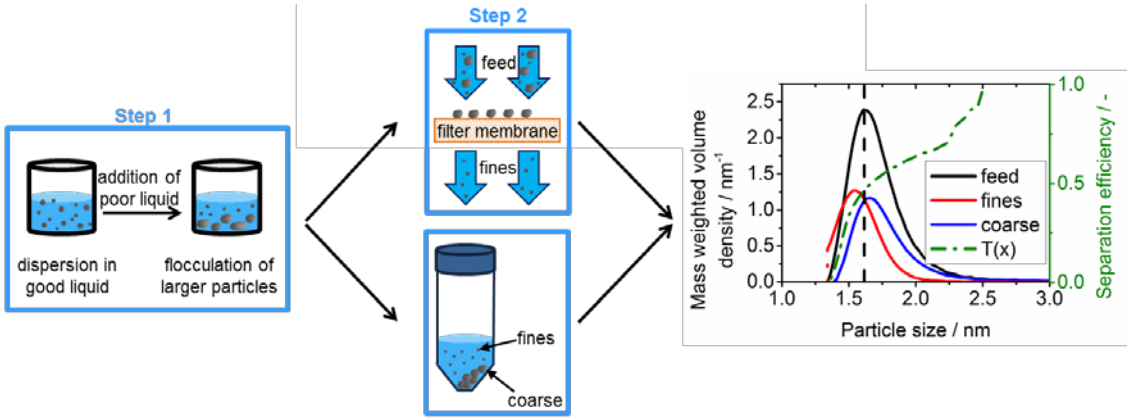

Figure 1: Summary of the two-step classification procedure (left and middle) and classification result with separation efficiency (right).

For filtration process design it is indispensable to know how stable the generated flocks are and how the flocks properties can be controlled. In a systematic parameter study we found out that the flocks are comparatively stable against shear forces generated at varying energy inputs, weakly affected by solvent polarity and that the flock diameter rises with increasing solid concentration. With this knowledge we designed a filtration process to separate flocks from the primary particles. After the flocculation of larger particles by addition of a poor liquid to a stable dispersion, the flocks were separated by filtration instead of centrifugation. Afterwards, the dried filter cake was proven to be redispersible in water. Thus, we were able to proof that it is possible to **replace the separation of flocks from the fines by centrifugation through filtration** during a nanoparticle classification experiment **without affecting the separation efficiency**.

4. Conclusions

Our work demonstrates for the first time the scalable classification of QDs < 10 nm by size selective precipitation. We successfully replaced the classical centrifugation step for flock separation by filtration without affecting the separation efficiency that is determined by the microprocesses. Noteworthy, this process is not restricted to classification by size, but can be extended towards multidimensional separation, e.g. size and composition or surface properties.

References

[1] D. Segets, S. Komada, B. Butz, E. Spiecker, Y. Mori, W. Peukert, J. Nanopart. Res. 15 (2013) 1486.
[2] D. Segets, C. Lutz, K. Yamamoto, S. Süß, Y. Mori, W. Peukert, J. Phys. Chem. C 119 (2015) 4009-4022.
[3] J. Nanda, S. Sapra, D. D. Sarma, Chem. Mater. 12 (2000) 1018-1024.
[4] D. Segets, J. Gradl, R. Klupp Taylor, V. Vassilev, W. Peukert, ACS nano, 3 (2009) 1703–1710.

ECCE12
The 12th EUROPEAN CONGRESS OF CHEMICAL ENGINEERING
Florence 15-19 September 2019

Manganese dioxide (MnO_2) based Janus nanoparticles for emulsion stabilization with potential application for enhanced oil recovery

Paula Rivera[1], Luz Ballesteros[1], D. Fabio Mercado[1], Dary Malagon[1]

[1] Centro de Investigaciones en Catálisis CICAT, Parque Tecnológico Guatiguará km 2 Vía el Refugio, Universidad Industrial de Santander, Piedecuesta (Santander), 681011, Colombia

*Corresponding author: paula.rivera.es@gmail.com

Highlights

- MnO_2 nanoparticles were synthetized with different phases and geometries.
- Different MnO_2 Janus nanoparticles were synthetized and characterized.
- The effect of amount surfactant in MnO_2 Janus nanoparticles were studied.

1. Introduction

In the Oil - thermal recovery processes, various techniques are employed to heat the residual oil in the formation, resulting in reduction of the viscosity of crude oil which improves its mobility, facilitating its fluidity toward production wells [1, 2]. These kinds of techniques are mainly divided into two types: steam injection and in-situ combustion (ISC) [3]. One of the most advantageous yet complex thermal methods is in-situ combustion (ISC) process [1].

The transport of ultradispersed catalysts in the reservoir is essential to bring this material into contact with the crude [4]; the catalysts used can be based on transition metal nanoparticles (NP), which have a high catalytic activity [5]. However, the transport of particles in very narrow reservoirs can be a challenge, an important factor to consider is the permeability of the reservoir. Manganese dioxide (MnO_2) is cheap and non-toxic [6], their diverse phases are successfully used in potential applications such as batteries, catalysis, water treatment, and chemical industry [7,8]. Additionally, when a material is present in a nanometric scale, it has larger surface areas compared to its macroscopic analogues [9].

Resasco [10] studied the application of hybrid nanoparticles in water/oil interfaces for improved recovery reactions and found that Janus particles are very effective to act as emulsion stabilizers and catalyst supports. It can be inferred that this type of nanomaterials could propagate in the flow of water through the porous media and reach the oleic phase [10]. The challenge of the oil industry is then to inject these catalysts into the reservoir through the porous medium without significantly affecting the permeability of the rock. For this purpose, it is essential that the catalytic systems form stable emulsions to transport them through the injector well [11]. Therefore, the main objective of this work is to formulate emulsions stabilized by Janus nanoparticles of manganese dioxide for their application in enhanced oil recovery.

2. Methods

α-MnO_2, β-MnO_2 and δ-MnO_2 nanoparticles (NP) were prepared by a redox hydrothermal method with some modifications [12]. An aqueous solution composed of $MnSO_4 \cdot H_2O$ and $(NH_4)_2S_2O_8$ with

different ratios of reagents was charged into a Teflon-lined autoclave. The autoclave was kept in an oven at different temperatures for certain period and then cooled at room temperature. The obtained black slurry was filtered and dried with water and ethanol. The NP were mainly characterized by FT-IR and DLS.

The as-obtained nanoparticles were selective surface functionalized through a Pickering emulsion [13] method in order to obtain Janus nanoparticles (JNP) and then a model emulsion was formed with an equal amount of oil and water.

With rheological tests as an index of fluency were chosen the best JNP for formulate emulsions and the percentage of functionalizing agent was varied to find a stable emulsion.

3. Results and discussion

An easy method was performed to synthesize MnO_2 nanoparticles from reagents with different charge ions, the characterization showed a narrow size distribution and the desired oxide on a nanometric scale. The synthesis also showed that the variation of reagent concentration and drying temperature affect the size and phase of nanoparticles, due to the change in the concentration of NH_4^+ and SO_4^- ions.

The synthesis of Janus manganese dioxide nanoparticles has not been widely studied, due to this finding the optimal fabrication conditions represented a challenge for the authors. The percentage of functionalizing agent was varied to analyze its effect on the JNP properties

4. Conclusions

In this work, the effect of the functionalizing agent in the stabilization of emulsions through Janus nanoparticles prepared by a Pickering emulsion method was studied. With this study, it is possible to understand the behavior of stable emulsions to be applied in different applications such as food, pharmaceutical, biochemistry, and the oil industry.

References

[1] A. Amrollahi, N. Hosseinpour, A. Bahramian, and A. Vatani, “In-situ upgrading of reservoir oils by in-situ preparation of NiO nanoparticles in thermal enhanced oil recovery processes,” *Colloids Surfaces A Physicochem. Eng. Asp.*, vol. 520, pp. 289–300, 2017.

[2] X. Kong, M. M. Ohadi, and T. Petroleum, “Applications of Micro and Nano Technologies in the Oil and Gas Industry- An Overview of the Recent Progress,” in *International Petroleum Exhibition & Conference*, 2010.

[3] S. M. Farouq Ali and S. Thomas, “The promise and problems of enhanced oil recovery methods,” *J. Can. Pet. Technol.*, vol. 35, no. 7, pp. 57–63, 1996.

[4] A. Zamani, B. Maini, and P. Pereira-almao, “Experimental Study on Transport of Ultra-Dispersed Catalyst Particles in Porous Media,” *Energy Fuels*, vol. 62, no. 8, pp. 4980–4988, 2010.

[5] N. N. Nassar, A. Hassan, and P. Pereira-Almao, “Comparative oxidation of adsorbed asphaltenes onto transition metal oxide nanoparticles,” *Colloids Surfaces A Physicochem. Eng. Asp.*, vol. 384, no. 1–3, pp. 145–149, 2011.

[6] Y. Tang, S. Zheng, Y. Xu, X. Xiao, H. Xue, and H. Pang, “Advanced batteries based on manganese dioxide and its composites,” *Energy Storage Mater.*, vol. 12, no. November 2017, pp. 284–309, 2018.

[7] J. Kawai and I. Ohtani, “A facile hydrothermal recovery of nano sealed MnO2 particle from waste batteries : An advanced material for electrochemical and environmental applications A facile

hydrothermal recovery of nano sealed MnO2 particle from waste batteries : An advanced mater," in *Materials Science and Engineering*, 2016.

[8] K. Kumar, Karikkat, "Synthesis , Characterization of Nano MnO2 and its Adsorption Characteristics Over an Azo Dye," *J. Mater. Sci.*, vol. 2, no. 1, pp. 27–31, 2014.

[9] K. H. Bae, K. Lee, C. Kim, and T. G. Park, "Surface functionalized hollow manganese oxide nanoparticles for cancer targeted siRNA delivery and magnetic resonance imaging," *Biomaterials*, vol. 32, no. 1, pp. 176–184, 2011.

[10] S. Drexler, J. Faria, M. P. Ruiz, J. H. Harwell, and D. E. Resasco, "Amphiphilic nanohybrid catalysts for reactions at the water/oil interface in subsurface reservoirs," *Energy and Fuels*, vol. 26, no. 4, pp. 2231–2241, 2012.

[11] R. Hashemi, N. N. Nassar, and P. Pereira Almao, "Nanoparticle technology for heavy oil in-situ upgrading and recovery enhancement: Opportunities and challenges," *Appl. Energy*, vol. 133, pp. 374–387, 2014.

[12] X. Wang and L. Yadong, "Synthesis and Formation Mechanism of Manganese Dioxide," Chem. - A Eur. J., vol. 9, no. 1, pp. 300–306, 2003. [13]E. Arenas-calderon, V. B. Medrano, and M. A. Guzmán, Chapter 3 - Catalytic applications of Janus nanoparticles. Elsevier Inc., 2018.

ECCE12
The 12th EUROPEAN CONGRESS OF CHEMICAL ENGINEERING
Florence 15-19 September 2019

Safe Drinking Water in Water Kiosks: Effect Of NOM on Virus Removal by Multiwalled Carbon Nanotubes (MWCNT).

Celine Jacquin[1,2], Kamila Domagala[3], Jacqueline Traber[1], Timothy R. Julian[2], Eberhard Morgenroth[1], Thomas Graule[3]

1 Department of Process Engineering, Eawag, Swiss Federal Institute of Aquatic Science and Technology, Überlandstrasse 133, 8600 Dubendorf, Switzerland
2 Department of Environmental Microbiology, Eawag, Swiss Federal Institute of Aquatic Science and Technology, Überlandstrasse 133, 8600 Dubendorf, Switzerland
3 Laboratory for High Performance Ceramics, Empa, Swiss Federal Laboratories for Materials Science and Technology, Überlandstrasse 129, 8600 Dübendorf, Switzerland

Highlights

- MS2 virus removal by adsorption is proportional to MWCNT mass.
- SRNOM adsorption onto MWCNT follows Freundlich isotherms.
- MS2 removal depends on SRNOM concentration.

1. Introduction

Safe drinking water access in low and middle-income countries is limited, especially in urban slums and rural area [1]. To increase safe water access and reduce waterborne diseases, water kiosks at community-scale were developed. For these decentralized water facilities, the water treatment technologies are selected according to their low costs, low maintenance, sustainability and ease of use [2]. In well operated and equipped water kiosks, bacterial removal is performed, while virus removal is seldom feasible [3]. It is therefore of major interest to develop solutions to increase virus removal and consequently decrease the waterborne diseases associated with these pathogens. The purpose of this study was to evaluate the interest of using MWCNT to produce filters that could be applied as a post-treatment in water kiosks, acting as a safe barrier against virus. In recent decades, the development of Carbon NanoTubes filters showed a high potential for water treatment and most specifically for virus removal in the case of electrochemical CNT filters [4]. However, NOM is expected to be a major limitation for virus removal, since it is also known to adsorb onto MWCNT. To better target the application of MWCNT for virus treatment, it is therefore important to better understand the competition mechanisms between virus and NOM.

2. Methods

MS2 (DSMZ 13767) were used as human virus pathogen surrogates due to their similitude with enteric viruses of human health concern. MS2 infectivity was evaluated using the MS2 plaque assays.

The MWCNT used in this study were purchased from CheapTubes. Their specific surface is equal to 116.63 m2/g, their diameter varies between 10-25nm, while their length is equal to 100µm.

SRNOM (IHSS) was used as a NOM surrogate to be able to compare our results with the existing literature. NOM characterization was performed using Liquid Chromatography with Organic Carbon Detector (LC-OCD) and TOCmeter.

Batch experiments were performed in glass vials of 25mL, using the bottle technique (one bottle corresponds to one point). After adding a fixed mass of MWCNT into MS2 stock solution, with or without SRNOM, the vials were mixed for 3h at 40rpm. After adsorption, samples were filtered with 0.45µm PES filters prior analysis.

3. Results and discussion

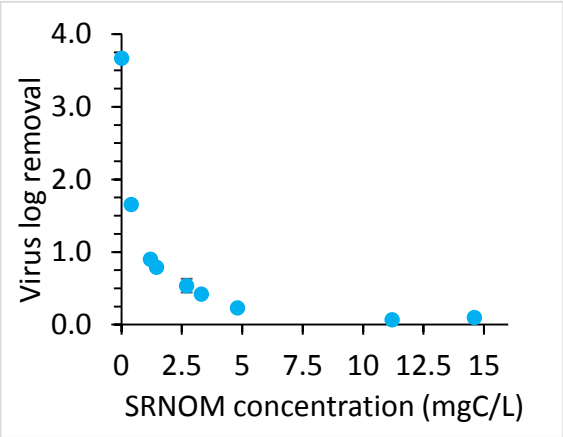

Figure 1: Virus removal by MWCNT as a function of Suwannee River Natural Organic Matter (SRNOM)

Batch experiments showed that MS2 removal is due to adsorption and is proportional to the mass of MWCNT. For pH between 5 and 8, the removal is equal to 0.3log/mgMWCNT. Batch experiments with SRNOM at different pH showed that SRNOM adsorbs onto MWCNT too, with a higher affinity at pH5. Competition between SRNOM and MS2 was tested with co-adsorption experiments and with preloading experiments. Figure 1 shows the results of the co-adsorption experiments, where the competitive effect of SRNOM even at low concentration. Virus removal drops by 38% at a concentration equal to 0.4mgC/L. This concentration corresponds to concentrations found in clean ground waters. Virus removal in low and middle-income countries using pristine MWCNT filters is highly compromised since a wide diversity of waters could be used for drinking water treatment.

4. Conclusions

The use of pristine MWCNT filters for virus removal is highly compromised by the presence of NOM that irreversibly adsorbs onto MWCNT. Saturation is quick since at a concentration of 5mgC/L of SRNOM, virus removal drops from 3.7log to 0.02log. MWCNT functionalization could be on option to limit NOM adsorption.

References

[1] Juma, M., Nuhu, S., Juma, F.B., 2018. Challenges of Water Accessibility in Peri-Urban Areas in Tanzania: A Case of Kigamboni Dar es Salaam. J. Soc. Sci. Res. 4, 47–54.

[2] Peter-Varbanets, M., Zurbrügg, C., Swartz, C., Pronk, W., 2009. Decentralized systems for potable water and the potential of membrane technology. Water Res. 43, 245–265. https://doi.org/10.1016/j.watres.2008.10.030.

[3] Gibson, K.E., 2014. Viral pathogens in water: occurrence, public health impact, and available control strategies. Curr. Opin. Virol., Virus entry / Environmental virology 4, 50–57. https://doi.org/10.1016/j.coviro.2013.12.005

[4] Vecitis, C.D., Schnoor, M.H., Rahaman, M.S., Schiffman, J.D., Elimelech, M., 2011. Electrochemical Multiwalled Carbon Nanotube Filter for Viral and Bacterial Removal and Inactivation [WWW Document]. https://doi.org/10.1021/es2000062

Micellar systems, embedding triplet-triplet annihilation active materials, as ratiometric and all-optical temperature sensing tool

Ralitsa Dimitrova[2], Yury Avlasevich[1], Katharina Landfester[1], Stanislav Baluschev[1,2]

1 Planck-Institute for Polymer Research, Ackermannweg 10, 55128 Mainz, Germany;

2 Sofia University "St. Kliment Ochridski", 5 James Bourchier Blvd, 1164 Sofia, Bulgaria

**Corresponding author: balouche@phys.uni-sofia.bg*

Highlights

- Include 3 to 4 highlights in bullets format. [Calibri 10].
- Max. 90 characters per highlight including spaces.
- Only the core results should be covered.
- Please do not change the selected fonts.

1. Introduction

Local temperature control in water environment is essential for both, soft matter- and life-science applications. The thermal sensing techniques developed are not directly applicable for thermal studies in water environment, particularly if simultaneously high thermal sensitivity, ratiometric and all-optical response are desired. A realistic temperature sensing alternative could be the process of triplet-triplet annihilation photon energy upconversion [1] in water environment (TTA – UC): It is inherently micro-scale sensing techniques – the sensing function is carried out by ensembles of organic macromolecules embedded in micelles of non-ionic surfactants. The TTA – sensing function is performed in all-optical regime by using a single excitation wavelength, although two characteristic optical signals (ratiometric response) are registered [2].

2. Results and discussion

Since the TTA – UC is a process controlled by the rotational diffusion of the interacting photo excited species it will depend extensively on the local mobility of the participating molecules, embedded in the hydrophobic core of the optically inactive micelles (Figure 1). Therefore, the dependence of the core viscosity on the sample temperature will lead to temperature dependence of both, the emitter delayed fluorescence and the residual sensitizer phosphorescence. Those two optical signals acting as ratiometric material response on the local temperature change ensure inherent & instantaneous compensation of the possible local changes of the sample parameters, and create non-ambiguous temperature calibration curve (Figure 2).

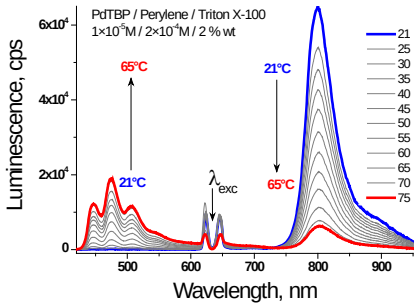

Figure 1: Dependence of the luminescence spectra of the micellar TTA-UC system in water environment on the sample temperature.

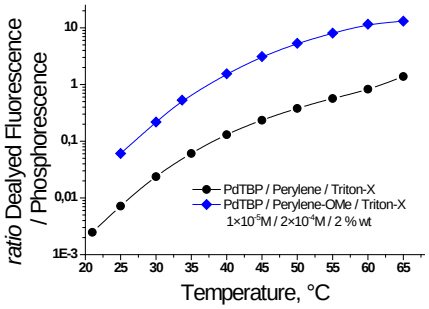

Figure 2: Calibration curve - dependence of the ratio of UC-delayed fluorescence versus residual phosphorescence on the sample temperature.

The influence of emitter hydrophobicity on the energetic and dynamical properties of process of TTA-UC in micelles of non-ionic surfactants, as well as identification of the non-ambiguous temperature calibration curves and measurement of local temperature in all-optical regime with sensitivity better than 0.05 K and temporal resolution of 200 µs will be demonstrated and discussed.

3. Acknowledgements

This work is performed under European Horizon 2020 research and innovation programme under grant agreement no. 732794 – project HYPOSENS.

References

[1] T. Ogawa, M. Hosoyamada, B. Yurash, T.Q. Nguyen, N. Yanai, N. Kimizuka, J. Am. Chem. Soc. (2018) 140, 28.

[2] S. Baluschev, K. Katta, Yu. Avlasevich, and K. Landfester, "Annihilation upconversion in nanoconfinement: solving the oxygen quenching problem", Mater. Horiz. (2016) 3, 478-486.

ECCE12
The 12th EUROPEAN CONGRESS OF CHEMICAL ENGINEERING
Florence 15-19 September 2019

A Computational Approach to Nose to Brain Drug Delivery from Nanoparticles Embedded in a Hydrogel Matrix

Athina Vasileiadou[1,2], Filippos Karageorgos[1,2], Stefania Serpetsi[2], Costas Kiparissides[1,2]

1 Department of Chemical Engineering, Aristotle University of Thessaloniki, Thessaloniki, Greece;
2 Chemical Process & Energy Resources Institute, Centre for Research and Technology Hellas, P.O. Box 60361, 57001 Thessaloniki, Greece

**Corresponding author: costas.kiparissides@cperi.certh.gr*

Highlights

- Sustained and controlled drug delivery.
- In situ hydrogel formation and swelling dynamics.
- Drug release from a population of drug-loaded particles.
- Drug diffusion through particle, hydrogel and biological barriers.

1. Introduction

Central nervous system (CNS) disorders (e.g., multiple sclerosis, Alzheimer's, Parkinson's or Huntington's disease, etc.) represent a growing public health issue, primarily due to the increased life expectancy and the aging population.

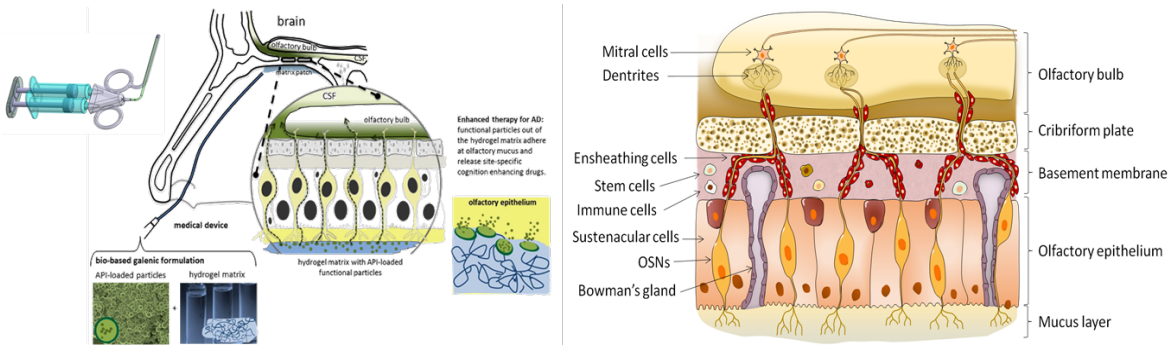

The role of the nasal cavity as an entry point for the brain-targeted delivery of various medications has been long identified as a potential alternative administration route to the intravenous delivery mode. Although highly advantageous due to its non-invasive nature, rapid onset of action and highly localized delivery resulting in low systemic exposure, the delivery of medications to the brain via the nasal cavity exhibits particular challenges, associated with the controlled and sustained release of biopharmaceutics across biological barriers or/and low drug stability attributed to the activity of enzymes residing in the nasal cavity.

In the present work, the development of an innovative nanotechnology-based formulation and application technology are described for the chronic treatment of CNS disorders. The novel drug formulation consists of biodegradable polymer nanoparticles (NPs) loaded with cognition enhancing drugs (e.g., long-acting insulin analogues). The drug loaded particles are embedded into

a biodegradable hydrogel matrix that is deposited, via a nasal endoscopic applicator as a thin liquid-gelling film, onto the olfactory region.

2. Computational Methods

A multi-scale modelling approach, comprising models at different time and length scales, is applied to quantify the fundamental physical, transport and biological processes in relation to the nose-to-brain delivery of biopharmaceutics from the embedded nanoparticles in a hydrogel film deposited onto the olfactory epithelium. In particular, a CFD-based model is developed to describe the flow and deposition of a reactive polymer solution, through an endoscopic applicator, onto the olfactory mucus/epithelium, in terms of a polymer solution flow, its viscoelastic properties, gelation kinetics, extruded volume and applicator diameter, in relation to the formation of a hydrogel film onto the olfactory cleft. Moreover, a hydrogel/mucus model is developed to predict the polymer solution spreading, hydrogel formation and degree of swelling. To predict the cross-linking kinetics of functionalized hyaluronic (HA-ox, HA-Tyr) and hydrogel swelling, a kinetic model is developed, in terms of the leading moments of the molecular weight distribution. The crosslinking kinetic model takes into account the effects of initial molecular weight of the polymer, pH and ionic strength of the medium. In order to examine the long term stability and detachment of the deposited hydrogel patch onto the olfactory region, the hydrogel swelling deformation is analyzed in terms of the environmental conditions in the olfactory region. A dynamic drug release model is developed to describe the drug release rate from the drug-loaded nano-carriers embedded in the hydrogel matrix in terms of molecular and morphological properties of polymeric carriers and hydrogel matrix. Finally, a drug release model is derived to calculate the drug release rate for a population of size-distributed particles and analyze the effects of particle size distribution, particle loading, particle swelling and polymer degradation on the drug release profile. Note that the derived model can simulate the observed phenomena including the observed burst in the drug release rate or/and delayed release from the drug-loaded particles. Moreover, the effects of system variables (i.e., gelation onset time, patch volume, particle size and particle drug loading, polymer and hydrogel degradation kinetics, etc.) on the drug release rate are assessed and compared with available experimental measurements.

3. Results and discussion

The various sub-models are numerically solved to calculate the drug mass transfer rate from the embedded nanoparticles in the hydrogel matrix through the mucus layer and epithelium to the olfactory bulb. It is shown that model predictions are in close agreement with experimental measurements obtained from nose to brain drug transfer experiments in rats reported in the literature.

4. Conclusions

A multi-scale mathematical modeling framework has been developed to aid the design, simulation and optimization of nose to brain controlled drug delivery for treatment of CNS disorders and maximize the drug efficacy and bioavailability.

5. Acknowledgments

The present research has been financially supported by the EU No. 721098 grant application under the Research and Innovation Horizon 2020 European Framework Programme.

Nanocellulose Based, facilitated transport membranes for carbon capture applications

Davide Venturi[1], Benjamin Dhuiège[2], Karim Missoum[2], Marco Giacinti Baschetti[1],

1) Alma Mater Studiorum – Università di Bologna, Via Terracini, 28, 40131 Bologna, Italy
2) INOFIB 461 rue de la Papeterie CS-10065 38402 Saint-Martin-d'Hères Cedex

**Corresponding author: marco.giacinti@unibo.it*

Highlights

- Nanofibrillated cellulose was used to prepare facilitated transport membrane for CO2 capture
- PVAm – Naocelllulose membrane showed interesting separation performance close to the 2008 upper bound for CO2/N2 separation.
- Arginine-Nanocellulose membranes were able to overcome 2008 upper bound for CO2/N2 separation.

1. Introduction

Carbon capture and storage (CCS) technologies represent an interesting medium-term solution to tackle climate change and CO2 emissions, removing the greenhouse gas before its release in the atmosphere. In order to make it a viable solution, high performance separation techniques must be applied, and gas separation membranes are a strongly investigated solution.

Within this work a new family of facilitated transport membranes (FTM) has been investigated that uses nanofibrillated cellulose (NFC) has matrix for the CO2 carriers. Thanks to its high hydrophilicity, the high mechanical resistance and the already interesting separation performances showed [1] this materials seems indeed a very interesting candidate to obtain high performing and stable Hybrid Facilitated transport membranes (HFTM).

A series of membranes loaded with different amounts amine based carriers such as L-Arginine and polyvinylamine (PVAm) were prepared and tested under humid conditions for CO2 and N2 permeability in order to assess their potential for post combustion carbon capture applications.

2. Methods

Two different types of nanocellulose were produced at inofib starting from the raw materials, namely the Carboxymethlated nanocellulose (NFC-CMC) where some of the idroxyl group on the fiber surface were substitute with carboxilyc acids and aminosilane modified Nanocellulose (NFC-AEAPTMS. L-Arginine was purchased from sigma adrich, while PVAm was obtained through a three step purification form the commercial product Lupamin® 9095 kindly provided by BASF Italia.

The membranes were produced by solvent casting from an aqueous solution obtained by adding the amine compound solution in a water dispersion of nanocellulose. Permeation test were carried out in humid condition in order to exploit the facilitated transport mechanisms which needs water

to be fully active. To that aim a purposely built apparatus was used [1] able to use well known barometric technique for gas permeability evaluation ls in presence of water vapor.

3. Results and discussion

The data obtained from the different experiments are shown in figure 1 a and b for the NFC-Arginine and for amonosilane treated NFC. It can be seen that the addition of the amino acid resulted in a significant increment of both permeability (from 29 to 220 Barrer) and ideal selectivity (from 56 to 185). Introduction of PVAm determined the formation of strong interactions with the NFC matrix, which reduced permeability respect to a pure mobile carrier, but improved stability at high relative humidity. Lastly, a chemically modified NFC, with amine-bearing moieties grafted onto the surface (NFC-AEAPTMS) was tested with a content of 20 wt% PVAm, also showing promising performances.

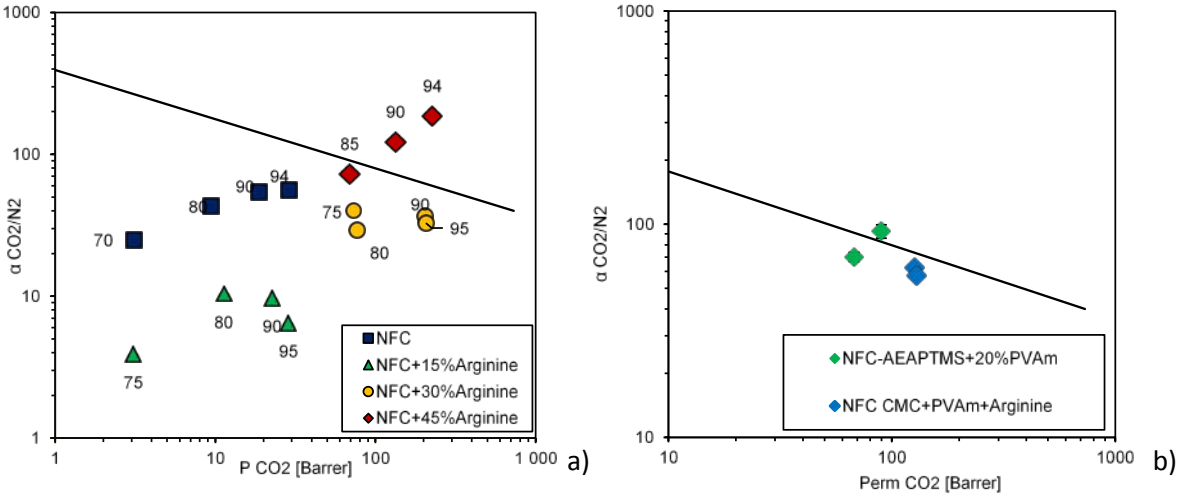

Figure 1 a) CMC-NFC permselectivity at different loadings of L-Arginine and relative humidity and b) of aminated NFC plus polyvinylamine at 100 RH% with respect to Robeson's Upper Bound [2]

4. Conclusions

In the present works a new type of nanocellulose based facilitated transport membranes were investigated for their use in post combustion carbon capture application. The general results showed that nanocellulose thanks to its hydrophilicity is a good candidate to be sed in facilitated transport membranes and is coupled with mobile carrier such as L-arginine it allows to obtine mebrane with separation performance well above the 2008 Robeson's Upper Bound.

Acknowledgements: This work has been performed in the framework of the European Project H2020 NANOMEMC^2 "NanoMaterials Enhanced Membranes for Carbon Capture", funded by the Innovation and Networks Executive Agency (INEA) Grant Agreement Number: 727734

References

[1] D. Venturi, D. Grupkovic, L. Sisti, M.G. Baschetti, Effect of humidity and nanocellulose content on Polyvinylamine-nanocellulose hybrid membranes for CO2capture, J. Memb. Sci. 548 (2018) 263–274.

[2] L.M. Robeson, The upper bound revisited, J. Memb. Sci. 320 (2008) 390–400.

ECCE12
The 12th EUROPEAN CONGRESS OF CHEMICAL ENGINEERING
Florence 15-19 September 2019

Sonochemical Synthesis of Dolomite ($CaMg(CO_3)_2$) for Utilize Seawater Resources and Application for Phosphor Material

Shinnosuke Kamei[1], Masakazu Matsumoto[2], Shigeki Furukawa[1]

1 Department of Sustainable Engineering, College of Industrial Technology, Nihon University, Chiba, Japan 275-8575; 2 Department of Liberal Arts and Basic Sciences, College of Industrial Technology, Nihon University, Chiba, Japan 275-8575

**kamei.shinnosuke@nihon-u.ac.jp*

Highlights

- A new synthetic approach of dolomite ($CaMg(CO_3)_2$) with ultra-sound irradiation by a liquid phase reaction was found.
- The average particle diameter was 470 nm.
- From energy dispersive X-ray spectrometry, dolomite of the high purity (Ca/Mg atomic ratio of 1.08) was successfully synthesized with the ultrasonic irradiation.
- Red-emitting Eu^{3+} doped dolomite phosphor and green-emitting Ce^{3+}-Tb^{3+} codoped dolomite phosphor were successfully synthesized by immersion treatment.

1. Introduction

Recently, ultrasonic irradiation assisted synthesis of inorganic materials has been actively conducted. On the other hand, synthesis of alkaline earth metal carbonate from the components dissolved in seawater is expected We focused on dolomite ($CaMg(CO_3)_2$). Dolomite is a double salt in which calcium carbonate ($CaCO_3$) and magnesium carbonate ($MgCO_3$) are regularly combined at a molar ratio of 1:1. By using ultrasonic irradiation, it is advantageous that the particle diameter obtained becomes nano-sized. Therefore, the synthesis of nanomaterial from seawater becomes possible. We introduce a new synthetic approach to obtain dolomite and report the synthesis of dolomite phosphor as an application material.

2. Methods

The preparation of $CaMg(CO_3)_2$ nano-powder was used $CaCl_2$, $MgCl_2$, $NaHCO_3$ and Na_2CO_3 powders as starting materials. Mixing of suspension was carried out by the mechanical stirring and the ultrasonic irradiation. With stirring and the ultrasonic irradiation (20kHz, 40W, 3-6mm horn diameter) reaction was maintained at 65°C for 1 hour. After reaction, the resulting suspension was filtered, washed with pure water, and dried at 40°C. Similarly, the same treatment was carried out using de-K ion bittern. The synthesis of dolomite phosphors used immersion method. The product was immersed in europium chloride solutions of 0.05～0.20 $mol \cdot dm^{-3}$ at room temperature, for 1 hours, with suspension concentration 1 mass%. Eu^{3+} doped dolomite phosphors were thus obtained. Using the same method, Ce^{3+}-Tb^{3+} codoped dolomite phosphors were obtained. Each sample was characterized by X-ray diffraction, scanning electron microscopy and Energy dispersive X-ray spectrometry. The fluorescence properties of the sample were measured using a spectrophotometer.

3. Results and discussion

Figure 1 shows the XRD patterns of the sample prepared with sonochemistry reaction. The diffraction patterns of the prepared samples showed good agreement with the powder patterns of dolomite and the single phase of dolomite was confirmed. In the case of using de-K ion bittern, the synthesis of dolomite was possible by controlling Ca concentration in de-K ion bittern. Figure 2 shows SEM image the sample prepared with sonochemistry reaction. The average particle diameter was 470 nm. Nano-sized particles are prepared easily made by sonochemistry reaction method. Moreover, from energy dispersive X-ray spectrometry, The Ca/Mg atomic ratio was 1.08. It was shown that dolomite of high purity can be easily synthesized. On fluorescence property of Eu^{3+} doped dolomite phosphor, the emission band was observed at 614 nm which is attributed to the $^5D_0$-$^7F_1$ transition of Eu^{3+} under excitation at 254 nm. In the case of Ce^{3+}-Tb^{3+} codoped dolomite phosphor, the emission band was observed at 544 nm which is attributed to the $^5D_4$-$^7F_5$ transition of Tb^{3+} under excitation at 254 nm. It was possible to make the prepared dolomite samples into phosphor materials.

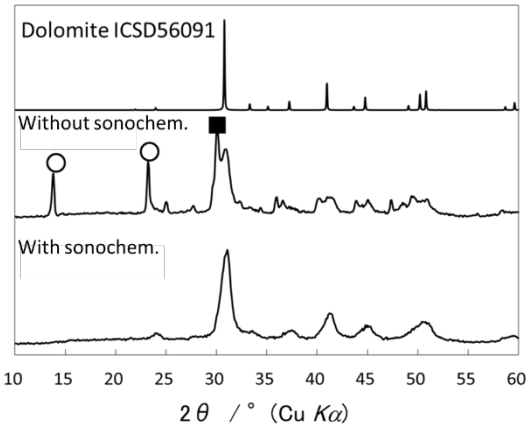

Figure 1. XRD patterns of the sample prepared with sonochemistry reaction.
○: Magnesium carbonate trihydrate
: Base-magnesium carbonate

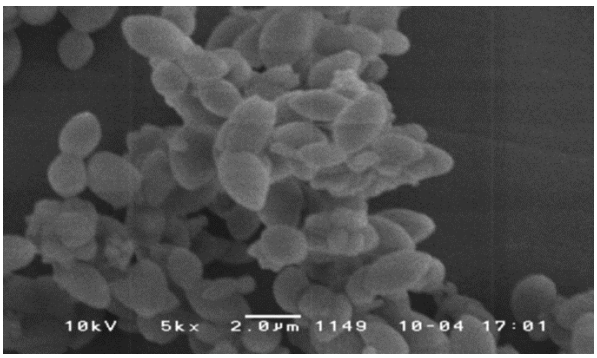

Figure 2. SEM image of the sample prepared with sonochemistry reaction.

4. Conclusions

We found a new synthesis of dolomite with ultrasonic irradiation under simple aqueous solution. Dolomite could be synthesized even using de-K ion bittern that is one of concentrated seawater. By immersion treatment, it was possible to synthesize dolomite phosphors showing the red or the green emission.

Reference

[1] S. Kamei, M. Matsumoto, S. Furukawa, The 7th Asian Particle Technology Symposium (APT 2017), Nanotechnology, PJ-8 (2017).

ECCE12
The 12th EUROPEAN CONGRESS OF CHEMICAL ENGINEERING
Florence 15-19 September 2019

Mesoscale Modeling and Experimental Study of Quercetin Organization as a Nanoparticles in Poly-Lactic-Co-Glycolic Acid/Water System.

Manel Slimane[1,2], Mohamed Ghoul[1,2], Latifa Chebil[1,2]

1 CNRS, Laboratoire Réactions et Génie des Procédés, UMR 7274, 2 avenue de la forêt de Haye, TSA 40602, Vandœuvre-lès-Nancy F-54518, France

2 Université de Lorraine, LRGP, UMR 7274, 2 avenue de la forêt de Haye, TSA 40602, Vandœuvre-lès-Nancy F-54518, France

**Corresponding author: latifa.chebil@univ-lorraine.fr*

Highlights

- Nanoparticles size is affected by the concentration of the different compounds of the system.
- Quercetin is encapsulated by poly-lactic-co-glycolic acid.
- Experimental investigations are in a good agreement with simulated ones.

1. Introduction

Quercetin (2-(3, 4-dihydrohyphenyl)-3, 5, 7-trihydroxy-4H-1-benzopyran-4-one) is a flavonoid widely distributed in plant kingdom. Quercetin has been reported to be an antioxidant and which is known for its anti-carcinogenic effect, antibacterial, anti- antihypertensive and anti-inflammatory properties [1]. Nevertheless, the solubility of quercetin in water and many organic solvents is very weak (<0.01 (g/L)) [2, 3]. Many strategies were developed to improve its solubility and stability by physicochemical approaches [4]. In this work, MesoDyn simulations were used to study the quercetin organization as a nanoparticles in poly-lactic-co-glycolic acid/water system. Results obtained from simulations were compared to experimental data. The effect of the concentrations of quercetin, PLGA, PVA (polyvinyl alcohol) and the lactic acid: glycolic acid ratio on the aggregation phenomena was studied.

2. Methods

2.1. Study of quercetin organization as a nanoparticles in poly-lactic-co-glycolic acid/water system by MesoDyn: in the MesoDyn method, the molecules are defined on a coarse-grained level as "Gaussian chains of beads". Each bead is of a certain component type representing covalently bonded groups of atoms (Figure 1). The solubility parameter-dependent method was used to calculate the Flory Huggins (χ_{ij}) parameter depending on the Hildebrand solubility of the different compounds. The interaction parameters that were used in the MesoDyn simulations were calculated using χ_{ij}. The aggregation and phase separation behavior of different beads was followed by the order parameter, P. P is a time dependent parameter obtained as an output of the MesoDyn simulation.

2.2. Nanoparticles preparation and characterization: PLGA nanoparticles loaded with quercetin were prepared by the solvent displacement method. The mean particle diameter and polydispersity index (PI) of the nanoparticles were determined by dynamic light scattering. The morphology of the PLGA-Q nanoparticles was examined by transmission electron microscopy.

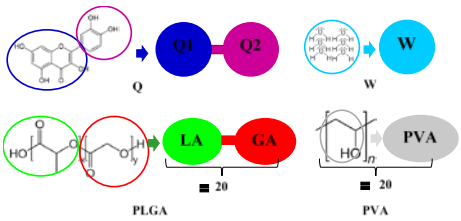

Figure 1. Coarse-grained model: molecules and monomer conversion into beads for Quercetin (Q), Poly (Lactic-co-Glycolic acid) (PLGA), Polyvinyl alcohol (PVA) and Water (W).

3. Results and discussion

Mesoscale simulations indicated that the studied systems allowed to produce nanoparticles well distributed in the continuous medium (water). The rapidity of the formation of nanoparticles is affected by the composition of the system. The fast kinetic of nanoparticle formation is reached with 10 g/L of poly-lactic-co-glycolic acid, 0.5 g/L of quercetin and 0.5% of polyvinyl alcohol. The increasing poly-lactic-co-glycolic acid and quercetin concentrations and LA content in poly-lactic-co-glycolic acid favor the formation of nanoparticles with large size. The formed nanoparticles were composed by quercetin (Q1 and Q2 parts) in the center of the system, poly-lactic-co-glycolic acid (lactic acid and glycolic acid) as a second layer and polyvinyl alcohol as third layer. The water is the continuous phase. The shape and the organization order of nanoparticles were checked experimentally. The obtained results showed that experimental investigations are in a good agreement with simulated ones (Figure 2).

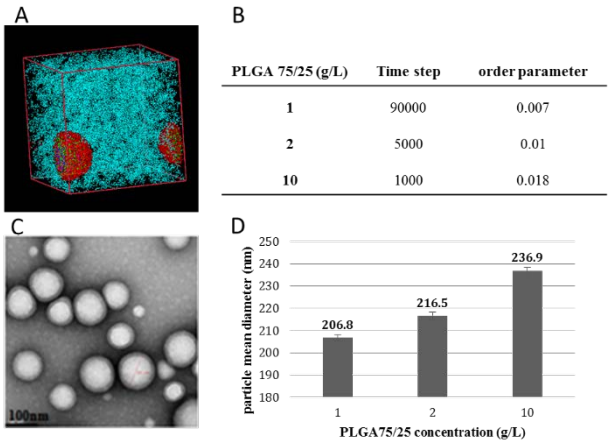

Figure 2. Main results obtained from mesoscale simulations (A, B) and experimental data (C, D).

4. Conclusions

Computational mesoscopic modeling approach can be used as a successful tool to understand and predict the behavior of quercetin/poly-lactic-co-glycolic acid/water systems under different operating conditions.

References

[1] C. Chen, J. Zhou, C.Y. Ji, Life Sci. 87 (2010) 333-338.
[2] L. Chebil, C. Chipot, F. Archambault, C. Humeau, J.M. Engasser, M. Ghoul, F. Dehez, J. Phys. Chem. B. 114 (2010) 12308-12313.
[3] M. Slimane, M. Ghoul, L. Chebil, Ind. Eng. Chem. Res. 57 (2018) 12519-12530.
[4] P. Calias, T. Galanopoulos, M. Maxwell, A. Khayat, D. Graves, H.N. Antoniades, M. D'Alarcao, Carbohyd. Res. 292 (1996) 83-90.

ECCE12
The 12th EUROPEAN CONGRESS OF CHEMICAL ENGINEERING
Florence 15-19 September 2019

Nanoemulsions Produced at Large Scale by Premix Membrane Emulsification – Influence of Process Parameters and Formulation.

Océane Alliod[1],Catherine Charcosset[1]

1 Univ Lyon, Université Claude Bernard Lyon 1, CNRS, LAGEP UMR 5007, 43 boulevard du 11 novembre 1918, F-69100, VILLEURBANNE, France

**Corresponding author: catherine.charcosset@univ-lyon1.fr*

Highlights

- Nanoemulsions were produced by premix membrane emulsification
- A high pressure syringe pump controlled the pressure and flowrate
- W/O nanoemulsions with droplet size down to 260 nm were obtained

1. Introduction

Nanoemulsions find a wide range of applications in cosmetics, pharmaceuticals or food industry and are defined by their droplet size which is smaller than 1000 nm, 500 nm or 100 nm, depending on the definition used [1]. Generally, nanoemulsions are oil-in water emulsions (O/W) as the oil phase is dispersed into the water continuous phase, but can also be water-in-oil emulsions (W/O) when the water phase is dispersed into the oil continuous phase. W/O and O/W nanoemulsions can be produced by sonication and high pressure homogenization.

Membranes can be used for emulsification either in direct membrane emulsification (DME) or premix membrane emulsification (PME) [2]. DME consists in injecting under mild pressure the dispersed phase through a microporous membrane to the continuous one, whereas PME relies on injecting a coarse emulsion through the membrane. PME produces emulsions of smaller size range and with greater flowrate but DME does not require a premix step.

However, the production of nanoemulsions by membrane emulsification is challenging. Bunjes et al. prepared nanoemulsions by PME with droplet size lower or around 200 nm with narrow size distribution with SPG membranes for volumes up to 10 mL [3]. In previous works, we produced O/W and W/O nanoemulsions by PME and SPG membranes at high flowrate and relatively large volumes up to 500 mL [4, 5]. The aim of this communication is to report the preparation at large scale of O/W and W/O nanoemulsions using PME.

2. Methods

The experimental set-up used for the preparation of nanoemulsions by PME is shown in Figure 1. The set-up was composed of a high pressure cylinder pump BTSP 500-5 (Floxlab, Nanterre, France). Hydrophilic and hydrophobic tubular SPG membranes were provided by SPG Technology Co. Ltd (Miyazaki, Japan). Hydrophilic SPG membranes were used for O/W nanoemulsion production and hydrophobic for W/O nanoemulsions. The continuous and dispersed phases were first prepared and then mixed under magnetic stirring for 10 min to produce the premix.

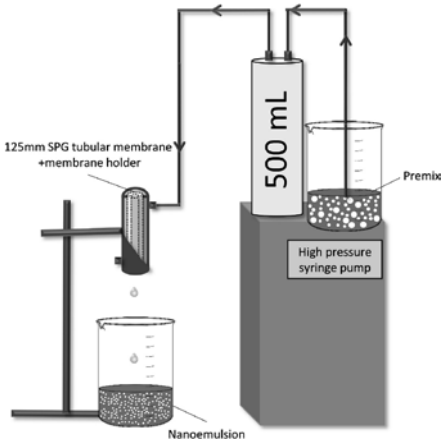

Figure 1. Experimental set-up of the high syringe pump with membrane holder and SPG membrane.

3. Results and discussion

The effect of several parameters was investigated: process parameters (scalability, cycle number, membrane pore size, flowrate) and formulation (oil and surfactant concentrations). Nanoemulsions were prepared at large scale up to 500 mL at production rate up to 200 mL/min, pressure below 60 bars and one cycle. The droplet size was linearly related to the membrane pore size and highly monodispersed nanoemulsions of around 260 nm in diameter and stable for 9 months at room temperature were achieved with the smallest pore size membrane (0.2 µm).

In addition, the effect of viscosities on pressure and droplet size was investigated: the water phase viscosity by increasing glycerol concentration, the oil phase viscosity with mineral oils of different viscosities and the overall emulsion viscosity by increasing the dispersed phase content of the emulsion. The pressure required to break up the droplets inside the membrane pores did not depend on viscosities, while the pressures generated by the flows through the pipe and the membrane were proportional to the viscosity of the overall emulsion. W/O nanoemulsions were more difficult to produce, they were obtained with mean droplets size around 600 nm and flowrate of 50 mL/min.

4. Conclusions

PME with SPG membranes produced O/W monodispersed nanoemulsions down to 260 nm with controlled size and very long stability over time. W/O nanoemulsions were produced with mean droplets size around 600 nm. W/O nanoemulsions were more difficult to produce and to characterize, but the different viscosities had the same influence on the membrane pressure as for O/W nanoemulsions.

References

[1] T. Tadros, P. Izquierdo, J. Esquena, C. Solans, Adv. Colloid Interface Sci. 108–109 (2004) 303–318,
[2] G. T. Vladisavljevic, Integrated Membrane Processes for the Preparation of Emulsions, Particles and Bubbles, in: Integrated Membrane Systems and Processes, Elsevier, pp. 79-140 (2016)
[3] S. Joseph, H. Bunjes, Eur. J. Pharm. Biopharm. 87 (1) (2014) 178–186
[4] O. Alliod, J.-P. Valour, S. Urbaniak, H. Fessi, D. Dupin, C. Charcosset,, Colloids Surf. A, 557 (2018) 76-84
[5] O. Alliod, L. Messager, H. Fessi, D. Dupin, C. Charcosset, Chem. Eng. Res. Des. 142 (2019) 87–99

ECCE12
The 12th EUROPEAN CONGRESS OF CHEMICAL ENGINEERING
Florence 15-19 September 2019

Effect of the solvation force and the van der Waals forces on the Pull-off between Two Slightly Rough Surfaces from a Molecular View.

Gerson E. Valenzuela[1*]

1 Chemical Engineering Department, Universidad de La Frontera, Av. Francisco Salazar, Temuco 01145, Chile; Centro de Excelencia de Modelación y Computación Científica CEMCC, Universidad de La Frontera, Temuco 01145, Casilla 54-D, Chile.

**Corresponding author: gerson.valenzuela@ufrontera.cl*

Highlights

- Water bridge effect on the pull-off.
- Solvation versus van der Waals forces.
- Molecular dynamics simulation of nanometric systems.

1. Introduction

The correct understanding of the interaction forces between particles and surfaces is determinant in technological development [1] and processes with nanoparticles. [2] Such interaction in the air is composed of the van der Waals and electrostatic forces, and the capillary and solvation forces because of water bridges. [3] The effect of humidity on the interaction force is expressed in the pull-off measurement obtained in force spectroscopy during retraction of the tip in atomic force microscopy. [4] Computer simulations have been shown the solvation force produces pull-off between smooth hydrophilic surfaces. [5]. In this work it is shown that, during a pull-off, the van der Waals forces between two slightly roughness surfaces can be hidden by the solvation force, depending on the size of the bridge. The systems and the results are of nanometric resolution.

2. Methods

Figure 1-A1 shows a general diagram of the system. Each substrate (S1 and S2) have a circular roughness of radius 3 nm and depth 0.25 nm (Fig. 1-A2). When S2 is moving down the water droplet (500 molecules) becomes in a water bridge. S1 and S2 are hydrophilic. Interaction parameters of the system can be reviewed in refs. [5] and [6], the droplet forms a contact angle of 57°. The simulations are performed with a program that has been used in previous works. [5, 6, 7] The water temperature is controlled at 298 K. The force laws are obtained according to the method developed in refs. [6] and [7]. The pull-off simulations are performed according to ref. [5]. Cross interaction S1-S2 is defined by the Lennard-Jones potential with parameters $\sigma_{S1-S2} = 0.3$ nm and $\epsilon_{S1-S2} = 5\mathrm{k_B}$, providing a Hamaker constant of $0.98x10^{-20}$ J (similar for glass [8]).

3. Results and discussion

The force laws in Fig. 1-B shows that the water bridge controls the adhesion between the smooth surfaces. The interaction of the two-layer bridge (B2) and the monolayer (B1) appears with repulsive walls at a higher distance of separation than the interaction of S1 and S2. When the substrates are roughness (Fig. 1-C) the force law of the water bridge displaces to the left (in *D* axis) due to the depth of the roughness, and the interaction of B2 develops in a similar range than the

interaction S1-S2. In an approach and retraction of S2, the pull-off simulation (Fig. 1-D) shows a small peak (P1) when interaction S1-S2 are on. From P1, S2 is pull-off out of the interaction domain S1-S2, but the attraction increases with the retraction because the pull-off is controlled by the bridge. The effect of the bridge is clear considering a smaller one (256 water molecules) which is fully trapped into the roughness (inset Fig. 1-E). Figure 1-E show the pull-off, the water bridge does not affect the maximum attraction between S1 and S2 showing in Fig. 1-C (red line).

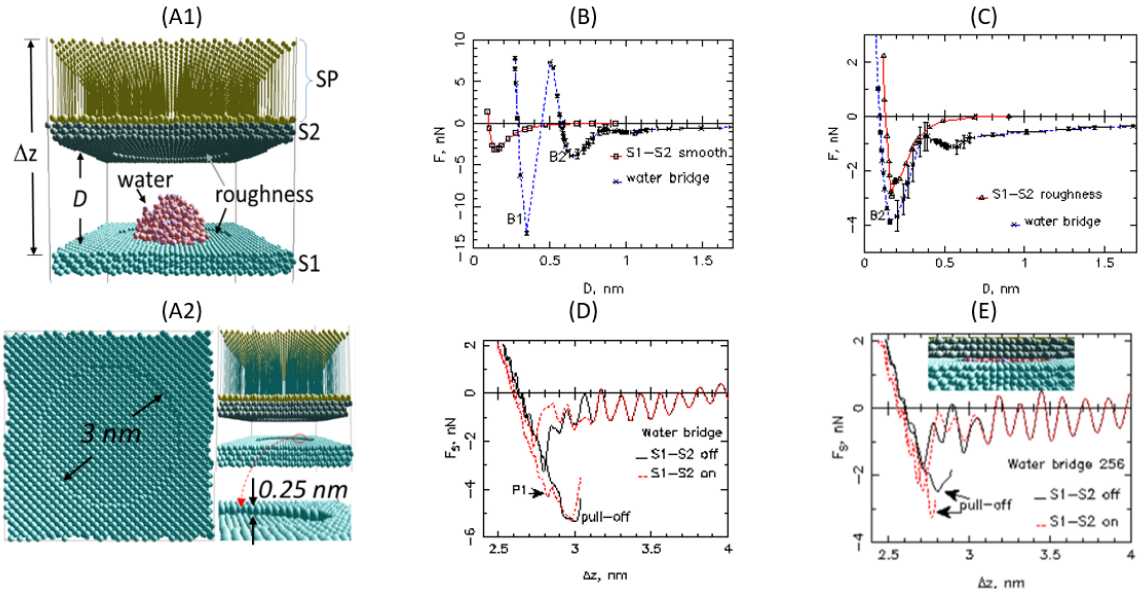

Figure 1. (A1) System. The force exerted by the bridge and the interaction S1-S2 is measured by the deflection of the SP. The "tip" (S2) is moved by displacing the top sites of the "cantilever" (SP) with constant speed, analogous to an AFM experiment; (A2) Detail of the roughness. (B) Force law for the interaction S1-S2 smooth alone (without a water bridge) and the force law for the bridge alone (interaction S1-S2 off) (C) Force laws between S1 and S2 roughness and for the bridge between them. (D) Pull-off for 500 water molecules (E) Pull-off for 256 water molecules.

4. Conclusions

The pull-off force between two smooth hydrophilic surfaces may be entirely dominated by a water bridge due to repulsive walls in the force law. For slightly roughness surfaces, the bridge affects the pull-off depending on its size. For a small bridge (250 water molecules) the van der Waals force between the surfaces is not affected by the solvation force, but for a bigger bridge (500 water molecules), the pull-off correspond to the solvation force.

References

[1] H.R. Moutinho, C.-S. Jiang, B. To, C. Perkins, M. Muller, M.M. Al-Jassim, L. Simpson, Sol. Energy Mater. Sol. Cells 172 (2017) 145-153.

[2] J. Laube, M. Dörmann, H.-J. Schmid, L. Mädler, L. Colombi Ciacchi, J. Phys. Chem C 121 (2017) 15294-15303.

[3] J.N. Israelachvili, Intermolecular and Surface Forces, Academic Press: San Diego, 2011.

[4] M. He, A. Szuchmacher, D.E. Astos, C. Buenviaje, R.M. Overney, R. Luginbühl, J. Chem. Phys 114 (2001) 1355-1360.

[5] G.E. Valenzuela, J. Phys. Chem C (2018) DOI: 10.1021/acs.jpcc.8b09907.

[6] G.E. Valenzuela, J.H. Saavedra, R.E. Rozas, P.G.Toledo, Phys. Chem. Chem. Phys. 18 (2016) 11176-11183.

[7] G.E. Valenzuela, R.E. Rozas, P.G. Toledo, J. Phys. Chem. C 121 (2017) 25986-25993.

[8] S. Acuña, P. Toledo, Langmuir 24 (2008), 4881-4887.

Analytical ultracentrifugation – A versatile tool for the multidimensional characterization of nanoparticles

Johannes Walter, Simon Wawra, Wolfgang Peukert

Institute of Particle Technology (LFG), FAU Erlangen-Nürnberg, Germany
Interdisciplinary Center for Functional Particle Systems (FPS), FAU Erlangen-Nürnberg, Germany

Knowledge about the size, shape and optical properties of nanoparticles (NPs) is of high importance for many processes because product properties are directly influenced by these parameters. So far, combined analysis of size and shape or the determination of size and shape dependent optical properties has been a major challenge for nanoparticulate systems. Scattering or microscopic techniques are often limited by statistics, resolution and applicability to broad particle size distributions (PSDs). Ensemble based measurement devices such as the benchtop UV/Vis spectrophotometer fail to provide spectral information about individual species and require narrow size fractions instead.

These ubiquitous challenges provide the motivation and basis for the studies presented in this contribution. We have shown that analytical ultracentrifugation equipped with an UV-Vis multiwavelength detector (MWL-AUC) is a powerful tool for the simultaneous analysis of hydrodynamic and optical properties without the necessity of doing any purification step beforehand.[1] AUC combines the fractionation of particles in a gravitational field with up to 280,000 g with UV-VIS spectroscopy. The distribution of particles in an optically accessible cell is measured in-situ using a CCD spectrometer, which captures full spectra ranging from 250 to 1000 nm at each radial position with very high temporal resolution during centrifugation.[2]

Sedimentation coefficients can be calculated for all species out of which PSDs can be derived. Our recent developments on the instrumentation, acquisition as well as the evaluation of MWL-AUC data allow us to significantly extend the possibilities of MWL-AUC.[1, 3-4] Information on the size of all species in a mixture can be directly linked to their optical properties. Either extinction spectra can be determined or optical information can be used to deconvolute PSDs consisting of chemically heterogeneous NPs. For CdTe semiconductor quantum dots it is shown that the size dependent band-gap is derived in a single experiment.[5] For plasmonic nanorods, a full 2D size and shape distribution is accessible using MWL-AUC.[6] This is possible as hydrodynamic properties can be directly linked to the extinction spectra without any up-stream processing.

In case of non-plasmonic anisotropic particles, AUC can be coupled with analytics in the gas phase for mobility analysis using a scanning mobility particle sizer.[7] This allows deriving the mean length and diameter of nanorods (e.g. ZnO). For mono-layered graphene oxide nanosheets, it will be shown that AUC is capable of resolving shape distributions with high accuracy, statistical confidence and experimental throughput, which makes it superior to the usually applied and very time consuming image analysis.[8] For polydisperse PSDs, excellent statistics are obtained due to the evaluation at multiple wavelengths.[4]

In summary, our contribution will demonstrate that MWL-AUC is a powerful technique, which provides multidimensional access to an extensive range of particulate systems not accessible so far by any other technique. The direct correlation of size, shape and optical properties of NPs in the range between 1 nm and 1 µm is highly relevant for a variety of new applications because targeted product design becomes possible.

References

1. Walter, J.; Löhr, K.; Karabudak, E.; Reis, W.; Mikhael, J.; Peukert, W.; Wohlleben, W.; Cölfen, H., Multidimensional Analysis of Nanoparticles with Highly Disperse Properties Using Multiwavelength Analytical Ultracentrifugation. ACS Nano 2014, 8 (9), 8871-8886.

2. Pearson, J.; Walter, J.; Peukert, W.; Cölfen, H., Advanced Multiwavelength Detection in Analytical Ultracentrifugation. Anal. Chem. 2018, 90 (2), 1280-1291.
3. Walter, J.; Sherwood, P. J.; Lin, W.; Segets, D.; Stafford, W. F.; Peukert, W., Simultaneous Analysis of Hydrodynamic and Optical Properties Using Analytical Ultracentrifugation Equipped with Multiwavelength Detection. Anal. Chem. 2015, 87 (6), 3396-3403.
4. Walter, J.; Peukert, W., Dynamic range multiwavelength particle characterization using analytical ultracentrifugation. Nanoscale 2016, 8 (14), 7484-7495.
5. Karabudak, E.; Brookes, E.; Lesnyak, V.; Gaponik, N.; Eychmüller, A.; Walter, J.; Segets, D.; Peukert, W.; Wohlleben, W.; Demeler, B.; Cölfen, H., Simultaneous Identification of Spectral Properties and Sizes of Multiple Particles in Solution with Subnanometer Resolution. Angew. Chem. Int. Ed. 2016, 55 (39), 11770–11774.
6. Wawra, S. E.; Pflug, L.; Thajudeen, T.; Kryschi, C.; Stingl, M.; Peukert, W., Determination of the two-dimensional distributions of gold nanorods by multiwavelength analytical ultracentrifugation. Nat. Commun. 2018, 9 (1), 4898.
7. Thajudeen, T.; Walter, J.; Srikantharajah, R.; Lübbert, C.; Peukert, W., Determination of the length and diameter of nanorods by a combination of analytical ultracentrifugation and scanning mobility particle sizer. Nanoscale Horiz. 2017, 2 (5), 253-260.
8. Walter, J.; Nacken, T. J.; Damm, C.; Thajudeen, T.; Eigler, S.; Peukert, W., Determination of the Lateral Dimension of Graphene Oxide Nanosheets Using Analytical Ultracentrifugation. Small 2015, 11 (7), 814-825.

ECCE12
The 12th EUROPEAN CONGRESS OF CHEMICAL ENGINEERING
Florence 15-19 September 2019

The Role of Surface-Ligand Interactions in Stability of All Inorganic Cesium Lead Halide Perovskite Nanocrystals.

Kiyoung Kim[1], Shin Ae Song[1], Sung Nam Lim[1], and Ju Young Woo*[,1]

1 Micro/Nano Scale Manufacturing R&D Group, Research Institute of Industrial Technology Convergence, Korea Institute of Industrial Technology (KITECH), Republic of Korea

**Corresponding author: jywoo@kitech.re.kr*

Highlights

- $CsPbX_3$ NCs prepared in typical synthetic procedure is unstable under air.
- The stability of $CsPbX_3$ NCs can be considerably enhanced by modifying the synthesis.
- Origin of enhanced stability of $CsPbX_3$ NCs can be interpreted in the context of modified surface.

1. Introduction

Recent drastic increase of interest in colloidal all inorganic cesium lead halide perovskite ($CsPbX_3$, X is Cl, Br, and/or I) nanocrystals have derived from their extremely bright photoluminescence (PL), narrow full width at half maximum (FWHM) of PL spectrum, band gaps which are tunable over entire visible spectrum, defect tolerance, and highly dynamic interaction between ligands and atoms on NC surfaces (surface-ligand interactions).[1,2] However, the NCs are significantly unstable under air, hence further investigation is strongly hampered.[2] Here we present new synthesis of $CsPbX_3$ NCs with modified surfaces, thus considerably enhanced air stability. Also, the origin of instability (and stability) of $CsPbX_3$ NCs is revealed in the context of surface-ligand interactions.[3]

2. Methods

The synthesis are described in previously reported studies.[1,2] For the synthesis of typical $CsPbBr_3$ NCs, hot Cs-oleate solution is injected into degassed mixture solution of $PbBr_2$, oleic acid (OA), and oleylamine (OLA) in 1-octadecene (ODE) at 170 °C. The NCs are immediately formed upon the injection and the flask containing reaction mixture is rapidly cooled in an ice bath. For the synthesis of surface modified and air-stable $CsPbBr_3$ NCs, the mixture solution is formed by adding additional metal bromides (e.g., $ZnBr_2$) to $PbBr_2$, OA, and OLA in ODE. And other procedures are carried out identically with typical $CsPbBr_3$ NCs. After the synthesis, the NCs are purified by multiple centrifugations with or without polar antisolvent (e.g., methyl acetate). Finally the $CsPbBr_3$ NCs are dispersed in organic solvents such as hexane and toluene, or stored in the form of films for further characterizations.

3. Results and discussion

The typical $CsPbBr_3$ NCs prepared without additional metal halides fused along (110) direction when the NCs were exposed to air in the form of films. Also, the PL QY of typical $CsPbBr_3$ NCs decreased drastically under air condition possibly due to relaxed confinement of exciton upon

fusion of the NCs.[4] In contrast, $CsPbBr_3$ NCs synthesized with additional of additional metal bromide are highly stable without nearly no sign of fusion in air. In addition, the PL QY of the NCs relatively well retained compared to typical NCs (Figure 1).[2]

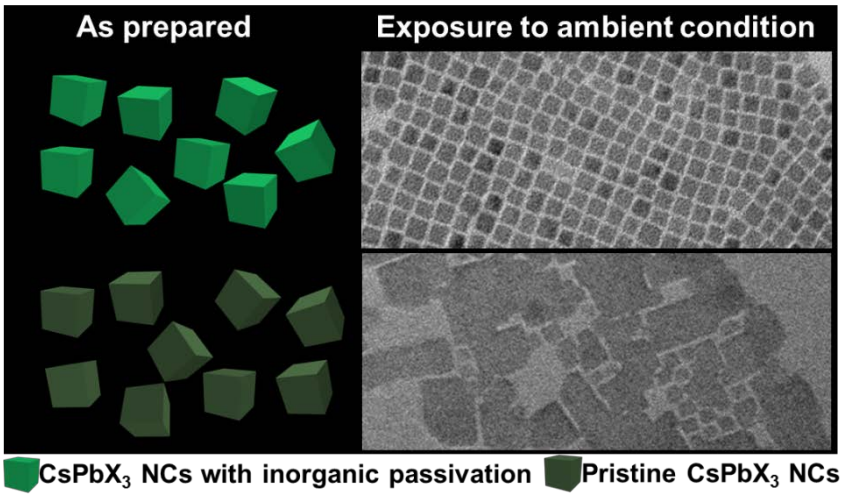

Figure 1. Schematic illustration and TEM images of typical (bottom) and modified (upper) $CsPbBr_3$ NCs.

4. Conclusions

In conclusion, we successfully present $CsPbX_3$ NCs with dramatically enhanced stability under air by adding additional metal halides in the synthesis.[2] Further study will be presented to reveal the origin of instability (stability) of $CsPbX_3$ NCs in the context of modified surface-ligand interactions with the addition of additional metal halides during the synthesis.

References [Calibri 10]

[1] L. Protesescu, S. Yakunin, M. I. Bodnarchuk, F. Krieg, R. Caputo, C. H. Hendon, R. X. Yang, A. Walsh, M. V. Kovalenko, Nano Lett. 15 (2015) 3692−3696.
[2] J. Y. Woo, Y. Kim, J. Bae, T. G. Kim, J. W. Kim, D. C. Lee, S. Jeong, Chem. Mater. 29 (2017) 7088−7092.
[3] J. De Roo, M. Ibanez, P. Geiregat, G. Nedelcu, W. Walravens, J. Maes, J. C. Martins, I. Van Driessche, M. V. Kovalenko, Z. Hens, ACS Nano 10 (2016) 2071−2081.
[4] H. Cho, S.-H. Jeong, M.-H. Park, Y.-H. Kim, C. Wolf, C.-L. Lee, J. H. Heo, A. Sadhanala, N. Myoung, S. Yoo, S. H. Im, R. H. Friend, T.-W. Lee, Science 350 (2015) 1222-1225.

ECCE12
The 12th EUROPEAN CONGRESS OF CHEMICAL ENGINEERING
Florence 15-19 September 2019

Stability of nanobubble dispersions in liquids of various composition and physicochemical properties

Karol Ulatowski, Paweł Sobieszuk*, Tomasz Ciach

Warsaw University of Technology, Faculty of Chemical and Process Engineering, Warynskiego 1, Warsaw, Poland

**Corresponding author: Pawel.Sobieszuk@pw.edu.pl*

Highlights

- Gas nanobubbles are stable even in deionized water.
- The stability of nanobubbles varies in liquids of different polarity.
- Nanobubbles are stable for low absolute values of zeta potential (under 30 mV).
- Diameter of bubbles is different for each gas phase used.

1. Introduction

Bulk nanobubbles are spherical gas domains in liquid which are characterized by diameter under 1 µm. In consequence, the rising velocity of nanobubbles is extremely low (according to Stokes law) and their internal pressure is high as for Laplace equation [1]. What is more, nanobubbles are reported to be stable for a long time (weeks to months) in aqueous dispersions [2-4]. However, the investigation of generation in non-polar liquids and systematic research of stability of bubbles in aqueous solutions with salt or surfactant additions is still to be done. This study aims to show the results of research of stability of bubbles generated in mentioned liquid phases.

2. Methods

Nanobubbles were generated in the system presented schematically in Figure 1. Gas from the cylinder squeezes through the pores of the ceramic membrane and forms hemispherical domains which are cut off by the flowing liquid. Several gases were used, including nitrogen, oxygen and air among others. The two-phase flow was returned to the storage tank. Liquid stored in tank was sucked by the rotary pump which induced the flow of the liquid inside the cylindrical membrane. Liquids ranged from pure (deionized) water, through water with salt and surfactant additions up to nonpolar organic liquids.

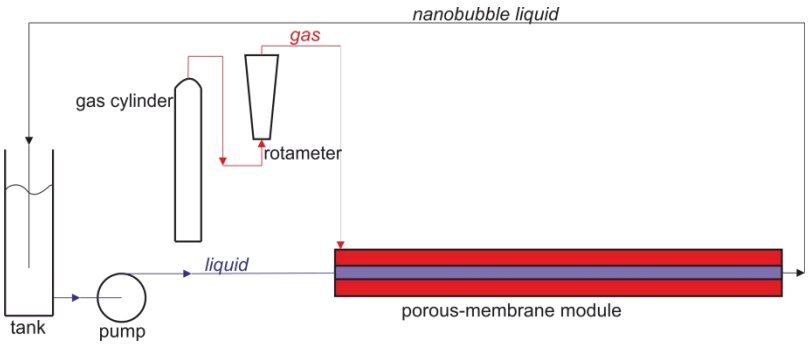

Figure 1. Scheme of the experimental setup

The distribution density of bubbles and zeta potential was measured using Malvern Zetasizer Nano ZS using DLS technique. For each measurement the Sauter diameter (d_{32}) was calculated.

3. Results and discussion

In Figure 2 one can see the exemplary results of Sauter diameter obtained for nitrogen and oxygen nanobubbles with deionized water as a liquid phase. It is clear that the diameter of bubbles over time is nearly constant. Another interesting fact is that oxygen nanobubbles are about two times smaller than the nitrogen nanobubbles. The reasons for such extraordinary stability of nanobubbles are not clear. Ulatowski et al. [2] proposed the possible explanation of this phenomenon, linking it with the reduction of surface tension due to accumulation of charge on nanobubble surface (analogously to reduction of surface tension on charged drop proposed by Lord Rayleigh theory). Another theory proposed by Ohgaki et al. [4] states that water molecules form hard shells around bubbles, due to their hydrophobicity. That leads to a reduction in diffusivity of gas through the gas-water interface and increase of surface tension. The stability of nanoobjects is linked to zeta potential value. For solid nanoparticles, the absolute value of zeta potential which indicates high stability of dispersion is assumed as 30 mV. In this work, the stable nanobubbles were obtained for low value of zeta potential of about –15 mV.

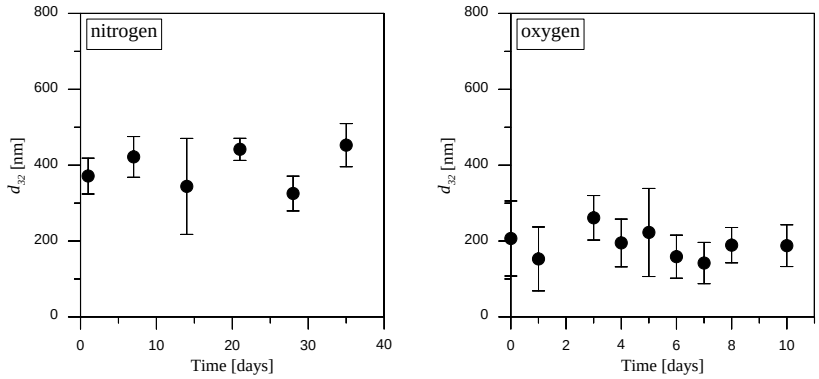

Figure 2. Sauter diameter of bubbles as a function of time for nitrogen and oxygen nanobubbles in pure water

4. Conclusions

Investigation of reasons of nanobubble stability is not a closed case. There is much to discuss and investigate in future. This works aims to investigate the stability of nanobubbles in various liquids of different polarity, ions presence and other physicochemical properties.

Acknowledgements

This work was supported by the National Science Centre, Poland (grant number 2018/29/B/ST8/00365).

References

[1] H. Tsuge, Micro- and Nanobubbles. Fundamentals and Applications, Pan Stanford Publishing, Boca Raton, 2015.

[2] K. Ulatowski, P. Sobieszuk, A. Mróz, T. Ciach, Chem. Eng. Process. Process Intensif. 136 (2019) 62-71.

[3] K. Ulatowski, P. Sobieszuk, Chem. Process Eng. 39(2018), 335-345

[4] K. Ohgaki, N. Q. Khanh, Y. Joden, A. Tsuji, T. Nakagawa, Chem. Eng. Sci. 65 (2010) 1296-1300

Fluorescent Nanomaterials for Optical Bioimaging and Beyond.

Dan Wang[1,2,*], Yuan Pu[1], Jie-Xin Wang[1,2], Jian-Feng Chen[1,2]

1 Research Center of the Ministry of Education for High Gravity Engineering and Technology, Beijing University of Chemical Technology, Beijing 100029, China; 2 Beijing Advanced Innovation Center for Soft Matter Science and Engineering, State Key Laboratory of Organic-Inorganic Composites, Beijing University of Chemical Technology, Beijing 100029, China

**Corresponding author: wangdan@mail.buct.edu.cn*

Fluorescent nanoparticles have received intense scientific attention and offer promising applications in many fields from optoelectronic devices to cancer treatment[1]. The development of robust mass-scale nanoparticle synthesis methods is one of key materials challenges in moving towards fluorescent nanoparticles for commercialization and advanced applications.[2] In this talk, I will summarize our work on green and scalable synthesis of fluorescent nanoparticles, including biomass-derived carbon dots[3], subcritical water technology for nanonization of organic compounds[4] and preparation of inorganic nanoparticles by high-gravity process intensification technology[5]. The applications of related fluorescent nanoparticles in biomedical imaging and therapy from cells to animals will be introduced. A brief overview of this exciting field, along with some challenges and opportunities, will also be presented.

References

[1] D. Wang, L. Zhu, J.-F. Chen, L. Dai, Angew. Chem. Int. Ed., 2016, 55, 10795-10799.
[2] Y. Pu, F. Cai, D. Wang, J.-X. Wang, J.-F. Chen, Ind. Eng. Chem. Res., 2018, 57, 1790-1802.
[3] D. Wang, Z. Wang, Q. Zhan, Y. Pu, J.-X. Wang, N. R. Foster, L. Dai, Engineering, 2017, 3, 402-408.
[4] Y. Pu, Y. Li, D. Wang, N. R. Foster, J.-X. Wang, J.-F. Chen, Powder Technol., 2017, 308, 200-205.
[5] X. He, Z. Wang, Y. Pu, D. Wang, R. Tang, S. Cui, J.-X. Wang, J.-F. Chen, Chem. Eng. Sci., 2019, 195, 1-10.

ECCE12
The 12th EUROPEAN CONGRESS OF CHEMICAL ENGINEERING
Florence 15-19 September 2019

Subcritical water processing for fluorescent organic nanodots

Rina Su[1,2], Yuan Pu[2], Dan Wang[*,1]

1 Beijing Advanced Innovation Center for Soft Matter Science and Engineering, State Key Laboratory of Organic-Inorganic Composites, Beijing University of Chemical Technology, Beijing 100029, China;

2 Research Centre of the Ministry of Education for High Gravity Engineering and Technology, Beijing University of Chemical Technology, Beijing 100029, China

** Corresponding authors: Dan Wang (Tel: +86-10-64449453; E-mail: wangdan@mail.buct.edu.cn)*

Abstract

Fluorescent nanomaterials have received intense scientific attention and offer promising applications from molecular sensors through cancer diagnosis agents to optoelectronic devices. Aggregation-induced emission (AIE), which effect is exactly opposite to the notorious ACQ (aggregation-caused quenching), are among the most attractive of fluorescent nanomaterials, offering possibility with any concentration for bioassays in the use of dye solutions. However, most AIE materials, such as hexaphenylsilole (HPS), are soluble in toxic organic solvents (e.g. tetrahydrofuran), and insoluble in green solvents (such as water), which limited the further application of biological applications. The high pressure reactors widely used in supercritical/subcritical fluid technique, can generate subcritical water (SBCW) referring to liquid water with pressure in the temperature range of 373.15 K to 647.15 K, which can be used as the solvent to eliminate the use of organic solvents and provide a green route to synthesize fluorescent nanomaterials. In this work, we reported a green process for the synthesis of AIE fluorescent nanoparticles via solvent anti-solvent precipitation, in which the SBCW and cold water were used as the solvent and anti-solvent respectively. The obtained AIE fluorescent organic nanodots showed an average size less than 10 nm with uniform distribution, and exhibited good optical performance and well-dispersion in aqueous solution. The use of SBCW as the solvent overcomes the limitations of using toxic organic solvents during solvent anti-solvent precipitation, offering a green method of manufacturing AIE fluorescent nanoparticles, as well as other poor water soluble fluorescent nanomaterials, and it is also more convenient for real-time monitoring of the temperature and pressure in the reaction system and more reliable for scalable mass-production.

Controllable Preparation of Multi-scale Silica Using High-gravity Technology Combined with Spray Drying Process for Dental Restoration Application

Dan-Lei Yang[1,2], Hao Niu[1,2], Dan Wang[1,2], Jie-Xin Wang*[1,2]

1 State Key Laboratory of Organic–Inorganic Composites; 2 Research Center of the Ministry of Education for High Gravity Engineering and Technology, Beijing University of Chemical Technology, Beijing 100029, PR China

**Corresponding author: wangjx@mail.buct.edu.cn*

Abstract

Resin-based composites have been frequently used in dental restoration because of their outstanding esthetics, mechanical performances, biocompatibility, and clinical operability. The particle size, dispersity and structure of inorganic filler are decisive for the properties of resin composite. In this study, monodisperse silica nanoparticles (MSNPs) with a controllable diameter were efficiently prepared with high-gravity technology in an internal circulation rotating packed bed (ICRPB), and then the spray-drying technology was used to efficiently construct micron-scale nanoparticle clusters (MSNCs). The results indicated that the particle size, morphology and dispersion of silica nanoparticles were influenced by the rotating speed of ICRPB and the concentration of reactants. Compared with traditional stirred tank reactor, the hydrolyzation process in ICRPB had one-third descent in reaction time and the size of MSNPs dramatically decreased. The prepared nanodispersions could be stably conserved for over 12 months without any changes in particle size, transparency and monodispersity. After being modified by the silane coupling agent, the MSNPs were mixed with the resin matrix to preparing the resin composites. The effects of filler content, particle size and structure on mechanical performances were further examined. It could be found that the mechanical properties of composites were significantly improved with the increased filler content from 40 to 70 wt.%, and enhanced first and then dropped with increasing particle size when the MSNPs were used as the fillers. Due to the excellent dispersity, the maximum content of MSNPs was 30% higher than that of commercial silica nanoparticles with the same size, thereby resulting in better properties of the composites. Furthermore, compared with silica microparticles with the similar average size and the MSNPs, the MSNCs showed an obvious improvement in flexural strength and compressive strength due to its steady porous structure inside, which was capable to produce a stronger interlocking between organic resin and inorganic fillers. This method could be applied to the preparation of hydroxyapatite, zinc oxide and zirconia nanoparticle clusters, and will provide a new idea for the controlled preparation of high-performance multifunctional fillers for dental restorative resin composites.

Multi-stimuli-responsive liquid marbles for miniature reactors

Zhijian Zhao[1,2], Yuan Pu[1,2], Dan Wang[1,2,*]

1 Beijing Advanced Innovation Center for Soft Matter Science and Engineering, State Key Laboratory of Organic Inorganic Composites, Beijing University of Chemical Technology, Beijing 100029, China;

2 Research Center of the Ministry of Education for High Gravity Engineering and Technology, Beijing University of Chemical Technology, Beijing 100029, China

** Dan Wang (wangdan@mail.buct.edu.cn)*

Liquid marbles (LMs) were first reported by Aussilous and Quéré in 2001 to realize the microfluidic motion without wetting solid surface[1] and this has attracted increasing research interest. LMs prevent the contact of encased liquid inside with supporting plan so that the problem of surface contamination is avoided and surface friction is significantly reduced. As a new approach to manipulating liquid, LMs can be driven by external forces, such as gravity, electricity, light, based on the liquid or component attributes; However, most LMs reported, as far as we are aware, respond to a single external stimulus only with limited prospects. The formation of LMs triggered by various stimuli is important for its potential application, which, however, are still problematic.LMs used as droplet reactors have also been adopted recently due to the advantages of compartmentalization, miniaturization, mono-dispersity, and high throughput, which can reduce the use of chemical reagents and solvents with confined micro-environments and controllable reaction conditions. However, existing research almost is based mainly on the static properties of LMs without turbulent mixing, or basically perform LM-based microreactions with the encapsulation of all reagents in an individual reaction system; this limits the performance of LMs as microreactors, since mass transfer and molecular mixing are crucial for chemical engineering processing. The interactions between LMs vary depending on the properties of the coating particles and liquid encapsulated within them, particularly. LMs coalescence is one of the most essential manipulation schemes to functionalize microfluidics with an application like micro-mixing and microreaction. When two LMs are placed in contact, they will not coalesce naturally even pressed against each other. However, the surface deformation during collision will convert the kinetic energy to an accumulated impetus for triggering and even intensifying reaction processes. A number of techniques have been reported to collide LMs such as magnetic force and DC voltage. However, the coalescence that intensifies a microreaction in LMs is rarely reported. In this talk, we report a set of LMs which were multi-stimuli-responsive to light, electricity, ultraphonic and magnetism. Therefore, LMs-based microreactors can be manipulated in different ways accordingly. The effects of drop size and collision on both reaction rate and nanomaterials size were investigated by both theoretical calculation and experimental studies. This work opens the way to for expand the functions of LMs, and offers analysis tools to study the mechanisms of micromixing in a large variety of applications.

Designing hybrid nanocomposites of molybdenum disulphide/carbon nanomaterials

Zuzanna Bojarska[1], Marta Mazurkiewicz-Pawlicka[1], Monika Arasimowicz[2], Łukasz Makowski[1]

1 Faculty of Chemical and Process Engineering, Warsaw University of Technology, Waryńskiego 1, 00-645 Warsaw, Poland; 2 Centre of New Technologies, University of Warsaw, Banacha 2c, 02-097 Warsaw, Poland

**Corresponding author: 6701@pw.edu.pl*

Highlights

- Method of the producing MoS_2 nanoparticles on carbon nanomaterials has been developed.
- Effect of carbon materials on properties of the obtained composite was investigated.

1. Introduction

In recent years, remarkable interest has been focused on the 2D nanomaterials and their applications, due to their unique properties. Designing and manufacturing new nanostructures with improved properties using modern techniques is a tempting prospect for nanotechnology. One of the most famous 2D nanomaterials is graphene. It is an amazing material, which has a large theoretical specific surface area (2630 m^2g^{-1}), high intrinsic mobility (200 000 $cm^2v^{-1}s^{-1}$), high Young's modulus (~1.0 TPa) and thermal conductivity (~5000 $Wm^{-1}K^{-1}$). It also has very high optical transmittance (~ 97.7%) and good electrical conductivity. Graphene and its derivatives such as graphene oxide (GO) or reduced graphene oxide (rGO) are new nanomaterials that have recently found numerous applications, such as graphene-based electronic devices, catalysts, transparent conductive electrodes and others [1]. Similarly, molybdenum disulphide (MoS_2) is a widely used 2D nanomaterial. Molybdenum disulphide has a crystal structure consisting of layers of S–Mo–S where a layer of molybdenum atom is sandwiched by two layers of sulphur atoms. Individual layers of S–Mo–S are coupled together by weak van der Waals forces, which could move relatively easily against each other. Furthermore, MoS_2 is a widely studied semiconductor, with a large band gap of around 1.8 eV. Thanks to the above-mentioned properties MoS_2 found numerous applications such as a dry lubricant, in hydrogen evolution reaction catalysis, hydrogen storage and others [2]. In addition, MoS_2 can be an excellent candidate for being combined with carbon nanomaterials to obtain new hybrid nanocomposites with outstanding properties including higher photocatalytic activity, increase of the adsorption of pollutants, and improved rheological properties [3].

2. Methods

The aim of the conducted research was the preparation of hybrid nanocomposites formed from molybdenum disulphide and carbon nanomaterials such as graphene oxide (GO), reduced graphene oxide (rGO), graphene oxide modified with ammonia (GO-NH_3), and reduced graphene oxide modified with ammonia (rGO-NH_3). Graphene oxide was synthesized from graphite powder,

following modified Hummer's method [4]. Reduced graphene oxide was prepared by the chemical reduction method using a 50% hydrazine solution. Furthermore, GO and rGO materials were modified with ammonia solution, which led to the addition of nitrogen-containing groups in the structure. Molybdenum disulphide nanoparticles were synthesized in the turbulent micromixer with coaxial geometry, using ammonium molybdate tetrahydrate, citric acid and ammonium sulfide as the substrates for the reaction. Physicochemical analysis of obtained carbon nanomaterials and molybdenum disulphide was carried out, using various analytical techniques: Fourier-transform infrared spectroscopy, thermogravimetric analysis, X-ray Diffraction, elemental analysis, particle sizing analysis, and electron microscopy. Molybdenum disulphide/carbon materials hybrid nanocomposites were obtained by: a) mixing both materials in an ultrasonic bath, followed by an ultrasonic homogenizer, b) a precipitation process in the turbulent micromixer. The full analysis of the samples was carried out. In addition, the optical properties of the obtained nanocomposites were evaluated by UV-vis spectroscopy, following the degradation of methylene blue (MB) under solar-like irradiation and under UV irradiation.

3. Results and discussion

Reduction of GO leads to partial removal of oxygen groups from GO (the content of oxygen in GO was 43.71 wt.%, and in rGO was 17.51 wt.%). Modification of GO with ammonia resulted in an enrichment of the GO structure with nitrogen (from 0.58 wt.% to 3.67 wt.%). Modification of rGO with ammonia solution resulted in an enrichment of the rGO structure with nitrogen (from 0.00 wt.% to 0.53 wt.%). The dispersion using an ultrasonic bath, followed by an ultrasonic homogenizer is a good method to obtain hybrid MoS_2/carbon nanomaterials, which was confirmed by XRF and TGA method. The precipitation method that allows controlled heterogeneous nucleation of primary nanoparticles of MoS_2 on graphene particles still needs improvement, due to the excess of sulphur present in the final product. The conducted research has shown the hybrid nanocomposites have better photocatalytic activity toward the photodegradation of methylene blue compared to pure MoS_2.

4. Conclusions

The aim of the presented research was the preparation process of hybrid MoS_2/carbon nanomaterials. Carbon nanomaterials including graphene oxide, reduced graphene oxide, graphene oxide modified with ammonia, and reduced graphene oxide modified with ammonia have been tested for this purpose. The obtained hybrid nanomaterials possess both favorable features and disadvantages and still needs further research. Although, the degradation of MB tests allowed to state that the presence of the carbon nanomaterials in the hybrid materials improve photocatalytic activity.

This work was supported by the National Science Centre [No.2017/27/B/ST8/01382].

References

[1] S. Cravanzola, F. Cesano, G. Magnacca, A. Zecchina, RSC Adv. (2016) 59001–59008.
[2] Z. He, W. Que, Applied Materials Today (2016) 23-56.
[3] Y. Zhu, S. Murali, W. Cai, X. W. Li, J. Suk, J. Potts, Advanced Materials (2010) 3906-3924.
[4] L. Stobinski, B. Lesiak, A. Malolepszy, M. Mazurkiewicz, B. Mierzwa, J. Zemek, P. Jiricek, I. Bieloshapka, Journal of Electron Spectroscopy and Related Phenomenon (2014) 195, 145-154.

ECCE12
The 12th EUROPEAN CONGRESS OF CHEMICAL ENGINEERING
Florence 15-19 September 2019

Continuous synthesis and characterization of hydroxyapatite nanoparticles modified with lecithin

Joanna Latocha, Michał Wojasiński, Paweł Sobieszuk*

Warsaw University of Technology, Faculty of Chemical and Process Engineering, Warynskiego 1, Warsaw, Poland

**Corresponding author: Pawel.Sobieszuk@pw.edu.pl*

Highlights

- Y-shaped millireactor application to the continuous synthesis of hydroxyapatite
- Lecithin used as a surfactant to control the morphology of particles
- Synthesis provides carbonated hydroxyapatite with a spherical shape
- The aging temperature affects the particles size

1. Introduction

Hydroxyapatite (HAp) is the main inorganic part of human hard tissue (bones and teeth) [1]. Therefore synthetic HAp is a common material in regenerative medicine, particularly in bone tissue regeneration [2]. Those applications create a demand for new methods of HAp synthesis. Among all the methods for producing hydroxyapatite powders, synthesis in a continuous reactor seems to be a promising way to obtain better control over the reaction conditions. Production of hydroxyapatite nanoparticles using ultrasonic tubular microreactor, meso-oscillatory flow reactor, tube-in-tube microchannel reactor, among the others, has been reported in the literature [3]. We present results of HAp nanoparticles synthesis using a Y-type millireactor. For this purpose, we use 3D printing technology to produce a continuous reactor with 1 mm inner hydraulic diameter and 10 mm in length of the outlet channel. We investigated the influence of the lecithin concentration used in the synthesis and the aging conditions on the properties of the powders.

2. Methods

We synthesized hydroxyapatite in the presence of lecithin (HAp-LE) by chemical precipitation method using a solution of $Ca(NO_3)_2 \cdot 4H_2O$ and solution of $(NH_4)_2HPO_4$ in ultra-pure water as starting media [4]. Ca/P molar ratio was maintained at 1.67 as in a stoichiometric HAp. The synthesis was conducted in Y-shaped continuous reactor (1 mm inner hydraulic diameter and 10 mm in length of the outlet channel) under atmospheric pressure with each starting media flow rate of 500 ml/h. The resulting suspension of hydroxyapatite was aged in an aging reactor for 24 h at room temperature (RT) or at 60 °C, or directly centrifuged without aging (wa). After the aging process, the suspensions were centrifuged, washed with fresh water and then dried in an oven at 50°C for 24 h. Four different concentrations of lecithin were tested: 1, 3, 5 and 15 g/L in the reaction mixture. Resulting powders were characterized by X-ray diffraction (XRD), Fourier transformed infrared spectroscopy (FTIR), scanning electron microscopy (SEM), nanoparticle tracking analysis (NTA), dynamic light scattering (DLS) and zeta potential measurement.

Moreover, we implemented the method of Chemical Oxygen Demand (COD) analysis to the quantitative determination of lecithin concentration in powders.

3. Results and discussion

Results of investigation of phase purity (XRD) and chemical composition (FTIR) show that we obtained carbonated hydroxyapatite regardless of the aging conditions and the amount of lecithin used. COD measurements confirm predicted increase in the concentration of lecithin in the final product with an increasing concentration of lecithin used in synthesis. SEM images show structure consisting of spherical particles with size 10-25 nm. The sizing techniques used (NTA and DLS) demonstrate broad particle size distribution indicating particles agglomeration with sizes to about 500 nm in NTA and about 1 000 nm in DLS. The values of the zeta potential around –5 mV explain instability and tendency of particles to agglomerate. Of the parameters tested here, the aging temperature has the greatest influence on the final properties of the HAp-LE. An increase in aging temperature causes higher crystallinity, larger crystal size, and larger particle sizes. What is more, we obtain a minimum particle size depending on the lecithin concentration - for samples aged at room temperature with a lecithin concentration of 5 g/L (around 10 nm), and for samples aged at 60 °C and without aging with a concentration of 3 g/L (around 15 nm).

4. Conclusions

The continuous process of hydroxyapatite precipitation in a 3D-printed millireactor was achieved and the final products were characterized. We present a simple and low-cost method to produce spherical nanoparticles modified with lecithin. Among tested parameters, the aging temperature has the most significant influence on powders properties (size, crystallinity). The concentration of lecithin also has an influence on the size of the resulting HAp-LE particles. Therefore, we conclude that lecithin is an addition that permits control over the size of the obtained particles. Summarizing, when planning the production of hydroxyapatite using the proposed approach, it is essential to control the lecithin concentration and the temperature in the post-processing reactor.

Acknowledgements

Authors acknowledge funding within the project: “Innovative polymer composites for filling bone defects”-INPOLYBOND. NCBR/EC, Smart Growth Operational Program for 2014-2020 of European Regional Development Fund, (POIR.04.01.04.00-0133/15).

References

[1] S. Marković, L. Veselinović, M.J. Lukić, L. Karanović, I. Bračko, N. Ignjatović, D. Uskoković, Synthetical bone-like and biological hydroxyapatites: A comparative study of crystal structure and morphology, Biomed. Mater. 6 (2011) 1-13

[2] J. Lu, H. Yu, C. Chen, Biological properties of calcium phosphate biomaterials for bone repair: a review, RSC Adv. 8 (2018) 2015–2033.

[3] J. Latocha, M. Wojasiński, P. Sobieszuk, T. Ciach, Synthesis of hydroxyapatite in a continuous reactor : A review, Chem. Process Eng. 39, 3 (2018) 281-293

[4] J. Latocha, M. Wojasiński, K. Jurczak, S. Gierlotka, P. Sobieszuk, T. Ciach, Precipitation of hydroxyapatite nanoparticles in 3D-printed reactors, Chem. Eng. Process. - Process Intensif. 133 (2018) 221–233.

Controllable Preparation of Monodispersed ZrO_2 Nanocrystals Using High-Gravity Reactive Precipitation Combined with Solvothermal Treatment

Yi Xia[1,2], Dan Wang[1], Jie-Xin Wang[1,2,*], Jian-Feng Chen[1,2]

1 State Key Laboratory of Organic–Inorganic Composites; 2 Research Center of the Ministry of Education for High Gravity Engineering and Technology, Beijing University of Chemical Technology, Beijing 100029, PR China

**Corresponding author: wangjx@mail.buct.edu.cn*

Abstract

The controllable synthesis of monodisperse nanocrystals has attracted broad attentions because of their scientific and technological applications. In this study, a novel route was presented to controllably prepare transparent dispersions of monodispersed ZrO_2 nanocrystals with inexpensive inorganic zirconium salt under an acid aqueous surrounding by using high-gravity reactive precipitation in a rotating packed bed reactor combined with solvothermal treatment. By altering reaction conditions, the controllability for the crystalline forms from monoclinic to tetragonal phases, the average particle size from 3 to 20 nm, the shapes of sphere, rice, spindle, rod, and cube can be achieved. The as-prepared monodispersed ZrO_2 nanocrystals can be readily dispersed in many solvents including water, alcohols, esters, cycloalkanes, oils, etc, thereby forming highly-concentrated (>60 wt%), highly-stable (>18 months) and highly-transparent nanodispersions. Furthermore, highly transparent polyvinyl alcohol (PVA)/ZrO_2 and polystyrene (PS)/ZrO_2 nanocomposite films with high refractive index were conveniently prepared with a simple solution mixing route. The refractive index can be tuned from 1.53 to 1.75 (@ 589 nm) by changing the mass fraction (0-80 wt.%) of ZrO_2 in transparent nanocomposite films. It could be envisioned that such highly dispersed ZrO_2 nanocrystals would be potential in many areas including LED encapsulation, dental ceramics, solar cells, catalysts and so forth.

ECCE12
The 12th EUROPEAN CONGRESS OF CHEMICAL ENGINEERING
Florence 15-19 September 2019

Study of interfacial adhesion between a nanoparticle coated natural fiber and a thermoset matrix

German Díaz-Ramírez[1(*)], Enrique Mejía-Ospino[2], Rafael Cabanzo[3], Brayan Arenas[4], Ricardo Cruz[5]

1-5 School of Civil engineering, Universidad Industrial de Santander, Bucaramanga, Colombia; 1-2-4 Laboratory of atomic and molecular spectroscopy (LEAM), Universidad Industrial de Santander, Bucaramanga, Colombia; 3 Grupo de Investigación en Tomografía y Tecnologías Emergentes, Universidad Industrial de Santander, Bucaramanga, Colombia

**Corresponding author: german.diaz1@correo.uis.edu.co*

Highlights

- The study focuses on the Interfacial shear strength (IFSS) in polymer composites reinforced with natural fiber yarns
- This study proposes a quantitively method for the evaluation of the IFSS
- The results indicated that there is a relationship between the IFSS and the type of chemical treatment performed on the natural fibers
- The NaOH treatment and coating with reduced oxygen graphene (rGO) increase the IFSS to a thermoset matrix in 80 % approximately

1. Introduction

Recently, natural fibers (NF) used as reinforcement for polymeric and cementitious composites have gained interest among researchers in materials engineering, mainly due to their specific tensile properties, such as their elasticity modulus, low costs, sustainability, high socio-economic impact on farming communities and reduction of the environmental impact mostly generated by the use of inorganic fibers such as glass, asbestos or carbon [1], [2]. Fique *"furcraea macrophylla"* fibers are obtained from the leaves of an agave plant with the same name, they are similar to Brazilian sisal and Mexican henequen fibers. In Colombia, they are cultivated mainly in the Andean areas such as Santander, Antioquia and Nariño. [3]

One of the most important properties used to analyse the mechanical performance of polymer composites is the adherence between the phases (matrix and reinforcement), that property is also known as interfacial shear strength (IFSS). The performance of a polymer composite reinforced with NFs like fique, can be compromised in the medium to long term because of the hydrophilic behaviour of fibers; to evaluate the IFSS, both qualitative and quantitative methods are used, which lately seek to establish the efficiency of different treatments on NFs such the previously mentioned among others, one of the most accepted methods is the uniaxial pull-out test, which has been researched mainly on inorganic singular fibers because the for the ease and precision in carrying out the calculations. The main advantage of this method is that it is a quantitative method of direct measurement, which allows to evaluate in a more accurate way the mechanical composite performance. However, due to the irregularity in the geometry of NFs, both longitudinally and transversally directions, such as fique fibers, this type of experiment can yield results with high degrees of dispersion.

2. Methods

In this work, uniaxial pull-out tests using fique fibers yarns (multifilament fibers) [4] instead of singular fibers, is proposed. The influence of three different treatments: NaOH cationization, nanoTiO_2 and rGO fibers coating on the IFSS in a thermoset composite was evaluated. 5 specimens of each type of modification were tested. The initial length was 100 mm (±0.5 mm). The tensile tests were performed using 2 mm/min displacement speed and at room temperature (≈25º C). For the critical immersion length determination, fique yarns with 20, 15, 10, 5, 2 and 1 mm of immersion were tested. The IFSS were calculated for the different types of modified yarns and the influence of the treatments on the IFSS was analysed.

3. Results and discussion

The main purpose of the multifilament probes instead of singular fibers or filaments was to reduce the dispersion on the obtained data and adjust the results to the commercial products that are marketed in Colombia for the company "Coohilados del fonce". The tensile tests showed a maximum resistance between 374,5 and 433,8 MPa for the fique yarns, similar to other natural fibers as sisal or henequen [5,6]. Table 1 shows the results of maximum resistance, elasticity modulus and deformation percentage at break for fique fibers yarns.

Table 1. Tensile test results for fique yarns

Treatment	σ_{max}	E	ε_{break}
	MPa	GPa	%
Untreated	433,8 ± 81,2	13,0 ± 4,5	0,0272 ± 0,005
NaOH	400,8 ± 122,2	12,4 ± 2,3	0,0301 ± 0,007
NaOH + TiO2	374,5 ± 62,1	11,4 ± 2,8	0,0321 ± 0,003

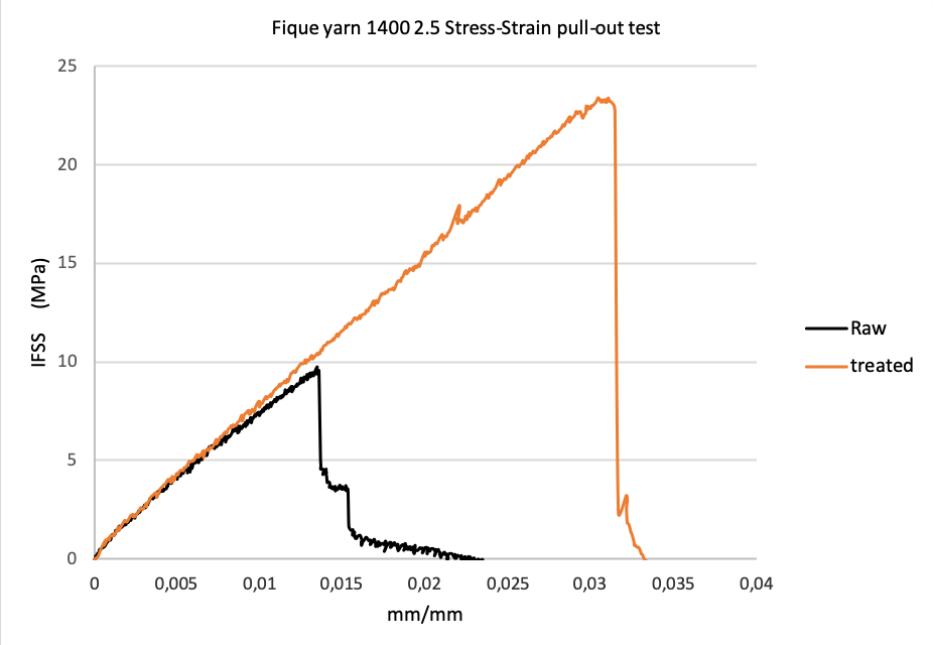

Figure 1. Interfacial shear strength vs strain tensile curve on raw and rGO coated fique natural yarns

The results from the uniaxial tensile test of IFSS are shown in Fig.1. The figure shows a typical IFSS stress strain curve, in this case obtained for the fique yarns tests, the curve indicates that the maximum IFSS stress for fique yarns increase from 9,75 MPa on raw fibers to 23,2 MPa on chemical treated fibers [7].

4. Conclusions

The results indicated that there is a relation between the IFSS and the type of treatment performed on the fique fibers, that is how fique fibers IFSS values increases with the treatments performed from 9,78 MPa for raw fique fibers to more that 20 MPa for the NaOH+rGO coated fibers average for the single fibers, assuming a circular cross section of 82 μm; for fique yarns the same values increase from 25, 5 MPa to 27,4 MPa, by calculating the cross section al area of 0,2278 mm^2 for raw yarns.

This study proposes the application of a direct measurement method of IFSS to achieve a more accurate evaluation of the interfacial adhesion properties for fique fibers and their derivate products.

References

[1] D. N. Saheb, J. P. Jog, D. Nabi Saheb, and J. P. Jog, "Natural Fiber Polymer Composites/: A Review,• *Adv. Polym. Technol.*, vol. 18, no. 4, pp. 351–363, 1999.

[2] K. H. Y. Cheung, "Natural fiber-reinforced polymer-based composites," *Nat. Fiber-Reinforced Biodegrad. Bioresorbable Polym. Compos.*, pp. 1–18, Jan. 2017.

[3] P. Gañán and I. Mondragon, "Surface modification of fique fibers. Effect on their physico-mechanical properties," *Polym. Compos.*, vol. 23, no. 3, pp. 383–394, 2002.

[4] A. Orue, A. Jauregi, J. Labidi, A. Eceiza, and A. Arbelaiz, •Composites/: Part B The effect of surface modifications on sisal fiber properties and sisal / poly (lactic acid) interface adhesion," *Compos. Part B*, vol. 73, pp. 132–138, 2015.

[5] S. Rocha, F. De Andrade, P. Roberto, L. Lima, R. Dias, and T. Filho, "Effect of fiber treatments on the sisal fiber properties and fiber – matrix bond in cement based systems," *Constr. Build. Mater.*, vol. 101, pp. 730–740, 2015.

[6] M. N. Cazaurang-Martinez, P. J. Herrera-Franco, P. I. Gonzalez-Chi, and M. Aguilar-Vega, "Physical and mechanical properties of henequen fibers," *J. Appl. Polym. Sci.*, vol. 43, no. 4, pp. 749–756, Aug. 1991.

[7] S. Zhandarov and E. Mäder, "Characterization of fiber/matrix interface strength: Applicability of different tests, approaches and parameters," *Compos. Sci. Technol.*, vol. 65, no. 1, pp. 149–160, 2005.

ECCE12
The 12th EUROPEAN CONGRESS OF CHEMICAL ENGINEERING
Florence 15-19 September 2019

Investigating Ion-Exchange Adsorption of Proteins through Experiments and Molecular Dynamics Simulations

Marine Tournois[1,*], Jérémy Esque[1], Isabelle André[1], Stéphane Mathé[1], Maria A. Fernandez[1]

1 LISBP, Université de Toulouse, CNRS, INRA, INSA, Toulouse, France

**Corresponding author: marine.tournois@insa-toulouse.fr*

Highlights

- The adsorption of α-chymotrypsin on SP Sepharose FF is investigated.
- The steric mass action model is used to describe single adsorption isotherms.
- MD simulations using all-atom models are performed.
- Results from MD simulations are in good agreement with macroscopic experiments.

1. Introduction

Chromatographic processes, especially Ion Exchange Chromatography (IEC), are extensively used in protein purification. However, their industrial scale-up remains under-optimized and is still based on empirical methods. Today, their cost represents up to 80-90% of the global cost for protein production. The protein adsorption on chromatographic media has been thoroughly investigated over the past decades, in terms of surface properties, influence of pH and/or ionic strength as well as protein characterization in single and multicomponent systems. The aim of this work is to better understand the binding mechanisms of proteins on adsorbents using Molecular Dynamics (MD) simulations. Indeed, MD simulations are a powerful tool and allow the study at the atomic level without requiring microscopic experimental techniques. The steric mass action (SMA) model [1], which accounts for the steric hindrance of the protein, is widely used to describe single adsorption isotherms and depends on different parameters such as the characteristic charge of the protein, the steric factor and the equilibrium constant. These parameters were obtained both experimentally and through MD simulations [2][3] for a protein (α-chymotrypsin) and a well-known resin (SP Sepharose FF) chosen as models. It allows validating the relevance of microscopic simulations to predict the protein adsorption behavior in adsorbents and then avoid long and costly experiences. This, in turns, enables simulation-based improvement of protein purification process which may have strong industrial impacts.

2. Methods

Experiments and molecular dynamics simulations were performed to study the ion-exchange mechanism from macroscopic and microscopic scales. Breakthrough curves measurements were performed by loading a protein solution, at controlled pH and ionic strength, into an IEC column, for determination of experimental adsorption isotherms. The SP Sepharose FF ionic capacity was also measured. Then, fitting of the experimental results by the SMA model allowed for the estimation of the characteristic charge, the steric factor and the equilibrium constant.

MD simulations were run using all-atom model [4]: a simulation box, containing the protonated protein (pH=5), the charged ligands (the agarose matrix is not represented), ions (Na^+ and Cl^-) and water molecules, was created. The protein is free to move in the box and the ligands are restrained to form a layer at the bottom. Then, long simulations (+100 ns) were performed with GROMACS 2018.3 simulation software and analyzed. Different starting orientations of the protein were also investigated and several simulations were run to obtain a reliable set of data.

3. Results and discussion

The results obtained through macroscopic experiments (presented in Figure 1.a) and microscopic simulations, especially the characteristic charge and the steric factor, were compared. Figure 1.b. shows an example of simulation box at initial conditions.

(a) (b)

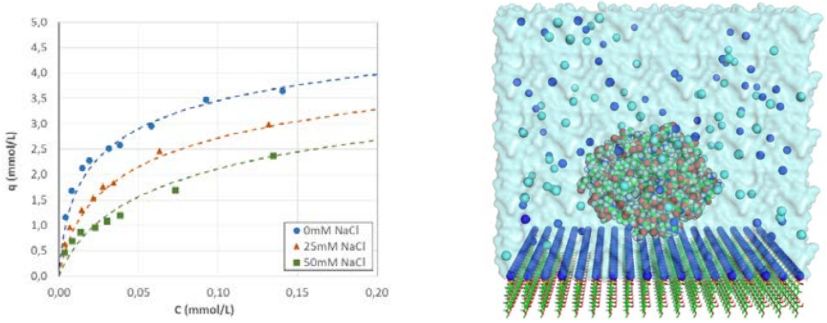

Figure 1. (a) Adsorption isotherms of α-chymotrypsin on SP Sepharose FF (pH=5): experiments vs SMA model (dotted line). **(b)** MD simulation box at initialization. Charged sites are represented at the bottom of the box (324 ligands); positively and negatively charged ions are colored in blue and cyan respectively.

All MD simulations led to an adsorption of the protein on the chromatographic surface, with exchange of Na^+ counter-ions, and the binding residues were also identified. Moreover, free binding energies of interaction were calculated and used to highlight the most favorable binding sites of α-chymotrypsin.

4. Conclusions

α-chymotrypsin and SP Sepharose FF were used to investigate the adsorption mechanism at the atomic scale, combining macroscopic experiments and MD simulations. The two parameters from the SMA model (charge and steric factor), obtained through the simulations, are in good agreement with those obtained from experiments. Thus, MD simulations seem to be a reliable tool to predict the protein retention with a chromatographic surface, in a single-component system. The influence of ionic strength, pH or ligand density is still under investigation, as well as the proteins behavior in multi-component system.

Acknowledgements

This work was granted access to the HPC resources on the TGCC-Occigen supercomputer and the Computing mesocenter of Région Midi-Pyrénées (CALMIP, Toulouse, France).

References

[1] C. A. Brooks, S. M. Cramer, AIChE J. (1992) 1969-1978.
[2] J. Liang, G. Fieg, F. J. Keil, S. Jakobtorweihen, Ind. Eng. Chem. Res. (2012) 16049-16058
[3] J. Liang, G. Fieg, S. Jakobtorweihen, Chem. Ing. Tech. (2015) 903-909
[4] F. Dismer, J. Hubbuch, J. Chromatogr. A (2010) 1343-1353

ECCE12
The 12th EUROPEAN CONGRESS OF CHEMICAL ENGINEERING
Florence 15-19 September 2019

Adsorption of elemental mercury from waste gases

Jonas Ambrosy[1], Christoph Pasel[1], Michael Luckas[1], Margot Bittig[2], Dieter Bathen[1,2]

[1]University of Duisburg-Essen, Chair of Thermal Process Engineering, Duisburg Germany

[2]IUTA Institute of Energy & Environmental Engineering, Duisburg, Germany

*Corresponding author: Jonas.ambrosy@uni-due.de

Highlights

- Thermodynamics of physical adsorption from 25 to 100 °C
- Determination of isosteric heats of adsorption
- Fitting of diffusion coefficients by mathematical modelling
- Investigation of chemical adsorption by temperature programmed desorption experiments

1. Introduction

Sources of mercury pollution such as coal-fired power plants, cement plants and waste incineration plants are subject to tightening of regulatory limits. In addition, a stronger focus is given to mercury emission from discontinuous processes e.g. in metal refining or crematoria. While in continuous processes, established technologies like absorptive gas scrubbing or flue gas adsorption are applied, for discontinuous emissions only fixed-bed adsorption with activated carbon is suitable from an economic point of view. For the design and optimization of such processes, a good knowledge of the adsorption thermodynamics and kinetics is necessary. Measurement of mercury adsorption is difficult because mercury is toxic, adsorbs chemically on the surface of many materials (e.g. metal surfaces of pipes and valves) and reproducible supply of mercury vapor requires thorough experimental care. Accordingly, only few data of mercury adsorption has been published.

The aim of this work is to better understand the mechanisms involved in the adsorption of mercury. This understanding particularly applies to the interactions of mercury with the surface of the adsorbents and the influence of the pore size distribution on equilibrium and kinetics.

2. Methods

The adsorption of Hg^0 from a N_2 carrier gas stream is studied on commercial activated carbons. Single and cumulative breakthrough curves are measured in a fixed bed at temperatures of 25 °C to 100 °C and mercury concentrations of 50 to 1000 µg/m^3. From the measured adsorption isotherms isosteric heats of adsorption are determined. In addition, desorption experiments are conducted to distinguish the contributions of physisorption and chemisorption. A dynamic simulation of experimental breakthrough curves yields diffusion coefficients which are discussed with respect to the concentration and temperature dependence of diffusion mechanisms in mercury physisorption. For detailed investigation of mercury chemisorption temperature programmed desorption (TPD) experiments employing activated carbon loaded with mercury are

carried out. During the experiments, the adsorbents are heated from 30 to 500 °C with a constant heating rate of 5 °C/min.

3. Results and discussion

The activated carbons AC 01 and AC 02 are good examples to investigate in detail the dynamics and equilibria during pure mercury physisorption. The measured equilibrium isotherms almost show Henry behavior. A significant increase in capacity is observed when temperature decreases and/or concentration increases. This pronounced temperature and concentration dependence is typical for physisorptive adsorption mechanisms. The calculated isosteric heats of adsorption of Hg^0 only amount to 50 % of the enthalpy of evaporation. This shows that the adsorption of Hg^0 is exothermic, but the interactions of mercury with the surface of the activated carbon are significantly weaker than the interactions between mercury atoms in the condensed mercury phase. This phenomenon can be explained by the strong forces in liquid mercury. At room temperature, liquid mercury forms strong van-der-Waals clusters, whose bonding energies lie between dispersion interactions and covalent bonds [1]. The experimental breakthrough curves can be described by dynamic simulations with good accuracy. The results demonstrate that surface diffusion is the rate-determining diffusion process. Surface diffusion of Hg^0 on the activated carbons exhibits no concentration dependence but a strong dependence on temperature typical for activated processes.

Both, physisorptive and chemisorptive mechanisms play a role in mercury adsorption on non-impregnated activated carbons AC 03 and AC 04. Ultimate analysis proves a high oxygen content of AC 03 and a high chlorine content of AC 04. The type and number of oxygen-containing functional groups are determined by Boehm titration. It is assumed in literature that the presence of oxygen-containing functional surface groups and chlorine favors chemisorption [2,3,4]. Therefore, TPD experiments are carried out to investigate the desorption kinetics and to obtain information on the surface chemistry of chemisorbed mercury. For AC 03, concentration peaks are detected in the temperature range from 120 to 350 °C, which can be assigned to individual functional oxygen groups. The results for AC 04 show a single peak at 420 °C and above. The reaction order and adsorption enthalpy can be determined by dynamic simulations.

4. Conclusions

The physisorptive and chemisorptive adsorption and desorption behavior of four commercial activated carbons was systematically investigated by experimental measurements and dynamic simulations.

References

[1] K. Sattler, Handbook of Nanophysics, Clusters and fullerenes, 2018.

[2] S. Krishnan, B. Gullett, W. Jozewicz, Sorption of Elemental Mercury by Activated Carbons, Environ. Sci. Technol., 1994.

[3] P. Sun, B. Zhang, X. Zeng, G. Luo, C. Li, H. Yao, C. Zheng, Deep study on effects of activated carbon's oxygen functional groups for elemental mercury adsorption using temperature programmed desorption method, Fuel Processing Technology, 2017.

[4] E. Olson, A. Azenkeng, J. Laumb, R. Jensen, S. Benson, M. Hoffmann, New developments in the theory and modeling of mercury oxidation and binding on activated carbons in flue gas, Fuel Processing Technology, 2009.

ECCE12
The 12th EUROPEAN CONGRESS OF CHEMICAL ENGINEERING
Florence 15-19 September 2019

Membrane separation of co-products in hydroaminomethylation reactions in thermomorphic multiphase systems

Stefan Schlueter[1], Annika Koenig[1], Bettina Scharzec[1], Jens Dreimann[2], Mirko Skiborowski*[1]

1 TU Dortmund University, Department of Biochemical and Chemical Engineering, Laboratory of Fluid Separations, Emil-Figge-Str. 70, 44227 Dortmund, Germany

2 TU Dortmund University, Department of Biochemical and Chemical Engineering, Laboratory of Industrial Chemistry, Emil-Figge-Str. 66, 44227 Dortmund, Germany

**Corresponding author: mirko.skiborowski@tu-dortmund.de*

Highlights

- Innovative separation of co-products by membrane filtration
- Applicability to aqueous and organic solvent systems
- Polyamide membranes favorable in aqueous solvent systems
- Low MWCO membranes required for separation in organic solvent systems

1. Introduction

Homogeneous catalysis offers high yields and selectivity at mild reaction conditions but requires the challenging separation and recovery of the valuable homogeneous catalyst. In previous work, it was shown that a combination of thermomorphic multiphase systems (TMS) and organic solvent nanofiltration (OSN) enables effective catalyst recovery in the hydroformylation of long chain olefins [1]. In this combination, a TMS of at least two solvents, which are homogeneous at high temperature in the reactor, forms a two-phase system at lower temperature. This system is first separated by a decanter into a catalyst-rich polar phase and a product-rich apolar phase, which is further processed by OSN to recover remaining catalyst and recycle it back to the reactor.

This contribution focuses on an alternative membrane-assisted TMS concept, which addresses the separation of polar co-products, such as water in hydroaminomethylation (HAM) reactions. Due to its high polarity water accumulates in the polar catalyst phase. Since this accumulation can influence the phase stability of the mixture and thereby negatively affect the reaction as well as the subsequent phase separation, the water content should be controlled. For this purpose, the implementation of a second pressure-driven membrane separation in the recycle stream is proposed. However, the specific type of membrane separation and membrane material selection depend on the TMS for the HAM. This consists of different solvents, depending on the substrates, which are two organic solvents, if the substrates are rather non-polar [2], or an organic solvent and water if more polar substrates are used [3]. In the case of an organic system, OSN is a possible choice, whereas reverse osmosis (RO) represents a suitable choice in case of the aqueous system. The current work presents the results of dedicated membrane-screening experiments for organic and aqueous solvent systems. For a range of solvents, which were selected based on literature data [2 - 4], a number of membranes were screened based on high rejection of the catalyst and selective water removal.

2. Methods

Concentrations of the catalyst and the co-product were estimated based on literature data and mass balances. Several commercially available membranes were selected. The experiments were conducted in cross-flow pressure cells. At least three different membrane sheets were measured for each membrane. For the organic system, dimethylformamide (DMF) and methanol (MeOH) as polar solvents were investigated, while a combination of water as the polar and 1-butanol (1-BuOH) as the non-polar solvent was investigated for the aqueous system. The applied ligands were the comparatively small triphenylphosphine (TPP) and tri-sulfonated triphenylphosphine (TPPTS), respectively.

3. Results and discussion

For the aqueous system, TPPTS rejections above 99% were measured for all membranes in water. Rejections decreased slightly when 1-BuOH was present in the mixture (Fig. 1a). Membranes made of polyamides are preferential for the selective separation of water since they combine a high rejection of TPPTS with a high rejection of 1-BuOH. Cellulose acetate membranes, however, show a negative rejection of 1-BuOH (Fig. 1b). For both membrane types, a high flux decrease was observed when 1-BuOH was present in the system (Fig. 1c). Based on the screening results a suitable PA membrane was identified and can be used for further investigations.

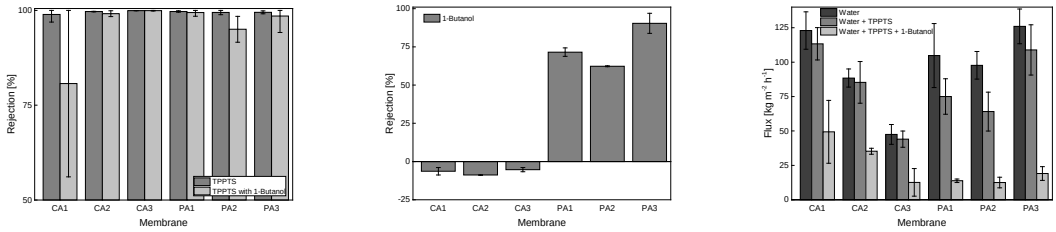

Figure 1. Rejection of TPPTS (a), rejection of 1-butanol (b) and total flux (c) for the aqueous solvent system. Feed pressure p_{Feed}=30 bar, ligand concentration w_{Ligand}=0.003 g g^{-1}, $w_{1\text{-}BuOH}$=0.04 g g^{-1}.

For the organic system, several commercial membranes were screened in a similar way. TPP rejections of 97% and higher were observed for a polyimide membrane with a molecular weight cut-off (MWCO) of 150 Da. The same membrane showed the best results in MeOH as well as DMF. Furthermore, selective water separation was possible with water rejections down to – 50%.

4. Conclusions

The current results show high prospect for the realization of the targeted co-product separation in HAM reactions in aqueous and organic solvent mixtures. Different OSN and RO membranes were suitable in the corresponding solvent systems. High catalyst rejections and selective water separation were achieved leading to a feasible process concept. Further investigations will focus on the implementation of the membrane separation into a continuously operated miniplant.

References

[1] J. Dreimann et al., Ind. Eng. Chem. Res. 56 (2017) 1354–1359.
[2] A. Vorholt et al., Eur. J. Lipid Sci. Technol. 119 (2017) 1600211.
[3] T. Faßbach et al., Adv. Synth. Catal. 360 (2018) 1473-1482.
[4] A. Vorholt et al., Chem. Ing. Tech. 85 (2013) 1540-1547.

ECCE12
The 12th EUROPEAN CONGRESS OF CHEMICAL ENGINEERING
Florence 15-19 September 2019

Experimental and modelling approach for the optimal design of a hydrogen permeation process in a gas-Ni-Na system

Pietro Brazzale[1], Aurélien Chassery[1], Thierry Gilardi[1], Christian Latgé[1], Xuan Meyer[2], Xavier Joulia[2]

1 CEA, DEN, Cadarache, DTN, F-13108 Saint-Paul-lez-Durance, France

2 Laboratoire de Génie Chimique, Université de Toulouse, CNRS, INP, UPS, Toulouse, France

**Corresponding author: pietro.brazzale@cea.fr*

Highlights

- Hydrogen introduction inside a liquid sodium loop by permeation through a Nickel membrane
- Set up of an experimental facility for the process analysis and validation
- Measurement of the stationary hydrogen permeation flux through the membrane
- Experimental and modeling approach
- Data reconciliation

1. Introduction

In the framework of SFRs (Sodium Fast Reactors), the contamination of the liquid sodium circulating in the secondary circuit with tritium produced in the core is one main process issue. In order to capture and recuperate this tritium, a certain amount of hydrogen dissolved in liquid sodium is necessary. Until now, the hydrogen is produced by steel corrosion and by hydrazine decomposition inside the steam generator, then it diffuses to sodium through the steel walls; to better control the hydrogen concentration, an external and independent process to introduce safely and in a controlled way a hydrogen flux into liquid sodium is necessary.
The permeation through a Nickel dense membrane has been individuated as the most suitable technical solution. Hydrogen permeation through Nickel has been widely studied when a gas phase is present on both side of the membrane [1]–[4]and some applications based on Nickel membranes were developed for SFRs to detect the hydrogen content inside sodium [5]. However, a more detailed study on hydrogen transfer from a gas phase to liquid sodium is necessary, considering not only the permeation through a Nickel membrane but also the mass transfer inside gas and sodium phases as main influential phenomena.

2. Experimental results

In this study, a device constituted by four Nickel tubular membranes (or “permeator”) is designed to transfer a continuous hydrogen flux from a gas mixture (Ar+H_2 at 3% molar) circulating inside the tubes to the external side of the tubes (shell) by permeation. The permeator is installed on a closed sodium loop, with the capability to purify sodium and to warm it up to a temperature of 450 °C. The permeator is tested at different temperatures, gas pressures and flowrates in order to obtain different hydrogen permeation fluxes, depending on the operating conditions. It is tested both in a gas-gas configuration (i.e. shell maintained under vacuum) and in a gas-sodium configuration (i.e. sodium circulating inside the shell), in order to identify the sodium resistance effect on the global hydrogen mass transfer.

Measurements of the main process parameters (pressure, temperature, flowrate) are carried out, as well as a hydrogen concentration measurement on the gas retentate side by a gas chromatograph. Moreover, a measurement of hydrogen concentration inside the sodium loop takes place, by means of a second Nickel membrane coupled to a mass spectrometer.
A data reconciliation method is applied to adjust the values of raw measurements, taking into account the system redundancy and the instrumentation uncertainties, in order to generate reconciled data which satisfy the hydrogen mass balance.

3. Simulation results

Under the hypothesis of steady state conditions, a simplified model of the permeator is set up in COMSOL Multiphysics®, as an instrument supporting the experience design. It includes the permeation Richardson's law[6] for the Nickel membrane, the hydrogen mass balances and the convective mass transport into the gas and liquid sodium phases. Thanks to this model, preliminary results can be produced by simulating the overall process.

4. Conclusions

The reconciled data allow comparing the calculated and the experimental hydrogen permeation flux under given operating conditions. Therefore, it is possible to validate the main hypotheses at the basis of the model and to evaluate the real influence of the operating parameters on the permeation.

References

[1] R. W. Webb, 'HYDROGEN PERMEATION THROUGH METALS', *Other Information: Orig. Receipt Date: 31-DEC-64*, 27-Apr-1964. [Online]. Available: https://digital.library.unt.edu/ark:/67531/metadc865810/. [Accessed: 12-Dec-2017].

[2] J. K. Gorman and W. R. Nardella, 'Hydrogen permeation through metals', *Vacuum*, vol. 12, no. 1, pp. 19–24, Jan. 1962.

[3] W. M. Robertson, 'HYDROGEN PERMEATION, DIFFUSION AND SOLUTION IN NICKEL.', *Z. Fuer Met. Res. Adv. Tech.*, vol. 64, no. 6, pp. 436–443, 1973.

[4] A. K. Altunoglu, N. S. J. Braithwaite, and D. M. Grant, 'A Study of Hydrogen Trapping in Cold-Worked Pure Nickel and Nickel-Thoria by a Pressure Modulation Technique*', *Z. Für Phys. Chem.*, vol. 181, no. 1–2, pp. 133–141, 1993.

[5] D. R. Vissers, J. T. Holmes, L. G. Bartholme, and P. A. Nelson, 'A Hydrogen-Activity Meter for Liquid Sodium and Its Application to Hydrogen Solubility Measurements', *Nucl. Technol.*, vol. 21, no. 3, pp. 235–244, Mar. 1974.

[6] O. W. Richardson, J. Nicol, and T. Parnell, 'I. The diffusion of hydrogen through hot platinum', *Lond. Edinb. Dublin Philos. Mag. J. Sci.*, vol. 8, no. 43, pp. 1–29, Jul. 1904.

ECCE12
The 12th EUROPEAN CONGRESS OF CHEMICAL ENGINEERING
Florence 15-19 September 2019

Influence of Fiber Diameter Distribution on the Filtration Performance of Depth Filter.

Kevin Hoppe[1,2], Lukas Wischemann[2], Gerhard Schaldach[2], Dirk Renschen[3], Markus Thommes[2], Damian Pieloth[1,2]

[1] University of Applied Science Köthen, 06366 Köthen, Germany; [2] TU Dortmund University, Laboratory of Solids Process Engineering, 44227 Dortmund, Germany; [3]DMT GmbH & Co.Kg, 45307 Essen, Germany

*Corresponding author: kevin.hoppe@hs-anhalt.de

Highlights

- Modeling of filtration performance of depth filter
- Investigation of fiber diameter distribution of depth filter media
- Influence of fiber diameter distribution on pressure drop and filtration efficiency
- Improved prediction of filtration performance

1. Introduction

The separation of particles from gas streams having low to medium loadings is an essential task in various civil (e.g. cabin air filters) or industrial (e.g. particulate air filter for clean rooms in aseptic production areas) applications. A high efficiency combined with a low pressure drop is desired to realize cost- and energy efficient separations. For the task of optimization the filter media, knowledge about the connection of macroscopic parameters of fibrous depth filter (e.g., pressure drop and filtration efficiency) to their microscopic properties (e.g., fiber diameter distribution or porosity) is evident [1]. In recent simulations, the fiber diameter distribution (FDD) within the filter media is often neglected and replaced by a medium or averaged value [2]. In this work, the impact of this parameter is in focus.

2. Methods

The FDD of a fine filter (F7, Trox GmbH, Neunkirchen-Vluyn, Germany) based on glass fibers (Filter A) and a coarse dust filter (TH 300-T2, Afprofilter GmbH, Bönen, Germany) based on polyester fibers (Filter B)were investigated using scanning electron microscopy (SEM), (H-S4500 FEG, Hitachi High Technologies Europe, Krefeld, Germany). The FDD was analyzed by digital image analysis. For that purpose, the open source software diameterJ [3] was used. 24 SEM-images of each material at clean- and raw-gas side were considered and the fiber diameter at around 20.000 positions in each image was evaluated. Those data were implemented in an in-house developed model for calculation filtration performance which is computed using Matlab (Matlab 2016a, The Mathworks, Nivack, USA). Filtration performances were measured according to the VDI 3926 using aluminum oxide as test dust (Pural NF, Sasol, Brunsbüttel, Germany).

3. Results and discussion

The FDD of both considered filter media was obtained by digital image analysis. The spans of the distributions, as well as the medium fiber diameter (MFD), were derived from these data. Since no significant deviations between the raw- and clean-gas sides were found, a constant FDD inside the filter was assumed for calculations. Calculations of the filtration efficiency were carried out and results are compared for using the MFD and the FDD (figure 1). A high influence of the FDD on the calculation of the filtration efficiency can be figured out. It is shown that implementing the FDD increases the calculated filtration efficiency (up to more than 50%) in comparison to using the MFD. Furthermore, it was found that this parameter becomes more significant in the region were inertial deposition of the dust can be assumed than in the diffusional dominate region at smaller particle diameter. Also, an influence on the pressure drop was figured leading to higher values for both filter media by considering the fiber diameter distribution. A comparison to experimental data results in an improved prediction of filtration efficiency. This emphasizes the importance of this parameter regarding investigating the filtration of particles in fibrous depth filter.

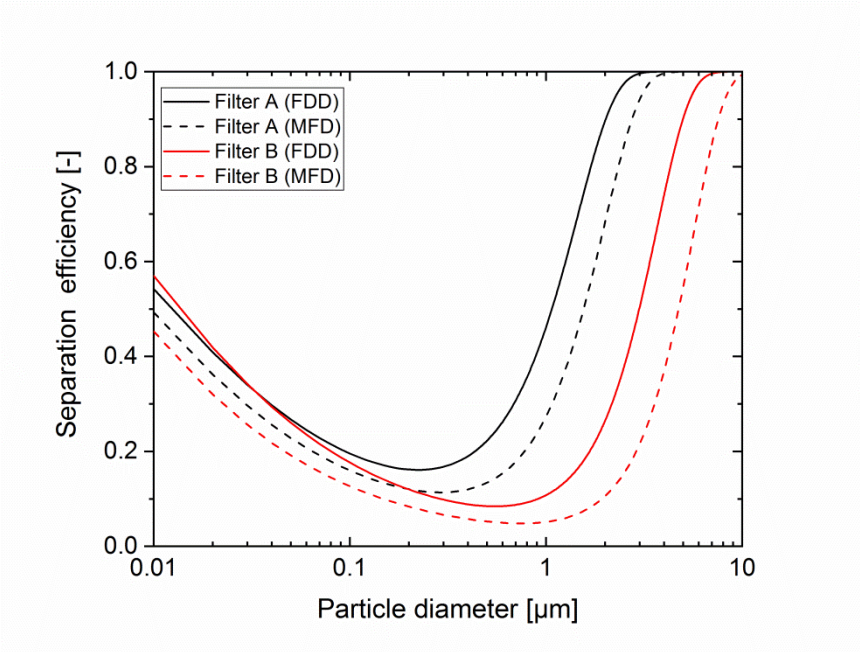

Figure 1. Calculation of filtration efficiency with and without considering the fiber diameter distribution

4. Conclusions

The FDD of two fibrous depth filter media were successfully determined combining SEM and digital image analysis. The influence of that parameter was theoretical investigated, implemented into an in-house developed model and compared with experimentally determined filtration efficiencies and pressure drops. From those results the importance of considering these data in modeling the filtration efficiency was emphasized.

References

[1] F. Theron, E. Lys, A. Joubert, F. Bertrand, L. Le Coq, Powder Technology 320 (2017), 295-303.
[2] S.A. Hosseini, H.V. Tafreshi, Powder Technology 201 (2010), 153-160.
[3] N.A. Hotaling, K. Bharti, H. Kriel, C.G. Simon, Biomaterials 61 (2015), 327-338.

Novel design of magnetophoretic microdevices for extracorporeal sepsis treatment

Cristina González-Fernández*, Jenifer Gómez-Pastora, Eugenio Bringas, Inmaculada Ortiz

Chemical and Biomolecular Engineering Department

ETySIIT, University of Cantabria, Avda. De los Castros, 39005, Santander, Spain

**Corresponding author: gonzalezferc@unican.es*

Highlights

- Magnetic bead separation from human whole blood is analyzed
- CFD approach is used for modeling magnetic bead magnetophoresis from blood
- Effect of fluid flow rates in the recovery of magnetic beads is modeled
- We report the rational design of magnetophoretic microfluidic devices

1. Introduction

The removal of disease-causing agents from bloodstream is considered to be the most direct conceivable treatment for infectious illness such as sepsis. In this regard, the coupling of functionalized magnetic microparticles and continuous flow microfluidic devices has attained outstanding attention for the extracorporeal toxin and pathogen isolation from blood. The laminar flow pattern developed in microfluidic devices allows co-flow of parallel streams with stable interface, while the magnetic beads provide the selective adsorption of the target substance on their surface and promote their recovery by external magnetic fields generated by rare-earth magnets [1, 2]. Nevertheless, the performance of such magnetophoretic-microfluidic devices has not been addressed yet because of the complexity of their mathematical description.

2. Methods

The current study presents both the experimental and computational based design of a two-phase continuous-flow extracorporeal magnetic blood cleansing microdevice for maximizing bead recovery while keeping impaired blood quality. In such system, a suspension (0.2 $g{\cdot}L^{-1}$) of fluorescent magnetic microparticles (4.9 µm) in Human Whole Blood (HWB) and a buffer solution are continuously injected through different inlets of a Y-Y shaped glass microchannel. The deflection of the particles and their collection in the buffer stream is achieved through the application of an external magnetic field by a permanent rectangular (10 x 5 x 3 mm^3) neodymium (NdFeB) magnet parallel to the microchannel. Experimentally, the use of fluorescent beads allows the quantification of the particle recovery by fluorescence microscopy, using a custom Matlab code for image analysis. For the numerical analysis, a Computational Fluid Dynamics (CFD)-based Eulerian-Lagrangian approach, using the commercial software FLOW-3D, linked to a Fortran code for magnetic field and forces calculations was employed. The numerical method reported here involves magnetic and fluidic models that describe the motion of the beads and can be used to

study critical details of the separation process, including the trajectories of individual particles and the stability of the blood/buffer interface.

3. Results and discussion

The complete bead recovery and fluids separation at the channel outlet requires a careful study of both magnetic and fluidic forces. For that purpose, a dimensionless number (J) that relates the variables that affect such forces (i.e. bead and fluids properties, magnetic field applied, selected flow rates) was employed.

The influence of fluids flow rates on both flow patterns and capture efficiency of the microseparator, expressed as particle recovery, is illustrated in Fig. 1. Because of the rheological properties of HWB, low flow rates of approximately 0.005 $\mu L \cdot s^{-1}$ are required to obtain high recovery (higher than 90%). This flow rate leads to similar values of magnetic and fluidic forces (J-value of 1.2) and corresponds to an average velocity of 0.65 $mm \cdot s^{-1}$ and a residence time of 3s, which is low enough to prevent diffusion of blood components to the buffer stream, thus ensuring that these low flow rates can be safely used since the properties of the blood are not affected. The experimental results fitted adequately to simulated data provided by the theoretical model (error lower than 10%).

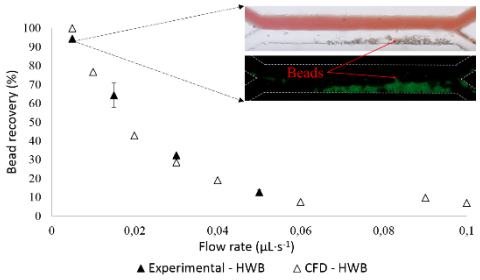

Figure 1. Magnetic bead recovery (experimental and theoretical approaches) from human whole blood as a function of the applied flow rate.

The improvement of the system performance requires the treatment of high contaminated blood volumes. Thus, several channel lengths (2, 5 and 10 mm) and cross sections were computationally tested in order to find the best geometrical conditions that allow the use of higher flow rates while achieving high bead recovery.

4. Conclusions

The theoretical and experimental methodology developed in this work provide insight into the design of magnetophoretic-microfluidic devices for biomolecules separations and can be adapted to a broad range of magnetically-enabled microfluidic applications.

Acknowledgements

Financial support from the Spanish Ministry of Economy and Competitiveness under the projects CTQ2015-72364-EXP/AEI and CTQ2015-66078-R is acknowledged. C. González-Fernández thanks the Concepción Arenal postgraduate research grant from the University of Cantabria.

References

[1] I. K. Herrmann, A. A. Schlegel, R. Graf, W. J. Stark, J Nanobiotechnol, 13 (2015) 49
[2] J. Gómez-Pastora, E. Bringas, M. Lázaro-Díez, J. Ramos-Vivas, I. Ortiz, in: From Materials to Medical Devices: Drug Delivery Systems, World Scientific, 2017.

Ultrafiltration of Protein Based Solution. Study of Selectivity and Protein Conformation.

Simona M. Miron, Patrick Dutournié, Arnaud Ponche

Institut de Science des Matériaux de Mulhouse (IS2M), UMR 7361 CNRS, Université de Strasbourg, Université de Haute Alsace, 3 bis rue A. Werner, 68098 Mulhouse Cedex, France

**Corresponding author: simona-melania.miron@uha.fr*

Highlights

- Membrane hydraulic and selectivity properties modified by lysozyme
- Lysozyme suffers changes in the hydrodynamic radius after filtration
- Denaturated form of lysozyme present after filtration

1. Introduction

With a growing market for them, proteins are intensively used in industry where they undergo different operations of separation, concentration and purification. A classical process used for such necessities is the membrane process.

Membrane processes use mild conditions of operation, have low energy consumption, no need for additives and can operate continuously. A key point to all the mentioned advantages is the possibility to modify the membrane properties to fit the need or demand of the industry. Thus, depending on the final outcome of the industry, membrane processes can give higher quality of the processed products. Nevertheless, membrane processes performances can be jeopardized by membrane fouling. Membrane fouling is a phenomenon in which, molecules from the liquid phase start to deposit or adsorb at the surface of the membrane or inside its pores. Fouling influences the membrane performances and in consequence, can affect the outcome of the process - economically and quality.

Our work consists in analyzing how proteins behave in membrane processes taking into account the evolution of the membrane performances and the transformation of the protein molecule.

2. Methods

Filtration of protein solutions was performed in a laboratory pilot-plant [1] using a tubular, ceramic asymmetric ultrafiltration membrane. In order to focus on the effect of the constrains generated by the change in pressure, temperature and flow rate are maintained constant.

The membrane performances after protein filtration were asset by determination of the selectivity (rejection rate) and of the hydraulic properties (permeability) using a neutral solution of Vitamin B12.

The possible change of the protein conformation after filtration was asset by High Performance Liquid Chromatography (HPLC) study, an analysis based on size-exclusion.

3. Results and discussion

A pre-established sequence of filtration was used in the current work as presented in Table 1. Between the lysozyme filtration tests series, neutral solution of Vitamin B12 followed by pure water filtration were performed to analyze the evolution of the membrane performances. It was found that the selectivity of the membrane increase with each filtration test while the permeability decreases. This behavior is specific to the phenomenon of adsorption. Thus, the lysozyme molecule could be adsorbed at the surface of the membrane or in the pores of the membrane. Further tests confirm this hypothesis.

Table 1. Sequence of filtration test with respective concentration, observed rejection rate and hydraulic permeability

Protein Solution	**Concentration (mM)**	**R max (%)**	**Lp ($10^{-14}m^3.m^{-2}_{memb}$)**
VB12	9,22E-03	40	5.7
Lysozyme I	0,025	90	4.7
Lysozyme II	0,025	95	4.5
Lysozyme III	0.025	97	4.0
VB12	9,22E-03	73	4.0

Analyses on the retentate (fraction of the feeding solution rejected by the membrane) and permeate (fraction of the feeding solution passing through the membrane) by HPLC confirm the change of the hydrodynamic radius of the molecule after passing through the membrane. Peak fitting performed on the HPLC chromatograms shows the different forms of lysozyme present in the permeate (native and denaturated) as opposed to the retentate, which shows only one form (native).

4. Conclusions

The current study gives a frame on the evolution of the membrane properties when using a protein solution, taking into account the protein behavior after filtration. The study confirms the adsorption of the lysozyme molecule in the pores, while making a further observation on the change of the protein molecule after filtration.

References

[1] J. Bikai, L. Limousy, P. Dutournie, L. Josien, W.Blel, C. R. Chim. 18 (2015) 56-62.

Mass Transfer in Bacterial Cellulose Synthesis and Their Use as Oxygen Vectors in Bioreactors

Tanase DOBRE

University Politehnica of Bucharest, Department of Chemical and Biochemical Engineering,

Bacterial Cellulose (BC) is a very interesting biodegradable biopolymer with very important mechanical, physical and chemical properties. It is a versatile polymer that could be changed or by biosynthesis or after that. It could also be used to obtain composite materials. B C and its composites are currently being studied for use in various biomedical applications, but bacterial cellulose shows considerable potential for other technical applications as well, electronic paper, transparent composites, conductive and resistive membranes, bio molecularly imprinted polymers, special membranes, etc. Most of these applications are still looking. In this work it is given results which show the use of the specific methods of chemical engineering in many directions characterizing the synthesis and use of bacterial cellulose. For synthesis of the bacterial cellulose he attracted attention with several statistical models developed to identify the culture medium composition and the operating conditions to have static reactors in work with good productivity [1]. The importance of oxygen transfer is not completely elucidated. Here, in BC synthesis the simplex regular method is illustrated for optimization of drum reactor where the process kinetics depend of over 6 factors . The problem of swelling of membranes and composites based on bacterial cellulose, contained in some proper work [2, 3], is analyzed using a new model, capable of finding the most common models. In intensification of oxygen transfer in aerobic bioreactors various strategies has been used in order to obtain a good efficiency of aerobic fermentation processes. The paper focuses on studies concerning the influence of solid carrier addition in the liquid phase on oxygen volumetric mass transfer coefficient in a stirred and aerated tank bioreactor. The selected oxygen carriers (vectors) can be easily separated and they have no harmful effect on the microbial population implied in bioprocesses. Fine particle of activated carbon, silicon oil impregnated activated carbon, bacterial cellulose, magnetite, and bacterial cellulose-magnetite composite were used as oxygen-vectors. An enhancement of oxygen transfer was indicated by an increase in volumetric mass transfer coefficient, k_la, which was determined by a dynamic method. A significant improvement of oxygen mass transfer in the presence of magnetite and bacterial cellulose-magnetite composite was highlighted. Important correlations was obtained. The experiments of aeration of active mud from polluted water shows that the biocellulose magnetite composite improves the efficiency of this bioreactor types.

References

[1] Dobre T.,Anicuta Stoica, Oana Parvulescu, Marta Stroescu, Iavorschi G., *Factors influence in bacterial cellulose growth in static reactors*, Rev. Chim (Bucharest), 59,5, 1092-1100, 2008

[2] Anicuta Stoica-Guzun, Marta Stroescu, Jinga I. S., Iuliana Jipa, Dobre T., *Microwave assisted synthesis of bacterial cellulose- calcium carbonate composites*, Ind. Crop Prod, 3, 414-422, 2013

[3] Chiciudean T. G., Anicuta Stoica, Dobre T., M van Torren *Synthesis and characterisation of poly(viny alchool)-bacterial cellulose composites*, UPB Sci. Bull., Series B, 2,73, 17-30, 2011

[4] Dobre T., Brandusa Sandu Ohreac, Oana Parvulescu, Danciu T., *Effect of sollid carriers on oxygen mass transfer in a stirred tank bioreactor*, Rev.Chim (Bucharest), 65,4, 489-496, 2014

Modelling and characterization of electrodialysis systems for multi-ionic solutions.

Antonino Campione[1], Andrea Cipollina[1], Luigi Gurreri[1], I. David L. Bogle[2], Michele Tedesco[3], Alessandro Tamburini[1], Giorgio Micale[1]

1 Dipartimento di Ingegneria, Università degli Studi di Palermo, viale delle scienze ed. 6, 90128 Palermo, Italia; 2 Centre for Process Systems Engineering, Department of Chemical Engineering, University College London, Torrington Place, London WC1E 7JE, UK; 3 Wetsus, European Centre of Excellence for Sustainable Water Technology, Oostergoweg 9, 8911 MA Leeuwarden, The Netherlands

**Corresponding author (A. Cipollina): andrea.cipollina@unipa.it*

Highlights

- Modelling of electrodialysis for multi-ionic solutions.
- Estimation of multicomponent membrane properties.
- Assessment of membrane properties effect on multi-ionic systems

1. Introduction

Membrane desalination processes play a crucial role in the current scenario of drinking water production. In particular, electrodialysis (ED) is currently spreading as a viable alternative to other membrane desalination processes, so that plenty of modelling and simulation works have been published in the last few years [1–3]. However, most of modelling and experimental works assume that the feed solution contains dissolved NaCl only. In fact, real feeds always contain additional ions that can substantially affect process performances [4].

When multiple ions systems have to be modelled, the estimation of a much larger number of parameters related to membrane properties is required. Therefore, in this work a simplified approach for the modelling of an ED system operating with multi-ionic solutions is presented. The main parameters required to fully characterize the system and the criticalities arising in their experimental determination are highlighted. In particular, salt diffusion permeability, membrane resistance and transport numbers are discussed.

2. Methods

A hierarchical semiempirical model for ED process operating with multicomponent solutions is developed. The low-hierarchy of the model (i.e. the cell pair) has a one-dimensional structure and incorporates the main transport phenomena occurring through membranes. Each ion flux is described, accounting for the salt back diffusion as well as for water transport. In addition, cell pair voltage is estimated through both Ohmic (i.e. membrane and channels resistances) and non-Ohmic (i.e. membrane potential) contribution. Particular attention is given to the expression of the membrane potential that changes significantly compared to the single-salt scenario. The high-hierarchy model (i.e. the stack) links a series of cell pairs with the electrodes and it is devoted to computing the main performance parameters (i.e. energy consumption, current efficiency, water productivity…). In addition, a geochemical database (PHREEQC, *USGS*) is used for the estimation of

the main thermodynamic parameters, such as activity coefficients, conductivities and saturation indexes of potential solid phases.

Empirical information on membrane properties are purposely collected via laboratory-test rigs: (i) salt diffusion permeability is estimated through batch diffusion dialysis experiments; (ii) membrane resistance is assessed via indirect measurement through an ED stack equipped with only one type of membrane (either anion or cation exchange membrane).

Finally, membrane transport numbers have been estimated through ED measurements according to Hittorf's method [5].

3. Results and discussion

Figure 1 shows, as an explanatory example, simulation results for an ED unit fed with a NaCl, $MgCl_2$ and $CaCl_2$ ternary solution. A preliminary estimation of transport numbers and diffusion permeabilities is used as simulation input. The figure shows the concentration profile of the cations along the channel length. It is worth noting how the membrane properties can strongly affect the magnitude of each ion removal, resulting in this case in a much larger removal of sodium ions.

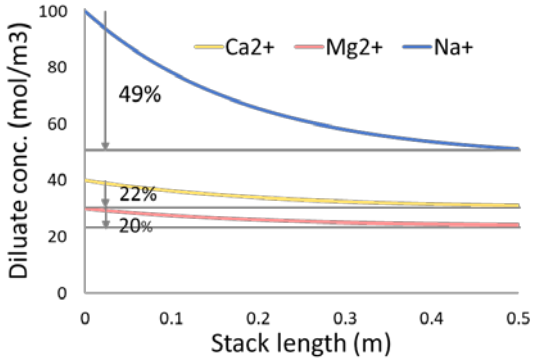

Figure 1. Concentration profiles inside a 0.1 x 0.5 m^2 electrodialysis stack desalinating a solution containing Na^+, Mg^{2+}, Ca^{2+} and Cl^-. Channels 270 µm thick, 2A current, 1 cm/s flow velocity. Transport numbers in cation exchange membrane: 0.25 (Ca^{2+}), 0.15 (Mg^{2+}), 0.55 (Na^+) and 0.05 (Cl^-). Transport numbers in anion exchange membrane: 0.01 (Ca^{2+}), 0.01 (Mg^{2+}), 0.03 (Na^+) and 0.95 (Cl^-). Salt diffusion permeability are assumed equal to $4 \cdot 10^{-12}$ m^2/s for each salt.

4. Conclusions

The development of an efficient simulation tool for multi-ionic ED results into the possibility of estimating the effect of multiple components in the feed solutions. The effect of the characterization-parameters as the membrane properties is crucial for a reliable prediction of the system performance, thus justifying the need for properly estimating them.

References

[1] N. C. Wright, S. R. Shah, S. E. Amrose and A. G. Winter, *Desalination*, 2018, **443**, 27–43.

[2] B. A. Qureshi and S. M. Zubair, *Desalination*, 2018, **430**, 197–207.

[3] A. Campione, A. Cipollina, I. D. L. Bogle, L. Gurreri, A. Tamburini, M. Tedesco and G. Micale, *Desalination, 2019 (under review).*

[4] J. Moreno, V. Díez, M. Saakes and K. Nijmeijer, *J. Membr. Sci.*, 2018, **550**, 155–162.

[5] C. Larchet, L. Dammak, B. Auclair, S. Parchikov and V. Nikonenko, *New J. Chem.*, 2004, **28**, 1260.

ECCE12
The 12th EUROPEAN CONGRESS OF CHEMICAL ENGINEERING
Florence 15-19 September 2019

On the potential of adsorption processes for low-carbon hydrogen production with carbon capture

Anne Streb[1], Mijndert van der Spek[1], Matteo Gazzani[2], Marco Mazzotti[1*]

1 ETH Zurich, Zurich/Switzerland; 2 Utrecht University, Utrecht/the Netherlands

**Corresponding author: marco.mazzotti@ipe.mavt.ethz.ch*

Highlights

- Adsorption processes developed for the simultaneous production of H_2 and CO_2
- Process intensification achieved: single stage for two separation tasks
- Competitive energy consumption
- Suitable for a variety of multicomponent feedstreams

1. Introduction

Carbon neutral hydrogen is expected to play an important role in future energy systems, especially in industry, transportation and heating applications. Today, hydrogen is used at large scale in many industrial processes, e.g. ammonia and methanol production and oil refining. However, it is mainly produced through conversion of fossil fuels, e.g. via steam methane reforming (SMR) followed by water gas shift (WGS) and pressure swing adsorption purification (PSA), resulting in high CO_2 emission intensity. Adding carbon capture and storage (CCS) to fossil fuel based H_2 production is a means to produce large amounts of low-carbon H_2 in a timely manner thereby paving the way towards an energy system where H_2 plays a pivotal role as low carbon energy carrier. We have developed a promising process integrating both H_2 purification and CO_2 separation within a single adsorption cycle. This option does not require an additional separation stage potentially reducing capital cost and energy requirement compared to the alternative of a separate downstream CO_2 separation process.

2. Methods

We have developed various cycles for integrating the production of high purity H_2 and CO_2 based on heuristics and on the use of a non-isothermal one-dimensional model for an adsorber column. The model was validated for a variety of conditions and cycles [1,2]. The feedstream composition, pressure and temperature are representative for the outlet of a WGS reactor consisting of mainly H_2 and CO_2 with CH_4, CO and N_2 as relevant impurities. The most promising cycles in terms of the key performance indicators, namely the purity and recovery of hydrogen and CO_2, the productivity and the energy consumption, are optimized by combining the use of the simulation tool with that of a multi-objective optimization routine [3].

3. Results and discussion

For all cycles, there exists a tradeoff between H_2 purity and recovery at a given CO_2 purity and recovery (and vice versa). Notably, three of the developed cycles can purify hydrogen to greater than 99.97 %, as required for fuel cells for transportation, with a recovery of > 90 % while coproducing CO_2 at > 90 % recovery and > 96 % purity, as required for CO_2 transportation and

storage. The cycles are flexible regarding the feedstream composition: the specifications given above can be reached for a feedstream with a high CO content (~5 %) representative of the outlet of a high temperature WGS reactor as well as for a feedstream with a lower CO content (< 0.5 %) representative for the outlet of a low temperature WGS reactor.

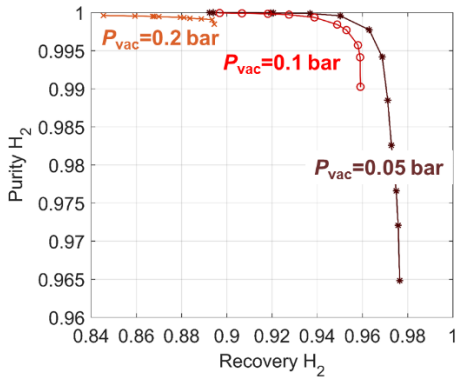

Figure 1. Optimized separation performance for a vacuum pressure swing adsorption cycle at different evacuation pressures, inlet: SMR + HT-WGS, coproduction of CO_2 at > 90 % recovery and > 95 % purity

To achieve the separation requirements, a subatmospheric pressure is required to withdraw CO_2. Lowering this pressure enhances the separation performance and increases the productivity at the expense of a higher energy consumption. The required hydrogen purity is another important factor: the minimum energy consumption increases with higher required hydrogen purities while the productivity decreases. For a hydrogen purity of 99.97 % with a recovery > 90 % (coproduction of CO_2 at > 90 % recovery and > 96 % purity), a minimum energy consumption for the separation of below 0.4 MJ/kg CO_2 separated (below 2.3 MJ/kg H_2 separated) can be obtained. This energy requirement is significantly lower than the energy required for pre-combustion capture using absorption, e.g. with MDEA, which is in the range of 2 MJ/kg CO_2 [4]. The energy required in the latter, however, is mainly steam whereas the former requires electricity for vacuum pumps. The equivalent electricity consumption for both processes assuming a conservative conversion efficiency of 20 % from steam to electricity is similar, but the adsorption process only requires a single process instead of two.

4. Conclusions and outlook

Advanced adsorption processes show promise for process intensification in the context of hydrogen production with CCS. Several cycles have been developed for the coproduction of high purity CO_2 and hydrogen. The equivalent electricity consumption is similar to commercial processes but an entire separation stage is now avoided. Moreover, the cycles are particularly promising due to a high flexibility towards different feedstream compositions. Layering of different adsorbents or the use of advanced adsorbent materials like MOFs leaves room for further process improvement.

References

[1] Schell J., Casas N. and Mazzotti M. (2012), Ind. Eng. Chem. Res., 52 (2013) 8311-8322
[2] Marx, D. et al., Ind. Eng. Chem. Res., 55 (2016) 1401-1412.
[3] F. Capra, M. Gazzani, L. Joss, M. Mazzotti, and E. Martelli, Ind. Eng. Chem. Res., 57 (2018) 9977–9993
[4] Meerman et al., IJGGC, 9(2012)

Utilizing the photo-induced hydrophilicity of TiO_2 to enhance permeate flux of composite membranes

Duc-Trung Tran, Julie Mendret*, Jean-Pierre Mericq, Catherine Faur & Stephan Brosillon

IEM (Institut Européen des Membranes), UMR 5635 (CNRS-ENSCM-UM), 34095 Montpellier, France

**Corresponding author: julie.mendret@umontpellier.fr*

Highlights

- Photo-active PVDF-TiO_2 composite membranes were prepared by NIPS method.
- Membrane WCA decreased upon UV irradiation due to photo-induced hydrophilicity of TiO_2.
- Permeate flux increased during filtration with UV irradiation (photo-filtration).
- Photo-filtration method offers potential benefits in operating cost.

1. Introduction

Other than being a photocatalyst for chemical reactions, TiO_2 also possesses an important property called photo-induced superhydrophilicity, in which its surface can become extremely hydrophilic upon UV irradiation [1]. As such, composite membranes containing TiO_2 nanoparticles have become very attractive prospects due to their excellent anti-fouling and self-cleaning properties. In addition, when membrane filtration is coupled with UV irradiation (photo-filtration), the permeate flux can be further enhanced thanks to said photo-induced effect [2]. In this study, that phenomenon was comprehensively investigated to explore the mechanism behind such flux enhancement and estimate the potential benefits in cost/efficiency balance of this new filtration method.

2. Methods

PVDF-TiO_2 membranes were prepared by the nonsolvent-induced phase separation (NIPS) method. The PVDF concentration was 20 wt% while the mass ratio of TiO_2 to PVDF was 1:5. The distribution of TiO_2 on membrane surface was characterized by energy-dispersive X-ray (EDX) mapping, while the water contact angle (WCA) was measured for membranes before and after UV irradiation. Photo-filtration tests were performed with pure water, humic acids (HA) and sodium alginate (SA) solutions in a crossflow filtration cell built with a Quartz window on top, so that the membrane could be irradiated by a 365-nm UV lamp. Filtration was performed in constant pressure mode, while irradiation mode was varied in terms of UV cycle (UV on/off time ranging from 15 to 90 min) and irradiance (I = 0.04-1 $mW.cm^{-2}$). The advantages of photo-filtration was demonstrated by comparing the behavior of normalized flux (the ratio between the flux at a given time (J) and the initial flux at the beginning of the test (J_0)) when UV was and was not utilized.

3. Results and discussion

Via EDX mapping, it can be seen that TiO_2 nanoparticles were dispersed uniformly on the surface of the membranes (Fig. 1a), suggesting photo-induced effects could occur once the membranes

were exposed to UV irradiation. Indeed, as the WCA was 77.4±1.2° for the membrane in normal condition (Fig. 1b), as opposed to 68.2±1.8° after it was irradiated by UV for 30 minutes (Fig. 1c). The decrease in WCA indicates an increase in membrane hydrophilicity, which was believed to be responsible for the rise in pure water flux during photo-filtration, as shown in Fig. 2.

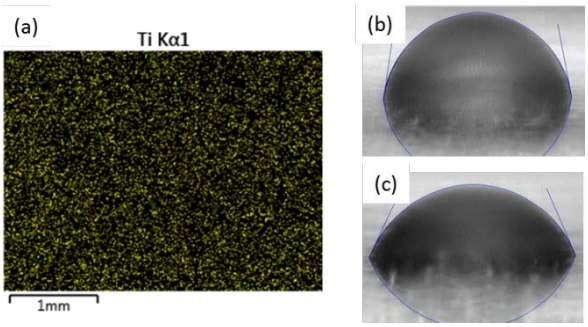

Figure 1. (a) Distribution of Ti on membrane via EDX mapping; and WCA of membranes in (b) normal condition and (c) post-UV-irradiated condition

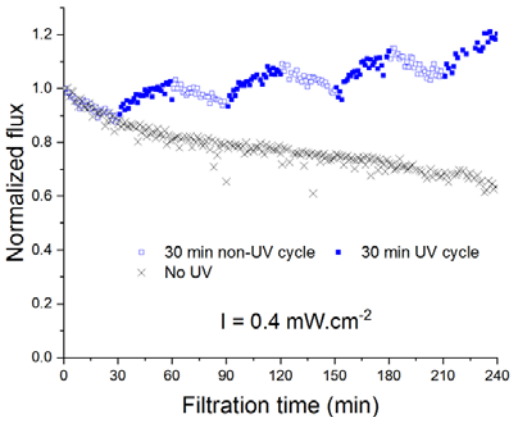

Figure 2. Permeate flux of water during photo-filtration with 30-min on/30-min off UV cycle

Despite that the membrane suffered an inherent flux decline due to compaction, every time UV was activated, a considerable rise in pure water flux could be observed. Even if UV was only utilized for 50% of the filtration time, a significant increase in water output could be achieved for the photo-filtration method compared to normal filtration, thanks to the flux "memory effect" in which the flux remained higher than usual even after UV was deactivated (Fig. 2). The permeate flux increase was also obtained for photo-filtration tests of HA and SA solutions, given the foulant concentration did not exceed 5 ppm for HA and 50 ppm for SA, with a rejection rate of 64% for HA and 90% for SA. Although UV irradiation increases energy consumption, the total operating cost for the whole process could be reduced, taking into account the extra water output. By varying the irradiation mode, several photo-filtration conditions were tested with pure water at lab scale, and the obtained experimental data were extrapolated to a large-scale water processing system (capacity 3000 m^3/day). It was estimated that, to achieve the same water output, utilizing photo-filtration in appropriate modes (for example, a moderate UV irradiance of 0.4 $mW.cm^{-2}$ and UV irradiation cycle of 30 minutes) could reduced the daily total operating cost up to 8.3% compared to normal filtration.

4. Conclusions

When PVDF-TiO_2 composite membrane was irradiated by UV, its hydrophilicity increased thanks to the photo-induced hydrophilicity effect of TiO_2, which led to a steady increase in permeate flux during photo-filtration. Thus, photo-filtration proved to be a promising method to improve the cost/efficiency balance of the filtration process in terms of water output, let alone the benefits from photocatalysis.

References

[1] R. Wang, K. Hashimoto, A. Fujishima, M. Chikuni, E. Kojima, A. Kitamura, M. Shimohigoshi and T. Watanabe, Nature 388 (1997) 431-432.

[2] J. P. Mericq, J. Mendret, S. Brosillon and C. Faur, Chem. Eng. Sci. 123 (2015) 283-291.

ECCE12
The 12th EUROPEAN CONGRESS OF CHEMICAL ENGINEERING
Florence 15-19 September 2019

Cellulose-developed Carbon Molecular Sieving Hollow Fiber Membranes for Gas Separation

Linfeng Lei[1], Arne Lindbråthen[1], Magne Hillestad[1], Xuezhong He[1],*, Marius Sandru[2], Xiangping Zhang[3] Evangelos P. Favvas[4]

1 Department of Chemical Engineering, Norwegian University of Science and Technology, NO-7491 Trondheim, Norway; 2 SINTEF Industry, SINTEF AS, NO-7465 Trondheim, Norway; 3 Beijing Key Laboratory of Ionic Liquids Clean Process, Institute of Process Engineering, Chinese Academy of Sciences, P.O. Box 353, Beijing 100190, China; 4 Institute of Nanoscience and Nanotechnology, National Center for Scientific Research "Demokritos", Aghia Paraskevi 153 41, Athens, Greece

**Corresponding author: xuezhong.he@ntnu.no*

Highlights

- Carbon hollow fiber membranes were developed from sustainable cellulose.
- 239 Barrer CO_2 permeability and 186 CO_2/CH_4 selectivity were obtained.
- The membrane exhibited attractive performances in 10% CO_2 -90% CH_4 mixed gas.

1. Introduction

Membrane systems are expected to apply in different gas separations such as oxygen recovery from air, natural gas sweetening and CO_2 capture from flue gas, thanks to the small footprint, low energy consumption, low capital and operating cost and process flexibility. Among different membrane materials, carbon molecular sieving (CMS) membrane is one of the most promising materials due to its high separation performance and good compatibility in some harsh operating situations (such as high pressures, high temperatures). Different polymers, like polyimide[1], cellulose acetate[2] and cellulose[3], have been employed as precursors for CMS membranes. Cellulose, as an inexhaustible and biorenewable material, could be a suitable precursor for large-scale producing CMS membranes. In this work, cellulose-based carbon hollow fiber membranes (CHFMs) were developed from cellulose/ionic liquid system.

2. Methods

Microcrystalline cellulose (MCC) was dissolved in 1-Ethyl-3-methylimidazolium acetate (EmimAc) and dimethyl sulfoxide (DMSO) solution at 50 °C with mechanical stirring in a glove box as a dope solution for spinning. Then, the defect-free cellulose hollow fiber precursors were fabricated by a dry-wet spinning, as shown in Figure 1a. The dried cellulose hollow fibers were carbonized in a tubular furnace by applying a specific carbonization protocol for preparing the CHFMs. Single gas permeation data were determined at room temperature with a feeding pressure of 2 bar. CO_2/CH_4 separation performance was evaluated by mixed gas tests (10% CO_2/90% CH_4) at different temperature and pressures.

3. Results and discussion

XRD and FTIR characterization confirmed that a crystalline structure transition from cellulose I (MCC) to cellulose II (cellulose hollow fibers) occurred during the cellulose dissolution and spinning process. Additionally, due to the transition of crystalline structure, the cellulose hollow fibers retained a higher carbon yield of 22.9% than the MCC after carbonization[3]. Single gas (e.g., CO_2, O_2, N_2, and CH_4) permeation testing indicated that the molecular sieving mechanism is dominating the gas transport through the CHFMs. In addition, the CO_2 permeability and CO_2/CH_4 selectivity of 239 Barrer and 186 were obtained in the single gas permeation, which presents a high separation performance cross the 2008 Robeson Upper Bound as shown in the Figure 1b. Moreover, it maintains attractive CO_2/CH_4 separation performances in 10% CO_2 -90% CH_4 mixed gas permeation testing at increasing temperatures and raising pressures.

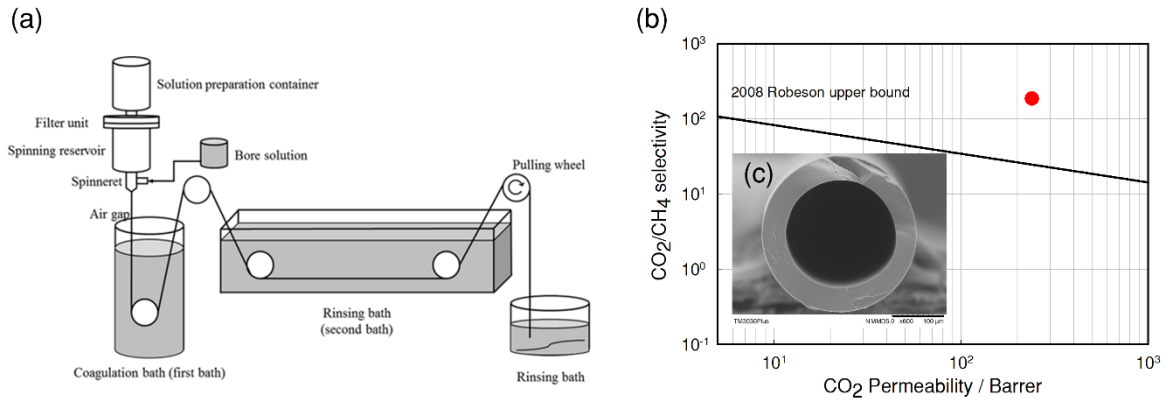

Figure 1. Schematic diagram of the spinning process, b) Gas permeation results for CO_2/CH_4 in prepared CHFM and comparison with the 2008 upper bound plot, c) Cross-sectional SEM images of a fabricated CHFM.

4. Conclusions

This study provides a suitable way to directly fabricate CHFMs using cellulose hollow fiber precursors spun from cellulose/(EmimAc + DMSO)/H_2O ternary system. The developed novel CHFMs shows attractive separation performance especially CO_2 removal from high pressure natural gas, as well as provides a new way for fabricating CMS membranes from sustainable and green materials.

Acknowledgement

The authors acknowledge the Research Council of Norway (Norges forskningsråd) for funding in the CO2Hing project (#267615) through the Petromaks2 programme.

References

[1] C. Zhang, W.J. Koros, Ultraselective Carbon Molecular Sieve Membranes with Tailored Synergistic Sorption Selective Properties, Advanced Materials, 29 (2017) 1701631.

[2] X. He, M.-B. Hägg, Hollow fiber carbon membranes: From material to application, Chemical Engineering Journal, 215-216 (2013) 440-448.

[3] L. Lei, A. Lindbråthen, M. Sandru, M. Gutierrez, X. Zhang, M. Hillestad, X. He, Spinning Cellulose Hollow Fibers Using 1-Ethyl-3-methylimidazolium Acetate–Dimethylsulfoxide Co-Solvent, Polymers, 10 (2018) 972.

ECCE12
The 12th EUROPEAN CONGRESS OF CHEMICAL ENGINEERING
Florence 15-19 September 2019

Supercritical water desalination (SCWD) for treatment of multicomponent brine streams.

Surika van Wyk[1], Aloijsius G.J. van der Ham[1], Sascha R.A. Kersten[1]

1 Sustainable Process Technology. Faculty of Science and Technology, University of Twente, Drienerlolaan 5, Posbus 217, 7500 AE, Enschede, The Netherlands

**Corresponding author: s.vanwyk@utwente.nl*

Highlights

- Desalination of multicomponent waste streams with zero liquid discharge.
- Phase behavior of various multicomponent brines under supercritical conditions.
- Selective removal of different salts from multicomponent brines.

1. Introduction

Supercritical water desalination (SCWD) is a promising zero liquid discharge (ZLD) technology that utilizes the non-polar nature of water under supercritical conditions (T > 374 ºC, Pressure > 22.1 MPa). SCWD is based on the formation of vapour-liquid equilibrium (VLE) where a supercritical water (SCW) phase (< 750 ppm NaCl) is separated from a concentrated liquid brine phase (30 – 40 wt.% NaCl). This approach to desalination has been investigated on both laboratory and pilot plant scale for different feed concentrations of NaCl (3.5 – 16 wt.%)[1]. Most large scale studies have been done with aqueous type I salt solutions such as NaCl and $CaCl_2$, however, in industry brine streams contain multiple salts. Different salts exhibit varying phase behaviour under supercritical conditions such as VLE or vapour (fluid) - solid equilibrium (VSE)[2]. As stated, VLE needs to be established for SCWD and therefore the formation of VSE could be problematic as this will lead to plugging and equipment failure. A manner in which this can be overcome, is to dissolve the formed solids in the brine originating from the presence of a type I salts[2,3]. In this manner VLE can be re-establish. This presentation will focus on the separation and treatment of typical brine waste streams found in industry namely, NaCl (type I) -Na_2SO_4 (type II) -H_2O (mining industry), NaCl (type I)-$CaCl_2$ (type I)-H_2O (desalination waste) and NaCl (type I)-KCl (type I)-H_2O (dairy industry). Firstly, the separation efficiency of water from the concentrated brine streams will be investigated. Subsequently, the feasibility of separating different salts from the multicomponent concentrated brine streams will be studied. The solubility of different salts in supercritical water can be easily manipulated by varying temperature and pressure and could therefore be used for the selective removal of certain salts from multicomponent brines.

2. Methods

The experimental procedure is divided into two steps, namely qualitative (step 1) and quantitative (step 2) analysis. Qualitative experiments are performed using quartz capillaries to ensure that all the solids are dissolved in the brine during separation, so as to avoid plugging of the system. Once it has been ensured that a VLE system will be obtained at the selected separation conditions (250 – 350 bar; 370 – 450 ^{o}C) for the given mixtures, quantitative phase equilibria measurements are

done, using a laboratory scale SCWD unit [4]. During the quantitative analysis salt composition and concentration of each phase is measured and the separation efficiency for each step is calculated.

3. Results and discussion

The qualitative capillary results for different NaCl:Na_2SO_4 ratios are shown in Figure 1.

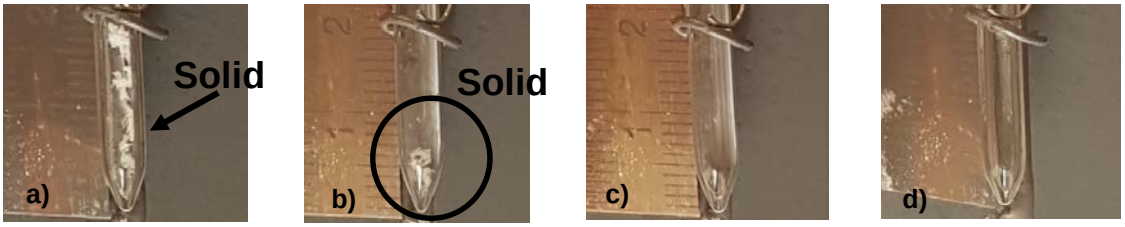

T_{wall} = 427 ºC
(P~ 376 bar)
Na_2SO_4 - 3.5 wt.%

T_{wall} = 431 ºC
(P~ 320 bar)
NaCl: Na_2SO_4 – **6:4**
Total salt - 3.5 wt.%

T_{wall} = 431ºC
(P ~ 316 bar)
NaCl: Na_2SO_4 – **7:3**
Total salt - 3.5 wt.%

T_{wall} = 429 ºC
(P ~ 250 – 350 bar)
NaCl - 3.5 wt.%

Figure 1. Phase behaviour of NaCl-Na_2SO_4-H_2O mixtures a) VSE b) vapour-liquid-solid equilibrium (VLSE) c) VLE d) VLE

The results show that for NaCl-Na_2SO_4-H_2O mixtures with mass ratios of 7:3 (NaCl:Na_2SO_4) 8:2 and 9:1, VLE is achieved. The quantitative results show that under supercritical conditions, Na_2SO_4 remains in the concentrated liquid phase and that the SCW phase has a low concentration of NaCl (400 - 1100 ppm) and trace amounts of Na_2SO_4. In general, the SCW concentration and recovery is comparable to that for NaCl-H_2O systems for the given operating conditions. Separation of the remaining concentrated NaCl-Na_2SO_4-H_2O brine will be further investigated. For the other multicomponent streams, the same procedure will be followed *i.e.* qualitative screening to ensure VLE followed by quantitative phase equilibria measurements to determine the separation efficiency of water from brine and that between different salts.

4. Conclusions

The conclusions made based on the experimental results for NaCl-Na_2SO_4-H_2O systems, is that water can be separated from the brine solutions, using the currently developed SCWD process for the treatment of brine streams with ZLD. An additional step will have to be added to separate certain salts for the remaining concentrated brine depending on solubility. The selective removal of salts from multicomponent brine could present an additional benefit to SCWD and could be an alternative method of separation to retrieve certain salts.

References

[1] S.van Wyk, A.G.J. van der Ham, S.R.A. Kersten, Desalination. 439 (2018) 80-92.
[2] M.M. DiPippo, K. Sako, J.W. Tester, Fluid Phase Equilibria. 157 (1999) 229-255.
[3] V.M. Valyashko, Pure & Applied Chemistry. 69 (1997) 2271-2280.
[4] S.O. Odu, A.G.J. van der Ham, S. Metz, S.R.A. Kersten, Ind. Eng. Chem. Res. 54 (2015) 5527-5535.

Olefin-Paraffin Separation with Customized Amorphous Fluoropolymer (CAF) Facilitated Transport Membranes

William Charlton, Hannah Murnen, Sudip Majumdar, Ken Loprete, Ken Pennisi

Compact Membrane Systems, Newport, DE, U.S.A.

Highlights

- The silver containing Facilitated Transport Membranes has shown high flux and olefin/paraffin selectivity in the laboratory over a period of >600 days.
- Facilitated Transport Membrane stability have been evaluated and proved stable in the presence of known poisons.
- Over the past year, CMS has been operating a pilot utilizing these silver based Custom Amorphous Fluoropolymer membranes on a refinery distillation column.
- CMS is partnering with an industry leader to field test commercial scale membranes in a petrochemical facility.
- CMS has expanded research to include C_4 separations, with initial results showing good performance and longevity.

1. Introduction

Ethylene and propylene are major chemical industry raw materials and consume a great deal of energy in their production. The separations of these materials are some of the costliest, most energy intensive, and most technically difficult separations in the industry due to the very similar size and nature of the molecules being separated. The technology currently employed for the separation of ethylene and propylene from paraffins is distillation and is estimated to consume 250 trillion BTU/year of energy.

A membrane based olefin-paraffin separation process would provide substantial economic benefit to petrochemical processes and drastically reduce the energy required. Membrane processes utilizing facilitated transport membranes for separating ethylene/ethane or propylene/propane have been extensively studied and described in the literature. While separations have been demonstrated in the laboratory, problems with membrane stability have prevented development of commercial systems.

Compact Membrane Systems has developed a customized amorphous fluoropolymer (CAF) facilitated transport membrane (FTM) containing silver ions that selectively transport olefin molecules from a mixture of olefin and paraffin that has shown stable performance in both laboratory testing and field pilot trials.

2. Methods

Over the past year, CMS has been operating a pilot utilizing these silver based CAF membranes on a distillation column at the Delaware City Refining Company. The Delaware City pilot is operated on a low concentration olefin stream (i.e., 10-20 wt% propylene in the feed) with the goal of achieving an HD5 quality propane (<.05 wt% propylene) and an enriched propylene stream. In addition, CMS has entered into a project with Dow Chemical through RAPID, a manufacturing institute funded by the U.S. Department of Energy. The goal of the work with Dow is to operate at the other end of the concentration spectrum where the feed is greater than 80% propylene and the target is an upgraded olefin-rich stream from the permeate. A pilot unit is installed in a Dow facility and we will share the latest results from our tests there.

3. Results and discussion

The silver containing FTM has shown high propylene flux and propylene/propane selectivity in the laboratory over a period of >600 days. Similar results were also obtained with ethylene and ethane gas mixtures. We have also evaluated membrane stability in presence of known process poisons such as hydrogen sulfide, acetylene, MAPD and hydrogen and will provide guidance on the appropriate concentration of these species for membrane applications.

CMS will also discuss initial results on laboratory testing of butane streams. This includes mixed gas separation of n-butane and 1-butene. We will share results for a number of operating conditions and will highlight several exciting C_4 separation applications including those with isomer streams. CMS will also provide an overview on the results of our pilot field trials with the Delaware City Refinery Company and the Dow Chemical Company.

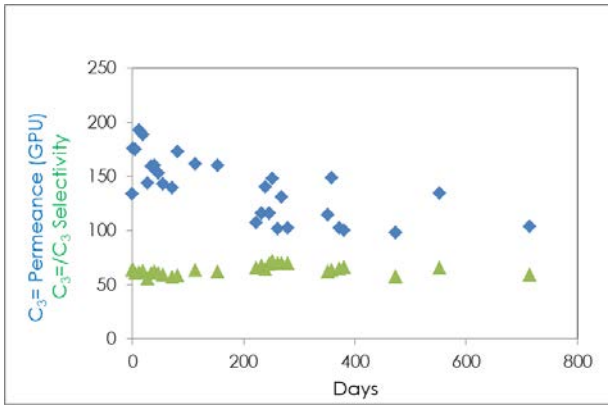

Figure 1. Long term Facilitated Transport Membrane aging study

4. Conclusions

A membrane based olefin-paraffin separation technology has the potential to provide substantial economic benefit to petrochemical industry and drastically reduce the energy required to complete these essential separations. In addition, membrane systems are scalable, allowing their implementation for smaller, stranded streams where distillation columns have not previously been installed due to limited economic value.

ECCE12
The 12th EUROPEAN CONGRESS OF CHEMICAL ENGINEERING
Florence 15-19 September 2019

Aromatic/aliphatic separation by liquid-liquid extraction with ionic liquids: an overview process analysis with the COSMO-based/Aspen Plus approach

Pablo Navarro[1], Daniel Moreno[1,2], Marcos Larriba[3], Julián García[3], Francisco Rodríguez[3], Roberto I. Canales[2], José Palomar[1,*]

1 Universidad Autónoma de Madrid, 28049 Madrid, Spain; 2 Pontificia Universidad Católica de Chile, 8331150 Santiago de Chile, Chile; 3 Universidad Complutense de Madrid, 28040 Madrid, Spain

**Corresponding author: pepe.palomar@uam.es*

Highlights

- More than 100 ionic liquids evaluated in the whole extraction + recovery process.
- Close relationship found between extractive properties and process insights.
- Cyano-based ionic liquids stand as the most potential solvents.
- The separation is enhanced but the costs are increased with the number of cyano groups.

1. Introduction

Ionic liquids (ILs) are non-conventional salts that are liquid below 373 K, showing negligible vapor pressure and an interesting liquid range of use only limited by their thermal stability [1]. Among other purposes, ILs have been frequently evaluated in a high number of separation cases as solvents in liquid-liquid extraction processes [1]. Focusing the attention in the aromatic/aliphatic separation, which is one of the most prolific and hopeful research lines using ILs [2], a feasible process was evidenced in the literature referring not only to the core separation (liquid-liquid extraction) but also including side-separations and purifications to enhance aromatic standards and recycle the solvent [3,4]. The aforementioned claim is supported by experimental data at laboratory and pilot plant scales [3-5] but also by process simulation [6,7]. Although large experimental liquid-liquid equilibrium data is available, vapor-liquid equilibrium data is scarce and simultaneous modelling liquid-liquid and vapor-liquid equilibria was not revealed to be easy; thus, a proper overview process analysis lighting the more convenient IL-based solvents is still not available in the literature.

According to this, a systematic process analysis for the aromatic/aliphatic separation seems to be interesting to evaluate, for this example, the real applicability of these neoteric solvents at industrial scale. To do this, COSMO-based/Aspen Plus methodology was selected because of its outstanding power and availability to deal with more than 100 ILs in a wide range of conditions, all in the framework of a commercial process simulator. After validating COSMO predictions against all reliable experimental data regarding liquid-liquid extraction and distillation units involved in the process, the methodology was deployed to better understand the aromatic/aliphatic separation.

2. Methods

Integrated COSMO-based-Aspen Plus methodology was deployed to simulate the aromatic/aliphatic separation process, which involves the extractor and three flash distillation

units; the first two flashes are destined to purify the aromatics, whereas the last one is aimed at separating the aromatics and the IL. The COSMOSAC property model was selected to calculate the activity coefficients in the simulations, specifically the modification to the Lin and Sandler model (mode 3 of COSMOSAC model) developed by Lin, Mathias et al. (2002) because that approach better represented available experimental data. Regarding the modules, EXTRACT and FLASH 2 were selected in the simulation.

3. Results and discussion

After properly selecting the input/output matrix and executing more than 5000 simulations, the results were summarized and analyzed. As exemplified in Fig 1 to representative ILs, it is difficult to find an IL with good performance in both aromatic recoveries and purities, even more complex considering recycling streams. Although [4mbpy][TCM] shows a very competitive performance in the more realistic conditions, the direct proportionality between aromatic distribution ratio and utilities costs makes the analysis even more complex. Taking into account process simulation performance, utilities costs and typical ILs' limitations as viscosity and thermal stability, cyano-containing ILs stand as the more potential ILs nowadays.

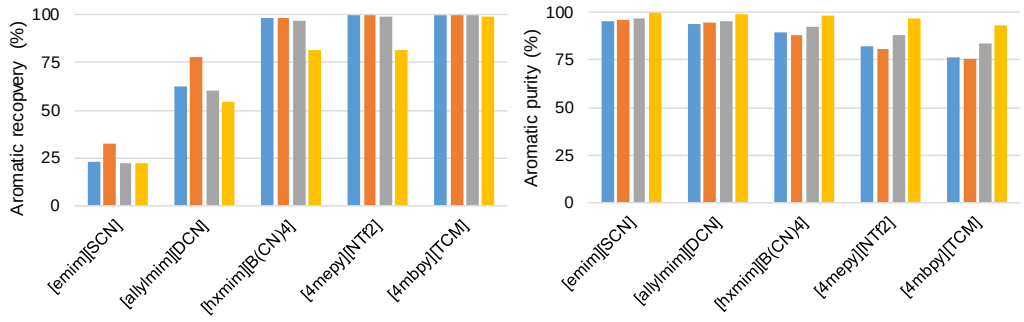

Figure 1. Aromatic recovery and purity with selected ILs in several scenarios. Toluene/n-heptane separation: only extraction, blue; whole process, grey. BTX removing from pyrolysis gasoline: only extraction, red; whole process, yellow.

4. Conclusions

The overview process analysis of the aromatic/aliphatic separation by liquid-liquid extraction with ILs has provided a useful guide to evaluate the global and partial impact of the extractive and physical properties related to available and future IL species on relevant process insights. A clear correlation between ILs features and process simulation insights, such as utilities costs, recoveries and purities, has permitted to give recommended standards for the solvents that will easy the search of even better solvents than cyano-containing ILs for the petrochemical industry.

References

[1] N.V. Plechkova, K.R. Seddon, Chem. Soc. Rev. 37 (2008) 123-150.
[2] R.I. Canales, J.F. Brennecke, J. Chem. Eng. Data 61 (2016) 1685-1699.
[3] M. Larriba, P. Navarro, E.J. González, J. García, F. Rodríguez, Fuel Process. Technol. 137 (2015) 269–282.
[4] P. Navarro, M. Larriba, J. García, F. Rodríguez, EnergyFuels 31 (2017) 1035-1043.
[5] G.W. Meindersma, A.B. de Haan, Chem. Eng. Res. Des. 86 (2008) 745–752.
[6] M. Larriba, J. de Riva, P. Navarro, D. Moreno, N. Delgado-Mellado, J. García, V.R. Ferro, F. Rodríguez, J. Palomar, Sep. Purif. Technol. 190 (2018) 211-227.
[7] J. de Riva, V.R. Ferro, D. Moreno I. Díaz, J. Palomar, Fuel Process. Technol. 146 (2016) 29–38.

ECCE12
The 12th EUROPEAN CONGRESS OF CHEMICAL ENGINEERING
Florence 15-19 September 2019

Confined liquid distribution in structured packings: Study of liquid films around a perforated topography

Manasa IYER[1,2], Hervé DUVAL[1], Joel CASALINHO[1], Jacopo SEIWERT[2], Mikael WATTIAU[2]

1 Laboratoire LGPM, CentraleSupélec, Université Paris-Saclay, Gif-sur-Yvette, 91190, France ;
2 Centre de Recherche Paris-Saclay, Air Liquide Research & Development, 1, chemin de la Porte des Loges, Les Loges-en-Josas - BP 126, 78354 Jouy-en-Josas, France

**Corresponding author: manasa.periyapattana@airliquide.com*

Highlights

- Film thickness profile over a perforated plate.
- Characterisation of different flow regimes.
- Critical flow rate at which the fluid fills the perforation.

1. Introduction

Falling films on structured packings are extensively studied because of their increased application in the distillation and absorption industries. A class of structured packings consists in stacks of metal sheets. These sheets usually comprise of various complex geometrical intricacies such as corrugations, perforation of various shapes that play a significant role in the local fluid redistribution. The unique flow paths of the liquid and the gas phases over the structured packing, caused by their complex geometry, gives motivation to investigate the physics of the fluid distribution over these topologies. The presence of a topography perturbs the fluid free surface and in a short time, several instabilities can be observed through the deformation of the free surface. The effect of perforations and micro-texture on liquid spreading over the surface of corrugated packing was examined experimentally by Pavlenko et al. (2017). Zhao & Cerro (1992) performed an experimental work over macro and micro structures in which he characterized the mechanics of the viscous film flows by measuring film thickness profiles, streamline patterns and free-surface velocities. More recently, Xie et al. (2018) have studied the liquid flow patterns over several shaped open window at different flow rates. However, in their experiments, perforated plates are supplied with liquid only on one side whereas supply of liquid is maintained on both sides of the metal sheets in real distillation conditions.

In our experimental study, we focus on the fluid redistribution mechanism specific to these topographies in order to clearly understand its contribution towards the spreading of the liquid over a packing. We aim to measure and characterise the local deformation of the film around the topography over a perforated aluminium plate while the fluid supply is maintained on both faces of the plate. The concept of two-face supply of the fluid over such a topographical plate has not been tested before and thus brings new insights on the film behavior around the topographical surfaces.

2. Methods

The film topology and the film pattern in and around the perforation is visualized by using a high speed camera (Phantom v310). With this method, characteristic flow patterns in the perforation and preferred flow paths around the perforation are qualitatively investigated. To measure the free surface topography, Confocal Chromatic Imaging (CCI) (Kofman et al. 2014) technique is used.

3. Results and discussion

The effect of the topography is studied for various aspect ratio of the perforation (diameter d, thickness t) for a range of Reynolds number Re (2 - 63) using three different liquids (Kapitza number Ka = 3, 63, 342). For each configuration, the flow transition from the state of fluid passing around the perforation to the state of fluid filling the perforation is

observed. For all configurations, we measure the critical flow rate at which the fluid fills the perforation. Regime transition occurs at a critical value of the Reynolds number (built with the critical rate) which depends on the Kapitza and Bond number (built with the perforation characteristic length).

Complete two-dimensional map of the free-surface shape of a liquid film in the vicinity of the topography is being constructed by measuring the film thickness using CCI.

Figure 1. Superimposed image of the thin falling film over a perforated plate seeded with silver coated particles to visualise the free surface streamlines for a low Re flow (Re = 0.5) for silicone oil of ν = 100 cSt.

4. Conclusions

In the present work, flow patterns specific to the perforated topography is investigated qualitatively and quantitatively to gain better understanding of the fluid distribution in microscale flow phenomena that may occur on the structured packing. This permits us to optimise the design of structured packings and thereby it could reduce the pressure drop in the column and thus the energy consumption.

References

- H. Xie, J. Hu, C.Wang, and G. Dai. Liquid flow transition and confined free film formation on a vertical plate with an open window. *Experimental Thermal and Fluid Science*, 92:174–183, 2018.
- A. N. Pavlenko, O. A. Volodin, and A. S. Surtaev. Hydrodynamics in falling liquid films on surfaces with complex geometry. *Applied Thermal Engineering*, 114:1265–1274, 2017.
- L. Zhao and R. Cerro. Experimental characterization of viscous film flows over complex surfaces. *International journal of multiphase flow*, 18(4):495–516, 1992.
- N. Kofman, S. Mergui, and C. Ruyer-Quil. Three-dimensional instabilities of quasi-solitary waves in a falling liquid film.Journal of Fluid Mechanics, 757:854–887, 2014.

Generating maximal mass transfer in highly curved helical hollow fiber membranes: a CFD study.

Omran Abushammala*[1], Rainier Hreiz[1], Cécile Lemaître[1], Éric Favre[1]

[1]*Laboratoire Réactions et Génie des Procédés, Université de Lorraine, CNRS, LRGP, F-54000 Nancy, France.*

Omran.abushammala@univ-lorraine.fr

Highlights

- CFD investigation of mass transfer in hollow fiber membranes of helical geometry
- The mass transfer efficiency is positively correlated to the helix curvature
- Mass transfer in highly curved helixes is up to 10 times higher than in straight tubes

1. Introduction

Membrane separation is widely used for the separation of homogeneous liquid or gaseous mixtures, and is one of the most promising intensification technologies for gas-liquid absorption processes. The design and operation of membrane modules have been the focus of many scientific researches aiming to improve the separation efficiency.

The mass transfer in membrane modules can be intensified by using helical pipe geometries instead of classic straight membranes. Indeed, the hydrodynamics in helical geometries is characterized by the occurrence of secondary flows, called Dean vortices, which considerably increase the mass transfer efficiency.

The present study addresses mass transfer in highly curved helical pipes, i.e. helical geometries with small helical radius and pitch. Figure 1 presents the limits of the so-called forbidden region in the (R_H^* , p*) space, where R_H^* and p^* are the reduced helix radius and pitch respectively, both nondimensionalized by the pipe diameter, d. The forbidden region corresponds to the zone where it is not possible to design helical shapes. Its frontier, which equation has been determined by Przybył et al. [1], corresponds to closely packed helices, i.e. helices which pitch cannot be further decreased because the consecutive turns of the helix would intersect/overlap one with/on another. Some helix designs are shown in Figure 1. They illustrate the fact that the helical pipe geometry tends toward that of a straight at three asymptotic limits: (i) when the dimensionless pitch *p** tends to infinity; (ii) when the dimensionless helix radius R_H^* tends to infinity; (iii) when the dimensionless helix radius R_H^* tends to zero.

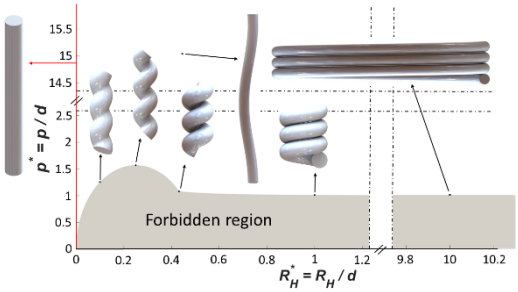

Figure 1: Limits of the forbidden region in the (R_H^* , p*) space (adapted from Przybył et.al [1]) and some representative helices.

2. Methods

In this paper, CFD (Computational Fluid Dynamics) is used to investigate the mass transfer efficiency in helical membranes. Simulations were conducted for various helix designs ($1.25 \leq p^* \leq 15$ and $0.05 \leq R_H^* \leq 10$). The computational mesh consisted of hexahedral cells only, with a boundary layer mesh in the near-wall zone for more accurate calculation of the steep gradients in that area. The commercial CFD code FLUENT 16.0 was used to simulate the mass transfer within the helical membranes. A Newtonian fluid was considered, and the flow, treated as laminar and incompressible, was described using the steady Navier-Stokes and continuity equations. The mass transfer equation was solved assuming a dilute medium and a uniform concentration at the walls.

3. Results and discussion

For each simulation performed, $\mathrm{Sh}_\mathrm{H}^\infty$, the asymptotic Sherwood number (i.e. in the region where the concentration profile gets fully developed) was calculated. Figure 2 shows the contour plot of $\mathrm{Sh}_\mathrm{H}^\infty/\mathrm{Sh}_\mathrm{S}^\infty$ for a Reynolds number of 400 and different Schmidt number values. $\mathrm{Sh}_\mathrm{S}^\infty$ denotes the asymptotic Sherwood number in straight pipes which equals 3.65 under a uniform wall concentration boundary condition.

The contour plots in Figure 2 were obtained using a triangulation-based cubic interpolation of the CFD results. The geometric parameters for which simulations were performed are represented by black dots: at these points, the values of Sh_H^∞/Sh_S^∞ that are displayed on the contour plots are exactly the same than those provided by CFD. Although the interpolated data exhibit some irregularities that are inherent to interpolation, these contour plots provide valuable information: (1) There is a positive correlation between Sh_H^∞ and the pipe curvature. Indeed, highly curved helices involve the highest Sherwood numbers, which is explained by the fact that they engender the most intense Dean-type recirculations. (2) For each dimensionless pitch, p^*, there exists a dimensionless helical radius, R_H^*, at which the Sherwood number is maximal. The ratio Sh_H^∞/Sh_S^∞ tends to one when R_H^* tends to zero or infinity, since the helical geometry approaches that of a straight pipe. (3) The mass transfer efficiency is extremely sensitive to the pitch value in the case of high curved helixes. For an infinite pitch, Sh_H^∞/Sh_S^∞ tends to one since the helical geometry tends to a straight pipe. (4) The mass transfer enhancement is the highest in the case of highly curved helixes and increases when the Schmidt number is increased.

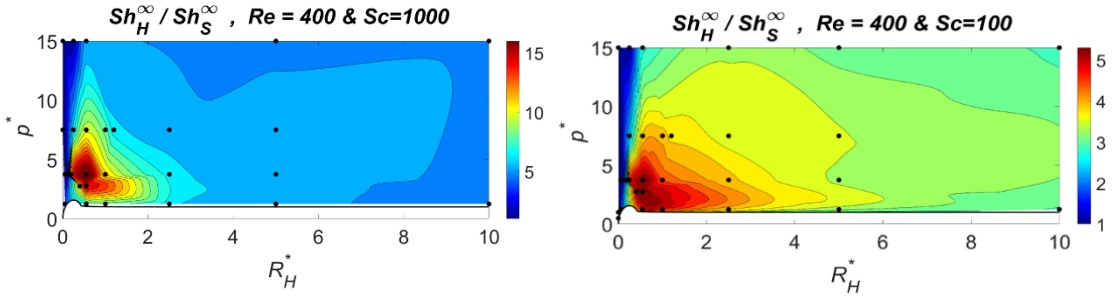

Figure 2: Contour plots of $\boldsymbol{Sh_H^\infty}$ to $\boldsymbol{Sh_S^\infty}$ ratio at different Schmidt numbers and a Reynolds number of 400. The data is interpolated from CFD results marked with black dots.

References

[1] Przybył, S., & Pierański, P. (2001). Helical close packings of ideal ropes. The European Physical Journal E, 4(4), 445-449.

ECCE12
The 12th EUROPEAN CONGRESS OF CHEMICAL ENGINEERING
Florence 15-19 September 2019

Formulating preliminary design optimization problem of an agrifood process using expert knowledge: application to milk microfiltration

Maëllis Belna[1,3,4], Anne-Laure Marie[1], Franck Sfiligoï-Taillandier[2], Amadou Ndiaye[3], Geneviève Gésan-Guiziou[4]

1 Boccard, Développement technologique, 35360 Montauban de Bretagne, France; 2 I2M, Université de Bordeaux, 33400 Talence, France; 3 I2M, Université de Bordeaux, INRA, 33400 Talence, France ; 4 STLO, Agrocampus Ouest, INRA, 35000 Rennes, France

**Corresponding author: maellis.belna@inra.fr*

Highlights

- Expert knowledge was used for formulating a process design optimization problem
- Expert knowledge makes easier the choice of relevant optimization objectives
- Causal map of optimization's objectives is an easy-to-understand graphic representation

1. Introduction

Modelling and optimizing food processes is a complicated task due to the high complexity of the food product itself, the lack of knowledge concerning mechanisms limiting process performances [1], and to the heterogeneity of the involved variables (ordinal, cardinal, discrete or continuous variables). This is the case for skim milk crossflow microfiltration with 0.1 µm pore size (MF 0.1 µm). This operation is commonly used in dairy industry to separate proteins: native casein micelles (retentate) are used in cheese making while serum proteins (permeate) are mainly used in food formulations for specific populations (elderly people, infants, etc). Despite the high interest in MF in the dairy sector, this process is not optimized by considering the different conflicting objectives of the industry such as maximizing protein recovery in the permeate fraction while minimizing economic costs. The choices of membrane configurations, processing designs and operating conditions are based on the know-how of operators and the available expert knowledge. This knowledge is partial and does not take into account links between the process operating variables, product state variables and optimization objectives. When the optimization of MF 0.1 µm is performed, it is often described as mono-objective and empirical problem [2] or as study cases showing the influence of one variable on a group of chosen variables [3]. This article presents a methodology for collecting, collating and representing expert knowledge necessary to the design of food processing multi-objective optimization problems focusing on skim milk MF.

2. Methods

The proposed methodology has four steps: formulation of the multi-objective optimization problem, modelling optimization objectives as functions, optimization of objective functions and choice of a solution to implement [4]. In this work, the focus is on the problem formulation. The

MF 0.1 µm optimization problem is multidisciplinary and the knowledges necessary to formulate and solve the problem are shared between several experts. By dividing the problem domain into domains of knowledge, the identification of experts and the knowledge collection are easier [5]. The semi-structured interview was used to elicit know-how and knowledge from experts. The influence relations between variables and objectives were collected from the interviews and represented as causal maps. Graphical representation allows expert to exchange easily about influence relations. After validations, maps of the same knowledge domain were merged, discussed and validated by the group of the domain experts. Maps represent the knowledge models to use for formulating the optimization objectives as functions from the literature or experimental data.

3. Results and discussion

In this work, the operational objective is to be able to compare optimized microfiltration systems within a global process that can accept different membranes, processing designs and operating conditions. Optimization objectives were defined with the stakeholders: ten experts and decision makers. First, ten objectives were defined and reduced to six regarding industrial issues (maximization of the retentate composition, permeate composition, permeate protein recovery and stability of the permeation flux and minimization of the investment cost and operating cost). The MF 0.1 µm optimization problem domain was divided into nine knowledge domains: membrane properties, performance of the filtration, operating variables, permeate fraction, retentate fraction, process design, costs and environmental impacts. Each knowledge domain benefited from two to seven experts. Knowledge was collected during 36 interviews representing 14h30 of audio recording. For each knowledge domain, a causal map by expert was established and the whole merged as the causal map of the domain. After validations, each domain causal maps were discussed and validated by the different domain experts (industrialists, scientists, equipment manufacturers). One very important point of this step was to define a shared glossary and a generic process scheme representative of all the specific schemes. By the end, the extracted causal relations between variables were represented in 9 maps using approximately 250 variables.

4. Conclusions

The optimization problem studied is complex with conflicting objectives and heterogeneous variables. The integration of expert knowledge allows the identification of relevant objectives regarding to industrial issues. The MF process is considered from conception to performances with the identification of lack of knowledge in order to plan new experiments. Causal maps allow an easy to understand representation of the influences between the variables and make it possible to establish which variables influence which objectives. Based on these maps, the objective functions will be formalized allowing to perform the optimization.

References

[1] G.Trystam, J. Food. Eng. 110 (2012) 269-277
[2] C.E Jorgensen, et al., J. Dairy. Sci. 99 (2016) 6164-6179
[3] G. Gésan-Guiziou, et al., J Membr Sci Technol. 158 (1999) 211-222
[4] E.G. Talbi, Metaheuristics: from design to implementation, John Wiley & Sons, Hoboken, 2009
[5] M.H. Hobbalah et al., Expert. Syst. Appl. 92 (2018) 95-105

Modelling of heat transfer in open cell foam described as graphs associated to the solid network using Port-Hamiltonian Systems.

Haithem Louati[1], Tobias Scheuermann[2], Bernhard Maschke[1], Marie-Line Zanota[3], Jerome Vicente[4], Paul Kotyczka[2], Isabelle Pitault[1]

1 Univ. Lyon, Université Claude Bernard Lyon1, CNRS, LAGEPP UMR 5007, 43 boulevard du 11 novembre 1918, F-69100 Villeurbanne, France; 2 Technical University of Munich, Department of Mechanical engineering, Chair of Automatic Control, Boltzmannstraße 15, 85748 Garching, Germany; 3 Univ. Lyon, CNRS, CPE Lyon, UCBL, LGPC UMR 5285, 43 boulevard du 11 novembre 1918, F-69100 Villeurbanne, France; 4 IUSTI, CNRS UMR 7343, Université de Aix-Marseille, Marseille 13453, France;

**Haithem Louati: haithem.louati@univ-lyon1.fr*

Highlights

- Modelling of heat transfer in metallic open-cell foam.
- New network approach based on Port-Hamiltonian Systems.
- Graph representation are obtained using *X-ray CT* and *iMorph*.

1. Introduction

This paper deals with the modelling of the heat transfer in metallic open-cell foams using their geometric and topological properties. Several works have considered simplified geometries such as regular paving by Kelvin's cell [1] or random cellular morphologies based on the weighted-Voronoi (Laguerre) tessellations [2]. These approaches, however, fail to represent accurately the actual, often non-homogeneous and non-regular, structure of foams and may lead to poor estimation of their effective properties. Another approach is to use, X-ray CT (Computed Tomography) to construct 3D realistic structure which can be used in a CFD software and perform a numerical simulation of the heat transfer equations using finite elements or finite volume methods (FEM, FVM). The main two drawbacks of this approach are (1) the discretization of the computational domain, which leads to numerical models of extremely high complexity (2) the use of staircase boundary approximations, which may lead to inconsistent results.

In this paper, we follow an alternative approach, based on the derivation of two graphs representing the solid and fluid phases obtained using X-ray CT and image analysis [3]. From these two dual graphs, we derive the Port Hamiltonian formulation [4] of the heat diffusion. In a first instance, the work presented here is limited to modelling of the heat transfer in the solid phase.

2. Methodology

From 3D images and using iMorph software [3] (as shown in **Fig. 1**), two graphs are derived. For the graph of solid, one associates nodes to adjacent half-struts and edges to interfaces. For the graph of fluid, one associates nodes with finite volumes and edges to surfaces at the interface of two volumes. Furthermore, some geometrical properties such as strut lengths and diameters, are extracted and associated with the elements of the graph.

The heat diffusion in the solid phase may be formulated as the Port Hamiltonian System $\begin{pmatrix}\frac{\partial u}{\partial t}\\ F\end{pmatrix} = \begin{pmatrix}0 & -div\\ -grad & 0\end{pmatrix}\begin{pmatrix}\tau\\ \phi\end{pmatrix}$ and $\begin{pmatrix}f^b\\ e^b\end{pmatrix} = \mathrm{tr}\begin{pmatrix}\tau\\ \phi\end{pmatrix}$ where u is the internal energy density, τ is the reciprocal temperature, ϕ the heat flux and $\begin{pmatrix}f^b\\ e^b\end{pmatrix}$ denotes the port boundary variables where tr is the trace operator at the boundary of the spatial domain. The Hamiltonian function is the total entropy $H_0 = S$, the state variable is the internal energy density u and the co-state variable is the reciprocal temperature , $\tau = \frac{\delta S}{\delta u}$ corresponding to Gibbs-Massieu equation $ds = \tau\, du$. The heat flux is obeying Fourier's law hence , $\phi = -\frac{\lambda}{\tau^2}F$ with the heat conductivity λ.

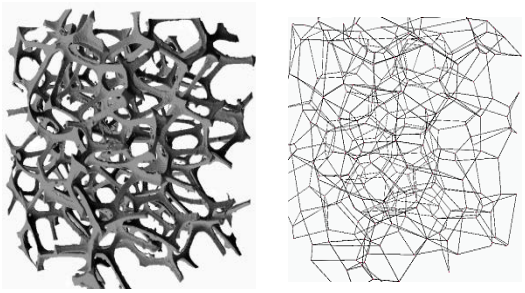

Figure 1. X-ray CT image reconstruction and the solid graph associated (623 nodes and 203 cells).

Writing the set of discrete balance equations, $\frac{d}{dt}\int_{V_i} u_i\, dv = -\int_{\partial V_{ij}} \phi_{ij}\, ds$, for every finite volume V_i associated with node n_i with boundary faces ∂V_{ij} associated with the edges e_{ij}, yields the finite-dimensional Port Hamiltonian Systems [5]:

$$\begin{pmatrix}\frac{du_i}{dt}\\ F_{ij}\end{pmatrix} = \begin{pmatrix}0 & D\\ -D^T & 0\end{pmatrix}\begin{pmatrix}\tau_i\\ \phi_{ij}\end{pmatrix} + \begin{pmatrix}D_b\\ 0\end{pmatrix}\phi_b \quad \text{and} \quad F_b = -D_b^T\tau_i$$

where D and D^T are the incidence and co-incidence matrices of the open graph of the solid. Simulations will be presented in comparison with experimental results [6].

3. Conclusions & perspectives

We have presented the Port Hamiltonian model of the heat conduction in the solid phase of a metallic foam, based on its graph structure obtained by image analysis and tomography. Thereby we take account of the real structure of the foam, the non-regularity of its geometry. Future work will consider the dual graph of the fluid phase and the coupling with the fluid phase and complete the heat transport with mass transport.

Acknowledgments: *Authors acknowledge the support collaborative research DFG & ANR project INFIDHEM.*

References

[1] K. Boomsma, D. Poulikakos, Int. J. Heat Mass Tran. 44 (2001) 827-836.
[2] A.M. Kraynik, Ad. Eng. Mat. 8 (2006) 900-906.
[3] E. Brun, J. Vicente, F. Topin, R. Occelli, iMorph: a 3D Morphological tool to fully analyze all kind of cellular materials in Cellmet'08, Dresden, Germany, 2008.
[4] A. Macchelli, B. Maschke in V. Duindam et al. (Eds.), Infinite-Dimentional Port-Hamiltonian Systems, Springer, Berlin Heidelberg, 2009, pp. 211-271.
[5] A. J. Van Der Schaft and B. M. Maschke, SIAM J. Control Optim. 51 (2013) 906-937.
[6] M. Zanota, I. Pitault, J. Gerardin, F. Bornette, R. Phillippe, D. Edouard, Réacteurs catalytiques structurés: Caractérisation des milieux poreux tel que les mousses métalliques, JEMP, Anglet, France, 2006.

Enhancing the separation performance of glassy poly(2,6-dimethyl-1,4-phenylene oxide) (PPO) with the addition of molecular sieves

Francesco M. Benedetti[1,2], M. Grazia De Angelis[1,2,*], Micaela Degli Esposti[1], Paola Fabbri[1], Alessandro Orsini[3], Alberto Pettinau[3]

1 Department of Civil, Chemical, Environmental and Materials Engineering (DICAM), University of Bologna, Via Terracini 28, 40131, Italy; 2 National Interuniversity Consortium of Materials Science and Technology (INSTM), Italy; 3 Sotacarbo S.p.A, Grande Miniera di Serbariu, 09013 Carbonia, Italy

**Corresponding author: grazia.deangelis@unibo.it*

Highlights

- PPO-based MMMs can be effectively implemented for CO_2 capture applications.
- Inclusion of selective adsorbents such as ZIF-8 and Zeolite 3A remarkably improved gas transport properties of the glassy polymer.
- Increasing temperature enhanced H_2/CO_2 separation, ideal for IGCC application.

1. Introduction

Membrane technologies represent an alternative to address relevant issues such as global warming and energy efficiency, leaving a smaller footprint than traditional technologies. The use of readily available materials to be combined in Mixed Matrix Membranes (MMMs) to improve the performance for gas separation applications, is one of the solutions to achieve large-scale applications.[1] The use of H_2-selective materials in IGCC plants can reduce the energy consumption associated to post-separation CO_2 compression and provide a hydrogen-enriched stream ready to be used as a fuel for power production.[2] To this purpose, we fabricated robust MMMs based on poly(2,6-dimethyl-1,4-phenylene oxide) (PPO) and different molecular sieves such as ZIF-8 and Zeolite 3A. The membrane preparation was optimized to allow the formation of films up to 45 wt.% of filler. Permeation, diffusion and sorption of He (used as a model for H_2), N_2, CH_4, CO_2 were investigated at 35, 50, 65 °C. Pure and composite materials were characterized from the morphological and calorimetrical point of view. Simple mathematical models were applied to evaluate the permeability of gases in the MMMs.[3]

2. Methods

Membranes were casted by solution casting technique under quick solvent evaporation conditions. MMMs were thermally annealed at 200 °C to remove residual solvent and activate the filler particles. To verify the complete solvent removal from the casting step and evaluate the thermal stability, TGA and DSC experiments were performed. Gas permeation was determined by means of a manometric technique and diffusion coefficients were evaluated with the time-lag method in the framework of the solution-diffusion model.[4] Diffusion coefficients were also evaluated from the diffusion kinetics while measuring sorption isotherms in a pressure decay apparatus. The quality of the adhesion between the filler and the polymer was determined through FEG-SEM images. Density

of membranes was measured by means of the buoyancy method. Maxwell-Wagner-Sillar (MWS) model was used to understand whether the membranes follow an additive rule.

3. Results and discussion

SEM images showed good adhesion between the polymer matrix and filler particles. The dispersion of the filler was homogeneous, especially at low loadings. DSC and TGA analysis revealed that membranes were solvent free after the thermal annealing and thermally stable. Remarkable gas transport results were showed, in particular by PPO/ZIF-8 MMMs, which revealed an increase of He permeability of around 800% with respect to the pure PPO and a He/CO_2 selectivity which was up to 15% higher. Permeability of each gas was successfully described with the Maxwell-Wagner-Sillar model in the range of validity of the model (**Figure 1**). MMMs sorption isotherms followed the additive rule. The effect of temperature further enables the gas separation properties, indeed both He permeability and He/CO_2 selectivity increase sharply with increasing temperature. The activation energy of the permeation and diffusion were evaluated as function of the filler content.

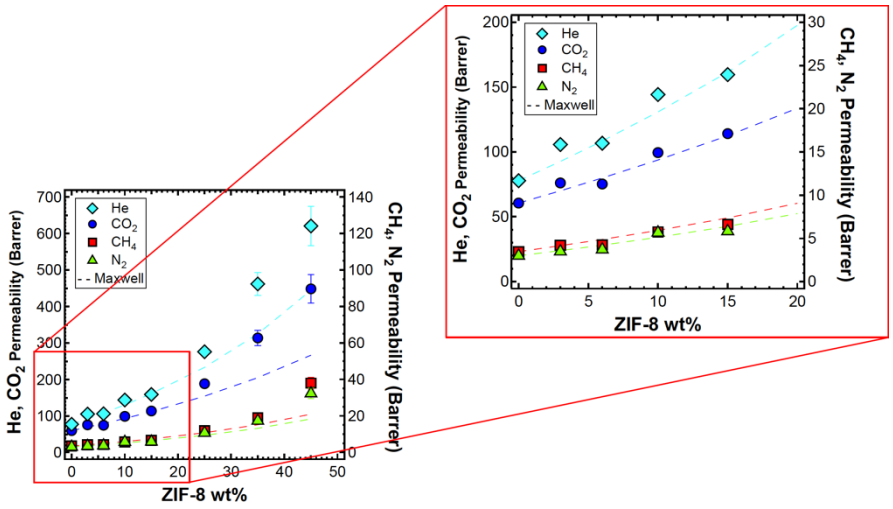

Figure 1. Enhanced gas permeability in PPO/ZIF-8 MMMs. Experimental data (markers) and MWS model (dashed lines).

4. Conclusions

MMMs prepared using PPO and ZIF-8 revealed significantly enhanced transport properties without compromising the processability of the polymer. Density measurements, solubility additive behaviour and Maxell modelling show the ideal behaviour of these MMMs. Higher than ideal permeability at high filler loading may be attributed to percolation phenomenon. Favourable effect on transport properties as the temperature increase make these materials interesting for industrial applications.

References

[1] J. Dechnik, J. Gascon, C.J. Doonan, C. Janiak, C.J. Sumby, Mixed-Matrix Membranes, Angew. Chemie Int. Ed. 56 (2017) 9292–9310.

[2] T.C. Merkel, M. Zhou, R.W. Baker, Carbon dioxide capture with membranes at an IGCC power plant, J. Memb. Sci. 389 (2012) 441–450.

[3] H. Vinh-Thang, S. Kaliaguine, Predictive models for mixed-matrix membrane performance: A review, Chem. Rev. 113 (2013) 4980–5028.

[4] J.G. Wijmans, R.W. Baker, The solution-diffusion model : a review, J. Memb. Sci. 107 (1995) 1–21.

ECCE12
The 12th EUROPEAN CONGRESS OF CHEMICAL ENGINEERING
Florence 15-19 September 2019

Continuous acetic acid extraction from dilute aqueous solutions with supercritical CO_2: experiments and simulation of external extract reflux

Astrid Novella*, Séverine Camy, Jean-Stéphane Condoret

Laboratoire de Génie Chimique, Université de Toulouse, CNRS, INPT, UPS, Toulouse, France

**astrid.novella@ensiacet.fr*

Highlights

- Supercritical fractionation of acetic acid-water mixtures was experimentally studied
- Performances of extraction of AA are low due to thermodynamic limitation
- Simulation of external reflux of extract was performed with Prosim Plus software
- Use of reflux significantly increased the mass fraction of AA in the extract

1. Introduction

Because of emergence of bio-refineries, recovery of valuable products from fermentation broths, such as carboxylic acids, is an important issue to deal with. Conventional purification processes like distillation or solvent extraction present drawbacks that could be alleviated by alternative processes such as supercritical carbon dioxide ($scCO_2$) extraction. $ScCO_2$ was already proposed for purification of alcohol-water mixtures[1] but rarely for recovery of organic acids[2]. Recovery of acetic acid (AA) from dilute aqueous solutions (5% w/w) using a $scCO_2$ countercurrent packed column was experimentally studied at laboratory scale and compared with modelling using a so-called rate-based model[3]. Experimentally, best results were obtained at 40°C and 15 MPa with a solvent-to-feed ratio S/F equal to 11 (according to experimental limits of the set-up), resulting in 43% w/w AA in the CO2-free extract with an AA recovery ratio equal to 36%[4]. This remains low as compared to performances of conventional processes and this is mainly due to the low partition coefficient of AA between CO_2 and water. However, for such systems with unfavorable thermodynamic behavior, use of reflux of extract is likely to allow significant increase of the extract composition. In the present work, performance of this configuration with reflux is assessed by using the commercial process simulation software Prosim Plus (ProSim SA, France), where the column is described as a set of theoretical stages. Thermodynamics of the CO_2-AA-water ternary system is described by an homogeneous approach with Boston-Mathias modified SRK equation of state with PSRK mixing rule and UNIQUAC coefficient activity model (EoS/G^E). For this system, depending on pressure and temperature conditions, so-called type I or type II ternary diagrams can be observed. In this study, design is proposed in terms of reflux ratio and number of theoretical stages for the recovery of AA from water with $scCO_2$, for two sets of operating conditions, corresponding to type I and type II ternary behavior.

2. Methods

Two sets of operating conditions were studied, 45°C and 10 MPa (type I diagram) and 65°C, 12.8 MPa (type II diagram) with and without external extract reflux. From ternary diagrams of figure 1, about 90% w/w of acetic acid in the extract could theoretically be reached at 45°C, 10 MPa, using

external reflux (Fig.1 left) and 100% w/w at 65°C and 12.8 MPa (Fig.1 right). To reach these separation objectives, minimal reflux ratio was graphically determined. Then, value of operational reflux, CO_2 flow-rate and number of theoretical stages were varied to approach these high separation performances.

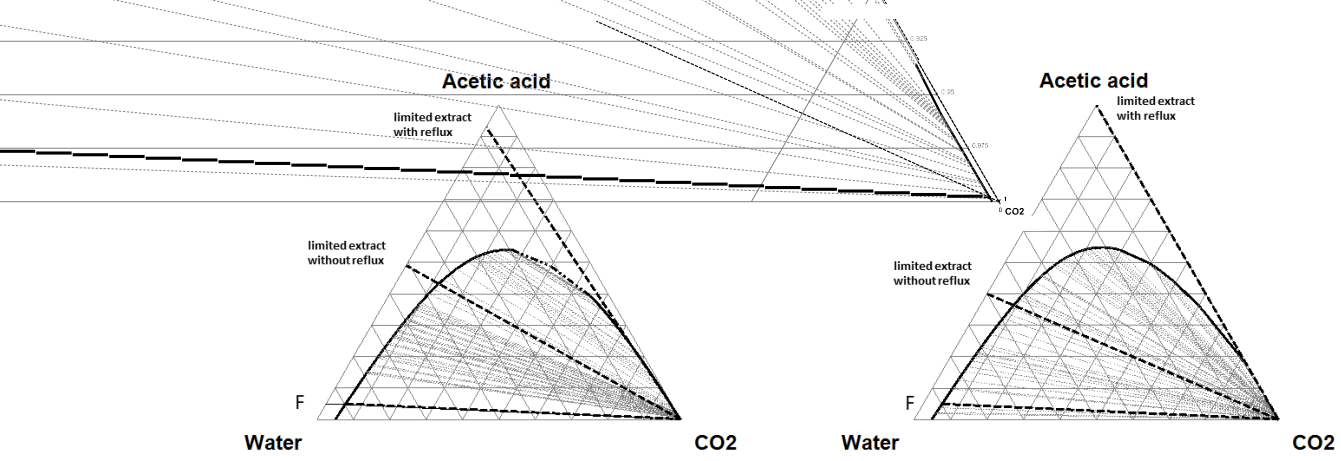

Figure 1. Left : 45°C 10 MPa (type I diagram) & Right : 65°C 12.8 MPa (type II diagram)
Equilibrium curves (solid lines), construction for limited extract in simple and reflux configurations (dotted lines)

3. Results and discussion

At 45°C and 10 MPa, using a S/F=10 with 10 theoretical stages and a reflux ratio=15.5, 87% w/w AA in the extract could be obtained, with a 23% recovery ratio whereas in the conventional extraction without reflux, only 30% w/w of AA in the extract are achieved. At 65°C and 12.8 MPa, 85% w/w AA (with a recovery ratio of 23%) in the extract could be obtained (same S/F and number of stage and with reflux ratio=18.2) whereas only 24% is reached without reflux. These results evidence the theoretical possibility to reach high separation performances for the recovery of dilute acetic acid in water.

4. Conclusions

In this work, supercritical CO_2 extraction for recovery of acetic acid, as an alternative to conventional processes, such as distillation or solvent extraction, was studied. Using conventional configuration of a packed column, *i.e.,* without extract reflux, high purity and high recovery ratio cannot be obtained due to thermodynamic barrier whereas modeling indicated that use of extract reflux could significantly improve separation performances. A larger range of operating conditions has to be considered now to find the optimal design of the contactor (S/F, number of stages, position of feed, reflux ratio). Nevertheless, these theoretical findings remain to be experimentally validated using a lab scale contactor[5]and this work is in progress in our lab.

References

1. M. Budich, G. Brunner, J. Supercrit. Fluid **2003**, 25, 45-55
2. B. G. Garrett, K. Srinivas, B. K. Ahring, J. Supercrit. Fluid **2014**, 95, 243-251
3. N. Gañán, J. Morchain, S. Camy, J.-S. Condoret, J. Supercrit. Fluid **2018**, 135, 168-179
4. A. Novella, N. Gañán, S. Camy, J.-S. Condoret, Proceeding for ISSF **2018**, http://supflu2018.fr/pdf/PF02.pdf
5. R. Lalam, S. Chamali, S. Camy, D. Rouzineau, R. Kessas, J.-S. Condoret, J. Supercrit. Fluid **2015**, 101, 24-35

ECCE12
The 12th EUROPEAN CONGRESS OF CHEMICAL ENGINEERING
Florence 15-19 September 2019

Novel catalytic distillation processes for a sustainable chemical industry

Anton A. Kiss[1,2]

1 School of Chemical Engineering and Analytical Science, The University of Manchester, Sackville Street, Manchester, M13 9PL, United Kingdom; 2 Sustainable Process Technology Group, Faculty of Science and Technology, University of Twente, PO Box 217, 7500 AE Enschede, The Netherlands

**Corresponding author: tony.kiss@manchester.ac.uk*

Highlights

- Novel reactive distillation processes

1. Introduction

Reactive distillation (RD) is an efficient process intensification technique that integrates catalytic chemical reaction and distillation in one single apparatus acting as a multi-functional reactor. [1] When a heterogeneous catalyst is used, the process is known as catalytic distillation (CD). RD/CD technology has many key advantages such as reduced capital investment and significant energy savings, as it can surpass equilibrium limitations, simplify complex processes, increase product selectivity and improve the separation efficiency.[2] However, reactive distillation is constrained by key thermodynamic requirements (e.g. related to volatility differences and heat of reaction), overlapping of the reaction and distillation operating conditions, and the availability of catalysts that are active, selective and with sufficient longevity to ensure economical operation.

2. Methods

This lecture aims to give an overview of the challenges and opportunities for catalytic distillation processes, the requirements in terms of hardware and catalyst engineering, and it also provides some industrially relevant examples. The potential of reactive / catalytic distillation processes to transform the chemical process industry is assessed from a techno-economic and sustainability perspective. Moreover, the role of the chemical engineering community in enhancing the applicability range of catalytic distillation technology will be addressed and discussed.

3. Results and discussion

The detailed examples presented in this study show that catalyzed RD processes can drastically improve the production of important chemicals such as: acrylic and methacrylic monomers, unsaturated polyesters resins, alkyl ethers (dimethyl ether, di-n-pentyl ether), fatty esters, and other short chain alkyl esters. Various RD configurations can be used, as illustrated in Figure 1. [3] The main drivers for such novel reactive distillation applications are: economical (large reduction of costs and energy use), environmental (lower CO2 emissions, no or reduced waste) and social (improved safety and health due to lower reactive content, reduced footprint and run away sensitivity). Hence RD technology strongly contributes to all three pillars of sustainability in the chemical process industry.

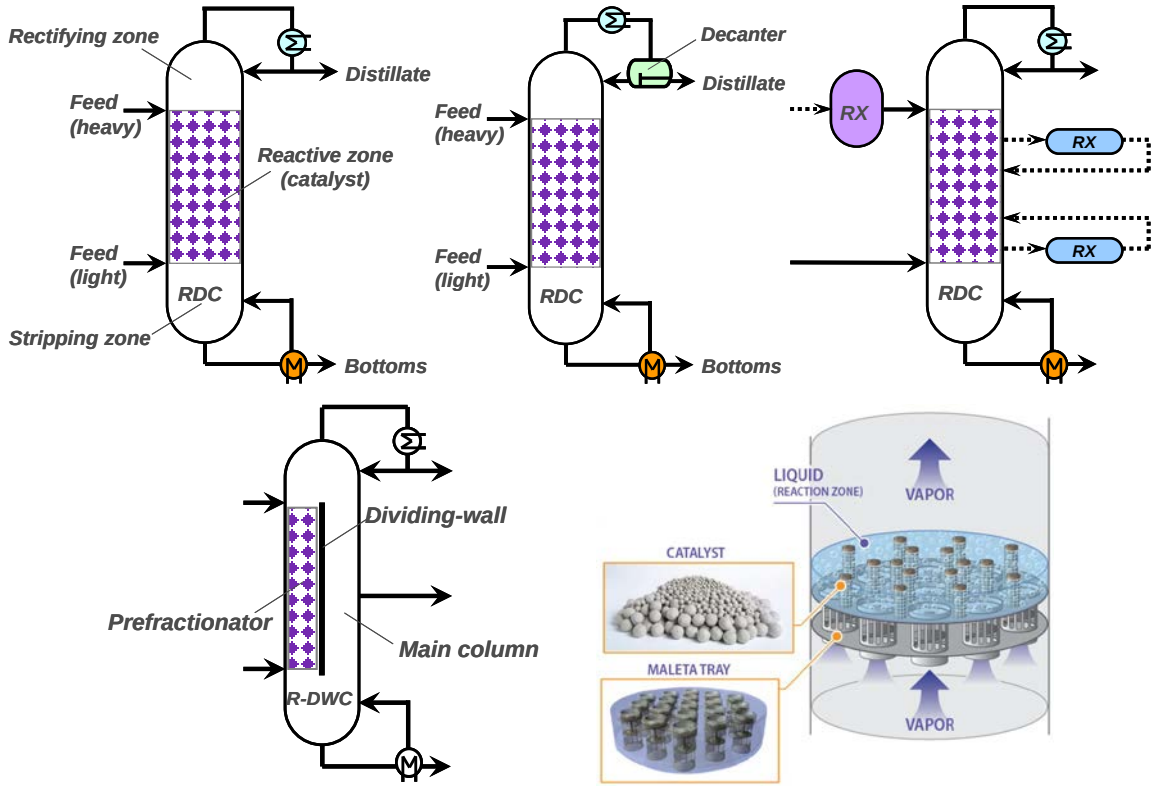

Figure 1: Configurations of reactive distillation processes: classic RD, azeotropic RD, RD with pre-reactors and side-reactors, reactive dividing-wall column (R-DWC), catalytic cyclic distillation internals (Maleta trays).

4. Conclusions

Despite the relatively complex design, control and equipment, RD remains one of the best process intensification technologies that fulfils all the principles of green engineering: design for separation, maximize efficiency, use renewable vs depleting sources, prevent instead of treat, meet need and minimize excess, integrate local material and energy flows, output-pulled vs input-pushed, and design for a commercial afterlife. RD offers key unique features such as: low number of processing units, enhanced overall rates, overcome unfavorable equilibrium, avoid difficult separations, improved selectivity, reduced energy use, less CO2 emissions, low or no solvent use. Considering the outstanding progress in equipment development, modeling and simulation, design and control strategies, real time optimization, and the rapid pace of exploring new applications, RD remains an important PI technique capable to bring green chemistry and sustainable engineering into the chemical process industry.

References

[1] A. A. Kiss, Topics in Catalysis (2019) DOI: 10.1007/s11244-018-1052-9
[2] A. A. Kiss, Journal of Chemical Technology and Biotechnology, 89 (2014) 479-498.
[3] A. A. Kiss, Advanced Distillation Technologies - Design, Control and Applications, Wiley, 2013.

ECCE12
The 12th EUROPEAN CONGRESS OF CHEMICAL ENGINEERING
Florence 15-19 September 2019

Investigating reverse osmosis membrane fouling and scaling by membrane autopsy.

Nishtha Dhunnoo[1], Luiza C. Campos[2], Pablo García-Triñanes [1]

[1] *Flow, Heat and Reaction Engineering Group (FHRENG), School of Engineering, University of Greenwich, Medway, ME4 4TB, United Kingdom;*
[2] *Department of Civil, Environmental and Geomatic Engineering, University College London, Gower Street, London WC1E 6BT, United Kingdom*
**Corresponding author: p.garciatrinanes@gre.ac.uk*

Highlights

- The study involved performing membrane autopsy and carrying out a series of tests to investigate the mitigation of fouling and scaling.
- Diatoms, pseudomonas and polysaccharides were the main biofoulants identified.
- Analysis revealed aluminium, calcium and silica as the main elements contributing to inorganic scaling.
- The findings pointed out flaws in pretreatment system of the household water treatment equipment.

1. Introduction

Population bloom, economic growth, industrialisation, climate change and water mismanagement are contributing to diminution of water globally. Many countries have adopted seawater reverse osmosis (RO) desalination to cope with increasing water demand [1]. However, fouling and scaling are crucial problems in the implementation of desalination which increases the cost of running this technology. Reduced efficiency is experienced in terms of a decrease in product output and permeate flux, high energy demand, increased operating pressure and reduced membrane lifetime [2]. The purpose of this research involves the study of proactive methods to mitigate RO membrane fouling and scaling.

2. Methods

This research involves investigating a desalination equipment used in household water treatment. Visual inspection was first carried out to observe the physical integrity to visually identify potential foulants. This step is important in determining subsequent analyses. Scanning electron microscopy (SEM) analysis was then performed to determine the topography and morphology of samples. This was conducted in conjunction with Energy Dispersive Spectroscopy (EDS) to identify and quantify the composition of the sample based on its element. Fourier Transform Infrared (FTIR) spectroscopy was then carried out to compare the wavelength of the foulant to identify the chemical bonds present. This was followed by three microbiological tests, namely catalase test, gram stain and API (Analytical Profile Index) test, to identify the bacteria causing biological fouling.

3. Results and discussion

Through visual inspection, Reverse Osmosis (RO) membrane fouling was visible as an irregularly distributed, thin and watery fouling layer. Scanning Electron Microscopy (SEM) characterization showed inorganic scaling in the form of salt crystal deposits. Different types of diatoms were also identified. Energy Dispersive Spectroscopy (EDS) analysis showed high concentration of Oxygen (O) and Carbon (C) suggesting deposits of organic and biological materials, with composition of C varying from 3.7% to 52.2% while that for O varying from 17% to 60% in the first membrane. Inorganic elements identified in the fouling layer through EDS are Al, Ca and Si. The spectrum obtained from Fourier Transform Infrared (FTIR) characterisation is shown in Figure 1. Amine group, amide group, proteins, polysaccharides, nucleic acid and aromatic compound were identified though interpretation of the frequency bands [3,4]. Different pseudomona species were identified through microbiological test analyses, confirming bacteria as one of the main causes for biofouling.

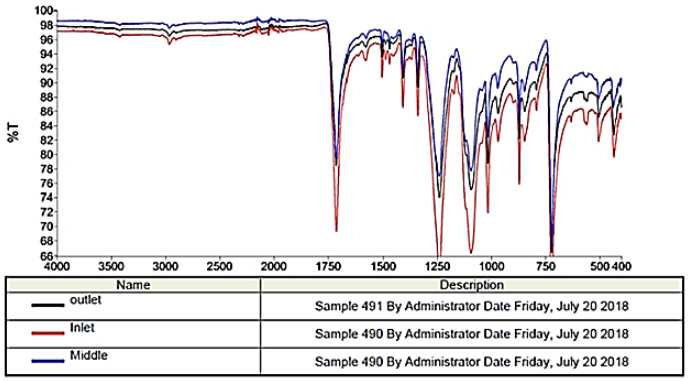

Figure 1. FTIR spectrum of membrane for outlet, middle and inlet sample.

4. Conclusions

Conclusions drawn through interpretation of membrane autopsy analyses indicate that biofouling is very pronounced due to the high number of diatoms, bacteria and the presence of carbon and oxygen. Inorganic scaling has also taken place in the membrane. The current pretreatment system being used in the water treatment equipment proves to be inefficient and inadequate. Additional pretreatment is required to protect the membrane from fouling and scaling. This need to be implemented based on the water quality flowing through the equipment.

References

[1] United Nations. (2018). Report of the Inter-agency Task Force on Financing for Development, New York: United Nations publication.

[2] Goh, P., Lau, W., Othman, M., Ismail, A. (2018). Membrane fouling in desalination and its mitigation strategies. *Desalination*, Volume 425, pp. 130-155.

[3] Jung, J., Ryu, J., Choi, S.Y., Park, K.Y., Song, W.J., Yu, Y., Jang, Y., Park, J., Kweon, J. (2018). Autopsy study of irreversible foulants on polyvinylidene fluoride hollow-fiber membranes in an immersed microfiltration system operated for five years. *Separation and Purification Technology*, Volume 199, pp. 1-8.

[4] Yu, T., Meng, L., Zhao, Q., Shi, Y., Hu, H., Lu, Y., (2017). Effects of chemical cleaning on RO membrane inorganic, organic and microbial foulant removal in a full-scale plant for municipal municipal wastewater reclamation. *Water Research*, Volume 113, pp. 1-10.

ECCE12
The 12th EUROPEAN CONGRESS OF CHEMICAL ENGINEERING
Florence 15-19 September 2019

Separation of SiO_2 Nanoparticles by Preparative Agarose Gel Electrophoresis with and without Limitation by Mesh Size.

Matthäus Barasinski[1], Georg Garnweitner[1]

1 Technische Universität Braunschweig, Institute for Particle Technology and Laboratory for Emerging Nanometrology, 38106 Braunschweig, Germany

**Corresponding author: m.barasinski@tu-bs.de*

Highlights

- Size fractionation of SiO_2 nanoparticles (10-300 nm) by agarose gel electrophoresis
- Particle migration is observed following a limited and an unlimited regime:
  - Limited migration of particles for sizes similar to gel mesh size
  - Unlimited migration of smaller particles according to zeta potential

1. Introduction

Monodisperse nanoparticles (NP) with completely uniform properties regarding size and morphology are essential already today e.g. for optical (plasmonic) applications. In future, such particles will be necessary for use in further areas, for example all complex nanosystems involving self-assembly processes. There these uniform NP promise structures with highest precision.
Since the required narrow particle size distribution or monodispersity typically is not reached after the synthesis at industrial scale, purification steps are needed. In most cases the high diffusion rates of NP are problematic for a practicable separation with conventional methods. For this reason, we investigate the use of gel electrophoresis for preparative purification, which provides the opportunity of a highly selective separation of synthesized NP by size and morphology. Thereby, the NP are spatially separated in an appropriate gel according to their different electrophoretic mobilities, with the gel matrix substantially reducing the NP diffusion. In principle, the mobility can be simply calculated by the measurement of zeta potential and utilization of the Henry formula.

2. Methods

The movement of the NP is traced during the migration by a simple camera and subsequent image processing, for correlation of the experimental data to the calculated electrophoretic mobility. Besides this, the separation of NP with regard to size and morphology is evaluated with SEM, TEM and small angle X-ray scattering (SAXS) inside the gel.

3. Results and discussion

After the Stöber-synthesis of silica NP under different ammonia concentrations, sizes and zeta potentials ζ were measured via DLS. The measured data show that bigger particles have greater absolute values of zeta potential. Once the voltage was set on, particles start to migrate from gel pockets through the gel from cathode to anode (here: due to negative zeta potential from top down). In Figure 1 different samples can be seen due to scattered light in a 0.2 wt-% agarose gel

after 50 minutes at an applied voltage of 40 V. Two different migration regimes can be distinguished: the unlimited and the limited case. If there is no limitation by too small mesh sizes of the gel, bigger particles migrate faster due to their greater absolute value of zeta potential (samples A and B) than smaller ones. In contrast, sample D is influenced by the mesh size which limits its migration although this sample has the most negative zeta potential. For sample C both cases are valid because the particle size distribution is quite large. Bigger particles within sample C seem to be limited by mesh sizes whereas smaller ones show unlimited and fast migration on the basis of their zeta potential.

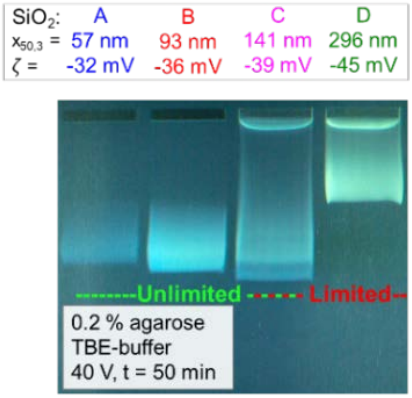

Figure 1. Migration of SiO_2-NP with different sizes in a 0.2 wt-% agarose gel after 50 minutes and an applied voltage of 40 mV.

As an example, in Figure 2 the migration of two SiO_2 samples and a separation of their binary mixture are presented. Sample D with the higher absolute value of zeta potential migrates much slower than sample B, because the mesh size of this specific agarose gel limits its migration speed. Here, the limited case is applied which acts like a sieve to separate the two fractions. After the electrophoretic experiment the particle sizes of the fractions were confirmed with dried gel samples by SEM images.

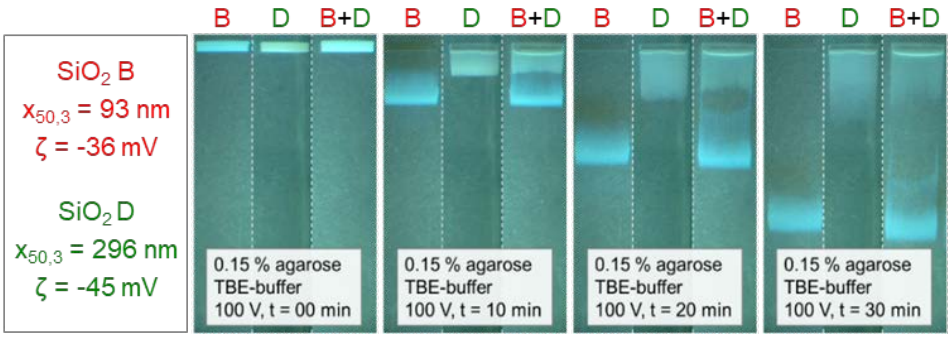

Figure 2. Separation of SiO_2-NP by limitation of sample D (bigger particles) in a 0.15 wt-% agarose gel at 100 V and different times (t = 0, 10, 20 and 30 min).

4. Conclusions

The influence of particle size and zeta potential on the migration behavior of particles inside an agarose gel was investigated and binary mixtures were successfully separated. After the electrophoretic experiment, particles were characterized by SEM, TEM and SAXS inside the gel.

ECCE12
The 12th EUROPEAN CONGRESS OF CHEMICAL ENGINEERING
Florence 15-19 September 2019

Direct observation of particle accumulation on a model filter: analysis of the morphology of solid particles and yeast cakes.

Alberto Valencia[1], Philippe Schmitz[1*], Christine Lafforgue-Baldas[1], Jeffrey Morris[2]

1 Université de Toulouse, INSA, LISBP, Avenue de Rangueil, 135, F-31077 Toulouse, France;
2 Levich Institute, CUNY City College of New York, 140th Street and Convent Avenue, New York, NY 10031
**Corresponding author: schmitz@insa-toulouse.fr*

Highlights

- A new microfluidic device for direct observation of particle accumulation.
- Use of image processing for particle tracking and concentration profile
- Growth of cakes of spherical solid particles and yeast cells.
- Compressibility effects of the yeast cake.

1. Introduction

Particle transport and capture are widely encountered in many applications, from living to environmental and manufactured systems. In the particular case of filtration of living cells such as microorganisms, the fouling phenomenon, partly related to cell accumulation at the filter surface, should still be better understood to improve the performance of a number of devices. Experiments in model systems have exhibited complex behaviors of the microorganisms due to their specific properties (shapes, mechanical properties, physiological state) that drastically depend on the local environment. A new microfluidic device was thus developed to study the morphology of filtration cakes through the direct observation of particle accumulation. Particle trajectories, velocity and concentration fields were all studied during cake growth.

2. Methods

The setup consists of a transparent photoetched microfluidic device with a rectangular channel (1mm x 20 to 30 µm) having a filtering structure of multiple slots and a microscope connected to a computer (Figure 1A). Different filter geometries were obtained by varying the width of the slots and the pitch (Figure 1B). Two model suspensions were used: monodispersed spherical solid particles (8.2µm) purchased from Thermoscientific, and cultivated yeast cells (mean diameter 6µm). Filtration experiments were performed at low flow rates (1 to 20 µl/min). The images of particle transport and capture and pressure drop were recorded during filtration. Dedicated image processing modules were developed for particle tracking, velocity and concentration fields and fluid/cake interface tracking.

3. Results and discussion

The effect of the filter geometry on the final position of the first arriving particles and the subsequent blockage of the slots was carefully analyzed. First, particles can eventually protect neighbor slots from blockage as function of the ratio between particle size and pitch (Figure 2A).

The same results were previously obtained in the case of microsieves (provided by Aquamarjin) made of regular arrangement of circular pores [1]. Then the permeability of the resulting first layers of accumulated particles depends on the filter geometry.

The mean porosity of the cake was calculated from the cake observed thickness and the mass of particles accumulated, taking into account the time variation of the particle concentration field above the cake. As can be expected it is about 50% in the case of spherical solid particles. However, it is lower in the case of yeast suspensions and slightly decreases with time of filtration, exhibiting a compressibility effects of yeast cakes. This phenomenon was observed as an increase of the cake thickness when the flow rate is stopped (Figure 2B). Analog results were previously obtained and explained by the deformation of the yeast under pressure [2].

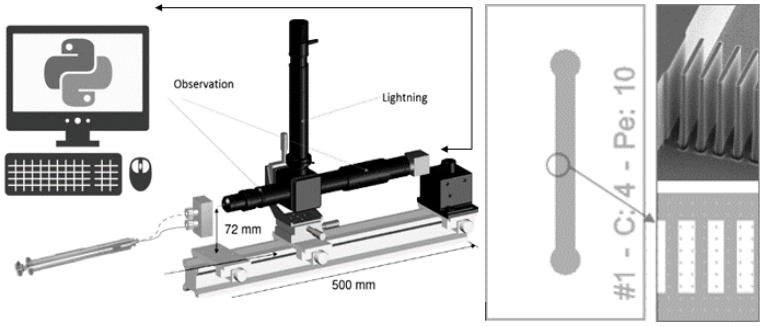

Figure 1. A) Experimental setup. B) Details of the filter geometry

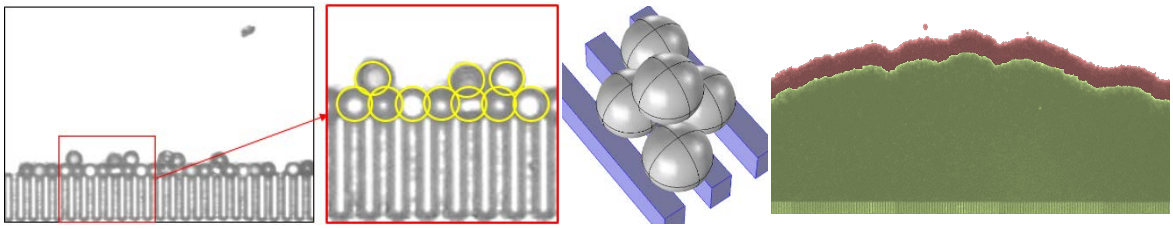

Figure 2. A) Visualization and sketch of first particle layer deposition. B) Compressibility effects of the yeast cake

4. Conclusions

A new microfluidic filtration device was developed to scrutinize the particle accumulation on a model filter. The results allow for better understanding of the first step of cake formation and the morphology of the cake, especially for yeast suspensions. Discussions should be strengthened by future experiments with non-spherical solid particles (snowman shape, for example) and yeast cells obtained from different states of cultivation.

References

[1] I. Ben Hassan, C. Lafforgue, A. Ayadi, P. Schmitz, J. Membr. Sci. 454 (2014) 283–297.
[2] M. Meireles, M. Clifton, Michael, P. Aimar, Desalination. 147 (2002) 19-23.

ECCE12
The 12th EUROPEAN CONGRESS OF CHEMICAL ENGINEERING
Florence 15-19 September 2019

Simulation of the AMP process for the purification of a flue gas stream from a power plant

Stefania Moioli[1], Ricardo R. Wanderley[2], Laura A. Pellegrini[1], Hanna K. Knuutila[2]

1 GASP, Group of Advanced Separation Processes and GAS Processing, Dipartimento di Chimica, Materiali e Ingegneria Chimica "Giulio Natta", Politecnico di Milano, Piazza Leonardo da Vinci 32, I-20133 Milano, Italy;
2 Department of Chemical Engineering, NTNU, N-7491 Trondheim, Norway
**Corresponding author: stefania.moioli@polimi.it*

Highlights

- Carbon dioxide removal needs to be applied for climate change mitigation.
- AMP is a sterically hindered amine which can be used for CO_2 removal.
- Simulation of non-precipitating aqueous AMP process for CO_2 absorption.
- Future development of precipitating pseudo-solvents based on literature data for AMP.

1. Introduction

Carbon dioxide is the greenhouse gas which produces the strongest effect on global warming and several methods for its removal have been developed, with chemical absorption (usually by aqueous solutions of alkanolamines) being generally recognized as a suitable technology in particular when applied to treatment of gaseous streams as flue gases from power plants. The formation of solids upon CO_2 absorption is a feature of many alternative amine systems and precipitation may actually be considered advantageous [1], as outlined in studies on potassium taurate [2,3], and by the UNO MK 3 process [4,5]. Notwithstanding these efforts, not enough attention has been paid on methodically outlining which particularities arise when moving from regular monophasic solvents to precipitating solvents. Issues such as increases in equipment complexity and sizing, the handling of viscous slurries, the shifting in rates of absorption upon precipitation are easily overlooked. Furthermore, the main energetic benefits of this process will be wasted if plant designers forget to adapt the typical absorption-desorption process structure to the specific context of precipitating solvents. With the aim of mapping the opportunities and challenges of employing precipitating solutions, a token solvent of aqueous 2-amino-2-methyl-1-propanol (AMP) has been selected. AMP is a sterically hindered primary alkanolamine with a tertiary carbon atom attached to the amino group. It presents good absorption capacity, absorption rate, selectivity and degradation resistance if compared to traditional amines [6]. Recently, Svensson et al. [7,8] have focused a lot of effort in developing a precipitating solvent based on AMP plus N-methyl-2-pyrrolidinone (NMP). For that reason, AMP is a good starting point for this analysis. In order to study this type of solvents, the first step, on which this work focuses, is to provide an accurate process design for a CO_2 capture plant based on aqueous AMP, for which only few papers in the literature [6,9-12] can be found.

2. Methods

ASPEN Plus® has been employed as tool for simulation. The thermodynamic model has been selected considering that the system is strongly non-ideal because of the chemical reactions

occurring in the liquid phase and generating ions and validated by comparison with experimental data. Kinetics and mass transfer have been taken into account for the simulation of the absorption and desorption units.

3. Results and discussion

The purification of a flue gas from a 500 MW coal-fired power plant has been considered for removal of 90% of carbon dioxide. The obtained results show that the profiles of the absorber are characterized by the same trends typical of the ones of traditional amines. Similar trends occur also in the regeneration section, though being the required energy different.

4. Conclusions

This works has focused on the study of AMP for use as solvent for the chemical absorption of carbon dioxide from flue gas of a 500 MW coal-fired power plant, which is removed with the aim of reducing the greenhouse gas emissions to the atmosphere. ASPEN Plus® has been validated and used for the simulation of the system, providing an accurate representation of the system, which can be used as a basis for the future developments of the work.

References

[1] U.E. Aronu, I. Kim, G. Haugen, Evaluation of Energetic Benefit for Solid-liquid Phase Change CO_2 Absorbents, Energy Procedia 63 (2014) 532-541.

[2] E. Sanchez-Fernandez, E.L.V. Goetheer, DECAB: process development of a phase change absorption process, Energy Procedia 4 (2011) 868-875.

[3] S. Moioli, M.H. Ho, D.E. Wiley, L.A. Pellegrini, Thermodynamic Modeling of the System of CO_2 and Potassium Taurate Solution for Simulation of the Process of Carbon Dioxide Removal, Chem. Eng. Res. Des. 136 (2018) 834-845.

[4] C. Anderson, B. Hooper, A. Qader, T. Harkin, K. Smith, K. Mumford, J. Pandit, M. Ho, A. Lee, N. Nicholas, Indrawan, J. Gouw, J. Xiao, N. Thanumurthy, N. Temple, G. Stevens, D. Wiley, Recent Developments in the UNO MK 3 Process–A Low Cost, Environmentally Benign Precipitating Process for CO_2 Capture, Energy Procedia 63 (2014) 1773-1780.

[5] K. Smith, A. Lee, K. Mumford, S. Li, Indrawan, N. Thanumurthy, N. Temple, C. Anderson, B. Hooper, S. Kentish, G. Stevens, Pilot plant results for a precipitating potassium carbonate solvent absorption process promoted with glycine for enhanced CO_2 capture, Fuel Processing Technology 135 (2015) 60-65.

[6] M. Afkhamipour, M. Mofarahi, Sensitivity analysis of the rate-based CO_2 absorber model using amine solutions (MEA, MDEA and AMP) in packed columns, Int. J. Greenh. Gas Control 25 (2014) 9-22.

[7] H. Svensson, J. Edfeldt, V. Zejnullahu Velasco, C. Hulteberg, H.T. Karlsson, Solubility of carbon dioxide in mixtures of 2-amino-2-methyl-1-propanol and organic solvents, Int. J. Greenh. Gas Control 27 (2014) 247-254.

[8] H. Svensson, C. Hulteberg, H.T. Karlsson, Precipitation of AMP Carbamate in CO_2 Absorption Process, Energy Procedia 63 (2014) 750-757.

[9] J. Gabrielsen, M.L. Michelsen, E.H. Stenby, G.M. Kontogeorgis, Modeling of CO_2 absorber using an AMP solution, AIChE J. 52 (2006) 3443-3451.

[10] H. Mehdizadeh, M. Gupta, I. Kim, E.F. Da Silva, T. Haug-Warberg, H.F. Svendsen, AMP–CO_2–water thermodynamics, a combination of UNIQUAC model, computational chemistry and experimental data, Int. J. Greenh. Gas Control 18 (2013) 173-182.

[11] D. Tong, J.P.M. Trusler, G.C. Maitland, J. Gibbins, P.S. Fennell, Solubility of carbon dioxide in aqueous solution of monoethanolamine or 2-amino-2-methyl-1-propanol: Experimental measurements and modelling, Int. J. Greenh. Gas Control 6 (2012) 37-47.

[12] S.K. Dash, A.N. Samanta, S.S. Bandyopadhyay, (Vapour+liquid) equilibria (VLE) of CO_2 in aqueous solutions of 2-amino-2-methyl-1-propanol: New data and modelling using eNRTL-equation, The Journal of Chemical Thermodynamics 43 (2011) 1278-1285.

ECCE12
The 12th EUROPEAN CONGRESS OF CHEMICAL ENGINEERING
Florence 15-19 September 2019

Strategies to improve the performance of Membrane Distillation.

Alessandra Criscuoli*

Institute on Membrane Technology (ITM-CNR), via P. Bucci 17/C, 87036 Rende (CS)

**Corresponding author: a.criscuoli@itm.cnr.it*

Highlights

- Different Membrane Distillation configurations were integrated.
- Different designs of membrane modules were realized.
- A feed-side heated flat membrane module was designed.

1. Introduction

Membrane Distillation (MD) is a thermal membrane separation technique based on the use of microporous hydrophobic membranes. The evaporation of the liquid feed occurs at the liquid-membrane interface, because of the hydrophobic membrane properties that prevent the liquid phase to permeate, and the vapor moves through the membrane micropores thanks to a difference of vapor pressures (driving force) established across the membrane. Depending on the way the driving force is created, different MD configurations can be obtained. The potential of MD as an efficient separation technique has been demonstrated in many fields (seawater and brackish water desalination, wastewater treatment, purification of physiological solutions, etc.). Complete rejection of non-volatile species can be, in fact, obtained working at lower operating temperatures and equipment size than traditional distillation columns. The high specific thermal energy consumption (ratio between the thermal energy supplied and the permeate produced) is, however, one of the main drawbacks of the technique, that is limiting its implementation at large scale. In this respect, this works aims at presenting some possible strategies to improve the performance of MD, in terms of higher permeate flux and lower energy consumption. In particular, the simplest and most investigated MD configuration, the Direct Contact Membrane Distillation (DCMD), was considered in the present study.

2. Methods

Three strategies were investigated to improve the performance of DCMD:

1. The coupling of the DCMD unit with an Air Gap Membrane Distillation (AGMD) unit, where the feed exiting from DCMD was heated up in AGMD [1];

2. The realization of new DCMD flat membrane modules presenting baffles at the feed side [2];

3. The design of a feed-side heated DCMD flat membrane module.

For each case, experiments were carried out by varying operating temperatures and flow rates, and the best conditions were identified.

3. Results and discussion

The investigated approaches allowed to reach positive results, like:

1. lower specific thermal energy consumption and higher permeate production for the integrated MD system;
2. better heat transport and higher permeate flux for the new DCMD designs.

4. Conclusions

The results obtained in this work confirmed the validity of the proposed strategies to improve the efficiency of DCMD. As future research, the combination of the three approaches could be explored to further enhance the performance of this promising separation technology.

References

[1] A. Criscuoli, Chem. Eng. Res. Des. 111 (2016) 316–322.
[2] A. Criscuoli, ICOM2017, July 30-August 4, 2017, San Francisco.

ECCE12
The 12th EUROPEAN CONGRESS OF CHEMICAL ENGINEERING
Florence 15-19 September 2019

STRATEGIES FOR PARACETAMOL WITH 4'-CHLOROACETANILIDE PURIFICATION AND CRYSTALLIZATION

Leila Keshavarz, Rene Steendam, Lian Blijlevens, Patrick Frawley

The striking ability of impurities to significantly influence crystallization processes is a topic of paramount interest in the pharmaceutical industry. Despite being present in small quantities, impurities tend to considerably change a crystallization process as well as the final crystalline product. In the present work, the effect of two markedly different impurities 4-nitrophenol and 4'-chloroacetanilide on the solubility, nucleation and crystallization of paracetamol are described. In the first part of this work, the fundamentals are outlined and show that although each impurity led to a small increase in solubility of paracetamol, their effect as a nucleation inhibitor was much more pronounced. Induction time experiments were used in conjunction with the classical nucleation theory to show that the impurities did not affect the solid-liquid interfacial energy but instead significantly reduced the kinetic factor, overall resulting in reduced nucleation rates. Intriguingly, both impurities influenced the solubility and nucleation of paracetamol in a similar fashion despite their significant differences in terms of molecular structure, solubility and ability to incorporate into the crystal structure of paracetamol. In the second part of this work, the incorporation of 4'-chloroacetanilide into the solid phase of paracetamol was investigated. The presence of 4'-chloroacetanilide in the solid phase of paracetamol significantly increased the compressibility of paracetamol, resulting in improved processability properties of paracetamol. The compressibility efficiency of paracetamol could be controlled using the amount of incorporated 4'-chloroacetanilide. Therefore, an experimental design space was developed and utilized to select the most important process parameters for impurity incorporation. Intriguingly, the number of carbon atoms in the aliphatic chain of the alcohol solvent strongly correlated to the impurity incorporation efficiency. As a result, it was feasible to accurately control the compressibility and the amount of 4'-chloroacetanilide in the solid phase of paracetamol by simply choosing the required alcohol as the solvent for crystallization. Thus, the present work comprehensively shows how different impurities impact the key crystallization mechanisms and properties of a pharmaceutical product. Rational process control over the incorporation of impurities and additives allows for advanced manufacturing of products with tailored specifications.

ECCE12
The 12th EUROPEAN CONGRESS OF CHEMICAL ENGINEERING
Florence 15-19 September 2019

Improved FOS fractionation using inhomogeneous membrane cascades

Zulhaj Rizki[1,*], Anja Janssen[1], Remko Boom[1] and Albert van der Padt[1]

1 Wageningen University, Food Process Engineering Group, the Netherlands

**Corresponding author: zulhaj.zulhajrizki@wur.nl*

Highlights

- Inhomogeneous filtration cascades fractionated FOS into 3 fractions vary in sizes.
- Separation was improved using more stages and altering configurations.
- Optimizing the process considering all performance indicators was done using a multi-criteria decision making approach.

1. Introduction

Fractionating fructo-oligosaccharides (FOS) into multiple fractions that vary in degree of polymerization (DP) is beneficial to produce prebiotics with different functionalities. Membrane separation becomes a favorable option for fractionating FOS due to its mild condition and high selectivity. However, a single stage membrane can only produce 2 fractions at a time and its maximum achievable purity is limited. Using a cascaded multi-stage membrane system overcomes that purity limitation and opens a possibility to extract multiple products at once. We used an inhomogeneous membrane cascade system to fractionate FOS into 3 different products rich in monosaccharides (DP1), DP3 and DP≥5 simultaneously using a side-stream approach (Figure 1.a). Differentiating from the firstly introduced ideal cascade [1], the inhomogeneous cascades allow us to use different set up at each stage [2] resulting a better separation performance. Having an independent system and multiple products raise new design questions: Which set up to use at each stage? And which (product) parameter should be optimized? Aided by a mathematical model, we simulated various possible setups and developed a method to select the best setup using a multi-criteria decision making approach.

2. Methods

A model based on characterization of 3 types of membranes (GE, GH and GK from GE Osmonic, USA, model 1812) was developed to predict the performance of single stage membranes. Such model was later expanded for cascaded systems [3]. A set of combinations was used to simulate the purities, yields and separation factors of products that are rich in DP1, DP3 and DP≥5. The simulated values were then used to develop an optimization procedure to select the best setup with compromised performance. Applying this procedure, we optimized the process by using 4 and 5 stages and altering the configurations (S- and L-strategies) while keeping the stage number at 3.

3. Results and discussion

The fractionation cascades with side stream approach were able to fractionate FOS into 3 different products with enhanced purity compare to the feed having maximum purities of 66% for DP1 (from 9%), 33% for DP3 (from 24%) and 54% for DP≥5 (from 34%). These maxima were achieved by using

a 4-stage design. The 4-stages designs create asymmetric configurations towards the top or bottom region resulting in a more specific separation. Similar considerations were used in the S- and L-strategies to improve the purities further while keeping the stage number at 3.

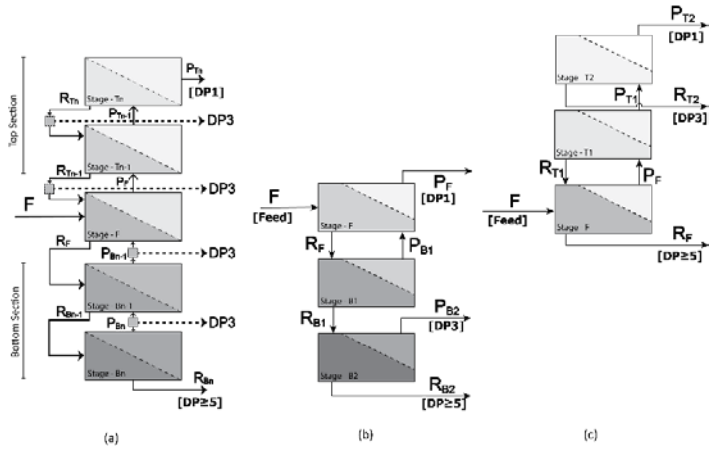

Figure 1. Configuration of (a) generalized fractionation cascades with side streams and example modification with (b) S-strategies and (c) L-strategies for 3 products.

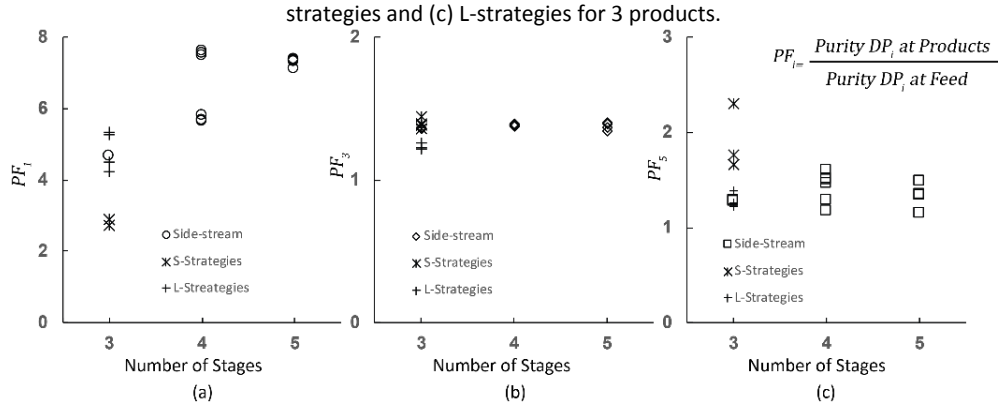

Figure 2. Maximum purification factor of (a) DP1, (b) DP3 and (c) DP≥5 achieved by membrane cascade system using side-stream approach for 3, 4 and 5 stages and modification of 3 stage cascades with S- and L-strategies.

Achieving those maximum purities could only be done by sacrificing the purities of other components or the yields. Using the multi-criteria decision making approach, a setup that is giving compromised performance indicators (purities, yields and separation factors) could be chosen.

4. Conclusions

Fractionating FOS into 3 products was performed using membrane cascaded systems. The system was improved by using more stages and altering the configuration. The approach to improve and optimize a fractionation process that we described here is applicable for other processes (not limited to membrane systems). A predictive model for a single process is required. This single stage model has to be expanded in the comprehensive model to predict the whole system. This comprehensive model needs to be used for optimization.

References

[1] E.N. Lightfoot, et.al. , Biotechnol. Prog. 24 (2008) 599–605.
[2] V. Aguirre Montesdeoca, et.al., J. Memb. Sci. 520 (2016) 712–722.
[3] Z. Rizki, et.al, Sep. Purif. Technol. 221 (2019) 183–194.

ECCE12
The 12th EUROPEAN CONGRESS OF CHEMICAL ENGINEERING
Florence 15-19 September 2019

Design aAnd Experimental Study oOf aA Milli-Channel Vaporizer.

G. Henry[1,] *, A. Pere-Gigante[1], J-M. Commenge[1], J. Seiwert[2], S. Valentin[2], M. Wagner[2]

1 Université de Lorraine, CNRS, Laboratoire Réactions et Génie des Procédés, UMR 7274, Nancy, F-54000 France; 2 , Air Liquide, Centre de Recherche Paris-Saclay, 1 chemin de la Porte des Loges, Les Loges-en-Josas, BP 126, 78354 Jouy-en-Josas, France

**Corresponding author: guillaume.henry@univ-lorraine.fr*

Highlights

- High-quality vaporization of liquid water in millichannels is studied experimentally
- Dedicated test bench is used to study influence of flow rates, temperatures and pressure
- Flow regimes, vapor quality and heat-transfer coefficients are estimated
- High-quality vaporization is reached at low flow rate and large temperature difference

1. Introduction and context

Steam is largely used in industry as an energy vector and is currently generated in large tubular heat exchangers coupled to a vessel in a thermosiphon system. Process intensification mainly aims at increasing the process efficiency by reducing the size of the equipment: the smaller the size, the better the control of the operating conditions, for instance the heat transfer. The case of the water vaporizer in hydrogen production is the focus of the present study. However, the results of this study could be used in other applications as long as heat has to be valorized, such as in the case of hot gases outgoing from the reactor of the Steam Methane Reforming (SMR) process.

The intensification of this process could enable to reach total vaporization of the water flow and a significant simplification of the installation. A plate milli-channel heat exchanger is studied in this work, although some other technologies could have been used in this application such as brazed plates-and-fins exchangers.

The main goal of this work is to develop a sizing tool for intensified vaporizers in order to meet the expectations of the steam production needs on SMR plants. It is developed thanks to an experimental study of the hydraulic and thermal phenomena occurring during phase change in the milli-structured device.

2. Test Bench and Methods

A test bench has been set up for this study. Convection of hot oil was chosen as the heating mode for the water vaporization to avoid the risks induced by a hot gas convection loop at lab scale. The test bench presents three different loops of fluids: one for the process water, another one for the hot oil and the last one for the condensation of the produced vapor. Several parameters are measured, namely, the flowrates, the temperatures of fluids and the absolute and differential pressure inside the vaporizer for the water. A particular attention is given to the wall temperature between the oil and the water, measured at six positions along the millimeter-size channels. The semi-circular cross section of the channels was chosen to enable the visualization of the boiling

fluid, through a 1 cm thick borosilicate window. Unfortunately, the vapor quality cannot be directly measured; nevertheless, it can be estimated using a heat balance on the vaporizer. A specific study on the heat losses was performed to minimize the uncertainty related to this heat balance.

3. Results and discussion

The vaporizer has been operated under various operating conditions: the water flowrate varied between 0 and 6 L/h, the oil flowrate between 0.5 and 4.5 L/min, the inlet temperature of oil between 100 and 190°C and the pressure on the water side between 1 and 5 bars. The resulting vapor quality (Figure 1.b), the pressure drop and the hydraulic regime, highlighted by image analysis of high frequency movies, are studied for all operating conditions. This work presents an analysis of this experimental campaign, completed with high-speed visualization, to characterize properly the "two-phase" thermal transfer coefficient in milli-structures (Figure 1.a), which is one of the keystones to design a vaporizer.

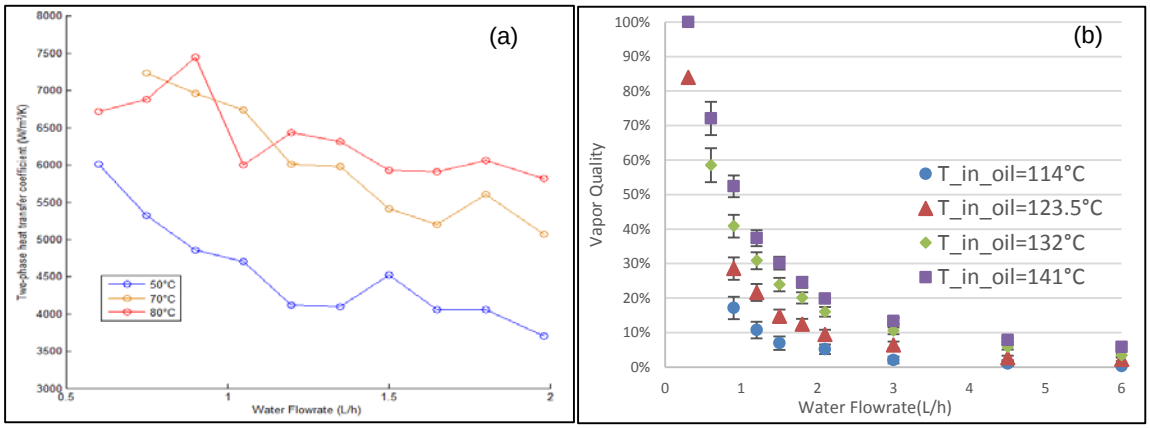

Figure 1. Influence of the pre-heating temperature on the two-phase heat transfer coefficient (a), Influence of the oil flowrate on the vapour quality (b)

The magnitude of the "two-phase" heat transfer coefficient ~~estimated in the milli-channels~~ is similar to what can be found in the literature [1]. Since the boiling in the vaporizer creates a high frequency oscillating flow, further investigations are needed to validate the evolution of these coefficients. Concerning the vapor quality, the geometry of straight milli-channels is not able to produce high quality at "high" water flowrates. However, it has been shown that the thermal gradient between the oil and the boiling water is the main way to step up the vapor quality.

4. Conclusions

The vaporizer studied enables the production of steam by heat recovery from a hot flow. The vapor quality produced is improved by low water flowrates and high differences of temperature between the hot and water flows.

References

[1] S. G. Kandlikar, Fundamental issues related to flow boiling in minichannels and microchannels, Experimental Thermal and Fluid Science, 26, 2002, pp 389-407

ECCE12
The 12th EUROPEAN CONGRESS OF CHEMICAL ENGINEERING
Florence 15-19 September 2019

KRAFT, BCTMP and TMP dewatering in a screw press: A statistical modeling.

Bouchaib El idrissi[1*], Éric Loranger[1], Robert Lanouette[1], Jean-Pierre Bousquet[2], Mark Martinez[3]

1 UQTR, Trois-Rivières. Canada; 2 Valmet, Montréal. Canada; 3 UBC, Vancouver. Canada

**Corresponding author: bouchaib.el.idrissi@uqtr.ca*

Highlights

- The pulp behavior is very similar regardless the type of the pulp.
- The behavior is predicted statistically with a good approximation.
- The screw rotational speed is the most significant factor.

1. Introduction

Screw presses are used for solids/liquids mechanical separation. As dewatering is one of the most important unit operations in the pulp and paper industry, this study was conducted to establish a statistical relationship between the operational parameters and the main outputs of the screw press.
The objective of this study was to analyze statistically the main outputs and try to find a predictive model of the screw press.

2. Methods

For this study, we used JMP from SAS for experimental design and statistical analysis.
The screw press used in this study is a Thune SP23 screw press from Voith. Four pressure sensors and fourteen filtrate baskets were installed along the screw press to track the pressure variation and filtrate characteristics.

3. Results and discussion

- At first, the designs were including the quadratic effects. After analysing all the data on JMP, the design can be reduced in most cases to having just the interactions parameters.
- For Kraft pulp, the R squares varied from 0.89 to 0.97 in the interactions model. The BCTMP model gives R squares from 0.85 to 0.98, and for TMP the R squares varies from 0.72 to 0.97.
- JMP allows us to see the effect of the parameters using a profiler for each pulp. In our case, we have chosen to observe the effect on the pulp outlet consistency and inlet flow; the filtrate consistency and flow rate; the screw press production; the pressure in the basket 4 near to the discharge end and finally the screw torque.
- The outlet consistency is mainly affected by the screw rotational speed. For the three-pulp studied, the outlet consistency decreases with increasing the rotational speed. Increase the rotational speed implies a reduction in the residence time, thus not enough time for the pulp to dewater, especially in the first section of the press. Comparing the three pulps, the rotational speed effect is more pronounced for BCTMP and TMP compared to KRAFT. This can be explained by the fact of the fibres size, the KRAFT fibres are almost twice longer than those of TMP and BCTMP, thus, the filtration process is faster and even when increasing the rotational speed, the filtration stage is less affected.

The other difference is for BCTMP, the outlet consistency increases more when increasing the freeness, by knowing that both KRAFT and TMP fibres are softwood and BCTMP fibres are hardwood, we can expect this difference is due to the fibres inner properties. The fiber length, the quantity of fines and the flexibility of the long fibers are to be considered.

- The filtrate flow rate increases with increasing the screw press and the feed pressure. This flow increase was observed to happen at the same rate for the three pulps and it can be explain by the fact, when increasing the rotational speed and the pressure, the pulp moves faster, giving a dilute suspension behind the screw flights, allowing the pulp to drain faster in the first section of the press. The drainage is more important when operating with higher freeness, so in this case the inlet flow increases when increasing the freeness, this was observed for KRAFT and TMP, for BCTMP we do not notice any variation. As mentioned before, KRAFT and TMP are softwood, and TMP is a hardwood, this can explain the difference observed when varying the freeness. On the other hand, when increasing the consistency, the pulp is more compact, and the fibres form a network that slows the drainage, thus giving a lower filtrate flow rate.
- The filtrate consistency increases with increasing the rotational speed, since when increasing the rotational speed, the perforated barrel is rapidly cleared off by the screw moving flights, allowing the fines and some fibres to slip from the screw press. The filtrate consistency is influenced by the feed consistency as well, increasing the feed consistency will give a more compact suspension rapidly, thus blocking the fines and fibres from sliding out of the press. The KRAFT and TMP response to the parameters variation is similar, whereas, the BCTMP is more sensible to the parameters variations, the slop is more important.
- It is obvious when increasing the rotational speed, we increase the inlet flow. On the other hand, when feeding the screw press with a more concentrated suspension, the inlet flow is lower for a same production rate, increasing the consistency will increase the shears in the screw press, thus implying a lower screw linear advance and lower inlet flow rate. These observations are the same for the three pulps studied, the only exception is the freeness, where it has no effect for the BCTMP.
- The screw press production increases with increasing the rotational speed, the pressure, the freeness and the feed consistency. The behavior is identic for the three pulps studied.
- The pressure does not change much in the screw press, only near to the discharge end where we have a noticeable increase. The rotational speed is the most significant factor, increasing the rotational speed implies a less important pressure near to the discharge end. Increasing the rotational speed pushes the pulp faster to the discharge end, thus the pulp drains by filtration and we do not have enough time for pressure build up. The three pulps react the same way to each variation.
- The screw press torque decreases when operating with high rotational speed because the shear is lower. The degree of variation is the same for the all the pulps studied.

4. Conclusions

- The rotational speed is the main factor that has the biggest influence in the screw press.
- The pulp behavior is very similar in the screw press for the three studied pulps. There is only a slight difference when changing the pulp type (softwood or hardwood) or fines or short fibers content.
- JMP analysis shows that the screw press outlets can be predicted with a very good approximation for each pulp.

ECCE12
The 12th EUROPEAN CONGRESS OF CHEMICAL ENGINEERING
Florence 15-19 September 2019

Dewatering of Cellulose Nanofibrils (CNF) Suspensions using Centrifugation

Jennifer Astorsdotter[1], Eva Ålander[1], Maria Sedin[1]

1 RISE Bioeconomy, Stockholm, Sweden; 2 Affiliation and address

**Corresponding author: maria-sedin@ri.se*

Highlights

- It is possible to dewater CNF using centrifugation with industrial relevant *g*-forces.
- Addition of NaCl or decreased pH improves the dewatering of carboxymethylated CNF.
- Final concentrations achieved was 5.3 w% for enzymatic CNF.
- Final concentrations achieved was 4.4 w% for carboxymethylated CNF using NaCl.

1. Introduction

Dewatering and thickening of cellulose nanofibrils (CNF) suspensions are challenging. Traditional filtration-based dewatering processes are very time-consuming. Once the solids of the suspension start forming a network, the permeability is very low due to small size-scale of the particles and the compressibility of the fibre network. In centrifugation the dewatering flow counteracts the compression of the network, thus maintaining a higher permeability during the thickening process. Therefore, centrifugation may be a viable alternative separation method.

2. Methods

Two qualities of CNF were produced by passing either enzymatic pre-treated (CNF1) or carboxymethylation pre-treated (CNF2) pulps through a high-pressure homogeniser yielding CNFs at 2 w% with different size distributions and charge densities [1, 2]. An analytical centrifuge [3] was used to study the dewatering behaviour. The height of the supernatant was determined during centrifugation from *in-situ* light transmittance measurements at 25°C and the average sediment concentration was calculated. The influence of *g*-force, initial concentration, pH and ionic strength were investigated.

3. Results and discussion

The average concentration of the sediment at 2320*g* is shown Fig. 1 for CNF1 and CNF2. In the figure it can be seen that for CNF1 a final concentration greater than 5 w% could be achieved whereas the final concentration for CNF2 could not be increased if the initial concentration was greater than approximately 0.5 w%. This is due to the highly charged particles, 600 μeq./g, attained with carboxymethylation. For comparison CNF1 has a total charge of approximately 60 μeq./g. The time required to reach the final concentration is given in Fig. 1. For CNF1 the time was about 30–60 s but CNF2 required at least 2 min or more if the separation was possible.

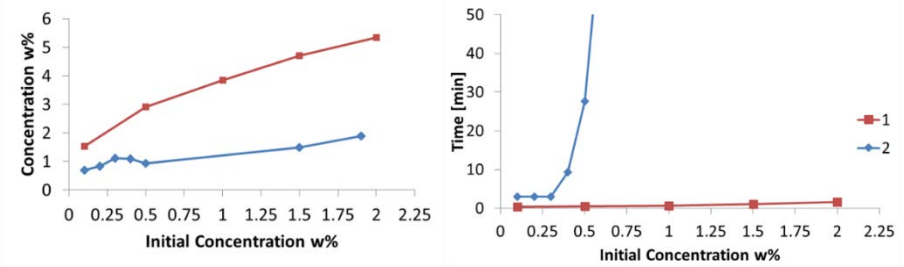

Figure 1. Effect of initial concentration on final concentration and separation time at 2320*g* for CNF1 and CNF2.

To improve the separation of CNF2, the pH and ionic strength of the suspension were changed. In Fig. 2 the effect of decreasing the pH is shown for 1.5 w% CNF1 and CNF2 suspensions. pH has a negligible effect for CNF1 on final concentration and separation time. On the other hand, the pH affects CNF2 significantly if the pH is less than 5; the final concentration is almost 4 w% and the separation time is comparable to CNF1 or even less. This is due to the protonation of the carboxyl group introduced in CNF2; pK_a approximately 4. Decreasing the pH will therefore reduce the electrostatic repulsion between CNF2 particles and improve the separation. The effect of adding NaCl to the suspension showed the effect of shielding the charges on the particles. At 0.1 and 0.5 M NaCl the final concentration at 2320*g* was 3.7 and 4.4 w%, respectively, for CNF2 whereas NaCl had a negative effect on CNF1. The effect of pH and NaCl on CNF2 was also visible in the light transmittance measurement: a zone with a concentration gradient was observed for CNF2 but not for CNF2 with NaCl added or pH adjusted.

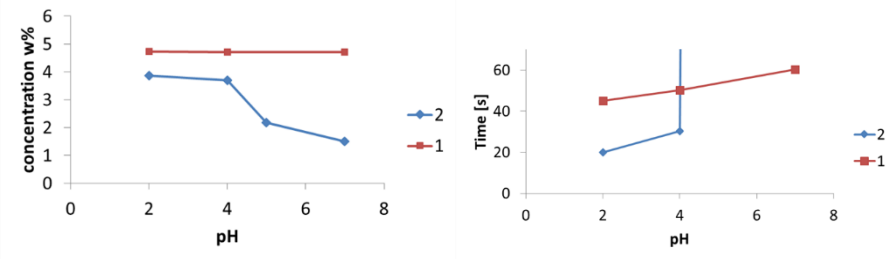

Figure 2. Effect of pH on final concentration and separation time at 2320*g* for CNF1 and CNF2 with initial concentration of 1.5 w%.

4. Conclusions

With centrifugation it is possible to increase the concentration of CNF1 (enzymatic) to more than 5 w% with a separation time of less than 60 s at 2302*g*. At an initial concentration above 0.5 w%, it is not possible to dewater the carboxymethylated CNF2, but with addition of electrolyte (shielding of charges) or decreasing the pH (protonation) 4 w% and a comparable separation time as CNF1 is reached.

References

[1] Pääkko, M., M. Ankerfors, H. Kosonen, A. Nykänen, et al., Biomacromolecules 8(6) (2007) 1934–1941.
[2] Siró, I., D. Plackett, M. Hedenqvist, M. Ankerfors, et al., J. Appl. Polym. Sci. 119(5) (2011) 2652–2660.
[3] Sobisch, T. & D. Lerche, Colloids Surf. A 331(1–2) (2008) 114–118.

ECCE12
The 12th EUROPEAN CONGRESS OF CHEMICAL ENGINEERING
Florence 15-19 September 2019

Development of a high velocity co-flowing stratified microfluidic process to obtain kinetic constants for reactive liquid-liquid extraction.

Florian Corne[1], Anne Lélias-Vanderperre[1*], Alastair Magnaldo[1], Christian Sorel[1], Nathalie Di Miceli Raimondi[2], Laurent Prat[2]

1 CEA - DEN, DMRC, Research Service for Dissolution and Separation Processes, Laboratory of Conception of Extraction Processes, F-30207 Bagnols-sur-Cèze, France; 2 Laboratoire de Génie Chimique, Université de Toulouse, CNRS, INPT, UPS, Toulouse, France

**Corresponding author: anne.lelias@cea.fr*

Highlights

- Uranium(VI) extraction from nitric acid by TBP 30% with contact time lower than 50 ms.
- Estimation of the chemical mass transfer constant using the microfluidic device: over 4.2 10^{-4} $m.s^{-1}$.
- Difference between the results and a 2D COMSOL model: presence of an acceleration factor?

1. Introduction

Kinetic constants in reactive liquid-liquid extraction processes are generally determined using constant interfacial area methods such as the single drop method the Nitsch cell or the Lewis cell. These techniques only allow reaching the overall kinetics of the process that is the result of two basic phenomena: the intrinsic reaction and the overall mass transfer of the components that participate to the reaction. The determination of the intrinsic kinetics of the reaction is necessary for the design and extraction process modelling. Mass transfer limitation is quite hard to be restrained in a device to determine intrinsic chemical kinetics since molecular diffusion contributes in majority to the overall mass transfer resistance. Hence, the field of microfluidic devices appears as an interesting way to study such kinetics by reducing the molecular diffusion. In this context, our study considers the well-known solvent TBP 30% in TPH used to reprocess nuclear spent fuels as a reference solvent to study mass transfer kinetics [1-4].

2. Methods

The extraction of uranium(VI) in nitric acid by tributylphosphate (TBP) diluted at 30% in TPH (hydrogenated tetrapropylene) was carried out using a Y-Y microfluidic chip with a 1.25 cm straight microchannel (dolomite). Two stratified flows in co-flowing configuration were generated with high fluid velocities to aim chemical kinetics constant determination, thanks to both diffusive length reduction and fine flow control in the microfluidic technology. Liquid-liquid stratified flow configuration with a centered interface avoids any tangential convective movements. Therefore, the hydrodynamics in the device is perfectly controlled and predictable using CFD codes, as for the mass transfer phenomenon. The experimental hypothesis of a centered interface along the microchannel depth was validated thanks to confocal experiments.

3. Results and discussion

First, the influence of inlet uranium concentration and total fluid velocity on the extraction yield has been studied as shown in Figure 1. The observed extraction yields are quite good considering the short contact time inside the microchip (lower than 0.05 s).

Then the results have been exploited to determine if diffusion still occurs in such conditions thus allowing the estimation of the chemical mass transfer constant (k_e), which is expected to be over 4.2 10^{-4} m.s^{-1} for a 0.12 M U(VI) aqueous solution. The results hardly fit with a preliminary 2D COMSOL model even by increasing the supposed k_e twice and the U(VI) molecular diffusion coefficient (DU) by a decade. Another solution to fit the experimental results consists on taking into account an acceleration factor, provided whether from a Hatta acceleration or from Marangoni instabilities.

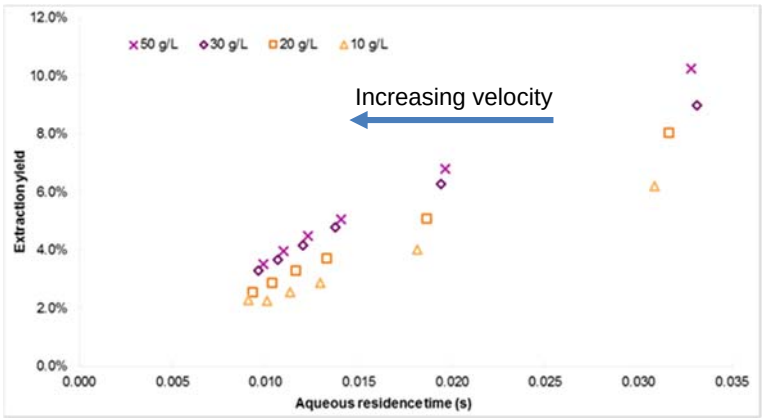

Figure 1. Comparison between the extraction rates of uranium(VI) in HNO_3 3M extracted by TBP 30% in TPH.

4. Conclusions

Attempts to determine the chemical kinetics constant of uranium(VI) from nitric acid by TBP 30% in TPH were carried out by means of microfluidics device at high flow velocities in order to limit the impact of diffusion phenomena on the global mass transfer. The intrinsic chemical kinetic constant was performed thanks to COMSOL modelling. When only chemical phenomenon is taken into account, all the numerical results are below the experimental data in the process modelling. Hence, both reaction and molecular diffusion have to be taken into account in the modelling of the microfluidic experiment through the presence of an acceleration phenomenon enhancing the overall kinetic constant.

References

[1] B. Dinh, PhD thesis from Ecole centrale des Arts et Manufactures, Paris, 1987.
[2] D. Horner et al., Ind. Eng. Chem. Fundamen., 19 (1980) 103-109.
[3] J.-P. Jasmin et al., Solvent Extr. Ion Exch., 35 (2017) 174-186.
[4] M. Yamamoto et al., J. Sep. Sci., 38 (2015) 1807-1812.

ECCE12
The 12th EUROPEAN CONGRESS OF CHEMICAL ENGINEERING
Florence 15-19 September 2019

7th Symposium on Product Design and Engineering

Functional analysis of selected ion electrically conductive hydrogel production and applications in seawater treatment

Mohamed H. Sorour, Marwa M. El Sayed*, Abdelghani M. G. Abulnour, Hayam, F. Shaalan, Heba A. Hani, Shadia R. Tewfik

Chemical Engineering and Pilot Plant Department, National Research Centre, Cairo, Egypt

El-Buhouth Street, Dokki; P.O. Box 12622 Phone: +201096170061, Fax: +20-2-33370931

**Corresponding author:eng_marwa06@yahoo.com*

Highlights

- Desalination technology is associated with various technological challenges
- Hydrogel composite is used for removal of seawater hardness.
- The characteristics of the composite and performance via adsorption of Ca^{++} and Mg^{++} have been determined.
- The electro-regeneration has been also explored.

1. Introduction

Seawater desalination is becoming a crucial intervention for mitigating water shortage in numerous Middle East countries. Desalination technology is associated with various technological challenges that should be resolved to maintain plant sustainability and performance. For instance, seawater hardness is recognized as a challenge for recent large scale desalination plants. Optional technologies including chemical treatment, adsorption and membrane filtration have been developed for hardness removal and recovery of Ca^{++} and Mg^{++}.

2. Methods

This paper addresses the development and application of a new conductive polymeric hydrogel composite exhibiting electrically tunable characteristics. The developed hydrogel composite comprises especially treated zeolite, polyacrylate, polyaniline, hydrolyzed polyacrylamide and special processing aids. The characteristics of the composite have been determined via scanning electron microscopy, Fourier transform infrared spectroscopy and electric conductivity measurements in addition to swelling ratio. Impact of composition and processing conditions on conventional and electrochemically enhanced adsorption experiments have been presented and analyzed. The electro-regeneration has been also explored.

3. Results and discussion

The promising features of this novel hydrogel composite are elucidated by the removal and recovery of hardness causing elements in simulated seawater and brines.

4. Conclusions

It is concluded that the developed hydrogel is initially qualified for upstream seawater softening. Additional endeavors are still needed for downstream brine management to overcome apparent osmotic effects.

References

(a) R. Ratheesh and K. Viswanathan, IOSR Journal of Applied Physics (IOSR-JAP) 2278-4861. Volume 6, Issue 1 Ver. II PP 01-09, (Feb. 2014).

(b) J. Stejskal and R. G. Gilbert, Pure Appl. Chem. 74, 857 (2002)

(c) lin lin and Qingsheng Wu , Improved Conductivity of Polysaccharide-co-Polyacrylate / Polyaniline Conducting Hydrogels , Polymers & Polymer Composites, Vol. 20, No. 4, 2012.

(d) Betul Tasdelen, Preparation and characterization of conducting hydrogel composite made of polyaniline, polyacrylamide and kaoline, Materials Today: Proceedings 5 (2018) 15983-15989.

(e) Wang Y., Jing X.: Intrinsically conducting polymers for electromagnetic interference shielding. Polymer for Advanced Technologies, 16, 344–351 (2005).

(f) A. K. Bajpai*, J. Bajpai, S. N. Soni, " Preparation and characterization of electrically conductive composites of poly(vinyl alcohol)-g-poly(acrylic acid) hydrogels impregnated with polyaniline (PANI), eXPRESS Polymer Letters Vol.2, No.1 (2008) 26–39.

(g) Mohamed H. Sorour , Heba A. Hani*, Hayam F. Shaalan, Marwa M. El Sayed, Mayyada M.H. El-Sayed, Softening of seawater and desalination brines using grafted polysaccharide hydrogels, Desalination and Water Treatment 2014- 55(9):1-9

ECCE12
The 12th EUROPEAN CONGRESS OF CHEMICAL ENGINEERING
Florence 15-19 September 2019

Membrane Flux of Representative Volatile Organic Compounds in Polydimethylsiloxane Membrane at Various Experimental Conditions

Lenka Moravkova, Karolina Machanova, Petr Stanovsky, Zuzana Petrusova

Institute of Chemical Process Fundamentals of the Czech Academy of Sciences, Rozvojova 135, 165 02, Prague 6, Czech Republic

**Corresponding author: petrusova@icpf.cas.cz*

Highlights

- PDMS was chosen as representative membrane for VOC removal from polluted air
- Permeability of representative VOCs were studied in PDMS membrane
- Linear alkane (hexane) was found to be the most permeable in PDMS membrane
- Membrane flux was studied at various experimental conditions

1. Introduction

Gas separation technology is a mature topic, while the vapor permeation (VP) process still needs some development. It can be presumed that VP will become extensively applied in the future, thanks to its economic and ecological advantages. VP can be successfully applied for example for removal of volatile organic compounds (VOCs) from polluted air (Figure 1) [1].

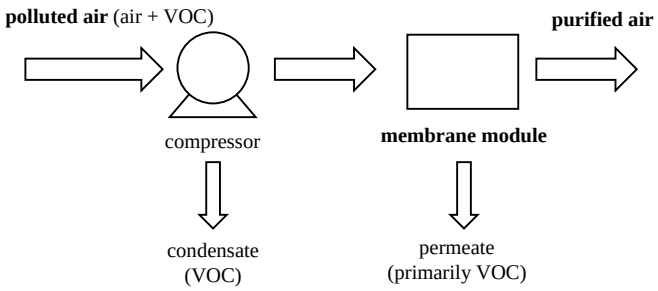

Figure 1. Scheme of VOC separation from polluted air.

2. Permeation experiments

Dense polydimethylsiloxane (Elastosil PDMS, Silicones and more) membrane was prepared by casting-knife method. The membrane thickness was 100 microns. The feed stream contained either pure nitrogen or nitrogen saturated by representative VOC (hexane, isooctane, and ethanol). Permeation experiments were carried out at temperature (25–35) °C and at feed pressure (100–250) kPa while the permeate pressure was always kept at 50 kPa. The basic test apparatus was described previously in a detail [2].

3. Results and discussion

The influence of long-term exposure of representative VOCs was studied at various experimental conditions. The membrane flux was studied for representative VOC to simulate purification of

polluted air by organic vapors (Figure 2A). The highest flux showed the representative linear hydrocarbon (hexane) while the branched hydrocarbon (isooctane) showed significantly lower flux that was less depended on VOC feed concentration. The lowest membrane flux was observed for chosen alcohol (ethanol). The flux of isooctane and ethanol depended similarly on VOCs feed concentration.

The membrane flux always increased with the VOC feed concentration as expected for PDMS membrane. The influence of temperature and trans-membrane pressure was studied for all representative VOCs (see temperature influence for the most permeable hexane in Figure 2B).

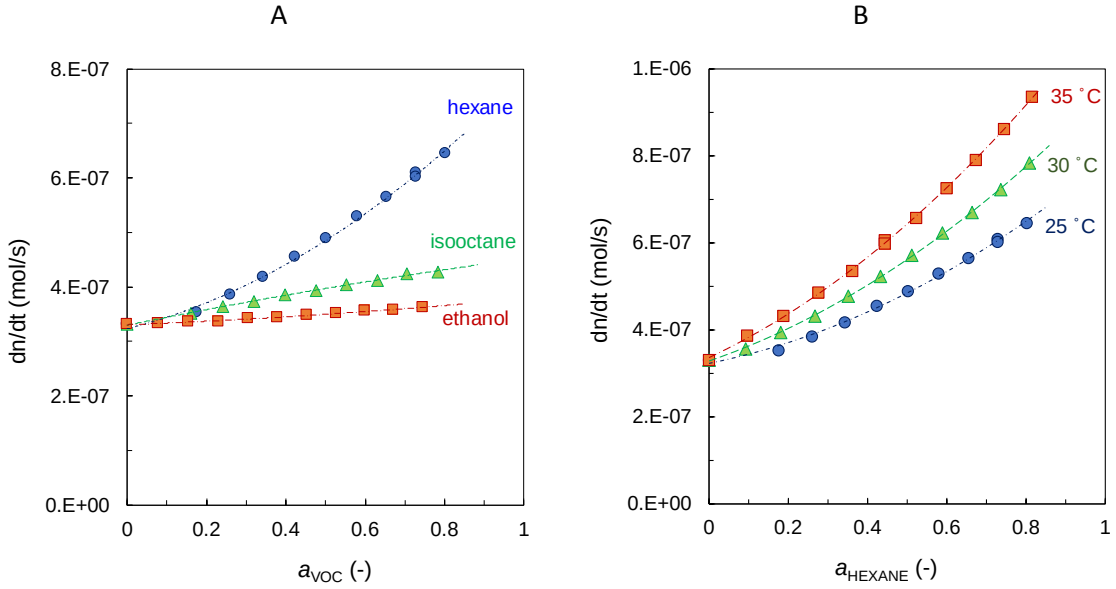

Figure 2. A) Comparison of molar flux of VOC + nitrogen in PDMS membrane as the function of VOC feed concentration at 25 °C and trans-membrane pressure of 150/50 kPa (ethanol – squares, isooctane – triangles, hexane – circles), B) Influence of temperature on hexane + nitrogen flux in PDMS membrane at the trans-membrane pressure of 150/50 kPa (25 °C – circles, 30 °C – triangles, 35 °C – squares).

4. Conclusions

It was found that prepared PDMS membrane is suitable for long-term separation of various volatile organic compounds from polluted air. The influence of input parameters (such as VOC feed concentration, temperature and pressure) has been discussed. Interestingly, the membrane increased with VOC feed concentration while the decrease was observed for a thicker PDMS film.

Acknowledgement

The financial support of the Czech Science Foundation (Junior Project 17-03367Y) is acknowledged.

References

[1] Z. Petrusova, K. Machanova, P. Stanovsky, P. Izak, Sep. Purif. Technol. 217 (2019) 95–107.
[2] Z. Petrusová, Z. Vajglová, L. Morávková, J. C. Jansen, J. Vejrazka, P. Izak, Chem. Biochem. Eng. Q. 31(2) (2017) 145–160.

ECCE12
The 12th EUROPEAN CONGRESS OF CHEMICAL ENGINEERING
Florence 15-19 September 2019

Purification of Volatile Fatty Acids from waste-derivative fermentation broth using nanofiltration

Yin Zhu[1], Claire Dumas[2], Sylvain Galier[1], Hélène Roux-de Balmann[1*]

[1] *Laboratoire de Génie Chimique, Université de Toulouse, CNRS, INPT, UPS, Toulouse, France*

[2] *LISBP, Université de Toulouse, CNRS, INRA, INSA, Toulouse, France.*

**Corresponding author: roux@chimie.ups-tlse.fr*

Highlights

- The retentions of VFAs increase with solution pH
- Separation factor between Ac and Bu increase with pressure and decrease with total concentration
- The best Separation is achieved at pH 8, 20 bar and total concentration of 0.1 M

1. Introduction

Volatile fatty acids (VFAs) are promising chemical building blocks that can be obtained by fermentation of biomass in the biorefinery concept. The present project aims to use Municipal solid waste (MSW), as raw material to produce VFAs. Previous investigations pointed out that the purification of VFAs is still a major challenge since the characteristics of the produced VFAs are similar and the fermentation broth contains many other components [1].

Nanofiltration (NF) is a pressure-driven membrane process, considered as environmentally friendly, that was already successfully used in the separation of many organic solutes like lactate and glucose [2]. Only a few reports concerning VFAs separation have been published [3], showing the necessity to improve the selectivity. The objective of this work is then to investigate the feasibility of NF for the selective recovery of VFAs from a waste-derived fermentation broth.

2. Methods

An experimental study is carried out using a dead-end stirred cell with a Filmtec (Dow) NF-45 membrane. The retention of the solutes is measured and the separation factor is calculated in order to characterize the separation efficiency. Synthetic solutions with various total concentration (from 0.1 mol to 0.5 mol) and pH (from 3 to 8) as well as a real fermentation broth are investigated.

3. Results and discussion

The results show that the individual retention of VFAs follows their molecular weight (acetate < propionate < butyrate) for all the conditions investigated (concentration and pH). The lowest VFAs retention is observed at pH 3 whereas the highest retention is obtained at pH 8, with an intermediate retention at pH 5.6 (*Fig. 1*). This phenomenon is due to the charge effects since the VFAs charge (due to the dissociation) as well as the fixed charges on the membrane surface increase with the pH. Thus, the increase of the electrostatic repulsion between the solutes and the membrane with the pH leads to the decrease of the VFAs transfer through the membrane, i.e. to the increase of their retention.

Separation factor is defined as the ratio of two solutes in the feed divided by their ratio in the permeate. At pH 8, the separation factor between Ac and Bu increase with transmembrane pressure and decrease with the total concentration of the solution (*Fig. 2*). The same trends are observed for the other pH investigated. It is also observed that a higher separation factor is achieved at higher retention.

The separation factor slowly increases as the pH increase from 3 to 5.6. However, a sharp increase is observed from a higher pH *(Fig. 3*). The highest separation factor between Ac/Bu is 2.2, and it is obtained at a total concentration of 0.1 mol, a transmembrane pressure of 20 bar and a pH of 8.

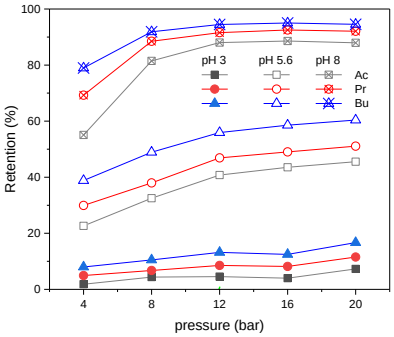

Figure 1 Individual VFAs retention versus transmembrane pressure in ternary solutions (Ac:Pr:Bu=33%:33%:33%, total concentration of 0.1 mol) at different pH

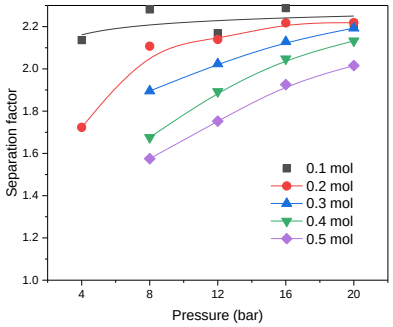

Figure 2 Separation factor of Ac/Bu versus transmembrane pressure for ternary solutions (Ac:Pr:Bu=33%:33%:33%, pH 8) at different total concentration

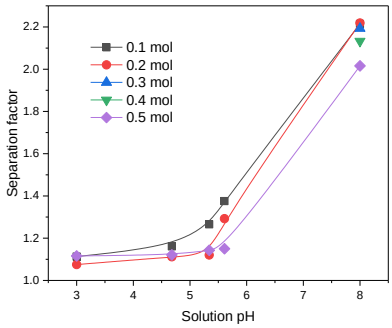

Figure 3 Separation factor of Ac/Bu in ternary solutions (Ac:Pr:Bu=33%:33%:33%) at different pH and total concentration

4. Conclusions

It is proved that NF could be used for the recovery of VFAs from a waste-derived fermentation broth. The selectivity of the recovered fractions strongly depends on the pH and total concentration of the fermentation broth, but further investigation is required to improve the efficiency of the separation.

References

[1] M. Atasoy, I. Owusu-agyeman, E. Plaza, Z. Cetecioglu, Bioresour. Technol. 268 (2018) 773–786.

[2] C. Umpuch, S. Galier, S. Kanchanatawee, H. Roux-de Balmann, Process Biochem. 45 (2010) 1763–1768.

[3] M.-P. Zacharof, S.J. Mandale, P.M. Williams, R.W. Lovitt, J. Clean. Prod. 112 (2016) 4749–4761.

ECCE12
The 12th EUROPEAN CONGRESS OF CHEMICAL ENGINEERING
Florence 15-19 September 2019

Improvement of a CDI System Concerning the Adsorption of Organic Acids by Investigation of the Potential Free Adsorption.

Robin Wagner[1], Matthias Franzreb[2]

1 Karlsruhe Institut of Technology, Kaiserstraße 12, 76131 Karlsruhe; 2 Karlsruhe Institut of Technology, Kaiserstraße 12, 76131 Karlsruhe

**Corresponding author: robin.wagner@kit.edu*

Highlights

- Adsorption Isotherms of an organic acid for various pH-values.
- Presentation of an easy way to improve adsorption capacities.
- Influence of co-ions on the adsorption process.

1. Introduction

Capacitive Deionization (CDI) is an easy to use method, which is suitable for the separation of ions or charged molecules in solutions. The advantages of this method are that it is already established for desalination and therefore available at low cost. Furthermore, it offers the opportunity to concentrate a charged species in a solution without additives [1]. Therefore, CDI can also be an interesting alternative for the purification and concentration of larger molecules like organic acids, which gained importance e.g. due to their use for the production of biopolymers [2]. Here we present a method to determine an appropriate pH-value and concentration for electrosorption purposes, by investigating the potential free adsorption properties of the carbon material. Furthermore, the influences of co-ions on the adsorption process are described. Afterwards the predicted optimum for the electrosorption of weak organic acids was checked by further experiments.

2. Methods

An organic acid solution with a specific pH-value was pumped through the CDI system without the application of an external electrical potential until an equilibrium between the molecules in the solution and the adsorbed molecules was reached. The moment when the conductivity stopped to change was taken as the state of equilibrium. After a sample was taken an equal amount of a high concentrated stock solution was added to increase the concentration and the process was repeated. Based on the results of the adsorption of the organic acids on the carbon surfaces due to potential free adsorption the best operation conditions for the electrosorption could be derived. For electrosorption experiments a potentiostat was attached to the CDI unit and different experimental series applying constant current or constant voltage mode were conducted.

3. Results and discussion

The adsorption isotherms of an organic acid onto an activated carbon based CDI electrode are plotted in Fig. 1. It shows that the isotherms mainly split into two groups with isotherms representing high capacities at pH-values ≤ 5.5 and isotherms representing small capacities at pH-

values ≥ 6.5. The fast variation of the potential free adsorption capacity in-between these pH-values directly correlates with the second dissociation constant of this organic acid. In the presentation the strong effect of this potential free adsorption onto the achievable electrosorption will be theoretically discussed and experimentally validated.

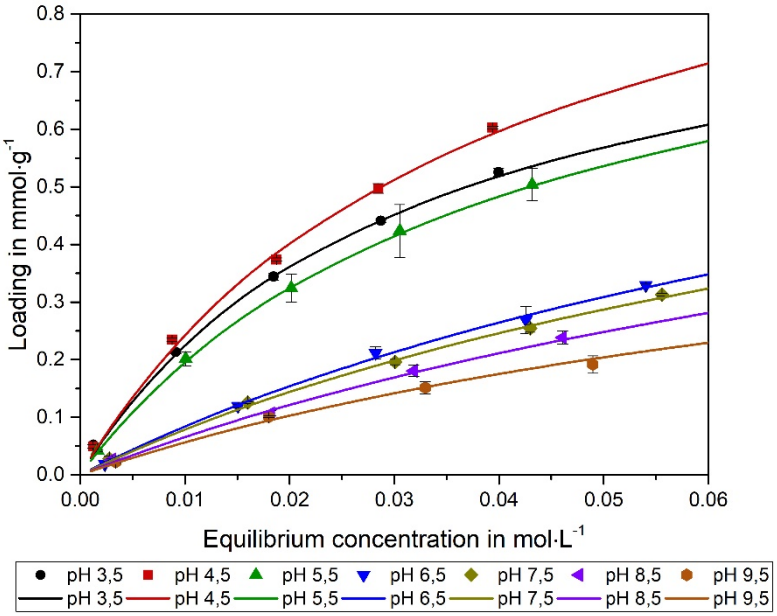

Figure 1. Adsorption isotherms of an organic acid for different pH-values and concentrations, fitted following the approach of Langmuir.

In addition to the pH also the concentration and type of strong electrolytes present, e.g. sodium chloride, show a clear effect onto the potential free and potential driven adsorption of weak organic acids. A generalized, thermodynamics based model will be presented which simulates these effects.

4. Conclusions

The electrosorption of weak electrolytes onto carbon materials shows a strong dependence onto the adjusted pH and the presence of other ions. In order to explain these effects, the dissociation behavior as well as potential free adsorption effects must be taken into account, resulting quickly in a relatively complex network of adsorption and chemical equilibria in combination with electrostatic effects. Detailed investigation of potential free adsorption data and literature based chemical equilibrium constants built the basis to understand this network and predict optimum operation windows for electrosorption processes.

References

[1] M. E. Suss, S. Porada, X. Sun, P. M. Biesheuvel, J. Yoon and V. Presser, Energy Environ. Sci 2015, **8**, 2296
[2] P. Liu, L. R. Jarboe, Computational and Structural Biotechnology Journal 2012, **3** (4), e201210011

ECCE12
The 12th EUROPEAN CONGRESS OF CHEMICAL ENGINEERING
Florence 15-19 September 2019

The sea as an open sky mine for minerals extraction

Enrico Drioli[1,2], Francesca Macedonio[1]

1 Institute on Membrane Technology - National Research Council (ITM–CNR), Via Pietro BUCCI, c/o The University of Calabria, cubo 17C, Rende (CS), 87036, Italy; 2 University of Calabria - Department of Environmental and Chemical Engineering, Rende (CS), 87036, Italy

**Corresponding author: e.drioli@itm.cnr.it*

Highlights

- Membrane assisted crystallization (MCr) was utilized for brine exploitation.
- New membranes were tested in MCr process.
- MCr performance was analyzed in terms of resistance to wettability and crystals properties.

1. Introduction

Membrane assisted crystallization (MCr) is an innovative process which combines crystallization process with membrane technology. This operation uses hydrophobic microporous membranes for promoting solvent evaporation from a feed solution thus concentrating it above its saturation limit and attaining a supersaturated environment where crystals may nucleate and grow. In a membrane crystallizer the membrane matrix acts as a selective gate for solvent evaporation, modulating the final degree and the rate for the generation of the supersaturation. Hence, acting on the transmembrane flux, either by changing the driving force of the process or by choosing membrane with proper characteristics, allows controlling the crystallization process very precisely.

2. Methods

The description of the lab scale apparatus utilized for performing the tests can be found elsewhere [1]. In all the tests, solution was charged in the crystallizer and recirculated through the membrane modules. The membrane-crystallization unit aims to induce supersaturation in solution by removing solvent in the vapour phase. The solvent evaporates at the interface of microporous hydrophobic membranes on the warm (retentate) side, diffuses through the pores and condenses on the opposite (distillate) side. In Table 1 the list of the utilized membranes can be found.

Table 1. Membrane utilized in MCr tests.

Membrane material and configuration	Type
Flat sheet Hyflon/PVDF composite membrane	AD40H_010, AD40H_022, AD40H_045
Hollow fiber ceramic membranes	CM-L, CM-S
Hybrid Bi2Se3/PVDF flat sheet composite membrane	Bi2Se3/PVDF

PVDF flat sheet membrane	PVDF

3. Results and discussion

All the tested membranes showed stable performance, without any wetting, during crystallization. Visual observation of the obtained NaCl crystals showed cubic shape whereas the analysis of their crystal size distribution proved their low dispersion (i.e., CV). Moreover, a secondary nucleation was observed which occurred simultaneously with crystal growth due to the contact of the growing crystals with the different parts of the plant. This effect was more evident for the membranes with the highest trans-membrane flux due to the highest rate in achieving supersaturation degree, supersaturation rate, nucleation and secondary nucleation. Furthermore, the inclusion of Bi2Se3 fillers in PVDF membranes, assisted the crystal-growth for NaCl, leading to a faster crystal growth and a higher uniformity of the crystal size.

4. Conclusions

All the analyzed membranes proved their suitability for MCr process whose performance can be controlled acting on the chemical–physical properties of the membranes and process parameters (temperature, concentration, flowrate, etc.). These aspects would be of undoubted benefit because allow modulating the final properties of the crystals produced both in terms of structure (polymorphism) and morphology (habit, shape, size, and size distribution).

References

[1] Cui, Z., Li, X., Zhang, Y., Wang, Z., Gugliuzza, A., Militano, F., & Macedonio, F. (2018). Testing of three different PVDF membranes in membrane assisted-crystallization process: Influence of membrane structural-properties on process performance. Desalination, 440, 68-77.

[2] Chia-Chieh Ko, Aamer Ali, Enrico Drioli , Kuo-Lun Tung, Chien-Hua Chen, Yi-Rui Chen, Francesca Macedonio. (2018). Performance of ceramic membrane in vacuum membrane distillation and in vacuum membrane crystallization. Desalination, 440, 48-58.

[3] Macedonio, F., Politano, A., Drioli, E., & Gugliuzza, A. (2018). Bi 2 Se 3-assisted membrane crystallization. Materials Horizons, 5(5), 912-919.

ECCE12
The 12th EUROPEAN CONGRESS OF CHEMICAL ENGINEERING
Florence 15-19 September 2019

ON THE EFFECT OF STEAM AS SWEEP GAS IN PALLADIUM SUPPORTED MEMBRANE

Maria Nordio[1], Jon Melendez[2], Alfredo Pacheco[2], Martin Van Sint Annaland[1], Fausto Gallucci[1]

1 Inorganic Membranes and Membrane Reactors, Sustainable Process Engineering, Chemical Engineering and Chemistry, Eindhoven University of Technology, Eindhoven, The Netherlands

2 TECNALIA, Energy and Environment Division, Mikeletegi Pasealekua 2, 20009 San Sebastian-Donostia, Spain

**Corresponding author: f.gallucci@tue.nl*

Highlights

- Steam induces additional mass transfer limitation in the alumina porous support
- Hydrogen permeation is strongly influenced by steam in the permeate side
- High temperatures reduce the mass transfer resistance induced by steam

1. Introduction

In recent years palladium membranes received increasing interest due to their extremely high selectivity and permeability and for the possibility to integrate into membrane reactors for hydrogen purification and production. There are two possible ways to increase the permeation of hydrogen at fixed feed pressure: decreasing the thickness of the membrane to increase the permeance, at the expenses of the selectivities, or to raise the driving force of the process via either a vacuum or a sweep gas in the permeate side of the membrane. Steam is generally suggested as sweep gas as it can afterward be easily separated by condensation. The effect of steam on the permeate side of a membrane is however not fully understood and it is the topic of this work.

2. Methods

An ultra-thin Pd-Ag membrane was deposited on asymmetric porous α-alumina tubes (100 nm pore size, from Rauschert) using simultaneous electroless plating (ELP) technique [1]. Thicknesses were defined by controlling the time of plating process. The membranes have been sealed and placed in the setup for its permeation characterization. The gases have been fed in the membrane module through mass flow controllers that can work until 10 l/min. The permeate side of the membrane has been analysed with flow meters in order to determine the gas permeances (H_2, CH_4, H_2O, N_2) and with gas chromatographer for measuring the H_2 purity in the permeate side. After a pure gas test to calculate the permeance and the selectivity of the membrane, a mixture of 10% H_2-90% CH_4 was fed in the retentate side while in the permeate side, counter-current sweep gas was applied. A validated model for the description of the membrane, which includes concentration polarization in the retentate, permeate and mass transfer limitation in the porous support was used for comparing and understanding the experimental results [2]. N_2 and H_2O was applied in the permeate side changing the sweep gas flow rate and the steam concentration from 0 to 93.5%.

The working temperature was changed from 350 °C to 500 °C and the retentate pressure between 1 and 5 bar.

3. Results and discussion

As depicted in Figure 1, the negative influence of steam as sweep gas is deduced because of the decreasing hydrogen permeation obtained when steam flow rate is increased. An additional effect apart from the concentration polarization and the mass transfer limitation in the porous support is clearly present in case of steam. Indeed, as shown in Figure 2, the model (that included a dusty gas model for the permeate side) could predict the behavior of the membrane in case of nitrogen as sweep gas but overestimates the hydrogen permeation in the presence of steam as sweep gas. The possible explanation could be found in the adsorption capacity of alumina which it could be relevant even at 400 °C. The XRD of the alumina support sample, moreover shows Si traces, which could represent an additional reason for the adsorption capacity of the support. Therefore, the temperature plays an important role because the lower the temperature, the more remarkable the negative steam effect. At 500 °C the steam adsorption on the alumina support seems to be negligible and indeed the model then predicts well the experimental results.

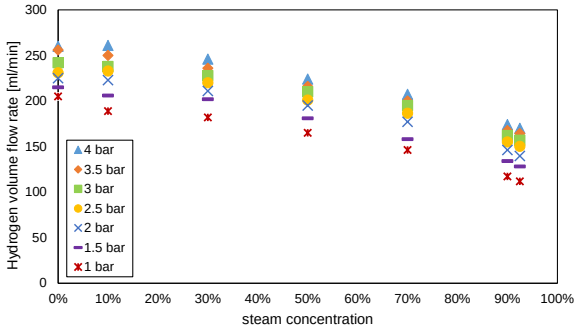

Figure 1. Hydrogen permeation trend with steam concentration

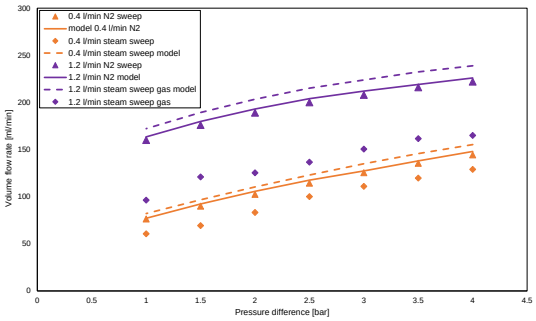

Figure 2. Comparison between experimental and model results in presence of N_2 and H_2O as sweep

4. Conclusions

The driving force of a Pd membrane when feeding steam as sweep gas is decreased between 350-450 °C because of steam adsorption on the support. Indeed the temperature plays an important role on the decreased hydrogen permeation in presence of steam. No influence of the steam on the retentate side was found in the experimental results.

Acknowledgment

This project has received funding from the Fuel Cells and Hydrogen 2 Joint Undertaking under grant agreement No 700355. This Joint Undertaking receives support from the European Union's Horizon 2020 research and innovation.

References

[1] J. Melendez, E. Fernandez, F. Gallucci, M. Van Sint, P. L. Arias, and D. A. Pacheco, "Preparation and characterization of ceramic supported ultra-thin (~ 1 µm) Pd-Ag membranes," *J. Memb. Sci.*, vol. 528, no. December 2016, pp. 12–23, 2017.

[2] P. Pinacci and F. Drago, "Influence of the support on permeation of palladium composite membranes in presence of sweep gas," *Catal. Today*, vol. 193, no. 1, pp. 186–193, 2012.

Poly(ionic liquid)/ionic liquid composite membranes with anions based on fluorosulfonyl derivatives: characterization and CO_2/H_2 separation

Andreia S. L. Gouveia,[1,2] Alexander S. Shaplov,[3] Liliana C. Tomé,[2,4,*] and Isabel M. Marrucho[1,*]

1 Centro de Química Estrutural, Instituto Superior Técnico, Universidade de Lisboa, Avenida Rovisco Pais, 1049-001 Lisboa, Portugal; 2 Instituto de Tecnologia Química e Biológica António Xavier, Universidade Nova de Lisboa, Av. da República, 2780-157 Oeiras, Portugal; 3 Luxembourg Institute of Science and Technology (LIST), 5 avenue des Hauts-Fourneaux, L-4362 Esch-sur-Alzette, Luxembourg; 4 POLYMAT, University of the Basque Country UPV/EHU, Joxe Mari Korta Center, Avda. Tolosa 72, 20018 Donostia-San Sebastian, Spain.

**Corresponding authors: liliana.tome@itqb.unl.pt; isabel.marrucho@tecnico.ulisboa.pt*

Highlights

- Poly(ionic liquid)s containing anions based on fluorosulfonyl derivatives were synthesized.
- PIL–IL composite membranes were prepared by solvent casting.
- Pure PILs and ILs and their composites were characterized by different techniques.
- The CO_2/H_2 separation through the studied PIL–IL membranes was evaluated.

1. Introduction

Despite the recognized potential of biohydrogen ($bioH_2$) for sustainable development, there are still issues regarding its production and purification, such as the elimination of CO_2, N_2, and other impurities (H_2O and H_2S), so that an enriched H_2 stream can be obtained for efficient energy generation [1].

Ionic liquids (ILs) have been used as a successful platform to design novel task-specific materials for CO_2 separation [2]. In an effort to improve the CO_2 permeability and permselectivity properties of supported ionic liquid membranes (SILMs), we recently reported the CO_2/N_2 separation performance of different ILs based on the $[C_2mim]^+$ cation and different fluorinated-based anions, such as $[TFSAM]^-$ or $[C_4F_9SO_3]^-$. The results showed that both $[C_2mim][TFSAM]$ and $[C_2mim][FSI]$-based SILMs present remarkable CO_2 permeabilities and CO_2/N_2 permselectivities [3]. However, and considering that the long-term stability and industrial operation of SILMs are still compromised due to the risk of IL draining from the membrane pores, different studies have been unveiling that the use of poly(ionic liquid)s (PILs) and their composites (PIL–IL) is a powerful strategy to design improved CO_2 separation membranes [2].

In this work, PIL–IL membranes composed of pyrrolidinium-based PILs with $[TFSAM]^-$, $[FSI]^-$ and $[TSAC]^-$ anions were prepared by the incorporation of ILs containing the same anions. The composite membranes as well as both PIL and IL components were characterized by different techniques (TGA, DSC, FT-IR and RAMAN) and their CO_2/H_2 separation performance was evaluated using the time-lag method at biohydrogen production conditions.

2. Methods

The free-standing PIL–IL membranes were prepared by solvent casting. The 6 (w/v)% solutions were

mixed until complete dissolution of the PIL and IL components and then poured into Petri dishes for slow evaporation of the solvent. The gas permeation properties were evaluated using the time-lag method at *T*=35°C and P_{feed} of 1 bar.

3. Results and discussion

From the thermogravimetric analysis results, and depending of the PIL used, different trends were observed for degradation temperatures of the PIL–IL composites with the addition of free IL, which led to the conclusion that the thermal stability of the studied PIL–IL membranes not always follows a simple mixing rule.

From CO_2 and H_2 permeation results, and taking into account that it was not possible to prepare PIL–IL composites with more than 40 wt% of free IL incorporated, both PIL TFSAM – 40 IL TFSAM and PIL FSI – 40 IL FSI membranes presented higher CO_2/H_2 selectivities (Figure 1) compared to the already reported PIL–IL membranes containing the conventional $[NTf_2]^-$ anion with 60 wt% of free IL.

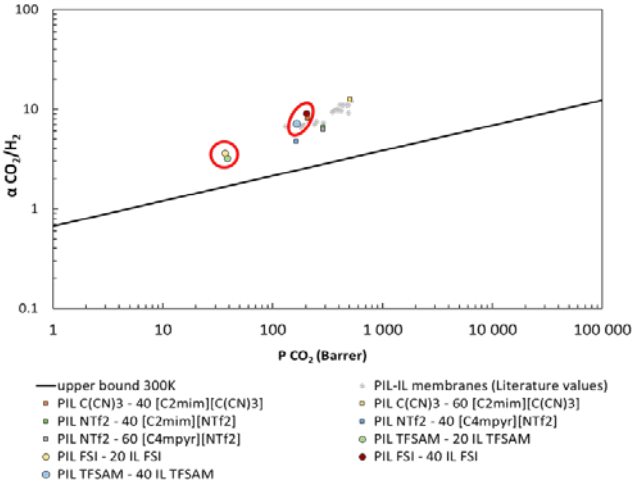

Figure 1. CO_2/H_2 separation performance of the PIL–IL membranes studied.

4. Conclusions

PILs and ILs containing anions based on fluorosulfonyl derivatives were synthesized and characterized. PIL–IL membranes were prepared to evaluate their CO_2/H_2 separation performance. In sum, higher CO_2/H_2 selectivities were obtained for both PIL FSI– 40 [C_2mim][FSI] (α = 9.0) and PIL TFSAM– 40 [C_2mim][TFSAM] (α = 7.1) compared to those of composites containing the conventional $[NTf_2]^-$ anion (PIL NTf_2 – 40 [C_2mim][NTf_2] (α = 6.5) and PIL NTf_2 – 60 [Pyr_{14}][NTf_2] (α = 6.3).

References

[1] Merkel T.C., Zhou M., Baker R.W., J. Memb. Sci., 389 (2012) 441–450.

[2] Tomé L.C., Marrucho, I. M., Chem. Soc. Rev., 45 (2016) 2785.

[3] Gouveia A.S.L., Tomé L.C., Lozinskaya E.I., Shaplov A.S., Vygodskii Y.S., Marrucho I. M., Phys. Chem. Chem. Phys., 19 (2017) 28876-28884.

Acknowledgments

Andreia S. L. Gouveia is grateful to FCT (Fundação para a Ciência e a Tecnologia) for her Doctoral (SFRH/BD/116600/2016). This work was supported by FCT through the project PTDC/CTM-POL/2676/2014 and R&D units UID/QUI/00100/2013 (CQE) and UID/Multi/04551/2013 (GreenIT). This project has received funding from the European Union's Horizon 2020 research and innovation programme under the Marie

Sklodowska-Curie grant agreement No 745734.

Adsorption of sulfur and nitrogen compounds present in commercial diesel.

Marco Figueiredo*, Luana Baia, Wallace Souza, Cláudia Veloso and André Costa.

State University of Rio de Janeiro, Rio de Janeiro, Maracanã, BRASIL.
* Corresponding author: mgaya@uerj.br

Highlights

- Higher removal of sulfur compounds by silica in isothermal and kinetic tests.
- Clay showed higher affinity for nitrogen compounds.
- The adsorption capacity of nitrogenous compounds was greater than that of sulphides

1. **Introduction**

In order to mitigate the damages caused by man's action on the environment, more restrictive legislation has been created, one of which is to reduce the sulfur content in fuels, in order to reduce the emission of SOx to the environment. This is responsible for the formation of acid rain, besides being directly harmful to human health, particularly in relation to the respiratory tract [1 and 3]. At the beginning of this century, regulations in different countries reduced the sulfur content to 15 mg kg-1 (USA, EU and Japan) [1] and 10 mg kg-1 (Brazil) [2]. The process used to remove sulfur compounds is hydrotreatment which is highly severe in energy and hydrogen consumption. Alternative processes with lower cost are being studied in order to remove this contaminant, being the adsorption one of these processes. In the present work, the adsorption of nitrogenous and sulfur compounds present in diesel samples was evaluated in three commercial adsorbents: silica, clay and coal. Kinetic curves and adsorption isotherms were obtained. In the modeling of the kinetic curves was used mass transfer model and isotherm data were adjusted by the Langmuir-Freundlich Model.

2. **Methods**

The adsorbents were characterized as texture properties, thermogravimetric data, chemical composition and acidity. The kinetic and isothermal tests were performed in a Dubnoff bath, where in the kinetic tests the ratio of diesel volume / adsorbent mass used was 2: 1 (mL / g), at 40 ° C, shaking of 2.5Hz and range of between 30 and 360 minutes. The isotherm tests were performed by varying the diesel / mass ratio of adsorbent between 1.25: 1 and 100: 1 (mL / g), time of 420 minutes and using the same agitation and temperature of the kinetic tests.

3. Results and discussion

The silica sample was the one that removed the largest quantity of sulfur compounds among the studied adsorbents, while the clay was the second adsorbent with the highest removal of this contaminant. In the equilibrium range studied between 1.25: 1 and 10: 1 mL of diesel: g adsorbent, the amount of sulfur compounds removed by silica ranged from 3.03 to 7.74 mmol of sulfur / kg adsorbent for the range studied.

The following sequence for the adsorption capacity of the nitrogen compounds was obtained: clay> silica> coal for the entire concentration range in the studied fluid phase. The ratio of volume (mL) of diesel per mass (g) of adsorbent ranged from 1.25: 1 to 100: 1 and an adsorption capacity of 1.48 to 34.43 mmol of nitrogen / kg of adsorbent was obtained. In order to adjust the adsorption isotherms, the Langmuir-Freundlich model was the most suitable for the treatment of the equilibrium data.

The experimental data for the nitrogen compounds presented a satisfactory fit, while for the sulfur compounds some points showed a greater dispersion. It is observed a greater removal of nitrogen compounds by the clay, while the silica presents a greater removal of the sulphur compounds, as already observed in the adsorption isotherm tests using the same charge and adsorbent. It is also noted that both nitrogen and sulfur compounds reach equilibrium faster in silica than in clay, which may be associated with the higher pore volume of this material.

The results show that the diffusive resistance is higher for sulfur compounds (lower diffusion coefficient) in relation to nitrogen ones, and silica presented the lowest diffusive resistance, in the removal of both contaminants in relation to the clay. This lower resistance to silica adsorption may be due to the fact that this material has the highest pores volume.

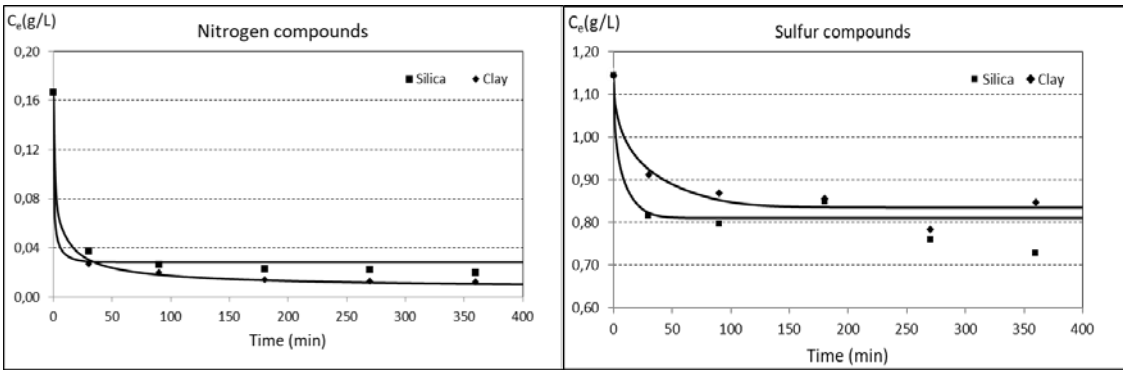

Figure 1. Kinetic curve of adsorption of nitrogen and sulfur compounds.

4. Conclusions

The results showed a higher affinity of the adsorbents for the nitrogen compounds in relation to the sulfur compounds. In equilibrium isotherm tests with diesel, silica and clay removed the largest amount of sulfur and nitrogen compounds, respectively. The effective diffusivity values estimated in the kinetic curves indicated a lower resistance of the sulfur and nitrogen compounds to the diffusion in the presence of silica.

References

[1] A. Stanislaus, A. Marafi, M.S. Rana. Catalysis Today, v. 153, n. 1-2, p. 1-68, 2010.

[2] J.M.P.F. Silva, E.B. Silveira, A.L.H. Costa, C.O. Veloso, C.A. Henriques, F.M.Zotin, M.L.L. Paredes, R.A.Reis, S.S.X. Chiaro. Ind. & Eng. Chem. Res., v. 53, p. 16000−16014, 2014.

[3] S.W. Lee, J.W. Ryu, W.Min. Catalysis Surveys from Asia, v. 7, n. 4, 2003.

Overcoming the Influence of HMF Reaction Mixture Constituents on Extraction Solvent Performance.

André B. de Haan[1]

1 Delft University of Technology, Chemical Engineering, Van der Maas Weg 9,

2629 HZ Delft, The Netherlands

**Corresponding author: a.b.dehaan@tudelft.nl*

Highlights

- Effect of ionic liquid, deep eutectic solvent and fructose on HMF extraction by MIBK and 2-pentanol was evaluated.
- All reaction mixture constituents decreased extraction performance.
- Monovalent salts can overcome decreased solvent performance.

1. Introduction

HMF (5-hydroxymethylfurfural) is a promising bio-based platform chemical that is obtained from hexose dehydration and can be used to produce biofuels and various chemical products [1]. The hexose dehydration reaction is equilibrium limited, reversible and the HMF formed in this reaction can decompose into levulinic acid (LA) and formic acid (FA).

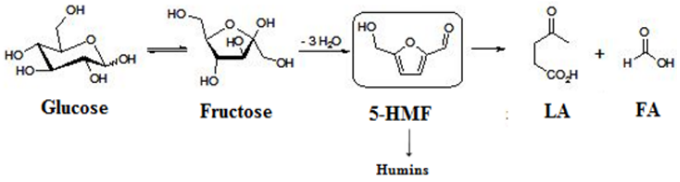

Figure 1. Reaction scheme for HMF formation.

In order to avoid HMF degradation, extensive research has been performed on biphasic systems wherein the catalytic dehydration reaction is coupled with direct extraction of the HMF into an organic solvent to increase the selectivity as well as conversion [2].

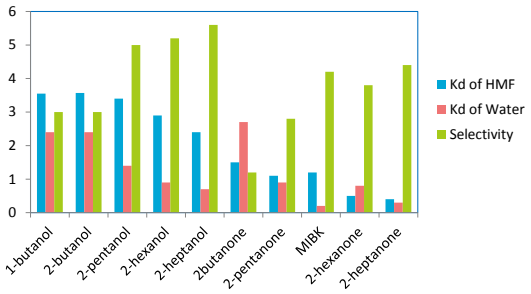

Figure 2. Comparison of various solvents for HMF extraction.

The focus of this work is a systematic study how the constituents of the reaction mixture affect the extraction performance of organic solvents. A solvent screening has shown that in addition to the

widely studied solvent methyl isobutyl ketone (MIBK), 2-pentanol is a promising alternative with comparable selectivity but significantly higher distribution coefficient. Next to water and HMF the reaction mixtures typically contain the hexose substrate (glucose, fructose), salts, catalyst (acid) and co-solvents (DMSO, ionic liquids, deep eutectic solvents) [1]. All these constituents will influence the extraction performance (distribution coefficient, selectivity) of the solvent. However, while using these complex reaction mixtures in studying the effect on conversion and selectivity of the dehydration reaction, there are to our knowledge no studies that have systematically investigated the combined effect of these constituents on the solvent performance.

2. Methods

The study has been executed by determining liquid-liquid phase equilibrium data for the ternary systems HMF, water, and solvent (MIBK or 2-pentanol) at 313.15 K (40^{o}C) and atmospheric pressure. Inorganic salts (NaCl, KCl, Na2SO4, KCl, K2SO4), [EMIM][BF4] as ionic liquid, 1:2 molar ratio mixture of choline chloride/urea as deep eutectic solvent and fructose were added to the aqueous phase. All data obtained were correlated using the NRTL model. The effects on solvent performance (HMF distribution coefficient and the selectivity) were derived from the LLE data.

3. Results and discussion

The results indicated that higher distribution coefficients are achieved in the 2-pentanol-HMF-water system compared to the MIBK-HMF-water system. On the other hand, the separation ability of MIBK is better than that of 2-pentanol. Adding up to 10 wt% inorganic salts to the system enhanced the distribution coefficient of HMF into the organic phase as well as the selectivity up to 2 times confirming the salting-out ability of the studied salts. The addition ionic liquid showed the opposite effect. At 30 wt% [EMIM][BF4] the HMF distribution coefficient as well as selectivity were reduced to 1/3 of the original value. This salting in effect is caused by the specific interactions between the HMF and ionic liquid that is known to increase the reaction selectivity by complexing with the hydroxyl groups of HMF. For the deep eutectic solvent a comparable effect as with the ionic liquid was observed. Also the introduction of fructose in the system reduced the HMF distribution coefficient and selectivity. Typically substrate concentrations up to 30 wt% are applied and at these conditions a significant decrease in solvent performance is observed. Finally it was observed that the presence of HMF and fructose in the system reduced the solubility of especially the divalent inorganic salts.

4. Conclusions

Overall monovalent salts like NaCl and KCl are the most suitable candidates to overcome the negative effects of co-solvents (ionic liquid, deep eutectic solvent) and hexose substrate on the solvent performance.

References

[1] Van Putten, R. -J.; Van der Waal, J. C.; De Jong, E.; Rasrendra, C. B.; Heeres, H. J.; De Vries, J. G., Chem. Rev. 2013, 113, 1499-1597

[2] E.C. Sindermann, A. Holbach, A.B. de Haan, N. Kockmann, Chem. Eng. J. 2016, 283, 251-259A. Bianchi, N.C. Jones, Chem. Eng. J. 157 (2019) 326–337.

ECCE12
The 12th EUROPEAN CONGRESS OF CHEMICAL ENGINEERING
Florence 15-19 September 2019

Experimental Investigation of Mass Transfer in a Miniplant Scale Rotating Packed Bed.

Matthias Hilpert[1], Jens-Uwe Repke[1]

1 Process Dynamics and Operations Group, Technische Universität Berlin, Sekr. KWT-9, Str. des 17. Juni 135, D-10623 Berlin, Germany

**Corresponding author: matthias.hilpert@tu-berlin.de*

Highlights

- RPB miniplant test stand constructed
- liquid side mass transfer coefficient evaluated from O2-stripping from water
- gas side mass transfer coefficient determined by distillation of binary alcohol mixtures

Rotating Packed Beds (RPBs) provide one approach to intensification of absorption and distillation processes by enhancing heat and mass transfer through intensified micromixing and increased effective specific surface area. Furthermore, much higher throughputs can be achieved without flooding. This leads to an up to 10-fold reduction in equipment size and thus lower space requirements and capital expenditure, as compared to conventional packed columns [1]. The RPB consists of packing material in the shape of a hollow cylinder clamped between two plates that rotate at speeds up to about 2000 min^{-1}. As illustrated in Figure 1, liquid is fed in the center near the axis of rotation and flows through the bed at multiples of normal gravity, while gas in countercurrent flows radially inward. The high centrifugal forces and thus the possibility to use high surface area packing that would flood in conventional columns lead to the aforementioned process intensification.

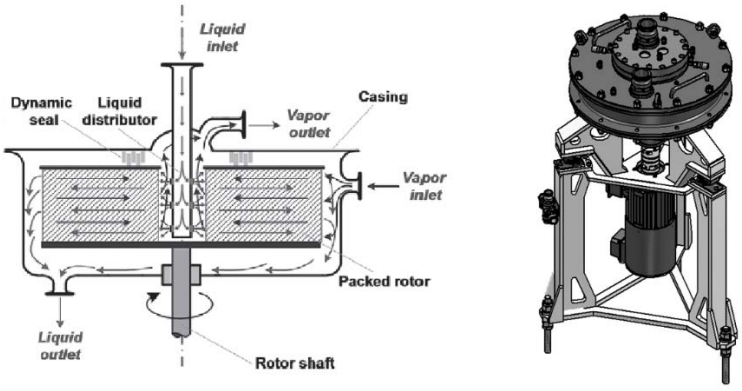

Figure 1. Flow pattern inside a single-stage horizontal RPB (left) [1], CAD-model of the constructed RPB (right).

Despite the potential of RPBs there are still few reported distillation applications in the European chemical industry which is among other factors due to the lack of validated design models for predicting RPB separation performance. While some studies regarding the distillation of binary

mixtures have been published, to the best of our knowledge no publications on multi-component mixtures exist up to now. These however are necessary to validate models of the required complexity. Furthermore, the existing studies report processed results in the form of correlations or specific NTU-values that are of limited use to the development of new correlations. Therefore, a test stand has been built at our institute to generate the required data.

The RPB test stand enables distillation, absorption and desorption experiments over a broad range of operating parameters at a semi-industrial scale. Different bed types, depths and heights, as well as different options for liquid distribution can be employed. Distillation under infinite and finite reflux conditions is possible.

To develop a validated model for multicomponent distillation in the RPB, the following systematic approach is chosen, as illustrated in Figure 2. Mass transfer inside the RPB takes place during the very short residence time of less than 1 s. Therefore, a rate-based modeling approach is adopted, requiring correlations for liquid and vapor side mass transfer coefficients. Liquid side coefficients are determined from desorption of oxygen from water into nitrogen atmosphere. Overall mass transfer coefficients are derived from distillation of binary mixtures of lower-chain alcohols at infinite reflux. Gas side mass transfer coefficients will be back-calculated and correlated using the results. To test the validity of the model, binary and ternary ideal and non-ideal mixtures will be distilled and modeled.

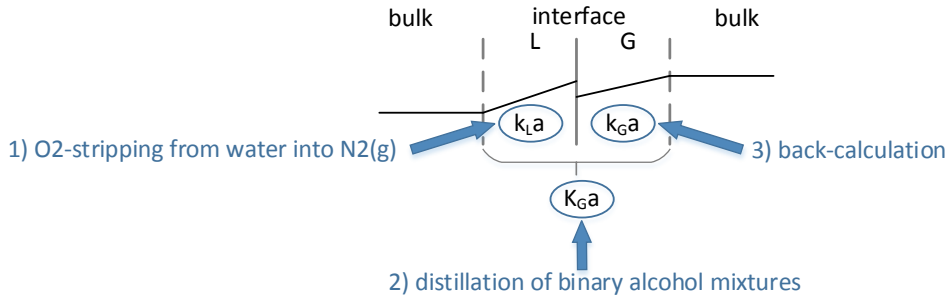

Figure 2. Schematic of approach for determination of mass transfer coefficients.

The contribution presents details of the RPB test stand and the experimental design. Results from desorption experiments and from binary distillation runs will be shown, which form the basis for the development of mass transfer coefficient correlations.

References

[1] G.E. Cortes Garcia, J. van der Schaaf, A.A. Kiss, J. Chem. Technol. Biotechnol. 92 (2017) 1136–1156.

ECCE12
The 12th EUROPEAN CONGRESS OF CHEMICAL ENGINEERING
Florence 15-19 September 2019

Model Performances Evaluated for Infinite Dilution Activity Coefficients Prediction At 298.15K.

Thomas Brouwer*, Boelo Schuur
University of Twente, Faculty of Science and Technology, Sustainable Process Technology group, PO Box 217, 7500AE, Enschede, The Netherlands.
Corresponding author: t.brouwer@utwente.nl

Highlights

- Eight models were evaluated for infinite dilution activity coefficient prediction.
- The most accurate model depends on each specific solute-solvent pair
- An accurate hydrogen bond description is essential for an accurate prediction
- An extended MOSCED model could be a potential approach for ionic liquids

1. Introduction

The global community relies on the chemical industry for the production of goods from complex raw materials, such as oil and biomass. The separation processes required in these production routes account for up to 50 % of the total energy costs in refineries[1] and improving the efficiency of separations can significantly reduce the environmental impact of the chemical industry. This can only be made by achieved by understanding the separation processes on molecular-level, which includes a good description of thermodynamic equilibria. An accurate description of these equilibria are possible with models like UNIQUAC and NRTL, but require labour intensive experimental data. Alternative predictive models can provide engineers with first estimates for molecular behaviour with less experimental data. In this manuscript, we explore different predictive models in predicting a molecular descriptor, the infinite diluted activity coefficient, γ_i^∞. This descriptor can be used in combination with predictive models to make a first estimate on the thermodynamic behavior in separation processes. Several types of models are known to be able to predict the γ_i^∞, for instance the Hildebrand parameter[2], Hansen Solubility Parameters[3], various Group Contribution Methods (UNIFAC), the Conductor like Screening Model for Real Solvents (COSMO-RS) model[4], Abraham model[5] and the Modified Separation of Cohesive Energy Density (MOSCED) model.[6] The aim of this manuscript is to compare the performance of these fundamentally different approaches in prediction the γ_i^∞ of (a)-polar solutes in (a)-polar (ionic) solvents. The relative performance of all evaluated models will be linked to the fundamental assumption incorporated in the various models.

2. Methods

For all γ_i^∞ predictions a systematic assessment was done at 298.15K and all model specific parameters were imported from literature sources. The overall average relative deviation (ARD) was determined both overall for all models as for specific solute-solvent combinations.

3. Results and discussion

A larger ARD was observed for Ionic Liquids (ILs) than for molecular solvents due to the additional ionic interactions. Overall averaged, the MOSCED model was the most accurate model for the prediction of γ_i^∞ of all solute classes in molecular solvents with an ARD of 16.2±1.35%. The UNIFAC Group Contribution Methods (GCMs), COSMO-RS and the Abraham models perform comparably with ARDs of 24.3-32.2%. Models using the Hildebrand parameter and the Hansen Solubility Parameters are significantly less accurate due to an insufficient description of intermolecular interactions such as hydrogen bonds. For predicting the γ_i^∞ in ILs, the Abraham model is overall the most accurate model with an ARD of 65.1±4.50%. The GCMs are less accurate with ARDs of 86.2-122%, while COSMO-RS is far less accurate with an ARD of 182±16.7%, due to a deficient description of long-range interactions.

Upon classification of solutes and molecular solvents, the evaluating for each of the solvent and solute classes was performed. Each model predicts most accurately, with the exception of the Hildebrand parameter and Hansen Solubility Parameters, the γ_i^∞ for specific classes of binary solute-solvent pairs. Though the accuracy decreases with the polarity of the solute. For ILs, the Abraham model is overall averaged most accurate, though several cations are more accurately described with mod. UNIFAC (Ly) or mod. UNIFAC (Do). The large ARDs from the UNIFAC models and the Abraham model are mainly due to large ARDs for bis(trifluoromethylsulfonyl)imide ($[NTF_2]$), tetrafluoroborate ($[BF_4]$) and the 2-(2-Methoxyethoxy)ethyl sulfate ($[MDEGSO_4]$) anions. Hence, improving the prediction of these anions will greatly increase their overall prediction accuracy. Additionally, the most accurate model for molecular solvents, MOSCED, could not be assessed for ILs. Therefore, an extension of MOSCED towards ILs may become an accurate tool in predicting accurate γ_i^∞ in ILs.

4. Conclusions

Based on the evaluation results, it can be concluded that choosing the most accurate model for estimation of γ_i^∞ depends on both the solute and solvent categories under evaluation. Using a predicted γ_i^∞ for IL screening should be done with caution, as these on average easily exceed deviation of 65%.

References

1. Kiss, A.A., et al., *Separation technology–Making a difference in biorefineries.* Biomass and Bioenergy, 2016. **95**: p. 296-309.
2. Hildebrand, J. and R. Scott, *The solubility of nonelectrolytes*, *Reinhold Pub.* Co., New York, 1950. **3**.
3. Hansen, C.M., *The three dimensional solubility parameter.* J. Paint Technol, 1967. **39**: p. 105.
4. Eckert, F. and A. Klamt, *Fast solvent screening via quantum chemistry: COSMO-RS approach.* AIChE Journal, 2002. **48**(2): p. 369-385.
5. Abraham, M.H., *Scales of solute hydrogen-bonding: their construction and application to physicochemical and biochemical processes.* Chemical Society Reviews, 1993. **22**(2): p. 73-83.
6. Thomas, E.R. and C.A. Eckert, *Prediction of limiting activity coefficients by a modified separation of cohesive energy density model and UNIFAC.* Industrial & Engineering Chemistry Process Design and Development, 1984. **23**(2): p. 194-209.

ECCE12
The 12th EUROPEAN CONGRESS OF CHEMICAL ENGINEERING
Florence 15-19 September 2019

Reactive Separation Concept for Valorizing Low Molecular Weight Carboxylic Acids from Aqueous Media.

Andreas Toth[1], Susanne Lux[1], Daniela Painer[1], Matthäus Siebenhofer[1]

1 Institute of Chemical Engineering and Environmental Technology, Graz University of Technology, Inffeldgasse 25C/III, 8010 Graz

**Corresponding author: andreas.toth@tugraz.at*

Highlights

- Valorization of dilute, biobased carboxylic acids is possible.
- Solvent regeneration rates above 75 % are feasible.
- Concept insensitive to residual acid in the regenerated solvent.

1. Introduction

Valorization of low molecular weight carboxylic acids (e.g., acetic acid, formic acid) of biogenic origin is associated with various problems. Originating mostly within biorefinery processes, the carboxylic acids show up at low concentration in aqueous broths. The main problems to be dealt with are (quasi-)azeotropic behavior, high water content and unfavorable combinations of substance properties (e.g., boiling points). While conventional separation technologies struggle with these problems, reactive separation technologies are promising alternatives. [1] For dilute acetic acid in particular and low molecular weight carboxylic acids in general, the concept of chemical conversion in emulsions with in-situ extraction of the products was developed. [2] Homogeneously catalyzed esterification with a higher aliphatic alcohol in the solvent phase (e.g., 1-octanol) addresses the liquid-liquid equilibrium partition by separation of the hydrophobized derivatives of the carboxylic acids. Reactive distillation with transesterification (octyl ester to methyl ester) was investigated for solvent regeneration and product isolation. The surfactant type catalyst 4-dodecylbenzenesulfonic acid accelerates esterification. 4-dodecylbenzenesulfonic acid is also reported to be a potent catalyst for transesterification by Hagen et al. [3]. A proof of concept was performed in batch operation mode.

2. Methods

The laden solvent after esterification was mixed with methanol in a batch reactive distillation column in lab-scale. Laden solvent with and without residual acetic acid from the esterification step was used. The setup consisted of a 500 ml three-neck flask, a 30 cm Vigreux column with a condenser and a reflux splitter. Total reflux ratio was applied until reflux from the condenser was fully developed, then the reflux ratio was set to 10. Distillate was withdrawn from the product funnel every 30 min and analyzed by gaschromatography. The experiments were performed until distillate formation stopped.

For the proof of concept, the molar ratio of methanol as well as the performance of the catalyst were investigated.

3. Results and discussion

Regeneration performance was evaluated via methyl ester yield and amount of volatile residues in the regenerated solvent phase. Figure 1 displays a comparison of methyl acetate yield for different stoichiometric ratios of methanol to octyl acetate. 3-fold excess of methanol allows a methyl acetate yield of 75.6 % and about 1.5 wt.% residual volatile components in the regenerated solvent. While increased excess of methanol is beneficial for yield and regeneration rate, energy demand for excess methanol removal multiplies.

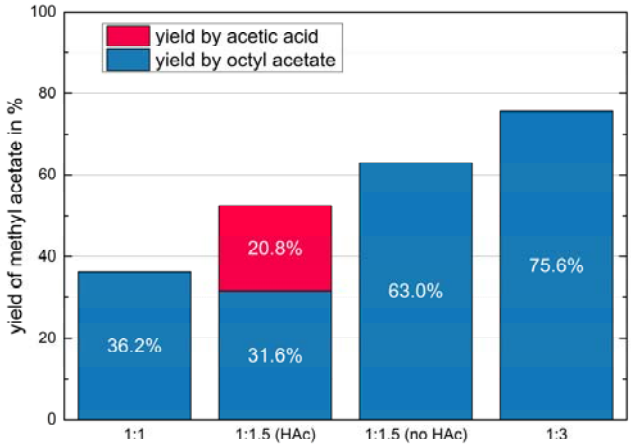

Figure 1. Methyl acetate yield of transesterification in batch reactive distillation

For 1.5-fold excess of methanol the impact of 2 wt.% residual acetic acid in the laden solvent was investigated. As shown in figure 1, less octyl acetate is converted, but more than 99 % of the acetic acid is esterified. Direct esterification (acetic acid to methyl acetate) is preferred over transesterification (octyl acetate to methyl acetate) as a consequence of a lower Gibbs free enthalpy for the esterification. In order to increase the performance a higher excess of methanol is needed, if residual acetic acid is present in the laden solvent.

4. Conclusions

The combination of reactive extraction (esterification in emulsion) and reactive distillation (transesterification) has proven feasible for valorizing low molecular weight carboxylic acids in lab-scale. Solvent regeneration with transesterification in reactive distillation allows regeneration rates in the order of 75 %. The favorable vapor-liquid equilibria between high and low boiling components enable reducing the amount of low boiling residues in the regenerated solvent to below 0.5 wt.%.

References

[1] V. D. Talnikar and Y. S. Mahajan, Korean J. Chem. Eng. (2014), 31, 1720–1731.
[2] A. Toth, S. Lux, D. Painer, M. Siebenhofer, React. Chem. Eng. (2018), 3, 905-911.
[3] J. Hagen, D. Henke, Chemie Ing. Tech. (2009), 81 (9), 1429–1438.

ECCE12
The 12th EUROPEAN CONGRESS OF CHEMICAL ENGINEERING
Florence 15-19 September 2019

Hydrocarbon Mass Transfer in Ionic Liquids.

Noemí Delgado-Mellado[1], Miguel Ayuso[1], Julián García[1], Francisco Rodríguez[1]

1 Department of Chemical Engineering, Complutense University of Madrid, 28040 Madrid, Spain

**Corresponding author: noemidelgado@ucm.es*

Highlights

- Determination of hydrocarbon diffusion coefficients at infinite dilution in ILs
- Hydrocarbon diffusion is highly influenced by the ionic liquid viscosities
- A modified Wilke-Chang correlation successfully predicts the diffusion coefficients

1. Introduction

The experimental values of diffusion coefficients are of special importance in the theory of transport properties and to predict the rate-limiting factor for chemical processes and engineering design [1]. Herein, the Taylor dispersion method has been used for the first time to measure the diffusion coefficients at infinite dilution of *n*-heptane and toluene in two ionic liquids (ILs), namely 1-ethyl-3-methylimidazolium dicyanamide ([emim][DCA]) and 1-ethyl-4-methylpyridinium bis(trifluoromethylsulfonyl)imide ([4empy][Tf_2N]). The importance of both ILs lies in their remarkable extraction properties in the aromatic/aliphatic separation process by liquid-liquid extraction [2]. A correlation based on the Wilke-Chang equation has been proposed to estimate the diffusion coefficients that satisfactorily predicts the temperature dependence.

2. Methods

The experimental equipment consists of a KDS Legato 200 metering pump which provides a constant and a laminar flow, a PEEK diffusion tubing (10 m length and $0.375 \cdot 10^{-3}$ m inner radius) located in a thermostatic incubator, and a Refractive Index Detector Agilent 1260 Infinity II which records the concentration gradient signal at the end of the diffusion tubing. The experiments were performed at temperatures between (298.2 and 333.2) K and a constant laminar flow of 50 $\mu L \cdot min^{-1}$ for 20 μL of samples with a hydrocarbon concentration of (0.02-0.10) $mol \cdot dm^{-3}$ in excess.

3. Results and discussion

Toluene presents higher values of diffusion coefficients than *n*-heptane in the [emim][DCA] IL because of the lower toluene molecular volume, meanwhile both toluene and *n*-heptane show similar values in the [4empy][Tf_2N] IL due to high effect of the solvent viscosity on the hydrocarbon diffusion (Figure 1). Meanwhile at a temperature of 298.2 K the [emim][DCA] IL has a viscosity of 15.1 mPa·s, the [4empy][Tf_2N] viscosity presents a much higher value of 34.5 mPa·s [3]. Therefore, the higher [4empy][Tf_2N] viscosity leads to a lower influence of the solute molecular volume on the diffusion coefficients.

It has been observed that the Wilke-Chang correlation [4] does not correctly predict these diffusion coefficients; it tends to underestimate them at low temperatures and overestimate

them at high temperatures, with an average deviation of 17.5%. The association parameter seems to be a nonconstant value influenced by the temperature in ILs, therefore a modified Wilke-Chang equation is proposed and expressed as:

$$D_{12} = 7.4 \cdot 10^{-8} \cdot \frac{(\varphi_{\mathrm{mod}}(T) \cdot M)^{0.5} \cdot T}{\eta \cdot V^{0.6}}$$

being $Æ_{mod}(T)$ the association parameter dependent on temperature as $Æ_{mod}(T)=a_1 \cdot T+a_2$. The modified Wilke-Chang equation correctly represents the temperature effect on the diffusion coefficients and estimates them with an average deviation of 2.6% (Figure 1).

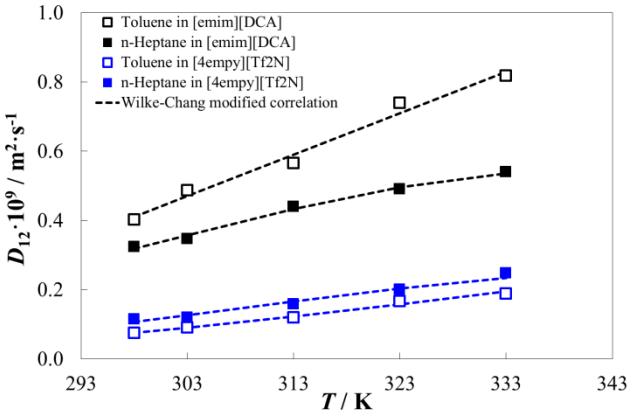

Figure 1. Diffusion coefficient at infinite dilution of *n*-heptane and toluene in [emim][DCA] and [4empy][Tf2N] ILs and dotted lines for Wilke-Chang modified correlation.

4. Conclusions

The hydrocarbon diffusion is faster in [emim][DCA] because of the much lower values of its viscosity, and the difference between *n*-heptane and toluene diffusion coefficients are due to their respective molecular volume. On the contrary, the high viscosity of [4empy][Tf_2N] IL leads to lower and similar diffusion coefficients of both hydrocarbons, prevailing the effect of the viscosity over the effect of the hydrocarbon molecular volume. The Wilke-Chang correlation, the most common one used to estimate the diffusion coefficients, unsuccessfully predicts the temperature dependence with an average deviation of 17.5%. A modified Wilke-Chang correlation has been proposed to properly estimate the dependence of the temperature on the association parameter. This correlation has shown a good fit in the studied temperature range with an average deviation of 2.6%.

References

[1] A. Safi, C. Nicolas, E. Neau. J. L. Chevalier, J. Chem. Eng. Data 53 (2008) 444-448.
[2] M. Larriba, P. Navarro, J. García, F. Rodríguez, J. Chem. Eng. Data 59 (2014) 1692–1699.
[3] M. Larriba, P. Navarro, J. García, F. Rodríguez, Sep. Purif. Technol. 120 (2013) 392–401.
[4] C. R. Wilke, P. Chang, AIChE Journal 1 (1955) 264-270.

ECCE12
The 12th EUROPEAN CONGRESS OF CHEMICAL ENGINEERING
Florence 15-19 September 2019

Mass transfer intensification in wastewater aeration system with novel conical mixer

Anastasia Grigoreva[1,2], Rufat Abiev[2]*

1 Asterion Ltd, Saint-Petersburg, Russia;
2 St. Petersburg State Institute of Technology, Moskovskii pr.26, 190013, Saint-Petersburg, Russia;

**Corresponding author: abiev.rufat@gmail.com*

Highlights

- New conical mixer has been elaborated and tested.
- New conical mixer has the same mass transfer efficiency as Ruston turbine, but lower power consumption.

1. Introduction

The practice of operating wastewater treatment plants shows that 60-80% of expences depends on the efficiency of the aeration system [1]. This is the most energy-consuming process. Rushton turbine is recognized as the most effective mixer for gas dispersing [2]. We have recently developed aeration system with new type of impeller, which shown in the Fig.1.

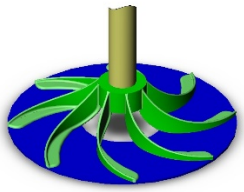

Figure 1. New type conical mixer.

This mixer has more streamlined shape, the blades are rounded, therefore hydraulic losses are minimized.

2. Methods

All tests were hold in plexiglass vessel with volume of 44 litres. In present work we analyzed bubbles' sizes using photographic method. From 5300 to 7300 bubbles were captured and calculated. Mass transfer was determined by method, described in [3]. Sodium sulfite was added to the tap water for deoxygenation. The oxygen content in the liquid was measured with oxygen sensor (Expert, Type 009, Russia). Volumetric Mass Transfer Coefficient (K_La) defined as

$$K_La = \frac{1}{t2-t1} ln \frac{d1}{d2}$$

Where d2 and d1 – oxygen deficiency at the moment of time moments of t2 and t1. Power consumption were measured with stand, which described in [4]. SOTE and SAE were chosen as criteria of efficiency [5].

3. Results and discussion

Oxygen content in the water during experiments shown in the Fig. 2. The main results are presented in the Table 1.

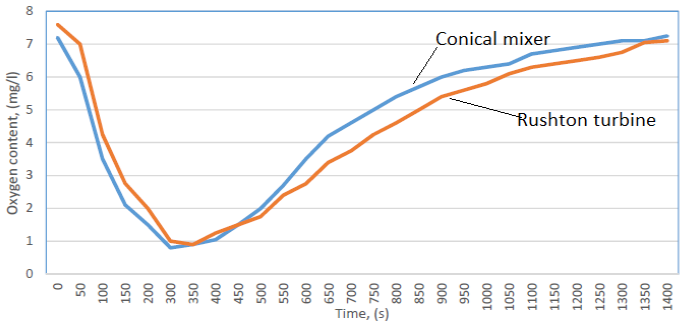

Figure 2. Oxygen content during experiments with conical mixer and Rushton turbine.

Table 1. Mass transfer characteristics of water oxidation

The name of calculated parameter	Rushton turbine	Conical mixer
Volumetric Mass Transfer Coefficient Kla,	11.06	15.62
Oxygen dissolution rate, kg/h	21.25	29.99
Oxygen use percentage SOTE, %	13.60	19.19
The ratio of the amount of oxygen dissolved in a liquid to the amount of electricity used SAE	0.35	0.64

4. Conclusions

Conical mixer shows SAE efficiency 1.82 times more than Rushton turbine. This is because the new type of mixer has a more streamlined shape, contributing to reduced power consumption. The proposed aeration system is a good alternative to the existing pneumatic aeration, especially in shallow tanks (up to 3 meters deep). Installing this kind of mixer will significantly reduce operating costs and avoid problems with clogging of small (approx.. diameter of 0.1 mm) pores in aerators (spargers).

References

[1] S.Yu.Andreev, A.M.Isayeva, T.V.Malyutina, I.V.Pantyushov, Regional Architecture and Construction, 2 (2008) 63-69 (in Russian).

[2] E.L. Paul, V.A. Atiemo-Obeng, S.M. Kresta, Handbook of industrial mixing: science and practice. Wiley, 2003

[3] Ya.A. Karelin, D.D. Zhukov, V.N. Zhurov, B.N. Repin, Treatment of industrial wastewater in aeration tanks., Stroyizdat, Moscow, 1973 (in Russian).

[4] R.S. Abiev. A.N Grigorieva, Trans. SPSIT (TU), 45 (2018) 94-97.

[5] *Merkblatt DWA-M 229-1. Systeme zur Belueflung und Durchmischung von Belebungsanlagen- Teil 1: Planung, Ausschreibung und Ausfuerung,* September 2017.

ECCE12
The 12th EUROPEAN CONGRESS OF CHEMICAL ENGINEERING
Florence 15-19 September 2019

Molecular dynamics simulations of the adsorption of partially hydrolyzed polyacrylamide on kaolinite edge surfaces in saltwater for a range of pH values: Effect of temperature

Quezada GR[1]*, Rozas RE[2], Toledo PG[3]
[1]*Water Center for Agriculture and Mining (CRHIAM), University of Concepción, Concepción, Chile*
[2]*Department of Physics, University of Bío-Bío, Concepción, Chile*
[3]*Chemical Engineering Department and Surface Analysis Laboratory (ASIF), University of Concepción, Concepción, Chile*

The adsorption of partially hydrolyzed polyacrylamide (HPAM) polymer chains on kaolinite particles is key in solid-liquid separation processes that seek to recover water in mineral processing. In this work, computational molecular dynamics is used to study the water-kaolinite interface in the presence of HPAM under conditions of high salt concentration and wide pH range. The salts used are some of the most common in seawater. Water clarification processes occur at very different temperatures at different times of the year, however the effect of temperature has practically not been studied. First, quantum mechanical calculations are used to describe the negative charging on the edge surfaces of the kaolinite at and above its point of zero charge. Then, molecular simulations are used to evaluate the effect of temperature on the adsorption of ions and HPAM chains on the edges of kaolinite particles. The saltwater contains different salts, where the anion is chloride and the cation an alkali metal or alkaline-earth metal, in all cases concentration is as high as 0.6 M. It is also considered a brine that imitates seawater, with an ionic strength of 0.6 M and the simultaneous presence of Cl^-, Na^+, $SO4^{2-}$, Mg^{2+}, Ca^{2+} and K^+. The pH range of the simulations is 7 to 11 and the temperature range is 273 to 313 K. The results show that the ions compete for the edge surfaces of the kaolinite, although water-structure maker ions always adsorb better than water-structure breaker ions. An interesting result is that the adsorption of HPAM is promoted by the salts with maker cations and is hindered by the salts with breaker cations. Temperature has a significant impact. We hope these results can contribute to the decision making in water clarification processes in mineral treatment.

Acknowledgement: We thank Centro CRHIAM through Project Conicyt/Fondap/15130015 for financial support and The Southern GPU-cluster (SGPU- C) UDEC funded by FONDEQUIP EQM150134 for computational support.

ECCE12
The 12th EUROPEAN CONGRESS OF CHEMICAL ENGINEERING
Florence 15-19 September 2019

Extraction of Glycyrrhetinic acid from Dried Licorice Root by using Supercritical Carbon Dioxide.

Kohei Wada and Masanao Imai*

Course of Bioresource Utilization Sciences, Graduate School of Bioresource Sciences, Nihon University, 1866 Kameino, Fujisawa, Kanagawa-pref. 252-0880, Japan
**corresponding author: XLT05104@nifty.com*

Highlights

- Glycyrrhetinic acid was extracted by supercritical carbon dioxide from dried Licorice.
- Extracted amount was increased with increasing pressure and decreasing with temperature.
- Extracted amount was correlated with estimated density of supercritical carbon dioxide.
- Lower energy required for extraction led higher extracted amount of glycyrrhetinic acid.

1. Introduction

Licorice is one of major medicinal herbs expecting anti-inflammatory and anti-cancer[1-3]. Pharmaceutical effects have been brought by glycyrrhetinic acid. In the licorice root, glycyrrhetinic acid is contained as an aglycone and glycyrrhizin is also included glycoside. In this work, glycyrrhetinic acid was focused as a target component. Supercritical carbon dioxide ($SCCO_2$) has been anticipated as lowest risk solvent and non-residual character in products. The aim of this study is to measure of effect of temperature and pressure on extracted amount of glycyrrhetinic acid. Extracted amount was correlated with the estimated density of supercritical carbon dioxide. Energy required for extraction was preliminary evaluated and then correlated with the extracted amount of glycyrrhetinic acid.

2. Methods

Licorice root was purchased from Uchida Wakanyaku Ltd. (Tokyo, Japan). Pure glycyrrhetinic acid (98%) was purchased from FUJIFILM Wako Pure Chemical Industries, Ltd (Osaka, Japan). It was used to determine the calibration curves to measure the concentration of glycyrrhetinic acid by high performance liquid chromatography. The mean size of the powdered licorice root was varied from 200 to 990 µm. The $SCCO_2$ extraction apparatus was presented in Fig.1[4]. The extraction was operated as batch mode. Extraction period was 30 min. throughout this study.

3. Results and Discussion

Extracted amount in this study was expressed as [mol-target･(g-dried-sample)$^{-1}$･(mol-$SCCO_2$)$^{-1}$]. Liquid-solid extraction by ethanol was employed as a primary experiment. Extracted amount was 6.0 [mol-target･(g-dried-sample)$^{-1}$･(mol-$SCCO_2$)$^{-1}$] at 303K.

The extracted amount was decreased with increasing temperature (Fig.2). It was remarkably decayed in the range of 313-318 K. The extracted amount was gradually increased with increasing pressure (Fig.3). Density of supercritical carbon dioxide was estimated by Bender's empirical equation[5]. The extracted amount was strongly depended on the density within 0.71-0.93 [g·cm^{-3}]. Energy required for extraction was evaluated from the square of difference of solubility parameters between $SCCO_2$ and glycyrrhetinic acid. Lower required energy led higher extracted amount of glycyrrhetinic acid.

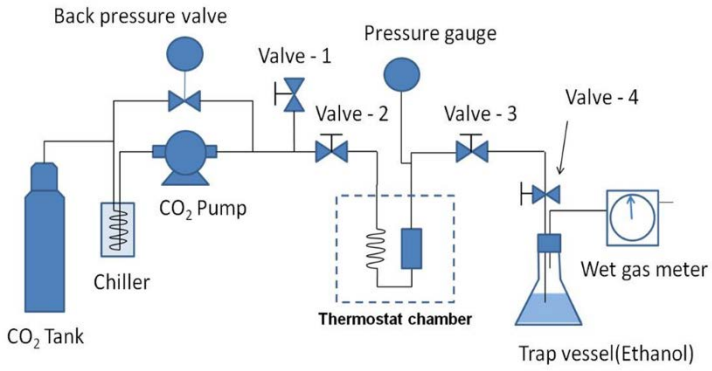

Fig. 1. Schematic illustration of $SCCO_2$ extraction process

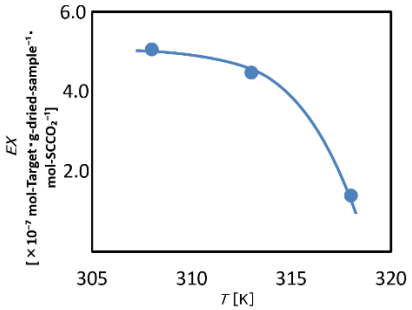

Fig. 2. Effect of temperature on the extracted amount

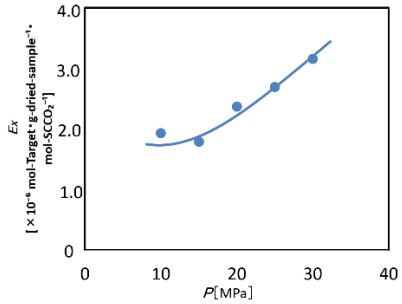

Fig. 3. Effect of pressure on the extracted amount

4. Conclusions

Glycyrrhetinic acid was successfully extracted by supercritical carbon dioxide from dried Licorice root ranging 308-318K and 10-30MPa. Extracted amount was increased with increasing pressure and decreasing with temperature. Extracted amount was closely correlated with the estimated density of supercritical carbon dioxide. Energy required for extraction was estimated from solubility parameter of supercritical carbon dioxide and glycyrrhetinic acid. Lower energy required led higher extracted amount of glycyrrhetinic acid.

References

[1] Nomura T, Fukai T, Akiyama T., Pure. Appl. Chem. 74(2002) 1199-1206.
[2] Cao L, Ding W, Jia R, Du J, Wang T, Zhang C, et al., 64 (2017) 234-242.
[3] Wang L, Yang R, Yuan B, Liu Y, Liu C., Acta Pharm Sin B 5 (2015) 310-315.
[4] Saotome,Y.and Imai,M., Food Sci. and Technol. Res. 24 (2018) 63-73 .
[5] Bender,E., 5th Symposium on Thermophysical Properties,New York (1970) 227-235.

ECCE12
The 12th EUROPEAN CONGRESS OF CHEMICAL ENGINEERING
Florence 15-19 September 2019

Multicomponent separation of nadolol stereoisomers combining different preparative technologies and chiral and achiral-chiral strategies

Rami Arafah[1,2], António Ribeiro[1,2], Alírio Rodrigues[3], Luís Pais[1,2]

1 Centro de Investigação de Montanha (CIMO), Instituto Politécnico de Bragança, Campus de Santa Apolónia, 5300-253 Bragança, Portugal; 2 Laboratory of Separation and Reaction Engineering, School of Technology and Management, Polytechnic Institute of Bragança, Bragança, Portugal; 3 Laboratory of Separation and Reaction Engineering – Laboratory of Catalysis and Materials, Associate Laboratory LSRE-LCM, Faculty of Engineering, University of Porto, Rua Dr. Roberto Frias s/n, 4200-465 Porto, Portugal.
**Corresponding author: pais@ipb.pt*

Highlights

- Strategies for the complete preparative separation of nadolol chiral drug.
- Optimization of different solvent compositions using chiral and achiral adsorbents.
- Experimental chiral separation by preparative and SMB chromatography.

1. Introduction

Nadolol is a common prescribed pharmaceutical drug for the relieve of several cardiovascular diseases and represents a very interesting case-study of multicomponent chiral separation since it is composed by four stereoisomers, being two pairs of enantiomers. In this way, it introduces the possibility of alternative strategies, using different kind of preparative separation sequences and techniques, the use of different packings (chiral and achiral stationary phases), and the corresponding mobile phase optimization at both normal and reversed-phase modes.

When considering preparative and multicomponent separation, the complexity deeply increases by introducing the necessity of multi-step separation sequences (or a much more complex multi-region separation process), by opening the possibility to combine chiral and achiral stationary phases (when in presence of stereoisomers instead of just one pair of enantiomers) and to combine different separation techniques (fixed-bed and simulated moving bed (SMB) related processes). The design of the complete preparative separation of nadolol stereoisomers asks for a global experimental and simulation methodology considering both the characterization and optimization of each separation step and its sequences to achieve the four nadolol components pure. New strategies using combinations of achiral and chiral stationary phases and sequences of different separation techniques will be presented. Extensive experimental and simulation results for the complete separation of all the four nadolol stereoisomers using Chiralpak IA (chiral) and different Waters C18 (achiral) stationary phases will be presented.

2. Methods

For the analytical measurements, an analytical Knauer HPLC was equipped with one Smartline 1050 pump, a 10 mL pump head and two detectors in series: a Smartline UV detector 2520 a polarimeter detector (Chiralser IBZ, Messtechnik, Germany). These measurements were performed using a Chiralpak IA column obtained from Daicel and a XBridge C18 column obtained from Waters. Both columns have the same analytical dimensions (250 mm L × 4.6 mm ID) and

packed with 5 μm particle size materials. For the preparative measurements, a preparative Knauer HPLC system equipped with a Smartline UV detector 2520, two Smartline 1050 pumps with 50 mL pump heads, was used. Three different preparative columns (100 mm L × 20 mm ID) were used, a Chiralpak IA (particle size diameter 20 μm), a SiliaChrom XT18 and a XBridge C18 column (both with a particle size diameter of 10 μm). The pseudo-binary SMB separation of nadolol stereoisomers was performed on a laboratory-scale SMB unit built on the LSRE group, Faculty of Engineering, University of Porto. The SMB unit was operated using a [1-2-2-1] column configuration. The SMB unit was operated with six Chiralpak IA columns for the pseudo-binary enantiomer separation and six XBridge C18 columns for the binary separation of the two nadolol racemates. Additionally, a commercial Azura Fixed-Bed prep HPLC system obtained from Knauer was also used for the binary separation of nadolol racemates. This system was equipped with two preparative HPLC pumps P2.1L model with 250 mL/min pump heads, one UV detector UVD2.1L model and a unique Waters XBridge prep C18 column (30 mm ID x 250 mm L) with particle size diameter of 10 μm.

3. Results and discussion

An extensive set of experimental and simulation results will be presented (see Fig. 1). Results will include the identification of the stereoisomers present in both nadolol racemates by means of using UV and polarimeter detectors in series. Then, a complete methodology developed during the last years by our group will be explained and applied to scale-up the separation process from analytical to preparative scales [1-3].

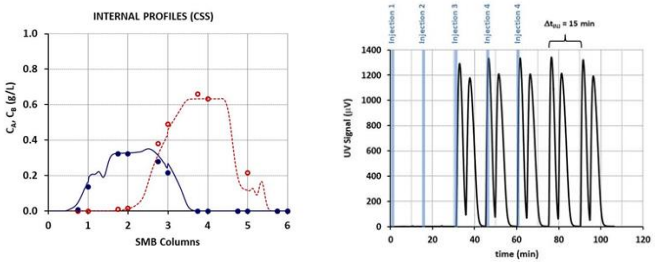

Figure 1. Experimental preparative separations of nadolol racemates using (left) Flex-SMB unit and (right) Fixed-Bed Azura pilot unit, both with achiral adsorbent under reversed-phase mode.

4. Conclusions

The results recently obtained by our research team for this topic clearly support the capacity to enhance the knowledge on the chromatographic separation of chiral pharmaceuticals using fixed-bed and SMB preparative chromatography. In this communication, it will be introduced original and innovative challenges through the real separation of multicomponent (quaternary) chiral mixtures which represents an important step forward for the pharmaceutical industry.

Acknowledgments

This work is a result of project "AIProcMat@N2020-Advanced Industrial Processes and Materials for a Sustainable Northern Region of Portugal 2020," with the reference NORTE-01-0145-FEDER-000006, supported by Norte Portugal Regional Operational Program (NORTE 2020), under the Portugal 2020 Partnership Agreement, through the European Regional Development Fund (ERDF), and of project POCI-01-0145-FEDER-006984-Associate Laboratory LSRE-LCM funded by ERDF through COMPETE2020-Programa Operacional Competitividade e Internacionalização (POCI)—and by national funds through Fundação para a Ciência e a Tecnologia (FCT).

References

[1] A.E. Ribeiro, A.E. Rodrigues, L.S. Pais, Chirality 25 (2013) 197-205.
[2] R.S. Arafah, A.E. Ribeiro, A.E. Rodrigues, L.S. Pais, Chirality 28 (2016) 399-408.
[3] R.S. Arafah, A.E. Ribeiro, A.E. Rodrigues, L.S. Pais, Chirality 31 (2019) 62-71.

ECCE12
The 12th EUROPEAN CONGRESS OF CHEMICAL ENGINEERING
Florence 15-19 September 2019

Electrokinetics of ion-exchange systems for electrodialysis and electrodeionization.

Zdeněk Slouka[1,2,*], Tomáš Belloň[1], Petr Polezhaev[1], Lucie Vobecká[1], Miloš Svoboda[1,2]

1 University of Chemistry and Technology Prague, Department of Chemical Engineering, Technická 3, Prague 6, 16628, Czech Republic, 2 University of West Bohemia, New Technologies - Research Centre, Univerzitní 8, Plzeň 30614, Czech Republic

**Corresponding author: sloukaz@vscht.cz*

Highlights

- Electrodialysis at overlimiting currents as a way of intensification.
- Investigation of overlimiting mechanisms in a specific cell.
- Electroconvection tracked by particle image velocimetry.
- Water splitting detected mostly at anion-exchange systems.

1. Introduction

Intensification of processes can bring significant savings both economical and ecological. With the advent of techniques allowing the investigation of the overlimiting region at ion-exchange membrane and with better understanding of the occurrence of overlimiting current, the scientist started to work on the development of electrodialysis units working in this high intensity current regime. Until now, these processes have been operated under much smaller currents, which in turn requires much larger units.

The typical current voltage curve (CVC) of ion-exchange systems displays three parts: (i) underlimiting, (ii) limiting, and (iii) overlimiting. The underlimiting region occurs at small current densities. The increase in the current density leads to depletion of ions on one side of the membrane which is manifested as limiting region on the CVC. However, further increase in the current results in the occurrence of physical mechanisms that partially destroy the region of depleted ions. There are two major mechanisms, and these are: (i) electroconvection, and (ii) water splitting. Unlike other separation processes (e. g. pressure driven), the overlimiting region overcomes the limitation given by concentration polarization. For the engineers to be able to exploit this advantage in the industrial applications, they need in-deep understanding of the ion-exchange system behavior in this region. We have developed a special cell, that allows to (i) visualize electroconvection in the system and (ii) measure pH changes associated with the water splitting reaction. Our work should contribute to the proper understanding of aforementioned mechanisms and their dependence on the structure of ion-exchange system and the composition of the desalted electrolyte

2. Methods

We manufacture a fluidic cell that incorporates either a small piece of an ion-exchange membrane or a single ion-exchange resin particle. This cell allows one to characterize the systems electrochemically (current-voltage curves, chronopotentiometric and amperometric curves) and

at the same time observation of the processes that occur at the interface between the ion-exchange system and the desalted electrolyte [1]. The electroconvection is tracked by solid microparticles and the results are evaluated by particle image velocimetry, the extent of water splitting reaction is directly measured by changes in pH of the respective electrolytes.

3. Results and discussion

Figure 1 depicts the results of a single experiment performed on a single cation-exchange particle. In a similar way these experiments can be carried out for any other ion-exchange system or for any other type of the measurement. In this particular case, we show that the underlimiting region is accompanied by formation of ion-depleted zone within which an array of vortices is formed upon reaching the limiting current. With further increase in the polarization current the vortices grow and start to affect the boundary created by the tracking particles. This growth gives rise to the appearance of the overlimiting current (first region), which is characterized by increasing slope. However, upon reaching a certain critical current, the system will transition into a second part of the overlimiting region that is characterized by constant slope of the CVC. This transition will form four large vortices on the system. We also showed that the water splitting is negligible on the cation-exchange particle. Very similar results were obtained for a small piece of a heterogenous cation-exchange particle. By contrasts, the anion exchange systems, although also showing occurrence, are easily prone to the water splitting reaction.

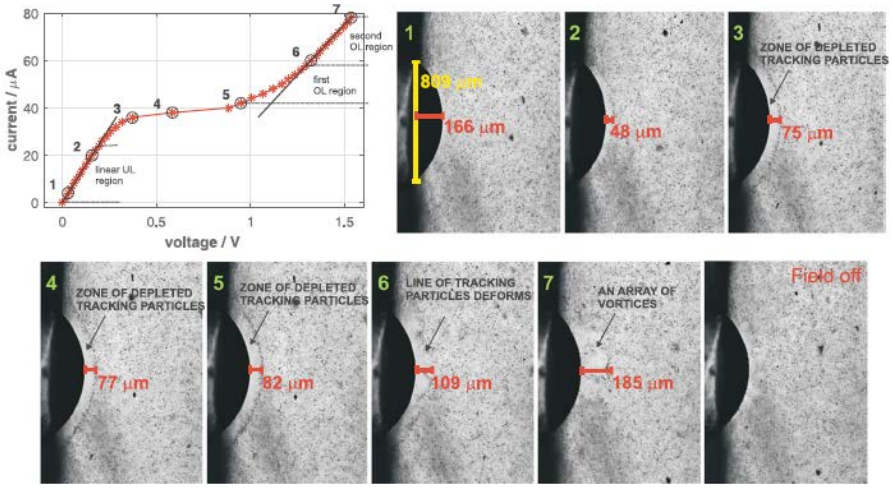

Figure 1. Current-voltage curve measured on a single cation-exchange particle and the set of images capturing the situation at the system-electrolyte interface under various polarization currents [2].

4. Conclusions

We monitored the processes occurring on the ion-exchange systems during polarization. Our observation confirmed the generation of the ion-depleted region followed by formation of the electroconvective vortices that are responsible for the overlimiting current exhibited by these systems. The water splitting reaction was shown to have small effect in cation-exchange membranes and reached much larger extent in anion-exchange system.

References

[1] L. Vobecka, M. Svoboda, J. Beneš, T. Belloň, Z. Slouka, J. Mem. Sci., 2018. 559: p. 127-137.
[2] T. Belloň, P. Polezhaev, L, Vobecká, M. Svoboda, Z. Slouka J. Mem. Sci., 2019. 572 p. 607-618.

ECCE12
The 12th EUROPEAN CONGRESS OF CHEMICAL ENGINEERING
Florence 15-19 September 2019

Contribution of Pervaporation in Eco design of Processes

Oleksandr DIMITROV[1], Evelyne NEAU[1], Isabelle RASPO[1], Pierrette GUICHARDON[1*], Alfred TESTA[2]

1 Aix Marseille Université, CNRS, Centrale Marseille, M2P2 UMR 7340, Technopôle de Château-Gombert, 38 rue Frédéric Joliot-Curie, 13451 Marseille, France ;

2 INNOVACLEAN, 73, rue du Douard, F-13685 Aubagne, France

**Corresponding author: pierrette.guichardon@centrale-marseille.fr*

Highlights

- Dehydration of organic solvents by pervaporation
- Pervaporation data treatment using solution-diffusion approach coupled with an accurate vapor-liquid equilibrium model
- Comparison of pervaporation and distillation efficiency in terms of separation and energy consumption

1. Introduction

In the modern conditions of constantly growing market demand and product consumption, the world leading industries shift progressively towards the eco design approach. That means a production with an attentive consideration for the environmental impacts of a product during its lifecycle, low material and energy resources consumption and using of the environmentally friendly solutions. Chemical engineering is not an exception. The situation becomes especially sensitive in separation technologies as the chemical waste treatment and recycling remains one of the most important problems of the humanity. For example, in the alcohols and organic solvents dehydration, robust and durable processes, such as distillation, are mainly used. Regardless of its durability and high product output, the overall results obtained by distillation may be far from expected. Its separation efficiency may be limited by the vapor-liquid equilibria (azeotropes, relative volatility etc). The modified processes such as azeotropic or extractive distillation are able to deal with these drawbacks generally at the expense of increased complexity and operational costs. Moreover, one should not ignore the high energy consumption of distillation.

The pervaporation, a membrane separation process, can be an excellent alternative to distillation. Though it is a relatively young technology, the attention of industries towards it increases every year mainly due to its low energy consumption and high separation performance. The main advantage of pervaporation is that the separation efficiency is independent of vapor-liquid equilibria and is only limited by the membrane material and operating conditions. A large number of researches on membrane materials have significantly decreased the costs of membrane modules which makes pervaporation even more attractive for separation of liquid mixtures.

The aim of our work was to emphasize the new horizons of solvent dehydration technology and mark the contribution of pervaporation in process eco design. We have experimentally and

theoretically studied the pervaporation applied to a dehydration of an aqueous mixture of three glycol ethers which are widely used in different chemical industries all over the world. The interest was mainly pointed towards the separation efficiency and energy consumption. The results were compared to those of distillation for the same mixture. The modeling of both processes was also performed in order to optimize operating conditions and increase the efficiency.

2. Methods

A mixture of three organic solvents and containing 10%wt of water was dehydrated by pervaporation using commercial dense membranes with a cross-linked polyvinyl-alcohol (PVA) active layer. The pervaporation was carried out at 30, 50 and 70°C. The permeate fluxes were measured by weighing and the permeate composition was determined by a gas chromatography method. The membrane permeances were calculated by the solution-diffusion approach coupled with accurate liquid-vapor equilibria data. The energy consumption of the process was determined as well.

A dehydration of the same mixture by distillation was carried out in parallel at the pressures of 1.013 bar, 0.2 bar and 0.05 bar. The modeling of the distillation process was made using ProSim Pro software.

3. Results and discussion

Results obtained were encouraging. The permeate analysis has indicated the presence of only pure water which means that the membrane is 100% selective to water and no solvent passed through it. The process was compared with the distillation in terms of separation efficiency and energy costs. While the distillation has offered high product flows, the separation was much less efficient because of the limit in vapor-liquid equilibrium; moreover, the energy consumption was very important.

4. Conclusions

In this work we have shown the potential of pervaporation to replace classic separation methods such as distillation while dehydrating organics. A highest separation rate and low energy expenses were achieved. An ideal permeate flux can be obtained by choosing a membrane module with an appropriate working area. Experimental and modeling results were used for further development of an industrial-scale applied process.

ECCE12
The 12th EUROPEAN CONGRESS OF CHEMICAL ENGINEERING
Florence 15-19 September 2019

Separation of mixtures containing SO_2, CO_2 a CH_4 using membranes based on polymers with intrinsic microporosity

Petr Stanovsky[1*], Andrea Zitkova[1], Magda Karaszova[1], Pavel Izak[1],
Bibiana Comesaña Gándara[2], Neil McKeown[2]

[1] *Instit. of Chem. Proc. Fund. CAS, Rozvojova 135, 165 02 Prague 6 – Suchdol, Czech Republic;*
[2] *Univ. Edinburgh, Sch. Chem., EaStCHEM, David Brewster Rd., Edinburgh EH9 3FJ, Midlothian, Scotland*

**Corresponding author: stanovsky@icpf.cas.cz*

Highlights

- Separation of CO_2 from CH_4 is efficient and overcome the Robeson upper bound 2008
- Permeability of SO_2 and CO_2 is very high but SO_2/CO_2 selectivity is low for industrial use.
- Selectivity of aged PIM membrane increased after testing with pure CO_2.

1. Introduction

Membrane separation of gases offer several advantages compared to common industrial methods as such as energy efficiency, safety and no additional waste production. One of the recent progressive direction in the field of polymer membrane science is a new class of ultrapermeable polymers based on inefficient packing of the two-dimensional chains – polymers with intrinsic microporosity (PIM).

2. Methods

Membranes were made of polymer with intrinsic microporosity based on tetramethyltetrahydronaphthalene combined with triptycene PIM-TMN-Trip (P5) casted from chloroform solution and further treated with methanol. The procedure of membrane preparation is described in detail in publication Rose et al [1].

Permeation of selected gases and its mixtures was tested using two apparatuses. First allows to set SO_2 concentration in mixture of air, N_2, CO_2 [3]. Second apparatus allow mixing CH_4, N_2, CO_2 or real biogas. The both allows analyzing either retentate or permeate stream via set of electrochemical and infrared detectors.

Membranes were tested for different values of SO_2 concentration ranging from 500 to 2500 ppm at temperature 25°C in mixture of 20% vol. CO_2 and dry air under 100 kPa of upstream and 90 kPa of downstream pressure. Further separation of mixture with 1800 ppm under increasing upstream pressure varying from 200 up to 500 kPa. Another tests with single gas as CO_2 and CH_4, their mixtures and real biogas from wastewater treatment plant were done at upstream pressure ranges from 100kPa to 500 kPa and 98 kPa of downstream pressure.

3. Results and discussion

Tested PIM-TMN-Trip membrane has shown superior separation properties for CO_2/CH_4 mixture. Combined ideal selectivity and permeability of single gases (gray circles in Fig. 1) lies above Robeson bound [2]. However, the membrane have shown lower values of permeability for CO_2 than similarly

prepared membrane by Rose [1]. Permeability of CH_4 slightly increase with increasing trans-membrane pressure; on the other hand, CO_2 permeability remain almost constant over all range of trans-membrane pressure. Mixtures of CO_2 with CH_4 and real biogas with traces of H_2S and siloxanes (red triangles and blue diamonds in Fig. 1) have shown the same permeability for CO_2 with mixed gas selectivity higher than ideal selectivity of particular gases similarly as for polymer PIM based on spirobifluorene unit. Mixed gas selectivity decreased with increasing trans-membrane pressure. Moreover, as the measurement was done for mixtures and afterwards for single gases with CO_2 as the last one; we observed afterwards big increase in selectivity without change of CO_2 permeability. This CO_2 sorption-induced ageing improved selectivity of separation considerably (empty circles in Fig. 1).

Separation of SO_2 from dry stream containing initially 1800ppm SO_2 in mixture of air and 20 % vol. CO_2 is rather low (selectivity is approx. 2) and basically similar to our recent results of water-swollen thin film composite membrane Toray [3] in terms of selectivity but it have much higher permeability for SO_2. Permeability of SO_2 decreased with increasing trans-membrane pressure.

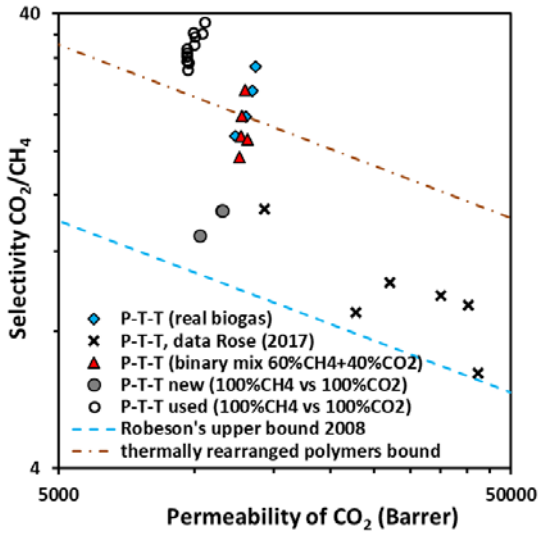

Figure 1. Selectivity CO_2/CH_4 vs permeability of CO_2

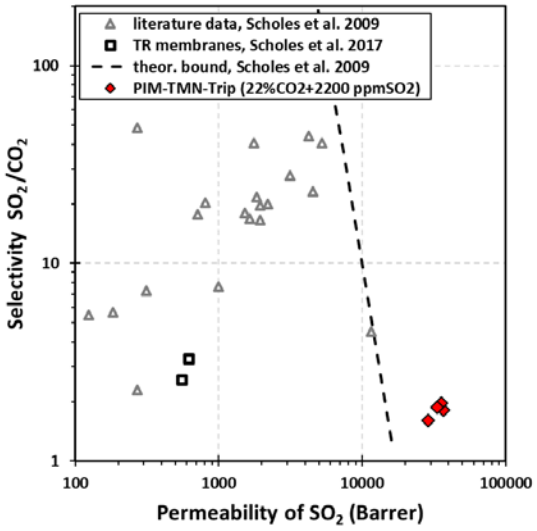

Figure 2. Selectivity SO_2/CO_2 vs permeability of SO_2

4. Conclusions

Tested PIM-TMN-Trip membrane have shown superior separation properties for mixture of CO_2/CH_4 mixture (CO_2 permeability 10-12.10^3 Barrer, selectivity 13-15, selectivity of used and likely aged membrane 30-38). Permeability of SO_2 from air-CO_2 mixture was very high (29-37.10^4 Barrer) but selectivity of SO_2 separation from CO_2 was small (1.6-2.0).

5. Acknowledgement

The support of Czech Science Foundation (project No. 18-05484S) is gratefully acknowledged.

References

[1] I. Rose, C.G. Bezzu, M. Carta, et al., Nature Mat. 16 (2017) 932-937.
[2] L.M. Robeson, J. Membrane Sci. 320 (2008) 390-400.
[3] A. Zitkova, M. Karaszova, P. Stanovsky, J. Vejrazka, P. Izak, Chem. Eng. Tech. 42 (2019) 1304-1309.
[4] C.A. Scholes, S.E. Kentish, W.S. Stevens, Sep. Purif. Rew. 38 (2009) 1–44.

ECCE12
The 12th EUROPEAN CONGRESS OF CHEMICAL ENGINEERING
Florence 15-19 September 2019

Selective separation of n-butanol from ABE solutions with polymeric inclusion membranes

Carla A. Arregoitia[1], Marcos Fallanza[1], Daniel Gorri[1], Inmaculada Ortiz[1]

[1] University of Cantabria, Santander, Spain;

*Corresponding author: cadriana.arregoitia@unican.es

Highlights

- The addition of IL into the polymeric matrix improves the membrane selectivity
- Permeation fluxes highly depend on the operation temperature
- Fabricated membranes show improved behavior with respect to commercial membranes

1. Introduction

Biobutanol is considered as an attractive commodity and it is used as a solvent for different applications and as a biofuel, it has many advantages [1]. Biobutanol can be produced via ABE fermentation from renewable feedstocks by Clostridia bacteria, the most commonly used microorganism. Yet, the very low yield in final concentration, the severe butanol toxicity to microorganisms and the high-energy consumption are still some challenges that prevent the process from being more competitive over the petrochemical route [2].

Among the many advantages of the Pervaporation (PV) membrane separation technique is the fact that it does not affect microorganisms, and prevents nutrients and substrates loss [3]. Alcohol perm-selective PV membranes are usually composite membranes [4] and are made with a thin and dense active layer on a porous substrate. Ionic liquids (ILs) in membrane techniques have been investigated and although they have a good potential for butanol separation; the application for separation of butanol from ABE solvents by PV has not been fully investigated. This work aimed to develop and evaluate polymeric inclusion membranes made of different amounts of polymer and IL for the recovery of butanol from aqueous solutions by PV

2. Methods

Different composite flat-sheet membranes based on polyether block amide (PEBA) and the ionic liquid 1-Hexyl-3-methylimidazolium tris (pentafluoroethyl) trifluorophosphate (HMImFAP) were prepared by using the TIPS technique (temperature induced phase separation). They were characterized using FTIR and SEM methods. They showed the membranes with the IL fully integrated into the polymer matrix. The resulting membranes were dense flat sheet membranes with an average thickness of 10 μm. Butanol recovery experiments from ABE mixtures (2% butanol, 1% ethanol, 1% acetone) were performed by a PV unit and the transport parameters of the membranes for each component were obtained. Finally, the Pervaporation Separation Index (PSI) allowed a comparison of the performance results between the prepared membranes and the commercial membranes.

$$PSI = J \cdot (\alpha_{i/j} - 1)$$

3. Results and discussion

It was observed that the transmembrane flux is highly dependent on both, membrane composition and operating temperature. Membranes with higher content of ionic liquids are more permeable and the transmembrane flux was observed to increase as the temperature increases.

Based on the obtained results, the addition of a small amount of ionic liquid into the polymeric matrix shows an important decrease of the water flux while the butanol permeation remains almost unaffected. Finally, the efficiency of the membranes prepared in this study for the recovery of butanol was measured in terms of pervaporation separation index (PSI), offering results up to 8 times better than those from commercial membranes.

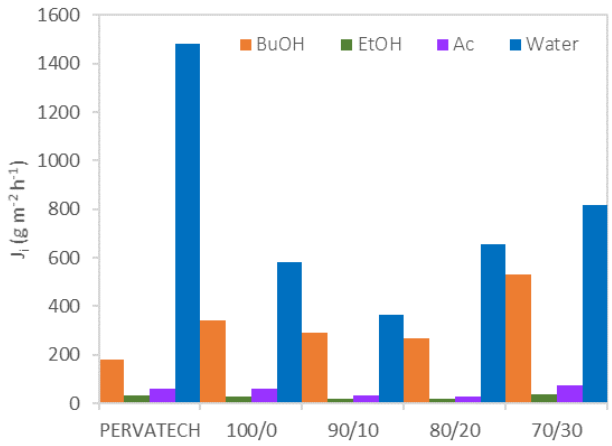

Figure 1. Flux comparison of commercial membrane PERVATECH and PEBAX/ HMImFAP polymeric membrane

4. Conclusions

Polymeric inclusion membranes were made of different amounts of polymer/IL for the recovery of butanol from aqueous solutions by PV process. It was observed that the flux increased as the temperature increased. Adding IL to the membrane showed an improvement by increasing the butanol flux and decreasing the water in the permeate stream. Finally, the influence of the composition of the membranes in the separation of butanol-water mixtures was studied and the performance of the membranes was compared with other commercial membranes showing a significant improvement.

Acknowledgements: This research has been funded by the Spanish Ministry of Economy and Competitiveness (Projects CTQ2015-66078-R and CTQ2016-75158-R). Carla Arregoitia also thanks for a PhD scholarship.

References

[1] D. Cai, H. Chen, C. Chen, S. Hu, Y. Wang, Z. Chang, Q. Miao, P. Qin, Z. Wang, J. Wang, T. Tan, Gas stripping-pervaporation hybrid process for energy-saving product recovery from acetone-butanol-ethanol (ABE) fermentation broth, Chem. Eng. J. 287 (2016) 1–10.

[2] N. Abdehagh, F.H. Tezel, J. Thibault, Separation techniques in butanol production: Challenges and developments, Biomass and Bioenergy. 60 (2014) 222–246.

[3] W. S. Winston Ho, and Kamalesh K. Sirkar, Membrane handbook, New York, Elsevier, 1992.

[4] S. Manshad, M.G. Mohd Nawawi, Membranes with favorable chemical materials for pervaporation process: A review, J. Membr. Sci. Technol. 06 (2016).

ECCE12
The 12th EUROPEAN CONGRESS OF CHEMICAL ENGINEERING
Florence 15-19 September 2019

Nano-structural modification of calcium alginate membrane for high performance separation of mono/oligosaccharide

Kaito Yoshida[1], Keita Kashima[1†], Masanao Imai[2]

1 Department of Materials Chemistry and Bioengineering, National Institute of Technology, Oyama College, 771 Nakakuki, Oyama, Tochigi, 323-0806, Japan;

2 Graduate School of Bioresource Sciences, Nihon University, 1866 Kameino, Fujisawa, Kanagawa, 252-0880, Japan

Corresponding author: † keitakashima@oyama-ct.ac.jp

Highlights

- Calcium alginate membrane for mono/oligosaccharide separation was successfully prepared.
- The structure of membrane was modified using polyethylene glycol in low-molecular-weight.
- Improvement of water permeability and sustention of glucose rejection were achieved.

1. Introduction

High-yield purification of monosaccharide and oligosaccharide is still demanded for advanced research in biological chemistry and bioengineering. Separation membrane from calcium alginate known as biopolymer has promising ability for molecular-size-screening of monosaccharide and oligosaccharide. [1-2] This study demonstrates nano-structural modification of calcium alginate membrane using polyethylene glycol in low-molecular-weight (PEG, M_n = 200 Da) for high-performance separation of mono/oligosaccharide.

2. Methods

2.1 Preparation of the calcium alginate membrane

A mixed solution of 10 g L^{-1} of the sodium alginate and 0 to 13 g L^{-1} of PEG was placed in a petri dish (ϕ 90 mm), which was dried at 303 K for 48 h in an electrical drying machine. The dried membrane was immersed in 20 mL of 1 M aqueous calcium chloride solution to cross-link alginate polymer for 40 min. The formed calcium alginate membrane was washed to remove PEG with 100 mL of deionized water at 333 K for 30 min repeated twice within a shaking bath.

2.2 Membrane permeation of aqueous solution of glucose

The prepared membrane was installed in a membrane holder (KST-90-UH, ADVANTEC). 10 mM glucose aqueous solution was permeated to the membrane with an operating pressure of 300 kPa using nitrogen gas. The mass of glucose solution permeated through the membrane was measured by electrical balance and was converted to permeated volume using density. The volumetric permeation flux, J_V [$m^3 \cdot m^{-2} \cdot s^{-1}$] was determined using the following equation (1).

$$J_v = \frac{V}{At} \qquad (1)$$

Where, V, A, and t are the volume of permeated solution [m^3], permeation area [m^2] (A = 0.00453 m^2), and permeation time [s], respectively. In addition, the concentration of permeated glucose solution was quantified through a mutarotase-glucose oxidase method with UV-Visible

spectrophotometer (λ= 505 nm). The rejection of glucose molecules (R [-]) by the calcium alginate membrane was evaluated from the equation (2).

$$R = 1 - \frac{C_s}{C_f} \qquad (2)$$

Where, C_s and C_f are the concentration of permeated solution [M] and the concentration of feed solution [M].

3. Results and discussion

Figure 1 shows the effect of added/removed PEG concentration on the permeation flux of glucose aqueous solution. The permeation flux remarkably increased with the increase of added concentration of PEG when the membrane was prepared. The water permeation was improved by the structural modification of membrane.

Figure 2 depicts the effect of added/removed PEG concentration on the rejection of glucose. The rejection was almost constant although the permeation flux was increased by the PEG modification, which indicates the size of mass transfer channel for glucose permeation was kept as well as the volume of channel increased. Addition and removal of low-molecular-weight PEG performed nano-structural modification.

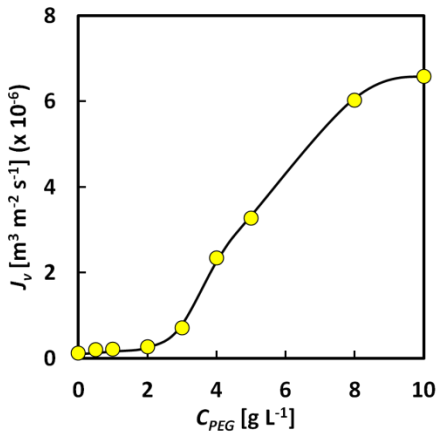

Fig. 1 Effect of the added/removed concentration of PEG (C_{PEG}) on the permeation flux of glucose aqueous solution (J_V)

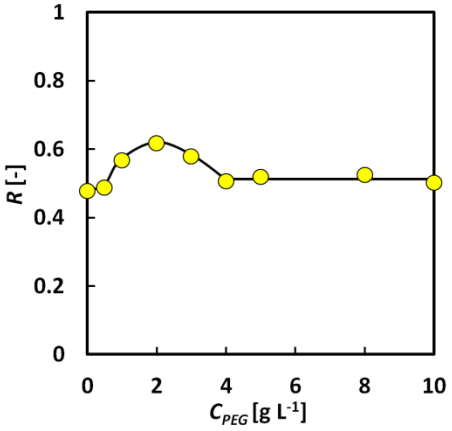

Fig. 2 Effect of the added/removed concentration of PEG (C_{PEG}) on the rejection of glucose molecules (R)

4. Conclusions

The improvement of water permeability and the sustention of glucose rejection were achieved by the nano-structural modification of calcium alginate membrane using low-molecular-weight polyethylene glycol. The modified membrane is expected to exert high performance on the separation of monosaccharide and oligosaccharide.

References

[1] K. Kashima, M. Imai, *Desalination and Water Treatment*, **34** (2011) 257-265.
[2] K. Kashima, M. Imai, *Food and Bioproducts Processing*, **102** (2017) 213-221.

Solvent extraction of La(III) complex using [bmim][Tf2N] and a β-diketone as extractant and its stripping with supercritical carbon dioxide.

Angélica Quintriqueo L*[1], Julio Romero[1] and Esteban Quijada-Maldonado[1]

1Laboratory of Membrane Separation Processes (LabProSeM), Department of Chemical Engineering, University of Santiago de Chile, Av. Libertador Bernardo O 'Higgins 3363, Estación Central, Chile

**Corresponding author: angelica.quintriqueo@usach.cl*

Highlights

- Solvent extraction La(III) complex using ionic liquid
- Stripping of La(III) complex using carbon dioxide

1. Introduction

Lanthanide elements are comparatively abundant in the earth's crust than other commonly exploited elements but are not sufficiently concentrated to make them easily exploitable. This is due to the similarity in their ionic radio, which makes them interchangeable in most minerals, and are very difficult to separate. In recent decades, lanthanide tris- β-diketones, Ln (β-diketone)$_3$ have attracted a lot of attention because of their spectroscopic properties (Binnemans, 2005). Lanthanum was chosen as an exemplifier of the rare earth (REE) series in this study because it is the most abundant trivalent REE that is found in major host rocks for REE minerals, and it also shows the closest match with respect to trivalent actinides among the other REEs in terms of ionic radio in 6-fold coordination (e.g., rLa 1.13 Å and rAc 1.18 Å) (Fricker, 2006). Solvent extraction (SX) is the most effective method to enrich metal ions, including rare earth. The counter current extraction process permits the separation of substances with different distribution coefficients (Mekki et al., 2006). Since the toxic and flammable characteristics of many organic solvents are detrimental to the environment, eco-friendly substitutes have been investigated. As an example, ionic liquids (ILs). The ionic liquids (ILs) have been considered as alternative solvents for solvent extraction processes because of their properties such as low volatility, low flammability, good chemical stability and adjustable miscibility and polarity (Kikuchi, Matsumiya, & Kawakami, 2014). The synergistic enhancement of the extractability depends largely on the type ligand, in this case, trioctyphosphine oxide (TOPO) was used. The chemical structure TOPO is responsible for its properties. Its strong coordinating abilities result from the presence of a single oxygen atom within the molecule (Anitha, Ambare, Singh, Singh, & Mohapatra, 2015).

There are some studies reported in literature on the extraction of metal ions using supercritical fluids (Wang, 1997) and ILs coupled to supercritical fluids (Mekki et al., 2006). In our previous contribution (Sepúlveda et al., 2017) we have tested an extraction technique to recover Cu(II) from aqueous solutions based on the use of an organic phase formed by an imidazolium-based ionic liquid as solvent and a β-diketone as extractant agent. In this framework, the aim of this work involves the improvement of the extraction and stripping of complex La(III) from an aqueous solution using [bmim][Tf2N] as solvent containing a fluorated β-diketone as extractant and dense carbon dioxide as stripping phase. This study is focused on the effect of the concentration of

extractant, phase contact time, volumetric Organic/Aqueous (O/A) ratio and overall volume of dense CO_2 on the whole process efficiency.

2. Methods

The organic phase was prepared with ionic liquid [bmim][Tf2N], as the solvent and β-diketone (HFOD) as the extractant. The aqueous solution was prepared by dissolving 1.0 g/L of La in deionized water (18.2 mΩ). The desired concentration of the salt was reached by using an analytical balance. The pH of these solutions was measured before and after extraction test using a pH meter. The removal of La(Beta-diketona)$_3$ complex from the aqueous solutions was carried out by means of the same procedure reported in our previous work(Castillo et al., 2014; Sepúlveda et al., 2017). The solvent extraction experiments were conducted by contacting 3 mL of aqueous solution with 3 mL of organic phase, where the phases were mixed in a horizontal mechanical shaker (Jin Yi ® model Hj-4B) at 140 rpm for 40 minutes. Then, the phase separation was achieved by centrifugation (Gemi Industrial Corp® model PLC-01) at 1000 rpm for 40 minutes. After phase separation, the final values of pH in the aqueous phase were measured. All the experiments were conducted at room temperature (25°C). Once these phases were completely separated, the concentration of the La(III) in the aqueous phase was quantified by means of Atomic Absorption Spectrophotometry (AAS) (GBS® Scientific Equipment model SensAA dual beam, equipped with a 4mA lamp (single element) Photron International ®). All the experiments were realized with duplicate samples.

The removal of La(III) complex from the aqueous solutions has been carried out by means of the same procedure reported in our previous work(Castillo et al., 2014). Thus, solvent extraction tests were achieved by contacting 2 mL of aqueous solution with 2 mL of organic phase formed by [bmim][Tf2N], beta-diketone and TOPO for 45 min in order to reach the equilibrium conditions. After phase separation the final values of pH and the concentration of La(III) complex in the aqueous phase were measured with a pH-meter and by AAS, respectively. From the results previously reported in literature (Castillo et al., 2014), it has been verified that the extraction of La(III) complex from an aqueous phase using [bmim][Tf2N] as diluent and beta-diketona as extractant is governed by the following reaction, which describes the cation exchange with formation of a neutral complex La(β-diketone)$_3$TOPO.

$$La^{+3} + 3(\beta\text{-diketone}) + 1\ TOPO \longleftrightarrow La(\beta\text{-diketone})_3TOPO + 3H^{+} \quad (1)$$

3. Results and discussion

This research is still being studied, we do not have data.

4. Conclusions

[1] Binnemans, K. (2005). Rare-earth beta-diketonates. *Handbook on the Physics and Chemistry of Rare Earths*, *35*(05), 107–272. https://doi.org/10.1016/S0168-1273(05)35003-3

[2] Castillo, J., Teresa, M., Fortuny, A., Navarro, P., Sepúlveda, R., & María, A. (2014). Hydrometallurgy Cu (II) extraction using quaternary ammonium and quaternary phosphonium based ionic liquid. *Hydrometallurgy*, *141*, 89–96. https://doi.org/10.1016/j.hydromet.2013.11.001

[3] G., A.-C. (2014). Review: Lanthanide coordination chemistry: from old concepts to coordination polymers. *Journal of Coordination Chemistry*, *67*(23–24), 3706–3733. https://doi.org/10.1080/00958972.2014.957201

ECCE12
The 12th EUROPEAN CONGRESS OF CHEMICAL ENGINEERING
Florence 15-19 September 2019

Membrane Filtration of Pickering Emulsions for Continuous Liquid/liquid Catalysis – Influence of Membrane Material and Nanoparticle Type

Anja Drews[1], Maresa Kempin[1], Tina Skale[1]

1 HTW Berlin, School of Life Science Engineering, Wilhelminenhofstr. 75A, 12459 Berlin, Germany

**Corresponding author: anja.drews@htw-berlin.de*

Highlights

- Membrane/nanoparticle/solvent combination influences nature of filtration behaviour.
- Gel-forming HDK H20 nanoparticles result in increased permeabilities.
- Suspension filtration can help to explain interactions of solid and liquid phases.

1. Introduction

Water-in-oil Pickering emulsions (PE) are currently receiving increased interest as a promising alternative to dispersions or surfactant stabilized emulsions in two-phase (bio-)catalysis. While batch PE catalysis has been demonstrated for a variety of reactions and catalysts, the separation of the two liquid phases and thus continuous operation has been identified as a main challenge [1]. Since then, the feasibility of using membrane filtration for the retention of catalyst containing droplets has been demonstrated [2-3]. In a proof-of-concept, the biocatalyst was still active after more than 8 residence times with feasible space-time-yields of 0.64 g/(Lh) [4]. After these first results, this works aims at investigating the influences of membrane material and type of stabilizing nanoparticles (NP) to yield more generally valid conclusions and to be able to explain individual interactions of present liquid and solid phases.

2. Methods

The desired amount of silica NP (HDK H20, H18 or H2000 by Wacker AG) was dispersed in the continuous phase (e.g., dodecene, CPME etc.) and PE were prepared by emulsifying the desired water phase fraction using a rotor/stator homogenizer Ultra-Turrax (UT, IKA GmbH) or ultrasonication (US, Branson Sonifier). In addition, NP suspensions were investigated.

A stirred cell (Merck, V_{max} = 91 mL, A_{eff} = $1.23 \cdot 10^{-3}$ m^2) was used for filtration trials. When pressure was applied to a connected surge tank, solvent was continuously transported to the completely filled stirred cell, which displaced permeate at the same rate. Recorded permeate weight was used to calculate flow rate. Membranes were soaked in solvent and pre-pressurized prior to use. Different ultrafiltration and organic solvent nanofiltration (OSN) membranes were used. Microscopic pictures of PE samples before and after filtration were taken and image analysis software (SOPAT GmbH) was used to measure droplet size distribution. Rheology was measured using a MCR 302 rotational rheometer (Anton Paar GmbH).

3. Results and discussion

First results showed that with permeabilities of up to around 40 L/(m² h bar) a large variety of PE could be filtered and concentrated to up to 80% water phase fraction [2-4]. As can be seen in Fig. 1 (left), an unexpected disproportionate flux behaviour with increasing pressure was repeatedly observed for filtration of different PE through a 1 kD PVDF membrane [2-3] which could neither be explained by drop coalescence nor membrane abrasion or swelling. In addition, filtration of a dodecene/H20-PE resulted in higher permeabilities than filtering dodecene alone. This was confirmed for a CPME/H20-PE and a 10 kD membrane [4] and might due to the gel- and network-forming nature of these NP [5]. In contrast, H2000 do not form such networks and result in different behaviour in both emulsion and suspension filtration as well as in rheology.

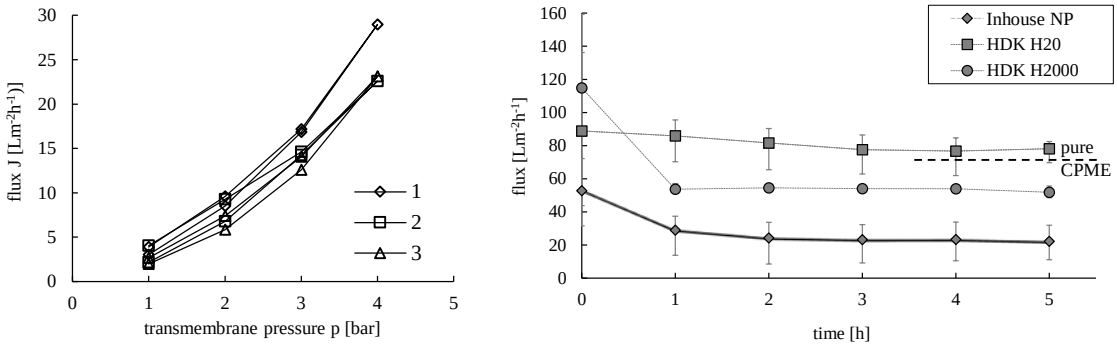

Figure 1. Left: Pressure stepping (dodecene PE, 2 g/$L_{dispersed\ phase}$ HDK H20, US, PVDF 1 kD, [3]). Right: Flux over time for different NPs (CPME PE, UT, PES 10 kD, 2 bar, [4]).

For all suspensions, almost linear flux increases were found. This means that drops add to the interactions, e.g., by adsorbing otherwise unbound residual NP at their interface but also by influencing the rheological behaviour. As opposed to the 1 kD ultrafiltration data shown above, first results indicate that using an OSN membrane with a similar MWCO (900 D) yields feasible permeabilities of around 3 L/(m² h bar), linear relationships and PE fluxes that are lower than pure solvent fluxes.

4. Conclusions

Membrane filtration was shown to be a promising process concept for the separation of aqueous PE droplets from continuous organic phases and thus for continuous liquid/liquid reactions in PE. The gel-forming H20 particles yield unexpected and different filtration behavior than other NP. Separating the influences of all present materials will help to understand individual interactions of all phases which is required for optimum material selection and robust process design.

Acknowledgments

Financial support by the German Research Foundation DFG (collaborative research centre InPROMPT TRR 63, B6) is gratefully acknowledged. We thank Wacker Chemie AG for kindly providing free particle samples.

References

[1] M. Pera-Titus, L. Leclercq, J.-M. Clacens, F. De Campo, V. Nardello-Rataj, Angew. Chem. Int. Ed. 54 (2015) 2006-2021.
[2] T. Skale, D. Stehl, L. Hohl, M. Kraume, R. von Klitzing, A. Drews, Chem. Ing. Tech. 88 (2016) 1827-1832.
[3] T. Skale, L. Hohl, M. Kraume, A. Drews, J. Membr. Sci. 535 (2017) 1-9.
[4] A. Heyse, C. Plikat, M. Ansorge-Schumacher, A. Drews, Catalysis Today (in press).
[5] L. Hohl, S. Röhl, D. Stehl, R. von Klitzing, M. Kraume, Chem. Ing. Tech. 88 (2016) 1815-1826.

ECCE12
The 12th EUROPEAN CONGRESS OF CHEMICAL ENGINEERING
Florence 15-19 September 2019

Investigation of interfacial mechanisms during organic acid reactive extraction through dynamic interfacial tension measurements

Ana-Karen Sánchez-Castañeda[1], Florian Chemarin[1,2], Marwen Moussa[1], Violaine Athes[1], Ioan-Cristian Trelea[1]*.

1 UMR 782 GMPA, AgroParisTech, INRA, Université Paris Saclay, 78850 Thiverval-Grignon, France; 2 URD Agro-Biotechnologies Industrielles, AgroParisTech 51110 Pomacle, France.

**Corresponding author: cristian.trelea@agroparistech.fr*

Highlights

- Interfacial phenomena during liquid-liquid reactive extraction are analyzed
- Dynamic interfacial tension is proposed as an easy method to monitor interfacial reactions
- A mathematical model gives insights in interfacial reaction mechanisms

1. Introduction

3-Hydroxypropionic acid (3-HP) is an attractive platform molecule that can be converted to several materials, such as acrylic acid and biodegradable polymers. Its production by bioconversion has made remarkable advances, but its industrial commercialization is still limited by low productivities caused by product inhibition. *In situ* liquid-liquid reactive extraction assisted by a hollow fiber membrane contactor (HFMC) is a promising strategy to intensify 3-HP bioconversion [1,2]. Several points remain to be better understood, however, to develop a continuous extraction system coupled to bioconversion and maintain a low acid concentration in the medium. 3-HP extraction performed on a hollow fiber membrane contactor occurs at the interface formed inside the pores of the membrane, between two immiscible liquids. Proper interface stabilization is an important factor to avoid emulsions and direct contact of the organic phase with cells. It is also known that extraction rates can be markedly affected by interfacial mass transfer. All this highlights the need to better understand the interfacial phenomena involved during 3-HP extraction. In this study dynamic Interfacial Tension (IFT) was used to monitor concentration of the chemical species at the interface. This allows investigating the mechanisms of mass transfer during 3-HP reactive extraction, by developing a mathematical model that relates IFT with interfacial concentration of species, in addition to usual bulk concentration measurements.

2. Methods

The studied system consisted of 3-HP at 7 different initial concentrations (0 to 50 g/L) in the aqueous phase, and Trioctylamine (TOA) diluted in n-decanol at 20% v/v as the organic phase. For IFT measurement, both phases were put in contact in a Pendant Drop Tensiometer, putting the 3-HP solution in a syringe that creates a pendant drop inside the organic phase. In membrane contactors, mass transfer is mainly controlled by diffusion in the membrane pores. Such a configuration mimics mass transfer conditions at the interface situated in membrane pores. A previously developed mathematical model that successfully describes interfacial equilibrium of the chemical species in the considered extraction system [3] was combined with a mass transfer model

adapted to the geometry and physical conditions of the pendant drop method. Then, the Gibbs equation that relates IFT with interfacial species concentration combined with the Langmuir-Freundlich adsorption isotherm were used to compare model predictions with dynamic IFT measurements.

3. Results and discussion

Dynamic IFT values were chiefly related to interfacial 3-HP/TOA complex concentration formed in reactive extraction, calculated by the model. IFT value of the organic phase with water was 10.24 mN/m, and this value decreased when 3-HP initial concentration increased. The lowest measured value was 6.36 mN/m with an initial concentration 3-HP of 50 g/L. These values are low enough to make potentially difficult the interface stabilization in the pores. Results showed that observed mass transfer in the pendant drop tensiometer could not be explained by molecular diffusion only and involved local convection in the organic phase [4]. The model allows one to estimate adsorption and desorption rates of chemical species at the liquid-liquid interface and the interfacial concentration of the acid-amine complex, the main surface-active species. Insights in the interfacial reaction mechanisms obtained in this study will be useful to determine the rate-limiting mechanisms (adsorption, desorption, reaction, diffusion, convection) in HFMC.

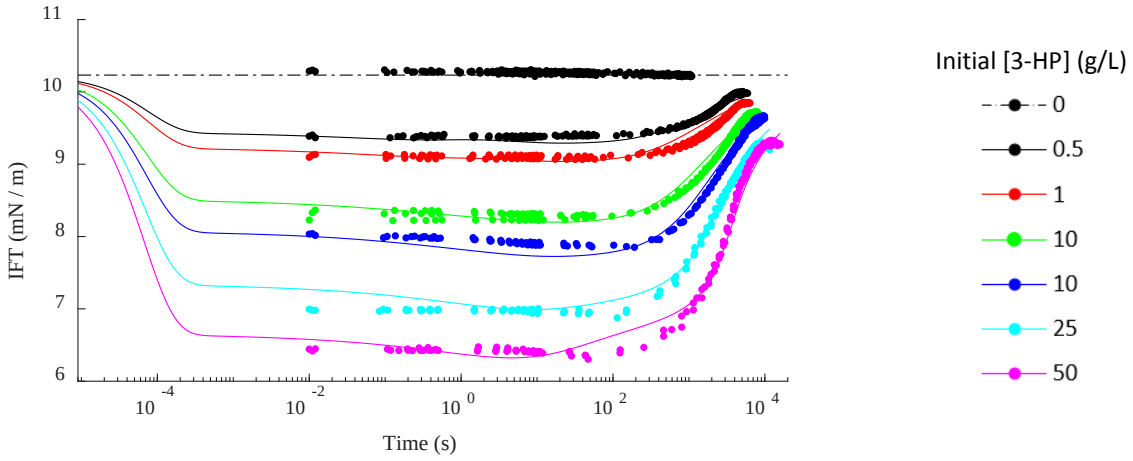

Figure 1. Dynamic Interfacial Tension at different initial 3-HP concentrations. Filled circles: experimental values. Lines: model results.

4. Conclusions

Information obtained from this study validates assumed mass transfer and reaction mechanisms and sets the stage for model-based process optimization in the HFMC configuration.

References

[1] G. Burgé *et al.*, J. Chem. Technol. Biotechnol. 92 (2017) 2425–2432.
[2] Z. Jin, S.-T. Yang, Biotechnol. Prog. 14 (1998) 457–465.
[3] F. Chemarin et al., Sep. Purif. Technol. 189 (2017) 475–487.
[4] P.M. Gassing *et al.*, Colloids Surf. A. 436 (2013) 1103–1110.

ECCE12
The 12th EUROPEAN CONGRESS OF CHEMICAL ENGINEERING
Florence 15-19 September 2019

Separation and Recovery of Vinyl Chloride Monomer using a Multitubular Adsorber

Paulo Carmo[1], Ana Ribeiro[1], Alírio Rodrigues[1], Alexandre Ferreira[1]

1 Laboratory of Separation and Reaction Engineering Associated Laboratory, LA/LSRE-LCM, Faculdade de Engenharia Universidade do Porto, Rua Dr. Roberto Frias s/n 4200-465, Porto, Portugal

**Corresponding author: paulo.carmo@fe.up.pt*

Highlights

- A 2D TPSA model was developed to separate an industrial scale VCM/N_2 mixture.
- A MTA geometry was used to increase the heat transfer rate of the system.
- A 6-step TPSA system with 3 MTAs was designed for the required separation.
- The system produces VCM with 95% purity and N_2 with less than 8 ppm of VCM.

1. Introduction

Vinyl chloride (VCM) is the main monomer in the production of polyvinyl chloride (PVC), as well as, a toxic and carcinogenic agent. As the polymerization reaction is not complete, the unreacted VCM must be stripped from the polymer, separated, and recycled. Prior art [1,2] details the use of activated carbon for the adsorption based separation of a VCM/nitrogen (N_2) mixture using steam purge regeneration. Drawbacks include a high temperature profile during the adsorption step, a high temperature requirement for regeneration and the creation of a contaminated condensed water stream. A design that overcomes these requirements is one that follows the geometry of a multitubular heat exchanger (MTA), in which the adsorbent material is split up and packed into several tubes, while the heat transfer fluid flows on the outer shell side. In this work, a 2D model of a TPSA system coupled with a MTA geometry will be designed to separate and purify a 40% (v/v) VCM rich mixture in N_2, using the activated carbon Pittsburgh type PCB. This process must produce a VCM stream with high enough purity to be recycled into the reactor feed (95% (v/v)) and a N_2 stream with a VCM composition that complies with the regulated gas emission levels (8 ppm (w/w)).

2. Methods

To simulate a 2D multicomponent TPSA model in a MTA, a set of mass, energy, and momentum balances must be specified, and some considerations must be made: the gas phase follows the ideal gas behaviour; the internal mass transfer resistance is expressed with the Linear Driving Force model; the external mass and energy transfer resistances are expressed with the film model; the column porosity, cross section and particle density are constant along the column; the temperature profile is homogeneous inside the particle; the Ergun equation is valid locally; the header tube arrangement achieves uniform flow distribution; the shell heat transfer performance is similar over all the tubes in the shell cross section; the shell side energy transfer resistance in the neighbourhood of each tube is negligible. Based on these considerations, the MTA geometry can be represented by the translation symmetry of each packed tube. As such, to calculate the performance of the proposed equipment, only the tube side of the equipment needs to be

simulated. The dimensions of this equipment were mostly based on values found in literature, to both guarantee an executable design and to facilitate size and parameter estimations.

3. Results and discussion

As illustrated by Figure 1a, the proposed TPSA cycle consists of six steps. In the Feed step, the gas mixture is feed into the packed tubes to produce a N_2 stream at a pressure P_{high}. During this step, the exothermic high-pressure adsorption of VCM heats up the adsorbent material, and, therefore, must be continually cooled down by the shell side heat transfer fluid at T_{low}. In the Rinse step, part of the recovered VCM stream is refeed into the packed tubes. In the Blowdown step, the tubes are radially heated up by the shell side heat transfer fluid at T_{high}, and blown down counter currently to the low-pressure P_{low}, producing a VCM rich stream. In the Purge step, the packed tube is further regenerated by a counter current N_2 product purge. In the Cooldown step, the tubes are cooled down back to T_{low} and are repressurized to P_{high} using the N_2 product, in the Pressurization step.

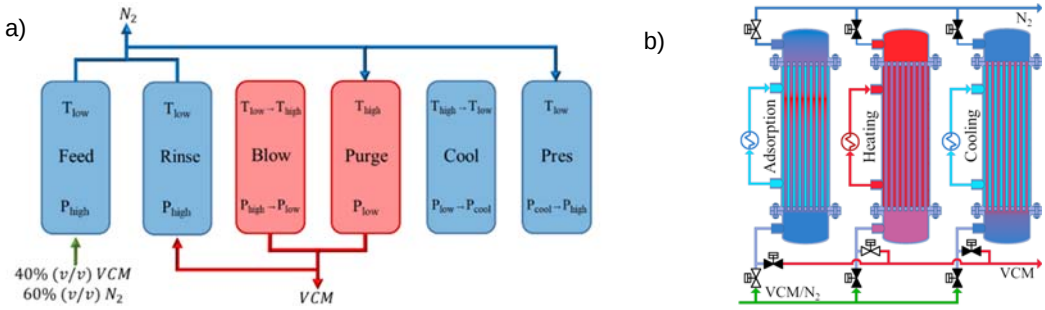

Figure 1. a) Outline of the TPSA cycle steps b) Schematic of the STHX-TPSA cyclic system.

It was set that each MTA should have 230 tubes with an outer diameter of 32 mm, thickness of 1.2 mm and 6 m length, for a total of 500 kg of adsorbent material. Following a square pitch design with a clearance of 8 mm, the shell diameter was estimated at 80 cm. The Feed step lasts 1800 s, the Rinse step 200 s, the Blowdown step 600 s, the Purge step 1400 s, the Cooling step 600 s and with a Pressurization step of 800 s the present model can be extended to a triple MTA system to guarantee a continuous feed consumption and purified stream production, as exemplified in Figure 1b. For this system, the high and low pressure, and temperature were, respectively, 100 kPa and 50 kPa, and 393 K and 293 K, which enables the use of pressurized water as the heat transfer fluid. In cyclic steady state, the purified N_2 stream contains 2.1 ppm (w/w) of VCM, and the VCM stream with a purity of 95.1% was obtained. This system reports a thermal energy consumption of 5.07 MJ/kg_{VCM}, which includes the thermal duties of the MTA and the electric energy consumption of the gas pressurization and vacuum, and liquid pumps.

4. Conclusions

A 2D multicomponent TPSA model following a MTA geometry was developed and successfully applied for the equilibrium adsorption separation of a VCM/N_2 mixture. The proposed equipment is successfully able to produce a VCM stream with a 95 % (v/v) purity, and a N_2 stream with a VCM content below the 8 ppm (w/w) emission level, with an energy consumption of 5.07 MJ/kg_{VCM}.

References

[1] P.J. Patel et al. U.S. Patent 3,984,218, 1976
[2] L. Raduly, U.S. Patent 3,796,023, 1975.

ECCE12
The 12th EUROPEAN CONGRESS OF CHEMICAL ENGINEERING
Florence 15-19 September 2019

Modeling solid-state deracemization via temperature cycles

Brigitta Bodák*, Francesca Breveglieri, and Marco Mazzotti

Institute of Process Engineering, ETH Zurich, 8092 Zurich, Switzerland

**Corresponding author: bbodak@ethz.ch*

Highlights

- Mathematical model of solid-state deracemization via temperature cycles was developed.
- The effect of the model parameters was investigated.
- Favorable conditions were identified as a function of the model parameters.

1. Introduction

Although preferential crystallization is a standard industrial process to obtain enantiopure crystals of conglomerate forming compounds, its maximum theoretical yield is 50%, unless one adds to it recycle and racemization steps [1]. On the contrary, one can produce an enantiopure powder from an initially racemic one through solid-state deracemization by exploiting several techniques [1,2]. Among such techniques, that based on temperature cycles is a promising candidate for industrial applications due to the simplicity of the setup required [1, 3, 4]. Because of the complexity of the process, its optimal implementation requires an accurate and reliable mathematical model [3].

Extending our isothermal population balance based model of attrition-enhanced deracemisation [3], we have developed a non-isothermal model to provide a clear explanation of the phenomena involved in the process [5]. Moreover, this model aims at explaining the sensitivity to variations in the model parameters, such as the breakage rate, the agglomeration rate, etc. that is challenging to be experimentally investigated.

2. Methods

We describe the evolution of the crystals during temperature cycles using a population balance model. The model describes the interplay of several phenomena (size-dependent solubility, crystal growth and dissolution, agglomeration, attrition and racemization) accounting for the dependence of their thermodynamic and kinetic parameters on the crystal size and on the temperature.

3. Results and discussion

We have developed a non-isothermal model, assuming to operate with an ideal temperature controller, hence the specified time-dependent temperature profile can be used instead of modeling heat transfer and temperature evolution through an energy balance. By identifying the relevant variables and their corresponding characteristic values, we have also derived the non-dimensional equations associated to the non-isothermal model. The nondimensional model allows to study the deracemization process in a quasi-universal manner, without the knowledge of the physical and chemical parameters, which are dependent on the specific system considered.

Using the PBE-model that we have introduced, we have simulated temperature cycles in batch crystallizers. The model is characterized by several physicochemical parameters, additionally, the outcome of the process depends on the initial and on the operating conditions. The effect of the process parameters was shown to compare well qualitatively with the experimental results that were investigated in a systematic way previously by our group [1]. The focus of this contribution is to investigate the effect of the model parameters on the process, e.g. the rate of breakage, the parameters of the agglomeration kernel, the rate of racemization, etc.

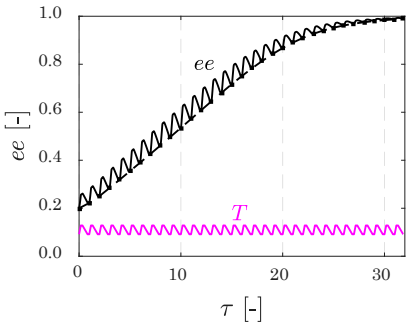

Figure 1. Evolution of the enantiomeric excess along the nondimensional time during deracemisation via temperature cycles. The magenta line indicates the generally utilized temperature profile (the line is not in scale with the values of the enantiomeric excess).

Various research groups studied experimentally how varying the operating temperature range or changing the cooling rate influence the process for different model compounds [1,4]. A thorough system parameter analysis can provide information on how to apply the role of initial asymmetry for different compounds to obtain the pure enantiomer. This analysis requires numerous simulations varying the model parameters that are associated with the chemicophysical properties of various model systems and their relative values that can vary for each substance. Therefore, we performed simulations to analyze the response of the system in a wide range of model parameters. With the help of the model these effects were evaluated and quantified based on the productivity.

4. Conclusions

We investigated the influence of several model parameters on deracemization via temperature cycles. Using the model the feasible and the optimal design spaces were identified.

References

[1] F. Breveglieri, G. M. Maggioni, M. Mazzotti, Cryst. Growth Des. 18 (2018) 1873-1881.
[2] W. L. Noorduin, W. J. P van Enckevort, H. Meekes, B. Kaptein, R. M. Kellogg, J. C. Tully, J. M. McBride, E. Vlieg, Angew. Chem., Int. Ed. 49 (2010) 8435-8438.
[3] M. Iggland and M. Mazzotti, Cryst. Growth Des. 18 (2011) 4611-4622.
[4] K. Suwannasang, A. E. Flood, C. Rougeot, G. Coquerel, Org. Process Res. Dev. 21 (2017) 623-630.
[5] B. Bodák, G.M. Maggioni, M. Mazzotti, Cryst. Growth Des. 18 (2018) 7122-7131.

This research has received funding as part of the CORE project (October 2016 – September 2020) from the European Union's Horizon 2020 research and innovation programme under the Marie Sklodowska-Curie grant agreement No 722456 CORE ITN

ECCE12
The 12th EUROPEAN CONGRESS OF CHEMICAL ENGINEERING
Florence 15-19 September 2019

The Role of Competitive Sorption in CO_2/CH_4 Separation with Membranes

Eleonora Ricci[1], Francesco Maria Benedetti[1], Maria Grazia De Angelis[1,*]

1 Department of Civil, Chemical, Environmental and Materials Engineering, University of Bologna, Via Terracini 28, 40131, Bologna, Italy

**Corresponding author: grazia.deangelis@unibo.it*

Highlights

- Sorption of CO_2/CH_4 mixtures in glassy polymers is characterized by strong competitive effects.
- Competition enhances the solubility-selectivity, improving membrane separation.
- Sorption has a greater influence on the separation than diffusion in multicomponent conditions.

1. Introduction

Gas separation with membranes is described by the solution-diffusion model, according to which the process is governed by a combination of solubility and diffusivity factors. When a moderately condensable gas, like CO_2, is involved in the separation, the solubility contribution plays a significant role in the process. Membrane materials characterization is often performed with pure gases. However, gas transport in mixed-gas conditions generally deviates from the pure-gas case. Competitive and synergistic effects are responsible for significant non-idealities, that cannot be properly evaluated with pure-gas measurements. Therefore, to uncover the relevant physical effects and assess the membrane performance closer to actual operating conditions, multicomponent tests are necessary.

In this work the sorption of CO_2/CH_4 mixtures in several high-performance glassy polymers was characterized experimentally, by means of a modified pressure-decay apparatus [1], and modelled using thermodynamic-based and empirical models, with the aim of identifying a reliable predictive tool, to reduce or complement the experimental effort. Finally, mixed-gas sorption measurements and literature multicomponent permeation data were coupled to evaluate gas diffusivity in multicomponent conditions and its effect on the separation.

2. Methods

Sorption of CO_2/CH_4 mixtures in several high free volume glassy polymers (PIM-1, TZ-PIM, PIM-EA-TB, PTMSP, Thermally Rearranged polymers) was evaluated at different compositions (10-50 mol.% CO_2) at 35 °C and up to 30 bar, using a dual-chamber pressure-decay apparatus coupled to a gas chromatograph [1]. Modelling of mixed-gas sorption data was performed with the NELF model (non-equilibrium extension of the Sanchez-Lacombe equation of state) [2] and with the Dual Mode Sorption model [3]. Both models require only pure-gas data in order to be parameterized and can be used to calculate multicomponent behavior predictively. Using the solution-diffusion model, diffusivity coefficients were calculated in the mixed-gas case, in order to evaluate the diffusivity contribution to the overall selectivity.

3. Results and discussion

The tests showed that the key feature of mixed-gas sorption in glassy polymers is the reduction of the solubility of both species with respect to the pure-gas case, due to competitive effects. However, the extent of this reduction is markedly different for the two gases, and is a function of mixture composition, temperature and pressure of the system, as it can be observed in **Figure 1** for the case of PIM-1. In particular, in the presence of a second component, the less condensable gas (CH_4) is excluded from the membrane to a much higher extent than CO_2.

This effect has a positive impact on the separation performance of the membrane materials, because it enhances the solubility-selectivity with respect to the ideal value, especially at high pressures, leading to increased ease of separation.

Both models used to calculate mixed-gas sorption were capable of capturing this reduction in solubility, however the NELF model showed a higher robustness and better quantitative agreement with the experimental data, also in the prediction of the solubility contribution to selectivity.

CH_4 diffusivity at multicomponent conditions was found to be systematically higher with respect to the pure-gas case, due to the simultaneous presence of a swelling agent (CO_2), which promotes a faster diffusion of CH_4. As a result, the diffusivity differences contribute only slightly to the selectivity of the membrane materials in real multicomponent operating conditions.

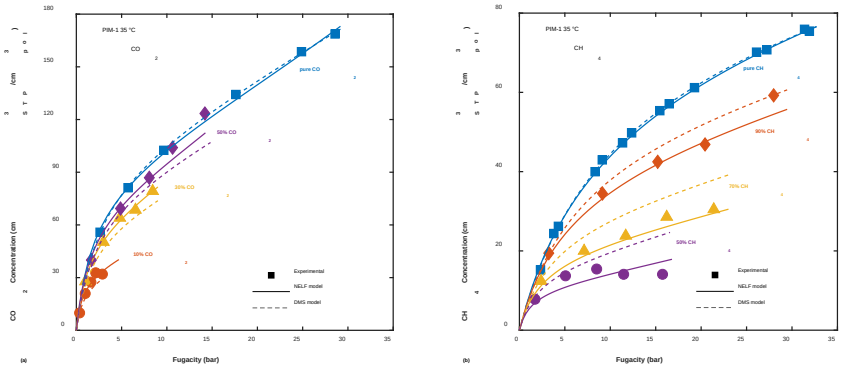

Figure 1. Sorption of CO_2/CH_4 mixtures in PIM-1 (symbols, [4]) at 35 °C and various mixture compositions, together with NELF model predictions (solid lines) and Dual Mode Sorption model predictions (dashed lines).

4. Conclusions

Sorption of CO_2 and CH_4 mixtures was measured in several glassy polymers suitable for CO_2 separation. The main effect in these systems is competitive sorption, which leads to a strong exclusion of the less condensable gas (CH_4) and results in an increased solubility-selectivity of the membrane. The NELF model successfully predicted this behavior, capturing also the effects of temperature and composition on the equilibrium, using only pure-gas parameters as input. Finally, a combined analysis of our measurements of mixed-gas sorption and multicomponent permeability data from the literature, allowed to establish that sorption is the most significant factor for CO_2/CH_4 separation with these membrane materials.

References

[1] O. Vopička, M.G. De Angelis, G.C. Sarti, J. Membr. Sci., 449 (2014) 97–108
[2] F. Doghieri, G.C. Sarti, Macromolecules, 24 (1996) 7885–7896
[3] R.M. Barrer, J.A. Barne, J. Slater, J. Polym. Sci., 27 (1958) 177-197
[4] O. Vopička, M.G. De Angelis, N. Du, N. Li, M.D. Guiver, G.C. Sarti, J. Membr. Sci., 459 (2014) 264–276

ECCE12
The 12th EUROPEAN CONGRESS OF CHEMICAL ENGINEERING
Florence 15-19 September 2019

Development of organic solvent nanofiltration membrane with high durability

Masanobu Nakata[1], Hideki Yamamoto[1], Sadao Araki[1]*

1 Kansai University, Department of Chemical, Energy and Environmental Engineering, 3-3-35 Yamate-cho, Suita-shi, Osaka 564-8680 Japan

**Corresponding author: araki_sa@kansai-u.ac.jp*

Highlights

- We succeeded in the preparation of silica membranes with hydrophobic functional groups.
- The prepared membrane showed higher durability than the previously reported polymeric membrane.

1. Introduction

Many nanofiltration membranes, which show the molecular weight cut-off (MWCO) of 200-2000, are used for the separation of water form aqueous solutions. Development of organic solvent nanofiltration (OSN) membranes, which can permeate organic solvents, is desired for recovery and recycling solvents in pharmaceuticals and petrochemical industries. This membrane technology can greatly reduce the waste solvents which need multiple separation steps and associated costs. However, polymeric membranes generally have a low durability for organic solvents. In this research, silica was used as a membrane material in order to improve the durability for organic solvents. We investigated the effect of the type of solute on the OSN performance of the silica membranes. In addition, short-time durability of the silica membrane was confirmed.

2. Methods

Membrane preparation

Propyl-functionaized silica membranes (PrFS membranes) were prepared on porous supports consisted of zirconia substrates (outer diameter: ϕ 2 mm, inner diameter: ϕ 1 mm) with γ-alumina interlayers[1]. A propyltrimethoxysilane (PrTMS) silica sol was prepared by hydrolysis and copolymerization of the PrTMS. The PrTMS (0.1 mol) was added to the solution consisted of cetyltrimethyl-ammoniumbromide (CTAB) (0.008 mol) and 25 mL of EtOH with gentle stirring. 7.5 mL of 1 mol $L^{-1}HNO_3$ was delivered by drops into the solution to promote the hydrolysis and condensation reactions of the PrTMS. Then, the solution was stirred continuously at room temperature for 6 h. The porous support was dipped into the PrTMS solution for 60 s and then pulled out at a speed of 1 cm min^{-1}. The support was dried at room temperature for 3 h and calcined at 453 K for 3 h. The membrane was then washed with ethanol to remove CTAB.

Nanofiltration test

Rose bengal(RB)/ethanol (EtOH), brilliant blue/EtOH, tartrazine(TZ)/EtOH and methyl orange/EtOH solution were used as the feed solution. Concentration of solutes in the feed solutions

was 35 µmol l^{-1}. The concentrations of the feed and permeate solutions were measured using an absorbance meter (ASUV 6300PC, ASONE corporation). Feed pressure was 5 bar.

3. Results and discussion

The MWCO of the PrFS membrane and average permeance in the solute are shown in Fig. 1. The MWCO of the PrFS membrane was 492. The permeance was highest in the case that TZ was used as the solute. It is considered that the affinity between the solute and the membrane surface may be related to this phenomenon. Fig. 2 shows the relationships between time and permeance in RB/EtOH system. The permeance reached 200 g m^{-2} h^{-1} bar^{-1} in about 60 min, and was nearly constant until end of the 420 min durability test. Since the PrFS membrane is based on the siloxane network, it is considered the durability against organic solvent is relatively high.

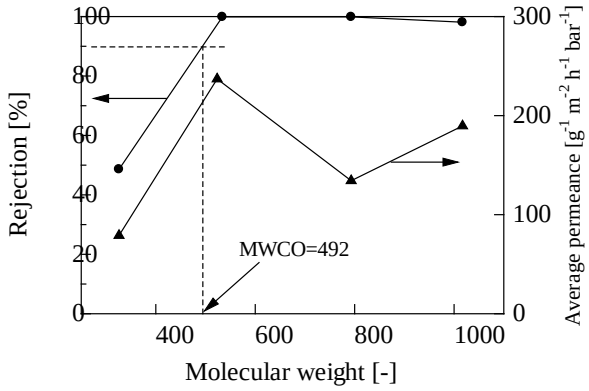

Fig. 1 The MWCO of the PrFS membrane and the relationships between molecular weight and permeance about PrFS membrane

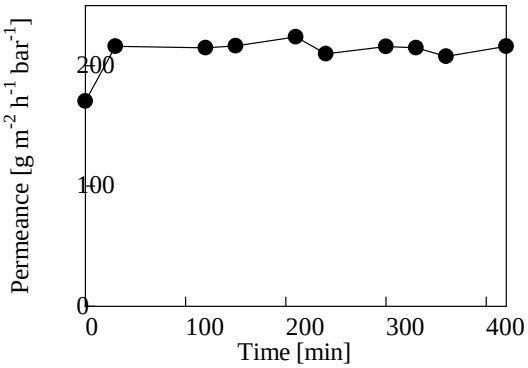

Fig. 2 The relationships between time and permeance in RB/EtOH system

4. Conclusions

The MWCO of the PrFS membrane was 492. The permeance was highest in the case that TZ was used as the solute. It is considered that the affinity between the solute and the membrane surface may be related to this phenomenon. The permeance was nearly constant form 60 min until end of the test in the RB/EtOH system.

References

[1] S. Araki, et al., J. Memb. Sci. 380 (2011) 41-47

ECCE12
The 12th EUROPEAN CONGRESS OF CHEMICAL ENGINEERING
Florence 15-19 September 2019

Selective recovery of nickel and copper from spent acids by chelating resins

Laura Ulloa*, Eugenio Bringas, María Fresnedo San Román

Chemical and Biomolecular Engineering Department

ETySIIT, University of Cantabria, Avda. De los Castros, 39005, Santander, Spain

**Corresponding author: laura.ulloa@unican.es*

Highlights

- Chelating resins are able to separate and recover Ni and Cu from acid media
- Equilibrium is described by the Langmuir model
- pH allows to control the selectivity of Ni/Cu separation
- Selective recovery of both metals is achieved by using H_2SO_4 and NH_3

1. Introduction

The management of metal-containing acidic effluents is usually performed by conventional treatment methods which exhibit some limitations such as the lack of selectivity, limited efficiency to reach the required concentration limits, waste generation, etc.; therefore, novel technologies are needed not only to overcome the aforementioned limitations, but also to recover valuable metals for further use. Generally, spent acids are complex wastes that contain high concentrations of metals and mineral acids, usually sulfuric or hydrochloric acids. In this work, spent acids containing nickel, copper and iron in sulphate media were provided by a local waste management industry. The selective removal and recovery of nickel and copper was experimentally analyzed using the chelating resin MTS9600® (bis-picolylamine functionalization) (Purolite). After describing the adsorption equilibrium, the influence on the process kinetics of different operation variables namely pH and solid/liquid (S/L) ratio was analyzed. Finally, the regeneration of the loaded resins allowing the independent recovery of both metals was assessed using H_2SO_4 and NH_4OH as regeneration agents.

2. Methods

In the adsorption equilibrium experiments, a certain amount of resin was contacted during 24 hours and constant temperature (25ºC) with spent acids with the following average composition: $[Ni^{2+}]$=9 g/L, $[Cu^{2+}]$=3 g/L, $[Fe^{2+}]$=24 g/L and pH≈1). The equilibrium concentrations of nickel, copper and iron in the aqueous phase were analyzed by Plasma-Atomic Emission Spectrometer (4210 MP-AES, Agilent Technologies®) being the values fitted to theoretical equilibrium isotherms. Kinetic experiments were carried out at 25ºC in a flask with continuous stirring during 3 hours under uncontrolled and controlled pH conditions using NaOH 5M. The S/L to liquid ratio varied from 1/10 to 1/2.5 mg/mL and the pH set point was set to values in the range between 1.5 to 3. Samples were taken at different times during the process and metal concentrations were measured. Regeneration was performed by contacting during 1 hour loaded resins with H_2SO_4 and after NH_3 at different concentrations and S/L ratio.[1],[2]

3. Results and discussion

Equilibrium data for both metals, nickel and copper, followed the Langmuir equilibrium model with values of the maximum adsorption capacity (q_{max}) of 50761 mg Ni/Kg dry resin and 97087 mg Cu/kg dry resin. However, the equilibrium constant for copper (K_L=0.063 L/mg) is more than 40 times higher than the value for nickel (K_L=1.47 10^{-3} L/mg) thus confirming the preferential affinity of the resin towards copper ions. On the other hand, Figure 1 shows the influence of pH on nickel and copper kinetics. In the case of copper, it is observed that kinetics and removal percentages at equilibrium conditions, near 100%, do not depend on the pH. However, in the case of nickel, removal yields decreased from 90% at pH≥2 to values lower than 50% at pH<2. By varying the S/L ratio it is concluded that the lower the ratio, the slower the nickel kinetics and the smaller the extraction percentages (20% for S/L=1/2.5 and 90% for S/L=1/10). However, copper kinetics are only affected at low values of the S/L ratio. The results from the regeneration experiments proved the selectivity of the proposed methodology, since only nickel was found in the stripping solution after one step of regeneration with H_2SO_4 1 M (43% recovery, 957,81 mg/L solution) and only copper was detected after the second regeneration stage with NH_3 2 M (45% recovery, 614,06 mg/L solution).

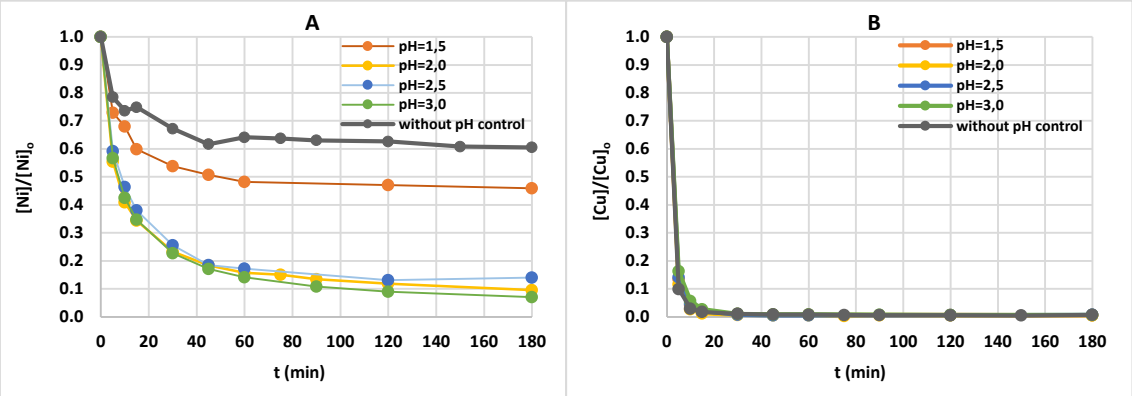

Figure 1. Time profiles for the removal of nickel (A) and copper (B) from spent acid wastes with MTS9600® resin.

4. Conclusions

From the experimental results it is concluded that the chelating resin MTS9600® is a suitable separation agent to recover transition metals from aqueous industrial wastewater at low pH values, since it reports removal percentages of nickel and copper of≈90% and ≈100% . It was also proved that the methodology proposed can lead to two high purity solutions of each metal after two in series regeneration stages with H_2SO_4 1 M and NH_3 2 M.

References

[1] Liebenberg, C.J. *et al.* (2013). The recovery of nickel and cobalt from a sulphate bioleach solution using Dow M4195. *The Southern African Institute of Mining and Metallurgy Base Metals Conference 2013*, pp. 269 – 282.

[2] Wolowitcz, H. (2012). The use of the chelating resin of a new generation Lewatit Monoplus TP-220 with the bis-picolylamine function. *Chemical Engineering Journal*, 197, pp. 493 – 508.

ECCE12
The 12th EUROPEAN CONGRESS OF CHEMICAL ENGINEERING
Florence 15-19 September 2019

Analysis of gas-liquid mass transfer around ascending microbubbles

Audrey Devatine[1], Carine Julcour[1], Anne-Marie Billet[1]

[1]*Laboratoire de Génie Chimique, Université de Toulouse, CNRS, INPT, UPS, Toulouse, France*
**Corresponding author: audrey.devatine@ensiacet.fr*

Highlights

- Experimental device that generates a chain of individual sub-millimeter bubbles
- Coupled experimental techniques: ombroscopy and optical recording of dissolved oxygen concentration
- Mass transfer model accounting for the composition variation of the rising bubbles
- Evaluation and analysis of the liquid-side mass transfer coefficient associated to microbubbles

1. Introduction

Gas-liquid transfer using micro bubbles (i.e. smaller than 1 mm) is a specific operation which is encountered for instance in wine processing or for oxygenation of stress sensitive cell culture. However, mass transfer performance obtained with a swarm of microbubbles has been rarely studied (Chiciuc et al., 2010; Devatine et al., 2013) and available correlations for millimeter-sized bubbles are usually extrapolated to this case. In this work, we have designed a dedicated device allowing studying mass transfer around a single ascending microbubble. The liquid-side mass transfer coefficient is then obtained by interpreting the experimental results with a convenient model. The resulting values of the liquid-mass transfer coefficient are compared with conventional correlations for mass transfer around a rigid sphere.

2. Methods

The experimental device is illustrated in Figure 1. It consists in a square transparent column of 1cm wide by 5cm high. Pure nitrogen or air is injected at the bottom, via a capillary (50 µm inner diameter) with a beveled cut orifice to generate sub-millimeter bubbles. The size and generation frequency of the ascending microbubbles are determined from image analysis of video records using a fast camera (Micron M20 – frame rate = 200 Hz). Oxygen absorption or desorption experiments are performed and the time evolution of the dissolved oxygen concentration is determined using a non-intrusive optical sensor located at the top of the column (Presens – Pst3: 0-45 mg.L^{-1}).

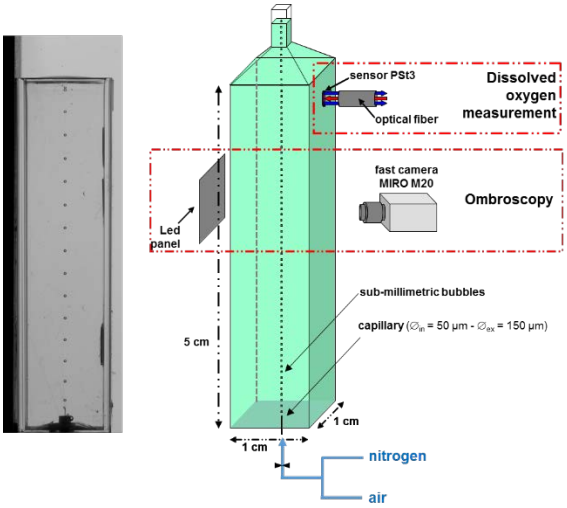

Figure 1. Experimental device.

3. Results and discussion

A quasi-steady state one-dimensional model evaluates the evolution of the bubble composition during its rise, thus the axial variation of the interfacial concentration. The average value is then accounted for in the mass balance describing the time-evolution of dissolved oxygen (DO) in the liquid bulk, which is considered perfectly mixed.

This approach gives access to the liquid-side mass transfer coefficient k_L according to the following equation:

$$k_L = -\frac{H_c V_b}{A_b H_L / \nu_b} \ln\left(1 + m \frac{V_L}{r_b H_c V_b}\right)$$

with k_L liquid-side mass transfer coefficient ($m.s^{-1}$)
H_c Henry's constant (referring to concentrations)
V_L liquid volume in the cell (m^3)
A_b bubble area (m^2)
H_L liquid height (m)
ν_b bubble velocity ($m.s^{-1}$)
V_b bubble volume (m^3)
r_b bubble frequency (s^{-1})
m slope of the regression line of $\ln(C_i/C) = f(t)$ for desorption experiment

where C_i DO concentration at initial time ($kg.m^{-3}$)
C DO concentration ($kg.m^{-3}$) during desorption

An example of time evolution of DO concentration is given in Figure 2 in the case of desorption by nitrogen bubbles. Figure 3 shows the linear regression of the DO data that gives the slope m for use in the above equation.

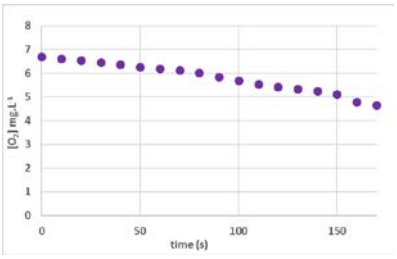

Figure 2. Oxygen desorption by nitrogen bubbles.

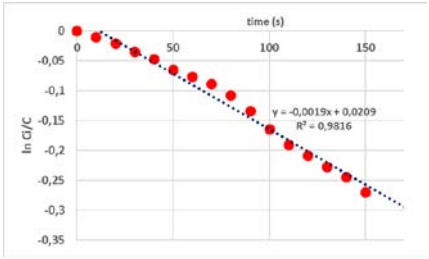

Figure 3. Mathematical processing of desorption data.

4. Conclusion and perspectives

The liquid-side mass transfer coefficient of individual ascending bubbles has been determined, showing a good agreement with that measured for a swarm of bubbles in our previous works (Devatine et al., 2013). Moreover, these values are well fitted by conventional mass transfer correlations established for rigid spheres.

References

[1] I. Chiciuc, V. Farines, M. Mietton-Peuchot, A. Devatine, Int. J. Food Eng., Vol. 6 (6), 9, 2010

[2] A. Devatine, I. Chiciuc, P. Guiraud, G. Hebrard, M. Mietton-Peuchot, *SFGP congress*, Lyon (France), 2013

ECCE12
The 12th EUROPEAN CONGRESS OF CHEMICAL ENGINEERING
Florence 15-19 September 2019

Chiral Symmetry Breaking and Deracemization of Sodium Chlorate in Taylor Vortex Flow

Jaekyu Ahn[1], Bowen Zhang[1], Gerard Coquerel[2], Woosik Kim[1]

1 Department of Chemical Engineering, Kyung Hee University, Yongin-si Kiheung-ku Soechun-dong 1, Kyungki-do, Korea, 2 SMS Laboratory EA3233, University of Rouen Normandy, F-76821 Mont Saint Aignan CEDEX, France

**Woosik Kim: wskim@khu.ac.kr*

Highlights

- Taylor vortex flow promoted the chiral symmetry breaking and deracemization.
- Initial chiral symmetry breaking was enhanced by increasing the rotation speed.

1. Introduction

Due to the significant difference in pharmacological and biological effect of enantiomers of a chiral compound, the synthesis of chiral substance with a single chirality is of great value. A pioneer study for chiral symmetry breaking was reported by Kondepudi et al.[1] Enantiomerically pure crystals of sodium chlorate was obtained in evaporation crystallization with stirring, whereas symmetric chiral crystals were produced without stirring. Meanwhile, abrasive grinding using glass beads and temperature swing were demonstrated as highly effective techniques for promoting deracemization. [2] [3] According to Ahn et al study on the cooling crystallization of sodium chlorate, it was shown that the initial chiral symmetry breaking strongly depended on the turbulent fluid motion, because the turbulent eddy flow directly dictated the secondary nucleation during the induction period.[4] Thus, the initial chiral symmetry breaking was enhanced by increasing the agitation speed. Also, the final deracemization was determined by initial chiral symmetry breaking. So, the complete deracemization was achieved when the high initial chiral symmetry breaking occurred. It was already known that the periodic Taylor vortex flow was highly effective for the induction of nucleation and phase transformation in polymorphic crystallizations [5]. So, in the present study, Taylor vortex flow was applied to promote the chiral symmetry breaking and deracemization in cooling crystallization of sodium chlorate.

2. Methods

The cooling crystallization of sodium chlorate was carried out in a Couette-Taylor (CT) crystallizer. The feed solution of 96 g-$NaClO_3$/100 ml was prepared at a saturated temperature of 26 ºC, and then filtered with micro-filter paper. The feed solution in CT crystallizer was cooled from 26 ºC to 13 ºC at a constant cooling rate for cooling crystallization. After the feed solution reached at 13 ºC, the CT crystallizer was further run for the deracemization. Suspension samples were taken intermittently and quickly filtered using a vacuum pump, then dried in a convection oven. The chirality of crystals was analysed using polarized microscope (Olympus, BX53M, Japan). The

crystal enantiomeric excess (CEE) was defined as (CEE = ($N_{major} - N_{minor}$) / ($N_{major} + N_{minor}$)), where N_{major} and N_{minor} meant crystal numbers of major and minor forms, respectively.

3. Results and discussion

The effect of the Taylor vortex flow on the chiral symmetry breaking and deracemization of sodium chlorate was investigated. As shown in Figure 1(a), initial chiral symmetry breaking (initial CEE) at low rotation speed of 100 rpm occurred at around 50%, and then, increased finally up to 80% (final CEE) by deracemization of chiral crystals. As increasing the rotation speed over 300 rpm, initial chiral symmetry breaking was enhanced over 80% and the complete deracemization was achieved within 7 hours. When considering the results in random turbulent flow, Taylor vortex flow was much effective for initial chiral symmetry breaking and deracemization of chiral crystal due to its unique periodic fluid motion. That is, Taylor vortex was much effective for the secondary nucleation during the induction period, resulting in high initial chiral symmetry breaking. Also, it promoted the deracemization of chiral crystals, bringing about the enantiomeric pure crystals within several hours. The cooling rate was also an influential factor in chiral symmetry breaking and deracemization, as shown Fig. 1(b). Initial chiral symmetry breaking was about 60% at high cooling rate of 0.295 °C/min, and it increased by decreasing the cooling rate. So, 91% of initial chiral symmetry breaking occurred at 0.0738 °C/min of cooling rate due to long induction period for the secondary nucleation. The deracemization also depended on cooling rate. Due to low initial chiral symmetry breaking at high cooling rate (0.295 °C/min), it took about 11 hours for complete of deracemization. However, it was reduced to 6 hours by decreasing the cooling rate to 0.0738 °C/min.

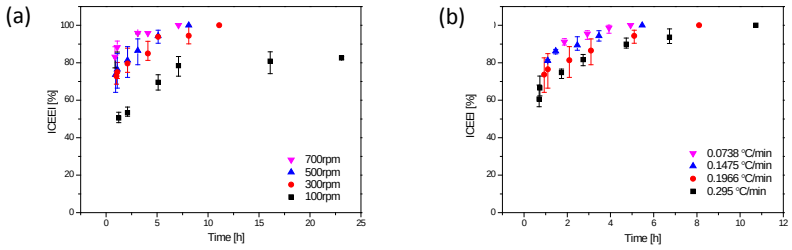

Figure 1. (a) Deracemization of sodium chlorate when varying rotation speed in cooling crystallization, The cooling rate was fixed at 0.197 °C/min; (b) Deracemization of sodium chlorate when varying cooling rate in cooling crystallization, The rotation speed was fixed at 500rpm [Calibri 9].

4. Conclusions

The Taylor vortex flow was highly effective for the secondary nucleation, resulting in high initial chiral symmetry breaking in the cooling crystallization of sodium chlorate. So, initial CEE was enhanced by increasing the rotation speed. As initial CEE increased, the deracemization was also facilitated. So, complete deracemization was achieved with initial CEE over 60%

References

[1] D. K. Kondepudi, R. J. Kaufman, N. Singh, Science, 250 (1990) 975–976.
[2] C. Viedma, Phys. Rev. Lett., 94 (2005) 065504.
[3] K. Suwannasang, A. E. Flood, C. Rougeot, G. Coquerel, Cryst. Growth. Des, 13 (2013) 3498-3504.
[4] J. K. Ahn, D. H. Kim, G.Coquerel, W. S. Kim, Cryst. Growth Des, 18 (2018) 297-306.
[5] S. A. Park, S. Lee, W. S. Kim, Cryst. Growth Des, 15 (2015) 3617-3627.

ECCE12
The 12th EUROPEAN CONGRESS OF CHEMICAL ENGINEERING
Florence 15-19 September 2019

Recovery of lignin from deep eutectic solvents by liquid-liquid extraction

Dion Smink[1], Sascha R.A. Kersten[1], Boelo Schuur[1]*

1 Department of Science and Technology (TNW), Sustainable Process Technology group, University of Twente, 7500 AE Enschede, The Netherlands

**Corresponding author: b.schuur@utwente.nl*

Highlights

- Lignin was recovered from DES by liquid-liquid extraction
- 2-MTHF is a suitable, bio-based extractant for lignin
- Addition of water greatly enhances lignin extraction by 2-MTHF

1. Introduction

Deep eutectic solvents (DES) are composite solvents that exhibit deep eutectic behavior upon mixing, and are often biocompatible, biodegradable and have a low toxicity.[1] Regeneration of deep eutectic solvents is most often performed by precipitation of either the solute or solvent in an anti-solvent. Especially in biomass fractionation, large amounts of water are required as anti-solvent for the precipitation of lignin.[2] We propose liquid-liquid extraction as an alternative method for the recovery of lignin from DES.

2. Methods

DES, solvent and any lignin were equilibrated in a shaking bath at overnight. The phases were separated and the concentrations of the DES constituents and solvent analyzed by high pressure liquid chromatography (HPLC). The lignin concentrations were analyzed as function of the molar weight by gel permeation chromatography (GPC). The lignin distribution coefficient was calculated as follows:

$$D = \frac{[lignin]_{Solvent}}{[lignin]_{DES}}$$

3. Results and discussion

The equilibria between the lactic acid - choline chloride DES and 2-MTHF were determined at three different temperatures. The phase equilibria are shown in figure 1. From this figure it can be seen that the temperature dependence of the equilibria is very small. Also, high amounts of choline chloride are required to create a phase split. All DES phases contained more than 27 wt.% choline chloride, but no choline chloride was found in the DES phases.

The lignin distributions between the 1.7:1 lactic acid - choline chloride DES and 2-MTHF were determined at 50 °C. Since water has a great influence on the lignin solubility in both DES[3] and low-hydrogen bond accepting solvents -such as 2-MTHF-, its influence on the lignin distribution was studied. It was found that the distribution coefficient increases with increasing amounts of water. Also, the effect of water is greater on the extraction of the higher molar weight fractions of the lignin. The results are shown in figure 2.

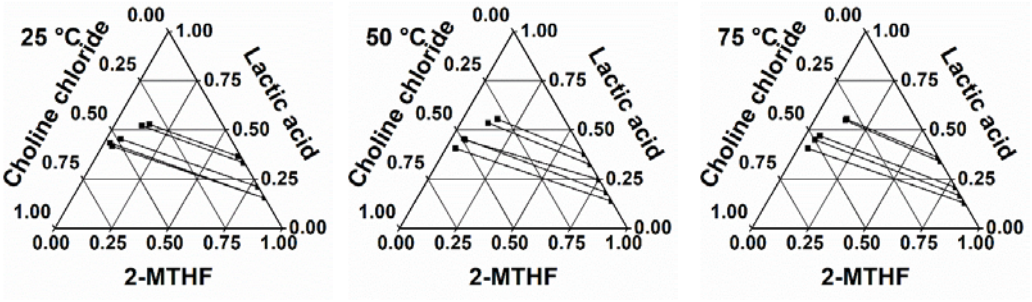

Figure 1. Phase diagram with liquid-liquid equilibrium data between choline chloride, lactic acid and 2-MTHF at 25, 50 and 75 °C. The axis show the mass fractions of the constituents.

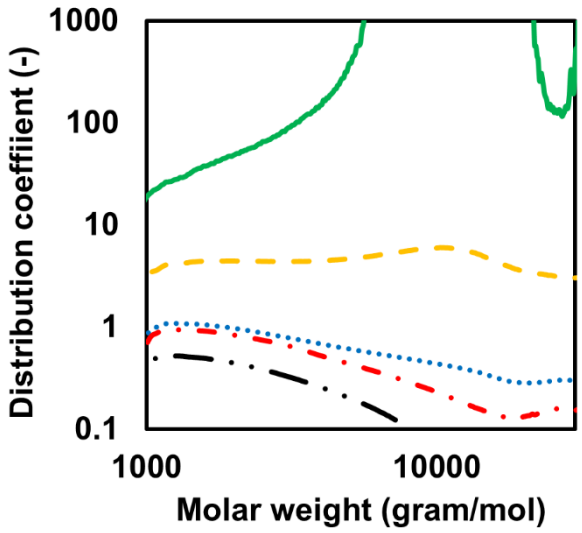

Figure 1. Distribution of lignin between DES and 2-MTHF at 50 °C. Various amounts of water were added to the DES: 50% (green-solid), 25% (yellow-dashed), 10% (blue-dotted), 5% (red-dash-dotted) and dry (black-dot-dot-dashed). For the parts of the green line that are out of the graph, no lignin fractions were found in the DES phase, and thus the distribution coefficient is infinite.

4. Conclusions

2-MHTF is a suitable extractant for lignin from DES. Addition of choline chloride to the DES is required to form two liquid phases and addition of more choline chloride decreased leaching of lactic acid to the 2-MTHF phase. The extraction lignin was studied and increases with increasing amounts of water.

References

[1] Macário, I.P.E.; Jesus, F.; Pereira, J.L.; Ventura, S.P.M.; Gonçalves, A.M.M.; Coutinho, J.A.P.; Gonçalves, F.J.M., Chemosphere 212 (2018) 890-897

[2] Alvarez-Vasco, C.; Ma, R.; Quintero, M.; Guo, M.; Geleynse, S.; Ramasamy, K.K.; Wolcott, M.; Zhang, X., Green Chem. 18 (2016) 5133–5141

[3] Soares, B.; Tavares, D.J.P.; Amaral, J.L.; Silvestre, A.J.D.; Freire, C.S.R.; Coutinho, J.A.P., ACS Sustain. Chem. Eng. 5 (2017) 4056–4065

ECCE12
The 12th EUROPEAN CONGRESS OF CHEMICAL ENGINEERING
Florence 15-19 September 2019

Influence of Temperature and Pressure on Isooctane Permeability in Polydimethylsiloxane Membrane

Lenka Moravkova, Karolina Machanova, Petr Stanovsky, Zuzana Petrusova

Institute of Chemical Process Fundamentals of the Czech Academy of Sciences, Rozvojova 135, 165 02, Prague 6, Czech Republic

**Corresponding author: moravkova@icpf.cas.cz*

Highlights

- Separation ability of flexible PDMS is influenced on operation conditions
- Isooctane permeability depends significantly on trans-membrane pressure
- Isooctane permeability is negligible influenced by process temperature
- Reproducibility of isooctane permeability is within 5 %
- Membrane flux does not show any hysteresis for the change of feed concentration

1. Introduction

Generally, sorption and diffusion are the key parameters for gas and vapor permeation in the polymeric dense membrane. The diffusivity is higher for smaller molecules, while sorption is stronger for larger condensable molecules. The permeability mainly depends on the VOC concentration in the feed stream as well as the condensability of the relevant VOC. One of the main applications is the separation of volatile organic vapors from a permanent gas [1].

2. Isooctane and nitrogen permeability in PDMS membrane

The membrane was prepared by a casting knife from Elastosil polydimethylsiloxane (PDMS, Silicones and more) as a dense film with the thickness of 100 microns. Nitrogen and (isooctane + nitrogen) permeation experiments were carried out at three temperatures: 25°C, 30°C and 35°C and at four trans-membrane pressures: 100/50 kPa, 150/50 kPa, 200/50 kPa and 250/50 kPa. The membrane flux was determined from the increase of permeate pressure in time. The basic test apparatus was described previously in a detail [2].

3. Results and discussion

The representative figures of membrane flux are shown at various experimental conditions in Figure 1. PDMs polymer is a flexible material and it can be expected that operation conditions will influence the membrane flux. The temperature and trans-membrane pressure were changed within 25–35°C and 50–200 kPa. It was found that the flux increases with the isooctane feed concentration as expected because of a high solubility of organic vapors in polymeric membranes. The temperature influence was found to be small (Figure 1A) while the trans-membrane pressure influenced the membrane flux significantly (Figure 1B).

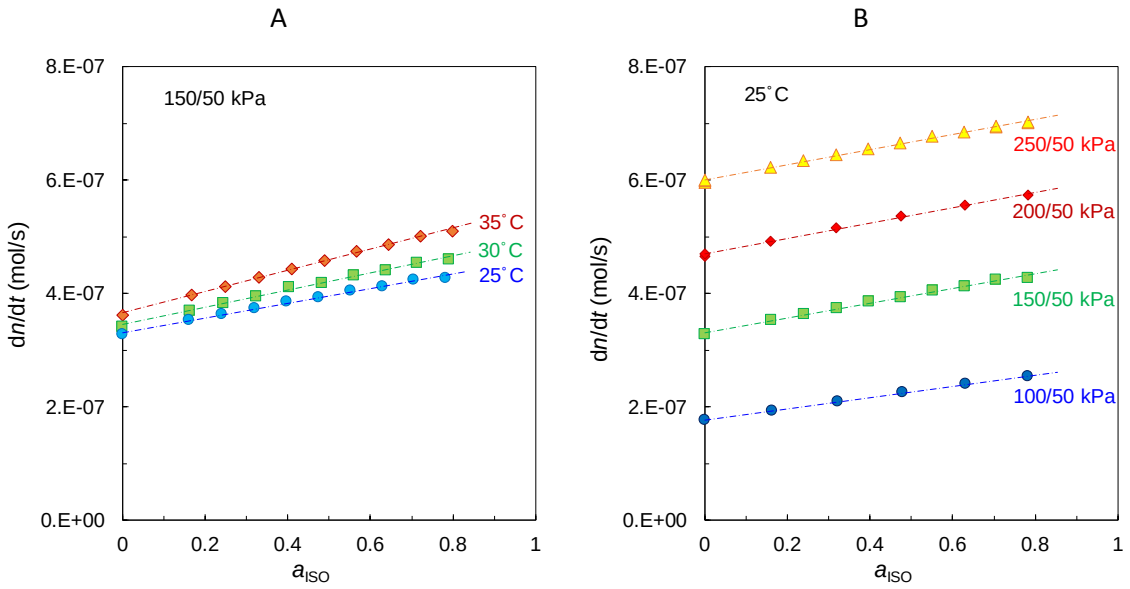

Figure 1. Influence of temperature (A) and trans-membrane pressure (B) on (isooctane + nitrogen) flux in PDMS.

4. Conclusions

It was found that the trans-membrane pressure has a significantly bigger influence on the flux in flexible PDMS polymeric membrane than temperature. None hysteresis was observed when the isooctane feed concentration increased and then decreased.

The increase of transmembrane-pressure from 50 kPa to 200 kPa caused almost three times higher membrane flux. While the membrane flux increased only negligible when the temperature increased from 25 °C to 35 °C. Interestingly, the increase of membrane flux was 40 % with the increasing isooctane feed concentration at the highest temperature while the membrane flux increased less at the highest trans-membrane pressure (by 17 %).

Acknowledgement

The financial support of the Czech Science Foundation (Junior Project 17-03367Y) is acknowledged.

References

[1] Z. Petrusova, K. Machanova, P. Stanovsky, P. Izak, Sep. Purif. Technol. 217 (2019) 95–107.
[2] Z. Petrusová, Z. Vajglová, L. Morávková, J. C. Jansen, J. Vejrazka, P. Izak, Chem. Biochem. Eng. Q. 31(2) (2017) 145–160.

ECCE12
The 12th EUROPEAN CONGRESS OF CHEMICAL ENGINEERING
Florence 15-19 September 2019

Effect of membrane profiles on the Limiting Current Density in Electrodialysis.

Mariagiorgia La Cerva[1], Luigi Gurreri[1], Michele Tedesco[2], Andrea Cipollina[1*], Alessandro Tamburini[1], Michele Ciofalo[1], Giorgio Micale[1]

1 Dipartimento di Ingegneria, Università degli Studi di Palermo – viale delle Scienze Ed. 6, 90128 Palermo, Italia; 2 Wetsus, European Centre of Excellence for Sustainable Water Technology, Oostergoweg 9, 8911 MA Leeuwarden, The Netherlands

**Corresponding author: andrea.cipollina@unipa.it*

Highlights

- LCD measurements in real ED stacks are presented.
- Different profiled membranes are tested.
- LCD performance of profiled and flat membranes are compared.

1. Introduction

Limiting Current Density (LCD) is a crucial parameter in electrodialysis (ED), and depends mainly on membrane surface properties [1] and on concentration polarization phenomena [2]. The latter are influenced by fluid dynamic aspects related, above all, to the characteristics of the spacers used in the channels. When profiled membranes [3] are used to create the channel thickness in stacks without spacers, the modification of the membrane surface and the presence of active membrane areas in directions not orthogonal to the current affect the LCD. Also the profile type is expected to have an effect on the LCD. In the present work, we experimentally investigated the effect of different membrane profiles on the LCD, testing also different operating conditions. The performance of profiled membranes and flat membranes (with spacers in the channels) were compared. The results were also used to validate our ED process model.

2. Methods

A crossflow ED stack, consisting of 10 cell pairs, with an active area of 10×10 cm^2 was used. Fujifilm membranes profiled with pillars or with overlapped cross filaments were tested. Inlet concentrations of NaCl ranging from 0.5 to 60 g/l and inlet velocities in the range 0.25 – 2 cm/s were examined. Current-voltage curves were built by chronopotentiometric measurements, thus identifying the LCD. Results obtained with profiled membranes were compared with data previously obtained with flat membranes and spacers [4]. Moreover, the experimental results were compared with the predictions of a one-dimensional process model [4], in which all the non-ideal transport phenomena through the membranes (osmosis, electro-osmosis, salt diffusion) are considered. The model predicts also concentration polarization by correlations for the Sherwood number obtained from computational fluid dynamics (CFD) simulations.

3. Results and discussion

We observed that the current-voltage curves show different trends depending on the membrane profile type present in the diluate compartment. In particular, when the profiles of the anion exchange membrane (AEM) are in the diluate compartment (blue symbols in Figure 1), the *i-V* curve changes slope at higher currents, thus leading to higher LCD values. However, this configuration exhibits lower LCD values compared to a stack equipped with flat membranes and net spacers (empty symbols in Figure 1), which can be attributed, at least in part, to a poorer mixing promotion.

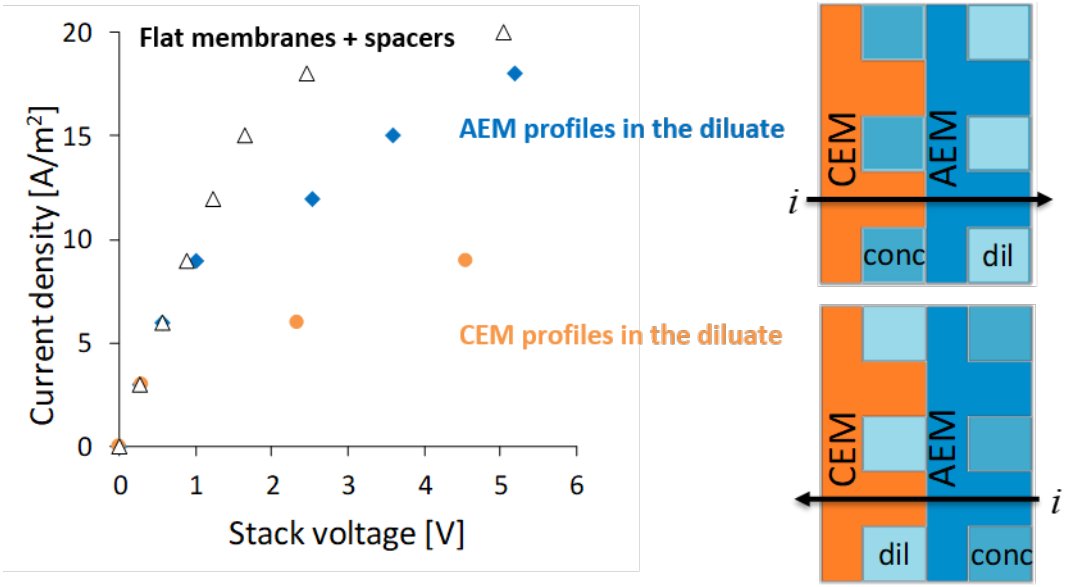

Figure 1. Current-voltage curves obtained with AEM profiles in diluate (blue symbols), with CEM profiles in the diluate (orange symbols) and with flat membranes and spacers (empty symbols). NaCl inlet concentration was equal to 0.5 g/l in both the concentrate and the diluate. Velocity was equal to 2 cm/s in both compartments.

4. Conclusions

In this work, we studied the influence of the membrane profiles on the LCD in ED units. We observed that the configuration with AEM profiles in the dilute channel is preferable, as provides higher LCD values. However, improved geometries have to be designed in order to enhance the performance with respect to conventional net spacers.

Acknowledgments

This work has been performed within the REvivED water project (*Low energy solutions for drinking water production by a REvival of ElectroDialysis systems*), Horizon 2020 programme, Grant Agreement no. 685579, www.revivedwater.eu.

References

[1] N. D. Pis'menskayaa, V. V. Nikonenko, N. A. Mel'nik, G. Pourcelli, G. Larchet, Russian Journal of Electrochemistry 48 (2012) 610–628.

[2] F. Li, W. Meindersma, A.B. de Haan, T. Reith, Journal of Membrane Science 208 (2002) 289–302.

[3] L. Gurreri, M. Ciofalo, A. Cipollina, A. Tamburini, W. Van Baak, G. Micale, Desalin. Water Treat. 55 (2015) 3404–3423.

[4] M. La Cerva, L. Gurreri, M. Tedesco, A. Cipollina, M. Ciofalo, A. Tamburini, G. Micale, Desalination 445 (2018) 138–148.

ECCE12
The 12th EUROPEAN CONGRESS OF CHEMICAL ENGINEERING
Florence 15-19 September 2019

Heat Transfer Problem for Different Densities Layered Gypsum Products in Influences of Fire.

Aivars Aboltins[1*], Harijs Kalis[2], Kristaps Pulkis[3]

1 Latvia University of Life Sciences and Technologies, Institute of Agricultural Machinery, Cakstes bulv.5, Jelgava LV-3001, Latvia; 2 Institute of Mathematics and Computer Sciences of University of Latvia, Raina bulv.29, Riga, LV-1459; 3 Latvia University of Life Sciences and Technologies, Faculty of Environment and Civil Engineering, Akademijas str.19, Jelgava, LV-3001

**Corresponding author: Aivars.aboltins@llu.lv*

Highlights

- A mathematical model of heat transfer with specific heat and thermal conductivity coefficients dependence on temperature for a 3-layer environment is offered.
- Modeling of heat transfer process for 3-layer sandwich wall, made of gypsum materials with different densities, in case of fire is done.
- Theoretical model shown good connection with experimental burning results.

1. Introduction

The use of gypsum materials in construction is well known. The requirements for lighter materials with good thermal insulation are increasing. This material is foam gypsum, the technology of which makes it possible to obtain a product with a density of less than 200 kgm^{-3} [1]. Nowadays not only energy efficiency but also demands of better living comfort highly increase sound and fire safety requirements of building components. Lot of construction materials for acoustic and fire safety characteristics are gypsum based which can improved changing properties of the material. Sandwich type gypsum materials with different densities are widely used in construction. The objective of this study is to develop a mathematical model of heat transfer through sandwich type gypsum materials (gypsum board and foam gypsum layer) in fire conditions.

2. Methods

The 3-layer sandwich type wall in which the foam gypsum layer is bounded by gypsum boards is considered. It is assumed that the specific heat c_p and thermal conductivity *K* coefficients depends on temperature *T* similarly in [2]. The cubic spline interpolation for $c_p(T)$ and *K(T)* is used. In the case of three layers (N=3) we obtain the system of three PDEs

$$\begin{cases} D_1(T)\dfrac{\partial^2 T_1(x,t)}{\partial x^2} = \dfrac{\partial T_1(x,t)}{\partial t} \\ D_2(T)\dfrac{\partial^2 T_2(x,t)}{\partial x^2} = \dfrac{\partial T_2(x,t)}{\partial t} \\ D_3(T)\dfrac{\partial^2 T_3(x,t)}{\partial x^2} = \dfrac{\partial T_3(x,t)}{\partial t} \end{cases} \quad (1)$$

where $D_i(T) = \dfrac{K_i(T)}{\rho_i c_{pi}(T)}$, $i = 1,2,3$ are thermal diffusion coefficients depending on *T*. For the initial condition for *t=0* are given $T_1(x,0) = T_2(x,0) = T_3(x,0) = T_0$, where $T_0 = 20\ ^0C$. Following boundary and continuous conditions are used :

$$\begin{cases} D_1(T)\frac{\partial T_1(0,t)}{\partial x} - \alpha(T_1(0,t) - T_a) = 0\,,\ T_3(L,t) = T_b + T_l(t), \\ T_1(x_1,t) = T_2(x_1,t)\,,\quad D_1(T)\frac{\partial T_1(x_1,t)}{\partial x} = D_2(T)\frac{\partial T_2(x_1,t)}{\partial x} \\ T_2(x_2,t) = T_3(x_2,t)\,,\quad D_2(T)\frac{\partial T_2(x_2,t)}{\partial x} = D_3(T)\frac{\partial T_3(x_2,t)}{\partial x} \end{cases} \quad (2)$$

where α are the constant mass transfer coefficients, $T_l(t) = 345 \cdot lg(8t + 1)$ in minutes, $T_a = T_b = 20\ ^0C$.

Conservative averaging method for reduce problem (1)-(2) to an initial problem for system of ODEs [3] is used. The problem (1)-(2) is solved by using MathLab.

3. Results and discussion

Experiments were done with a wall of foam gypsum ($\rho = 450kgm^3$) inside separated by 6.5 mm gypsum boards ($\rho = 900kgm^3$). The thickness of the foam gypsum layer was 23 and 30 mm. Experimental and theoretical temperature distribution on both sides of wall and inside are shown at fig.1a and fig.2a. ,where the number means the distance to the fire in millimeters. Theoretical temperature distribution in the wall depending on the burning time at one of the edges is shown in the pictures 1b and 2b.

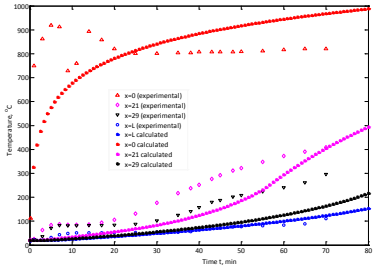

Figure 1a Temperature distribution in wall with thickness 36 mm.

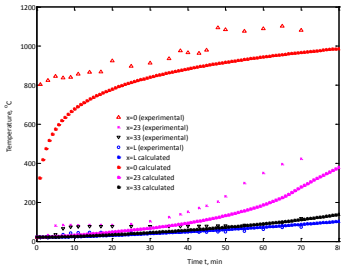

Figure 2a Temperature distribution in wall with thickness 43 mm.

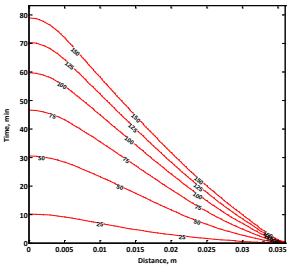

Figure 1b Theoretical calculated temperature distribution inside wall with thickness 36 mm.

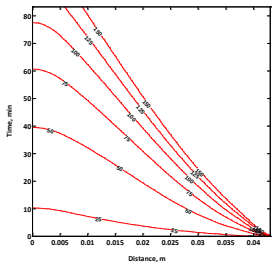

Figure 2b Theoretical calculated temperature distribution inside wall with thickness 43 mm.

4. Conclusions

Proposed mathematical model (1)-(2) can be used for more in-depth research of different material layer heat transfer problem. Theoretical model shown good connection with practical experimental burning results.

References

[1] J. Skujans, Technological Means of Foam Gypsum Production, Kraskovo, 1987, p 24 (in Russian)

[2] I. Rahmanian, Y.C. Wang, A combined experimental and numerical method for extracting temperature-dependent thermal conductivity of gypsum boards. Construction and Building Materials 26, (2012) 707- 722

[3] A. Aboltins, H. Kalis, K. Pulkis., J. Skujans., I. Kangro, Mathematical modelling of heat transfer problem for two layered gypsum board products exposed to fire. Proceedings of International conference "Engineering for Rural Development" Jelgava, Latvia, 2017, pp.1369-1376

ECCE12
The 12th EUROPEAN CONGRESS OF CHEMICAL ENGINEERING
Florence 15-19 September 2019

Recovery of cobalt from acidic solutions by ion exchange through electrodialysis.

Gerardo Cifuentes[1], Gonzalo Muñoz, Belén Garrido, *Jorge Manríquez[1], Magdalena Cifuentes-Cabezas[2]

[1] *Full Professor, Metallurgical Engineering Department, University of Santiago of Chile, Avda. L. B. O'Higgins 3363, Estación Central, Santiago, Chile.* [2] *Department of Chemical and Nuclear Engineering, University Research Institute for Industrial, Radiophysical and Environmental Safety (ISIRYM), Universitat Politècnica de València, C/Camino de Vera s/n, 46022 Valencia, Spain*

**Corresponding author: jorge.manriquez@usach.cl*

1. Introduction

During copper extraction processes from oxidized minerals to produce cathodic copper the cobalt is accumulated in the refine and in leaching piles by means of mechanical drag and electrolytic purges, reaching concentrations of 60 to 110 mg/L. However, during the electrodeposition process, cobalt salts are added to the electrolyte to stabilize the surface of lead anode with a layer of $PbO_2 - \beta$, improving its quality and, consequently, reducing the formation of ladder slats that provide an increase in the cathodic quality. This article presents the results of study of cobalt recovery through electrodialysis using ionic exchange membrane cationic.

2. Methods

The electrodialysis circuit consists of a cubic cell of two chambers with a cation exchange membrane were placed between the electrodes, at a distance de 10 cm, to form a separate anolyte and catholyte chambers (see Figure 1). Catholyte of volume 1 dm^{-3} containing 1 to 1,6 mol dm^{-3} H_2SO_4 and two anolytes 3 dm^{-3} in volume containing, the first: cobalt ions at a concentration of 100 mg dm^{-3} and 0,1 mol dm^{-3} HCl and the second: cobalt ions at a concentration of 100 to 1,000 mg dm^{-3} and 0.1 to 0.5 mol dm^{-3} H_2SO_4. Catholyte and anolyte were circulated to each chamber using separate pumps. The flow rate of both electrolytes was kept constant at 1 dm^{-3} min^{-1}. A stainless-steel cathode was used. The electrolytes are fed from the lower and the outlet is from top by gravity.

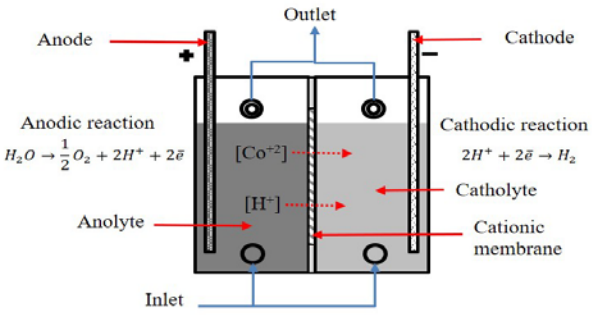

Figure 1. Scheme Electrodialysis cell

Anodic overpotential curves (SPA) to determine the material of anodic electrode were realized (graphite or titanium) in order to avoid the formation of chlorine gas. To determine the current intensity of work potential-current curves (CVC) were realized to the cationic membrane.

Finally, electrodialysis test was carried out for 8 h at 25 and 40°C and different current intensity depending on the results of the SPA and CVC curves, the parameters are show in Table 1.

Table 1 Parameters of electrodialysis test

Test	Current intensity (A)	T (°C)	Acid in anolyte (M)	H_2SO_4 in Catholyte (M)	Cobalt (mg dm^{-3})
1	0.02	25	0.1 HCl	1	100
2	0.02	25	0.1 H_2SO_4	1.6	100
3	0.02	25	0.1 H_2SO_4	1.6	1,000
4	1.5	40	0.5 H_2SO_4	1.6	1,000
5	3	40	0.5 H_2SO_4	1.6	1,000

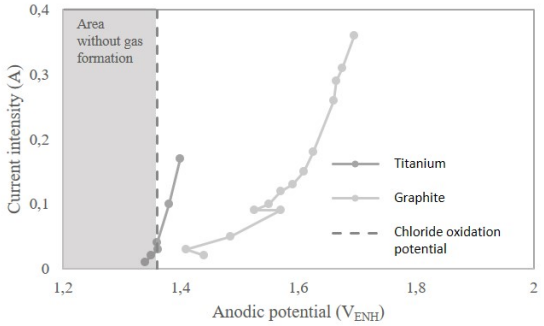

Figure 2. Anodic overpotential for titanium and graphite anode, and the area without gas formation.

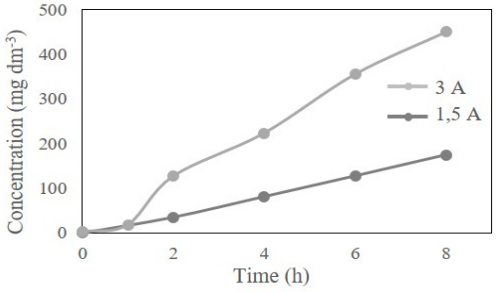

Figure 3. Profile concentration of cobalt in catholyte, mol dm^{-3}.

3. Discussion and Conclusions

The results of SPA curves (Figure 2) indicate that there is no gas formation to 0.03 A, using titanium anode while if using graphite anode there is gas formation according to the equation $2Cl^- \rightarrow Cl_2 + 2\bar{e}$ $(E° = -1.36V_{ENH})$. On the other hand, the CVC curves indicate that there was not limit current in the 0 to 3 A section for all solutions (Figure 3). Then, a test was performed at 0.02 A in chloride medium (test 1), however, no cobalt traces were found in the catholyte. The test 2 and 3 was performed at 0.02 A in sulphate medium to different cobalt concentrations, but no cobalt traces were found in the catholyte.

The test 4 and 5 were developed using a cationic membrane with less electrical resistance, it can see from in figure 3 that it was found cobalt in the catholyte in concentrations of 173.3 and 449.2 mg dm^{-3}, respectively. In conclusion, is possible recovery cobalt from acid solutions through ionic exchange with recovery rate of 21.7 and 55.85 mg dm^{-3} h^{-1} to 1.5 and 3 A, respectively with 0.45 and 0.48 Wh mg^{-1} specific energy consumption. These results give foot to continue the study of this processes and achieve recoveries on 1,000 mg dm^{-3}, optimizing the process with the use of electrodes and membranes of less electrical resistance.

References

[1] Cooper, W.C.,1985. Advances and future prospects in copper electrowinning, 789-805.

[2] Boss, F. E. E. et.al., 1927. Means for protecting storage battery grids. US Patent No. 1,826,724.

[3] Krivolapova V. et. al., 1941. An investigation of the corrosion of lead in oxidizing media, 335-341.

[4] Koch,D.F.A., 1959. The effect of cobalt on a lead anode in sulfuric acid. Electrochim, 32-38.

[5] Collana M., 2009. Desarrollo de módulos de electrodiálisis para la desalinización de aguas salobres, determinación de parámetros físicos y evaluación experimental de modelo difusional, Lima, Perú.

[6] J. J. Krol, M. Wessling, H. Strathmann, 1991. Concentration polarization with monopolar ion exchange membranes: current-voltage curves and water dissociation, 145-154.

[7] Cifuentes, G., et al. , J. Chil. Chem. Soc. 60 (2015) 4, 2711-2715.

[8] Rubinstein y Shtilman, 1979. Voltage against current curves of cation-exchange membranes, 231-246.

ECCE12
The 12th EUROPEAN CONGRESS OF CHEMICAL ENGINEERING
Florence 15-19 September 2019

In situ monitoring of the formation of mixed CO_2/CH_4 gas hydrates via Raman spectroscopy

Andreas S. Braeuer[1]

1 Institut für Thermische Verfahrenstechnik, Umwelt- und Naturstoffverfahrenstechnik, Technische Universität Bergakademie Freiberg, Freiberg, 09599, Germany

**Andreas.Braeuer@tu-freiberg.de*

Highlights

- *In situ* analysis of gas hydrate formation.
- Gas separation

1. Introduction

Gas hydrates are crystalline ice-like solids that consist of a three dimensional network of hydrogen bonded water molecules stabilized by the incorporation of small guest molecules, such as carbon dioxide (CO2) or methane (CH4).

Hydrate formation is a promising technology for gas separation processes, due to the gas specific thermodynamics of incorporation. For example, at certain pressure and temperature, the incorporation of CO2 molecules is preferred compared to CH4 molecules, which can be utilized for the separation of shale gas, biogas or the capture of CO2 from flue gas. In order to improve the separation process, fundamental understanding of the formation kinetics of the mixed gas hydrates on a molecular level is crucial.

2. Setup and Measurements

Here we present an experimental study on the formation kinetics of the formation of mixed CO2/CH4 gas hydrates. The experimental setup allows for the in situ monitoring of the composition of the gas phase as well as the hydrate phase during hydrate formation. The influence of initial gas composition, temperature and pressure on the evolution of the composition in the gas and in the hydrate phase is analyzed.

3. Conclusions

With our study, we aim to contribute further inside into the formation kinetics of mixed gas hydrates.

Acknowledgement

The project leading to this contribution has received funding from the European Union's Horizon 2020 research and innovation programme under ERC Starting Grant agreement No. 637654 (Inhomogeneities).

Separation of methycyclohexane – toluene mixture in the presence of ionic liquids

Elena Graczová*, Dávid Molnár, Pavol Steltenpohl

Institute of Chemical and Environmental Engineering, Faculty of Chemical and Food Technology, Slovak University of Technology in Bratislava, Radlinského 9, 812 37 Bratislava, Slovakia
elena.graczova@stuba.sk

1. Introduction

Modern chemical research is focused on the use of alternative, green, solvents as the traditional ones show numerous adverse properties including human health risk, volatility and flammability. Moreover, stringent legal requirements adopted recently oblige chemical and pharmaceutical companies to re-evaluate and adapt existing processes.

Since the 90th, there is an enormous increase in the number of studies regarding application of ionic liquids (ILs). ILs are a new type of solvents, often denoted as green solvents. They possess outstanding physical-chemical properties; they are liquid in a large region of temperatures, non-flammable, chemically and thermally stable. They act as liquid salts and due to their negligible vapor pressure, ILs are environment friendly and relatively easy to be regenerated [1].

Elevated polarity of ILs influences the properties of mixtures to be separated; in homogeneous systems it affects relative volatility of components of the original mixture, in case of heterogeneous systems, ILs polarity influences the components solubility and selectivity towards the extracted component. Hence, there is potential of ILs use in the separation of azeotropic and close boiling point mixtures, e.g. in extraction distillation and liquid phase extraction [2].

ILs are considered substitutes for traditional organic solvents in extraction of aromatics from their mixtures with aliphatic hydrocarbons. Thanks to their high selectivity, ILs can be used to separate aromatics by liquid extraction from mixtures containing less than 20 mass % of aromatics [1].

2. Methods

Aim of this work was to propose the process of **separation for methylcyclohexane–toluene model mixture in the presence of ionic liquid** (IL). Production line was composed of a counter-current liquid-phase extraction column coupled with single effect evaporator for extraction solvent regeneration and distillation column used to purify toluene. Mathematical models of individual devices were based on material and enthalpy balances taking into account phase equilibrium, too. Organic part of the equipment model simulation was energetic analysis of this complex systems including heat integration. Calculations were carried out partly in ASPEN+ simulation software and partly employing proprietary programs elaborated in Matlab.

3. Results and discussion

In the work, three ionic liquids (1-ethyl-3-methylimidazolium bis trifluoromethylsulfonyl imide ([Emim][NTf_2]); 1-hexyl-3-methylimidazolium tetracyanoborate ([Hmim][TCB]) and 1-butyl-3-methylimidazolium tetracyanoborate ([Bmim][TCB])) were used.

Based on experimental and calculated LLE data [3, and our experiment], capacities and selectivities of individual solvents were evaluated. Selectivities of [Bmim][TCB] and [Hmim][TCB] ILs were comparable, both ILs reached high capacity value (k_B > 1,2). [Emim][NTf_2] exhibited the lowest selectivity and capacity values amongst the ILs studied.

The input parameters of the extractor design calculations were the composition of the feed (methylcyclohexane–toluene mixture containing 10 mole % of toluene) and the extraction solvent composition (containing 99 % of IL). The required purity of the raffinate was maximum 0,5 mole % of toluene in the raffinate. The desired purity of toluene in the bottom product of the distillation column was 99,8 %.

The yield of methylcyclohexane in raffinate (99,98 %) was reached regardless the IL used. Assuming yield of toluene in the bottom product of distillation column, the values ranged from 95,50 % (for [Emim][NTf_2]) to 95,92 % (in case of [Hmim][TCB].

Solvent-to-produced methylcyclohexane mass ratio values were as follows: the lowest value (2,54 kg/kg) was obtained when [Hmim][TCB] was used as extraction solvent. In case of [Bmim][TCB] the value was somehow higher (2.69 kg/kg) and the highest value (9,38 kg/kg), i.e. the largest amount of solvent necessary for the model mixture separation was obtained in case of [Emim][NTf_2].

The energetic analysis of the process has shown that the largest heat demand was associated with evaporator operation, where almost 10 times more heat was consumed compared to that in the distillation column reboiler. The highest cooling demand was observed in cooler of the recirculated ionic liquid.

Total energy consumption for heating and cooling of the individual devices was comparable for simulations assuming [Bmim][TCB] and [Hmim][TCB] as extraction solvents (1,01 MJ and 1,05 MJ per kg of methylcyclohexane produced). Use of [Emim][NTf_2] ionic liquid for this purpose was connected with more than two-times higher heat and cooling demand.

The last part of the design was the thermal integration of the process. It was found that proper heat integration allows up to 72 % reduction of the overall energy demand.

4. Conclusions

Energetic analysis has clearly shown suitability of both [Bmim][TCB] and [Hmim][TCB] ionic liquids for their use in methylcyclohexane–toluene mixture separation.

References [Calibri 10]

[1] G.W. Meindersma, A.B. de Haan, Chem. Engineering research and design 86 (2008) 745–752.

[2] J.P. Gutiérrez, G.W Meindersma,., A.B & de Haan, Industrial & Engineering Chemistry Research 51, (2012) 1518–11529.

[3] J.P. Gutierrez, W. Meindersma, A.B. de Haan, J. Chem. Thermodynamics 43 (2011) 1672–1677.

Acknowledgments: This work was supported by Agency APVV (APVV-0858-12 and APVV APVV-0232-18).

ECCE12
The 12th EUROPEAN CONGRESS OF CHEMICAL ENGINEERING
Florence 15-19 September 2019

Crystallization fundamentals and industrial processes

Intensified stereoselective secondary nucleation in solid state deracemization via microwave-assisted temperature cycles

Fabio Cameli[1], Christos Xiouras[1,2], Georgios D. Stefanidis[1]

1 Process Engineering for Sustainable Systems (ProcESS), Department of Chemical Engineering KU Leuven, Celestijnenlaan 200F, 3001 Leuven, Belgium

2 Crystallization Technology Unit (CTU), Janssen Pharmaceutical Companies of Johnson & Johnson, Janssen Research & Development, Tournhoutseweg 30, 2340, Beerse, Belgium

** georgios.stefanidis@kuleuven.be*

Highlights

- The high supersaturation ratios attained through the sharp thermal cycles performed in a microwave set-up favor the occurrence of secondary nucleation.
- Enantioselective secondary nucleation greatly affects deracemization rate in temperature cycling-induced deracemization.

1. Introduction

The need for single enantiomers is becoming central in the pharmaceutical and fine chemical industry. To this direction, various methods have been designed to produce single handed compounds, either by asymmetric synthesis or by downstream separation of a racemic mixture [1]. The latter approach has proved more efficient in terms of industrial feasibility, as cost effective and established separation techniques, such as crystallization processes (in the framework of deracemization methods) allow for high productivity of the target compound.

Among the most promising solid-state deracemization techniques, substantial attention has been lately given to temperature cycling-induced deracemization. This technique is based on thermal fluctuations, which induce partial dissolution and subsequent crystallization of a racemic suspension, whose liquid phase is maintained in a chemical equilibrium by a catalyzed racemization reaction [2].

As the process time of this kind of techniques is intrinsically long, cycle duration can be significantly reduced by efficient heating and fast cooling which can be easily performed, for example, in a microwave apparatus [3]. On the other hand, the high supersaturation levels achieved upon cooling are likely to result in the generation of secondary nuclei. Up to date, the occurrence of secondary nucleation as main pathway for the depletion of the solute supersaturation has been regarded as detrimental for deracemization due to the expected racemic nature of the produced crystals. However, a thorough evaluation of the handedness of the generated particles has not been performed yet, therefore this study aims at establishing the role of secondary nucleation in the framework of temperature cycling-induced deracemization and the connection between the magnitude of secondary nucleation and deracemization rate.

2. Methods

A chiral suspension of conglomerate crystals of 2-isopropyl-3-hydroxy-3-phenylisoindolin-1-one in toluene with catalytic amount of 1,8-diazabicyclo[5.4.0]undec-7-ene (DBU) was subjected to temperature cycles in a monomode microwave reactor capable of attaining rapid thermal cycles in which dissolution and crystallization phases can be run isothermally at the two temperature limits of the sweeps. Thus, the extreme operating windows employed in this study allow for investigation into the main factors affecting the occurrence of secondary nucleation which are namely:

- Solute supersaturation ratio
- Suspension density
- Stirring rate

3. Results and discussion

The sharp temperature cycles performed in the microwave apparatus induce high solute supersaturation ratios that are responsible for the generation of secondary nuclei during the low temperature period. The deracemization rate is positively affected by the increase in supersaturation up to a certain threshold, beyond which competition between stereoselective and non-stereoselective secondary nucleation hinders the rate of the process. On the other hand, increasing suspension density intensifies the stereoselective production of new particles leading to higher deracemization rate per unit mass. Lastly, vigorous stirring can deliver extensive generation of secondary nuclei that contribute to higher specific surface area of the overall crystals population (Figure 1a). The chirality of the new particles is seemingly influenced by the parent crystals in an autocatalytic manner resulting in enhanced deracemization as displayed in Figure 1b.

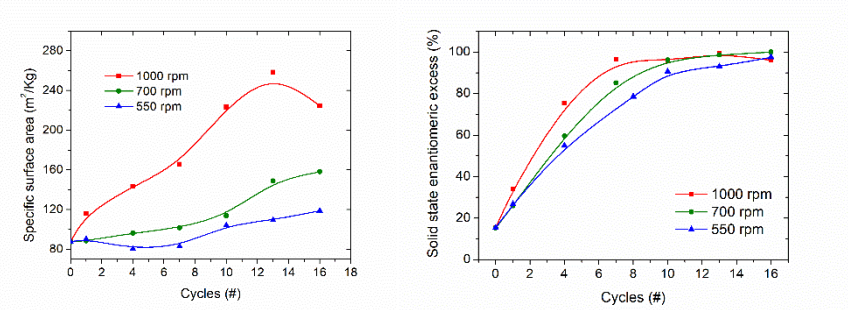

Figure 1. (a) Specific surface area and (b) enantiomeric excess trends of the particles obtained from experiments run under the same thermal profile but with different agitation conditions (in legend).

4. Conclusions

Enantioselective secondary nucleation plays a crucial role in solid-state deracemization via temperature cycles under intensified running conditions attainable within a microwave set-up. This physical phenomenon is greatly affected by operating parameters such as solute supersaturation, suspension density and agitation rate. Therefore, by optimizing these factors the total process time can be significantly enhanced.

References

[1] Lorenz, H. and Seidel-Morgenstern, A., Angew. Chem. Int. Ed., 2014, 53, 1218 – 1250.
[2] K. Suwannasang, A. E. Flood, C. Rougeot, and G. Coquerel. Cryst. Growth Des. 2013, 13, 3498−3504.
[3] F. Cameli, C. Xiouras, and G. D. Stefanidis. CrystEngComm, 2018, 20, 2897.

ECCE12
The 12th EUROPEAN CONGRESS OF CHEMICAL ENGINEERING
Florence 15-19 September 2019

Solketal purification by Supercritical Fluid Simulated Moving Bed technology

Pedro M. Walgode, Rui P. V. Faria, Alírio E. Rodrigues

LA LSRE-LCM, Department of Chemical Engineering - FEUP – University of Porto
*Rua Dr. Roberto Frias, s.n., 4200-465 Porto, Portugal *Corresponding author: pwalgode@fe.up.pt*

Highlights

- Adsorption experiments using HBEA-25 as adsorbent and $ScCO_2$ as eluent.
- k_{ads}, Q_{sat}, k_L estimated using acetone, solketal and water pulse perturbations data.
- Water and solketal separation using a four zones SF-TMB.
- Solketal productivity of 8 kg/L·day at 150 bar, 353 K and 99% purity outlet streams.

1. Introduction

Increasing world's biodiesel production is leading to the accumulation of crude glycerol, a reaction byproduct with almost no economic value. A glycerol valorization route is reacting it with acetone over an acid catalyst, yielding water and 2,2-dimethyl-1,3-dioxolane-4-methanol (solketal) with almost full selectivity. Solketal is a high added value product and is considered a green fuel additive[1]. Solketal industrial production is not yet economic viable, and despite the scientific community efforts, almost no work was found concerning solketal separation process. In this work, supercritical CO_2 ($ScCO_2$) is proposed as an efficient and environmental friendly separation eluent for solketal separation process from water and unreacted acetone, to overcome equilibrium and mass transfer problems. $ScCO_2$ is cheap, safe, nontoxic, nonflammable, its critical point is readily attainable, has well-established industrial use and it is easily separated and recycled by depressurizing the system below CO_2 critical point[2-4]. The aim of this work is to design a supercritical fluid simulated moving bed (SF-SMB) to separate solketal from water, using a high water affinity HBEA-25 zeolite as adsorbent. For that, a supercritical fluid true moving bed supercritical (SF-TMB) was simulated using data obtained by single solute pulse experiments with $ScCO_2$ as eluent in a supercritical chromatographic fixed bed column (SF-FBC), under different operating conditions.

2. Methods

Mono component pulse perturbations at the inlet concentration were performed using $ScCO_2$ as eluent and zeolite HBEA-25 (from Süd-chemie, SiO_2/Al_2O_3 molar ratio of 25:75, particle diameters between 600 and 1180 nm) as adsorbent in a SF-FBC with dimensions 4 x 125 mm, bulk porosity of 0.438, particle porosity of 0.326 and total volumetric flow of 2 mL min^{-1}. A SF-FBC model was developed in gPROMS software assuming: plug flow model with axial dispersion and isothermal process and the adsorption is described by Langmuir competitive equilibrium isotherm model. The model was used to adjust the experimental pulse data, allowing the estimation of the Langmuir adsorption isotherm parameters, k_{ads} and Q_{sat}, and overall mass transfer coefficients, k_L. SF-TMB process was designed and optimized through numerical simulations using the data obtained and estimated for SF-FBC.

3. Results and discussion

Water solketal and acetone mass transfer coefficients and the adsorption isotherm parameters were estimated three different conditions: 150 bar and 313 K; 150 bar and 353 K; and 200 bar and 313 K (Figure 1 a) to c)). As expected, water presented the highest retention times, independently of the conditions tested. The SF-FBC model was able to accurately describe the experimental results obtained for the water, solketal and acetone pulse experiments.

A four zone SF-TMB was optimized through a simulation study for the three operating conditions, using columns similar to SF-FBC (except for the length, which was set to 37.5 cm) and considering the following parameters: safety factor of 0.4, solid flow velocity of 3.75 cm min^{-1}, raffinate and extract purity above 99 %. The best separation performance was achieved operating at 150 bar and 353 K (Figure 1 d)). A solketal productivity of 8.4 $kg/L_{Ads}{\cdot}d$ and an eluent consumption of 99.9 L_{Des}/kg_{solk} were estimated.

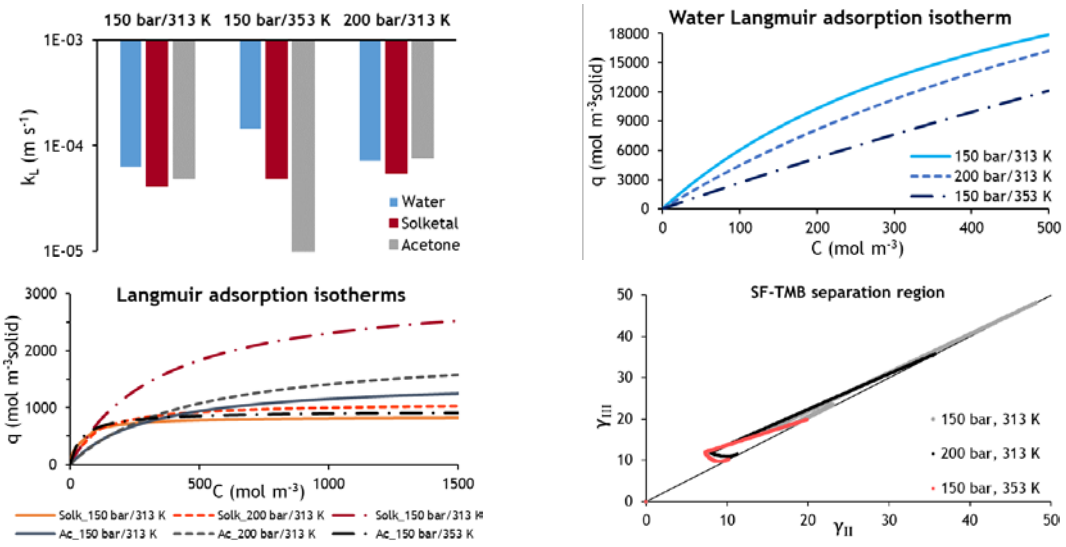

Figure 1 – a) Water, solketal and acetone estimated k_L. **b)** Water, **c)** solketal and acetone Langmuir equilibrium adsorption isotherms using the estimated K_{ads}, Q_{sat} at the three operating conditions, **d)** SF-TMB separation regions.

4. Conclusions

Through the present work it was possible to estimate k_L, K_{ads} and Q_{sat} for water solketal and acetone using SF-FBC pulse experiments. A four-zone SF-TMB unit was simulated, and the optimum operating conditions were found at 150 bar and 353 K. The zeolite HBEA-25 is also a strong acid catalyst for glycerol ketalization into solketal and its dehydration properties may overcome reaction equilibrium limitations by adsorbing water from the reaction media, allowing a possible future process intensification with reaction and separation in the same unit, such as a reactive SF-SMB.

References

[1]Nanda, M. R.; Zhang, Y.; Yuan, Z.; Qin, W.; Ghaziaskar, H. S.; Xu, C. C., *Renewable and Sustainable Energy Reviews* **2016,** *56*, 1022-1031.

[2]Majewski, W.; Valery, E.; Ludemann-Hombourger, O., *Journal of liquid chromatography & related technologies* **2005,** *28* (7-8), 1233-1252.

[3]dos Santos, B. A. V. Process Intensification in the Synthesis of the Green Chemical Dimethyl Carbonate. Department of Chemical Engineering, Faculty of Engineering, University of Porto, Portugal, 2014.

[4]Puiggené, J.; Larrayoz, M.; Recasens, F., *Chemical Engineering Science* **1997,** *52* (2), 195-212.

ECCE12
The 12th EUROPEAN CONGRESS OF CHEMICAL ENGINEERING
Florence 15-19 September 2019

A comparison of different amino acid solutions for CO_2 capture using a membrane contactor

Vida Sang Sefidi[1], Inès Winand[1], Patricia Luis[1]

[1] *Materials & Process Engineering (IMMC-IMAP), UCLouvain, Place Sainte Barbe 2, 1348 Louvain-la-Neuve, Belgium*

**Corresponding author: vida.sangsefidi@uclouvain.be*

Highlights

- Comparison of performance of five different amino acids with membrane contactor.
- Similar performance between arginine and NaOH solvents.
- Better performance of amino acid salts than amino acids alone.

1. Introduction

The growing concern about the global warming has triggered the public attention to the main greenhouse gas contributor namely carbon dioxide (CO_2) [1]. The most extended post combustion CO_2 capture technologies rely on absorption columns. Alkanolamines are typical solvents due to low cost and high absorption rates [2]. However, amine-based systems have high energy requirements for solvent regeneration and large solvent losses due to amine vaporization [3]. Lower energy consumption would be achievable using a different kind of technology: membrane contactors, which also allow an ease control of operating conditions, large contact area and scale-up flexibility [4]. In addition, the use of novel absorption solvents have been proposed in membrane contactors. For example, solvents with similar functionality as amines, such as amino acid salts (AAS) [5,6]. AAS are positively characterized by their high surface tension, non-volatility , etc., and their kinetics is defined by zwitterion reaction [7]. While an amino acid is initially inactive in the solution, it can be activated by addition of sodium hydroxide (NaOH), potassium hydroxide (KOH) and sodium carbonate (Na_2CO_3) [8,9].

In this work, five different amino acids have been studied for CO_2 capture. The CO_2 capture feasibility is studied in the membrane contactor using the amino acid salts solutions as the solvent, activated with NaOH. The process performance using the amino acids was compared to that using only NaOH in solution.

2. Methods

Serine (Alfa Aesar, >95%), methionine (Sigma Aldrich,>98%), Arginine(Sigma Aldrich,99%), 6-aminohexanoic acid (Alfa Aesar,99%) and Valine (Acros Organics, 99%) and sodium hydroxide (VWR,>98 %) were acquired and used without further purification. All amino acids were neutralized with an equilibrium molar amount of sodium hydroxide.

A hollow fiber membrane contactor (MiniModule 1x5.5 G543, liquid-Cel, Membrane GmbH, Germany) was used for the chemical absorption process. The inlet and outlet volume percentage

of CO_2 was measured via the CO_2 gas analyzer (Rosemount™ X-stream enhanced XEGK countinuous gas analyzer, Emerson, Germany).

3. Results and discussion

The overall mass transfer coefficient (K_{ov}) and process performance using amino acids and amino acid salts were studied. All amino acids saturated shortly after the start of experiments except arginine. The results could be explained since acid dissociation constant (pKa) for some amino acids is low. However, similar performance of arginine to NaOH is related to their comparable high pKa values.

The amino acid absorption improves after the activation with a base. As all amino acid have a primary amine group for the CO_2 capture, it is expected to observe a similar performance when they are activated. However, not all amino acids show same absorption rate for CO_2 capture, which is related to the difference in structure of amino acids. In addition, the absorption rate is higher when an amino acid is activated with a base that has higher pKa. A stronger base has higher capability of activation of amino acids.

4. Conclusions

This work uses a membrane contactor with amino acid salts for chemical absorption. The performance of different amino acids was compared to NaOH solution based on the mass transfer coefficient. Arginine performed similar to NaOH in the non-active form suggesting its direct application for CO_2 capture.

References

[1] A. S. Brierley and M. J. Kingsford, *Current Biology*. 2009.

[2] P. Luis, *Desalination*. 2016.

[3] E. I. Koytsoumpa, C. Bergins, and E. Kakaras, *J. Supercrit. Fluids*, vol. 132, pp. 3–16, Feb. 2018.

[4] P. Luis and B. Van Der Bruggen, *Greenhouse Gases: Science and Technology*. 2013.

[5] F. Weisler, *Ultrapure Water*, no. June, pp. 27–31, 1996.

[6] J. Van Holst, J. P. M. Niederer, G. F. Versteeg, and F. Science, vol. 31, no. 5. 2012.

[7] S. Shen, X. Feng, R. Zhao, U. K. Ghosh, and A. Chen, *Chem. Eng. J.*, vol. 222, pp. 478–487, 2013.

[8] J. van Holst, G. F. Versteeg, D. W. F. Brilman, and J. A. Hogendoorn, *Chem. Eng. Sci.*, vol. 64, no. 1, pp. 59–68, 2009.

[9] J. Van Holst, S. R. A. Kersten, and K. J. A. Hogendoorn, *J. Chem. Eng. Data*, vol. 53, no. 6.

ECCE12
The 12th EUROPEAN CONGRESS OF CHEMICAL ENGINEERING
Florence 15-19 September 2019

Synthesis and Gas Adsorption Properties of Hypercrosslinked Styrene-based Polymer for CO_2 capture

Kateřina Setničková[1]*, Karel Jeřábek[1], Tomáš Strašák[1], Petr Uchytil[1]

1 Institute of Chemical Process Fundamentals of the CAS, v. v. i., Department of Bioorganic Compounds and Nanocomposites, Rozvojová 2/135, CZ-165 02 Prague 6 – Suchdol, Czech Republic

**Corresponding author: setnickova@icpf.cas.cz*

Highlights

- Hypercrosslinked styrene-divinylbenzene porous material have been prepared.
- The resulting porous network exhibited the high surface area around 800 m^2/g.
- The CO_2/H_2, CO_2/N_2 selectivity of the polymer were 22 and 5 at 298 K, respectively.
- Promising material for mixed matrix membranes preparation usable to gas separation.

1. Introduction

The continuous and increasing release of carbon dioxide to the atmosphere due to human activities, being damaging to the environment and the earth, has initiated considerable interest in the development of new materials and technologies for CO_2 capture. To date, a cheap alternative solution to effective CO_2 capture has been developed by design and synthesis of microporous organic polymers (MOPs) categorized into four classes according to the types of organic reactions and the chemical structures [1]: polymers of intrinsic microporosity (PIMs), hypercrosslinked polymers (HCPs), conjugated microporous polymers (CMPs), and covalent organic frameworks (COFs). These organic porous materials generally possess low skeletal density, in which the precise control over the material's chemical composition and textural properties can lead to a significant enhancement in gas storage. In this study, we report on the synthesis of hypercrosslinked styrene-divinylbenzene microporous material and its application for CO_2 capture, gas separation.

2. Methods

The gas adsorption ability in new materials was determined using an apparatus based on the volumetric method. Simplified, the weighted amount of sample was placed in the adsorption chamber and evacuated. Then the chamber is filled with a gas at a certain pressure, the pressure value inside apparatus was monitored by computer. The pressure decrease corresponded to the adsorption of gas in the studied material.

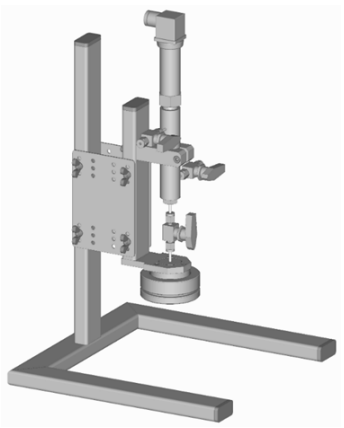

Figure 1. Design of the experimental apparatus for gas adsorption capacity measurement in materials.

After reaching the equilibrium the pressure is subtracted and used to determination of absorbed amount of gas in material. The constant temperature of the whole system during the absorption experiment was provided by a heated box.

3. Results and discussion

The results of adsorption capacities measurement of synthetized hypercrosslinked styrene-divinylbenzene microporous polymer for four tested gases is depicted in Fig.2.

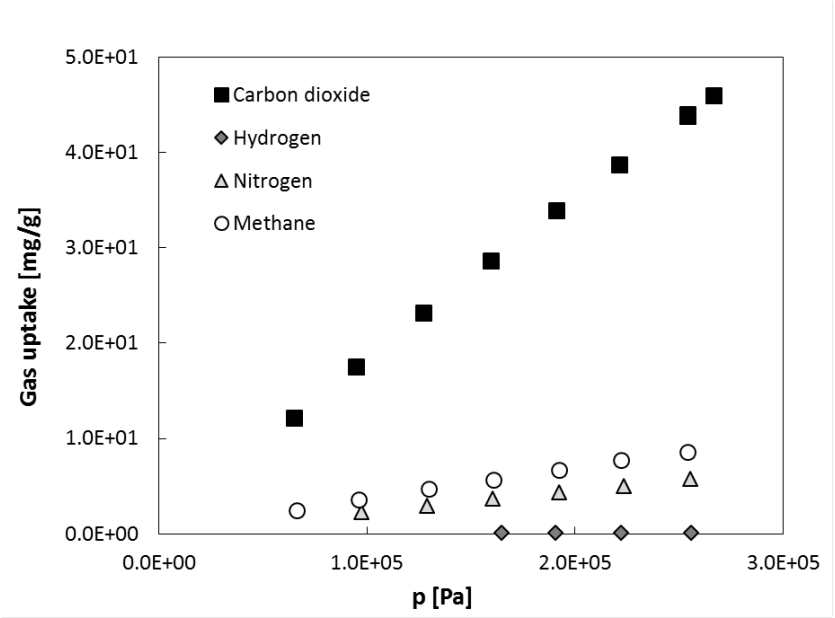

Figure 2. Gas adsorption isotherms in tested material.

4. Conclusions

The synthesis, characterization, and the CO_2 adsorption performance of new hypercrosslinked styrene-divinylbenzene based polymer exhibiting a high apparent surface area and very good sorption properties is reported in this study.

References [Calibri 10]

[1] YL. Luo, BE. Tan, Porous Materials for Carbon Dioxide Capture Book Series: Green Chemistry and Sustainable Technology (2014) 143-180.
[2] P. Veverka, K. Jeřábek, React. Funct. Polym. 41 (1999) 21–25.

ECCE12
The 12th EUROPEAN CONGRESS OF CHEMICAL ENGINEERING
Florence 15-19 September 2019

Process Intensification of the Hydrolysis of Cellulosic Fiber Wastes Using Membrane Bioreactors for Catalyst and Enhancer Recycle

Surya N. Jampana[1], Bandaru V. Ramarao*,[2]

1, 2 Department of Bioprocess Engineering, State University of New York ESF, SYRACUSE NY 13210

**Corresponding author: bvramara@esf.edu*

Highlights

- Recycled paper fibers are enzymatically hydrolyzed using cellulases.
- Surfactants are necessary to combat inhibition activity of mineral particulates.
- Better kinetics and yields are achieved using membrane separation in an MBR.
- Process modeling enables optimization of the operation of the MBR.

1. Introduction

Mixed office waste paper (MOW) and other grades of fine and packaging paper are widely reused to produce recycled tissue and packaging paper. Recycled pulp is made by dispersing the wastepaper in water and removing the ink and mineral particles by air flotation. However, fiber fragments also float and are rejected in the waste streams and up to 60% of such wastes can be such cellulosic particles. Furthermore, as fibers are recycled multiple times, they become brittle and fragment during pulp preparation. The fragments are a hindrance to paper manufacture. They clog the paper mats and wires during dewatering and drying, significantly slowing down the paper machine reducing the production rate. Modern paper machines are operated at very high speeds (in excess of 60 mph) and any hindrance can have significant impact on profitability. Recycled pulp fines also reduce bonding within the paper sheets and reduce the strength and quality of the final product. However, the rejection of such pulp fines into the waste stream increases the waste volume and its organic load imposing large disposal costs to the paper mills, negatively impacting the environment and the sustainability footprint of the paper products. Reduction of this waste stream through its utilization presents a great opportunity.

In recycled paper mills, these waste fines are usually rejected into the rejects stream which is eventually dewatered and the solids landfilled. However, there is increasing pressure on landfilling due to environmental degradation and increasing costs of transportation. Therefore, any effort to reduce the volume of these solid wastes can be economically attractive with a positive impact on the environment. Waste fibers (WF) represents an attractive biomass due to its cellulosic fibers content and the fact that its structure is feasible for bioconversion without pretreatment. Waste Fiber composition is diverse depending on the substrate and pulping and paper making processes but is mostly composed with 40-65% of sugars, 10-40% of ash and low portion of other materials such as lignin, plastics, or synthetic fibers [1-3]. These waste fibers are advantageous because the biomass particle size has already been reduced to the micrometer range (in fiber diameters) and the fact that the bulk of the lignin has been removed in the wood pulping process itself. However, high ash content in the WF inhibits the ability to convert its carbohydrates and reduces the productivity of processes. The heterogeneity of paper sludge results in low product concentration by limitation of solid loading]. Among the fillers, calcium carbonate ($CaCO_3$) is reported as the strongest inhibitor reducing enzymatic activity effecting on hydrolysis yield by pH drift. The inhibitory effect of $CaCO_3$ could also be potentially related to non-productive enzyme binding. The affinity of $CaCO_3$ is much higher towards enzyme more than the affinity of clay, and precipitated calcium carbonate (PCC) shows much higher binding affinity than ground calcium carbonate (GCC)].

2. Methods

Samples of waste fibers were procured from a recycled linerboard-manufacturing mill (RF). A synthetic model of this waste rejects was also prepared in the laboratory by grinding a sample of unbleached softwood kraft pulp (UKP) fibers. This was mixed with different quantities of clay and precipitated calcium carbonate. The hydrolysis was carried out in hydrolysis flasks placed in a shaking incubator (Reciprocal Shaking Bath 51221080, Precision Scientific Co., Denver CO) and hydrolyzed at 50°C up to 72 h at 130 rpm. The cellulase enzyme used was commercially available Cellic CTec2 (Novozymes USA) in 5% consistency using 0.05M sodium acetate buffer (pH 5). The hydrolyzate was removed after fixed time and samples withdrawn and analyzed with HPLC or NMR. For the calcium ion solution test, the PCC was dissolved in the prepared sodium acetate buffer and acetic acid was added to bring the pH to 5 (SU). The solid residue was filtered on Whatman filter paper #1 and the filtered solution was supplied for UKP hydrolysis to measure the effect of dissolved calcium ions. Tween 80 (Amresco®) was selected for non-ionic surfactant test for this study.

A continuous membrane bioreactor configuration was set up and used for experiments.

3. Results and discussion

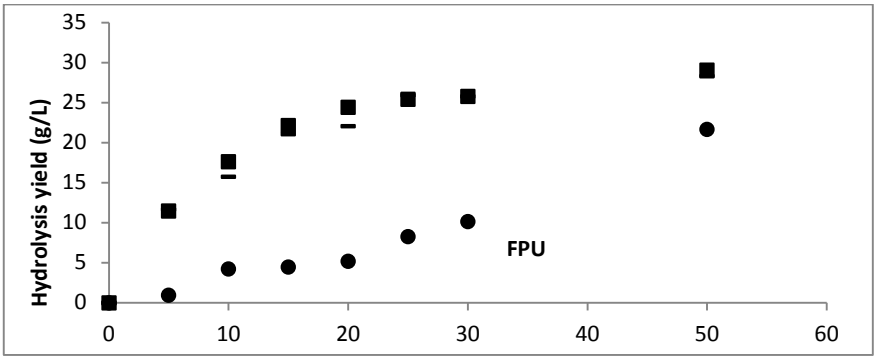

Figure 1. Hydrolysis of fibers as a function of enzyme concentration in FPU. Effect of surfactant.

The continuous separation of sugars as hydrolysis products from the reaction vessel allows faster kinetics and a reduction in the size of the reactors. Optimization of the reaction conditions by kinetic modeling is currently underway.

4. Conclusions

A membrane bioreactor is able to improve yields and kinetics of the enzymatic hydrolysis and also enable enzyme and promoter recycling, contributing to effectiveness and economical production costs of the process.

References

[1] B. C. Min, S. N. Jampana, C. M. Thomas, B. V. Ramarao. 'Study of buffer substitution using inhibitory compound in Enzymatic hydrolysis of paper mill waste fines.' J Korea TAPPI, 50, 2, 77-82 (2018).

[2] B C Min, B. V. Ramarao. 'Mechanisms of the inhibition of enzymatic hydrolysis of waste pulp fibers,' Bioprocess and Biosystems Engineering, 40, 6, 799-806. (2017).

[3] BC Min, BV Bhayani, VS Jampana, BV Ramarao. 'Enhancement of the enzymatic hydrolysis of fines from recycled paper mill waste rejects,' Bioresources and Bioprocessing 2 (1), 1, (2016).

ECCE12
The 12th EUROPEAN CONGRESS OF CHEMICAL ENGINEERING
Florence 15-19 September 2019

Improving the simulated moving bed separation of oleanolic and ursolic acids with a C30 stationary phase

I.S. Azenha[1], J.P.S. Aniceto[1,*], A. Mendes[2], C.M. Silva[1]

1 CICECO, Department of Chemistry, University of Aveiro, 3810-193 Aveiro, Portugal; 2 LEPABE-Faculdade de Engenharia, Universidade do Porto, 4200-465 Porto, Portugal

**joseaniceto@ua.pt*

Highlights

- C30 column and methanol/water were best phases to separate oleanolic and ursolic acids.
- Equil. & mass transfer constants of pure compounds were validated for binary mixture.
- An SMB using C30 columns is capable of separating the two acids with purities of 99.9 %.
- This is a significant improvement over previous results obtained with C18 columns.

1. Introduction

Eucalyptus globulus is a predominant species in the Portuguese forest [1] and a vital resource for the pulp and paper industry. The bark residues are usually burned for energy production without any further valorization. Recently, the bark has been identified as a source of triterpenic acids (TTAs) such as oleanolic and ursolic acids [2]. These compounds are known to possess a wide spectrum of bioactivities, including anti-oxidative, antitumoral, anti-inflammatory, anti-hyperlipidemic, and anti-microbial effects [3]. Thus, under the scope of the biorefinery concept, *E. globulus* bark is a potential candidate to extract high-value compounds such as TTAs. However, their separation after extraction is challenging as oleanolic and ursolic acids are two structurally related isomers and occur simultaneously in the same natural matrix. Simulated moving bed (SMB) chromatography is a continuous adsorption technique, which appears as an efficient alternative to batch elution chromatography. The SMB continuous countercurrent mode of operation maximizes the mass transfer driving force, providing improved productivity and reduced solvent consumption [4]. Thus, an SMB process may be a potential candidate for TTAs separation.

2. Methods

A series of impulse experiments were conducted to select appropriate mobile phases for the separation of oleanolic and ursolic acids. Experimental breakthrough curves were measured in a custom laboratorial installation. Breakthrough of pure components were conducted to determine equilibrium and mass transport parameters, by fitting a chromatographic model to the experimental data. Parameters were validated through the successful prediction of breakthrough assays of binary mixtures.

3. Results and discussion

From a series of several impulse tests methanol/water 95/5 (%, v/v) emerged as the most favorable mobile phase to conduct their continuous separation by SMB providing a value of selectivity of 1.08. The C30 column demonstrated a remarkable separation capacity for the triterpenic acids, enabling

simultaneously higher selectivities and faster analysis times, when compared with previous results using a C18 packing material and the same mobile phase [5]. Equilibrium and mass transport parameters obtained from breakthrough experiments of pure acids (and validated for a binary mixture) were used to design the SMB separation of a representative mixture of oleanolic and ursolic acids from a natural extract of *E. globulus*. A classical SMB scheme was simulated and optimized using a Design of Experiments – Response Surface Methodology. Purity requirements were defined while the productivity was maximized. Rigorous phenomenological simulation results, of which the concentration profile in the SMB at cyclic steady state is presented in Figure 1, demonstrated that the SMB is able to attain purities levels of 99.9 %, for both extract and raffinate outlets, and productivities of 1.705 kg/($m^3_{adsorbent}$ day) with 2-2-2-2 configuration. This is a significant achievement as previous results with a C18 stationary phase showed that purities of 99.4 % and 99.1 % for ursolic and oleanolic acids, respectively, were achievable at the expense of using three columns per section (3-3-3-3), and consequently at the expense of extremely low productivities [5]. The work presented here with the C30 column represents important improvements towards the successful chromatographic separation of these triterpenic acids.

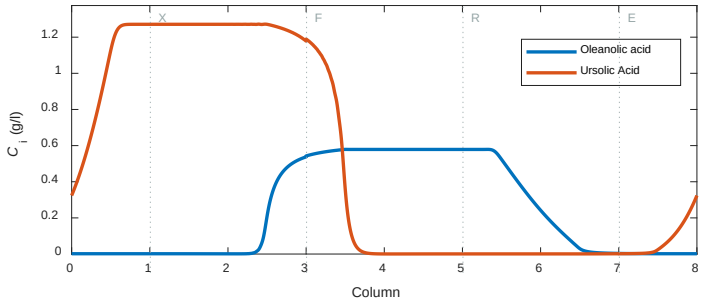

Figure 1. Simulation results of SMB operation at cyclic steady state for the isolation of oleanolic (blue line) from ursolic acid (orange line). E – eluent; F – feed; X – extract; R – raffinate.

4. Conclusions

The separation of oleanolic and ursolic acids by SMB was enhanced by applying C30 columns and a methanol/water 95/5 (%, v/v) mobile phase. The SMB unit with two columns per section, which was optimized combining the design of experiments and response surface methodologies with phenomenological computer simulations, attained purities of 99.9 %. This represents a significant improvement in terms of purity and productivity when compared with previous results obtained with C18 columns, which required a 3-3-3-3 configuration to attain purities of 99.4 %.

Acknowledgements

CICECO (FCT Ref. UID/CTM/50011/2019); Multibiorefinery project (POCI-01-0145-FEDER-016403); LEPABE - POCI-01-0145-FEDER; I.S. Azenha thanks PhD grant SFRH/BD/126509/2016.

References

[1] J.S. Uva, Instituto da Conservação da Natureza e das Florestas (2013) p. 3.
[2] M.M.R. de Melo, E.L.G. Oliveira, A.J.D. Silvestre, C.M. Silva, J. Supercrit. Fluid., 70 (2012), pp. 137-145.
[3] J. Liu, J. Ethnopharmacol. 49 (1995) 57–68.
[4] J.P.S. Aniceto, C.M. Silva, Sep. Purif. Rev., 44 (2013), pp. 41-73.
[5] J.P.S. Aniceto, I.S. Azenha, F.M.J. Domingues, A. Mendes, C.M. Silva, Sep. Purif. Technol. 192 (2018) 401–411.

ECCE12
The 12th EUROPEAN CONGRESS OF CHEMICAL ENGINEERING
Florence 15-19 September 2019

CO_2 solubility on ionic liquid + tetraglyme mixtures.

D. Hospital-Benito*, J. Lemus, R. Santiago, J. Palomar

Chemical Engineering Department. Universidad Autónoma de Madrid. 28049, Madrid, Spain

**Corresponding author: daniel.hospital@uam.es*

Highlights

- Ionic liquids (ILs) with chemical absorption show outstanding results for CO_2 capture application.
- Tetraglyme (TGM) is an effective additive in reducing ILs viscosity that also has a high CO_2 solubility.
- TGM/IL mixtures were found to be suitable for CO_2 capture application.

1. Introduction

The study of carbon dioxide (CO_2) solubility in different composition mixtures of ionic liquid (IL) and tetraglyme solvent (TGM) is interesting for the development of carbon capture and storage technologies [1]. In the present work, it was used four kind of ionic liquids, with different chemical and physical properties, implying different kinetic and thermodynamic results [2]. The ILs used in this study were two with chemical absorption by CO_2, such as [Bmim][Acetate] and [P66614][CNPyr], and two others with physical CO2 absorption, [Bmim][TCM] and [Bmim][$MeSO_4$].

2. Methods

The experiments were carried out using a high pressure termobalance that let us obtain high-pressure solubility of CO_2 in a wide range of TGM/IL mixtures (from 0 to 90 wt% TGM), measured at 303 K and at different pressures, from 1 up to 20 bar. The CO_2 capture performance of all composition mixtures of IL and TGM was evaluated using Aspen Plus commercial process simulator. To model the absorption operation in Aspen Plus using the ILs with chemical absorption by CO_2, a multiscale COSMO-based methodology developed in our group was used to include them into the simulator database. [Bmim][TCM] and [Bmim][$MeSO_4$] are contained in ILAUM database [4] and TGM and its COSMOSAC parameters are already included in Aspen Plus by default. The absorption column was simulated as a packed column using the RAD-FRAC rigorous model in Rate-Based mode. The solvent mass flow needed to achieve a capture rate of 90% was calculated.

3. Results and discussion

Tetraglyme as co-solvent improves the mass transfer kinetics by reducing viscosity and enhances CO_2 physical absorption. Promising TGM/IL mixtures were found using ILs with chemical absorption because of their high CO_2 solubility compared with TGM, so minimum solvent needs can be achieved as can be seen in Figure 1. Otherwise, ILs with physical CO_2 absorption due to their lower CO_2 solubility are useful at high operating pressures so do not seem a good alternative to TGM.

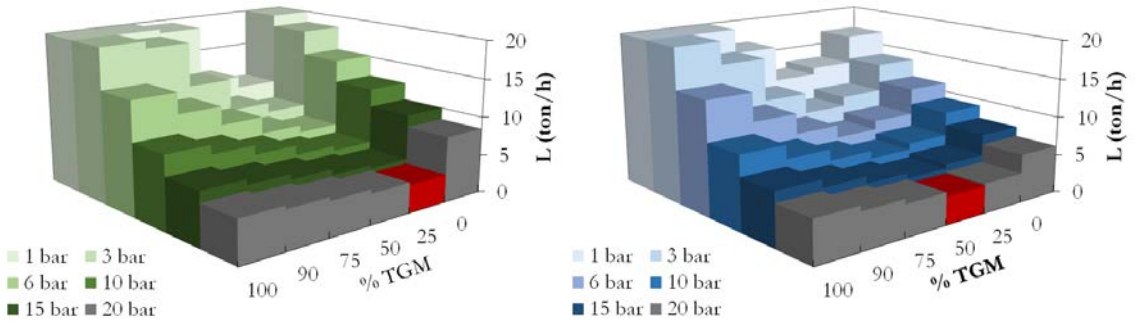

Figure 1. Solvent flow needed to reach a 90% CO2 captured rate by the solvent as a function of the CO2 partial pressure and compositions mixtures IL/TGM calculated by Rate-based RADFRAC model using [P66614][CNPyr] (left) and [Bmim][Acetate] (right).

4. Conclusions

It can be concluded that although ILs with chemical absorption show outstanding results for CO_2 capture application, their relatively high viscosity presents a challenge for the mass transfer properties [3]. In this sense, this work shows that TGM, which has a relatively low vapor pressure at temperatures of interest for these applications, is an effective additive in reducing viscosity of the IL tested, improving drastically the kinetic of the process, without high weakening of the absorption capacity. In the case of ionic liquids with physical absorption, they present low solubility compared with TGM and they have to be used at high operating pressures.

References

[1] (Journal) Amaral M, Crespo EA, Dariva C, Vega LF, Carvalho PJ, Coutinho JAP. High-pressure solubility of CO2 in glymes. Chemical Society Reviews. 2018; 219:120-125.

[2] (Journal) Santiago R, Lemus J, Moreno D, Moya C, Larriba M, Alonso-Morales N, Gilarranz MA, Rodríguez JJ, Palomar J. From kinetics to equilibrium control in CO2 capture columns using Encapsulated Ionic Liquids (ENILs). Chem Eng. J. 2018; 348:661-666.

[3] (Journal) Fillion JJ, Bennett JE, Brennecke JF. The Viscosity and Density of Ionic Liquid + tetraglyme Mixtures and the Effect of Tetraglyme on CO2 Solubility. J. Chem. Eng. Data 2017;62:608−622.

[4] (Journal) Ferro V. R, Moya C, Moreno D, Santiago R, de Riva J, Pedrosa G, Larriba M, Diaz I, Palomar J. Enterprise Ionic Liquids Database (ILUAM) for Use in Aspen ONE Programs Suite with COSMO-Based Property Methods. Ind. Eng. Chem. Res. 2018; 57, 3:980-989.

Absorption of Natural Aromas in a Rotating Packed Bed.

Ilya Lukin[1], Gerhard Schembecker[1]*

1Laboratory of Plant and Process Design TU Dortmund University, Emil-Figge-Strasse 70, D-44227 Dortmund/Germany

**Corresponding author: gerhard.schembecker@tu-dortmund.de*

Highlights

- The faster rotation speed of an RPB increases the absorption efficiency
- Variation of the rotation speed allows flexible throughput at equal efficiency
- RPB can be operated with highly viscous absorbents at a low pressure drop

1. Introduction

An increasing demand for natural aromas enhances the role of a biochemical production as an alternative to the natural feedstock extraction [1]. A combination of in-situ product stripping and absorption in a Rotating Packed Bed (RPB) is a novel potent technique to overcome downstream challenges during the recovery of natural aromas from crude biochemical mixtures (Figure 1).

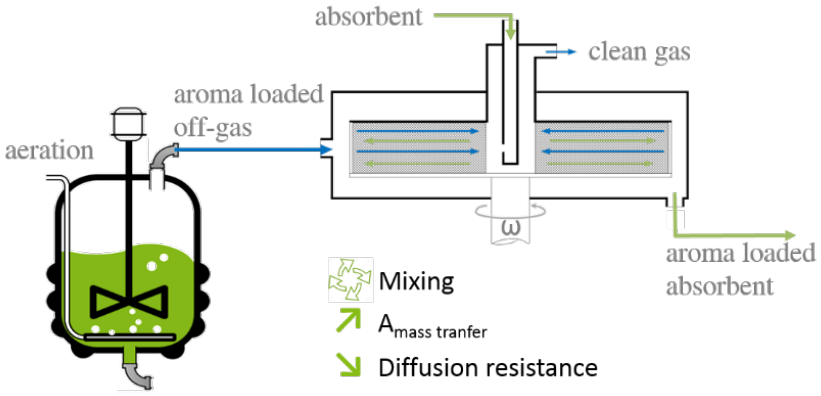

Figure 1: Schematic process of the recovery of natural aromas using Rotating Packed Bed technology

Inside a rotating circular packing of an RPB, the centrifugal force leads to an intensified gas-liquid mixing increasing the mass transfer of a target compound[2-4]. In order to investigate the influence of process parameters on the recovery of aromas, a newly designed small-scale RPB was integrated into a laboratory aroma stripping and absorption plant.

2. Methods

A stripping column was used in order to mimic a bioreactor. Inside the stripping column, the air was loaded with the desired aroma and then brought into contact with the absorbent in the rotating packing of the RPB. The results of gas and liquid phase analytics were used for the calculation of absorption efficiency, pressure drop and mass transfer resistances.

3. Results and discussion

The results show that the absorption efficiency of an aroma compound decreases with the increased gas throughput implicating some mass transfer limitations (Figure 2). Due to the intensified mixing at higher rotation speed the later could be overcome leading to an increased efficiency. Altogether, the variation of the rotation speed enables larger gas loadings at constant absorption efficiencies leading to higher space-time productivity of the recovery process.

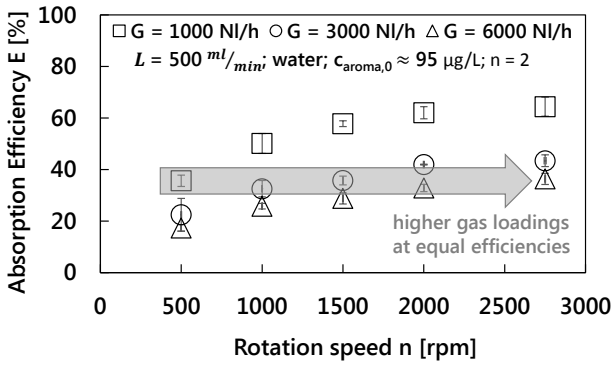

Figure 2: Effect of the rotation speed of an RPB on the absorption efficiency of benzaldehyde in water at varying gas throughputs.

A further efficiency increase is expected when stronger hydrophobic absorbents, e.g. plant oils, are used. The often challenging distribution of highly viscous oils in conventional absorption columns can be assisted by the generated centrifugal field allowing the operation of the RPB at moderate pressure drops (Figure 3) decreasing the process costs.

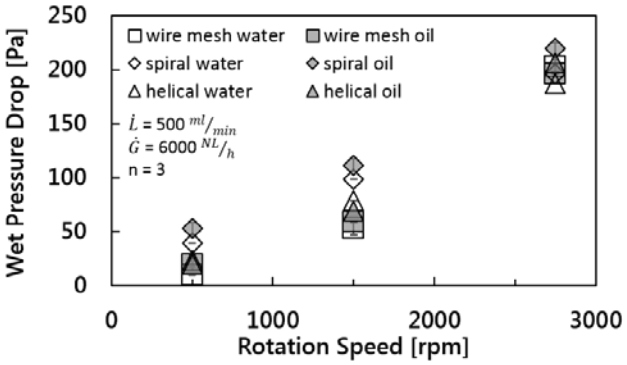

Figure 3: Wet pressure drop of different packings inside an RPB for water and rapeseed oil at varying rotation speed.

4. Conclusions

The use of the centrifugal field inside the packing of a Rotating Packed Bed helps to overcome mass transfer limitations leading to the improvement of the recovery process. Rotation assisted liquid distribution expands the selection of absorbents towards highly viscous plant oils.

References

[1] V.F. Cataldo, J. López, M. Cárcamo, E. Agosin, Appl. Microbiol. Biotechnol. 100 (2016) 5703-5718.
[2] C. Ramshaw, Chem. Eng. (1983) 13-14.
[3] L. Agarwal, V. Pavani, D.P. Rao, N. Kaistha, Ind. Eng. Chem. Res 20 (2010) 10046-10058.
[4] Y.S. Chen, F.Y. Lin, C.C. Lin, C.Y.D. Tai, H.S. Liu, Ind. Eng. Chem. Res. 20 (2006) 6846-6853.

ECCE12
The 12th EUROPEAN CONGRESS OF CHEMICAL ENGINEERING
Florence 15-19 September 2019

An investigation of the controllability of optimal reactive distillation processes

A. Tsatse[1)], S.R.G. Oudenhoven[2)], A. J. B. ten Kate[2)], E. Sorensen[1)*]

1) Department of Chemical Engineering, University College London, Torrington Place, WC1E 7JE London, United Kingdom; 2) Nouryon, Zutphenseweg 10, 7418 AJ Deventer, the Netherlands

** Corresponding author: e.sorensen@ucl.ac.uk*

Highlights

- The reactive distillation column superstructure is solved based on an economic objective function
- The impact of the reaction kinetics on the final process design and associated cost is investigated
- The controllability of the design alternatives is evaluated in the frequency domain
- This work provides a methodology on how to synthesize a reactive distillation process, including its control system

1. Introduction

Over the last few decades, there has been an increasing focus on process intensification in an effort to reduce environmental impact and to improve the economic performance of chemical processing plants. Reactive distillation combines reaction and separation into one single unit, offering significant energy and capital savings as well as improvements in reaction selectivity and yield[1-2]. The combination of the two different phenomena in a single unit, however, makes the design, operation and control of the process more demanding due to the interactions between the reaction and the separation[3]. Although research has shed light on many aspects of reactive distillation, the extension of conventional distillation design techniques to reactive systems is still a challenge and thus, a rigorous method of reactive distillation systems design, which also includes consideration of the controllability of the system, has not yet been fully established[4].

2. Methods

The concept of distillation column superstructures has been successfully applied in the past for the design of distillation columns[5]. In this work, this approach will be extended to consider reactive distillation column superstructures[6] in order to determine structural and operational decisions, including but not limited to, total number of stages, feed stages location, reactive zones, existence of additional units (pre/side/post reactors) etc. Case studies are considered with different kinetic characteristics. The Mixed-Integer Non-Linear Optimization Problem (MINLP) formed aims to minimize the total (capital and operational) cost of the process, subject to constraints such as

maximum number of stages, product purity etc. gPROMS ProcessBuilder is used for the simulation and the optimization due to its rigorous optimization capabilities. The optimal design is then considered in dynamic mode and the controllability indices of the dynamic system are finally generated within the frequency domain in MATLAB in order to investigate the controllability and stability of the optimal design alternatives.

3. Results and discussion

It will be shown how the existence of fast or slow reaction kinetics inside the distillation column impacts on the optimal process design and control. In addition, the difference in the optimal total cost found for the various systems will be evaluated in order to explore how reaction kinetics impact on the total cost of the process and whether this can be a reason to render reactive distillation less economically attractive for systems with certain reaction characteristics. Moreover, the controllability analysis in the frequency domain will demonstrate how fast or slow kinetics impact on the stability and controllability of a process, and how controllability can determine whether a process alternative is selected for further investigation or not.

4. Conclusions

In this work, a Mixed-Integer Non-Linear Optimization Problem (MINLP) is solved, based on the superstructure method, for the synthesis of an economically optimal design of a reactive distillation column given a specific separation duty (target product purity). Different case studies are considered (slow/fast kinetics) and the impact of reaction kinetics on the optimal process design and cost is evaluated. The controllability and stability of the design alternatives are also evaluated. This work provides a methodology for how to select the most suitable reactive distillation process design, based on the minimum total cost as well as on the controllability of the process, especially in cases when more than one process design configuration exists.

References

1. Luyben, W. L. and Yu, C. C., *Reactive Distillation Design and Control*, Wiley, New Jersey, **2008**.
2. Kiss, A. A., *Advanced Distillation Technologies: Design, Control and Applications*, Wiley, Chichester, **2013**.
3. Harmsen, G. J., *Reactive distillation: The front-runner of industrial process intensification: A full review of commercial applications, research, scale-up, design and operation*, Chem. Eng. Process., 46, 774–780, **2007**.
4. Wang, S. J. et al., *Plantwide Design of Ideal Reactive Distillation Processes with Thermal Coupling*, Ind. Eng. Chem. Res., 49, 3262-3274, **2010**.
5. Dünnebier, G. and Pantelides, C.C, *Optimal Design of Thermally Coupled Distillation Columns*, Ind. Eng. Chem. Res., 38 (1), 162-176, **1999**.
6. Panjwani, P. et al., *Optimal design and control of a reactive distillation system*, Eng. Optimiz., 37(7), 733-753, **2005**.

ECCE12
The 12th EUROPEAN CONGRESS OF CHEMICAL ENGINEERING
Florence 15-19 September 2019

Ultrafiltration System Optimisation for Nuclear Decommissioning

Kyriacos Hadjidemetriou[1,2], Jay J. Dunsford[2], Genevieve Boshoff[2], Claudio P. Fonte[1], Thomas L. Rodgers[1].

1 School of Chemical Engineering and Analytical Science, The University of Manchester, UK.

2 National Nuclear Laboratory, Workington, UK.

Corresponding author: kyriacos.hadjidemetriou@postgrad.manchester.ac.uk

Highlights

- Ultrafiltration optimisation using modelling and experimental work.
- Ferric floc filtration properties in the ultrafiltration process.
- Effluent treatment in nuclear decommissioning.
- Fouling control and cleaning methods for UF tubular membranes.

1. Introduction

The decontamination process of waste radioactive effluent in the Enhanced Actinide Removal Plant (EARP) at the Sellafield Site (UK) has been operating for more than 20 years. The plant has successfully generated and separated ferric flocs with incorporated radioactive components produced from acidic feeds arising from upstream spent nuclear fuel reprocessing plants. The EARP treatment process focuses on the chemical precipitation (CP) of ferric floc and an ultrafiltration (UF) process, in which separation of ferric floc is achieved in a two dewatering stage process [1].

UF technology performance and longevity are affected by the fouling deposition on the surface and inside the pores of the membrane. The development of a UF rig will be used for experimental work on the separation of flocs and the validation of the computational models [2].

2. Methods

Computational modelling work to build the 1D and CFD models has been utilised to predict the UF rig system performance under various operating conditions. The Darcy's law and the Poiseuille model for calculating the permeability coefficient were incorporated in the equations to build the 1D model across a tubular metallic membrane, as well as the friction factor for the loss of pressure through the membrane [3].

$$J_M = \frac{K\Delta P_{TM}}{\mu\delta} \quad (1) \qquad K = \frac{d_0^2\varepsilon}{32} \quad (2)$$

The laminar interface for the laminar flow and the k-epsilon model for the turbulent flow were used on building the 2D CFD model of the membrane. The experimental data from the developed UF system will be used to validate and improve the 1D and CFD model and the fouling resistance effects. The average pore diameter, d_0, and the porosity of the membrane, ε, were measured by using ESEM and porosimetry analysis- Porolux 1000.

3. Results and Discussions

The CFD results show the fluid behaviour inside the membrane and the fluid pulsations happening at the inlet of the membrane due to the pipe - membrane different diameter and the extra shear stresses being caused at the inlet of the membrane and the high fluid velocity, Figure 1.

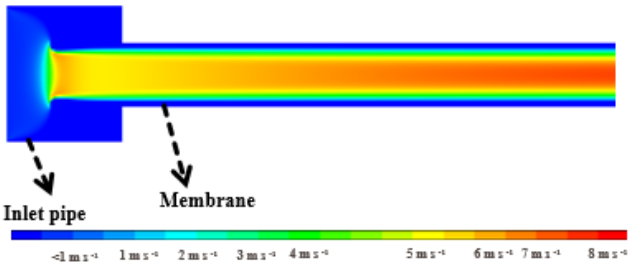

Figure 1: Velocity results of the fluid behaviour in the UF membrane.

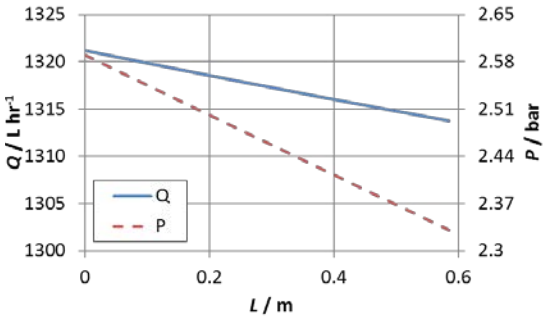

Figure 2: Volumetric flowrate and pressure across the membrane.

A 1D model is generated based on equation 1 and 2 using the experimental measurements of pore size and porosity and checked with the CFD model. Figure 2 shows the volumetric flowrate reduction along the membrane as permeate is generated and the pressure drop along the membrane. Table 1 compares the predictions of this 1D model with the obtained experimental data for the pressure drop and the total percentage of the inlet flow as permeate generation across the membrane.

Table 1: Pressure loss through membrane and permeate generation comparison of the 1D model and experimental data.

	1D Model	**Experiment**
Pressure Loss:	0.26 bar	0.26 bar
Total % as permeate generation:	0.56%	0.50%

4. Conclusions

Initial 1D and CFD models share similar results with the experimental data obtained from the UF system. The two models can predict the flux generation across the membrane, the volumetric flowrate and the pressure differences in the presence of membrane resistances. Further experimental work on the UF rig can potentially prepare fouling control and cleaning methods to reduce the fouling build-up in the system and improve the membrane longevity.

References

1. Weatherill, J., Iron Oxyhydroxide Formation in the Enhanced Actinide Removal Plant. 2018, The University of Manchester p. 245.
2. K. Wang, L., et al., Membrane and Desalination Technologies. 2011.
3. Nagy, E., 7 - Transport of Fluid Phase in a Capillary Membrane, in Basic Equations of the Mass Transport through a Membrane Layer, E. Nagy, Editor. 2012, Elsevier: Oxford. p. 177-192.

ECCE12
The 12th EUROPEAN CONGRESS OF CHEMICAL ENGINEERING
Florence 15-19 September 2019

Preparation of graphene oxide/silica composite membranes and their application for nanofiltration

Kojiro Ueda[1], Masanobu Nakata[1], Hideki Yamamoto[1], Sadao Araki[1*]

1: Kansai University, Department of Chemical, Energy and Environmental Engineering, 3-3-35 Yamate-cho, Suita-shi, Osaka 564-8680 Japan

**Corresponding author: araki_sa@kansai-u.ac.jp*

Highlights

- Graphene oxide/Silica composite (GO/SiO_2) membrane was prepared by using hydrolysis and polycondensation reaction of tetraethoxysilane.
- GO and GO/SiO_2 membranes showed high rejection of rose bengal.
- GO/SiO_2 membrane showed high adhesion properties compared to GO membrane.

1. Introduction

Graphene oxide (GO) multi-layered membranes have high permeability and good separation properties. However, since it is formed just by laminating GO on a support, GO layers easily peel off in plug flow type modules and the performance is remarkably decreased. In this study, to solve this issue of GO membranes, graphene oxide/Silica composite (GO/SiO_2) membranes were focused. It is expected that silanol groups react with hydroxyl groups of GO. Therefore, it is thought that GO/SiO_2 membranes have high durability compared with GO and polymer composite membranes. We prepared the GO/SiO_2 membranes and their nanofiltration properties was confirmed. In addition, the effect of composite of GO and silica on their adhesion was evaluated.

2. Methods

2.1 Preparation of GO membrane

GO suspension was synthesized using a modified Hummerś method and its concentration was 0.05 g/L [1]. Yttrium stabilised zirconia (YSZ) hollow fiber support with dead-end structure was soaked in the suspension. GO layers were deposited on the support by vacuuming inside of the support for 30 minutes. Then, the membrane was dried in air for 2 days.

2.2 Preparation of GO/SiO_2 membrane

0.1 mol of tetraethoxysilane (TEOS) as a silica source was added to 50 ml of ethanol. As an acid catalyst, 15 ml of 1 mol/ml nitric acid was added at a dropping rate of 1 ml/min. By stirring for 3 h, silica sol was prepared. GO was dispersed in the silica sol at a concentration of 0.05 g/L, and GO/SiO_2 membrane was prepared by the same procedure as the GO membrane.

2.3 Nanofiltration test

GO and GO/SiO_2 membranes were tested by connecting them in a pressure vessel filled with 35 µM rose bengal aqueous solution. The filtration tests were conducted at 5 bar. The permeation flux was calculated from the weight of the permeate. The dye concentration of the permeate was determined by using a UV-spectrometer (ASUV-6300PC, Shimadzu). The rejection rate calculated from the concentration ratio of permeate to feed solution. In addition, to confirm the adhesion of GO and GO/SiO_2 membranes, the pressure of 2 bar was added from inside of the fiber. Then, their nanofiltration properties were confirmed by 35 µM rose bengal solution.

3. Results and discussion

Table 1 shows nanofiltration results of GO and GO/SiO_2 membranes. The permeance of GO/SiO_2 membrane was reduced to one-third of the GO membrane. It is thought that SiO_2 inhibited permeation of water molecules. The rejections of both GO and GO/SiO_2 membranes was almost 100%. Table 2 shows nanofiltration results of GO and GO/SiO_2 membranes after the applying counter pressure. The rejection of GO membrane was reduced to 0% because GO layers were peeled off. On the other hand, GO/SiO_2 membrane kept a high rejection rate. From the above results, compared to the GO membrane, the adhesion properties of the GO/SiO_2 membrane were improved by the siloxane network.

Table 1. NF results of GO and GO/Si membranes.

Membrane	Permeance[L m^{-2} $h^{-1}$$bar^{-1}$]	Rejection[%]
GO	0.686	99.9
GO/Si	0.23	99.9

Table 2. NF results of GO and GO/Si membranes conducted durability test.

Membrane	Permeance[L m^{-2} $h^{-1}$$bar^{-1}$]	Rejection[%]
GO	11.3	0
GO/Si	0.32	97.2

4. Conclusions

GO/SiO_2 membrane was prepared to improve the adhesion properties of GO membranes. GO/SiO_2 membrane showed a high rejection of rose bengal, which is similar with the GO membrane. After the addition of counter pressure, the rejection of rose bengal for GO membrane was dramatically reduced. On the other hand, GO/SiO_2 membrane kept the rejection after the applying counter pressure.

References

[1] Liu. Hong. et al, J. Ferroelectrics. 528 (2017) 15-21

ECCE12
The 12th EUROPEAN CONGRESS OF CHEMICAL ENGINEERING
Florence 15-19 September 2019

Preparation and formation mechanism of AFX zeolite

Koki Maekawa[1], Satoshi Imasaka[2], Koji Kida[2], Hideki Yamamoto[1], Sadao Araki[1*]

1 Kansai University, Department of Chemical, Energy and Environmental Engineering, 3-3-35 Yamate-cho, Suita-shi, Osaka 564-8680 Japan

2 Hitachi Zosen Corporation, 2-11, Funamachi 2-Chome, Taisho-ku, Osaka 551-0022, Japan

**Corresponding author: araki_sa@kansai-u.ac.jp*

Highlights

- Effect of hydrothermal synthesis time on the preparation of thee AFX zeolite was confirmed.
- The FAU zeolite could be completely converted to the AFX zeolite for 7 h.
- The shape of AFX zeolite is hexagonal cylinder with bipyramidal tips at each ends.

1. Introduction

Zeolite is a crystalline oxide composed of silicon and aluminum. Zeolite generally shows high chemical and mechanical stabilities. Moreover, since zeolite has regularly arrayed pores of 1 nm or less, they can selectively separate certain materials by the difference of their molecular diameters. Among them, AFX zeolite can be expected for N_2 (0.36 nm)/ CH_4(0.38 nm) separation because the AFX zeolite has the pore structure of 0.36 × 0.34 nm. However, the formation mechanism of the AFX zeolite has not been clarified and optimized the synthesis conditions. In this study, AFX zeolite was prepared by using 1,1'-(1,4-butanediyl)bis(1-azonia-4-azabicyclo[2,2,2]octane)dication (Dab-4^{2+}), and synthesis time for obtaining AFX zeolite was examined in detail.

2. Methods

A synthesis gel was prepared by mixing sodium silicate, deionized water, 40 wt % Dab-4Br_2, 48 wt % sodium hydroxide, and FAU zeolite particles to be predicted molar composition. The obtained mixture was sealed in an autoclave and heated at 150 °C for 0 h, 3 h, 6 h, 7 h, 9 h, and 12 h. After the hydrothermal synthesis, the obtained solid product was filtered, washed, and dried at 80 ℃ overnight. These products were evaluated using X-ray diffraction and Field Emission Scanning Electron Microscopy（FE-SEM）.

3. Results and discussion

The FE-SEM images and XRD patterns of the products synthesized at each time (0 h, 3 h, 6 h, 7 h, 9 h, 1 2 h) are shown in Fig. 1 and Fig.2, respectively. As shown in Fig.2, XRD patterns of the products prepared for 0 h and 3 h were only FAU phase. In addition, no change for the shape and particle size of FAU zeolite was observed for the samples of hydrothermal synthesis of 0 h and 3 h, as shown in Fig. 1. For the XRD pattern of the product prepared for 6 h, the peak intensity of the FAU zeolite decreased and the peaks of the AFX zeolite were confirmed. Moreover, the crystals of hexagonal

cylinder with bipyramidal tips of AFX zeolite with crystal sizes ranging from 2 to 3 µm were observed with FAU zeolite particles, as shown in Fig. 2. At first, the agglomeration of FAU zeolite particles was occurred and then it turned to AFX zeolites, as shown yellow circle in Fig.1. The products of 7 h hydrothermal synthesis, the peaks of AFX zeolite were only confirmed. In addition, crystal size and shape of these products were similar. This result suggests that the FAU zeolite could be completely converted to the AFX zeolite for 7 h in this condition.

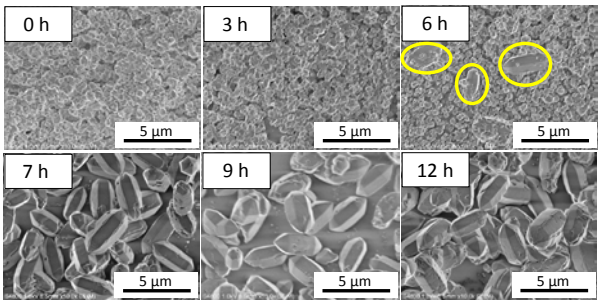

Figure. 1 FE-SEM images of zeolite synthesized at different hydrothermal times(0 h, 3 h, 6 h, 7 h, 9 h and 12 h).

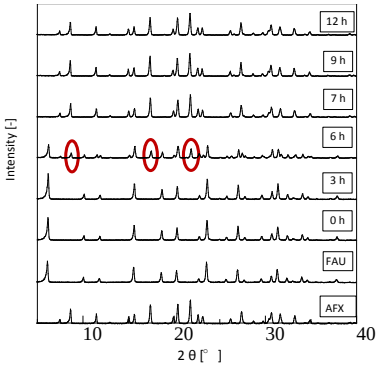

Figure. 2 XRD patterns of zeolite synthesized at different hydrothermal times (0 h, 3 h, 6 h, 7 h, 9 h and 12 h).

4. Conclusions

Conversion of FAU zeolite as a starting material to AFX zeolite was confirmed at 6 h hydrothermal synthesis. In addition, after 7h hydrothermal synthesis, FAU zeolite completely converted to AFX zeolite.

References

[1] Yusuke Naraki, et al., Micro.Mesopor.Mater.,254, 160-169, (2017)
[2] S.I.Zones, et al., Chem.Master.,8,2409-2411,(1996)

ECCE12
The 12th EUROPEAN CONGRESS OF CHEMICAL ENGINEERING
Florence 15-19 September 2019

Design, analysis and optimization of batch distillation processes using BatchColumn software

Olivier Baudouin[1*], Stéphane Déchelotte[1], Philippe Guittard[1], Rodolphe Sardeing[1], Benjamin Wincure[2]

1 ProSim SA, Immeuble Stratège A, 51 rue Ampère, F-31670 LABEGE, France

2 ProSim, Inc., 325 Chestnut Street, Suite 800, Philadelphia, PA 19106, USA

**Corresponding author: olivier.baudouin@prosim.net*

Highlights

- Thermodynamic server;
- Complex mixtures;
- Modeling and simulation;
- Batch distillation.

Batch distillation is an important unit operation in the batch processing industry and is used in a wide range of applications: fine chemical industries, pharmaceuticals, specialty chemicals, biochemical, essential oils, alcohols… The great flexibility of batch distillation allows for the separation of complex mixtures with a single column. This flexibility, combined with the inherent unsteady state nature of the process, poses challenging design and operation problems [1]. There is no 'rule of thumb' to achieve the optimal solution (reduced operating time, good product separation, minimum energy consumption…) and dedicated tools are required.

BatchColumn software [2] allows for the detailed representation almost any kind of distillation column, e.g. azeotropic and close boiling separation using heterogeneous or homogeneous entrainers [3, 4, 5, 6], batch distillation with a middle vessel column [7], etc. The software takes into account the associated equipment technology (middle vessels, boiler, condenser…) and column hydrodynamics. It provides the evolution through time of all parameters of interest such as compositions, temperature, pressure, reflux ratio… Through the creation and analysis of operating scenarios, it enables the identification of the best resources management policies, recipes for product quality optimization and cost reduction. BatchColumn allows modeling of complex systems by taking advantage of the power of Simulis Thermodynamics (thermodynamic properties server) which offers an extensive set of thermodynamic models with a pure components database of more than 2,300 pure components (AIChE's DIPPR® database [8]). The main features and strengths of BatchColumn are highlighted on various application examples.

References

[1] U.Diwekar, Batch Distillation – Simulation, Optimal Design and Control, CRC press, 2nd ed. (2012)

[2] http://www.prosim.net/en/index.php

[3] I. Rodriguez-Donis, V. Gerbaud, X. Joulia, Ind. Eng. Chem. Res., 40, 12, 2729-2741 (2001)

[4] I. Rodriguez-Donis, V. Gerbaud, X. Joulia, Ind. Eng. Chem. Res., 40, 22, 4935-4950 (2001)

[5] S. Pommier, S. Massebeuf, B. Kotai, P. Lang, O. Baudouin, P. Floquet, V. Gerbaud, Chem. Eng. Process., 47, 3, 408-419 (2008)

[6] I. Rodriguez-Donis, V. Gerbaud, X. Joulia, AIChE J., 48, 6, 1168-1178 (2002)

[7] I. Rodriguez-Donis, V. Gerbaud, X. Joulia, Feasibility Analysis and Reflux Policies for the Heterogeneous Batch Distillation in a Middle Vessel Column, SIMO 2002 (2002)

[8] R.L. Rowley, W.V. Wilding, J.L. Oscarson, N.F. Giles, DIPPR® Data Compilation of Pure Chemical Properties, Design Institute for Physical Properties, AIChE, New York, NY (2011)

ECCE12
The 12th EUROPEAN CONGRESS OF CHEMICAL ENGINEERING
Florence 15-19 September 2019

Dynamics and process parameters evaluation of citric essential oils vapor distillation extraction

Esperanza Medina[1], Luis Miranda[2], Yaimi Cordova[3], Jhoan Velazquez[4]

1 San Agustín National University of Arequipa. emedinale@unsa.edu.pe; 2 San Agustín National University of Arequipa. lmirandaz@unsa.edu.pe

**Esperanza Medina: emedinale@unsa.edu.pe*

Highlights

- The study was carried out at a pilot plant level.
- The extraction dynamics differed significantly from one citrus to another
- Steam pressure/packing factor of the bed, determined the extraction dynamics

1. Introduction

This work evaluates at a pilot plant level, the dynamics of the process of extraction by steam distillation of essential oils in citrus (*citrus sinensis*, *citrus limetta*, *citrus latifolia* and *citrus reticulata*) from different Peruvian regions. The processing conditions have been determined in the extraction and phase separation units, ensuring efficiency while maintaining a high oil quality. The steam distillation method of extraction has been selected, because it is the only one that is normalized and that is widely used in industry [1]. New technologies for extracting essential oils are being tested, but they do not necessarily provide better results than the steam distillation method[2,3], if oil quality and process yield are main guidelines.

The dynamics of extraction, may be represented by the model developed by Ho & Oumarou [4]:

$$\frac{dCt}{dt} = k(Cs - Ct)^2$$

Where:

k second order constant of velocity of extraction ($Lg{-}1 - min{-}1$);
Cs concentration of oil in saturation ($gL{-}1$);
Ct concentration of oil in the solution at any time instant ($gL{-}1$) t (min)

2. Methods

The steam distillation process of extraction took place in a 15 L pilot plant provided with pressure and temperature sensors. Oil production was monitored with a precision of 0.2mL. The following variables have been manipulated: the packing factor of the citrus peel in the extractor, the inlet pressure of the steam and its flow, as well as the extraction time. Also, in order to understand the mass transfer mechanism of the essential oil located in the citrus peels to the vapor phase, microscopic analysis have been performed to the skin of the citrus materials.

3. Results and discussion

The process of extraction presents a dead time (θ) that depends on the citrus species, vapor pressure (u) and packing factor (ϕ). We have formulated a model including these variables, based

on the approach of transfer functions for process control. The model we obtained is characterized by the equation $y(t) = \{1\text{-exp}\,[-(t-\theta)/\tau]\}$ K Δu(t).

Both the gain *K* and the time constant τ depend fundamentally on the type of citrus material. Our results showed a substantial difference (up to 80%) in the dynamics of orange with respect to other citrus species. The optimal time for extraction for all four citrus materials is very much alike, in the range of 10 to 15 minutes, where 80% of the essential oil has been already extracted.
The relation between vapor pressure and packing factor as a function of oil yield is exponential for the orange, hence an optimal point for maximal efficiency can be obtained. However, for the other citrus species it has a linear inverse relation, therefore the best results are obtained with a minimal relation between steam inlet pressure versus packing factor.

In the oil extraction process the dead time could indicate the time required to meet the conditions for the oil to flow out of the glandular trichomes where it is contained, in order to be dragged by the vapor flowing across de bed. These conditions refer to the pressure for breaking the walls of the trichomes, and the temperature to vaporize the essential oil. The measured dead time is in the range of 1.5 to 3 minutes.
Along the extraction, a convective process takes place since there is a continuous vapor flow through the extraction bed; and a diffusive process as well, with the oil flowing across the solid phase due to a concentration gradient. Therefore the gain *K* might represent a mixed transfer coefficient that accounts for both, the convective and diffusive phenomena pointed out, that will be helpful in determining a global efficiency of the extraction process. On the other hand, the time constant is referred to the velocity of the extraction, and indicates the time needed to extract most of the oil. This parameter allows estimation of extraction process ending.

4. Conclusions

The dynamics of the extraction of essential oils from citrus is best explained considering a first-order model with dead time, process gain and time constant. These parameters account for bed resistance, convective/diffusive coefficient, and extraction velocity, respectively. A critical zone was achieved where maximum efficiency is obtained, which lies in the range of 10 to 15 minutes of extraction time. The relation between steam inlet pressure and packing factor is a good indicator of the extraction process dynamics.

References

[1] Limones piuranos. Callelos Naranjos 272, Urb. Sta. Isabel, Piura, Perú. http://www.limonespiuranos.com/eng/contact.html

[2] Ayub, M., Hanif, M., et al. Biological activity of Boswellia serrafa Robxb. Oleo gum resin essential oil: effects of extraction by supercritical carbon dioxide and traditional methods. International Journal of Food Properties. 21(1) (2018) 808-820

[3] Prado, JM., Veggi, PC., et. al. 2014. Supercritical fluid extraction of Lemon Verbena (sf Aloysia triphylla): Process Kinetics and Scale-Up, Extract Chemical Composition and Antioxidant Activity, and Economic Evaluation. Separation Science and Technology. 49 (4) 569-579.

[4] Ho, Y. Oumarou, H. Kinetic and model building of leaching of water-soluble compounds of Tilia Sapwood. Separation and Purification Technology 2005; 169-173.

ECCE12
The 12th EUROPEAN CONGRESS OF CHEMICAL ENGINEERING
Florence 15-19 September 2019

Multidimensional fractionation of finely dispersed particles using the cross-flow filtration with superimposed electric field

Philipp Lösch, Kai Nikolaus, Sergiy Antonyuk

Institute of Particle Process Engineering, Technische Universität Kaiserslautern, 67663 Kaiserslautern

**Corresponding author: Philipp.loesch@mv.uni-kl.de*

Highlights

- Fractionation of fine particles by hydrodynamic effects
- Affect the separation method by adding additives
- CFD simulation of a crossflow filtration with electric field

1. Introduction

The separation of particle fractions with highly specific physical properties from suspensions has great importance for process success in various engineering processes. The physical properties of a particle collective are directly related to the particle size, particle shape, surface properties and chemical composition of the individual particles. Frequently, suspensions form highly complex particle collectives, which contain all of these features in different distributions. Since the characteristic dimensions of the technical structures in the raw materials are continuously decreasing, ever finer, more highly specific particle systems will be produced, processed and recycled. In known separation processes, such as e.g. Sedimentation, filtration or centrifugation, the particles are either classified according to a certain grain size or sorted by a physical characteristic. However, in many applications in which finely dispersed multicomponent mixtures of particles with sizes < 10 µm with different properties are to be separated in industrially relevant quantities, the use of a single separating feature is often no longer sufficient. Therefore this present study focusses on the utilization of multiple separating features to amplify the separation process.

2. Methods

In this research project, a novel cross-sectional superficial electric field filtration technique is being developed, which is a promising method for the highly specific separation of micro- and sub-micron suspensions. The particles are thus subject both to an electric field and to the lift and drag force. The method not only allows fractionation with regard to the particle size, but also the particle shape, the chemical composition and the physical properties of the individual particles. In most theoretical and experimental studies, individual separation features were only studied separately, but the development of a multidimensional fractionation method requires knowledge of the relationships between the superimposed effects. The construction and operation of suitable facilities should be made possible by the knowledge gained in the research project.

3. Results and discussion

First studies on the hydrodynamic effects of different particle distributions and concentrations showed, that a classification is possible. To achieve a multidimensional fractionating, an electric field across the filter media add an electrophorese force. The multidimensional fractionation of a suspension according to the separation characteristics grain size, particle shape and zeta potential can be achieved by the combination of lift force, drag force and electrophoretic force. Therefore, the isoelectric point and the charge of the particles of the used stable suspensions were investigated.

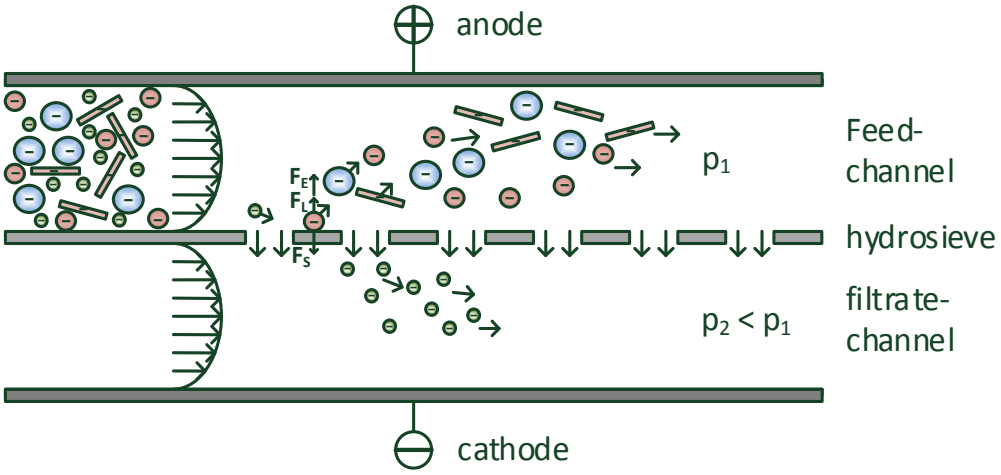

Figure 1. scheme of the fractionation process

Beside the experiments, the adjustment of the macroscale particle transport process is supplemented by CFD simulations with the Euler-Lagrange approach. This will help to find the operation point for the experimental investigations.

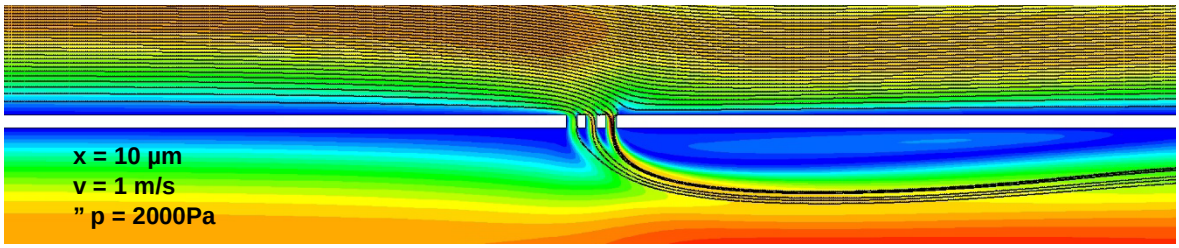

Figure 2. CFD simulation of the flow channel with particle tracking

Here, with the flow velocity and the electric field strength the hydrodynamic and electrophoretic forces can be adjusted, to achieve a classification.

4. Conclusions

A new method of fractionation finest particles using the crossfow-filtration is investigated. The effect of a hydrodynamic classification is shown. By using CFD-methods, the operating parameters are figured out. Due to the scalability of the process, which is based on membrane technology, the large-scale feasibility of the process is guaranteed. The individual effects used in the process and plant components needed for the process are known from filtration and membrane technology, but are still not used today for fractionation.

ECCE12
The 12th EUROPEAN CONGRESS OF CHEMICAL ENGINEERING
Florence 15-19 September 2019

Simulation of a two-stage membrane system for the recovery of hydrogen from a flue gas stream

Fernando Pardo*, Gabriel Zarca, Ane Urtiaga

Department of Chemical and Biomolecular Engineering, University of Cantabria,

Av. de Los Castros s/n. Santander 39005, Spain

**Corresponding author: pardof@unican.es*

Highlights

- Efficiency of the overall process was evaluated in terms of H_2 purity and recovery.
- Operation conditions can be optimized towards H_2 purity or H_2 recovery.
- Maximum H_2 purity of 95% could be achieved at feed gas pressure of 12 bar.
- Maximum recovery of 83% could be achieved at feed gas pressure of 12 bar.

1. Introduction

Given the current global context of progressive depletion of fossil fuels and increasing environmental concerns for global warming, research efforts towards shifting from a linear production model to a circular economy model are a priority. In this sense, industrial processes must look for a better efficiency of resource use and waste management, not only to minimize their environmental impact, but also to increase the competitiveness of the productive process. In particular, this study is focused on the valorization of the flue gas generated in carbon black manufacturing. Considerable amounts of hydrogen (up to 20% vol on dry basis) can be found in this type of gaseous stream [1], thus its recovery could provide a competitive advantage towards a more sustainable production. In this sense, membrane technology offers a cost-effective alternative over other separation technologies such as cryogenic distillation and pressure swing adsorption. There is extensive knowledge in the use of H_2 selective materials for hydrogen recovery from ammonia purge gas, syngas ratio adjustment or H_2 recovery in the steam methane reforming process. Nevertheless, available data for the material valorization of tail gas from the carbon black manufacturing process is scarce. Therefore, the novelty of this work focuses its attention on the simulation of a two-stage membrane process with recirculation (Figure 1) to improve both material and energy management of the carbon black manufacturing process. The effect of critical variables such as feed pressure, permeation area and type of polymeric material on the effectiveness of the overall process, evaluated in terms of H_2 purity in the permeate stream and H_2 recovery, is assessed.

2. Methods

The tail gas data composition considered in this work corresponds to reference values included in the Best Available Techniques for the manufacture of carbon black [1]: water vapor (30–50%), N_2 (30–50%), H_2 (7–14%), CO (6–12%), CO_2 (1–5%) and CH_4 (0.1-1 %), as well as traces of sulphur and nitrogen compounds. Membrane modules of polyphenylene oxide (PPO) and polyimide (PI) in

hollow fiber configuration were considered [2]. Permeability values for N_2, H_2, CO, CO_2 and CH_4 gas were obtained from literature [3,4]. A mathematical model describing gas permeation through the hollow fiber membrane module has been implemented in Aspen Custom Modeler. Permeation of gases though the polymeric material are described by the solution-diffusion model [5]. This model was then exported to Aspen Plus to simulate the gas separation processes with a two stage membrane system.

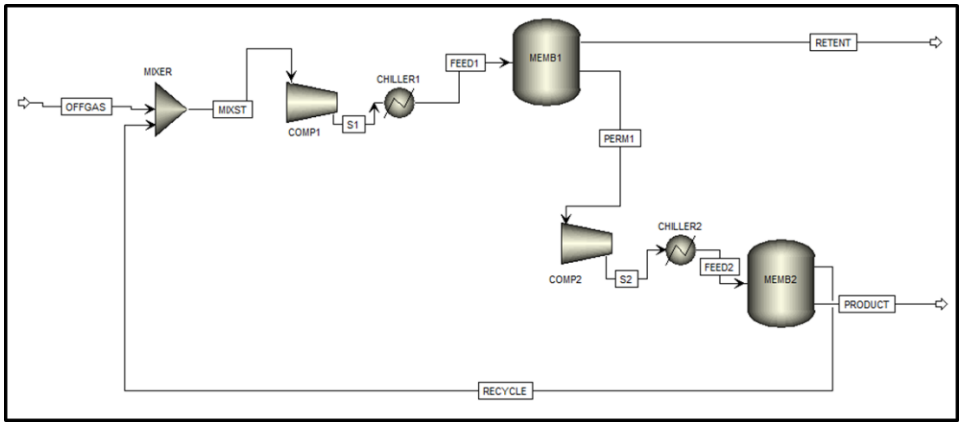

Figure 1. Configuration of the two-stage membrane process.

3. Results and discussion

According to the simulated results, 95% H_2 purity can be obtained in the product stream at a reachable feed pressure up to 12 bar using a 2-stages system consisting of two polyimide hollow fiber membrane modules. The highest hydrogen recovery (80%) was obtained when the PPO polymer was used as material for the first membranes module.

4. Conclusions

This work provides valuable data of the extent of the potential application of membrane technology for the recovery of hydrogen from a tail gas stream. Despite the limitations to deal with the trade-off between H_2 purity and recovery, the results show that polymer membrane technology can be successful for obtaining H_2 enriched streams with sufficient quality to be used in applications that do not require ultra-high purity H_2 as feedstock, such as hydrodesulphurization or hydrocracking.

Financial support from the Spanish Ministry of Economy and Competitiveness (CTM2016-75509-R and CTQ2015-66078, MINECO-AEI/FEDER) is gratefully acknowledged.

References

[1] European Commission, Integrated Pollution Prevention and Control, best available techniques for the manufacture of large volume inorganic chemicals – Solids and Other. August 2007.
[2] L. Wang, Doctoral Thesis. Cyclic Membrane Gas Separation Processes. July 2012.
[3] A. Alentiev, E. Drioli, M. Gokzhaev, G. Golemme, O. Ilinich, A. Lapkin, V. Volkov, Yu. Yampolskii, Journal of Membrane Science 138 (1998) 99-107.
[4] O. C.David, D. Gorri, K. Nijmeijer, I. Ortiz, A. Urtiaga, Journal of Membrane Science 419–420 (2012) 49–56.
[5] G. Zarca, A. Urtiaga, L. Biegler, I. Ortiz, Journal of Membrane Science 563 (2018) 83–92.

ECCE12
The 12th EUROPEAN CONGRESS OF CHEMICAL ENGINEERING
Florence 15-19 September 2019

Comparative Studies of Molecularly Imprinted Polymers (MIPs) Synthesized from Different Monomers for the Purification of Lincomycin

Youhong Zhang[1,2] , Yinan Lu[1,2], Jiliang Zhong[1,2], ***Kean Wang***[3,4,*]

[1]*School of Environmental Ecology and Bioengineering*,

[2]*Key Laboratory for Green Chemical Process of Ministry of Education, Wuhan Institute of Technology, Wuhan 430205, China*

[3]*Chemical Engineering Department*

[4]*Center for Separation and Catalysis (CeCAS)*

Khalifa University of Science & Technology

United Arab Emirates

**Corresponding author: kean.wang@ku.ac.ae*

Highlights

- Molecularly imprinted polymers (MIP) were synthesized for the purification of lincomycin (an antibiotic) in chloroform solution.
- Three monomers (methacrylic acid, trifluoromethyl acrylic acid, and acrylamide) were investigated, respectively, for their performance in related MIPs.
- Separation mechanisms, equilibrium, kinetics and operation parameters were studied. Industrial fermentation solution was used to examine the performance of the MIPs.

1. Introduction

With strong antibacterial effect against gram-positive bacterium and inhibitory effect to mycoplasma, lincomycin has attracted strong interest in global pharmaceutical industries [1, 2]. It possesses such advantages of: broad antimicrobial spectra, strong antibacterial ability, low toxicity and convenient administration, etc.. The industrial purification process of lincomycin involves mainly the extraction of fermentation products with butyl-alcohol or mixed alcohol[2, 3]. The crude product is obtained by crystallization process, following repeatedly extracting, concentrating and bleaching processes. A few companies utilized the hydrochloric acid stripping technique after extraction, thereafter the crystals are obtained by bleaching/crystallizing with acetone. These technologies suffered from such disadvantages as: high cost, low yield, high material and energy consumption, and environmental pollutions, etc. [3]. The fermentation solution of Lincomycin

contains mainly lincomycin A, as well as a few analogues such as lincomycin B, C and D, which are known for less antibacterial activity but toxic side effects. Therefore, new technology is needed for high purity and low-cost production of the antibiotics.

Molecular imprinting is a new technology to prepare adsorbents with highly specific affinity (selectivity). The molecularly imprinted polymers (or MIPs), whose spatial structure and binding sites were designated to match with the template molecules, shed new lights for the separation of large/biomolecules out of the complicated mixture solutions[4]. The spatial structure and physicochemical properties of the template molecules are created in the MIP which can identify the template molecules effectively from a complex mixture solution [5, 6]. This technology has found numerous application in chemical[7-9], biological [10], medicine[11-13] and other fields.

2. Methods

Lincomycin was used as the template molecule, ethylene glycol dimethacrylate as the cross-linker. Three MIPs were synthesized, respectively, with different functional monomers (namely, methacrylic acid, trifluoromethyl acrylic acid, and acrylamide) via a two-step swelling method, and grown on the polystyrene microspheres. The related non-imprinted polymers (NIP) were also synthesized using the same procedures as MIPs, nut without adding the template molecules. The 6 samples were denoted as: $MIP_{TF\text{-}MAA}$ and $NIP_{TF\text{-}MAA}$; MIP_{MAA} and NIP_{MAA}; MIP_{AM} and NIP_{AM}, respectively.

The MIP/NIP samples were structurally characterized using a number of instruments (SEM, FTIR, XRD, Particle size analyser, etc.), which suggested that the MIP was successfully grown on the substrates with homogeneous structure. Adsorption studies were performed in aqueous solution, chloroform solution and industrial extracts solutions, respectively. Fixed bed column breakthrough experiments were also performed to examine the kinetics and reusability of the MIPs.

3. Results and discussion

Figure1a shows the adsorption of lincomycin on MIPs prepared by different functional monomers. The initial concentration was fixed with a dosage of 50mg-adsorbents/20ml-chloroform solutions. We see that the adsorption capacity increases steadily with the lincomycin concentration, while the adsorption on NIPs gradually approaches to its saturation. Regardless of MIPs or NIPs, the

adsorption capacity is gradually decreasing in order of TF-MAA, MAA, and AM. This is mainly attributed to the molecular structure of lincomycin. Lincomycin shows alkaline because of an amino group in molecule, so the imprinted polymer prepared by acid functional monomer has better adsorption capacity, especially the TF-MAA with three fluorine atom substituents. To MIPs and NIPs prepared by the same functional monomer, the binding capacity of MIPs is obviously higher than NIPs; this gap increases with lincomycin concentration's increase. It indicated that the spatial structure and binding sites matched with lincomycin formed in the synthesis process, which made MIPs better adsorbents than NIPs, which are absent of the special recognition ability for lincomycin.

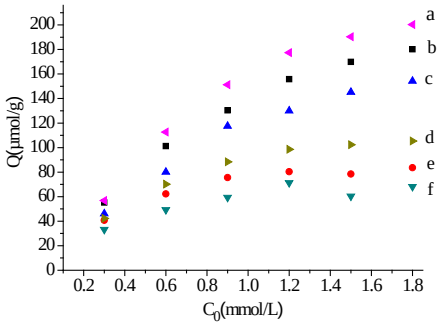

Figure 1. Adsorption isotherms of $MIP_{TF\text{-}MAA}$ (a,d) and $NIP_{TF\text{-}MAA}$, (b,e)--Adsorption isotherm of MIP_{MAA} and NIP_{MAA}, (c,f)--Adsorption isotherm of MIP_{AM} and NIP_{AM}

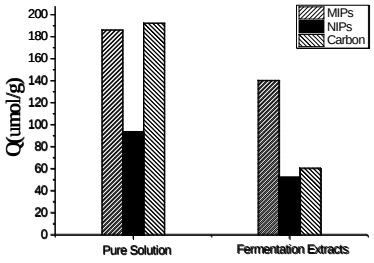

Figure 2 The adsorption capacities of lincomycin on MIP, NIP, and activated carbon in two solutions (left: pure lincomycin solution from Lab; right: raw fermentation extracts solution from industry)

Figure 1b shows the comparative studies for MIP with activated carbon and the NIPs. It was found that MIP presented a moderately higher capacity in pure solution of lincomycin, but a significantly higher capacity (more than doubled) in the practical lincomycin fermentation solution extracts, confirming the superior performance (specific affinity/selectivity) of the MIP over NIP and carbon for this application.

The adsorption/desorption kinetics were also studied on MIP_{MA} in a fixed bed column. The breakthrough curves were found to be well fitted by the Thomas model and the fixed bed has the good regeneration capability with the elution ratio > 93%.

4. Conclusions

With lincomycin as the template molecule, 3 different MIPs were prepared using TF-MAA, MAA and AM as functional monomers, respectively. Adsorption studies showed that MAA as the optimal functional monomer for this application. By comparing the lincomycin adsorption on MIP, NIP, as well as on activated carbon, it was found that MIPs gave better specific recognition and an adsorption capacity upto 180 μmol/g, which is higher than NIP and carbon in pure solution This

difference became much higher (~ 2.5 times) for the adsorption in the practical fermentation solution extracts. Column adsorption experiment indicated that MIP had good separation effect for lincomycin. The fitting results of the kinetic model indicated that Thomas model gave a good correlation to the breakthrough curves (R^2=0.98). Elution-regeneration experiments showed that the adsorption column had good desorption and regeneration capacities, with an elution ratio of 93.8 % while the breakthrough curves little changed in many cycles. These results proved that the MIP is a promising adsorbent for industrial separation and purification of lincomycin.

References

[1] X.-n. Jiang, W.-p. Li, Y.-h. Zhang, X.-w. ZHU, J. CHEN, and T.-j. SU, "Preparation and properties of lincomycin A molecular imprinted polymer microspheres," *J Wuhan Inst Technol,* vol. 34, no. 5, p. 16, 2012.

[2] Z. X. L., " Progress in Lincomycin Hydrochloride Purification Process " *Hebei Chemical Industry,,* vol. 5, p. 3, 2003.

[3] Q. P. Y. Zhou T, Miao Y, et al., " A Review on lincomycin Extraction Process " *World Notes on Antibiotics,,* vol. 20, no. 2, p. 4, 1999.

[4] B. Sellergren, *Molecularly imprinted polymers: man-made mimics of antibodies and their application in analytical chemistry*. Elsevier, 2000.

[5] C. Baggiani, C. Giovannoli, L. Anfossi, C. Passini, P. Baravalle, and G. Giraudi, "A connection between the binding properties of imprinted and nonimprinted polymers: a change of perspective in molecular imprinting," *Journal of the American Chemical Society,* vol. 134, no. 3, pp. 1513-1518, 2012.

[6] T. Renkecz, G. n. Mistlberger, M. Pawlak, V. Horváth, and E. Bakker, "Molecularly imprinted polymer microspheres containing photoswitchable spiropyran-based binding sites," *ACS applied materials & interfaces,* vol. 5, no. 17, pp. 8537-8545, 2013.

[7] Y. Zhao, Y. Shen, L. Bai, R. Hao, and L. Dong, "Synthesis and CO2 adsorption properties of molecularly imprinted adsorbents," *Environmental science & technology,* vol. 46, no. 3, pp. 1789-1795, 2012.

[8] Y. Fuchs, A. V. Linares, A. G. Mayes, K. Haupt, and O. Soppera, "Ultrathin selective molecularly imprinted polymer microdots obtained by evanescent wave photopolymerization," *Chemistry of Materials,* vol. 23, no. 16, pp. 3645-3651, 2011.

[9] C. Xu, K. M. A. Uddin, X. Shen, H. S. N. Jayawardena, M. Yan, and L. Ye, "Photoconjugation of molecularly imprinted polymer with magnetic nanoparticles," *ACS applied materials & interfaces,* vol. 5, no. 11, pp. 5208-5213, 2013.

[10] E. Turiel and A. Martín-Esteban, "Molecularly imprinted polymers for sample preparation: A review," *Analytica Chimica Acta,* vol. 668, no. 2, pp. 87-99, 2010/06/04/ 2010.

[11] A. J. Hall, M. Quaglia, P. Manesiotis, E. De Lorenzi, and B. Sellergren, "Polymeric receptors for the recognition of folic acid and related compounds via substructure imprinting," *Analytical chemistry,* vol. 78, no. 24, pp. 8362-8367, 2006.

[12] E. P. Herrero, E. M. Martín Del Valle, and N. A. Peppas, "Protein imprinting by means of alginate-based polymer microcapsules," *Industrial & Engineering Chemistry Research,* vol. 49, no. 20, pp. 9811-9814, 2010.

[13] M. Peeters *et al.*, "Impedimetric detection of histamine in bowel fluids using synthetic receptors with pH-optimized binding characteristics," *Analytical chemistry,* vol. 85, no. 3, pp. 1475-1483, 2013.

ECCE12
The 12th EUROPEAN CONGRESS OF CHEMICAL ENGINEERING
Florence 15-19 September 2019

Thermodynamics of stereoisomer mixtures. Identification of ambiguously defined substances and interpretation of their properties.

Vladimir Diky[1], Andrei Kazakov[1]

1 Material Measurement Laboratory, National Institute of Standards and Technology,

325 Broadway, Boulder CO 80305, USA

**Corresponding author: diky@nist.gov*

Highlights

- Thermodynamic properties of stereoisomer mixtures have been analyzed.
- Magnitudes and nature of deviations from the component properties has been revealed.
- Principles of identification of ambiguously defined compounds have been developed.
- They can be adopted in chemical engineering.

1. Introduction

Accurate knowledge of thermophysical properties is critical for process simulation and other engineering applications. One of the sources contributing to data errors is incorrect identification of substances which are actually mixtures of components or species, and subsequent misinterpretation of their properties. Those substances can be mixtures of stereisomers (e.g., 2,3-butanol) or isomers (e.g., xylene) or undergo reversible chemical transformations (e.g., carbohydrates or nitrogen dioxide). While some properties of such substances (typically, fluid properties) are close to those of their components, the others (such as entropy, molecular, formation, solid-state properties, and phase equilibria involving solid phase) are not or are even not applicable to mixtures. Special care has to be taken when dealing with properties of mixtures containing similar substances as even correctly measured values can be assigned to inappropriate phenomena and cause apparent inconsistencies, misleading recommendations, and wrong expectations.

2. Methods

A thorough analysis of the available property data for ambiguously defined substances and their components has been performed at Thermodynamics Research Center (TRC) of the National Institute of Standards and Technology (NIST). The analysis involved about 1000 pairs of stereoisomers and 50 composition-explicit mixtures of stereoisomers. That analysis was possible because of the availability of a large thermodynamic data collection presently containing over 6.6 million distinct property values (SOURCE database [1, 2]), detailed molecular structures stored in that database, and structure comparison algorithms based on the molfile, InChI, and other representations.

3. Results and discussion

The available property data for composition-explicit mixtures of stereoisomers revealed the patterns of the composition-dependent properties and the magnitudes and of their deviations from the properties of the components. The nature of those deviations can only be interpreted if such substances are treated as mixtures. The presentation will include an overview and give typical examples. Numerous ambiguities and inconsistencies have been identified and explained, such as the spread of the available data on the melting temperature of 2,3-butanediol. Many of them can be avoided if the type of each substance (pure species, equilibrium or non-equilibrium mixture) is defined and the results of experimental measurements are correctly interpreted. That is done in the TRC databases, where the relations of the ambiguously defined compounds to their components or species are also maintained. The type of a substance not only controls interpretation of its experimentally measured properties, but also defines specific requirements to the substance characterization, as well as measurements and reporting of its properties. That is important, in particular, for reviewing experimental reports and for design of processes involving solid substances.

4. Conclusions

The principles and methods of identification of ambiguously defined substances have been developed at TRC on the basis of the analysis of molecular structures and available thermodynamic property data. They allow resolving apparent inconsistencies and obtaining a more accurate knowledge. Being adopted in chemical engineering, they can provide better understanding and higher fidelity of process simulation.

References [Calibri 10]

[1] M. Frenkel, Q. Dong, R.C. Wilhoit, K.R. Hall, Int. J. Thermophys. 22 (2001) 215-226.

[2] A. Kazakov, C. D. Muzny, K. Kroenlein, V. Diky, R. D. Chirico, J.W. Magee, I. M. Abdulagatov, M. Frenkel, Int. J. Thermophys. 33 (2012) 22–33.

ECCE12
The 12th EUROPEAN CONGRESS OF CHEMICAL ENGINEERING
Florence 15-19 September 2019

Experimental Influence of Thermodynamic Inhibitors on the Phase Equilibria of Carbon Dioxide Hydrates Above the Q_2 Point

Jose Carlos Cordeiro Jr.[1], Moisés A. Marcelino Neto[1]*, Rigoberto E. M. Morales[1], [2] Amadeu K. Sum

[1]*NUEM Multiphase Flow Research Center, Graduate Program in Mechanical and Materials Engineering, Federal University of Technology - Paraná (UTFPR), Curitiba, PR, Brazil;*
[2] *Hydrates Energy Innovation Laboratory, Colorado School of Mines, 1500 Illinois Street, Golden, CO, USA*

**Corresponding author: mneto@utfpr.edu.br*

Highlights

- Some oilfields can have very high concentrations of CO_2.
- Experimental data for condensed CO_2 hydrates are scarce in literature.
- New data for CO_2 hydrates above the Q_2 point with MEG and NaCl is presented.

1. Introduction

Due to high pressures and low temperatures achieved in oil and gas industries, the formation of hydrates can block pipelines, causing damage and preventing normal operations. Hydrates are a solid non-flowing phase that forms by the combination of water molecules that trap a molecule of a second type. A common practice in the industry is the use of thermodynamic inhibitors, such as Monoethylene Glycol (MEG), which can change the conditions at which hydrates form, preventing their appearance. In offshore oil and gas extraction, the water that accompanies the production is naturally inhibited by the presence of salts. These salts, such as sodium chloride (NaCl), acts similarly to MEG, lowering the activity of water and consequently causing the conditions for the formation of hydrates to be more severe [2]. Some oilfields, for instance in the Brazilian pre-salt region, can have very high concentrations of carbon dioxide (CO_2), changing the conditions at which hydrate formation occurs. Due to these high CO_2 concentrations, the condensation of the vapor phase becomes possible. This causes the appearance of an upper quadruple point (Q_2) in the phase equilibria, which is characterized by the presence of four phases: Liquid CO_2 / Vapor CO_2 / Liquid Water / Hydrate [3]. This work presents new experimental data for carbon dioxide hydrates above Q_2 formed with the presence of MEG, NaCl and their mixtures in the aqueous phase. For validating the experimental procedure, data for CO_2 hydrates with pure water was obtained and compared with data available in literature with good agreement.

2. Methods

To determine the hydrate equilibrium temperature for a given pressure, an isobaric experimental procedure was performed. A stainless steel equilibrium cell was connected to a syringe pump, which added or removed CO_2 in order to keep a constant pressure. The formation was induced by lowering the temperature of the cell; next, the temperature was increased, promoting hydrate

dissociation. Data for the change in volume of the pump and the temperature inside the cell were collected and the equilibrium temperature was determined graphically. The equilibrium conditions for a given pressure was determined as the temperature of which hydrates no longer exist.

3. Results and discussion

Experimental results obtained in this work are shown in Figure 1. For evaluating MEG (blue symbols), mass concentrations of 10%, 20% and 30% were used. For NaCl, mass concentrations of 5% and 10% were considered. The concentrations of 5% NaCl and 10% of MEG were found to be practically equivalent. In addition, the mixture of 5% of NaCl + 10% of MEG had an inhibition effect slightly higher when compared to the single inhibitors concentrations.

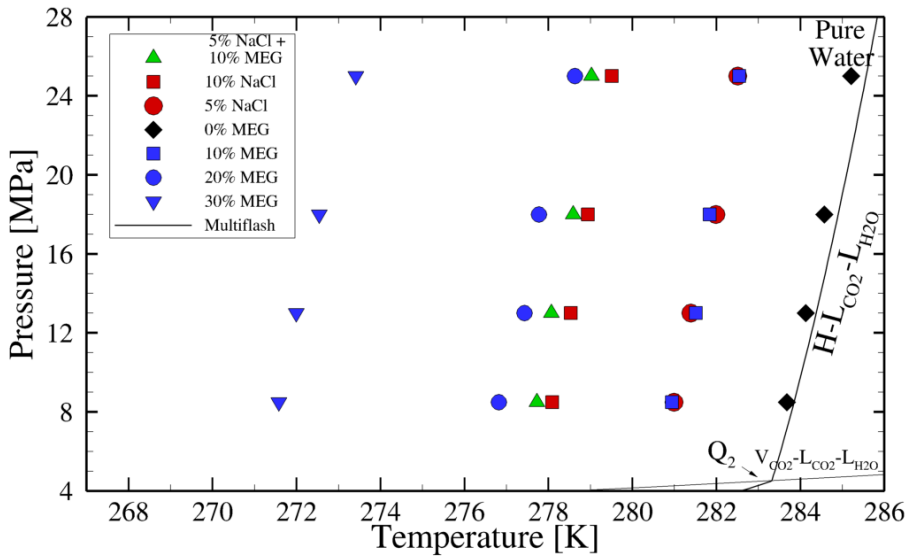

Figure 1. Liquid water-liquid carbon dioxide-hydrate equilibrium condition. The line is prediction done using Multiflash [3]. Blue symbols are data for MEG. Red symbols are for NaCl. Green symbols are for the 5% NaCl + 10% MEG mixture. All concentrations are in mass base.

4. Conclusions

In order to evaluate the influence of thermodynamic inhibitors, NaCl and MEG aqueous solutions were prepared and the equilibrium for carbon dioxide hydrates was experimentally determined above the upper quadruple point. As expected, higher concentrations of inhibitor caused a higher decrease in the equilibrium temperature. Lastly, the mixture of NaCl and MEG resulted in a higher inhibition effect than the simple sum of the temperature decrease caused by the aforementioned single inhibitors concentrations.

References

[1] E.D. Sloan, C.A. Koh, Clathrate Hydrates of Natural Gases, CRC Press/Taylor & Francis, 2008.
[2] Melo, C. L.; Thedy, E. A.; Rocha, P. S.; Almeida, A. S. De; Paula, A., The challenges on the CCGS monitoring in the development of Santos Basin Pre-salt Cluster. Energy Procedia., 4, 3394–3398,2011.
[3] Multiflash 6.1, KBC Processing Technologies Products, 2017.

ECCE12
The 12th EUROPEAN CONGRESS OF CHEMICAL ENGINEERING
Florence 15-19 September 2019

Thermodynamic prediction of the glass transition temperature in polymers and polymer blends

Margarete Roericht, Sabine Enders*

Karlsruhe Institute of Technology, Institute of Technical Thermodynamics and Refrigeration Engineering, Engler-Bunte-Ring 21, 76131 Karlsruhe, Germany.

**Corresponding author: sabine.enders@kit.edu*

Highlights

- Calculation of the glass transition temperature with an equation of state.
- Comparison of the results with experimental data from the literature.
- Application of the theory to various examples e.g. miscible/immiscible blends.

1. Introduction

The development of reliable approaches for the prediction of the thermodynamic properties of polymer systems is crucial for the reasonable design of polymer materials and polymer processing in a wide range of polymer applications (for example composites, electronics, food, controlled drug delivery systems, medical devices). Glasses are disordered materials that lack the periodicity of crystals but behave mechanically like solids.

The assumption that the glass transition is basically thermodynamic in nature was used to derive a theoretical framework for the calculation of the glass transition temperature (T_G) of polymers, copolymers and polymer blends [1,2,3]. The theory is a synthesis of a thermodynamic equation of state suitable for polymers, the generalized entropy theory for glass-formation in polymer materials, and the rigorous Kirkwood-Buff theory for concentration fluctuations in binary mixtures [2,3].

2. Methods

In the present contribution the above described framework is applied in order to compare the theoretical results with experimental data taken from the literature. Hereby the Sanchez-Lacombe equation of state (SL-EOS) [4] was used, because the pure-component parameters for several different polymers (polystyrene, (PS); poly(vinyl methyl ether), (PVME); poly(methyl methacrylate), (PMMA); poly(p-phenylene oxide), (PPO)) as well as for the statistical copolymer consisting of styrene and acrylonitrile (PSAN) are available. Unfortunately, the parameters for polyacrylonitrile (PAN) are not available, because no PVT (pressure, volume, temperature) data can be measured with high accuracy. The reason for this finding is the thermal instability of this polymer. Therefore, the pure-component parameter for PAN were estimated using PS and PSAN data simultaneously.

3. Results and discussion

Using the above mentioned theoretical framework [1,2,3] the T_G of pure polymers was calculated as function of the molecular weight, and compared to experimental data. The analysis shows, that

one adjustable parameter per pure polymer is required to match experimental T_G data. Regarding the molecular weight dependency, the theory predicts correctly that the T_G tends towards a limiting value for high molecular weight polymers. This concept can also be applied to statistical copolymers (i.e. PSAN), where the T_G is predicted as function of the chemical composition in good agreement with experimental data taken from the literature [5].

Furthermore the theoretical method can be applied for polymer blends, where the Kirkwood-Buff formalism serves for the determination of the concentration fluctuation. These calculations were performed for immiscible blends made of PS and PVME, where the T_G was investigated as function of blend composition. The results are compared with experimental data [6,7] in Figure 1. Blends made of PS and PPO serve as an additional example for miscible blends, where experimental data are taken from [8].

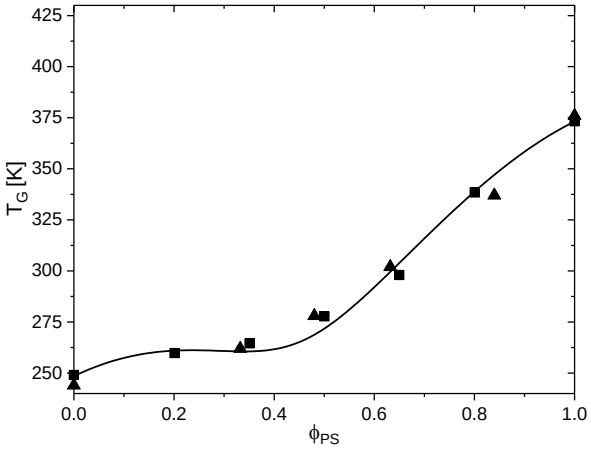

Figure 1. Calculated (solid line) and experimental data from the literature (squares [6], triangles [7]) for the glass transition temperature in a PS-PVME blend.

4. Conclusions

It is shown that the calculation of T_G in polymers and polymer blends can be done with an equation of state e.g. SL-EOS. Hereby the application of the Kirkwood-Buff formalism allows to combine thermal and concentration fluctuations in polymer blends. The results are in good accordance with experimental data and can be applied for different systems e.g. miscible/immiscible polymer blends.

References [Calibri 10]

[1] J. Dudowicz, K.F. Freed, J.F. Douglas, Adv. Chem. Physics 137 (2008) 125.
[2] J. Dudowicz, J.F. Douglas, K.F. Freed, J. Chem. Phys. 140 (2014) 244905.
[3] J. Dudowicz, J.F. Douglas, K.F. Freed, J. Chem. Phys. 141 (2014) 234903.
[4] I.C. Sanchez, R.H. Lacombe, Macromolecules 11 (1978) 1145.
[5] L. Fan, D. Zhao, C. Bian, Y. Wang, G. Liu, Polym. Bull. 67 (2011) 1311.
[6] E. Leroy, A. Alegría, J. Colmenero, Macromolecules 35 (2002) 5587.
[7] Y. Miwa, K. Usami, K. Yamamoto, M. Sakaguchi, M. Sakai, S. Shimada, Macromolecules 38 (2005) 2355.
[8] W.M. Prest, R.S. Porter, J. Polym. Sci. A-2 10 (1972) 1639.

ECCE12
The 12th EUROPEAN CONGRESS OF CHEMICAL ENGINEERING
Florence 15-19 September 2019

Non-ideal Multicomponent Adsorption in Thermally-rearranged Polybenzoxazole (TR-PBO) Membranes by Reactive Vacancy Solution Theory

Alessio Caravella[1*], Adele Vaccaro[1], Carmen Rizzuto[2], Giuseppe De Marco[3], Elena Tocci[4]

[1]*Department of Environmental and Chemical Engineering, University of Calabria, Via P. Bucci, Cubo 44A, Rende (CS), 87036, Italy*

[2]*Department of Physics, University of Calabria, Via P. Bucci, Cubo 31C, Rende (CS), 87036, Italy*

[3]*Information Technology Center (ICT), University of Calabria, Via P. Bucci, Cubo 22B, Rende (CS), 87036, Italy*

[4]*National Research Council - Institute on Membrane Technology (ITM-CNR), Via P. Bucci, Cubo 17C, Rende (CS), 87036, Italy*

**Corresponding author: alessio.caravella@unical.it*

Highlights

- Binary-mixture membrane adsorption isotherms are obtained by molecular dynamics
- The Reactive Vacancy Solution Theory is used to model the gas mixture adsorption
- Activity coefficients and selectivity are calculated up to 20 bar in non-ideal conditions
- Our approach allows a precise description of multi-adsorption at high pressure

1. Introduction

Polymeric membranes are nowadays the class of membranes mostly used in gas separation at moderate temperatures due to their relatively low cost compared to the ceramic ones. Thus, a considerable research work has been carried out to create polymeric films with high values of permeability and selectivity. In particular, the TR-PBO membranes have been extensively studied [1-4], reporting a detailed analysis on the free volume and its relation to solubility, diffusivity and permeability. These studies conclude that TR-PBO has high permeability mainly due to a high diffusivity owing to the higher amount of the free volume. However, the behaviour of these membranes in non-ideal conditions subject to multicomponent sorption at high pressure has not been considered yet in the literature, which is indeed the aim of our work.

2. Mathematical approach to adsorption model

The *Reactive Vacancy Solution Theory* (*RVST*) [5] is paired with the Wilson activity model for the adsorbate phase to predict the membrane behaviour at high pressure in non-ideal conditions. To do that, the single-gas isotherms of four light gases of interest (H_2, N_2, CH_4, CO_2) and their six binary-mixture isotherms were obtained by means of molecular dynamics at 35°C. Then, these data are used to calculate the parameters of the RVST by means of a robust in-house routine.

3. Results and discussion

Some results are shown in Figure 1 as adsorbate activity coefficients and adsorption selectivity. We can see that the activity coefficients are significantly different from the unity, this stating the strong system non-ideality, which thus cannot be modelled by an ideal adsorption model.

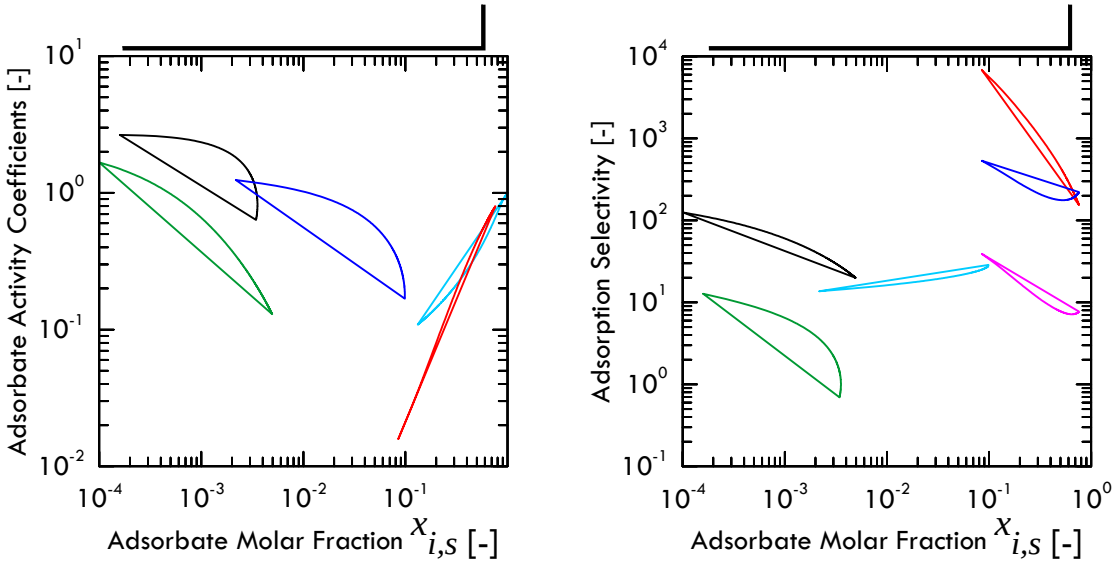

Figure 1. a) Adsorbate activity coefficients and b) Adsorption Selectivity as functions of the adsorbate molar fraction for an equimolar four-species gas mixture at 35°C. The adsorbate composition refers to the upper species in the selectivity definition and is let vary by changing the total pressure within [0.01, 20] bar.

Furthermore, interesting values of adsorption selectivity are found, with the CO_2/H_2 and CO_2/N_2 ones that are respectively estimated around 150 and 210 at a total pressure of 20 bar. These observations suggests possible applications of these materials to gas separation also as adsorbents rather than as membranes, since their perm-selectivity is expected to be lower than the adsorption selectivity due to their relatively high free volume.

4. Conclusions

In this work, the multicomponent adsorption of light gases – H_2, N_2, CH_4, CO_2 – in thermally-rearranged Polybenzoxazole (TR-PBO) membranes was described using the *Reactive Vacancy Solution Theory* (*RVST*) in order to deal with high-pressure and non-ideal conditions. For this purpose, both single-gas and binary-mixture isotherms were obtained by means of molecular dynamics techniques at 35°C. Afterwards, we interpreted these data by the reactive vacancy solution theory (RVST) paired with the Wilson activity model for the adsorbate phase, developing an in-house robust routine to calculated the model parameters.

Our approach, which can be generally applied to all membranes, allow us to predict the real adsorption behaviour of multicomponent mixtures at high pressure (at least up to 20 bar) and in non-ideal cases, where simple Langmuirian models used within the Ideal Adsorption Solution Theory (IAST) cannot satisfactorily describe the mutual adsorbate-adsorbate-adsorbent interactions present in conditions of interest for process industry.

References

[1] Y. Jiang, F.T. Willmore, D. Sanders, Z.P. Smith, C.P. Ribeiro et al., Polym. 52 (2011) 2244-2254.
[2] K.S. Chang, Z.C. Wu, S. Kim, K.L. Tung, Y. M. Lee, Y.F. Lin, J.Y. Lai, J. Membr. Sci. 454 (2014) 1-11.
[3] C.H. Park, E. Tocci, S. Kim, A. Kumar, Y.M. Lee, E. Drioli, J. Phys Chem., B 118 (2014) 2746-2757.
[4] S. Kim, J.G. Seong, Y.S. Do, Y.M. Lee, J. Membr. Sci., 474 (2015) 122–131.
[5] Munakata K., Surf. Sci., 616 (2013) 1–11.

CO_2 sorption modelling in humidified Polyvinyl amine (PVAm) with PC-SAFT

Riccardo Rea[1], Maria Grazia De Angelis[1,*], Marco Giacinti Baschetti[1]

1 Department of Civil, Chemical, Environmental and Materials Engineering (DICAM), University of Bologna, Via U. Terracini, 28, 40127, Bologna

**Corresponding author: grazia.deangelis@unibo.it*

Highlights

- H_2O sorption in PVAm modelled with PC-SAFT EoS
- CO_2 physical solubility predicted in the ternary systems PVAm / H_2O / CO_2

1. Introduction

Carbon dioxide emissions represent one of the main environmental issue of our time. The greenhouse gases atmospheric loading, due to anthropogenic activities, are causing a continue rise of global temperature. In the field of CO_2 capture from gas streams, membrane technologies are promising alternative to the more common operations. Among these, Facilitated Transport Membranes show high performances in terms of CO_2 permeabilities and selectivities even at low pressures by coupling a simple solution diffusion transport mechanism and a reversible chemical reaction with a carrier agent. Polyvinyl amine (PVAm) binds one primary amino group for each monomer along the chain, showing high hydrophilicity and affinity to CO_2. In this work we use the PC-SAFT [1] Equation of State to model the H_2O uptake and the solubility of CO_2 in the ternary system of PVAm / H_2O / CO_2.

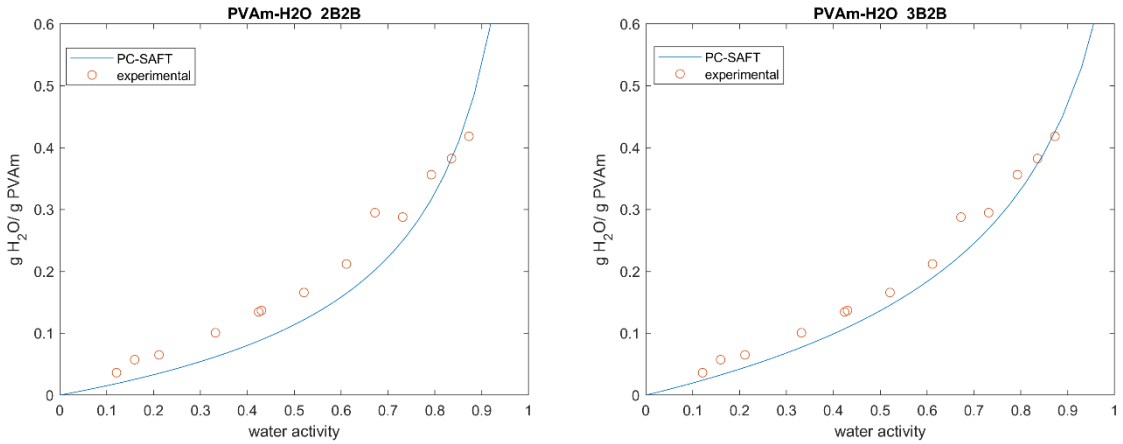

Figure 1. Water uptake in PVAm at 35°C. Circles are experimental data, lines are model calculations.

2. Methods

Within the PC-SAFT, each species is pictured as a series of chained spheres, interacting each other by dispersive, repulsive and associative forces. In the present work, the water has been treated as

a self associative species, with 2 association sites (2B). The same scheme, together with the 3B [2], has been tested also for the PVAm. Besides the non associative case, two sites have been hypothesized for carbon dioxide to better consider the physical interactions among CO_2 and H_2O.

3. Results and discussion

In the figure 1 above, the uptake of water at 35°C in purified PVAm is reported, experimental points are the red circles while the blue lines are the model calculation. Both the association scheme used can describe the actual behaviour of the system in quantitative agreement with the experimental data. The scheme 3B (right) agree better over all the water activity range in respect to the 2B one. The physical sorption prediction (without considering explicitly the chemical reaction(s)) of CO_2 in the ternary system is reported in figure 2 below.

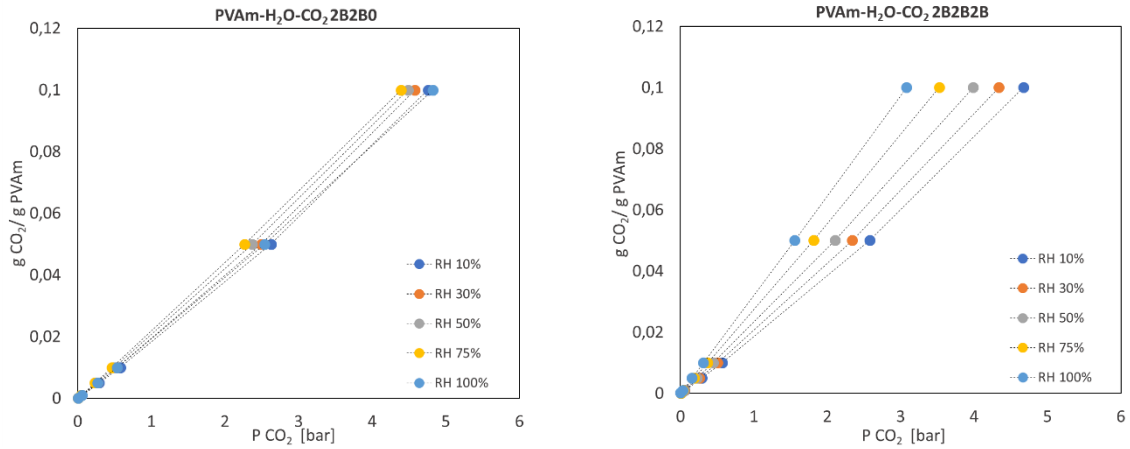

Figure 2. Prediction of CO_2 physical sorption in humidified PVAm.

In the non associative case (left figure) the relative humidity of water does not influence the uptake of CO_2 ; the presence of two sites, instead, elucidate the role of relative in humidity in the system . The higher the water activity, the higher the gas uptake, as we could expect for the system under study.

4. Conclusions

Both the two associative scheme used, 2B and 3B, are able to describe the behaviour of the membranes in terms of H_2O sorption. Moreover the physical solubility of the carbon dioxide in the ternary system of PVAm / H_2O / CO_2 is predicted and the role of relative humidity is elucidated by the presence of two possible associative sites on CO_2. A deeper investigation on the reacting ternary system is undergoing by the use of extended PC-SAFT [3] for polyelectrolyte.

Acknowledgements: This work has been performed in the framework of the European Project H2020 NANOMEMC^2 "NanoMaterials Enhanced Membranes for Carbon Capture", funded by the Innovation and Networks Executive Agency (INEA) Grant Agreement Number: 727734

References

[1] J. Gross, G. Sadowski, Ind. Eng. Chem. Res. 40 (2001) 1244–1260.
[2] S.H. Huang, M. Radosz, Ind. Eng. Chem. Res. 29 (1940) 2284-2294.
[3] S. Naeem, G. Sadowski, Fluid Ph. Equilibria 299 (2010) 84-93.

ECCE12
The 12th EUROPEAN CONGRESS OF CHEMICAL ENGINEERING
Florence 15-19 September 2019

Phase Equilibrium and Density of Highly Asymmetric Gas-Oil Mixtures at High Temperatures and High Pressures

Yiqun. Liu, Teresa Regueira, Erling H. Stenby, Wei Yan*

CERE, Department of Chemistry, Technical University of Denmark, DK-2800 Kgs. Lyngby, Denmark

**Corresponding author: weya@kemi.dtu.dk*

Highlights

- Density and phase equilibrium of CH_4, N_2 and CO_2-oil mixtures systematically measured up to 190 ℃ and 1400 bar.
- Measured data most valuable for modeling highly asymmetric reservoir fluids.
- The more theoretical PC-SAFT model evaluated using the data against the classical cubic models with and without volume translation.

1. Introduction

The global demand for oil is still increasing and expected to stay at a high level for the near future. This has driven many production activities to deep reservoirs at high pressures and high temperatures (HPHT). Accurate description of phase equilibrium and thermophysical properties is of paramount importance to reduce the technical and economic risks in developing HPHT reservoirs. This study is a continuation of our previous work on measuring and modeling asymmetric hydrocarbon systems relevant to reservoir fluids[1][2]. Although we measured binary, ternary and multiple component systems, it is found that the well-defined mixtures are not sufficiently representative for reservoir fluids. Hence, we here conducted a systematic measurement using the mixtures of a stock tank oil with various gases (CH_4, N_2 and CO_2). The measurement includes phase equilibrium and density data up to 190 ℃ and 1400 bar. Since the systems mimic reservoir fluids better, the obtained data provide a more relevant evaluation of various thermodynamic models in describing highly asymmetric reservoir fluids. We evaluated classical cubic models SRK and PR, and the more theoretical PC-SAFT EoS with a heptanes plus characterization method specially developed for it[3].

2. Methods

The density measurement was conducted in an Anton Paar DMA-512P high pressure oscillating tube densimeter following a modified Lagourette et al. method[4][5]. Densities of CH_4-oil, N_2-oil, and CO_2-oil mixtures with different compositions were measured at six temperatures from 25 to 190 ℃ and at six pressures from 400 to 1400 bar. A full visibility cell ST PVT 240/1500 was used to measure the saturation pressure and liquid fractions in the two-phase region for the same gas-oil mixtures. The cell has a motor-driven piston to vary the system pressure and a sapphire window at its bottom to allow full visual observation of phenomena inside the cell and determination of phase fractions. At six temperatures from 25 to 190 ℃, gas (CH_4, N_2, or CO_2) was added to the oil stage by stage to prepare mixtures with increasing gas mole fraction. The classical cubic models SRK and PR were compared with the more theoretical PC-SAFT EoS in modeling the measured data. For SRK and PR, calculation results with and without volume translation were presented.

3. Results and discussion

Our measurement has produced over 270 density points and over 70 saturation pressure points. Figure 1 shows the phase envelopes for three selected mixtures with a gas mole fraction of 0.2. All models predict the correct trend but SRK and PR show large deviations for N_2-oil. Overall, three models show comparable deviations for the C_1-oil and CO_2-oil but PC-SAFT is better for N_2-oil. Some typical density modelling results are shown in Figure 2 for mixtures with a gas mole fraction of 0.2. PC-SAFT is clearly more accurate than SRK and PR without volume translation, but the volume translated SRK and PR show comparable and sometimes even better results than PC-SAFT.

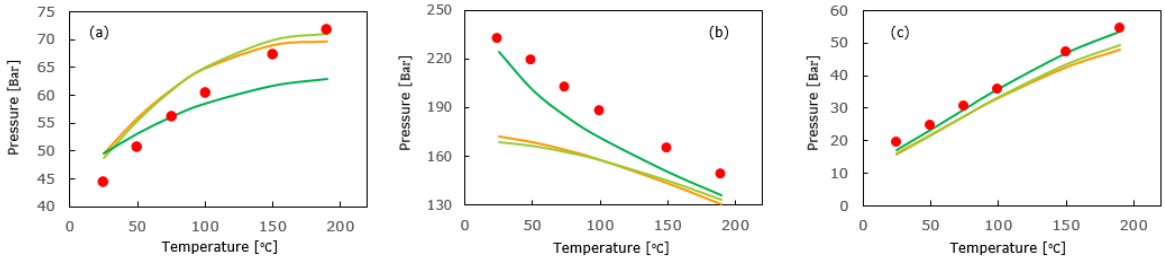

Figure 1. Phase envelope of C_1-oil (a), N_2-oil (b), CO_2-oil (c): data (●); prediction by SRK (—), PR (—) and PC-SAFT (—).

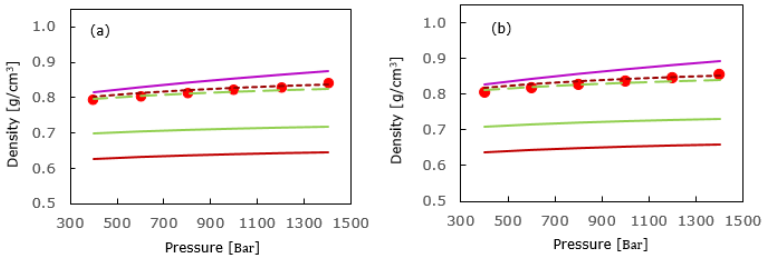

Figure 2. Density for C_1-oil (a) and N_2-oil (b) at 25 °C: data (●); prediction by SRK (—), PR (—), PC-SAFT (—), SRK-VT (- -), and PR-VT (– –).

4. Conclusions

This study has produced valuable HPHT density and phase equilibrium data of highly asymmetric C_1-oil, N_2-oil and CO_2-oil mixtures in a wide composition range. The data are particularly valuable for evaluating and further improving thermodynamic models for HPHT reservoir fluids since well-define mixtures turned out useful but not sufficiently representative in our previous study. The model comparison of PC-SAFT with classical models show that the more theoretical PC-SAFT has some advantages but may not be superior to PR (VT) and SRK (VT) in density modelling. For a more comprehensive evaluation, it is worthwhile to compare these models using other derived properties like excess volume and compressibility data.

References

[1] T. Regueira, G. Pantelide, W. Yan, E.H. Stenby, Fluid Phase Equilibria 428 (2016) 48-61.
[2] T. Regueira, M.L. Glykioti, E.H. Stenby, W. Yan, J. of Chem. & Eng. Data 63 (2018) 1072-1080.
[3] F. Varzandeh, E.H. Stenby, W. Yan, Fluid Phase Equilibria 433 (2017) 97-111.
[4] M.J.P. Comuñas, J.P. Bazile, A. Baylaucq, C. Boned, J. of Chem. & Eng. Data 53 (2008) 986-994.
[5] B. Lagourette, C. Boned, H. Saint-Guirons, P. Xans, H. Zhou, Measurement Sci. and Tech. 1992, 3, 699.

ECCE12
The 12th EUROPEAN CONGRESS OF CHEMICAL ENGINEERING
Florence 15-19 September 2019

Combination of different methods to characterize surface chemistry of activated carbons

Johanna Muthmann[1], Christian Bläker[1], Christoph Pasel[1], Michael Luckas[1], Dieter Bathen[1,2]

[1]Chair of Thermal Process Engineering, University of Duisburg-Essen, Lotharstr. 1, 47057 Duisburg, Germany, [2]Institute of Energy and Environmental Technology e. V. (IUTA), Bliersheimer Str. 60, 47229 Duisburg, Germany

**Corresponding author: johanna.muthmann@uni-due.de*

Highlights

- New and improved methods for characterization of surface chemistry
- Chemical modification changes surface chemistry but not structural properties
- Increasing number of acidic oxidic surface groups increases polarity
- Change in surface chemistry shows hardly any effect on the heat of adsorption

1. Introduction

Carbonaceous adsorbents such as activated carbons are used in many technical adsorption processes. Depending on the raw material and the activation conditions, these materials may have different properties. Adsorption is significantly influenced by structural properties and surface chemistry. To characterize structural properties well established methods are available like mercury porosimetry and nitrogen adsorption. At the same time, the impact of surface chemistry on adsorption is not well understood for activated carbons. The aim of the project is to improve the characterization of the surface chemistry of activated carbons and to distinguish between the influence of surface chemistry and structural properties on adsorption.

2. Methods

In this project activated carbons are investigated, which differ systematically in surface chemistry due to chemical modification. To characterize surface chemistry, new and improved methods such as Boehm titration, the measurement of excess isotherms as well as the coupling of volumetric and calorimetric measurements are used. The structural properties are analyzed by nitrogen adsorption

Boehm titration enables quantitative determination of acidic oxidic surface groups of activated carbon using different bases. The ratio of polar, non-polar and aromatic surface groups can be described by excess isotherms [1]. These isotherms reflect the adsorption preference between two competing sample molecules as a function of mole fraction in the liquid phase and thus provide additional information about surface polarity. By coupled volumetric and calorimetric measurements the adsorption enthalpy can be determined, which is a parameter for the strength of interactions in adsorption and allows an energetic characterization of the adsorbent surface [2].

3. Results and discussion

The activated carbon surface was oxidized using nitric acid (HNO_3). The chemical modification changes the surface chemistry whereas structural properties largely remain the same. Boehm titration shows that the number of acidic oxidic surface groups increases with increasing concentration of HNO_3.

In excess isotherms the rising number of acidic oxidic surface groups leads to an increasing ratio of adsorbed polar component over adsorbed aromatic and non-polar components. The increased affinity for the polar adsorptive indicates an increasing polarity of the activated carbon.

In contrast, the heats of adsorption of acetone, toluene and n-heptane are almost identical for the original and for the chemically modified activated carbons . This suggests that the strength of the interactions between surface and adsorptive molecules are dominated by the energetically heterogeneous multimodal pore size distribution of the activated carbon. The surface chemistry plays only a minor role.

To investigate the influence of structural properties in detail, activated carbons manufactured under different activation conditions will be characterized.

4. Conclusions

The combination of different methods enables to distinguish between the influence of structural properties and surface chemistry on adsorptive properties. The investigations were carried out on activated carbons with the same structural properties but different surface chemistry. A rising number of acidic oxidic surface groups results in an improved adsorption of a polar component in a binary mixture and increases the polarity of the activated carbon. In contrast, an influence of surface chemistry on the strength of the interactions between surface and adsorptive molecules could not be detected.

References

[1] J. Treese, C. Pasel, M. Luckas, D. Bathen, Chem. Eng. Technol. 39 (2016) 1144–1150.
[2] C. Bläker, C. Pasel, M. Luckas, F. Dreisbach, D. Bathen, Microporous and Mesoporous Materials 241 (2017) 1–10.

ECCE12
The 12th EUROPEAN CONGRESS OF CHEMICAL ENGINEERING
Florence 15-19 September 2019

Preferential Adsorption in Electrolyte Mixtures

Max F. Döpke[1], Remco Hartkamp[1]

1 Process & Energy Department, Delft University of Technology, Leeghwaterstraat 39, 2628 CB Delft, The Netherlands

**Corresponding author: r.m.hartkamp@tudelft.nl*

Highlights

- Preferential adsorption is driven by a balance between interactions
- Different surface sites show preference to different electrolytes

1. Introduction

Interfaces between aqueous solutions and oxide surfaces are critical to a plethora of industrial and biological systems. Solutions typically contain various monovalent and multivalent electrolytes. However, countless studies have considered solutions with only a single electrolyte to represent systems in which the concentration of one electrolyte is dominant, such as seawater.

Although such an approach may be appropriate for the study of bulk fluid properties, local properties at the solid-liquid interfaces can be highly ion specific. Consequently, even electrolytes that are present in small quantities can dominate the electric double layer (EDL) and thus play a key role in nanofluidic transport, sensing,[1] energy storage, sensing and electrochemical processes.

This study reveals the origin of preferential ion adsorption onto an amorphous oxide surface. Furthermore, we show how traditional electric double layer models fall short in predicting or fitting the ion distribution in the case of electrolyte mixtures.

2. Methods

Experimental techniques often rely on fitting measurement data to EDL models (such as variants of the Gouy-Chapman model) and macroscopic transport relations to infer quantities that cannot be directly measured.[2] Such simplified models disregard ion specificity and assume that the solid surface is flat and homogeneous and that fluid transport coefficients are constant in space. Alternatively, molecular dynamics (MD) simulations can provide detailed insight into the three-dimensional EDL structure and local transport properties, without the need for an assumed EDL model. As such, MD offers an appealing approach to gain detailed insight into interfacial properties and can aid in improving models and assumptions used for interpreting experimental measurements.

3. Results and discussion

Using all-atom MD simulations[3] of NaCl-$CaCl_2$ solutions in a charged oxide nanochannel (Figure 1), we found that Na^+ and Ca^{2+} ions were simultaneously adsorbed to the surface, with some surface

sites showing a distinct preference for Na^+ and others for Ca^{2+}. Although Ca^{2+} ions experience stronger electrostatic attraction to the negatively charged surface sites, their large and strong hydration shell forms a steric hindrance at some of the surface sites, whereas the hydration shell of the Na^+ ions does not suffer from the same hindrance. Using a metric to quantify the geometry of surface sites, ion-specific adsorption can be successfully predicted.

Turning to adsorption kinetics, Ca^{2+} ions were found to be adsorbed much longer than Na^+, with adsorption times depending on the specifics of the surface site. As such, the presence of even small quantities of preferentially adsorbed ions can dramatically alter interfacial dynamics, including fluid-wall slip, interfacial viscosity enhancement, and conductance.

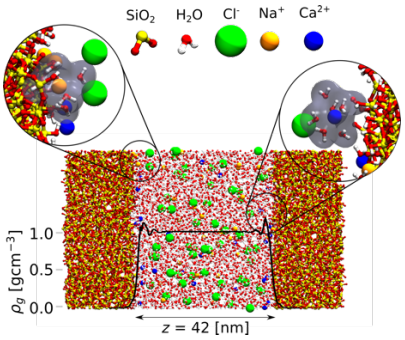

Figure 1. Channel configuration for simulations with fluid density overlaid on the channel. The left inset shows Na^+ adsorption, with the hydration shell penetrating the wall. Right inset shows Ca^{2+} adsorption, with the hydration shell remaining intact.

4. Conclusions

Surface roughness, as well as placement and orientation of surface sites, severely impacts preferential adsorption. Insight from MD simulations into the relation between surface structure and preferential adsorption can help to interpret experimental measurements and can also be used to microengineer surfaces with selectivities for specific ions.

References

[1] R. Sivakumarasamy, R. Hartkamp, B. Siboulet, J.-F. Dufreche, K. Nishiguchi, A. Fujiwara, N. Clement, Nature Mater., 17, 464-470 (2018)

[2] R. Hartkamp, A.-L. Biance, L. Fu, J.-F. Dufreche, O. Bonhomme, L. Joly, Curr. Opin. Colloid Interface Sci., 37, 101-114 (2018)

[3] M.F. Döpke, J. Lützenkirchen, O.A. Moultos, B. Siboulet, J.-F. Dufreche, R. Hartkamp, in preparation

ECCE12
The 12th EUROPEAN CONGRESS OF CHEMICAL ENGINEERING
Florence 15-19 September 2019

Molecular-Thermodynamic Correlation of Solubility Data for 20 Amino Acids in Water, in Ethanol and in Water-Ethanol Mixtures.

Nathan Bowden[1], Marieke E. Bruins[2], Johan Sanders[3], John M. Prausnitz[4]

1 Institute for Sustainable Process Technology, Groen van Prinstererlaan 37 3818JN Amersfoort, the Netherlands; 2 Wageningen Food & Biobased Research, Bornse Weilanden 9, 6107WG Wageningen University and Research, The Netherlands; 3 Biobased Chemistry and Technology Group, AFSG, Bornse Weilanden 9, 6708WG Wageningen, Wageningen University and Research, The Netherlands; 4 Department of Chemical & Biomolecular Engineering, Gilman Hall, University of California, Berkeley, CA 94720-1462, USA

**Corresponding author: Nathan.bowden@ispt.eu*

Highlights

- The solubilities of some amino acids show maxima in a water-ethanol mixed solution
- These calculated maxima, predicted by the model, are in agreement with experiments
- Solubility of amino acids depends its on $(f^s/f^L)_{pure}$ ratio and its solvent interaction
- Amino acids with the lowest interaction parameters are not necessarily the most soluble
-

1. Introduction

Models have been proposed for amino acid solubility in aqueous solution [1] and for the solubility of amino acids in salt solutions [2]. A few empirical models with regressed parameters have been proposed to describe the solubility of α-amino acids in ethanol/water systems [3,4]. In this work, we apply the van Laar equation for the molar excess Gibbs energy to all 20 proteinogenic amino acids in ethanol, in water and in ethanol-water mixtures.

2. Methods

For each amino acid, T_m and Δh_{T_m} are estimated using the method proposed by Marrero and Gani [4]. To predict the solubility of an amino acid in mixtures of water and ethanol, we must determine the interaction parameters, A_{ij}, of an amino acid (i) in water (j) or ethanol (j) and of water (i) and ethanol (j) in a solute free solution, where i and j are all possible binary combinations of solute (1), water (2) and ethanol (3). To obtain the A_{ij} parameters, we used the van Laar equation obtained from Wohl's expansion for the molar excess Gibbs energy of a binary solution.

We then obtain the saturated mole fraction of the amino-acid solute, x_1^S by simultaneously solving the model with the mass balance $x_1 + x_2 + x_3$= 1.00. The ratio $(f^s/f^L)_{pure}$ at 25 °C is obtained.

$$x_1^S = (f^s/f^L)_{pure}\left(exp\left[\frac{x_2{}^2 A_{12}\left(\frac{A_{21}}{A_{12}}\right)^2 + x_3{}^2 A_{13}\left(\frac{A_{31}}{A_{13}}\right)^2 + x_2 x_3 \frac{A_{21}A_{31}}{A_{12}A_{13}}(A_{12}+A_{13}-A_{32})\left(\frac{A_{13}}{A_{31}}\right)}{\left(x_1 + x_2\frac{A_{21}}{A_{12}} + x_3\frac{A_{31}}{A_{13}}\right)^2}\right]\right)^{-1} .$$

This calculation is not explicit in x_1^S. Solution of Equation is achieved by a simple iterative computer program.

3. Results and discussion

The Normalized Root Mean Square Variance for 16 of the 20 proteinogenic amino acids were lower than 0.100, indicating very good agreement with the solubility data. This group of amino acids includes L-tyrosine, whose maximum solubility occurs when the solute-free mixed solvent contains 91.1 mole% water and 8.90 mole% ethanol, higher than that at 100 mole% water. For L-isoleucine, L-tryptophan, L-phenylalanine and L-proline, NRMVs are lower than 0.220, indicating good agreement with the solubility data.

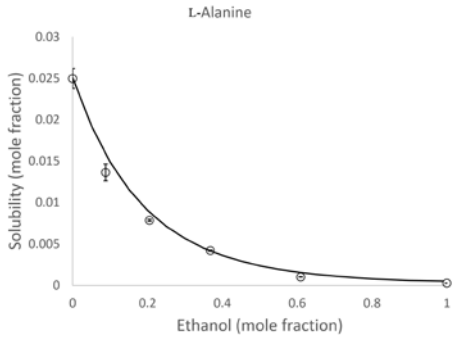

Figure 1: Predicted (solid line) and experimental (circles) solubilities of L-alanine in water-ethanol mixtures at 25 ˚C.

4. Conclusions

The ternary form of the van Laar equation for the molar excess Gibbs energy is useful for predicting the solubilities of amino acids in water-ethanol mixtures at 25 °C. The calculated solubilities of some amino acids show maxima in a water-ethanol mixed solution. These calculated maxima, predicted by the van Laar model, are in agreement with experiments.

The advantage of the thermodynamic technique used in this work is scale-up. A good solubility of a solute in a binary solvent (i.e. a ternary system) can be calculated based on only binary information.

References

[1] Gude, M. T.; Meuwissen, H. H. J.; van der Wielen, L. A. M.; Luyben, K. C. A. M., Partition Coefficients and Solubilities of α-Amino Acids in Aqueous 1-Butanol Solutions. *Industrial & Engineering Chemistry Research* **1996**, 35 (12), 4700-4712;

[2] Held, C.; Prinz, A.; Wallmeyer, V.; Sadowski, G., Measuring and modeling alcohol/salt systems. *Chemical Engineering Science* **2012,** *68* (1), 328-339;

[3] Gude, M. T.; van der Wielen, L. A. M.; Luyben, K. C. A. M., Phase behavior of α-amino acids in multicomponent aqueous alkanol solutions. *Fluid Phase Equilibria* **1996,** *116* (1–2), 110-117.

[4] Bowden, N. A.; Mendez Sevillano, D.; Sanders, J. M. P.; Bruins, M. E. Modelling the effects of ethanol on the solubility of the proteinogenic amino acids with the NRTL, Gude and Jouyban-Acree models. *Fluid Phase Equilibria* **2017** 459: 158-169

[5] Marrero, J.; Gani, R.; Group-contribution based estimation of pure component properties *Fluid Phase Equilibria* **2001**, 183-208

ECCE12
The 12th EUROPEAN CONGRESS OF CHEMICAL ENGINEERING
Florence 15-19 September 2019

Development of a new experimental method to determine inherent dissolution properties of active pharmaceutical ingredients

Dominik Sleziona[1], Amelie Mattusch[1], Sebastian Klosa[1], Gerhard Schaldach[1], David R. Ely[2], Gabriele Sadowski[3], Markus Thommes[1]

[1] TU Dortmund, Department of Biochemical and Chemical Engineering, Laboratory of Solids Process Engineering, Emil-Figge-Str. 68, 44227 Dortmund, Germany; [2] Ivy Tech Community College, 3101 S Creasy Ln, Lafayette, IN 47905, USA; [3] TU Dortmund, Department of Biochemical and Chemical Engineering, Laboratory of Thermodynamics, Technical University Dortmund, Emil-Figge-Str. 70, 44227 Dortmund, Germany

**Corresponding author: markus.thommes@tu-dortmund.de*

Highlights

- Drug release can be limited by diffusion or surface reaction kinetics.
- A flow channel was constructed to ensure well-defined fluid conditions.
- Intrinsic material data were derived by analyzing four different drugs.
- A model that accounts for diffusion- and surface reaction limited drug release was developed.

1. Introduction

The dissolution behavior is a crucial factor in novel drug substance formulation. The two main factors limiting the dissolution kinetics of active pharmaceutical ingredients are diffusion (Fick, 1855) and surface reaction kinetics (Paus et al., 2015).

2. Methods

Dissolution experiments such as the intrinsic dissolution test described in the pharmacopeia (European Pharmacopoeia Commission, 2017) have been performed for many years. To overcome the disadvantages of the intrinsic dissolution test, a flow channel was constructed and evaluated to ensure well defined flow conditions. The mass transfer rates from a flat, solid surface into the solvent flowing over the solid surface within the flow channel were used to derive a mathematical model that distinguishes between diffusion limited and surface reaction limited drug release.

3. Results and Discussion

A rectangular flow channel was designed (Shah and Nelson, 1975) (Figure 1, left) based on fluid dynamics calculations (Ansys CFX® 19.1, Ansys Inc., Canonsburg, USA). A rectangular surface with a width to height ratio of 5 was chosen (Ward-Smith, 1980). The characteristic velocities for a flow of Re 250 are color coaded. The powder sample was compress into a die resulting in a well-defined sample surface. The sample concentration in the dissolution media was measured by UV spectroscopy. The right-hand image in Figure 1 shows the weight flux from the sample as function of the Reynolds number. For particularly low Reynolds numbers, the weight flux is limited by diffusion (intercept with the ordinate (Re=0); J^{w}_{D}). For high Reynolds numbers (Re > 150) the

weight flux begins to level out indicating it is limited by the surface reaction. Between those stages the weight flux depends on the flow conditions and is a function of the Reynolds number.

$$J_{diss}^{w} = \left(0.5 \cdot sgn\left(\left(0.03 \cdot \sqrt{\lambda} \cdot Re \cdot Sc^{\frac{1}{3}} \cdot J_D^w + J_D^w\right) - \frac{k_{SR} \cdot \rho_{solid}}{\delta_{SR}}\right) + 0.5\right) \cdot \frac{k_{SR} \cdot \rho_{solid}}{\delta_{SR}}$$
$$+ \left(0.5 \cdot sgn\left(\frac{k_{SR} \cdot \rho_{solid}}{\delta_{SR}} - \left(0.03 \cdot \sqrt{\lambda} \cdot Re \cdot Sc^{\frac{1}{3}} \cdot J_D^w + J_D^w\right)\right) + 0.5\right) \cdot \left(0.03 \cdot \sqrt{\lambda} \cdot Re \cdot Sc^{\frac{1}{3}} \cdot J_D^w + J_D^w\right)$$

The weight flux from pure diffusion is quite similar for the two tested model substances. This is unsurprising based on their similar molecular size, which is used to predict diffusivity via the Stokes-Einstein correlation. Theophylline shows a much higher flux at high Reynolds number compared to benzocaine, which indicates a faster surface reaction for theophylline. The reason is not clear yet and needs to be investigated further. The linear correlation between flux and Reynolds number (0 < Re < 150) can be attributed to convection and is captured by an approach based on Prandlt's work (Brauer and Mewes, 1971).

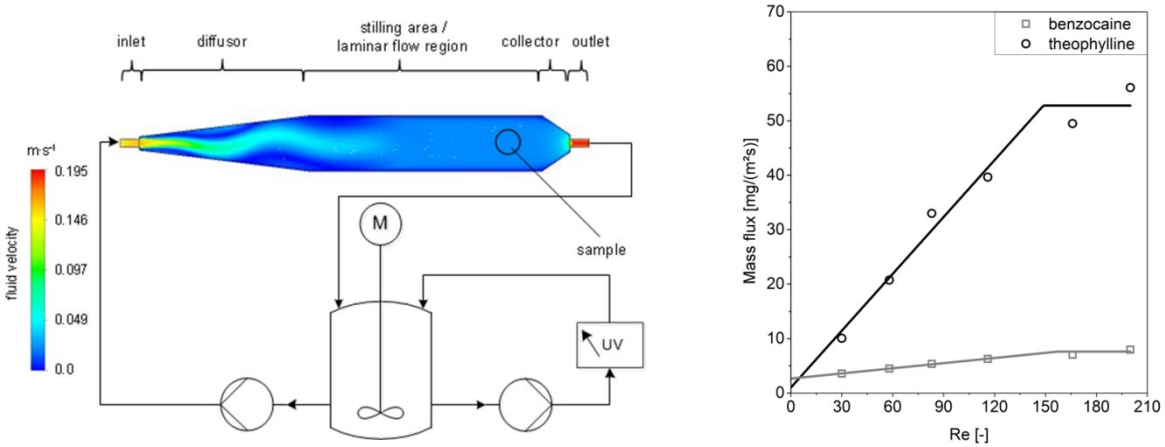

Figure 1. Set up of the flow channel dissolution experiment (left) and the resulting weight flux of benzocaine, theophylline as a function of the Reynolds numbers (av, n = 3).

4. Conclusions

A new intrinsic dissolution setup has been deigned in order to overcome the limitations of the pharmacopeia test. This enables diffusion- and surface reaction limited regimes for drug release to be determined experimentally. Two model drugs were tested and differences were observed.

References

[1] European Pharmacopoeia Commission (2017) European pharmacopoeia, Vol. 9.0, Council of Europe.
[2] Fick, A. (1855) Ueber Diffusion, Annalen der Physik 170, 59-86.
[3] Paus, R., Ji, Y., Braak, F.,Sadowski, G. (2015) Dissolution of crystalline pharmaceuticals: experimental investigation and thermodynamic modeling, Industrial & Engineering Chemistry Research 54, 731-742.
[4] Shah, A. C. and Nelson, K. G. (1975) Evaluation of a convective diffusion drug dissolution rate model, Journal of Pharmaceutical Sciences 64, 1518-1520.
[5] Ward-Smith, A. J. (1980) Internal Fluid Flow-The fluid dynamics of flow in pipes and ducts, Nasa Sti/recon Technical Report A 81.
[6] Brauer, H., Mewes, D. (1971),Stoffaustausch enschließlich chemischer Reaktionen, Sauerländer.

Molecular Dynamics Simulations of Confined Water inside Stacked Graphene Oxide Membranes

One-Sun Lee
Qatar Environment and Energy Research Institute, Hamad Bin Khalifa University, Doha, Qatar

Stacked graphene oxide (GO) is an emerging membrane with the application of desalination. However, the structure and dynamics of water molecules and ions inside GO membrane is not known, and this has proven to be a hindrance in understanding how this system functions. Here, we investigate the dynamic behavior of water inside GO membrane using computational approach. We developed four different models of GO membrane with different interstice distance (*d*) between GO sheets (*d* = 7, 9, 11, and 13 Å in Figures 1 (A) and (B)), and performed molecular dynamics simulations of water (SPC/E model) inside each membrane. The measured diffusion coefficients (in unit of $\times 10^{-5}$ cm^2/sec) of water are 0.3 (*d* = 7 Å), 0.9 (*d* = 9 Å), 1.2 (*d* = 11 Å), and 1.5 (*d* = 13 Å). To understand the retarded diffusion of water with narrower interstice distance, we analyzed the hydrogen bond autocorrelation relaxation and the rotational relaxation. The molecular rotation is described by the first and second-rank Legendre polynomials,

$$P1_i(t) = \left\langle \vec{u}_i(0) \cdot \vec{u}_i(t) \right\rangle = \left\langle \cos\theta_i(t) \right\rangle \quad (1)$$

$$P2_i(t) = \left\langle \frac{3}{2}\left(\vec{u}_i(0) \cdot \vec{u}_i(t)\right)^2 - \frac{1}{2} \right\rangle \quad (2)$$

using the molecular body-fixed axes (See Figure 1(C)). We found that the hydrogen bond lifetime is longer in the GO membrane with the narrower interstice distance, and the rotation relaxation of water is also slower in the GO membrane with the narrower interstice distance (Table 1). Therefore, we concluded that the diffusion of water is retarded by the hydrogen bond with the hydroxyl or epoxy groups of GO membrane. Our simulation result would be a useful theoretical source for designing new carbon-based membranes for desalination.

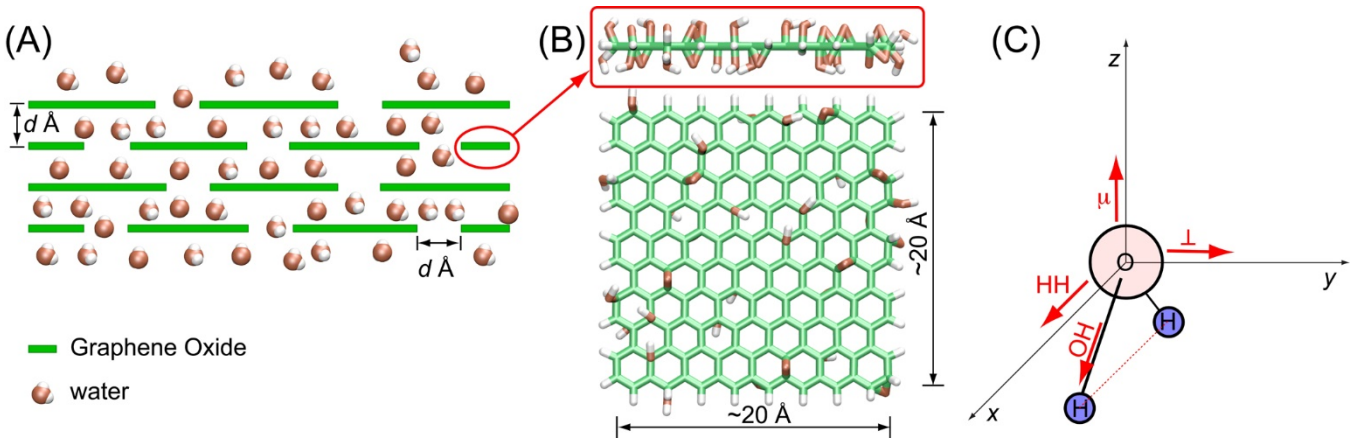

Figure 1. (A) Schematic representation of the penetration of water through the interstices of stacked GO membrane. (B) Snapshots of the side and top view of GO used in the simulations. (C) Coordinates of water molecule for the analysis of rotation dynamics.

Table 1. Rotational correlation time (ps) of water inside stacked graphene oxide

d (Å)	7	9	11	13	• *	• **
τ_1^{HH}	12.2	6.9	5.7	5.3	4.3	-
τ_1^{μ}	31.8	11.1	7.9	6.8	4.7	4.76[1]
$\tau_1^{\perp}$	10.9	5.1	4.2	3.7	2.9	-
τ_1^{OH}	18.5	8.3	6.5	5.7	4.5	-
τ_2^{HH}	14.8	4.9	3.4	2.9	2.0	2.0[2]
τ_2^{μ}	18.3	6.1	3.8	2.8	1.6	1.92[1]
$\tau_2^{\perp}$	32.4	9.2	4.8	3.2	1.2	-
τ_2^{OH}	13.4	4.8	3.3	2.7	1.8	1.95[3]

• * Bulk water (simulation)
• ** Bulk water (experiment)

References:

1. Sansom, M. S. P.; Kerr, I. D.; Breed, J.; Sankararamakrishnan, R., Water in channel-like cavities: Structure and dynamics. *Biophys. J.* **1996,** *70* (2), 693-702.
2. Halle, B.; Wennerstrom, H., Interpretation of magnetic-resonance data from water nuclei in heterogeneous systems. *J. Chem. Phys.* **1981,** *75* (4), 1928-1943.
3. Ludwig, R., NMR relaxation studies in water-alcohol mixtures - the water-rich region. *Chem. Phys.* **1995,** *195* (1-3), 329-337.

ECCE12
The 12th EUROPEAN CONGRESS OF CHEMICAL ENGINEERING
Florence 15-19 September 2019

Phase Behavior of Bio-based Ionic Liquid Crystal Mixtures based on Choline and Fatty Acids

Ariel Toledo-Hijo[1], Guilherme Maximo[1], Jorge Pereira[2], Felipe Ferrari[1], Mariana Costa[3], Antonio Meirelles[1,*]

[1] School of Food Engineering, University of Campinas, Campinas, São Paulo, Brazil, 13083-862; [2] School of Pharmaceutical Sciences, Universidade Estadual Paulista, Araraquara, São Paulo, Brazil, 14800-903; [3]School of Chemical Engineering, University of Campinas, Campinas, São Paulo, Brazil, 13083-852

**Corresponding author: tomze@unicamp.br*

Highlights

- Remarkable wide ILC temperature domain of systems containing bio-based ILs
- Mixing ILs and fatty acids improved their physical and thermal properties
- The investigated mixtures form solid solutions
- Mixtures presented high MP depression and high decrease in ILC temperature domain

1. Introduction

Bio-based ionic liquids (ILs) are promising compounds and their synthesis by using compounds obtained from natural sources has been considered as an alternative way to overcome the toxicity aspect and expand their applications in food and cosmetic industries [1]. This is the case of ILs based on fatty acids and choline. Fatty acids are considered GRAS substances and food additives with functional properties (e.g. omega fatty acids) [2], which makes them interesting precursors to produce low toxic and possible edible ILs. Choline cation belongs to the B-complex vitamins, that can be found in several foods and is considered as essential and nontoxic nutrient.

Mixing ILs have been considered an alternative way to improve their thermal and physical properties, but studies on such approaches using ILs obtained from natural compounds are still scarce [3]. The phase behavior of mixtures containing such ILs are far from be fully evaluated, especially those systems with liquid crystalline mesophases. In this context, new possibilities toward the design of bioproducts by using compounds of interest for food and cosmetic industries, such as lipidic based products, have been encouraged.

The aim of this work was to characterize the Solid-Liquid-crystal-Liquid thermodynamic Equilibrium (SSLcLE) of two binary mixtures of bio-based ILs and fatty acids.

2. Methods

The two systems comprises ILs with their fatty acid precursor: cholinium stearate + stearic acid ($[Ch][C_{18}OO] + C_{18}OOH$) and cholinium oleate + oleic acid ($[Ch][C_{18:1}OO] + C_{18:1}OOH$). The melting temperatures were determined using a DSC8500 calorimeter (PerkinElmer, USA) in a cooling-heating cycle at 1 K min^{-1}. The liquid crystalline mesophases (LCMs) were evaluated using a polarized optical thermomicroscope (Leica, Germany) in a 0.1 K min^{-1} heating run.

3. Results and discussion

Phase equilibrium data indicated two phase transition regions S-LC and one LC-L, presenting three solid phases with solid solutions SS, one mesophase LC and one isotropic liquid phase L. This behavior is commonly observed for ILs. Furthermore, the investigated mixtures form solid solutions. This work also revealed a remarkable wide ILC temperature domain of ILs derived from choline and fatty acid. The system [Ch][C_{18}OO] + C_{18}OOH presented lower decrease on their ILC temperature domain and lower depression of the melting points (MPs). This could be related to higher anion-cation interactions and layered structures, as well as mesophases-forming ability due to their long alkyl chain length and linearity. Otherwise, systems containing molecules with unsaturation in their structures presented a higher decrease on ILC temperature domain and a higher MP depression.

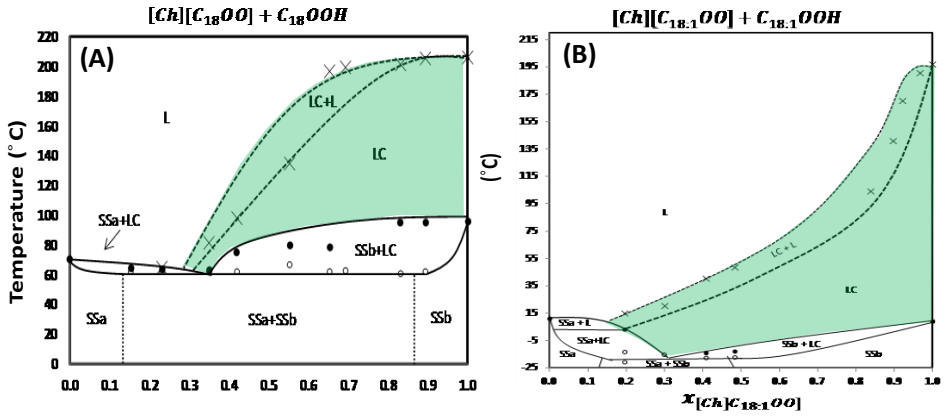

Figure 1. Phase equilibrium of the binary mixtures of ILs and fatty acids: cholinium stearate + stearic acid ([Ch][C_{18}OO] + C_{18}OOH) (A) and cholinium oleate + oleic acid ([Ch][$C_{18:1}$OO] + $C_{18:1}$OOH) (B).

4. Conclusions

The results reported in this work show a decrease on the ILC temperature domain and melting temperature by mixing bio-based ILs and fatty acids. The tunability on the thermal and physical properties of the mixtures are related to the concentration and presence of unsaturation in the molecular structure of their components. The melting profile exhibited the formation of very well define liquid crystalline mesophases in a wide temperature range. These results open perspectives on the applications of ILs for the design of lipid-based structuration agents or industrial applications in processes at high temperatures.

Acknowledgements: Authors thank FAPESP, CNPq and CAPES for financial support and scholarships.

References

[1] A.A.C. Toledo Hijo, G.J. Maximo, M.C. Costa, E.A. Batista, A.J.A. Meirelles, ACS Sustainable Chem. Eng. 4 (2016) 5347–5369.

[2] A.A.C. Toledo Hijo, G.J. Maximo, M.C. Costa, R.L. Cunha, J.F.B. Pereira, K.A. Kurnia, E.A. Batista, A.J.A. Meirelles, J. Phys. Chem. B 127 (2017) 3177–3189.

[3] A.A.C. Toledo Hijo, G.J. Maximo, R.L. Cunha, F.H.S. Fonseca, L.P. Cardoso, J.F.B. Pereira, M.C. Costa, E.A. Batista, A.J.A. Meirelles, Phys. Chem. Chem. Phys. 20 (2018) 6469–6479.

ECCE12
The 12th EUROPEAN CONGRESS OF CHEMICAL ENGINEERING
Florence 15-19 September 2019

PC-SAFT Prediction of Amino-Acid Solubility with New Experimental Melting Properties.

Hoang Tam Do [1], Yeong Zen Chua[2], Christoph Schick[2], Dzmitry Zaitsau[2], Christoph Held[1*]

[1]Laboratory of Thermodynamics, Department of Biochemical and Chemical Engineering, TU Dortmund University, Emil-Figge Str. 70, 44227 Dortmund, Germany

[2] Institute of Physics, University of Rostock, Competence Centre CALOR, Faculty of Interdisciplinary Research, University of Rostock, Albert-Einstein-Str. 25, 18051 Rostock, Germany

*Christoph Held: christoph.held@tu-dortmund.de

Highlights

- **New experimental melting properties of amino acids**
- **Prediction of aqueous solubility of amino acids with PC-SAFT**
- **Transfer of the method to peptides**

1. Introduction

The solubility of amino acids plays an essential role for the production and purification of amino acids, especially for crystallization processes. The solubility affects product yield and purity as well as the choice of solvent for the process. Further, several (bio)chemical operations are processed at homogenous conditions, i.e. amino-acid precipitation has to be avoided; this also requires solubility data. The experimental measurement of solubility is time-consuming and expensive considering the nearly uncountable different conditions in biological solutions (pH-value, temperature, type and concentration of co-solutes and co-solvents). Therefore, the prediction of solubility using thermodynamic models is desired, which however requires activity coefficients and the melting properties of the considered solute. However, measuring the enthalpy of fusion and the melting temperature of biomolecules such as amino acids is usually not possible using conventional differential scanning calorimetry due to decomposition of the solid during the measurement.

2. Methods

Application of fast scanning calorimetry (FSC) overcomes the problem of decomposition, and FSC was used in this work to measure the melting properties. The measurements were performed under an inert atmosphere of nitrogen with a sample mass less than 100 ng. Figure 1 shows the temperature-time profile used in this study.
The profile is divided into three measurements stages. (i) Sample mass determination (#1-#4), (ii) sample melting and quenching (#5-#7) and (iii) reheating of supercooled sample (#8-#11). In this work the enthalpy of fusion and melting temperature were measured for a series of amino acids.

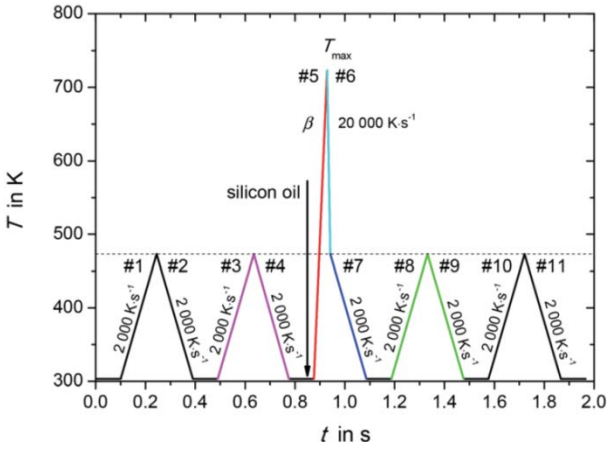

Fiure. 2: Temperature-time profile for determination of melting properties with fast scanning calorimetry.

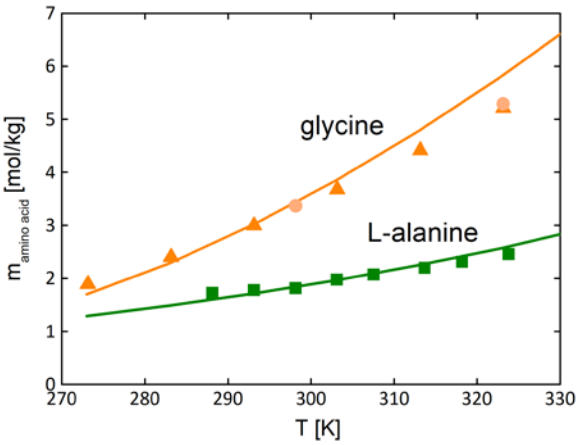

Figure 1 Glycine and L-alanine solubility in water as molality vs. temperature. Symbols represent experimental data (circles[3], triangle[4], squares[5]). Lines represent PC-SAFT predictions.

2. Results and discussions

The solubility measurements of amino acids were performed in aqueous solution. The PC-SAFT pure-component parameters for the amino acids as well as the water parameters were taken from literature [2]. Additionally, one binary interaction parameter k_{ij} was used between amino acid and water. The values for k_{ij} were fitted to experimental osmotic-coefficient data of aqueous amino-acid solutions at 298.15 K and atmospheric pressure. As shown in Figure 2 the temperature-dependent solubility of glycine and L-alanine in water were predicted with PC-SAFT using the melting properties measured from FSC in very good agreement to the experimental data. The method could be successfully transferred to peptide solutions as well as to solubility of amino acids in water-alcohol mixtures.

4. Conclusions

In this work it was the goal to predict solubility of components that decompose before melting, e.g. amino acids or peptides. The predictions require PC-SAFT parameters and melting data. All PC-SAFT parameters were taken from literature or fitted to new solubility-independent thermodynamic properties such as osmotic coefficients. Melting properties were measured using FSC. The results revealed that amino-acid solubilities can be accurately predicted over a broad temperature range. The combination between PC-SAFT and FSC generally allows the predicting solubility of molecules that decompose before melting.

References

[1] Y.Z. Chua, H.T. Do, C. Schick, D. Zaitsau, C. Held, *RSC Advances*, 8, 6365-6372; (**2018**)
[2] C. Held, L.F. Cameretti, G. Sadowski, Ind- Eng- Chem. Res., 50, 131-141; (**2011**)
[3] J. P. Amend, H. C. Helgeson, Pure Appl. Chem, 69, 935-942, (**1997**)
[4] H. Sober, Handbook of Biochemistry, Selected Data for Molecular Biology, CRC Press, (**1973**)
[5] T. H. Lilley, Physical Properties of Amino Acids, ed. G.C. Barret, 591-624, (**1985**)

ECCE12
The 12th EUROPEAN CONGRESS OF CHEMICAL ENGINEERING
Florence 15-19 September 2019

A Discrete Modeling Approach for Excess Gibbs-Energy Models Coupled with Random Sampling of Molecules.

Christoph Mayer[1], Thomas Wallek[1]

1 Graz University of Technology, Institute of Chemical Engineering and Environmental Technology, Inffeldgasse 25/C, 8010 Graz, Austria

**Corresponding author: cmayer@tugraz.at*

Highlights

- Condensed phase equilibrium calculations
- Ab initio distinction between isomers
- Intrinsic configurational information

1. Introduction

Thermodynamic models for fluid phase equilibria calculations, such as equations of state and activity coefficients, are being challenged by the need to describe complex and/or strongly oxygenated molecules. In this context, previous papers proposed 'discrete modeling' as a novel approach to incorporate a more detailed molecular picture into thermodynamics from scratch. The approach is characterized by the rigorous use of Shannon information as thermodynamic entropy. As a proof of concept, the thermal and caloric equations of state, heat capacity and Maxwell-Boltzmann distribution for ideal gas were derived on the basis of discrete states of individual molecules [1-2]. To further extend this approach to strongly interacting condensed-phase systems [3], a previous application of discrete Markov-chains to thermodynamic modeling [4] was modified and extended from a flat lattice towards a three-dimensional, Ising-type lattice model. The initial step of this model was the description of spherical molecules [5]. In this paper, it is extended and coupled with a force field-based random sampling algorithm to account for real substances, beyond spherical molecules.

2. Methods

From the whole lattice system, a small, three-dimensional subgroup resp. cluster of sites is picked out as a representative part of the system and the basis for thermodynamic modeling. Its stepwise formation is described by starting from one lattice site and successively adding further nearest-neighbor sites using conditional probabilities in terms of discrete Markov-chains. Such clusters can be treated as statistically independent subsystems, yet account sufficiently for cooperative effects due to molecular interactions inside the cluster. The according probability of occurrence of clusters can more vividly be rewritten in terms of probabilities of pairwise interactions which are also used by the quasi-chemical approximation by Guggenheim and derived approaches. Next, the internal energy and the Shannon entropy of the system are formulated on the basis of these pairwise probabilities. The Shannon entropy is then used equivalently to thermodynamic entropy. Constrained minimization of the free energy yields the equilibrium distribution for the probabilities of pairwise interactions. For non-spherical molecules, a random sampling algorithm is used to determine energetic interactions between molecules in a cluster together with its respective probability of occurrence.

3. Results and discussion

First, the model is derived for spherical molecules of equal size with uniform surface properties. For given system parameters like composition and interchange energies, the resulting equilibrium properties of the system, i.e. internal energy and entropy, are compared to those derived from Monte-Carlo simulations and to the quasi-chemical approximation by Guggenheim [6]. The latter represents an important limiting case, because practically all state-of-the art activity coefficient models reduce to the Guggenheim approach in the case of uniform spheres. Figure 1 compares the new model to data from Monte-Carlo simulations for spherical molecules. It is evident that the new approach considerably improves representation of Monte-Carlo data, compared to the quasi-chemical approximation, particularly at strong molecular interactions. Consequently, the new model could be used as a more precise alternative to the quasi-chemical approximation. In order to allow more realistic molecule models, it is coupled with a force field-based random sampling algorithm.

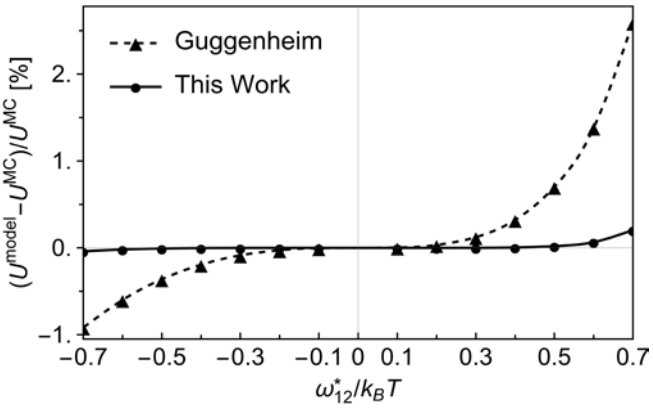

Figure 1. Relative deviation for the internal energy, U, between the models and Monte-Carlo (MC) data for a simple cubic lattice with 50^3 sites at a global composition of $x_1 = 0.3$. ω^*_{12}/k_BT is the dimensionless interchange energy.

4. Conclusions

Due to its better representation of spherical molecules and its intrinsic ability to distinct between isomers by using clusters as modeling basis, the proposed approach is a promising basis for further developing the method towards an activity coefficient model for liquid mixtures.

References

[1] Pfleger M., Wallek T., Pfennig A. Constraints of Compound Systems: Prerequisites for Thermodynamic Modeling Based on Shannon Entropy. Entropy 2014, 16, 2990-3008.

[2] Pfleger M., Wallek T., Pfennig A. Discrete Modeling: Thermodynamics Based on Shannon Entropy and Discrete States of Molecules. Ind. Eng. Chem. Res. 2015, 54, 4643-4654.

[3] Wallek, T., Pfleger, M., Pfennig, A. Discrete Modeling of Lattice Systems: The Concept of Shannon Entropy Applied to Strongly Interacting Systems. Ind. Eng. Chem. Res. 2016, 55, 2483–2492.

[4] Vinograd V.L., Perchuk L.L. Informational Models for the Configurational Entropy of Regular Solid Solutions: Flat Lattices. J. Phys. Chem. 1996, 100, 15972-15985.

[5] Wallek, T., Mayer, C., Pfennig, A.: Discrete Modeling Approach as a Basis of Excess Gibbs-Energy Models for Chemical Engineering Applications, Industrial and Engineering Chemistry Research 2018, 57, 1294–1306.

[6] Guggenheim E.A. Mixtures. Oxford at the Clarendon Press, 1952.

ECCE12
The 12th EUROPEAN CONGRESS OF CHEMICAL ENGINEERING
Florence 15-19 September 2019

A Thermodynamic Approach to Predict the Combined Influence of High-Pressure and Co-Solvents on Reaction Kinetics of a Peptide Hydrolysis.

Michael Knierbein[1], Anton Wangler[1], Christoph Held[1], Trung Quan Luong[2], Roland Winter[2], Gabriele Sadowski[1]*

1 Laboratory of Thermodynamics, TU Dortmund University, 44227 Dortmund, Germany
2 Physical Chemistry I, TU Dortmund University, 44227 Dortmund, Germany

**Corresponding author: gabriele.sadowski@tu-dortmund.de*

Highlights

- Application of a thermodynamic activity-based approach to enzyme kinetics.
- Prediction of combined high-pressure and co-solvent effects on reaction kinetics.
- Molecular interactions explain observed high-pressure and co-solvent effects.

1. Introduction

To optimize biotechnological production processes, knowledge about the effects of the reaction medium (temperature, pH, concentration and co-solvents [1]) on reaction yield and kinetics is very important. Even though liquid-phases are generally assumed to be incompressible, pressure is also an important influence factor to tune enzyme-catalyzed reactions taking part in liquid aqueous systems [2]. Certain enzymes are known to be pressure tolerant and additionally piezophile (i.e. pressure has a positive effect on enzyme activity) [3]. Consequently, the thermodynamic variable pressure should be an important influence factor, similar to temperature. In this work, the enzyme-catalyzed peptide hydrolysis of SPNA (N-succinyl-L-phenylalanine-p-nitroanilide) was investigated. The effects of high pressure and of co-solvents on the reaction kinetics were studied and explained by thermodynamics (interactions in the liquid phase).

2. Methods

In this work, experimental kinetic studies were performed at 20 °C for pressures of 1 bar and 1500 bar and the high-pressure influence on reaction kinetics was determined. Experimental data was analyzed according to the Michaelis-Menten procedure yielding the observed Michaelis constant K_M^{obs} and the turnover number k_{cat}^{obs}. Further, the thermodynamic model PC-SAFT (Perturbed-Chain Statistical Associating Fluid Theory) [4] was used to predict co-solvent effects on the reactive system. For this purpose, the constants K_M^a and k_{cat}^a were determined based on thermodynamic activities instead of concentrations in order to be independent of solvent effects, which requires activity coefficients: $K_M^a = K_M^{obs} \cdot \gamma_{substrate}$ and $k_{cat}^a = k_{cat}^{obs} \cdot \gamma_{enzyme}^*$.

The substrate's activity coefficient $\gamma_{substrate}$ as well as the enzyme's activity coefficient γ_{enzyme}^* were obtained by PC-SAFT. These account for molecular interactions that are expected to determine co-solvent effects on reaction kinetics. The kinetic constants were measured only in the neat cosolvent-free system while PC-SAFT was then applied to predict the kinetic constants in a reactive system of different composition or in different solvents. Applying the exponential

pressure dependence of K_M and k_{cat} additionally allowed for predicting the pressure influence on reaction kinetics.

3. Results and discussion

Experimental results showed the positive influence of high pressure on the reaction kinetics. For increasing pressures up to 2000 bar, K_M was found to decrease indicating a higher affinity of the substrate towards the enzyme. Furthermore, k_{cat} increased for increasing pressure indicating a faster product formation. In contrast, the co-solvents under investigation (0.5 mol kg^{-1} TMAO, 1 mol kg^{-1} urea and 4.2 mol kg^{-1} DMSO) had a negative effect on reaction kinetics (see Figure 1). These effects were rather small for TMAO and urea by only slightly increasing K_M and decreasing k_{cat}. However, DMSO strongly increased K_M, indicating a weaker affinity of the substrate towards the enzyme. k_{cat} was also considerably decreased by DMSO.

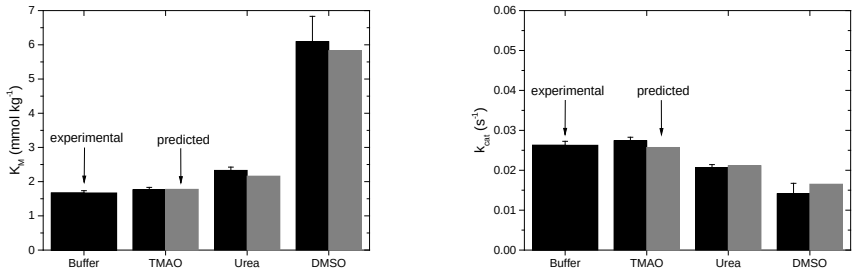

Figure 1. Left: Experimentally determined K_M (black) and PC-SAFT predicted K_M (grey) in mmol kg^{-1}, right: Experimentally determined k_{cat} (black) and PC-SAFT predicted k_{cat} (grey) in s^{-1} plotted against co-solvent at 500 bar and 20 °C.

PC-SAFT predictions of high-pressure and co-solvent effects on reaction kinetics were performed. For these predictions, the combined high-pressure and co-solvent effects on reaction kinetics were of special interest (see Figure 1). The PC-SAFT predicted Michaelis constants K_M are in almost quantitative agreement with experimental data for all co-solvents as well as for all observed pressures. The fact that PC-SAFT successfully predicts the combined co-solvent and high-pressure effects on K_M is a proof that the observed effects are dominated by molecular interactions. Additionally, even though the combined co-solvent and pressure effects on k_{cat} are small, PC-SAFT predictions agree very well with experimental data.

4. Conclusions

Applying a thermodynamic activity-based approach allows predicting the combined high-pressure and co-solvent effects on reaction kinetics of the investigated peptide hydrolysis. Predictions and experimental results were in very good agreement. That is, molecular interactions (substrate/co-solvent) are mainly responsible for the experimentally-observed effects of high pressure and co-solvent on reaction kinetics.

References

[1] A. Wangler, G. Sadowski, Phys. Chem. Chem. Phys. 20 (2018) 11317-11326.
[2] T.Q. Loung, R. Winter, Phys. Chem. Chem. Phys. 17 (2015) 23273-23278.
[3] M.J. Eisenmenger, J.I. Reyes De Corcuera, Enzyme Microb. Technol. 45 (2009) 331-347.

[4] J. Gross, G. Sadowski, Ind. Eng. Chem. Res. 40 (2001) 1244-1260.

ECCE12
The 12th EUROPEAN CONGRESS OF CHEMICAL ENGINEERING
Florence 15-19 September 2019

Phase- and Interfacial Properties of Aqueous Binary Mixtures.

Annika Reinhardt[1], Niklas Haarmann[2], Gabriele Sadowski[2], Sabine Enders[1*]

[1] *Karlsruhe Institute of Technology, Institute of Technical Thermodynamics and Refrigeration Engineering, Engler-Bunte-Ring 21, 76131 Karlsruhe, Germany.;*

[2] *TU Dortmund, Chair of Thermodynamics, Emil-Figge-Str. 70, 44227 Dortmund, Germany*

**Corresponding author: sabine.enders@kit.edu*

Highlights

- new data for the interfacial tension for aqueous binary mixtures were provided
- modelling of interfacial properties using DGT in combination with PCP-SAFT
- occurring maxima of interfacial tension is captured by the model

1. Introduction

Renewable resources like natural oils and fats are of great importance to combat the depletion of fossil fuel. Natural fats and oils primarily consist of triglycerides that are the basis for long-chain molecules like fatty alcohols, fatty amines and fatty acids. To characterize aqueous binary mixtures with these renewable substances the knowledge of phase- and interfacial properties are crucial in process engineering applications. Challenges arise in particular when water is mixed with a slightly polar or associating long-chain molecules (LCM), such as fatty acids, fatty acid methyl esters and fatty alcohols. Recently, the miscibility gap of water + n-alkanes could be modelled with a very high accuracy using PCP-SAFT approach [1]. This holds true for the solubility of n-alkane in water, the solubility of water in n-alkane as well as the solubility minima were captured [1]. The phase behavior of mixtures made of water and polar compounds, like aldehydes or esters, could be also modelled very close to experimental data, where the hetero-segmental version of PCP-SAFT was utilized [2]. The mixtures made of n-alcohol + water exhibit self-association as well as cross-associations. If these effects were included in the PCP-SAFT framework, the phase behavior can also modelled very close to the experimental data [3]. The aim of the present study consists of experimental and theoretical investigation of the interfacial properties of these mixtures, where these properties can be modelled by the density gradient theory (DGT) in combination with the above mentioned PCP-SAFT.

2. Methods

The binary phase behavior and the interfacial properties of the aqueous mixtures were modeled by a combination of DGT with PCP-SAFT [4]. Both the hetero-segmental and homo-segmental approach of PCP-SAFT are investigated and presented for this purpose. In case of the hetero-segmental approach, the n-alkylic residue within a homologous series was modeled using the PCP-SAFT parameters of n-alkanes and the binary interaction parameters, k_{ij}, were taken from water + n-alkane mixtures. Applying the hetero-segmental approach, polar and associative interactions among the identical head domains were explicitly taken into account. Due to its group-contribution-

like character, the hetero-segmental approach enables the prediction of thermodynamic properties of various compounds within a homologous series. The influence parameters occurring in the DGT of LCM were adjusted to the surface tensions. However, the influence parameter for water must be slightly readjusted. The spinning drop tensiometer was used to measure the interfacial tension of the binary LCM-water mixtures at different temperatures.

3. Results and discussion

Interfacial tension were measured for mixtures, where already data exist in the literature [5,6]. These data base was extended to different temperatures. Furthermore, interfacial tension data of so far non-investigated LCM-water mixtures (water + n-amines, water + methyl ester) were generated.

The solubility of LCM in water shows usually a solubility minima and consequentially the tie line runs through a maxima as function of temperature. One example is depicted in Figure 1. In Figure 1, it can be recognized that the experimental data, taken from the literature [7], as well as the modelled interfacial tension show a maximum value at a temperature, where the solubility minima occurs. Similar results were obtained for all investigated mixtures.

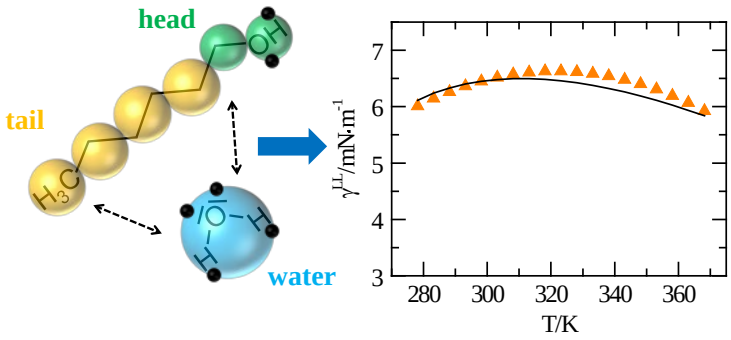

Figure 1 Interfacial tension γ^{LL} of the binary n-hexanol + water mixture at atmospheric pressure as a function of temperature T obtained with hetero-segmental approach of PCP-SAFT [3] .

4. Conclusions

It could be shown, that the suggested theoretical framework allows the modelling of the phase behavior and the interfacial properties close the experimental data.

References

[1] N. Haarmann, S. Enders, G. Sadowski, Fluid Phase Equilibria 470 (2018) 203-211.
[2] N. Haarmann, S. Enders, G. Sadowski, Ind. Eng. Chem. Res., in press.
[3] N. Haarmann, A. Reinhardt, A. Danzer, G. Sadowski, S. Enders, Ind. Eng. Chem. Res., in preparation.
[4] E. Schäfer, S. Enders, G. Sadowski, Fluid Phase Equilibria 362 (2014) 151-162.
[5] R. Aveyard, B.J. Briscoe, J. Chapman, J. Chem. Soc., Faraday Trans. 1 68 (1972) 10-16.
[6] I. del Pozo, M. Cartes, F. Llovell, A. Mejía, J. Chem. Thermodynamics 121 (2018) 121-128.
[7] D. Villers, J.K. Platten, J. Physi. Chem. 92 (1988) 4023-4024.

ECCE12
The 12th EUROPEAN CONGRESS OF CHEMICAL ENGINEERING
Florence 15-19 September 2019

Maximum bubble size in aqueous solutions of methyl isobutyl carbinol and NaCl

Jorge Saavedra[1*], Renato Quezada [2], Pedro Toledo[2]

1 Departamento de Ingeniería en Maderas, Universidad del Bío-Bío, Concepción, Chile
2 Departamento de Ingeniería Química, Universidad de Concepción, Concepción, Chile

**Corresponding author: jsaavedra@ubiobio.cl*

Highlights

- Scarcity of fresh water requires to find new sources.
- Electrolytes affects the behavior of frothers in floatation process.
- New explanation for the bubble size generation.

1. Introduction

Due to water scarcity mining copper industries in the north of Chile as in many other countries are using new sources of water like groundwater, recirculating water and seawater. These sources of water have salt electrolytes which have unknown effects on reagents as frothers and collectors in the floatation process, where the valuable mineral is separated from the gangue. In the floatation process, frothers avoid bubble coalescence and provide foam stability. It is known that salt electrolytes like NaCl modify properties of the air-liquid interface of aqueous solution with frothers like methyl isobutyl carbinol, one of the most frequently used frothers in floatation [1]. Bubble size is reduced as frother and salt concentration increases [2]. According to a conventional explanation this phenomenon can be explained due to the reduction of bubble coalescence [3,4]. Here we present a new way to understand this behavior evaluating the maximum stable bubble size and their relationship with surface tension and wettability.

2. Methods

Aqueous solutions were prepared with distilled water and different concentrations of methyl isobutyl carbinol (MIBC) as a frother and NaCl. The maximum stable bubble size was determined in an optical tensiometer Theta from Attention. Bubbles were generated passing small amounts of air in a hooked needle with a blunt needle point submerged in a transparent glass vessel containing the aqueous solution. Bubble volumes and their surface tensions were obtained by fitting the edges of the bubble to the Young-Laplace equation.

3. Results and discussion

Figure 1a shows the maximum stable bubble size for different concentrations of MIBC, for pure water and a solution of NaCl 2M, for an instant measurement and for a measurement realized after two hours of exposure of the solution to the needle pore. Bubble size decreases with increasing MIBC concentration and with the presence of salt. Figure 1a also shows that measurements for the condition of two hours of exposure have a significant reduction of the maximum stable bubble size.

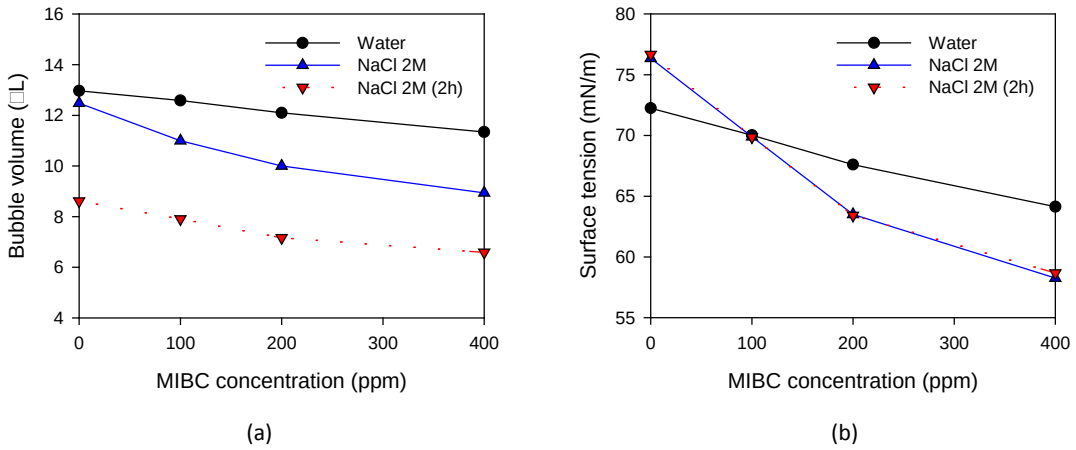

(a) (b)

Figure 1. (a) Maximum stable bubble volume and (b) surface tension at different MIBC concentration for pure water and NaCl 2M. NaCl 2M (2h) means the solution was in contact with the needle for 2 hours.

These results reveals that the generation of bubbles is influenced by surface tension of the solution and the time the solution is in contact with the pore substrate or the needle, which in turn is a manifestation of change in the wettability of the liquid over the substrate. A long exposure of the liquid over the needle pore increases its wettability. A detailed view of the analyzed images reveals that in the case of the instant measurement the base of the bubble fits with the outer area of the needle pore, and that in the measurements with two hours of exposure the base of the bubble has a reduced area. Figure 1b shows the surface tension for the same solutions revealing that the results of NaCl 2M are not affected by the bubble size, as expected.

4. Conclusions

The salt electrolyte NaCl has a significant impact on the decreasing of the maximum stable bubble size. These results reveals that the effect of the MIBC and NaCl in the decreasing of the bubble size is not only related to the reduction of the coalescence of bubbles, it is also related to the generation of the bubble; where surface tension, wettability of the solution over the porous and the size of the porous determine the size of the bubbles. In particular, the effect of the frother and the electrolytes over the wettability of the aqueous solutions over the different solids involved in a flotation cell can lead to an unexpected performance of the process.

References

[1] Castro, S., Miranda, C., Toledo, P., & Laskowski, J. S. (2013). *International Journal of Mineral Processing*, *124*, 8-14.
[2] Wang, L. (2015). *International Journal of Mineral Processing*, *134*, 41-49.
[3] Bournival, G., e Souza, L. D. O., Ata, S., & Wanless, E. J. (2015). *Chemical Engineering Science*, *131*, 1-11.
[4] Samanta, S., & Ghosh, P. (2011). *Chemical engineering science*, *66*(20), 4824-4837.

ECCE12
The 12th EUROPEAN CONGRESS OF CHEMICAL ENGINEERING
Florence 15-19 September 2019

H_2 Solubility in Gamma-Lactones for Hydrodeoxygenation to Biofuel Components

José Luis González Escobedo[1*], Petri Uusi-Kyyny[1], Riikka L. Puurunen[1], Ville Alopaeus[1],

1 Department of Chemical and Metallurgical Engineering, Aalto University, P.O. Box 16100, 00076 Aalto, Finland
**Corresponding author: jose.gonzalezescobedo@aalto.fi*

Highlights

- Gamma-Lactones are derivatives and model compounds of biorefinery platform compounds.
- H_2 solubility is important in liquid-phase Hydrodeoxygenation for biofuel production.
- In γ-nonalactone, solubility increased more from 200 to 250 °C than from 250 to 300 °C.
- The solubility of H_2 was greater in γ-nonalactone than in γ-heptalactone.

1. Introduction

Levulinic acid (LA) dimers are a potential platform stream in lignocellulose biorefineries [1]. LA dimers are slightly branched C_{10} molecules, containing lactone, carbonyl, and carboxyl moieties, which cannot be blended in fuel. However, valorization could be possible by heterogeneously catalyzed hydrodeoxygenation (HDO). Recently, the HDO of LA dimers has been assessed through the study of a relevant model compound, γ-Nonalactone (GNL), at 6 MPa H_2 and at 200-280 °C [2]. Because HDO is performed in three phases, H_2 can only reach the catalyst after its dissolution from the gas phase into the liquid reaction mixture. Due to lack of empirical data on the solubility of H_2 in GNL, it is difficult to clarify the effect of hydrogen on the reaction. Thus, in the present work, the solubility of gaseous H_2 in liquid lactones was studied at temperatures and pressures relevant to HDO. The length of the aliphatic side chain was thought to improve the solubility. Hence, both γ-heptalactone (GHL) and GNL were studied.

2. Methods

The lactones were purified by vacuum distillation at 60 mbar before use. The solubility measurements were performed in a continuous flow apparatus with temperature and pressure control. The saturation point was identified by the appearance of gas bubbles in the liquid flow, which was monitored in an optical cell. Saajanlehto et al. [3] described the apparatus and the procedure in detail. For each lactone, H_2 solubility was measured at 200, 250, and 300 °C and for pressures in the range of 3 to 10 MPa. The isotherms (H_2 mole fraction vs. pressure at selected constant temperatures) are expected to intercept the y axis at a value equal to the vapor pressure of the pure lactone at the given temperature. Thus, the vapor pressures were calculated based on literature [4] and added to the isotherms. The 6 MPa measurements of GNL at 200 and 250 °C were repeated at different residence times in order to verify that the system was operated at steady state.

3. Results and discussion

The measured saturation points are presented in Figure 1 with regression lines. The standard deviations of the repeated measurements at different residence times were $4.43 \cdot 10^{-4}$ on average, i.e. two orders of magnitude lower than the values of the measurements. The saturation mole fractions in GNL were 10% to 41% higher than in GHL. However, when accounting for molecular mass, the differences were only 4% to 16% and in some cases, the solubility per lactone mass was greater in GHL. It is worth noting that the solubility of H_2 at 250 °C for GHL had an intermediate position between the solubilities at 200 and 300 °C, whereas for GNL, the H_2 solubility at 250 °C was closer to the solubility at 300 °C than to the solubility at 200 °C. At 6 MPa, the solubility in GNL went from 0.049 at 200 °C to 0.058 at 250 °C and to 0.064 at 300 °C. That is, it increased by ~20% from 200 to 250 °C and by ~10% from 250 to 300 °C. In order to provide a rough picture of the solubility, Henry's law solubility constants can be estimated from the reciprocals of the regression slopes (Table 1).

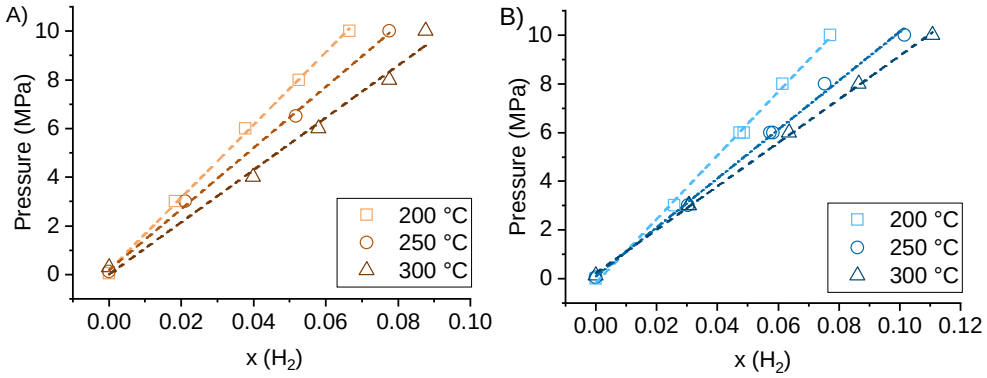

Figure 1. Solubility of H_2 in A) γ-heptalactone and B) γ-nonalactone at pressures and temperatures relevant to hydrodeoxygenation. The isotherms present the saturation pressures at given H_2 mole fractions.

Table 1. Slopes of regression lines.

	GHL slopes (MPa)	GNL slopes (MPa)
200 °C	149.3	130.7
250 °C	125.5	100.4
300 °C	107.4	89.2

4. Conclusions

The H_2 mole fractions in GNL at the HDO conditions studied in [2] were between 0.049 and 0.058. There was a strong dependence on temperature and pressure and, in the case of GNL, the solubility increase was more marked from 200 to 250 °C than from 250 to 300 °C. This observation might be significant for HDO kinetics. On the other hand, H_2 was more soluble in GNL than in GHL.

References

[1] M. Käldström, M. Lindblad et al., Ind. Eng. Chem. Res. 56 (2017) 13356-23366.
[2] J. L. González Escobedo, E. Mäkelä et al., Top.Catal. (2019) https://doi.org/10.1007/s11244-019-01161-6
[3] M. Saajanlehto, P. Uusi-Kyyny, V. Alopaeus, Fluid Phase Equilib. 382 (2014) 150-157.
[4] V. N. Emel'yaneko, S. A. Kozlova, et al., J. Chem. Thermodyn. 40 (2008) 911-916.

ECCE12
The 12th EUROPEAN CONGRESS OF CHEMICAL ENGINEERING
Florence 15-19 September 2019

In situ determination of vapor-liquid-equilibria via Raman-Spectroscopy in a microcapillary setup

Michael H. H. Fechter[1], Andreas S. Braeuer[1*]

1 Institut für Thermische Verfahrenstechnik, Umwelt- und Naturstoffverfahrenstechnik, Technische Universität Bergakademie Freiberg, Freiberg, 09599, Germany

**Andreas.Braeuer@tu-freiberg.de*

Highlights

- *In situ* analysis of VLE under high temperature and high pressure

1. Introduction

Due to the invasiveness of most of the analytical methods, the determination of vapor-liquid-equilibria under high temperature and high pressure is a challenging task. Another aspect is the danger that high pressure reactors might present if ignitable mixtures are analyzed. With the microcapillary setup that is presented here, real time VLE measurements are safely and easily feasible using *in situ* Raman-Spectroscopy. Thereby data such as *T-x*- and *p-x*-diagrams are obtained, that are scarce in literature for ignitable mixtures under high temperature and high pressure.

2. Setup and measurements

The setup consists of an optically accessible microcapillary, in which pressure and temperature are adjusted and controlled by a heating system and syringe pumps. The investigated mixture components with a global composition inside the two-phase region are unified in a T-junction, leading to a phase-separation and a flow of alternating liquid and vapor segments, depending on pressure and temperature. Light barrier technology is applied, using the difference in optical density of the vapor and liquid phases, to obtain an oscilloscope signal that is directly matching to the segmented flow. A piezoelectric system can be triggered to this oscillation, passing phase selectively only Raman signal of the investigated phase to the spectrometer.

3. Conclusions

We aim to contribute with our past and future research to the scarce data of VLE under high pressure and temperature.

Acknowledgement

The project leading to this contribution has received funding from the European Union's Horizon 2020 research and innovation programme under ERC Starting Grant agreement No. 637654 (Inhomogeneities).

ECCE12
The 12th EUROPEAN CONGRESS OF CHEMICAL ENGINEERING
Florence 15-19 September 2019

Novel Hydrate-Based Gas Separation: A Process Design and Phase Equilibria Calculations

Muhammad Khan[1,2], Sheraz Bashir[1], Cor J. Peters[2], Carolyn A Koh[2]

[1]*University of Hafr Al Batin, Chemical Engineering Department, Hafr Al Batin, Kingdom of Saudi Arabia.*

[2]*Colorado School of Mines, Chemical & Biological Engineering Dept., Center for Hydrate Research, Golden, CO 80401, USA*

**Corresponding authors: Cor J. Peters (cjpeters@mines.edu)*

Highlights

- A Novel design for separation of high CO_2 and H_2S contents from sour gas mixture
- Implementation of GEM algorithm for gas separation process design
- # of stages required for desired separation dependent on process conditions

1. Introduction

Removal of acidic gases from natural gas mixtures is one of the prime objectives of industry. Depending upon the nature of separation and contaminants present in gas mixtures, there are various separation techniques available, e.g.: cryogenic fractionation, polymeric membranes, metal organic frameworks. Among them adsorption and absorption processes are the most common. Removal of high H_2S and CO_2 contents require adequate methods to isolate them from natural gas (*NG*) mixtures. However, economic factors, high energy consumption and effective removal from the *NG* mixture is a restraining step [2-8]. To achieve an efficient separation, several attempts were made to find a reliable and energy efficient alternative compared to conventional separation methodologies [9]. The use of hydrate formation for acidic gases removal can be a promising technique over a range of *T*, *P* and acidic gas contents. The separation of H_2S & CO_2 gases from acid gaseous mixture can be achieved via gas hydrate formation and as represented by the simplified scheme shown in Figure 1 [1].

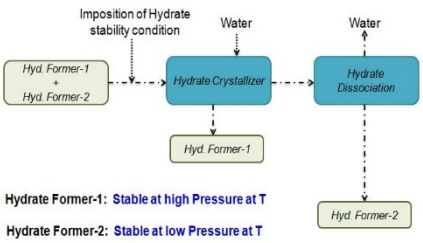

Figure 1. Conceptual picture for gas separation using hydrate formation [1].

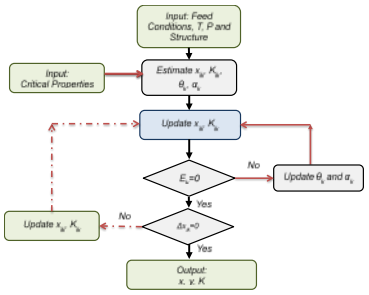

Figure 1. Gibbs free energy minimization algorithm.

2. Methods

Phase equilibria calculations were carried out using the modified vdWP model + Gibbs energy minimization algorithm over a range of temperature, pressure and CO_2/H_2S concentrations. Simplified algorithm for the Gibbs energy minimization algorithm was demonstrated in Figure 2 [1].

3. Results and discussion

The enclathration of carbon dioxide, hydrogen and natural gas are key applications for gas hydrates, since clathrates can adsorb gases in high concentrations. Hence, gas hydrates can provide an effective removal of acidic gases from natural gas mixtures. In this work gas separation via hydrate formation was proposed and a statistical thermodynamic model was used for hydrate

phase equilibria calculations to validate the performance of a hydrate-based separation process. During hydrate-based separation, gas mixtures with various acidic gas contents were brought in direct contact with brine or pure water under low temperature and high-pressure conditions to attain stable conditions for hydrate crystals nucleation. Multiphase equilibria calculations were also performed for various gas mixtures ($CH_4 + CO_2$, $CH_4 + H_2S$, $CO_2 + CH_4 + H_2S$ and $CO_2 + CH_4 + C_2H_6 + H_2S + N_2$) over a range of compositions and T, P conditions to establish the suitable region for separation. In addition, the fractional cage occupancy and the compositions of gases in each phase were also calculated to support the optimal selection of separation temperature and pressure conditions. Recovery and selectivity for gaseous mixtures were found to be significantly dependent on the hydrate former polarity and process conditions. Furthermore, a novel process design diagram (*PDD*) was also proposed for various gas mixtures to be separated and process conditions.

4. Conclusions

A process design has been proposed for removal of acidic gases from natural gas mixtures to achieve desired selectivity in gas mixtures, where removal of H_2S & CO_2 is carried out based on a component's ability to form hydrate crystals. Moreover, hydrate phase equilibria calculations for hydrates of CO_2, H_2S with various hydrocarbons compositions are calculated to locate optimum separation conditions. Fractional cage occupancy and acidic gas fractions were calculated in all the possible phases present to determine separation *T* and *P* conditions. Recovery and separation factor for various acidic gas mixtures were found to be strongly dependent on process conditions and feed gas compositions. A detailed analysis of the hydrate-based separation leads to the fact that the number of stages required to attain a desired separation efficiency was dependent on the nature of the gas mixture and the hydrate stability.

5. References

1. Khan, M.N., *Phase equilibria modeling of inhibited gas hydrate systems including salts: applications in flow assurance, seawater desalination and gas separation*. 2016, Colorado School of Mines. Arthur Lakes Library.
2. Aaron, D. and C. Tsouris, *Separation of CO2 from flue gas: a review.* Separation Science and Technology, 2005. **40**(1-3): p. 321-348.
3. Kang, S.P. and H. Lee, *Recovery of CO2 from flue gas using gas hydrate: thermodynamic verification through phase equilibrium measurements.* Environmental science & technology, 2000. **34**(20): p. 4397-4400.
4. Klara, S.M. and R.D. Srivastava, *US DOE integrated collaborative technology development program for CO2 separation and capture.* Environmental progress, 2002. **21**(4): p. 247-253.
5. Linga, P., R. Kumar, and P. Englezos, *Gas hydrate formation from hydrogen/carbon dioxide and nitrogen/carbon dioxide gas mixtures.* Chemical engineering science, 2007. **62**(16): p. 4268-4276.
6. Linga, P., R. Kumar, and P. Englezos, *The clathrate hydrate process for post and pre-combustion capture of carbon dioxide.* Journal of Hazardous Materials, 2007. **149**(3): p. 625-629.
7. Linga, P., *Separation of carbon dioxide from flue gas (post-combustion capture) via gas hydrate crystallization*. 2009, University Of British Columbia.
8. Adeyemo, A., et al., *Capture of carbon dioxide from flue or fuel gas mixtures by clathrate crystallization in a silica gel column.* International Journal of Greenhouse Gas Control, 2010. **4**(3): p. 478-485.
9. Azari, A., S. Atashrouz, and H. Mirshekar, *Prediction the Vapor-Liquid Equilibria of CO 2-Containing Binary Refrigerant Mixtures Using Artificial Neural Networks.* ISRN Chemical Engineering, 2013. **2013**.

ECCE12
The 12th EUROPEAN CONGRESS OF CHEMICAL ENGINEERING
Florence 15-19 September 2019

Vapor-Liquid Phase Equilibrium for Binary Systems Containing 1,2,4-Trimethylbenzene and Aromatic Compounds

Salal Hasan Khudaida, Ming-Jer Lee*

Department of Chemical Engineering, National Taiwan University of Science and Technology
43 Keelung Road, Section 4, Taipei 106-07, Taiwan

Corresponding author e-mail: mjlee@mail.ntust.edu.tw

Highlights

- **The isothermal VLE data were measured for 1,2,4-trimethyl benzene + *m*-xylene and 1,2,4-trimethyl benzene + *p*-xylene systems at temperatures from 363.15 K to 473.15 K using a static apparatus.**
- **Experimental VLE data were correlated well with the NRTL-HOC model.**

1. Introduction

For conducting the process simulation for an oil refinery plant, we need vapor-liquid equilibrium (VLE) data of the mixtures containing alkyl aromatics and xylenes. Among several others, the VLE data of binary mixtures of 1,2,4-trimethylbenzene + *m*-xylene and + *p*-xylene are still unavailable from open literature. In this work, the total pressure method was used to measure the isothermal VLE data for the binary systems of 1,2,4-trimethylbenzene with *m*-xylene or *p*-xylene at 363.15 K, 393.15 K, 433.15 K, and 473.15 K with 8:2/6:4/4:6/2:8 in mole ratios of the consituent compounds in the liquid phase. Using the NRTL-HOC model, we determined the optimal values of the binary interaction parameters for each investigated system via data correlation.

2. Methods

The Isothermal VLE data were measured for the binary systems of 1,2,4-trimethylbenzene + *m*-xylene and + *p*-xylene by using total pressure method with a static apparatus. The operation of this static apparatus is briefly described as follows. The air impurities were adequately evacuated from the cell with a vacuum pump (Model GLD-N136, a minimum pressure of 6.7×10^{-1} Pa, ULVAC). The high-purity chemicals were degassed to remove the non-condensable dissolved gases before use. Each of binary mixture was prepared from the degassed compounds with an electronic balance (Model FA-2204C, Chrom Tech Co., Ltd., Taiwan), which can be accurate to ± 0.1 mg and then mixed well by using magnetic stirrer under a certain composition. The prepared solution was then charged into the evacuated equilibrium cell by pressure difference between vaccum and atmospheric pressure [1]. The charging process was terminated before the liquid level in the degassing bottle lower than the bottom of the feeding tube to prevent non-condensable gas from entering the equilibrium cell. After the charging process, the temperature of the bath was adjusted to the desired value. Since this equipment has no circulating pump, it is necessary to shake the cell manually to accelerate the system to achieve a vapor-liquid equilibrium state. As the equilibrium state is attained, the pressure reading will reach a constant value, which was recorded as the equilibrium pressure (P) at the specific temperature (T). The equilibrium pressure was measured at different temperatures by an increment of about 30 K. Additonally, the

composition of each loaded liquid sample was analyzed by gas chromatography. The uncertainties of the reported equilibrium temperature, pressure, and liquid phase composition are estimated to be 0.1 K, 0.01 bar, and 0.005 in mole fraction, respectively.

3. Results and discussion

The total pressures (P) at given T and liquid composition (x_i) were measured for 1,2,4-trimethylbenzene + m-xylene and 1,2,4-trimethylbenzene + p-xylene at 363.15 K, 393.15 K, 433.15 K, and 473.15 K over the entire composition range. The experimental results show that equilibrium pressure increases as increasing temperature and no azeotrope was formed in both two systems. The VLE data were correlated using the (γ-ϕ) method. The NRTL model [2] and the two-term virial equation of state with Hayden-O'Connell method [3] for estimation of the second virial coefficient (HOC) were adopted to represent the non-idealilties of liquid and vapor phases, respectively. Figures 1 and 2 indicate that the NRTL-HOC model correlates satisfactorily the VLE data. The average absolute relative deviations (AARDs) between measured and calculated values are 0.003 % and 0.14 % for the systems containging *m*-xylene and *p*-xylene, respectively.

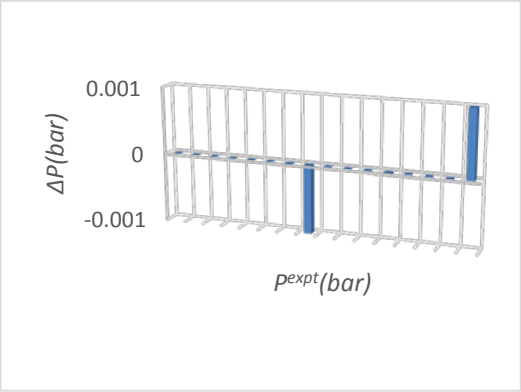

Figure 1. Deviation distribution of the calculated values from the NRTL-HOC model with the measured values for 1,2,4-trimethylbenzene + *m*-xylene system.

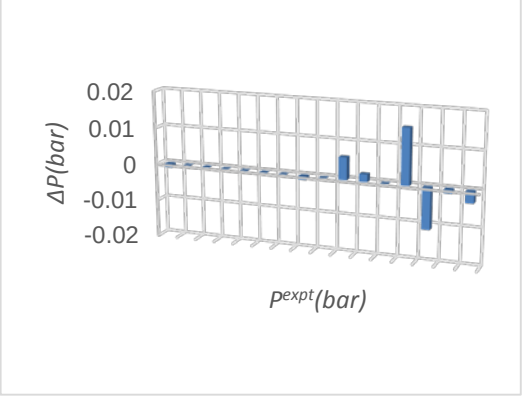

Figure 2. Deviation distribution of the calculated values from the NRTL-HOC model with the measured values for 1,2,4-trimethylbenzene + *p*-xylene system.

4. Conclusions

In the present study, the VLE data of 1,2,4-trimethyl benzene + *m*-xylene and 1,2,4-trimethyl benzene + *p*-xylene were measured at temperatures from 363.15 K to 473.15 K. The experimental results exhibit no azeotropic behavior over whole temperature ranges studied here. The calculated results reveal that the NRTL-HOC model can accurately represent the VLE behaviour for these two investigated systems. These experimental data are fundamentally important to conduct the optimal process simulation and design for an oil refinery plant.

References

[1] I. Khoiroh, M. L. Lee, Chem. Thermodynamics. J. 56 (2013) 99–105.
[2] H. Renon, J. M. Prausnitz, AIChE.J.14 (1968) 135-144.
[3] J. G. Hayden, J. P. O'Connell, Ind. Eng. Chem. Process Des. Dev. 14 (1975) 209-216.

ECCE12
The 12th EUROPEAN CONGRESS OF CHEMICAL ENGINEERING
Florence 15-19 September 2019

On Passive thermal regulation for application to closed solar photobioreactor Algofilm©: An experimental approach

Kashif Hussain MANGI, Jack LEGRAND, Jeremy PRUVOST, El-Khider SI-AHMED*
University of Nantes, CNRS, ONIRIS, GEPEA, UMR-6144, 37 Bd de l'université, BP406, 44602 Saint-Nazaire, France
*Corresponding author: el-khider.si-ahmed@univ-nantes.fr

Highlights

- Passive thermal regulation technique for Algofilm Photobioreactor
- Experimental Study for Quantification of Condensation for estimation of Condensate Film thickness
- Droplet size evolution as a function of inclination

1. Introduction

Thermal regulations in Solar Photobioreactors has been a major problem specifically for overheating of microalgae culture due to variable weather factors such as year-round operation, and day/night cycles (Pruvost *et al.*, 2017). In Algofilm Photobioreactor, the phenomenon of evaporation-condensation has been observed (Goetz *et al.*, 2011), which allows a thin film of condensate to be developed on the inner surface of optical cover. It can absorb some amount of infrared radiations which results reduction in energy requirement to regulate the temperature of Microalgae culture inside the Algofilm. Subsequently water (condensate) has an ability of transmitting the visible light spectrum which is essentially required for microalgae. So, an autoregulation technique of the AlgoFilm temperature through a condensate film on the inner surface of reactor has been hypothesized. In first step the experiments for quantification of condensation have been conducted on lab-scale Algofilm© by optimizing the water flowing film temperature, inclination angle and the flowing film thickness, because absorption of solar radiation (Infrared range) is the function of condensate film thickness.

2. Methods

Experimental study on Lab-scale Algofilm for quantification of condensation is carried out by varying the fluid temperature and inclination angle to investigate their effect on the condensate and dripping volume. Temperature measurements were obtained through LabVIEW software and (ICP.CON Data Acquisition Model i-7019R), thermocouples were installed at glass, condensate film, humid air medium, flowing liquid and bottom surface. Flowing liquid thickness measurement was carried out for each inclination angle, and inclination angle was measured with digital inclinometer (Sensorex ALPHA 4000). Condensed volume of water was collected in a container placed under the Algofilm PBR.

3. Results and discussion

The thickness of the flowing water was measured at every inclination angle and it remained under the suggested limit of 2mm by (Goetz *et al.*, 2011; Pruvost *et al.*, 2017). Experimental results have shown encouraging condensation which indicated the possibility to develop considerable condensate film thickness, which will filter some amount of the Infrared radiations.

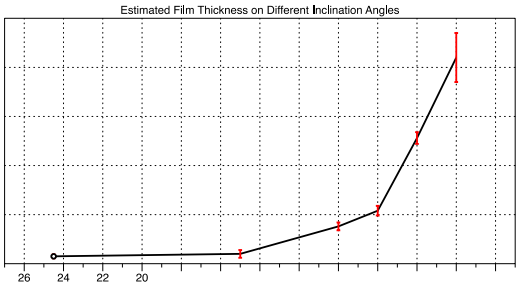

Figure 1:Film thickness as function the inclination angle

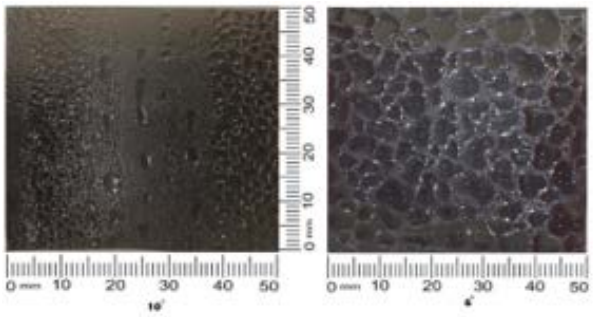

Figure 2. Droplets size evolution as a function of Slope after 4 hours at Different Angles

It is also observed during experiments that decreasing the inclination angle resulted a notable increase on the overall film thickness (figure 1), by increasing the droplet size as shown in figure 2 which will ultimately increase the absorption of Infrared radiations. However, the operational inclination angle for Algofilm is around 2° as per previous study on Algofilm by (Le Borgne, 2014), where condensate flowrate was almost equal to zero, so it is assumed that the condensed volume will be remained at glass cover and bigger droplets will be formed. Moreover, experiments for hourly condensation mass flux at different temperatures were also conducted and the percentage of the dripping flow could be deduced as shown in figure 3. This data will be of interest in the modelling aspect.

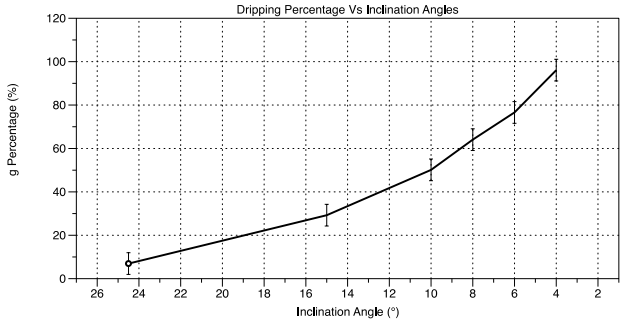

Figure 3 Dripping percentage as function of the inclination angle

4. Conclusions

The optimum objective of current study is to develop a passive thermal regulation for microalgae production in solar conditions through condensate film which will absorb the Infrared radiations. Results of experimental study for the condensation and dripping with variations of flowing liquid temperature and inclination angles of Algofilm Photobioreactor have shown that inclination angle is in direct relationship with the condensate flowrate and inversely with the dripping volume. Results are very favourable on lower inclination angle to achieve higher film thickness of condensate in which higher amount of infrared radiations would be absorbed. Furthermore, the simulation study is undergoing to validate these experiments and further experimental study is being conducted on the estimation of Infrared radiation absorption on the basis of these condensation rate results. This thermal regulation technique can be effective for Algofilm type photobioreactors to reduce the energy requirements to regulate the inside temperature.

References

[1] Le Borgne, F. (2014) *Development of an Intensified Solar Photobioreactor for Large Scale Production of Microalgae Biomass*. PhD Thesis, University of Nantes.

[2] Goetz, V. *et al.* (2011) 'A generic temperature model for solar photobioreactors', *Chemical Engineering Journal*. Elsevier B.V., 175, pp. 443–449. doi: 10.1016/j.cej.2011.09.052.

[3] Pruvost, J. *et al.* (2017) 'Development of a thin-film solar photobioreactor with high biomass volumetric productivity (AlgoFilm©) based on process intensification principles', *Algal Research*. Elsevier B.V., 21, pp. 120–137. doi: 10.1016/j.algal.2016.10.012.

ECCE12
The 12th EUROPEAN CONGRESS OF CHEMICAL ENGINEERING
Florence 15-19 September 2019

Ionic Liquid's Structural Variations inside Nano-slit by Molecular Dynamic Simulations

Lili Shi[1], Linghong Lu[1*], Changxun Dong[2]

1 College of Chemical Engineering, Nanjing Tech University, Nanjing 211816, China; 2 College of Sciences, Nanjing Agricultural University, Nanjing 210095, China

**Corresponding author: Linghonglu@njtech.edu.cn*

Highlights

- the [Emim][DCA] IL behave differently both in the charged and uncharged graphene interface.
- The number density of anion near the interface is always greater than the cation when the pore size is 0.8 nm in both charged and uncharged systems.
- imidazolium rings prefer to lie parallel to the graphene surface in narrow silt pore.
- imidazolium rings gradually tends to be perpendicular to the surface as the pore width increases.

1. Introduction

Exploring ionic liquids (ILs) / graphene charged interface is importance in the energy collection and storage devices, because the structural properties and transportation of ILs at the interface have great influence on the performance of energy collection and storage devices. Unfortunately, it is still challenging to directly detect the interface properties of nanoconfined ILs by experimental methods. Therefore, we present a molecular dynamics(MD) simulation study of 1-ethyl-3-methylimidazolium dicyanamide ([Emim][DCA]) ionic liquid confined by two charged graphene planar surfaces with different pore widths. Graphene surfaces with positive and negative charges can be imagined as positive and negative electrodes of capacitors, respectively.

2. Methods

MD simulation for [EMIM][DCA]-graphene system were carried out using the LAMMPS software. Ionic liquids ([EMIM][DCA]) were confined to two parallel interfaces of graphene, respectively. Four different slit pore sizes were considered with 3.6、2.4、1.6、0.8nm, separately. Graphene sheets were modeled as rigid entities along all the considered simulations. The box size for the xy plane was reach to 49.12×48.22 $Å^2$, as a consequence, it can accommodate enough ion pairs to obtain dependable statistically significant results. According to previous reports, all the four systems have a comparable IL density to the bulk value.[1] Therefore, 270、190、130 and 65 [EMIM][DCA] ion pairs were randomly placed in the two-dimensional graphene slits with the pore size of 3.6, 2.4, 1.6, and 0.8nm, respectively. The force field parameter for [EMIM][DCA] ions was obtained from literature.[2,3] The Lennard-Jones (L-J) parameter and partial atomic charges used for graphene in this work were taken from literature.[4]

3. Results and discussion

We find that the [Emim][DCA] IL behave differently both in the charged and uncharged graphene interface. The number density profiles of [Emim][DCA] IL along the direction perpendicular to the graphene wall indicates that the anion DCA- peak intensity is always greater than the cation Emim+ when the pore size is 0.8 nm in both charged and uncharged systems. The 3D orientation analysis of cations and anions close to the graphene surface indicates that imidazolium rings prefer to lie parallel to the graphene surface, and imidazolium rings gradually tends to be perpendicular to the surface as the pore width increases. Finally, their diffusion coefficients exhibit anomalies in negatively charged pores.

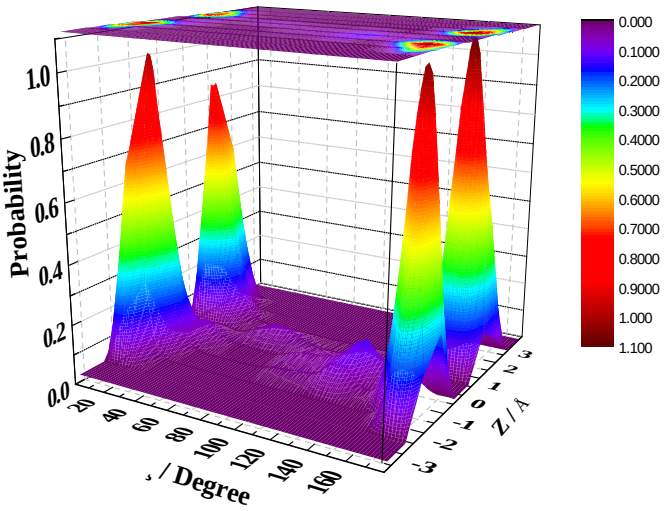

Figure 1. The probability distribution of angle orientation in a silt pore with charge density of 2.29 e/nm^2 (pore size= 0.8 nm).

4. Conclusions

The research work aimed at interface nanostructures is helpful for the design of electrode materials. From the results of simulation we found pore size is important for the Ionic Liquid's Structural Variations and diffusion coefficient inside Nano-slit, which are critical to the performance of energy collection and storage devices such as electrochemical capacitance.

References

[1] Weber, Henry, Barbara Kirchner, The Journal of Physical Chemistry B. 120.9 (2016) 2471-2483.

[2] Atilhan, Mert, Santiago Aparicio, The Journal of Physical Chemistry C. 122.3 (2018) 1645-1656.

[3] Canongia Lopes, José N., Agílio AH Pádua, The Journal of Physical Chemistry B. 110.39 (2006) 19586-19592.

[4] Jorgensen, William L., David S. Maxwell, Julian Tirado-Rives, Journal of the American Chemical Society. 118.45 (1996) 11225-11236.

ECCE12
The 12th EUROPEAN CONGRESS OF CHEMICAL ENGINEERING
Florence 15-19 September 2019

Asphaltene deposition experiment and modeling in the service of thermodynamics

Mohamed Saidoun[1,2], Hervé Carrier[1], Jean-Luc Daridon*[1], Cláudio Vilas Boas Fávero[4], Thierry Palermo[2], Nicolas Passade-Boupat[2], Roel Belt[2], and H. Scott Fogler*[3]

1 Laboratoire des Fluides Complexes et leurs Réservoirs-IPRA UMR5150, CNRS/TOTAL/Univ Pau & Pays Adour, 64000 PAU, France ;
2 TOTAL SA, CSTJF Avenue Larribau - 64018 PAU Cedex, France ;
3 Department of Chemical Engineering, University of Michigan, Ann Arbor, Michigan 48109-2136, USA;
4 Exponent, 9 Strathmore Road, Natick, Massachusetts 01760, USA
**Corresponding authors: jean-luc.daridon@univ-pau.fr & sfogler@umich.edu*

Highlights

- Monitoring asphaltenes deposition using a fully immersed Quartz Crystal Resonator
- Experimental identification of deposition mechanism by liquid alkane titrations
- Experimental identification of deposition mechanism by depressurization of gas-dissolved oils
- Deposition modeling and comparison to experimental data

1. Introduction

Asphaltenes destabilization and deposition are mainly caused by the expansion of dissolved light alkanes, such as methane, during the petroleum extraction. Based on experimental observations replicating the expansion of light-ends by flowing fixed concentration mixtures of petroleum and liquid alkanes at ambient conditions; deposition models have been developed[1,2]. In those cases, diffusion-limited equations were computed with measured and realistically fitted input parameters in order to match the experimental observation. Upscaling the diffusive principles of these models to the flow of gas-dissolved oils implies calculations of multiple pressure dependent parameters instead, which increases uncertainties. Additionally, the nature of the precipitant showed a significant effect on the asphaltenes destabilization[3]. Experimental verifications of the modeled deposition of asphaltenes destabilized by the expansion of light alkanes are very limited in the current literature.

2. Methods

Two different apparatus were used to measure the deposited mass of asphaltenes destabilized by addition of liquid n-alkanes:

(i) a packed bed of beads apparatus recently developed[1] in which an isothermal mixture is continuously flowing at a controlled flow rate.

(ii) a continuously stirred reactor containing a fully immersed Quartz Crystal Resonator (QCR) indirectly recording asphaltenes deposited mass on its surface during isothermal titrations of liquid n-alkanes.

The QCR is an advantageous technique that requires very few deposit (sensitive to nano grams) and working in pressurized fluids[4]. Therefore, we also performed isothermal constant mass expansions of gas-dissolved systems while recording the deposition with the QCR. In parallel, a centrifugation method was used to measure the mass concentration of aggregated unstable asphaltenes for multiple mixtures of oil and liquid n-alkanes. The interplaying effects of time and evolution of the composition were studied. Based on experimental investigations, the initial goal was to verify the first principles of the existing models and apply them to the QCR geometry.

3. Results and discussion

The comparison of the concentration of unstable asphaltenes (obtained by centrifugation) with the deposition experiments, along with an analysis of the deposition profiles at several conditions enables an identification of the fraction of asphaltenes that can deposit. The possible deposition mechanisms are discussed based on experimental results, i. e. diffusion-limited and reaction-limited. Consequently, this work provides insights for a new model by proposing corrections on the key parameters. Computed deposition rates are then evaluated against the experimental results.

4. Conclusions

The validation of a novel deposition model is presented using experimental data recorded from a QCR sensor at ambient pressure and at gas-dissolved conditions. This study provides a major step in the understanding of asphaltenes deposition in industrial conditions, it helps identifying the predominant parameters and the mechanism of their deposition rate. This work does not only provide a validation of the deposition mechanism but mass transport equations combined to high pressure immersed QCR signal interpretation also give us access to a crucial information for the understanding of asphaltenes behavior: the concentration of unstable asphaltenes at all conditions. Thermodynamic models can therefore be challenged against implicitly measured quantities thanks to the findings.

References

[1] C. Vilas Bôas Fávero, A. Hanpan, P. Phichphimok, K. Binabdullah, and H. S. Fogler, Energy Fuels, 2016, 30 (11), pp 8915–8921

[2] A. S. Kurup, J. Wang, H. J. Subramani, J. Buckley, J.L. Creek, and W. G. Chapman Energy Fuels, 2012, 26 (9), pp 5702–5710

[3] N. Haji-Akbari, P. Teeraphapkul, A. T. Balgoa, and H. Sc. Fogler, Energy Fuels, 2015, 29 (4), p 2190–2196

[4] M. Cassiède, J.-L. Daridon, J. H. Paillol, and J. Pauly, Journal of Applied Physics 108, 034505 (2010)

Honorary lecture for Philipp Rudolf von Rohr: Multiphase Reaction and Transport Processes in Microreactor Systems.

Klavs Jensen[1]

1 MIT, Department of Chemical Engineering,

**Corresponding author: kfjensen@mit.edu*

Highlights

- Lecture honoring the contributions of Professor Rudolph Von Rohr ETH-Zurich.
- Insights into multiphase reaction and transport processes in microreactors.
- Automation for extracting kinetics and performing process optimization.
- Process intensification and steps towards autonomous chemical manufacturing.

Abstract

Chemical synthesis in microreactors has matured over the two past decades from simple demonstration examples to applications in pharmaceuticals and fine chemicals. Advantages of controlled mixing, enhanced heat and mass transfer, expanded reaction conditions, and safety have driven adoption of continuous flow techniques and the related process intensification. The field has moved beyond single transformations to continuous multistep synthesis of fine chemicals and active pharmaceutical ingredients by incorporating in-line workup techniques.[1]

The first part of this lecture reviews the understanding of multiphase reaction and transport processes in microstructured systems we gained from studies initiated by Professor Rudolph Von Rohr ETH-Zurich. Emphasis is placed on multiphase mass transfer in microreactors and packed beds along with membrane based extraction techniques. Presented examples include both experimental studies and computational fluid dynamic simulations.

The second half of the lecture focus on process intensification and automation, which offer opportunities for faster development and more efficient production[1] Automated optimization in continuous flow based on feedback of information is shown to be efficient for extracting chemical kinetic models and optimizing performance over continuous variables (*e.g.*, temperature, residence time, and concentrations).[2],[3] Use of microliter-scale droplets enables consideration of discrete variables (e.g., catalyst species, base, and solvents) in addition to the continuous ones without requiring system reconfiguration.[2],[4]

On demand production of pharmaceuticals serves to illustrate potential advantages of process intensification. The platform enables multistep chemical synthesis at elevated temperatures and pressures to enhance reaction rates in a plug-and-play, manually reconfigurable, refrigerator-sized manufacturing platform of integrated unit operations. As

a consequence, the resulting residence times are on the order of minutes, in contrast to the multiple hour-long processes typically needed for batch processing. [5,6]

Finally, integration of robotics with machine learning represents a step toward autonomous manufacturing. Computer-aided organic synthesis based on machine learning of millions of reactions in data databases predicts reaction paths to a given molecular target from purchasable starting materials. [7] With expert user input, the synthesis planning outcomes are converted into recipes executed by a modular continuous flow platform that is automatically configured by a robotic arm to setup the required unit operations and execute reactions.

References

[1] K. F. Jensen, AlChE J. 2017, 63 (2017) 858-869.

[2] B. J. Reizman, K. F. Jensen, Acc. Chem. Res. 49 (2016) 1786-1796.

[3] A.-C. Bédard, A. Adamo, K.C. Aroh, M.G. Russell, A.A. Bedermann, J. Torosian, B. Yue, K.F. Jensen, T.F. Jamison, Science 361, 1220–1225 (2018)

[4] L. Baumgartner, C. W. Coley, B. Reizman, K. Gao, K.F. Jensen, React Chem Eng, 3 (2018) 301–311

[5] P. Zhang, N. Weeranoppanant, D. A. Thomas, K. Tahara, T. Stelzer, M. G. Russell, M. O'Mahony, A. S. Myerson, H. K. Lin, L. P. Kelly, K. F. Jensen, T. F. Jamison, C. H. Dai, Y. Q. Cui, N. Briggs, R. L. Beingessner, A. Adamo, Chemistry-a European Journal 2018, 24, 2776-2784.

[6] A. Adamo, R.L. Beingessner, M. Behnam, J. Chen, T.F. Jamison, K.F. Jensen, J.-C. M. Monbaliu, A.S. Myerson, E.M. Revalor, D.R. Snead, T. Stelzer, N. Weeranoppanant, S.Y. Wong, P. Zhang, Science, 352 (2016) 61-66.

[7] C. W. Coley, W. H. Green, K. F. Jensen, Acc. Chem. Res. 51 (2018) 1281-1289.

ECCE12
The 12th EUROPEAN CONGRESS OF CHEMICAL ENGINEERING
Florence 15-19 September 2019

A new optical sensor for bubble velocity and size measurements in heterogeneous bubbly flows.

Anthony Lefebvre[1], Stéphane Gluck[1], Yann Mezui[2], Martin Obligado[2], Alain Cartellier[2]

*1 A2 Photonic Sensors, 38016 Grenoble, France ; 2 Univ. Grenoble Alpes, CNRS, Grenoble INP**, LEGI, 38000 Grenoble, France.*

**Corresponding author: alefebvre@a2photonicsensors.com*

** Institute of Engineering Univ. Grenoble Alpes

Highlights

- A new sensor devoted to complex bubbly flows has been developed.
- The sensor combines phase detection and bubble velocity measurements.
- Bubble velocity distributions are measured in homogeneous and heterogeneous regimes.
- Bubble velocity statistics conditioned on local void fraction become accessible.

1. Introduction

Bubble columns are routinely exploited in industry and are often operated in the heterogeneous regime with gas hold-up up to 40%. Despite intense research since the 70's, the hydrodynamics of these buoyancy driven bubbly flows is still poorly understood. As shown by the numerous correlations proposed in the literature [1], there is no consensus on the influence of the column size or of the gas superficial velocity on key variables. Beside simulations based on two-fluid models still require ad-hoc closures, and the scale-up from lab units to industrial units still relies on empiricism. That situation is evolving thanks to new measuring techniques, to well-controlled experiments and to progress in modelling. For example, the relative velocity in the heterogeneous regime has been shown to widely exceed the bubble terminal velocity [2]. That has prompted the use of a swarm factor that diminishes the drag with void fraction: this correction neatly improves the prediction capability [3]. This relative velocity modification is possibly due to the presence of clusters (with local void fraction up to 10 times the mean gas hold-up) and of voids (with local void fraction down to 0.1 times the mean): such meso-scale structures generate strong concentration gradients and are reminiscent of buoyancy instabilities in turbulent convention [2]. To progress further, there is a crucial need to gather information on bubble velocity. Such measurements are difficult and remain scarce [4-6]. The present contribution deals with the development of a new bubble velocity sensor and with its test in the heterogeneous regime.

2. Sensor development and preliminary measurements

The new sensor combines conical optical probes that are efficient phase detectors [7] with velocity measurements based on Doppler shift. The latter arises from a light wave reflected at the (fixed) probe tip combined with a light wave that exits the probe, interacts with a moving interface and enters back the fiber. The recorded signal is modulated at the Doppler frequency $f_D=2V\cos(\alpha)/\lambda$ where V is the interface displacement velocity, α the angle between the interface velocity and the fiber axis, λ the wavelength in the external medium. The measure of f_D directly

provides the velocity. That principle has been exploited on gas slugs [8], on micro-bubbles [9], on capillary waves [10] and on solid particles [11]. Yet, all previous works used cleaved fibers that are not adapted to phase detection. Instead, we exploited conical tips whose shape was optimized (Fig.1) to enhance the Doppler amplitude. All prototypes were manufactured from 8.2µm core diameter single mode fibers. A signal processing was implemented to select meaningful Doppler signals detected at the bubble exit (Fig.1) based on the number of successive periods and on their stability. An analysis of the sensor response, including necessary optical conditions for obtaining Doppler signals, indicate that this sensor provides the translation velocity of the bubble mass center projected on the fiber axis with a 10% uncertainty. The sensor was exploited in a bubble column (0.4m I.D., 3m high). Bubble velocity distributions in homogeneous and in heterogeneous regimes gathered at H/D=3.62 above injection are presented Fig.1. For these data sets, 12000 bubbles were detected among which 60% (resp. 30%) provided a velocity in the homogeneous (resp. heterogeneous) regime. Note that bubble's velocities up to 3m/s are recorded in the latter case: such magnitude is expected as liquid velocities up to 2m/s are observed in the same conditions, and since the actual relative velocities are about 2 to 3 times the terminal velocity [2].

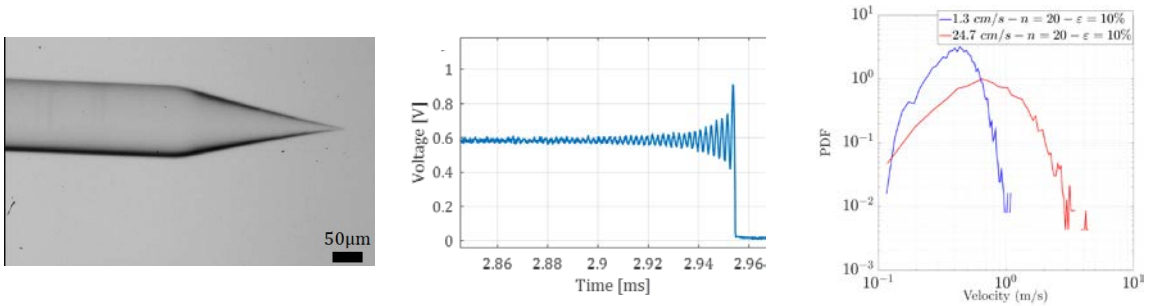

Figure 1. Conical fiber tip (left). Doppler signal collected at an air-water transition (middle). Bubble velocity distributions in homogeneous (blue) and heterogeneous (red) regimes (right).

3. Conclusions

A new sensor has been successfully developed that combines phase detection and bubble velocity measurements. Applied to a bubble column, the sensor indeed provides velocity distributions both in the homogeneous and in the heterogeneous regimes. Future work will be devoted to gather statistics on gas velocity conditioned by the local concentration in order to evaluate the impact of meso-scale structures on the relative velocity.

References

[1] P. Maximiano Raimundo, A. Cloupet, A. Cartellier, D. Beneventi, F. Augier, Chem. Eng. Sci. 198 (2019) 52-61.
[2] L. Gemello, V. Cappello, F. Augier, D. Marchisio, C. Plais, Chem. Eng. Research and Design, 136 (2018) 846-858.
[3] J. Xue, M. Al-Dahhan, M. Dudukovic, R. Mudde, The Canadian Journal of Chemical Engineering 81 (2003) 375-381.
[4] H. Chaumat, A.M. Billet-Duquenne, F. Augier, C. Mathieu, H. Delmas, Exp. Therm. Fluid Sci. 31(2007) 495–504.
[5] D.D. McClure, J.M. Kavanagh, D.F. Fletcher, G.W. Barton, Chem. Eng. Sci., 170 (2017) 91-97.
[6] J. Vejrazka, M. Vecer, S. Orvalho, Ph. Sechet, M. Ruzicka, A. Cartellier, Int. J. Multiphase Flow 36 (2010) 533-548.
[7] K. Sekoguchi, M. Takeishi, H. Kano, K. Hironaga, T. Nishiura, 2nd Int. Conf. on Laser Anemometry, 2-4 July, Lisbon, Portugal (1984).
[8] R. Wedin, L. Davoust, A. Cartellier, A. Dahlkild, 10th Int. Symp. on Appl. of Laser Tech. to Fluid Mech., 10-13 July (2000), Lisbon, Portugal.
[9] L. Davoust, J.-L. Achard , A. Cartellier, Progress in Colloid and Polymer Science 115 (2000) 249-254.
[10] K.-A. Chang, H.-J. Lim and C.B. Su, Rev. Sci. Instrum. 74 (7) (2003) 3559-3565.

ECCE12
The 12th EUROPEAN CONGRESS OF CHEMICAL ENGINEERING
Florence 15-19 September 2019

Bubble breakup induced by interaction with vortex-ring.

Maria Zednikova[1], Petr Stanovsky[1], Sandra Orvalho[1], Tereza Travnickova[1]

1 Institute of Chemical Process Fundamentals of the CAS, v.v.i., Rozvojova 135, CZ-165 02 Prague, Czech Republic

**Corresponding author: zednikova@icpf.cas.cz*

Highlights

- Interactions of single bubble with single vortex-ring are studied experimentally.
- Vortex-ring is characterized combining experiments and numerical simulations.
- Bubble deformation and breakup efficiency is investigated using high-speed camera.
- Results show the present data comparable with data obtained in homogeneous turbulence.

1. Introduction

Breakup of fluid particles (bubbles or drops) in a turbulent flow is a phenomenon encountered in many industrial applications. The understanding of the mechanism is essential to improve the modelling of complex multiphase flows by numerical methods [1]. To provide a controllable experiment where the bubble will break in a defined turbulent flow is quite difficult task because the turbulence has stochastic nature and huge amount of data needs to be treated to achieve a satisfactory level of accuracy. Therefore, more deterministic approach in the bubble breakup studies is needed.

The interaction of a single bubble with a vortex-ring can be assumed as more deterministic system simplifying the collision of bubble with turbulent eddy [2, 3]. Revuelta [2] found that the large vortex rings causes bubble deformations following the shapes identified in turbulent flow and he demonstrated, that the bubble breakup issuing from bubble-vortex-ring interactions can be used as idealized situations of bubble breakup in turbulent flow. However, the conclusion was obtained using numerical simulations and it should to be proved also experimentally. The aim of the contribution is to provide the experiments on bubble breakup induced by interaction with vortex-ring in order to contribute the understanding of the bubble breakup process in turbulent flows and to provide the reliable breakup parameters.

2. Methods

The experiment is based on the production of single bubble and single vortex-ring both moving against each other since they interact (Fig. 1). Vortex-ring is generated by pulse-flow from an immersed nozzle (1.2 in diameter, duration of pulse-flow is typically 25 ms). Bubble of defined size (ranging from 0.8 to 2.5 mm in diameter) is produced by the generator based on movable capillary [4]. The collision process is observed by high-speed camera in order to tract the mother bubble and all the daughter bubbles arising from breakup. Breakup frequency, number and size distribution of daughter bubbles are determined in dependence on mother bubble size and vortex-ring energy.

The vortex-ring energy is defined by the circulation strength of the vortex-ring, which is obtained combining the experimental visualizations and numerical simulations of the vortex-ring generation based on the same convective velocity of the vortex-ring (ranging from 0.9 to 1.5 m/s).

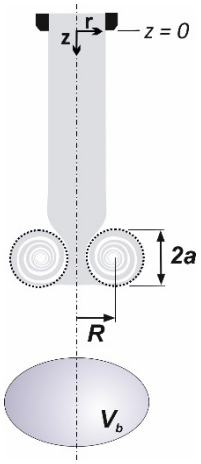

Figure 1. Illustration of coordinate system.

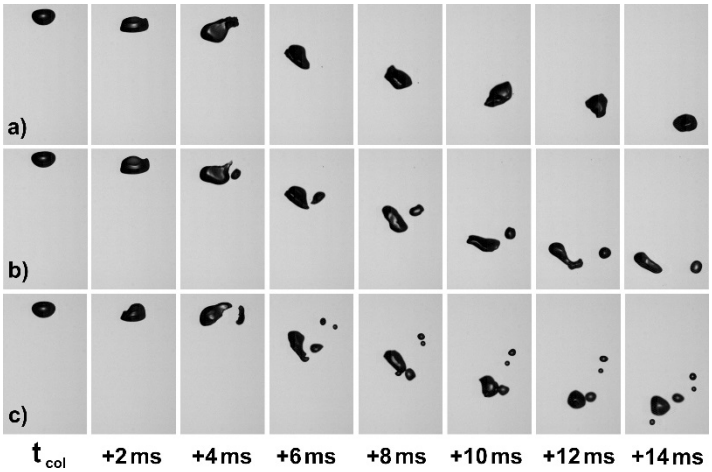

Figure 2. Examples of possible events after the bubble-vortex-ring interactions, a) no bubble breakup, b) binary breakup, c) multiple breakup

3. Results and discussion

The problem of bubble-vortex ring collision can be characterized by Weber number *We*, which is the ratio of vortex-ring energy and surface energy of the bubble. For low *We* ≈ 3, the bubble breakup efficiency is about 50%, where no breakup events (Fig. 2a) are of the same probability as the bubble breakup preferably into two daughter bubbles (Fig. 2b). Increasing the Weber number (*We* > 5), the breakup efficiency is nearly 100% and preferably breakages into multiple daughters occurs (Fig. 2c).

The breakup parameters obtained from the bubble-vortex-ring interactions are compared with breakup parameters obtained in homogeneous turbulent flow [5]. The results show satisfactory agreement in data of breakup frequency and also in number of daughter size distribution.

4. Conclusions

The comparison of present experimental data obtained for interactions of single bubble with single vortex-ring and the data obtained in homogeneous turbulence proved that the bubble-vortex-ring interaction can be assumed as an idealizes situation of collision of bubbles with eddies in turbulent flow.

The financial support by the Czech Science Foundation through project 19-09518S is gratefully acknowledged.

References

[1] J. Solsvik, S. Tangen, H.A. Jakobsen, Rev. Chem. Eng. 29 (2013) 241-356.
[2] A. Revuelta, Eur. J. Mech. B-Fluids 29 (2010) 119-126.
[3] C. Martinez-Bazan, J. Fluid Mech. 780 (2015) 1-4.
[4] J. Vejrazka, M. Fujasova, P. Stanovsky, M.C. Ruzicka, J. Drahos, Fluid Dyn. Res. 40 (2008) 521-533.
[5] J. Vejrazka, M. Zednikova, P. Stanovsky, AIChE J. 64 (2018) 740-757.

ECCE12
The 12th EUROPEAN CONGRESS OF CHEMICAL ENGINEERING
Florence 15-19 September 2019

Transport processes in disperse multiphase systems in the presence of surfactants: A single drop study

Joschka M. Schulz*, Matthias Kraume

Technische Universität Berlin, Chair of Chemical and Process Engineering, Ackerstraße 76, 13355 Berlin, Germany

**Corresponding author: j.schulz@tu-berlin.de*

Highlights

- Prediction of mass transfer rates by consideration of drop movement
- Spatially resolved concentration field measurement by Rainbow Schlieren Deflectometry
- Interfacial phenomena due to the presence of surfactants
- Evaluation of drop production phase

1. Introduction

The presented work focuses on the interaction between mass transfer and fluid dynamics in disperse liquid/liquid systems in the presence of surfactants and is part of the Collaborative Research Center Integrated Chemical Processes in Liquid Multiphase Systems financed by the German Research Foundation. In industrial processes surfactants occur intentionally or as an impurity and change the interfacial behavior. The induced interfacial phenomena such as Marangoni convection or adsorption may lead to a change of important process parameters. Since these phenomena have contrary effects on the mass transfer in multiphase systems, the prediction of their occurrence and the resulting mass transfer rates is a challenging task. To get a deeper insight into the transient mass transfer processes, fluid dynamic measurements of single droplets are used as an indicator for the prediction of interfacial phenomena and mass transfer rates. Furthermore, the mass transfer during droplet production is considered and a refractive index-based optical measuring technique is applied for the non-invasive in situ visualization of the concentration field in the continuous phase.

2. Methods

For experimental purposes a single drop rising test cell with a length of 700 mm is used. Samples are taken at different contact times and the rising speed and path of the droplets are determined optically with a high-speed camera. For detailed analysis, the experimental setup introduced in Merker et al. [1] is used, which extends the concept of the rising test cell by adding a vertical traverse system with real-time control, thus enabling the three-dimensional measurement of shape, velocity and trajectory of the particle during the ascent with high temporal and spatial resolution. Additionally, mass transfer during drop production is measured separately. An experimental setup applying Rainbow Schlieren Deflectometry has been developed for non-

invasive real-time measurement of the concentration field in liquid/liquid systems and is used for the visualization of interfacial phenomena.

3. Results and discussion

Figure 1 (left) the shows the transient drop rise velocity of single 1-octanol droplets in water for varying surfactant concentrations of Butyldiglycol, which is chosen as a model surfactant. The terminal drop rise velocity decreases with increasing surfactant concentration showing good agreement with the calculated velocity of a movable interface (Feng and Michaelides [2]) for negligible surfactant concentrations. For high surfactant concentrations the velocity is reduced to the value for rigid spheres (Martin [3]). In case of deformation, the measured velocities can decline even further. Although the observed effect is in good agreement with the literature, the mass transfer rates show contrary behavior due to the occurrence of Marangoni convection, which can be identified by detailed consideration of the drop movement.

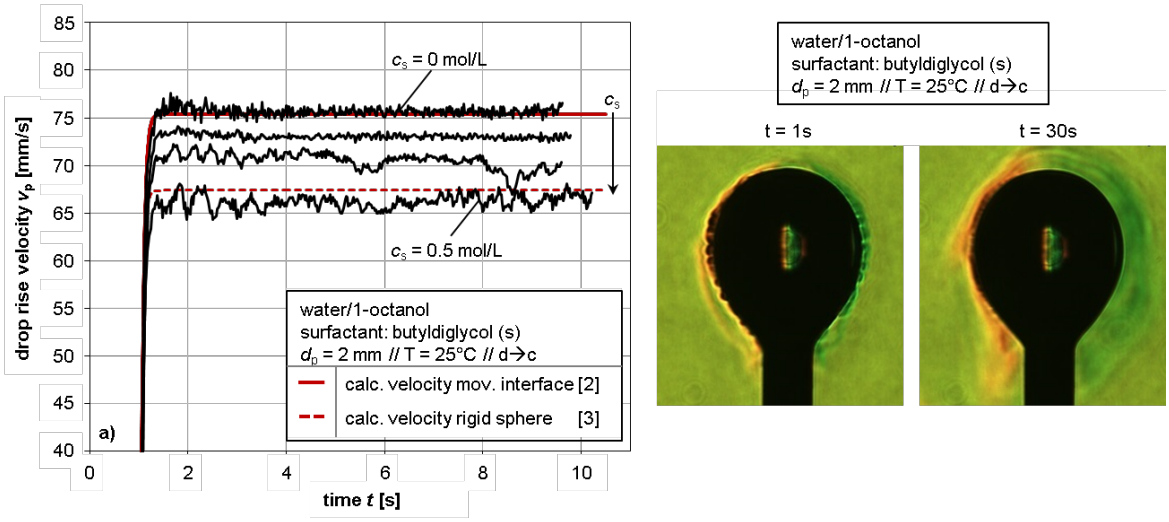

Figure 1. Left: Experimental drop rise velocity of 2 mm 1-Octanol droplets in water for varying surfactant concentration. Right: Concentration gradient field for mass transfer of model surfactant for different contact times visualized with Rainbow Schlieren Deflectometry.

Experimental results for the visualization of the instationary concentration gradient field of the surfactant butyldiglycol around a stagnant 1-octanol droplet in water are shown exemplary in Figure 1 (right) for different contact times. The different color values indicate differing values of concentration and result from the application of Rainbow Schlieren Deflectometry.

4. Conclusions

Fluid dynamic measurements and application of Rainbow Schlieren Deflectometry show great potential for a deeper insight into mass transfer processes and interfacial phenomena induced by surfactants and may lead to a better description of transport processes in multiphase systems.

References

[1] D. Merker, L. Böhm, M. Oßberger, P. Klüfers, M. Kraume, Chem. Eng. Technol., 2017, 40, 1391-1399.
[2] Z.-G. Feng, E. E. Michaelides, J. Fluids. Eng., 2001, 123, 841-849.
[3] H. Martin, Chem. Ing. Techn., 1980, 52, 199-200.

ECCE12
The 12th EUROPEAN CONGRESS OF CHEMICAL ENGINEERING
Florence 15-19 September 2019

Tomographic visualization of droplet break-up during high-pressure homogenization with orifices in a scaled test section

Benedikt Mutsch[1], Christian J. Kähler[2]

1 Institut for Fluid Dynamics and Aerodynamics, Bundeswehr University Munich, Werner-Heisenberg-Weg 39, 85577 Neubiberg, Germany; 2 Institut for Fluid Dynamics and Aerodynamics, Bundeswehr University Munich, Werner-Heisenberg-Weg 39, 85577 Neubiberg, Germany

**Corresponding author: benedikt.mutsch@unibw.de*

Highlights

- Flow field measurements inside a scaled high-pressure homogenizer.
- Droplet and droplet breakup visualization method.
- Tomographic reconstruction of droplets during breakup
- Determination of droplet breakup regions and mechanisms.

1. Introduction

Emulsions are produced and used in chemical, pharmaceutical and food technology. Since the droplet size and the droplet size distribution have an important influence on the properties of the emulsion, these parameters are of special importance. Drop sizes in the range from 100 nm to 10 µm can be produced by means of high-pressure homogenization.

This process uses high pressure to press the raw emulsion through small channels in the disintegration unit to break the coarse droplets of the raw emulsion into fine droplets of the desired size. However, the physical mechanism responsible for the break up is not known as the accurate visual inspection of the tiny droplets in space and time is not possible due to the small size.

In order to visualize the disintegration process, and to understand the physical phenomena responsible for the droplet break-up, high-speed images of well defined and reproducible droplets emerging from an orifice plate scaled to a scale factor of 50 were taken using the shadow image method. In order to investigate not only the geometric similarity but also a physically similar model, the material parameters density and viscosity of the model material system and the operating pressure are adapted so that the diameter, viscosity and density ratio as well as the Reynolds number and the Weber number are kept constant in comparison to the original process.

For a better understanding of the processes, these images were taken from several angles of view, so that a 3D model of the drop deformation during disintegration could be created for the first time.

The correlation of the drop break-up measurements with 2D2C-PIV measurements shows that the local turbulence intensity has a large influence on the break-up.

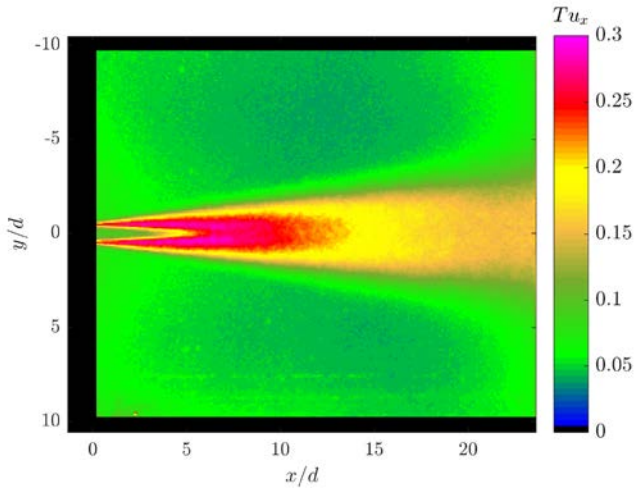

Figure 1. Local mean turbulence intensity behind the orifice

The drop emerges as an elongated filament from the Orifice in the core of the free jet. The images show that the drop is hardly deformed in this area due to the low turbulence. At the transition of the drop from the core area of the free jet to the shear layer, the drop begins to oscillate and meander. As a result of this incipient deformation, the droplet is strongly deformed in the shear layer, resulting in twisting and swirling of the filament. Ultimately, the deformed droplet decays into individual areas that are further deformed until a mist of fine droplets is formed.

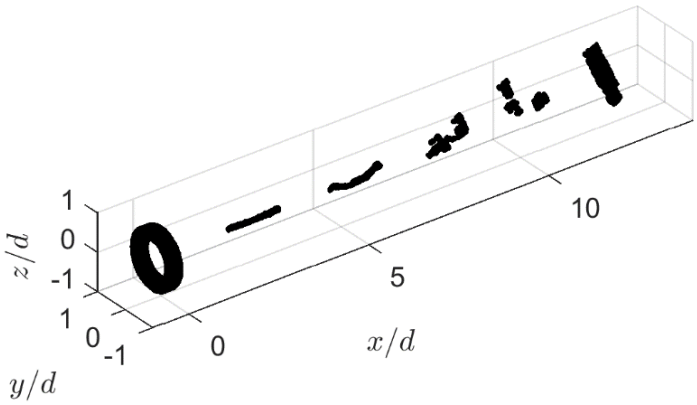

Figure 2. 3D reconstruction of the droplet breakup evolution behind an orifice from a long filament to a spray of small droplets

In order to investigate the droplet break-up mechanisms more closely, further investigations will be carried out. On the one hand, the droplet feed position is varied so that the droplet emerges from the orifice at different radial positions. This allows the expanded droplet to experience the local turbulence of the shear layer earlier and with a different intensity. The result is that the point of break-up shifts towards the orifice.

Furthermore, the Reynolds number is varied in the experiments so that the limits of drop break-up can be investigated with regard to the required turbulence intensity. Depending on the Reynolds number and the resulting different elongation of the droplet, different break-up mechanisms can be observed which have to be investigated in further investigations. The results of the various experimental investigations will be discussed and explained on physical grounds.

ECCE12
The 12th EUROPEAN CONGRESS OF CHEMICAL ENGINEERING
Florence 15-19 September 2019

Impact of Additives on Mass Transfer in Gas/liquid/liquid Systems

Marc Petold[1], Nona Afraz[2], Kristin Hecht[2], Lutz Böhm[1], Matthias Kraume[1]

1 Technische Universität Berlin, Chair of Chemical and Process Engineering, Ackerstraße 76, 13355 Berlin, Germany; 2 Otto-von-Guericke Universität Magdeburg, Institute of Instrumental and Environmental Technology, Universitätsplatz 2, 39128 Magdeburg, Germany

**Corresponding author: m.petzold@tu-berlin.de*

Highlights

- Characterization of complex behavior of micellar solvent systems and Pickering emulsions
- Influence of phase behavior on the mass transfer in innovative solvent systems
- Quantification of the effect of coverage and drop sizes on the transfer process

1. Introduction

Homogenously catalyzed reactions in multiphase systems, as they are used for example in the Ruhrchemie/Rhône-Poulenc process, offer a promising approach to produce base chemicals from renewable resources. The organic and gaseous educts react with the catalyst, which is designed to be soluble in water to provide a good separation from the likewise organic products. In the resulting gas/liquid/liquid systems, the reaction is controlled through interfacial and transport phenomena. These processes fail for long chained Olefins – e.g. vegetable oils and fats - because of their low solubility in water. Surfactants or nanoparticles can be added as emulsifier to form innovative solvent systems – micellar solvent systems (MSS)[1] or Pickering emulsions (PE)[2] respectively – and increase reaction speed [3,4] and phase separation [5]. The additives adsorb at the interface, increase the mass transfer area but add an additional mass transfer resistance. Furthermore, MSS form up to three liquid phases, depending on temperature and composition, whereas one phase is always a microemulsion. In consequence, the mass transfer in these systems is complex. This work focuses on the quantification of the impact of additives on the mass transfer in these innovative solvent systems.

2. Methods

For simplification reasons, measurements were conducted focusing on the non-reactive system consisting of long chained oils and water with either a non-ionic surfactant or silica nanoparticles. The Gas/liquid mass transfer was measured in a pressurized stirred tank reactor for several temperatures and compositions. Using the dynamic pressure method [6] the k_La values could be determined. The phase behavior of the MSS was characterized using settling experiments and by measuring the conductivity of the emulsions. To determine the interaction of the disperse phases in the stirred reactor, drop and bubble sizes were recorded using optical endoscope measurements [7]. Influence of occurring liquid/liquid mass transfer could be determined with single rising drop experiments [8]. A high speed camera was used to record the fluid dynamics of the drops. A tracer

component was added and the drops were collected at different heights to analyze the mass transfer.

3. Results and discussion

For the gas/liquid mass transfer, the k_La values rose with temperature in pure liquids but experienced a sudden change upon adding small amounts of a liquid dispersed phase. Depending on the formation of a water-in-oil or oil-in-water emulsion, the k_La experienced an increase or decrease, respectively. The change can be credited to the interaction of bubbles and drops. In MSS the mass transfer is up to two times faster. With rising temperature, a first decreases happens and is followed by a mass transfer acceleration and another decrease. For higher surfactant concentrations, a third region with constant k_La follows (see Fig. 1). The behaviour can be credited to the phase behaviour of MSS, where the continuous phase changes with temperature from aqueous to bicontinuous microemulsion to organic phase.

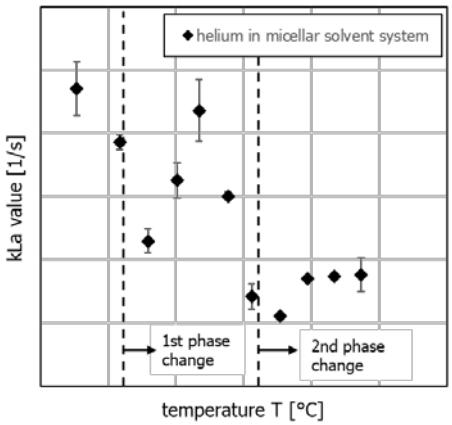

Figure 1. k_La value of micellar solvent system for different temperatures

Liquid/liquid mass transfer showed strong reduction due to interfacial coverage in both solvent systems, partly even falling below the expected results of a fully covered drop.

4. Conclusions

Phase behavior as well as drop and bubble interactions and coverage play an important role for the gas/liquid mass transfer in a stirred system with several dispersed phases. Both effects can significantly change the mass transfer and therefore reaction rates.

References

[1] M. Kahlweit, R. Strey, Angew. Chem. Int. Ed. Engl. 24 (1985), 654-668.
[2] S. U. Pickering, J. Chem. Soc. Trans. 91 (1907), 2001-2021.
[3] T. Pogrzeba, M. Schmidt, N. Milojevic, C. Urban, M. Illner, J.-U. Repke, R. Schomäcker, Ind. Eng. Chem. Res. 56 (2017), 9934-9941.
[4] R. v. Klitzing, D. Stehl, T. Pogrzeba, R. Schomäcker, R. Minullina, A. Panchal, S. Konnova, R. Fakhrullin, J. Koetz, H. Möhwald, Y. Lvov, Adv. Mater. Interface 4 (2017).
[5] L. Hohl, M. Knossalla, M. Kraume, Chem. Eng. Sci. 171 (2017), 76-87.
[6] A. Lekhal, R. V. Chaudhari, A. M. Wilhelm, H. Delmas, Chem. Eng. Sci. 52 (1997), 4069-4077.
[7] S. Maaß, N. Paul, M. Kraume, Chem. Eng. Sci. 76 (2012), 140-153.
[8] M. Wegener, N. Paul, M. Kraume, Int. J. Heat Mass Transfer 71 (2014), 475-495.

ECCE12
The 12th EUROPEAN CONGRESS OF CHEMICAL ENGINEERING
Florence 15-19 September 2019

Numerical Modelling of Emulsion Preparation Through CFD.

Guido Lupieri[1*], Adam J. Kowalski[1] and Jo J.M. Janssen[2]

1 Unilever R&D, Port Sunlight Laboratory, Quarry Road East, Bebington, Wirral CH63 3JW, UK;

2 Unilever Research and Development, Olivier van Noortlaan 120, 1330 AC Vlaardingen, The Nederlands

**Corresponding author: Guido.Lupieri@unilever.com*

Highlights

- High shear mixing and emulsification processes in high phase volume products
- Experimental models for numerical applications
- Population balance and instability

1. Introduction

Experiments and numerical modelling are considered crucial steps to control production in modern industrial processes since ensure the best quality of the product and the repeatability at the desired scale. These ideas apply also to the study of product preparation, when suited models of emulsification, viscosity, oil droplet distribution and size have been obtained in experimental sessions by one of the authors [1] or from existing computing libraries [2], [3]. This work concerns the modelling through Computational Fluid Dynamics instruments and scales of a step in the complex mixing process necessary to prepare the high phase volume emulsions in a standard [4] rotating geometry. The final goal is to control some of the most important properties of the emulsion like creaminess and taste.

2. Computing methods

The problem considers and simplifies the geometry of Figure 1 (a) in a computing domain discretized with polyhedral cells as in Figure 1 (b) where a multiphase segregated flow reproduces product and oil droplet. Finite Volume approach is assumed to resolve a set of differential equations for mass transport, momentum (and eventually energy) of each phase. All the phases share a common pressure field while for each one is defined a volume fraction according to VOF (Volume of Fluid) approach [3]. Interaction between phases is also assumed with models for drag force and droplet length scale, S-gamma [2] particle breakage and coalescence is adopted, the flow is considered and modelled in turbulent regime. A constitutive equation for viscosity is obtained from a Cross model modified according to the results in [1].

3. Results and discussion

Among the results, the oil droplet size at the outlet of the mixer is compared with the measures. An interesting feature of this flow is the possible development of instabilities in the small gap between the rotor and the cone mill walls as shown in Figure 1 (c).


(a)

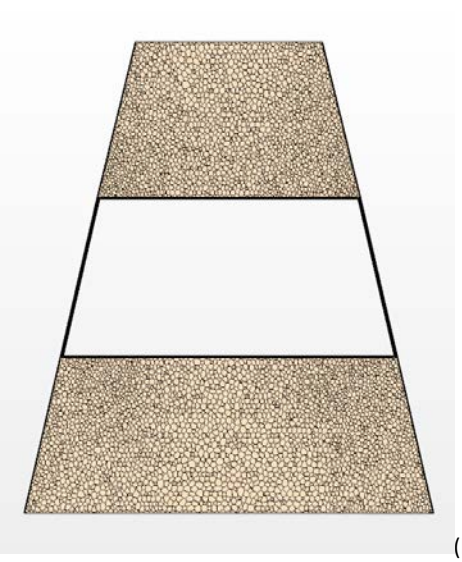
(b)

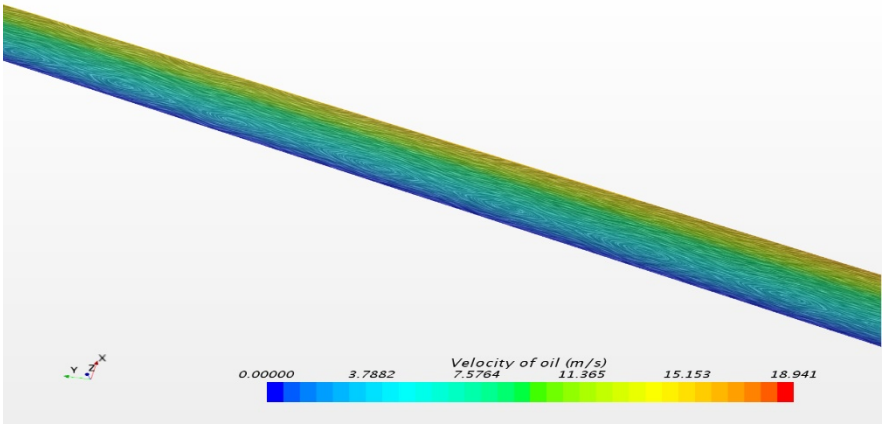

(c)

Figure 1. IKA cone mill from [4] on (a). A sketch of the computing domain on (b). Instability patterns of oil droplet patterns on (c).

4. Conclusions

By varying the rotation speed of the mixer, some numerical simulations have been conducted vs experiments in order to validate the approach and provide an affordable instrument for further analysis on in-house production processes.

References

[1] A. Dubbelboer, Jo J.M. Janssen, H. Hoogland, E. Zondervan, J. Meuldijk (2016). Chemical Engineering Science, 148, pp. 32-43.

[2] S. Lo and D. Zhang (2009). Modelling of Break-up and Coalescence in Bubbly Two-Phase Flows. J. Comp. Multiphase Flows, 1, pp. 23-38.

[3] C.W. Hirt and B.D. Nichols (1981). Volume of Fluid (VOF) Method for the Dynamics of Free Boundaries. Journal of Computational Physics, 39, 201-225.

[4] IKA Group. IKA Process Technology Brochure. www.ikausa.com

ECCE12
The 12th EUROPEAN CONGRESS OF CHEMICAL ENGINEERING
Florence 15-19 September 2019

Coalescence modelling for settler design

David Leleu, Andreas Pfennig

University of Liège, Department of Chemical Engineering - Products, Environment, and Processes (PEPs), Quartier Agora, Allée du six Août, 11, Liège, Belgium,]

dleleu@uliege.be, andreas.pfennig@uliege.be

Highlights

- single-drop based (ReDrop) concept to predict the settling of liquid dispersion for settler design
- consistent coalescence model for ReDrop, developed on the fundamental analysis of the phenomena
- Settling experiments with iso-optical system used to validate the model

1. Introduction

Continuous and batch settlers are used in processes in order to separate liquid-liquid dispersion. Their design can be challenging, e.g. quantitatively predicting the remaining fraction of fine drops found at settler outlet as function of the operating conditions. For batch settler design, a numerical tool has been developed, which is based on considering the behavior if individual representative drops (ReDrop concept) [1]. This tool, which applies a Monte-Carlo method to solve the drop-population balances, allows to simulate the separation of liquid-liquid dispersions and thus to optimize the design of continuous settlers. Sedimentation and coalescence are evaluated for a sufficiently large ensemble of representative individual drops at each time step. The information obtained is then collected to determine e.g. the required settler size. In these simulations, the coalescence modeling is a major challenge due to the complex interactions of drops upon approach and coalescence.

2. Coalescence model

As shown in Figure 1, the probability that two drops coalesce depends on three contributions. The first is the frequency with which they meet, defined by the so-called collision rate. The second parameter is the bouncing probability. It characterizes the probability that the drops stay in contact during the time following the collision. If they are not, the collision leads to the direct bouncing without any chance to coalesce. The final variable influencing the coalescence probability is the efficiency with which the drops coalesce once they met. The coalescence efficiency in turn depends on the time, during which the drops stay in contact and the time they would need to coalesce. The developed equation describing the coalescence efficiency is fundamentally different from the model of Coulaloglou and Tavlarides, which is inconsistent at a basic level.

It turns out that solely the fluid dynamics of the regarded equipment determines the frequency with which drops meet, the bouncing probability and the time they stay in contact. The differences in equipment to which this model is applied characterize the fluid dynamics, which thus has to be characterized only once for a given type of equipment. The time the drops need to coalesce on the other hand only depends on the specific material system used [2].

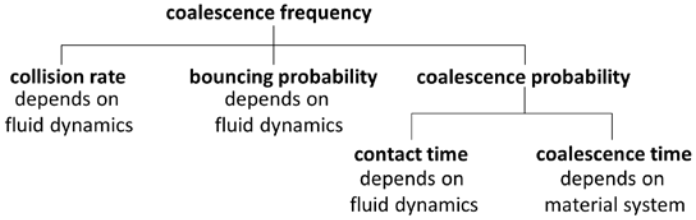

Figure 1. Coalescence model developed

3. Experimental device

The coalescence time can be evaluated experimentally from any suitable settling experiment. Here the experiments are conducted in the standardized settling cell proposed by Henschke [3]. It consists of a glass vessel with a capacity of 800ml, with 2 shafts for stirring with 4 stirrers on each shaft. A SOPAT probe is used to measure the drop-size distribution in situ. Iso-optical two-phase systems are analyzed and the settling after dispersing followed over the time. A dye present in one of the two phase allows to measure the local holdup. The experimental results are used to validate the model and the numerical approach.

4. First results and outcome

First experiments were performed with a system of paraffin oil droplets dispersed in water. The results depicted in Figure 2 show on the right hand side a simulation performed with the ReDrop program. The model parameters were fitted in order to follow the experimental data shown by the black dots. The latter represent the sedimentation and the coalescence curves observed visually from the movie recording of the settling experiment. The initial drop-size distribution used in the simulation was measured with the SOPAT probe. It is represented on the left side of Figure 2.

This results of the ReDrop simulation is in good agreement with the experimental data and shows good basis for the further experiments, detailed evaluation, and model validation using iso-optical systems.

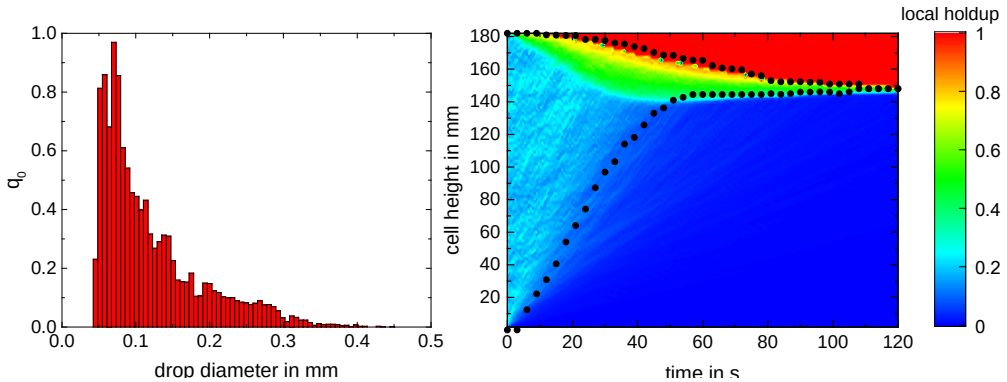

Figure 2. Fitting of experimental results (right) with the initial drop-size distribution measured with the SOPAT probe (left)

References

[1] J. Ayesteràn, N. Kopriwa, F. Buchbender, M. Kalem, A. Pfennig, Chem Ing. Tech., 38, (2015) 1894-1900.
[2] N. Kopriwa, A. Pfennig, Solvent Extraction and Ion Exchange, 34, (2016) 622-642.
[3] M. Henschke, L. H. Schlieper, A. Pfennig, Chem. Eng. J., 85 (2002), 369-378.

ECCE12
The 12th EUROPEAN CONGRESS OF CHEMICAL ENGINEERING
Florence 15-19 September 2019

Impact of nanoparticles and surfactants on drop size distribution and phase separation in liquid/liquid systems

Susanne Röhl[1], Lena Hohl[1], Maresa Kempin[2], Matthias Kraume[1]

1 Technische Universität Berlin, Chair of Chemical & Process Engineering,

Ackerstraße 76, 13355 Berlin, Germany

2 University of Applied Sciences Berlin, Chair of Process Engineering in Life Science,

Wilhelminenhofstraße 75A, 12459 Berlin, Germany

**Corresponding author: s.roehl@tu-berlin.de*

Highlights

- Detailed analysis of nanoparticles and surfactants as emulsion additives.
- Impact of additives on coalescence investigated via transient drop size distributions and phase separation curves.
- Self-similarity of drop size distributions and impact on the separation process.

1. Introduction

To optimize industrial processes it is often crucial to know the dispersion and coalescence behaviour, respectively the resulting drop size distribution, of liquid multiphase systems. Nanoparticles or surfactants can be used as innovative additives to reduce the droplet size in agitated multiphase systems and enhance the interfacial area available for mass transfer [1,2]. Beside a high interfacial area, the separation of the phases and a subsequent recycling of components is mandatory for economic efficiency [3]. For both agitated systems and the separation process different modeling approaches exist, but the description of additives often is realized using system-specific fit parameters since their actual impact on dispersion and coalescence is not yet fully understood. Aim of this work is a detailed analysis of liquid/liquid systems with nanoparticles [5, 6] and/or surfactants [7, 8] as additives including a detailed description of the droplet size distributions and their impact on the separation process.

2. Methods

Drop size distributions are experimentally determined in-situ in a stirred tank set up using an endoscope measurement technique in combination with an image analysis tool and automated drop detection (SOPAT GmbH). With an external camera, the dynamic phase separation is recorded after agitation stop and the overall separation time and phase separation curves are determined [1]. The system composition is described using the mass fraction of nanoparticles in the dispersed phase and the oil/water ratio $\alpha = m_{oil}/(m_{oil}+m_{water})$.

3. Results and discussion

The dynamic behaviour of the Sauter mean diameter after changes in agitation speed are shown in Figure 1 (left). The o/w emulsion consisted of water, n-heptan and different weight percent of

fumed silica nanoparticles (HDK H20, Wacker). With rising nanoparticle concentration, the coalescence rate after the reduction of agitation speed clearly diminishes. This is caused by the presence of nanoparticles at the liquid/liquid interface and its increased resistance against deformation [5, 6]. The dynamic phase separation curves after a complete agitation stop are shown in Figure 1 (right). The swarm sedimentation towards its continuous phase is illustrated via the sedimentation curve and the height of the completely coalesced interface via the coalescence curve. Higher particle concentrations clearly lead to higher separation times.

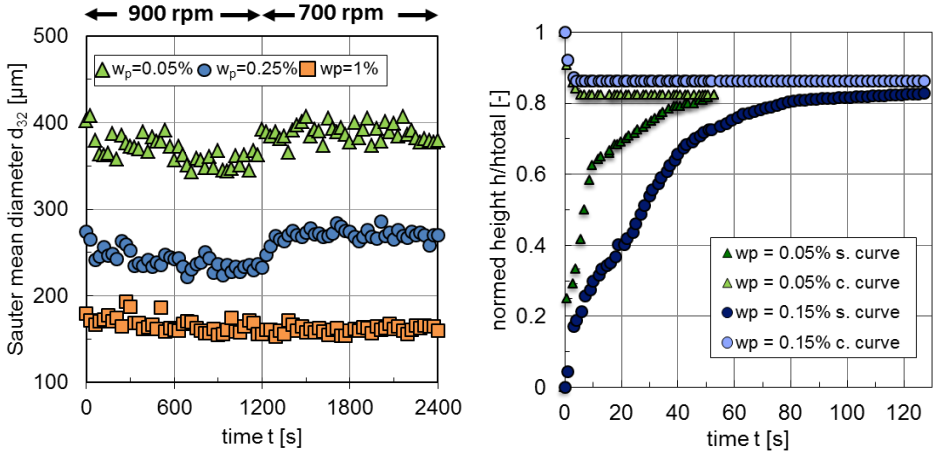

Figure 1. Transient Sauter mean diameters in agitated systems (left) and phase separation after agitation stop ($n_{initial}$ = 900 rpm) (right) in a water, n-heptane, silica nanoparticle HDK H20 system (o/w emulsions, α = 0.15, T = 20°C).

4. Conclusions

Nanoparticles and surfactants are promising additives for homogeneously catalysed liquid/liquid reactions. A detailed analysis of the coalescence behaviour under different flow conditions can be performed using the combination of endoscope measurements and separation curve analysis. Although both additives reduce the coalescence, the mechanisms are quite different due to their adsorption energy, size, shape and molecular structure. With the presented measurements and a detailed analysis of the complete drop size distributions, crucial information for the modeling approaches can be achieved.

References

[1] A. Rost, M. Müller, T. Hamerla, Y. Kasaka et al., Chem. Eng. Process. Process Intensif. 67 (2013) 130-135.
[2] R. von Klitzing, D. Stehl, T. Pogrzeba, R. Schomäcker et al., Adv. Mater. Interfaces, 1600435 (2016)
[3] T. Pogrzeba, D. Müller, M. Illner, M. Schmidt et al., Chem. Eng. Process. Process Intensif. 99 (2016), 155–166
[4] M. Henschke, L. H. Schlieper, A. Pfennig, Chem. Eng. J. 85 (2002), 369-378
[5] B. P. Binks, Curr. Opin. Colloid Interface Sci. 7 (2002) 21-41
[6] L. Hohl, S. Röhl, D. Stehl, R. von Klitzing, M. Kraume, Chem. Ing. Tech., 88 (2016), 1815-1826
[7] J.-L. Salager, R. E. Anton, D. A. Sabatini, J H. Harwell, et al., Surfactants Deterg. 8 (2005), 3-21
[8] L. Hohl, M. Kraume, Chem. Eng. Res. Des. 129 (2018), 89-101

ECCE12
The 12th EUROPEAN CONGRESS OF CHEMICAL ENGINEERING
Florence 15-19 September 2019

The Similarity of Power and Flow In Batch and Inline Rotor-Stator Mixers.

Thomas John[1], Adam J Kowalski[2], Tom L Rodgers[1], Claudio P Fonte[1].

1 University of Manchester, Manchester, M19 2FT, UK; 2 Unilever R&D, Wirral, CH63 3JW, UK.

**Corresponding author: thomas.john@manchester.ac.uk*

Highlights

- Inline and batch rotor-stators modelled using CFD.
- Power and flow numbers investigated for various screen hole sizes.
- Inline and batch rotor-stators can be characterized using the same model
- A correlation is developed to predict the recirculating flow in inline mixers.

1. Introduction

Rotor-stator mixers are mixing widely used across many industries for emulsification and de-agglomeration which can be operated in batch or inline mode. Often, the scaling of rotor-stators involves a change from batch to continuous mode, so it is highly desirable to understand how the power and flow characteristics differ between the two modes of operation. Power number in inline mixers can be characterized using the following equation[1].

$$\mathrm{Po} = \mathrm{Po_Z} + k_1 \mathrm{N_Q} \quad (1)$$

However, no such model has been developed or tested for batch mixers. The primary aim of this study was to investigate how this characterization differs between the two modes of operation.

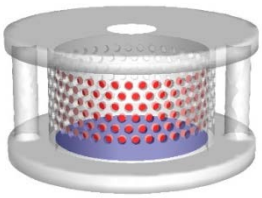

Figure 1. Surfaces across which flow was measured.

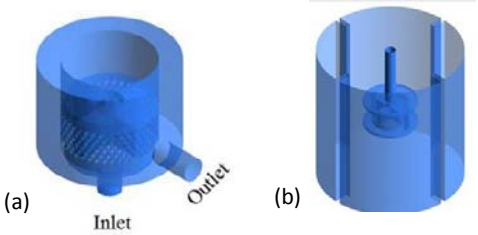

Figure 2. CFD geometries for (a) inline and (b) batch

2. Methods

The mixer studied was the Silverson L5M with standard emulsor head (Figure 1 and 2). Fluent v18.1 was the software used in this study. The standard k-ε turbulence model was utilized along with third order MUSCL discretization schemes for special discretization of momentum and turbulence. Rotation of the rotor was modelled using the multiple reference frame technique. Flow rate was measured across the red and purple surfaces shown in Figure 1. Power was measured from the bending moments on the rotor. In this study, using CFD, we were able to change the flow number in the batch configuration by constricting the base hole of the stator in small increments.

3. Results and discussion

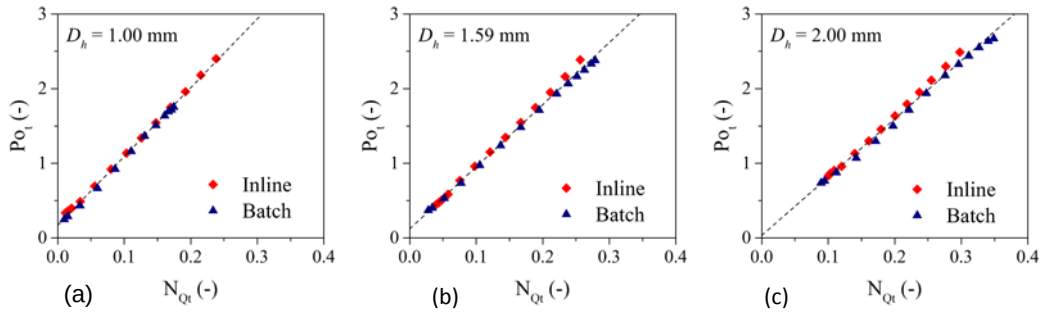

Figure 3. Power number vs flow number for both modes and hole sizes of (a) 1.00 mm, (b) 1.59 mm, and (c) 2.00 mm.

Figure 3 shows the power number as a function of the total flow number for the batch and inline simulations with various screen hole sizes. It can be seen that there is no difference between batch and inline RSMs in terms of power characterization. These results could suggest that with the same flow number, there will be no difference in the droplet size of an emulsified product, something which has also been suggested by Carillo De Hert[2].

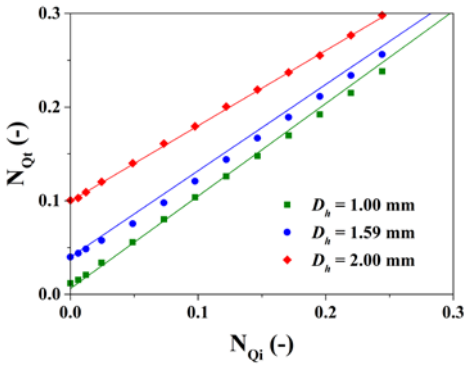

Figure 4. Total flow number vs imposed flow number for inline. Symbols - CFD data, lines - prediction by Equation 2.

Figure 4 shows the total flow number as a function of the imposed inlet flow number in the inline mixer. Since obtaining the total flow number would usually require CFD or PIV, a correlation was developed in order to predict the total flow number from imposed flow number and the geometry of the mixer using the following equation. The predicted results are shown in Figure 4.

$$N_{Qt} = N_{Qi} + 0.33\left(\frac{Area\ holes}{Rotor\ diameter^2}\right)^2 [0.51 - N_{Qi}] \quad (2)$$

4. Conclusions

Batch and inline rotor stators share the same characterization of agitation power. We have developed a correlation which enables the prediction of the total flow number from the imposed inlet flow number for inline rotor stators. This predicts how much flow recirculates back into the holes of the screen, and provides us with the true flow number that matches the batch data.

References

[1] A.J. Kowalski, Chem. Eng. Process: Process Intensif. 48 (2009) 581–585.
[2] S. Carrillo De Hert, Drop Size Distribution Analysis of Mechanically Agitated Liquid-Liquid Dispersions, University of Manchester, UK., 2017.

ECCE12
The 12th EUROPEAN CONGRESS OF CHEMICAL ENGINEERING
Florence 15-19 September 2019

Population Balance Modelling in Bubble Columns Operated in Heterogeneous Regime: From 3D URANS QMOM Simulations to the Development of a Stable Sauter Diameter Model.

Frédéric Augier[1,*], Luca Gemello[1,2], Cécile Plais[1], Daniele Marchisio[2]

*1 IFP Energies nouvelles, Rond-point de l'échangeur de Solaize, 69360 Solaize (69), France, 2 Dipartimento di Scienza Applicata e Tecnologia, Istituto di Ingegneria Chimica, Politecnico di Torino, Corso Duca degli Abruzzi 24, 10129 Torino, TO, Italy. *Corresponding author: frederic.augier@ifpen.fr*

Highlights

- Efficient CFD modeling of Bubble Columns coupled with Population Balance
- Identification of a set of kernels validated over a wide range of cases
- Dimensionless analysis and proposal of a simple 0D approach to screen kernels

1. Introduction & Methods

This project aims at developing a bubble column model that couples CFD 3D Unsteady Reynolds Averaged Navier-Stokes equations (3D URANS) with a Population Balance (PB) approach. Experimental data obtained in a former work[1] including gas holdup, liquid velocity and bubble size measurements have previously been used to validate a 3D URANS CFD model[2] without PB, thanks to the use of a specific drag law[2]. Now the Quadrature Method of Moments (QMOM) is applied[3] to solve PB. This method allows to calculate, at low CPU cost, the k-first moments (m_k) of the Bubble Size Distribution (BSD), and thus the Sauter mean diameter d_{32} (=m_3/m_2). We propose to present 1) the validation of breakage and coalescence kernels for this application, and 2) a model simplification and analysis that points out the link between physical models and the resulting Sauter mean diameter. The CFD and QMOM equations are solved with the commercial software ANSYS Fluent® 18.2.

Transport equations of the moments of the BSD are synthetized in Figure 1:

$$\frac{\partial m_k}{\partial t}+\frac{\partial\left(m_k \boldsymbol{u}_g\right)}{\partial x}=\frac{1}{2}\sum_{i=1}^{3} w_i \sum_{j=1}^{3} w_j h\left(L_i,L_j\right)\left[\left({L_i}^3+{L_j}^3\right)^{\frac{k}{3}}-L_i^k-L_j^k\right]+\sum_{i=1}^{3} w_i g\left(L_i\right)\left(\bar{b}_i^k-L_i^k\right) \quad (1)$$

$$h\left(L_i,L_j\right)=h_0\left(L_i,L_j\right)\cdot\lambda\left(L_i,L_j\right)$$

$$h_0\left(L_i,L_j\right)=C'_2\,\gamma\,\Pi\left(L_i+L_j\right)^2\varepsilon^{1/3}\sqrt{{L_i}^{2/3}+{L_j}^{2/3}}$$

$$\gamma=\frac{\alpha_{max}}{\alpha_{max}-\alpha}$$

$$\Pi=1-e^{\left(-C\frac{\alpha_{max}^{1/3}\,\alpha^{1/3}}{\alpha_{max}^{1/3}-\alpha^{1/3}}\right)}$$

$$\lambda\left(L_i,L_j\right)=u_{crit}/u_{rel}$$

$$u_{rel}=\sqrt{2}\,\varepsilon^{1/3}\sqrt{{L_i}^{2/3}+{L_j}^{2/3}}$$

$$g\left(L_i\right)=C_1\varepsilon^{1/3}erfc\left(\sqrt{\frac{C_2\sigma}{\rho_L\varepsilon^{2/3}{L_i}^{5/3}}+\frac{C_3\mu_L}{\sqrt{\rho_G\rho_L}\varepsilon^{1/3}{L_i}^{4/3}}}\right)$$

$$\bar{b}_i^k=\int_0^{L_i}\beta(L,L_i)L^k dL=\frac{3240L_i^k}{(k+9)(k+12)(k+15)}$$

$$\beta(L,L_i)=180\left(\frac{L^2}{L_i^3}\right)\left(\frac{L^3}{L_i^3}\right)\left(1-\frac{L^3}{L_i^3}\right)^2$$

Figure 1. Scheme of the moment transport equations.

where L (m) is the bubble diameter, i and j are the indices of the 3 nodes of the quadrature method. w_i (m^{-3}) is the bubble density of the node i. h ($s^{-1}m^3$) is the coalescence kernel and g (s^{-1}) is the breakage kernel. h_0 ($s^{-1}m^3$) is the collision frequency model, λ (-) is the coalescence efficiency, β (m^{-1}) is the distribution of the daughter bubbles after the breakage of a parent bubble and ε is the dissipation rate (W/kg). α is the gas volume fraction, u_{rel} (m/s) is the turbulent

relative velocity and u_{crit} (m/s) is the critical approach velocity between bubbles above which coalescence is not possible. γ and Π are dimensionless correction factors to include the effect of gas volume fraction on collision frequency. α_{max} is the maximum gas volume fraction, taken equal to 0.8. C_{xx} are the constants of the different involved models. At each time step and in each spatial location, wi and Li are reconstructed from the m_0 to m_5 moments by a Product-Difference algorithm. Breakage and coalescence contributions to the moments are computed with the 3 nodes (w_i, L_i) in the source (right) term of Eq. (1) in Fig. 1.

3. Results and discussion

Comparing simulations and experimental data obtained in the breakage-dominated regime[2], it is possible to validate the breakage model of Laakonnen[4]. Concerning the coalescence model, the best agreement is obtained by coupling the collision frequency model suggested by Wang[5] and the coalescence efficiency of Lehr[5], based on the critical approach velocity model (Fig.1) . Sauter diameter radial profiles are well predicted over a wide range of operating conditions (not shown). Besides, as equation (1) is very complex, a drastic simplification is considered to analyse the consistency of the kernel with our phenomenology. In Eq. (1) the source term is computed by considering only a single bubble diameter (L=d_{32}) to calculate the right-hand term. Consequently i=j=1 in the transport equations, and the bubble density is equal to $w = 6\alpha/(\pi L^3)$. Note that m_3 is always equal to $6\alpha/\pi$ whatever the BSD. The steady state of the equation (1) for k=2 is strongly simplified and becomes a dimensionless relation:

$$\tau_b/\tau_c = 6\alpha.h(L,L)/(g(L).\pi.L^3) = \left(1-\bar{b}^2/L^2\right)/\left(2^{-\frac{1}{3}}-1\right) \quad (2)$$

where $\tau_b = 1/g(L)$ is the characteristic breakage time and $\tau_c = 1/w.h(L,L) = \pi L^3/(6\alpha.h(L,L))$ is the characteristic coalescence time. The term $\bar{b}^2/L^2$ depends only on the shape of the daughter-bubble distribution β and not on L^2. Using the β model of Laakonnen leads to $\tau_b/\tau_c \approx 1.15$. This equation only depends on L, α and ε and physical properties . It can be used to calculate directly the stable d_{32} and to compare various models of breakage and coalescence. α and ε can be computed by using CFD simulations for instance. d_{32} calculated from Eq. (2) is successfully compared both to the complete CFD+QMOM model and experimental results in Figure 2. This shows that the strong assumptions done to develop the Eq. 2 are acceptable if only the Sauter mean diameter of the BSD is required.

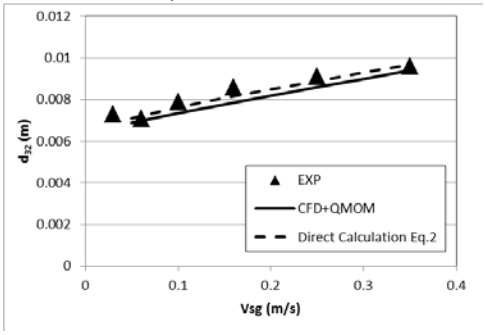

Figure 2. d_{32} comparison between CFD, Eq. (2) and experiments[1] (0.4 m column diameter, demineralized water)

References

[1] L. Gemello, C. Plais, F. Augier, A. Cloupet, D.L. Marchisio, Chem. Eng. Sci. 184 (2018) 93-102.
[2] L. Gemello, V. Cappello, F.Augier, D.L.Marchisio, C. Plais, Chem. Eng. Res. Des. 136 (2018) 846-858.
[3] D.L. Marchisio, R.D. Vigil, R.O. Fox, J. Coll. Interf. Sci. 258 (2003) 322-334.
[4] Y.Liao, Lucas, Chem. Eng. Sci. 64 (2009) 3389-3406.
[5] Y.Liao, Lucas, Chem. Eng. Sci. 64 (2010) 2851-2864.

ECCE12
The 12th EUROPEAN CONGRESS OF CHEMICAL ENGINEERING
Florence 15-19 September 2019

Numerical modelling of micromixing in a T-mixer flow at low Reynolds numbers

Cláudio P. Fonte[1], Joelle Aubin[2], Pierrette Guichardon[3], David F. Fletcher[4,*]

1 School of Chemical Engineering and Analytical Science, The University of Manchester, Oxford Road, Manchester, M13 9PL, United Kingdom; 2 Laboratoire de Génie Chimique, Université de Toulouse, CNRS, Toulouse, France; 3 Aix Marseille Université, CNRS, Centrale Marseille, M2P2 UMR 7340, Technopôle de Château-Gombert, 38 rue Frédéric Joliot-Curie, 13451 Marseille, France 4 School of Chemical and Biomolecular Engineering, The University of Sydney, Sydney, Australia

**Corresponding author: david.fletcher@sydney.edu.au*

Highlights

- CFD simulations are performed to study micromixing in a laminar microfluidic flow.
- Segregation indices are calculated using the Villermaux-Dushman protocol.
- Micromixing is modelled directly with CFD and indirectly with a lamellar model.
- The two solutions are compared in terms of computational cost and analysis times.

1. Introduction

Micromixing, i.e., the full homogenisation of mixtures of two or more components down to the molecular level, is a particularly important phenomenon in systems that involve fast and competitive chemical reactions, since it will directly impact on the achieved conversion and selectivity [1]. Directly modelling micromixing in laboratory or industrial equipment using Computational Fluid Dynamics (CFD) can, however, be computationally expensive. This is due to the need to resolve all the mixing scales down to those at which molecular diffusion becomes the dominant mechanism for the dissipation of concentration gradients. In the past 50 years [2], many efforts have been made to develop sub-grid models capable of describing micromixing in turbulent flows with Reynolds-Averaged Navier-Stokes or Large Eddy Simulations. Laminar flows have, however, received far less attention from the CFD community. In this work, we show that, in spite of their apparent simplicity, direct simulation of micromixing in the laminar regime can still be a challenging task when complex chaotic motions are present in the flow. Micromixing is assessed using the well-known Villermaux-Dushman reaction protocol in a milli-sized T-mixer with square bends. Direct numerical simulations of micromixing from the CFD flow field are compared with the predictions using a lamellar mixing model and previous experimental results.

2. Methods

The mixer geometry and flow conditions used in this work were chosen to replicate the experimental investigation of Commenge and Falk [3]. The flow domain has been discretised with hexahedral meshes with 20 and 40 cells across the duct. The continuity and momentum conservation equations were solved with ANSYS Fluent 19.0 to obtain 3D steady state flow fields in the microchannel at low Reynolds numbers ($60 \leq \mathrm{Re} \leq 300$). The transport and reaction of the species involved in the Villermaux-Dushman protocol have been directly solved using the built-in

Stiff Chemistry solver directly integrated with the CFD flow field. The segregation index, X_S, has been calculated from the concertation of all the species as described by Commenge and Falk [3] as the metric to assess micromixing.

The flow field obtained from the CFD simulations was additionally used to perform a Lagrangian tracking of the position and deformation of infinitesimal fluid elements injected at the inlets. These results were further processed to obtain an average rate of decay of the striation thickness of laminas of fluid necessary to model micromixing in the microchannel using a lamellar-structure mixing model as described by Ottino *et al.* [4]. Up to 800 particles were tracked with an adaptive 7^{th}-8^{th} order explicit Runge-Kutta method. The lamellar mixing model equations were solved using the pdepe function in MATLAB. It is worth mentioning that both developed models of micromixing in this work are fully-predictive and have no adjustable parameters, requiring only information on the kinetics of the Villermaux-Dushman reaction scheme found in the literature [3].

3. Results and discussion

The obtained simulation results for both models are in quite good agreement with experimental data of Commenge and Falk [3] (see Figure 1). The lamellar model tends to over predict micromixing at the lower range of Reynolds numbers but predicts well the rate of decay of the segregation index with the increase in Re. The direct numerical simulations of the species transport and reaction show quite good agreement with experimental results in the lower part of the Re range but seem to over predict the degree of micromixing in the upper part of the range, indicating that further refinement might still be necessary for those flow conditions.

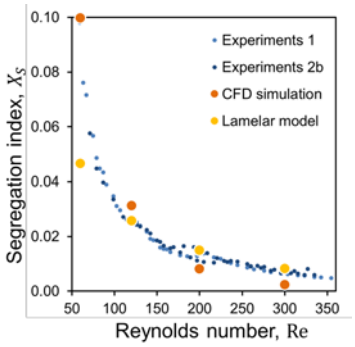

Figure 1. Comparison between the segregation index obtained experimentally by Commenge and Falk [3], the direct CFD simulation of the species transport and reaction, and the simulations using the lamellar mixing model.

The direct numerical simulations of micromixing using the CFD flow field have been found to be computationally very costly, requiring very fine meshes (up to 11.5 million elements).

4. Conclusions

CFD simulations have been successfully used in this work to simulate the flow and micromixing in a T-mixer with square bends in the laminar regime. This work shows that, even for simple geometries and low Re, the direct simulation of micromixing can be very computationally expensive when chaotic structures are produced by the flow. The use of micromixing models can offer an attractive alternative to direct simulations.

References

[1] Baldyga J., Bourne J.R., *Turbulent Mixing and Chemical Reactions*, Wiley-Blackwell (1999)

[2] Santos R.J., Dias M.M., Lopes J.C.B., *Mixing through half a century of chemical engineering*, in: Single and Two-phase Flows on Chemical and Biomedical Engineering, Bentham Science, pp. 79–112 (2012)

[3] Commenge J.-M., Falk L., *Villermaux–Dushman protocol for experimental characterization of micromixers*, Chemical Engineering and Processing: Process Intensification, 50 (10), pp. 979-990 (2011)

[4] Ottino J.M., Ranz W.E., Macosko C.W., *A lamellar model for analysis of liquid-liquid mixing*, Chemical Engineering Science, 34 (6), pp. 877-890 (1979)

ECCE12
The 12th EUROPEAN CONGRESS OF CHEMICAL ENGINEERING
Florence 15-19 September 2019

Development and validation of an experimental based particle breakup model for Lagrangian CO_2 dry-ice simulations

Arthur Rudek[1,2], Rudolf Kombeitz[1], David Muckenhaupt[1], Thomas Zitzmann[1], Gerald Russ[1] and Barry Duignan[2]

1 Hochschule Darmstadt, Haardtring 100, 64295 Darmstadt, GERMANY
2 Technical University Dublin, Bolton Street, Dublin-1, IRELAND

**Corresponding author: arthur.rudek@h-da.de*

Highlights

- Experimental insight into CO_2 dry-ice particle impact and breakup behaviour
- Development of a new particle breakup model for Lagrangian particle tracking
- Wind-tunnel experiment for the validation of the new particle breakup model

1. Introduction

A new particle breakup model is presented for Lagrangian particle tracking, which was developed in the context of the design process of a new CO_2 dry-ice based cleaning system for commercial aircraft engines. Particle breakup resulting from solid wall impacts is considered. The model is based on a large statistical database, which is derived from experimental particle impact data captured using two high speed cameras. In this work, approximately 4000 primary particles were recorded impacting a solid wall with various wall temperatures and using a range of impact velocities and impact angles. The recordings were post-processed by in-house-developed digital image processors to obtain secondary particle numbers, sizes and velocities. These secondary particle characteristics are discussed in the context of the experimental parameters and show significant dependence on impact angle and velocity and negligible dependence on target temperature. Using this data, a mass- and energy-based formulation is applied to predict particle breakup statistics in numerical simulations. The approach chosen is shown to be mass-, momentum- and energy conservative and is implemented in the commercial numerical code Ansys CFX. An additional validation experiment for the new particle breakup model is presented, in which a dilute dry-ice laden air flow is established in a wind-tunnel set-up containing a flat plate target. Particle collisions upon this plate are recorded using two high speed cameras and post-processed as described above. A comparison of the experimental data with numerical predictions of the same situation shows satisfactory overall agreement. The limitations of the new model are discussed and future developments are addressed based on these results.

2. Methods

The procedure presented is mainly influenced by the extensive investigations towards dry-ice by KRIEG [1], REDEKER [2] and HABERLAND [3] and the most recent water-ice particle breakup studies by HAUK et al. [4], VARGAS et al. [5] and those from PAN and RENDER [6] and GUEGAN et al. [7]. The modelling assumption used is comparable to what was introduced by CHAPELLE et al. [8]. The particle breakup process is governed by an overall mass- and energy balance of the impacting particles. It is derived from a theoretical model analysis and simplified based on a sensitivity analysis. A fundamental HSC experiment is made, where single dry-ice

particles are recorded while impacting solid walls at a range of impact velocities, angles and wall temperatures. The data acquired from post-processing of these recordings represents the statistical database for the new particle breakup model and the model is used in numerical simulations in the Lagrangian particle tracking toolbox in Ansys CFX.

3. Results and discussion

Representative experimental particle data and total results are presented. The dry-ice breakup process is discussed in physical terms, such as shown for example in Fig. 1, left. The main validation study compares numerical particle numbers and sizes to experimental results. The predictive capabilities of the new model implementation are determined in conjunction with simulation set-ups of the validation case; a numerical example is shown in Fig. 1, right.

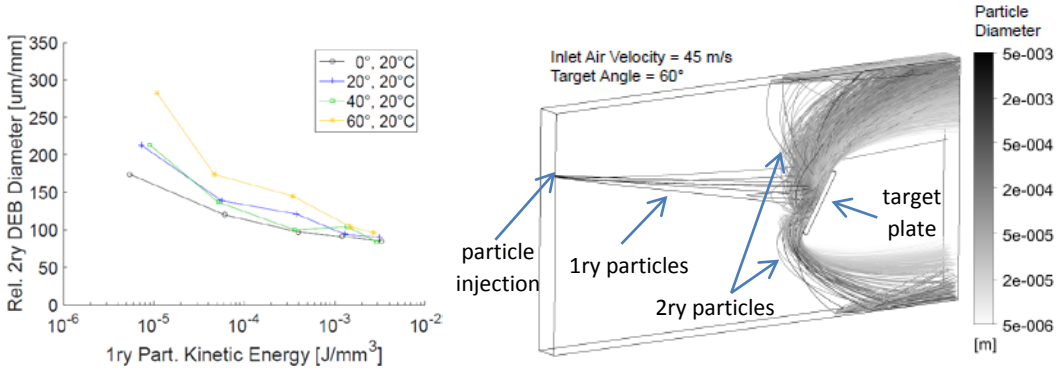

Figure 1: Particle sizes after 1ry particle breakup (left), particle breakup simulation in wind-tunnel setup (right).

4. Conclusions

A single particle experiment was presented to generate breakup statistics for dry-ice particles which are typically used in aircraft defouling applications. The statistical database was analyzed and it was found that the secondary particle numbers, sizes and velocities are mainly dependent on the primary particle impact velocity and on the impact angle. There was almost no dependency found on the target temperature, however, additional temperature effects at high impact velocities cannot be ruled out. Secondly, a wind-tunnel validation study of the new model was presented in which predicted values were compared to corresponding experimental data. Mean deviations of 5 to 10 % are encountered for the prediction of the secondary particle sizes. The prediction of the particle sizes of specific size classes is more precise than the prediction of the overall particle size. This can be attributed to more significant inaccuracies in the predictions of the numbers of secondary particles, which show mean deviations as high as 27 %.

References

[1] M. C. Krieg, Analysis of the effects of dry-ice blasting (in German), PhD-Thesis, TU Berlin, 2008.
[2] C. Redeker, Erosion and removal by dry-ice blasting (in German), PhD-Thesis, Univ. Hannover, 2003.
[3] J. Haberland; Cleaning and deburring with dry-ice (in German), PhD-Thesis, Univ. Bremen, 1999.
[4] T. Hauk, Investigation of the impact & melting process of ice particles, PhD-Thesis, TU Darmstadt, 2016
[5] M. Vargas et al., Ice particle impacts on a flat plate, IN: SAE Technical Paper 2099: pp 1–23, 2015.
[6] H. Pan and P. M. Render, Impact characteristics of hailstones simulating ingestion by turbofan aeroengines, IN: J. of Propulsion and Power, 12: pp 457–462, 1996.
[7] P. Guegan et al., Experimental investigation of the kinematics of post-impact ice fragments, IN: Int. J. of Impact Engineering, 38: pp 786–795, 2011.
[8] P. Chapelle et al., Computational model for prediction of particle degradation during dilute-phase pneumatic conveying, IN: Advanced Powder Technology, 15: pp 13–29, 2004.

ECCE12
The 12th EUROPEAN CONGRESS OF CHEMICAL ENGINEERING
Florence 15-19 September 2019

Application of microCT for the visualization of multiphase phenomena in small ducts

Julia Schuler[1], Norbert Kockmann[1]

[1]TU Dortmund University, Equipment Design, Emil-Figge-Straße 68, 44227 Dortmund, Germany

*Corresponding author: julia.schuler@tu-dortmund.de

Highlights

- Micro CT system for the investigation of liquid/liquid flows
- 2D and 3D investigation of liquid/liquid interfaces and transport phenomena
- Detailed analysis in MATLAB

1. Introduction

For process intensification in chemical engineering, miniaturization of equipment to the millimeter or micrometer range offers great potential for high mass and heat transfer and, thus, safer processes. Multiphase applications are often occurring and allow for executing gas/liquid reactions or liquid/liquid separation processes. To ensure successful process intensification via miniaturization, knowledge about the interfaces between the phases is crucial. Usually, interfaces in miniaturized equipment are examined by optical cameras, but often optical access is limited. To overcome this limitation, micro computed tomography (micro CT) is used to investigate interfaces and transport phenomena in miniaturized equipment in this contribution.

Nowadays, computed tomography CT is widely used not only in medical diagnosis [1], but also in material science [2] and geology [3]. Even in the field of process engineering, CT increasingly becomes an important tool, for example for the investigation of the distribution of liquid distribution in packed columns [4,5,6]. However, the extension of CT imaging to the field of micro process engineering needs high spatial resolution. In this work, we present a methodology that enables 2D and 3D investigation of multiphase flows in capillaries. The focus is set on liquid/liquid applications.

2. Methods

Image acquisition is carried out with the Bruker Skyscan 1275 (RLJ Micro & Analytics, Germany), that allows resolutions up to 4 µm. It is equipped with a stationary X-ray source and detector and a rotating sample stage, as shown in figure 1. For safety reasons, the image acquisition unit along with the mounted sample equipment is enclosed in a lead housing. For liquid

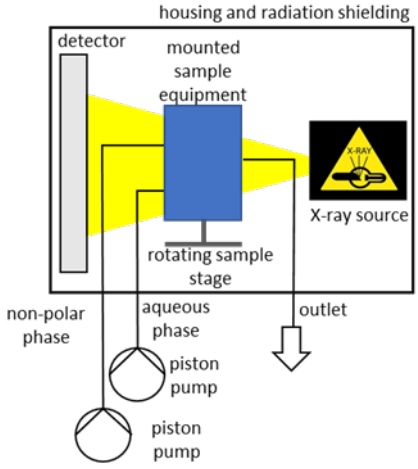

Figure 1. *Schematic of the experimental set up for the investigation of multiphase phenomena in small ducts.*

supply and liquid removal, it is additionally equipped with fluorinated ethylene propylene hoses. An aqueous and a non-polar phase are pumped through the scanner using piston pumps and contacted inside the scanner in a narrow duct.

After image acquisition, the images are reconstructed using *NRecon*, the reconstruction software that comes along with Bruker Skyscan 1275, to obtain 3D information and analyzed using a self-developed procedure in MATLAB. For 2D investigation, image analysis can be performed directly after image acquisition.

3. Results and conclusion

The presented procedure allows the 2D and 3D investigation of liquid/liquid interfaces. Figure 2a) shows a liquid/liquid interface extracted from a stack of reconstructed projection images. In figure 2 b) a 2D projection image of a liquid/liquid bubbly flow in a low density polyethylene hose (inner diameter 1.5 mm), generated by a stainless steel cannula is shown.

Future work will incorporate a more detailed investigation of liquid/liquid interfaces in different flow regimes, such as parallel flow or periodic bubbly or slug flow. This will be supplemented by first mass transfer experiments inside the CT.

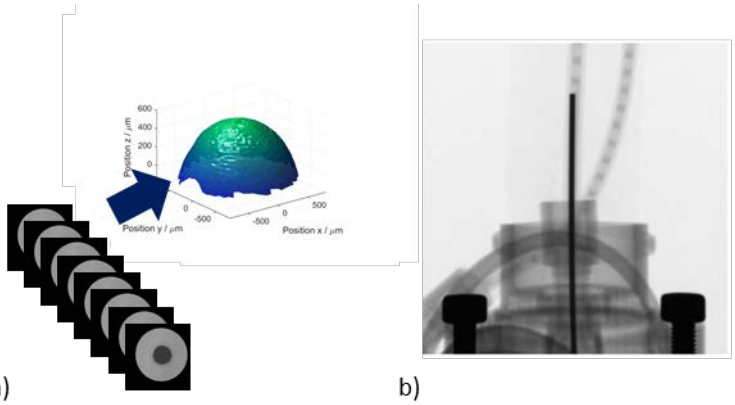

Figure 2. *a) Stationary liquid/liquid interface extracted from a stack of reconstructed slices, b) Projection image of the experimental set up for the generation of a liquid/liquid drop flow in a low density polyethylene hose generated by a cannula.*

References

[1] D. W. Holdsworth and M. M. Thornton, Trends in Biotechnology, 2002, 20, S34-S39.
[2] J. Bock and A. M. Jacobi, Materials Characterization, 2013, 75, 35–43.
[3] M. Andrew, B. Bijeljic and M. J. Blunt, Advances in Water Resources, 2014, 68, 24–31.
[4] S. Aferka, A. Viva, E. Brunazzi, P. Marchot, M. Crine and D. Toye, Chemical Engineering Science, 2011, 66, 3413–3422.
[5] D. Toye, P. Marchot, M. Crine, A.-M. Pelsser and G. L'Homme, Chemical Engineering and Processing: Process Intensification, 1998, 37, 511–520.
[6] A. Janzen, J. Steube, S. Aferka, E. Y. Kenig, M. Crine, P. Marchot and D. Toye, Chemical Engineering Science, 2013, 102, 451–460.

ECCE12
The 12th EUROPEAN CONGRESS OF CHEMICAL ENGINEERING
Florence 15-19 September 2019

Comparison of numerical approaches for drop breakup in microporous channels

Tobias Wollborn[1,2], Alexander Schulz[1,2], Udo Fritsching[1,2]

1 Leibniz Institute for Materials Engineering - IWT; 2 Particles and Process Engineering, University of Bremen, Germany

**Corresponding author: ufri@iwt.uni-bremen.de*

Highlights

- Comparison of numerical studies. Volume-of-Fluid vs. Lattice-Boltzmann
- Drop breakup is related to interfacial shear stress and pore geometry
- Generic simulations are performed to analyze the breakup processes in complex structures
- Stress related breakup mechanisms enable opportunities in membrane design

1. Introduction

Emulsions are widely used in industrial applications. In particular in the food technology and in the pharmaceutical industry the quality of the emulsion is relevant. The membrane emulsification process obtains the advantage to adjust the droplet size distribution according to the pore structure and the geometry of the membrane. The membrane emulsification process is a low stress process which is relevant for the handling of shear sensitive media (i.e. in biological systems). Whereas the emulsification process and influence of the membrane structure and geometry on the final product is well investigated, the liquid deformation and liquid dispersion process inside of the membrane structure is quite unknown. In particular the shear and strain stress at the droplet interface is important, especially in combination with adsorption processes of surfactants. Local stresses determine the droplet deformation and eventually the breakup. On the other hand, shear and strain stresses can influence the adsorbed structures (surfactants) at the interface, in example proteins. In this work numerical investigations with the Volume-of-Fluid-Method were performed to understand stress related breakup mechanisms in microporous structures. Furthermore Lattice-Boltzmann studies were carried out to investigate the effect of non-Newtonian fluid on the breakup process. The results of both methods are complemented to get an overall understanding of the complex breakup mechanisms in membrane emulsification processes.

2. Methods

A Volume-of-Fluid method formulation within OpenFOAMS InterFoam solver was implemented. This model enables the calculation of local shear and strain conditions (stress tensor) at the interface of a liquid-liquid system. With this extension the stress residence time behavior at the liquid-liquid interface in idealized pore structures and elementary flow constrictions has been analyzed. The parameters influence on the droplet deformation is carried out and critical shear and strain stresses for droplet breakup are analyzed. The simulation procedure was extended to real membrane pore geometries and compared to the stress conditions and break up mechanisms received from the idealized pore geometries. The inter-particle Shan Chen Lattice Boltzmann model for immiscible fluids is used to analyze the droplet dynamics in porous model structures and real

membrane structures. Furthermore, models for shear-thinning and viscoelastic fluids are used to study the differences in the break-up mechanism. Newtonian droplets in non-Newtonian continous phases and vice versa are investigated at different Deborah numbers. Parameters in both numerical studies were varied by the pore geometry, capillary number, contact angle and droplet size.

3. Results and discussion

An example of the porous structures investigated and a simulated (VOF) drop within this structure is shown in Fig. 1. For the Volume-of-Fluid Method the results show that liquid-liquid (disperse-continuous) interface stress determines the drop deformation process rather than liquid-solid (disperse-wall) interface stress. The main stress related drop breakup mechanisms were derived. At a critical capillary number the drop detaches from the pore wall based on contact line instabilities, followed by a deformation of the droplet at the liquid-liquid interface due to stress and strain histories, ending up in the breakup of the droplet due to local constrictions. The analysis of local and integral interfacial stress condition gives insight of the geometry and time dependent drop deformation behavior. [1]

The results of the Lattice-Boltzmann studies show that the feedback of the viscoelastic fluid changes the breakup process and thus the resulting drop size distribution. This leads to smaller drop sizes. The local shear rates in the membrane structure induce local shear thinning of the non-Newtonian fluid, which results in a change of the local stress conditions and hence of the drop deformation behavior.

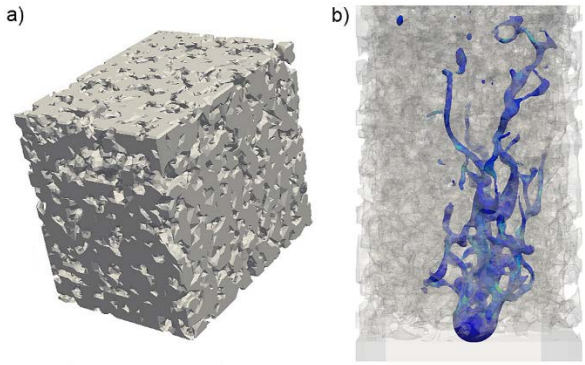

Figure 1. CT-scan of a porous membrane structure (a) and a simulated droplet within the membrane structure (b) [1]

4. Conclusions

The analysis of the stress dependent drop breakup mechanisms in micro-pores and the investigation of the effect of non-Newtonian fluid on the breakup process enable new opportunities in the design of porous structures to reduce the stress conditions during the emulsification process for the utilization stress sensitive media and for the formulation of certain emulsion properties.

Acknowledgement

This project has been funded by the German Research Foundation (DFG) within the SPP 1934 “DiSPBiotech” (Tobias Wollborn) and the MIMENIMA Graduate School (Alexander Schulz) at the University of Bremen. The resources for the numerical calculations have been provided by The North-German Supercomputing Alliance (HLRN).

References

[1] T. Wollborn, L. Luhede, U. Fritsching, in: Phys. Fluids 31 (2019) doi: 10.1063/1.5064858

ECCE12
The 12th EUROPEAN CONGRESS OF CHEMICAL ENGINEERING
Florence 15–19 September 2019

Computational fluid dynamics analysis of 3D flow patterns in a stirring blade turning space in a wide range of Reynolds number

T. Hakamada[1], R. Misumi[*1], M. Kaminoyama[1]

1 Yokohama National University, 79-5, Tokiwadai, Hodogaya-ku, Yokohama-shi, Kanagawa, 240-8501, Japan

**misumi-ryuta-zm@ynu.ac.jp*

Highlights

- We used CFD to qualify 3D flow patterns in the stirring blade turning space.
- We validated the CFD results from PIV measurements in the blade turning space.
- Effects of viscosity on the flow pattern were ascertained for a wide range of *Re*.

1. Introduction

During mixing operations, the flow pattern in the stirring blade turning space affects the circulation flow in the tank. The pattern is linked directly to the success or failure of the operation. However, because it is difficult to measure the flow pattern in the turning space, the flow pattern in the turning space has not been revealed sufficiently. Especially in the transitional regime, the effects of the fluid viscosity, vessel size, and impeller speed on the flow pattern have remained unclear. Computational fluid dynamics (CFD) is a very useful technique to predict fluid flow. However, when using CFD, validation with reliable experimental data is fundamentally important. For this study, the three-dimensional fluid velocity distribution in the turning space of a six-blade paddle in a non-baffled vessel was quantified by CFD from the laminar, transitional, and then to turbulent regime. Furthermore, horizontal two-dimensional particle image velocimetry (2D-PIV) in the turning space was performed in the rotational coordinate system. The CFD analysis was validated based on the PIV data.

2. Methods

Software (Fluent 18.0; ANSYS Inc.) was used for CFD analysis. For this study, a non-baffled cylindrical tank with a flat bottom of inner diameter T = 0.20 m was used. The blade diameter and width were, respectively, D = 0.10 m and b = 0.02 m. The rotational speed was N = 2 s^{-1}. The fluid depth was H = 0.25 m. The blade height was h = H/2. Water or glycerin aqueous solution was assumed as the working fluid. We performed CFD analysis at Re = 24, 177, 511, and 22,400 by changing the glycerin solution viscosity. Laminar, transition-SST, DES, and LES models were adapted for each flow regime. Polyhedral mesh was adapted, and two conditions of 390,000 and 890,000 cell number were prepared. The radial, tangential, and axial velocities in the rotational coordinate system were calculated. Time-averaged velocities were quantified for 4 s under a steady state.

2D-PIV measurements were taken under the same conditions as those used for CFD. The tracer particle motion was captured continuously for 2 s using a high-speed video camera. Fluid velocity distributions in the Cartesian coordinate system were analyzed from 2000 images using PIV

software (Flow Expert 2D2C; Kato Koken). Then, the radial velocity $u_{r,ro}$ and the tangential velocity $u_{\theta,ro}$ synchronized with the impeller rotation were calculated using the original MATLAB® program.

3. Results and discussion

3.1 Radial velocity distribution between two blades in the rotational coordinate system

Fig. 1 shows the relation between time-averaged radial velocity $\overline{u_{r,ro}}$ normalized with the blade tip velocity v_{tip} and circumferential angle θ_{ro} [rad] at the center height of blade at *Re* = 177. Laminar, transition-SST, and LES were used with 390,000 cells at *Re* = 177. Fig. 2 shows the parity plot of $\overline{u_{r,ro}}$ between PIV and CFD by the transition SST model. Fig. 1 and Fig. 2 show the PIV measurements can be predicted most accurately by transition-SST model. Their accuracy is confirmed as approximately ±16%. Similar procedures were used for other *Re* number conditions.

3.2 Quantification of three-dimensional flow pattern

Fig. 3 shows the isosurface of $\overline{u_{r,ro}}$ = 0.3 v_{tip} of the CFD result in the wide range of *Re*. The isosurface shows the distribution of discharge flow from blades. At *Re* = 24, the fluid is pushed out by the blade and is discharged from the front side of the blade. At *Re* = 177, the fluid is discharged from both the front and back sides of the blade. At *Re* = 511, the discharge flow is mainly induced around the back sides, and at *Re* = 22400, the radial flow velocity from the back sides decreases. In other words, results show that the discharge flow shifts from the front side to the back side of the blade as the flow regime changes from laminar, transitional, and then to turbulence.

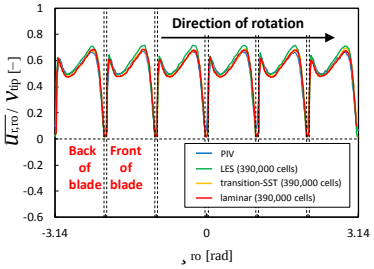

Figure 1. Relation between $\overline{u_{r,ro}}/v_{tip}$ and θ_{ro} (*Re* = 177, at the blade center height)

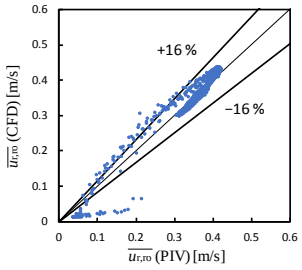

Figure 2. Parity plot of $\overline{u_{r,ro}}$ between PIV and CFD (*Re* = 177 with transition-SST model)

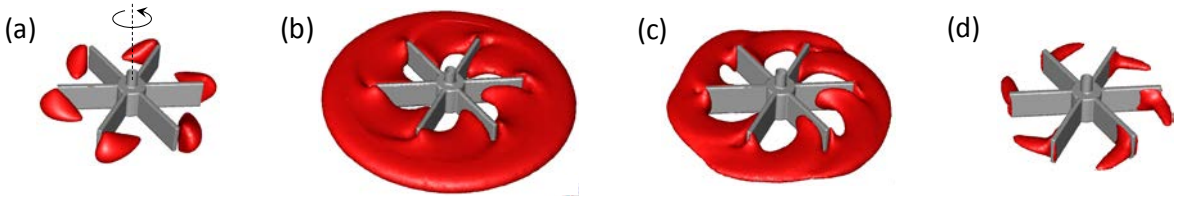

Figure 3. Isosurface of $\overline{u_{r,ro}}$ = 0.3v_{tip} ((a) *Re* = 24, (b) *Re* = 177, (c) *Re* = 511, (d) *Re* = 22400)

4. Conclusions

This study quantified three-dimensional flow patterns in the turning space of the stirring blades from laminar, transitional, and to a turbulent regime by CFD. Moreover, to confirm the validity of CFD, the discharge flow velocity distribution in the turning space was quantified using horizontal 2D-PIV. The accuracy of CFD results with various analytical models was evaluated for the respective *Re* number conditions. The most accurate CFD results showed that the discharge flow shifts from the front side to the back side of the blade as the flow regime change from the laminar, transitional, and then to turbulence.

This study was supported by JSPS KAKENHI (Grant Nos. 19K05118 and 17K06886).

ECCE12
The 12th EUROPEAN CONGRESS OF CHEMICAL ENGINEERING
Florence 15-19 September 2019

Simulation of Developing Bubbly Pipe Flows with a Coupled Multi-Fluid/Population Balance Solver

Mohsen Shiea[1], Marco Vanni[1], Daniele Marchisio[1], Antonio Buffo[1]

1 Dipartimento di Scienza Applicata e Tecnologia, Politecnico di Torino, 10129 Torino, Italia.

**Corresponding author: mohsen.shiea@polito.it*

Highlights

- CFD with population balance equation is a powerful tool to simulate bubbly flows.
- QMOM with two-fluid approach predicts the average bubble size satisfactorily.
- Multi-fluid approach is necessary when the bubble size distribution is wide.

1. Introduction

Comprehensive CFD simulation of disperse gas-liquid flows requires the knowledge about the evolution of the disperse phase, i.e. gas bubbles, that can be achieved by solving the population balance equation (PBE) along with the relevant governing equations, which are limited, in this work, to mass and momentum balance equations. The PBE can be solved to predict how the population of the bubbles are distributed over the properties of interest, e.g. bubble size and bubble velocity. If the bubble size is the only property under study, i.e. assuming constant velocity for bubbles of different sizes, then the PBE can be integrated into a two-fluid model (TFM) solver. However, if the constant velocity assumption is not valid, for instance if the bubble size distribution (BSD) is wide, bubbles of different sizes should be transported with different velocities, hence the necessity of adopting a multi-fluid approach. This work aims at analyzing and comparing the simulation predictions of a developing turbulent air/water pipe flow using both two-fluid and multi-fluid approaches. The comparison of the predictions in this specific system is interesting since the lift force plays an important role in the radial distribution of the air as the flow develops. On the other hand, both the magnitude and the direction of the lift force depend on the bubble size [1]. Therefore, the effect of considering different velocities for bubbles of different sizes can be studied.

2. Methods and Experimental Data

The experimental data was adopted from the work by Bayer and co-workers [2]. The setup is a vertical air/water pipe flow with the inner diameter of 0.1953 (m). The air enters from the injection points located on the wall into the upward-flowing water. The flow develops gradually until it reaches a wire-mesh sensor that measures air volume fraction, air velocity and bubble size distribution. The injection points have different distances from the sensor, therefore, the information about how the flow develops in the pipe is available.

The simulations are performed with both two- and multi-fluid approaches. The two-fluid model consists of the momentum balance equations for the liquid and gas phases in addition to the volume fraction balance equation for the gas phase. The interfacial forces and corresponding models are selected based on some preliminary mono-disperse simulations, which include drag,

lift, turbulent dispersion and wall lubrication. The PBE is solved using the Quadrature method of moments (QMOM). It considers the effects of hydrostatic pressure, bubble coalescence and bubble breakage (modelled on the assumption of homogeneous isotropic turbulence) on the BSD. In this work, the QMOM approximates the BSD with three groups of bubbles (three-node quadrature). In multi-fluid model, the balance equations are written for each group as if there are three disperse phases with different characteristic lengths. All the simulations were performed using the modified versions of *twoPhaseEulerFoam* and *reactingMultiphaseEulerFoam* solvers of OpenFOAM v5.0 and v6.0. Further details of the implementation are described by Buffo and co-workers [3].

3. Results and discussion

Figure 1 depicts the radial profile of the air volume fraction (left) and the axial changes of the Sauter mean diameter, SMD, (right) obtained by the two-fluid approach for the operating condition with the inlet water and air velocities equal to 0.405 and 0.0368 m/s respectively. The predicted radial profiles of the air volume fraction show good agreement with the experimental data, particularly at the higher section where the flow is almost developed. The discrepancies, such as those seen at the lower section, could be attributed to fact that according to the experimental data, the BSD near the air injection point is wider in comparison to the higher sections, where the flow is more developed. It suggests using the multi-fluid approach to allow the bubbles to move with different velocities and assess its effect on the radial air distribution. Nevertheless, the PBE coupled with the two-fluid approach provides satisfactory predictions for the change of the SMD in the axial direction by using coalescence/breakage kernels based on the homogeneous isotropic turbulence.

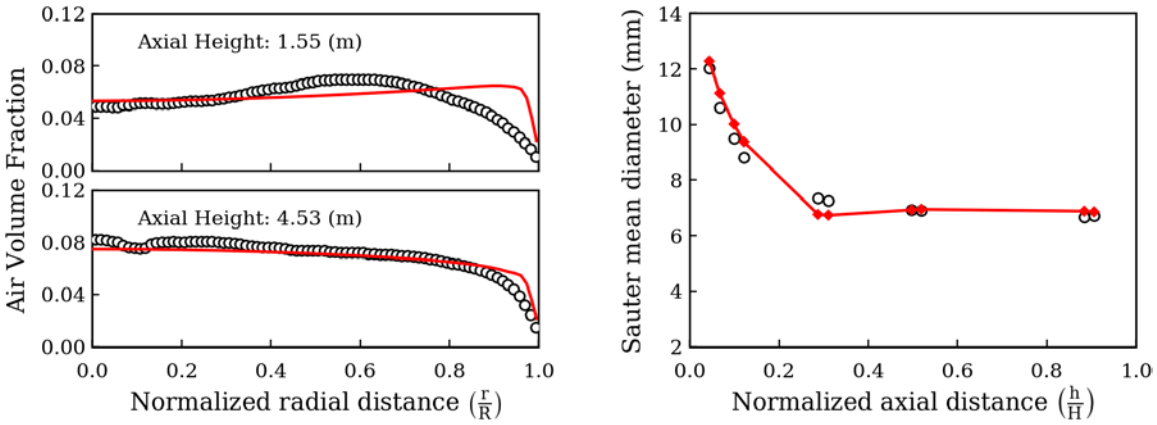

Figure 1. The radial profiles of the air volume fraction at two axial heights (left) and the axial profile of the average SMD (right) predicted by the two-fluid approach. Experimental measurements are shown by the circular markers.

4. Conclusions

A developing turbulent bubbly pipe flow was simulated using CFD-PBE method. Satisfactory predictions, particularly for higher sections (developed flow) were obtained by assuming one velocity for bubbles of different sizes. The multi-fluid approach will be used to assign different velocities to bubbles of different sizes, which is necessary when the BSD is wide.

References

[1] A. Tomiyama, H. Tamai, I. Zun, S. Hosokawa, Chem. Eng. Sci. 57 (2002) 1849–1858.
[2] M. Beyer, D. Lucas, J. Kussin, P. Schütz, Report FZD-505, 2008.
[3] A. Buffo, D. Marchisio, Rev. Chem. Eng. 30(1) (2014) 73–126.

ECCE12
The 12th EUROPEAN CONGRESS OF CHEMICAL ENGINEERING
Florence 15-19 September 2019

Characterization of a Microfluidic Device Manufactured by Reactive Ion Etching

Jens Bobers[1*], Maurice Hesselmann, Arndt-Christian Schneider, Jakob Zimmermann[2], Norbert Kockmann[1]

1 TU Dortmund University, Biochemical and Chemical Engineering, Laboratory of Equipment Design, Emil-Figge-Str. 68, 44227 Dortmund, Germany;

2 TU Dortmund University, Electrical Engineering & Information Technology, Intelligent Microsystems Institute, Emil-Figge-Str. 68, 44227 Dortmund, Germany

**Corresponding author: jens.bobers@tu-dortmund.de*

Highlights

- New manufacturing process for microstructured devices.
- Etch rate of the RIE process increased by increasing SF_6 and oxygen flow rates at higher pressure.
- Resulting surface roughness minimized with high gas flow rates at high pressure.
- Linear relation between pressure drop and Reynolds number indicates laminar flow.

1. Introduction

Two-phase droplet flow in microchannels is of great potential providing high specific surface, low liquid hold-up and, intensified chemical reactions. A new manufacturing process for polyimide-based microfluidic devices was developed. Reactive ion etching (RIE) was used as production technique obtaining anisotropic etching and high spatial resolution. Polyimide (PI) withstands most solvents, acids and bases and is suitable for RIE. The combination of RIE and PI for microfluidic devices provides high geometric flexibility, reproducibility and, wide range of applications. The production process was applied on microfluidic geometry for droplet generation. [1–3]

2. Methods

The etching gas for the RIE process contains sulphur hexafluoride (SF_6), oxygen (O_2), and argon (Ar). A 2^4 full factorial designed experiment was used to analyze the effects of the investigated parameters on the surface roughness and etch rate and to determine the interactions between these parameters. The experiments were performed with an RIE apparatus Plasmalab® µEtch (Oxford Instruments plc, Abingdon, UK). The gas composition during the RIE process and the total pressure were varied between 133 and 266 Pa. The pressure drop of the manufactured geometry was measured as an indicator of the prevailing flow regime (see Figure 1, left).

3. Results and discussion

The physical etching during RIE is caused chiefly by the argon ions and partly by the oxygen atoms. The chemical etching is performed by fluoride ions generated from SF_6. The optimal parameter

settings was found with all parameters on high level since the positive effect on the etch rate exceeds the minor increase of roughness. A value of 0.7137 µm min^{-1} was found for the etch rate and for mean surface roughness 0.5878 µm were measured with a mean etch depth of 50 µm. The measured pressure drop was compared to calculated values using the Darcy Weisbach equation for flow inside a tube and with a fitted constant, respectively (see Figure 1, right). The linear course of the pressure drop indicates laminar flow regime and only a minor influence of the surface roughness and the channel widening on the liquid flow [4].

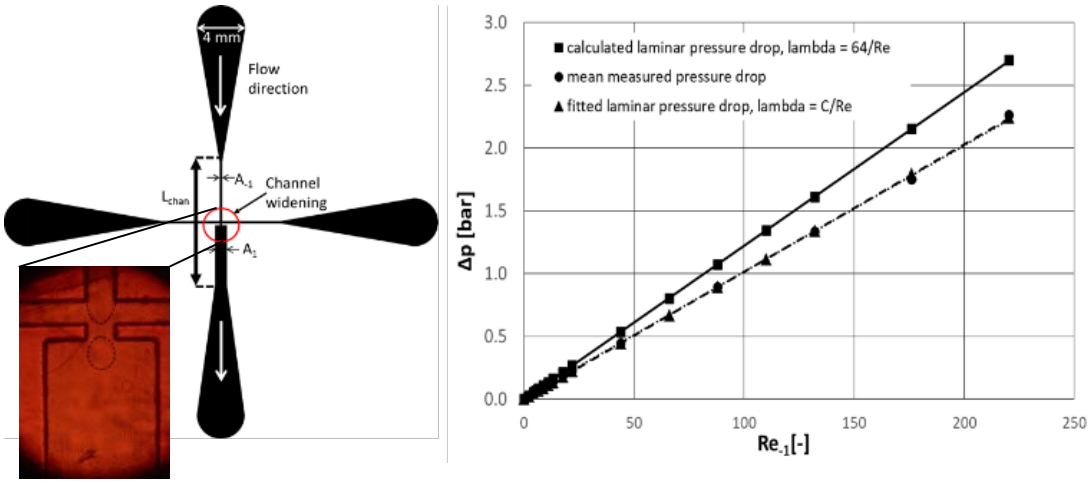

Figure 1: Manufactured geometry (left) with observed drop flow for water/silicone oil (0.01 ml min^{-1}/0.1 ml min^{-1}), measured and calculated single-phase (water) pressure drop plotted against the highest Reynolds number (right), constant C fitted on the measured values and found as 53

4. Conclusions

A RIE manufacturing process for microstructured devices was developed and characterized regarding to the etch rate and surface roughness. A microstructured droplet generator with a widening from 100 µm to 300 µm was manufactured with the optimized parameter settings and drop flow was observed for water in silicone oil. The course of the pressure drop implicates a laminar flow regime for the investigated flow rates. The linear part of the Darcy Weisbach equation dominates the pressure drop in contrast to the contribution of the quadratic part. This indicates that the small straight channel have the greatest impact on the total pressure drop in contrast to the surface quality and other geometric influences.

References

[1] Hwang, Y.-J., Coley, C. W., Abolhasani, M., Marzinzik, A. L., Koch, G., Spanka, C., Lehmann, H. and Jensen, K. F. "A segmented flow platform for on-demand medicinal chemistry and compound synthesis in oscillating droplets." *Chem. commun.* Vol. 53 No.49 (2017) pp. 6649 – 6652.

[2] Buder, U., Klitzing, J.-P. v. and Obermeier, E. "Reactive ion etching for bulk structuring of polyimide." *Sensors and Actuators A: Physical* Vol. 132 No.1 (2006) pp. 393 – 399.

[3] Dittrich, P. S. and Manz, A. "Lab-on-a-chip." *Nature rev. Drug discovery* Vol. 5 No.3 (2006) pp. 210 – 218.

[4] Agarwal, N., Ponoth, S., Plawsky, J. and Persans, P. D. "Roughness evolution in polyimide films during plasma etching." *Appl. Phys. Lett.* Vol. 78 No.16 (2001) pp. 2294 – 2296.

ECCE12
The 12th EUROPEAN CONGRESS OF CHEMICAL ENGINEERING
Florence 15-19 September 2019

Influence of impeller geometry on hydromechanical stress in agitated bioreactors

Chrysoula Bliatsiou[1], Robert Panckow[1], Philipp Waldherr[1], Lutz Böhm[1], Matthias Kraume[1]

1 Chair of Chemical and Process Engineering, Technische Universität Berlin, Fraunhoferstr. 33-36 10587 Berlin, Germany

**Corresponding author: c.bliatsiou@tu-berlin.de*

Highlights

- Hydromechanical stress crucial for shear-sensitive filamentous microorganisms.
- Impeller geometry determining factor for particle breakage in bioreactors.
- Quantification of particle breakage by means of in situ endoscopic technique.
- Investigation of novel impellers.

1. Introduction

As part of the DFG priority program SPP 1934 DiSPBiotech, this study focuses on the characterization of local mechanical stresses occurring in stirred tank bioreactors and their effect on biological agglomerates. This work intends to identify and develop low-shear stirrers for cultivations of filamentous microorganisms. As case study, the cultivation of the filamentous fungi *Aspergillus niger* is used. Direct measurements of mechanical stresses in real cultivation broths are barely possible. Thus, the investigations are carried out by using model systems [1], which simulate the most significant properties of the biological system (broth rheology, bio-agglomerates morphology). Conventional and newly developed stirrer types are characterized in terms of particle stress, which is quantified by measuring particle breakage in the agitated reactor by means of an in situ particle size measuring technique. The interpretation of the breakage mechanisms in the stirred vessel succeeds through quantification of shear and elongation stresses by using Particle Image Velocimetry (PIV).

2. Methods

Experiments were conducted in a 3-L lab scale baffled agitated tank, geometrically similar to a fermenter. 15 impellers were used for the investigations. Among the conventional agitators (Rushton, pitched blade turbines etc.), five novel agitators were developed in cooperation with EvoLogics GmbH (Fig. 1).

Development of model systems: As particulate systems fluid/fluid and solid/fluid systems were used. Particularly, droplets of silicon oil and clay/polymer flocs were chosen as dispersed phase to approximate a wide range of *Aspergillus* morphology (spherical pellets and mycelial forms). The cultivation broth appears to be low viscous up to a specific level of biomass concentration and then it develops a shear thinning behavior. Water and a Xanthan gum solution were used as model fluids for the continuous phase to approximate the broth rheology at initial and later cultivation phases.

In situ particle size measurement: An in situ analysis method was used to monitor the particle breakage kinetics in the stirred tank. The photo-optical SOPAT measurement technique for particle sizing (SOPAT GmbH) uses endoscopic probes, capable to obtain two-dimensional images of a disperse phase during a process and measure the sizes and shapes by an automated image analysis [2].

Fluid dynamic investigations: Mechanical stress is quantified by recording the velocity vector field by means of Particle Image Velocimetry (PIV) and calculating shear/elongation gradients in the tank.

3. Results and discussion

The particle breakage caused by the investigated stirrers was measured in the stirred tank for the developed particulate model systems. The particle stress caused by each stirrer is quantified as a function of a steady state characteristic particle diameter with the average energy dissipation rate. Fig. 2 indicates that an axial propeller causes stronger breakage, producing smaller droplets in comparison to a radial Rushton turbine, which in the biotechnological field has been wrongly considered as high shear impeller. Through PIV measurements, the particle breakage caused by 15 stirrer types is further analyzed. Fig. 3 shows that mixing with a propeller produces significantly high shear gradients, inducing consequently stronger particle breakage as depicted in Fig. 2.

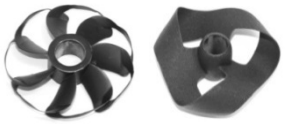

Figure 1. Patent pending novel impeller geometries; Bionic Loop (left) and Wave-Ribbon impeller (right) (EvoLogics GmbH)

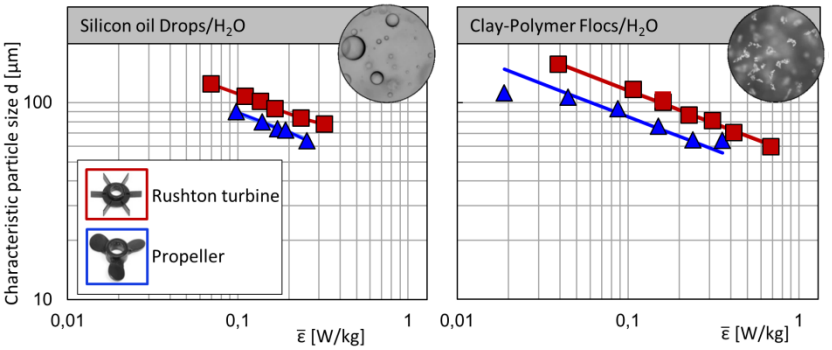

Figure 2. Steady state particle diameter as a function of the av. energy dissipation rate for two impellers; drops dispersion (left) and flocs suspension (right)

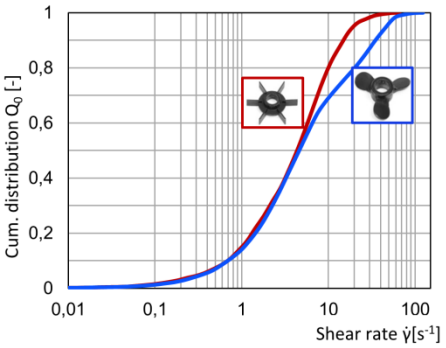

Figure 3. Cum. distribution of the shear rates produced by two impellers for $\bar{\varepsilon}$=0,1 W/kg

4. Conclusions

The results of the abovementioned experimental work contribute significantly in the design of low-shear impellers to be used for the cultivation of shear sensitive filamentous microorganisms.

References [Calibri 10]

[1] Henzler, H-J.,2000 Particle Stress in Bioreactors. In: Schügerl K. et al. (eds) Influence of Stress on Cell Growth and Product Formation. *Adv. Biochem. Engin./Biotechnol*. 67, Springer.

[2] Panckow, RP., Reinecke, L., Cuellar, MC., Maaß, S., 2017. Photo-Optical *In-Situ* Measurement of Drop Size Distributions: Applications in Research and Industry. *Oil Gas Sci. Technol.* 72, 3, 14.

ECCE12
The 12th EUROPEAN CONGRESS OF CHEMICAL ENGINEERING
Florence 15-19 September 2019

Visualization of Mixing Performance and Measurement of Power Input in Aerated Stirred Tank Reactors on a lab and industrial scale

Jürgen Fitschen[1], Annika Rosseburg[1], Johannes Wutz[2], Thomas Wucherpfennig[2], Michael Schlüter[1]

1 Institute of Multiphase Flows, Hamburg University of Technology, Hamburg, Germany; 2 Boehringer Ingelheim Pharma GmbH & Co. KG, Biberach an der Riß, Germany

**Corresponding author: juergen.fitschen@tuhh.de*

Highlights

- Deep insights into industrial scale aerated stirred tank reactors
- Comparison of mixing performances for different scales
- Challenges of scale-up process from lab- to industrial scale

1. Introduction

Aerated stirred tank reactors (STR) are often used for mixing, heat- and mass transfer processes in chemical and biochemical engineering due to their robust operation and extensive description in the past. However, in case of mammalian cell expression systems special requirements have to be fulfilled. Beside media and feed, the hydrodynamic properties like power input, mixing and mass transfer performance have to be customized for each individual cell line [1] as well as reactor size during the upstream process.

Commonly used scale up parameters are constant geometrical ratios, constant volumetric power input P/V, constant superficial gas velocities w^0_g as well as constant volumetric gassing rates vvm. Whereas the scale-up of stirred tank reactors is still challenging justified by the fact that most design criteria as well as correlations are based on measurements on small scale reactors [3]. Especially for mixing time correlations, most investigations are based on operation conditions for bacterial or yeast fermentation with power inputs over 100 W/m^3 and gas flow rates over 1 vvm [2].

To overcome this gap, an acrylic glass reactor has been designed and erected on industrial scale (15 m^3) at Hamburg University of Technology in cooperation with Boehringer Ingelheim Pharma GmbH & Co.KG. With the help of the acrylic glass reactor (Figure 1) of industrial scale it is possible to visualize global and local flow structures and to investigate the influence of heterogeneities of the flow on the mass transfer as well as the mixing time. Furthermore, it is possible to investigate the influence of different stirrer geometries and configurations on the hydrodynamic behavior of an industrial scale aerated stirred tank reactor.

Figure 1: 15 m3 acrylic glass reactor at TUHH

2. Methods

The acrylic glass reactor with an inner diameter of D = 2 m and a total volume of V_R = 15 m^3 is equipped with a bottom mounted magnetic agitator as well as three baffles. The agitator can be equipped with either up to three Rushton turbines or pitched blade turbines (d/D = 1/3). An open tube sparger is used, which is located below the Rushton turbine [2].

The gas flow rate is controlled by an F-203AV mass flow controller from Bronkhorst®. The power input is measured at the stirrer shaft using a DR-3000 torque measuring instrument from Lorenz®.

The mixing time is determined by a decolorization method in combination with a high spatial and time resolution image processing [2].

3. Results and discussion

First investigations have been performed with a two stage impeller system. In figure 2 two different mixing processes of two different flow regimes are presented. On the left hand side a homogeneous bubbly flow is present where the bubbles are rising homogeneously dispersed over the cross section. The axial mixing is reduced and two compartments are forming.

This leads further to a high mixing time. On the right hand side a heterogeneous flow regime with large bubbles is presented. These large bubbles are rising with a much higher velocity and are not equally dispersed over the cross section of the reactor. This leads to a buoyancy driven flow structure and thus better axial mixing [2].

Further investigation into the hydrodynamics of different impeller combinations will be presented.

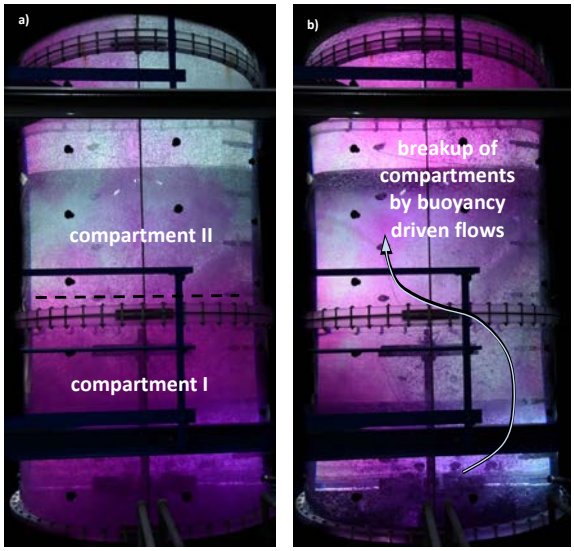

Figure 2: Exemplary decolourization processes after t = tmix · 0.5 for two different flow regime: homogeneous (left), heterogeneous (right).

4. Conclusions

A first characterization can be done by taking into account buoyancy driven flows superimposing the flow induced by the impeller. A correlation is presented to estimate the transition between a loading and flooding regime on large scale. This correlation enables the calculation of mixing times for a wide range of stirrer frequencies and superficial gas velocities. Furthermore, this presentation will emphasize the challenges of scale-up on the basis of laboratory experiments in small scale.

Reference

[1] Lalonde, M. & Durocher Y. Therapeutic glycoprotein production in mammalian cells, Journal of Biotechnology, Volume 251, 2017, Pages 128-140

[2] Rosseburg, A., Fitschen J., Wutz, J., Wucherpfennig, T. & Schlüter, M. Hydrodynamic inhomogeneities in large scale stirred tanks – Influence on mixing time, Chemical Engineering Science, Volume 188, 2018, Pages 208-220

[3] Nauha, E. K., Visuri, O., Vermasvuori, R. & Alopaeus, V. A new simple approach for the scale-up of aerated stirred tanks, Chemical Engineering Research and Design, Volume 95, 2015, Pages 150-161

ECCE12
The 12th EUROPEAN CONGRESS OF CHEMICAL ENGINEERING
Florence 15-19 September 2019

Flow regimes of immiscible liquid-liquid systems in stirred vessels

Francesco Maluta[1*], Teresa Megna[1], Giuseppina Montante[2], Alessandro Paglianti[1]

[1] DICAM, Università di Bologna, via Terracini 34, Bologna, Italy; [2] CHIMIND, Università di Bologna, via Terracini 34, Bologna, Italy

*Corresponding author: francesco.maluta2@unibo.it

Highlights

- Drawdown and dispersion of oil droplets in water are investigated by ERT.
- A procedure for liquid-liquid flow maps identification in stirred tanks is proposed.
- The flow map for moderately concentrated water-diesel fuel systems is presented.

1. Introduction

The impeller speed required to successfully disperse one immiscible phase in another in stirred vessels is a very important process parameter, which experimental determination is not straightforward [1], particularly in dense liquid-liquid systems. This work has the goal to suggest a new procedure to obtain the flow map of immiscible liquid-liquid systems, based on the measurements of the dispersed phase distribution by Electrical Resistance Tomography (ERT).

2. Methods

The investigation concerns a moderately concentrated immiscible liquid-liquid system, consisting of diesel oil of density, ρ_{oil}, equal to 810 kg/m^3 at ambient conditions, and demineralized water, containing 0.5 g/L of NaCl for enhancing the conductivity difference with the non-conductive oil phase, as required by the ERT technique. The dispersion is obtained in a flat bottomed fully baffled tank of diameter, T, equal to 232 mm stirred with a Rushton turbine of diameter, D, equal to T/3, placed at the clearance, C, equal to T/2. The distribution of the diesel fuel in water is observed at different impeller speeds, N, going from complete segregated conditions to fully dispersion. Data are collected at different average oil volume fractions in the vessel, varying from 0.05 to 0.14, keeping the total liquid height, H_L, in still conditions always equal to T. The analysis is based on the time-averaged conductivity data on four horizontal vessel sections (axial elevations, z, equal to 60, 110, 160, 210 mm), consisting on 316 values per plane, with a square mesh with each cell of 11.5 mm side. For each condition, the time-averaged conductivity is obtained from 1000 instantaneous measurements. The ERT instrumentations and the data acquisition systems are similar to those adopted in previous investigations [2].

3. Results and discussion

Different flow conditions have been identified through the analysis of the time-averaged conductivity data on the four measurement planes. Starting from the complete segregated

conditions, the just drawdown and the complete dispersion of the oil have been detected subtracting the mean conductivity value obtained at fixed impeller speed from the value recorded at N=0 on the plane at z=160mm, being this plane just below the liquid-liquid interface at N=0. By monitoring the local maximum absolute value of the conductivity difference from the completely segregated condition (N=0) on the plane at z=160 mm at increasing N, an evolution curve is obtained, as shown in Fig.1, relevant to diesel fuel volume fraction of 0.14.

As shown in Fig.1, through a linearization procedure of the experimental data (open circles), we identified the just drawdown impeller speed as the intersection of the two lines, highlighted in red, and the just completely dispersed impeller speed as the intersection highlighted in black. The homogeneous dispersion condition was identified once the variation of the conductivity on the four measurement planes reached an asymptotical value. By the procedure described above, a flow map of the different regimes can be identified.

The flow map relevant to the conditions investigated in this work is shown in Fig.2, where the Froude number, Fr; [3] is defined as:

$$Fr=\frac{DN^2}{g}\left(\frac{\rho_{water}}{\rho_{water}-\rho_{oil}}\right)^{0.42}\left(\frac{D}{T}\right)^{3.65}.$$

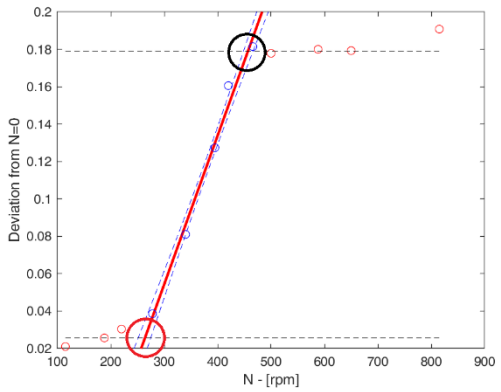

Figure 1. Experimental data and identification of the drawdown and completely dispersed impeller speeds.

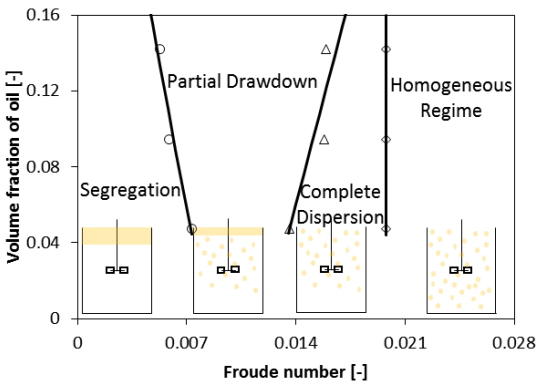

Figure 2. Flow map for the diesel fuel-water system.

4. Conclusions

A novel method is proposed for obtaining the flow map of immiscible liquid-liquid systems in stirred tanks based on the collection and a suitable analysis of ERT data. The method can be easily applied to any vessel size and liquid volume fraction, thus providing a useful guideline for the selection of the operating conditions of stirred vessels.

References

[1] D.A. Brown, P.J. Jones, J.C. Middleton, G. Papadoloulos, E.B. Arik, in Handbook of Industrial Mixing, Chapter 4 (2014), 189.
[2] A. Paglianti, C. Carletti, A. Busciglio, G. Montante, Can. J. Chem. Eng. 95 (2017) 1789–1799.
[3] G.E.H. Joosten, J.G.M Schilder, A.M. Broere, Trans. Inst. Chem. Eng. 55 (1977) 220–222.

ECCE12
The 12th EUROPEAN CONGRESS OF CHEMICAL ENGINEERING
Florence 15-19 September 2019

Euler-Euler Simulation of Bubbly Flow in Stirred Tanks

Roland Rzehak[1], Pengyu Shi[1,2]

1 Helmholtz-Zentrum Dresden – Rossendorf, Institute of Fluid Dynamics, Bautzner Landstrasse 400, D-01328 Dresden, Germany;
2 Technische Universität Dresden, Faculty of Mechanical Engineering, Institute of Power Engineering, D-01062 Dresden, Germany

**Corresponding author: r.rzehak@hzdr.de*

Highlights

- A previously established baseline model for bubbly flow is applied to stirred tanks.
- One extension found necessary is the use of a Reynolds stress turbulence model.
- A second one is a correction factor to describe turbulence effects on drag.
- Good agreement is found for a comprehensive dataset from different literature sources.

1. Introduction

Aerated stirred tanks are frequently used equipment in industries ranging from chemical engineering and biotechnology to minerals processing. In principle, CFD simulation of such equipment on industrial scales is feasible within the Euler-Euler framework of interpenetrating continua. Practical application, however, requires suitable closure models to account for phenomena on the scale of individual bubbles, which are not resolved in this approach. Validation of such models is the purpose of the present contribution.

2. Methods

Starting point for the investigation is a baseline closure model that has previously been used in a large number of CFD studies on bubbly pipe flows and flow in bubble columns [1]. The model comprises drag, lift, wall, virtual mass and turbulent dispersion forces. Previous work from other researchers has shown that due to the high levels of turbulence in stirred tanks, a modification of the drag force is required [2], which is included in the present simulations. For the liquid turbulence an isotropic k-ω SST model has been adopted in the baseline model, however, it turned out that only rather poor agreement with experimental could be achieved for stirred tanks. To overcome this, two common variants of anisotropic Reynolds stress models are applied due to Launder, Reece, and Rodi (LRR, [3]) and Speziale, Sarkar, and Gatski (SSG, [4]). Correspondingly, anisotropic source terms modeling the bubble-induced turbulence are used [5].

3. Results and discussion

To validate the model, a database is accumulated from different literature sources, which comprises measurements of gas fractions and average velocities data relating to fluctuating velocities such as turbulent kinetic energy or Reynolds stress. In addition, information on the bubble size is needed, which appears in virtually all sub-models. For the present purpose the

average value suffices since only monodisperse simulations will be performed. Extensive study of numerical parameters has been undertaken such as grid-size, time-step and location of the boundary between rotating and fixed domains. Comparison between simulation and experiment for singlephase flows shows that mean velocities are captured well by the Reynolds stress models but turbulent fluctuations tend to be somewhat underpredicted. For the multiphase flows, the peak in radial mean velocities is underpredicted by the turbulence k-ω SST model (Figure 1a), which neglects the anisotropic effects, and the axial component of mean gas velocity is too small if the turbulent modification of the drag force is omitted (Figure 1b). If both effects are taken into account, similar agreement is obtained between simulation and experiment as for the singlephase flows. A detailed account of the results has been given in [6].

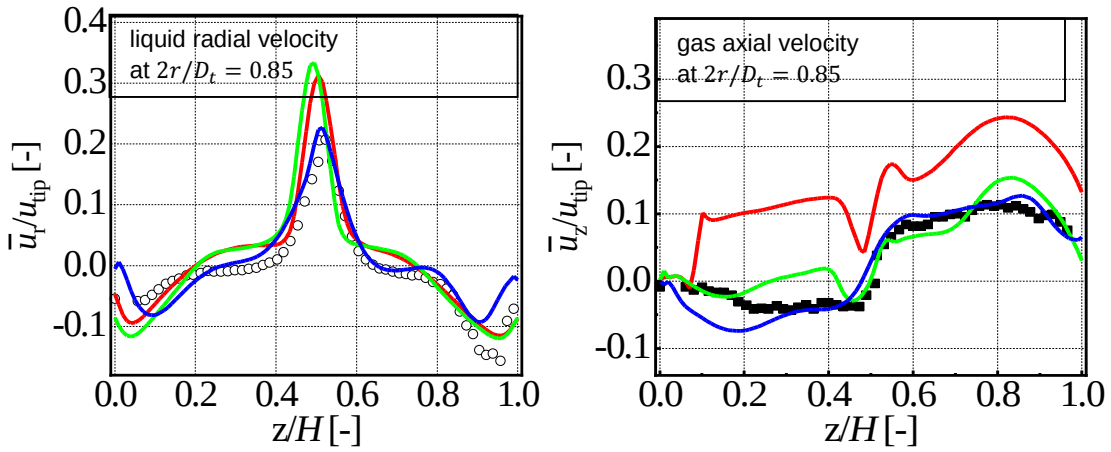

Figure 1. Comparison between simulations using different models (red: k-ω SST model without drag correction, green: k-ω SST model with drag correction, blue: SSG model with drag correction) and experiments (symbols) from [7].

4. Conclusions

With the modification factor for the drag force due to [2] and a Reynolds stress model with anisotropic source terms modeling the bubble-induced turbulence [6] reasonable agreement with the experimental data can be achieved. A slight preference for the SSG over the LRR turbulence model is identified. Concerning further model development, improvement of the BIT modeling appears most promising to improve the model predictions. The development of better models should be accompanied by the acquisition of improved experimental data for model validation. In particular the availability of mean liquid and gas velocities, turbulent fluctuations and gas fractions for the same configuration would be very beneficial to interpret the simulation results.

References

[1] Rzehak, R., Ziegenhein, T., Kriebitzsch, S., Krepper, E., and Lucas, D., Chemical Engineering Science 157, (2017) 147–158.
[2] Lane, G. L., PhD thesis, University of Newcastle, New South Wales, 2006.
[3] Launder, B. E., Reece, G. J. and Rodi W., Journal of Fluid Mechanics 68 (1975) 537–566.
[4] Speziale, C. G., Sarkar, S. and Gatski, T. B., Journal of Fluid Mechanics 227 (1991) 245–272.
[5] Parekh, J. and Rzehak, R., International Journal of Multiphase Flow 99 (2018) 231–245.
[6] Shi, P. and Rzehak, R., Chemical Engineering Science 190 (2018) 419–435.
[7] Montante, G., Horn, D., and Paglianti, A., Chemical Engineering Science 63 (2008) 2107–2118.

ECCE12
The 12th EUROPEAN CONGRESS OF CHEMICAL ENGINEERING
Florence 15-19 September 2019

Investigation of reactive mass transfer processes at single rising gas bubbles by means of Time-Resolved Scanning Laser-Induced Fluorescence

Felix Kexel, Sven Kastens, Jens Timmermann, Marko Hoffmann, Alexandra von Kameke, Michael Schlüter

1 Hamburg University of Technology, Institute of Multiphase Flows, Eissendorfer Str. 38, 21073 Hamburg, Germany;

**Corresponding author: michael.schlueter@tuhh.de*

Highlights

- O_2 mass transfer
- 3D wake structure
- Time Resolved Scanning Laser Induced Fluorescence (TRSLIF)

1. Introduction

The mass transfer from a gaseous, dispersed phase into the surrounding liquid phase is a major task for chemical industry as well as for bio-, food- or environmental engineering. Nevertheless a reliable and exact design of multiphase reactors is one of the unsolved challenges in process engineering, since local mass transfer process could not be easily investigated within dense bubble swarms.

Therefore the empirical and semi-empirical correlations like for the dimensionless Sherwood number

$$Sh = 2 + C_1 Re^a Sc^b \quad (1)$$

based on integrally measured data, like Sauter bubble diameter, bubble rise velocity (Reynolds number Re) and the material system with liquid viscosity ν and diffusion coefficient of the gaseous species D (Schmidt number Sc) (Brauer, 1979). In contrast to these assumptions, today the dispersed gas phase is more and more considered as individual gas bubbles with local mixing elements and a major contribution to meso mixing in multiphase flows.

To gain a deeper knowledge of local mass transfer phenomena in bubbly flows the planar laser induced fluorescence (p-LIF) technique was widely and successfully used in different experimental arrangements, which was recently reviewed by Rüttinger (Rüttinger et al., 2018). Nevertheless, the applicability of this technique is limited to an accurate and reproducible bubble rise. Due to this limitation, the accurate investigation of 3D mass transfer processes close to deforming fluidic boundary layers at free rising bubbles is a challenging task. The Time Resolved Scanning Laser-Induced Fluorescence (TRS-LIF) enables such deeper insights into local processes in bubbly flows.

2. Methods

The basic setup has already been used in a slightly different configuration by Timmermann (Timmermann et al. 2017, Kastens et al. 2018). As measuring technique, the TRS-LIF is used. A scheme of top view of the setup for TRS-LIF, based on the work of (Soodt et al., 2012), is shown in Fig. 1, left. In contrast to the investigation with p-LIF, the laser sheet is reflected from a rotating

polygon (20 or 38 faces) into the volume of interest. With a precise synchronization of rotational speed and laser pulse emission, light sheets with reproducible deflection could be observed and parallelized by a cylindrical lens to obtain equidistant spacing. By variation of the laser pulse rate, polygon rotational speed and the number of pulses per polygon mirror, the generated light stacks are adjustable to the experimental scales, like bubble rise velocity and rise trajectory expansion. It should be noted, that the parameters are interlinked, where a higher sheet number reduces the maximum achievable volume scan rate, limited by the maximum rotational speed of the polygon of 10,000 rpm and the maximum pulse rate of the laser of 20,000 Hz.

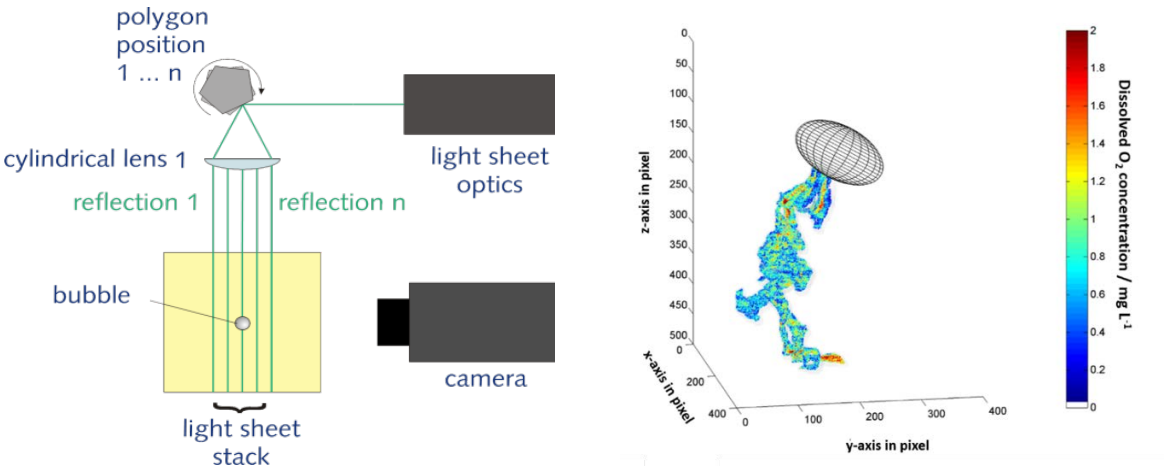

Figure 1. left: Schematic top view of the experimental setup for Time-Resolved Scanning LIF, **right:** 3D reconstruction of the oxygen concentration field within the wake of a free rising wobbling bubble (Timmermann, 2018).

Upgrading the number of faces on the polygon is a key parameter to optimize the temporal and/or spatial resolution for the realization of nearly instantaneous 3D scans.

3. Results and discussion

Fig. 1, right shows an example of the reconstructed wake structure behind a rising ellipsoidal O_2 bubble. Experiments are obtained at 20°C and atmospheric pressure. The two-dimensional images have been recorded with a frequency of approx. 15,000 fps. This leads to a volume scan rate of 335 Hz for one entire stack. The reconstructed 3D dissolved O_2 concentration within the wake structure shown in Fig. 1, is calculated by using calibration equations for each plane, allowing the determination of the concentration with uncertainties lower than 1 ppm. The mixing within the wake structure is in focus, where vortices with an enriched oxygen concentration are mixed with the bulk phase. The vortex shedding and mixing intensity depends on bubble shape and fluid properties, which are varied in this work. Moreover, a more precise analyzing method using online and parallel oxygen concentration calibration in the reaction vessel. Combined with analyzing each pixel within a plane the uncertainties are decreased below 0.2 ppm.

4. Conclusions

By investigating parallel-consecutive chemical reactions it is expected, that the times-scales of mass transfer and mixing will influence the local yield and selectivity within the bubble wake. With the TRS-LIF method a measurement system has been developed and successfully applied, that allows the analyzation of instantaneous 3D concentration fields within the wake of free rising bubbles. This method enables more detailed information about the influence of local hydrodynamic conditions in gas-liquid flows on yield and selectivity, which will be clarified in near future.

References

[1] Brauer, H., Particle/fluid transport processes. Fortschritte der Verfahrenstechnik, 17, 61-99 (1979)
[2] Glaeser, H. Brauer, H. Berechnung des Impuls- und Stofftransports durch die Grenzfläche einer formveränderlichen Blase, VDI-Verlag, (1977).
[3] Kastens, S. Timmermann, J. Hoffmann, M. Schlüter, M.; Influence of boundary layer deformations on mass transfer and chemical reaction. E-proceeding 19th Lisbon Symposium 2018
[4] Ohl, C. D. Generator for single bubbles of controllable size, Review of Scientific Instruments, 72(1), 252-254. (2001). DOI: 10.1063/1.1329900.
[5] Rüttinger, S. Spille, C. Hoffmann, M. Schlüter, M.: Laser-induced Fluorescence in Multiphase Systems. ChemBioEng Reviews, 2018, 5, 253-269. (2018)
[6] Sone, D., Sakakibara, K. Yamada, M. Sanada, T. Saito, T. Bubble motion and its surrounding liquid motion through the collision of a pair of bubbles, Journal of Power and Energy Systems, 2(1), 306-317, (2008). DOI: 10.1299/jpes.2.306.
[7] Soodt, T. Schröder, F. Klaas, M. van Overbrüggen, T. Schröder, W. Experimental investigation of the transitional bronchial velocity distribution using stereo scanning PIV. Experiments in Fluids, 52(3), 709-718. (2012). DOI: 10.1007/s00348-011-1103-5.
[8] Timmermann, J. Hoffmann, M. Schlüter, M. Influence of Bubble Bouncing on Mass Transfer and Chemical Reaction. Chemical Engineering & Technology, 39(10), 1955-1962. (2016). DOI: 10.1002/ceat.201600299.
[9] Timmermann, J. Experimental analysis of fast reactions in gas-liquid flows. Dissertation. Hamburg, 2018.

ECCE12
The 12th EUROPEAN CONGRESS OF CHEMICAL ENGINEERING
Florence 15-19 September 2019

Predictive Direct Numerical Simulation of Peclet number in small fixed beds

Matthieu ROLLAND[1], Vittorio Petrazzuoli[1], Vasileios Sassanis[1], Vincent Ngu[1], Lionel Gamet[1]

1 Process Intensification dept, IFP Energies Nouvelles, 69360 Solaize, France

**Corresponding author: matthieu.rolland@ifpen.fr*

Highlights

- CFD workflow to compute Pe in small size fixed beds using DEM and OpenFOAM
- Accurate prediction of Pe numbers using first two moments of age distribution
- Local Pe depends on local structural features
- CFD prediction allows to study small trends without experimental errors

1. Introduction

Over the decades, fixed bed reactors for catalyst testing have faced a reduction in size and now they commonly have diameters below 1 cm, the limit being the catalyst pellet size (~1-3 mm). The advantages of these reactors are numerous: less catalyst used, less amount of reactant used and of wastes produced, better temperature control, reduced safety risks and easier implementation of parallel reactor systems [1]. Those reactors were designed for catalyst screening, so that hydrodynamics was not really an issue as long as the ranking and uncertainty were correct. As those reactors produce a large amount of data, a new question arises: can we use those results to build models for catalyst performance prediction? This work aims at improving our understanding of the hydrodynamics of these small reactors using CFD tools.

2. Methods

The work is based on a workflow mimicking the real usage of fixed bed reactors. In a first step, we pack spherical particles in cylindrical reactors using a Discrete Element Method package (Grains3D [2], Figure 1). Then we compute the steady state hydrodynamics in those reactors using the `simpleFoam` solver (Figure 1) from the OpenFOAM suite [3] augmented with the simulation of the moments of age distribution [4]. The outputs of the simulation are the mass flux weighted averages of the first and second order moments of age in many cross-sections of the reactors. Using the classical formula, we then compute the Peclet number (Pe) for any sub-volume in the reactor as:

$$Pe = 2\,\frac{\tau^2}{\sigma^2} = 2\,\frac{(m_{1,outlet} - m_{1,inlet})}{(m_{2,outlet} - m_{1,outlet}^2) - (m_{2,inlet} - m_{1,inlet}^2)}$$

Simulations have carried out for a common cylindrical reactor of 7.75 mm diameter and 187 mm long packed with spheres of 2 to 7 mm in diameter. Two layers, with 3mm thickness each, and free of particles, have been added at the top and bottom sides of the packing, respectively, to facilitate the numerical simulation of flow conditions near the inlet and outlet regions.

3. Results and discussion

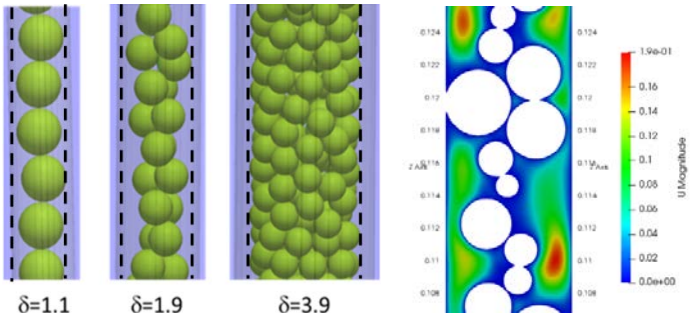

Figure 1: Left: Examples of packing, $\delta = D/d_p$, - Right : Velocity magnitude in a reactor cut (d_p = 4 mm)

The CFD results match very well experimental data based on RTD [5] (Figure 2 - left). Local packing structures have a staircase impact on local Pe evolutions (Figure 2 - middle). The effect of molecular diffusion on Bodenstein number (Bo =Pe d_p/L) matches the literature [6] in the global shape and effect of Schmidt number (Figure 2 - right).

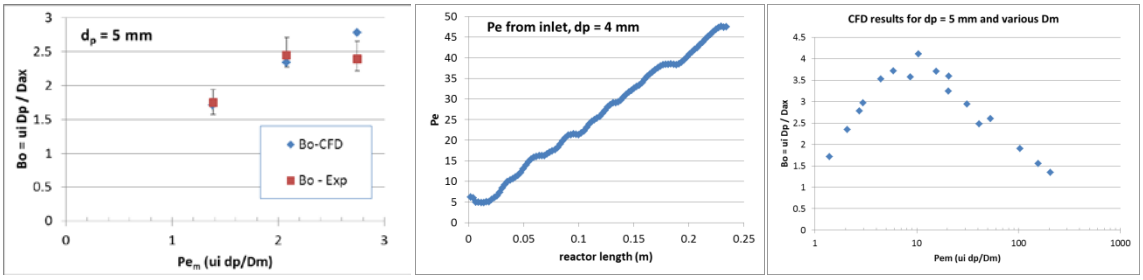

Figure 2: Left: Comparison experiments / CFD – Middle: plot of the evolution of Pe from inlet – Right: parametric study on velocity and molecular diffusion.

4. Conclusions

Our simulation workflow matches very well the experimental data and will be used to study precisely the effects of molecular diffusion, inlet velocity and reactor-to-particle diameter ratio on the plug flow behavior of fixed beds. We also plan to study the randomness effects on the results when the packings are repeated.

References

[1] Moulijn J., Pérez-Ramírez J., Berger R., Hamminga G., Mul G., Kapteijn F. (2003) High-throughput experimentation in catalyst testing and in kinetic studies for heterogeneous catalysis, *Catalysis Today* 81, 3, 457–471W.

[2] Wachs, A., Girolami, L., Vinay, G., & Ferrer, G. (2012). Grains3D, a flexible DEM approach for particles of arbitrary convex shape—Part I: Numerical model and validations. Powder Technology, 224, 374-389.

[3] Pozzobon, V., Colin, J., & Perré, P. (2018). Hydrodynamics of a packed bed of non-spherical polydisperse particles: A fully virtual approach validated by experiments. Chemical Engineering Journal, 354, 126-136.

[4] Liu, M., & Tilton, J. N. (2010). Spatial distributions of mean age and higher moments in steady continuous flows. *AIChE journal*, 56 (10), 2561-2572.

[5] Petrazzuoli, V., Rolland, M., Mekki Berrada, A., Schuurman, Y. (2019) Choosing the right packing in millimetric packed bed reactors, submitted at ECCE12.

[6] Delgado, J. M. P. Q. (2006). A critical review of dispersion in packed beds. *Heat and mass transfer*, 42(4), 279-310.

ECCE12
The 12th EUROPEAN CONGRESS OF CHEMICAL ENGINEERING
Florence 15-19 September 2019

Mass transfer at rising single nitric oxide bubbles in reacting iron ligand systems

David Merker*, Lutz Böhm and Matthias Kraume

Technische Universität Berlin, Chair of Chemical and Process Engineering, Sekr. FH 6-1, Fraunhoferstraße 33-36, 10587 Berlin, Germany

**Corresponding author: david.merker@tu-berlin.de*

Highlights

- Liquid phase reaction
- Mass transfer enhancement
- Bubble fluid dynamic

1. Introduction

The design of gas liquid reaction is still a challenging task. In addition to the reaction itself, the fluid dynamics of the phases and thus the changed mass transfer conditions must also be taken into account. Occurring processes are not completely understood yet. To be able to describe a complex gas liquid, the DFG Priority Program 1740 "Reactive Bubbly Flows" SPP1740 focuses on different substance systems and scales. In this project the complexity is reduced by first analyzing single bubbles with a high spatial and temporal resolution.

2. Methods

The experimental setup built in this project can be seen in Figure 1. The main part is a 2 m long glass tube, in which a single bubble can rise freely through a stagnant fluid. [1]

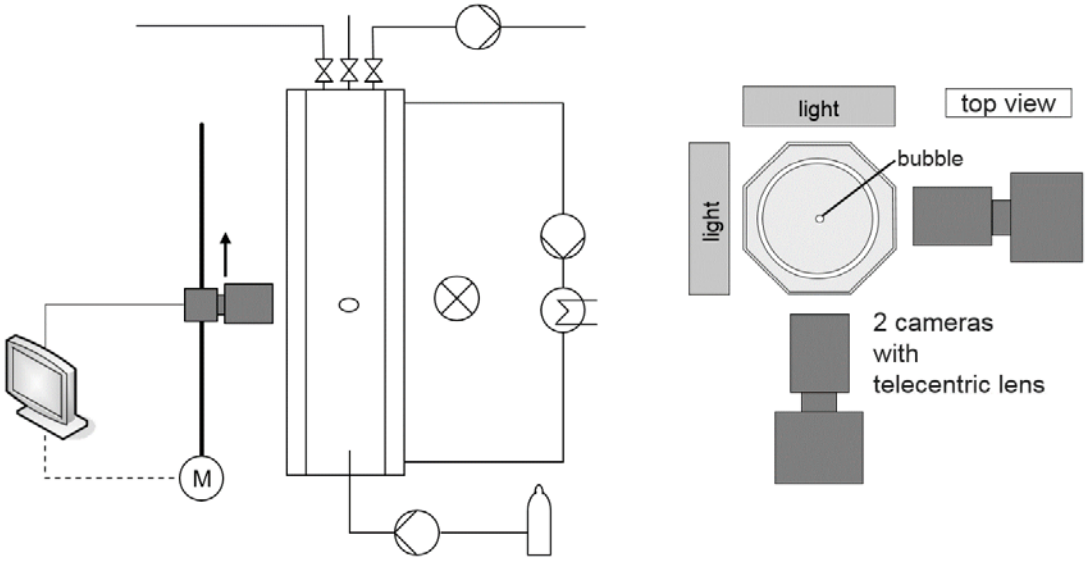

Figure 1. Experimental setup: schematic sketch (left), single bubble rises in a temperature-controlled glass tube (h = 2m) observed with high-speed cameras; Cross section of the system (right)

The temperature is controlled with an acrylic glass jacket that also provides a better optical access. The bubble is tracked with two high-speed cameras, which are moved along with the rising bubble. It is possible to perform experiments under a protective atmosphere. Apart from the solution of carbon dioxide (CO_2) in water/$NaOH_{aq}$, experiments with different iron complexes reacting with nitric oxide (NO) as the gas phase were carried out. The choice of ligand influences the reaction rate of the system.

3. Results and discussion

Figure 2 shows a nitric oxide bubble in an iron sulfate edta solution ($FeII(edta)_{aq}$). The product is colored and can be detected in the wake of the bubble. The two images were taken at the same time by the two cameras with an offset of 90°. The size, shape and 3D rising path can be resolved with a high temporal and spatial resolution.

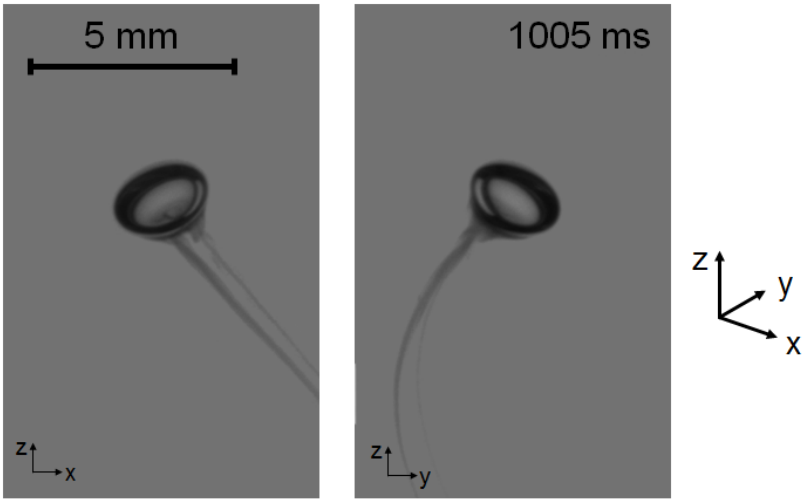

Figure 2. nitric oxide (NO) bubble in $FeII(edta)_{aq}$ with a concentration of 75 mmol/l, view from the two cameras simultaneous

The changing fluid dynamics of the dissolving bubble can be tracked. Different initial diameters were investigated. Various ligands have an influence on the reaction rate, as well as on the shape and fluid dynamics.

4. Conclusions

It is possible to measure the volume change and thus evaluate the mass transfer of a bubble depending on the contact time. Due to the detailed measurements, enhancement factors can be measured depending on the ligand and educt concentration.

Acknowledgements

The authors gratefully acknowledge the financial support provided by the German Research Foundation within the Priority Program ‘‘Reactive Bubbly Flows’’, SPP 1740.

References

[1] D. Merker, L. Böhm, M. Oßberger, P. Klüfers, M. Kraume, Chem. Eng. Technol. 40 (8) (2017) 1391-1399.

ECCE12
The 12th EUROPEAN CONGRESS OF CHEMICAL ENGINEERING
Florence 15-19 September 2019

Influence of microbubble aeration on hydrodynamics and mass transfer in a lab scaled Stirred Tank Reactor

Simon Matthes[1], Benjamin Thomas[2], Paul Bubenheim[2], Andreas Liese[2], Koichi Terasaka[3], Michael Schlüter[1]

1 Institute of Multiphase Flows, Hamburg University of Technology, Germany;
2 Institute of Technical Biocatalysis, Hamburg University of Technology, Germany;
3 Department of Applied Chemistry, Keio University, Japan

**Corresponding author: simon.matthes@tuhh.de*

Highlights

- Mass transfer measurements for microbubble aerated systems.
- Comparison of microbubble aeration and conventional aeration.
- Determination of the influence of BSD on the performance of gas-liquid systems.

1. Introduction

Many chemical and biocatalytic reactions are consuming gaseous species like oxygen, provided by the mass transfer across interfaces of multiphase contact apparatuses. In large-scale processes the gas is often supplied to the liquid bulk phase by bubble aeration. Especially for biocatalytic reactions the macroscopic aeration can lead to reduced enzyme activity by foaming and induced shear forces. For fast chemical reactions in multiphase flows, the mass transfer limitation is often the bottleneck for a process optimization and becomes “a critical factor in equipment sizing” [2]. Considering bubbles with diameters less than 100 µm, large volume-specific interfacial areas a and therefore high mass transfer rates $k_L a$ of the gaseous reactant on its way to the bulk phase are offered. In addition the high Laplace pressure at that size is leading to an acceleration of the mass transfer. Compared to large-scale bubble aeration, the potential of using bubbles with diameters smaller than 100 µm is less explored so far.

At that point this project starts investigating the aeration with fine bubbles, due to the rising demand in process engineering for aeration with high mass transfer performance, low pressure drop, low shear stress and the avoidance of foaming.

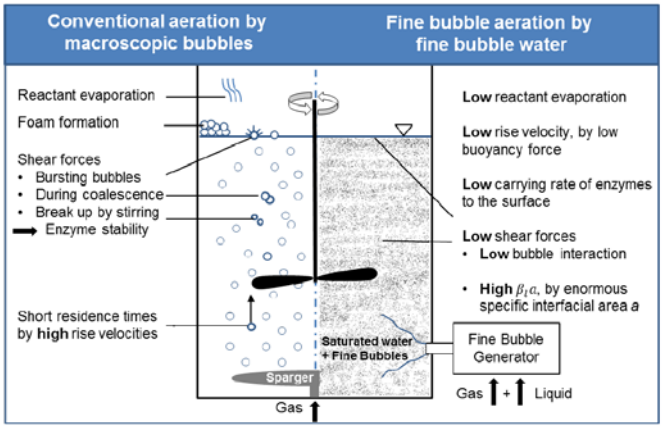

Figure 1. Comparison between conventional aeration and fine bubble aeration in biocatalytic processes in a STR.

Furthermore, the rise velocity of a bubble decreases with decreasing bubble diameter leading to higher residence time and low induced shear stress. To determine the potential of fine bubbles for biocatalytic processes, the promising properties of fine bubble aeration compared to conventional aeration (as shown in figure 1) is under investigation in close collaboration with the Institute of Technical Biocatalysis (ITB) at the Hamburg University of Technology and Prof. Koichi Terasaka from Keio University, Japan.

2. Methods and results

To quantify the influence of fine bubble aeration on the hydrodynamics and the mass transfer, measurements of the bubble size distribution (BSD) and the mass transfer rates from oxygen into the liquid phase are executed in a 3 L stirred tank reactor. The BSD is measured near by the stirrer using an endoscopic probe by SOPAT GmbH. The effect of different stirring speeds and gas flow rates are determined for the reference system deionized water/ air and the two aqueous solutions of glucose (133 mmol/L), with and without 67 mg/L bovine serum albumin (BSA), and rhododendrol (10 mmol/L) as bioactalytic model systems which are also aerated with air. All investigations took place in a turbulent state at stirrer speeds of 400, 600 and 800 rpm and gas flow rates from 25 mL/min up to 100 mL/min. Different fine bubble generators working under the principle of the pressurized dissolution and the spiral liquid flow method are used [1]. The microbubble aeration is compared with conventional aeration by membranes of pore sizes from 0.5 µm up to 2 µm regarding their performance and influence on the liquid systems. A well mixing of the system and therefore a homogeneous distribution of the bubbles is assumed. Figure 2 shows the BSD for the 2 µm membrane and its mass transfer performance.

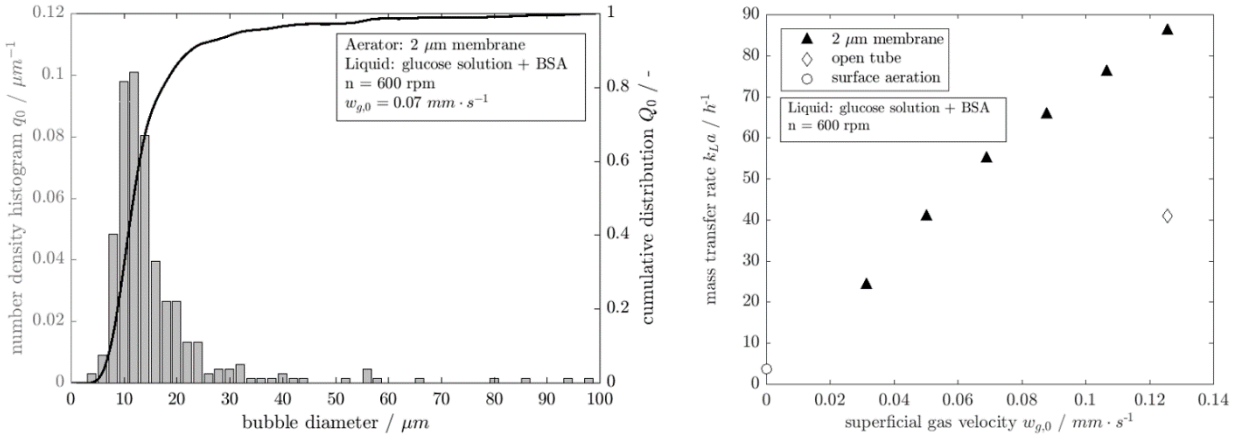

Figure 2. Bubble size distribution measured via SOPAT-VI Pl (left) and mass transfer rates for different gas flow rates for a sinterstone with a pore size of 2 µm producing microbubbles (right).

4. Acknowledgement

The authors gratefully acknowledge the financial support provided by the Deutsche Forschungsgemeinschaft (DFG) within the project (SCHL-617_LI-899).

References

[1] K. Terasaka et al., Chem. Eng. Sci. 66 (2011) 3172-3179.
[2] P. Zehner, P. Kraume, Bubble Columns, Wiley-VCH Verlag GmbH & Co. KGaA, Weinheim, 2005.

ECCE12
The 12th EUROPEAN CONGRESS OF CHEMICAL ENGINEERING
Florence 15-19 September 2019

Fine and ultrafine particle deposition in packed-bed catalytic reactors

Gianluca Boccardo[1], Rajandrea Sethi[2], Daniele Marchisio[1]

1 Department of Applied Science and Technology, Politecnico di Torino, Torino, Italy;

2 Department of Environment, Land and Infrastructure Engineering, Politecnico di Torino, Torino, Italy

**Corresponding author: gianluca.boccardo@polito.it*

Highlights

- CFD simulations of fine filtration in packed beds are performed
- In-silico generated random packings are used to successfully represent packed beds.
- Polydisperse particles are considered: results very different from theoretical predictions.

1. Introduction

In this work (whose main results were recently accepted for publication [1]) we have performed an extensive CFD simulation campaign studying particle transport and deposition in different catalytic systems and under different conditions. Two types of geometric models representing different porous media were created. The first is a number of random packings of spheres created via rigid body simulations: this approach was tested and validated in previous studies [3]. The second is a regular arrangement of spheres, which was also successfully employed in previous works to study fine particles dispersion. Using these random packings, simulations of particle deposition have been performed at different operating conditions. In the first part we calculated values of particle deposition efficiency and compared our results with the classical filtration theory, highlighting the issues in the use of the simplified models upon which the theory is based. In the second part we have studied the effect of polydisperse particle populations: this is also missing in the classical filtration theory, which always considers the transport of particles with uniform diameter. Thus, we have performed population balance modelling simulations for particle deposition, employing the quadrature method of moments (QMOM) [2]. Even more clearly in this case, the results show that the description of polydisperse populations has a very noticeable effect on the macro-scale description, which would dramatically improve the understanding of particle transport and deposition in filtration and catalytic processes.

2. Methods

The first step in this study is the creation of the random packing geometry: this was done via rigid-body simulations using the open-source code Blender, following a procedure described in detail in a previous published work [3]. Then, CFD simulations of fluid flow and particle transport simulations were performed, using the open-source CFD code OpenFOAM (version 4.0): a snapshot of a simulation can be seen in Fig. 1. The effect of gravitational settling was considered by the addition of the particles settling velocity to the advective term of the transport equation. In each case (with and without gravitational settling), a new and improved constitutive equation for the prediction of filtration efficiency was proposed. Then, in the second part of the work, we solved the population balance equation in order to consider the evolution of the full population of particles (expressed in terms of distribution of particle diameter).

3. Results and discussion

Simulation results were expressed in terms of particle filtration efficiency, extracted from the ratio between outlet and inlet particle concentration. Both in the case of normal diffusion, and when the gravitational effect is added, the newly proposed constitutive equation for filtration efficiency is very different from the theoretical expectation [1].

Also, when the population balance equation is solved, the resulting filtration efficiency for the polydisperse case as a function of the system Peclet number is quite different from both the CFD results for the monodisperse case and the theoretical laws, highlighting another point where the classical predictions can be improved upon, as it can be seen in Fig. 2.

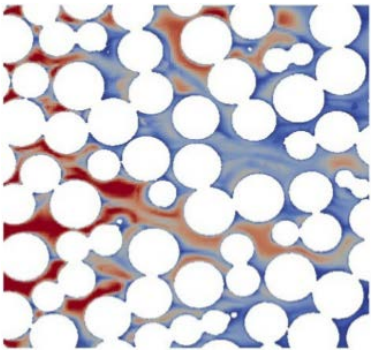

Figure 1. Contour plots of particle concentration in a median section of the domain.

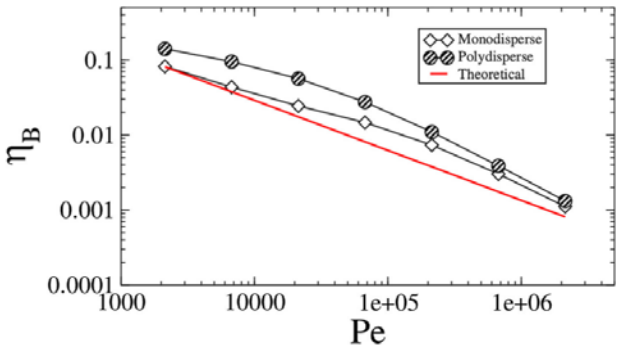

Figure 2. Contour plots of particle concentration in a median section of the domain.

4. Conclusions

This work employs an innovative technique for the generation of random packing, useful to represent a variety of random media, and specifically packed bed reactors, improving on the classical filtration theory, which is based on simplified models of arranged spherical collectors. Then, the main modelling advance of this work is presented, which is the description of the polydispersity of the particle population: this was done here via the solution of the population balance equation, solved by the quadrature method of moments. The results from these simulations show a marked difference with respect to the theoretical predictions and evidence the pitfalls of the simplified description valid for monodisperse populations, evidencing how the proposed model can greatly improve the description of particle transport and deposition in real filtration and catalytic processes.

References

[1] Boccardo, G., Sethi, R. and Marchisio, D.L., 2018. Fine and ultrafine particle deposition in packed-bed catalytic reactors, *Chemical Engineering Science*, In press.

[2] Marchisio, D.L. and Fox, R.O., 2013. *Computational models for polydisperse particulate and multiphase systems*. Cambridge University Press.

[3] Boccardo, G., Augier, F., Haroun, Y., Ferre, D. and Marchisio, D.L., 2015. Validation of a novel open-source work-flow for the simulation of packed-bed reactors. *Chemical Engineering Journal*, *279*, pp.809-820.

ECCE12
The 12th EUROPEAN CONGRESS OF CHEMICAL ENGINEERING
Florence 15-19 September 2019

The effect of improved liquid distribution on the gas-liquid contacting in a rotating packed bed

Jasper Hacking[1 *], Michiel de Beer[2], John van der Schaaf[1]

1 - Chemical Reactor Engineering group, Department of Chemical Engineering and Chemistry, TU Eindhoven, De Rondom 70, 5612AZ Eindhoven, The Netherlands; 2 – Expert Capability Group – Process Technology, Akzo Nobel Chemicals B.V., Zutphenseweg 10, 7418AJ Deventer, The Netherlands

**Corresponding author: j.hacking@tue.nl*

Highlights

- Introduction of redistribution rings in a rotating packed bed reactor.
- Improved liquid distribution in angular and axial direction.
- Results show that angular maldistributions of up to 90° can be mitigated.

1. Introduction

Rotating packed beds (RPB) have been a promising technology for process intensification since their introduction [1][2], enabling increased gas-liquid mass transfer rates [3] due to the application of a centrifugal field. Although a significant amount of possible applications have been reported in literature [4], a major challenge in industrial application of the technology is the absence of proper design correlations leading to ineffective scale-up of the RPB. The effectiveness of gas-liquid mass transfer decreases with increasing radius [3], mainly due to severe maldistribution in the tangential direction at large radii [5][6]. In the current work, a novel design rotating packed bed reactor is proposed, which employs redistribution rings at regular radial intervals, similar to redistributor plates in conventional columns.

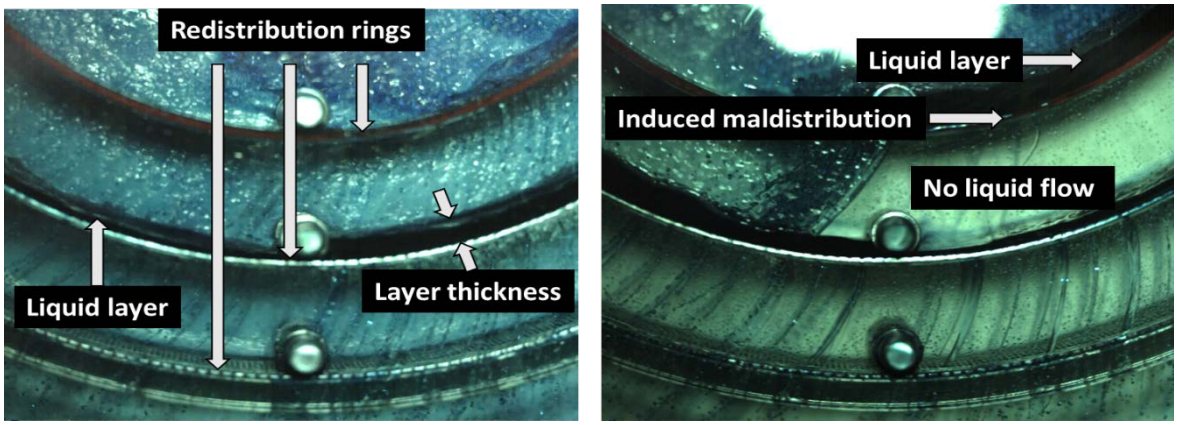

Figure 1. Experimental view of the water layer at a rotational speed of 1200 RPM and a liquid flow of 1000 L/h with (A) no induced maldistribution and with (B) a 90° induced maldistribution.

2. Methods

Perforated rings are placed at regular intervals inside the bed to redistribute the liquid both in angular and axial direction. This is shown in the top-down image in Figure 1A, where the liquid layer

accumulates against the ring and is subsequently redistributed. To further test the effectiveness of the redistribution rings a maldistribution was induced in the inner of the three rings and the effect of the liquid distribution in the other two rings was analyzed. An example of an induced maldistribution of 90° can be found in figure 1B.

3. Results and discussion

The mean and deviation of the liquid layer thickness in the middle ring are used to determine the effectiveness of the redistribution rings: the smaller the standard deviation, the more even the liquid is spread angularly, and consequently, the more uniform the liquid flow. An example of the results for an experiment with no maldistribution can be seen in Figure 2A, where the fitted normal distribution yields both the average liquid layer thickness (14.16 mm) and the standard deviation of this layer (1.10 mm). An induced maldistribution of 90° at the same process conditions yields the results as shown in Figure 2B. Without redistribution rings the results would show two peaks: one around 0 mm corresponding to the area behind the maldistribution and one at the average water layer. These results clearly show a single normal distribution with a slightly larger standard deviation as compared with the reactor without induced maldistribution.

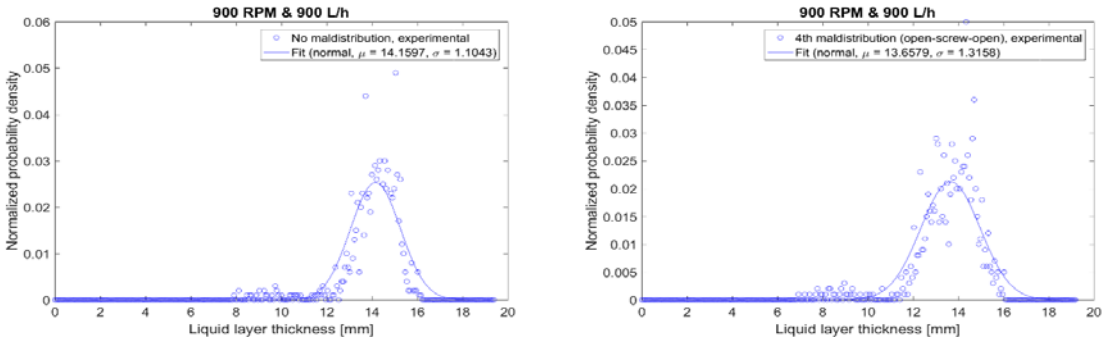

Figure 2. Results of the experiments at a rotational speed of 900 RPM and a liquid flow of 900 L/h for an experiment with (A) no induced maldistribution and with (B) an induced maldistribution of 90°.

4. Conclusions

The efficacy of the redistribution rings is demonstrated here without a packing present, mainly for visualization purposes. Experiments with a packing present have shown a similar behavior, indicating the redistribution rings can also be applied to actual rotating packed beds. It is therefore concluded that the redistribution rings improve the liquid distribution over the entire radial length of the packed bed, which in turn results in a more efficient use of the packing and a higher overall gas liquid mass transfer rate. Therefore, the novel design is a promising tool in enabling a more efficient scale-up of rotating packed beds.

References

[1] C. Ramshaw and R. H. Mallinson, “Mass transfer process,” US4283255, 27-Nov-1978.
[2] C. W. Pilo and S. W. Dahlbeck, US2941872, 09-Jun-1959.
[3] Y.-S. Chen, C.-C. Lin, and H.-S. Liu, Ind. Eng. Chem. Res., vol. 44, no. 20, pp. 7868–7875, Sep. 2005.
[4] K. Neumann et al., Chem. Eng. Res. Des., vol. 134, pp. 443–462, Jun. 2018.
[5] J. R. Burns and C. Ramshaw, Chem. Eng. Sci., vol. 51, no. 8, pp. 1347–1352, Apr. 1996.
[6] K. Groß et al., Chemie Ing. Tech., no. 00, pp. 1–10, 2019.

ECCE12
The 12th EUROPEAN CONGRESS OF CHEMICAL ENGINEERING
Florence 15-19 September 2019

Numerical prediction of a turbulent diffusion flame by rhoReactingFoam.

Esteban Maya[1], Jairo Valdés[1], Alexander Ladino[1*], Omar López[2]

1 School of Mechanical Engineering, Universidad del Valle, Calle 13, No. 100-00, Cali 760032, Colombia

2 Department of Mechanical Engineering, Universidad de los Andes, Cra 1 Este N 19A-40, Bogotá, Colombia

**Corresponding author: jair.ladino@correounivalle.edu.co*

Highlights

- Density-based solver *rhoReactingFoam* was validated against experimental and computational data.
- Flame prediction performed via RANS, one step global reaction and PaSR as combustion model
- Four single step global reactions evaluated.
- *rhoReactingFoam* provides good agreement with available data for the reaction kinetics considered
- *rhoReactingFoam* is capable to predict small diffusion flames at low-moderate Re.

1. Introduction

One of the most basic structure in combustion is a flame, widely used as heating mechanism in industry equipment like boilers and furnaces. However, even for the simplest geometries, its nature of turbulent combustion and flame instability downstream represents a complex process cannot be treated analytically but numerical models widely validated with experimental data.

In this work, experimental data from the literature of SANDIA D flame [1] was used to validate the numerical model of density-based thermodynamics package compressible reacting flow solver *rhoReactingFoam*, implemented in OpenFOAM package. Numerical model implemented involves Reynolds Averaged Navier-Stokes equations and k-ε for turbulence modeling, Partially Stirred reactor (PaSR) for chemistry-turbulence interaction with a single-step global reaction considered [2]. Finally, the *rhoReactingFoam* results for flame temperature and species were compared with experimental data [1] and previous computational studies widely developed by Lysenko and given in [3].

2. Methods

The Sandia flame D [1], is a piloted free non-premixed methane-air burner in which the flame is established between an internal flow of fuel and an external flow of a lean mixture of methane and air. The Main fuel jet is composed of 25% methane and 75% air by volume with a Reynolds number at the burner exit of 22400. The pilot is a lean mixture ($\varphi = 0.77$) of methane and air.

Numerical implementation in *rhoReactingFoam* involves an axisymmetric domain, spatial discretization of first/second order TVD schemes for advection and second order central differences for diffusion terms. Also, a stabilized local time-step (STLS) and Rosenbrook23 schemes for temporal

discretization were employed for transport equations and species reaction rates respectively. Convergence criteria were 10^{-6} and 10^{-10} for transport quantities and reaction rate respectively.

3. Results and discussion

The Figure 1 shows results for mean temperature and methane mass fractions at flame centerline of this study for the global reaction that best fits the experimental data given [1] and also the results given by Lysenko in [3] which used the Eddy Dissipation Concept (EDC) as chemistry-turbulence interaction, one-step global reaction mechanism and Large Eddy Simulation (LES) for turbulence modelling. Results show that *rhoReactingFoam* reproduces the dynamics of the flame as [3], but in reasonable agreement with the experimental data due to the restriction of the limited reaction kinetics simulated which involves only a one step global reaction.

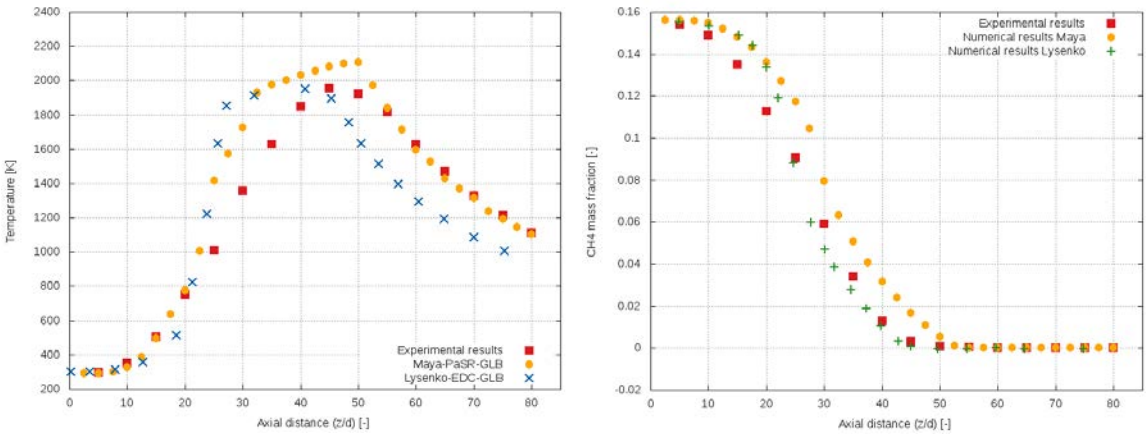

Figure 1. Mean flame temperature (left), and methane mass fraction (right) at centerline. This study: One step global reaction A=6.7x10^{12}, E_a=48.4, a=0.2, b=1.3. See Table II [2].

4. Conclusions

Overall agreement between the simulated results, computational ones from [3] and the experimental data given [1], validate the *rhoReactingFoam* solver for small methane diffusion flames. The coupling of RANS k-ε, PaSR model with single-step reaction demonstrates to provide reliable results as same as [3] for axial temperature with some over prediction of peak temperature but with better performance at flame positions downstream from that point. Also, the most relevant discrepancy is the reactant mixing prediction mainly due to turbulence formulation but in agreement with other studies and solvers. Finally, further research involves the validation and testing of *rhoReactingFoam* with GRI detailed chemistry.

References

[1] R. Barlow and J. Frank, “Piloted CH4 /Air Flames C, D, E, and F Release 2.1,” 2007.

[2] C. K. Westbrook and F. L. Dryer, “Simplified reaction mechanisms for the oxidation of hydrocarbon fuels in flames,” *Combust. Sci. Technol.*, vol. 27, no. 1–2, pp. 31–43, 1981.

[3] D. A. Lysenko, I. S. Ertesvag, and K. E. Rian, “Numerical Simulations of the Sandia Flame D Using the Eddy Dissipation Concept,” *Flow Turbul. Combust.*, vol. 93, pp. 665–687, 2014.

ECCE12
The 12th EUROPEAN CONGRESS OF CHEMICAL ENGINEERING
Florence 15-19 September 2019

UV/Vis Computed Tomography based 3D Concentration Measurement in Bubble Columns

Jajnabalkya Guhathakurta[1], Günter Rinke[2], Manfred Kraut[2], Sven Simon[1]

1 Institute for Parallel and Distributed Systems (IPVS), Department of Parallel Systems, Universitätsstr. 38, 70569 Stuttgart; 2 Institute for Micro Process Engineering (IMVT), Karlsruhe Institute of Technology, Hermann-von-Helmholtz-Platz 1, 76344 Eggenstein-Leopoldshafen, Germany

**Corresponding author: jajnabalkya.guhathakurta@ipvs.uni-stuttgart.de*

Highlights

- In-situ concentration measurement in bubble columns.
- Measurement based on UV/VIS computed tomography.
- High spatial and temporal resolution.
- Selectivity measurement for Fe(edta)NO system.

1. Introduction

Bubble columns play a crucial role in the chemical industry for two phase systems and are primarily relevant for reactions like oxidation, hydrogenation, alkylation etc. However, a realistic description and prediction of the reaction kinetics and mass transfer are still a major bottleneck in industrially relevant reactive bubble columns. Furthermore, localized concentration measurement are difficult to achieve due to the fast reactions and reduced access. This work aims at developing a spatially and temporally resolved 3D concentration measurement technique in reactive bubble columns using UV/Vis computed tomography.

Another important challenge for chemical and process engineers is determining the selectivity in a two phase reaction system. This is considered as a primary design goal in our measurement technique. The system utilizes multiple wavelengths and fast switching light sources to simultaneously and separately measure the concentration of both the products in a competitive consecutive reaction and deduce the selectivity of the reaction from it.

2. Experimental Setup

The developed UV/Vis computed tomography system accumulates absorption projections from different angles around the bubble column (Blue circle in Fig. 1 middle). These directional absorption projections are then fed into an iterative reconstruction algorithm to obtain a 2D concentration field perpendicular to the direction of flow. The measurement technique can be applied to any chemical system having distinct peak for products in the absorption spectrum e.g. Fe(edta)NO system represented by the spectrum in Fig 1 (left). In this system one wavelength (472 nm) is used for measuring the first product P, another wavelength (696 nm) is used for measuring the consecutive product S and a reference wavelength (540 nm) is used at the isosbestic point. Projection data from all the wavelengths are captured within 1 ms and the process is repeated to get high temporal resolution of the 2D concentration field one after the other.

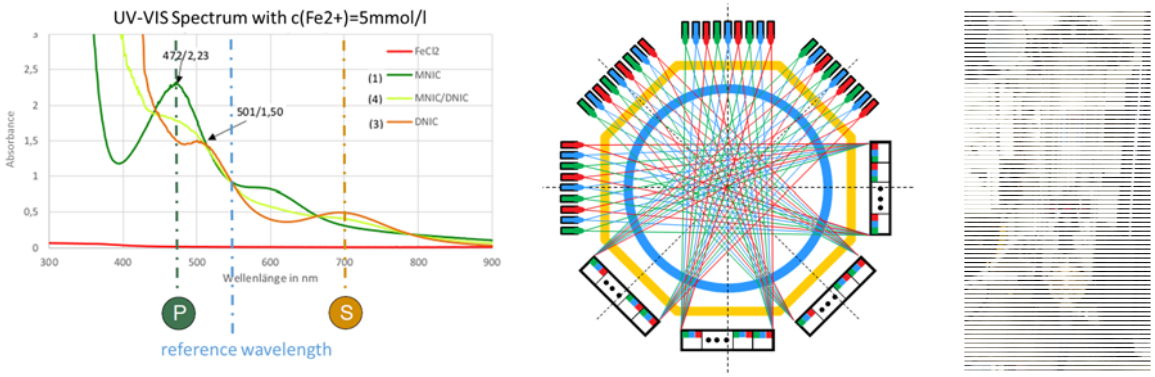

Figure 1. (left) UV/Vis spectrum for Fe(EDTA)NO system [1], (middle) cross section of 75mm diameter bubble column with octagonal refractive index matching mantle showing directional projections, (right) actual bubble column

3. Results and discussion

The setup was optically simulated with Zeemax ray tracing software in order to verify the setup (Fig. 2 left). A collimated laser beam directed by a polygon scanner meets a micro cylindrical lens array which generates the fan beam that is made to travel through the bubble column. The absorption of this fan beam is captured by line sensors on the other end to get the directional projection of the corresponding product. These projections are fed to an iterative reconstruction algorithm uses total variation which performs the best in case of extremely low number of projections as needed by our setup. The functionality of algorithm is verified in simulation where a simulated concentration field in a bubble column is used and the reconstructed field is compared with the original data (Fig 2. right). It can be seen from the cross section that the reconstructed data plot (orange) approximately follows the original data.

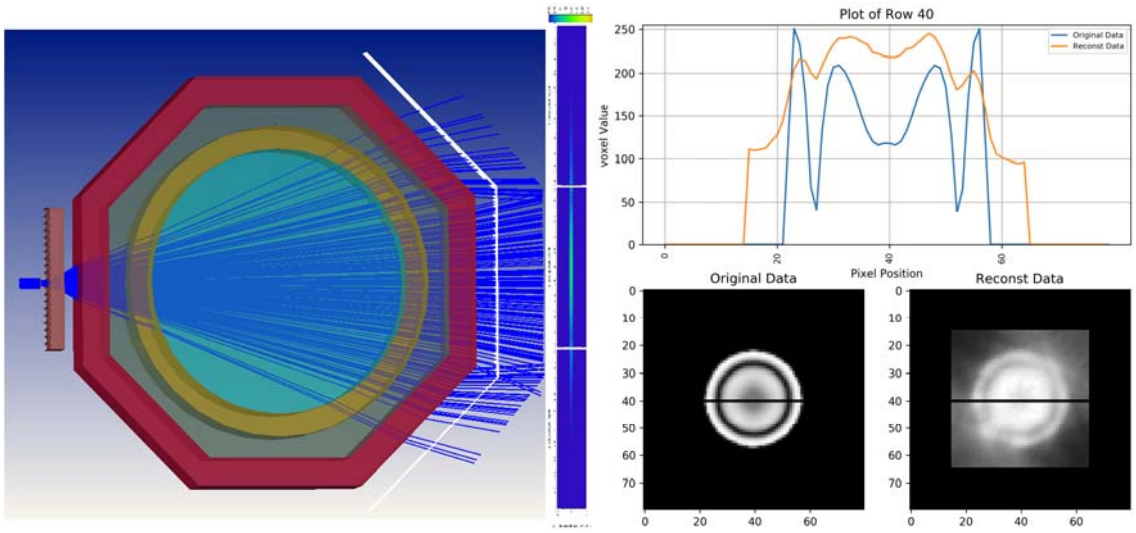

Figure 2. (left) Zeemax ray tracing simulation for each projection [1], (middle) Reconstructed concentration field on simulation data in bubble columns.

4. Conclusions

A novel technique to measure 3D concentrations in bubble columns has been proposed in this work based on UV/Vis computed tomography. The experimental setup along with the iterative reconstruction results and simulations have been presented. Obviously the reconstructed CT data correspond to the ground truth sufficiently with respect to the considered cases.

ECAB 5
The 5th EUROPEAN CONGRESS OF APPLIED BIOTECHNOLOGY
Florence 15-19 September 2019

The Challenge of Continuous Multiphase Flow For Heterogeneously Catalyzed Reactions with Liquid-Liquid Extraction.

Annika Grafschafter[1*], Matthäus Siebenhofer[1]

1 Graz University of Technology, Institute of Chemical Engineering and Environmental Technology, Inffeldgasse 25C/II, 8010 Graz, Austria

**a.grafschafter@tugraz.at*

Highlights

- Successfully implemented continuous multiphase flow.
- Heterogeneously catalyzed reactions with liquid-liquid extraction.
- Hydrodynamic investigation.

1. Introduction

The economic isolation of constituents from dilute aqueous effluents, as can arise in downstream processing of the biobased industry, may be achieved by the combination of reactive separations (e.g. esterification) with liquid-liquid extraction. By simultaneous extraction of the target product with a suitable solvent, equilibrium composition will shift and conversion can be enhanced. Slow chemical reactions, such as esterification reactions, require catalytic acceleration. For continuous operation, heterogeneous catalysts are very suitable since they are simple to separate via sedimentation. The implementation of continuous heterogeneously catalysed reactions combined with liquid-liquid extraction requires adequate apparatus design. Although different equipment is available on the market, equipment design and optimization is still a challenge, especially when targeting continuous multiphase flow. The Taylor-Couette Disc Contactor (TCDC) [1], a hybrid of the Rotating Disc Contactor (RDC) and the Taylor-Couette Reactor (TCR) satisfies the requirements for intensive continuous multiphase operation. The design of internals provides flexible operation under harsh operation conditions. The design is similar to the RDC, but with increased shaft diameter and without stator rings, whereby dead zones for accumulation of solid catalysts can be avoided. At convenient operation conditions, the shaft and rotor discs of the TCDC induce banded flow pattern, providing appropriate mixing of the liquid phases and the solid phase, and providing sufficient residence time for the solid catalysts.

2. Methods

Continuous liquid-liquid-solid flow has been implemented in a TCDC with 50 mm column diameter and 700 mm active mixing height. For the hydrodynamic investigation, ShellSol-T was used as solvent phase, deionized water as continuous phase and Amberlyst15® as solid phase. The hydrodynamic parameters dispersed phase holdup, solid phase holdup, mean droplet size as well as the on-set behavior of appropriate three phase operation have been investigated for varying rate of rotation (0 – 1100 rpm), hydraulic load (5-15 $m^3\ m^{-2}h^{-1}$) and mass load of the catalyst. Since the

continuous phase of this system is the driving force for appropriate mixing behavior, single phase CFD simulations of the continuous phase were conducted and evaluated.

3. Results and discussion

Beyond a critical rotational speed, the vorticity of the continuous phase overcomes sedimentation force of the dispersed phase and the solid phase and ensure intensive phase contact in the single compartment. The solid phase is dragged by the toroidal vortexes, and even in the presence of the dispersed phase the catalyst particles remain within the single compartment for reasonable residence time. The catalyst can easily be separated at the bottom of the column by sedimentation. Via the Q-criterion (CFD simulations) the vortexes inside the TCDC column can be pictured and the vorticity can be evaluated. Figure 1 depicts the vorticity of the counterrotating vortexes at increasing rate of rotation and varying hydraulic load. The vorticity increase with increasing rate of rotation. The increase of the hydraulic load does (nearly) not affect the vorticity.

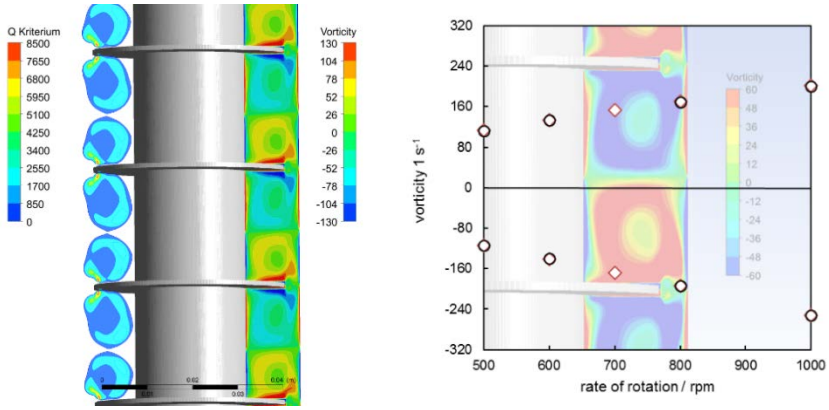

Figure 1. Q-Criterion and vorticity of the toroidal vortexes inside the compartment of a Taylor-Couette Disc Contactor.

4. Summary

The design principle of the TCDC offers intensive phase contact without hydrodynamic dead zones. Continuous multiphase flow was successfully implemented in the TCDC. Hydrodynamic investigations confirm applicability of this column design for intensifying heterogeneously catalyzed reactions combined with liquid-liquid extraction.

References

[1] E. Aksamija, C. Weinländer, R. Sarzio, and M. Siebenhofer, Sep. Sci. Technol. (2015) 2844-2852.

ECCE12
The 12th EUROPEAN CONGRESS OF CHEMICAL ENGINEERING
Florence 15-19 September 2019

Choosing the Right Packing in Millimetric Packed Bed Reactors.

Vittorio Petrazzuoli[1], Matthieu Rolland[1], Adrien Mekki Berrada[1], Yves Schuurman[2]

1 IFP Energies nouvelles, Rond-point de l'échangeur de Solaize, BP 3, 69360 Solaize - France
2 IRCELYON, CNRS, University Lyon 1, 2 Av. Albert Einstein, 69626 Villeurbanne - France
**Corresponding author: vittorio.petrazzuoli@ifpen.fr*

Highlights

- Gas solid RTD measurements in millipacked beds show a steep Pe increase for $D/d_p > 4$
- Insertion of fine inert powder in the bed porosity improves Pe, but the effect is not appreciable for very small reactor diameters (~2 mm)
- Reactive performances are improved by the use of inert powder

1. Introduction

Over the decades, fixed bed reactors for catalyst testing have faced a reduction in size and now they commonly have diameters below 1 cm, the limit being the catalyst pellet size (~1-3 mm). The advantages of these reactors are numerous: less catalyst used, less amount of reactant used and of wastes produced, better temperature control, reduced safety risks and easier implementation of parallel reactor systems [1-3]. Those reactors were designed for catalyst screening, so that hydrodynamics was not really an issue as long as the ranking and uncertainty were correct. As those reactors produce a large amount of data, a new question arises: can we use those results to build models for catalyst performance prediction? This work aims at improving our understanding of these small reactors. Do we need to use a hydrodynamic model? When is it interesting to use fine powder to fill the porosity between the catalyst pellets? The results of two experimental campaigns will be presented:

- Measurements of residence time distributions for gas-solid millireactors with reactor (D) to particle (d_p) diameter ratio less than 8, with and without porosity filler;
- Effect of packing on reactive performances.

2. G/S RTD measurements

2.1 Methods

RTD measurements are performed using the concentration step technique, with N_2 as carrier gas and He as tracer. The reactor and particle dimensions are varied between 1-7 mm. The particles are non-porous, in spherical or cylindrical form. The tests are performed with superficial velocities between 0.013-0.06 m/s. A 1D dispersion model is used in order to estimate the void fraction (ε) and the axial dispersion coefficient (D_{ax}) of the reactors.

2.2. Results and discussion

The results of the RTD studies show that, at constant flow rate, it is preferable to work under conditions of $\delta=D/Dp > 4$ (Figure 1). We relate this to the change from structured to random packing that occurs when increasing δ: structured packings offer more potential for channeling

than random beds. Provided that the bed is long enough, the Pe number is sufficient to consider the reactors as ideal (plug flow) for most applications. The addition of inert powder to lower the bed porosity improves the Pe number but the RTD shows an additional contribution. An explanation can be the presence of dead volumes in case of the use of a porosity filler. For very small reactor diameters (~2 mm), the improvement is no longer appreciable.

3. Effect of the packing on n-heptane reforming reaction

The effect of the packing is measured by comparing the conversion in reactors with different packings in a 8-parallel reactor system (Avantium FLOWRENCE). The reaction is the n-heptane reforming over chlorinated Pd/Alumina catalyst at 10 barg, T=450-500 °C with conversions in the range of 60-90%. The reactor internal diameters are 2 mm, and they are packed with cylindrical catalyst particles (d_p=1.6 mm). The parameters investigated are the fine powder size and type. N-heptane conversion increases when adding inert powder to the catalytic bed, with even better results for finer and rounder particles (Figure 1). As at this conversion levels the reactor is always ideal, this difference cannot be explained by an improvement of the Pe number, but may be due to a better heat control or a better mass transfer.

4. Conclusions and perspectives

Gas phase RTD measurements indicate that, if long enough, millipacked bed reactors exhibit a pseudo-ideal behavior. The value of D/d_p has an effect probably related to the passage from structured to random beds. This aspect will be further investigated by CFD.

Addition of small spherical powder showed an improvement of the performance of a gas-solid mass transfer limited reaction. Next step is to discriminate between thermal and mass transfer effects.

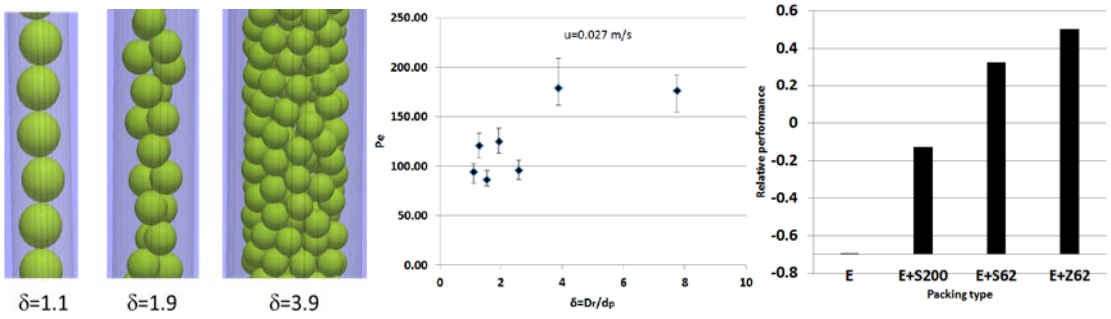

Figure 1. Left: Example of packing. Middle: Effect of δ=D/dp on the Pe number for spheres (L=18.2 cm, u=2.7 cm/s). Right: Relative performance of different packings on n-heptane conversion

References

[1] Zhang J., Teixeira A.R., Jensen K.F. (2017) Automated measurements of gas-liquid mass transfer in micropacked bed reactors, *AIChE J.* 36, 8, 3292.

[2] Moonen R., Alles J., Ras E.j., Harvey C., Moulijn J.A. (2017) Performance Testing of Hydrodesulfurization Catalysts Using a Single-Pellet-String Reactor, *Chem. Eng. Technol.* 40, 11, 2025–2034.

[3] Moulijn J., Pérez-Ramírez J., Berger R., Hamminga G., Mul G., Kapteijn F. (2003) High-throughput experimentation in catalyst testing and in kinetic studies for heterogeneous catalysis, *Catalysis Today* 81, 3, 457–471W.

ECCE12
The 12th EUROPEAN CONGRESS OF CHEMICAL ENGINEERING
Florence 15-19 September 2019

Power consumption and mixing dynamics for Newtonian and non-Newtonian across different single-use mini bioreactor configurations

Anne de Lamotte[1], Martina Micheletti[1]

1 Department of Biochemical Engineering, University College London, Gower Street, WC1E 6BT London, UK;

**Corresponding author: a.delamotte@ucl.ac.uk*

Highlights

- Accurate power consumption measurements by the use of a dynamometer
- Detailed mixing dynamics assessment by means of the pH dual colorimetric technique
- Characterization of the impact of rotating speed and viscosity on Newtonian and non-Newtonian fluids
- Evaluation of the influence of baffles and internals on axial- and radial-flow configurations

1. Introduction

The biopharmaceutical manufacturing industry has created a pull for advancing high-throughput, automated technologies for process development and optimisation such as disposable multi-parallel miniature bioreactor platform. Actually, the latter are increasingly used within the industry, not only as screening tools but also as scale-down models. Among the current commercially available small-scale bioreactor systems, the stirred-tank design has again become prevailing. In stirred-tank bioreactors, hydrodynamics governs bulk fluid mixing. The understanding of these two key physical aspects and of their interactions are required within the framework of scale-translation models. The selection of agitation configuration and operating conditions has then to meet two objectives. On the one hand, the influence of process variables on bioreactor performance has to be properly understood. On the other hand, hydrodynamics and mixing, as well as their coupling, need to be assessed in relation to the bioreactor design and scale. In this context, engineering characterisation is required to understand and quantify these multiscale transport phenomena for better bioreactor design. This work aims at gaining a better understanding of the mixing effectiveness within different single-use mini bioreactor configurations for both Newtonian and non-Newtonian fluids.

2. Methods

Measurements are performed in the mini bioreactor systems ambr® 250 (Sartorius Stedim Biotech). The reactor with a working volume of 250 mL has been fitted with either two Rushton turbines (20 mm diameter, 30 mm spacing), or two pitched-blade impellers (26 mm diameter, 30 mm spacing, up- and down-pumping) with or without four equally-spaced baffles. The internals (pH probe and gas sparger) are also used to study their influence on mixing and power characteristics. The working fluids are water and aqueous solutions of glycerol (viscous), sodium alginate (low

shear-thinning) and xanthan gum (highly shear-thinning) of different concentrations. Rheological measurements are carried out using a Kinexus Lab+ rheometer (Malvern Panalytical).

The power draw in the different ambr® 250 configurations is measured by the use of a dynamometer based on a pneumatic bearing allowing rotation without friction. More information about the technique is provided in [1].

The Dual Indicator System for Mixing Time (DISMT) technique, based on a fast acid–base reaction in presence of pH indicators [2], is used to assess the mixing dynamics by using a camera. A description of the DISMT methodology and of the image-processing algorithm used to evaluate the mixing time can be found in [3].

3. Results and discussion

Power consumptions experiments with Newtonian fluids are carried out for providing the common thread of this work, and for characterizing the power curve of shear-thinning fluids within ambr® 250 configurations by means of the Metzner-Otto [4] and Rieger-Novak [5] methods.

The DISMT experiments are used to identify the main structures in the flow within ambr® 250 configurations, and to determine the macro-mixing time, the mixing time of segregated regions in the flow and the rate of reduction in size of the slow mixing regions for fluids with separate rheological behaviour [6].

The influence of Reynolds numbers on power consumption and mixing characteristics of baffled and unbaffled bioreactors is presented for operating conditions corresponding to non-aerated regime (no gas entrainment from the free surface). The impact of impeller type and of internals presence is investigated to assess the functional dependence of the power and mixing numbers on geometrical features under any fluid dynamic regime.

Finally, the mixing and power datasets are combined to determine and compare the mixing effectiveness of the agitation systems in relation with the operating conditions (rotating speed, working fluid).

4. Conclusions

The coupled analysis of power and bulk mixing characteristics of fluids with distinct rheological properties in different single-use mini bioreactor configurations, allows a first step towards a more systematic approach toward scale-down models development. An improved understanding of fluid dynamics and flow properties enables a more adequate application of key engineering parameters, in particular the power input.

References

[1] G. Ascanio, B. Castro, E. Galindo, Chem. Eng. Res. Des. 82 (2004) 1282-1290.
[2] L. A. Melton, C. W. Lipp, R. W. Spradling, K. A. Paulson, Chem. Eng. Commun. 189 (2002) 322-338.
[3] G. Rodriguez, T. Anderlei, M. Micheletti, M. Yianneskis, A. Ducci, Biochem. Eng. J., 82 (2014) 10-21.
[4] A.B. Metzner, R.E. Otto, AIChE J. 3 (1957) 3-10.
[5] F. Rieger, V. Novák, Chem. Eng. Sci. 29 (1974) 2229-2234.
[6] G. Rodriguez, M. Micheletti, A. Ducci, Chem. Eng. Res. Des. 132 (2018) 890-901.

ECCE12
The 12th EUROPEAN CONGRESS OF CHEMICAL ENGINEERING
Florence 15-19 September 2019

Investigating Deep-Sea Oil Spills – Transfer of Engineering Methods to an Environmental Issue in Experiments and Modeling

Simeon Pesch[1*], Claire Paris[2], Zachary Aman[3], Philip Jaeger[4], Marko Hoffmann[1], Michael Schlüter[1]

1 Hamburg University of Technology, Institute of Multiphase Flows, Eissendorfer Str. 38, 21073 Hamburg, Germany; 2 University of Miami, Rosenstiel School of Marine and Atmospheric Science, 4600 Rickenbacker Causeway, Miami, FL 33149, USA; 3 University of Western Australia, Dept. of Chemical Engineering, 35 Stirling Hwy., Perth WA 6009 Australia; 4 Eurotechnica GmbH, An den Stücken 55, 22941 Bargteheide, Germany

**Corresponding author: simeon.pesch@tuhh.de*

Highlights

- Scale-up of oil-in-water DSD and effects of pressure are examined experimentally.
- New approach for prediction and scale-up of jet DSD based on TKE dissipation rate.
- Rise of gas-saturated oil droplets is accelerated by pressure-induced degassing.

1. Introduction

The depletion of readily accessible oil reservoirs in conjunction with the unabated demand for fossil fuels leads to the exploration and production of remote deposits, esp. in deep-sea regions. Such operations at hard-to-reach locations far beyond atmospheric conditions are extremely challenging and associated with elevated risk, which became clear when the Deepwater Horizon drilling rig ignited and sank in 2010 in the Gulf of Mexico, causing one of the largest oil spills in human history. The depiction and prediction of the multiphase plume's behavior under deep-sea conditions and the oil fate is critical for the development of mitigation strategies in case of a subsea blowout. Some of the most important input parameters for accurate oil fate modeling are the ensuing droplet size distribution (DSD), the rise velocity of the present droplets and bubbles plus the physical properties and phase behavior of the involved substances. The highly turbulent flow structure and the multiphase nature of the system as well as the specific deep-sea conditions must be accounted for when experimental facilities are designed or when oil-spill models are developed and tuned[1].

2. Methods

Extensive experimental research on the oil and gas behavior under ambient and in-situ conditions is done at Hamburg University of Technology (TUHH). The DSD of oil-in-water free jets at varying nozzle sizes, measuring positions and exit velocities as well as appropriate scale-up rules for the prediction of the DSD are investigated under ambient conditions. For this purpose, a lab-scale and a pilot-plant-scale experimental plant with direct optical access have been designed, commissioned and used, covering nozzle diameters from 1 mm to 74 mm and volume flow rates from 0.28 to 200 L/min. Particle image velocimetry is applied for the investigation of flow characteristics like the turbulent kinetic energy (TKE) dissipation rate. A colorized white oil (H&R PIONIER 7467) is used as dispersed and DI water as continuous phase. The DSD is determined by means of endoscopic imaging techniques. A high-pressure counter-current flow cell is used in order to simulate the rise

of gas-saturated crude oil droplets (Louisiana Sweet Crude oil, saturated with CH_4, in seawater). Reservoir conditions (~250 bar) and depth-dependent hydrostatic pressures of up to 150 bar, corresponding to the 1,500 m water column of the Deepwater Horizon blowout, can be adjusted. Temperatures range from 4 to 25 °C, also corresponding to the real conditions. The droplet's size, shape and motion is captured by means of high-speed imaging and evaluated over time[1].

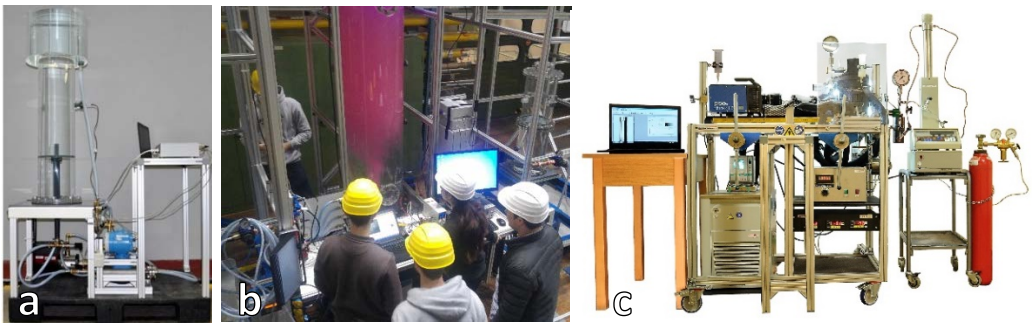

Figure 1. Experimental facilities for the investigation of submarine oil spills at TUHH: a. Lab-scale jet facility with direct optical access and variable nozzle size; b. Oil-in-water jet experiment in the pilot-plant-scale jet facility; c. High-pressure counter-current flow cell for the investigation of single rising live-oil droplets under simulated deep-sea conditions.

3. Results and discussion

The recorded droplet sizes of the oil-in-water jets are approximately log-normally distributed. In collaboration with the University of Western Australia, a new model correlation for the prediction and scale-up of the jet DSD based on the TKE dissipation rate (TDR) and incorporating the recent experimental results as well as older datasets is developed at TUHH. The model correlates the mean diameter with the TDR, which is calculated by means of literature equations, using a power-law function. The results are independent of the nozzle size but scale with the TDR value, which enables scale-up. In contrast to models available in literature, this quite fundamental correlation is capable of accounting for high-pressure effects, like pressure drop at the blowout site and outgassing of dissolved natural gas from the liquid oil. In the drop-rise experiments, gradually decreasing the pressure leads to the formation of gas bubbles inside the initially gas-saturated but purely liquid crude oil droplets. This internal degassing causes a substantial growth of the two-phase particles and a significant decrease of their average density. Both effects lead to an increased buoyancy and therefore a higher rise velocity of the droplets. The enhanced buoyancy of gas-saturated droplets is implemented into the 3D Lagrangian oil fate model by Paris et al. at the University of Miami[2].

4. Conclusions

The presented experimental results and modeling approaches help to understand and predict the fate of the oil masses in case of a subsea blowout. The multiphase nature of the oil and gas jet in question that determines the droplet size distribution as well as pressure-dependent effects like enhanced buoyancy due to degassing are critical for accurate oil fate modeling. This research was made possible by a grant from the Gulf of Mexico Research Initiative, C-IMAGE III.

References

[1] S. Pesch, P. Jaeger, A. Jaggi, K. Malone, M. Hoffmann, D. Krause, T.B.P. Oldenburg, M. Schlüter, Environ. Eng. Sci. 35(4), 2018, 289–299.

[2] C. Paris, M. Le Henaff, Z. Aman, A. Subramaniam, J. Helgers, D.-P. Wang, V. Kourafalou, A. Srinivasan, Environ. Sci. Technol. 46(24), 2012, 13293–13302.

ECCE12
The 12th EUROPEAN CONGRESS OF CHEMICAL ENGINEERING
Florence 15-19 September 2019

Experimental investigation of hydrodynamics and mass transfer of viscous non-Newtonian fluids in stirred tanks.

Haider Ali[1], Jannike Solsvik[1]

[1]Department of Chemical Engineering, NTNU-Norwegian University of Science and Technology, Trondheim, Norway

*Corresponding author: jannike.solsvik@ntnu.no

Highlights

- Hydrodynamic and mass transfer of viscous non-Newtonian fluid in a stirred tank.
- Bubble size distribution changes with the height of tank.
- Bubbles size reduces in the stirrer vicinity.
- Rheology of liquids affects the bubble distribution in a stirred tank.

1. Introduction

Stirred tanks massively attract the bioprocess and chemical industries because of their cost-effectiveness. Improved mixing conditions and high heat and mass transfer rates are the prominent characteristics that make stirred tanks suitable for the fluids with complex rheology (non-Newtonian behavior) [1]. A mechanical stirrer enhances the mixing in the stirred tank by breaking the gas bubbles and increasing the turbulence of the liquid. However, the use of highly viscous non-Newtonian fluids significantly reduces the mixing process that consequently affects the performance of a stirred tank [2].

The objective of this study is to experimentally investigate the hydrodynamics and mass transfer characteristics of viscous non-Newtonian fluid in a stirred tank. A more detailed analysis of bubble-liquid mass transfer is obtained in this work because of the combined use of the two types of probes. That is, with the knowledge of the local dissolved concentration of oxygen along with the local bubble size distribution, the overall mass transfer coefficient can be analyzed in further details by splitting it into its components of liquid side mass transfer coefficient and interfacial area. In contrast to previous studies, where an overall bubble size is assumed for the whole tank unit, this study provides detailed information on the bubble size distribution at various local tank positions. Improved knowledge on mass transfer in non-Newtonian liquids is crucial for operation of many fermentations processes. The experiment is first performed to measure the hydrodynamics and mass transfer properties of Newtonian (water) liquid. Then viscous Newtonian (glycerol), and non-Newtonian (Carboxymethylcellulose sodium) fluids will be experimented to examine the effects of fluid rheology. Various gas volumetric flow rates, stirrer speeds, and probe positions are considered to examine their effects on the bubble size distribution, gas holdup, and mass transfer coefficient.

2. Methods

This study used a 15.0 L laboratory scale stirred tank made of plexiglass and with a working volume of 11.0 L. The gas was bubbled in the stirred tank by a ring sparger with 0.06 m diameter. The

sparger consists of 32 holes with a diameter of 0.0005 m. A Rushton turbine stirrer with six blades (0.07 m in diameter) and clearance of 0.045 m was used to prompt stirring in the tank. Dissolved oxygen concentration and bubble size distribution were measured at four different vertical positions (0.055 m apart) of the stirred tank. The gas volumetric flow rate and stirring speed varied from 1.0×10^{-4} to 1.4×10^{-4} m^3/s and 10 to 13.33 1/s respectively. An optical dissolved oxygen probe (InPro 6870i Mettler Toledo, Switzerland) and photo optical probe (VI Kr SOPAT, Germany) were used to measure dissolved oxygen concentration and bubble size distribution. The overall mass transfer coefficient was measured with the dynamic gassing-in method [3]. The rheological properties (apparent viscosity etc.) of the viscous liquids will be measured using rheometry.

3. Results and discussion

Figure 1 shows the bubble size distribution for the different vertical probe positions. The volumetric gas flow rate is 1.0×10^{-4} (m^3/s), stirrer speed is 10 (1/s), and the frame rate of the optical probe is 5 (Hz) for these results. The breaking of the bubble by the stirrer produces significantly small size bubbles in the first position (stirrer vicinity). The size of bubbles starts to increase as they move away from the stirrer (second position) because of the coalescence. The large size bubbles recorded at the third and fourth positions suggest that the bubble coalescence is dominant in these regions. The Sauter mean diameter is 0.95 mm for the first position, 1.78 mm for the second position, 2.15 mm for the third position, and 2.04 mm for the fourth position.

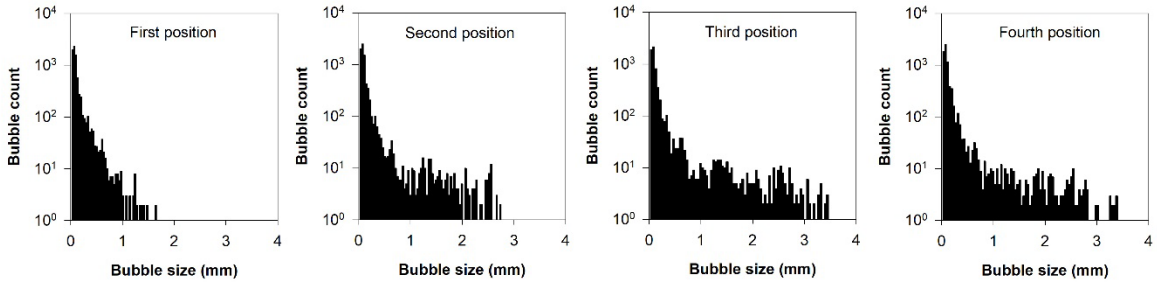

Figure 1. Bubble size distribution for different probe positions.

4. Conclusions

This experimental study investigates the hydrodynamics and mass transfer characteristics of viscous non-Newtonian fluid in a stirred tank. The study uses different gas volumetric flow rates, impeller speeds, and probe or positions to examine their effects on the bubble size distribution, gas holdup, and mass transfer coefficient. Initially, the bubble size distribution in the water was measured at four different probe positions. The coalescence produces large size bubbles in the regions that are quite distant from the stirrer. Use of viscous Newtonian and non-Newtonian fluids will increase the coalescence that consequently affects the bubble distribution in the tank. Therefore, experiments will be carried out to measure hydrodynamics and mass transfer of viscous Newtonian and non-Newtonian fluids.

References

[1] S. S. de Jesus, J. Moreira Neto, R. Maciel Filho, Biochem. Eng. J. 118 (2017) 70–81.
[2] A. Story, Z. Jaworski, M. Major-Godlewska, G. Story, Chem. Eng. Res. Des. 138 (2018) 398–404, 2018.
[3] F. Garcia-Ochoa, E. Gomez, Biotechnol. Adv. 27 (2009) 153–176.

ECCE12
The 12th EUROPEAN CONGRESS OF CHEMICAL ENGINEERING
Florence 15-19 September 2019

Thin gap bubble column with a non-Newtonian liquid phase: study of the hydrodynamics and gas-liquid mass transfer

Sikandar ALMANI[1], Abdallah HAYDAR[1], Walid BLEL[1], Emilie GADOIN[1], Caroline GENTRIC[1*]
[1]*GEPEA, CNRS-UMR 6144, Saint-Nazaire Cedex, France.*
*Corresponding author: caroline.gentric@univ-nantes.fr

Highlights

- Mimicking microalgae culture at high concentration using shear thinning liquid phase.
- Identification of flow regimes and their transition.
- Determination of mixing time and gas liquid mass transfer coefficient.
- Optimization of hydrodynamic conditions for higher biomass productivity.

1. Introduction

Bubble column technology is particularly adapted to photosynthetic microorganism culture because the injection of air enriched with CO_2 allows mixing as well as feeding the culture with inorganic carbon. Nevertheless, technological advances are still required to reduce production costs and environmental impacts. In this context, intensification of performances *via* an increase of culture concentration in photosynthetic microorganisms is a promising way to optimize production systems. However, it has been shown that the increase in cell concentration is accompanied by the increase of the viscosity and the modification of the rheological properties of the microalgae suspension [1]. Moreover, to reach high cell concentration, reducing PBR thickness is required to ensure light availability on the whole reactor gap. Confinement and rheological characteristics impact the bubbling effect on hydrodynamics and gas-liquid mass transfer [2]. The objective of this work is to characterize hydrodynamics as well as gas-liquid mass transfer for non-Newtonian liquid phase in a 2D bubble column having gap of 4 mm [2], for different gas injection conditions (sparger size and gas flow rate). For this purpose, non-Newtonian shear thinning solutions are used to mimic the high concentration of *Chlorella vulgaris* cultures at 30-40 g/L. Solutions of Xanthan gum (XG) and Carboxymethyl cellulose (CMC) are used respectively at the concentrations of 1 g/L and 2 g/L. The rheological characterization is performed using the PAAR Physica® MCR500 rheometer and the power law equation is used for modelling the rheological behaviour. Gas sparging is achieved using 15 capillaries which can have 5 different diameters (0.1016, 0.254, 0.508, 0.762 and 1.016 mm) in order to vary the size of the injected bubbles. A wide range of superficial gas velocities is also explored to investigate the effect of sparging on the global hydrodynamics of a non-Newtonian liquid phase in this thin gap bubble column.

2. Methods

Experimentally, the gas phase is characterized locally through the shadowgraphy method using DANTEC DYNAMICS Shadow Strobe, which allows to obtain the size, the shape and the velocity of bubbles. The hydrodynamics of the continuous phase is characterized by Particle image velocimetry (PIV) technique. Secondly, flow regimes and their transitions are investigated by studying gas holdup determined by liquid height or by hydrostatic pressure measurements. Identification of regime transition is obtained from gas holdup using three different methods based on gas retention as a function of superficial gas velocity or swarm velocity method or drift method. The mixing time characterization is carried out using a tracer method which consists in the injection of 2 mL of NaCl Solution at 200 g/L and follow-up the conductivity of the liquid over time until stabilization. Finally, to determine the volumetric mass transfer coefficient, kLa, the classical dynamic gassing-out gassing-in method is employed [2]. The obtained results are compared to those presented in the literature for non-Newtonian solutions in unconfined bubble columns in order to emphasize the confinement effect on hydrodynamics and gas-liquid mass transfer[3].

3. Results and discussion

Figures 1 and 2 present respectively gas holdup and mixing time *vs* the superficial gas velocity for an injection with capillaries of 0.508 mm of diameter. Whatever the nature of the fluid, three flow regimes are observed: homogeneous, transition and heterogeneous regimes. For the three tested liquids, the overall gas holdup increased with the increase of the superficial gas velocity. Besides, at the same superficial gas velocity, the overall gas holdup in non-Newtonian liquids was larger than those in the water [Fig 1]. This result disagrees to one available in the literature ([3][4]and[5]) using unconfined column operating with non-Newtonian fluids. This result could be explained by the effect of the confinement between bubbles and column walls. Indeed, the experiments for an isolated bubble in this column showed that low terminal velocities have been observed in the case of non-Newtonian phase compared to the Newtonian one. Consequently, higher residence time of bubbles is observed with CMC and XG solutions. Comparison between the two non-Newtonian fluids shows that CMC and XG have similar gas hold-ups, certainly due to their similar rheological properties. It could be noted that the regime transitions between the homogeneous and the intermediate regimes appear at lower superficial gas velocity with non-Newtonian fluids due to their coalescence tendency. Higher gas hold-up is obtained in the XG solution than in the CMC, this phenomenon was already observed by [3] which they explained by elastic effects of XG solution.

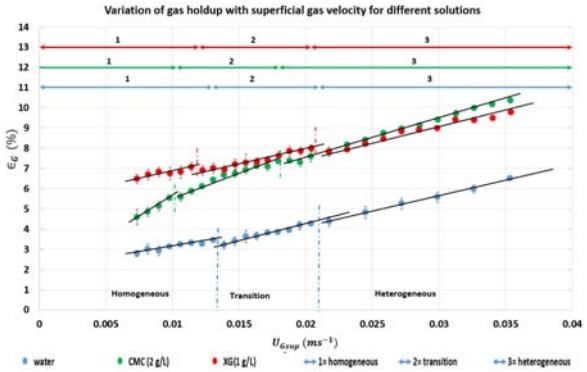

Figure 1. Effect of superficial gas velocity on gas holdup.

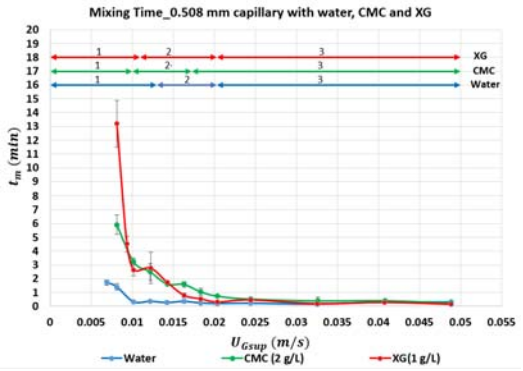

Figure 2. Effect of superficial gas velocity on mixing time

Concerning the mixing time, Fig 2 shows a decrease of this parameter with the increase in the superficial gas velocity. The mixing time in water decreases rapidly during the homogeneous regime ($U_{Gsup} < 0.01$ m.s^{-1}) and then is quite constant for higher values of U_{gsup}. For CMC and XG solutions, the important decrease is observed during the homogeneous and the transition regimes. Increasing the capillary diameter generates large bubbles which leads to the lower mixing times for all solutions. With all capillaries studied, the mixing time in XG solution is higher than in the two other solutions, especially in homogeneous regime.

4. Conclusions

Global hydrodynamics characterization of a thin gap bubble column shows that the gas holdup in non-Newtonian liquid phase is higher than Newtonian one due to the higher residence time. The regime characterization, performed using various methods, shows that regime transitions for non-Newtonian liquids appear at slightly lower superficial gas velocities than the Newtonian one. The mixing time experiments show that mixing in non-Newtonian liquids is quite poor at low gas flowrates, especially during the homogeneous and transition regime with mixing time values up to 10-15 times higher than those observed in the heterogeneous regime. An important increase of the mixing time with the viscosity was also observed. The work for gas liquid mass transfer and experiments with PIV technique are in process to determine the other aspects that can affect hydrodynamics in this thin gap bubble column with non-Newtonian liquid in order to optimize culture conditions for higher biomass productivity.

References

[1] A. Souliès, J. Pruvost, J. Legrand, C. Castelain, and T. I. Burghelea, "Rheological properties of suspensions of the green microalga Chlorella vulgaris at various volume fractions," *Rheol. Acta*, vol. 52, no. 6, pp. 589–605, Jun. 2013.

[2] C. Thobie, E. Gadoin, W. Blel, J. Pruvost, and C. Gentric, "Global characterization of hydrodynamics and gas-liquid mass transfer in a thin-gap bubble column intended for microalgae cultivation," *Chem. Eng. Process. Process Intensif.*, vol. 122, pp. 76–89, 2017.

[3] A. Esmaeili, C. Guy, and J. Chaouki, "The effects of liquid phase rheology on the hydrodynamics of a gas – liquid bubble column reactor," *Chem. Eng. Sci.*, vol. 129, pp. 193–207, 2015.

[4] M. Mokhtari and J. Chaouki, "New technique for simultaneous measurement of the local solid and gas holdup by using optical fiber probes in the slurry bubble column," *Chem. Eng. J.*, vol. 358, pp. 831–841, 2019.

[5] E. Fransolet, M. Crine, P. Marchot, and D. Toye, "Analysis of gas holdup in bubble columns with non-Newtonian fluid using electrical resistance tomography and dynamic gas disengagement technique," *Chem. Eng. Sci.*, vol. 60, no. 22, pp. 6118–6123, 2005.

ECCE12
The 12th EUROPEAN CONGRESS OF CHEMICAL ENGINEERING
Florence 15-19 September 2019

Overview for real time monitoring devices: measurements of bubble and drop size distributions and phase inversion

Sebastian Maaß[1], Jörn Emmerich[1,2] and Matthias Kraume[3]

1 SOPAT GmbH, Berlin, Germany; 2 Technische Universität Berlin, bioprocess engineering; 3 Technische Universität Berlin, chemical engineering

**Corresponding author: Sebastian.maass@sopat.de*

Highlights

- Introduction of new automation technique for multiphase applications
- General overview of inline techniques for the particle characterization given
- ISO standards are applied to the evaluation and show the advantages of image analysis

1. Introduction

The exact knowledge of drop size distributions (DSD) plays a major role in liquid-liquid extraction, for controlling and optimizing processes and separation efficiency as well as reducing residence times. Many efforts have been made to measure the size of liquid dispersed droplets. The techniques can be divided into those that require a sample to be withdrawn from the vessel, column or pipe and those that take the measurement in situ. The next step forwardc is the control of the fluid particle size in such systems. Therefore, fast information acquisition is needed but difficult to obtain. While many users are confronted with these requirements an adequate measurement technique for all applications is needed but has not yet been developed. A further difficulty handling such dispersed systems is the possible danger of a phase inversion (PI). Does this phenomenon occur spontaneously during a process, it can have fatal consequences for the process and/or equipment.

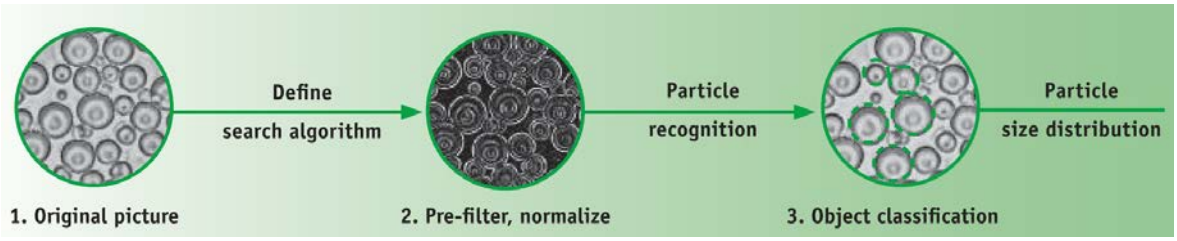

Fig. 1: Photo-optical Measuring Method for Particle Size Distributions

2. Methods

An overview is given for already existing measurement techniques. They are divided into three main groups: sound, laser and photo based techniques. The FBRM® [1], the 2-D ORM® [2] and the PARSUM IPP 30 [3] which all give online and in-situ information together with an in house developed photo optical technique SOPAT-VR® [4, 5] will be discussed in detail. They have been tested for different applications in various multiphase system (liquid-liquid, gas-liquid-liquid, gas-

liquid-liquid-solid). The results achieved by the different measurement techniques are compared with each other. As proposed in literature, image analysis is used as the standard method that all other techniques are compared with. The photo-optical SOPAT measuring technique for particle sizing is capable of acquiring raw data (two-dimensional images) of the dispersed phase (here: droplets) during the process and measure the sizes by means of automated image analysis, see Fig. 1. This study demonstrates the capability of a photo-optical measurement method by taking the example of a separation apparatuses after a mixer.

3. Results and discussion

Fig. 2 exemplarily shows the measured DSDs for the separation process. The experiments showed clearly that the initial droplet size is of major importance for the separation efficiency. The studies, varying volume flow, dispersed phase concentration as well as dispersed phase are shown and its influence determined. Additionally it could not only detect the required DSD, but also was able to distinguish between different dispersed phases, for example disturbing bubbles and furthermore the beginning of PI have been detected and therefore the measurement system could be used as a warning for PI. As the results are available inline and in real time, a closed control loop can be established.

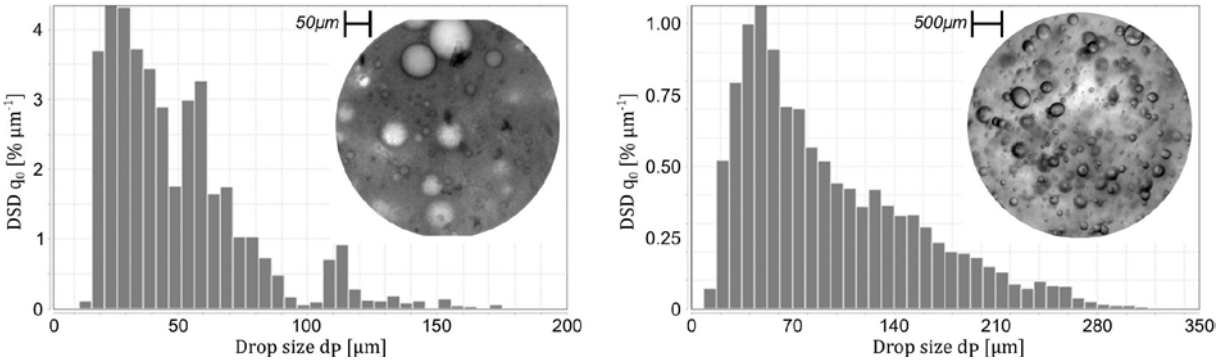

Fig. 1: Measured DSD for w/o (left) and o/w separation process (right) with exemplary photo-optical image data

References

[1] Ruf et al., Modeling and experimental analysis of PSD measurements through FBRM. Part. Part. Sys. Char., 17 (2000) 167-179.

[2] Lovick, J., Mouza, A.A., Paras, S.V., Lye, G.J. and Angeli, P., 2005. Drop size distribution in highly concentrated liquid-liquid dispersions using a light back scattering method. J. Chem. Technol. Biotechnol., 80(5): 545-552.

[3] Petrak, Simultaneous measurement of particle size and particle velocity by the spatial filtering technique. Part. Part. Sys. Char., 19 (2002) 391-400.

[4] Maaß, S., Rojahn, J., Hänsch, R. and Kraume, M., (2012); Automated drop detection using image analysis for online particle size monitoring in multiphase systems. Comp. Chem. Eng., 45: 27-37

[5] Panckow, R. P., Comandè, G., Maaß, S. and M. Kraume (2015). Determination of Particle Size Distributions in Multiphase Systems Containing Nonspherical Fluid Particles. Chem. Eng. & Technol. 38 (11), 2011-2016.

ECCE12
The 12th EUROPEAN CONGRESS OF CHEMICAL ENGINEERING
Florence 15-19 September 2019

Real-time planar temperature measurement of fluidized particle aggregates heated by high radiation flux

Wanxia Zhao[1,2], Kimberley Kueh[2,3], Graham Nathan[2,3], Zeyad Alwahabi[1,2,*]

1 School of Chemical Engineering, University of Adelaide, Adelaide, South Australia 5005, Australia;
2 Centre of Energy Technology, University of Adelaide, Adelaide, South Australia 5005, Australia;
3 School of Mechanical Engineering, University of Adelaide, Adelaide, South Australia 5005, Australia

** Corresponding author: zeyad.alwahabi@adelaide.edu.au*

Highlights

- The fast-moving aggregates were heated by well-characterized multi-diode laser.
- The *in situ* planar aggregate temperature was determine by PLIP technique.
- Averaged particle aggregates temperatures were compared at several fluxes.

1. Introduction

Heat transfer within particle-laden flow strongly influence the process heat flow, energy conversation and the system's reliability of chemical engineering processes [1]. Thus, the understanding of heat transfer in two phase flow and precise temperature measurement of particles are important in improving such process efficiencies. Nowadays, the heat transfer of two-phase flow is still not fully understood because the temperature measurements of suspended particles in the gas flow are extremely difficult. Therefore, planar laser-induced phosphorescence (PLIP) technique has been developed to offer the non-invasive temperature measurement for both static and moving surfaces with higher accuracy [2]. In this work, the temperature measurement of particle aggregates, heated by high radiation flux, has been investigated. PLIP technique has been applied to yield accurate non-intrusive surface temperature of fluidized aggregates. The radiation was supplied by the well-characterized high radiation multi-diode laser system that recently developed at the University of Adelaide [3].

2. Methods

The experiment setup was divided into three parts, which are the high radiation multi-diode laser system to generate high radiation flux, the fluidized bed to provide particle-laden flow, and imaging system for signal collection. $BaMg_2Al_{10}O_{17}$:Eu (BAM) was selected as thermographic phosphor due to its large temperature sensitivity up to 1300 K. The Nd:YAG laser excited phosphorescence emission signals from particles were directed to the imaging system. An imaging splitter transferred two images, which captured at two different wavelengths, into a single ICCD camera. Both images were collected simultaneously with the advantages of minimizing the error during the image processing. The real-time particle aggregates temperature is determined by the emission intensity ratio at two different wavelengths, namely 400 nm and 460 nm.

3. Results and discussion

Single-shot particle aggregates temperature measurement was performed at 7 different heating fluxes. For each flux, 300 images were recorded by the ICCD camera during the heating period. Figure 1 presents the typical example of particle aggregates temperature derivation. Column A and column B are the individual particle aggregates images taken with the 400 ± 20 nm filter and 460 ± 7 nm filter respectively, while column C shows the inferred particle temperature. The final temperature distribution of particle aggregates is obtained by dividing the intensity on two sub-images pixel-by-pixel using MATLAB code.

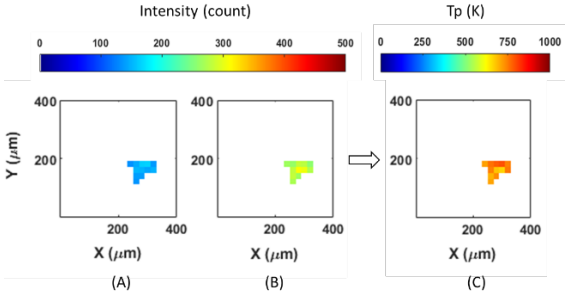

Figure 1: Example of single shot aggregates temperature distribution images deriving from two raw sub-images

Figure 2(a) presents the example of aggregates temperature distribution over 300 images, while Figure 2(b) shows the average aggregates temperature at 7 different fluxes. The average aggregates temperature has the linear increasing trend. As heat flux increasing, the maximum BAM average temperature is achieved more than 700 K when the heat flux at 27.28 MW/m².

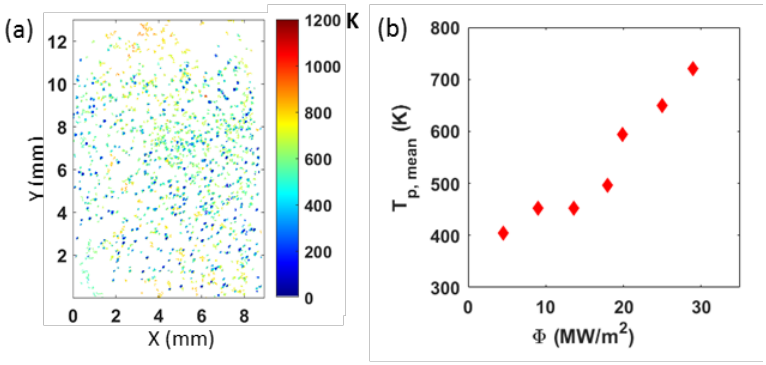

Figure 2: (a) Real particle aggregates temperature distribution in measurement area by overlap particles over 300 images at heating flux of 24.97 MW/m². (b) Mean BAM particle aggregates temperature at various heat fluxes

4. Conclusions

Real-time planar temperature measurement of fluidized BAM aggregates was performed by planar laser induced phosphorescence (PLIP) technique with using a single ICCD camera and imaging split system. Averaged particle aggregates temperatures were compared at several fluxes. At the highest heating flux, the average aggregates temperature was increased to more than 700 K.

References

[1] W. Lipiński, J.H. Davidson, S. Haussener, J.F. Klausner, A.M. Mehdizadeh, J. Petrasch, A. Steinfeld, L. Venstrom, Journal of Thermal Science and Engineering Applications 5 (2013) 021005-021014.

[2] M. Aldén, A. Omrane, M. Richter, G. Särner, Progress in Energy and Combustion Science 37 (2011) 422-461.

[3] Z. T. Alwahabi, K. C. Kueh, G. J. Nathan, and S. Cannon, Opt Express 24 (2016) A1444-A1453.

ECCE12
The 12th EUROPEAN CONGRESS OF CHEMICAL ENGINEERING
Florence 15-19 September 2019

Numerical simulations supporting process models of chemical engineering: applications for membrane systems.

Luigi Gurreri[1]*, Imen El Mokhtar[2], Salah Al Tahar Bouguecha[2], Mariagiorgia La Cerva[1], Alessandro Tamburini[1], Andrea Cipollina[1], Michele Ciofalo[1], Giorgio Micale[1]

1 Dipartimento di Ingegneria, Università degli Studi di Palermo, viale delle scienze ed. 6, 90128 Palermo, Italia; 2 Water, membrane and environmental biotechnology laboratory, Water Researches and Technologies Center, Borj-Cedria Technopark Tourist Route of Soliman Nabeul, 8020 Soliman, Tunisia

**Corresponding author: luigi.gurreri@unipa.it*

Highlights

- Spacer features affect significantly transport phenomena.
- Electrical resistance and deformation can be effectively predicted.
- Results are easily integrated in multi-scale process models.

1. Introduction

In the last years, the scientific community has been exhibited a growing interest towards several separation processes based on membrane technologies. For the development of novel and optimized designs, the implementation of robust and reliable process models is a challenge. An effective modelling strategy, able to provide accurate predictions with a sustainable computational demand, is represented by a multi-scale modelling approach [1]. In a structured separation of scales, numerical simulations analyze in detail transport phenomena at the lowest scale of modelling and provide correlations to the higher scale models, which simulate the whole membrane/channel assembly, unit and plant.

This work presents computational fluid dynamics simulations aimed at characterizing flow and mass/heat transport mechanisms in spacer-filled channels for membrane processes, with particular reference to (reverse) electrodialysis and membrane distillation. Further kinds of numerical simulations were performed in order to assess aspects poorly studied so far, i.e. electrical "shadow" effects of spacers and membrane deformations.

2. Methods

Spacer-filled channels and profiled-membrane channels were simulated by the periodic unit cell approach, i.e. assuming fully developed conditions. The basic set of differential equations includes continuity and Navier-Stokes equations, transport of enthalpy and convective-diffusive transport of solute. Equilibrium, compatibility and constitutive equations were solved in simulations aimed at finding configurations deformed under an imposed load mimicking a trans-membrane pressure. Finally, the Laplace equation for the electric potential was solved in simulations assessing the Ohmic resistance. Grid-sensitivity of results was assessed, in order to present results practically unaffected by the discretization degree. The finite-volume Ansys-CFX code and the finite-element Ansys-Mechanical code were used.

3. Results and discussion

Dimensionless quantities were computed from CFD simulation results, namely Darcy friction factor (*f*), Sherwood number (Sh) and Nusselt number (Nu). Figure 1 reports some typical results for different configurations. It can be observed that woven spacers enhance mass/heat transfer compared to overlapped spacers, but at the expense of larger pressure drops. The *P/H* value has straightforward effects only in the case of woven spacers. SST *k-ω* turbulence model predictions for non-steady flows fairly agree with laminar simulation trends, but direct numerical simulations would be more appropriate for incipient turbulence regimes. Nu and *f* predictions were validated against experimental data and exhibited a good agreement.

Significant effects of membrane deformation were observed: friction and mass transfer coefficients increased in the compressed channel, while they decreased in the expanded channel.

The spacer shadow factor for the Ohmic resistance was found to be close to the reciprocal of the average between porosity and open area, in agreement with experimental findings.

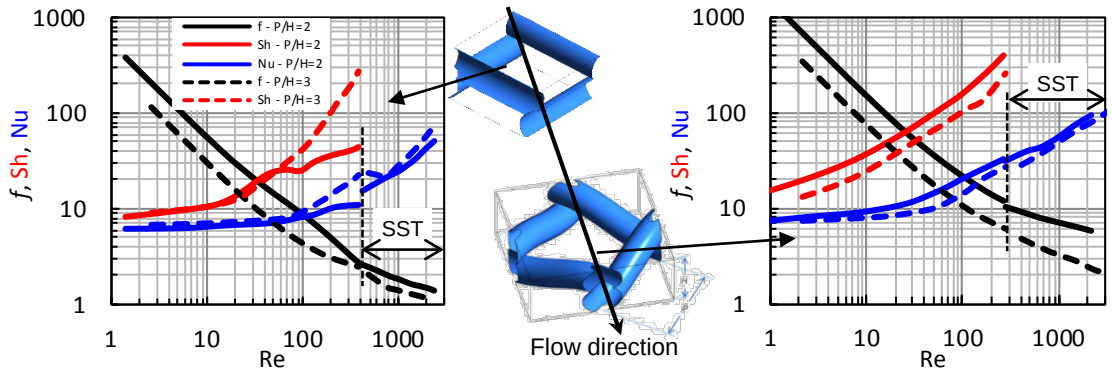

Figure 1. *f*, Sh and Nu in spacer-filled channels as functions of the Reynolds number (Pr=4.33, Sc=600).

4. Conclusions

Simulation tools implementing well-established and validated physical models and numerical methods were presented. CFD predictions showed that spacer features can significantly affect flow and heat/mass transfer characteristics. Novel models showed to be effective in the simulation of aspects poorly investigated so far, such as the mechanical response and the electrical resistance.

The present outcomes provide correlations to integrated process simulators in order to calculate pressure drop, temperature/concentration polarization effects, electrical resistance and fluid-structure interactions. The present numerical simulations represent basic predictive tools for optimization studies and for the development of novel designs and concepts.

Acknowledgments

This work has been performed within the REvivED water project (*Low energy solutions for drinking water production by a REvival of ElectroDialysis systems*), Horizon 2020 programme, Grant Agreement no. 685579, www.revivedwater.eu.

References

[1] A. Campione, L. Gurreri, M. Ciofalo, G. Micale, A. Tamburini, A. Cipollina, Desalination 434 (2018) 121–160.

ECCE12
The 12th EUROPEAN CONGRESS OF CHEMICAL ENGINEERING
Florence 15-19 September 2019

Investigating Coarse-Graining Effects on CFD-DEM Simulations of Fluidized and Spouted Bed Reactors

Thomas Eppinger[1], Nico Jurtz[2], Felix Klippel1, Leonard Becker1, Oleh Baran[3], Ravindra Aglave[3], Matthias Kraume[2]

1 Siemens Industry Software GmbH, Nürnberg, Germany; 2 Berlin Institut of Technology, Chair of Chemical & Process Engineering, Berlin, Germany; 3 Siemens PLM, Houston, TX, USA
**Corresponding author: Thomas.eppinger@siemens.com*

Highlights

- Effect of different coarse-graining methods and factors are investigated
- Comparison against experimental data shows good agreement with averaged quantities
- Differences in the dynamic behavior are quantified

1. Introduction

Since its introduction [1], the Discrete Element Method (DEM) has proven to be a valuable method for the analyzing and understanding particulate flows. Supported by the continuously increasing computational power, CFD-DEM simulations have found their way into the chemical and process industry for various applications like solid suspension in mixing vessels, fluidized and spouted beds, granular transport and coating applications in rotary drums [2,3].

The major shortcoming of DEM, however, is its computational cost that increases with the amount of particles involved, their material properties (stiffness) and size. This hinders the application of CFD-DEM simulation to large-scale systems of industrial size. To overcome this shortcoming a coarse grain (CG) model has been described [4]. Using straightforward scaling rules, a group of particles gets replaced by a representative coarse parcel. This effectively reduces the number of particles that need to be processed and subsequently shortens the computational time. On the other hand they introduce a modeling error into the simulation. In this study we are investigating different coarse graining models and quantify the effect on different parameters and their fluctuation like pressure drop and expansion height in a fluidized and spouted bed.

In this work two different contact scaling methods are examined for a fluidized and for a spouted bed reactor. The results are compared against experimental results and against a DEM simulation without coarse graining.

2. Methods

In this investigation the software tool Simcenter STAR-CCM+ was used for the coupled CFD-DEM simulation. The built-in DEM solves for each particle Newton's law of motion in each time step. The particle-particle and particle-wall interaction is taken into account based on Hertz-Mindlin model (spouted bed) or the linear-spring-dashpot model (fluidized bed). Momentum exchange between the background gas phase and the DEM particles is calculated based on Gidaspow drag model and

three different coarse graining (CG) approaches were used: Particle-based CG with l3-scaling, Parcel-based CG with l3-scaling and Parcel-based CG with l2-scaling.

3. Results and discussion

Exemplarily the results for the fluidized bed are shown here, but similar results were also found for the spouted bed. Figure 1 shows a snapshot in time of the different CG methods. In general it can be stated that bed expansion and pressure drop are well predicted for all investigated CG methods, but depending on the CG factor the dynamic of the system cannot be captures which can be seen in Figure 2 as deviations in the RMS values for the respective parameter.

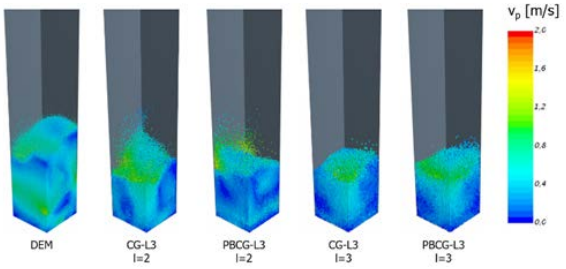

Figure 1. Comparison of the particle dynamics for different CG methods

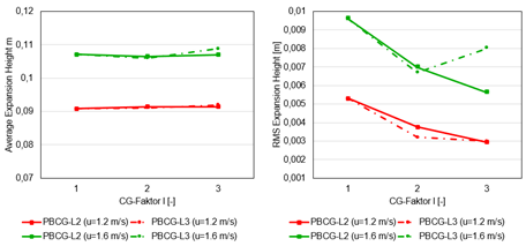

Figure 2: Average and RMS expansion height for different CG methods

4. Conclusions

Coarse-graining is a promising method to increase the number of particles in CFD-DEM simulations and simultaneously reducing the runtime by orders of magnitude. The predictivity is slightly affected in terms of the particle dynamics while overall properties are still predicted accurately in the investigated CG range.

References

[1] P.A. Cundall, O.D.L. Strack, Geotechnique, 29 (1979), 47

[2] T. Eppinger, O. Baran, R. Aglave, S. Lo, Simulating Solid Suspension in Stirred Vessels with a Fully Coupled CFD-DEM Algorithm (161d), AIChE Annual Meeting 2017, Minneapolis

[3] O. Baran, R. Aglave, M. Tandon, A. Karnik, S. Lo, Numerical Simulation of Dense Gas-Solid Fluidized Beds: Comparison Between Eulerian Multiphase and Discrete Element Methods, AIChE Annual Meeting 2015, Salt Lake City, UT.

[4] M. Sakai, Y. Yamada, Y. Shigeto, K. Shibata, V.M. Kawasaki, S. Koshizuka, Numerical Methods in Fluids 64 (2010), 1319

[5] V. Salikov, V., S. Antonyuk, S. Heinrich, V.S. Sutkar, N.G. Deen, J.A.M. Kuipers, Pow. Tech.270 (2015), 622

ECCE12
The 12th EUROPEAN CONGRESS OF CHEMICAL ENGINEERING
Florence 15-19 September 2019

Advection-dominated reactive species transport at fluid interfaces via data-driven Subgrid-scale modeling

Andre Weiner[1], Dennis Hillenbrand[1] , Holger Marschall[1] , Dieter Bothe[1]*

1 Institute for Mathematical Modeling and Analysis, TU Darmstadt

Alarich-Weiss-Straße 10, 64287 Darmstadt

**Corresponding author: bothe@mma.tu-darmstadt.de*

Highlights

- Subgrid-scale modeling for reactive concentration boundary layers
- Data-driven approach for approximate functions
- Significant reduction of mesh resolution and computation time

The transport of chemical species close to the gas-liquid interface of a rising bubble is typically characterized by strong advection along the interface and molecular diffusion normal to it. Consequently thin boundary layers form, which have to be resolved in numerical methods to evaluate local reaction-engineering quantities like enhancement factor, selectivity or yield accurately. In [1,2] we introduced a non-reactive subgrid-scale (SGS) model that mitigates this high-Schmidt-number problem significantly. This model was used successfully in [3] to validate numerical simulations against experimental results of species transport at small rising bubbles. The basic idea is to derive an analytical solution for a substitute problem which describes the main features of an advection-dominated boundary layer. This analytical solution is used to correct diffusive and convective fluxes in interface cells of the numerical simulation.

However, in the general case of reactive boundary layers it is not possible to derive closed-form solutions. Our new approach to extend the SGS modeling for reactive systems is based on a machine-learning algorithm which represents an approximate solution of the substitute problem over a chosen range for characteristic parameters like Peclet or Damkohler numbers. The machine learning algorithm - a multi-layer-perceptron - has adjustable weights which are optimized to reflect the numerical input data. As before, the approximate solution is used to correct the numerical fluxes near the interface in simulations. This approach was validated for the transport of a specie from a rising axisymmetric bubble followed by a first-order decay reaction in [4]. Figure 1 shows the improvement of the species transport via the local Sherwood number profile along the polar angle of the bubble. The flux corrections from the data-driven SGS model enable the representation of the reference profile even for coarse meshes. Additionally, the evaluation of the data-driven SGS model produces almost no computational overhead. This results in a significant reduction of computation time while introducing an error of less than 5% for the overall species transport. Due to the flexibility of this approach it can be adjusted to the required parameter ranges and extended to more complex reaction systems.

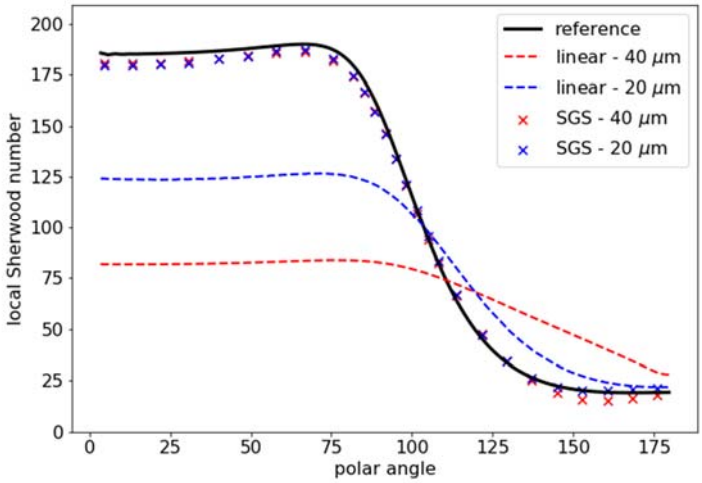

Figure 1. Local Sherwood number profiles for coarse meshes with and without using the SGS model.

References

[1] C. Pesci, A. Weiner, H. Marschall, D. Bothe, Computational analysis of single rising bubbles influenced by soluble surfactant, Journal of Fluid Mechanics, vol. 856, (2018), 709–763.

[2] A. Weiner, D. Bothe, Advanced subgrid-scale modeling for convection-dominated species transport at fluid interfaces with application to rising bubbles, J. Comput. Phys., 347, (2017), 261-289.

[3] A. Weiner, J.Timmermann, C. Pesci, J. Grewe, M. Hoffmann, M. Schlüter, D. Bothe, Experimental and numerical investigation of reactive species transport around a small rising bubble, arXiv e-prints, p. arXiv:1811.03851, Nov. 2018

[4] A. Weiner, D. Hillenbrand, H. Marschall, D. Bothe, Data-driven subgrid-scale modeling for convection-dominated reactive boundary layers, submitted 2019

ECCE12
The 12th EUROPEAN CONGRESS OF CHEMICAL ENGINEERING
Florence 15-19 September 2019

Unconventional pressure dependence of Ibuprofen solubility in binary mixture of water and organic solvent

Mirko D'Auria[1], Andreas S. Braeuer[1*]

1 Institute of Thermal-, Environmental-, and Resources' Process Engineering (ITUN), Technische Universität Bergakademie Freiberg (TUBAF), 09599 Freiberg, Germany

**Andreas.Braeuer@tu-freiberg.de*

Highlights

- Solubility of Ibuprofen at elevated pressures
- Hydrogen bond network

1. Introduction

Unexpectedly we found that the solubility of Ibuprofen, a hydrophobic compound, in mixtures of water and organic solvent can increase with increasing pressure. This behaviour can be exploited for particle precipitation strategies that are based on a rapid pressure changes.

We therefore characterized the solubility of ibuprofen in binary mixtures of water and organic solvent (here acetone and acetonitrile) up to 20 MPa. The obtained results are interpreted based intermolecular interactions revealed using Raman spectroscopy and on thermodynamic considerations revealed by measuring the partial molar volumes of the solvents and the dissolved ibuprofen.

This kind of binary mixtures also show an ambiguous behaviour in the hydrogen bond network that changes with temperature and pressure. According to "iceberg theory", water and organic solvent molecules can organise themselves creating regions rich and others poor in water.

2. Setup

For the determination of the solubility data at high pressure, the setup consists of a high pressure variable volume view cell (HPVVVC), where pressure can be fixed by increasing/decreasing the volume and temperature can be adjusted by a heating system.

3. Conclusion

We aim to contribute with this study in the implementation of a precipitation process by pressure variation.

Acknowledgement
The project leading to this contribution has received funding from the European Union's Horizon 2020 research and innovation programme under ERC Starting Grant agreement No. 637654 (Inhomogeneities).

ECCE12
The 12th EUROPEAN CONGRESS OF CHEMICAL ENGINEERING
Florence 15-19 September 2019

Modelling of binary nucleation in Laminar Co-Flow Tube.

Tereza Trávníčková[1], Jaromír Havlica[1,2], Jan Hrubý[3], Vladimír Ždímal[4]

1 Institute of Chemical Process Fundamentals of the CAS, v. v. i., Department of Multiphase Reactors, Prague, Czech Republic; 2 University of Jan Evangelista Purkinje, Ústí nad Labem, Czech Republic; 3 Institute of Thermomechanics of the CAS, v. v. i., Department D 2 - Thermodynamics, Prague, Czech Republic; 4 Institute of Chemical Process Fundamentals of the CAS, v. v. i., Department of Aerosols Chemistry and Physics, Prague, Czech Republic

**Corresponding author: travnickovat@icpf.cas.cz*

Highlights

- Binary nucleation of H_2SO_4 and H_2O
- Measuring at Laminar Co-Flow Tube.
- Numerical and analytical models comparison.

1. Introduction

Particle nucleation is one of the important phenomena encountered in both chemical engineering and environmental studies. The Laminar Co-Flow Tube (LCFT) was designed for experimental measurement of binary and ternary nucleation of mixtures of atmospheric aerosols at laboratory conditions, most often H_2SO_4 + H_2O + amines (MEA, TEA)/terpenes (α-pinene, limonene). When nucleating components are entrained co-currently with H_2S0_4 in the axial flow, a clearly defined nucleation zone can be formed in the axial region of the chamber. As a result, the losses of the formed particles on the device walls are minimized. Laminar flow allows mathematical modeling of velocity and partial pressure profiles in the chamber. From these, it is then possible to predict the shape and size of the nucleation zone and subsequently the nucleation rate. Two models were used for mathematical modeling of momentum and mass transfer in the LFDC; 2D axisymmetric CFD model and simplified 1D analytical model. A parametric study was carried out using both models and the influence of the individual simplifications of analytical model on overall behavior of the system was discussed.

2. Methods

The measurement of H_2SO_4 nucleation with water vapor using LCFT is described in detail in publication [1]. The LCFT device consists of two coaxial tubes. A mixture of nitrogen (inert gas) with sulfuric acid is led into the inner tube. A nitrogen mixture with water vapor flows parallel within the inner and outer tube annulus. When laminar profiles are developed, axial flow merges with the annular one. The magnitudes and ratio of flow rates are set, so that the flow remains laminar after opening of the inner tube and both mixtures are in diffusional contact. When the concentrations of H_2SO_4 and water vapors are sufficiently high, in the nucleation zone, stable clusters are formed at a nucleation rate *J*. The nucleated particles grown to detectable size are counted by PSM (Particle Size Magnifier) counter.

To obtain nucleation isotherms, the experimental measurements were supplemented with numerical CFD simulations. 2D axisymmetric CFD model solves Navier-Stokes equations with equation of continuity and component mass balance equations. Simplified analytical 1D model assumes uniform (plug flow) velocity profile and negligible diffusion in axial direction. For nucleation rate modeling, a model of Wyslouzil et al. was used [2]. All results were normalized for relative humidity *Rh* = 0.38.

3. Results and discussion

The resulting nucleation isotherms obtained by experiment and subsequent modeling using the numerical model (v_z=$v_z(r)$) and analytical model with three different choices of plug flow velocities v_z=v_{avg} (average val. of radial laminar vel. profile), v_z=v_{max} (maximum of radial vel. profile in co-flow section), v_z=$v_{i,max}$ (maximum of inner tube radial vel. profile) are clearly illustrated in the figure 1.

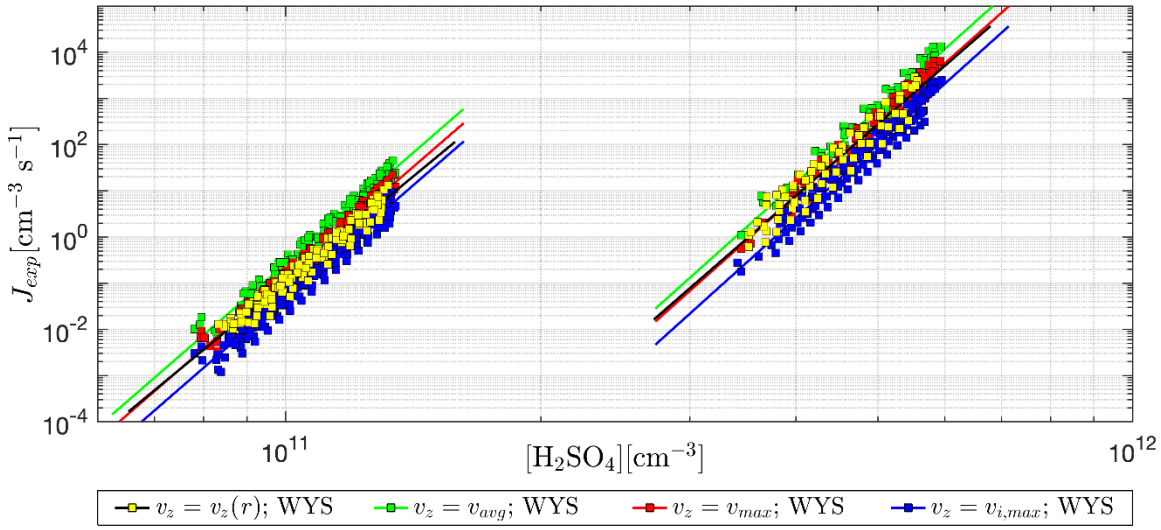

Figure 1. Comparison of nucleation isotherms 15 and 27°C computed by CFD numerical model v_z=$v_z(r)$ and analytical model with different plug flow velocities: v_z=v_{avg}, v_z=v_{max} *and* v_z=$v_{i,max}$.

Deviations in the maximal experimental nucleation velocity are caused by different modeling of gas flow in the region of nucleation zone. For most of our experimental flow rate settings, plug flow rate $v = v_{max}$ is the best choice, when the experimental nucleation rate can be underestimated down to 0.3 times and overestimated up to 2.3 times in comparison to 2D axisymmetric numerical model.

4. Conclusions

By appropriately selecting value of the plug flow rate in the analytical model, it is possible to achieve, that the location and shape of the nucleation zone will be similar and also the resulting nucleation rates will be estimated with sufficient precision. Usage of the analytical model is suitable for this type of nucleation experiments with the advantage of a significant saving the computing time.

Acknowledgement: This work was supported by the Czech Science Foundation [grant number 17-19798S]

References

[1] T. Travnickova, L. Skrabalova, J. Havlica, P. Krejci, J. Hruby, V. Zdimal, Tellus B, 70 (2018).
[2] B.E. Wyslouzil, J.H. Seinfeld, R.C. Flagan, K. Okuyama, J. Chem. Phys., 94 (1991) 6842-6850.

ECCE12
The 12th EUROPEAN CONGRESS OF CHEMICAL ENGINEERING
Florence 15-19 September 2019

Effects of flow structure on mixing related processes.

Jerzy Bałdyga* Michał Kotowicz

1Faculty of Chemical and Process Engineering, Warsaw University of Technology, ul. Waryńskiego 1, 00-645 Warsaw, Poland
** jerzy.baldyga@pw.edu.pl*

Highlights

- Effects of flow structure on mixing, mass transfer and emulsion behavior are considered.
- The rate-of-strain and rate-of-rotation tensors characterize flow structure.
- The invariants of the rate-of-strain and rate-of-rotation tensors are used in modeling.

1. Introduction

Details of micro- and meso-scale flow structures affect the course of many processes of industrial importance. Most often effects of hydrodynamics on processes and products are expressed in terms of such variables like the rate of energy dissipation or the Reynolds number.
Objectives of this work are to characterize the flow structure and show its effect on micromixing in single-phase systems and mass transfer in two-phase systems. Also effects of flow structure on drop breakup and rheolology of dense emulsion will be briefly considered.
A difference in breaking droplets in simple shear and hyperbolic flows is well known. It has been often interpreted and generalized using a simple two-dimensional linear flow approximation [1].

$$\mathbf{S}=\frac{G}{2}\begin{bmatrix}1+\alpha & 0 & 0\\ 0 & -1-\alpha & 0\\ 0 & 0 & 0\end{bmatrix}\quad \mathbf{\Omega}=\frac{G}{2}\begin{bmatrix}0 & 1-\alpha & 0\\ -1+\alpha & 0 & 0\\ 0 & 0 & 0\end{bmatrix} \tag{1}$$

where **S** and **Ω** are the deformation and rotation tensors**,** *G* is the scalar velocity gradient, and *α* determines the flow type: *α* = 0 for simple shear flow, *α* = 1 for plane hyperbolic flow and *α* = -1 for pure rotation.

2. Models for flow structure dependent processes.

In 3D flows instead of eq.(1) one can characterize the flow using the second invariants of the rate-of-strain tensor II_D and the rate-of-rotation tensor II_Ω, ω_i being component of vorticity vector :

$$II_D=-\frac{1}{2}S_{ij}S_{ij}=\frac{1}{2}\left[\left(S_{ii}\right)^2-\left(S_{ii}^2\right)\right]\quad II_\Omega=\frac{1}{2}\Omega_{ij}\Omega_{ij}=\frac{1}{4}\omega_i\omega_i \tag{2}$$

The second invariant II_D characterizes deformation rate and is proportional to the local rate of viscous dissipation of kinetic energy. In turbulence, high values of viscous dissipation are concentrated in sheet-like and ribbon-like structures. II_Ω is proportional to the enstrophy density (enstrophy is the integral of the square of vorticity). In turbulent flows regions of high enstrophy form tube-like structures. Both, deformation and rotation affect micromixing rate [2] and micromixing efficiency [3]. In Figure 1 relative energetic efficiency is presented for the flow defined as elongation in direction 1 and contraction in directions 2 and 3 $\gamma_1'=\alpha'\cdot s=\alpha'\cdot\left(\varepsilon_T/(3\nu)\right)^{1/2}$ and $\gamma_2'=\gamma_2'=-(1/2)\alpha'\cdot s=-(1/2)\alpha'\cdot\left(\varepsilon_T/(3\nu)\right)^{1/2}$ and including effect of Sc; here α' represents effect of reduction of deformation due to rotation effect. In fact α' is similar to the energetic efficiency by Ottino [4].

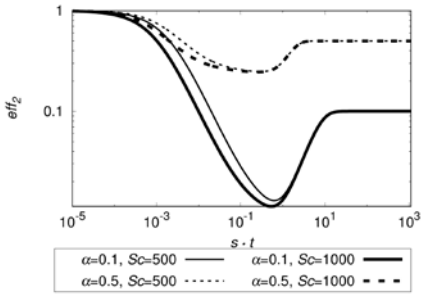

Figure 1. Effect of deformation rate *s* and Schmidt number on relative efficiency of mixing in 3-dimensional flow

In typical models of mass transfer between droplets and continuous phase, the Sherwood number is proportional to $Pe^{1/2}$ with coefficients of proportionality dependent of flow structure. More universal approach, including application of the second invariant, was proposed by Polyanin [5].

$$Sh = \frac{k_L d}{D} = 0.620\left(\frac{1}{K+1}\right)^{1/2} Pe^{1/2}; \quad Pe = \frac{d^2\sqrt{|II_D|}}{D} \tag{3}$$

where *K* represents the viscosity ratio μ_d/μ_c and *D* is the coefficient of molecular diffusion.
However, this approach neglects effects of rotation on mass transfer coefficient. Batchelor [6] has shown that for solid particles at high *Pe* the Sherwood number depends on the ratio of extension rate to rotation rate, s_1/Ω; for small s_1/Ω it affects the Sherwood number for any value of the Péclet number and becomes asymptotically independent of s_1/Ω at high values of this ratio. A real challenge is to generalize this effects by using the second invariants of the rate-of-strain tensor and the rate-of-rotation tensor. At present we can show that for high *Pe* and high II_Ω/II_D the region of closed streamlines around a droplet across which the transfer by molecular diffusion takes place becomes a shell of thickness proportional to $R\cdot\left(II_\Omega/II_D\right)^{1/2}$. Hence, the external mass transfer coefficient can be expressed as $k_L \propto DR^{-1}\cdot\left(II_D/II_\Omega\right)^{1/2}$. As $II_D/II_\Omega \to \infty$ the values to which the mass transfer coefficient tends are $k_L \propto D^{1/2}\left(K+1\right)^{-1/2}\left(II_D\right)^{1/4}$.
Application of both second invariants enables description of drop breakage in 3D laminar flows of emulsions, extension to turbulence and linking to CFD. Rheology of dense emulsions depends on the maximum packing volume fraction that increases with increased deformation of droplets.

3. Conclusion

It has been shown that flow structure affects several chemical engineering processes. A possible way to model these effects is to use the second invariants of the rate-of-strain tensor and the rate-of-rotation tensor. Examples of new results based on proposed approach are presented.

The authors acknowledge the financial support from Polish National Science Centre (Grant agreement number: UMO-2017/27/B/ST8/01323)

References

[1] J. M. Rallison, Ann. Rev. Fluid Mech. 16 (1984) 45-66.
[2] J. Baldyga, J.R. Bourne, Turbulent Mixing and Chemical Reactions. Wiley, Chichester, 1999.
[3] J. Bałdyga, M. Jasińska, Chem. and Process Eng. 38 (2017) 433-444.
[4] J.M. Ottino, Chem. Eng. Sci. 35 (1980) 1454–1457.
[5] A.D. Polyanin, Zhurnal Prikladnoi Mekhaniki i Tekhnicheskoi Fiziki, 4 (1984)71-81.
[6] G.K Batchelor, J . Fluid Mech. 95(2) (1979) 369-400.

ECCE12
The 12th EUROPEAN CONGRESS OF CHEMICAL ENGINEERING
Florence 15-19 September 2019

Energy and Chemical Engineering

Impact of variation of rheological properties on pressure drop calculation

Ehsan Farno[1], Nicky Eshtiaghi[1,*]

1 Chemical and Environmental Engineering, School of Engineering, RMIT University, VIC, 3000, Australia

**Corresponding author: nicky.eshtiaghi@rmit.edu.au*

Highlights

- Impact of variation of rheological properties on pressure drop calculation
- Adopted Re3 friction loss model from mineral industries into sewage sludge

1. Introduction

Wastewater treatment is an integral part of the sustainable development of modern cities. Factors such as population growth, water shortage and stricter environmental regulations demand a considerable increase in increasing the capacity of treatment plants as well as improving its efficiency [1].

A large portion of the total energy consumption in wastewater treatment plants is used for pumping wastewater sludge within the treatment processes [2]. Although the energy usage of the sludge transportation systems is critically important, pumping systems are not commonly operating in their best efficiency points. By improving the pumping systems, better energy efficiency of treatment processes can be achieved. Several reasons underlies the inefficient operation of sludge pumping systems. One of them is the variation of sludge rheology which sometimes can be an order of magnitude difference. It is vitally important to identify the impact of rheological variations on the variation in pressure drop of sludge pipeline to be designed. This is even more important for concentrated sludge as it is highly non-Newtonian and, because of that, the pressure drop is more sensitive to the variation of rheological parameters. This paper investigates the impact of variation of sludge rheology on the calculation of pressure drop for highly concentrated sludge pipeline.

2. Methods

Digested sludge was collected at the concertation of about 2% from Eastern Treatment Plant, Melbourne over one year. Sludge was concentrated to 4% and 5.5% using vacuum filtrations process. Samples flow curve was measured using controlled-stress rheometer equipped with a cup-and-bob (with 1 mm gap) and a vane-and-rough cup (with 8 mm gap) geometries for dilute and concentrated sludge, respectively. Flow curve was fitted with the Herschel-Bulkley model using the robust least-squares method of MATLAB.

3. Results and discussion

Figure 1.a depicts the variation in rheological parameters of sludge over the measurement period. And Figure 1.b shows the variation in calculated pressure drop for a typical sludge pipeline resulted from the variation of rheological parameters.

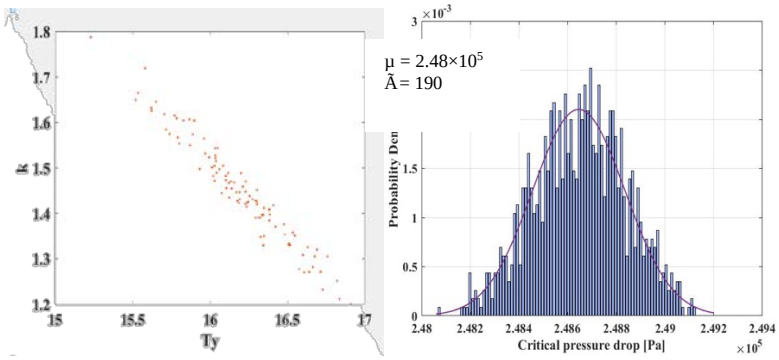

Figure 1. (a) Variation in rheological parameters of sludge (b) variation in calculated pressure drop

Table 1 presents a sensitivity analysis of the pressure drop calculation procedure in respect to variation in the model parameters. As shown in Table 1 [3], pressure drops were mostly correlated to the variation of *k* while variation in τ_H was the least influential factor on the calculated pressure drop.

Table 1. sensitivity analysis of pressure drop calculation procedure

Model parameter	τ_H	*k*	*n*
Sensitivity	*5%*	*60%*	*33%*

Table 2 shows variations of pressure drop as a results of increasing solid concentration. This is almost four times when solid content of sludge increases from 2.3% to 4% and it is doubled for increase of solid content from 4% to 5.5%. Besides, the flow regime will change from turbulent to laminar as Reynolds number drops to below 1600 and 800 for 4% and 5.5% digested sludge, respectively.

Table 2. variation in calculated pressure drop [kPa] for the nominated pipeline

TS	24.6 L/s	40.8 L/s	$Reynolds_3$*
2.3%	263 ±50	263 ±50	8500 - 20000
4%	1041 ±80	1041 ±80	300 - 1600
5.5%	1914 ±100	2034 ±100	150 - 800

4. Conclusions

Results compare the variation in the calculated pressure drop between different sludge concentrations. This study shows that a small variation in rheological parameters of concentrated sludge creates large variations in pressure drop calculation. This variation needs to be considered for the accurate design of sludge pipelines.

References [Calibri 10]

[1] Munro-Smith, H. (2018). IBISWorld Industry Report Waste Treatment and Disposal Services in Australia.

[2] Longo, S., B. M. d'Antoni, M. Bongards, A. Chaparro, A. Cronrath, F. Fatone, J. M. Lema, M. Mauricio-Iglesias, A. Soares and A. Hospido (2016). "Monitoring and diagnosis of energy consumption in wastewater treatment plants. A state of the art and proposals for improvement." Applied Energy 179: 1251-1268.

[3] Farno, E., K. Coventry, P. Slatter and N. Eshtiaghi (2018). "Role of regression analysis and variation of rheological data in calculation of pressure drop for sludge pipelines." Water Research 137: 1-8.

ECCE12
The 12th EUROPEAN CONGRESS OF CHEMICAL ENGINEERING
Florence 15-19 September 2019

Comparison between a Rocking and a Stirred Bioreactor Concerning Particle Stress in a Liquid-Liquid Model System

Robert Panckow[1]*, Chrysoula Bliatsiou[1], Lutz Böhm[1], Michael Muthig[2], Sebastian Maaß[2], Matthias Kraume[1]

1 Chair of Chemical and Process Engineering, Technische Universität Berlin, Fraunhoferstr. 33-36, 10587 Berlin, Germany; 2 SOPAT GmbH, Boyenstraße 41, 10115 Berlin

**Corresponding author: panckow@tu-berlin.de*

Highlights

- Mixing concept determines hydro-mechanical stress on particles in bioreactors.
- Liquid-liquid model system substitutes biological system.
- New image analysis by neural networks provides faster and more accurate results.
- Particle analysis tool provides distinction between different disperse phases.

1. Introduction

High mechanical power input to achieve fast heat and mass transfer can damage a present disperse phase, with cells and cell agglomerates being of interest in biotechnology. An efficient mixing system which gives even suspension with gentle stirring and does not generate high shear forces results in a homogeneous culture environment. In this study, fluid-mechanical particle stress is characterized by application of a two-phase model system with liquid disperse phase.

2. Methods

Comparatively, the investigations were carried out in a rocking single-use bioreactor (CELL-tainer® 20L, Celltainer Biotech BV) and in a DN160 stirred tank with torispherical bottom, see **Fig. 1**.

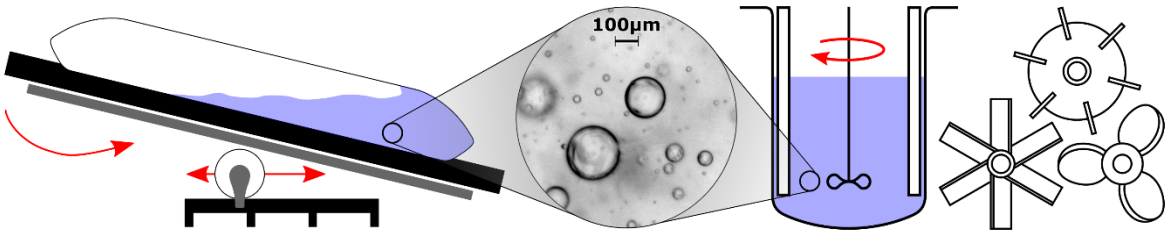

Figure 1. Motion concept of CELL-tainer® 20L (left), recording of drop sizes (middle), DN160 stirred tank with torispherical bottom (right).

The disperse droplet phase consisted of Mobil EAL Arctic 22 refrigerator oil having a density similar to the continuous phase [1]. By variation of working volume V, rotational frequency k and rocking angle φ (CELL-tainer) as well as stirrer geometry and stirrer frequency n (stirred tank), the droplet sizes of the disperse phase were recorded in situ by means of photo-optical particle analysis technology from SOPAT GmbH [2, 3], see **Fig. 1** (middle). Measurement of the two-dimensional raw image data by automated image analysis provided the droplet size distribution. New

implementations of image analysis algorithms based on neural networks yielded faster and more precise size measurements with classification of the detected particles.

The fluid dynamic investigations by particle image velocimetry (PIV) in the stirred vessel and by computational fluid dynamics (CFD) for both reactors support the understanding of the experimentally determined droplet breakage. In the stirred vessel, only the liquid phase was modeled, whereas in the CELL-tainer simulations the volume of fluid (VOF) method was applied to describe the two-phase flow. For both reactors, the RANS-based k-ε turbulence model was used. The velocity vector fields provide the basis for a coordinate transformation towards the flow direction along the streamlines to calculate shear and elongation gradients.

3. Results and discussion

The droplet breakage caused by different wave motion due to various operating points in the CELL-tainer and by the investigated stirrers in the stirred tank was monitored for the model system. The dynamic destruction kinetics were recorded, with the steady-state droplet diameter characterizing the particle stress. Noticeable, the measured drop sizes in the CELL-tainer show higher values as compared to the stirred tank for the investigated range of operating conditions and thus, indicate less particle stress. For the comparison of different stirrer geometries, axial stirrers show higher droplet breakage than radial pumping ones.

4. Conclusions

Due to the high sensitivity of the photo-optical measurement system, a precise differentiation of operating points was possible. The new algorithms could not only detect the desired droplets, but also were able to distinguish between different dispersed phases, for example disturbing bubbles. The dynamic destruction kinetics for different operating points of both reactor types in combination with the particular flow fields give new insights into the transferability of cell cultivation between the two reactor types.

References

[1] S. Wollny, R. Sperling, Partikelbeanspruchung in gerührten Behältern. Chem. Ing. Tech. 79 (3), 2007, pp. 199–208.

[2] Maaß et al., Automated Drop Detection Using Image Analysis for Online Particle Size Monitoring in Multiphase Systems. Comput. Chem. Eng. 45, 2012, pp. 27–37.

[3] Panckow et al., Determination of Particle Size Distributions in Multiphase Systems Containing Nonspherical Fluid Particles, Chem. Eng. Technol. 38 (11), 2015, pp. 2011–2016.

ECCE12
The 12th EUROPEAN CONGRESS OF CHEMICAL ENGINEERING
Florence 15-19 September 2019

Effect of bubble dynamics and bubble induced turbulence (BIT) on chemically reacting bubbly flows

Manuel Taborda, Martin Sommerfeld

Multiphase Flow Systems, Institute for Process Engineering, Otto-von-Guericke-University Magdeburg; Zeppelinstraße 1, 06130 Halle (Saale), Germany

**Corresponding author: e-mail: manuel.taborda@ovgu.de*

Highlights

- Point-particle Euler/Lagrange method for reacting bubbly flows.
- Tumbling bubble rise model and shape oscillations.
- Sub-grid-scale Turbulence modification modeling.
- Validation for single bubble rise with mass transfer.
- Validation for a laboratory column with chemisorption of CO_2 in NaOH solution.

1. Introduction

Bubble columns as multiphase reactors are commonly used in industry since they yield a high contact area, which affects directly the required mass transfer. Nevertheless, the flow structure and bubble behaviour are very complex so that appropriate modelling in the frame of numerical calculations is still today a challenge, especially when mass transfer and chemical reactions are involved. Bubbles from a certain size show oscillations in the shape and a zig-zag/helical motion, which cannot be captured by classical Lagrangian models anymore. In order to do so, the bubble dynamics should be taking into account not only for the momentum, but also for the mass transfer and chemical reactions.

2. Numerical method and modelling

Based on the Euler/Lagrange approach, numerical predictions of bubble columns were conducted, where all the relevant forces acting on bubbles, such as drag, transversal lift, virtual mass, fluid inertia, wall, Basset and naturally gravity/buoyancy were considered. A stochastic modification of bubble eccentricity and motion angle is used to mimic oscillations (Sommerfeld et al., 2018). The effects of such bubble dynamics on mass transfer were modeled through a dynamic Sherwood number (Montes et al., 1999). Large Eddy Simulation (LES) was used for modeling flow and turbulence of the carrier phase, considering not only the effect of sub-grid-scale (SGS) turbulence on bubble motion (Lipowsky & Sommerfeld, 2007), but also BIT modification by bubbles (Lain et al.; 2002, Sommerfeld, 2001; Sato & Sekoguchi, 1975). SGS turbulence effects were also taken into account through modification of the diffusion coefficient in the species equation. With an analogy to the turbulent dispersion model, SGS variations on the bulk concentration seen by the bubble were also considered.

3. Results and discussion

The model validation was performed by comparing the results with experimental data (hydrodynamic and species transport) present in the Literature (Sommerfeld and Bröder, 2009; Merker et al., 2017; Darmana et al., 2007). The performance of the involved different models, bubble induced turbulence, bubble dynamics, dynamic Sherwood number were tested for these different cases. Good agreement with the experimental observations, not only with regard to the liquid dynamics but also with volume change of single bubbles in time and concentrations of participating species in the bubble column. This was only possible when bubble dynamics in the frame of Euler-Lagrange approach was considered, even with point-particle approximation. The decay of volume from CO_2 single bubbles rising in water were compared with data presented in the literature and good agreement was found. A comparison with experiments of bubble swarms and chemical reactions was also realized. In this case, the predicted decay of pH due to chemisorption of CO_2 in a NaOH solution was satisfactory only when bubble dynamics and enhancement factor were considered.

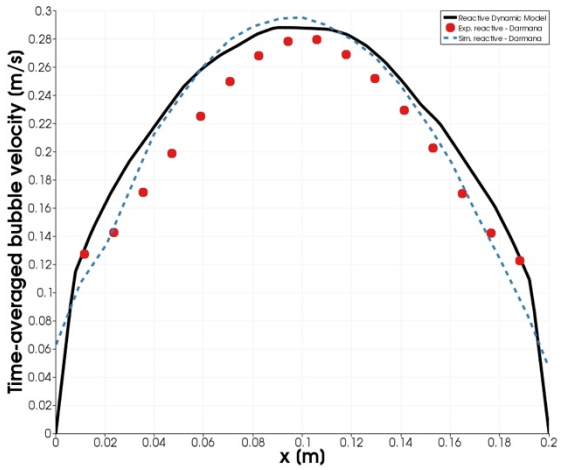

Figure 1. Time-averaged bubble velocity profile at z/H = 0.75.

References

Sommerfeld, M., Muniz, M. and Reichardt, T.: On the importance of modelling bubble dynamics for point-mass numerical calculations of bubble columns. *Journal of Chemical Engineering of Japan*, Vol. 51 301–317 2018.

Montes, F.J., Galan, M. A, Cerro, R.L.: "Mass transfer from oscillating bubbles in bioreactors", *Chemical Engineering Science*, vol. 54, 3127-3136, 1999.

Lipowsky, J. and Sommerfeld, M.: LES-simulation of the formation of particle strands in swirling flows using an unsteady Euler-Lagrange approach. *Proceedings of the 6th International Conference on Multiphase Flow*, ICMF2007, Leipzig Germany, Paper No. S3_Thu_C_54, 2007.

Lain, S., Bröder, D., Sommerfeld, M. and Göz, M.F.: Modelling hydrodynamics and turbulence in a bubble column using the Euler-Lagrange procedure. *International Journal of Multiphase Flows*, Vol. 28, 1381-1407, 2002.

Sato, Y and Sekoguchi, K.: Liquid velocity distribution in two phase bubble flow. *International Journal of Multiphase Flow.* Vol. 2, no. 1, 79-95, 1975.

Sommerfeld, M., Bröder, D.: Analysis of hydrodynamics and microstructure in a bubble column by planar shadow image velocimetry, Ind. Eng. Chem. Res. 48, 330–340, 2009.

Darmana, D., Henket, R., Deen, N. and Kuipers, J.: Detailed modelling of hydrodynamics, mass transfer and chemical reactions in a bubble column using a discrete bubble model: Chemisorption of CO2 into NaOH solution, numerical and experimental study. *Chemical Engineering Science*, Vol. 62, 2556–2575, 2007.

ECCE12
The 12th EUROPEAN CONGRESS OF CHEMICAL ENGINEERING
Florence 15-19 September 2019

Shape and Velocity Prediction of Slug Bubbles in Vertical Pipes.

Alexandre Boucher[1], Roel Belt[2], Alain Liné[1]

1. *INSA Toulouse, Transfer-Interface-Mixing, LISBP - 135 avenue de Rangueil, 31077, Toulouse, France,*
2. *TOTAL S.A., PERL, Pôle Economique 2 – B. PP 47, 64170 Lacq, France.*

**Corresponding author: aboucher@insa-toulouse.fr*

Highlights

- Vertical slug flow in stagnant and flowing liquids.
- Semi-analytical methods for slug bubble shape determination.
- Effect of inertia, surface tensions, and viscosity on bubble shape and velocity.

1. Introduction

Co-current vertical slug flow is present in numerous fields of applications, among which the transportation of hydrocarbons into pipelines, the promotion of mixing in reactors, the filtration through membranes, or emergency cooling of nuclear reactors are some practical examples. Simplified mechanistic models together with adequate closure laws seem to model satisfactorily vertical slug flow for most industrial purposes. Hence, a prolific number of closure relations have been developed on the terminal slug bubble velocity or the slug void fraction, but few focused on the characterization and the prediction of the slug bubble shape. However, terminal velocity and the shape of the nose are intimately linked, and most closure relations can benefit a better characterization of the slug bubble shape. Semi-analytical (the final analytical set of equations is solved numerically) methods have been reviewed and predictive slug bubble shapes have been computed with respect to flowing liquid velocities and surface tensions. Extended methods to include viscous forces into the predictions have also been studied.

2. Results and discussion

Dumitrescu [5] was one of the first to derive the slug bubble shape and velocity using a couple resolution of the Stokes stream function $\psi(\xi,\eta)$ given by potential flow theory and Bernoulli's equation on the bubble surface. He concluded with an impressive accuracy that the square of the rising velocity U_B of an elongated bubble in a stagnant liquid with negligible surface tension was proportional to the acceleration due to gravity g and the pipe diameter D, leading to a Froude number $Fr = 0.351$.

Ever since, his methodology was extensively used ([4], [9], [3], [1], and [8]) on problems with increasing complexity, taking for instance into account the effects of a flowing liquid ([9], [3], [1], and [8]) and turbulent velocity profiles ([3], and [1]) in terms of Reynolds number, and the effects of surface tension ([9], [1], and [8]) in terms of Eötvös number. These works can be grouped in two resolution methods: the Power Series resolution (PSR) used in [1], [4], [5] and [9], and the Total Derivative method (TDM) used by [3] and [8]. It is also worth mentioning that more recently the viscous potential flow theory was used in [7] and [6] in order to determine the shape and the

velocity of a deformable spherical cap and an ovary ellipsoid respectively. The bubble shape for an air bubble in stagnant water was computed on Fig. 1 using the PSR solution. This result can be extended to different values of surface tensions as shown in Fig. 2 where the resulting velocity is compared to experimental data for different methods of resolution.

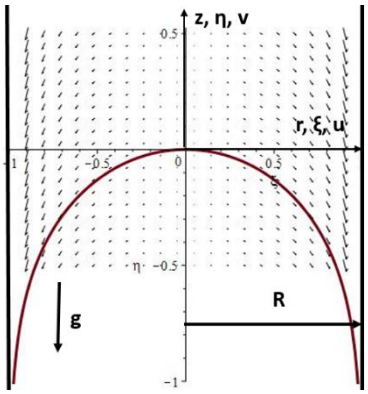

Figure 2. Computed bubble shape and velocity field around it in the moving frame coordinate system.

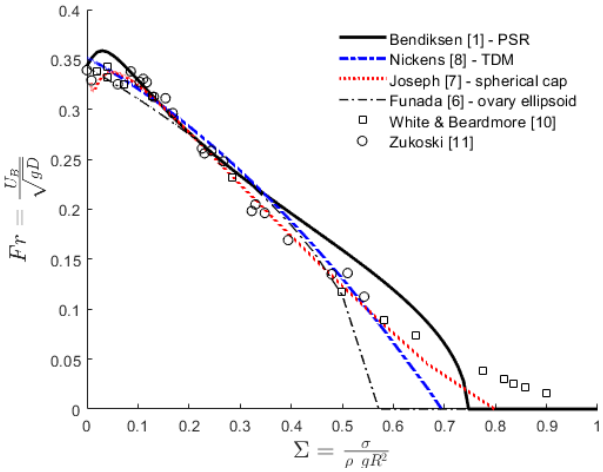

Figure 1. Dimensionless slug bubble velocity in function of surface tensions. Comparison to experimental data.

3. Conclusions and perspectives

The slug bubble shape can be computed using semi-analytical methods and the resulting rising velocity seems to be in agreement with experimental data for small values of surface tensions. For smaller tube diameters, the curvature of the bubble surface and the increasing importance of the liquid film (viscous zone) is in contradiction with potential flow hypothesis and require a specific theory of the kind of Bretherton's [2] in order to accurately predict the film thickness of the developed zone. A new resolution method can thus be found considering both potential flow at the vicinity of the bubble nose and the effects of the draining film at a binding distance $l_{nF}(Eo, Re, Mo)$ of the bubble tip depending on the properties of the system.

References

[1] K. H. Bendiksen, 'On the motion of long bubbles in vertical tubes', *IJFM* vol. 11, no. 6, (1985) 797–812.
[2] F. P. Bretherton, 'The motion of long bubbles in tubes', *JFM*, vol. 10, no. 2, pp. 166–188, Mar. 1961.
[3] R. Collins, F. F. D. Moraes, J. F. Davidson, and D. Harrison, 'The motion of a large gas bubble rising through liquid flowing in a tube', *JFM*, vol. 89, no. 3, pp. 497–514, Dec. 1978.
[4] R. M. Davies and G. I. Taylor, 'The mechanics of large bubbles rising through extended liquids and through liquids in tubes', *Proc. R. Soc. Lond. A*, vol. 200, no. 1062, pp. 375–390, Feb. 1950.
[5] D. T. Dumitrescu, 'Strömung an einer Luftblase im senkrechten Rohr', *ZAMM - JAMM / Zeitschrift für Angewandte Mathematik und Mechanik*, vol. 23, no. 3, pp. 139–149, Jan. 1943.
[6] T. Funada, D. D. Joseph, T. Maehara, and S. Yamashita, 'Ellipsoidal model of the rise of a Taylor bubble in a round tube', *IJFM*, vol. 31, pp. 473–491, Apr. 2005.
[7] D. D. Joseph, 'Rise velocity of a spherical cap bubble', *JFM*, vol. 488, pp. 213–223, Jul. 2003.
[8] H. V. Nickens and D. W. Yannitell, 'The effects of surface tension and viscosity on the rise velocity of a large gas bubble in a closed, vertical liquid-filled tube', *IJFM*, vol. 13, no. 1, pp. 57–69, Jan. 1987.
[9] K. W. Tung and J.-Y. Parlange, 'Note on the motion of long bubbles in closed tubes-influence of surface tension', *Acta Mechanica*, vol. 24, no. 3, pp. 313–317, Sep. 1976.
[10] E. T. White and R. H. Beardmore, 'The velocity of rise of single cylindrical air bubbles through liquids contained in vertical tubes', *Chemical Engineering Science*, vol. 17, no. 5, pp. 351–361, Jan. 1962.
[11] E. E. Zukoski, 'Influence of viscosity, surface tension, and inclination angle on motion of long bubbles in closed tubes', *JFM*, vol. 25, no. 4, pp. 821–837, Aug. 1966.

ECCE12
The 12th EUROPEAN CONGRESS OF CHEMICAL ENGINEERING
Florence 15-19 September 2019

Enhancement of CO_2 Absorption by Ionic Liquid Electrospray

Hidemasa Takana[1], Nozomi Hara[1], Takashi Makino[2] and Mitsuhiro Kanakubo[2]

1 Institute of Fluid Science, Tohoku University, 2-1-1 Katahira Aoba-ku, Sendai 980-8577, JAPAN

2 National Institute of Advanced Industrial Science and Technology (AIST), JAPAN

**takana@tohoku.ac.jp*

Highlights

- Ionic liquid electrospray characteristics have been clarified by high speed imaging. Ionic liquid electrospray behavior can be categorized into four modes depending on applied voltage and feeding flow rate.
- Ionic liquid electrospray produces nano droplets and it was successfully demonstrated that ionic liquid electrospray enhances CO_2 absorption even at low CO_2 concentration.
- The absorbed amount of CO_2 for 20 minutes increases by 220 % by ionic liquid electrospray.

1. Introduction

Ionic liquids (ILs) are ambient temperature molten salts, which generally consist of a bulky organic cation and organic/inorganic anion. ILs exhibit unique characteristics such as non-volatility, non-flammable, thermal and chemical stability. Moreover, ILs have drawn great attention as a potential CO_2 absorbents. ILs capture CO_2 chemically and reversibly desorb CO_2 by heating.

Since CO_2 chemical absorption occurs at the gas-liquid interface, the absorption rate can be enhanced by increasing the specific surface area. In this study, nano order IL droplets are generated by electrospray with aiming enhanced CO_2 chemisorption. The characteristics of IL electrospray were experimentally evaluated and the effect of applied voltage on the CO_2 absorption performance was discussed with correlating to spray behavior.

2. Methods

Schematic illustration of experimental setup is shown in Fig. 1. Both upper and lower flanges of an acrylic chamber with volume of 50.3 cm^3 has gas inlet and outlet ports of 4 mm in diameter. The CO_2/N_2 gas (1.03% CO_2) and N_2 gas (≥ 99.999%) is introduced in the changer and flows out from the outlet port. CO_2 concentration is monitored by CO_2 analyzer (VAISALA GMP252) at downstream of outlet port. The capillary tube made of a fused silica (ID: 100 µm, OD: 375 µm, GL Sciences) was used as a nozzle. Positive DC high voltage was applied to the capillary nozzle with the counter ring electrode grounded. The electrode gap distance between the center of ring electrode of nozzle tip was set to be 6 mm. 1-ethyl-3-methylimidazolium acetate

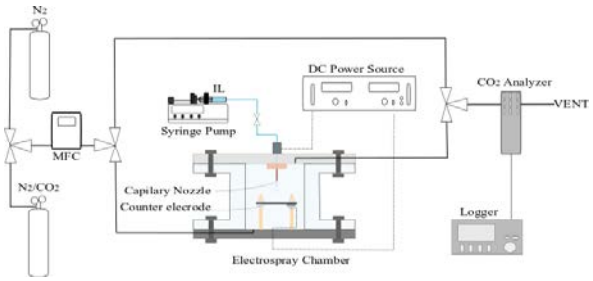

Figure 1. Schematic illustration of experimental setup.

([EMIM][Ac], ≥ 95.0%, SIGMA-ALDRICH) was used in this study as an absorbent. Droplet size distribution was optically measured by aerosol spectrometer (WELAS 2070 PALAS) for the sampling time of 30 seconds. Electro spray behavior was characterized by taking high-speed shadow graph images at the flame rate of 4000 fps (FASTCAM SA-X2, Photron). In the CO_2 absorption experiments, CO_2/N_2 premixed gas was supplied at a constant flow rate of 20 ml/min.

3. Results and discussion

Fig. 2 shows shadow graph images taken by high speed camera. IL spray can be categorized into 4 modes depending on applied voltage and flow rate. The mode I is referred to as "dripping mode" with rather large droplets of ~0.2 mm. The mode Ⅱ generates not only large droplets like mode I but also fine droplets through breakup of the liquid thread extended from the Taylor cone. In mode Ⅲ, ultrafine droplets are continuously generated from the liquid thread tip due to electrostatic repulsion. The typical droplet size distribution of model III is shown in figure 3. The peak diameter of 255 nm is generated in this mode. The mode Ⅳ is observed at a relatively high voltage when corona discharge appears around the Taylor cone. Since ionized gas layer shields electric field at the tip of the ionic liquid thread, larger droplet is primary generated just like mode II followed by finer droplets generation by secondary breakup due to high electric field. In the following experiments, the ionic liquid flow rate was fixed at 2 mL/h.

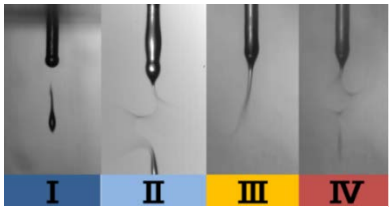

Figure 2. Observed spray modes in ionic liquid electrospray.

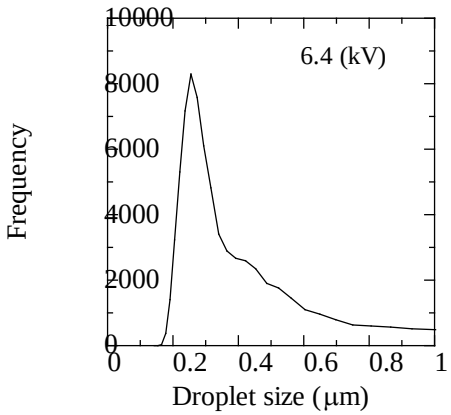

Figure 3. Droplet size distribution in mode III.

Fig. 4 shows the time traces of CO_2 concentration. When 8.0 kV is applied (mode IV), CO_2 concentration rapidly decreases at the initial period. The reaction rate in this case enhanced by approximately 10 times compared to the case without applied voltage. The absorbed amount of CO_2 for 20 minutes also increases by 220 %. When shutting down IL supply and applied voltage, CO_2 concentration recovers. Slower increase in 8.0 kV is because of the attached fine droplets remains on the chamber wall. From this result, it has been clearly shown that atomization of ionic liquid by electrostatic spray enhances the CO_2 absorption even under low CO_2 concentration conditions.

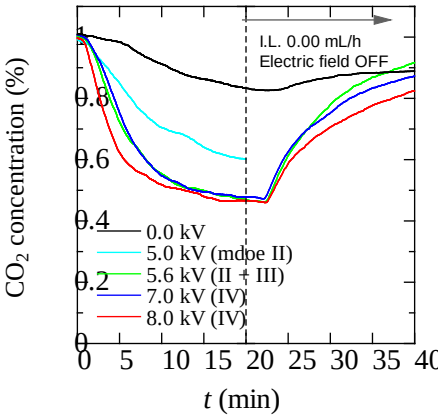

Figure 3. Time traces of CO_2 concentration with various applied

4. Conclusions

The characteristics of IL electrospray was clarified using high-speed imaging and the effect of IL electrospray on CO_2 absorption was shown with correlating to the spray characteristics.

Acknowledgment

Part of this research was supported by JSPS KAKENHI Grant Number 16H04262.

ECCE12
The 12th EUROPEAN CONGRESS OF CHEMICAL ENGINEERING
Florence 15-19 September 2019

Mixing and its influence on the precipitation of organic nanoparticles from the liquid phase: A Lagrangian perspective

Tobias Schikarski[1]& Holger Trzenschiok[1], Marc Avila[2], Wolfgang Peukert[1*]

1 Institute of Particle Technology, Friedrich-Alexander Universität Erlangen-Nürnberg; 2 Center of Applied Space Technology and Microgravity, Universität Bremen

**Corresponding author: wolfgang.peukert@fau.de*

Highlights

- Precipitated nanoparticles of Ibuprofen down to 25nm
- Precise simulations of liquid mixing in a T-mixer
- Prediction of trend of particle size and shape of PSD with Lagrangian mixing

1. Introduction

Mixing is key for the fast precipitation of organic **[1]** and inorganic **[2]** compounds because it determines the supersaturation build-up, which in turn governs the primary particle formation steps such as nucleation and diffusion-limited growth **[1,2].** Due to the naturally very small diffusivities of liquid mixtures, turbulence is primarily chosen to impose fast and well mixing because of its spatio-temporal randomness and the cascade of various length scales. To accurately model precipitation, turbulent mixing needs to be well captured in simulations.

In our recent study **[3]**, we achieved excellent qualitative agreement in the mixing efficiency of a simple T-mixer between experiments and direct numerical simulations (no turbulence modeling) over a wide range of Reynolds numbers *Re=(100,4000).* Despite the newly gained insights into the mixing process, analysis of the influence of the mixing on the particle size distribution (PSD) of organic nanoparticles, resulting from precipitation experiments at various flow rates, is still missing. In doing so, we study the mixing behavior along Lagrangian trajectories and relate the findings to the experimentally obtained PSDs. It appears that this approach allows to qualitatively predict the trend of the mean particle size as well as the width of the PSD without any precipitation modeling, which is very challenging itself.

2. Methods

A simple T-mixer is used to mix an alkaline aqueous ibuprofen solution with an acidic aqueous Zirconium chloride solution, which triggers the precipitation of Ibuprofen while Zr-ions stabilize the formed particles. The resulting stable nanoparticle suspensions are analyzed with dynamic light scattering to obtain the PSD. Note that the fluid properties of the water-water mixture are not affected by the chemicals as well as the excellent particle stability prevents ripening or aggregation. The numerical approach consists of direct numerical flow simulations of the mixing process solving for the Navier-Stokes (velocity) and the convection-diffusion equation (composition). An empirical-free approach is here applied which does not require any turbulence modeling. Lagrangian trajectories are computed by solving $\frac{\partial x_i}{\partial t} = \boldsymbol{u_i}$, where x_i and $\boldsymbol{u_i}$ are the

position and velocity vector of the i^{th} trajectory, respectively. Details on the mixing and precipitation experiments as well as on the flow simulations can be found in **[3,4]**, respectively.

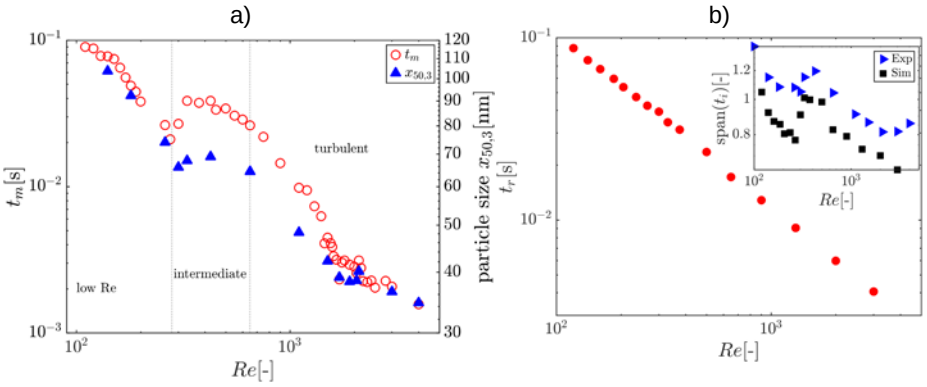

Figure 1. (a) Experimentally measured and computationally estimated mixing time t_m (left y-axis) and median particle size $x_{50,3}$ (right y-axis) as a function of Reynolds number Re. (b) Mean residence time t_r as a function of Reynolds number Re. The inset compares the width of PSD to that of the RTD.

3. Results and discussion

The supersaturation is the thermodynamic driving force of precipitation, which is determined by the rate the two fluids are brought in contact with each other. Thus, the primary particle formation steps nucleation and growth are mixing controlled under the assumption of fast chemical reactions, and the outcome should reflect the mixing efficiency when a sufficient stabilization is applied. This prevailing view is substantiated in Fig. 1a), which depicts a nearly perfect alignment of the experimentally determined mixing efficiency t_m by the Villermaux-Dushman reaction **[3]** with the median particle size $x_{50,3}$ as Reynolds number increases.

In the chemical engineering community, it is common to relate the reaction outcome with the residence time and its distribution. Having a large number of Lagrangian trajectories, the residence time distribution (RTD) can be precisely calculated by simulations. Fig. 1b) shows the mean residence time t_r as a function of the Reynolds number. It turns out that the qualitative trend of the mixing efficiency and likewise of the median particle size induced by alteration of flow structures are not featured by the mean residence time. However, comparing the widths of PSDs with these of RTDs, the qualitative trend is very well captured. This finding suggests that the shape of the PSD is determined by the spatial distribution of large-scale flow structures while the trend of the mean particle size depends primarily on local changes of the fluid composition.

4. Conclusions

In the talk, we will detail the experimental and numerical findings of the comparative study of the precipitation and Lagrangian mixing, respectively. In particular, we will demonstrate how to analyze the fluid composition to predict the qualitative trend of the median particle size. Furthermore, we will address the influence of inflow condition and different mixing fluids.

References

[1] A. A. Thorat, S.V. Dalvi, Chem. Eng. J. 181 (2012) 1-34.
[2] S. M. D'Addio, R.K. Prud'homme, Adv. Drug. Deliv. Rev. 63 (2011) 417-426.
[3] T. Schikarski, H. Trzenschiok, W. Peukert, M. Avila, Reac. Chem. Eng. (2019)
[4] H. Trzenschiok, M. Distaso, W. Peukert. Chem. Eng. J. 361 (2019) 429-438.

ECCE12
The 12th EUROPEAN CONGRESS OF CHEMICAL ENGINEERING
Florence 15-19 September 2019

Flow Regimes in Slurry Bubble Columns.

Sandra Orvalho[1], Masaaki Hashida[2], Maria Zednikova[1], Petr Stanovsky[1], Marek C. Ruzicka[1], Akio Tomiyama[2]

1 Department of Multiphase Reactors, Institute of Chemical Process Fundamentals, Czech Academy of Sciences, Rozvojova 135, 16502 Prague, Czech Republic; 2 Department of Mechanical Engineering, Kobe University Graduate School of Engineering, Kobe, Japan

**Corresponding author: orvalho@icpf.cas.cz*

Highlights

- Detailed experiments on slurry bubble columns hydrodynamics
- Flow regimes in slurry bubble column and their transitions: effect of liquid level and solid particles concentration
- Modelling slurry bubble columns hydrodynamics under HoR, TrR, HeR and PHeR

1. Introduction

Bubble columns and sparged gas-liquid systems have wide application in chemical industry and in biotechnology, being slurry bubble column (SBC) is a special case of three-phase gas-liquid-solid. In most applications, SBC are operated under pure heterogeneous hydrodynamic regime (non-uniform, churn turbulent). However, operation of slurry bubble columns (SBC) in homogeneous regime (uniform, laminar) may be preferred in some cases like in the intensification of catalytic reactors using special distributors [1] or to secure low level of shear stresses in some bioapplications [2]. Most of the research on SBC is however dedicated to pure heterogeneous regime (PHeR) and very little attention has been paid to HoR. In the present contribution we will present a systematic study of the hydrodynamic behavior of SBC equipped with “fine sparger”, able to give homogeneous and heterogeneous regime and transition between them.

2. Methods

This experimental study focused on the flow regimes and gas holdup behavior in a lab-scale slurry bubble column (vertical plexiglass cylinder, diameter 0.14 m, total height 2 m). The gas distributor was a fine perforated brass plate (orifices with 0.5 mm diameter, free plate area 0.19 %), producing both homogeneous (HoR) and heterogeneous (HeR) flow regimes, and the transition between them (TrR). The three-phase gas-liquid-solid mixture was composed of local air, tap water and fine porous silica particles (size 100 µm). The gas holdup e was measured by bed expansion method, using free layer height evaluated visually or by digital image analysis. Three experimental parameters were tested: gas input q, initial slurry layer height H and concentration of solid particles c.

3. Results and discussion

The gas holdup e depends on the gas input q, layer height H and solid content c. From the holdup data measured, flow regimes were identified and the transition points were determined. The reference system for our study is the two-phase system c = 0 % and 0.8 m layer height, presented

in Fig 1 (a). In this system, the bubble column gives three regimes with two transition points, depending on the gas input q. Increasing the layer height and the solid load reduces the gas holdup and destabilizes HoR. At low solid load (c < 3%) all three regimes exist, depending on q. At solid load higher than c ≥ 3% only one regime exists, pure heterogeneous regime. The main findings are resumed in the flow regime map in Fig. 1 (b). Existing model equations, derived for two phase systems [3], were adapted to take in consideration the presence and concentration of the third phase (suspended particles). The parameters of the models have physically meaningful parameters such as terminal velocity or factor of flow non-uniformity and they can be proved by auxiliary visualization experiments.

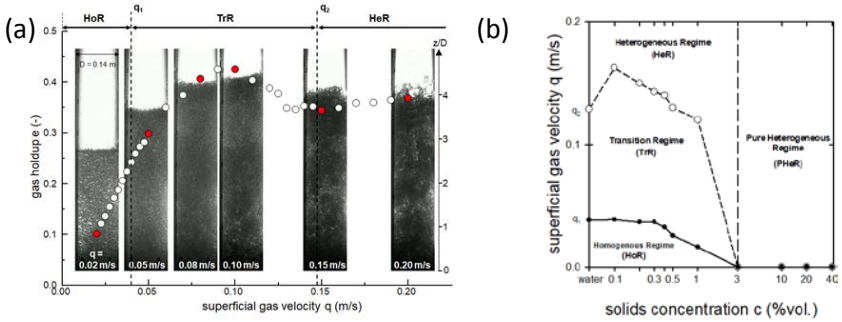

Figure 1. (a) Identification of flow regimes (HoR, TrR, HeR) and critical points (q1 and q2) of flow transition, based on images of bubble column and gas holdup data; (b) Flow regime map for slurry bubble column (SBC).

4. Conclusions

The present study is based on visualization experiments, for determination of gas holdup and flow regimes, and intends to improve our understanding of the dynamics of slurry bubble columns generated by “fine spargers”. The main result of the study is a flow regime map with three parameters, q, H and c.

The financial support by the Czech Science Foundation through project 19-09518S, and by the Graduate School of Engineering, Faculty of Engineering, Kobe University during Mr. Hashida work stay in Prague, are gratefully acknowledged.

References

[1] N. Hooshyar, P.J. Hamersma, R.F. Mudde, J.R. van Ommen, Can. J. Chem. Eng. 88 (2010) 533-542.
[2] A. Mota, A.A. Vicente, J. Teixeira, Chem. Eng. Sci. 66 (2011) 3350-3357.
[3] M.C. Ruzicka, J. Zahradnik, j. Drahos, N.H. Thomas, Chem. Eng. Sci. 56 (2001) 4609-4626.

ECAB 5
The 5th EUROPEAN CONGRESS OF APPLIED BIOTECHNOLOGY
Florence 15-19 September 2019

Integrated Biofilm Reactor-Separator Using a Rotating Spiral Channel

Jordan MacInnes and Esther Karunakaran

Chemical and Biological Engineering, University of Sheffield, Mappin Street, Sheffield S1 3JD

**Corresponding author: j.m.macinnes@sheffield.ac.uk*

Highlights

- Rotating spiral channel controls liquid-liquid contact between media and solvent
- Allows continuous control of nutrient and product concentration
- Preliminary result will be presented to demonstrate feasibility

1. Introduction

Industrial biotechnology aims to use microorganisms to transform one chemical species to another. Engineering systems to control the supply of nutrient species and the removal of product species must optimise production rate per cost. For continuous processing by biofilms - an aggregate of microorganisms attached to an abiotic surface[1] - a surface must be provided with access to a flow of aqueous media to both sustain the biofilm and remove waste. The aqueous flow should be even over the biofilm, have a thickness that allows all of the media to be accessed and have a flow rate that is suited to the biofilm production rate. Indeed, the media supply may be used to optimise production conditions. It may also be helpful to bring a second, immiscible, liquid into contact with the aqueous phase to help control conditions in the medium, not least to separate the product species.

A rotating spiral channel allows such an arrangement of biofilm, aqueous media and an immiscible solvent liquid. The spiral channel rotating around its axis segregates the two fluid phases into parallel-flowing layers of adjustable flow rate and interface position. Fig. 1a shows a schematic of a typical cross-section of the channel. The biofilm is shown on the left hand side wall, stabilised there by the strong radial acceleration ($r\Omega^2$) and in contact with the denser aqueous media, which in turn is in contact with an organic solvent. The media and solvent are flowing in the direction perpendicular to the section, either co-currently or counter-currently.

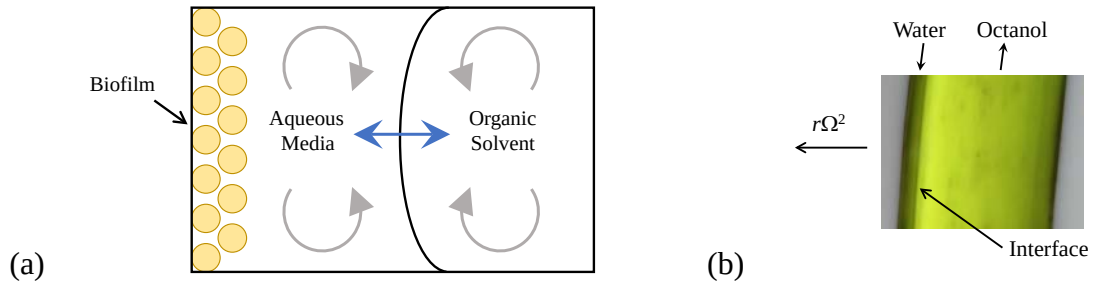

Figure 1. (a) Channel section with biofilm (on the left), aqueous media and solvent. Grey arrows indicate the secondary flow[5] (from centrifugal and Coriolis accelerations) that assist species transfer. (b) Photograph taken from below of water and octanol flowing counter-currently in a rotating spiral channel.

2. Background

Rotating spiral channels allow contacting of two immiscible fluids at the optimum flow rate ratio of the two phases and ratio of the thicknesses of the two fluid layers[2]. Mass transfer coefficients that are orders of magnitude greater than those with conventional contacting methods have been demonstrated[3]. While that work considered gas-liquid contacting, ideal theory[4] predicting interface position and flow rates in relation to fluid properties, rotation rate, pressure gradient and channel size applies equally to liquid-liquid and gas-liquid flows. Indeed, a number of informal tests with the same apparatus used for the gas-liquid work[2,3] confirm it handles liquid-liquid contacting equally well. Fig. 1b shows an image from a test with water and octanol contacting counter-currently. The relatively high viscosity of the octanol means it occupies the majority of the channel cross section for the conditions of the test. This is predicted by the model which also shows that the interface could be moved to other positions by suitable choices for pressure gradient and rotation rate, while maintaining correct solvent flow rate, e.g. that to fully remove the product.

3. Concentration control

Product concentration will vary with position (z) along the channel both as it accumulates from biofilm production and as the product transfers to the solvent. Co-current flow of the solvent results in a steadily increasing product concentration (C) along the channel (Fig. 2a). By contrast, with counter-current flow of the solvent phase the concentration in the aqueous phase first increases rapidly as product is gained from the loaded solvent and then decreases as pure inlet solvent is encountered (Fig. 2b). Consequently, the biofilm media will have a more uniform bulk concentration. Increasing solvent flow rate is expected to reduce product concentration levels in the aqueous phase; decreasing channel size is expected to increase concentration uniformity. Thus, considerable control of product concentration in the biofilm environment should be possible.

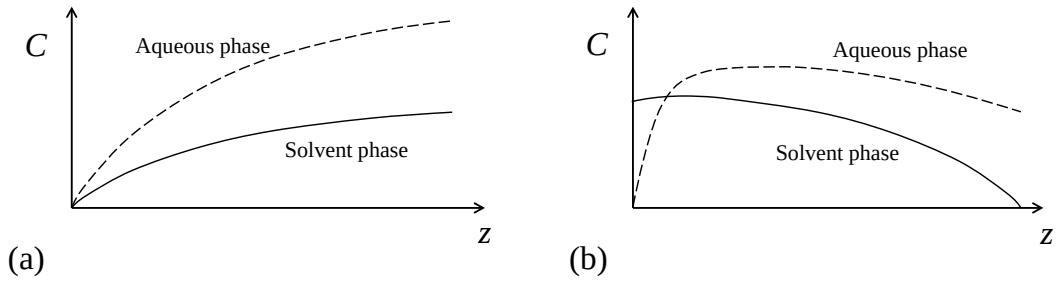

Figure 2. Product concentration profiles along the channel for (a) co-current and (b) counter-current flow of solvent.

4. Conclusions

An existing and proven apparatus[2.3] will be used to produce continuous biofilm processing in a rotating spiral channel with simultaneous product extraction into a counter-flowing solvent stream. A preliminary assessment will be presented at the congress.

References

[1] E. Karunakaran, B. Ramalingam, J. Mukherjee, C. A. Biggs, Appl. Micro. Biotech. 90 (2011) 1869 – 1881.
[2] J.M. MacInnes, M.K.S. Zambri, Chem. Eng. Sci. 126 (2015) 427-439.
[3] J.M. MacInnes, A.A. Ayash, Chem. Eng. Sci. 175 (2018) 320-334.
[4] J.M. MacInnes, M.J. Pitt, G.H. Priestman, R.W.K. Allen, Chem. Eng. Sci. 69 (2012) 304-315.
[5] M. Selmi, K. Nandakumar, W.H. Finlay, J. Fluid Mech. 262 (1994) 353-375.

ECCE12
The 12th EUROPEAN CONGRESS OF CHEMICAL ENGINEERING
Florence 15-19 September 2019

Numerical simulation of a high-shear cone mill mixer for food emulsions production

Antonio Buffo[1], Marco Ferrari[1], Gianluca Boccardo[1], Daniele Marchisio[1]

1 Department of Applied Science and Technology, Politecnico di Torino, Torino, Italy

**Corresponding author: antonio.buffo@polito.it*

Highlights

- A CFD analysis of a cone-mill mixer for food emulsions production is carried out
- Development of an open simulation platform for a modelling marketplace
- Qualitative analysis of the result sees a match with experimental data

1. Introduction

Mayonnaise belongs to the family of high disperse phase liquid-liquid emulsions and the prediction of the final droplet size distribution is crucial for determining the properties of the final product, such as structure, stability over time, taste and color. The production of mayonnaise is a typical mixing process, in which the ingredients (i.e. egg yolk, vinegar, oil and water) are first brought together and mixed in large stirred vessels at moderate rotational speed. Then the formed emulsion is finally fluxed into a high-shear mixer, where the droplets undergo breakage until the final size distribution is reached; this last step is crucial to fine tune the droplet size distribution, in order to have a final product with the desired features. In this work, we aim to simulate the last step of the production process by means of a Computational Fluid Dynamics approach coupled with a Population Balance Model (CFD-PBM) [1], to properly describe both the non-Newtonian dynamics of the emulsion and the evolution of the droplet size distribution. This methodology is eventually validated with experimental data available in the literature [2,3]. This work focuses on the macroscale of a more complex multiscale simulation, where the interfacial properties and the rheology of the emulsion are also predicted using a numerical approach. This particular workflow will be useful to develop an open simulation platform for generic multiscale and multiphysics simulations, where the computational codes aiming at different parts of the physics are linked and coupled. This will be the main component of a marketplace for modelling of materials and chemical processes.

2. Methods

A schematic representation of the investigated high-shear mixer, i.e. a cone mill mixer, is reported in Fig. 1. As it can be seen, it is constituted of a solid conical frustum rotor inside of a slightly larger stator of the same shape, forming a small gap in which the emulsion flows (moving from the lowest radii section to the largest) and experiences high-shear rates.

From a computational point of view, this geometry was preliminarily reproduced using a two-dimensional grid, exploiting the intrinsic symmetry of this system. The fluid was considered as a

shear thinning pseudo single phase, with an apparent viscosity evaluated through a power law model fitted with experiments [2]. However, the feasibility of more sophisticated approaches (such as three-dimensional simulations and two-phase models) will be evaluated in the future. The simulations are carried out with the open source CFD code OpenFOAM (version 6.0).

3. Results and discussion

As expected, the preliminary simulations show a high velocity gradient due to the high rotational speed, in particular the highest velocity corresponds to the tip velocity of the rotor: this can be seen in Fig. 2. Another interesting result is reported in Fig. 3, where the axial velocity profile at the middle section is reported: as it can be seen the emulsion flows in the downward direction but there is a small backflow close to the stationary wall, which is evidence of the presence of recirculation patterns typical of these systems. A qualitative analysis shows good agreement with the experimental data.

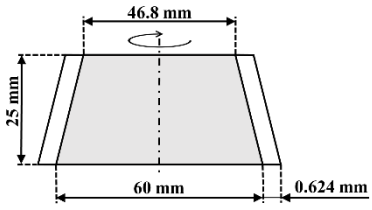

Figure 1. Sketch of the cone mill mixer.

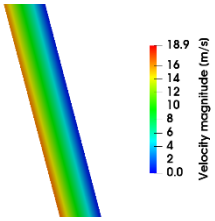

Figure 2. Contour plot of velocity magnitude magnified around the central part of the mixer

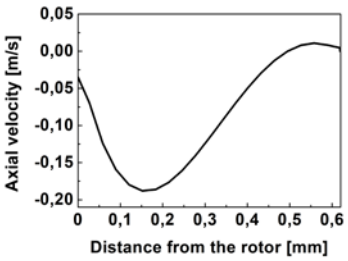

Figure 3. Axial velocity profile at the middle section

4. Conclusions

The first results regarding the fluid dynamics description of the cone mill are promising, as the behavior of the high-shear mixer is properly reproduced. The next step will be the solution of the Population Balance Equation (PBE), in order to account for the droplet breakage induced by the high-shear rates inside the mixer. This will be useful to predict the final droplet size distribution by using a fully-predictive approach.

Acknowledgements

The project leading to this application has received funding from the European Union's Horizon 2020 Research Innovation Programme under Grant Agreement n. 760907.

References

[1] D. Li, Z. Gao, A. Buffo, W. Podgorska, D.L. Marchisio, AIChE J. 63 (2017) 2293–2311.

[2] A. Dubbelboer, J.J.M. Janssen, H. Hoogland, E. Zondervan, J. Meuldijk, Chem. Eng. Sci. 148 (2016) 32–43.

[3] A. Dubbelboer, Towards optimization of emulsified consumer products: modeling and optimization of sensory and physicochemical aspects, (PhD Thesis) Eindhoven: Technische Universiteit Eindhoven, 2016.

ECCE12
The 12th EUROPEAN CONGRESS OF CHEMICAL ENGINEERING
Florence 15-19 September 2019

Experimental analysis on the mixing of two parallel bubbly flows.

Corné Muilwijk*[1], Harry E. A. Van den Akker[1,2]

[1]Bernal Institute, University of Limerick, V94 T9PX, Limerick, Ireland

[1,2]Transport Phenomena Lab, Department of Chemical Engineering, Delft University of Technology, Van der Maasweg 9, 2629 HZ, Delft, The Netherlands

*Corresponding author: Corne.Muilwijk@ul.ie

Highlights

- Mixing of two parallel vertical bubbly flows of various superficial liquid/gas velocity
- Bubble image velocimetry approach to study mixing patterns
- Gas fraction and bubble velocity measurements using optical fiber probes

1. Introduction

Gas liquid contacting is one of the most important operations in the chemical and biochemical industry. Aerated vessels offer a high degree of mixing, heat and mass transfer, while local shear rates are relatively low. Computational Fluid Dynamics are widely used to assist in the design of new (bio)-reactors. The on-going development of these numerical models, often on the basis of a single bubble size, requires precise experimental data for validation purposes. We present experiments on the mixing pattern of two parallel bubbly flows with an almost uniform (initial) bubble size distribution.[1] We studied mixing patterns of both a uniformly and non-uniformly aerated rectangular flow channel, with and without vertical liquid co-flow.

2. Methods

Fig. 1 shows a sketch of the bubbly flow channel. Two separate parallel bubbly streams (Left and Right) are mixed in a rectangular flow channel after the trailing edge of the splitter plate. The superficial gas and liquid velocities, for each of the inlet compartments, is in the range 0.5-6.25 and 0-50 cm/s, respectively. Large uniform bubbles, 4-8 mm in diameter, are formed by needle spargers[2] to yield an overall void fraction in the range 2 - 25 %. We studied the mixing pattern

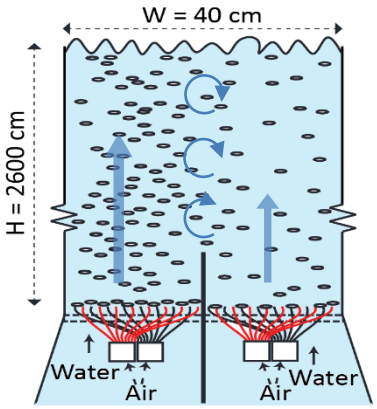

Figure 1. Sketch (not on scale) of the mixing of two parallel bubbly flows with different superficial liquid/gas velocities.

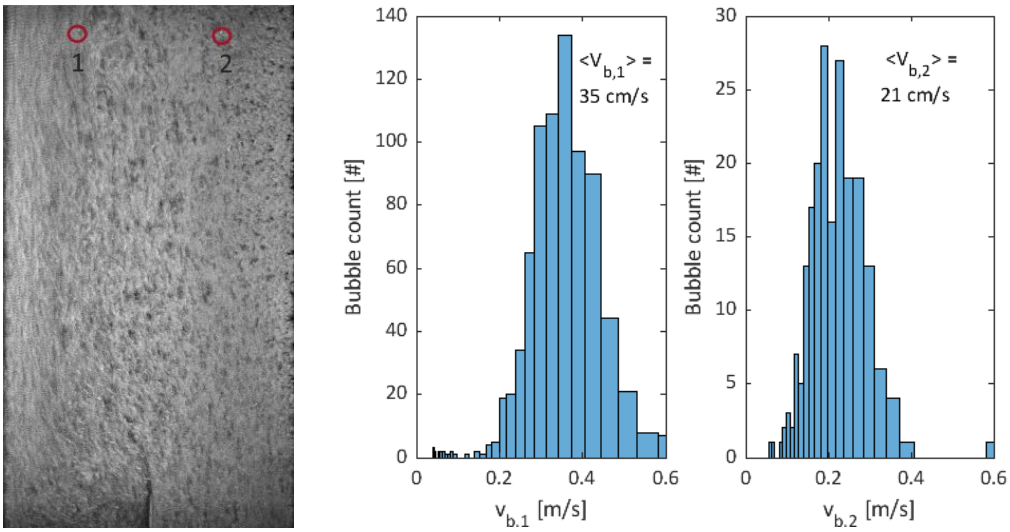

Figure 2. Left: Visualization of bubble streaks. Higher superficial gas velocity on the left size of the column. Bubble probe positions are denoted with a circle. Right: bubble velocity histograms of both monitoring points.

downstream the trailing edge of the splitter plate as a function of the inlet superficial gas and liquid velocities using dual-tip optical fiber probes (local void fraction, bubble velocities and bubble chord lengths), Bubble Image Velocimetry (macroscale mixing pattern) and Laser Doppler Velocimetry (local liquid velocities and turbulence levels).

3. Results and discussion

Fig. 2 (left) shows bubble streaks of an in-homogeneously aerated column (no liquid co-flow). The inlet superficial gas velocities on the left and right side of the column are 1.38 and 1.12 cm/s respectively. A recursive image correlation technique is adopted to calculate the displacement of bubble parcels to obtain local gas velocities for a range of operating conditions. Large self-organizing flow structures arise as a function of the difference in both (left, right) inlet conditions.

Bubble probes are installed in the flow channel as denoted in Fig. 2 by point 1 (left) and point 2 (right) and the measured time-averaged gas fraction (500 s) for both probes is 5.7 and 4.5 % respectively. The right side of Fig. 2 shows the bubble velocity distributions. For the case shown, we observe normally distributed bubble velocities of 35±10 cm/s on the left and 21±6 cm/s on the right, while the bubble chord length distributions are almost identical for both probes. For larger differences in superficial gas velocities between both inlets (left, right), local bubble velocities may start to deviate significantly from vertically up, due to entrainment in a self-organized vortex, and bubble velocity measurements of a dual-tip bubble probe then are subjected to a large measurement uncertainty.

4. Conclusions

We studied mixing patterns of two parallel bubbly flows using a novel bubble image velocimetry approach and dual-tip optical fiber probes. Precise data are obtained on spatial distributions of the local gas fraction, chord lengths and gas velocities with the view of validating CFD simulations.

References

[1] C. Muilwijk, H.E.A. Van den Akker, Chem. Eng. Res. Des. (2019). submitted
[2] C. Muilwijk, H.E.A. Van den Akker, Chem. Eng. Sci. 202 (2019) 318–335.

ECCE12
The 12th EUROPEAN CONGRESS OF CHEMICAL ENGINEERING
Florence 15-19 September 2019

Considering the Entire Turbulence Spectrum in Breakage and Coalescence Kernel Formulation.

Simone Castellano[1,2], Lorenzo Carrillo[1], Nida Sheibat-Othman[2], Daniele Marchisio[3], Antonio Buffo[3], Sophie Charton[1*]

1 CEA, DEN, Research Department on Mining and Fuel Recycling Processes, SA2I, Bagnols-sur-Cèze, France;

2 Université Claude Bernard Lyon 1, CNRS, UMR 5007, LAGEP, 43 b 11 Novembre 1918, Villeurbanne, France

3 Politecnico di Torino, DISAT, Corso Duca degli Abruzzi 24, Torino, Italy

**Corresponding author: sophie.charton@cea.fr*

Highlights

- 0D Population Balance Equation model.
- Breakage and Coalescence kernels formulation.
- Second order structure function accounting for the entire turbulence spectrum.

1. Introduction

Liquid-liquid extraction is a common unit operation in the chemical, food, pharmaceutical and nuclear industries. In order to optimize and control this operation, the knowledge of the droplet size distribution or the Sauter mean diameter is needed. These two properties could be determined through the Population Balance Equation (PBE), whose accurate solution depends on the modeling of its source terms, *i.e*. the breakage and coalescence kernels. The kernels are of fundamental importance since they express the number of droplets breaking or coalescing per unit time. In the case of turbulent dispersions, these models generally assume the droplets to have dimension in the inertial subrange of turbulence, where the Kolmogorov theory applies. Therefore, shear stresses and characteristic times are expressed in agreement with the results of this theory. However, since in a solvent extraction process the droplet diameter varies from microns to millimeters, many droplets will have dimension in other turbulence ranges (Dissipation, Energy-containing). Therefore, general breakage and coalescence models that account for the entire spectrum of turbulence are proposed and experimentally validated.

2. Methods

Coulaloglou and Tavlarides proposed breakage and coalescence kernels considering the droplet to have dimension in the inertial subrange of turbulence. In this work, these models are extended to the entire turbulence spectrum implementing the second-order structure function (SOF) proposed by Davidson [1]:

$$\langle[\Delta u(r)]^2\rangle \approx \frac{4}{3}\int_0^\infty E(\kappa)\left\{1-3\left[\frac{sin(\kappa r)}{(\kappa r)^3}-\frac{cos(\kappa r)}{(\kappa r)^2}\right]\right\}d\kappa$$

The Pope energy spectrum $E(\kappa)$ [2] is considered, since it accounts for the eddy energy distribution in the entire turbulence spectrum. This model depends on the continuous phase viscosity and the turbulent dissipation rate ε. This latter is usually not uniform in the liquid-liquid contactor. Therefore, in the employed 0D PBE model, the ε inhomogenenities were considered through a probability density function obtained from CFD simulation [3]. Finally, the proposed kernels were tested on turbulent liquid-liquid dispersion experiments performed in a stirred tank of 1L volume equipped with a Mixel-TT impeller. Distilled water was used as the dispersed phase, while the continuous phase consisted of a mixture of Isane 175 (1.2 cP) and Marcol 82 (12 cP). The experiments were carried out at varying impeller rotation speeds (600-700-800rpm), dispersed phase volume fractions (1-2%) and continuous phase viscosities (1.2 – 4.1 cP).

3. Results and discussion

The results of the general model (Fig. 1, green) were compared to the ones of the previous model (dashed blue) based on the inertial subrange assumption [3]. At 1.2 cP (pure Isane, left), both models were able to predict the time evolution of the Sauter mean diameter. At 2.4 cP (Isane 70%-Marcol 30%, centre) and 4.1 cP (Isane 70%-Marcol 30%, right), while the simulations based on the general model are in good agreement with the experimental data, the original model underestimate the Sauter mean diameter. Indeed, at higher viscosities, the inertial subrange of turbulence is reduced and most of the droplets have dimension in the Dissipation subrange. In this subrange, the dampening effect of the continuous phase viscosity on the eddy turbulent kinetic energy is more and more important approaching the Kolmogorov scale. Therefore, the model based on the inertial subrange assumption, which do not account for the continuous phase viscosity effects, overestimates the turbulent kinetic energy of the eddies and consecutively the breakup rate.

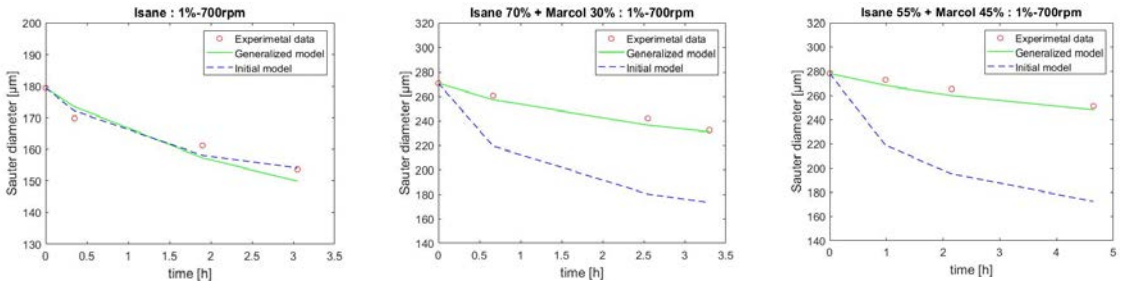

Figure 1. Caption. [Calibri 9].

4. Conclusions

In this work, general breakage and coalescence kernels, accounting for the entire spectrum of turbulence, are proposed. The new model is based on a refined second-order structure function and an energy spectrum considering all the domains of turbulence. The model shows good agreement with experimental data measured in liquid-liquid dispersions at increasing viscosity.

References

[1] A. P. Davidson, Turbulence: an introduction for scientists and engineers, Oxford University Press, 2004.
[2] S. B. Pope, Turbulent flows, Cambridge University Press, 2000.
[3] S. Castellano, N. Othman, D.L. Marchisio, A. Buffo, S. Charton, Chem. Eng. J. 354 (2018), pp. 1197-1207.
[4] S. Castellano, L. Carrillo, N. Othman, D.L. Marchisio, A. Buffo, S. Charton, Chem. Eng. J. (2019), *accepted*

ECCE12
The 12th EUROPEAN CONGRESS OF CHEMICAL ENGINEERING
Florence 15-19 September 2019

Hydraulic Characterization of Water-Air Flows in Cooling-Tower Packing.

Nicolas Jourdan[1,2], Mohamed Kanniche[1], Thibaut Neveux[1], Olivier Potier[2]

1 EDF R&D, EDF Lab Chatou, 6 quai Watier 78400 CHATOU FRANCE
2 LRGP, CNRS UMR 7274, Université de Lorraine, 1 rue Grandville, 54000 NANCY FRANCE

**Corresponding author: nicolas.jourdan@edf.fr*

Highlights

- Study of wet-cooling tower packing hydrodynamics
- Experimental characterization of falling water films: thickness and instabilities
- Benchmark of CFD approaches for simulations of water films

1. Introduction

Industrial wet-cooling towers are used in various industrial fields such as power plants, refineries or chemical plants. These cooling towers are filled with packing to increase heat and mass transfer between hot water and counter-current air flow [1]. Despite numerous investigations of heat transfer performances and pressure losses [2], hydraulic characteristics such as wetting ratios or water film thicknesses –prerequisite for study of fouling phenomena– are yet to be determined. This study aims at presenting both experimental and numerical characterization of packing hydrodynamics using a dedicated pilot-plant and CFD simulations.

2. Methods

To obtain local information on the flow characteristics along the cooling tower packing, a small scale transparent cooling tower pilot-plant was designed and built, with attention put on the representativeness of water and air distributions. Falling films along the packing channels are observed using a fast camera system tangent to the packing surface. The transparent walls allow the visualization all around the packing structure on different spots. The water film is isolated by subtracting images with and without water with the help of a specific program and Matlab Image Analysis toolbox. The global characterization of the packing is obtained by a statistical analysis film thickness over time and location in the various flow conditions (liquid load, air flow rate, temperature and humidity).

In the same time, CFD simulations are performed on simplified geometry, taken from literature [3], in order to investigate the ability of different CFD approaches to predict correctly falling water films along vertical surfaces.

3. Results and discussion

With the experimental apparatus, data on the flow characteristics are obtained and particularly on water films thickness. One example of post-treatment is shown on Figure 1. From the videos, two phenomena are observed: the wavy film instabilities that came from the flow regime and drops falling along the wall significantly increasing the film thickness. Film thickness evolution is one main parameter influencing fooling phenomena such as kinetics of calcium carbonate precipitation and biofilm development. The wavy film instabilities are estimated by plotting the film thickness over time and processing data with a harmonic analysis using Matlab.

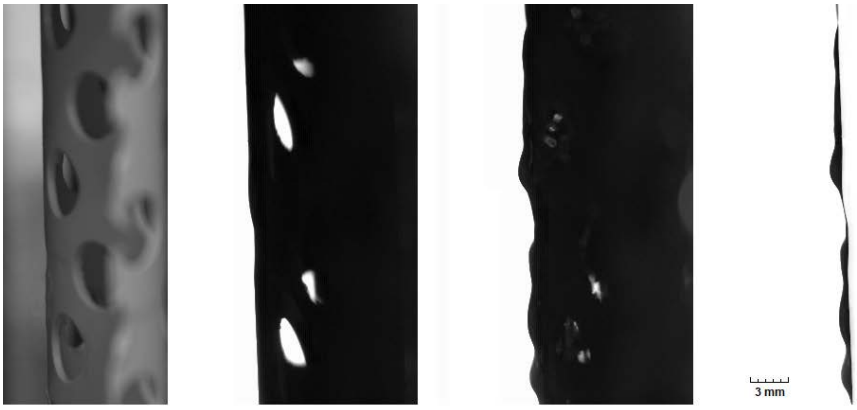

Figure 1. (a) Picture of packing. (b) Reference dry frame. (c) Picture of wetted packing. (d) Subtracted frames to obtain the resulting water film

CFD simulations were performed with two different approaches: Eulerian-Eulerian two-phase model with interface tracking using NEPTUNE_CFD software [4] and VOF method using OpenFOAM software. First results showed that the VOF method is more suitable for falling film simulations because it takes into account the contact angle with the wall for better prediction of wettability, near-wall velocity profiles and shear-stress that influence fouling phenomena (Figure 2).

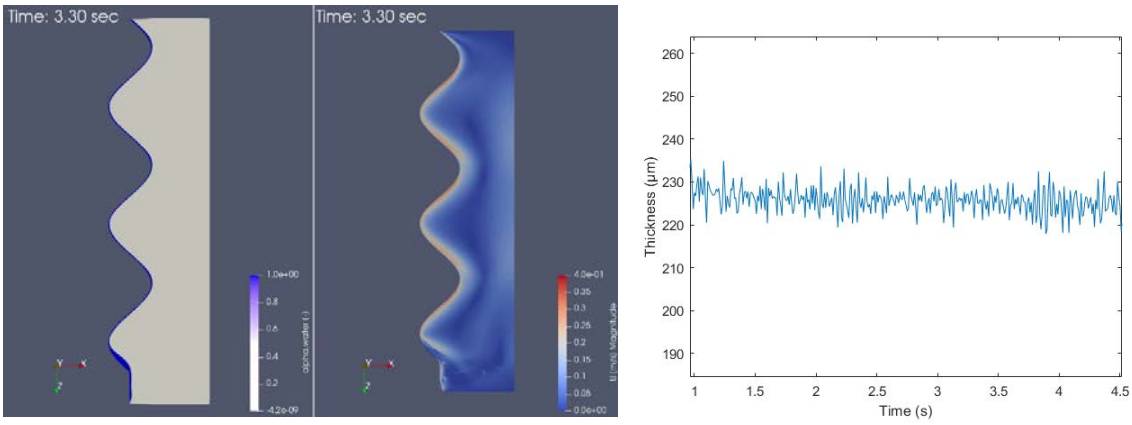

Figure 2. VOF simulations results (a) Water phase rate and air velocity (b) Water film thickness (z=13mm)

4. Conclusions

The experimental setup allows the characterization of falling water on cooling tower packing surface. The water films thickness and their variations were pointed out and the instabilities characteristics were estimated to better understand the phenomena that depend on hydrodynamics. The CFD simulation is promising methods to complete experimental data towards predictive results. These two approaches are complementary to model phenomena of interest such as mass transfer, heat transfer or chemical reactions.

References

[1] R. Terblanche, H.C.R Reuter, D.G. Kröger, Appl. Therm. Eng., 29 (2009) 1552–1560.
[2] M. Lemouari, m. Boumaza, A. Kaabi, Energ. Conv. Manag., 50 (2009) 1610-1617
[3] S. Negny, M. Meyer, M. Prevost, Int. J. Heat Mass Tran., 44 (2001) 2137-2154
[4] P. Coste, Nuc. Engin. Design., 255 (2013) 38-50

ECCE12
The 12th EUROPEAN CONGRESS OF CHEMICAL ENGINEERING
Florence 15-19 September 2019

Single Drop Rising and Salt Effects in Low Interfacial Tension System.

Jiyizhe Zhang[1], Yundong Wang[1], Geoffrey W Stevens[2] , Weiyang Fei[1]

1 The State Key Laboratory of Chemical Engineering, Department of Chemical Engineering, Tsinghua University, Beijing 100084, China , 2 Department of Chemical and Biomolecular Engineering, The University of Melbourne, Parkville, Victoria 3010, Australia

**Corresponding author: wangyd@mail.tsinghua.edu.cn*

Highlights

- Terminal velocities were evaluated for the low interfacial tension system.
- By plotting d_e-v_t-Re in a three dimensional way, application range of implicit correlation can be observed apparently.
- Influences caused by salt addition was investigated.

1. Introduction

Liquid-liquid extraction plays an important role in petrochemical, pharmaceutical, hydrometallurgical, as well as post-processing in nuclear industry. Single drop rising is one of the most fundamental behaviors which influences the terminal velocity and affects mass transfer rate ultimately. However, the motion of droplet is sensitive to contaminations, like salt ions, surfactants or solid particles, which are usually unavoidable in industrial operations. In general, drop terminal velocities can be predicted in three ways [1]: explicit correlations and models in the form of $v_t=f(d_e)$, implicit correlation of $C_D=f(Re)$ and generalized graphical correlation in terms of Eötvös number, Reynolds number and Morton number. Although different methods have been adopted for calculating terminal velocity, few of them are validated in low interfacial tension system. In addition, contaminations like surfactants have been investigated, but limit work has been done to determine the influence caused by salt ions, e.g. salt concentration and type.

In this study, single drop rising in low interfacial tension system (i.e. butanol-water system) was recorded by high speed camera to obtain terminal velocity. Then the terminal velocities were compared to the predictions by correlations from literature, both explicit and implicit. Furthermore, salt effect was determined by adding different salt with various concentrations into continuous phase.

2. Methods

As proposed by European Federation of Chemical Engineering (EFCE), n-butanol/water was chosen as the standard low interfacial tension system and the two phase were mutually saturated before use. Different type of salts were used, e.g. NaCl, Na_2SO_4, NaAc, NaI, $MgCl_2$, $MgSO_4$, and $AlCl_3$. Droplet rising was accomplished in a lab-scale column and was recorded by high speed camera. Images were analyzed by software ImageJ to derive drop diameter and terminal velocity.

3. Results and discussion

For the low interfacial tension system, correlations for terminal velocity were evaluated both explicitly and implicitly. For implicit correlation given as C_D=f(Re), by plotting d_e-v_t-Re in a three dimensional way, the application range of the correlation can be viewed obviously.

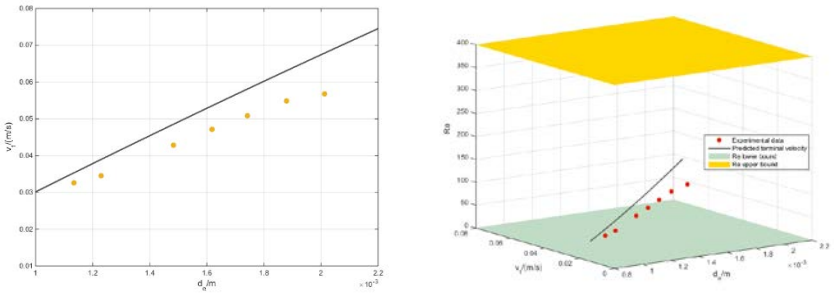

Figure 1. Terminal velocity predicted from Saboni drag coefficient correlation[2]

The addition of salt changes the physical properties of the system and influences the hydrodynamic behaviors of droplet consequently. From a general view in Figure2, the terminal velocity increases with concentration. When the concentration is low, the increase of terminal velocity is not obvious. In this case, ions absorb at the interface and slightly decreases the interfacial tension. However, as the concentration increase further, the increase of terminal velocity becomes apparent. This is because the interface becomes saturated and subsequently addition of salt increases the bulk concentration as well as density.

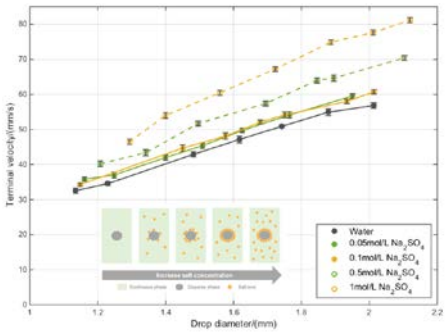

Figure 2. Influence of Na_2SO_4 concentration on terminal velocity

4. Conclusions

Terminal velocities for n-butanol drop rising in water as well as in salt solution have been investigated experimentally. Various explicit and implicit correlations for terminal velocities were evaluated. For the implicit correlations, the application range was considered carefully by plotting d_e-v_t-Re in a three dimensional way. Influence of ions showed that physical properties change caused by salt addition should be analyzed at the same time.

References

[1] M. Wegener, N. Paul, and M. Kraume, International Journal of Heat and Mass Transfer, 71 (2014) 475-495.

[2] A. Saboni, S. Alexandrova, AIChE journal, 48(2002), 2992-2994.

ECCE12
The 12th EUROPEAN CONGRESS OF CHEMICAL ENGINEERING
Florence 15-19 September 2019

Engineering Method for Calculating of an Axial Valve Separator with an External Location of the Locking Part.

Anna Kapranova[1], Sergey Neklyudov[2], Anton Lebedev[1], Alexander Meltser[2], Dmitriy Voronin[2]

1 Yaroslavl State Technical University, Moskovsky Prospect, 88, Yaroslavl, 150023, Russia; 2 JSC «Regulyator», Gagarin Street, 68a, Yaroslavl, 150023, Russia

**Corresponding author: kapranova_anna@mail.ru*

Highlights

- Proposed a block diagram of the calculation of the axial valve separator.
- The required valve flow capacity is taken into account.
- The results of stochastic modeling of the hydrodynamic cavitation are the basis.
- An example of the calculation of the axial valve separator is made.

1. Introduction

Improving engineering methods for calculating valves is a pressing issue in the field of pipeline fittings design. The task of reducing the intensity of cavitation effects in the flow part of the valve can be successfully solved by throttling fluid flows. Axial valves provide a straight-line flow of fluid with minimal resistance when opened. The design of the axial valve proposed by the authors [1] assumes a coaxial arrangement of the separator and the movable external locking member, which have the form of hollow cylindrical shells (fig. 1). Thus, the throttle round holes of the fixed separator overlap when the cylindrical shell obeys along its outer surface. This shell can be set in motion as a rack and a crank mechanism.

2. Methods

The purpose of the work is to develop a scientifically based method for calculating the effective ranges of the design parameters of the throttle part of the axial valve. Earlier, the authors used the stochastic approach with the equilibrium representation of the states of the energetically closed macrosystem [2] within the framework of the Ornstein-Uhlenbeck random process [3] to form the model of the bubble formation process in the separator at the initial stage of hydrodynamic cavitation. The proposed stochastic models [4-8] allowed us to obtain differential distribution functions of the number of cavitation bubbles formed during the initial stage of the evolution of hydrodynamic cavitation, according to their size [4-6] and the degree of opening of the axial valve [7, 8]. The expression obtained using this model [4] for calculating the average over the ensemble of the diameter D_{sb} for the macrosystem of cavitation bubbles [5, 6] takes into account the physical and mechanical properties of the working medium, as well as the main design and operating parameters of the axial valve. Another model [7, 8] made it possible to establish a connection between the critical value of the Reynolds number Re_{cr} in the case of a complete opening of the valve and its design parameters. So, these expressions for D_{sb} [5, 6] and Re_{cr} based on [7, 8], as well

as the obtained expressions for the energy parameter of the stochastic model [8] and the hydraulic resistance coefficient [9] are used in the proposed engineering method.

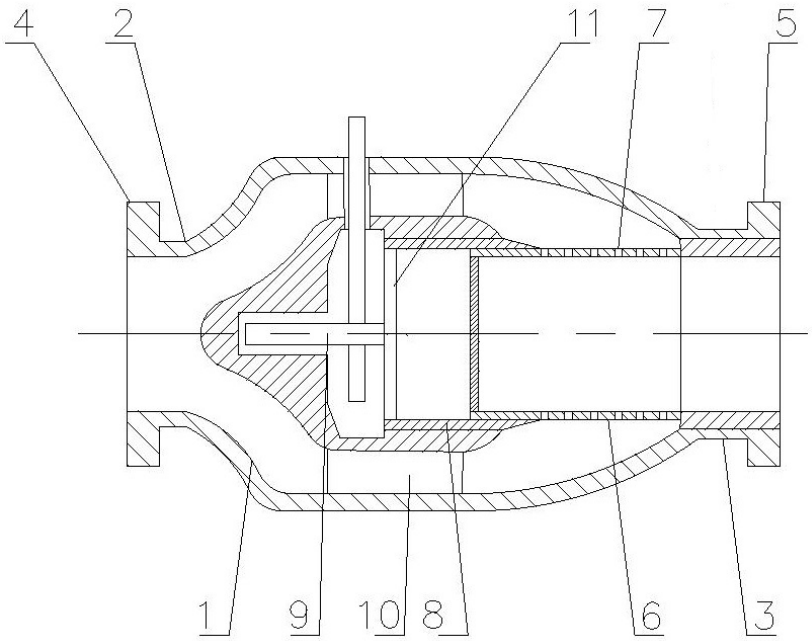

Figure 1. Schematic diagram of an axial valve with an external positioning of the locking member:

1 - outer case, 2 and 3 - inlet and outlet nozzles, 4 and 5 - flanges, 6 - separator, 7 - throttle holes, 8 - cylindrical conical, 9 - rack and pinion mechanism, 10 - cavity of the inner housing, 11 - radial partitions

3. Results and discussion

The proposed block diagram (fig. 2, 3) consists of 25 main blocks for calculating 13 effective values of the design parameters of an axial valve separator. For example, the required parameters include: diameter of round throttle holes d_0, arc distance between the holes in one row, distance between rows of these holes, separator thickness, number of holes for one row, number of these rows, diameter of the outlet of the separator, its perforated part length, bevel angle for the cylindrical part of the shell, etc. Specified operating parameters are the maximum attainable fluid flow through the regulating device at a given value of the medium temperature, the minimum pressure drop, the maximum pressure in the center of the bubble, which corresponds to the minimum value of its radius, the saturated vapor pressure of the medium, the velocity of the fluid in the pipeline. The input parameters for the calculation are the maximum attainable flow rate of the medium, the temperature of the medium, the limits of variation of the minimum pressure drop and the velocity of the fluid in the pipeline. The output parameter is the required valve capacity K'_{vy}. The flowchart proposes a phased calculation of various approximations of the desired design parameters depending on the selected intervals for changing the maximum value of the valve throughput. The specified intervals are refined three times (blocks 3, 10, 21), taking into account the required value of capacity K'_{vy} with the choice of safety factors. For the first time, this is done at specified intervals of change in the minimum pressure drop (block 3), in the second - after calculating Re_{cr} based on [7, 8, 10] to determine correction factors for medium viscosity (block 10), in the third - after estimating the hydraulic resistance coefficient ζ_y^* [9] from the condition of minimal D_{sb} value (block 21) [5, 6].

4. Conclusions

According to the performed calculation example, with K'_{vy}=6,0 m^3/h; Re_{cr}=5209,58; ζ_y^*=0,119 obtained rational ranges of changes of the desired parameters, in particular, the average value of d_0 from the specified range is 5.05x10^{-3} m with a separator outlet diameter of 4.19x10^{-2} m and the length of its perforated part 8.21x10^{-2} m. The main practical value of this work is the possibility of reducing the intensity of cavitation in an axial valve when throttling fluid flows, as a result, extending the service life of regulating devices of this type.

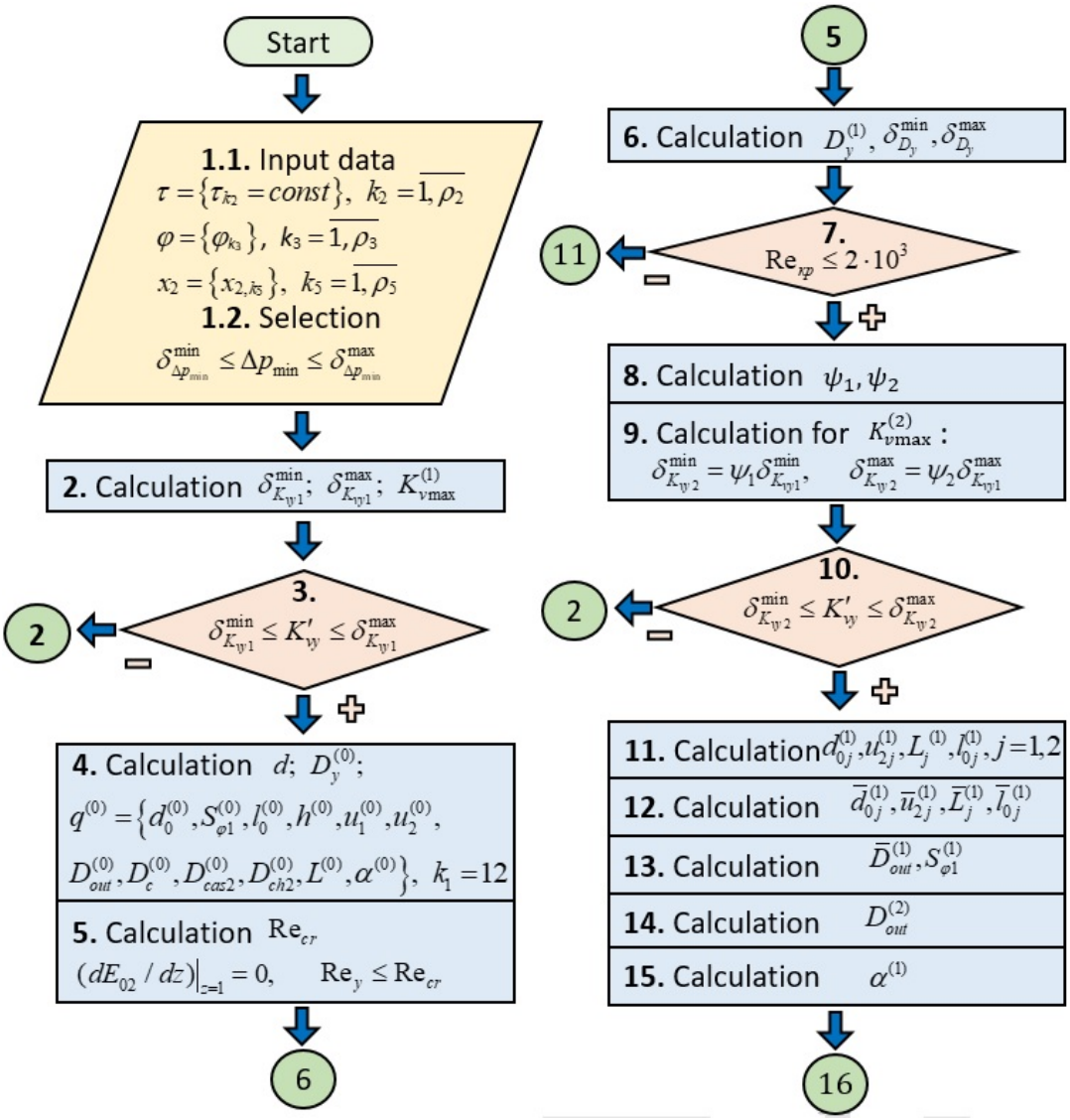

Figure 2. Conventional block diagram of the calculation of the design parameters of the axial valve separator with the external location of the locking member (Part 1)

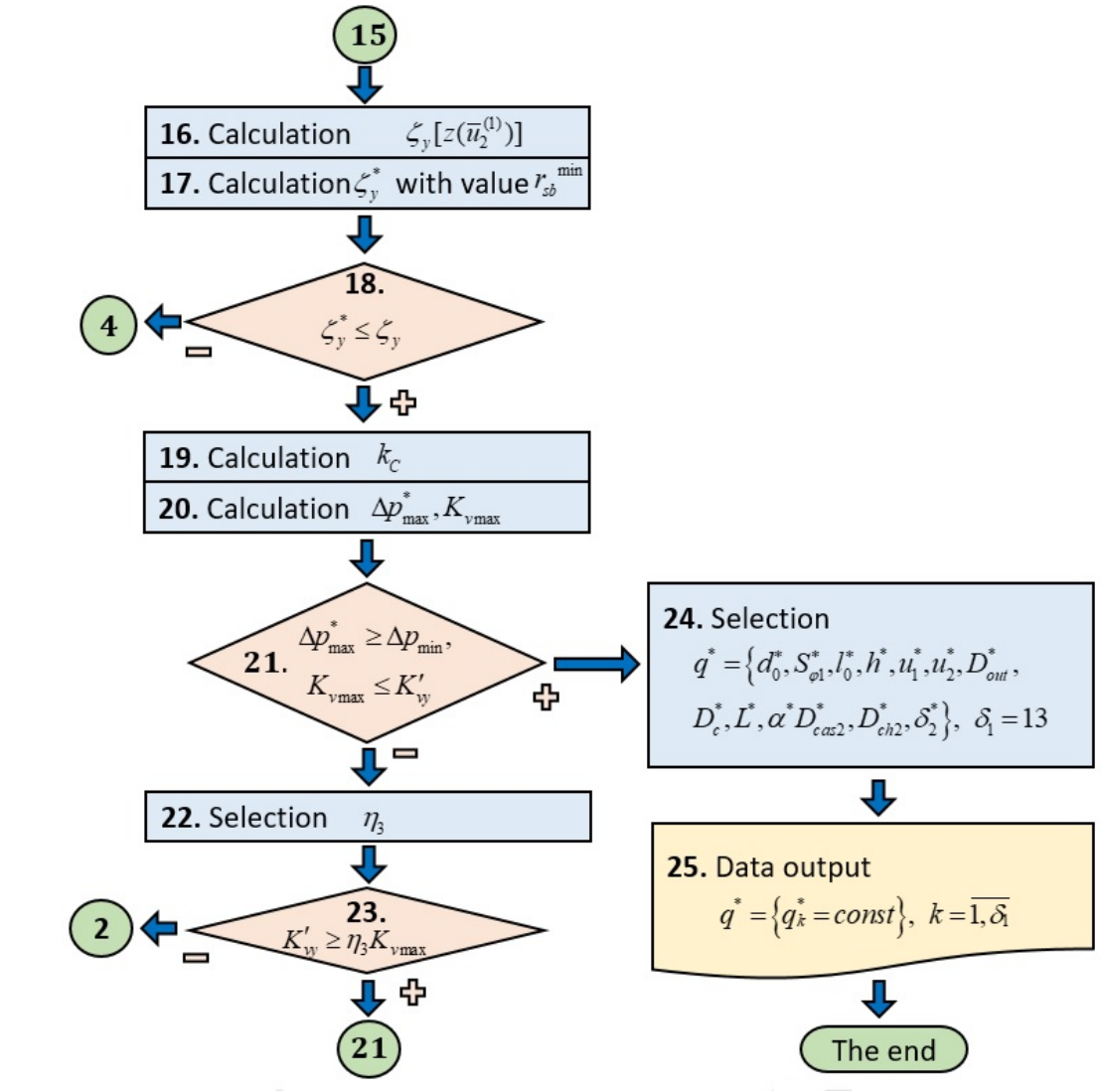

Figure 3. Conventional block diagram of the calculation of the design parameters of the axial valve separator with the external location of the locking member (Part 2)

References

[1] A.E. Lebedev, A.B. Kapranova, A.M. Meltser, S.A. Solopov, D.V. Voronin, S.V. Neklyudov. Patent on the model 175776 Russian Federation, IPC F16K 1/12, F16K 47/14, F16K 3/24. Direct-acting control valv. May 2018.

[2] Y.L. Klimontovich, Turbulent Motion and Chaos Structure: A New Approach to the Statistical Theory of Open Systems, LENAND, Moscow, 2014.

[3] A.B. Kapranova, A.E. Lebedev, A.M. Meltser, S.A. Solopov, Czas. Tech. Mech. 113 (2, 2016) 136-144.

[4] A.B. Kapranova, A.E. Lebedev, A.M. Meltser, S.V. Neklyudov, Vestn. IGEY Her IGEY. 4 (2016) 94-107. doi:10.17588/2072- 2672.2016.4.024-029.

[5] A. Kapranova, A. Lebedev, A. Meltser, S. Neklyudov, Int. J. Mech. Eng. Technol. 9 (3, 2018) 25-31.

[6] A.B. Kapranova, A.E. Lebedev, A.M. Meltser, J. Chem. Eng. Process Technol. 8(5 (Suppl), 2017). doi:10.4172/2157-7048-C1-009.

[7] A.B. Kapranova, J. Chem. Eng. Process Technol. 9 (2018). doi:10.4172/2157-7048-C3-016

[8] A. Kapranova, S. Neklyudov, A. Lebedev, A. Meltser, Int. J. Mech. Eng. Technol. 9 (8, 2018) 160-166.

[9] A. Kapranova, S. Neklyudov, A. Lebedev, A. Meltser, Int. J. Mech. Eng. Technol. 9 (8, 2018) 153-159.

[10] A. Kapranova, A. Miadonye, J Oil Gas Petrochem Sci. 2(2, 2019) 70-75. doi:10.30881/jogps.00026.

ECCE12
The 12th EUROPEAN CONGRESS OF CHEMICAL ENGINEERING
Florence 15-19 September 2019

CFD-DEM Simulation of The Breakup of Carbon Black Agglomerates in an Internal Mixer.

Graziano Frungieri[1], Gianluca Boccardo[1], Antonio Buffo[1], Daniele Marchisio[1], Marco Vanni[1]

[1] *Dept of Applied Science and Technology, Politecnico di Torino, Corso Duca degli Abruzzi 24, Torino*

**Corresponding author: graziano.frungieri@polito.it*

Highlights

- Novel approach for modelling the compounding of rubber materials.
- CFD simulation of an internal mixer for rubber compounding.
- Stokesian Dynamics of carbon black agglomerates.

1. Introduction

The compounding of rubber materials frequently requires the incorporation of solid filler particles, in order to enhance the mechanical properties of the final product. Carbon black particles are among the most commonly used; they generally exist in the form of large agglomerates (up to hundreds of micrometers) which, during the mixing process, are broken down into smaller fragments and uniformly distributed into the rubber matrix.
Previous studies have generally focused on the investigation of the flow field in the mixing equipment and only few attempts have been made in the analysis of the breakup behavior of the agglomerates, with most of them adopting severe simplifications on the aggregate morphology and the breakup mechanism [1].
In this work we adopt a numerical approach which couples a computational fluid dynamics (CFD) simulation of the flow field in a typical mixing equipment with detailed Discrete Element Method (DEM) simulations, able to fully count for the agglomerate morphology and to predict accurately the occurrence of breakup.

2. Methods

A 2D section of an actual rubber internal mixer has been used for the current investigation. The flow field inside the mixing equipment is computed using the open-source CFD code Code_Saturne. The rheology of the rubber medium is modelled according to the Bird-Carreau model. At this stage, agglomerates are treated as point particles, whose trajectories are recorded together with the viscous stress experienced during the motion.
This piece of information is used by a DEM code built in the framework of the FTS (force-torque-stresslet) formulation of Stokesian Dynamics [2]. At this stage the disordered structure of the agglomerates is modeled in detail; the DEM is thus able to evaluate the hydrodynamic forces acting on each constituent monomer and to evaluate the internal stress acting on each single intermonomer contact, in terms of normal force, transverse force and bending moment. The occurrence of breakup can be then readily determined by comparing the internal stresses with the single bond resistance.

3. Results and discussion

Figure 1 shows an overview of the simulation results. In the top figure a snapshot of the instantaneous velocity contour plot is reported. As expected, the regions of highest shear are located in the narrow gap between the rotor tip and the chamber wall. The bottom left figure reports the intensity of the hydrodynamic force acting on each single monomer. It is apparent that larger forces act on the most external monomers. On the contrary, inner monomers experience lower hydrodynamic forces because of the screening effect induced by the surrounding ones. However, the most stressed bonds are generally located in the inner parts of the agglomerate (bottom right figure); this is in line with the expectation that the stress induced by the flow field propagates from the peripherical to the internal region of the agglomerate and accumulates in some critical locations. [3]

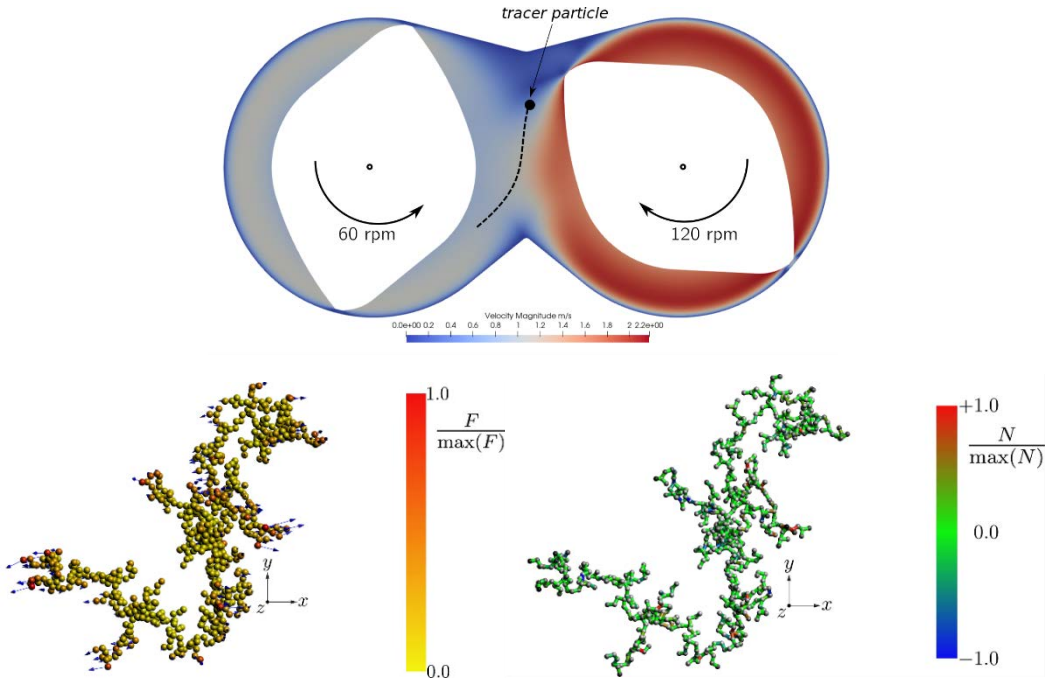

Figure 1. (top) Instantaneous velocity contour plot in a 2D section of an internal mixer. The gap between the rotor tip and the chamber wall is 1 cm wide. (bottom left) Instantaneous hydrodynamic forces acting on a model carbon black agglomerate. The agglomerate has fractal dimension equal to 1.7 and gyration radius equal to 30 micrometers. (bottom right) Instantaneous normal stress acting on the monomer-monomer bonds. Positive values indicate tensile stress.

4. Conclusions

In this work a combined CFD-DEM approach is adopted to investigate the compounding process of rubber composites. Results provide new insights into the breakup mechanism and may be useful for the design and the choice of operative conditions of internal mixers.

The project leading to this application has received funding from the European Union's Horizon 2020 research and innovation programme under grant agreement No 760907.

References

[1] I. Manas-Zloczower, Mixing and compounding of polymers: theory and practice, second ed., Hanser Publishers, Munich, 2009.
[2] G. Frungieri, M. Vanni, Can. J. Chem. Eng. J. 95 (2017) 1768-1780.
[3] M. Vanni, A. Gastaldi, Langmuir 27 (2011) 12822-12833.

ECCE12
The 12th EUROPEAN CONGRESS OF CHEMICAL ENGINEERING
Florence 15-19 September 2019

Intensifying the Re-carbonation Process of Water.

Gabi Altabash[1], Mahmoud Al-Hindi[1], Fouad Azizi[1*]

1 Dept. of Chemical and Petroleum Eng. American University of Beirut, POBox: 1107 2020 Beirut, Lebanon

**Corresponding author: fouad.azizi@aub.edu.lb*

Highlights

- An attempt to intensify CO_2 absorption in water was undertaken,
- Two different measurements techniques were employed,
- High k_La values were obtained in short residence times at low energy consumption,

1. Introduction

Several reactor types are used for gas-liquid mass transfer operations; however, many of which remain improperly designed because of their complex hydrodynamics. A new type of static mixing element was recently introduced in which woven mesh screens or grids are used to repetitively superimpose an adjustable uniformly distributed turbulence field on the nearly plug flow conditions encountered in high velocity pipe flows. These mixers were found to be very effective at processing multiphase operations [1, 2]. These screens are typically used as a source or sink for turbulence and are characterized by their wire size, mesh opening, and fraction open area. This study therefore aims at employing them to intensify the absorption of CO_2 in RO water without chemical reactions. Its success would allow achieving smaller reactor volumes and introducing various economical and safety enhancements. Faster and more efficient re-carbonation processes can thus be conducted at lower energy consumption and space requirements. In addition, the intensification of these processes will also impact the design of photo-bioreactors by providing CO_2-rich waters for the cell cultures in very short residence times and influence various applications of biogas upgrading.

2. Methods

In order to meet the research objectives, a plug flow reactor design (length = 560 mm and inner diameter = 25 mm), equipped with screen type static mixers was employed to test and quantify the transfer rates of CO_2 into RO water. To analyze the data, the amount of absorbed CO_2 was quantified using two different measurement techniques, namely, pH measurements and another direct measurement technique using a CO_2 analyzer (Anton Paar®, model CarboQC). The method of analysis was that proposed by Kordač and Linek [3]. The experiments were conducted using 8 screen elements placed at 70 mm apart. The total superficial velocity was varied between 1 and 2 m/s while testing for three different gas volume fractions (ϕ = 10, 20, and 30%). Under these conditions, the residence time of the mixture in the mixing section varied between 0.28 and 0.56 s.

3. Results and discussion

The efficiency of the reactor was evaluated from the calculated volumetric mass transfer coefficients, k_La, that were determined from the dissolved concentrations of CO_2 in water. The two

measurement techniques differed by less than 10% when comparing pH measurements to pH values back-calculated from direct CO_2 measurements. Similarly, to many other studies, k_La increased with an increasing U_T and ϕ (cf. Figure 1). It reached a maximum value of 1.01 s^{-1}. These values were obtained at low energy consumption rates. The latter was characterized using the specific energy consumption per unit mass of liquid treated, E_{spm} [1]. This parameter was found to vary between 0.002 and 0.019 kWh/tonne and always decreased with an increase in ϕ because of the subsequent reduction in the total pressure drop. For a detailed comparison with other gas-liquid contactors, the reader is referred to [1]. Furthermore, to better differentiate the effect of changing the screens, it was critical to choose the Reynolds number characteristic length with respect to the screen geometry and not rely on the empty pipe Re (cf. Figure 2).

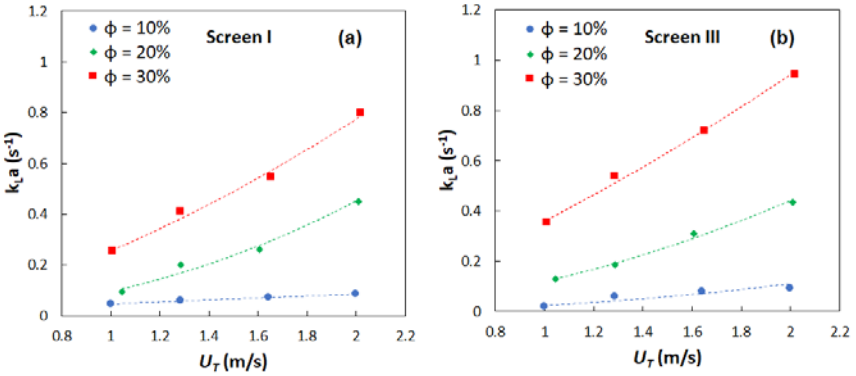

Figure 1. Effect of superficial velocity and gas holdup on the volumetric mass transfer coefficient.

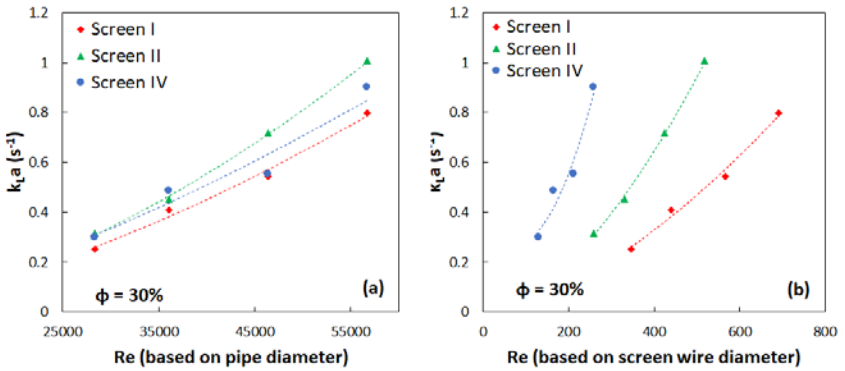

Figure 2. Effect of changing Re characteristic length on interpretation of results.

4. Conclusions

Intensifying CO_2 absorption in RO water was investigated using a tubular reactor equipped with screen-type static mixers. k_La values were affected by screen geometry where higher values were recorded when using screens characterized by small open area, small wire diameter and mesh size. The values obtained in the present work were found to be one to two orders of magnitude higher than conventional gas-liquid contactors such as mechanically agitated tanks and bubble columns and were in the same order of static mixers and advanced flow reactors.

References

[1] F. Azizi, A.M. Al Taweel, Ind. Eng. Chem. Res., 54 (2015) 11635–11652.
[2] A.M. Al Taweel, F. Azizi, G. Sirijeerachai, Chem. Eng. Proc.: Proc. Intens. 72 (2013) 51–62.

[3] M. Kordac, V. Linek, Ind. Eng. Chem. Res., 47 (2008) 1310–1317.

ECCE12
The 12th EUROPEAN CONGRESS OF CHEMICAL ENGINEERING
Florence 15-19 September 2019

Crystal Growth Simulation in a Continuously Operated Helically Coiled Tube.

Viktoria Wiedmeyer[1], Andreas Voigt[1], Kai Sundmacher[1,2]

1 Otto von Guericke University Magdeburg, Magdeburg, Germany; 2 Max Planck Institute for Dynamics of Complex Technical Systems, Magdeburg, Germany

**Corresponding author: viktoria.wiedmeyer@ovgu.de*

Highlights

- The crystal size distribution width stays constant in the helically coiled flow tube.
- The crystal product-to-seed ratio attains a saturation level at increasing tube length.
- For a tube length of up to 150 m, the crystal residence time is in the order of minutes.

1. Introduction

Continuous crystallization can be advantageous in continuous process chains when a constant product quality is required. The product quality is influenced by the product crystal size distribution. A narrow size distribution and a low number of additives are often preferred considering downstream steps in the process chain as solid liquid separation. Hence, cooling crystallization is selected. Among the continuous crystallizers, tubes offer narrow residence time ranges and thus narrow product crystal size distributions may be reached through crystal growth. Breakage and abrasion are negligible compared to setups with active mixing. Among the tubes, helically coiled flow tubes (HCTs) have a compact geometry and mixing properties, which are necessary to realize narrow residence time distributions. The potential of this novel crystallization device and a reasonable operation regime regarding residence times and tube lengths are estimated.

2. Methods

A simulation study is carried out for varying flow rates and crystallizer lengths. The model is a coupled population balance equation (PBE) system that is based on experimental results. The system consists of a PBE that is dominated by (1D) growth [1] and (1D) convection along the axis of the HCT and of mass balances for the continuous phase. The partial differential equations are solved by discretization on an equidistant grid of finite volumes using a slope limiter. Numerical diffusion can be adjusted by the number of control volumes to reflect hydrodynamic dispersion and growth rate dispersion. The investigated model substance is univariate potash alum. For this substance, experiments showed that aggregation could be neglected [2]. Further, the model includes experimentally measured size-dependent crystal residence times at two selected laminar fluid velocities of 0.27 m/s and 0.35 m/s [3]. The laminar flow range is selected to realize sufficient residence times at reasonable tube lengths. The inlet temperature was 41 °C. It was assumed that the temperature profile decayed exponentially along the tube to 35 °C while it reached 35.5 °C at a tube length of 10 m.

3. Results and discussion

As expected, the mean product size and mass increase with the tube length. The width of the crystal size distribution stays constant in the simulations due to the size-dependent crystal velocity despite growth rate dispersion. At a length of 25 m, the mean crystal size increased from 80 µm to 119 µm at the low flow rate. At a length of 100 m, it increased only slightly more to 124 µm while the standard deviation of the product crystal distribution was still equal to the initial standard deviation of 15 µm. Similarly, the crystal product-to-seed mass ratio saturates with the tube length in Figure 1. Since the temperature profile is fixed along the HCT, the supersaturation approaches the equilibrium solubility with an increasing tube length and the driving force for crystal growth diminishes. For a tube length of 25 m, the crystals occupy 9 % of the HCT volume at steady state while they occupy 11 % for a tube length of 100 m. For a tube of 25 m length, the crystal residence time is about 8 min while it is about 30 min for 100 m. For the higher fluid flow rate, the residence time is only about 10 min at 100 m. Only for large tube lengths, the product to seed mass ratio is higher than for the low flow rate.

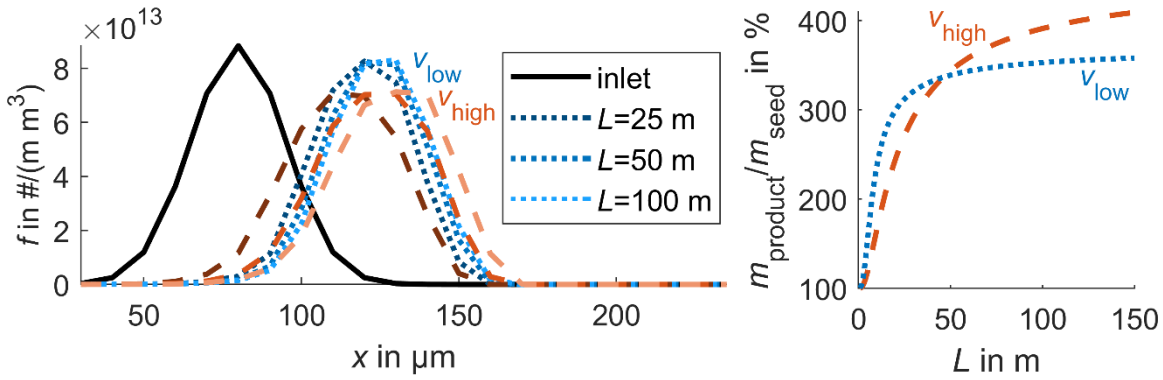

Figure 1. Left: Crystal number distribution per second at steady state in the feed and in the product over crystal size for two laminar flow rates at varying tube length. Right: Ratio of product to seed crystal mass at steady state over tube length for two laminar flow rates under fixed conditions.

4. Conclusion

Continuously operated helically coiled flow tubes can produce narrow crystal size distributions. For a fixed temperature profile, the product to seed mass ratio saturates with the tube length. When the product crystal mass shall be maximized, it depends on the tube length whether low or high flow rates are advantageous assuming that sedimentation is avoided. In this case, a tube of 0.06 m diameter and of up to 25 m length for the low flow rate and up to 100 m length for the high flow rate seems to be reasonable.

The financial support of the DFG (Deutsche Forschungsgemeinschaft) within the priority program SPP 1679 "Dynamic simulation of interconnected solid processes DYNSIM-FP" is gratefully acknowledged.

References

[1] C. Y. Ma, J. Wan, X. Z. Wang, Powder Technol. 227 (2012) 96–103.
[2] V. Wiedmeyer, A. Voigt, K. Sundmacher, Chem. Eng. Technol. 40 (2017) 1584–1590.
[3] V. Wiedmeyer, F. Anker, C. Bartsch, A. Voigt, V. John, K. Sundmacher, Ind. Eng. Chem. Res. 56 (2017) 3699–3712.

ECCE12
The 12th EUROPEAN CONGRESS OF CHEMICAL ENGINEERING
Florence 15-19 September 2019

Selectivity of gas-liquid reactions in straight and coiled capillaries and CFI

Julia Grühn[1], Norbert Kockmann[1]

1 TU Dortmund University, Biochemical and Chemical Engineering, Laboratory of Equipment Design,

Emil-Figge-Str. 68, 44227 Dortmund, Germany

**Corresponding author: julia.gruehn@tu-dortmund.de*

Highlights

- Deeper understanding of gas-liquid reactions with mass transfer
- Optical measurement technique for mass transfer and selectivity
- Correlations between flow behavior and chemical selectivity

1. Introduction

Two-phase flow and gas-liquid reactions in particular are of great importance in the chemical industry and, therefore, subject of current research since they are often limited by mass transfer or show low selectivity [1]. Investigations of Krieger *et al.* based upon the consecutive oxidation of leuco-indigo carmine [2]. To visualize local gas-liquid mass transfer in capillary plug-flow a colorimetric technique was used there. For studies on selectivity it is essential that the oxidation passes two detectable color changes. Further investigations on flow behavior have shown three relevant flow regimes depending on different operating conditions [2]. Since the selectivity in bio-catalytic reaction systems is an important field in research as well, investigations of bio-catalytic parallel reactions were performed, too**.** Beyond that, suitable reaction systems from the DFG-SPP1740 "Reactive Bubbly Flows" [3] were tested and an optical measuring method was established.

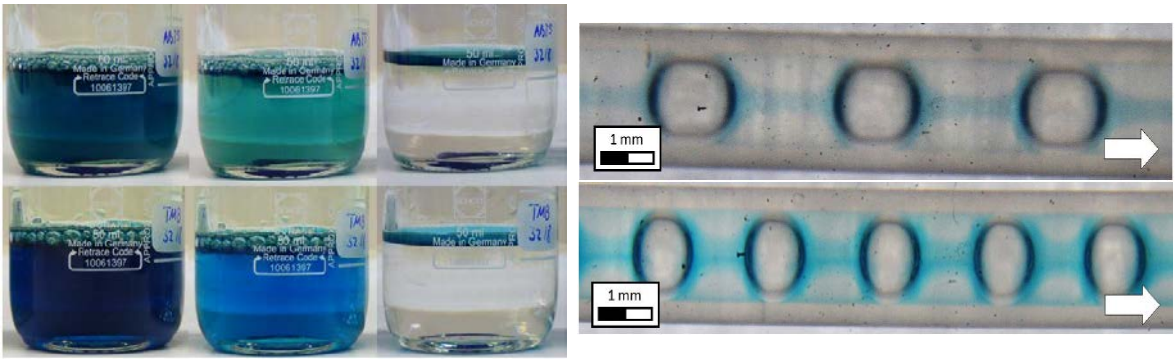

Figure 1. Top left: Enzymatically solution of glucose oxidase and ABTS (2,2´-azino-bis(3-ethylbenzothiazoline-6-sulphonic acid)) as dye. Completely oxidized (l.), 35 s after oxidation (m.), completely reduced (r.). Top right: Gas-liquid capillary flow with the enzymatically solution and ABTS as dye. Bottom left: Enzymatically solution of glucose oxidase and TMB (3,3´,5,5´-Tetramethylbenzidine) as dye. Completely oxidized (l.), 45 s after oxidation (m.), completely reduced (r.). Bottom right: Gas-liquid capillary flow with the enzymatically solution and TMB as dye.

2. Methods

The experiments of the two-phase flow in capillaries were performed according to the approach of Krieger *et al*., in which the flow regime is dominated by Taylor vortices. The experimental setup consists of a straight capillary build of FEP (fluorinated ethylene propylene) with 1.6 mm inner diameter. Furthermore, the experiments were performed in a PMMA box (Poly(methyl-methacrylate)) filled with deionized water [2]. Since FEP and water have nearly the same refractive index, it can be assumed that disturbances caused by deviating refractive indices are negligible. Beyond this, the experimental setup is temperature-adjustable. Building on this, investigations on gas-liquid reactions in coiled capillaries and coiled flow inverters (CFI) follow for suitable bio-catalytic systems as well as for chemical systems from the DFG-SPP1740 “Reactive Bubbly Flows” [3]. For analytical evaluation an optical measurement system is required to avoid flow disturbances. The colorimetric technique used by Krieger *et al*. was adapted to the respective reaction system [2].

3. Results and conclusion

Finally a deeper understanding on selectivity of gas-liquid reactions in general is developed by comparing the experimental results of the consecutive oxidation of leuco-indigo carmine with the bio-catalytic parallel reaction and other reaction systems from the DFG-SPP1740 “Reactive Bubbly Flows”. Furthermore, the studies on the different reactor types (straight capillary, coiled capillary and CFI) provide information about the correlation between flow behavior and selectivity for gas-liquid reactions.

References

[1] P.V. Danckwerts, Gas-liquid reactions, McGraw-Hill, New York, 1970.

[2] W. Krieger, J. Lamsfuß, W. Zhang, N. Kockmann, Chem. Eng. Technol. 2017, 40 (11), 2134-2143.

[3] SPP-1740: *Reactive Bubbly Flows* http://www.dfg-spp1740.de/ [Online] Accessed: 14.01.2019

ECCE12
The 12th EUROPEAN CONGRESS OF CHEMICAL ENGINEERING
Florence 15-19 September 2019

Development of a Novel Atomization Process using Liquid Carbon Dioxide

Clara Lauscher*, Gerhard Schaldach, Markus Thommes

TU Dortmund, Laboratory of Solids Process Engineering, Emil-Figge-Str. 68, 44227 Dortmund, Germany

**Corresponding author: clara.lauscher@tu-dortmund.de*

Highlights

- Fabrication of droplets in the small micrometer range.
- Dispersing a liquid in liquid carbon dioxide.
- Expansion of the CO_2 emulsion.

1. Introduction

Atomization is used in many industrial processes like in spray drying. Unfortunately, atomization is limited regarding small droplet sizes. A new approach to overcome this limitation is to disperse two liquid phases into each other rather spraying a liquid into a gas. Since the droplet size also depends on the continuous phase, using emulsification could be beneficial for achieving the desired size reduction. Indeed, in addition to spraying, there are various methods of emulsification and the milk industry has already proven that it is possible to produce droplets smaller than 1µm. The aim of this study is to investigate the potential to produce an aerosol using emulsification. Therefore, an emulsion of liquid carbon dioxide and a non-miscible liquid will be produced. Afterwards, due to the expansion of the emulsion a fine aerosol will have been prepared.

2. Methods

Based on the idea an aqueous system will be emulsified with liquid carbon dioxide using various emulsification processes. Therefore, a high-pressure emulsification system will be constructed utilizing HPLC equipment. Following, the high-pressure emulsion will be evaporated through a special nozzle.

3. Results and Discussion

As the emulsification system needs to be constructed, first experiments were conducted by using silicon oil (η = 1mPas) instead of liquid carbon dioxide as the continuous phase. Demineralized water is the disperse phase. The disperse phase (water) was pumped through a capillary (d = 0.3mm) with a volume flow rate of 50ml/min leading to a Reynolds number of 3500.

The Reynolds number of the continuous phase was calculated based on the physical properties of the continuous phase and drawn in Ohnesorge/Reynolds diagram (figure 1a). As shown in the diagram, the disintegration regime changes from the Rayleigh regime to second wind induced regime by changing the continuous phase from air to silicon oil. By spraying into air a droplet size of about 570µm can be expected [1]. In case of spraying the water into silicon oil the average droplet diameter ($d_{50,3}$) measured in the preliminary experiment is about 110µm as shown in

figure 1b. The emulsion was analyzed using laser diffraction technique (Malvern Spraytec, Harrenberg, Germany).

In general, the Reynolds number of the continuous phase increases with decreasing viscosity and increasing density. Consequently, dispersing in a liquid phase can cause higher Reynolds numbers and result in smaller droplet sizes.

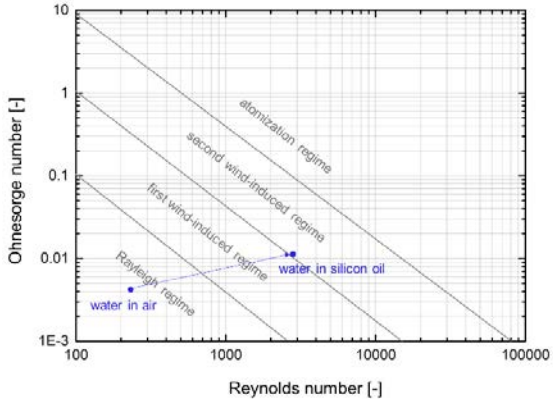

Figure 1a. Ohnesorge/Reynolds diagram for dispersing water in silicon oil versus in air.

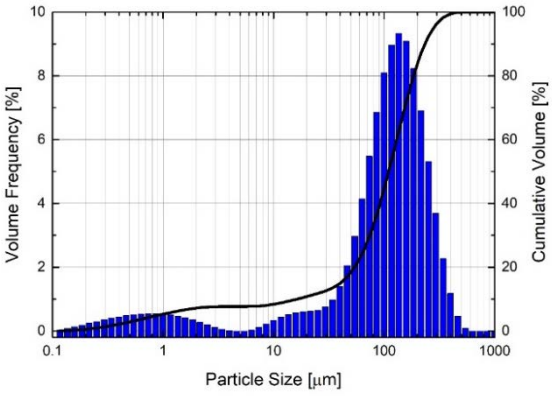

Figure 1b. Particle Size Distribution Dispersing water in silicon oil (η= 1mPas) through a capillary nozzle (d=3mm).

4. Conclusions

The idea to emulsify liquid carbon dioxide seems to be a promising approach to produce fine droplets. The low viscosity will increase the Reynolds number significantly. In addition, liquid carbon dioxide facilitates spraying of the emulsion and is non-toxic. Liquid carbon dioxide vaporizes rapidly as soon as the pressure drops below the saturated vapour pressure and should support the production of even smaller droplets.

References

[1] Walzel, P., 2012, "Spraying and Atomizing of Liquids," Ullmann´s Encyclopedia of Industrial Chemistry, 34, pp. 79-98.

ECCE12
The 12th EUROPEAN CONGRESS OF CHEMICAL ENGINEERING
Florence 15-19 September 2019

The effect of liquid film thickness on the mass transfer of a single catalyst pellet in a scaled down trickle bed reactor

Jonathan White[1], Frans Muller[1], Thomas Chamberlain[1], Richard Bourne[1], Colin Brennan[2], David Taylor[2]

1 Institute of Process Research & Development, University of Leeds, Leeds, LS2 9JT, UK; 2 Syngenta, Jeallot's Hill International Research Centre, Bracknell, Berkshire, RG42 6EY, UK

**Corresponding author: cp15jpw@leeds.ac.uk*

Highlights

- Single pellet trickle bed reactor presented
- Liquid film thickness limits hydrogen diffusion to the catalyst
- Model relating mass transfer rate of hydrogen to liquid flow rate developed

1. Introduction

Heterogeneous hydrogenations are an important class of catalytic reactions, used extensively within the fine chemical, agrichemical and pharmaceutical industries [1]. Though these reactions are often performed in batch due to better understanding of the limiting regimes, continuous hydrogenation has the potential to offer increased economic, safety and quality improvements [2]. Trickle bed reactors (TBR) are an attractive option for continuous manufacturing due to simple operation and lower back mixing enhancing selectivity. However, due to the complex relationship that exists between the kinetics and hydrodynamics, these reactors can be challenging to study at laboratory scale [3]. This article presents a method for scaling a TBR down to the scale of a single catalyst pellet to investigate the effects of liquid film thickness during the reduction of styrene.

2. Methods

A single pellet TBR was developed by immobilizing a 1% Pd/C extrudate within a packed bed of glass beads (shown in Figure 1). A reactor column of similar diameter to the length of the extrudate was used to minimize liquid bypassing. Hydrogen gas and a styrene solution in methanol were passed co-currently through the bed and the styrene conversion was monitored via gas chromatography. Liquid flow rates were chosen based on the liquid holdup within the reactor and corresponded to Reynolds numbers between 1 and 5. The gas flow rate remained constant throughout this study. To examine the extent to which diffusion though the liquid film effects the overall mass transfer rate of hydrogen (MTR_{H2}), hydrogenations were conducted with both hydrogen saturated and unsaturated methanol. To visually investigate the film thickness as liquid trickles over the catalyst, a small number of pellets were glued together to form a stack. Liquid was passed over the stack at various flow rates and filmed using an optical microscope to observe changes in the film thickness.

3. Results and discussion

The film thickness and single pellet TBR results are shown in Figure 1. As confirmed by the pellet stack experiment, at increased liquid flow rates the methanol film on the surface of the catalyst

becomes thicker. When unsaturated, hydrogen must diffuse through this film and the increase in thickness is thought to give rise to the apparent decease in MTR_{H2}. With liquid presaturation the MTR_{H2} increases almost linearly with increasing liquid flow rate. As diffusion through the film is no longer limiting the reaction, increased turbulence is thought to enhance mass transfer and contribute to the observed increase in MTR_{H2}.

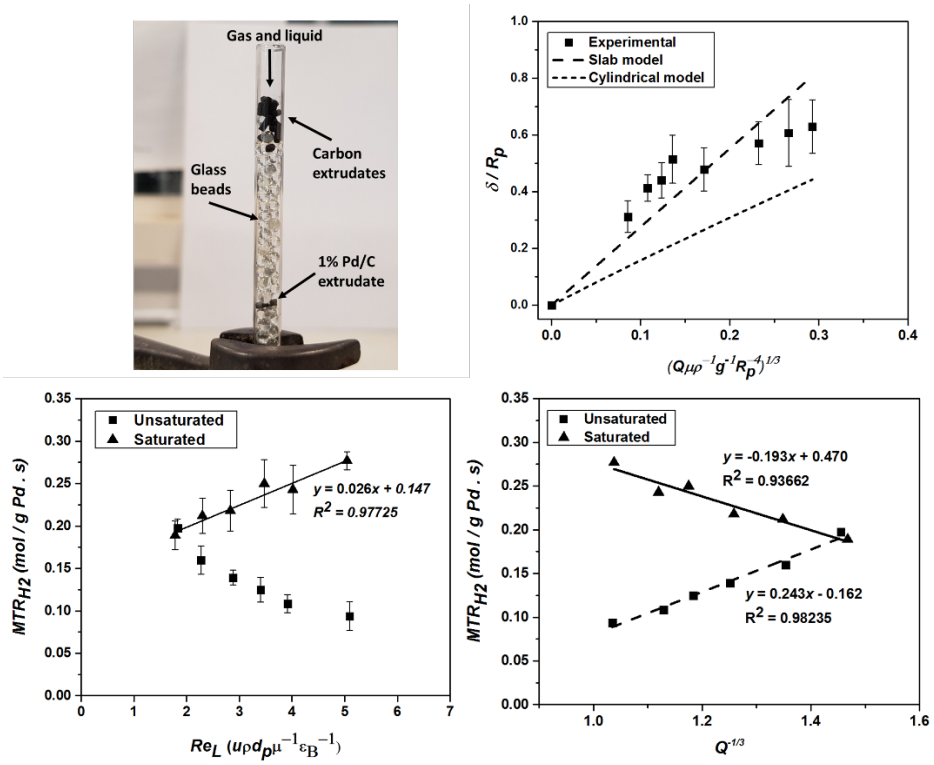

Figure 1. Top left; the single pellet TBR used. Top right; recorded liquid film thickness on the pellet stack at various liquid flow rates. Bottom left; mass transfer rate of hydrogen against different liquid flow rates. Bottom right; correlation between the mass transfer rate of hydrogen and the reciprocal cubic root of liquid flow rate.

The effect of volumetric liquid flow rate on film thickness was modelled and subsequently a relationship between the MTR_{H2} and liquid flow rate was found. This model was shown to fit both the liquid film and single pellet TBR experimental data well.

$$MTR_{H2} = \frac{ADC_{H2,l}}{\delta} \; and \; \delta = \sqrt[3]{\frac{3\mu Q}{\rho g S_A}} \; \therefore MTR_{H2} \propto \frac{1}{\sqrt[3]{Q}}$$

4. Conclusions

A single pellet trickle bed reactor has been used to investigate the liquid film thickness trickling over a catalyst pellet. Increasing the liquid flow rate results in a thicker film and thus exhibits a greater limiting effect due to the increased diffusion distance. A model was developed to describe the relationship between the overall mass transfer rate and the volumetric liquid flow rate.

References

[1] A. Faridkhou, J.-N. Tourvieille and F. Larachi, *Chem Eng Process*, 110 (2016) 80-96.
[2] J.G.V. Alsten, M.L. Jorgensen and D.J. am Ende, Org. Process Res. Dev., 13 (2009) 629-633.
[3] F.S. Mederos, J. Ancheyta and J. Chen, Appl. Catal., A., 355 (2009) 1-19.

ECCE12
The 12th EUROPEAN CONGRESS OF CHEMICAL ENGINEERING
Florence 15-19 September 2019

A computational workflow to study particle transport in porous media: coupling CFD and deep learning

Gianluca Boccardo[1], Agnese Marcato[1], Daniele Marchisio[1]

[1]*Department of Applied Science and Technology, Politecnico di Torino, Torino, Italy;*

**Corresponding author: gianluca.boccardo@polito.it*

Highlights

- CFD simulations of fine filtration in packed beds are performed
- Deep-learning methods are used for feature extraction and parameter identification
- Effectiveness of different machine-learning setups are presented

1. Introduction

The study of particle transport in porous media is of the utmost importance as it touches a wide variety of different fields: from the study of contaminant transport in aquifers to the design of effective packed bed reactors in chemical engineering. One of the difficulties lies in the many parameters characterizing the porous media (which are generally geometric), and whose impact and synergy of action can be impossible to analytically predict. These particularities, which render the problem of particle transport in random media difficult to treat, at the same time make it a prime candidate for machine learning (ML) and specifically deep-learning (DL) approaches. These techniques are particularly suited to extract essential features hidden in data, and are making their way from computer science to "hard sciences", e.g. in chemical engineering [1]. In this work we couple our recent CFD work exploring fluid flow and particle transport and deposition [2] with a variety of different classes of classical and deep neural networks (NNs and DNNs).

2. Methods

The first step was the creation of the geometry: first, randomly arranged distributions of non-overlapping circular elements are generated, then, CFD simulations of fluid flow and particle transport and deposition were performed, using the open-source CFD code OpenFOAM: a snapshot of a simulation can be seen in Fig. 1. One thousand of these fully solved CFD realizations are used for generating the datasets, each differing in a random variation of the defining spatial features: porosity, grain diameter, channel width. Reynolds and Peclet numbers (respectively via the imposed pressure drop and the mass diffusion coefficient) were also randomly varied.

3. Results and discussion

Using the obtained "fully-solved" CFD dataset described earlier, a parameter identification analysis was performed by employing differently built NNs and DNNs (using Matlab Machine Learning Toolbox). First, a single layer NN was used for prediction of permeability and particle deposition efficiency. When a new, random set of parameters (inside the training range) was given to the NN, the result prediction was almost perfect (error <0.5%) as the parity diagrams in Fig. 3 show. Different number of neurons were used, from 10 to 100, with 20 neurons giving the best results: this fits with the expected trade-off between a too coarse prediction with fewer neurons and overfitting with too many. Then, deep-neural networks with different arrangements of 20 neurons in 1-, 2-, and 3-layered fully-connected networks were tested, without appreciable differences in prediction accuracy, showing that for these number of features a simple 1-layer

network suffices. Then, we tested the obtained neural network to make predictions using input data from outside the range where the network was trained: as it is to be expected, the predictions degrade in quality the further the input data is from the training range. Nonetheless, as it can be seen in Fig. 2, reasonable accuracy (<10% error) can still be obtained even when all input parameters are well below (or above) the limits of the data range: this shows the wide range of applicability of this approach.

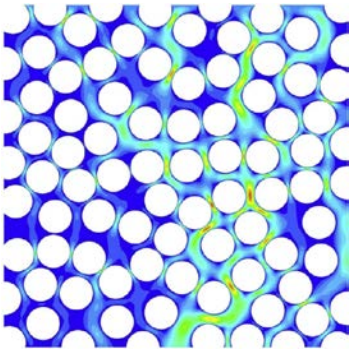

Figure 1. CFD contour plots of velocity magnitude for the 2D random arrangement of circles

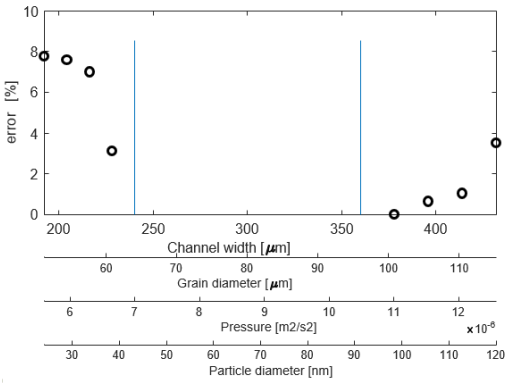

Figure 2. Prediction errors when input data (quantitities on the different scales) is outside the training range of the neural network, indicated by the vertical lines (inside of which error is circa 0%, as seen in Fig. 2).

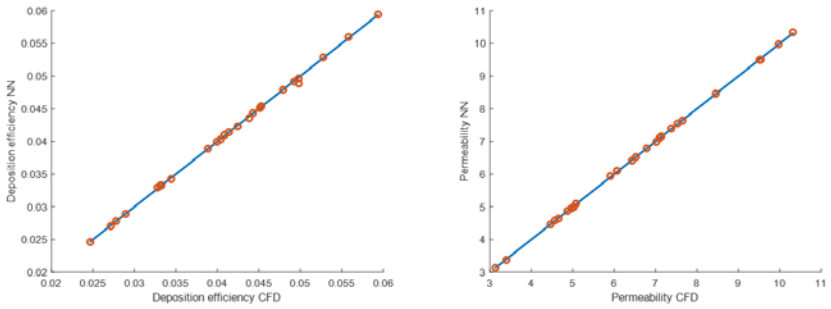

Figure 3. Parity diagrams comparing actual CFD simulations with NN-predicted results.

4. Conclusions

Different types of neural networks are used to predict both fluid dynamic and mass transfer properties in porous media: the results show that this approach is very successful, reducing the cost of property prediction by orders of magnitude (CFD: around 10 minutes, NN: around a second). This allows for fast reactor/filter prototyping, on-line process control (analyzing process response in real time) and makes tightly-coupled multi-scale modelling possible by means of efficient, machine-learning powered, surrogate models for pore-scale transport.

References

[1] Chu, X.,et al., 2018. A computationally light data-driven approach for heat transfer and hydraulic characteristics modeling of supercritical fluids: From DNS to DNN. *International Journal of Heat and Mass Transfer*, *123*, pp.629-636.

[2] Boccardo G., Marchisio D.L., Sethi R., 2014, Microscale simulation of particle deposition in porous media, *Journal of Colloid and Interface Science*, 417, pp. 227-237.

ECCE12
The 12th EUROPEAN CONGRESS OF CHEMICAL ENGINEERING
Florence 15-19 September 2019

Comparison of Miniaturized Draft Tube Baffle and Coiled Flow Inverter Crystallizer Construction

Mira Schmalenberg*[1], Anna Nocon[1], Felix Buckmann[1], Norbert Kockmann[1]

1 TU Dortmund, Emil-Figge-Straße 68 44227 Dortmund

**Corresponding author: mira.schmalenberg@tu-dortmund.de*

Highlights

- Continuous crystallization for process development
- Comparison of design methods
- Down-scale of a draft tube baffle crystallizer
- Residence time behavior in comparison

1. Introduction

To develop processes as quickly and easily as possible, continuous apparatuses are required even for very small quantities. This is especially valid for crystallization, which is still frequently carried out in batch mode[1].
The procedure for constructing two different cooling crystallizers is to be compared here. A Draft Tube Baffle (DTB) crystallizer as a stirred tank is compared to a Coiled Flow Inverter Crystallizer (CFIC), which belongs to the tube crystallizers. In addition to the different construction methods, the main features of the crystallizers will also be compared.

2. Methods

In order to ensure a homogeneous suspension flow in the CFIC, Hohmann et al. [2] has already developed a flow chart to identify homogenous suspension flow. The CFIC presented here has been developed on the basis of this map[3]. The most important parameter here is the densimetric Froude number based on flow velocity and density difference between fluid and solid.

Regarding the DTB an already known DTB[4] crystallizer has been down scaled from 1100 L to 1 L to allow the same suspension characteristics. With the help of different particles (glass particles and acetylsalicylic acid) and solid weight fractions it is possible to determine an operating range for the DTB. Here the densimetric Froude number is an important parameter, too.

3. Results and discussion

A tube-in-tube CFIC has been designed with an internal process tube diameter d_i of 1.6 mm (Figure 1, left). This was designed for a suspension flow rate of 15 – 20 g·min^{-1}. The CFIC can be varied by identical units so that the coiled tube length (7.8 - 54.6 m) and thus the mean residence time (1 – 7 min) can be varied. The special feature of this crystallizer is the very narrow residence time distribution, which is close to an ideal plug flow. [3]

In contrast, the constructed DTB (Figure 1, right) obviously behaves similarly to the residence time distribution of an ideal continuous stirring vessel. Thus, despite a similar mass flow rate (around 15 g·min^{-1}), significantly longer residence times of about 67 min are possible. This should make it possible to produce much larger crystals than in the CFIC.

The special feature of the DTB is that it has a classifying function. This is induced by the baffles so that fine grain can be removed and a narrower crystal size distribution (CSD) be reached. In this work, the achievable CSD, which should be narrow, of the two crystallizers will be compared although the crystallizers are of two different types.

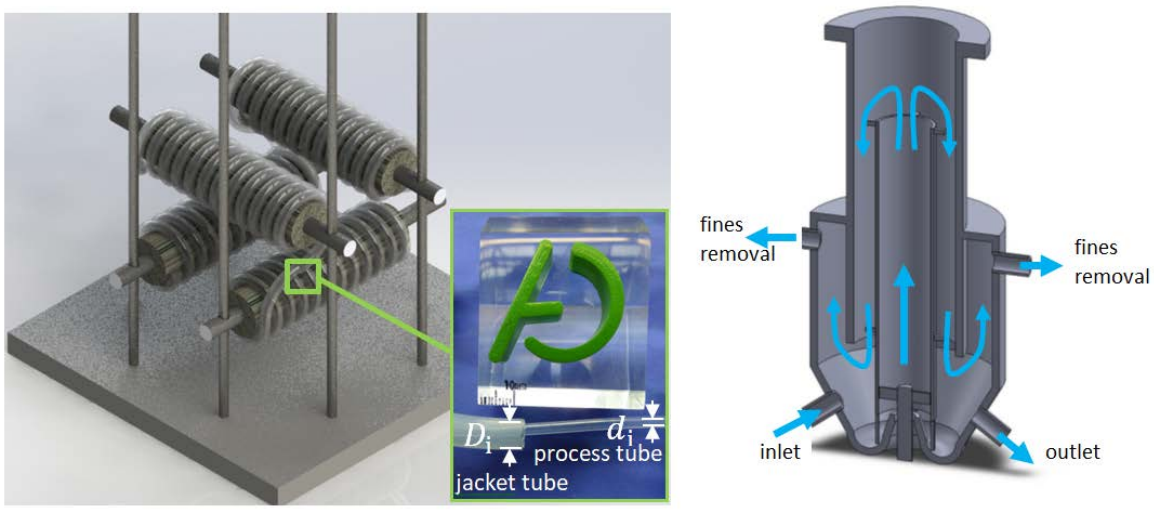

Figure 1. Single CFIC unit with coiled tube length of 7.8 m with tube-in-tube construction of the CFIC (left); Down-scaled DTB prototype with flow direction (right)

4. Conclusions

Two different continuous cooling crystallizers have been designed for small quantities of about 15 g·min^{-1}, where for both a complete homogenous suspension behavior is a design criterion. To characterize the crystallizers, the residence time behavior was compared. This shows that the different apparatuses are suitable for various crystallization tasks.

The German Federal Ministry for Economic Affairs and Energy (BMWi) is acknowledged for funding this research as part of the ENPRO2.0 initiative. (Support code: 03ET1528A)

References

[1] P. Kleinbudde, J. Khinast, J. Rantanen, Continuous Manufacturing of Pharmaceuticals, 2017.
[2] L. Hohmann, M. Schmalenberg, M. Prasanna, M. Matuschek, N. Kockmann, Chemical Engineering Journal, 2018
[3] M. Schmalenberg, L. Hohmann, N. Kockmann, ASME ICNMM2018-7660, 2018
[4] A. ten Cate, S. K. Bermingham, J. J. Derksen, H. M. J. Kramer, 10th European Conference on Mixing, 2000

ECCE12
The 12th EUROPEAN CONGRESS OF CHEMICAL ENGINEERING
Florence 15-19 September 2019

Power and Flow Characteristics of the in-line Rotor-Stator Ytron ZC1

James M. Mitchell, James C. Bacon, Nabeel Umar#, Chris D. Rielly, N. Gül Özcan-Taskin*
Loughborough University, Dept. of Chemical Engineering, Loughborough, LE11 3TU, UK
#Now at: 3M Derby Road, Loughborough UK
**Corresponding author: N.Ozcan-Taskin@lboro.ac.uk*

Highlights

- The suction performance of an in-line rotor-stator used for powder incorporation into a liquid, the Ytron ZC1, showed an optimum range of operation avoiding liquid flow into the powder inlet for both 1.5 and 3.0 mm gap heads
- Power characteristics of the Ytron ZC1 were determined and two expressions were obtained for 1.5 and 3.0 mm gap rotor-stator heads
- Results obtained will form the basis for further studies on incorporation and deagglomeration

1. Introduction

Nanoparticles incorporated in novel formulations have been shown to improve product properties or achieve properties and performance that cannot be achieved otherwise. Abrasion-resistant coatings, pharmaceuticals, catalysts, paints and coatings with increased colour brilliance and increased protection from sun creams are examples of such products. Final or intermediate products in the form of nanoparticulate dispersions in a liquid require initially the incorporation of the dry nanoparticle powder into the liquid, which is often performed using a stirred tank[1]. The pre-dispersion formed is then deagglomerated using a power-intensive device, such as a rotor-stator. In this study, the performance of an in-line rotor-stator, Ytron ZC, used for powder incorporation, is assessed in terms of its power and suction characteristics.

2. Experimental

Experiments were conducted using a variable speed Ytron ZC1 operated up to 6,500 rpm in the recirculation loop of a 0.58 m diameter stirred tank equipped with a hydrofoil (Figure 1). The liquid volume was 100 l. The Ytron ZC1 rotor-stator head shown in Figure 2 is available with gap sizes of either 1.5 or 3.0 mm; the stator teeth had a length of 9.19 mm. Power input was determined using a calorimetry technique. The suction performance of the device was determined by making air velocity measurements with an anemometer at the powder inlet.

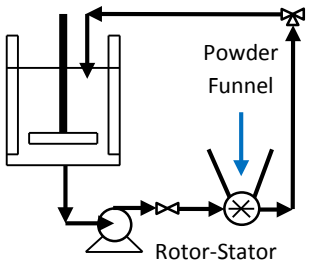

Figure 1. Experimental set up

Figure 2 Ytron ZC mixer head stator, on the left, of diameter 0.089 m and rotor, on the right, of diameter 0.095 m

3. Results and discussions

Figure 3 shows that the liquid flow rate through the rotor-stator is not affected by the rotor speed or teeth gap, which suggests that the Ytron YC1 has negligible pumping action and therefore

requires an external pump.

The liquid flow through the rotor-stator head induces suction from the powder inlet to achieve incorporation when dry powder is added. It can be seen from the air velocity results (Figure 4) that at a given rotor speed, the air velocity increases slightly as the liquid flow rate is increased, then tends to a plateau which corresponds to the optimum operating range.

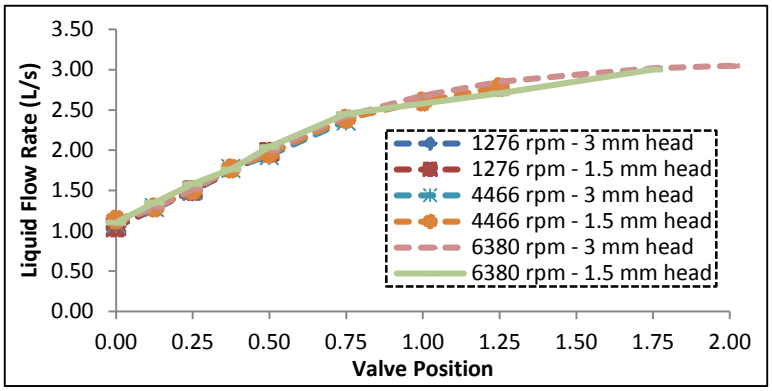

Figure 3 Liquid flow rates for a range of rotor speeds using the Ytron-ZC1

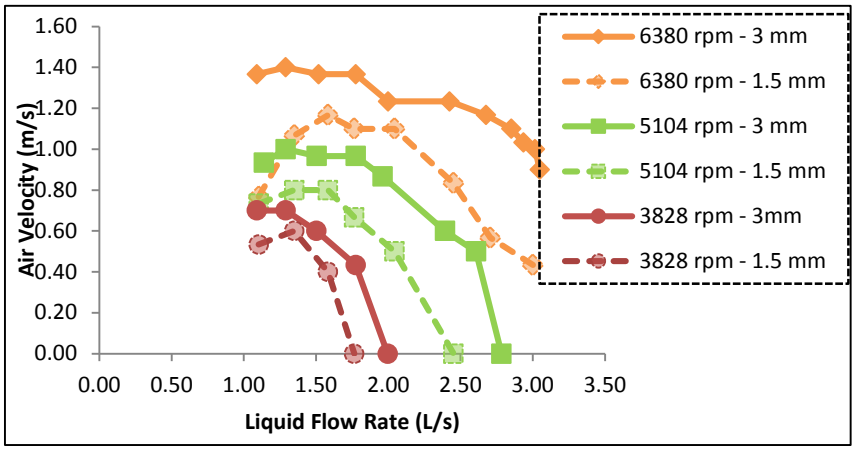

Figure 4 Air velocities over a range of conditions for Ytron-ZC1 and ZC0

Further increases in the liquid flow rate decreases the suction performance (Figure 4). This reduction in suction at high liquid velocities is caused by the flooding of the powder inlet by the liquid, which is highly undesirable as the wetted powder can form clumps and cause blockage. Increasing the rotor speed increased the air velocity, resulting in improved suction performance. The 3.0 mm gap head has a higher suction air velocity and is therefore better suited for powder incorporation.

From the data obtained, the following relationships were obtained in which the values for Po_1 and Po_2 ($P = Po_1 \rho N^3 D^5 + Po_2 \rho N^2 D^2$) were of the same order of magnitude as those reported for other in-line rotor-stators[2]:

$$P = 0.28\rho N^3 D^5 + 13.95\,\rho N^2 D^2 Q \qquad \text{for 3.0 mm head and}$$
$$P = 0.20\rho N^3 D^5 + 15.07\rho N^2 D^2 Q \qquad \text{for 1.5 mm head.}$$

4. Conclusions

The suction performance of an in-line rotor-stator used for powder incorporation, the Ytron ZC1 was determined over a range of rotor speeds and liquid flow rates, which demonstrated that there is an optimum range over which powder incorporation can be achieved. The effect of gap width could be identified. In addition, the study on the power characteristics of the device allowed two relationships to be obtained for the different gap sizes. These will form the basis of further work on incorporation and deagglomeration.

References

[1] Özcan-Taskin, N.G. (2013) *Chemical Engineering Research and Design,* pp. 1-7 (DOI: 10.1016/j.cherd.2013.03.019)

[2] Özcan-Taşkin, N. G. Padron, G., Kubicki, D. (2011) *Canad. Jrnl of Chem Eng.*Vol. 89, Issue: 5, p:1005-1017 (DOI 10.1002/cjce20553)

ECCE12
The 12th EUROPEAN CONGRESS OF CHEMICAL ENGINEERING
Florence 15-19 September 2019

Performances of a Compact Static Mixer for Turbulent Flows in Pipelines

Alessandro Paglianti[1], Francesco Maluta[1], Giuseppina Montante[2]

1 DICAM – Università di Bologna, via Terracini 34, 40131 Bologna, Italy; 2 CHIMIND – Università di Bologna, via Terracini 34, 40131 Bologna, Italy

**Corresponding author: giuseppina.montante@unibo.it*

Highlights

- Good mixing with limited energy requirements is achieved by a very compact static mixer.
- Enhancement of blending is ensured without modification in existing pipelines.
- Effective mixing with limited space requirement helps continuous process intensification.

1. Introduction

Static mixers for turbulent flows are adopted in several industrial operations, ranging from synthesis of pharmaceuticals [1], to mass transfer in bioreactors [2], emulsification [3] and heat transfer [4], just to mention a few examples. In this work, the mixing performances and the energy requirements of a novel static mixer, whose main characteristics with respect to other traditional designs are the easiness of the installation and a very compact geometry, are investigated by Computational Fluid Dynamics (CFD). The validation of the computational results based on the comparison with experimental pressure drops and tracer homogenization data is presented. The investigation can be easily extended to any industrial application, for the preliminary identification of the most effective geometrical and operating conditions for achieving the desired production target.

2. Methods

The velocity flow field, the pressure drops and the pipe length required to achieve the blending of two miscible liquid streams are obtained by the numerical solution of the Reynolds-Averaged conservation equations of mass, momentum and scalar concentration for incompressible, isothermal and steady-state flow of Newtonian liquids. The Reynolds stress and the Reynolds flux terms are modelled using the eddy viscosity and the eddy diffusivity hypotheses, respectively. The computational domain consists of a pipe of diameter, D, equal to 90 mm and length, L, equal to 10×D placed horizontally and equipped with one compact static mixer element of the TWIN-P series designed by Pittaluga s.r.l. It is a very compact static mixer, being its width, W, equal to D/7, consisting of six 45° pitched blades fixed to the external surface of a Venturi section. Blending is ensured by a double-mechanism, due to the combined action of the blades and of the Venturi section, and is particularly suitable for treating streams of very different flowrates. The domain discretization is performed through an unstructured grid consisting of about 4.3×10^6 cells. The grid effect on the mean velocity field, on the turbulent variables and on the degree of homogenization is also considered. The simulations replicate a parallel experimental investigation, considering different flow rates of the main liquid water stream, Q, varying from 4 to 35 m^3/h and a single flow rate of the secondary stream, Q_s, that is an aqueous solution of Rhodamine of 10 L/h. The pressure

drops and tracer concentration data adopted as a benchmark for the simulation results are measured by pressure transducers and Planar Laser Induced Fluorescence (PLIF), respectively, placing the static mixer in a test rig consisting of a 7 m long plexiglass pipe, a storage tank and a centrifugal pump.

3. Results and discussion

The energy requirements and the mixing performances of the TWIN-P static mixer are shown in Figure 1, by means of the parameter K at different water flow rates and of the Coefficient of Variation (CoV) of the Rhodamine concentration along the pipe axis. The K value is defined as:

$$K = \Delta P / \left(\frac{1}{2}\rho V_s^2\right) \tag{1}$$

where ΔP is the absolute pressure difference across the mixer, ρ is the fluid density and V_s is the fluid superficial velocity. The CoV at selected pipe cross sections is calculated as:

$$CoV = \sqrt{\frac{\sum_{i=1}^{N}(C_i - C_{mean})^2}{N-1}} \frac{1}{C_{mean}} \tag{2}$$

where c_i is local Rhodamine concentration at the i-th evaluation point, c_{mean} is the mean concentration on the cross section, N is number of evaluation positions at the cross section.

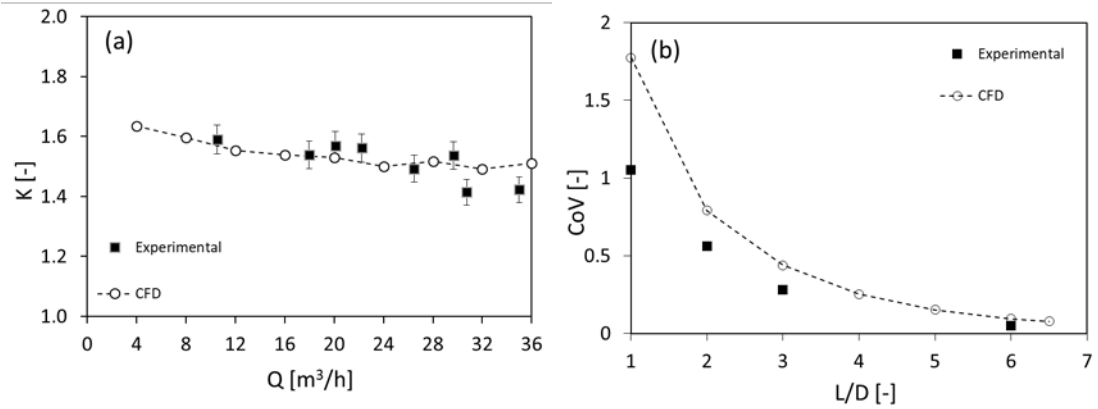

Figure 1. Comparison of CFD and experimental results. (a) K vs Q; (b) CoV at different cross sections downstream the mixer outlet section, Q=20 m³/h.

Based on the experimental data and the comparison with the performances of other static mixers for similar applications[5], the investigated TWIN-P static mixer is found to ensure low pressure drops and good mixing performances. The CFD results fairly agree with the experiments. As a result, the fully predictive three-dimensional CFD modelling approach considered in this work is confirmed an industrially viable and reliable method for turbulent static mixing design and optimization.

References

[1] C. Brechtelsbauer, F. Ricard, Organic Process Research and Development 5 (2001) 646-651.
[2] C.U. Ugwu, J.C. Ogbonna, H.Tanaka, Applied Microbiology and Biotechnology 58 (2002) 600-607.
[3] F. Theron, N.L, Sauze, Int. J. Multiphase Flow 37 (2011) 488-500.
[4] R. Rakoczy, S. Masiuk, M. Kordas, P. Gradzik, Chem. Eng. Proc. Proc. Int. 50 (2011) 959-969.
[5] S.M. Hosseini, K. Razzaghi, F. Shahraki, AIChE J. 65 (2019) 1126-1133.

ECCE12
The 12th EUROPEAN CONGRESS OF CHEMICAL ENGINEERING
Florence 15-19 September 2019

CFD Analysis of Direct Contact Condensation (DCC) of Superheated Gas Jets into a Vertically Flowing Liquid Channel.

K N Jayachandran[1], Arnab Roy[2], Parthasarathi Ghosh[1]

1 Cryogenic Engineering Centre, Indian Institute of Technology, Kharagpur, India-721302; 2 Department of Aerospace Engineering, Indian Institute of Technology, Kharagpur, India-721302

**Corresponding author: knjayachandran93@gmail.com*

Highlights

- Two fluid model used for simulation of DCC in R123 gas-liquid flows.
- Mean bubble diameter correlation will be developed for low Jakob (Ja) number liquid flows.
- Numerical model will be validated with experimental data of Zhu *et al.,* [1].

1. Introduction

In a typical staged combustion cycle based LOX/kerosene semi-cryogenic rocket engine, the liquid oxygen booster turbine is driven by the oxidizer-rich combustion products from the pre-burner [2,3]. The turbine driving gas comes in direct contact with the liquid oxygen stream from the booster pump after the booster turbopump exit and gets condensed [4]. Very few studies are reported in the above complicated case of direct contact condensation, which demands further investigation in this area [3]. The purpose of the present study is to understand the GOX-LOX DCC by exploring the DCC of R123 fluid with similar flow (low liquid Ja) and geometry configuration as reported in Zhu *et al.,* [1] by the use of numerical methods.

2. Methods

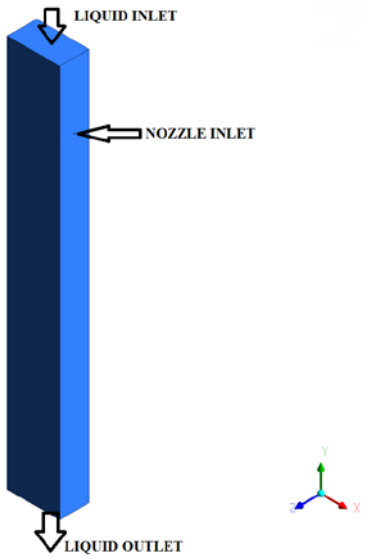

Figure 1. Geometry with gas and liquid boundaries.

Table 1. Boundary conditions.

Parameter	Value
Nozzle inlet mass flow rate (g/s)	1.22
Nozzle inlet temperature (K)	346.98
Liquid inlet velocity (m/s)	1
Liquid inlet temperature (K)	311.98
Domain pressure (MPa)	0.175

A two-fluid model with thermal phase change model for predicting condensation effects has been implemented in the present study using the commercial CFD package ANSYS CFX®. The geometry has been taken from the experimental data of Zhu *et al.,* [1] as shown in Fig. 1. The nozzle has a diameter of 2mm whereas the liquid domain is of dimensions 45mm x 80mm x 600 mm. The boundary conditions are reported in Table 1.

3. Results and discussion

Initially, steady state simulations are performed and the gas volume fraction contours are plotted as shown in Fig. 2. It can be observed that the gas exits through the nozzle and comes in contact with liquid R123. Further, transient simulations have to be performed to understand the dynamic condensation process.

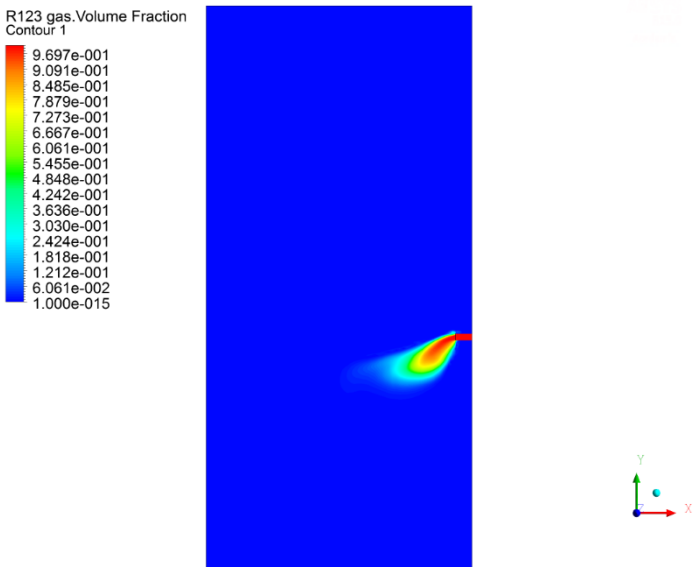

Figure 2. Gas volume fractions after steady state simulations.

4. Conclusions

A two-fluid model used to simulate the DCC of R123 gas-liquid flow. Further, the different sets of experimental data will be simulated to validate the numerical model. It has been observed by the authors in the previous works that the mean bubble diameter correlation by Anglart *et al.,* [5] may not be applicable for all cases of DCC. Hence, based on the simulations, a correlation for mean bubble diameter will be developed.

References

[1] K. Zhu, L. Yanzhong, M. Yuan, J. Wang, L. Wang, C. Li, Exp. Therm. Fluid. Sci. 98 (2018) 1-11.
[2] Z. Kang, L. Yanzhong, L. Gang, W. Jiaojiao, X. Fushou, M. Yuan, Asia-Pac. J. Chem. Eng. 13 (2018) 1-13.
[3] K. N. Jayachandran, A. Roy, P. Ghosh, Indian J. Cryogenics. 43 (2018) 124-130.
[4] K. N. Jayachandran, A. Roy, P. Ghosh, IOP Conf. Ser.: Mater. Sci. Eng. 171 (2017) 012052.
[5] H. Anglart, O. Nylund, Nucl. Eng. Des. 163 (1996) 81-98.

ECCE12
The 12th EUROPEAN CONGRESS OF CHEMICAL ENGINEERING
Florence 15-19 September 2019

Rheological characterization and flow simulation of a thixotropic toothpaste.

A. Makhmet[1], W. Bourguiba[1], C. Lemaitre[1*], P. Marchal[1], R. Mercade[2], R. Erkassov[3]

1 LRGP, Université de Lorraine-CNRS, UMR 7274, 1 rue Grandville, Nancy F-54001, France

2 School of Engineering, Nazarbayev University, 53 Kabanbay Batyr Ave, 010000 Astana, Kazakhstan

3 Department of Chemistry, Eurasian National University, 2 Satpaev st., 010008 Astana, Kazakhstan

**Corresponding author: cecile.lemaitre@univ-lorraine.fr*

Highlights

- Rheological measurement on a toothpaste showed yield stress and thixotropy
- Kinetic and a rheological model selected and optimized to fit the experiments
- Rheological models implemented in ANSYS Fluent to simulate the toothpaste flow in an agitated tank.

1. Introduction

Due to their multi-ingredients composition, toothpastes are shear thinning (decreasing viscosity with increasing shear rate), they display a yield stress τ_y (no flow for stresses lower than τ_y) and they are thixotropic (time evolving viscosity under constant solicitation, due to progressive evolution of the material structure) [1]. Toothpaste SIGNAL® Complete 8 was used in the present study.

2. Rheological characterization

A rotative strain-imposed rheometer ARES provided by TA Instrument is used to perform the measurements. The sample is placed between 2 parallel disks of 25 mm or 40 mm diameter, distant of about 1 mm. The operating temperature is set to 20°C.

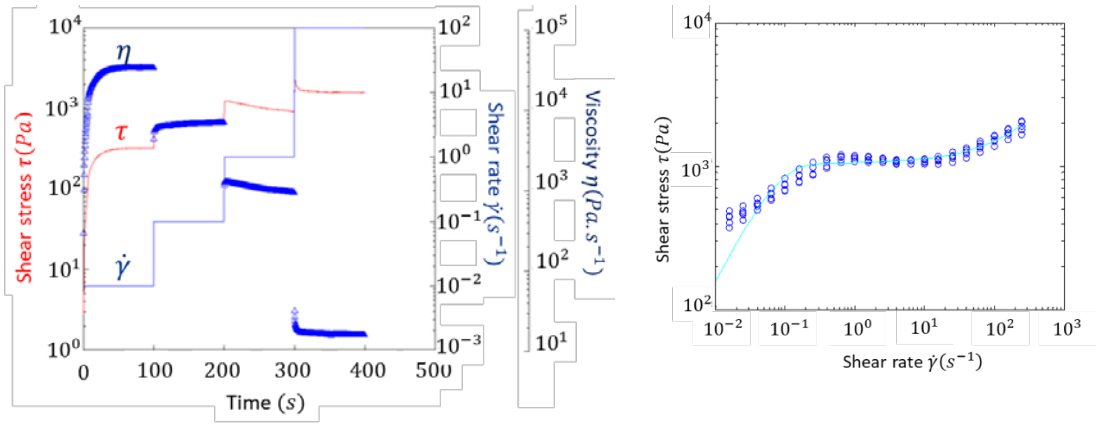

(a) (b)

Figure 1. (a) Transient tests presented as a function of time. (blue line) imposed shear rate steps ; (red line) measured stress; (blue triangles) measured viscosity. (b) Steady tests: shear stress $\tau\ (Pa)$ as a function of the shear rate $\dot{\gamma}\ (s^{-1})$.

Two types of tests were conducted: transient and steady. During the transient tests, shear rate $\dot{\gamma}$ steps were imposed to the sample and the shear stress τ and viscosity η were recorded in time. As for the steady tests, the τ and η values at long times are measured for each imposed value of $\dot{\gamma}$.

The transient tests, Fig. 1(a), evidenced the thixotropic behavior of the toothpaste. The steady tests, presented in Fig. 1(b), show a shear thinning character, with a yield stress $\tau_y \approx 10^3$.

Following [2], a kinetic and a rheological model were optimized to describe best the structural evolution in time of the toothpaste and the evolution of viscosity as a function of the shear rate.

3. Flow simulation

The purpose of the simulations was to reproduce the flow of a toothpaste sample in a tank equipped with a ribbon agitator, shown in Fig. 2(a), integrated to the ARES rheometer.

The geometry, designed with ANSYS Design Modeler, consists of two volumes: a cylindrical volume V1 containing the ribbon and an annular volume V2, surrounding V1, at the tank walls Fig. 2(b). Two meshes were generated with ANSYS Meshing, of 2,365,013 and 6,060,741 tetrahedral cells, refined near the walls. Both meshes were divided into two sub-meshes, one in V1 and the other in V2.

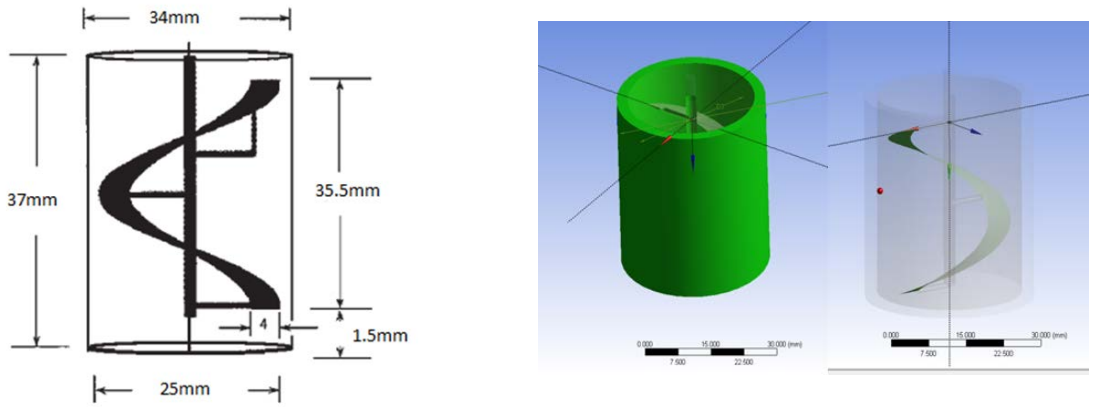

(a) (b)

Figure 2. -(a) Dimensions of the geometry. (b) Geometry used for the sliding-mesh simulations.

The simulations were conducted with ANSYS Fluent. The rotational velocity of $N = 0.573\ rps$ yielded a Reynolds number $Re = 4.66 \times 10^{-3}$, indicating laminar flow for a Newtonian fluid. The V1 sub-mesh was rotated at N, sliding against the static V2 sub-mesh. No-slip conditions were enforced at the tank and ribbon walls. On the free surface the shear stress was set to zero. The rheological model determined above was parametrized in Fluent. Navier-Stokes equations were solved using QUICK and central-difference schemes.

We will present the velocity vectors and profiles for different times. The calculated torque on the agitator will be compared to the one obtained experimentally.

References

[1] Laba D. Rheological properties of cosmetics and toiletries. New York : M. Dekker, 1993. 426 p.(Cosmetic science and technology, 13)

[2] Ardakani a, E. M. (2011). Thixotropic flow of toothpaste through extrusion dies. Journal of Non-Newtonian Fluid Mechanics.

ECCE12
The 12th EUROPEAN CONGRESS OF CHEMICAL ENGINEERING
Florence 15-19 September 2019

Parametric study of customizable 3D-printed droplet-microfluidic device

Jan Klusák, Jan Mucha, Marek Večeř*

VSB-Technical University Ostrava, FMT, department chemistry,
Tr. 17. listopadu 15, 70833, Ostrava-Poruba, Czech Republic

**Corresponding author: marek.vecer@vsb.cz*

Highlights

- 3D printed droplet generator is enough accurate to produce droplets with single modal PSD.
- Clear effect of output channel geometry at the same flow conditions.
- Individual and collective behavior of droplets–limiting flow rate ratio of O/W phase.
- Correlation of droplet size on to the volumetric flow rater ratio.

1. Introduction

Droplet-microfluidic devices are becoming more and more powerful platform in chemical, material, biological and pharmaceutical applications where small, highly controllable droplets and particles with uniform size are essential. 3D printing provides effective tool for rapid production of cheap and complex 3-dimensional droplet generators. We apply FDM (fused deposition modeling) 3D printing technology to fabricate customizable microfluidic device [1] with droplet chips which allows production of highly monodisperse droplets, emulsions and double emulsions (droplet-in-droplet) in this work. By varying the channel diameter and droplet chips geometry we are able to generate W-O-W and O-W-O droplets with defined parameters. Several types of material have been tested to find optimal transparency of droplet fluidic chips. Customizable 3D printed microfluidic device with different types of fluidic chips was successfully tested over a range of flow conditions.

2. Methods

Water droplets was prepared in the flow of oil continuous phase. Density, viscosity and interfacial tension was determined for both used liquids. FDM 3D printing technology was used for manufacturing microfluidic chips with various width of output channel. High speed visualization and advanced image analysis [2] was used for droplet primary data treatment.

3. Results and discussion

Four 3D printed microfluidic chips was evaluated under similar flow conditions. CT scan of each channel was performed to obtain actual information about channel profile geometry. Primary geometrical parameters of droplet was detected and statistical evaluation of results was performed. Droplet size normalized by channel width as a function of ratio of volumetric flow rate of dispersed phase to the volumetric flow rate of continuous phase gives single line (1) showed in Figure 1.

$$\frac{d}{h} \approx 1.8\left(\frac{Q_D}{2Q_C}\right)^{0.2} \quad (1)$$

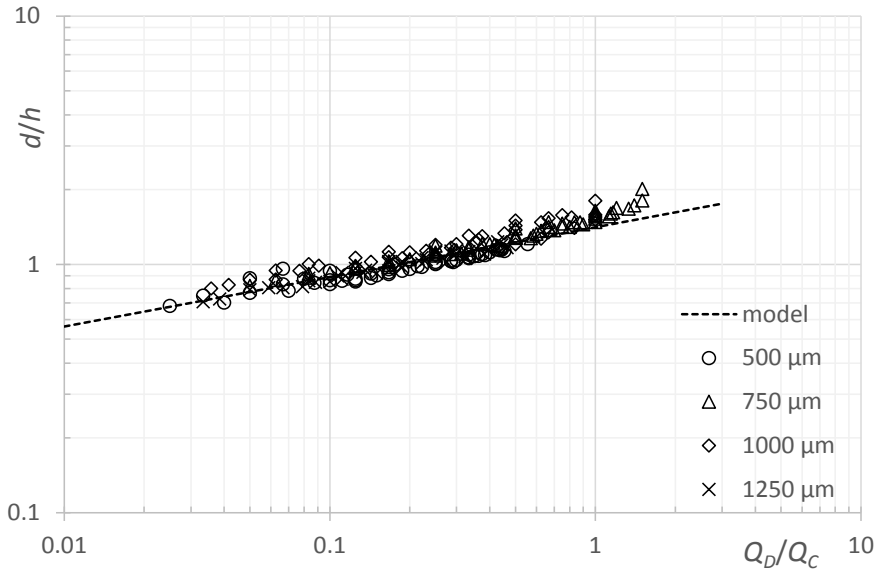

Figure 1. Equivalent droplet size normalized by channel width as a function of volumetric flow rate ration of dispersed to continuous phase.

4. Conclusions

Simple method of 3D printing was used for manufacturing of droplet generator with sufficient accuracy. Image analysis was used to evaluation of experiments. Effect of surface tension, viscosity and effect of different surface active agents was evaluated and satisfactory correlation of droplet size on the volumetric flow rate ratio was obtained.

References [Calibri 10]

[1] J. Klusák, J. Mucha, M. Večeř, 23rd International Congress of Chemical and Process Engineering CHISA 2018 Prague. 25.-29.2018.D6.2 Customizable 3D-printed droplet-microfluidic device for defined emulsion preparation.

[2] Z.Z. Chong, S.B. Tor, A.M. Gaňán-Calvo, Z.J. Chong, N.H. Loh, N.-T. Nguyen and S.H. Tan. Microfluidics and Nanofluidics. 20(4) (2016) 1-14.

ECCE12
The 12th EUROPEAN CONGRESS OF CHEMICAL ENGINEERING
Florence 15-19 September 2019

SIMULATION OF FLUIDIZED BED DRYER FOR COPPER CONCENTRATE THROUGH CFD + DEM.

Sebastian Perez, Javier Norambuena, Yerko Aguilera, Juan Pablo Vargas, Juan Jarufe

Abstract:

The fluidized bed drying equipment has the function of drying the copper concentrate containing 8 to 10% moisture, to leave it with a humidity less than 0.2%. The process consists in the transfer of heat, through the fluidization air, which is a mixture of combustion gases plus fresh air, this is transferred through a bed of gravel. The flow is extracted by a fan by dragging the dry concentrate, which is separated from the stream by a dust collector located outside the equipment. The equipment studied is part of a copper smelter in Chile and has a processing capacity of 123 t / h of dry concentrate, this dry concentrate is able to enter the copper converter to be melted and continue with the process until reaching to be metallic copper.

A computational fluid dynamic simulation (CFD) of the equipment was performed, which allowed us to see the behavior of the fluidization air through the pressure profiles, velocity vectors. Then a coupling of the CFD simulation was carried out with a discrete element modeling program (DEM) to study the behavior of the concentrate particles interacting with the fluid dynamics condition.

The results obtained from the simulations are presented in the form of figures showing the velocity vectors and the orientation of the flows reached both by the fluid and by the particles of the concentrate.

The validation of the results was carried out indirectly comparing the results of the sensors located inside the equipment on an industrial scale with the results observed in the simulation. The variation between the simulated model and the measured operational condition shows differences less than 1.7% for the parameter measured.

Conclusion

The study of a fluidized bed dryer is a highly complex process, however, making simplifications, and applying numerical methods using computational tools such as Ansys Fluent or Rocky DEM, it is possible to know the internal behavior of the flows with acceptable margins of error for engineering equipment design.

ECCE12
The 12th EUROPEAN CONGRESS OF CHEMICAL ENGINEERING
Florence 15-19 September 2019

Numerical Study of Fluid Mixing at Different Inlet Flow Rate Ratio

Md Readul Mahmud[1], Vladimir Viktorov[2], Carmen Visconte[2]

1 SECS, Independent University, Bangladesh (IUB); 2 DIMEAS, Politecnico di Torino, Turin, Italy

**mahmud.readul@iub.edu.bd*

Highlights

- A new Y-Y passive SAR mixer is designed and analyzed.
- Numerical simulation is done using Fluent for inlet flow rate ratio from 1 to 3.
- Mixing efficiency, flow pattern and pressure drop is calculated.
- Y-Y mixer shows the lowest pressure drop and have 90% mixing efficiency.

1. Introduction

Micromixer is a device which mix fluids regardless of their properties and nature such as density, viscosity, surface tension etc. in micro-scale. Micromixers and micro reactors are used in a wide range of chemical reactions, biochemical reactions, drug development and delivery, medical diagnosis, chemical synthesis and food industries [1] [2]. In micro scale the flow is typically laminar due to low Reynolds number [3]. In this paper, we designed a new SAR Y-Y mixer, and mixing performance and pressure drop is performed numerically by varying the inlet flow-rate ratio (1 to 3). In order to have a point of reference, the Y-Y micromixer was compared to the already established Chain, Tear drop and H-C micromixers.

2. Micromixer Design

The detailed geometrical configuration of Chain, Tear-drop, H-C and Y-Y micromixers is shown in Figure 1. All mixers are made of four identical elements which are connected with each other in various way to maximize mixing performance. The minimum dimension of all mixers is 4 mm.

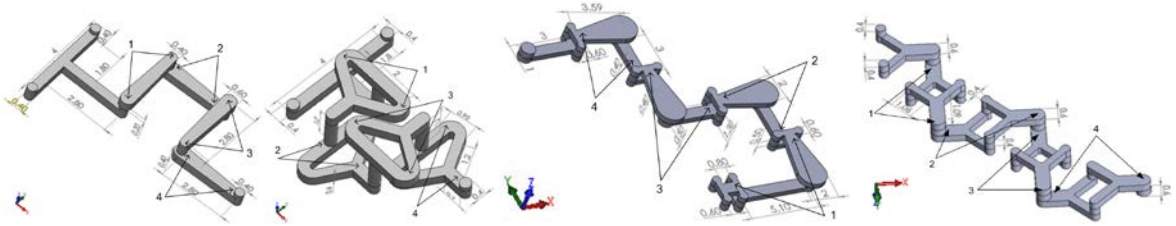

Figure 1. Design of the (a) Chain (b) Tear-drop and (c) H-C (d) Y-Y mixers with important parameters (unit in mm)

3. Numerical Method

ANSYS FLUENT 15, a commercial computational fluid dynamics software was employed to numerically determine mixing efficiency and pressure drop. The value of Reynolds numbers was used as one of the primary parameters for this study and is calculated as $Re = \frac{\rho v d}{\mu}$. Where ρ and μ are the fluid density and dynamic viscosity, respectively, v is the fluid velocity evaluated at the rectangular channel, and d is the characteristic length. A cut-cell Cartesian method was used to generate hexahedral cells suitable for the complex geometry used in computational fluid dynamics

(CFD) simulations. Standard deviation of species concentration was calculated at a cross-section of the mixing channel to evaluate the mixing efficiency using the standard equations [4]. The grid dependency test for all mixers were performed varying numbers of grids.

4. Result and Discussion

Figure 2 revels the efficiency of all four mixers curves for different inlet flow-rate ratios and the curves show the same trend, the efficiency slightly increases for higher inlet flow-rate ratios, especially at $30 \leq Re \leq 100$. The overall mixing efficiency is more than 90% at all Reynolds numbers, regardless of the inlet flow-rate ratios. The numerical data are in line with experimental values.

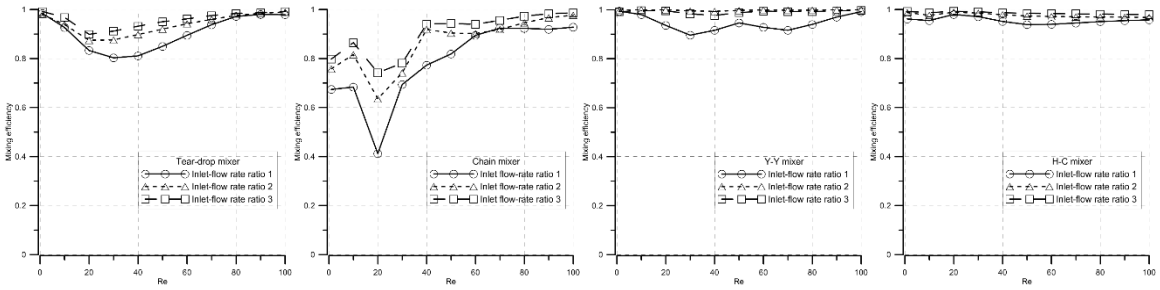

Figure 2. Numerical mixing efficiency of the mixers at the exit of the fourth element (Ratio 1 to 3)

As demonstrates in Figure 3, numerical curves of all mixers have the same trend, i.e. pressure-drop increases with the increase of flow rate. It is also clear that Y-Y has the lowest pressure drop.

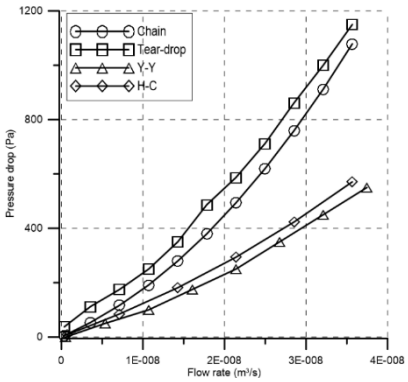

Figure 3. Numerical pressure drop of the four micromixers, varying flow rate

5. Conclusions

Four passive mixers, which uses fluid folding, rotation, expansion and construction along with splitting and recombination to improve mixing, is presented. The numerical model was used to analyze the effect of different inlet flow-rate ratios (1 to 3) at $1 \leq Re \leq 100$. The results showed that mixing efficiency depends on the Reynolds number as well as inlet flow rate ratio. The mixing efficiency of the Y-Y and H-C mixers is very good (greater than 90%) over the entire examined range of Reynolds numbers but Y-Y has the lowest pressure drop among the all presented micromixers.

References

[1] V. Khaydarov, E. S. Borovinskaya, Appl. Sci. 8 (2018) 1-16
[2] M. A. Ansari, K. Y. Kim, S. M. Kim, micromachine 9 (2018) 1-14
[3] J. M. Park, D. S. Kim, T. H. Kang, Micro. And Nano. 4 (2008) 513-523
[4] N. Solehati, J. Bae, A. P. Sasmito, Computers & Fluids 96 (2014) 10-19

ECCE12
The 12th EUROPEAN CONGRESS OF CHEMICAL ENGINEERING
Florence 15-19 September 2019

Mathematical and Computational Modelling of Anodic Oxidation of Oxygen in Copper Refining with Arc Electrolysis.

Jorge Manríquez[1], Gerardo Cifuentes[1], Cristian Vargas[1], Alejandro Gutierrez[2]

1 Full Professor, Metallurgical Engineering Department, University of Santiago of Chile, Avda. L. B. O'Higgins 3363, Estación Central, Santiago, Chile; 2 Full Professor, Mechanical Engineering Department, University of Santiago of Chile, Avda.L.B. O'Higgins 3363, Estación Central, Santiago, Chile.

**Corresponding author: jorge.manriquez@usach.cl*

1. Introduction

The common route of refining the impurities of copper and other non-ferrous metals is pyrometallurgical. The penalties in the price of copper for the level of impurities vary from 0.9 to 4.1 US/lb. The classic equipment of operation is the rotatory furnace of pyrorefining. The operation involves two sequential process steps: (a) oxidation - complexing; according to reaction of Eq(1):$\underline{S}+O_2 = SO_2$, and (b) reduction, according to reaction of Eq(2): $\underline{C} + \underline{O} = CO$. Refining with arc electrolysis is considered an alternative means of removing impurities from the molten copper without introducing deoxidizing agents. The use of this electrochemical method replaces the chemical reactions involved in the oxidation and reduction processes by electrochemical reactions. In this work, we will be studied the dynamic behavior of the anodic oxidation of the oxyanion as the supply of oxidizing agent of impurities in the blister copper through modeling and simulation using program Comsol.

2. Methods

The arc electrolysis furnace consists of a cylindrical crucible (see Figure 1). The crucible is contained in a furnace of silica refractory bricks heated with silicon carbide electrodes. A single graphite electrode enters through the top seal of the crucible. Copper blister and slag are fed from the top prior to heating and sealing the crucible.

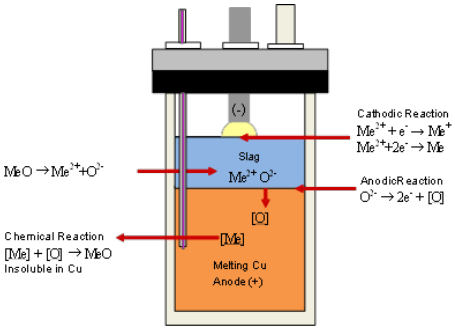

Figure 1. Scheme Arc Electrolysis Furnace

The mesh was refined at the walls and slag – metal and arc -slag interfaces. Complete mesh consists of 6,274 elements, minimum quality of 0.1208 and average quality of 0.8981. The system consists of 5 domains, 19 edges and 15 points. The physical properties of the subdomains of the system are given in the following Table 1. Where k, is the thermal conductivity, h is the heat transfer coefficient by convection. Q, u, and v are values that are obtained by simultaneously solving the equation of the conductive medium DC and Navier-Stokes, respectively. To solve the energy equation the temperature at which the furnace is initially located is 1500 K and to evaluate the heat transfer by radiation $\varepsilon = 0.5$ and $\sigma = 5.67 \times 10^{-8}$ [W/m²K⁴].

Table 1. Physical properties of the subdomains.

Subdomain	Crucible	Copper	Slag	Arc	Electrode
k, W/mK	3	400	3	50	30
ρ, kg/m³	3000	7800	3500	10	2000
C_p, J/kgK	1900	500	1200	10	2000
h, W/m²K	20	-	20	30	40
Q, W/m³	0	ec.Qh	ec.Qh	ec.Qh	ec.Qh
u	-	u	u	-	-
v	-	v	v	-	-

To solve the mass equation the oxygen concentration at which the slag is initially is 2,446 mol/m³, Value obtained by the stoichiometric oxygen contained in the Cu_2O in the slag and the volume of the slag. In Eq(3):

$$N_O\left[\frac{mol}{m^2 s}\right] = V_{slag}\,[m^3] \times c_O\left[\frac{mol}{m^3}\right] \times \frac{1}{z_O F[C]} \times J_z\left[\frac{A}{m^2}\right]$$

The oxygen diffusivities (Fukunaka et al, 1991) in the slag and oxygen in the blister copper are 10^{-7} m²/s and 10^{-6} m²/s, respectively. The metal-slag interface is modeled as a boundary condition of flow discontinuity where it is entered Faraday's Law, the mass transfer of oxygen to this interface is by natural convection and is modeled by its coupling with momentum transfer and is generated by temperature gradients modeled by its coupling with transfer heat. Where C_0 is the concentration of oxygen in the slag obtained from the mass transport equation and *Jz* is the total current density obtained from the coupling with the conductive medium DC equation for the *z* component of the current density.

3. Conclusions

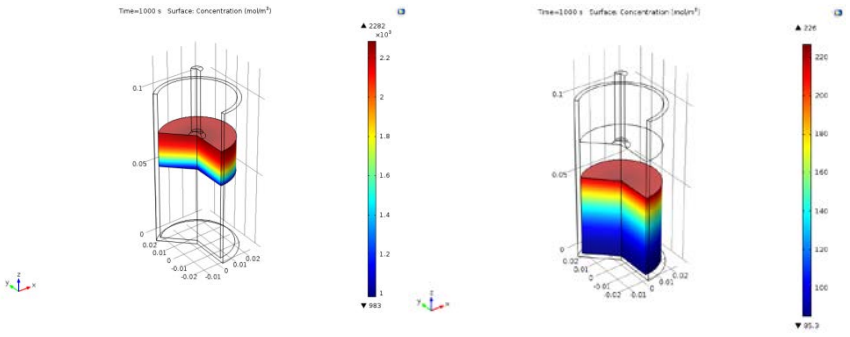

The simulation results in an arc temperature of 2,067 K that forms a movement created by natural convection generated by temperature gradients that in turn generate concentration gradients.

Figure 2. *Profile Concentration of oxygen in Slag, mol/m³ (left) and in Blister Copper, mol/m³ (right).*

In the slag speed reaches a maximum of 6.79 x 10^{-7} m/s, and in the molten copper 10^{-10} m/s. In Figure 2, the simulation of the oxygen mass transport in the slag shows that the initial oxygen with a concentration of 2,446 mol/m³ develops after 1,000 s of simulation a profile with a maximum of 2,282 mol/m³ in the slag - gas interface that goes down to 983 mol/m³ in the metal slag interface where the electrochemical oxidation reaction occurs. The simulation of mass oxygen transport in copper shows that the oxygen not present initially, as a result of the electrochemical oxidative oxidation reaction, develops a profile with a maximum of 226 mol/m³ in the metal slag interface in that descends to reach 85.3 mol/m³ at the bottom of the crucible.

Acknowledgments. The authors thank to the DICYT 051714MF(2017) and Project 155LD of the USACH.

References

[1] D.R. Gaskell, 1997, Structural Aspects of Slags, Molten slags, fluxes and salts '97 conference, 11-26.
[2] T. R. Shelley and J. A. Charles, Transactions of the Institute of Mining & Metallurgy, (1974), C18-C24.
[3] COMSOL Multiphysics 4.3b, License Number: 2079130, (2013) Version: 4.3b, Stockholm, Sweden.
[4] Y. Fukunaka, K. Nishikawa, H.S. Sohn, And Z. Asaki, Metallurgical Transactions B, 22B (1991), 5–11.
[5] Q.G. Reynolds, R.T. Jones, and B.D. Reddy, 2010, The Journal of The Southern African Institute of Mining and Metallurgy, 110 (2010), 733–742.
[6] A. Powell and D.Dussault, Scandinavian Journal of Metallurgy 32(2003), 33–36.

ECCE12
The 12th EUROPEAN CONGRESS OF CHEMICAL ENGINEERING
Florence 15–19 September 2019

Lagrangian simulation of particle properties and stirring condition effects on solid particle distributions in stirred tanks with different size

S. Imai[1], M. Kuroda[1], R. Misumi*[1], M. Kaminoyama[1]

1 Yokohama National University, 79-5, Tokiwadai, Hodogaya-ku, Yokohama-shi, Kanagawa, 240-8501, Japan

**misumi-ryuta-zm@ynu.ac.jp*

Highlights

- The vertical distribution of particle concentration was calculated using CFD-DEM.
- A parameter was found to ascertain the dispersion state in the tank.
- An equation was proposed to predict particle concentration at the vertical height.

1. Introduction

Solid–liquid mixing is widely used in crystallizers and chemical reactors with catalysis. In these processes, some difficulties occur by which solid particles aggregate and collide with stirring blades. Particle collision causes particle breakage and abrasion. Furthermore, when scaling up to the scale to industrial equipment, the particle dispersion state usually becomes insufficient. It is important to qualify the solid particle concentration distribution in the tank and to ascertain the dispersion state to solve these problems. However, it is difficult to measure the detailed particle concentration in the tank under many conditions. Therefore, for this study, Euler–Lagrangian simulations were performed with various particle diameters, particle densities, impeller speeds, impeller diameters, and tank diameters to qualify the vertical distribution of solid particle concentrations in the vessel. We also identified the factors affecting the dispersion state.

2. Analytical method

The Euler–Lagrangian approach, which tracks all particle motion, was used. Turbulent flow in the vessel was represented by Large Eddy Simulation. The particle–particle and particle – solid surfaces interactions were modeled using distinct element method. Simulations were conducted using Computational Fluid Dynamics software (FLUENT 18.0; ANSYS Inc.). The simulated system was a flat-bottom cylindrical vessel with four baffles and a six-blade paddle impeller. Tank diameter T was changed from 10 cm to 30 cm with geometrical similarity. The diameter was equal to liquid height H. The impeller diameter D was $T/2$. Blade width b was $T/10$. The impeller bottom clearance was $T/3$. The impeller speed N was 4.0–6.0 s^{-1}. The fluid was presumed to be water. The solid particle density was changed from 1011 to 2500 kg/m^3. The diameter of the 5000 particles varied: 100–400 µm. The tank interior was divided into 50 zones in the vertical direction. The particle concentration in each zone at height C_i and the particle concentration of the entire tank C_{av} were calculated. The standard deviation of particle concentration σ_c was calculated using C_i and C_{av}. The time-averaged values of σ_c, $\sigma_{c,av}$ were used as particle dispersion state evaluation indexes for the vessel.

3. Results and Discussion

Fig. 1 portrays the relation between $\sigma_{c,av}/C_{av}$ and $u_t/(N D^{0.8})$. Here, u_t, N, and D respectively represent the terminal velocity of a single particle, impeller speed, and impeller diameter. Results from Fig. 1 show that $\sigma_{c,av}/C_{av}$ is correlated with the value of $u_t/(N D^{0.8})$, irrespective of the particle properties, impeller speed, and vessel size. Furthermore, results show that the particles are well dispersed in the tank in the range of at $u_t/ND^{0.8} < 0.03$, and that most of the particles are deposited on the bottom in the range of $u_t/ND^{0.8} > 0.06$. These results demonstrate that using the scale-up factor of '$ND^{0.8}$ = constant' enables the change of dispersion state in the small tank to be reproduced when scaling up to the large tank. The vertical component of fluid velocity near the bottom is presented in Fig. 2. The y-axis shows $\overline{v_z}/(ND^{0.8})$, which was of the time-averaged value $\overline{v_z}$ of the vertical velocity near the tank bottom (z/H = 0.1) along the tank centre section divided by $N D^{0.8}$. The figure shows that the distributions of vertical fluid velocities have nearly the same profile, irrespective of the impeller speed or tank diameter. The uniformity of particle concentration in the vertical direction, $\sigma_{c,av}/C_{av}$ can be arranged according to the ratio of u_t to $ND^{0.8}$, probably because the distribution of $\overline{v_z}/(ND^{0.8})$ near the bottom, which is the fluid flow suspending the particles, shows a similar profile.

Fig. 3 portrays the vertical distribution of particle concentration in the range of $0.03 < u_t/(ND^{0.8}) < 0.06$. This figure shows that the dispersion state of the particles varies greatly in this range. Because $\sigma_{c,av}/C_{av}$ depends strongly on $u_t/(ND^{0.8})$, the particle concentration C/C_{av} is normalized by $u_t/(ND^{0.8})$ in that range, as portrayed in Fig. 4. Results show that, by multiplying $u_t/ND^{0.8}$, it is integrated roughly into one line. Fitting was performed using an exponential function for $0.03 < u_t/(ND^{0.8}) < 0.06$. The following equation was found.

$$(C/C_{av})\, u_t/(ND^{0.8}) = 0.0297 + 0.0427 \exp(-7.12\, z/H) \qquad (1)$$

Using equation (1), the particle concentration at the vertical height can be predicted at ±30 % irrespective of the particle property, impeller speed, and vessel size.

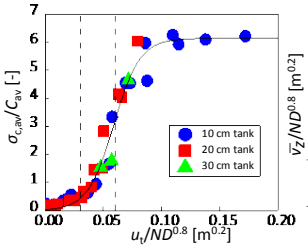

Fig. 1 Relation between $u_t/ND^{0.8}$ and $\sigma_{c,av}/C_{av}$

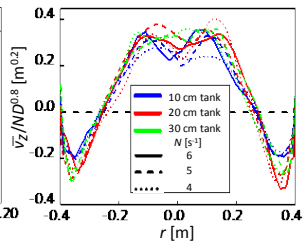

Fig. 2 Distribution of $\overline{v_z}/ND^{0.8}$ at z/H =0.1 in r-z plane

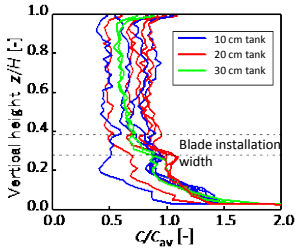

Fig. 3 Particle concentration at $0.03 < u_t/ND^{0.8} < 0.06$

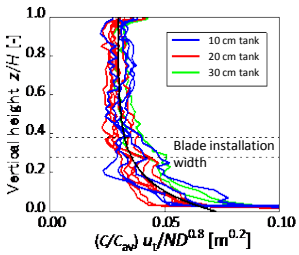

Fig. 4 Particle concentration normalized by $u_t/ND^{0.8}$

4. Conclusions

The vertical distribution of the particle concentration in the stirred vessel was analyzed using Euler–Lagrangian method. Results show that the deviation of particle concentration is correlated with the ratio of terminal velocity of single particle u_t to $ND^{0.8}$. In addition, in the range of $0.03 < u_t/(ND^{0.8}) < 0.06$, an equation (Eq. (1)) was established as capable of predicting the particle concentration distribution in the vertical direction based on $u_t/(ND^{0.8})$.

This study was supported by JSPS KAKENHI (Grant Nos. 19K05118 and 17K06886).

ECCE12
The 12th EUROPEAN CONGRESS OF CHEMICAL ENGINEERING
Florence 15-19 September 2019

OIL/WATER FLOW IN A HORIZONTAL PIPE EXPERIMENTAL AND SIMULATION - DISPERSEDED FLOW PATTERN

D. S. SANTOS[1], M.G. RASTEIRO[1], P.M. FAIA[2], F.A.P. GARCIA[1]

[1]Chemical Process Engineering and Forest Products Research Centre (CIEPQPF), Department of Chemical Engineering, University of Coimbra, Portugal,

[2]Center of Mechanical Engineering, Materials and Processes (CEMMPRE), Electrical and Computers Engineering Department, University of Coimbra, Portugal.

In multiphase fluids flow, the formation of dispersed patterns, where one of the phases is completely dispersed in the other one (continuous medium) is common, for example, in crude oil extraction and during the transport of water/oil mixtures.

In this work, experimental and numerical studies were carried out for the flow of an oil/water mixture in a horizontal pipe, the dispersed liquid being a paraffin (oil with density 843 kg.m^{-3} and viscosity 0.025 Pa.s) and the continuous medium a water solution doped with NaCl (1000 $\mu S.\,cm^{-1}$). The tests were made for oil concentrations of 0.01, 0.13 and 0.22 v/v and velocities of the mixture between 0.9 and 2.6 m.s^{-1}. Experimental work was performed in a pilot rig equipped with an Electrical Impedance Tomography (EIT) system. Information on pressure drop, EIT maps, volumetric concentrations in the vertical diameter of the pipe and flow images were obtained. Simulations were performed in 2D geometry using the Eulerian-Eulerian approach and the k-ε model for turbulence modelling. The model was implemented in a Computational Fluid Dynamics (CFD) platform with the program COMSOL Multiphysics version 5.3. The simulations were carried out using the Schiller-Neumann correlation for the drag coefficient and two equations for the viscosity calculation: Guth and Simba (1936) and Pal (2000). For the validation of the simulations, the pressure drop was the main control parameter.

The simulations predicted the fully dispersed flow patterns which were confirmed experimentally and the pressure drop calculated when using the Pal (2000) equation for the viscosity calculation showed the best fit. By withdrawing samples of the oil/water mixture for different positions on the vertical diameter, which were later analysed through optical microscopy, it was possible to confirm the dispersion of the oil phase in the water phase, the size of the oil drops being dependent on the oil concentration and flow velocity. The results of the images of the flows obtained by the photographs, EIT and simulations were in good agreement, the same being observed for the 1D concentration profiles referred to the vertical pipe diameter.

Keywords: Oil/water flows, dispersed flow pattern, pressure drop, Euler-Euler model.

ECCE12
The 12th EUROPEAN CONGRESS OF CHEMICAL ENGINEERING
Florence 15-19 September 2019

Enhancing the Thermal Efficiency of Hydrogen Compressor by the use of LOHC Falling film.

Arian Shoshi[1]*, S. Ehsan Emamjomeh[1], Eberhard Schlücker[1]

1 Institute of Process Machinery and Systems Engineering, Friedrich-Alexander-Universität Erlangen-Nürnberg (FAU)
**Corresponding author: arian.shoshi@fau.de*

Highlights

- Transient CFD Simulations for compressing hydrogen gas.
- LOHC falling film investigation inside compressor chamber.
- Optimizing LOHC layer for the increase of volumetric efficiency.

1. Introduction

Liquid Organic Hydrogen Carriers (LOHCs) are chemical compounds, which they store hydrogen by bonding it chemically during the hydrogenation process in chemical reactors. The hydrogenation process to take place, heat, is required relatively to high temperatures at elevated pressures. The release of hydrogen during the dehydrogenation process requires more energy in terms of heat at even higher temperatures. By compressing hydrogen gas to very high pressures up to 1000 bar in hydrogen compressors, very high discharge temperatures are reached since the compression process undergoes close to the adiabatic process. The generated heat during the compression in the most cases is wasted to the surrounding. The current research represent an approach for using this heat. LOHCs are stable in liquid state up to 300 °C and there is no risk in vapor formation. Therefore, they offers an excellent use as a cooling liquid in hydrogen compressors, in this way improving the thermal efficiency and the volumetric efficiency of the compressor. The new prototype of this compressor designed at Institute of Process Machinery and Systems Engineering is currently carrying out the first tests with very promising results.

2. Methods

The described compressor is a plunger type operating always upward and use a LOHC falling film as coolant liquid formed along at the inner walls of compressor chamber for absorbing the compression heat. The flow of falling film from the top to bottom dead center of the compressor form a LOHC layer above the front end of the plunger. This LOHC layer has a crucial role in preventing hydrogen to leak outside the compressor chamber. Falling film ensures cooling of the walls in order to avoid also the heating of hydrogen gas brought during the suction phase. Beside this, LOHC liquid level above the plunger in a significant way decrease the detrimental space, by filling this clearance between the compressor head and the piston, which is left in order to prevent the mechanical collusion. The detrimental space therefore is nearly “zero”. A thin layer of the hot LOHC together with the compressed hydrogen by the end of the stroke is discharged in the separator, for separating hydrogen form LOHC. Hot LOHC afterwards follows the dehydrogenation process in reactor. The high-pressure hydrogen can be used wherever is required but the best

example of use is in mobility since the LOHCs plays an important role in hydrogen logistic as well. This compressor is an important component of a new hydrogen storage system or hydrogen transport system for making the hydrogen available with high pressures and without wasting energy in terms of heat. For better understating and validating the results, in parallel simulations and experimental tests are investigated. For observing the behavior of LOHC falling film and optimizing the LOHC layer, a Plexiglas cylinder same as the real compressor chamber were used. The figure 1 shows formation of the LOHC layer above the plunger

3. Results and discussion

Ongoing research represent results only for the transient state operation. Due to the safety issues, for the early phase, nitrogen gas and loaded LOHC is used during the all experiments. Until now, pressures up to 630 bar are reached with one stroke starting from 2 bar absolute pressure. The presented compressor is driven with a hydraulic unit at relative low velocities starting from 10-40mm/s. The results depicted in Figure 2 shows a temperature rise of nitrogen gas above 110 °C by 630 bar. Compressing a diatomic gas such as nitrogen, hydrogen, undergoing an adiabatic process from 1 bar (abs) to 1000 bar, results in temperature rise of gas above 2000 K.

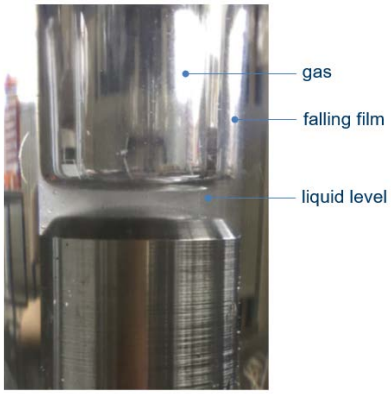

Figure 1. LOHC Falling film.

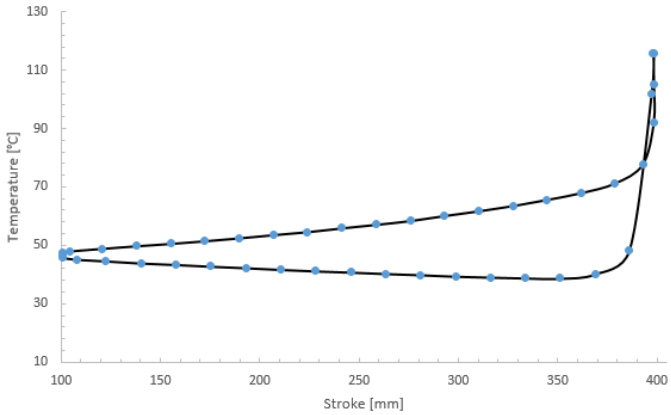

Figure 2. Temperature rise of nitrogen gas during compression up to 630bar.

4. Conclusions

This conceptual research describes a way of internal cooling of a hydrogen compressor for enhancing the thermal efficiency. Currently are running tests still with nitrogen for the higher pressures and as long it is reached a safe and a stable state hydrogen will be used. Thereafter, the validation of the data take place to justify the thermal efficiency.

References

[1] O. Singh, Applied Thermodynamics, third ed., 2009.
[2] I.L. Spain, J. Paauwe, High Pressure Technology, Vol. 1, New York and Basel, 1977.
[3] R. N. Brown, Compressors: Selection and Sizing, third ed., Elsevier, 2005
[4] Th. Bergman, A. Lavine, F. Incropera, D. Dewitt, Fundamentals of Heat and Mass Transfer, John Wiley & Sons, 2011

ECCE12
The 12th EUROPEAN CONGRESS OF CHEMICAL ENGINEERING
Florence 15-19 September 2019

Quality by Design for Fused Deposition Modeling 3D Printing: Extrudate Mass Flow Control.

Tim Feuerbach, Markus Thommes

TU Dortmund University, Laboratory of Solids Process Engineering,

Emil-Figge-Str. 68, 44227 Dortmund, Germany

**Corresponding author: tim.feuerbach@tu-dortmund.de*

Highlights

- Filament diameter variations affect the obtained extrudate mass flow
- Feedback control of filament feeding velocity based on filament diameter
- Implemented control strategy results in more uniform extrudate mass flow

1. Introduction

Fused Deposition Modeling (FDM) is a promising manufacturing method for customized pharmaceutical products, such as patient-specific implants [1]. In FDM, thermoplastics in form of a filament are used as a feedstock material. In addition to the imposed mechanical requirements on the filaments, there are also geometrical requirements [2]. The main reason is the utilization of the nominal diameter to determine the required filament feed velocity to achieve the desired extrudate mass flow. Since there is no feedback control in FDM printers, variations of the filament diameter directly translate into inconsistent flowrates [3], as indicated in Figure 1 (left). These inconsistencies can lead to excess material or to voids and cavities that can influence the object porosity, geometry and mechanical strength. The aim of this study was to evaluate if extrudate mass flow variations can be compensated by adjusting the filament feed velocity based on measured filament diameters to obtain consistent extrudate mass flow.

2. Methods

Commercial grade acrylonitrile butadiene styrene (ABS) filament (White ABS 1.75mm 1 KG, RepRap Austria, Neuhofen/Krems, Austria) was used as received. The filament diameter was measured with a laser gauge (Laser 2025T, Sikora GmbH, Bremen, Germany). The filament was discretized into 1 mm compartments and each compartment was assigned with a representative diameter. A custom-built FDM printer [4] was used to extrude the material. The extruded material was analyzed gravimetrically with an analytical scale (Cubis® MCM66, Sartorius, Göttingen, Germany).

3. Results and Discussion

The printing process was conducted with a constant filament feed velocity, assuming a filament diameter of 1.75 mm. The diameter variations were similarly introduced into the extrudate mass flow. Assuming a worst-case scenario of a 0.05 mm systematic error, a mass deviation of 6 % would be introduced into the product, as shown in Figure 1 (right). For most pharmaceutical

products containing at least one drug, this would lead to an intolerable deviation from the nominal drug dosage.

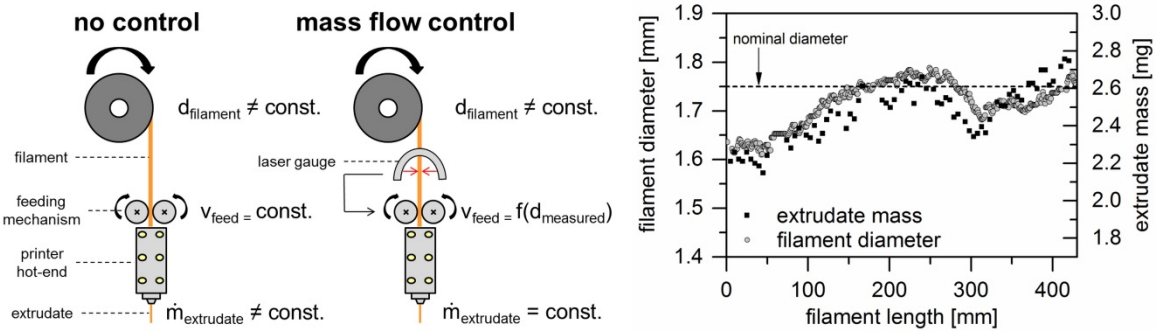

Figure 1. Schematic of the printing process with and without mass flow control (left) and measured filament diameter and corresponding extrudate mass without mass flow control (right).

In a next step, the measured filament diameter was used to adjust the filament feed velocity to obtain the desired extrudate mass flow. A constant diameter of 1.75 mm would have led to sample weights of m_{set} = 48.1 mg, as indicated in Table 1. However, the utilized filament piece for this experiment had a diameter of 1.699 ± 0.021 mm (arithmetic mean ± standard deviation, n = 7). Based on this deviation from the nominal diameter, a theoretical mean sample weight of $m_{no\ control}$ = 45.33 mg was expected for each compartment, which is similar to a mass deviation of approximately -5.8%. The applied control strategy led to an improved mean sample weight of $m_{controlled}$ = 47.31 mg, which is similar to a mass deviation of only -1.6%.

Table 1. Expected extrudate mass and measured extrudate mass with mass flow control.

m_{set} [mg]	$m_{no\ control}$ [mg]	$m_{controlled}$ [mg]
48.1	45.33 ± 1.11 (n = 7)	47.31 ± 0.90 (n = 7)

4. Conclusions

Systematic and random deviations from the nominal filament diameter were successfully compensated by the presented control strategy, which resulted in a more uniform extrudate mass flow. This is particularly important for 3D printing of pharmaceutical products to control the drug dosage. The control strategy can be integrated as a Quality by Design tool into the printing process and allows the application of a wider range of filaments.

References

[1] Espalin, D.; Arcaute, K.; Rodriguez, D.; Medina, F.; Posner, M. and Wicker, R. Fused deposition modeling of patient-specific polymethylmethacrylate implants. Rapid Prototyping Journal, 16, 164-173 (2010).

[2] Feuerbach, T.; Callau-Mendoza, S. and Thommes, M. Development of Filaments for Fused Deposition Modeling 3D Printing with Medical Grade Poly(Lactic-Co-Glycolic Acid) Copolymers. Pharmaceutical Development and Technology, DOI: 10.1080/10837450.2018.1514522 (2018).

[3] Rane, K.; Cataldo, S.; Parenti, P.; Sbaglia, L.; Mussi, V.; Annonio, M.; Giberti, H. and Strano, M. Rapid Production of Hollow SS316 Profiles by Extrusion based Additive Manufacturing. AIP Conference Proceedings, 1960, DOI: 10.1063/1.5035006 (2018).

[4] Feuerbach, T.; Kock, S. and Thommes, M. Characterisation of fused deposition modeling 3D printers for pharmaceutical and medical applications. Pharmaceutical Development and Technology, DOI: 10.1080/10837450.2018.1492618 (2018).

ECCE12
The 12th EUROPEAN CONGRESS OF CHEMICAL ENGINEERING
Florence 15-19 September 2019

Online monitoring of emulsion polymerization by SRS and Raman spectroscopies

Manis Gheghiani[1*], Noémie Caillol[2], Serge Henrot[2], Timothy McKenna[3], Nida Sheibat-Othman[1]

1 University of Lyon, University Claude Bernard Lyon 1, CNRS, LAGEPP UMR 5007, F-69100, Villeurbanne, France ; 2 Axel'One, Solaize, France ; 3 Université Claude Bernard Lyon 1, CPE Lyon, CNRS, UMR 5265, C2P2-LCPP group, Villeurbanne, France

**Corresponding author: manis.gheghiani@univ-lyon1.fr*

Highlights

- Monitoring of emulsion polymerization with NIR and Raman spectroscopies
- Spatially resolved spectroscopy (SRS) for heterogeneous process
- Prediction of the polymer fraction and particle size with PLS

1. Introduction

Online monitoring of polymerization processes is essential to ensure the process security, product quality and process productivity by allowing process control and reconfiguration of the operating conditions when necessary. Monitoring of emulsion polymerization is particularly challenging due to the multiphase nature of the reaction. In this kind of systems, it is important to monitor the different concentrations (monomer, polymer, and surfactant) as well as the key product properties, like the polymer molecular weight or the particle size. Currently, calorimetry constitutes the primarily online technique used for monitoring of polymerization processes. Spectroscopies, like Raman and Near Infrared (NIR), are becoming widely employed online. Based on NIR spectroscopy, the Spatially Resolved Spectroscopy (SRS) has been developed to study heterogeneous media and obtain information related to the light scattering and thus the particle. SRS and Raman spectroscopies are investigated in this study to evaluate the potential of SRS to predict the polymer fraction and the particle size online in emulsion polymerization.

2. Methods

A batch polymerization period was first conducted, during which polymer particles were nucleated, followed by a semi-continuous reaction to allow their growth follows. The reactions were done in a 1 L reactor with mechanical stirring, between 300-400 rpm. First, the surfactant was dissolved in water and degassed using nitrogen and the mixture was heated to 70 °C using a thermostated bath with silicon oil. The co-monomer mixture was then added and the polymerization was initiated by adding the initiator, KPS. During the reaction, the nitrogen gas flow was moved out of the reaction medium to the top of the reactor to maintain an atmosphere saturated with nitrogen. At the end of particle nucleation, the semi-continuous phase was started by adding the monomer mixture under starved conditions. Samples were collected at specific time intervals to measure the solids content (SC, i.e. mass fraction of solid) using a thermobalance and the particle size using dynamic light scattering (DLS, Malvern Nano ZS®).

Throughout the reaction, online analysis was provided with Raman spectroscopy using an OceanOptics QE65000 and an immersion probe with a wavelength laser excitation of 785 nm. SRS spectroscopy, based on NIR spectroscopy, from Indatech-Chauvin Arnoux was used with angles of measurement to the light source at 180° (for transmission), 175°, 170° (for scattering) and 30° (for backscattering).

3. Results and discussion

The results presented in the following figure show the prediction of masse fraction of polymer by both the SRS and Raman spectroscopy. Extensive data analysis combined with multivariate calibration using Partial Least Square (PLS) regression was necessary to exploit the online data. The figure shows that the prediction of the polymer fraction can be established by both spectroscopies and fits well with the reference measurement made offline on the thermobalance.

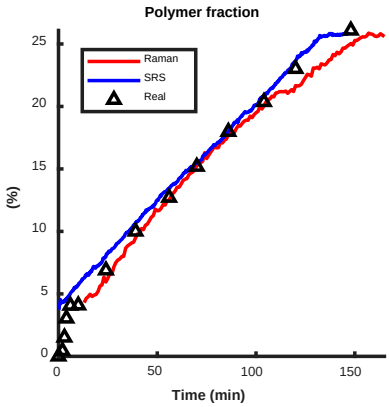

Figure 1. Polymer fraction estimated by gravimetry, Raman and SRS.

The prediction of the diameter of particles was also investigated by both spectroscopies. The SRS was more adapted for this study than Raman spectroscopy mainly due to the specific probe configuration that makes it particularly sensitive to light scattering due to particles and is therefore sensitive to the particle size distribution.

4. Conclusions

Online monitoring of the polymer fraction and the diameter of polymer particles was established by using Raman and SRS spectroscopies. Both methods gave rather good predictions of the chemical information, like the polymer fraction, but the SRS was more suitable for the prediction of physical parameters like the mean diameter of particles.

References

[1] W. K. Silva, D. L. Chicoma, R. Giudici, Polym. Eng. Sci. 10, (2011), 2024-2034.
[2] O. Elizalde, M. Azpeitia, M. Reis, J. Asua, J. Leiza, Ind. Eng. Chem. Res., 18, (2005), 7200-7207.
[3] A. Cherfi et G. Févotte, Macr. Chem. and Phy. 203, 9, (juin 2002), 1188.
[4] Gossen, Paul D., J. F. Macgregor, et Robert H. Pelton. App. Spec. 47, 11 (novembre 1993): 1852‑70.

ECCE12
The 12th EUROPEAN CONGRESS OF CHEMICAL ENGINEERING
Florence 15-19 September 2019

Effect of flow regimes on reaction yield in a T-shaped micro-reactor.

Matteo Antonelli, Alessandro Mariotti, Chiara Galletti, Maria Vittoria Salvetti, Roberto Mauri, Elisabetta Brunazzi*

Dipartimento di Ingegneria Civile e Industriale, Università di Pisa, Largo L. Lazzarino 2, 56122 Pisa, Italy

**Corresponding author: elisabetta.brunazzi@unipi.it*

Highlights

- Experimental and numerical reaction yields in a T-shaped micro-reactor.
- Reaction yield depends on both Reynolds number, Re, and Damköler number, Da.
- With segregated flow regimes, the reaction yield decreases with increasing Re.
- In the engulfment regime, the reaction yield increases with increasing Re.

1. Introduction

Micro-devices, constituted by channels with typical dimensions < 1 mm, are well suited for many applications ranging from mixing to chemical reaction, dispersion and emulsification. Micro-reactors could allow a large intensification of many pharmaceutical and fine-chemistry processes, due to continuous operation, enhanced heat transfer and well controlled residence time, resulting in an increase of the reaction yield. A key role is played by the mixing that, however, should be promoted with special techniques because the flow in micro-channels is laminar; a simple way to enhance mixing is to design micro-devices where the flow symmetries are broken, and a transverse convection is induced. A large variety of micro-mixer geometries has been proposed. The simplest configuration is the T-shaped micro-rector, whose mixing behavior has been largely characterized in literature both experimentally and numerically by feeding it with water. Although its simplicity, several complex flow regimes, even time periodic ones, have been found, depending on Reynolds number, i.e. Re [1][2]. So far, large attention has been payed to the characterization of the mixing process in these regimes, but there is scarce knowledge about their effect on the yield of a chemical reaction. In particular, the reaction yield is affected not only by the manner the reactants come into contact (i.e. mixing), but also by the reaction kinetics (chemical reaction). Hence, an important role is played by the Damköhler number, i.e. *Da*, representing the flow to chemical time-scale ratio.

The present work is aimed at investigating the effect of *Da* and *Re* on the yield of a chemical reaction in a T-junction, by combining experiments and computational fluid dynamics (CFD).

2. Methods

A T-shaped micro-reactor, shown in Fig. 1a, is used to carry out flow visualization experiments. The reaction that has been chosen is A+B→C+D and a large excess of B was used to have a pseudo-first order kinetic, i.e. $\frac{dC_A}{dt} = -kC_A$, where C_A is the concentration of A. Moreover, the reaction is catalyzed by an acid E, so that the kinetic constant $k = f(C_E)$. The reaction can be

observed experimentally through flow visualization as the reactant A has a color that disappears while converting into products. A syringe pump feeds the mixer inlets with equal flow rates. One inlet stream is an aqueous solution of A and E, while the other stream is an aqueous solution of B. By arranging the concentrations of B and E, the kinetic constant k is varied in the range from 1 to 20 s^{-1} to span a range of Da in addition to Re.

An upright microscope with a magnifying lens of 4x and a halogen lamp are used to observe the mixing of the streams inside the mixer. The images are collected by using a monochromatic high-speed camera having a resolution of 920x2048 pixels and a frame rate up to 387 frames/s. Flow visualization images are processed off line to convert pixel intensities into normalized depth-averaged A concentration images [1] and thus to estimate the reaction yield.

Numerical modeling was carried out by solving continuity, momentum and chemical species transport equations using ANSYS Fluent v19 code [3]. In order to better capture the reaction region, the grid was refined in the region of high reaction rates through the mesh adaption technique.

3. Results and discussion

Both the numerical and the experimental investigations were carried varying the *Re* from 10 to 260 and *k* from1 to 22 s^{-1}. Fig. 2b shows for example the average concentration of A along the mixing channel as estimated from the CFD and from the experimental image analysis for k = 10 s^{-1} and for different *Re*, in the range *Re* = 10-60. A good agreement between experiments and CFD can be observed. Moreover, with increasing *Re*, the concentration of A in the outlet increases indicating lower yield. This is due to the lower residence time in the reactor.

(a) 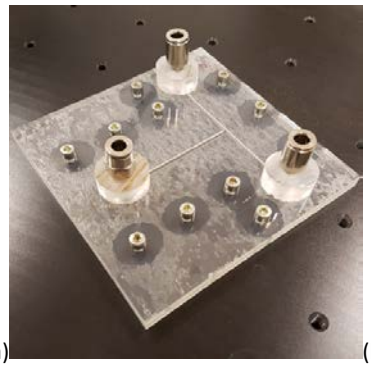

(b) 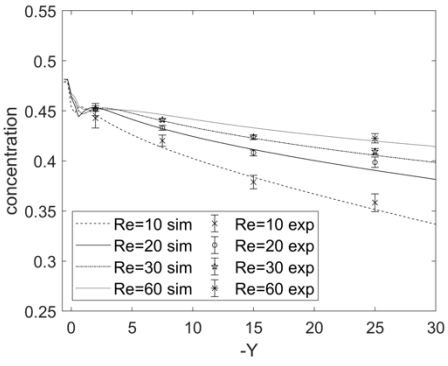

Figure 1. (a) T-junction. (b) Concentration of A along the mixing channel as a function of Re.

4. Conclusions

The effect of both *Da* and *Re* on the reaction yield in a T-junction is investigated experimentally and numerically. At low *Re*, with segregated flow regimes, the reaction yield decreases with increasing *Re* because of the lower residence time. Instead, increasing *Re* in the engulfment regime, leads to an increase of reaction because the enhanced mixing.

References

[1] A. Mariotti, C. Galletti, R. Mauri, M.V. Salvetti, E. Brunazzi, Chem. Eng. J. 341, (2018) 414-431.
[2] C. Galletti, E. Brunazzi, R. Mauri, Chem. Eng. Sci. 164 (2017) 333-343.
[3] C. Galletti, A. Mariotti, L. Siconolfi, R. Mauri, E. Brunazzi, Can. J. Chem. Eng. 97 (2019) 528-541.

ECCE12
The 12th EUROPEAN CONGRESS OF CHEMICAL ENGINEERING
Florence 15-19 September 2019

Scale-up strategies for the blending of miscible liquids with large viscosity differences

Nur Azmina Hadirah Binti Hamdan[1], Joelle Aubin[1*], Martine Poux[1], Catherine Xuereb[1]

1 Laboratoire de Génie Chimique, Université de Toulouse, CNRS, Toulouse, France
**Corresponding author: joelle.aubin@ensiacet.fr*

Highlights

- $N.t_m$ versus Re* allows identification of stirrer or added liquid regimes
- Re* does not allow $N.t_m$ to be replicated across scales
- Impeller tip speed or specific power replicate $N.t_m$ better across scales

1. Introduction

Blending of small quantities of additives that have higher viscosity and/or density than the bulk is a common operation in the process industries (personal care, food, water treatment), it is however a difficult task. A few studies have addressed the subject and it was found that a modified Reynolds number, $Re^* = \rho N D^2/\mu_a$ allows identification of whether the added liquid has an effect on mixing time compared with turbulent blending [1, 2]. [2] also looked the effect of scale on blend time in these systems and found that large viscosity differences may affect small scale more than in large scale vessels and that depending on the scale the operating regimes (stirrer controlled or added liquid controlled) may change. Whilst correlating dimensionless mixing time ($N.t_m$) with Re* may be useful for determining if turbulent blending correlations can be used for these systems, it does not provide guidance for scaling-up or down. The objective of this work is to identify which stirred tank operating parameters should be kept constant to replicate blending miscible liquids with large viscosity ratios across equipment scales.

2. Methods

Experimental set-up. The tanks employed in this work are dish-bottomed cylindrical tanks with dimensions, $T_1 = H_1 = 0.19$ m and $T_2 = H_2 = 0.6$ m, which correspond to volumes of 5 L and 171 L, respectively. The tanks are equipped with four equally spaced Perspex baffles of width $w = T/10$ placed 90º to each other. An axial flow Mixel TT impeller ($D = T/2$) used to blend the liquids with an off-bottom clearance of $C = T/3$, where C is defined as the distance from the vessel bottom to the lowest horizontal plane swept by the impeller.

Fluids and operating conditions. The fluid in the bulk of the tank was tap water at 20°C. The impeller speed was in the range 130-400 rpm for the 5 L tank and 90-185 rpm for the 171 L tank, which correspond to fully developed turbulent flow. The viscous additive was a solution of carboxymethyl cellulose (CMC) at concentrations ranging from 1% w/w to 7% w/w. For CMC solutions with concentrations less than 2% w/w, the rheological behaviour was quasi-Newtonian and the viscosity ranged from 0.1 to 1.3 Pa.s. However, for higher concentrations, the additive had an increasingly shear-thinning behaviour. The apparent viscosity at 10 s^{-1} (approximate shear rate in injection zone)

was taken as a reference, being 11 Pa.s, 35 Pa.s, 580 Pa.s and 820 Pa.s for 4-7% CMC solutions. Nevertheless, the amount of viscous fluid added to the bulk was relatively small, being 1 mL or 10 mL, and this was assumed to have no impact on the turbulent flow regime in the tank.

Mixing time measurements. Macro mixing time was determined using a coloration-decolouration method based on an oxido-reduction between sodium thiosulfate and iodine. The water in the tank is initially coloured brown with an iodine solution. CMC is dissolved in sodium thiosulfate and this solution is then injected into the bulk at the liquid surface using a large syringe, midway between the shaft and the tank wall and midway between two baffles. The sodium thiosulfate solution decolours the brown iodine solution. The macro mixing time is evaluated visually and is determined as the time taken for all of the iodine to have disappeared. For each operating condition, the experiment was repeated four times and an average value was used for analysis.

3. Results and discussion

Figure 1 (left) shows a constant dimensionless mixing time in the 5L tank for Re* ≥ 10 corresponding to the stirrer controlled regime, whilst for decreasing values of Re* lower than this limit, $N.t_m$ increases, which corresponds to the added liquid controlled regime. Indeed, for viscosity ratios $\mu_a/\mu_b < 10^3$–10^4, mixing time may be predicted by conventional correlations for turbulent blending. It is noted however that this does not hold when working in the 171L tank, suggesting that Re* may not be the appropriate scale-up invariant. On the other hand, for a given viscosity ratio, $N.t_m$ is better replicated at both scales when impeller tip speed (Figure 1, right) or power per unit volume are kept constant, at lease for lower viscosity ratios.

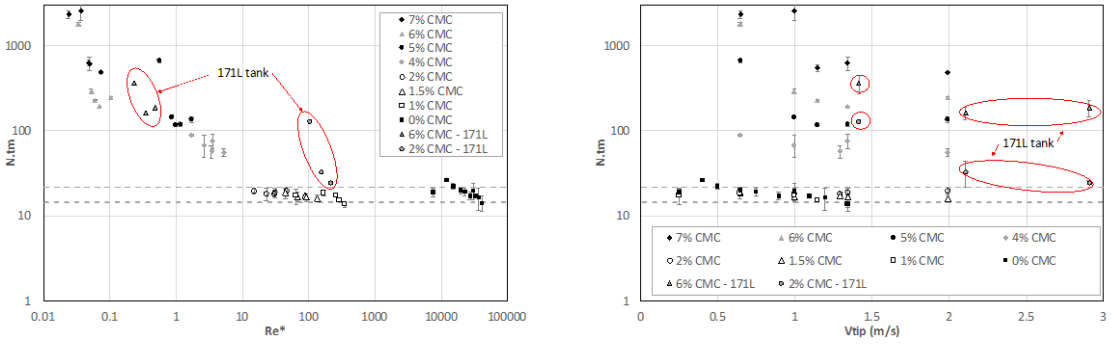

Figure 1. Dimensionless mixing time in the 5L and 171L tanks as a function of Re* (left) and impeller tip speed (right).

4. Conclusions

Mixing time is unaffected by additive viscosity for $\mu_a/\mu_b < 10^3$–10^4, however it increases significantly for higher ratios. Also, $N.t_m$ is not constant over the entire turbulent flow regime as the viscosity ratio increases. $N.t_m$ correlates better with the modified Re* based on the viscosity of the added liquid although Re* does not seem to correctly replicate $N.t_m$ across scales when at large viscosity ratios. $N.t_m$ appears to better replicated at both scales at constant impeller tip speed or power per unit volume.

References]

[1] S.S.H. Burmeister, C.D. Reilly, M.F. Edwards, 7th Euro. Conf. Mixing, Brugge, Belgium (1991) 9-16.
[2] P.N. Jones, G.N. Ozcan-Taskin, Chem Eng Tech. 28 (2005) 908-914.

ECCE12
The 12th EUROPEAN CONGRESS OF CHEMICAL ENGINEERING
Florence 15-19 September 2019

Characterization of gas-liquid flow photoreactors at the micro- and milli-scale

Anca Roibu, Tom Van Gerven, Simon Kuhn*

Department of Chemical Engineering, KU Leuven, Celestijnenlaan 200F, 3001 Leuven, Belgium

**Corresponding author: simon.kuhn@kuleuven.be*

Highlights

- Photon flux per liquid volume increases with gas transport fraction.
- Optical pathlength is smaller in gas-liquid phase in comparison to single phase.
- Actinometry has potential for quantification of scattering and liquid residence time.

1. Introduction

Flow photo microreactors are a promising tool for gas-liquid photoreactions such as photooxidations and fluorinations due to their small penetration depth and the promotion of segmented flow which leads to good mass transfer of the gas in the liquid [1,2]. However, reaction condition optimization in microreactors and scale-up to milli-reactors requires an extensive parameter study [4,5]. Nevertheless, the optimal light source intensity, reagent concentration and total flow rate are determined by photon transport and hydrodynamics in the employed gas-liquid photoreactors. When these phenomena are understood at a fundamental level, the optimization and the scale-up procedure become faster and cost efficient. Chemical actinometry is an important tool to characterize photoreactors and was previously used to determine the optical pathlength and photon flux in single liquid phase in a microstructured reactor [6]. However, the observations found in single-phase may not apply to two-phase flow due to the light scattering at the gas-liquid interface and hydrodynamics determined by the presence of the gas bubbles. The aim of this study is to experimentally determine the optical pathlength and photon flux in gas-liquid micro- and milli-scale photoreactors and compare it with the case of single liquid phase.

2. Methods

The microreactor used in this work consists of a glass plate with a serpentine channel characterized by a volume of 0.6 mL and a diameter of 1 mm. The milli-scale reactor is a Corning Advanced-Flow G1 Photo Reactor which is composed of heart-shaped elements and is characterized by a volume of 8 mL and a channel height of 1.1 mm. Both reactors are irradiated by green Light-Emitting Diodes (LEDs). The photon flux and the optical pathlength are experimentally determined by visible-light actinometry following a methodology previously reported [6]. The actinometric measurements are performed in single liquid phase and in gas-liquid two-phase flows. The total flow rate is 1.3 $mLmin^{-1}$ in the microreactor and between 35 and 42 $mLmin^{-1}$ in the milli-scale reactor. Nitrogen is used as inert gas with volumetric gas transport fractions (β_G) comprised between 0.2 and 0.9 in the microreactor and between 0.2 and 0.5 in the milli-scale reactor.

3. Results and discussion

To ease the comparison, the values of the photon flux per liquid volume obtained in two-phase flow are normalized by the values found in single phase. As shown in Figure 1, the photon flux in two-phase flow experiences an exponential increase with the gas transport fraction reaching 240% at β_G=0.9 in the microreactor and 54% at β_G=0.5 in the milli-scale reactor. This increase can be caused by light scattering. Another possibility is that the liquid residence time is higher than considered in calculations due to the slip and occurrence of local back flow through the liquid films [7]. Currently, a residence time distribution investigation is carried out in order to experimentally determine the mean liquid residence time. Moreover, it was found that the optical pathlength in two-phase flow is 31% smaller at β_G=0.9 compared to the single phase microreactor and 17% smaller in the milli-scale reactor irrespective of the gas fraction.

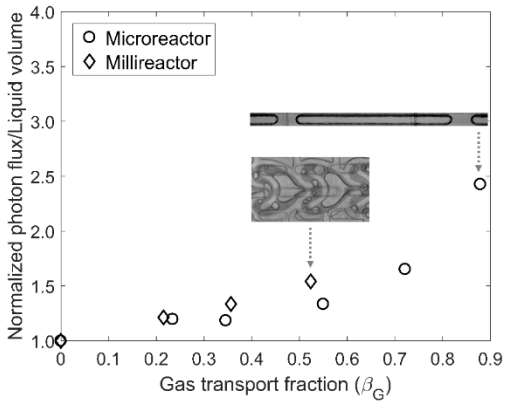

Figure 1. The variation of normalized photon flux per liquid volume with the gas transport fraction (β_G) in the microreactor and the milli-scale reactor. The insets illustrate the flow pattern at β_G = 0.88 in the microreactor and at β_G = 0.52 in the milli-scale reactor.

4. Conclusions

Our study shows that the presence of gas bubbles has a significant impact on the amount of photons received by the liquid phase and on the distance travelled by photons within the reactor at both micro- and milli-scale. The correlation of the actinometric measurements with the photon transport and hydrodynamics could extend the application of actinometry to the quantification of light scattering and liquid residence time in two-phase photoreactors.

References

[1] D. Cambié, C. Bottecchia, N. J. W. Straathof, V. Hessel, T. Noël, Chem. Rev. 116 (2016) 10276–10341.
[2] A. Gavriilidis, A. Constantinou, K. Hellgardt, K. K. (Mimi) Hii, G. J. Hutchings, G. L. Brett, S. Kuhn, S. P. Marsden, React. Chem. Eng. 1 (2016) 595-612.
[3] A.Woitalka, S.Kuhn, K.F.Jensen, Chem. Eng. Sci. 116 (2014) 1–8.
[4] C. Mendoza, N. Emmanuel, C. A. Páez, L. Dreesen, J.-C. M. Monbaliu, B. Heinrichs, J. Photochem. Photobiol. A 356 (2018) 193-200.
[5] N. Emmanuel, C. Mendoza, M. Winter, C. R. Horn, A. Vizza, L. Dreesen, B. Heinrichs, and J.-C. M. Monbaliu, Org. Process. Res. Dev. 21 (2017) 1435–1438.
[6] A. Roibu, S. Fransen, M. E. Leblebici, G. Meir, T. Van Gerven and S. Kuhn, Scientific Reports 8 (2018) 1-10.
[7] A. A. Kulkarni, V. S. Kalyani, Ind. Eng. Chem. Res., 48 (17) 2009.

ECCE12
The 12th EUROPEAN CONGRESS OF CHEMICAL ENGINEERING
Florence 15-19 September 2019

Non-linear rheology of granular matter under large amplitude oscillatory shear

Rishab Handa[1], Christian Wagner[1] and Jorge Fiscina[1]

1 Experimental Physics, University of Saarland, 66123 Saarbrücken, Germany

rishabhanda93@gmail.com

Keywords: Chebyshev polynomial, Lissajous-Bowditch curve, nonlinear rheology

The structure and dynamics of granular materials is a problem of fundamental and industrial interest. Investigating the granular flow near jamming transition can yield insight into the energy landscape of granular media. Large amplitude oscillation shear rheometry is a well-defined technique that offers to shear material at rates similar to huge deformation that occurs in industrial processing operations. In this study, we show that the viscosity of granular materials can be significantly tuned by orders of magnitude by applying normal force of an order of few Newton. Also our comparative study of dry and wet granular systems confirms that dry granular media flow considerably slower than wet granular systems, contradicting to the common assumption of wet granular material being more viscous than dry granular material. We have utilized a new framework to characterize the non-linear stress-strain response and seemingly have identified different dynamical regimes of granular materials in the context of LAOS rheometry.

ECCE12
The 12th EUROPEAN CONGRESS OF CHEMICAL ENGINEERING
Florence 15-19 September 2019

Hollow Fiber Membrane Bioreactor for the Liver Tissue Engineering

Loredana De Bartolo[1], Haysam Mohamed Magdy Ahmed[1,2], Simona Salerno[1], Antonella Piscioneri[1], Shervin Khakpour[1,2], Lidietta Giorno[1] and Enrico Drioli[1,2]

[1]*Institute on Membrane Technology, National Research Council of Italy, ITM-CNR, via P. Bucci cubo 17/C,* [2]*Department of Chemical Engineering and Materials (DIATIC), University of Calabria, Rende, Italy*
**Corresponding author: l.debartolo@itm.cnr.it*

Highlights

- Liver microtissue spheroids were cultured in a HF membrane bioreactor
- Membrane bioreactor enabled the maintenance of cell functions up to 25 days
- O_2 concentration profiles into the spheroids and bioreactor were evaluated
- A proper oxygenation was proven by oxygen uptake and mass transfer

1. Introduction

The development of bioartificial devices that are able to favour the liver reconstruction is still challenging[1]. Our strategy was to create human liver microtissue spheroids metabolically active by using an optimized crossed HF membrane bioreactor whose design and structural features ensure a uniform microenvironment and adequate oxygenation[2]. When culturing large spheroids, the lack of a perfusing vascular network, as occurs in vivo, could imply a reduced supply of oxygen and nutrients leading to impairment of cell viability and functions. The bioreactor consists of two bundles of hollow fiber (HF) polyethersulfone (PES) membranes cross-assembled in alternating manner. One bundle of HF membranes provides cells nutrients and metabolites whereas the other HF bundle removes catabolites from cell compartment mimicking in this way the in vivo arterious and venous blood vessels. The combination of these two fiber set creates three compartments: two intraluminal compartments of PES HF in which the medium flows and one extraluminal compartment represented by extracapillary network formed by the fibers in which spheroids are cultured.

2. Methods

The bioreactor consists of two bundles of PES HF membranes cross-assembled in alternating manner and potted with polyurethane adhesive within glass housing. The membranes were characterised in order to establish the physico-chemical, structural and transport properties. The bioreactor fluid dynamics were characterized in terms of cumulative residence time distribution (RTD). Spheroids of primary human hepatocytes were realized in agarose mold and then cultured in the extralumen compartment of the bioreactor. The oxygen uptake, urea synthesis and albumin production rates as well as biotransformation functions were evaluated with time. The oxygen concentration profile inside the spheroids and in the extra-capillary space was determined through mathematical modelling of the mass and momentum transfer under steady-state conditions. A periodic unit element (750×750×500 μm) representative of the perfusion system in

the bioreactor was chosen to decrease the computational complexity of the model. The equations were numerically solved using COMSOL Multiphysics®.

3. Results and discussion

Human hepatocyte spheroids with uniform size and shape were formed through self-assembling and cultured into the bioreactor (Fig.1). Adjacent spheroids fused, giving rise to larger microstructures around the fibers forming liver-like tissue, which retained functional features in terms of urea synthesis, albumin production, and diazepam biotransformation up to 25 days. The metabolic function data strongly corroborates that within the bioreactor a proper oxygenation and supply of nutrients were provided to the cells ensuring a physiological amount even in the spheroids core. The oxygen uptake rate and the mathematical modelling of the mass transfer directly elucidated that liver microtissue spheroids are not exposed to any oxygen mass transfer limitation. The minimum oxygen concentration reached at the center of multiple spheroids with diameter of 200 μm is significantly higher than the one of the perivenous zone in vivo (42-49 μmol/L), while for larger microtissues (400 μm diameter) the oxygen concentration drops to values that are equal to the maximum concentration found in the liver periportal zone (Fig. 1). Both experimental and modelling investigations led to the achievement of significant results in terms of liver cell performance. Indeed, the creation of a permissive microenvironment inside the bioreactor supported the formation and long-term maintenance of functional human liver microtissues.

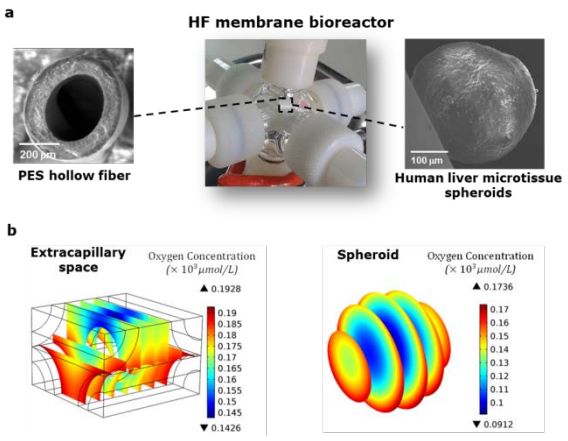

Figure 1. a) Hollow fiber membrane bioreactor used for culture of liver microtissue spheroids; b) oxygen concentration profiles in a large spheroid within a unit element of the bioreactor and in the extra-capillary space in the element.

4. Conclusions

The bioreactor provided a well-controlled microenvironment at molecular level thanks to the selective permeable properties of the membranes and fluid dynamics conditions. The oxygen concentration profiles into the spheroids and in the extracapillary space giving a microscopic view over the cellular microenvironment confirmed the capability of the bioreactor to provide adequate oxygenation to the microtissues.

References

[1] HMM. Ahmed, S. Salerno, S. Morelli, L. Giorno, L. De Bartolo. Biofabrication 9 (2017) 025022A.
[2] S. Khakpour, A. Di Renzo, E. Curcio, F. Paolo Di Maio, L. Giorno, L. De Bartolo. J. Memb. Sci 544 (2017) 312-322.

ECCE12
The 12th EUROPEAN CONGRESS OF CHEMICAL ENGINEERING
Florence 15-19 September 2019

Comparison of functional membranes of PCL doped with different graphene-based nanomaterials to modulate neural differentiation

Nazely Diban[1], Olga Tapia[2], Maria Teresa Berciano[3], Miguel Lafarga[2], Ane Urtiaga[1]

1 Dpt. of Chemical and Biomolecular Engineering, University of Cantabria-IDIVAL (Spain); 2 Dpt. of Anatomy and Biology and CIBERNED, University of Cantabria-IDIVAL (Spain); 3 Dpt. of Molecular Biology, University of Cantabria-IDIVAL.

**Corresponding author: dibann@unican.es*

Highlights

- Polycaprolactone (PCL)/Graphene-based nanomaterial (GbN) membranes favor cell response
- Differentiation of C6 cells to astrocytes on PCL/GbN membranes was better than on PCL
- Different oxygen content on the GbNs affects the cellular response
- Chemical defects in GbNs could be involved in the mechanism of neural activation

1. Introduction

Recent studies in tissue engineering and regenerative medicine have demonstrated that graphene-based nanomaterials used as scaffolds for in vitro stem cells cultures, induce cell differentiation toward specific tissues [1]. Furthermore, in our previous work we observed that graphene oxide (GO), and particularly reduced graphene oxide (rGO) doped in the matrix of polymer membranes of polycaprolactone (PCL), induced a significant improvement on neural differentiation of human Neural Progenitor Cells (hNPC) towards neurons, as well as a higher neural functional activity after maturation [2]. However, there is a lack of data in the literature covering the comparison of the effect of incorporating graphene-based nanomaterials with different chemical and physical characteristics on polymer scaffolds for the modulation of neural differentiation. The aim of this work is to broaden the comparison of different type of GbNs immersed on PCL/GbN composite membranes to be able to find out more information about the potential properties of GbNs that might trigger the differentiation of stem cells to neural cells.

2. Methods

In this study flat composite membranes with PCL and GO, with different oxygen content and produced using different exfoliation procedures, were used. The nanomaterials produced by anodic exfoliation contained either 2% (GO2%Ox) or 20% (GO20%Ox) of oxygen groups respectively (supplied by the Carbon Institute, INCAR-CSIC, Oviedo) [3]. Furthermore, GO was also produced using a modified Hummer's method, followed by a reduction of oxygen groups by a hydrothermal process, forming rGO. Then flat PCL/Graphene-based Nanomaterials (GbN) composite membranes (PCL/GO2%Ox, PCL/20%Ox, PCL/rGO) were fabricated using phase inversion following the procedure described elsewhere [4]. Plain PCL membranes were also produced for comparison.

Membranes were characterized by SEM, Raman and cyclic voltammetry. Furthermore, C6 cell cultures were carried out on every type of membrane and the differentiation degree was quantified by assessing the nuclear size, length and number of cellular processes and percentage of cells that could express GFAP protein (an astrocyte's specific protein marker).

3. Results and discussion

Figure 1 shows confocal microscopy images showing the proliferation (Figures 1a-e) and differentiation (Figures 1f-j) stages of C6 seeded on the different membranes and in tissue control plate (TCP) as control. At day 1, TCP showed better cell proliferation (Figure 1a), though interestingly at day 3 (Figure 1f), C6 cells on TCP differentiated towards fibroblast instead of astrocytes. The differentiation to astrocytes was particularly better for PCL/rGO membranes (Figure 1j) and, at a lower extent, in PCL/GO20%Ox membranes (Figure 1i). Contrary to expectations, despite GO2%Ox nanomaterials have the closest Raman spectrum to CVD-quality graphene [3], PCL/GO2%Ox membranes presented the worst cell differentiation among the PCL/GbN membranes (Figure 1h).

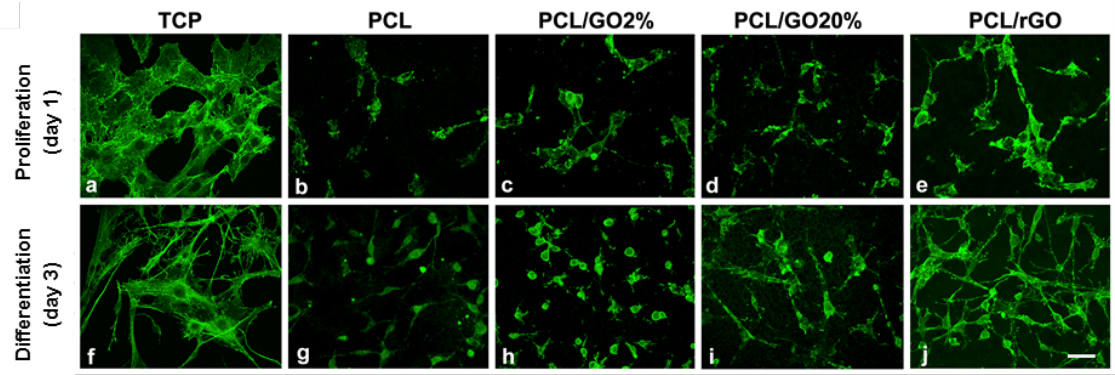

Figure 1. Confocal images showing the length of emitted projections of non-differentiated (day 1) and differentiated (day 3) C6 cells (F-Actin staining in green). Cell morphology at day 3 on TCP corresponded to fibroblasts. The emitted projections (astrocyte-like) on PCL/rGO and PCL/GO20%Ox were significantly longer than in the rest of membranes. (Scale bar 30 μm)

4. Conclusions

The evidences shown in this work highlight that graphene based nanomaterials with chemical defects on PCL/GbN composite membranes might be more favorable than pristine graphene to modulate the differentiation towards neural cells for neural in vitro models. However, the actual mechanisms behind the effect of GbNs on neural stimulation need to be explained, and therefore, further studies have to be performed.

Financial support through project InnVal17/20 (IDIVAL, Spain) and nanomaterials supply by Carbon Institute, INCAR-CSIC, are gratefully acknowledged.

References

[1] O. Akhavan, J. Mater. Chem. B 4 (2016) 3169-3190
[2] Sánchez-González, S. Diban, N, Bianchi F., Ye, H. Urtiaga, A. Macromol. Biosci. doi: 10.1002/mabi.201800195 (2018)
[3] Munuera, J.M., Paredes, J.I., Villar-Rodil, S., Castro-Muñiz, A., Martínez-Alonso, A., Tascón, J.M.D (2018) Appl. Mater. Today 11 (2018) 246–254
[4] Diban, N., Sánchez-González, S. Lázaro-Díez, M., Ramos-Vivas, J., Urtiaga, A. J Membr. Sci. 540 (2017) 219–228

ECCE12
The 12th EUROPEAN CONGRESS OF CHEMICAL ENGINEERING
Florence 15-19 September 2019

Adsorption of uremic toxins onto Mixed Matrix Membranes Adsorbers (MMMAs)

Matilde De Pascale[1*], Maria Grazia De Angelis[1], Monica Faria[2], Maria Norberta de Pinho[2], Cristiana Boi[1]

1 Department of Civil, Chemical, Environmental and Materials Engineering (DICAM), University of Bologna, via Terracini 28, Bologna, Italy; 2 Instituto Superior Técnico, Chemical Engineering Department, Lisbon, Portugal

**Corresponding author: matilde.depascale2@unibo.it*

Highlights

- Preparation of Cellulose Acetate-zeolite (HEU) Mixed Matrix Membranes Adsorbers (MMMAs).
- MMMAs removal efficiency is enhanced compared to the one of the pristine adsorbent.
- MMMAs permeability increases with respect to the one of pure polymeric membrane.

1. Introduction

Renal failure is a debilitating and chronical condition in which kidneys are no longer able to remove toxins and excess fluid from the body. For patients with terminal kidney disease, that were approximately 3.2 million at the end of 2017 [1], haemodialysis is the primary support treatment. Two of the main drawbacks of the therapy are the massive use of water, about 120 L per patient per treatment, and the uncomplete removal of uremic toxins from blood. Our work is focused on the preparation and characterization of novel porous Mixed Matrix Membranes Adsorbers (MMMAs) to remove the toxic compounds present in the spent dialysate. The purified water might be reused, to produce new dialysis fluid for the same patient, in order to reduce substantially the amount of pure water required for a single dialysis treatment.

2. Methods

Porous MMMAs based on Cellulose Acetate (Sigma Aldrich®) and ZUF (HEU) zeolite (Zeolith-Bentonit-Versand.de®) were prepared through the phase inversion casting technique [2], [3]. MMMAs with different amounts of ZUF were fabricated and characterized to investigate the removal of uremic toxins (urea, creatinine and uric acid) from aqueous solutions. Adsorption tests were performed in batch and in continuous mode (Fast Protein Liquid Chromatography). MMMAs removal capacity from aqueous solution was evaluated for the single uremic toxin and for a mixture of them.

3. Results and discussion

Results of the permeation tests showed the increase of the hydraulic permeability with the filler (ZUF) loading: the water permeability coefficient B_0 (m^2) is enhanced from 6.6E-16 m^2 to 1.2E-15

m^2 going from the pure cellulose acetate membrane to the MMMAs (30% ZUF). In Figure 1 is reported the urea and uric acid percentage removed from aqueous solution as a function of the ZUF wt%. The results are obtained in batch adsorption mode.

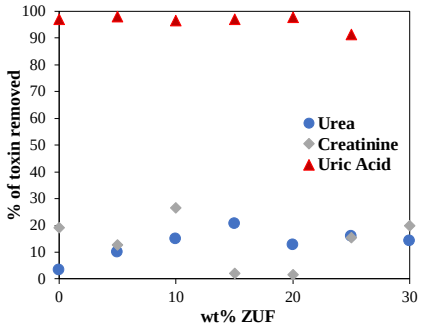

Figure 1. Percentage of uremic toxin removed as a function of ZUF wt%.

The removal of uric acid is easy, and it is almost independent on the loading of zeolite present in the membrane while for urea the percentage of ZUF plays and important role in the adsorption process. From the results shown in Figure 1, is also understandable that the membrane itself is actively involved in the adsorption mechanism.

4. Conclusions

MMMAs with ZUF were successfully prepared and tested to evaluate their removal capacity and their hydraulic permeability. The preliminary results indicate the potentiality of porous materials and MMMAs in toxin removal for the hemodialysis process and justify the future investigation of other combinations of polymers and fillers.

References

[1] G. Lesaffer, R. De Smet, N. Lameire, P. Duym, R. Vanholder, Nephrol. Dial. Transplant 15 (2000) 50-57.
[2] E. Salijoughi, M. Sadrzadeh, T. Mohammadi, J. Memb. Sci. 326 (2013) 252-258.
[3] J.T. Chen, C.C. Shih, Y.J. Fu, S.H. Huang, C.C Hu, K.R. Lee, J.Y. Lai, Ind. Eng. Chem. Res 53 (2014) 2781-2789.

ECCE12
The 12th EUROPEAN CONGRESS OF CHEMICAL ENGINEERING
Florence 15-19 September 2019

Use of salinity gradients for the recovery of valuable components from wastewater

Marie-Charlotte Sparenberg, Israel Ruiz Salmón, Patricia Luis[1]

1 UCLouvain, Materials & Process Engineering (iMMC-IMAP), Place Sainte Barbe 2, 1348 Louvain-la-Neuve, Belgium

**Corresponding author: patricia.luis@uclouvain.be*

Highlights

- Osmotic membrane distillation-crystallization allowed the recovery of target salts from synthetic wastewater.
- The economic evaluation showed the potential benefit of recovery.
- Optimal operation conditions are essential to achieve economic viability.

1. Introduction

Osmotic membrane distillation-crystallization is a novel technology that makes use of salinity gradients as the driving force to concentrate solutions until reaching the saturation concentration and thus, allowing the crystallization of target components. In this study, osmotic membrane distillation-crystallization is applied to recover sodium carbonate, potassium nitrate and sodium sulphate from synthetic industrial wastewater solutions. The technical viability of the process [1], discussed in terms of transmembrane fluxes, mass transfer coefficients and crystals purity, is completed with an economic study. The key operation conditions that determine the economic viability of the crystallization process are evaluated for each recovered salt [2].

2. Methods

The osmotic membrane distillation–crystallization contactor used in this study was the hollow fiber membrane contactor 2.5 × 8 Extra-Flow Module from LiquiCel (Membrana GmbH, Germany). The feed solution (*i.e.,* aqueous solution of pure Na_2CO_3, Na_2SO_4, KNO_3, or mixtures) was pumped to the membrane through the lumen side (inside of the hollow fibers) of the membrane. The osmotic stream (NaCl) circulated in counter-current mode through the shell side (outside of the hollow fibers). The influence of concentrations of the feed and osmotic solutions as well as the flow rates on the process performance was studied. In order to assess the economic viability of the process, the annual costs and salt sale profits were evaluated and the final benefit of salt recovery was determined as a function of the operation conditions.

3. Results and discussion

The experimental results showed that varying the concentration of the osmotic solution was the main parameter affecting the transmembrane flux. The concentration of the three salts in the feed had slight influence while no significant effect was observed when flow rates in both the feed and

the osmotic side were varied. High purity crystals of $Na_2CO_3.10H_2O$, $Na_2SO_4.10H_2O$ and KNO_3 was obtained (Figure 1).

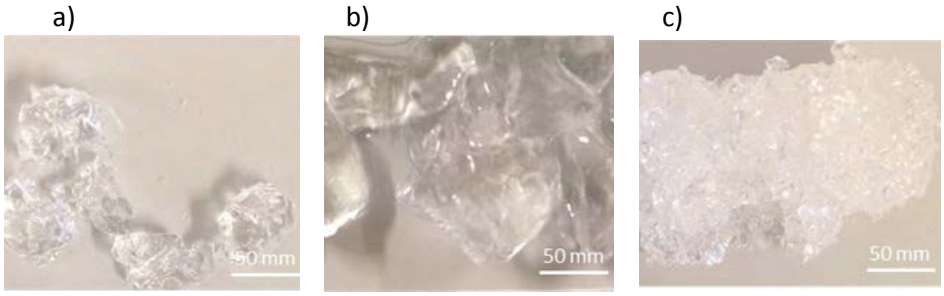

Figure 1. Crystals of a) $Na_2CO_3.10H_2O$; b) $Na_2SO_4.10H_2O$; and c) KNO_3

Figure 2 illustrates the influence of the initial osmotic concentration (ranging from 100 to 300 g L^{-1}) on the economics of the process for the three salts, with initial feed concentration and flow rate of 100 g L^{-1} and 500 L h^{-1} respectively and initial osmotic flow rate of 27 L h^{-1}. It can be clearly seen that the osmotic concentration has a major impact on the economic viability of the process. Increasing this concentration leads to a higher driving force hence a higher flux, less membrane area and lower costs.

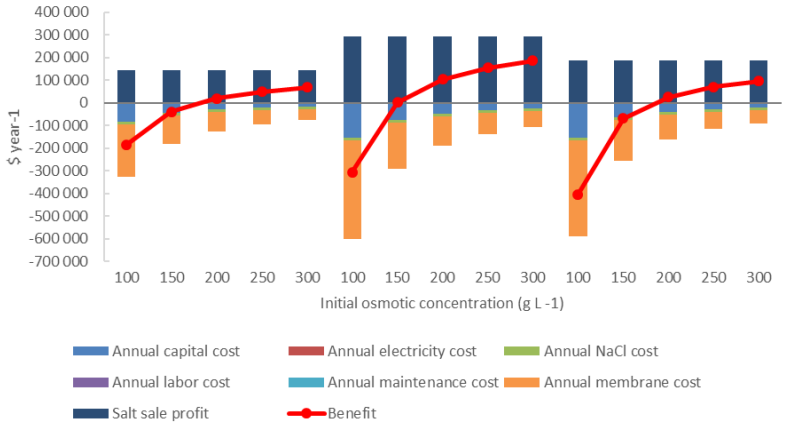

Figure 2. Costs, salt sale profit and benefit for the crystallization of the three salts. Initial feed concentration and flow rate are 100 gL^{-1} and 500 Lh^{-1} respectively and osmotic flow rate is 27 Lh^{-1}.

4. Conclusions

High purity crystals of $Na_2CO_3.10H_2O$, $Na_2SO_4.10H_2O$ and KNO_3 were obtained using osmotic membrane distillation-crystallization in synthetic wastewater. Using the highest possible concentration of osmotic solution (limited by the solubility of the salt i.e. 358 g L^{-1} at room temperature for NaCl) is desired because of its marginal costs and high impact on the economics.

References

[1] I. Ruiz Salmón, K. Simon, C. Clérin, P. Luis, Salt recovery from wastewater using membrane distillation-crystallization, Crystal Growth & Design 18 (2018) 7275–7285.

[2] M-C. Sparenberg, I. Ruiz Salmón, P. Luis, Economic evaluation of salt recovery from wastewater via membrane distillation-crystallization, Desalination, submitted.

ECCE12
The 12th EUROPEAN CONGRESS OF CHEMICAL ENGINEERING
Florence 15-19 September 2019

Bipolar membrane (reverse) electrodialysis acid/base flow battery for energy storage: a multi-scale model for increased efficiency.

A. Culcasi, A. Zaffora, L. Gurreri, A. Cipollina, A. Tamburini*, G. Micale
Dipartimento di Ingegneria, Università degli Studi di Palermo (UNIPA) - Viale delle Scienze Ed.6, 90128 Palermo, Italia

**Corresponding author: alessandro.tamburini@unipa.it*

Highlights

- A 4-scale model ranging from the channel scale to the plant scale was developed.
- Pressure drops and polarization have minor effects on the process performance.
- Ionic short-circuit currents *via* manifolds may halve the Round Trip Efficiency.

1. Introduction

The renewable energy market is rapidly increasing. Most of renewable energy sources are intermittent, e.g. wind and solar among them. This has led to the need for new large scale energy storage systems. In this regard, the Acid/Base Flow Battery (AB-FB) represents an innovative, safe and sustainable way to store energy with high performances [1]. The energy density accumulated in an AB-FB, in the form of pH and salinity gradients, can theoretically reach 7 kWh/m^3 which is higher than the values relevant to the most used technologies (e.g. pumped hydropower and compressed air). The core of the battery is the stack where two membrane separation processes are carried out: bipolar membrane electrodialysis during charge phase and its opposite bipolar reverse-electrodialysis during discharge. A stack consists of repetitive units called cells or “triplets”, composed by a cation exchange membrane, a salt solution, an anion exchange membrane, an acidic solution, a bipolar membrane and a basic solution. The aim of this work is to develop a simulation tool able to predict the operation and performances of the battery.

2. Methods

The modelling tool was developed using a multi-scale approach. The lowest scale is the single channel. At this level, all variables are discretized along the main flow direction and correlations coming from Computational Fluid Dynamics [2] are implemented in the model in order to evaluate the concentration polarization effects and the channel pressure loss. The medium-low scale simulates the triplet, computing its electrical behavior and all fluxes through the membranes (ohmic, diffusive, osmotic and electro-osmotic). The medium-high scale simulates the stack and predicts its pressure losses and ionic short circuit currents *via* manifolds [3]. The highest scale simulates the external hydraulic circuit, the electrolyte solutions storage tanks and the transient behavior of the battery. All the levels of the multi-scale model are fully integrated and predict the distribution of the process variables as well as meaningful performance parameters, such as the Round Trip Efficiency (RTE).

3. Results and discussion

Preliminary experiments show a good agreement with the model predictions. Thus, a sensitivity analysis was performed in order to assess the effect of stack features and operating conditions. Under most conditions simulated, pumping power and voltage drop due to concentration polarization have only minor effects on the process efficiency. Conversely, ionic short circuit currents *via* manifolds affects significantly the system performance. Just as an example, Figure 1 reports simulation results concerning the impact of the parasitic currents on the cell currents, triplet by triplet: the lower the ratio reported in the y-axis of the figure the higher the parasitic currents impact. Each line refers to a different electric current supplied to an external circuit (discharge, Fig.1a) or coming from it (charge, Fig.1b). As the external current decreases, the impact of parasitic current losses becomes more important (see distance from the horizontal line at $I_{cell}/I_{cell,max}$ =1). RTE reduction due to ionic short circuit currents ranges from 13 to 46 % (RTE range 21–31 %).

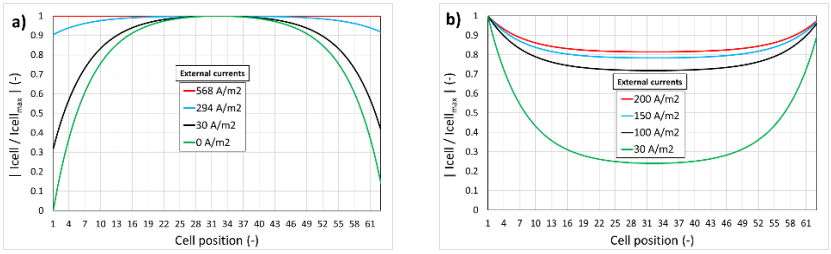

Figure 1. Ratio between cell current and maximum cell current along the stack for discharge (a) and charge (b). Stack of 63 triplets, membrane area 0.19x0.21 m^2, spacer thickness 500 µm, manifolds diameter 8 mm, mean flow velocity 0.4 cm s^{-1}, starting composition: acid 1M HCl-0.25M NaCl, base 1M NaOH-0.25M NaCl, salt 0.02M HCl, 0.25M NaCl.

4. Conclusions

A mathematical multi-scale tool was developed in order to simulate AB-FB units. From a sensitivity analysis, pumping power and polarization were found to slightly affect the battery performance. On the other hand, ionic short-circuit currents represent the major issue, leading up to almost halved values of RTE (~30 %). These preliminary results provide important insights for improved designs, and further studies are ongoing to achieve competitive RTE values, e.g. larger than 70%.

Acknowledgements

This work was performed in the framework of the BAoBaB project (*Blue Acid/Base Battery: Storage and recovery of renewable electrical energy by reversible salt water dissociation*). The BAoBaB project has received funding from the European Union's Horizon 2020 Research and Innovation program under Grant Agreement no. 731187 (www.baobabproject.eu).

References

[1] W.J. van Egmond, M. Saakes, I. Noor, S. Porada, C. J. N. Buisman, H.V.M. Hamelers, Int. J. Energy Res. (2017) 1-12.
[2] M. La Cerva, M. Di Liberto, L. Gurreri, A. Tamburini, A. Cipollina, G. Micale, M. Ciofalo, J. Membr. Sci. 541 (2017) 595-610.
[3] J. Veerman, J.W. Post, M. Saakes, S.J. Metz, G.J. Harmsen, J. Membr. Sci. 310 (2008) 418-430.

ECCE12
The 12th EUROPEAN CONGRESS OF CHEMICAL ENGINEERING
Florence 15-19 September 2019

How the fouling can affect the transport and energy generation in PRO process

Endre Nagy[1*], Imre Hegedüs[1]

[1]*University of Pannonia, Research Institute of Biomolecular and Chemical Engineering, Laboratory of Chemical and Biochemical Processes, Egyetem u. 10, H-8200, Veszprem, Hungary*;
**Corresponding author: Nagy@mukki.richem.hu*

Highlights

- Developing new expressions involving the fouling layer.
- This layer forms quickly and lowers essentially the performance..
- Seawater/river water pair provide not enough energy.
- An alternate solute might be the switchable polarity ionic liquid.

1. Introduction

Accumulation of a foulants on the membrane layer (or inside it) during energy generation by pressure retarded osmosis process, applying e.g. seawater/river water pair affects strongly the transport process and the power generation. Several paper studied the efficiency of the energy generation by seawater/river water pair [1,2]. The conclusion was, that the commercially available membrane does not provide nowadays enough selectivity and water transport to make this process economic. On the other hand, the mass transport through the transport layers, including the fouling layer, should accurately be described to be able to predict reasonably the process efficiency. In a study we have shown how the literature models have been extended for the fouling layer, as well [3]. Accordingly, this new transport model describes the real effect of the fouling layer on the mass transport process, namely on the solute and the water transport. Equations developed involve also the separate expression of the internal interface concentrations, thus they make possible to predict the osmotic pressure difference, and thus the power density more accurately than the literature expressions.
On the other hand if one wants to use draw solution with much higher solute concentrations than the seawater than the solution used should be regenerated for its repeated usage. It seems that a switchable polarity solvent might be suitable to it. For its investigation, high molecular weight dibutyl-(2-(2-metoxyethoxy)-ethyl)-amine was prepared, which forms water soluble ionic liquid in water+CO_2 system. This ionic liquid can then switch back to the molecular (non-water soluble) form by expelling CO_2 at 90 ^oC.

2. Methods

Organic fouling experiments using alginate are used to validate the model and observe the effects of feed salinity, cross-flow velocity, membrane orientation, feed spacers on foulant accumulation rates. Increasing feed salinity and cross flow velocity both lead to a decrease in foulant accumulation in PRO orientation. It will also be shown deviances in the osmotic pressure

difference, using the individual interface concentrations of the active layer, and the literature approach. On the other hand, we have measured the energy generation with the ionic liquid prepared. Its regeneration have also been investigated.

3. Results and discussion

During the building the fouling layer, the water flux was significantly decreased, depending on the thickness of the fouling layer. Figure 1 illustrates the power density as a function of the draw side osmotic pressure, at three different thickness of the fouling layer, S_c. Its decrease is essential.

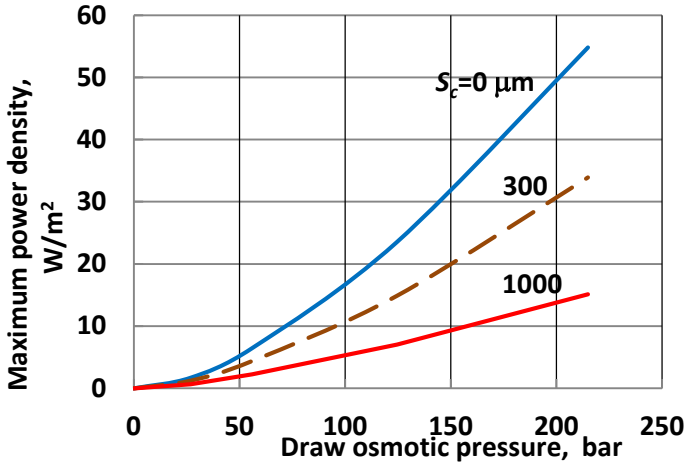

Figure 1. Maximum power density as a function of draw solution osmotic pressure and cake structural parameters in PRO system for a river water feed Parameters used were: C_f =0.862 g/L (0.015 mol/L; river water); k_d = 8.43 × 10^{-5} m/s; k_f = 2.07 × 10^{-5} m/s; A = 1.8 × 10^{-7} m/s-bar; B = 5 × 10^{-7} m/s (A, B are water and solute (NaCl) permeabilities)

It will also be shown the effect of the ionic concentration on the energy generation and results will be compared with those obtained with NaCl solution. On the other hand, the regenerability of the ionic liquid will be discussed as alternative solution to the seawater/river water pair. Namely, the easy regeneration of the solutes would enable to use high concentration draw solution, which can produce much higher energy density than the seawater/river water pair.

4. Conclusions

The production of the “blue” energy needs still essential improvement to become more economic. This presentation try to answer some questions to be solved for it.

References [Calibri 10]

[1] A.P. Straub, A. Desmuckh, M. Elimelech, Environ. Sci. Technol., 9 (2016) 21-48.
[2] G. O’Toole, L. Jones, C. Coutinho, C. Hayes, M. Napoles, A. Achilli, Desalination 389 (2016) 39-51.
[3] E. Nagy, I. Hegedüs, E.W. Tow, J.H. Lienhard, J. Membr. Sci., 565 (2018) 450-462..

Stimuli-Responsive DNA-Aptamer Gating Membranes

Thomas Schäfer[1,2*], Beñat Olave[1], Iliane Rafaniello[1]

1 POLYMAT, University of the Basque Country, Donostia-San Sebastián, Spain; 2 IKERBASQUE, Basque Foundation for Science, Bilbao, Spain

**Corresponding author: thomas.schafer@ehu.es*

Highlights

- The conformational change of DNA-aptamers can be used as nanovalves in membrane pores.
- DNA-aptamer gating membranes respond to a molecular rather than a bulk stimulus.
- DNA-aptamers are versatile building blocks for bioinspired nanostructured hybrid membranes.

1. Introduction

Aptamers are oligonucleic acids that can be selected to specifically interact with in principle any kind of target molecule. An important asset of aptamer conjugates is the fact that upon specific binding, their spatial conformation may change drastically, depending on a fine equilibrium between mainly electrostatic and hydrophobic interactions. Recently, if has been shown that this specific conformational change can be exploited for controlled release applications in particles and membranes, where aptamers serve as a "nanovalve" which selectively triggers the opening or closing of a nanopore depending on the presence of a target molecule [1]. Such systems add an important degree of freedom in the design of stimuli-responsive systems which conventionally respond to bulk stimuli such as pH, temperature, light or electrical and magnetic fields. Figure 1 schematically shows as an example the conformational which an AMP-aptamer undergoes upon target binding.

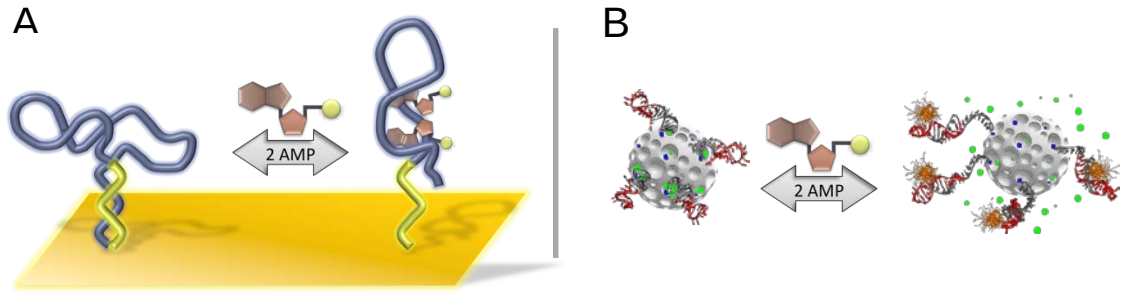

Figure 1. Conformational change of a DNA-Aptamer upon molecular target recognition (A, here: AMP) and use for gating the solute permeation in nanoporous matrices (B).

2. Methods

The build-up of the DNA-aptamer gating membrane was monitored in real-time by quartz crystal microbalance with dissipation monitoring (QCM-D) and multi-parameter surface plasmon

resonance (MP-SPR). The DNA-aptamer used was specifically recognizing adenosine monophosphate (ATP) but not guanine monophosphate (GTP, negative control). DNA/AAO membranes were manufactured by surface modification of the AAO membrane that allow subsequent self-assembly of the DNA. The permeability of the DNA-aptamer gated AAO membranes was measured spectrofluorometrically using a single-photon counting spectrofluorimeter and fluorescein as a tracer dye. Successful and selective gating was proven by (1) using GTP as negative control and (2) using a scrambled sequence of the DNA-aptamer which has no specificity for the molecular target ATP.

3. Results and discussion

The AAO membranes were modified with a DNA-aptamer that specifically recognizes ATP as a small molecular target. Upon target recognition as a molecular stimulus, the DNA-aptamer gated membranes responded with a nanopore opening whose degree depended on the target (ATP) concentration (Figure 2, left) and was according to the K_D of the DNA-aptamer (Figure 2, right).

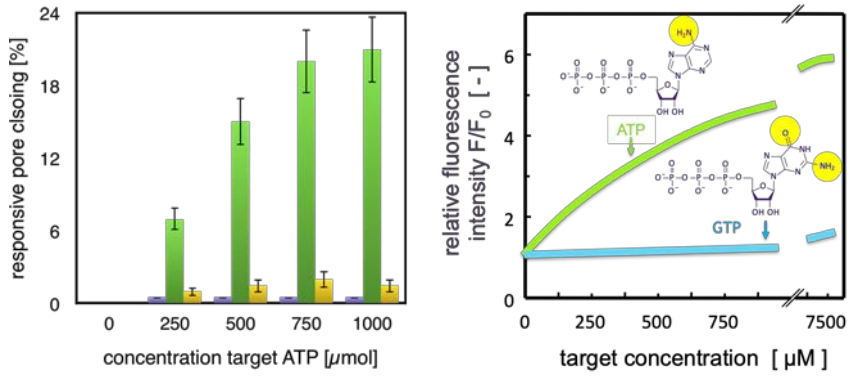

Figure 2. Left: Permeation of fluorescein across a DNA-aptamer gated AAO membrane as a function of the concentration of the DNA-aptamer molecular target ATP; Right: Dissociation constant K_D of the DNA-aptamer for ATP and GTP, respectively.

The scrambled sequence of the DNA-aptamer and the molecular target GTP did not result in any response of the membrane, i.e., the membrane pores remained closed (Figure 2, left), corroborating that the conformational change of the DNA-aptamer upon specific target recognition was the sole trigger for modulating permeation of fluorescein across the membrane.

Owing to the reversibility of the conformational change of the DNA-aptamer, permeate flow of fluorescein could be repeatedly switched on and off depending on the concentration of ATP, simulating in this way to a certain extent the function of transporter proteins in biological membranes.

4. Conclusions

DNA-aptamers are highly versatile building blocks for creating bioinspired stimuli-responsive membranes. The conformational change of the DNA-aptamer is highly specific and reversible, allowing to modulate permeation of solutes across the membrane based on a molecular stimulus.

References

[1] T.Schäfer and V.C. Özalp. Chem Commun, 2015, 51, 5471.

ECCE12
The 12th EUROPEAN CONGRESS OF CHEMICAL ENGINEERING
Florence 15-19 September 2019

Preparation of high CO_2 permeable CHA type zeolite membrane using TEAOH.

Sadao Araki[1*], Yuto Okubo[1], Imasaka Satoshi[2], Hideki Yamamoto[1]

1 Kansai University, Department of Chemical, Energy and Environmental Engineering, 3-3-35 Yamate-cho, Suita-shi, Osaka 564-8680 Japan

2 Hitachi Zosen Corporation, 2-11, Funamachi 2-Chome, Taisho-ku, Osaka 551-0022, Japan

**Corresponding author: araki_sa@kansai-u.ac.jp*

Highlights

- A high-silica CHA-type zeolite membrane was prepared by using TEAOH.
- The CO_2 permeance of the membrane showed 3.5×10^{-6} mol m^{-2} s^{-1} Pa^{-1}.
- The CO_2 permeance was 2-fold value of that of TMAdaOH.

1. Introduction

At the present time, carbon dioxide is generally separated by chemical absorption. As an alternative to the chemical absorption, membrane separation technologies have attracted much attention due to their low energy consumption and compact device designs. Among the large number of membrane materials, zeolite have been extensively studied owing to their high chemical and mechanical stabilities. Particularly, CHA-type zeolite membranes show the excellent CO_2 permeability and high selectivity because the CHA-type zeolite has a suitable pore size (0.38×0.38 nm) for CO_2/CH_4 owing to the effects of molecular sieving.

In our previous study, it was found that the CHA membrane with a high Si/Al ratio showed of a high water flux for water/ethanol pervaporation and high CO_2 permeance for CO_2/CH_4 gas separation [1]. On the other hand, there were few reports about the preparation of CHA zeolite with a high Si/Al ratio using organic structure directing agents (OSDAs) except for N,N,N-trimethyl-1-adamantammonium hydroxide(TMAdaOH). In this study, we prepared a high silica CHA membrane using tetraethyl ammonium hydroxide (TEAOH) as OSDA. The gas permeances and separation properties for this membrane were determined by gas permeation test.

2. Methods

The high-silica CHA-type zeolite seed crystals were prepared by the following literature [2]. High-silica CHA-type zeolite seed crystals were applied to the outer surface of a porous α-alumina support tube (pore size: 0.5–1.0 μm; Hitachizosen Corp.) by rubbing. The membrane synthetic gel was prepared with TEAOH, ion exchanged water, sodium hydroxide, and FAU-type zeolite. The α-alumina support tube with the high-silica CHA type zeolite seed crystals was placed in a Teflon container, and immersed in the synthesis gel. After installing the Teflon container in an autoclave, the hydrothermal treatment was performed at 160 ℃ for 3 days. The membranes were characterized by XRD and FE-SEM. The single gas permeance of N_2, CO_2, and CH_4 for the CHA membranes were measured at 40 ℃. Gas separation properties for the membranes were confirmed

by the gas permeance (mol m^{-2} s^{-1} Pa^{-1}) which was calculated as the permeate flow rate of each gas divided by the partial pressure difference and membrane area.

3. Results and discussion

Fig. 1 shows XRD patterns of the CHA membranes prepared by TEAOH. The peaks at 2θ=9.4°, 20.5°, and 30.4° correspond to (1 0 0), (2 0−1), and (3−1−1) planes of the CHA-type zeolite and large peaks appearing at 2θ=35.2°, 37.9°, and 43.2° are related to the α-alumina support. Typical peaks positions of the FAU-type zeolite (2θ=6.8°, 11.9°, and 15.6°) were not observed. This result indicates that a CHA type zeolite layer was successfully formed on the surface of the α-alumina support by using TEAOH. Fig. 2 shows cross-sectional FE-SEM images of the CHA membrane. The thickness of the polycrystalline zeolite layer was ca. 10 µm.

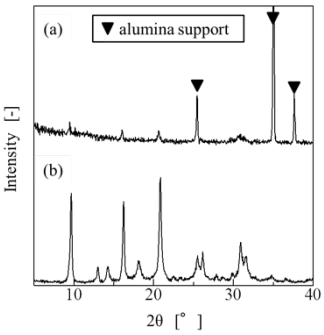

Fig.1 XRD patterns of (a) CHA membrane and (b) CHA seed crystal

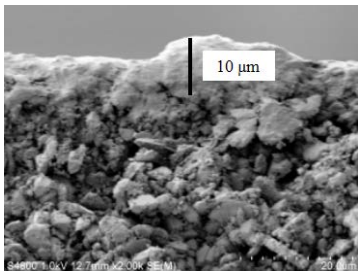

Fig.2 FE-SEM image of CHA membrane

Table 1 shows the comparison of gas permeation properties for CHA membranes prepared using TEAOH and TMAdaOH [1]. The CHA membrane of TEAOH showed the two-fold CO_2 permeance than that of TMAdaOH with the similar CO_2/CH_4 selectivity. Generally, the permeance is proportional to the reciprocal of the membrane thickness. The thickness of the CHA membrane of TMAdaOH reported to be about 3.0 mm. Therefore, the increase of CO_2 permeance by using TEAOH is not due to the membrane thickness. This reason might be the differences of pore structure caused by OSDAs.

Table1 Gas permeances and selectivity of CHA membranes prepared using TEAOH and TMAdaOH

Membrane		TEAOH	TMAdaOH [1]
Permeance [mol m^{-2} s^{-1} Pa^{-1}]	CO_2	3.5×10^{-6}	1.7×10^{-6}
	N_2	3.4×10^{-7}	1.2×10^{-7}
	CH_4	3.6×10^{-8}	1.8×10^{-8}
Selectivity [-]	CO_2/CH_4	97	98

4. Conclusions

In this study, the high-silica CHA-type zeolite membrane was synthesized on the α-alumina support tube by TEAOH as OSDA. The membrane showed the excellent separation performance for CO_2/CH_4 gas.

References [Calibri 10]

[1] S. Imasaka et al., Sep. Purif. Technol. 199 (2018) 298-303.
[2] N. Kosinov et al. , J. Mater. Chem. A, 2 (2014) 13083-13092

ECCE12
The 12th EUROPEAN CONGRESS OF CHEMICAL ENGINEERING
Florence 15-19 September 2019

Micro-computed tomography for structural analysis of heterogenous ion-exchange membranes.

Miloš Svoboda[1,2*], Jan Beneš[2], Lucie Vobecká[1], Zdeněk Slouka[1,2]

1 University of Chemistry and Technology Prague, Department of Chemical Engineering, Technická 3, Prague 6, 16628, Czech Republic, 2 University of West Bohemia, New Technologies - Research Centre, Univerzitní 8, Plzeň 30614, Czech Republic

**Corresponding author: milossvo@ntc.zcu.cz*

Highlights

- Micro-CT for structural analysis of ion-exchange membranes in their swollen state.
- Membrane swelling caused by the resin, shrinkage with increasing concentration.
- Method allows determination of ion-exchange area of heterogenous membranes.
- Sand equation shown not to hold for small pieces of the membranes.

1. Introduction

Electromembrane separation processes based on the use of ion-exchange membranes (IEM) play a very important role in production of potable water and increasingly in areas of waste water treatments. It is known that the performance of the whole process largely depends on the quality of the IEMs. These membranes can be classified into two major groups: (i) homogeneous, and (ii) heterogeneous. While homogenous generally posses better electrochemical properties they suffer from low mechanical and chemical stability. In these two aspects, they are outperformed by heterogenous ones which is however, at the expense of electrochemical performance. One of the ways how to improve the properties of heterogenous IEMs is too understand the relation between their structure and the exhibited behavior and later design membranes with optimal properties for a given application. This puts a requirement on having available analytical techniques that would allow to reconstruct 3D structure of these membranes and describe its composition quantitatively and qualitatively. At the same time these analyzed membranes should be practically tested regarding their performance.

To address the aforementioned problem we developed a technique which reconstructs 3D structure of membranes by micro-computed tomography and quantifies the composition not only in terms of volumetric composition but also in terms of surface composition which in turn provides very important data on the available ion-exchange area. Our method can work with both dry and wet (fully swollen) membranes which also allows one to study structural changes of membranes associated with swelling. We test our approach on testing the suitability of the Sand equation for determination of the fraction of conductive (ion-exchange) domains by combining our analytical technique with electrochemical measurement performed in a specific fluidic cell.

2. Methods

We developed a specific cell which allows microCT scanning of the samples in both dry and wet state. The details of this technique along with description of the evaluating methods can be found in [1]. Later the same piece of analyzed membrane can be integrated within a fluidic chip that allows electrochemical characterization. In this work, we measured so called transition times which are later used in the Sand equation to evaluate fraction of conductive domains. The details can be found in [2].

3. Results and discussion

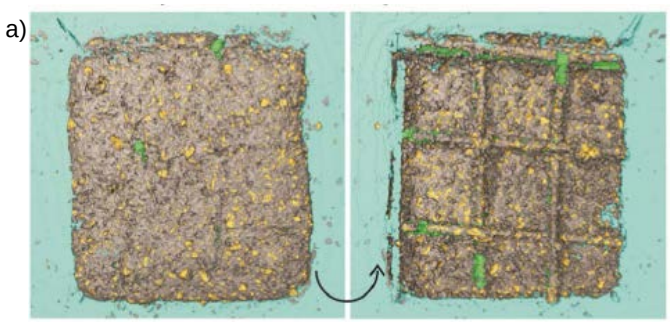

Figure 1. MicroCT surface analysis of a heterogeneous cation-exchange membrane.

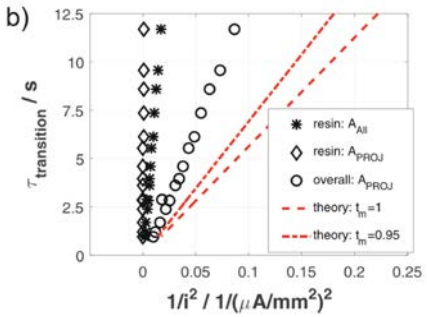

Figure 2. Measurement of the transition times in the dependence of the applied electric current.

Figure 1 and 2 show respective results of our studies focused on estimation of the ion-exchange area with two methods. The first one is based on the analytical reconstruction of the surface area by micro-CT and the other one on electrochemical measurement of transition times and substitution into the Sand equation. While microCT analysis is a direct technique that can locate the ion exchange-resin particles responsible for the actual ion-exchange (yellow color in Figure 1), the measurement of transition times is indirect technique that relies on several simplifications. Our results show that the electrochemical technique, although it might provide reasonable numbers, does not agree with results from microCT (compare red lines with black ones in Figure 2). Unlike that the Sand equation works very well for ion-exchange resin particles which can be considered as homogeneous and satisfies conditions under which Sand equation works.

4. Conclusions

Our technique based on micro-computed tomography allows to analyze the volumetric and surface structure of the heterogenous ion-exchange membrane, which are essential in electromembrane separation processes. By using this technique, we are able to characterize studied membranes in terms of composition and geometry. When combined with electrochemical measurements, we can relate the behavior of the membranes to the exhibited behavior.

References

[1] L. Vobecka, M. Svoboda, J. Beneš, T. Belloň, Z. Slouka, J. Mem. Sci., 2018. 559: p. 127-137.
[2] M. Svoboda, J. Beneš, L. Vobecká, Z. Slouka, J. Mem. Sci., 2017. 525: p. 195-201.

On-line monitoring of membrane fouling at the nanoscale combining advanced surface-sensitive techniques

Iliane Rafaniello[1], Thomas Schäfer[1,2]

1 POLYMAT, University of the Basque Country, San Sebastián, Spain; 2 IKERBASQUE, Basque Foundation for Science, Bilbao, Spain & Surphase, San Sebastián, Spain

**Corresponding author: iliane.rafaniello@polymat.eu*

Highlights

- Combination of QCM-D/MP-SPR enables fast screening of membrane antifouling properties.
- Fouling observed on QCM-D/MP-SPR sensors concurs with that in ultrafiltration tests.
- QCM-D and MP-SPR are powerful methods for predicting fouling in membrane separations.

1. Introduction

Water membrane filtration processes are commonly affected by membrane fouling which until today is accepted to be to a certain degree inevitable. Therefore, attempts are being made to at least minimize the impact of fouling by either modifying the membrane surface chemically, or by adopting adequate operation strategies. Finding the right strategy, however, is often based on a time-consuming trial-and-error approach. Hence, on one hand, accurate, fast, and non-invasive techniques would be desirable in order to verify the efficiency of the membrane surface modification. On the other hand, real-time monitoring of the early-stage development of membrane fouling would enable adapting the optimal process operating conditions.

Unfortunately, current monitoring techniques neither reach such efficiency nor sensitivity. For example, it has so far been impossible to reliably detect the very first adsorbed layers of foulants, which occur at the nanoscale but play a crucial role on the subsequent development of the fouling phenomenon. Furthermore, conventional characterization techniques, such as contact angle measurements, are indirect and prone to lead to false conclusions about the anti-fouling strategy adopted.

This work presents an approach of overcoming the limitations of conventional methods by combining two advanced surface-sensitive techniques for monitoring membrane fouling, namely quartz crystal microbalance with dissipation monitoring (QCM-D) and multi-parameter surface plasmon resonance (MP-SPR). It will be shown that these non-invasive techniques are both highly feasible for characterizing the build-up of the very first fouling layers at the nanoscale, and that they possess a high potential of significantly accelerating the screening of the efficiency of membrane modifications.

2. Methods

As a model membrane polymer, polyamides (PA) modified with polyethylene glycol (PEG, n=12) at different degrees (0, 25, 50, and 75%, respectively) were tested as these had been employed

previously as the membrane material in an ultrafiltration (UF) process [1]. Ultra-thin films of these polymers were cast onto QCM-D and MP-SPR sensors by spin-coating. QCM-D and MP-SPR sensors had an area of less than 1 cm^2. Bovine serum albumin (BSA) was used as a model foulant in the UF process, as well as for the combined QCM-D/MP-SPR monitoring system.

3. Results and discussion

Non-invasive and real-time monitoring of adsorption of BSA on the PA films revealed that QCM-D and MP-SPR enable a very fast detection with high temporal resolution. As an example, Figure 1 (left) illustrates how almost 90% of the steady-state signal was reached in an interval of only 40 seconds.

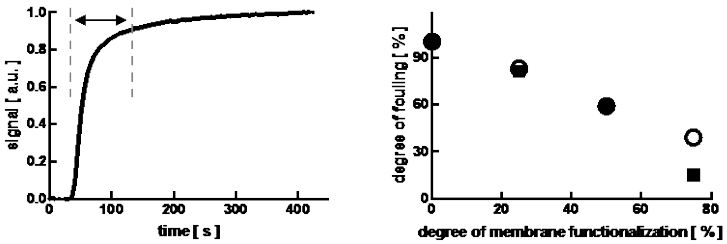

Figure 1. Left: Response of an ultra-thin PA film to the exposure to 100 $mg \cdot l^{-1}$ of BSA in water as measured by QCM-D. The arrow indicates the time interval needed to reach 90% of the signal. Right: Degree of fouling measured on polyamides with different degrees of functionalization by PEG and deposited as ultra-thin films on QCM-D (open circles) and MP-SPR (filled squares) sensors.

Both QCM-D and MP-SPR detected in very good agreement how the fouling tendency was reduced significantly with increasing content of PEG in the polyamides (Figure 2, right). This corroborates that QCM-D/MP-SPR are excellent and fast screening tools for studying membrane antifouling properties.

Although the working principle of both techniques is entirely different, QCM-D and MP-SPR proved to be highly complementary: protein fouling layers were tendentially detected to be of higher mass by QCM-D than by MP-SPR. The underlying reason for this phenomenon is the amount of associated water which is detected by QCM-D, but not so by MP-SPR. Nevertheless, and most importantly, it was observed that the degree of fouling measured for different PA-PEG films in QCM-D and MP-SPR was in very good agreement with fouling data obtained during independent UF experiments using the very same membrane materials [2].

4. Conclusions

QCM-D and MP-SPR are powerful techniques to reliably monitor the build-up of the very first membrane fouling layers even at the nanoscale. A further advantage of this sensorial screening system is that it not only saves time, but also resources: the deposition of ultra-thin PA films on the sensors requires only a few microliters of polymer solution and the microfluidic set-up saves sample volume, which in principle allows a high-throughput screening.

A strategy for implementing QCM-D/MP-SPR as a water membrane filtration monitoring tool will be presented, and the operating window of this approach will be critically discussed.

References

[1] S. Molina, P. Carretero, S. B. Teli, J. G. de la Campa, A. E. Lozano, J. De Abajo, J. Mem. Sci. 454 (2014) 233–242.

[2] I. Rafaniello, T. Schäfer, PCT and EP “Monitoring device for membrane fouling”, 2019 (submitted)

ECCE12
The 12th EUROPEAN CONGRESS OF CHEMICAL ENGINEERING
Florence 15-19 September 2019

Development of a new process for preparing polymeric membranes without the use of organic solvent

K-W. Li[1], J-P.Mericq[1], C. Faur[1], D. Quemener[1], A. Deratani[1], D. Bouyer*[1]

[1] *Institut Européen des Membranes, IEM – UMR 5635, ENSCM, CNRS, Univ Montpellier, Montpellier, France*

**Corresponding author: denis.bouyer@umontpellier.fr*

Highlights

- Green membranes (without organic solvent)
- New process for preparing polymeric membranes
- Coupling thermally induced phase separation and cross-linking

1. Introduction

Phase separation using non-solvent coagulation bath of a polymer solution is the most widespread industrial process to manufacture membranes. During the industrial process, large quantities of organic solvent are used that may lead to crucial environmental and health problems. Our objective in this work was to develop a novel process for membrane mass production in agreement with the principles of green chemistry. HydroxyPropyl Cellulose (HPC), a biosourced and water-soluble polymer was therefore used in this work, thus preventing the use of classical organic solvent, such a NMP, DMAc, DMF etc. Mastering this phase separation process was very appealing, but needed the following requirements:

- Fully understand how phase separation proceeds in water as temperature is above LCST
- Establish the relationship between PS, evaporation and crosslinking mechanism
- Determine the permeation performances of the obtained membranes

2. Methods

Starting from a polymer solution composed pf HPC and water (weight ratio 20%/80%) a phase separation was induced by increasing the temperature above the lower critical solution temperature (LCST) (Fig. 1). Then, a chemical crosslinking using Glutaraldehyde (GA) was performed to prevent the re-solubilization of the membrane during further use for water filtration. A porous morphology was finally obtained and observed by SEM. The membranes were fully characterized (stability, porosity, mechanical properties…) and the filtration properties were tested using a dead-end filtration system.

3. Results and discussion

The flat membrane obtained using the original phase separation process used in this work (LCST-TIPS process) showed porous morphologies, showing a phase separation by spinodal decomposition (Fig. 1). After several weeks in water, the membrane exhibited a perfect stability, i.e. no re-solubilization was observed.

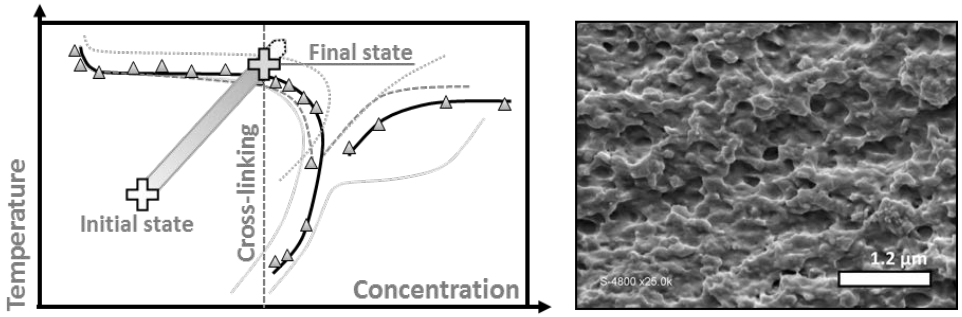

Figure 1. Phase diagram of HPC and behavior during membrane elaboration process; SEM of HPC membrane section.

A first filtration stage exhibited a flux was between 0 and 40 $L.h^{-1}.m^{-2}$ at 3.5 bar. After a thermal treatment, a flux up to 160 $L.h^{-1}.m^{-2}$ was obtained (Figure 2a). Hysteresis filtration experiment was then performed: the transmembrane pressure was raised slowly until it reaches the maximum value of 3 bars, then it was decreased to its initial value. Figure 2b represents normalize flux versus pressure, showing that the transmembrane flux was unchanged after the conditioning step.

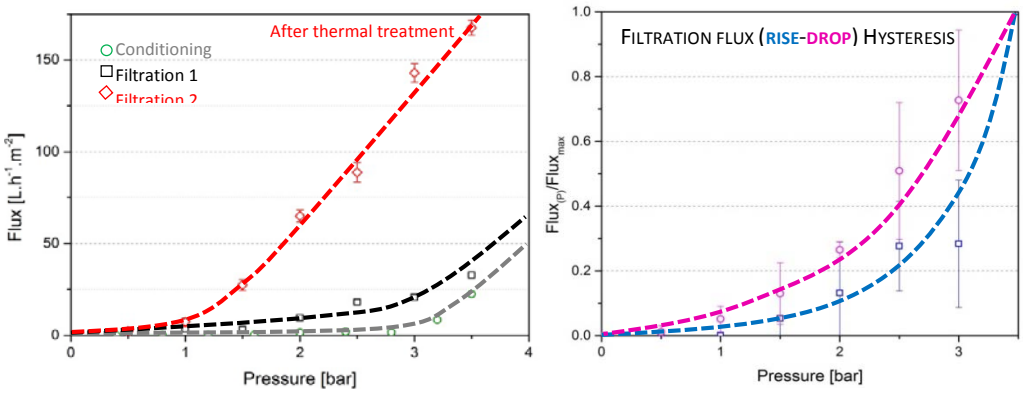

Figure 2. Flux measurement for HPC membrane, conditioning, filtration at room temperature and second filtration after a thermal treatment.

4. Conclusions

This work demonstrated that a porous and stable membrane can be obtained from water-soluble and biosourced polymer, i.e. without organic solvent in the formulation. An original phase inversion process was developed, based on a LCST-TIPS process coupled to chemical cross-linking.

References

[1] Guido, S. (1995). Phase behavior of aqueous solutions of hydroxypropyl cellulose. Macromolecules, 28 : 4530-4539.

[2] Larez-V, C., & Crescenzi, V. (1995). Phase separation of rigid polymers in poor solvents 1 : hydroxypropyl cellulose in water. Macromolecules, 28 : 5280-5284.

[3] Makarova, V.-V., & Kulichikhin, V. (2012). Application of interferometry to analysis of polymer-polymer and polymer-solvent interaction. Interferometry - Research and Application in Science and Technology, 426.

[4] Vshivkov, S.-A., Adamova, L.-V., Rusinova, E.-V., Safronov, A.-P., Dreval, V.-E., & Galyas, A.-G. (2007). Thermodynamics of liquid-crystalline solutions of hydroxypropyl cellulose in water and ethanol. Polymer science series A, 49 : 5, 578-583.

ECCE12
The 12th EUROPEAN CONGRESS OF CHEMICAL ENGINEERING
Florence 15-19 September 2019

Engineering of biohybrid systems by membrane emulsification

Emma Piacentini*, Lidietta Giorno

Institute on Membrane Technology, National Research Council, ITM-CNR, via P. Bucci, 17/C, I-87030 Rende (Cosenza), Italy

**Corresponding author: e.piacentini@itm.cnr.it*

Highlights

- Membrane emulsification is a suitable technology to design biohybrid-engineered systems
- Enzyme-loaded PVA microspheres were produced by membrane emulsification
- Improved operational stability and optimal enzyme-substrate interaction was accessed
- Droplets with controlled structure and glucose-sensitive release properties were developed

1. Introduction

Membrane emulsification is a micro-manufacturing process that allow designing micro-nanostructured multi-material components with target particle size and sizing distribution and complex 3D structures []. The method offers many advantages in the micro-manufacturing of particles able to meet modern demand for a new generation of dispersed materials able to assist or replace important physiological functions by cell encapsulation and/or biomolecules delivery. In particular, membrane emulsification is emerging as a more promising formulation method to produce monodispersed particles with target size in mild operative conditions and with low energy consumption.

The present work will demonstrate the suitability of membrane emulsification process for the development of micro-nanostractured biohybrid systems for biomedical applications. The introduction of new strategies in membrane emulsification method to decrease the shear stress conditions maintaining high productivity will be illustrated to promote the use of membrane emulsification when biological systems, living organisms or derivatives thereof are used. Enzyme-loaded particles and glucose-responsive delivery systems will be described as cases study. The general idea is to functionalize droplet interface by using a biomolecule with a specific biological activity to design advanced biohybrid devices.

2. Methods

Microporous membranes have been used for liquid droplets production (emulsion). One phase (referred as dispersed phase), containing target biomolecules, is dispersed into the other (referred as continuous phase) by forming droplets at the membrane pore opening, where the two phases meet, as a result of the pressure gradient driving force and the interfacial tension existing between the dispersed phase and the membrane wetted by the continuous phase. The integration of membrane emulsification technology with appropriate secondary reactions (cross-linking) allowed

extending to the production of micro-/nano-carriers with different architecture and physical structure. Lipase has been used as a model enzyme to demonstrate the potential of the use of membrane emulsification process in the production of enzyme-loaded PVA particles. A multiple emulsion, containing a bio-receptor (Con A) that specifically recognizes and interacts with an artificial ligand (Glucose), was manufactured by the membrane process and used as a model system. Structural properties of the produced particles (i.e. size, size distribution, surface properties) as well as the functional activity (i.e. catalytic activity for the enzyme loaded particles and glucose-sensitive release for the drug delivery systems) have been evaluated

3. Results and discussion

Uniform droplets (span = 0.4) with a size equal of three times the pore size of the membrane has been produced at the optimized fluid-dynamic conditions by membrane emulsification.

The method allow to obtain a specific activity comparable with the one of the free enzyme when has been used for enzyme-loaded particles production. This can be explained considering the structural properties of the enzyme. Lipase is an interfacial enzyme and exhibit the active form in the presence of a water/oil interface. When enzyme immobilization was carried out by entrapment, the carrier is formed in the presence of the enzyme. The lipase is oriented at the interface in the open form that is also the active form.). On the other end, Con A is able to promote marker substance release as a function of glucose stimulus when membrane emulsification has been employed for biomolecule-responsive particles fabrication. The high affinity between Con A and glucose determined a preferential preferential interaction between them, causing the protein displacement from emulsion interface with phase separation and marker substance release.

4. Conclusions

An effective approach for cell and/or biomolecules encapsulatuion and delivery as well as the construction of carriers with tailored properties are crucial for biohybrid sistems engineering. Results demonstrated that the mild operative conditions applied extend the application of membrane emulsification toward the encapsulation of shear-sensitive compounds such as proteins (antibody or enzyme) and cells. It is expected that membrane emulsification can improve the use of particulate materials for many applications in bioscience and bioengineering by tuning the structural and functional properties of micro/nanostructured biohybrid particles.

References

[1] E. Piacentini, M. Dragosavac, L. Giorno, Current Pharmaceutical Design 23(2) (2017) 302-318
[2] E. Piacentini, E. Drioli, L. Giorno, J Membr Sci 468 (2014) 410-422.

ECCE12
The 12th EUROPEAN CONGRESS OF CHEMICAL ENGINEERING
Florence 15-19 September 2019

Energy from pH and salinity gradients: An experimental study of an Acid/Base battery

Andrea Zaffora*, Andrea Culcasi, Alessandro Cosenza, Luca Muratore, Andrea Cipollina, Alessandro Tamburini, Monica Santamaria, Giorgio Micale

Università degli Studi di Palermo, Dipartimento di Ingegneria, Viale delle Scienze, Ed. 8, Palermo, Italia.

**Corresponding author: andrea.zaffora@unipa.it*

Highlights

- A novel flow battery, based on pH and salinity gradients, is presented.
- Ion exchange membrane parameters are estimated by electrochemical measurements.
- The performances of the device are promising for an efficient electrical energy storage.

1. Introduction

Electrodialysis (ED) and Reverse Electrodialysis (RED) are processes based on the selective transport of ions through ion exchange membranes (IEMs). The former, in which electrical energy is used to desalinate brackish water to produce fresh water, is one of the most valuable alternative to the common membrane desalination processes. The latter is used to produce electrical energy by directly converting salinity gradient energy. The combination of RED and ED processes leads to an electrical energy storage system [1], i.e. a concentration gradient flow battery that converts electrical energy into salinity gradients (charge phase) and recovers the energy exploiting the salinity gradient (discharge phase).

A higher energy density can be obtained using both salinity and pH gradients. This new technology is called Acid/Base Flow Battery (AB-FB) where bipolar membranes (BPMs) and typical IEMs are used to obtain acid and base streams during the charge phase and to produce electrical energy from electrolytes with different pH and salinity during the discharge phase. The use of hydrochloric acid and sodium hydroxide solutions (1 M) leads to an electromotive force (EMF) over the BPM of 0.83 V, one order of magnitude larger than the EMF that can be extracted from salinity gradients [2].

In the present work the performances of this new AB-FB were studied by changing operating conditions such as feed solutions composition and number of repeating units. Electrochemical measurements have been also carried out to study monopolar membranes properties.

2. Methods

A lab-scale setup (provided by Fumatech, Germany) equipped with a variable number of triplets (Acid/Base battery repeating unit) with a membrane active area of 10 x 10 cm^2 was used for the experimental campaign. The triplet was composed by a cation exchange membrane (CEM), an anion exchange membrane (AEM) and a BPM, each one separated from the adjacent by a spacer

500 μm thick. Two DSA electrodes were used in the end-compartments to convert ionic fluxes into electric fluxes. A cross-flow arrangement was adopted for feeding solutions that were prepared by using demineralized water and NaCl, HCl and NaOH. The aqueous electrode rinse solution was 0.25 M in Na_2SO_4. The performances of the AB-FB have been experimentally studied under different charge and discharge conditions with different acid and base concentrations.

Electrochemical measurements (among these, Electrochemical Impedance Spectroscopy, EIS, was used) have been carried out in order to investigate the effect of electrolytes composition on membranes permselectivity, membrane and interface resistances of the monopolar membranes.

3. Results and discussion

Open Circuit Voltage (OCV) values of the device were recorded by changing the concentration of acid and base aqueous solutions (reaching 1 M). These solutions were mixed with NaCl in order to reduce the concentration gradient of NaCl over the monopolar membranes. During the discharge phase, too high current density values can lead to delamination of bipolar membranes with consequent device failure. At high number of triplets, part of the electrical energy generated can be dissipated due to the onset of parasitic currents inside the stack. Charge-discharge flow battery cycles have been also studied starting from “pure” NaCl solutions (beginning of charge phase), then estimating round-trip efficiency of the system as function of operating conditions.

Membranes resistance were estimated by data fitting (with an appropriate electric equivalent circuit) of the electrochemical impedance spectra recorded by changing solution compositions and flow velocity. Membrane resistance was not so influenced from flow velocity whilst values of boundary layer resistance changes by changing the hydrodynamic conditions.

4. Conclusions

A novel flow battery based on pH and salinity gradients is presented. Feeding more concentrated acid and base solutions leads to an increase of the obtainable energy from the device, although at high number of triplets part of the generated energy is dissipated in parasitic currents. During discharge phase, too high current density values cannot be reached due to possible delamination phenomena of bipolar membranes. Membranes characteristics were estimated by electrochemical measurements and they could be used as input in system modelling activity. Further experimental studies are necessary to improve the efficiency of the system.

References

[1] W.J. van Egmond et al., J. Power Sources 325 (2016) 129–139.
[2] W.J. van Egmond et al., Int. J. Energy Res. 42 (2018) 1524-1535.

Acknowledgments

This work was performed in the framework of the BAoBaB project (*Blue Acid/Base Battery: Storage and recovery of renewable electrical energy by reversible salt water dissociation*). The BAoBaB project has received funding from the European Union’s Horizon 2020 Research and Innovation program under Grant Agreement no. 731187 (www.baobabproject.eu).

ECCE12
The 12th EUROPEAN CONGRESS OF CHEMICAL ENGINEERING
Florence 15-19 September 2019

Mass Transfer Associated to the Metabolic Clearance of Uremic Toxins in a Surrogate System of the Artificial Kidney.

Mónica Faria[1], Tiago Eusébio[1], Pedro Brogueira[1], Maria Norberta de Pinho[1]

1 Universidade de Lisboa Instituto Superior Tecnico, CeFEMA and Department of Chemical Engineering, Av. Rovisco Pais, 1049-001 Lisbon, Portugal; 2 Universidade de Lisboa Instituto Superior Tecnico, CeFEMA and Department of Physics, Av. Rovisco Pais, 1049-001 Lisbon, Portugal

**Corresponding author: monica.faria@tecnico.ulisboa.pt*

Highlights

- Innovative membrane synthesis coupling phase inversion and sol-gel techniques
- Asymmetric monophasic hybrid (CA/SiO_2) membranes with enhanced hemocompatibility
- High water fluxes with total urea removal and total albumin rejection

1. Introduction

Artificial organs associated to clinically well-established membrane-based treatments assure in extracorporeal blood circulation devices the metabolic functions of a failing organ like the hemodialyzer for the kidney. The hemodialysis (HD) membrane is the key component of the artificial kidney as it is responsible for removing accumulated uremic toxins, excess ions and water while simultaneously retaining vital components from the blood of End Stage Renal Disease (ESRD) patients [1,2]. The technical and medical progress of the artificial kidney depends on two major factors: 1) hemocompatibility of the membrane/blood interfaces, and 2) enhancement of the flow management/mass transfer associated to the metabolic functions of the artificial kidney.

The present study reports the synthesis and characterization of hybrid CA/SiO_2 membranes containing 5 wt.% silica via the coupling of the phase inversion and the sol-gel techniques taking into account a two-fold goal: 1) development of integrally skinned asymmetric CA/SiO_2 ultrafiltration (UF) membranes with high water permeability, preferential permeation of uremic toxins and total retention of vital blood components; 2) tailoring of membranes with hemocompatible surface morphologies.

2. Methods

The surface morphology of the membranes was characterized by Scanning Electron Microscopy (SEM). Mass transfer studies associated to the metabolic functions of the kidney are conducted in a custom-made benchmark device with a membrane surface area of 60 cm^2 as a surrogate system of the artificial kidney. Permeation experiments are carried out to yield hydraulic permeability (Lp), Molecular Weight Cut Off (MWCO) and rejection coefficients (*f*) to a set of reference solutes including urea, creatinine, uric acid and Bovine Serum Albumin (BSA).

3. Results and discussion

Monophasic hybrid integrally skinned asymmetric membranes containing 5 wt.% of silica, CA/SiO_2-5, were synthesized by a novel method that combines phase inversion with acid-catalyzed sol-gel process [3]. Fig. 1 displays the SEM image of a monophasic asymmetric cross section of the CA/SiO_2-5 membrane characterized by a very thin dense layer and a much thicker porous substructure. Permeation studies reveal that the hydraulic permeability of the hybrid CA/SiO_2-5 membrane is 82 kg/h/m2/bar, which is approximately 2.5 times higher than the value of the pure CA membrane (32 kg/h/m^2/bar), total permeation of urea and complete retention of bovine serum albumin (BSA).

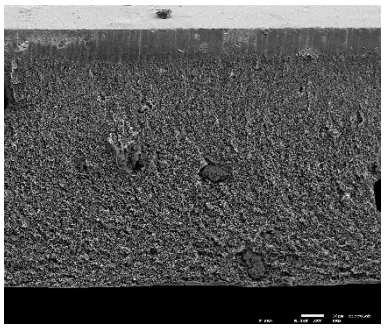

Figure 1. SEM image of the cross section (500x) of the hybrid integral asymmetric CA/SiO_2-5 [3].

4. Conclusions

In this work hybrid CA/SiO_2 membranes containing 5 wt.% silica were synthesized via the coupling of the phase inversion and the sol-gel techniques. Permeation studies show that the integration of silica into CA membranes by the innovative phase inversion/sol-gel method results in high flux ultrafiltration membranes with enhanced mass transfer properties pertaining to the metabolic functions of the kidney. In particular, the study shows that the CA/SiO_2-5 membrane is capable of complete removal of urea, the surrogate marker for small molecular weight uremic toxins while simultaneously retaining the vital protein found in blood, albumin. The versatility of the novel synthesis method allows further tailoring of structures and permeation properties of CASiO_2 membranes for the Artificial Kidney with high efficiency for specific removal of other critical uremic toxins.

References [Calibri 10]

[1] N.S. Hakim, ed., Artificial Organs, Springer-Verlag, London, 2009. //www.springer.com/gp/book/9781848822818.

[2] J. Vienken, Membranes in Hemodialysis, in: Membr. Life Sci., Wiley-Blackwell, 2010: pp. 1–48.

[3] G.Mendes, M. Faria, A. Carvalho, M.C. Gonçalves, M.N. de Pinho, Structure of water in hybrid cellulose acetate-silica ultrafiltration membranes and permeation properties, Carbohydr. Polym. 189 (2018) 342–351

ECCE12
The 12th EUROPEAN CONGRESS OF CHEMICAL ENGINEERING
Florence 15-19 September 2019

Nanofiltration removal of perfluorohexanoic acid: the role of salts concentration and pH

Álvaro Soriano, Daniel Gorri, Ane Urtiaga

Department of Chemical and Biomolecular Engineering, University of Cantabria. Av. Los Castros 46, Santander 39005, Spain

** Corresponding author: urtiaga@unican.es*

Highlights

- The removal of PFHxA from industrial process waters by two NF membranes was studied.
- Excellent PFHxA rejection and intermediate fluxes when treating model PFHxA solutions were observed.
- Presence of salts in the water matrix severely decreased PFHxA rejection.

1. Introduction

Perfluoroalkyl substances (PFASs) are a family of man-made organic compounds classified as persistent organic pollutants due to their recalcitrance in the environment and their high bioaccumulation potential [1]. For these reasons, chemical manufacturers are progressively replacing regulated long-chain PFASs by 6:2 fluorotelomers and shorter-chain perfluoroalkyl homologues such as perfluorohexanoic acid (PFHxA) [2]. On the other hand, PFHxA can also be a 6:2 fluorotelomer alcohol biodegradation product [3]. Thus, increasing production of substitutive compounds is leading to rising concentrations of persistent PFHxA in the environment. Since conventional wastewater treatments are ineffective in PFASs treatment, current research efforts are focused on separation (nanofiltration (NF), reverse osmosis and adsorption) and advanced oxidation technologies. However, most of the studies focus on already phased-out long-chain PFASs at very low concentrations. Treatment of industrial process streams, that constitute the major source of PFASs emissions to the environment, is rarely studied. Hence, this work studies the separation of PFHxA by nanofiltration at industrial emission levels

2. Methods

PFHxA ($C_5F_{11}COOH$) molecular weight is 314.05 g mol^{-1}. Accordingly, two NF commercial membranes, ESNA1-LF and ESNA1-LF2 (Hydranautics), recommended for water softening and pesticides removal were selected. The NF membranes were evaluated in terms of PFHxA rejection and permeate flux, in the pressure range 2.5-20 bar. The flat-sheet membrane coupons were housed in a cross-flow filtration test cell (SEPA-CF, GE Osmonics). The feed solution was maintained at constant temperature (20°C) in a jacketed tank connected to a refrigeration system and the cross-flow velocity was kept at 24.7 cm s^{-1} using a variable-speed diaphragm pump. Two types of feed samples were prepared: (i) 100 mg L^{-1} PFHxA aqueous solutions at neutral pH, and (ii) model solutions to emulate the salts content of real process waters with 100 mg L^{-1} of PFHxA, 36 mg L^{-1} of NaCl, 575 mg L^{-1} of $CaSO_4$, and 98 mg L^{-1} of $NaHCO_3$, at pH = 7.84 ± 0.1. PFHxA was quantified using UPLC-MS/MS.

3. Results and discussion

Figure 1 shows the influence of the water matrix on the PFHxA observed rejection (R_{obs}) and the volumetric flux (J). For both membranes, PFHxA rejection was severely affected by the chemistry of the solution while the permeability remained reasonably constant. Whilst very high PFHxA rejection values were obtained when treating pure PFHxA aqueous solutions (ESNA1-LF: 96.1 – 99%; ESNA1-LF2: 95.4 – 97.9%), the presence of salts considerably reduced the rejection performance (ESNA1-LF: 67.2 – 70.4%; ESNA1- LF2: 70.2 – 76.5%). This could be attributed to the high counter-ion concentration in the feed side of the membranes that could induce a shielding effect on the negatively-charged surface of the two NF membranes. Thus, the diminished electrostatic repulsion between the charged NF membranes surface and the perfluorohexanoate anion form of PFHxA in solution at neutral pH, would leave the steric-exclusion role as the dominant separation mechanism.

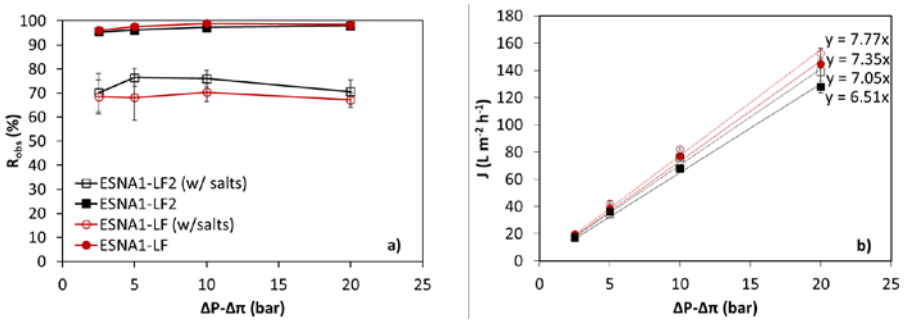

Figure 1. (a): PFHxA observed rejection (R_{obs}) and (b): water flux (J_v) versus the effective pressure gradient. 100 mg L^{-1} of pure PFHxA aqueous solutions and PFHxA synthetic process water feed with salts.

4. Conclusions

Two nanofiltration membranes (ESNA1-LF and ESNA1-LF2, Hydranautics) were tested in the separation of persistent perfluorohexanoic acid (PFHxA) at concentration levels typically found in industrial process waters. Both membranes showed excellent PFHxA rejection performance and intermediate water productivity when treating pure aqueous PFHxA solutions at neutral pH. However, the presence of salts in the water matrix severely decreased PFHXA rejection. These findings point to a drastic change in the electrostatic repulsion mechanism between the dissociated PFHxA and the charged membranes surfaces, negatively influenced by the presence of positive divalent counter-ions. Decontamination of complex water matrixes impacted with PFHxA that are generated in the chemical process industry could need tighter and more selective nanofiltration or reverse osmosis membranes.

Acknowledgments. Funding of project CTM2016-75509-R (MINECO Spain/FEDER) is gratefully acknowledged

References

[1] Á. Soriano, D. Gorri, A. Urtiaga, Water Res. 112 (2017) 147–156.
[2] A. Urtiaga, Á. Soriano, J. Carrillo-Abad, Chemosphere 201 (2018) 571–577.
[3] A. Soriano, D. Gorri, A. Urtiaga, Sep. Purif. Technol. 208, (2019) 160–168.

ECCE12
The 12th EUROPEAN CONGRESS OF CHEMICAL ENGINEERING
Florence 15-19 September 2019

Enhanced permeate flux through nano-filtration Polyphenylsulfone membrane using modified silica nanoparticles

Mohammad Mehdi Zarei[1,3], Frances Neville[2], Roberto Moreno-Atanasio[1,3], Grant B. Webber[1,3]

1 *School of Engineering, The University of Newcastle, Callaghan, NSW 2308, Australia*
2 *School of Environmental and Life Sciences, The University of Newcastle, Callaghan, NSW 2308, Australia*
3 *Priority Research Centre for Advanced Particle Processing and Transport, The University of Newcastle, Callaghan, NSW 2308, Australia*

**Corresponding author: Mohammadmehdi.zarei@uon.edu.au*

Highlights

- Manufacturing new mixed matrix membranes (PPSU/SiO_2).
- Preparation of silica nanoparticles incorporated with PEI.
- The antifouling performance of PPSU membranes greatly improved.
- The nanocomposite membrane presented excellent removal efficiency of copper ions.

1. Introduction

Polyphenylsulfone membranes (PPSU) are a promising option for separation applications due to their high versatility to control pore size distribution and their chemical and thermal stability. However, the applications of PPSU membrane are limited due to their hydrophobicity which decreases water permeability and increases membrane fouling in an aqueous environment [1].
During the past decade, blending of the membranes with organic/inorganic modifiers such as nano-particles and copolymers has become the most common approach to improve membrane performance. Specially nanocomposite membranes which are composed of polymers and nanoparticles have received special attention [2]. Silica nanoparticles (SNPs), due to their low cost and surface OH moieties, may be selected as a promising filler for membrane modification as they improve the hydrophilicity [3] and water flux capacity of the membranes [4, 5].
In the present work, PPSU membrane will be fabricated by addition of modified silica nanoparticles. The performance of the prepared membrane will be analysed. Then the results will be used to enhance the membrane rate of water transport, hydrophilicity and copper rejection. Finally, the comparison of the performance of synthesised membranes will be presented.

2. Methods

All PPSU blended membranes were prepared using the non-solvent induced phase inversion method [6]. In the preparation of the blend membranes, PPSU with different concentration of SiO_2 nanoparticles was employed as the membrane bulk material. The morphology, the distribution of the silica nanoparticles and the presence of chemical functional groups in the prepared membranes have been investigated via field emission-scanning electron microscopy (FE-SEM) and attenuated total reflectance Fourier-transform infrared spectroscopy (ATR-FTIR). Finally, the performance of the prepared membranes were characterised and compared in terms of hydrophilicity, water flux, fouling resistance and copper rejection.

3. Results and discussion

Water flux over time of the prepared membranes was investigated at 500 kPa constant pressure (Fig. 1). As shown in the figure, water flux of PPSU/SiO_2 membrane is remarkably higher than that of the neat PPSU membrane due to its higher hydrophilicity and higher pore size as these characteristics were enhanced with the addition of silica nanoparticles. In addition, it is quite clear that the water flux declined which may be due to clogging of the membrane pores by the presence of copper ions. Also, the result of copper rejection is shown in Figure 2. As can be seen in the figure, the copper rejection of the neat PPSU membrane was reported 43%. However, the results were altered to about 57% and 79% for 0.2 wt% and 0.4 wt% of PPSU/SiO_2 membranes, respectively. These changes indicated that silica nanoparticles played a significant role in enhancing the copper rejection ratio of the blended membranes.

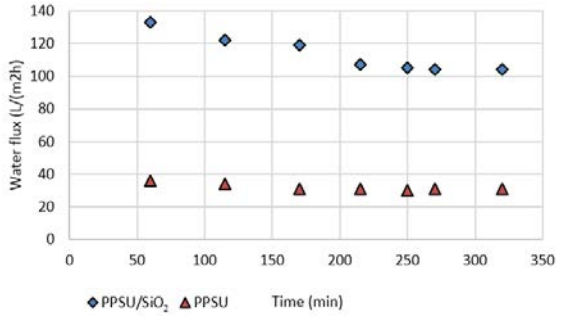

Figure 1. Water flux of PPSU membranes

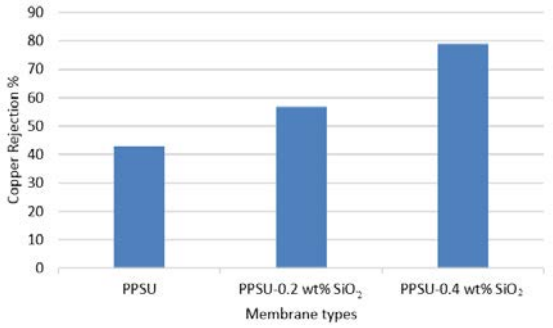

Figure 2. Copper rejection of PPSU membranes

4. Conclusions

A new approach was used to modify PPSU membrane using a phase inversion method in order to improve the membrane properties such as hydrophilicity and anti-fouling. The addition of modified silica nanoparticles to the polymer casting solution resulted in a considerable improvement in the fabricated membrane hydrophilicity and water flux.

References

[1] Daraei, P., et al., Novel polyethersulfone nanocomposite membrane prepared by PANI/Fe_3O_4 nanoparticles with enhanced performance for Cu (II) removal from water. Journal of Membrane Science, 2012. 415: p. 250-259.

[2] Yurekli, Y., Removal of heavy metals in wastewater by using zeolite nano-particles impregnated polysulfone membranes. Journal of Hazardous Materials, 2016. 309: p. 53-64.

[3] Dong, H., et al., Superhydrophilic Surfaces via Polymer−SiO_2 Nanocomposites. Langmuir, 2010. 26(19): p. 15567-15573.

[4] Shen, J.-n., et al., Preparation and characterization of PES–SiO_2 organic–inorganic composite ultrafiltration membrane for raw water pretreatment. Chemical engineering journal, 2011. 168(3): p. 1272-1278.

[5] Yu, L.-Y., et al., Preparation and characterization of PVDF–SiO_2 composite hollow fiber UF membrane by sol–gel method. Journal of Membrane Science, 2009. 337(1): p. 257-265.

[6] Hwang, L.-L., H.-H. Tseng, and J.-C. Chen, Fabrication of polyphenylsulfone/polyetherimide blend membranes for ultrafiltration applications: The effects of blending ratio on membrane properties and humic acid removal performance. Journal of Membrane Science, 2011. 384(1): p. 72-81.

ECCE12
The 12th EUROPEAN CONGRESS OF CHEMICAL ENGINEERING
Florence 15-19 September 2019

Environmental benefits of SGE-RED energy recovery using LCA

Carolina Tristán, Marta Rumayor, Marcos Fallanza, Antonio Dominguez, Raquel Ibañez, Inmaculada Ortiz

Chemical and Biomolecular Engineering Department, Universidad de Cantabria, Av. Los Castros s/n 39005 Santander, Spain

**Corresponding author: inmaculada.ortiz@unican.es*

Highlights

- The SGE-RED process environmental benefits are proved by a cradle-to-gate LCA method.
- The best RO desalination plant-RED scenario, regarding environmental issues, is found.
- LCA results will enable to identify the SGE-RED process bottlenecks and challenges.

1. Introduction

Salinity gradient energy (SGE) is a promising alternative source of energy, currently attaining growing attention among the scientific community. Reverse Electrodialysis (RED) is arising as one of the most advantageous membrane-based technologies for recovering energy from the controlled mixing of two solutions of different salinities. At present, research efforts are mainly focused on RED technical development as well as modelling and optimisation [1, 2]. Nonetheless, the environmental sustainability of an SGE-RED system must be compared against other energy renewable sources to verify the potential environmental benefits.

In this regard, the Life Cycle Assessment (LCA) is an effective tool used to evaluate the environmental sustainability of products, processes or services against a well-known benchmark [3]. Our research group is currently addressing the evaluation of the potential environmental benefits of SGE-RED units for the recovery of energy from desalination discharge effluents. The study comprises the evaluation of the use of natural resources and the carbon footprint associated with an SGE-RED energy recovery process to partially substitute fossil-fuelled based supply to a reverse osmosis (RO) desalination plant, which features an intensive energy use

2. Methods

A “cradle-to-gate” LCA methodology has been applied in this study. First, a simple system (System-1) comprised by an SGE-RED is analysed (Figure 1(a)). The impacts related to the generation of a 1 kWh from the SGE-RED unit —defined as the functional unit in the LCA methodology— have been assessed and compared with other renewable power resources. The second system (System-2) integrates the SGE-RED unit in a RO desalination plant (Figure 1(b)). The energy supply required to treat 1 m^3 of seawater (SW) or brine water (BW) in the RO plant is partially delivered by the SGE-RED unit and the RO untreated brine by RED is directly released to the marine environment.

A mathematical model has been built for each system. The EGS-RED model consists of a set of mass and energy balances and experimental parameters obtained in previous activities [2]. The inputs and outputs obtained from the model are collected in the LCI. The infrastructure influence is evaluated by modelling the construction of an SGE-RED unit considering the lifetime of the membrane as the main variable.. A sensitivity analysis is performed including the following variables: flow water streams; streams concentrations; temperature; and membrane lifetime to evaluate different operation scenarios.

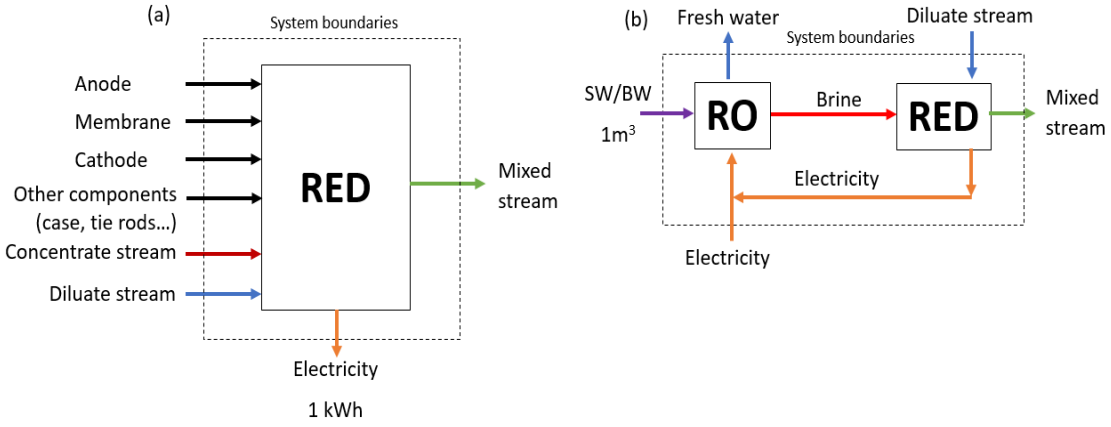

Figure 1. Boundaries of (a) System-1 (RED design) and (b) System-2 (RED integrated in a reverse osmosis (RO) plant)

LCA is completed using the GaBi Professional software applying the mid-point method CML 2001. In this project, global warming and brine discharge impacts are considered. Global warming potential (GWP) is assigned as the main impact indicator to assess the carbon footprint of the analysed alternatives. The potential damage caused by concentrated brine effluents is evaluated by a new impact category developed within the study.

3. Results and discussion

LCA results enable to identify the bottlenecks and challenges of SGE-RED process and its implementation in a RO desalination plant. The System-1 results shows the environmental effects of a 1,0 kWh SGE-RED system and allow their comparison with other renewable power sources. The System-2 results demonstrate the potential environmental benefits of the RO-RED hybrid system in the different proposed scenarios. The sensitivity analysis indicates the combination of the tested variables that ensures that the process is beneficial from an environmental perspective when compared with similar process options.

4. Conclusions

The LCA tool enables the quantitative assessment of the environmental benefits of the SGE-RED technology in a systematic way, and helps in finding the optimum environmental related RO-RED scenario.

5. Acknowledgements

Financial support from project: Gradisal “RM16-XX-046-SODERCAN/FEDER” and the projects CTQ2015-66078-R and CTM2017-87850-R is acknowledged.

References

[1] R.A. Tufa, S. Pawlowski, J. Veerman, K. Bouzek, E. Fontananova, G. di Profio, S. Velizarov, J. Goulão Crespo, K. Nijmeijer, E. Curcio, App Energy. 225 (2018) 290–331.

[2] R. Ortiz-Imedio, L. Gomez-Coma, M. Fallanza, A. Ortiz, R. Ibañez, I. Ortiz, Desalination (accepted; 2019; DOI: 10.1016/j.desal.2019.01.005).

[3] M. Rumayor, A. Dominguez-Ramos, A. Irabien, Sustainable Production and Consumption. 18 (2019) 72–82.

ECCE12
The 12th EUROPEAN CONGRESS OF CHEMICAL ENGINEERING
Florence 15-19 September 2019

Long-term assessment of Energy Recovery from Salinity Gradients

Lucia Gómez-Coma, Victor Ortiz-Martínez, Carolina Tristán, Marcos Fallanza, Alfredo Ortiz, Raquel Ibañez, Inmaculada Ortiz*

Chemical and Biomolecular Engineering Department, University of Cantabria, Avda de los Castros s/n 39005, Santander, Spain

**Corresponding author: inmaculada.ortiz@unican.es*

Highlights

- Salinity Gradient Energy from desalination and wastewater treatment plant streams
- Mathematical modelling tool for evaluation of different scenarios.
- RED Technology for energy recovery and biomedical applications.

1. Introduction

Salinity Gradient Energy (SGE) is considered one of the most attractive renewable energy sources since it is completely clean and sustainable with no toxic gas emissions [1]. The main technology to harvest the SG energy is Reverse Electrodialysis (RED), which has emerged as a promising membrane-based technology for renewable energy generation by mixing two solutions of different salinity. The state of the art and technical challenges for a wider implementation of the technology have been excellently reviewed in a recent work [1]. Besides, the proximity of two streams with different salinity is important for its final implementation; apart from the well-known mixing between sea and river waters different scenarios have been analyzed such as, the mixing of desalination streams, brine with brackish water, seawater and WWTP streams, respectively. More recently the downscaling of the RED technology has addressed the development of new lab-on-a-chip (LOC) biomedical devices, e.g. medical implants powered by RED technology [2] concluding that RED technology offers great opportunities for new, long-lasting and safer biomedical devices.

In this sense, the development of robust model tools for the study of SG power generation and RED performance under diverse scenarios and different operational and system conditions is still essential for the optimization of this technology. Thus, we aim to contribute to the wider implementation of the SGP-RED technology by advancing comprehensive models supported by the experimental evidence. For this purpose, in this work we have evaluated, theoretical and experimentally, the performance of a SGP-RED laboratory plant for the long-run applied to the energy recovery from desalination wastes and we have defined the maintenance protocol.

2. Methods

The experiments were performed using a RED stack composed of 20 cation and anion exchange membrane pairs with membrane areas per cell of 200 cm^2 and polyethersulfone spacers, both supplied by Fumatech®. The electrode rinse solution (ERS) was constantly flowed in a closed loop. The schematic setup is shown in Figure 1. Experiments were performed by using an electronic load device (Chroma Systems Solutions 63103A, USA) [3]. The stack was continuously fed with stream solutions coming from desalination plants. To perform the modelling of the process, the software Aspen Custom Model V9 (AspenTech) was used based on the equations that describe the phenomena occurring inside the cell, establishing the following assumptions: (i) co-current flow

distribution, (ii) purely sodium chloride aqueous solutions and (iii) evaluation of the parameters at the average conditions between inlet and outlet [3].

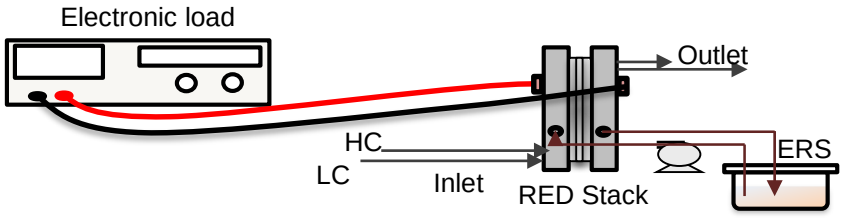

Figure 1. Experimental setup. HC: high concentration solution; LC: low concentration solution.

3. Results and discussion

First, we performed the analysis of the energy recovery by mixing two solutions of different characteristics. Figure 2.a displays the gross power (W/m^2) achieved under different scenarios and the experimental results against current (A), showing that predicted curves are in concordance with lab scale results. The deviation between simulated and experimental results over time was lower than 10%. In view of the simulated data for the experimental assessment we worked with 2 industrial streams, S1 and S2, with a concentration of NaCl of 0.94 M and 0.04 M respectively, together with other ions and we tested the stability of the plant with time. Figure 2.b) depicts the results obtained over one month of continuous operation. Gross Power remained constant for this period when a simple maintenance protocol was applied.

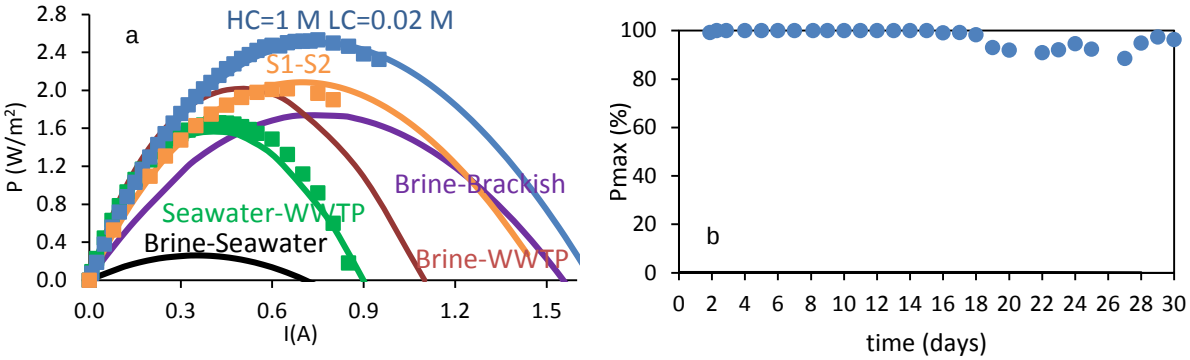

Figure 2. a) Power performance resulting from the combination of different scenarios; b) Long-run testing of RED stack fed with water streams from desalination plants.

4. Conclusions

A stable performance of the SGP-RED technology working with rejections of desalination plants has been proved in continuous operation with a simple maintenance protocol. The good agreement between the experimental results and simulated data with the mathematical model validated the design tool that can be expanded to down-scale operations using miniaturized devices.

Acknowledgments

Financial support from the projects: Gradisal "RM16-XX-046-SODERCAN/FEDER", CTQ2015-66078-R, and CTM2017-87850-R and are gratefully acknowledged.

References

[1] R.A. Tufa, S. Pawlowski, J. Veerman, K. Bouzeka, E. Fontananova, G. di Profio, S. Velizarov, J.G. Crespo, K. Nijmeijer, E. Curcio, Appl. Energy. 225 (2018) 290–331.

[2] J. Hestekin, C. Hestekin, C. Smith, B. Rodgers, P.R. Lima-Vieira. Patent: WO 2018/049333 Al (2018).

[3] R. Ortiz, L. Gomez-Coma, M. Fallanza, A. Ortiz, R. Ibañez, I. Ortiz, Desalination, doi:10.1016/j.desal.2019.01.005.

ECCE12
The 12th EUROPEAN CONGRESS OF CHEMICAL ENGINEERING
Florence 15-19 September 2019

Transfer behavior of saccharides in thermoresponsive polymer layered membrane.

Hiromu Kashiwazaki[1], Kazumitsu Naoe[1*], and Masanao Imai[2]

1 Dept. of Materials Sci. & Chem. Eng., National Institute of Technology, Nara College, Yamato-Koriyama, Nara 639-1080, Japan; 2 Graduate School of Bioresource Sci., Nihon University, Fujiwara, Kanagawa 252-0880, Japan

**Corresponding author: naoe@chem.nara-k.ac.jp*

Highlights

- The water permeation rate through the polymer layered membrane was linearly proportional to the pressure indicating the permeation mechanism was Hagen-Poiseuille flow.
- The water permeation rate steeply increased at around 30 °C.
- The effective diffusion coefficient of model components in the membrane increased with temperature.

1. Introduction

Membrane separation is separation technology that selectivity separates materials via pores and/or tiny gaps in the membrane structure. And membrane technology plays an important role in conserving energy during purification process. Especially, separation of saccharides is an important issue in the production process of food industry. On the other hands, smart responsive polymer has various types such as thermoresponsive, photo-responsive, pH-responsive and etc. Especially thermoresponsive polymers are easy to control[1]. In this study, thermaoresponsive polymer layered membrane is prepared and its permeation behaviors of solvent and model saccharides through the membrane are investigated.

2. Methods

The polymer system composed of polyacrylamide and poly (acrylic acid) was used as a positive thermoresponsive polymer exhibiting an upper critical solution temperature (UCST). Acrylic acid/acrylamide monomer solution was deposited onto a support membrane and thermally polymerized. This operation was repeated to prepare the thermoresponsive polymer layered membrane. The water permeation rate of the prepared membrane was determined from the water mass flux with N_2 gas pressure. The overall mass transfer coefficient (K_{OL}) was determined from a measurement of mass transfer flux of methyl orange or saccharides in the glass cells sandwiching the membrane. The effective diffusion coefficient (D_{eff}) in the membrane was evaluated from the membrane mass-transfer coefficient (k_m) obtained under fully turbulent conditions. The mass transfer experiment of the model components was investigated at different temperature conditions (25 °C and 60 °C)

3. Results and discussion

The water permeation rate through the polymer layered membrane was linearly proportional to the pressure indicating the permeation mechanism was Hagen-Poiseuille flow. The effect of temperature on the water permeation through the membrane was examined. The water permeation rate steeply increased at around 30 °C (Fig. 1), indicating that the membrane showed UCST behavior. The D_{eff} of model components in the membrane increased with temperature. The increase in the D_{eff} was larger than the contributions of temperature and viscosity to the bulk diffusion coefficient. This supposed that the polymer framework of the membrane swelled with increasing temperature, which led to the reduction of mass transfer resistance. These findings indicated that positive thermosensitive control of mass transfer was successfully achieved using the polymer layered membrane.

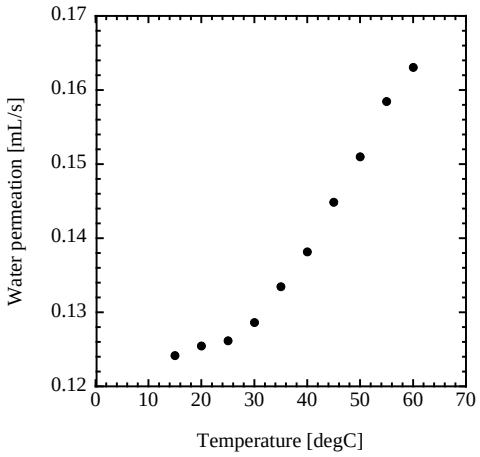

Figure 1. Water permeation through the polymer layered membrane at various temperatures (pressure: 0.1 MPa).

4. Conclusions

Thermaoresponsive polymer layered membrane were prepared, and its permeation behaviors of solvent and model components through the membrane were investigated. In water permeation through the membrane, UCST thermoresponsive behavior was successfully shown. In mass transfer behavior of model components through the membrane, it is possible to control K_{OL} and D_{eff} by temperature and suggesting of possibility of separation.

References

[1] Yang, W. et al., ACS Appl. Mater. Interfaces, 6, 0146−10152 (2014)

ECCE12
The 12th EUROPEAN CONGRESS OF CHEMICAL ENGINEERING
Florence 15-19 September 2019

MEMBRANE (MF and UF) APPLIED IN THE 2,3-BUTANEDIOL PURIFICATION PROCESS

Beal, Lademir Luiz[1]; Beux, Assis Reinaldo Dariva[2]

1 and 2 University of Caxias do Sul; Address: Francisco Getúlio Vargas 1130, Caxias do Sul, Brazil

**Corresponding author: llbeal@ucs.br*

Highlights

- The pressure is strongly correlated with the resistance
- The pressure was not a determinant effect to increase the permeate flux.
- There were no significant differences between the flux of permeate in MF and UF.

1. Introduction

In an effort to reduce global dependence on fossil fuels, biofuels have been gaining more space. Biodiesel can partially or completely replace diesel. A byproduct of biodiesel is glycerol, a substrate that can be exploited in the chemical industry and produce other biofuels such as biohydrogen and biomethane. Among its uses is the production of 2,3-butanediol, which can be obtained by fermentative processes, especially using Klebsiela pneumoniae. The production of 2,3-butanediol is well established for batch processes. Some difficulties inherent to fermentative processes with pure cultures, such as contamination, prevent the effective use of obtaining this compound in CSTR. The use of membranes can be interesting as a step of the purification process or used in continuous processes (MBR), reducing the risks of contamination, and providing a greater reduction. Gupta et al. (2005) using flat sheet cellulose acetate MF membrane obtained results where the increase of permeate flux were from 54% to 146% for different gas flow rate. The main goal of this paper is to discuss the different hydraulic behavior using MF and UF membrane, both with hollow fiber configuration, to separate Klebsiella pneumoniae cells and macromolecules compounds.

2. Methods

Two modules of PVDF membranes (UF and MF), in hollow fiber configuration, of asymmetric morphology, contact angle with water of 66º, moderate hydrophobicity and filter area of 0.047 m² were used. The membranes of UF were made in porous support medium, since MF membranes are extruded integrals. Before each cycle of tests, the membranes were subjected to compaction and hydraulic characterization. Total resistance during the fermented assay was assayed at pressures of -400, -250, -150 and 60 mbar for MF and -400, -250, -150 mbar for UF. The test pilot was set at 30 ° C with air injection at the base of the module for cleaning. The flow was measured for 3 hours. The total resistance to filtration was obtained through Equation $J = \Delta P / (\mu \times R_{tot})$, where J is the flow, μ is the absolute viscosity of the permeate and R_{tot} is the total resistance to filtration.

3. Results and discussion

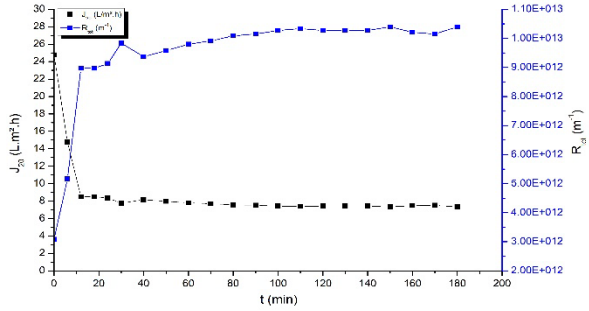

Figure 1 – Flux in MF250.

The partial result obtained had showed that both membrane, MF and UF, have a good and similar behavior when is compared the permeate flux. The permeate flux in 20 minutes decrease almost 60 % and after this moment is practically stable as shown in the Figure 1 (an example of the graphic obtained).

Analyzing the results presented in Table 1 to MF tests it is possible to conclude that the pressure was not a determinant effect to increase the permeate flux, since from 60 to 250 mbar the values were very similar, but when is analyzed the results to 400 mbar the percentage of the permeate flux reduction was higher than the others and the resistance increase percentage was higher than other as well.

Table 1: Behavior of MF and UF modules.

	P (mbar)	Jo ($L.h^{-1}.m^{-2}$)	Ju ($L.h^{-1}.m^{-2}$)	% decrease	Ro (m^{-1})	Ru (m^{-1})	% increase
MF	60	21.6	7.10	67	8.3E+11	2.6E+12	216
	150	30.8	8.20	73	1.5E+12	5.6E+12	277
	250	24.8	7.30	71	3.1E+12	1.0E+13	238
	400	73.9	6.70	91	1.6E+12	1.8E+13	997
UF	50	10.9	6.80	22	1.5E+12	2.2E+12	68
	150	25.3	5.60	78	1.8E+12	8.2E+12	353
	250	36.5	5.40	85	2.1E+12	1.4E+13	579
	400	59.9	6.40	89	2.0E+12	1.9E+13	841

The reduction of the permeate flux in the UF tests were higher than the MF tests and the increase of the resistance was higher than MF as well. The permeate flux (Ju) values were very similar but the pressure effect was more significant for the increasing of resistance than the flux.

4. Conclusions

It is possible conclude that the pressure is strongly correlated with the resistance (r=0.992 to MF and r=0.980 to UF). It is not interesting to use high pressure in this process since there is not positive effect on the permeate flux. The permeate flux is higher in the MF membrane than the UF membrane but without significant differences.

References [Calibri 10]

[1] B. Sen Gupta, M. A. Hashin, K. B. Ramachandran, I Sen Gupta, and Z. F. Cui. Eng. Life Sci. 5 (2005) 54-57.
[2] Y. Satyawali, K. Vanbroekhoven, and W. Dejonghe Biochemical Engineering Journal 121 (2017) 196-223.
[3] X. Ji, H. Huang, and P. Ouyang. Microbial 2,3-butanediol production: A state-of-the-art review Biotechnology Advances 29 (2011) 351–364.

ECCE12
The 12th EUROPEAN CONGRESS OF CHEMICAL ENGINEERING
Florence 15-19 September 2019

Pervaporation characteristics of PVA-alumina hollow fiber composite membrane for the recovery of by-product in the epoxy resin manufacturing process

Seung-Eun Nam*, Yong Sung Kwon, Ahrumi Park, Young Mi Kim
HoSik Park, You-In Park,

Membrane Research Center, Korea Research Institute of Chemical Technology,
141 Gajeongro, Yuseong, Daejeon 34114, Korea
* *Corresponding author: senam@krict.re.kr*

1. Introduction

Pervaporation is a membrane separation technology with high efficiency and energy saving benefits for liquid mixture separation, in particular, for the separation of close boiling or azeotropic mixtures [1]. One of the most frequent industrial application areas of pervaporation is dehydration of solvents that form an azeotrope with water e.g. ethanol, isopropanol, tetrahydrofurane. The membrane contacts with the liquid mixture on the feed side, while permeate is removed as a vapor. The mass transport is driven by the vapor pressure difference between the feed solution and the permeate vapor. The chemical potential gradient across the membrane is the driving force for the mass transport. The driving force and be created by applying either a vacuum or an inert sweep gas on the permeate side to maintain the permeate vapor pressure lower than the partial pressure of the feed liquid. Mass transport in the pervaporation membrane can be explained by the solution-diffusion model [2]. Pervaporation is a well-known alternative method to classical distillation due to its high selectivity and low operational cost. Since the pervaporation is normally applied to remove a minor component of a liquid mixture, high permselectivity is essential for competing with convential means such as distillation and extraction.

Epichlorohydrin (ECH) containing epoxide and organochlorine moieties is a highly reactive electrophilic compound used in the production of glycerol, plastics, and epoxy resins [3]. Epoxy resin is prepared by polymerization of ECH with phenol, Bisphenol-A (BPA) is used as a phenol resin and isopropanol (IPA) is used as solvent. Excess ECH is included in the raw material to control the molecular weight of the produced epoxy resin. After reaction, ECH, IPA, a series of chlorine impurities, and water is remained and distillation process has been widely applied for the recovery of these by-products. However, the impurity content gradually increases after repeated reuse. During the recovery of ECH and IPA by distillation, ECH and IPA form a ternary azeotropic mixture with water impurities, and the recovery of high purity ECH and IPA is difficult only by distillation process. Therefore, in terms of energy efficiency and reuse of unreacted materials, improvements to this process are required. Furthermore, ECH can cause environmental hazards because it is carcinogenic in nature and can have serve adverse effects on ecological systems if its effluent comes into contact with the environment. A hybrid process involving moisture removal by pervaporation and recovery and purification of ECH and IPA *via* distillation can improve the ecofriendly energy efficiency and the product competitiveness by reducing the cost associated with the epoxy resin manufacturing process.

In this study, pervaporation performance and stability of the prepared PVA-alumina hollow fiber composite membrane was evaluated at various operational condition in a highly reactive ECH-containing ternary mixture feed system of ECH/IPA/Water(50/30/20 wt%).

2. Methods

Selection of stable polymeric membrane material for pervaporation in the ECH/IPA/water feed system is a challenging task because ECH is a highly reactive chemical. Poly(vinylalcohol) (PVA, M.W. 85000-124000 g/mol) as active layer material for dehydration aqueous organic solution has excellent membrane forming properties, a high tensile strength, and stability in organic solvents. The crosslinking reaction of PVA was carried out at 50^{o}C for 2hr and the composition of the crosslinking agent was GA/IPA/Water/HCl = 5/89.5/5/0.5 vol%. Pervaporation performance and chemical stability of the prepared composite membrane was evaluated at various operational condition in a highly reactive ECH-containing ternary mixture feed system of ECH/IPA/Water (50/30/20 wt%).

3. Results and Discussion

Figure 1 shows the SEM pictures of (a) the surface and fractured cross-section of the alumina hollow fiber support and (b) the fractured cross-section of PVA-alumina hollow fiber composite membranes. PVA active layer was observed to be a have uniform thickness of less than 2 μm.

The prepared PVA-alumina hollow fiber composite membranes, in this study, showed excellent pervaporation dehydration performance with the feed comprising an ECH/IPA/Water (50/30/20 wt%) azeotropic mixture in long-term stability test: the permeate flux of above 0.135 kg/m^2 hr and separation factor was above 3500 at 30 ^{o}C. As shown in Figure 2, the composite membrane was operated for 500 hours with no observed decrease in performance.

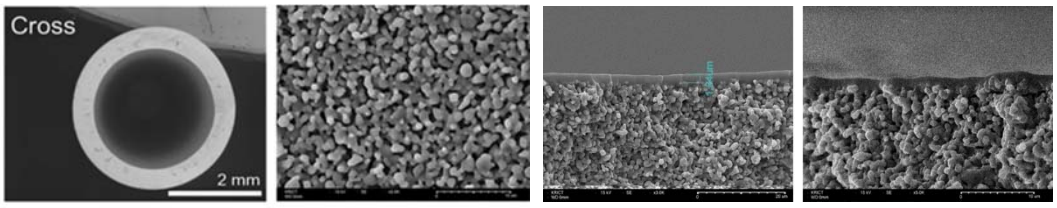

(a) (b)

Figure 1. SEM pictures of (a) alumina hollow fiber support (b) PVA-alumina composite membrane.

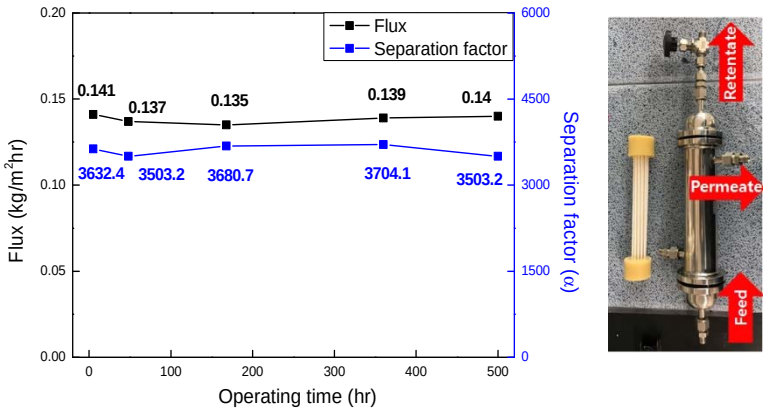

Figure 2. Pervaporation performance of the PVA/alumina composite membrane.

4. Conclusions

The stability and pervaporation performance of PVA-based composite membranes in a highly reactive ECH-containing ternary mixture feed system showed remarkable pervaporation dehydration efficiency. To reduce energy cost, make possible a difficult separation, and improve the degree of separation, pervaporation-based hybrid process are very promising especially in cases where high product purities are required.

References

[1] P.D.Chapman, T.Oliveira, A.G.Livingston, K.Li, *J. Membrane. Sci.,* **318** (2008) 5.
[2] J.G.Wiljmans and R.W.Baker, *J. Membrane. Sci*., **107** (1995) 1.
[3] C.Chang and W.Lee, *J. Appl. Poly. Sci.,* **116** (2010) 2065.

ECCE12
The 12th EUROPEAN CONGRESS OF CHEMICAL ENGINEERING
Florence 15-19 September 2019

Addressing limitations to implement ternary phase diagrams into the systematic prediction of membrane morphology by phase inversion

Marta Romay[1*], Nazely Diban[1], Ane Urtiaga[1]

1 Chemical and Biomolecular Engineering department, University of Cantabria, Santander, Spain

**Corresponding author: romaym@unican.es*

Highlights

- Assessment of morphology membrane prediction based on Flory-Huggins model.
- Thermodynamic evaluation of the ternary system PVDF/solvent/water.
- Addressing the systematic determination of solvent-non-solvent interaction parameters.

1. Introduction

Phase inversion by Non-solvent Induced Phase Separation (NIPS) is a widely implemented technique for the synthesis of polymeric membranes [1]. This mechanism is thermodynamically explained through the Flory-Huggins theory based on the Gibbs free energy and interaction parameters of the components: polymer, solvent and non-solvent. Moreover, solvent/non-solvent miscibility importantly affects the rate of their exchange that will ultimately define the membrane morphology. Overall, the membranes morphology prepared by NIPS strongly depends on both thermodynamics and kinetics of the ternary system.

Traditionally, membranes by NIPS have been prepared by arbitrarily selecting the set of components polymer/solvent/non-solvent, which implies an experimental trial-and-error procedure. Currently, several works have attempted to find ways to systematize the selection of the components based on thermodynamic and/or kinetic interactions and tried to correlate these data with morphological parameters of different NIPS-prepared membranes [2-4]

Binodal curves of ternary systems, which represent the polymer/solvent/non-solvent composition ratios, where a polymeric solution precipitates, are usually obtained experimentally and fitted to Flory-Huggins model. However, interaction parameters are usually estimated through different empirical equations or by estimation procedures which depend importantly on the experimental points of the binodal curves. In order to systematize this as a design tool for the synthesis of membranes by NIPS techniques, broadly valid empirical equations for the estimation of interaction parameters should be defined. Moreover, the revision of the best methodology for the experimental determination of the binodal cloud points should be done.

2. Methods

In the present work, the production of PVDF membranes by NIPS is selected as a case study to explore the potential of the ternary phase diagrams in the prediction of certain membrane morphology.

The Flory- Huggins model for a ternary mixing is already developed in the literature [2,3]. The Flory-Huggins interaction parameters for the studied system were obtained before a comprehensive review of the literature. Different strategies were developed to determine the interaction parameters among polymer/solvent/non-solvent simultaneously [3]. However, it was founded a huge amount of different empirical equations that describes solvent/non-solvent interaction parameter. The search of the empirical equation that could be valid over a broad range of systems and conditions was done from the comparison of different equations proposed in the literature using Aspen Custom Modeler as solving software.

3. Results and discussion

The comparison of the experimental binodal curves reported in the literature for different systems PVDF/solvent/water, where the solvent could be dimethyleacetamide (DMAc), N-methylpirrolidone (NMP) and dimethylformamide (DMF), has been done. Broad differences could be found among different authors for the same ternary system. Thus, see for instance in Figure 1 the experimental points of the binodal curves for the system PVDF/NMP/water, reported by different authors. This experimental uncertainty hampered model fitting. Therefore, a detailed study of the experimental methodologies of the literature has been done in order to propose a reliable procedure to implement in following works.

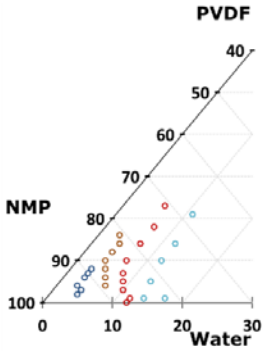

Figure 1. Comparison of experimental points of the binodal curves for the ternary system PVDF/NMP/Water attained from the literature [4-7]

4. Conclusions

The uncertainty in the experimental data of binodal curves due to the experimental difficulty limits the ability to determine broadly valid empirical equations for interaction parameters. Therefore, an experimental protocol to determine the binodal curves has to be proposed out of a thorough literature revision.

Financial support of project CTM2016-75509-R (MINECO-FEDER) and FPI grant BES-2017-081112 are acknowledged.

References

[1] S. Mohsenpour, F. Esmaeilzadeh, J. Mol. Liq. 224 (2016) 776–785
[2] Y. Wei, Z. Xu, Desalination 192 (2006) 91-104
[3] L. Xu, F. Qiu, Polymer 55 (2014) 6795-6802
[4] A. Bottino, G. Camera-Roda, J. Memb. Sci. 57 (1991) 1-20
[5] H. Fashandi, A. Yegane, Fibers Polym. 6(2) (2015) 326-344
[6] M. Enayatzadeh, T. Mohammadi, J. App. Polym. Sci. 135 (27) (2018)
[7] F. Liu, N. Awanis, J. Memb. Sci. 375 (2011) 1-27

ECCE12
The 12th EUROPEAN CONGRESS OF CHEMICAL ENGINEERING
Florence 15-19 September 2019

Towards the recovery of refrigerant gases from end-of-life equipment: study of the separation performance of polymer membranes

Fernando Pardo*, Gabriel Zarca, Ana Urtiaga

Department of Chemical and Biomolecular Engineering, Universidad de Cantabria,

Av. de Los Castros s/n. Santander 39005, Spain

**Corresponding author: pardof@unican.es*

Highlights

- Two fluorinated gases have been considered for this study (R-32 and R-134a).
- Gas permeability and gas pair selectivity were compared for material discrimination.
- Rubbery polymers have shown promising properties for the recovery of fluorinated gases.
- Fluorine in the hydrocarbon chains has a remarkable effect on membrane performance.

1. Introduction

Hydrofluorocarbon gases (HFCs) are the third generation of fluorine-based refrigerants. The absence of chlorine atoms in their molecular structures makes HFCs to be considered as ozone-friendly gases. Despite this fact, HFCs are powerful greenhouse gases and the new regulations (EU No 517/2014 and Kigali Amendment to the Montreal Protocol in 2016) are looking for an 85% reduction in their production and consumption by 2047. In this context, research efforts should be dedicated to the development of new separation technologies to facilitate the reuse and recycling of these compounds. Therefore, the application of membrane technology, a cost-effective alternative to cryogenic distillation and pressure swing adsorption, is envisaged to play an important role in the reduction of HFCs emissions.

Membrane technology has reached a state of maturity in the recovery of several gases, such as H_2 from ammonia purge gas or from refinery flue gases, or the recovery of CO_2 from natural gas mixtures, etc [2]. Nevertheless, there is a lack of research data in the separation of fluorinated-based refrigerant gases. In this sense, this work aims at providing novel information about the permeation properties of some of the most used refrigerant gases, R32 and R134a.

Therefore, this work shows the permeation properties of the aforementioned fluorinated-based gases in different membranes (glassy and rubbery polymers) for the first time.

2. Methods

The polymeric films were synthetized by the solvent casting method. The resulting films had an average thickness below 100 µm. Single and mixed gas permeation tests were performed with H_2,

N_2, R32 and R134a at several temperatures (303 - 353 K) and feed pressures (1 - 5 bar). The experimental setup, based on continuous permeation of gases, is described in previous works [3].

3. Results and discussion

This work reports on the effect of pressure and temperature on the refrigerant permeation properties through rubbery polymeric membranes (different PEBAX grades and PVDF-HFP). The experimental results show a linear increase of the permeability of all gases with pressure, a common effect of organic vapors and condensable gases. The activation energy of permeation of the different gases on the polymers which offered the best separation performances was also calculated. This work also presents the study of the effect of the fluorine substitution in the molecular structure by comparing the permeability of the fluorinated gases with their respective hydrocarbon analogues (CH_4, C_2H_6 and C_3H_6).

4. Conclusions

In light of these results, polymer membranes are presented as potential candidates with exceptional properties for the recovery of fluorinated gases.

Acknowledgements

This research is supported by Project KET4F-Gas – SOE2/P1/P0823, which is co-financed by the European Regional Development Fund within the framework of Interreg Sudoe programme. Also, financial support from the Spanish Ministry of Economy and Competitiveness (CTM2016-75509-R, MINECO-AEI/FEDER) is gratefully acknowledged.

References

[1] Regulation (EU) No 517/2014 of the European Parliament and of the Council of 16 April 2014 on fluorinated greenhouse gases and repealing Regulation (EC) No 842/2006. Official Journal of the European Union, May 20th, 2014, 150, 195-230.

[2] P. Bernardo, E. Drioli, G. Golemme, Industrial Engineering Chemistry Research, 48 (2009) 755-761.

[3] G. Zarca, I. Ortiz, A. Urtiaga, Journal of Membrane Science, 438 (2013) 38-45.

ECCE12
The 12th EUROPEAN CONGRESS OF CHEMICAL ENGINEERING
Florence 15-19 September 2019

Hydrophilic and hollow nanocubes functionalized thin film nanocomposite membrane with enhanced nanofiltration performance

Zhipeng Liao, Jiansheng Li

Affiliation and address: Nanjing University of Science and Technology, Nanjing 210094, P.R .China

**Corresponding author: lijsh@njust.edu.cn*

Highlights

- Hydrophilic hollow nanocubes (HHNs) nanofillers were obtained by etching ZIF-8 with tannic acid.
- HHNs were incorporated into the polyamide layer to form thin film nanocomposite (TFN) membranes.
- The prepared TFN membranes exhibit improved permeability and antifouling performance.
- The enhanced performance stems from the structural and compositional characteristics of the incorporated nanofillers

1. Introduction

Nanofiltration has prevailed in water desalination, and is mainly applied to the removal of divalent salts. However, the application of nanofiltration membrane is limited by the intrinsic defects, such as low permeability and poor antifouling property. Incorporation of nanoparticles into the selective layer of composite membrane is an ideal strategy to resolve the dilemma. The structure and composition of nanoparticles are detrimental to the performance of the fabricated composite membrane. Herein, hydrophilic and hollow nanocubes (HHNs) were prepared and incorporated into the selective layer of the composite membrane. The fabricated composite membrane presents excellent permeability, selectivity as well as antifouling property.

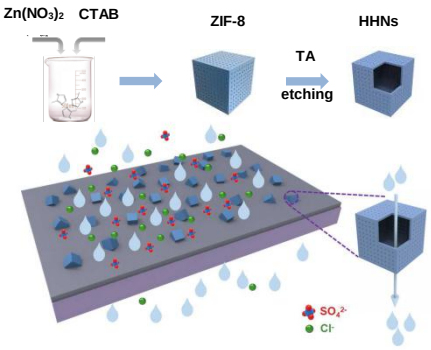

Figure. 1 Schematic diagram of the TFN-4H membrane.

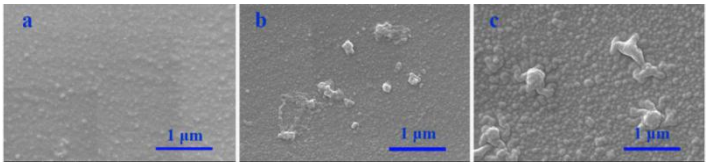

Figure. 2 SEM images of various membranes: TFC (a), TFN-4H (b) and TFN-4S (c) .

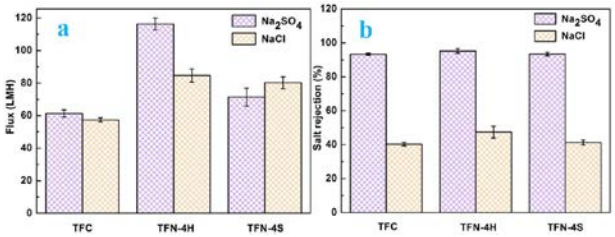

Figure. 3 Performances of various membranes: water flux (a) and salt rejection (b) tested with 1 g/L Na_2SO_4 and NaCl solution at ambient temperature and 6 bar.

2. Methods

Hydrophilic and hollow nanocubes were prepared by etching hydrophobic zeolitic-imidazolate-framework-8 (ZIF-8) using tannic acid. 0.04 wt% HHNs was added to the organic phase and introduced into the selective layer of the nanofitration membrane via interfacial polymerization, the prepared nanocomposite membrane was denoted as TFN-4H (Figure. 1). To highlight the influence of the structure and composition of nanofillers to the performance of composite membrane, equal dose of solid and hydrophobic ZIF-8 was incorporated into the selective layer, the final membrane was denoted as TFN-4S. The filtration performances of the fabricated composite membranes were investigated by Na_2SO_4 and NaCl solution. Meanwhile, the antifouling properties of the composite membranes were studied using humic acid and bovine albumin as the simulated pollutants.

3. Results and discussion

As shown in Figure 2, more and larger nodular structures present on the surface of the composite membranes after the introduction of nanofillers into the selective layer. Besides, there are some incorporate nanofillers exist on the membrane surface. The observed nanofillers are embedded in the selective layer of the composite membranes. It can be concluded from Figure 3, the permeabilities and selectivities of composite membranes modified by nanofillers are better than that of the control membrane. Moreover, the performance of the TFN-4H membrane is much better than that of the TFN-4S membrane. With the introduction of HHNs, the flux and Na_2SO_4 rejection of the TFN-4H membrane increased up to 116.4 L/(m^2·h) (LMH) and 95.24 %, respectively. However, the flux and Na_2SO_4 rejection of the TFN-4S membrane only increased to 71.6 LMH and 93.4 %, respectively. In addition, the TFN-4H membrane presents excellent antifouling property. Oppositely, the antifouling property of TFN-4S membrane is undesirable and even poorer than the control membrane.

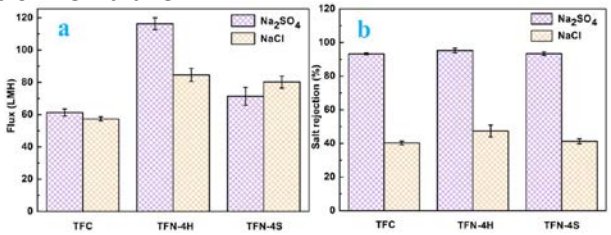

Figure. 4 Time-dependent relative water flux of various membranes tested with 1 g/L Na2SO4 and 1 g/L Na2SO4 + 1 g/L HA solution (a) and 1 g/L Na2SO4 and 1 g/L BSA solution (b) at ambient temperature and 6 bar.

4. Conclusions

The incorporation of HHNs significantly enhanced the permeability and selectivity of the nanocomposite membrane. Compared with the solid and hydrophobic ZIF-8, the prepared hollow and hydrophilic HHNs are more favorable for the improvement of the membrane performance. More importantly, the introduction of HHNs elevated the antifouling property of the composite membrane.

References

[1] J. Zhu, L. Qin, A. A. Uliana, et al, ACS Appl Mater Interfaces, 9 (2017) 1975-1986.
[2] R. R. Choudhury, J. M. Gohil, S. Mohanty et al, J. Mater. Chem. A, 6 (2018) 313-333.
[3] Z. Liao, X. Fang, J. Li, et al, Sep. Purif. Technol, 207 (2018) 222-230.

ECCE12
The 12th EUROPEAN CONGRESS OF CHEMICAL ENGINEERING
Florence 15-19 September 2019

Fabrication and Characteristics of PSS / G-Ch Hybrid Membrane for DMFC

Tomoki Takahashi[1]*, Naotake Horimatsu[2], Katsuto Otake[2]

1 College of Industrial Technology, Nihon University, 1-2-1 Izumicho, Narashino, Chiba 275-8575 Japan;

2 Faculty of Engineering, Tokyo University of Science, 1-3 Kagurazaka, Shinjyuku, Tokyo 162-8601, Japan

**Corresponding author: takahashi.tomoki@nihon-u.ac.jp*

Highlights

- PSS / G-Ch hybrid membranes were prepared.
- The methanol permeability of membranes suppressed by GA cross-linked.
- Fabricated membrane have about equal methanol permeability with Nafion 117.

1. Introduction

The direct methanol fuel cell (DMFC) have attracted considerable attention in fuel cell technology owing to their stable operation, high energy efficiency, portable power source and low environmental burden for mobile electronic devices [1-3]. Protons transfers from anode to cathode are important components in a polyelectrolyte membrane (PEM) with a DMFC system. In addition, methanol crossover (MCO) is another important component. MCO is phenomenon that methanol is transported to the cathode, which decreases the fuel cell efficiency [4, 5]. Thus, both high proton conductivity and low methanol permeability are required for PEM of DMFC. However, these two factors are trade-off relationship. Because, though existence of water is indispensable for protons transfers so that water has methanol and high affinity. In our study, a glycol chitosan (G-Ch) and a sodium salt of polystyrene sulfonate (PSS) were selected as materials of membrane [6]. G-Ch, which is water-soluble derivative of chitosan, can prepare uniform aqueous solution without an acetic acid. This characteristic is used in a protonation of amino groups after mixture of anionic polymer. In addition, we expected to PSS having many sulfonate groups gives PEM the high proton conductivity. We investigated about preparation methods and characteristics in PSS/G-Ch hybrid membrane cross-linked with glutaraldehyde (GA). In addition, we estimated superiority of the hybrid membrane by comparison with Nafion 117.

2. Methods

The PSS powder and G-Ch powder of predetermined quantity were added to ion exchanged water, and it was stirred and was dissolved at 298 K for 24 hours. This PSS and G-Ch mixture solution was cast on the glass petri dish and placed at 298 K for three days. Subsequently, dry membrane was immersed by acetic acid/methanol aqueous solution (volumetric ratio, 5:80:15) for 24 hours to form polyionic complexes between the sulfonate group of PSS and the amino group of G-Ch , as shown in Scheme 1 (a). Furthermore, it was immersed by GA/methanol solution of predetermined concentrations for 24 hours to cross-linked between amino groups of G-Ch, as shown in Scheme 1 (b). Finally, the free-standing membrane was obtained by desorption from glass petri dish with immersing in ion-exchanged water for 24 hours. The obtained membrane was saved in ion-exchanged water. In this work, notation of a membrane sample is described as follows; PSS/G-Ch/GA. The number of notation stands for the gravimetric concentration of PSS in cast solution, the

gravimetric concentration of G-Ch in cast solution, and the volumetric concentration of GA in methanol solution, respectively.

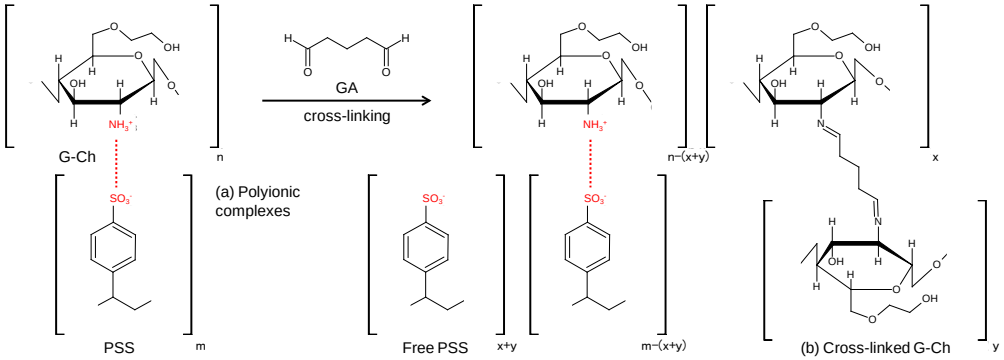

Figure 1. The scheme of the formation of polyionic complexes between PSS and G-Ch and the cross-linked G-Ch.

3. Results and discussion

In this study, we prepared PSS/G-Ch cross-linked by GA hybrid membrane for DMFC, and measured structure of hybrid membrane, water content, methanol permeability, and proton conductivity. From the values of proton conductivity and methanol permeability, we calculated the selectivity parameter. Higher selectivity parameter means that a performance of a hybrid membrane is superior. Table 1 shows the properties of PSS/G-Ch hybrid membranes and Nafion 117 membrane [7]. For the membrane cross-linked by GA, the swelling of PSS/G-Ch hybrid membrane controlled, the methanol permeability reduced, and the proton conductivity increased. The experimental results revealed that the 4/2/2 hybrid membrane exhibited high performance compared to the other composition membranes.

Table 1. The properties of PSS/G-Ch hybrid membranes and Nafion 117 membrane.

membrane (PSS/G-Ch/GA)	thickness [μm]	water content [%]	methanol permeability [$cm^2\ s^{-1}$]	proton conductivity [$S\ cm^{-1}$]	selectivity [$S{\cdot}s{\cdot}cm^{-3}$]
4/2/1	165	89.3	5.4×10^{-6}	0.0061	1136
4/2/1.5	102	71.8	2.4×10^{-6}	0.0120	5003
4/2/2	97	67.3	2.1×10^{-6}	0.0130	6003
Nafion 117	183	23	2.0×10^{-6}	0.1000	-

4. Conclusions

It reveals that the chitosan based hybrid membrane of polyionic complexes have higher proton conductivity value than that of the other polyionic complexes membranes, but lower than that of Nafion membrane, and have just about equal methanol permeability as compared with Nafion. From now on, we think of using the other cross-linking agent to decrease the water content and methanol permeability, more and more PSS to increase the proton conductivity.

References

[1] C. Zhao, H. Lin, H. Na, Int. J. Hydrogen Energy 35 (2010) 2176–2182.
[2] H. Li et al., J. Power Sources 195 (2010) 6443–6449.
[3] M. Higa, M. Sugita, S. Maesawa, N. Endo, Electrochem. Acta 55 (2010) 1445–1449.
[4] C.C. Yang, S.J. Chiu, K.T. Lee, W.C. Chien, C.T. Lin, C.A. Huang, J. Power Sources 184 (2008) 44–51.
[5] M. Helen, B. Viswanathan, S.S. Murthy, J. Power Sources 163 (2006) 433–439.
[6] N. Horimatsu, et al., Desalination and Water Treatment 51 (2013) 5254-5259.
[7] W.C. Choi, J.D. Kim, S.I.Woo, J. Power Sources 96 (2001) 411.

ECCE12
The 12th EUROPEAN CONGRESS OF CHEMICAL ENGINEERING
Florence 15-19 September 2019

Investigating the effect of TiO_2 nanoparticles on the performance of Nanocomposite Membranes from PAN for Produced Water Treatment

Hamid Reza Shahriari[1], Seyed Saeid Hosseini *[1,2]

1 Membrane Science and Technology Research Group, Department of Chemical Engineering, Tarbiat Modares University, Tehran, Iran; 2 Nanotechnology and Water Sustainability Research Unit, College of Science, Engineering and Technology, University of South Africa, Johannesburg, South Africa

**Corresponding author: Saeid.Hosseini@modares.ac.ir*

Highlights

- PAN nanofiltration membranes developed for effective produced water treatment.
- The effect of inclusion of TiO_2 nanoparticles was examined by RSM.
- Membranes with improved separation efficiency were obtained for treating oily wastewater.

1. Introduction

Many governments have regulated discharge limit concentrations in order to at least alleviate the destructive impacts of contaminants on the environment. Several stand-alone or integrated systems are currently in operation for produced water treatment. Among these common systems, membrane filtration offers indisputable advantages while maintaining the high process efficiency. These have attracted researchers to utilize different kinds of membranes for the produced water treatment.

2. Methods

Dope solutions containing prescribed amounts of polymer (22 wt.%), organic and inorganic additives were prepared by moderately dissolving PAN, TiO2 and citric acid in DMF. Dope solutions were cast onto the nonwoven polyester substrates using a knife casting at 70˚C. After a distinct time spans of solvent evaporation, nascent films were submerged in coagulation bath containing pure water with different temperatures. Membranes were characterized by various methods.

3. Results and discussion

Figure 1 shows the cross-section morphology of NF membranes with TiO2 variation. All membranes were asymmetric having both macrovoid and sponge-like structures. It was found that increasing the TiO2 concentration in the dope solution, the porosity of NF membranes was increased from 45.74% to 63.28%. Moreover, both mean macrovoid size and area fraction of macrovoids increased from 29.06 to 51.60 µm and from 0.28 to 0.34 respectively. Also, an increment in TiO2 concentration led to a decrease in contact angle of NF membranes. It is worth mentioning that the reduction of membrane contact angles is not only attributed to the presence of TiO2, but also the surface roughness of the membrane plays an important role in determining the terminal contact angle values. It was also clear that owning to the agglomeration of nanoparticles on the surface of

membrane, number and height of the surface curvatures was increased as the TiO2 content of the dope solution was increased. As stated by Cassie-Baxter theory, the surface hydrophilicity of a pristine hydrophilic surface intensifies when it gets rougher. Therefore, the final contact angle values of NF membranes are determined by the superimposition of surface roughness and modification effects. The emerged changes in the membrane structure might be related to the hydrophilicity enhancement of membrane surface due to the presence of TiO2 nanoparticles which led to the instantaneous demixing process.

Based on the results, the PWF was enhanced from 108.8 to 131.5 (lit.m-2.h-1) through TiO2 addition to dope solution up to 1wt.%. This might be demonstrated by the reduction in the surface contact angles of NF membranes. Despite the positive effect of TiO2 addition on membrane flux, the intensity of PWF variations diminishes at high TiO2 concentrations. The observation could be explained due to the fact that nanoparticles tend to agglomerate on the surface of the membrane, considering their hydrophilic nature. High concentrations of TiO2 in the dope solution, reduces the distance between nanoparticles due to the presence of different forces (i.e.: hydration, bridge, Van der Waals) which provides the chance for them to agglomerate and reduce their surface energy. Also, increasing the TiO2 concentration resulted in an increment in CaSO4 rejection and elevated the rejection from 73.5% to 83%. Considerable changes in the membrane salt rejection could be conceived by the aggregation of nanoparticles on the surface of the membrane. Higher contents of TiO2, increase the viscosity of the polymeric film which delays the demixing process and provides the opportunity for the nanoparticles to form aggregates on the membrane surface to plug the surface pores and reduce the effective membrane mean pore size.

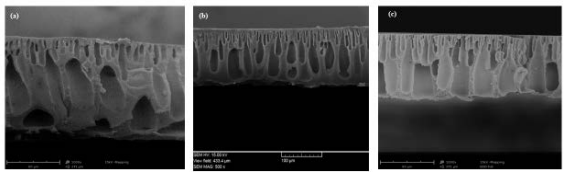

Figure 1. Cross-Sectional images of PAN NF membranes containing (a) (TiO2: 0 wt.%) (b) (TiO2: 0.5 wt.%) (c) (TiO2: 1 wt.%) (Conditions: PAN: 22 wt.%, citric acid: 0.75 wt.%, solvent evaporation time: 2 min)

4. Conclusions

The effect of several fabrication and design parameters including the concentration of TiO2, on the PWF of PAN NF membranes was assessed. RSM technique was employed to explore the effect of the selected variables on the performance and characteristics of PAN NF membranes. Zeta potential and surface hydrophilicity of NF membrane were also intensified. As the TiO2 nanoparticles were added to the dope solution, the area fraction and the membrane porosity were increased. Considering the effect of TiO2 on the membrane performance, both the PWF and the salt rejection of membranes were promoted via the enhancement of membranes hydrophilicity and nanoparticles agglomeration on the surface of membranes.

References

[1] M. Höök, R. Hirsch, K. Aleklett, Giant oil field decline rates and their influence on world oil production, Energy Policy, 37 (2009) 2262-2272.

[2] R.L. Hirsch, The inevitable peaking of world oil production, Bulletin of the Atlantic Council of the United States, 16 (2005) 1-10.

[3] C. Clark, J. Veil, Produced water volumes and management practices in the United States, in, Argonne National Laboratory (ANL), 2009.

ECCE12
The 12th EUROPEAN CONGRESS OF CHEMICAL ENGINEERING
Florence 15-19 September 2019

Effect of the diamine monomer on the structural and desalination properties of thin film composite membranes.

Isam Aljundi[1]

1 Chemical Engineering Department, King Fahd University of Petroleum and Minerals, Dhahran, Saudi Arabia.

*Corresponding author: aljundi@kfupm.edu.sa

Highlights

- Thin Film Composite membranes were prepared from different diamine monomers.
- Polypiperazine membrane showed the highest salt rejection.
- Strong correlation was found between the operating temperature and the salt rejection.
- Increasing the operating pressure or the feed velocity have positive impact on the permeate flux.

1. Introduction

Interfacial polymerization (IP) is the most important method for commercial fabrication of thin-film composite (TFC) RO and NF membranes. The first interfacially polymerized TFC membranes were developed by Cadotte et al. [1] and represented a breakthrough in membrane performance for RO applications. Since then, several methods have been adopted to improve the performance of the polyamide selective layer in terms of enhancement of permeate flux, salt rejection, fouling and chlorine resistance. Among those methods is to change the diamine monomer used in the IP aqueous phase. However, a systematic study on the effect of the side chain of on the aromatic or cycloaliphatic diamine monomers is lacking in the literature. In this project, the effect of the diamine side-chain was investigated in terms of the structure and desalination properties (salt rejection and permeate flux) of the membrane.

2. Methods

The selective polyamide layer of the membrane was prepared by reacting the diamine (2 wt% in distilled water) with TMC in hexane (0.2 g TMC in 100 mL hexane) on top of a previously prepared polysulfone layer. The membranes were dried in a muffle furnace at 75 °C for 5 min for further crosslinking.

The permeate flux and rejection were measured using a cross-flow setup with an effective membrane area of 14 cm2 at different operating conditions of temperatures and pressures. Four diamine were used: Piperazine (PIP), m-xylenediamine (XLN), 1,4-Bis(3-aminoprpyl)piperazine (DAPP), 1-(2-Aminoethyl)piperazine (EAP).

In addition, the effect of operating conditions (T, P, feed velocity, and salt concentration) on the performance of the membranes were also investigated.

3. Results and discussion

The surface morphology of the prepared membranes is shown in Figure 1. It reveals rough surfaces with typical ridge and valley structures of polyamide membranes.

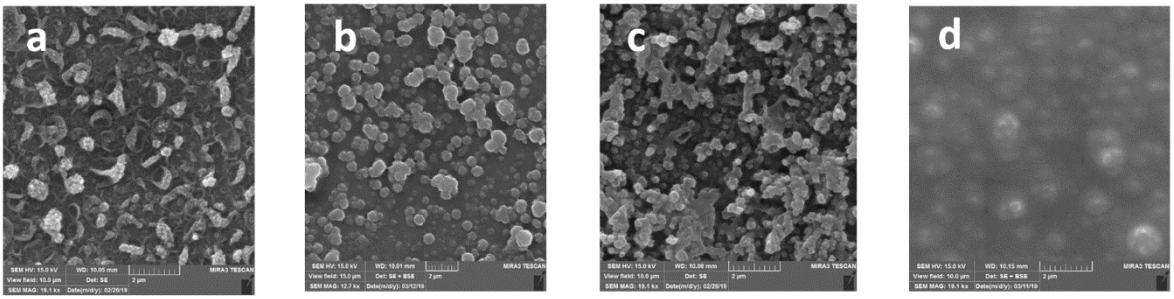

Figure 1. SEM images of the (a) PIP, (b) EAP, (c) XLN, (d) DAPP membranes.

The performance of each membrane was evaluated using different salts. PIP membrane showed the best performance among all membranes where the sulfate rejection was higher than 97%. However, the rejection of sodium chloride was about 73% which is considered high for a nano-filtration membrane. The overall performance was poor for the XLN membrane, however it showed the lowest rejection of NaCl which is advantageous in some applications such as the treatment of fracturing fluids.

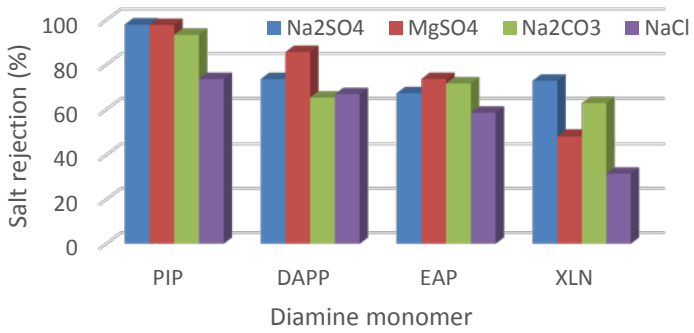

Figure 2. Salt rejection of membranes prepared from different diamine monomers.

4. Conclusions

Four different diamines were used to prepare nanofiltration membranes. The best performing membrane was the one with PIP monomer which showed high rejection along with excellent permeate flux. The hydrodynamics study of the desalination process showed a strong correlation with Reynold's number. In addition, results showed that increasing the operating pressure and Temperatures has positive impact on the permeate flux. However, the salt rejection deteriorated as the temperature increased. Changing the salt concentration in the feed water did not show significant effect on the membrane performance.

References

[1] J. Cadotte, R. Forester, M. Kim, R. Petersen, T. Stocker, Desalination 70 (1988) 77–88.

ECCE12
The 12th EUROPEAN CONGRESS OF CHEMICAL ENGINEERING
Florence 15-19 September 2019

Concentration, pH, counter ion and charge effect of metal ions in the treatment of heavy metals using nanofiltration.

Luis Pino[1], Catalina Vargas[1], Florencia Saravia[2], Alex Schwarz[1], Harold Horn[2] and Rodrigo Bórquez[1*]

1 Facultad de Ingeniería, departamento de Ingeniería Química, Universidad de Concepción; 2 Water Chemistry, Engler-Bunte-Institut, Karlsruher Institut für Technologie; 3 Facultad de Ingeniería, departamento de Ingeniería Civil

**Corresponding author: rborquez@udec.cl*

Highlights

- Zeta potential measurements reveal important information on electrostatic rejection.
- Increase the cation valence shows an inverse charge of the membrane.
- The co-ion showed an important change in the membrane IEP.

The presence of heavy metal ions in the environment has received important attention due to increased discharge, toxicity in the environment, and other adverse effects which heavy metal ions have on receiving waters [1]. In Chile, copper mining is one of the main industrial activities and has become one of the major discharging heavy metal wastewater. One of this kind of wastewater is associated with the generation of acid mine drainage (AMD). AMD is formed by oxidation of sulfide minerals such as pyrite when it is placed in direct and simultaneous contact with water and oxygen [2]. The main characteristics of this dangerous pollutant are the high degree of acidity (pH of 2-4), the elevated concentrations of sulfate (1-20 g/L), and the presence of metals such as iron, copper, calcium and aluminium, among others [3].

In the literature are reported many methods for the treatment of acid mine drainages such as neutralisation, ion exchange, bioadsorption, biological treatments and solvent extraction [2, 4, 5]. However, all these technologies have disadvantages in their application; most of them have many serious economic, technical, environmental, and efficient limitations. An alternative such as membrane-based technologies such as pressure-driven processes has high performances in the removal of ions and contaminants. Nanofiltration (NF) is an attractive membrane separation technology more used to wastewater treatment and industrial applications. NF offers the advantage of operating at lower pressure and obtaining high permeate flux, leading to lower capital investment and decreasing the cost of operation and maintenance.

The application of NF membranes to treat AMD has been previously studied [3, 6-10]. The performance depends on the constituent membrane characteristics. Typically, NF are thin-film composites (TFC) made from various polymers such as polyamides, polysulfone, sulfonated polysulfone, polyamide and poly(piperazine amide) [11]. The separation mechanism of NF membranes includes the diffusion and convection transport in addition to electromigration related to the charge of the functional groups of the surface of the membrane. The charge acquired on the

surface membrane can be by mechanisms as adsorption of ions, adsorption of polyelectrolytes, ionic surfactants and charged macromolecules [Artug]. Interfacial attraction and adhesion forces are expressed as the electrostatic, acid-base, van der Waals, and hydrophobic forces between the surface of the membrane and feed stream ionic contaminants. Therefore, electrokinetic surface properties are of vital importance to understand the phenomena of electrostatic rejection of NF membranes.

At present, zeta potential can be measured by electrophoresis or measuring streaming potential methods. Electrophoresis method can be used to describe the migration and separation of charged particles (ions) under the influence of the electric field. In contrast, the streaming potential is the potential difference at zero current produced by the convective flow of an electrolyte solution through a stationary capillary or porous plug. Streaming potential measurements have been widely used to characterise charged materials such as membranes [12-17], root surface [18], textile [19], fibres [20] and polymers [21]. Several studies were dedicated to evaluating the performance of a commercial NF with electrolyte solutions containing divalent ($MgSO_4$, $CaSO_4$, $MgCl_2$, and $CaCl_2$) and monovalent (NaCl, KCl, LiCl, and K_2SO_4) ions relating to their behaviour to the surface charge by zeta potential measurement. However, the behaviour of electrolytic solutions of metals such as copper, calcium and aluminium has not been fully studied.

In the present work, the retention properties of a negatively charged commercial NF membrane are investigated with three electrolytes (calcium, copper and aluminium) having co-ion of sulphate and chloride at acid and normal pH condition. The concentration or ionic strength of sulphate electrolyte solution on membrane zeta potential and the effect of co-ion (chloride) were investigated using a combination of streaming potential measurements and theoretical modelling.

ECCE12
The 12th EUROPEAN CONGRESS OF CHEMICAL ENGINEERING
Florence 15-19 September 2019

Modelling and optimization of a reactive distillation column to obtain high pure cyclohexanone in caprolactam production process.

David Lorenzo[1*], Aurora Santos[1], Carlos Pérez-Galván[2], Cristian Triana[2], Arturo Romero[1], I. David L. Bogle[2]

1. Dpto. Ing. Química y de Materiales, Universidad Complutense de Madrid, Avda. Complutense S/N, 28040 Madrid, Spain; 2. Dpt. Chemical Engineering. University College London, Torrington Place. London WC1E 7JE

**Corresponding author: dlorenzo@ucm.es*

Highlights

- 2-ciclohexen-1-one is easily removed using a reactive distillation.
- NaOH is used as catalyst in a reactive distillation to produce high pure cyclohexanone.
- The reactive distillation model is experimentally validated.
- A reactive distillation model is used to optimize the production of cyclohexanone.

1. Introduction

Cyclohexanone (CX-ONE) is the main compound used in the caprolactam production which is the monomer of nylon 6. The most common cyclohexanone production process starts oxidizing cyclohexane to produce a mixture of cyclohexanol, cyclohexanone and other organic impurities [1-3]. Cyclohexanone purification process involves three distillation columns and a reactor where the cyclohexanol is dehydrogenated to cyclohexanone. However, some of the organic impurities (formed either during cyclohexane oxidation or cyclohexanol dehydrogenation) cannot be removed by a standard distillation because their boiling point are close to cyclohexanone. One of those is 2-cyclohexen-1-one (CX-ENONE), it has drastic effects in the nylon fiber because it can produce a rubber during the polymerization. To reduce the amount of this impurity in the pure cyclohexanone a reactive distillation (RD) step has been proposed using NaOH. Sodium hydroxide promotes the condensation of the impurity and cyclohexanone yielding a dione compound [4]. Dione boiling point is higher than cyclohexanone and can be easily removed within the purification process. Nevertheless, the presence of alkali in the reaction medium also promotes the self-condensation of cyclohexanone, which is a non-desirable loss of cyclohexanone. In this work the RD process is modelled and optimised in order to select the operating conditions that guarantee the removal CX-ENONE with minimum losses of CX-ONE.

2. Methods

The RD column is modelled considering both the physical and chemical processes taking place in the column trays, condenser and reboiler. The RD model developed was validated using experimental data obtained at the laboratory-scale distillation packed column. The selfconstructed model was used to simulate and optimized the RD column operating at industrial-scale which

ensure the minimal unit total cost (UTC), defined as the production cost of a unit of mass of pure cyclohexanone. A mixed non-linear programming problem (MINLP) was formulated and solved using the optimization algorithm which is available in gPROMS[5].

3. Results and discussion

To study the operating condition range and the UTC, different case studies were carried out. Those cases depend on the CX-ENONE amount which is presented in the pure CX-ONE stream within the range 5-15 mg/kg of impurity. The results are summarized in Table 1. They show the optimal operation conditions to obtain a high purity cyclohexanone product with the minimum unitary total cost.

Table 1.

Parameter	Value		
Case	1	2	3
$C_{CX-ENONE,D}$, mg/kg	15	10	5
Pressure, bar	0.12	0.10	0.09
$C_{CX-ONE,D}$, %w:w	99.56	99.83	99.85
Reflux Rate	2.52	2.42	2.36
UTC, \$/kg$_{CX-ONE}$	0.76	0.77	0.75
$C_{NaOH}\ mmol/kg$	33.1	36.3	40.0
Nstrip	21	20	23
Nrect	19	19	20
Ntrays	41	40	44
Number of reaction trays	37	37	38
d_{col}, m	2.31	2.41	2.36

4. Conclusions

Following validation, the reactive distillation model was used to optimize conditions of operation. The objective function used was the minimization of the unitary total cost to produce a kg of pure cyclohexanone. The model was implemented as a MINLP problem which was solved using the optimiser within gPROMS. The optimal values of NaOH concentration, number of reaction stages, number of trays, pressure, and reflux rate were obtained. Using this information, other design and operation variables were obtained. The model is a powerful tool to study the design of the purification unit to produce high pure cyclohexanone in the caprolactam production process.

References [Calibri 10]

1. Jodra, L.G., et al., *Impurity content and quality definition of commercial epsilon-caprolactam.* Ind. Eng. Chem. Prod. Res. Dev., 1981. **20**(3): p. 562-566.
2. Burlone, D.A., et al., *A Method o Minimizing Aldehyde-Based Impurities in a Process Stream*. 2006.
3. Meier, H.P., E.J. Van, and E. Terweduwe, *Purification of cyclohexanone*. 1993, Bayer Antwerpen N.V., Belg. . p. 5 pp.
4. Wyatt, L., A.H. Benneker, and A.P.H. Schouteten, *Process for reducing the aldehyde concentration in a mixture comprising cyclohexanone and one or more aldehydes*. 2004, Koninklijke DSM N.V., Neth. . p. 8 pp.
5. Tanvir, M.S. and I.M. Mujtaba, *Optimisation of design and operation of MSF desalination process using MINLP technique in gPROMS.* Desalination, 2008. **222**(1): p. 419-430.

ECCE12
The 12th EUROPEAN CONGRESS OF CHEMICAL ENGINEERING
Florence 15-19 September 2019

Solvent Selection Methods and Tool.

Patrick M. Piccione[1,*], Julia Baumeister[1], Thomas Salvesen[2], Yannick Flores[1], Christophe Grosjean[1], Vikrant Murudi[4], Ashok Shyadligeri[4], Olga Lobanova[3], Christian Lothschütz[1,†]

[1] Syngenta, 4333 Münchwilen, Switzerland; [2] Syngenta, 1870 Monthey, Switzerland; [3] Syngenta, Bracknell, RG42 6EY, UK; [4] Syngenta, Corlim, Goa, 403110, India † Current address: DSM, 4334 Sisseln, Switzerland

**Corresponding author: patrick.piccione@syngenta.com*

Highlights

- A solvent selection tool developed at Syngenta is described through examples.
- Its guiding principles are ease of use, flexibility, and empowerment of chemists.
- Its interactive visualizations help exploring the solvent parameter space efficiently.

1. Introduction

Chemical manufacturing processes, especially for fine chemicals, often take place in the liquid phase. Solvents facilitate reactions, enable separations, and lower viscosity for convenient transport. Where possible, water is typically used, but many phenomena require different properties, better provided by organic solvents. The multitude of possible functional groups leads to even more numerous property combinations. Solvent selection is thus an important decision in chemical process development. Many methods have been put forward to optimize this selection, from high throughput screening to predictive models. The latter typically rely on physicochemical descriptors and can be made more accessible by embodiment in software tools [1, 2]. To get the most value from such tools, the corresponding theories and assumptions must be understood. To achieve both prediction and insight, an in-house tool was built at Syngenta and is described here.

2. Methods

Solvent selection methods have been researched by chemists as well as process systems engineers [3, 4]. Information technology skills are required to produce robust, attractive, and sustainable tools. A multi-functional project team was thus assembled (see Table 1). The basic philosophy was to build a tool empowering trained chemists to explore the process space – not a prescriptive tool with definite decisions, but a *suggestive* one. A main use thereof is defining the next iteration of solvents to try in the laboratory.

Chemists: Main user community	**Process engineers**	**Statisticians**	**Data scientists**
Definition of usage criteria Data for repository	Theories for property/phenomena correlations Functionalities and workflows	Fitting techniques	IT implementation

Table 1. Experts' roles on the project team

Physical and other properties were compiled for approximately 130 solvents in a spreadsheet ("the database"), from the following broad categories: identifiers; measured properties; physicochemical derived descriptors; HSE scores. The following calculations were then automated in the software R-Shiny: 1) similarity and difference searching using hierarchical cluster analysis; 2) multi-criteria

searching in property value space; 3) principal component analysis (PCA) for visualization as maps. All these functions allow dynamic, real time selection of the properties of interest by the user.

To underpin the *use* of the tool, several theories were used; in particular, solvatochromic / Abraham [5] and Kamlet-Taft [6] descriptions. The corresponding sets of properties were selectable together for convenient access to the occasional user.

3. Results and discussion

The R-Shiny tool appears as a typical browser interface. Parameter and visualization choices are set in a "start" tab, leading to real-time calculations in various results tabs. The tool is designed to be usable in many different ways. Cluster analyses yield solvents similar, to, or different from, a specific one. Multidimensional filtering allows several property ranges (e.g., solubility parameters and boiling point) to be matched simultaneously (Fig. 1a). PCA maps based on parameters known to matter for a process (e.g., Kamlet-Taft α, β, π* + boiling point, Fig. 1b) also provide alternatives.

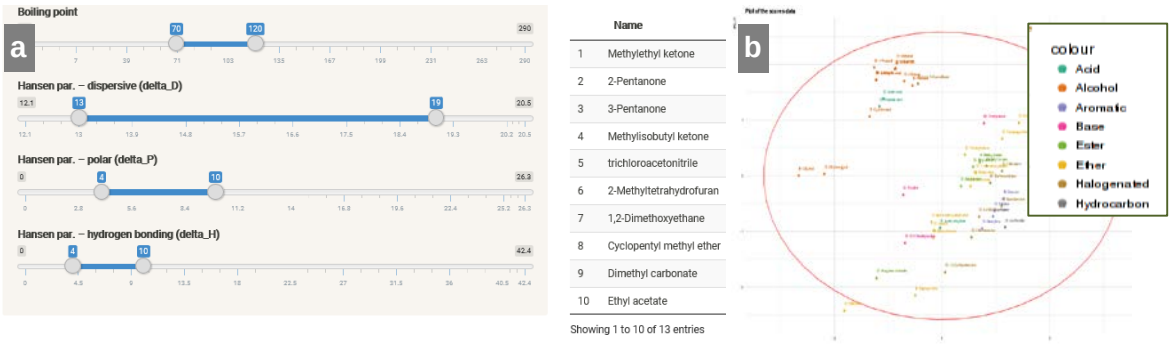

Figure 1. Screenshots of the matching (a) and PCA (b) tabs in the tool.

4. Conclusions

Different scientific specialisms lead to different languages and approaches. Tool development was found to be more intrinsically iterative than originally expected. While physical properties are a Rosetta stone for the meeting of chemists, engineers, and statisticians, progress required real usage cases. It was far easier to discuss mock-ups and share user stories than to write requirement specifications, leading to the mantra "show, don't tell". To remain meaningful to physical scientists, graphs and points required extensive labelling. Several concrete examples of use are documented in [7]. Possible improvements were continuously identified. Two important directions are: further incorporation of chemical theories; increased tool interactivity and filtering capability.

References

[1] L.J. Diorazio, D.R.J. Hose, N.K. Adlington, Org. Proc. Res. Dev., 2016, 20, 760–773.
[2] C.M. Alder, J.D. Hayler, R.K. Henderson, A,M. Redman, L. Shukla, L.E. Shuster, H.F. Sneddon, Green Chem., 2016, 18, 3879-3890.
[3] D. Curzons, D.J.C. Constable, D.N. Mortimer, V.L. Cunningham, Green Chem., 2001, 3, 1–6.
[4] P.M. Murray, F. Bellany, L. Benhamou, D.-K. Bučar, A. Tabor, T.D. Sheppard, Org. Biomol. Chem. 2016, 14, 2373-2384.
[5] M.J. Kamlet, J.-L.M. Abboud, M.H. Abraham, R.W.Taft, J. Org. Chem. 1983, 48, 2877-2887.
[6] M.H. Abraham, Chem. Soc. Rev. 1993, 73-83.
[7] P.M. Piccione, J. Baumeister, T. Salvesen, C. Grosjean, Y. Flores, E. Groelly, V. Murudi, A. Shyadligeri, O. Lobanova, C. Lothschütz, Org. Proc. Res. Dev. 2019, 23, 998-1016.

ECCE12
The 12th EUROPEAN CONGRESS OF CHEMICAL ENGINEERING
Florence 15-19 September 2019

OPC UA-based Concept for Online Implementation of Model-based Advanced Process Control Tools

Volodymyr Kozachynskyi[1], Saskia Bublitz[1], Markus Illner[1], Joris Weigert[1], Christian Hoffmann[1], Erik Esche[1], Jens-Uwe Repke[1]

1 Technische Universität Berlin, Fachgebiet Dynamik und Betrieb technischer Anlagen, Berlin, Germany

**Corresponding author: volodymyr.kozachynskyi@tu-berlin.de*

Highlights

- A concept for the online application of APC tools on plants in real time is proposed
- This concept utilizes an OPC UA standard for efficient data exchange
- The implementation of the concept is successfully demonstrated in a case study

1. Introduction

The structural implementation and application of model-based advanced process control tools based on methods such as data reconciliation, state estimation, sequential optimal experimental design or dynamic real-time optimization is a complicated and time-consuming task. It requires the development of a methodology for coupling of the tools with a process model, selection of a solver and implementation of a data-processing algorithms. The robust online application of these tools brings even more challenges for a developer. Solution must ensure that the APC tool can (i) read current and historical data from the plant in real-time, (ii) indicate relevant information to the plant operator, and (iii) influence the operation of the plant by manipulating variables, e.g. set points of the controllers.

This gap between the development of an APC tool and its efficient online implementation is being addressed in this contribution. The proposed data communication model is independent from the specific plant and APC tool and is based on the OPC UA standard [1], which fulfills all requirements for Industry 4.0 communication [2].

2. Methods

The data communication concept is shown in Fig.1. The connection between a plant and an APC tool is achieved via an intermediate aggregating OPC UA server, which is the main feature of the concept. It mirrors data from the real plant, stores it in a database and assures a bidirectional communication between the plant and the APC tool. Complex data types, provided by a server, specify a communication data model for APC tools allowing for a standardized data handling. The process model and the APC tool based on it are generated with the web-based modeling platform MOSAICmodeling [3]. The latter contains information about mapping of process variables (sensors, actuators, etc.) and model variables.

3. Case Study and Results

In order to check the applicability and potential of the developed concept, a case study has been conducted. Real-time plant operation is mimicked by the simulation of a dynamic model of a continuously stirred tank reactor with a chemical reaction of the second order. This simulation is connected to an aggregating OPC UA server, which constantly stores measurements in a database. This data is accessed by different APC tools, which are based on the same dynamic model: moving horizon state estimation, dynamic optimization of plant trajectories, and parameter estimation. The concept has been implemented in Python [4] and successfully tested. Simulation and state estimation have been running in parallel for twenty hours, while all the generated data has been stored in the database. No data has been lost during the experiment and no bottlenecks that hinder long lasting experiments were found. This allows for further investigations of the concept applicability on a real mini-plant for homogeneously catalyzed liquid multiphase reactions at TU Berlin operated by the SIMATIC PCS 7 distributed control system.

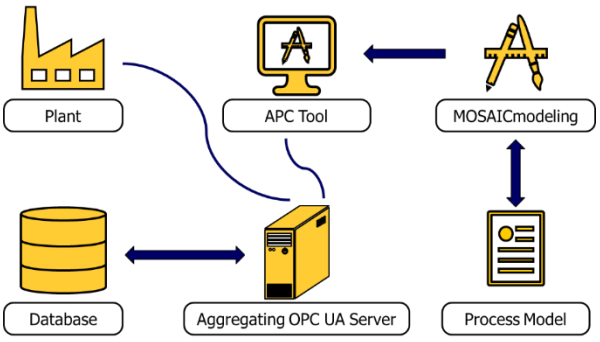

Figure 1. Proposed data communication concept.

4. Conclusions

Online implementation of APC tools is a complex task, which requires an efficient and easily applicable solution. On the one hand, this solution must be robust and secure, while on the other hand it must be easy in use and flexible. The concept presented in this contribution, fulfills these requirements. Based on results it is suggested that the OPC UA standard is to be used as a base layer for online application of APC tools, while the proposed concept and its Python implementation are a good example of a possible generalized solution of the highlighted challenge.

Acknowledgment

This work is part of the Collaborative Research Center "Integrated Chemical Processes in Liquid Multiphase Systems" (subproject D2, D4) coordinated by the Technische Universität Berlin. Financial support by the German Research Foundation (Deutsche Forschungsgemeinschaft, DFG) is gratefully acknowledged (TRR 63).

References

[1] https://opcfoundation.org/developer-tools/specifications-unified-architecture
[2] F. Pethig, S. Schriegel, A. Maier, J. Otto, S. Windmann, B. Böttcher, O. Niggemann, J. Jasperneite. (2017). Industrie 4.0 Communication Guideline Based on OPC UA.
[3] E. Esche, C. Hoffmann, M. Illner, D. Müller, S. Fillinger, G. Tolksdorf, H. Bonart, G. Wozny, J.-U. Repke (2017) “MOSAIC – Enabling Large-Scale Equation-Based Flow Sheet Optimization”, Chemie Ingenieur Technik, DOI: 10.1002/cite.201600114
[4] https://www.python.org/

ECCE12
The 12th EUROPEAN CONGRESS OF CHEMICAL ENGINEERING
Florence 15-19 September 2019

Generic Model-based Framework for Predictive Particle Monitoring using Advanced Image Analysis and Deep Learning

Rasmus Fjordbak Nielsen[1], Krist V. Gernaey[1], Seyed Soheil Mansouri[1]

[1]*Process and Systems Engineering Centre (PROSYS), Department of Chemical and Biochemical Engineering, Technical University of Denmark, Sølvtofts Plads, Building 229, DK-2800 Kgs. Lyngby, Denmark*

**Corresponding author: seso@kt.dtu.dk*

Highlights

- Generic modeling framework for particle processes using real time imaging
- Using raw images and deep neural network to estimate particle birth/growth rates
- Estimating particle size distribution measurement uncertainty
- Including measurement uncertainty to enhance model robustness

1. Introduction

Particle processes has gained significant importance in chemical and biochemical engineering in the last two decades. Especially within fermentation, flocculation, crystallization, there has been an increased industrial focus on optimizing and enhancing controllability of these processes. At the same time, both optics and image-analysis algorithms have improved significantly. It is now possible to analyze sample particle populations in real-time. This can be done by automatically sampling particle suspensions from the production tank to a mono-layer lab-on-a-chip device, where microscopy images are taken and analyzed using automatized advanced image analysis.

In this work, a deep neural network is used to estimate the birth and growth rates of the given particle process in real-time. Here we use the raw image, the results from the image analysis, and the measured and controlled process variables as inputs. When using deep neural networks, there is a greater risk of overfitting [1]. To accommodate this, it has previously been suggested to add random noise to the input data [2]. Here we utilize the prior knowledge on the inherent sampling error from the image analysis, and show how it is possible to reduce the risk of overfitting the neural network model. At the same time, we also account for the measurement uncertainty already during the model generation.

2. Methods

The suggested model structure can be seen in Figure 1. The network consists of a range of dense neural network layers, one generic population balance model and a loss function. Here we evaluate the performance of the model by calculating the mean absolute error (MAE) of the predicted relative size distribution. By adding Gaussian, zero-mean, random noise to the size-distribution data during training, with the same standard deviance as the known sampling error of the image analysis, the risk of overfitting can be reduced. At the same time, the uncertainties of the measurements are included in the process model during model generation, resulting in a more robust model. This will work for even crude errors, as long as the measurement uncertainty is correctly estimated.

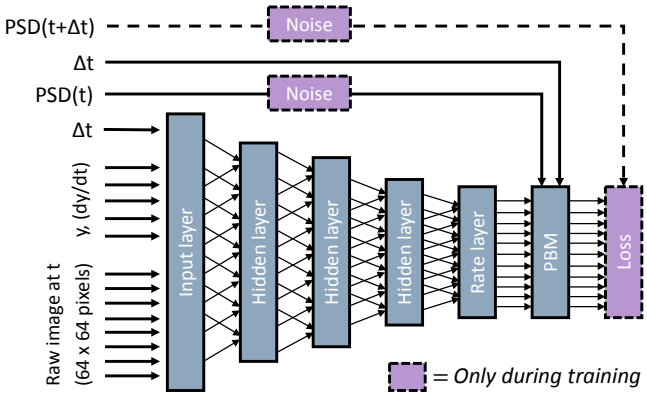

Figure 1. Modelling structure, where y represents measured and controlled variables. The time-derivative data of y is only supplied for controlled variables. The number based particle size distribution is abbreviated as PSD.

The sampling error of image analysis is here be estimated by assuming a random and unbiased sampling, where total sample size $\sum_i N_i$ (number of particles detected on the image) is much smaller than the total number of particles in process tank [3]: $\sigma = \sqrt{N_i \cdot (1 - N_i / \sum_i N_i)}$

3. Results and discussion

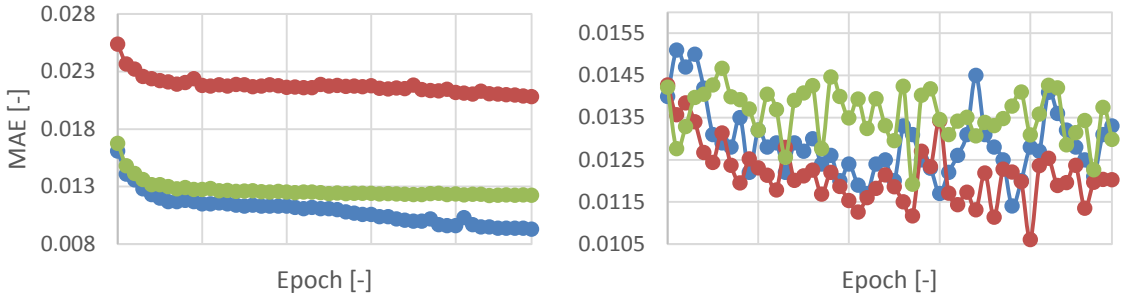

Figure 2. Training error (left) and validation error (right). ● Without noise ● Random noise ● Measurement specific noise

By applying the presented framework on a case study of lactose crystallization, where the temperature is the only measured and controlled process variable, it is here shown that the generated model is able to predict the evolution of the crystal size-distribution with high precision. As can be seen in Figure 2, by adding measurement-specific noise, compared to no noise addition and random noise, the model precision is increased. Furthermore, the tendency to overfitting is also shown to be reduced.

4. Conclusions

With the presented framework, it is shown possible to model a particle process using advanced image analysis and deep learning, giving accurate predictions of the size-distribution evolution. Here, the image analysis uncertainty is already taken into account during model training, showing to give even better predictions.

References

[1] X. Meng, C. Liu, Z. Zhang, D. Wang, IEEE ChinaSIP, 16-20, 2014
[2] Y. Grandvalet, S. Canu, IEEE Trans Syst Man Cybern 25 (4) 678–681, 1995
[3] S. Singh, Advanced Sampling Theory with Applications, Springer 71-136, 2003

ECCE12
The 12th EUROPEAN CONGRESS OF CHEMICAL ENGINEERING
Florence 15-19 September 2019

Development and validation of a model of the fructose metabolism across the liver sinusoid.

Yunjie Liao[1], David Bogle[1], Nathan Davies [2]

1 Department of Chemical Engineering, University College London, London, WC1E 7JE, United Kingdom;

2 Institute for Liver and Digestive Health, Division of Medicine, University College London, Royal Free Campus, London, NW3 2PF, United Kingdom

**Corresponding author: d.bogle@ucl.ac.uk*

Highlights

- Novel use of Process Systems Engineering techniques.
- A model of reaction mechanisms for fructose metabolism in the human liver.
- The model predicts the effects of novel therapeutic interventions.

1. Introduction

The liver is one of the most complicated processing organs in human body. It performs a broad range of biochemical functions for maintaining metabolic and energetic homeostasis of the whole body. Fructose, a daily dietary ingredient metabolised in the liver, had been proposed as a beneficial sweetener and recommended as a desired replacement for glucose for the obese and for diabetics. Yet both clinical and experimental studies recently have suggested a causal relationship between fructose over-consumption and damaged metabolism inducing hepatic steatosis [1-3]. However, neither animal models nor immortalised (HepG2) cell line studies have provided biologically accurate information relevant to human subjects due to species differences and the lipid build-up characteristics of HepG2 cells, respectively. Further, little is known on the effects of fructose on differential metabolic zones across the sinusoid. Therefore, a computational model based upon a systems biology approach is an attractive option to acquire a more comprehensive insight into the potential pathophysiological mechanisms of high fructose intake.

2. Methods

A kinetic model of hepatic fructose (± glucose/sucrose) metabolism was developed in MATLAB (Mathworks, MA, USA) based on modified Michaelis-Menten and Hill equations. The model includes literature identified biochemical components and reactions within distinct pathways, e.g. gluconeogenesis, *de novo* lipogenesis, beta-oxidation and triglyceride synthesis. The model parameters were determined and refined by comparison to literature values and also *in vitro* and *in vivo* studies (including a range of samples from healthy and diseased cases).

3. Results and discussion

In our *in silico* model, eight graded compartments including the fructose metabolism were constructed to represent hepatic heterogeneity along the periportal to perivenous axis. The simulations predicted increasing production of pyruvate, fatty acid and triglycerides on a 12-hour

periodic basis after fructose feeding, showing good association with published values [4,5]. The model also shows sensitivity at a number of control loci that may represent therapeutic intervention points such as fructokinase and peroxisome proliferator-activated receptors (PPARs).

4. Conclusions

We have adopted a systems engineering approach to investigate the fructose metabolism across the liver sinusoid and to determine the rate of pathophysiological consequences that develop as a result of an affected metabolism. The results suggest that the model is robust and reliably predicts the behaviour of the fructose metabolism, showing an accumulation of lipid within the hepatocyte as a direct consequence of fructose feeding. The model is further expected to predict the effects of novel therapeutic interventions based upon identified regulatory points which can then be corroborated by experimental studies.

We believe that organ modelling *in silico* model systems will have numerous applications in developing future therapeutic strategies and are a future growth area for Process Systems Engineers in collaboration with clinical colleagues.

References

[1] T. Jensen, et al. "Fructose and sugar: a major mediator of nonalcoholic fatty liver disease." *Journal of hepatology*, 2018.

[2] X. Ouyang, et al. "Fructose consumption as a risk factor for non-alcoholic fatty liver disease." *Journal of hepatology,* 48(6), 2008, pp. 993-999.

[3] L. G. Sánchez-Lozada, et al. "Comparison of free fructose and glucose to sucrose in the ability to cause fatty liver." *European journal of nutrition,* 49(1), 2010, pp. 1-9.

[4] A. Asipu, et al. "Properties of normal and mutant recombinant human ketohexokinases and implications for the pathogenesis of essential fructosuria." *Diabetes*, 52(9), 2003, pp. 2426-2432.

[5] K. L. Stanhope, et al. "Twenty-four-hour endocrine and metabolic profiles following consumption of high-fructose corn syrup-, sucrose-, fructose-, and glucose-sweetened beverages with meals–." *The American journal of clinical nutrition*, 87(5), 2008, PP. 1194-1203.

ECCE 12
ECAB 5

ECAB 5
The 5th EUROPEAN CONGRESS OF APPLIED BIOTECHNOLOGY
Florence 15-19 September 2019

Machine Learning in the context of the Modifier Adaptation Methodology for Real Time Optimization.

Daniel Navia[1], Felipe Moreno[1]

1 Universidad Técnica Federico Santa María, Av. Vicuña Mackenna 3939, Santiago de Chile, Chile

**Corresponding author: daniel.navia@usm.cl*

Highlights

- Machine learning implemented in the modifier adaptation method.
- Rejection of disturbances and modelling mismatch in real time optimization.
- Method allows tracking the optimum of an uncertain process in spite of disturbances.

1. Introduction

Real Time Optimization (RTO) with Modifier Adaptation method (MA) allows finding the optimum of a process ($\boldsymbol{u}_p^\star$) when the model of the process presents structural mismatch. To do so, MA updates the decision variables ($\boldsymbol{u}$), solving iteratively a modified model-based optimization problem, updated with first ($\boldsymbol{\lambda}$) and zeroth ($\boldsymbol{\varepsilon}$) order corrections in the objective function (J) and in the inequality constraints ($\boldsymbol{C}$). $\boldsymbol{\lambda}$ are calculated using process gradients with respect to $\boldsymbol{u}$ [1]. As the process is uncertain, the experimental gradients are calculated with historical data. In real processes unmeasured disturbances ($\boldsymbol{\xi}$) can affect the process outputs, i.e. $J_p(\boldsymbol{u},\boldsymbol{\xi})$ and $\boldsymbol{C}_p(\boldsymbol{u},\boldsymbol{\xi})$. Therefore, the process derivatives calculated only with past information of $\boldsymbol{u}$ can be erroneous, which implies that the MA may not find $\boldsymbol{u}_p^\star$ [2]. To avoid the estimation of the process gradients, MA has been reformulated as a nested optimization problem (NMA) [3]. NMA uses an upper optimization layer to update $\boldsymbol{\lambda}$, looking for the minimization of the Lagrangean of the process ($\mathcal{L}_p \coloneqq J_P(\boldsymbol{u},\boldsymbol{\xi}) + \boldsymbol{\mu}^T\boldsymbol{C_P}(\boldsymbol{u},\boldsymbol{\xi})$). As $\boldsymbol{\xi}$ can affect the outputs, it is expectable that $\boldsymbol{u_p^\star(\xi)}$**.** Machine Learning (ML) is a subset of artificial intelligence algorithms that uses statistical techniques to give computers the ability to learn with data. It allows overcoming the uncertainty related with the modeling-mismatch of a process building internal surrogated models based in statistical analysis. It relays in the idea of sequential queries to the real process, each of them calculated solving an optimization problem with the surrogated model. At each evaluation in the process, the model uses the gathered data to increase the knowledge of the uncertain system. The objective of this work is the implementation of algorithms based in ML in the upper layer of NMA (ML-NMA) to give the MA the ability to track the value of $\boldsymbol{u}_p^\star(\boldsymbol{\xi})$ in real time.

2. Methods

For a given steady state k, the upper layer proposes $\boldsymbol{\lambda}_{k+1}$ solving Eq.(1), where $f_{GP_k}(\cdot)$ is the available mapping of $\mathcal{L}_p$. f_{GP_k} is obtained with the Gaussian Process approach (GP). GP is a nonparametric regression method to find an approximation of $\mathcal{L}_P$ with the available data.

$$\min_{\boldsymbol{\lambda_{k+1}}} f_{GP_k}\left(\mathcal{L}_p\left(\boldsymbol{u}(\boldsymbol{\lambda_{k+1}}),\boldsymbol{\mu}(\boldsymbol{\lambda_{k+1}})\right)\right), s.t.: Eq.(2) \quad (1)$$

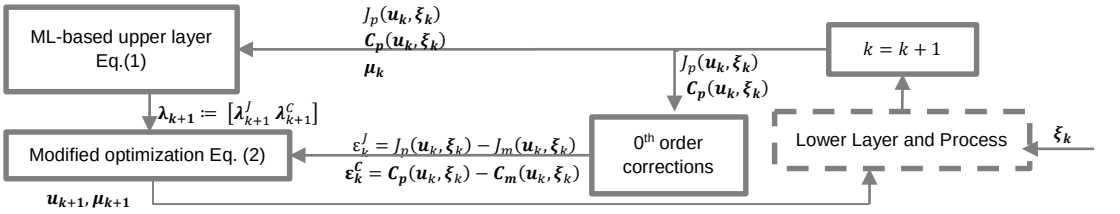

Figure 1. Developed algorithm of NMA with ML (ML-NMA).

The value of $\boldsymbol{\lambda}_{k+1}$ and $\boldsymbol{\varepsilon_{k+1}}$, are used to solve the modified optimization from Eq.(2). The outcome of Eq.(2) is implemented into the process. Once the steady state is reached, the outputs of the process are measured to update f_{GP_k} and solve Eq.(1). The update of f_{GP_k} gives the ML-NMA the ability to adapt the MA to the changing conditions of $\boldsymbol{\xi}$.

$$\min_{\boldsymbol{u}\in\boldsymbol{U}} J_m(\boldsymbol{u},\boldsymbol{\alpha}) + \left(\boldsymbol{\lambda}^J_{k+1}\right)^{\boldsymbol{T}}(\boldsymbol{u}-\boldsymbol{u}_k) + \varepsilon^J_{k+1}$$
$$s.t.: \boldsymbol{C}_m(\boldsymbol{u},\boldsymbol{\alpha}) + \left(\boldsymbol{\lambda}^C_{k+1}\right)^{\boldsymbol{T}}(\boldsymbol{u}-\boldsymbol{u}_k) + \boldsymbol{\varepsilon}^C_{k+1} \le 0 \qquad (2)$$

3. Results and discussion

The ML-NMA was tested in the Otto-Williams reactor. The process consisted of an isothermal CSTR working at a given temperature T_R with two influents (F_A and F_B). Inside the CSTR three chemical reactions are produced, while in the approximated model of the process only two of them are considered. The decision variables of the process are T_R and F_B. In this work we have considered F_A as an unmeasured disturbance changing over time. The RTO looks for F_B and T_R those optimize the economic benefit of the process inside a feasible region [4]. The main result of this work was that the evolution of F_B calculated with ML-NMA followed the trajectory of the optimum of the process closer than other MA approaches, while T_R was better estimated by the DUAL-MA SSKF (Figure 2). Nevertheless DUAL-MA SSKF depends on the accuracy in $\boldsymbol{\xi}$ estimation.

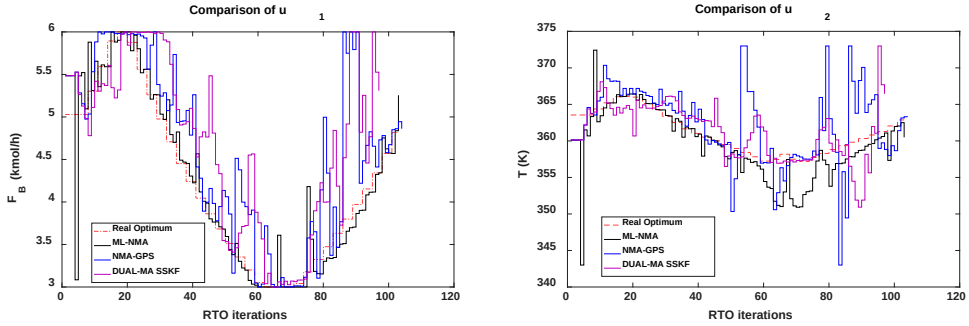

Figure 2. Evolution of F_B and T_R: ML-NMA (black solid line), real optimum of the process (red dotted line), NMA using Generalized Pattern Search (blue solid line), MA with dual approach and Steady-state Kalman Filter (magenta solid line)

4. Conclusions

It has been demonstrated that ML-NMA allows tracking the optimum of an uncertain process which is affected by unmeasured disturbances.

References

[1] Marchetti A, Chachuat B, Bonvin D. , J Proc. Cont. (2010) 20(9):1027–37.
[2] Navia D, Puen A, Quintanilla P, Bergh L, Briceño L, de Prada C., Comp. Aided Chem. Eng. (2018) 43.
[3] Navia D, Briceño L, Gutiérrez G, De Prada C., Ind Eng Chem Res. (2015) 54(48).
[4] Rodríguez-Blanco T, Sarabia D, Navia D, de Prada C., Comp. Aided Chem. Eng (2017) 40.

ECCE12
The 12th EUROPEAN CONGRESS OF CHEMICAL ENGINEERING
Florence 15-19 September 2019

Synthesizing Temperature Control System for Binary Distillation Columns.

Lu Liu[1], Kejin Huang[2], Yang Yuan[3], Xing Qian[4], Haisheng Chen[5]

College of Information Science and Technology,
Beijing University of Chemical Technology, Beijing 100029, People's Republic of China

**Corresponding author:2017210320@mail.buct.edu.cn*

Highlights

- Sensitivity analysis and minimum deviation methods give inconsistent outcomes.
- The new method balances the static and dynamic behaviors of rectifying section.
- The new method suppresses sensitivities to pressure variations of stripping section.
- The new method renders better static and dynamic behaviors than the former two methods.

1. Introduction

Based on the sensitivity analysis and minimum deviation methods, the synthesis and design of temperature inferential control systems for three ethanol/butanol binary distillation columns with, respectively, low, intermediate, and high product purities are addressed in this work. The temperature inference control systems based on the sensitivity analysis method focusing on dynamic behaviors and the minimum deviation method focusing on static behaviors are difficult to give satisfactory control effects under high product purity conditions. Through in-depth analysis of the static and dynamic behaviors of the controlled stages in the rectifying section and the stripping section, we explain why these two methods fail to give consistent control effects at low, intermediate, and high product purities, followed by verification in closed loop control.

2. Methods

The controlled stages by the sensitivity analysis method usually exhibit quick dynamic responses but only in the case of low product purities can their temperatures display satisfactory corresponding relationships with product compositions. For the controlled stages by the minimum deviation method, their temperatures usually display satisfactory corresponding relationships with product compositions. In the case of high product purities, because the controlled stages are quite near in locations to the ends of the distillation column, degraded process dynamics is introduced in the rectifying section and great sensitivity to pressure variations occurs in the stripping section, both worsening the performance of the temperature inferential control system. Therefore, in order to achieve tight inferential control of product qualities, it is necessary to develop a new method that can compensate for changes in system characteristics. In order to compromise the static and dynamic behaviors in the rectifying section, the controlled stage should be selected between the top stage and the sensitive stage. The temperature difference between the two lowest stages in the stripping section should be used as the controlled variable to achieve the most effective compensation for pressure changes.

3. Results and discussion

Let us take the example of an ethanol/butanol binary distillation column with an intermediate product purity of 99%. The closed loop response processing a ±20% step change of feed composition and a ±20 % step change of feed flow rate is shown in Figures 1 and 2, respectively. The closed loop response based on the sensitivity analysis, minimum deviation and new methods are labeled as CS1, CS2 and CS3, respectively. The positive responses are represented by black curves and negative responses by gray curves. In Figure 1, although the CS2 greatly reduces the steady-state deviations compared to the CS1, its dynamic behaviors of the top and bottom products are deteriorated. In Figure 2, the CS2 not only has larger steady-state deviations than CS1 in the bottom product, but also deteriorated dynamic behaviors. Compared with CS1, CS3 not only reduces the steady-state deviation of the top product concentration, but also reduces the transient and steady-state deviations of the bottom product concentration. Although the CS3 has slightly larger steady-state deviations than CS2 processing ±20% step change in feed composition, its static and dynamic behaviors are balanced.

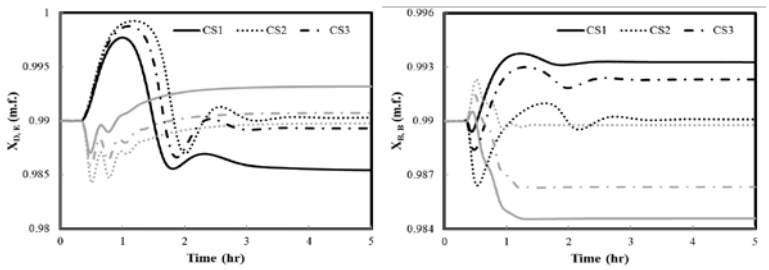

Figure 1. Closed-loop responses in case of a ±20% step change in feed composition.

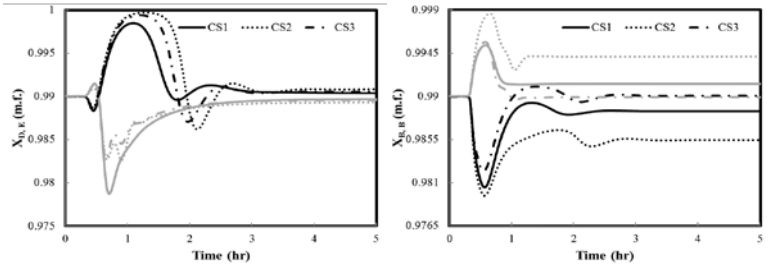

Figure 2. Closed-loop responses in case of a ±20% step change in feed flow rate.

4. Conclusions

Sensitivity analysis and minimum deviation methods give inconsistent outcomes. Therefore, we develop a systematic method that can not only compromise the static and dynamic behaviors of the rectifying section but also suppress the sensitivity to pressure variations in the stripping section. The obtained results have confirmed that the new method can render better static and dynamic behaviors than the sensitivity analysis and minimum deviation methods.

References

[1] W.L. Luyben, Evaluation of Criteria for Selecting Temperature Control Trays in Distillation Columns, Process Control. J. 2006, 16, 115.

[2] L.J. Zang, K.J. Huang, T. Guo, Temperature inferential control of a reactive distillation column with double reactive sections, Chinese Journal of Chemical Engineering. J. 2018, 1333-1342.

ECCE12
The 12th EUROPEAN CONGRESS OF CHEMICAL ENGINEERING
Florence 15-19 September 2019

Multi-Objective Optimization in Process Simulation using Stochastic Algorithms

Fabian Zapf[1,*], Thomas Wallek[1]

1 Institute of Chemical Engineering and Environmental Technology, Graz University of Technology, Inffeldgasse 25C, 8010 Graz, Austria

**Corresponding author: fabian.zapf@tugraz.at*

Highlights

- Multi-objective optimization
- Process simulation
- Scalarization methods
- Genetic algorithm

1. Introduction

The use of a variety of commercial process simulators is state of the art, offering the possibility for calculating mass transfer phenomena, thermodynamics and reaction kinetics of single processes, individual production plants and entire production sites. The last step in process simulation is the optimization of the design and/or operating parameters of the plant in view of economy, operational safety, environmental impacts and social aspects. As these aspects are often conflicting each other, this frequently implies a multi-objective optimization (MOO) problem, also called Pareto optimization. MOO problems always include two or more objectives, common examples for that are investment costs vs. operational costs and profitability vs. environmental aspects.

Popular process simulators, like Aspen Plus, Aspen HYSYS, CHEMCAD and gProms, include optimization modules, which are capable of performing only single objective optimization (SOO). To overcome this drawback, introducing MOO in process simulators is commonly realized by coupling the process simulator with an external application which runs the optimization algorithm. In general, there exist two groups of optimization algorithms: deterministic and stochastic algorithms.

Deterministic optimization algorithms require gradient information of the optimization problem, which makes them very fast compared to stochastic algorithms. Gradient information in process simulators is only available when they are running in equation orientated simulation mode via the equation set object, defined by the CAPE-OPEN standard. [1]

Stochastic optimization algorithms, on the other hand, require only information about the dependent variables (objectives or output of the system) and the independent variables (process parameters to be optimized). Therefore, they are suitable for optimizing black-box functions, such as process simulators running in sequential modular mode. Their main disadvantage is the

relatively slow convergence, due to many evaluations of the objective functions in the course of evaluation runs of the process simulator.

In this work, several approaches for applying MOO in process simulation are compared among their effort for realization and their suitability for optimization in process engineering. They are implemented in the framework of Wolfram Mathematica, which is coupled with KBC PetroSIM as a process simulator via a COM Interface.

2. Methods

Scalarization methods, which transform a MOO problem (vector) into a SOO problem (scalar) are very popular due to the fact that they are easy to implement and the broad availability of built-in SOO algorithms in nearly every mathematical program. [2] Therefore, as a first step, popular scalarization methods, such as the weighting method and ε-constraint method are implemented and their resulting SOO problems are solved by the built-in global SOO algorithms, i.e., simulated annealing, differential evolution and Nelder-Mead. [3]

As a second step, a genetic algorithm is implemented. Genetic algorithms are population based and a group of them is able to handle MOO problems directly. One of the most popular algorithms is the Non-dominated Sorting Genetic Algorithm II (NSGA-II). This standard-algorithm is implemented together with several adaptions for handling integer variables. Additionally, five different jumping-gene operators as well as the hyper-volume of the Pareto front as a convergence measure are implemented as extensions to NSGA-II. [2,4]

3. Application

To compare these different implementations and variations for MOO, they are applied to the example of a steam reformer located in a European refinery, optimizing the process in view of specific hydrogen production (kg H_2/kg natural gas) and HPS (high pressure steam) production. Using this example, strengths and weaknesses of the aforementioned approaches are analyzed and recommendations for their application are given.

3. Conclusion

The presented work demonstrates the workflow and efforts to enable MOO in process simulators with the example of optimizing a steam reformer in view of process flexibility. Beyond the typical application of MOO for economic optimization, it gives the possibility of evaluating the increasing demand of process flexibility and load-shift capability of plants and processes.

References

[1] C.A.M. Lopez, D. Telen, P. Nimmegeers, L. Cabianca, F. Logist, J. V. Impe, A process simulator interface for multiobjective optimization of chemical processes, Computers and Chemical Engineering, Vol 109, 2018, pp. 119-137

[2] G.P. Rangajah, Introduction, Multi-Objective Optimization, Advances in process systems engineering, Vol 5, 2016, pp 1-27

[3] R.T. Marler, J.S. Arora, Survey of multi-objective optimization methods for engineering, Structural and Multidisciplinary Optimization, Vol 26, 2004, pp 369-395

[4] M. Ramteke, S.K. Gupta, Multi-Objective Genetic Algorithm and Simulated Annealing with the Jumping Gene Adaptations, Multi-Objective Optimization, Advances in process systems engineering, Vol 5, 2016, pp 93-133

ECCE12
The 12th EUROPEAN CONGRESS OF CHEMICAL ENGINEERING
Florence 15-19 September 2019

Global optimization of catalyst recovery in a thermomorphic multiphase system using surrogate models

Christian Kunde[1,*], Tobias Keßler[1], Steffen Linke[2], Kevin McBride[2], Kai Sundmacher[1,2], Achim Kienle[1,2]

1 Otto von Guericke University Magdeburg, Universitätsplatz 2, 39106 Magdeburg, Germany
2 Max Planck Institute for Dynamics of Complex Technical Systems, Sandtorstraße 1, 39106 Magdeburg, Germany

**Corresponding author: christian.kunde@ovgu.de*

Highlights

- Global optimization of catalyst recovery in an extraction cascade.
- Complex LLE and catalyst distribution models replaced by artificial neural network.
- Implicit model formulation reduces the input dimension of the surrogate model.
- Surrogate model quality is improved by optimization based bound tightening during preprocessing.

1. Introduction

The aim of using renewable resources for chemical processes and improving their energy efficiency calls for the exploration of novel and integrated process concepts. Thermomorphic multiphase systems (TMS) enable favorable reaction conditions as well as efficient catalyst recycling for homogeneously catalyzed reactions. A TMS is homogeneous at reaction conditions and a subsequent decrease in temperature results in biphasic behavior: a catalyst-lean product phase and a catalyst-rich phase that is recycled back to the reactor. If the separation of catalyst from the product phase in one step is not sufficient, the process can be extended by additional extraction stages to further increase recovery of valuable catalyst.

Mathematical optimization can be used to find the economically most viable realization of such a process. For nonlinear models with continuous decision variables this leads to nonlinear programs (NLP), which are typically hard to solve and may possess multiple local minima. Therefore, deterministic global optimization is required to avoid suboptimal design decisions based on poor local solutions. Thermodynamic models employed to predict the phase equilibrium of TMS and the catalyst distribution are often computationally difficult to handle within optimization problems, even in the case of local optimization. Replacing thermodynamic models with suitable surrogates provides the means to trade model accuracy for better computational tractability.

As an example, the hydroformylation of long-chain aldehydes with homogeneous catalysts using a TMS for catalyst recovery is considered in [1]. In that work, the thermodynamic models are replaced by a Kriging model to avoid convergence problems within the local optimization of the overall hydroformylation process. However, the resulting surrogate model comprises a large number of relatively complex nonlinear terms, which renders it computationally unfavorable for deterministic global optimization.

To overcome this problem, we present modifications to the surrogate construction aimed at reducing the number of nonlinear expressions and thus the computational complexity of the model. Globally optimal solutions of the resulting model are identified using BARON [2].

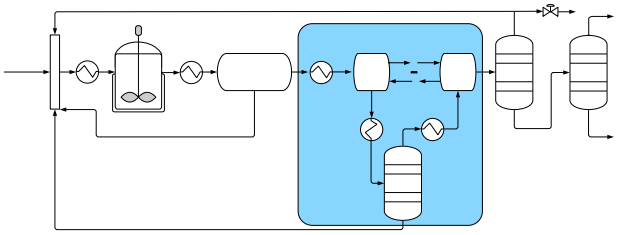

Figure 1. Flowsheet of the hydroformylation process considered in [1]. The highlighted area shows a multistage extraction cascade with solvent recycle.

The following methods are applicable for processes dealing with liquid-liquid-equilibria. However, we focus on a subprocess taken from [1], highlighted in Figure 1, as a case study. Catalyst is recovered from a product stream by an extraction solvent in a series of decanter units in a countercurrent setup. The extraction solvent is regenerated using a distillation column. As in [1], the reference data of the temperature dependent liquid-liquid equilibrium of a four-component mixture and distribution of catalyst between the separate phases is generated using a modified UNIFAC Dortmund model and COSMOtherm. The economic cost function comprises refrigeration, decanter units, catalyst loss, and costs for a short-cut distillation column.

2. Methods and results

A number of methods for data-driven surrogate modeling is available in the literature, see e.g. [3,4] for an overview. Based on testing with various Kriging formulations and artificial neural networks (ANN), an ANN with a single hidden layer and tangent hyperbolic activation function was selected to replace the thermodynamic reference models. The input dimension of the surrogate is reduced in comparison to [1] by choosing the position on the binodal curve as an input instead of the feed composition. This strategy, illustrated in Figure 2, results in an implicit model, but it simplifies the definition and modeling of valid input values. The quality of the ANN is further improved by reducing the range of input values with optimization based bound tightening in a preprocessing step. Error bounds for a least-squares fitted second order polynomial are chosen such that all available data points lie within the relaxed model. The polynomial surrogate model may have larger error bounds than an ANN, but computational effort is significantly lower. BARON is then utilized to calculate tighter bounds on the input variables based on the relaxed model.

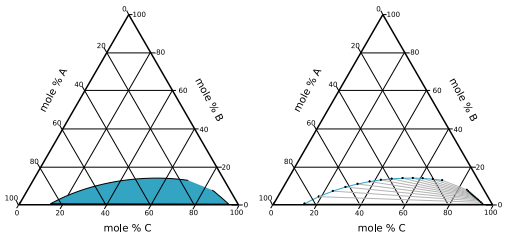

Figure 2. Ternary phase diagram with a two-phase region. Input space highlighted for explicit (left) and implicit (right) model formulation.

These combined methods reduce the computation time and increase the accuracy of global optimization with surrogate models in the considered case study. The global optimization results also verify the findings presented in [1]. Application to other processes will be tested in the future.

References

[1] K. McBride, N. M. Kaiser, K. Sundmacher, 2017. Computers & Chemical Engineering 105, 212–223.
[2] M. R. Kılınç, N. V. Sahinidis, 2018. Optimization Methods and Software 33 (3), 540–562.
[3] M. J. Asher, B. F. W. Croke, A. J. Jakeman, L. J. M. Peeters, 2015. Water Resour. Res. 51 (8), 5957–5973.
[4] A. Bhosekar, M. Ierapetritou, 2018. Computers & Chemical Engineering 108, 250–267.

ECCE12
The 12th EUROPEAN CONGRESS OF CHEMICAL ENGINEERING
Florence 15-19 September 2019

Effect of Boiling Point Rankings on the Optimal Feed Locations of Reactive Distillation Columns.

Rahma Muthia[1], Aloijsius G. J. van der Ham[2], Megan Jobson[1], Anton A. Kiss[1,2]

1 School of Chemical Engineering and Analytical Science, The University of Manchester, Sackville Street, Manchester, M13 9PL, United Kingdom; 2 Sustainable Process Technology Group, Faculty of Science and Technology, University of Twente, PO Box 217, 7500 AE Enschede, The Netherlands

**Corresponding author: tony.kiss@manchester.ac.uk*

Highlights

- Conceptual design of reactive distillation (RD) processes
- Effect of boiling point orders on the applicability of RD
- Evaluation of the applicability of RD to quaternary systems

1. Introduction

Reactive distillation (RD) is an attractive process intensification unit as it offers multiple benefits, such as higher conversion, improved selectivity, energy savings and lower costs [1]. However, the number of its commercial applications was limited by the assessment of RD applicability and operation [2, 3]. To deal with this problem, we proposed a mapping method to comprehend and predict the applicability of RD [4]. The present work employs this method to determine the optimal feed locations of RD columns (lower energy usage) in quaternary systems (A + B ⇄ C +D) with different boiling point (T_b) rankings: 1) group I_p ($T_{b,C} < T_{b,A} < T_{b,B} < T_{b,D}$), 2) group III_p ($T_{b,C} < T_{b,A} < T_{b,D} < T_{b,B}$), and 3) group III_r ($T_{b,A} < T_{b,C} < T_{b,B} < T_{b,D}$). The group's naming convention follows the rules as set by Luyben and Yu [5]. Other boiling point rankings are not considered because they are not promising for the application of a single RD column [6]. To the best of our knowledge, this is the first study that provides essential insights into the optimal feed locations of RD considering the effect given by the boiling point rankings.

2. Methods

The main feature of the mapping method is the applicability graphs plotting the reflux ratio (RR) vs number of theoretical stages (NTS). They are produced from generic reactions under assumptions of ideal thermodynamics and constant key parameters, i.e. relative volatilities (α) and chemical equilibrium constant (K_{eq}). The lowest RR possible for each NTS forms a boundary line in each graph that splits applicable and not-applicable areas. To construct an applicability graph, the numbers of rectifying, reactive and stripping stages of any RD configurations are varied, while the feed locations of each reactant are always fixed at both end-sides of reactive zone. Afterwards, a representation of RD with the lowest RR and $NTS=2 \cdot NTS_{min}$ is selected and its feed locations are optimized to further reduce the reflux ratio (lowering energy requirement). All simulations in this work are carried out with Aspen Plus v8.6 software.

3. Results and discussion

Figure 1 depicts reflux ratios based on varied feed stages of both reactants. The optimization of feed locations decreases RRs by 15% in group I_p, 37% in group III_p and 23% in groups III_r. In group I_p, positioning both feed inlets close to the centre of the reactive zone is favorable. In group III_p, lower RRs are achieved by placing the feed inlets at the top of the reactive section. In contrast, for group III_r, it is more beneficial to set the feed stages at the bottom of the reactive zone.

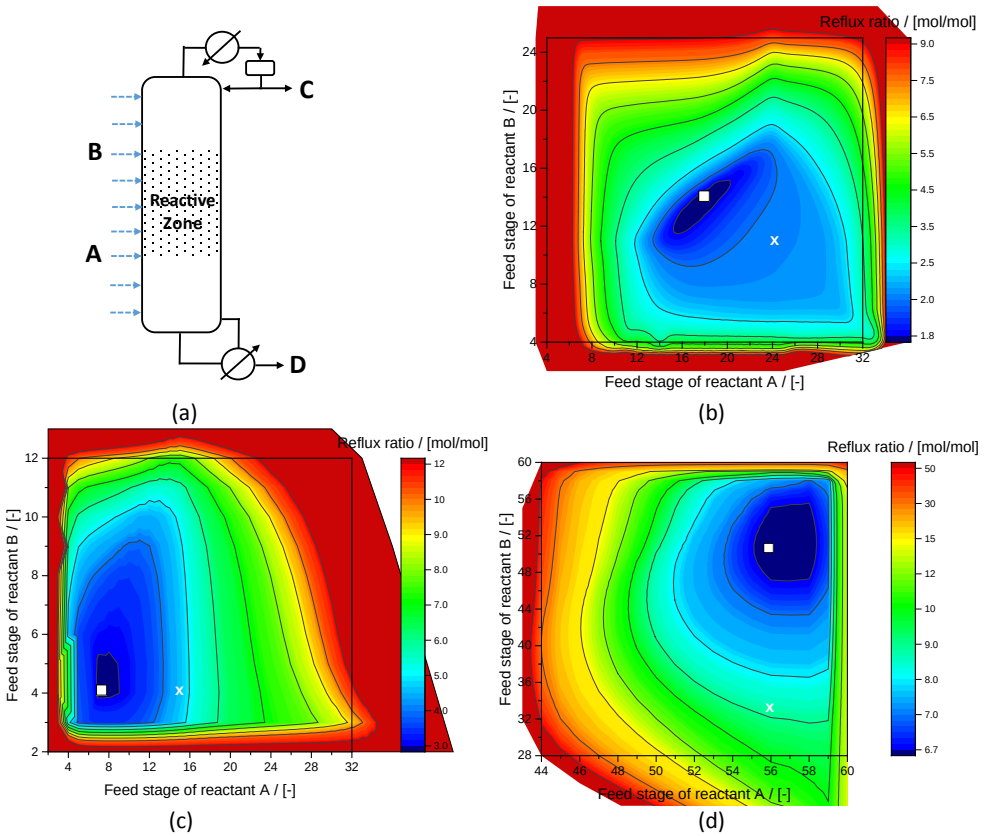

Figure 1. RD setup with varied feed locations (a). Contour plots of RRs in (b) group I_p, (c) group III_p and (d) group III_r with α_{AB}=2, α_{CD}=6 and K_{eq}=1. Cross and square marks indicate the feed locations before and after the optimization [7].

4. Conclusions

The boiling point rankings determine the location of the optimal feed stages of RD columns. The findings in this work suggest that positioning the feed inlets close to each other improves the RD performance (lowering reflux ratios), but placing both reactants at the same stage results in a competition between reaction and separation, which hinders an effective RD process.

References

[1] A. A. Kiss, Top. Catal. (2019) 1-17.

[2] M. Shah, A. A. Kiss, E. Zondervan, A. B. de Haan, Chem. Eng. Process. Process Intensif. 60 (2012) 55-64.

[3] J. G. Segovia-Hernández, S. Hernández, A. B. Petriciolet, Chem. Eng. Process. Process Intensif. 97 (2015) 134-143.

[4] R. Muthia, A. G. T. Reijneveld, A. G. J. van der Ham, A. J. B. ten Kate, G. Bargeman, S. R. A. Kersten, A. A. Kiss, Chem. Eng. Process. Process Intensif. 128 (2018) 263-275.

[5] W. L. Luyben, C.-C. Yu, Reactive Distillation Design and Control, John Wiley & Sons, Inc., USA, 2008.

[6] R. Muthia, A. G. J. van der Ham, A. A. Kiss, Comput. Aided Chem. Eng. 43 (2018) 827-832.

[7] R. Muthia, A. G. J. van der Ham, M. Jobson, A. A. Kiss, submitted to Chem. Eng. Res. Des. (2019).

ECCE12
The 12th EUROPEAN CONGRESS OF CHEMICAL ENGINEERING
Florence 15-19 September 2019

Comparison of process synthesis methods: case study of the design of membrane separation processes

Thibaut Neveux[1*], Bernardetta Addis[2], Christophe Castel[3], Veronica Piccialli[4], Eric Favre[3]

1 EDF R&D, EDF Lab Chatou, F-78400 Chatou, France ; 2 Université de Lorraine, CNRS, LORIA, F-54000 Nancy, France ; 3 Université de Lorraine, CNRS, LRGP, F-54000 Nancy, France ; 4 University of Rome Tor Vergata, 00133 Rome, Italy

**Corresponding author: thibaut.neveux@edf.fr*

Highlights

- First systematic and critical comparison of process synthesis strategies
- Rigorous coupling of module simulation and optimization is key
- Novel process designs are identified through process synthesis
- Guidelines for selection of the best process synthesis approach are proposed

1. Introduction

In the field of process synthesis (or process design), various methods have been proposed to select a set of equipment with their operational conditions and their interconnection in a process flowsheet. These methods may vary from empirical approaches (where the "process designer" proposes an architecture based on his/her expertise or using hierarchical decomposition methods and then uses a simulation tool to validate the proposed design by means of sensitivity analysis) to optimization-based approaches (where the process synthesis problem is posed as a mathematical problem) [1].

In this paper, it is proposed to compare several methods from the field of Process System Engineering (PSE) on a common process synthesis problem.

2. Methods

Three methods, developed by the paper's authors, are selected for the comparison (see Table 1).

Table 1. Process synthesis approaches and mathematical formulation chosen in this paper.

SYNTHESIS APPROACH	MATHEMATICAL FORMULATION	SOFTWARE TOOL	REF.
Superstructure-based	Global optimization NLP	AMPL + Knitro	[2]
Superstructure-based	MINLP solved by Ant Colony Optimization	Prosim + MIDACO	[3]
Ab-initio (no superstructure)	Evolutionary Programming	Dedicated	[4]

These approaches differs in the synthesis approaches (based or not on a superstructure, i.e. a virtual process including various structural alternatives) and mathematical formulations used to solved the optimization problem.

The comparison procedure is summarized as follows:

- Definition of the synthesis problem (all): available components, unit operations, associated degrees of freedom and their range, objectives and constraints.
- Problem formulation (approach-specific) to fit the method's requirements.
- Calibration (all): check that the physico-chemical models for unit operation and process simulation give the same results by performing parametric screening (crucial step).

- Optimization (approach-specific): run each algorithm and isolate optimal solutions.
- Validation (all): simulation of the optimal solutions within a process simulator.

The results can be then compared on the basis of various criteria such as: best solutions, exclusivity of solutions (process structure and parameters), computational time, ease of use for a process engineer, etc.

3. Case study: O_2/N_2 separation

A case study of N_2 production from air using membranes is chosen for the comparison. Results are analysed from both structural (number of stages and recycles) and design/operational parameters (membrane surfaces, pressure ratio) points of view. The design is performed using an economic objective function considering capital costs (turbomachineries, membranes, heat exchanger) and operational and maintenance costs (energy, membrane replacement, operation), together with technological constraints and minimal levels of purity for produced N_2 from 90% up to 99.9%.

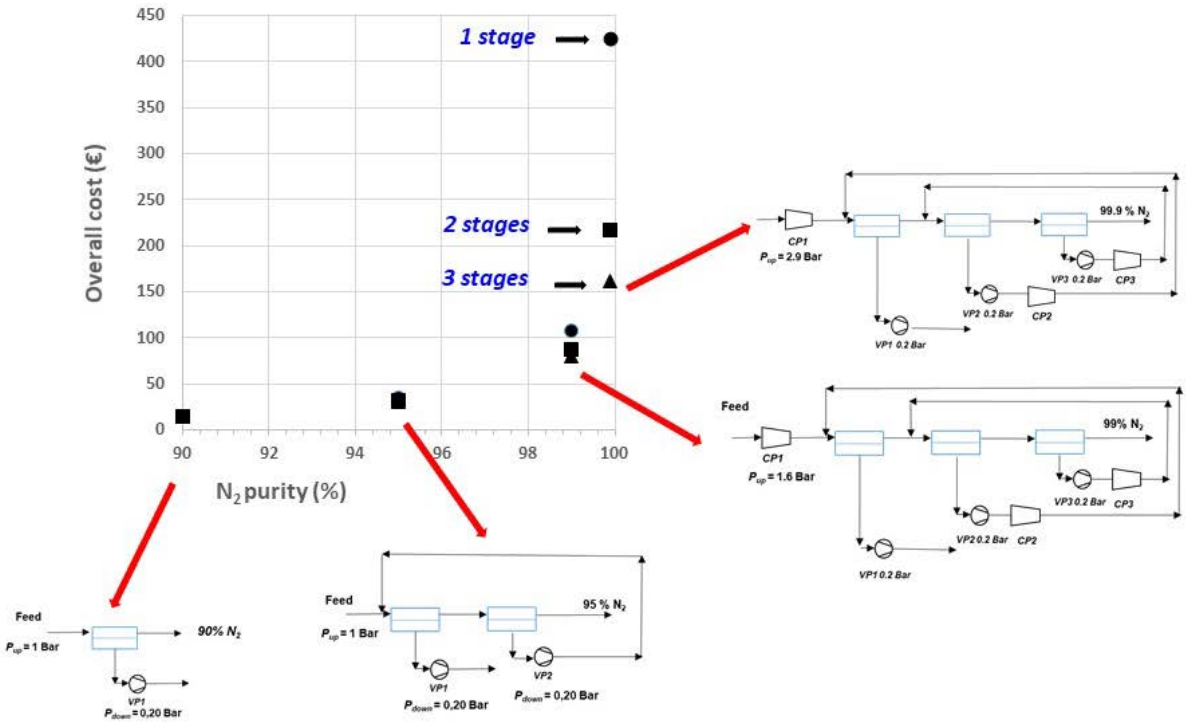

Figure 1. Example of configurations for O_2/N_2 separation for several recoveries and purities [2].

References

[1] Q Chen, O Grossmann, Ann Rev Chem Biomolec Eng 8 (2017), 249–283
[2] A Ramirez-Santos, M Bozorg, B Addis, V Piccialli, C Castel, E Favre, J Membr Sci 566 (2018), 346-366
[3] Q Zhao, T Neveux, M Mecheri, R Privat, P Guittard, JN Jaubert, Comput Aided Chem Eng 43 (2017), 767-772
[4] T Neveux, Chem Eng Sci 185 (2018), 209–22

ECCE12
The 12th EUROPEAN CONGRESS OF CHEMICAL ENGINEERING
Florence 15-19 September 2019

Comparison of sequential and simultaneous draining in periodic cycled separation columns

Jess Rasmussen, Seyed Mansouri, Jens Abildskov, Jakob Huusom*

PROSYS, Department of Chemical and Biochemical Engineering, Technical University of Denmark, Søltofts Plads, Building 229, 2800 Kgs. Lyngby, Denmark

**Corresponding author: jkh@kt.dtu.dk*

Highlights

- Development of models for sequential and simultaneous drained cyclic distillation
- Comparison of tray efficiency for different draining methods
- Comparison of developed models with theoretical expectations

1. Introduction

Periodic (or cyclic) distillation is an intensified distillation process first proposed in the 1960's [1], where the liquid and the vapor phase flows are divided in two separate periods [2,3]. The two periods are a vapor flow period (VFP) and a liquid flow period (LFP). During the VFP, the liquid holdup(s) on the trays are in fixed positions, while vapor flows through the column. During the LFP, the liquid is drained from one tray to the tray below, followed by a new VFP and so forth. By operating a distillation in cyclic mode, the separation efficiency has been shown to be higher than for conventional distillation [3]. When replacing a conventional distillation column with a cyclic distillation column, a smaller column with fewer trays is needed for the same separation [1]. Depending upon the design, energy consumption may also be reduced. This expands the range of options for designs [2,3].

The theory of cyclic distillation was developed during the 20th century. However, industrial applications are only slowly coming along [3]. A serious problem with the first generation of realizations was the need for improved liquid flow control. This problem was solved in different ways during the 1980s. In recent years, new trays [4] have made it possible to operate any size column in periodic mode and thus making cyclic distillation feasible in large scale. With this tray design there is still an issue regarding the need for interrupting the vapor flow during LFPs. This can cause significant pressure dynamics. An alternative tray design has been developed that implies draining of the trays occur sequentially instead of simultaneously [5].

The currently available models are relatively simple. These models are often based on mass balances and neglect effects of pressure drop, energy transfer and variations of the point efficiency. Furthermore, it is only the more recent models that allows multi-component mixtures and non-linear phase equilibrium. In addition to this, (nearly) all existing models address simultaneous draining, which means there is a need for models that describes the sequential draining for comparison

2. Methods

Simple linear phase equilibrium models for binary mixtures are developed for both the sequential and the simultaneous draining method. These simple models are suitable for describing stripping, absorption and high-purity distillation and are convenient for analysis.

With the developed models, the efficiencies for the two draining methods are compared to each other and to theoretical expectations.

3. Results and discussion

With the developed models, the two draining methods presented for cyclic distillation have been compared to each other and theory. There are currently no comparisons available in the literature. The comparisons are focused on the tray and the overall separation efficiencies.

The difference in draining methods is expected to have an effect on the separation efficiency. When a column is drained sequentially, there is an empty tray at greater fractions of time. This will affect the overall tray efficiency. On the other hand, the rest of the trays still undergo VFP when another tray is being drained, which could be an advantage. Our analysis will investigate these conflicting effects.

4. Conclusions

Cyclic distillation is an intensified process that increases the separation efficiency compared to conventional distillation. There are two liquid draining methods available, sequential and simultaneous draining, which each have its own advantages and disadvantages. Simple models have been developed to describe a cyclic distillation process with either sequential or simultaneous draining. The developed models for the two draining methods are compared to each other and to the theoretical expectations.

References

[1] M.R. Cannon, Ind. Eng. Chem. 53 (1961) 629.
[2] A.A. Kiss, Advanced Distillation Technologies, first ed., Wiley, Chichester, 2013.
[3] C.S. Bîldea, C. Pătruţ, S.B. Jørgensen, J. Abildskov, A.A. Kiss, J. Chem. Technol. Biotechnol. 91 (2016) 1215-1223.
[4] V.N. Maleta, A.A. Kiss, V.M. Taran, B.V. Maleta, Chem. Eng. Process 50 (2011) 655-664.
[5] B. Toftegård, C.H. Clausen, S.B. Jørgensen, J. Abildskov, Ind. Eng. Chem. Res. 55 (2016) 1720-1730.

ECCE12
The 12th EUROPEAN CONGRESS OF CHEMICAL ENGINEERING
Florence 15-19 September 2019

Flexible and efficient process synthesis and optimization based on Aspen Plus simulations - MTBE production case study.

Maximilian Cegla[1], Tim Janus[1], Stephen Tlatlik[2], Peter Krause[3], Thomas Bäck[3], Axel Gottschalk[2], Sebastian Engell[1]

1 TU Dortmund University; 2 SUPREN GmbH; 3 Divis Intelligent Solutions GmbH

**Corresponding author: Maximilian.cegla@tu-dortmund.de*

Highlights

- Global optimization using Aspen Plus flowsheet simulations
- Memetic algorithm
- Flexible customizable cost function
- Reduction of the total cost compared to expert solution

1. Introduction

The decisions taken during process development are critical for the economic success of process engineering projects. The design engineer needs to screen, develop and evaluate a large number of process alternatives. Even when sophisticated software tools are applied for modelling and analysis, iteratively carrying out the design usually requires month to years. Due to the strong involvement of human work force, high personnel costs are incurred and the results depend on the experience of the developers. Obviously, also the risk of human errors e.g. by prematurely ruling out alternative solutions is always present.

Marking a breakthrough in boosting the efficiency of process development a novel process optimization tool has been established in a joint project between divis, SUPREN and TU Dortmund. Starting from an existing simulation flowsheet that was created by a design engineer, a memetic algorithm is applied to investigate, globally optimize and assess alternative process configurations and conditions in an automated fashion. The tool supplements the process understanding and creativity of an engineer with the reliability and efficiency of optimization. Replacing human labor by computations, the repetitive work in the course of process development is accelerated while the related costs decrease.

2. Methods

This contribution presents the results of the application of our computer-aided optimization procedure to the production of methyl tert-butyl ether (MTBE) (world production volume 18 Mtons/year in 2005) that is inspired by the Oxeno-technology [1]. A memetic algorithm is applied because of its capabilities to act as a global solver and to handle integer design variables. The memetic algorithm used combines an evolutionary algorithm, e.g. an evolution strategy (ES), with a local solver. At the beginning of the optimization procedure the ES gen erates a population (a set of individuals) with integer design variables and continuous operation parameters within given bounds. For this first population, using the widely used simulation tool Aspen Plus, process

simulations are performed. The results are evaluated automatically with regard to customizable – often economic – objective functions. Based on the results of the ES, the memetic algorithm generates new individuals (offspring) by the recombination and mutation of two of the afore-investigated individuals. This procedure is repeated until the convergence criteria are met. [2]

The optimization problem discussed includes 22 continuous and 7 integer design variables and 3 process constraints. Based upon objective functions that are available in the library of the tool along with problem-specific information, the economics of the process alternatives are assessed.

3. Results and discussion

Commencing from a previously optimized solution created by an experienced engineer for an industrial client, the optimizer achieves a further improvement of 1.2% of the overall costs. Exploiting the simulation file present from the manual investigation, about 2 hours of time are needed to define the optimization problem. Afterwards, without interaction with an expensive design engineer, 3 days of computation time are required to reach the results presented in Figure 1. Multiple runs of the stochastic optimization establish the uniqueness of the result.

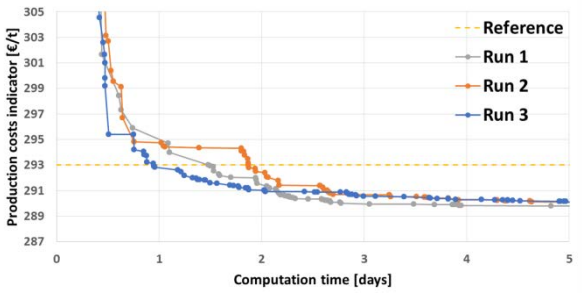

Figure 1: Improvements of the economic cost function with the expert solution as reference.

Due to the use of a commercial simulation environment the required computation time is high, but the advantage is the flexibility of the approach. Changes to the flowsheet such as the introduction of additional process equipment can be performed easily and fast. For the current case, modifications of the model were tested and realized in timespans of well under 30 minutes of human work and 3 days of calculation time. Thanks to a fully automated documentation, the results of the optimization run are summarized in the form of easily accessible spreadsheets and the corresponding Aspen simulation files are stored. Based on this information, each individual solution or the optimization run can be analyzed in detail with regard to the identified operation and design parameters as well as to the objective functions.

4. Conclusions

The presented approach is capable of enhancing the process development workflow using the reliable and efficient memetic algorithm in combination with the creativity and knowledge of the process engineer. Due to the use of a commercially available simulation tool, industrially trusted results are generated. In summary, the application of the tool leads to overall better process designs involving the engineer primarily in the creative development process rather than in repetitive and tedious elements of the workflow.

References

[1] M. Winterberg et al.: „Methyl Tert-Butyl Ether”, Ullmann's Encyclopedia of Industrial Chemistry, Electronic Release, chap. 4, Wiley-VCH, Weinheim, 2010.

[2] Urselmann, M. et al.: „A memetic algorithm for global optimization in chemical process synthesis problems.” IEEE Transactions on Evolutionary Computation 15 (5) (2011), 659-683.

ECCE12
The 12th EUROPEAN CONGRESS OF CHEMICAL ENGINEERING
Florence 15-19 September 2019

Flexibility Analysis and Economic Assessment of a Distillation Train

Martina Raymo[2], Alessandro Di Pretoro[1,2], Ludovic Montastruc[1], Flavio Manenti[2], Xavier Joulia[1]

1. Laboratoire de Génie Chimique, Université de Toulouse, CNRS/INP/UPS, Toulouse, France.
2. Politecnico di Milano, Dipartimento di Chimica, Materiali e Ingegneria Chimica "Giulio Natta", Piazza Leonardo da Vinci 32, 20133 Milano;
** ludovic.montastruc@ensiacet.fr*

Highlights

- Under perturbated conditions the flexibility analysis assesses the system performance.
- The price of an higher flexibility is a system oversizing.
- The total cost vs flexibility trend helps the engineer decision making.

1. Introduction

In process engineering the leading separation process is distillation. The standard procedure for distillation columns design is based on the economic and operational aspects. However, this optimal design is strictly related to the operating conditions, i.e. perturbations, when present, can seriously turn the tables.

Flexibility analysis is an important part of process design seldom included in the standard procedure. Even if sometimes a sensitivity analysis is performed afterwards, there are some differences between the two that can't be neglected.

The flexibility, for a chemical plant, is defined as the ability of the system to cope with any change of the operating conditions. To achieve higher values of flexibility it is necessary to perform a structured analysis. The analysis can be applied to existing plants and to plants in the design phase [1]. These higher values guarantee a reduction of the risk of money losses and of the stand-by period.

2. Methods

From the available literature about this topic it is clear that the flexibility analysis has been deeply studied and well defined as well as the resulting economic considerations.

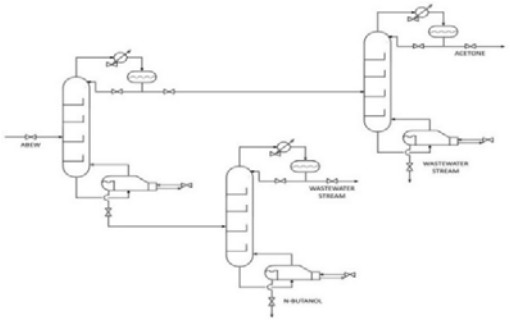

Figure 1: Distillation columns in a midsplit configuration

The mathematical procedure used to assess the flexibility of the selected case study system is the one developed by Saboo and Morari [2], i.e. the Resilience Index (RI). It is assessed by calculating the largest total disturbance load, independent from the direction of disturbance, a system is able to withstand without becoming unfeasible. The RI is then defined as the lowest of the aforementioned withstood perturbations so that every parameter value can change within the +/- RI range without compromising the system operation. This index has been applied to a complex system made of three distillation columns in a midsplit configuration, used to separate a water, ethanol, n-butanol and acetone mixture. Figure 1 shows the system under study.

3. Results and discussion

The flexibility analysis has been carried out and the maximum withstood load for each variable has been assessed. The most constraining parameters result to be water (8%) and butanol (13%), while ethanol and acetone flexibility limits can be neglected, since they are 32% and 45%. The price for a higher flexibility is linked to a system oversizing (column diameter, condenser and reboiler exchanger surface). The economic assessment has been performed and the corresponding total cost vs flexibility trend is plotted in Figure 2 as suggested by Di Pretoro et al (2019) [3].

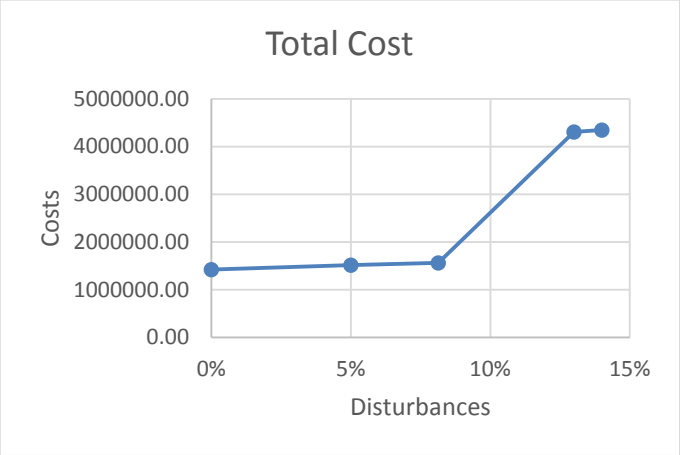

Figure 2. Total Cost

4. Conclusions

The article shows that an a priori flexibility analysis can lead the designer engineer to the optimal compromise between a flexible plant and an affordable investment.

References [Calibri 10]

[1] I. E. Grossmann and M. Morari, 'Operability, Resiliency, and Flexibility: Process Design Objectives for a Changing World', Department of Chemical Engineering, (1983).
[2] A. K. Saboo, M. Morari, and D. C. Woodcock, `Design of Resilient Processing Plants .8. a Resilience Index for Heat-Exchanger Networks', Chemical Engineering Science, 40.8 (1985), 1553-65.
[3] A. Di Pretoro , L. Montastruc, F. Manenti, X. Joulia, 2019, 'Flexibility analysis of a distillation column: indexes comparison and economic assessment', Submitted to Computers and Chemical Engineering.

ECCE12
The 12th EUROPEAN CONGRESS OF CHEMICAL ENGINEERING
Florence 15-19 September 2019

Development of Hybrid Membrane Separation-Distillation Processes for Propylene-Propane Separation

Takehiro Yamaki[1*], Keigo Matsuda[2,3], Akira Endo[1]

1 Research Institute for Chemical Process Technology, National Institute of Advanced Industrial Science and Technology (AIST), 305-8565 Ibaraki, JAPAN; 2 Department of Chemistry and Chemical Engineering, Graduate School of Science and Engineering, Yamagata University, 992-8510 Yamagata, JAPAN; 3 Renewable Energy Research Center, National Institute of Advanced Industrial Science and Technology (AIST), 963-0298 Fukushima, JAPAN

**Corresponding author: takehiro-yamaki@aist.go.jp*

Highlights

- Evaluation of energy consumption of hybrid membrane separation-distillation processes
- Energy consumption of the hybrid process is 83% less than that of distillation process
- Capital cost divided by the payback time of membrane separation unit was estimated

1. Introduction

Energy-saving of separation process is a problem in order to reduce greenhouse gas emission, because the separation process accounts for about half of the energy consumption in the chemical industry [1]. In the chemical industry, diversification of raw materials is proceeding. An as example, in propylene production, the propylene content in the mixture fed to the propylene purification column is 98% for the ethylene center, whereas it is 90% for the propane dehydration process. Although distillation is widely used for these separations, reduction of the propylene content leads to increase of energy consumption. Therefore, it is necessary to develop an alternative energy-efficiency separation process. As an energy-efficiency separation process, membrane separation has attracted attention [1]. However, since membrane separation is not suitable for high throughput, it is difficult to replace the distillation process of propylene separation with membrane separation. To solve this problem, there is hybridization of membrane separation and distillation as one of the candidates. In the design of hybrid process, it is necessary not only to clarify the configuration that can reduce the energy consumption but also to achieve cost reduction. This study clarifies the influence of the configuration of the hybrid process on energy consumption for separation of propylene/propane mixture and discusses the cost of the separation membrane unit.

2. Simulation model

For a case study, the propylene content in the feed was set as 90 mol%, and the feed flow rate was constant at 1433 kmol/h. As the product specifications, the propylene content was 99.5 mol%, and the recovery ratio of propylene was 99.5%. The thermodynamic properties were estimated using the Peng-Robinson model. **Figure 1** shows the schematic diagrams of hybrid membrane separation-distillation processes. The hybrid process consists of one distillation column and one membrane separation unit. The stage numbers of the distillation column was fixed at 230 stages. The pressure of the distillation column was 2040 kPa. As membrane separation performances, the propylene

permeability was 1×10^{-6} mol/($m^2 \cdot s \cdot Pa$), and the propylene selectivity was 100. The pressures of permeate and feed side were 2040 and 200 kPa. All simulation were performed by Pro/II (ver. 9.4).

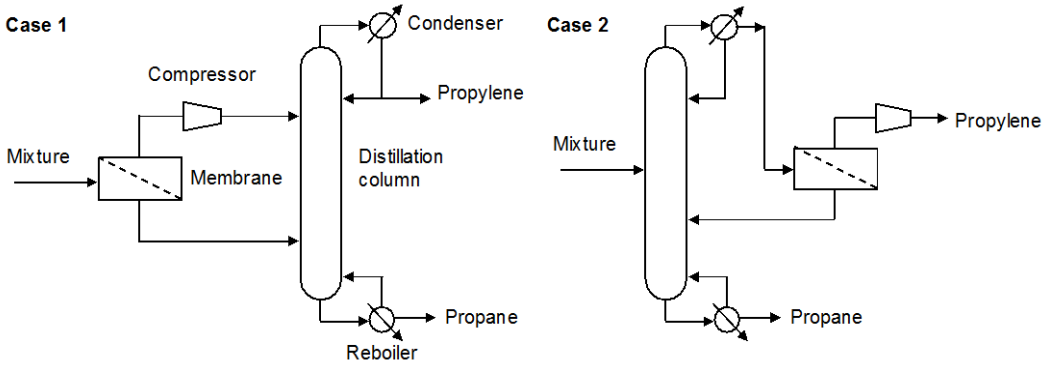

Figure 1. Schematic diagrams of hybrid membrane separation-distillation processes.

3. Results and discussion

The energy consumptions including duties of reboiler and compressor of Case 1 and 2 were minimized when the membrane areas were 355 and 413 m^2, respectively. The energy consumption of Case 1 and Case 2 were 50.5 and 48.1 GJ/h. There results correspond to energy saving of approximately 82 and 83% compared to the distillation process. Based on the results, this study estimated the cost reduction by reducing energy consumption. Here, the costs of the steam and the electricity was assumed to be 13.28 and 16.8 $/GJ [2]. The operating time per year was set to be 8322 hours [2]. As a result, the annual operating costs for the distillation process, Case 1 and 2 were 3.09×10^7, 6.12×10^6, and 5.87×10^6 $, respectively. If the difference of operating cost between the distillation and the hybrid process is greater than the equipment cost divided by the payback time, total annual cost (TAC) of the hybrid process is reduced. Therefore, the upper limit of the equipment cost divided by payback time for Case 1 and 2 are 2.48×10^7 and 2.50×10^7 $.

4. Conclusions

This study evaluated the energy consumptions for the hybrid processes of Case 1 and 2, and found that energy savings of 82 and 83% can be achieved in Case 1 and 2, respectively. Based on the results, this study estimated the upper limit of the equipment cost divided by the payback time of the membrane separation unit.

References

[1] D. S. Sholl, R. P. Lively, Nature, 532 (2016) 435–438.
[2] R. Turton, R. C. Bailie, W. B. Whiting, J. A. Shaeiwitz, Analysis, Synthesis, and Design of Chemical Processes, Second ed., Prentice Hall, New York, 2007.

Acknowledgment

This work was partially supported by NEDO, JAPAN, in the project of “Development of energy-efficient basic chemical production processes with innovation separation technologies”.

ECCE12
The 12th EUROPEAN CONGRESS OF CHEMICAL ENGINEERING
Florence 15-19 September 2019

Systematic System Identification and Analysis of Operability for Surfactant Containing Multiphase Reaction Media

Markus Illner[1*], Volodymyr Kozachynskyi[1], Erik Esche[1], Jens-Uwe Repke[1]

1 Process Dynamics and Operations Group, Technische Universität Berlin, Straße des 17. Juni 135, D-10623

**Corresponding author: markus.illner@tu-berlin.de*

Highlights

- Microemulsion systems as enabler for homogeneous catalysis of long-chained substrates
- Soft sensor implementation to access immeasurable states
- Long-term mini-plant operation
- Moving horizon state estimation and dynamic optimization

1. Introduction

Homogeneous catalysis provides highly desirable reaction performance features, such as high chemo- and regio-selectivities and is thus widely applied in process industry[1]. To allow for recycling, applied valuable catalysts are often reallocated to an aqueous phase via ligand modification. However, for the conversion of long-chained substrates this triggers contradicting design features of the reaction system. On the one hand, perfect miscibility of substrate and catalyst phase is required for the reaction. On the other hand, perfect separability for downstreaming and catalyst recycling is desired. To this end, surfactant containing multiphase system can be applied to overcome this hurdle. Surfactants are used as phase transfer agents to enable efficient conversion of nonpolar substrates. Moreover, the specific phase separation behavior of these microemulsion systems can be exploited for catalyst recovery and product separation. Due to their complexity, such novel process concepts pose a variety of operational challenges and reliable plant operation is only possible by applying model-based advanced process control. Especially for microemulsion systems, profound theoretical descriptions are absent and thus a detailed experimental investigation is inevitable to obtain suitable models to aid process operation. Regarding this, we present a systematic approach for the efficient identification and operability analysis of such systems to enable the fast track development of semi-empiric models to be used in process control.

2. Methods

As a case study, the hydroformylation of 1-dodecene in a microemulsion system formed with an aliphatic nonionic surfactant is applied and tested in a fully automatized mini-plant, holding a high-pressure reactor-settler setup and 3 individual recycles[2]. The systematic system identification and analysis firstly focusses on the reaction itself. Here, a mechanistic microkinetic model is adapted regarding relevant influences of the component system on reaction performance. Secondly, the dynamic phase separation behavior of the microemulsion is systematically studied to identify the relevant set of influencing factors and suitable operation regions for plant operation. Additionally, the controllability of the system regarding monitoring of relevant states is analyzed. From this, an

updated experimental series is conducted gaining the relevant results for the modeling the three phasic separation of the microemulsion system. This information is merged into a fully dynamic mini-plant model and used within optimal control strategies comprising moving horizon state estimation and dynamic real-time optimization.

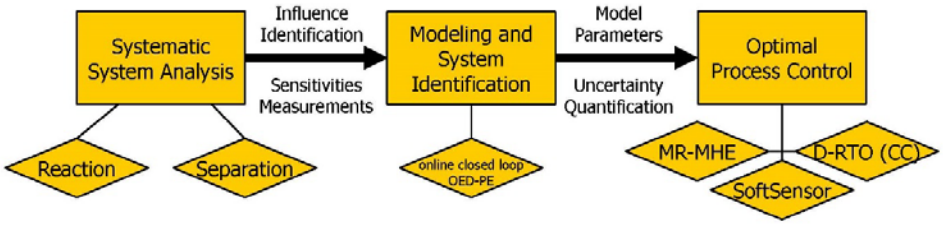

Figure 1. Workflow for systematic system analysis and development of advanced process control strategies for reactions in microemulsion systems

3. Results and Discussion

The systematic system analysis was successfully applied. A new macrokinetic model was derived and parameterized, which is able to describe undesired byproduct formation induced by local concentration changes in the microemulsion system. Furthermore, the analysis of the phase separation system revealed that the surfactant concentration, the most sensitive influence factor on the separation state, is immeasurable and a stable process operation is not possible. To cope with this, a model-bases soft-sensor was developed, which is based on optical observation of the phase evolution in the microemulsion system. The applicability of developed optimal process control strategies was then tested in long-term continuous mini-plant campaigns of up to 200 h. Control of the critical phase separation step was tested for different operation modes and overall good oil phase purities of up to 99,5 % (amount of oily components in the separated oil phase) were observed. The reaction performance was validated against preliminary lab-scale investigations, wherein a product yield of 40 % and an overall selectivity of 95 % were achieved.

4. Conclusions

Within this contribution, a procedure for the systematic system identification and operability analysis of surfactant containing multiphase systems has been proposed. Based on this, semi-empiric models have been formulated to describe the system dynamics and applicable operation regions. Especially, the identification of immeasurable states has been enabled by a model-based soft sensor. From the application of developed models for state estimation and the calculation of plant trajectories from a dynamic optimization a stable mini-plant operation with successful reaction and separation was achieved.

Acknowledgment

This work is part of the Collaborative Research Center "Integrated Chemical Processes in Liquid Multiphase Systems" (subproject D2, D4) coordinated by the Technische Universität Berlin. Financial support by the German Research Foundation (Deutsche Forschungsgemeinschaft, DFG) is gratefully acknowledged (TRR 63).

References

[1] F. Franke, D. Selent, A. Börner, Applied Hydroformylation, Chem. Rev, 2012, 112 (11), 5675-5732.
[2] M. Illner, D. Müller, E. Esche, T. Pogrzeba, M. Schmidt, R. Schomäcker, G. Wozny, J.-U. Repke, Ind. Eng. Chem. Res, 55 (31) (2016) 8616−8626.

ECCE12
The 12th EUROPEAN CONGRESS OF CHEMICAL ENGINEERING
Florence 15-19 September 2019

Critical CO_2 Carnot Engine for Industrial Waste Heat Recovery and Utilization

Sarah Makuc[1], Eldred Chimowitz[2]

1,2 University of Rochester Chemical Engineering Department, Rochester, NY

Highlights

- Critical CO_2 Carnot cycle maximizes low-grade heat harnessing and utilization
- Small (~1.5 L) engines can utilize waste heat, generating power
- Increased energy savings, decreased energy bills, and environmental emissions

1. Introduction

Industrial processes regularly discard large volumes of low-grade waste heat to the environment. Harnessing this heat and transforming it into usable power would be environmentally and economically advantageous for industries. An overlooked solution to utilizing this waste heat is the use of a Carnot cycle to generate work with supercritical CO_2 as the working fluid. Supercritical CO_2 is a novel working fluid for a Carnot engine as its critical temperature (31.1°C) is much lower than the boiling point of water. This allows for the lower isotherm of the Carnot cycle to be constructed at the critical temperature, resulting in a sizable Carnot cycle with a near flat lower isotherm and upper isotherm just below the temperature of the low-grade heat. Thus, this type of Carnot cycle encompasses a larger area on a P-V diagram than any other thermodynamic conditions, thereby optimizing the amount of work that can be converted to power using a relatively small engine. We describe this approach of waste heat harnessing and illustrate ideas for utilizing the waste heat from an industrial toluene process. The impact of compression ratio, upper isotherm temperature, and pressure in the engine are investigated. Resulting savings amount to hundreds of thousands of kWh/year, thereby reducing cooler loads, electricity bills, and environmental emissions.

2. Methods

The developed and validated Excel program can analytically calculate the work of the Carnot cycle using the following equations derived from the Van der Waals equation of state and the critical parameters for CO_2. The calculated work is then used to find the size/frequency of an engine necessary to harness all of the available work and transform it to usable power.

$$Q_H = \int_{V_1}^{V_B} \frac{RT_H}{V-b} = RT_H ln(\frac{V_B - 1}{V_1 - b}) \text{ where } b = \frac{1}{8}\frac{RT_c}{P_c} \quad \textbf{Equation 1}$$

$$W = Q_H(1 - \frac{T_C}{T_H}) \quad \textbf{Equation 2}$$

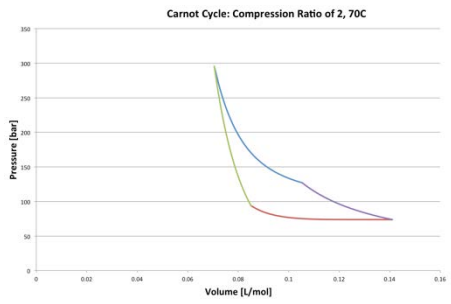

Figure 1. Typical Carnot Cycle Program Output

Required program inputs include cooler size, isotherm temperatures, compression ratio, frequency, and starting volume. Outputs include work available, engine size,

pressure, and, if applicable, the necessary cooler size still required. An alternative program takes in the engine size and outputs the required frequency. Reversible adiabatic and isothermal steps have been assumed.

3. Results and discussion

Program outputs for specific examples found in the disproportionation of toluene process indicate a large potential for utilizing waste heat. With a decrease in upper isotherm temperature, the work available, and thus power, increases and engine size decreases, but the analogous increase in pressure is a limiting factor. With the increase in engine size, the required frequency of the engine, measured in Hertz, decreases. Process specific findings include the ability to harness 135.49kW from one stream in the toluene process, cooling it roughly 39°C. This leads to a net annual production of 975,528 kWh of energy, amounting to over $50,000/year in cost savings.

Upper Isotherm (°C)	Work (J/mol)	Power (kW/mol)	Maximum Volume (L/mol)	Engine Size (L)	Pressure (bar)
60	224.14	11.21	0.141	2.01	266
70	264.00	13.20	0.141	1.45	296
100	270.56	13.53	0.141	0.644	386

Table 1. Data for a 135.48 kW Power Production.

Electricity Source	Price [*U.S. EIA estimates]	Cost Savings per Year ($)
U.S. National Average	$0.0724/kWh	70,628
Conventional Coal	$98.7/MWh	96,285
Biomass	$95.3/MWh	92,968
Onshore Wind	$48/MWh	46,825
Solar Thermal	$126.6/MWh	123,502

Table 2. Annual Energy Savings from a 135.49 kW Engine

4. Conclusions

It is found that with a relatively small engine and frequency, on the order of 1.5 L and 50 Hz, moderate upper isotherm temperature, and a compression ratio of 2, almost 1 million kWh can be saved each year from the integration of a single Carnot cycle into the disproportionation of toluene process. Considering various electricity sources, the production of 1 million kWh of electricity can save the industrial plant over $50,000/year and decrease environmental emissions. Carnot cycles therefore represent an underutilized resource to harness low grade waste heat present in numerous industrial processes.

References

[1] J.T. Banchero, B.D. Smith (Ed.), R.J. Hengstebeck. *Disproportionation of toluene*, 1969.
[2] Eldred H. Chimowitz Madeleine R. Laitz, F. Douglas Kelley. *Critical CO_2 Carnot Cycle for Waste Heat Utilization*, 2017.

ECCE12
The 12th EUROPEAN CONGRESS OF CHEMICAL ENGINEERING
Florence 15-19 September 2019

Towards a Circular Economy: A Systems Engineering Approach

Styliani Avraamidou[1], Efstratios N. Pistikopoulos[2]

1 Postdoctoral Research Associate, Texas A&M Energy Institute, Artie McFerrin Department of Chemical Engineering, Texas A&M University

2 Director, Texas A&M Energy Institute, TEES Eminent Professor, Artie McFerrin Department of Chemical Engineering, Texas A&M University

**Corresponding author: stratos@tamu.edu*

Highlights

- Circular Economy (CE) can be a solution to resource degradation and scarcity.
- To achieve CE a system's engineering approach is needed for optimal decision making.
- A system's engineering framework towards CE is developed and presented.
- Case studies indicate that the approach can supply optimal solutions towards a CE.

1. Introduction

Natural resources play a critical role in the development and wealth of societies. They are vital for the provision of energy, food, shelter, transport and all basic functions of our societies. Population growth, welfare growth and the constant need of an increasing standard of living, means that more natural resources are used, leading to resource degradation, increased landfill wastes caused be the increased consumption, and negative environmental impact caused by the production and consumption of resources.

Circular Economy (CE) can be a solution to this resource challenge. CE is an economy that is restorative and regenerative by design and aims to keep products, components, and materials at their highest utility and value at all times [1]. CE operates at three levels, the micro level (products, companies, consumers), meso level (eco-industrial parks) and macro level (city, region, nation and beyond) [2]. To achieve such an economy, four actions have been suggested: reuse, repair, remanufacturing, and recycling (Figure 1) [3, 4]. These actions close loops and connect different stages of the supply chain of a product that in a linear economy are discreate. These interconnections along with the players and stakeholders connected with them make decision making for CE supply chains very challenging. A holistic systems engineering approach is thus clearly needed to navigate the multi-scale, multi-faceted and interconnected CE supply chain, identify opportunities for synergistic benefits and systematically explore interactions and trade-offs.

2. Methods

We present the foundations of a systems engineering framework and quantitative decision-making tools for the analysis and trade-off optimization of interconnected resource networks to achieve a CE. The framework combines data analytics and mixed-integer modelling and optimization methods to establish (i) the interconnections between different stages of the supply chain, (ii) the potentially

competing interests amongst various stakeholders, and (iii) policy, regulation and societal issues. A multi-objective optimization strategy is followed for the analysis of the trade-offs empowered by the introduction of composite metrics for CE that include waste, energy and resource use minimization, as means to facilitate decision making and compare alternative process and technological options. The versatility, potential and applicability of the proposed framework will be demonstrated through a case study on the supply chains of coffee [6].

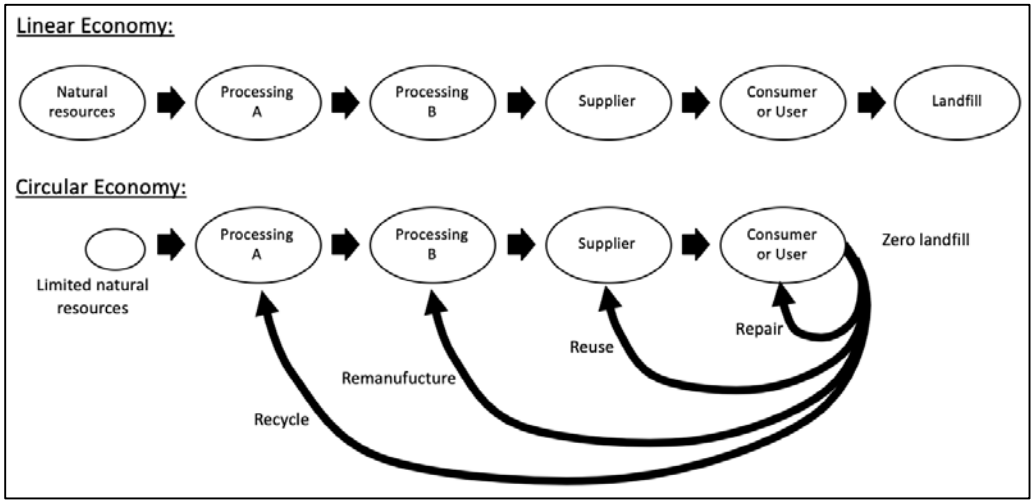

Figure 1. Linear and Circular Supply Chain

3. Results and discussion

Computational results of the two case studies indicate that the proposed approach is capable of supplying the decision makers with different optimal trade-off solutions and pathways towards a CE supply chain.

4. Conclusions

CE supply chain systems call for a systematic methodology that considers conflicting objectives, multiple scales and stakeholders for optimal decision making. This work presents a system's engineering framework for the analysis and trade-off optimization of supply chains towards a CE.

References

[1] Ellen MacArthur Foundation, Intelligent assets: Unlocking the circular economy potential, 2016.
[2] J. Kirchherr, D. Reike, M. Hekkert. Conceptualizing the circular economy: An analysis of 114 definitions, Resources, Conservation and Recycling, 127 (2017) 221-232.
[3] M. Lieder, A. Rashid. Towards circular economy implementation: a comprehensive review in context of manufacturing industry, Journal of Cleaner Production, 115 (2016) 36-51.
[4] R. De Angelis, M. Howard, J. Miemcyk. Supply Chain Management and the Circular Economy: towards the Circular Supply Chain, Production Planning and Control, 29 (2017) 425-437.
[5] S. Avraamidou, A. Milhorn, O. Sarwar, E. N. Pistikopoulos. Towards a quantitative Food-Energy-Water Nexus metric to facilitate decision making in process systems: A case study on a dairy production plant, 28th European Symposium on Computer-Aided Process Engineering (ESCAPE-28), Elsevier, (2018) 391-396.
[6] G. A. Figueroa, T. Homann, H. M. Rawel. Coffee Production Wastes: Potentials and Perspectives, Austin Food Science, 1(3) (2016) 1014.

ECCE12
The 12th EUROPEAN CONGRESS OF CHEMICAL ENGINEERING
Florence 15-19 September 2019

Green Solvent Selection and Early Stage Process Design for the Homogeneously Catalyzed Reductive Amination of Long-chain Aldehydes

Steffen Linke[1,*], Kevin McBride[2], Karsten Hans Georg Rätze[1] Kai Sundmacher[1,2]

1 Otto-von-Guericke University Magdeburg, Chair for Process Systems Engineering, Universitätsplatz 2, 39106 Magdeburg, Germany; 2 Max Planck Institute for Dynamics of Complex Technical Systems, Process Systems Engineering, Sandtorstraße 1, 39106 Magdeburg, Germany

**Corresponding author: linke@mpi-magdeburg.mpg.de*

Highlights

- Integrated computer-aided solvent selection and process design.
- Performance evaluation in terms of thermodynamic and environmental criteria.
- Application of the methodology to a challenging, complex reaction.

1. Introduction

One of the major challenges facing chemical engineering today is the transition from fossil-based resources towards renewable alternatives. In pursuit of this goal, difficulties arise connected to the conversion of biomass into useful substrates. Not only this, but there are additional questions regarding how to efficiently use the long chained molecules gained from such biomass conversions [1]. This leads to the need for new process concepts. One such promising approach for the functionalization of long chained molecules is homogeneous catalysis. The use of homogeneous catalysts enables mild reaction conditions, higher selectivities with respect to the target products, and high reaction rates. However, the most critical step in homogenously catalyzed processes is usually the recovery of the often expensive transition metal catalysts (e.g. Rhodium). Liquid extraction can efficiently solve this separation problem using a suitable solvent as extraction agent [2]. In most cases, the choice of the solvent is made on the basis on expert's knowledge and predictive tools, like the Hansen parameters or COSMO-RS that explore the direct functionality of the solvent without consideration of the efficiency of the entire process.

In this work, we present a new approach to compare systematically the performance of different solvents – determined by computer-aided solvent screening – on the process level, and exemplify it for the reductive amination of long chained aldehydes [3]. Besides thermodynamic properties, our approach includes environmental, health and safety criteria (EHS) in order to select a green solvent, and it estimates the technological-economic process performance of green solvents.

2. Methods

For the generation of possible solvent candidates, screening of approx. 7800 molecules using COSMO-RS was performed, thereby taking into account the boiling point, the solubility of the Rhodium-based catalyst and the size of the liquid-liquid miscibility gap wherein liquid-liquid extraction of the catalyst can be performed. For the evaluation of the EHS criteria, we took various QSAR models found in the VEGA toolbox [4] and created from these several ensemble models to

represent each predicted characteristic. Finally, the ensemble model results were compressed into a single, overall green solvent index in order to efficiently rank solvents. EHS end-points considered are carcinogenicity, mutagenicity, fish toxicity, biodegradability, persistence, among others. After identifying a set of suitable solvents, process design based around these candidate solvents is performed. The separation task is defined by the composition formed after the reaction; there may be one or two liquid phases depending on the solvent used in the reaction. For the downstream process, we consider liquid-liquid and vapor-liquid separations. The split factor for each separation step is calculated with COSMO-RS due to the lack of experimental data at this design stage.

3. Results and discussion

In figure 1, the general design methodology is illustrated starting with the thermodynamic and EHS solvent screening, and ending with the process design.

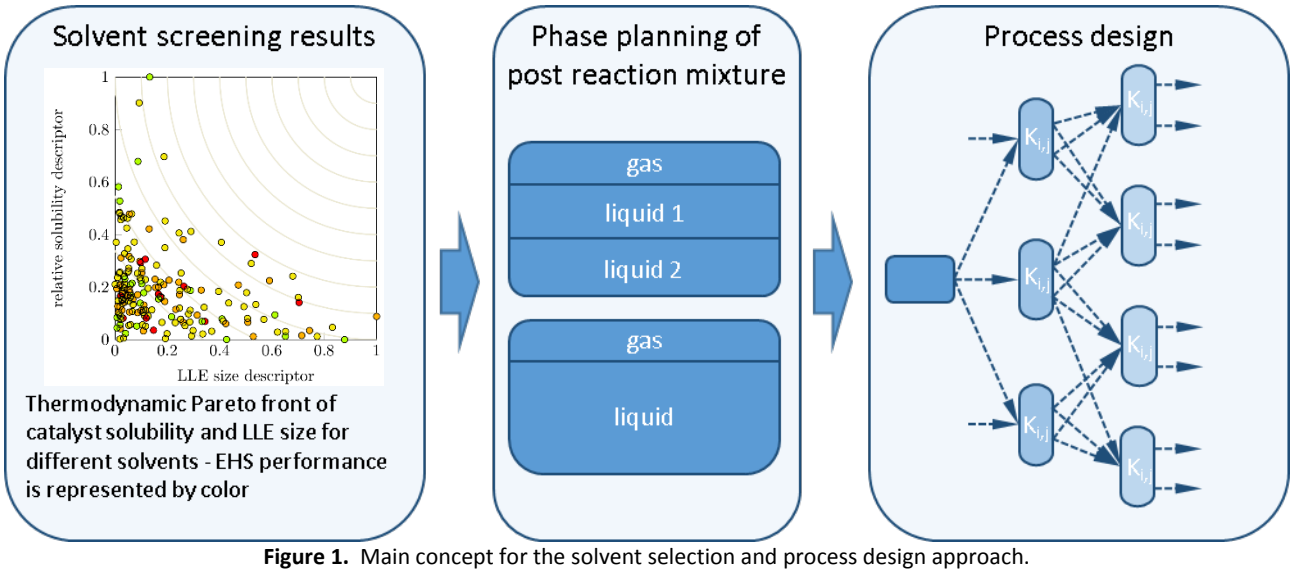

Figure 1. Main concept for the solvent selection and process design approach.

4. Conclusions

We present a combined solvent-process design approach for homogeneously catalyzed reactions and discuss the benefit of early stage process design compared to simple solvent screening methodologies. Simultaneously, the performance potential of green solvents is evaluated.

Acknowledgement

This research work was conducted within the Collaborative Research Centre “InPROMPT: Integrated Chemical Processes in Liquid Multiphase Systems” (Project B9). The financial support from the German Research Foundation (DFG) under the grant SFB/TRR 63 is gratefully acknowledged. S.L. is also affiliated with the „International Max Planck Research School for Advanced Methods in Process and Systems Engineering (IMPRS ProEng, Magdeburg)”.

References

[1] A. Behr, A.J. Vorholt, Homogeneous Catalysis with Renewables, Springer Nature, 2017
[2] K. McBride, N.M. Kaiser, K. Sundmacher, Comput. Chem. Eng. 105 (2017), pp. 212-223.
[3] A. Behr, R. Roll, J. Mol. Catal. A: Chem. 239 (2005), pp. 180-184.
[4] E. Benfanati, A. Manganaro, G. Gini, CEUR workshop proceedings Vol. 1107 (2013)

ECCE12
The 12th EUROPEAN CONGRESS OF CHEMICAL ENGINEERING
Florence 15-19 September 2019

Multi-step Automated Heat Exchanger Network Retrofit Planning

Timothy G. Walmsley[1], Nathan Lal[2], Petar S. Varbanov[1], Jiří J. Klemeš[1]

1 Sustainable Process Integration Laboratory – SPIL, NETME Centre, Faculty of Mechanical Engineering, Brno University of Technology, Brno, Czech Republic; 2 Energy Research Group, School of Engineering, University of Waikato, Hamilton, New Zealand

**Corresponding author: walmsley@fme.vutbr.cz*

Highlights

- Heat Exchanger Network retrofitting is becoming increasingly more urgent
- The Automated Retrofit Targeting algorithm is further developed
- A petrochemical example is analysed, developing many retrofit investment plans
- The best three-step retrofit option saved 7.3 MW with a profit of 1.3 M EUR/y

1. Introduction

Ever-rising energy costs and environmental concern drives a cycle of continuous process energy improvement in the chemical and process industries. To remain competitive, industrial companies and sites need to retrofit and revamp their technology to keep pace with more energy-efficient new plants. Such options include disruptive projects – e.g. new reactor installation – and incremental improvement – e.g. new heat exchangers [1]. Due to the capital intensity of disruptive change, most companies favour incremental, low-risk retrofit. Recent efforts have focused on graphical retrofit techniques based on individual process stream mapping [2] and the Energy Transfer Diagram [3] as well as mathematical optimization techniques [4].

This paper presents an extension to the recently developed Automated Retrofit Targeting – ART algorithm [5]. A unique feature of the algorithm is the comprehensive search function that systematically looks at all practicable pathways for energy retrofits. This algorithm is now extended in this work to a multi-step approach, exponentially increasing the number of retrofit options while providing a long-term investment guide for energy projects. To help counteract the increase in complexity, the extended ART determines the Pareto optimal solutions, together with logical and thermodynamic constraints [6], reducing the search space to a manageable size.

2. Methods

The ART algorithm was previously developed and explained by Walmsley et al. [5] and further refined by Lal et al. [6]. To main brevity, please refer to these works for method details. Two changes are proposed in this work. First, the extension implements an outer iterative loop to obtain multi-step retrofit solution, detailing the retrofit action required at each step. Second, the extension finds the Pareto optimal solutions using

$$\max \quad \left\{ k\frac{Q_i}{Q_{max}} + j\frac{(Q/A)_i}{(Q/A)_{max}} + (1-j-k)\frac{(Q/n)_i}{(Q/n)_{max}} \right\}, \quad 0 \le j \le 1, \quad 0 \le k \le 1, \quad j+k \le 1 \tag{1}$$

by varying values of *k* and *j* at steps of 0.1. In Eq. 1, *Q* is the heat savings, *A* is the required new heat transfer area, and *n* is the number of new heat exchanger units (modifications). The approach intentionally relied on non-economic results that are key dimensions that affect economics.

3. Results and discussion

This work re-examines the petrochemical case study of Walmsley et al. [5]. The number of retrofit "steps" was limited to 3. Figure 1 presents the results with the various colours representing each of the sequential steps with the "best" solution (i.e. the most profitable). The algorithm selected the retrofit option with the shortest payback (1.1 y) as the first step. The 48 possible first retrofit steps are not shown due to provide better clarity. Figure 1A shows the general trend that as successive retrofit steps are taken, the ratio Q/A decreases, i.e. diminishing returns with the additional area.

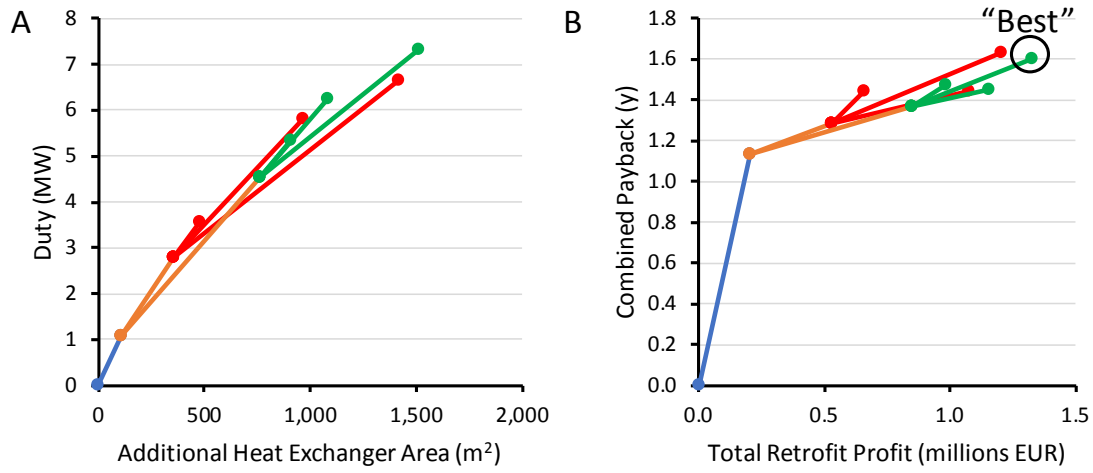

Figure 1. Pareto front of Heat Exchanger Network retrofit options - (A) Trade-off between area and heat recovery duty. (B) Economic performance.

4. Conclusions

The extended multi-step Automated Retrofit Targeting algorithm, combined with the identification of the Pareto front, has enabled a new tool for retrofit investment planning. A petrochemical plant example is solved, providing multiple options for investment in Heat Exchanger Network retrofit with an estimated final profit of 1.3 M EUR/y and a payback of 1.6 y for the best solution. With a heat savings of 7.3 MW, the estimated greenhouse gas emission reduction is 11,800 t/y.

The new Automated Retrofit Targeting algorithm has many facets that will continue to be developed in future work. Some directions include heat pump integration, lifecycle analysis, detailed heat exchanger design, and network simulation.

References

[1] L. Čuček, S. Boldyryev, J.J. Klemeš, Z. Kravanja, G. Krajačić, P.S. Varbanov, N. Duić, Journal of Cleaner Production 211 (2019) 884–894.
[2] Y.Q. Lai, Z.A. Manan, S.R. Wan Alwi, Energy 155 (2018) 1113–1128.
[3] J.-C. Bonhivers, B. Srinivasan, P.R. Stuart, Applied Thermal Engineering 119 (2017) 659–669.
[4] N. Jiang, W. Han, F. Guo, H. Yu, Y. Xu, N. Mao, Energy Conversion and Management 177 (2018) 477–492.
[5] T.G. Walmsley, N.S. Lal, P.S. Varbanov, J.J. Klemeš, Frontiers of Chemical Science and Engineering 12 (2018) 630–642.
[6] N.S. Lal, T.G. Walmsley, M.J. Atkins, M.R.W. Walmsley, J.R. Neale, 1 70 (2018) 1951–1956.

ECCE12
The 12th EUROPEAN CONGRESS OF CHEMICAL ENGINEERING
Florence 15-19 September 2019

Process design and economic analysis of a biomass-based integrated gasification combined cycle (BIGCC) system

Fang Wen[1], Bin Shi[1], Wei Wu[2,1*]

[1]Department of Chemical Engineering, Wuhan University of Technology, Wuhan 430070, China;
[2]Department of Chemical Engineering, National Cheng Kung University, Tainan 70101, Taiwan

*Corresponding author: weiwu@gs.ncku.edu.tw

Highlights

- A heat-integrated IGCC polygeneration plant using SCL is presented.
- The investing in BIGCC is superior to the conventional IGCC power plant.

1. Introduction

Recently, the IGCC power plants were combined with the clean coal technologies which were used to reduce CO_2 emissions and remove other pollutant emissions such as sulfur dioxide (SO_2) and nitrogen oxides (NOx). The oxy-fuel combustion with the aid of the air separation unit (ASU) could effectively reduce NOx and increase the concentration of CO_2 in the flue gas, but the high cost and the high energy penalty of ASU would obviously enhance the levelized cost of electricity (LCOE) [1]. To improve the overall efficiency of the IGCC system, an elevated-pressure ASU had significant potential option [2]. Regarding the reduction of energy penalty of ASU, a new technology based on coal gasification integrated with the syngas chemical looping (SCL) was validated to reduce the energy penalty as well as the capital cost of the cryogenic air separation unit (CASU). This work show a few results (i) a heat-integrated IGCC polygeneration plant using SCL is presented, (ii) the SCL contributes to generate electricity, H_2, and CO_2-rich gas, (iii) the net energy efficiency of the proposed design can achieve about 60% if ASU and CCS are removed, (iv) the BIGCC using 20% biomass in place of coal can reduce the yields of hydrogen and methanol by 8.3% and 10.7%, respectively.

2. Methods

The proposed BIGCC power plant connecting the syngas chemical-looping (SCL) shown in Fig. 1 is carried out the process simulations in the Aspen Plus environment.

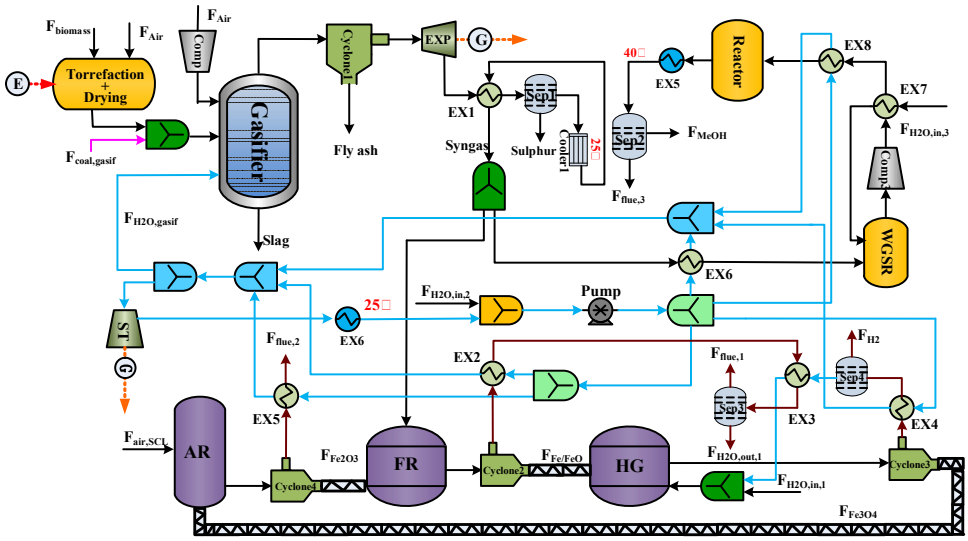

Figure 1. Schematic of BIGCC power plant connecting the syngas chemical-looping (SCL)

3. Results and discussion

This study is emphasized on the reactor design in the chemical looping, where the fast fluidized bed reactor and the moving bed reactor can be validated by some experiments. Through the system integration, the new polygeneration processes with biomass gasification is proposed and its performance in terms of hydrogen yield, hydrogen thermal efficiency, net power efficiency, and the overall system efficiency is evaluated. Based on the prescribed economic model with different scenarios and conditions, the economic indicators such as the levelized cost of electricity, net present value, and internal rate of return carry out the complete economic assessment. Finally, it is expected that the BIGCC has a few economic benefits. In the research, the integration of Aspen Plus® and Matlab® is used to execute the simulation task.

4. Conclusions

To remove the high energy duty of the air separation unit such as CASU are investigated, the BIGCC polygeneration plant connecting can increase the net energy efficiency output since it connects the syngas chemical looping to generate electricity and hydrogen simultaneously. The corresponding net efficiency would be up to 60% if the heating values of fuels of hydrogen and methanol are taken into account.

References

[1] D.Y.C. Leung, G. Caramanna, M.M. Maroto-Valer. Renew Sust Energ Rev 39 (2014) 426-443.
[2] B. Shi, E. Wu, W. Wu, Energy 134 (2017) 449-457.
[3] L. Zhu, F.. Wang, Z. Zhang, Chem Eng Process 106 (2016) 33-41.
[4] B. Shi, W. Xu, E. Wu, W. Wu, P.-C. Kuo, Journal of Cleaner Production 195 (2018) 176-186.

ECCE12
The 12th EUROPEAN CONGRESS OF CHEMICAL ENGINEERING
Florence 15-19 September 2019

A Simulation-based Support System for the Planning and Design of Modular Logistics in Chemical Production Processes.

Christian Sonntag[1,*], Dominik Wolff[1], Markus Zajac[2]

1 INOSIM Consulting GmbH, Joseph-von-Fraunhofer-Str. 20, 44227 Dortmund, Germany
2 Fraunhofer-Institut für Materialfluss und Logistik, Joseph-von-Fr.-Str. 2-4, 44227 Dortmund, Germany
**Corresponding author: christian.sonntag@inosim.com*

Highlights

- Modular plant logistics are essential to realize the full potential of modularization.
- A new planning support tool enables efficient design of modular logistic systems.
- Material flow simulation quickly provides quantitative KPIs for decision support.

1. Introduction

In process industries, there is a constantly growing trend towards increasing product differentiation, shorter product life cycles, and increasing market volatility [1]. The reason for that lies in increasing market uncertainty: While in the past, usually only a few products were demanded constantly over long periods, nowadays markets require permanent innovation. This enforces raised industrial standards in production planning and logistics. To address these uncertainties, modular production concepts are receiving wide-spread attention since they allow industry to adjust their production processes quickly to changing market environments and enable a reduction in reconfiguration and adjustment times [2]. To realize the full potential of modularization, it must be extended beyond production itself to include the process logistics, including e.g. the plant supply chain, packaging, and shipping.

The increased flexibility that is provided by modular logistics systems requires new approaches for planning, engineering, and validation. In the scope of the research and innovation project LEGOLAS [3], we are developing a new planning support system for the simulation-based design of such modular logistics systems. This talk provides an overview of this system and illustrates its features on a challenging case study, the filling/packaging section of an herbicide/fungicide production plant.

2. The Planning Support System for Modular Production Logistics

The planning support system provides an environment to quickly design and validate modular logistics systems, covering scenarios such as from-scratch design, re-configuration, disturbance and fault analysis, and turnaround management.

Fig. 1 provides an overview of the iterative workflow that is supported by the planning support system. First, the user creates a set of system alternatives in a graphical drag-and-drop environment. These alternatives are then transformed into material flow models and analyzed using the INOSIM process simulation software to generate quantitative KPIs that the user then uses to choose a process alternative that fulfills all requirements or, if all alternatives are discarded, to return to the system design step to create more alternatives.

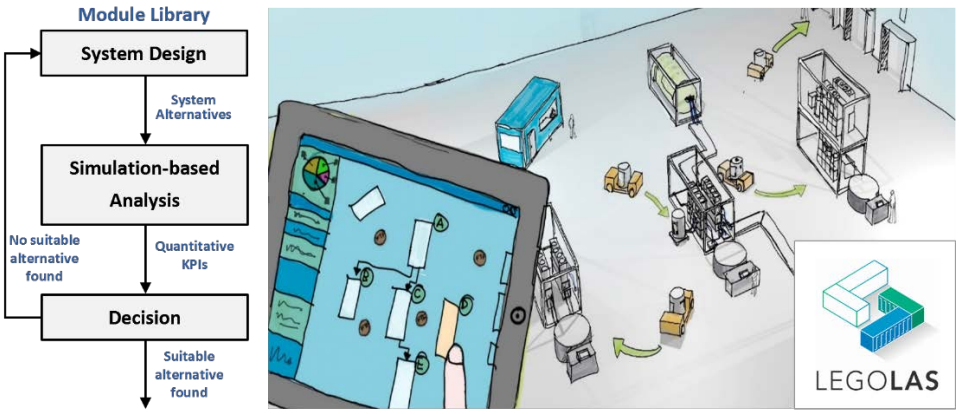

Figure 1. Conceptual workflow supported by the LEGOLAS planning support system.

3. Decision Support based on Material Flow Simulation

To illustrate the features of the planning support system, it has been applied to a challenging case study, the modular filling/packaging section of an herbicide/fungicide plant (see Fig. 2) by the German logistics provider Imperial Logistics. In this talk, the demonstration focuses on the simulation-based decision support step which is based on the dynamic simulation of modular logistics systems using the INOSIM process simulator and its new packaged-goods simulation engine, enabling the user to model complex batch and mixed processing plants and their logistical elements seamlessly within the same environment.

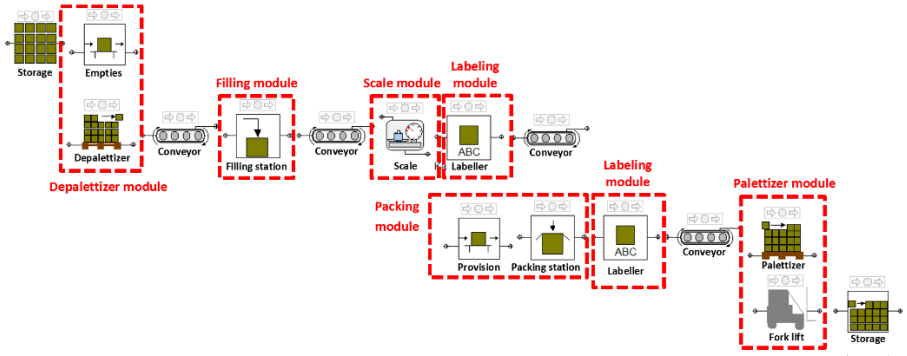

Figure 2. Flowsheet of a modular filling/packaging section of an herbicide/fungicide plant in the INOSIM process simulator.

4. Conclusions

The LEGOLAS planning support tool enables the efficient engineering of modular logistics systems based on material flow simulation for quantitative decision support. The next step is to validate it and illustrate its potential on a number of other challenging case studies.

References

[1] DECHEMA / VDI ProcessNet Work Group on Modular Plants: Flexible Chemical Production by Modularization and Standardization – Status Quo and Future Trends. White Paper, 2016, ISBN: 978-3-89746-191-2, available at: http://processnet.org/dechema_media/ModularPlants_2016-p-20002425.pdf
[2] F3 Factory: Flexible, Fast, and Future Production Processes. EU FP7 Project, 2009-2013, GA No. 228867.
[3] LEGOLAS: Planning Support System For Modular Industry 4.0 Plants in the Process Industries. R&I Project funded by the European Regional Development Fund (EFRE.NRW), 2017-2020.
[4] INOSIM Software GmbH: The INOSIM Process Simulation Suite. www.inosim.com.

ECCE12
The 12th EUROPEAN CONGRESS OF CHEMICAL ENGINEERING
Florence 15-19 September 2019

Benefits of Using Macrokinetic Bioreactor Models in Rigorous Flowsheet Simulators

Jan C. Schöneberger[1*], Armin Fricke[1], M. Nicolas Cruz Bournazou[2]

1 Chemstations Europe GmbH, Berlin, Germany; 2 Department of Chemistry and Applied Biosciences, ETH Zürich, Swizerland

**Corresponding author: js@chemstations.eu*

Highlights

- Simulation of coupled up- and downstream processes
- Rigorous First-Principal modelling of biotechnological processes
- Economic analysis and optimization of complete biotechnological processes

1. Introduction

The number of biotechnological processes that are realized in large-scale dimensions is steadily increasing. In addition to food technology applications such as breweries or biofuel applications like biogas and bioethanol plants, biorefineries for the production of basic and specialty chemicals are becoming more important. In classical EPC business, flowsheet simulators are used to solve the mass and energy balances of the processes taking into account the laws of thermodynamics. The results from the simulation form the basis for equipment dimensioning and plant wide process optimization.

The apparatus models used in biotechnology differ from the apparatus models used in classical chemical processes. Reactors or fermenters in biotechnological processes are often operated discontinuously. Downstream processes can be operated batch wise, but depending on the amount of product, a continuous process is often the more economical solution.

In the modeling of bioreactors, the high number and complexity of biochemical intracellular reactions makes it difficult to accurately describe the dynamic behavior of the reactor. In addition, the properties of the microorganisms are subject to constant change. Macrokinetic models can be used to describe these reactions at least for a certain time period or a specific state of the bacteria's life cycle. However, these models commonly need to be adjusted and model parameters must be updated regularly.

2. Methods

In this work two approaches are presented for including macrokinetic models in a flowsheet simulator, a mass-balance based approach and a mole-balance based approach. The different simulation results of these approaches are discussed in detail by means of a simple example from Fogler [1]. The mole-balanced approach is then applied to an Escherichia coli based production process for 1,3-Propanediol (PDO). Therefore, a more complex macrokinetic is used, similar to the one published by Anane et al. [2]. The PDO process is modelled in CHEMCAD as a combination of

four batch fermenters and a continuous downstream process with filtration section, ion exchanger, and distillation section. The flowsheet is depicted in Figure 1.

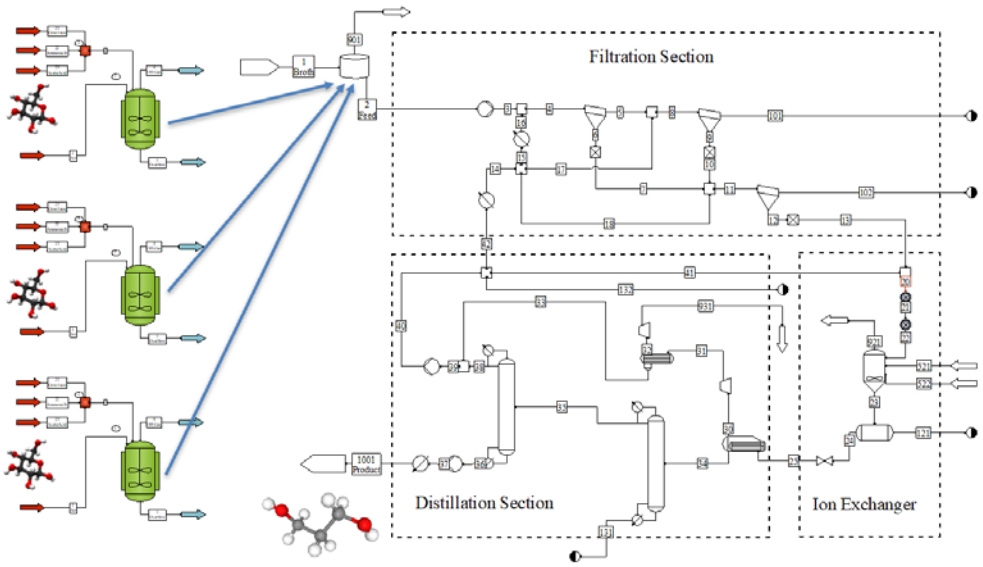

Figure 1. Simulation flowsheet of a bacteria based PDO production process.

3. Results and discussion

The simulation of the complete production chain from cane juice to PDO allows a detailed estimation of the operational expenditures (OPEX), considering the costs of the feed (cane juice, ammonia, and acetic acid), the utilities (electricity, steam, and cooling water), chemicals (caustic soda and sulfuric acid), and the revenues gained with the produced PDO as a function of the final product quality. Such calculations enable an economic optimization of the production process.

The maximization of the PDO plant's benefit was the task of the Process Simulation Cup 2018 [3], where students from all over the world were allowed to change predefined design variables. Table 1 shows the development of the calculated profit by enabling over the one year's runtime of the cup the design variables of the different sections.

Table 1. Achieved profit of the PDO plant during the different stages of the PSC2018.

Initial Solution	Optimization of the distillation section	Optimization of the distillation section and the recycle flows	Optimization of the substrate flows with fixed downstream	Optimization of the substrate flows + air flow with fixed downstream	Optimization of the coupled process
-387 $/h	191 $/h	422 $/h	695 $/h	1.192 $/h	1.408 $/h

4. Conclusions

The results given it Table 1 demonstrate impressively, how the usage of microkinetic bioreactor models in rigorous flowsheet simulators help to find optimal or at least improved operation parameters for biorefineries.

References

[1] H.S. Fogler, Elements of Chemical Reaction Engineering, 5th Edition, Prentice Hall, 2016
[2] E. Anane, D. Lopez, P. Neubauer, M.N. Cruz, Biochemical Engineering Journal 125 (2017) 23–30
[3] www. process-simulation-cup.com\psc2018 (Last called 03.01.2019)

Chemical Engineering Education in Botswana

Paul Serban Agachi[1]

1 Botswana International University of Science and Technology

**Paul Serban Agachi: agachip@biust.ac.bw*

Highlights

- Education and Higher Education in Botswana
- Chemical Engineering Education in Southern Africa.
- Botswana International University of Science and Technology. Chemical Engineering Department in Botswana.
- Challenges and successes

1. Higher Education in Botswana

Botswana is newly formed country, gaining its independence in 1966. Previously, the former state organizational form was Bechuanaland Protectorate under British rule, established in 1885 in the arid Kalahari Desert. Since it was a very poor territory (the diamonds were not discovered) there was practically no interest for development. Until 1982, Botswana did not have its own, autonomous HE institution. In 1964 the common University of Botswana, Lesotho and Swaziland (UBLS) was established and operated until 1974, with its headquarters in Lesotho. Then, the University of Botswana and Swaziland (UBS) functioned in Swaziland between 1975 and 1976. In 1982, the University of Botswana (UB), the first autonomous institution of HE in the country, was established and was totally focused on the "education of educators". At the time of liberation, there were only 677 qualified primary school teachers. And that was all teachers' body in Botswana. It is touching how UB was established through public donations: each family donated as much as it could from their household: a cow, a goat … Only in 1991, the next professional technical university was established, the present Botswana University of Agriculture and Natural Resources and, long time after, in 2005 (but practically operating from 2012), Botswana International University of Science and Technology [1].

2. Chemical Engineering Education in Southern Africa.

Southern Africa is the southernmost region of Africa, comprising Botswana, Lesotho, Namibia, South Africa and Swaziland. There are 9 Bachelor's Degree programs of Chemical Engineering/ Chemistry and Chemical Engineering/ Physical Metallurgy in South Africa only, plus one program in Namibia and one in Botswana. It is somehow unnatural that these countries with such luxury of minerals to remain exporters of small value added materials.

3. Botswana International University of Science and Technology. Chemical Engineering Department in Botswana.

The conception of the Botswana International University of Science and Technology (BIUST) can be traced to the national strategic shift that came with the Revised National Policy on Education (RNPE)

of 1994. Unlike the country's first Education Policy of 1977 dubbed 'Education for Kagisano' whose thrust was 'access and equity', the RNPE shifted focus to 'quality' and emphasized an education system geared at the world of work [2].

RNPE recognised Science and Technology as the driving engines in transforming the country from a pre-dominantly agro-based economy to an industrial economy, hence the subsequent establishment of a National Science and Technology Policy in 1998.

The first program of Chemical Engineering in Botswana was a logic consequence of the Botswana Economic Development Plan and was established in 2015 [3]. To build it from scratch was a real struggle.

4. Challenges and successes

Although it was a struggle to build the results are promising: next year 20 Batswana students graduate in this field. The curriculum had to be adapted at what Botswana needs most. There are plans of research and real research projects which are supposed to bring real benefit for the country.

References

[1] Tertiary Education at a Glance, Botswana, Human Resource Development Council, 2015
[2] History of BIUST, https://www.biust.ac.bw/about-us/history/
[3] BEng Program of Chemical Engineering, http://intranet.biust.ac.bw/Site/view.cfm?siteID=2002234

Influence of Different CO_2 Concentrations in Aeration Air During Thermophilic Fermentation Of *Bacillus Caldolyticus.*

Milan K. Popovic[1], Larissa Skelac[1], Sandra Wewetzer[1], Axel Karschöldgen[2], Johannes Bader[1]

1 Beuth University of Applied Science Berlin, Germany; 2) Kreienbaum Wissenschaftliche Messsysteme, Langenfeld, Germany
**Corresponding author: popovic@beuth-hochschule.de*

Highlights

- Optical dissolved CO_2-probe at 70 °C
- Fermentation of thermophilic bacterium
- Beneficial effect of increased CO_2 concentrations
- Increased yield by reduced aeration rate

1. Introduction

In fermentation processes, the concentration of CO_2 is a relevant parameter for the control of the metabolic function of microorganisms in the bioreactor. In most cases, CO_2 is determined in the exhaust-gas-stream as a sum parameter of the metabolic activity in the bioreactor. In large scale bioreactor inhomogenities exist, which can influence product yield and product quality. Whereas small amounts of dissolved CO_2 have advantageous effects on the production of amylase and proteases (Popovic *et al*., 2009 [1]; Bader *et al*., 2015 [2]), increased CO_2 concentrations result in a decreased pH value in the cells followed by altered metabolic activity. Hence, it is beneficial to measure directly in the fermentation broth, instead of using the exhaust-gas-analysis. A slight increase of CO_2-concentration can be achieved by a reduction of the aeration rate combined with a pressurized fermentation. Hence, aeration costs may be reduced and the yield can be increased simultaneously (Popovic et al. 2014 [3]).

2. Methods

Fermentation of *Bacillus caldolyticus* DSM 405 was performed in stirred tank reactor Biostat E (Sartorius AG, Germany) at 70 °C in batch mode. Amylase and protease activities were determined according to Manning and Campbell (1961) [4] and Strydom *et al.* (1986) [5]. The amount of dissolved carbon dioxide was calculated by the exhaust air composition (Sidor, Sick Maihack GmbH, Reute, Germany). CO_2 measurement by in-situ probe was carried out by using YSI 8500 CO2 Monitor (YSI Inc., Yellow Springs, USA).

3. Results and discussion

In the Biostat E bioreactors a congruent response of in-situ probe and exhaust gas analysis could be observed (Figure 1).

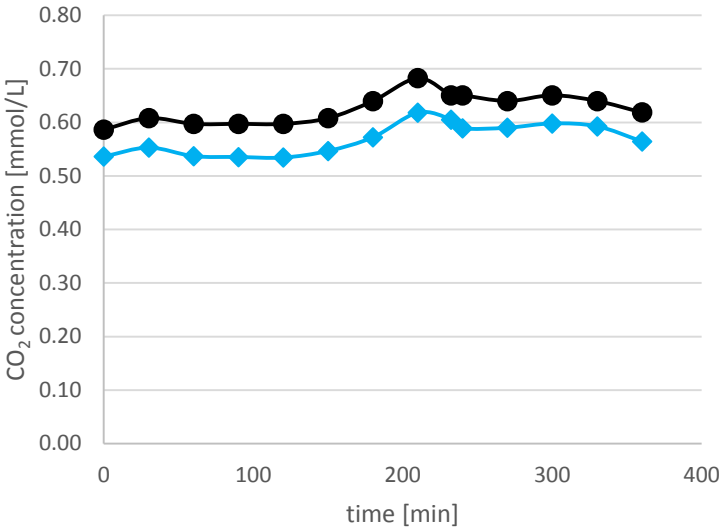

Figure 1. Comparison of the CO_2-quantification by in-situ probe (black dot) and exhaust gas measurement (blue diamond) (Bader *et al.*, 2015) [2])

At atmospheric CO_2 concentration, an amylase concentration of 5.5 U/mL was observed after 300 minutes whereas the increase in CO_2 concentration to 5% (v/v) resulted in a maximal amylase concentration of 6 U/mL after only 180 min. Comparable effects of the increased CO2 concentration were observed for the protease production. Without increased CO_2 concentration, 1.2 U/ml of protease were observed. At 5% (v/v) CO_2, 2 U/ml were secreted after 210 min.

These results indicate to importance of reliable CO_2 measurement during fermentation processes. Especially in large scale bioreactors these effects have to be taken into account due to high hydrostatic pressure and known inhomogenities.

4. Conclusion

In the presented work, the reliability of an optical dissolved CO_2-probe was evaluated during the fermentation of the thermophilic microorganism *Bacillus caldolyticus* at a temperature of 70 °C over a period of 10 hours. The results were compared with exhaust-gas-analysis measurement. The applied optical dissolved CO_2-probe showed comparable and reliable results during the whole fermentation process. This indicated the possibility of using this in-situ measurement even under high temperatures.

References

[1] M.K. Popovic, M. Senz, J. Bader, New Biotechnol. 25s1 (2009) 193
[2] J. Bader, C. Brigham, M.K. Popovic [Eds. Horst W. Doelle, Stefan Rokem, Marin Berovic], in Encyclopedia of Life Support Systems (EOLSS), Developed under the Auspices of the UNESCO, Eolss Publishers, Paris, France, 2015 [http://www.eolss.net]
[3] M.K. Popovic, M. Senz, J. Bader, L. Skelac, W. Schilf, R. Bajpai, New Biotechnol. (2014) 31 (2): 141-149
[4] G.B. Manning, L.L. Campbell, J. Bio. Chem 236 (1961) 2952-2957
[5] E. Strydom, R.I. Mackie, D.R. Woods, Appl. Microbiol. Biotechnol. 24 (1986) 214-217

ECCE12
The 12th EUROPEAN CONGRESS OF CHEMICAL ENGINEERING
Florence 15-19 September 2019

The Quality Monitoring of Vinyl Chloride Polymerization by Soft Sensor and OPC Technology.

Haitian Pan[1*], Pengfei Zhu[2], Mengfei Zhou[1], Luyue Xia[1]

1 College of Chemical Engineering, Zhejiang University of Technology, Hangzhou, Zhejiang 310014, PR China;
2 Zhejiang Longsheng Chemical Research Co. Ltd., Shaoxing, Zhejiang 312368, PR China

**Corresponding author: htpan@zjut.edu.cn*

Highlights

- A multi-model fusion modeling method
- A soft sensor application scheme by OPC technology
- The operation load of the entire monitoring system is light and stable

1. Introduction

In the vinyl chloride polymerization process, it is essential to monitor the polymerization rate and the conversion rate online for the sake of product quality, process optimization and safety [1]. Traditional off-line measurement methods cannot meet the real-time control requirements. A soft sensor method with multi-model is used for the polymerization process monitoring by OLE for Process Control (OPC) technology.

2. Methods

The development of modern control theory and artificial intelligence enriches the soft sensor technology [2,3]. According to the characteristics of vinyl chloride polymerization, a multi-model fusion modeling method, based on an improved Kalman filter algorithm, is proposed, as shown in Figure 1.

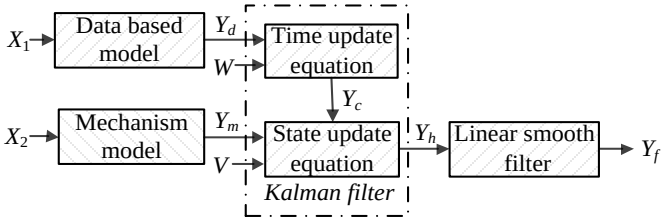

Figure 1. Multi-model fusion modeling structure

where， X_1, Y_d, X_2, Y_m are inputs and outputs. The update equations are as follows:

$$Y_t=Y_{t-1}+(Y_{d,t}-Y_{d,t-1})+w_{t-1} \quad (1)$$

$$Z_t=Y_{m,t}=HY_t+v_t \quad (2)$$

where t is the time, Y is the state variable, Z is the observation variable, H is the gain of state variable to observation value, w, v are the process noise and the measurement noise respectively, and the corresponding variances are W and V. In the recursive framework of the Kalman filtering algorithm, the combined weights are automatically adjusted online. The predictive value of combination model Y_h is obtained. Moreover, a linear sliding smoothing filter is applied to stabilize Y_h and the final prediction value Y_f is obtained. However, the application of the method takes much computing resource if this program is run in the control system. Thus, a soft sensor application scheme by OPC technology is proposed, the structure is shown in Figure 2. The server station and the operation station constitute the communication network through the industrial Ethernet. The real-time process parameters of DCS control system are sent by OPC server. The server computer runs soft

sensor module program. The target variables are sent back to the control system. The monitoring software obtains the data by the OPC client.

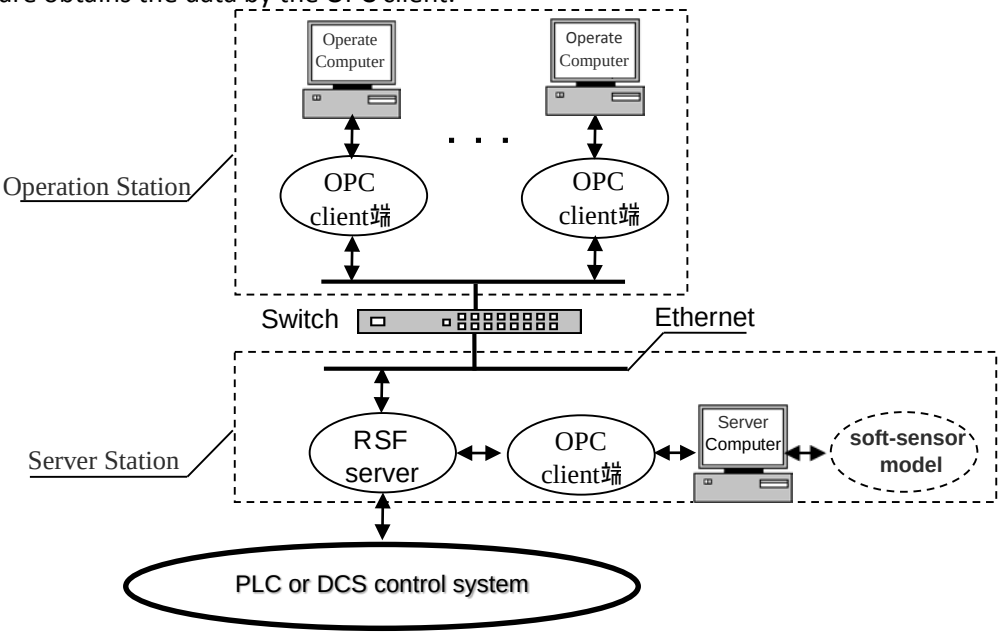

Figure 2. Structure of a soft sensor application scheme by OPC technology

3. Results and discussion

The multi-model fusion modeling method and OPC technology are applied to the soft-sensing of the polymerization rate in vinyl chloride polymerization. First, a data-driven modeling method is used by combining mixtures of Kernels Principal Component Analysis (K_2PCA) with Artificial Neural Network (ANN). The input variables are polymerization time *t*, polymerization temperature T_r, inlet and outlet temperature of jacket cooling water T_{Ji} and T_{Jo}, flow rate of jacket cooling water F_J. The output variable is polymerization rate. Second, a mechanism model based on the heat balance model of the reactor is proposed by calculating the thermal equilibrium parameters. The thermodynamic mechanism model is as follows:

$$Y_m = \frac{dx}{dt} = \frac{F_J \rho_w c_{p,w}(T_{Jo} - T_{Ji}) + F_w \rho_w c_{p,w}(T_r - T_{in})}{(-\Delta H_r) m_m} \tag{3}$$

The final value *of* polymerization rate Y_f is obtained through a series of mentioned techniques. Then, the polymerization conversion *X* can be obtained by integral.

$$X = \int_0^t Y_f \, dt \tag{4}$$

4. Conclusions

The OPC application result is satisfactory. The soft sensor technology solves the problem of online monitoring of the polymerization quality. The OPC technology solves the data switching problem between different software and hardware. The application in the vinyl chloride polymerization process proves the stability and reliability of the method.

References

[1] J. Zeaiter, V. G. Gomes, J. A. Romagnoli, et al. Chemical Engineering Journal,2002,89 (1-3) 37-45.
[2] F. S. Mjalli, A. S. Lbrehem. Chemical Engineering Research and Design, 2011, 89 (7) 1078-1087.
[3] G. Zahedi, A. Lohi, K. A. Mahdi. Fuel Processing Technology,2011, 92 (9) 1725-1732.

ECCE12
The 12th EUROPEAN CONGRESS OF CHEMICAL ENGINEERING
Florence 15-19 September 2019

Application of Iterative Real-time Optimization in an Intensified Continuous Plant at Pilot Plant Scale.

Anwesh Reddy Gottu Mukkula[1*], Sebastian Engell[1]

1 Process Dynamics and Operations Group, Technische Universität Dortmund, Germany

**Corresponding author: anweshreddy.gottumukkula@tu-dortmund.de*

Highlights

- A lithiation process performed in an intensified tubular reactor is optimized.
- Modifier adaptation with quadratic approximation (MAWQA) is used.
- MAWQA identifies the plant optimum in the presence of plant-model mismatch.
- Concentrations are measured using an online NMR developed by BAM, Berlin.

1. Introduction

It is always of great interest to identify the optimal point of a plant and to operate it at this point. Usually, the optimal operating point of a plant is identified by solving a model-based optimization problem. Developing an accurate mathematical model and estimating its parameters require a large amount of time and effort. Sometimes it may not be possible at all to develop an accurate model due to the complex phenomena that take place in the plant. Modifier adaptation with quadratic approximation (MAWQA) [1] is an iterative optimization scheme which uses measurements from the plant to drive the plant to its true optimum in spite of the presence of significant plant-model mismatch.

2. Methods

In MAWQA, the iterative gradient-modification optimization (IGMO) method is combined with a derivative free optimization (DFO) method to estimate the plant gradients along with an additional surrogate model. We refer to [1] for a detailed description of the MAWQA algorithm. The process under consideration is a lithiation reaction that takes place in a tubular reactor in a containerized pilot plant. The pilot plant setup has been developed in the European project F3-Factory [2]. The reaction mechanism and its kinetic parameters are not precisely known. The overall reaction is depicted in Figure 1.

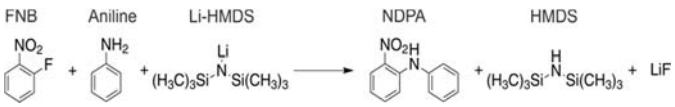

Figure 1: Overall lithiation reaction scheme

Due to the unavailability of the complete reaction information, the mathematical model of the process is incomplete and does not represent the behavior of the plant accurately.

The aim of the controller is to operate the process at its economically optimal operating point. This is enabled by real-time concentration measurements from a novel online NMR device that was developed by BAM, Berlin [3], in the context of the EU-funded project CONSENS [4].

The maximized plant profit function is: $\text{profit} = \frac{M_4 C_4 w_4}{\rho} \sum_i^3 u_i - \sum_i^3 w_i u_i$. M_4, C_4 are molar mass $[\frac{kg}{mol}]$ and concentration $[\frac{mol}{m^3}]$ of Li-NDPA. u_1, u_2, u_3 are feed flowrates $[\frac{kg}{h}]$ of Aniline, Li-HMDS and FNB. w_1, w_2, w_3, w_4 are relative costs of reactants Aniline, Li-HMDS and FNB and product Li-NDPA. ρ is the density $[\frac{kg}{m^3}]$ of the reaction mixture.

3. Results and discussion

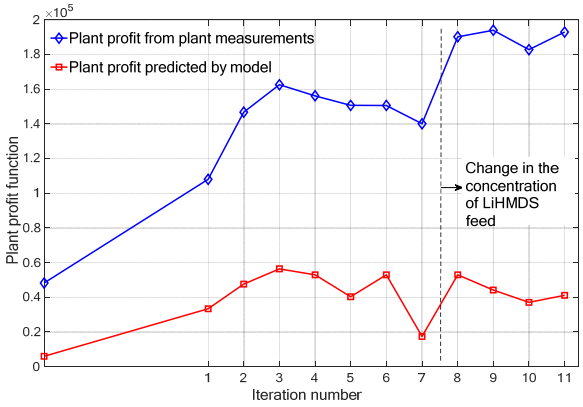

Figure 2: Plant cost over MAWQA iterations in the validation experiment performed at the pilot plant in INVITE, Leverkusen

The evolution of the plant profit during the iterative optimization using the NMR measurements is shown in Figure 2. The blue line indicates the real plant profit as computed from the measurements whereas red line represents the plant profit as computed from the nominal model which has both structural and parametric plant-model mismatch. After an unknown change of the feed concentration of Li-HMDS, the algorithm managed to improve the plant profit (blue line) significantly. In contrast, the plant profit function that was predicted by the model drops as a fixed value for the feed concentration is assumed.

4. Conclusions

In summary, it was validated that the combination of the NMR measurements with the iterative optimization algorithm MAWQA could drive the plant to an optimal operation despite significant deviations between the plant model and the true plant behavior. MAWQA reacted quickly to changes in the process conditions and responded by making input moves to identify the true process optimum. Measurement delays caused by low sample flow rates and long piping between the reactor and the NMR device can be compensated using the methods proposed in [5].

References

[1] W. Gao, S. Wenzel and S. Engell, “A reliable modifier-adaptation strategy for real-time optimization,” Computers & Chemical Engineering, pp. 318-328, 2016.

[2] “Final Report Summary - F³ FACTORY (Flexible, Fast and Future Production Processes),” [Online]. Available: https://cordis.europa.eu/project/rcn/92587/reporting/en. [Accessed 12 01 2019].

[3] S. Kern, K. Meyer, S. Guhl, P. Gräßer, A. Paul, R. King and M. Maiwald, “Online low-field NMR spectroscopy for process control of an industrial lithiation reaction---automated data analysis,” Analytical and Bioanalytical Chemistry, vol. 410, no. 14, pp. 3349--3360, 2018.

[4] “Consens,” [Online]. Available: http://www.consens-spire.eu/. [Accessed 12 01 2019].

[5] A. R. Gottu Mukkula, S. Wenzel and S. Engell, “Active Perturbations Around Estimated Future Inputs in Modifier Adaptation to Cope with Measurement Delays,” in IFAC-PapersOnLine, 2018.

ECCE12
The 12th EUROPEAN CONGRESS OF CHEMICAL ENGINEERING
Florence 15-19 September 2019

Optimization of Heat Exchanger Network in the Dehydration Process by Using the Utility Pinch Analysis.

Choon-Hyoung Kang[1]*, Moon Jeong[2], Seon Gyun Rho[3], In-Ju Hwang[4]

1 School of Applied Chemical Engineering, Chonnam National University, 77 Yongbong-ro, Buk-gu, Gwangju 500-757, Korea; 2.CES Co. Ltd. 166, Gosan-ro, Gunpo-si, Gyeonggi-do,15850, Kore; 3 Department of Fire Service Administration, Honam University, 417, Eodeung-daero, Gwasan-gu Gwangju, 62399, Korea; 4 Environment Engineering Research Division, Korea Institute of Construction Technology, 283 Goyangdae-ro, Ilsanseo-gu, Goyang-si, Gyeonggi- do 10223, Korea
**Corresponding author: chkang@jnu.ac.kr*

Highlights

- Perform modeling and pinch analysis for water removal process of natural gas.
- Process improvement in consideration of energy and economy in the water removal process of natural gas

1. Introduction

Many energy plants using processing system are trying to improve its efficiency and lessen the production of greenhouse gasses. In this study, the pinch analysis of the water removal process using triethylene glycol (TEG-$C_6H_{14}O_4$) was performed for the water removal process of the LNG plant. From the results of this study, the improvement factors of the heat flow were identified, and the applicability was evaluated by optimizing the pinch point on the composite diagram.

2. Methods

The economic feasibility was examined using the results of energy targeting using the pinch analysis. Energy costs were evaluated by using the following equation.

$$\mathrm{E \cdot C} = \sum\left(C_h \times Q_{h,min}\right) + \sum\left(C_c \times Q_{c,min}\right) \qquad (1)$$

C_h and $\mathrm{C_c}$ are utility costs of hot and cold temperatures, respectively. Also $\mathrm{Q}_{h,min}$ and $\mathrm{Q}_{c,min}$ are target energy values (kW) of hot and cold temperatures, respectively. Equation 2 was used to calculate the initial installation cost (C.C) of optimized heat exchanger network that can supply the minimum heat and cold utility values corresponding to energy target temperature (ΔT_{min}).

$$\mathrm{C \cdot C} = \mathrm{a} + \mathrm{b} \times \left(\frac{Area}{Shells}\right)^{C} \times Shells \qquad (2)$$

Finally, the total annual cost(TAC) is calculated from Eq(3) [1].

$$\mathrm{A \cdot C} = \mathrm{A} \times \left(\sum C \cdot C\right) + E \cdot C \qquad (3)$$

$$A = \frac{(1+ROR/100)^{PL}}{PL} \qquad (4)$$

Rate of return (ROR) is fixed at 10% as investment-return rate. In addition, the heat exchanger network plant life was assumed to be 15 years.

3. Results and discussion

The static process model for the water removal process and utility system is shown in Fig. 1.

Furthermore, an attempt was made to see whether it is viable to replace high-pressure steam to either mid (175 ℃, 1,500 kPa) or low (125 ℃, 500 kPa) pressure steam. We set 8.5 ℃ as the lowest allowable temperature and applied various steam pressures to create balance composite curve and utility composite curve as seen in Figs. 2 and 3. As a result, it was possible to replace with 102.9 MJ/h (61%) of low pressure steam and 21 MJ/h (13%) of mid pressure steam, which account for 74% of overall heat supply in the plant.

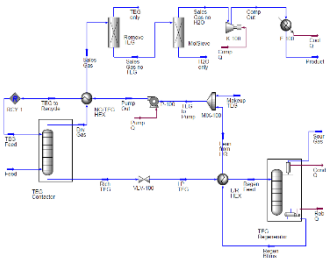

Fig. 1. The process flow diagram of the hydration process.

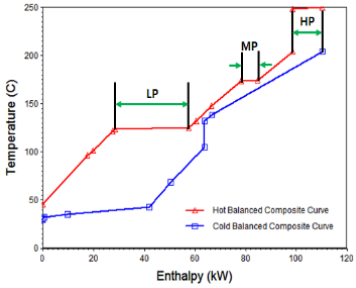

Fig. 2 Balanced composite curve with 3 utility.

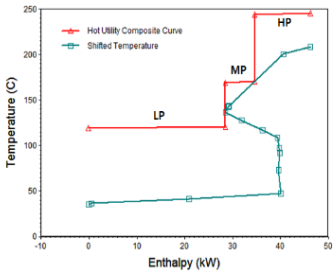

Fig. 3 Utility composite curve with 3 utility.

4. Conclusions

Defining hot and cold stream utilities during the dehydration process was in order, followed by carrying out static process modeling in the utility system. The data resulted from these steps allowed producing composite curves of various utility usage levels, which can be helpful in planning a reduction strategy of the heat exchange temperature in the dehydration process.

References

[1] S. G. Yoon, Applied Thermal Engineering, 27(2007) 886-893.

ECCE12
The 12th EUROPEAN CONGRESS OF CHEMICAL ENGINEERING
Florence 15-19 September 2019

Applying Stochastic Optimization to Demand-Side Management of a Combined Heat and Power Plant.

Egidio Leo[1], Keivan Rahimi-Adli[1,2], Benedikt Beisheim[1,2], Ralf Gesthuisen[2], Sebastian Engell[1]

1 Process Dynamics and Operations Group, Department of Biochemical and Chemical Engineering, Technische Universität Dortmund, EmilFigge-Str.70, 44221 Dortmund, Germany; 2 INEOS Manufacturing Deutschland GmbH, Alte Str. 201,50769 Köln, Germany

**Corresponding author: egidio.leo@tu-dortmund.de*

Highlights

- Development of an MILP model for Industrial Demand Side Management.
- Approximation of Multi-stage problems as a series of two-stage problems.
- Novel aggregated formulation for power contract optimization.
- Application of risk measures to an industrial-size power plant.

1. Introduction

Integrated production sites in the chemical industry typically consist of many large-scale plants which are highly interconnected through material (e.g. base chemicals or intermediates) and utility networks [1]. A power plant is of major significance, as it provides utilities to the plants, e.g. electricity and process steam. Furthermore, power plants are able to collect off-gases from other plants and use them as fuels. The importance of power plants is also acknowledged by the European Union with the CHP Directive (Directive 2004/8/EC, 2004) that sets a framework to promote growth of cogeneration plants.

In this work we address the integrated electricity procurement and operation of a power plant that supplies steam and power to a chemical process and interacts with the power grid. Adopting a stochastic mixed-integer programming formulation, the aim of this work is to optimally determine for a planning horizon of one week:

- the amount of electricity purchased from power contracts;
- a daily day-ahead commitment with hourly discretization to purchase electricity from the day-ahead market under time-sensitive prices;
- the hourly production levels of steam and electricity;
- the amount of fuels stored and the off-gases incinerated.

2. Methods

To integrate electricity procurement and operation of the power plant, we adopted a multi-stage stochastic mixed-integer programming approach taking into account day-ahead electricity price uncertainty [2, 3]. To overcome the large computational effort needed to solve an industrial-size multi-stage stochastic program, we adopt an approximation strategy that solves a series of two-stage stochastic programs within a rolling-horizon framework. The rolling horizon framework not only reduces the problem size but also makes it possible to react to new information available

regarding the amount of off-gases to be incinerated. The proposed approximation strategy drastically reduces the computational burden and renders possible the application of multi-stage programs to industrial-size optimization problems.

Considering even a low probability of large losses as not acceptable, we integrate the concept of risk into the optimization problem adopting the Conditional-Value at Risk measure.

3. Results and discussion

Fig.1 shows the electricity purchase profiles and the electricity produced by the power plant obtained solving the proposed multi-stage stochastic program with the described approximation strategy. The risk-averse solution follows the time-sensitive electricity price and purchases electricity from the power contracts when the price variation is higher to reduce the risk measure. The computation of a positive Value of the Stochastic Solution estimates the savings that the power plant could obtain adopting a stochastic formulation instead of a deterministic one.

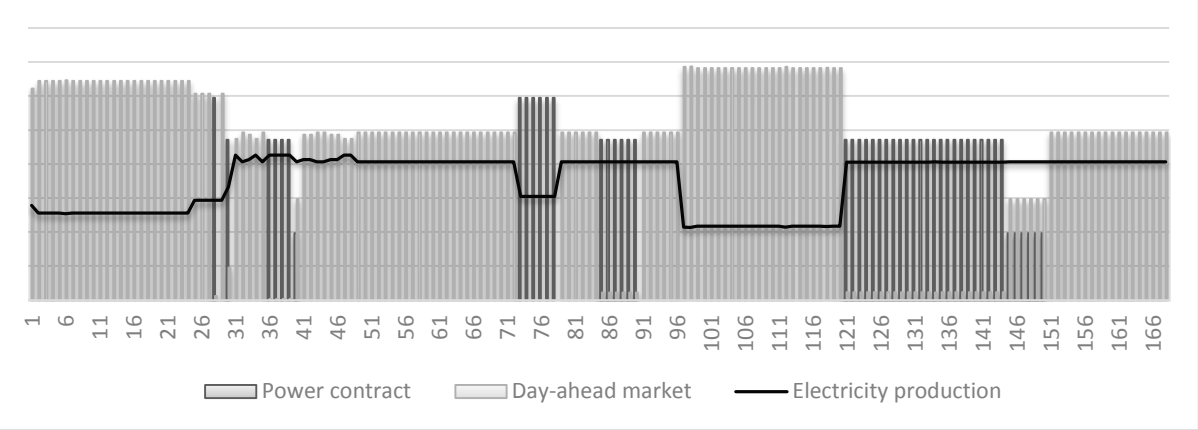

Figure 1. Optimal electricity procurement.

4. Conclusions

This work addresses the integrated electricity procurement and operation for an industrial-size power plant. A multi-stage mixed-integer stochastic program is proposed to model electricity commitments taking into account electricity price uncertainty. An approximation strategy is proposed to solve efficiently industrial size optimization problems.

Acknowledgements- The financial support from the Marie Sklodowska-Curie Horizon2020 project "PRONTO" (Contract No: 675215) is gratefully acknowledged.

References

[1] Wenzel et al, “Optimal resource allocation in industrial complexes by distributed optimization and dynamic pricing”, Automatisierungstechnik 2016; 64(6): 428–442
[2] Leo, E and Engell, S. “Multi-stage integrated electricity procurement and production scheduling.” In: International Symposium on Process Systems Engineering – PSE 2018.
[3] Leo, E and Engell, S. “Integrated day-ahead energy procurement and production scheduling“ Automatisierungstechnik 2018;66(11):950–963
[4] Mitra, S et al. “Optimal scheduling of industrial combined heat and power plants under time-sensitive electricity prices.” In: Energy 54 (2013), pp. 194–211.

ECCE12
The 12th EUROPEAN CONGRESS OF CHEMICAL ENGINEERING
Florence 15-19 September 2019

Price-based coordination of shared resources with external suppliers

Christian Klanke[1*], Lukas S. Maxeiner[1], Sebastian Engell[1]

1 Process Dynamics and Operations Group, Department of Biochemical- and Chemical Engineering, TU Dortmund University, 44221 Dortmund

**Corresponding author: Christian.klanke@tu-dortmund.de*

Highlights

- Ecological and economical savings via coordination of plants at chemical production sites
- Incorporation of access to global commodity markets
- Confidentiality in case of competing enterprises by employing a distributed coordination scheme

1. Introduction

Worldwide, chemical production sites are significant consumers of energy and resources and improving their efficiency has been pursued continuously over the past decades. Optimizing plant operations is an economically attractive way of improving their efficiency because the investments are relatively low, and the duration of the projects is not overly long. In large chemical sites, the plants are interconnected by networks of raw and intermediate materials and of carriers of energy, especially steam at different pressure levels. Coordinating the production and consumption of these shared resources provides an impactful lever towards a more efficient production.

While the site-wide optimization of the operation of the interconnected plants is theoretically feasible, practically it is desirable to perform a distributed optimization with some central coordination. One strong argument in favour of such schemes is that information on the internals of the individual plants, e.g. their demands, revenues and profit functions does not have to be shared so that such schemes can also be applied if the plants are operated by different business units. This can be achieved by so-called *price-based coordination* schemes in which a central coordinator balances the networks by adapting the transfer prices, which enter in the individual cost functions [1].

A limitation that the previously proposed coordination schemes suffer from is that many of the shared resources produced and/or consumed on the site are also available via external suppliers on short notice or can be sold on the spot market.

Such exchanges of materials and carriers of energy are subject of medium- or long-term contractual agreements. What we propose here is a scheme that determines dynamic transfer prices in the context of such agreements without providing the parties involved access to sensitive data, thus improving flexibility and enhancing fairness. This is an essential agreement of the practical implementation of industrial symbiosis.

2. Methods

A dual decomposition-based method entitled *price-based coordination* forms the core approach within this work [2]. Mathematically speaking, it is based on dual decomposition, interpreting the Lagrange multipliers as correct transfer prices of the resources and utilities under consideration [3]. As a result of applying dual decomposition the mass balances that govern the connecting networks are transformed into economical incentives for the individual plants. This way the network balances are satisfied and confidentiality is guaranteed [4].
The scheme uses a gradient-based update step that computes the equilibrium prices in an iterative procedure. At these equilibrium prices, the network balances are satisfied.

3. Results and discussion

Based upon an industrial case study, existing *price-based coordination* schemes have been extended to deal with complex pricing structures that are imposed by suppliers on external commodity markets. The investigated pricing structure covers two resources, where the purchase price of one resource depends on the purchase amount of both resources and vice versa.
Despite of this coupling of the purchase prices, it is possible to derive a distributed coordination algorithm, which finds the optimum of the resulting mixed-integer problem. The algorithm reliably converges to equilibrium prices, as can be seen in Figure 1 right. At the equilibrium price, the supplies and demands of all resources match, as shown in Figure 1 on the left. At the same time, optimal amounts of external purchases of both resources are determined.

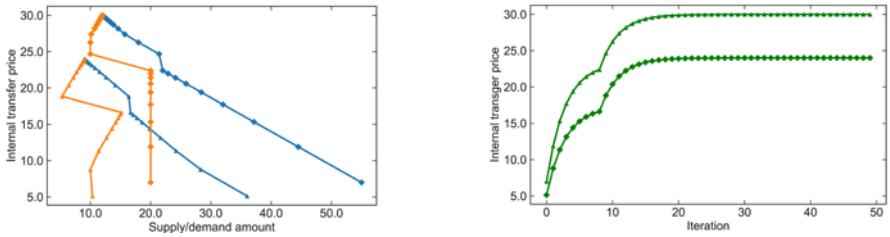

Figure 1. Supply (/) and demand (/) curves of two resources depending on the internal transfer price (left). Internal transfer price (/) plotted against iteration number for both resources (right).

4. Conclusions

By characterizing the solution structure of the centralized solutions to the coordination problem taking access to external markets into account, it is possible to find operating conditions and purchases at which the site operates optimally. Future work will include how to distribute the savings between the participating units on the site.

Acknowledgement

The project leading to this publication has received funding from the European Union's Horizon 2020 research and innovation programme under grant agreement No 723575 (CoPro, spire2030.eu/copro) in the framework of the SPIRE PPP.

References

[1] S. Wenzel, R. Paulen, G. Stojanovski et al., at – Automatisierungstechnik 64 (2016) 428-442.
[2] L.S. Maxeiner, S. Wenzel, S. Engell, Computer Aided Chemical Engineering 40 (2017) 1897-1902
[3] D. Palomar, M. Chiang, IEEE Journal on Selected Areas in Communications 24 (2006) 1439-1451
[4] R. Jose, L. Ungar, AIChE Journal 46 (2000) 575-587

ECCE12
The 12th EUROPEAN CONGRESS OF CHEMICAL ENGINEERING
Florence 15-19 September 2019

Computational fluid dynamics model of internally cooled bubbling fluidized-bed reactor for CO_2 methanation process

Son Ich Ngo[1], Young-Il Lim[1,*], Doyeon Lee[2], Kang Seok Go[2], Myung Won Seo[2]

1 Center of Sustainable Process Engineering (CoSPE), Department of Chemical Engineering, Hankyong National University, Gyeonggi-do, Anseong-si, Jungang-ro 327, 17579 Korea

2 Climate Change Research Division, Korea Institute of Energy Research, Daejeon, Yuseong-gu, Gajeong-ro 152, 34129 Korea

**Corresponding author: limyi@hknu.ac.kr*

Highlights

- A CFD model was proposed for CO_2 methanation in bubbling fluidized-bed (BFB).
- An internal helical heat exchanger was employed to the BFB reactor.
- Heterogeneous reaction kinetics and multiphase heat transfer were applied.
- Temperature, solid holdup, gas composition and reaction heat were analyzed.

1. Introduction

Power-to-gas (PtG) processes are being considered as one of the most promise alternatives to integrate renewable energy resources into a current energy grid [1] via CO_2 methanation process. Computational fluid dynamics (CFD) has become a suitable tool for design and hydrodynamics evaluation of chemical processes [2,3]. Kopyscinski et al., [4] did the first attempt to apply the fluidization technology for CO methanation. Recently, Sun et al., [5] evaluated the full-loop circulating fluidized-bed using CFD for CO methanation. However, few CFD studies on bubbling fluidized-bed (BFB) reactor have been done for CO_2 methanation with H_2.

This study focuses on the design of an internally-cooled BFB (IC-BFB) reactor for CO_2 methanation with H_2 using CFD model. A heterogeneous reaction kinetics from the literature and gas-solid heat transfer model are employed to the CO_2 methanation with a Ni-based catalyst. The CFD model results on pressure, velocity, temperature, solid volume fraction, CH_4 composition, and reaction heat are presented.

2. CFD model and boundary condition

The IC-BFB includes the two domains: (1) fluidized-bed reactor with diameter of 80 mm and height of 500 mm, where the catalyst bed height is about 250 mm; (2) helical coil heat exchanger (HCHE) with a tube diameter of 6 mm and a center diameter of two coils of 30 and 60 mm, respectively.

A commercial CFD code ANSYS Fluent R19 (ANSYS Inc., USA) was used, the reaction kinetics from Xu and Froment [6] was employed via a user-defined function. The material properties and boundary conditions are summarized in Table 1. The 2D CFD domains were discretized into 39,000 cells. The time step of the unsteady-state gas-solid Eulerian two-fluid flow model was set to 1×10^{-4} s. The CFD domains and mesh structure are shown in Figure 1a.

Table 1. Material properties and boundary conditions.

Material type	Properties					
	Diameter [μm]	ρ [kg/m³]	λ [W/m/K]	C_p [J/kg/K]	Diff. [m²/s]	Viscosity [kg/m/s]
Catalyst	100	2350 kg/m³	0.67	880	-	1.789e-5
Gas mixture	-	SRK real gas	Ideal-gas mixing-law	Mixing law	Kinetic-theory	Ideal-gas mixing-law
BC name	Boundary conditions					
	BC type	T [K]	HTC [W/m²/K]	P [Pa]	Velocity [m/s]	$CO_2/H_2/N_2$ [mole %]
Inlet	Velocity inlet	673	-	5e5	0.13 m/s	0.2/0.8/0
Outlet	Pressure outlet	673	-	5e5	-	0/0/1
Reactor wall	Wall	353	0.3	-	-	-
Coil wall	Wall	470	135	-	-	-

3. Results and discussion

The snapshots at t = 60 s for the contours of pressure, velocity, solid volume fraction, temperature, CH_4 mole fraction, and heterogeneous reaction heat are displayed in Figure 1b, c, d, e, f and g. Reactions are more intensive at the core of the reactor, while gas-solid mixing is enhanced by HCHE to become almost even distribution of temperature in the whole catalyst bed. The product dry gas compositions of $CO_2/H_2/CH_4$ = 0.079/0.329/0.592 are similar to literature [7].

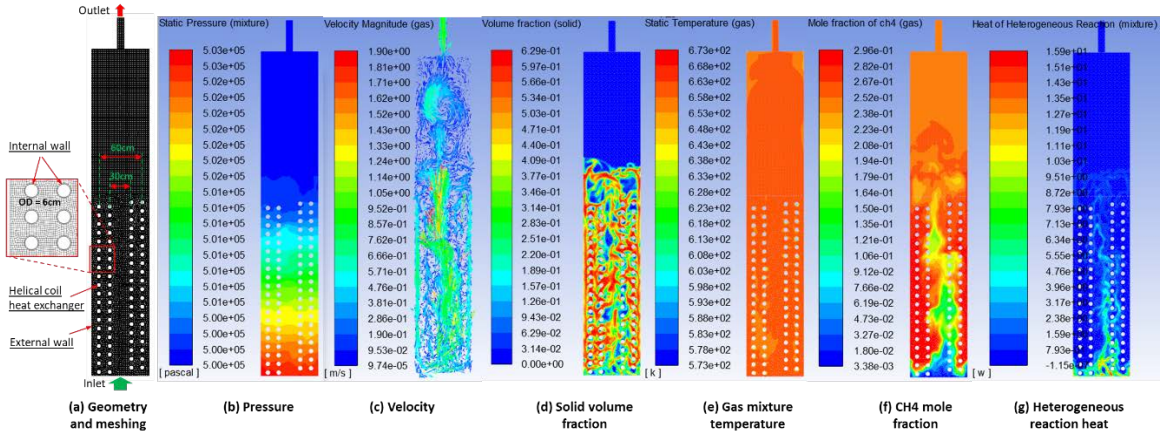

Figure 1. CFD domain and meshing, and CFD results.

4. Conclusions

An IC-BFB was modeled using a 2D Eulerian two-fluid CFD model for CO_2 methanation. The CFD model demonstrated the excellent heat and mass transfer capability of the IC-BFB reactor.

Acknowledgements

This work was conducted under framework of the research and development program of the Korea Institute of Energy Research (B9-2446).

References

[1] S.G. Jadhav, P.D. Vaidya, B.M. Bhanage, J.B. Joshi, J. Energy Chem. 25 (2014) 2557–2567.
[2] S.I. Ngo, Y.-I. Lim, W. Kim, D.J. Seo, W.L. Yoon, Appl. Energy. 236 (2019) 340–353.
[3] S.I. Ngo, Y. Il Lim, B.H. Song, U. Do Lee, J.W. Lee, J.H. Song, Powder Technol. 275 (2015) 188–198.
[4] J. Kopyscinski, T.J. Schildhauer, S.M.A. Biollaz, Chem. Eng. Sci. 66 (2011) 924–934.
[5] L. Sun, K. Luo, J. Fan, Fuel. 231 (2018) 85–93.
[6] J. Xu, G.F. Froment, AIChE J. 35 (1989) 88–96.
[7] S. Rönsch, J. Köchermann, J. Schneider, S. Matthischke, Chem. Eng. Technol. 39 (2016), 208–218.

ECCE12
The 12th EUROPEAN CONGRESS OF CHEMICAL ENGINEERING
Florence 15-19 September 2019

Optimization of water mist system in refinery process

Hyundo Park[1, 2], Junghwan Kim[1,*]

1 Green Materials & Processes Group, Korea Institute of Industrial Technology, Ulsan, Republic of Korea

2 Department of Chemical and Biomolecular Engineering, Seoul National University of Science and Technology, Seoul, Republic of Korea

**Corresponding author: kjh31@kitech.re.kr*

Highlights

- Development of CFD model and pilot plant based on the actual refinery process.
- Optimization of flow rate, number of nozzles and mist size.
- Reduction of the number of nozzles (20%) or amount of water (25%).

1. Introduction

At the CCR/Platforming process, which is operated by commercial refinery company, heat exchange is performed using an air-cooled heat exchanger. Unlike a water-cooled heat exchanger, an air-cooled heat exchanger uses air for heat exchange. Therefore, it is affected by ambient air temperature. Especially in the summer, when the temperature is high, a problem occurs that the heat exchange efficiency is reduced.

To solve this problem, many refinery companies are using water mist system. Water mist system is that sprays water finely to absorb heat in the ambient air. However, there is a problem with this system. That is, the corrosion of refinery device because of spraying excessive water.

In this study, we developed the CFD model to find out variables that affect water mist system and optimize the water mist system to solve the problem.

2. Methods

2.1 CFD modeling

The flow analysis model was developed based on the actual operational process using computational fluid dynamics (CFD). In this model, Lagrangian analysis and unsteady state flow conditions are simulated. There are 8 fans (2 fans/1 set) and 640 nozzles (80 nozzles/a fan) in the actual process. The CFD model is develop with 1/2 fan and 40 nozzles.

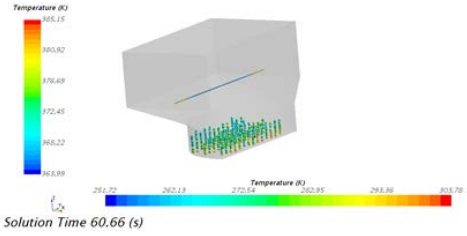

Simulator	Star CCM+ v12.04.011
Analysis time	60 seconds
Computational time	144hours/case (CPU 2.1GHz 64GB RAM)

Figure 1. CFD model of water mist system.

2.2 Pilot plant configuration

We made a pilot plant to observe the cooling effect of water mist system. The size of pilot plant is 2165mm (length) x 1670mm (width) x 2543mm (height).

3. Results and discussion

3.1 CFD simulation results

Table 1 shows two results. First, when the number of nozzles is decreased by 20%, the cooling effect increases by 6%. Second, when the total flow rate is increased by 16.7%, the cooling effect increases by 23.1%.

Table 1. Result of CFD simulation.

Case	Number of nozzles	Flow rate per nozzle	Total flow rate	Cooling effect [K]
1	64	15L/hr	960L/hr	-9.31
2	80	12L/hr	960L/hr	-8.78
3		14L/hr	1120L/hr	-10.81

3.2 Pilot plant test results

Table 2 shows no difference between nozzle A and B of cooling effect. Although the total flow rate of nozzle B is about 75% of nozzle A, they have almost same cooling effect. Because water mist size and distribution of nozzle B is smaller and better than nozzle A.

Table 2. Cooling effect by operating pressure.

	Input [K]	Output [ΔK, 30bar]	Output [ΔK, 40bar]	Output [ΔK, 50bar]	Output [ΔK, 60bar]
Nozzle A	387.15	45	45	45	45
Nozzle B		45	45	45	46

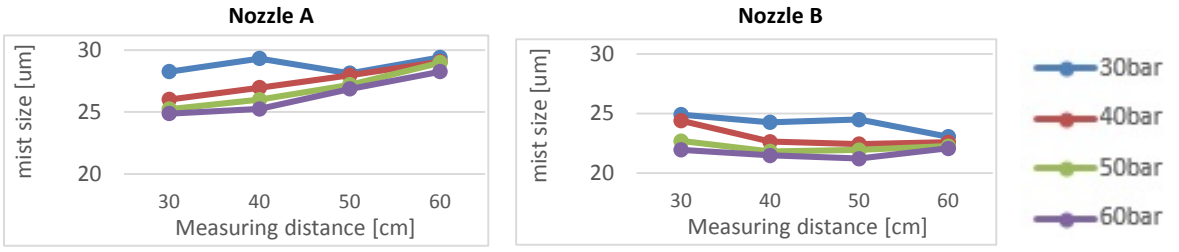

Figure 2. Water mist size by pressure.

4. Conclusions

We developed CFD model and optimized water mist system in refinery process. Pilot scale experiment for water mist system is conducted to find out mist size distribution and cooling effect depending on the nozzle A and B. Finally, we reduce the number of nozzles by 20% or amount of water by 25% to optimize the water mist system.

References

[1] Yan Hou, Yujia Tao, Yu Zou, Dongliang Sun, Numerical simulation of multi-nozzle spray cooling heat transfer, International Journal of Thermal Sciences. 125 (2018) 81-88

[2] Hideki Yamada, Gyuyoug Yoon, Masaya Okumiya, Hiroyasu Okuyama, Study of Cooling System with Water Mist Sprayers: Fundamental Examination of Particle Size Distribution and Cooling Effects, Building Simulation. 1(3) (2008) 214-222

ECCE12
The 12th EUROPEAN CONGRESS OF CHEMICAL ENGINEERING
Florence 15-19 September 2019

Immobilization of lipase onto micro tubular reactor for efficient production of (S)-ibuprofen.

Masakazu Naya*, Yuri Ikazaki, Katsuto Otake, Atsushi Shono

Department of Industrial Chemistry, Faculty of Engineering, Tokyo University of Science, Kagurazaka 1-3, Shinjuku-ku, Tokyo,162-8601, Japan

**Corresponding author: m.naya@ci.kagu.tus.ac.jp*

Highlights

- The activity of lipase on (S)-ibuprofen was confirmed by batch system.
- The immobilized lipase onto micro tubular has been prepared by multi-layer deposition.
- The reactivity of immobilized lipase was well conserved during repeated uses.

1. Introduction

Ibuprofen is an important drug material of NSAIDs and is sold as a racemate in the market. (S)-Ibuprofen has been reported to be 160 times more reactive than the (R)-ibuprofen. Currently established (S)-ibuprofen production methods involve complex organic synthesis. Lipases have been paid attention to lipid modifications [1]. They catalyzed hydrolysis, alcoholysis, acidolysis, amidolysis, and esterification in food and pharmaceutical industry. Some studies reported lipase reactivity for enantio synthesis of (S)-ibuprofen from racemate [2]. In spite of interesting performance of lipases, their application in industrial level is limited because of their cost and requires reuse of lipase for a practical process. We focused on immobilizing lipase onto micro tube and aimed to develop the reactivity of lipase for (S)-ibuprofen producing.

2. Methods

The polydopamine layer was used as a primer layer in polytetrafluoroethylene (PTFE) micro tube to provide inner surface of micro tube reactable groups. Polyethylenimine and *Candida rugosa* lipase were adsorbed on the PTFE surface by the layer-by-layer method. (S)-Ibuprofen production was initiated to introduce ibuprofen ester racemate as substrate into PTFE micro tubular reactor (Fig.1). The (S)-ibuprofen produced was analyzed quantitatively with HPLC.

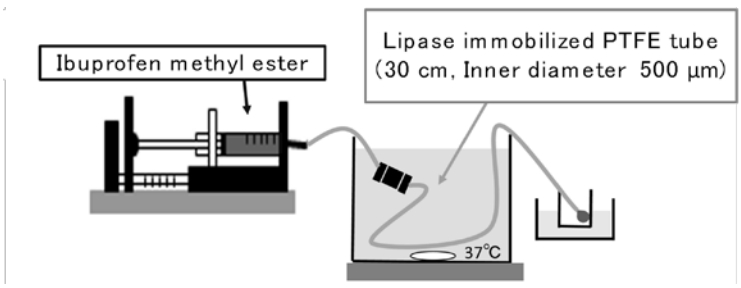

Figure 1. The experimental apparatus of (S)-ibuprofen production by immobilized lipase.

3. Results and discussion

The amount of loading lipase kept increasing as the number of layers increased by the 8th layer (Fig.2). The production yield of immobilized lipase on micro tubular reactor was developed than the yield prediction of batch system. The reactivity of immobilized lipase on tubular reactor (loading 3400 μg lipase) was determined by repeated reactions. The reactivity was well conserved during 8th repeated uses. It retained almost 80% of that of first reaction. The results successfully demonstrated that the immobilized lipase on PTFE inner surface was stable throughout the repeated uses.

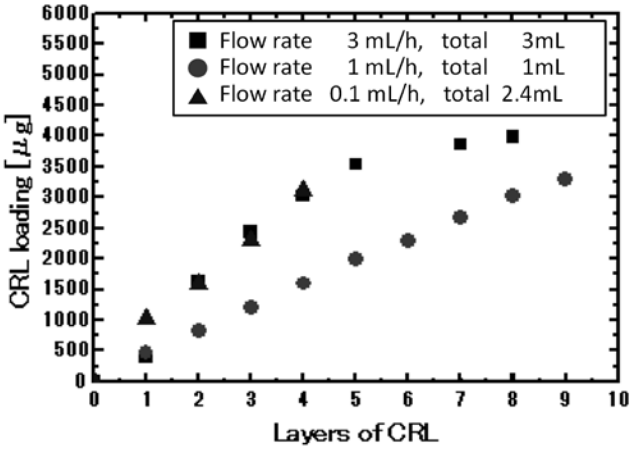

Figure 2. The amount of loading lipase by the multi-layer deposition on PTFE. The lipase loading kept increasing as the number of layers increased by the 8th layer.

4. Conclusions

The immobilized lipase onto micro tubular reactor has been successfully prepared by multi-layer deposition. Efficient performance of immobilized micro tubular reactor for production of (S)-ibuprofen was developed.

References

[1] Masakazu Naya, Masanao Imai, Journal of Chemical Technology and Biotechnology, 91, Issue 10 (2016) 2620-2630.
[2] Ozlem Sahin et al. Applied Cat A:General, 369 (2009) 36-41.

ECCE12
The 12th EUROPEAN CONGRESS OF CHEMICAL ENGINEERING
Florence 15-19 September 2019

Integration of power-to-gas concepts with biomass gasification in the Swedish electricity grid

Johan M Ahlström[1*], Viktor Johansson[1], Lisa Göransson[1], Stavros Papadokonstantakis[1]

[1] *Chalmers University of Technology, 412 96 Gothenburg, Sweden*

**Corresponding author: johanah@chalmers.se*

Highlights

- A gasifier combined with an electrolyser implemented in an energy systems model
- The value of process flexibility is compared to hydrogen storage
- Results highlight the benefits of a flexible biomass gasification process

1. Introduction

The variability of wind and solar electricity generation will demand a flexible electricity system in the future. Simultaneously, increased demand for fuels and chemicals produced from biomass is expected in the future in response to climate change mitigation goals [1]. A power-to-gas concept, which produces H_2 and O_2 can contribute to balancing the electricity grid while increasing the output of biofuel production processes [2]. In the present study we suggest a concept where generated H_2 is utilized to increase the output of methane from a biomass gasification plant by converting CO_2 effluent from the gasification cold gas, using the Sabatier process. The purpose is to evaluate the value of having a direct, oxygen blown, gasification process that can use H_2 to increase production when it is economical, in relation to a process with constant H_2 demand.

2. Methods

In a previous study, four process configurations were assessed for the upgrading of the produced gas to biomethane [3]. The considered configurations differ in terms of how CO_2 separation and H_2 separation are placed in relation to the Sabatier reactor in the flowsheet. Here, two gasification processes are considered, a flexible gasification process which can utilize H_2 to increase production if it is beneficial from an economical perspective, and a non-flexible process that requires a constant feed of H_2. Data generated from a sensitivity analysis over model parameters is used to create a linear surrogate model for CAPEX, OPEX and biomethane production as a function of CO_2 recirculation and H_2 addition (applying the partial least squares method). The equations are implemented in a cost-minimizing regional electricity system model [4]. Actual wind, solar and load data from Sweden is applied. The model optimizes the cost of the total electricity system and can produce biomethane with or without H_2 addition; the biomass supply is limited to 100 TWh/year.

3. Results and discussion

Figure 1 shows the total H_2 production and the electricity price over one year for the two types of gasifiers, the flexible one that can use H_2 to enhance production of biomethane, and the one which requires a constant feed of H_2 to generate biomethane of sufficient quality. For both cases, the model produced biomethane using all available biomass. In the flexible case, H_2 is injected at 44% of the hours of the year, for the second case it is constantly required. The gasifier configuration

with an adjustable hydrogen demand (Fig. 1 a)) uses electricity for hydrogen production at an average price of 4.5 €/MWh. The electrolysers in the adjustable gasification process are dimensioned to meet the maximal hydrogen demand from the process. To avoid electricity generation in gas turbines, the electrolysers are used with a storage to produce fuel for fuel cells if the biomethane price is above 70€/MWh. Implying, that it becomes cheaper to generate electricity at peak-load with fuel cells rather than using biomethane as fuel in gas turbines.

For the configuration with a constant demand for process hydrogen (Fig. 1 b)), the average electricity price for hydrogen production is 47 €/MWh. When high priced electricity is used for H_2 production the value increases and there is an incentive to store hydrogen. Therefore, the optimized electrolyser is dimensioned with approximately 10% higher capacity than the maximum H_2 input. Both the adjustable process and the process with constant demand increase the value of wind power contra the value of thermal generation techniques.

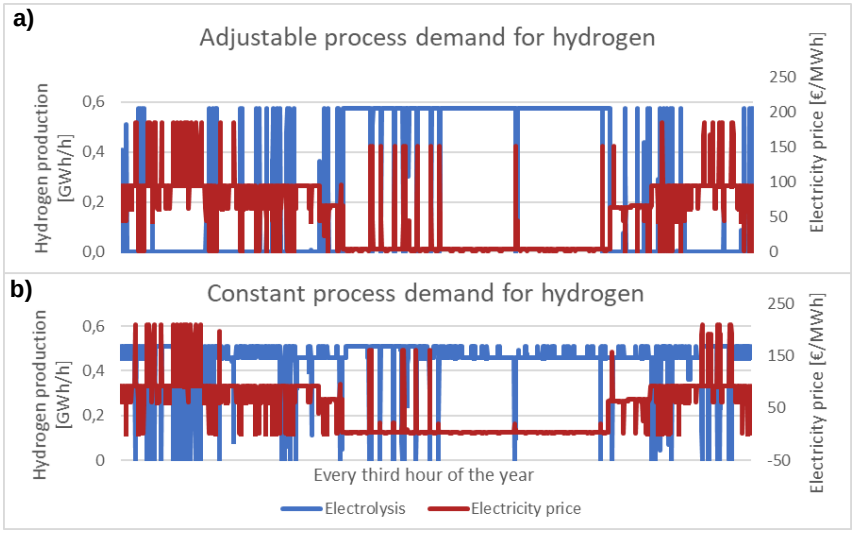

Figure 1. Hydrogen production and electricity price with a three-hour time resolution over 1 year. a) is a process configuration that can use H_2 flexibly, b) is a process configuration that need constant feed of H_2 to operate.

4. Conclusions

The adjustable gasification process uses low-priced electricity to increase methane production and the process with a constant H_2 demand avoids H_2 generation at the hours with highest electricity price by using storage. Both a static and flexible H_2 demand increases the economic benefits of constructing variable electricity generation. Thus, there is economic incentive to combine electrolysers with biomass gasification from a process perspective while it constitutes a driving force to increase wind power capacity. Future work will include analysis of the possibilities to include CCS in the gasification process and sensitivity analysis on important economic parameters, e.g. biomass price.

References

[1] D. Connolly, B.V. Mathiesen, and I. Ridjan, Energy, 2014. 73: p. 110-125.
[2] V. Johansson, L. Göransson, Impacts of variation management on cost-optimal investments in wind power and solar photovoltaics. Renewable Energy Focus, Under review.
[3] J.M Ahlström, S. Harvey, and S. Papadokonstantakis, Computer Aided Chemical Engineering, 2018. 44: p. 109-114.
[4] L. Göransson, et al.,. Applied Energy, 2017. 197: p. 230-240.

ECCE12
The 12th EUROPEAN CONGRESS OF CHEMICAL ENGINEERING
Florence 15-19 September 2019

Discrimination criteria for early decision-making between uncoupled or multifunctional reactor and membrane units

Jean-Marc Commenge[1], Camilo Ruiz[1], Jean-François Portha[1]

1 Université de Lorraine, Laboratoire Réactions et Génie des Procédés, UMR 7274, 1 rue Grandville, BP 20451, 54001 Nancy Cedex, France.

**Corresponding author: jean-marc.commenge@univ-lorraine.fr*

Highlights

- Superstructures for RSR loop and membrane reactor are optimized for maximal yield
- Dimensionless numbers (Da, Pe) are explored to define optimality domains of structures
- Discrimination criteria are built to delimit the optimality zone of membrane reactors

1. Introduction

The development of a sustainable industry for a successful energetic transition requires rethinking existing processes and/or designing innovative processes by applying Process System Engineering methodologies. Intensified devices and multifunctional units have been extensively studied in the last decades and have demonstrated their interest for cost minimization and plant optimization. Unfortunately, they are not systematically considered in conventional design approaches[1,2], whereas the early steps in process design are critical to define the technologies, utilities, control strategy, etc. and to assess the OPEX and CAPEX of a project.

The main objective of this work is to define quantitative criteria to choose the most interesting combination between a reaction step and a membrane separation unit, even at the early phases of the process synthesis. To do so, two cases are studied, optimized and compared: (i) a membrane separator in a Reactor-Separator-Recycle loop (RSR) and (ii) its integrated equivalent, a membrane reactor.

2. Methods

Two superstructures have been designed including either a reactor and a membrane unit, or an integrated membrane reactor (Figure 1). Both superstructures are parameterized by 4 and 2 split factors respectively, and characterized by physical data, such as the reaction stoichiometry and kinetics, reactor volume, membrane area, permeability and pressures. Numerical resolution of the mass balances gives access to all flow rates, compositions and performance criteria such as the overall yield of both processes. For a given chemical system, the split factors of each structure are optimized to maximize the yield. The single-pass conversion and two separation efficiencies are calculated for further comparison and criteria definition. Particular attention is drawn to multiple solutions and, if equivalent, the simplest solution in terms of structure is favored.

To generalize the investigation, the set of parameters is made dimensionless by introducing the permselectivity, the pressure ratio, the Damköhler number and the Péclet number: these

numbers enable to easily compare the reaction time, the space time and a characteristic time of the separation[3,4].

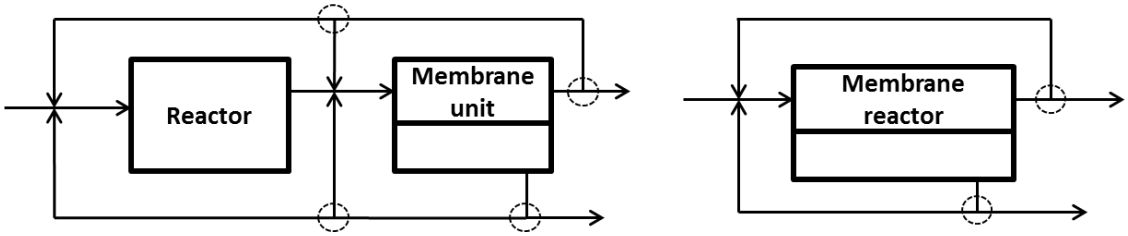

Figure 1. Superstructures studied for the RSR loop (left) and the membrane reactor (right). Dashed circles indicate the positions of split factors.

3. Results and discussion

Concerning the RSR superstructure, for a given chemical system, only a few non-trivial recycle schemes (among 49 possibilities) are optimal with respect to the overall yield: these optimal substructures can be directly related to the local efficiencies and can be discriminated by a simple criterion that describes the frontiers between their optimality domains.

Comparison of both structures confirms the technical superiority of the membrane reactor with respect to the overall yield for all studied cases: the multifunctional unit systematically exhibits a higher criterion than the RSR structure. Nevertheless, the possible gain is not significant over the whole range of dimensionless numbers: both optimized structures may exhibit very similar yields depending on the dimensionless numbers.

For definition of appropriate discrimination criteria, the existence of trivial and multiple optimal solutions requires exploring only a relevant part of the dimensionless space: the Da number should be large enough to enable sufficient single-pass conversion, the permselectivity and pressure ratio should be coherent with typical values, etc. On this basis, the zone of significant superiority of the membrane reactor can be circumscribed.

4. Conclusions

Two superstructures and corresponding balance equations describing the overall efficiency of a RSR loop and a membrane reactor have been studied, enabling to determine the maximum attainable yield and the associated optimal structure to solve a generic reaction separation problem. Exploration of the parameter space enabled to define discrimination criteria and optimality domains, with respect to this technical criterion.

Even if the overall efficiency described in this work is an important parameter in the decision-making procedure for process design, further works should focus on including economic aspects as main criteria for decision-making between uncoupled and multifunctional units.

References

[1] M. Baldea, Comp. Chem. Eng. 81 (2015) 104–114.
[2] J.-F. Portha, L. Falk, J.-M. Commenge, Chem. Eng. Process. Process Intensif. 84 (2014) 1–13.
[3] W. S. Moon, S. B. Park, J. Memb. Science. 170 (2000) 43-51.
[4] S. Battersby, P. W. Teixeira, J. Beltramini, M. C. Duke, V. Rudolph, J. C. Diniz da Costa, Cat. Today 116 (2006) 12-17.

ECCE12
The 12th EUROPEAN CONGRESS OF CHEMICAL ENGINEERING
Florence 15-19 September 2019

Investigation of control and on-line optimisation opportunities of a wastewater treatment plant

Harry Laing[1 *], Chris O'Malley[1], Mark J. Willis[1], Anthony Browne[2]

1 Newcastle University, School of Engineering, Merz Court, Newcastle University, Newcastle upon Tyne, NE1 7RU, United Kingdom; 2 Northumbrian Water, Boldon House, Wheatlands Way, Pity Me, Durham, DH1 5FA

**Corresponding author: h.j.laing@ncl.ac.uk*

Highlights

- A Mixed Integer Linear Programming approach is applied to Biogas Production
- Retrospective Optimisation reveals potential annual savings of over 11%
- An optimal operational strategy is provided for plant operators

1. Introduction

Northumbrian Water (NW) anaerobically digests up to 40,000 tonnes of sewage sludge (dry solids) annually at their plant on Tyneside, producing renewable Biogas. Typically, Biogas produced on a wastewater Anaerobic Digestion (AD) plant in the UK is used to generate electricity only. Many sites are looking to upgrade to produce Biomethane for injection into the National Gas grid to take advantage of the government's Renewable Heat Incentive [1]. The Tyneside Advanced Anaerobic Digestion (AAD) plant is a rare case in that it has three possible uses for Biogas produced on site: upgrade for injection into the national gas grid; burning it in Combined Heat and Power (CHP) Engines; or burning it in Steam Boilers for the thermal hydrolysis plant. There are three CHP Engines, three Steam Boilers and one Gas Upgrade/Injection plant on site. If required, the plant may flare excess biogas. In addition, to ensure overall sludge processing remains unimpeded the plant may draw Natural Gas from the national gas grid to be used in the CHP Engines or Steam boilers.

Currently, there is no model on site to advise the optimal distribution of Biogas produced or how much Natural Gas is required to be purchased to ensure optimal cost and sludge processing performance. This work develops an optimal site gas distribution strategy, to enable operators to validate and make improved decisions.

2. Methods

Each unit is able to process a maximum volume of Biogas or Natural Gas on a daily basis. These processing limits were determined thorough retrospective analysis of plant operational data and are different for Biogas and Natural Gas volumes. Work reported in [2] was adapted to apply a Mixed Integer Linear Programming (MILP) approach to minimise total plant operational cost, T_C:

$$T_c = \sum_{t=1}^{H_t}(C_b\, B_{CHP}\, z_i) + \left(C_n N_{CHP}(1-z_i)\right) + \sum_{t=1}^{H_t}(C_b\, B_S\, z_i) + \left(C_n N_S(1-z_i)\right) + \sum_{t=1}^{H_t}(C_I\, B_I\ + \sum_{t=1}^{H_t}(C_f\, B_f)$$

C_b C_n C_I and C_f is the cost of burning Biogas, Natural Gas, Biomethane Injection and flaring Biogas retrospectively, B_{CHP} B_S B_I and B_f are biogas volume to CHP Engines, Steam Boilers, Injection and

Flaring respectively, N_{CHP} and N_S are Natural Gas to CHP Engines and Steam Boilers respectively, and z_i is a binary variable used to ensure only one of each gas type is used by each unit, subject to $z_i \in \{0,1\}$, $(\forall\, t = 1 \ldots H_t)$, where H_t is the operation horizon in one day intervals.

The optimiser was implemented using MATLAB's *intlinprog* function to minimise plant costs.

3. Results and discussion

The optimiser takes total daily biogas production on site and optimises the overall gas distribution, providing the operator with a visual operation strategy (Figure 1). Each daily optimisation also has an associated operational cost, which is used to perform Retrospective Optimisation (RO) of plant operations.

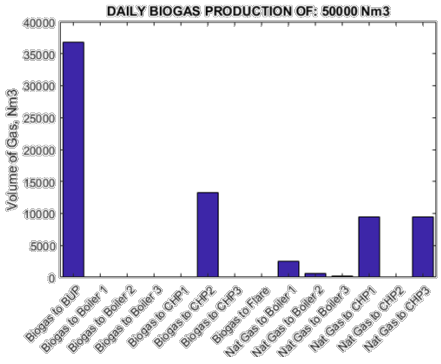

Figure 1. Optimal Gas Distribution on site for daily production of 50,000 Nm3 of Biogas

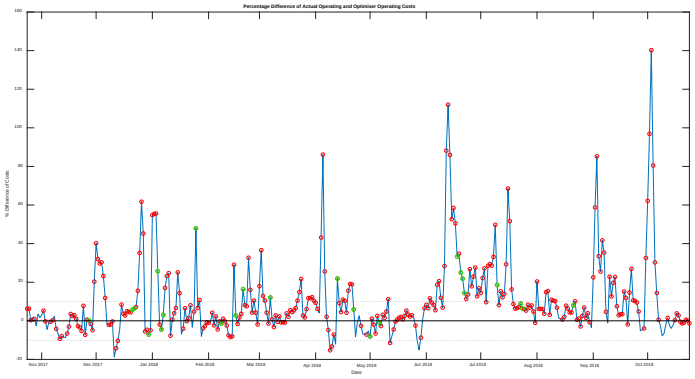

Figure 2. Daily RO result over 12 month period. 0% Difference is optimal. Red dots indicate days where flaring occurred but was unnecessary. Green dots indicate optimal performance.

RO of the daily optimal operational cost compared to the actual historical operational cost was performed for the 12 month period Nov 2017 to Oct 2018 (Figure 2). Initial RO results indicate potential annual operational cost savings >11% (>£0.5m). At times the plant operates more efficiently than the optimiser predicts. This is due to the static nature of model parameters that are an average of overall annual performance, and will be rectified in future work.

4. Conclusions

Our work indicates there are potential annual savings of over 11% to operational costs that could be achieved through improved operational strategies; the daily optimal operation strategy is provided to the operators in visual form, though weekly strategies are also possible if required. Further work is to be carried out to provide operators with a full sludge processing optimisation model, including a biogas production model to allow for improved operational forecasting.

References

[1] M. Hale, Maximizing biomethane use in sewage plants, Filtr. Sep. 54 (2017) 26–27. doi:10.1016/S0015-1882(17)30082-4.

[2] T. Cummings, R. Adamson, A. Sugden, M.J. Willis, Retrospective and predictive optimal scheduling of nitrogen liquefier units and the effect of renewable generation, Appl. Energy. 208 (2017) 158–170. doi:10.1016/j.apenergy.2017.10.055.

Optimization of wastewater treatment processes using a rheological approach

Jamal HAMDANI[1,3], Nicolas ROCHE[2], Isabelle SEYSSIECQ[3]

1 University Mohammed 6 Polytechnic, Benguerir, Morocco ; 2 Aix Marseille Univ, CNRS, IRD, INRA, Coll France, CEREGE, Aix-en-Provence, France ; 3 Aix Marseille Univ, CNRS, Centrale Marseille, M2P2, Aix-en-Provence, France

**Jamal HAMDANI: jamal.hamdani@um6p.ma*

1. Introduction

Biological processes such as classical activated sludge treatment or membrane bioreactors (MBR) are the process the most used for the treatment of wastewater within the last decades. In recent years however, we are witness to an increase of global inflows entering wastewater treatment plants (WWTP), whereas authorized levels of pollutants in the outflows get more and more reduced. To face this context, WWTP new units have to become more and more efficient and a great attention is now paid to the optimization of treatment processes of both wastewater and excess wastewater sludge. In the present work, rheological approach is investigated to optimize wastewater treatment plan using a bench test device specially developed for the purpose of this work.

2. Methods

The rheological bench used consists in a bioreactor equipped with a double helical ribbon impeller fixed on a motor (HRI system) and a recirculation loop in which the sludge flows in pipes (pipe system) of 2 different diameters used to measure the "in situ" rheological behavior of activated sludge. The pipe system is equipped with two differential pressure transmitters and a flow meter to measure the pressure drop and the volumetric flow rate. This permit to draw the rheograms of sludge in pipes. For each solid concentration (TSS) studied, the parameters (τ0, K and n) of the Herschel-Bulkley model are determined based on the reference rheograms measured by the Couette rheometer (AR550). These rheograms are then compared to the one obtained with the different in situ configurations (HRI and pipes).

3. Results and discussion

HRI rheograms always show a good agreement with the reference one. On the contrary, pipes rheograms do not always match the reference. Wall slips phenomena are observed for each TSS concentrations, notably depending on the pipe diameter. At low concentration, slip is only observed for the pipe with the smaller diameter whereas at high concentration slip is present with both pipe configurations. Slip phenomena have been taken into account using slip correction calculations. Plotting the slip velocity curves as a function of the wall shear stress, we can distinguished two types

of phenomena responsible for wall slip: the static depletion and the particle migration. The occurrence of each mechanism is dependent on interparticles interactions via the TSS concentration.

References

[1] Ohanessian – 2016 - Développement d'un outil de caractérisation in situ d'écoulements de boues de station d'épuration

[2] Seyssiecq et Al. - 2015 - In Situ Rheological Characterisation of Wastewater.

[3] Seyssiecq et Al. - 2003 - State-of-the-art: Rheological characterisation of wastewater treatment sludge

[4] Mori, M.; Isaac, J.; Seyssiecq, I.; Roche, N. Effect of Measuring Geometries and of Exocellular Polymeric Substances on the Rheological Behaviour of Sewage Sludge. Chem. Eng. Res. Des. 2008, 86 (6), 554–559. https://doi.org/10.1016/j.cherd.2007.10.013.

[5] Wang, H.-F.; Hu, H.; Yang, H.-Y.; Zeng, R. J. Characterization of Anaerobic Granular Sludge Using a Rheological Approach. Water Res. 2016, 106, 116–125. https://doi.org/10.1016/j.watres.2016.09.045.

[6] TIXIER, N. Approche des propriétés rhéologiques de suspensions biologiques floculées. 160.

[7] AL-DAWERY, S. K.; REDDY, S. S. AN EXPERIMENTAL STUDY ON THE RHEOLOGICAL PROPERTIES OF CONDITIONED MUNICIPAL ACTIVATED SLUDGE. 2017, 12, 18.

[8] Ratkovich, N.; Horn, W.; Helmus, F. P.; Rosenberger, S.; Naessens, W.; Nopens, I.; Bentzen, T. R. Activated Sludge Rheology: A Critical Review on Data Collection and Modelling. Water Res. 2013, 47 (2), 463–482. https://doi.org/10.1016/j.watres.2012.11.021.

[9] Liang, F.; Sauceau, M.; Dusserre, G.; Arlabosse, P. A Uniaxial Cyclic Compression Method for Characterizing the Rheological and Textural Behaviors of Mechanically Dewatered Sewage Sludge. Water Res. 2017, 113, 171–180. https://doi.org/10.1016/j.watres.2017.02.008.

ECCE12
The 12th EUROPEAN CONGRESS OF CHEMICAL ENGINEERING
Florence 15-19 September 2019

Root cause diagnosis of multiple process faults: Integrating pattern matching with active simulation

Weijun Li[1], Xiangping Zhang[2], Sai Gu[1], Tao Chen[1]*

[1] Department of Chemical and Process Engineering, University of Surrey, Guildford GU2 7XH, United Kingdom; [2] Beijing Key Laboratory of Ionic Liquids Clean Process, Institute of Process Engineering, Chinese Academy of Sciences, Beijing 100190, China

*Corresponding author: t.chen@surrey.ac.uk

Highlights

- A novel and effective framework for root cause diagnosis.
- Applicable to both single fault and multiple faults.
- Integrating mechanistic model, pattern matching and optimisation.

1. Introduction

With increasing demand on process safety, fault detection and diagnosis (FDD) has attracted considerable attentions [1]. Despite the significant success in fault detection and isolation, root cause analysis remains a challenge for data-driven methods [2]. On the other hand, dynamic process simulations, based on mechanistic models, encapsulate a large amount of process knowledge especially the causal information, thus could be an effective tool in root cause diagnosis. Although hybrid mechanistic-empirical modelling is well known, its application in FDD for medium-to-large scale industrial processes has not been well explored. In this work, a generic root cause analysis method applicable to both single and multiple faults is developed by use of mechanistic model and pattern matching technique. Case study with the Tennessee Eastman (TE) process [3] is conducted to demonstrate its effectiveness, and the current limitations and potential solutions are discussed.

2. Methods

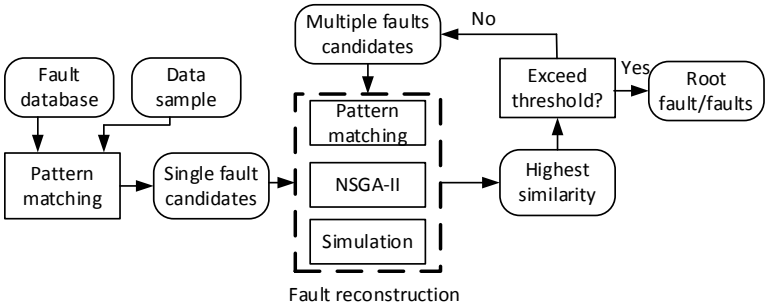

Figure 1. Flowchart of the proposed root cause analysis method.

The proposed strategy is summarised in Figure 1. Firstly, a fault database is built by simulating process faults at different magnitudes offline. Then, the operational data sample is compared with the database to screen fault candidates. From the candidates, the root cause is further confirmed

by use of an optimisation based fault reconstruction method, in which a multi-objective optimisaiton algorithm (NSGA-II: Non-dominated Sorting Generic Algorithm II [4]) is used to search for the root cause of the fault based on pattern matching [5] and process simulations. Two similarity metrics are employed in the pattern matching, i.e. PCA similarity (Spca) and Mahalanobis distance similarity (Sdist). Spca measures the similarity between datasets by relative angles between their principle components while Sdist by the distance between their centers.

3. Results and discussion

Figure 2(a) and 2(b) show the results in diagnosing single fault (caused by IDV1) and multiple faults (caused by IDV1+IDV7), respectively, in which IDV indicates the disturbances as described in [3]. Similarities (Spca and Sdist) displayed in Figure 2 represent the average values over individuals at each iterations in the optimisation. Figure 2(a) successfully identifies IDV1 as root cause of the single fault due to its much improved similarity values after optimisation. In Figure 2(b), the similarities of all the candidates are still low (symbols connected by solid line) after optimisation. Considering multiple faults scenario, we further evaluate candidate combinations and identify IDV1+IDV7 (the red dotted line) as the root cause due to its much improved similarities.

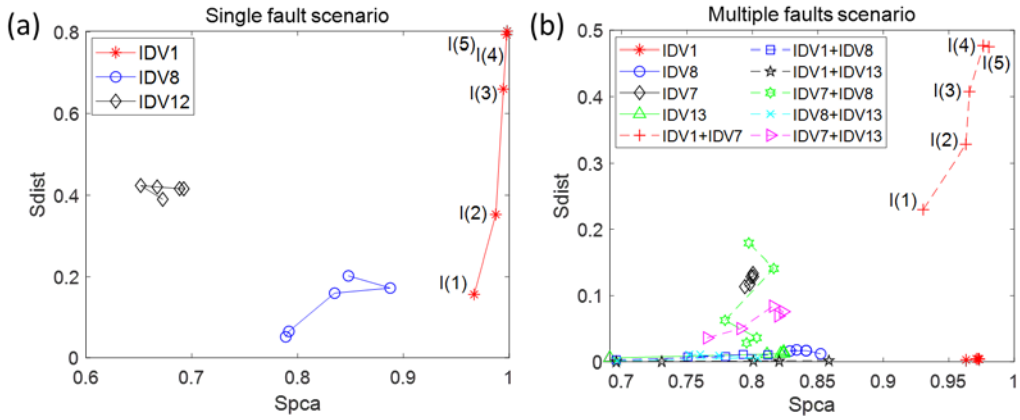

Figure 2 Similarity of candidates after fault reconstruction; I(i) indicates the i-th iteration during the optimisation.

4. Conclusions

This work proposes a novel root cause diagnosis method and demonstrated its effectiveness with the TE process. It is worthy to note its effectiveness depends largely on two aspect: 1) real-time model update technique to lessen model-plant mismatch; 2) pattern matching method effectively extracts similar features between operational and simulated dataset.

Acknowledgement

This work has been partially supported by the UK EPSRC (EP/R001588/1), BBSRC (BB/S020896/1), and the Unilever-IPE-Surrey collaborative doctoral training (CDT) programme.

References

[1] B. He, J. Zhang, T. Chen, and X. Yang, Ind. Eng. Chem. Res. 52 (2013) 7784-7794.
[2] B. He, T. Chen, and X. Yang, Comput. Chem. Eng. 64 (2014) 167–177.
[3] J. Downs and E. Vogel, Comput. Chem. Eng. 3 (1993) 245–255.
[4] K. Deb, A. Pratap, S. Agarwal, and T. Meyarivan, IEEE T. Evolut. Comput. 6 (2002) 182-197.
[5] A. Singhal and D. Seborg, IEEE control systems 22 (2002) 53-63.

ECCE12
The 12th EUROPEAN CONGRESS OF CHEMICAL ENGINEERING
Florence 15-19 September 2019

Optimization Study to Maximizing Heavy Naphtha Draw from a Condensate Distillation Unit

Mohammad Shamsuzzoha*, Mohammad Abdur Rakib, Mohamed Al-Musharfy

Research Centre Division, ADNOC Refining, Post Box: 3593, Abu Dhabi, UAE

**Corresponding author:* mshamsuzzoha@adnoc.ae

Highlights

- A rigorous simulation model has been developed in rating mode for an existing condensate distillation column to obtain the optimal condition.
- The calibrated model has been run for different cases to obtain the optimal seniors to maximize the deep cut naphtha.

1. Introduction

Steady-state process simulations provide powerful insights into the plant behaviour which can be used to enhance designs, safety and operations of oil refinery units. The process simulation model can be utilized in several ways from design stage to operation in oil refinery i.e., efficient and profitable designs, achieve consistent product quality, analyse plant operations, monitor & optimize operations and real-time optimization etc.

In order to explore sources of increased demand of heavy naphtha for increasing the throughput of heavy naphtha reformer for an additional heavy naphtha reformer, a rigorous simulation model was developed in process simulation software for an existing condensate distillation column. The model was tuned using test run data. Assays information for various sources of the condensate feed mix were studied, and implemented in the feed definitions to see the impact of different feed mix ratios. Since monitoring the benzene precursors for the downstream section is an important requirement, special attention was given to include detailed naphtha component analysis while defining the assays for the different condensates. A Peng-Robinson (PR) Equation of State was utilized while developing the rigorous tray-to-tray model. The model captures detailed heat exchanger networks with heat recovery from the column pump arounds. Hence the model was capable of evaluating different scenarios and studying the equipment limitations, especially the heat exchangers. An optimum scenario was thereby proposed to maximize heavy naphtha yield with details of benzene precursors for the downstream heavy naphtha reformer.

2. Methods

The calibrated model has been run for different cases to obtain the optimal seniors to maximize the deep cut naphtha. The heat duty of the overhead section of the main fractionation column has been main constraint in the column. The column overhead section constitutes both the air and trim cooler to achieve required reflux temperature.

3. Results and discussion

Therefore, in last three cases, the limiting overhead duty of 40 Gcal/hr has been restraint to keep draw adequacy and limitation of the unit overhead section.

Case 1: Calibrated model with plant data.
Case 2: Deep cut heavy naphtha 100-180°**C** EP.
Case 3: Heavy naphtha flow rate of 175 m^3/hr.
Case 4: Heavy naphtha flow rate of 155 m^3/hr, limiting overhead duty of 40 Gcal/hr.
Case 5: Heavy naphtha flow rate of 165 m^3/hr, limiting overhead duty of 40 Gcal/hr.
Case 6: Heavy naphtha flow rate of 175 m^3/hr limiting overhead duty of 40 Gcal/hr.

4. Conclusions

One the basis of the equipment adequacy and limitations, Case 5 has been selected for the design purposes. This case has heavy naphtha draw rate of 165 m^3/hr and limiting overhead duty of 40 Gcal/hr. The predicted results have been compared with the plant data, for yields and different other properties e.g, SG, flash point, freezing point and pour point. The products qualities show that the results are in line with expectation as.

References

[1] A.-F. Chang, K. Pashikanti and Y. A. Liu, Refinery Engineering: Integrated Process Modeling and Optimization, Wiley-VCH Verlag GmbH & Co. KGaA, 2012.

[2] K. Anitha, T. Shuwana and V. R. Kumar, "Simulation of Atmospheric and Vacuum Crude Units Using Aspen Plus," *Petroleum Science and Technology,* vol. 29, p. 1885–1894, 2011.

[3] R. K. More, V. K. Bulasara, R. Uppaluri and V. R. Banjara, "Optimization of crude distillation system using aspen plus: Effect of binary feed selection on grass-root design," *Chemical Engineering Research and Design,* vol. 88, no. 2, pp. 121-134, 2010.

[4] M. Shamsuzzoha, H. Kelani, A. M. Rakib and M. Al Musharfy, "Systematic Procedure for Simulation of a Crude Distillation Unit," in *6th TRC-JCCP/Idemitsu International Symposium, 10th - 11th February 2016, TRC,*, Sas Al Nakhl, Abu Dhabi, 2016.

ECCE12
The 12th EUROPEAN CONGRESS OF CHEMICAL ENGINEERING
Florence 15-19 September 2019

Conceptual study on coal power plant transformation to metal power plant; A look into the future

P. Awad[1*], R.G. Baltazar[1], I.D. Garcia[1], E. Dijkman[1], P.L.J. Swinkels

TU Delft, Chemical Engineering Department, Van der Maasweg 9, 2629 HZ Delft, Netherlands

**Corresponding author: p.w.a.awad@tudelft.nl*

Highlights

- Iron oxide power plant conceptual design
- Reduced carbon emission power plant
- Reduction of iron oxide with carbon monoxide from dry methane reforming

1. Introduction

Greenhouse gases have been exhibiting a rapid increase recently. Coupled with the will to ensure security of energy supply, governments are trying to change the source of energy to other fuels, reducing the production and emission of these gases. As part of these efforts the Dutch government decided in May 2017 to stop using coal for electricity generation in the very near future.

The objective of this work is to assess the feasibility of a swift shift from coal-fired power plants to metal fuels power plants. A preliminary conceptual design is performed taking as a reference the existent Uniper's coal power plant in Rotterdam, the Netherlands.

2. Methods

For this project the Delft Design Map method is used [1]. The general approach of this method is to explore a wide range of options hierarchically. It consists of different design levels, from which the following are used in this work: Project Framing, Costumer Wants, Input-Output Structure, Subprocesses, Task Network, Unit Network and Process Integration.

Regarding the design itself, current assets of the existing coal plant was maximized. Preliminary and shortcut design methods were used whenever appropriate and preliminary cost estimations (±35%) were applied. Three main critical design decisions characterize the project outline, reflecting the final process design and the respective economic evaluation.

1- Input-output structure.

Process options are examined using input-output diagrams to decide on metal fuel type(s), regeneration need, extent and percentage of regeneration. Low cost of iron ore (mainly FeO), coupled with its oxidation stability and geographic availability are the main reasons for selecting it as the main raw material. It was also decided to use regeneration to FeO instead of reduction to pure Fe after some high-level mass balance and cost analysis calculations. Iron Oxide regeneration allows for a significant reduction of both required metal fuel needed as well as the waste stream.

A number of reducing agents and methods for regenerating the Fe_2O_3 combustion product were evaluated: hydrogen, carbon monoxide, iron electrolysis, micro-organisms and biomass. Then, carbon monoxide produced from dry methane reforming was selected due to the advanced

development stage of the reduction reaction and low investment. The production of CO is advantageous since it uses carbon dioxide to produce carbon monoxide, with hydrogen as by-product. A cyclic process was designed in order to minimize CO_2 emissions and introduce a flexibility of using CH_4 potentially from a bio source as a supplementary fuel to the process.

2- Process thermodynamics

Introduction of the Brayton cycle to the current existing Rankine cycle was another important decision. Furthermore, using exhaust gases from the furnace to heat the medium pressure steam results in a higher energy produced per raw material consumed. The absence of any carbon source creates an opportunity to use a turbine in this stream due to higher density providing higher separation efficiency upstream of the turbine. The combination of these two factors result in an increase in efficiency from 47% to 60%, primarily caused by the steam temperature upgrade.

3- Waste treatment

The purge stream from the iron cycle is considered as an added-value stream to the steel industry. Compared to the conventional inlet iron ore stream, produced iron oxide waste (Fe_2O_3) from this process is richer in oxygen and has a lower impurity content. Therefore, it can be sold at an interesting price to the steel industry. Furthermore, this reduces the demand for mining in the steel industry.

3. Results and discussion

Preliminary design and cost evaluation for this conceptual design resulted in a -1300 M€ NPV which is unacceptable for an investment. Raw material demand proved to be the largest cost driver. However, the project was initiated with future scenario's in mind. It was already known at the start that currently it is not yet economically feasible. The question was how far from economic feasibility it actually is, and what needs to change before it will become economically feasible, and when this is expected to take place. Carbon tax used in this work was set around €50/ton but it is uncertain when this will shift to higher values. A significant reduction on the raw material price would change NPV drastically. This can be achieved by researching other sources for the raw material, such as metal scraps from the car industry.

4. Conclusions

A metal fuel power plant as a replacement for a coal-fired power plant proved to be economically infeasible under the current circumstances and market values. However, when compared to conventional coal power plant, of which NPV is zero for €72/ton carbon tax, it reaches the same (negative) NPV once carbon tax is €103/ton. Figure 1 shows the relationship between NPV values and carbon tax values for both a conventional coal power plant and metal fuel one.

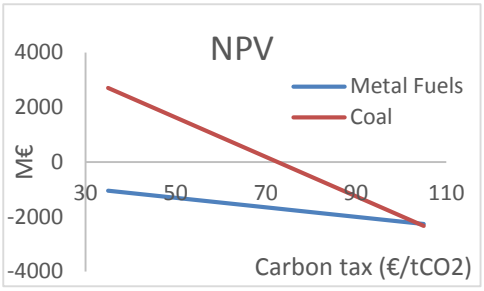

References

[1] J. Harmsen, A.B. de Haan, P.L.J.Swinkels, Product and Process Design, De Gruyter, Berlin, 2018

ECCE12
The 12th EUROPEAN CONGRESS OF CHEMICAL ENGINEERING
Florence 15-19 September 2019

Effect of the Hydrodynamic Conditions on the Precipitation Process of Particles Generated from Electrochemical Cr(VI) Removal Process.

Clara G. Escárcega-Ramírez[1], Sergio A. Martínez-Delgadillo[2], Ricardo López Medina[3], Israel González-Neria[4], Gabriela Rivadeneyra-Romero[5], J. Antonio Yáñez-Varela[4*].

1 Ingeniería Química, Universidad Autónoma Metropolitana, Av. San Pablo No. 180, Azcapotzalco, CDMX. C.P. 02200. México; 2 Depto. de Ciencias Básicas Universidad Autónoma Metropolitana, Av. San Pablo No. 180, Azcapotzalco, CDMX. C.P. 02200. México; 3 Depto. de Energía, Universidad Autónoma Metropolitana-Azcapotzalco, Av. San Pablo No. 180, Azcapotzalco, CDMX. C.P. 02200. México; 4 Posgrado en Ingeniería de Procesos. Universidad Autónoma Metropolitana, Av. San Pablo No. 180, Azcapotzalco, CDMX. C.P. 02200. México; 5 Ingeniería de Petróleos, Universidad del Istmo, Ciudad Universitaria S/N, Tehuantepec, Oax. México.

**Corresponding author:* jayanezv@outlook.com

Highlights

- Precipitation process of particles generated from electrochemical Cr(VI) removal process is studied.
- The effect of the average velocity gradient on the sedimentation velocity was evaluated.
- The produced sludge form the Cr(VI) reduction was characterized.
- The sludge from the electrochemical process has chromite, which have potential reuse.

1. Introduction

Wastewaters from the chromate conversion coating have high concentrations of Cr(VI), which is a high toxic substance. Electrochemical process has been applied to remove the Cr(VI) from the industrial wastewaters [1]. During the process Fe(II) ions are released from a sacrifice iron electrode. These ions reduce the Cr(VI) to Cr(III) and the Fe(II) is oxidized to Fe(III) form. Both, Cr(III) and Fe(III) are precipitated at basic pH. There are no studies to evaluate the effect of the hydrodynamic conditions on the precipitation process of particles generated from electrochemical Cr(VI) removal process, which is important to reduce the sludge volumetric index (SVI) and optimize the coagulation and flocculation conditions, such as the reagents use, the agitation velocity and the precipitation pH. During flocculation the hydrodynamic behavior have important effects on the flocs characteristics. The velocity gradient is an important parameter that affects the flocs characteristics, because its size depends on the balance between the flocs agglomeration due to de mixing and the breaking of them because the energy kinetic dissipated [2]. Both effects depend on the agitation power supplied. To characterize the performance of agitated tanks used in fluctuation process, the average velocity gradient in the vessel (G_{ave}), is used (equitation 1).

$$G_{ave} = \left(\frac{\varepsilon_{ave}}{\nu}\right)^{1/2} = \left(\frac{N_p N^3 D^5}{V\nu}\right)^{1/2} \quad (1)$$

where: μ_{ave} = average energy dissipation rate, ½= kinematic viscosity, N_P = power number, $\acute{A}$ = density of liquid, N = rotational speed of impeller, D = impeller diameter.

In this work, the effect of the G_{ave} on the precipitation process of particles generated from electrochemical Cr(VI) removal process is studied. In addition, the sludge obtained was characterized.

2. Methods

The experimental tests were performed in a jar test apparatus with square transparent vessel of 2 L of capacity, with paddles of 7.6 cm of diameter. The sample was taken from a laboratory electrochemical reactor used to remove the Cr(VI) from wastewater. The wastewater was prepared with $K_2Cr_2O_7$. The pH was increased with NaOH 8M. During the tests, a rapid mixing at 200 or 100 rpm during 60s was applied, followed of a slow mixing at 50 or 25 rpm during a flocculation time (t_f). The t_f tested were 5,10, 20 and 30 minutes. After this, the sedimentation velocity (V_s) was evaluated. The sludge obtained was characterized by Raman spectroscopy.

3. Results and discussion

Figure 1a, shows the results obtained of the V_s variation as a function of the accumulated G_{ave} (G_{ave}·t_f). As can be seen, as G_{ave}·t_f (is reduced until about 200 the V_s drops, but it increases linearly until values of accumulated G_{ave} of 75, reaching a V_s = 0,42ms^{-1}, where after this value the V_s is almost the same (0.45ms^{-1}) at lower G_{ave}·t_f, which means that the agglomeration and breaking flocs forces are in equilibrium [2]. On the other hand, figure 1b, shows the results of the characterization of the produced sludge form the Cr(VI) reduction electrochemical process.

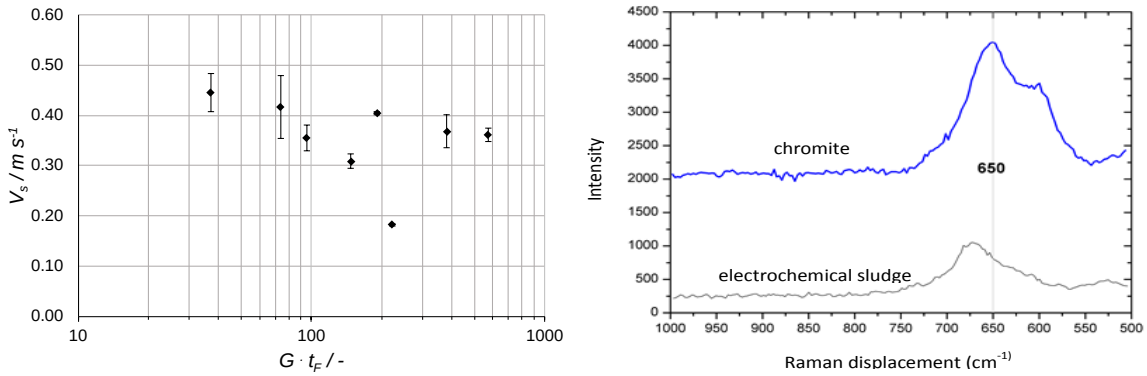

Figure 1. a) V_s variation as a function of the accumulated G_{ave} (G_{ave}·t_f), b) characterization of the produced sludge.

As it is shown, the sludge has chromite, which have potential reuse.

4. Conclusions

Based on the results, the G_{ave} to operate satisfactorily the flocculation process were obtained. The sludge produced during the electrochemical process has chromate which can be reused.

References

[1] C.E. Barrera-Díaz, V. Lugo-Lugo, B. Bilyeu, , J. Hazard. Mater. 223–224 (2012) 1–12.
[2] W. He, Z. Zhao, J. Nan, Z. Xie, W. Lu, J. Environ. Chem. Eng. 6 (2018) 3041–3053.

ECCE12
The 12th EUROPEAN CONGRESS OF CHEMICAL ENGINEERING
Florence 15-19 September 2019

Simulation of methanol production from different point sources of CO_2

Tina Kegl[1], Blaž Likozar[2], Anita Kovač Kralj[1], Rok Gomilšek[3], Gregor Kravanja[1], Lidija Čuček[1]

1 Faculty of Chemistry and Chemical Engineering, University of Maribor, Smetanova 17, Maribor, Slovenia; 2 National Institute of Chemistry, Hajdrihova 19, Ljubljana, Slovenia; 3 Talum Inštitut d.o.o., Tovarniška cesta 10, Kidričevo, Slovenia

**Corresponding author: lidija.cucek@um.si*

Highlights

- Methanol production is a promising option for significant CO_2 emission reduction
- Influences of impurities and concentrations from point sources of CO_2 are studied
- Various catalysts and the dynamics of catalyst deactivation are analyzed
- Sensitivity analysis is performed to obtain simple economic bound of alternatives

1. Introduction

Human activities have led to an increased concentration of greenhouse gas emissions in the atmosphere, mainly by burning of fossil fuels [Vooradi et al., 2018]. Since the beginning of the industrial revolution the concentrations of CO_2, the principal greenhouse gas, has risen from 280 ppm to 400 ppm [Zhang and Huisingh, 2017]. In order to stabilize the global CO_2 concentration in the atmosphere, carbon capture and sequestration are estimated to play a major role in the reduction of CO_2 emissions [Kravanja et al., 2018]. However, more sustainable and economically-promising option for greenhouse gas emission reduction is CO_2 utilization [Roh et al., 2016], which is also in line with industrial ecology and circular economy. Captured CO_2 at different large point sources [Meylan et al., 2015] could be converted by chemical pathways [Rafiee et al., 2018] into commercial products such as syngas, methane, methanol, ethanol, organic acids and many other fuels and chemicals [Norhasyima and Mahlia, 2018]. It could also be used directly (by physical pathway) [Rafiee et al., 2018] in carbonated beverages, fire extinguishers, as a refrigerant, extractant, in enhanced oil and gas recovery, in algae farms and other applications [European Commission, 2018]. CO_2 emission reduction opportunities from point sources are shown in Figure **1**.

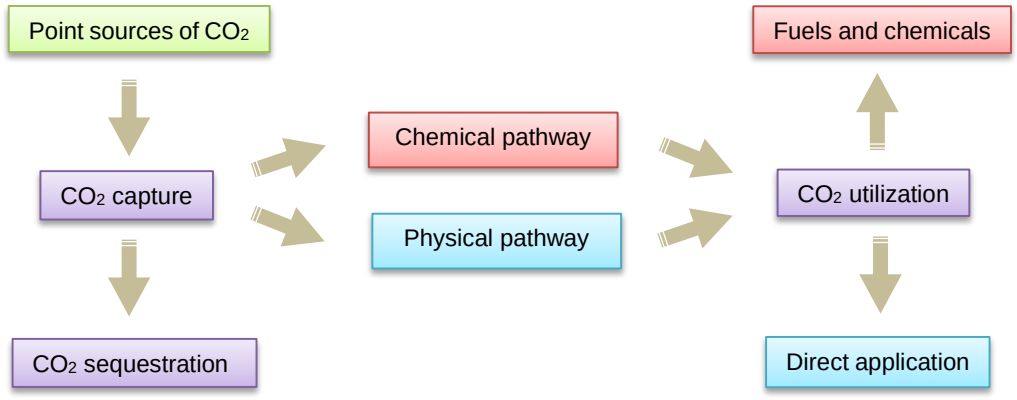

Figure 1: Schematic of CO_2 capture, sequestration and utilization from point sources

2. Methodology and results

This contribution presents simulation of methanol production as a promising option for significant CO_2 emission reduction. Methanol, as one of the most useful products, has multiple industrial applications, such as it could be used for production of formaldehyde, acetic acid, dimethyl ether and other chemicals [Van-Dal and Bouallou, 2013], as a fuel, solvent, energy carrier and in many other applications [Dalena et al., 2018]. Simulation is performed for different point sources of CO_2, from power plants, cement factories and aluminium industry. Influences of impurities and CO_2 concentrations in the flue gas on methanol production are investigated. As the feasibility of the process largely depends on the catalyst, simulation also considers various catalysts and the dynamics of catalyst deactivation. Finally, sensitivity analysis is performed in terms of CO_2 capture cost, prices of CO_2 allowances and methanol prices to obtain simple economic bound [Biegler et al., 1997] of various studied alternatives.

Preliminary results show that by MEA absorption about 50 % CO_2 was captured from flue gas, and methanol conversion from captured CO_2 was around 30 %. Furthermore, the effect of impurities content on the methanol productivity was determined in the packed bed reactor. It was found, that the reaction rate of methanol formation decreased significantly with the addition of higher percentages of impurities. In terms of the stability of catalyst in the parallel packed bed reactor in the aging tests, it was found that aging does not influence CO_2 conversion significantly.

Acknowledgments

The authors are grateful for the financial support from the Slovenian Research Agency (PhD research fellowship contract No. 1000-18-0552 and core research funding No. P2-0412, P2-0032, P2-0152 and P2-0046).

References

[1] R. Vooradi, M.-O. Bertran, R. Frauzem, S.B. Anne, R. Gani, Chemical Engineering Research and Design 131 (2018) 440-464.
[2] Z. Zhang, D. Huisingh, Journal of Cleaner Production 142 (2017) 1055-1064.
[3] G. Kravanja, Ž. Knez., M. Knez Hrnčič, International Journal of Greenhouse Gas Control 71 (2018) 142–154.
[4] K. Roh, R. Frauzem, T.B.H. Nguyen, R. Gani, J.H. Lee, Computers & Chemical Engineering 91 (2016) 407-421.
[5] F.D. Meylan, V. Moreau, S. Erkman, Journal of CO_2 Utilization 12 (2015) 101-108.
[6] A. Rafiee, K.R. Khalilpour, D. Milani, in: K.R. Khalilpour (Ed.), Academic Press, Elsevier Inc., 2019, pp. 213–246.
[7] R.S. Norhasyima, T.M.I. Mahlia, Journal of CO_2 Utilization 26 (2018) 323-335.
[8] European Commission <s3platform.jrc.ec.europa.eu/carbon-capture-and-utilization> (2018) Accessed: 28.4.2019.
[9] É.S. Van-Dal, C. Bouallou, Journal of Cleaner Production 57 (2013) 38-45.
[10] F. Dalena, A. Senatore, A. Marino, A. Gordano, M. Basile, A. Basile, in: A. Basile, F. Dalena (Eds.), Elsevier, 2018, pp. 3-28.
[11] L.T. Biegler, I.E. Grossmann, A.W. Westerberg, Prentice Hall, PTR, New Jersey, USA, 1997.

ECCE12
The 12th EUROPEAN CONGRESS OF CHEMICAL ENGINEERING
Florence 15-19 September 2019

Environmental evaluation of renewable formaldehyde for production of melamine non-woven material

Annamaria Vujanović[1], Tina Kegl[1], Damjan Murn[2], Christoph Kindler[2], Rok Gomilšek[3], Igor Mihelič[4], Lidija Čuček[1]

1 Faculty of Chemistry and Chemical Engineering, University of Maribor, Smetanova 17, Maribor, Slovenia; 2 SmartMELAMINE d.o.o., Tomšičeva cesta 9, Kočevje, Slovenia; 3 Talum Inštitut d.o.o., Tovarniška cesta 10, SI-2325 Kidričevo, Slovenia; 4 MELAMIN d.d., Tomšičeva cesta 9, Kočevje, Slovenia

**Corresponding author: lidija.cucek@um.si*

Highlights

- Formaldehyde is sourced from methanol and air and used for melamine non-woven material
- Environmental evaluation of renewable formaldehyde from biomass and waste is performed
- OpenLCA software, ecoinvent 3.1 database and data from Aspen Plus models are used
- Environmental evaluation is compared with non-renewable formaldehyde from natural gas

1. Introduction

Melamine Etherified Resin (MER) non-woven, commercially known as smartMELAMINE, have a great potential for various applications, such as mobility, as a construction material, for thermal protection (fire blocker, thermal protective clothing, thermal insulation), filtrations and other industrial applications. To produce MER non-woven, mainly formaldehyde and ammonia are used as raw materials. Both could be produced from renewable sources and offer great potential for reducing environmental burdens. Formaldehyde is produced from methanol and air, where methanol could be sourced from various waste materials, while ammonia could be produced from nitrogen by using renewable sources (renewable hydrogen and electricity).

2. Scope

In this contribution environmental evaluation of formaldehyde is performed, which is sourced from renewable methanol, to be used to produce melamine non-woven material. Various waste materials for formaldehyde production are considered, such as wet and dry biomass, waste plastics and waste CO_2. Environmental evaluation is performed with OpenLCA software using the ecoinvent 3.1 database and the data from process models developed using Aspen Plus simulator. Environmental burdens are further compared with those using natural gas as a raw material for formaldehyde production.

Acknowledgments

Authors would like to acknowledge financial support from the Ministry of Education, Science and Sport of Republic of Slovenia and European Regional Development Fund for the project No. 5442-1/2018/106 and Slovenian Research Agency (PhD research fellowship contract No. 1000-18-0552 and core research funding No. P2 0412). This project has also received funding from the European Union's Horizon 2020 research and innovation programme under grant agreement No. 756081.

ECCE12
The 12th EUROPEAN CONGRESS OF CHEMICAL ENGINEERING
Florence 15-19 September 2019

Wastewater Treatment Optimization of Nitration of Aromatics

Ákos Korbács[1], Alexandra Jakab-Nácsa[1], Károly Fodor[1], Árpád Markó[1], Nan Zhao[1]

1 BorsodChem Ltd., Bolyai tér 1, H-3700 Kazincbarcika, Hungary

**Corresponding author: akos.korbacs@borsodchem.eu*

Highlights

- Extraction, optimal extracting agent – Laboratory & ChemCAD simulations.
- Distillation, energy demands calculations – Laboratory & ChemCAD simulations.
- Pretreatment of waste water – Reaction & Chemical quantity optimization.
- Green chemistry – viewpoints and goals.

1. Introduction

Whether an aromatic chemical is nitrated via mixed acid processes [1] the nitrated products are washed with acidic, neutral and alkaline waters in order to purify them. Almost all water soluble side products will be dissolved from the products and will appear in the water phase in form of its salts [2].

The waste waters will have also products dissolved, which are unfavorable thus extraction is carried out. Product specific extraction is needed thus undesirable chemicals would not be extracted back. Optimization of extraction is a main target of our experiments, so intermediates and starting materials were tested to measure its capacity and selectivity.

2. Methods

First the technology and possibilities was checked. Alternative chemicals were measured, data were put into ChemCAD. After the data refresh, simulations were carried out [Figure 1]. Optimal solutions were tested in laboratory; results were measured by various analytical methods, HPLC, GC, UV-VIS and FTIR [3].

Energy optimizations and toxicity measurements were tested in ChemCAD and laboratory plant seed tests respectively.

3. Results and discussion

More comparison happened with the extracted waste waters, which was focused on alkaline washing water which is the richest in side-products. The main key factors were the distillation possibilities of the extracting agent, and the pre-treatment investigation related with Fenton oxidation.

Green chemistry factors were checked and examined, and we can say, with optimal extraction agent 60 wt% more products can be extracted from the waste water, which would be more pure because of better selectivity. The distillation energy needs is 80% less for the optimal extracting agent [4]. The pre-treatment requires 30 wt% less oxidation agent, and the total nitrate amount

would decrease by 25 wt% in the alkaline waste water [5]. The toxicity of the waste water is reduced by 20% [5].

Fenton oxidation catalyst optimization might cause also reduced amount of waste iron catalyst in the pre-treatment system.

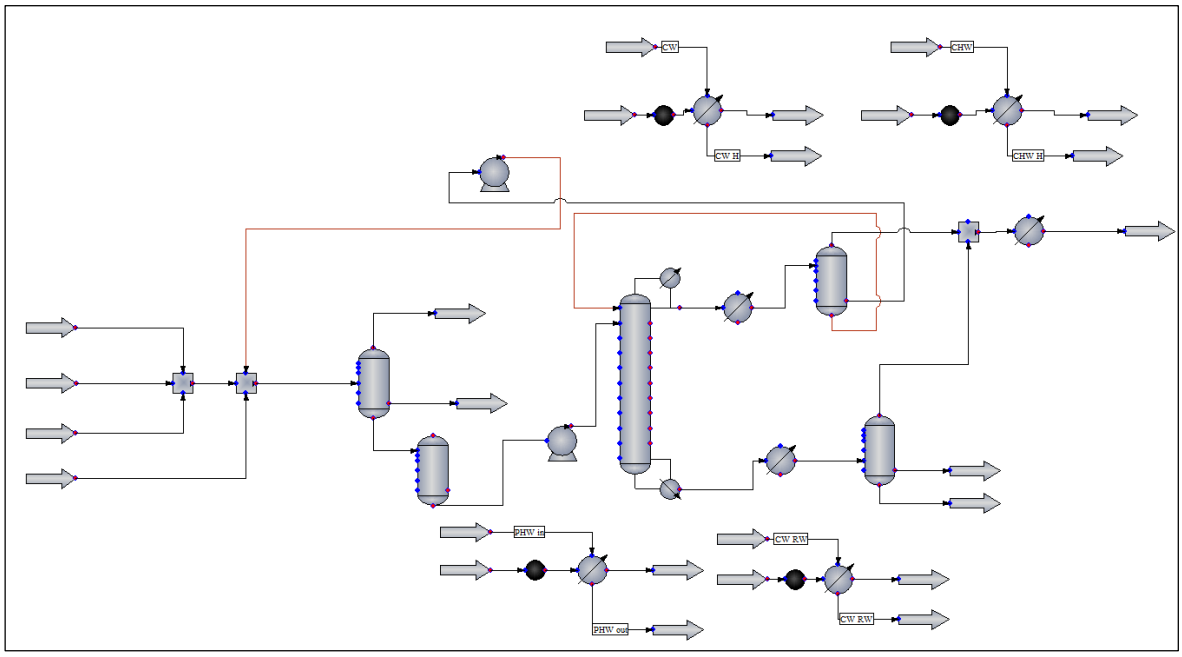

Figure 1. Simulations were set up in ChemCAD environment.

4. Conclusions

When choosing a good extracting agent, it is really important to follow the steams until it is disposed or treated in biological systems. Choosing the best can be difficult, but whether the data are correct that people have, it is recommended to calculate, measure and upscale if possible, before applying one technology. By using computational methods and simulations, cost reduction can appear, it makes easier to find the optimal chemical processes.

References

[1] W. J. Mazzafro, S. I. Clarke, M. S. Simpson, and R. Van Court Carr, “Weak acid process for producing dinitrotoluene - EP 0 903 336 B1,” 2003.

[2] D. J. L. Prak and D. W. O. Sullivan, “Solubility of 4-Nitrotoluene, 2,6-Dinitrotoluene, 2,3-Dinitrotoluene, and 1,3,5-Trinitrobenzene in Pure Water and Seawater,” J. Chem. Eng., pp. 2446–2450, 2007.

[3] F. Fiedler, H.-J. Schöbel, and M. Otto, “Identification of Nitrogen Compounds from Degradation of Dinitrotoluene and Toluylenediamine Isomers Within an Industrial Purification Plant,” Microchim. Acta, vol. 135, no. 1–2, pp. 1–7, 2000.

[4] Á. Korbács, B. R. Zsanett, A. Rodriguez, and L. Farkas, “Reducing of DNT Content in Red Water Formed During TDI Production,” Mater. Sci. Eng., vol. 43, no. 1, pp. 71–78, 2018.

[5] Á. Korbács, É. Szabó, Á. Markó, K. Fodor, and L. Farkas, “Development option for industrial waste water treatment at BorsodChem Ltd. TDI plant in order to decrease the nitrate anion concentration,” in 24th International Conference on Chemistry, PhD Student Plenary Presentations, Applied and Chemical Engineering Section, 2018.

First Attempt for Robust Bubble/Dew Problem Solution with Bender EoS

Filippo Bisotti[1], Flavio Manenti[1*]

1 Politecnico di Milano, DMIC Department "Giulio Natta", Piazza Leonardo da Vinci, 32, 20133, Milan, Italy;

**Corresponding author: flavio.manenti@polimi.it*

Highlights

- Thermodynamic package available only for Air Separation Unite
- Attractive to be used in simulation environment
- Presence of twenty fitting parameters makes Bender EoS very flexible and efficient
- Development of numerical tricks to avoid any trivial and unfeasible solutions

1. Introduction

The Bender Equation of State is a specific thermodynamic package available for Air Separation Unit. Bender EoS is essentially composed by twenty fitting parameters which let very flexible and efficient prediction of thermodynamic of air mixture. The model has been implemented to solve bubble/dew problems. The main difficulty is to avoid the convergence of the system toward trivial solution, which is actually unfeasible. In addition, strong nonlinearities in the formulation of the Equation of State and in the mixing rules make the solution quite stiff (Figure 1), where for very small change of the density value, pressure solution rapidly diverges. Therefore, some tricks have to be applied in order to drive the system toward the right solution

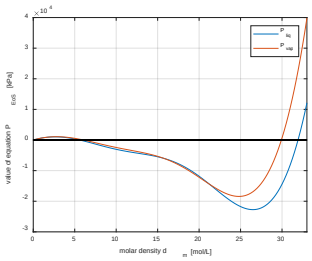

Figure 1 – pressure prediction with Bender EoS for liquid (blue line) and vapor phase (red)

2. Methods

In order to solve a vapor-liquid equilibrium the following nonlinear system has to be solved

$$\begin{cases} f_k^{vap} - f_k^{liq} = 0 & for\ k = 1\ (N_2), 2\ (Ar), 3\ (O_2) \\ P - P_B^{vap} = 0 \\ P - P_B^{liq} = 0 \\ \sum_{k=1}^{3} x_k - 1 = 0\ \vee\ \sum_{k=1}^{3} y_k - 1 = 0 \end{cases}$$

According to the thermodynamic model, pressure is function of temperature, density and composition of the phase (m): temperature and pressure dependence appear in mixing parameter

$$P_m = d_m T \left[R + \left(a_1 - \frac{a_2}{T} - B \right) d_m + C d_m^2 + D d_m^3 + E d_m^4 + F d_m^5 + (G + H d_m^2) d_m^2 \cdot \exp(-a_{20} d_m^2) \right]$$

To prevent any possible divergence of the solution due to nonlinearities, a sensitivity analysis on the several mixing coefficients and, finally, on the global term appearing inside the square brackets has been done. This clearly depicts that exists for both phases a feasibility region owing to that absolute pressure cannot be negative. Obviously, this criterion is adopted to remove any potential unfeasible behavior of the model in any iteration during the nonlinear system solution. The system has been solved in VSC++ 2013 combined with the BzzMath Library numerical tools.

3. Results

Figure 2 compares the solutions of dew problem in pressure for dry air with the results of other EoS directly implemented in Aspen-Hysys: Peng-Robinson, BWR and Bender one. The experimental data are taken from NIST experimental campaigns' results published in literature

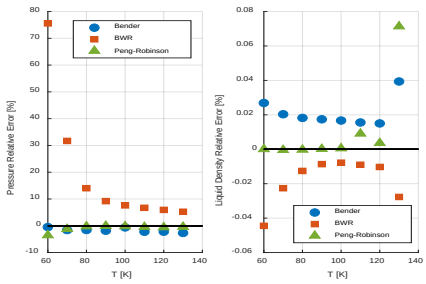

Figure 2 – relative error comparison of pressure and liquid density prediction with three different EoS

4. Conclusion and future developments

Bender model is an effective thermodynamic tool to predict the behavior if air components mixtures and its results are comparable to those obtained from commonly used Equation of State in ASU design. Indeed, it is also accurate near both the triple and the critical points of the mixture. In addition, more reliable results and convergence are ensured by forcing the solver to avoid the unfeasible region. Therefore, considering that Bender EoS's parameters directly derive from a numerical fitting, the partial loss of physical meaning can be overcome by properly selecting and imposing physical constraints on the thermodynamic model itself. In the future, further numerical tricks may be applied not only to increase the predictive capacity and help the convergence but major efforts should be focus on decreasing the computational time without loss in accuracy and precision.

References

[1] E. Bender, The Calculation of Phase Equilibria from a Thermal Equation of State Applied to the Pure Fluids Argon, Nitrogen, Oxygen and their Mixtures, C.F. Verlag Muller, Karlsruhe, 1973

[2] E. Bender, An equation of state for predicting vapour-liquid equilibria for system N_2-Ar-O_2, *Cryogenics*, 13(1), 1973

[3] G. Buzzi-Ferraris, F. Manenti, Nonlinear Systems and Optimization for Chemical Engineer – Solving numerical problems, Wiley-VCH, 2014

[4] E.W. Lemmon, R.T. Jacobsen, S.G. Penoncello, D.G. Friend, Thermodynamic Properties of Air and Mixtures of Nitrogen, Argon and Oxygen From 60 to 2000K at Pressures to 2000MPa, *J. Phys. Chem. Ref. Data*, 29(3), 2000

ECCE12
The 12th EUROPEAN CONGRESS OF CHEMICAL ENGINEERING
Florence 15-19 September 2019

Ionic Liquid Design and Process Simulation for Shale Gas Separation

Xinyan Liu[1], Yuqiu Chen, Xiangping Zhang[2], Suojiang Zhang[2], Xiaodong Liang[1], Rafiqul Gani[3], Georgios M. Kontogeorgis[1*]

1 Department of Chemical & Biochemical Engineering, Technical University of Denmark, DK 2800 Kgs. Lyngby, Denmark;

2 Beijing Key Laboratory of Ionic Liquids Clean Process, CAS State Key Laboratory of Green Process and Engineering, Institute of Process Engineering, Chinese Academy of Sciences, Beijing 100190, China;

3 PSE for SPEED, Skyttemosen 6, DK-3450 Allerod, Denmark

**Corresponding author: gk@kt.dtu.dk*

Highlights

- A three-stage framework for IL-based shale gas separation is proposed.
- Two ILs are selected and designed based on a database and UNIFAC-IL model.
- An IL-based hybrid separation scheme for shale gas model has been designed with a potential energy-saving objective.
- IL-based gas separation has the potential to achieve a low energy consumption and economic cost.

1. Introduction

Shale gas, considered as the clean energy and a substitute for coal, has attracted increasing attention in recent years. It needs to go through a series of processing units to obtain the upgrading commercial gas. Traditional common technologies for shale gas separation include energy intensive distillation and solvent based absorption. Distillation is usually applied for light hydrocarbon gas separation in which the separated gas is recognized as an important raw gas for synthesizing many industrial chemicals. The process includes columns with large numbers of trays to get a high purity product at low temperatures and high pressures resulting in a high energy consumption and negative environmental impact. The solvent-based absorption technology is widely used for separating gases such as CO_2, H_2S which need to be removed in order to satisfy the emission standard of air pollutants. Having some advantages of non-volatility, flexible designing, ionic liquid (IL) has been paid much attention. It is reported that different ILs can be used for different gases absorption[1]. Therefore, a strategy for a five-gas shale gas model separation process synthesis where both traditional distillation and IL-based absorption are employed has been developed. However, the numerous combinations of cation and anion make it a challenging task to search for the optimal one for this shale gas separation. Then selection-screening methods are proposed first. The associated process simulation and evaluation are performed.

2. Methods

In this work, we first establish an experimental database on gas solubility and Henry's law constant in various ILs. Then database is applied for the predicted model development including corrected COSMO-RS model and UNIFAC-IL model. The activity coefficients of gas in ILs are calculated based on these predicted models so that the gas solubility in new ILs which is not

included in experiments could be predicted [2]. A three-stage methodology proposed for the shale gas separation process design and evaluation will be highlighted. The first stage involves IL screening, where two options are applied. One is only based on the experimental database. The other is a computer-aided method which could be used to automatically obtain the optimal IL on the group contribution basis. The second stage is process design, where the important design issues are determined. Then overall separation scheme is generated. The third stage is process simulation and evaluation. Rigorous process simulation is conducted after the development and verification of related thermodynamic model. Here, a model shale gas containing five gases is assumed as a case study to highlight the application of this methodology.

3. Results and discussion

A five-component shale gas model, which consists of 80% CH_4, 7% CO_2, 7% C_2H_6, 3% C_2H_4, 3% H_2, is assumed in this work. Based on the experimental database, it's found only CO_2 could be absorbed by IL. One optimal IL-a ([thtdp][phos]) has been selected with both high solubility of CO_2 and high selectivity of CO_2/CH_4. Besides, another IL-b ([MMPy][eFAP]) is designed based on a UNIFAC-IL model with a higher selectivity of CO_2/CH_4 than IL-a. Both these two ILs are applied for further simulation to be evaluated. Then a shale gas separation scheme is proposed including two parts: IL-based process for CO_2 removal and traditional distillation columns for other light hydrocarbon gas separation. Evaluated results for total energy consumption and economical cost are shown in Fig.1. IL-b based process gives an improved energy-based technology.

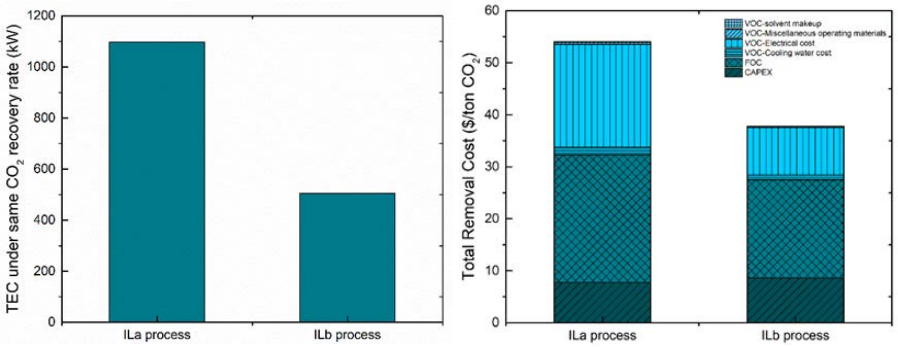

(a) (b)

Figure 1. Process evaluation on a) total energy consumption and b) total CO_2 removal rate

4. Conclusions

This work proposes a hybrid IL-based technology for shale gas separation where the IL is used to remove CO_2 and distillation is applied to obtain the desired final products. A three-stage methodology, in which systematic IL screening, process design and simulation, and process evaluation, is established. Two ILs are selected through two options. IL-b with its good separation results provides a promising recommendation for future solvent development of gas separation process. Future work would focus on further removing the hydrogen for syngas production combining with the removed CO_2 as well as separation and use of C_2H_4 and C_2H_6.

References

[1] Lei, Z., Dai, C. & Chen, B. *Chem. Rev.* 114, (2014) 1289–1326.
[2] Liu, X., Zhou, T., Zhang, X. *et al. Chem. Eng. Sci.* 192, (2018) 816–828.

ECCE12
The 12th EUROPEAN CONGRESS OF CHEMICAL ENGINEERING
Florence 15-19 September 2019

From Conceptual Design to Process Design Optimization: Future research challenges

Ludovic Montastruc[1], Ségolène Belletante[2], Alexandre Pagot[2], Stéphane Negny[1], Ludovic Raynal[2]

1Université de Toulouse, Laboratoire de Génie Chimique UMR CNRS/INPT/UPS France,
2IFP Energies nouvelles, Rond-point de l'échangeur de Solaize - BP 3,69360 Solaize,France

**Corresponding author: ludovic.montastruc@ensiacet.fr*

Highlights

- The new role of Process Systems Engineering (PSE) focusing on process synthesis.
- Future research challenges that process synthesis will have to face.

1. Introduction

Process synthesis is a dynamic research domain widely explored by the process systems engineering (PSE) community. This topic was first put forth 60 years ago. Westerberg in his retrospective on design and process synthesis, has defined process synthesis as the part of engineering "where one invents the structure and operating levels for a new chemical manufacturing process"[1]. Process synthesis applies to both the design of a completely new process flowsheet and the retrofit and optimization of an existing process. Furthermore, process synthesis is the assembly and interconnection of unit operations into a process network involving different physical and chemical phenomena to transform a material into desired products for given energy inputs with the goal of optimizing either economic, environmental, and/or social objectives [2]. This dynamics of this research will be further increased due to the future research challenges that process synthesis will face, e.g., biomass transformation, shale production, embedded process, modular plant design, and intermittent production of energy.

2. Methods

A systematic literature review method composed of a search strategy and an analysis of the collected documents are performed. The purpose is to identify the main methods and approaches developed in the literature and to examine them thoroughly. The PSE research groups several topics or subjects: continue or batch, simulation or optimization, Linear Programming or No Linear Programming with or without integer variables, mono or multi- objective….. We identify the most influential research teams and papers that played major roles. In the considered period2011-2016, 1288 articles were published, and 16 research teams wrote 95% of them only. While these teams are all working on process and conceptual design, from figure 1, one can identify a first category of authors who are more focused on optimization methods, i.e., Barton, Biegler, Floudas, and Grossmann. For these groups, process synthesis is one application of the optimization methods that they develop in their research teams because the conversion of process alternatives into mathematical models often results in MINLPs that are difficult to solve. For other authors, mono- or multiobjective optimization is often a tool that is included in their methodology. One major

observation from this figure is that the authors study the process synthesis under the domain of their scientific backgrounds. Indeed, You, Puigjaner, and Srinivasan are more focused on supply chain; Klemes, Kravanja, El Hawagi, and Marechal on heat integration aspects, whereas Maravelias tackles the problem with his vision as a scheduling specialist. A majority of authors are more on the process design area except for two of them who are more focused on conceptual design, i.e., Gani and Engell. Finally, another category of researchers, composed of Marquardt and Ng, try to have a more comprehensive approach that seeks to integrate all previous elements.

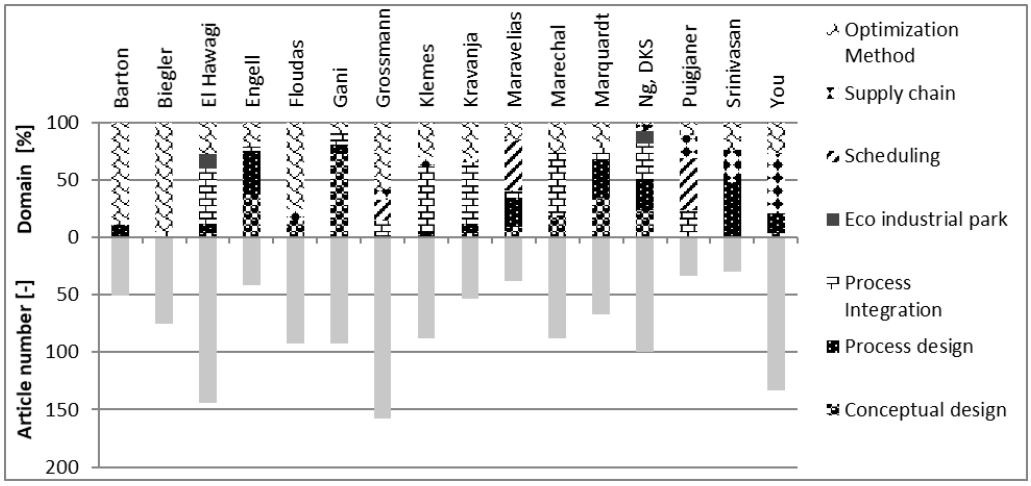

Figure 1. Relationship between domain clusters and research teams

3. Conclusions

In addition to these future challenges, theoretical advances are also required. Obviously, the development of optimization methods and algorithms must continue to provide solutions to the global optimization problem. Either conventional or intensified unit operations require more detailed models to introduce small-scale phenomena, which influence the performance of unit operations. Such an approach leads to the introduction of multiscale information in the design process. The development of methods to handle uncertainties is also a crucial challenge. During the process design stages via optimization approaches, hybrid approaches, or through metamodeling (multiparametric approach, “surrogate model,” etc.), the introduction of inaccuracies and/or uncertainties on data is performed by local sensitivity studies or calculation of flexibility indices. In recent years, new methods of global sensitivity (e.g., Sobol method and chaos polynomials) have emerged, allowing the effective modeling and propagation of uncertainties in numerical simulation. Similarly, machine-learning methods have expanded considerably, for example, in the treatment of partitioning or discrimination problems. Furthermore, the modeling of poorly known data remains a major asset of the fuzzy logic. A possible strategy of renewing the methods for design processes could be the use of these three techniques, separated or combined, in order to reach more robust solutions that can allow inaccuracies/uncertainties inherent to the design stage, but at the same time, deal with hazards during process operation.

References

[1] Westerberg, A. W. (2004). A retrospective on design and process synthesis. Computers & Chemical Engineering, 28(4), 447–458.

[2] Chen, Q., & Grossmann, I. E. (2017). Recent Developments and Challenges in Optimization-Based Process Synthesis. Annual review of chemical and biomolecular engineering, 8, 249–283.

ECCE12
The 12th EUROPEAN CONGRESS OF CHEMICAL ENGINEERING
Florence 15-19 September 2019

H_2-CCS Chain Tool and Evaluation Methodologies for Integrated Chains.

D. Iruretagoyena[1,*], N. Sunny[1], C. Antonini[2], R. de Kler[3], N. Mac Dowell[1], N. Shah[1,*]

[1] Department of Chemical Engineering, Imperial College London, South Kensington, London, SW7 2AZ, UK

[2] ETH Zurich, Institute of Process Engineering, Sonneggstrasse 3, CH-8092 Zurich, Switzerland

[3] TNO Science and Industry, Leeghwaterstraat 46, 2628 CA Delft, The Netherlands

*Corresponding authors: n.shah@imperial.ac.uk, d.iruretagoyena09@imperial.ac.uk

Highlights

- An open-source design tool for a fully integrated H_2-CCS chain is developed
- Combining SMR, CCS and salt caverns enables to meet heating and CO_2 emissions regulations in the UK
- Dynamic behavior of a CCS plant shows smooth responses to SMR load fluctuations
- Large flow fluctuations are not desirable for the compressor train operation

1. Introduction

Carbon Capture and Storage (CCS) is currently considered as the "most important technology" to decarbonize the industrial sector by the International Energy Agency (IEA). This technology can in principle be integrated with industrial process plants, separate out the carbon dioxide and transport it to a suitable location for long term underground storage. Similarly, hydrogen (H_2) will play an important role to decrease the carbon emissions from fossil fuel combustion, primarily due to its use as an ultraclean fuel in the heating and transportation sectors, as well as a process feedstock.[1] Contrary to natural gas that produces about 180 gm/kWh CO_2, hydrogen emits no GHGs (at the point of use). However, steam reforming of methane (SMR) and coal gasification, which are currently considered to be the most feasible and economic routes to large-scale H_2 production, also produce significant quantities of CO_2.[2] Therefore, it is crucial to develop strategic H_2-CCS infrastructure to meet the targets in the Paris 2016 Climate Agreement, which have resolved to reduce carbon emissions by over 80% by 2050.[3] The ELEGANCY project enables the evaluation of integrated H_2-CCS chains with respect to technological and economic efficiency, operability and environmental impact. To this end, this contribution is focused on the development of an open-source systems modelling framework with a steady-state design mode and a dynamic operational mode. The methodology developed is applied to five national case studies: Netherlands, Switzerland, United Kingdom, Germany and Norway.

2. Methods

The modelling toolkit developed involves two modes: *(1) Design mode:* Steady state model where the user can explore the time evolution of system design (e.g. choice, scale and location of key technologies and network structure for H_2 and CO_2). For this purpose, we use the Resource-technology network (RTN) methodology, which integrates key elements such as space, time, resources, technologies, infrastructure/Networks to obtain optimal H_2-CCS configurations in terms

of costs (CAPEX and OPEX). The Mixed Integer Linear Programming (MILP) models are developed using Python software. QGIS is used for geographical visualization. (2) *Operational mode:* This enables the user to simulate dynamic behavior of the designed system including intermittent operation. The ranges of key systems variables such as flowrate, temperature, pressure and impurity profiles are quantified. Different technologies for H_2 production are assessed including steam methane reforming and autothermal reforming. The models are developed using OpenModelica software and are compared to relevant ASPEN, gPROMS and Matlab codes.

3. Results and discussion

An open source H_2-CCS steady-state model based on the RTN framework has been successfully developed. The toolkit provides the location, type, number and capacities of process and storage technologies, the distribution infrastructure linking one region to another and the retrieval rates of all resources in the system in every location in the time horizon. Figure 1a shows an example of the implementation of the model to the UK as a case study. It is found that combining SMR with salt cavern technologies enables the production of sufficient amounts of H_2 to meet the heating demands in the UK. The integration of SMRs with CCS technologies is able to reduce the carbon emissions content from 180 gCO_2/kwh in natural gas to approximately 50 gCO_2/kwh from H_2, resulting in a 73% reduction in overall emissions.[4] Regarding the operational mode, a dynamic model for integrated SMR-CCS processes is successfully developed. A scheme of the dynamic model of a CCS plant in OpenModelica is shown in Figure 1b. Some key results indicate that the CCS section has a smooth response to load fluctuations of the SMR plant, and the required stabilization time of the CCS plant is closely related to its liquid residence time. Large flow fluctuations are not desirable for the compressor train operation. Simulations showed that a single compressor train with recycle valve surge control is able to meet the desired performance.[5]

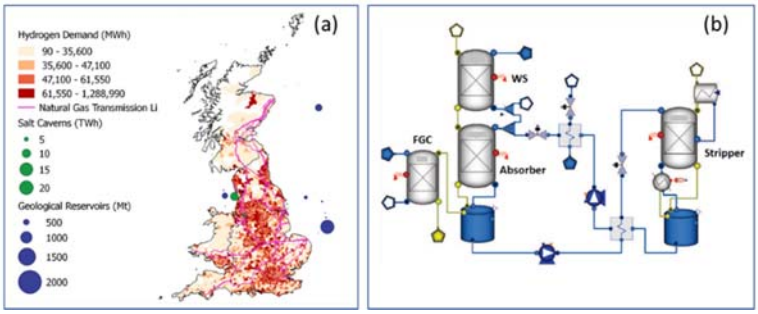

Figure 1. (a) Design mode, H_2-CCS, UK Case study. (b) Operational mode, Dynamic model of CCS plant.

4. Conclusions

In this study, we describe an open-source system modelling framework with a steady-state design and a dynamic operational modes that has been developed in the Elegancy project. The modelling toolkit is applied to five national case studies providing particular strategies to implement efficient H_2-CCS networks. The results obtained for the UK case study are relevant to accelerate implementation of the low-carbon gas network for Leeds.

References

[1] R. Anantharaman, et al., Hydrogen production with CCS, Int. J. Hydrog. Energy, 41 (2016) 4969-4992.
[2] N. Shah, et al., Optimal transition towards a large-scale hydrogen infrastructure for the transport sector: The case for the Netherlands, 36 (2011) 4619-4635.
[3] Committee on Climate Change, Next steps for UK heat policy, (2016).
[4] H21 North of England, H21 NoE Report/2018
[5] R. de Kler et al., Dynamic behaviour CO_2 capture and compression: an assessment, Energy Procedia, 63 (2014) 2727-2737.

ECCE12
The 12th EUROPEAN CONGRESS OF CHEMICAL ENGINEERING
Florence 15-19 September 2019

Optimal performance membrane processes for nitrogen separation from air

Marjan Bozorg[1, 2, 3], Bernardetta Addis[2], Veronica Piccialli[3], Álvaro A. Ramírez-Santos[1], Christophe Castel[1], Eric Favre[1, *]

1 Université de Lorraine, CNRS, LRGP, F-54000 Nancy, France; 2 Université de Lorraine, CNRS, LORIA, F-54000 Nancy, Franc; 3 Dipartimento di Ingegneria Civile e Ingegneria Informatica, Universitá degli Studi di Roma Tor Vergata, viale

**Corresponding author: Eric.Favre@univ-lorraine.fr*

Highlights

- Nitrogen production
- Membrane separation process
- Membrane material
- Process synthesis

1. Introduction

Membrane processes are one of the key technology for gas separation applications. They combine a series of key advantages that can result in energy efficient, small sized and environmental friendly processes. Among those processes, nitrogen production from air by membrane gas separation processes is a mature technology, which is applied in numerous industrial sectors (chemistry, food, aeronautics, space...). Depending on the nitrogen purity requirements (typically between 90 and 99.9%), single stage or multi-stage membrane process configurations are used. The main challenge is then to be able to build and provide tools to optimally design membrane processes that is mainly the answer of the question: what is the best membrane material and the best process architecture to achieve my separation targets?

A very large number of advanced membrane materials have been recently reported, showing increasing permeability and/or selectivity for air separation applications (i.e. trade-off limits of dense polymeric materials for the O_2/N_2 pair gas [1]) compared to the commercially available membranes. The interest of these new materials in terms of nitrogen production cost and their impact in terms of process configuration have never been reported through a process synthesis study. The results of the optimization (process synthesis) are expected to generate useful guidelines for membrane material development: is it better to push selectivity or permeance in order to decrease NEA production cost? Is it interesting to combine different membranes in a multi-staged unit, in order to achieve lower production costs? This is what this study is aimed to answer.

2. Methods

Based on a tailor made global optimization methodology and program [2], optimal process configurations achieving minimal production cost are first identified for standard and commercial O_2/N_2 separation membranes (PSf [3] and PPO[4]) for four different levels of N_2 purity. (90, 95, 99, 99.9%). The same strategy is then performed with membrane materials considered as a variable of the system, with the possibility to combine different materials in multi-staged systems. The choice of the membrane materials can be freely made in the domain delimited by the trade-off limit. The

impact in terms of nitrogen production cost for the different purities and the corresponding optimal membrane materials and process configurations are discussed.

3. Results and discussion

The acceptable domain for O_2/N_2 separation membranes considered based on [1] (the green region in the Figure 1). Consequently, the optimal process configuration with associated operating conditions and the lowest N_2 production cost is obtained while converging to the optimal membrane performances for different nitrogen purity levels.

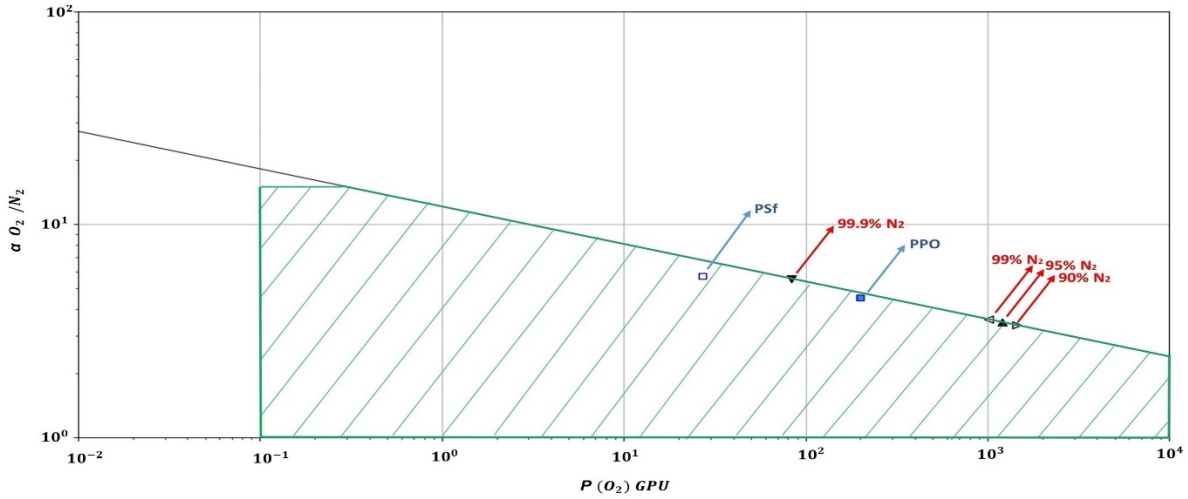

Figure 1. Commercial available membrane materials (blue squares) and the optimal performance membranes for different nitrogen purity levels indicate with triangles.

4. Conclusions

Surprisingly, a medium membrane selectivity combined to a high permeability is shown to systematically offer the best set of performances, for mono or multistage systems. In contrast with current practice, vacuum operation and recycling loops are shown to generate lower N_2 production costs with high performance membranes. For the set of parameters tested in our study, it seems that the use of different membranes in a multistage system does not offers attractive improvement potentialities. It is obvious that this statement does not systematically hold for gas permeation and should be reconsidered from case to case.

References

[1] L. M. Robeson, The upper bound revisited, Journal of Membrane Science 320 (2008) 390–400.

[2] Álvaro A. Ramírez-Santos, M. Bozorg, B. Addis, V. Piccialli, C. Castel, E. Favre, Optimization of multistage membrane gas separation processes. Example of application to CO2 capture from blast furnace gas, Journal of Membrane Science 566 (2018) 346–366.

[3] H. M. Ettouney, H. T. El-Dessouky, W. Abou Waar, Separation characteristics of air by polysulfone hollow fiber membranes in series, Journal of Membrane Science 148 (1998) 105-117.

[4] S. McConnell, Heavy-duty diesel engine NO_x reduction with nitrogen-enriched combustion air (2010).

ECCE12
The 12th EUROPEAN CONGRESS OF CHEMICAL ENGINEERING
Florence 15-19 September 2019

Tar Removal by Catalytic Cracking in Biomass and Waste Gasification

Juma HAYDARY*, Jakub HUSAR, Patrik ŠUHAJ

Institute of Chemical and Environmental Engineering, Slovak University of Technology in Bratislava, Radlinského 9, 812 37 Bratislava

* juma.haydary@stuba.sk

Highlights

- Thermal and catalytic cracking of tar from biomass and waste gasification was studied
- Different types of clay based and char based cheap catalysts were characterized and tested
- Both calcined and Ni impregnated clay catalysts reduced the tar content
- Char based catalysts showed large catalytic effect in the reduction of tar

1. Introduction

Gasification of biomass or solid waste produces combustible gases consisting mainly of H_2, CO and CO_2. Air, oxygen, steam or their mixtures can be used as a gasifying agent [1]. Although much attention has been devoted to gasification in recent years, there are still a number of challenges to full commercialization of biomass and solid waste gasification [2].

One of the critical issues in biomass and waste gasification is the quality of produced gas. To be used in internal combustion engines or turbines, the gas should fulfil relatively strict requirements for gas composition, heating value and tar content. Production of fuel quality gas requires the removal of tar from the producer gas. This work deals with secondary catalytic tar cracking in the gasification of biomass and waste, using low cost catalysts. Different types of catalysts based on two different types of materials (red clay (RC), tire pyrolytic char) have been prepared by calcination (carbonization) at different conditions and/or impregnation with Ni. The catalysts were tested by using toluene and p-Xylene as model tar components and also by experiments with gasification of RDF (Refused-Derived Fuel) samples.

2. Methods

The catalysts were characterized by pore structure and specific surface measurement (before and after use), thermogravimetric analysis, elemental analysis and X-ray diffraction analysis. In the first step, the catalyst activity was tested by cracking of a model organic compound at different conditions. In the next step, the catalysts were used for cracking of tars in a two stage laboratory scale gasification unit, where the composition of producer gas and gas tar content were observed for different process conditions and catalyst types. As the raw material in these experiments, RDF, a fraction of municipal solid waste, MSW was used. The gas composition was measured by gas chromatography GC. Tar content of the gas was measured using a standard method based on tar capture in isopropanol and subsequent distillation at specific conditions and gravimetric measurement.

3. Results and discussion

Char based catalysts were thermally stabilized (carbonized) at temperatures from 800 to 1000 °C. Ni impregnated char catalysts were prepared by impregnation of carbonized char catalysts. Specific surface area of char catalysts increased from 28 m^2/g to 105 m^2/g due to carbonization. Char based catalysts showed large catalytic effect also in the reduction of tar in the gas from the RDF gasification. Char catalysts prepared by carbonization at 900 °C reduced the tar content of producer gas by 92.3 % compared to the non-catalytic (thermal) decomposition process.

The red clay containing mainly SiO2 and some amounts of Al_2O_3, Fe_2O_3, $CaCO_3$, $MgCO_3$ and others [3] had the initial specific surface area of around 100 m^2/g; however, its surface area decreased by calcination up to 35 m^2/g. Both calcined and Ni impregnated clays reduced the tar content of the gas up to 80 and 91.8%, respectively. An example of tar yield versus clay catalyst to RDF ratio is shown in Figure 1. Ni impregnation of both clay on char catalysts resulted in higher H_2 content of the produced gas [4].

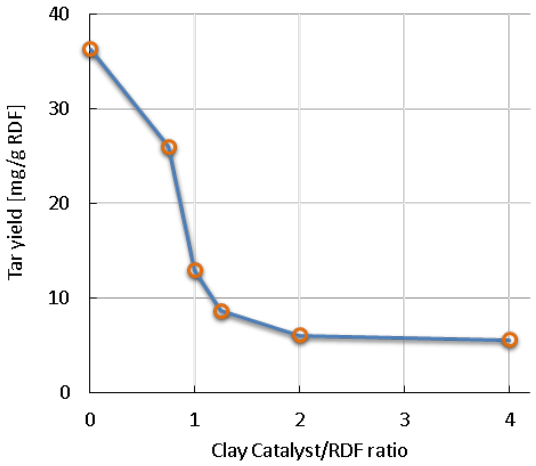

Figure 1. Tar yield versus catalyst/RDF ratio (Temperature: 800°C)

4. Conclusions

Calcined red clay and carbonized pyrolytic char can serve as low cost catalyst in the removal of tar from gas produced by the gasification of solid waste and biomass. Impregnation of these catalysts with Ni leads to better char removal and higher content of H_2 in the gas, however it can also represent additional costs related to catalyst preparation and after use treatment.

Acknowledgement

This work was supported by the Grant APVV-15-0148 provided by the Slovak Research and Development Agency

References [Calibri 10]

[1] N. Antoniou, G. Stavropoulos, and A. Zabaniotou, Ren. & Sust. En. Rev., 39, (2014), 1053-1073
[2] J. Haydary, Chem.l Eng. Trans., 61, (2017) 1465-1470
[3] J. Haydary, D. Susa, and J. Dudáš, Waste management 33 (5), (2013), 1136-1141
[4] P.Šuhaj, J. Haydary, J. Husár, P. Steltenpohl, I. Šupa, Waste Management 85 (2019) 1–10

ECCE12
The 12th EUROPEAN CONGRESS OF CHEMICAL ENGINEERING
Florence 15-19 September 2019

A Population Balance Model for the Dynamic Simulation of Enzymatic Hydrolysis of Lignocellulosic Biomass in Batch or Fed-Batch Bioreactors.

Vasileios Margaritopoulos[1], Christos Chatzidoukas[1,*]

[1] *Chemical Engineering Department, Aristotle University of Thessaloniki (AUTH), 54142, Thessaloniki, Greece*

**Corresponding author: chatzido@auth.gr*

Highlights

- Endo- and exoglucanases synergy-the role of cellulose chain length distribution.
- Continuous varying substrate accessibility to the enzymes.
- Hydrolysis yield improvement from batch to fed-batch operation of bioreactors.

1. Introduction

Biomass hydrolysis is a critical step in biochemical processes where cellulose is degraded to glucose for the production of biofuels and useful chemical products. Enzymatic hydrolysis is a promising method for glucose production due to its low energy demand and mild operating conditions [1]. However, the multiple phenomena that occur make the hydrolysis process complex, impeding the comprehension of the exact mechanism. Thus, the commercialization of the process is still considered a challenge. Detailed mathematical models provide the means for further elucidating the dominant mechanisms and process optimization. Various semi-empirical models have been developed, however they usually suffer an over-parameterization or their predicting capability is confined within certain experimental conditions due to a simplified and macro-scale approach of the problem. In this work a mechanistic model is developed deepening further on meso- and micro-scale phenomena involved in the hydrolysis of lignocellulosic biomass, while accounting for critical substrate characteristics such as particle size, cellulose chain length distribution and lignin content. The dynamic evolution of the substrate accessibility to the enzymes is efficiently captured by the model in order to prove the hydrolysis yield reduction [5], experimentally observed in bioreactors of high solids loading compared to those of lower solids loading, demonstrating the model handiness for the operational design of fed-batch bioreactors.

2. Methods

Biomass hydrolysis refers to the degradation of cellulose to its oligomers, meaning glucose and cellobiose. The enzymatic hydrolysis is catalyzed by two types of cellulases named endo- and exo-glucanases. Endoglucanase attacks β-1,4-glycosidic bonds within the cellulose chain with random chain scission, while exoglucanase removes single units of cellobiose with chain end scission [3,4]. A population balance technique is applied [2,3,4] to describe the dynamic evolution of cellulose chain length distribution, from the distinct action of each enzyme as is described below:

$$x_{mer} \xrightarrow{endoglucanase} y_{mer} + (x-y)_{mer} \qquad x_{mer} \xrightarrow{exoglucanase} (x-2)_{mer} + cellobiose$$

The model emphasizes on the fractional accessibility of the substrate to the surrounding enzymes adopting a layer-by-layer exposure of the cellulose chains and a binding mechanism of the enzyme

on these chains. The Langmuir isotherm is employed to describe the adsorption of soluble enzymes on both surficial cellulose and lignin of the insoluble biomass particles to account for the heterogeneity of the hydrolysis mechanism. The entire dynamic model is developed and solved with the gPROMS® simulation platform.

3. Results and discussion

Endoglucanase is responsible for generating quickly cellulose chains of shorter length and providing to exoglucanase additional chain ends. Exoglucanase, hydrolyzes the substrate by generating soluble oligomers. Cellulose hydrolysis would be practically unaccomplished in the case where only endoglucanase was used, however, its role is not negligible since the generation of shorter chains increases the exoglucanase efficiency. The derived model uncovers these phenomena, the synergy between the two types of enzymes and the way endogenous traits of the substrate, such as particle radius, cellulose chain length distribution and lignin content are involved in the hydrolysis reaction rate. Precisely, as the hydrolysis proceeds new substrate layers of non-degraded cellulose chains, tangled with lignin, are exposed. The hydrolysis rate takes its maximum value at the beginning of the process since the quantity of enzymes that can bind effectively on the biomass is the maximum possible. Progressively, the particle radius is reduced and less amount of enzyme is adsorbed on the particle's surface. Moreover, the lignin fraction in the particle increases, leading to the reduction of the effectively bound enzymes and finally the total rate of hydrolysis, without any product inhibition effect being necessary for such a response.

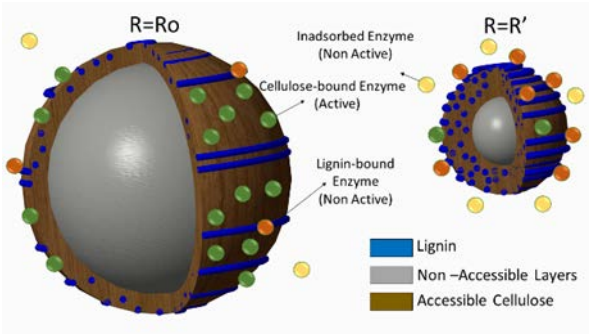

Figure 1: Graphical representation of particle hydrolysis.

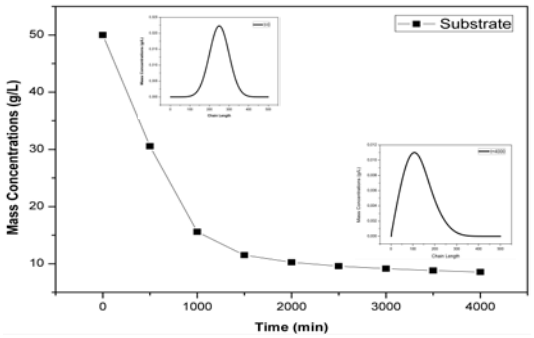

Figure 2: Time profile of cellulose hydrolysis.

4. Conclusions

A generic mechanistic model, which takes into consideration factors like chain length distribution, lignin content, particle size and specific surface area, has been built up. The influence of substrate characteristics on the catalytic efficiency of the enzyme highlights the importance of the pre-treatment the lignocellulosic biomass is subjected to. A model-based investigation of the optimal dynamic operation of fed-batch hydrolysis bioreactors can be essentially supported by the proposed mathematical model.

References

[1] Bansal, P., Hall, M., Realff, M., Lee, J. and Bommarius, A. (2009). *Biotechnol. Adv.*, 27(6), pp.833-848.
[2] Griggs, A., Stickel, J. and Lischeske, J. (2011). *Biotechnol. Bioeng.* 109(3), pp.665-675.
[3] Hosseini, S. and Shah, N. (2011). *Biomass and Bioenergy*, 35(9), pp.3830-3840.
[4] Hosseini, S. and Shah, N. (2011). *Biomass and Bioenergy*, 35(9), pp.3841-3848.
[5] Kristensen, J., Felby, C. and Jørgensen, H. (2009). *Biotechnol Biofuels*, 2(1), p.11

ECCE12
The 12th EUROPEAN CONGRESS OF CHEMICAL ENGINEERING
Florence 15-19 September 2019

Enzymatic hydrolysis of Cytisus striatus: acid sulfite pretreatment optimization.

Álvaro Vaz[1*], Tânia Gomes[2], Rogério Simões[1]

1 FibEnTech Research Unit, University of Beira Interior, Rua Marquês D'Ávila e Bolama 6201-001 Covilhã, Portugal; 2 University of Beira Interior, Rua Marquês D'Ávila e Bolama 6201-001 Covilhã, Portugal

**Corresponding author: avaz@ubi.pt*

Highlights

- Pretreatment conditions affect total recovered sugars (6% up to 69%) and generated degradation products.
- For a given sulfite load, more acidic conditions lead to higher sugar release and further material fragmentation, increasing degradation products.
- Moderate loads of sodium bisulfite (1%) and sulfuric acid (2.25%), release practically all hemicelluloses.

1. Introduction

Ethanol production from lignocellulosic material includes three major steps: biomass pretreatment, which fragments the lignocellulosic matrix to facilitate the enzymes access to the substrate; hydrolysis, where the polysaccharides are converted into fermentable sugars (e.g. glucose and xylose) [1]; and finally, fermentation that produces ethanol or other biologically based chemicals (e.g. lactic acid, succinic acid) [2]. The aim was to study the effect of pretreatment operative variables, namely sodium bisulfite and sulfuric acid loadings, temperature and time, on released sugars in Cytisus striatus enzymatic hydrolysis with a Novozymes® cocktail. Pre-treatment intends lignin and hemicelluloses removal, reduced cellulose crystallinity and lignocellulosic network porosity increase in order to facilitate enzyme access.

2. Methods

Cytisus striatus was chipped with a Retsch Mühle knife mill with 10 mm x 10 mm sieve, being fines removed with 18 mesh screens, resulting a material with 1-2 mm width and 10 mm long. Chips were then submitted to different reaction conditions, with a central composite experimental design 2^4+star, exploring the following variables: sulfuric acid charge (0-3%), sodium bisulfite charge (0-4 %), maximum temperature (150-190ºC) and time at maximum temperature (0-30 minutes). For each assay, 30 g (o.d.) broom chips were treated in 200 mL stainless steel reactors with 5/1 (v/w) liquid-to-wood chip ratio. The temperature profile was as follows: after impregnation at 90ºC (60 min.), the temperature was raised to its maximum in 90 minutes, remaining at that temperature for 30 minutes. The reactors were then suddenly cooled down with tap running water, and acid hydrolysates were recovered and the solid residues were mechanically disintegrated and thereafter subjected to enzymatic hydrolysis with an enzymatic cocktail from Novozymes® including 6 different enzyme solutions (cellulase complex: 5%, xylanase: 0.25%, β-glucosidase: 0.6%, enzyme complex: 0.4%, hemicellulose: 2%, glucoamylase: 0.06%) suitable for lignocellulosic materials

hydrolysis purporting bioethanol production. The cellulase loading (NREL procedure) was 6.6 FPU/mL. The never-dried pre-treated solid residues were placed in 50 mL falcon tubes at 1% solid content (0.4 g o.d. solids/tube) and adjusted with citrate 50 mM buffer solution of pH 5.5 up to a total volume of 40 mL per tube, improving agitation with 0.3 mm glass spheres. All tubes were homogenized in a vortex and inserted horizontally into a 50ºC water bath. Solids were subjected to enzymatic hydrolysis for 7, 15, 24, 48 and 96 hours and the enzymatic hydrolysates sugar content was determined by HPLC.

3. Results and discussion

The different factors effect (NaHSO3 load [A], H2SO4 load [B], temperature [C] and time at T_{max} [D]) on different response variables was mathematically established. As examples, the equations corresponding to the XMG (Xylose + Mannose + Galactose) and to the released sugars are shown:

$$XMG = 14{,}0 + 0{,}39A + 3{,}06B + 1{,}54C + 0{,}54D - 0{,}12A^2 - 0{,}96AB - 0{,}65AC - 0{,}08AD - 0{,}04B^2 - 5{,}38BC - 2{,}40BD - 1{,}80C^2 - 2{,}30CD - 0{,}74D^2 \quad \text{(Eq. 1)}$$

$$Sugars = 32{,}5 + 7{,}17A + 13{,}02B + 26{,}54C + 8{,}94D + 4{,}73A^2 + 0{,}66AB + 1{,}96AC + 0{,}78AD + 2{,}54B^2 - 1{,}743BC - 0{,}55BD + 1{,}62C^2 + 1{,}58CD - 0{,}23D^2 \quad \text{(Eq. 2)}$$

Standard effects and yield surface response were also obtained and analysed, as seen in Fig. 1 and Fig. 2:

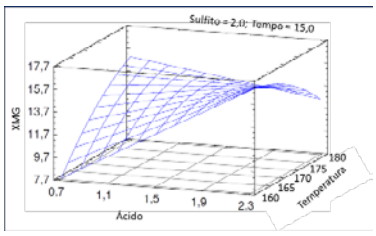

Figure 1. XMG surface response.

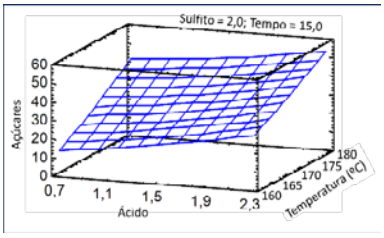

Figure 2. Sugar surface response.

4. Conclusions

Biomass pretreatment with sodium bisulfite in acid environment alters the feedstock structure and composition, making it more suitable for enzymatic treatment. The pretreatment conditions produce an effect on the amount of total recovered sugars and on the generated degradation products. For a given sulfite load, more acidic conditions lead to higher sugar release and further material fragmentation, but also to an increase in degradation products. Moderate loads of sodium bisulfite (1%) and sulfuric acid (2.25%), release practically all hemicelluloses of the raw material. The enzymatic treatment showed to be very sensitive to the pretreatment conditions. The released sugars percentage in the enzymatic hydrolysis ranged from 6.0% to 68.9%. More acidic conditions increase the rate and extent of the enzymatic hydrolysis of the polysaccharides.

References

[1] V. Costa, T. Gomes, R. Simões, J. Wood Chem. & Tech. 36-1 (2019): 63-75.
[2] N. Gil, F.C. Domingues., M.E. Amaral, A.P. Duarte, J. Biobas. Mat. & and Bioener. 6-3 (2012) 292-298.

ECCE12
The 12th EUROPEAN CONGRESS OF CHEMICAL ENGINEERING
Florence 15-19 September 2019

Bio-Economy:
Chances, Challenges, and Perspective of the System as a Whole.

Andreas Pfennig

University of Liège, Department of Chemical Engineering - Products, Environment, and Processes (PEPs), Quartier Agora, Allée du six Août, 11, Liège, Belgium,]

andreas.pfennig@uliege.be

Highlights

- Faster growth of world population than expected results in increased challenges for sustainable development.
- Bio-based economy competes with food production for land area, third-generation biomass cannot fulfill the demands.
- Bio-based economy will have sufficient options to be globally realized.
- Bio-energy will strongly compete with food production.

1. Introduction

Humanity is facing grand challenges: we have to reduce the consumption of fossil resources and replace them with sustainable technologies. This implies the use of sustainable raw materials in the chemical industry as well, such as bio-based raw materials or carbon dioxide. Much has been published on the various options for raw materials and technologies to be used. Why one or the other of the many options is more promising than another may not always be obvious.

2. Approach taken

In order to get a realistic insight, balances on available resources are used to gain a holistic picture allowing to answer, how the demands of humanity can be fulfilled. The considerations take into account the general challenges of mankind, namely climate change, energy utilization, and world hunger. The balances build on publicly available data like the FAOSTAT database of the UN. The limits considered are the carbon-dioxide emissions to the atmosphere and the land area required for production of food, bio-energy, and feedstock for the chemical industry. The main raw-material and technology options are discussed and related to these boundary conditions and among each other. For the chemical industry the focus is on mass products such as plastics. Some promising main routes are described, and the practical challenges of their realization are addressed, e.g. supply, conversion and distribution. From these interrelationships the societal responsibilities can directly be deduced.

3. Conclusions

It turns out that the global population growth is significantly faster than usually considered, because major studies don't take the continual slight upward shift in the projection of the UN – which are typically applied – into account. Thus the demand side for resources and the waste produced are underestimated. A high population growth has to be considered at least as one bounding scenario.

Based on different population perspectives, the energy demand is considered and coupled with projections on sustainable energy transition. The results show that the energy transition may be possible but will be significantly more demanding than e.g. projected by the Intergovernmental Panel on Climate Change. The efforts, i.e. the rate at which fossil energy systems are replaced by renewable energy technologies, need to be increased by a factor of five in the EU and a factor of almost 10 worldwide. This means that the time-scale of the change has to be some few decades at most, during which also a bio-economy would need to be established.

Considering land area as scarce resource shows that food supply will be challenging, even, if the agricultural efficiencies are continually increased. Thus, bio-energy should not be fostered to a degree proposed in various scenarios, e.g. also those of the EU.

Finally, these considerations set the scene to discuss the available options for bio-based feedstock for the chemical industry. Different crops are compared and combined with different technological options to analyse, if it will be possible to develop a bio-economy without further increase in world hunger. The results show e.g. that third generation biomass will not be sufficient to supply a majority of the feedstock required. Thus competition with food production for land area is unavoidable. At the same time various options exist which will allow bio-based products with only limited land-area use, see Fig. 1. Of course a suitable mix of the different options wll finally be realized, taking into account climate and soil situation. The options are discussed and related, also considering technological maturity of the resulting processes.

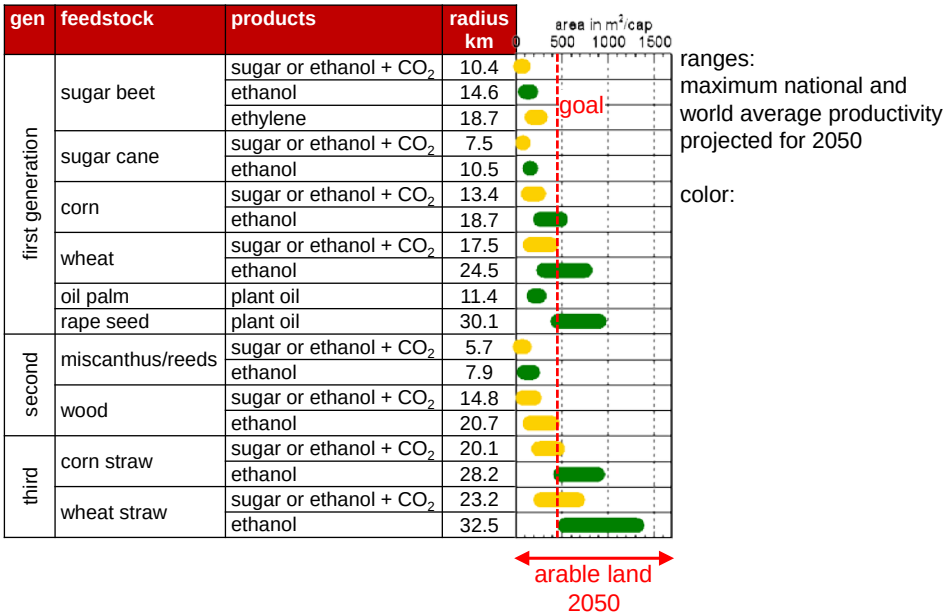

Figure 1. Required land area for a bio-based economy assuming that each path supplies individually the required feedstock.

Along the way, also the utilization of carbon dioxide is evaluated, which can obtained from the atmosphere in a sustainable economy. For the chemical activation of carbon dioxide, energy, presumably in the form of hydrogen is required, which in turn needs a significant additional contribution from renewable energies. This is related to the effects and consequences of bio-economy.

ECCE12
The 12th EUROPEAN CONGRESS OF CHEMICAL ENGINEERING
Florence 15-19 September 2019

e-BioPond® – added value from food industry secondary products and wastewater for a sustainable Spirulina production

Andrea Schievano[1], Francesca Girotto[2*], Laura Piazza[2]

1 e-BioCenter – DESP, Università degli Studi di Milano, Via Celoria 2, 20133, Milano (Italy);

2 DESP, Università degli Studi di Milano, Via Celoria 2, 20133, Milano (Italy).

**Corresponding author: francesca.girotto@unimi.it*

Highlights

- Arthrospira platensis is sustainably grown on food industry wastewaters.
- Microbial electrochemical technologies are introduced through the e-BioPond®.
- Inorganic carbon and dissolved nutrients from the oxidized wastewater are the growth medium.

Abstract

Organic-rich **secondary products** of food industry and **wastewaters** are important sources of nutrients which should be valorised as an important resource rather than being disposed as a waste. We propose a technological application to recover these nutrients for a sustainable Spirulina (*Arthrospira platensis*) cultivation. Spirulina is a microalgae culture whose nutritional value and properties have attracted the attention of both researchers and industrialists. Commonly microalgae cultures are grown is an inorganic medium, which negatively affects the costs of the process. Through the alternative **sustainable microalgae cultivations** using the **e-BioPond**, **microbial electrochemical technologies** are introduced.

In **e-BioPond** (***patent pending Italian deposit 102018000010683 - Nov 29th, 2018***), a separation between the microalgae culture and wastewater is obtained using low-cost composite membranes (***international patent pending n. 102017000110538 - ref E0116619***), with the shape of pipes or panels (**microbial electrochemical pipe/panel, MEP**). The pore dimensions of such materials (<500 nm) is smaller than the microbial cells. This keeps the two environments separated in terms of **microbial contamination**.

Within the inner volume of MEPs, a conductive material acts like a **bioanode**, where wastewater flows and electroactive microorganisms anaerobically oxidize the organic fractions and liberate CO_2/HCO_3- and minerals (NH_4^+, NO_3^-, etc.). On the microalgae-side, another conductive layer acts like a **biocathode**, where electroactive microorganisms reduce the photosynthetic oxygen.

Simultaneously, **inorganic carbon and dissolved nutrients** are allowed to diffuse through the MEP to the cathodic chamber, where they are used as growth medium by microalgae.

In particular, the first lab scale tests enabled to grow around 40 mg_{TSS} $L^{-1}d^{-1}$ of Spirulina when the anodic chamber was fed with 12 gCOD/L. COD removal rate was 0.65 gCOD L^{-1} d^{-1}, dissolved

oxygen in the cathodic chamber ranged between 15 and 18 ppm, and the measured electrical power density was 4 W/m^2.

The final goal of the project would be to test the **quality** of the **Spirulina biomass** that can still be obtained from this sustainable system and, consequently, proceed with the extractions of **proteins** and **pigments** to be used in food, pharmaceutical and feed industries.

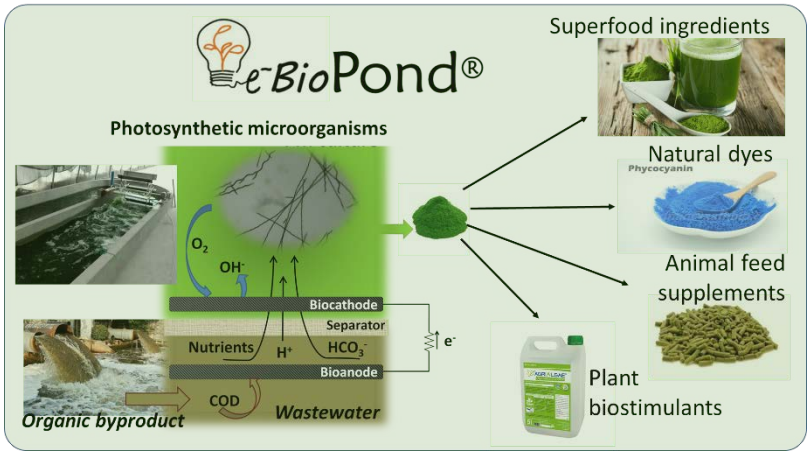

Figure 1. e-BioPond® mechanism.

ECCE12
The 12th EUROPEAN CONGRESS OF CHEMICAL ENGINEERING
Florence 15-19 September 2019

Towards Sustainable Marine Biorefineries: Macroalgae Continuous Fractionation with Pulsed Electric Fields and Mechanical Press.

Alexander Golberg, Klimentiy Levkov

Porter School of Environment and Earth Sciences Tel Aviv University, Tel Aviv, Israel.

**Corresponding author: agolberg@tauex.tau.ac.il*

Highlights

- Pulsed electric field generator with gravitation press electrodes was developed
- PEF parameters 4kV, 1kAmp, 1-100µs duration and total power dissipation of 20W
- Macroalgae *Ulva* sp. was electroporated with ~2kV/cm, 12µs duration 200A.

1. Introduction

Of the major technological challenges for bioeconomy is biomass fractionation, or biorefining: similar to oil or gas cracking or refining. An important step in those biomass fractionation processes is the breakdown of cell membranes. This breakdown allows for efficient separation of water from organic material (drying) and also it enables to extract for various uses intercellular components such as proteins, amino acids, lipids, carotenoids and other molecules each of which already has significant market values. One type of these technologies is based on the use of high voltage, short pulsed electric fields (PEF) [1]. However, unique physical characteristics of each species of plant biomass, the dynamics and nature of their changes in the process of electroporation require case by case adaptation of PEF parameters such as applied voltage, number of pulses, pulse duration, frequency and temperature for successful and energy efficiency biomass fractionation. The goal of this work was to develop a laboratory device with adaptive electrical and mechanical components to allow electroporation of the marine macroalgae biomass, an emerging feedstock for biorefinery. Indeed, macroalgae fractionation with pulsed electric fields, once available, could lead to non-thermal, chemical-free extraction of valuable phytochemicals from cells such as proteins, amino acids and carbohydrates [2]. In this work, we report on the development of a laboratory PEF system with asymmetric voltage multiplying and gravitation-press electrode device that enables electroporation of a highly conductive marine macroalgae, a promising but challenging feedstock for the biorefinery.

2. Methods

2.1 Macroalgae *Ulva* sp. Biomass. *Ulva* sp.was grown under controlled conditions in using 40 L macroalgae photobioreactors (MPBR) incorporated in a building's south wall under daylight conditions. Nutrients were supplied by adding ammonium nitrate (NH_4NO_3) and phosphoric acid (H_3PO_4), (Haifa Chemicals Ltd, IS) to maintain 6.4 g m^{-3} of total nitrogen and 0.97 g m^{-3} of total phosphorus in the seawater. The sole CO_2 source was bubbled air.

2.2 *Ulva* sp. biomass electroporation. *Ulva* sp. biomass was harvested and centrifuged in the manual kitchen centrifuge to remove the surface water 3 times for 2 min. The biomass was loaded in the electroporation cell, pressurized with the moving the electrodes and exposed to the external constant electric field from generated by the applied voltage of 600 – 4000 Volt and the 1 – 20 mm

gaps between the electrodes. The voltage drop was measured at the electroporation cell and at the resistor connected in series with a known resistance (5Ohm). Voltages and currents were measured with a PicoScope 4224 Oscilloscope with a Pico Current Clamp (60A AC/DC) and analyzed with Pico Scope 6 software (Pico technologies Inc., UK). Extracted juice was collected at the bottom of the device. The experiment was repeated three times.

3. Results and discussion

The developed system, allows applying for up to 4kV, 1kAmp pulses with 1-100µs and total power dissipation of 20W and up to 10kg of mechanical load. The system has two novel elements: asymmetric voltage charger for energy consumption minimization (**Fig. 1a**) and gravitation-driven press electrode device for continuous fractionation (**Fig. 1b**). The developed device uses a charge source, which consists of a step-up transformer of 220/2000 Volts, a voltage doubler, and an ESC voltage regulating unit. The developed device uses an asymmetric voltage doubling circuit (**Fig. 1a**), which consists of two high-voltage diodes and two capacitors allowing to control the applied voltage at each pulse. This is a new feature, we did not found in the literature. The first is a charging capacitor that, in addition to the voltage doubling function, performs the function of current limitation when the ESC is charged. The second capacitor is the ESC. Images of the voltage and current pulses as recorded applying 2kV (field ~2kV/cm), 12µs duration 200A on 10 g of wet macroalgae are shown in **Fig. 1c.** This is in the range of electric field requirement shown in our previous work to extract proteins from this biomass [3].

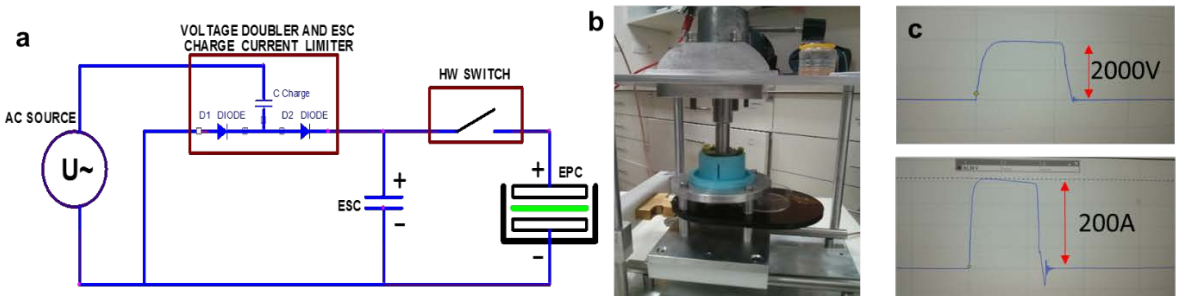

Fig. 1. a. Principle components of the develop laboratory biomass electroporation device. **b.** The gravitational press-electrode device with loaded biomass. **c.** Voltage (top image) and current (bottom image) of Ulva biomass exposed to pulsed electric fields of 2kV

4. Conclusions

Macroalgae biomass is the most challenging feedstock for PEF application in industry because of high salinity which leads to very low resistance of the biomass and very high currents in the system at fields that lead to cell membrane permeabilisation. In this work we developed the device which enables the control over the applied voltage at each pulse, reducing the energy consumption of the electroporation-driven biomass fractionation.

References

[1] A. Golberg, M. Sack, J. Teissie, G. Pataro, U. Pliquett, G. Saulis, T. Stefan, D. Miklavcic, E. Vorobiev, W. Frey, S. Töpfl, D. Miklavcic, E. Vorobiev, W. Frey, Energy Efficient Biomass Processing with Pulsed Electric Fields for Bioeconomy and Sustainable Development., Biotechnol. Biofuels. 9 (2016) 1. doi:10.1186/s13068-016-0508-z.

[2] A. Robin, A. Golberg, Pulsed Electric Fields and Electroporation Technologies in Marine Macroalgae Biorefineries, (2016) 1–16. doi:10.1007/978-3-319-26779-1_218-1.

[3] M. Polikovsky, F. Fernand, M. Sack, W. Frey, G. Müller, A. Golberg, Towards marine biorefineries: Selective proteins extractions from marine macroalgae Ulva with pulsed electric fields, Innov. Food Sci. Emerg. Technol. (2016). doi:10.1016/j.ifset.2016.03.013.

ECCE12
The 12th EUROPEAN CONGRESS OF CHEMICAL ENGINEERING
Florence 15-19 September 2019

Investigations of molybdenum-promoted manganese-based solid sorbents for H_2S capture

Jianyu Ma[1], Kumar R. Rout[2], Maximilian Sauer[3], Mehdi Mahmoodinia[1], Edd A. Blekkan[1*]

1 Dept. of Chemical Engineering, Norwegian University of Science and Technology (NTNU), NO-7491 Trondheim, Norway

2 SINTEF Industry, NO-7465 Trondheim, Norway

3 Technical University of Munich, Germany

**Corresponding author: edd.a.blekkan@ntnu.no*

Highlights

- Mo-promoted Mn-based solid sorbents for desulphurization were studied
- Real-time residence H_2S concentration was monitored on-line
- Mo addition promoted sorbent capacity and stability significantly

1. Introduction

Biomass gasification and subsequent fuel synthesis is a realistic route to 2nd generation biofuels. However, the produced syngas contains undesired species and contaminants (tar, alkali, sulfur species etc.) that has severe detrimental effects on downstream equipment and catalysts [1]. Therefore, gas cleaning and gas conditioning are important steps. From a process design point of view high-temperature gas cleaning is beneficial in terms of energy efficiency and investment cost. A key contaminant in biomass-based syngas is hydrogen sulfide, and this contaminant must be removed in order to avoid rapid deactivation of catalysts for fuel synthesis, e.g. cobalt-based Fischer-Tropsch catalysts [2]. Several materials have been proposed for high-temperature sulfur removal and manganese is reported to be a promising candidate based on thermodynamics (calculated sorption properties at high temperatures) as well as other chemical features (resistance to reduction, volatilization and carbide formation) [3]. The properties of sorbents can be improved by addition of promoters. Molybdenum oxide is selected in this study as a promoter on account of its ability to provide higher desulphurization capacity and improve stability of catalysts [4].

2. Methods

A series of Mo-promoted manganese sorbents supported on alumina were prepared by incipient wetness impregnation method using Mn-nitrate and ammonium molybdate as precursors. The samples were dried at 90°C and calcined at 700°C to decompose the salt. The nominal Mn loading was 15 wt% and Mo loadings were 2wt%, 5wt% or 8wt%, and 8wt% made using 2-step impregnation. Their H_2S sorption properties were investigated in a laboratory setup, see [5] for further details. The sorption was done on pre-reduced samples at 600°C using a dry gas mixture containing 0,4 vol% H_2S and 40% H_2, the balance being inert gases (Ar, N_2). The regeneration was done at 650°C and ambient pressure, using a gas containing 25 vol% air. The testing was performed as 10 cycles of sorption - regeneration. The residual H_2S level was monitored at different sorption temperatures with a specific sulphur analyzer, Thermo-Fisher 450i.

3. Results and discussion

All the samples initially adsorbed H_2S down to a very low level. After some time the concentration of H_2S in the exit gas started to increase (breakthrough), the sorption was then terminated by flushing the reactor with inert gas. The sorbent capacity before breakthrough were calculated from the amount H_2S adsorbed. Subsequently the sorbent was regenerated by diluted air. The only sulfur species detected in the gas phase during regeneration was SO_2. The initial sorption capacities declined in the following order: 15Mn5Mo-Al_2O_3> 15Mn8Mo-Al_2O_3> 15Mn8Mo-2step-Al_2O_3>15Mn2Mo-Al_2O_3>15Mn-Al_2O_3, indicating that addition of Mo increases sorbent initial capacity. After one cycle, the capacities for sorbent 15Mn8Mo-Al_2O_3 and 15Mn8Mo2step-Al_2O_3 increased obviously and remained stable for subsequent cycles. However, the capacity of 15Mn2Mo-Al_2O_3 suffered large deactivation and turned to be even lower than sorbent without Mo. The sorption capacity after 10 cycles declined in the following order: 15Mn8Mo-2step-Al_2O_3> 15Mn8Mo-Al_2O_3> 15Mn5Mo-Al_2O_3>15Mn-Al_2O_3>15Mn2Mo -Al_2O_3.

The residence H_2S concentration after sulfidation by 15Mn8Mo-Al_2O_3 was as low as around 1.95ppm at a sorption temperature of 400°C. At 600°C, the residual concentration increased to around 2.65ppm. In contrast, the 15Mn-Al_2O_3 showed a similar result at 400°C, 2.4ppm, however, a significantly higher value of 11ppm was recorded at 600°C sorption temperature.

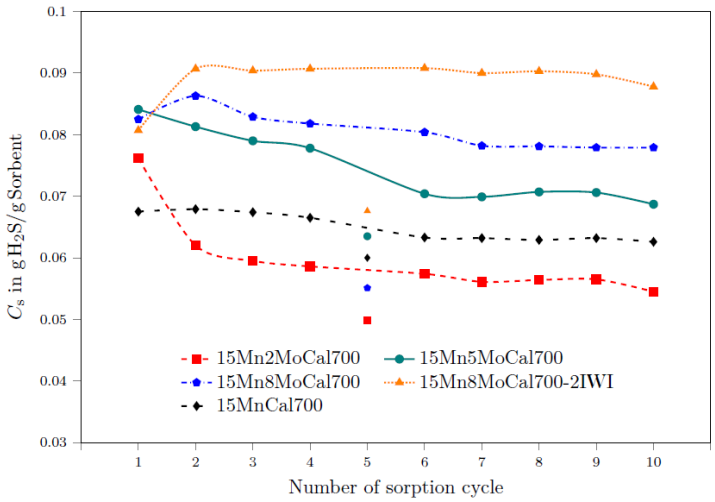

Figure 1. Capacities of Mn-based sorbents promoted with Mo.

4. Conclusions

The addition of Mo is found to be beneficial for Mn-based sorbents, in terms of capacity, stability and residual H_2S concentration in the gas phase after sorption.

References

[1] G.W. Huber, S. Iborra, A. Corma, Catal, Eng, Chem. Rev. 106 (2006) 4044–4098.
[2] A.H. Lillebø, A. Holmen, B.C. Enger, E.A. Blekkan, WIREs Energy. Environ. 2 (2013), 507–524.
[3] W.F. Elseviers, H. Verelst, Fuel 78 (1999) 601–612
[4] Laosiripojana, N., and S. Assabumrungrat. Applied Catalysis A: General, 290.1-2 (2005): 200-211.
[5] S. Chytil, M. Kure, R. Lødeng, E.A. Blekkan, Fuel, 196 (2017) 124–133.

ECCE12
The 12th EUROPEAN CONGRESS OF CHEMICAL ENGINEERING
Florence 15-19 September 2019

Full-field assessment of gaseous flow within open-cell foams: comparison of µCT-based CFD simulations and magnetic resonance velocimetry results

Mehrdad Sadeghi[1], Mojtaba Mirdrikvand[2], Georg Pesch[1], Wolfgang Dreher[2], Jorg Thöming[1]

[1]University of Bremen, Faculty of Production Engineering, Chemical Process Engineering, Bremen, Germany
[2]University of Bremen, Faculty of Chemistry, in-vivo MR group, Bremen, Germany
*Corresponding author: sadeghi@uni-bremen.de

Highlights

- µCT-based CFD simulations of gaseous flow within open-cell foams were performed.
- CFD simulations are based on real structure of open-cell foams in a foam reactor.
- Magnetic resonance velocimetry (MRV) method was used for flow mapping and verification of CFD results within the open-cell foams.

1. Introduction

Open-cell foams, which are also known as solid sponges, enjoy beneficial morphological properties such as a low pressure drop, a high thermal conductivity and an excellent soli-gas heat and mass transfer which make them a good choice as monolithic catalyst supports. Computational fluid dynamics (CFD) simulations have been employed as a cost-effective and reliable numerical tool for the study of transport phenomena through catalytic sponges; however, their irregular and complex geometries demands high computational effort. Nevertheless, the complexity of the geometry is a major cause for the good performance of the solid sponge. It significantly controls flow pattern and the sponge's heat and mass transfer characteristics. Apart from detailed experimental studies, this fact requires in-depth numerical studies which spatially resolve transport phenomena in the sponge locally [1]. Magnetic resonance velocimetry (MRV) is a non-invasive method which has been applied for measurement of flow within solid sponges. In this study, the obtained flow fields and velocity profiles form CFD simulations were compared with magnetic resonance velocimetry (MRV) measurements.

2. Methods

In this study, we simulated the entire fully-resolved geometry of sponges which were obtained from micro computer tomography (µCT) imaging of real samples. The Procedure is summarized in Figure 3 in the Appendix. Due to highest investigated Reynolds number (based on reactor diameter, 25 mm) for the flow rate of 1.5 Sl min^{-1} (Re= 76.49, u_{in}=0.051 ms^{-1}), laminar flow regime and incompressible condition was considered. To ensure the simulations are grid-independent, a grid analysis was carried out for different meshing densities. To guarantee that the simulated flow results are physically correct, they were validated against pressure loss correlations for foams at flow rates from 0.5 to 20 SL min^{-1}. Subsequently, CFD results containing 41.1 millions of computational cells were validated by experimental velocimetry measurements and literature correlations. We investigated numerically and experimentally the incompressible gas flow within three cylindrical (25 × 68 mm) 20 PPI Al_2O_3 open cell foams in a row (See Table 1 in Appendix for

morphological properties). A gas flow of methane at different flow rates of 0.5, 1 and 1.5 L min^{-1} was examined. In this study, CFD simulations are based on the real, large segments of sponges. This allows us to measure the differences between CFD simulations and full-field MRV measurements. The computational cell size and MRV voxels are 0.1 and 0.8 mm, respectively.

3. Results and discussion

In comparison with homogeneous (porousSimpleFoam solver of OpenFOAM) models, µCT-based CFD results (solved using the simpleFoam solver from OpenFOAM) showed the sensitivity of velocity profiles to the local morphology of open cell foams (Figure 4 in Appendix). The obtained flow fields form CFD simulations and MRV measurements are presented in Figure 1. We compared axial velocity profiles of CFD and MRV results for the middle section of porous structure. The results showed remarkable agreement with an accuracy of ±10% (see Figure 2). Furthermore, the obtained average radial velocity profiles from CFD and MRV data are in good agreement together (see one example in Figure 5 in Appendix). This justifies the use of CFD of large sponge segments as an adequate and reliable tool for the study of gaseous flow within porous structures.

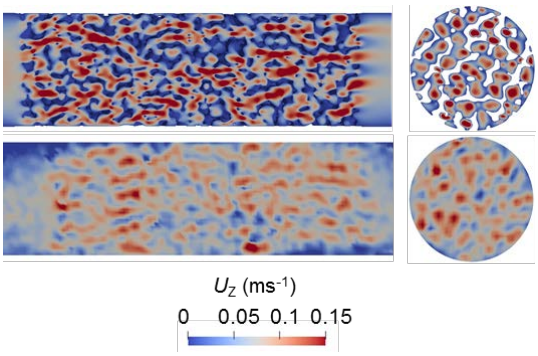

Figure.1. Obtained flow fields form CFD simulations (top) and MRV measurements (bottom)

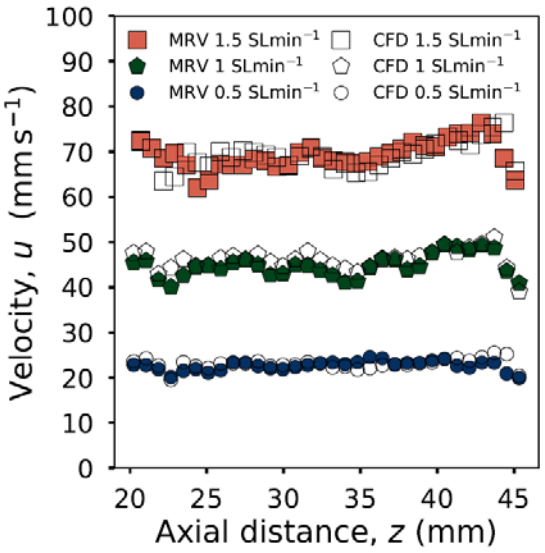

Figure.2. Obtained average axial velocity profiles within the middle Al_2O_3 sponge from CFD simulations and MRV measurements for different flow rates of 0.5, 1 and 1.5 L min^{-1}.

4. Conclusions

The quantitative agreement between CFD and MRV results amplifies the reliability of CFD simulations and underpins the capability of NMR-based measurements for *in-situ* temperature and concentration measurements. Obtaining similar results with both methods improves the reliability of either method. Finally, full-field numerical and NMR-based experimental studies of heat transfer and chemical reactions within catalytic sponges are on the way.

Appendix

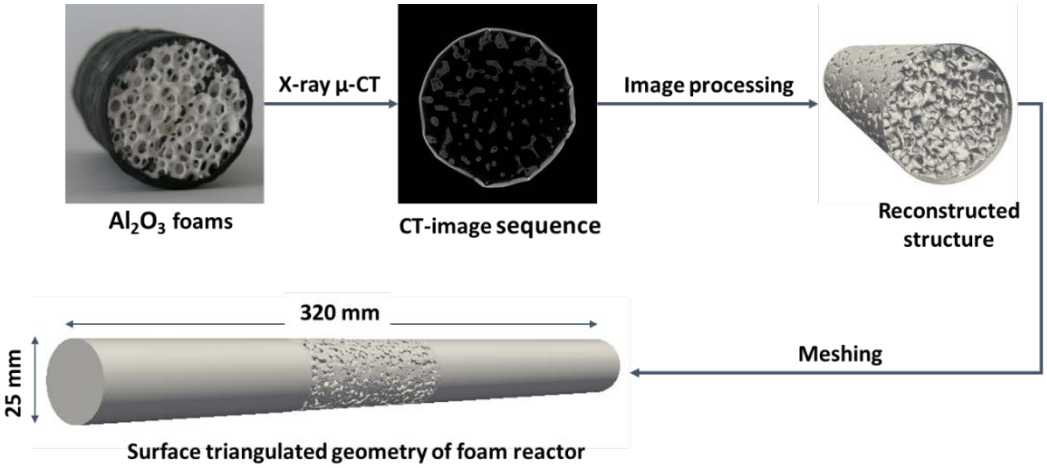

Figure 3. Procedure for preparation of foam reactor geometry

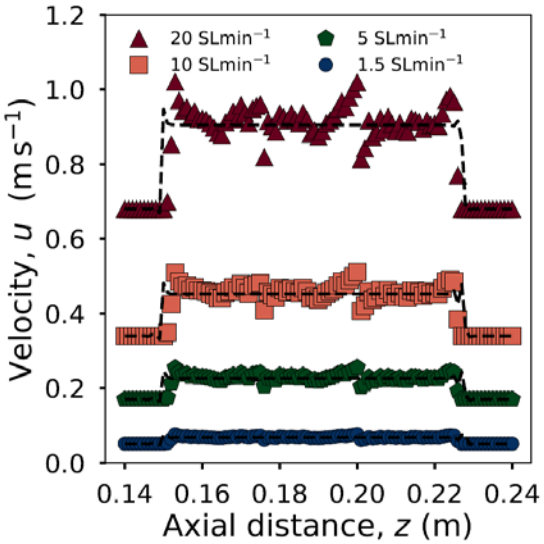

Figure 4. Calculated averaged axial velocity profiles within foam reactor from heterogeneous model (the color markers) and homogeneous model (dotted lines) for different flow rates of 1.5, 5, 10 and 20 SL min^{-1}

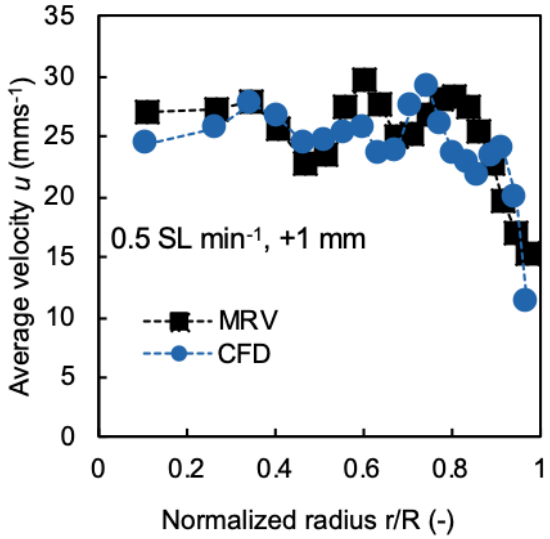

Figure 5. The obtained radial velocity profiles from CFD and MRV for the flow rate of 0.5 SL min^{-1} and 1 mm after the beginning of second sponge

Table 1. Morphological properties of utilized 20 PPI open cell foams for simulation and experimental velocimetry measurements. Obtained from: 1) processing of CT-images and 2) literature correlation

Quantity	Symbol	Value
Open porosity	ε_o	0.752 (1)
Pore diameter $.10^{-3}$ m	d_p	3.41±0.6 (1)
Window diameter $.10^{-3}$ m	d_w	1.904±0.3 (1)
Specific surface area $m^2\ m^{-3}$	S_v	852.3 (2)

References

[1] Jürgen Ulpts, Wolfgang Dreher, Lars Kiewidt, Miriam Schubert, JorgThöming. 2016, Catalysis Today, pp. 91-98.

ECCE12
The 12th EUROPEAN CONGRESS OF CHEMICAL ENGINEERING
Florence 15-19 September 2019

Design of Continuous Confined Impinging Jets for Emulsions

Margarida Brito[1], Cláudio Fonte[2], Ricardo Santos[1,*]

1 Laboratory of Separation and Reaction Engineering – Laboratory of Catalysis and Materials (LSRE-LCM), Faculdade de Engenharia, Universidade do Porto, Rua Dr. Roberto Frias, 4200-465 Porto, Portugal; 2 School of Chemical Engineering and Analytical Science, The University of Manchester, Oxford Road, Manchester M13 9PL, U.K.

**Corresponding author: rsantos@fe.up.pt*

Highlights

- Mixing of dissimilar fluids in CIJs is described for a viscosity ratio range 1:2-1:60
- Mixing of dissimilar fluids is studied at flow rate ratios ranging from 1:1 to 1:4
- New design equation for CIJs mixers is proposed with an extended validity range

1. Introduction

Confined Impinging Jets (CIJs) mixers are one of the most energy efficient devices for mixing flow streams because the full power of the inlet streams is focused on the opposed jet at an impingement point. CIJs in the 10 mm scale range are able to generate mixing scales as small as 10 µm in less than 100 ms [1]. The most efficient operation of CIJs occurs at a specific flow regime, the chaotic flow regime that onsets above a critical jets Reynolds number $Re_c \approx 120$ [1]. The fast decrease of the mixing scales at this regime is associated to the formation of a vortex street in the mixing chamber. Fonte et al. [2] clearly shows that the chaotic flow regime for $Re > Re_c$ was only possible if the jets were balanced at the mixing chamber axis. Figure 1 shows Planar Laser Induced Fluorescence (PLIF) images of the mixing of a dyed and clear fluid in CIJs. The best mixing performance is associated to the chaotic flow regime with the onset of the vortex street (Figure 1b).

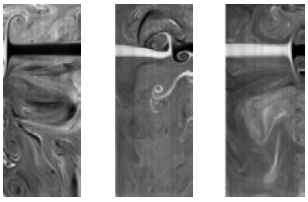

(a) **(b)** **(c)**

Figure 1. PLIF images of mixing of equal fluids, with one jet at $Re = 304$ and for three different flow rate ratios [1].

Fonte et al. [2] developed the Elastic Analogue Model (EAM) based on the balance of the jets kinetic energy rate to predict the position where the opposed jets contact in the mixing chamber, i.e., the impingement point position. EAM was validated from Computational Fluid Dynamics (CFD) simulations and experimentally for the mixing of fluids with the same viscosity. EAM enables the description of the jets balancing for jets with different flow rates, for CIJs with different diameter of the opposed injectors, and of fluids with different viscosities. Because of that, this model enables the design of CIJs for many processes, such as, emulsification processes in food (e.g. mayonnaise), pharmaceutical and cosmetic industries.

Recently, the validation of EAM was extended for mixing of fluids having different viscosities [3]. These results showed some divergence from EAM, and so application of this model to design the mixing of dissimilar fluids still needs further studying. In this work, the previous EAM model is further developed from the balance of jets momenta and compared with the numerical and experimental data. The objective is the development of a rigorous tool capable to design CIJs which can be used to mix fluids with different viscosities.

2. Methods

CFD simulations described in this work was studied using ANSYS Fluent and the CIJs model presented by Brito et al. [3]. Thus, mixing was studied with CFD setting the Volume-Of-Fluid (VOF) model which tracks the interface between two immiscible fluids with no surface tension. Only the impact of viscosity on the impingement point position is studied and, because of that, the surface tension between fluids was neglected. The experimental flow visualizations were obtained from PLIF images using the setup described in Brito et al. [3].

3. Results and discussion

Figure 1 shows the plots of the non-dimensional jets' impingement point position, ξ, as function of jets kinetic energy ratio, ϕ_K, for one of the case studies, the mixing of two fluids with viscosity ratio 1:2 at $Re = 50$ and $Re = 100$. The modification of EAM (new model) corrects the deviation between EAM and experimental and CFD results that was reported by Brito et al. [3]. The new model enhances the description of the flow providing a valuable design tool for industrial applications.

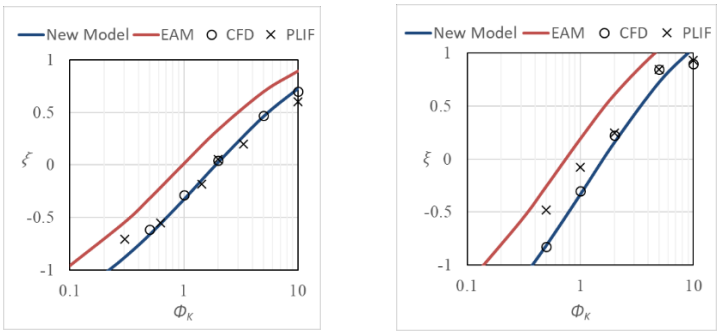

Figure 1. Impingement point position at a) Re=50 and b) Re=100 for mixing of two fluids with viscosity ratio 1:2.

4. Conclusions

A new model is proposed to predict the balancing position of jets impingement point in CIJs. Results show that the new model enhances the CIJs flow prediction for dissimilar fluids. This model enables the optimal design of CIJs, as far as mixing is regarded, changing the flow rate ratios and jets' diameter for industrial applications involving dissimilar fluids, such as, emulsification processes.

References

[1] C.P. Fonte, M.A. Sultan, R.J. Santos, M.M. Dias, J.C.B. Lopes, Chem. Eng. J. 260 (2015) 316-330.
[2] C.P. Fonte, M.A. Sultan, R.J. Santos, M.M. Dias, J.C.B. Lopes, AICHE J. 62 (2016) 2200-2212.
[3] M.S.C.A. Brito, L.P. Esteves, C.P. Fonte, M.M. Dias, J.C.B. Lopes, R.J. Santos, Chem. Eng. Res. Des. 134 (2018) 392-404.

ECCE12
The 12th EUROPEAN CONGRESS OF CHEMICAL ENGINEERING
Florence 15-19 September 2019

Characterizing the dispersion of Cellulose Micro/Nanofibers hydrogels

Jose L. Sanchez-Salvador, M. Concepcion Monte, Ana Balea, Angeles Blanco*, Carlos Negro

*Chemical Engineering and Materials Department, Universidad Complutense de Madrid, Avda. Complutense s/n, 28040 Madrid, Spain. *Corresponding author: ablanco@ucm.es*

Highlights

- Gel point is used to evaluate CMF/CNF dispersion
- Stirring speed modifies CMF/CNF hydrogels network
- CMF/CNF dispersion affect to their application efficiency

1. Introduction

Cellulose micro/nanofibers (CMF/CNF) have gained attention due to their desirable properties as high strength, stiffness, high surface area or low toxicity [1,2]. The methods to disintegrate cellulose fibers into substructures are well-known. However, CNF characterization is an area still under development [3]. The history of CNF before its use has a significant effect on their efficiency. Therefore, the dispersion of CNF hydrogels is an important parameter to understand and optimize their effectiveness in several applications, e.g. strength additive or wastewater treatments. Nowadays, there is not a methodology to quantify how stirring speed influence on the CNF network in suspensions. For this reason, the adaptation of a parameter used to measure NC sedimentation, the gel point (ϕ_g), is proposed [4-6]. ϕ_g, the volume concentration in the boundary between dilute and semi-dilute region, may be considered the lowest volume fraction at which all primary flocs are interconnected throughout the container, and form a self-supporting network [5]. The aim of this work is to show how CNF/CMF hydrogels perform at different stirring speed using the ϕ_g as parameter to quantify the dispersion in hydrogels.

2. Methods

CMF/CNF were obtained from recycled old newspaper. It was disintegrated in a pulp disintegrator at 30,000 revolutions before soaking. CNF were obtained using TEMPO-mediated oxidation with 10 mmol of NaClO/g dry pulp and 4 steps of homogenization at 600 bars in a homogenizer. CMF were obtained by refining the pulp in a PFI mill at 5,000 revolutions and 6 homogenization steps. Both products were characterized [1]. ϕ_g was evaluated with 250 mL of CMF/CNF suspensions at different concentrations (C_o), stirred with a 3-bladed propeller stirrer at several speeds for 10 min. Crystal violet was used as dye to visualize suspensions. Then, they were settled for 2 days (CMF) or 8 days (CNF) to claim fibers deposition. The curve C_o vs. the relation deposit height / initial height (H_s/H_o) was fitted with a quadratic equation for each speed. The linear term gives the ϕ_g [4-6].

3. Results and discussion

Figure 1 shows C_o vs. H_s/H_o for CMF/CNF at different stirring speeds. Gel point values were obtained from the fit of quadratic equations and Figure 2a shows Gel point for each stirring speed.

$ø_g$ decreases slightly in both cases with stirring speed until a minimum value and then, $ø_g$ increases. The suspensions with the stirring speed that produce the lower $ø_g$, have the higher Hs/Ho relation (Figure 2b). The opening of the network increase with stirring speed until the lower $ø_g$ in which the fibers start to break and destroy the structure, decreasing H_s/H_o relation. The results were compared using Electronic Microscopy. An opening network would be the more effective state to applicate CNF/CMF hydrogels in applications as strength additive in cardboard or water-based inks treatment.

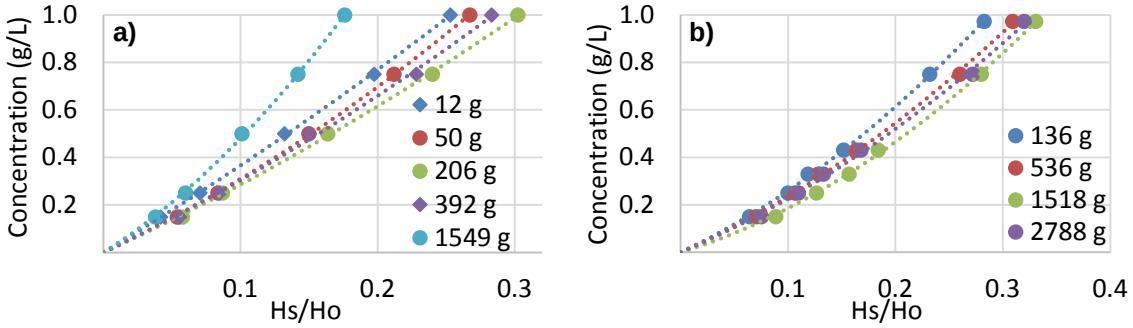

Figure 1. Gel point representation: a) CNF; b) CMF.

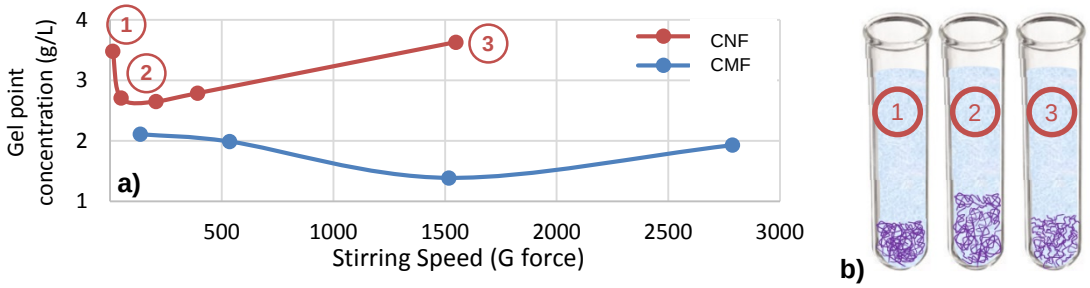

Figure 2. a) Influence of CNF/CMF gel dispersion on Gel point; b) CMF network representation with stirring speed.

4. Conclusions

$ø_g$ of CNF/CMF at different stirring speeds have a minimum for each material with a lower stirring speed in CNF due to the high fibrillation and an easy break. Suspensions stirred when $ø_g$ is minimum have the most opening network and they would be the most effective state to applicate the hydrogel. However, higher stirring speeds break the fibers and destroy the networks. Gel point methodology can be used in other cellulosic materials to obtain the optimal network configuration.

Acknowledgement

The authors wish to thank the Economy and Competitiveness Ministry of Spain for the support of the project (CTQ2017-85654-C2-2-R) as well as UCM and B. Santander for the grant of J.L. Sanchez-Salvador (CT17/17).

References

[1] A. Balea, N. Merayo, E. Fuente, P. Mutje, A. Blanco, C. Negro. Bioresources, 11 2016 3416-3431.
[2] D. Klemm, E.D. Cranston, D. Fischer, M. Gama, ... K. Petzold-Welcke. *Materials Today*, 21 2018 720-748.
[3] A. Blanco, M.C. Monte, C. Campano, A. Balea, N. Merayo, C. Negro. In Handbook of Nanomaterials for Industrial Applications, Elsevier, 2018, pp. 74-126.
[4] W.K. Mosse, D.V. Boger, G.P. Simon, G. Garnier. Langmuir, 28(7) 2012 3641-3649.
[5] P. Raj, A. Mayahi, P. Lahtinen, S. Varanasi, G. Garnier, D. Martin, W. Batchelor. *Cellul.* 23 2016 3051-3064.
[6] P. Raj, S. Varanasi, W. Batchelor, G. Garnier. *J. Colloid Interface Sci.* 447 2015 113-119.

ECCE12
The 12th EUROPEAN CONGRESS OF CHEMICAL ENGINEERING
Florence 15-19 September 2019

Development of an intensified heat exchanger reactor manufactured by 3D printing for acrolein synthesis.

Jean-François Portha[1*], Mathieu Chateau[1], Éric Schaer[1], Guillaume Gauthier[2], Catarina Rocha[3], Virginie Bellière-Baca[3], Karima Gahfif[1]

[1] *Université de Lorraine, Laboratoire Réactions et Génie des Procédés, UMR 7274, 1 rue Grandville, BP 20451, 54001 Nancy Cedex, France.*

[2]*Solvay, Research and Innovation, Rue de Ransbeek 310, 1120 Brussels, Belgium*

[3]*Adisseo France SAS, Antony Parc 2-10, Antony, France*

**Corresponding author: jean-francois.portha@univ-lorraine.fr*

Highlights

- The catalytic oxidation of propylene into acrolein is studied.
- Kinetic parameters are identified by optimization.
- A milli-channels heat exchanger reactor is developed to intensify heat transfer.
- Numerical validations by CFD calculations are performed.

1. Introduction

Acrolein synthesis is a key stage in the multi-step methionine production process, which is an amino acid used as a nutritional additive for animal feed. Acrolein is produced by heterogeneous and exothermic catalytic oxidation of propylene in gaseous phase. Numerous side reactions can occur leading to a moderate acrolein yield. The conventional industrial reactor is a multitubular fixed bed cooled by molten salt. The axial temperature profile in tubes presents a quite large hot spot which is partly responsible for the promotion of side reactions. The use of an intensified milli-channels heat exchanger reactor (HEXR), in which the catalyst is wash-coated on the wall, is then required especially to better control the temperature profile and to avoid the use of hazardous molten salts. Besides, additive manufacturing offers the opportunity to develop new HEXR configurations and to avoid solder joints by manufacturing the device in one unique piece. Then, the HEXR is built by metal 3D printing. This work consists in:

- the determination of a precise kinetic model to enhance catalyst performance prediction,
- the sizing of the new milli-channels HEXR,
- the validation of the device by CFD calculations.

2. Kinetic modelling

The first step of the work is therefore to improve the prediction of the kinetic model with respect to the experimental data. A first reaction scheme was established by Arntz *et al.*[1] from measurements of initial formation rates of products. A more complete kinetic model, containing 10 species and 10 chemical reactions, was also developed by Redlingshöfer *et al.*[2]. A new kinetic model was then established by taking into account information from literature and experimental observations. This kinetic model considers the propylene adsorption and the oxidation ratio of the

catalyst surface. Experimental data were collected on a catalytic screening platform consisting in isothermal fixed bed reactors coupled by on-line gas chromatography. Influences of temperature, gas hourly space velocity and oxygen to propylene molar ratio have been studied. A one-dimensional plug flow pseudo-homogeneous reactor model has been developed in order to interpret the 200 performed experiments. A set of kinetic parameters, minimizing the difference between the experimental results and those obtained by the model, is found by an optimization method.

3. Design and validation of the HEXR

The optimal operating conditions based on this new kinetic model have been determined in order to maximise acrolein yield. The yield is optimal for isothermal conditions, which is confirmed by the literature[3]. This isothermal behaviour can be achieved in an intensified HEXR[4]. The HEXR is designed by taking into account different constraints (process specifications, safety constraints, catalyst wash-coating constraints and maximal dimensions of the 3D printing machine) and then by calculating and studying different items:

- the number of channels required to convert the fixed mass flow rate of reactants,
- the fluid flow configuration (cross flow or co-current),
- the shape of fluid distributors and collectors,
- the temperature profile of the reactive and coolant sides.

Finally, after sizing the HEXR, some validations concerning safety aspects have been performed by CFD calculations. The influence of a potential thermal runaway is simulated in a section of the device to confirm the efficiency of the heat transfer. Besides, to evaluate the mechanical strength of the HEXR, a study is performed by using the temperature profile of the nominal case and by applying it to calculate the mechanical constraints on the structure. The same work is performed by considering a pressure gradient between both fluid sides.

4. Conclusions

An intensified mini-channel HEXR, presenting interesting performances, has been designed and manufactured by metal 3D printing. A complete simulation, coupled with the kinetic model, for a fraction of the device, as well as experiments on the manufactured unit, have yet to be done.

References

[1] D. Arntz, K. Knapp, G. Prescher, Catalytic air oxidation of propylene to acrolein: modeling based on data from a fixed bed reactor, ACS symposium (1982) 3-14.
[2] H. Redlingshöfer, A. Fischer, C. Weckbecker, K. Huthmacher, G. Emig, Kinetic modeling of the heterogeneously catalyzed oxidation of propene to acrolein in a catalytic wall reactor, Ind. Eng. Chem. Res., 42 (2003) 5482–5488.
[3] M. Lei, F. Lesage, M.A. Latifi, S. Tretjak, Optimization of acrolein production in a fixed-bed reactor system, Proceedings of Int. Conf. on Process Control, 2 (2013) 421–426.
[4] Z. Anxionnaz, M. Cabassud, C. Gourdon, P. Tochon, Heat exchanger/reactors (HEX reactors): concepts, technologies: state-of-the-art, Chem. Eng. Process. PI, 47 (2008) 2029-2050.

ECCE12
The 12th EUROPEAN CONGRESS OF CHEMICAL ENGINEERING
Florence 15-19 September 2019

A Power-to-Liquid Process – An alternative Process for the Production of (Poly-)Oxymethylene Dimethyl Ether (OME) based on Methanol.

Lara Theiss[1,2], Mohamed Ouda[1], Franz K. Mantei[1], Achim Schaadt[1], Robert Güttel[2]

1 Fraunhofer Institute for Solar Energy Systems ISE, Heidenhofstraße 2, 79110 Freiburg, Germany
2 Institute of Chemical Engineering, Ulm University, Albert-Einstein-Allee 11, 89081 Ulm, Germany

**Corresponding author: lara.theiss@ise.fraunhofer.de*

Highlights

- Methanol (MeOH) oxy-dehydrogenation to dimethoxymethane (OME_1) and formaldehyde (FA) shows high potential for efficient OME synthesis
- Reasonable MeOH conversions with high OME_1 and FA selectivities
- Successful water separation *via* membranes, as one of the crucial steps in all OME synthesis processes

1. Introduction

Due to their interesting thermo-physical and intrinsic combustion properties, (poly)oxymethylene dimethyl ethers (OMEs) have a high potential as diesel fuel alternative, "green" solvents or as CO_2 absorbent [1, 2]. The greatest challenge for introducing OME into the market is the lack of an energy-efficient, economically feasible and scalable industrial process for the synthesis of OME with a certain chain length. A promising synthesis route includes the formation of formaldehyde (FA) and dimethoxymethane (OME_1) by oxidative dehydrogenation of methanol (MeOH) in a single reactor first, using a porous solid catalyst providing both acidic and redox sites. Subsequently, FA and OME_1 are converted into higher OMEs, e.g. $OME_{3\text{-}5}$. The crucial issue in the first step is the stoichiometric by-product water, which limits the equilibrium yield and has to be removed prior to the second higher OME synthesis step. Thus, the water management plays a major role in the overall process. However, due to several azeotropes in mixtures containing FA, MeOH, water and OME_1, separation by distillation is cumbersome. Therefore, alternative processes like the application of membranes gain a lot of interest [3], which is aimed at in the present contribution.

2. Methods

In order to investigate the oxidative dehydrogenation of MeOH and the water removal by membrane technology systematically, a Design of Experiment (DoE) is applied. This allows quantitively evaluation of the correlation between input parameters, such as temperature, pressure and membrane material, and the most important target parameters, e.g. yield or water separation efficiency. The experiments are performed in two stages: A continuously operated plug flow reactor using a self-made bifunctional catalyst was used for MeOH dehydrogenation at 200-300°C and 1 bar. The obtained product mixture was continuously subjected to two membrane units. Moreover, a short cut model for the reaction and the separation step is applied, in order to simulate the whole process for addressing scale up issues.

3. Results and discussion

First results of the oxidative dehydrogenation of MeOH and the subsequent separation of water by selected hydrophilic membranes show promising results. **Figure 1** shows the molar fractions of the oxidative dehydrogenation reaction product (denoted with "Reaction"), which is subsequently directly introduced into the membrane unit during the test run. The molar fractions of the retentate (denoted with "Retentate") shows that almost a complete separation of water could be achieved at different ratios of sweepgas to reaction product stream (denoted with "R"). Moreover it is found that the amount of the other components does not change significantly in the retentate, which indicates a rather selective water separation. During reaction, MeOH conversion of about 40% and OME_1 and FA selectivities of 20% and 50% could be determined. Molar ratios of OME_1 to FA of 0.4 - 0.8 were obtained, which is a crucial target parameter for the subsequent synthesis for higher OMEs.

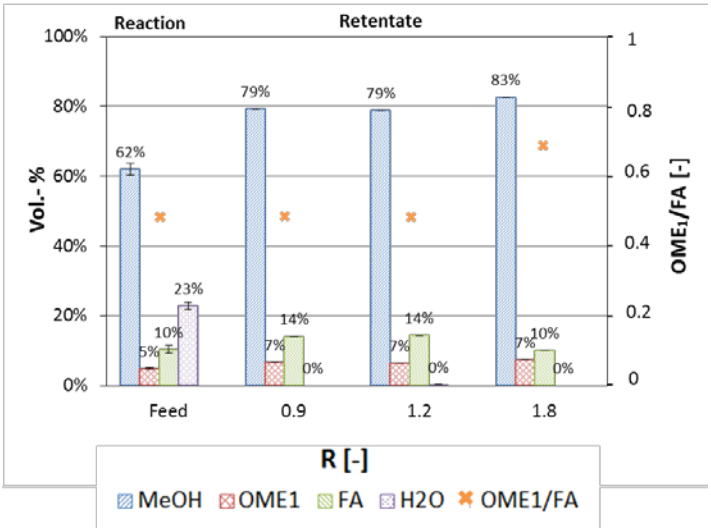

Figure 1. Exemplary combined reaction and separation test run, performed in a plug flow reactor and using a hydrophilic membrane. The initial molar fraction of methanol is 40%. R is the ratio of sweepgas to the membrane feedgas.

4. Conclusions

The oxidative dehydrogenation of MeOH directly into OME_1 and FA shows promising results. By producing OME_1 and FA in one synthesis step, a simple, efficient and scalable synthesis pathway for the production of higher OME can be provided. The separation of water, as one of the biggest challenges in OME synthesis, could be achieved successfully by applying hydrophilic membranes. Maximizing the MeOH conversion, without changing selectivities, as well as the long-term stability of the membrane performance will be investigated successively.

References

[1] M. Schappals, T. Breug-Nissen, K. Langenbach, J. Burger, H. Hasse, *J. Chem. Eng. Data* **2017**. DOI: 10.1021/acs.jced.7b00718.

[2] K. Gaukel, D. Pélerin, M. Härtl, G. Wachtmeister, *Internationales Wiener Motorensymposium* **2016**, *37*, 193 – 223.

[3] N. Schmitz, C. F. Breitkreuz, E. Ströfer, J. Burger, H. Hasse, *Journal of Membrane Science* **2018**, *564*, 806 – 812. DOI: 10.1016/j.memsci.2018.07.053.

ECCE12
The 12th EUROPEAN CONGRESS OF CHEMICAL ENGINEERING
Florence 15-19 September 2019

Highly active, stable and selective (Ru)Ni catalysts for CO_2 methanation

Joana A. Martins[1], Ana C. Faria[1], M.A. Soria[1], Carlos V. Miguel[1], A.E. Rodrigues[2], Luís M. Madeira[1]*

[1]*LEPABE-Laboratory for Process Engineering, Environment, Biotechnology and Energy, Faculty of Engineering - University of Porto, Porto, Portugal;* [2]*Laboratory of Separation and Reaction Engineering-Laboratory of Catalysis and Materials (LSRE-LCM), Faculty of Engineering - University of Porto, Porto, Portugal*

**Corresponding author: mmadeira@fe.up.pt*

Highlights

- Activity experiments over CO_2 methanation catalysts were performed.
- Ruthenium, nickel and bimetallic catalysts were prepared and tested.
- Nickel-based catalysts presented higher activity, selectivity and stability.

1. Introduction

Power-to-Methane is an attractive solution for the storage of the surplus renewable energy from intermittent and fluctuating natural sources (e.g. sun, wind), by the conversion of the electric energy into a chemical. To this end, the surpluses are firstly transformed into H_2 (via water electrolysis), and afterwards into methane that can be stored and transported through the existing natural gas grid [1]. Methane is produced through the Sabatier reaction (Eq. 1) using the renewable H_2 and captured CO_2, the latter being available from emission sources such as power plants, cements kilns or oil refineries [1-2].

$$CO_2 + 4H_2 \rightleftharpoons CH_4 + 2H_2O \qquad \Delta H_{298K} = -165\ kJ \cdot mol^{-1} \qquad (1)$$

Due to the exothermic nature (and negative change in number of moles), the Sabatier reaction is thermodynamically favored at low temperatures (and high pressures). To overcome kinetic limitations and achieve acceptable rates and selectivity, especially at low temperatures, highly active catalysts are required [2]. In this work, metal-based heterogeneous catalysts for the CO_2 methanation were screened regarding to their activity, CH_4 selectivity and stability.

2. Methods

2.1 Catalyst synthesis

Catalytic tests were performed on 4 materials: in-house synthesized Ru(2%)/SiO_2, Ni(34%)MgAl, Ru(0.5%)/Ni(34%)MgAl and a commercial catalyst supplied by Degussa (Ru(1%)/Al_2O_3).
Ni(34%)MgAl was prepared by the co-precipitation method, while Ru(0.5%)/Ni(34%)MgAl was prepared by wetness impregnation over the nickel-aluminum derived hydrotalcite. Ru(2%)/SiO_2 was obtained by wetness impregnation over a commercial SiO_2 support (Sigma Aldrich).

2.2 Catalyst screening

The experiments were conducted using *ca*. 100 mg of catalyst particles sized between 200-250 µm and diluted in inert beads that were loaded into a tubular fixed-bed reactor (*L*=12 cm; I.D.= 0.72 cm). The reactor was warmed up at a heating rate of 5 $^oC \cdot min^{-1}$ until 300 ^oC or 650 ^oC and held 1 or 2 hours at that temperature, for the Ru or (Ru)Ni catalysts, respectively. Catalyst activation was performed using a stream of 10 vol. % H_2 balanced in N_2. Activity tests were conducted sequentially

at 250, 300 and 350 °C using a reactant stream made of N_2 (30 mL_n/min), H_2 (16 mL_n/min) and CO_2 (4 mL_n/min) that was fed for 75 minutes. Catalyst stability was assessed at 350 °C during 24 hours before decreasing the temperature and submitting the catalyst to new activity measurements at 300 °C and 250 °C. CO_2 conversion (X_{CO2}) and CH_4 selectivity (S_{CH4}) were calculated according to Eq. 2 and Eq. 3, respectively, with F_{CO2}^{in} being the CO_2 inlet molar flow rate, and F_{CO2}^{out}, F_{CH4}^{out} and F_{CO}^{out} the outlet molar flow rates of CO_2, CH_4 and CO, respectively.

$$X_{CO2} = \frac{F_{CO2}^{in} - F_{CO2}^{out}}{F_{CO2}^{in}} \quad (2)$$

$$S_{CH4} = \frac{F_{CH4}^{out}}{F_{CH4}^{out} + F_{CO}^{out}} \quad (3)$$

3. Results and discussion

Nickel-based catalysts Ni(34%)MgAl and Ru(0.5%)/Ni(34%)MgAl were the most promising materials with the highest CO_2 conversion ($X_{CO2,MAX}$ = *ca*. 81-92 % at 300-350 ºC) and CH_4 selectivity (≥ 99 %) (cf. Fig. 1). They also revealed stable performances after 24 hours on stream (cf. Fig. 1a). However, CO_2 conversion is lower for the bimetallic Ni-Ru catalyst compared to the Ni(34%)MgAl sample, particularly at 250 °C (62.5 % vs. 36.6 % - cf. Fig. 1a). The undesired formation of CO was limited with both Ni(34%)MgAl and Ru(0.5%)/Ni(34%)MgAl; the maximum CO fraction obtained was 587 ppm, and was null at 300 °C. Regarding to the other ruthenium catalysts tested, it was found that CH_4 selectivity drops abruptly after 24 hours on stream (cf. Fig. 1b). These catalysts become more active towards carbon monoxide with CO selectivity reaching 34.1 % and 41.3 % at 300 °C for the Ru(1%)/Al_2O_3 (Degussa) and Ru(2%)/SiO_2, respectively (cf. Fig. 1b).

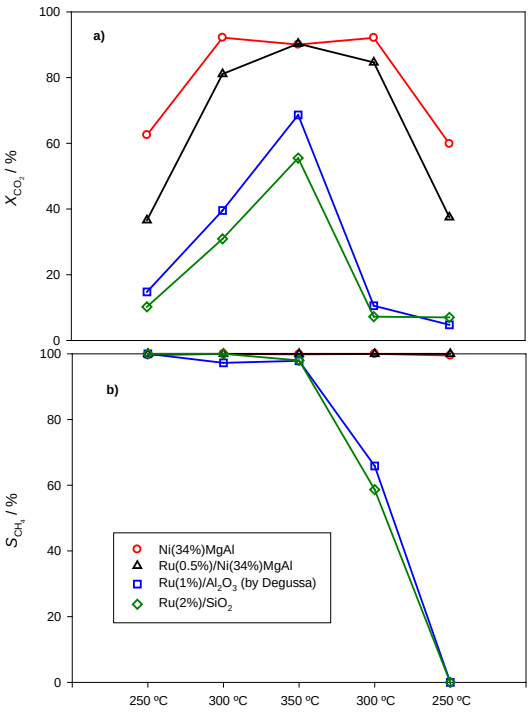

Figure 1 - CO_2 conversion (a) and selectivity to CH_4 (b) attained at the different temperatures.

4. Conclusions

The nickel-based catalysts, Ni(34%)MgAl and Ru(0.5%)/Ni(34%)MgAl, presented higher activity, selectivity and stability, when compared to the commercial Ru(1%)/Al_2O_3 and prepared Ru(2%)/SiO_2 catalysts. Ongoing detailed physical-chemical characterization will help establishing relationships between catalytic performances.

Acknowledgments

This work was financially supported by: i) Project UID/EQU/00511/2019 – LEPABE, funded by national funds through FCT/MCTES (PIDDAC); ii) Project POCI-01-0145-FEDER-030277, funded by the European Regional Development Fund (ERDF) through COMPETE2020 – Programa Operacional Competitividade e Internacionalização (POCI) and by national funds (PIDDAC) through FCT/MCTES and iii) Project "LEPABE-2-ECO-INNOVATION" – NORTE-01-0145-FEDER-000005, funded by Norte Portugal Regional Operational Programme (NORTE 2020), under PORTUGAL 2020 Partnership Agreement, through ERDF.

References

[1] C.V. Miguel, A. Mendes, L.M. Madeira, Energies 11 (2018) 3259-3279.
[2] K. Ghaib, F.Z. Ben-Fares, Renew. Sustain. Energy Rev 81 (2018) 433–446.

ECCE12
The 12th EUROPEAN CONGRESS OF CHEMICAL ENGINEERING
Florence 15-19 September 2019

CO_2 methanation activated by Ni/MgO catalysts

Astrid Loder[1]*, Susanne Lux[1], Matthäus Siebenhofer[1]

1 Institute of Chemical Engineering and Environmental Technology, Graz University of Technology, Inffeldgasse 25/C/II, 8010 Graz, Austria

**Corresponding author: astrid.loder@tugraz.at*

Highlights

- Ni/MgO catalysts are active for the CO_2 methanation and 100 % selective to CH_4.
- Higher Ni load leads to higher CO_2 conversion.
- The rate law shows a correlation between frequency factors and Ni load.

1. Introduction

Carbon dioxide hydrogenation utilizes CO_2 to produce hydrocarbons and carbon monoxide. The product selectivity is influenced by the catalyst and the process parameters. If methane is the main product, the process is called CO_2 methanation. [1] CH_4 can be transported in already existing pipelines for natural gas and acts as a chemical hydrogen storage.

$CO_2 + 4\ H_2 \rightarrow CH_4 + 2\ H_2O$

A bifunctional nickel magnesium oxide catalyst was investigated. Nickel provides the adsorbent capacity for hydrogen and is highly selective to CH_4. [2] MgO activates carbon dioxide and suppresses possible catalyst deactivations. [3] MgO reduces the negative impact of water on the catalyst. The Ni/MgO catalyst is a cheap, highly active, easy to synthesize and robust catalyst. [4] The reaction kinetics for the CO_2 methanation and the catalysts activity were investigated to describe the reaction for a future industrial application.

2. Methods

The Ni/MgO catalysts were prepared via wet impregnation. Calcined magnesium oxide was mixed with a solution of nickel nitrate hexahydrate ($Ni(NO_3)_2*6H_2O$) and water. The catalysts were dried, calcined and reduced in hydrogen atmosphere. Four Ni/MgO catalysts were prepared with 11, 17, 21 and 27 w% nickel load.

The CO_2 methanation experiments were performed in a bench scale fixed bed tubular reactor. The product gas was continuously analyzed by a Caldos27 thermal conductivity analyzer for H_2 and Uras26 infrared photometer for CO_2, CO and CH_4. The H_2:CO_2:N_2 ratio of the feed gas flow was 56:14:30 and ambient pressure was applied. Steady state experiments were performed between 533 to 648 K and 1.2 $m^3\ kg^{-1}\ h^{-1}$ to 14.9 $m^3\ kg^{-1}\ h^{-1}$.

3. Results and discussion

A high nickel load leads to a higher CO_2 conversion. The highest CO_2 conversion was achieved at 598 K with a 27 w% Ni/MgO catalyst. At higher temperature the CO_2 conversion drops caused by

the lower equilibrium conversion. Nickel loads over 30 w% are only beneficial for temperatures lower than 600 K. The methane selectivity was 100 % for every Ni/MgO catalyst.

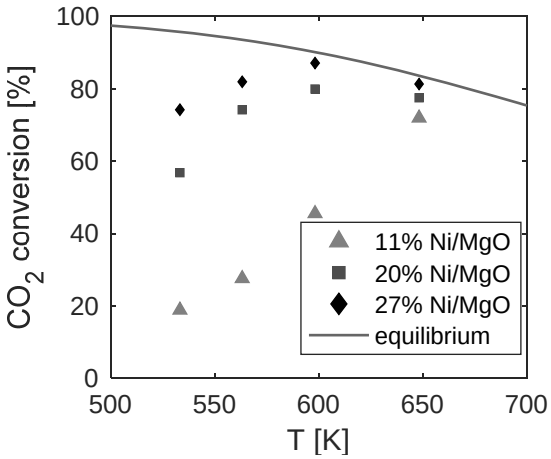

Figure 1. CO_2 conversion for the carbon dioxide methanation with catalysts of varied Ni load at 3.7 $m^3\ kg^{-1}\ h^{-1}$ and the equilibrium CO_2 conversion.

The rate law of the CO_2 methanation consists of a forward reaction, a backward reaction and an adsorption term. The temperature dependence was modelled by an Arrhenius approach. The frequency factors show a correlation to the Ni load of the catalyst.

4. Conclusions

The CO_2 methanation is an opportunity to reduce CO_2 emissions. A bifunctional Ni/MgO catalyst is active for the CO_2 methanation and 100 % selective to CH_4. Higher nickel loads result in higher CO_2 conversions up to 30 w% nickel load and 600 K.

References

[1] G. Centi and S. Perathoner, Opportunities and prospects in the chemical recycling of carbon dioxide to fuels, Catal. Today, vol. 148, no. 3–4, pp. 191–205, 2009.

[2] Y. Yan, Y. Dai, H. He, Y. Yu, and Y. Yang, A novel W-doped Ni-Mg mixed oxide catalyst for CO2 methanation, Appl. Catal. B Environ., vol. 196, pp. 108–116, 2016.

[3] M. Guo and G. Lu, The effect of impregnation strategy on structural characters and CO2 methanation properties over MgO modified Ni/SiO2 catalysts, Catal. Commun., vol. 54, pp. 55–60, 2014.York, 2009, pp. 181–304.

[4] G. Baldauf-Sommerbauer, S. Lux, W. Aniser, B. Bitschnau, I. Letofsky-Papst, and M. Siebenhofer, Steady state and controlled heating rate methanation of CO 2 on Ni / MgO in a bench scale fixed bed tubular reactor, J. CO2 Util., vol. 23, pp. 1–9, 2017.

ECCE12
The 12th EUROPEAN CONGRESS OF CHEMICAL ENGINEERING
Florence 15-19 September 2019

Are steady-state kinetics sufficient for the simulation of the transient CO_2 methanation?

Bjarne Kreitz[1], Jan Martin[1], Steffen Flaischlen[1], Gregor Wehinger[1], Thomas Turek[1]

1 Institute of Chemical and Electrochemical Process Engineering, Clausthal University of Technology, Leibnizstr. 17, 38678 Clausthal-Zellerfeld

**Corresponding author: kreitz@icvt.tu-clausthal.de*

Highlights

- Transient operation of the Sabatier reaction on Ni catalysts
- Dynamic simulation the methanation in a Berty reactor
- Storage effects on the catalyst are visible during concentration forcing
- Steady-state kinetics fail to describe the transient behavior

1. Introduction

Heterogeneously catalyzed processes are usually operated in steady state. The coupling of these processes to renewable energy sources, such as the methanation of CO_2 in the Power-to-Gas process, may require a dynamic operation of the reactor. Reaction kinetics resulting from steady-state measurements, mostly in the form of Langmuir-Hinshelwood-Hougen-Watson approaches, are typically used for the reactor design or the investigation of suitable operating conditions. The simulation of the periodic operation of a methanation reactor based on steady-state kinetics predicted dramatic effects of the inlet composition on temperature profile and outlet composition [1]. However, the underlying description of the reaction rate is a strong simplification of the actual processes on the catalyst surface. A detailed description of the transient and steady-state operation can be achieved by microkinetic models [2]. But microkinetics are rarely applicable for simulation and design on the reactor scale. Therefore, the aim of this study is dedicated to the detailed experimental investigation of the dynamic methanation on Ni catalysts in order to verify whether steady-state kinetics can describe the observed transient phenomena.

2. Methods

In order to develop a proper kinetic approach, measurements with a Ni catalyst in a Berty reactor are carried out. At temperatures of 200 - 400°C and pressures up to 30 bar, this reactor can be regarded as an ideally mixed continuous stirred tank reactor (CSTR). Through online analysis of the gas composition with a mass spectrometer, both stationary and dynamic measurements can be performed with high temporal resolution. For the investigation of the dynamic behavior of the methanation reaction, concentration pulses and steps are applied to the system. The high frequency of the step changes also allows for a periodic modulation of the system. During the dynamic catalyst operation, storage effects of adsorbed educts and intermediate products become visible. Additionally, the storage capacity is studied via the adsorption of CO_2 and H_2 at reaction temperatures by volumetric and dynamic adsorption methods, which allows the determination of adsorption isotherms and adsorption kinetics. Based on the experiments, approaches for the reaction kinetics (steady-state, dynamic) are developed. These are used in a model of the Berty

reactor to explore the limits of steady-state kinetics and the applicability of simplified dynamic kinetics. The Berty reactor is modelled as a CSTR taking the catalyst as a separate solid phase into account.

3. Results and discussion

The bang-bang operation of a Ni/Al_2O_3 catalyst, where the reactor inlet composition is alternated between pure H_2 and CO_2, can be described with a relatively good accuracy by using a published steady-state reaction kinetics [3]. Figure 1 shows the transient operation of the same catalyst with a flush of He between the step changes in order to remove the remaining CO_2 from the gas phase. Switching to H_2 then leads to desorption of adsorbed CO_2 and methane formation sets in. This simple experiment nicely illustrates the failure of the steady-state reaction kinetics. Since H_2 and CO_2 do not simultaneously occur in the reactor, the calculated reaction rate is always zero. The observed methane formation reveals that significant quantities of CO_2 and/or carbon containing intermediates are adsorbed on the catalyst surface, which is also evidenced by the adsorption measurements.

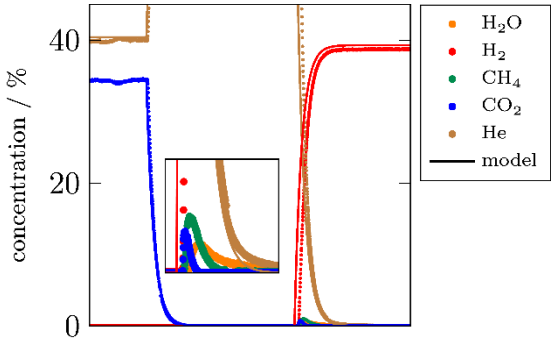

Figure 1. Experimental (dots) and simulation (solid) results when the Berty-reactor is flushed with He for 10 min between a change from CO_2 to H_2. The zoom is located at the step change of H_2. Conditions: 20 wt.-% Ni/Al_2O_3, 0.5 g, 250 °C, 2 bar, 200 mL_N/min.

4. Conclusions

The comparison of the reactor simulation and kinetic experiments shows, that steady-state kinetics are able to predict transient phenomena of the Berty reactor when both reactants are present in the gas phase. If, however, a component is missing, as shown in the experiment, the steady-state kinetics cannot correctly reproduce the behavior of the reactor. In order to be able to reproduce the transient results, it is necessary to develop dynamic kinetic approaches which can also be used on the reactor scale.

References

[1] B. Kreitz, G.D. Wehinger, T. Turek, Chem. Eng. Sci., 195 (2019) 541-552.
[2] C. Seidel, A. Jörke, B. Vollbrecht, A. Seidel-Morgenstern, A. Kienle, Chem. Eng. Sci., 175 (2018) 130–138.
[3] F. Koschany, D. Schlereth, O. Hinrichsen, Appl. Catal., B, 181 (2016) 504–516.

ECCE12
The 12th EUROPEAN CONGRESS OF CHEMICAL ENGINEERING
Florence 15-19 September 2019

Direct epoxidation of linseed oil by hydrogen peroxide: thermal risk assessment

Wander Y. Pérez-Sena[1,2], Pasi Tolvanen[2], Lionel Estel[1], Tapio Salmi[2], Sébastien Leveneur[1,2]

1.Normandie Univ, INSA Rouen, UNIROUEN, LSPC, EA4704, 76000 Rouen, France

2.Johan Gadolin Process Chemistry Centre, Åbo Akademi University, Åbo/Turku, Finland.

**Corresponding author: sebastien.leveneur@insa-rouen.fr*

Highlights

- Adiabatic experiments for the epoxidation.
- Thermal risk assessment for different epoxidation routes.
- Kinetic model for the direct epoxidation.

1. Introduction

The use of vegetable oil as industrial feedstock could be a promising substitute to petroleum-derived sources. For instance, production of biodiesel from transesterification of vegetable oils is a well-developed process at the industrial level. Vegetable oils are used in industry because they are renewable, biodegradable, non-toxic and abundant.

One of the first step is the epoxidation of vegetable oils. Epoxidized vegetable oils can be seen as platform molecules because they can be transformed into different chemicals [1] such as polyols, carbonated vegetable oils [2] and polyurethanes [3-4].

Conventionally, production of epoxidized vegetable oils is done by the Prileschajew method. It is a liquid-liquid reaction system, with several consecutive and parallel exothermic reactions [5]. The first step is the production of percarboxylic acid in the aqueous phase. Then, the percarboxylic acid diffuses into the organic phase to epoxidize the unsaturated groups. Due to the presence of several exothermic reactions, the risk of thermal runaway exists [6-7].

The issues of the Prileschajew method are:

-production of organic waste during the process;

-acidity of the reaction mixture favors the side reaction of ring-opening;

-separation step and waste treatment are more demanding;

-formic and acetic acids are the most used and can cause some corrosion.

Hence, direct epoxidation of vegetable oil by oxygen and hydrogen peroxide is seen as the best option concerning thermal safety, waste treatment and selectivity. The objective of this study is to compare the thermal risk for the epoxidation of linseed oil by three chemical systems: Prileschajew oxidation by using peracetic acid, Prileschajew by using performic acid and by the direction epoxidation of hydrogen peroxide on alumina. For the evaluation of the thermal risk on the epoxidation of linseed oil, the TMR_{ad} (Time to Maximum Rate under adiabatic conditions) was

chosen as a reliable safety parameter to identify the probability of hazardous scenarios. The adiabatic calorimeter ARSST standing for Advanced Reactive System Screening Tool was used [8] to determine TMR_{ad}. We have decided to use the most conservative assumption implying to determine the TMR_{ad}(Tp) at the initial temperature Tp by using the zero- order approximation.

2. Methods

Experiments were performed in a pseudo-adiabatic calorimeter: ARSST (Advanced Reactive System Screening Tool) following the heat loss compensation principle by using and electrical heating supply [8]. To decrease the evaporation, experiments were performed under high pressure of nitrogen.

3. Results and discussion

We have tested the influence of different parameters on the thermal risk parameter TMR_{ad} such as concentrations of reactants or catalyst. Figure 1 shows the evolution of TMR_{ad} at different catalyst concentrations for the Prileschajew by formic acid catalyzed by sulfuric acid, Prileschajew by acetic acid catalyzed by sulfuric acid and epoxidation by Al_2O_3.

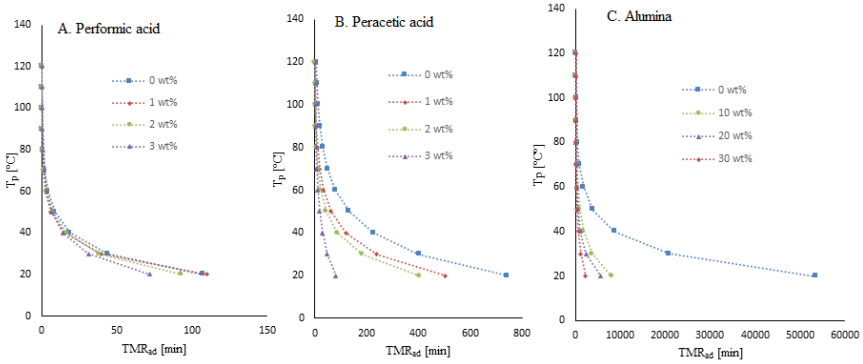

Figures 1. Process temperature Tp versus TMRad for the epoxidation by performic acid (A); by peracetic acid (B) and direct epoxidation by hydrogen peroxide over alumina (C) with different weight percentage of catalyst.

4. Conclusions

Figure 1 shows that direct epoxidation by alumina is thermally safer than the Prileschajew ones. The continuation of this work is the kinetic modeling of these reactions to know which process is more efficient from a kinetic viewpoint.

References

[1] S. Danov, O. Kazantsev, A. Esipovich, A. Belousov, A. Rogozhin, E. Kanakov, Catal. Sci. Technol. 7 (2017) 3659-3675.
[2] X. Cai, J.-L. Zheng, J. Wärnå, T. Salmi, B. Taouk, S. Leveneur, Chem. Eng. J. 313 (2017) 1168-1183.
[3] M. Ahmad Sawpan, J. Polym. Res. 25 (2018) 184-199.
[4] W. Pérez-Sena, X. Cai, N. Kebir, L. Vernières, C. Serra, T. Salmi, S. Leveneur, Chem. Eng. J. 346 (2018) 271-280.
[5] J.-L. Zheng, J. Wärnå, F. Burel, T. Salmi, B. Taouk, S. Leveneur, AIChE J. 62(3) (2016) 726-741.
[6] C. Vianello, E. Salzano, G. Maschio, Process Saf. Environ. Prot. 116 (2018) 718–726.
[7] S. Leveneur, L. Estel, C. Crua, J. Therm. Anal. Calorim. 122 (2015) 795–804.
[8] L. Vernières-Hassimi, A. Dakkoune, L. Abdelouahed, L. Estel, S. Leveneur, Ind. Eng. Chem. Res. 56 (2017) 13040-13049.

ECCE12
The 12th EUROPEAN CONGRESS OF CHEMICAL ENGINEERING
Florence 15-19 September 2019

Determination of the Factors Responsible for Stabilization in Hydrotreating.

Ngoc Yen Phuong Cao[1], Benoit Celse[1*], Denis Guillaume[1], Isabelle Guibard[1], Joris W. Thybaut[2]

1 IFP Energies nouvelles, Rond-point de l'échangeur de Solaize, BP 3, 69360 Solaize, France; 2 Ghent University, Laboratory for Chemical Technology, Technologiepark 914, Ghent, B-9052, Belgium

**Corresponding author: benoit.celse@ifp.fr*

Highlights

- Stabilization is due to chemical phenomena and depends on feed and operating conditions
- Stabilization follows a first-order transfer function
- A characteristic time parameter is defined for stabilization

1. Introduction

Hydrotreating is a catalytic conversion process in petroleum refineries, among others for removing organic nitrogen, sulfur and oxygen from hydrocarbon streams. A kinetic model is mandatory for the design and simulation of this process. It is usually developed based on data acquired at steady state conditions. A significant challenge in this respect is that establishing the steady state requires several days, leading to long duration to acquire sufficient experimental data for kinetic model construction. However, during the transient state, effluent analyses are carried out at regular time intervals to determine whether the steady state has been reached. The aim of this work is to have a better understanding of the stabilization behavior by estimating the influential factors, such that the data acquired in this period can also be employed for kinetic modelling.

2. Methods

The experimental data are obtained using the hydrodenitrogenation pilot plant operating in a continuous manner in IFP Energies Nouvelles. The total catalyst volume in the reactor is 50 cm^3. Operating conditions are switched after having reached the steady state corresponding with the previous operating conditions. Data cover 11 Vacuum Gas Oil (VGO) feeds over two catalysts. Liquid Hourly Space Velocities (LHSV) vary between 0.5 and 4 h^{-1}, the total pressure between 50 and 140 bar and the temperature between 350 and 410 °C. The data are measured as the *'liquid product nitrogen content'* with time on stream, including 920 measurements, see Figure 1. One *'episode'* is defined as a series of points corresponding to one experimental run.

A hydrodynamics study on the pilot plant has been done using a tracer technique. Stabilization evolution is assessed via exploratory data analysis [1]. It resulted in a first-order transfer function as shown in Equation (1). The characteristic time τ of each episode presented in the equation is estimated via nonlinear least-squares problem (solid line in Figure 1). A multiple linear regression

with interaction technique is then used for τ prediction to evaluate the phenomena underlying the transient data. The most influential input variables are estimated via variable selection technique *'leaps'* [2].

$$N = N_{init} + (N_{final} - N_{init})\left(1 - e^{\left(\frac{-(TOS - TOS_{init})}{\tau}\right)}\right) \quad (1)$$

Where:

- N : product nitrogen at a specific TOS (ppm)
- N_{init} : first point of episode (ppm)
- N_{final} : last point of episode (ppm)
- TOS : time on stream (h)
- TOS_{init} : TOS corresponding to N_{init} (h)
- τ : characteristic time (h)

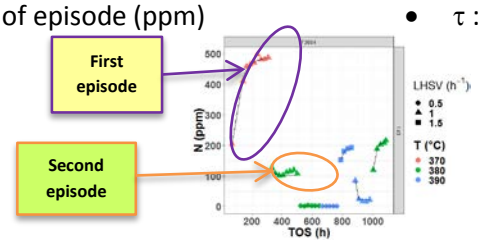

Figure 1. Data representation (Feed F3884, P = 140 bar, point : experimental data, solid line : model fitting Equation (1))

3. Results and discussion

The stabilization evolution of the tracer component is significantly faster than the stabilization of hydrodenitrogenation. Chemical phenomena are therefore involved in the stabilization. τ reflects the time required to reach the steady state. First episodes take more time to stabilize than other episodes. Two linear models for τ were built: one for first episodes (model M1) and another for other episodes (model M2). Model M1 was achieved with a R^2 of 0.83, see Figure 2. It contains three variables (LHSV, feed resin, pressure) and one interaction term LHSV*resin. An inverse relationship between LHSV and τ was found. The interaction term shows that the impact of LHSV on τ depends on the value of feed resin which is the polar components with high molecular weight. A direct relationship between pressure and τ was observed. Temperature is not an influential parameter for stabilization. However, stabilization of other episodes seems more complex. Model M2 relies by not only on the operating conditions and feed properties but also on the operating conditions of the previous episode.

Figure 2. Parity plot with 95% confidence interval for model M1 *(left, R^2 = 0.83)* and model M2 *(right, R^2 = 0.66)*

4. Conclusions

Stabilization behavior is a critical point for hydroprocessing experiments. Two models (one for the first episode, another for the others) were built to predict the stabilization time and assess the most influential parameters (LHSV, resin, pressure). The models will be tested against new data.

References

[1] J. W. Tukey. Exploratory Data Analysis, *Addison-Wesley, Reading, MA*, 1977.

[2] G. M. Furnival, R. W. Wilson, Jr. Regressions by Leaps and Bounds, *Technometrics*, 1974, 499-511.

ECCE12
The 12th EUROPEAN CONGRESS OF CHEMICAL ENGINEERING
Florence 15-19 September 2019

Supercritical Water: a Roadmap to Biorefineries Through Innovation.

María José Cocero, Tijana Adamovid, Luís Vaquerizo, Celia Martínez.

Bioecouva Research Institute, High Pressure Processes group. Valladolid University

**Corresponding author: mjcocero@iq.uva.es*

Highlights

- Ultrafast supercritical water (SCW) hydrolysis to avoid hydrolysis products degradation.
- Ultrafast preheating to avoid hydrolysis products during the heating step.
- From the conventional hydrothermal ionic reaction media to the non-ionic SCW media.
- Efficient lignocellulosic biomass fractionation in sugars and lignin.

1. Introduction

The selective fractionation of the lignocellulosic biomass in its main components (hemicellulose, cellulose and lignin) is a challenge of the sustainable biorefineries development that has not been solved yet. The complexity of the biomass and its structure limit the process by mass transfer. In addition, the crystallinity of cellulose complicates its dissolution in conventional solvents. Water at temperature and pressure above the critical point (374ºC and 22MPa) has physical properties that allow dissolving the cellulose. The water ionic product changes from 10-12 at 300ºC to 10-19 to 374ºC, so at subcritical water conditions the ionic reactions mechanisms are favoured and at SCW conditions the radical mechanism predominates. The decrease of the ionic mechanism reaction avoids the loss of selectivity that occurs in the conventional hydrothermal processes. Additionally, SCW has low viscosity and high diffusivity that facilitate the penetration of water into the complex structure of the lignocellulosic matrix, whilst its low dielectric constant, similar to non-polar organic solvents, enhances solubility of organic compounds. Under these conditions, the hydrolysis of biomass fractions is extremely rapid and presents a means to achieve a significantly more process intensive fractionation of biomass.

Reaction speed – while being an advantage to process intensification – is also a significant disadvantage to selectivity at longer reaction times, leading to degradation of hydrolysis products and resulting in complex reaction mixtures. To take advantage of the properties of the SCW and avoid the degradation of hydrolysed products, we have introduced the ultrafast process by operation at residence times below 1 second. This process allows the hydrolysis of the cellulose, but avoids the hydrolysis of the sugars. The control of the residence time is possible by our innovative reactor design: the sudden expansion micro reactor that preheats the biomass in residence times below 10ms, by direct mixture of the SCW and the biomass suspension, and cools the reaction effluent by the Joule Thomson effect that takes place during the depressurization.

This process allows fractionating lignocellulosic biomass in the next stages: i) separation of extractives as polyphenols, antioxidants, starch, proteins or oils; ii) hydrolysis of hemicellulose to

produce hemicelluloses oligomers and C5 sugars; iii) hydrolysis of the cellulose fraction to produce a liquid effluent, mainly C6 sugars, and a solid effluent, mainly lignin (1).

2. Methods

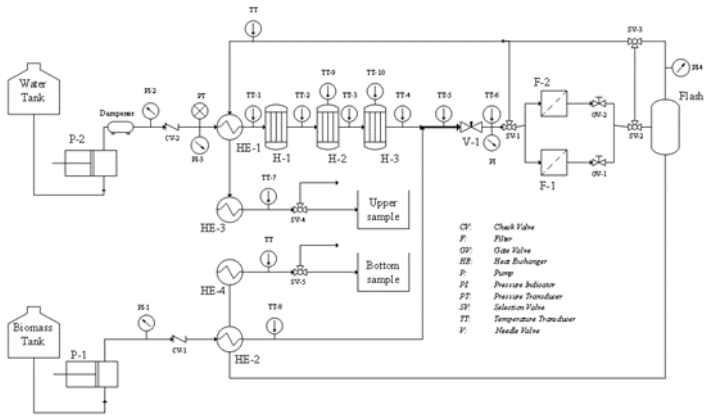

Figure 1 presents a pilot plant flow diagram for lignocellulosic biomass fractionation. The pilot plant operates at temperatures of 400ºC, pressures of 25 MPa and biomass suspension flow of 10 kg/h. The pilot plant has four units: 1) biomass pumping, 2) SCW production, 3) reaction and 4) heat integration and energy recovery (2)

3. Results and discussion

The fractionation of pulp sugar beet is presented as an example of lignocellulosic biomass fractionation. The effect of the residence time on the composition of the liquid effluent sugars is presented in Figure 2. Sugar beet pulp has a concentration of pectin of 27%; although the pretreatment extracts the pectins, the remaining pectins hinder the flow of SCW into the complex biomass matrix, requiring longer residence times. These residence times increase degradation, but even at residence times of 230ms, the C6 yield is higher than 80%, significantly higher than the conventional processes (3).

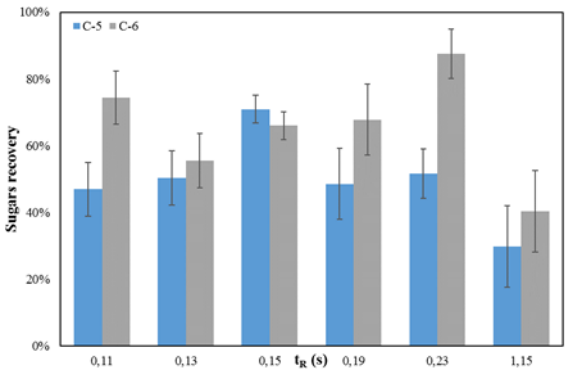

Figure 2. Beet pulp SCW hydrolysis at 390°C and 25 MPa. C-6 and C-5 liquid concentration at different reaction times.

4. Conclusions

The SCW ultrafast hydrolysis is a selective process for the fractionation of lignocellulosic biomass in a liquid effluent of C5 and C6 sugars than can be used for fermentation, and a solid effluent that is mainly a lignin composite. Any HMF is produced.

Acknowledgements

The authors thank the Spanish Ministry of Economy and Competitiveness for the Project CTQ2016-79777-R. TA thanks Valladolid University for its FPI-UVA grant.

References

[1] M.J. Cocero, Á. Cabeza, N. Abad, T. Adamovic, L. Vaquerizo, C.M. Martínez, M.V. Pazo-Cepeda, J. (2018) Supercrit. Fluids, 133 pp 550-565.

[2] Martínez, C.M., Adamovic, T., Cantero, D.A., Cocero, M.J. (2019) Journal of Supercritical Fluids, 143, pp. 242-250.

[3] Martínez, C.M., Cantero, D.A., Cocero, M.J. (2018) Journal of Cleaner Production, 204, pp. 888-895.

ECCE12
The 12th EUROPEAN CONGRESS OF CHEMICAL ENGINEERING
Florence 15-19 September 2019

Hydrothermal CO_2 Reduction and Biomass Valorization in One-Pot Reaction.

María Andérez-Fernández,[1]*Gareth Davies,[2] Justin Driver,[2] Cynthia Kartey,[2] Eduardo Pérez,[1] Ángel Martín,[1] James McGregor,[2] M. Dolores Bermejo,[1]

[1]*BioEcoUva. Research Institute on Bioeconomy. High Pressure Process Group. Department of Chemical Engineering and Environmental technology. Universidad de Valladolid, Valladolid, 47011, Spain, Spain*

[2]*Department of Chemical Engineering, University of Sheffield, Sheffield, S1 3JD, United Kingdom*

**Corresponding author: mariaanderezfernandez@gmail.com*

Highlights

- It is the first time that $NaHCO_3$ hydrothermal reduction is performed using non-edible biomass.
- A higher extent of liquefaction of biomass was achieved by adding $NaHCO_3$.
- Biomass with high-content in holocelluloses (sugar bagasse) achieved higher yields.

1. Introduction

Production of fuels and chemicals from renewable sources is extensively investigated due to the low level of fossil fuels reserves and their impact on environment. Among the different technologies hydrothermal valorization of lignocellulosic biomass has been intensely investigated. High temperature water (HTW) exhibits outstanding properties c, playing different roles in the reaction, such as reactant, solvent and catalyst.

Increasing carbon dioxide (CO_2) levels are having harmful consequences for the environment. Different processes have been envisioned as effective methods for CO_2 conversion into useful chemicals and fuels, being hydrothermal processing one of the most innovative. CO_2 hydrothermal reduction has already been studied using metals and organic model compounds[1,2]. Combining both processes of hydrothermal biomass valorization and hydrothermal CO_2 reduction to produce useful chemicals would lead to an optimized and greener process.

In this research, CO_2 conversion to formic acid in hydrothermal media was carried out using non-edible lignocellulosic biomass (pine needles and sugarcane bagasse), demonstrating the possibility for the first time the use biomass residues as a reductant for CO_2 reduction in a one-pot reaction.

2. Methods

Reactions were performed in a 100 mL batch reactor with a magnetically driven impeller. Biomass (pine needles, PN, or sugarcane bagasse, SB) were presoaked overnight in 25mL of distilled water, and placed afterwards in the reactor, adding extra 25 mL of water and sodium bicarbonate ($NaHCO_3$) as a CO_2 source. After sealing and purging the reactor, the reactor was placed in a heating jacket, previously preheated, and setting this point as t=0'. After the desired reaction time, the reactor was cooled and liquid and solid samples were collected. Liquid samples were analyzed using HPLC and TOC techniques, while solid samples were analyzed through FTIR and SEM.

3. Results and discussion

To study whether biomass residues can convert $NaHCO_3$ into formic acid in one-pot reaction, both PN and SB were treated with and without $NaHCO_3$ for 30 min at 250ºC (0.50M $NaHCO_3$ and 1.0g of biomass). Results showed that not only a higher production of formic acid when $NaHCO_3$ was added in both cases, but also to a higher content of dissolved organic carbon in liquid samples, achieving a higher extent of biomass liquefaction. Comparing both biomass types, SB achieved a better yield to formic acid (referenced to the initial amount of biomass) than PN. This may be caused by a higher amount of holocelluloses (sugar-based biopolymers) in SB than in PN.

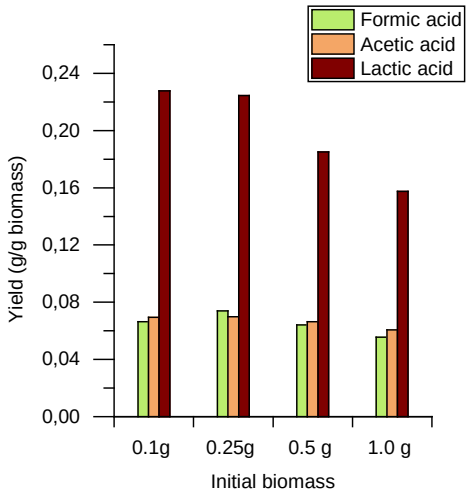

Figure 1. Influence of the amount of initial SB at 250ºC for 30 min.

Thus, selecting SB as reductant, different reaction parameters were optimized, such as initial amount of biomass (0.10g, 0.25g, 0.50g and 1.00 g, results shown in Figure 1), temperature (225ºC, 250ºC and 275ºC) and time (15 min, 30 min, 60 min, 90 min and 180 min). The best yield to formic acid was achieved using 0.25 g of SB in a 50 mL solution of 0.50M $NaHCO_3$ at 250ºC for 180 min (0.10g of formic acid per gram of initial sugar bagasse). Among the different by-products resulting from the biomass liquefaction and hydrolysis, acetic acid, lactic acid, glycolaldehyde and glyceraldehyde were detected in the highest concentrations.

4. Conclusions

For the first time, the possibility of converting $NaHCO_3$ as CO_2 in hydrothermal media was accomplished using biomass residues. Despite future work should study in the mechanism of the reaction and the implementation of the processes in a continuous pilot plant, this work is a promising starting point for a novel method of CO_2 and biomass valorization.

Acknowledgments

This project has been funded by Junta de Castilla y León through project VA248P18. MAF acknowledges Junta de Castilla y Leon for predoctoral position (Orden EDU/520/2017). MDB thanks MINECO for Ramon y Cajal position.

References

[1] Z. Shen, Y. Zhang, F. Jin, Green Chem. 13 (2011) 820-823
[2] M. Andérez-Fernández, E. Pérez, A. Martín, M.D. Bermejo, J. Supercrit. Fluids 133 (2018) 658-664

ECCE12
The 12th EUROPEAN CONGRESS OF CHEMICAL ENGINEERING
Florence 15-19 September 2019

The Kinetics of Ethylene Oxide and Its Substituents in the Autocatalytic Reaction with Fatty Amines.

Pia Müller[1*], Wyatt Winkenwerder[2], John van der Schaaf[1]

1 Department of Chemical Engineering and Chemistry, Eindhoven University of Technology, P.O. Box 513, 5600MB, the Netherlands; 2 Nouryon, Brewster, New York 10509, United States

**Corresponding author: p.muller@tue.nl*

Highlights

- Ethylene-, propylene- and butylene oxide follow one reaction mechanism
- Lower or no substitution of the epoxide ring increases the reaction rate

1. Introduction

The reaction of fatty amines with two equivalents of epoxide is an industrial process producing surface-active compounds used in several applications, such as paints, corrosion inhibitors, and textiles. The reaction follows an S_N2 mechanism, which is auto-catalyzed by the formed intermediate (SEC) and the end product (TERT) shown in Figure 1.

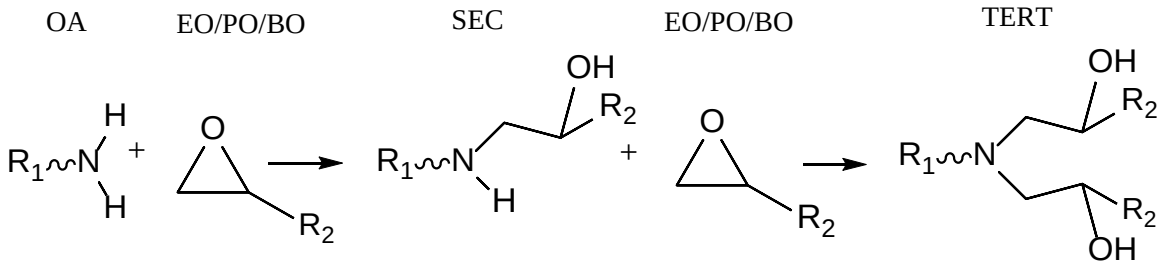

R_1=C_8 alkyl chain
R_2= H (EO), CH_3 (PO), CH_2-CH_3 (BO)

Figure 1. Reaction scheme.

As described by Smith [1], the reaction is catalyzed by alcohol groups, such as the formed products. Sundaram and co-worker found that butylene- (BO), propylene- (PO), and ethylene oxide (EO) react with organic amines in an aqueous phase following the same mechanism [2]. Furthermore, the reaction rates decrease for increasingly substituted epoxides. In this work we aim to proof this correlation for the reaction with fatty amines without the influence of external catalysts or solvents.

2. Methods

Butylene- (BO) and propylene oxide (PO) reacted with octylamine (OA) as model substrate in a microchannel (10 ml). The reaction was carried out at 130 - 160 °C and pressurized to 10 bar. The data was collected by the switch flow method. For EO the system was, due to safety reasons, built inside a glovebox with a set pressure of 60 bar. The products were analyzed by GC, NMR and FTIR.

3. Results and discussion

For the reaction of PO with OA experimental data were collected in flow (Figure 2). Based on preliminarily experimental data a kinetic model was fitted. The overall reaction for PO was 1.5 times as fast as for BO. It is expected for EO an increase in rate by at least a factor 2 compared to PO. The reaction proceeds slowly until significant amounts of SEC are formed. This could be avoided by using a CSTR or recycle system to further increase the process efficiency. Compared to the industrial process the continuous set-up is superior due to the higher saturation of the amine with epoxides.

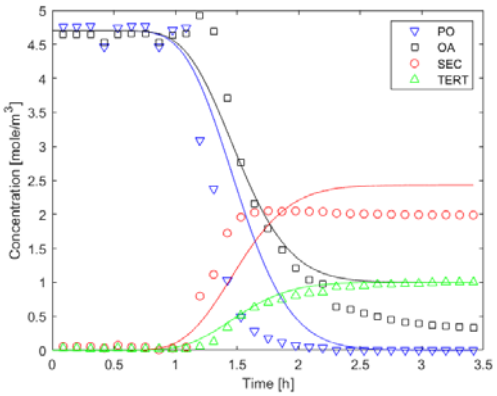

Figure 2. Exemplary reaction of PO with OA in a 1/1 ratio at 140 °C and 10 bar.

4. Conclusions

A kinetic model fitting the experimental data for the reaction of BO, PO, and EO with amines was found and shows a rate dependency towards the substitution degree. The kinetic data collected are of high importance for the intensification of the industrial process. Using a continuous flow system, the intrinsic safety risks associated to the process could be overcome and different options for advanced process engineering can easily be tested and predicted.

References

[1] I. T. Smith, Polymer, vol. 2 (1961) 95–108.
[2] P. K. Sundaram and M. M. Sharma, Bull. Chem. Soc. Jpn. vol. 42 no. 11(1969) 3141–3147.

ECCE12
The 12th EUROPEAN CONGRESS OF CHEMICAL ENGINEERING
Florence 15-19 September 2019

Woody and Agricultural Biomass Torrefaction: Modelling Solid Conversion and Volatile Species Release by Extracted Macromolecular Components.

María Gonzalez Martinez[1,2,3*], Capucine Dupont[4], Sébastien Thiery[1], Denilson Da Silva Perez[5], Xuân-Mi Meyer[2,3], Christophe Gourdon[2,3]

1 Université Grenoble Alpes, CEA, Laboratoire de Préparation des Bioressources, F-38054 Grenoble cedex, France; 2 Université de Toulouse, INPT, UPS, Laboratoire de Génie Chimique, F-31432 Toulouse, France; 3 CNRS, Laboratoire de Génie Chimique, F-31432 Toulouse, France; 4 IHE Delft Institute for Water Education, Delft, the Netherlands; 5 FCBA, InTechFibres Division, CS 90251, F-38044, Grenoble, France

**Corresponding author: maria.gonzalez-martinez@cea.fr*

Highlights

- 14 woody and agricultural biomasses were deeply characterized in torrefaction.
- Extracted cellulose, hemicelluloses and lignin from five biomasses were also torrefied.
- Biomass characterization and family type strongly impacted its behavior in torrefaction.
- Biomass behavior in torrefaction was better represented by the extracted components.

1. Introduction

Due to its diversity and dispersion, biomass waste is currently underexploited. To face this issue, the European project MOBILE FLIP proposes to develop mobile conversion processes, among which torrefaction. This mild thermal treatment (200-300°C, 10min to 1h, default-oxygen atmosphere) gives rise to a solid with optimized processing properties and condensable coproducts with high-added value as “green” chemicals.

Biomass is a highly diverse resource, whose properties are very different from a coniferous to a deciduous wood, or from an agricultural by-product to an herbaceous crop. This diversity may impact biomass thermochemical conversion, together with biomass macromolecular composition in cellulose, hemicelluloses and lignin [1]. The upscaling of biomass torrefaction to industrial units requires therefore the modelling of both solid conversion and gases released versus feedstock type and its macromolecular composition. Up to now, only few studies, typically based on a reduced number of biomasses, have characterized and modelled both solid and condensable species during torrefaction versus biomass type. Furthermore, torrefaction tests on macromolecular components are scarce and based on commercial constituents [1,2].

The objective of this study is to develop a torrefaction model able to predict both solid and volatile species yields versus operating conditions and biomass type. Experimental data is obtained from extracted macromolecular components from 5 woody and agricultural biomasses.

2. Methods

14 biomasses were selected as representative of the European diversity and of the main biomass families: pine, pine forest residues, Scot pine bark (coniferous wood); ash wood, beech, poplar, willow (deciduous wood); miscanthus, reed canary grass (herbaceous crops); corn cob, grape seed cake, sunflower seed shells and 2 wheat straws (agricultural by-products) [3]. From them, five were identified as reference biomasses for analyzing the impact of biomass characteristics in torrefaction and further modelling: ash-wood, beech, miscanthus, pine and one wheat straw. An optimized extraction procedure was proposed to recover cellulose-, hemicellulose- and lignin-

based fractions from the five reference biomasses. The extracted fractions and the raw biomasses were characterized in terms of sugar composition (except lignin) and torrefaction behaviour.

Experiments were performed on a thermogravimetric analyzer coupled to a gas chromatography mass spectrometer device through a heated storage loop system (TGA-GC/MS). Solid degradation and volatile species release were studied in torrefaction experiments in chemical regime [4].

3. Results and discussion

The results obtained with the raw biomasses confirmed that their macromolecular composition strongly influences their behaviour in torrefaction. The heterogeneity of the resource, particularly in the case of agricultural biomasses, highlights this result [3].

A very different behaviour was observed for the extracted components compared to commercial compounds, particularly in the case of cellulose. This suggests that a limitation could be induced by the common use in literature of commercial compounds for torrefaction modelling. Macromolecular component properties were shown to strongly impact their behaviour in torrefaction, particularly hemicellulose sugar composition and cellulose crystallinity.

Furthermore, differences in release kinetics of volatile species during torrefaction were observed, even for volatiles belonging to the same chemical family (acids, furans, ketones).

Derived from these results, a torrefaction model based on the additive contribution of extracted cellulose, hemicelluloses and lignin to biomass behaviour in torrefaction was proposed, and this for the 5 representative biomasses. Two levels of detail were proposed (mod 1 and mod 2), in function of the extracted fractions considered (Figure 1, models for pine and wheat straw).

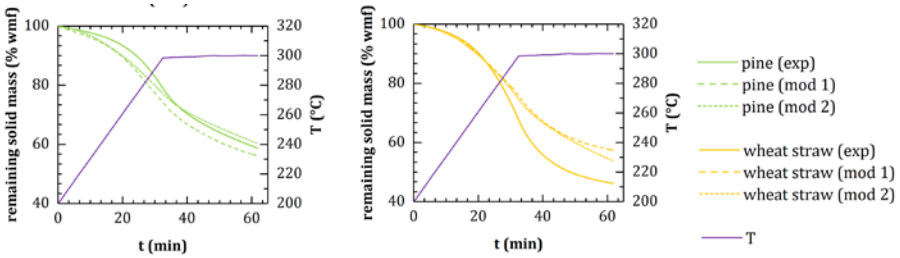

Figure 1. Remaining solid mass loss versus temperature and time in torrefaction for pine and wheat straw in TGA-GC/MS (exp) and modelled through the first-level model (mod 1 curves) and the second-level model (mod 2)

An improved representation of the behavior of biomass in torrefaction in terms of solid mass loss kinetics was achieved with the proposed model. This improvement was especially remarkable for deciduous and coniferous wood, while the representation was less accurate for agricultural biomasses. This torrefaction model was extrapolated to the 14 raw biomasses initially selected.

4. Conclusions

Biomass family and macromolecular composition were shown as key factors determining biomass behavior in torrefaction. Compared to previous models based on commercial compounds, the use of macromolecular components directly extracted from different biomasses through an optimized procedure allowed improving the representation of raw biomass behaviour in torrefaction.

References

[1] Nocquet T., Dupont C., Commandre J-M., Grateau M., Salvador S.: Energy, 72, 188–194 (2014).

[2] Chen, W-H., Peng, J., Bi, X.T.: Renewable Sustainable Energy Rev., 44, 847-866 (2015).

[3] González Martínez M., Dupont C., Meyer X.-M., Gourdon C., Biomass Bioenergy, 119, 43–53 (2018).

[4] González Martínez M., Dupont C., Meyer X.-M., Gourdon C., Chem. Eng. Trans., 50, 61–66 (2016).

ECCE12
The 12th EUROPEAN CONGRESS OF CHEMICAL ENGINEERING
Florence 15-19 September 2019

Modelling and simulation of a sorptive reactor unit for Power-to-Gas applications featuring CO_2 capture and utilization (CCU)

Carlos V. Miguel[1], Jonathan C. Gonçalves[2], Alírio E. Rodrigues[2], Luís M. Madeira[1]

[1]*LEPABE - Laboratory for Process Engineering, Environment, Biotechnology and Energy, Faculty of Engineering, University of Porto, Portugal;* [2] *Laboratory of Separation and Reaction Engineering - Laboratory of Catalysis and Materials (LSRE-LCM), Faculty of Engineering of University of Porto, Portugal*

**Corresponding author: mmadeira@fe.up.pt*

Highlights

- The proof-of-concept of a sorptive reactor for CCU was performed.
- Process intensification improves CO_2 desorption capacity and kinetics.
- A model for reactor simulation and optimization was proposed.

1. Introduction

Power-to-Gas concept (PtG) relies in the chemical storage of electrical energy surpluses in the form of a gas, with hydrogen and/or methane commonly considered the most suited options [1]. The electricity generated powers H_2O electrolysis to produce H_2 (and O_2) which, in turn, can be further converted to CH_4 through the CO_2 methanation reaction (Eq. 1).

$$CO_2 + 4H_2 \rightleftharpoons CH_4 + 2H_2O \qquad \Delta H_{298K} = -165\ kJ{\cdot}mol^{-1} \tag{1}$$

A sorptive reactor for PtG applications able to capture and convert CO_2 to methane in the same unit is presented and modeled to describe its operation.

2. Methods

2.1. Experimental

The sorptive reactor consists in a tube with *L*=15 cm and ID=2.07 cm, packed with alternating layers of a K-promoted hydrotalcite and a Ni-based catalyst with a sorbent/catalyst ratio of 3.15. A synthetic flue gas stream (15 mol % of CO_2 in N_2) was fed to the bed and CO_2 retained by the sorbent. The sorption step ended when the feed was switched to pure H_2 for the reactive regeneration step, where CO_2 desorbs and is converted to CH_4 (and H_2O) at the catalyst layers (cf. Eq. 1). Experiments were performed at low pressure (≤2.5 bar) in a range of *T*=300-350 ˚C.

2.2. Reactor model assumptions

Reactor model assumptions are: 1) ideal gas behavior, 2) axially dispersed plug flow, 3) absence of radial profiles, 4) presence of heat and mass resistances between gas and solid phases and the reactor wall, 5) CO_2 sorption occurs only at the hydrotalcite material, 6) CO_2 sorption equilibrium is described by the dual-site Langmuir model [2], 7) CO_2 sorption kinetics described by the linear driving force model [2], 8) CO_2 methanation kinetics described by the rate equation given in [3], 9) mass transfer in the radial direction of catalyst spheres is described by pore diffusion, 10) pressure drop follows Ergun equation, 11) constant porosity assumed within each layer. Model validation against experimental is ongoing and the gProms software used to solve model equations.

3. Results and discussion

Fig. 1a shows the CO_2 desorption curves during cycle 5 and 6, where N_2 or H_2 were used as purge gas, respectively. Fig. 1a highlights that the desorption kinetics was faster when H_2 was used (i.e. cycle 6) because the reaction of desorbed CO_2 with H_2 at the catalyst layers produces H_2O (cf. Eq. 1), that is known for its ability to regenerate hydrotalcites [2]. Besides faster desorption kinetics, the *in situ* H_2O formation leads also to the complete reestablishment of the initial CO_2 sorption capacity (i.e. cycle 0 vs. cycle 7 in Fig. 1b).

The proof-of-concept of the sorptive reactor concept was successfully performed; the sorbent retained 0.30 moles of CO_2 per each kg (with T=350 ˚C and p_{CO2}=0.20 bar), and the catalyst was able to convert 99 % of captured CO_2, mostly into CH_4 (n_{CH4}/n_{CO}≈25,000).

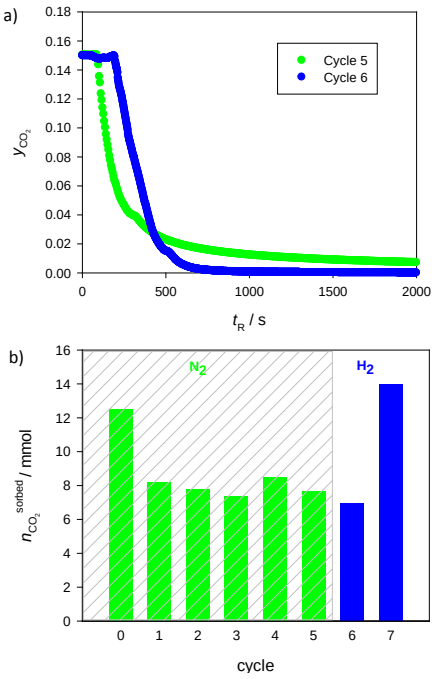

Figure 1. a) CO_2 desorption curves during regeneration in cycles 5 (with N_2) and 6 (with H_2) and b) CO_2 sorption capacity with cycling. T=350 ˚C and P=1.34 bar.

4. Conclusions

The performance of a sorptive reactor for PtG applications was presented. The experimental data highlights that the CO_2 capture step benefits from process intensification. Ongoing modelling and simulation work will provide the key to optimize and boost the reactor performance, while reducing the experimental effort, particularly to find the best operation conditions and bed configurations to enhance the CH_4 purity at the reactor outlet and comply with the natural gas grid specifications (data not shown).

Acknowledgments

This work was financially supported by: i) Project UID/EQU/00511/2019 - LEPABE funded by national funds through FCT/MCTES (PIDDAC); ii) Project POCI-01-0145-FEDER-030277, funded by ERDF through COMPETE2020 – Programa Operacional Competitividade e Internacionalização (POCI) and by national funds (PIDDAC) through FCT/MCTES; iii) Project POCI-01-0145-FEDER-006984 – Associate Laboratory LSRE-LCM – funded by ERDF through COMPETE2020 - (POCI) – and by national funds through FCT; iv) Project "LEPABE-2-ECO-INNOVATION" – NORTE-01-0145-FEDER-000005, funded by Norte Portugal Regional Operational Programme (NORTE 2020), under PORTUGAL 2020 Partnership Agreement, through ERDF; v) Project "AIProcMat@N2020 - Advanced Industrial Processes and Materials for a Sustainable Northern Region of Portugal 2020", with the reference NORTE-01-0145-FEDER-000006, supported by NORTE2020, under the Portugal 2020 Partnership Agreement, through ERDF. The authors also acknowledge Clariant and Sasol for supplying, respectively, the catalyst and sorbent materials used.

References

[1] C.V. Miguel, A. Mendes, L.M. Madeira, Energies 11 (2018) 3259-3279.
[2] E.L.G. Oliveira, C.A. Grande, A.E. Rodrigues, Sep. Purif. Technol. 62 (2008) 137-147.
[3] C.V. Miguel, A. Mendes, L.M. Madeira, J. CO2 Util. 25 (2018) 128-136.

ECCE12
The 12th EUROPEAN CONGRESS OF CHEMICAL ENGINEERING
Florence 15-19 September 2019

Plastic Waste Catalytic Pyrolysis in a Reactive Semi-Batch Distillation

Everton Santos[1], Bruna Rijo[1], Maria Amélia Lemos[1*], Francisco Lemos[1]

1 CERENA, Dep. Eng. Química, Instituto Superior Técnico, Universidade de Lisboa, 1049-001, Lisbon, Portugal

**E-mail: mandal@tecnico.ulisboa.pt*

Highlights

- The use of the ZSM-5 catalyst caused a significant increase in the gas and liquid fractions of products.
- Increasing the temperature, the gas and liquid formation increased, and solid yield decreased.
- The composition of liquid formation, in catalytic pyrolysis, was mostly in the range of gasoline.

1. Introduction

The generation of plastic waste is constantly increasing. In the context of processing waste from electric and electronic equipment (WEEE), recycling plastics from electric cable waste has attracted increasing attention in recent years. Although the priority is generally given to the recycling of the conducting metal, due to its higher value, large amounts of plastic from electric cable waste are released into the environment without an effective disposal [1]. This incorrect disposal causes great problems to the environment, since, plastics (part of electric cable) are not easily degraded and remain in the environment for a long time if disposed in a landfill [2]. A large part of this waste may also be incinerated [3]. New processes are needed to increase the percentage that is recycled. The use of feedstock recycling, for example by resorting to pyrolysis may be an attractive alternative. It allows us to obtain a broad distribution of products, including char, oil/wax and combustible gases from plastic wastes [4]. In this work, the influence of temperature on the catalytic pyrolysis of the electrical cables waste (ECW) will be analysed.

2. Methods

The ECW were provided by Pyroplas. The samples were washed and crushed into coarse grains. The catalytic pyrolysis experiments were carried out using an unstirred glass distillation reactor in semi-batch operation at atmospheric pressure. The catalyst used was a ZSM-5 and ratio catalyst/plastic was 1%. The reactor was initially flushed with N_2, then about 10 g of the plastic waste material were placed in the reactor which was heated at 10 °C min^{-1} to a final temperature ranging from 450 to 500°C. The final temperature was maintained for 90 min. On top of the reactor there is liquid collection vessel below the condenser where the coolant water was fed at 20 °C to control the product that escaped into the gaseous phase. The gases that escaped the condenser were collected in a gas-burette.

3. Results and discussion

The mass yield of the products obtained for catalytic pyrolysis are described in Figure 1, for the three temperatures studied the reaction time was 90 min after reaching the final temperature.

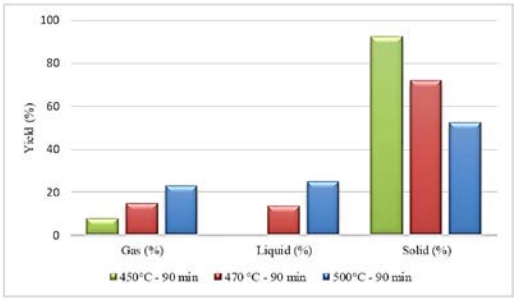

Figure 1: Variation of the yield of products for catalytic pyrolysis of ECW at different temperatures.

It is observed from the results of Figure 1 that the largest amount of products formed is in the solid phase (wax), results which are in accordance with Chaala [5]. For the lowest temperature (450 °C) it was not possible to collect any liquid phase products. It is important to note that the increase of 50 °C in the system did not cause any significant changes in the yield of the products in the liquid and gaseous phase.

The distributions of the products collected in the gas and liquid phase for the catalytic pyrolysis are shown below in Figures 2a and 2b respectively. The wax products obtained were also characterized by TG/DSC.

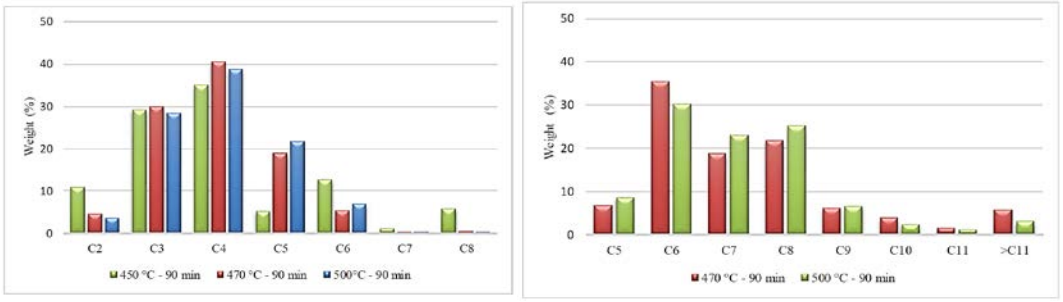

Figure 2: Product distribution (a) Gas phase and (b) Liquid phase.

4. Conclusions

The reactive distillation system was able to reach around 50 % conversion into liquids and gases. Increasing the temperature, the gas and liquid formation increased, and solid yield decreased. The gas phase has a composition in the range from C2 to C8. It is possible to observe that the increasing the temperature there was an increase of C4 and C5 formation and decrease C2 and C6 formation. Heavier fractions of the gas products (C6-C8) were converted into the light products with the increase in temperature of 50 °C in the set-point temperature, which evidences the increase in the C5 for this variation. In liquid phase, the increase of temperature, caused a decrease of the heavier compounds formation (> C11) and increase production of the components of C5, C7, and C8.

References

[1] Chen, R.; Lu, S.; Zhang, Y.; Lo, S. Energy Conversion and Management 2017, 153, 83–92.
[2] Mastral, J. F.; Berrueco, C.; Ceamanos, J. Journal of Analytical and Applied Pyrolysis 2007, 80, 427–438.
[3] Stelmachowski, M. Energy Conversion and Management 2010, 51, 2016–2024.
[4] Chen, D.; Yin, L.; Wang, H.; He, P. Waste Management 2014, 34, 2466–2486.
[5] Chaala, A.; Darmstadt, H.; Roy, C. Journal of Analytical and Applied Pyrolysis 1997, 39, 79-96.

ECCE12
The 12th EUROPEAN CONGRESS OF CHEMICAL ENGINEERING
Florence 15-19 September 2019

The Role of Eucalyptus Pre-treatment on Co-Pyrolysis with PE Wastes

Filomena Pinto*[1], Luís C. Duarte[1], Filipe Paradela[1], Joana Marques[1], Paula Marques[1], Paula Costa[1], Rui. André[1], Florbela Carvalheiro[1] Diogo Costa[1]

1 LNEG, Estrada do Paço do Lumiar, 22, 1649-038 Lisboa, PORTUGAL

**Corresponding author: filomena.pinto@lneg.pt*

Highlights

- Co-Pyrolysis of pre-treated eucalyptus blended with PE Wastes.
- Comparison of different eucalyptus pre-treatments on its pyrolysis.
- In general acid hydrolysis was the most effective pre-treatment.

1. Introduction

Eucalyptus globulus waste was selected for this study, because this species has been largely used in pulp and paper industry in Iberian Peninsula, which has generated high amounts of wastes. Pyrolysis has been widely applied to biomass for the production of bio-oils. Though, bio-oils yields up to 60-75% have been reported [1], the produced bio-oils have some adverse characteristics, like: high contents of solids, ash, oxygen-containing compounds and water and chemical instability, which prevents them from being directly used in fuel conventional engines. Though the quality of the bio-oils may be improved after upgrading catalytic processes, the overall costs are economically prohibitive. In contrast, polyethylene (PE) wastes pyrolysis produce liquids contents up to 85%, containing mainly hydrocarbons suitable to be used in conventional engines after minor upgrading [2]. Thus, co-pyrolysis of biomass and plastics may help to solve the problems associated to bio-oils disadvantages. As a different approach, eucalyptus waste was pre-treated before pyrolysis by auto-hydrolysis and acid hydrolysis to start molecular gradation and easing pyrolysis chemical bonds break-down. These pre-treatments removed hemicellulose and produced added-value products, like: oligosaccharides with applications in the food and pharma industries. Pre-treatments remaining solids were blended with different contents of PE wastes and co-pyrolysed to be converted into pyrolysis liquids to be used as biofuels or as raw materials.

2. Methods

Eucalyptus was pre-treated by different processes: acid hydrolysis and auto-hydrolysis. In acid hydrolysis, eucalyptus wastes were pre-treated at 130°C with an aqueous solution of 1.5 % H_2SO_4, using a liquid/solid ratio of 7 (w/w) at 130°C. While, in auto-hydrolysis only water was used, the same liquid/solid ratio was tested, but at temperatures of 190° and 210°C. The liquid fraction and the solid residue (cellulolignin), obtained after these pre-treatments, were separated at room temperature using a hydraulic filter press (up to 200 bar). The solid was washed with water, pressed again and dried at 45°C. Untreated eucalyptus and pre-treated by all these processes were blended with of PE wastes and co-pyrolysed. Eucalyptus content changed from 0 to 100 wt%. Co-pyrolysis experimental work was carried out in an autoclave at the following conditions: 400ºC, 30 minutes and nitrogen initial pressure of 0.6 MPa. Gases, liquids and solids were analysed according to previous work [3].

3. Results and discussion

There was a significant decrease in hemicellulose content after all treatments, thus yielding cellulose enrichment. As expected auto-hydrolysis pre-treatment at 210°C was more effective than that done at 190°C. Specifically, hemicellulose was completely removed for auto-hydrolysis at 210°C, thus lignin content increased around 30%, together with an increase in the cellulose content, in relation to pre-treated material. Regarding the acid hydrolysis, extractives and soluble ash were removed from the solid phase, together with hemicellulose (near to 85% removal). Thus, there was an increase in the lignin and glucan fractions, that accounted for more than 40 %, each, of the recovered solid material (dry basis). Acid hydrolysis and auto-hydrolysis at 210°C led to the recovery of hemicellulose as soluble saccharides (mainly monomeric pentoses) that can be upgraded by fermentation. While, auto-hydrolysis at 190°C led mainly to soluble oligosaccharides that are directly marketable added-value products. As such, a more integrated upgrade approach can be obtained to yield synergies between the thermochemical and biochemical routes. Though no great changes were observed in Figure 1, in general, acid hydrolysis was the most effective pre-treatment, as it led to the highest contents of liquids, to the highest conversions and to the lowest solids contents. Both auto-hydrolysis led to similar liquids yields, while the lowest liquids contents were obtained for untreated eucalyptus. However, with the rise of PE content, the effect of eucalyptus pre-treatment decreased, because PE is easier to pyrolyse than biomass.

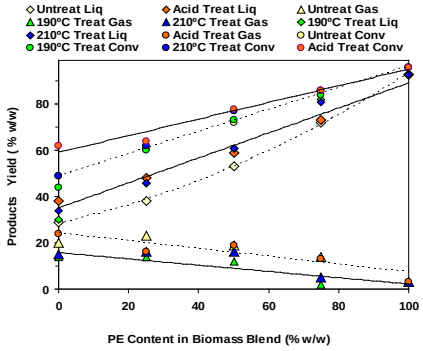

Figure 1. Effect of eucalyptus content and type of pre-treatment on products yields obtained by co-pyrolysis at 400ºC, and 30 min. Solid lines refer to pre-treated eucalyptus and dashed lines to untreated eucalyptus.

4. Conclusions

Eucalyptus pre-treatments weakened initial macromolecular structure and eased pyrolysis. Acid hydrolysis was the most effective pre-treatment, leading to the recovery of hemicellulose as soluble saccharides and to the highest pyrolysis liquids. As PE was easier to pyrolyse, the effect of pre-treatment on co-pyrolysis was more important with lower contents of PE wastes.

Acknowledgments

This article is a result of the project BIOFABXXI - POlisboa-01-0247-FEDER-017661, supported by Operational Programme for Competitiveness and Internationalization (COMPETE2020) and by Lisbon Portugal Regional Operational Programme (Lisboa 2020), under the Portugal 2020 Partnership Agreement, through the European Regional Development Fund (ERDF).

References

[1] A.V. Bridgwater, Biomass and Bioenergy 38 (2012) 68 – 94.
[2] F. Pinto, P. Costa, M. Miranda, Fuel 174 (2016) 153 – 163.
[3] F. Pinto, F. Paradela, F. Carvalheiro, L. C. Duarte, P. Costa, et al., Chem. Eng. Trans. 65 (2018) 211 – 216.

ECCE12
The 12th EUROPEAN CONGRESS OF CHEMICAL ENGINEERING
Florence 15-19 September 2019

Fast pyrolysis of Ecuadorian biomass for obtaining chemical precursors

Diana C. Vargas[12], Sebastian Salazar[1], Carolina Andino O.[1] Kevin M. Van Geem[2], Daniela Almeida Streitweiser[1]

[1] *Institute for Development of Alternative Energies and Materials – Department of Chemical Engineering, Universidad San Francisco de Quito USFQ, Av. Diego de Robles s/n, Campus Cumbayá. Quito, Ecuador, Quito, Ecuador*

[2] *Laboratory for Chemical Technology, Ghent University, Technologiepark-Zwijnaarde 121 - 9052 Ghent, Belgium*

**Corresponding author: dalmeida@usfq.edu.ec*

Highlights

- Different lignocellulosic biomass from agricultural processes are pyrolyzed to obtain bio oil.
- Fast Pyrolysis technology in a free fall tubular reactor.

1. Introduction

During the last years, biomass has drawn attention as a promising feedstock for its conversion into renewable fuels. The thermochemical process of pyrolysis under which biomass is converted into gas, bio-oil and char has drawn also attention for the different compounds found in bio-oil. Ecuador due to its biodiversity and different climate has different crops with a wide range of compositions, which have shown a great potential for pyrolysis feedstock. Bio-oils obtained from biomass appear to be an attractive option to obtain chemical precursors that have been synthetized from fossil fuels. In this study, we explore the advantages not only about the recovery of chemical precursors from the biomass pyrolysis products, but also the environmental impact of biomass residual waste used as feedstock.

2. Methods

A free fall fast pyrolysis equipment has been designed and constructed to study fast pyrolysis. The equipment consist on a quartz reactor with an oven, which can rapidly heat the sample (40 – 1200C). The outlet streams passes through a cyclone to remove the solid char. The gaseous stream passes through two traps the first trap at -20°C collects the volatiles liquid and the second trap at -10 collects the C2 fractions. The rest of the gasses are directly injected into the GC coupled with two detectors (FID and TCD) for its characterization and quantification. The piping used in the equipment is stainless steel 1/4" for the feed system and the purge separation line. For the online analysis stream after the purge, a 1/8" stainless steel pipeline is used which reaches direct to the GC (Thermo Fisher Scientific, TRACE 1310).

The feedstock used are four different types of Ecuadorian residual biomasses, which were characterized to find the cellulose, lignin, protein, fat and ash content. These biomasses were palm fiber, coffee husks, rice husks and palm rachis. Cellulose content was determined using the protocol

described by Dominguez [1]. Lignin content was determined using the official method AOAC 973.18 [2]. The Kjeldahl method was used to quantify the amount of protein in the samples using a digester DK6 VLEP Scientifica and a semiautomatic distillation unit UDK 139 based on the official method AOAC 960.52 [2]. A modified version of the official method AOAC 2003.05 and 2003.06 [2], which uses a solvent extractor equipment VELP Scientifica SER 148, was followed to determine the fat content in the samples. Finally, ash content was determined using the official method AOAC 942.05 [2]. A Leica DM500 microscope was used to analyze the size and geometry of the fiber of samples. Pictures were taken using the Leica ICC50 HD camera and the fibers were measured with the software Leica Application Suite EZ.

The setup has a solids feeding system that consists of a glass tube with three Teflon ball valves. Valve 1 is used to purge the feed system, valve 2 is used to insert the carrier gas and purge the system, and valve 3 is used to insert the solid sample, with the carrier gas, inside the reactor. For this investigation, the biomass samples were pyrolyzed in a ceramic tubular vertical free-fall reactor using helium as carrier gas. The reaction temperatures used were 500, 550 and 600.

3. Results and discussion

Biomass characterization

The characterization of four types of Ecuadorian residual biomasses were performed to find the cellulose, lignin, protein, fat and ash content. The characterization shows that the samples have a significant amount of cellulose in a range between 15-33 wt% of dry biomass. The biomasses were observed in the microscope to have a reference of their shape and size. Palm rachis morphology showed a cylindrical uniform shape, rice husk a powder heterogeneous distribution and coffee husks and pal fiver showed spherical uniform distributions.

Composition of liquid products of pyrolysis

The liquid products are retained in the liquid trap at −10°C, collected and analyzed using GC-MS/FID/TCD. Preliminary characterization of the products show the presence of C2 gases, acetic acid, hydroxytaldehyde, levoglucosan, levogluconsanone, phenol and various poly phenols. Depending on the pyrolysis temperature the amount of the products varies.

Analysis of the solid products of pyrolysis

The solid products were characterized using a Leica DM500 optical microscope. The observations done after selecting random fibers for each biomass shown a shrinkage of 30% in length and of 1% to 17% in diameter for all temperatures.

4. Conclusions

The wide range of the composition of liquid bio-oils products obtained from Ecuadorian fast pyrolysis show a great potential to obtain chemical precursors for further upgrading processes.

References

[1] M. M. Domínguez Domínguez, A. Alvarez-Castillo, T. Castrejón-Rosales, M. J. Granados Baeza, F. J. Hernández Campos, V. H. Alcalá Octaviano, and J. C. Tapia Picazo, “Estudio de la cinética de la hidrólisis ácida de bagazo de caña de azúcar sin pretratamiento para la obtención de azúcares reductores,” *Rev. Iberoam. Polímeros*, vol. 12, no. 3, pp. 153–159, 2011.

[2] AOAC, *Official Methods of Analysis of AOAC International*. Gaithersburg: AOAC International, 2012.

Biomass hydrothermal liquefaction: use of metal catalysts, Zn and Ni, to enhance bio-oil yield and quality.

Benedetta de Caprariis[1], Paolo De Filippis, Lingyu Tai, Paola Bracciale

1 Department of Chemical Engineering, Sapienza University of Rome

**benedetta.decaprariis@uniroma1.it*

Highlights

- The use of Zn and Ni in HTL of oak wood improves oil yields of about 20 %.
- Zn is completely oxidized during the reaction and the obtained bio-oil is richer in H.
- Ni is not oxidized and the resulting oil has higher amount of C (15 % more)

1. Introduction

Hydrothermal liquefaction (HTL) is one of the most promising technologies for the production of bio-oils from biomass. HTL process works at medium temperature (250-400 °C) and high pressure (10-25 MPa) in presence of water which at the used operative conditions acts as a reagent in the biomass decomposition reactions. With respect to the traditional thermochemical processes such as pyrolysis HTL does not need expensive biomass drying pre-treatments and furthermore, the obtained bio-oil has lower oxygen content and thus higher calorific value [1]. HTL has been extensively studied in literature in batch mode and in the last years the first continuous plants have been developed [2,3]. The use of catalysts in order to increase the yields and quality of the bio-oil is of fundamental importance. Alkaline catalysts such as Na2CO3, NaOH, K2CO3, KOH and Ca(OH)2 have been widely employed to enhance bio-oil yields but they do not have any effect on its composition [4]. The use of metal catalyst, in particular Fe, have demonstrated to lead to bio-oil quality improvement by the production of hydrogen in the reaction mass which is used for in situ hydrogenation reactions of bio-oil fragments [5,6].

In this work for the first time the use of Ni and Zn as catalysts for HTL of oak wood was investigated in a range of temperature of 260-340 °C. The effect of the addition of catalysts on the bio-oil yield and quality was attributed to the oxidation of the metal in the reaction condition and thus in the formation of hydrogen.

2. Methods

The tests were conducted in small autoclave having a volume of 10 mL; the reactors were heated in a sand bath with a heating rate of 60 °C/min. The biomass was loaded into the reactor with water in a ratio of 1:5. The amount of catalyst was fixed to 10 % with respect to the biomass weight. The reaction time was set to 15 min. At the end of the reaction time the reactors were quenched, the four products, gas, water insoluble organic phase (bio-oil), water phase containing the soluble organics and solid residue (catalyst+char), were separated as described in [ref]. The bio-oils were characterized with GC-MS and elemental analyses. The state of the metal after the reaction was

evaluated by X-ray diffraction. The organic content of the water phase was measured with TOC analysis.

3. Results and discussion

The results reported in Fig 1a show that the use of catalysts lead to higher bio-oil yields. The highest production of oil is reached with Ni at 330 °C (36 % with respect to the biomass weight). The use of Zn leads to lower increase of the oily phase but promotes the formation of organic compounds soluble in water, in fact the TOC of the water phase obtained using Zn at 330 °C is 21100 ppm compared with 17000 ppm and 15000 ppm obtained using Ni and without catalyst, respectively. The elemental analyses of the oils reported in Fig 1b point out a slight enhancement of the bio-oil quality in terms of decrease of oxygen content. It has to be noted that in the case of the use of Ni this decrease is due to a higher carbon amount in the oil while for the oil produced using Zn the oxygen decrease is related to an increase of the hydrogen amount. This result is consistent with the XRD analyses which report that Zn is completely oxidized to ZnO, demonstrating the H2 production, while Ni is still in its metallic form.

a) b)

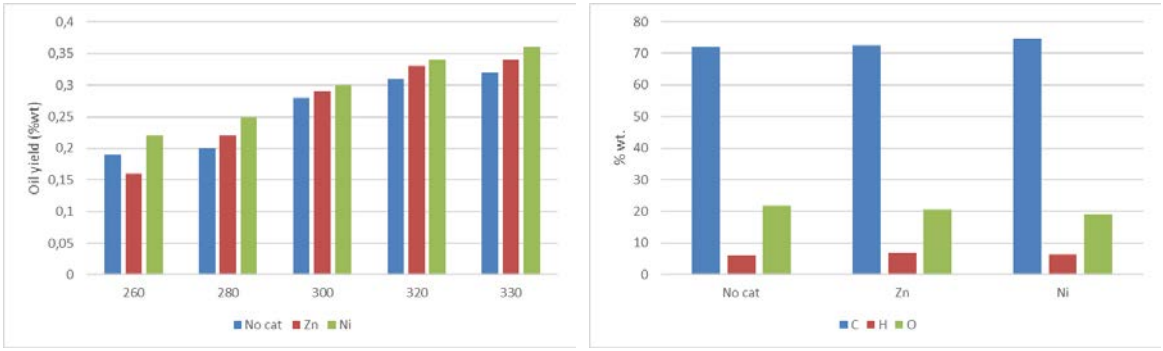

Figure 1. a) Oil yields as a function of catalysts and temperature b) Elemental oil composition.

4. Conclusions

Metal catalysts promotes the formation of the oily phase in the HTL of oak wood; with Ni the enhancement is about 25 % while with Zn 15 %. The quality of the oil is improved, the oxygen amount decrease leading to an increased calorific value which is 28.1 MJ/kg and 30.4 MJ/kg for the oils obtained without catalyst and Ni, respectively.

References

[1] L. Yang, L. Nazari, Z. Yuan, K. Corscadden, C.C. Xu, Q.S. He, Biomass Bioenerg 86 (2016) 191-198.
[2] I.M. Sintamarean, I.F. Grigoras, C.U. Jensen, S.S. Toor, T.H. Pedersen, L.A. Rosendahl, Biomass Convers. Biorefinery 7 (2017) 425–435.
[3] D.C. Elliott, T.R. Hart, G.G. Neuenschwander, L.J. Rotness, G. Roesijadi, A.H. Zacher, J.K. Magnuson, ACS Sustain. Chem. Eng. 2 (2014) 207–215.
[4] A. Dimitriadis, S. Bezergianni, Renew. Sustain. Energy Rev. 68 (2017) 113–125.
[5] Y. Miyata, K. Sagata, M. Hirose, Y. Yamazaki, A. Nishimura, N. Okuda, Y. Arita, Y. Hirano, Y. Kita, ACS Sustain. Chem. Eng. 5 (2017) 3562–3569
[6] B. de Caprariis, I. Bavasso, M.P. Bracciale, M. Damizia, P. De Filippis, M. Scarsella, J Anal Appl Pyrolysis 139 (2019) 123-130.

ECCE12
The 12th EUROPEAN CONGRESS OF CHEMICAL ENGINEERING
Florence 15-19 September 2019

Steam and Hydro-Thermal Gasification of Canola Hull and Canola Meal Fuel Pellets.

Ramin Azargohar[1], Sonil Nanda[2], Ajay Dalai[1,*], Janusz Kozinski[3]

1 University of Saskatchewan, Saskatoon, SK, Canada; 2 Western University, London, ON, Canada; 3 New Model in Technology & Engineering, Hereford, United Kingdom

**Corresponding author: ajay.dalai@usask.ca*

Highlights

- Canola hull and meal were pelletized using bio-additives with optimized concentrations.
- Steam gasification showed suitable range (1.2-1.6) of H_2/CO ratio for untreated syngas.
- Hydro-thermal gasification of pellets is suitable technique for hydrogen production.
- Steam-gasified biochars showed compact aromatic structure and high surface area.

1. Introduction

Conversion of agricultural wastes to value-added products such as fuel pellets has economic and environmental advantages. Use of abundant agricultural residues such as canola hull and canola meal can benefit both agriculture and industry sections. In this research work, bio-additives including lignin, glycerol, and L-proline were used for production of hydrophobic fuel pellets with high mechanical strength. The concentration of bio-additives in the pellet formulation was optimized based on the relaxed density and mechanical strength of pellets. Then, gasification was used for production of synthesis gas (syngas) and hydrogen from these fuel pellets. For steam gasification, effects of gasification temperature and equivalence ratio (ER) were investigated on the gasification products. For hydro-thermal gasification, the effects of gasification temperature, feed concentration (biomass/water mass ratio), and residence time were studied.

2. Methods

Canola hull and canola meal were provided by the Milligan Biofuels Inc. (SK, Canada). For pelletization, biomass particle size in the range of 100-1,750 µm was preferred. Alkali lignin (as binder), pure and crude glycerol (as lubricant), and L-proline (as plasticizer) were used as bio-additives. Samples were densified in a lab scale single-pelleting unit. Two-stage fixed-bed gasifier and batch reactor were used for steam and hydro-thermal gasification, respectively. A wide range of characterization techniques were used to probe properties of feedstocks, pellets, gas product, and biochars. Central composite design (CCD) was used to design the experiments.

3. Results and discussion

Optimization study for canola hull showed that durability (measured by drop test) and relaxed density of pellets, respectively, were in the ranges of 51-99% and 647-1,110 kg/m^3. This study showed that pellet made of 6, 4, 6, 17 wt/wt % of lignin, glycerol, L-proline, and water, respectively, had the largest relaxed density (1,110 kg/m^3) and durability (99%). An increase in water content up to 17 wt% resulted in better performance for alkali lignin as a binder in

densification process. The pellets' relaxed density and mechanical durability increased with an increase in the moisture content, for the entire range of lignin concentration. Glycerol showed lubricating effects in the form of 10-20 % decrease in pelletization's compression energy. L-proline worked as a plasticizer to increase the mechanical strength of pellet. For canola meal, the optimum formulation identified included 8 wt% alkali lignin, 8 wt% glycerol, 2 wt% L-proline, and 4 wt% water. It had relaxed density of 1,050 kg/m^3 and durability of 99%. As shown in Fig. 1, synchrotron 3-D imaging technique was used to visualize the internal void structure (blue color area) of pellets which is an influential parameter on the relaxed density and mechanical strength of pellets. Fig. 1 shows effects of alkali lignin, glycerol, and water on the internal porosity of canola meal pellets.

For steam gasification with an increase in temperature, concentration of hydrogen (H_2) and carbon monoxide (CO), in the gas product, increased for all ERs. Effect of ER on the gas component concentrations was more intense at the highest temperature (850 ^{o}C), especially in case of increase in hydrogen concentration. In hydro-thermal gasification, with the rise in temperature from 350 to 650°C, H_2 and CO_2 yields increased , due to the enhancement of water-gas shift reaction at higher temperatures in hydro-thermal conditions. The same effect was observed with an increase in residence time (from 15 min to 60 min). However, these yields decreased with an increase in feed concentration. Hydro-thermally produced biochars showed characteristics of amorphous char at high gasification temperatures (≥550 °C). For steam-gasified biochars, higher BET surface area indicated the development of composite char at all gasification temperatures.

4. Conclusions

Use of bio-additives resulted in the production of mechanically durable and hydrophobic fuel pellets. Due to the increasing amount of lignin, glycerol and amino acids obtained, respectively from the pulp and paper industries, biodiesel refineries, and corn wet milling industries, they are promising bio-additives for production of fuel pellets. Steam gasification produced syngas with the suitable range of H_2/CO molar ratio. In addition, it produced biochars with developed porous characteristics which can be used as adsorbent or catalyst. Hydro-thermal gasification produced larger H_2/CO ratio and is more useful for hydrogen production.

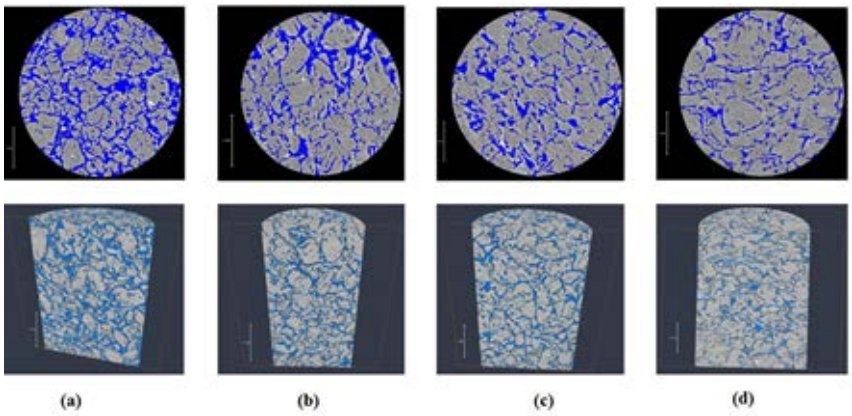

Figure 1. Effects of lignin, glycerol, and water on pellet porosity in the cross section and longitudinal section for the canola meal pellets produced using the optimum formulation as follows: (a) without water, (b) without lignin, (c) without glycerol, and (d) including all ingredients.

ECCE12
The 12th EUROPEAN CONGRESS OF CHEMICAL ENGINEERING
Florence 15-19 September 2019

On the modeling of the kinetics of high-functionality biopolymers. Application to the polycondensation of sugars

Dimitrios Meimaroglou[1], Sandrine Hoppe[1], Baptiste Boit[2]

1 Laboratoire Réactions et Génie des Procédés,Université de Lorraine,CNRS,

LRGP, F-54000 Nancy, France; 2 Roquette Frères, Lestrem, FR

**Corresponding author: dimitrios.meimaroglou@univ-lorraine.fr*

Highlights

- Industrial polycondensation process of sugar syrups of various compositions.
- Kinetic/topological Monte Carlo modeling framework.
- Dynamic evolution of the exact position and type of each bond of all species.
- Generalized framework, not limited to low-degree oligosaccharides.

1. Introduction

Polycondensation reactions of oligosaccharides are important in several application fields, such as fuel synthesis or food processing. They are generally carried out in the presence of acid catalysts, in temperatures varying roughly within the range of 100 ^{o}C – 200 ^{o}C. Nevertheless, despite their industrial importance, only few kinetic modeling studies are found in the literature [1]. In fact, the primary monomer unit of these reactions is glucose, dominantly found in the form of glucopyranose, which is a cyclic molecule containing five –OH groups, all susceptible to react. Hence, the –OH group in the position 1 of the molecule (i.e., with respect to the anomeric carbon atom) is prone to receive a proton from the –OH group of another glucose molecule, thus eventually forming a glucosidic bond with the parallel release of a water molecule. Such bonds can be formed between the C1 atom of the first glucose and any other C atom of the second glucose, found in positions 1, 2, 3, 4 or 6. In addition, the stereochemistry of the formed bond can be either in α- or β- position, resulting in two kinds of stereoisomer products from each type of bond. This means that nothing but the simple reaction between two single glucopyranose units may result in as much as 11 different disaccharides. At the same time, a series of internal ring-closure reactions of the glucose units that result in structurally different, inert anhydrosugars, further complicate the landscape of this reaction system, before even attempting to extend the study to the reactions of disaccharides, trisaccharides, etc. In the present work, a novel modeling framework is proposed for the simulation of the polycondensation reactive systems of sugars, capable of taking into account the above-described complexity.

2. Methods

The complexity of the system relies primarily on the fact that the each type of glucosidic bond that is formed during the reaction (i.e., α-1-1, β-1-1, α-1-2, etc.), is dictated by a different formation and hydrolysis rate (i.e., mainly due to steric factors). In this respect, in order to be able

to accurately follow the dynamic kinetic developments in the reactor, with respect to the operating conditions and the initial syrup composition, it is crucial to follow all the relevant information concerning the different species concentrations as well as their specific structural characteristics. The first of the above is relatively trivial to achieve via the implementation of any modeling framework that defines the problem through a population-balance perspective. On the contrary, the tracking of the structural information requires an approach capable of treating, in addition to the species concentrations, the associated multi-dimensionality (i.e., expressed in terms of the different bonding positions and stereochemistry of the glucose units). Such a modeling approach has been previously developed and applied on the industrial polymerization paradigm of low-density polyethylene (LDPE) [2]. The developed kinetic/topology Monte Carlo (MC) algorithm, which was implemented in this case to follow the branching architectural developments of LDPE, is adapted in this work to the specificities of the sugars polymerization system.

3. Results and discussion

The modeling predictions were compared against a series of experimental data produced in an industrial pilot-scale reactor, under varying conditions. Some preliminary results on the evolution of the average molecular weight and the molecular weight distribution are given in Figure 1.

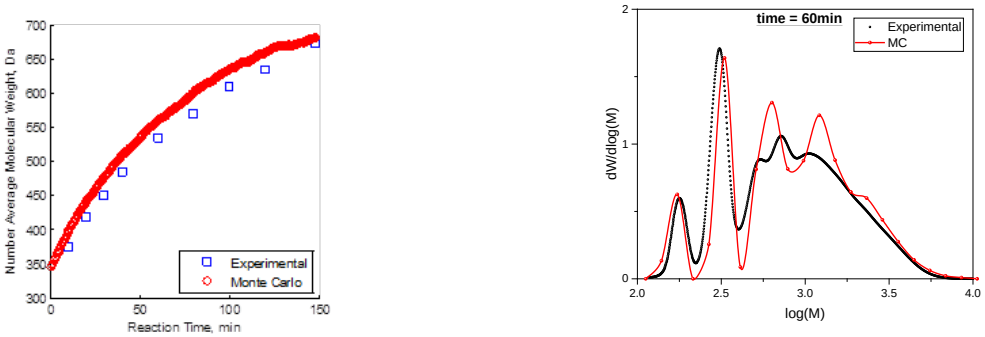

Figure 1. Evolution of the a) number-average molecular weight and a) molecular weight distributions of the formed oligosaccharides. Comparison between experimental data and MC simulations.

4. Conclusions

In the present work, a novel modeling framework is proposed for the kinetic developments of the polycondensation of sugars. This modeling framework relies on the implementation of a powerful kinetic/topological Monte Carlo technique, previously applied for the description of the molecular architecture of industrially-produced highly-branched LDPE. The preliminary results of the study show that, for the first time, an accurate description of the system can be achieved and the compositional and molecular weight evolution can be accurately tracked even for oligosaccharides of relatively high degree of polymerization.

References [Calibri 10]

[1] H.M. Pilath, M.R. Nimlos, A. Mittal, M.E. Himmel, D.K. Johnson, Glucose Reversion Reaction Kinetics, J. Agric. Food Chem. 58 (2010) 6131–6140. doi:10.1021/jf903598w.

[2] D. Meimaroglou, C. Kiparissides, A Novel Stochastic Approach for the Prediction of the Exact Topological Characteristics and Rheological Properties of Highly-Branched Polymer Chains, Macromolecules. 43 (2010) 5820–5832. doi:10.1021/ma1005233.

ECCE12
The 12th EUROPEAN CONGRESS OF CHEMICAL ENGINEERING
Florence 15-19 September 2019

Kinetics of acid-catalyzed hydrolysis of oat β-glucan to produce short chain polysaccharides with controlled degree of polymerization

Tuomo Sainio[1*], Hoang Nguyen[1], Markku Laatikainen[1], Jari Heinonen[1]

1 LUT University, Department of Separation and Purification Technology, Yliopistonkatu 34, FI–53850 Lappeenranta, Finland

**Corresponding author: Tuomo.sainio@lut.fi*

Highlights

- Mechanistic model developed for acid hydrolysis of beta-glucan from oat
- The non-random structure of the polysaccharide is included in the model
- Evolution of the molecular weight distribution during hydrolysis is explained

1. Introduction

Natural beta-glucan is a linear, nondigestible polysaccharide composed of D-glucose monomers linked by β-glycosidic bonds. Beta-glucan from cereals (oat and barley) consists of mixed-linkage β-(1,3) and β-(1,4)-D-glucose monomers, whereas β-glucan from yeasts or mushrooms is composed of mixed-linkage β-(1,3) and β-(1,6)-D-glucose units [1, 2]. Enzymatic or acid hydrolysis of β -glucan produces oligosaccharides and short chain polysaccharides that can be used as prebiotic food ingredients.

It is desirable to produce short chain polysaccharides (e.g. DP = 30…50) rather than oligosaccharides from large plant polysaccharides. To achieve this, the reaction conditions and operation of the reactor should be optimized such that degradation to oligosaccharides is minimized. In this work, an accurate kinetic model for acid hydrolysis is developed and validated using experimental data.

2. Methods

Homogeneous acid-catalyzed hydrolysis of oat β-glucan was studied at 323 K and 353 K using HCl and H_2SO_4. The kinetic experiments were carried out in a jacketed glass reactor (Orb system, Syrris Ltd., United Kingdom). The molecular weight distribution (MWD) of β-glucan was measured using SEC–MALLS on HPLC system (Agilent 1200 Infinity series) with an RI detector and a multi-angle laser light scattering detector. To deal with low intensity of small molecules in the samples, a two-step method was used. In this method, the samples withdrawn from the reactor were first fractionated in preparative scale SEC column and the MWD of each fraction was determined using the HPLC SEC-MALLS.

β-(1,4) and β-(1,3) glycosidic bonds are known to have different reactivity in acid hydrolysis [3]. A structured kinetic model was developed that takes into account the difference in the reactivity of

β-(1,4) and β-(1,3) glycosidic bonds as well as their positions in the polysaccharide chain. Numerical solution of the large ODE system was accelerated by using an adaptive Jacobian matrix approach.

3. Results and discussion

The number average molecular weight of oat beta-glucan changes during acid hydrolysis in a manner consistent with assumption of first order kinetics. However, a random scission model does not explain the formation rates of oligosaccharides. The structured model presented here can explain the observations within good accuracy.

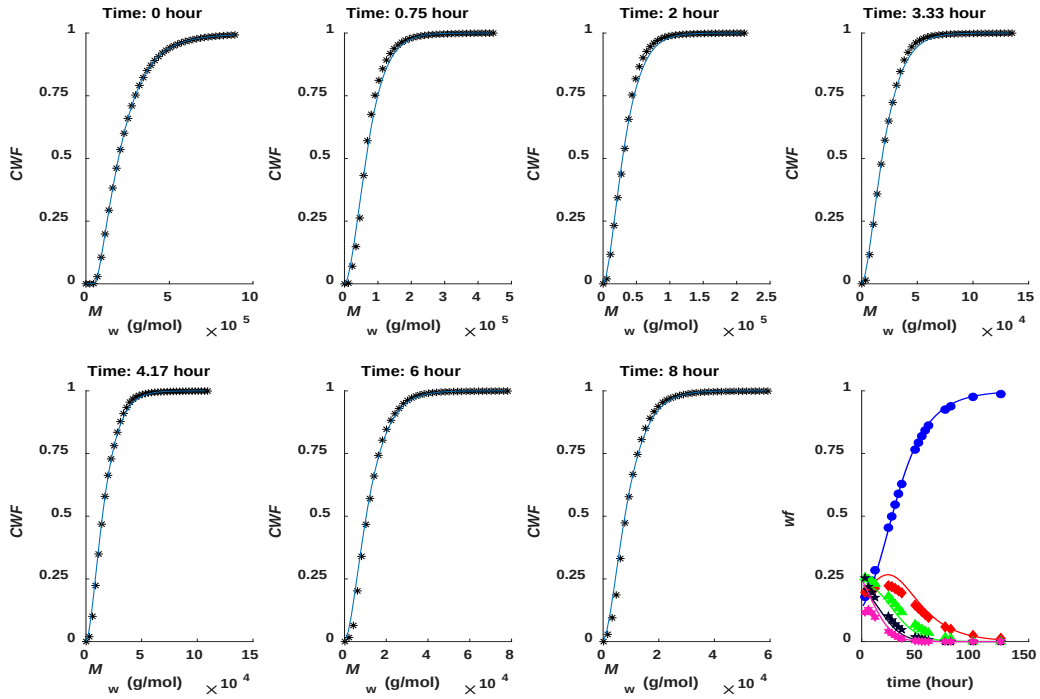

Figure 1. Evolution of the molecular weight distribution of β-glucan with HCl 0.05 M with HCl 0.25 M at 353 K. Oligosaccharides are shown in bottom left: blue = DP 1, red = DP 2, green = DP 3, black = DP 4, magenta = DP 5.

4. Conclusions

The simulation of β-glucan hydrolysis with the new model was in good agreement with the experimental data and shows improvement over existing non-structured models for hydrolysis of plant polysaccharides.

References [Calibri 10]

[1] Ahmad A, Anjum FM, Zahoor T, Nawaz H, Dilshad SMR. Beta Glucan: A Valuable Functional Ingredient in Foods. Crit Rev Food Sci Nutr. 2012;52:201-212.

[2] Daou C, Zhang H. Oat Beta-Glucan: Its Role in Health Promotion and Prevention of Diseases. Compr Rev Food Sci Food Saf. 2012;11:355-365.

[3] Nguyen, H.S.H., Heinonen, J., Sainio, T., Acid hydrolysis of glycosidic bonds in oat β-glucan and development of a structured kinetic model, AIChE J., 64(2018), 2570-2580

ECAB 5
The 5th EUROPEAN CONGRESS OF APPLIED BIOTECHNOLOGY
Florence 15-19 September 2019

Acceleration of a kinetic Monte Carlo Master Equation Solver for Gas Phase Chemical Kinetics

Andrea Landella[1*], Carlo Cavallotti[2]

1 Via Cividale 23, 20017 Rho, Milano; 2 Politecnico di Milano, Via Luigi Mancinelli 7, 20131, Milano

**Corresponding author: andreagiuseppe.landella@mail.polimi.it*

Highlights

- The MCRRKM stochastic master equation solver is adaptively accelerated.
- Speedup factors reach 1E+25 for low temperature simulations (300 K).
- Rate constant computation is now feasible in the full temperature range.
- Calculated k(T,P) with acceleration are accurate within a factor of 1.2.

1. Introduction

The calculation of pressure and temperature dependent rate constants of gas phase reactions requires the solution of a Master Equation, which describes the energy transfer dynamics between molecules as a continuous time Markov Process[1]. The stochastic approach, or kinetic Monte Carlo (kMC) integration[2], allows to directly extract rate coefficients, but suffers from intrinsic time scale separation between reaction events and internal energy relaxation by strong collisions. The Markov process converges on rare event dynamics[3] and molecules reach thermodynamic equilibrium. In these cases, especially at low temperatures, the stochastic simulation explores energies well below the reaction thresholds, requiring approximately 10^{20} iterations before reaching a reactive event. It is therefore necessary to search and implement solutions that will allow a speedup, or acceleration, of the stochastic simulation algorithm while maintaining high accuracy for the extracted rate coefficients. As such, a validation must be performed with existing solvers, possibly with method-independent (deterministic) ones, to eliminate sources of statistical error.
This problem also arises for deterministic solvers, e.g. MESS[4], that numerically solves the Master Equation as a linear matrix ODE problem, exploiting the physics of the reactive system. Different approaches have been proposed to speed up master equation solvers; the most commonly used one is the Reservoir State Approximation[5], as it defines a fictitious set of energy states, called reservoir, which is treated as a single macrostate. The reactant energy distribution within that state is assumed at thermal equilibrium, thus described with the Boltzmann distribution.
The reservoir dimensions, or the number of lumped energy states under a threshold, are usually taken as an input data and are inherently system dependent. They are directly linked to the reaction barrier energies, thus the chemical mechanism or energy profile. It should be preferable to skip the setting of the reservoir threshold by an adaptive calculation, employed within the code.

2. Methods

The present work examines an existing RRKM Master Equation solver, called MCRRKM[6], which adopts the stochastic solution method. MCRRKM is a research code, developed by prof. Cavallotti at the Applied Physical Chemistry Lab. An acceleration protocol was developed that allows speeding up the kMC integration by introducing an analytical correction for the time the random walkers spend in the Boltzmann equilibrated portion of the energy distribution function.

3. Results and discussion

The acceleration protocol was implemented within MCRRKM with an adaptive calculated threshold, the Thermal Energy Limit, below which energy levels are treated as populated according to the Boltzmann distribution and binned as a single macrostate. The Speedup was found to be dependent only on thermodynamic quantities: the partition function ratio of the unperturbed and perturbed energy states. Below are two main results of the acceleration protocol on two test reactions:

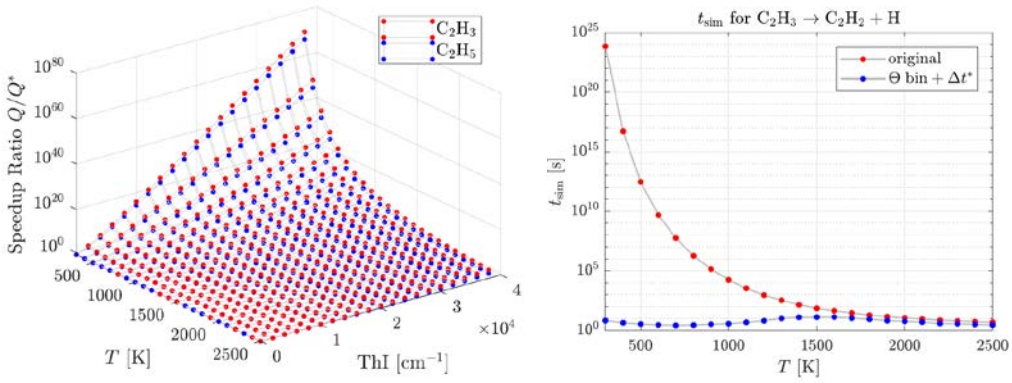

Figure 1. (left) Speedup factor as a function of simulation temperature and thermal energy limit (in 1/cm) for two reactions [C2H3 = $C_2H_3 \rightarrow C_2H_2 + H$, and C2H5 = $C_2H_5 \rightarrow C_2H_4 + H$]. The speedup is super-exponential with temperature, thus at low temperatures the rare-event dynamics problem is solved. The acceleration protocol is effective at low T. (right) estimated simulation time [red] and actual simulation time [blue] for the reaction $C_2H_3 \rightarrow C_2H_2 + H$ at 0.1 bar.

4. Conclusions

This work led to the development of a new acceleration protocol for the Monte Carlo integration of the master equation for reactive systems that drastically reduces computational times, from approximately 10^{20} to 10^{2} iterations to reach a reactive event, making the stochastic solution of the Master Equation feasible at all temperatures. The protocol was validated with respect to MESS, a solver developed by Georgievskii and Klippenstein[4], employing the deterministic approach over two reactions of combustion interest: hydrogen dissociation from vinyl (C_2H_3) and ethyl (C_2H_5) radicals. With temperature and pressure ranges of 300-2500 K and 0.001-1000 bar, rate constants differ by a maximum 1.2 factor (0-20% relative error) from MESS results in all cases.

References

[1] Montroll, E. W., & Shuler, K. E. (1957). The application of the theory of stochastic processes to chemical kinetics. *Advances in Chemical Physics*, 361-399

[2] Rao, C. V., & Arkin, A. P. (2003). Stochastic chemical kinetics and the quasi-steady-state assumption: Application to the Gillespie algorithm. *J. Chem. Phys*, *118*(11), 4999

[3] Rubino, G., *et al.* (2009). Rare event simulation using Monte Carlo methods (Vol. 73). New York: Wiley.

[4] Georgievskii, Y. and S. J. Klippenstein (2015). *Master Equation System Solver (MESS)*. url: http://tcg.cse.anl.gov/papr/codes/mess.html

[5] Glowacki, D. R., *et al.* (2012). "MESMER: An Open-Source Master Equation Solver for Multi-Energy Well Reactions". *The Journal of Physical Chemistry A* 116.38, pp. 9545–9560.

[6] Barbato, A., C. Seghi, and C. Cavallotti (2009). "An ab initio Rice-Ramsperger-Kassel-Marcus master equation investigation of SiH4 decomposition kinetics using a kinetic Monte Carlo approach". *The Journal of chemical physics* 130.7, p. 074108

ECCE12
The 12th EUROPEAN CONGRESS OF CHEMICAL ENGINEERING
Florence 15-19 September 2019

Implementation of catalytic descriptors within kinetic models. How to predict the nC7 aromatisation selectivity obtained with a new catalyst?

Olivier Said-Aizpuru[1], Florent Allain[1], Aurélie Dandeu[1], Fabrice Diehl[1], David Farrusseng[2] and Jean-François Joly[1]

1 IFP Energies Nouvelles, Rond-point de l'échangeur de Solaize, BP3, 69360 Solaize Cedex, France

2 IRCELYON, CNRS, 2 Avenue Albert Einstein, 69100 Villeurbanne, France

**Corresponding author: olivier.said-aizpuru@ifpen.fr*

Highlights

- Integration of catalyst active phase descriptors into kinetic models
- High Throughput catalytic testing for intrinsic kinetics studies
- Bi-functional n-heptane aromatisation catalysis

1. General context and motivations

Several refining or petrochemical catalytic processes show a strong dependence of overall performances upon catalytic active phase composition and structure. Their development requires the identification of the relevant dimensioning parameters of the catalyst that are referred to as "descriptors". Kinetic models provide an indispensable tool for an accurate design of catalytic processes. Extensive descriptions of the active phase behaviour within kinetic models were investigated over the past decades, usually through sophisticated models based on theoretical calculations or more often on advanced characterisations. Yet, the simplicity and a limited amount of parameters of a kinetic model are necessary in order to handle frequent changes in catalytic formulation. There is therefore a deep interest in identifying global catalytic activity descriptors that could be easily measured and controlled by a dedicated catalyst synthesis. We and others have shown that fitting the kinetic parameters of a well-known (*i.e.* model) reaction is an efficient approach to probe and quantify the overall activity of a catalyst. This work addresses the possibility to perform catalytic tests on a model reaction in order to identify relevant and independent descriptors.

2. Objectives and strategy

The frame of this study is to set up a methodology in order to implement active phase descriptors within a lumped kinetic model for the n-heptane reforming reaction (see Figure 1). Aromatisation of n-heptane requires a bi-functional catalysis enabling proton and hydrogen transfer. Thus, a typical naphtha reforming catalyst comprises a metallic phase (sub-nanometric Pt or Pt alloys particles) supported on a mild-acidic support (chlorinated γ-Al_2O_3). A collection of twenty-one active phase formulations specifically prepared in order to exhibit various inter-sites (acid-acid or metal-acid) distances as well as different site ratios is first gathered. Both Pt only and Pt-Sn catalysts are tested and different ranges of Pt (0.3-1%$_{wt}$) and Cl (0.1-1.4%$_{wt}$) are considered. Three objectives are then successively targeted: i) Probing the intrinsic surface reactivity over a variety

of reforming catalysts ii) Determining the effect of a systematic formulation change over the kinetic parameters for different reforming reaction families iii) Finding statistical correlations between kinetic parameters and physico-chemical properties.

A standard catalytic test protocol was designed to investigate intrinsic n-heptane transformation at the surface of the catalyst. Tests were carried out on a high-throughput Flowrence™ (Avantium) device allowing the use of small sample amounts (see Figure 2). The geometry of the reactors allows for a well-defined hydrodynamics and the unit is used close to isothermal mode.

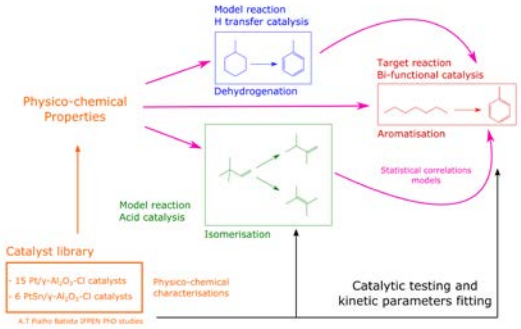

Figure 1. General experimental strategy followed for the identification of catalytic activity and selectivity descriptors.

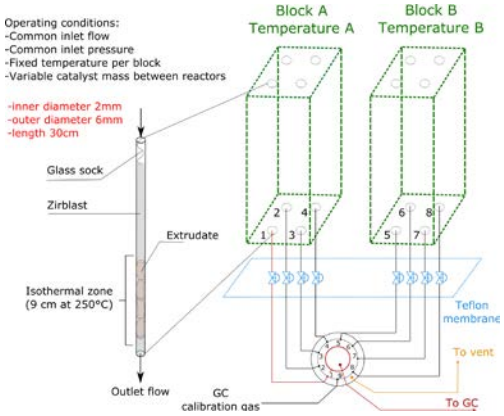

Figure 2. Simplified scheme of the reactive section of the High Throughput Experimental device used for catalytic tests.

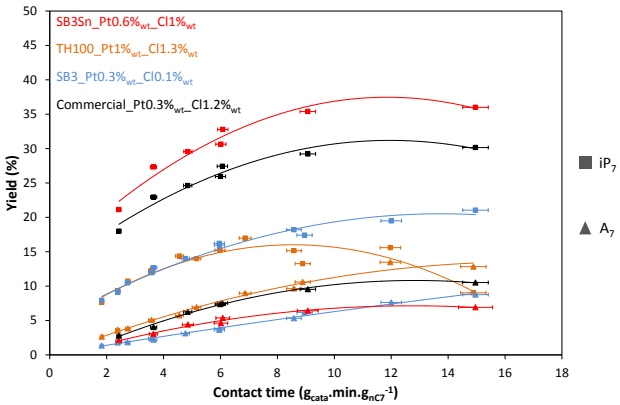

Figure 3. Yield structures obtained at 430°C, 10 barg and H2/HC molar ratio equal to 3. A_7 stands for toluene and iC_7 for paraffinic isomers. SB3 and TH100 are commercial γ-Al_2O_3.

3. First results and outlooks

As shown on Figure 3, there is a strong dependence of the reaction scheme selectivity over the amount of chlorine, the amount of platinum and the presence of a second metal (Sn). Competition between sites could be responsible for aromatisation interception by other reactions such as isomerisation or cracking. Then, the challenge in identifying reforming selectivity descriptors lies in understanding which catalytic parameters rule the interactions between sites.

Once the explicit description of the active phase is included in the kinetic model, it will be validated by comparison with results from catalysts with new active phase formulations, demonstrating the possibility of pre-screening catalysts with the model before moving on to traditional experimental screening.

ECCE12
The 12th EUROPEAN CONGRESS OF CHEMICAL ENGINEERING
Florence 15-19 September 2019

Reaction and kinetic studies of homogeneously catalyzed benzyl alcohol oxidation in a gas-liquid slug flow microreactor

Jun Yue*, Arne Hommes, Bas Disselhorst

Department of Chemical Engineering, Engineering and Technology Institute Groningen, University of Groningen, Nijenborgh 4, 9747 AG Groningen, The Netherlands

**Corresponding author: Yue.Jun@rug.nl*

Highlights

- Aerobic oxidation of benzyl alcohol was studied over a homogeneous Co/Mn/Br catalyst.
- Wetted and dewetted gas-liquid slug flows were identified in the microreactor.
- A kinetic expression of benzyl alcohol oxidation to benzaldehyde was established.
- A reactor model was developed under mass transfer limited conditions.

1. Introduction

Slug flow processing in microreactors brings significant transport intensification (e.g., enhanced heat and mass transfer rates) and precise process control (e.g., regular flow pattern, narrowed residence time and uniform reaction temperature) that benefit chemical synthesis in multiphase systems. Thus, it represents an attractive means for the intensification of a variety of gas-liquid reactions (including typically selective oxidation and hydrogenation reactions), as well as kinetic investigations thereof [1-3]. In this work, a model reaction, the aerobic oxidation of benzyl alcohol to benzaldehyde in the presence of a homogeneous Co/Mn/Br catalyst, has been studied in a microreactor in the gas-liquid slug flow regime. The microreactor performance has been experimentally characterized under various slug flow conditions, which was interpreted based on the developed kinetic expression and reactor model.

2. Methods

The reaction was performed in a capillary microreactor made of polytetrafluoroethylene, using benzyl alcohol (dissolved in acetic acid) as the substrate, oxygen or air as the oxidant, a mixture of $Co(OAc)_2$, $Mn(OAc)_2$ and NaBr as the homogeneous catalyst. The reaction temperature was up to 150 ^oC and pressure up to 5 bar. The pictures of slug flow were recorded with a digital camera. The collected liquid samples from the microreactor outlet were analyzed by gas chromatography.

3. Results and discussion

Under the investigated conditions, the reaction was found highly selective towards benzaldehyde. Two different types of gas-liquid slug flow were identified: wetted flow (characterized by a complete liquid film surrounding the bubble) and dewetted flow (characterized by a partially wetting liquid film surrounding the bubble); the latter flow suffered from a limited interfacial area available for mass transfer. The transition from wetted to dewetted slug flow depended on the flow velocity and gas-liquid flow ratio (i.e. the bubble length). By a fine tuning of the reaction

temperature and mass transfer (i.e., via the presence of wetted or dewetted flow), the reaction behaviour fell in either kinetic or mass transfer limited conditions. The experimental results at lower reaction temperatures were used to develop a simplified kinetic expression. The experimental results at higher reaction temperatures were well described by the developed microreactor model. The model considers a fast reaction regime, where mass transfer details (under wetted and dewetted slug flows) are based on the literature correlations and the reaction kinetics is based on the current work.

4. Conclusions

Aerobic oxidation of benzyl alcohol to benzaldehyde was studied over a homogeneous Co/Mn/Br catalyst in the microreactor operated under wetted and dewetted gas-liquid slug flows. The reaction was found under either kinetic or mass transfer limited conditions, depending on the reaction temperature. The experimental results at lower temperatures allowed to establish a simplified kinetic expression. This expression, with a further consideration of mass transfer details in slug flow, enabled the formulation of a microreactor model describing the experimental results at higher temperatures.

References

[1] M.N. Kashid, A. Renken, L. Kiwi-Minsker, Chem. Eng. Sci. 66 (2011) 3876–3897.
[2] L. Vanoye, M. Pablos, C. de Bellefon, A. Favre-Réguillon, Adv. Synth. Catal. 357 (2015) 739–746.
[3] J. Yue, Catal. Today 308 (2018) 3–19.

ECCE12
The 12th EUROPEAN CONGRESS OF CHEMICAL ENGINEERING
Florence 15-19 September 2019

Intensification of Fatty Acid Epoxidation in a Loop Reactor in the Presence of Microwave Radiation and Heterogeneous Catalysts.

Adriana Freites Aguilera[1*], Pasi Tolvanen[1], Kari Eränen[1], Johan Wärnå[1], Sébastien Leveneur[1,2], Tapio Salmi[1].

1 Laboratory of Industrial Chemistry & Reaction Engineering, Department of Chemical Engineering, Johan Gadolin Process Chemistry Centre, Åbo Akademi University, FI-20500 Åbo-Turku, Finland
2 Laboratoire de Sécurité des Procédés Chimiques, Institut National des Sciences Appliquées de Rouen, FR-76800 Saint-Étienne-du-Rouvray, France. Email: sebastien.leveneur@insa-rouen.fr

**Corresponding author: adriana.freites@abo.fi*

Highlights

- Epoxidized vegetable oils are environmentally friendly chemical intermediates
- An extensive study of the epoxidation kinetics of vegetable oils was conducted in a loop reactor
- Microwave irradiation and heterogeneous catalysts enhanced the process considerably
- A detailed mathematical model for the multiphase system was developed

1. Introduction

Epoxidized vegetable oils are chemical intermediates to valuable products, such as lubricants, plasticizers or non-isocyanate polyurethanes [1]. Tall oil obtained from forest biomass is a good source for vegetable oils, because it does not compete with the food chain. Epoxidation by the Prileschajew method implies the substitution of a double bond by an oxirane ring caused by a percarboxylic acid that is formed *in situ* from a carboxylic acid and hydrogen peroxide. Two liquid phases are present (oil and aqueous phases) and four reactions proceed simultaneously: formation of percarboxylic acid (perhydrolysis in aqueous phase), decomposition of the percarboxylic acid (aqueous phase), epoxidation of fatty acid (oil phase) and opening of the oxirane ring (oil phase) [2]. The principal method for vegetable oil epoxidation is well known but most of the studies published hitherto are qualitative in their character. Only few modelling studies have been published e.g. [3-4]. For process design, a detailed mathematical model for the complex multiphase system is necessary. The principles of the model and the essential modelling results are reported here.

2. Methods

A tailored recycle reactor system consisting of a vigorously stirred tank reactor, a circulation loop and a microwave source was constructed (Figure 1). The glass reactor was connected to a loop including a microwave cavity (Sairem) and a heat exchanger. Experiments were carried out both in the absence and presence of heterogeneous catalysts to reveal the potential intensifying effect of the catalysts. The cation exchanger Amberlite IR-120 was used as the main heterogeneous

catalyst. The reaction temperatures were 40–70°C and the oil-H_2O_2- acetic acid ratio was varied in the experiments. The organic phase content was 32–45 %v/v.

3. Results and discussion

The main observations from the experiments were: epoxidation of vegetable oils (e.g. model component oleic acid) occurs spontaneously in the absence of the catalyst, but the reaction rate can be considerably enhanced by exposing the system to microwave irradiation and incorporating a catalyst. The benefit of the use of a heterogeneous catalyst (ion-exchange resin) is obvious compared to a homogeneous catalyst (e.g. mineral acid), because the catalyst separation problem is completely avoided when the heterogeneous catalyst is used. An example of an epoxidation experiment is given in Figure 1. A detailed mathematical model was developed for the system, consisting of mass balances of all the reacting components in both aqueous and oil phases. The set of differential equations in the model was solved numerically during parameter estimation. The accuracy of the parameters was checked by standard mathematical analysis and a Markov Chain Monte Carlo (MCMC) method. An example of experimental data and model fit is provided in Figure 2. In general, the model fit was good and the estimated parameters had a good accuracy. The model can be used for prediction of the progress of epoxidation in the absence and presence of microwave irradiation and catalysts.

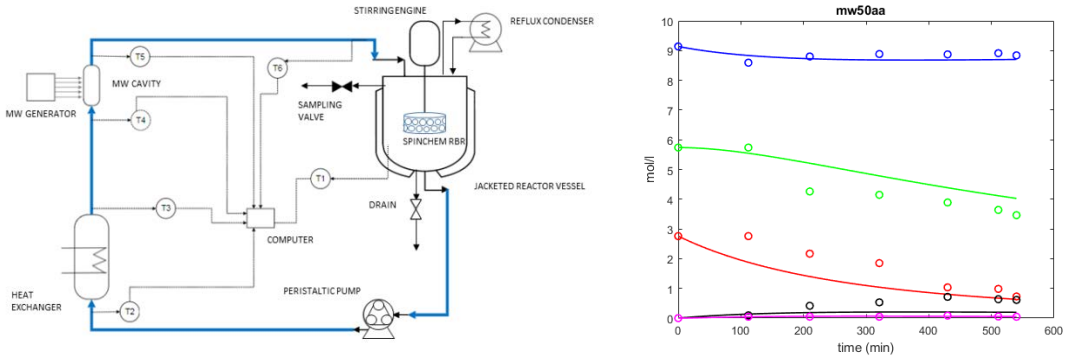

Figure 1. Tailored loop reactor system (left), model fit to experimental data (right); microwaves, 50ºC. In **black**: epoxidized oleic acid, pink: peracetic acid, red: oleic acid, green: hydrogen peroxide and blue: acetic acid.

4. Conclusions

An extensive set of kinetic experiments were carried out for the epoxidation of vegetable oils in a tailored reactor system. Microwaves and heterogeneous catalysts were successfully used to enhance the epoxidation process of a model compound, oleic acid and real tall oil mixtures. A multiphase reactor model was developed and applied to the experimental data. The model gave a good description of the experimental data and thus provides a perspective for process scale-up.

References

[1] S.G. Tan, W.S. Chow, Polymer-Plastics Technology and Engineering. 49 (2010) 1581-90.
[2] A. Campanella, M.A.Baltanás, European Journal of Lipid Science and Technology 106 (2004) 524-30.
[3] E. Santacesaria, R. Tesser, M. Di Serio, R. Turco, V. Russo V, D. Verde, Chemical Engineering Journal 173 (2011) 198-209.
[4] Z Wu, J Fang, Q. Xie, T. Zheng, L. Wu, M. Lu, et al. Industrial Crops and Products 122 (2018) 266-76.

ECCE12
The 12th EUROPEAN CONGRESS OF CHEMICAL ENGINEERING
Florence 15-19 September 2019

Micromixing efficiency in a rotor-stator Spinning Disc Reactor for liquids with different viscosities

Arturo Neissen Manzano Martinez[1], Melissa Assirelli[2], John van der Schaaf*[1]

1 Laboratory of Chemical Reactor Engineering, Department of Chemical Engineering and Chemistry, Eindhoven University of Technology, P.O. Box 513, 5600 MB Eindhoven, The Netherlands
2 Nouryon Specialty Chemicals, Deventer, The Netherlands

* j.vanderschaaf@tue.nl

Highlights

- Micromixing efficiency of three liquids with different viscosities is presented
- Segregation index decreases with increasing rotational speeds in all situations
- Compared to a stirred vessel, rs-SDR enhances mixing for liquids with different viscosities

1. Introduction

In the last years, Process Intensification (PI) and the development of novel equipment have become key approaches for engineers and scientist to address the challenges of the modern era, e.g reducing waste generation, emissions, energy consumption, etc. However, for a full implementation of new technology in the chemical industry, sufficient knowledge is needed in order to make it attractive and to guarantee functionality in real situations.

One way of reducing the energy-intensive separation steps in a process is by improving selectivity towards desired products, which may be difficult for fast reactions competing for a limiting reagent. In these cases, micromixing – the homogenization of the system at the smallest scale – plays a crucial role. [1]

Previous results proved that the rotor-stator Spinning Disc Reactor (rs-SDR) can enhance selectivity for fast reactions, with estimated micromixing times ranging between 1×10^{-4} to 1×10^{-2} seconds. [2] However, since industrial processes often involve reagents of different properties, the characterization of micromixing efficiency of liquids with different viscosities needs to be investigated.

2. Methods

The "Villermaux-Dushman protocol for experimental characterization of micromixers" [3] was performed with two modifications. Instead of Sulfuric Acid, Perchloric acid was chosen for being a strong, monoprotic acid [4]. Since the kinetics of the system have been a great deal of controversy, the iodide-iodate reaction was studied resulting in an empirical equation for the reaction rate [5] that is in agreement with a previous kinetic study [6].

The experimental setup for the rs-SDR was reported previously [2]. In order to compare with traditional equipment, the protocol was performed under the same conditions (temperature, concentrations, etc) in a 5 L tank, stirred with a propeller stirrer set at 900 and 1200 RPM.

To achieve a comparison on micromixing efficiency between an aqueous system and a viscous/non-viscous system, only the viscosity of the acid solution was increased using 10-20%vol of glycerol.

3. Results and discussion

The preliminary results are summarized in Figure 1. As expected, segregation Index decreases with an increase in rotational speeds. Furthermore, an increase in viscosity reduces the micromixing efficiency as expected. Surprisingly, at low rotational speeds the effects of an increment in viscosity seem to be less than at high rotational speeds. Further investigation is ongoing to explain these results. When comparing the estimated micromixing times in the rs-SDR with the ones obtained in a stirred vessel for the range of local energy dissipation rates used, the rs-SDR exhibits a better performance, due to the high energy input that can be transferred into a very small volume.

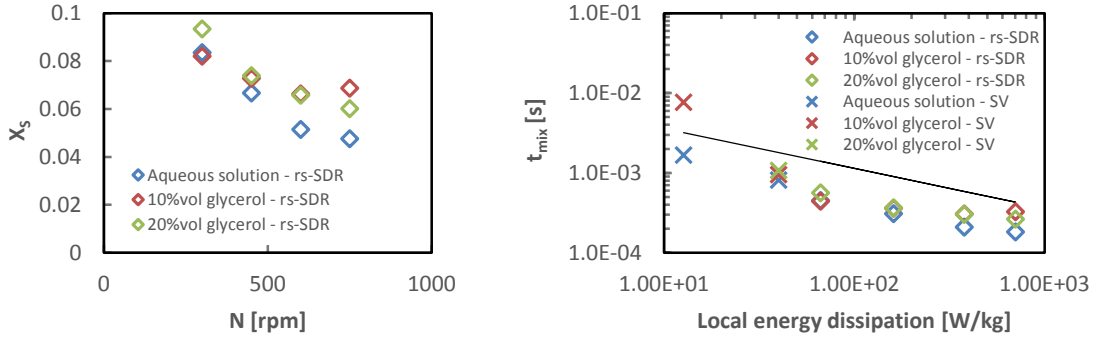

Figure 1. (a) The effect of segregation index with varying rotational speeds for two different viscosities of the injected acid in two different reactors and (b) the estimated micromixing times as a function of energy dissipation rate.

4. Conclusions

The rs-SDR not only shows better micromixing efficiency when compared to a stirred vessel, but it is also less affected by the addition of a liquid of higher viscosity.

References

[1] Bourne, J. R. (2003). Mixing and the Selectivity of Chemical Reactions. Organic Process Research & Development, 7(4), 471–508. https://doi.org/10.1021/op020074q

[2] Manzano Martínez, A. N., Van Eeten, K. M. P., Schouten, J. C., & Van Der Schaaf, J. (2017). Micromixing in a Rotor-Stator Spinning Disc Reactor. Industrial and Engineering Chemistry Research, 56(45), 13454–13460. https://doi.org/10.1021/acs.iecr.7b01324

[3] Commenge, J. M., & Falk, L. (2011). Villermaux-Dushman protocol for experimental characterization of micromixers. Chemical Engineering and Processing: Process Intensification, 50(10), 979–990. https://doi.org/10.1016/j.cep.2011.06.006

[4] Baqueiro, C., Ibaseta, N., Guichardon, P., & Falk, L. (2018). Influence of reagents choice (buffer, acid and inert salt) on triiodide production in the Villermaux–Dushman method applied to a stirred vessel. Chemical Engineering Research and Design, 136, 25–31. https://doi.org/10.1016/J.CHERD.2018.04.017

[5] Kinetic study of the iodide-iodate reaction for micromixing characterization. / Manzano Martinez, A.N.; Haase, Sander; van der Schaaf, J. 2018. Poster session presented at CHAINS 2018 (CHemistry As INnovating Science), Veldhoven, Netherlands.

[6] Palmer, D. A., & Lyons, L. J. (1989). Kinetics of iodine hydrolysis in unbuffered solutions. Retrieved from https://inis.iaea.org/search/search.aspx?orig_q=RN:22075560

ECCE12
The 12th EUROPEAN CONGRESS OF CHEMICAL ENGINEERING
Florence 15-19 September 2019

Process intensification in direct amide synthesis with catalytic packed-bed milli-reactors operated under induction heating

Evgeny Rebrov[1], Nikolay Cherkasov[1], Pengzhao Gao[2]

1 University of Warwick, Coventry, CV4 7AL, UK; 2 Hunan University, Changsha, 410082, China

**Corresponding author: e.rebrov@warwick.ac.uk*

Highlights

- Induction heating improved catalytic activity by 1.5 times in a direct amide synthesis reaction.
- The initial reaction rate over core-shell catalysts was further increased by 1.7 times r as compared to a mechanical mixture.
- Thermal gradients in a packed bed milli-reactor under RF heating have been analyzed.
- Design criteria for a near-isothermal milli-reactor have been suggested.

1. Introduction

The fact that small-scale and distributed chemical manufacturing systems are proved to offer advantages such as lower capital expenses, compactness of equipment, relatively small energy consumption, and reduced by-product formation has led to the growing interest in newer process intensification methods using reactors with channel diameter in the millimeter range (milli-reactors). These reactors can be heated by induction heating of magnetic microparticles placed inside the reactor to generate heat rapidly and uniformly within the bed, while eliminating hot spots and large radial temperature gradients. Induction heating utilizes easier scalable hardware such as magnetic materials and induction coils connected to an RF generator.

Under RF heating, the composite magnetic catalyst should provide both high heating and reaction rates. A core-shell structure is often used because the shell layer often acts as a catalyst and protects the magnetic core from chemical erosion and aggregation. Over the last few years, we developed a series of core-shell composites for direct amide synthesis, which is one of the most important reactions in pharmaceutical industry [1-3]. The catalytic activity was determined in a reaction between aniline and phenylbutyric acid in a fixed bed flow reactor under induction heating.

2. Methods

The catalytic activity was compared in the reaction between 4-phenylbutyric acid and aniline. A glass reactor (Omnifit HiT, i.d 6.6 mm, 250 cm long) was used. Two HPLC pumps were used to feed the solutions of 4-phenylbutyric acid and aniline in p-xylene to the reactor. The flow reactor was packed with the catalyst pellets (fraction size: 125–250 μm) and it was placed in the center of an 8-turn RF coil operated at 300 kHz. A 5-mm preheating zone was packed with Fe_3O_4 pellets of the same size. A fiber optic temperature sensor was attached to the outer surface of catalytic zone to control the temperature using a PID controller.

3. Results and discussion

Under near-isothermal conditions, no products other than the amide were identified [3]. The reaction kinetics is the first order in respect to both amine and acid and it is controlled by strong product inhibition at conversion levels above 50%. However, even a small deviation of the catalyst temperature from an isothermal operation results in a substantial decrease of selectivity. Because of their small dimensions, larger contributions of axial conduction and heat losses to the environment were observed in the millireactor and, accordingly, the temperature profiles deviate from those observed in large-scale reactors that follow adiabatic operation. Therefore we developed quantitative criteria for the absence of axial temperature gradients in the reactor [4].

The method was applied to control the temperature in the reactor. It was necessary to split up the catalytic bed in several heating sections with additional sections of nonmagnetic catalyst in order to obtain near-isothermal conditions. One nonmagnetic catalytic zone and one heating zone with composite magnetic catalyst forms a single periodic unit that is repeated in the axial direction. Further adjustments were made by varying the position and the length of the individual heating zones. The approach allows to obtain a temperature non uniformity inside the catalyst bed within 2K.

Under isothermal operation, the induction heating resulted in a higher reaction rate as compared to conventional heating. Furthermore, the initial reaction rate was 1.7 times higher over the composite catalyst as compared to the mechanical mixture of the same composition without major changes in the deactivation kinetics. This indicates the importance of the close contact between the magnetic core and the catalytic shell in the composite catalysts. The initial reaction rate decreased by 36% after a period of 55 h on stream. The catalyst activity was restored after a treatment with a H_2O_2 solution.

4. Conclusions

Determination of the temperature profile in an RF-heated catalytic packed-bed milli-reactor is essential for interpretation of kinetic data in these systems. The short distance between the heating source and the catalyst provides an excellent temperature uniformity, and decreases heat losses which are the main problems in conventional heating. This, together with the possibility of fast plant startup, holds promise for these reactors to replace classical batch reactors as well as to be used as remote chemicals plants in a future economy driven by electricity obtained from sustainable energy sources.

References

[1] Y. Liu, N. Cherkasov, P. Gao, J. Fernández, M.R. Lees, E.V. Rebrov, J Catal. 355 (2017) 120-130
[2] Y. Liu, P. Gao, N. Cherkasov, E.V. Rebrov, RSC Adv. 6 (2016) 100997–101007
[3] T.K. Houlding, K. Tchabanenko, M.T. Rahman, E.V. Rebrov, Org. Biomol. Chem. 11 (2013) 4171–4177
[4] S. Chatterjee, T.K. Houlding, V.Yu. Doluda, V.P. Molchanov, V.G. Matveeva, E.V. Rebrov, Ind. Eng. Chem. Res. 56 (2017) 13273-13280.

ECCE12
The 12th EUROPEAN CONGRESS OF CHEMICAL ENGINEERING
Florence 15-19 September 2019

Chaotic Mixing in the NETmix Reactor

Joana Matos[1], Ricardo Santos[1], Madalena M. Dias[1], José Carlos B. Lopes[1*]
1 LA LSRE-LCM. Rua Dr. Roberto Frias, 4200-465 Porto, Portugal
**Corresponding author: lopes@fe.up.pt*

Highlights

- NETmix is an industrial reactor constituted by chambers and channels.
- The ratio between chamber diameter and channel width is crucial on mixing.
- Different structures of strange attractors can be related with mixing in chambers.

1. Introduction

NETmix is a novel static mixer reactor composed by a meso or micro sized network of mixing chambers interconnected by channels (Figure 1a) [1]. The NETmix network can be obtained by the repetition of the NETmix Unit Block (NUB) (Figure 1b). NETmix is used in industry for continuous production of nanoparticles [2] and other applications are being developed, namely: continuous production of CO2 hydrates [3] and photo-oxidation processes in water treatment [4]. Mixing in NETmix depends on the reactor geometry which influences the flow dynamics. Mixing will be evaluated using particles injections: the best mixture occurs when the particles out fraction is 0.5. The ratio between chambers diameter and channels width, *D*/*d*, (Figure 1b) is studied along with the vorticity history dynamics from phase diagrams that show different structures of strange attractors which are related to the degree of mixing in NETmix.

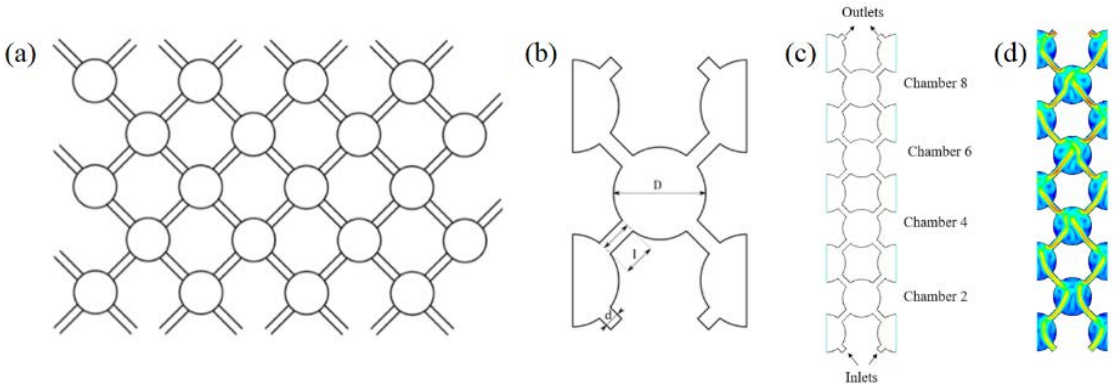

Figure 1. (a) NETmix network, (b) NUB, (c) ExtendedNUB, (d) velocity magnitude contour.

2. Methods

2D CFD simulations (time step, Δt = 1.14× 10^{-4} m/s) with water were performed for Re = 300, using the ExtendedNUB geometry in Figure 1c. The channel width is *d* = 1.00 mm and the chamber diameter varied from *D* = 5.75 to 7.25 mm. The simulated velocity flow-fields (e.g. for *D*/*d* = 6.55 in Figure 1d) were used for particle tracking with Lagrangian Mixing Simulation (LMS). LMS is an algorithm developed by Matos et al. [5] where the mixing interface between two fluids is tracked. Blue particles were positioned at left inlet and red particles at right over the initial velocity field of chamber 6. Along with the flow-time, the particles change their position: Figure 2a for 8.00× 10^{-4} s and Figure 2b for 3.50× 10^{-3} s. Note that in LMS, the number of particles in each series (blue and red) increases to represent accurately the mixing dynamics.

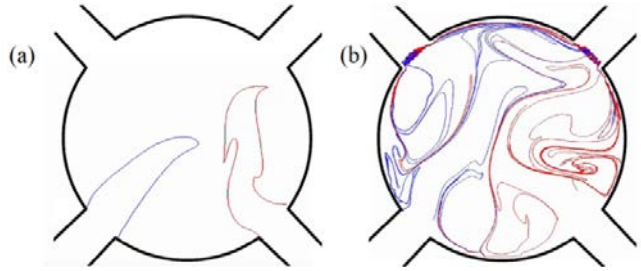

Figure 2. Particles injection in chamber 6 with LMS at different flow-times: (a) 8.00× 10^{-4} s and (b) 3.50× 10^{-3} s.

To study the mixing inside the chamber, the fraction of blue and red particles that leave chamber 6 through right or left channel was recorded using batch particles injections, i.e., maintaining the initial number of particles.

3. Results and discussion

For *D/d* = 5.75 to 5.95, the fraction of particles that go out through the same side from where they were injected is 0.9. This shows that only 10% of the particles are advected to the opposite side of the chamber. When *D/d* is between 6.55 and 6.95, the particles outlet distribution is 0.5 which represents complete mixture between the inlet streams. For larger *D/d* the particles out fraction grows apart from 0.5 again, e.g., at *D/d* = 7.25 the fraction is 0.8, i.e. only 20% of the particles are advected to the opposite side. Phase diagrams show different structures of strange attractors which can be related to the mixture inside the chamber. Figure 3 shows that a good mixture is associated to a strange attractor while a poor mixture is represented by a disorganized structure. The structures clearly show the transition between turbulent (*D/d* = 5.75 and 7.25) and chaotic (*D/d* = 6.55 and 6.78) laminar flows and the best mixing in NETmix (50/50 outlet distribution) is obtained with chaotic flows.

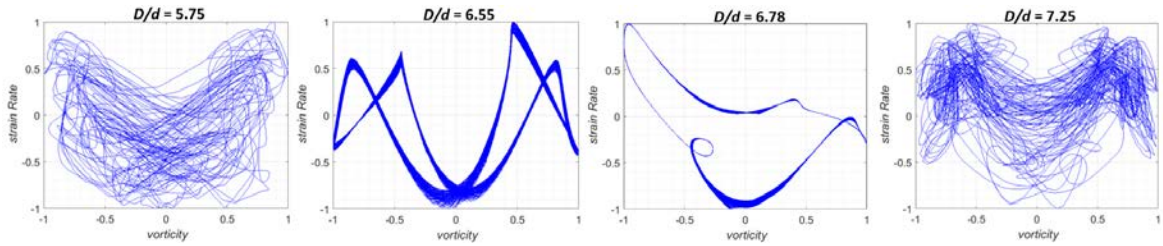

Figure 3. Normalized *Strain Rate* vs *Vorticity* for *D/d* = 5.75, 6.55, 6.78 and 7.25 in the centre of chamber 6.

4. Conclusions

The ratio *D/d* has an optimal range from 6.55 to 6.95 for mixing in NETmix. The optimal degree of mixing is represented by strange attractors.

Acknowledgements

Financed by: NORTE-01-0145-FEDER-000006 - funded by NORTE2020 through PT2020 and ERDF; Associate Laboratory LSRE-LCM - UID/EQU/50020/2019 - funded by national funds through FCT/MCTES (PIDDAC).

References

[1] P. E. Laranjeira, NETMIX Static Mixer, PhD Thesis of University of Porto, 2005.
[2] V. Silva, P.A. Quadros, P.E. Laranjeira, M.M. Dias, J.C.B. Lopes, J. Disper. Sci. Technol. 29 (2008) 542-547.
[3] M. F. Costa, The NETmix® Technology, Applied to Gas Hydrates Production. PhD Thesis of U. Porto, 2017.
[4] M. J. Lima, A.M.T. Silva, C.G. Silva, J.L. Faria, J.C.B. Lopes, M.M. Dias, Chem. Eng. J. 287 (2017) 419-424.
[5] J. Matos, M.S.C.A. Brito, M.M. Dias, J.C.B. Lopes, R.J. Santos, Chem. Eng. Sci. 192 (2018) 199-210.

ECCE12
The 12th EUROPEAN CONGRESS OF CHEMICAL ENGINEERING
Florence 15-19 September 2019

Experimental study and CFD simulation of a new reactor for hybrid catalysis.

Myriam Frey[1], Léo Violet[1], Serge Simoëns[2], Dominique Richard[1*], Pascal Fongarland[1]

1 LGPC UMR 5285 (CNRS, CPE Lyon, UCB Lyon 1), Université de Lyon, 3, rue Victor Grignard F-69616, Villeurbanne, cedex ; 2 LMFA UMR 5509 (CNRS, ECL, INSA Lyon, UCB Lyon 1), Université de Lyon, 36 av. G. de Collongues, F-69130 Ecully

**Corresponding author: dri@lgpc.cpe.fr*

Highlights

- A new double-basket reactor for hybrid catalysis has been designed.
- A $k_L.a$ of 0.035 s^{-1} is achieved for O_2 gas-liquid transfer.
- Simulated flow field are compared with PIV derived experimental values.
- A.ΔT of up to 15 K in the reactor is achieved through use of wall and coil T control.

1. Introduction

The use of enzymes in fine chemistry has been the subject of much research in the last decades. Among these works the concept of **hybrid catalysis** has recently emerged : the coupling of conventional chemical catalysis with enzymatic catalysis [1,2]. The aim of the GLYCYBRIDE project, on which this study is based, is to develop a synergy between enzymatic and heterogeneous catalysis in a one-pot reactor with the end-application of transforming glycerol into value-added chemicals.

The feasibility of a model one-pot reaction in three-phase hybrid catalysis, one step being an oxidation has been shown [3]. The model reaction proposed is a two-step reaction : an enzymatic catalyzed isomerization of fructose to glucose followed by a heterogeneously catalyzed oxidation of glucose to gluconic acid.

The aim of the present work is to study the design of a double-basket reactor allowing the implementation of the tri-phasic hybrid system. The main challenge lies in the optimal reaction conditions (temperature, hydrodynamics, substrate concentration) that differ between the different catalysis. The design of the reactor (Fig. 1) must thus allow the maintenance of some heterogeneity between the different reactive zones, while ensuring sufficient matter transfer between them.

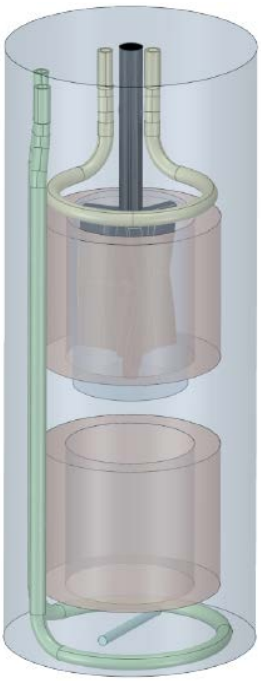

Figure 1: Scheme of the double-basket reactor

2. Methods

The hydrodynamics of the reactor has been characterized by physical methods such as : kLa of O_2 measurement (dynamic method with O_2 probe), mixing time measurement and RTD (NaCl used as a tracer). PIV velocity measurements have also been performed to determine the velocity of the flow field in the different areas of the reactor.

A CFD modeling of the hydrodynamics and thermal behavior of the reactor has been carried out with the Fluent© software (Ansys) using the realizable k − ε turbulence model associated to Multiple Reference Frame model to deal with rotating parts [4].

3. Results and discussion

Values of kLa between 0.02 s^{-1} and 0.035 s^{-1} are measured, consistent with values of single basket reactor reported in the literature. Mixing times of 15 to 20 s are observed for stirring rates above 500 rpm, in good agreement with the one calculated by CFD simulation. RTD measurement showed a behavior very close to the one expected for an ideal CSTR.

The CFD simulation provided the values of velocities in the different parts of the reactor, with velocities reduced in the basket holding the catalysts as expected (Fig. 2). These values are discussed in relation with the experimental one derived from PIV measurements.

The simulation of the thermal behavior of the reactor showed that: (1) Influence of the coils is largely inferior compared to the reactor walls, (2) Magnetic bar stirring rate has a negative but very weak influence, (3) Impeller stirring rate has a negative influence, (4) A large temperature gap between cooling and warming temperatures is necessary (80-100 K) to obtain a gap of 10-15 K in the reactor.

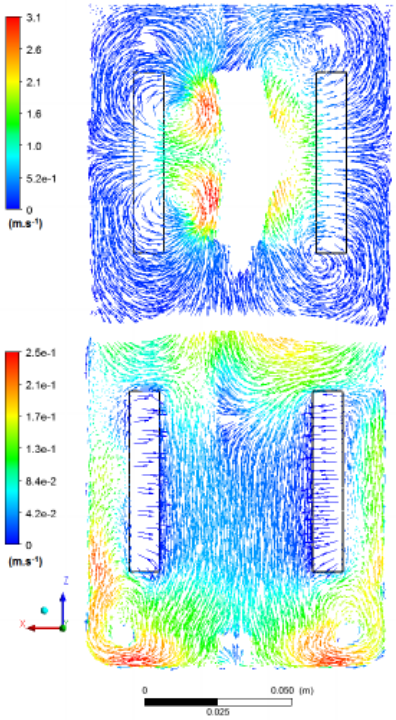

Figure 2: Flow fields on a vertical plane at y = 0 cm. Vector length is normalized. Stirring rates at 1100 rpm for the impeller, 300 rpm for the magnetic bar.

4. Conclusions

A novel double-basket reactor designed for hybrid catalysis has been first characterized for its physical transfer properties such as k_L.a, mixing time and RTD and simulated using CFD. Values of k_L.a measured are consistent with values of single basket reactor reported in the literature. The CFD simulation provided the values of velocities in the different parts of the reactor which have been compared with PIV measurements. The mixing time obtained by simulation are similar to the experimental ones. The simulation of the thermal behavior of the reactor showed that it is possible to obtain two zones in the rector, a "cold" one and a "hot" one with a ΔT of up to15 K while keeping an efficient stirring allowing for good mass transfer.

References

[1] O, Långvik, T. Saloranta, D. Y. Murzin, R. Leino, ChemCatChem 7 (2015) 4004-4015
[2] F. R. Bisogno, M. G. López-Vidal, G. de Gonzalo, Advanced Synthesis & Catalysis, 359 (2017) 2026-2049
[3] M. Frey, L. Seyidova, D. Richard, P. Fongarland, submitted to Catalysis Today, 2018
[4] V. Santos-Moreau, L. Brunet-Errard, M. Rolland, Chemical Engineering Journal, 207-208 (2012) 596-606

ECCE12
The 12th EUROPEAN CONGRESS OF CHEMICAL ENGINEERING
Florence 15-19 September 2019

3D printed continuous reactors for exothermic and corrosive reactions.

Terje Didriksen and Carlos A. Grande

SINTEF. Forskningsveien 1. 0373 Oslo, Norway

**Corresponding author: carlos.grande@sintef.no*

Highlights

- A novel 3D printed reactor was designed for flow chemistry applications.
- Sulfonation of anisole and dilution of sulfuric acid were tested as model reactions.
- Batch and commercial 3D printed reactor used as benchmark.
- Computational fluid dynamics was used to assist in reactor design.

1. Introduction

Exothermic and corrosive reactions are normally carried out in batch units manufactured with expensive steel alloy materials and sometimes with high dilution. Additive manufacturing can be used for continuous reactor design with tailored properties for matching mass and heat transfer rates. Additionally, the possibility of printing in titanium can lead not only to smaller volumes and thus increased safety, but also to higher rates of heat transfer.

Design of tailored reactors is a new area of flow chemistry that can allow higher interplay between design and possibilities to tailor mass, heat and momentum transfer (mixing). This can result in reactors having the properties of micro-reactors but with the advantage of being millimeter size.

Exothermic reactions are present in almost all fields of chemistry. Unfortunately, often the increase of temperature resulting from the reaction not only accelerates the reaction that was targeted, but also triggers other reactions resulting in a net loss of selectivity and reducing conversion towards desired products.

In last years, additive manufacturing has proven that it allows great flexibility in the design of customized pieces. The customization of shapes that is possible to achieve with some 3D printing techniques, can lead to advanced reactors where traditional constrains and trade-offs are displaced to other more profitable design and modes of operation.

2. Methods

We have made batch reactions of sulfuric acid dilution and sulfonation of anisole. We have also used a continuous process in a commercial 3D printed reactor (Innosyn) as a reference.

To manufacture our customized reactor, we have used a genetic algorithm to design optimized shapes for Hartridge-Roughton mixers which are good for mixing at intermediate Reynolds. We have designed a reactor with enhanced heat-transfer properties that was 3D printed using commercial titanium alloy.

3. Results and discussion

Using a genetic algorithm we have designed a Hartridge-Roughton mixer with optimized surface area per unit volume of reactor. Although multi-parametric 3D optimization is required, the computational time required for this task is still larger than finding semi-optimal solutions and test the flow quality experimentally. Once a satisfactory design was achieved, we have made CFD simulations of a single reactor as shown in Figure 1.

Based on the simulation results and on the need of extending the production of products, we have designed a reactor that has 4 parallel reactors and that has enhanced heat exchanger properties. A cut-off of the reactor is shown in Figure 2.

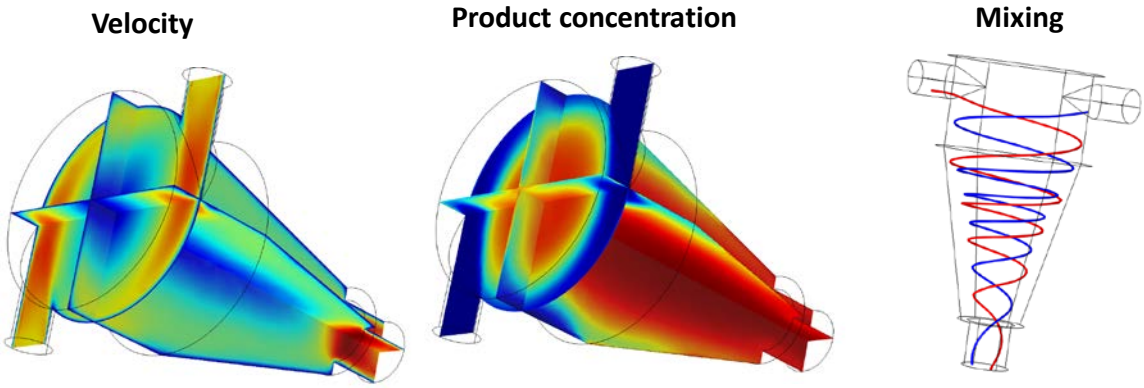

Figure 1. Detailed 3D simulations in the designed mixers.

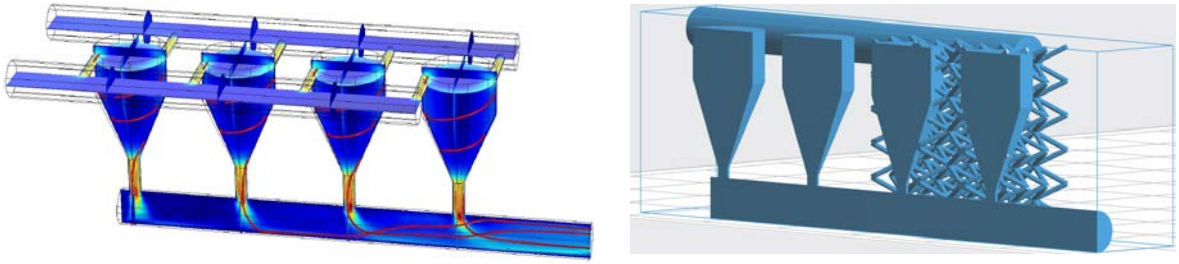

Figure 2. 3D simulations and cut-off of the 3D printed reactor for sulfonation reactions.

4. Conclusions

3D printing allows us to produce tailored reactors that can equilibrate rates of reaction and heat transfer in order to pursue continuous operation even in very exothermic conditions. It is very difficult to make multi-parametric 3D optimization for determining optimal shapes, but some simplifications can be made to reach suitable reactor designs.

ECCE12
The 12th EUROPEAN CONGRESS OF CHEMICAL ENGINEERING
Florence 15-19 September 2019

Experimental Study of Inductive Heating-Assisted Catalytic Hydrocracking of Naphthalene and Tetralin as Model Compounds of Heavy Oil.

Abarasi Hart [1*], Mohamed Adam [2], John P. Robinson [2], Sean P. Rigby [2] and Joseph Wood [1]

[1] *School of Chemical Engineering, University of Birmingham, Edgbaston, Birmingham B15 2TT, UK*
[2] *Faculty of Engineering, University of Nottingham, Nottingham NG7 2RD, UK*
** Corresponding author:a.hart@bham.ac.uk*

Highlights

- Hydrogenation upgrades poly-aromatics into light hydrocarbon components.
- Dehydrogenation causes condensation of poly-aromatics exemplar of heavy oil.
- Ni enhanced the hydrogenating activity of the catalyst compared with Co.
- The rate of naphthalene hydroconversion is higher than tetralin.

1. Introduction

The demand for transportation fuels is rising with the major source of supply being declining crude oil reserves. To meet the demand-supply gap, the exploitation of lower quality but abundant deposits of heavy oil and bitumen is necessary, while waiting for the transition to renewable fuels. Partial upgrading of heavy oil can be achieved in situ through Toe-to-Heel Air Injection (THAI) and its catalytic variant CAPRI; however, to attain the required temperature in the catalytic zone necessitates a rapid heating method such as inductive heating [1].

Poly-aromatic hydrocarbons account for remarkable portion of heavy oil and bitumen, and give them high viscosity and low American Petroleum Institute (API) gravity. In the process of catalytic upgrading, the poly-aromatics are readily condensed to form coke, especially in a hydrogen limited environment which rapidly deactivates and plugs the catalyst pores [1,2].

The hydrocracking of poly-aromatics in heavy oils with inductive heating-assisted catalysis was studied. Typical hydrotreating catalysts (e.g., $NiMo/Al_2O_3$ and $CoMo/Al_2O_3$) were evaluated for hydrocracking reactions. The formation of coke based on the number of aromatic rings was also studied using naphthalene and tetralin. This study is conducted as part of the evaluation of incorporating inductive heating to augment the temperatures in the vicinity of the catalyst zone in the THAI-CAPRI process in order maximise catalyst performance and increase upgrading.

2. Methods

Commercial catalysts $NiMo/Al_2O_3$ and $CoMo/Al_2O_3$ quadra-lobe shaped (AkzoNobel) with dimensions (5 ± 2.1 mm × 1.4 mm × 1.21 mm) were used. The feedstock was naphthalene (99+%, Alfa Aesar), tetralin (99.5%), solvent n-hexadecane (99%, Alfa Aesar) and H_2 supplied by BOC, UK.

The inductive heating system comprises of a fixed bed reactor of quartz glass tube (440 mm × 20 mm i.d × 40 mm o.d) rated 20 bar pressure (Inductelec Ltd and assembled by C-Tech Innovation, UK). The height of the induction coil wound around the tube is 230 mm, which also represent the catalytic bed height. The catalyst bed is heated inductively by steel balls susceptors of size 3 mm mixed the catalyst in a volume ratio of 70% (v/v). The steel balls convert the electromagnetic field into heat, to heat the catalyst bed volumetrically. The reactants were preheated to 200 °C with the aid of trace heater cable wrapped around the line and mixed with hydrogen prior to being

delivered into the reactor from the top. A hydrogen flow rate of 200 mL.min^{-1}, temperature 300 ^{o}C, catalyst-to-steel balls ratio (CTSBR) 70% (v/v), pressure 18 barg, and LHSV 0.75 h^{-1} condition obtained from optimisation were used in the experiment.

The liquid product was analysed using an Agilent 6890N GC equipped with a capillary column HP-5 (30 m × 0.320 mm × 0.25 µm), and a thermogravimetric analyser, TGA (TG 209 F1 Iris® instrument, NETZSCH-Geratebau GmbH) was used to determine the amount of coke on the catalyst.

3. Results and discussion

Induction heating provided an effective means of heating the catalyst bed, with 70 %v/v CTSBR the bed could be heated to 250°C within about 3 minutes. In previous study with NiMo/Al_2O_3 alone, we found that with induction heating the catalytic activity was enhanced and the spent catalyst coke content was lower when compared to conventional heating. Figure 1 shows hydrogenation of naphthalene and tetralin. The NiMo/Al_2O_3 exhibited a superior hydrogenating activity than CoMo/Al_2O_3, which promoted further hydrogenation from tetralin to (*trans*/*cis*) decalins and thus significantly improved the selectivity to decalins (Figure 1a).

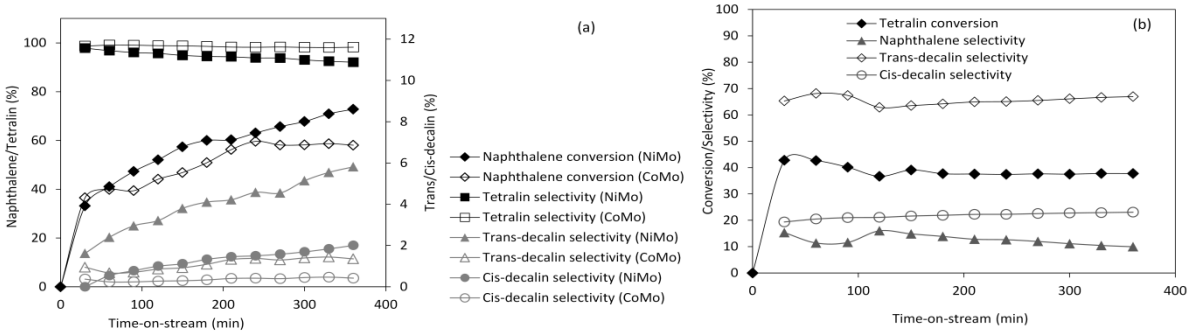

Figure 1. The hydrogenation of (a) naphthalene with NiMo/Al_2O_3 and CoMo/Al_2O_3 and (b) tetralin with NiMo/Al_2O_3 at 300 ^{o}C, 18 bar, 0.75 h-1 and CTSBR 70% (v/v).

The sequential reaction scheme shown in Figure 2, can be confirmed in Figures 1a and b, the intermediate tetralin can either undergo further hydrogenation to (*trans*/*cis*) decalins or dehydrogenation to naphthalene. However, the direction of the reaction is largely dependent on the catalyst type and the process conditions.

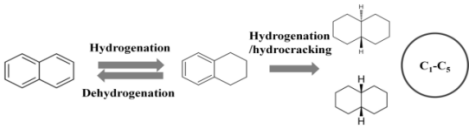

Figure 2. Reaction scheme

4. Conclusions

Induction heating of catalytic bed was studied for hydrogenation and hydrocracking of typical poly-aromatics found in heavy oil. Alumina supported NiMo and CoMo catalysts were investigated, while Ni increased the production of *trans*- and *cis*-decalins than Co, the rate of naphthalene hydroconversion was higher than tetralin for NiMo/Al_2O_3 catalyst.

References

[1] A. Hart, J. Wood, Energies. 11 (2018) 636.

[2] P.A. Rautanen, M.S. Lylykangas, J.R. Aittamaa, A.O.I. Krause, Ind. Eng. Chem. Res. 41 (2002) 5966-75.

ECCE12
The 12th EUROPEAN CONGRESS OF CHEMICAL ENGINEERING
Florence 15-19 September 2019

Aqueous Oxidation of Xylose to Xylonic Acid and Xylaric Acid over Synergistic PtAu and PtCu Catalysts Using Molecular O_2.

Jie Ding[1], Mengyuan Liu[1], Tianqi Fang[1], Chaohe Yang[1], Jian Shen[2], Xin Jin[1*]

1 College of Chemical Engineering, China University of Petroleum, Huangdao District, Qingdao, Shandong Province 266580; 2 College of Environment and Recourses, Xiangtan University, Xiangtan, Hunan Province 411105

**Corresponding author: jamesjinxin@upc.edu.cn*

Highlights

- Selective oxidation of xylose using O_2 in base-free medium at 80 °C.
- Bimetallic PtAu and PtCu catalysts display synergistic performances.
- Combined selectivity towards xylonic and xylaric acid is approximately 85%.

1. Introduction

Carboxylic acids are important industrial chemicals for a variety of different everyday products. Catalytic conversion of inexpensive sugars to value-added acids provides an alternative route to fossil-based products. Xylaric acid ($ 2,650/g), produced from xylose ($ 0.07/g), has been identified as one of the top ten value-added chemicals for biomass conversion, with wide applications in fine chemicals, agriculture, medicine, and architecture [1].

Xylaric acid is conventionally produced using nitric acid as the oxidant, generating significant amounts of toxic by-products such as N_2O and NO. While oxidation of xylose to xylaric acid using molecular O_2 is environmental-friendly compared with mineral acid method, very limited work has been published on catalyst design for xylaric acid synthesis. One of the most recent results reported by Saha and colleagues showed that oxidation of xylose with O_2 to xylaric acid can be realized over supported monometallic Pt, Pd, Au, Ru and Cu catalysts with 64% yield [2]. The correlation of catalyst structures, including particle size, surface composition and metal-support interaction, with catalytic activity and selectivity, however, has yet to be fully understood in this area. Therefore, in this work, we reported a series of Pt-based mono- and bimetallic catalysts for effective oxidation of xylose to xylonic and xylaric acids. Influence of catalyst morphologies on conversion and selectivity will be particularly discussed in this work, with the aim to provide further insights into effective catalyst design for xylaric acid synthesis from xylose.

2. Methods

The catalysts were prepared by traditional method involving use of $NaBH_4$ as the reducing agent [3]. Metal loading was approximately 2wt%. In a typical oxidation experiment, 20 mL of aqueous xylose solution (0.07 mol/L) was added to the reactor and mixed with 0.05 g of catalyst. Reaction was conducted at 80 ℃ and 1 MPa O_2. The product solutions were analyzed by HPLC equipped with both RID-10A and SPD-20A detectors.

3. Results and discussion

Several TiO_2 supported Pt based mono and bimetallic catalysts were screened to evaluate their performances for xylose oxidation. Among other candidates, bimetallic PtAu catalyst shows enhanced conversion of xylose (X ~ 85%) and selectivity of xylaric acid (S ~ 18%, Figure 1a). PtCu catalysts also display interesting behaviors during xylose conversion. It is found that, $PtCu/ZrO_2$ catalyst exhibits higher conversion compared with $PtCu/TiO_2$, CeO_2, and AC with good selectivity towards xylaric acid being 19.6% at 80 °C. The preliminary results clearly suggest bimetallic catalysts show promising performances compared with monometallic ones.

We also observed other co-products such as tartaric, glyceric, glycolic and formic acids, suggesting that xylose and xylonic acid might undergo C_1-C_4 and C_2-C_3 cleavage during oxidation reactions. Therefore, in this presentation, the influence of particle size of bimetallic PtAu and PtCu catalysts, and metal-support interaction on catalytic activity and product distribution during xylose oxidation will be discussed in details. BET, XRD, TEM and XPS characterization data will be correlated with experimental results from batch studies to establish possible structure-performance relation.

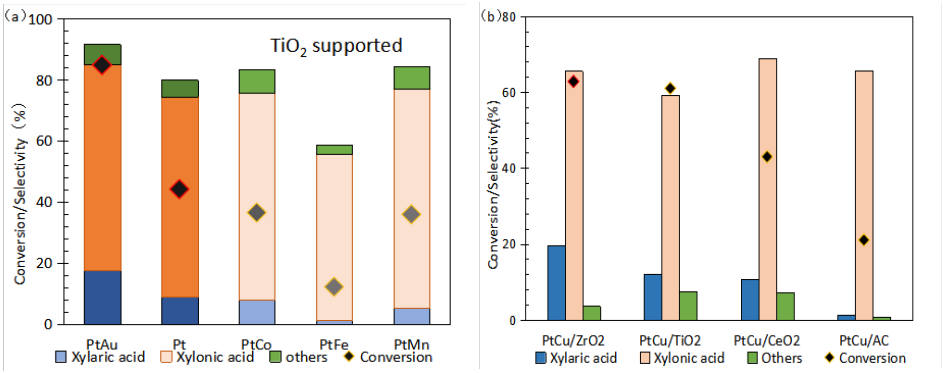

Figure 1. Activity and product distribution of Pt based mono and bimetallic catalysts (reaction conditions: 0.15 g xylose, 0.05g catalyst, 2wt.%, 2wt.%–2wt.% metal loading, 80 ℃, 10 h and 1 MPa O_2).

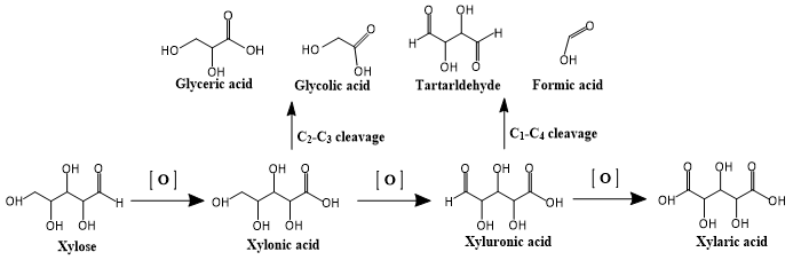

Scheme 1. Proposed reaction pathways of xylose Oxidation.

4. Conclusions

Bimetallic PtAu and PtCu catalysts exhibit synergistic catalytic performance in terms of activity and selectivity towards xylonic and xylaric acids during xylose oxidation.

References

[1] T. Werpy, G. Petersen, U.S. Department of Energy, 2004.
[2] S. Sadula, B. Saha, ChemSusChem, 2018.
[3] H. Shi, P. S. Thapa, B. Subramaniam, R. V. Chaudhari, Organic Process Research & Development, 2018.

ECCE12
The 12th EUROPEAN CONGRESS OF CHEMICAL ENGINEERING
Florence 15-19 September 2019

Methanol Synthesis with Steel-Mill-Gases: Simulation and Practical Performance Investigations

Kai Girod*, Klaas Breitkreuz, Stefan Schlüter, Thomas Marzi, Stefan Kaluza

Fraunhofer UMSICHT, Osterfelder Straße 3, 46047 Oberhausen, Germany

**Corresponding author: kai.girod@umsicht.fraunhofer.de*

Highlights

- Impact of different syngases from steel mills on MeOH productivity
- Catalyst stability at high CO_2 and H_2O concentrations
- Synthesis in close-to-practice test reactor system with intrinsic heat gradients
- Optimization of test conditions by sophisticated process simulation

1. Introduction

State-of-the-art steel mills as large and highly integrated sites comprise different sources of CO_2, CO and hydrogen. Besides the current energetic utilization, these gases provide promising potential to be utilized as feedstock for bulk chemical production, while simultaneously reducing the CO_2 footprint of the steel mill. The commercial Cu-based catalyst applied in industrial methanol synthesis is optimized for constant gas streams of high purity and fixed composition. The scope of this work is to evaluate the possibility of applying a commercial methanol synthesis catalyst in the conversion of synthesis gas derived from steel mill exhaust gases exhibiting fluctuating compositions [1]. The present contribution deals with the influence of altering CO/CO_2-ratios as well as the influence of high water concentrations in the inlet gas stream on the performance of the catalyst. In addition, gas streams with specific compositions from different steel mill production sites are investigated, including CO_2- and nitrogen rich blast furnace gases as well as gas streams originating from steel processing (converter gas). These gas streams have to be enriched with H_2 from electrolysis or coke oven gas. The ongoing investigations were performed within the scope of the project Carbon2Chem®, funded by the German Federal Ministry of Education and Research (BMBF).

2. Methods

Catalyst development and testing is usually performed with rather small amounts of catalyst [2]. However, transferring the results about performance and lifetime of the catalyst to industrial relevant pilot-scale application is hardly feasible. Here, larger amounts of differently shaped catalyst particles are usually applied resulting in a non-ideal temperature distribution and transport phenomena that can influence the overall performance of the catalyst. In order to close the gap between lab-scale and large-scale catalyst testing a new test system was developed [3]. In addition, a large scale methanol synthesis process simulation was developed including a kinetic model for the heterogeneously catalyzed methanol synthesis reaction. The theoretically identified operating points were subsequently applied in practice using two different test facilities. The first system is

close to the industrially applied geometry. A second complementary test system with a total reactor volume of 15 ml is characterized by a higher grade of automatization.

3. Results and discussion

The ongoing research focuses on technically and economically feasible gas compositions and their impact on the overall catalyst performance. The carbon efficiency describes the total carbon utilization of the process and is shown in figure 1. The recycle ratio has to be kept in an economically reasonable range in order to enable high reactor efficiency. The CO_2/CO-ratio has a crucial effect on the catalyst performance.

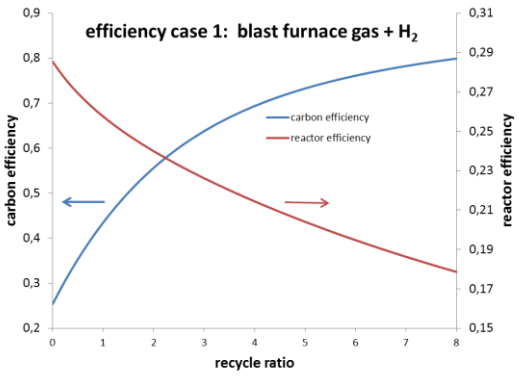

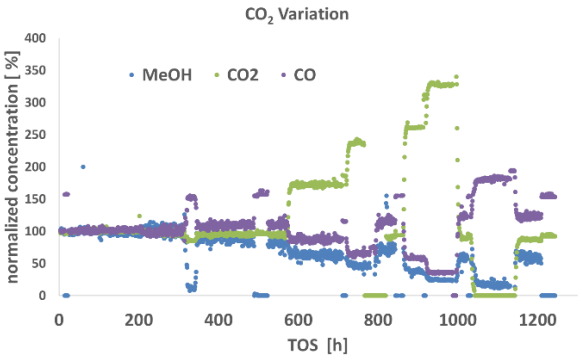

Figure 1: carbon and hydrogen process efficiency as a function of the recycle ratio (left)

Figure 2: MeOH formation depending on CO_2/CO (right)

As expected, the methanol productivity decreased with increasing CO_2 concentration (figure 2). A minimum CO_2 concentration is required for a high catalyst activity, as the lowest methanol productivity was obtained for pure CO. Apparently high water and CO_2-concentrations reduce the lifetime of the commercial MeOH-synthesis-catalyst.

4. Conclusions

The obtained results proof that methanol synthesis with H_2-enriched steel mill gases as feedstock is possible. However, for the same MeOH plant capacity a synthesis with steel mill gases requires a larger reactor due to lower catalyst productivity.

References

[1] J. Schittkowski, H. Ruland, D. Laudenschläger, K. Girod, K. Kähler, S. Kaluza, M. Muhler, R. Schlögl, Methanol Synthesis from Steel Mill Exhaust Gases: Challenges for the Industrial Cu/ZnO/Al_2O_3 Catalyst, Chemie Ingenieur Technik, Volume 90, Issue 10 (2018)

[2] J. Haber, J. H. Block, B. Delmon, *Methods and Procedures for Catalyst Characterization*, in Handbook of Heterogeneous Catalysis, 8 Volume Set, 2nd Edition (Eds: G. Ertl, H. Knözinger, F. Schüth, J. Weitkamp), Wiley VCH, Weinheim **2008**

[3] K. Girod, K. Breitkreuz, A. Gerstner, T. Marzi, T. Schulzke, S. Kaluza, Close-to-Practice Investigations of Heterogeneously Catalyzed Syngas Conversions in Slurry and Fixed-Bed Reactor Systems, Chemie Ingenieur Technik, Volume 90, Issue 5 (2018) 690-695

ECCE12
The 12th EUROPEAN CONGRESS OF CHEMICAL ENGINEERING
Florence 15-19 September 2019

Model-based Solvent Screening for a Reductive Amination.

Fabian Huxoll[1], Jonas Bianga[2], Thomas Seidensticker[2], Dieter Vogt[2], Gabriele Sadowski[1]*

1 Laboratory of Thermodynamics, TU Dortmund University, 44227 Dortmund, Germany
2 Laboratory of Industrial Chemistry, TU Dortmund University, 44227 Dortmund, Germany

**Corresponding author: gabriele.sadowski@tu-dortmund.de*

Highlights

- Application of an activity coefficient-based approach for a fast solvent screening.
- Solvent influence on reaction equilibrium and reaction rate can be predicted.
- No experimental reaction data needed.
- Promising solvents could be confirmed by experiments.

1. Introduction

Reaction equilibrium and reaction rate of chemical reactions are significantly influenced by the solvent used. Therefore, to optimize the equilibrium position, to increase the selectivity towards the product of interest and to enhance the reaction rate, it is important to consider the solvent influence on a reaction [1, 2]. State-of-the-art lab screening is highly time-consuming and therewith cost-intensive.

In this work, the RA (reductive amination) of undecanal and diethylamine to DEAU (1-diethylamino-undecan) and water was investigated. Appropriate solvents were identified using a thermodynamic approach and subsequently validated by experiments.

2. Methods

The thermodynamic equilibrium constant K_a, which does NOT depend on the solvent nor on the reactant concentrations, was used as the starting point of this approach. K_a is the product of K_x, which contains the equilibrium concentrations x_i, and of K_γ, which contains the activity coefficients γ_i. As the activity coefficients may strongly depend on the solvent whereas K_a does not, K_x is also strongly influenced by the solvent.

According to equation 1, increasing activity coefficients of the reactants lead to an increase of product concentrations at the reaction equilibrium. Moreover, high activity coefficients of the reactants imply a high reaction rate (2). Accordingly, the aim of this approach is to identify solvents which lead to high activity coefficients of the reactants.

$$K_a = \frac{x_{Product,1} \cdot x_{Product,2}}{x_{Reactant,1} \cdot x_{Reactant,2}} \cdot \frac{\gamma_{Product,1} \cdot \gamma_{Product,2}}{\gamma_{Reactant,1} \cdot \gamma_{Reactant,2}} \quad (1)$$

$$r = k \cdot x_{Reactant,1} \cdot \gamma_{Reactant,1} \cdot x_{Reactant,2} \cdot \gamma_{Reactant,2} \quad (2)$$

For the solvent screening, a wide range of different solvents was investigated. Using the modified group contribution method UNIFAC [3], the activity coefficients were predicted without using any reaction data. Solvents were identified that lead to the highest possible reactant-activity coefficients. Afterwards, the most promising solvents of the screening were validated regarding reaction equilibrium and reaction rate.

3. Results and discussion

Based on the predicted activity coefficients, it could be shown that the applied solvents significantly influence the reaction rate and the reaction equilibrium. The activity coefficients of the reactants deviated from each other by a factor of up to 20. Out of 14 investigated solvents, methanol, DMF (*N,N*-dimethylformamide) and ACN (acetonitrile) turned out to be the most promising ones (see Figure 1).

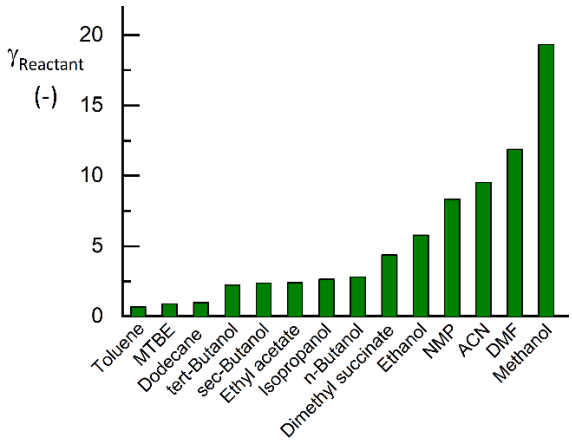

Figure 1. RA-reactant activity coefficient for reaction mixtures in different solvents.

To validate these results, experiments were performed in these solvents at 30 bar and 100 °C. Results showed that the highest product concentrations and reaction rates were indeed achieved in the three top solvents of the screening. Furthermore, using this approach it was possible to qualitatively predict the influence of initial substrate concentrations on reaction yield and kinetics.

4. Conclusions

Applying a thermodynamic approach allows a fast solvent screening without the need of any experimental reaction data for parameter estimations. Predictions and experimental results were in very good agreement, showcasing the advantages of thermodynamic models in order to screen possible solvents over the experimental and thus time and cost consuming lab screening.

References

[1] M. Lemberg, R. Schomäcker, G. Sadowski, Chem. Eng. Sci. 176 (2018) 264-269.
[2] C. Reichardt, T. Welton, Solvents and solvent effects in organic chemistry, VCH, Weinheim, 2010.
[3] J. Lohmann, R. Joh, J. Gmehling, Ind. Eng. Chem. Res. 40 (2001) 957-964.

ECCE12
The 12th EUROPEAN CONGRESS OF CHEMICAL ENGINEERING
Florence 15-19 September 2019

An in Situ FTIR and Raman Study of MOF MIL-53(Al) Formation Under Solvothermal Conditions

Heidemarie Embrechts[1,2], Martin Kriesten[3], Wolfgang Peukert[1,2], Martin Hartmann[3], Monica Distaso[1,2]

[1] *Department of Chemical and Biological Engineering, Institute of Particle Technology, Cauerstr. 4, 91058 Erlangen, Germany* *heidemarie.embrechts@fau.de
[2] *Interdisciplinary Center for Functional Particle Systems, FAU Erlangen-Nürnberg, Haberstr. 9a, 91058 Erlangen, Germany*
[3] *Erlangen Catalysis Resource Center, Egerlandstr. 3, 91058 Erlangen, Germany*

Highlights

- The formation steps of the MOF MIL-53(Al) are studied with in situ FTIR and Raman spectroscopy in a specially designed solvothermal reactor.
- The formation of prenucleation building units, MIL-53 nuclei, MIL-53 formation, and the decomposition of the solvent DMF to formic acid are observed in situ.
- The MIL-53 particle size is linked to the accumulation of prenucleation building units which influences the supersaturation of MIL-53 prior to particle formation.

1. Introduction

Metal-organic frameworks (MOFs) are a class of porous coordination polymers formed by the self-assembly of polydentate bridging ligands and metal-oxo clusters.[1] Due to their remarkably high surface areas, highly-ordered microporous networks, and structural diversity, MOFs exhibit great promise in the fields of catalysis, sensing, drug delivery, gas separation, and gas storage.[2]

Although there has been much research on the properties of metal-organic frameworks and numerous novel structures have been synthesized to date, there are only few reports focusing on the MOF formation steps prior to precipitation. Optimization of MOF synthesis protocols has, in consequence, been largely governed by serendipity. An understanding of the individual formation steps would allow for the development of improved strategies for the targeted engineering of MOF materials with defined crystal structures tailor-made to fit a variety of specific applications.

2. Methods

Such mechanistic understanding is achieved by monitoring MOF synthesis with Raman and FTIR spectroscopy in a 1.5 L solvothermal reactor specially designed to enable in situ monitoring of the reaction solution.[3] MIL-53(Al), one of the most-studied MOFs with interesting breathing behaviour and high thermal stability, serves as a model system.[4] MIL-53(Al) is synthesized in N,N-Dimethylformamide/water mixtures from aluminum salts and terephthalic acid. In situ observations are complemented with detailed ex situ analysis of the synthesized MOFs with N_2 sorption, x-ray diffraction, SEM imaging, thermogravimetric analysis, and solid state FTIR measurements.

3. Results and discussion

The formation of prenucleation building units (PNBUs) consisting of one linker molecule and one aluminum atom, MIL-53(Al) nuclei, crystalline MIL-53(Al) and the decomposition of DMF to formic acid is followed over time.[3] By comparing the kinetic profiles of the PNBUs $[Al(H_2O)_4–HBDC]^{2+}$ and the solid MIL-53(Al) phase at various synthesis temperatures, the rearrangement of the PNBU to form the metal-organic framework is identified as the rate-limiting step of synthesis. The calculated activation energy of formation of the PNBU (65.5 kJ mol^{-1}) is significantly lower than that of MOF formation (90.4 kJ mol^{-1}). This information is used to contruct a proposed MIL-53 formation pathway (Figure 1).

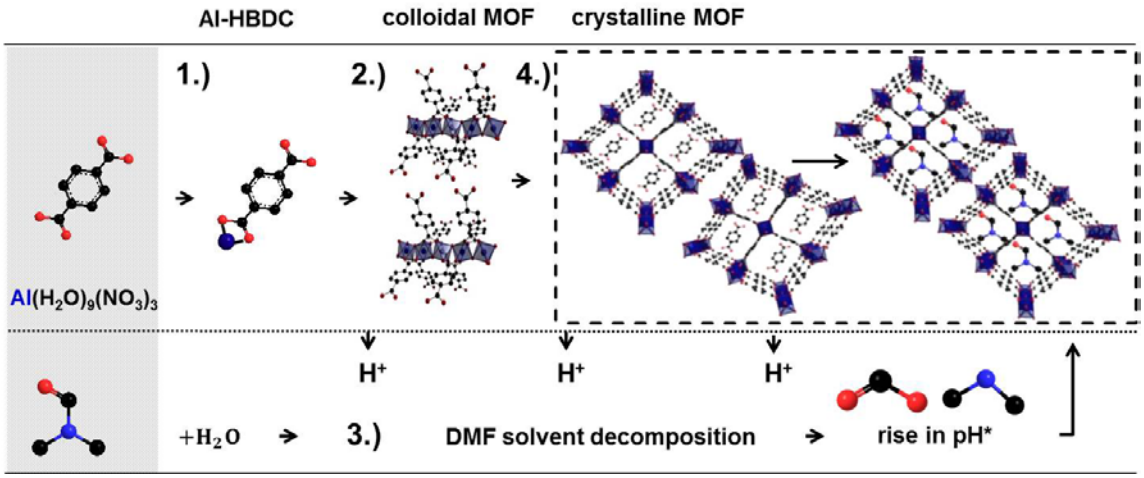

Figure 1. Proposed MIL-53 formation mechanism with reaction steps observed in situ.

The synthesized MIL-53 particle size is found to depend on the accumulation of prenucleation building units in solution prior to precipitation of the solid MIL-53(Al) phase. PNBU accumulation preferentially occurs when both the metal center and linker precursors are initially free to coordinate. A larger accumulation of prenucleation building units prior to MIL-53 precipitation results in a higher supersaturation, larger burst of nucleation, and the formation of nanoMOFs. Conditions less favorable to PNBU accumulation result in the formation of micron-sized particles.

4. Conclusions

This information gained from this study can be used as a tool to rationally understand the effect of various parameters on the MOF MIL-53(Al) formation process. The methodology described here could also be applied to rationally understand the formation of other MOF structures.

References

[1] A. Schneemann, V. Bon, I. Schwedler, I. Senkovska, S. Kaskel, R. A. Fischer Flexible metal–organic frameworks. Chem. Soc. Rev. 43 (2014) 6062.
[2] G. Férey. Chem. Soc. Rev. 37 (2008) 191–214.
[3] H. Embrechts, M. Kriesten, K. Hoffmann, W. Peukert, M. Hartmann, M. Distaso. J. Phys. Chem. C. 122 (2018) 12267-12278.
[4] Maurin, G.; Serre, C.; Cooper, A.; Férey, G. Chem. Soc. Rev. 46 (2017) 3104–3107.

ECCE12
The 12th EUROPEAN CONGRESS OF CHEMICAL ENGINEERING
Florence 15-19 September 2019

Kinetic analysis of the steam reforming of biomass derived oxygenates over Ni and Rh catalysts: Investigation of support effects

Marinela D. Zhurka, Panagiotis N. Kechagiopoulos*

Chemical and Materials Engineering Group, School of Engineering, University of Aberdeen, Aberdeen, AB24 3UE, UK.

**Corresponding author: p.kechagiopoulos@abdn.ac.uk*

Highlights

- Steam independent kinetic pathways over oxide supports for ethanol reforming
- Sepiolite's structure memory-effects revealed to influence rate determining step
- Rh shows an optimal performance in the steam reforming of phenolic compounds

1. Introduction

The steam reforming of oxygenates originating from biomass pyrolysis has received wide research attention in relation to the sustainable production of H_2. Bio-oil produced from biomass pyrolysis comprises of a complex mixture of organic compounds. Research to date has focused on reforming of model compounds of the aqueous phase of bio-oil, such as acetic acid, however much less work has been carried out in relation to lignin-derived aromatic compounds. In the current work, an extensive kinetic study of ethanol, phenol and hydroquinone reforming is presented over single metal (Ni and Rh) and bimetallic (Ni-Co) catalysts. Various supports, ranging from SiO_2 and γ-Al_2O_3, to mixed oxides of CeO_2, ZrO_2 and La_2O_3, to natural sepiolite, are utilized to probe support effects on the kinetic mechanism in combination with the active metal chosen.

2. Methods

The kinetic analysis was carried out using a fully automated reaction system by PID Eng & Tech (Micro Activity-effy unit). An HPLC pump (Gilson 307) was used to feed the water/organics mixture, the latter evaporated and mixed with N_2 prior reaching the catalyst bed. A stainless steel (SS316) fixed bed reactor (9.1 mm i.d, total length 304.8 mm) was used heated by a single-zone furnace. The gases were analyzed in an HP5890 GC equipped with a TCD detector and MS-5A and HS-T columns, while the liquids were analyzed in a Thermo Scientific TRACE 1300 GC using an FID detector and a WAXMS A column. Catalysts were prepared via wet impregnation.

3. Results and discussion

Concerning ethanol steam reforming, the effect of temperature for both Ni and Rh revealed dehydrogenation and decomposition reactions to be dominant at lower temperatures whereas higher temperatures promoted reforming and water gas shift reactions. Ni catalysts supported on SiO_2 and sepiolite showed a high methane selectivity at lower temperatures suggesting a metal-depended reaction pathway due to Ni's known methanation activity at these conditions [1]. On Rh no methane was detected, with the metal effectively promoting the dehydrogenation pathways of CH_x groups [2]. Identification of primary and secondary products on Ni catalysts revealed at lower temperatures acetaldehyde as a primary product, originating from ethanol dehydrogenation, with

CH_4 and CO being secondary products, emerging from acetaldehyde's decomposition, and CO_2 from the water gas shift reaction primarily and acetate species decomposition to a smaller degree. Strong support effects were observed in terms of the reaction pathway for ethanol reforming. A particularly low methane selectivity was observed over the CeO_2-ZrO_2-La_2O_3 mixed oxide supported catalysts, attributed to known activity of CeO_2 to form surface and bulk oxygen vacancies than can be replenished by water from the feed, hindering the development of CH_x to CH_4 and contributing to the elimination of the deposited carbon [3]. Interestingly, the catalyst supported on natural sepiolite exhibited a positive reaction order to water and negative to ethanol, in contrast to the rest of the supports. The calcination temperature of this catalyst was further revealed to have a critical impact on the reaction network, attributed to the memory-effect the structure of sepiolite exhibits when the mineral has not been exposed to temperatures higher than 530°C. Water preferentially adsorbs in sepiolite's structural channels, replacing the absent water and unfolding its structure, but also restricting the transfer of water from the support to the metal [4], resulting in steam activation being the rate determine step at low temperatures (Figure 1a). The lack of water derived species on the metal potentially further leads to a surface saturation by ethanol derived species explaining the negative order observed on ethanol (Figure 1b). Increasing the calcination temperature to 550°C (Figure 1c) or the reaction temperature to 500°C (Figure 1d) leads to the permanent collapse of sepiolite's structure, inhibiting water from entering its channels and facilitating the transfer of water to the metal for the promotion of the reforming reactions [5].

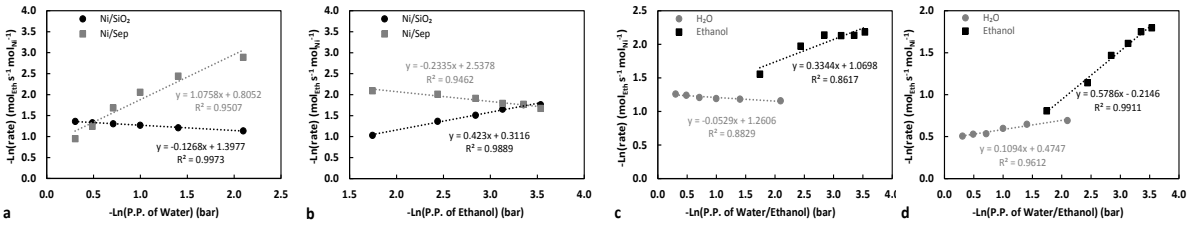

Figure 1. Partial reaction orders of ethanol steam reforming over Ni/SiO_2 and Ni/Sepiolite at 400°C (P = 0.9 bar, V_{tot} = 160 cm^3 min^{-1}) for (a) water and (b) ethanol. Partial reaction orders of ethanol steam reforming for water and ethanol at (c) 400°C on pre-treated Ni/Sepiolite catalyst at 550°C and (d) 500°C over untreated Ni/Sepiolite.

Reforming of phenol and hydroquinone, over Rh and Ni-Co catalysts supported on γ-Al_2O_3, revealed the effective conversion of the aromatic compounds to H_2 and CO_x at high temperatures (>500°C) and H_2O/C ratios (>8). Ongoing work at low temperatures focuses on liquid products analysis to elucidate the mechanistic pathways of these compounds.

4. Conclusions

The steam reforming reaction pathways of different classes of biomass derived oxygenates over a wide range of conditions and catalysts were investigated. For ethanol, the production of acetaldehyde is strongly related to the operating temperature. Ni promotes methanation reactions while Rh favors dehydrogenation reactions. On all oxide supports a steam-independent pathway is observed. Unique support effects are observed with sepiolite related to the interaction of water with the internal channels of the clay, restricting water from transferring to the metal and resulting on a steam-dependent kinetic mechanism. Current work extends the study to aromatic compounds.

References

[1] M. D. Zhurka, A. A. Lemonidou, J. A. Anderson, P. N. Kechagiopoulos, React. Chem. Eng. 3 (2018) 883–897.
[2] J. Zhang, Z. Zhong, P. Hu, M. B. Sullivan, L. Chen, ACS Catal. 4 (2013) 448–456.
[3] M. Patel, T. K. Jindal, K. K. Pant, Ind. Eng. Chem. Res. 52 (2013) 15763–15771.
[4] Y. Grillet, J. M. Cases, M. Francois, J. Rouquerol, J. E. Poirier, Clays Clay Miner. 36 (1988) 233–242.
[5] C. Serna, J. L. Ahlrichs, J. M. Serratosa, Clays Clay Miner. 23 (1975) 452–457.

ECCE12
The 12th EUROPEAN CONGRESS OF CHEMICAL ENGINEERING
Florence 15-19 September 2019

Effect of temperature on $NiAl_2O_4$ catalyst stability in the steam reforming of raw bio-oil

Aingeru Remiro*, Naiara García-Gómez, Beatriz Valle, Lide Oar-Arteta, Javier Bilbao, Ana G. Gayubo

Dept. Chemical Engineering, University of the Basque Country, 48080 Bilbao, Spain

**Corresponding author: aingeru.remiro@ehu.eus*

Highlights

- 600 and 700 ºC are suitable temperatures for enhancing $NiAl_2O_4$ catalyst stability
- Ni sintering is avoided at 600 ºC and coking is minimized at 700 ºC
- Temperature significantly affects the nature of the coke and its impact on catalyst porous structure
- Coke deposition affects more severely the porous structure at 650 ºC, thus causing a faster deactivation

1. Introduction

Among the alternatives for sustainable hydrogen production, the steam reforming (SR) of bio-oil obtained by pyrolysis of lignocellulosic biomass is a promising route with a low environmental impact because of neutral CO_2 balance [1]. One of the main problems of bio-oil SR is the deposition of carbonaceous material that causes reaction equipment clogging and rapid catalyst deactivation. In order to improve its economic viability, research effort has been focused on the development of process strategies that improve the operability (minimizing clogging) and new catalysts with high resistance to deactivation and capability to be completely regenerated. In a previous work [2], the suitability of a bulk $NiAl_2O_4$ catalyst was highlighted, especially for its efficient regeneration at high temperature. The aim of this work is to establish an optimum reaction temperature for enhancing the H_2 production and attenuating deactivation of bulk $NiAl_2O_4$ catalyst in the SR of bio-oil.

2. Methods

The raw bio-oil, obtained by flash pyrolysis of pine sawdust, was supplied by BTG Bioliquids BV (The Netherlands). The bulk $NiAl_2O_4$ catalyst (with 33 wt% Ni) was synthesized by the co-precipitation method, calcined at 850 ºC for 4 h and sieved between 150-250 µm. Fresh and deactivated catalysts have been characterized by N_2 adsorption-desorption (porous structure), transmission electron microscopy (TEM) and X-ray diffraction (XRD) (metal properties) and temperature programmed oxidation (TPO) (amount and nature of the coke). The catalytic runs were performed in an automated reaction equipment (Microactivity Reference) provided with two steps (thermal +catalytic) in series [3]. The controlled deposition of pyrolytic lignin in the thermal step at 500 ºC minimizes operation problems and catalyst deactivation in the subsequent catalytic step. The latter has been carried out in a fluidized bed, with steam/carbon (S/C) molar ratio of 6 and space time of 0.15 $g_{catalyst}/g_{bio\text{-}oil}$. Prior to each reaction, the catalyst is reduced *in situ* (with 10% v/v of H_2 in N_2) for 4 h at 850 ºC.

3. Results and discussion

The evolution with time on stream (TOS) of bio-oil conversion and H_2 yield for different reaction temperatures (Figure 1a) show a slower and similar deactivation rate at 600 and 700 ºC, whereas the deactivation is faster at 650 ºC. This unusual result differs from that previously reported in bio-oil SR with Ni/La_2O_3-αAl_2O_3 supported catalyst [4], whose deactivation was attenuated by increasing temperature in the 600-700 ºC range. This different kinetic behavior suggests different deactivation mechanism for bulk $NiAl_2O_4$ catalyst and Ni/La_2O_3-αAl_2O_3 supported catalyst.

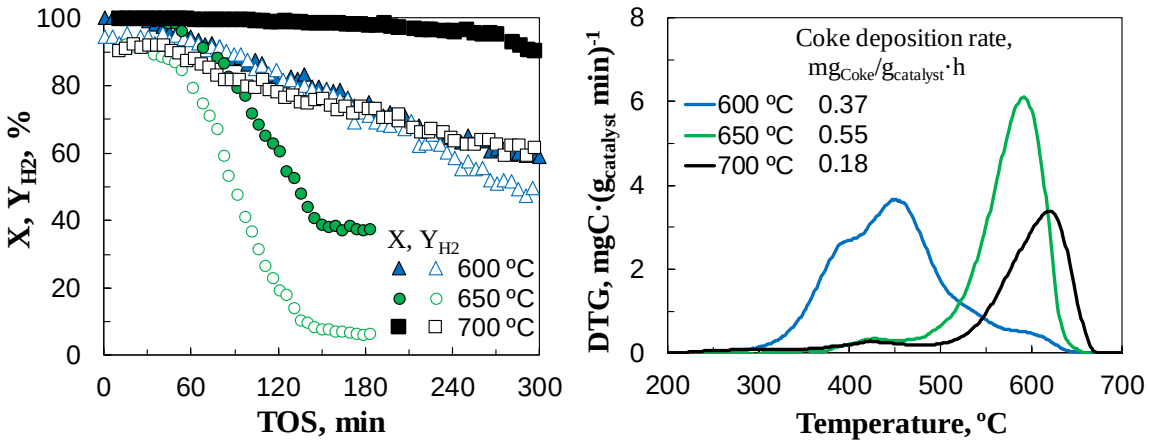

Figure 1. Effect of temperature on the evolution with TOS of conversion and H_2 yield (a) and on the TPO profile of the deactivated catalyst (b). Reaction conditions: S/C = 6, space time of 0.15 $g_{catalyst}/g_{bio\text{-}oil}$.

The XRD analysis of deactivated catalysts evidences that Ni sintering is incipient at 650 ºC and noticeable at 700 ºC. TPO analysis (Figure 1b) shows the formation of two different types of coke, which depends on the reaction temperature. An encapsulating coke that burns at low temperature is deposited at 600 ºC, whereas at 650 and 700 ºC a more condensed coke is deposited on the support, which partially blocks the porous structure. Both types of coke contribute to catalyst deactivation. The lower deactivation observed at 700 ºC compared to 650 ºC is explained by the promotion of coke gasification and a lower impact of coke on the porous structure of the catalyst.

4. Conclusions

The bulk $NiAl_2O_4$ catalyst undergoes greater deactivation during the SR of bio-oil at 650 ºC compared with that observed at 600 ºC and 700 ºC, because Ni sintering is avoided at 600 ºC, whereas coke deposition is attenuated at 700 ºC. It is concluded that 600 ºC is the optimum temperature for SR of bio-oil with bulk $NiAl_2O_4$ catalyst because it is suitable for attaining slightly higher H_2 yield than at 700 ºC (because of WGS promotion), with lower energy requirement, and moreover, it is also suitable for strategies that enhance H_2 selectivity (e.g., sorption enhanced steam reforming and membrane reactor).

References

[1] W. Nagban, T.A.T. Abdullah, R. Mat, B. Nabgan, Y. Gambo, M. Ibrahim, A. Ahmad, A.A. Jalil, S. Triwahyono, I. Saeh, Renew. Sust. Energy Rev. 79 (2017) 347–357.
[2] A. Remiro, A. Arandia, L. Oar-Arteta, J. Bilbao, A.G. Gayubo, Appl. Cat. B 237 (2018) 353–365.
[3] A. Remiro, A. Arandia, J. Bilbao, A.G. Gayubo, Energy Fuels 31 (2017) 7147–7156.
[4] B. Valle, B. Aramburu, M. Olazar, J. Bilbao, A.G. Gayubo, Fuel 216 (2018), 463–474

ECCE12
The 12th EUROPEAN CONGRESS OF CHEMICAL ENGINEERING
Florence 15-19 September 2019

Control of Temperature Uniformity for Exothermic Liquid Reaction in Structured Passages

Mohammed Msaed, Jordan MacInnes* and Annette Taylor

Chemical and Biological Engineering, University of Sheffield, Mappin Street, Sheffield S1 3JD

**Corresponding author: j.m.macinnes@sheffield.ac.uk*

Highlights

- Spatially-resolved temperature measurement using a fine-wire thermocouple
- Computation predicts the measured temperature profiles
- Buoyancy significant for the 5 mm passage size and flow rates used

1. Introduction

Exothermic reaction may cause temperature to exceed limits associated with preventing unwanted product formation or runaway reaction. Yet for efficient use of reactor volume it is important to operate as near to the temperature limit as possible to maximize reaction rate. Thus, an important engineering objective is minimizing temperature non-uniformity during the reaction process.

Reactors employing small-scale passages to increase relative heat transfer area have been widely advocated[1] but structuring the passage geometry to get the best performance out of a given size has received little attention. The present approach uses spatial temperature measurements within the flow passages, by traversing a fine-wire thermocouple, to assess the capability of predictive computation, thereby allowing probing at other scales and for other geometries than those used in the experiments. Spatial temperature measurement has not been attempted within the flow in small passages. Those reported are either of exterior temperature of the device, e.g. using infrared thermometry [2], or require sensor size approaching that of the passage, therefore not local and only at the passage walls[3,4].

The 'F' mixer geometry[5,6] shown in Fig. 1a is considered here. Only the first four elements of a multi-element reactor are studied as the first few elements are where the reactant streams mix, the largest concentrations prevail and hence the greatest challenge to thermal control occurs. The experiment uses relatively large passage size to enable accurate local resolution of temperature by the measurement. The size is large enough for buoyancy to be significant, although at the smaller size passages envisioned for best thermal control, buoyancy will have reduced importance.

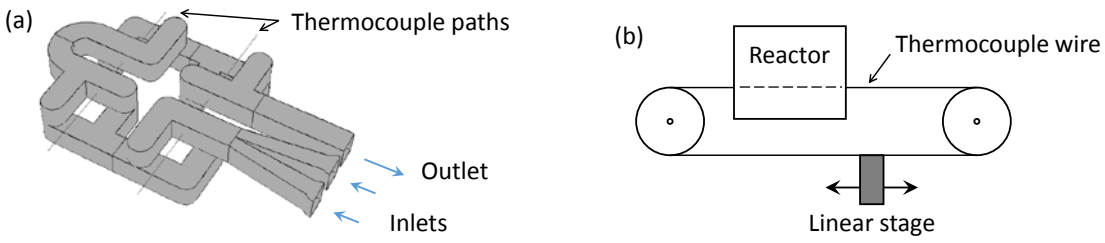

Figure 1. (a) Reactor geometry and (b) temperature measurement arrangement.

2. Methods

In the experiment, two separate streams are supplied at uniform temperature to four F elements placed in series. The element passages are milled from PEEK, covered top and bottom by 1 mm stainless steel sheets coated on the passage side with a thin PFA layer and sandwiched between two copper plates containing cooling water passages. Temperature profiles are measured along linear paths passing through the passages by traversing a 75 micron diameter butt-welded K-type thermocouple (Fig. 1b). Calculations of wire temperature in a flow with sinusoidal fluid temperature variation along the wire suggest conduction error is less than 1% of field temperature difference with this wire size. Computations use ANSYS 16 to solve the Navier-Stokes, energy and species equations in the experimental geometry, the domain including the solid regions surrounding the passage. Boundary conditions are uniform temperature, composition and velocity at the inlets, uniform temperature at the top and bottom boundaries (although with a heat transfer coefficient representing the thermal resistance of the PFA-coated cover sheet) and zero heat flux at other external boundaries. The apparatus is design to deliver these with good approximation.

3. Results and discussion

Fig. 2a shows a typical result for computed and measured temperature profile with water flow (no reaction). In this case a warm inlet (46 °C) is cooled by the top and bottom plates (25 °C). The importance of buoyancy is clear from the computed result with gravity switched off (dashed line). Fig. 2b shows successful measurement of temperature with reaction occurring (18 °C adiabatic temperature rise) from inlet reagent streams at 25 °C with plates at (35 °C). Computations of the reacting cases are underway and could provide a route to deducing models for reaction kinetics.

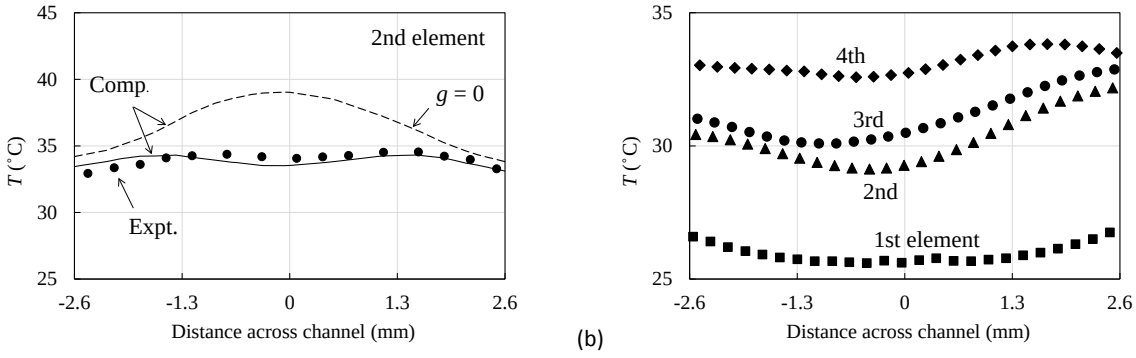

Figure 2. Temperature along wire path (a) in Element 2 for water flow with heating and (b) reaction of 0.35 M sodium chlorite and 0.10 M potassium tetrathionate with 0.002 M sodium hydroxide.

References

[1] L. Brocken, P.D. Price, J. Whittaker, I.R. Baxendale, React. Chem. Eng. 2 (2017) 662-668.
[2] H. Ammar, B. Garnier, A. Ould El Moctar, H. Peerhossani, ICNMM2012-73103, Puerto Rico (2012).
[3] D. Hamadi, B. Garnier, H. Willaime, F. Monti, H. Peerhossaini, Lab. Chip. (2012) 652-658.
[4] A. Zribi, M. Barthes, S. Begot, F. Lanzetta, J.Y. Rauch, V. Moutarlier, Sens. Act. A 245 (2016) 26-39.
[5] H. Chen, J.C. Meiners, Appl. Phys. Lett. 84(12) (2004) 2193-2195.
[6] J.M. MacInnes, A. Vikhansky, R.W.K. Allen, Chem. Eng. Sci. 62 (2007) 2718-2727.

ECCE12
The 12th EUROPEAN CONGRESS OF CHEMICAL ENGINEERING
Florence 15-19 September 2019

Bio-Cascading of Heat-Treated Wood after Service Life to Obtain Lignocellulosic Derivatives

Eduardo Robles*, Pedro L. De Hoyos Martínez, Javier Fernández, René Herrera, Oihana Gordobil, Jalel Labidi

Biorefinery Processes Group, Chemical and Environmental Engineering Department, Faculty of Engineering Gipuzkoa, University of the Basque Country UPV/EHU, Plaza Europa 1, 20018 Donostia, Spain

**joseeduardo.robles@ehu.eus*

Highlights

- Include 3 to 4 highlights in bullets format. [Calibri 10].
- Max. 90 characters per highlight including spaces.
- Only the core results should be covered.
- Please do not change the selected fonts.

1. Introduction

The use of wood-based products in Europe is projected to increase threefold worldwide between 2010 and 2050. The need for innovative products from fewer resources to help reducing pressure on forests is attracting the attention of scientific community to provide a value-added use of wood-based products after their traditional service life. In this sense, cascading of wood is an efficient use of these resources from the point of view of natural resource higher value uses that allow the reuse and recycling of products and raw materials. In this work, heat-treated wood (*Pinus radiata* L., 212 ºC) after one year of weathering exposure was subjected to a multi-stage lignocellulosic fractioning following the cascading and the biorefinery principles. This fractioning allowed the obtaining of hemicelluloses and lignin as chemical precursors, which were analyzed in their yield and quality. To determine the quality of the obtained products, the same fractioning was done to natural wood and heat-treated wood with no weathering exposure, as well as the natural wood after being exposed to the same conditions.

2. Methods

Monterey pine (Pinus radiata D. Don) was harvested from the forest areas of the Basque Country (Spain) was debarked, sawed, stored and conditioned before the heat-treatment. Pine boards were thermally modified according to industrial production standards a heat-treatment chamber with steam presence and under inert N_2 atmosphere [1]. Monterrey pine samples (natural and thermally modified) were exposed to natural weather [2].

Organosolv process was conducted using a mixture of ethanol/water (65:35 v/v) as white liquor, at 200 ºC during 90 min and a fiber to liquid ratio of 1:10 (w/v) 0.05M MgSO4 was used as catalyst. Liquid fraction was separated via filtration and the solid fraction was washed several times until driving the remaining fibers to a neutral pH level. Lignin (L1) was precipitated by adding 2 volumes

of acidified water (pH 2), after which solid fraction was filtered with a 0.22 µm membrane. Filtrate was concentrated and then added to 4 volumes of ethanol and kept at 3 ºC during 24 h, precipitated solid (H2) was separated by centrifugation.

A Totally Chlorine Free Bleaching (TCF) sequence was selected, which was based on two alkaline oxygen stages, (E_O), one peroxide stage (P) with secondary chelating reaction (P_{OQ}) and an alkaline peroxide stage under oxygen atmosphere (P_O). Lignin was precipitated from the first liquor (L2) by acidifying them dropwise until pH ~2.

3. Results and discussion

Lignin yields showed a higher recovery of lignin during Organosolv process (Table 1) especially in the case of pine, either weathered or not. I In case of lignin from P extracted during organosolv, it can be seen that Pw has a lower recovery (~16% less) regarding the original mass. Organosolv lignin from thermotreated wood showed lower yields than that of normal pinewood in absolute values. Table 1 also presents the content of acid insoluble lignin (AIL), acid soluble lignin (ASL), carbohydrates, ashes, molecular weight (Mw) and polydispersity index (Mw Mn^{-1}).

Table 1. main purity indicators of the recovered lignins.

		Yield [%]	AIL [%]	ASL [%]	Carbohydrates [%]	Ashes [%]	Mw [g mol^{-1}]	Mw Mn^{-1}
Po	L1	17.92	93.37	0.88	1.84	1.13	5534	4.43
	L2	8.67	83.34	1.46	3.01	1.15	2772	2.94
Pw	L1	15.03	93.89	0.53	1.83	0.29	7401	5.32
	L2	5.29	93.05	1.20	4.44	0.65	10049	8.68
To	L1	8.54	93.36	0.74	1.73	0.51	1453	2.36
	L2	9.06	92.82	1.08	5.27	1.06	3477	4.16
Tw	L1	9.80	94.62	0.95	2.58	0.25	4307	3.71
	L2	7.14	89.92	1.29	6.11	0.49	3465	3.88

4. Conclusions

The recovery of lignin from Organosolv treatment and mild-alkaline bleaching sequence resulted in very different technical lignins, with different possible applications.

References

[1] Herrera, R.; Erdocia, X.; Llano-Ponte, R.; Labidi, J. J. Anal. Appl. Pyrolysis 107, 256–266, 2014. https://doi.org/10.1016/J.JAAP.2014.03.010.

[2] Herrera, R.; Arrese, A.; de Hoyos-Martinez, P. L.; Labidi, J.; Llano-Ponte, R. Constr. Build. Mater., 172, 233–242, 2018.

ECCE12
The 12th EUROPEAN CONGRESS OF CHEMICAL ENGINEERING
Florence 15-19 September 2019

ENHANCEMENT OF HYDROCRACKING ACTIVIY OF DISCARDED FCC CATALYST BY MEANS OF ACIDITY MODIFICATION

Alazne Gutiérrez[1,*], Idoia Hita[1], Roberto Palos[1,2], Francisco J. Vela[1], José M. Arandes[1]

1 Department of Chemical Engineering, University of the Basque Country UPV/EHU, PO BOX 244, 48080 Bilbao, Spain; 2 Department of Chemical and Environmental Engineering, University of the Basque Country UPV/EHU, Plaza Europa 1, 20018 Donostia-San Sebastian, Spain

**Corresponding author: alazne.gutierrez@ehu.eus*

Highlights

- Noble metal-based catalysts with different acidities are employed
- Acidity plays a key role in the second stage of the LCO upgrading
- Lifespan of equilibrated FCC catalysts is extended

1. Introduction

Nowadays the oil market is especially volatile, thus the refining industry is working hard to find the most optimum way to process the heavier and sourer crude while maintaining its economics and profitability together with meeting the growing demand of high-quality fuels [1]. With the aim of intensifying the oil valorization, high efforts are being done to adapt the already installed and amortized units for the processing of non-conventional feedstocks, such as LCO. Considering the units available in the refineries, the best perspectives are focused on the usage of hydroprocessing units due to their multiple advantages [2]. Moreover, hydroprocessing in two stages, a first stage of hydrotreating (HT) with transition metal-based catalysts and a second stage of hydrocracking (HC) with noble metal-based catalysts, has proved to be a very suitable way of upgrading these streams [3]. In this work, the possibilities of using equilibrated FCC catalysts as support for catalysts used in the second hydrocracking stage of LCO valorization has been studied, extending, in this way, the life cycle of one of the highly produced residua of the refineries.

2. Methods

The feedstock consists of a previously hydrotreated light cycle oil (LCO_{HT}). Two in-house prepared catalyst have been used: (i) Pt-Pd/HY and (ii) Pt-Pd/HY-Al_2O_3, with the same Pt-Pd metal loading (0.5-0.5 wt%) and using as supports a HY ultra-stable zeolite (SiO_2/Al_2O_3 = 12) and an equilibrated commercial FCC catalyst (HY- Al_2O_3), respectively. In this work, apart from these two catalysts a physical mixture of them (50 wt%) has been employed, also. A deep characterization of the catalysts have been done [3]. Hydrocracking runs have been carried out in a down-flow fixed bed reactor in the following conditions: 400 °C; 65 bar; H_2/LCO_{HT} ratio, 1000 NmL_{H2} mL_{LCO}^{-1}; space velocity (WHSV), 0.21 h^{-1}; time on stream (TOS), 8 h. Products have been analyzed by chromatographic means.

3. Results and discussion

In the studied process, all the catalysts, before reaching a pseudo-equilibrium state, show an initial fast deactivation period as a consequence of both coke deposition and the stabilization of the metallic phases [4]. The length of this initial period has varied depending on the catalyst employed: the Pt-Pd/HY catalyst reached it after 2 h, whereas both Pt-Pd/HY-Al_2O_3 catalyst and the physical mixture of catalysts needed c.a. 4 h. Since the metallic phase is the same for the three catalysts, the coke formation rate seems to be related to the properties of the support, i.e., acidity and porous structure. Besides, as it has been widely demonstrated, the acidity of the catalyst is a key factor controlling the hydrocracking activity and selectivity of noble metal-based catalysts in the hydrocracking of secondary streams [5]. Figure 1 depicts the dependence between the hydrocracking (HC) and hydrodearomatization (HDA) conversions and the acidity of the catalyst employed. This way, the HC activity of the catalysts is linearly dependent of their acidity in the pseudo-stationary state, reaching for acidities higher than 0.16 $mmol_{NH3}$ g^{-1} total conversions at zero time of reaction. On the other hand, the HDA activity has not clear acidity dependence, so, for this route, porous structure appears to be a key factor. One more time, at zero time of reaction values of 100 % of HDA conversion are achieved. Comparing the performance of the different catalysts, the intermediate behavior of the physical mixture offers promising results, as the products stream is composed of c.a. 50 wt% of naphtha and diesel fractions with high HDA and HC activities. This fact reveals that adding a high acidity catalyst to the spent FCC catalyst is a good way of improving the behavior of the discarded FCC support and extending its lifespan.

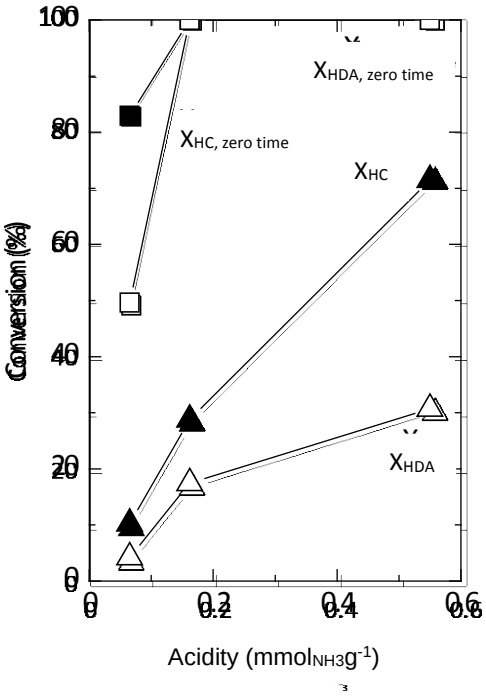

Figure 1. Dependence between the hydrodearomatization (HDA) and the hydrocracking (HC) conversions with the acidity of the catalysts.

4. Conclusions

Using the spent FCC catalyst mixed with a high acidic fresh catalyst in the second stage of hydrotreatment of LCO is a good way of extending the life cycle of highly produced residua of the refineries. The addition of this highly acidic catalyst leads to an enhancement of the acidity, which is the key factor controlling the hydrocracking activity and selectivity, producing a stream with a good quantity of naphtha and diesel. Besides, the hydrodearomatization activity, controlled also by other physical properties of the catalyst like pore volume, is improved.

References

[1] N. Chandak, A. George, A. Hamadi, M. Dakhan, A. Chaudhry, G. Singaravel, S. Morin Catal. Today. (2018), in press, DOI: 10.1016/j.cattod.2018.10.040.
[2] T. Xing, A. Alvarez-Majmutov, J. Chen, Fuel. 235 (2019) 696–702.
[3] R. Palos, A. Gutiérrez, J.M. Arandes, J. Bilbao, Fuel. 216 (2018) 142–152.
[4] A. Gutiérrez, J.M. Arandes, P. Castaño, A.T. Aguayo, J. Bilbao, Energy Fuels. 25 (2011) 3389–3399.
[5] A. Gutiérrez, J.M. Arandes, P. Castaño, M. Olazar, J. Bilbao, Fuel. 94 (2012) 504–515.

ECCE12
The 12th EUROPEAN CONGRESS OF CHEMICAL ENGINEERING
Florence 15-19 September 2019

CO_2-Reforming for production of CO rich synthesis gas at low steam to carbon ratio in industrial scale

Kim Aasberg-Petersen*, Peter Mølgaard Mortensen, Marené Rautenbach, Peter Seier Christensen

1: Haldor Topsøe A/S, Haldor Topsøes Allé 1, DK-2800 Lyngby, Denmark

**Corresponding author: kap@topsoe.com*

Highlights

- New process for CO_2-reforming
- Uses traditional Nickel catalysts
- Reduces size of steam reformer
- Almost any H_2/CO-ratio can be produced

1. Introduction

Many bulk chemicals such as methanol are produced in a multiple step process. The first step is normally conversion of natural gas or similar feedstock to produce hydrogen or synthesis gas (a mixture with mainly hydrogen and carbon monoxide) followed by the actual synthesis and purification. The synthesis gas production is often carried out by steam reforming of the feedstock with steam and carbon dioxide (in the following referred to as CO_2-reforming). Carbon dioxide reforming is an environmentally interesting process as it in theory offers a way of using CO_2, which in many industries is considered as a waste product and is a polluting greenhouse gas. Overall, CO_2-reforming is one of few chemical processes which can be designed with an overall negative CO_2-emission, as the process can be designed to utilize more CO_2 than what is produced from the process. The process could therefore play an important role in combination with CO_2 capture technologies, which are receiving much attention currently.

CO will make up a significant fraction of the produced synthesis gas when CO_2 is imported to the plant. Depending upon the process and amount of imported CO_2, synthesis gas with H_2/CO ratios in the range from 0.5-3 can be produced. Large amounts of CO are used within the chemical industry for example for production of higher alcohols, synthetic fuels, or acetic acid. There are also needs for carbon monoxide in especially the polymer industry in production of polycarbonates and polyurethane, among others.

A key challenge in the development of CO_2-reforming is to define (economical) operating conditions in combination with a suitable catalyst to avoid carbon formation. Carbon formation in a steam reformer is largely dictated by thermodynamics. In Fig. 1 the carbon limits are illustrated for various feed feed compositions with methane, steam, and CO_2. In the typical design of a reformer, it is a requirement that there is no affinity for carbon formation anywhere in the catalyst bed. This means that a sufficient amount of steam must be added to the process feed gas to avoid potential for carbon formation. In the case of the classical fired reformer, the process gas may enter the reformer at 450-600°C while leaving the reformer at an average temperature often

in the range 850-950°C. Hence, when designing a steam reformer, there must not be an affinity for carbon formation anywhere between 400°C and ca. 1000°C.

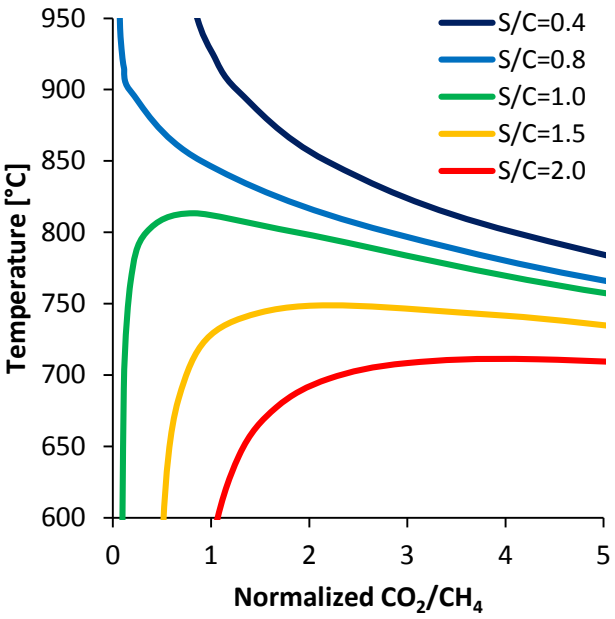

Fig. 1: Thermodynamic evaluation of carbon limit as a function of normalized H_2O/CH_4 (S/C), CO_2/CH_4, and temperature. A point placed below a curve in the graph will have a potential for carbon formation

In most cases, Nickel-based catalysts are used in a steam reformer. Nickel is relatively cheap compared to the alternative noble metals based catalyst. On the other hand, noble metals based catalysts have a lower affinity for carbon formation and a higher activity for steam and CO_2-reforming. However, very high raw material prices of these material makes them unattractive for extensive use in industrial scale. Consequently, nickel based catalyst are established as the preferred catalyst for industrial use for CO_2-reforming although the needed steam to avoid carbon formation is excessive compared to optimal design. This makes the process plants relatively expensive and there is an incentive to develop an improved concept still allowing for use of Nickel based catalysts.

2. New high temperature reactor for CO production

In the current work, a new reactor configuration is presented where hot CO_2 is added directly downstream a reformer and equilibrated in an adiabatic reactor. One possible configuration is illustrated in Fig. 2. This concept utilizes the high temperature of the reformer product gas and detailed understanding of the underlying thermodynamic and kinetic mechanisms to circumvent the carbon formation area. This allow for a method to tailor the product toward practically any H_2/CO ratio without the risk of carbon formation, while still using a cost-efficient nickel based catalyst. The adiabatic reactor may in principle be added downstream any reformer type and be used both for grassroot and revamp cases. Experiments have been carried out to demonstrate carbon free operation with the new reactor concept at significantly lower steam-to-carbon ratios than is possible with stand-alone CO_2-reforming. In Fig. 3 the gas composition profiles in the adiabatic reactor are provided illustrating significant conversion of CO_2 to CO and the resultant low H_2/CO-ratio in the product gas.

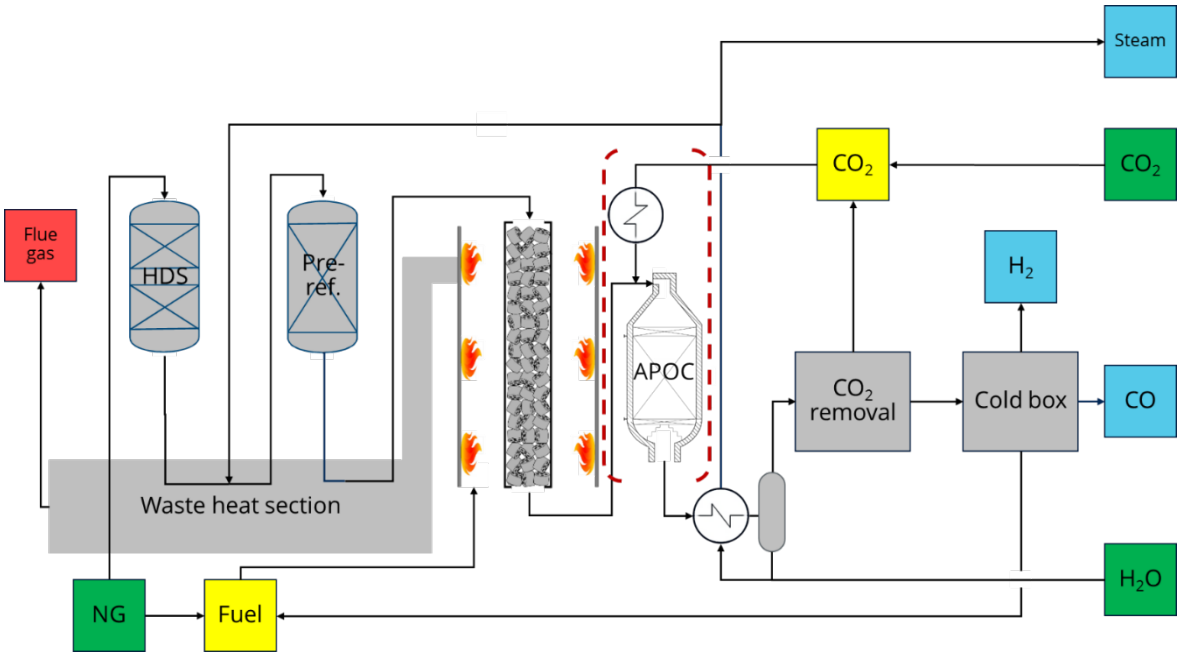

Fig. 2: Process concept with new technology utilizing an adiabatic reactor (APOC) downstream the steam reformer in a plant for producing CO and H_2.

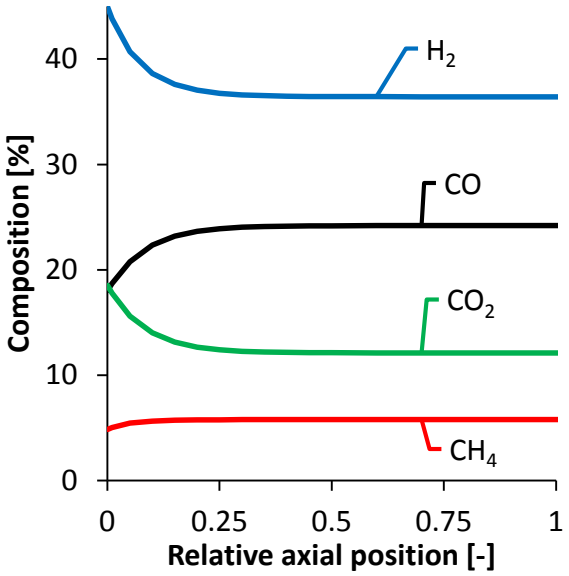

Fig. 3: Gas composition profiles in the adiabatic reactor (APOC) downstream the steam reformer

A series of process economic calculations have been carried out to illustrate the benefits of the new technology. Selected results include:

- The size of a steam reformer can be reduced by up to ca. 25%. Alternatively, the plant capacity can be boosted accordingly.

- The carbon for the CO product originates to a large extent from the CO_2 in the feed and the plant consequently has a large net use of CO_2.
- Practically any H_2/CO ratio can be supplied in the product synthesis gas.

3. Conclusion

In conclusion, the new high temperature CO production reactor is a promising technology for producing synthesis gas with a high content of CO at a low steam to carbon ratio. The technology can for example be used to retro-fit an existing production towards more CO production or included in new projects. In the presentation, the new technology will be described and the benefits will be illustrated with specific examples.

ECCE12
The 12th EUROPEAN CONGRESS OF CHEMICAL ENGINEERING
Florence 15-19 September 2019

Superior performances of Fe-FER compare to Fe-ZSM5 in NO_x and N_2O abatements for Nitric acid plant

Michele Corbetta[1], Alberto Garbujo[1*], Roberto Lanza[2], Emmanuel Rohart[3], Arnaud Lahougue[3], Grégoire Gaudry[2], Raffaele Ostuni[1], Pierdomenico Biasi[1].

1 Casale SA, Lugano, Switzerland; 2 Verdant, Stockholm, Sweden; 3 Alsys, Ploemeur, France.
**Corresponding author: a.garbujo@casale.ch*

Highlights

- Fe-FER, CASALE and ALSYS catalyst, shows better catalytic activity then Fe-ZSM5.
- Fe-FER, CASALE and ALSYS catalyst, has lower deactivation than Fe-ZSM5 under aging treatment.
- The results obtained point out the Fe-FER as the best industrial solution for Nitric acid plant.

1. Introduction

Nitric acid is one of the most produced commodity worldwide. It is mainly used as a strategical chemical for the synthesis of fertilizers and in 2013 the production reached 78 million tons[1] [2]. In recent years, the higher awareness in the greenhouse effect and in the environmental pollution, have highlighted the importance of a new development in the nitric acid tail gas treatment, especially concerning the N_2O and NO_x species [1]. Many metal oxide and zeolite catalysts have been developed for N_2O and NO_x abetment, each one with benefits and drawbacks. The state of the art materials are based on Fe-zeolites which both show NO_x and N_2O abatement with the same catalyst. Many Fe zeolites have been explored, such as Ferrierite (FER), ZSM5 and BEA [3].

In this paper, the comparison of fresh and laboratory aged Fe-FER and Fe-ZSM5 industrial catalysts, both supplied by ALSYS, has been carried out. Fe-FER catalyst is a proprietary catalyst of CASALE and ALSYS and is used in nitric acid plants [4]. The results from field and laboratory showed that Fe-FER will allow customers to benefit from a higher catalytic activity and greater stability compare to the current commercial solution with Fe-ZSM5.

2. Methods

The extruded catalysts tested were prepared at industrial scale, from process production to quantity scale, by ALSYS. The catalytic tests were carried out in an Inconel reactor under industrial nitric acid plant conditions. The feed compositions are reported in figure 1 caption. The GHSV used was 25,000 h^{-1}. Very high space velocity was chosen with the purpose to highlight the differences in catalytic activity among the catalysts tested. The hydrothermal aging treatment was performed for 150h at ambient pressure at two temperatures (600 and 700°C) with a feed of 12% of O_2 and 6% of H_2O with a GHSV of 5000 h^{-1}. The detector used was FT-IR coupled with a lambda probe for oxygen measurement.

3. Results and discussion

Fe-FER and Fe-ZSM5 extruded catalysts have been subjected to a simulated aging procedure to investigate the catalytic behavior under stressed condition. The catalysts show a uniform cylindrical shape with a diameter close to 2 mm (with typical composition and shape of industrial catalyst). The catalytic tests were performed under relevant industrial deN_2O and deNO_x reaction conditions. The results (figure 1) display the higher catalytic activity of Fe-FER compared to Fe-ZSM5. The superior Fe-FER catalytic activity becomes particularly significant after the aging procedure where a different catalytic behavior is observed. Fe-FER, slightly decreased its activity, after the aging treatment, while the Fe-ZSM5 dramatically dropped its performances. In addition, N_2O formation is detected under deNO_x condition for Fe-ZSM5, while the Fe-FER does not exhibit any N_2O formation. The characterizations performed revealed that the reduced activity of Fe-ZSM5 compared to the Fe-FER is due to the Fe species present in the catalyst.

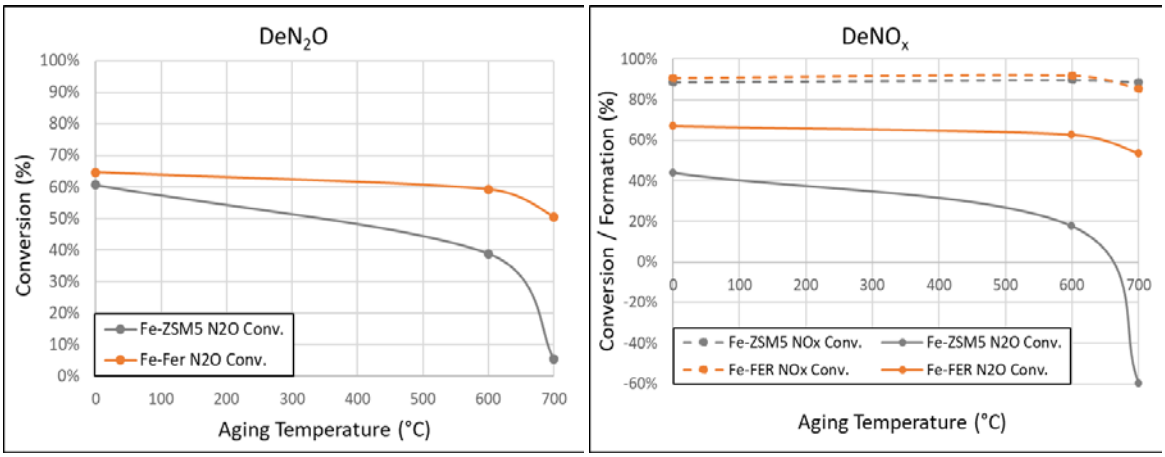

Figure 1. (Left) deN_2O condition: NO 70 ppm, NO_2 30 ppm, N_2O 900 ppm, O_2 3.0%, H_2O 0.3% and N_2 balance. (Right) deNO_x condition: NO 325 ppm, NO_2 325 ppm N_2O 40 ppm NH_3 650 ppm, O_2 3.0%, H_2O 0.3% and N_2 balance.

4. Conclusions

In this work, representative industrial catalysts were investigated in industrial conditions before and after severe aging treatments. Results showed that Fe-FER is the most stable catalyst and high performance that can be used for tail gas treatment in nitric acid plants. Moreover Fe-FER is extremely selective in N_2 even after severe aging while the Fe-ZSM5 exhibited a larger undesired N_2O formation. The Fe-FER catalyst for deN_2O and deNO_x applications has superior performances compared to the Fe-ZSM5.

References

[1] M. Thiemann, E. Scheibler, and K. W. Wiegand, “Nitric Acid, Nitrous Acid, and Nitrogen Oxides,” Ullmann’s Encycl. Ind. Chem. Vol. 24, vol. 2003, Vol 24. 177-223.
[2] C. A. Grande et al., Ind. Eng. Chem. Res., vol. 57, no. 31, pp. 10180–10186, 2018.
[3] K. Skalska, J. S. Miller, and S. Ledakowicz, Sci. Total Environ., vol. 408, no. 19, pp. 3976–3989, 2010.
[4] C. Hamon, D. Le Guern, O. Le Lamer, and L. Navascues, EP1918016B1, 2006.

ECCE12
The 12th EUROPEAN CONGRESS OF CHEMICAL ENGINEERING
Florence 15-19 September 2019

Parametric analysis of particle entraining in the freeboard zone of a moving bed melting gasifier

Federica Fusco[1], Alessia Borgogna[1], Annarita Salladini[2], Gaetano Iaquaniello[2], Maria Cristina Annesini[1]

[1]Dip. Ingegneria Chimica Materiali e Ambiente, Sapienza Università di Roma, Via Eudossiana 18, 00184 Roma (Italy)

[2]NextChem s.r.l., Via di Vannina 88, 00156, Rome (Italy)

*Alessia Borgogna: Alessia.borgogna@uniroma1.it

Highlights

- 2D simplified dynamic system has been analytically resolved.
- 3D analysis has been developed in Comsol Multiphysics environment.

1. Introduction

Gasification is a well-known thermal conversion process, which in recent years has been applied to convert renewable feedstock such as biomass and waste. More specifically, gasification of Refuse Derived Fuel (RDF) in a high temperature melting gasifier has been employed for energy production, and applications for chemical production have been extensively studied [1-2]. Compared with biomass gasification, gasification of RDF faces several issues related to its intrinsic heterogeneity, such as the non-homogenous structure of the bed reactor, which entails a more significant solid particles release in the freeboard zone compared to the predictable occurrence. Once released, solid particles could be entrained with the gas flow or deposit on reactor wall producing crusts, as experimentally observed. This peculiar release of solid particle can be related to the occurrence of complex dynamic phenomena in the bed, for which solid particles could be released with an initial velocity higher than that of the gas [3]. In this work we introduce a discussion regarding conditions which may cause particle entrainment of deposition. The analysis has been developed in two steps: - a preliminary study to identify the conditions of entrainment of particles released with an initial velocity v_p^0 in a cylindrical gasifier, where gas moves upwards with a velocity v_g; - a more detailed model of particle behavior with the geometry and operating conditions of an industrial gasifier developed using Comsol Multiphysics.

2. Methods

2.1 Preliminary study

In order to gain some preliminary knowledge about the entrainment of solid particles ejected from the bed with an initial velocity, v_p^0, we firstly consider a very simple 2D model of a cylindrical gasifier, with a 3.4m diameter and 14 m height over the solid bed, working with a gas flow rate of 12.000 Nm^3 (see Fig.1-a). Two limit conditions have been considered based on the values of: particle diameter, d_p, density, ρ_p, and initial velocity, v_p^0. The first one is defined with reference to the terminal particle velocity, v_p^t: particles with $v_p^t > 0$ are always entrained by the gas and flow outside

the reactor; while, the destination of particles with $v_p^t < 0$ depends on dynamics. Thus, a second limit condition has been considered: for each pair of values (ρ_p, d_p) there exists an initial value of particle velocity, $v_p^{0,l}$, for which particles arrive at the top of the reactor with velocity equal to 0.

2.2 3D simulation

A more rigorous analysis accounting for the true reactor geometry and velocity field requires 3D simulation (see fig.1-b) for which Comsol Multiphysics has been used. A one-way approach has been followed: first the fluid dynamic of the syngas inside the reactor has been resolved, then the particle tracking module has been applied for particle dynamics. Interactions between particle and surfaces of the domain are described by sticky boundary condition.

3. Results and discussion

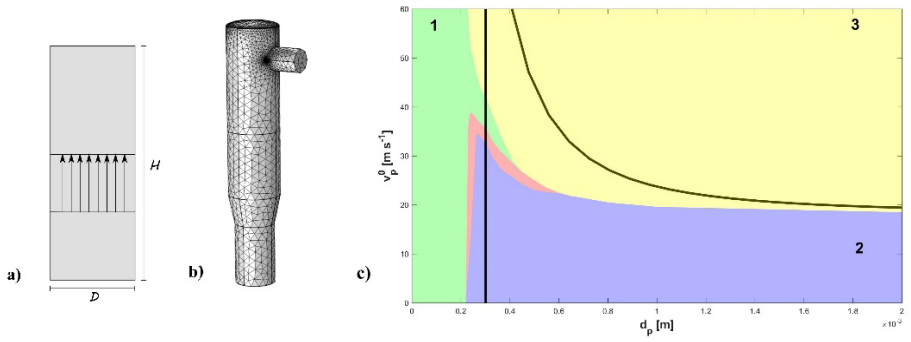

Figure 1. a) and b) Simulation domain, respectively, 2D and 3D; c) Comprehensive results representation (see text).

The analytical results show that particle density plays a less significant role compared to other parameters, so in what follows a mean particle density of 1500 kg m^{-3} has been considered.
With the analytically defined limiting conditions different particle behaviors can be recognized as a function of particle parameters (d_p , v_p^0). In fig.1-c black lines distinguish three characteristic zones resulting from the preliminary analysis. The one on the left (1) represents particles (v_p^t>0) entrained and flowing out with the gas; on the right side (v_p^t<0), the zone below the black curve (2) represents particles falling back on the bed, while the zone above (3) represents particles whose destination is strictly related to reactor geometry. Considering all the simplifying assumptions made, the preliminary results show good agreement with those from the 3D simulation, represented by the colored areas depicted in fig.1-c. Indeed, green and violet areas represent particles with the same behavior, respectively, to those in zones (1) and (2). Further distinctions can be made for other particles, which can stick on the upper (yellow) and lateral (pink) walls of the reactor.

4. Conclusions

Comparison of the results with experimental surveys from industrial gasifier can allow an assessment of the magnitude of particle “ejection” and provide a strategy for the reduction of particle entrainment and crusts formation.

References

[1] Iaquaniello, G., Centi, G., Salladini, A., Palo, E., Perathoner, S. and Spadaccini, L., (2017). Bioresource Technology, 243, pp.611-619.

[2] Antonetti, E., Iaquaniello, G., Salladini, A., Spadaccini, L., Perathoner, S. and Centi, G., (2017) ChemSusChem, 10(5), pp.912-920.

[3] Scala, F. and Salatino, P., 2002. Chemical engineering science, 57(7), pp.1175-1196.

ECCE12
The 12th EUROPEAN CONGRESS OF CHEMICAL ENGINEERING
Florence 15-19 September 2019

Liquid-phase synthesis of *sec*-butyl levulinate by esterification of levulinic acid with 1-butene over Amberlyst-15

J.H. Badia, E. Ramírez*, R. Bringué, C. Fité, M. Iborra, J. Tejero, F. Cunill
Chemical Engineering and Analytical Chemistry Department, Faculty of Chemistry, University of Barcelona, Martí i Franquès 1 11, 08028 Barcelona, Spain
*Corresponding author: eliana.ramirez-rangel@ub.edu

Highlights

- Esterification of levulinic acid with 1-butene over Amberlyst-15 is technically feasible
- The proposed reaction pathway entails very low byproducts formation
- High temperature and excess of levulinic acid gives high yield of sec-butyl levulinate
- Amberlyst-15 is a promising catalyst for the *sec*-butyl levulinate production

1. Introduction

Liquid-phase synthesis of *sec*-butyl levulinate (SBL) by esterification reaction of levulinic acid with 1-butene over an acidic ion-exchange resin (Amberlyst 15) has been studied in a batch reactor. The use of SBL in transportation fuels formulation is of interest due to some of its properties, which make SBL a potential candidate for blending in both diesel and gasoline fuels. For instance, when blended in diesel, butyl levulinates reduce vapor pressure and improve the lubricity, conductivity, and cold flow properties of the fuel, which leads to cleaner combustion, and are completely soluble below the diesel cloud point (around −25.8 °C) [1]. However, levulinates exhibit low cetane numbers, which entails that their inclusion in diesel formulation requires additional cetane-enhancing additives. With respect to gasoline, high blending octane quality is achieved by adding butyl levulinates. For instance, blending values of RON and MON of 107 and 98, respectively, have been reported for 10 %vol. addition of SBL [2].

On the other hand, since levulinates are synthesized from levulinic acid (LA), which is a non-edible lignocellulose derivative, SBL can contribute in achieving the biofuel target in current EU legislation, which sets a minimum 10 %vol. of biomass-based oxygenates to improve fuel automobile quality by 2020 [3].

Conventional production of butyl levulinates is achieved by: 1) esterification of LA with butanol, 2) furfuryl alcohol-butanol alcoholysis, and 3) direct butanolysis of saccharides or polysaccharides; all of which are acid-catalyzed reactions. In most cases, ester formation is limited due to side reactions responsible for the formation of, for instance, dialkylether, water and polymerization products. Alternative pathway synthesis for butyl levulinates involves replacing the alcohol for an olefin as the esterification agent, which poses lower byproducts formation than conventional pathways. In addition, residual refinery streams containing “spent” C4 compounds, which are usually regarded as low-value streams, can be re-valorized by using them as the olefin source, taking advantage of the fact that these streams are usually rich in linear butenes, butane, and isobutane.

Therefore, and given the scarce number of literature references on the proposed synthesis reaction using ion-exchange resins as catalysts, the present work is aimed at determining the optimal reaction conditions for the batch-mode liquid-phase synthesis of *sec*-butyl levulinate over Amberlyst-15, in terms of temperature and initial reactants concentration.

2. Methods

Reactants were LA (>98 %wt., Across Organic) and 1-butene (>99.9 %GC, Air Liquide). Amberlyst-15 (The Dow Chemical Company) was used as the acidic ion-exchange resin catalyst (acid capacity of 4.81 meq H^+/g, BET surface area of 42.1 m^2/g, BET pore volume of 0.328 cm^3/g, and maximum operating temperature of 393 K).

Experiments were performed following a two-factor face-centered experimental design in which temperature ranged from 323 to 373 K and initial AL to olefin molar ratio was varied between 0.5 and 2.0. The catalyst load was set at 5 g (about 3 %wt.). All experiments were carried out in a 200 cm^3 stirred-tank reactor equipped with a six-blade magnetic stirrer operated in batch mode. The pressure was set at 2.5 MPa by means of N_2. Samples were taken in-line at different reaction times and analyzed by GC-MS using a capillary column (HP-PONA 19091S-001, J&W Scientific; 100% dimethylpoly-siloxane, 50m×0.20mm×0.50 µm). The typical duration for every experimental run was of 5 h, at least.

3. Results and discussion

Almost complete conversion of 1-butene was achieved in all of the experiments, whereas some LA remained unreacted at the end of the runs. In fact, 1-butene readily isomerizes to *cis*- and *trans*-2-butenes, which in turn react with LA to give the corresponding ester, SBL. Results showed only minimal side reactions extension regardless of the assayed experimental conditions, being the sum of all formed byproducts, mainly 2-butanol and olefin dimers, always below 5 %GC. Table 1 lists main results in terms of yield towards SBL from 1-butene. As seen in the table, higher yield is achieved at high temperature and high initial molar ratio.

Table 1. Yield (Y) of SBL from 1-butene.

***T* (K)**	***R*°$_{A/O}$**	Y [a] **(%)**
323	0.5	21
323	2.0	54 ± 6
373	0.5	88
373	2.0	98
348	1.0	89

[a] Yield calculation is based on GC areas.

4. Conclusions

The feasibility of the proposed chemical reaction pathway is strongly supported by the low amount of formed byproducts, which is the main drawback of conventional synthesis of butyl levulinates. The highest assayed temperature (373 K) and an excess of levulinic acid in the reactants mixture favors the formation of the desired product. Amberlyst-15 is a promising catalyst for the proposed reaction, since it allows high conversions at relatively low temperature while being an inexpensive catalyst.

References

1. E. Christensen, A. Williams, S. Paul, S. Burton, R.L. McCormick, Energy Fuels 25 (2011) 5422–5428.
2. H. Jungbluth, K. Gottlieb, R. Wessendorf, Flüssige Kraftstoffe, WO1994021753A1, 09/29/1994.
3. European Directives 2009/28/EC and 2009/30/EC of 23 April 2009.

ECCE12
The 12th EUROPEAN CONGRESS OF CHEMICAL ENGINEERING
Florence 15-19 September 2019

Calcium looping for thermochemical energy storage: Kinetic modeling of limestone calcination

Athanasios Scaltsoyiannes[1], Andy Antzara[1], Tom Hills[2], Mark Sceats[2], Angeliki Lemonidou*[1]

[1] Department of Chemical Engineering, Aristotle University of Thessaloniki, University Campus, Thessaloniki, GR-54124, Greece; [2] Calix Europe Limited, Old Library Chambers, 21 Chipper Lane, Salisbury, SP1 1BG, UK

*Corresponding author: alemonidou@cheng.auth.gr

Highlights

- Kinetic experiments of calcination in a fixed-bed reactor.
- Calcination completed in less than 15 sec under conditions tested.
- A modified RPM (GRPM) describes adequately the reaction.

1. Introduction

Thermochemical energy storage (TCES) is of growing interest especially for concentrated solar power plants (CSP). The current technology is based on storage of sensible thermal energy using molten salts which "suffer" from short period storage, crystallization at temperatures lower than 200°C and degradation at temperatures higher than 550°C. A promising alternative is the calcium looping (CaL) due to the highly exothermic carbonation reaction and the higher operating temperatures (~850°C). Other advantages are the non-toxicity and availability of raw materials (e.g. limestone) and their capability to be stored for long periods at ambient conditions.

$$CaO + CO_2 \leftrightarrow CaCO_3 \qquad \Delta H = -178\ kJ/mol$$

Accordingly, the solar energy can drive the endothermic reaction in a calciner reactor while the reverse carbonation reaction will produce energy via a power cycle (e.g. Rankine cycle). The reaction kinetics is of great importance as it affects the overall efficiency of the process.
This work focuses on the kinetic measurements and modeling of the calcination reaction as well as on the deactivation evolution of limestone through the cycles. A fixed bed reactor flow unit was used for the experiments in order to achieve efficient gas-solid contact and eliminate the control by external transfer phenomena. A two stage mechanism was adopted for the kinetic modeling [1]. For comparison, two different models were used, namely a Prout Tompkins equation and a Generalized Random Pore Model (GRPM), which is a modified version of the RPM described by Gavalas [1, 2].The evolution of the deactivation through cycling was described with existing models [3].

2. Methods

The evaluation of reaction kinetics of the samples was performed in a bench scale laboratory unit operating near atmospheric pressure. The unit consists of the gas feed inlet section, a fixed bed quartz reactor (10mm ID) and a mass spectrometer (Omnistar TM GSD 320, PFEIFFER)). The material used was a limestone (Granicarb 0.1/0.8 provided by OMYA) with a particle size of 45-75μm. The tests were conducted using superficial velocity >12 cm/s to avoid the influence of mass

transfer to the observed rates. For the calcination kinetic experiment the sample was calcined under 20% CO_2/N_2 (GHSV=22500h^{-1}, P=1.5atm, T=950°C). The multicycle experiment (10 cycles, cycle time duration: 6min) for the deactivation assessment comprised carbonation under pure CO_2 flow (27000h^{-1}, P=1.7atm, T=890°C) and calcination under 20% CO_2 in N_2 (GHSV=22500h^{-1}, P=1.5atm, T=890°C).

3. Results and discussion

Figure 1 (A) presents the evolution of calcination expressed as a function of time. The calcination of limestone is very fast at 950°C and is completed in 15sec. Almost 80% of the conversion is achieved in less than 7sec. The two models provide good fitting to the experimental data obtained from a fixed bed reactor apparatus. The GRPM describes better the calcination reaction compared to the P-TM especially for low conversions. It is based on the evolution of the available surface area, so it is more realistic compared to the P-TM, which is a symmetrical sigmoidal curve. For both models the pre-exponential factor k_0 was the fitted parameter (GRPM: k_0=0.41m/s, P-TM: k_0=4.69 $10^9 s^{-1}$). Due to intense sintering, the multicycle performance deteriorates as the material loses 65% of initial capacity after 10 cycles (B). The deactivation was adequately described with a semi-empirical equation with a deactivation constant of k_d=0.48.

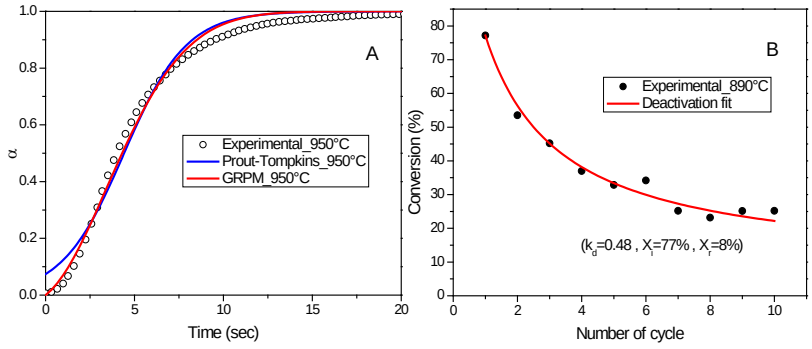

Figure 1. Calcination of limestone at 950°C along with P-TM and GRPM curves (A); Deactivation evolution of limestone through 10 cycles and modeling (B).

4. Conclusions

Calcination reaction as well as deactivation of limestone were studied experimentally in a fixed bed reactor unit and kinetically modeled. Two models were used for describing the experimental data. The GRPM better fits to the results compared to the P-TM. Calcination under the studied conditions is completed in a few seconds, rendering limestone appropriate as a solid heat carrier for CSP-TCES applications.

Acknowledgments

This work has received funding from the European Union's Horizon 2020 research and innovation program under grant agreement No 727348, project SOCRATCES.

References

[1] J.M. Valverde, P.E. Sanchez-Jimenez and L.A. Pérez-Maqueda, J. Phys. Chem. C, 119 (2015) 1623-1641.
[2] G.R. Gavalas, AIChE J., 26(4) (1980) 577-585.
[3] C. Ortiz, J.M. Valverde and R. Chacartegui, ACS Sustain. Chem. Eng., 6 (2018) 6404-6417.

ECCE12
The 12th EUROPEAN CONGRESS OF CHEMICAL ENGINEERING
Florence 15-19 September 2019

Design of the metal oxide catalysts for highly efficient and low temperature oxidation of VOCs

Marina Duplančić[1], Vesna Tomašić[1], Stanislav Kurajica[1], Zoran Gomzi[1], Albin Pintar[2]

1 University of Zagreb, Faculty of Chemical Engineering and Technology, Marulićev trg 19, Zagreb, Croatia;

2 National Institute of Chemistry, Department for Environmental Sciences and Engineering, Hajdrihova 19, Ljubljana, Slovenia

**marina.duplancic@fkit.hr*

Highlights

- Low temperature oxidation of VOCs.
- Mixed manganese and copper oxide catalyst.
- Fixed bed reactor *vs.* metal monolith reactor.
- Toluene as a model VOC component.

1. Introduction

The quality of the air and thus the quality of life is greatly affected by excessive emissions of volatile organic compounds (VOCs) which are recognized as the major contributors to global air pollution [1]. VOCs are emitted from different industrial plants and motor vehicles. Process intensification methodology, which most often involves the integration of catalytic and adsorption processes, and the development and application of structured catalysts, in particular monolith reactors, was used to develop highly efficient monolith reactors for low temperature oxidation of VOCs. The aim was to develop a metal monolith catalyst/reactor for catalytic oxidation of toluene as a representative volatile organic compound. Toluene was chosen as a model component because it is used in various industries (such as the automotive and pharmaceutical industries), and is often emitted in the environment as a result of the production and use of organic chemicals, solvents, dyes and similar products.

2. Methods

Mixed manganese and copper oxide in powder form ($MnCuO_x$) was prepared by the co-precipitation method [2]. Detailed characterization included the nitrogen adsorption-desorption analysis (BET), scanning electron microscopy (SEM), X-ray diffraction (XRD) analysis, differential scanning calorimetry (DSC) and Fourier Transform Infrared Spectroscopy (FTIR). Catalytic properties of the prepared catalyst were tested in a fixed bed reactor for toluene oxidation at various working conditions (temperature, reaction mixture flow rate).

Preparation of metal monolith catalysts/reactors included deposition of stabile catalytically active layer of $MnCuO_x$ on the surface of the corrugated metal monolith support (Al). In order to prepare metal monolith structure for a stable catalytic layer deposition, two-sided anodization of aluminum tiles was used. Catalytically active layer composed of manganese and copper oxides was

washcoated onto the metal monolith support (Al/Al_2O_3) [2]. The influence of working conditions, such as temperature and reaction mixture flow rate was tested.

Appropriate kinetic and reactor models for both, fixed bed and monolith reactor, were proposed and tested.

3. Results and discussion

The BET analysis showed textural properties of the prepared mixed oxide catalyst. With specific surface area of 23.7 $m^2 g^{-1}$, total pore volume of 0.10 $cm^3 g^{-1}$ and the average pore diameter of 16.5 nm the obtained catalyst can be classified as a mesoporous material, according to the IUPAC standards. The morphology of the $MnCuO_x$ oxide catalyst in powder form was further checked by the scanning electron microscopy (SEM) and it can be seen that the surface of the powder catalyst consists mostly of the spherical clusters with typical dimensions of about 1 micron. X-ray diffraction (XRD) of the powder $MnCuO_x$ mixed oxide identified four phases CuO, $CuMnO_4$, MnO_2 and Mn_2O_3. Differential scanning calorimetry over a wide range of temperatures (298-823 K) was used to investigate the thermal properties of $MnCuO_x$ mixed oxides it was found that in the temperature range from 523 K to ca. 655 K $MnCuO_x$ catalyst changes its crystalline structure which is accompanied by the release of energy of -209 J g^{-1}. In line with these observations before testing the catalyst activity for toluene oxidation the catalyst was pre-treated (calcined) at the temperature of 523 K for 2 h and then for 3 h at the temperature of 773 K. The DCS curve after pre-treatment shows no structural changes in the observed temperature range indicating that the catalyst obtained after pre-treatment is structurally stable in this temperature range and as such suitable for catalytic experiments. FTIR analysis confirmed that during the toluene oxidation over $MnCuO_x$ oxide catalyst there was no significant adsorption of possible reaction intermediates or reactants on the surface of the catalyst. Specific T_{90} values (90% toluene conversion) for powder $MnCuO_x$ vary from 431 to 480 K depending on the reaction mixture flow rate and T_{90} values for monolith catalysts, Al/Al_2O_3-$MnCuO_x$ are even lower, from 432 to 468 K depending on the reaction mixture flow rate.

4. Conclusions

Toluene oxidation over manganese and copper mixed oxide catalyst in powder and monolith form was studied. The high specific surface area, mesoporous structure along with high catalytic activity at relatively low temperatures demonstrates that this catalyst is suitable for the catalytic oxidation of toluene at different operation conditions.

The prepared powder $MnCuO_x$ and monolith Al/Al_2O_3-$MnCuO_x$ catalysts show extremely high activity for the toluene oxidation. It is particularly important to point out that the observed high conversions of toluene are achieved at relatively low temperatures (< 432 K) depending on the reaction mixture flow rate, which is important for the practical application of the catalyst in real systems. Applied mathematical models give satisfactory results for the oxidation of toluene in the experimental system described in this work.

References

[1] M. S. Kamal, S. A. Razzak, M. M. Hossain, Atmos. Environ. 140 (2016) 117–134.
[2] M. Duplančić, V. Tomašić, Z. Gomzi, Environ. Technol. 39 (2018) 2004 – 2016.

ECCE12
The 12th EUROPEAN CONGRESS OF CHEMICAL ENGINEERING
Florence 15-19 September 2019

Reactor concept for continuous milli-reactors

Marlies Moser, Esteban Rosasco, Norbert Merkel, Alain Georg

Fluitec mixing + reaction solutions AG, Seuzachstrasse 40, 8413 Neftenbach, Switzerland

**Corresponding author: mm@fluitec.ch*

Highlights

- Scale-up of exothermic reactions up to 2500 – 4300 t y^{-1}.
- Concept for a safe reactor design.
- Countercurrent safety purge system.
- Control system with a standard operating manual.

1. Introduction

Flow Chemistry at production and pilot scale presents new challenges to plant manufacturers. Scale-up of highly exothermic and fast reactions requires reliable safety measures. This work shows a reactor concept with safety elements for hazardous reactions including technical and electronic solutions to prevent an excessive temperature and pressure.

2. Methods

This pilot plant was designed and manufactured by Fluitec. Also, programming was done by Fluitec using Siemens PLC.

3. Results and discussion

The DN50 reference pilot plant for 2500 – 4300 t y^{-1} consists of two dosing systems, a tubular reactor containing static mixer heat exchangers [1], the safety purge system and a quench tank (Figure 1). Its underlying concept merges directives and standards of four fields: mechanical engineering (PED 2014/68/EU, MD 2006/42/EC, ATEX 2014/34/EU), chemical engineering (thermal safety concepts from F. Stoessel [2]), electrical engineering and safety (functional safety SIL according to EN 61511).

With this plant, three protection goals are met: dosing, inadmissible temperature and pressure. The devices are monitored by multiple mass flow meters, axial temperature sensors along the reactor, SIL approved temperature sensors and pressure sensors. In the case of a failure, the SIL approved safety purge system will empty out the reactor within a few seconds and direct the media to the quench tank, where it will be immediately inertised. This countercurrent safety purge was developed as an event preventing safety device. Besides this also damage limiting devices were installed such as rupture discs and a safety valve.

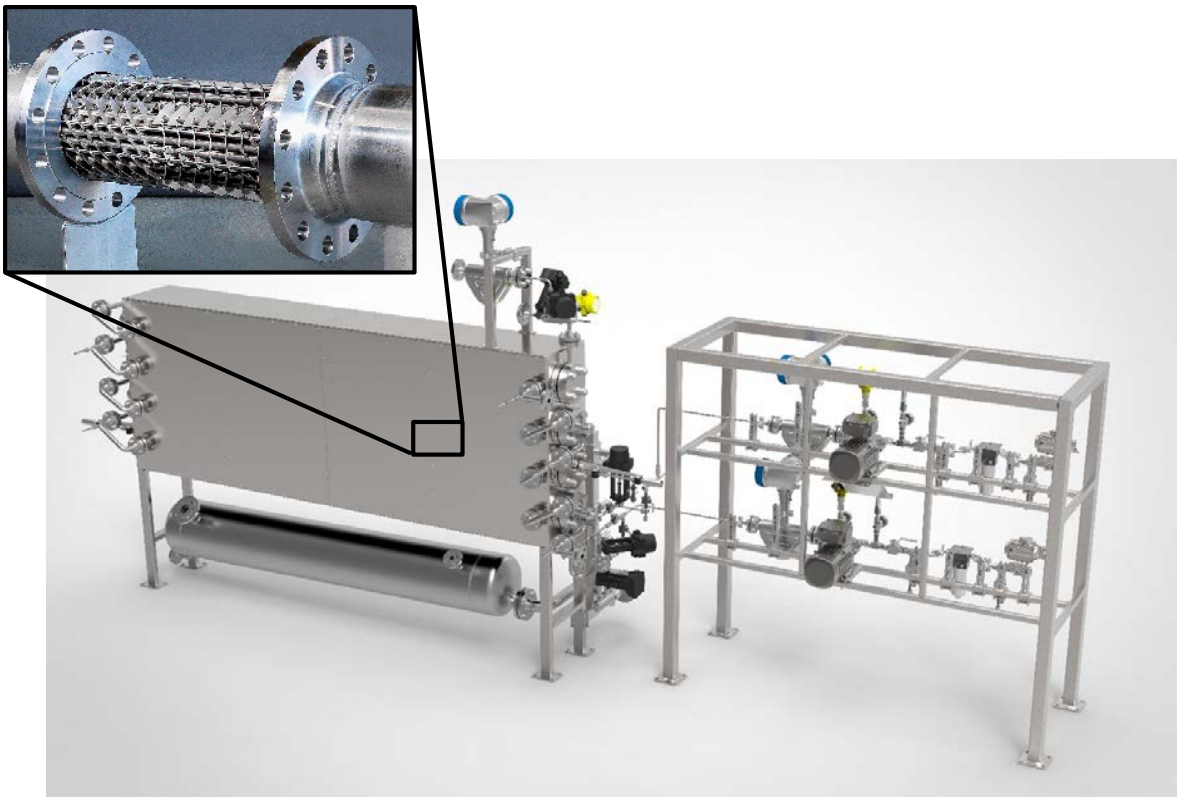

Figure 1. Reference pilot plant (2500 – 4300 t y^{-1}) containing two dosing systems, DN50 mixer heat exchangers and the safety purge system with quench tank.

4. Conclusions

This concept together with the scalable bundle mixer heat exchanger provides a way to tackle the scale-up problem of highly exothermic reactions in tubular reactors. The reactor and programming of the control system needs to be adjusted according to the characteristic temperature levels of the desired and decomposition reaction.

References

[1] A. Georg, M.B. Daescher, Chem. Ing. Tech. 2005, 77 (6), 681-693.

[2] F. Stoessel, Thermal Safety of Chemical Processes: Risk Assessment and Process Design, John Wiley & Sons, Weinheim 2008.

ECCE12
The 12th EUROPEAN CONGRESS OF CHEMICAL ENGINEERING
Florence 15-19 September 2019

A Bayesian approach for continuous improvement of kinetic parameter estimates

Karsten H. G. Rätze[1], Kevin McBride[2], Kai Sundmacher[1,2]

1 Otto von Guericke University, Magdeburg; 2 Max Planck Institute for Dynamics of Complex Technical Systems, Magdeburg

**Corresponding author: raetze@mpi-magdeburg.mpg.de*

Highlights

- Optimal experimental design (OED) with Bayesian parameter estimation
- Continuous improvement of estimation quality via repeated OED and experiments
- Optimal control trajectories for parameter estimation of the Hydroformylation of 1-decene

1. Introduction

Estimation of kinetic model parameters requires experimental data which needs to be gathered over multiple experiments with varying reaction conditions. As a consequence, building a mechanistic reaction model is labor intensive and requires significant financial investments. Combining optimal experimental design (OED) with dynamic perturbation experiments [1] improves the data generation while reducing the overall experimental effort. By embedding the OED in a sequential approach of repeated experimental design, execution of experiments and subsequent parameter estimation, the amount of necessary experiments is reduced to a minimum. However, implementing the proposed procedure requires repeated usage and updates of prior information on the kinetic parameters. Bayesian parameter estimation is one possible solution by incorporating prior information of different sources in the parameter estimation process while simultaneously providing a measure of the estimation quality.

2. Methods

The parameter estimation procedure may be exemplified using four steps. Initially, a structurally viable, dynamic kinetic model is required with initial values for the model parameters. To improve the quality of the error bounds of the parameter estimations, measurment errors of the experimental equipment are required. Initially, OED generates dynamic control profiles respective to the chosen optimality criterion (A-, D- or E-optimality). Additionally, optimal measurement times need to be calculated that incorporate physical limitations of the experimental equipment and procedure. After performing the experiment, the prior information is used to perform the parameter estimation using Monte Carlo Marcov Chain simulations.

3. Results and discussion

To exemplify the proposed procedure, the hydroformylation of 1-decene is chosen as example reaction. Based on mechanistic models from literature [2] a selected set of unknown parameters

$p = [A_{\mathrm{Iso1}}, B_{\mathrm{Iso2}}]$ is chosen for parameter estimation. An initial guess is provided which deviates from the true parameter values $p_{\mathrm{true}} = [11.04, 18.53]$ found in [2]. Besides limiting the measurment data to two of the reactants, dodec-1-ene and dodec-2ene, the limitations of the experimental equipment are incorporated by enforcing a two minute time interval between measurments and limiting the rate of change of the reaction temperature $|\frac{\mathrm{d}T}{\mathrm{d}t}| \leq 2\,\mathrm{K/min}$. A normal distribution is chosen with $\mu = [10, 17]$ and $\sigma = [0.5, 0.5]$ as prior information for the parameters.

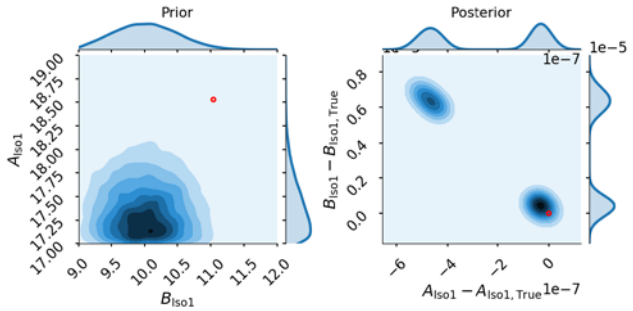

Figure 1. Probability density function improvement of A_{Iso1} and B_{Iso1} after one experiment.

Figure 1, depicts the improvement of the parameter probability density functions. In addition to the adequate approximation of the true parameter values via the density mean, the standard deviation of both probability density functions indicate a significant improvement of the estimation quality.

4. Conclusions

The proposed procedure shows a fast convergence to the true parameter values while simultaneously providing an indicator for the estimation quality. The standard deviation may be used as a stopping criterion for determining the necessary amount of experimental data, thereby reducing the development time for reaction kinetic models and improving economics.

Acknowledgements

This work is part of the Collaborative Research Center/Transregio 63 „Integrated Chemical Processes in Liquid Multiphase Systems“ (subproject B1). Financial support by the Deutsche Forschungsgemeinschaft (DFG, German Research Foundation) is gratefully acknowledged. The corresponding author is also affiliated to the „International Max Planck Research School for Advanced Methods in Process and Systems Engineering”.

References

[1] P. Heidebrecht, K. Sundmacher, L.T. Biegler, AIChE Journal 57 (2011) 2888–2901.
[2] A. Jörke, T. Gaide, A. Behr, A. Vorholt, A. Seidel-Morgenstern, C. Hamel, Chemical Engineering Journal 313 (2017) 382–397.

ECCE12
The 12th EUROPEAN CONGRESS OF CHEMICAL ENGINEERING
Florence 15-19 September 2019

CFD studies on the hydrodynamics in systems with open-cell foam internals

José D. Araújo*[1], João Barbosa[1], Manuel A. Alves[1] and João M. Campos[1]

[1] CEFT, Department of Chemical Engineering, Faculty of Engineering of the University of Porto

Rua Dr. Roberto Frias, 4200-465 Porto, Portugal

*Corresponding author: daraujo@fe.up.pt

Highlights

- Open-cell foams based on cubic cells with different tilt angles were investigated
- Residence time distribution was computed by CFD techniques
- Mass dispersion coefficients and pressure drop per unit length were estimated

1. Introduction

Fixed bed reactors are among the most relevant operation units in chemical industries, and the design of the internals is a subject that gathers particular attention. In the past, random or unstructured packings were mostly used which largely limited the freedom of design. Nowadays, this freedom is continuously increasing due to the application of more ordered structures, which can be even more potentiated by the implementation of 3D printing in the reactors intensification [1]. Following this trend, open-cell foams place themselves as a very attractive option suitable to enhance a wide range of industrial applications [2]. However, there is still a lack of detailed investigations about the hydrodynamics in fixed beds based on open-cell foams. Regarding chemical engineering, computational fluid dynamics (CFD) is widely used to simulate specific phenomena and also the combination of features that occurs on entire production units like chemical reactors. Overall, CFD tools can provide great flexibility for parametric studies and sufficient detail to describe different phenomena with distinct spatial and temporal characteristic scales.

The present work consists on a parametric and systematic study of the hydrodynamics of single phase flows through open-cell foams with cubic cell topology. CFD techniques are used to numerically replicate tracer experiments for the prediction of several characteristic parameters, such as mass dispersion and pressure drop.

2. Methods

The present numerical study was based on a CFD approach entirely open-source: OpenFOAM® CFD package to perform the numerical simulations; Blender® to generate the geometry/domain in the form of STL files; and SnappyHexMesh tool of OpenFOAM® to create the computational mesh. The domain under consideration (total length of 4.5 cm and diameter of 2.0 cm) is a portion of a cylindrical tube filled with ordered open-cell foam structure with different configurations derived from the repetition of unitary cubic cells. The space between struts (pore size) varied from 0.2 to 0.3 cm corresponding to porosities in the range of 0.60-0.95.

The simulated systems replicate tracer tests in order to produce residence time distribution data, i.e., it consists on liquid phase flow (water properties) through the foam with a feed of solute in the

core of the inlet cross-section (step input). The model includes the Navier-Stokes equations and the mass balance equation for the tracer. A large set of simulations was performed with different superficial velocities and cubic cells orientations.

3. Results and discussion

The main raw data to extract from the CFD simulations are the velocity, pressure and concentration fields. Based on this data for each simulation, it is possible to determine the pressure drop per unit length, produce the cumulative residence time distribution (Figure 1a) and estimate axial and radial mass dispersion coefficients (Figure 1b). These coefficients are obtained from fitting the numerical data to Danckwerts [3] and Hiby and Schummer [4] equations. The first step was to perform mesh independency tests to define a proper density (around 1300000 mesh elements) to apply throughout the work. It was verified that the mesh density affects mainly the dispersion coefficients results and the estimation of stagnant regions.

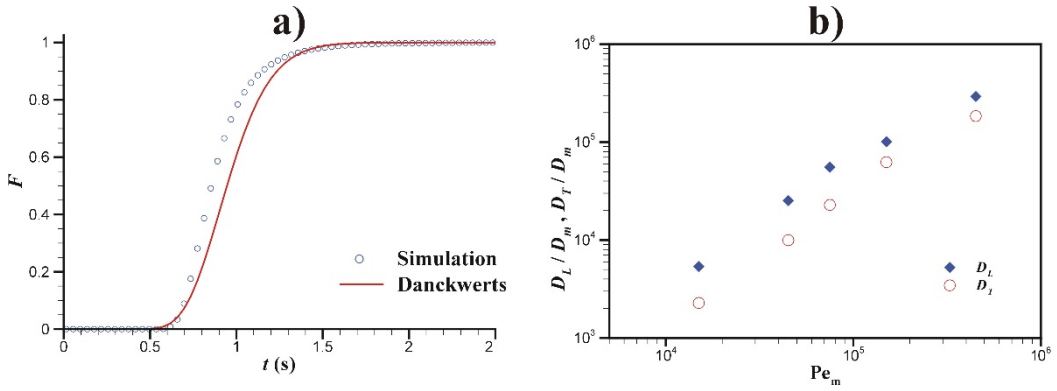

Figure 1. Cumulative residence time distribution for a system with a superficial velocity of 0.03 m/s (a) and dimensionless axial and radial dispersion coefficients as a function of molecular Peclet number (b).

The results in Figure 1 are illustrative of what will be obtained in this study, since the work is still under active development. More detailed and extensive results will be presented and comparisons will be made with available experimental and/or correlation data. Furthermore, there is the possibility of including a last set of simulations addressing illustrative homogeneous and surface reactions in some selected foam structures.

4. Conclusions

The implementation of open-source computational tools to simulate the flow inside tubes filled with open-cell foams was carried out. Single phase flow simulations were performed to replicate tracer experiments and produce important hydrodynamic information such as mass dispersion coefficients and pressure drop. A parametric study will be presented about the influence of the superficial velocity and tilt angles of the foam unitary cubic cells on the referred hydrodynamic parameters.

References

[1] https://www.sintef.no/projectweb/printcr3dit/.
[2] E. Bianchi, W. Schwieger, H. Freund, Adv. Eng. Mater. 18 (2016) 608-614.
[3] P.V. Danckwerts, Chem. Eng. Sci. 2 (1953) 1-13.
[4] J. Hiby, P. Schümmer, Chem. Eng. Sci. 13 (1960) 69-74.

ECCE12
The 12th EUROPEAN CONGRESS OF CHEMICAL ENGINEERING
Florence 15-19 September 2019

Gas-liquid hydrogenation in continuous flow for process intensification and rapid process optimization

Nikolay Cherkasov[1,2*], Evgeny V Rebrov[1,2]

1 Stoli Catalysts Ltd, Coventry, UK; 2 University of Warwick, Coventry, UK

**Corresponding author: n.cherkasov@stolicatalysts.com*

Highlights

- Catalyst-coated tube reactors provide no mass transfer limitations in hydrogenation
- Compared to packed-bed reactors, the coated tubes show 14-25 times higher throughput
- Quick mass transfer in catalyst-coated tubes provides excellent product selectivity
- Low-cost refractory sensors provide process automation and faster process development

1. Introduction

The fine chemicals industry relies on batch reactors which are inefficient in terms of space-time yield and safety. Flow chemistry solves these problems, provides a possibility for process intensification, and allows for production with lower capital requirements. Additionally, flow chemistry offers opportunities for process automation. In the work we present the application of catalyst-coated tube reactors in continuous flow hydrogenation of alkynes, alkanes, imines, and unsaturated aldehydes and their advantages compared to batch and fixed bed reactors in terms of mass transfer and product selectivity.

2. Methods

The tube reactors wall-coated with 12 wt% Pt/SiO2, 5 wt% Pd/ZnO, 5 wt% Pd/C catalysts were provided by Stoli Catalysts Ltd [1]. The solid catalysts were obtained by removal of the catalyst coatings. The reactions were performed in a flow system containing an HPLC pump for a substrate solution, mass flow controllers for H_2, an oven with the catalyst-coated tube, an Equilibar gas-liquid back-pressure controller downstream followed by a fraction collector. The reaction was operating autonomously using a pre-defined set of steps collecting samples for offline GC analysis controlled with OpenFlowChem automation platform [2].

3. Results and discussion

We studied the effect of mass transfer and residence time distribution on semi-hydrogenation reaction of alkyne (2-methyl-3-butyn-2-ol) and full hydrogenation of ethyl cinnamate. The catalyst-coated tube reactors showed no external mass transfer limitations, in contrast to packed beds, and a substantially narrower residence time distribution. The Peclet number in the tube reactor was above 100 indicating an ideal plug-flow behaviour in contrast to the packed-bed (Figure 1A). As a

result, the alkyne semi-hydrogenation in packed-bed reactors was a factor of 25 slower less selective (60% vs 95%). The full hydrogenation reaction was 14 times slower in packed-bed compared to catalyst-coated tube. Similarly, the packed-bed reactor filled with a 12 wt% Pt/SiO2 catalyst was inferior to the catalyst-coated tube with the selectivity towards unsaturated alcohol of 20% vs 90% likely due to elimination of mass transfer limitations and excellent control of residence time [3].

The continuous-flow hydrogenation can benefit from process automation. We demonstrated that low-cost (<10$) refractory liquid sensors can be used to accelerate process development and optimisation [4]. An example of dehydrolinanool hydrogenation in Figure 1B shows that the approach provides consistent and reproducible results.

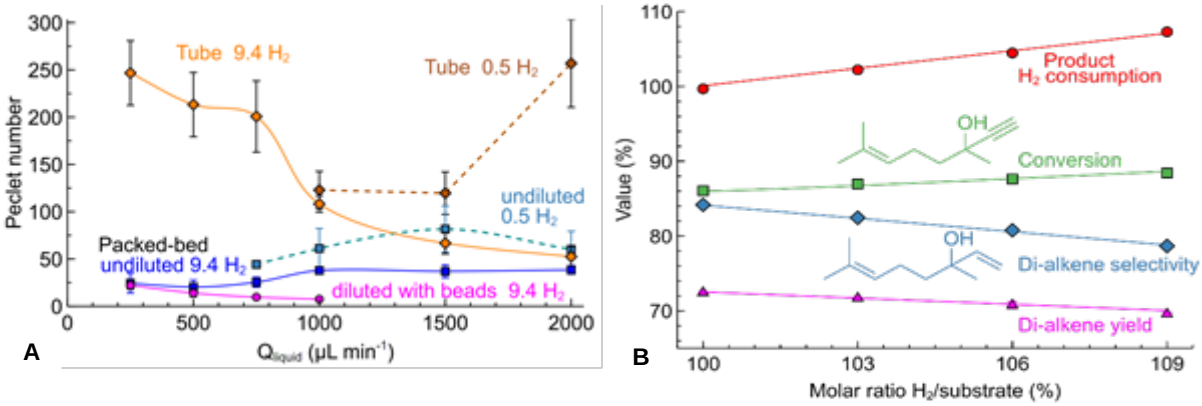

Figure 1. (A) Effect of the liquid flow rate on the Péclet number obtained in the tube and packed-bed reactors. (B) Dehydrolinalool semi-hydrogenation in a 2.3 wt% Pd/ZnO catalyst-coated tubes at various H_2/substrate feed ratios at 95% H2 absorption.

4. Conclusions

The results show that the catalyst-coated tube reactors provide excellent control of hydrogenation reaction conditions without external or internal mass transfer limitations. This results in a substantially higher throughput, a factor of 14-25 and higher selectivity in case of selective hydrogenation reactions. Using online analytics such accelerates the process development.

References

[1] N. Cherkasov, A.O. Ibhadon, E. V. Rebrov, Lab Chip. 15 (2015) 1952–1960.
[2] N. Cherkasov, Y. Bai, A.J. Exposito, E. V. Rebrov, React. Chem. Eng. 3 (2018) 769–780.
[3] Y. Bai, N. Cherkasov, S. Huband, D. Walker, R. Walton, E. Rebrov, Catalysts. 8 (2018) 1–18.
[4] N. Cherkasov, A. Exposito, Y. Bai, E. V Rebrov, React. Chem. Eng. 4. (2018) 112-121.

ECCE12
The 12th EUROPEAN CONGRESS OF CHEMICAL ENGINEERING
Florence 15-19 September 2019

Continuous scalable synthesis of reactive intermediates: Grignard Reagents and Grignard Reaction

M. G. Menges-Flanagan*, E. Deitmann, L. Gössl, C. Hofmann, P. Löb

Fraunhofer Institute for Microengineering and Microsystems IMM, Carl-Zeiss-Str. 18-20, 55129 Mainz, Germany

**Corresponding author: Gabriele.menges-flanagan@imm.fraunhofer.de*

Highlights

- Continuous synthesis of industrially relevant Grignard reagents.
- Grignard reaction immediately following the reactive intermediate synthesis.
- Scalable processes allowing throughputs of tens of liters per hour.
- Improved product quality and flexible production to improve time-to-market.

1. Introduction

For over 100 years, Grignard reagents (RMgX) and their either simultaneous (Barbier reaction) or subsequent reaction (Grignard reaction) with other halides, aldehydes, ketones, etc. have been a most useful tool for process chemists seeking to form new C-C bonds.[1] However, drawbacks such as variable incubation periods for their initial formation, high exothermicity requiring effective heat management, as well as side reactions such as Wurtz coupling pose challenges to be overcome when aiming at large scale industrial production of such compounds. Here, continuous processing will benefit the Grignard reagent formation and Grignard reaction through improved heat management and the continuous provision of a large Mg excess with the aim to significantly suppress unwanted side product formation.

2. Methods

All solvents and reagents were purchased from commercial suppliers and were used without further purification. The set-up consists of Postnova syringe pumps while tempering of the reactors is achieved by the use of thermostatic baths. Progress of the reactions could be followed by recording the temperatures within the reactors. The family of reactors used for the continuous Grignard reagent formation spanning a wide range of accessible flow rates is given in Figure 1. Titration of the Grignard reagent was done following the method of Lin and Paquette[2] or Krasovskiy and Knochel[3].

3. Results and discussion

Initially, a laboratory scale reactor was established by 3D laser melting and tested for the continuous synthesis of a number of common Grignard reagents *via* processing of solid/liquid mixtures. In contrast to conventional processing of Grignard reagents, in this case a large excess of Mg within the reactor with integrated mechanical Mg activation, was used to suppress unwanted side reactions and allow for full halide conversion within one passage through the reactor with residence times on the order of 3-30 minutes depending on concentration and

reactivity. A broad applicability of this approach was established by synthesizing multiple alkyl and aryl Grignard reagents at varying concentrations in qualities comparable to commercially available products. Additionally, a number of Grignard reactions were also performed on the laboratory scale using freshly prepared Grignard reagents omitting the need for storage of these rather reactive intermediates. Lastly, results will be presented on scale-up efforts undertaken to build a larger scale pilot reactor set-up allowing for halide throughputs of up to 20l/h as well as again including an immediate second step (Grignard reaction) after online detection of Grignard reagent quality formed.

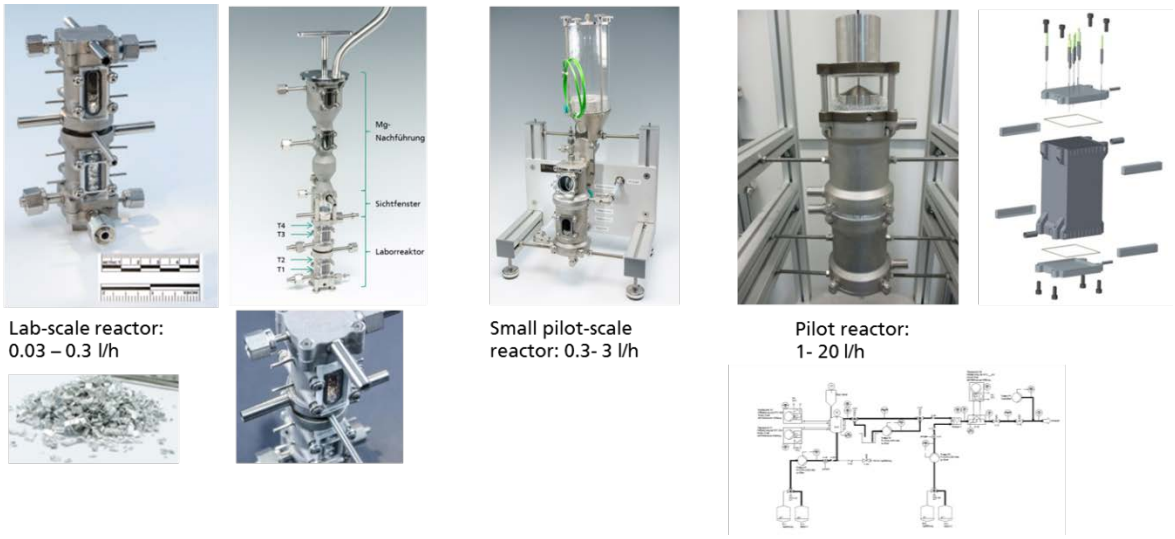

Figure 1. Family of scalable 3D laser sintered reactors for Grignard reagent formation and Grignard reaction.

4. Conclusions

In conclusion, a continuously operating laboratory set-up for Grignard reagent formation manufactured *via* 3D laser melting was established and tested in the optimization of process parameters for scalable continuous Grignard reagent formation. It was aimed at full halide conversion within a single reactor passage with the goal of achieving maximum throughput with minimal energy input (heating/cooling). After Grignard reagent formation was established continuously, it was immediately followed by Grignard reactions consuming the reactive intermediate omitting the need to store this reagent over prolonged time periods. Finally, efforts are underway to scale-up the two steps to pilot-scale throughputs to halide solution flow rates of up to 10-20l/h.

References

[1] V. Grignard, in CR Hebd. Séances Acad. Sci., Ser. C. 130, 1900, pp 1322–1324.
[2] H.-S. Lin, L. A. Paquette, Synth. Commun. 1994, 24(17), 2503-2506.
[3] A. Krasovskiy, P. Knochel, Synthesis 2006, 5, 890-891.York, 2009, pp. 181–304.

ECCE12
The 12th EUROPEAN CONGRESS OF CHEMICAL ENGINEERING
Florence 15-19 September 2019

Biohydrogen from waste wood hemicellulose hydrolysate

*Atte Aho[1], Irina Simakova[3], Juha Ahola[2], Jani Kangas[2], Juha Tanskanen[2], Dmitry Yu. Murzin[1], Tapio Salmi[1], Henrik Grénman[1]**

[1]*Laboratory of Industrial Chemistry and Reaction Engineering, Johan Gadolin Process Chemistry Centre, Åbo Akademi University, Turku/Åbo, Finland*

[2]*Chemical Process Engineering, University of Oulu, Oulu, Finland*

[3]*Boreskov Institute of Catalysis, Novosibirsk, Russia*

**Corresponding author: henrik.grenman@abo.fi*

Highlights

- APR performed directly on sugar solutions has been a challenge hindering the development
- Experiments were performed with model solutions followed by actual hydrolysates
- 100% conversion was obtained with tailor made catalysts
- The selectivity of the process could be steered by choice of catalyst

1. Introduction

Currently, one of the key processing operations in the versatile utilization of biomolecules to value added products is hydrotreatment e.g. the stabilization and refining of bio-oils originating from biomass pyrolysis and liquefaction lead typically to different hydrotreatments and the valorization of "waste" lignin requires hydrotreatment in many pathways [1-2]. One potential source for the hydrogen used in the hydrotreatments is biohydrogen produced from waste wood and wood hydrolysates. In this study we investigate biohydrogen production applying first selective reactive/catalytic extraction of hemicellulose from waste wood to monosaccharides. After the reactive extraction we evaluate if the monosaccharides can be used directly, or first after hydrogenation to sugar alcohols, as a raw material to produce hydrogen using aqueous phase reforming (APR) over a solid catalyst. Aqueous phase reforming of sugar alcohols, and more generally polyols, to hydrogen and light alkanes can be performed over various supported metal catalysts at relatively mild operating conditions (ca. 225 °C, 30-50 bar) [3,4].

2. Methods

The reactive extraction experiments were performed using ground softwood (Pinus sylvestris) particles. Extraction solvent was a mixture of water and formic acid, which acted as the catalyst. The effects of operation conditions (reaction time, temperature and acid concentration) and particle size to the quality of the hydrolysate were investigated in an Accelerated Solvent Extraction equipment.

To enable initial evaluation of the characteristics and feasibility of the selected biohydrogen production route from wood hemicellulose, APR experiments were performed using a water

solution of xylitol, mixtures of xylitol and xylose, and finally with a mixture of xylose and formic acid. The actual extracts were tested after the evaluation with the model mixtures. Commercially available and tailor made catalysts were employed in the experiments. The effects of temperature, residence time and gas flow through the reactor on the conversion and selectivity to hydrogen and CO_2 were investigated. The fixed bed continuous reactor was operated in co-current trickle flow and the gas analysis was performed online with micro-GC while the liquid phase was analyzed with HPLC.

3. Results and discussion

Based on the reactive extraction experiments, formic acid catalyzed hemicellulose extraction results in the recovery of hemicellulose as monosaccharides with the efficiency ranging from 60%-75% at the optimal extraction time. Maximum recovery is relatively independent on the reaction temperature or formic acid concentration, when temperature is over 140 °C and formic acid concentration is over 4 wt-%.

In the APR experiments, it was observed that in order to achieve high conversion of xylitol the temperature should be preferably above 225°C. Additionally a three phase system with a flow of inert gas is very beneficial for increasing the conversion. No significant changes in selectivity to hydrogen was observed at different xylitol conversions obtained at varying experimental condition. Mixtures with different ratios of xylose and xylitol were tested in the same experimental conditions with the idea that the hydrogen produced from the xylitol could in situ hydrogenate the xylose and initiate the further APR reaction. All of the experiments resulted in the same conclusion; the mixture caramelized rapidly and blocked the reactor due to humine formation. Attempts to hydrogenate the sugar mixture were unsuccessful as the formic acid prevented the hydrogenation. Experiments were then performed with the xylose and formic acid mixtures. Promising results were obtained at relatively mild conditions, but even at higher temperatures the caramelization due to humine formation was avoided utilizing a tailor made catalyst and 100% conversion was obtained.

4. Conclusions

These results show that Aqueous phase reforming can be performed on actual hydrolysate sugar solutions directly, which is a significant advancement in the field. It enables the flexible supply of biohydrogen in locations that process biomass with side streams of sugars and .

References

[1] Wildschut, J. et al. 2009. Hydrotreatment of fast pyrolysis oil using heterogeneous noble-metal catalysts. Industrial & Engineering Chemistry Research 48(23), 10324–10334.

[2] Wang, H., Male, J. & Wang, Y. 2013. Recent advances in hydrotreating of pyrolysis bio-oil and its oxygen-containing model compounds. ACS Catalysis 3(5), 1047–1070.

[3] Coronado, I. et al. 2016. A review of catalytic aqueous-phase reforming of oxygenated hydrocarbons derived from biorefinery water fractions. International Journal of Hydrogen Energy 41(26), 11003–11032.

[4] Murzin, D.Yu. et al. 2017. Kinetics, Modeling, and Process Design of Hydrogen Production by Aqueous Phase Reforming of Xylitol. Industrial and Engineering Chemistry Research 56, 13240–13253.A. Bianchi, N.C. Jones, Chem. Eng. J. 157 (2019) 326–337.

ECCE12
The 12th EUROPEAN CONGRESS OF CHEMICAL ENGINEERING
Florence 15-19 September 2019

Preparation of Hydrogen Source COx-free Fuel Cell by Ammonia Decomposition using ZA-5 Wustite Catalyst

Huazhang Liu, Chao Huo*

Institute of Industrial Catalysis, Zhejiang University of Technology, Hangzhou 310014, P.R. China

**Corresponding author: chaohc@zjut.edu.cn*

Highlights

- ammonia decomposition, ZA-5 $Fe_{1-x}O$ based catalyst, hydrogen fuel.
- The performance of ZA-5 wustite-based catalyst for ammonia decomposition to produce hydrogen is studied in this paper. The technology of ZA-5 wustite-based catalyst is ripe with low cost. Ammonia decomposition has obvious advantages in process technology, product composition and production cost.
- The ammonia conversion was over 99.9% and the hydrogen production rate reached 189.58 mol H_2/(gcat·h).

1. Introduction

Hydrogen is regarded as a clean energy source with broad application prospects. Hydrogen fuel cells are the most promising new generation energy supply system[1-3]. Currently, hydrogen production and storage technologies are solved by ammonia decomposition. In other word, storage of hydrogen is in liquid ammonia.

At present, the widely used catalysts for ammonia decomposition in industry are Ru or Ni catalysts supported on MgO and $A1_2O_3$. Although the Ru-based catalyst has high activity, it is costly and the Ni-based catalyst consumes a large amount of electricity and is severely corroded. Therefore, this paper uses a new low-temperature and high-efficiency ammonia synthesis ZA-5 $Fe_{1-x}O$ catalyst to study the performance of ammonia decomposition hydrogen production.

2. Methods

Promoters and fine magnetite powder and the reduced iron powder was mixed uniformly. Then the mixture is putted into the electric melting furnace at one time. After melting, the high temperature slurry is rapidly poured into the cooling tank with water jacket and cooled to room temperature, then broken and sifted to the desired particle size.

3. Results and discussion

The effect of the main factors of reaction temperature and space velocity on the ammonia decomposition activity of ZA-5 $Fe_{1-x}O$-based catalyst was carried out. The effects of temperature (450-600 °C) and space velocity (900-7800 h^{-1}) on the ammonia decomposition activity over ZA-5 $Fe_{1-x}O$- based catalyst were investigated.

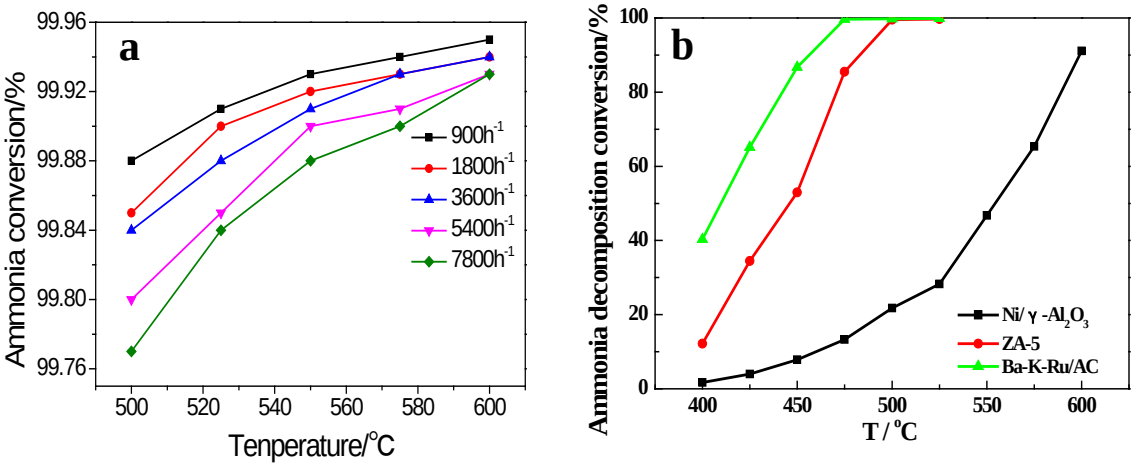

Figure. 1(a)The conversion of ammonia over ZA-5 $Fe_{1-x}O$-based catalyst as a function of reaction temperature at different space velocity; (b) Comparison of ammonia decomposition conversion for ZA-5, Ru/AC and Ni catalysts

It is observed from Figure.1a that the conversion of ammonia decomposition increases with the increase of temperature and decreases with the increase of space velocity. When the temperature reaches 500°C, the ammonia conversion reaches more than 99.7% at all investigated space velocity. If the temperature continues to rise, the ammonia conversion will have little difference, which because the ammonia conversion is close to the equilibrium conversion.

The activity of ZA-5, Ru/AC and Ni/γ-Al_2O_3 catalyst produced by an enterprise was determined under the same conditions. The conversion is shown in Figure.1b. It can be seen from Figure.1b that the low temperature activity of Ru/AC catalyst below 500 °C is obviously higher than that of ZA-5 catalyst, but the difference is not significant above 500 °C and the price is high. While the activity of Ni/ γ-Al_2O_3 catalyst is very bad.

4. Conclusions

The performance of ZA-5 $Fe_{1-x}O$ based catalyst for ammonia decomposition was studied. The results showed that the ammonia conversion was over 99.9 % and the hydrogen production rate reached 189.58 mol H_2/(gcat·h), and compared with Ru/AC and Ni catalysts. The cost of raw material, catalyst and investment cost of industrial plant for ammonia decomposition hydrogen production were analyzed. H_2 obtained from ammonia decomposition does not contain harmful substances such as CO_x, SO_x, NO_x. Ammonia is liquid at room temperature and 0.8 MPa with high energy density per unit volume. Therefore, the combination of ammonia and Fe catalysts with fuel cells is a perfect combination.

References

[1] A. S. Chellappa, C. M. Fischer, W. J. Thompson. Applied Catalysis A: General, 227 (**2002**) 231–240.

[2] C. K. Dyer. J. Power Sources, 106 (**2002**) 31–34.

[3] D. R. Palo, J. D. Holladay, R. T. Rozmiarek, Consuelo E. Guzman-Leong, Yong Wang, Jianli Hu, Ya Huei Chin, Robert A. Dagle, Eddie G. Baker. J. Power Sources, 108 (**2002**) 28–34.

ECCE12
The 12th EUROPEAN CONGRESS OF CHEMICAL ENGINEERING
Florence 15-19 September 2019

Evaluation of the Catalytic Activity of Red Mud for Olive Mill Wastewater Tretament by Fenton's Process

E. Domingues, J. Gomes, D. Lopes M..J. Quina, R. M. Quinta-Ferreira, R. C. Martins
[1]*CIEPQPF – Chemical Engineering Processes and Forest Products Research Center, Department of Chemical Engineering, Faculty of Sciences and Technology, University of Coimbra, Pólo II – Rua Sílvio Lima, 3030-790 Coimbra, Portugal, Portugal;* [2]*CICECO –Aveiro Institute of Materials, Department of Materials and Ceramic Engineering, University of Aveiro, 3810-193 Aveiro Portugal.*

Highlights

- Fenton, photo-Fenton, Red-mud, low cost catalyst

1. Introduction

Fresh OMW is considered phytotoxic because it has in its constitution phenolic compounds. The traditional physical chemical treatments only solve part of the problem since the contaminants are not destroyed but rather phase changed. Thus, an oxidation (chemical or biological) treatment is necessary to complete the treatment of the effluent. In this work, a low-cost catalyst, red mud, was applied in the Fenton process with the objective of reducing the costs of operation and reusing a waste that is currently produced in large quantities. Red-mud richness in iron and aluminium as well as some rare metals can enhance the Fenton´s process. In this context, the aim of the present research was to analyze the efficiency of red-mud as a solid catalyst in Fenton's process for OMW treatment.

2. Methods

Red mud was characterized morphologically by scanning electron microscopy (SEM) with a Hitachi S-4100 microscope. Particle size distribution was performed with a Coulter LS 230 (0.040 - 2000 µm). Specific surface area by the Brunauer-Emmett-Teller (BET) method was studied with a Micromeritics Germini 2380. X-ray diffraction was used to ascertain the crystallography of the powder with a PANalyticalXPert PRO diffractometer (2θ =10-80°, CuKα radiation), where a Panalytica lHigh Score Plus 4.1 (PDF-4) was used for phase identification.

The simulated OMW was prepared by dissolving 100 mg/L of each of the following phenolic acids in ultrapure water: trans-cinnamic, 3,4-dimethoxybenzoic, 4-hydroxybenzoic, 3,4,5-trimethoxybenzoic and 3,4-dihidroxybenzoic acid.

Dark and photo-Fenton's experiments were carried out in a glass spherical reactor (500 mL). A high-pressure sodium grow lamp (LUMATEK 600 W) was used for photo-Fenton's experiments.

3. Results and discussion

SEM images of RM are shown in Figure 1, where the waste seems to be formed by agglomerates with heterogeneous shape and size of particles (Figure 1 a)). Regardless the shape, the particles seem to be around 1.00 µm (Figure 1 b)), in average. Particle size analysis showed that the average size of particles is 1.10 µm, with a mean size (D_{50}) of 0.58 µm (Figure 2a), where 10% of particles have a particle diameter lower than 0.17 µm (D_{10}) and 90% of particles have a diameter lower than 2.86µm (D_{90}). The waste catalyst has a surface

area of BET of 10.57 m^2/g and 0.02cm^3/g of pore volume. XRD studies (Figure 2b) confirm the presence of several phases, in accordance with SEM results.

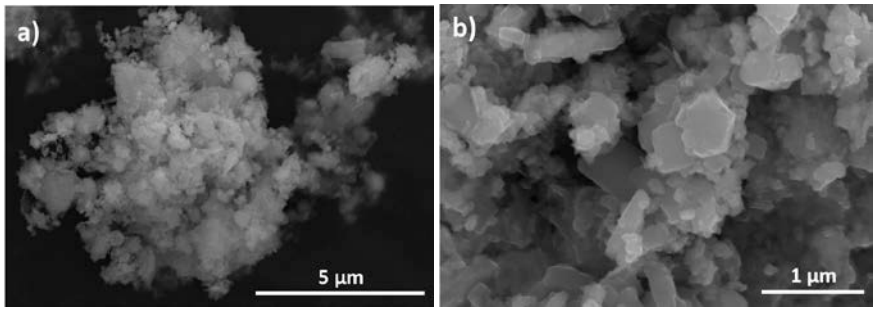

Figure 1. SEM of the red mud powder.

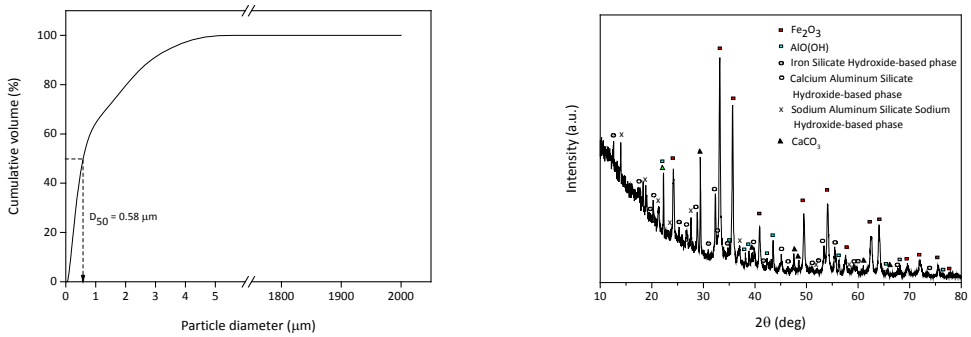

Figure 2. a) Cumulative volume (%) of red mud particles. b) XRD pattern of red mud.

Fenton's experiments showed that red mud is a suitable low-cost catalyst for the removal of the phenolic content. The operating parameters were optimized and the impact of Fenton's process over the treated wastewater ecotoxicity was evaluated.

4. Conclusions

Fe_2O_3 is the major constituent of RM, followed by AlO(OH) and an iron silicate hydroxide phase. Minor compositions of SiO_2, TiO_2, Ca_3SiO and $Al(OH)_3$ are present.

The presence of visible radiation in Fenton´s process decreased the efficiency of the process, probably led to the decomposition of hydrogen peroxide into non-reactive species with contaminants such as water and oxygen. The catalyst load above 1 g / L shows that the scavenger effect of the catalyst prevails. It has been found that increasing the concentration of hydrogen peroxide to 100 mg / L favors the process by increasing the rate of degradation of the phenolic acids.

References

[1] A. Bianchi, N.C. Jones, Chem. Eng. J. 157 (2019) 326–337.

[2] W. Black, E.B. White, The Elements of Science, third ed., MacCluski, New York, 1987.

[3] G.R. Pangar, L. Liu, in: N.C. Jones, A. Bianchi (Eds.), The Electronic Technology, E-Publishing Inc., New York, 2009, pp. 181–304.

[4] Khairul, M.A., Zanganeh, J., Moghtaderi, B. (2019). The composition, recycling and utilisation of Bayer red mud.Resources, Conservation & Recycling 141, 483–498.

ECCE12
The 12th EUROPEAN CONGRESS OF CHEMICAL ENGINEERING
Florence 15-19 September 2019

Predictive Model of Delayed Coker Unit for Studying Variations in Feed.

Hala Kelani[1], Dr. Mohammad Abdur Rakib[2], Mohamed AL Musharfy[3]

[1,2,3] ADNOC Refining Research Center, PO Box 3593, ADNOC Refining

Abu Dhabi, United Arab Emirates

*Corresponding author: hkelani@adnoc.ae

Highlights

- *Delayed Coker*
- *Process Simulation*
- *Scenario studies*
- *Feed flexibility*

1. Introduction

Delayed Coking is a thermal process in which a residuum material from a vacuum distillation unit in a refinery is rapidly heated in a furnace and then thermally cracked in coke drums under appropriate conditions of temperature and pressure. Typical products from a Delayed Coker unit include Sour Off Gas, Sour LPG (C3s and C4s), full range of Stabilized Coker Naphtha, Light Coker Gas Oil (LCGO), Heavy Coker Gas Oil (HCGO), and Coke (Green Coke). In ADNOC Refining, the Delayed Coker Unit is designed for a feed blend of Vacuum Residue (VR) and Hydrotreated RFCC (Residue Fluidized Catalytic Cracker) Slurry. Depending on the availability of feed from its upstream units, and depending on dynamic market scenarios, the feed to a Delayed Coking unit might vary in terms of quality due to variation of blend ratios, as well as in feed rate. Hence, as reported in this present study, a predictive model was developed using a commercial simulation software to conduct scenario studies for various feeding scenarios (feed throughputs and blend ratios) to assess the expected impacts on the products yield and properties, prior to introducing these in real operations.

2. Methods

Delayed coking is a highly endothermic reaction with the furnace supplying the necessary heat of reaction. The exact mechanism of coking is quite complex and determination of the chemical reactions occurring would be quite challenging.

A commercial simulation software was utilized in the current study, whereby a base case was calibrated using a design case, denoted as Design Case 1. Data required for this calibration of the base model included: (a) Feed analysis for each stream in the feed blend, e.g. specific gravity, distillation curves, sulfur and metals content etc., (b) detailed operating conditions for each equipment of the unit including delayed coker furnace, coke drums, and the separation column, and (c) product analysis and yields for each product stream from the unit.

This calibrated model was validated by testing the model against another design scenario, denoted as Design Case 2, in addition to a set of operating data denoted as Scenario 3. The prediction for

these cases indicated a very good match, and henceforth the calibrated model was utilized for prediction of an additional scenario, denoted as Scenario 4. Feed for theese cases are as in Table 1.

Table 1: Feed blend percentage for each case

	Flow Rate Percentage (%)			
Feed	**Design Case 1**	**Design Case 2**	**Scenario 3**	**Scenario 4**
Vacuum Residue	85	85	83	85
RFCC Slurry (0.1 wt% S)	15	-	-	-
RFCC Slurry (0.2 wt% S)		15	-	-
Hydrotreated Atmospheric Residue	-	-	17	15

3. Results and discussion

Tabulated below are results for these predicted scenarios.

Table 2: Products yields simulation results for different feed scenarios compared to the calibrated case

	Yields (wt%)			
Products	**Design Case 1**	**Design Case 2**	**Scenario 3**	**Scenario 4**
Gas	4.7	4.7	4.21	4.191
LPG	4.82	4.82	5.64	5.596
Light Coker Naphtha	16.67	16.52	18.94	18.659
Heavy Coker Naphtha	8.71	8.623	9.8335	9.713
Light Coker Gas Oil	26.53	26.29	29.93	29.68
Heavy Coker Gas Oil	6.25	6.31	5.68	5.72
Coke	32.14	32.7	25.1	25.74

The presentation will include a detailed discussion of these results and the source of these variations of the individual yields.

4. Conclusions

A commercial Delayed Coker unit was simulated, whereby one set of design data were used to calibrate the model, and validated using a second set of design data and actual operating data. Parametric prediction cases were performed and validated directionally to provide operational guidelines to the refinery process engineers for assessing unit performance and limits of feed flexibility for the various feeding scenarios. The coke product yield has been significantly impacted while using hydrotreated atmospheric residue in the feed blend. These step-out predictions have also been made available for refinery production planning personnel to generate Linear Programming (LP) vectors for input for production planning software.

References

[1] Delayed Coker Operating Manual, ADNOC Refining, 2014.

ECCE12
The 12th EUROPEAN CONGRESS OF CHEMICAL ENGINEERING
Florence 15-19 September 2019

Fast Pyrolysis of Agricultural Eggplant Stalk Waste

Merve Atıl, H. Ferdi Gerçel

Department of Chemical Engineering, Eskişehir Technical University, Eskişehir 26555, Turkey

**Corresponding author: hfgercel@eskisehir.edu.tr*

Highlights

- Pyrolysis experiments of the eggplant stalk were carried out in the nitrogen gas atmosphere.
- The effects of pyrolysis temperature on the pyrolysis product yields were investigated.
- The highest liquid product yield was obtained as 28.16 wt.%.

1. Introduction

Pyrolysis is one of the thermochemical conversion methods of biomass, carried out in the complete or near complete absence of an oxidizing agent (air or oxygen), typically at 400–700°C to provide complex fractions of gases, condensable liquids (tars), and char (solid residue) [1]. Fast pyrolysis is the rapid thermal decomposition of biomass in the absence of oxygen. The main product of fast pyrolysis is a dark brown and viscous liquid, known as bio-oil [2, 3]. In this study, eggplant stalk was investigated as a source of biomass, pyrolysis was carried out in a nitrogen gas atmosphere and the effect of pyrolysis temperature on yields of the pyrolysis product was investigated.

2. Methods

Agricultural waste eggplant stalk was collected from Kızılinler village around the city of Eskisehir, which is located in central Anatolia, Turkey. Prior to use, the sample was dried at moisture free and shade conditions, ground with a high-speed rotary cutting mill and then sieved to a uniform size (0.425–0.6 mm). Pyrolysis experiments were carried out in a 310 stainless steel, fixed bed tubular reactor in an inert gas atmosphere. Pyrolysis of the eggplant stalk conducted in nitrogen atmosphere flowing at a rate of 100cm^3/min, at temperatures of 400, 450, 500, 550, 700°C with a heating rate of 300°C/min. After pyrolysis, the resulting solid char was separated, weighed and the char yield was calculated. The amount of water, collected from the liquid product-water mixture in the cooling containers, was determined. The tar was removed by washing with dichloromethane, then the solvent was removed in the rotary evaporator to calculate the liquid product yield and also the pyrolysis conversion from the weight loss in the reactor. Gas yield was calculated from the total mass balance. Chemical composition of liquid was determined by liquid column chromatographic fractionation. The liquid product was separated into two fractions as n-pentane soluble and insoluble compounds by using 100 mL pentane. The pentane soluble material was further separated on activated silica gel, pretreated at 105°C for 2 h prior to introduction into a 20 cm high and 25 mm i.d. column. The column was eluted with n-pentane, toluene, and methanol to produce

aliphatic, aromatic, and polar fractions successively. Chemical characterization of liquid, n-pentane eluate, toluene eluate and methanol eluate samples were carried out using potassium bromide (KBr) disks in a Fourier transform infrared spectrophotometer (FTIR, Perkin Elmer Frontier) in a scanning range of 4000-400 cm^{-1}.

3. Results and discussion

Pyrolysis product yields at different pyrolysis temperatures are presented in Figure 1. The highest overall conversion of 76.05 wt.% was obtained at the final pyrolysis temperature of 700°C under the nitrogen, flowing at a rate of 100 cm^3/min. The liquid yield also increased as pyrolysis temperature was raised from 400 to 500–550°C, although a decrease in the liquid yield was observed at higher pyrolysis temperature of 700°C.

FTIR spectra of the n-pentane, toluene, methanol eluate and the liquid product samples are presented in Figure 2. The O-H stretching vibrations between 3200 and 3400 cm^{-1} indicate the presence of phenols and alcohols; the C-H stretching vibrations, observed between 2800 and 3000 cm^{-1} and C-H deformation vibrations between 1350 and 1475 cm^{-1} indicate the presence of alkanes. The C=O stretching vibrations between 1650 and 1750 cm^{-1} indicate the presence of ketones or aldehydes. The absorbance peaks between 1575 and 1675 cm^{-1} represent C=C stretching vibrations are arising from the presence of alkenes and aromatics.

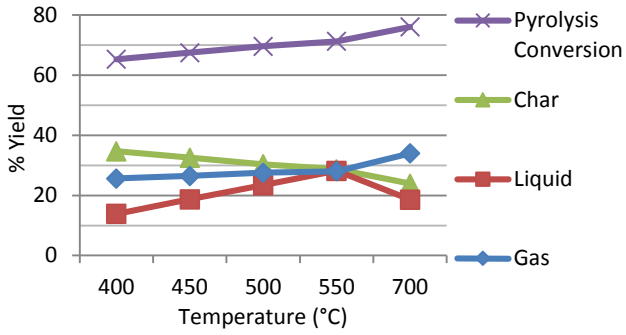

Figure 1. Pyrolysis product yields at different pyrolysis temperatures

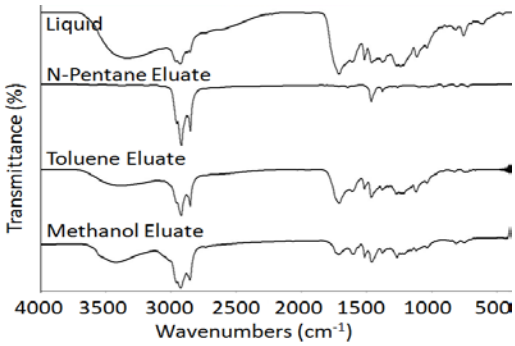

Figure 2. FTIR spectra of the n-pentane, toluene, methanol eluate and the liquid product samples.

4. Conclusions

FTIR spectra of the n-pentane, toluene, methanol eluate and the liquid product samples demonstrated that the functional groups of the liquids are consistent with those of the liquids and the chromatographic fractions obtained from eggplant stalk. The maximum liquid yield from eggplant stalk were achieved at the pyrolysis temperature of 550°C, under 100 cm^3/min nitrogen flow rate. The highest overall conversion of 76.05 wt.% was obtained at 700°C.

References

[1] R. Alén (Eds.), Biorefining of Forest Resources, Paper Engineers' Association, Finland, 2011, pp. 55–114.

[2] A.V. Bridgwater, G.V.C. Peacocke, Renew. Sustain. Energy Rev. 4 (2000) 1–73.

[3] M.R. Rover, Fuel 153 (2015) 224–230.

ECCE12
The 12th EUROPEAN CONGRESS OF CHEMICAL ENGINEERING
Florence 15-19 September 2019

Catalytic Performance Investigations of the Direct DME Synthesis with Variable $CO/CO_2/H_2$ Feeds.

Stefan Wild[1], David Guse[2], Karla Herrera Delgado[1], Matthias Kind[2], Stephan Pitter[1], Sabrina Polierer[1] and Jörg Sauer[1]

1 Institute for Catalysis Research and Technology (IKFT); 2 Institute of Thermal Process Engineering (TVT) Karlsruhe Institute of Technology (KIT) D-76131 Karlsruhe/Germany

**Corresponding author: Stefan.wild@kit.edu*

Highlights

- Highly active CZZ/zeolite catalyst system with high CO_2 tolerance
- Good long-term stability under variable operating conditions

1. Introduction

Synthesis gas, a mixture of H_2, CO and CO_2 with variable composition, is the preliminary stage for many basic chemicals. Synthesis gas can be produced from a variety of feedstocks, resulting in a wide range of $CO/CO_2/H_2$ ratios[1]. Methanol (MeOH) and Dimethylether (DME) formed from synthesis gas are promising energy carriers in the "Power to Fuels" (PtF) concept[2]. Using CO_2 as a COx source would lead to a CO_2 recycle system and to CO_2-neutral fuels.

2. Methods

Within this study, the direct DME synthesis is investigated in a fixed-bed reactor aiming at dynamic processing with variable feed compositions. For initial methanol formation $Cu/ZnO/ZrO_2$ (CZZ) catalysts prepared at KIT-IKFT/TVT are used. Different solid-acid components such as γ-Al_2O_3, H-FER and H-MFI realize the dehydration of MeOH to DME. Experiments have been carried out under following reaction conditions: 483-523 K; 50 bar; gas hourly space velocity (GHSV) between 18.000 and 42.000 $ml_N/(g*h)$; initial $CO_2/(CO_2+CO)$ inlet-ratio between 0 and 1.

3. Results and discussion

Figure 1 (left) shows that CZZ catalyst enables up to 76 % higher DME productivity compared to a commercial $Cu/ZnO/Al_2O_3$ (CZA) sample material. DME productivity can be even increased at 503 K by raising the CO_2 content in the feed. At higher reaction temperature, the thermodynamic equilibrium becomes more noticeable, reflected by lower DME productivity for CO_2-rich feed compositions. More CO_2 in the feed generally favors water formation by reverse water-gas shift reaction, what also leads to a reduction of DME productivity[3]. In a long-time experiment over nearly 600 h time on stream (ToS) using a CZZ/H-FER catalyst system a total decrease of 29 % in DME yield is observed. Figure 1 (right) shows the deactivation during the first 100 h under constant reaction conditions, followed by periods of variable dynamic changes subjected to varying temperatures, residence times and feed compositions.

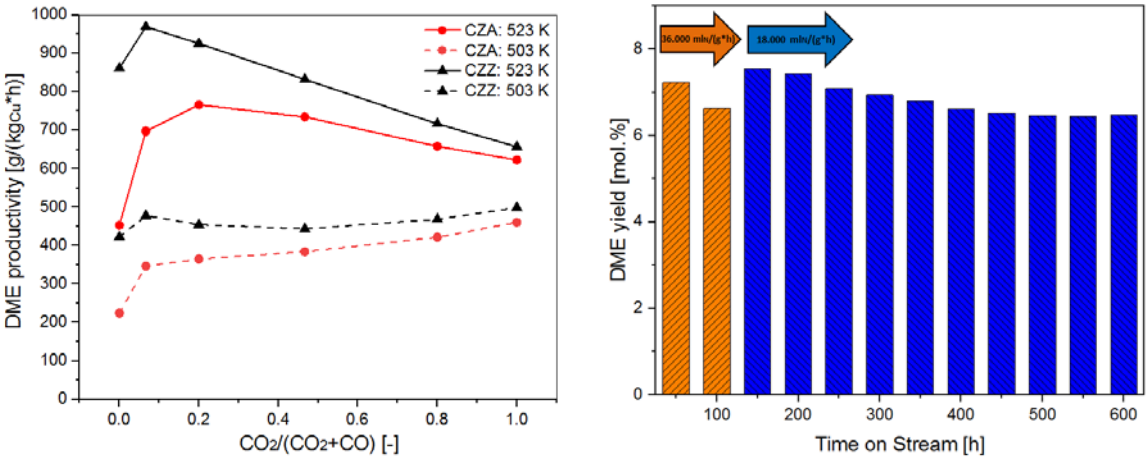

Figure 1. DME productivity of CZZ/H-FER and a commercial CZA/H-FER catalyst system (left). DME yield in a long time test of the CZZ/H-FER system (right).

4. Conclusions

The CZZ/H-FER system prepared at IKFT shows an enhanced performance compared to a commercial CZA/H-FER system and is a promising material for the conversion of syngas to DME with variable composition of $CO/CO_2/H_2$. With the appropriate choice of reaction conditions it is possible to make the DME productivity almost independent of the $CO_2/(CO_2+CO)$ inlet-ratio.

References

[1] Ahmad, A.A., et al., Renewable and Sustainable Energy Reviews, 2016, 53: p. 1333-1347
[2] Niethammer, B., et al., Chemie Ingenieur Technik, 2018, 90(1-2), p. 99-112
[3] Ateka, A., et al., Reaction Kinetics, Mechanisms and Catalysis, 2018, 124(1): p. 401-418.

ECCE12
The 12th EUROPEAN CONGRESS OF CHEMICAL ENGINEERING
Florence 15-19 September 2019

DFT, microkinetic and experimental study of lignin model compound hydrotreatment over noble metals on C

Miha Grilc[1], Ana Bjelić[1], Matej Huš[1], Blaž Likozar[1]

1 Department of Catalysis and Chemical Reaction Engineering, National Institute of Chemistry, Hajdrihova 19, 1000 Ljubljana, Slovenia

**Corresponding author: Miha.Grilc@ki.si*

Highlights

- Experimental and ab-initio study of eugenol HDO over Pt, Pd, Rh, Ru on C.
- Micro-kinetics modelling of adsorption, desorption, bulk and surface reactions.
- The lowest hydrogenation/deoxygenation ratio found for Ru/C, the highest for Pd/C.
- Ru closest to the top of the volcano dependency: TOF vs. eugenol adsorption energy

1. Introduction

The present study represents an integrated theoretical and experimental assessment of the catalytic hydrotreatment of eugenol, a representative lignin monomer model compound, over the Ru/C catalyst. A micro-kinetic model has been developed to describe experimental observations at more fundamental level accompanied by DFT calculations.

2. Methods

Experiments have been performed in a cylindrical stainless steel slurry reactor (Autoclave Engineers) in a completely batch regime. A typical experiment was performed with 5 wt% (4.5 g) of eugenol, 0.2 wt% (0.2 g) of the Ru, Pd, Pt, Rh on C and 94.8 wt% (85.3 g) of the solvent (hexadecane) at 275 °Ca and 5 MPa of initial hydrogen pressure under vigorous mixing of 1000 min^{-1}. Reactions proceeded for 3 h at the final temperature (heating up period 30 – 45 min). During the experiment, sampling of the liquid and gas phase took place. Liquid samples were analyzed by using a gas chromatograph with flame ionization detector (GC–FID) coupled with a mass spectrometer detector (GC–MS), while gas samples were analyzed by using gas chromatography (GC) and Fourier Transform Infrared (FTIR) Spectroscopy.

Based on a reaction pathway network, proposed according to the experimentally-determined intermediates and DFT study, a microkinetic model of hydrotreatment in a three-phase slurry reactor has been developed, that includes the influence of i) thermodynamics, ii) hydrodynamics, iii) mass transfer (gas – liquid, liquid – solid surface), iv) adsorption and desorption kinetics, v) surface reaction kinetics, vi) reaction kinetics in bulk phase on the global reaction rate [1-3]. Mass balances for each component in every phase (gas, liquid, catalyst surface) have been written as a set of ordinary differential equations (ODE) and were solved numerically. Kinetic, mass transfer and thermodynamic parameters were obtained either by empirical correlations, DFT calculations or regression analysis.

Density functional theory calculations have been performed in a Quantum Espresso open-source software using computationally-cheap approaches, specifically; Plane-Wave DFT with Perdew–Burke–Ernzerhof functional (PBE) and Grimme-D2 for van der Waals interactions. Unit cell consisted of 96 Ru atoms (4x6x4). Approximately 500.000 core-hours were spent for 500 stable and transition-state structures search and optimization [2].

3. Results and discussion

Ru/C catalyzed hydrotreatment of eugenol yielded 2-methoxy-4-propylphenol (HMPB), 4-propylphenol (HPB), 2-methoxy-4-propylcyclohexanol (HMPC), 4-propylcyclohexanol (HPC), propylbenzene (PB), propylcyclopentane (PCP), propylcyclohexane (PC), 4-propylcyclohexanone (KPC), 4-propyl-1,2-cyclohexanediol (HHPC), trans-isoeugenol (IHMAB), 2-metyl-1-propylcyclopentate (MePCP) and 2-methoxy-4-propylcylohexanone (KMPC). Blank experiment reviled that allyl double bond isomerization and hydrogenation proceed also without the catalyst, what has been supported by DFT calculations. Reaction network of eugenol hydrotreatment over the Ru/C has been established based on the product evolution over the reaction time and experiments performed with intermediates [1]. The proposed reaction network has been confirmed by the DFT calculations.

Temperature variation influenced the product distribution the most significantly. Hydrogenation reactions took place predominantly at lower temperatures as a consequence of low activation energies (approx. 50 kJ mol^{-1}) estimated by the model. On the other side, deoxygenation reactions were significantly promoted at higher temperatures due to greater activation energies (approx. 100 kJ mol^{-1}). Pressure change affected primarily the yield of hydrogenated products. Agitation speed variation indicated absence of the external mass transfer limitations in the tested range. The catalyst loading promoted all reactions, as expected. Demethoxylation and dehydroxylation rate constants have been estimated 36- and 42-fold higher for aromatics relative to oxygen-containing cycloalkanes. Energy diagram, determined for HMPC deoxygenation by the DFT, has been provided in Fig 2a, while Fig. 2b demonstrats integrated experimental and micro-kinetic model results obtained for the experiment performed at 275 °C.

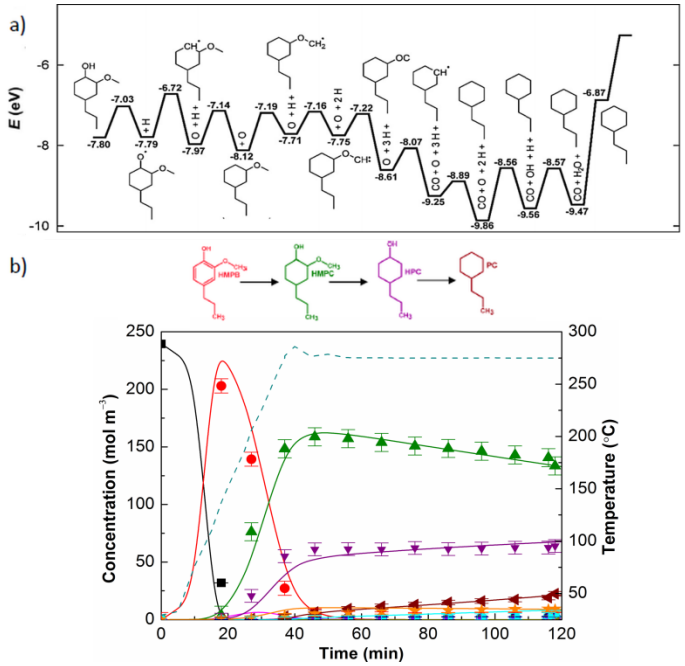

Figure 1. a) Potential energy surface for the minimum energy pathway of the HMPC deoxygenation obtained by the DFT b) eugenol hydrotreatment over the Ru/C at 5 MPa H_2.

References

[1] A. Bjeli•, M. Grilc, B. Likozar, Chemical Engineering Journal 333 (2018) 240-259.

[2] M. Hua, A. Bjeli•, M. Grilc, B. Likozar, Journal of Catalysis 358 (2018) 8-18.

[3] A. Bjeli•, M. Grilc, S. Gyergyek, A. Kocjan, D. Makovec, B. Likozar, Catalysts 8 (2018) 425.

ECCE12
The 12th EUROPEAN CONGRESS OF CHEMICAL ENGINEERING
Florence 15-19 September 2019

Experiment Design, Modeling and Comparative Design Optimization of the Pretreatment of Wheat Straw for the Sustainable Production of Xylitol

Nikolaus I. Vollmer[1], Celina K. Yamakawa[2], Krist V. Gernaey[1], Solange I. Mussatto[2], Gürkan Sin[1] *

1 PROSYS, Department of Chemical and Biochemical Engineering, Technical University of Denmark;

2 Biomass Conversion and Bioprocess Technology Group, Novo Nordisk Foundation Center for Biosustainability, Technical University of Denmark.

**Corresponding author: gsi@kt.dtu.dk*

Highlights

- Pretreatment of Lignocellulosic Biomass with Dilute Acid Pretreatment (DAc) vs. Liquid Hot Water Pretreatment (LHW)
- Design Optimization with Response Surface Methodology vs. Artificial Neural Network - Genetic Algorithm
- Predictive Modelling to use in Process Design for Sustainable Production of Xylitol

1. Introduction

Xylitol has manifold beneficial health properties, e.g. possessing a low insulin index, while tasting similarly to sucrose and thus being perfectly suitable as sugar substitute for diabetics [1]. Its currently predominant production process involves extensive purification and separation steps, which makes it highly cost-expensive [2]. The feedstock for this process is lignocellulosic biomass, whose hemicellulosic fraction consists to major parts of xylose. Rather than pursuing a chemical reaction, the xylose can also be converted to xylitol by fermentation. Consequently, a sustainable, biotechnological production process for xylitol represents a possible alternative [3]. One of the bottlenecks remains the pretreatment of the lignocellulosic biomass in order to partition the hemicellulosic fraction optimally from the biomass. Therefore, the scope of this work comprises a comprehensive analysis of a pretreatment experiment design: Two pretreatment methods are analyzed in two respective design of experiments. Furthermore, the design is optimized comparatively by means of a) Response Surface Methodology (RSM) and b) an Artificial Neural Network (ANN) coupled with a Genetic Algorithm (GA), in order to provide a statement on optimal process conditions for a maximal xylitol production. This is complemented by a sensitivity analysis of both approaches [4]. On basis of the optimized design, one of the pretreatments is chosen to be implemented as a model in order to serve in an overall process design routine.

2. Methods

The two methods Liquid Hot Water (LHW) pretreatment and Dilute Acid (DAc) pretreatment are considered as base cases. An experimental design with a fixed temperature range for both pretreatment methods is chosen and, subsequently, for each chosen temperature experiments with both pretreatments are done. The variable considered for LHW is time, and the variables

considered for DAc are time and the concentration of acid. The experiments are conducted with wheat straw as lignocellulosic biomass, chopped in a defined particle size interval. All experiments are conducted in stainless steel reactors under defined conditions. The acid used for DAc is sulfuric acid. Measured process variables are time, the concentration of xylose, glucose and the concentration of common inhibitors, such as furfural, HMF, acetic acid and phenolics [4].

The measured data from these experiments is then used to optimize the design with both RSM and the hybrid approach employing ANN-GA, with the twofold objective of a maximal xylose production and simultaneously low inhibitors formation. A local and global sensitivity analysis concludes the procedure. After the analysis of the optimized results, the pretreatment is then implemented as model based on the work of Prunescu et al. [6] and afterwards calibrated and validated with the experimental data.

3. Results and discussion

LHW tends to be conducted at higher temperatures than DAc. This is due to the reason of better solubility of the hemicellulosic fraction. With increasing temperature and/or acid concentration, DAc tends to yield higher concentrations of inhibitors during the course of pretreatment [5]. A main drawback of LHW is however the production of large amounts of oligomers instead of xylose monomers [4].

The main objective of the pretreatment is, as mentioned, the fractionation of the biomass. It should therefore yield a maximum amount of monomeric xylose. Other factors indicating the qualitative superiority of a pretreatment method is the amount of inhibitors produced, as well as the costs for heat and acid. In order to provide a sufficient answer for the choice of one pretreatment method or another, the design optimization gives a sufficient answer. The optimization of the design with RSM and respectively with the hybrid ANN-GA yields optimal process parameters for a maximal xylose production during the pretreatment. The comparison between both methodologies show certain differences in overall accuracy, sensitivity and optimal result. DAc yields higher amounts of monomeric xylose, although the use of acid involves cost, but still outruns LHW performance wise. The implemented, calibrated and validated model shows good predictive abilities.

4. Conclusions

The comprehensive analysis of the LHW and DAc pretreatment of wheat straw as lignocellulosic biomass yields ambiguous data in terms of favorability of one of them. The optimization of the design with RSM and with ANN/GA display different results considering their performance, but indicate that DAc should be chosen. This method is therefore supposed to be implemented as model for an overall process routine. Therefore, choosing DAc under optimal conditions for the pretreatment step for the biotechnological production of xylitol surmounts the bottleneck best, which makes it suitable for a sustainable process alternative.

References

[1] S.I. Mussatto, in: S. da Silva, A. Chandel (Eds.), D-Xylitol. Springer, Berlin, Heidelberg, 2012, pp. 309-323.
[2] J.C. Pajaró, H. Domínguez, J.M. Domínguez, Bioresoure Technology 65 (1998) 191-201.
[3] T.L. de Albuquerque, I.J. da Silva Jr., G.R. de Macedo, M.V.P. Rocha, Proc. Biochem. 49 (2014) 1779-1789.
[4] F.M. Girío et al, in: S. da Silva, A. Chandel (Eds.), D-Xylitol. Springer, Berlin, Heidelberg, 2012, pp. 3-37.
[5] A.K. Kumar, S. Sharma, Bioresources and Biopreocessing 4:7 (2017)
[6] R.M. Prunescu et al, AIChE Journal 61 (2015) 4235-4250.

ECCE12
The 12th EUROPEAN CONGRESS OF CHEMICAL ENGINEERING
Florence 15-19 September 2019

Optimal conditions of dolomite pre-reforming step for enhancing catalyst stability in the steam reforming of raw bio-oil

Naiara García-Gómez, Beatriz Valle*, Aingeru Remiro, Javier Bilbao, Ana G. Gayubo

Dept. Chemical Engineering, University of the Basque Country, 48080 Bilbao, Spain

**Corresponding author: beatriz.valle@ehu.eus*

Highlights

- Dolomite activity depends highly on temperature and changes composition of raw bio-oil
- H_2 yield is enhanced at 400 °C due to conversion of acids and levoglucosan into ketones
- Severe pre-reforming conditions lead to alkyl-phenols formation and faster deactivation

1. Introduction

Steam reforming (SR) of the bio-oil produced by fast pyrolysis of biomass is an interesting route for renewable and sustainable production of hydrogen [1]. However, direct valorization of raw bio-oil is hampered by its complex composition, high corrosivity and thermal instability. Poly-substituted phenols (e.g., catechols, guaiacols, syringols) are the main undesired components in bio-oil, which undergo condensation reactions leading to the formation of carbonaceous material, which may cause clogging of the reactor and severe catalyst deactivation [2]. Several Ni-based catalysts have been tested under a wide range of operating conditions, which despite achieving high yields of H_2 undergo a rapid deactivation. Selection of operating conditions and strategies that minimize catalyst deactivation is essential for the industrial feasibility of raw bio-oil SR. The on line two-step (thermal-catalytic) reaction system has proved to be effective for attenuating deactivation [3], and the use of dolomite as a pre-reforming catalyst has been addressed as a low-cost way of protecting the more expensive reforming catalysts [4].

In this work, the influence that temperature and dolomite space-time has on the subsequent reforming step has been studied with the aim of establishing optimal pre-reforming conditions with dolomite for enhancing H_2 production and attenuating deactivation.

2. Methods

Raw bio-oil (obtained by fast pyrolysis of pine sawdust) was continuously fed (0.1 ml/min) into the first thermal/pre-reforming unit (Pre-SR) where the previously calcined dolomite (at 850 °C for 5h) was located in a fixed bed reactor. The resulting volatile stream entered the fluidized bed reforming reactor (SR), where a Ni-spinel catalyst ($NiAl_2O_4$ with 33 wt % Ni) was located. The pre-reforming step was studied at 400-700 °C and two values of space-time (1.4 and 2.8 $g_{dolomite}h/g_{bio-oil}$), whereas conditions for steam reforming were settled at 700 °C and 0.15 $g_{catalyst}h/g_{bio-oil}$. Additional water was co-fed with bio-oil to have a steam-to-carbon ratio (S/C) of 3. Product stream was analyzed by on-line GC and GC/MS of the liquids collected at the outlet of the Pre-SR and SR reactors. The coke deposited on the $NiAl_2O_4$ catalyst was quantified by temperature-programmed oxidation (TPO).

3. Results and discussion

The effect of pre-reforming (Pre-SR) on the evolution with time on stream of the overall H_2 yield is studied in Figure 1, where the results are also compared with that obtained without dolomite in the first unit (black circles) and those corresponding to the Pre-SR unit outlet (dotted lines). For the same amount of dolomite (Figure 1a), the $NiAl_2O_4$ catalyst stability was enhanced when the pre-reforming was performed at 400 °C. Figure 1b also revealed that half the amount of dolomite was necessary to improve H_2 production (compared to the conventional SR) when the pre-SR was conducted at 700 °C. The faster catalyst deactivation observed as the pre-reforming temperature was raised from 400 to 700 °C was attributed to a higher coke deposition (from 4 to 18 wt %).

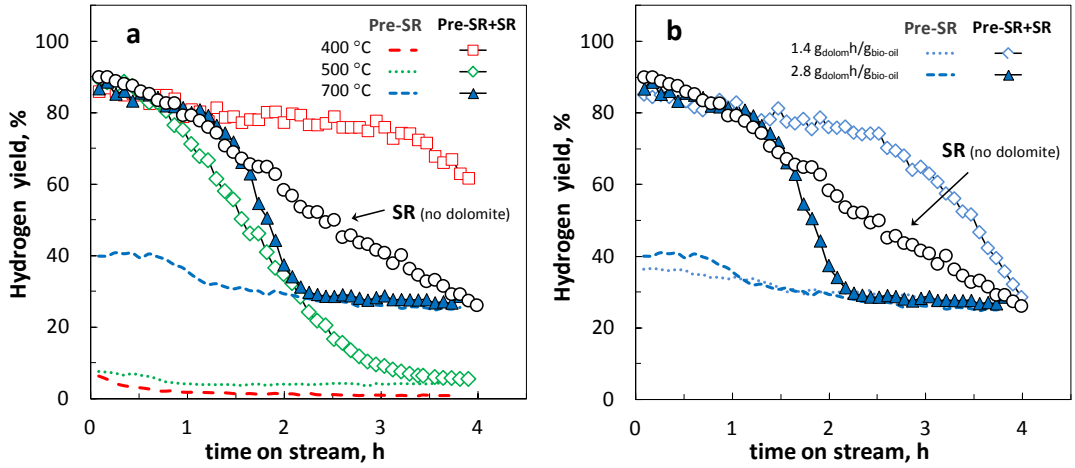

Figure 1. Effect of pre-reforming (Pre-SR) temperature (Graph a, 2.8 $g_{dolomite}h/g_{bio\text{-}oil}$) and dolomite space-time (Graph b, 700 °C) on the overall hydrogen yield. Conditions on the steam reforming (SR) step: 700 °C, 0.15 $g_{catalyst}h/g_{bio\text{-}oil}$.

These results were explained by differences in the composition of the oxygenated stream caused by the dolomite activity for ketonization, steam reforming, WGS, cracking and H_2 transfer reactions, whose relative prevalence depends on the operating conditions [5]. At 400 °C, acids and levoglucosan were mainly converted *via* ketonization leading to acetone, 2-butanone and cyclic ketones as majority compounds. Dolomite activity for reforming reactions was favored by temperature and space-time, although cracking and hydrodeoxygenation of poly-substituted phenols were also promoted, resulting in oxygenated stream with alkyl-phenols and aromatics as majority compounds.

4. Conclusions

The pre-reforming with dolomite at low temperature (400 °C) or low space-time is effective to attenuate the deactivation by coke of the Ni-spinel catalyst in the reforming step, due to the conversion of acids and levoglucosan contained in raw bio-oil into ketones, whereas more severe pre-reforming conditions promote formation of alkyl-phenols that cause faster deactivation.

References

[1] P. Nikolaidis, A. Poullikkas, *Renew. Sust. Energy Rev.*, **67** (2017) p. 597.
[2] A. Ochoa, B. Aramburu, B. Valle, D.E. Resasco, L. Bilbao, A.G. Gayubo, P. Castaño, *Green Chem*., **19** (2017) p. 4315.
[3] A. Remiro, B. Valle, A.T. Aguayo, J. Bilbao, A.G. Gayubo, *Energy Fuels*, **27** (2013) p. 7549.
[4] F. Lónyi, J. Valyon, E. Someus, J. Hancsók, *Fuel*, **112** (2013) p. 23.
[5] B. Valle, B. Aramburu, C. Santiviago, J. Bilbao, A.G. Gayubo, *Energy Fuels*, **28** (2014) p. 6419.

ECCE12
The 12th EUROPEAN CONGRESS OF CHEMICAL ENGINEERING
Florence 15-19 September 2019

Light activated dehydrogenation of Liquid Organic Hydrogen Carriers.

Alexander Wunsch[1], Michel Bartsch[1], Marek Grzelczak[2], Roland Dittmeyer[1], Peter Pfeifer[1], Alexander Navarrete[1]

1 Institute for Micro Process Engineering, Karlsruhe Institute of Technology, Eggenstein-Leopoldshafen, Germany;
2 Donostia International Physics Center (DIPC), Paseo Manuel de Lardizabal 4, Donostia – San Sebastián 20018, Spain

**Corresponding author: alexander.navarrete@kit.edu*

Highlights

- Renewable energy has great potential but fluctuation and storage are always a challenge.
- Long-term storage of hydrogen can connect high-energy potential with demand.
- We propose a process to release hydrogen from LOHCs using solar energy.
- Concept and initial results are introduced.

1. Introduction

Potential for renewable energy based society is big but it cannot achieved without an appropriate energy storage infrastructure that copes with the fluctuating nature of the renewable sources [1-3].

Long-term hydrogen storage by means of Liquid Organic Hydrogen Carriers (LOHCs) is based on cycles of hydrogenation- dehydrogenation. This provides an option, which is potentially cheap, safe and easy to handle in order to connect regions with high-energy generation potential to regions with large energy demand. The sustainability of the process requires to recover the hydrogen using a heat source that do not emit CO_2 [4]. Solar light is an abundant resource that can be used for this purpose. Nevertheless the technology is not yet developed.

We make use of a plasmonic composite in order to capture the light energy and locally activate the dehydrogenation of LOHCs. For this, we have developed a dedicated reaction system, which will be described here.

2. Methods

2.1. Reaction setup and catalyst integration:

The reactor allows the illumination of the plasmonic composite while the flow and temperature of the LOHC is controlled. The plasmonic catalyst is deposited on the transparent slides by means of a layer-by-layer method. Optical profilometry and UV-Vis spectroscopy are used to characterize the surface. Electronic microscopy is used to study the catalytic nanostructure.

2.2. Reaction test:

The reactor is tested under white light with different flow rates. The production of hydrogen is followed by the degradation of the LOHC by means of refractometry.

3. Initial results

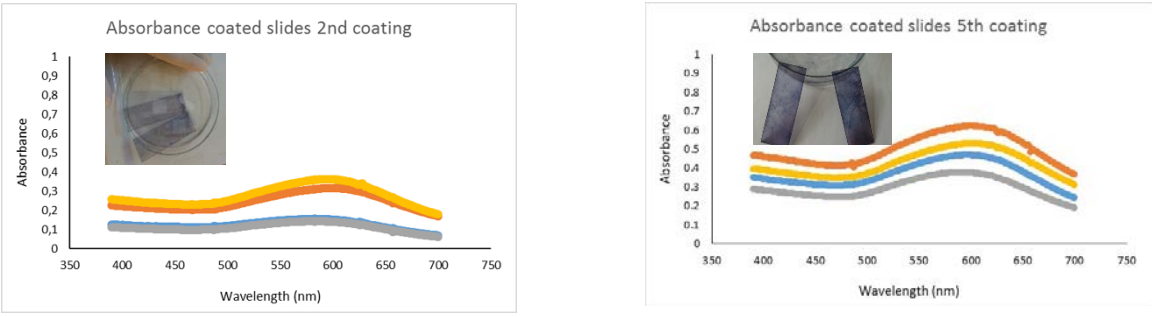

Figure 1. Catalyst deposition evolution.

The layer-by-layer method is appropriate to deposit catalyst with controlled optical characteristics that allow to absorb solar energy. This work provides evidence on the possibility of storing and releasing hydrogen using renewable energy during the storage-supply cycle. In particular, hydrogen could be recovered using solar energy in future processes based on LOHCs.

References

[1] K. F. Kalz, R. Kraehnert, M. Dvoyashkin, R. Dittmeyer, R. Gläser, U. Krewer, K. Reuter, J.-D. Grunwaldt, ChemCatChem. 9 (2017) 17-29.

[2] P. Lanzafame, S. Abate, C. Ampelli, C. Genovese, R. Passalacqua, G. Centi, S. Perathoner, ChemSusChem, 10 (2017) 4409-4419.

[3] A. Navarrete, G. Centi, A. Bogaerts, Á. Martín, A. York, G. D. Stefanidis, Energy Technol. 5 (2017) 796-811.

[4] M. Niermann, S. Drünert, M. Kaltschmitt, K. Bonhoff, Energy Environ. Sci. (2019) accepted. DOI: 10.1039/C8EE02700E.

ECCE12
The 12th EUROPEAN CONGRESS OF CHEMICAL ENGINEERING
Florence 15-19 September 2019

A Manganese Modified Fe_3O_4 Microsphere Catalyst with Effective Active Phase of Forming Light Olefins From Syngas.

Yi Zhang* and Yi Liu

1 [a]State Key Laboratory of Organic-Inorganic Composites, Beijing University of Chemical Technology, Beijing, 100029, China
**Corresponding author: yizhang@mail.buct.edu.cn*

Highlights

- The MnOx dispersed on the surface of Fe3O4 microsphere.
- The unique promoter-on-iron structure of obtained catalyst.
- The θ-Fe3C phase plays crucial roles in enhancing the light olefins selectivity.

1. Introduction

Light olefins (C_2-C_4) are key building blocks of the chemical industry and typically produced by steam cracking naphtha [1]. The direct conversion of syngas into light olefins via the Fischer-Tropsch synthesis (FTS) process is a promising route to meet the increasing demand for chemical feed-stocks [2]. It is well know that iron carbide is recognized as the active phase for the FTS reaction [3]. Herein, a manganese modified Fe_3O_4 microsphere catalyst was developed as illustrated in **Figure 1A**, where the MnOx dispersed on the surface of Fe_3O_4 microsphere to avoid the porous structure and solely modify the carburization of the catalysts.

2. Methods

The Fe_3O_4 microspheres were prepared by a solvothermal method [4]. For preparation of Mn/Fe_3O_4 catalyst, in order to improving the dispersion of supported Mn, an ethylene glycol solution of $Mn(NO_3)_2 \bullet 4H_2O$ was impregnated onto the Fe_3O_4 microspheres [5], followed by drying at 473 K under vacuum. The obtained catalysts were characterized by STEM-Mapping, HRTEM, XAFS, XPS, and Mössbauer spectroscopy.

3. Results and discussion

Figure 1B shows SEM image of the Fe_3O_4 microspheres, which possess uniformly spherical shape of ~300 nm. N_2 adsorption-desorption isotherms show representative type-Ⅱ curves, which is normally obtained with non-porous adsorbents [6]. Meanwhile, it was found that the MnO_x located at the edge of Fe_3O_4 microspheres as shown in **Figure 1C**. Hence, MnO_x should locate on the surface of the Fe_3O_4 microspheres as designed. It is considered that this unique promoter-on-iron structure of obtained catalyst would contribute to enhancing the promotional effects of manganese and clarifying the different role of iron carbides.

The prepared Fe_3O_4 microsphere catalysts were applied to FTS reaction for 50 h under 1.0 MPa, 593 K, and H_2/CO ratio of 1. The Mn/Fe_3O_4 catalyst with moderate amount of Mn (6 wt %) exhibits the best C_2-C_4 olefins selectivity (60.1 %) and lowest CH_4 selectivity (9.7 %) with better stability

compared with un-promoted Fe_3O_4 catalyst. The unprecedented efficiency of converting syngas to light olefins could be attributed to the special surface carbonaceous species, as confirmed by in situ XPS. The results on the activated catalysts show that the presence of significantly different surface carbonaceous species, and the charge of surface carbon atom was influenced by the Mn promoter. It is proposed that a specific carbide phase could be formed on the surface of Fe_3O_4 microsphere due to the presence of Mn promoter. This is also confirmed by Mössbauer spectroscopy and EXAFS. As shown in Mössbauer spectroscopy (Figure 2), a new carbide phase, identified as cementite (ϑ-Fe_3C), was discerned when Mn was added. Fourier transforms of the EXAFS spectra at the Fe K-edge **(Figure 1D)** show that, the Fe formed another carbide phase, ϑ-Fe_3C, in addition to χ-Fe_5C_2. Thus, it is reasonable to conclude that the ϑ-Fe_3C phase plays crucial roles in enhancing the light olefins selectivity.

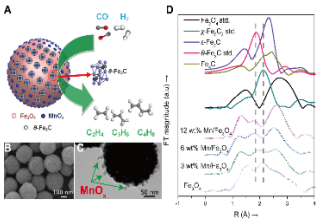

Figure 1 (A) Structural model for the Mn/Fe3O4 catalyst; (B) SEM images of the fresh Fe3O4 microspheres; (C) TEM images of the 6 wt % Mn/Fe3O4 catalyst after reduction; (D) Fourier transformed (FT) k3-weighted χ(k)-function of the EXAFS spectra. Solid lines denote reference samples of Fe3O4, χ-Fe5C2, ε-Fe3C, θ-Fe3C and Fe4C.

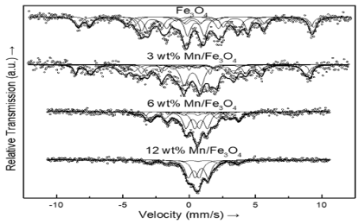

Figure 2 Mössbauer spectra of the iron-based catalysts after reduction.

4. Conclusions

The non-porous structure combined with dispersed manganese on the Fe_3O_4 microsphere surface contributes to enhancing the promotional effects of Mn and clarifying the different role of iron carbides. It was found that the ϑ-Fe_3C plays important role to enhance the selectivity of C_2-C_4 olefins during the FTS reaction.

References

[1] B. Hu, S. Frueh, H. F. Garces, L. Zhang, M. Aindow, C. Brooks, E. Kreidler, S. L. Suib, Appl. Catal. B, 2013, 132-133: 54.

[2] H. M. T. Galvis, J. H. Bitter, C. B. Khare, M. Ruitenbeek, A.I. Dugulan, K.P. de Jong, Science. 2012, 335: 835.

[3] S. Li, R. J. O'Brien, G. D. Meitzner, H. Hamdeh, B. H. Davis, E. Iglesia, Appl. Catal. A 2001, 219: 215.

[4] J. Liu, Z. K. Sun, Y. H. Deng, Y. Zou, C. Y. Li, X. H. Guo, L. Q. Xiong, Y. Gao, F. Y. Li, D. Y. Zhao, Angew. Chem. Int. Ed. 2009, 48: 5875.

[5] Y. Liu, J. F. Chen, J. Bao, Y. Zhang, ACS Catal. 2015, 5: 3905.

[6] K. S. W. Sing, Pure. Appl. Chem. 1985,57: 603.

ECCE12
The 12th EUROPEAN CONGRESS OF CHEMICAL ENGINEERING
Florence 15-19 September 2019

Mathematical modeling of the hydrolysis process of sucrose

Vittorio Romano*[1], Brunella Ascione[1], Rino Apicella[1]

1 University of Salerno, Department of Industrial Engineering

**Corresponding author: vromano@unisa.it*

Highlights

- Hydrolysis process of sucrose
- Michaelis-Menten equation with enzymatic inhibitions
- Mathematical modeling
- Finite Element Method

1. Introduction

Simulations of the enzymatic hydrolysis of sucrose were conducted for a Michaelis-Menten kinetic with product and substrate inhibitions in a tubular reactor with axial and radial dispersion.

2. Methods

The sucrose enzymatic hydrolysis process was modeled as a laminar flow with average velocity v_m inside a tubular reactor of radius R=0.04 m and length L=0.3 m, triggered by a pressure drop between inlet and outlet sections, that generates a velocity component v_z (r,t). The transient sucrose concentration and temperature profiles result to be dependent both on the radial and the axial direction: Cs (r, z, t); T (r, z, t). The unsteady equations of mass and energy, including molecular and convective transport, were developed on a differential volume $\Delta V = 2\pi r\, \Delta r\, \Delta z$, considering a cylindrical coordinate system (r, θ, z).

$\mu\left(\frac{1}{r}\frac{\partial}{\partial r}\left(r\frac{\partial v_z}{\partial r}\right)\right)+\frac{P_{in}-P_{out}}{L}=\rho\frac{\partial v_z}{\partial t}$							
$-2v_m\left[1-\left(\frac{r}{R}\right)^2\right]\frac{\partial C_s}{\partial z}+\mathfrak{D}\frac{\partial^2 C_s}{\partial z^2}+\mathfrak{D}\left(\frac{1}{r}\frac{\partial C_s}{\partial r}+\frac{\partial^2 C_s}{\partial r^2}\right)-(-r_s)=\frac{\partial C_s}{\partial t}$							
$-2\rho c p v_m\left[1-\left(\frac{r}{R}\right)^2\right]\frac{\partial T}{\partial z}+k\frac{\partial^2 T}{\partial z^2}+k\left(\frac{1}{r}\frac{\partial T}{\partial r}+\frac{\partial^2 T}{\partial r^2}\right)-(-r_s)(-\Delta H_r)+16\mu {v_m}^2\frac{r^2}{R^4}=\rho c p\frac{\partial T}{\partial t}$							
$(-r_s)=\frac{K_3 C_{eT} C_S}{k_m\left(1+\frac{C_{S0}-C_S}{k_I}\right)+C_S+\frac{C_S^2}{k_{III}}}$							
$t=0$	$v_z=0$	$C_S=C_{S0}$	$T=T_0$				$\forall z, \forall r$
$r=0$	$\frac{\partial v_z}{\partial r}=0$	$\frac{\partial C_s}{\partial r}=0$	$\frac{\partial T}{\partial r}=0$	$r=R$	$v_z=0$	$\frac{\partial C_s}{\partial r}=0$	$\frac{\partial T}{\partial r}=0$	$\forall z, \forall t>0$
$z=0$	$C_s=C_{s0}$	$T=T_0$		$z=L$	$\frac{\partial C_s}{\partial z}=0$	$\frac{\partial T}{\partial z}=0$		$\forall r, \forall t>0$

The differential equations system was solved numerically by the finite element method.

3. Results and discussion

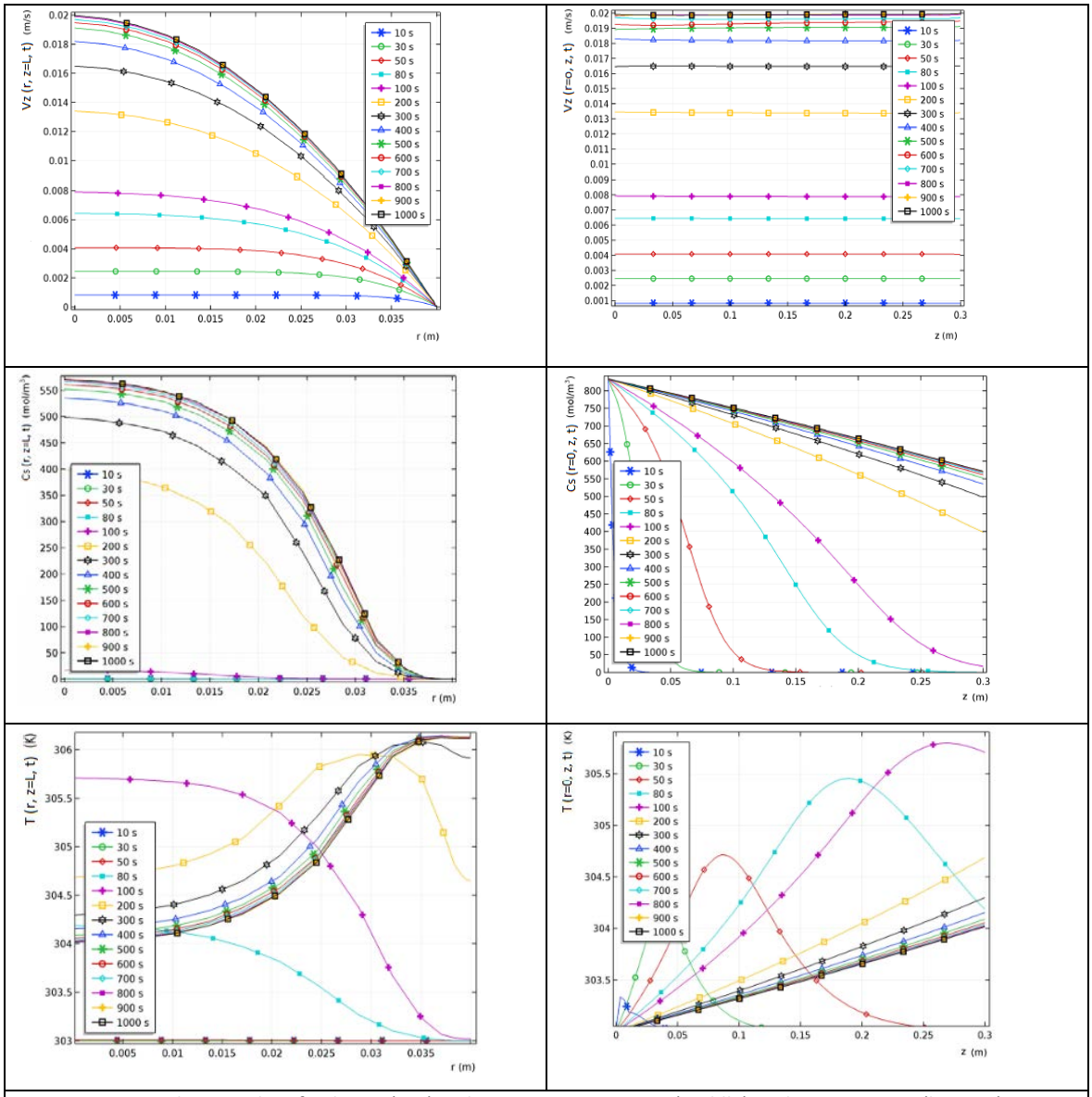

Time parametric line graphs of velocity (top), substrate concentration (middle) and temperature (bottom) against radial direction (left) and axial direction (right)

4. Conclusions

The radial concentration distribution is strongly influenced by the velocity profile, whereas along axial direction the only effect is due to the temporal evolution of the velocity. On the other hand, the temperature increasing for long times derives from the concentration consumption, considering that the reaction is exothermic.

References

[1] D.M. Himmelblau and K.B. Bischoff, Process analysis and simulation

[2] L.Bowski, R. Saini, Kinetic modeling of the hydrolysis of sucrose by invertase (1971)

[3] D.Combes ,P.Monsan, Sucrose hydrolysis by invertase. Characterization of product and substrate inhibition (1982)

[4] Y. Queneau, A Jarosz et Al., Sucrose chemistry (2007)

[5] S.M. Cuesta, S.A. Rahman, et Al.,The classification and evolution of enzyme function (2015)

[6] Z. I. Kertesz, J. Amer. Chem. Soc. 1935, 57, 1277-1279.

ECCE12
The 12th EUROPEAN CONGRESS OF CHEMICAL ENGINEERING
Florence 15-19 September 2019

BIONICO Project – A Case Study of Chemical Reactors Development & Prototyping at ICI Caldaie.

Carlo Tregambe

ICI Caldaie S.p.A. via G.Pascoli 38 , 37059 Campagnola di Zevio (VR) Italy

**Corresponding author: carlo.tregambe@icicaldaie.com*

Highlights

- Reactors development and prototyping
- Industrialization: from lab scale (TRL 4) to turnkey transportable reactors (TRL 9)
- Complete system integration and testing

1. Introduction

In the H2020 BIONICO project, a novel reactor concept that integrate H2 production and separation in a single vessel is been built by ICI Caldaie and will be demonstrated at TRL 6 at a real biogas plant, with a H2 production capacity of 100 kg/day. Main characteristics of the novel reactor are the utilization of fluidized bed catalyst for reforming reaction and Pd based membrane for pure H2 separation.

2. Methods

Synergies and deep cooperation between project partners were essential for the obtainment of the results.

Politecnico di Milano (coordinator): modelling and optimization of the innovative fuel processor - **TECNALIA:** Development of Pd-based supported membranes and membrane characterization - **Eindhoven Unversity of Technology:** Design, construction and testing of the lab scale membrane reformer - **Johnson Matthey:** development, characterization and testing of novel fluidizable reforming catalysts - **ICI Caldaie:** design, manufacturing and integration of the novel reactor at full size - **Quantis:** research on adapting environmental life cycle assessment (LCA) - **Rauschert:** Development of ceramic porous supports for the membranes - **ENC POWER:** field testing of the novel reactor in the ENC biogas plant.

3. Results and discussion

The activity of ICI Caldaie started 60 years ago in the business of high temperature and high pressure boilers (up to 950°C and 50 bar).

In the early 2000' ICI Caldaie became aware that chemical reactors were the proper and natural way to exploit the high level reached by its R&D department and started a dedicated laboratory called "ICI LAB".

Since the beginning of the activity “ICI LAB” created synergies between its academic partners and the industrial department of ICI CALDAIE, becoming a player able to have an holistic approach to the reactors business, starting from joint design solutions, through feasibility studies and up to the manufacturing, industrialization and integration of the reactors. Partnerships with universities, research centers and other industries all over the world have led to many projects (Internal 1, National 2,3, European 4,5) focused on the realization of chemical reactors and its integration in complex systems like CHP and production plant.

The first field of application was identified in the onsite hydrogen production from natural gas and Bio gas. Different reactors for hydrogen production were developed according to different sizes (from 3 to 50 Nm3/h) and different grades of purity for different hydrogen applications.

Together with hydrogen production and purification, the experience and knowhow acquired so far range from “CO2 capture and sequestration”, “gas to liquid reactors” to several other systems

Figure 1. BIONICO membrane reactor

Figure 2. Installation of H2FC cogeneration system prototype

4. Conclusions

Thanks to ICI manufacturing capability and proven ability of good knowledge transfer between industry and university, ICI is now screening new markets in reactor manufacturing business.

References

[1] Sidera30 – (http://www.icicaldaie.com/sidera-30.asp)
[2] Microgen30 – (Progetto EE01_00013 – Bando Efficienza Energetica – Decreto di concessione D.M. n° 00019EE01 del 26/05/2011) - (http://www.h2it.org/it/2009/industria-2015-progetto-microgen-30)
[3] STAR – (Prot. CCSE n° 4609 del 03/07/2009 – Decreto MISE del 16/02/2010) – (http://www.icicaldaie.com/progetti.asp)
[4] CISTEM - (FCH JU, Grant number 325262) – (http://www.project-cistem.eu/)
[5] BIONICO - (FCH2 JU, Grant number 671459) – (http://www.bionicoproject.eu/)

ECCE12
The 12th EUROPEAN CONGRESS OF CHEMICAL ENGINEERING
Florence 15-19 September 2019

Methyl Lactate Production from the Degradation of Polylactic Acid By a Zinc Complex.

Luis A. Román-Ramírez[1], Paul McKeown[2], Matthew D. Jones[2] and Joseph Wood[1,*]

1 School of Chemical Engineering, University of Birmingham, Edgbaston, Birmingham B15 2TT, United Kingdom.

2 Department of Chemistry, University of Bath, Claverton Down, Bath BA2 7AY, United Kingdom.

**Corresponding author: j.wood@bham.ac.uk*

Highlights

- Oxygen stable Zn(II) complex used for the depolymerization.
- Main operating parameters identified through design of experiments.
- Reaction mechanism and kinetic modelling presented.
- Membrane separation process for product purification.

1. Introduction

Biodegradable-biorenewable polymers such as polylactic acid (PLA) are suitable candidates to replace synthetic oil-derived polymers. However, PLA can be still a potential source of environmental pollution. Chemical recycling presents an alternative to mechanical recycling or composting for end-of-life PLA that not only results in value-added products but that could also reduce production costs [1]. Although chemical recycling methods have been demonstrated in the literature (hydrolysis, acid-base depolymerization and transesterification) [2, 3], these processes are characterized for high temperatures (up to 260 °C). Milder operating conditions can be achieved in the transesterification reaction by using a complex metal catalyst. In this project, a Zn(**1**)$_2$ complex was used for the PLA degradation to produce methyl lactate (Me-La). Main operating parameters for the process were studied by a design of experiments. A preliminary evaluation of the use of membranes and distillation for the purification step is also presented.

2. Methods

Small Initial trials of the PLA degradation were performed in a Schlenk flask, with 0.25 g of PLA and 22.4 mg catalyst at 50 °C. THF was selected as the solvent whereas methanol as the reactant. Zn(**1**)$_2$ was first tested for oxygen stability. Me-La production was traced by GC and ^{1}H NMR. Polymer disappearance was confirmed by GPC. With the aim to show scalability of the process, reactions were then performed in a 300 mL SS-316 stirred batch reactor. Operating parameters for the Taguchi design of experiments were: polymer concentration, polymer molecular weight, catalyst concentration and reaction temperature. Additionally, mass transfer limitations of the process were studied by including polymer particle size and stirring speed. The effects studied were: PLA conversion, Me-La selectivity, Me-La yield and maximum amount of Me-La produced. Sensible values of the range of operating parameters were included in the model. The effects were statistically analyzed. The progress of all the reactions was traced by withdrawing samples at

different time intervals. Membrane separation studies were performed in a cross-flow system with a commercial membrane (Duramem 150), by varying pressure and temperature. Samples of the permeate were analyzed by GC and ^{1}H NMR.

3. Results and discussion

Zn(**1**)$_2$ was shown to be oxygen stable and easy to produce in large quantities. The statistical analysis of the results revealed that the main factors affecting conversion, selectivity and yield are temperature and catalyst concentration. No mass transfer limitations of the process were found. The maximum amount of Me-La produced only depends on the initial concentration of PLA. The observed experimental data was characteristic of two consecutive reactions showing formation of an intermediate and with the second reaction being reversible (Figure 1). The corresponding set of differential equations for the mass balance and rate equations were solved numerically coupled with a fitting procedure to get the kinetic constants for the different conditions studied. The temperature dependency of the kinetic constants for the PLA degradation step was evaluated by an Arrhenius type form. The activation energies obtained were in the range: 39 – 65 kJ/mol^{-1}, which are of the order of magnitude of other PLA degradation processes that require higher temperatures. Preliminary separation studies show the possibility of removing intermediate products by a commercial membrane. Solvent and alcohol can be recovered by distillation.

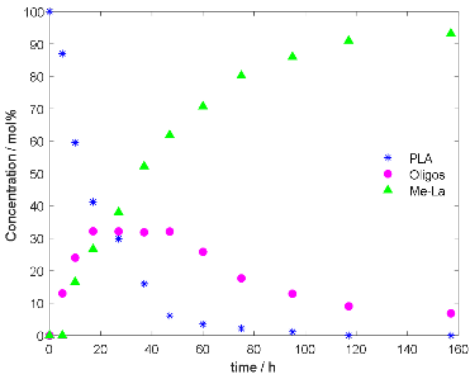

Figure 1. PLA degradation experimental data.

4. Conclusions

Complete degradation of PLA was demonstrated by the use of a metal complex catalyst which is stable in the presence of oxygen and that can be easily scalable. A valuable chemical (methyl lactate) was produced from this degradation. The main operating parameters of the process were identified and a kinetic model proposed. Kinetic constants and activation energies were calculated from the model that can be used for reactor design and optimization.

References

1. Hong, M. and E.Y.X. Chen, *Chemically recyclable polymers: a circular economy approach to sustainability.* Green Chemistry, 2017. **19**(16): p. 3692-3706.
2. Petrus, R., D. Bykowski, and P. Sobota, *Solvothermal Alcoholysis Routes for Recycling Polylactide Waste as Lactic Acid Esters.* ACS Catalysis, 2016. **6**(8): p. 5222-5235.
3. Piemonte, V. and F. Gironi, *Kinetics of Hydrolytic Degradation of PLA.* Journal of Polymers and the Environment, 2013. **21**(2): p. 313-318.

ECCE12
The 12th EUROPEAN CONGRESS OF CHEMICAL ENGINEERING
Florence 15-19 September 2019

Effect of Process Conditions in The Reduction of CO_2 Captured By Ammonia.

Juan I. del Río[1,2], David León[1], Eduardo Pérez[1], Ángel Martín[1], M.D. Bermejo [1,*]

1 BioEcoUva. Research Institute on Bioeconomy. High Pressure Process Group. Department of Chemical Engineering and Environmental technology. Universidad de Valladolid, Valladolid, 47011, Spain, Spain

2 Grupo Procesos Químicos Industriales, Facultad de Ingeniería, Universidad de Antioquia UdeA, calle 70 No.52-1, Medellín, Colombia

**Corresponding author: mdbermejo@iq.uva.es*

Highlights

- CO_2 as ammonium carbamate can be reduced to formic acid in hydrothermal media with a yield up to 38%
- Catalyst content, temperature and time are the relevant variables
- The formic acid yield is indirectly proportional to the initial concentration of carbamate
- The aluminum-water splitting reaction is feasible for reducing capture CO_2 without dry H_2

1. Introduction

The rapid population growing is making necessary the use of fossil fuels for the production of electricity, as well as fuel in the automotive industry, and will be still extended for many years [1]. This situation have encouraged to put the efforts in finding solutions concerning the mitigation of CO_2 emissions, such as CO_2 capture and storage technologies (CCS), and the Carbon Capture Utilization (CCU). The amine based CCS technology is one of the most attractive solutions nowadays, but the high cost of the desorption step entails to consider further possibilities. For instance, the French Company Alston developed a technology known as "Chilled Ammonia" [2]. In this technology, combustion gases are absorbed into an ammonia aqueous solution (28%wt) at low temperature (2-10˚C), to absorb CO_2 as carbonate, bicarbonate and carbamate of ammonia. Regeneration step consists also in desorption at temperatures between 100-150˚C, being less energetic than those from amines. Nevertheless, to completely avoid this step, our proposal is to reduce CO_2 captured in aqueous media as a carbamate with or without gaseous hydrogen. The last is achieved by the implementation of an environmentally friendly and economical hydrogen production technology like Aluminum-water splitting, and other reducers like zinc or biomass derivatives, which have proven to be effective in reducing sodium bicarbonate in hydrothermal media with efficiencies of up to 60% [3]. In the present work, the main product of the absorption of CO_2 in ammonia, the ammonium carbamate (AC), is transformed into formic acid in hydrothermal media, using metallic aluminum powder as reductant and Pd (5% wt) supported in activated carbon as catalyst, at temperatures from 80 to 200˚C and pressures above the saturation of water.

2. Methods

For stablishing the effect of the process variables on the production of formic acid (FA), several assays, under inert atmosphere of N_2, varying the temperature (80-300˚C), time (0.5-5 h), Al:AC molar ratio (3-9), catalysts content (7.5-60 wt% with respect to carbamate), liquid filling (50-85% of the total volume of the vessel) and initial concentration of aqueous AC solution (0.5-2.0M) were conducted in an stainless steel stirred reactor from Parr instruments, with autogenic pressure. The variation of the variables was performed based on a central point of reaction conditions (120˚C, 2h, Al:AC ratio of 6, 15% catalyst, 70% filling and 0.5 M of AC). The concentration of AC and FA were determined by means of HPLC (Waters, Alliance separation module e2695), using an Aminex 87H (Bio-Rad) column and RI detector (Waters, 2414 module).

3. Results and discussion

As observed in figure 1 (selectivity and conversion not disclosed), the time positively affects the yield, reaching 27% after 4 h of reaction and tends to level off, but with the depletion of selectivity. The highest selectivity (72%) is achieved at 0.5 h, indicating that the FA is formed faster than other possible compounds. The increase of initial concentration appears to not have a positive impact, since we observed a drop in the yield from 25% (0.5M) to 12% (2.0M). The temperature (not shown) presents a maximum yield of 20% between 120-150˚C. The catalyst content behaves similarly than time, allowing to obtain a yield as high as 38%, with a high selectivity of 85%, and conversion of 40% (not shown).

On the other hand, the Al:AC molar ratio does not have a great impact on the process. The liquid filling level also plays a positive effect over the process as the final autogenic pressure increases.

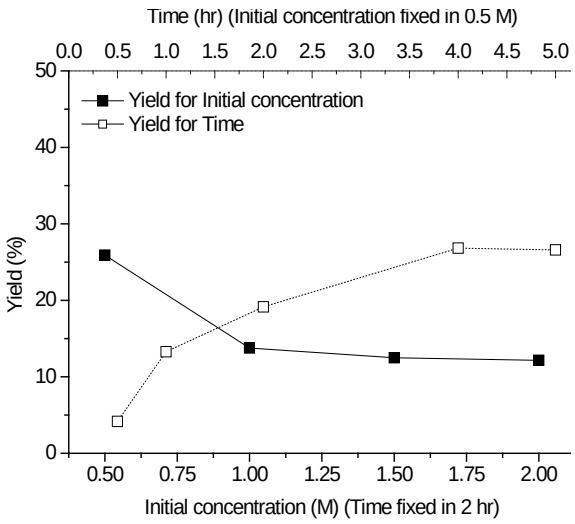

Figure 1. Effect of time and Initial concentration over Yield of FA

4. Conclusions

In the process to obtain formic acid, from the capture of CO_2 in aqueous ammonia solution, the variables that mostly affect the yield are the catalyst content, temperature and time. The reduction reaction can be achieved without the use of gaseous hydrogen with a yield up to 38% with an AC initial concentration of 0.5M. Scarce works have been found in the hydrothermal reduction of carbamates without dry hydrogen for producing value-added chemicals, representing a promising field of innovation.

Acknowledgments

This project has been funded by Junta de Castilla y León through project VA248P18. Juan Ignacio del Río acknowledges Universidad de Valladolid for the predoctoral fellowship. M. Dolores Bermejo thanks MINECO for Ramon y Cajal position.

References

[1] T. Covert, M. Greenstone, C.R. Knittel, J Econ Perspect. 30 (2016) 117-138.
[2] E. Gal, Patent No. WO2006022885, (2006).
[3] M. Andérez-Fernández, E. Pérez, A. Martín, M. Bermejo, J Supercrit Fluid. 133 (2017) 658–664.

ECCE12
The 12th EUROPEAN CONGRESS OF CHEMICAL ENGINEERING
Florence 15-19 September 2019

Microstructured Reactor Development and Detailed Investigation into Catalyst Performance for Decentralized Power-To-Gas Applications.

Sarvenaz Farsi*, Wolfgang Olbrich, Peter Pfeifer, Roland Dittmeyer

Karlsruhe Institute of Technology, Eggenstein-Leopoldshafen/ Germany

**Corresponding author: Sarvenaz.farsi@kit.edu*

Highlights

- A detailed study of the methanation kinetics was carried out.
- A novel microreactor with internal cooling structure for hot spot control in methanation was developed and validated.
- Influence of different process parameters on reactor performance was studied.

1. Introduction

The growing interest in renewable energies calls for development of energy storage processes which support a balanced energy supply and demand and provide a stable power grid. In order to meet the problem of storing energy from renewable sources and to be carbon dioxide neutral, Power-to-Gas (PtG) applying CO_2 as carbon source is recognized as a promising future technology. The resulting synthetic natural gas (SNG) from methanation reaction can be either stored or injected without limits unlike H_2 into a natural gas grid, since the infrastructure for its transportation and storage already exists [1]. Moreover, steam generated from the highly exothermic methanation of carbon dioxide may be used for considerably increasing the overall process efficiency by feeding a steam electrolysis unit.

In the framework of Kopernikus project Power-to-X, we study the methanation reaction of carbon dioxide from both, reaction fundamentals as well as reactor development point of view.

2. Methods

To reveal the underlying kinetics of the methanation reaction, a microstructured packed bed reactor with highly efficient internal cross-flow cooling obtained at IMVT-KIT has been fabricated.

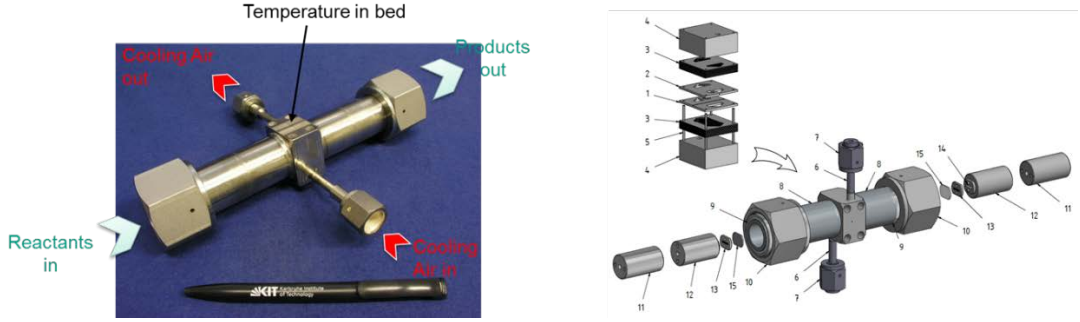

Figure 1 Packed-bed microstructured reactor used for kinetic measurements

Another focus of the work is dedicated to development and examination of a novel and compact evaporation cooled microstructured packed bed reactor for catalytic methanation of pure CO_2 for syngas throughputs of up to 2 Nm^3/h. The reactor (Figure 1) consists of two parallel reaction chambers in form of rectangular ducts. The heat management is accomplished by means of cooling channels above/below the reaction chambers and five heating cartridges between the reaction slits [2].

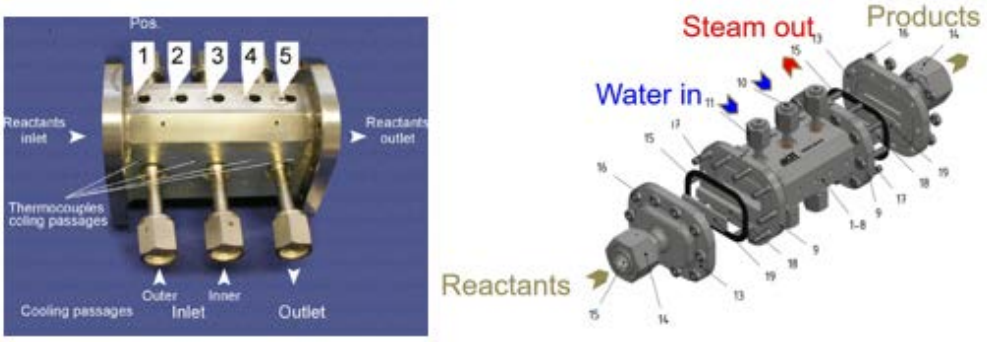

Figure 2 The microstructured reactor designed for methanation with two cooling inlets and one cooling outlet

3. Results and discussion

In the kinetic studies, the operation temperature, composition of the components in reaction and WHSV were varied to investigate their influence on reaction rate and stability of the catalyst. The results contributed to validation of the models for the catalytic methane production based on literature data for a stable and selective Ni_3Fe catalyst [3].

With regard to evaporation cooling, efficient heat removal and hot spot control by variation of the parameters of water feed were investigated. To assess the reactor behavior in cooperation with INERATEC GmbH, supply of pressurized water up to 20 bar to the cooling structures in different amount and distribution between the inlets was tested.

4. Conclusions

The in the current contribution parameters for reliable models for a wide range of process conditions are developed. The derived model can be applied to a microstructured reactor with internal evaporation cooling. The latter was also validated through this study.

References

[1] M. Götz, J. Lefebvre, F. Mörs, A. McDaniel Koch, F. Graf, S. Bajohr, R. Reimert, T. Kolb, J. Renewable Energy 85, 1371−1390, 2016.
[2] M. Belimov, D. Metzger, P. Pfeifer, J. AIChE 63, 120-129, 2017.
[3] B. Mutz, M. Belimov, W. Wang, P. Sprenger, M-A. Serrer, D. Wang, P. Pfeifer, W. Kleist, J.-D. Grunwaldt. ACS Catalysis 7 (10), 6802-6814, 2017.

ECCE12
The 12th EUROPEAN CONGRESS OF CHEMICAL ENGINEERING
Florence 15-19 September 2019

Dynamic Adsorptive Chromatographic Reactor Model.

Vincenzo Russo[1], Riccardo Tesser[1], Tapio Salmi[2], Martino Di Serio[1]

1 Università di Napoli Federico II, Complesso Universitario M.S. Angelo, via Cintia 4, IT-80126 Napoli.; 2 Åbo Akademi, Piispankatu 8, FI-20500 Turku/Åbo

**Corresponding author: v.russo@unina.it*

Highlights

- A new chromatographic reactor model was developed.
- Methyl acetate hydrolysis was simulated.
- Full conversion and product separation were predicted.

1. Introduction

The esterification of carboxylic acid with alcohols is a hot topic of the modern bio-refinery, to produce, for example, solvents, plasticizers [1]. Nowadays, a lot of effort is in progress to optimize the synthesis of several esters. The right reactor should optimize the physical characteristics of the system that is, as before mentioned, a liquid-solid reaction: i.e. Mazzotti et al. [2], used the simulated moving bed reactor (SMBR) packed with Amberlyst-15 catalyst to perform acetic acid esterification to ethylacetate, demonstrating that the resin can be used both to catalyze the reaction and separate the stream. It is important to underline that to design such apparatus, accurate and reliable models are needed, involving profiles along different coordinates (time, reactor radius, reactor axis and catalyst radius) [3], the knowledge of physical and chemical properties, and powerful tools to reach a reliable solution. In the present work, the development of a reactor model, that can be used to interpret experimental data collected in chromatographic reactors will be presented. Methyl acetate hydrolysis catalyzed by DOWEX 50W-X8 catalyst was chosen as case study [4].

2. Methods

The developed model can be considered an advancement respect to the recent efforts published in the literature [4]. The breakthrough idea is to develop a model where no rate-determining-step is considered, writing the opportune mass balance equations on both the liquid bulk and intraparticle phases. All the physical parameters were calculated from existing correlations. The liquid bulk and intraparticle mass balance equations are respectively reported in Eqs. 1-2.

$$\frac{\partial C_{i,B}}{\partial t} = -u\frac{\partial C_{i,B}}{\partial z} + D_z\frac{\partial^2 C_{i,B}}{\partial z^2} - k_m a_{sp}\left(C_{B,i} - C_{i,L}\big|_{r_P=R_P}\right) \quad (1)$$

$$\varepsilon\frac{\partial C_{i,L}}{\partial t} + (1-\varepsilon)K_i\frac{\partial C_{i,L}}{\partial t} = \varepsilon\frac{D_P}{r_P^s}\frac{\partial}{\partial r_P}\left(r_P^s\frac{\partial C_{i,L}}{\partial r_P}\right) + (1-\varepsilon)\frac{D_S}{r_P^s}\frac{\partial}{\partial r_P}\left(r_P^s\frac{\partial K_i C_{i,L}}{\partial r_P}\right) + (1-\varepsilon)\nu_{ij}r_j \quad (2)$$

The model was implemented in gPROMS ModelBuilder v.4 software, solving the axial and particle radial partial derivatives with a centered finite difference method with respectively 150 and 25 discretization points.

3. Results and discussion

Methyl acetate (MA) hydrolysis kinetic rate laws with related parameters are fixed and directly taken from literature [4]: the authors carried out different experiments by fixing the flow-rate at 0.75 mL/min and injecting pulses of 100 µL of a 0.5 mol/L solution of methyl acetate in water, at different temperatures (from 298 to 328 K). The results are reported in Fig. 1-left, together with the model predictions. As revealed, a temperature increase corresponds to an increase of the reaction conversion (the MA area decreases) with the related formation of the two products (M and A). Parameter estimation was carried out to obtain the surface diffusivity for each component, obtaining that the surface diffusivity values follow the order MA>M>A. The trend is due to the different acidity of each component, interacting with the acid solid phase. A parametric investigation was conducted evaluating the effect of different operation conditions on both the acid conversion and product separation (Fig. 1-right). It was possible to achieve complete MA conversion and product separation fixing the reactor length to L=2.50 m and T=323K, demonstrating high performances of the chromatographic reactor.

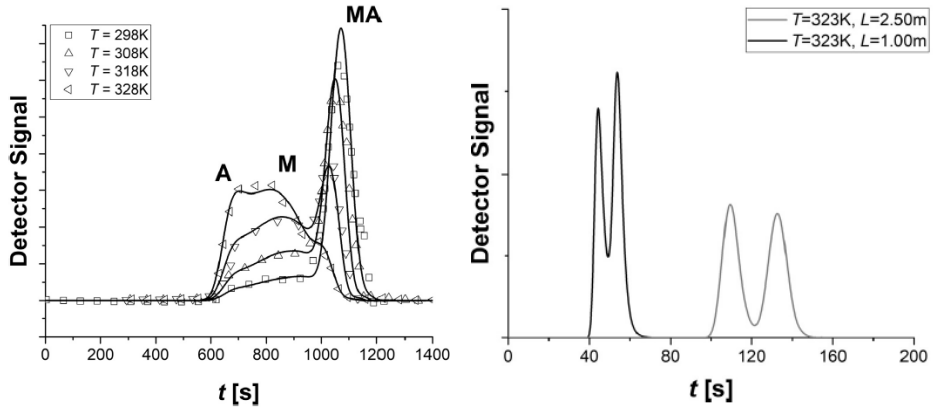

Figure 1. (Left) Description of experimental data taken from literature [4]: symbols are experimental data, lines the model description. (Right) Simulation of full conversion and total product separation.

4. Conclusions

A novel chromatographic reactor model was developed to interpret experimental data dealing both with the esterification of carboxylic acids and with the hydrolysis of organic esters. The model is advanced respect to the state of the art because no rate-determining steps are considered. All the physical and chemical phenomena are considered. In perspective, the model can be applied in optimizing the esterification/hydrolysis processes.

References

[1] D.R. Fernandes, A.S. Rocha, E.F. Mai, C.J.A. Mota, V.T. da Silva, Appl. Catal. A-Gen. 425 (2012) 199-204.

[2] M. Mazzotti, A. Kruglov, B. Neri, D. Gelosa, M. Morbidelli, Chem. Eng. Sci. 51 (1996) 1827-1836.

[3] V. Russo, R. Tesser, C. Rossano, R. Vitiello, R. Turco, T. Salmi, M. Di Serio, Chem. Eng. J. (2018). DOI: 10.1016/j.cej.2018.08.078

[4] T.D. Vu, A. Seidel-Morgenstern, J. Chromatogr. A 1218 (2011) 8097-8109.

ECCE12
The 12th EUROPEAN CONGRESS OF CHEMICAL ENGINEERING
Florence 15-19 September 2019

IMPACT OF HYDROTHERMIC BIOMASS WASHING ON THE ENZYMATIC HYDROLYSIS

Ariane S. S. Pinto[1,2], Marcelo P. A. Ribeiro[1], Roberto C. Giordano[1], Cristiane S. Farinas [1,2]

[1] *Graduate Program of Chemical Engineering, Federal University of São Carlos, São Carlos, Brazil;*

[2] *Embrapa Instrumentação, São Carlos, Brazil*

**Corresponding author: arianesbrice@gmail.com*

Highlights

- 2G ethanol bioconversion process still needs to overcome process challenges.
- Inhibitors from lignin degradation hinder the biochemical reactions.
- Removal of soluble inhibitors improved the conversion of the hydrolysis.

1. Introduction

The large scale production of 2G ethanol is still under development and needs to overcome obstacles such as high solids loading in the reactors, in addition to inhibitors impairing the biochemical reactions (1). Inhibitors released from both chemical degradation of lignin and cellulose/hemicellulose during the pretreatment process negatively impacts the subsequent steps (2). During enzymatic hydrolysis of biomass, the phenolic inhibitors from lignin degradation deactivate and/or inhibit the biological catalysts (3-4), increasing the amount of enzymes required. In this context, the configuration of the overall processes with a detoxification of soluble inhibitors is a possible strategy for contributing to the feasibility of large-scale process (3). Washing the pretreated biomass with hot water, for instance, has been shown a high removal of inhibitors from steam pretreated hardwood (5). Thus, the purpose of this work was to investigate a feasible protocol for washing pretreated sugarcane bagasse in order to improve the enzymatic hydrolysis process.

2. Methods

Hydrothermal pretreatment of sugarcane bagasse was carried out at 195 ° C, 10 minutes and 15% solids (w:w). The washing protocols were carried out using hot water at 90 °C. The first procedure consisted in homogenization of the mixture water and biomass at 10% solids (t_{MIX} < 1 minute), followed by filtration for 2 and 3 washing steps. The second washing process was conducted using a batch with 3% solids during 10 minutes for 6 washing steps (assuring the stabilization of the pH of the washing water). Subsequently, the enzymatic hydrolysis was performed at 50°C, 15% solids (w:w) and 10 FPU/g of dry bagasse in sodium citrate buffer (50 mM, pH = 5.0). Glucose was determined using a D-glucose enzymatic assay kit (Liquiform®, Brazil).

3. Results and discussion

The enzymatic hydrolysis conversion of washed pretreated biomass from first washing procedure with 2 washing steps removed the soluble inhibitors and improved up to 30.2% the conversion during enzymatic hydrolysis.

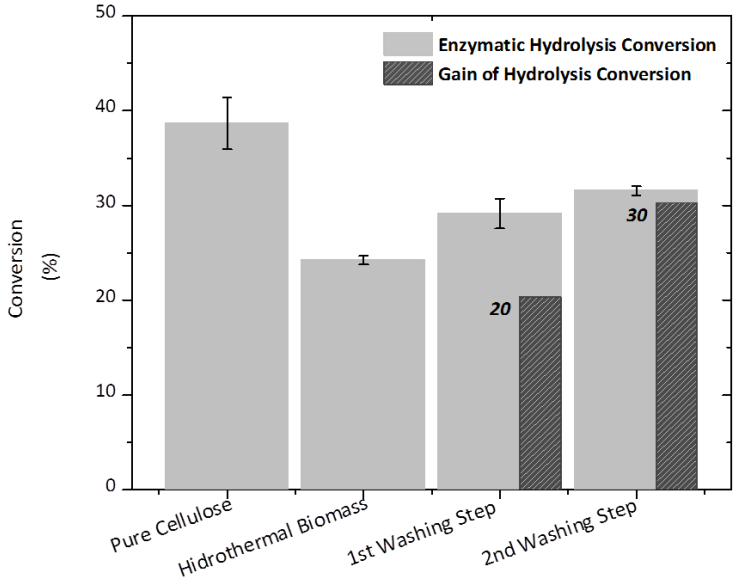

Figure 1. Conversion in the hydrolysis stage for each biomass processing and the conversion gain for the unwashed hydrothermal bagasse (52.41 % of cellulose).

On the other hand, the severe conditions of time and the many stages of washing with a lower solids loading (3% w:w) showed a negative impact on the enzymatic hydrolysis reaction (second protocol). This washing procedure not only removed the soluble inhibitors, but also helped to solubilize and disperse the remaining lignin in the biomass, resulting in the blocking of biomass to the action of the enzymes.

4. Conclusions

The results suggest that for improving the enzymatic conversion, the study of different washing proceedings is crucial to optimize the removal of soluble inhibitors during the production of 2G ethanol.

References

[1] L. H. d. S. Martins, S. C. Rabelo, A. C. d. Costa, Effects of the pretreatment method on high solids enzymatic hydrolysis and ethanol fermentation of the cellulosic fraction of sugarcane bagasse. *Bioresource Technology* **191**, 312-321 (2015).

[2] L. J. Jönsson, C. Martín, Pretreatment of lignocellulose: Formation of inhibitory by-products and strategies for minimizing their effects. *Bioresource Technology* **199**, 103-112 (2016).

[3] L. Qin *et al.*, Inhibition of lignin-derived phenolic compounds to cellulase. *Biotechnology for Biofuels* **9**, 70 (2016).

[4] S. Sun, Y. Huang, R. Sun, M. Tu, The strong association of condensed phenolic moieties in isolated lignins with their inhibition of enzymatic hydrolysis. *Green Chemistry* **18**, 4276-4286 (2016).

[5] Y. Kim, T. Kreke, R. Hendrickson, J. Parenti, M. R. Ladisch, Fractionation of cellulase and fermentation inhibitors from steam pretreated mixed hardwood. *Bioresour Technol* **135**, (2013).

ECCE12
The 12th EUROPEAN CONGRESS OF CHEMICAL ENGINEERING
Florence 15-19 September 2019

Reaction pathway network and kinetic model development for catalytic HDO of furfural over Ru/C and Rh/C

Rok Šivec[1], Miha Grilc[1], Blaž Likozar[1]

1 Department of Catalysis and Chemical Reaction Engineering, National Institute of Chemistry, Hajdrihova 19, 1000 Ljubljana, Slovenia

**Corresponding author: Miha.Grilc@ki.si*

Highlights

- Furfural is used as a renewable source for value added product production.
- Hydrodeoxygenation of furfural was carried out in a stirred three-phase reactor.
- Ru/C and Rh/C catalysts were used.
- A microkinetic model was developed and fitted to experimental data.

1. Introduction

Furfural is a very promising platform chemical, which can be produced from renewable sources, such as lignocellulosic (LC) biomass. The use of LC materials is increasing due to demand, and so are its residues (wastes), which are produced in millions of tons annually. [1] As a result, furfural is already produced in large quantities (close to 300 kTon annually). Furfural can be used as a valuable bio-derived source for many value added chemicals and biofuels. [2]

The hydrodeoxygenation (HDO) reaction of furfural with gaseous hydrogen was studied, by using different heterogeneous catalysts, such as Ru/C and Rh/C, in a high-pressure three-phase batch reactor system. Neat furfural and its iso-propanol solutions were used and various process parameters were varied. Furthermore, the reaction mechanism is being studied and a microkinetic model developed. The model will be fitted to experimental data. The use of different catalysts will also be compared.

2. Methods

A three-phase batch reactor was used, consisting of a 300 mL vessel, Rushton turbine stirrer and sampling lines for liquid and gaseous phase. 100 mL of liquid medium was used, composed of pure furfural as the main reactant or furfural dissolved in iso-propanol, while the latter has not only the role of a solvent but also participates in the reaction as a hydrogen donor. A solid catalyst (Ru/C or Rh/C) was added afterwards. The reaction vessel was closed, flushed with N_2 and pressurized under pure hydrogen at high pressure (50 bar at room temperature). The convective heat and mass transfer was assisted with vigorous stirring at 500 rpm. The reaction mixture was heated-up with a heat-up rate of 5 K min^{-1} to the temperatures of plateau at 175 °C, 200 °C and 250 °C, respectively. Liquid and gas samples were taken during the experiment and analysed by GC-MS/FID and NMR (liquid samples), and by GC-FID/TCD and FTIR (gaseous samples). At the end of the experiment, the reaction vessel was rapidly cooled down and flushed with N_2.The microkinetic model is being developed in Matlab software according to the proposed reaction sheme in Figure 1.

3. Results and discussion

100% conversion of furfural was achieved during the reaction (Figure 2), leading to numerous intermediates and products, such as Furfuryl alcohol, 2-methylfuran, 2-methyltetrahydrofuran, Tetrahydrofurfuryl Alcohol, 2,2'-[oxybis(methylene)]difuran and others. According to the microkinetic model, furfural is firstly hydrogenated to furfuryl alcohol. Three parallel reactions occur afterwards: a) furfuryl alcohol hydrogenation to tetrahydrofurfuryl alcohol and subsequent hydrodeoxygenation to 2-methyltetrahydrofuran, b) furfuryl alcohol hydrodeoxygenation to 2-methylfuran and subsequent hydrogenation to 2-methyltetrahydrofuran and c) furfuryl alcohol oligomerization to 2,2'-[oxybis(methylene)]difuran with subsequent hydrogenation to furfuryl alcohol and 2-methylfuran, which are further converted as already mentioned.

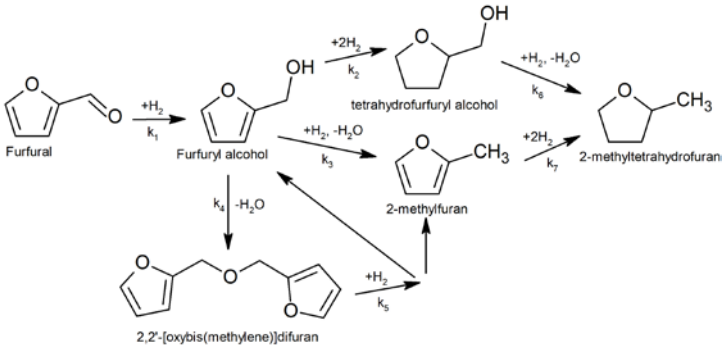

Figure 1. Proposed reaction scheme.

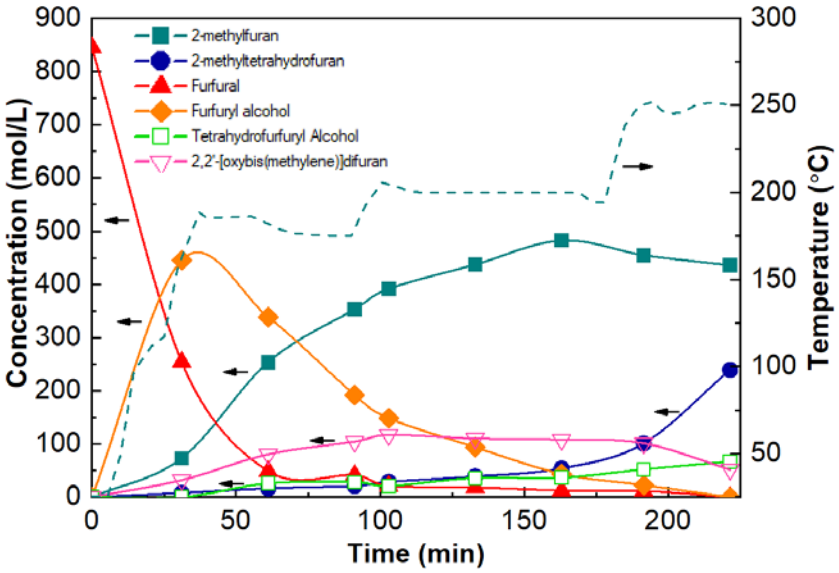

Figure 2. Experimental data of furfural conversion over Rh/C catalyst.

4. Conclusions

Experiments of furfural hydrodeoxygenation were carried out with the use of Ru/C and Rh/C catalyst. The results are promising for 2-methylfuran and 2-methyltetrahyfdrofuran production. The developed microkinetic model will be fitted to experimental data points and used to predict the reaction at different conditions.

References

[1] M. Dashtban, A. Gilbert, and P. Fetehi, J-FOR, 2(4) (2012) 44–53.

[2] R. Mariscal, P. Maireles-Torres, M. Ojeda, I. Sádaba, and M. López Granados, Energy Environ. Sci., 9(4) (2016) 1144–1189.

Methanol synthesis in a stirred batch reactor – application of the total pressure method and reaction-diffusion modelling

Pasi Tolvanen[1], Vincenzo Russo[1,2], Kari Eränen[1], Tapio Salmi[1*],

1 Laboratory of Industrial Chemistry & Reaction Engineering, Department of Chemical Engineering, Johan Gadolin Process Chemistry Centre, Åbo Akademi University, FI-20500 Åbo-Turku, Finland
[2]Università di Napoli ''Federico II'', Chemical Science Department, IT-80126 Napoli, Italy

**Corresponding author: tapio.salmi@abo.fi*

Highlights

- The theory for the total pressure method applied on the study of heterogeneously catalyzed kinetics was presented
- Experiments on methanol synthesis was carried out in a intensively stirred batch reactor
- The reaction-diffusion model for porous particles were used to interpret the data and to determine the kinetic parameters
- The applicability of the total pressure method was demonstrated for methanol synthesis and generic examples

1. Introduction

The total pressure method is well-known for the measurement of the kinetics of homogeneous gas-phase reactions. If the number of molecules change in a gas-phase process, the total pressure in a closed reactor vessel changes indicating the progress of the reaction. The total pressure method can be applied to heterogeneously catalyzed gas-phase reactions, too. In this work, the general theory for the interpretation of kinetic data in stirred batch reactors is presented. The concept was applied to the synthesis of methanol from carbon monoxide and hydrogen on a commercial copper-based catalyst.

2. Methods

The catalyst particles were placed in a spinning impeller which rotated at high speed, typically 300-600 rpm. The volumes of the autoclave reactor and the gas phase were constant. Catalyst particles of equal sizes were used in all the experiments and isothermal conditions prevailed. The reaction temperatures and pressures were 150-250ºC and 10-30 bar, respectively. The classical modelling approach, based on simultaneous chemical reactions and diffusion in porous media was applied. This implies that that separate mass balances are valid for the gas-phase components in the gas bulk and in the catalyst pores. The catalyst particles were presumed to be chemically (activity, number of active sites) and physically (particle size, porosity, tortuosity, surface area) equal. Thus the aspects of particle size distribution and chemical inhomogeneity of the catalyst surface were ignored.

The model for the catalyst particles in the rotating device is

$$\varepsilon_P \frac{dc_i}{dt} = \frac{D_{ei}}{R^2}\left(\frac{d^2c_i}{dx^2} + \frac{s}{x}\frac{dc_i}{dx}\right) + r_i\rho_P$$

where x = the dimensionless particle coordinate, R = particle radius, s = shape factor, r_i= the generation rate of component i, ρ_P = particle density, ϵ_P = particle porosity, D_{ei} = effective diffusion coefficient. For the gas bulk surrounding the spinning impeller, the balance equation is given by

$$\frac{dc'_i}{dt} = -\frac{D_{ei}}{V_G R}\left(\frac{dc_i}{dx}\right)_{x=1} n_P A_P$$

where n_P and A_P denote the number of particles and their outer surface area, respectively. V_G is the gas volume. The model was solved numerically and the parameters were estimated from collected total pressure data.

3. Results and discussion

The results of the sensitivity analysis of the model revealed that the increase of the kinetic constant leads to a faster decrease of the overall pressure. The initial pressure plays an activating role on the reaction kinetics as well. By working at higher H_2/CO ratio, a lower rate is observed. Examples of the intraparticle profiles of carbon monoxide and hydrogen are displayed in Figure 1, which confirms the role of the internal diffusion effect in the catalyst pores as concentration gradients appear inside the particles.

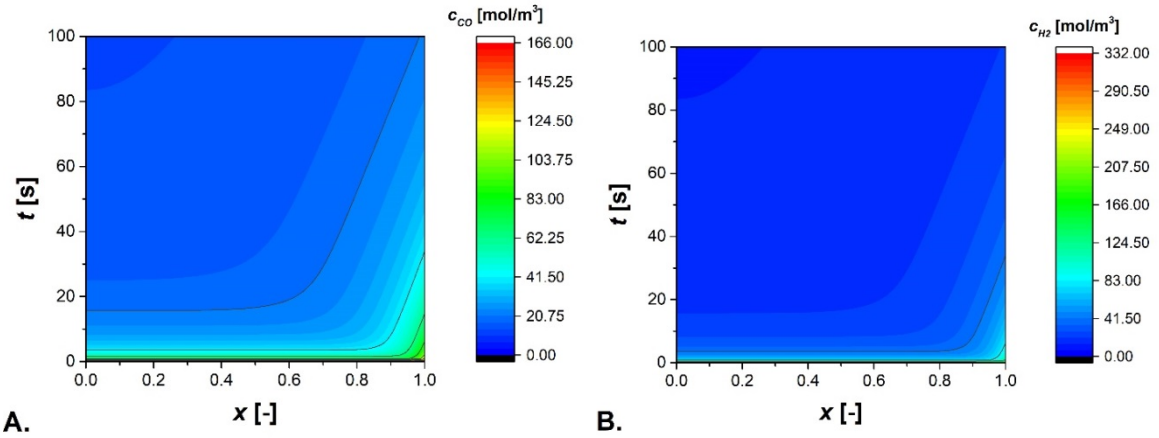

Figure 1. CO (A) and H_2 (B) concentration profiles inside the catalyst particle.

4. Conclusions

Rapid methods are very valuable in the determination of the kinetic and mass transfer effects for heterogeneously catalyzed reactions. The total pressure method is a classical tool in the measurement of the kinetics of gas-phase reactions. It can be successfully applied to the kinetics of gas-phase processes enhanced by solid catalysts. A general theory for the analysis of heterogeneously catalyzed gas-phase kinetics in stirred batch reactors was presented for the case of the kinetic control and combined kinetic-diffusion control. The concept was successfully applied to gas-phase synthesis of methanol from carbon monoxide and hydrogen.

ECCE12
The 12th EUROPEAN CONGRESS OF CHEMICAL ENGINEERING
Florence 15-19 September 2019

Kinetics and modeling of Ibuprofen removal in the absence and presence of heterogeneous catalysts

Soudabeh Saeid[1], Vincenzo Russo[2], Pasi Tolvanen[1], Narendra Kumar[1],

Jyri-Pekka Mikkola[3], Tapio Salmi[1]

1 *Laboratory of Industrial Chemistry and Reaction Engineering, Johan Gadolin Process Chemistry Centre, Åbo Akademi University, FI-20500 Åbo/Turku, Finland*
2 *University of Naples "Federico II", Chemical Sciences Department, IT-80126 Naples, Italy*
3 *Technical Chemistry, Department of Chemistry, Chemical-Biological Centre, Umeå University, SE-90187 Umeå, Sweden*
**Corresponding author: ssaeid@abo.fi*

Highlights

- The degradation of ibuprofen by catalytic ozonation was studied.
- A kinetic model was developed.
- The model gave a valid description of data.

1. Introduction

Pharmaceuticals are continuously entering surface waters due to the growing worldwide consumption which is a health risk to humans as well as the environment [1]. Hundreds of different compounds – painkillers, inflammatory mediators, hormones and antibiotics are eluted to the seas, because conventional water treatment plants cannot eliminate these compounds from wastewaters. Ozonation is a good treatment upon removal of micropollutants; however, low mineralization, peril by-products, limited ozone solubility and low stability in water are the main shortcomings of ozonation. The limitations of using ozone alone can be avoided by combining solid catalysts with ozonation which promotes the of ozone reactivity and the formation of hydroxyl radicals, and eventually a complete mineralization becomes possible [2]. In order to progress towards process design, a detailed mathematical model for the three-phase system is required.

2. Methods

Semibatch ozonation experiments were conducted in a double jacketed glass reactor (1100 ml) connected to an ozone generator (Fig. 1). The experiments were managed in a gas-liquid reactor system which consisted of the aqueous phase containing IBU, ethanol and deionized water in batch, while the gas mixture containing ozone was continuously bubbled from the bottom into the solution through a disperser. In case a catalyst was used, it was immobilized inside the stirrer, which is a special mixing device (Spinchem™ Rotating Bed Reactor) that maximizes the mass transfer between all phases. The operating conditions were: concentration of ibuprofen (IBU): 10 mg/L, ethanol 10ml/L, gas flow range: 250-1100 ml/min, mixing rate: 900-1070 rpm, temperature: 5-30˚C and the reaction time was typically 2-4 h. For the catalytic experiments, a preset amount of 0.25-0.5 g catalyst (zeolites) were used in a rotating mixer.

3. Results and discussion

The kinetic model for catalytic ozonation of IBU was implemented in gPROMS, which helped to describe and evaluate the reaction kinetics. The dissolved ozone concentration and the kinetic parameters were modeled based on the experimental data, and the data were utilized to model the ibuprofen decomposition using a number of experiments performed under various conditions. An improved understanding on the complex behavior of the reaction system was successfully achieved thanks to the model.

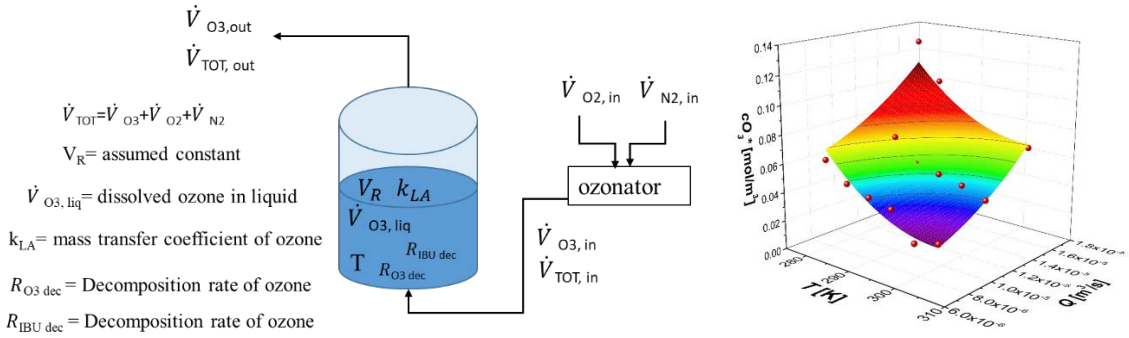

Figure 1. Left: The reactor setup and considered parameters for modeling. Right: fitting of the dissolved ozone concentration vs T(°C) and gas flow rate.

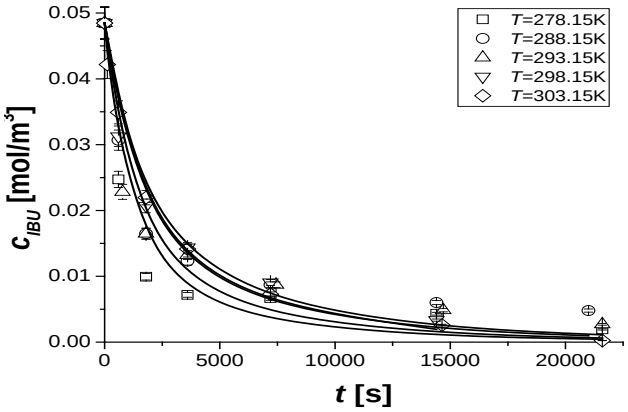

Figure 2. IBU ozonation experiments conducted at different temperatures without heterogeneous catalyst. Symbols represent the experimental data, lines the calculated profiles.

A preliminary interpretation was achieved to describe the experiments conducted in the absence of heterogeneous catalysts. The calculations were performed by fixing a power-law rate expression, finding apparent reaction orders of 1.5 for ibuprofen and 3 for ozone, suggesting a complex reaction mechanism. The activation energy was determined to 100kJ/mol. The results are portrayed in Figure 2. As revealed, a good fit was obtained. The model was further developed to describe the ozonation system in the presence of heterogeneous catalysts, where the catalyst amount, the mixing intensity and the active metal species were shown to have an important role.

Conclusions

An extensive study of ibuprofen removal was carried out. The ozonation system and the ibuprofen decomposition with and without heterogeneous catalyst was successfully modeled.

References

[1] Rosal, R.; Rodríguez., A.; Gonzalo, M. S.; García-Calvo, E. Appl. Catal. B Environ. 2008, 84 (1–2), 48–57.
[2] Saeid, S.; Tolvanen, Salmi, T.et al., Appl. Catal. B Environ. 2018, 230 (January), 77–90.

Lignin fractionation by means of organic solvents.

Nagore Izaguirre[1], Oihana Gordobil[1], Laíse Guerreiro[2], Jalel Labidi[1]

[1] *Chemical and Environmental Engineering Department. University of the Basque Country UPV/EHU. Plaza Europa, 1, 20018. San Sebastian, Spain*
[2] *Postgraduate Program of Science and Engineering of Materials, Federal University of Pelotas, Gomes Carneiro street, 1, Pelotas, Brasil*
**Corresponding author: jalel.labidi@ehu.eus*

Highlights

- Efficient fractionation method with organic solvents widely used in industry and with low boiling point
- Obtaining of different molecular weight fractions
- Lignin fractionated with different structure and properties

1. Introduction

In current times, the utilization of materials from renewable resources has been severely promoted, as well as the revalorization of industrial wastes for the production of high added value materials. Therefore, biorefineries of lignocellulosic materials are key not only for the pollution reduction, but also for the sustainable development, being the means of obtaining fuels, chemicals and renewable materials[1]. For all these reasons, it can be predicted that all the main components of biomass (lignin, hemicellulose and cellulose) will significantly contribute to the global bioeconomy[2].

Lignin is one of the most interesting components of lignocellulosic materials. It is the most abundant aromatic compound on earth as well as having high availability and low price. However, it has great heterogeneity, and its properties, linked with composition and structure, also vary. Consequently, its uses are limited and in order to incorporate lignin in added value applications, its fractionation is an essential requirement to be used as feedstock in the industry[3].

One of the most promising methods is the use of organic solvents. This method allows separating lignin in different fractions to obtain fractions with specific properties by the successive utilization of different organic solvents. Apart from that, it was also taken in consideration the fact that these organic solvents were environmentally friendly and they could be bio-derived[4]. Therefore, the main objective of this work was to study the fractionation of industrial kraft lignin, as well as organosolv lignin, to separate it in more homogeneous fractions and characterize their structure and composition.

2. Methods

The fractionation was conducted using two types of lignin, kraft (from local industrial waste) and organosolv (commercial provided by *chemicalpoint*). They were dissolved firstly in ethyl acetate, the organic solvent with the lowest capacity to dissolve lignin. The insoluble fraction was obtained by filtration whilst the soluble fraction (F1) was obtained by rotavaporation of the solvent. The

next step was followed with the insoluble fraction with the next solvent with the lowest solubility, ethanol. The same procedure was followed, except for the fact that the soluble fraction (F2) was obtained by precipitation with acidified water. The sequence was finished after using acetone and methanol, respectively, to obtain the two remaining fractions (F3 and F4).

The obtained fractions were analyzed to determine their structural and thermal properties. Gel Permeation Chromatography (GPC) was conducted to know the molecular weight of both lignins and their fractions. Fourier Transformed Infrared was also performed, as well as the spectrophotometric method of Folin-Ciocalteau to calculate the total phenolic content, Py-GC-MS to identify the main components, and the glass transition temperature and thermal stability were determined.

3. Results and discussion

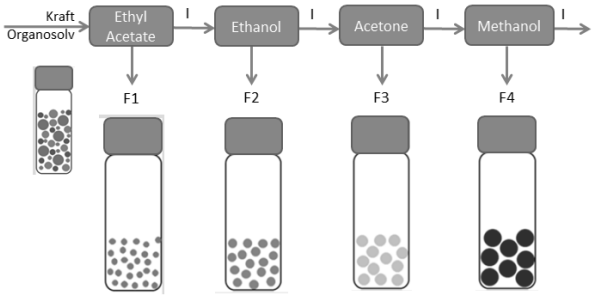

Mw		F1	<	F2	<	F3	<	F4
OH content		F1	>	F2	>	F3	>	F4
Py	S/G	F1	>	F2	>	F3	>	F4
	Purity	F1	>	F2	>	F3	>	F4

Figure 1. Schematic representation of the fractionation process and summary of the results obtained.

Although the kraft and the organosolv lignin have different characteristic, the same tendency could be observed during the fractionation process, obtaining molecules of the smallest molecular weights first and the biggest ones last.

It can also be observed the influence of the fractionation in the total phenolic content, since the molecules with the smallest weight had the largest phenolic content. From the pyrolysis analysis it was noticed that the purity increased after the fractionation method and that he first fractions (F1 and F2) contained a higher syringil derived components quantity.

4. Conclusions

It can be concluded that the fractionation method is efficient. First of all, it could be observed that the molecular weights of the fractions increased along the solubility parameter of the organic solvent used. Moreover, the content of phenolic hydroxyl groups diminished, which leads to an increase in the content of condensed compounds.

References [Calibri 10]

[1] A. Chandel, V. Garlapati, A. Singh, Bioresources Technology, 264 (2018) 370-381
[2] A. Chandel, O. Singh, G. Chandrasekhar, Journal of Commercial Biotechnology, 3 (2010) 239-257
[3] A. Naseem, S. Tabasum, K. Mahmood, International Journal of Biological Macromolecules, 93 (2016) 296-313
[4] D. Prat, A. Wells, J. Hayler, Green Chemistry, 18 (2015) 288-296

ECCE12
The 12th EUROPEAN CONGRESS OF CHEMICAL ENGINEERING
Florence 15-19 September 2019

Esterification of myristic acid with methanol using functionalized mesoporous SBA-15

Darja Pečar*, Petra Kotnik, Andreja Goršek

University of Maribor, Faculty of Chemistry and Chemical Engineering
Smetanova 17, SI-2000 Maribor, Slovenia

**Corresponding author: darja.pecar@um.si*

Highlights

- Propyl-sulfonic acid functionalized SBA-15 catalyst was synthesized.
- The catalyst characterization was performed.
- The esterification reaction of myristic acid with methanol was conducted.
- Kinetic parameters of the reaction were determined.

1. Introduction

Acid catalysis is one of the most important catalytic processes in the chemical industry. Industrially important organic transformations include esterifications and transesterifications [1,2]. Solid acid catalysts present an alternative to dangerous and corrosive mineral acid catalysts used in the industry. They contain more environmentally benign components, while providing higher activity and selectivity in comparison with existing homogeneous catalysts.

Mesoporous silicas, a type of solid acid catalyst, are solid inorganic carriers with large surface areas and relatively large ordered pores. Catalysts based on silica are inexpensive, simple to synthesize, and insoluble in most organic solvents, which allow them to be recycled. One type is modified mesoporous silica SBA-15, which is applicable for a wide variety of organic reactions [3].

In this study, mesoporous silica SBA-15 was functionalized with sulfonic acid, a very suitable catalyst for acid-catalyzed reactions. We used a slightly modified single-step synthesis based on simultaneous hydrolysis and condensation. After extensive characterization, the catalyst was tested performing the esterification reaction of myristic acid with methanol.

2. Methods

Propyl-sulfonic acid functionalized SBA-15 was synthesized by the one-step co-condensation procedure. The catalyst characterization was performed applying XL-30 scanning electron microscope from Philips and ZetaSizer Nanoseries from Nano, a Tristar II 3020 porosimeter from Micromeritics, FTIR IRAffinity-1 from Shimadzu and TA4000 from Mettler Toledo.

All experiments were performed in a batch reactor at different temperatures, ϑ = (55, 60 and 64.5) ºC and stirrer speed, f_s = 600 min^{-1}, loading of the catalyst, m = (0.2, 0.4 and 0.6) g and 10 mL of myristic acid solution in methanol with an initial concentration, γ = 15 g/L. The analyses of myristic acid were performed on a Shimadzu GC-2010 equipped with an autosampler AOC-20s and a flame ionization detector (FID).

3. Results and discussion

The myristic acid conversion was calculated from determined concentration of myristic acid in the reaction medium. The results at 55 °C are presented in Fig. 1. At 55 °C the conversion of myristic acid after 1 h was 49.9, 68.2, 81.7 % and 93.7, 98.7, 99.0 % after 5 h, applying 0.2, 0.4 and 0.6 g of the catalyst, respectively. We can observe that at the beginning of the reaction the conversion is highly dependent on the amount of catalyst used, while at the end those differences are not so pronounced.

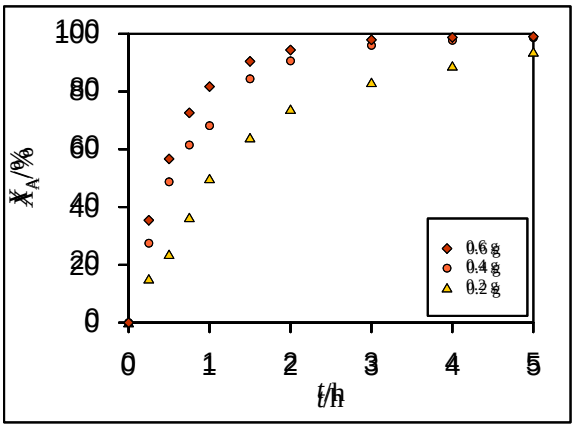

Figure 1. Conversion of myristic acid versus time at different catalyst loadings, ϑ = 55 °C and f_s = 600 min^{-1}.

In order to calculate reaction rate constants, the Langmuir-Hinshelwood-Hougen-Watson model was applied. The plots $\ln((M - X_A)/M\,(1 - X_A))$ versus t were constructed for all sets of experimental data. The reaction rate constants were then obtained from the slopes of the lines divided by c_{A0} $(M - 1)$ term. The Arrhenius equation was used to calculate activation energies and pre-exponential factors form the determined values of reaction rate constants at different temperatures. The average activation energy for myristic acid esterification was found to be E_a = 32.2 kJ/mol.

Three subsequent reactions were performed with each batch of the catalyst to test the deactivation between individual repeated reaction. The results revealed that used catalyst is highly resistant to deactivation, because there were practically no differences in the conversion for the 1st, 2nd or 3rd reaction.

4. Conclusions

Functionalized mesoporous silica SBA-15 containing sulfonic groups was synthesized with a modified one-step procedure. The results of catalyst characterization reveal that SO_3H functional groups are incorporated in the structure of homogenous particles with a random distribution. The catalyst has high catalytic activity in esterification reaction and is easily separated from the reaction medium. We confirmed the high potential of the catalyst's reuse with no significant loss of activity between consecutive reactions. Additionally, the kinetic parameters of the reaction were determined and they are in accordance with the literature data.

References

[1] M. Trejda, B. Pokora, and M. Ziolek, Catal. Today 254 (2015) 104-110.
[2] W. Xue, H. Zhao, J. Yao, F. Li, and Y. Wang, Chin. J. Catal. 37 (2016) 769-777.
[3] B. Chang, Y. Tian, W. Shi, J. Liu, F. Xi, and X. Dong, J. Porous Mater. 20 (2013) 1423-1431.

ECCE12
The 12th EUROPEAN CONGRESS OF CHEMICAL ENGINEERING
Florence 15-19 September 2019

Oxidative coupling of methane: performance comparison of powdered, pelletized and 3D printed catalysts at miniplant scale

Tim Karsten[1], Vesna Middelkoop[2], Hamid Reza Godini[3], Jens Uwe Repke[1]

[1]*Process Dynamics and Operation Group, Sekr, KWT-9, Technische Universität Berlin, Germany.*
[2]*Flemish Institute for Technological Research, VITO NV, Boeretang 200, Mol, Belgium.*
[3] *Dept. Chemical Engineering and Chemistry, Eindhoven University of Technology, Eindhoven, The Netherlands.*

**Corresponding author: tim.karsten@tu-berlin.de*

Highlights

- 3D structured catalysts show promising performance and low pressure drop
- Examined correlation between pressure profile and reactor performance
- Performance of a scaled up reactor for OCM demonstrated

1. Introduction

Powdered catalysts in most cases offer high reactivity and specific surface area, both for oxidative coupling of methane (OCM) and other gas phase reactions. However, powdered catalysts have significant drawbacks too. Their use often results in high specific pressure drops and they are difficult to handle and maintain. This is the reason that powdered catalysts are rarely used in large-scale applications. On the other hand, pelletized catalysts are conventionally used, as they are easier to work with and show a decent compromise between reactivity and pressure drop. The use of modern 3D printers opens up the possibility to print catalyst material directly. 3D printed catalysts represent a real alternative to pellets with tuneable porosity, high surface area, low pressure drop and improved heat and mass transfer.

The aim of this work is a comparative investigation into powdered, pelletized and 3D structured catalysts on a miniplant scale using the example of the oxidative coupling of methane.

The OCM reaction is a promising way to produce ethylene directly from natural gas or biogas. It presents an attractive alternative to naphtha cracking as it can utilizes different and more widely available feedstock.

2. Methods

For all the experiments that were carried out, MnNa2WO4/SiO2, provided by Johnson Matthey, was used as catalyst for the OCM reaction testing. The powder was first pressed and subsequently ground to obtain a particle size range of dp=400-600µm. The pellets, provided by Johnson Matthey too, were produced through extrusion with a particle size of 2.7mm. The catalyst powder was printed by VITO into catalyst structures with periodic lattices, using a direct write technique that offers a high degree of control over the composition, surface area and geometry.

The structures, pellets and source powder (Figure 1) were tested in a miniplant scale reactor at TU Berlin with a total reactor volume of 1.8l. The performance in terms of C2 yield was assessed under different temperatures and feed rates. Other parameters, such as the CH_4 to O_2 ratio, pressure and dilution were kept constant.

In order to examine the possible loss of reactivity due to the fabrication process, a second set of experiments was performed. The pellets and structures were ground back to a powder with the same particle size as the source material. Subsequently, the three powder samples were tested in a smaller size fixed bed reactor under the same operating conditions.

Figure 1. MnNa2WO4/SiO2 catalysts for OCM reaction tests; powdered (left), pelletized (middle), 3D printed structures (right)

3. Results and discussion

The main design considerations in the scaled-up reactor were (1.) facilitating the stacking of the 3D printed structures and (2.) ensuring a robust seal between the perimeter of the structures and the inner wall of the reactor tube in order to prevent gas from bypassing along the length of the reactor. The resulting scaled-up reactor demonstrates the design modularity and ability to perform OCM reactions in applications that are larger than lab scale.

The preliminary results of testing the structured catalysts are promising when compared to the conventional packed bed configurations. The influence of the different catalyst shapes on the pressure drop along the reactor was examined and quantified showing a correlation between the specific surface area and the reactivity, or C2 yield. Furthermore, it can be seen to what extent the production process of the pellets and 3D printed structures influence the reactivity of the catalyst.

4. Conclusions

In this work, the different shapes of OCM catalysts and their influence on C2 yield have been quantified and compared. It has been shown that 3D printed structures have the potential to provide tailor-made catalysts for large-scale applications, offering increased accessibility of the active sites within their engineered porosity.

Acknowledgments

This project has received funding from the European Union's Horizon 2020 research and innovation programme under grant agreement No 679933

ECCE12
The 12th EUROPEAN CONGRESS OF CHEMICAL ENGINEERING
Florence 15-19 September 2019

Continuous reactive distillation for the esterification between glycolic acid and butan-1-ol

Carole Mutschler[1], Clémence Nikitine[1], Pascal Fongarland[1]

1 Laboratoire de Génie des Procédés Catalytiques, Université Claude Bernard Lyon 1, CPE Lyon, CNRS,43 bd du 11 novembre 1918, B.P. 82077, 69616 Villeurbanne cedex, FRANCE

**Corresponding author: cmu@lgpc.cpe.fr*

Highlights

- Characterization of a reactive distillation column
- Reaction between glycolic acid and butanol in a continuous reactive distillation in the transient state

1. Introduction

The production of bio-based carboxylic acids have aroused considerable interest in industrial field as intermediate products. By oxidizing glycerol in aqueous phase, formic acid, oxalic acid and alpha hydroxy acids such as lactic, glycolic, glyceric and tartronic acids were obtained [1,2]. These acids have low volatility with each other, and some of them are subject to thermal degradation at higher temperature (tartronic acid, glycolic acid …). Hence, their separation tend to be difficult by simple distillation. To overcome that issue it has been decided to esterify those acids with an alcohol. Using reactive distillation to esterify alpha hydroxy acids has already been developed in order to remove water and then shift the chemical equilibrium [3,4].
In first instance, it has been decided to focus our research on the esterification of glycolic acid with butan-1-ol by reactive distillation in order to get butyl glycolate and water as presented in Figure 1

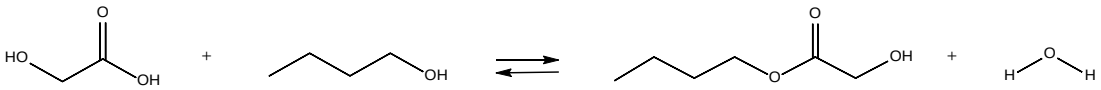

Figure 1 : Esterification between glycolic acid and butan-1-ol

2. Methods

A preliminary study was carried out in order to evaluate the feasibility of producing butyl glycolate through reactive distillation. A model of reactive residue curve maps was developed on Matlab®. In these reactive residue curve maps, the butyl glycolate is a stable node. A residue highly concentrated in butyl glycolate can therefore be obtained. However, a distillation boundary split the area into two regions. In order to get a residue of mainly butyl glycolate the feed should be in large excess of butanol.
Experiments were conducted in a laboratory distillation column of 1m high and with an internal diameter of 32mm designed by Pignat® (Figure 2). The column is divided into three different sections filled with random packing (glass bead

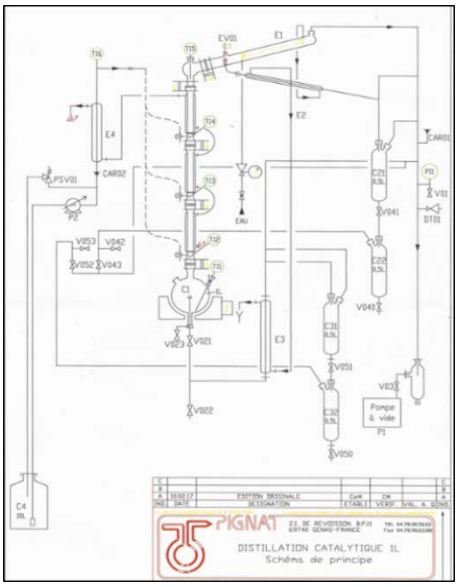

Figure 2 : Catalytic distillation column designed by Pignat®

of 7 mm) or foam. Catalysts (amberlyst36 or TiO_2-WOx) used are directly filled in those sections or coated on a foam.

The column was first characterize. The number of theoretical plates of the column was determined by a mixture of isopropanol and ethanol at atmospheric pressure and infinite reflux in batch mode. Three theoretical plates are counted (4 if the boiler is considered). The heat supplied to the boiler was determined by the evaporation of pure water with no reflux and is about 71 W. Simulations with Prosim Plus® have given the same results as the characterization.

Esterification experiments were conducted continuously at 390mbar with a feed composed of glycolic acid and butanol 1:10 wt./wt. The boiler was first filled with pure butan-1-ol. The analysis of both distillate and residue was operated by HPLC with a Phenomenex® Kinetex XB-C18 column, equipped with a Refractive Index (RI) and an UV detector.

3. Results and discussion

Results shown in Figure 3 correspond to a reaction carried out without any catalyst. After 3h of reaction, the steady state is not achieved as the composition of the residue is still evolving, but the mass balance has been established. However, the ester is produced through the operation even without any catalyst. In order to get the steady state quicker, it will be needed to start the reactive distillation with a composition at the boiler close to the steady-state composition of the residue.

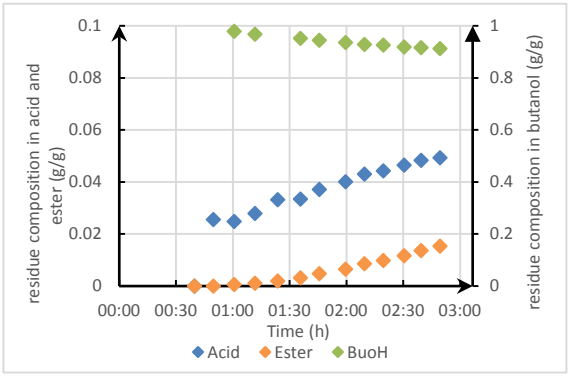

Figure 3 : Composition at the residue in butan-1-ol, glycolic acid and butyl glycolate

In one hour batch distillation, 22% and 88% of acid conversion have been observed without and with catalyst respectively. Moreover, simulations with Prosim Plus© showed that acid conversion is close to 100 % after one theoretical plate. So, it is possible to obtain a residue concentrated in butyl glycolate by using catalysts in one section of the column. Hydrodynamic and liquid-gas contact with foam or glass bed packing are similar. Hence, foam coated on TiO_2-WOx is a proper catalyst for this reaction in this process.

4. Conclusions

To conclude, our column has been characterized and first tests for the esterification of glycolic acid with butan-1-ol in reactive distillation have been performed. It shown that the production of butyl glycolate through reactive distillation is feasible without any by-product. Different catalytic packing (Amberlyst 36 beds, TiO_2-WOx pellets or coated on foam) are tried which represent a commonly known issue in reactive distillation as it needs to be efficient in both distillation (G/L contact, pressure drop) and reaction (good conversion). Results in simulation always show a good conversion (more than 90%) and separation of the products.

References

[1] SKRYNSKA E., DUMEIGNIL F., CAPRON M. et DUHAMEL L. WO2014199256 A1, 2014.
[2] CAPRON M., DUMEIGNIL F. et SKRZYNSKA E. WO2015055942 A3, 2015.
[3] HILDEBRANDT R., VOLLMER H-J., ALSCHER A., HOLTMANN W. US20050096481 A1, 2004.
[4] TERRILL D. L., MORAN K. M., FALLING S. N. US20130310598 A1, 2013

ECCE12
The 12th EUROPEAN CONGRESS OF CHEMICAL ENGINEERING
Florence 15-19 September 2019

Kinetic modeling of catalyst deactivation in the rhodium diphosphite catalyzed hydroformylation of long chain olefins

Martin Gerlach[1]*, Maximilian Wendt[1], Andreas Seidel-Morgenstern[1,2], Christof Hamel[1,3]

1 Otto von Guericke University, Institute of Process Engineering, Magdeburg, Germany; 2 Max Planck Institute for Dynamics of Complex Technical Systems, Magdeburg, Germany; 3 Anhalt University of Applied Sciences, Department of Applied Biosciences and Process Engineering, Köthen, Germany

**Corresponding author: martin.gerlach@ovgu.de*

Highlights

- Kinetic study of industrially relevant impurities
- Detailed experimental investigation of deactivation kinetics
- Operando FTIR spectroscopic validation of catalyst deactivation
- Extension of mechanistic kinetic models by deactivation model

1. Introduction

In the Collaborative Research Center Transregio 63 of the German Research Foundation the concept of thermomorphic multi component solvent systems (TMS systems) is investigated for the Rh/BIPHEPHOS-catalyzed hydroformylation of long chain olefins and esters. For a TMS system consisting of *N,N*-dimethylformamide (DMF), decane and 1-dodecene reaction kinetics and solvent effects on the chemical equilibrium were investigated in detail [1,2,3]. Previous studies on feed impurities revealed a significant kinetic influence of hydroperoxides on the isomerizing hydroformylation network of long chain olefins [4]. In particular, a loss of active ligand specific n- to iso-aldehyde production could be correlated to the decomposition of the diphosphite ligand which was observed by ^{31}P NMR [4]. In parallel, industry is facing reduced aldehyde space-time yield and selectivity by decomposition of catalyst due to unavoidable traces of peroxides in the olefin feed [5]. This work aims to contribute to a better understanding of the deactivation kinetics which is necessary to be optimized in the rhodium catalyzed hydroformylation process using highly active diphosphite ligands.

2. Methods

Hydroformylation experiments were carried out in a high pressure reactor system equipped with temperature and pressure controllers. The TMS system consisted of 1-dodecene ($c^0_{substrate}$ = 0.9 mol L^{-1}), decane and DMF. Rh(acac)(CO)$_2$ and BIPHEPHOS were used as catalyst precursor and ligand (Rh/ligand = 1:3, c_{cat} = 13 ppm), respectively. Two hydroperoxide species, *tert*-butyl hydroperoxide and a mixture of unsaturated hydroperoxides, generated by autoxidation of 1-dodecene, were used as model and substrate derivative hydroperoxides, respectively. These hydroperoxides were separately spiked to 1-dodecene according to different peroxide/ligand ratios. The hydroformylation was performed at temperatures ranging from 95 °C to 115 °C at a constant CO/H$_2$ (1:1) pressure of 30 bar. In addition, operando FTIR hydroformylation experiments were conducted at 60 °C and 10 bar CO/H$_2$ (1:1) in toluene using an increased catalyst concentration of c_{cat} = 500 ppm.

3. Results and discussion

The kinetic influences of hydroperoxides on the hydroformylation of terminal olefins were investigated at different temperatures and different hydroperoxide to ligand ratios (Fig. 1a). Both hydroperoxide species revealed different activity in the hydroformylation experiments.

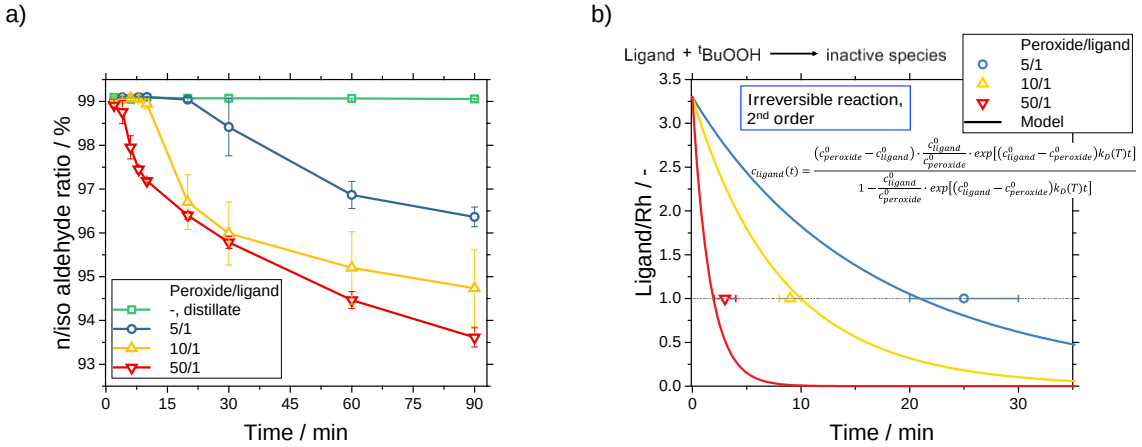

Figure 1. Results of the kinetic deactivation study for the Rh/BIPHEPHOS-catalyzed hydroformylation of 1-dodecene at 105 °C and 30 bar CO/H_2 (1:1) for different peroxide/ligand ratios: a) n/iso Aldehyde regioselectivity, b) Simulation of ligand decomposition

The decomposition of the ligand BIPHEPHOS by hydroperoxides was assumed to proceed as a second order irreversible reaction. Thus, a kinetic model for the decomposition could be derived and parameterized. The resulting simulation of ligand/Rh ratio shows a good correlation to the experimental findings (Fig. 1b) whereas a decline of the ligand/Rh ratio below 1 is supposed to significantly change the regio- and chemoselectivity of the catalysis. In addition, a change of the catalytic species could be observed during the decomposition using FTIR spectroscopy.

4. Conclusions

The kinetic influence of industrially relevant hydroperoxides was studied in detailed kinetic experiments. The kinetic data was used to derive and parameterize a kinetic model for a mathematical description of decomposition of the ligand as well as the corresponding deactivation of the catalyst. Thus, already existing mechanistic kinetic models for Rh/BIPHEPHOS-catalyzed hydroformylation could be extended to an improved prediction of the reaction kinetics allowing a description, simulation and optimization of the reactor behaviour using real feedstocks in industry.

References

[1] G. Kiedorf, D. M. Hoang, A. Müller, A. Jörke, J. Markert, H. Arellano-Garcia, A. Seidel-Morgenstern, C. Hamel, Chem. Eng. Sci., 115 (2014), 31-48.

[2] M. Lemberg, G. Sadowski, M. Gerlach, E. Kohls, M. Stein, C. Hamel, A. Seidel-Morgenstern, AIChE J., 63 (2017), 4576-4585.

[3] A. Jörke, T. Gaide, T. A. Behr, A. Vorholt, A. Seidel-Morgenstern, C. Hamel, Chem. Eng. J., 313 (2017), 382-397.

[4] M. Gerlach, D. Abdul Wajid, L. Hilfert, F. T. Edelmann, A. Seidel-Morgenstern, C. Hamel, Catal. Sci. Technol., (7) 2017, 1465-1469.

[5] D. Hess, D. Ortmann, O. Moeller, K.-D. Wiese, D. Fridag, W. Bueschken, Evonik Oxeno GmbH, US7495134 B2, 2009.

ECCE12
The 12th EUROPEAN CONGRESS OF CHEMICAL ENGINEERING
Florence 15-19 September 2019

Kinetic modelling for hydrogenation of levulinic acid and its esters.

Yanjun WANG[1], Mariasole CIPOLLETA[2], Lamiae VERNIERES-HASSIMI[1], Valeria CASSON-MORENO[2], Sébastien Leveneur[1,3]

1.Normandie Univ, INSA Rouen, UNIROUEN, LSPC, EA4704, 76000 Rouen, France

2.Dipartimento di Ingegneria Chimica, Civile, Ambientale e dei Materiali, Alma Mater Studiorum—Università di Bologna, via Terracini 28, 40131 Bologna, Italy

3.Johan Gadolin Process Chemistry Centre, Åbo Akademi University, Åbo/Turku, Finland.

**Corresponding author: yanjun.wang@insa-rouen.fr*

Highlights

- Mass transfer study
- Kinetic modelling for hydrogenation of levulinic acid and its esters.
- Relationships between reactivity and structure.

1. Introduction

Nowadays, biomass valorization has attracted great interests as its products have shown potential to substitute the fossil-oriented products. Conversion of biomass to biofuels and chemicals is one of the hot topic in chemical engineering. Levulinic acid (LA) is regarded as one of the top 12 building-block molecules from biomass. Besides, hydrogenation of levulinic acid and its esters leads to γ-valerolactone (GVL) [1], which is also another important platform molecule for biofuel production and industrial applications. GVL can also be used as industrial solvent, fuel additives, food and pharmaceutical industries.

From our previous research, the safe operation conditions for hydrogenation of levulinic acid to γ-valerolactone were determined from thermal risk assessment, which could provide an operational guide for further study of this process [2]. However, as LA is corrosive to the reactor system, a comparison of kinetic for hydrogenation of LA and its esters, such as methyl levulinate (ML), ethyle levulinate (EL) and butyl levulinate (BL) which could be obtained by alcoholysis of cellulose, is important for a better optimization of GVL synthesis.

The hydrogenation process of LA and its esters in GVL has two steps: the first step is the hydrogenation of the ketone group to the intermediates and the second step is the intra-molecule cyclization to get the final product GVL and its corresponding water or alcohol. The objective of this study is to study the kinetic modelling for hydrogenation of levulinic acid and its esters. Then, we will determine a relationship between the structure of the different substrates and their kinetics.

2. Methods

Experiments were performed in a Parr reactor equipped with efficient gas entrainment impeller, hydrogen reservoir, pressure and temperature recording system. GC-MS and GC were used to identify and quantify the compositions of the sample.

3. Results and discussion

Due to space limitation, we did not include the mass transfer study. Based on this study, we were able to determine the value of the mass transfer coefficient and Henry's constants at different temperature.

For the kinetic study, different parameters such as substrate concentration, catalyst loading, pressure and temperature were studied for hydrogenation of levulinic acid and its esters to GVL. Figure 1 shows the good fit of simulated data to the experimental data.

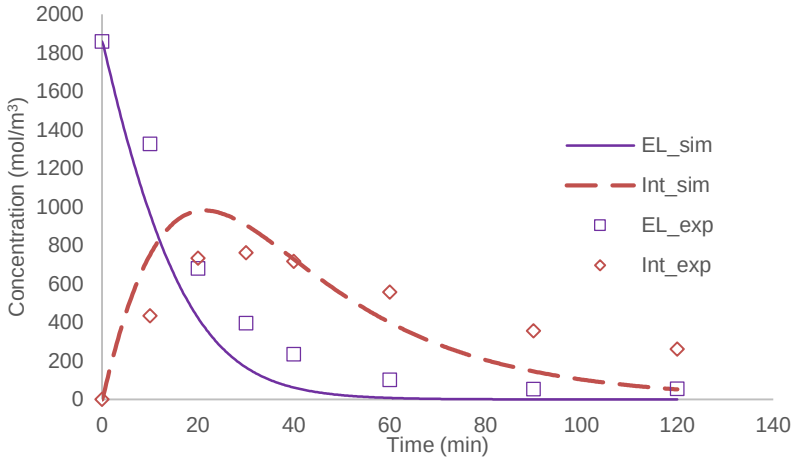

Figures 1. The fit of simulated data to experimental data for Ethyl levulinate hydrogenation. Reaction conditions: EL 2mol/L, Ru/C catalyst 1.4g, Hydrogen pressure 20bar, Temperature 413K, stirring speed 1000rpm.

4. Conclusion

Figure 1 shows that the simulated data from kinetic model could fit the experimental data. The continuation of this work is to compare the kinetic between the different substrates to find a more efficient hydrogenation process and look for a possible relationship between the reactivity and structure.

References

[1] Alonso DM, Wettstein SG, Dumesic JA. Gamma-valerolactone, a sustainable platform molecule derived from lignocellulosic biomass. Green Chem 2013;15:584.

[2] Wang, Y., Vernières-Hassimi, L., Casson-Moreno, V., Hébert, J. P., & Leveneur, S. (2018). Thermal risk assessment of levulinic acid hydrogenation to γ-valerolactone. Organic Process Research & Development, 22(9), 1092-1100.

ECCE12
The 12th EUROPEAN CONGRESS OF CHEMICAL ENGINEERING
Florence 15-19 September 2019

Production of 5-hydroxymethylfurfural from fructose in a heterogeneous reaction using supported triazolium-based ionic liquids.

Claudio Araya-Lopez[1], Gabriel Abarca[2], Cristian Valdebenito[1], Ricardo Salazar[1], Julio Romero[1]*

1 University of Santiago de Chile, Av. Libertador Bernardo O'Higgins 3363, Estación Central, Santiago, Chile
2 Universidad Mayor, Camino la Pirámide 5750, Huechuraba, Santiago, Chile
**Corresponding author: julio.romero@usach.cl*

Highlights

- Dehydration of fructose to produce 5-hydroxymethylfurfural.
- Supported triazolium-based ionic liquid catalysts.
- Click chemistry for the synthesis of triazolium salts.

1. Introduction

5-hydroxymethylfurfural (5-HMF) is considered a furan-type platform chemical derived from the dehydration of hexoses, along with being a versatile and critical intermediate in biofuel chemistry and an important building block to produce plenty of chemical compounds, such as dimethylfuran (DMF), 2,5-diformylfuran (DFF) among others. Nevertheless, the reaction to produce 5-HMF shows the disadvantage of promoting side-reactions with undesired by-products. Furthermore, the rehydration of 5-HMF takes place frequently forming levulinic and formic acid. In order to produce 5-HMF, a wide range of conditions has been assessed, from homogeneous to heterogeneous catalyst as well as the use of monophasic or biphasic systems that are coupled with different separation techniques. The main technical challenge is to achieve the efficient production of 5-HMF through cleaner and greener chemical reactions and separation steps, due to the exponential growth of the green chemistry and its benefits to chemical processes [1]. In this framework, ionic liquids (ILs) are one of the most promising green solvents, specially triazolium-based ionic liquids, which are synthesized under click chemistry concepts by 1,3 dipolar cycloadditions, acting as a chemically supported Bronsted acidic ILs [2]. This work is based on the study of a new family of triazolium-based ionic liquids supported on silica or alumina to be used as a catalyst in the dehydration of fructose. Moreover, the 5-HMF production yield was quantified in this work as well as the reaction kinetic in order to identify the best-operating conditions.

2. Methods

Synthesis of supported triazolium-based ionic liquids: a first triazolium salt was synthesized pouring together sodium azide and benzyl bromide in water (2mL); meanwhile, iodo tris(triphenylphosphine) copper (I) was used as catalyst. After stirring of 30 min, 3-butyn-sulfonate was added, and the reaction was kept at room temperature for 24h. A second triazolium salt was also synthesized pouring together the 3-azidopropane sulfonate and phenylacetylene at the same conditions, using the same reaction solvent and catalyst of the previous reaction. The anchoring of triazolium salt was carried out putting the triazolium salt together (iodobutyl) trimethylsilane-functionalized silica or alumina (the triazolium salt mass corresponded to 20% with respect to

support mass) refluxing in toluene for three days. The obtained product was a supported triazolium-based ionic liquid. Finally, to functionalize the ionic liquid with $[HSO_4]^-$, H_2SO_4 was used according to the procedure reported by Zhang and coworkers [3].

Dehydration reaction of fructose: 2%(w/w) of fructose was pouring in DMSO (4mL) and 20%(w/w) of supported triazolium-based ionic liquid catalyst with respect to the fructose. The reaction was left at 100°C for 2h. The produced 5-HMF was quantified by UV-HPLC.

3. Results and discussion

The main idea for synthesizing this new type of ILs considers that the 1,2,3-triazolium salts can be produced under click chemistry concepts, being greener, cleaner and closer to green chemistry processes. As far as the reaction of fructose is concerned, this is carried out under acid conditions; this characteristic is provided by the $[HSO_4]^-$ anion, which was functionalized with the ionic liquids, owing to its acid characteristics. Figure 1 and 2 show the structures of both catalysts, which were supported in SiO_2. For the case of Al_2O_3 support, the same ILs were anchored. The chosen solvent was DMSO as it is highly polar and capable to stabilize 5-HMF [4]. Therefore, it allows comparing the catalysts with each other avoiding the rehydration reaction to some extent.

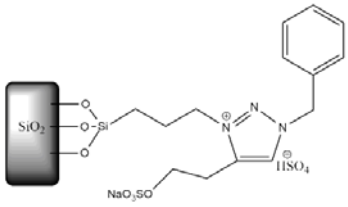

Figure 1. First supported triazolium-based ionic liquid, TR1-Si-HSO_4

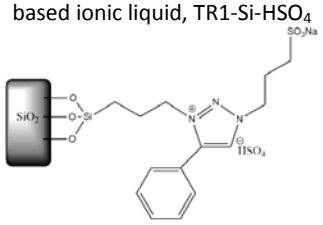

Figure 2. Second supported triazolium-based ionic liquid, TR2-Si-HSO_4

The results presented in figure 3 show that the silica support allows obtaining better yields than alumina support after 2h, being of 80% and slightly lower than 70%, respectively, in comparison with the others, which around 60%. Moreover, the kinetic reaction was faster using silica support.

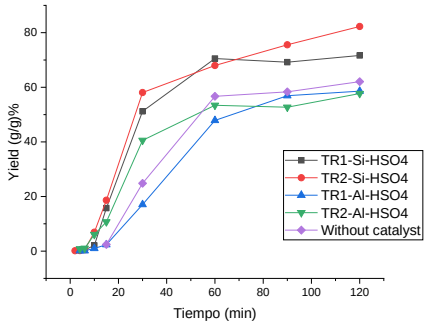

Figure 3. Reaction kinetic of 5-HMF, yield vs reaction time

As far as the triazolium ionic liquid is concerned, independently of the support, the second triazolium presented better results than its counterpart, probably due to the steric/electronic effect produced by the aromatic group attached directly to the triazolium ring, which could modify the physicochemical properties of the ionic liquid. This fact could favour the interaction between the anion and the HMF, via transfer of electron density from the O to OH groups, that is a crucial step to break the inter and intramolecular hydrogen bonding. However, these results were obtained considering just a few amounts of catalyst mass, so that the results could improve, and the yields may be higher than the non-catalyst case when the mass of catalyst increases.

4. Conclusions

The use of a new kind of ionic liquids based on triazolium salts anchored in different supports could represent a promising alternative supported catalyst for greener processes. Furthermore, these catalysts could be used to obtain high yield in the dehydration of fructose to produce 5-HMF.

References

[1] R. Van Putten, J. Van der Waal et. al., Chem. Rev. 2013, 113, 3, 1499-1597.
[2] Zekarias Yacob and Jürgen Liebscher (October 10th 2011). 1,2,3-Triazolium Salts as a Versatile New Class of Ionic Liquids, Ionic Liquids, Scott T. Handy, IntechOpen.
[3] Qiang Zhang, Jun Luo and Yunyang Wei. Green Chem. 2010, 12, 2246-2254.
[4] Quanxi Bao, Kun Qiao et. al., *Catalysis Communications, 2008, 9*(6), 1383-1388

ECCE12
The 12th EUROPEAN CONGRESS OF CHEMICAL ENGINEERING
Florence 15-19 September 2019

Zeolite-supported FeMoP catalysts for the hydrodeoxygenation of a raw black poplar bio-oil towards hydrocarbons

Idoia Hita[1], Tomás Cordero-Lanzac[1], Giuseppe Bonura[2], Catia Cannilla[2], Francisco J. Vela[1], José M. Arandes[1], Francesco Frusteri[2], Javier Bilbao[2]

1 Department of Chemical Engineering, University of the Basque Country (UPV/EHU), PO Box 644-48080, Bilbao, Spain; 2 CNR-ITAE, Istituto di Tecnologie Avanzate per l' Energia "Nicola Giordano", Via S. Lucia sopra Contesse, 5-98126, Messina, Italy

**Corresponding author: idoia.hita@ehu.eus*

Highlights

- Zeolite supports enhance dehydration/condensation reactions
- The acidity features of the catalyst play a primary role in their performance
- The FeMoP/ZSM5 catalyst is the most selective towards aromatics

1. Introduction

In the recent years, bio-oil has been attracting great research attention given its potential as a sustainable source of fuels and platform chemicals [1]. When aiming for the production of chemicals (*i.e.*, aromatics, phenolics), hydrodeoxygenation (HDO) has proven to be a versatile approach for achieving an efficient conversion of the most refractory bio-oil components [2]. In this context, phosphided catalysts are known to provide high HDO activities [3]. However, no studies with raw bio-oil are reported to date.

2. Methods

The supported FeMoP catalysts (20 wt. %) were prepared by impregnation of three zeolites of different topology (*i.e.*, HZSM-5, Hβ and HY) with an aqueous citric acid solution in which were previously added Fe, Mo and P. A "bulk" FeMoP catalyst was also prepared as a reference. The catalysts were characterized by means of ICP-MS, N_2 adsorption-desorption, NH_3-TPD, and XRD. The bio-oil hydrodeoxygenation runs were carried out in a downflow fixed bed reactor described elsewhere [2] at 450 °C, 65 bar, space time, 0.15 g_{cat} h $g^{-1}_{bio\text{-}oil}$; 90 ml min^{-1} H_2; and time on stream, 0-8 h. Organic liquid products were assessed through two-dimensional Gas Chromatography coupled with Mass Spectrometry (GCxGC-MS).The water content in the aqueous product phase was quantified by Karl-Fischer titration.

3. Results and discussion

In contrast to the negligible specific surface of the bulk FeMoP, the FeMoP/ Hβ and FeMoP/HZSM-5 catalysts showed a specific surface of 356-366 m^2 g^{-1} (Table 1), with this value being significantly higher for the FeMoP/HY catalyst (750 m^2 g^{-1}) due to a much higher microporosity. The latter catalyst was also the most acidic (1.11 $mmol_{NH3}$ g^{-1}) and with a higher proportion of medium-

strong acidic sites (66 %). The FeMoP/ Hβ catalyst was the least acidic (0.27 $mmol_{NH3}$ g^{-1}) with a higher contribution of weak-medium acidic sites (35 %).

Table 1- Physico-chemical properties of the fresh catalysts

	FeMoP/Hβ	FeMoP/HZSM-5	FeMoP/HY	Bulk FeMoP
S_{BET} (m^2 g^{-1})	365.9	355.9	750.3	6.0
$V_{micropore}$ (cm^3 g^{-1})	0.084	0.082	0.207	0.002
Total acidity ($mmol_{NH3}$ g^{-1})	0.27	0.57	1.11	0.24
Weak-medium (%)	65	47	34	48
Medium-strong (%)	35	53	66	52

In Figure 1a, an increase was observed in carbon products upon incorporating the zeolite support (22.8-27.0 wt%) in contrast to the bulk FeMoP phase (16.5 wt%), due to the enhancement of dehydration/condensation reactions performed by the zeolites. The highest total acidity and stronger nature of the acidic sites of the FeMoP/HY zeolite enhanced HDO reactions (higher amount of water being formed), leading to lower carbon product yields. On the other hand, the highest carbon product yields were attained with the FeMoP/HZSM-5 catalyst, likely due to a compromise between total acidity and a moderate content of stronger acidic sites. Moreover, FeMoP/HZSM-5 catalyst is also the most selective towards phenol and phenolic compounds (Figure 1b, 12.6 wt% total phenolics), as well as aromatics (13.5 wt% total aromatics).

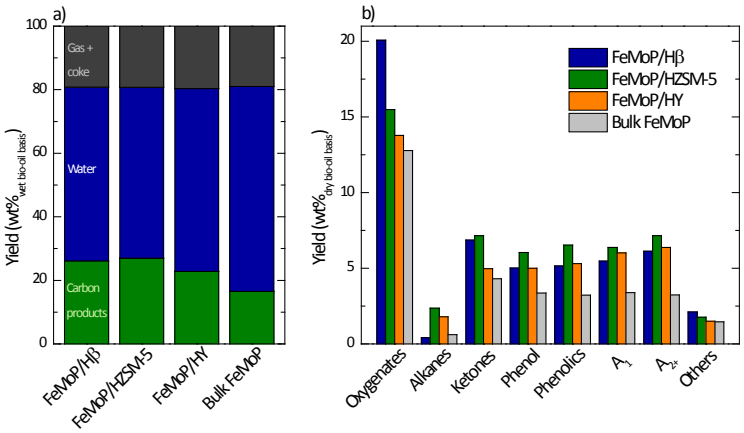

Figure 1. a) Total product yields (in a wet basis) and b) carbon product lump yields (in a dry basis) obtained with the different zeolite-supported catalysts and bulk FeMoP at TOS = 8 h.

4. Conclusions

The total acidity of the catalyst and an equilibrium between weak-medium and medium-strong acidic sites are the dominant catalyst property on the HDO of a raw bio-oil towards hydrocarbons, with shape selectivity playing a secondary role. The FeMoP/HZSM-5 catalyst was the most suitable, providing the highest yield of total carbon products, and also the most selective towards the formation of aromatics, phenol and phenolic components.

References

[1] A.R.K. Gollakota, M. Reddy, M.D. Subramanyam, N. Kishore, Renew. Sustain. Energy Rev. 58 (2016) 1543–1568.

[2] T. Cordero-Lanzac, R. Palos, J.M. Arandes, P. Castaño, J. Rodríguez-Mirasol, T. Cordero, J. Bilbao, Appl. Catal. B Environ. 203 (2017) 389–399.

[3] Z. Si, X. Zhang, C. Wang, L. Ma, R. Dong, Catalysts. 7 (2017) 169.

ECCE12
The 12th EUROPEAN CONGRESS OF CHEMICAL ENGINEERING
Florence 15-19 September 2019

DEVELOPPING A KINETIC MODEL FOR THE CONVERSION OF BIOETHANOL INTO 1,3-BUTADIENE OVER A ONE-STEP HFZN/SiO_2 CATALYST.

G.M. Cabello González[1*], J.R. López Beltrán, A. L. Villanueva Perales[1], M. Campoy Naranjo[1], F. Vidal Barrero[1], A. Martínez[2], P. Ollero[1]

[1]*Departamento de Ingeniería Química y Ambiental - Universidad de Sevilla (España)*
[2]*Instituto de Tecnología Química - Universidad Politécnica de Valencia (España)*
**Corresponding author: gcabello3@us.es*

Highlights

- A kinetic model was developed for the one-step ethanol to butadiene process.
- The kinetic model includes the effect of co-feeding water.
- The experimental observations were explained through the model parameters.

1. Introduction

1,3-Butadiene is an important building block for the manufacture of synthetic rubber, resins, and elastomers. In the last years, the increasing use of ethane as steam cracking feedstock instead of heavier fractions has decreased the production of 1,3-butadiene, but its demand continues growing, so 1,3-butadiene short-term demand is not expected to be satisfied by the current capacity of oil refineries. In that context, the production of 1,3-butadiene from renewable sources, such as bioethanol, rises as an environmentally friendly alternative that may help solving demand issues.

In spite of the potential relevance of this process, very few studies have attempted to propose a kinetic model of the ethanol to 1,3-butadiene conversion, and none of these studies considered the most supported ethanol to 1,3-butadiene pathway, which includes ethanol dehydrogenation into acetaldehyde and its posterior aldo-condensation to crotonaldehyde, crotyl alcohol production from ethanol and crotonaldehyde MPVO reduction, and crotyl alcohol dehydration into 1,3-butadiene. That way, we aim to generate a formal kinetic model describing the main reaction pathway that can predict the catalyst performance in a range of operating conditions around the optimum. Besides, this kinetic model includes the effect of co-feeding water among with the ethanol feedstock, what has never been reported so far for this process.

2. Methods

The catalyst was prepared following the methodology reported in the work of De Baerdemaeker et al. [1]. Catalytic tests were carried out in a continuous flow fixed-bed reactor at 340-380 ºC, 1.12-9.8 h^{-1}, 0-15% w/w water in the feedstock, ethanol partial pressure of 0.21 bar and atmospheric pressure. The bed was divided into three sections. The top section was a SiC bed, the middle one comprised a bed of catalyst (0.3-0.5 mm) diluted in the necessary amount of SiC to

obtain a bed length of 13 cm, and the bottom section was also a SiC bed. All sections were separated by a glass wool plug. The ethanol was fed with an HPLC-pump and N_2 was used as carrier gas. The reactor output line was electrically traced and insulated to avoid product condensations before analysis by an Agilent 7890A on-line gas chromatograph (GC) equipped with two flame ionization detectors (FID) and a thermal conductivity detector (TCD).

3. Results and discussion

Making use of the tests carried out in the laboratory-scale reactor, a power-law model was developed, and the statistically significant variables in the rate expression for the generation of each product were found. The reaction scheme considered for the calculation of the balance is a simplification of the one proposed in our previous work [2]. The considered reaction rates are based on exponential rate equations or Langmuir-Hinshelwood kinetic.

The differential mole balance equations were solved obtaining an initial guess of the kinetic parameters assuming constant molar flow along the reactor and solving the algebraic system. These rough parameters were used as initial guess values for solving the differential mole balance along the reactor.

- Main reactions: $C_2H_5OH \rightarrow C_2H_4O + H_2$
  $C_2H_5OH + C_2H_4O \rightarrow C_4H_6 + 2H_2O$
- Ethanol dehydration: $2C_2H_5OH \rightarrow (C_2H_5)_2O + H_2O$
  $C_2H_5OH \rightarrow C_2H_4 + H_2O$
- Butanol formation: $2C_2H_5OH \rightarrow C_4H_9OH + H_2O$
- Butenes formation: $C_4H_9OH \rightarrow C_4H_8 + H_2O$
- Heavy compounds formation (diphenylketone) : $6.5\ C_2H_4O \rightarrow C_{13}H_{10}O + 5.5H_2O + 2.5H_2$

4. Conclusions

The formation of 1,3-butadiene over a Hf-Zn catalyst was evaluated. The main products observed were acetaldehyde, butadiene, ethene, diethyl ether, butanol, butenes and heavy compounds. A Langmuir−Hinshelwood type of kinetic model was developed for the equations involving acetaldehyde production and consumption. The model can be used to predict the rates of formation of the products and the predictions agree with the experimental data, as well as to design an industrial facility.

References

[1] T. De Baerdemaeker, M. Feyen, U. Müller, B. Yilmaz, F.S. Xiao, W. Zhang, T. Yokoi, X. Bao, H. Gies, D.E. De Vos, ACS Catal. 5 (2015) 3393–3397.

[2] G.M.Cabello, R.Murciano, A.L.Villanueva, A.Martínez, F.Vidal-Barrero, M.Campoy, App. Catal. A. 570 (2019) 96-106.

ECCE12
The 12th EUROPEAN CONGRESS OF CHEMICAL ENGINEERING
Florence 15-19 September 2019

Photocatalytic decomposition of ethylene released from agricultural products

Fumihide Shiraishi*, Yuichi Akimoto, Toshiaki Koto, and Masashi Iwanaga

Section of Bio-process design, Department of Bioscience and Biotechnology, Graduate School of Bioresource and Bioenvironmental Sciences, Kyushu University, Motooka 744, Nishi-ku, Fukuoka 819-0395, Japan

**Corresponding author: fumishira@brs.kyushu-u.ac.jp*

Highlights

- The present reactor can reduce the ethylene concentration to below 40 ppb.
- Agricultural products releasing ethylene at a low speed can be kept fresh at least for 9 days.
- It is difficult to maintain the quality of fruit synthesizing ethylene quickly by only its decomposition.

1. Introduction

Ethylene released from fruits greatly lowers the quality of not only themselves but also agricultural products in their neighbourhood [1], which causes a serious problem when one stores the agricultural products or conveys them kept in containers by ship or truck. For solving the problem, it is necessary to keep the ethylene concentration in air at a low level. Although the extent of decrease in the ethylene concentration is different according to the kind of agricultural products, it should be fundamentally set as low as possible [2]. Unfortunately, there is no promising technique by which the ethylene concentration can be decreased to a very low concentration level.

Application of UV-excited titanium dioxide (TiO_2) to air purification has been actively investigated in the past two decades. One of the advantages of this application is that the VOC concentration can be reduced to almost zero (for example, below 40 ppb for toluene) if the reaction field on the TiO_2 surface is precisely controlled [3]. It is thus natural to apply the photocatalytic technique to the decomposition of ethylene released from agricultural products. It is known that this decomposition is strongly influenced by the moisture in the air. Therefore, this fact should be taken into consideration in applying photocatalytic technique.

In the present study, based on our accumulated knowledge and experience, we attempt to develop a photocatalytic reactor to rapidly decompose ethylene released from agricultural products. A photocatalytic reactor with three coiled glass tubes and six 6-W UV lamps was used to maintain the quality of agricultural products and the performance of the reactor was investigated.

2. Methods

An nanosized TiO_2 (Degussa P25)-coating solution containing H_2PtCl_6 was prepared by the same method as described elsewhere [4].This solution was poured into a coiled Pyrex glass tube and applied to its inside surface, which was then heated in an electric maffle furnace at 300 °C for 30 min. The same operation was repeated three times, so that a TiO_2 film was formed on the inside

surface. Three coiled glass tubes with TiO_2 were prepared in the same manner. A 6-W blacklight blue fluorescent lamp with a wavelength range of 300–400 nm was inserted into the center of each coiled glass tube. Three immobilized TiO_2 glass tubes thus prepared were vertically arrayed in a triangular framework. Furthermore, three UV lamps were put between the glass tubes to enhance UV irradiation. The photocatalytic reactor constructed was connected to an acrylic box (1.17×10^5 cm^3) via an air pump to circulate the air in the container. An apple, banana, persimmon, cucumber and cabos were put in the container. The UV lamps were switched on to start the decomposition. The experiment was performed over 9 days. A similar experiment was performed using an atemoya over 7days. For comparison, the experiment without treatment was carried out simultaneously. The temperature in the container was always kept at about 20 °C. The ethylene concentration was measured with a gas chromatograph equipped with a flame ionization detector. The detection limit of ethylene was 40 ppb for this analytical system.

3. Results and discussion

When the air was photocatalytically treated, ethylene released from agricultural products (mainly from the apple) was always kept at a very low level (below 40 ppb). Consequently, the qualities of all products were kept high at about 20 °C, at least, for 9 days. When no air was treated, on the other hand, the ethylene concentration constantly increased, attaining to 2.7ppm, which significantly lowered the qualities of persimmon and cucumber. Although the apple did not change apparently, it lost sweetness completely.

The atemoya was found to release ethylene five-times as fast as the apple did. The present reactor decreased the ethylene concentration to below 350 ppb, but the atemoya changed its surface color from green to brown after one week regardless of treatment. This result suggests that it is difficult to maintain the quality of fruit that synthesizes ethylene at a very high speed, by only decomposing ethylene.

4. Conclusions

The photocatalytic reactor with three coiled glass tubes is useful to reduce the concentration of ethylene released from agricultural products to a very low level, thereby making it possible to keep the qualities of agricultural products at a high speed over a long period of time. By contrast, for the agricultural products synthesizing ethylene quickly, the use of the present treatment technique is probably difficult to apply to even when the ethylene concentration is significantly reduced. In this case, we consider that the products should be kept refrigerated.

References

[1] M. L. V. de Chiara et al., Biosys. Eng. 132 (2015) 61-70.
[2] S. P. Burg, E. A. Burg, Plant. Phys. 37 (1962) 179-189.
[3] F. Shiraishi, D. Maruoka, Y. Tanoue, Sep. Purif. Technol. 175 (2017) 185-193.
[4] Y. Tanoue, F. Shiraishi, Eco-Eng. 29 (2017) 39-44.

ECCE12
The 12th EUROPEAN CONGRESS OF CHEMICAL ENGINEERING
Florence 15-19 September 2019

Dealing with Structural Uncertainties in Lumped Reaction Networks

Zoltán Till[1,*], Tamás Varga[1], János Sója[2], Norbert Miskolczi[2], Tibor Chován[1]

[1]University of Pannonia, Department of Process Engineering
10 Egyetem Street, H-8200 Veszprém, Hungary

[2]University of Pannonia, Department of Hydrocarbon and Coal Processing
10 Egyetem Street, H-8200 Veszprém, Hungary

*Corresponding author: tillz@fmt.uni-pannon.hu

Highlights

- The definition of the pseudocomponents contributes to the uncertainty of the model.
- In principle, this effect can be separated from the other components of the model error.
- Therefore, the lumping scheme can be optimized within certain limits.

1. Introduction

Complex chemical processes are often modeled using lumped reaction networks [1]. Dealing with these models, however, involves some uncertainties. Firstly the overall predictive ability of the lumped kinetic model is limited (due to bias, variance, etc.). Secondly, the kinetic parameters can have broad confidence intervals, mainly because there are a number of alternative pathways in a lumped chemical reaction network that cannot be observed separately. Thirdly, there is an uncertainty in the lumping scheme, i.e. in how we define the pseudocomponents themselves.

In this work, we would like to deal with the latter. Given an experimental data set (of thermo-catalytic pyrolysis of real plastic waste) and number of pseudocomponents to follow (e.g. solids, at least two liquid fractions, gas) we measure the changes of model uncertainty as a function of how these pseudocomponents are actually defined.

The aim of our work is to measure and minimize the model error related to the lumping scheme in case of fixed structural complexity, i.e. for a certain number of lumps and reactions between them.

2. Methods

Pyrolysis of real plastic waste was carried out in a two-stage laboratory reactor system with 50 g shredded HDPE/LDPE/PP feedstock using various zeolite-based catalysts at different temperature levels (425/455/485 °C in the 1st stage and 380 °C in the 2nd stage). The gaseous product was driven through a water cooled heat exchanger. Condensate was collected and analyzed by gas chromatography at given time intervals, while the volume of the remaining gas was measured using a gas flow meter [2].

For the kinetic study, we propose a lumped chemical network in which the solid (polymer, coke), liquid (C_6-C_{30+}) and gaseous (C_0-C_5) products are distinguished. Here we would like to consider a

straightforward lumping scheme where we group the liquid components into a lighter and heavier fraction (L– and L+) and investigate how this classification affect the uncertainty of the model. It is a somewhat improved model derived from our previous work [3].

3. Results and discussion

After minimizing the uncertainty in connection with the identification process and the lumped chemical reaction network and then carrying out the identification procedure consecutively by changing the boundary between the two defined liquid lumps, we were able to relate the change in the squared error between the experimental and calculated data to the uncertainty in the model structure. Apparently, the definition of these pseudocomponents does have an impact on the error of the model, as you can see in Figure 1.

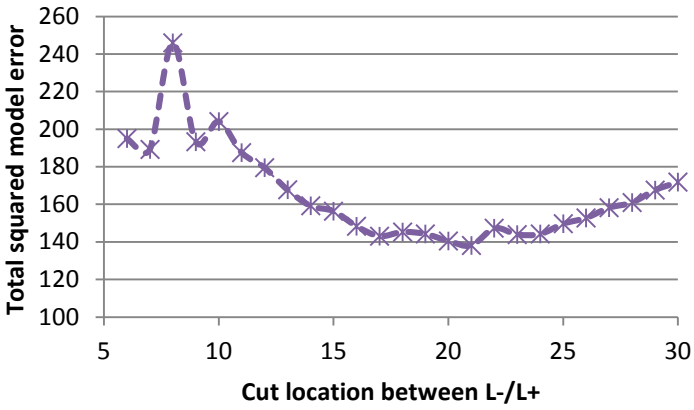

Figure 1. Development of total model error while moving the boundary between the two liquid pseudocomponents.

Undoubtedly, there is a limitation in how we define these two lumps, given that we would like to follow the concentrations of specific components, e.g. the boundary between gasoline and Diesel fuel is somewhere between C_{10}-C_{12}; nevertheless, this effect worth not to look over.

4. Conclusions

Our results already indicate that the uncertainty inherent to the model structure can be quantified. Nevertheless, there is much to be done. We would like to find the adequate measure of the complexity of the model. There are plenty of these in the literature and we have to find a select the most representative indicator. Moreover, the remaining uncertainty in the reaction network needs to be separated from the uncertainty of the lumping scheme. In any case, the proposed approach appears to be particularly promising and feasible to continue.

References

[1] L. P. de Oliveira, D. Hudebine, D. Guillaume, J. J. Verstraete, Oil Gas Sci. Technol. – Rev. D'IFP Energ. Nouv. 71(3) (2016) 45.
[2] N. Miskolczi, J. Sója, E. Tulok, J. Anal. Appl. Pyrolysis 128 (2017) 1–12.
[3] Z. Till, T. Varga, J. Sója, N. Miskolczi, T. Chován, Energy Convers. Manag. 173 (2018) 320–330.

ECCE12
The 12th EUROPEAN CONGRESS OF CHEMICAL ENGINEERING
Florence 15-19 September 2019

Experimental studies on ammonium heptamolybdate reaction with ammonium sulfide in turbulent micromixers

Michał Wojtalik, Wojciech Orciuch, Łukasz Makowski

Faculty of Chemical and Process Engineering, Warsaw University of Technology, Warsaw, Poland

** Michał Wojtalik: michal.wojtalik.dokt@pw.edu.pl*

Highlights

- Precipitation of molybdenum disulphide nanoparticles has been investigated in semi-batch and turbulent micromixers
- Particles size distribution has been evaluated in terms of precipitation kinetics

1. Introduction

One of the promising ways to obtain molybdenum disulfide for special purposes such as catalyst, lubricant additives [1] or semiconductors is wet chemical synthesis using ammonium heptamolybdate and ammonium sulfide [2]. In such a process, one can produce an amorphous product of molybdenum disulphide containing sulfa. Further recrystallization and purification by heat treatment can be used to improve product crystallographic properties. Obtained product due to its high surface area can be much more valuable than natural origin.

For advanced applications such as catalyst high quality and purity is crucial. Synthesis carried out in turbulent micromixers allows to control the process and make it continuously. In this work, authors focused on precipitation kinetics in turbulent micromixers and semi-batch system.

2. Methods

Synthesis of molybdenum disulphide nanoparticles was carried out in the turbulent micromixers with coaxial and tangential geometry and also in the semi-batch system shown in Fig. 1. Ammonium molybdate tetrahydrate $(NH_4)_6Mo_7O_{24}\cdot 4H_2O$ (HMA), citric acid $C_6H_8O_7$ (CA), and ammonium sulphide $(NH_4)_2S$ (AS) were used as substrates of the reaction [3]. Firstly, ammonium molybdate tetrahydrate and citric acid were dissolved at 90°C and mixed for at least 30 minutes with Mo:CA ratio of 1:2. This ratio was found best for the synthesis during previous tests in a batch procedure, due to the high selectivity of the reaction (up to 60% of MoS_2) and absence of sulphonic groups detected in obtained particles. Just before reaction, both prepared solutions were filtrated using 220 nm filters.

Produced particles were measured using LS Beckman&Coulter LS 13 320 analyzer, which uses PIDS – polarization intensity light scattering and LD – laser diffraction. Obtained particle size distribution was analyzed and used to calculate possible kinetics of the precipitation.

SEM imaging was also performed to determined particles agglomeration and morphology.

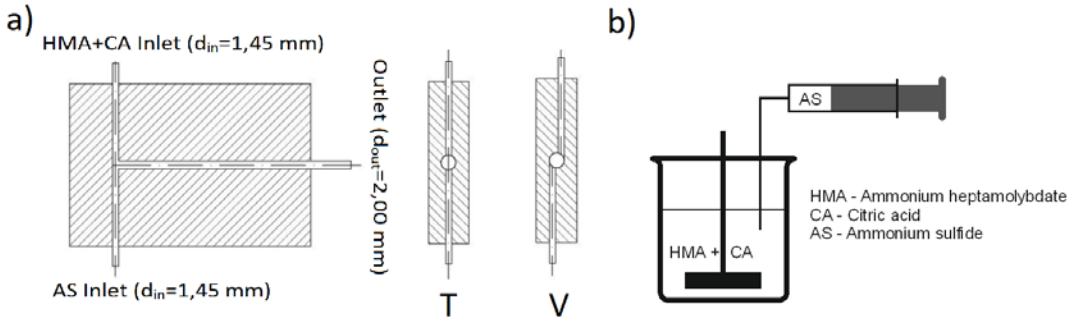

Figure 1. Turbulent micromixers (a) and semi-batch system (b) used in experiments

3. Results and discussion

The volume-weighted mean particle size D_{43} of obtained particles and an example of particle size distribution were shown in Fig. 2. Only the primary particles were taken into account. On Fig. 2. One can see that the average size is close to 200 nm regardless of flow and reactor type.

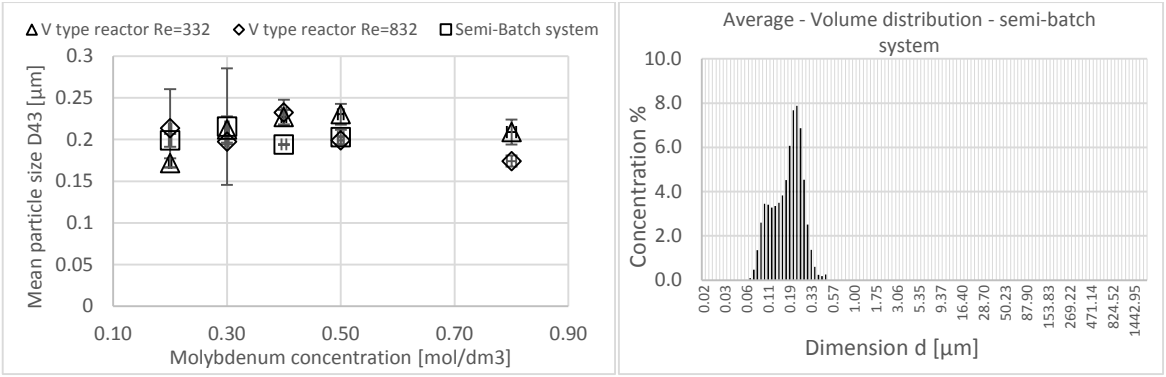

Figure 2. Mean particle sizes of particles (left). Example of particles size distribution obtained (right)

4. Conclusions

Molybdenum disulphide can be obtained by wet chemical synthesis in the turbulent micromixers. However, it is highly contaminated with sulpha and unreacted substrates. Due to contamination, it is not possible to use produced molybdenum disulphide directly after the reaction. Therefore, proper separation techniques have to be developed.

Mixing conditions appears to have a small impact on product size in the applications. The initial concentration and Reynolds number impact on precipitation process have not been observed.

Acknowledgements

This work was supported by the National Science Centre [No.2017/27/B/ST8/01382]

References

[1] M.F. Sgroi, M. Asti, F. Gili, F.A. Deorsola, S. Bensaid, D. Fino, G. Kraft, I. Garcia, F. Dassenoy, Engine bench and road testing of an engine oil containing MoS2 particles as nano-additive for friction reduction, Tribol. Int. 105 (2017).

[2] F.A. Deorsola, N. Russo, G.A. Blengini, D. Fino, Synthesis, characterization and environmental assessment of nanosized MoS 2 particles for lubricants applications, Chem. Eng. J. 195–196 (2012).

[3] G. Santillo, F.A. Deorsola, S. Bensaid, N. Russo, D. Fino, MoS2 nanoparticle precipitation in turbulent micromixers, Chem. Eng. J. 207–208 (2012).

ECCE12
The 12th EUROPEAN CONGRESS OF CHEMICAL ENGINEERING
Florence 15-19 September 2019

Total Oxidation of VOC on Palladium Catalyst Supported on Activated Carbon from Cocoa Pod Husk

Karel Soukup[1], Pavel Topka[1], Vladimír Hejtmánek[1], Gerardo J.F. Cruz[2], Olga Šolcová[1]

1 Institute of Chemical Process Fundamentals of the CAS, v. v. i., Rozvojová 135, CZ–165 02 Prague 6, Czech Republic; 2 National University of Tumbes, Department of Forestry Engineering and Environmental Management, Av. Universitaria s/n, Campus Universitario, Pampa Grande – Tumbes, Peru

**Corresponding author: soukup@icpf.cas.cz*

Highlights

- Activated carbon was prepared from cocoa pod husk by chemical activation
- Palladium nanoparticles were supported on activated carbon
- Catalytic activity and selectivity in the oxidation of ethanol was studied
- At 99% ethanol conversion, the selectivity to CO_2 was higher than 95% for all catalysts

1. Introduction

Volatile organic compounds (VOCs) represent one of the most significant contributors to the air pollution [1]. Catalytic oxidation is recognized as an efficient, cost-effective and environmentally friendly way to treat VOC emissions [2]. Total catalytic oxidation of VOCs especially at low concentrations is a promising method to convert VOCs to water and carbon dioxide. Moreover, in contrast to thermal oxidation, dangerous reaction by-products such as NO_x are not formed [3].

2. Methods

For preparation of activated carbon samples, which will be further referred to as CPH–AC, cocoa pod husk was used. The cocoa beans, gathered in Tumbes Region (coastal region in north western Peru), were mixed with an activating agent ($ZnCl_2$) in a weight ratio of 1:1. Then, the mixture was directly carbonized under nitrogen atmosphere at 600 °C for 2 h with heating rate 10 C min^{-1}. After fast cooling with pressurized indirect air, the prepared samples were washed with 0.15 mol L^{-1} water solution of HCl and with hot and later cold distilled water. Prepared activated carbon was impregnated with the impregnation solution consisting of palladium(II) acetate (99.9% purity, Aldrich, USA) dissolved in the mixture of acetone and methanol (volumetric ratio 2:1) and 3.5 wt% of citric acid. The initial concentration of palladium acetate in the impregnation solution was the same in all cases (0.34 wt.%). The volume of the impregnation solution was adjusted to obtain 0.28 wt.% Pd, 0.61 wt.% and Pd, 2.64 wt.% Pd, for the 0.28Pd/CPH-AC, 0.61Pd/CPH-AC and 2.64Pd/CPH-AC catalysts, respectively.

3. Results and discussion

Conversion curves of ethanol oxidation are shown in Figure 1. The catalytic performance increased in the order of CPH-AC < 0.28Pd/CPH-AC < 0.61Pd/CPH-AC < 2.64Pd/CPH-AC (corresponding T_{50} was as follows: 249 °C, 206 °C, 158 °C, and 123 °C, respectively). The selectivity to CO_2 can be even

more important than catalyst activity due to the fact that some by-products of ethanol oxidation (e.g., acetaldehyde) can be even more detrimental for the environment and human health compared to ethanol itself. At 95% ethanol conversion, the selectivity to CO_2 decreased in the order of CPH-AC < 0.28Pd/CPH-AC < 2.64Pd/CPH-AC < 0.61Pd/CPH-AC (94%, 79%, 40%, and 33%, respectively). Ethylene, acetaldehyde, ethylacetate and traces of acetic acid were observed as the reaction by-products. However, it should be noted that at 99% ethanol conversion, the selectivity to CO_2 was higher than 95% for all catalysts.

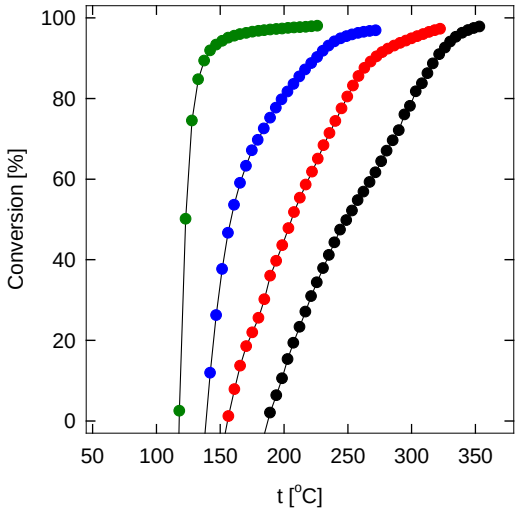

Figure 1. Conversion curves of ethanol during oxidation reaction over CPH-AC (●), 0.28Pd/CPH-AC (●), 0.61Pd/CPH-AC (●) and 2.64Pd/CPH-AC (●) catalysts

4. Conclusions

The activated carbon was prepared from cocoa pod husk using $ZnCl_2$ as an activating agent and employed as a catalyst support. Palladium nanoparticles were introduced by impregnation with palladium acetate in the presence of citric acid. In contrast to typical Pd/activated carbon catalysts, we were able to prepare catalysts with large palladium nanoparticles (~23 nm), which may be beneficial for oxidation catalysis. Moreover, these Pd nanoparticles were present on the external surface of the support and can be prepared even at low Pd loading (0.28 wt. %).

Acknowledgment

The financial support of the Technology Agency of the Czech Republic (The Competence Centre, project TE01020080 and the National Centres of Competence, project TN0100048/5) is gratefully acknowledged.

References

[1] H. Huang, Y. Xu, Q. Feng, D.Y.C. Leung, Catal. Sci. Technol. 5 (2015) 2649–2669.
[2] P. Topka, M. Klementová, Appl. Catal. A-Gen. 522 (2016) 130–137.
[3] A.C. Gluhoi, B.E. Nieuwenhuys, Catal. Today 119 (2007) 305–310.

ECAB 5
The 5th EUROPEAN CONGRESS OF APPLIED BIOTECHNOLOGY
Florence 15-19 September 2019

Screening of biomass degrading enzymes from *Aureobasidium pullulans*, using non-synthetic nitrogen sources

Matheus Maitan Vieira[1], Silvio Silvério da Silva[1], Felipe Antônio Fernantes Antunes[1], Anuj Kumar Chandel[1]

1 Department of Biotechnology, Engineering School of Lorena, University of São Paulo, postal code 12602-810, Lorena, SP, Brazil

**Corresponding author: maitan.matheus@usp.br*

Highlights

- *A.pullulans* can be a cellulolytic enzyme producer
- Enzymes can be produced by non-synthetic medium
- Submerged fermentation showed to be a good method to produce these enzymes
- Soybean represent the best non-synthetic nitrogen source in this process

1. Introduction

With the increasing demand for renewable fuels and bioproducts, with a view to sustainable development, lignocellulosic biomass has become an important compound to be applied in bioprocesses due to its low cost and high availability. Brazil generates foreseeable amount of lignocellulosic biomass primarily agro-residues such as sugarcane bagasse (SB), sugarcane straw (SS), corn stover (CS) and *Eucalyptus* residues round the year (LYND *et al.* 2002). These lignocellulosic residues are excellent feedstock for second-generation (2G) sugars production which could be utilized for liquid fuels and value-added products such as biopigments, biopolymers and several other biochemicals based on biorefinery concept. However, for the cost competitive production of these products, the most important concern is the economic production of 2G sugars, as these sugars act as building block in biorefineries (FERNANDES, 2006). For 2G sugars production, efficient cellulases production and their concerted action on lignocellulosic residues is vital. Commecial cellulases are available in the market but due to their high costs, limited supply and monopoly of certain industries, this is necessary to focus on in-house production of stable and complete cellulolytic enzyme cocktails. The objective of this work was to study the production of cellulolytic enzymes from the microorganism *Aureobasidium pullulans* using sugarcane bagasse residues and soybean meal, corn and rice as a source of nitrogen.

2. Methods

The investigations of the production of cellulase by the yeast *Aureobasidium pullulans* were carried out in order to evaluate sugarcane as carbon source using non-synthetic nitrogen source. Nonsynthetic nitrogen sources were soybean meal, corn bran and rice bran at 1.8 g/L, as well as for synthetic nitrogen sources in Mandel's medium, which obtained a total weight of 1.8 g/L total. For the fermentation 1mL of the isolate stock was transferred to a pre-inoculum in 50mL of Sabouroud dextrose broth in shaker 30ºC and 200 rpm for 48 hours. Subsequently, $1.6x10^6$ CFU were transferred to erlenmeyers containing 100 mL of the minimal Mandel medium with only one nitrogen source with 1% of the carbon source (sugarcane bagasse) and kept at 30°C for 96 h with shaking at 200 rpm. Samples were withdrawn every 24 hours with 5 minutes rest for decantation and 1mL of the supernatant was withdrawn for the reducing sugar test according to Ghose (1987).

3. Results and discussion

The maximum activity also occurred during 60 h, for CMCase soybean meal was 6.865 U/mL and for FPase 2,449 U/mL corn meal and rice meal with CMCase of 3.692 U/mL and FPase of 1.407 U/mL, and CMCase of 3.842 U/mL and FPase of 1.425 U/mL, respectively. The figure shows the enzymatic activity as a function of the bioprocessing time from the use of organic nitrogen sources as the only factor of nitrogen in the process of submerged fermentation for the production of enzymes of the cellulolytic complex. These nitrogen sources have different proportion of proteins and sugars (MARTINIANO *et al.*, 2017) and the results indicate that the protein source is important for the production of crude enzyme extract, however, not being the only factor, considering that these brans have very close amounts of protein (g/L). Ilmén *et al* (1997) questioned the action of nitrogen as an inducer in suggesting that the induction of nitrogen does not alter at the genetic level the production of enzymes, altering only the cell mass and, consequently, the production of enzymes. Non-synthetic nitrogen sources have been used in the literature to improve the cellulase synthesis conditions (AHAMED and VERMETTE, 2008), due to their low cost and to be, as well as sugarcane bagasse, a sub-agroindustrial product.

4. Conclusions

The submerged fermentation of non-synthetic sources (soybean, corn bran and rice bran) can be used to improve the productivity of a CMCase and Fpase by using *A. pullulans* as producer. This nitrogen sources have advantages as low cost, availability and efficiency on submerged fermentation for cellulase production. This study is a preliminary study for further proteomic approach.

References

[1] AHAMED A, VERMETTE P. Enhanced enzyme production from mixed cultures of *Trichoderma reesei* RUT-C30 and *Aspergillus niger* LMA grown as fed batch in a stirred tank bioreactor. **Journal of Biochemichal. Engineering**. v.42, p.41-46, 2008.

[2] FERNANDES, M. L. M. **Produção de lipases por fermentação no estado sólido e sua utilização em biocatálise**. (Tese de Doutorado) - Setor de Ciências Exatas, Universidade Federal do Paraná, 2006.

[3] GHOSE, T.K. Measurement of cellulase activities. **Pure and Applied Chemistry**, v.59, p.257-268, 1987. doi10.1351/pac198759020257.

[4] ILMÉN, MARJA & SALOHEIMO, ANU & L ONNELA, M & PENTTILÄ, MERJA. Regulation of Cellulase Gene Expression in the Filamentous Fungus**. Applied and environmental microbiology**, v.63, p.1298-306, 1997.

[5] LYND, L.R.; WEIMER, P.J.; VAN ZYL, W.H.; PRETORIUS, I.S. Microbial cellulose utilization: fundamentals and biotechnology**. Microbiology and Molecular Biology Reviews**, v.66(3), p.506–577, 2002.

[6] MARTINIANO, S. E.. Produção de leveduras enriquecidas com selênio a partir de resíduos vegetais. Lorena: Escola de Engenharia de Lorena, Universidade de São Paulo, 2017. PhD tesis in applied microbiology.

ECCE12
The 12th EUROPEAN CONGRESS OF CHEMICAL ENGINEERING
Florence 15-19 September 2019

Modified catalysts for a low-aromatic Dimethyl ether-To-Gasoline process

Benjamin Niethammer[1], Ulrich Arnold[1], Jörg Sauer[1]

[1]Karlsruhe Institute of Technology (KIT), Institute of Catalysis Research and Technology (IKFT)
Hermann-von-Helmholtz-Platz 1, 76344 Eggenstein-Leopoldshafen, Germany
*Corresponding author: benjamin.niethammer@kit.edu

Highlights

- Lab-scale investigation of miscellaneous acid zeolite catalysts.
- Catalysts with high selectivity to branched alkanes.
- Catalyst modification for an improved lifetime.

1. Introduction

The Dimethyl ether-To-Gasoline (DTG) process employs zeolite catalysts for the production of gasoline from dimethyl ether (DME). DME can be produced from renewable feedstocks, like biomass. This enables gasoline synthesis in a closed CO_2 cycle. Established DTG approaches generate a highly aromatic liquid product fraction. Due to their high octane numbers, aromatics can be used as anti-knock additives for gasoline, without increasing the oxygen content and lowering the heating value. On the other hand, aromatics are known to be precursors of soot formation in the engine combustion chamber. One approach to counteract this effect could be a change of the fuel composition to a reduced aromatics content in gasoline. Thereby, the reduction of greenhouse gases and the reduction of harmful particulate emissions in the transport sector could be addressed hand in hand. The intention of this work is to modify the DTG process to a low aromatic content and a large fraction of highly branched alkanes in the product spectrum [1].

2. Methods

Catalytic tests were performed in a continuously operated laboratory plant. DME, synthesis gas (H_2 and CO) and the inert gases N_2 and He can be fed as educt streams in a fixed bed reactor. The gaseous products of the catalytic conversion are transferred through a heated pipeline to a gas chromatographic (GC) online analysis. The GC (Agilent 7890) is equipped with a flame ionization detector (FID) and a thermal conductivity detector (TCD). Thereby, the educt conversion can be determined and an overview of the catalyst selectivity can be obtained. Subsequently, the gas stream is transferred into a cold trap, where the hydrocarbons in the range C_{5+} are liquefied. Analysis of the composition of the liquid samples is then carried out via gas chromatography according to the ASTM D6730-01 (2016) standard test method.

3. Results and discussion

Different acid zeolite morphologies were tested in the lab-scale plant. The catalysts were assessed and compared regarding their selectivity to non-aromatic C_{5+} components. The main focus was to

increase the content of highly branched alkanes, with high octane numbers, in the boiling range of gasoline. Promising zeolite types were identified, but these catalysts revealed only short lifetimes.

The conversion of DME to hydrocarbons is shown in equation 1, whereby -[CH_2]- represents the average composition of the product spectrum.

$$CH_3OCH_3 \rightarrow 2\ \text{-}[CH_2]\text{-} + H_2O \quad (1)$$

Consequently, the reaction comprises the formation of unsaturated components, which can as precursors of coke deposits that deactivate the catalyst. To improve the lifetime, modified zeolite catalysts were prepared and tested. The zeolites were loaded with hydrogen-active metals and H_2 was added to the educt feed. Thus, the formation of unsaturated hydrocarbons is reduced or prevented in the DTG chain-growth mechanism and alkanes (C_nH_{2n+2}) can be formed without organic byproducts, as shown in equation 2.

$$CH_3OCH_3 + H_2 \rightarrow C_nH_{2n+2} + H_2O \quad (2)$$

The lifetime of these catalysts clearly exceeded that of the unmodified catalysts, while maintaining or even improving the favorable product selectivity.

4. Conclusions

Modified zeolite catalysts that are able to incorporate co-fed H_2 into the chain-growth mechanism of the DTG process can improve the catalyst lifetime and the selectivity during the reaction with the intent to increase the content of branched alkanes in the product spectrum.

References

[1] B. Niethammer, S. Wodarz, M. Betz, P. Haltenort, D. Oestreich, K. Hackbarth, U. Arnold, T. Otto, J. Sauer, Chem. Ing. Tech. 90 (2018) 99–112.

ECCE12
The 12th EUROPEAN CONGRESS OF CHEMICAL ENGINEERING
Florence 15-19 September 2019

Kinetic model development of special hydrocracking of sunflower oil and petroleum mixture

Omar Péter Hamadi[1], Tamás Varga[1], Zoltán Till[1], Zoltán Eller[2], Jenő Hancsók[2]

1 Department of Process Engineering, University of Pannonia, Veszprém, Hungary; 2 Department of MOL Hydrocarbon and Coal Processing, University of Pannonia, Veszprém, Hungary

**Corresponding author: hamadio@fmt.uni-pannon.hu*

Highlights

- Sunflower oil and petroleum mixture special hydrocracking.
- 5-lump trickle bed reactor model development.
- Considering the change in hydrogen solubility along the reactor.

1. Introduction

Based on our previous work, a 5-lump kinetic and a simple reactor models were developed and validated against measurements in case of special hydrocracking of sunflower oil and petroleum mixture. In the model the effect of pressure has not considered and different parameter sets were determined for each pressure. The aim of that work was to characterize the catalyst fouling phenomena and its effect on the overall performance of the reactor. In this work the model is improved with the consideration of multiple phases and the mass transportation between these phases. Based on Korsten and Hoffmann reactor model [1]. Due to the reactions the composition of the reaction mixture changes along the reactor which has effect on the solubility of the hydrogen. The model of this effect is also built into the reactor model.

2. Methods

Experiments

A fixed-bed tubular reactor (diameter: 29 mm, length: 700 mm) was applied to perform the special hydrocracking reactions of the investigated oil mixture. The feedstock was the mixture of kerosene and sunflower oil in a mass ratio of 3:7. In the experimental system the temperature, the pressure and the LHSV can be controlled, so the hydrocracking experiments were performed at 533-613 K, 30-70 bar, 1.0-2.0 h^{-1} employing Pt/H-mordenite catalyst (Pt content: 0.45%, specific area, BET: 451 m^2/g, micropore volume: 0.18 ml/g, Si/Al ratio from XRF: 19 mol/mol, acid sites by ammonia TPD: 0.82 mmol/g, particle diameter: 1.4 mm). The measurements were performed after reaching a steady state condition.

Modeling

The pseudo (lumped) components in the developed kinetic model was determined by their boiling point range. Since the experimental data contains 5 pseudo components (triglycerides, diesel, kerosene, gasoline, and gas fractions), the kinetic model was developed using these lumps. For further improvement, the mass transportation of hydrogen was built in the model through

applying the Langmuir Hinshelwood mechanism and Henry's law. The unknown parameters of the proposed reactpr model were estimated based on measurement data with the application non-linear global optimization algorithm.

3. Results and discussion

In Figure 1 the validation of our previously described kinetic model for the mentioned material system can be seen. As the processes take place in the reactor are described in more details in the improved model we think that catalyst fouling effect can characterized much more precisely. The more we know about catalyst fouling the higher production efficiency can be achieved in the reactor.

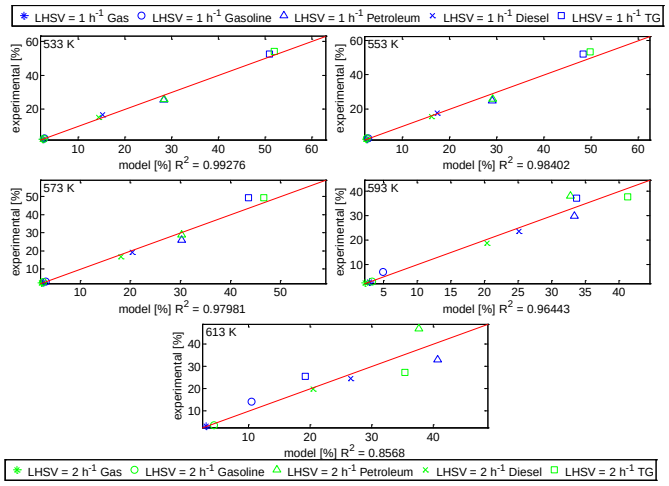

Figure 1. Parity plot for the previously described kinetic model at 30 bar

4. Conclusions

Our previous analysis of the investigated system revealed that there is a significant effect of catalyst fouling on the product composition. We consider the thermodynamic phases and the connections between each phase to improve the proposed reactor model. In the proposed model the effect of liquid composition on the hydrogen solubility was also considered. The performed model improvements support us to characterize the catalyst fouling phenomena.

References

[1] Korsten H, Hoffmann U. AlChE J 1996; 42:1350–60.

Acknowledgment

The authors acknowledge the financial support of the project of the Economic Development and Innovation Operative Programme of Hungary, GINOP-2.3.2-15-2016-00053: Development of liquid fuels having high hydrogen content in the molecule (contribution to sustainable mobility). The Project is supported by the European Union and co-financed by Széchenyi 2020.

ECCE12
The 12th EUROPEAN CONGRESS OF CHEMICAL ENGINEERING
Florence 15-19 September 2019

Influence of fluid dynamic conditions on the course of precipitation reactions in a static mixer

Agata Małysiak[1], Przemysław Gidziela[1], Karolina Rurarz[1], Kamila Tomala[1], Piotr Synowiec[1]

1 Department of Chemical Engineering and Process Design, Silesian University of Technology, Strzody 7, 44-100 Gliwice, Poland

**Corresponding author: Agata.Malysiak@polsl.pl*

Highlights

- Three different salts were precipitated.
- Kenics static mixer was used as a multifunctional reactor.
- Influence of fluid dynamics on reaction kinetics and obtained crystals was investigated.

1. Introduction

In recent years there is a growing need to produce systems of small particle diameters with the desired and reproducible qualities and characteristics in an economical and easily scalable way. This is especially visible in the case of nanoparticles applications: the great desire is for pharmaceutics, cosmetics, medicinal imaging and diagnostics. Taking all that into account the natural choice would be precipitation. This reaction is simple, inexpensive and efficient thus the economy is favorable [1]. For the precipitation reaction the residence time is not of crucial importance, as the reaction is very fast. More significant will be high mixing efficiency and uniform unit power input in order to avoid an uncontrolled supersaturation regions [2]. For those reasons the precipitation could be successfully conducted in static mixers [3, 4]. In comparison to tank reactors they are much easier scalable and takes a lot less space, but their applicability is limited.

2. Methods

In this study precipitation of three compounds were considered: $CaSO_4$, CaC_2O_4 and $BaSO_4$. The production of those salts was conducted according to the equations:

$$Na_2SO_4 + CaCl_2 + 2H_20 \rightarrow CaSO_4{\cdot}2H2O\downarrow + 2NaCl$$

$$C_2O_4H_2 + CaCl_2 + H_2O \rightarrow CaC2O_4{\cdot}H_2O\downarrow + 2HCl$$

$$Na_2SO_4 + BaCl_2 \rightarrow BaSO_4\downarrow + 2NaCl$$

The substrates were aqueous solutions of Na_2SO_4, $CaCl_2$, $H_2C_2O_4$ and $BaCl_2$ respectively, introduced in stoichiometric proportions. Investigated salts are characterized by different solubility product and thus the relative supersaturation is maintained at the same level in order to investigate the influence of fluid dynamics on reaction kinetics and product characteristics.

The selected multifunctional reactor was Kenics static mixer with six inserts. Its total length was equal to 0.165 m and inner diameter was 0.0136 m. Change of fluid dynamic conditions was assured by investigating Reynolds numbers in the range of 500 to 2000.

The laboratory setup is presented in figure 1. It consisted of two tanks (1) in which solutions of two reagents were prepared and stored. Solutions were pumped to the reactor (3) using peristaltic pumps (2). The obtained suspension was collected in storage tank.

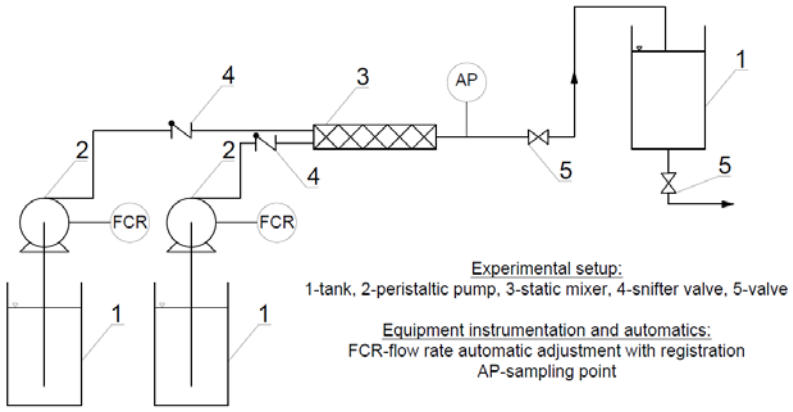

Figure 1. Experimental setup.

3. Results and discussion

The precipitation of three different insoluble salts was performed assuring the same fluid dynamic conditions in form of range selected range of Reynolds number and similar level of relative supersaturation. Each of investigated compounds was characterized by different solubility and product characteristics. The results show that there is a noticeable influence of fluid dynamic conditions on precipitation kinetics and product characteristics.

4. Conclusions

Different characteristics in terms of solubility of precipitated compounds results in very different kinetics of the reaction. The influence of fluid dynamic conditions on product characteristics is also undeniable.

Acknowledgment

This research was supported by the Polish National Science Centre (NCN) under Grant No. 2016/21/D/ST8/01714.

References [Calibri 10]

[1] E. Gavi, D.L. Marchisio, A.A. Barresi, M.G. Olsen, R.O. Fox, Chem. Eng. Res. Des., 88 (2010) 1182-1193.

[2] A. J. Alvarez and A. S. Myerson, Cryst. Growth Des., 10 (2010) 5, 2219–2228.

[3] R.K. Thakur, Ch. Vial, K.D.P. Nigam, E.B. Nauman, G. Djelveh, Trans IChem Eng. Part A, 81 (2003) 787-826.

[4] A. Cybulski, K. Werner, Int. Chem. Eng., 26 (1986) 1, 171-180.

ECCE12
The 12th EUROPEAN CONGRESS OF CHEMICAL ENGINEERING
Florence 15-19 September 2019

Characterization of macrophyte *Eichhornia crassipes*: potentiality of wetlands pruning wastes in thermo-conversion processes.

Eliane Cristina Braga Martins Gonçalves[1], Francisco José Moura[1*], Marcos Alexandre Teixeira[2]

[1]Department of Chemical and Materials Engineering, Pontifical Catholic University of Rio de Janeiro (PUC-Rio), Rio de Janeiro, Brazil; [2]Department of Agricultural and Environmental Engineering, Fluminense Federal University (UFF), Niterói, Brazil.

**moura@puc-rio.br*

Highlights

- Evaluate of thermal conversion potential of *E. crassipes*.
- Physical-chemical characterization of the biomass.
- Determination of the biomass thermal properties.
- Potential use of the biomass for bioenergy production.

1. Introduction

In the search for a more sustainable and equitable energy for the future, the use of biomass residues from anthropic action arises as valuable source of raw material for bio or thermo-conversion, economically viable and ecologically sustainable. In this sense, aquatic macrophytes become interesting from the standpoint of their valorization as biomass source for energy production [1]. The objective of this paper was the fully characterization of the pruning wastes from macrophyte *Eichhornia crassipes* from secondary sewage treatment of wastewater treatment plant, in order to investigate the potential of the use of wetlands management control pruning residues for use as a renewable fuel.

2. Methods

The plant samples were analysed as a single whole fraction, including inflorescence, sheets, root and petioles. The characterization tests were based on the methodologies proposed by Soxhlet [2], Doc236 [3] and ASTM [4]. The thermogravimetric analyses were carried out in a simultaneous thermal analyser, model Netzsch STA449 - F3 Jupiter, according to following parameters: sample mass of approximately 10 mg, temperature programming (from 20°C to 900°C), inert gas (N_2), and heating rates of 10°C.min^{-1}, 15°C.min^{-1} and 20°C.min^{-1}.

3. Results and discussion

The bromatological and chemical analyses are essential for the evaluation of this source of biomass for thermal-conversion processes. The bromatological composition values obtained were: extractive content (4.06 wt%), lignin (9.99 wt%), cellulose (20.11 wt%) and hemicellulose (28.59 wt%). As expected for aquatic biomass, carbon (40.24 wt%) and oxygen (35.28 wt%) presented the highest content. Hydrogen and nitrogen average values obtained were 5.03 wt% e 5.71 wt%, respectively. The analysed macrophyte presented high moisture (95.19 wt%), as

expected. After forced drying, the moisture remained above 10 % (11.52 wt%) for the sample analysed. The high average value of ash content (16.07 wt%) can be attributed to the contribution of roots, which usually retain in their tissues high concentrations of insoluble materials such as silicates. *E. crassipes* samples also presented average values of 80.96 wt% for combustibility, 70.01 wt% for volatiles, 13.91 wt% for fixed carbon, with the ratio volatile/fixed carbon higher than 3.50. The higher heat value (HHV) is directly related to biofuels effectiveness. Biomasses with ash contents of less than 25% and HHV higher than 14.65 $MJ.kg^{-1}$ are considered energetically efficient [6]. The samples presented HHV average value of 15.89 $MJ.kg^{-1}$. According to thermogravimetric analysis of biomass (Figure 1), the TGA/DTG curves presented three distinct regions of mass loss relating to moisture reduction (I), hemicellulose and cellulose degradation (II) and lignin degradation (III). The region II presented the highest mass loss (39 - 44 %), due to the lower thermal stability of hemicellulose and cellulose. The increase of the heating rate changes the maximum mass loss of biomasses to higher temperatures.

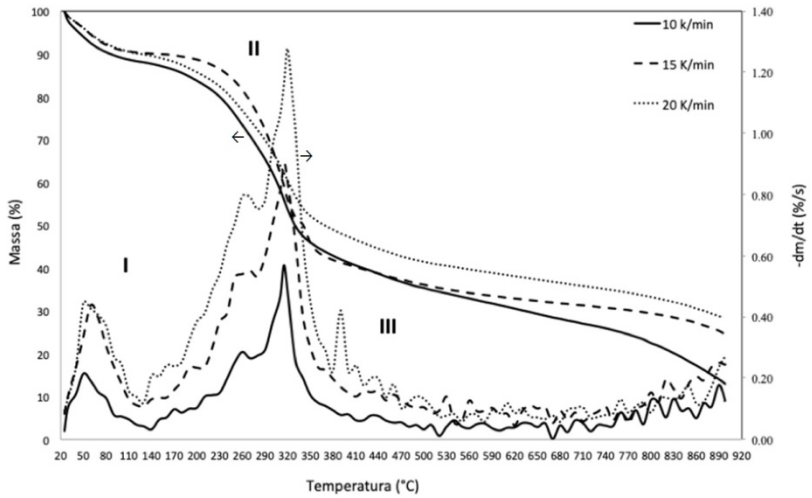

Figure 1. Influence of heating rates on TGA / DTG thermogravimetric curves.

4. Conclusions

The samples characterizations suggest that *Eichhornia crassipes* control pruning residues have potential for bioenergy production, especially biochar, associated with gasification rather than direct combustion process (due high ash content). High carbon and hydrogen contents affect positively the higher heat value of the biomass. High volatiles content (> 70%) increase the gas production. The biomass analysed presented HHV value of 15.89 $MJ.kg^{-1}$.

References

[1] Wetzel, R.G. (2011). Limnology: lake and river ecosystems, Londres: Academic Press, 850.
[2] Soxhlet, F. (1879). Die gewichtsanalytische bestimmung des milchfettes, Polytechnisches Journal, Erlangen, 232, 5, 461-465.
[3] EMBRAPA (2010). Documento 236: procedimento para análise lignocelulósica, Campina Grande: Centro Nacional de Pesquisa de Algodão, Embrapa.
[4] ASTM (2009). Standard D240: standard test method for heat of combustion of liquid hydrocarbon fuels by bomb calorimeter, West Conshohocken: ASTM, 10.1520/D0240-09.
[5] Pompêo, MLM., Moschini-Carlos, V. (2003). Macrófitas aquáticas e perifíton – aspectos ecológicos e metodológicos, São Carlos: Rima.
[6] Morais, S.A.L. de, Nascimento, E.A. do, Melo, D.C. de. Chemical analysis of *Pinus oocarpa* part I: quantification of macromolecular components and volatile extractives, Árvore, 29, 3, 461-470.

Study of the economic feasibility for the implementation of a sustainable biorefinery in the production of bioethanol

Alma Hortensia Serafin-Muñoz [1]*, Berenice Noriega-Luna[1], Julio C. Leal-Vaca[1], Luis-Enrique Mendoza Puga[1], Israel Cabrera-Barron[1].

[1] *Engineering Division, Campus Guanajuato. University of Guanajuato. Juárez No.77, Col. Centro. C.P.36000. Guanajuato, Gto. Mexico.*
**sermuah@ugto.mx*

1. Introduction

The preoccupations about climate change and sustainability have driven the exploration of the production of alternative fuels. Bioethanol currently dominates the market and contributes 65% of the world's biofuel production [1, 2]. In this work, the feasibility of obtaining bioethanol from the lignocellulosic biomass in Guanajuato (Mexico) was studied, integrating SWOT tools and sustainability indicators of the reproduced processes into the study, that could be taken as a model in other cases of study at a national or international level under the same perspective.

2. Methods

The proposed methodology was divided into three stages: 1. Agricultural zones, 2. Reproducibility of the processes, 3. Analysis of the feasibility. **Agricultural zones (obtaining and quantification of raw material)**. The quantification of residual biomass from corn crops was carried out based on the model obtained by Bentsen [3], in which the waste index (WI) is exponentially proportional to the yield (Y) : $WI = a \cdot e^{bY}$, where a = 2656, b = -0.000103 ha· year · kg^{-1} and yield (Y) is given in units kg · ha^{-1} · $year^{-1}$. Waste produced (W) from the production of a certain crop is proportional to the volume produced (V) according to the relation $W = V \cdot WI$. Following the relation $W = P \cdot WI$, the expression to estimate the produced volume of waste in kg is: $W = V \cdot 2{,}656 \cdot e^{-0.000103\,Y}$.To measure the volume of waste from each municipality of the study area, the yield (Y) and production values recorded by the Secretariat of Agriculture, Livestock, Rural Development, Fisheries and Food (SAGARPA) [4]. **Reproducibility of the processes**. This was carried out based on the established methodology, figure 1 [5,6].

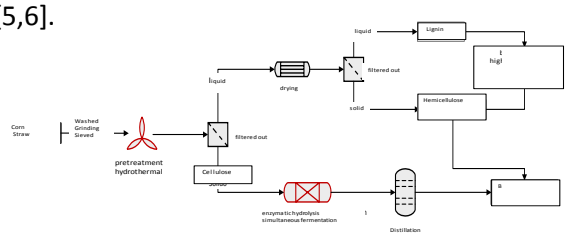

Figure 1. Scheme of the productive chains for the obtaining of bioethanol [6].

Analysis of the feasibility.

The indicators of sustainability were developed as indicated by the methodology of Indicators of Sustainable Development [7]. The SWOT matrix was developed by four types of strategies: strength-opportunity, weakness-opportunity, strength-threat, weakness-threat, that can be raised to convert weaknesses into strengths and threats into opportunities. The analysis of attractiveness was made based on the business template PNESINSO / strategy planning model, Innova Solutions

[8]. Based on the results obtained in the three stages, the feasibility of a sustainable biorefinery of the production for bioethanol was analyzed and discussed.

3. Results and discussion

The Guanajuato States was divided into geographical farming zones (Figure 2). The map shows the biomass potential within the state of Guanajuato in relation to corn residues ranging from 2,800 + 320 tons / year, representing a high energy potential of the production for biofuels and identifies the municipalities that contribute this biomass. The identification of these municipalities is the first step to evaluate the current availability of biomass and accurately estimate the bioenergy production capacity of waste derived from corn agricultural crops. The reproducibility of the pretreatment and delignification processes was performed to get a way cheaper to feasibility to the economy, that was analyzed base on the SWOT tools (Figure 3), and the sustainability indicators of from reproduced processes (Table 1).The results indicate that bioethanol production cost is 1.65±2.1 USD/gallon and potential production is 60.14 MM gallon/year using corn straw, which indicates that to reduce these costs should be optimized the processes.

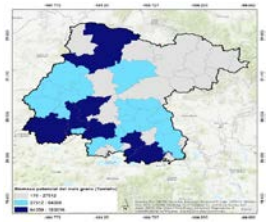

Figure 2. The residual corn biomass potential

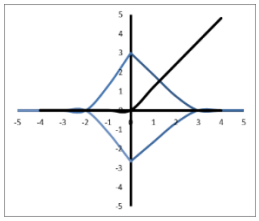

Figure 3. Graph resulting from the analysis of the Attractiveness [8].

Table 1. Indicators of sustainability

Policy in issue in NSDS	Indicator	Type of reference
Agriculture	Quantification of straw or residual biomass	SAGARPA, INIFAP, FINNOVATEG-CFINN0186 Project
Bioenergy	Index of projects related to Bioenergy	SICES CONACYT, SENER
Biorefinery	Cost analysis in productive chains	FINNOVATEG-CFINN0186 Project
Air quality	Air pollution from burning straw or residual biomass from agricultural crops	Pro Air of the State of Guanajuato Secretary of the Environment and Territorial Planning
GHG emissions	GHG and CO_2 emissions	FINNOVATEG-CFINN0186 Project, Pro Air of the State of Guanajuato Secretary of the Environment and Territorial Planning
Energy	Renewable energy use as a proportion of total	National Development Plans, State Innovation Agenda
Energy	Generation of biofuels	National Development Plans, State Innovation Agenda , SENER
Global responsibility	Environmental quality certification standards	ISO 14000

4. Conclusions

The pretreatment represented the stage of greatest cost in the conversion of biomass to ethanol, the investigations are focused on developing pretreatments of delignification, clean technologies and innovation methodologies. However, the cost of a liter of bioethanol is 48% below the current price of gasoline in Mexico. In parallel, the analysis with the tools SWOT and Sustainability Indicators, let us know the project has highly feasible to implement in Mexico, as an alternative to use the agricultural residues had been generated representing a high potential to obtaining new biofuels.

References

[1] Biofuels Production. www.bp.com/en/global/corporate/energy-economics/statistical-review-of-world-energy/renewableenergy/biofuels-production.html. Accessed 2 Jun 2017.

[2] Vermuë, M. H., et al. Multi-product microalgae biorefineries: from concept towards reality. Trends in biotechnology 36.2 (2018): 216-227.Bentsen, A. Bianchi, N.C. Jones, Chem. Eng. J. 157 (2019) 326–337.

[3] https://www.gob.mx/agricultura

[4] Muñoz, Alma Hortensia Serafín. Characterization and integrated process of pretreatment and enzymatic hydrolysis of corn straw." Waste and Biomass Valorization 10.7 (2019): 1857-187

[5] Cabarcas G. and Serafin Muñoz A., et. al. Prototipo de diseño sustentable para la obtención de biocombustibles bajo el esquema de biorrefinerías." jóvenes en la ciencia 3.2 (2017): 2225-2229.

[6] Hák, Tomáš, Svatava Janoušková, and Bedřich Moldan. Sustainable Development Goals: A need for relevant indicators. Ecological Indicators 60 (2016): 565-573.

[7] https://mx.linkedin.com/in/gerardo-pati%C3%B1o-zamudio-8794a451

ECCE12
The 12th EUROPEAN CONGRESS OF CHEMICAL ENGINEERING
Florence 15-19 September 2019

Experimental Investigations on Dynamic co-Methanation of CO/CO_2 mixtures using Ni/Al_2O_3 Catalysts

Dominik Meyer[1], Jannik Schumacher[1], Jens Friedland[1], Robert Güttel[1]

1 Institute of Chemical Engineering, Ulm University, Ulm, Germany

**Corresponding author: dominik.meyer@uni-ulm.de*

Highlights

- Transient turn-over frequency calculated for unsteady-state co-methanation.
- Dynamic regimes in reactor behavior identified based on frequency response.
- Critical switching frequency identified for pseudo-steady-state behavior.
- Criterion deduced for tolerant operation under transient conditions.

1. Introduction

The increasing utilization of regenerative resources in the chemical value chain induces new challenges in the operation strategy of chemical reactors. As an example, the chemical storage of regenerative energy via the power-to-X process (PtX) provides an option to store fluctuating electrical energy via water electrolysis and subsequent hydrogenation of carbon oxides. The formed methane can be stored and transported in the existing gas grid. However, this scenario implies a dynamic behavior of the process chain, depending on the installed storage capacity. As the storage of large quantities of electrical energy and hydrogen is not yet feasible, the necessity of an unsteady-state operation of the methanation reactor becomes likely.

An interesting carbon source for PtX are industrial exhaust gases, such as coke oven gas, which consist of a mixture of CO and CO_2 [1], which can be subject to strong fluctuations in composition. For the steady-state case the co-methanation mechanism is widely investigated [2]. However, for the unsteady-state case only little is known, even though a profound understanding of the dynamic methanation of CO/CO_2 mixtures is essential for the implementation of the co-methanation in a sustainable energy scenario based on renewables. The present contribution will discuss the strong interrelation between the unsteady-state behavior of the reactor and the frequency of feed composition alteration for methanation on a Ni/Al_2O_3 catalyst. Based on experimental results, conclusions on the effect of the frequency on the underlying transport mechanisms will be drawn.

2. Methods

The experiments are performed in an isothermal packed-bed reactor (length 20 mm, diameter 2 mm) using a self-prepared Ni/Al_2O_3 catalysts (Ni loading 5 wt%, particle size 800 µm, 200 mg). Two gas lines with different compositions (line 1: 0.8 H_2/0.1 CO_2/0.1 He; line 2: 0.8 H_2/0.1 CO/0.1 Ar) are switched by means of a 4-way valve with a frequency between 0.0083 and 0.25 s^{-1} and a split of 0.5. Both gas lines contain a different inert gas as internal standard for measuring the residence time behavior under reaction conditions. The effluent was analyzed by a mass spectrometer with sampling time of 0.5 s providing sufficient temporal resolution. Prior to dynamic experiments, the as-made catalyst was reduced and the catalytic behavior was studied under steady-state conditions

for various feed compositions and in a temperature range of 260 to 310 °C and 2 bar. The dynamic experiments were then performed under the same conditions.

3. Results and discussion

Figure 1 shows selected results in the phase plane. The fraction of either reactants or products at the reactor outlet are displayed as a function of the internal standard, according to our previous work [3]. The deviation of the profiles from a linear function between the steady-state conditions allow to conclude on the inherent transient system behavior. For example, the negative deviation of the CO fraction from the linear correlation in the increasing branch (Figure 1 a), lower red curve) indicates either a stronger adsorption of CO at the Ni surface or a more pronounced conversion into methane compared to CO_2. Since the mass balance is fulfilled and a limit cycle is reached for several consecutive periods, the data can be evaluated quantitatively. In this regard, Figure 1 b) indicates an increase in methane productivity upon periodic operation, as indicated be the upward shift of the limit cycle compared to the expected steady-state system.

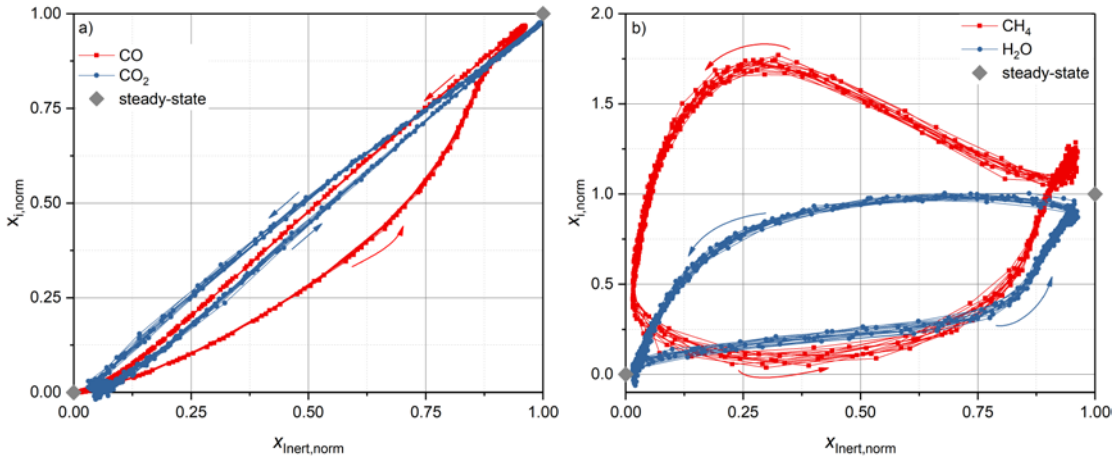

Figure 1. Limit cycle of the reactants (a) and products (b) in the phase-plane upon periodic exchange of CO with CO_2, period duration 30 s, T = 573 K, p = 2 bar, H_2/carbon source/inert = 8/1/1.

4. Conclusion

We present experimental results on the dynamics of the CO/CO_2 co-methanation on Ni-based catalysts. The different behavior of the reactive species indicates differences in interaction strength between those species and the active catalyst surface, which allows to deduce on the basic reaction mechanism. By quantitatively analyzing the dynamic change in the molar flow rate, we are able to determine a transient turn-over frequency (TOF) for methane formation and to compare it to the steady-state case value. Finally, we link the frequency response of each of the reactants to either the quasi steady-state, the full transient regime or the relaxed steady-state according to [4]. This provides to identify a tolerant operation window for fluctuating inlet compositions.

References

[1] M.A. Schöß, A. Redenius, T. Turek, R. Güttel, Chem. Ing. Techn. 86 (2014) 734–739.
[2] G.D. Weatherbee, C.H. Bartholomew, J. Catal. 77 (1982) 460–472.
[3] B. Kreitz, J. Friedland, R. Güttel, G. Wehinger, T.Turek, Chem. Ing. Techn. (2019) in press.
[4] D. Meyer, J. Friedland, T. Kohn, R. Güttel, Chem. Eng. Technol. 40 (2017) 2096–2103.

ECCE12
The 12th EUROPEAN CONGRESS OF CHEMICAL ENGINEERING
Florence 15-19 September 2019

Application of the integrated supercritical fluid extraction-impregnation process for incorporation of *Melissa officinalis* extract into cotton gauze

Ivana Lukić[1*], Jelena Pajnik[1], Erika Vági[2], Edit Szekely[2], Irena Žižović[3]

1 University of Belgrade, Faculty of Technology and Metallurgy, Belgrade, Serbia;

2 Budapest University of Technology and Economics (BME), Department of Chemical and Environmental Process Engineering, Budapest, Hungary;

3 Wroclaw University of Science and Technology, Faculty of Chemistry, Wroclaw, Poland.

**Corresponding author: ivanal888@yahoo.co.uk*

Highlights

- Cotton gauze was impregnated with *M. officinalis* extract using SFE-SSI process.
- Three different process modes were tested.
- FTIR analysis confirmed the presence of *M. officinalis* extract on cotton gauze.

1. Introduction

Lemon balm (*Melissa officinalis*) has long been used in herbal medicine due to its numerous biological activities including antioxidant, antimicrobial and antiviral [1].When there is a need to impregnate a solid material with a supercritical extract, merging of the supercritical fluid extraction (SFE) and supercritical solvent impregnation (SSI) into the one, integrated, SFE-SSI process enables energy savings as well as minimization of the extract losses [2-4]. The goal of this study was to obtain cotton gauze functionalized with *Melissa officinalis* extract for potential topical application by the integrated SFE-SSI process. The influence of different processing modes on the obtained impregnation yield was studied.

2. Methods

M. officinalis folium was milled in a blender and sieved prior the experiments. Integrated SFE-SSI process was performed on laboratory scale unit (High Pressure Extraction Adsorption (HPEA) 500, Eurotechnica, Germany), whereby both, extraction and impregnation, were performed at 10 MPa and 40 °C. Detailed equipment description and possible processing modes are presented elsewhere [3, 4].

3. Results and discussion

Three types of processing modes were performed in order to obtain maximal impregnation yield (I). **Mode I:** Batch mode - supercritical fluid was circulated through the system (extractor and adsorber) for 5 h. **Modes II and III:** Circulation of supercritical fluid through the system was performed in cycles (Table 1). Between the cycles, a continuous CO_2 flow (10 g/min) through the extractor and adsorber was maintained during 5 minutes.

Introduction of fresh CO_2 positively influenced the yield of impregnation (defined as the mass fraction of the extract in the functionalized material). Introduction of fresh CO_2 while maintaining the total process time approximately equal, enabled 6.5 times higher impregnation yield when

Mode III (2.24%) was applied compared to Mode I (0.34%). The introduction of fresh CO_2 positively affected the efficiency of extraction process, leading to the higher amount of the extract available for the SSI. Further increase in contact time led to the decrease of the impregnation yield.

Table 1. Impregnation yield of *M. officinalis* extract for different processing modes

	No of cycles	Cycle duration, h	Total contact time	I, %
Mode I	1	5	5 h	0.34±0.035
Mode II	3	2+2+1	5 h + 10 min flow	1.48±0.127
Mode III	5	1	5 h + 20 min flow	2.24±0.141

The FTIR spectra show the main differences between the impregnated and control cotton gauze in the range 3000–2800 cm^{-1} and around 1700 cm^{-1} attributed to C–H and C=O stretching vibrations, respectively, confirming that the balm extract was effectively impregnated into the gauze.

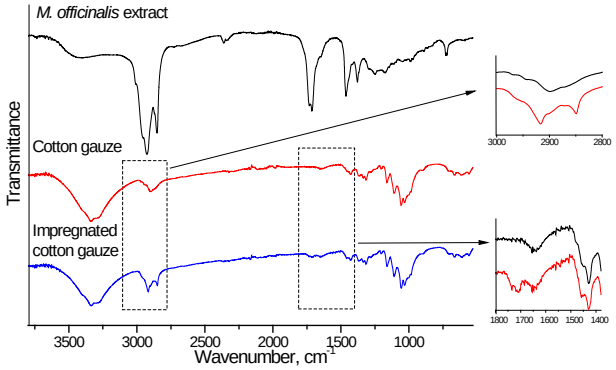

Figure 1. FTIR spectra of pure *M. officinalis* extract, control and impregnated cotton gauze.

4. Conclusions

Cotton gauze was successfully impregnated with *M. officinalis* extract using the integrated SFE-SSI process at 10 MPa and 40 °C. In order to optimize the process, three different processing modes were tested. The presence of extract on the surface of cotton gauze was confirmed by FTIR analysis.

Acknowledgement

This work was financially supported by the Ministry of Education, Science and Technological Development of the Republic of Serbia (Project No III 45001 and III45017), as well as the Higher Education Excellence Program of the Ministry of Human Capacities in the frame of Biotechnology research area of Budapest University of Technology and Economics (BME FIKP-BIO).

References

[1] A. Shakeri, A. Sahebkar, B. Javadi, J.Ethnopharmacol. 188 (2016) 204–228.

[2] M. A. Fanovich, J. Ivanovic, D. Misic, M. V. Alvarez, P. Jaeger, I. Zizovic, R. Eggers, J. Supercrit Fluids 78 (2013) 42–53.

[3] J. Ivanovic, S. Milovanovic, M. Stamenic, M. A. Fanovich, P. Jaeger, I. Zizovic, in: J. Osborne (Ed.), Handbook on Supercritical Fluids, Fundamentals, Properties and Applications, Nova Science Publishers, Hauppauge, NY, 2014, pp 257–280.

[4] S. Maksimović, V. Tadić, J. Ivanović, T. Radmanović, S. Milovanović, M. Stanković, I. Žižović, Chem. Ind. Chem. Eng. Q., 24 (2)(2018) 191–200.

ECCE12
The 12th EUROPEAN CONGRESS OF CHEMICAL ENGINEERING
Florence 15-19 September 2019

Modelling and Simulation of Porous Catalyst Pellets for Unsteady-State co-Methanation of CO/CO_2 mixtures: Comparison of Diffusion Models

Jannik Schumacher[1], Dominik Meyer[1], Jens Friedland[1], Robert Güttel[1]

1 Institute of Chemical Engineering, Ulm University, Ulm, Germany

**Corresponding author: Jannik.schumacher@uni-ulm.de*

Highlights

- Unsteady-state methanation is modelled and simulated on the pellet scale.
- Different diffusion models are compared with respect to their dynamic effects.
- The exchange of CO_2 with CO is used as a model experiment of a dynamic process.

1. Introduction

The methanation process is a promising part of a sustainable energy supply and infrastructure via the power-to-gas (PtG) process. However, since the availability of renewable energy and carbon sources is fluctuating, the methanation has to work under unsteady-state conditions as well, depending on the upstream storage capacities [1]. One of the main challenges arising from this situation is the dynamic behavior of the porous catalyst pellets used for methanation, where heat and mass transfer occur simultaneously with the chemical reaction. Dynamically changing spatial profiles of temperature and concentrations develop, which are coupled non-linearly. Since the measurement of those profiles, especially under operando-conditions is very challenging [2], modelling and simulation provides a powerful tool for analyzing the occurring dynamic processes. Among methanation of pure CO_2 and CO a mixture of both carbon oxides is of interest especially when considering process gases, such as coke oven gas, as carbon source. However, when switching from CO_2 to CO-methanation or between various mixtures of both, the dynamic profiles change in an unpredictable way, which originates from the different reaction mechanism for CO and CO_2 hydrogenation. Thus, the present contribution analyses the dynamic behavior at particle scale based on modelling and simulation.

2. Methods

This work puts emphasis on the comparison of different diffusion models under isothermal and unsteady-state methanation conditions as a basis for reliable simulation results. The compared diffusion models comprise, but are not limited to, the models by Fick and Wilke-Bosanquet as well as the dusty-gas model [3]. The models are evaluated based on accuracy and numerical effort. Due to a lack of experimental data for validation the dusty-gas-model is assumed as the most accurate model, since it is the most complex one and thus probably considers all relevant effects on diffusion. Thus, the alternative (and simpler) models are compared to the results of the dusty-gas model as benchmark. The model equations for the unsteady-state reaction-diffusion problem are implemented to Aspen Custom Modeler for simulation. The diffusion models in accordance to Solsvik et al. [4] are used, while the reaction kinetics are taken from Xu and Froment [5]. For simulation typical

methanation conditions are chosen with respect to temperature, pressure and reactant composition. The catalyst pellet is assumed to be isothermal, in order to avoid super-imposed temperature influences. The effects at reactor scale are neglected, as well as external heat and mass transfer resistances, in order to isolate the diffusion effects. The dynamic profiles when exchanging CO_2 with CO are calculated with respect to the different diffusion models.

3. Results and discussion

As example Figure 1a shows the simulated steady-state profiles of the methane molar fraction in the CO_2-methanation process for different diffusion models. It is obvious that the choice of the diffusion model is a critical part in the modelling and simulation process. Although the concentration profiles calculated with the dusty gas model and the Wilke-Bosanquet are highly different, the surface methane fluxes and consequently the effective reaction rates are quite similar (Figure 1b). Based on the systematic evaluation of diffusion models under steady-state conditions, the dynamic behavior of the concentration profiles is analyzed by changing the switching frequency between H_2/CO and H_2/CO_2 as well as for different H_2/CO_x gas mixtures (not shown in abstract). From the obtained results the impact of mass transport on the behavior of the catalyst pellet is evaluated.

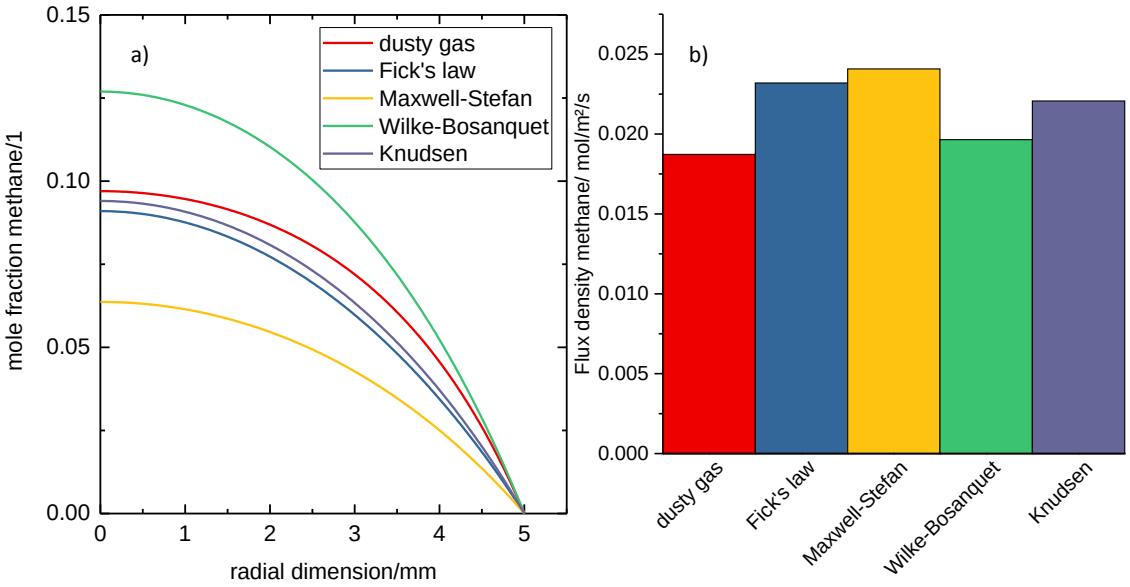

Figure 1. a) Steady-state methane concentration profiles for CO_2-methantion with different diffusion models, b) steady-state flux density of methane across the external surface of the catalyst pellet.

4. Conclusions

While the effective reaction rates in the CO_2-methantation process are quite similar for the studied diffusion models, the dynamic behavior of the profiles is expected to differ, since the concentrations are highly different.

References

[1] J. Lefebvre, M. Götz, S. Bajohr, R. Reimert, T. Kolb, Fuel Process. Technol. 132 (2015) 83–90.
[2] T. Titze, C. Chmelik, J. Kullmann, L. Prager, E. Miersemann, R. Gläser, D. Enke, J. Weitkamp, J. Kärger, Angew. Chem. 127 (2015) 5148–5153.
[3] R. Krishna, J.A. Wesselingh, Chem. Eng. Sci. 52 (1997) 861–911.
[4] J. Solsvik, S. Tangen, H.A. Jakobsen, Ind. Eng. Chem. Res. 51 (2012) 8222–8236.
[5] J. Xu, G.F. Froment, AIChE Journal 35 (1989) 88–96.

ECCE12
The 12th EUROPEAN CONGRESS OF CHEMICAL ENGINEERING
Florence 15-19 September 2019

Homogeneous, Continuous and Highly Selective mono-Bromination of 3-Methylanisole in a Microreactor System

Pei Xie[1], Kai Wang[2], Jian Deng[3], Guangsheng Luo[4]

The State Key Laboratory of Chemical Engineering, Department of Chemical Engineering, Tsinghua University, Beijing 100084, China

**Guangsheng Luo, gsluo@tsinghua.edu.cn*

Highlights

- Synthesize continuously 4-bromo-3-methylanisole in a microreactor system.
- Improve dramatically mono-brominated selectivity in a homogeneous reaction.
- Simplify greatly the purification process of crude 4-bromo-3-methylanisole.

1. Introduction

4-Bromo-3-methylanisole (BMA) is mainly used to synthesize ODB-2 which is the most important heat-sensitive dye in the manufacture of thermal paper. [1-2] In industry, BMA has been mass-produced by mono-bromination of MA with Br_2 - aq. HBr (Scheme 1). The crude BMA has to be distilled to remove high boiling point bis/tris-brominated byproducts (PB) because of the low mono-brominated selectivity in a heterogeneous reaction system. Therefore, the microreactor technology is expected to intensify the mixing and heat exchange of bromination reaction to reduce PB content in a homogenous reaction system and simplify the purification process of crude BMA.

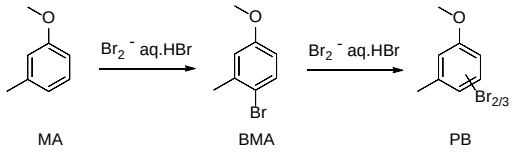

Scheme 1. Heterogeneous Brominated Reaction

2. Methods

The homogeneous bromination of MA in $CHCl_3$ was performed in the microreactor system (Figure 1) whose core components are the micro-sieve dispersion reactor (Figure 2). Considering the corrosiveness of Br_2 and HBr, the tubes, M1 and M2 are made of PTFE. [3-4]

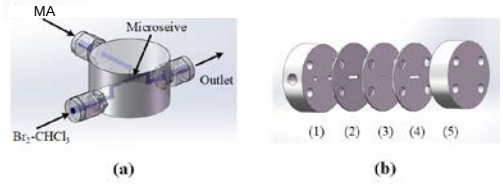

Figure 1. Structure of Micro-sieve Dispersion Reactor

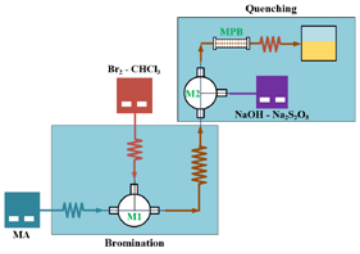

Figure 2. Microreactor System

3. Results and discussion

The mono-brominated selectivity (Figure 3) and BP content (Figure 4) were compared in the heterogeneous and homogeneous reaction system.

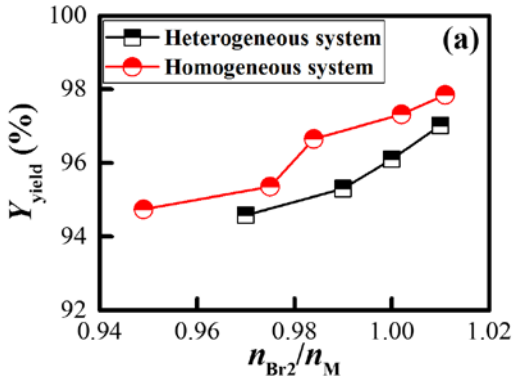

Figure 3. The Comparison of BMA Yield

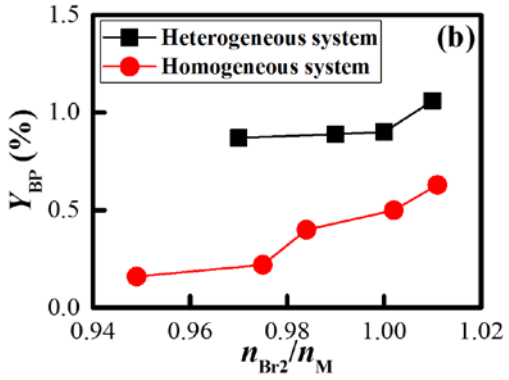

Figure 4. The Comparison of PB Content

4. Conclusions

BMA was synthesized continuously in a microreactor system under homogeneous conditions. The PB content can be controlled below 0.5% at a mild temperature (20-25 °C) in a minute residence time. Finally, the distillation purification of crude BMA is unnecessary as result of higher mono-brominated selectivity.

References

[1] Qian M, Wang H, Xu X. Summary of Methods to Produce 4-Methoxy-2-methyl-N-phenylaniline. Zhejiang Chemmical Industry. 2012; 43 (8): 9-13.

[2] https://en.wikipedia.org/wiki/Thermal_paper.

[3] Xie P, Wang K, Wang P, Xia Y, Luo G. Synthesizing bromobutyl rubber by a microreactor system. AIChE Journal. 2017; 63 (3): 1002-1009.

[4] Wang K, Li L, Xie P, Luo G. Liquid–liquid microflow reaction engineering. Reaction Chemistry & Engineering. 2017; 2 (5): 611-627.

ECCE12
The 12th EUROPEAN CONGRESS OF CHEMICAL ENGINEERING
Florence 15-19 September 2019

Analyses of a non-isothermal simulated moving bed reactor based on Multi-objective optimization

Jian Wang, Weifang Yu*, Jin Xu*

College of Chemistry and Material Engineering, Wenzhou University

**Corresponding author: ywf@wzu.edu.cn; xujin@wzu.edu.cn*

Highlights

- Non-isothermal operations of an SMBR for methyl acetate synthesis were evaluated by multi-objective optimization.
- In addition to unit throughput and product purity, solvent consumption was also considered.
- Effects of kinetic parameter and adsorption strength of reactant were investigated by sensitivity study.
- The feasibility of applying non-isothermal operations was systematically investigated.

1. Introduction

Simulated moving bed reactor (SMBR) couples in-situ adsorptive separation with chemical reaction. Conversion of a reversible reaction can be increased beyond the limit of thermodynamic equilibrium and, as the same time, pure product can be directly collected, simplifying the downstream purification processes [1]. SMBR consists of a series of columns packed with solid phase materials with both catalytic activity and adsorptive selectivity. Typically, inlet and ourlet ports divide the columns into four zones, each playing a specific functional role.

Efficiency of the onsite separation is crucial for the success an SMBR. VariCol and PowerFeed technologies that have been originally developed for SMB separation were proven to be effective for the improvement of SMBR performance [2,3]. Gradient operation by introducing different adsorptive strength into different zones according to their functions has been extensively used to reinforce SMB separation processes.

The ongoing work in this group and colleagues is aimed at examining the feasibility of applying temperature variance on an SMBR. For this purpose, synthesis of methyl acetate catalyzed by amberlyst 15 was used as the model reaction. It has been shown by both theoretical and experimental studies that complete conversion and separation can be achieved [4,5].

One of our previous study investigated the effects of temperature gradient under the frame of Triangle Theory [6]. Maximum unit throughput for complete conversion and separation was acquired by fixing conservative flowrates in zones I and IV and searching the two dimensional parametric plane consisting of flworates in zones of II and III. In this work, zones I and IV were also taken into consideration. Multi-objective optimizations were carried to evaluate SMBR performance in terms of unit throughput, product purity and solvent consumption as well.

2. Methods

Mathematical model and model parameters for the simulation of an SMBR reactor were established in previous publications [5,6]. A four zone SMBR has five independent operating parameters, namely, switching time and the four flowrate. The maximum flowrate that is limited by column pressure was assigned to zone I as a scaling factor. Simultaneous maximization of unit throughput and product purity was pursued by tuning the other four parameters that had been converted to dimensionless flowrate ratios. As in general, operating conditions have contradicting effects on these two objectives and the solutions form a pareto curve. Non-dominated sorting genetic algorithm (NSGA-II) was used to acquire the solutions.

3. Results and discussion

Pareto solutions of an SMBR operated under various modes are compared in Figure 1. Minimization of solvent consumption was then pursued by both parametric sensitivity analyses and 3-objective optimizations. Using the same procedure, effects of kinetic rate, adsorption strength of reactant and reaction heat on the SMBR performance were also investigated. More detailed results and discussions omitted here for conciseness will be presented in the conference.

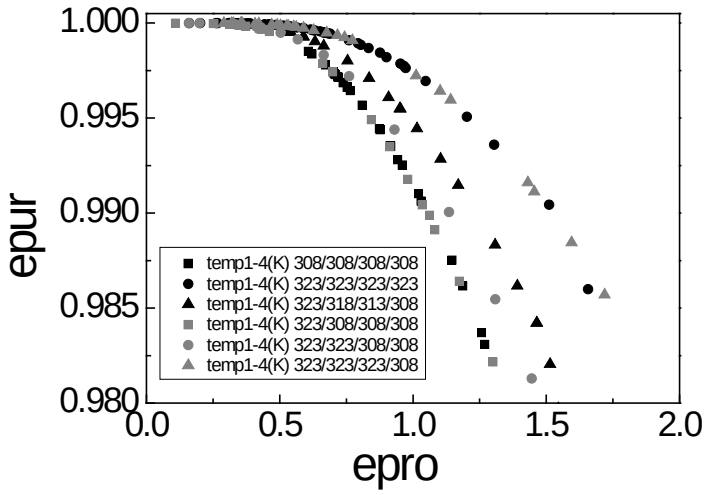

Figure 1. comparison of pareto solutions acquired for SMBR with several temperature distributions

4. Conclusions

Temperature may have both synergy and contradicting effects on reaction kinetics and separation in different zones. As a result, temperature gradient operation can be conditionally but not generally applied to improve SMBR performance.

References [Calibri 10]

[1] A.K. Ray, R.W. Carr, Chem. Eng. Sci. 50 (1995) 3033–3041.
[2] W. Yu , K. Hidajat , A.K. Ray, Chem. Eng. J. 112 (2005) 57-72.
[3] J.S. Hariprasad , K. Hidajat , A.K. Ray, Comput. Chem. Eng. 27 (2003) 1883–1901.
[4] W. Yu , K. Hidajat , A.K. Ray, Ind. Eng. Chem. Res. 42 (2003) 6743–6754.
[5] W. Yu , K. Hidajat , A.K. Ray, Appl. Catal. A: Gener. 260 (2004) 191–205.
[6] J. Xu, Y. Liu, G. Xu, W. Yu, A. K. Ray, AIChE J., 59 (2013) 4705-4714.

ECCE12
The 12th EUROPEAN CONGRESS OF CHEMICAL ENGINEERING
Florence 15-19 September 2019

The Differential Gibbs and Helmholtz Reactors for Ideal and Non-Ideal Gases and Selected Applications

Sindre Bakke Øyen[1], Tore Haug-Warberg[1], Hugo Atle Jakobsen[1], Jannike Solsvik[1]

1 Norwegian University of Science and Technology, Sem Sælands vei 4

**Corresponding author: sindre.b.oyen@ntnu.no*

Highlights

- Fluid mechanics combined with thermodynamics in continuity equations
- Rate expressions in classical reactors substituted out for minimizing Gibbs free energy
- A theoretical upper limit at all points throughout the reactor

1. Introduction

In chemical process design, equilibrium calculations are frequently carried out to explore whether the construction of a production plant is profitable or not. Simulation tools, such as Aspen HYSYS, provide the tools for this kind of calculation: the equilibrium reactor or the Gibbs reactor. Both obtain chemical reaction equilibrium by minimizing Gibbs free energy at the specified temperature and pressure, displaying the theoretical maximum production. However, this does not account for the real conditions in a reactor such as temperature, pressure and velocity gradients. This work is a continuation of the differential Gibbs and Helmholtz reactors presented by Solsvik et al. [1], where the idealized plug flow reactor, e.g. Fogler [2], with ideal gas conditions were used to illustrate a chemical reactor combined with the thermodynamic equilibrium condition, i.e. minimum Gibbs energy [3]. The reactor displays a maximized production at each point throughout the reactor, giving insight on both the deviation from optimality as well as how high/low the temperature can get at its extremes.

2. Methods

The idealized plug flow reactor model with Ergun's equation used by Solsvik et al. [1] is still used. The ideal gas model is used initially, and after successfully converging this problem, the model is extended to also consider equations of state for non-ideal gas behavior. This affects both the reactor models as well as the thermodynamic equilibrium calculation. The simulations are repeated for several chemical systems, numerical schemes and for both the differential Gibbs and Helmholtz reactors. The results are then compared to classical reactor models with rate expressions to see how the compositions differ throughout the reactor. The numerical scheme chosen will impact the complexity of the algorithm for solving the reactor model and, hence, the choice of energy surface to minimize, e.g. Gibbs or Helmholtz energy.

3. Results and discussion

Results presented here include the production of methanol from synthesis gas, a mixture of H_2, CO and CO_2. Results obtained with the differential Gibbs reactor are presented below. As seen, the immediate equilibrium next to the inlet yields a steep rise in temperature. The exothermic reaction also makes the density drop, which by continuity makes the velocity rise. The methanol production is however inhibited by the high temperature, and hence, the mole fraction of methanol is not at its maximum value. As the reactor is cooled, the mole fraction slowly rises, and at approximately 4 meters, the value stabilizes. The density rises to this point as well, causing the velocity to drop. After 4 meters, only the pressure drop from Ergun's equation affects the velocity and density to some degree. However, this has no significant impact on the equilibrium composition, since the pressure drop is relatively small.

The apparent bump in carbon dioxide mole fraction is caused by the following reaction reversing:

$$CO_2 + 3H_2 = CH_3OH + H_2O$$

while the following reaction is shifted towards right:

$$CO + H_2 = CH_3OH$$

Therefore, only the mole fraction of H_2O and CO_2 is visually apparent.

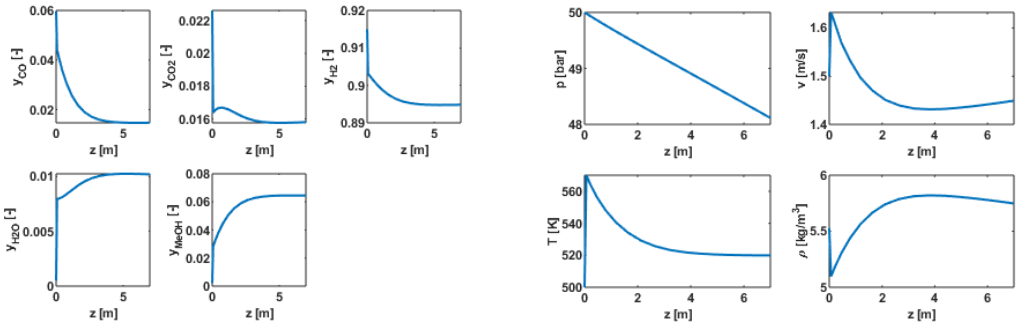

4. Conclusions

The model considered suggests an approach for combining fluid flow with thermodynamic equilibrium. The thermodynamic part is a useful tool in the lack of reaction rate kinetics and in a process design feasibility study, while the fluid dynamic part retains the effects of fluid flow. The profiles from the fluid dynamic part can also be used to characterize worst-case scenarios, such as steep temperature rise, and therefore in risk assessment and online operation, making the model a proactive choice.

References

[1] Solsvik, J., Haug-Warberg, T., & Jakobsen, H. A. (2016). Implementation of chemical reaction equilibrium by Gibbs and Helmholtz energies in tubular reactor models: Application to the steam-methane reforming process. Chemical Engineering Science, 140, 261–278. https://doi.org/10.1016/j.ces.2015.10.011

[2] Fogler, H. S. (2016). Elements of chemical reaction engineering. Boston: Prentice Hall.

[3] Haug-Warberg, T. (2006). Den termodynamiske arbeidsboken (1st ed.). Fornebu: Kolofon Forlag AS.

ECCE12
The 12th EUROPEAN CONGRESS OF CHEMICAL ENGINEERING
Florence 15-19 September 2019

Influence of operating parameters on the single pass removal efficiency during the photocatalytic degradation of acrylonitrile.

Henrietta Essie Whyte[1], Cécile Raillard[1], Albert Subrenat[1], Valérie Héquet[1]

1 GEPEA UMR CNRS 6144, IMT Atlantique, DSEE, 4 rue Alfred Kastler CS 20722, 44307 Nantes, France

**Corresponding author: Valerie.hequet@imt-atlantique.fr*

Highlights

- Single-pass removal efficiencies can be improved according operating parameters
- A complete mineralization can be reached irrespective of initial pollutant concentration
- Conversion vs. mineralization rates show the probable formation of intermediates

1. Introduction

The hospital is a place where the air quality is very important as it plays an important role in the health of both patients and hospital staff. Microbial contamination in relation to nosocomial infections has been at the fore front of hospital air quality whilst chemical contamination is rarely studied [1]. One of the most demanding areas in terms of the air quality is the operating room (OR). Surgeons and operating theatre staff are routinely exposed to pollution from the surgical smoke. The chemicals present in greatest quantity in surgical smoke are hydrocarbons and nitrile compounds among which is acrylonitrile. Barret and Garber [2] reported acrylonitrile concentrations to be between 1 and 1.6 ppm. In ORs air quality is assured mostly by HVAC. However, this is not always enough thus additional treatment devices can be used to purify air. Stand-alone devices that use photocatalytic oxidation (PCO) are becoming increasingly popular to treat indoor air. The aim of this work is to assess if PCO is efficient for removing acrylonitrile and to study the influence of three operational parameters (air velocity, light intensity and initial concentration) on the photocatalytic removal efficiency of acrylonitrile.

2. Methods

A 420 L multi-pass dynamic photocatalytic reactor was used to carry out the PCO experiments. It has been described and modelled in a previous articles [3],[4]. The media used was supplied by Saint-Gobain Quartz (QUARTZEL®) and consisted of quartz fibers coated with TiO_2 deposited through a sol-gel method. The media was irradiated with two 18-W UVC fluorescent tubes (Phillips PL-L series). Acrylonitrile was supplied from a certified commercial gas cylinder produced by Air products. The cylinder contained 150 ppm of acrylonitrile balanced in nitrogen at a pressure of 150 bars. The selected average light intensities (I) ranged from 1 to 4.5 $mW.cm^{-2}$. The air velocities corresponding to the selected flow rates (73 - 216 $Nm^3.h^{-1}$) varied from 0.5 to 1.5 $m.s^{-1}$ and were determined as the ratio between the air flow rate and the cross-sectional area (0.04 m^2) of the photocatalytic module. Initial concentrations (C_0) chosen for the experiments ranged from 0.5 to 10 ppm which were representative of concentrations reported in the literature. The relative humidity (RH) was maintained at 50% at 20°C to be representative of average humidity levels found in operating rooms in European countries.

3. Results and discussion

First results showed that acrylonitrile is degraded within 1h based on the experimental conditions of C_0=2ppm, v=1 m.s^{-1} and I = 4.5mW.m^{-2} (Fig. 1). It was observed that the degradation followed a first order kinetic. The experimental points were then fitted to the model developed by Dumont and Héquet. The model describes the first order decay relationship of concentration vs. time and helps to determine the single pass removal efficiency. It is as follows:

$$\mathbf{C} = \boldsymbol{C_0}\,\mathbf{exp}\left\{-\frac{\boldsymbol{t}}{\boldsymbol{\tau_R}}\Big|[\mathbf{1}-\mathbf{exp}(-\boldsymbol{\alpha})]\right\} \qquad \textbf{(1)}$$

In Eqn. 1 the term α is the single pass removal efficiency and represents the fraction of the total flow treated during the time τ_R (residence time in the reactor). C is the pollutant concentration at time t and C_0 is the initial pollutant concentration. Numerical resolutions are carried out using Excel® Solver which is based on the least- square method.

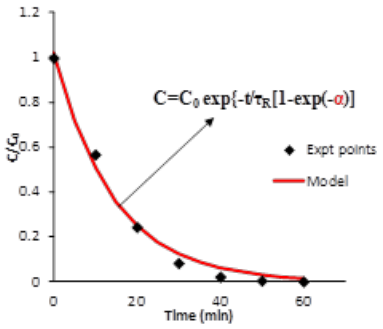

Figure 1. Experimental degradation curve of acrylonitrile fitted to model (C_0 = 2 ppm; v = 1 m.s^{-1}; I = 4.5 mW.cm^{-2}).

4. Conclusions

Conclusively, PCO is able to degrade acrylonitrile. The experimental points are well fitted to the model and enable the calculation of the one-pass removal efficiency. Since the global objective is to study the effect that the operating parameters have on the single pass removal efficiency, experiments are conducted at the selected air velocities, light intensities and initial concentrations to determine their influence.

Acknowledgements: the authors thank ATA Medical company and IMT-Atlantique for their financial support.

References

[1] C.-C. Jung, P.-C. Wu, C.-H. Tseng, H.-J. Su, Indoor air quality varies with ventilation types and working areas in hospitals, Build. Environ. 85 (2015) 190–195.
[2] W.L. Barrett, S.M. Garber, Surgical smoke: a review of the literature, Surg. Endosc. Other Interv. Tech. 17 (2003) 979–987.
[3] A. Maudhuit, C. Raillard, V. Héquet, L. Le Coq, J. Sablayrolles, L. Molins, Adsorption phenomena in photocatalytic reactions: The case of toluene, acetone and heptane, Chem. Eng. J. 170 (2011) 464–470.
[4] É. Dumont, V. Hequet, Determination of the Clean Air Delivery Rate (CADR) of Photocatalytic Oxidation (PCO) Purifiers for Indoor Air Pollutants Using a Closed-Loop Reactor. Part I: Theoretical Considerations, Molecules. 22 (2017).

ECCE12
The 12th EUROPEAN CONGRESS OF CHEMICAL ENGINEERING
Florence 15-19 September 2019

Reductive amination in different solvent systems: reaction network analysis and kinetics

Sabine Kirschtowski[1], Christof Kadar[2], Andreas Seidel-Morgenstern[1,3], Christof Hamel[4]

1 Otto von Guericke University, Institute of Process Engineering, Magdeburg, Germany
2 Nuremberg Institute of Technology, Faculty of applied Chemistry, Nuremberg, Germany
3 Max Planck Institute for Dynamics of Complex Technical Systems, Magdeburg, Germany
4 Anhalt University of Applied Sciences, Processing Engineering, Köthen, Germany
**Corresponding author: sabine.kirschtowski@ovgu.de*

Highlights

- Formulation of a reaction network for the reductive amination
- Good performance of the RA in homogeneous and thermomorphic solvent systems
- Kinetic description of the RA in two different solvents

1. Introduction

The Collaborative Research Center Transregio 63 of the German Research Foundation (DFG) develops methods and strategies to adapt established reactions to substrates from renewable raw materials. Focus of this project is the evaluation of the potential of complex homogeneously catalyzed tandem reactions using the example of the rhodium-catalysed hydroaminomethylation (HAM) of 1-decene. This reaction offers a direct and efficient synthesis of various pharmaceuticals, natural products, agrochemicals and fine chemicals [1]. To acquire detailed knowledge regarding the overall reaction the sub-network of the reductive amination (RA) step is analysed separately.
To recover the expensive Rh-catalysts from the homogeneous reaction solution thermomorphic solvent systems (TMS) are applied. In TMS the separation between products and catalysts is realized by using temperature dependent miscibility gaps in mixture of solvents of different polarity [2]. With regard to process development and optimization detailed knowledge of the reaction rates is necessary. We will report about a kinetic model to describe the reactions in homogeneous solvents and the transferability to TMS systems.

2. Methods

RA experiments were conducted in a high-pressure batch reactor system equipped with a gas supplying system and pressure and temperature controllers. The RA was investigated in three different solvent systems (2 homogeneous, 1 TMS) considering the reactants undecanal and diethylamine (DEA) ($c_{undecanal}$ = 0,18 mol/L, n_{DEA}:$n_{undecanal}$=4:1 and 1:1). The homogeneous solvent systems constituted of isopropyl or methanol (with 1 wt-% dodecane as internal standard respectively), whereas the TMS constituted of methanol and dodecane (w_{MeOH} : $w_{dodecane}$ = 50 : 50). The ligands triphenylphosphine (TPP) and Xantphos (XPH) were investigated, so that the catalyst is formed by Rh(acac)COD and the corresponding ligand (n_{Rh}:n_P:$n_{undecanal}$ = 1:2:1000). Kinetic experiments were carried out in the temperature and H_2 pressure ranges between 85°C…115°C and 10 bar…30 bar, respectively.

3. Results and discussion

Based on the experimental results a reaction network for the reductive amination is postulated considering four groups of compounds (Figure 1): the desired product n-amine, the intermediate n-enamine and the side products n-alcohole and aldole.

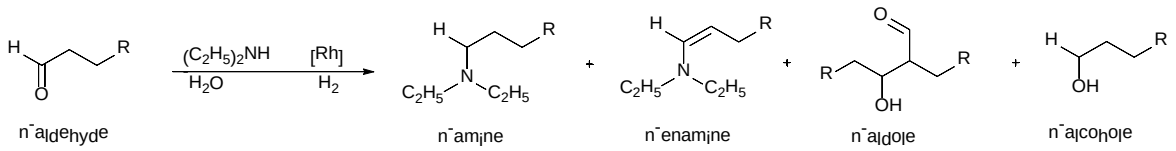

Figure 1. Main and side products of the rhodium-catalysed reductive amination of a linear aldehyde

Concerning the RA performed in methanol with the ligand XPH significant conversion X of the reactant and a high yield Y with respect to the n-amine were observed after 120 min ($X_{undecanale}$ = 100 %, Y_{amine} = 91 %, Figure 2a). The RA carried out in isopropyl revealed a different behavior. With the ligand TPP the reactant conversion is significantly lower ($X_{undecanal}$ = 90 %) and the yield is only Y_{amine} = 63 % (Figure 2b). In this case the hydrogenation of the enamine to the amine is clearly inhibited. The reductive amination carried out in the TMS methanol:dodecane = 50:50 showed similar conversions ($X_{undecanal}$ = 100 %) and yields (Y_{amine} = 85 %) as for the homogeneous solvent methanol.

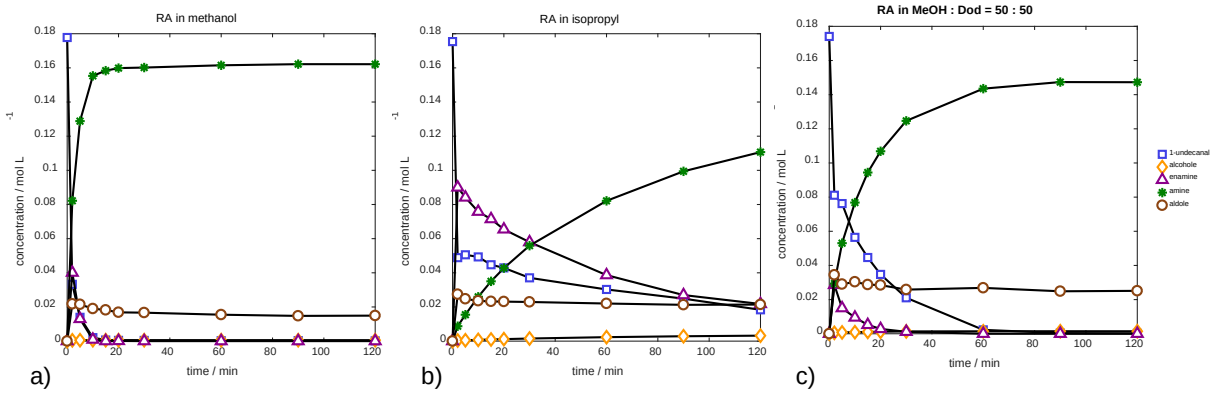

Figure 2. Reductive amination of 1-undecanale at T = 100 °C, p_{H2} = 20 bar. a) in methanol with XPH, DEA:Sub = 4 b) in isopropyl with TPP, DEA:Sub = 4 c) in TMS (MeOH:dodecane = 50 : 50) with XPH, DEA:Sub = 1

4. Conclusions

To describe the experimentally observed trends with a suitable kinetic model, the influence of the solvent composition needs to be considered. Currently the inhibition of the hydrogenation of the enamine to the amine is quantified in more detail in order to provide a quantitative kinetic model for the reaction carried out in the TMS.

References

[1] P. Eilbrecht et al., *Chem. Rev.* **1999**, 11, 3329-3366

[2] T. Gaide, A. Jörke, K.E. Schlipköter et al., *Appl. Catal. A* **2017**, 532, 50-56

ECCE12
The 12th EUROPEAN CONGRESS OF CHEMICAL ENGINEERING
Florence 15-19 September 2019

Utilization of extraction methods for practical applications

Stanislav Sabata[1], Milena Rouskova[1], Ywetta Maleterova[1], Jiri Hanika[1], Olga Solcova[1], Milena Stranska[2]

1 Institute of Chemical Process Fundamentals of the CAS, v.v.i., Prague 6, Czech Republic;

2 University of Chemistry and Technology Prague, Prague 6, Czech Republic

**Corresponding author: sabata@icpf.cas.cz*

Highlights

- Recovery of biomass components was studied.
- Extraction techniques for the isolation of valuable substances (antioxidants, carotenoids, waxes, fragrances) from plant sources was developed.
- Waste-less treatment is nowadays required for sustainable economy

1. Introduction

Bio-refining is a perspective branch that focuses on the development of separation methods for recovery of valuable substances from biomass or also for the processing of bio-waste from agriculture. The goal of the research was to propose a procedure for the waste-less treatment of plant material or the acquiring of health-beneficial substances suitable as e.g. dietary supplements.

2. Methods

Two ways of separating the monitored components from the solid matrix into a liquid solvent were tested. The first one was the extraction using Soxhlet´s apparatus, a highly efficient multistage process. The second more gentle process was a single-stage extraction in a stirred system at room temperature in an absence of light under inert atmosphere. From analytical methods mainly (U-)HPLC/MS was applied. The antioxidant activity of waste marc was determined using three methods: ABTS, DPPH and Folin-Ciocalteu.

3. Results

The aim of the study was the development of extraction technique for the isolation of carotenoids from medicinal plants (*Calendula officinalis, Tagetes sp.*), the separation of waxes from *Miscanthus sp.* stalks or the obtaining of fragrances from *Magnolia* × *pruhoniciana* blooms. From the waste biomass, the residual fresh marc after vine grapes pressing was processed to obtain resveratrol and other substances with antioxidant activity.

Raw processed biomass is shown on Figure 1.

Figure 1. Processed biomass. *Calendula* (a), *Tagetes* (b), *Miscanthus* (c), marc of white and red grapes (d), *Magnolia* × *pruhoniciana* blooms (e).

4. Conclusions

Carotenoids, especially lutein, contained in larger quantities in *Calendula* and *Tagetes*, are used as a component of poultry feed or as a dye in food supplements. It plays an important role in human nutrition as it has antioxidant effects in neutralizing free radicals causing degenerative changes in the retina.

Tall stems of *Miscanthus* contain a broad spectrum of various substances being potentially exploitable in cosmetics. Waste biomass has, after being pressed into the form of pellets, the potential for energetic utilization as “green fuel”.

Wine grape marc as an agricultural waste was tested on the antioxidant activity and resveratrol content. It is a rich source of polyphenolic substances with the influence on heart and blood vessel diseases.

Fragrant essences obtained by extracting fresh flowers of *Magnolia* × *pruhoniciana* have been tested as face creams and fragrant ingredients and they could be useful for other various cosmetic products.

All processes were designed to maximize the biomass utilization with a view to waste-less eco-recovery of valuable bio-material substances.

Acknowledgement

Financial support of the Technology Agency of the Czech Republic the Competence Centre BIORAF (project No. TE01020080) and the National Competence Centre Biocirtech (project No. TN010000048) is acknowledged

ECCE12
The 12th EUROPEAN CONGRESS OF CHEMICAL ENGINEERING
Florence 15-19 September 2019

Hydrodeoxygenation of bio-oil model compounds over the nickel phosphide catalysts

Jundong Wang[1], Lokmane Abdelouahed[2], Luis Reyes[3], Bechara Taouk[4]

1-5-Normandie Univ, INSA Rouen Normandie, UNIROUEN, Laboratoire de Securité des Procédes Chimiques (LSPC EA 4704)

** bechara.taouk@insa-rouen.fr*

Highlights

- Detailed analysis of gas and liquid product of hydrodeoxygenation of model compounds
- Hydrodeoxygenation of model compounds
- Effect of temperature on hydrodeoxygenation of model compounds

1. Introduction

Multifarious efforts have been focused on the production of renewable and clean biofuels and chemicals to meet growing energy demand and environmental and sociopolitical concerns arising from a current heavy global dependence on fossil fuels. Biomass is considered as sustainable and abundant feedstock which can be effectively converted into liquid fuels via fast pyrolysis technologies. Unfortunately, although fast pyrolysis is a promising method to obtain bio-oil, the high content of oxygenated molecules (ketones, aldehydes, organic acids, furans, phenolic derivatives and lignin-derived oligomers) decrease its chemical and thermal instability [1]. It is unsuitable for direct use as a transportation fuel (or as a fuel additive) because of its low heating value and high corrosiveness caused by the presence of significant oxygenated compounds. These organic compounds are highly reactive, promoting the formation of ethers, acetals, hemiacetals and heavier organics through condensation reactions, resulting in some problem in bio-oil application, for example, coke formation. Therefore, it requires the investigators to improve the pyrolysis bio-oil to obtain an upgraded liquid fuel or some useful chemicals with proper properties which can be suitable for the global transport infrastructure.

In this paper, hydrodeoxygenation (HDO) experiments of the bio-oils model compounds upgrading reaction over the Ni_2P/HZSM-5 and Ni_2P/SiO_2 will be studied. Here presents an experimental study of influence of different reaction parameters, such as feedstock state, residence time, reaction temperature and reaction pressure (H_2 partial pressure) etc.

2. Methods

Supported nickel phosphide catalysts (Ni_2P/HZSM-5 and Ni_2P/SiO_2) were prepared by incipient wetness impregnation and a temperature programmed reduction (TPR). The XRD and elemental analyzer was used to characterize the catalysts. The model compounds feedstock (acetic acid, 4-Ethylguaiacol) vapor phase was introduced into a continuous fix-bed reactor under the high hydrogen pressure. The liquid phase feedstock had been conducted in a batch reactor. The gas

chromatography-mass spectrometer (GC-MS) and GC/FID will be used to analyzed the gas and liquid products to compare the results between different types of reaction.

3. Results and discussion

Figure 1 shows the main oxygenated compounds (CO, H_2O) content in the gas and liquid products of acetic acid HDO reaction. It indicated that the CO content in the gas products was decreased with the reaction pressure increasing. This can be explained by the promotion of the reaction CO and H_2 given that the H_2 partial pressure was increased. In addition, figure 1 also shows that the moisture content increase due to the increasing of reaction pressure. It means that more oxygen was removed by the hydrogenation reaction.

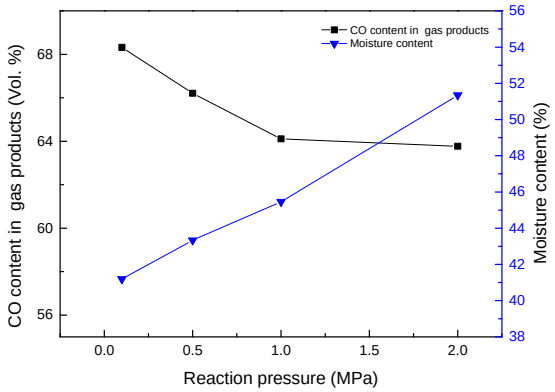

Figure 1. The CO content in gas products and moisture content in the liquid products under different reaction pressure.

4. Conclusions

In this work, the HDO reaction of different model compounds where studied in different experimental conditions (temperature, contact time and pressure) and catalysts. Results show that the pressure of hydrogen has a conspicuous influence on the HDO reaction. It had a promoted effect on the hydrogenation. The liquid products moisture was higher using the Ni_2P/HZSM-5 catalysts and relative lower using the Ni_2P/SiO_2 catalysts. It was possible that the conversion and products selectivity were higher when the HDO reaction took place in the continuous fix-bed reactor with the vapor phase hydrodeoxygenation of model compounds.

References

[1] A. Berenguer, James A. Bennett, Catalytic hydrodeoxygenation of m-cresol over Ni2P/hierarchical ZSM-5, Catalysis Today, 304, 2018, 72-79.

[2] N. Koike, S. Hosokai, Upgrading of pyrolysis bio-oil using nickel phosphide catalysts, Journal of Catalysis, 333, 2016, 115-126.

[3] M.V. Bykova, D.Yu. Ermakov, Ni-based sol–gel catalysts as promising systems for crude bio-oil upgrading: Guaiacol hydrodeoxygenation study, Applied Catalysis B: Environmental, 113-114, 2012, 296-307.

ECCE12
The 12th EUROPEAN CONGRESS OF CHEMICAL ENGINEERING
Florence 15-19 September 2019

Application of Near-Infrared Spectroscopy and Chemometrics for In-line real-time monitoring during a chlorophyll extraction process

Corro-Herrera, V.A.*[1], Aguilar-Uscanga, M.A[2]., Lienqueo, M.E.[1]

1 Centre for Biotechnology and Bioengineering (CeBiB); Institute for Cell Dynamics and Biotechnology (ICDB) Department of Chemical Engineering, Biotechnology and Materials, University of Chile, Beauchef 851, CP 8370456, Santiago, Chile.
2 Bioengineering Laboratory of Food Research and Development Unit; Veracruz Institute of Technology, Calzada M.A. De Quevedo 2779, Veracruz, CP 91860, Mexico.
**Corresponding author: corroherrera@gmail.com*

Highlights

- NIRS and Chemometrics applied to extraction process.
- Highly accurate prediction model. (R^2 = 0.967, SEP = 2.823 mg/L; ε = 5.04 %.
- The technical feasibility of the methodology was proved successfully.

1. Introduction

The applications and the importance of In-line real-time monitoring using Near-Infrared Spectroscopy (NIRS) and Chemometrics, as a Process Analytical Technology (PAT) in the Pharmaceutical and Food Industries, have increased through the years, due to their advantages and the results obtained (Scarff *et al*., 2006). Another interesting application for this technology is the chemical process of extraction. Liquid extraction using organic solvents is a very widespread technique for obtain molecules of industrial interest from biomass, *e.g.*, chlorophyll, that uses as colorant and additive. It is therefore interesting to search new sources of this molecule, one of this sources could be the pine needles, that left behind the forest exploitation, and have no apparent use. For this reason, the application of NIRS and Chemometrics for the real-time monitoring of chlorophyll extraction from pine needles is an alternative to improve the process and generate applicative knowledge.

2. Methods

Chlorophyll extraction process. Extractions were carried out according to the Lichtenthaler method (2001). Extraction conditions were optimizing with a Box-Behnken design, variables were: temperature (50 ºC), ethanol concentration (95 %) and time (240 min).
Reference method. Analyses were performed on an Agilent 1,100 liquid chromatographic system equipped with a diode-array UV/ vis detector. A 250 mm x 4.6 mm i.d., 5 µm particle size Inertsil ODS 2 column (Sugelabor) was used. Elution was performed at a flow rate of 1.0 mL/min at room temperature, using as the mobile phase a mixture (8:2 v/v) of methanol/water containing 0.025 % ammonium acetate and 0.05 % triethylamine as phase A and methanol/acetone (1:1 v/v) as phase B. Concentration is expressed in milligrams of chlorophyll by liter of extract.
NIRS measurements. Spectra were acquired with a Near-Infrared Spectrophotometer XDS Process Analytics (Foss- NIRSystems, Silver Spring, USA) using an in-situ fiber optic transflection probe, 3 mm pathlength. The samples were scanned in duplicate over the whole NIR range (800–2,200 nm)

every 20 min until the kinetic extraction was ended. The spectra were then averaged and derived (second derivative) in order to reduce the signal/noise ratio (Corro-Herrera *et al*., 2016).

Model development and validation. Linear models were constructed using Partial Least Squares Regression (PLSR 1). Ten extraction batches were used to collect the samples spectra. Development of all PLS models was carried out by Vision software (v 3.5, Foss-NIRSystems, Sylver Spring, USA). To avoid overfitting due to many factors or latent variables (LVs), the software predicts residual error sum of squares (PRESS) calculated from random subsets cross validation; a lower PRESS value indicates an adequate number of factors in the model. To assess the prediction capacity of the models, the coefficient of determination (R^2), standard error of calibration (SEC), standard error of prediction (SEP) and error (ε %) were used as quality parameters.

3. Results and discussion

Model quality parameters for calibration are R^2 = 0.974, SEC = 2.453 mg/L and for validation R^2 = 0.967, SEP = 2,823 mg/L; ε = 5.04 %. LVs = 4 (Figure 1a and 1b, respectively). Considering the SEC and SEP as first quality parameter, they are consistent according to the same magnitude order of the value. For R^2 of both, the values are close to the unit, showing the good correlation between the data and for validation.

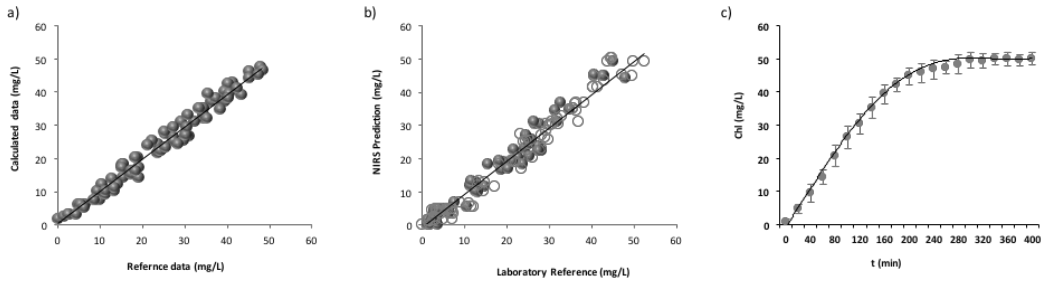

Figure 1. a) Calibration curve and b) Validation curve: (●) laboratory reference, (○) NIRS prediction. c) Real-time monitoring of chlorophyll concentration during the extraction, using the prediction model. (●) Experimental data, (—) prediction of the model.

Once the model was validated, it was now used to the real-time monitoring during the extraction process. 10 batches were carried out for collect the data shows in the Figure 1c. Fitting of the model is quite good with a R^2 =0.987. Chemometric model has the sufficient robustness to predict the concentration of chlorophyll throughout the process. Furthermore, this model fits to the variability of the process, and in addition to expresses the process kinetic behavior.

4. Conclusions

The technical feasibility of real-time monitoring through an immersion transflection probe, of chlorophyll extraction matrix, employing NIRS and Chemometrics, has been demonstrated. This assertion is based on the generation of a functional and robust prediction model for chlorophyll concentration, with R^2 values close to 1 and low SEC and SEP.

References

[1] M. Scarff, S.A. Arnold, L.M. Harvey, B. McNeil, Crit. Rev. Biotechnol. 26 (2006) 17-39.
[2] H. K. Lichtenthaler, C. Buschmann, Current Protocols in Food Analytical Chemistry. (2001) F4.3.1-F4.3.8.
[3] V. A. Corro-Herrera, J. Gómez-Rodríguez, P.M. Hayward-Jones, D.M. Barradas-Dermitz, M.G. Aguilar-Uscanga, Biotechnol. Prog. 32 (2016) 510-517.

ECCE12
The 12th EUROPEAN CONGRESS OF CHEMICAL ENGINEERING
Florence 15-19 September 2019

Combined Enzymatic Decarboxylation and Pd-catalyzed Heck Coupling in Continuous Flow

Bianca Grabner[1], Anna K. Schweiger[2], Kristian Gavric[1], Robert Kourist[2], Heidrun Gruber-Woelfler[1*]

1 Institute of Process and Particle Engineering, Graz University of Technology, Graz, Austria
2 Institute of Molecular Biotechnology, Graz University of Technology, Graz, Austria

**Corresponding author: woelfler@tugraz.at*

Highlights

- A fully integrated two-step flow process combining metal- and biocatalysis
- Use of deep eutectic solvent (DES) to overcome the problem of solvent compatibility
- Full conversion for both decarboxylation and subsequent Heck coupling
- The two-step process was successfully operated for more than 16 h

1. Introduction

Tandem-catalytic reactions are promising routes for the synthesis of high-value products in fine-chemical, agrochemical and pharmaceutical industry. Therefore, they have attracted the attention of researchers in the past decade. [1] Based on recent findings [2], in this work we present a fully integrated two-step flow setup consisting of an enzymatic decarboxylation followed by a Heck reaction coupling the decarboxylation product to an aryl halide as shown in Figure 1 to synthesize asymmetric stilbene derivatives. The most prominent derivatives of stilbenes are resveratrol and its analogues. Their conjugated double bond system gives the molecule anti-oxidant, anti-inflammatory, antidiabetic, antiaging and anticancer properties. [3]

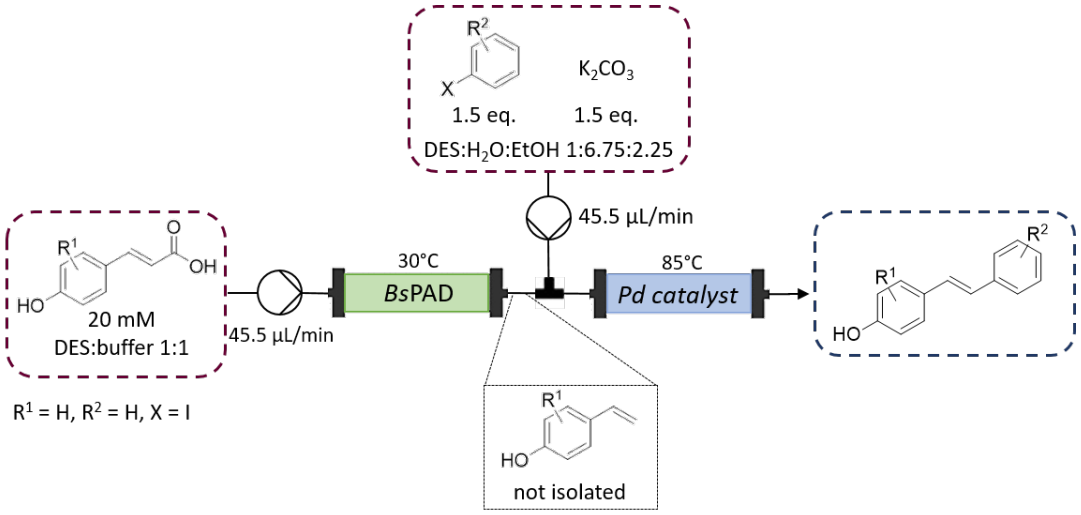

Figure 1. General reaction scheme for enzymatic decarboxylation with a phenolic acid decarboxylase from *Bacillus subtilis* (*Bs*PAD) yielding a 4-hydroxystyrene derivative, which serves as substrate for a Pd-catalyzed cross-coupling reaction with an aryl halide, resulting in a 4-hydroxystilbene product.

2. Methods

A cell-free extract (CFE) of phenolic acid decarboxylase from *Bacillus subtilis* (*Bs*PAD) was immobilized in 2 % alginate beads and employed in a 1:1 (v/v) mixture DES (Choline chloride:glycerol 1:2 (mol/mol)) with potassium phosphate buffer (50 mM, pH 6.0) to decarboxylate *para*-coumaric acid. [4] For the second step, the Heck coupling of the decarboxylation product to iodobenzene, an in-house developed heterogeneous Pd-catalyst (Pd-substituted cerium-tin-oxide with the composition $Sn_{0.79}Ce_{0.29}Pd_{0.01}O_{2-\delta)}$ was applied. [5] The reaction was conducted in a solvent mixture of DES (30 vol%), buffer (25 vol%), ethanol (34 vol%), and water (11 vol%) For the continuous mode, both catalysts were packed in stainless steel columns and heated to 30 °C (PAD) and 85 °C (Pd-catalyst) in a water bath, respectively.

3. Results and discussion

The residence time in the reactors was calculated to be 30 min for the decarboxylation and 45 minutes for the Heck coupling. The conversion of the first step could be followed visually as CO_2 bubbles left the reactor as soon a full conversion of the substrate was achieved. In continuous mode, full conversion was reached for both decarboxylation and Heck coupling. The two-step process was successfully operated for more than 16 h. While the continuous mode allowed to conduct both reaction at their optimal temperature, DES proved to be a solvent compatible with both reactions.

4. Conclusions

These results are important steps towards chemo-enzymatic reactions in continuous flow and should be further investigated in the near future. The results show the importance of DES to overcome obstacles like substrate solubility and solvent compatibility in chemo-enzymatic tandem reactions.

References

[1] a) F. Rudroff, M. D. Mihovilovic, H. Gröger, R. Snajdrova, H. Iding, U. T. Bornscheuer, Nat. Catal. 1 (2018) 12-22; b) J. Enoki, C. Mügge, D. Tischler, K. Miyamoto, R. Kourist, Chemistry 25 (2019) 5071-5076; c) S. Schmidt, K. Castiglione, R. Kourist, Chem. Eur. J. 24 (2018) 1755-1768; d) J. M. Sperl, J. M. Carsten, J.-K. Guterl, P. Lommes, V. Sieber, ACS Catal. 6 (2016) 6329-6334.

[2] Á. Gómez Baraibar, D. Reichert, C. Mügge, S. Seger, H. Gröger, R. Kourist, Angew. Chem. Int. Ed. 55 (2016) 14823-14827.

[3] a) H.-Y. Tsai, C.-T. Ho, Y.-K. Chen, J. Food. Drug. Anal. 25 (2017) 134-147; b) W. Nawaz, Z. Zhou, S. Deng, X. Ma, X. Ma, C. Li, X. Shu, Nutrients 9 (2017); c) M. Savio, D. Ferraro, C. Maccario, R. Vaccarone, L. D. Jensen, F. Corana, B. Mannucci, L. Bianchi, Y. Cao, L. A. Stivala, Sci. Rep. 6 (2016) 19973.

[4] a) Z. Maugeri, P. Domínguez de María, ChemCatChem 6 (2014) 1535-1537; b) J. Paris, N. Ríos-Lombardía, F. Morís, H. Gröger, J. González-Sabín, ChemCatChem 10 (2018) 4417-4423; c) L. Cicco, N. Ríos-Lombardía, M. J. Rodríguez-Álvarez, F. Morís, F. M. Perna, V. Capriati, J. García-Álvarez, J. González-Sabín, Green Chem. 20 (2018) 3468-3475

[5] a) G. J. Lichtenegger, M. Maier, J. G. Khinast, H. Gruber-Wölfler, J. Flow Chem. 6 (2016) 244-251; b) G. J. Lichtenegger, M. Maier, M. Hackl, J. G. Khinast, W. Gössler, T. Griesser, V.S.P. Kumar, H. Gruber-Woelfler, P. A. Deshpande, J. Mol. Catal. A-Chem 426 (2017) 39-51.

ECCE12
The 12th EUROPEAN CONGRESS OF CHEMICAL ENGINEERING
Florence 15-19 September 2019

Yeast biomass as biotechnological strategy for detoxification of hemicellulosic hydrolysate of sugarcane byproducts for xylitol production

Fanny Jofre[1], Sarah Queiroz[1], Andres Hernandez-Perez[1], Henrique dos Santos[1], Júlio dos Santos[1], Maria das Graças de Almeida Felipe[1].

[1] *Escola de Engenharia de Lorena da Universidade de São Paulo EEL-USP, Departamento de Biotecnologia, Estrada Municipal do Campinho, s/n, CEP 12602810, Lorena, SP, Brasil.*

**Corresponding author: mgafelipe@usp.br*

Highlights

- Xylitol production using yeast biomass as detoxification agent.
- Use of sugarcane bagasse and straw for biotechnological production of xylitol.
- Yeast biomass is a promisor raw material for detoxification procedures.

1. Introduction

New technologies which use the exploitation of lignocellulosic materials have been contributed for the development of bioprocesses in the context of biorefineries for example the sugar and alcohol sector. The production of biomolecules from its constituent fraction in this material such as hemicellulose have been studied for example xylitol [1, 2, 3]. Xylitol is a sugar-alcohol important in industry of food, pharmaceutical, cosmetic and odontological), which industrial production occurs by chemical route. Investigations have been done for development of technology of its biotechnological production and it was also stablished parameters such as pH, temperature, aeration. The detoxification before fermentation is required in function of toxic compounds resultant from plant cellular wall deconstruction usually done by diluted acid hydrolysis [4]. Usually detoxification is made with vegetal activated charcoal which contributes for the reduction of toxic content of the hydrolysate such as phenolic compounds [5]. Alternative for charcoal can be proposed as exploitation of residual cellular biomass from the production process of xylitol. The use of non-viable microbial cells in detoxification has as objective its utilization as adsorbent, which can occur the interactions between toxic compounds (adsorbate) and functional groups of the cell and/or its cellular wall (adsorbent) [6]. This research proposes the use of yeast cellular biomass of *Candida guilliermondii* FTI 20037 as detoxification agent of hemicellulosic hydrolysate from the mixture of sugarcane bagasse and straw for xylitol biotechnological production.

2. Methods

The hemicellulosic hydrolyzate from the mixture of sugarcane bagasse and straw (HHSBS) was obtained by diluted acid hydrolysis (1% w/v of H_2SO_4) [5] followed by vacuum concentration to increase its sugars content. For detoxification it was used residual dry biomass of *Candida guilliermondii* FTI 20037 from a previous xylitol production in HHSBS. The detoxification process occurs in HHSBS (adjusted pH for 2), 5% (w/v) dry biomass of *Candida guilliermondii*, temperature 30°C, in Erlenmeyer flasks at 100 rpm to 24 hours. The control with activated charcoal 1% (w/v), pH 2.5, 60°C for 30 minutes was also realized [5]. The fermentation occurred in detoxified hydrolysates,

with addition of nutrients (gL^{-1}): solution of rice bran extract (20), $(NH_4)_2SO_4$ (2), $CaCl_2 \cdot 2H_2O$ (0.1), for 46 hours. The determination of sugar concentration in hydrolysate was done by liquid chromatography, while phenolics by spectrophotometry [2].

3. Results and discussion

In the Table 1 are shown the results of fermentation of HHSBH with the use of dry biomass of *Candida guilliermondii* FTI 20037 as detoxifying agent as well the use of activated charcoal. The use of dry biomass of *Candida guilliermondii* residual of xylitol bioproduction indicates its potential as detoxification agent since removed 27% of phenolic compounds present in HHSBH compared with 40% when used activated charcoal. According the values shown in Table 1 the maximum value of yield and productivity was achieved in 46 hours, which were for yield ($g.g^{-1}$) 0.83 and 0.66; and productivity ($g.L^{-1}.h^{-1}$) of 0.46 and 0.63, for HHSBS detoxified with dry biomass and activated charcoal, respectively.

HHSBS detoxified with yeast biomass					
Time (h)	Biomass (gL^{-1})	Xylose consumption (%)	Xylitol (gL^{-1})	Y p/s (gg^{-1})	Qp ($gL^{-1}h^{-1}$)
22	7.15	14.85	6.97	0.19	0.42
46	9.95	48.69	21	0.83	0.46
70	13.37	81.74	29.45	0.69	0.42
HHSBS detoxified with activated charcoal					
Time (h)	Biomass (gL^{-1})	Xylose consumption (%)	Xylitol (gL^{-1})	Y p/s (gg^{-1})	Qp ($gL^{-1}h^{-1}$)
22	6.93	33.53	9.37	0.47	0.43
46	9.97	74.06	28.87	0.66	0.63
70	12.96	89.24	34.14	0.65	0.49

Table 1. Fermentative parameters from xylitol production by *Candida guilliermondii* FTI 20037 grown in HHSBS detoxified with dry cell biomass or activated charcoal.

4. Conclusions

The utilization of residual dry biomass from xylitol bioproduction in hemicellulosic hydrolysate of sugarcane bagasse and straw has potential to be used as detoxificant agent of this hydrolysate as economical strategy in relation to activated charcoal usually used in this bioprocess, besides the capacity of remove the toxics and promising fermentative parameters reached.

References

[1] P.V. Arruda et al. Journal of Industrial and Engineering Chemistry, 47 (2017) 297-302.
[2] T. Silva-Fernandes et al, Bioresource Technology, 243 (2017) 384-392.
[3] A.F. Hernandez-Perez et al, Bioresource Technology, 200 (2016) 1085-1088.
[4] M.G.A. Felipe in: B. Saha, K. Hayashi (Eds) Lignocellulosic biodegradation, (2004) 300-315.
[5] Marton et al. Brazilian Journal of Chemical Engineering, 23 (2006) 9-21.
[6] M. Fomina, G.M. Gadd, Bioresource Technology, 160 (2014) 3-14.

ECCE12
The 12th EUROPEAN CONGRESS OF CHEMICAL ENGINEERING
Florence 15-19 September 2019

Kinetics and mass transfer for biomass reductive catalytic fractionation

Alexei Kramarenko, John van der Schaaf, *Fernanda Neira d'Angelo**

Eindhoven University of Technology

** M.F.Neira.dAngelo@tue.nl*

Highlights

- Biomass reductive catalytic fractionation is studied in a flowthrough reactor
- A kinetic model that successfully fits the experimental data is proposed
- The different reaction steps are studied step-wise by using both native lignocellulose as well as monomer model compounds

1. Introduction

Lignin is one of the main components of biomass, together with cellulose and hemicellulose. Despite its rich chemical structure and high aromatic content, it is the most underutilized fraction of biomass. This is due to the severe degradation of lignin during biomass fractionation. Innovative fractionation approaches such as reductive catalytic fractionation (RCF) enable the valorization of lignin by preserving the native structure of lignin. For optimal results during RCF (i.e., maximal yields of lignin-monomers), the RCF reactor should allow for a well-tuned balance between the following reaction steps: 1) lignin extraction from the biomass feedstock and depolymerization using liquid solvents (i.e., a solid-liquid process); and 2) immediate stabilization of lignin monomers using solid catalyst (i.e., a gas-liquid-solid process). Despite the promising results reported so far on RCF, understanding the dynamics of such complex multiphase system is very limited. By following a step-wise approach, we investigate the kinetics of the separate steps using lignocellulosic biomass and lignin-monomer model compounds. Integration of this kinetic information with multiphase transport rates, we propose a reactor model that can successfully predict product yield and product distribution as a function of various reaction parameters. Special emphasis is put on the effect of internal/external mass transfer under different operating conditions.

2. Methods

Experiments were carried out in a gas-liquid-solid fixed bed reactor containing a biomass bed and a metallic supported catalyst (Pd/C). The reactor was fed with cocurrent flows of hydrogen and liquid solvent. The studied experimental variables were: reaction temperature, catalyst weight, biomass particle size, residence time and gas/liquid flow ratio. The reaction samples were analyzed using HPLC, GC, GPC and NMR respectively. An heterogeneous 1-D steady state model of the reactor was built in MATLAB accounting for reaction kinetics and mass transfer between the different phases.

3. Results and discussion

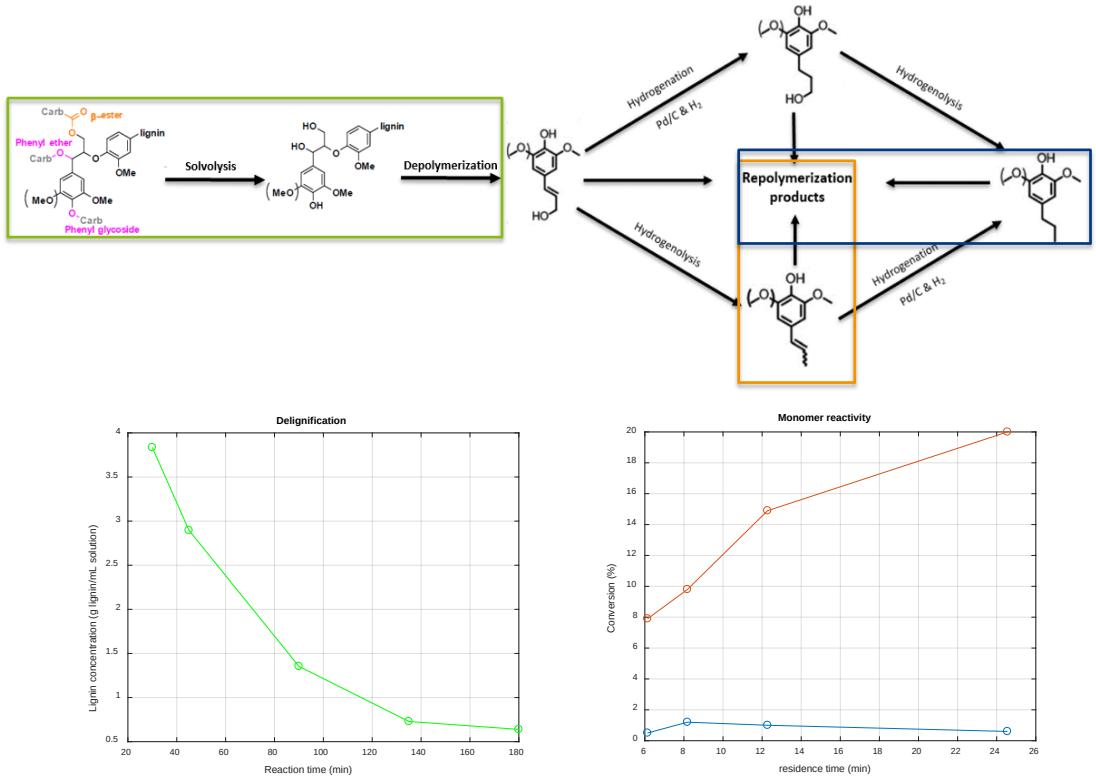

Figure 1: RCF reaction mechanism and experimental results corresponding to reactions (plot series colors match respective color boxes in the mechanism scheme)

4. Conclusions

This work provides a crucial understanding of the reaction mechanism. Kinetic parameters have been successfully extracted for the different steps of the complex reaction scheme, as well as relevant insights in the different mass transfer steps involved. The reactor model can successfully predict the experimental data, constituting a powerful tool for further process optimization

References

[1] T. Renders, a E. Cooreman, B. F. Sels, 2018. Catalytic lignocellulose biorefining in n-butanol/water: a one pot approach toward phenolics, polyols, and cellulose. Green Chem. 20, 4607-4619

[2] J. Zakzeski, P. Bruijnincx, A. Jongerius, B. Weckhuysen, 2010. The Catalytic Valorization of Lignin for the Production of Renewable Chemicals. *Chem. Rev.* 110 (6), pp 3552–35

ECCE12
The 12th EUROPEAN CONGRESS OF CHEMICAL ENGINEERING
Florence 15-19 September 2019

Energy efficient bulk polymerization

Roland Kunkel)*, Dr. Daniel Witte

LIST Technology AG Berstelstrasse 23 CH 4422 Arisdorf Switzerland

**Corresponding author: roland.kunkel@list.ch*

Highlights

- Solvent free Polymerization
- Devolatilization to 300 ppm
- Process Simulation

1. Introduction

The goal of most polymerization processes is to create a high molecular weight material with a specific structure. However, these polymerization processes are often highly exothermic and the final polymer is very viscous. The conventional production process for polymers requires large volumes of excess solvent and / or monomer to absorb the heat of reaction and to dilute the polymer to a low viscosity that can be processed. The LIST Kneader are able process extremely viscous materials, while adding or removing large amounts of heat, and this makes them an ideal alternative to the conventional processes.

A typical process using LIST Kneader consists of two stages. The first stage LIST Kneader is used to polymerize the monomers and catalyst in a highly concentrated, solvent-free phase. Conversion rates of 90% to 99% can be easily reached. In the second stage Kneader, the polymer is directly devolatilized to a residual monomer content of 1000 ppm or lower.
Especially in exothermic bulk (co)- polymerization processes, the large heat exchange surface of LIST Kneader in combination with evaporative cooling helps to precisely control the product temperature. The unique geometry of the mixing elements provides constant surface renewal which optimizes the heat transfer while minimizing product accumulation and dead zones. High quality polymer can be produced with low remaining monomer without solvent.

2. Methods

During the polymerization, conventional stirred-tank reactors require solvents to transfer heat and facilitate mixing of the viscous mass. After polymerization, solvents – whose concentrations can reach 90% – must be removed. Additionally, the conversion rate is limited [1].
The Kneader however, is designed to operate without or with little solvent, reaching a polymer concentration between 40 and 99%. In the case of polymerization without solvent, the conversion rate can exceed 99%. The polymer mass can then be directly devolatilized, to 100 – 500 ppm or lower.

3. Results and discussion

The technology is suitable for solvent-free living and free-radical polymerization with a polydispersity index less than 2. The unique design of the kneader provides constant surface renewal that improves heat transfer, allows excellent temperature control, and minimizes the diffusion and mass transfer limitations – particularly effective for exothermic bulk the polymerizations. The conversion rate in the polymerization step is up to 98,5% and monomer content in the final product after the devolatilization reaches 100 to 500 ppm. For the devolatilization a simulation program is used to scale the industrial process units.

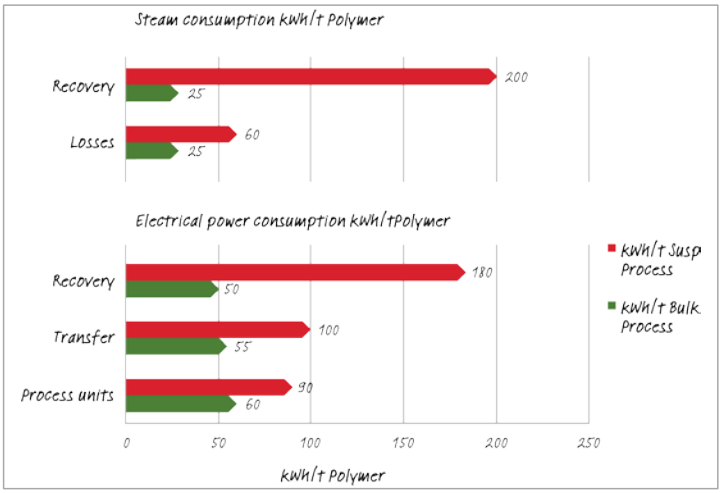

Figure 1. Energy consumption for the production of a meth acrylic polymer in bulk compared to suspension prcessing

The process intensification leads to savings in the entire process chain. Compared to the suspension polymerization, in bulk in total up to 65% of energy can be saved.

4. Conclusions

Due to this process intensification, process steps can be eliminated and the recovery step can be simplified. The result is a recreated or new process solution leading to the savings of raw material, operational costs, with improved product qualities and with a much smaller carbon footprint.

References

[1] Zahev Todmor, Costas G. PRINCIPLES OF POLYMER PROCESSING, Viley.com, ISBN 0-471-36770-3 pp 620-624

ECCE12
The 12th EUROPEAN CONGRESS OF CHEMICAL ENGINEERING
Florence 15-19 September 2019

Evaluation of extraction of fermentable sugars from banana peels (*Musa cavendish*)

María Lara Triana[1], Edna Méndez Mondragón[1], Dionisio Malagón-Romero[2*], Mauricio Bernal Morales[3], Dolly Montoya Castaño[3]

1 Semillero Procesos Industriales, Universidad ECCI; 2 Universidad Santo Tomás-Universidad ECCI; 3 Instituto de Biotecnología, Universidad Nacional de Colombia

**Corresponding author: dionisiomalagon@usantotomas.edu.co*

Highlights

- The banana peel is a waste rich in fermentable sugar.
- The best sugar extraction is with water.
- The extraction is not the best method to use all banana peel.

1. Introduction

Due to the high volumes of banana production in Colombia, large amounts of waste have been generated (97.8 million boxes by the end of 2017, which represents approximately 29.3 million waste generated) [1]. The banana peel is a valuable source of bioactive compounds according to researchers[2] and constituting 30%-40% of a banana fruit[3], thus it is necessary to develop new alternatives to convert this waste generated into value-added products. Due to the high amount of soluble sugars, recent researches have been showing that banana peel is used as substrate to produce animal feed, organic acids, bio fertilizer, industrial enzymes, medicinal uses and energies clean by biological processes[4]. Through the development of this project, it is desired to use this waste for the extraction of fermentable sugars which can be a useful source of sugars.

2. Methods

Banana Peel was washed, dried, ground, sieved, and then was subjected to a granulometric analysis. It was collected about 20 kg of waste in different plantations near Bogotá (Colombia). Waste collected was characterized for determining humidity content and dry matter using the procedure described in the literature consulted[5]. The morphology and the content of carbon, nitrogen, and oxygen were determined from scanning electron microscopy with energy dispersive X-ray spectrometry (SEM-EDS) of samples of the banana peel to obtain an approximate data. Finally, the extractions of sugar in the pretreated material was carried out by the alkaline hydrolysis, acid hydrolysis and with water, evaluating the temperature and concentration parameters in a reflux system. The design of experiment was done for the alkaline hydrolysis with NaOH where two temperatures (40°C and 70°C) and two concentrations of the base (1% and 2%) were evaluated. The extraction with water was done at the same temperatures, finally, the extraction with acid hydrolysis was carried out with HCl at a concentration of 0,29M at 40°C. Additionally, all samples were exposed during 90 minutes in duplicate to evaluate the kinetics of the process taken samples every 30 minutes. Samples were centrifuged, the sugar extracted was determined by DNS according to the guide protocol[6].

3. Results and discussion

The average particle size was 0.9727 mm ± 0.115 for the Banana peel. The banana peel have a high percentage of moisture (86.84 % ± 1.56). This value is similar to reported by Dormond [7]. The nitrogen present in the peel is about 9.26-9.36%, the oxygen is about 64.78-69.54% and the carbon is approximately 6.89-6.99%. The picture 1.d) shows the morphology of the different particles that appear with an irregular size. For the alkaline hydrolysis the best results were obtained at a concentration of 1% and a temperature of 40 °C as shown in Figure 1.a). The acid hydrolysis is shown in Figure 1.b). Results obtained have shown a better extraction compared to the alkaline extraction at 40 °C. In both hydrolysis shows a decrease in the sugar concentration over time this could be due to the denaturing of carbohydrates due to the high concentration. Finally, the extraction with water showed the best results in the hole experiment, as it shows the figure 1.c). The best condition was obtained at 70°C. For this extraction, it was calculated that 0.2 grams of sugar are obtained for each gram of processed banana peel and the total sugars obtained was 6.1252 g/L which is the expected because is similar with reported by Kurto• lu and Yildiz[8]. Between the extraction protocols observed, there are no significant differences in fermentable sugars extracted because the approximation of the maximum value is 6 g / L for all of them. However, the high extraction of fermentable sugars begins at zero minutes with water.

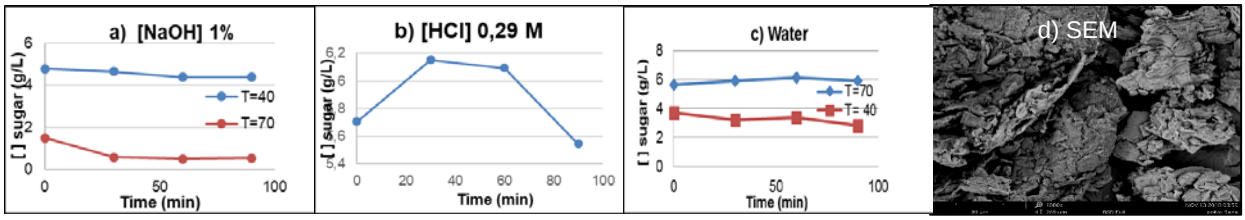

Figure 1. Kinetics of the different extractions.

4. Conclusions

It was observed that the amount of soluble sugars is higher with water compared with alkaline and acid treatment. Additionally, in alkaline conditions and water assays at initial time presents the higher extraction of fermentable sugars. These sugars could be used as substrate for fermentative process.

References

[1] G. Jaramillo and L. Zapata, "Aprovechamineto de los residuos sólidos orgánicos en Colombia," Universidad de Antioquia, 2008.

[2] P. D. Pathak, S. A. Mandavgane, and B. D. Kulkarni, "Fruit peel waste : characterization and its potential uses," vol. 113, no. 3, 2017.

[3] P. D. Pathak, S. A. Mandavgane, and B. D. Kulkarni, "Valorization of banana peel : a biorefinery approach," vol. 32, no. 6, pp. 651–666, 2016.

[5] B. K. Dadzie and E. Orchard, "Evaluación rutinaria postcosecha de híbridos de bananos y plátanos : criterios y métodos," *International Network for the improvement of Banana and plantain*. pp. 1–75, 1997.

[5] G. L. Miller, "Use of Dinitrosalicylic acid reagent for determination of reducing sugar," *Analytical chemestry*, vol. 31, no. 3, pp. 426–428, 1959.

[6] U. D. C. Rica *et al.*, "Evaluación preliminar de la cáscara de banano maduro como material de ensilaje, en combinación con pasto King Grass (Pennistetum purpureum. (Nota técnica)," p. 21, 2011.

[7] G. K. Ğ. Lu and S. Yildiz, "Extraction Of Fructo-Oligosaccaride Components From Banana Peels," vol. 24, no. 4, pp. 877–882, 2011.

ECCE12
The 12th EUROPEAN CONGRESS OF CHEMICAL ENGINEERING
Florence 15-19 September 2019

Catalytic Oxidation Kinetics of Arabinose on Supported Gold Nanoparticles.

Leolincoln Correia[1], Johan Wärnå[1], Henrik Grénman[1], Tapio Salmi[1], Dmitry Murzin[1*]

1 Laboratory of Industrial Chemistry and Reaction Engineering, Johan Gadolin Process Chemistry Centre (PCC), Åbo Akademi University, 20500 Turku, Finland

**Corresponding author: dmurzin@abo.fi*

Highlights

- A novel kinetic model for aqueous-phase arabinose oxidation on Au catalysts is proposed.
- Influence of oxygen flowrates, pH values and temperature was adequately described.
- The model shows adequate results for both D- and L-arabinose oxidation.

1. Introduction

In order to decrease the high dependency on fossil feedstock, lignocellulosic biomass has been considered as a renewable resource alternative. Representing 15-30% of the total lignocellulosic biomass, hemicelluloses are the second most abundant carbohydrate polymers [1-2]. Selective oxidation of sugars, such as arabinose, to their corresponding aldonic acids is one of the most important lignocellulosic biomass valorization processes. Several articles have demonstrated that supported gold nanoparticles as a sugar oxidation catalyst under alkaline conditions result in high selectivity towards aldonic acids [3,4,5,6]. In the previous work [3], kinetic data for oxidation of arabinose were generated and a kinetic model was developed. However, there were some systematic deviations in the description of the experimental data and the role of hydroxyl groups in the reaction kinetics was not explained and molecular adsorption of oxygen and contribution of different forms of sugar were not considered. The objective of this work is to revisit the data reported in ref. [3], evaluate the reaction kinetics and to propose a new kinetic model based on the plausible reaction mechanism for arabinose oxidation over gold supported on alumina.

2. Methods

All the experimental results, setup and catalyst characterization data concerning L-arabinose oxidation over supported gold catalyst used for modelling were obtained from the work of Kusema *et al*. [3,6]. In order to bring the reaction to a more practical level, an experiment in a standard batch reactor with D-arabinose was carried out. The novel model was developed taking into account the different forms of sugar in aqueous solutions, molecular adsorption of oxygen and production of H_2O_2. The set of differential equations representing concentrations of the reagents and products was solved numerically during the parameter estimation using the Levenberg-Marquardt or Simplex methods incorporated in the ModEst software [7].

3. Results and discussion

The fit of the proposed kinetic model to the experimental concentration profiles is presented in Figure 1, clearly illustrating a good correspondence between experimental and calculated data (R^2 = 99.35 %). There were no systematic deviations in the description of experimental data compared to the work of Kusema *et al.* (R^2 = 98.70 %). Moreover, simulation of D-arabinose oxidation in a conventional batch described very well the experimental data (Fig 2).

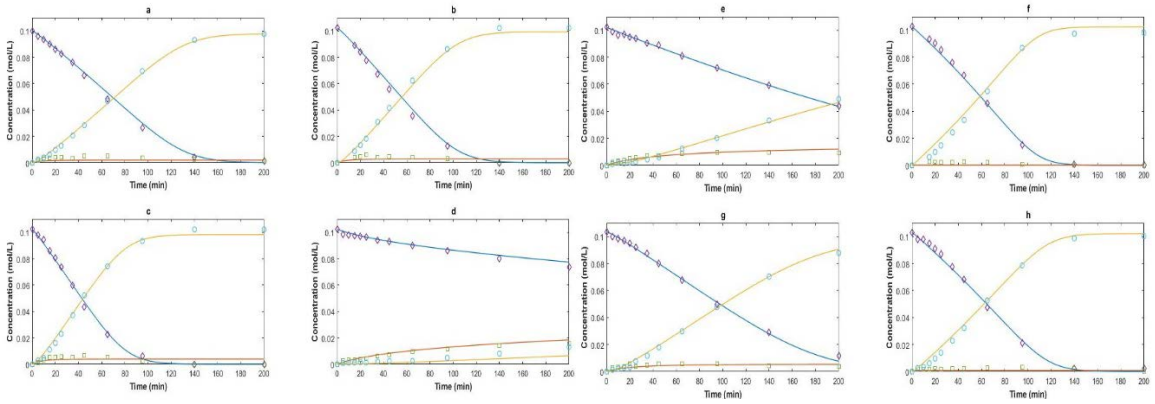

Figure 1. Experimental (dots) [3] and calculated (lines) concentrations profiles (◊→ L-arabinose, □ → arabinolactone, ○ → arabinonate) in arabinose oxidation over 1 wt% Au/Al_2O_3, m=0.25g. (a) 60°C, 2.5mL/min O_2, pH 8; (b) 60°C, 3.5mL/min O_2, pH 8; (c) 60°C, 5.0mL/min O_2, pH 8; (d) 60°C, 2.5mL/min O_2, pH 6; (e) 60°C, 2.5mL/min O_2, pH 7; (f) 60°C, 2.5mL/min O_2, pH 9; (g) 50°C, 2.5mL/min O_2, pH 8; (h) 70°C, 2.5mL/min O_2, pH 8.

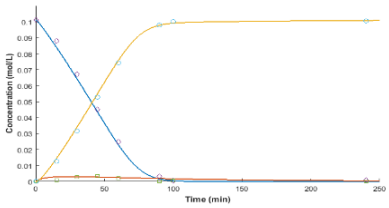

Figure 2. Experimental (dots) and calculated (lines) concentrations profiles (◊→ D-arabinose, □ → arabinolactone, ○ → arabinonate) in arabinose oxidation in a batch reactor over 2 wt% Au/Al_2O_3, m= 0.5g, T= 60°C, P_{O2} = 0.125 bar and pH=8.

4. Conclusions

A novel kinetic model for the aqueous-phase selective oxidation of L-arabinose over gold catalysts was proposed considering different forms of sugar in the solution. The parameter estimation was successfully carried out revealing that the calculated values are in good correspondence with the experimental behaviour. In general, oxidation kinetics for both D- and L-arabinose was successfully represented by the proposed elementary reaction mechanism.

References

[1] A. C. Canos, S. Iborra, A. Velty, Chem. Rev. 107 (2007) 2411–2502.
[2] M.N. Belgacem, A. Gandini, Monomers, Polymers and Composites from Renewable Resources, Elsevier, 2008.
[3] B.T. Kusema, J.-P. Mikkola, D.Y. Murzin, Catal. Sci. Technol. 2 (2012) 423–431
[4] O.A. Simakova, B.T. Kusema, B.C. Campo, A.-R. Leino, K. Kordás, V. Pitchon, P. Mäki-Arvela, D.Y. Murzin, J. Phys. Chem. C 115 (2011) 1036–1043.
[5] B.T. Kusema, B.C. Campo, O.A. Simakova, A.R. Leino, K. Kordás, P. Mäki-Arvela, T. Salmi, D.Y. Murzin, ChemCatChem 3 (2011) 1789–1798.
[6] B.T. Kusema, B.C. Campo, P. Mäki-Arvela, T. Salmi, D.Y. Murzin, Appl. Catal. A Gen. 386 (2010) 101–108.

[7] H. Haario, ModEst User's Guide, Prof. Math Oy. Helsinki (2001).

ECCE12
The 12th EUROPEAN CONGRESS OF CHEMICAL ENGINEERING
Florence 15-19 September 2019

Overall Reaction Rate of Oximation of Impurities in the Production Process of Caprolactam.

David Lorenzo*, Aurora Santos, Laura del Arco, Arturo Romero

Dpto. Ingeniería Química y de Materiales, Universidad Complutense de Madrid. Avda. Complutense S/N 28040 Madrid.

**Corresponding author: dlorenzo@ucm.es*

Highlights

- Impurities oximation using hydroxylamine sulfate as reagents.
- Reaction routes the main impurities formed in the caprolactam production process.
- Kinetic models of oximation reaction the main impurities in cyclohexanone.

1. Introduction

Caprolactam is used as a monomer in the nylon 6 production process. The most common caprolactam production process is promoted by oxidation of cyclohexane to obtain a reaction mixture known as KA-oil, which contains cyclohexanone, cyclohexanol and other impurities [1-3]. Cyclohexanone, after being purified, reacts with hydroxylamine, and subsequently epsilon-caprolactam is obtained by Beckmann rearrangement of cyclohexanone oxime [4]. The quality of the nylon 6 fibers is closed affected by type and amount of the impurities presented in ε-caprolactam. Leading companies in the production sector are currently examining the origin and the development of those impurities, to reduce their formation or to promote their elimination. The characterization of the quality of the ε-caprolactam, by means of the quantification and identification of its impurities is a complex task. Main difficulties in the determination of the impurities are their variety, low concentration and lack of information due to the confidenciality of the processes. Based on available information in literature the main impurities in cyclohexanone that could be transformed in the oximation step affecting the quality of ε-caprolactam have been selected. The scope of this work is the study of the transformation of these impurities found in the pure cyclohexanone in the oximation reaction step.

2. Methods

The impurities selected were n-heptanones (n=2,3), hexanal, n-methylcyclohexanones (n=2,3,4), 2-methylcyclopentanone, 2-cyclohexen-1-one. These ketones are in appreciable amounts in the purified cyclohexanone and have significant negative effects on the final nylon 6.

The oximes of these impurities were synthesized from their commercial ketone. They were identified by NMR and gas chromatography using a mass detector (GC/MSD) to obtain the stereoisomeric proportions that is produced in the oximation reaction. Oximation runs were carried out in an isothermal semicontinuous stirred reactor where NH_3 solution was continuously fed to neutralize the acid promoted to keep a constant pH. The reactions were carried out using hydroxyl ammonium sulfate as reactant (82 °C, atmospheric pressure and pH 5,5). In addition, it was studied the oximation reaction kinetics of those impurities that are in higher concentration in pure

cyclohexanone or have greater effect on the quality of ε-caprolactam. The experimental conditions used were closed to the industrial. The kinetic study of 2-heptanone, 2-cyclohexen-1-one and 2-methylcyclohexanone was carried out. Samples were taken at different reaction times to quantify the amount of reacted ketone.

3. Results and discussion.

A kinetic model was proposed to obtain an overall oximation rate, under the industrial operation conditions. The model was developed assuming the reaction takes place in the interphase of the organic and aqueous phases and it does not exist mass transfer limitations at each phase, because of the high agitation used. Good agreement between experimental and predicted values was found, which means to validate the model proposed and the model assumptions. The model proposed can be summarized as follows:

$$\frac{dX_{ONA}}{dt} = S \cdot k_{ap} \frac{(1-X_{ONA})}{V_{org}} \left(\frac{N_{SHA_0} - 1/2\,(N_{ONA_0}(1-X_{ONA}))}{V_{aq}} \right)^{1/2} \quad \therefore \quad k_{ap}{}' = \frac{S \cdot k_{ap}}{V_{org}} \qquad \text{Eq.(1)}$$

An apparent kinetic constant was proposed including the kinetic constant of the oximation rate of each respective impurity and the pH influence. In Table 1 the values of the apparent kinetic constant at 82 ºC and pH=5.5 are listed. It was found up that the oximation rate of 2-cyclohexen-1-one is the lowest one, followed by 2-heptanone, and finally, 2-methylcyclohexanone, whose apparent constant doubles the value of the 2-heptanone constant.

Table 1. Apparent constant values for the model proposed in Eq.1

Compund	$k_{ap}{}'$ ($kg_{aq}^{0,5} \cdot mmol^{-1,5} \cdot min^{-1}$)	SQR	% VE
2-heptanone	0.033± 0.002	0.098	96
2- methylcyclohexanone	0.066±0.006	0.078	97
2-cyclohexen-1-one	0.0057±0.0003	0.120	97

4. Conclusions

The importance the quality of caprolactam has been increased last few years due to development of new technologies. However, the information about the impurities which can affect the quality of the final product is limited. In this work, the main impurities present in the cyclohexanone used as intermedia in the caprolactam process were synthesized and identified by GC/MS and NMR. Besides a kinetic model of the most important impurities was proposed. Kinetics constants obtained provide helpful information useful for the analysis of the purification steps.

References

[1.] Jodra, L.G., A. Romero, F. Garciaochoa and J. Aracil, Ind. Eng. Chem. Prod. Res. Dev. 20(1981): p. 562-566.

[2.] Burlone, D.A., R.M. Sink, J. Lanza and K. Gust, *A Method o Minimizing Aldehyde-Based Impurities in a Process Stream*. 2006.

[3.] Meier, H.P., E.J. Van and E. Terweduwe, *Purification of cyclohexanone*. 1993, Bayer Antwerpen N.V., Belg. . p. 5 pp.

[4.] Romero, A., A. Santos and P. Yustos, Ind. Eng. Chem. Res. 43(2004): p. 1557-1560.

ECCE12
The 12th EUROPEAN CONGRESS OF CHEMICAL ENGINEERING
Florence 15-19 September 2019

Reaction engineering approach to the preparation of sodium hydride and sodium borohydride

Tapio Salmi[1*], Vincenzo Russo[1,2]

1 Laboratory of Industrial Chemistry & Reaction Engineering, Department of Chemical Engineering, Johan Gadolin Process Chemistry Centre, Åbo Akademi University, FI-20500 Åbo-Turku, Finland
[2]Università di Napoli ''Federico II'', Chemical Science Department, IT-80126 Napoli, Italy

**Corresponding author: tapio.salmi@abo.fi*

Highlights

- Sodium hydride and sodium borohydride are industrially important reducing agents
- Mathematical models for two complex multiphase processes were developed: synthesis of sodium hydride and sodium borohydride
- Experimental data obtained in laboratory scale were used in the modelling
- The advanced multiphase model is useful in process simulation and optimization

1. Introduction

Sodium hydride and sodium borohydride are strong reducing agents with widespread industrial applications. The synthesis of sodium hydride (NaH) and sodium borohydride ($NaBH_4$) are very demanding multiphase and multistep processes. Sodium hydride is produced industrially by letting melt sodium to react with gaseous hydrogen. In spite of many attempts to develop new processes for the industrial production of sodium borohydride, the procedure discovered by Schlesinger and Brown in 1940's and 1950's is still the dominant one. The process is based on the use of sodium hydride and trimethyl borate ($B(OCH_3)_3$) as raw materials. The reaction steps are carried out in dispersions of inert mineral oil at elevated temperatures. A typical reaction temperature for the preparation of NaH is 230-260°C, while temperatures 250-270°C are typical for the synthesis of $NaBH_4$. In spite that these processes are very classical, a vast majority of the published literature is of qualitative character only. Nowadays the understanding of complex multiphase processes has advanced very much and the modelling and computational tools enable a reaction engineering approach to these industrially important and technically demanding systems. Mathematical modelling of the reactions $4Na(l) + 2H_2(g) \rightarrow 4NaH(s)$ and $4NaH(s) + B(OCH_3)_3(l) \rightarrow NaBH_4(s) + 3NaOCH_3(s)$ is considered in the present work.

2. Methods

Both reactions are carried out in semibatch reactors. The processes were modelled based on plausible surface reaction mechanisms. The hypothesis for the formation of NaH was that it proceeds through a surface reaction between adsorbed hydrogen atoms on the droplets of finely dispersed Na in mineral oil. Solid NaH particles are formed and they react in the next step in a surface reaction with dissolved $B(OCH_3)_3$ in the oil phase forming $NaBH_4$ and $Na(OCH_3)$. A

partially hydrogenated intermediate (X1) is detected in the $NaBH_4$ formation step. Based on these mechanistic hypotheses, rate equations were derived and they were coupled to the mass balances of the components, taking into account the interfacial mass transfer effects.

The rate equation for the formation of NaH is, including two adjustable parameters (k' and K') only: $r=k' c_H^{1/2} /(1+K' c_H^{1/2})$

For the formation of $NaBH_4$, the rate equation is (B=$B(OCH_3)_3$) and X1=reaction intermediate)

$r=k'' c_{X1}/(1+ K_B c_B + K_{X1} c_{X1})$

The mass balances for the multiphase systems were described by taking into account the transfer of hydrogen from the gas phase to the mineral oil and from the mineral oil to the Na droplets. In the synthesis of $NaBH_4$, the mass transfer of $B(OCH_3)_3$ from mineral oil to the surfaces of the NaH particles was included. The correlations for Sherwood numbers were used to obtain expressions for the interfacial mass transfer coefficients. The behaviours of the Na droplets and the dispersed NaH particles were described with the generalized shrinking particle model developed by our group. The experimental data collected previously by us was used in the modelling.

3. Results and discussion

Examples of the modelling results of the NaH and $NaBH_4$ formation processes are provided in Figure 1. As revealed by the figure, the model describes well the behaviour of the system at a wide range of rotation speeds of the disperser. The yields of the main product (P=$NaBH_4$) and the reaction intermediate (X1) are very well predicted by the complex multiphase model.

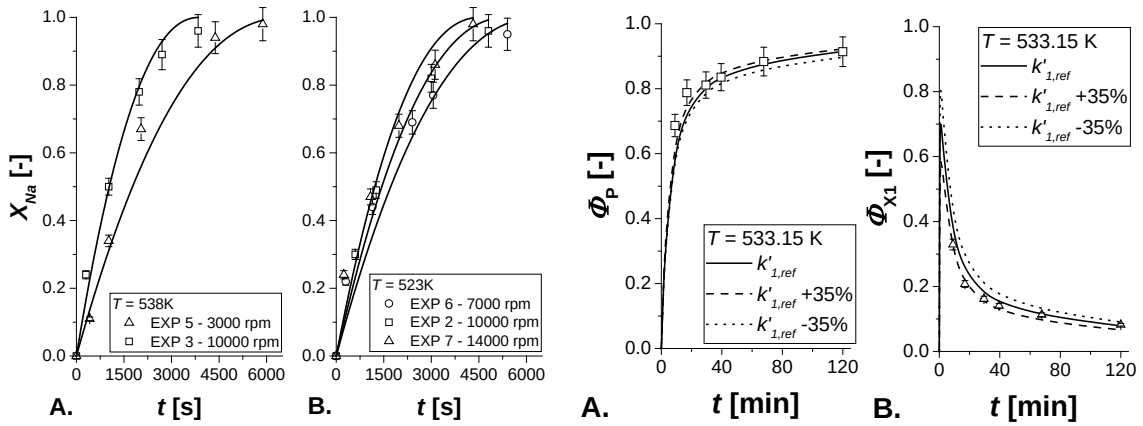

Figure 1. Effect of the stirring rate on the sodium conversion (X) to NaH and sensitivity analysis of the yields of $NaBH_4$ and X1 (Õ) Continuous lines represent model predictions.

4. Conclusions

New multiphase models were developed for the industrial synthesis of NaH and $NaBH_4$. The model parameters were determined from experimental data obtained from laboratory-scale semibatch reactors. The models can be used for process design and optimization.

ECCE12
The 12th EUROPEAN CONGRESS OF CHEMICAL ENGINEERING
Florence 15-19 September 2019

Experimental Validation of the Production of PolyVinyl Acetate in a Pilot Reactor – A Case of Optimization

Andrés Augusto Herrera Morales, Bibiana Raba Mora, Iván Darío Gil Chaves, Gerardo Rodriguez Niño & Manuel Florez
[a] *Chemical and Biochemical Processes Group, Department of Chemical and Environmental Engineering, Universidad Nacional de Colombia, Bogota, Colombia.*
idgilc@unal.edu.co*

Highlights

- Validation of an emulsion polymerization.
- Polymer properties continuous determination during reaction time.
- Time reaction reduction up to 30% from a standard procedure.

1. Introduction

Polyvinyl acetate is obtained through an exothermic reaction in a process of free-radical emulsion polymerization. Polyvinyl acetate is widely used in the adhesives industry, and it is also largely implemented in the generation of sub products. For example, it is a film-forming ingredient in water-based (latex) paints; it is used in adhesives, varnishes and lacquer, paper coatings, fabric adhesives, resin bases, among others[1]. The demand for new latex products has rapidly increased, together with research efforts in modeling, optimization and control of the manufacturing process. In the past few years, multiphase models have been developed, reflecting factors like nonlinear behavior and the sensitivity to perturbations[2][3]. A pilot scale emulsion polymerization was developed on a 75L stirred tank reactor based on a model that describes emulsion polymerization phenomena such as initiation, propagation and termination stages. Temperature reactor, viscosity, solids content and particle size distribution were determined in order to validate the model.

2. Methods

At first, a dynamic model was proposed where by a control strategy to assess an optimal condition was defined. The purpose of this model is to minimize the reaction time by varying the heating/cooling flows fed through the reactor jacket. In turn, the model made it possible to estimate the effect of the initiator and the monomer dosage, as well as the influence of temperature on the reaction. Then, a description of the properties was made in order to follow up on the reaction and determine its quality in terms of the solids content, viscosity, distribution of size particle and residual monomer. Solids content and viscosity were determined based on a Colombian Technical Standard, temperature was measured and recorded in Siemens 1200 PLC and Particle size distribution was determined by a dynamic light scattering method with a Zetasizer Nano equipment. [4][5][6][2]

3. Results and discussion

A total of seven tests were conducted for the validation of the model: two under normal operation conditions and five reproducing the optimal profile. The profiles obtained through the

a: NTC 5003
b: NTC 2790

experimentation shows an approximation to the model values, allowing to conclude that the model studied is accurate to real heterogeneous phenomena.

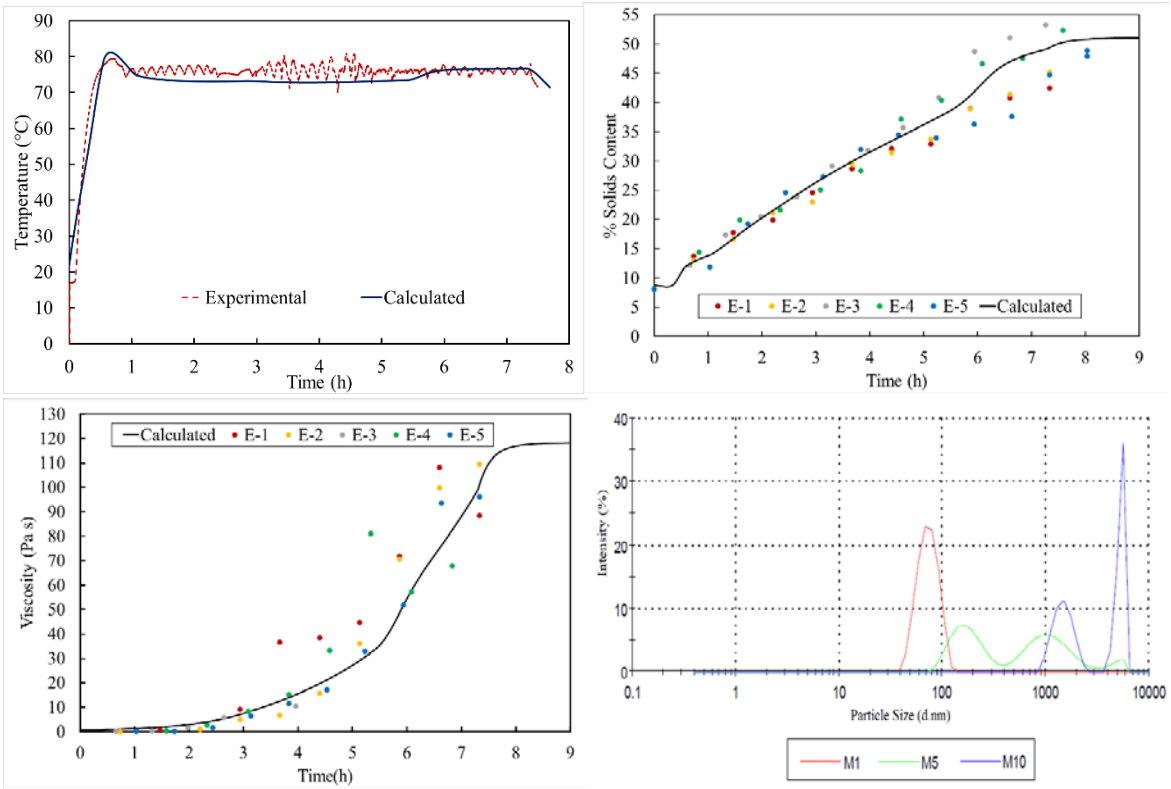

Figure 1. Temperature, solids content, viscosity and particle size distribution from an experimental data of an optimal time emulsion polymerization reaction.

4. Conclusions

From the data obtained from the temperature profile and the product's final properties it was possible to confirm that through the control strategies proposed for the temperature control optimization model it is possible to reduce the reaction time by 20%, taking as reference the reaction that is currently conducted in the industrial sector.

It was possible to implement strategies like the addition of the monomer and the initiator at different time intervals, as well as the variation of the heating/cooling flows feeding the reactor jacket in a pilot reactor (65 liters), where transport and mass transfer phenomena found in an industrial reactor, at a larger scale, were also present.

The results obtained for each one of the properties make it possible to ensure that the quality of the final polymer obtained through the optimized model is like the one obtained through the conventional process. The model used employed an optimal control, which is designed to track the temperature in the reaction system despite typical perturbations like initiator injections of the monomer.

References

[1] Market, E. C. (2008). Polyvinyl Acetate and Polyvinyl Alcohol. A review of the CIS Production Eurasian Chemical Market (Vol. 11).

[2] Penlidis, A., MacGregor, J.F., Hamielec, A.E., 1985. Dynamicmodeling of emulsion polymerization reactors. AIChE J. 31,881–889.

[3] Dimitratos, J.; Eliçabe, G.; Georgakis, C. Control of emulsion polymerization reactors. AIChE J. 1994, 40, 1993−2021.
[4] ICONTEC.: Adhesivos. Determinación del contenido de sólidos convencional y delcontenido de sólidos a masa constante. Bogotá: Norma Técnica Colombiana NTC5003, 2010.
[5] ICONTEC.: Adhesivos. Métodos de ensayo para determinarla viscosidad Bogotá: Norma Técnica Colombiana NTC 2790, 2010.
[6] Benyahia, B., Latifi, M.A., Fonteix, C., Pla, F., 2011. Multicriteriadynamic optimization of an emulsion copolymerizationreactor. Comput. Chem. Eng. 35, 2886–2895.

ECCE12
The 12th EUROPEAN CONGRESS OF CHEMICAL ENGINEERING
Florence 15-19 September 2019

Characterization of edible oil foams with a fast inline measurement using acoustic and ultrasound spectroscopy

Lorenzo Metilli[1], Mathew Francis, Megan Povey, Aris Lazidis, Stephanie Marty-Terrade, Elena Simone

[1] School of Food science and Nutrition, University of Leeds, UK; [2] Nestlè PTC York, UK

*Corresponding author: fslme@leeds.ac.uk, e.simone@leeds.ac.uk

Highlights

- Edible oil foams are used for reducing caloric density and modify food texture.
- The physical properties of foams affect rheology and stability of the final products.
- Acoustic techniques can be used to assess the physical properties of foams.

1. Introduction

Because of the dramatic rise of obesity in UK in the last three decades, several food companies have committed to design and manufacture healthier foods with reduced caloric content. An effective way of achieving this goal is by using edible oil-based foams (oleofoams) to prepare aerated confectionary food (e.g., mousses) [1].. The main constituents of edible oleofoams are a liquid oil phase, air bubbles and a further high-melting, crystalline fat phase, which stabilizes the bubbles via a Pickering effect. Such complex microstructure determines the macroscopic physical and nutritional properties of oleofoams [2]. Therefore, a correct characterization and continuous monitoring and control of oleofoams microstructure during process design and manufacturing is essential to ensure the quality of the final food product. Ultrasound spectroscopy is a fast and affordable monitoring technique, characterized by non-intrusiveness and non-destructive behaviour, which is particularly promising for inline, in situ characterization of oleofoams. The aims of this work are: (1) identify a methodology based on multiple offline techniques to characterize the microstructure of oleofoams and (2) find a robust correlation between the physical properties and microstructure of oleofoams and specific characteristic acoustic measurements.

2. Methodology

High oleic sunflower oil and cocoa butter were used to prepare the oleofoams. Melted cocoa butter was mixed to sunflower oil and recrystallized (oleogel phase) by cooling in a jacketed vessel equipped with temperature control. Aeration was performed using a Kitchen Aid whipping machine. The structures of oleogels and oleaofoams were characterized using several offline techniques including polarized and confocal microscopy, x-ray scattering and tomography as well as differential scanning calorimetry. Acoustic measurements were carried out using an airborne acoustic microscope, with two focused transducers at three variable frequencies.

3. Results and discussion

The experiments showed that both foamability and foam stability are dependent from cocoa butter content, with heavier (20-30%) oleogels reaching equilibrium air content later compared to lighter ones (10%). Confocal microscopy was proven successful to image surface layers of the foams, allowing an estimate of bubble size distribution. Figure 1 shows how air bubbles can be easily detected by this technique. Finally, samples were analyzed with the acoustic microscope and a positive correlation between the intensity of the reflected signal and the content of cocoa butter crystals in the samples was found.

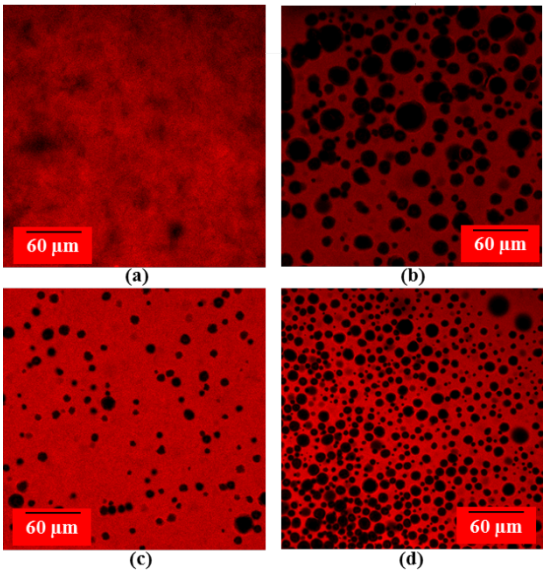

Figure 1. Confocal microscope images of four samples at (a) 0%, (b) 70% (c) 175% and (d) 200% overrun.

4. Conclusions

Oleogels and oleofoams were characterized with offline techniques as well as acoustic measurements. Initial finding showed the applicability of acoustic spectroscopy in detecting and quantifying fat crystals within oleofoams. In fact, acoustic reflectivity increased with increasing solid fat content in such foams.

References

[1] Campbell, G. M., & Mougeot, E. (1999). Creation and characterisation of aerated food products. *Trends in Food Science and Technology*, *10*(9), 283–296.

[2] Heymans, R., Tavernier, I., Dewettinck, K., & Van der Meeren, P. (2017). Crystal stabilization of edible oil foams. *Trends in Food Science and Technology*, *69*, 13–24

ECCE12
The 12th EUROPEAN CONGRESS OF CHEMICAL ENGINEERING
Florence 15-19 September 2019

In situ real-time rheological characterization of calcium alginate hydrogels

Ioanna Besiri[1], Thomas Goudoulas[1], Natalie Germann[1*]

1 Fluid Dynamics of Complexed Biosystems Group, Maximus-von-Imhof-Forum 2, School of Life Sciences Weihenstephan, Technical University of Munich, 85354 Freising, Germany

**Corresponding author: natalie.germann@tum.de*

Highlights

- Design of a custom-made geometry for the rheological study.
- *In situ* gelation kinetics of sodium alginate and calcium chloride.
- Understanding the initial phase of the reaction kinetics.

1. Introduction

Polysaccharides are among the fundamental components of biosystems, and they are responsible for a variety of functions. Alginate is an important polysaccharide and forms hydrogels. [1,2] As a linear negatively charged high-molecular-weight copolymer of two monosaccharides, it reacts with multivalent cations (e.g. Ca^{2+}, Ba^{2+}) in aqueous solutions and forms hydrogels through ionic crosslinking, also referred to as ´´egg-box`` structural formation. [3] The motivation was to develop an understanding of the fast gelation kinetics of this model system using a custom-made rheometric setup. In the future, this investigation can be extended to similar reactions and controlled drug delivery studies.

2. Methods

We studied the kinetics of the *in situ* gelation of alginate in the presence of Ca^{2+} ions during the initial gelation phase using a custom-made cone and plate geometry (Figure 1a). The lower plate has been altered, providing a cavity where the Ca^{2+} solution can exist. Only upwards flow to the surface can be achieved where the alginate solution is placed. The alginate solution covered the lower plate and the upper cone was adjusted at the corresponding gap. Using a volumetric syringe to supply the appropriate volume of the Ca^{2+} solution, instant gelation can be achieved and the rheological response can be recorded. In this study, $CaCl_2$ solutions were utilized with concentrations up to 200 mM and volumes between 0.1 to 0.25 mL. We performed small amplitude oscillatory shear time sweeps at alginate concentrations up to 4 wt.%, by applying 3% strain amplitude at 1 rad/s angular frequency. In all measurements, injection occurred after the initiation of the oscillatory time sweep.

3. Results and discussion

We found that with a sampling rate of 3 points per second, the rheometer can successfully record the fast gelation reaction during the initial ten seconds (Figure 1b, indicated area). For increased volumes of the injected Ca^{2+} solution, the elastic modulus G´ increases continuously in time while

the loss modulus G'' forms a plateau (Figure 1b). Moreover, the magnitudes of the dynamic moduli were significantly higher. When the injection volume was constant, the same effect was noticed for the Ca^{2+} concentration. For instance, by supplying twice the $CaCl_2$ concentration, the storage modulus of the hydrogel was doubled. At the end of the experiments, a macroscopic evaluation was performed and typical flowable soft gels were observed in all cases.

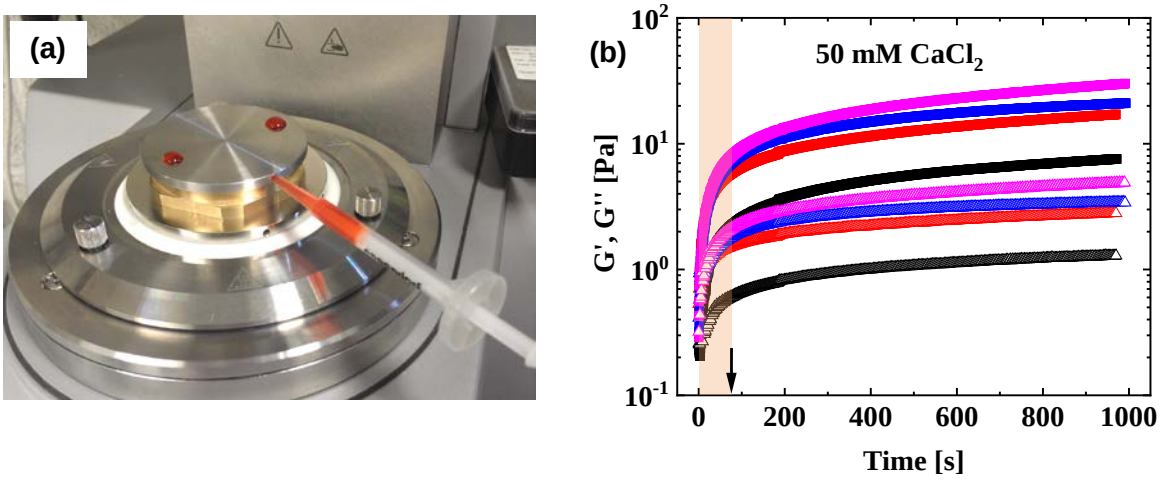

Figure 1. (a) Custom-made lower plate placed on rheometer. A volumetric syringe is used for supplying a tracing liquid through the internal cavity and the two micro-holes (approx. 250 µm) to the surface of the lower plate. (b) Storage modulus (G', filled square symbols) and loss modulus (G'', nonfilled triangle symbols) vs. time. The *in situ* conditions correspond to 1 wt.% sodium alginate and 50 mM calcium chloride for injected volumes of 0.10 mL (black), 0.15 mL (red), 0.20 mL (blue), and 0.25 mL (magenta).

4. Conclusions

In this work, we present a method for recording *in situ* real-time gelation kinetics, like fast changes of storage and loss moduli. By studying the Ca^{2+}/alginate system at various concentrations and volumes, we found that two distinct regions exist. The initial rapid region seems to be independent of the applied Ca^{2+} volume while the plateau region indicates a quasi-stable structure. The knowledge gained using this probing technique in this research can be applied in many engineering fields, such as food technology or tissue engineering.

References

[1] M. Matyash, F. Despang, C. Ikonomidou, M. Gelinsky, Tissue Eng. Part C Methods 20 (2014) 401–404.
[2] B. Larsen, J. Bjørnstad, E. Pettersen, H. Tønnesen, J. Melvik, BMC Biotechnology 15 (2015) 15-29.
[3] G. Grant, E. Morris, D. Rees, P. Smith, D. Thom, Febs Letters, 32 (1973) 195-198.

ECCE12
The 12th EUROPEAN CONGRESS OF CHEMICAL ENGINEERING
Florence 15-19 September 2019

Engineering hemicellulose-lignin complexes' extraction for obtaining emulsion stabilizing hydrocolloids

Jussi Rissanen[1], Maarit Lahtinen[2], Kirsi Mikkonen[2], *Henrik Grénman[1]

[1] *Laboratory of Industrial Chemistry and Reaction Engineering, Johan Gadolin Process Chemistry Centre, Åbo Akademi University, Turku/Åbo, Finland*

[2]*Department of Food and Nutrition, University of Helsinki, Helsinki, Finland*

**Corresponding author: henrik.grenman@abo.fi*

Highlights

- Wood based compounds have the potential to be excellent stabilizers in food, pharmaceutics, and cosmetics
- Spruce GGM displayed exceptional capacity to inhibit lipid oxidation and act as a multifunctional stabilizer
- GGM was extracted with hot water using an additive, which is suitable for the alimentary and cosmetics industry
- The extraction rate was enhanced with the additive and amphiphilic water soluble lignin-hemicelluloses were formed

1. Introduction

The performance of hemicellulose-based compounds from lignocelluloses in the potential products is determined largely by the chemical composition and the structure of the molecules. The objective in the extraction processes has mostly been to obtain completely pure fractions of hemicellulose, lignin, and cellulose. However, a controlled mixed structure of the compounds can be an advantage in certain applications.

Recently researchers has shown, that galactoglucomannan (GGM) based compounds have the potential to replace the "golden standard" food stabilizer gum Arabic (GA) in food, pharmaceutics, and cosmetics. [1, 2] In these studies, GGM displayed exceptional capacity to inhibit lipid oxidation and act as a multifunctional stabilizer, enhancing both the physical and oxidative stability of emulsions. The higher content of phenolic residues in GGM compared to GA was concluded to contribute to GGM's excellent oxidation inhibition capacity. The exact mechanisms behind the beneficial influence of lignin residues in the GGM are unclear, as is the influence of the structure and composition of the lignin-hemicellulose complexes (LCC) on their performance. The basic phenomenon has been established, but many of the details are in the dark.

2. Methods

In our recent study, hemicellulose-lignin complexes from spruce were extracted with pressurized hot water (PHWE) in a batch reactor using a well separable additive, which is suitable for the alimentary and cosmetics industry. Detailed GC analysis and NMR were used in the characterization of the extracted compounds. The complexes were utilized for emulsion stabilization studies in

collaboration with specialists in alimentary research and emulsions. Different wood species combined with varying reaction conditions were tested and their performance as emulsion stabilizers and anti-oxidizing agents was evaluated.

3. Results and discussion

The results clearly demonstrated that the extraction rate was considerably enhanced with the additive (Fig. 1) and about 10-15% more lignin (Klason lignin in solid) was dissolved compared to normal PHWE. Moreover, the NMR results indicated that lignin stays covalently bound to the dissolved hemicelluloses forming amphiphilic water soluble LCC. The extraction method also influenced e.g. the molar mass of the obtained macromolecules as displayed in Figure 2. Clear differences in emulsification and antioxidant properties were observed between the samples. Revealing the detailed mechanisms of dissolution combined with understanding the mechanisms of emulsion stabilization are key factors for being able to tune the properties of the extracted compounds by varying the experimental conditions.

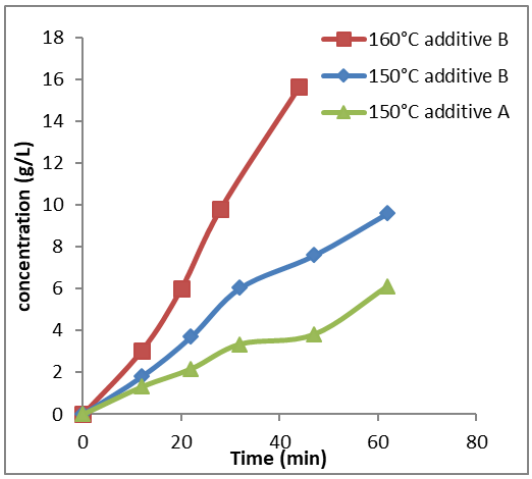

Figure 1. The enhancement of the extraction rate by selected additive.

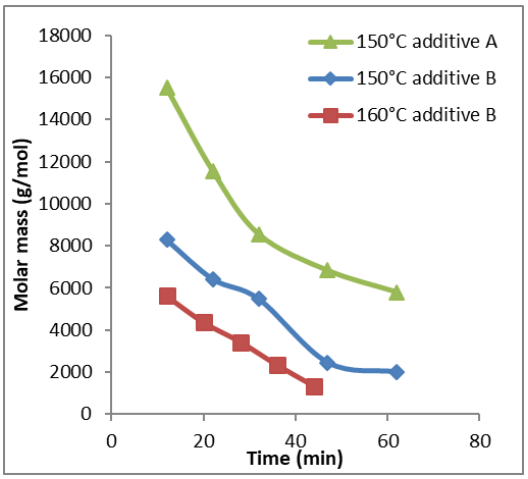

Figure 2. The influence of additive addition to the molar mass of the macromolecules.

4. Conclusions

The current interdisciplinary research focuses on building on a newly developed extraction method for enhancing hemicelluloses extraction, which enables tuning the lignin content and properties of the LCC. The work bridges the state of the art knowledge in the safely enhanced extraction of hemicelluloses-lignin compounds and the related reaction engineering (chemical engineering) and the utilization of the LCC for alimentary purposes (alimentary chemistry). Moreover, the potential utilization is by no means limited to the alimentary industry, but fields such as cosmetics and health products are highly viable.

References [Calibri 10]

[1] K. S. Mikkonen, C. Xu, C. Berton-Carabin, K. Schroën, *Food Hydrocolloid*. 52 (2016), 615-624.
[2] M. Lehtonen, S. Teräslahti, C. Xu, M. Madhav, A-M. Lampi, K. Mikkonen. *Food Hydrocolloids*, 58, (2016), 255-266

ECCE12
The 12th EUROPEAN CONGRESS OF CHEMICAL ENGINEERING
Florence 15-19 September 2019

Unravelling food thermal reactivity by an original methodology to analyze and model reactions during baking of a cake model

Jeehyun Lee, Stéphanie Roux, Barbara Rega, Catherine Bonazzi

UMR Ingénierie Procédés Aliments, AgroParisTech, Inra, Université Paris-Saclay, 91300 Massy, France

**Corresponding author: jeehyun.lee@agroparistech.fr*

Highlights

- Thermal reactions were followed in an inert cake model added with targeted precursors
- A wide range of markers were quantified fulfilling an observable reaction scheme
- Reactions were simulated by coupling stoechio-kinetics to heat and mass transfer models.

1. Introduction

In baked foods, process and formulation steps lead to the generation of a multitude of compounds responsible for quality: aroma, flavor, color and safety, through the activation of thermal reactions. However the link between composition, reactivity and quality determinants is not an easy task because of the interdependency of physical and chemical parameters and the complexity of real ingredients. Therefore, studying complex transformations in a food matrix under strictly controlled physical, structural and chemical conditions is of paramount help to verify the hypotheses formulated by many decades of results obtained in simple model systems (far from real foods) or in real products (with limited understanding on specific reaction pathways).

2. Methods

An inert model imitative of a sponge cake was developed in order to master the nature and the quantity of reaction precursors [1]. The cake model was added with targeted precursors to activate thermal reactions in a controlled way (caramelization in model G - glucose containing model; both caramelization and Maillard reactions in model G+L - glucose and leucine containing model). G and G+L models were submitted to controlled process conditions (140°C, 170°C or 200°C baking temperatures; high and low convection levels). Ten reaction markers (precursors, intermediates and products), were quantitatively analyzed during the course of baking (8 kinetic points) by a complementary sampling approach. Volatile markers (e.g. furanic compounds, pyrazines, Strecker's aldehydes, acids) were sampled from baking vapors by on-line sampling device and TD-GC-MS analysis while nonvolatile and water-soluble markers were extracted from the cake matrices and quantified as follows: reducing sugars by UHPLC-CAD, free amino groups by Sørensen formol titration, dicarbonyl intermediates by UHPLC-DAD/MS, furfural and 5-hydroxymethylfurfural by UHPLC-DAD. These markers were thus selected to fulfil the requirements for an observable reaction scheme and a stoechio-kinetic modeling.

Synchronous experimental data on heat and mass transfers and reactions were acquired under perfectly controlled conditions of thermal treatment (temperature and convective transfer coefficient) and used for the modelling of coupled transfers and reactions in the cake using Comsol™ and Matlab™.

3. Results and discussion

The only presence of glucose in the G model was sufficient to activate caramelization reaction with the production of high levels of furfural, 5-methylfurfural, 5-hydroxymethylfurfural, and acetic acid. These compounds showed a typical final product behaviour (exponential production) except from furfuryl alcohol (bell-shaped behaviour) and a dependency to baking temperatures and convection speed. These markers were also found in the G+L model where caramelisation and Maillard reaction could jointly occur. Interestingly, specific pathways were activated by the presence in the system of leucine and glucose: the quantification of 3-methylbutanal in high amounts showed the activation of the Strecker's degradation in model G+L. Moreover, when comparing the amounts of dicarbonyl intermediates, the higher generation rate of the 3-deoxyosone relatively 1-deoxyosone model suggested that the 1,2-enolisation pathway was favored compared to the 2,3-enolisation in the G+L model and showed that the higher the temperature and the convection level, the faster their degradation.

The stoechio-kinetic model was coupled with a mass and heat transfer model in order to predict markers content in the cake models during baking. Hence this joint approach provided an excellent opportunity to understand, model and control the kinetics of thermal reactions contributing to the generation of process-induced compounds in solid food.

4. Conclusions

An original methodology coupling chemical and physical on-line measurements was developed in order to follow a broad range of reaction markers and unravel Maillard and caramelization reactions under realistic but controlled processing conditions. Thanks to a solid food model (cake model) having a complex structure and technological history but only containing known amounts of one or two reactive precursors, two observable reaction schemes could be built and modelled into a stoechio-kinetic model, taking into account mass and heat transfer in the cake model. This model is helpful for capitalizing on knowledge about the impact of formulation and process on quality of baked products.

References

[1] J. Bousquières, C. Bonazzi, C. Michon, Food hydrocolloids. 63 (2017) 552-560

[2] R. Srivastava, J. Bousquières, M. Cepeda-Vásquez, S. Roux, C. Bonazzi, R. Rega, Food Chemistry. 267 (2018) 329-336.

ECCE12
The 12th EUROPEAN CONGRESS OF CHEMICAL ENGINEERING
Florence 15-19 September 2019

Optimization of conditions for the purification of chlorogenic acid from a sunflower meal co-product by macroporous resins: static and dynamic study

Thi Tuong Le[1], Irina Ioannou[1], Armelle Ropars[2], Arnaud Aymes[1], Jean-Pol Frippiat[2*], Romain Kapel[1*]

[1] *Laboratoire Réactions et Génie des Procédés, Université de Lorraine, CNRS, LRGP, F-54000 Nancy, France*

[2] *Stress, Immunity, Pathogens, Université de Lorraine, EA 7300, 9 avenue de la foret de Haye, Vandoeuvre-les-nancy, France*

**Corresponding author: romain.kapel@univ-lorraine.fr/ jean-Pol.frippiat@univ-lorraine.fr*

Highlights

- CGA adsorption on XAD 7 resin was described by pseudo-second-order and Langmuir model.
- Optimal capture conditions were the adsorption flow rate of 15 BV/ h and pH at 2.7 and desorption with ethanol 50% (v/v).
- CGA fraction from sunflower protein purification effluent had similar biological effects than commercial CGA

1. Introduction

The extraction/ purification of plant proteins for food applications yields a large volume of liquid effluent. Recently we developed a process for the production of sunflower proteins isolate. The purification step is made by ultrafiltration with a diafiltration step using NaCl solution. This effluent is composed of various organic micro-solutes (amino acids, organic acids, peptides, carbohydrates etc.). It also contains chlorogenic acid (CGA) which is the main sunflower polyphenol. Many reports show the great biological activities of this polyphenol (like anti-inflammatory properties [1, 2]). The capture of sunflower polyphenol and particularly CGA from ethanol or methanol extracts is well documented [3]. But the capture its capture from an aqueous media charged in hydro-soluble molecule and salts has never been performed to our knowledge.

This study presents the static adsorption/ desorption capacity of CGA in the effluent with macroporous resins. This allowed choosing the most appropriate resin for CGA capture. Then, we implemented a multi-objective optimization strategy to establish the best adsorption /desorption conditions for CGA capture in column. Finally, we studied the biological activity of the obtained fraction compared to commercial CGA.

2. Methods

Batch adsorption/ desorption of CGA was studied with five macroporous resins (XAD4, XAD7, XAD16, XAD1180 and HP20) by monitoring CGA in the liquid phase (SE-HPLC method). CGA in adsorbed on the solid phase was deduced by applying the mass balance. For the dynamic study (column), the effect of pH (2 – 5) and flow rate (5 – 15 BV/h) on dynamic binding capacity ($DBC_{10\%}$), productivity and recovery were modeled by nonlinear regression (Response Surface Methodology, RSM). For the desorption step, the effect of the ethanol concentration (30 - 90% v/v) on CGA purity

was also considered. The effects of these fractions on the viability of human THP-1 derived macrophages and wondered if they could moderate their LPS-induced inflammatory response.

3. Results and discussion

XAD 7, XAD 16 and HP 20 showed high CGA adsorption and desorption capacities at equilibrium. Four kinetic models are used to fit experimental CGA adsorption data. The pseudo-second-order model is the most suitable for describing the whole adsorption behavior. Four isotherm models were used to describe the adsorption properties of CGA on resins. The Langmuir model was the most favorable for describing the adsorption at equilibrium (Fig. 1A). For the dynamic study, XAD7 has been selected resin due to showing high specific surface adsorption capacity. The effect of the pH and charge step flow rate on $DBC_{10\%}$, CGA recovery and process productivity by DoE (Fig. 1B). R^2 obtained for the 3 criteria was higher than 0.9 meaning that the regression models appropriately fitted experimental data well. The multicriteria optimization strategy showed that the best conditions were a flow rate of 15 BV/ h and a pH of pH 2.7 and the most appropriate ethanol concentration was 50% (v/v). Fig. 1C demonstrates that CGA fraction (F1) and CGA standard did not affect cell viability on human THP-1 derived macrophages at dose 50-100 mM. Results revealed that TNF-α was inhibited approximately of 15-20% when we treated samples with LPS before and after 1 hr, similar to that obtained with CGA standard. These results suggested a newly discovered anti-inflammatory feature of CGA from by-products of protein extraction.

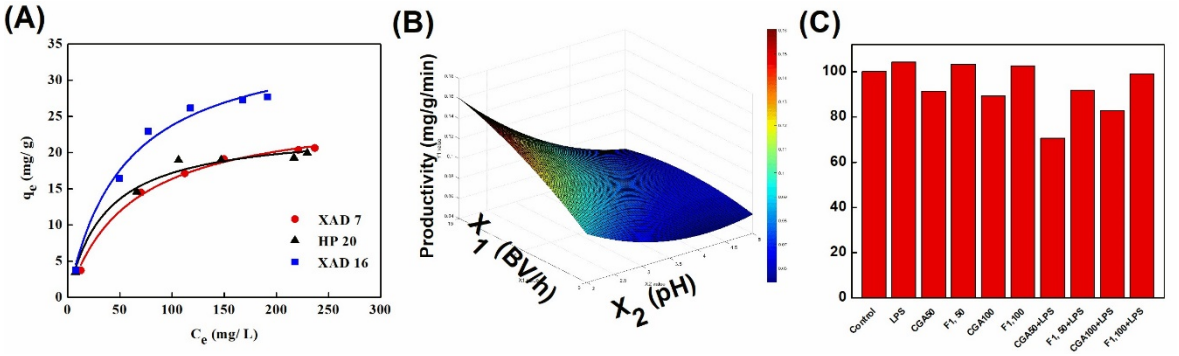

Figure 1. Illustrated results**.** A. Langmuir model; B. Response surface of productivity; C. Cytotoxicity on THP-1 cells line.

4. Conclusions

In the static study, the adsorption of CGA had a monolayer adsorption behavior. The pH of the starting effluent significantly affected the adsorption and desorption capacities. Based on RSM, the optimal conditions for purification of chlorogenic acid was defined. The obtained fractions and standard did not affect cell viability. This natural product may then be proposed as an alternative product that helps in preventing and treating inflammatory disorders. Studies are currently ongoing to evaluate the capacity of these fractions to reduce THP-1-derived macrophages inflammatory response.

References

[1] Szydlowska et al. 2010, J Argic. Food Chem, 58 : 7502-7509
[2] Weisz et al. 2013, IFSET Journal, 17: 169-179
[3] F.S. Taha et al. 2011, Am. J. Food Technol. 6: 1002-1020.

ECAB 5
The 5th EUROPEAN CONGRESS OF APPLIED BIOTECHNOLOGY
Florence 15-19 September 2019

Rheological and Tribological Characterization of Different Commercial Hazelnut Based Spreads

*Laura Principato[1], Gulliermo Duserm Garrido[1], Roberta Dordoni[1], Spigno Giorgia**

1 DiSTAS – Department for Sustainable Food Process, Università Cattolica del Sacro Cuore, Piacenza (Italy)

* *giorgia.spigno@unicatt.it*

Highlights

- 5 hazelnut-cocoa base spreads characterized for rheological properties
- Influence of used geometry on the obtained flow-curves
- Substantial differences in tribological behavior with both recipe and temperature

1. Introduction

The principal aim of this work was the knowledge development in the research area of rheological characterisation of food semi-solid systems as hazelnut-cocoa based spreads. Five commercial cocoa spreads with different hazelnut/fat compositions were selected and rheological and tribological tests were carried out. Bulk and lubrication properties were estimated to investigate the occurring of microstructural changes from handling and storage step to oral consumption, respectively.

2. Methods

Both rheological and tribological tests were carried out with a laboratory rheometer (Anton Paar MCR 302). Spread flow curves were obtained at different temperatures with different geometries. Oscillatory mode test was conducted to determine linear viscoelastic region (LVR) , storage and loss modulus (G' and G''), complex viscosity (η) and tan(δ). Three-run flow cycle was applied to estimate the variation of thixotropic properties with temperature. Finally, tribological Stribeck curves were evaluated.

3. Results and discussion

Rheological analysis highlighted a pseudo-plastic behaviour in all spreads with the elastic component prevalent on the viscous one (G'>G''). Rotational analysis showed the strictly dependency of flow curve from temperature in all cases. Moreover, geometry changing determined only flow index (n) value modification. Curves obtained with parallel plates showed n value lower than cup and bob device. Furthermore, in the same way as viscosity, consistency index (K)

decreased with temperature in all samples. The effect of temperature on K may be modelled by Arrhenius equation obtaining a linear correlation between ln(K) and 1/T. A stronger dependency of consistency index (K) on temperature may be related to higher sensitivity of microstructural change to thermal stress. Spread with greater K variation demonstrated a higher tendency of G' and G'' curves to cross-over at higher temperature. The occurring of cross-over point expressed the shift from solid-like to liquid-like behaviour due to melting of solid lipid fraction. In addition, a greater decrease of friction factor and more significant shape modification of the Stribeck curves highlight thermal structural changes. Three-run flow cycle showed that palm oil based spread exhibit higher thixotropic behaviour meanwhile the sample with the highest hazelnut percentage (45%) displays the narrowest hysteresis area. Finally by Casson regression, it was found plastic viscosity (η_{CA}) increase by decreasing the fat/sugar ratio. This latter result may be related to lower lubrication and emulsifying properties of fat layer around solid particle with consequently higher friction.

4. Conclusions

The principal aim of this work was the knowledge development in the research area of rheological characterization of food semi-solid systems as hazelnut-cocoa based spreads. Rheological analysis highlighted a pseudo-plastic behavior in all spreads with the elastic component prevalent on the viscous one (G'>G''). Rotational analysis showed the strictly dependency of flow curve from temperature in all cases. Moreover, geometry changing determined only flow index (n) value modification. Spread with greater K variation demonstrated a higher tendency of G' and G'' curves to cross-over at higher temperature. In addition, a greater decrease of friction factor and more significant shape modification of the Stribeck curves highlight thermal structural changes. Palm oil based spread exhibited higher thixotropic behaviour meanwhile the sample with the highest hazelnut percentage (45%) displayed the narrowest hysteresis area.

Acknowledgements

This work was supported by the Fondazione Cariplo and Regione Lombardia through the research project Cremona Food-LAB, grant n. 2015/1341.

ECCE12
The 12th EUROPEAN CONGRESS OF CHEMICAL ENGINEERING
Florence 15-19 September 2019

The influence of water addition in Pre-Treatment of Sugarcane Straw Using Three Different Ionic Liquids

Felipe Ferrari[1*], Ariel Hijo[1], Jorge Pereira[2], Marcus Forte[1*]

1 Faculty of Food Engineering, University of Campinas (UNICAMP), Campinas 13083-862, SP, Brazil; 2 School of Pharmaceutical Sciences, São Paulo State University (UNESP), Rodovia Araraquara-Jaú/Km 01, Campos Ville, 14800-903 Araraquara, SP, Brazil

**Corresponding author: ferrari.faf@gmail.com / forte@unicamp.br*

Highlights

- Acetate based ILs had better performance on dry straw pre-treatment.
- [Emin][Ac] showed the best aptitude to pre-treat the dry straw.
- [Emin][Ac] was the most impacted by water addition.
- [Mea][Hex] was the only IL positively affected by water addition, regarding enzymatic digestibility.

1. Introduction

The replacement of fossil fuels by renewable alternatives has been studied in order to mitigate the environmental impact of energy production. However, the use of lignocellulosic (LC) residues, such as sugar cane straw (SW) to the synthesis of biofuels, demands pre-treatment, due to its complexity. The recent use of ionic liquids (ILs) in this process emerges as a strategy to overcome the problems faced, such as high-energy demand and inhibitory compounds production [1]. The ILs´ aptitude to efficient pre-treat SW in presence of water is crucial since LC materials are highly hydrophilic, and water addition is one strategy to overcome the hurdle of IL cost.

2. Methods

Brazilian Bioethanol Science and Technology Laboratory (CTBE) provided the grinded straw. Sieves (between 16 and 24 mesh) were used as feedstock for pre-treatments. Chemical composition was assessed before and after each experiment using NREL31 methodology adapted from CTBE. 1-ethyl-3-methylimidazolium acetate ([Emim][Ac], 98 % pure) was purchased from Iolitec (Germany) and used as received. 2-hydroxyethylammonium acetate ([Mea][Ac]) and 2-hydroxyethylammonium hexanoate ([Mea][Hex]) were synthetized in Schott flasks through acid-basic neutralization. All other chemicals and standards were purchased from Sigma Aldrich (Germany) and used as received. Enzymatic hydrolysis was performed in 1.5 mL plastic tubes using Cellic CTec2 (Novozymes), at 5% (w/w) of solid loading and 10 FPU of enzyme per gram of biomass. Hydrolysis was carried out in pH 4.8, citrate buffer, for 48h. The enzymatic digestibility of cellulose and hemicellulose was calculated according the relationship between initial solid mass and sugars concentration from supernatant (adapted from NREL's LAP TP-510-4363031,32). Pre-treatment assays were done in triplicate. 0.6 g of dry SW was mixed with pure IL, and with IL 70 %(w/w) in H2O solution at 6% (w/w) solid loading, and then placed, in a convection oven at 90 °C for 12h. After the pre-treatment 10 g of water were added to each sample.

3. Results and discussion

The process using [Emin][Ac] had the best performance among the tested pure IL, entailing in 100 % of glucose realize after enzymatic digestion, followed by [Mea][Ac] and [Mea][Hex] 69 % and 46 %, respectively, without water addition. Both $[Ac]^-$ based IL had similar performance on hemicellulose digestibility, 54 % for [Mea][Ac] and 55 % for [Emin][Ac]. Although acetate based ILs are described as good enhancers on biomass pre-treatment [2], it is evident that changes of cations also play an important role on IL aptitude to pre-treat LC, mainly on cellulosic portion.

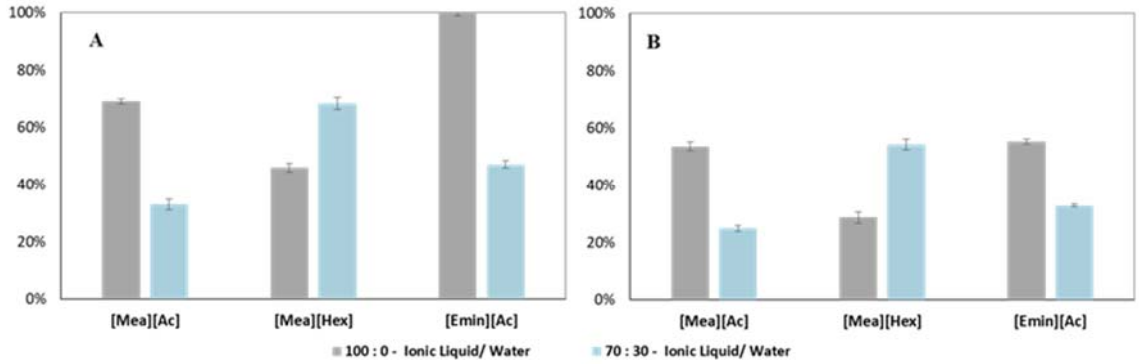

Figure 1. Enzymatic digestibility of cellulose (A) and hemicellulose (B) prevenient from residual solids after pre-treatment.

Nevertheless, in presence of water, [Mea][Hex] had the best performance among the tested IL, showing an opposite effect in this circumstance. Instead of the negative effect as observed in [Mea][Ac] and [Emin][Ac] process, water addition enhanced cellulose and hemicellulose digestibility in 49 % and 89 %, respectively. Acetate based ILs are good hydrogen bound acceptor, reason why IL species with this anion have good performance on LC pre-treatment [3], which also lead to higher interaction with water through hydrogen bound. Moreover, water tends to interact closely to the charged areas of IL (hydrophilic moiety) [4], the longer chain length of hexanoate anion my difficult the solvation of the molecule, thus allowing it to interact more efficiently with LC matrix than acetate in presence of water.

4. Conclusions

Considering enzymatic digestibility as criteria, [Mea][Hex] showed the best performance regarding water addition (the same values of cellulose and hemicellulose digestibility comparing with the pure [Mea][Ac]). The acetate based ILs were negatively impacted by water presence. Moreover, [Emin][Ac] had the worst stability regarding water addition, in the tested conditions, despite its good performance without water addition.

Acknowledges

The authors would like to acknowledge FAPESP for financial support, projects 2015/50612-8 and 2017/24520-4.

References

[1] Agbor, V. B.; Cicek, N.; Sparling, R.; Berlin, A.; Levin, D. B. Biomass Pretreatment: Fundamentals toward Application. Biotechnol. Adv. 2011, 29 (6), 675–685.

[2] Doherty, T. V.; Mora-Pale, M.; Foley, S. E.; Linhardt, R. J.; Dordick, J. S. Ionic Liquid Solvent Properties as Predictors of Lignocellulose Pretreatment Efficacy. Green Chem. 2010, 12 (11), 1967–1975.

[3] Brandt, A.; Gräsvik, J.; Hallett, J. P.; Welton, T. Deconstruction of Lignocellulosic Biomass with Ionic Liquids. Green Chem. 2013, 15 (3), 550–583.

[4] Sánchez, P. B.; García, J.; Pádua, A. A. H. Structural Effects on Dynamic and Energetic Properties of Mixtures of Ionic Liquids and Water. J. Mol. Liq. 2017, 242, 204–212.

ECCE12
The 12th EUROPEAN CONGRESS OF CHEMICAL ENGINEERING
Florence 15-19 September 2019

Development of capillary suspension by green tea powder and coconut oil to produce novel sol-gel characteristic functional food.

Hiroki Sato† and Masanao Imai*

Course of Bioresource Utilization Sciences, Graduate School of Bioresource Sciences, Nihon University, 1866 Kameino, Fujisawa, Kanagawa-pref. 252-0880, Japan
† present address: Iwai Pharma Tech Co.Ltd., 3-17-10 Higashi-Kojiya, Ota-ku,Tokyo 144-0033, Japan
**corresponding author: XLT05104@nifty.com*

Highlights

- Capillary suspension by green tea powder and coconut oil appears novel rheological food.
- When the volumetric fraction of additive water was 0.032, the fluid dynamics was changed.
- Apparent viscosity and shear stress were increased by small amount of additive fluid.

1. Introduction

Solid-liquid suspension was commonly appeared in foods, cosmetics and pharmaceutical supplements. Fluid dynamic character of conventional solid-liquid suspension was drastically changed by small amount of additive fluid[1]. That has been called as a capillary suspension illustrated by Fig.1. Networks of liquid bridges of additive fluid were looks like as a "capillary mesh"[2]. Some additive small amount of fluid was introduced into a conventional solid particles in oil suspension, fluid dynamics was drastically changed at the desired amount of additive fluid. It showed typical rheological character not Newtonian fluid. The aim of this study was to investigate change of fluid dynamic character of food based solid in oil suspension and capillary suspension[3]. It was promise for forthcoming novel rheological characteristic fluid applied for tubular packaged foods, cosmetics and pharmaceutical supplements[4].

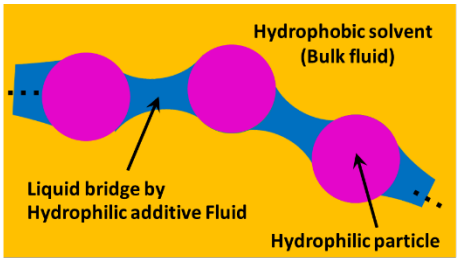

Figure 1. Network structure of capillary suspension.

Table 1. Definition of volume fractions.

$$\phi_{S/T2} = \frac{\text{Volume of particle}}{\text{Total volume}}$$

$$\phi_{L/T2} = \frac{\text{Volume of solvent}}{\text{Total volume}}$$

$$\phi_{AD/T3} = \frac{\text{Volume of Additive fluid}}{\text{Total volume}}$$

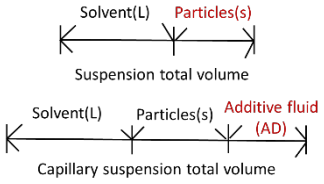

2. Methods

In this study, green tea powder and coconut oil was employed to make a conventional solid in oil suspension. Water was used as an additive fluid to make a capillary suspension. Green tea powder was purchased from Tsujiri Ltd. (Kyoto, Japan). Spherical assumed mean diameter was measured as 4.07 µm. Density of green tea powder in dried state was measured 1.12 [g·cm^{-3}]. Coconut oil

was purchased from Nissin Oillio Co. Ltd. (Tokyo, Japan). Density of coconut oil was measured 0.926 [g･cm^{-3}]. Coconut oil appeared liquid state at room temperature. Rheological character of suspension and capillary suspension was measured by ARES Rheometer, TA Instruments. Disc diameter was 8 mm. Gap was set at 0.5 mm, and the shear rate in measuring was ranged within 0.1 s^{-1} – 100 s^{-1}. Temperature was conveniently set at room temperature 298±1 K.

3. Results and discussion

Definition of volumetric fraction of green tea powder particle in coconut oil shows as $\Phi_{S/T2}$, where S indicates “solid” , L indicates liquid, and T2 means “2 components system”. Volumetric fraction of additive water shows as $\Phi_{AD/T3}$,where AD indicates “additive water”, and T3 means “3 components system”. Table 1 summarized these definitions.

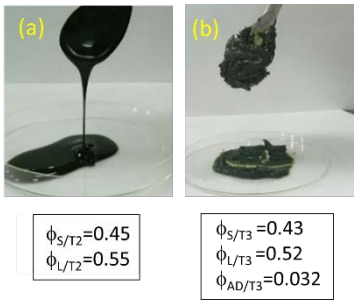

Figure 2. Preparation of capillary suspension

(a)Normal suspension (b) Capillary suspension.

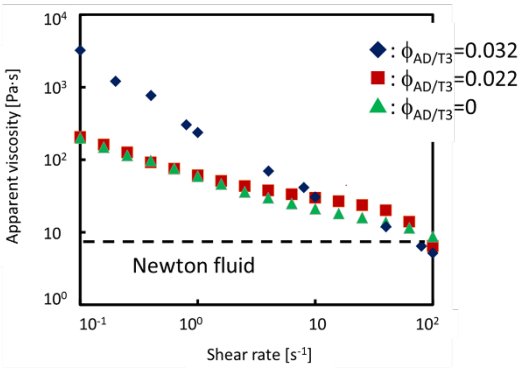

Figure 3. Apparent viscosity vs. Shear rate

When the volumetric fraction of additive pure water more than 0.032, the fluid dynamics of suspension was drastically changed to gel-like capillary suspension (Fig.2).

The rheological properties of the capillary suspension were measured by a strain-controlled rheometer. Apparent viscosity and shear stress were increased by adding a small amount of additive fluid (Fig.3). This indicated that capillary suspension has characteristic to keep the form.

4. Conclusions

Capillary suspension composed by green tea powder and coconut oil was successfully prepared. Apparent viscosity and shear stress were increased by small amount of additive fluid. When the volumetric fraction of additive water $\Phi_{AD/T3}$ was 0.032, the fluid dynamics was changed to gel like character. Novel rheological characteristic fluid was applied for tubular packaged foods, cosmetics and pharmaceutical supplements. They were promised as easy handling for chidden, older people and handicapped persons.

References

[1] Erin Koos, Norbert Willenbacher, Science. 331, 897, (2011)
[2] Erin Koos, Norbert Willenbacher, Soft Matter. 8, 3398, (2012)
[3] Susanne Wollgarten, Ceren Yuce, Erin Koos, Norbert Willenbacher, Food Hydrocolloids. 52, 167-174, (2016)
[4] Susanne Hoffmann, Erin Koos, Norbert Willenbacher, Food Hydrocolloids. 40, 44-52, (2014)

Ultrasonic Bath as a Complement to the Extraction of Bee Pollen Colorants

Suárez-Rivero, Deivis*[a]; Marin-Mahecha, Olga[a]; Guayabo-Miranda, Cristhian A.[a]; Marín Torres, Daniel[b]; Bermudez- Quintero, Sergio L.[c]; Ortiz-Aguilar, Jannet[c]
[a]Fundación Universitaria Agraria de Colombia – UNIAGRARIA.
[b]Universidad Nacional Abierta y a Distancia – UNAD.
[c]Universidad Cooperativa de Colombia – UCC.
*deivissr2000@hotmail.com

Nowadays, the importance of pollen is given by its great source of protein, colorants among other functional compounds that are incorporated into the human and animal diet; beyond pollination (fertilization process between similar plants) to improve them, make them resistant to pesticides, to dehydration or increase crop production. It's like that in this research we sought to determine the best type of extraction using the Soxhlet method with and without pretreatment through the use of an ultrasonic bath. Additionally, the influence of the type of solvent based on its polarity was analyzed, using acetone and ethanol. For this purpose, apicultural pollen collected from the municipalities of Tenjo and Zipaquirá was used, botanical origin, taken mainly from flowers *Taraxacum officinale* (L.) Weber and Eucalyptus sp. of native forest in the area. On the other hand, the second pollen was extracted from the municipality of Fundación, Magdalena, with a botanical origin especially from *Citrus* sp., *Theobroma* and *Coffea*. For both pollen processes, the preexperimental variables were % humidity, % dry mass, pH and ° Brix, where these gave similar values, while the obtained yields showed that the combination between ethanol and ultrasonic bath is the most suitable for extraction with values higher than 20 % yield. In this context, it was established that, with the use of the ultrasonic bath for the extraction of apicultural pollen dyes and depending on the botanical origin, the solvent used and the extraction method to be used will perform a marked action on the yields of the extracts that will be obtained.

ECCE12
The 12th EUROPEAN CONGRESS OF CHEMICAL ENGINEERING
Florence 15-19 September 2019

Review of results in sugar crystallization obtained at the University of Chemical Technology in Prague

Zdenek Bubnik*, Pavel Kadlec, Evzen Sarka, Vladimir Pour, Andrea Hinkova, Svatopluk Henke and Simona Gillarova

University of Chemical Technology, Technicka 3, 16628 Prague 6, Czech republic

**Corresponding author: zdenek.bubnik@vscht.cz*

Highlights

- Physical and chemical properties of sucrose and sugar solutions
- The growth kinetics of sugar crystals in pure and impure sugar solutions
- Simulation and mathematical modeling of new processes and technologies
- Experimental work for industry and cooperation with industrial partners

This paper represents a summary of most important research activities in sucrose crystallization, in which the Department of Carbohydrates and Cereals, part of the University of Chemistry and Technology (UCT) Prague, have been focused over the last 25 years. A wide range of these projects has been carried out in cooperation with many research institutes, universities and industrial partners.
These activities can be divided into four main research areas that are interconnected and support each other.

1st area: Physical and chemical properties of sucrose and sugar solutions

The main condition for a successful control of the crystallization process is knowledge of physical properties of sucrose, other sugars and their impure solutions. At the beginning, it was necessary to obtain and verify these data experimentally. The most important properties to measure were: *(a)* density of sugar solutions (cooperation with Prof. Dandar, STU Bratislava); *(b)* solubility of sugars in technical sugar solutions (cooperation with Dr. Parkin, the British Sugar Research Centre in Norwich); *(c)* the effect of impurities on a shape of sugar crystals (cooperation with prof. Mantovani and Prof. Vaccari, University of Ferrara); and *(d)* the increase of boiling point of sugar solutions (Dr. Sarka, UCT Prague). This work involved a modification and/or design of new experimental devices. The most important data and results have been published in professional and scientific papers; included in the SUGAR TECHNOLOGY MANUAL (authors: Bubnik, Bruhns, Kadlec, Urban); and presented in congresses, such as CITS, ESST and AvH.

2nd area: The growth kinetics of sugar crystals in pure and impure sugar solutions

This area included work on gathering kinetic data that describe the growth of sugar crystals under conditions simulating the industrial environment. Equations describing the crystallization process have been suggested and verified using the data obtained from the 1st research area. Newly designed and built experimental equipment have been also used in laboratory and pilot plant trials.

Ultrasonic techniques for measurement of properties of sugar solutions and suspensions as well as US methods for determination of the metastable zone width have been developed and applied for sucrose crystallization control.
In cooperation with Prof. Mathlouthi from the Universite de Reims Champagne-Ardenne, a new image analysis method has been developed for control of the crystal formation and evaluation of crystal size distribution in crystallization processes.

3rd area: Simulation and mathematical modeling of new processes and technologies

Physical data about sugar solution properties and kinetic equations became an indispensable condition for further work on creation of new technological diagrams; simulation and modeling of processes; and not least, design of new manufacturing process diagrams for industrial partners. These activities were carried out under the European project Copernicus SUCLEAN that has been focused on raw juice crystallization and design and modeling of new sugar processing diagram. Partners in this project were: University of Ferrara, UMIST Manchester (Dr. Klemes), UCT Prague and Politechnika Warszawska Fillie Plock (Prof. Urbaniec). An essential part of the research was a study of application of membrane filtration (MF and NF) for purification of sugar solutions before crystallization carried out in cooperation with LSU Baton Rouge, USA.

4th area: Experimental work for industry and cooperation with industrial partners

The fourth part of our activities involves application of experimental data in measurement and modeling of processes in real sugar manufactures. Significant cooperating partners were VUC Prague (continuous crystallizer, Dr. Gebler), sugar factory TTD Dobrovice and other Czech sugar plants, ZVU Hradec Kralove, Czech Technical University Prague, and the Mikropur Company Hradec Kralove (Dr. Pridal).

ECCE12
The 12th EUROPEAN CONGRESS OF CHEMICAL ENGINEERING
Florence 15-19 September 2019

Understanding freeze drying of sucrose solutions

Mercedeh Sadat Hosseinalipour, Luca Bosetti, Viktoria Wiedmeyer, Marco Mazzotti*

Institute of Process Engineering, ETH Zurich, 8092 Zurich, Switzerland

mhossein@ipe.mavt.ethz.ch

Highlights

- Freeze drying, a pharmaceutical unit operation to ensure prolonged product stability during storage
- Model study of sucrose, as one of the main excipients used in pharmaceuticals
- Importance of ice nucleation for freeze drying and final product structure

1. Introduction

Freeze-drying is a process, where a solvent, e.g. water, is removed from a frozen product under vacuum. Such a process, also called lyophilisation, is widely used in pharmaceutical industry to improve stability and long term storage of labile drugs [1]. Freezing and drying are the main two steps of the process, among which the latter can be further divided into primary and secondary drying. Controlling ice nucleation temperature during the freezing step is one of the most challenging aspects of the development of a lyophilisation cycle and it affects drying time, product morphology, protein preservation, intra-vial and vial-to-vial heterogeneity and process performance [2]. In order to overcome this challenge, understanding thermodynamics and kinetics of the product is of great importance.

In addition to being bulking agents, disaccharides, like sucrose, have proven to be most effective in stabilizing products such as liposomes and proteins during lyophilisation [3]. Since in many pharmaceutical preparations the bioactive content amounts to no more than a few percent, the freeze-drying characteristics of such formulations are often governed mainly by the physical and thermomechanical behaviour of the excipient mixture [4]. In the present work, sucrose-water solution has been chosen as a model solution to be freeze-dried regarding its wide usage in pharmaceutical formulations.

2. Methods

The basis to investigate thermodynamics and kinetics is the state diagram of sucrose-water solution with experimentally driven equations of solubility, solidification and glass transition temperature [5], which is shown in Figure 1.

Experiments were performed to investigate the effects of different thermal treatments, drying conditions and solution volume on the final freeze-dried product. XRD and TGA were used to study crystallinity and water content of different experiments.

3. Observations and discussion

Freeze-dried sucrose of all experiments were amorphous, as expected [5]. Samples with the same freezing treatment but different drying conditions resulted in very different specifications of the final product related to cake appearance, colour and stickiness. Regarding their characteristics, some of the products were classified as totally or partially collapsed cakes. These observations further clarified that sucrose, as an important component in pharmaceutical formulations, can present various states.

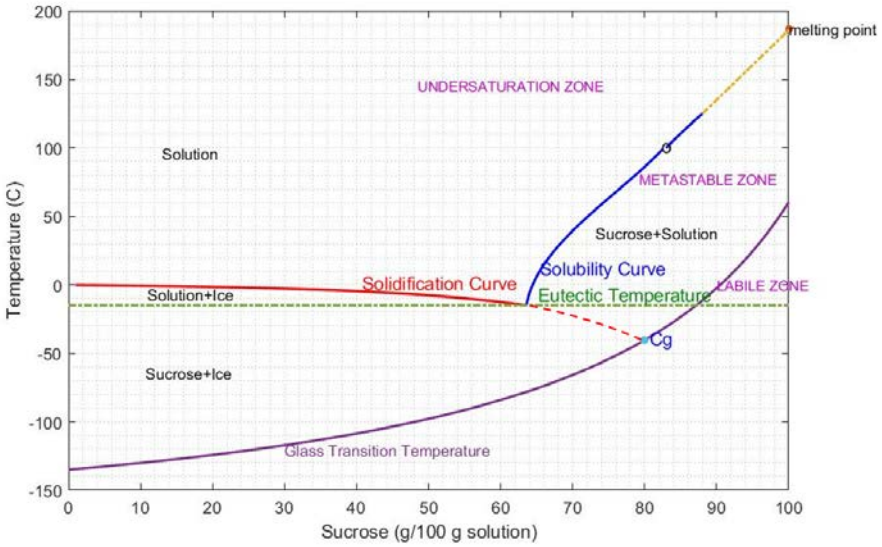

Figure 1. State diagram of sucrose-water [5]

4. Conclusions

In this work, it has been discussed how better understanding of the state diagram for a formulation to be freeze-dried can lead to a successful process. The importance of thermodynamics and kinetics is crucial to improve the design of a lyophilisation cycle of a formulation in a more predictable way.

References

[1] S. Nail, G. Gatlin, "Freeze drying: principles and practice," in *Pharmaceutical Dosage Forms - Parenteral Medications*, 2010, pp. 353-381.

[2] R. Pisano, "Alternative methods of controlling nucleation in freeze drying," in *Lyophilization of Pharmaceuticals and Biologicals*, New York, NY, Humana Press, 2019, pp. 79-111.

[3] S. Leslie, E. Israeli, B. Lighthart, J. Crowe and L. Crowe, "Trehalose and sucrose protect both membranes and proteins in intact bacteria during drying," *Applied and Environmental Microbiology,* vol. 61, no. 10, pp. 3592-3597, 1995.

[4] F. Franks, "Freeze-drying of bioproducts: putting principles into practice," *European Journal of Pharmaceutics and Biopharmaceutics,* vol. 45, pp. 221-229, 1998.

[5] M. Mathlouthi and P.Reiser, Sucrose, properties and applications, Chapman & Hall, 1995.

This project has received funding from the European Research Council (ERC) under the European Union's Horizon 2020 research and innovation programme under grant agreement No 2-73959-18.

ECCE12
The 12th EUROPEAN CONGRESS OF CHEMICAL ENGINEERING
Florence 15-19 September 2019

Prediction of hesperidin content in orange peel extract using artificial neural network model

Stela Jokić[1], Silvija Šafranko[1], Martina Jakovljević[1], Ana-Marija Cikoš[1], Mate Bilić[1], Maja Molnar[1]

[1]*Josip Juraj Strossmayer University of Osijek, Faculty of Food Technology Osijek, Franje Kuhača 20, 31000 Osijek, Croatia*

**Corresponding author: stela.jokic@ptfos.hr*

Highlights

- Citrus peel is a by-product, which represent a potential source of valuable components.
- A three layer FFBP-ANN was investigated for hesperidin prediction in orange peel extract.
- The ANN model was found to be a useful tool for hesperidin yield prediction.

1. Introduction

During industrial citrus processing, large quantities of waste material is produced mainly as citrus peels [1]. These food industry by-products represent a potential source of valuable components being important raw materials in the food, chemical and pharmaceutical industries. Hence, the utilization of these citrus residues rich in bioactive and functional components has become a study of interest. In recent years, artificial neural networks (ANNs) are receiving more attention from researchers as an effective predictive tool. It has also been reported that ANN models can be used to predict extraction yields [2]. So in this study, the prediction of hesperidin content as the main bioflavonoid in orange peel extracts was studied by ANN.

2. Methods

In this work, an ultrasound-assisted extraction (UAE) was performed from reused orange peel (after SC-CO_2 extraction) in order to obtain the extracts rich in hesperidin - bioflavonoid with wide range of pharmacological properties. A three-layer feed-forward backpropagation artificial neural network (FFBP-ANN) was proposed to investigate the influence of four operating parameters: extraction temperature (30, 50, 70 °C), time (15, 30, 45 min), ethanol/water ratio (20%, 50%, 80% v/v) and solvent-solid ratio (10, 30 and 50 mL/g) on the extraction yield of hesperidin in UAE extracts. The performance of the developed ANN predictive models was evaluated based on the obtained mean square error (MSE) and coefficient of determination (R^2) parameters. The experimental hesperidin yield was determined by reversed-phase high performance liquid chromatography (HPLC) and its content was in the range from 3.3 to 23.0 µg/mg.

3. Results and discussion

Comparing developed models based on the AAD (Average Absolute Deviation), MSE (Mean Square Error), and R^2 coefficient (Coefficient of determination), the best performing ANN model was determined. These statistical parameters are useful in assessing model performance. The obtained

AAD of 5.24 %, R^2 value of 0.9769 and 0.9837 and minimum MSE of 0.0108 and 0.00796 during training and testing stage indicated that developed 4-5-1 FFBP-ANN model is the best performing model in predicting the hesperidin yield for studied dataset.

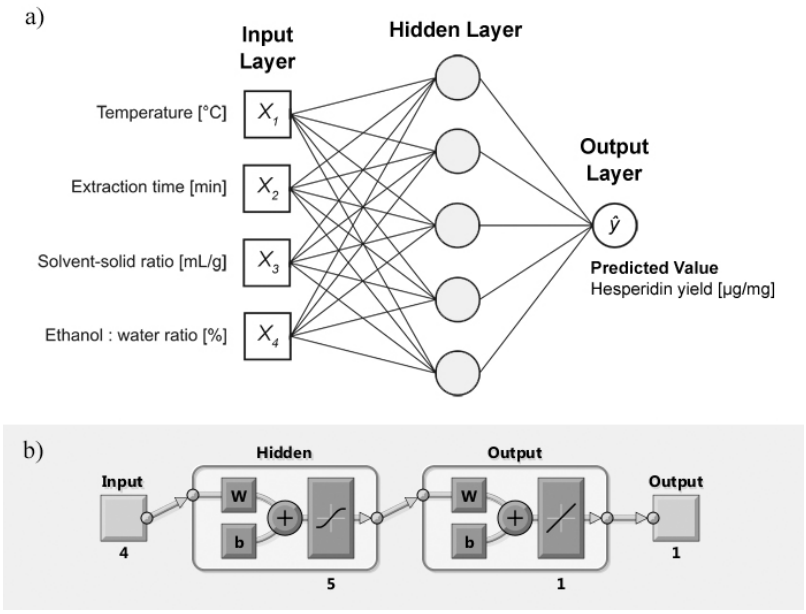

Figure 1. Configuration of the developed ANN [4-5-1], a) schematic representation and b) diagram automatically generated by MATLAB software.

4. Conclusions

Yield prediction of target components is of great importance and the first step for defining the optimal operating conditions, but also necessary for a successful regulation of extraction processes. It is well-known that citrus peel is a rich source of bioactive natural compounds, therefore it is essential to find an appropriate technique for optimization of extraction process. The ANN predictive model was found to be a suitable performing model for extraction hesperidin yield prediction from orange peel extract, as indicated by the statistical analysis.

Acknowledgments

This work has been supported by Croatian Science Foundation under the project “Application of innovative techniques of the extraction of bioactive components from by products of plant origin” (UIP-2017-05-9909)

References

[1] Y. Shan, Comprehensive Utilization of Citrus by-Products, first ed., Academic Press, London, 2016.
[2] A. Toboc, V. Lavric, Rev. Chim. 63 (2012) 743-748.

ECCE12
The 12th EUROPEAN CONGRESS OF CHEMICAL ENGINEERING
Florence 15-19 September 2019

Risk & Decision Making in Research Environment.

Anastasia Kalugina, Thierry Meyer

Ecole Polytechnique Fédérale de Lausanne

Institute of Chemical Sciences and Engineering; EPFL SB ISIC GSCP, CH-1015 Lausanne Switzerland

**Corresponding author: Thierry.meyer@epfl.ch*

Highlights

- Laboratory Risk profile is not limited by the number of Hazards.
- Underestimation of the Human Factor might lead to severe consequences.
- Real Risk Reduction Potential of the Measures is influenced by the Feasibility of them.

1. Introduction

During the last decades, many studies have been carried out on topics related to risk and decision-making (DM) in different sectors of economics. With an improvement in quality of life, as well as the introduction of Corporate Social Responsibility principles, more and more companies' resources are spent on safety enhancement. Generally, risk management (RM) and DM tools are only developed in the business environment. However, when talking about Academia, one has to consider this environment as safe. In order to keep such brand image, universities have to implement an effective system of risk management. An essential part of the RM process are the risk assessment and the DM steps. Due to the complexity of the Academia environment (different cultural background of the employees and students, high turnover, explicit professional features of the individuals and the important role of their creativity), the decision-making process becomes more complicated. Thus it requires a tool which takes into account the entire specific features of the environment and allocates resources according to the objectives, reducing the risk to an acceptable level. The objective of this project is to develop such a methodology which will allow making optimal decisions according to the settled objectives.

2. Methods

A combination of various qualitative and quantitative research methods has been used: unstructured interviews of safety experts, surveys, participant observations, case studies and simulations. Some of the qualitative data obtained have been transformed using semi-qualitative research methods such as FAHP (Fuzzy Analytical Hierarchy Process) and TOPSIS (Technique for Order of Preference by Similarity to Ideal Solution).

3. Results and discussion

In order to build a useful decision-making tool, it is important to have reliable outputs from the Risk Assessment step. The model is built in such a way that it considers the Risk as a 3-component phenomenon (fig. 1). The legal component of the risk [1] allows decision makers to choose among binding and optional measures. The introduction of the Human Factor [2] allows decision makers to choose among different corrective measures, those which are more suitable in the specific working environment. Furthermore, the Human Factor serves as a signal to act on the

improvement of the Safety Climate. Hazard indexes are evaluated based on the model proposed in the Laboratory Assessment Risk Analysis (LARA) method [3]. According to this method, the risk is calculated in relation to each particular Hazard and represents a combination of several parameters, which cumulatively give the value of the Laboratory Criticality Index (LCI).

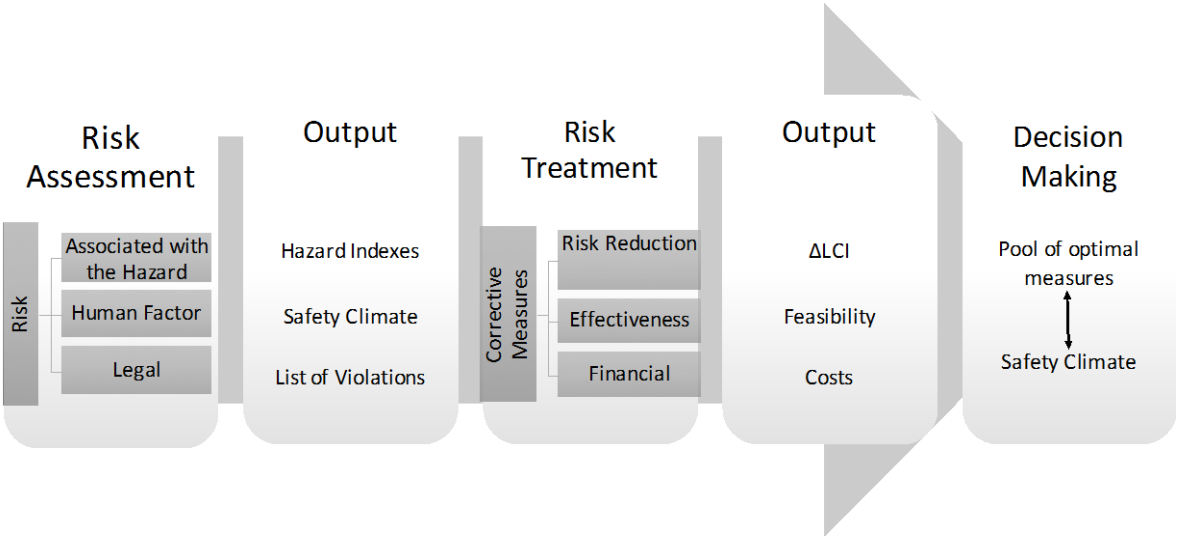

Figure 1. Decision-Making tool.

The next step of the RM process is the evaluation of the chosen corrective measures. It is important to consider their effectiveness from the risk reduction perspective, but also take into account how suitable they are in the specific working environment and in relation to the processes analyzed. Six parameters influencing the decision-making process have been identified based on the observations of the audits conducted by the OHS group at EPFL and following discussions with safety engineers or safety specialists. Two parameters describe characteristics of the measures which are affected by the Human Factor, three parameters address the technical effectiveness of the measures and one parameter is an indicator of cost-effectiveness. The six parameters are combined together in one parameter – Feasibility. Based on the results of the Risk Assessment and Evaluation of the measures, Fuzzy-TOPSIS is then used for a Resource Allocation optimization.

4. Conclusions

The model described here for Decision-Making in a research environment is a flexible tool that can be applied to different laboratories, where different safety climates, risk profiles and financial situations are present. This method allows decision makers to obtain optimal safety decisions depending on the settled objectives. It is multi-objective and can be used not only by experts but also by inexperienced users for interpretation.

References

[1] E. Marsden, Risk regulation, liability and insurance, APPORTS, 2014
[2] H. Ikin, Overcoming Human Limitations in Managing Risk, TMS Consulting, 2015
[3] A. Ouédraogo, A. Groso, Th. Meyer, Risk analysis in research environment – Part I: Modeling Lab Criticity Index, using Improved Risk Priority Number, Safety Science 49 (6): 778-784, 2011

ECCE12
The 12th EUROPEAN CONGRESS OF CHEMICAL ENGINEERING
Florence 15-19 September 2019

How hurricane Harvey affected the Chemical and Process Industry.

Valeria Casson Moreno[1], Noor Quddus[2], Alessio Misuri[1], Valerio Cozzani[1*]

1 University of Bologna, Department of Civil, Chemical, Environmental and Materials Engineering, Italy;
2 Texas A&M University, Mary Kay O'Connor Process Safety Center, College Station, United States
**Corresponding author: valerio.cozzani@unibo.it*

Highlights

- The effect of hurricane Harvey on Chemical and Process Industry was investigated
- The focus was on the release of chemicals from industrial installations
- Vulnerable equipment were identified
- A lack of effectiveness of physical safety barriers was revealed

1. Introduction

The number of climate related natural catastrophes is growing in last years (Hopper, 2016), arising the concern of stakeholders such as civil society, industry and insurance companies. Indeed, in the recent past, the impact of natural phenomena on industrial facilities has proved to be able of severe consequences and escalating scenarios (Krausmann and Cruz, 2016). For this reason, understanding NAtural events triggering a TECHnological scenario (NaTech) is becoming a crucial topic.
In this study, the effects of hurricane Harvey on Chemical and Process Industry were analyzed. Harvey was one of the most severe and costliest hurricane hitting the United States ever. It heavily affected the economy of the region: during Harvey, the estimated loss on U.S. refining capacity was of approximately 20 %.
The analysis is focused on the releases of hazardous substances during the hurricane. The aim was to identify the equipment and conditions involved. The key issues highlighted in the present research provide a valuable insight for better informed decision making during risk assessment and management of NaTech events.

2. Methods

The analysis of the events is based on the data available from the United States Coast Guard National Response Center (NRC) Database (http://nrc.uscg.mil/). The Database is aimed at the collection of information on oil spills and chemical releases. Among all the dataset available, the records included in the present analysis were those related to industrial facilities only and explicitly ascribable to hurricane Harvey.

3. Results and discussion

The total number of record selected from the NRC Database was 80. The majority of the records (91 %) are related to on-shore facilities and, in particular, the claimed loss of containment was from: (i) equipment (85 %) and (ii) pipelines (4%). In 2 cases, the release of chemicals took place from mobile trailers: one of the cases is the well-known Arkema incident (Chemical Safety Board, 2018). The remaining 9% of the cases described are related to off-shore facilities.

The analysis of the equipment involved in the loss of containment revealed that tanks are the most vulnerable equipment (see Figure 1). Nevertheless, it has to be noted that a similar share of events involved emergency gas flares: the release of chemical was not "accidental" but took place because of emergency shut-down (and following start-up) procedures as a consequence of the hurricane.
The majority of the releases recorded was to air (41 %, see Figure 2), followed by water (35 %) and soil (5 %). Unfortunately, in 6 cases only (8 %), the release was contained (e.g. in dikes or containment ponds), revealing a lack of effectiveness of physical safety barriers.

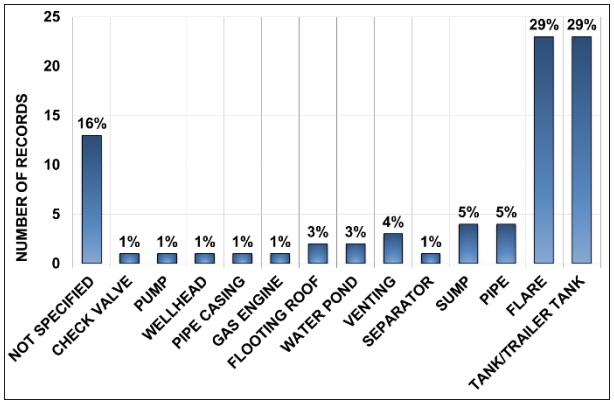

Figure 1. Analysis of the equipment involved in the release of chemicals during hurricane Harvey based on NRC data.

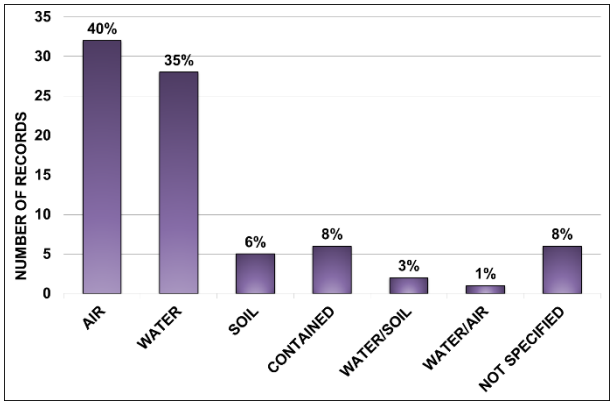

Figure 2. Analysis of the release to air, soil, and water environments during hurricane Harvey based on NRC data.

4. Conclusions

The analysis of data on the releases of chemicals during Harvey highlighted that tanks were the most vulnerable equipment during the hurricane. Of particular note was the role of flares during emergency shut-down and start-up operations. In general, a lack of effectiveness of physical safety barriers was observed.

References

[1] P. Hopper, Weather and Climate Extremes 11 (2016) 70-79.
[2] Krausmann, E., Cruz, A. M., Past Natech Events, Natech Risk Assessment and Management: Reducing the Risk of Natural-Hazard Impact on Hazardous Installations, 2016, 3-31.
[3] United States Coast Guard National Response Center: http://nrc.uscg.mil/ (accessed 10.1.18).
[4] Chemical Safety Board, Arkema Final Report, 2018. https://www.csb.gov/csb-releases-arkema-final-report/

ECCE12
The 12th EUROPEAN CONGRESS OF CHEMICAL ENGINEERING
Florence 15-19 September 2019

Fire and Explosion risk indexing methods analysis and application to chemical plants

Enrico Danzi[1], Luca Fiorentini[2], Giovanni Pinetti[2], Marta Farinella[2], Luca Marmo[1]

1 Applied Science and Technology Dept. Politecnico di Torino, Cso Duca degli Abruzzi 24, 10129, Turin (Italy); 2 TECSA SRL, Via Figino 101, Pero MI, (Italy)

**enrico.danzi@polito.it*

Highlights

- Fire and explosion risk assessment
- Chemical process plants
- Indexing methodologies

1. Introduction

Risk assessment in industrial workplaces is mandatory by a number of national and over national laws, directives and technical standards and it must consider the totality of potential hazards related to processes and manufacturing activities. Among them, fire and explosion hazards, and related risks, are present in most industries, particularly in chemical and process industry due to the hazardous properties of the substances handled as well as, often, the process conditions. Most common and simplified methods for oil & gas industry have been developed by Dow Chemical Company and Imperial Chemical Industries, namely Fire and Explosion Index (F&EI) [1] and the Mond Index [2]. Lately, Khan et al. have developed the SW&HI method (Safety Weighted & Hazards Index, [3])which could also apply to fire and explosion risk evaluation in chemical industrial realities. Both the methods allow a fast approach to fire & explosion risks given a number of indexes.

In the proposed work, aforementioned methods have been applied to a process plant to verify their similarities, discrepancies, and accuracy. The case study was a “chemical process” department of a chemical plant, where the main products are fine chemicals and powdered products. “Moderate” risk level have been obtained similarly by the different methods, the Mond Index being the highest among them. The most critical process for F&E risk in the facility, according to all the methods, has been identified in the the combustible powder packing operation.

A modification of the SW&HI index is proposed by the authors to overcome identified and discussed limits for a more versatile tool, to be used as a preliminary screening tool in the risk assessment workflow suitable. The new index method incorporates hazards related to solid substances having oxidizing, explosive and combustible properties. A critical and comparative analysis of the different incomes and application strategies of the three methods is given and a normalized risk index (NRI), is also proposed.

2. Methods

Plants not ruled by Seveso EU Directive, could although imply a high F&E risk, if any prevention/protection strategies are implemented. As to evaluate numerically this risk, indexing methods, devoted to risk evaluation screening procedure, could be applied. The SW&HI (Safety Weighted Hazard Index) method [3] has been developed as a quick and user-friendly tool for identifying hazards and assessing fire and explosion risk in the process industry. It represents an evolution of previous oil & gas based method, being more comprehensive and less time-consuming in the evaluation process.

3. Results and discussion

The chemical plant examined in this work is a North-western Italy company, the methods have been applied in the risk assessment of Department defined as “Chemical Product 1”, in which main products are plastic additives,

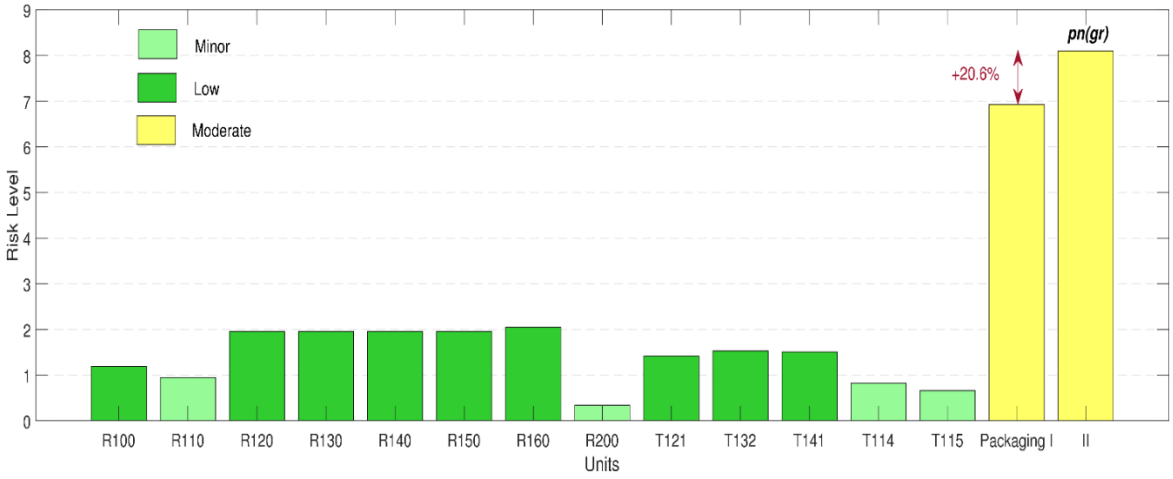

Figure 1. SW&HI results for case study, where packaging department is evaluated twice, before and after the algorithm modification imposed in this work (as to consider combustible powders).

Application of the Mond Index to the chemical department CP1 seemed to be most appropriate technique, due to its general approach in the identification of the substance (directly through physic-chemical characteristics, like ΔH_c) and the process hazards. F&EI application underlined how effectively different risk scenario could be mitigated: the measures adopted by the company manager demonstrate to be adequate with respect to actual potential hazards

4. Conclusions

A normalized risk index, defined here as NRI is introduced (Eq. 1), as to compare methods outputs: this value has to be considered as a preliminary risk level indication, or to be used in comparison with other department or chemical plants, while most hazardous areas (with a higher risk than NRI) has to be considered carefully and a detailed assessment is due to adopt the adequate protection measures. The algorithm modification of SW&HI evaluation implies an increase of about 20% of the risk level (as in Figure 1), which has not been accounted in the original method and gives the analysis a broader range of application and a more conservative approach.

$$NRI = \frac{\frac{Average\ SW\&HI}{Max\ SW\&HI} + \frac{Average\ F\&EI}{\mathrm{Max}\ F\&EI} + \frac{\ln Average\ Mond}{\ln Max\ Mond}}{4} \quad (1)$$

References

[1] DOW Chemical Company, Fire & explosion index DOW (F&EI), 6Th EDITION, AIChE, 1987.
[2] (ICI) Imperial Chemical Industries, The Mond Index, Second Edition. 1985.
[3] Khan, F. I., Husain, T. and S. A. Abbasi (2001), “Safety Weighted Hazard Index (SWeHI): A New, User-friendly Tool for Swift yet Comprehensive Hazard Identification and Safety Evaluation in Chemical Process Industries,” Process Saf. Environ. Prot., 79 (2) 65–80.

ECCE12
The 12th EUROPEAN CONGRESS OF CHEMICAL ENGINEERING
Florence 15-19 September 2019

How Heat Integrated Units become a Safely Integrated Plant

Tim Wezendonk*[1], Roel Ranzijn[1], Juan Huertas[2], Ana Cardoso Lopes[1], Ernst Visser[1] and Jelle Ernst Oude Lenferink[1]

1 Fluor B.V., Taurusavenue 155, 2132 LS Hoofddorp, The Netherlands;
2 SacyrFluor, Calle Ribera del Loira 16-18, 28042 Madrid, Spain

**Corresponding author: tim.wezendonk@fluor.com*

Highlights

- Development of improved relief scenarios for fully integrated Aromatics complex
- Simulation of vapor flow rates from columns with fired heater reboilers
- Mitigated relief loads resulting in considerably smaller flare header

1. Introduction

The design of Aromatic complexes has become increasingly more integrated over the years. The first process integration was achieved by removal of intermediate storage followed by feed-effluent heat integration. In recent years, a large degree of heat exchange between units has been applied. Together with the use of co-produced desorbent and a large amount of dividing wall columns, these developments have resulted in fully integrated aromatics complexes.

When developing relief scenarios for such an integrated complex, one should therefore look beyond the single-equipment envelop. In this paper, an example will be provided how power-failure scenarios were established and optimized for an integrated Aromatics plant.

2. Methods

The design of a 60” flare header resulting from large vapor flow rates in the Aromatics plant under relieving conditions triggered Fluor to establish a baseline relief load. Estimates from a simple black-box assessment, coupling the plant inventory to the residual heat, provided significantly lower relief loads for the governing relief scenarios. Therefore, Fluor assessed these scenarios in the various units of the complex heat-integrated Aromatics plant and established the basis for the combined relief load by development of a fully integrated plant scenario. The design data from the distillation columns, fired heaters and hydraulic circuits were used to simulate the vapor flow rates contributing to the combined relief load. By applying high integrity pressure protection systems (HIPPS) on the fired heater reboiled columns, an improved general power failure scenario provided the governing relief load and a new basis for the hydraulic calculations to perform flare header sizing.

3. Results and discussion

The basis for the general power failure scenario is a typical steady-state total unmitigated relief load resulting from the residual heat input of the fired heater reboilers into the isolated process at normal operating conditions with full loss of cooling capacity (**Figure 1**). Therefore, the relief

loads are result of the duty of the fired heaters and the available column inventory. As sizing of the individual relief valves serves the primary purpose of column protection, interaction between columns in the heat-integrated plant is not taken into account. This approach results in an overly conservative and often, cost prohibitive design of the flare header. Considering that there is a fixed amount of residual fired heater duty, the proper identification of heat integration and application of HIPPS provides an improved relief scenario and mitigated relief loads. The overall result is a more balanced design and a considerably smaller flare header of 32".

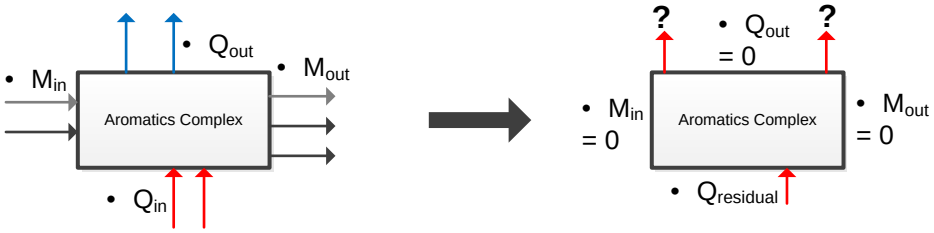

Figure 1. Sketch of the relief load resulting from the residual fired heater duty into the isolated process.

4. Conclusions

Column overpressure safety systems for completely heat-integrated plants should be carefully designed by looking beyond the single-equipment envelope. Only with a fully integrated plant scenario a proper assessment can be made for both column safety and the impact on the combined relief load for the governing relief scenario. In addition, mitigation of the combined relief load will lead to a substantial cost benefit in the design.

References

[1] API Standard 520 Part I, *Sizing, Selection and Installation of Pressure-relieving Devices, Part I – Sizing and Selection*, Ninth Edition, January 2014.

[2] API Standard 521, *Pressure-Relieving and Depressurizing Systems*, Sixth Edition, January 2014.

ECCE12
The 12th EUROPEAN CONGRESS OF CHEMICAL ENGINEERING
Florence 15-19 September 2019

Air quality assessment of smart-sustainable cities and innovative sensors system

Angela Poletti[1], Irina Tumini[2]

1 Politecnico di Milano Piazza Leonardo da Vinci, 32 Milan (Italy); 2 Indipendent researcher (Spain)

**Corresponding author: angela.poletti@polimi.it*

Highlights

- Novelty in environmental monitoring sensors.
- Bio- and chemo-sensoristic contribution to smart environment.
- Assessing smart-sustainable project of pollution reduction.
- Integration between Air Quality Monitoring (AQM) stations and crowdsourcing.

1. Introduction

Many studies describe different types of sensors and methods used for air quality monitoring, impact and exposure of an individual to air pollution, interpolation, and calibration techniques on collected data [1]. Pollution monitoring is of huge importance to environmental protection and in health effects estimates. The Air Quality Monitoring (AQM) stations network has limited ability to account for spatial variability of pollution levels in heterogeneous regions such as urban areas, which in return, renders exposure assessment a very difficult task [2]. The interest in widespread environmental monitoring is limited in the implementation of smart and sustainable city projects despite the great importance given to climate change. While monitoring technology is proliferating, thanks to the decrease in sensor costs and the diffusion of different types of technological devices, research to inform the translation of air sensor data into information that might guide an individual's decisions about daily activities remains limited [3]. At the same time, the demand for rapid detecting biosensor will increase in the near future [4].
Starting from the recent literature on bio-sensoristic and chemo-sensoristic devices for detection of environmental contaminants, the paper tries to highlight how without a quality monitoring and diagnostic system identifying chemical and biochemical substances in the environmental matrix the goal of a smart city will be missed. With this purpose, we examine a series of smart city projects focusing on the theme of environmental pollution and applied sensor technologies.

2. Methods

After selecting ten case studies in the Italian context, following the criteria of demographic dimension of the city and the presence in the first positions of the international rankings related to smart cities, we assess the smart environment (based on the Giffinger components of Smart City [5]). The assessment focuses on sensors technology and its applications in the case studies, and on the ability to make the city evolve towards greater environmental sustainability and quality of life of its inhabitants. The assessment approach is based on the multi-criteria decision aid theory, specifically using the Multi-Criteria Decision Aid Constructive Approach (MCDA-C).

3. Results and discussion

According to the literature, application of low cost sensors/monitors have already changed the paradigm of air pollution monitoring, and application of these technologies is set to grow. In real case study, the full potential of existing projects is not achieved. However, only by analysing what has been done and its impacts is it possible to identify existing problems and ensure that the integration of intelligent innovation helps users and service providers to make better decisions and take decision in real time. In this sense, the integration between monitoring networks and data collected by citizens is still in an ancillary phase, also due to the need for an expert intelligence that re-elaborates and provides suitable indicators to influence individual behaviour without creating alarmism.

4. Conclusions

The paper described an analysis of smart city projects for the sole component of environmental pollution and focused on the use of innovative sensors and sensor networks in Italy and on a sample of 10 cities selected according to the size demographic criterion and presence in national and international rankings on smart cities. The assessment of the projects was based on adherence to the achievement of sustainability and the quality of life of citizens. We have applied Multi-Criteria Decision Aid Constructive Approach (MCDA-C). The results showed a fair distance between the capacity of existing technologies and described in literature and reality.

References

[1] S. Singla, D. Bansal, A. Misra and G. Raheja, “Towards an integrated framework for air quality monitoring and exposure estimation—a review,” *Environment Monitoring and Assessment,* pp. 1-21, 2018.

[2] S. Rao, V. Chirkov, F. Dentener, R. Van Dingenen, S. Pachauri, P. Purohit, M. Amann, C. Heyes, P. Kinney, P. Kolp, Z. Klimont, K. Riahi and W. Schoepp, “Environmental modeling and methods for estimation of the global health impacts of air pollution.,” *Environmental Modeling & Assessment,* vol. 17, no. 6, pp. 613-622, 2012.

[3] B. J. Hubbell, A. Kaufman, L. Rivers, K. Schulted, G. Hagler, J. Clougherty, W. Cascio and D. Costa, “Understanding social and behavioral drivers and impacts of air quality sensor use,” *Science of the Total Environment,* pp. 866-894, 2018.

[4] G. Hernandez-Vargas, J. E. Sosa-Hernández, S. Saldarriaga-Hernandez, A. M. Villalba-Rodríguez, R. Parra-Saldivar and H. M. N. Iqbal, "Electrochemical Biosensors: A Solution to Pollution Detection with Reference to Environmental Contaminants," *Biosensors,* vol. 8, no. 29, pp. 1-21, 2018.

[5] R. Giffinger and H. Lü, The Smart City perspective: A necessary change from technical to urban innovation (First), Milano: Fondazione Giangiacomo Feltrinelli, 2015.

ECCE12
The 12th EUROPEAN CONGRESS OF CHEMICAL ENGINEERING
Florence 15-19 September 2019

Nanocellulose explosions: influence of the agglomeration and turbulence on the combustion rate-limiting step and flame propagation

Audrey Santandrea[1], Marine Gavard[1], Stéphanie Pacault[1], Alexis Vignes[2], Laurent Perrin[1], Olivier Dufaud[1]*

1 Laboratoire Réactions et Génie des Procédés, Université de Lorraine, CNRS, LRGP, F-54000 Nancy, France
2 INERIS, Parc Technologique ALATA, BP 2, F-60550, Verneuil-en-Halatte, France

**Corresponding author: olivier.dufaud@univ-lorraine.fr*

Highlights

- Great influence of agglomeration on the rate-limiting step of the combustion
- Consideration of the whole reactive surface area when evaluating explosivity
- Estimation of an unstretched burning velocity for nanocellulose

1. Introduction

Dust explosion risk assessment is relatively well established for micron-sized particles and requires the determination of key safety parameters representing the ignition sensitivity and explosion severity of the dust. When considering nanoparticles, the particle size distribution (PSD) is more likely to vary during the injection process, due to both the agglomeration phenomenon inherent to strong interactions and the fragmentation phenomenon due to flow shear stresses. As a consequence, safety parameters and their determination methods can differ significantly from micro to nanopowders. A peculiar attention has then to be given to the cloud characteristics (PSD, turbulence), more precisely at the exact moment of ignition. This work focuses on nanocellulose and aims at evaluating the influence of the agglomeration phenomenon and flow turbulence on the dust combustion. Flame propagation tests were performed to evaluate the unstretched burning velocity and explosions tests were carried out to estimate the combustion mechanisms involved.

2. Methods

A nanocellulose powder (NCC - CelluForce), with a specific surface area of 400 $m^2.g^{-1}$ and primary fiber dimensions of 3 nm width and an average length of 70 nm, was chosen for this study. The powder was mechanically pressed and then coarsely ground to form agglomerates. In addition to the pure nanocellulose, two ranges of agglomerate diameters were chosen in order to highlight the influence of particle agglomeration on dust explosion: 30-180 µm and 180-450 µm. Explosion tests were performed in a standard 20L sphere according to EN 14034-1 & -2 [1] and the combustion gases were collected and analysed by gas chromatography. The burning velocity was estimated by filming the flame propagation within a semi-opened tube and the flame stretching was analysed. In both the tube and the 20L sphere, the PSD was measured during the dispersion using in situ laser particle size measurement and the turbulence level was obtained using Particle Image Velocimetry.

3. Results and discussion

Dispersion and explosion tests were performed for the three samples to estimate the evolution of the PSD during the injection and its influence on the explosion severity. It appears that the maximum rate of pressure rise significantly decreases when the agglomerate size increases, whereas the maximum explosion pressure is less sensitive to the variation of PSD. Indeed, the particle size has a direct influence on the rate-limiting step, as the combustion can be controlled by surface reaction (small particles) or by the diffusion to the surface (agglomerates). By controlling the agglomerate size, it is then possible to highlight both limitations and their effects. Chromatographic analyzes performed on the gases collected after the combustion of nanocellulose (mainly CO_2, CO, H_2, CH_4, C_2H_4, N_2 and O_2) show that, when increasing the dust concentration, the remaining oxygen content decreases slower for a diffusion-controlled reaction than for a surface-controlled one. It also appears that if the representation of the explosion severity is very commonly done as a function of the mass concentration, considering the whole reactive surface area of the dust cloud leads to agreement when the explosion kinetics is controlled by a surface reaction.

Among their specific properties, nanoparticles exhibit low sedimentation rates. This particularity allows tests at a low turbulence and can lead to an estimation of the unstretched burning velocity, which is an intrinsic parameter of the mixture. By varying the ignition delay time t_v during the tests, the turbulence is modified and thus the flame stretching. Figure 1 shows the flame 20 ms after ignition for different ignition delay times. By increasing the latter, the turbulence decreases and the flame becomes smoother and similar to gases explosion (parabolic profile – Fig 1c). The spatial flame velocity was determined considering the flame kernel growth before the interactions with the walls, and an unstretched burning velocity of around 12 $cm.s^{-1}$ was determined for nanocellulose using the linear relation between the burning velocity and the Karlovitz factor [2].

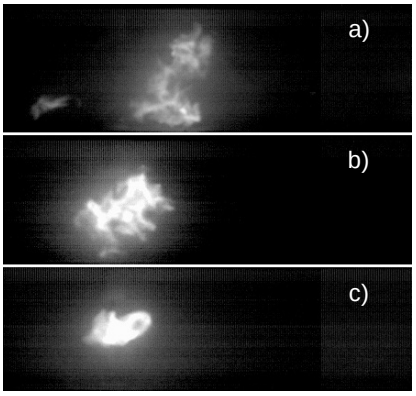

Figure 1. Flame propagation images 20 ms after inflammation for a) tv = 135 ms, b) 220 ms, c) 340 ms

4. Conclusions

Nanopowders tends to be naturally agglomerated. The size of their agglomerate depends on the turbulence of the dust cloud and plays a role on their combustion kinetics and thus on their explosion severity. Controlling these parameters and choosing the right parameter to represent the PSD helps to ensure a reliable explosion risk assessment. Finally, tests are currently performed to highlight the influence of dust agglomeration on the unstretched burning velocity of nanocellulose.

References

[1] EN 14034-1&2, Determination of explosion characteristics of dust clouds, Eur. Com. for Standard., 2011.
[2] G.H. Markstein, Non-steady Flame Propagation, Pergamon Press, Oxford, 1964.

ECCE12
The 12th EUROPEAN CONGRESS OF CHEMICAL ENGINEERING
Florence 15-19 September 2019

Visualization of aluminum dust flame propagation in two different lengths prototypes: some experimental considerations

Clement Chanut[1*], Frederic Heymes[1], Pierre Lauret[1], Elena Asquini[1], Pierre Slangen[1]

1 LGEI, IMT Mines Ales, Univ Montpellier, Ales, France]

**Corresponding author: clement.chanut@mines-ales.fr*

Highlights

- Aluminum dust flame propagation in two different lengths tubes: 70 cm and 218 cm
- Comparison of visualization and physical measurements (pressure): pulsating behavior
- Influence of rupture disk on flame propagation (pulsating behavior)
- Influence of optical properties of the walls (radiative thermal losses)

1. Introduction

Dust explosion is a major hazard for all industries dealing with powders, as all fine flammable dusts can cause an explosion when dispersed. These industries have to predict the consequences of potential explosions in given scenarios. To predict dust explosion consequences, models commonly used for gas explosions can be adapted. Although these models can be adaptable for organic dust explosions they are not accurate enough in case of metallic dusts [1]. Experimental studies are necessary to understand flame propagation mechanisms for these metallic dusts. Aluminum dust flame propagation is studied inside two prototypes of different lengths.

2. Methods

The first prototype is a vertical tube of 700 mm height and 150x150 mm square cross section. Walls are made of glass to visualize the dust dispersion and the flame propagation. The dust is dispersed by the discharge of two 1-liter compressed air vessels inside four vertical dust injection tubes, located in the corners of the tube. A fully characterized spark between two electrodes ignites the dust cloud. The energy of the spark is measured for each test. For the tests presented here, this energy is about 13 J. A rupture disc is located at the top of the prototype to limit the overpressure inside the prototype and also to keep control on the dust concentration. Details of this experimental setup can be found in [2].

The longest prototype is adapted from this first one. It consists of three parts of the previous prototype. Dust is injected on the two first stages. The rupture disc is located between the second and the third floor. No dust is initially present in the third floor, which is used to visualize the flame propagation after the rupture disc. Details of the second setup can be found in [3].

Aluminum powder with a mean diameter of 6.5 µm is studied. Flame propagation is analyzed thanks to fast camera and pressure sensors.

3. Results and discussion

Aluminum dust flame propagation is recorded in both prototypes. Pulsating behavior of light intensity is observed during the propagation of the flame. These light intensity pulsations correspond with the pulsations obtained with the different pressure sensors. Other authors also observed light pulsating behavior during aluminum dust flame propagation [4].

Complementary experiments are realized with the smallest prototype. First the influence of the rupture disc on flame propagation is investigated. This rupture disc has a weak rupture resistance (rupture around 35 mbar) to limit the influence of its rupture on the flame. Experiments are realized with and without the presence of this rupture disk. Diminution of the pulsating behavior of the flame is observed for the tests realized without the rupture disc.

In each prototype, the main pressure peak is recorded after the flame leaves the prototype, while the flame front is inside the exhaust duct. Change of optical properties of the walls is supposed to explain this main pressure peak. Inside the prototype, the walls are made of glass. The flame is supposed to present in this case important radiative thermal losses at the walls. On the contrary, the exhaust duct is made of galvanized steel. Inside this duct, the flame is supposed to present less radiative thermal losses leading to an acceleration of this flame. For this purpose, experiments are realized in the smallest prototype. Some walls of glass are covered of aluminum paper. With two opposite walls covered of aluminum paper, a more important pressure peak inside the prototype and a faster flame propagation are observed confirming the hypothesis of the influence of optical properties of the walls on aluminum dust flame propagation.

4. Conclusions

Aluminum dust flame propagation has been studied inside two different lengths prototypes. A pulsating behavior has been observed especially inside the longest porotype. Observations made inside this prototype conducted to realize complementary experiments inside the smallest one. This pulsating behavior decreases when the rupture disc is not present inside the prototype.

An important pressure peak has been recorded as the flame reached the exhaust duct with each prototype. This effect is probably linked to optical properties of the walls. The walls of the prototype are made of glass, presenting a potential thermal loss by thermal radiation for the flame. Inside the galvanized steel exhaust duct the flame is accelerated by decreasing the thermal losses of the flame. This observation emphasizes the importance of the properties of the walls for experimental investigation but also for comparison with numerical results. For safety purpose, this result underlines the importance of the material used for exhaust ducts inside industrial plant and its influence in case of accident.

References

[1] I. Kahlili, Sensibilité, sévérité et spécificités des explosions de mélanges hybrides gaz/vapeurs/poussières, dissertation, Université de Lorraine (2012).
[2] C. Chanut, F. Heymes, P. Lauret and P. Slangen, Chem. Eng. Trans. 67 (2018) 7–12.
[3] C. Chanut, Etude expérimentale de la propagation du front de flamme et de la vitesse de combustion d'une explosion de poussières d'aluminium, dissertation, IMT mines Alès (2018).
[4] P. Julien, J. Vickery, S. Goroshin, D.L. Frost and J.M. Bergthorson, Combust. Flame, 162 (11) (2015), 4241-4253.

ECCE12
The 12th EUROPEAN CONGRESS OF CHEMICAL ENGINEERING
Florence 15-19 September 2019

Selective Copper Leaching from End-Of-Life Printed Circuit Boards Using Ammonium Salt Solutions.

Carolina Silva, Carolina Pinheiro, Maria da Graça Rasteiro, Licínio Gando-Ferreira*

CIEPQPF, Department of Chemical Engineering, University of Coimbra, Rua Sílvio Lima, Pólo II, P-3030-790 Coimbra, Portugal

**Corresponding author: lferreira@eq.uc.pt*

Highlights

- Copper is the main element in PCB scrap.
- Ammonium salt solutions can selectively recover the copper.
- Influence of reagent concentration and liquid/solid ratio were studied.
- Copper recovery of 100% and a selectivity of 77% were achieved.

1. Introduction

End-of-life electrical and electronic equipment such as printed circuit boards (PCB) are becoming a major environmental problem due to their composition, which comprises toxic metals, polymers and ceramics. From an environmental and economic point of view, the amount of metals present, especially copper, makes this residue an interesting secondary source of metals.

The recovery of metals from electronic scrap using hydrometallurgical methods has attracted considerable attention in the literature for being effective and less harmful to the environment [1]. This process uses acid or basic solvents to extract the metals, which are then separated and purified using processes such as precipitation, solvent extraction, adsorption or ion-exchange.

In this context, this work aims at processing the metal containing fraction of PCB using hydrometallurgical processes. A solution of ammonia and hydrogen peroxide was used as oxidizing agent, in order to combine high levels of extraction efficiency as well as a low environmental impact.

2. Methods

The analyzed PCB scrap sample was provided by an E-waste Recycling Portuguese company, and was constituted by 4 kg of computer motherboards, RAM memories, mobile phones and processors. First, a mechanical/physical processing was performed, consisting in the dismantling and fragmentation of components using a guillotine and a sheet mill. Afterwards, a blade mill was used to reduce the PCI particle size, which was then separated into two fractions – oversize (>0.0707 mm) and undersize (<0.707 mm).

The chemical characterization was performed by x-ray fluorescence (XRF) model Rigaku Nex CG. Previously, acid digestions were performed in open systems by heating the waste with aqua regia reinforced with hydrogen peroxide. The Cu recovery tests were carried out in a closed cylindrical reactor, with a condenser attached, a termocouple and a mechanical stirrer. Two relevant operation conditions, namely liquid/solid (L/S) ratio and reagent concentration were studied using a 3 level full factorial design of experiments.

3. Results and discussion

The chemical characterization of the raw material is shown in Figure 1.

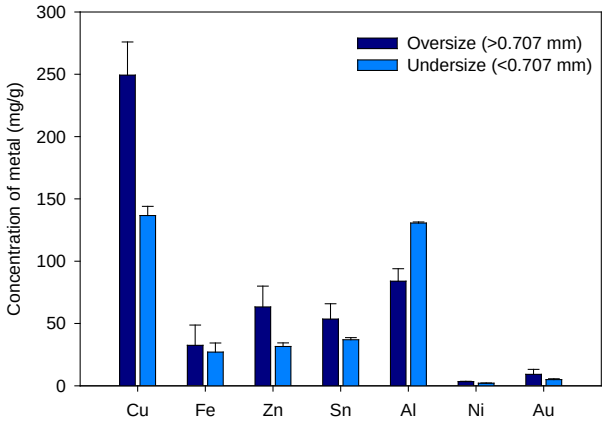

Figure 1. Chemical composition of the PCB components analyzed.

The results show that copper is the most abundant metal in PCB and is mostly found in the oversize fraction, with a maximum concentration of about 244 mg/g of waste. Precious metals such as gold are also present in promising quantities, which can also be recovered.

The influence of reagent concentration and L/S ratio on the recovery of Cu is reported in Table 1.

Table 1. Leaching yield and selectivity of the Cu recovery.

Run	L/S	C % (vol. %)	Yield (wt. %)	Selectivity (wt. %)
1	3	23.2	64.3	75.9
2	5	23.2	63.9	75.5
3	7	23.2	86.4	74.9
4	3	42.7	68.0	86.2
5	5	42.7	69.3	75.9
6	7	42.7	64.4	73.9
7	3	72.4	74.1	76.9
8	5	72.4	100	77.0
9	7	72.4	78.0	72.0

A yield of 100% and a selectivity of 77% was obtained for the copper extraction using a reagent concentration of 72.4% and a L/S ratio = 5. It can be concluded that the concentration and L/S ratio have a positive effect on the extraction efficiency. The higher the concentration and the smaller the amount of residue, the easier the dissolution of the metals with the reagents.

4. Conclusions

Copper is the main basic metal present in PCB scrap. The best yield for copper extraction was obtained at a maximal reagent concentration (about 72.4%) and a L / S ratio = 5. Recovery of almost 100 % of copper was achieved.

References

[1] F. Habashi, Hydrometallurgy 79 (2005) 15–22.

ECCE12
The 12th EUROPEAN CONGRESS OF CHEMICAL ENGINEERING
Florence 15-19 September 2019

Phase-Change Solvents For CO_2 Capture: Sustainability Aspects.

Gulnara Shavalieva[1], Stavros Papadokonstantakis[1]

[1] Chalmers University of Technology, SE-412 96 Gothenburg, Sweden

*Corresponding author: gulnara.shavalieva@chalmers.se

Highlights

- Sustainability assessment should be considered already during solvent selection
- Assumptions will significantly influence the results of the assessment
- Extra equipment might be required to guarantee safety of the workers

1. Introduction

2°C warming scenario requires widespread adoption of efficient carbon capture and storage technologies. Post-combustion CO_2 capture by chemical absorption is the most mature of existing ones. However, high energy requirement and associated costs of the capture process hinder the technology's diffusion and large-scale employment. Phase-change solvents is a novel solution to an energy penalty problem of post-combustion CO_2 capture. At certain temperatures the solvents generate two phases and one of them is recycled back to the absorber reducing the input to the energy-intensive stripping process.

While the improved performance processes using phase-change solvents are proven by various studies [1], [2] there is limited research done on the environmental and health aspects of such processes. Many of the phase-change solvents are new molecules with no or very limited occupational safety and health information that makes it challenging to perform a sustainability assessment. Potential hazards linked to the process use of the harmful molecules affect the cost and design of the process and need to be considered already during the selection of solvent.

2. Methods

The analysis was done with the help of literature study and a holistic method combining life cycle (LCA) and environmental, health and safety assessments (EHS). During the literature study problems associated with process use of CO_2 capture solvents were gathered and evaluated in terms of applicability to phase-change solvents. Additional challenges were also thought through. Since there is no data on industrial use of phase-change solvents, different scenarios and assumptions were generated to anticipate the different behavior of the system in terms of solvents loss and process specific hazards such as products of solvent degradation and volatile emissions.

3. Results and discussion

Two phase-change solvents were used for the study: MCA (N-methylcyclohexanamine), and a novel solvent S1N. The molecules are structurally similar chemicals, however MCA is a more volatile and S1N- more soluble in water. LCA impact of solvent manufacturing is lower for S1N solvent. EHS values for the chemicals are close, but MCA has worse S (safety) and H(health) values due to higher mobility of the chemical, whereas S1N performs worse in E (Environment) category. Losses of the

solvent during the capture process due to degradation, aerosol formation and vaporization and energy consumption of the process are the main contributors to the LCA impact in such categories as global warming potential, cumulative energy demand and ReCiPe endpoint indicator at the process level. The overall impact is highly influenced by the assumptions discussed below.

Due to low vapor pressure and high solubility in water S1N is expected to have the lowest loss of the solvent during the process operation [2]. It is more difficult to estimate loss of the solvent due to aerosol formation. It has been reported that aerosol formation can increase the emissions by 1-2 orders of magnitude if left uncontrolled [3]. Study performed by [4] states that substantial amine loss via aerosols can occur even for low volatility solvents, thus to recover and remove the significant part of the MCA and S1N solvents from the gas leaving to the atmosphere and control the escape of solvent degradation products a wash section was added to the process sheet.

Another complex phenomenon difficult to estimate is solvent degradation. MCA is a secondary amine, therefore expected to degrade significantly in presence of oxygen. MCA reported to degrade 1.5-3 times more than MEA [2]. To estimate the oxidative degradation potential of S1N, degradation data on structurally similar compounds was used for calculation. Thus, it was assumed that the degradation rate is 3-10 times of MEA. It is reported that a product of oxidative degradation for MCA is ammonia [2], S1N might also produce a different degradation compound, allylamine. Scenarios considered cases of 85% and 65% of degradation products being volatile and the rest - heat stable salts (HSS) for MCA and vice versa for S1N, since it is believed that the majority if the S1N degradation products will stay in the liquid phase. Phase-change solvents can be recovered at lower temperatures; therefore the thermal degradation is expected to be generally lower than for systems using MEA.

During the capture with phase-change solvents part of the process stream is recycled back to the absorber and some part of the degradation products formed in the absorber including dangerous to health substances like nitrosamines, can follow the stream back to the absorber avoiding their removal in the reclaimer and also the thermal process of stripping responsible for partial destruction of the hazardous substances [5]. Additional safety measures and an extra reclaiming point might be required.

4. Conclusions

There are several aspects of the CO_2 capture of the process using phase-change solvents that can significantly influence the result of sustainability assessment. Extra equipment might be required to guarantee safety of the process. This will lead to added costs and should be considered already during the solvent selection and early design phase of the carbon capture process.

References

[1] Y. Tan, “Study of CO 2 -Absorption into Thermomorphic Lipophilic Amine Solvents,” Technischen Universität Dortmund, 2010.
[2] J. Zhang, “Study on CO2 capture using thermomorphic biphasic solvents with energy-efficient regeneration.,” 2013.
[3] S. M. Fulk and G. T. Rochelle, “Modeling aerosols in amine-based CO2capture,” Energy Procedia, 2013.
[4] H. Majeed, H. Knuutila, M. Hillestad, and H. F. Svendsen, “Effect of Amine Volatility on Aerosol Droplet Development in Absorption Columns,” Energy Procedia, 2017.
[5] N. A. Fine, M. J. Goldman, and G. T. Rochelle, “Nitrosamine formation in amine scrubbing at desorber temperatures,” Environ. Sci. Technol., 2014.

ECCE12
The 12th EUROPEAN CONGRESS OF CHEMICAL ENGINEERING
Florence 15-19 September 2019

Fixed Bed Adsorption and Breakthrough Modelling of Activated Porous Carbon Derived from Compost for Post-Combustion CO_2 Capture

Mohsen Karimi[1], José A.C. Silva[2], Alírio E. Rodrigues[1]

1 Department of Chemical Engineering, University of Porto, Rua Dr. Roberto Frias, S/N, 4099-002, Porto, Portugal; 2 Department of Chemical and Biological Technology, Polytechnic Institute of Braganca, Campus de Santa Apolonia, 5300-857 Braganca, Portugal

**Corresponding author: mohsen.karimi@fe.up.pt*

Highlights

- Novel adsorbents were synthesized from derived compost in mechanical biological treatment.
- 5-samples were activated chemically and thermally in different procedures.
- Breakthrough experiments were performed in a fixed bed column.

1. Introduction

In the recent years, synthesis, preparation and development of valuable carbon materials have received much interest in the view of energy efficiency and sustainability for various applications in CO_2 capture, wastewater treatment and gas storage studies [1, 2]. On the other hand, based on European legislation to management of solid wastes and limiting the utilization of fertilizers from waste as well as finding approaches to manage these materials, novel approaches are required [3]. In this study, the obtained compost by mechanical biological treatment plant from municipal solid waste has been considered as a source of adsorbents for CO_2 capture.

2. Methods

The compost used was obtained in mechanical biological treatment plants for municipal solid waste, supplied by the company "Resíduos do Nordeste, EIM". In order to homogenize and remove the soluble compounds and suspended solids, the compost was first mixed with water and washed. Then, two different materials were prepared by carbonization at 400 (CMSW-400) and 800 ºC (CMSW-800). In addition, two materials were prepared with H_2SO_4 before and after the carbonization at 800 ºC (CMSW-S-800 and CMSW-800-S, respectively). Then, breakthrough measurements of CO_2 were carried at post combustion conditions (40ºC and 1-5 bar).

3. Results and discussion

Figure 1 shows the uptake capacity of proposed samples at 40 ºC. The results show the prepared sample by the subsequent treatments with acid sulfuric and thermal calcination has the higher uptake capacity than other ones and literature reports; which it can derived from several factors. Frist, better textural properties of proposed sample, including: higher external surface area (S_{ext}), microporous surface area (S_{microp}) and external surface area (S_{ext}). It can be also ascribed for desorption of weak superficial groups as consequence of the thermal treatment at 800 ºC.

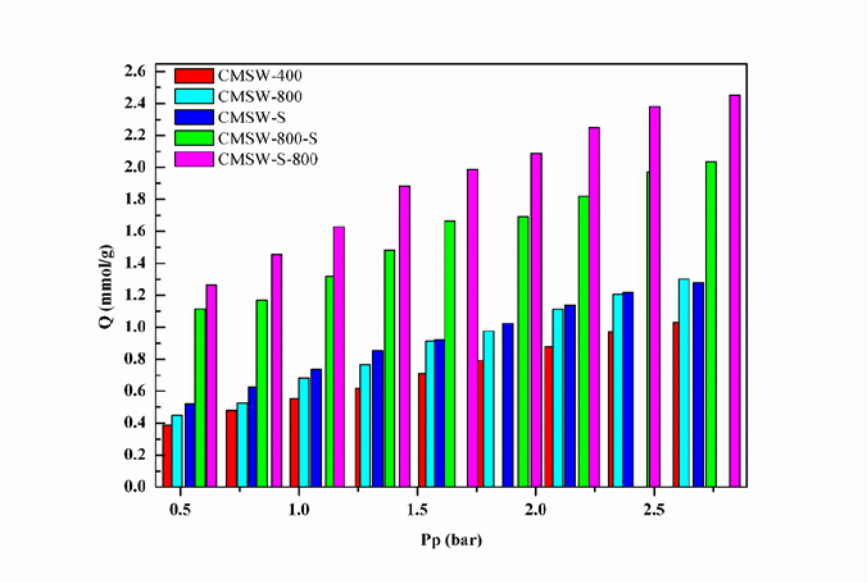

Figure 1. A comparison between CO_2 uptake capacity (mmol/g) of investigated adsorbents at 40 ^{0}C.

4. Conclusions

In this study, the potential of municipal solid wastes as a source of adsorbents for CO_2 capture were investigated at the post-combustion operational conditions. Then, the breakthrough measurements in the fixed bed adsorption column were performed. The equilibrium adsorption capacity of the considered samples revealed that the adsorption capacity of the sample which has been treated with the subsequent treatments with acid sulfuric and thermal calcination is the best one and its uptake capacity is comparable with commercial carbon materials. The results proved the proposed strategy can be a green route for integrated management of environment.

Acknowledgements – This work is a result of the projects "VALORCOMP" (0119_VALORCOMP_2_P), funded by FEDER through Programme INTERREG V A Spain - Portugal (POCTEP) 2014–2020, and "AIProcMat@N2020 - Advanced Industrial Processes and Materials for a Sustainable Northern Region of Portugal 2020", with the reference NORTE-01-0145-FEDER-000006, supported by NORTE 2020, under the Portugal 2020 Partnership Agreement, through FEDER; and POCI-01-0145-FEDER-006984 – Associate Laboratory LSRE-LCM funded by FEDER through COMPETE2020 - POCI – and by national funds through FCT.

References

[1] M. Karimi, M. R. Rahimpour, D. Iranshahi, J. Nat. Gas Sci. Eng. 17 (2014) 136-150.
[2] M. Karimi, J.A.C. Silva, C. Gonçalves, Ind. Eng. Chem. Res. 57 (2018) 11154-11166.
[3] G. Tchobanoglous, F. Kreith, Handbook of Solid Waste Management, second ed., Mc-Graw Hill, New York, 2002.

ECCE12
The 12th EUROPEAN CONGRESS OF CHEMICAL ENGINEERING
Florence 15-19 September 2019

Acid gas removal in waste-to-energy plants via high temperature reaction with calcined dolomite

Alessandro Dal Pozzo*, Giacomo Antonioni, Valerio Cozzani

LISES – DICAM, Alma Mater Studiorum - Università di Bologna, via Terracini n.28, 40131 Bologna, Italy

**Corresponding author: alessandro.dalpozzo3@unibo.it*

Highlights

- The furnace injection of calcined dolomite was tested as acid gas removal method
- The test run campaign demonstrated high reactivity towards both HCl and SO_2
- A model for HCl and SO_2 removal was calibrated on test run data
- Adding furnace injection can reduce the overall cost of flue gas treatment

1. Introduction

Acid gases like HCl and SO_2 are typical pollutants arising from the combustion of municipal or industrial waste fractions having Cl and S content. The upcoming revision of the BAT (Best Available Techniques) for waste incineration sets high standards for the emission control of these contaminants [1]. Old waste-to-energy (WtE) plants might require retrofitting to obtain a renewal of their environmental permits. In this framework, the injection of calcined dolomite (CD) in the combustion chamber, as solid reactant for acid gas abatement, has been proposed recently as a simple approach to retrofitting, with minimal investment cost and without the need for additional equipment [2]. The current study aims to investigate the cost-effectiveness of CD injection.

2. Methods

The performance of CD as high temperature reactant for acid gas removal was tested in two WtE plants. Both plants adopted the injection of sodium bicarbonate at low temperature (180 °C) as acid gas abatement stage, as commonly performed in several European WtE plants [3]. As sketched in Fig. 1a, the tested configuration consisted in the introduction of CD as an additional acid gas abatement stage directly in the combustion chamber (T ~ 1000 °C). The concentration of HCl and SO_2 in the flue gas was measured downstream of the furnace (point SMP). Therefore, in order to assess the effect of CD injection on the acid pollutants, “on/off tests” were performed by alternating periods of injection and interruption of the CD feed rate, as shown in Fig. 1b. The removal efficiency of CD towards HCl or SO_2 at different feed rates was calculated considering the reduction in acid gas concentration at point SMP compared to the periods without injection of reactant. A previously formulated model for dry acid gas removal [4] was calibrated on the experimental data. The calibrated model was used to simulate the operation of the WtE acid gas removal line (furnace injection of CD + downstream bicarbonate injection) at different feed rates of CD. The simulations allowed to identify the operating point of the plant that minimizes the operating costs of acid gas removal.

3. Results and discussion

The results of the test run campaign are summarized in Fig. 3c, where the acid gas removal efficiency (for HCl and for SO_2) is plotted as a function of the stoichiometric ratio (SR) of reactant. Dolomite appeared particularly reactive towards SO_2: at SR = 1 (i.e. reactant feed rate without stoichiometric excess), the removal efficiency for SO_2 and HCl was 81 % and 29 %, respectively. Calibrating a performance model (continuous lines in Fig. 1c) on the experimental data (dots) allowed to study the process optimization of the two-stage acid gas removal system (dolomite stage + bicarbonate stage). The performance model for bicarbonate was obtained through a dedicated analysis as in [4]. A typical flue gas composition (HCl = 800 mg/Nm^3, SO_2 = 200 mg/Nm^3) resulting from municipal waste combustion was considered as reference case. The overall operating costs of the two-stage line (cost of the reactants plus disposal of process residues) were assessed as a function of HCl conversion in the CD stage, as shown in Fig. 1d, while keeping constant the overall acid gas conversion in the two-stage system. The minimum of operating costs was found for a 25 % HCl conversion in the CD stage, which realizes a 14 % cost reduction compared to the single-stage sodium bicarbonate acid gas removal system without dolomite injection.

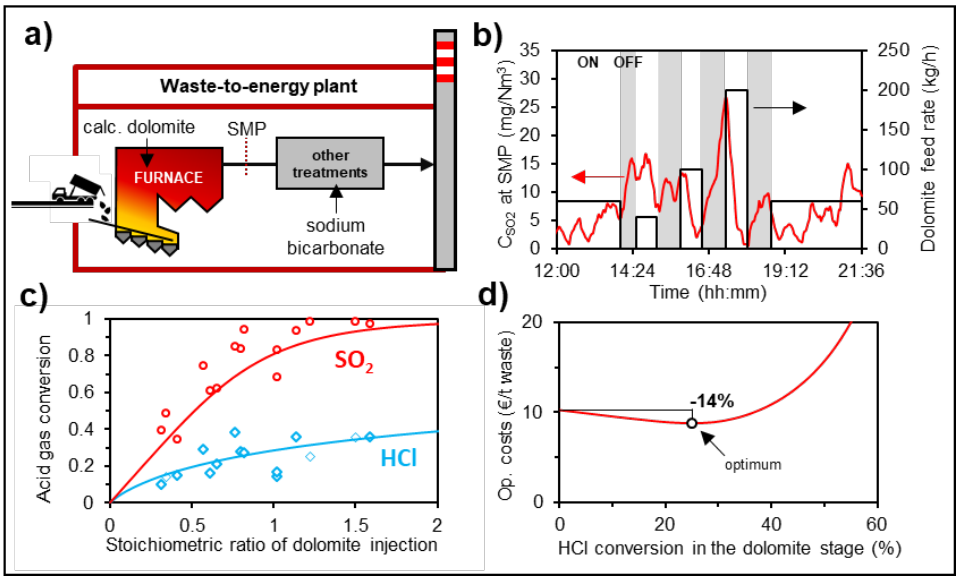

Figure 1. Framework of the study: a) sketch of the WtE plant configuration (dolomite + bicarbonate two-stage acid gas removal system); b) dolomite feed rate and SO_2 concentration over time during a typical test run; c) removal efficiency of calcined dolomite for HCl and SO_2; d) operating costs of the two-stage acid gas removal system as a function of HCl conversion in the dolomite stage.

4. Conclusions

The test run campaign conducted in WtE facilities demonstrated the cost-effectiveness of acid gas removal via the high temperature reaction with CD. Retrofitting a plant equipped with a sodium bicarbonate treatment stage with an additional dolomite stage as furnace injection can reduce the overall operating cost of acid gas treatment, if the feed rate of dolomite is properly optimized.

References

[1] European Commission, BREF Waste Incineration (draft), Dec 2018. Available at: https://bit.ly/2UTDHhl
[2] L. Biganzoli, G. Racanella, L. Rigamonti, R. Marras, M. Grosso, Waste Manage. 36 (2015) 98-105.
[3] J. Vehlow, Waste Manage. 37 (2015) 58-74.
[4] A. Dal Pozzo, M. Giannella, G. Antonioni, V. Cozzani, Chem. Eng. Trans. 67 (2018) 463-468.

ECCE12
The 12th EUROPEAN CONGRESS OF CHEMICAL ENGINEERING
Florence 15-19 September 2019

Adsorption of Active Trace Gases by Ensemble of Ultrafine Porous Particles with Impermeable Core.

Andrew Fominykh[1*], Itzhak Katra[2], Boris Krasovitov[1], Avi Levy[1]

1 Department of Mechanical Engineering, Ben-Gurion University of the Negev, P. O. B. 653, 8410501, Israel
2 Department of Geography and Environmental Development, Ben-Gurion University of the Negev, P. O. B. 653, 8410501, Israel

**Corresponding author: fominykh@bgu.ac.il*

Highlights

- Original model of gas adsorption by particles with non-uniform porosity is proposed.
- Effect of radioactive decay and kinetic effects on the rate of gas adsorption is studied.
- Gas adsorption by ensemble of particles is governed by integro-differential equation.
- Theoretical predictions are in good agreement with experimental results.

1. Introduction

Consider adsorption of atmospheric trace gas from a mixture with inert gas by a moving ensemble of porous particles. The size of the particles can be of the same order of magnitude as mean free path of molecules in air at normal conditions. The velocity of particles is equal to a gas velocity. At time t = 0 particles begin to adsorb active gas from the gaseous mixture. Gas adsorption inside a porous particle is determined by nonstationary equation of diffusion in spherical coordinates with a sink term. Equation of diffusion is supplemented by initial and boundary conditions – zero mass flux at a surface of impermeable core and to be determined from equation of mass balance for a unit cell time-dependent mass flux at gas-particle interface.

2. Methods

When the size of a particle have the same order of magnitude as a mean free path, the Fickian diffusion approach for the analysis of reactant molecules transport is not applicable. We overcome this difficulty applying the flux-matching theory (see [1]-[2]) which is a hybridization of the diffusion and the free molecule approaches. The concentration profile of radioactive gas far away from the particle is described by the diffusion equation. This profile coincides with the real one down to the distances of the order of the mean free path of molecules of adsorbate. A limiting sphere is then introduced inside of which the free molecule kinetics governs the adsorbate transport. Then the radius of the limiting sphere is obtained from the condition of equality of the fluxes in both zones.

3. Results and discussion

The developed model of radioactive gas adsorption by ultrafine porous particles is applied to investigation of scavenging of radioactive gases from a mixture with air by an ensemble of moving carbon-based aerosols. The results of calculations of concentration of I-132 gas in a gaseous phase as a function of time are shown in Figure 1. Calculations are performed for aerosol number density $1.2\cdot 10^{4}\,\mathrm{cm}^{-3}$, the specific surface area of a particle was assumed to be equal to $100\,\mathrm{m}^{2}\mathrm{cm}^{-3}$, and density of porous particle with radius a=50 nm is 1 $\mathrm{g}\cdot\mathrm{cm}^{-3}$. Analysis of Fig. 1 shows that

concentration of radioactive trace gas decreases rapidly at the initial stage of gas adsorption. Rapidly decreasing segment of the temporal dependence of concentration is followed by a shallow-slope segment. For large time the concentration of a radioactive trace gas vanishes due to radioactive decay. The slope of the curve at the steep-slope segment of the temporal dependence of concentration increases with an increase of Knudsen number. The magnitude of concentration at a shallow-slope segment of the curve decreases with a decrease of a Knudsen number. The larger the Knudsen number, the larger is a period of time required for concentration of active trace gas in a gaseous phase to reach a shallow-slope segment of the temporal dependence of concentration.

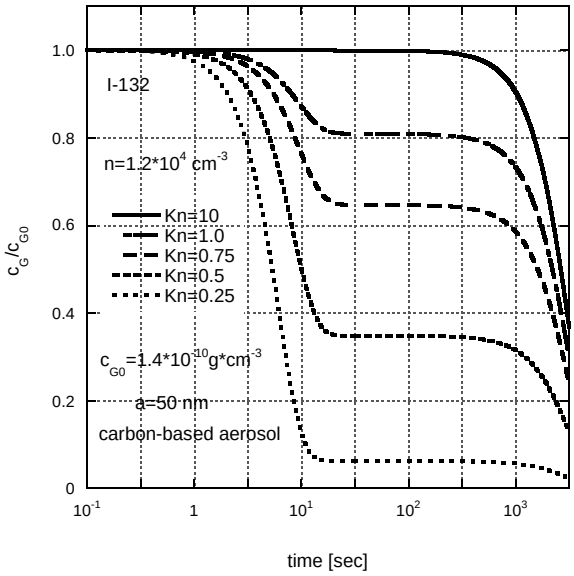

Figure 1. Concentration of active gas in a gaseous phase as a function of time.

4. Conclusions

We developed a model for adsorption of active atmospheric gases by an ensemble of solid porous particles taking into account radioactive decay in the dispersed and continuous phases. Using the developed model we calculated temporal dependences of concentration of adsorbed gas in a particle, concentration of radioactive gas in a gaseous phase and scavenging coefficient for adsorption of I-131, I-132, Rn-220 and Rn-222 by carbon-based aerosols. The obtained results can be summarized as follows:

1. Mass flux density at the particle interface is determined by integral equation while temporal evolution of concentration of an active trace gas in a gaseous phase is described by integro-differential equation.

2. Neglecting kinetic effects during gas adsorption by ultrafine particles leads to the overestimation of the rate of adsorption.

3. The developed model of radioactive gas scavenging by an ensemble of aerosols yields the same estimate of the dependence of the adsorbed amount of gaseous radioactive Iodine-131 in a particle vs. time as the measurements of Noguchi et al. [3].

References

[1] T. Elperin, A. Fominykh, B. Krasovitov, A. Lushnikov, Phys. Rev. E 87 (2013) 1–8.
[2] T. Elperin, A. Fominykh, I. Katra, B. Krasovitov, Meteorol. Atmos. Phys. (2018) 1-9.
[3] H. Noguchi, M. Murata, M, K. Suzuki, Japanese Journ. Health Phys. 25 (1990) 209-219.

ECCE12
The 12th EUROPEAN CONGRESS OF CHEMICAL ENGINEERING
Florence 15-19 September 2019

Development of a hybrid biological process for oilfield produced water treatment.

Nicolas Lusinier[1], Isabelle Seyssiecq[2], Cecilia Sambusiti[3], Matthieu Jacob[3], Nicolas Lesage[4] and Nicolas Roche[1,*]

1 Aix-Marseille Univ, CNRS, IRD, INRA, Coll France, CEREGE, Aix en Provence FRANCE ; 2 Aix-Marseille Univ, CNRS, Centrale Marseille, M2P2, Marseille France ; 3 TOTAL SA, PERL – Pôle d'Etudes et de Recherche de Lacq, Pôle Economique 2, BP 47 – RD 817, Lacq, France ; 4 TOTAL SA, CSTJF, Avenue Larribau, Pau, France

**Corresponding author: nicolas.roche@univ-amu.fr*

Highlights

- Amount of produced water from oil exploration and production is increasing.
- A hybrid biological process was developed to treat oil produced water.
- Enhancement of oxygen transfer occurs in the presence of a packing material.

1. Introduction

Crude oil extraction leads to the production of produced water (PW). PW flowrate increases with oil field lifetime, up to more than 20 times the flowrate of crude oil. Since the regulations regarding PW disposal becoming more stringent, there is a big challenge in developing efficient treatment processes (i.e. physico-chemical and/or biological treatments). Among them, biological treatments (i.e. conventional activated sludge processes) are commonly installed in the industrial sector, due to cheaper operation costs and higher removal efficiencies of biodegradable compounds compared to those obtained by chemical treatments. However, critical parameters, such as the PW composition (i.e. salinity and low biodegradability of some compounds) and technology compactness for offshore implementation, have to be taken into account. Hybrid processes defined here, as the combination of two biotreatment processes (i.e. fixed and suspended microbial biomass in the same reactor) showed promising performances in terms of oxygen transfer [3]. Furthermore, this combination enhances treatment efficiencies as both, the biomass concentration and the microorganisms variety increase in the bioreactor [4]. Thus, this study relates the development of a hybrid biological process for oilfield produced water treatment.

2. Methods

Experiments were carried out by using a laboratory pilot plant, consisting of two bioreactors (30 L of working volume) and two clarifiers (5 L of working volume) in parallel (Figure 1). Reactor columns have an inner diameter of 19 cm and a total height of 107 cm. The aeration is supplied by compressed air flowing into a membrane to provide fine bubbles. The packing material, confined into the bioreactors, is made of cylindrical solid rings (AnoxKaldnes®). The air flowrate is controlled by a flowmeter. Preliminary experimental tests were conducted to determine the oxygen transfer rate (K_La) on clear water and on a physico-chemical Newtonian suspension (i.e. 3g/L bentonite suspension), by varying the air flow rate (4-10-16 L/min) and the packing height (0-17-34 cm). The oxygen transfer measurements were carried out by using the disulfite deoxygenation method followed by a re-oxygenation phase [3].

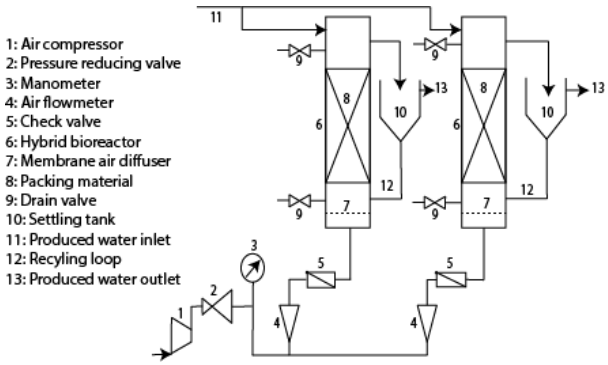

Figure 1. Experimental set-up of the two packed-bed bioreactors.

3. Results and discussion

Concerning the oxygen transfer, results showed that, in the presence of the physico-chemical Newtonian suspension (bentonite suspension) oxygen transfer is reduced compared to clear water at a same packing height and/or air flowrate (figure 2a and 2b). Furthermore, figure 2b shows that the oxygen transfer coefficient increases with the air flowrate (up to 60 %) but also with the packing height. Indeed, the presence of the packing bed is thought to induce a decrease in bubble coalescence, inducing in turn an increase in specific exchange area, thus of the K_La coefficient (up to 30 %).

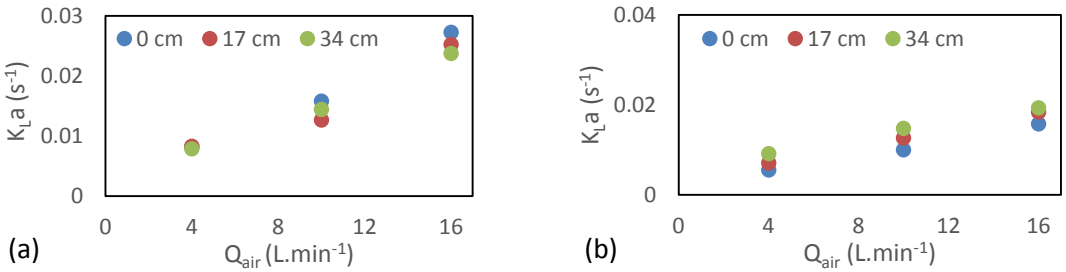

Figure 2. Evolution of oxygen transfer coefficient as a function of air flowrate and packing height for clear water (a) and bentonite suspension (b)

4. Conclusions

Results showed that the presence of the packing bed induce a 52-64 % increase in oxygen transfer for both clear water and bentonite suspension and for an identical energy input (constant air flow rate) due to the presence of the packing bed inducing a decrease of bubbles coalescence along the column. Further studies of oxygen transfer will be performed with a non-Newtonian bioflocs suspension, as well as biotreatment studies to assess the treatment efficiency of such a process for a synthetic produced water. During acclimation test, first results showed that the COD of produced water can be removed with high treatment efficiencies (>95 %).

References

[1] P. Baldoni-Andrey, P. Pedenaud, P.L. Dehaene, B. Segues, Society of Petroleum Engineers (2006).
[2] P. Pedenaud, P. Baldoni-Andrey, A. Breton, B. Segues, A. Demangel, M. Jacob, Society of Petroleum Engineers (2018).
[3] K. Zerari, I. Seyssiecq, D.E. Akretche, N. Roche, Journal of Chemical Technology & biotechnology 88 (2013) 1007-1013.
[4] V.S. Ruys, K. Zerari, I. Seyssiecq, N. Roche, Journal of Chemistry (2017) 1-7.

ECCE12
The 12th EUROPEAN CONGRESS OF CHEMICAL ENGINEERING
Florence 15-19 September 2019

Use of a filter press as a reactor for heterogeneous Fenton advanced oxidation: Experimental evaluation and CFD simulation

José Luis Trigueros Soto, J. Esteban Durán*

School of Chemical Engineering, University of Costa Rica, San José, 11501, Costa Rica

** Corresponding author: esteban.duranherrera@ucr.ac.cr*

Highlights

- A filter press was used as a reactor for heterogeneous Fenton AOP
- Caffeine degradation of 20% was achieved using 3 g of catalyst and 0.38 L/min
- CFD model provided insight on the hydrodynamics and multiphase interactions inside the reactor chambers

1. Introduction

Fenton process is a well-known technology that has been applied on the treatment of industrial wastewater containing non-biodegradable organic pollutants. However, because of the many drawbacks of conventional homogeneous Fenton process (e.g. sludge generation), considerable effort has been put in the development of heterogeneous Fenton systems. Unfortunately, most of the works has focused on catalyst development [1], and little research has been done on the development of proper reactor configurations for utilizing such heterogeneous catalysts. This study explores the use of a filter press as a heterogeneous catalytic reactor for the Fenton reaction utilizing iron-modified diatomite as catalyst [2]. Experimental data and computational fluid dynamics simulations (CFD) were used to characterize this novel reactor so it can be later scale up for commercial implementation.

2. Methods

Residence time distribution (RTD) experiments [3] using one filter press frame were performed in order to understand the hydrodynamics inside the reactor and to evaluate the CFD model. NaCl was used as a tracer; after a concentrated salt shot was spiked at the reactor inlet, its concentration was measured at the outlet with a conductivity meter. Also, CFD simulations of this same experiment were performed using Ansys Fluent.

Different experiments were performed to determine the effect of various operational factors (number of filter plates, catalyst load per plate, and flow rate) on the reactor performance. To assess the reactor performance, the degradation of caffeine (as model pollutant) was spectrophotometrically measured under steady state conditions. With these data, it was possible to approximate reaction kinetics and to compare experiments with CFD predictions. A multiphase Eulerian approach was used for the CFD model and transient state simulations were performed using Ansys Fluent.

3. Results and discussion

Using the RTD experiment measurements, it was possible to obtain the *C* and *E* curves to characterize the homogeneous hydrodynamics inside of the filter press. With these experimental data, it was possible to evaluate the steady state simulation. CFD simulations were in close agreement with the experimental curves. Good-mixing patterns are found in the reaction chambers, mainly due to the tangential inlet flow.

Fig. 1 shows a picture of the filter press with five frames, three of them loaded with the iron-modified catalyst. The side view allows seeing particle suspension and mixing promoted by the tangential inlet flow (bottom right-side). Caffeine conversions of 20% were obtained using 3 g of catalyst per chamber and 0.38 L/min flowrate.

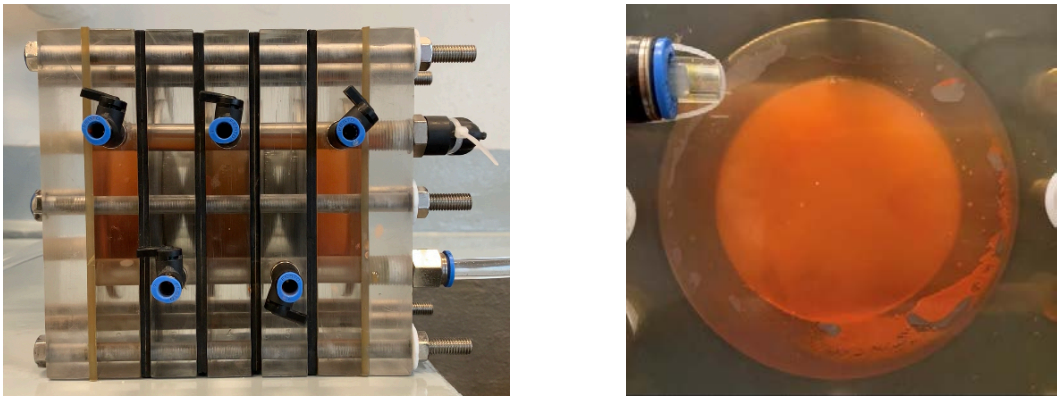

(a) (b)

Figure 1. Filter press reactor equipped with five frames, three loaded with iron-modified diatomite (a); side view of reaction chamber

In the congress presentation we will further discuss our experimental and simulation results.

4. Conclusions

A filter press used as a reactor for advanced oxidation processes using the heterogeneous Fenton reaction was characterized and simulated using CFD. The computational model was very useful for providing insight on the multiphase interaction and hydrodynamics inside the reaction chambers. It is recommended to further investigate the suitability of using this system in industrial scale water and wastewater treatment plants.

References

[1] P.V. Nidheesh, RSC Advances 5 (2015) 40552–40577.

[2] J.E. Duran, A. Araya, S. Arguedas, Proc. IOA & IUVA World Congress (2013).

[3] H.S. Fogler, Elements of Chemical Reaction Engineering, forth ed., Pearson Ed., New York, 2006.

ECCE12
The 12th EUROPEAN CONGRESS OF CHEMICAL ENGINEERING
Florence 15-19 September 2019

Assessment of Advanced Photocatalytic Oxidation process for Micropollutant Elimination in Municipal and Industrial Waste Water Treatment Plants.

Julien G. Mahy[1], Christelle Vreuls[2], Sophia Dircks[3], Andrea Börgers[3], Jochen Türk[3], Stéphanie D. Lambert[1*]

1 University of Liege, Department of Chemical Engineering – Nanomaterials, Catalysis, Electrochemistry, Liege, Belgium; 2 CELABOR, Research Centre, Environmental Departement, Herve, Belgium; 3 IUTA, Institut für Energie- und Umwelttechnik e.V, Bliersheimer Str. 58 – 60, Duisburg, Germany.

**Corresponding author: stephanie.lambert@uliege.be*

Highlights

- Organic synthesis pathways by sol-gel process for photocatalysts.
- Ag and/or P25 nanoparticles-doped TiO2 photocatalysts.
- Ozonation and Photodegradation of micropollutants in aqueous media.
- Very high degradation efficiency for all micropollutants in a pilot reactor.

1. Introduction

Pharmaceuticals, personal care products, pesticides and other chemicals used for domestic purpose or industrial or agro-food production are continuously discharged into wastewater and lead to global contamination of the aquatic environment all over Europe [1]. Removal during conventional wastewater treatment is unsatisfactory knowing that only 20 to 50% of micropollutants are removed in current waste water treatment plants [2].

The objective of the AOPTi project is to develop and validate an innovative technology to ensure efficient elimination of different types of micropollutants and toxic effects in waste water. The process is a tertiary treatment process, which can be easily integrated into municipal and industrial WWTPs. It is an economical physico-chemical treatment step after the conventional biological treatment [3]. The process is based on oxidation by ozone and a subsequent photocatalytic treatment. The technology is developed for companies involved in the water purification sector and for companies with toxic effluents loaded with micropollutants. Process parameters have to be determined depending on the type of waste water in order to lead to almost total degradation of all micropollutants and to ensure absence of toxicity of the resulting water. Treated water will be characterized in term of chemical transformation products (TPs) and toxicity.

2. Methods

At the pilot scale (flow rate = 150 L/h), 24 major micropollutants have been chosen to model waste water like pesticides (simazine, diuron, isoproturon, DTT, atrazine, lindane), plasticizers (DEHP, tributyl phosphate), brominated compounds (PBDE), pharmaceuticals (metoprolol, diclofenac, carbamazepine…), industrial chemicals (PFOS), contrast agent (iohexol, iopromide). Their degradations are quantified by GC-MS/MS and UHPLC-MS.

Photocatalysts have been synthesized by organic sol-gel methods [4] and deposited as thin transparent films by spray-coating inside the long alkaline-free tube for a pilot test: pure TiO2 and doped titanium dioxide (with Ag and/or commercial Evonik P25 nanoparticles). Samples were characterized by profilometry, GIRXD, UV-Vis transmission. The absence of leaching was characterized by ICP-AES and MS.

3. Results and discussion

The best photocatalyst for the degradation of the 22 micropollutants is TiO2 doped with 2 wt.% of Ag and 10 wt.% P25. The results are presented in Figure 1, in which the percentage of each micropollutant present in water is shown after different treatments (ozonation, adsorption and photocatalysis). In Figure 1 (on the left):

(i) Chlortoluron and isoproturon are totally degraded by ozonation for 30 min; (ii) atrazine, DDT and BDE are totally disrupted thanks to photocatalysis; (iii) for the other micropollutants, their percentage of degradation evolves from 10% to 90% after a photocatalytic treatment for 6 h.
In Figure 1 (on the right):

(i) Carmabazepine, diclofenac, sulfamethoxazole, clarithromicyn and terburtyn are totally degradated by ozonation for 30 min; (ii) metoprolol is partially degraded after a photocatalytic treatment of 6 h (about 12% remains); (iii) the other pollutants are totally disrupted thanks to the photocatalytic treatment and sol-gel coating.

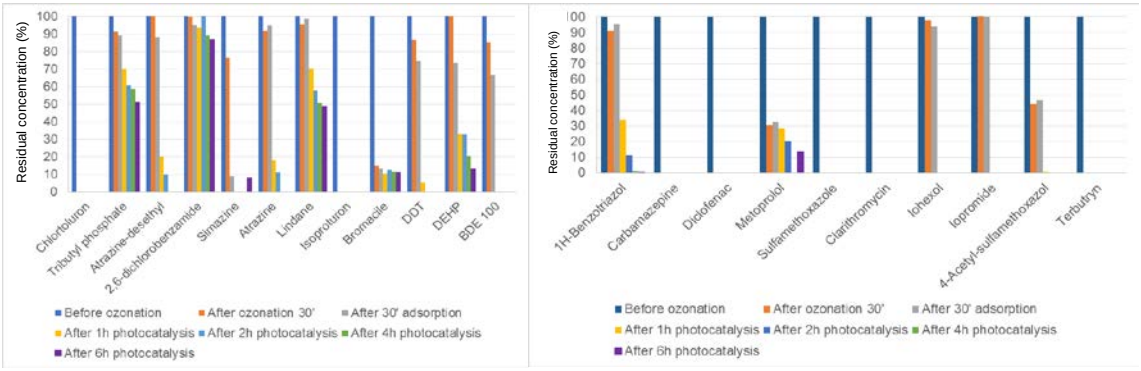

Figure 1. Evolution of 22 micropollutants concentrations during the ozonation and photocatalytic tests.

4. Conclusions

It is concluded that the use of an ozonation treatment followed by a photocatalytic treatment allow disrupting different micropollutants present in waste waters. And the toxicity of waters very strongly decrease during the AOP treatments.

References

[1] P. P. Amador, R. M. Fernandes, M. C. Prudêncio, M. P. Barreto, I. M. Duarte, J. Environ. Sci. Health., Part A 50 (2015) 26–39.

[2] S. Al-Bahry, I. Y. Mahmoud, J. R. Paulson, S. K. Al-Musharafi, Int. Arabic J. Antimicrob. Agents 4 (2014) 1–11.

[3] M. A. Sousa, C. Gonçalves, J. H. O. S. Pereira, V. J. P. Vilar, R. A. R. Boaventura, M. F. Alpendurada, Sol. Energy 87 (2013) 219–228.

[4] C. J. Bodson, B. Heinrichs, L. Tasseroul, C. Bied, J. G. Mahy, M. Wong Chi Man, S. D. Lambert, J. Alloys Compd. 682 (2016) 144–153.

ECCE12
The 12th EUROPEAN CONGRESS OF CHEMICAL ENGINEERING
Florence 15-19 September 2019

ADSORPTION OF FLUORIDE AND ARSENIC (V) FROM AQUEOUS SOLUTION ON BONE CHAR MODIFIED WITH IRON SULFATE

Diana E. Villela-Martínez, Roberto Leyva-Ramos*, Carolina Vazquez-Mendoza

Centro de Investigación y Estudios de Posgrado, Facultad de Ciencias Químicas, Universidad Autónoma de San Luis Potosí, Av. Dr. M. Nava 6, Zona Universitaria, 78260, San Luis Potosí, S.L.P., MÉXICO.
**Corresponding author: rlr@uaslp.mx*

Highlights

- Arsenic and fluoride can be removed from water by adsorption on bone char modified with iron sulfate.
- Solution pH plays a key role on the adsorption of these anions onto bone char.
- Adsorption of arsenic and fluoride is due to electrostatic interactions and ion exchange.

1. Introduction

The concentration of the arsenic in natural waters varies depending on the presence of arsenic species in the soil [1]. Diverse epidemiological studies have found that the exposure to arsenic via the consumption of drinking water can cause the illness hyperkeratosis and cancer in bladder, lungs, skin, kidneys, liver and prostate. Besides, arsenic exposure has been associated with cardiovascular, pulmonary, immunological, neurological, peripheral vascular and endocrine diseases. The presence of fluoride in drinking water is a crucial issue since both low and high concentrations can affect human health. When the fluoride concentration is less than 0.5 mg/L, the incidence of dental cavities increases considerably; however, consumption of water with fluoride concentrations ranging between 1.5 and 4 mg/L can cause dental fluorosis [2]. Another severe health problem caused by the fluoride excess ingestion is skeletal fluorosis [2].

The removal of these pollutants from drinking water can be accomplished by several separation processes. Nowadays, adsorption is considered one of the best methods available to eliminate arsenic and fluoride from drinking water because it can reduce the arsenic concentration to trace levels and its easiness of operation. However, it is necessary to find novel adsorbent materials, which have a high capacity for adsorbing arsenic and fluoride, and the novel adsorbents have to be inexpensive and efficient.

2. Methods

The granular bone char (BC) used in this work is commercially manufactured from cattle bones. The BC was modified (BCM) by contacting with a solution of $FeSO_4$ and $NH_4Fe(SO_4)_2{\cdot}H_2O$, and the modification procedure was similar to that described by Asfarama et al. [3].

The point of zero charge (pH_{PZC}) and surface charge distribution of the adsorbent was evaluated using the method described in Mendoza-Barron et al. [4]. The textural properties were determined using a surface area and porosimeter analyzer, Micromeritics, ASAP model 2020. A scanning electron microscope JEOL, model JSM-6610LV, was employed to analyze the surface morphology of BCM. The crystalline species were identified by employing an X-ray diffractometer Bruker, model D8 Advance.

3. Results and discussion

The pH_{PZC} of BCM is 10.3 indicating that the surface of the BCM is basic. The XRD analysis confirmed the presence of calcite, hydroxyapatite and sodium sulfate in the BCM. The BCM has an irregular morphology due to the agglomeration of the hydroxyapatite sheets and the iron deposited on the BC. The characterization revealed the BCM is mesoporous, and its surface was basic.

The adsorption of isotherms of As(V) on BC and BCM are depicted in Figure 1, and the adsorption capacity of BCM towards As(V) was enhanced about 10 times at an equilibrium concentration of As(V) of 100 µg/L. As shown in Figure 2, the capacity of BCM was almost enhanced 4 times compared to that of the BC. The effect of the solution pH on the adsorption of fluoride on BCM is also presented in Figure 2, and the capacity of BCM was decreased by raising the solution pH from 5 to 11. Similar behavior was observed for the adsorption of As(V) on BCM. At pH below the pH_{PZC}, the surface of BCM was positively charge due to the protonation of the phosphates and hydroxyl groups contained in the material and As(V) and fluoride were present as anions. Thus, the predominant adsorption mechanism was the electrostatic attraction between the anionic species in solution and the positive charge of the BCM.

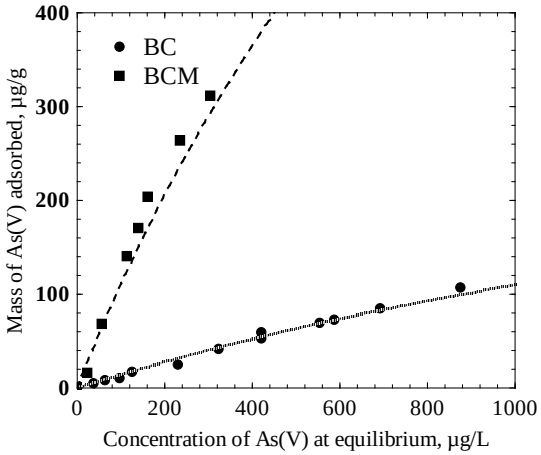

Figure 1. Effect of modification on the adsorption capacity of BC towards As(V) at T = 25 °C

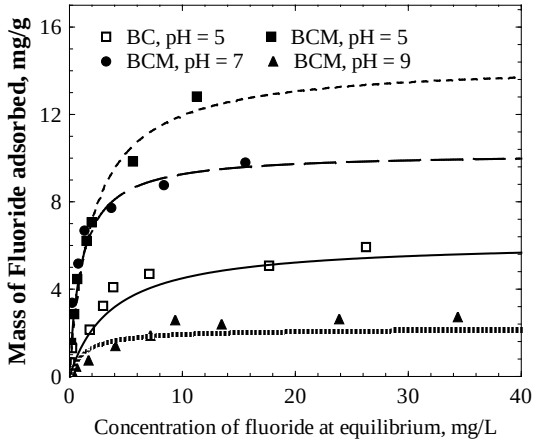

Figure 2. Effect of modification on the adsorption capacity of BC towards fluoride, and effect of pH on the adsorption capacity of BCM at T=25°C.

4. Conclusions

The modification of BC by $FeSO_4$ improved the adsorption capacity of BCM towards As(V) and fluoride considerably. The predominant adsorption mechanism was the electrostatic attraction between the anionic species in solution and the positive charge of the BCM. The adsorption capacity of BCM towards As(V) and fluoride was considerably reduced by increasing the solution pH.

References

[1] B.K. Mandal, K.T. Suzuki, Talanta 58 (2002) 201-235.

[2] N.A. Medellín-Castillo, E. Padilla-Ortega, L.D. Tovar-García, R. Leyva-Ramos, R. Ocampo-Pérez, F. Carrasco-Marín, M.S. Berber-Mendoza, Adsorption 22(7) (2016) 951-961.

[3] A. Asfarama, M. Ghaedi, S. Hajati, A. Goudarzi, Ultrason. Sonochem 32 (2016) 418-431.

[4] J. Mendoza-Barron, A. Jacobo-Azuara, R. Leyva-Ramos, M.S. Berber-Mendoza, R.M. Guerrero-Coronado, L. Fuentes-Rubio, J.M. Martinez-Rosales, Adsorption 17(3) (2011) 489–496.

ECCE12
The 12th EUROPEAN CONGRESS OF CHEMICAL ENGINEERING
Florence 15-19 September 2019

Efficient modification of montmorillonite with Sodium Lignosulfonate to adsorb Cd^{2+}.

Jianzhe Ma[1]

1 School of Chemical Engineering, Nanjing University of Science and Technology, Nanjing 210094, Jiangsu, China.

**Corresponding author: 748447353@qq.com*

Highlights

- Preparation of the modified Na montmorillonite with sodium
- Lignosulphonate-montmorillonite composites increase the heavy metal retention.
- The key parameters that control the chelation are determined.

1. Introduction

The remediation of wastewater containing Cd^{2+} has attracted much attention due to the harm of Cd^{2+} to the environment and human health[1]. Montmorillonite could be a kind of potential low cost sorbent for various kinds of heavy metals since it is abundant in nature and only needs little processing[2]. In spite of the huge amounts of papers reporting the use of untreated clay minerals for the heavy metal retention, the cation exchange capacity is not enough for large-scale applications. In order to increase the selectivity and the adsorption capacity for heavy metal cations, a promising adsorbent, functionalized montmorillonite modified with sodium lignosulphonate (Na-LS) was prepared under mild reaction conditions.

2. Methods

The Na-LS modified Ca-montmorillonite (denoted as NA-LS-MMT) was synthesized by mixing 5.00 g of Ca-MMT and 1.00 g of Na-LS in a 250-mL glass bottle. Then, the pH of the mixture of Na-LS and Ca-MMT suspension was adjusted to 5.0 using 1.0 M NaOH and 1.0 M HNO3 solutions. Afterwards, the suspension was shaken in a water bath shaker at 25 °C for 20 h. Subsequently, the resulting material was collected by centrifugation at 4000 rpm for 10 min, washed out the excess of Na-LS on the surface of Ca-MMT with deionized water for several times, so as to remove excess HA. Finally, the precipitate was air-dried at 45 °C, pulverized to pass through a 200-mesh sieve, and stored for future use.

3. Results and discussion

The batch adsorption experiments illustrated that the removal capacity of Cd^{2+} was crucially dependent on pH and the initial concentration of solution and it was favorable with an increase in pH in acidic solution. The adsorption thermodynamics of Cd^{2+} by NA-LS-MMT showed that the adsorption process was an endothermic reaction. The adsorption kinetics of NA-LS-MMT showed a better fit with the pseudo-second-order model. The adsorption isotherm data of NA-LS-MMT

followed the Freundlich isotherm better, which inferred that more than one kind of adsorption site happened on NA-LS-MMT (ion exchange and chelation).

4. Conclusions

In conclusion, composite adsorptive materials based on lignosulphonate and montmorillonite have been successfully prepared and characterized in depth. The raw montmorillonite and the composites were tested for heavy metal retention. The experimental results indicate the capacity of our composites to chelate heavy metal cations. Indeed, a high affinity between the lignosulphonate and all heavy metal cations was observed.

References

[1] Xueyan, G., Z. Shuzhen, and S. Xiao-quan, J. Hazard. Mater. 2008. **151**(1): p. 134-142.
[2] Abollino, O., et al. Water Res. 2003. **37**(7): p. 1619-1627.

ECCE12
The 12th EUROPEAN CONGRESS OF CHEMICAL ENGINEERING
Florence 15-19 September 2019

Ciprofloxacin photocatalytic degradation present in water using MOCVD deposition of TiO_2 and UVA LEDs

Thibaut Triquet[1], Claire Tendero[2], Romain Richard[1], Marie-Hélène Manero[1], Caroline Andriantsiferana[1*]

1 Laboratoire de Génie Chimique, Université de Toulouse, CNRS, INPT, UPS, Toulouse, France; 2 Centre Inter-universitaire de Recherche et d'Ingénierie des Matériaux, Université de Toulouse, CNRS, Toulouse, France
**Corresponding author:* caroline.andriantsiferana@iut-tlse3.fr

Highlights

- CIP is degraded by photolysis with 365 nm UV but not its intermediates
- Photocatalysis with TiO_2 deposits is efficient to mineralized CIP
- Very low quantities of TiO_2 are sufficient to degrade CIP and its intermediates.

1. Introduction

Nowadays, many toxic molecules particularly micropollutants (pharmaceuticals products such as antibiotics, anti-inflammatory, analgesic) are present in waterways and underground water, causing serious consequences for the environment. Advanced Oxidation Processes (AOP) and particularly the photocatalysis are promising processes to eliminate such molecules by generating powerful and non-selective radical oxidants through UV irradiation of the catalyst (commonly powder of titanium dioxide TiO_2) [1]. When implemented in water treatment process, an expensive filtration step is then necessary in order to remove the catalyst. In this context, a deposit of TiO_2 on a support could propose a competitive industrial implementation. In this study, two different morphologies of TiO_2 coating were studied to eliminate a target antibiotic: the ciprofloxacin (CIP). Both compact and columnar coatings were synthetized using Metal Organic Chemical Vapor Deposition (MOCVD) [2]. The aim of this study is to compare the efficiency of TiO_2 powder and both coatings on the degradation of CIP using LEDs (365 nm).

2. Methods

Analytical grade ciprofloxacin, $C_{17}H_{18}FN_3O_3$ (CIP, 98% purity) and TiO_2 powder (DEGUSSA-P25) were purchased from Sigma Aldrich. The deposition of TiO_2 on glasses surface were obtained by MOCVD [2]. Figure 1 represents the experimental set-up used for all photolysis and photocatalysis experiments. The top of the photo-reactor (130x10x12mm) is a window made of glass which is irradiated by LEDs (365 nm). The loop reactor is composed of the photo-reactor (V=15.6 mL) and a storage tank (V=100mL). The liquid flows via a peristaltic pump at a constant rate (200 mL/min). For each experiment, a 20mg/L CIP solution (100mL) was used and the temperature was maintained at 25°C (±1°C). For photolysis (without TiO_2), two irradiations were studied: 3mW/cm² and 10mW/cm². For photocatalysis (I=10mW/cm²), P25 was added (11.5mg and 5.6mg). In all experiments, an adsorption step of 1.5h was carried out before switching on the UV LEDs during 8h. The liquid samples were collected in the storage tank and filtered through a 0.45 µm membrane before being analyzed. The CIP concentration was

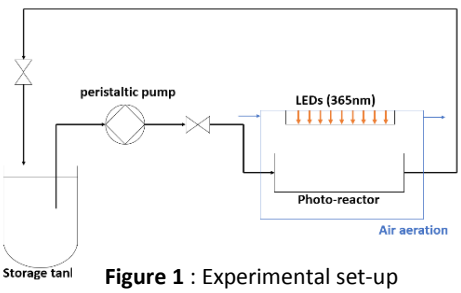

Figure 1 : Experimental set-up

determined by HPLC-UV (detector at 280 nm) and a C18 column. A measurement of Total Organic Carbon (TOC) was implemented before and after treatment.

3. Results and discussion

Figure 2a shows the evolution of CIP concentration for both photolysis and photocatalysis experiments with TiO_2 powder and using glass TiO_2 deposits. Without photocatalyst, after 10h, 75% of CIP is degraded. In presence of a small quantity of TiO_2 powder, 100% of CIP degradation was obtained after 2h (11.5mg) and 4h (5.6mg). After 8h of irradiation, the COT removal is higher than photolysis: 55-61% with P25 powder *vs* 8% without TiO_2. Even if the target molecule is easily degraded by photolysis, the problematic intermediates have not been eliminated [3]. In presence of low amount of catalyst, a total mineralization is not reached for both cases, in agreement with literature [4]. In addition, refractory aliphatic acids with small carbon chain remain generally in solution [4]. Indeed, as shown in Figure 1B, the areas, of the chromatogram pics associated to the intermediates, decrease and after 6h, these intermediates have almost disappeared. The efficiency of TiO_2 deposits is comparable to the one of P25: the amount of carbon removal is 55% for columnar coating and 64 % for the compact one. However, the degradation kinetic is slower than experiments with P25, probably due to a lower surface available for photocatalysis reaction. This could be explained by (i) the inaccessibility of the part of TiO_2 fixed on the glass and/or (ii) a possible recombination of the electron-hole pair due to the low quantity of O_2 near the glass.

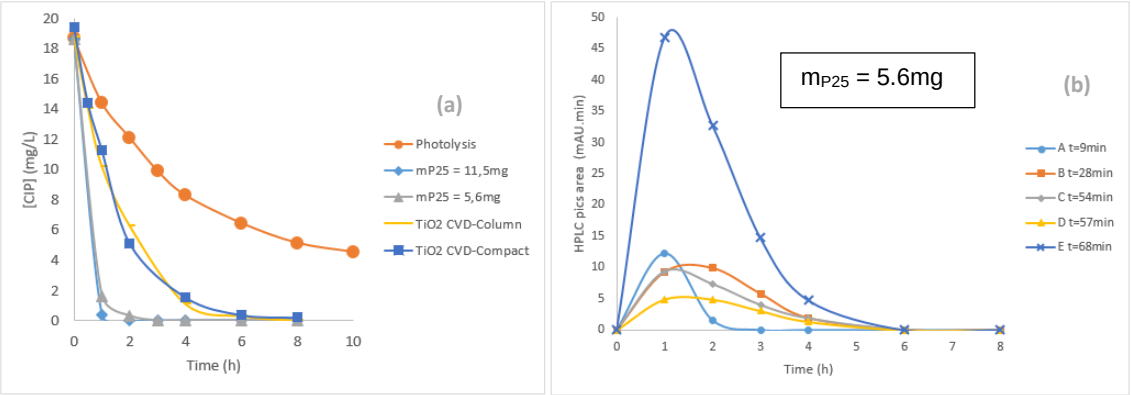

Figure 2 : Photolysis ant photocatalysis kinetics **(a)** and HPLC peaks area of principal intermediates A, B, C, D and E **(b)**

4. Conclusions

It has been shown that ciprofloxacin can directly react with 365 nm UV but a total mineralization of CIP cannot be achieved (8h/8%). In presence of a low TiO_2 powder quantity (11.5mg), photocatalysis is efficient: a total CIP degradation (2h) and a high TOC removal (8 h/61%). Both TiO_2 coatings on glass present the same photocatalytic activities and a total elimination takes 3 times longer than with powder. To go further, another support will be tested: activated carbon (AC). Indeed, previous studies have demonstrated the synergistic effect of AC and TiO_2 [5, 6].

References

[1] González-Labrada, Katia and al., Latin American Applied Research, 46(2016), 115-120
[2] F. Maury and F.D. Duminica F.D., Surf Coat Tech, 205 (2010) 1287
[3] Si Li. Jiangyong Hu and al., Water Research, 132 (2018), 320-330
[4] Muna Sh. Yahya and al., Chemosphere, 117 (2014) 447–454
[5] C. Andriantsiferana, E.F. Mohamed, H. Delmas, Env tech 35 (2014) 355
[6] C. Andriantsiferana, E.F. Mohamed, H. Delmas, Environ. Eng. Res. 20 (2015) 181

ECCE12
The 12th EUROPEAN CONGRESS OF CHEMICAL ENGINEERING
Florence 15-19 September 2019

A predictive operating control system based on Data Driven Bayesian Networks

Tomaso Vairo[a-b]*, Margherita Pettinato[b], Bruno Fabiano[b]

a ARPAL, Grandi Rischi, via Bombrini 8, 16149 Genoa Italy
b DICCA – Genoa University, via Opera Pia 15, 16145,Genoa, Italy

**Corresponding author: tomaso.vairo@edu.unige.it*

Highlights

- Data Driven Models
- Process control
- Dynamic risk management

1. Introduction

In these last years, on one hand the industrial world experienced radical technological advances in connection with communication and fast-developing societal progresses requiring further research and applications for sustainability and process safety improvement. On the other hand, especially in Europe, a large part of industrial process facilities date back to the 1960's and 1970's. Operational errors are identified as one of the most important causes of the deterioration of the plant equipment, consequently, the operational control is one of the main systems to manage and slow down the effects of aging [1],[2]. This paper reports a first step towards the implementation of a digital twin of an upper tier Seveso plant, which can predict the behavior of the system (failures, risks, malfunctions, errors) in order to operate effectively in safety. The system, based on machine learning algorithms and Bayesian reasoning, learns continuously from the data provided by the physical system. From the operational experience of the coastal storage facility, it is clear how most of the accidental events are due to a wrong arrangement of the valves, to abnormal transfer pressures, to pump failures and pipe deterioration. This paper is focused on building an operational management system, based on the operational instruction, suitable to predict operational errors and accordingly avoiding them and thus protecting asset integrity and improve aging management.

2. Methods

Data-driven modelling can be considered as an approach to modelling that focuses on using the Machine Learning methods in building models that would complement the "knowledge-driven" models describing physical behaviour. Bayesian Networks (BBNs) were proven to be a robust probability reasoning method under uncertainty, providing a tool for incorporating these types of evidence [3]. Starting from the operating manual, various coupled Bayesian Belief Networks were built. So, the asset integrity management was an upper layer which receive and send data to the lower levels. Top events and risk assessment for the case-study of the discharge of diesel oil from a ship moored at the "Beta-ponente" pier were evaluated. The BBNs were then updated, on one hand, with the reliability parameters (results of the inspections or failures on demand - hard evidences) and, on the

other one, with the evidences of the ongoing activities, which represent the likelihood coefficients (soft evidences).

3. Results and discussion

The decision-making network carried out the steps reported in Figure 1.a, which is the BBN structure as learned from the operating manual. The networks were then updated by the data from the plant (state of the valve – open, close, pressure in the pipelines), which are hard evidences and, on the other hand, with the evidences of the ongoing activities, which represent the likelihood coefficients (soft evidences).

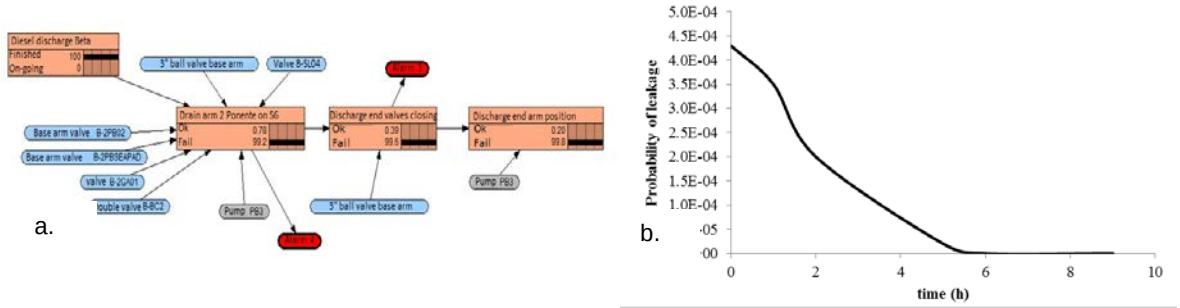

Figure 1. a) Decision-making BBN for ending the diesel discharge from BETA pier; b) "Good" evidences: trend of the posterior probability failures in the collectors pit.

The combination of the risk analysis BBNs and the operational BBNs allowed to manage the whole cycle of the operations, giving, step by step, the updated probability of failure (Figure 1.b). The proposed system represents a tool that in real time allows to manage the operations focusing on safety and, combined with proper advanced analytics applications, allows anticipating what should be done to avoid upcoming incidents.

4. Conclusions

Data Driven BNs are a robust method for modeling complex systems in the probability and uncertainty analysis. The results of the application of the method allow identifying which, among the basic failures, are the most influencing on the probability of the top events occurrence, and therefore, to have a more precise indication on the maintenance priorities. Additionally, the relationship between the risk trend represented as a probability function and the evidences during the operation in progress was analyzed. So both aspects (risk management and operational management) can be improved together.

References

[1] Vairo T., Reverberi A.P., Milazzo M.F., Fabiano B. 2018. Aging and Creeping Management in Major Accident Plants according to Seveso III Directive. Chemical Engineering Transactions 67, 403-408.
[2] Kalantarnia M., Khan F., Hawboldt K. 2009. Dynamic risk assessment using failure assessment and Bayesian theory, Journal of Loss Prevention in the Process Industries, 22, 600–606.
[3] Yang, M. Kahn, F., Lye, L. 2013. Precursor-based hierarchical Bayesian approach for rare event estimation: a case of oil spill accident. Process Safety and Environmental Protection, 91(5), 333-342.

ECCE12
The 12th EUROPEAN CONGRESS OF CHEMICAL ENGINEERING
Florence 15-19 September 2019

HazOp Analysis: going beyond traditional goals

Stefano Milanese[1], Andrea Casalli[2], Emanuele Salvador[1*], Michele Piola[1]

[1]*Arthur D. Little S.p.A., Corso Monforte 54, 20122 Milan (Italy)*

[2]*Eni SpA, Piazzale Enrico Mattei 1, 00144 Rome (Italy)*

**Corresponding author: salvador.emanuele@adlittle.com*

Highlights

- Arthur D. Little supported a major refinery in the EPC[1] phase HazOp[2] of a plant
- The review integrated several aspects (asset integrity operations, operating manual, safety report development, etc.) not typically included in such an assessment
- The integrated approach supported the client in managing the multiple activities required for the construction and startup phase, making up for some EPC delays.

1. Introduction

In 2018, risk management consulting firm Arthur D. Little was tasked to carry out a HazOp assessment on the EPC design of a plant in a major Italian refinery. The plant, built according to an innovative hydrocracking process, underwent major modifications: there was considerable interest at site, Business Unit and HQ levels to ensure a thorough HAZOP review.

In accordance with the client, Arthur D. Little's framework included additional discussions and analysis, allowing an early start on future activities such as asset integrity checks, alarm management, layers of protection improvement.

2. Methods

The HAZOP was carried out according to international standards ([1] and [2]). The analysis was «full recording», noting all discussions even when no credible scenarios would emerge. Both consequences on occupational and process safety, asset integrity and on operability have been taken into consideration. Therefore, a comprehensive assessment was carried out not only on Top-Events, but also on other scenarios typically not assessed during a HazOp due to time and resources constraints.

A comprehensive set of recommendations was issued regarding design and instrumentation modification to be implemented prior to start-up. Furthermore, suggested improvement actions gave relevant contribution on the following aspects:

- Asset integrity. Whenever a scenario was at risk of going beyond design conditions, the equipment and lines were included as "Safety Critical Elements" and/or "Operational Critical Elements" (SCE/OCE) to be subject to dedicated monitoring. Arthur D. Little also recommended additional verifications on the asset integrity whenever such alarms were activated (e.g. registration and analysis of integrity operating windows)

[1] Engineering, Procurement & Construction
[2] Hazard & Operability

- Transient states. Startup/shutdown procedures, as well as safety operations such as slow and fast depressurization, were included in the study. These operations typically involve less than 10% of the operating time, but account for more than 50% of incidents ([3]). Through the assessment of these procedures, some deficiencies were noticed and countermeasures were considered and included in the operating manuals
- Operating manuals. They had been issued in preliminary versions: the inclusion in the HAZOP highlighted the need of further integrations
- Training. A specific list of recommendations was drafted to ensure that future training programs included special operations following the activation of alarms or emergency procedures.
- Safety Report. The HazOp assessment was included in the Safety Report, as defined by European legislation Seveso-III-Directive [4]. From it, quantitative risk assessments were carried out on the key scenarios, using the Fault Tree Analysis methodology.

3. Results and discussion

The HAZOP team divided the recommendations in 10 categories and additional 35 sub-categories and conducted the complete follow-up activities.

The assessment was also fundamental to strengthen the interaction between the process design team (a mixed team with internal and external resources) and the production internal team.

4. Conclusions

Throughout this project, the fruitful collaboration between Arthur D. Little and client representatives allowed the HazOp assessment to go beyond its original goals. It can be used as a tool to highlight the “typical” deviations and also to assess and integrate in safety management several other aspects that are not typically considered in the traditional approach.

This way, the client got a head start on follow-up activities, allowing to recover the delay in the EPC process and to start construction activities as planned.

References

[1] IEC 61882 (all parts), 2016, Hazard and operability studies (HAZOP studies) – Application guide
[2] IEC 31010, 2009, Risk management — Risk assessment techniques
[3] Ostrowski S.W., Keim K.K., *Tame Your Transient Operations – Use a special method to identify and address potential hazards*, ExxonMobil Chemical Company, 2010
[4] European Commission, 2012, Directive 2012/18/EU of the European Parliament and of the Council of 4 July 2012 on the control of major-accident hazards involving dangerous substances, amending and subsequently repealing Council Directive 96/82/EC Text with EEA relevance, 2012/18/EU
[5] ISO, Asset Management, 55000:2014 series, 1st ed., International Organization for Standardization, Geneva, SUI, 2014
[6] CCPS, *Guidelines for Mechanical Integrity Systems*, 1st ed., Center for Chemical Process Safety, New York, USA, 2006
[7] CCPS, Guidelines for Risk Based Process Safety, 1st ed., Center for Chemical Process Safety, New York, USA, 2007.
[8] Hollifield B., *Understanding and Applying the ANSI/ISA 18.2 Alarm Management Standard*, PAS, 2010

ECCE12
The 12th EUROPEAN CONGRESS OF CHEMICAL ENGINEERING
Florence 15-19 September 2019

Wood Wastes Valorization Through the Development of Eco-Friendly Cellulose-Based Polyelectrolytes for Potential Industrial Applications.

Kinga Grenda[1,2], Julien Arnold[2], José Gamelas[1], Maria G. Rasteiro[1]

[1,2] University of Coimbra, Chemical Eng. Dep - CIEPQPF, Portugal, [2] AQUA+TECH Specialities, Geneva, Switzerland

*Corresponding author: mgr@eq.uc.pt

Highlights

- Wood wastes valorization, evaluation of influence of lignin content.
- An alternative replacement for traditional, oil-based, synthetic polyelectrolytes
- Environmental friendly cationic bio-polyelectrolytes for industrial applications.

1. Introduction

Low biodegradability, being harsh to the environment or to human health, are just some of the drawbacks when traditional synthetic polyelectrolytes (PEL) are used. There is then, a strong need for the replacement of oil-based materials by more eco-friendly, biodegradable, non-toxic, easy available solutions. Bearing in mind wood is the world's most important source for industrial purposes, not only for furniture or pulp and paper production, but also as a feedstock for the extraction and production of chemicals for various industries [1], the production of cellulose-based added value materials, reusing lignocellulosic wastes, appears as a viable and added value solution to deal with such wastes, and is going to be addressed here, especially production of cellulosic PELs.

Unmodified cellulose presents insolubility in water and in most organic solvents [2]. Consequently, introduction of new functional groups into the cellulose backbone is required to improve the cellulose properties, which will strongly depend on the types of substituent groups and on the degree of substitution (DS), as well as on their distribution in the cellulose backbone. As a result, new applications of cellulose can be achieved with potential replacement of oil-based materials. Regarding PELs production, the path of oxidation/cationization with sodium periodate and Girard's reagent T (GT) was used to produce highly charged water soluble cellulose based PELs. The aim of this study was to establish a procedure to successfully prepare cellulose-based PELs, with diverse DS, starting from more complex cellulosic raw materials with higher content of lignin and lower cellulose content, thus minimizing pre-extraction procedures. Some studies in the literature refer cationization of cellulose [3][4], but, as far as we know, these reactions have never been performed starting from highly complex cellulosic materials, with a low degree of cellulose purity.

2. Methods

Eucalyptus wood chips wastes were submitted to soft kraft pulping using 14 % or 19 % active alkali charges to previously hot water extracted and non-extracted wood. The produced pulps were thoroughly washed with water and dried. Resulting materials were characterized and corresponded to different lignin content based on kappa number, being 10.2 or 13.9 (pulps with hot water pre-

treatment) and 16.1 or 26.7 (pulps without hot water pre-treatment). Highly oxidized pulps were first produced from those raw materials, by oxidation using $NaIO_4$. After 3 h at 75 °C, the dialdehyde cellulosic product (DAC) was filtered and washed with water. The aldehyde content of DAC was determined based on the oxime reaction [5]. Cationization of non-dried DAC followed through reaction with GT in aqueous media [5]. After 1 h at 70 °C the soluble products from reaction mixture were precipitated with isopropanol and centrifuged and the cationic product was oven-dried. The GT/aldehyde ratio varied from 0.975 to 3.9 to obtain bio-PELs with different cationization degree.

3. Results and discussion

Modification of cellulosic-rich materials (obtained from *Eucalyptus* wood wastes with various lignin levels) by introduction of charged quaternary ammonium groups was chosen, as these groups are widely present in successfully applied synthetic PELs. The main objective was to allow the introduction of high content of ionic groups to obtain sufficiently charged cellulose-based materials. The pre-modification to DAC, by selective oxidation with periodate, allowed a high modification degree, since two highly reactive aldehyde groups were introduced per AGU unit. Finally, for the cationization, reaction of DAC with GT was conducted. This treatment allowed to introduce more than one cationic group per AGU unit, yielding highly charged end products which were soluble in in water at room temperature. The charge density and DS of the end product depended on the cationization conditions (temperature, time, pH, molar ratio GT/aldehyde) and also on the properties of the pre-treated cellulosic sample, used as starting material. Typically with the increase of kappa number the DS and charge of PEL decreases when applying the same GT/aldehyde ratio. However, even when using cooked pulp with the highest lignin content (kappa 26.7) and for the lowest GT/aldehyde ratio of 0.975, water soluble PEL with DS of 0.79 and zeta potential of 40±3 mV was produced. When applying the same low GT/aldehyde ratio to the hot water pre-treated/cooked pulp with the lowest kappa of 10.2, the produced PEL exhibited DS of 0.96 and zeta potential of 51±2 mV. Moreover, the obtained PELs, independently of the chemical complexity of raw pulp used in the modification procedure, showed high performance in the treatment of several model coloured effluents and in a real industrial effluent treatment, namely in colour removal.

4. Conclusions

Valorization of cellulosic wastes to provide end products with higher added value (PELs) by applying a sequence of two reactions, oxidation followed by cationization, was investigated. Cellulosic raw materials with different lignin content (kappa number 10.2-26.7) were used. The cationic bio-PELs proved to be efficient biopolymeric flocculation aids in the tested model waters and in an industrial effluent. The developed products can be considered as an alternative to traditional synthetic PELs.

References

[1] E. Guibal, J. Roussy, React. Funct. Polym. 67 (2007), 33–42.
[2] D. Klemm, B. Heublein, H. P. Fink, A. Bohn, Angewandte Chemie - Int.Ed. 44 (2005), 3358–3393.
[3] J. Sirviö, A. Honka, H. Liimatainen, J. Niinimäki, O. Hormi, Carbohydr. Polym. 86 (2011), 266–270.
[4] H. Liimatainen, J. Sirviö, O. Sundman, M. Visanko, O. Hormi, J. Niinimäki, Bioresour. Tech. 102 (2011), 9626–9632.
[5] K. Grenda, J. Arnold, J. A. F. Gamelas, M. G. Rasteiro, Water Sci. Tech. 76 (2017), 1490–1499.

Acknowledgements

The authors thank the financial support from Marie Curie Initial Training Networks (ITN) – European Industrial Doctorate (EID), Grant agreement FP7-PEOPLE-2013-ITN- 604825 and FCT, Pest/C/EQB/UI0102/2013.

ECCE12
The 12th EUROPEAN CONGRESS OF CHEMICAL ENGINEERING
Florence 15-19 September 2019

New persistent organic pollutants: polybrominated diphenyl ethers

Elisabetta Bemporad, Simona Berardi, Sabrina Campanari, Alessandro Ledda, Paolo Napolitano.

Inail, Dipartimento Innovazioni Tecnologiche e Sicurezza degli Impianti, Prodotti ed Insediamenti Antropici, via Roberto Ferruzzi 38/40, 00143 Roma, Italia.
**Corresponding author: e.bemporad@inail.it*

Highlights

- Persistent organic pollutants
- Polybrominated diphenyl ethers
- Environmental pollutants
- Health, safety and wellness

1. Introduction

Persistent Organic Pollutants (POPs) are a group of organic compounds that possess toxic properties, persist in the environment, bio-accumulate through the food web and pose a risk of causing adverse effects on human health and the environment. The European Union (EU) coordinates its Member States being parts to the global Stockholm Convention (SC) on POPs. The Conference Of the Parties (COP) to the SC is cooperating closely with the appropriate bodies under the Basel Convention (BC) on POPs waste to develop guidelines for what is considered Environmentally Sound Management (ESM) of POP containing waste and to establish destruction limits for such wastes. The BC is a global environmental treaty on the control of transboundary movements of hazardous wastes and their disposal. The POPs listed in the two Conventions are to date 26, including some of the PolyBrominated Diphenyl Ethers (PBDEs) (UNEP/POPS/COP.7/INF/27), an important class of Brominated Flame Retardants (BFRs). The last BDE listed in Annex A, to the SC (UNEP/POPS/COP.7/INF/27) in 2017 was decaBDE component (BDE-209) of c-decaBDE with specific exemptions for the production and use. Under the REACH Regulation, decaBDE was registered in 2011 and identified as a Persistent, Bioaccumulative and Toxic (PBT) and very Persistent and very Bioaccumulative (vPvB) substance (UNEP/POPS/COP.7/INF/22).
The Department of Technological Innovations (DIT) of INAIL, for several years, has been part of the Small Intersessional Working Group (SIWG) for the development of Technical Guidelines (TG) on the ESM of wastes consisting of, containing or contaminated with POPs. Considering this background, the present work summarizes and gives an overview on the commercial identity, production and use of POP-BDE potential exposure to them through environmental contamination and, in particular, management of waste contaminated by them, with particular reference to decaBDE. The main purpose of the present work is to make available, in aggregate and immediately usable form, information and useful data for identifying risks to health and the environment and for the adoption of suitable prevention interventions to protect the exposed receptors.

2. Methods

Starting from the regulatory framework with which the European Union implement the provisions of the Convention about substances, mixtures, and wastes, the sound management of the POP waste will be illustrated, including information and data for 1) Articles, waste and recycled materials containing PBDEs; 2) Uses and industrial productions; 3) Life-cycle; 4) PBDEs levels in the waste. Moreover, information about the latest activities on the TGs for the ESM of POP wastes as result of the most recent amendments to the Annexes of the Stockholm Convention will be given. Finally, advices about human health and the environment from the adverse effects of hazardous wastes will be provided.

3. Results and discussion

The production, marketing or use of decaBDE as a substance or as an element of other substances, in mixtures and in products, is set out in Annex XVII (list of limitations), of the REACH Regulation, which prohibits the production and placing on the market of decaBDE as a pure substance from March 2nd 2019. Directive 2011/65/EU (RoHS Directive) restricts the use of PBDEs, as a substance group, in Electrical and Electronic Equipment (EEE). As this directive restricts PBDEs as a substance group, it also applies to decaBDE. The maximum concentration value for PBDEs is 0.1 % by weight (1,000 mg/kg) in homogeneous materials. According to Annex VII of Directive 2012/19/EU on Waste Electrical and Electronic Equipment (WEEE), on the selective treatment of materials and components of EEE, plastics containing BFR have to be removed from any separately collected WEEE. If the total bromine concentration is below 2,000 mg/kg, it is considered that the treatment operator complies with the de-pollution requirements for BFR according to the WEEE Directive. Regarding ESM for WEEE plastics, there is a risk that contaminated recycles enter in the product cycle. The risk can be minimized as far as possible through a higher degree of separation of plastic WEEE containing decaBDE. The current POP Regulation does not yet include decaBDE, but in the specific TGs developed under the Basel Convention it was proposed to include deca-BDE for the sum of POP-BDEs, already limited to 1000 mg/kg

4. Conclusions

In waste streams are still introducing goods containing C-decaBDE. Emissions of c-decaBDE to the environment occur at all its life-cycle stages, but they are assumed to be the highest during service-life and during the waste phase. Production and use of c-decaBDE is decreasing but still ongoing in significant quantities. The production and use of the other commercial PBDEs has been stopped in the first decade of the 2000s at a global level. As a consequence, levels in products and wastes, as well as recycled (secondary) materials, are expected to decrease continuously in the coming years. In addition, an extensive POPs contamination of sites in Countries with transition or development economies has recently emerged. In these Countries POPs wastes are frequently exported, without being adequate capacity to manage them in safety, also due to the scarcity of the controls and to the inadequate implementation of the Conventions [1, 2].

References

[1] Weber R., Aliyeva G., Vijgen J., 2013. The need for an integrated approach to the global challenge of POPs management. Environmental Science and Pollution Research 20(4), 1901-1906.

[2] Bell L., Weber R., De Borst B., Paun M.C., Holoubek I., Kakareka S., Petrlík J., Watson A., Vijgen J., 2016. Assessment of POPs contaminated sites and the need for stringent soil standards for food and feed safety. Working document for UNEP Dioxin Toolkit and BAT/BEP group. Bratislava (Slo).

ECCE12
12th EUROPEAN CONGRESS OF CHEMICAL ENGINEERING
Florence 15-19 September 2019

Catalytic Wet Air Oxidation of Effluent Containing 2, 4, 6-Trichlorophenol Using Bimetallic Feru/Carbon Xerogel Catalyst.

Manjari Kumari, Anil K. Saroha*

Department of Chemical Engineering, Indian Institute of Technology, Delhi, India

**Corresponding author: aksaroha@chemical.iitd.ac.in*

Highlights

- A low-cost carbon xerogel was prepared using resorcinol, tannic acid and formaldehyde.
- Iron-ruthenium/carbon xerogel catalyst was used in CWAO of TCP solution.
- A TCP and COD removal efficiency of 95.82 % and 93.14 % respectively were obtained.

1. Introduction

Chlorophenols are a group of toxic and recalcitrant compounds commonly found in the effluent of industries such as pesticides, petrochemical, pulp and paper, dye, olive oil, pharmaceuticals, etc. (Olaniran & Igbinosa, 2011). The permissible limit of chlorophenols in drinking water is 10 µg/L (Pera-Titus et al., 2004). Therefore, it is mandatory to treat industrial effluent containing chlorophenol before its discharge in the environment. Advanced oxidation processes have proved to be a successful method for the treatment of high strength and toxic effluents. Wet air oxidation involves oxidation of pollutant at elevated temperature and pressure conditions but oxidation in presence of suitable catalyst, catalytic wet air oxidation (CWAO), can be performed at mild conditions of temperature and pressure leading to a substantial reduction in capital and operating costs. The use of carbon materials (activated carbon, carbon nanotubes, carbon gels, etc.) as catalyst support is advantageous as they are prepared from natural materials, possess high specific surface area and the precious active metals impregnated on the carbon support can be recovered from the spent catalyst (left over ash) by its oxidation in presence of oxygen (air). Carbon gels, commonly prepared from natural materials, are advantageous as they possess high surface area & pore specific volume, mechanical strength and are stable at high temperatures. The bimetallic catalysts, often referred to as 'alloy catalysts', show synergistic effect. The addition of a small amount of the second metal to a monometallic catalyst causes better dispersion of the metal particles and reduces the size of metal particles on the support surface resulting in an increase in active specific surface area of the catalyst which leads to better activity (Garrido-Ramirez et al., 2016). Thus, in the present study, the carbon xerogel (MCXO) based bimetallic (FeRu/MCXO) catalyst was prepared and used in the CWAO of an aqueous solution containing 100 ppm 2, 4, 6-trichlorophenol (TCP).

2. Methods

Xerogel was prepared by a sol-gel reaction of a natural precursor tannic acid (67 %), resorcinol (33 %) and formaldehyde. The water content of the wet organic gel was exchanged using a solvent (such as t-butanol, acetone, toluene and ethanol) of lower surface tension. Later, the carbon xerogel was modified using an acid (such as o-phosphoric acid, nitric acid and sulphuric acid) in order to enhance its surface properties. The active metals Fe and Ru were impregnated on the surface of the xerogel support material by co-impregnation method. The catalyst was characterized using various techniques such as BET, XRD, SEM & TEM analysis, FTIR, TGA, etc. The CWAO of TCP was carried out and the results were interpreted in terms of TCP and COD removal efficiencies. The effect of various operating parameters such as metal loading, initial pH of TCP solution, air flow rate, catalyst dose, reaction temperature and operating pressure on TCP and COD removal efficiencies was studied. The kinetics of the degradation of TCP was studied. The reusability and stability of the bimetallic catalyst was also studied.

3. Results and discussion

A low-cost carbon xerogel was prepared by partially replacing the costly resorcinol with a low-cost precursor tannic acid. The solvent exchange with t-butanol conserved the porosity of the xerogel and modification with o-phosphoric acid induced oxygenated functional groups on the surface of the carbon xerogel. The bimetallic catalyst (FeRu/MCXO) having a high specific surface area (562 m^2/g) and pore specific volume (1.51 cm^3/g) showed the maximum TCP and COD removal efficiency of 95.82 % and 93.14 % respectively at the optimum value of operating parameters. The optimum value of metal loading, initial pH of TCP solution, air flow rate, catalyst dose and operating pressure for FeRu/MCXO catalyst were found to be 4 wt. % iron and 0.3 wt. % ruthenium, 4, 3 L/min, 0.8 g/L and 1 bar respectively at 75 °C. The kinetics of the degradation of TCP by CWAO was studied and it was found that the reaction followed pseudo-first order kinetics with respect to the concentration of TCP in the aqueous solution. The FeRu/MCXO catalyst was found to be stable with a marginal decrease (3.11 %) in its activity after third reuse of the spent catalyst.

4. Conclusions

A novel bimetallic FeRu/MCXO catalyst was prepared having high specific surface area (562 m^2/g) & poro specific volume (1.51 cm^3/g). The CWAO of aqueous solution containing TCP resulted in good removal of TCP (TCP-95.82 % & COD-93.14 %) at the optimized value of operating parameters. The catalyst was found to be stable and suitable for use in continuous processes.

References

[1] A.O. Olaniran, E.O. Igbinosa, Chemosphere 83 (2011) 1297-1306.
[2] E.G. Garrido-Ramirez, J.F. Marco, N. Escalona, M.S. Ureta-Zanartu, Microporous Mesoporous Mater. 225 (2016) 303-311.
[3] M. Pera-Titus, V. Garcia-Molina, M.A. Banos, J. Gimenez, S. Esplugas, Appl. Catal., B47 (2004) 219-256.

ECCE12
The 12th EUROPEAN CONGRESS OF CHEMICAL ENGINEERING
Florence 15-19 September 2019

Electrochemical treatment for removal humic acids from aqueous solutions using platinum anodic electrode: effect of supporting electrolytes

Angelo Fenti[1], Sante Capasso[2], Pasquale Iovino[2,3], Stefano Salvestrini[2,3], Simeone Chianese[1,2*], Dino Musmarra[1,2]

1 Department of Engineering, University of Campania "Luigi Vanvitelli", 81031 Aversa (CE), Italy; 2 Environmental Technologies, University Spin-Off of University of Campania "Luigi Vanvitelli", Via Vivaldi, 43, Caserta, Italy; 3 Department of Environmental, Biological and Pharmaceutical Sciences and Technologies, University of Campania "Luigi Vanvitelli", via Vivaldi 43, Caserta, Italy

**Corresponding author: simeone.chianese@unicampania.it*

Highlights

- Electrochemical removal of humic acids was investigated.
- The effects of NaCl and NaClO4 electrolytes were studied.
- Humic acids removal was faster in the presence of NaCl.

1. Introduction

Humic acids (HA) are the soluble fraction of humic substances at alkaline and neutral pH and are produced by biotic and abiotic degradation of dead organic matter. HA have a broad molecular weight distribution and contain several functional groups such as aromatic, carboxylic and phenolic groups [1]. Owing to their solubility, HA are common water contaminants, hence procedures for their removal from water have been extensively investigated [2,3]. Among them, electrochemical treatment is very promising because of its efficiency and ease of use. Depending on the operating conditions and the type of pollutant, a diversity of reactions can occur at the electrodes and in solution [4]. Recently, the removal by electrocoagulation of humic acids (HA) has been analyzed using aluminum as sacrificial electrode, indicating that HA removal rate increased with ionic strength and electric current density [5].

2. Methods

In the present work, the electrochemical treatment of HA solutions has been investigated in the presence of different electrolytes (i.e. NaCl and $NaClO_4$) using a platinum-coated titanium anodic electrode and a graphite cathodic electrode, under amperostatic conditions. Investigations were carried out with the following experimental conditions: HA concentration = 50 mg L^{-1}; salt concentration = 0.08 mol L^{-1}; current density = 6.12 A m^{-2}; ΔV = 5.0 V; pH =7.0. HA concentration was measured by using spectroscopy technique.

3. Results and discussion

Fig. 1 shows the time-dependence of humic acids concentration, as determined by the absorbance signal at 320 nm, in the presence of NaCl and $NaClO_4$, respectively. As it can be seen, during the electrochemical process, HA concentration rapidly decreases with both electrolytes; interestingly, when NaCl is used, HA concentration reaches a stable value in about 2 h. The results indicate that

humic acids removal is faster in the presence of NaCl, probably as a consequence of chlorine formation by oxidation of Cl^-, which acts as oxidizing agent for HA. The UV-Vis spectra of HA at time zero and at the end of the electrochemical treatment are reported in Fig.2. The figure shows a marked blue shift of HA spectrum with both electrolytes, which is probably associated with the reduction of the conjugation of HA aromatic groups during the oxidation process. Detailed products characterization of the electrochemical treatment of HA is under investigation.

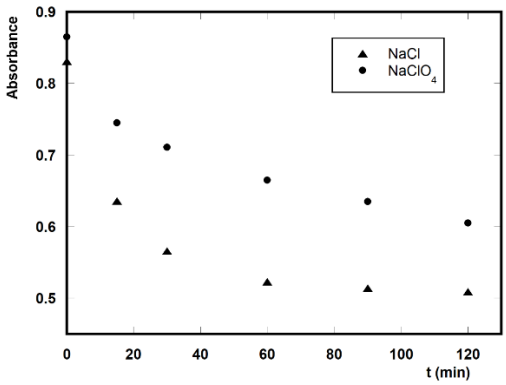

Figure 1. Time-dependence of HA concentration in the presence of different electrolytes; λ = 320 nm, [HA] = 50 mg L^{-1}, salt concentration = 0.08 mol L^{-1}, current density = 6.12 A m^{-2}, ΔV = 5.0 V, pH =7.0.

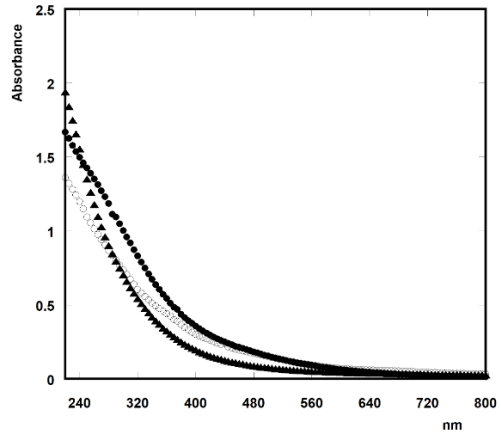

Figure 2. UV-Vis spectra of HA at time zero (●), in the presence of 0.08M NaClO4 at 2h (○) and in the presence of 0.08M NaCl at 2h (²); [HA] = 50 mg L-1, current density = 6.12 A m-2, □V = 5.0 V, pH =7.0.

4. Conclusions

The effects of NaCl and $NaClO_4$ electrolytes on HU removal from wastewater was investigated. Findings highlighted that with both electrolytes HA concentration rapidly reduced. In particular, humic acids removal was faster in the presence of NaCl. A blue shift of HA spectrum was observed probably due to the reduction of the conjugation of HA aromatic groups during the oxidation.

References

[1] W.M.A. Niesses, Liquid chromatography-mass spectrometry, third ed., CRC Press-Taylor and Francis, Boca Raton, 2006.
[2] P. Iovino, V. Leone, S. Salvestrini, S. Capasso, Desalin. Water Treat. 56 (2015) 55-62.
[3] V. Leone, D. Musmarra, P. Iovino, S. Capasso, Water Air Soil Pollut. 228 (2017) 136.
[4] H. Särkkä, A. Bhatnagar, M. Sillanpää, J. Electroanal. Chem. 754 (2015) 46-56.
[5] S. Capasso, S. Salvestrini, V. Roviello, M. Trifuoggi, P. Iovino, J. Chem. in press (2019).

ECCE12
The 12th EUROPEAN CONGRESS OF CHEMICAL ENGINEERING
Florence 15-19 September 2019

Potential formation of PCDD/Fs during TCS electrochemical oxidation. Influence of the operation variables

Claudia Solá-Gutiérrez, Sophie Schröder, María Fresnedo San Román, Inmaculada Ortiz

Biomolecular and Chemical Engineering Department, ETSIIT, University of Cantabria, Avda. De los Castros, 39005, Santander, Spain

**Corresponding author: solac@unican.es*

Highlights

- Electrochemical oxidation of triclosan in aqueous phase is investigated.
- The influence of initial concentration of triclosan, supporting electrolyte and presence of copper in the solutions has been studied.
- The formation of highly toxic PCDD/Fs congeners within the oxidation is assessed.

1. Introduction

Triclosan (TCS), 5-chloro-2-[2,4-dichlorophenoxy]-phenol, classified as a PPCP (pharmaceutical and personal care product) is widely used as a broad-spectrum antimicrobial and antifungal agent in many professional and personal products (deodorant soaps, toothpaste and mouthwash, plastic consumer goods…) [1]. Triclosan and related compounds are characterized by acute resistance to biodegradation, environmental persistence and high lipophilicity. Therefore, in order to protect the environment from the harmful effects caused by the discharge of wastewater containing triclosan, the application of efficient technologies able to mineralize this type of compounds becomes crucial. Advanced Oxidation Processes (AOPs) have emerged as powerful alternatives to remove many chlorinated organic compounds. Electrochemical oxidation, among them, has been successfully applied to remediate aqueous solutions containing TCS [2]. However, powerful oxidation media can favor the formation of minor and more harmful byproducts such as polychlorinated dibenzo-p-dioxins and furans (PCDD/Fs); thus, the traceability of the formation of this kind of by-products during the oxidation treatment has become an issue of concern [2,3]. In this work, the influence of the supporting electrolyte (NaCl and Na_2SO_4), the presence of copper in the aqueous solution and the initial concentration of TCS on the potential formation of PCDD/Fs has been studied. Finally, based on previous literature, a reaction mechanism describing the formation of PCDD/Fs from triclosan solutions in aqueous and gas phase is proposed.

2. Methods

The electrochemical oxidation experiments were carried out in batch mode in a laboratory system with a labELOX 1/176 cell (APRIA Systems S.L.). The cell consisted of two regular electrodes: BDD as anode and titanium as cathode. An initial volume of 1 L was treated. Initial concentrations of TCS were 10, 100 and 150 mg L^{-1}, and the current density applied was 6, 60 and 90 A m^{-2}, respectively. The concentration of the two supporting electrolytes was 56.34 mM NaCl and 21.11 mM Na_2SO_4. In the solutions were the copper salt was present, its concentration was 39.63 mg L^{-1} (10 mg L^{-1} of Cu). TCS removal has been quantified in a HPLC using the original standard. PCDD/Fs analysis have been performed following USEPA 1613 method by high-resolution gas chromatography coupled with high-resolution mass spectrometry (HRGC-HRMS) [3].

3. Results and discussion

Complete degradation of TCS was achieved after 2, 3 and 4.5 hours when its initial concentration was 10, 100 and 150 mg L^{-1}, respectively. Total concentration of PCDD/Fs achieved values up to 3.68 x 10^2, 3.42 x 10^4 and 1.64 x 10^5 pg L^{-1} when the initial concentration of TCS was 10, 100 and 150 mg L^{-1}, respectively. The results confirmed the dominance of tetrachlorodibenzo-p-dioxin (TCDD) in the homologue profile of the total PCDD/Fs, reaching values up to 1.11 x 10^5 pg L^{-1} in samples with initial TCS concentration of 150 mg L^{-1} and NaCl as electrolyte (Figure 1 (a)). The International Toxicity Factor (I-TEF), as expected, increased with the initial concentration of TCS from 4.8 to 379.7 pg L^{-1} for 10 and 150 mg L^{-1} TCS samples, respectively. This value is much higher than the maximum contaminant level established by the USEPA for drinking water, 30.0 pg L^{-1}. However, the presence of copper in the oxidation medium tends to reduce I-TEF values.

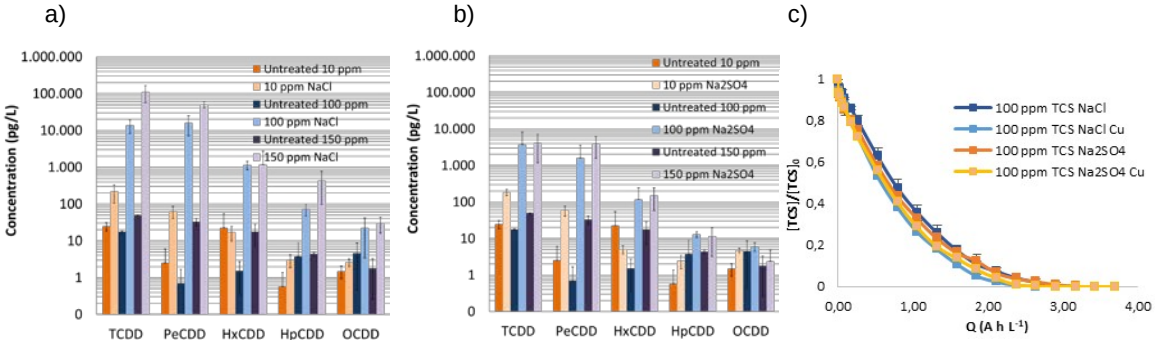

Figure 1. PCDD concentration after electrochemical oxidation of 10, 100 and 150 mg L^{-1} of triclosan using NaCl (a) and Na_2SO_4 (b) as supporting electrolytes; c) Influence of the supporting electrolyte and the presence of copper in the aqueous medium on the removal of triclosan with the specific charge.

The presence of copper did not show influence on the TCS degradation rate (Figure 1 (b)); however, the total concentration of PCDD/Fs was reduced by 55.26 % and 18.06 % for NaCl and Na_2SO_4 as supporting electrolytes, respectively. Finally, a detailed reaction mechanism describing the formation of PCDD/Fs from triclosan was proposed and supported by the experimental results [4,5].

4. Conclusions

Electrochemical oxidation allowed complete elimination of triclosan in all experiments. However, it has to be highlighted the increased concentration of PCDD/Fs in comparison with the untreated samples, specially the concentration of TCDD homologues. The comparison between the results obtained using two broadly applied electrolytes, NaCl and Na_2SO_4, emphasizes the role and importance of the chloride concentration on the formation of chlorinated byproducts during the electrochemical oxidation of triclosan; when NaCl was used as supporting electrolyte, I-TEF levels increased from values closed to zero for the untreated solution to 379,7 pg L^{-1} when complete removal of 150 mg L^{-1} triclosan was achieved. Finally, the reaction pathway leading to the formation of PCDD/Fs from TCS oxidation has been proposed.

References

[1] M. Muñoz, Z.M. de Pedro, J.A. Casas, J.J. Rodríguez, Chem. Eng. J. 198-199 (2012) 275-281.
[2] C. Solá-Gutiérrez, M.F. San Román, I. Ortiz, Sci. Total Environ. 626 (2018) 126-136.
[3] M. Vallejo, M.F. San Román, I. Ortiz, Environ. Sci. Technol. 47 (2013) 14200-12408.
[4] Y. Gao, Y. Ji, G. Li, T. An, Water Res. 49 (2014) 360-370.
[5] X. Zhang, C. Zhang, X. Sun, L. Kang, Y. Zhao, Int. J. Mol. Sci. 16 (2015) 8128-8141.

ECCE12
The 12th EUROPEAN CONGRESS OF CHEMICAL ENGINEERING
Florence 15-19 September 2019

Numerical studies of CO_2 capture by enhanced weathering of carbonate minerals

Lei Xing, Aidong Yang, Richard Darton

Department of Engineering Science, University of Oxford, Parks Road, Oxford, OX1 3PJ, United Kingdom

**Corresponding author: aidong.yang@eng.ox.ac.uk*

Highlights

- Weathering of calcite is used to model CO_2 capture in an aqueous environment.
- Intrinsic kinetics of calcite dissolution is coupled with mass transfer processes.
- Passive absorption and reinforced bubbling of CO_2 were numerically compared.
- Mass transfer of CO_2 from air to aqueous solution can be the rate-limiting step.

1. Introduction

The target of restricting global mean temperature rise to around 1.5 C will require draw-down of some 810 Gt CO_2 from the atmosphere by 2100 according to climate models [1]. The capture and storage of atmospheric carbon dioxide could thus become a very large industry later this century. Various methods and technologies have been suggested for this process, and have been recently reviewed [2,3]. The weathering of natural minerals like carbonate and silicate offers one possible route. The chemistry involves dissolution of CO_2 in water and subsequent reaction to bicarbonate and carbonate as balancing cations are solubilised from the rock. However, in order to play a significant role, this very slow natural process needs to be dramatically accelerated, affordably and without causing unacceptable environmental damage. A key aspect of designing and assessing a suitable reaction scheme and equipment is to identify the rate-limiting step in this three-phase system, so that further enhancement measures can be introduced accordingly.

2. Methods

In this work, we consider two reactor schemes with respect to gas supply. One uses passive diffusion of CO_2 at the air-water interface, the other is by active supply through gas bubbling. The three-phase bubble reactor provides greater gas/liquid contact area, and higher rates of CO_2 absorption [4]. The effect of mass transfer rate of CO_2 from atmosphere to aqueous solution on the overall reaction rate was numerically studied for the two schemes. Calcite ($CaCO_3$) is used as the model mineral for the calculations due to its relatively fast weathering rate. The reaction scheme and all chemical rate constants are taken from the work of Plummer et al [3].

Calcium ions are formed at the surface of the mineral particles, at a rate which depends on the composition of the bulk water phase. CO_2 which is transferred into the water through the gas/liquid interface is ionized to bicarbonate and carbonate. The kinetic scheme accounts for the presence of H^+, OH^-, HCO_3^-, CO_3^{2-}, in addition to physically dissolved CO_2 and Ca^{2+}. A charge balance is maintained. Diffusion of CO_2 from gas to liquid takes account of resistance in both gas and liquid phase, using the two-film theory.

3. Results and discussion

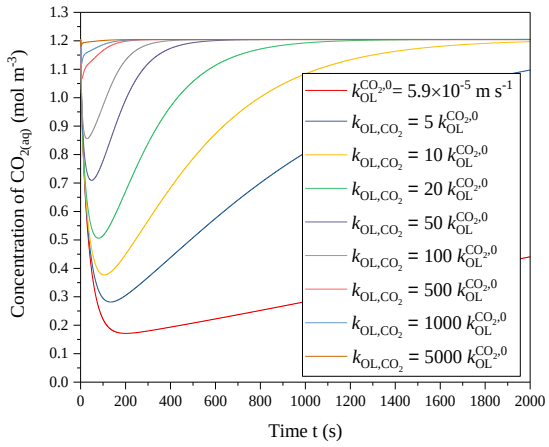

Figure 1. Dependence of $CO_{2(aq)}$ conc on k_{OL,CO_2}

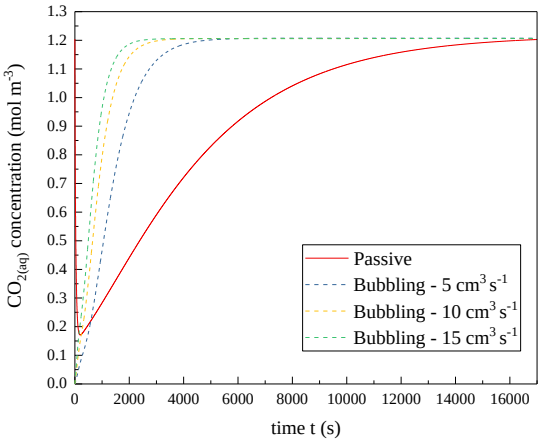

Figure 2. Effect of gas rate on $CO_{2(aq)}$ conc

Fig. 1 shows the concentration of aqueous CO_2 in the passive diffusion case. As the mass transfer coefficient increases, the aqueous CO_2 concentration approaches the equilibrium level at a steadily faster rate. This suggests that in this case the rate of absorption of CO_2 is the limiting factor, and not the rate of dissolution of mineral. The grinding of rock to create small particles, and thus high particulate surface area is an expensive process. It is thus important to establish, for any particular mineral and reactor configuration, what particle size is required. Fig. 2 compares the two CO_2 supply modes, passive diffusion and bubbling, and shows, as expected that gas bubbling improves the mass transport rate and leads to a faster process. In practice, given the very large scale of reactors that will be needed, the improved rate of absorption will have to be balanced against the extra cost of air compression for bubble injection. Further calculations, including a trickle-flow scheme that will be matched with experiment, are planned.

4. Conclusions

Calculations of CO_2 mass transfer rates in the absorption of atmospheric CO_2 during mineral weathering show that in passive diffusion it can be the rate-limiting step, rather than chemical reaction or mineral dissolution. An enhanced weathering reactor with air bubbling significantly improves the mass transport, but at the cost of greater cost and complexity. The mass transfer and mineral reaction model developed will be useful for scoping other, novel reactor designs.

Acknowledgement: Natural Environment Research Council, UK Grant NE/P01982X/1

References

[1] UNEP 2017. The Emissions Gap Report 2017. United Nations Environment Programme (UNEP), Nairobi

[2] National Academies of Sciences, Engineering, and Medicine. 2018. Negative Emissions Technologies and Reliable Sequestration: A Research Agenda. Washington, DC: The National Academies Press.

[3] Royal Society and Royal Academy of Engineering 2018 Greenhouse gas removal https://www.raeng.org.uk/publications/reports/greenhouse-gas-removal

[4] A. Yang. Ind. Eng. Chem. Res. 50 (2011) 11181-11192.

[5] L.N. Plummer, T.M.L. Wigley, D.L. Parkhurst. American J Sci. 278 (1978) 179-216.

ECCE12
The 12th EUROPEAN CONGRESS OF CHEMICAL ENGINEERING
Florence 15-19 September 2019

Preparation of Carbon Nitride Composite and Its Application in Electrochemical Detection.

Chenglong Chen, Wu Lei*

School of Chemical Engineering, Nanjing University of Science and Technology, Nanjing 210094, Jiangsu, China.

**Corresponding author: leiwuhao@njust.edu.cn*

Highlights

- Carbon nitride quantum dots is used to prepare electrochemical sensors for the determination of ascorbic acid.
- Optimized various factors affecting the electrochemical performance of the electrode to achieve the best detection results
- The proposed ascorbic acid sensor has outstanding sensitivity, wide linear range and low detection limit.

1. Introduction

Ascorbic Acid (AA) is an important antioxidant widely present in biological systems, which is an essential substance to maintain normal physiological function of human body. Abnormal contents of AA may cause several symptoms, including fatigue, infertility and scurvy. Therefore, it is imperative to develop a fast and sensitive analysis approach for AA quantitative determination.[1-6]

2. Methods

Carbon nitride quantum dots (CNQDs) were prepared by hydrothermal method using sodium citrate and urea as raw materials, and characterized by transmission electron microscopy (TEM) and fluorescence spectroscopy. Then, the electrochemical sensor (CNQDs/PEDOT/GCE) for the determination of ascorbic acid was prepared by in situ polymerization. The cyclic voltammetry was used to study the effect of ascorbic acid on the electrode electrochemical behavior.

3. Results and discussion

The optimum material ratio and the best experimental environment were obtained by the optimization experiment. The CVs of AA acquired at CNQDs/PEDOT/GCE were shown in **Fig. 1**. Under the optimal experimental conditions, the anodic peak current exhibited a linear response to the increasing concentration of AA in the range of 50-1500 μM and the linear equation can be elucidated as: $I_{pa,\ AA}$(μA) = 0.0185 C_{AA} (μM) - 0.1019 (R^2 = 0.9999). The limit of detect (LOD) were calculated as low as 6.38 μM for AA (S/N = 3).

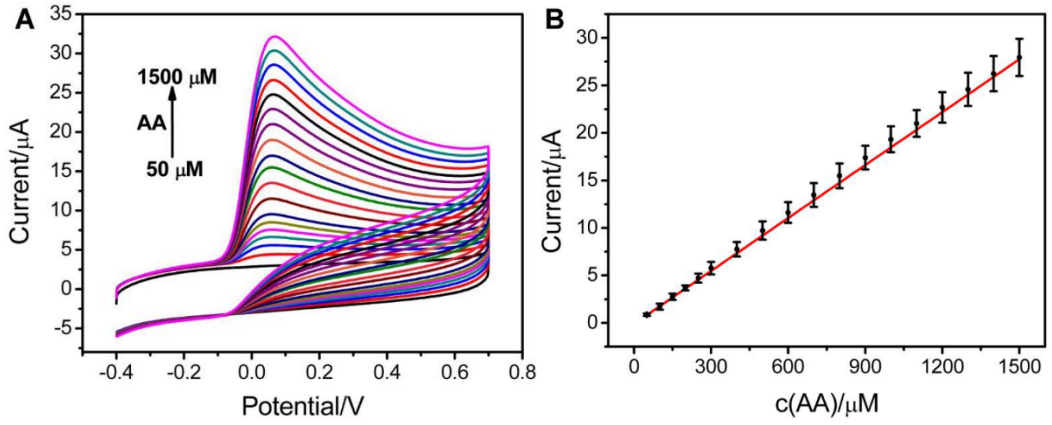

Figure 1. A) CVs at CNQDs/PEDOT/GCE in 0.2 M PBS (pH =7.4) containing different concentrations of AA from 50 μM to 1500 μM. D) The linear relationship between anodic peak current and the concentration of AA.

4. Conclusions

The results show that the modified electrode has many advantages, such as outstanding sensitivity, wide linear range, low detection limit and so on. Based on the excellent properties of carbon nitride quantum dots, a new type of electrochemical sensor was established to determine the concentration of ascorbic acid in human body.

References

[1] H. Ding, P. Zhang, T.Y. Wang, J.L. Kong, H.M. Xiong, NANOTECHNOLOGY, 25 (2014) 205604.
[2] M. Sadhukhan, S. Barman, J. Mater. Chem. A, 1 (2013) 2752-2756.
[3] A. Vinu, Adv. Funct. Mater., 18 (2010) NA-NA.
[4] J. Wen, J. Xie, X. Chen, X. Li, Appl. Surf. Sci., 391 (2017) 72-123.
[5] G. Xin, Y. Meng, J. Chem.,2013,(2012-11-4), 2013 (2012).
[6] G. Xin, Y. Xia, Y. Lv, L. Liu, B. Yu, Water Environ. Res., 88 (2016) 318.

ECCE12
The 12th EUROPEAN CONGRESS OF CHEMICAL ENGINEERING
Florence 15-19 September 2019

An Novel Electrochemical Sensor Based on ErGO/MWCNTs to Detect 2, 4-dinitroanisole.

Shasha Feng, Yong Ding, Wu Lei*

School of Chemical Engineering, Nanjing University of Science and Technology, Nanjing 210094, People's Republic of China

**Corresponding author: leiwuhao@njust.edu.cn*

Highlights

- Detection of 2, 4-dinitroanisole by the electrochemical method for the first time.
- Construct a sensor based on electrochemical reduced graphene oxide–multiwalled carbon nanotubes nanocomposite.
- Facile, cost-effective, and rapid manufacturing route.

1. Introduction

2, 4-Dinitroanisole (DNAN) as a low sensitivity melt-cast formulation, is a promising replacement for 2, 4, 6-trinitrotoluene (TNT). It is reported that DNAN is metabolized to 2, 4-dinitrophenol (2, 4-DNP) in the body, which is a chemical with high acute and chronic toxicity[1, 2]. Graphene is a two-dimensional material with a single layer of carbon atoms tightly arranged honeycomb lattice[3]. The conductivity of the electrochemical reduced graphene oxide (ErGO) is higher than that of graphene oxide[4]. Carbon nanotube is a kind of one-dimensional material, which is made of single-layer graphene reel[5]. The combination of the two materials not only preserves their respective properties, but also increases the energy transfer force of the electron and the binding sites to the electrically active substance[6]. The synergistic effect of ErGO and multiwalled carbon nanotubes (MWCNTs) obviously increases the catalytic activity for DNAN. In this work, a novel electrochemical sensor was developed based on ErGO/MWCNTs to detect DNAN by linear sweep stripping voltammetry (LSSV).

2. Methods

The prepared GO/MWCNT/GCE was electroreduced to obtain ErGO/MWCNTs/GCE by cyclic voltammetry. Sensitivity of the sensor was quantified through the LSSV method using electrochemical workstation. Measurements were taken at a constant potential of -0.4 V and in 0.1 M PBS (pH = 7.0, containing 0.1 M NaCl).

3. Results and discussion

Experimental conditions are optimized, such as accumulation time and accumulation potential. Under optimal experimental conditions, as depicted in Figure 1, the current linearly increased with incremental DNAN concentration from 0.1 to 30 μM, and the limit of detection (LOD) was calculated to be 0.084 μM（S/N = 3）.

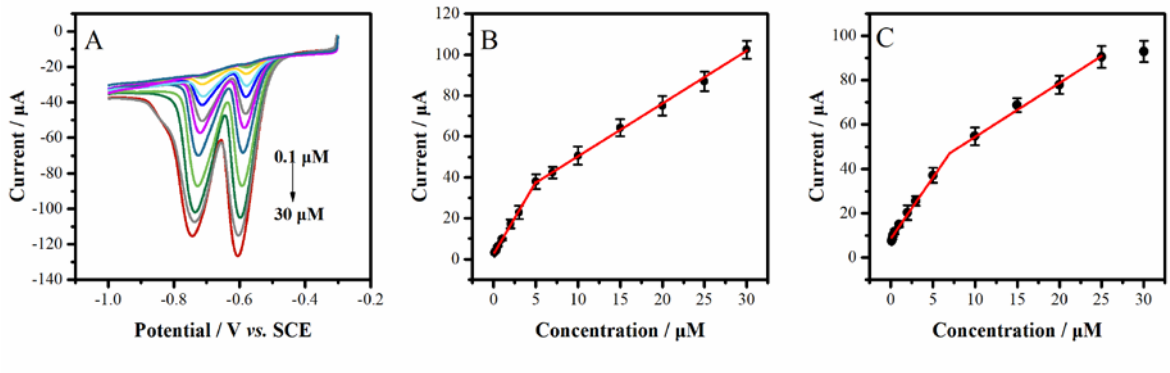

Figure 1. LSSV curves of the sensor in the presence of DNAN with different concentrations (A). The calibration curves for DNAN detection about peak α (B) and peak β (C). DNAN concentrations: 0.1, 0.2, 0.3, 0.5, 1.0, 2.0, 3.0, 5.0, 7.0, 10.0, 15. 0, 20.0, 25.0, 30.0 μM.

4. Conclusions

A novel efficient electrochemical sensor, ErGO/MWCNTs/GCE, was successfully constructed to analyse the low concentration levels of DNAN. The sensor got high sensitivity due to the excellent catalytic activity of ErGO/MWCNTs nanocomposite. The sensor was successfully applied to determine DNAN in water samples with the advantages of anti-interference performance, good reproducibility, and acceptable stability.

References

[1] N.N. Perreault, D. Manno, A. Halasz, S. Thiboutot, G. Ampleman, J. Hawari. Biodegradation. 23 (2012) 287-295.
[2] V.M. Boddu, K. Abburi, S.W. Maloney, R. Damavarapu. J. Chem. Eng. Data. 53 (2008) 1120-1125.
[3] V. Singh, D. Joung, L. Zhai, S. Das, S. I. Khondaker, S. Seal. Prog. Mater. Sci. 56 (2011) 1178-1271.
[4] M. Pumera. Chem. Soc. Rev. 39 (2010) 4146-4157.
[5] T. Nosaka, R. S. Lankone, Y. Bi, D. H. Fairbrother, P.Westerhoff, P. Herckes. Anal. Methods. 10 (2018) 1032-1037.
[6] Y. Vlamidis, I. Gualandi, D. Tonelli. J. Electroanal. Chem. 799 (2017) 285-292.

ECCE12
The 12th EUROPEAN CONGRESS OF CHEMICAL ENGINEERING
Florence 15-19 September 2019

Incipient Fault Detection Based on Exergy Efficiency and Support Vector Data Description.

Mengfei Zhou, Haitian Pan, Zhihong Liu

College of Chemical Engineering, Zhejiang University of Technology, Hangzhou, Zhejiang 310014, PR China

**Corresponding author: htpan@zjut.edu.cn*

Highlights

- Exergy-data abstraction using mutual information.
- Reduce complexity of the SVDD model based on process exergy efficiency
- Detect incipient faults with different severity based on EESVDD

1. Introduction

In the paper, a novel fault detection method based on exergy efficiency and support vector data description (EESVDD) for incipient fault is proposed. The complexity of the SVDD model is reduced based on process exergy-data abstraction using mutual information (MI) method. Additionally, the proposed method presents great fault detectability and isolability and can detect incipient faults with different severity and indicate the evolution direction of faults. The effectiveness of the proposed method is illustrated by an industry distillation column system.

2. Methods

Exergy loss is the opposite of exergy efficiency, which represents the loss of process effective energy. Actually, the concept of performance degradation is intrinsically included by exergy, which can be used to explain the performance changes of incipient fault processes. In our work, MI is used to get the correlation between measured variables and exergy efficiency. Generally, MI can be composed of marginal entropy and joint entropy, it is possible to use K-nearest neighbor statistic to estimate entropy and then to obtain MI value. It is meaningful to compare which of the measured variables contain more information of exergy efficiency. After the MI values are obtained between each measured variable and the exergy efficiency, a set of measured variables that are most relevant to exergy efficiency is identified for improving the validity of datasets according to the cumulative percent mutual information (CPMI).

And then, the corresponding SVDD state models can be established with the feature sample sets of different fault states. The main idea of SVDD is to find a sphere region that contains most of the target samples with the smallest volume. Given a train set $\mathbf{x}_i \in R^{N\times m}\ \ (i=1,2,\ldots,N)$, where N is the number of samples. The radius minimization problem of the sphere can be formulated as the following quadratic programming problem with inequality constraints.

$$\min F(R,\mathbf{a},\xi_i) = R^2 + C\sum_{i=1}^{N}\xi_i \tag{1}$$

$$\text{s.t.}\left\|\mathbf{x}_i-\mathbf{a}\right\|^2 \le R^2+\xi_i \qquad (\xi_i \ge 0) \tag{2}$$

where, C is a penalty factor and ξ_i are the slack variables. The sphere can be described by radius R and center $\mathbf{a}$. The fault can be detected according to the principle of minimum relative distance and identify qualitatively the severity of the fault.

The overall framework of the proposed method is shown in Figure 1.

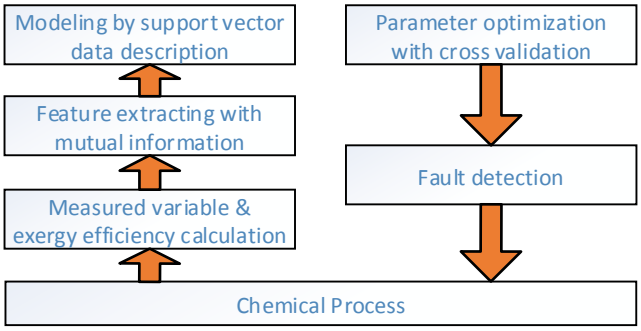

Figure 1. The overall framework of the proposed algorithm

3. Results and discussion

The proposed method has been illustrated by an industrial distillation process, which consists of two distillation columns which is used to separate propane and propylene, as shown in Figure 2. In this case, the faults are generated by stepping the fouling factor of the shell and tube side. And the different severities of fault can be also obtained. For the sake of convenience, the fault detection rate (FDR) is used to quantify the detection performance for different fault states. The FDRs of SVDD, principal component analysis and SVDD (PCA-SVDD), EESVDD in different incipient fault states have been compared in Table 1. From Table 1, it is obvious that the EESVDD method is better than the other two methods in the FDRs of three fault states. The exergy-data abstraction based method draws on the process physical and thermodynamic knowledge, and reveals the performance degradation information of process.

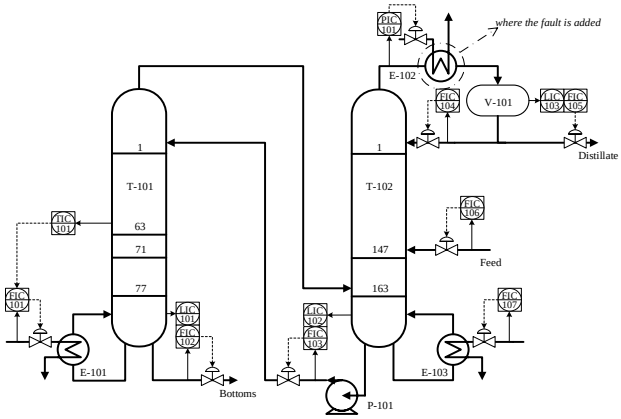

Figure 2. The flowchart of the industrial distillation columns

Table 1. The FDRs of SVDD, PCA-SVDD, EESVDD on different incipient fault states

	Normal condition	Moderate degradation	Severe degradation
SVDD	0.8654	0.9091	0.8830
PCA-SVDD	0.9038	0.9394	0.9474
EESVDD	0.9679	0.9848	0.9766

4. Conclusions

The key idea of the proposed method is that the relationship is constructed between the exergy efficiency and measured variables using MI method, and the SVDD detection model is established by replacing the principal component vectors with the exergy efficiency feature. Besides, the method can detect the severity of incipient faults and point out the evolution direction of faults. The method extends the application for incipient fault detection based on exergy-data abstraction. The case have been showed the effectiveness of the proposed method.

ECCE12
The 12th EUROPEAN CONGRESS OF CHEMICAL ENGINEERING
Florence 15-19 September 2019

Mass Transport of Micro- and Macro-Molecule Compounds of Phosphorous Base Fertilizer Fortified With Protein in Soil Matrix.

Maksymilian Olbrycht[1], Michał Kołodziej[1], Roman Bochenek[1], Mateusz Przywara[1], Maciej Balawejder[2], Dorota Antos[1]*, Wojciech Piątkowski[1]

1 Department of Chemical and Process Engineering, Faculty of Chemistry, Rzeszow University of Technology, 35-959 Rzeszow/PL; 2 Chair of Chemistry and Food Toxicology, University of Rzeszow, 35-601 Rzeszow/PL

**Corresponding author: dorota.antos@prz.edu.pl*

Highlights

- Microgranule phosphorous soil fertilizer based on a post-production waste was developed
- Diffusion of micromolecule components of the granule in soil matrixes was measured
- Degradation and diffusion of protein components in soli matrix was determined

1. Introduction

In recent years there has been a significant increase in the prices of phosphorous fertilizers, which made it necessary to seek alternative, more cost-effective solutions in the field of plant fertilization. Much cheaper fertilizers containing partially decomposed phosphorite, have become an alternative to the existing phosphorus sources, such as superphosphate [1-3].

Raw material for the production of such fertilizers can also be obtained from animal bones containing natural hydroxyapatite. The benefit of this natural source is the lack of fluoride in the raw material of animal origin, which greatly simplifies production. Therefore, we developed a mineral phosphate fertilizer based on ash obtained by incinerating the meat industry wastes. The fertilizer in the form of a microgranule was supplemented with additives sourced from natural raw materials, i.e., protein preparations based on post-production waste (milk serum, soy paste, eggs).

In this project we measured the mass transport of the microgranule components in two different model solid matrixes composed of sand and standardized soil. The mechanism of protein decomposition during the fertilization process was proposed.

2. Methods

Microgranules were prepared using a laboratory pan granulator. The granule was composed of incinerated and grounded bones, lake chalk and protein isolates from milk serum, soy and chicken egg proteins. A microgranule (0.5 g mass) was placed on the bottom of a 15-ML cylinder with piston and a matric scale on the side-wall. Seven identical cylinders were used for the experiments. The cylinders were filled with wet sand or wet standardized soil (both with a predefined moisture content) with the height of 4.5 cm. The samples of the solid matrixes (sand and soil) were withdrawn at different time intervals; 5 mL slices of matrixes were acquired at different distances from the microgranule (from the bottom of the cylinder). Next, the samples were mixed with 5 mL

of 0.1 M NaCl solution and vortex-homogenized. The supernatants obtained were subjected to HPLC, HPLC-SEC and Lowry method analyses, to determine the mass transport of ions and proteins through the matrix.

3. Results and discussion

Typical results of the concentration analysis of a protein from milk serum isolate and micromolecule components of microgranules in the matrix samples that were acquired at different distances from microgranule and different time intervals are presented in Fig.1 and Table 1. It can be observed that the maximum of the protein concentration is reached after 48 h at the distance of 1.5 cm from the microgranule. The concentration of the protein drops rapidly with increasing the distance, and practically vanishes at 4.5 cm away from the microgranule. Moreover, the concentration of the protein decreases in time, which is caused by its degradation. The latter is confirmed by increasing ammonia ion concentration with increase in time (Table 1). The concentration of other ions reaches quickly its maximum due to fast diffusivity of small ions in the solid matrix. The results obtained for other protein isolates were similar to those reported above.

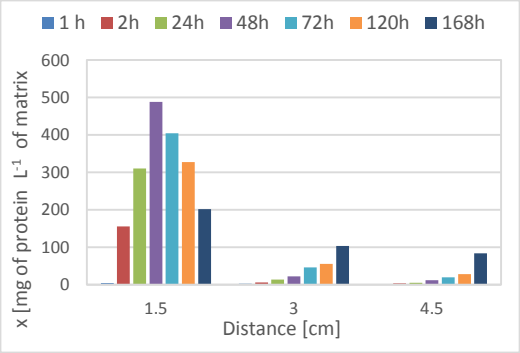

Figure 1. Protein concentration at different distances from microgranule containing milk serum isolate.

Table 1. Concentration of ions at the distance of 1.5 cm away from the microgranule measured at different time intervals.

Time	ammonium	potassium	magnesium	calcium	nitrate	phosphate	sulphate
[h]	mg of ion L^{-1} of matrix						
6	0.45	62.46	7.52	15.95	2.01	1.43	449
24	0.43	79.48	8.58	19.69	1.47	3.36	366
48	2.35	72.09	9.42	27.45	0.82	4.05	334
72	4.29	68.18	10.72	24.57	0.94	3.80	354
120	40.79	71.33	26.91	34.02	0.76	3.26	391
168	41.27	66.87	31.86	43.75	1.91	3.66	544

4. Conclusions

The macromolecule components of the microgranule fertilizer diffuse through the solid matrix very slowly. The transport of the proteins is accompanied with their degradation, which induces formation of ammonium ions. The maximum of the protein concentration and ammonia ions is reached at very close distance from the microgranule, therefore, the fertilizer granule should be placed in vicinity to the plant grain.

References

[1] S.H. Chien, L.I. Prochnow, S. Tu, Snyder C.S., Nut. Cyc. Agroecosys. 89 (2011) 229-255.
[2] P.K., Ghosh, K.K. Bandyopadhyay, R.H. Wanjari, M.C. Manna, A.K. Misra, M. Mohanty, A.S. Rao, J. Sustain. Agr., 30 (2007) 61-86.
[3] A.J. Weatherley, B.F. Quin, K.B. Dassanayake, J.S. Rowarth, Chemical Industry 92 (2013) 1289-1295

Financial support of this work by National Center for Research and Development, Poland (project BIOSTRATEG1/270963/6/ NCBR/2015) is gratefully acknowledged.

ECCE12
The 12th EUROPEAN CONGRESS OF CHEMICAL ENGINEERING
Florence 15-19 September 2019

Antimicrobial Effect of Extracts from Leaves of Native Brazilian Plants

Bárbara Ponzilacqua[1], Sarah Lee[1], Roice Rosim[1], Carlos Corassin[1], Carlos Oliveira[2]*

[1] *Department of Food Engineering, School of Animal Science and Food Engineering, University of São Paulo, Pirassununga, Brazil*

**Corresponding author: carlosaf@usp.br*

Highlights

- Leaves from sweet passion fruit and araçá tested against *S. aureus* and *A. parasiticus*.
- Crude and lyophilized extracts from Araçá had highest inhibitory activity on *S. aureus*.
- None of the extracts demonstrated effective results against *A. parasiticus*.

1. Introduction

Staphylococus aureus and *Aspergillus parasiticus* are important causative agents of foodborne diseases and mycotoxin-producing in cereals [1], respectively. In the food industry, antimicrobial agents are generally not permitted as additives in raw or processed products. Thus preventive measures to control the microbial contamination of foods are of particular importance to avoid foodborne infections. The possibility of using natural antimicrobial agents is an attractive alternative to control or reduce the bacterial and fungal load in food products, provided that they are biodegradable, environmental friendly, and biologically safe [2]. Previous studies indicated that essential oils and plant extracts containing secondary metabolites have antimicrobial properties similar to common antimicrobials [3]. The Brazilian native flora is very rich in diversity of species due to the presence of different regions and biomass in the country. A large number of Brazilian plants are popularly used as medicinal herbs, although the pharmacological bases of action for some plants are not completely understood. The objective of this study was to evaluate crude and lyophilized extracts of leaves from two Brazilian native plants with little information regarding their antimicrobial action, sweet passion fruit and araçá, regarding their *in vitro* antimicrobial effects on planktonic cells of *S. aureus* and *A. parasiticus*.

2. Methods

Leaves from *Passiflora alata* (sweet passion fruit) and *Psidium cattleianum* (araçá) were collected during the summer and fall period of 2017 in the Southern region of Brazil. Extracts were prepared according to recommendations of the Brazilian Pharmacopeia (20), after the leaves were dried, grinded and mixed (4 g) with 100 mL of ethyl alcohol (96 °GL). The organic solvent was evaporated by fractional distillation under reduced pressure in an evaporator (Heidolph, Schwabach, Germany). Next, the aqueous extract from each plant was divided into 2 aliquots, one (crude extract) reserved for direct evaluation of antimicrobial activity, and the other submitted to freeze-drying (lyophilized extract) (lyophilizer LC 1500, Terroni Equipment Ltda., São Carlos, Brazil) before running the antimicrobial evaluation. The concentrations of dry matter in crude extracts of

sweet passion fruit and araçá were 28.3 and 60.0 mg/mL, respectively. The lyophilized extracts were re-dissolved in sterile water at 40 mg/mL.

The antimicrobial activities of crude and lyophilized plant extracts were evaluated using strains of *S. aureus* (ATCC 29213) and *A. parasiticus* (NRRL 2999), previously cultured until reaching the turbidity of 0.5 on the McFarland scale. The minimum inhibitory concentration (MIC) of plant extracts was tested using the broth microdilution reference technique [4]. Data were analyzed by the MIXED procedure of Statistical Analyses System, considering $P<0.05$ (28).

3. Results and discussion

Table 1 presents the in vitro antibacterial activities of crude and lyophilized extracts against *S. aureus* and *A. parasiticus*. Extracts from sweet passion fruit had no antibacterial activity against the S. aureus strain tested, since its MIC values could not be determined (>14.15 and >20 mg/mL for crude and lyophilized extracts, respectively). However, crude and lyophilized extracts from leaves of araçá inhibited *S. aureus*. Similarly to results obtained in the antibacterial assays, both types of extracts from araçá had lowest ($P < 0.05$) MIC values against *A. parasiticus*.

Table 1. Mean values of minimal inhibitory concentration of plant extracts against *Staphylococcus aureus* (ATCC 29213) and *A. parasiticus* (NRRL 2999).

Plant extract	Minimum inhibitory concentration (mg/mL)	
	S. aureus	*A. parasiticus*
Crude extracts:		
Sweet passion fruit (*P. alata*)	> 14.15 [a]	> 14.15 [a]
Araçá (*P. cattleianum*)	0.39 [b]	3.12 [b]
Standard error	0.12	0.44
Lyophilized extracts:		
Sweet passion fruit (*P. alata*)	> 20.00 [a]	> 20 [a]
Araçá (*P. cattleianum*)	0.45 [b]	10 [b]
Standard error	0.11	0.31

[a-b] Mean values within each column with no common superscript differ significantly ($P < 0.05$).

4. Conclusions

Sweet passion fruit showed no action against any of the micro-organisms tested. However, crude and lyophilized extracts from Araçá had the highest antimicrobial effects against two microorganisms of public health importance, *S. aureus* and *A. parasiticus*. This is the first preliminary evidence of antibacterial effects of extracts from Araçá leaves.

References [Calibri 10]

[1] J.M. Jay, M.J. Loessner, D.A. Golden, Modern food microbiology, 7th ed, Springer, New York, 2005.
[2] J. Varma, N.K. Dubey, Curr Sci. 76 (1999) 172-179.
[3] R.R. Santo, M. Andrade, N.R. Melo, A. Sanches-Silva, Trends Food Sci Technol. 61 (2017) 132-140.
[4] National Committee for Clinical Laboratory Standards, Performance Standards for Antimicrobial Susceptibility Testing (2015) Vol. 26.

ECCE12
The 12th EUROPEAN CONGRESS OF CHEMICAL ENGINEERING
Florence 15-19 September 2019

Urban atmospheric dispersion modeling with artificial neural networks: using the Indianapolis data set.

Pierre Lauret[1], Frederic Heymes[1], Laurent Aprin[1]

[1] LGEI, IMT Mines Ales, Univ Montpellier, Ales, France

*Corresponding author: pierre.lauret@mines-ales.fr

Highlights

- Artificial neural networks are used to forecast dispersion concentrations
- Two dimensional model is used
- Results show improvement compared to Gaussian models while keeping low computing time

1. Introduction

Atmospheric dispersion modelling in complex environment is a tricky task because of the number of parameters involved. Indeed, dispersion in the free field is highly influenced by stability of the atmosphere. Moreover, when complex terrain is considered, the process of dispersion may be considered as non-linear due to the directivity of the flow with buildings. In order to evaluate the performance of atmospheric model, different data set are used. One of them is helpful to deal with dispersion around urban area. The Indianapolis dataset correspond to a 170 hours recording of SF6 concentration with 160 ground level monitors. The SF6 source was released from the top of an elevated stack inside the urban area. While Gaussian models are usually applied very fast, they present low level of performance. On the other hand, models from Computation Fluids Dynamics (CFD) are accurate but requires high expertise and important computer resources. In this paper, we investigate the potential of a neural network to predict concentrations in the urban field, using the Indianapolis experiments as a database for the training process.

2. Methods

The EPRI Indianapolis field study involved SF6 tracer releases from the 83.8 m stack at the Perry K power plant in Indianapolis, Indiana, USA in a typical urban area with many buildings within two kilometers of the stack. 170 hours of tracer data are available from September and October, 1985, and represent all stability classes and most wind speed ranges. Meteorological observations were taken from a 94 m height at the top of a building in the middle of the urban area. Concentrations were measured on a network of about 160 ground-level monitors on arcs at distances ranging from 0.25 to 12.0 km from the stack.

Before training the neural network, the example database has to be built from the initial one. Several recordings exist for the meteorological data. A correlation matrix including measured concentrations is made in order to established the weather station to use. The inputs selection is made through this use. Inputs used are related to the weather, the release and the location where the concentration has to be predicted. In order to compare ANN method to Gaussian models, we

use same inputs as Gaussian models to train a Multi Layer Perceptron (MLP). The training phase is optimized through the variation of three parameters: initialization, number of neurons in hidden layer and variable selection. Evaluation of the model performance is done through the use of Hanna and Chang criteria.

3. Results and discussion

To select the best model, several initializations are made. The influence of this parameter on the result is emphasized through the value of the coefficient of determination. Moreover, increasing the number of neurons in hidden layer shows an improvement in the results. For each best initialization, the best model is obtained with less than 10 neurons in hidden layer. Finally, the selection of the variables shows that the best variables to be selected as inputs are those traditionally used in Gaussian model. This model shows an improvement compared to Gaussian model.

4. Conclusions

The model presented here uses neural networks to forecast concentration on the two dimensional dispersion field. It improves the results of Gaussian models giving the maximum concentration by searching in the entire database of the Indianapolis data set. Finally, the model gives the opportunity of building a two dimensional map of the concentration through time.

References [Calibri 10]

[1] Lauret, P., Heymes, F., Aprin, L., Johannet, A., Munier, L., Lapébie, E., 2013. Near Field Atmospheric Dispersion Modelling on an Industrial Site Using Neural Networks. Chem. Eng. Trans. 31, 151–156.

[2] Pelliccioni, a, Tirabassi, T., 2006. Air dispersion model and neural network: A new perspective for integrated models in the simulation of complex situations. Environ. Model. Softw. 21, 539–546.study using the Indianapolis urban set. Inderscience Enterprises Ltd, Vol. 40, 2010

[3] Chang, J.C., Hanna, S.R., 2004. Air quality model performance evaluation. Meteorol. Atmos. Phys. 87, 167–196.

ECCE12
The 12th EUROPEAN CONGRESS OF CHEMICAL ENGINEERING
Florence 15-19 September 2019

Capture and mineralization of CO_2 to yield metal carbonates

Dalia Santa Cruz-Navarro [1], Miguel Torres-Rodríguez [2]*, Violeta Mugica-Álvarez[2], Mirella Gutiérrez-Arzaluz[2]

1 Posgrado en Ciencias e Ingeniería, Universidad Autónoma Metropolitana, Av. San Pablo No. 180 Azcapotzalco, C.P. 02200, Ciudad de México, México.

2 Área de Química Aplicada, Departamento de Ciencias Básicas, Universidad Autónoma Metropolitana, Av. San Pablo No. 180, Azcapotzalco, C.P. 02200, Ciudad de México, México.

**Corresponding author: trm@correo.azc.uam.mx;*

Highlights

- Capture and sequestration of CO_2 is priority for the coming years.
- Capture of CO_2 to form metal carbonates is an interesting mitigation of Climate Change.
- Perfect mixing semibatch reactor is a simple device for capturing CO_2.
- Metal carbonates are interesting in various industrial sectors.

1. Introduction

Climate change due to global warming is one of the most important problems that humanity currently faces, regionally and globally. The physico-chemical consequences associated with the absorption of infrared radiation and the amounts emitted by different sources are the main cause of global warming, as reported by the Intergovernmental Panel on Climate Change in recent years (1). There are several processes for the capture and sequestration of CO_2, (2) one of the simplest processes for the latter comprises its adsorption and chemical reaction. In this work, we present results of the capture and sequestration of CO_2 through metal hydroxides aqueous solutions to obtain metal carbonates.

2. Methods

The capture and sequestration tests via reaction between metals hydroxide solutions with gaseous CO_2, were performed in a perfectly mixed semibatch reactor, with 15.17 ml min^{-1} CO_2 continuous flow at atmospheric pressure and two reaction temperatures: 25 and 30 °C. In all the tests 250 ml of 0.06 and 0.07 M Sr, Ba, Mg hydroxide aqueous solution were used, which corresponds to the saturated solutions, the variation of pH, temperature and the mass of dry metal carbonate formed according to the reaction time. All the solids were characterized by X-ray Diffraction (XRD), Scanning Electron Microscopy (SEM), elemental analysis by means of Energy Dispersive Spectroscopy (EDS) and Fourier Transform Infrared Spectroscopy (FTIR).

3. Results and discussion

In each capture and sequestration test, the reaction between the gaseous CO_2 and the alkaline metal solutions formed solid precipitates, which after filtering, washing and drying were weighed to calculate the reaction yield; during the reaction, a decrease in the pH of the solution was observed, as well as an increase in temperature as a function of reaction time. The analysis of the

solids by XRD shows that the corresponding metal carbonate was formed, as shown in figure 1a, where the characteristic peaks of the metal carbonates can be identified, the analysis of the samples by SEM / EDS, shows that the solid formed presents different morphologies, such as that shown in figure 1b, where the solid appears as acicular crystals with longitudinal dimensions of 3 µm by 0.15 µm; the elemental analysis shows the presence of C, O and metal, which can be attributed to the carbonate formed, while the FTIR results shows the characteristic bands of the carbonates at the most intense wavelengths at 1442 cm^{-1} to 20 min, at 1440 cm^{-1} to 30 min and at 1452 cm^{-1} to 40 minutes of reaction and at 854 and 705 cm^{-1}, for all reaction times.

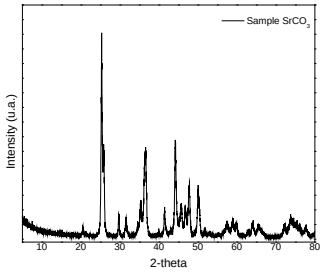

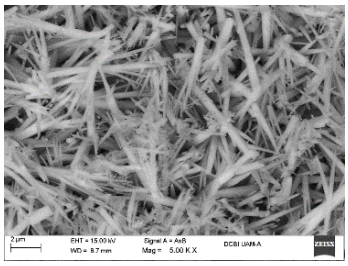

(a) (b)

Figure 1. a) XRD diffraction pattern, b) SEM microscopy of strontium carbonate

The capture of CO_2, to form strontium carbonate ($SrCO_3$) is of interest in various industrial sectors such as: in the refining of sugar and the manufacture of military rockets. Magnesium carbonate ($MgCO_3$) is used as a reinforcing agent in neoprene rubber, as a drying agent and for color retention in food and cosmetics, it is also used as an antiacid in medicine, these capture alternatives give value added to CO_2 sequestration products via carbonate formation

4. Conclusions

Through a simple system of perfectly mixed semibatch reactor, it is possible to capture CO_2 to form metal carbonates under simple conditions at atmospheric pressure and temperature, which represents a sustainable process due to its low energy consumption. According to the results of X-ray diffraction, the solids formed are the metal carbonates of the metal hydroxide solutions. The formed solids present different morphologies according to the results of scanning electron microscopy.

References

[1] The Intergovernmental Panel on Climate Change (IPCC), 2007, Geneva, Switzerland.
[2] Cuéllar, R. & Azapagic, A. Carbon capture, storage and utilization technologies: A critical analysis and comparison of their life cycle environmental impacts. *Journal of CO_2 utilization*, 2015, 82-102.
[3] Aresta M. *Carbon dioxide recovery and utilization*, The Netherlands, Kluwer Academic Publishers, 2003, 53-120.

ECCE12
The 12th EUROPEAN CONGRESS OF CHEMICAL ENGINEERING
Florence 15-19 September 2019

Challenges during the Start-up of Anaerobic Reactors for Wastewater Treatment

Borja Ojembarrena[1]; Noemi Merayo[1,2]; Angeles Blanco[1]; Carlos Negro[1]

1 Complutense University of Madrid, Dpt. Ingeniería Química y de Materiales, Avda. Complutense s/n, 28040, Madrid, Spain; 2 Universidad Politécnica de Madrid, ETSIDI, Dpt. Ing. Mecánica, Química y Diseño Industrial, Ronda de Valencia 3, 28012 Madrid, Spain

**Corresponding author: cnegro@ucm.es*

Highlights

- Start-up of anaerobic reactor is a critical stage
- Time required for start-up is one of the main limitations for anaerobic process
- Time required for the start-up depends on the scale of the treatment
- At full scale, start-up time increases regarding pilot plants and laboratory

1. Introduction

The start-up of the anaerobic reactors is a critical stage to assure a good performance of the anaerobic treatment during normal operation. Contrarily to aerobic reactors, anaerobic ones require long time to growth the appropriate consortia of microorganisms that are able to degrade the substrate provided (the wastewater) and additionally, to generate the maximum amount of biogas to be used as source of energy [1]. Not only are the anaerobic conditions that should be maintained constrain for the start-up process, but also the acclimatization and adaptation to a particular wastewater. The relevance of the start-up phase in anaerobic reactor is related to the operability of the reactor, because if the start-up is not well performed, this will affect the subsequent process operation [2].

2. Purpose

Both the lag between research and development levels, in terms of overall start-up strategies, and the challenge to obtain good quality anaerobic inoculum, particularly in developing countries, prove the necessity of further investigation in the field of the reduction of acclimation period [3].

Therefore, the aim of this work is to evaluate different factors of the anaerobic process, such as microorganism population, reactor design, treated wastewater, etc. that can affect the start-up of the anaerobic process; establishing the degree of influence they have on this step, considering the time required for the start-up, the stability of the microorganism population and any difficulties found. Furthermore, approaches to improve start-up step of the anaerobic treatment were analyzed and compare to show their actual effect.

3. Results and discussion

A successful start-up leads to improve methane production by the biomass, requiring at the beginning both low loads and long time for acclimatization and adaptation of the biomass [4].

Furthermore, the lack of acclimated biomass must be considered because it further leads to instability and failure, [5].

As it can be seen in figure 1, the scale of the treatment has a considerable effect on the time required for the start-up step of the anaerobic treatment. As long as the scale grows, the start-up time tends to increase as well. Therefore, it is important to consider that the results obtained at the laboratory scale for the start-up step of the process must be further checked at bigger volumes to predict what will happen at the full scale.

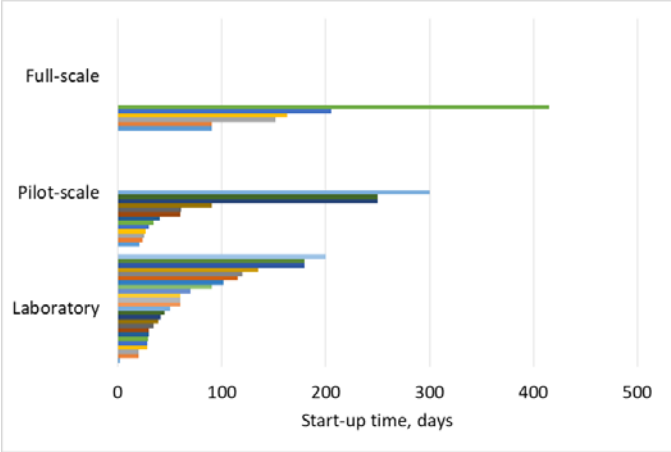

Figure 1. Effect of the scale of the anaerobic treatment on the time required for the start-up step.

The configuration and design of the anaerobic reactor also have a significant impact on the start-up of the process, such as the case of using of multistage reactors, which favors an acidification zone at the front of the reactor and a methanogenic zone at its end and improving the pH control in the reactor [6].

4. Conclusions

Start-up of the anaerobic treatment is a key factor to make this process available and easily implemental. In this communication, several factors will be presented and analysed to show their effect on the time required for the start-up step of the anaerobic treatment of wastewater.

References

[1] G. Skouteris, D. Hermosilla, P. López, C. Negro, A. Blanco, Chem. Eng. J. 198 (2012) 138-148.
[2] M.A. De la Rubia, V. Riau, F. Raposo, R. Borja, Crit. Rev. Biotechnol. 33 (2013) 448-460.
[3] R. Maroun, M. El Fadel, Environ. Sci. Technol. 41 (2007) 6808-6814.
[4] A. Akram, D.C. Stuckey. Environmental technology, Taylor & Francis, 2008, pp. 1053-1065.
[5] M. El-Fadel, P. Saikaly, S. Ghanimeh, Crit. Rev. Env. Sci. Tec. 43 (2013) 2685-2721.
[6] H.M. Zwain, S.R. Hassan, N.Q. Zaman, H.A. Aziz, I. Dahlan, J. Env. Chem. Eng. 1 (2013) 61-64.

ECCE12
The 12th EUROPEAN CONGRESS OF CHEMICAL ENGINEERING
Florence 15-19 September 2019

Zero-valent iron (ZVI) activation of persulfate (PS) for degradation of Para-chloronitrobenzene in soil

Changxun Dong [1], Linghong Lu [2*]

1 College of Sciences, Nanjing Agricultural University, Nanjing 210095, China];

2 College of Chemical Engineering, Nanjing Tech University, Nanjing 211816, China

** Corresponding author: Linghonglu@njtech.edu.cn*

Highlights

- The p-CNB removal rate increased significantly from 10.8% to 90.1% with an increase of ZVI dosage from 0.1 mmol•g-1 to 1.0 mmol•g-1..
- The p-CNB removal increased with the decrease of initial solution pH and a removal efficiency of 85.3% was obtained.
- the ZVI-persulfate system showed more sufficient p-CNB removal capacity and the removal rate of p-CNB was 88.7%.

1. Introduction

Para-chloronitrobenzene (p-CNB) in soil has posed significant health risks because of its persistence and high toxicity. Chemical oxidation by means of persulfate (PS) has received considerable attention for organically contaminated groundwater and soil remediation. Recently, it has been found that Zero-valent iron (ZVI) or metal iron can activate persulfate at room temperature, and it can gradually release Fe^{2+} to produce sulfate radicals during a long time length, via reactions with water and oxygen in air. ZVI can restore Fe^{3+} to Fe^{2+} while reducing hydroxide precipitation during the oxidation. Meanwhile, ZVI is an alternative source of Fe^{2+} and can serve as an electron donor for the reaction. The objective of this study was to determine the feasibility of p-CNB polluted soil remediation by ZVI-persulfate systems.

2. Methods

The naturally contaminated soil of p-CNB were prepared for each batch experiment. Several sets of the experiments were conducted to determine the effects of various parameters on p-CNB degradation. Dynamics experiments were performed to study the difference between the removal of p-CNB by single persulfate, ZVI and ZVI-persulfate system. The reactions were carried out in 100 mL centrifuge tube. Reaction mixtures were obtained by taking an appropriate amount of 50 g contaminated soil and mixed with the 50 mL deionized water on a rotary shaker at 125 rpm and 25°C. During the experiment, 1.0 mL of solution sample was periodically withdrawn from each reactor with a glass syringe and then filtered through a 0.45 μm membrane for immediate analysis. The pH value was monitored by a pH electrode.

3. Results and discussion

The results of initial ZVI dosage suggest that the degradation efficiency was heavily influenced by the ZVI when the concentrations of persulfate and p-CNB were fixed. In this system, ZVI play two

roles, reducing chloronitrobenzene to chloroaniline and providing Fe2+ for the activation of persulfate (Zhao et al. 2010). Higher initial ZVI dosage provided more active sites on ZVI surface to persulfate, and the persulfate was activated by the release of Fe2+ from Fe0 in the ZVI-persulfate system. Fe2+ is one of the strongest species that can catalyze persulfate to sulfate radicals, the Fe2+ is continuously supplied to the system to ensure the efficiency of degradation of p-CNB. However, at higher initial dosage (1.0 and 1.5 mmol g−1), the degradation rate was similar. Thus, for economic reasons, 1.0 mmol g−1 was chosen as the best dosage.

The removal rate was markedly increased when ZVI and persulfate coexist due to the generation of •OH and SO4−• in combine system. The increased ZVI dosages resulted in enhanced p-CNB degradation benefiting by increased activation of persulfate by ZVI. Combined with the results of SEM, the increase of ZVI could provide more reactive sites for the activation of persulfate, producing more SO4−• and increasing the efficiency of p-CNB degradation. The removal of p-CNB was advantageous in acid condition. At pH 3.0, 90.3% degradation was achieved in 8 h. The results of EPR showed that acidic conditions were beneficial to the activation of persulfate by ZVI to produce more sulfate radicals. In addition, acidic conditions reduce the precipitation of Fe2+ and Fe3+ facilitate reaction. MS analysis in combination with literature review of p-CNB degradation, intermediates identified in this work include p-chloroaniline, 1, 4-benzoquinone and 5-chloro-2-((3-chlorophenyl) diazenyl) phenol..

4. Conclusions

The p-CNB removal rate increased significantly from 10.8% to 90.1% with an increase of ZVI dosage from 0.1 mmol•g-1 to 1.0 mmol•g-1. The p-CNB removal increased with the decrease of initial solution pH and a removal efficiency of 85.3% was obtained at an initial pH value of 6.8 in this combined system. Compare three systems, the p-CNB removal rate in the persulfate oxidation system and the single ZVI system was 36.5% and 60.2%, while the ZVI-persulfate system showed more sufficient p-CNB removal capacity and the removal rate of p-CNB was 88.7%. Scanning electron microscopy (SEM) was adopted in order to observe the changes of surface morphology of ZVI before and after reaction. The results showed that with the reaction prolonging, the surface of ZVI changed from smooth to uneven. The generated radical species were identified by Electron paramagnetic resonance (EPR) technique, and the results showed that sulfate radicals (SO4-•) were predominant under acidic condition and hydroxyl radicals (•OH) were predominant under basic condition, revealing the potential reduction and oxidation reaction mechanism responsible for p-CNB removal by ZVI-Persulfate in soil..

References [Calibri 10]

[1] G.P. Anipsitakis, D.D. Dionysiou Environ Sci Technol 38 (2004) 3705
[2] J. Zhao, Y. Zhang, Q. Xie, S. Chen,Sep Purif Technol 71 (2010) 302–307
[3] A. Ghauch, G. Ayoub, S. Naim Chem Eng J. 228 (2013) 1168–1181
[4] M. Nie, C. Yan, M. Li, X. Wang, W. Bi, W. Dong. Chem Eng J (2015) 279 507–515

Assessment of the application enzymes in wastewater treatment.

Sara Dormido Delgado[1], Carlos A. Aragón Cruz[1], Álvaro Real Jimenez[1], Khalid Fahd Draissi[1], Isabel Martín García[1], Pablo Caballero-Jiménez[2] and Juan Parrado-Rubio[2].

1 Fundación CENTA. Autovía Sevilla-Huelva (A-49), km 28 - 41820 – Carrión de los Céspedes (Sevilla)
2 Facultad de Farmacia, Universidad de Sevilla. C/ Calle Profesor García González, 2 - 41012- Sevilla.

** sdormido@centa.es*

1. Introduction

Water is a basic resource for society, ecosystems and climate. Nevertheless, water is limited, both in quantity and quality terms, where climate change aggravates the situation. The Water Framework Directive (Directive 2000/60/CE) has supposed a radical change in the focus of management of water resources, changing utilitarian view to protective view of resource. Within main pressures which affects superficial subterranean water bodies in the UE, founding waste from urban and industrial wastewater. The control of waste and the protection of recipient mass of water was regulated with the directive 91/271/CEE, today in force, which bind an adequate treatment of all wastes generate by urban congestion regardless size. The Wastewater treatment (WWTP) is considered a crucial step in the safety and qualities of the environment, for that reason, some studies are focused on the improvement of depurative efficiency. One of them could be the addition of hydrolytic enzymes which stimulate the assimilation of organic matter.

The treatment of urban and industrial wastewater is commonly based on biological processes where determinate microorganisms digest organic or inorganic material from them, which uses for their metabolism. Degradation of organic contaminants by microorganisms requires the pass across cellular membrane of these substances. For that reason polymeric substances must be degraded previously by the actuation of hydrolytic extracellular enzymes (Nybroe et al, 1992).

The improvement is expected like in conventional system (activated sludges) as natural or extensive systems (constructed wetlands). Enzyme's hydrolysis has been applied in industrial effluents with high levels of fat and oils, with low level of biodegradability like alternative for conventional systems (Becker et al, 1999) and for sludge digestion (Aragón et al, 2009) to solubilize organic material reducing sludge production until 30% in pilot scale (Bermúdez et al, 2013). Nevertheless, enzyme catalysis in WWTP is limited by high cost of commercial enzymes. In this sense, previous works have allowed the production of enzymes from organic by-products' fermentation, like sludge from sewage treatment (Rodríguez-Morgado et al, 2015). The addition of these enzymes could improve the process, obtaining water with better quality, in less time and with a low price.

This study aims at (a) the determination of the optimum conditions for the application of enzymes in the wastewater treatment (b) the assessment of the effects on both intensive

(activated sludge) and extensive treatment systems (constructed wetlands) and (c) environmental protection.

2. Methods

In a first stage, lab scale pilot plants are employed for the assessment of the application enzymes to biological reactors. Both commercial enzymes and by-products of the sludge fermentation are being tested. Physicochemical and microbiological parameters are monitored. Besides, sludge production and "clogging" phenomena are being studied. Then, the results are being extrapolated to a several real scale treatment plants.

3. Results and discussion

Initial results show a slight increase in the treatment efficiency in both systems (larger organic matter removal) after the enzyme dosage. Besides, a reduction in sewage sludge production is observed in the SBR unit. Finally, it is observed a delay in the appearance of the clogging phenomenon in the horizontal flow constructed wetlands.

4. Conclusions

As The Water Framework Directive (Directive 2000/60/CE) aims protection of water bodies, that are highly contaminated due to conventional water treatment systems, innovative techniques are being studied. It has been proven that hydrolytic enzymes stimulate organic matter assimilation, so that the efficiency of the treatment increases. This research studies the effect of addition of hydrolytic enzymes in the treatment process. The results show that adding enzymes into the treatment system, supposes a very important improvement in the quality of effluents, providing water protection and a reduction in economic costs.

References

[1] Aragón, C. et al. (2009). Comparison of four chemical uncouples for excess sludge reduction. Environmental Technology, 30, 707-714.

[2] Becker P., et al. (1999). The biodegradation of olive oil and the treatment of lipid-rich wool scouring wastewater under aerobic thermophilic conditions. Water Research, Vol 33, Pages 653-660

[3] Bermúdez, G. et al. (2013). Minimización de la producción de biomasa generada en una unidad de lodos activos mediante la adición de material extracelular procedente de una digestión aerobia de lodos. TecnoAqua, nº 2.

[4] Directive 2000/60/EC. The Water Framework.

[5] Directive (91 /271 /CEE). Concerning urban waste water treatment.

[6] Nybroe O. et al. (1992). "Enzyme activities in waste water and activated sludge". Water Research 26 (5) 579-584.

[7] Rodríguez-Morgado, B. et al. (2015). Effect of pH on the production of hydrolytic enzymes of industrial interest by Bacillus licheniformis using sewage sludge as a low-cost culture medium. Meeting-Abstract. Fermentation Technology. Vol. 3. Núm. 2. Pag. 81-81. 10.4172/2167-7972.s1.003_021.

ECCE12
The 12th EUROPEAN CONGRESS OF CHEMICAL ENGINEERING
Florence 15-19 September 2019

Adsorption of Anionic Surfactant on Activated Carbon inside a Semipermeable Membrane.

Israel Chavez-Sumarriva[*,1,2], Teodardo Cardenas[1], Luz Eyzaguirre[2]

1 Faculty of Chemical and Textile Engineering. National University of Engineering. Av. Tupac Amaru 210. Rimac, Lima, Peru; 2 Graduate Unit of the Faculty of Petroleum, Natural Gas and Petrochemical Engineering. National University of Engineering. Av. Tupac Amaru 210. Rimac, Lima, Peru

**Corresponding author:*

Highlights

- Adsorption of Sodium dodecylbenzenesulfonate (SDBS) on activated carbon.
- Activated carbon was placed inside a semipermeable membrane.
- The adsorbed amount of SDBS does not decrease with the use of a semipermeable membrane.

1. Introduction

Surfactants are chemical compounds used in many chemical processes *e.g.* enhance oil recovery in petroleum industry, textile and paper industry, etc. Surfactants are also used in many products and formulations, such as detergents, cosmetics, paints, inks, etc.[1] Unfortunately, large usage of surfactants has led to water pollution. Sodium dodecylbenzenesulfonate (SDBS) is a widely used anionic surfactant. SDBS is biodegradable under anaerobic conditions[2] but the amount of this anionic surfactant in water is high and therefore is still difficult to eliminate them. Nowadays, SDBS is removed by different methods, such as chemical oxidation,[3] coagulation,[4] biological degradation,[5] electrochemical removal[6] and adsorption on soils,[7] clay[8] and carbonaceous materials.[9,10] Adsorption on carbonaceous materials such as activated carbon is widely used because is easy to operate and cheap but sometimes the activated carbon used for eliminate the SDBS can polluted the aqueous media. A solution is proposed in this research, the activated carbon is placed inside a semipermeable membrane for avoid pollution of the aqueous media.

2. Methods

Determination of SDBS Concentration

The SDBS concentration in solution before/after adsorption with activated carbon without/inside semipermeable membrane (regenerated cellulose) was determined using a Shimadzu UV−Vis spectrophotometer at 224 nm.

3. Results and discussion

Based on adsorption kinetics studies of activated carbon inside a semipermeable membrane, the time to reach the equilibrium adsorption capacity was 24 hours, a security factor was added and the time used in all adsorption tests was 30 hours. Adsorption tests were made (T = 298 K) to

determine if the semipermeable membrane decreases the equilibrium adsorption capacity. Figure 1 shows the adsorption tests of Sodium Dodecylbenzenesulfonate (SDBS) on activated carbon without / inside semipermeable membrane, it can be seen that the equilibrium adsorption capacity (q_{eq}) does not change when the activated carbon is placed inside a semipermeable membrane. The influence of temperature was studied with activated carbon inside a semipermeable membrane at 298 K, 308 K, 318 K and 328 K. The results showed that when the temperature increases the adsorption capacity decreases. The influence of pH was also studied with activated carbon inside a semipermeable membranes (T=298 K). The pH was varied between 4 and 11; the results showed that the adsorption capacity does not change with pH which confirms that there are no electrostatic interactions between the SDBS and the activated carbon. After determining the optimal adsorption parameters (time, pH, Temperature) an adsorption isotherm was made (see Figure 2). The adsorption capacity of activated carbon inside semipermeable membrane founded was *ca.* 271 $mg_{SDBS}\ g_C^{-1}$.

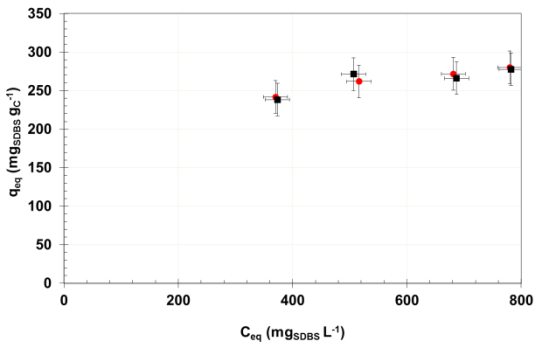

Figure 1. Effect of semipermeable membrane on the adsorption capacity of SDBS on activated carbon; red circles: without semipermeable membrane; black squares: with semipermeable membrane.

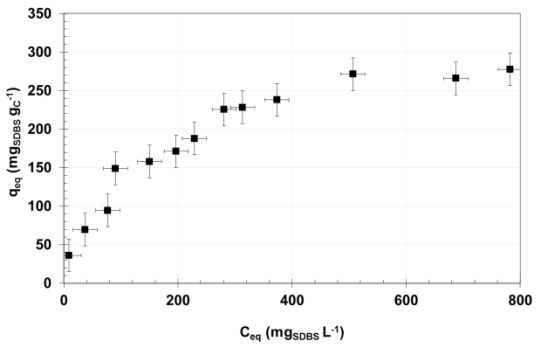

Figure 2. Adsorption isotherms of SDBS on activated carbon placed inside a semipermeable membrane (initial conditions; T=298 K, pH=7, 30 h contact time).

4. Conclusions

The results demonstrated that the amount absorbed of the anionic surfactant Sodium Dodecylbenzenesulfonate (SDBS) on activated carbon does not change with the use of a semipermeable membrane, therefore the proposed method could be used in industrial applications in which is needed to remove SDBS from an aqueous solution and it is not desired to contaminate this aqueous solution with small particles of activated carbon.

References

[1] M.J. Rosen, J.T. Kunjappu, Surfactants and Interfacial Phenomena, Fourth ed., John Wiley & Sons, Inc., Hoboken, 2012.
[2] D. Prats, F. Ruiz, B. Vázquez, M. Rodriguez-Pastor, Water Res. 31(1997) 1925-30
[3] J.D. Mendez-Diaz, M. Sanchez-Polo, J. Rivera-Utrilla, M.I. Bautista-Toledo. Water Res. 43(2009) 1621-9
[4] J. Beltrán-Heredia, J. Sánchez-Martín, C. Solera-Hernández, Chem Eng J. 153(2009) 56-61
[5] M.T. Garcia, E. Campos, I. Ribosa, A. Latorre, J. Sanchez-Leal, Chemosphere. 60(2005):1636-43
[6] E. Onder, A. Koparal, U. Ogutveren, Sep. Purif. Technol. 52(2007):527-32
[7] Z. Ou, A. Yediler, Y. He, L. Jia , A. Kettrup, T. Sun, Chemosphere. 32(1996) 827-39
[8] D.C. Rodríguez-Sarmiento, J.A. Pinzón-Bello, Appl Clay Sci. 18(2001) 173-81
[9] S.D. Gupta, S.S. Bhagwat, J Disper Sci Technol. 26(2005) 111-20
[10] E. Ayranci, O. Duman, J Hazard Mater 148(2007) 75-82

ECCE12
The 12th EUROPEAN CONGRESS OF CHEMICAL ENGINEERING
Florence 15-19 September 2019

Zeolitic imidazole frameworks-8 derived ZnO/carbon nanocubes: a broad-spectrum solid-phase microextraction coating

Xingru Hu, Jiansheng Li *

Key Laboratory of Jiangsu Province for Chemical Pollution Control and Resources Reuse, School of Environment and Biological Engineering, Nanjing University of Science and Technology, Nanjing 210094, China.

**Corresponding author: lijsh@njust.edu.cn*

Highlights

- ZIF-8 derived ZnO/C was prepared and used as adsorbent for SPME.
- The dispersed composition endows ZnO/C with broad-spectrum extraction capability.
- The double-shelled hollow structure is beneficial for the sensitive extraction.
- The resultant fiber is applied for the determination of the analytes from water samples.

1. Introduction

Development of high-efficient determination of the environmental pollutants is of great significance. [1] Solid phase microextraction (SPME), as a solvent-free extraction method, is very widely used for the sensitive detection of emerging pollutants.[2] The properties of the coating materials generally determine the extraction performance.[3] It is thus a marked research interest in developing a kind of SPME fiber coating that can provide sensitive extraction capability for broad-spectrum analytes from the complex samples. Recently, metal-organic frameworks (MOF) has been considered as the promising precursor to synthesize functional materials directly by high-temperature pyrolysis.[4] In order to broaden the utilization and improve the performance of the MOFs-derived materials, hollow structure with abundant active sites has been designed and fabricated.[5] Encouragingly, the MOF-derived double-shelled hollow materials seems to be a potential choice for the broad-spectrum and sensitive SPME of the environmental pollutants. In this study, we develop a SPME fiber based on zeolitic imidazole frameworks-8 (ZIF-8)-derived double-shelled hollow ZnO/carbon (ZnO/C) materials. The ZnO/C coated fiber is used to investigate its simultaneous extraction ability for polar and nonpolar compounds. The highly synergistic effect of carbon networks and ZnO crystals leads to the broad-spectrum extraction of the ZnO/C-F. Moreover, the double-shelled hollow structure improves the sensitive extraction for the analysts.

2. Methods

The ZIF-8 nanocubes were first prepared by mixing the HMI, Zn(NO3)2•6H2O and CTAB. After tannic acid etching treatment, these nanocubes could be converted into double-shelled hollow structure. Then the DSH-ZIF-8 experienced a thermal annealing at 500 °C to synthesis the ZnO/C. Finally, the resultant ZnO/C was directly coated on the SSW by the glue method to form the SPME fiber.

3. Results and discussion

As shown in Fig. 1a, the morphology of ZnO/C is kept after carbonization. Besides, the broken particle (inset in Fig. 1a) suggests the presence of the double-shelled structure. From TEM characterization (Fig. 1b,c), the void space and structure can be clearly testified. Obvious lattice fringes with an spacing of 0.25 nm in the high-resolution TEM image (Fig. 1d) and bright diffraction rings in SAED pattern (Fig. 1d inset) have been observed for the ZnO/C, corresponding well to the (101) planes of ZnO. The elemental mapping data presented in Fig. 1e reveals that the C, O and Zn elements are distributed uniformly on the particle. As shown in Fig. 1g, the sharp peaks of ZnO/C show the typical structure for ZnO crystal phase, which is consistent with the SAED pattern.

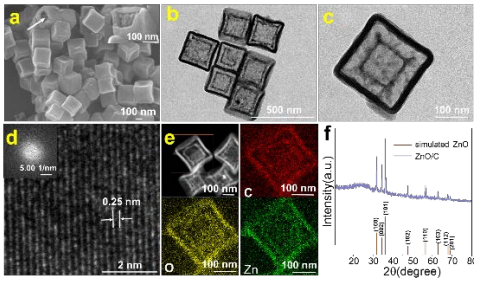

Figure 1. (a)SEM image, TEM images at low (b) and high (c) magnification, (d) high-resolution TEM image (inset: SAED pattern), (e) elemental mapping showing C, O and Zn of ZnO/C. (f) XRD patterns of simulated ZnO and ZnO/C.

To evaluate the extraction performance, ZnO/C-F was compared with the commercial PDMS/DVB fiber, which has been proved for SPME of both nonpolar and polar compounds. The ZnO/C-F displays a prominent advantage in extracting both the BTEX and CPs (Figure 2). The excellent performance could attribute to the combined effect of the ZnO/carbon composition and double-shelled hollow structure.

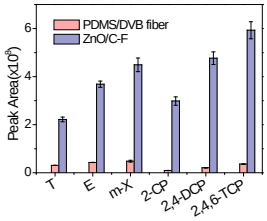

Figure 2. Peak areas comparison of ZnO/C-F with S-ZnO/C-F and commercial PDMS/DVB fiber.

4. Conclusions

In conclusion, the MOF-derived double-shelled hollow ZnO/C materials have been prepared. Then they were coated on the surface of a stainless steel wire to form the SPME fiber. Compared with the commercial fiber, ZnO/C-F displayed superior extraction efficiency owe to the combined effect of the ZnO/C composition and double-shelled hollow structure.

References [Calibri 10]

[1] E. Y. Zeng, J. A. Noblet. Environ. Sci. Technol. 36 (2002) 3385-3392.
[2] É. A. Souza-Silva, R. Jiang, Gionfriddo, J. Pawliszyn. TrAC Trends Anal. Chem.71 (2015) 224-235.
[3] F. Wang, J. Zheng, J. Qiu, S. Liu, G. Chen, G. Ouyang. ACS Appl. Mater. Interfaces 9 (2017) 1840-1846.
[4] H. B. Wu, B. Y. Xia, L. Yu, X. Yu, X. W. Lou. Nat. Commun, 6 (2015) 6512.
[5] L. Zhang, L. Shi, L. Huang, J. Zhang, R. Gao, D. Zhang. ACS Catal., 4 (2014) 1753-1763.

ECCE12
The 12th EUROPEAN CONGRESS OF CHEMICAL ENGINEERING
Florence 15-19 September 2019

Stability study as a basis for optimizing the extraction conditions of resveratrol and ε-viniferin

Ema Kosovic[1], Martin Topiař[1]

1 Institute of Chemical Process Fundamentals of CAS v.v.i., Rozvojová 135, Prague 6, 16502, Czechia

**Corresponding author: kosovic@icpf.cas.cz*

Highlights

- Comparison of several different extraction techniques under various conditions
- Performing the stability tests on extracted stilbenes
- Light induced formation of *cis*-viniferin by dimerization of resveratrol

1. Introduction

Czech Republic belongs among countries with long winemaking tradition. Unfortunately, the wine-processing industry produces large amounts of waste, which is usually burnt or used in compost [1]. However, wine waste formed during wine production can comprise valuable bioactive substances e.g., resveratrol and viniferin, important in food production and very useful in various branches of science including medicine, pharmacy and cosmetic industry thanks to their potential antioxidant activity [2]. The great interest in these compounds also stems from their biological properties and chemical stability. The mechanism that leads to production of these antimicrobial compounds synthesized and accumulated in different parts of the plant in response to biotic or abiotic stress is based on self-defense potential of the plants [3, 4]. This work is focused on the combination of several extraction techniques for the isolation of polyphenols with subsequent induction of stress conditions. Concern these factors, stability study is the basis for optimizing conditions of extraction methods of resveratrol and viniferin.

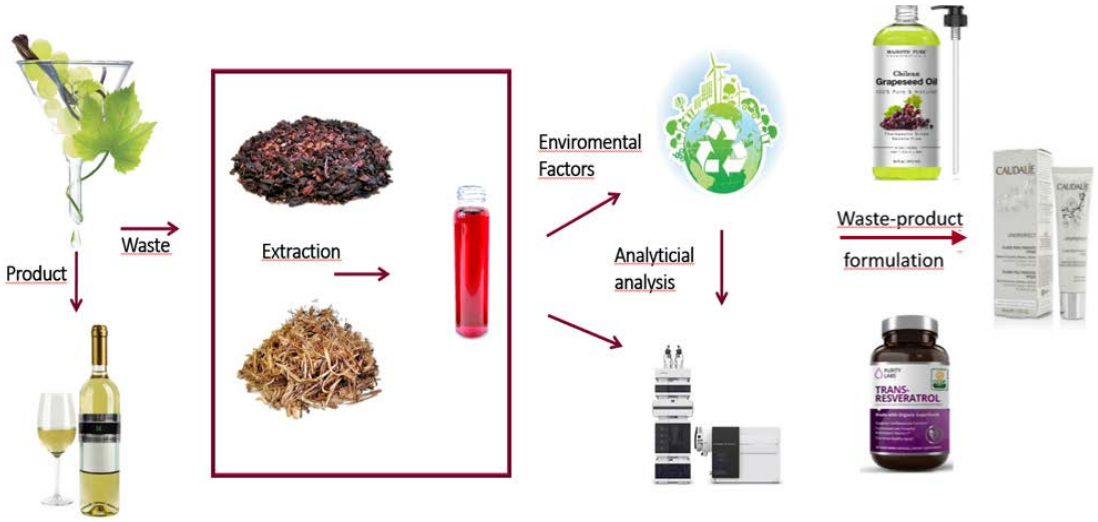

Figure 1. From grapes to main product and by-products.

2. Methods

To obtain a usable amount of stilbenes for subsequent processing it is essential to use highly effective extraction methods. Considering that, a comparison of several different extraction such as maceration, ultrasonic extraction, Soxhlet and pressured liquid extraction has been performed. The effects of stress conditions used in stability study were monitored and performed by newly developed HPLC-MS method, which is proved to be accurate, reproducible and efficient for determination of resveratrol and viniferin.

3. Results and discussion

Among extraction methods, the most noticeable results were obtained using maceration in dark and Soxhlet extraction method at atmospheric pressure providing the highest concentration of resveratrol. The outcome of stability study showed, that storage in dark didn't affect the concentration of monitored compounds but light exposure induced visible decreasing in resveratrol and *trans*-viniferin concentration while the concentration of *cis*-viniferin increased considerably. The explanation of this phenomenon is lying in possible dimerization of two molecules of resveratrol induced by light and also photoisomerisation of *trans* form of stilbenes into *cis*, resulting in observable concentration increase of *cis*-viniferin [5]. To confirm this thesis, the sample without *cis*-viniferin was exposed to sunlight and UV light for defined time intervals. Process of formation of *cis*-viniferin was confirmed as well as supposed distinction between sunlight and UV light: UV light accelerates the entire process. Already known fact that higher temperature leads to degradation of stilbenes was also confirmed. Nevertheless, the short-time exposure of plant material to heating in solution enhances the release of resveratrol from other plant structures, such as carbohydrates.

4. Conclusions

Based on the stability study, the optimal conditions for obtaining individual stilbenes from grape cane extracts of *Vitis vinifera* L. cv. Cabernet Sauvignon were determined. Results showed that light-induced dimerization of *trans*-resveratrol leads to inverse concentration change between viniferin and resveratrol, while high temperature test showed complete degradation of stilbenes. Following photoisomerisation of *trans*-stilbenes into *cis* form also induced by light, explained the increase of *cis* form versus *trans.* Due to this, the basis for optimizing extraction conditions of resveratrol and viniferin was obtained.

References

[1] C. Schonnenbeck, G. Trouve, M. Valente, P. Garra, J. F. Brilhac, Fuel 180 (2016) 324-331.
[2] G.Y. Tang at al., Molecules 23 (2018) 2598.
[3] M. Chalal et al., Molecules 19 (014) 7679-88.
[4] G. Armijo et al., Front. Plant Sci. 7 (2016) 382.
[5] L.M. Szewczuk, S.H. Lee, I.A. Blair, T.M. Penning, J. Nat. Prod. 68 (2005) 36-42.

Acknowledgments

The financial support from the Technological Agency of the Czech Republic via grant no. TJ01000249 is gratefully acknowledged.

ECCE12
The 12th EUROPEAN CONGRESS OF CHEMICAL ENGINEERING
Florence 15-19 September 2019

Explosibility characterization of combustible dusts from Italian industries

Luca Marmo[1], Almerinda Di Benedetto[2], Roberto Sanchirico[3], Valeria Di Sarli[3], Enrico Danzi[1]

1 Applied Science and Technology Dept. Politecnico di Torino, Cso Duca degli Abruzzi 24, 10129 Turin (Italy); 2 Dipartimento di Ingegneria Chimica, dei Materiali e della Produzione Industriale, Università Federico II Napoli, P.le Tecchio 80, 80125 Naples (Italy); 3 CNR IRC, P.le Tecchio 80, 80125 Naples (Italy)

**luca.marmo @polito.it*

Highlights

- Dust explosion hazard
- Testing the explosibility of industrial dust waste may not be completely fulfilled by current norm
- Explosion hazard assessment requires proper dust characteristics measurement

1. Introduction

The first documented dust explosion in the world is that occurred in Turin (Italy) in 1785. Many years have passed since then, but dust explosion phenomena are still being investigated as they pose several open issues. Literature studies have been mostly focused on how to deal and protect industrial equipment, where fine solid particles are involved, both as processing powder and as waste material to be disposed. Powdered materials could also be produced accidentally, due to mechanical or thermal stress, such as working operations aiming to refine or reduce shape of raw materials, but also when brittle solid materials are handled or stored. Most of the dusts generated by these operations are heterogeneous in shape and particle size distribution, as well as in volatile content and chemical composition. Testing combustible dusts coming from industries means to deal with samples which are mostly not pure, but mixture of combustible and inert materials. The assessment of the likeliness of a combustible dust to explode in certain conditions is not an easy task, even though several standards could be used to determine the explosive properties, such as the recent ISO 80079-20-2:2016. Nevertheless, dust explosion hazard is based on the known "pentagon", a side of which represents the dispersibility of the material that often plays a critical role. Non-spherical dusts, such as fibers, scraps or shavings from finishing operations are difficult to disperse with traditional testing procedures, but this could not a priori exclude their unsafe behavior in industrial equipment, or in peculiar conditions: dispersibility dynamics of such type of dusts is not well understood.

This paper summarizes results and draw conclusions obtained from the testing of over two hundred of dust samples, collected in industrial facilities from all over Italy, deriving from different type of processes, with different chemical nature and morphology.

2. Methods

Dust samples were subjected to preliminary characterization tests, as to measure those properties which could significantly influence dust explosivity parameters. Metal oxide content was measured when dealing with dust coming from metal industrial plants, while CHN analysis was performed on most organic dusts. Moisture content was also determined for all samples as to verify its inerting effect on the explosion strength of dusts. PSD was obtained for all samples, both through a pile of sieves, operated by a mechanical sieving machine, and by laser granulometric

analysis (ISO 13320:2009). Dust ignition sensitivity was evaluated through the measurement of Minimum Ignition Temperature (in cloud and in layer), Minimum Ignition Energy and with the Explosibility screening test (ISO 80079-20-2:2016). Dust explosion violence was measured according to EU standard 14034:2011, defining maximum rate of pressure rise (or K_{ST}, deflagration index), maximum pressure rise and Lower Explosibility Limit (LEL).

3. Results and discussion

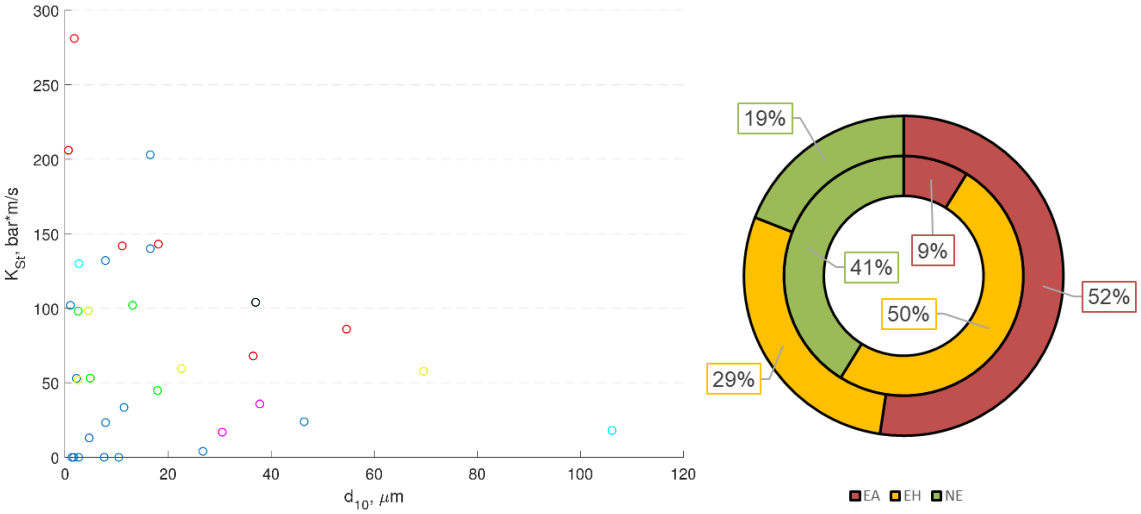

Figure 1. K_{St} value vs tenth percentile diameter of particles, where red dots represent plastic samples, blue metal, green textiles, black wood, yellow food, magenta feed, cyan others (left); Speditive explosibility test results sort by sample origin (inner ring inorganic samples, outer ring organic samples) (right).

4. Conclusions

Assessing the explosion hazards related to combustible dusts derived from industrial processes and waste is a challenging task for many reasons: samples are rarely pure dusts, but mixtures; PSD and morphology, among other variables, could vary extensively through the dust sample due to collecting procedures; actual industrial conditions and material handling are difficult to recreate in laboratory scale [1]. In this work, more than hundreds of samples were tested, deriving from different industrial realities: dusts produced by plastic manufacturing plants presented higher hazards in terms of explosion violence (K_{St} class 2), followed by samples from metal waste, with higher metallic content [2]. Organic samples constituted a potential explosion risk, as only about 20% of them did not imply an explosion behavior, while inorganic non explosible samples are two times higher. Care must be paid when dealing with non-traditional dusts (such as those generated from manipulation of textile fibers), as relative high value of K_{St} are registered, even though standard explosibility test devices could not disperse efficiently those type of samples [3].

References

[1] Danzi, E., Marmo, L., & Riccio, D. (2015). Journal of Loss Prevention in the Process Industries Minimum Ignition Temperature of layer and cloud dust mixtures. J. Loss Prev. Process Ind., 36, 326-334.

[2] Marmo, L., Riccio, D., & Danzi, E. (2017). Explosibility of metallic waste dusts. Process Safety and Environmental Protection, 107, 69-80.

[3] Marmo, L., Sanchirico, R., Di Benedetto, A., Di Sarli, V., Riccio, D., & Danzi, E. (2018). Study of the explosible properties of textile dusts. J. Loss Prev. Process Ind. 54, 110-122.

ECCE12
The 12th EUROPEAN CONGRESS OF CHEMICAL ENGINEERING
Florence 15-19 September 2019

NOx Trap and Removal Performance on Barium and Barium-Ceria Containing SCR Catalysts

JinWoo Kim[1,2], Bora Ye[1], Taewook Kim[1], Heesoo Lee[2], Hong-Dae Kim[1,*]

1 Green Materials and Processes Group, Korea Institute of Industrial Technology, Ulan 44413, Republic of Korea; 2 School of Material Science & Engineering, Pusan National University, Busan 46241, Republic of Korea

**Corresponding author: hdkim@kitech.re.kr*

Highlights

- Barium and barium-ceria containing V_2O_3-WO_3/TiO_2 SCR catalyst was synthesized.
- Baium-ceria containing catalyst has improved NOx storage performance than barium containing catalyst.
- NOx desorption occurs at SCR activation temperature range.
- No significant deactivation even after NOx desorption.

1. Introduction

Recently, the importance of reducing nitrogen oxides (NOx) has been emphasized because atmosphere regulations are enhanced [1,2]. Selective catalytic reduction (SCR) is a representative technology for converting harmful NOx into harmless water and nitrogen by reducing agents such as NH_3 [2,3]. The optimum activation temperature of the V_2O_5-WO_3/TiO_2 SCR catalysts (VWTi catalysts) is a range of 300-400 °C, which requires a lot of energy and time to raise the temperature. However, it generated under low-temperature operating conditions, such as start-up and shut-down procedures of equipment, is a problem as it is not removed by catalyst and released into the atmosphere [4]. Therefore, NOx trap technology is required at low temperatures.

Barium is an alkali metal having the NOx storage properties. In the case of alkaline and alkaline earth metals such as K and Cs except Ba, the NOx occlusion ability increases but the catalytic activity decreases by increasing the basicity. However, Barium oxide converts NOx to nitrate ($Ba(NO_3)_2$) form and stores NOx. Currently, it is used as NOx Trap material of Lean NOx Trap (LNT) catalyst [4,5]. Ceria is a coagulating agent that supplies oxygen needed for reaction to the active material [6]. In this study, Barium and Barium/Ceria are impregnated into VWTi catalyst, and the adsorption / desorption behavior of the catalyst was confirmed.

2. Methods

TiO_2, $Ce(NO_3)_3$, and BaO are dispersed in ethanol with stirring. Ammonium metavanadate (AMV), and Ammonium metatungstate (AMT) are separately stirred for 1 hour in a solution of oxalic acid dissolved in ethanol. The solutions are treated with ultrasonic for 1 h after mixing each solution. Then, they are stirred for 6 hours at 60 °C. After the evaporation of ethanol at 60 °C using a rotary evaporator, the synthesized powder is sintered at 500 °C with a rate of 3 °C/min for 2 hours. Figure

1 shows the experimental flow chart scheme for the preparation of the NOx Trap functional catalyst.

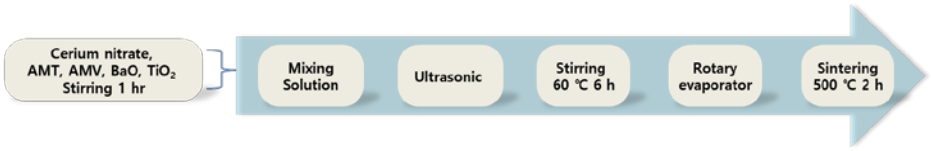

Figure 1. Experimental flow chart for preparation NOx trap functional catalyst

3. Results and discussion

The storage and desorption characteristics of Barium and Barium/Ceria doped VWTi catalyst are affected by reaction temperature, space velocity and catalyst content. Figure 2 shows the adsorption characteristics according to the composition of the catalyst at a space velocity of 36,000 h^{-1} and a temperature of 200°C. In the case of barium containing catalyst, barium increase the NOx adsorption property compared with the non-containing catalyst (VWTi catalyst). In addition, the barium-ceria containing catalyst showed better adsorption performance than barium containing catalyst.

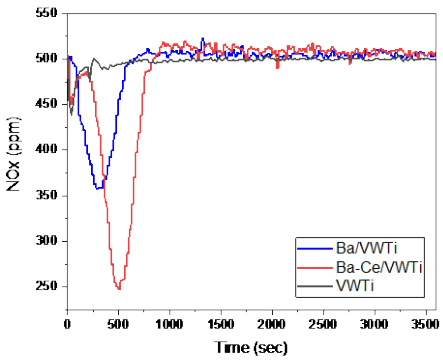

Figure 2. NOx adsorption profile of V_2O_5-WO_3/TiO_2 (VWTi), BaO/VWTi, and BaO–CeO_2/VWTi (SV : 36,000 h^{-1}, O_2 : 10 vol%, NOx : 500 ppm, N2 : Balance gas, 200 ℃)

Desorption behavior was occurred at 300-350 °C, which is the catalytic activation temperature range. Furthermore, about 90% efficiency was measured in the denitration rate evaluation. It was confirmed that the activity did not decrease after desorption.

4. Conclusions

Due to the additional role of ceria, the adsorption property of barium-ceria containing catalyst was found to be higher than that of Barium containing catalyst. NOx desorption was observed at 300 - 350 °C, which is the catalyst activation temperature, and it was confirmed that there was no decrease in the activity of the SCR reaction.

References

[1] L. Lietti, J. Svachula, P. Forzatti, G. Busca, G. Ramis, P. Bregani, Catalysis Today 17 (1993) 131–139.
[2] X. Zhao, L. Huang, H. Li, H. Hu, X. Hu, L. Shi, D. Zhang, Appl. Catal. B Environ. 183 (2016) 269–281.
[3] J.R. Strege, C.J. Zygarlicke, B.C. Folkedahl, D.P. McCollor, Fuel 87 (2008) 1341–1347.
[4] Y. Li, Y. Li, Y. Wan, S. Zhan, Q. Guan, Y. Tian, RSC Adv. 6 (2016) 54926–54937.

[5] C. Wang, L. Sun, Q. Cao, B. Hu, Z. Huang, X. Tang, Appl. Catal. B Environ. 101 (2011) 598–605.
[6] X. Wang, L, Lv, Q. Zhang, Y. Zhang, J. Wang, M. Shen, Catal. Sci. Technol., 2013, 3, 200-207

ECCE12
The 12th EUROPEAN CONGRESS OF CHEMICAL ENGINEERING
Florence 15-19 September 2019

Ferroniobium of the Colombian Guania Shield for obtaining rare earth metals: crystallographic analysis

Michelle Chico[1*], Aida Liliana Barbosa[2]

[1] Chemical Program. Faculty of Exact and natural sciences. Laboratory of research in catalysis and new materials (LICATUC). Universidad of Cartagena. Colombia.
abarbosal@unicartagena.edu.co

Highlights

- Niobium ore deposits in the Guinía-Colombia were studied founded niobium, zirconium, cobalt and titanium.
- The presence of radioactive elements in trace (uranium, thorium, curium, praseodymium) was evidenced in the materials using Raman spectroscopy and FRX.
- Solvometallurgy techniques were used for the separation of REEF and oxide of Nb and Ta, obtaining a solid yellow corresponding with the FeC_2O_4

1. Introduction

The Guinia Shield in the area of Inírida-Colombia has been found pirocloros with the presence of oxides of Ti, W, Ta and Nb often enriched with U, Hf, Zr and rare earth elements. 1

The most effective and frequently applied solution method for mineral specimens containing Ta and Nb implies the use of HF as a leachate reagent, experiencing the formation of different soluble metal fluoride complexes such as Heptafluoruros, Hexafluoruros or Oxifluoruros, [6]. Solvometalurgicos processes are presented as an alternative to conventional metallurgical, which impact environmentally by the use of polluting inorganic acids.

2. Methods

The samples of niobium ore were collected on "El Zancudo" Guinía (Colombia). The specimen was dried and pulverized, passed by sieve 100mesh and was characterized by stereoscopic microscopy, Laser-Raman spectroscopy, and X-ray diffraction powder (XRD) and X-ray fluorescence (FRX)). The extraction of Nb and Ta of Ferriniobio use solvents 2-octanol and Metilisobutilcetona, as extraction agents. [2.4]

3. Results and Discussion

FRX analysis showed high percentages of SnO_2, TiO_2, Nb_2O_5 and Ta_2O_5, percentages about 8% of Fe_2O_3 and ZrO_2, below 3% w/w MnO, W, Al_2O_3, SiO_2. Stereoscopic optical microscopy, show presence of transparent quartz, iron ore with uneven surface, grey metals with metallic sheen that were related to niobium, tungsten and zirconium.

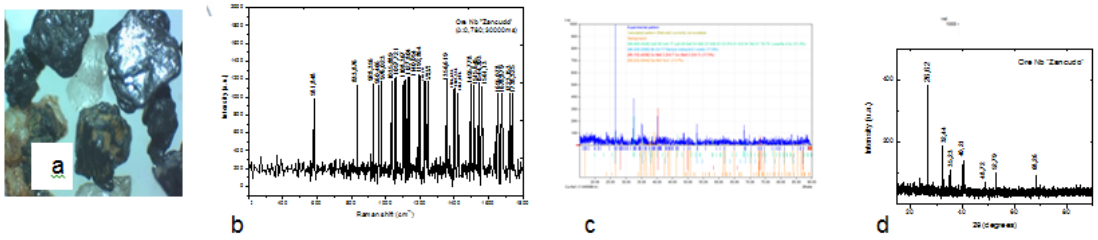

Figure 1. (a) External of optical microscopy Nb ore 3.5x. (b) Raman spectrum of outer layer (0.780- 30000ms). (c) and (d) DRX pattern Ore Nb

Feldspars were seen as subhedral-shaped crystals of white and pink color, together with magnetite with rhombic faces of metallic luster and black color. Raman signals features in 581.848 cm^{-1} it associated with stretch Nb-O, possibly of the NbO_2, one observes two bands located both with approximately 677cm^{-1}, assigned to phases of magnetite Fe_3O_4, the peaks or signals quite intense at 1037 cm^{-1}, 1113 cm^{-1} and 1235 cm^{-1} were characteristic of hematite Fe_2O_3, the band 833.876 cm^{-1} was reported to be consistent with uranium oxide [3]. XRD analysis record peaks in 2 θ = 26.62, 2 θ = 32.44, 2 θ = 35.23 and 2 θ = 40.21, were characteristic of metals such as zirconium, titanium, niobium and cobalt.

4. Conclusions

The method of extraction with solvents led to two major products one of them iron oxalate, which was extracted to treat the leachate with metil butyl ketone and the subsequent washing of the loaded metil butyl ketine, which allowed the obtaining of a solid Niobium white, when the solution reached pH 7 by adding ammonia. These results show that the proposed method is potential for the purification of the native mineral.

References

[1] Cramer, T, Et Al. Caracterización de depósitos aluviales con manifestaciones de tantalio y niobio (“coltán”) en las comunidades indígenas de matraca y caranacoa, Guainía. INGEOMINASUNAL. 2011.

[2] T. E. Amer, M. G. A. El-azm, and R. M. Issa, —Liquid – liquid extraction of tantalum and niobium by octanol from sulfate leach liquor, Arab. J. Chem., vol. 5, no. 1, pp. 31–39, 2012.

[3] A. Timofeev, A. A. Migdisov, and A. E. Williams-jones, —An experimental study of the solubility and speciation of tantalum in fluoride-bearing aqueous solutions atelevated temperature, Geochim. Cosmochim. Acta, vol. 197, pp. 294–304, 2017.

[4] Novoa, L,. Cortes, L. E, Gonzalez, E, Jimenez A,.Cortes,L.G, Ojeda,M and Barbosa,A.L Evaluation of Anticorrosive Effect of Niobium Carbide Coating Applied on Carbon Steel Chemical Engineering Transactions. 57 p.p 1386-1392,2017

Acknowledgement to Colciencias by grant project 004-2016. Geoscience Program.

ECCE12
The 12th EUROPEAN CONGRESS OF CHEMICAL ENGINEERING
Florence 15-19 September 2019

Development of Multi-site Microkinetic Model for the Methanol Synthesis Catalysts

Anže Prašnikar[1], Damjan Lašič[1], Venkata Dasireddy[1], Blaž Likozar[1]

1 Department of Catalysis and Chemical Reaction Engineering, National Institute of Chemistry, Hajdrihova 19, SI-1000 Ljubljana, Slovenia

**Corresponding author: anze.prasnikar@ki.si*

Highlights

- Tested Cu:M:Ti oxide catalysts (M=Sr, Ba, Ca) with various compositions.
- Investigated structural properties by CO_2 TPD, N_2O chemisorption and other techniques.
- Copper particle size and basicity important for the methanol synthesis.
- Observed trends incorporated into the multi-site microkinetic model.

1. Introduction

Methanol is important industrial chemical with the annual production of 110 Mton [1]. Development of new catalysts with enhanced properties is a key for an efficient methanol synthesis. Additionally, microkinetic models built on trends from experimental work, with reaction rate constants from quantum chemical calculation [2], can be used to obtain insights into catalytic reaction mechanisms and for further plant operation optimization.

The beneficial influence of the basicity of the copper catalyst on the methanol synthesis was previously reported [3,4]. In our work we prepared and tested different Cu:M:Ti oxide (M=Sr, Ba, Ca) catalysts. Catalysts were characterized by N_2 physisorption, N_2O pulse chemisorption, CO_2 TPD and H_2 TPR. We investigated structure-activity relationship for the preparation of the microkinetic model.

2. Methods

Catalysts were prepared by solution combustion synthesis with citric acid and calcined at 650 °C. We pelletized powders and reduced them at 300 °C for 12 h. For the catalytic tests, the temperature was varied at pressure 20 bar, GHSV = 6000, 12000 1/h and inlet gas composition H_2:CO_2 = 3:1. Outlet gas composition was determinate using gas chromatography. N_2 physisorption was performed using ASAP 2020, H_2 TPR was executed in 50 mL/min flow of 10% H_2/Ar gas with heating rate of 10 °C/min from 60 °C to 300 °C, N_2O pulse chemisorption was performed after H_2 TPR, in the 20 mL/min flow of He at 90 °C. The consumption of N_2O was determined using daily calibrated mass spectrometer. CO_2 TPD were performed from -40 °C to 600 °C with heating rate of 20 °C/min in the 20 mL/min of He. Mass spectrometer was also used to analyze results. N_2O pulse chemisorption, CO_2 TPD and H_2 TPR were performed on Autochem 2920.

3. Results and discussion

Methanol and carbon monoxide production at 220 °C and 20 bar were used and normalized to copper surface area obtained from N_2O pulse chemisorption to calculate turnover frequency (TOF). We tested catalysts at various copper loadings (Figure 1), different Sr/Ti ratio (Figure 2) and different earth alkaline metals (Ca, Sr, Ti) (Figure 3). We observe, that at different Cu loadings, Cu particle size increase which increases TOF for MeOH, while TOF for CO remains constant. This suggests that larger copper particles expose surfaces, which are more selective for MeOH synthesis. Turnover frequency for MeOH increases with increasing Sr/Ti ratio, while CO TOF remains almost constant. This suggests that Sr promotes adsorption of CO_2 and further reaction with adsorbed H* species through Langmuir-Hinshelwood mechanism. Much larger benefits are obtained using Ca, which much strongly adsorbs CO_2. Therefore for the development of the microkinetic model is important incorporation of multiple sites, such as basic sites with various copper metal sites.

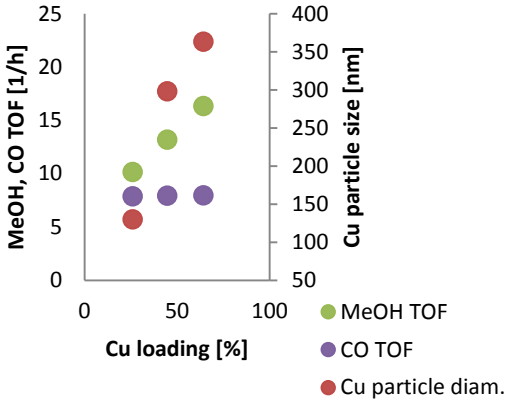

Figure 1. Influence of copper loading on TOF for MeOH and CO at constant Sr/Ti. (GHSV=6000 1/h)

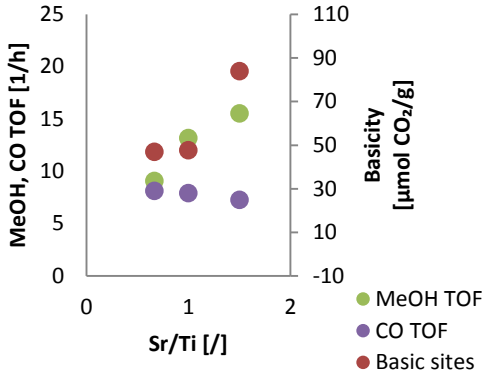

Figure 2. Influence of Sr/Ti ratio on TOF for MeOH and CO at constant copper loading 50 wt%.(GHSV=6000 1/h)

4. Conclusions

Important catalyst properties were investigated to obtain structure-activity relationships. We found out that the basic sites importantly influence the catalyst activity and should be included into microkinetic model, beside copper sites.

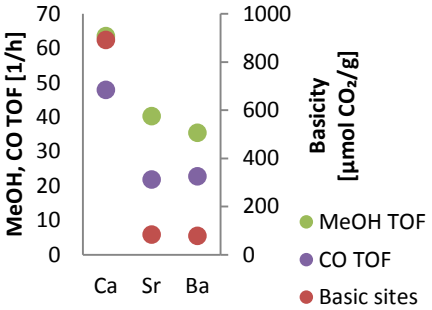

Figure 3. Influence of different earth alkaline metals for Cu:M:Ti=5:3:2. (GHSV=12000 1/h)

References

[1] https://www.methanol.org/the-methanol-industry/W. Black, E.B. White, The Elements of Science, third ed., MacCluski, New York, 1987. Accessed on 10.1.2019.

[2] M. Huš,D. Kopač, B. Likozar, ACS Cat.,9,(2019), 105-116.

[3] H . Zhan, F.. Li, P. Gao, N. Zhao, F. Xiao, W. Wei, Y. Sun, RSC Adv., 4, (2014), 48888–48896.

[4] E., Choi, K. Song, S. An Lee, M Youn, K. Park, S.Jeong, Kim, H. Korean J. Chem. Eng., 35,(2017), 73–81.

ECCE12
The 12th EUROPEAN CONGRESS OF CHEMICAL ENGINEERING
Florence 15-19 September 2019

AUTOMATIC DETECTION OF SCORCHED OR OTHER FOREIGN PARTICLES IN GRANULATION PROCESS USING INLINE PROBES

Mirco Wegener[1], Sebastian Maaß[1]

1 SOPAT GmbH, Boyenstraße 41, 10115 Berlin, Germany

**Corresponding author: mirco.wegener@sopat.de*

Highlights

- Live imaging ensures the view into the process
- Differentiation of different colors, shapes and sizes possible in a real time monitoring
- Quality assurance is used for optimization and feedback control

1. Introduction

Granulation, the process of particle enlargement by agglomeration technique, is one of the most significant unit operations in the production of pharmaceutical, chemical or food products. These process transforms fine powders into free-flowing, dust-free granules that are easy to compress. Nevertheless, granulation poses numerous challenges due to high quality requirement of the formed granules in terms of content uniformity and physicochemical properties such as granule size, bulk density, porosity, hardness, moisture, compressibility, nonexistence of foreign particles etc. together with physical and chemical stability of the drug, the chemical component or food ingredient.

Realtime monitoring of the named parameters using inline measurement technologies was discussed in general but not implemented throughout the industrial community due to severe technical challenges. Especially the measurement of granule size, granule shape and colour (implying scorched or other foreign particles) has not been implemented successfully in industrial granulation processes. The presentation will give a brief overview of existing measurement techniques developed for the above mentioned tasks, as different techniques based on different physical principles for measuring particle size distributions are available. The authors did compare several measurement techniques and will provide those results.

2. Methods

The mainly used system for this presentation is a newly developed photo optical in-line measurement technology combined with an innovative image processing and analysis software. These analyses show exactly the size, shape and colour of the granules. Additional parameters like local concentration or moisture can be derived from the image analysis. This makes it possible to monitor and to optimize granulation processes in a feedback loop, as the particle data are available in real time.

3. Results and discussion

The quality and variability in quality of the images obtained by the camera computer system (see Fig. 1) greatly influences the success of the automated interpretation. All important step will be discussed and presented in detail. A first example is given in the following figure.

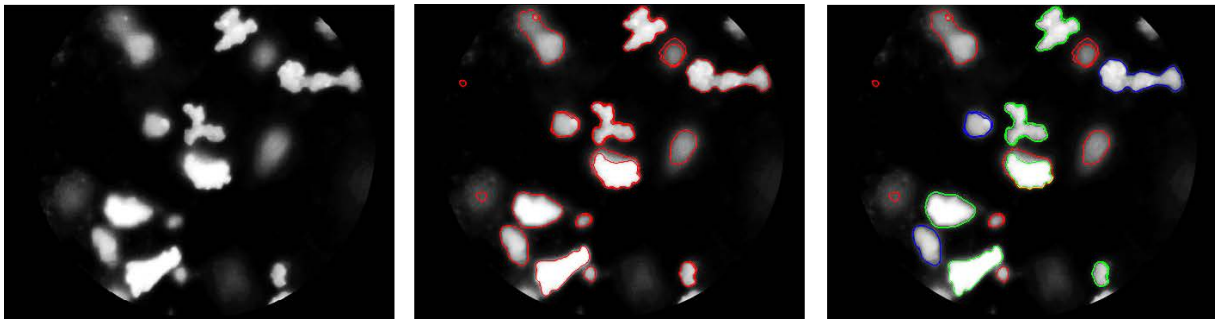

Fig. 1 image analysis steps for irregular shaped particles: (a) – original image; (b) – segmented image; (c) – classified image; only classified particles are used for the size distribution (green and blue; red are excluded)

The particle size and number are tracked over time and the information of the amount of foreign particles did lead to significant savings.

ECCE12
The 12th EUROPEAN CONGRESS OF CHEMICAL ENGINEERING
Florence 15-19 September 2019

Going digital changes the game – teaching fundamental chemical engineering for the digital age

I.-S. Porschewski[1]

1 Dr.-Ing. Ingrid S. Porschewski, Technische Hochschule Bingen, Berlinstr. 109, 55411 Bingen, Germany;

Highlights

- going digital requires a rethinking of education
- basic units have to be linked to show dependencies
- arrangement of knowledge and documentation of thoughts have to be dealt with

1. Introduction

Industrial settings change over time due to economic and environmental demands or new products. Today we find ourselves in a situation where data-sets and their interpretation is focused upon. The goal is to optimize process behavior as to stability of quality, maintenance and in case of multi-purpose-plants to switch the production process automatically. All this sounds familiar, although the working environment has changed. Modern software packages allow to simulate models, calculate statistics and look up data to manage the production on an everyday basis. This changes the speed of decision making and the kind and amount of knowledge which is needed to perform. On viewing this my colleagues and I decided to adapt the bachelor and master study courses accordingly. What followed was a turmoil of changes and a new concept of the courses which development is still in progress, since process engineering is on its way to create a digital twin.

2. Methods

In the former courses the topics were presented via static sheets, for each topic a problem was solved using a pocket calculator. Optimizations or variations of the problem were roughly estimated, some of the solutions were shown on slides or using an excel-worksheet. Graphs were drawn to show dependencies or to construct thermal stages. Handling of the pocket calculator, drawing the graphs and documenting the solution took more than 50% of the time. This led to a demonstration of idealized problems (only one basic unit in its clear definition). The students were in a receptive partly passive state and rarely interacted in a discussion. Yet, the lack of understanding was not clearly visible, routinely done calculations with some luck in guessing advanced questions was enough to pass the course. This dissatisfying situation was contradicted by experiences in supervising bachelor / master-thesis as well as lab-courses. Students worked in interdisciplinary teams, were interested in models and discussed their problems. A conceptual change was more than necessary.

For a deeper understanding of the theoretical background it is necessary to build a theoretical classification before working on an exemplary problem, otherwise a selective search for information or solutions would be hindered in future times [1]. Research on causes of study termination show that the main reasons are pressure to perform, dominance of formulas, irrelevance of topics and lacking supervision [2]. Countries with high scores in the TIMSS-study 2015 teach mathematics and

sciences by showing how the solution is achieved and allowing students time to try for themselves followed by a discussion and subsequent variations of the problem [3].

The idea was to create a course where the models can be used in a more creative way, this should lead to a way of technical thinking and posing the right questions. An independent working group found the same concept for a future work environment and called it “Funky Prototype” [4]. The idea to calculate with Excel-Worksheets was abandoned, although stage construction was quite comprehensive, because easy to use predefined functions and interdependence of worksheets was hard or impossible to handle. This would set a focus on programming skills not on mechanical and thermal engineering. The software used is MATLAB or for training at home the comparable freeware-tools OCTAVE and SCILAB. The models are held simple but can be used in a modular way, because they are included in predefined functions. Basic programming skills and commands to call for functions, graphs or other in- and output are taught in an introductory lecture. The first two solutions are explained in detail, then the way to solve the problem is briefly outlined before the students start on their own. The outcome is discussed and later an optimization or a different setting is explored.

3. Results and discussion

Most students are eager to follow and start to develop own questions and approaches while communicating more intensely with me and with each other. Insecure students need more support while interested students excel. The sensitivity of parameters is visible more easily and the problems later in the course resemble case studies. Surprisingly almost everything, including the presentation of the theory, had to be changed. Instead of bothering with an idealized approach, approximations are applied where thinking about a meaningful threshold value is important. Optimization and interpretation of the graphs is focused upon, which shows very clearly who understands the model and the concept. Usage of model-functions (e.g. thermal equilibrium, distributions of particles) is discussed in contrast with using experimental data.

4. Conclusions

The complexity of the problems is higher, which should to be handled with care. Control of basic units and consecutive units can be integrated in the future. The idea to create a learning environment like at starship “Enterprise” in the Star Trek series, where modular solutions are recommended by a board-computer and selected by an engineer who is solely responsible for arranging the information in a meaningful way, is enchanting. Questions as to how the decision is documented, data is treated and exams are to be taken are still discussed. Students need to acquire basic digital key competences as soon as possible but not later as during their Bachelor courses.

References

[1] Alfred Riedl, Andreas Schelten in R. Bader, P.F.E.Sloane, Lernen in Lernfeldern Theoretische Analysen und Gestaltungsansätze zum Lernfeldkonzept, Markt Schwaben: Eusl 2000, pp. 155-164

[2] Wibke Derhoven, Gabriele Winkler, „Tausend Formeln und dahinter keine Welt“. Eine geschlechtersensitive Studie zum Studienabbruch in Ingenieurswissenschaften in Beiträge zur Hochschulforschung, 32. Jahrgang 1/2010

[3] http://timssandpirls.bc.edu/timss2015/international-results/timss-2015/science/student-achievement/distribution-of-science-achievement/ from the 23.3.2019

[4] Norbert Kockmann, Chem. Ing. Tech. 2018,90, No.00,1-8

ECCE12
The 12th EUROPEAN CONGRESS OF CHEMICAL ENGINEERING
Florence 15-19 September 2019

Immersive learning: Way forward in chemical engineering education and operator training?

Jarka Glassey[1], Daniel Cermak-Sassenrath[2], Jean-Luc Dubois[3], Kevin Haelterman[4], Liesbeth Kester[5], Thies Pfeiffer[6], Michael Wilk[7], Tom van Gerven[8]

[1]School of Eng., Newcastle Uni, UK; [2]Center for Computer Games Research, IT Uni Copenhagen, [3]HR Dept, Arkema, [4]LuGus Studios, [5]Dept. of Education, Uni Utrecht, [6]Centre of Excellence for Cognitive Interaction Tech, Bielefeld Uni, [7]Performance Materials Operations Organics, Merk, [8]Dept of Chem Eng, KU Leuven

**Corresponding author: Jarka.glassey@ncl.ac.uk*

Highlights

- Benefits of immersive learning technologies in chemical engineering education highlighted.
- Overview of current attitudes to safety training provided.
- Challenges in measuring learning gain through these approaches discussed.

1. Introduction

Chemical engineering education is influenced not only by the significant changes in the process industries, including Industry 4.0 concept, but also in rapidly changing educational experiences and expectations of the future chemical engineers. A 2016 survey by Hanover Research and McGraw Hill Education shows that 84% of college students report that the use of technology improves their education, 81% report that digital learning technology helps save them time and be more efficient, and 81% claim that digital-learning technology is helping them boost their grades [1].

Digital game-based learning is an excellent tool to teach conceptual and procedural knowledge and competences in an interactive and participative manner, hence complementing conventional teaching methods in the acquisition of experience in meta-level thinking, on-going learning and constructive problem solving [2]. Digital games contribute to the intrinsic motivation of the student to learn; they appeal to intuition to learn complex and abstract concepts; and the methods that are applied are considered to be very relevant by the population under the age of 25, who are growing up in a digital and mediatized environment. Virtual reality (VR) technology increases implementation efficiency, as the interactive learning material is of a digital nature and can thus be distributed to (teams of) trainees more efficiently than physical training installations.

This contribution reports on a subset of activities of an MCSA ETN Charming, which addresses this challenge by developing learning strategies, content and prototypes for the application of games and VR/augmented reality (AR) for motivating, teaching and training children, students and employees in chemistry, chemical engineering and chemical operations (Fig 1). In particular, this contribution sets out to explore the benefits of games, VR and immersive learning in safety teaching and operator training. This research builds on the results of an EIT Raw Materials sponsored project, which explored the use of gaming in engaging young pupils in concepts of recycling and thus encouraging them into chemical engineering careers. The learnings from this project were invaluable in the development and the evaluation of the work reported here.

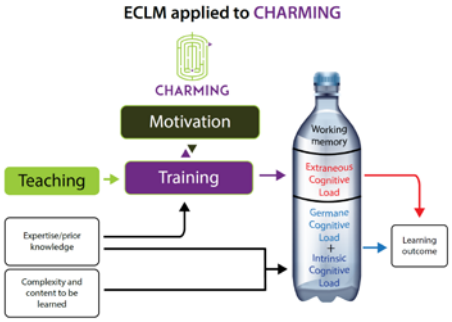

Figure 1. Motivation, Teaching and Training in the Updated and Extended Cognitive Load Model (adapted from [3]).

2. Methods

Review of current literature and case studies on the use of VR/AR in tertiary education and continuous professional development (CPD), together with latest developments in psychology, e.g. in the field of situational judgement, facilitated the development of the questionnaires to establish the current attitudes of students/operators to the use of technology for safety training. Statistical analysis of numerical responses, together with the thematic analysis of open text responses provides the starting point for the development of the VR/AR based safety training system.

3. Results and discussion

The previously mentioned research on gaming in inspiring young generation of chemical engineers by engaging them a highly topical area of recycling of various materials indicated high levels of engagement in an appropriately designed virtual environment can be achieved. With the technology savvy generation of University students and early stage professionals, this is a useful approach to engaging the professionals with the aim of increasing retention of knowledge. The analysis of industrial case studies using technology enabled safety training indicate positive impact of technology on retention of important concepts.

4. Conclusions

The VR training environment can present content for learning in new ways, thus providing grounds for creativity and innovation of new learning technologies based on an available platform. Simulation-based immersive VR training allows the trainees to explore the use of the simulated systems freely, learning about the effects and consequences, which provides them with more flexibility and deeper learning than case-based learning. This is particularly important in the highly ‘risk averse’ industry, such as the chemicals sector, where innovation is often stifled by (frequently overestimated) fear of safety issues associated with particular solutions. The results of the questionnaire analyses to establish current attitudes to technology enabled safety training will be presented. The challenges in measuring learning gain through these approaches will by highlighted in the context of these results and initial methodology of VR/AR enable training framework will be highlighted.

References [Calibri 10]

[1] Hanover Research and McGraw Hill Education (2016). Digital study trends survey. https://learn.mheducation.com/edtech_digital_study_trends.html
[2] C.I. Muntean, Proc. 6th Int. Conf. Virtual Learning ICVL, 2011, 323-329;
[3] H.H. Choi, J.J.G. van Merrienboer, F. Paas, Educational Psychology Review, 26 (2014), 225–244

ECCE12
The 12th EUROPEAN CONGRESS OF CHEMICAL ENGINEERING
Florence 15-19 September 2019

Birth of a Serious Escape Game for Chemical Engineering Labs

Lilian BEZARD[1], Marie DEBACQ[1], Astrid ROSSO[1]

1 Cnam, 292 rue St Martin, 75003 PARIS, France

**Corresponding author: marie.debacq@lecnam.net*

Highlights

- Increasing motivation to prepare labs.
- Promoting exchanges and cooperation between peers.
- Emulation through the game + emotions that promote learning.

1. Introduction

Starting from Japan, the United-States and different places in Europe, the escape rooms have flourished in the last decade, for fun adventure experiences with family or friends or for professional team building activities. Players work together in a team of few people, solve puzzles with the help of clues, in order to escape from a locked room, in a given period (usually about one hour). At the same time, the concept of gamification is developing in pedagogy. Nothing surprising indeed in the appearance of “serious escape games”.

It is often difficult to motivate learners to prepare the practical sessions. This is the starting idea of this project, currently under development: first experiment will take place in April-May 2019.

2. Methods

We first read some literature on the subject (for example [1-2]). Then we experimented card-based games such as Unlock [3] and Exit [4]. The playing team was composed of teachers and pedagogical engineers. During this stage, we tried to understand the “mechanics” of these games and identify types of enigmas that can be applied to a learning topic. The Mécanicartes [5] (under Creative Commons license BY-NC-SA and also provided in English and Dutch) are a relevant tool to understand and “husk” the game process. Then we set up a “scenario” for the game, based on reviews needed to prepare the labs and required preliminary calculations before moving to pilot plants experiments. We also found useful help on a French web site dedicated to pedagogical escape games [6].

3. Results, discussion and conclusions

are of course not currently available and will be presented during the congress.

References

[1] Alpár István Vita Vörös and Zsuzsa Sárközi, *Physics escape room as an educational tool*, AIP Conference Proceedings (2017) – https://aip.scitation.org/doi/pdf/10.1063/1.5017455

[2] Gaëlle Guigon, Jérémie Humeau and Mathieu Vermeulen, *A Model to Design Learning Escape Games: SEGAM*, Proceedings of the 10th International Conference on Computer Supported Education (2018) – https://hal.archives-ouvertes.fr/hal-01744860/

[3] https://www.spacecowboys.fr/unlock-demo
[4] https://www.iello.fr/fr/fiche/exit-le-jeu-le-laboratoire-secret
[5] http://www.mecanicartes.com/
[6] http://scape.enepe.fr/

ECCE12
The 12th EUROPEAN CONGRESS OF CHEMICAL ENGINEERING
Florence 15-19 September 2019

Mastering Digitized Chemical Engineering

Dr. Hermann J. Feise[1], Eric Schaer[2]
1 European Federation of Chemical Engineering, Rugby, United Kingdom and BASF SE, Ludwigshafen, Germany

2 Université de Lorraine, Nancy, France

**Corresponding author: Hermann.Feise@basf.com*

Highlights

- Digitization transforms the Chemical Industry rapidly across its entire chain
- New competencies will be required from chemical engineers to interact with new colleagues. The specific Engineering competencies needed for digitized Chemical Engineering are necessarily unknown, because of the fast-changing digital environment
- Data analytics tools will become standard engineering tools like CAD, FEM. The fundamentals will keep their importance, nevertheless.
- More and better lifelong learning will be required. Universities can and possibly must develop new offerings for the new learners.

1. Introduction

The chemical industry with its large world scale production units and its multi-purpose facilities is one of the energy-, raw materials- and capital-intensive industries, which currently face the challenges of the digital transformation. In these conditions, the chemical engineer's activities also have to evolve.

2. Digital Transformation

The digital transformation or Industry 4.0 is expected to change business models, allowing new efficiency gains and improving European competitiveness. In the chemical industry much of the key aspects of the digital transformation are not foreign: Internet of Things, Industrial Internet or automated ordering, have a strong history in process optimization and -automation. However, logistics and maintenance are the only two fields which have developed truly digital workflows. The way to a truly digitally transformed plant is still very long.

3. Skills and Competences

A digitally transformed chemical plant will lead to new challenges and new opportunities for chemical engineers. New tasks will be developed and colleagues with new competencies and different skills will work together with chemical engineers. This will require additive knowledge from the chemical engineer which are not part of today's engineering skill set, although some of them have been for previews generations of chemical engineers.

Drivers for the digital transformation can be found in various areas, e.g. data management systems, digital data, improved sensors for control, connectivity, simulation, spatial data. While the use of smart sensors for control has always been part of chemical engineering, neither their design or their use for simulation and optimization tools are mainstream chemical engineering tasks. Digital transformation will logically lead to the use and application of artificial intelligence systems in the industry, and should require, for example, strong knowledge and skills in (transient) simulation and optimization. This should also require an ability to critically evaluate the results provided by such systems.

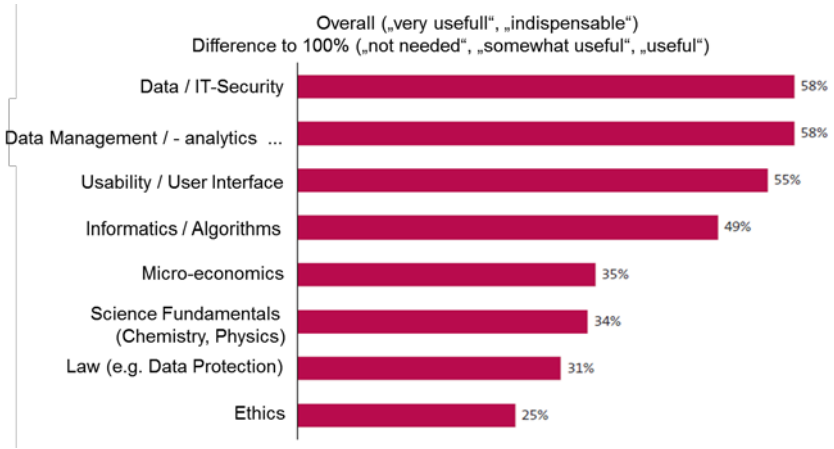

Figure 1. Industry 4.0 engineering knowledge outside the core [1]

4. Conclusions

The future chemical engineers will still have to demonstrate technical and management skills, taking into account ethics (global warming, resources depletion, well-being…) and economic aspects. The digital transformation should be seen as an opportunity, both for teaching and learning (use of virtual, augmented reality, contributions of artificial intelligence on acquisition of skills and knowledge…), as for the engineering practices, allowing to focus on innovation, interdisciplinarity and optimization.

The way to a truly digitally transformed plant is still very long, so far only logistics and maintenance have digitalized. Engineering competencies needed for digitized Chemical Engineering are necessarily unknown, because of the fast-changing digital environment. However, it will at least require: statistics, data models, data combination (vocabulary). Data analytics tools will become standard engineering tools like CAD, FEM. For the next decade we will still rely on data engineering experts, however.

Some new teaching topics should so be added in the curriculum, but as the first law of thermodynamics imposes, if the teaching duration remains unchanged, some other topics should then be removed. It is our responsibility, and interest to remain competitive and innovative, but also to meet social expectations, to think and anticipate these deep changes in the training of future chemical engineers.

References

[1] E Heidling et al.: Ingenieurinnen und Ingenieure für Industrie 4.0, Institut für Sozialwissenschaftliche Forschung e.V., München, 2019.

[2] VDI - Statusreport: „Bedeutung der digitalen Transformation für die chemische Industrie“, 2017.
[3] Wolfram Keller: Berufe 4.0 – Wie Chemiker und Ingenieure, in der digitalen Chemie arbeiten, Whitepaper, GDCh, 2018.

ECCE12
The 12th EUROPEAN CONGRESS OF CHEMICAL ENGINEERING
Florence 15-19 September 2019

Using supplementary screencasts in teaching computational tools to undergraduate chemical engineering students

Mazaher Molaei Chalchooghi*

Department of Chemical Engineering, University College London,
Torrington Place, London WC1E 7JE, United Kingdom
**m.chalchooghi@ucl.ac.uk*

Highlights

- Computational Tools in Chemical Engineering.
- Supplementary screencast videos.
- e-learning material.

1. Introduction

The application of screencast videos in teaching chemical engineering courses and their advantages have been reported [1], [2]. Screencasts are mainly used to enhance students' learning by giving them extra support through explaining certain topics or solving examples in short videos with narrations. One of the main advantages of using screencasts is that students with mixed abilities can benefit from these videos and replay them as many times as they need which will also increases student confidence [3]. This is also very useful for students with English as their second language, with hearing problem and dyslexic students.

Screencasts can either be used for flipping teaching approach [4], [5] or supplementary [6] to conventional teaching methods. In the latter, the videos are short (under 10 min) and are topic based to keep the attention of students. Also, short videos are more encouraging for students to go through this material. In this paper we will be reviewing the use of short screencast videos (~ 3 min each) as additional supplementary resources in teaching computational tools in chemical engineering.

2. Methods

In the Department of Chemical Engineering at University College London (UCL), we have already established using e-learning material to enhance students' learning in computational tools, and we have received very positive feedback from our students that it helped them to improve their learning [7]. Our undergraduate students receive some in–class lectures on use of computational tools (gPROMS, GAMS, MATLAB and Aspen Plus) followed by some computer lab tutorials. They also benefit from online-resources, which are particularly designed as supplementary material to give them extra support towards their learning, more specifically the details which cannot be covered during the in-class lectures due to the time restrictions.

After successfully implementing the use of e-learning material mainly in the form of self-learning lecture slides, the department has decided to also incorporate video learning materials in how we teach computational tools (gPROMS) in undergraduate core modules. The use of gPROMS in solving mathematical models, and in particular differential equations, of chemical process

engineering is integral to our undergraduate programmes, from Year 1 through to Year 4, during which they learn the main concepts and programming principles in gPROMS. The tool is introduced in an in-class lecture followed by two tutorials in Year 1. In Years 2 & 3 they experience advanced material only through the online resources. Yet more advanced topics are covered in Year 4 through a combination of in-class lectures and tutorials. This initial provision is now augmented by videos that have been developed by Process Systems Enterprise Ltd [8] and which are incorporated into, initially our Year 1, but will also be used for Years 2-4 going forward.

3. Results and discussion

The screencast material have very recently been introduced to our first year students and although we have received some positive feedback from those who have used this material, but we will receive more comprehensive feedback by end of the term. At the meantime, the main challenge could be encouraging students to go through this material as these are optional material and some students may not bother to approach the material. Details of students' feedback will be available to be presented in the congress. We will be reviewing students' performance through their in-class quiz (of gPROMS) and a coursework in a module known as Computational Modelling and Analysis. We will be comparing their performances to previous years which student did not have these screencast resources. We will also be tracking students' feedback and comments to Computational Modelling and Analysis, which usually happens at end of the term, and includes the use of gPROSM in solving model equations in this module.

4. Conclusions

The use of supplementary screencast material has been incorporated into teaching one of the computational tools for first year students in chemical engineering programme. So far, we have received positive feedback from students, but the details of the impact of these additional learning resources will be available by end of the term through their assessment results and also through the regular end of the term student survey.

References

[1] T. Pinder-Grover, K. R. Green, and J. M. Millunchick, "The efficacy of screencasts to address the diverse academic needs of students in a large lecture course," *Adv. Eng. Educ.*, vol. 2, no. 3, 2011.

[2] P. R. Hampson, "Use of screencasting to facilitate engineering course delivery," *Int. J. Mech. Eng. Educ.*, vol. 43, no. 3, pp. 191–206, 2015.

[3] G. . Nicodemus *et al.*, "Screencasts for enhancing chemical engineering education," *ASEE Annu. Conf. Expo. Conf. Proc.*, 2014.

[4] T. Marlin, "Flipping the Chemical Engineering Process Control Class with e-Lessons," no. 2014, pp. 1–24, 2018.

[5] M. V Jamieson *et al.*, "T HE U NIVERSITY OF A LBERTA C HEMICAL E NGINEERING C APSTONE D ESIGN C OURSE G OES F LIPPED !," pp. 1–6, 2015.

[6] C. M. Halupa and B. W. Caldwell, "A Comparison of Two Engineering Statics Courses: Traditional Lecture-based and Lecture-based with Online Supplemental Video," *Int. J. High. Educ.*, vol. 4, no. 1, 2015.

[7] M. Molaei Chalchooghi and E. Sorensen, "Supporting the use of PSE computational tools across a chemical engineering program," in *Computer Aided Chemical Engineering*, 2018, pp. 1651–1656.

[8] https://www.psenterprise.com/how-to-videos

ECCE12
The 12th EUROPEAN CONGRESS OF CHEMICAL ENGINEERING
Florence 15-19 September 2019

Education 4.0: Which changes can be foreseen regarding students, higher education institutions and industry?

Michael Wilk[1], Steve Rommel[2], Marcel Liauw[3], Willi Meier[4], Hans-Ulrich Moritz[5], Bernd Schinke[6], Horst-Werner Zanthoff[7]

1 Merck KGaA, Darmstadt, Germany; 2 Konica Minolta Business Solutions GmbH, Darmstadt, Germany; 3 RWTH Aachen, Aachen, Germany; 4 Dechema e.V., Frankfurt, Germany; 5 Universität Hamburg, Hamburg, Germany; 6 Hochschule Mannheim, Mannheim, Germany; 7 Evonik Technology & Infrastructure GmbH, Marl, Germany*

**Corresponding author: michael.wilk@merckgroup.com*

Highlights

- Need for change in education matters due to digital transformation / Industry4.0 highlighted.
- Changes in student learning behavior and expectations discussed.
- Changing role of HEI considered.
- Increasing significance of life-long-learning for industry reviewed.

1. Introduction

The impact of the 4th Industrial Revolution on our future working environment is supposed to be highly significant, which already triggered a broad social discourse. Apart from many more or less speculative assumptions around the magnitude of potential job losses or which job profiles will become obsolete, an intensified discussion on the essential change requirements in educational terms is observed.

Regarding process engineers (and similar education profiles), these change requirements have been discussed within the late 2017 “Educations Days” organized by the German ProcessNet section “Education and Innovation” and hosted by Dechema e.V. in Frankfurt.

2. Methods

A highly interactive discussion in World Café and Design Thinking formats was structured following three dimensions introduced by key notes:
a) HEI 4.0: what needs to be done to make higher education institutions more agile and adaptive?
b) Student 4.0: how can we describe the learning behavior of digital natives? What is the impact?
c) Industry 4.0: what is the need for change regarding life-long-learning during professional life?

3. Results and discussion

Results have been summarized in form of theses and a White Paper is under development.
Main theses will be presented in the conference.

4. Conclusions

Three theses may serve as examples of the outcome:

A) Mastering the engineering fundamentals will remain a core competency requirement for graduates from HEIs and must be addressed appropriately. Moving towards the “VUCA world” (volatile, uncertain, complex, ambiguous), this mastery will be key to assess and solve highly complex problems or those with very limited known facts.

B) “Digital Natives” have outstanding capabilities in using and learning from digital media and benefit strongly from collaborative learning environments. Therefore, certain modern teaching and learning formats are especially well suited to improve knowledge dissemination and maximize learning outcomes.

C) To maintain employability in times with ever increasing speed of knowledge development and changing job profile requirements, the life-long-learning framework needs to be fostered. HEIs are invited to develop educational programs and offers for professionals and need to be mandated for this purpose.

ECCE12
The 12th EUROPEAN CONGRESS OF CHEMICAL ENGINEERING
Florence 15-19 September 2019

An effective approach to embedded learning of professional skills contextualized in engineering practice.

Justin Siefker[1], Eva Sorensen[2]

1 Department of Chemical Engineering and Centre for Nature Inspired Engineering, University College London, London, United Kingdom;

2 Department of Chemical Engineering, University College London, London, United Kingdom

**Corresponding author: Justin.Siefker@ucl.ac.uk*

1. Introduction

Professional skills are an essential element of the modern engineering curriculum, and are required to provide graduates with the ability to competently approach the challenges of tomorrow. Even though professional skills are incorporated into engineering programs, employers still struggle to recruit graduates with sufficiently developed abilities. With industrial positions evolving in scope, do traditionally based educations adequately prepare students for the professional practice of engineering post-graduation? Unfortunately, even when professional skills are incorporated into engineering programs, this question persists as professional skills are often not embedded as integrated curricular themes facilitating continual, incremental development. While professional skills focused modules are essential for introducing new concepts, these modules are often non-technical in nature, and time-limited to a specific term. This approach routinely leads to a disjointed student experience, where professional skills are not applied within a real-world context and are disconnected from the broader curriculum, while constraining student development to a single term. On the other hand, directly embedding professional skills within core modules also leads to challenges, such as inconsistency of assessment format and evaluation criteria, tacit discouragement of incremental development, and application of professional skills in a manner not directly relevant to engineering in-practice. In particular, both approaches encourage the development of professional skills outside of a practical engineering or industrial context, and limit incremental development, as professional skills are practiced in unrelated contexts lacking a unified theme woven throughout the program. As a result, it is difficult to develop practical professional skills beyond a superficial level following these approaches.

In notable contrast to the above approaches, capstone design courses often foster significant development of practical professional skills. This often stems from the practical, integrated nature of engineering design. The quintessential design project incorporates and links core engineering theory, experimental results, process modelling, safety analyses, further impacts, and consideration of the broader context. The integration and delivery of such projects actively develops professional skills in a practical, professional context. Unfortunately, by this point of their studies, many students have already adopted poor habits, and must unlearn, acquire, and build professional skill competency within the duration of a single project. While capstone projects

enable effective development, due to their time-bound nature, they are not singularly adequate for preparing students to enter the engineering community.

2. Methods and discussion

Aside from industrial placements, design projects are often the closest to real-world practice students experience throughout their education. Acknowledgment of this reality provides the opportunity to develop an effective approach to embedding professional skills into an engineering curriculum from the onset of study. By embedding a coherent through-line of practical design, unified by a common theme and structure, the disadvantages of the classical approaches can be mitigated, and synergistic advantages arise. The elements to this approach include both professional skills focused modules and design projects embedded in core modules. Although, unlike the classical approach, the professional skill modules and embedded design projects serve only as part of a unified professional skills thread that builds rigor through the course of the program. In this manner, profession skills are holistically co-developed as essential elements of applied engineering in-practice.

3. Results and conclusions

An implementation of the discussed approach has become the favored method for professional skills development within the Department of Chemical Engineering at University College London (UCL). This approach has been enabled by the integration of a core through-line of practical design incorporate during each academic term. Multiple design projects are embedded in core modules each term and are facilitated as independent design sprints, with sequentially increasing rigor. The design projects are directly complimented by corresponding Design and Professional Skills modules, providing the requisite continuity for incremental development. The direct link between design projects and professional skills modules provides immediate context for taught professional skills, including engineering specific skills (e.g. safety evaluation, sustainability assessment, applied ethics). The success of this implementation is resultant of not only program structure, but also the structure of the design project sprints. Design projects are framed as a program nexus, with links throughout the program, and are perceived by students as independent milestones of the university experience. Herein, program structure and design project case studies will be critically discussed, focusing on both the successes and limitations of this approach.

ECCE12
The 12th EUROPEAN CONGRESS OF CHEMICAL ENGINEERING
Florence 15-19 September 2019

Systematizing experimental work by a template for electronic laboratory notebooks

Patrick M. Piccione[1,*]

[1] Syngenta, 4333 Münchwilen, Switzerland;

*Corresponding author: patrick.piccione@syngenta.com

Highlights

- The general structure of scientific experimental work was abstracted, and the necessary steps highlighted.
- A structured framework to facilitate planning and execution of laboratory work by supporting the scientific thought process was developed in an ELN environment.
- The resulting template is shared to enable further use and adaptation, together with a commented example.

1. Introduction

Science relies on "quality"[1] for the essential qualities that have led to its success: reproducibility, predictability, falsifiability. Careful experimentation can be very time-consuming. In today's team-based working environment, it is therefore valuable to share work approaches openly and consistently to maximize effectiveness and minimize misunderstandings.

Electronic laboratory notebooks (ELNs) have recently soared in popularity.[2] Prior contributions in this area have focused on procedural, hardware and information technology aspects.[3,4] In addition to practical benefits (storage, sharability, and integration), ELNs offer an opportunity to structure thought. Accordingly, a systematic framework was created and embedded in Syngenta's ELN. This article shares the methodology and template so as to enable adaptations and improvements.

2. Methods

The framework was developed with the assumptions of Table 1 in mind.

Philosophical considerations	The most general science is hypothesis driven. Scientific abstraction requires interpretation to be useful. A clear purpose optimizes the benefit of work.
Practical considerations	The framework must encourage discussion between several parties - by explicitly listing assumptions and approach is beneficial. A highly structured approach induces clarity of thought. Efficiency is a key driver, leading to advance planning

Table 1. Assumptions for template development.

These principles led to the general framework in Figure 1. Syngenta uses the "Electronic Laboratory Notebook" from Dassault Systèmes. A special tab was added, which by procedure must be discussed at least with the individual's manager before formal sign-off, and experimental work.

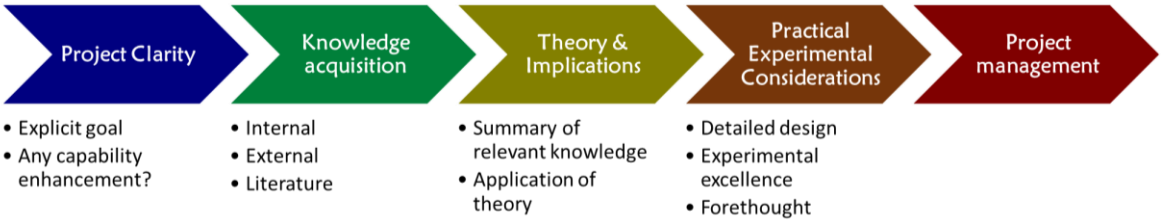

Figure 1. Successive steps in the ELN template.

3. Results and discussion

Actual experience, exemplified for mixing of a non-Newtonian fluid, showed that a compact document can be assembled with a moderate amount of effort. The compilation of relevant prior art and its implications enabled debate as well as the preparation of the later experimental work.

Strong managerial engagement to use and review the template during project discussions brought the approach alive. The best outcomes were obtained in "peer review"-type meetings. A mixed audience of both experimentalists and non-laboratory-based colleagues led to the best results. The ELN embedding allowed the framework to profit from the advantages thereof: sharability and formal validation steps; archival saving of additional insights and suggestions.

Some challenges in implementation also merit commentary. First, compiling and interpreting information takes time. Examples helped balance exhaustiveness and timeliness. Second, adoption was enhanced by writing the template steps in the natural order for performing the work.

The system has proven its value through use in many projects. By assisting scientific due diligence early on, it has ensured best long term use of resources. Specific examples include: pointing out the need for a more in-depth literature review; identifying additional measurements to be done; avoiding trials that were unlikely to lead to information; and emphasizing the calculations through which the information would ultimately be used.

Future opportunities include: the auto-generation of work reports; and modification for mathematical modeling. Different types of workflows, such as purely analytical work and academic exploratory work performed in the absence of theory, will also require adaptation.

4. Conclusions

A template has been devised to help systematize scientific work by clearly documenting: objectives; knowledge acquisition; relevant theory and its applications and expectations; and the resulting experimental considerations and plan. This framework, and its ELN implementation, enables systematic planning, as well as discussion and co-creation between researchers. The author invites others to adopt and adapt this new framework to systematize their own science workflows.

References

[1] R. Pirsig, Zen and the Art of Motorcycle Maintenance; William Morrow: New York, 1974.
[2] D. Garijo, O. Corcho, Y. Gil, Proceedings 7th international conference on knowledge capture 2013, 33-40.
[3] J. Zeng, H. Hillman, M. Arnold, Bioanalysis 2013, 3, 1501-1511.
[4] C. Bernlind, C. Urbaniczky, Org. Process Res. Dev. 2009, 13, 1059-1067.

ECCE12
The 12th EUROPEAN CONGRESS OF CHEMICAL ENGINEERING
Florence 15-19 September 2019

Are TRIZ and Mind Maps Two Sides of the Same Coin? Insights from a Chemical Product and Process Design Course

João Silva[1], Isabel João[2]

1 ISEL – Instituto Superior de Engenharia de Lisboa, Instituto Politécnico de Lisboa, CATHPRO/CQE, Instituto Superior Técnico, Universidade de Lisboa, Portugal; 2 ISEL – Instituto Superior de Engenharia de Lisboa, Instituto Politécnico de Lisboa, CEG-IST, Instituto Superior Técnico, Universidade de Lisboa, Portugal

**Corresponding author: jmsilva@deq.isel.ipl.pt*

Highlights

- TRIZ and Mind Maps (MM) for creative problem solving
- Creative product and process design teaching and learning with examples
- TRIZ and MM examples in Chemical Product and Process Design
- TRIZ and MM feature comparison to explore creativity development as a thinking skill

1. Introduction

In the last decades chemical engineering has undergone great changes due to the evolution of the so-called commodities for high value-added chemical products where the main issues are centered on its performance and quality [1]. Since many of the chemical products currently have little to do with the products developed a few decades ago, the portfolio of skills and technical knowledge required by the new chemical engineers has also been changing in recent years. Nowadays, chemical engineers work with a wide range of products not only commodity chemicals but mainly specialty chemicals, devices for chemical change and formulated products, this last classically classified to cover a large body of industrial sectors (e.g. paints, cosmetics, inks, pharmaceutical, personal care, household, food) [2]. It is central to prepare students for the more flexible, diverse and creative role that they are expected to perform in Chemical Product and Process Design (CPPD) activity, mainly because engineering students do not see their training as requiring much creativity [3].This work compares and contrasts TRIZ and Mind Maps to explore creativity development in ideas generation, a very important step in CPPD procedure.

2. Mind Maps and TRIZ in Chemical Product and Process Design

The TRIZ theory is based on the premise that creativity means finding a standard solution based on the premise that somebody somewhere has already solved the problem or one like it and adapting it to the current problem [4]. Genrich Altshuller developed TRIZ which is also known as TIPS and acronym of Theory of Inventive Problem Solving and known as Systematic Innovation because inventive solutions share common patterns, making TRIZ a problem-solving philosophy based on logic, data and research rather than on intuition. On the other hand, other types of creativity tools based mainly on intuition are widely used. Some of the methods usually applied for creativity enhancement are brainwriting and brainstorming that are used to develop creativity based on the assumption that a quantitative increase of ideas will bring a qualitative improvement and one

effective format to brainstorm generate ideas and get creativity development is the mind map [5] [6]. Looking at what is systematic innovation and for the intuitive processes of creativity it seems that these are at opposite poles with TRIZ suggesting a step by step excluding the intuitive approach and can be seen opposite to brainstorm and mind map techniques with try and error thinking. In this work we present examples from chemical product and process design course and we will use TRIZ and Mind Maps to explore creativity development and explore from the thinking skill perspective. Illustrative examples of mind maps are presented within the CPPD teaching and learning activities [7]. The potential of the maps to disclose students´ thinking about a topic of interest and to reveal connections and inter relationships between topics is highlighted as well as its role to develop student's creativity and thinking skills. Illustrative example of TRIZ in chemical Process Industry is presented with focus on the major challenges experienced by Chemical Process Industries to develop more sustainable processes [8]. Through a TRIZ illustration on how to deal with operational problems that can reduce energy efficiency of a distillation process the systematic innovation approach is explained (i.e. the contradiction matrix and the inventive principles).

Based on the examples developed within the DPP course, both creativity approaches (i.e. TRIZ and Mind Maps) are compared to identify the main differences and the linking issues. The main characteristics of each approach are described and the advantages of each are highlighted.

3. Conclusions

Despite the differences that exist between the systematic innovation of TRIZ and the intuitive processes of innovation where brainstorming and mind maps take place it can be concluded through the advantages identified in each method that the approaches are complementary and are the two sides of the same coin in creative problem solving and the combination can likely lead to creativity among students and development of higher order thinking skills.

References

[1] P.M. Saraiva, R. Costa, Trans IChemE, Part A Chem. Eng. Res. Des., 82(A11) (2004) 1474-1484.
[2] R. Costa, G.D. Moggridge, P.M. Saraiva, AIChE J., 52(6) (2006) 1976-1986.
[3] K.L. Hohn, in Proceedings of the 2010 Midwest Section Conference of the American Society for Engineering Education, http://www.asee.org/documents/sections/midwest/2010/19_Hohn.pdf.
[4] G.S. Altshuller, Creativity as an Exact Science. The theory of the Solution of Inventive Problems. Gordon and Breach Publishers, 1984.
[5] T. Buzan, Use Your Head. Innovative Learning and Thinking Techniques to Fulfil Your Mental Potential. BBC books, 1974.
[6] T. Buzan, B. Buzan, The Mind Map Book: How to Use Radiant Thinking to Maximize Your Brain's Untapped Potential. BBC books, 1993.
[7] IM. João, J.M. Silva, IJEP, 4(5) (2014) 42-48.
[8] I.M. João, J. M. Silva, IJoSI, 4(4) (2017) 15-25.

ECCE12
The 12th EUROPEAN CONGRESS OF CHEMICAL ENGINEERING
Florence 15-19 September 2019

Development of academics educating future generations of chemical engineers

Jarka Glassey[1], Fernando Russo Abegao[1], Sue Gill[2]

[1]School of Engineering, [2]Learning and Teaching Development Service,

Newcastle University, UK

*Corresponding author: Jarka.glassey@ncl.ac.uk

Highlights

- Benefits of a structured programme to assist engineering educators in their practice are highlighted.
- Overview of training activities is provided.
- Experiences of graduates of the programme demonstrate the added value of this training provision.

1. Introduction

Advances in learning technologies and the educational history and preferences of current generations of chemical engineering students increase the demands on the educators to develop their skills in new pedagogical methodologies, not just in technical aspects of their profession. In order to address current and future societal challenges, the future engineering professionals must be educated do develop into autonomous learners, capable of continuously acquiring new technical knowledge and essential professional competencies. Chemical engineering profession is particularly dependent on these characteristics to be fully developed in the graduates as soon as possible (preferably before graduation), although pedagogical literature clearly indicates the significant challenges in achieving these goals (e.g. [1]). Innovative pedagogical interventions, such as 'flipping' the classroom delivery and concentrating on the higher cognitive skills of the students have been identified as an effective method of deeper learning ([2], [3]). However, in order to achieve effective learning experience for the students, it is essential that the academics are confident not only in the technical aspects, but also pedagogical methodologies they need to implement. It is particularly pertinent with the move towards more technology enabled learning, when a range of tools and approaches is available to support the educators and the learners.

Newcastle University has been operating a structured programme of support and development of new-to-teaching academics for a number of decades now. This contribution will describe the structure of this training programme and highlight the experiences of the academics undertaking this course, both through the results of a survey of programme benefits and impact on the participants and through personal reflections of chemical engineering educators, who have completed the programme in recent years.

2. Programme structure

Certificate in Advanced Studies in Academic Practice (CASAP) programme aims to provide participants with the opportunity to critically reflect upon, evaluate, and develop their professional

practice as academics or support staff at Newcastle University in the light of relevant scholarship and research, responding positively to the institutional mission, the external context and the diversity of the student population. It also supports participants in developing appropriate knowledge and understanding, skills and professional values for academic practice; and the development of these, in alignment with the UK Professional Standards Framework [4]. In addition, it provides a fertile environment for participants to learn from and work effectively with colleagues from diverse academic backgrounds on matters of academic practice.

The programme brings together academics from all disciplines within the University, who undertake a series of modules including formal instruction of the latest pedagogical research developments in University-level education, technology enabled learning and assessment and practice these in active delivery of teaching. Participants are supported by experienced mentors (Faculty Programme Liaison Officers, FPLOs) – academics with long-standing experience and excellence in teaching. The assessment of the programme consists of a range of activities requiring reflection on personal practice that will be detailed during the presentation

3. Results and discussion

The effectiveness of the programme is regularly evaluated through the feedback questionnaires administered to the participants. In addition, a longitudinal evaluation of the programme was recently carried out to evaluate the long-term impact of this initiate upon the personal pedagogical practice of participants. These evaluations highlight that being observed and getting the feedback, meeting others from different backgrounds, having time to think about teaching and learning and having a professional standards adviser to talk with are highly valued by those that undertake this programme. In addition, the hands on delivery and 1:1 feedback from an observation, seeing others deliver in an engaging way, feedback on a video-recorded teaching activity, discussion and debate and working through ideas and issues with fellow teachers who do similar styles of teaching was seen a highly valuable practical support for future academic practice. In terms of pedagogical scholarship, learning about the range of learning theories and teaching methods that could extend my practice, talking to a range of teaching staff from other academic disciplines and having a teaching observation and the associated conversations and developing pedagogical vocabulary and familiarity with some teaching theories; sharing experiences; learning about new techniques; and being able to complete a project was highly valued. Detailed results and personal experiences of a chemical engineering participant will be shared during the presentation.

4. Conclusions

The importance of a structured training programme for new-to-teaching academics is highlighted through this contribution and supported by evidence from the participants. Details of the programme and the experiences of chemical engineering academics undertaking the training will be discussed in detail in the presentation.

References

[1] A. Mohan, D. Merle, C. Jackson, J. Lannin, S.S. Nair, IEEE Transactions on education, 53, (2009) 562-571
[2] M.B. Gilboy, S. Heinerichs, G. Pazzaglia J Nutrition education & behavior, 47, (2015) 109-114
[3] G.S. Mason, T.R. Shuman, K.E. Cooke, IEEE Transactions on education, 56, (2013) 430-435
[4] Higher Education Academy, (2011). The UK Professional Standards Framework for teaching and supporting learning in higher education. https://www.heacademy.ac.uk/ukpsf

ECCE12
The 12th EUROPEAN CONGRESS OF CHEMICAL ENGINEERING
Florence 15-19 September 2019

From Jamming to Fast Compaction Dynamics in Granular Binary Mixtures.

Salvatore Pillitteri[1,*], Geoffroy Lumay[1], Eric Opsomer[1], Nicolas Vandewalle[1]

1 GRASP, Institute of Physics, Building B5a, University of Liège, 4000 Liège, Belgium.

**Corresponding author: s.pillitteri@uliege.be*

Highlights

- The maximal compacity can be optimized with the relative mass fraction of the components.
- The compaction is highly dependent on the size ratio of the beads.
- A jamming transition is observed close to the percolation threshold.

1. Introduction

The compaction of granular materials under vibrations is a popular method for powder characterization [1]. The final compacity and the typical time of compaction of a powder can be correlated to its flowability [1,2]. While the compaction dynamics is often studied with identical spheres as model particles, the polydisperse case has been poorly investigated at our knowledge. In our study, we focused on binary mixtures of spherical glass beads. We analyzed the dynamics of those systems by measuring compaction, considering both the mass fraction of small beads f and the size ratio $\alpha = d_L/d_S$, d_L and d_S respectively the diameter of large and small beads.

2. Methods

In our study, we use the automated device GranuPack from GranuTools [1,3], illustrated on the left of the Figure 1. This instrument performs free falls of Δz and measures after each tap the height *h* of the granular column. The compacity η is obtained by dividing the bulk density $\rho_{bulk} = \frac{4m}{\pi h D^2}$ by the true density of the material, $\rho_{true} = 2500\ kg/m^3$ in our case. The compaction curve is then fitted with the logarithmic law (1), as seen on the right of the Figure 1, to obtain the final compacity η_∞ and the typical time of compaction τ.

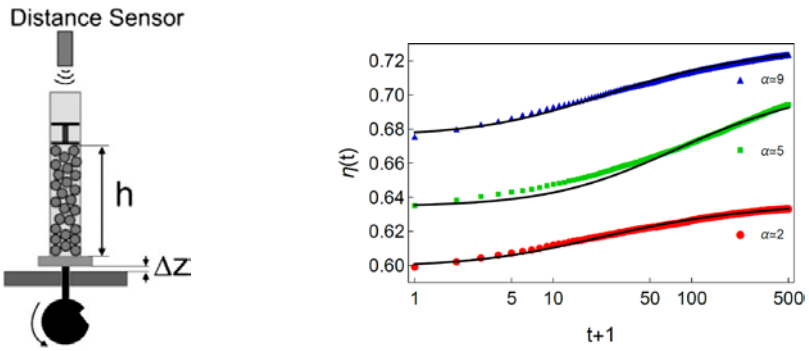

Figure 1. (left) Sketch of the experimental setup. (right) Exemples of three typical compaction curves for *f* = 0.2.

$$\eta(t) = \eta_\infty - \frac{\eta_\infty - \eta_0}{1 + \ln(1 + t/\tau)} \qquad (1)$$

3. Results and discussion

As many studies have shown, we observe that binary granular mixtures increase their maximal compacity with the size ratio of the beads. The evolution of η_∞ with f can be estimated by geometrical arguments [4,5], as seen on the left of Figure 2. Moreover, we observe experimentally a diverging typical time of compaction close to a critical size ratio $\alpha^* \approx 5.5$, as shown on the right of the Figure 2. This divergence appears in the vicinity of the percolation threshold $\alpha_c = 3 + 2\sqrt{3}$, when small particles can pass through the voids left by the large ones [6].

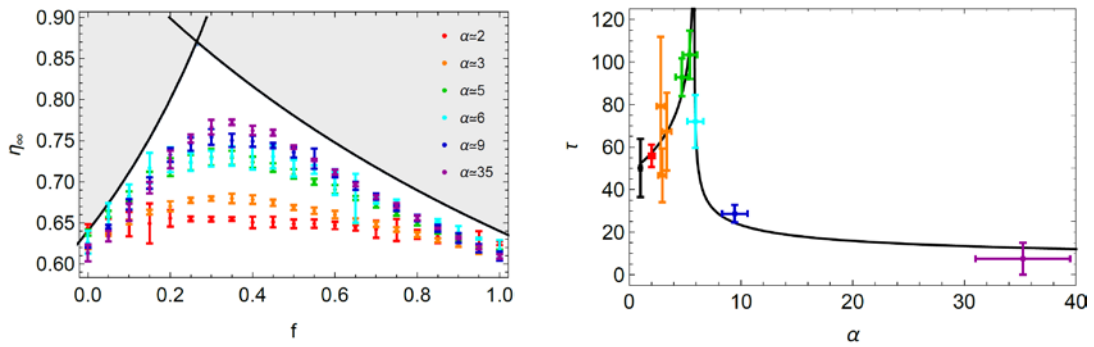

Figure 2. (left) Final compacity η_∞ depending on the fraction of small beads f for different size ratios α. (right) Typical time of compaction τ depending on the size ratio α for a fixed $f = 0.2$. The color code is the same for both graphics.

4. Conclusions

We studied the dynamics of compaction for various binary mixtures and evidenced a divergence of the typical time of compaction τ. This divergence seems to occur close to the percolation threshold and suggests that the jamming of the packing is maximum at this point.

References

[1] Lumay, G. et al. Measuring the flowing properties of powders and grains. *Powder Technol*. **224**, 19–27 (2012).
[2] Lumay, G., Vandewalle, N., Bodson, C., Delattre, L., & Gerasimov, O. Linking compaction dynamics to the flow properties of powders. *Applied physics letters* **89**, 093505 (2006).
[3] Traina, K. et al. Flow abilities of powders and granular materials evidenced from dynamical tap density measurement. *Powder Technol.* **235**, 842–852 (2013).
[4] Furnas, C. Grading aggregates-i.-mathematical relations for beds of broken solids of maximum density. Ind. *Eng. Chem.* **23**, 1052–1058 (1931).
[5] Prasad, I., Santangelo, C. & Grason, G. Subjamming transition in binary sphere mixtures. *Phys. Rev. E* **96**, 052905 (2017).
[6] Soddy, F. The kiss precise. *Nature* **137**, 1021 (1936).

Sustainable Performance and skills in Chemical Engineering 4.0

By Jean-Claude ANDRE and Eric SCHAER
LRGP-UMR7274 CNRS-UL, 1, rue Grandville – F54000 Nancy – France

When we enter in a process engineering classroom, what do we see? Is it in 2019 as in 2000 or 1960, close to the introduction of chemical engineering courses in France? The teacher stands at the front of the room, copying part of his/her notes, less and less often on the board, and more and more often using Power Point presentations, more or less personal, repeating aloud what he/she writes or presents on a screen.... Students sit, often passively, play with their mobile phones, a little less during the supervised exercises, which are essentially deductive, read more rarely, work on the homework of another class, or dream...

Understanding the learning environment invites us to consider the activity of today's learner in its intentional, instrumental and social components. This activity, in a formal or non-formal context, involves questioning the engineering of training systems, how to formalize processes, learning products and their evaluation. It is a complex set of approaches, not only because of the diversity of teaching methods on the one hand, but also because of the theoretical and epistemological frameworks used to describe and understand learning on the other. In Process Engineering, "teacher-researchers" are confronted with the lack of a framework for building their methods, both in terms of data production and analysis. What methods can be proposed? What criteria should be identified and defined to ensure their scientificity?

Today, the main axis of development of higher education institutions (and French Schools of Engineers) logically concerns the disciplines and contents of training. Graduates' professions are changing, sectors of activity are changing, and learners can no longer have the same skills and/or culture relative to the recent past. Among the current incremental trends, we retain the following aspects: occupation, sectors of activity, learners' cultures, the effects of spontaneous and stimulated pedagogical conservatism, etc. New knowledge is only placed on old knowledge without much change. Teaching is only partially successful: as soon as the conditions for learning are changed, common knowledge reappears. In other words, the student's mental representations are probably the main obstacle to teaching science subjects....

At the same time, our universe, which is globalized, but also weakened by different types of crises and trade wars, requires differentiated development of proactive, creative and supportive personalities: trained, through appropriate and varied accompaniments, to "juggle" variously with incessant new (artificial intelligence (AI)) or old topics, cognitive and methodological (complexity) objects, as well as material ones, without weighing down or bothering them, within a liberal and open civilization. Paradoxical tasks! Teachers and trainers can no longer be limited to mere masterful inculcations or binding and marginless imitations. They need a range of pragmatic modalities, gathered and certified cooperatively, following a progressive scientific research, in order to constitute a reasoned set of Methods and Instruments, Techniques and Values, Combinatorics and robust Modelling: that is, a varied, plural range of Engineering Sciences of training and education.

A forecasting analysis highlights various major trends (depletion of reserves, various types of pollution, clean processes, renewable energies, changes in trade, recycling, information inflation,

exploration of complexity, interdisciplinary projects, etc.). However, in the field of matter and energy transformation processes, we can observe the simultaneous presence of century-old processes (Sodium carbonate production, for example) at the same as recent activities in full development (additive manufacturing, some biotechnologies, etc.). How to manage such diverse temporalities and technological issues?

On this “simple” basis, the volume of information, which engineers are collectively called upon to know, is increasing considerably, faster than the ability of current curricula to take it into account.

This observation for an engineering domain that is rather difficult to attract students (in France), but which does not currently have any difficulty in placing graduates, raises a number of questions today:

1- How can the system of evaluating engineering education and training be made to understand the radical need to change working methods?
2- How can we anticipate a future that will have to take into consideration the complexity of the socio-technical systems covered by process engineering (PE)? How then can we support emerging problem-solving skills? How will the students be able to become successful researchers in PE?
3- How to encourage risk-taking and creativity in current training courses based on traditional deductive methods? How can it be adapted to anticipate and manage change?
4- With the development of the concept of Industry 4.0 and Artificial Intelligence, is there not a need to take this important contribution to training, saving time on basic teachings?
5- How to think about the transition concerning innovation on new processes resulting from research towards training?
6- How to take into account the notion of social and environmental responsibility in training?
7- Can we take into consideration the contributions of digital technologies to participate in training on the one hand, and in industrial development on the other? How to take into account the students' appetite for these new technologies?
8- How can we obtain "sustainable" engineers who will be able to participate in technological progress in their field of competence based on the answers to these various questions?

The increase in the knowledge required in the current disciplinary educational system, limited in time to a 3+2 year schooling, is not possible. Artificial intelligence can fill certain gaps, even more and better; it can then participate in an emerging process in the training of managers and in decision support. The emergence of AI is therefore an opportunity to rethink and relocate, in time and space, the exchanges between teachers and students, especially individualized ones. It is a world under construction that is becoming closer, going beyond the current “MOOC's” (Massive Open Online Course).

To achieve this objective, facilitators will be sought to develop the company's competitive subsidiarity, taking into account its processes and constraints (safety, supply, waste management, environment, society, etc.) as well as communication methods, a good estimate of current societal and technological movements, etc. So these are open proposals for reorienting the mission of process engineers?

It seems important that a student discovers the complexity of the subject matter of a practical question when leaving the (indispensable) disciplines learned, that he or she “goes beyond” the limits of his or her basic teaching to try to see the question in a way other than through disciplinary

filters. This is why it might be useful to introduce into a compartmentalized system the idea of a virtuous “circle” over various openings in order to achieve an updated performance... But in a world in profound change, are the characteristic times of the different changes compatible? To do nothing is a mistake, to do nothing is a risk taking! Then, let us follow Henri Bergson, a French philosopher who wrote: “Man is the only animal whose action is poorly assured, who hesitates and gropes, who forms projects with the hope of success and the fear of failure”. Let's dare...

The purpose of the presentation will concern, on the one hand, the factual elements present and envisaged in the future, but also proposals that could be the subject of questioning and debate with the GP audience.

ECCE12
The 12th EUROPEAN CONGRESS OF CHEMICAL ENGINEERING
Florence 15-19 September 2019

Analysis of Problem based learning (PBL) applied in heat transfer course for chemical engineering students.

Bustos-Gutiérrez Paola[1*], Saavedra Jorge[1], Reyes Laura[1]

1 Universidad del Bío-Bío, Departamento de Ingeniería en Maderas, Escuela de Ingeniería Química

Avenida Collao 1202, Casilla 5C, Concepción, Chile

**Corresponding author: pdbustos@ubiobio.cl*

Highlights

- PBL experience in heat exchanger design was successfully implemented.
- Third year students showed an important change in perception of acquired knowledge
- Leadership, autonomy and responsibility were determining aspects in collaborative work.
- Teams with good results were those with motivation and that saw their colleagues as source of knowledge.

1. Introduction

Today, Chemical process industries (CPI) have noticed that the difference between chemicals engineers they need and professionals who are being formed at universities is actually big [1]. CPI need people with skills like, team work, communication, creativity and critical think, among others. With this in mind, universities have gradually changed their educational models from "teacher centered" to "student centered". So, academics have been forced to change their classical lectures to the use of active methodologies.

Among many others, problem based learning (PBL) has shown be able to motivate students because PBL is based in real situations, so, students feel closer to professional world [2]. Also, specifically in engineering, it has been reported that PBL is an effective tool for significant learn and for acquire several soft skills needed in the current industry [3].

2. Methods

PBL intervention was done in heat transfer course for chemical engineering students who were in 3rd year (from 5,5 years). Teams with 4 o 5 students were formed and each one received a different practical problem. The main goal of all problems was the heat exchanger design. Students were characterized with Perry's inventory and a test of long learn skills [4]. PBL was performed in 8 sessions of 80 minutes each one. Teams analyzed problem, did brainstorming, defined learning objectives and thought about the best solutions that could be implemented. Evaluation was done in different ways and in different moments of PBL process, so, rubrics were constructed. Self and peer evaluations were considered too. At the end, students answered surveys that measured team work quality and their perception of acquired knowledge during the intervention.

3. Results and discussion

Perry's inventory shows the maturity of students in order to face PBL experience, in this work, they averaged a Perry´s level of 3,5±0,3, which is consistent with their academic level and implies they yet need some teacher accompaniment as guide learning [4]. Even this, it is important to mention that teams with the same Perry´s level did not always have the same performance.

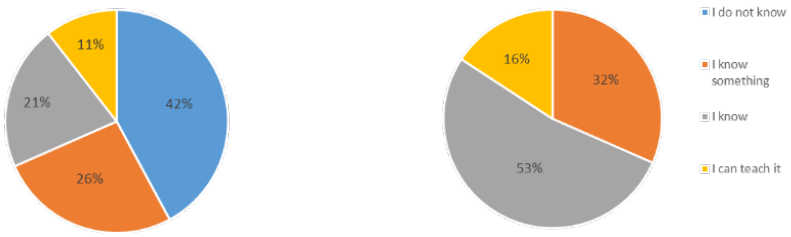

Figure 1. Percentage of responses to the statement "I know what overall heat transfer coefficient is"

Regarding the perception of knowledge, figure 1 shows the change produced in a particular conceptual aspect related to heat exchangers design. This behavior was repeated with other eight conceptual and proceeding aspects. There were no variations in attitudinal aspects, maybe because the time spent in this work was not so long. There were interesting changes in long learn skills, especially in seeing the peers as a reliable source of knowledge. Teams who improved in this aspect were who showed the best performance at the end of the experience. Concerning team work, leadership, was one of the important points associated to disagreement. Responsibility and autonomy in assigned tasks were an important source of conflict too. In spite of this, all teams finished the activity and 86% of students pointed PBL as a good methodology and strategy to do the connection between university courses theory and professional reality.

4. Conclusions

(i) In addition to Perry´s level, motivation and frustration management affected performance of the teams. (ii)The more conflictive aspects of collaborative work were: type of leadership, autonomy and responsibility. (iii) When students saw their peers as valid sources of knowledge, team work was improved. (iv) Most of students rated PBL experience as enriching, academic and personally.

References

[1] Ramírez, C. C., Zartha, J. W., Arango, B., & Orozco, G. L. (2016). Prospectiva 2025 de la Carrera de Ingeniería Química en algunos Países pertenecientes a la Organización de Estados Americanos (OEA). *Formación universitaria*, *9*(6), 127-138

[2] Northwood, M. D., Northwood, D. O., & Northwood, M. G. (2003). Problem-Based Learning (PBL): from the health sciences to engineering to value-added in the workplace. *Global J. of Engng. Educ*, *7*(2), 157-163.

[3] Hitt, J. (2010). Problem-based learning in engineering. Center for Teaching Excellence, United States Military Academy, West Point, NY.

[4] Woods,D.R (2006). Preparing for PBL. http://chemeng.mcmaster.ca/sites/default/ files/media/Woods-Preparing-for-PBL.pdf. Last access January 21th, 2019.

ECAB 5
The 5th EUROPEAN CONGRESS OF APPLIED BIOTECHNOLOGY
Florence 15-19 September 2019

A methodology to simulate the protein conversion rate and the degree of hydrolysis kinetics for enzymatic hydrolysis process

Sophie Beaubier[1,2], Claire Defaix[1,2], Xavier Framboisier[1], Olivier Galet[2], Romain Kapel[1]*

1 Laboratoire Réactions et Génie des Procédés, Université de Lorraine, CNRS, LRGP, F-54000 Nancy, France
2 Avril SCA, 11 rue de Monceau, F-75008 Paris, France
Corresponding author: * romain.kapel@univ-lorraine.fr

Highlights

- Identification of models for proteolysis kinetics was realized
- Kinetic terms were correlated with operating conditions (T, pH and E/S)
- Pareto front were generated toward cost and time of reaction

1. Introduction

Enzymatic proteolysis is an effective process to improve protein properties (digestibility and functionalities). However, the enzyme cost often remains a killer for industrial proteolysis implementation. Proteolysis kinetics and performances depend on several operating conditions (pH, temperature (T), ratio Enzyme/Substrate (E/S)). To date, there is a lack of rationality in proteolysis process implementation. Several approaches were proposed to model proteolysis kinetics. At the best, these approaches were able to predict degree of hydrolysis (DH) kinetics as a function of T and protein initial concentration or E/S. But to our knowledge, no methodology for multi-objective optimization (enzymatic cost and reaction duration) has ever been proposed.

The aim of this communication is to present a new methodology for establishing Pareto front (reaction duration vs enzymatic cost) of proteolysis with a given protease / protein couple at chosen protein conversion rate (Xp) or DH values. The proposed methodology was applied to the enzymatic hydrolysis of rapeseed albumins using Alcalase 2.4L. Because of its balanced amino acid profile and good functional properties [1], this isolate can be of interest as an alternative to animal proteins for food applications. However, its digestibility is poor, requiring a comprehensive study of its proteolysis.

2. Methods

The first part of the method consisted in a simulation of DH and Xp kinetics as a function of pH, E/S and T. In order to describe this complex system 3 assumptions were made: (i) Xp and DH kinetics follow 2nd order reaction models [2], (ii) maximum hydrolysis terms (Xp_{max} and DH_{max}) only depend on pH, (iii) hydrolysis kinetic terms (k_{Xp} and k_{DH}) depend on T, pH and E/S**.** Xp_{max} and DH_{max} were determined experimentally. k_{Xp} and k_{DH} were modelled as a function of the operating conditions by an original methodology. A full factorial design of experiments (DoE) with 3 factors (T, pH and E/S) was implemented. Proteolysis kinetics (Xp and DH) were monitored during 3 h in the conditions of the DoE matrix. Kinetics were monitored by a recently published method [3] and regressed using second order model to get the corresponding kinetic terms. Then, correlation models between operating conditions (T, pH and E/S) and kinetic terms were obtained by non-linear regressions. The second part of the method consisted in implementing the obtained models with genetic-evolutionary algorithms to generate the Pareto front. These front presented the best compromises between enzymatic cost and time of reaction for desired DH or Xp value.

3. Results and discussion

First, mean peptide size *vs* DH was studied in the operating pH and T range of Alcalase at E/S between 1/15 and 1/150 for rapeseed albumin hydrolysis by Alcalase. The same trend was observed, suggesting that the same proteolysis mechanism (one-by-one type) occurred whatever the operating conditions. Then the methodology described above was applied. Xp_{max} and DH_{max} varied between 89% and 100% and 15% and 23% respectively for pH ranging from 7 to 10. DoE methodology enabled to establish correlations between pH, T and E/S and the kinetic terms (k(Xp) and k(DH)). The ANOVA showed that the 2 models were reliable. R^2 for k(Xp) and k(DH) correlations were 0.9 and 0.85 respectively. Furthermore, p-value was inferior to 0.05 and no significant lack of fit was observed.

The simulation methodology was validated with experimental kinetics in two set of operating conditions totally different from DoE matrix and with different initial protein concentration. Relative errors less than 15 % were founded between the predicted and observed values of Xp and DH for the validation conditions (Figure 1A). Then, Pareto fronts were successfully generated for different DH and Xp values.

Finally, the best DH trade-off in terms of functional properties (emulsifying and foaming properties) and *in vitro* digestibility for rapeseed albumin hydrolysis with Alcalase was searched and found at 18% DH. The Pareto front was established as explained above (Figure 1B). The figure shows that 16 mg protease /g substrate could be saved for a prolongation of 1 hour of reaction (6 instead of 5 hours of hydrolysis) in order to get the targeted DH value.

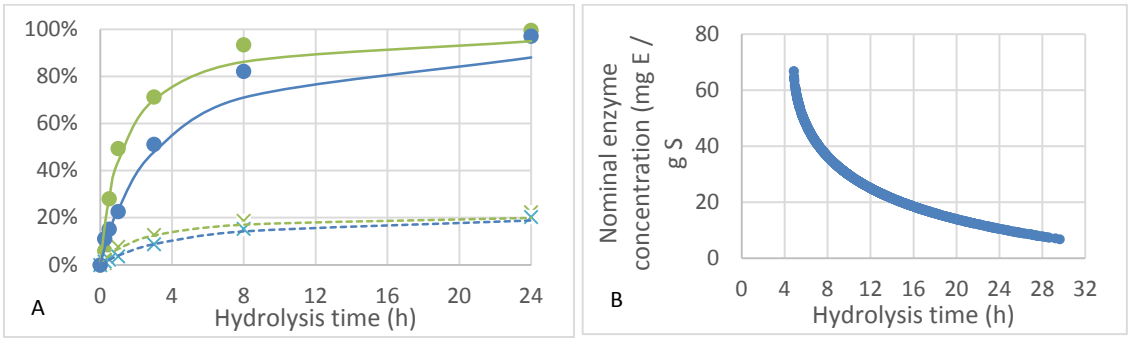

Figure 1. Experimental kinetics (cross type and round points) and predicted kinetics (dotted and solid lines) of Xp (round points; solid lines) and DH (cross type points; dotted lines) for validation points (S_0= 10 g/L in blue; S_0= 50 g/L in green) (A) and Pareto front generation (B) for DH value of the identified compromise digestibility/functionnalities.

4. Conclusions

The modelling study is a powerful tool to predict the Xp and DH values with defined operating conditions and for a given time in order to produce hydrolysates. That means significant time savings in order to characterize chosen hydrolysates toward functional properties or bioactivities (antimicrobial or antioxidant).

References

[1] Tan, S. H., Mailer, R. J., Blanchard, C. L., & Agboola, S. O. (2011). Canola proteins for human consumption: extraction, profile, and functional properties. *Journal of Food Science*, 76(1), R16-R28.
[2] Deng, Y., van der Veer, F., Sforza, S., Gruppen, H., & Wierenga, P. A. (2018). Towards predicting protein hydrolysis by bovine trypsin. *Process Biochemistry*, *65*, 81-92.
[3] Beaubier, S., Framboisier, X., Ioannou, I., Galet, O., Kapel, K. (2019). Simultaneous quantification of the degree of hydrolysis, protein conversion rate and mean molar weight of peptides released in the course of enzymatic proteolysis. *Journal of Chromatography B,* 1105, 1-9.

Hybrid modeling of bioprocesses: revisiting the direct identification method

José Pinto[1], Gerald Striedner[2], Rui Oliveira[1*]

1 REQUIMTE, FCT/Uni NOVA Lisboa, Portugal; 2 Dep. Biotechnology, BOKU University, Vienna, Austria

**Corresponding author: rmo@fct.unl.pt*

Highlights

- Modification of the direct identification method.
- Much faster and stable identification of hybrid models.
- Improved scalability of hybrid models to more complex biological systems.

1. Introduction

The general bioreactor hybrid model has been used many times to describe the dynamics of a bioprocess (e.g. Psichogios and Ungar, 1992, Oliveira, 2004). This model is primarily based on a set of material balance equations of the key substrates/products taking the form of a system of ODEs. The reaction kinetics such as the specific growth rate, m, substrate uptake, vs, and product synthesis rates, vp, are less defined parts of the model. They are the result of thousands of metabolic reactions regulated at different levels by genes, proteins and environmental factors. In hybrid models the rates are modeled by artificial neural networks (ANN) acknowledging the fact that they are too complex to be described mechanistically. The combination of ODEs with ANNs gives rise to so-called hybrid semiparametric models with particular identification challenges. Training the ANN linked with ODEs is not the same as a standalone ANN. There are two main methods to train the ANN: the direct (e.g. Tholudur & Ramirez, 1996) and the indirect method (e.g. Psichogios and Ungar, 1992). The indirect method is much more complex, slower and less flexible than the direct method but it typically produces more accurate and above all more stable results. For this reason it has been preferred in the literature.

2. Modified direct identification method

The direct identification is a two-steps method where the material balances and ANN are decoupled. In a first step the the biologic kinetic rates are calculated from the experimentally measured concentrations by solving the material balance equations (e.g. Tholudur & Ramirez, 1996). In the second step the calculated rates are used as target outputs for the training of the ANN. The training can proceed with standard techniques such as error backpropagation. In this study we propose the time integral of weighted least squares of volumetric reaction rates as cost function for ANN training in the second identification step.

3. Results and discussion

A synthetic data set was generated by simulation of a simple fed-batch bioprocess whereby biomass, X, grows on substrate, S, and produces product, P, over time, t. Gaussian noise was

added with a standard deviation of 0.3 g/L for all variables. These data are represented by the symbols in the upper panel plots of Fig. 1. The biologic kinetic rates were calculated from the concentrations by differentiation. Smoothing splines were applied to the concentrations X, S and P over time, followed by analytical differentiation of the splines function to obtain estimates of derivatives dX/dt, dS/dt and dP/dt at given time points. A Monte Carlo approach was adopted whereby the calculation of rates is repeated 100 times by adding Gaussian noise with s.d. of 0.3 g/L to the concentrations. This procedure resulted in the "experimental" reaction rates represented in the lower panel plots of Fig. 1. These data were set as target outputs of a 3-layered ANN with 1 input (substrate concentration, S) and 3 outputs (the specific rates). The results of the modified direct identification method are shown in the lower panel for the rates (full line is true property; dashed line is ANN prediction). Finally, the integration of ODEs coupled with the trained ANN resulted in the predicted concentrations shown in the upper panel plots (full line is true property; dashed line is ANN prediction)

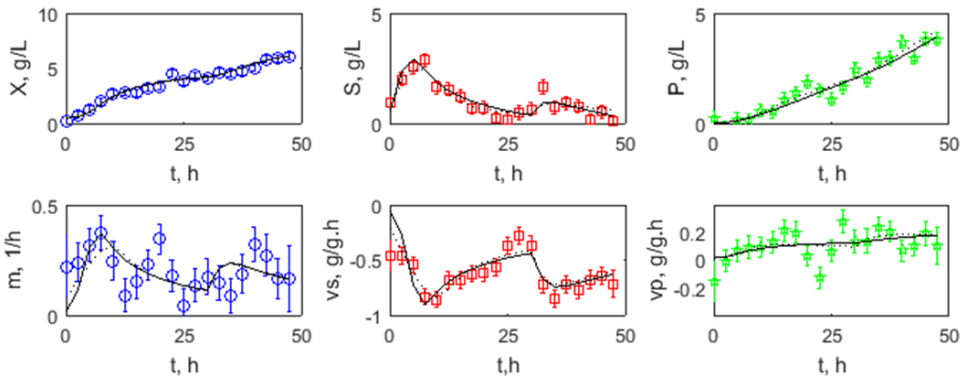

Figure 1. Hybrid modeling results using the direct identification approach. Symbols are measurements, full line is true property and dashed line is the respective hybrid model prediction. Upper panels from left to right represent concentrations of biomass (blue), substrate (red), product (green) over time. Lower panels represent from left to right the specific growth rates of biomass (blue), substrate (red) and product (green).

4. Conclusions

As seen in the results the modified indirect identification method enabled an almost perfect identification of the specific reaction rates (comparison between the full and dashed lines). Equivalent results are however also obtained with the classical direct approach. The most remarkable result is the fact that the integration of ODEs+ANN (i.e. the full hybrid model) resulted in almost perfect identification results in terms of concentrations. Opposed to this, the traditional direct identification method typically fails in the prediction of concentrations. Thus we conclude that the modified direct method has similar performance to the currently preferred indirect methods. This is very significant as the scale and complexity of hybrid models can be largely augmented by applying a much faster and much more flexible direct identification methods.

References

[1] D.C. Psichogios, L.H. Ungar, AIChE. J. 38 (1992) 1499–1511.
[2] R. Oliveira, Comp Chem Eng, 28 (2004) 755-766.
[3] A. Tholudur, W.F. Ramirez, Biotech. Prog., 12 (1996) 302-309

ECCE12
The 12th EUROPEAN CONGRESS OF CHEMICAL ENGINEERING
Florence 15-19 September 2019

Microalgal biorefinery approach: integration and co-optimisation of the different unit operations.

Imma Gifuni[1]*, Antoinette Kazbar[1], Luc Marchal[2], Anthony Massé[2], Jérèmy Pruvost[1,2], Olivier Lépine[1][Calibri 12]

1 AlgoSource Technologies, 37 boulevard de l'Université, 44600 Saint-Nazaire Cedex, France ;

2 Genie des Procédés en Environnement et Agroalimentaire, Université de Nantes, UMR CNRS 6144, CRTT, 37 boulevard de l'Université, 44600 Saint-Nazaire Cedex, France.

**Corresponding author: imma.gifuni@algosource.com*

Highlights

- Highest energetic performances of bead milling are for inlet cell concentration ≥ 50 g/L
- Separation and purification steps are negatively affected by the optimal BM parameters
- Integrated optimization is required as well as techno-economic analysis.

1. Introduction

In the last years microalgae production attracted rising interest and a peak of governmental and industrial investment mainly aimed at green and sustainable food/feed and pharmaceutics production. Large segment of the current market involves the production of raw and entire biomass and only few high-value products extractions. One of the issues limiting the use of algae feedstock for several industrial fields (food, beverages, bio-plastics and bio-materials, cosmetics) is the lack of optimized downstream technology for microalgae components fractionation at industrial scale [1]. In this study, the fractionation of soluble and not soluble product is investigated for the widely recognized microalga *Chlorella vulgaris*. In particular, bead milling is used as cell disruption technology then, centrifugation and membrane filtration are applied for water soluble product separation and purification.

2. Methods

Microalgal strain

The microalgal strain used in this study was *Chlorella vulgaris*. The biomass was gently provided by MIAL (Germany) in the form of paste 20% dry matter.

Bead milling cell disruption

Disruption experiments were performed by bead milling (*Dyno-mill multi lab*) operated in pendulum mode, at temperature of 20°C, flow rate of 200 mL min^{-1} and filling ratio of 80%. Beads density, beads diameters, the rotation speed and initial biomass concentration were varied in order to test different stress intensities. Specific energy requirement for the 90% of cell disruption was calculated according to Montalescot et al. [2]:

$$E_m \propto \frac{SN_{0.9} \cdot SI}{m}$$

Centrifugation

Centrifugation parameters (speed, g and time, min) were chosen in order to meet the availability in the existing large-scale facility of GEPEA (Algosolis): 8000 g for 20 min.

Membrane filtration

The filtration process was conducted with a pilot scale filtration plant. All membranes used (0.22 µm and 3 kDa) were made of ceramic to minimize interactions between the compounds and the membrane. The transmembrane pressure (TMP) was arbitrary fixed at 2 bar for 0.22 µm membrane and 5 bar for 3 kDa which corresponds to classical transmembrane pressures for such operation. The recirculation flow rate was fixed at 250 L h^{-1}.

Biochemical analysis

The entire biomass, the solid and liquid fractions obtained from the different downstream steps were analysed for proteins, pigments, sugars and lipids content according to AOAC methods.

Technoeconomic analysis

A complete biorefinery model was proposed for the adopted strain. The techno-economic feasibility of the process was tested using the software SuperPro Designer (Intelligen Inc.).

3. Results and discussion

The combination of bead milling/centrifugation/membrane filtration was analyzed for *Chlorella vulgaris*. Optimal bead milling parameters (0.5 mm glass beads, filling ratio 80%, rotational speed of 8 m/s) and biomass concentration (150 g/L) were identified for soluble proteins release in the water fraction and for low energy consumption related to disruption step. Theoretical and experimental studies showed the impossibility of processing the lysate obtained if the optimization is solely done on bead milling. Indeed, the following centrifugation at large scale produced a liquid fraction characterized by intense green colour, high viscosity, presence of numerous small particles. The nature of the liquid fraction also prevented the exploitation of membrane filtration as solvent-free purification technology. A new refining model was proposed and validated by techno-economic analysis.

4. Conclusions

The optimal yield and energetic performances of a single downstream step (bead milling) rarely produce the optimal raw material for the following purification or transformation steps. Different solutions have been proposed and the techno-economic feasibility of the new bio-refinery process was proved.

References

[1] I. Gifuni, A. Pollio, C. Safi, A. Marzocchella, G. Olivieri, Trends Biotechnol (2019).

[2] V. Montalescot, T.Rinaldi, R.Touchard, S.Jubeau, M.Frappart, P.Jaouen, P.Bourseau, L.Marchal, Biores Technol, 196 (2015), 339-346.

ECAB 5
The 5th EUROPEAN CONGRESS OF APPLIED BIOTECHNOLOGY
Florence 15-19 September 2019

Development of a Hybrid Ozone-Biological Process for the Treatment of Drill Cuttings: Microbial Consortium Characterization and Dynamics.

Argyro Tsipa[1], Ioannis Vyrides[1], Kostas Andreou[1], Giorgos Kazamias[2], Michalis Chatzicharalampous[2], Costas Varavvas[2], Michalis Koutinas[1]

1 Department of Environmental Science & Technology, Cyprus University of Technology, 30 Archbishop Kyprianou Str., 3036, Limassol, Cyprus; 2 Innovating Environmental Solutions Center, 33 Spyrou Kyprianou str, 3rd Industrial Area of Ypsonas, Ypsonas 4193, Limassol, Cyprus

**Corresponding author: michail.koutinas@cut.ac.cy*

Highlights

- Isolation of microorganisms adapted to drilling fluids.
- Microbial consortium characterization using next-generation sequencing.
- Monitoring of microbial consortium dynamics using quantitative polymerase chain reaction.

1. Introduction

The entire eastern Mediterranean is swimming in huge untapped oil and gas (O&G) reserves. Thus, drilling operations have recently increased considerably in Cyprus necessitating the safe disposal of drill cuttings (DC) currently posing important waste management and environmental problems mainly due to the vast quantities generated and the high content in contaminants. IESC Ltd and Cyprus University of Technology currently aim to develop an enhanced hybrid ozone oxidation-bioremediation system at pilot-scale for DC treatment producing added-value compost as well as a consortium of microorganisms with applicability in bioremediation of similar waste.

The study of population dynamics through qPCR may quantify the expression of specific metabolic routes involved in the biodegradation of different pollutants [1]. Furthermore, metagenomic methods, such as Next Generation Sequencing (NGS), employed for assessing the composition of entire environmental communities in a variety of microbial habitats have resulted in discovering new genes and gene products from uncultivated microorganisms, assembling whole genomes [2]. Recent NGS studies applied in hydrocarbon bioremediation processes have shown the crucial effect of these techniques in identifying, monitoring and estimating the proportions of degrading populations during soil bioremediation providing information for novel biocatalysts and enzymes involved [3].

The proposed waste management technology is expected to significantly reduce current thermal processing costs, while the company aims in eventually moving the novel technology for DC management to full scale and to increase its competitiveness through production of added-value commodities. The work is part of the OzoneBioPro project, which is funded from the Research Promotion foundation of Cyprus.

2. Methods

Operation of the pilot system: DC treatment involved ozonation in a 0.3 m^3 reactor followed by bioremediation (1 m^3 each installation) through composting with the addition of green waste and activated sludge. Various process parameters in ozonation and bioremediation were evaluated.

Molecular biology techniques: Total RNA isolation, cDNA synthesis and Quantitative Real-Time Polymerase Chain Reaction (Q-RT-PCR) was conducted as previously described [4].
Isolation of microbial degraders: Samples of untreated DC including oil contaminated soil and activated sludge, respectively, were used. The isolation procedure was conducted using minimal medium (M9) supplemented with drill cutting fluid following the procedure applied in [1]. The microbial isolates were identified through DNA extraction followed by PCR amplification, while the PCR products were sequenced using Next-Generation sequencing (Macrogen, the Netherlands). Analysis of obtained sequences was performed using the BLAST NCBI database.

3. Results and discussion

The objectives of the development of the hybrid ozone oxidation-bioremediation technology are explained in Fig. 1. Currently, the isolation of microbial degraders adapted to DC is finalized and the hybrid pilot unit has been designed and constructed at the premises of IESC Ltd in Limassol (Cyprus). The presentation will include evaluation of the performance of the ozonation-bioremediation system for DC treatment, evaluation of the microbial dynamics in the bioprocess using NGS and qPCR as well as characterization of the microbial consortium constructed for enhancement of DC bioremediation.

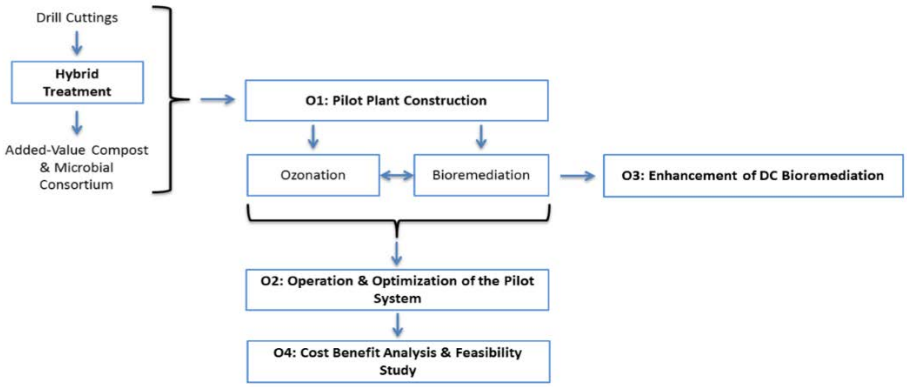

Figure 1. Outline of project objectives.

4. Conclusions

Application of NGS and qPCR for monitoring the microbial diversity, the genomes of all microorganisms incorporated and expression from specific metabolic routes in DC bioremediation will progress research beyond the current state-of-the-art through correlation of microbial diversity with the efficiency of bioremediation under different process conditions.

References

[1] E.M. Drakou, M. Koutinas, I. Pantelides, M. Tsolakidou, I. Vyrides, Int. Biodeterior. Biodegrad. 99 (2015) 85-94.
[2] J. Frias-Lopez, Y. Shi, G. W. Tyson, M. L. Coleman, S. C. Schuster, S. W. Chisholm, E. F. DeLong, Proc. Natl. Acad. Sci. U.S.A. 105 (2008), 3805-3810.
[3] G. Zafra, T. Taylor, A. E. Absalón, D. V.C ortés-Espinosa, J. Hazard. Mater. 318 (2016) 702-710.
[4] M. Koutinas, M. Lam, A. Kiparissides, R. Silva-Rocha, M. Godinho, A.G. Livingston, E.N. Pistikopoulos, V. De Lorenzo, V.A.P. Martins Dos Santos, A. Mantalaris, Environ. Microb. 12 (2010) 1705-1718.

ECAB 5
The 5th EUROPEAN CONGRESS OF APPLIED BIOTECHNOLOGY
Florence 15-19 September 2019

Aerosol Photobioreactors: a New Possibility for Cultivation of Phototrophic Biofilms.

Judith Stiefelmaier[1], Dorina Strieth[1], Björn Wrabl[1], Roland Ulber[1]*

1 Chair of Bioprocess Engineering, TU Kaiserslautern, Gottlieb-Daimler-Str. 49, 67663 Kaiserslautern, Germany

**Corresponding author: ulber@mv.uni-kl.de*

Highlights

- Terrestrial cyanobacteria are versatile organisms but only sparsely investigated.
- Aerosol photobioreactors for surface-associated cultivation of terrestrial biofilms.
- Investigation of biofilm growth under varied cultivation conditions possible.
- Investigation of surface-adhesion of biofilms on different substrates.

1. Introduction

Cyanobacteria, belonging to the oldest known microorganisms, are a diverse group of phototrophic bacteria with a wide product spectrum. For instance, cyanobacterial biomass is already used as food additive and pigments can be used as natural stains in foods, cosmetics or clothing, which fits costumer preferences. Several antimicrobial substances have already been discovered in different cyanobacterial strains and in their extracellular polymeric substances (EPS). In addition, EPS amongst others contain various polysaccharides. A subcategory of cyanobacteria represent the so-called terrestrial cyanobacteria. Those generally grow in biofilms embedded in EPS and are attached to air-exposed surfaces such as stone, soil or bark. However, due to a lack of suitable cultivation systems, terrestrial cyanobacteria have only been sparsely investigated. The emerse photobioreactors (ePBR) developed at the Chair of Bioprocess Engineering (TU Kaiserslautern, Germany) provide a possibility for the surface-associated cultivation of terrestrial cyanobacteria with media-supply via an aerosol [1]. This enables the more detailed investigation of terrestrial cyanobacteria with the prospect of finding new products.

2. Methods

The hexagonal emerse photobioreactor (hePBR) (see Figure 1 A) consists of a hexagonal glass vessel with a plastic lid, a holding for three variable cultivation surfaces and several connections. Due to the reactor geometry the biofilm on the cultivations surfaces can be lighted uniformly with LEDs. The aerosol for media-supply is generated in an extra vessel by an ultrasonic transducer based on a patent by Schmidt and Just [2] and subsequently transferred into the reactor vessel. After cultivation in the hePBR the cyanobacterial biomass was analyzed concerning EPS and pigment content. To evaluate biofilm adhesion to the cultivation surface, grown biofilms were overflown with liquid medium at different flow speeds. Biofilm deformation and peel off were documented by optical coherence tomography (OCT).

3. Results and discussion

Cultivations in the hePBR were conducted successfully at different temperatures, on different substrates and with different wavelengths of light. Hereby, the effect on biomass and EPS formation and pigment composition was investigated. Variations of cultivation conditions revealed a differing impact on biomass productivity as well as on EPS content (Figure 1 B). Furthermore, by varying light wavelengths pigment composition and content could be influenced (data not shown). Increasing adhesion of the biofilm to the cultivation surface during emerse cultivation could be shown by OCT while applying different flow velocities. This set-up allows the comparison of adhesion to different substrates and of different cyanobacterial strains.

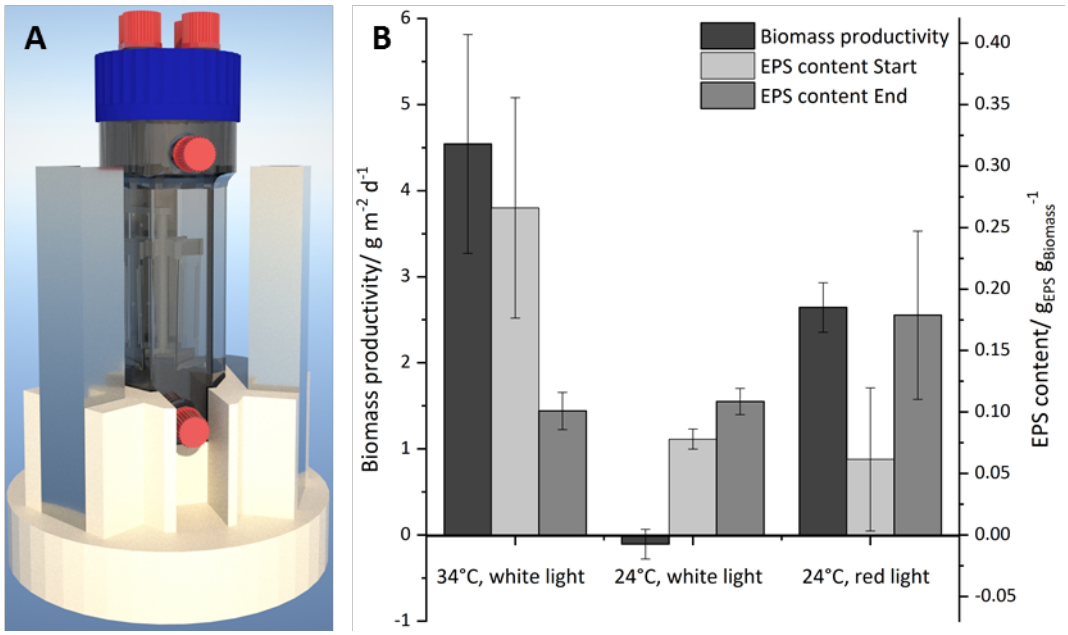

Figure 1. A: CAD model of the hePBR; B: Effect of different temperatures and light colors on biomass productivity and EPS content of *Coleofasciculus chthonoplastes*

4. Conclusions

The hePBR offers a possibility for surface-associated cultivation of terrestrial cyanobacteria. This allows the enhanced research of these microorganisms under conditions mimicking their natural habitat, which can help discovering further potential products.

References

[1] D. Strieth, J. Schwing, S. Kuhne, M. Lakatos, K. Muffler, R. Ulber, A semi-continuous process based on an ePBR for the production of EPS using *Trichocoleus sociatus,* Journal of biotechnology 256 (2017), 6–12.

[2] T. Schmidt, L. Just, Vorrichtung und Verfahren zur Kultivierung und Generierung von biologischem Material in einem Nährstoffnebel; 2006, WO2007068467A1

This project was financially supported by BMBF (031B0068D) and DFG (UL 170/16-1).

Simultaneous saccharification and fermentation of LX-cellulose for the production of high optical pure L(+)-lactic acid

Linda Schroedter[1], Friedrich Streffer[2], Peter Unger[1], Joachim Venus[1*]

1 Leibniz-Institute for Agricultural Engineering and Bioeconomy (ATB), Department of Bioengineering, Max-Eyth-Allee 100, 14469 Potsdam, Germany;
2 LXP Group GmbH, Rheinstr. 3, 14513 Teltow, Germany

**Corresponding author: jvenus@atb-potsdam.de*

Highlights

- L-lactic acid of optical purity >99% is produced from lignocellulosic biomass.
- Time of inoculation has influence on the overall yield of the SSF process.
- Using the SSF-process enables to decrease process durations <24 h.

1. Introduction

Lignocellulosic biomass is an abundant and inexpensive renewable material which does not compete with the production of food. Several lignocellulosic waste streams of agro-industrial processes yet bear the possibility to be valorized. In this study, lignocellulosic biomass was utilized as an alternative sugar source for the fermentative production of high optical pure L(+)-lactic acid (L-LA). The recalcitrant nature of the lignocellulose was overcome by the patented LX-pretreatment [1]. Mild process conditions reduce the formation of furfural or hydroxy-methylfurfural (HMF) which enhances the subsequent fermentation. Simultaneous saccharification and fermentation (SSF) is performed, employing the thermophilic bacterium *Bacillus coagulans*. Low pH and high temperature regime of the SSF allow the process to be operated under non-sterile conditions.

In classical SSF, enzymes and inoculum are added simultaneously to the vessel [2]. Additionally, fed-batch studies developed effective feeding schemes using various time points for supplement of enzyme or inoculum [3]. Nevertheless, a systematic approach is needed to understand the influence of delayed inoculum supplement to the enzyme reaction. This study aims to contribute to the development of optimized feeding schemes for SSF of lignocellulosic substrates.

2. Methods

The lignocellulosic feedstock that was used in our experiments was the fibrous effluent of an anaerobic digestion plant fed with corn silage. Pretreatment was done by the LXP Group GmbH at a dry matter content of approx. 80% employing the patented LX-method [1]. The lignocellulosic biomass was dissolved in 75 - 80% phosphoric acid at 60 to 75 °C at a ratio of approx. 1:3 (w/w) for 15 - 45 min at ambient pressure. After the dissolution was complete the carbohydrates were precipitated leading to a process stream referred to as LX-cellulose.

With this LX-cellulose, SSFs were carried out at ATB in 1 L-scale using the enzyme CellicCTec2® (Novozymes A/S, Denmark) and the thermophilic bacterium *B. coagulans* isolate A166 at 50 °C and pH 5 adding 10 g L^{-1} yeast extract as nutrient and 20% (w/w) NaOH for pH regulation. In contrast to classical SSF in which enzymes and inoculum are added at once, we also performed "delayed SSF" experiments by adding inoculum subsequently to the enzymes at different time points (0, 6 and 12 h).

3. Results and discussion

The "delayed SSF" strategy yielded in L-LA with 99.5% optical purity. Our experimental results showed that by delaying the addition of the inoculum an improvement on the overall yield of the process was achieved. Figure 1.A shows that a delay of 6 h can enhance overall yield to 10% (t = 12 h). The overall yield is given as produced lactic acid divided by the total sugars that could potentially be released from the substrate (in g_{LA} g_{Sug}^{-1}). Furthermore, from Figure 1.B it can be stated that with *B. coagulans* A166 SSF process durations of <24 h are possible. This is also due to the fact that the mild conditions of the LX-method reduce the formation of growth inhibitors during pretreatment.

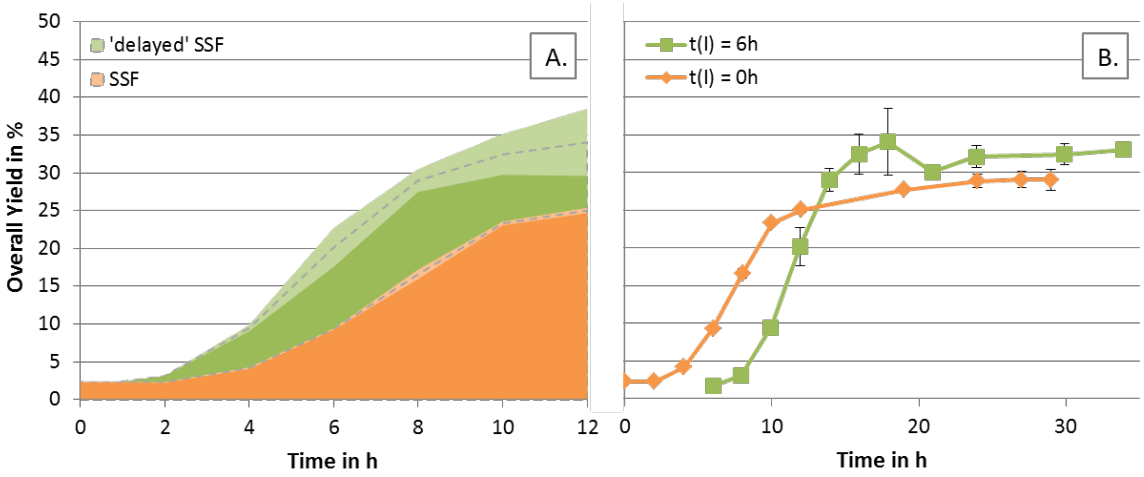

Figure 1. SSF of LX-pretreated corn silage digestate employing *B. coagulans* A166; comparison of inoculation at t(I) = 0 h and t(I) = 6 h ('delayed' SSF): A. yield over time of fermentation; B. yield over time of whole SSF process.

4. Conclusions

Our study aimed at producing high optical pure L-LA from corn silage digestate which was pretreated by the LX-method. The *B. coagulans* isolate A166 effectively fermented glucose and xylose to L-LA, reaching high productivity. The SSF experiments indicated that time of inoculation is crucial for the development of an optimal process. Final titers of around 20 g L^{-1} were obtained, with an optical purity of 99.5%.

References

[1] Streffer, F. (2009). Patent No PCT/EP2009/007583 Munich, Germany: European Patent Office.
[2] F. Cui et al., Bioresour. Technol. 102 (2011) 1831-1836.
[3] J. Hu et al., Bioresour. Technol. 182 (2015) 251-257.

Biotechnological production of succinic acid from lignocellulosic raw material.

Donatella Cimini[1], Lucio Zaccariello[2], Sergio D'Ambrosio[1], Michela Ventrone[1], Licia Lama[3], Olimpia Pepe[4], Chiara Schiraldi[1]

*1*University of Campania L. Vanvitelli, Department of Experimental Medicine, Via de Crecchio 7, 80138, Naples, Italy*; 2* University of Campania L. Vanvitelli, Department of Environmental, Biological and Pharmaceutical Sciences and Technologies, Via Vivaldi 43, 81100, Caserta, Italy; *3* National Research Council, Institute of Biomolecular Chemistry (ICB), Via Campi Flegrei, 34 - 80078 Pozzuoli, Naples, Italy; *4* Department of Agricultural Sciences, Division of Microbiology, University of Naples Federico II, Via Università 100, 80055 Portici (Naples), Italy

**Corresponding author: donatella.cimini@unicampania.it*

Highlights

- *B.succiniciproducens* produced 37 g/L of succinic acid on *A. donax* hydrolysate.
- *A fermentation efficiency of about 75% was demonstrated on pilot scale FB experiments*.
- *Effective and theoretical optimized process performance was assessed via material flow analysis.*

1. Introduction

Due to its wide range of applications in the food, pharmaceutical and chemical fields, microbial synthesis of succinic acid is receiving growing attention, generating already relevant industrial results, as well as fueling constant research for improvements. In order to develop a sustainable process, a special focus is now set on the exploitation and conversion of lignocellulosic biomasses into platform chemicals.

2. Methods

Fermentation experiments were performed on a Biostat C (150 L total volume) with a working volume of 70-80 L (Sartorius Stedim; Melsungen, Germany). All fermentations were carried out at 37°C on MH medium supplemented with *A. donax* hydrolysate. The culture was sparged with CO_2 at 0.1 vvm and agitation speed was set to 100-200 rpm and a constant pH of 6.5 was maintained. For the fed-batch phase a concentrated feeding solution containing sugars and yeast extract, was added to the broth in order to prolong growth. The feeding profiles provided addition of about 33-55 g/L of total sugars either pure or diluted in *A. donax* with a rate ranging from 0.2 to 1.2 g/L·h. The global evaluation of process efficiency considering the conversion of cellulose and hemicellulose to monosaccharides and their fermentation to succinic acid was performed [2].We carried out material flow analysis (MFA) by using the STAN software (published by TU Wien, Institute for Water Quality, Resource and Waste Management) that is a freeware that follows the Austrian standard ÖNorm S 2096 (Material flow analysis – Application in waste management).Shake flask experiments were conducted in 0.1 L bottles filled with 0.1 L of medium at 37°C and 140 rpm, in a rotary shaker incubator (model Minitron, Infors, Bottmingen, Switzerland). Bottles were sealed with stainless steel headpiece caps and sterile venting filters to insufflate CO_2, before starting the

experiment and during growth. Experiments were conducted on standard MH medium supplemented with lignocellulosic hydrolysates as C source.

3. Results and discussion

In the present work we used *Basfia succiniciproducens* BPP7 in separated hydrolysis and fermentation experiments with *Arundo donax* as starting material. We developed batch and fed-batch strategies, the latter showing a maximal production of about 37 g/L of succinic acid a productivity of 0.9 g/L·h on the pilot scale. Global mass balance calculations demonstrated a hydrolysis and fermentation efficiency of about 75%.

	SA (g/L)	LA+FA/SA (g/g)	AA/SA (g/g)	SA/TA (g/g)	TA/SA (g/g)	Fermentation efficiency (%)
FB1	26.5	0.30	0.18	2.06	0.48	46.9
FB2	21.0	0.36	0.22	1.77	0.56	67.0
FB3	24.0	0.22	0.20	2.37	0.42	49.2
FB4	37.0	0.29	0.17	2.16	0.46	75.4

Table 1-Fed-batch fermentations on pilot scale. SA, succinic acid; LA, lactic acid; FA, formic acid; AA, acetic acid; TA, LA+FA+AA.

A Material Flow Analysis was applied showing that, in the identified conditions 88.5 % of succinic acid per Kg of virgin biomass used, and 52% of product on the total generated output, were obtained. Considering an optimized process that uses *A. donax* as only C source, data indicated a potential yield of about 30% of product, and an unconverted residue of 31% mainly composed of lignin, a potentially valuable feedstock for bioenergy and biochemicals production.

4. Conclusions

The use of fed-batch strategies for the growth of *B. succiniciproducens* on *A. donax* improved the titer and productivity of succinic acid on a scale that is close to industrial application. Best experimental results were analysed by material flow analysis to evaluate another aspect of industrial development and assess the performance of the entire production process.
Currently, investigations on the possibility of using other lignocellulosic biomasses and microorganisms are in progress.

References

[1] A.A. Shatalov, H. Pereira. Carbohyd Pol. (2012) 87:210-217.
[2] D. Cimini, L. Zaccariello , S. D'Ambrosio,L. Lama, G. Ruoppolo, O. Pepe, V. Faraco, C. Schiraldi. Biotechnol. Biofuels. (2019) 12:22-36.

Increasing of the Nanowire FET Biochip Sensitivity to Virus Particles Using Dielectrophoresis.

Alexandr Safatov[1*], Vladimir Generalov[1], Konstantin Generalov[1], Galina Buryak[1], Olga Naumova[2], Boris Fomin[2], Elza Zaitseva[2]

1 Federal Budgetary Research Institution «State Research Center of Virology and Biotechnology "Vector"», Federal Service for Supervision of Consumer Rights Protection and Human Well-Being (Rospotrebnadzor), Koltsovo, Novosibirsk region, 630559, Russian Federation

2 A.V. Rzhanov Institute of Semiconductor Physics, Siberian Branch of the Russian Academy of Sciences, Novosibirsk, 630090, Russian Federation
**Corresponding author: safatov@vector.nsc.ru*

Highlights

- Biochip architecture including nanowire FETs, dielectrophoresis' electrodes is developed.
- Dielectrophoresis allows to concentrate antigens in the vicinity of nanowire sensor.
- Concentrating of antigens potentiates the biochip sensitivity.

1. Introduction

Real time detection of viruses in atmospheric bioaerosol samples may be done using devices based on nanowire FET [1], [2]. Viruses' concentration in aerosol is very low in some cases. It may lead to missing the viruses in the sample due to insufficient sensor's sensitivity. Viruses in the measuring chamber volume are distributed randomly. The vicinity of nanowire has a small part of the whole chamber volume and viruses predominantly from this volume easily interact with antibodies on the nanowire. It is proposed to use dielectrophretic forces [3] for viruses' concentration near nanowire for increasing the nanowire FET biochip sensitivity.

2. Methods

Preliminary experiments were conducted using vaccinia virus (LIVP strain was obtained from the FBRI SRC VB "Vector"'s Governmental Collection of viruses) stained with FITC dye (Thermo Fisher, USA) at room temperature. A droplet (volume of about 1 µL) of suspension with low virus concentration was placed between electrodes and luminescent particles behavior was observed using dark field microscope Stemi 2000 (Zeiss, Germany). Vaccinia virus is one of the largest viruses (its dimension is about 400 nm), so its movement may be readily seen under optical dark field microscope.

3. Results

Biochip architecture including as 12 nanowire FETs as electrodes for dielectrophoresis at each nanowire FET is developed, Figure 1. Preliminary experiments showed that viruses can be

effectively concentrated by dielectrophoresis near the electrodes, Figure 2. One of these electrodes is nanowire itself.

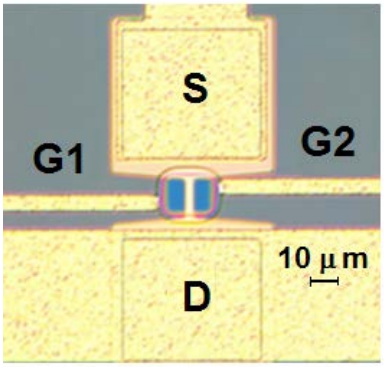

Figure 1. Top view of biochip's fragment. S – FET's source, D - FET's drain and nanowire between them; G1 and G2 - electrodes for dielectrophoresis.

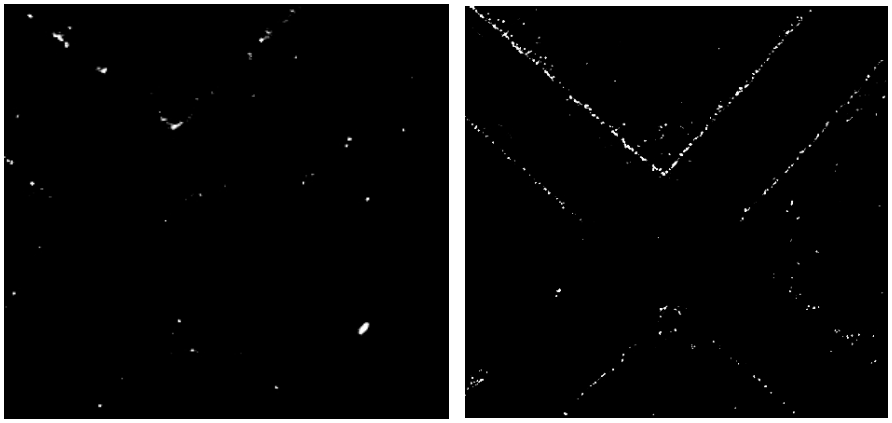

Figure 2. Distribution of vaccinia viruses (bright white dots) between perpendicular electrodes Left – no electric field applied. Right – electric field applied with frequency 200 kHz, voltage amplitude 5 V.

4. Conclusions

The results obtained visually demonstrates the possibility of viruses in bioaerosol samples to be concentrated near nanowire sensor. So the sensitivity of biochip may be increased using dielectrophoresis.

Acknowledgement

This work is supported by the Russian Science Foundation for Basic Research project # 18-29-02091\18 (in part of designing of biochip topology and calculation of electrical field parameters in it) and by state assignment GZ-11/16 (in part of concentration of viruses).

References

[1] Shen, F., et al. (2011). Environ. Sci. Technol., 45, 7473–7480.
[2] Park, K.-T., Cho, D.-G., Park, J.-W., Hong, S. & Hwang, J. (2015). Sci. Reports, 5, paper 17462.
[3] Generalov et al. Dielectrophoresis in diagnostics of infectious and noninfectious diseases, Ceris, Novosibirsk, 2011. (In Russian)

ECAB 5
The 5th EUROPEAN CONGRESS OF APPLIED BIOTECHNOLOGY
Florence 15-19 September 2019

Feasibility Study of Glycolysis Using New Thermodynamic Standard Data.

Thorsten Greinert[1], Christoph Held[1]

1 Laboratory of Thermodynamics, TU Dortmund University, 44227 Dortmund, Germany

**Corresponding author: christoph.held@tu-dortmund.de*

Highlights

- Thermodynamic approach to describe reaction equilibria.
- New consistent standard Gibbs energy of reaction for glycolytic reactions.
- Thermodynamic explanation of the feasibility of the glycolysis pathway.

1. Introduction

Thermodynamics has successfully been applied to many areas of biological systems. However, application of thermodynamics to examine entire metabolic networks remains a challenging task. A prominent example for such a network is the enzymatic reaction cascade of the glycolysis pathway. The feasibility of a pathway can be explained by means of second law of thermodynamics, i.e. by the rule that Gibbs energy of reaction $\Delta^R g$ has to be negative for each single reaction. Applying this to glycolysis leads to positive $\Delta^R g$ values for some reactions, i.e. thermodynamic analyses using literature standard data predict that glycolysis is not feasible [1]. We found [2] that reasons for this phenomenon are inconsistent published data on reaction equilibria of the single reaction steps.

2. Methods

The Gibbs energy of reaction $\Delta^R g$ is determined using standard Gibbs energy of reaction $\Delta^R g^0$ and the cellular metabolite activities (expressed as ratio of products and reactants Q) and solving $\Delta^R g = \Delta^R g^0 + RT\ln Q$. In recent works it was found that published $\Delta^R g^0$ values were not determined under standard conditions (hypothetically ideal solution) [2,3]. This causes inconsistent values for $\Delta^R g^0$ and thus also unreliable $\Delta^R g$ values. $\Delta^R g$ might even be positive though the reaction has been found to be feasible under the given conditions, which leads to wrong conclusions when examining metabolic networks. Thus, the main goal of this work was to understand the thermodynamics of each single reaction step within glycolysis. Therefore, reaction equilibria were measured in-vitro and influences of the reaction medium on reaction equilibria were determined experimentally. In order to bring these experimental conditions to standard state, activity coefficients of the metabolites were measured and modeled with the electrolyte Perturbed-Chain Statistical Associating Fluid Theory (ePC-SAFT) [4].

3. Results and discussion

Combination of experimental equilibrium concentrations and activity coefficients allowed establishing an activity-based approach to describe reaction equilibria while simultaneously providing consistent standard data $\Delta^R g^0$ for the single reactions of glycolysis. Based on the new $\Delta^R g^0$ values and the activity coefficients of the metabolites, the feasibility of glycolysis could be proven in this work. This is shown in Figure 1, in which $\Delta^R g$ values calculated from literature and from new $\Delta^R g^0$ values are compared. The comparison shows, that there is a significant difference between the literature and the new data. Using new data from the introduced approach does even result in negative $\Delta^R g$ values, where using literature data resulted in positive values, which shows the relevance of new high precision standard data. Additionally, applying the new $\Delta^R g^0$ values and the activity-based approach allows predicting the influence of the reaction medium (concentrations of the metabolites, salts, pH value, temperature and cosolutes) on reaction equilibria.

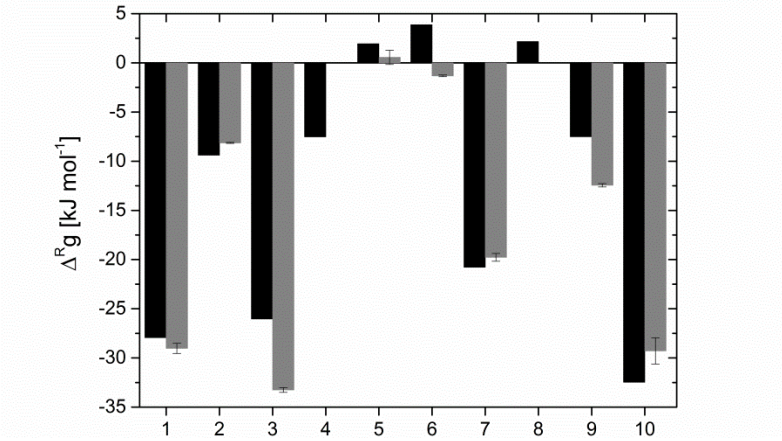

Figure 1. Gibbs energy of reaction calculated from literature (black) and new (grey) standard Gibbs energy of reaction for the ten single reaction steps of glycolysis pathway.

4. Conclusions

Inconsistent published data on reaction equilibria and standard Gibbs energy of reaction $\Delta^R g^0$ have been identified to be the reason why thermodynamic analyses failed to explain the feasibility of glycolysis. Thus, an activity-based approach has been developed which uses concentration-based equilibrium measurements and activity coefficients from modeling with ePC-SAFT in order to provide new consistent $\Delta^R g^0$ values. Based on this approach, the feasibility of glycolysis could be proven in this work. Additionally, applying the new $\Delta^R g^0$ values and the activity-based approach allows predicting the influence of the reaction medium on reaction equilibria.

References

[1] T. Maskow, U. von Stockar, Biotechnol. Bioeng. 92 (2005) 223-230.
[2] A. Wangler, C. Schmidt, G. Sadowski, ACS Omega. 3 (2018) 1783-1790.
[3] F. Meurer, M. Bobrownik, G. Sadowski, C. Held, Biochem. 55 (2016) 5665-5674.
[4] C. Held, T. Reschke, S. Mohammad, A. Luza, G. Sadowski, Chem. Eng. Res. Des. 92 (2014) 2884-2897.

ECAB 5
The 5th EUROPEAN CONGRESS OF APPLIED BIOTECHNOLOGY
Florence 15-19 September 2019

Process Analytical Technology Implementation for Protein Refolding: GCSF as a Case Study

Vishwanath Hebbi, Garima Thakur, and Anurag S. Rathore*

Department of Chemical Engineering, Indian Institute of Technology, 110016, Hauz Khas, India
**Corresponding author: asrathore@biotechcmz.com*

Highlights

- Implementation of Doe and PAT is demonstrated in refolding operation
- Real-time data of redox, temperature and pH was used to build SPC charts
- MVDA based statistical charts were used to monitor and control refolding of GCSF

1. Introduction

Process analytical technology is gaining interest in the biopharmaceutical industry as a means to enable consistency in processing and thereby in product quality via process control. Protein refolding is known to be significantly impacted by critical process parameters and feed material attributes including composition and pH of the solubilization and refolding buffers. Hence, in order to achieve robust process control and product quality, these attributes and parameters need to be monitored[1]. This paper presents an approach towards statistical process control and monitoring of protein refolding utilizing the measurements of online redox potential, temperature, and pH for development of a statistical model. The model has then been integrated with LabView to permit real time monitoring of the refolding process.

2. Methods

Refolding operations were conducted at lab scale in 50 mL and 500 mL glass beakers for solubilisation and refolding, respectively. Real-time data was collected using online probes of redox, ph and temperature. Critical variables were varied in design space and operating space and their implications on critical quality attributes were analysed using HPLC. Real-time data were used to build statistical control charts using multivariate data. The model was tested for operation in design space, operating space and potential deviations.

3. Results and discussion

Continuous measurements of ORP, pH, and temperature were performed during buffer preparation and protein addition steps. The ORP signal was found to be highly sensitive to each subsequent addition, as is evident from the changes to its profile as a function of time. Temperature and pH signals provide complementary measures of process changes. Simultaneous use of multiple sensors makes the PAT tool more robust as it effectively deals with issues that otherwise arise during commercial installation including signal-to-noise variability, drifting, and unexpected failure.

Characterization of time profiles of process variables within design space

The authors defined the design space for refolding to deliver refolding yield greater than 70%, oxidized impurities below 15%, and protein concentration above 0.18 mg/mL [2]. In the present study these

findings have been utilized for design of a suitable PAT application . Eight control runs were conducted around design space and were validated through HPLC analysis.

Detection and identification and implementation of deviations with SPC charts

Figure 1 shows the Hotelling's T2 plots of the deviation batches plotted using the training model. For the solubilisation buffer, the urea deviation appears at zero minutes and the DTT deviation appears at 46 minutes. In the refolding buffer, pH deviation appears at 37 minutes, and deviations caused due to the addition of improperly solubilized IBs (due to low urea or DTT) appear when the SIB is added at 40 minutes. Once a deviation is present in the system, errors in the SPC charts persist for future time intervals, as the changes in the online measured variables of ORP, pH and temperature persist in future stages of the batch. The overlay of analytical RP-HPLC profiles corresponding to the deviations has been shown in Figure 1(c).

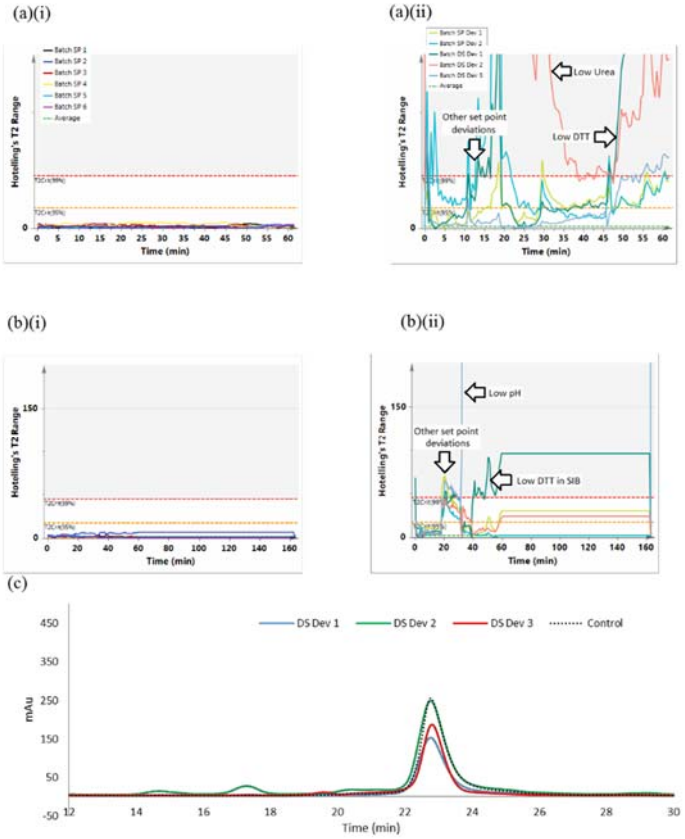

Figure 1 Hotelling's T2 charts for (a) solubilisation and (b) refolding for (i) control batches and (ii) deviation batches, (c) overlay RP-HPLC chromatograms of deviation runs and control run.

4. Conclusions

This study describes a PAT tool to monitor a complete refolding unit operation, from preparation of the solubilisation and refolding buffers to quenching of the refold. Data from online ORP, pH, and temperature probes are used to create a fingerprint of a typical refolding batch within the pre-defined design and operating spaces. A database of successful runs about a set-point is then created and used to develop statistical process control charts to monitor the evolution of the batch with respect to the addition of each subsequent component and are used in real-time monitoring for process deviations.

[1} M. Pathak, S. Dixit, S. Muthukumur and A.S. Rathore, “ Analytical characterization of in vitro refolding in the quality by design paradigm: Refolding of recombinant human granulocyte colony stimulating factor," Journal of pharmaceutical and biomedical analysis, vol. 126, pp. 124-131, 2016.
[2] P. D. Bade, S. P. Kotu, and A. S. Rathore, "Optimization of a refolding step for a therapeutic fusion protein in the quality by design (QbD) paradigm," Journal of separation science, vol. 35, pp. 3160-3169, 2012.

ECAB 5
The 5th EUROPEAN CONGRESS OF APPLIED BIOTECHNOLOGY
Florence 15-19 September 2019

Syngas Mass Transfer in a Membrane Bioreactor.

Marina Elisiário[1,2], Heleen De Wever[2], Wouter van Hecke[2], Henk Noorman[1,3], Adrie Straathof[1]

1 Department of Biotechnology, Delft University of Technology, van der Maasweg 9, 2629 HZ Delft, the Netherlands; 2 Flemish Institute for Technological Research (VITO), Boeretang 200, 2400 Mol, Belgium; 3 DSM Biotechnology Center, PO Box 1, 2600 MA Delft, The Netherlands

**Corresponding author: m.perdigaoelisiario@tudelft.nl*

Highlights

- Syngas fermentation is a promising route for bio-based production of commodity chemicals
- Syngas fermentation mass transfer limitations can be overcome in a membrane bioreactor
- Mathematical models can describe mass transfer and conversions in a membrane bioreactor

1. Introduction

Syngas can be obtained from sustainable and renewable processes such as biomass and municipal waste streams gasification, water and carbon dioxide electrolysis or directly from gaseous waste streams of heavy industry (e.g. steel industry) [1]. Syngas fermentation to commodity and fine chemicals is an emergent technology in biobased economy and it is foreseen to have an important contribution against climate change, by the reduction of greenhouse gas emissions and simultaneous valorization of waste streams. Syngas fermentation for ethanol production is a process currently being established at commercial scale. Novel microbial processes are developed to drive syngas biotechnological applications towards the production of more valuable multi-carbon compounds.

At the process side, the mass transfer limitation is the major resistance for gaseous substrate diffusion, due to the low aqueous solubilities of the gaseous substrates and reduced mass transfer coefficients. This is one of the urgent challenges to be tackled in syngas fermentation to building blocks, so that sufficient productivity and product titers can be achieved [2].

Membrane bioreactors are a promising configuration for overcoming gas to liquid mass transfer limitations in syngas fermentation [3]. High gas-liquid interfacial areas can be achieved in hollow fiber membrane modules given their geometry and higher driving force can be obtained by increased transmembrane pressure. However, so far the potential of membrane bioreactors has not been systematically explored for syngas fermentation.

2. Methods

Syngas fermentation in suitable membrane bioreactors is mathematically modeled using Comsol Multiphysics, using chemostat data and literature data. This allows computational fluid dynamics calculations. Model-based optimization incorporates syngas feed rate and composition, nitrogen

source feed rate, pressure, cell concentration, product concentration, and liquid flow rate. Additionally, the model optimization results will be used for design of experiments of the membrane bioreactor at lab scale and further validation of the model.

3. Results and Discussion

The syngas substrates are fed in hollow fiber lumens and the microorganisms are maintained on the shell surface, that is, on the liquid contacting side of the membrane fibers. At many conditions, the microorganisms can form biofilms. The gaseous substrates permeate across the hollow fiber wall toward a biofilm, where the microorganisms convert the gaseous substrates into the product, which then diffuses to the liquid phase.

4. Conclusions

At sufficiently high membrane area, mass transfer kinetics does not remain limiting. Therefore, other relevant phenomena need to be taken into account as well, such as fluid dynamics, fermentation stoichiometry and kinetics, and biofilm formation kinetics.

References

[1] Liew, F., Martin, M. E., Tappel, R. C., Heijstra, B. D., Mihalcea, C., & Köpke, M. (2016). Gas Fermentation—A Flexible Platform for Commercial Scale Production of Low-Carbon-Fuels and Chemicals from Waste and Renewable Feedstocks. Frontiers in Microbiology, 7(694).

[2] Bengelsdorf, F. R., Beck, M. H., Erz, C., Hoffmeister, S., Karl, M. M., Riegler, P., . . . Dürre, P. (2018). Chapter Four - Bacterial Anaerobic Synthesis Gas (Syngas) and CO2+H2 Fermentation. In S. Sariaslani & G. M. Gadd (Eds.), Advances in Applied Microbiology (Vol. 103, pp. 143-221): Academic Press.

[3] Yasin, M., Jeong, Y., Park, S., Jeong, J., Lee, E. Y., Lovitt, R. W., . . . Chang, I. S. (2015). Microbial synthesis gas utilization and ways to resolve kinetic and mass-transfer limitations. Bioresource Technology, 177, 361-374.

ECAB 5
The 5th EUROPEAN CONGRESS OF APPLIED BIOTECHNOLOGY
Florence 15-19 September 2019

Surfactin production optimization in biofilm bioreactors using genetically modified *Bacillus subtilis 168* strains with improved adhesion capacities

Hannah Brück[1,2], François Coutte[2], Frank Delvigne[1], Pascal Dhulster[2], Philippe Jacques[1,2]*

1 MiPI, TERRA Teaching and Research Centre, Gembloux Agro-Bio Tech, University of Liège, Avenue de la Faculté, 2B, B-5030, Gembloux, Belgium; 2 Univ. Lille, INRA, ISA, Univ. Artois, Univ. Littoral Côte d'Opale, EA 7394 - ICV - Institut Charles Viollette, F-59000 Lille, France

**Corresponding author: philippe.jacques@uliege.be*

Highlights

- The presence of exopolysaccharide improves significantly the support colonization
- The surfactin productivity of immobilized cells is higher in a continuous process mode
- A high dilution rate enhances biofilm formation on the reactor support

1. Introduction

Biofilm bioreactors have shown to be efficient cultivation systems for the production of bacterial biosurfactants [1]-[3]. They provide improved productivity and process stability through cell immobilization while avoiding foam formation. The widely known Gram-positive bacterium *B. subtilis* 168 is a potential producer of a very powerful biosurfactant, surfactin, with many applications in different industrial sectors [4]. The genome of *B. subtilis* 168 is completely sequenced and the strain can easily be genetically modified [5]. However, as a result of its domestication process, this laboratory strain is not able to produce surfactin anymore due to genetic mutations in the *sfp* gene coding for a co-factor required for the synthesis [6]. Furthermore, *B. subtilis* 168 possesses only poor biofilm formation capacities. This is mostly due to a deficiency in exopolysaccharide production [7]. In this work, different surfactin producing mutants of *B. subtilis 168* with increased adhesion and biofilm formation capacities have been investigated for the cultivation in a trickle-bed biofilm reactor [2].

2. Methods

The used *B. subtilis* 168 mutants contained all a functional *sfp* gene necessary for surfactin production. Firstly, a mutant with restored exopolysaccharide production (*epsC+*) has been selected to optimize the natural immobilization of the bacterial cells on the bioreactor support. Secondly, cell filamentation has been additionally provoked through the deletion of the *sepF* gene which is involved in the cell division process [8]. The idea was to promote further the initial cell adhesion step as well as the support colonization through this change of cell shape. The surfactin productivity and biofilm formation capacity of these mutant strains have been studied under batch and continuous process conditions in a trickle-bed biofilm reactor containing a structured metal packing with a high specific surface area for the cell colonization [1], [2]. Moreover, the effect of the dilution rate on biofilm formation has been examined.

3. Results and discussion

As expected, the *epsC+* mutants showed significant improved attachment capacities on the biofilm bioreactor support resulting in an increased surfactin productivity compared to the control strain. The restoration of the exopolysaccharides permitted the cells to produce a biofilm matrix which helps to stick the cells together for their immobilization on the reactor support. The surfactin productivity could be further increased through the transition from a batch to a continuous production mode. An increased dilution rate (D=0.5 h^{-1}) permitted to enhance the biofilm formation and thus higher cell densities on the reactor support could be achieved. By choosing a dilution rate higher than the maximum specific growth rate, the number of suspended cells could be reduced by washing out the cells. Microscope images of biofilm samples of the *epsC+ ΔsepF* mutant revealed strongly filamentous cells. The deletion of *sepF* did not affect the cell metabolism and had a minor impact on the support colonization in comparison to the presence of exopolysaccharides.

4. Conclusions

A continuous production mode is more favorable for surfactin production than the production in a batch reactor. A dilution rate that is higher than the maximum specific growth rate permits to reduce suspended cells and increase the biofilm formation in the trickle-bed biofilm reactor and thus improve the surfactin productivity. Exopolysaccharide production is important for an increased support colonization by *B. subtilis 168* whereas induced morphological changes seem to have a lower impact on the final biofilm formation but may facilitates initial adhesion on the reactor support.

References

[1] Q. Zune et al., Chem. Eng. Sci., vol. 170, pp. 628–638, 2017.
[2] Q. Zune et al., J. Chem. Technol. Biotechnol., vol. 89, no. 3, pp. 382–390, 2013.
[3] F. Coutte et al., Biotechnol. J., vol. 12, no. 1600566, pp. 1–10, 2017.
[4] P. Jacques, in: G. Soberon-Chavez (Ed.), Biosurfactants, Microbiology Monographs, Vol. 20, Springer Verlag Berlin Heidelberg, 2011, pp.57–91.
[5] R. Gallegos-Monterrosa et al., Microbiology, pp. 1–11, 2016.
[6] F. Coutte et al., J. Appl. Microbiol., vol. 109, no. 2, pp. 480–491, 2010.
[7] A. L. McLoon et al., J. Bacteriol., vol. 193, no. 8, pp. 2027–2034, 2011.
[8] L. W. Hamoen et al., Mol. Microbiol., vol. 59, no. 3, pp. 989–999, 2006.

ECAB 5
The 5th EUROPEAN CONGRESS OF APPLIED BIOTECHNOLOGY
Florence 15-19 September 2019

Designing scale down fermentations: strategies and challenges

Amit Deshmukh[1], Cees Haringa[1], Wouter van Winden[1], Boris Zacchetti[2], Maria Metheniti[3]
Luis Portela[3], Frank Delvigne[2], Henk Noorman[1]
1 DSM Biotechnology Center, Alexander Fleminglaan 1, 2613 AX Delft, The Netherlands
2 Université de Liège, Avenue de la Faculté, 2B, B-5030 Gembloux, Belgium
3 Chemical Engineering Department, Delft university of Technology, Delft, The Netherlands

Corresponding author: Amit.Deshmukh@dsm.com

Highlights

- Scale down simulator design based on CFD-CRD model
- Following life lines of organism, seeing through microorganism view
- Microfluidics techniques studying single cell and population heterogeneity

1. Introduction

In microbial fermentations, it is frequently observed that upon scaling up of processes there is a loss in performance (yields/productivity/titers) due to lack of homogeneity in industrial fermentors. It is now generally recognized that a good scale down (SD) protocol is necessary to capture the inhomogeneities (for C-source, oxygen, precursors, pH, temperature, or shear stress) due to realistic mixing times at production scale. Depending on the characteristic times, one or more of these gradients may have impact on the performance of strain/process in fermentation. Developing a scale down protocol for lab-scale environment that reflects industrial heterogeneities is challenging due limited knowledge of said heterogeneity. Traditionally, a scale down protocol mimicking the heterogeneity based on characteristic times alone is insufficient as this method lacks spatial resolution.

2. SD simulator design approach

An alternative solution that was proposed was a scale down approach using a novel methodology integrating computational fluid (CFD) and reaction dynamics (CRD) modelling of industrial fermentors [1]. In these simulations, the multiphase flow and transport phenomena taking place inside the bioreactor are simulated and integrated with the microbial reaction kinetics (e.g. substrate uptake) [2]. The microorganisms inside the reactor are followed along their trajectories, where they experience a changing environment. This approach resulted in metabolic response from the microorganism point of view and provided input for experimental design of scale down simulators.

3. Strategies and Challenges

This CFD-CRD coupling is an improvement over the traditional approach for designing scale down experiments, though it brings its own challenges that need to be addressed [2]. On the CFD side, the bioreactor hydrodynamics such as macro-mixing, gas–liquid interaction, and microbial reactions are often considered dominant. However, for specific cases it may be necessary to consider to look

into meso-mixing, eddy micro mixing, film diffusion for viscous processes, including non-Newtonian rheology. On the CRD side, currently, the models coupled with CFD are limited to metabolic models but that can be extended to a broader spectrum of cellular responses (eg. transcription and translation dynamics, protein formation, cell cycles), provided the resolved timescales are sufficient to capture such dynamics. Furthermore, the CRD models should be designed by keeping its coupling with CFD in mind such as to avoid instabilities eg. noisy rates or non-zero rates at zero pool size. Computational advances are required to enable full fermentation duration, and real-time simulations.

Actual design of SD simulators is guided by the lifeline structure (smooth changes versus discrete jumps) and practical considerations. In a single vessel SD-simulator, which is straightforward to operate and analyse, all organisms see the same extracellular environment and the effect of extreme fluctuations cannot be captured. On the other hand, a multi-vessel simulator accounts for a distribution of the exposure time to the various conditions by design, but not for the distribution of the amplitude. Additionally, the operational challenges will remain such as pumping issues for shear-sensitive and complex rheology systems. While current SD simulators operating at industrial biomass concentration may capture dynamics at the average level, more rapid dynamics at the individual cell level are unattainable. Some of these challenges cannot be overcome in single system and the selection of the SD simulator will depend on the case study at hand. It was shown that single and multiple compartments do not show similar microbial response for identical extracellular disturbances [4].

The challenges still remain for the SD simulators such as to decouple rate-of-change from consumption, to impose the full range of amplitudes and (stochastic) durations, and that each cell undergoes a different experience similar to the industrial scenario. Some of these can further be tackled using advancements in microfluidic devices, using fluorescent techniques.

4. Conclusions

Integrating computational fluid (CFD) and reaction dynamics (CRD) modelling of industrial fermentors allows improved design of SD simulators. Some of the challenges remain such as improving the simulation of bioreactor hydrodynamics, coupling of CFD-CRD models, and lack of industrial scale data for model validation. Some of the issues can be solved by increasing computational power, efficient CFD-CRD models, and scaling down further to microfluidics level.

References

[1] Haringa, C., Tang, W., Deshmukh, A. T., Xia, J., Reuss, M., Heijnen, J. J., Mudde, R. F. and Noorman, H. J. (2016). "Euler-Lagrange computational fluid dynamics for (bio)reactor scale down: An analysis of organism lifelines." Engineering in Life Sciences **16**(7): 652-663.

[2] Haringa, C., Tang, W., Wang, G., Deshmukh, A. T., van Winden, W. A., Chu, J., van Gulik, W. M., Heijnen, J. J., Mudde, R. F. and Noorman, H. J. (2018). "Computational fluid dynamics simulation of an industrial P. chrysogenum fermentation with a coupled 9-pool metabolic model: Towards rational scale-down and design optimization." Chemical Engineering Science **175**: 12-24.

[3] Haringa, C., Mudde, R. F. and Noorman, H. J. (2018). "From industrial fermentor to CFD-guided downscaling: what have we learned?" Biochemical Engineering Journal **140**: 57-71.

[4] Wang, G., Zhao, J., Haringa, C., Tang, W., Xia, J., Chu, J., Zhuang, Y., Zhang, S., Deshmukh, A. T., van Gulik, W., Heijnen, J. J. and Noorman, H. J. (2018). "Comparative performance of different scale-down simulators of substrate gradients in Penicillium chrysogenum cultures: the need of a biological systems response analysis." Microbial Biotechnology: **11**(3): 486-497.

ECAB5
The 12th EUROPEAN CONGRESS OF CHEMICAL ENGINEERING
Florence 15-19 September 2019

Continuous manufacturing

DESIGN OF A CONTINUOUS SEMI-PARTITION BIOREACTOR FOR *IN-SITU* (EXTRACTIVE FERMENTATION) PRODUCT REMOVAL

George .M. Teke [1], Robert .W. Pott[1]

Department of Process Engineering, University of Stellenbosch, South Africa

**Corresponding author: rpott@sun.ac.za*

Highlights

- A novel adapted bioreactor for *in-situ* product recovery (ISPR) was design and demonstrated.
- Separation profile, mixing and settling studies were conducted and evaluated.
- Mathematical model was demonstrated for mass transfer and flowrate characterization.

1. Introduction

Fermentation technology involves the use microorganism to convert simple substrates to valuable products, which find use in a variety of industries, from pharmaceuticals to fine chemicals. While fermentation technologies are commonly used, and represent a mature technology, there are nonetheless still challenges, particularly with regards low product yield and productivity caused by product inhibition, high energy consumption, mass transfer and selective metabolic issues [1], [2]. Extractive fermentation was introduced in the 1960's, as a mechanism to combat several of these issues. The technique is based on product removal while it is been formed (*in-situ*). This technology has developed over years, with usage of different separation techniques such as gas stripping, pervaporation, adsorption and liquid-liquid extraction. For the most part, many of these systems have been developed to run on batch mode operation. While development of fed-batch or continuous production systems has not received as much attention. Continuous systems, in particular, can be attractive, since yield, productivity and economies of scale can be improved over batch operation (although other operational challenges remain) [3], [4].
To give biotechnologists another operational mode from which to select from, more research needs to be focused on a robust *in-situ* design on the continuous systems of production, to be implemented for industrial use. This project presents the design and evaluation of adapted bioreactors for usage during *in situ* liquid-liquid extractive fermentation.

2. Methods

Reactor operation

The designed bioreactor is shown in Figure 1 below, this design permitted the continuous mixing and settling of two immiscible liquids. The mixing region used a Continuous stirred tank bioreactor (CSTR) while the settling region was an insert. As an exemplary two-phase system, 10 wt% of polyethylene glycol (PEG-8000) and 10wt% potassium phosphate solutions where added to the system of deionized water and stirred continuously. The addition of New Coccine dye to the mixture permits the recording of the separation profile of the liquids which was based on settling heights of the top and the bottom phases with respect to time.
Tracer solutions of 0.1M NaCl salt was used that permitted the validation and parameter fitting of a mathematical model derived to obtain the mass transfer and inter-compartmental flux values. Also, a mixing time studies was done using this tracer solution to understand the homogeneity of the systems. All experiments were done in triplicates for errors minimization.

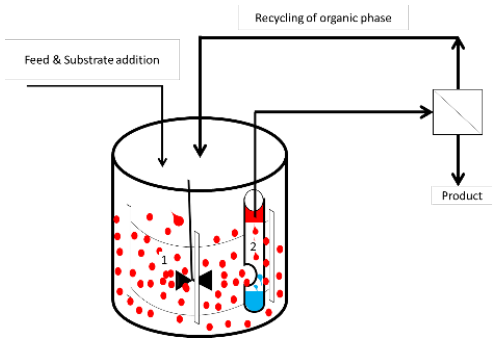

Figure 1: A Semi-Partitioning Bioreactor Diagram, 1- CSTR (Mixer) and 2- Inserted tube (settler)

3. Results and discussion

In Figure 2 below, 2(A) demonstrate a mixing and settling capacity of the designed bioreactor which is in line with other works on phase separation [5]–[7]. These previous studies demonstrate a phase boundary after settling which is not our case because the driving force of the impellers into the settler still permits some mixing as demonstrated by S (figure 2A). This indicates the possibility of a continual mixing, settling, potential substrate addition, cell or organic phase recycling, and a possibility of product/ by-product removal from the top organic phase there by reducing production cost. 2(B) demonstrated a perfectly fitted model that generates a 0.005 $l(\text{sec})^{-1}$ and 1.53 $lm^{-2}(\text{sec})^{-1}$ of flowrate and mass transfer (K_L) values respectively of the system (Semi-partitioning bioreactor) after triplicate runs. This high rate of exchange of materials is evident as there is a rapid homogeneity of the system as shown in the mixing time (t_m) curves in 2(C) with t_m being 112 seconds and 9 seconds of the settler and mixer sections respectively.

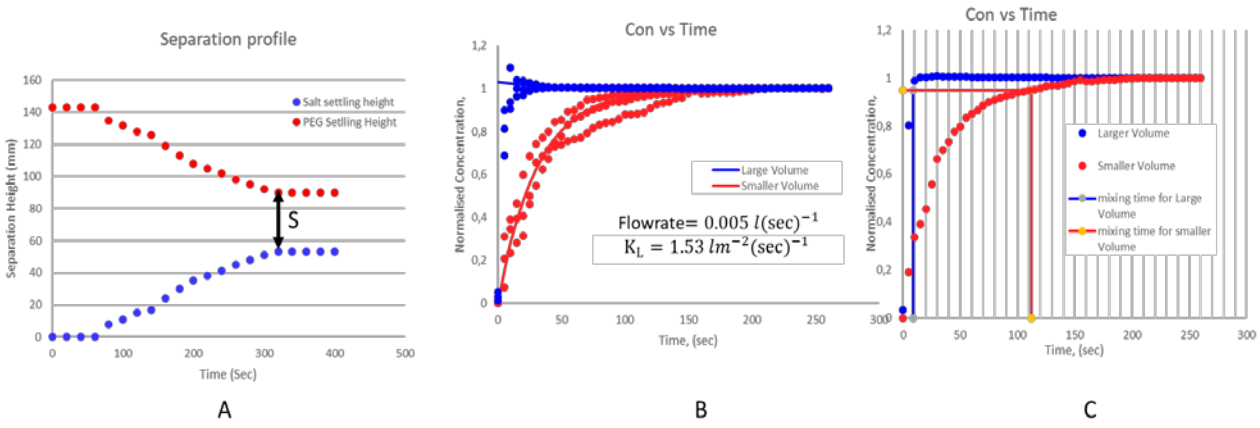

Figure 2:A Brief result summary (A)-Separation Profile, (B)- Mathematical model for Flowrate and Mass Transfer obtained (C)- Extent of mixing (Mixing time). Large volumes - mixer section while smaller volume - settler section.

4. Conclusions

The results above have demonstrated the possibility of designing a mixer-settler bioreactor which would be applicable for *in-situ* product removal. This implies there would be a continuous addition of substrate in the mixer section with a spontaneous removal of the product through settling section of the bioreactor. A mathematical model was generated for the system which made us better understand the extent of mixing or the fast rate of homogeneity in the system.

References

[1] A. Kuila and V. Sharma, *Principles and Applications of Fermentation Technology*, First. Martin Scrivener and Phillip Carmical, 2018.

[2] P. F. Stanbury, A. Whitaker, and S. J. Hall, *Principles of fermentation technology*, Third. Joe Hayton, 2017.

[3] D. Stark and U. von Stockar, "In Situ Product Removal (ISPR) in Whole Cell Biotechnology During the Last Twenty Years," in *Process Integration in Biochemical Engineering*, vol. 80, 2003, pp. 149–175.

[4] W. Van Hecke, G. Kaur, and H. De Wever, "Advances in in-situ product recovery (ISPR) in whole cell biotechnology during the last decade," *Biotechnol. Adv.*, vol. 32, no. 7, pp. 1245–1255, 2014.

[5] E. Barnea and J. Mizrahi, "Separation mechanism of Liquid-Liquid Dispersions in a deep-Layer Gravity Settler: Part IV - Continuous Settler Characteristics.," *Trans. Inst. Chem. Eng.*, vol. 53, pp. 83–92, 1975.

[6] J. A. Asenjo, S. L. Mistry, B. A. Andrews, and J. C. Merchuk, "Phase Separation Rates of Aqueous Two-Phase Systems : Correlation with System Properties," 2002.

[7] J. Golob and R. Modic, "Coalescence of liquid/liquid in dispersions in Gravity Settler," *Trans. Inst. Chem. Eng.*, vol. 55, pp. 207–211, 1977.

STABILITY OF MICROEMULSIONS WATER IN OIL (W / O) TO CHANGES OF PH CHARGED WITH CANTOCYANINS OF *Ardisia compressa* K.

Elvia Joaquín-Cruz [1], Landy Hernández-Rodríguez[2], Rubén Jiménez-Alvarado[3], Jaime Vernon- Carter[1], Angélica Román-Guerrero [1]*

[1]*Departments of Biotechnology and Process Engineering and Hydraulics, Autonomous Metropolitan University, San Rafael Atlixco 186, Col. Vicentina, Cd. de México, 09340, México.*

[2] *Agricultural High School, Autonomous University Chapingo, Chapingo, Estado de México. 56230, México.*

[3] *Institute of Agricultural Sciences, Autonomous University of the State of Hidalgo, Tulancingo, Hidalgo, 43600, México*

**Corresponding author: elviajoce@gmail.com*

Highlights

- It shows three formulations containing dispersed phase mass fractions of 10, 20 and 30% respectively.
- Summarizes the stability presented by the microemulsions at pH changes
- Provides detailedde accelerated stability profiles

1. Introduction

The fruit of ACK presents a high content of total phenolic compounds, mainly anthocyanins; These compounds have functional properties as antioxidant activity and with potential for their use as natural dyes. However, due to their high reactivity they are highly susceptible to degradation against environmental factors such as light, temperature, pH, among others. In this way, the incorporation of these compounds in encapsulation systems allows not only provide a means of transport, but also protection and release. EM´s are translucent, optically isotropic and thermodynamically stable dispersions, which have a small droplet size (5-50 nm) and low surface tension, which can result in better permeation and high absorption of compounds. Scientifically, ME is a dispersion of oil, surfactant and water [1] and are found in such concentrations that they form spontaneously, and whose formation depends on the thermodynamic equilibrium between the aqueous, oily phases, and the surfactant. The ME can be a good liquid membrane carrier for the transport of hydrophilic substances through the lipoidal media and for transporting the hydrophobic substances through the aqueous medium [2]. In this sense, the pH of the aqueous phase has a significant effect both on the type of the emulsion and on its stability and functionality. So the objective of this research is to evaluate the kinetic stability of $ME_{W/O}$ when subjected to pH changes by determining the change in D_{hd} and its stability against sedimentation phenomena.

2. Methods

Ethanolic extracts of ACK (5 g of ACK in 50 mL of EtOH 75% v / v) were obtained. $ME_{W/O}$ were obtained by means of a low energy method, where the ethanolic extract of ACK [10-30%] was dripped in the oil phase constituted by rosemary essential oil (due to its functional properties; AER) [40-80%], and Tween 80 (T80) and Span 80 (S80) [50:50, 10-30%] as surfactants. The obtained emulsions were adjusted in their initial pH (5.0) and characterized according to their D_{hd} in a

dynamic light scattering size analyzer (NanoSizer ZS) and accelerated stability in a Lumisizer dispersion analyzer, operated at 2000 rpm with 250 measurements every 30 s [3]. From these data the sedimentation velocities were obtained for each emulsion.

3. Results and discussion

The fresh $ME_{W/O}$ presented an initial pH of 5, with purple colorations. The D_{hd} ranged from 1.82 to 3.36 nm, where at a higher concentration of aqueous phase and surfactant showed a significant reduction in droplet size ($P < 0.05$). When carrying out the pH modification it was observed that in acidic conditions the D_{hd} presented changes in all emulsions, observing significant difference for 10 and 20% concentrations of extract and surfactant. For the pH of 7 there was a significant increase in D_{hd}, of ME2, followed by ME1 (Figure 1). It is worth mentioning that ME3 was the system with the lowest pH effect. This may be due to the fact that the presence of the different counterions (OH -, H +) present in the medium, can induce the destabilization of the equilibrium reached during the formation of the ME and that, under a certain level of concentration of both extract and of surfactant, this effect is minimized. Table 1 shows the values obtained for the sedimentation rate as an accelerated stability evaluation method derived from the transmission profiles of the ME, for the ME3 it was stable, while for the ME2 it increased in the two pHs (3 and 7).

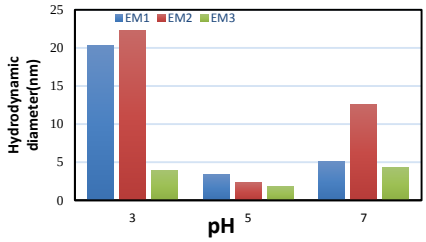

Figure 1. Effect of pH on the D_{hd} of the $ME_{O/W}$.

Tabla 1. Sedimentation rate of the $ME_{O/W}$

	Sedimentation rate (s^{-1})		
	pH 3	pH 5	pH 7
ME1	-0.1536 ±0.09	0.1156±0.04	-0.0731±0.06
ME2	0.3212±0.10	0.1707±0.02	0.3142±0.08
ME3	0.1148±0.01	0.1651±0.02	0.1497±0.09

4. Conclusions

The ME containing 30% ACK extract and 30% surfactant showed the best physical and kinetic stability with respect to pH change, while ME2 showed the highest change in its D_{hd} and higher sedimentation rates followed by ME1. The above can be attributed to the fact that the stability of these dispersed systems depends on the equilibrium achieved between the different phases involved, so that the modification of the ionic strength in the medium promotes the generation of new equilibriums that impact stability and potentially functionality of these systems. The above opens the guideline to the evaluation of the chemical stability of the materials trapped in the ME´s.

References

[1] G. Dixit, V. B. Mathur, Asian J. Pharm. Clin. Res. 8 (2015) 7-17.

[2] A. Muhammad, N. Tehreem, M. Abbas, S. Nazir, N. Younas, S. Majeed, N. Qureshi, N.A. Muhammad, Colloid and Interface Science Communications 28 (2019), 41-48

[3] A. Zielińska, C. Martins-Gomes, N.R. Ferreiraa, A.M. Silvac, I. Nowak, E.B. Souto, Int. J. of Pharmaceutics 553 (2018) 428–440.

Tracking phenotypic traits correlated with glycolytic flux capacity as a strategy for directing cell population

Thai Minh Nguyen[1]*, Hosni Sassi[1]*, Samuel Telek[1], Guillermo Gosset[2], Alexander Grünberger[3,4], Frank Delvigne[1]

1 Terra research and teaching centre, Microbial Processes and Interactions (MiPI), Gembloux Agro-Bio Tech, University of Liège, Gembloux, Belgium.
2 Departamento de Ingeniería Celular y Biocatálisis, Instituto de Biotecnología, Universidad Nacional Autónoma de México, Cuernavaca, Morelos, México.
3 Forschungszentrum Jülich GmbH, IBG-1: Biotechnology, Jülich, 52425, Germany
4 Multiscale Bioengineering, Bielefeld University, Universitätsstraße 25, 33615 Bielefeld, Germany

Corresponding author : F.Delvigne@uliege.be
** equal contributors*

1. Introduction

Phenotypic diversification has been the focus of intensive researches during the last decade that have led to a coherent mathematical and experimental framework of molecular stochasticity in prokaryotic and eukaryotic systems. This framework has been notably used in order to decipher the impact of regulatory network structure on possible metabolic specialization in clonal population of bacteria upon diauxic shift [1][2], but we are still far from applying these knowledges to more specific case studies, e.g. bioprocess optimization where control of phenotypic diversification is desired [3]. This is partly due to the fact that most of these researches have been conducted at low spatio-temporal resolution, i.e. either on a limited numbers of cells, or focused on given time point.

2. Methods

Phenotypic diversification dynamics of E. coli strains displaying different glycolytic fluxes (i.e., either wild-type strain E. coli W3110, mutant strains ΔptsG and ΔptsGΔmanX displaying reduced glycolytic flux or mutant strain ΔompC exhibiting increased glycolytic flux) have been investigated based on automated flow cytometry [4]

.3. Results and discussion

ΔompC strain, exhibited considerably increased diversification rate in chemostat cultivation. By comparison with the other strains, a correlation between the intensity of the glycolytic flux and the phenotypic diversification rate has been established. Interestingly, this effect was increased when strains were exposed to a succession of diauxic shifts in continuous culture, suggesting the occurence of a cell-decision making process in front of environmental fluctuations.

4. Conclusions

Phenotypic diversification rate is correlated to glycolytic flux in E.coli population. This study suggest. a step forward for managing the heterogeneity of microbial systems.

References [Calibri 10]

1. Kotte O, Volkmer B, Radzikowski JL, Heinemann M. Phenotypic bistability in Escherichia coli's central carbon metabolism. Mol Syst Biol. 2014;10.
2. Solopova A, van Gestel J, Weissing FJ, Bachmann H, Teusink B, Kok J, et al. Bet-hedging during bacterial diauxic shift. Proc Natl Acad Sci U S A. 2014;111:7427–32.
3. Binder D, Drepper T, Jaeger K-E, Delvigne F, Wiechert W, Kohlheyer D, et al. Homogenizing bacterial cell factories: Analysis and engineering of phenotypic heterogeneity. Metab Eng. 2017;42:145–56.
4. Sassi H, Nguyen Minh T, Telek S, Gosset G, Grunberger A, Delvigne F. Segregostat: A novel concept to control phenotypic diversification dynamics on the example of Gram-negative bacteria. BioRXiv. 542704.

Enhanced butanol production from Isopropanol-Butanol-Ethanol (IBE) fermentation by an integrated gas stripping-pervaporation process.

Eloísa Rochón[1], María Teresa García Cubero[2], Mario Daniel Ferrari[1], Mónica Coca[2], Claudia Lareo[1]

1 Universidad de la República, Facultad de Ingeniería, Departamento de Bioingeniería, Montevideo, Uruguay; 2 Departamento de Ingeniería Química y Tecnología del Medio Ambiente, Universidad de Valladolid, España.

**Corresponding author: merochon@fing.edu.uy*

Highlights

- Isopropanol-butanol-ethanol fermentation joined to gas stripping-pervaporation system
- *C. beijerinckii* DSM6423 fermented successfully industrial sugarcane-sweet sorghum juices
- 559 g/L of butanol were obtained in an IBE fermentation with gas striping-pervaporation

1. Introduction

n-Butanol is a four-carbon alcohol used as an advanced biofuel as well as a commodity chemical. It can be produced through the acetone-butanol-ethanol (ABE) or isopropanol-butanol-ethanol (IBE) fermentation by various *Clostridium* spp. in which a solvent mixture is produced. The production of isopropanol instead of acetone, which is corrosive, makes the produced mixture of solvents (IBE) to be used as fuel [1]. The raw material used for biobutanol production and the energy consumption are the major costs in an ABE [2] or IBE fermentation. Both sugarcane and sweet sorghum are crops which have high amount of soluble fermentable sugars. The low product concentrations reached in the fermentation broth, which is probably a consequence of cell toxicity by butanol, cause an intensive energy consumption. In order to overcome this problem gas stripping and pervaporation are the main recovery techniques studied for *in situ* butanol recovery process. Pervaporation coupled directly to the fermentation can present fouling in the membrane. The aim of this work was to evaluate a hybrid *in situ* gas stripping-pervaporation process to recover butanol of a batch fermentation of sugarcane and sweet sorghum juices using *C. beijerinckii* DSM 6423. Gas stripping was used to continuously remove butanol from fermentation broth, followed with pervaporation to further condense butanol.

2. Methods

Batch fermentation from the industrial medium of sugarcane and sweet sorghum juices was performed in a 2.5-L bioreactor using *Clostridium beijerinckii* DSM 6423. Fermentation conditions were: 35 ºC, initial pH 6.0 and 150 rpm. Gas stripping started at 23 h at a gas flowrate of 0.7 vvm and condenser temperature 0 ºC. Sugars were determined by HPLC using a Shodex SUGAR KS-801 column at 55 ºC and 0.7 mL/min. Organic acids and solvents were determined by GC equipped with a flame ionization detector and a fused silica column. Pervaporation assays were done with a

polydimethylsiloxane (PDMS) membrane. Pervaporation conditions were: flow rate 50 mL/min, vacuum 20 mbar, feed and condensation temperature 70 and -6 °C, respectively. An IBE aqueous solution with the same condensate composition as that obtained from the fermentation coupled with *in situ* gas stripping (I-B-E: 46-36-6 g/L) was used as the feed solution. Isopropanol, butanol and ethanol were determined by HPLC using an Aminex 87-H column at 30°C and 0.6 mL/min. To evaluate the pervaporation performance, partial permeation flux and selectivity were calculated.

3. Results and discussion

Sugar and solvent profiles are shown in Fig. 1. A sugar conversion of 98% was obtained in 158 h which demonstrated that the gas stripping system successfully mitigated butanol inhibition. As expected, sugar conversion was reflected in higher solvent concentration. Butanol and isopropanol concentrations reached were 7.8 and 10.9 g/L, respectively (total solvent as IBE 19.6 g/L). The average solvent concentration in the condensate was 47.5 g/L isopropanol, 33.1 g/L butanol, 4.9 g/L ethanol. Neither acetic nor butyric acids were detected in the condensate.

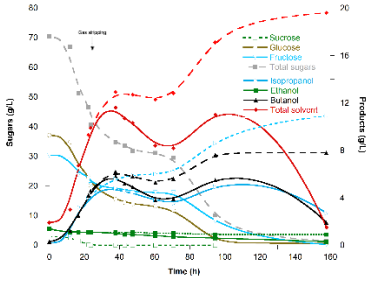

Figure 1. Fermentation batch profiles with *in situ* gas stripping from sugarcane-sweet sorghum juices. Dashed lines indicate the total production including products collected in the gas stripping condensate and those remained in the fermentation broth. The arrow indicates when the gas stripping started.

The condensate was then submitted to pervaporation for further butanol dehydration. At the beginning of the pervaporation butanol and IBE fluxes were 100 and 134 g/hm^2 respectively, which declined to 39 and 52 g/hm^2 after 38 h because of the decrease in their retentate concentrations. Isopropanol and ethanol fluxes were lower (9-32 and 1-2 g/hm^2, respectively). Butanol selectivity varied between 50-78, while for isopropanol and ethanol were stable at less than 6. The hydrophobic characteristic of the PDMS contributed to the high selectivity for butanol and low selectivity for isopropanol and ethanol. The separation efficiencies and concentration in the condensate during 38 h were: 16, 83 and 8 % and 140, 559 and 10 g/L for isopropanol, butanol and ethanol, respectively. Results showed that the membrane was effective to recover butanol from feed with high butanol concentration.

4. Conclusions

The strategy used allows alleviating butanol inhibition and to recuperate a condensate containing high butanol concentration (559 g/L), which could reduce energy consumption in the final product recovery.

References

[1] S. Bankar, G. Jurgens, S. Survase, H. Ojamo, T. Granstrom, Fuel. 136 (2014) 226-232.
[2] D. Cai, Y. Wang, C. Chen, P. Qin, Q. Miao, C. Zhang, P. Li, T. Tan, Bioresour. Technol. 211 (2016) 704-710.

Economic evaluation of sugarcane industry integrated to cogeneration system and bio-oil hydrotreatment for diesel and gasoline production.

Edvan Gonçalves[1], Lucas Rocha[1], Mara Scaliante[1], Marcelino Gimenes[1], Sérgio Faria[1], Marcos Souza[1]

1 State Universit of Maringá, Paraná, Brazil

**Corresponding author: eq.evgoncalves@gmail.com*

Highlights

- There are some technical obstacles that must be overcomed in order to become pyrolysis of biomass financially viable in front of cogeneration in the sugarcane industry.
- Advances in the area of catalysis may allow the production of diesel and gasoline through catalytic hydrotreatment of bio-oil.
- A new integrated plant concept estimates the production of diesel and gasoline from renewable sources at a very competitive price in the Brazilian market.

1. Introduction

Considering its potential for products generation, the pyrolysis of biomass has been shown to be a field of research that arouses and deserves great attention of scientific community. Such process consists of thermochemical decomposition of biomass under reduced atmosphere and results in the synthesis of three main fractions: pyrolysis liquid, biochar and gases (carbon oxides, hydrogen and hydrocarbons) [1, 2].

The chemical composition of bio-oil delimits its physical properties and its quality in the steps of storage, handling and combustion. Thus, to be used as a liquid fuel, bio-oil needs to satisfy several technical and market barriers, complying with constraints and standards of quality, and safety related to their properties (pH, viscosity, homogeneity, water content, calorific potential, acidity, among others) [3]. Therefore, several researches are being developed with proposes of improving deficiencies found in bio-oil, calling attention the process of deoxygenation by hydrogenation and catalytic hydrogenation for hydrocarbons production, which meet the composition range of diesel and gasoline [4, 5].

Nsaful et al. [6] investigated the integration of the cogeneration power system to a rapid pyrolysis process with the possibility of convert biomass energy into bio-oil or electricity. Furthermore, the results showed that it is preferable, from the economic point of view, to allocate all excess of bagasse to the generation of electricity in cogeneration systems. In constrast, it is possible to observe that the research of Dutta et al. [5] show promising results of the economic feasibility of integrating lignocellulosic pyrolysis processes with hydrotreatment and bio-oil catalytic hydrocracking for production of biofuels. Overall, considering what has been exposed, and taking account that in Brazil the sugar and ethanol plants jointly offer more than 186 million tonnes of sugarcane bagasse on the market annualy and the effects of inflation and reduction of non-

renewable fuels, this work has been proposed to study the technical and economic viability of integrating systems of energy cogeneration of sugarcane industry to the processes of rapid pyrolysis in fluidized bed coupled to hydrotreatment of bio-oil, aiming the production of diesel and gasoline.

2. Methods

The synthesis, simulation and economic evaluation of integration of energy cogeneration system of a sugar and alcohol production plant to the processes of pyrolysis of sugarcane bagasse, hydrotreatment and catalytic hydrocracking of bio-oil for the production of diesel and gasoline, product separation and vapor reforming of non-condensable gases for hydrogen production were performed using Aspen Plus™ software. The effect on financial indicators results was investigated considering the variation of biomass feed division for energy cogeneration and pyrolysis systems. The sensitivity analysis for the results of bagasse split by 50% for cogeneration and 50% for pyrolysis was developed considering variation of financial and operational parameters.

3. Results and discussion

In general, the results show that the internal rate of return on capital investment is greater for production of diesel and gasoline than for energy cogeneration. The cogeneration system shows internal rate of return of 6.9% a year while pyrolysis and hydrotreatment transformation demonstrated 12.4%. For the net sales revenues prices of fuels produced, it was possible to estimate $0.64/L (maximum of $0.70/L in sensitivity analysis), while the value practiced in the Brazilian market, in September 2018, was estimated in the range of $0.72/L and $0.88/L.

4. Conclusions

The implementation of the new concept of integration requires the commitment of greater financial resources than the current used cogeneration system. Despite this, in view of all the proposals investigated, the highest values of economic viability have been estimated for the production of diesel and gasoline through pyrolysis and catalytic hydrotreatment. The results showed that it is possible to supply these products to the Brazilian market with very competitive prices.

References

[1] D. Mohan, C. Pittman, P. Steele. Energ. Fuels. 20 (2006) 848-889.
[2] E. Gonçalves, C. Teodoro, F. Seixas, E. Canesin, M. Scaliante, M. Gimenes, M. Souza. Can. J. Chem. Eng. 95 (2017) 2249-2257.
[3] Y. Solantausta, A. Oasmaa, K. Sipilä, C. Lindfors, J. Lehto, J. Autio, P. Jokela, J. Alin, J. Heiskanen. Energ. Fuels. 26 (2012) 233-240.
[4] F. Zheng, J. Chang, Y. Fu. Fuel. 157 (2015) 107-114.
[5] A. Dutta, A. Sahir, E. Tan, D. Humbird, L. Snowden-Swan, P. Meyer, J. Ross, D. Sexton, R. Yap, J. Lukas. Process Design and Economics for the Conversion of Lignocellulosic Biomass to Hydrocarbon Fuels: Thermochemical Research Pathways with In Situ and Ex Situ Upgrading of Fast Pyrolysis Vapors. National Renewable Energy Laboratory – Pacific Northwest National Laboratory, 2015.
[6] F. NSAFUL, J. GÖRGENS, J. KNOETZE. Energy Convers. Manag. 74 (2013) 524-534.

ECAB 5
The 5th EUROPEAN CONGRESS OF APPLIED BIOTECHNOLOGY
Florence 15-19 September 2019

Techno-Economical Evaluation of the Rotating Packed Bed Technology for the Recovery of Natural Aromas from Fermentation Broth .

Ilya Lukin[1], Gerhard Schembecker[1]*

1Laboratory of Plant and Process Design TU Dortmund University, Emil-Figge-Strasse 70, D-44227 Dortmund/Germany

Dortmund/Germany

**Corresponding author: gerhard.schembecker@tu-dortmund.de*

Highlights

- RPB showed larger investment and operation costs for small-scale processes
- The cost analysis revealed the limitations of the novel technology
- The flexibility analysis covers the recovery of differently volatile aroma mixtures

1. Introduction

An increasing supplementation of products with aromas leads to an enhanced interest in biochemical production as an alternative to natural feedstock extraction[1]. Although advantageous, the economic success of aroma fermentation is still often limited by the challenging downstream process. An in-situ stripp-absorption using a Rotating Packed Bed (RPB) presents a novel approach for the recovery of natural aromas from crude biochemical broth. Our recent research shows that the mass transfer limitation of the absorption of volatile aromas can be overcome in a centrifugal field of the RPB increasing the process productivity. However, the rotation of the packing causes additional cost compared to the conventional techniques. Moreover, the lack of experience in operational boundaries and scale up parameters is yet a hurdle on the way to broad industrial application. Thus, the competitiveness of this novel technology needs to be evaluated in terms of its flexibility and costs.

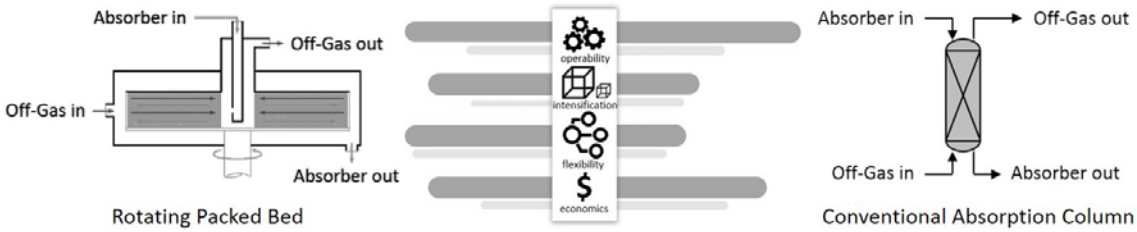

Figure 1. Techno-Economical comparison of a Rotating Packed Bed and conventional recovery techniques

2. Methods

The profitability is evaluated in terms of investment and operational costs, which are calculated in dependence of the separation task scale and difficulty. Experimental results support the analysis of the influence of the production stage parameters as well as of the physico-chemical properties of the target compound. The operational boundaries of the RPB absorption are analyzed using flexibility maps[2].

3. Results and discussion

At the conditions for the absorption of a model aroma compound from an exemplary fermentation process investigated in this study, the small scale RPB showed larger costs than a simple bubble column (Fig 2).

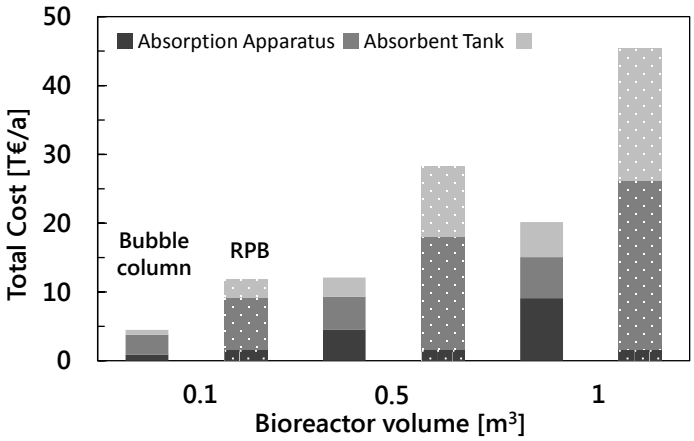

Figure 2. Total costs for the recovery of model aroma from the bioreactor off-gas for the Rotating Packed Bed and conventional Bubble Column (based on an exemplary fermentation process (100 h, 1 vvm aeration, constant aroma release, 95 % recovery) after the scale-up form laboratory experiments).

The analysis revealed that the costs of the RPB process were mainly driven by the large volume of water used as absorbent. Although low, the energy costs of RPB were three times higher than that of a bubble column. Obviously, the RPB could not fully display its advantages at operation with water. In order to reduce the absorbent consumption, the more hydrophobic liquids like plant oil were used. On the one hand, the enormous recovery increase is expected due to the rotation assisted mass transfer enhancement. On the other hand, only minor increase of operational costs is expected due to moderate pressure drop increase. Especially when dealing with highly viscous liquids like plant oil the RPB should be superior to other recovery techniques.

Further expansion to the broad range of aroma compounds of different volatility classes as well as to aroma mixtures will lead to more elaborated understanding of the technological potentials and limitations for the recovery of different products.

4. Conclusions

The stripp-absorption with Rotating Packed Bed presents a novel approach to the recovery of biochemically produced aromas. The results of the techno-economical evaluation of this potent technique will be presented. The flexibility analysis will reveal the potential and limitations of the RPB use for different classes of biotechnological aromas in comparison to classical downstream techniques.

References

[1] V.F. Cataldo, J. López, M. Cárcamo, E. Agosin, Appl. Microbiol. Biotechnol. 100 (2016) 5703-5718.
[2] D. Sudhoff, M. Leimbrink, M. Schleinitz, A. Górak, P. Lutze, Chem. Eng. Res. Des. 94 (2015) 72-89.

ECAB 5
The 5th EUROPEAN CONGRESS OF APPLIED BIOTECHNOLOGY
Florence 15-19 September 2019

Anaerobic digestion of model food waste at high and low concentration for the production of chemicals

Davide Dionisi,* Claudia Fernandez Martin, Serena Simonetti

University of Aberdeen, School of Engineering, Chemical and Materials Group, Aberdeen AB24 3UE, Aberdeen, Scotland, UK

**Corresponding author: davidedionisi@abdn.ac.uk*

Highlights

- Anaerobic digestion of model food waste was investigated with waste concentration in the range 25-400 gCOD/l
- The total product yield at the end of the experiments was in the range 10-13 % (COD basis), unaffected by the feed concentration
- Lactic acid and acetic acids were the main products in experiments at high and low feed concentration, respectively.

1. Introduction

Short-chain organic acids (e.g. acetic, propionic, butyric, lactic) and alcohols are usually commercially produced from fossil fuels (e.g. natural gas) or food crops (e.g. bioethanol production from corn). The production of these chemicals from the anaerobic digestion of organic waste would be in principle a more attractive and sustainable process [1, 2]. So far research on the production of these chemicals using anaerobic digestion has been mainly carried out at relatively low feed concentration, with, correspondingly, low concentration of the products, low process productivity and high separation costs. This study aims to investigate the effect of feed concentration on the anaerobic fermentation of model food waste, with the aim at achieving the highest possible product concentration and yield and process productivity.

2. Methods

The model food waste was prepared based on the estimated composition of unavoidable food waste in the UK [3]. The composition of the most concentrated waste (feed A) included the following: yeast extract 80 g/l; wheat grass powder 72.1 g/l; sucrose 66.6 g/l; oleic acid 52.6 g/l; starch 45.7 g/l; peptone 26 g/l. Distilled water was used to prepare feed A (which had a concentration of 429 gCOD/l) and the diluted feeds B (1:2 dilution, 214 gCOD/l), C (1:4, 107 gCOD/l), D (1:8, 54 gCOD/l), E (1:16, 27 gCOD/l). The batch tests were carried out in agitated 300 ml glass vessels, operated at room temperature (24-26 ^{O}C), with uncontrolled pH and inoculated with the effluent of a completely-mixed commercial digester fed with organic and food waste. The batch tests lasted 42 days and were run in duplicate.

3. Results and discussion

Figure 1 shows the main results. The concentration of total products generally increased over time and reached 40 g/l with the most concentrated feed. Interestingly, the total product yield was

virtually unaffected by the feed concentration, being in the range 10-13 % COD/COD. The pH dropped rapidly and remained acidic for feed A-D, while it increased to approximately 6.5 in the reactor with the most diluted feed (feed E), indicating some conversion of the acids into methane. A strong effect of feed concentration was observed on product distribution. The reactors with the most concentrated feeds (A, B) produced mainly lactic acid (about 80 % of the total products). The most diluted feeds (C, D, E) produced a wider spectrum of products, acetic acid being the main product, with low lactic acid concentrations. COD removal (not shown) from the liquid phase was very low with the concentrated feeds (A, B) and was the highest for the most diluted feed (E) (30 % COD removal), confirming that for this feed concentration some of the COD was converted to methane.

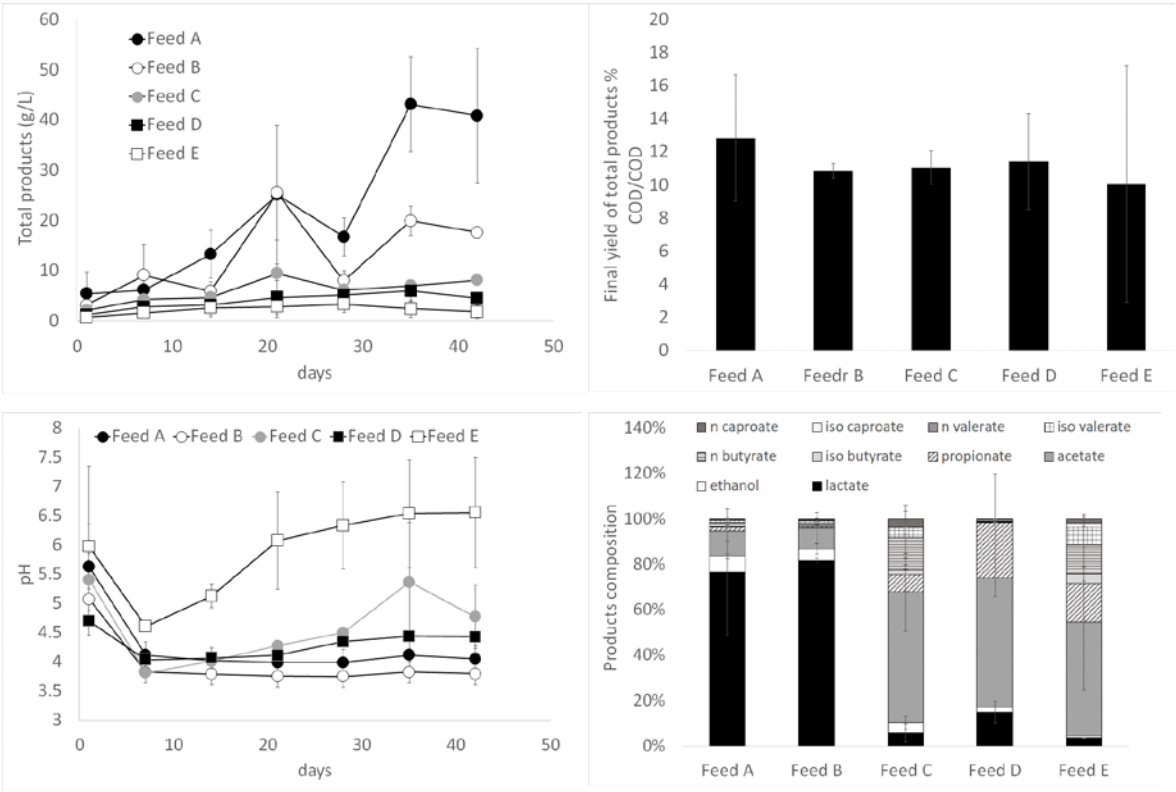

Figure 1. Main results of the batch tests

4. Conclusions

The results indicate that anaerobic digestion of food waste for the production of chemicals is feasible even with very high concentrations of the feed and with no pH correction, with no inhibition observed even a feed concentration of up to 429 gCOD/l. The research is ongoing with the aim to increase the product yield, concentration and productivity, using a combination of batch tests and SBR (Sequencing Batch Reactors) runs.

References

[1] D. Dionisi, I.M.O. Silva, Rev. Env. Sci. Biotechnol. 15 (2016) 213–242.

[2] J. Placido, Y. Zhang, Biom. Conv. Bioref. 8 (2018), 621-634.

[3] WRAP, 2009, Household Food and Drink Waste in the UK. Report prepared by WRAP. Banbury (UK).

ECAB 5
The 5th EUROPEAN CONGRESS OF APPLIED BIOTECHNOLOGY
Florence 15-19 September 2019

Reactive coupling: A novel approach for glycerol free biodiesel production.

Ibrahim A. Mohammed, Jonathan G.M. Lee, and Adam P. Harvey

School of Engineering, Newcastle University

**i.a.mohammed2@ncl.ac.uk*

Highlights

- Simultaneous production of biodiesel and polyglycerol.
- Reduction in the use of methanol during biodiesel production.
- Conversion of the excess methanol to added value product.

1. Introduction

Using conventional processes, biodiesel production is necessarily accompanied by the production of a low value glycerol-rich co-product. There is currently a substantial worldwide surplus of this coproduct, and it is of low value due to its low quality (due to the high level s of impurity present) and oversupply. The aim of this project was to develop a process to convert the glycerol produced into polyglycerol, a higher value product, in situ. In principle, this could improve the economics of biodiesel production. The improvement would not only be via the increased coproduct value, but also by reducing the methanol requirement of the process, which would reduce the load on the distillation column (used to recycle the methanol).

The "reactive coupling" proposed is given below:

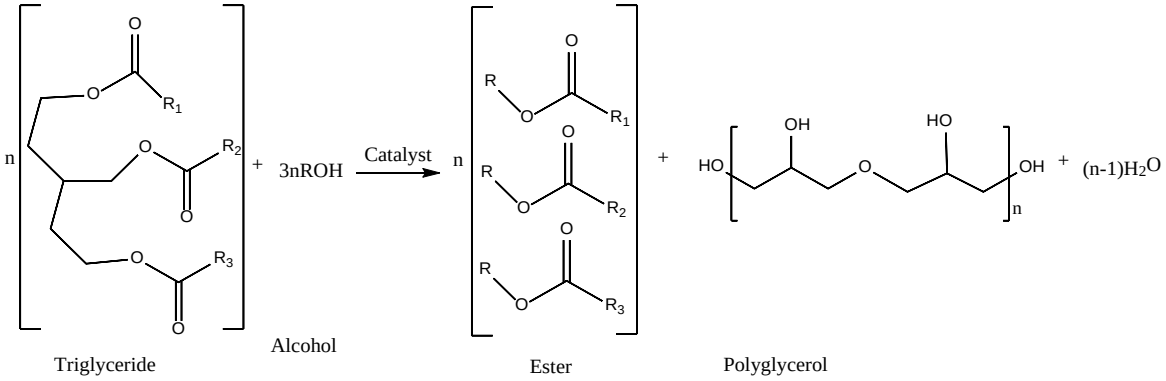

2. Methods

The coproduct will undergo step-growth polycondensation in the same pot to produce polyglycerol and water. The reaction was performed in a pressurized vessel at 130 – 160 °C with sulfuric acid as the catalyst. The effect of reaction temperature, catalyst concentration and molar ratio of triglyceride to methanol was studied. Both FAME, polyglycerols and gas sample produced were analyzed using gas chromatography. Methyl heptadecanoate (C17) was used as internal standard for the FAME and N,O Bis(trimethylsilyl)trifluoroacetamide with trimethylchlorosilane (BSTFA) was used to silylate the polyglycerol sample before analysing with the GC.

3. Results and discussion

Conversion of the triglyceride of approximately 100% was achieved. The glycerol were majorly converted to diglycerols. The glycerol conversion increased with increasing temperature and with decreasing mole ratio. The diglycerols peaks are similar to previous reports (Barros *et al.* 2017, Guerrero-Urbaneja *et al.* 2014, Ayoub and Abdullah 2013) with the α,α diglycerols isomer more predominant than the α,β diglycerols and the β,β diglycerols. A high signal around 6 minutes was observed, which was presumed to be the cyclic diglycerols with two hydroxyl groups while the glycerol and diglycerols have three and four hydroxyl group attached to them respectively.

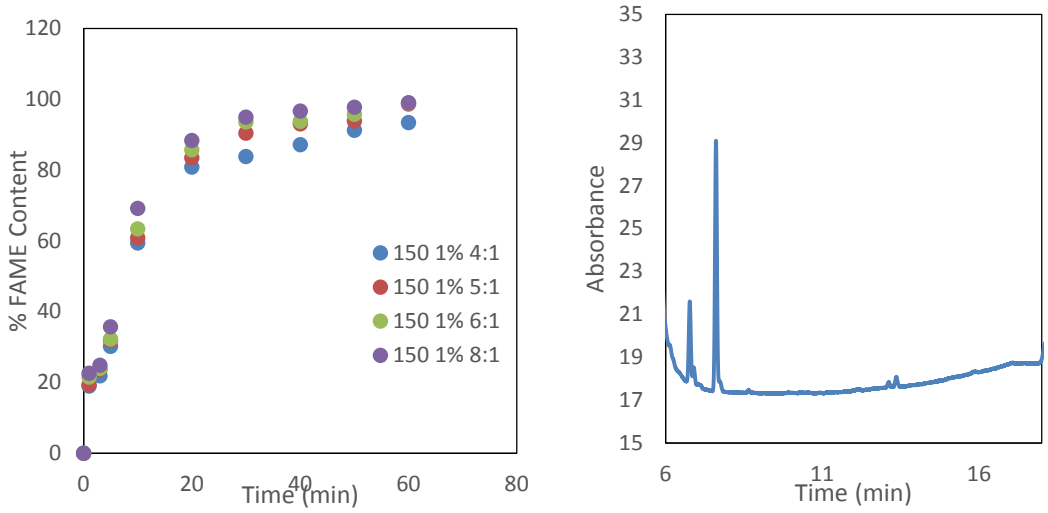

Figure 1. (a) Percentage FAME content after analysis with GC and (b) GC of the coupled glycerol during combined transesterification and reactive coupling showing the glycerol and isomers of diglycerols peaks.

The gas sample analysed were mostly methanol with few percentage of dimethyl ether (DME). This might be due to dehydration of the excess methanol in the reaction.

4. Conclusions

A proof-of-concept has been developed for this process to achieve high triglyceride conversion at low methanol-to-oil molar ratio and polyglycerols as the co-product of the reaction. The α,α diglycerols linear isomer was predominant among linear diglycerols which indicate the high selectivity of the homogeneous catalyst towards the etherification.

References

[1] F.J.S Barros, R.Moreno-Tost, J.A. Cecilia, A.L. Ledesma-Munoz, L.C.C. de Oliveira, F.M.T. Luna, R.S. Vieira, Molecular Catalysis, 433 (2017) 282–290.

[2] P. Guerrero-Urbaneja, C. Garcia-Sancho, R. Moreno-Tost, J. Merida-Robles, J. Santamaria-Gonzalez, A. Jimenez-Lopez, P. Maireles-Torres, Applied Catalysis A: General, 470 (2014) 199–207.

[3] M. Ayoub, A.Z. Abdullah, Chemical Engineering Journal 225 (2013) 784–789.

ECAB 5
The 5th EUROPEAN CONGRESS OF APPLIED BIOTECHNOLOGY
Florence 15-19 September 2019

Enhancing the Biochemical Methanation Potential of Sugarcane Bagasse using VoDCa (Vortex based Devices for Cavitation) Pre-treatment

Sanjay Nagarajan and Vivek Vinayak Ranade*

Multiphase flows, reactors and process intensification group, School of Chemistry and Chemical Engineering, David Keir Building, Queen's University Belfast, Belfast – BT9 5AG, United Kingdom.

** Corresponding author: v.ranade@qub.ac.uk*

Highlights

- A patented Vortex based Device for Cavitation was used for bagasse pretreatment
- Effect of additives prior and during cavitation was quantified.
- Biochemical methanation potential (BMP) of untreated & pretreated bagasse were compared.
- 1st order kinetic model (with time delay) was used to describe BMP.

1. Introduction

Anaerobic digestion (AD) for biogas production is an established technology for the production of biofuels combined with waste minimisation. AD was firstly used for wastewater sludge treatment, its application was however extended to biogas production from food waste, organic fraction of municipal solid waste, agri residues, animal slurries and other lignocellulosic biomass (LCB) later. Especially, with the recent climate agreement, global interest in AD to intensify biogas production is on the rise. Although a mature technology, process instability is of concern deterring its expansion.

The predominant hindering factor is the recalcitrance of LCB feedstock. To overcome the recalcitrance and to improve its digestibility, a range of pre-treatments have been reported [1-2]. Amongst the methods available, a physico-chemical method known as cavitation was utilised in this work to pre-treat sugarcane bagasse (SCB) for enhanced biogas production. Acoustic or hydrodynamic cavitation (HC) have been reported in literature for the purpose of pre-treatment of a range of LCB's. HC is energetically favourable and relatively easier to scale up when compared to ultrasonication and hence preferred [3-5]. Conventional HC treatment were predominantly performed using orifice plates or venturi tubes as HC devices. However, these devices exhibit problems such as erosion and clogging. A recently patented device by Ranade *et al;* – vortex diode, could however be used as an alternative to conventional devices for this purpose [6]. These Vortex based Devices for Cavitation (VoDCa) have been reported to be superior than the conventional devices for simulated waste water treatment [7], and now its application has been extended for LCB pre-treatment.

In this work, we report the use of VoDCa for the pre-treatment of SCB. SCB was selected as the feedstock due to its availability, for instance, Indian sugar industries generate ~80 million tonnes annually. Additional HC investigations were performed with additives prior or during bagasse cavitation to achieve enhanced pre-treatment. Biochemical methanation potential (BMP) of the samples were then compared and the optimal pre-treatment combination was identified.

2. Methods

HC experiments were conducted in a rig with a configuration shown in Figure 1 with SCB as feedstock. Additional experiments with additives such as alkalis and H_2O_2 prior or during the HC pre-treatment were performed. Solids were characterised using a range of techniques before and after treatment. Liquid phase was analysed using a HPLC. The solids were then subjected to 1 week BMP tests to quantify the enhanced BMP due to pre-treatment. A 1st order kinetic model (with time delay) was developed and used to describe the BMP data.

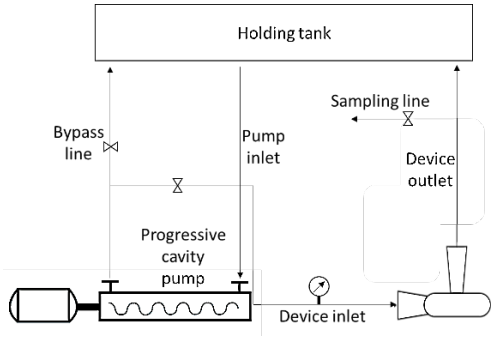

Figure 1. Experimental rig of VoDCa for bagasse pre-treatment

3. Results and discussion

There have been reports in literature that have presented results on LCB delignification using alkali (or H_2O_2)-conventional device HC combined pre-treatment of a variety of LCB for bioethanol or biogas production. Delignification is required, as the lignin, when present and broken down to phenolics, have the capability to inhibit methanogensis. It is expected that the combined pre-treatment in this case using novel VoDCa would be efficient in delignifying bagasse as well as hydrolyse a part of the polysaccharides enhancing its biodigestibility. It was shown that the model parameters obtained from 7 days of BMP data were able to simulate BMP data for longer durations. The model was then used to quantitatively understand the influence of pre-treatment combinations on delay time as well as maximum BMP. The approach and results will be useful to develop optimal pre-treatment for bagasse and other LCB valorization.

4. Conclusions

VoDCa based pre-treatment was found to enhance BMP of bagasse. The approach and results presented here are useful for developing an effective pre-treatment method for bagasse which can be easily scaled-up.

References

[1] A.T.W.M. Hendriks, G. Zeeman, Bioresour. Technol. 100 (2009) 10-18.
[2] Y. Zheng, J. Zhao, F. Xu, Y. Li, Prog. Energy. Combust. Sci. 42 (2014) 35-53.
[3] M.J. Madison, G. Coward-Kelly, C. Liang, M.N. Karim, M. Falls, M.T. Holtzapple, Biomass. Bioenergy. 98 (2017) 135-141.
[4] R. Terán Hilares, G.F. de Almeida, M.A. Ahmed, F.A.F. Antunes, S.S. da Silva, J. Han, J. Santos, Bioresour. Technol. 235 (2017) 301-308.
[5] P.N. Patil, P.R. Gogate, L. Csoka, A. Dregelyi-Kiss, M. Horvath, Ultrason. Sonochem. 30 (2016) 79-86.
[6] V.V Ranade, A.A Kulkarni, V.M Bhandari, US patent US9422952B2, 2016.
[7] P.G Suryawanshi, V.M. Bhandari, L.G. Sorokhaibam, J.P.Ruparelia, V.V. Ranade. Environ. Prog. Sustain. Energy. 37 (2017) 295-304.

ECCE12
The 12th EUROPEAN CONGRESS OF CHEMICAL ENGINEERING
Florence 15-19 September 2019

High throughput screening of methanogens under high pressure

Sara Zwirtmayr[1,*], Patricia Pappenreiter[1], Lisa-Maria Mauerhofer[2], Sébastien Bernacchi[3], Arne H. Seifert[3], Alexander Krajete[3], Simon K.-M.R. Rittmann[2], Christian Paulik[1]

1 Institute for Chemical Technology of Organic Materials, Altenbergerstraße 69, Johannes Kepler University/Linz/Austria;
2 Archaea Biology and Ecogenomics Division, Department of Ecogenomics and Systems Biology, Althanstraße 14 (UZA I), University Vienna/Austria

3 Krajete GmbH, Linz, Austria

**sara.zwirtmayr@jku.at*

Highlights

- Biological methane production (BMP).
- Simultaneous bioreactor system (SBRS).
- CO_2-hydrogenotrophic methanogenic strains.

1. Introduction

The biological methane production (BMP) is a promising technology for CO_2 neutral energy production and storage. Usually methanogens, an archaeal group of microorganisms, are applied in biotechnological process to produce methane (CH_4), water and biomass from hydrogen (H_2) and carbon dioxide (CO_2) according to (1). There are two ways to perform the process, either in continuous or discontinuous mode. A further possibility is to use pure or industrial emission waste gas for the biomethanation [1-4].

$$CO_2 + 4\ H_2 \rightarrow CH_4 + 2\ H_2O \quad (1)$$

Primarily the bioprocess is limited by the gas-liquid mass transfer step [4-5]. This is also influenced by different factors like the geometry and velocity of the stirrer, the sparger system or gas flow rates. The prevailing partial pressure in the system is an additional coefficient. Therefore, we developed the simultaneous bioreactor system (SBRS), which operates at elevated pressure to increase the dissolved concentration of H_2 and CO_2 during the reaction. Different CO_2-hydrogenotrophic methanogenic strains were cultivated in the SBRS at a pressure of 10 and 50 bar relative.

2. Methods

The SBRS has four identical reactors. Each of them has a total volume of 160 mL, which can be used for screening of methanogens in closed batch cultivation mode at pressure up to 50 bar relative. Five different methanogenic strains are tested in the SBRS at 10 and 50 bars.

- *Methanothermobacter marburgensis* DSM 2133
- *Methanobacterium thermaggregans* DSM 3266
- *Methanobacterium palustre* DSM 3108

- *Methanobacterium subterraneum* DSM 11074
- *Methanocaldococcus villosus* DSM 22612

The microorganisms are obtained from “Deutsche Stammsammlung für Mikroorganismen und Zellkulturen”. In addition, five hyperthermophilic strains will be tested. The following key aspect were used for the experiments: they were performed with a H_2:CO_2 (4:1) substrate gas mixture, a simplified medium composition for each strain (60 mL) was used, a $Na_2S \cdot 9\ H_2O$ solution (1 v/v%) was injected and the SBRS is mounted on a laboratory shaker instead of using a stirrer.

At the end of each experiment, gas- and liquid samples were taken through the respective valves. The obtained gas samples were measured with a gas chromatograph to determine the methane off-gas concentration, while the liquid samples get reconditioned for scanning electron microscope (SEM) pictures. In addition, the biomass samples were taken, after releasing the overpressure from the SBRS. The biomass is washed by centrifugation with water and finally dried over night (105°C) to determine the dry weight.

3. Results and discussion

To describe the CO_2-BMP process different parameters like the turnover rate, the methane evolution rate (MER) and the maximum conversion rate, were selected. Calculating the turnover rate is an alternative way to determine the CH_4 productivity indirectly [6]. *M. villosus* showed an increased conversion rate, turnover rate, and MER results at 50 bar compared to 10 bar.

Through the online measurement of the pressure, it can be shown that the methanogenic CH_4 production leads to a pressure drop. The production of CH_4 was also checked by GC measurements for each experiment.

4. Conclusions

Our developed SBRS is a suitable high throughput bioreactor system for fast characterization of methanogens and gas converting microorganisms at 10 and 50 bar. All strains were successfully cultivated at 10 bar and until now also the two strains *M. Marburgensis* and *M. Villosus* were successfully cultivated at 50 bar. Further experiments with the remaining strains are planned. It has been demonstrated that gas conversion and biomethane production can be achieved in each experiment.

References

[1] L.-M. Mauerhofer, B. Reischl, T. Schmider, B. Schupp, K. Nagy, P. Pappenreiter, S. Zwirtmayr, B. Schuster, C. Paulik, S. K.-M. R. Rittmann, Appl. Microbiol. Biotechnol. 102(17) (2018) 7643-7656.
[2] S. K.-M. R. Rittmann, A. H. Seifert, A. Krajete, BIOspektrum 20(7) (2014), 816-817.
[3] B. Lecker, L. Illi, A. Lemmer, H. Oechsner, Bioresource Technology 245 (2107) 1220-1228.
[4] E. Inkeri, T. Tynjälä, A. Laari, T. Hyppänen, Applied Energy 209 (2018) 95-107.
[5] S. Bernacchi, A. Krajete, C. Herwig, AIMS Microbiology 2(3) (2016), 262-277.
[6] R.S. Taubner, P. Pappenreiter, J. Zwicker, D. Smrzka, C. Pruckner, P. Kolar, Nature Communications 9 (2018), 748.

ECAB 5
The 5th EUROPEAN CONGRESS OF APPLIED BIOTECHNOLOGY
Florence 15-19 September 2019

Optimization of batch aqueous two-phase extraction and centrifugal partition chromatography in purification of monoclonal antibodies

Wojciech Marek, Wojciech Piątkowski, Dorota Antos

Rzeszow University of Technology, Faculty of Chemistry, Department of Chemical and Process Engineering, Powstańców Warszawy Ave. 6, Rzeszów

**wmarek@prz.edu.pl*

Highlights

- Aqueous Two-Phase extraction (ATPE) was applied for purification of a monoclonal antibody.
- ATPS containing PEG and ammonium sulfate was used.
- The efficiency of a batch single-stage and multi-stage ATPE (CPC) was compared.

1. Introduction

The most expensive step in downstream processing of monoclonal antibodies is protein A chromatography. Therefore, to reduce the cost of the chromatographic step, an alternative prepurification method can be used. In this work, a method based on coupling aqueous two-phase extraction (ATPE) and centrifugal partition chromatography (CPC), which is a multistage-extraction process, was developed. The subject of the study was a CHO cell-culture supernatant (Harvest), which contained a monoclonal antibody IgG1. ATPE was used for clarification, concentration and capture of the target product and partial separation of impurities in one or two stages.

Alternatively, CPC, comprising several hundreds of extraction stages, was applied. The bottom phase (BP-1) produced in the first ATPE-stage (Fig. 1) was further processed in a CPC system (Fig. 2). Fractions collected from the ATPE (BP-1 and BP-2) and CPC (F-CPC) stages were analyzed by protein A chromatography (AC) and size exclusion chromatography (SEC) for the antibody concentration and purity.

An optimization of the process was performed subject to purity of the target product, the residence time (or flow rate of the mobile phase) and possibility of recycling of the ATPS-phases.

2. Methods

ATPE and CPC were performed in systems containing polyethylene glycol (PEG, 3350 Da) and ammonium sulfate dissolved in water. The CPC mobile phase was the bottom phase from ATPE, whereas the CPC stationary phase was the ATPE-upper phase, the rotor speed was 1800 rpm, the rotor volume was 100 mL.

The *SEC purity* was calculated as the ratio of the peak area recorded for the IgG monomer and the sum of the area of IgG peak and peaks of all impurities.

The *level of impurities* in the factions was determined from the AC analysis as the area of the flow-through peak (FT) divided by the area of the FT-peak received for BP-1.

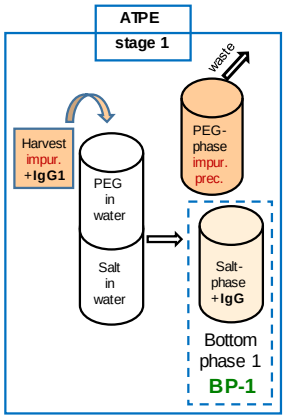

Figure 1. Single-stage batch extraction for antibody capture and precipitation of impurities

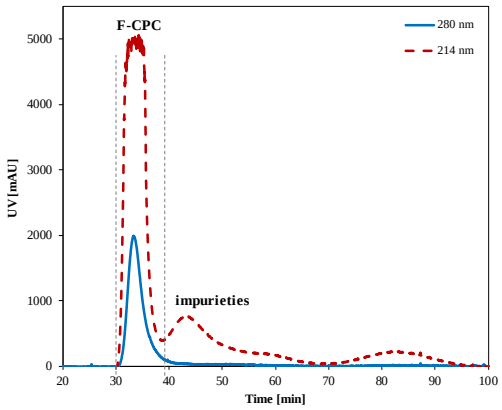

Figure 2. Example of a chromatogram from CPC purification of the ATPE-bottom phase BP-1. F-CPC – fraction of the target protein

3. Results and discussion

Impurities with low solubility were precipitated and removed in the first ATPE-stage, in which extraction was accompanied with precipitation of impurities (Fig.1). The bottom phase (BP-1), contained the target product (IgG1), and a high amount of impurities. That amount was reduced by ca. 40% after purification in the second ATPE-stage (see BP-2 in Table 1). Processing of BP-1 by CPC allowed us to further reduce the level of impurities by more than 80%. The fractions of the target product collected after two ATPE-stages and after CPC were analyzed by SEC. They contained low molecular weight impurities and very low amount of IgG-aggregates (<1%).

The CPC stationary and mobile phases (without the target product) were reused in the first ATPE-stage preceding CPC. In case of batch ATPE-extraction stages only the upper phase (e.g. BP-2) was recycled. The recycling conditions were optimized to reduce the solvent consumption.

Table 1. Purity of the target product fractions. The level of impurities was referred to BP-1 (assigned as 100%), BP-2 is the bottom phase fraction after the second ATPE-stage, F-CPC is the fraction collected after CPC.

Fractions	BP-1	BP-2	F-CPC
Level of impurities	100%	58%	12%
SEC purity	29%	42%	78%
IgG recovery	99%	99%	82%

4. Conclusions

- High recovery of the antibody was achieved due to selective extraction of the target product into the ATPE-bottom phase
- Significant reduction of impurities in CPC step was observed in comparison to two-stage ATPE.
- Recycling of phases in both ATPE and CPC operations allows reducing solvent consumption and the total cost of the operation.
- ATPE and CPC fractions can be further directly processed by HIC process due to high kosmotropic salt concentration in post-extraction solutions. Such sequential operations have a potential to substitute protein A chromatography.

We would like to acknowledge Polpharma Biologics for providing the biological material.

Thermodynamics Based Design Method of Aqueous Two-Phase Systems for Extractive Purification of Biomolecules

Maximilian Wessner[1], Mike Nowaczyk[1], Christoph Brandenbusch[1]

1 Laboratory of Thermodynamics, TU Dortmund University, 44227 Dortmund, Germany

**Corresponding author: christoph.brandenbusch@tu-dortmund.de*

Highlights

- Thermodynamics based design method for aqueous two-phase systems
- Prediction of biomolecule partitioning in aqueous two-phase systems
- Process tailored purification systems for selective extraction of biomolecules

1. Introduction

The downstream processing of biotechnological products such as therapeutic proteins is a challenging task. It has been shown recently, that Aqueous Two-Phase Systems (ATPS) offer mild processing conditions and a biocompatible environment for the purification of biomolecules due to their high water content of 70-90 wt% [1]. ATPS consist of two hydrophilic components, termed phase formers, (most likely either polymer – polymer or polymer – salt) dissolved in water above a critical concentration, forming two immiscible liquid phases. State of the art identification of ATPS is based on trial-and-error screening methods. In order to circumvent these cost intensive methods, a novel target-oriented method has to be available. This presentation will introduce a thermodynamics based design method [2] dramatically minimizing the experimental effort for ATPS design, and giving rise to a predictive description of the intermolecular interactions between low-molecular components and biomolecules. Based on the knowledge of the interactions of the molecules in solution, the critical concentration of the phase formers, aggregation propensity of the biomolecules, and the partition coefficients of the biomolecules are estimated.

2. Methods

In a first step phase equilibria data, either determined experimentally or modeled applying the ePC-SAFT equation of state [3], is used to determine the minimal concentration of phase formers that allow for the formation of an ATPS. This provides an access to the interactions between the low-molecular components. In order to take the interactions of the biomolecules in the ATPS into account, the osmotic virial coefficients B_{22} (biomolecule - biomolecule interactions) and B_{23} (biomolecule - solute interactions) are measured using composition gradient multi-angle light scattering (CG-MALS) for different concentrations of phase formers (polymers, salts) and displacement agents (e.g. neutral salts). Osmotic virial coefficients lower than zero indicate attractive interactions, values higher than zero indicate repulsive interactions. CG-MALS setup comprises of a Calypso II mixing unit, an Optilab T-rEX refractive index and a DAWN HELEOS 8^+ light scattering detector from Wyatt Technology (Santa Barbara, CA). Subsequently an in-house model [2] is used to predict the partition coefficient of the biomolecules in the ATPS.

3. Results and discussion

In order to identify an optimal ATPS for a given target component, investigations were performed for five phase formers. However, only the results for tri-sodium citrate (Na_3Cit), sodium glutamate (NaGlu) and polyethylene glycol 2000 (PEG2000) are briefly discussed in this abstract. At first, phase equilibria data were measured experimentally (figure 1 left side) and evaluated with respect to the critical concentration of phase formers required to form an ATPS. Furthermore, a model was used to characterize the interactions between the low-molecular components in the ATPS. The measurements show that the critical concentration of phase formers needed is comparable for all combinations investigated. Afterwards B_{22} values of Immunoglobulin G (IgG) in presence of the respective phase former were measured using CG-MALS to determine the interactions between the biomolecules (figure 1 right side). It is shown that B_{22} values of IgG in presence of NaGlu are dramatically higher compared the values for Na_3Cit. Based on these results the attractive interactions between IgG molecules in presence of NaGlu are significantly lower and as a consequence, the aggregation propensity of IgG is reduced. Thus, by choosing the NaGlu-PEG2000-ATPS at the respective concentrations indicated in Figure 1 the thermodynamics based design method was successfully applied to identify a process tailored purification of IgG.

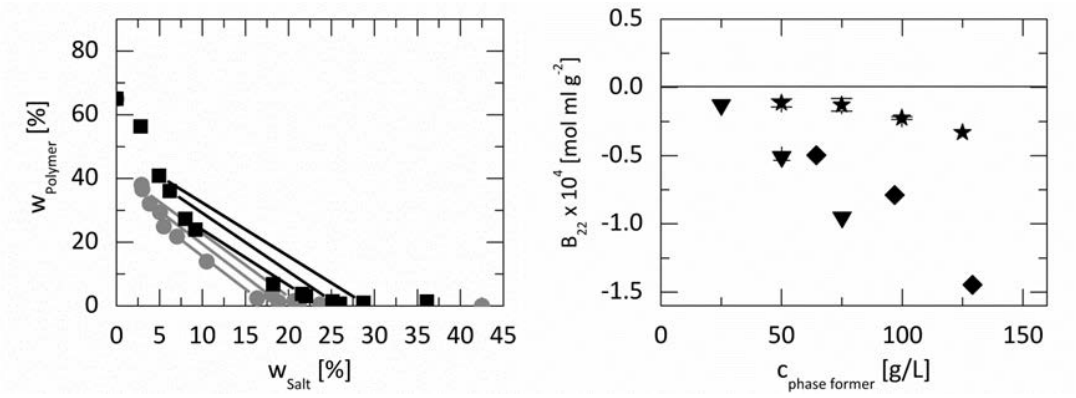

Figure 1. Left: Phase equilibria and binodal curve of ATPS containing sodium glutamate / polyethylene glycol 2000 (■) and tri-sodium citrate / polyethylene glycol 2000 (●) at pH of 7 and 298.15 K. Right: B_{22} values of Immunoglobulin G in presence of the phase former tri-sodium citrate (◆) [4], sodium glutamate (★) and polyethylene glycol 2000 (▼) in an aqueous 50 mM K_2HPO_4-NaH_2PO_4 solution with pH of 7 and 298.15 K.

4. Conclusions

Within this work, we present a thermodynamics based design method selecting suitable phase former for the extractive purification of IgG. Conventional design approaches fail, due to the fact that knowledge on the interactions between the molecules in an extraction process is limited. It was shown that the description of these interactions is the key factor for establishing a process tailored design of a suitable ATPS. The new method allows for an estimation of the aggregation propensity as well as the partitioning of the biomolecule in the ATPS. It has been proven that the method is a powerful tool and can be used for variety of biomolecular components.

References

[1] P. Albertsson, Advan. Protein Chem. 24 (1970) 309-341.
[2] C. Kress, G. Sadowski, C. Brandenbusch, J. Biotechnol. 233 (2016) 151-159.
[3] C. Held, T. Reschke, S. Mohammad, A. Luza, G. Sadowski, Chem. Eng. Res. Des. 92 (2014) 2884-2897.
[4] C. Kress, C. Brandenbusch, J. Pharm. Sci. 104 (2015) 3703-3709.

ECCE12
The 12th EUROPEAN CONGRESS OF CHEMICAL ENGINEERING
Florence 15-19 September 2019

Novel Solvents and Processes for the Bio-Safe Biorefinery.

Vittoria Sapone[1], Agnese Cicci[2], Giorgia Sed[1], Marco Bravi[1*]

1 Dipartimento di Ingegneria Chimica, Materiali e Ambiente, via Eudossiana 00184, Roma; 2 Bio-P s.r.l., via di Vannina, 00156, Roma

**Corresponding author: marco.bravi@uniroma1.it*

1. Introduction

Novel modifiable solvents can play a key role in obtaining the maximum value from biomass, increasing sustainability of current biorefinery processes, and avoiding regulatory issues. Switchable solvents ability to reversibly change their nature (hydrophobic-hydrophilic, and/or polar-non polar) can be used to improve existing liquid-solid extraction unit operations thanks to pretreatments simplification and reduction of their energy requirement. Natural Deep Eutectic Solvents (NaDESs) feature an assignable (by proper choice of their components) and in some cases tunable hydrophilicity. Most commonly, NaDES are hydrophilic, but hydrophobic NaDES have been discovered and a NaDES-based SHS has been introduced. Novel SHS- and NaDES-based biorefining concepts and techniques have been developed targeting two major current and forthcoming biomass resources: lignocellulosic materials (LCM) and microalgal biomass. Here we give account of two promising green approaches exploring paradigmatic shifts in biorefinery.

2. Methods

So far, SHS have only been used in their hydrophobic form to extract hydrophobic solutes. During the hydrophobic-to-hydrophilic switch, dissolved hydrophobic solutes separate as a second (hydrophobic) phase which is easily collected. However, the treated biomass might also contain hydrophilic solutes that can be easily removed by treating the residue of the hydrophobic extraction with the hydrophilic form of the very same SHS. Subsequent back-switch to the hydrophobic form leaves a hydrophilic phase constituted by water and water-loving solutes behind, whereby the cyclic extraction can restart. The biomass extraction can begin with either the hydrophobic or the hydrophilic form of the solvent and may continue with the other form. The operation sequence starting with a hydrophobic extraction was denoted by the inventors as Forward-Mode extraction (FME) and the opposite sequence (hydrophilic extraction first, then hydrophobic) was called Backward-Mode Extraction (BME) [1] (Figure 1A). This dual use of SHS, denoted as “Circular Extraction”, has been touted to increase the utility of the extraction process and of the solvent itself. Recently, the first NaDES-based switchable system was developed (“NaDES-Y”) [2] to address the toxicity issues of other SHS (such as DMCHA) in the food and other regulated domains. The present paper compares its performance in microalgae extraction to that of DMCHA (DimethylCycloHexylAmine) under said “Circular Extraction” approach. Choline chloride-based NaDES are of hydrophilic nature and exhibit polarity higher than water that can be tuned by adjusting water content in the NaDES formulation. Choline chloride-based NaDES are able to solubilise lignocellulose. However, a recent quantum leap forward in NaDES-based processing has demonstrated [3] revolutionary closed-cycle fractionation of LCM into cellulose, hemicellulose and lignin.

3. Results and discussion

As far as microalgal biomass biorefining is concerned, Sed at al. (2018) used the "Circular Extraction" protocol to assess NaDES-Y potential in extracting useful biological fractions compared to DMCHA, a well-known SHS. Results are shown in Table 1.

FME Extraction stage	Metabolite extraction in FME			BME Extraction stage	Metabolite extraction in BME		
	Proteins	Carbo-hydrates	Lipids		Proteins	Carbo-hydrates	Lipids
I - Hydrophobic	4 (7)	8 (42)	88(96)	I - Hydrophilic	4 (7)	8 (42)	88(96)
II - Hydrophilic	32 (34)	25 (9)	0 (0)	II - Hydrophobic	32 (34)	25 (9)	0 (0)
Total	36 (41)	33 (51)	88 (96)	Total	36 (41)	33 (51)	88 (96)

Table 1. Extraction efficiency in FME with NaDES-Y compared to (DMCHA)

LCM biorefining by NaDES can be carried out in closed-cycle [3] based on a first extraction, which dissolves lignin and hemicellulose, followed by two selective precipitations, the former obtained by tuning NaDES polarity by adding water (lignin precipitates), and the latter obtained by adding acetonitrile as an antisolvent (xylan precipitates) (Figure 1B). Although acetonitrile still taints the "intrinsically bio-safe" concept, researchers will hopefully find a bio-safe antisolvent alternative.

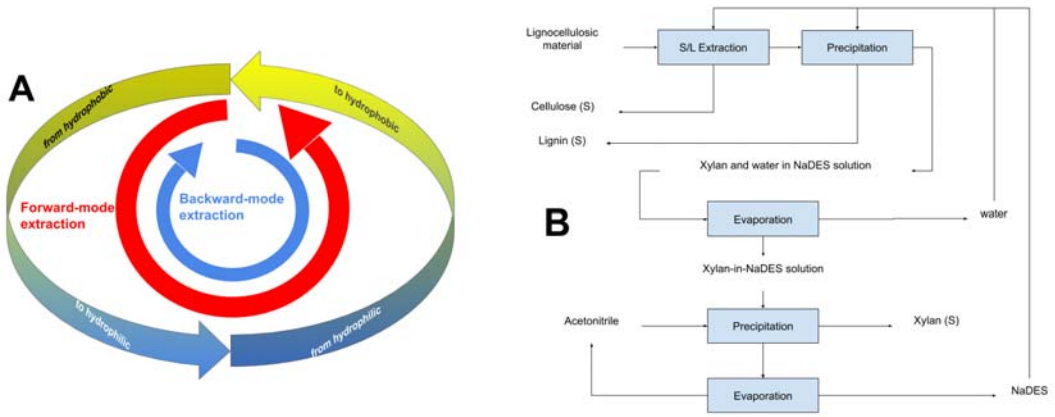

Figure 1. FME and BME approaches (A) and NaDES-based LCM biorefining (B).

4. Conclusions

Solvent extraction of a complex biomass containing an array of compounds should be treated with an array of solvents. With the aid of novel solvents which may change intrinsic features at the user's will the "one-solvents-fits-all" target might come into the biorefinery range.

References

[1] Cicci, A., Sed, G., Jessop, P. G., Bravi, M. (2018). Circular extraction: an innovative use of switchable solvents for the biomass biorefinery. Green Chemistry, 20(17), 3908-3911.

[2] Sed, G., Cicci, A., Jessop, P. G., Bravi, M. (2018). A novel switchable-hydrophilicity, natural deep eutectic solvent (NaDES)-based system for bio-safe biorefinery. RSC Advances, 8(65), 37092-37097.

[3] Kumar, A.K., Sharma, S., Shah, E. and Patel, A., 2018. Technical assessment of natural deep eutectic solvent (NADES) mediated biorefinery process: A case study. Journal of Molecular Liquids, 260, pp.313-322.

Organic phase selection for *in situ* membrane-assisted reactive extraction of 3-hydroxypropionic acid produced by bioconversion.

Ana-Karen Sánchez-Castañeda, Marwen Moussa, Luther Ngansop, Ioan-Cristian Trelea, Violaine Athès*.

UMR 782 GMPA, AgroParisTech, INRA, Université Paris Saclay, 78850 Thiverval-Grignon, France.

**Corresponding author: violaine.athes-dutour@inra.fr*

Highlights

- A solvent selection strategy including extraction performance and biocompatibility is proposed.
- Flow cytometry results are used as a quick assessment of solvents' biocompatibility.
- The effects of active and inert diluent on extraction and biocompatibility are studied.

1. Introduction

3-Hydroxypropionic acid (3-HP) is an attractive platform molecule that can be converted into several compounds such as acrylic acid and biodegradable polymers. Thanks to the increasing interest in the use of renewable resources in order to develop more sustainable processes, research on its production by bioconversion with microorganisms has made remarkable advances [1]. However, its industrial commercialization is still limited by low yields caused by product inhibition. Previous studies have shown that *in situ* reactive extraction assisted by a hollow fiber membrane contactor (HFMC) is a promising strategy to intensify glycerol bioconversion to 3-HP by a selected strain of *Lactobacillus reuteri* and simplify its recovery and purification [2-4]. However, there are some process limitations that need to be better understood in order to develop a system that allows continuous and *in situ* extractive bioconversion. Notably, the biocompatibility of the extraction system together with a good extraction performance are key factors. The objective of this work is to study a selection strategy to choose an adequate organic phase composition.

2. Methods

A screening of solvents was performed using trioctylamine (TOA) as the extractant compound. This tertiary amine is able to react with the organic acid in the aqueous media. It was mixed with different fatty alcohols with chain lengths from 8 to 18 carbons (active diluents) and alcanes (decane and dodecane, as inert diluents) at different proportions. Each mixture was evaluated in terms of 3-HP extraction performance and biocompatibility with respect to *Lactobacillus reuteri*. Extraction performance was determined by the extraction yield of a 3-HP solution at 5 g/L and 25°C, and the viscosity of the organic phase. A good extraction performance requires a high extraction yield and a low viscosity, which is related to a faster mass transfer in HFMC. In addition, biocompatibility with a selected strain of *Lactobacillus reuteri* [5] was evaluated by flow cytometry using two fluorescence probes simultaneously, carboxyfluorescein diacetate (cFDA) and propidium iodide (PI), that are able to assess respectively the enzymatic activity and the membrane integrity

of the cells put in contact with different organic mixtures. Bioconversions of 5 g/L of glycerol in contact with the organic phase molecules were also performed in order to compare substrate consumption and metabolites production. Substrate and metabolites' concentrations were determined by HPLC.

3. Results and discussion

Extraction yield and viscosity of the mixtures were used to select the type of inert diluent to use and its concentration. It was determined that there was no significant difference between the extraction yield using decane and dodecane at the same concentration. Moreover, although the viscosity of mixtures with decane were slightly lower, dodecane was selected, since it was expected to be more biocompatible in a HFMC because it is less soluble in water. The proportion of 20% TOA, 40% decanol and 40% dodecane was selected for comparison of the different active diluents maintaining the same molar proportion between TOA and the active diluent. Figure 1 shows that between the most biocompatible mixtures, the one with dodecanol 47% (2.1 mol/L) is the most interesting for *in situ* extraction since it has a lower viscosity than oleyl alcohol 80% (2.5 mol/L) and a higher extraction yield than 2-hexyl-1-decanol 61% (2.1 mol/L). The interest of dodecanol was corroborated by flow cytometry and 3-HP production results.

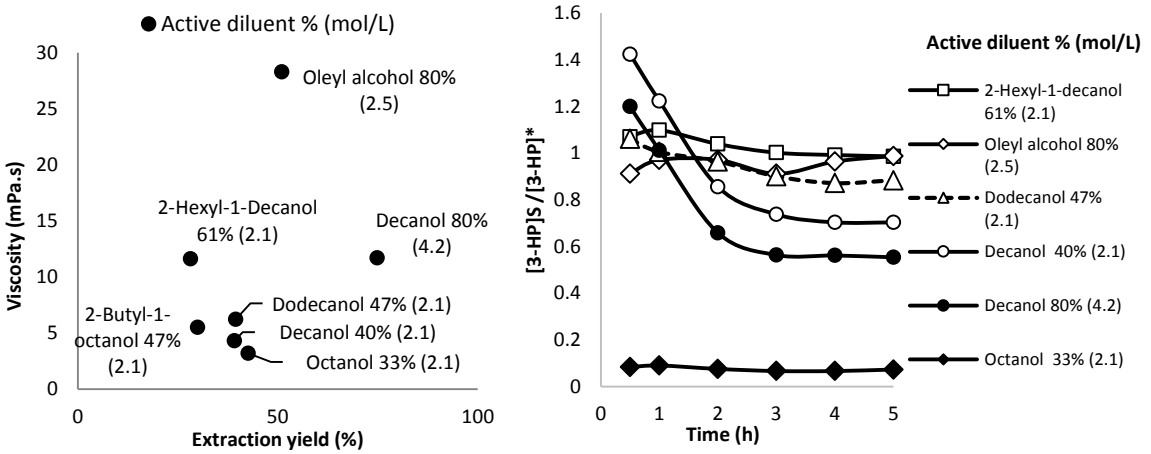

Figure 1. Extraction performance (yield and viscosity) and biocompatibility (3-HP production ratio) of the evaluated organic solvent mixtures. [3-HP]s = 3-HP produced in contact with solvents molecules. [3-HP]* = 3-HP produced in control (without contact with solvents molecules).

4. Conclusions

The selection methodology developed in this study is a useful tool for process optimization, because it compares solvent properties important for reactive extraction that are relatively easy to evaluate. After this preliminary screening, the number of organic phases to be tested in bioconversion coupled to HFMC *in situ* extraction system is considerably reduced, saving experimental effort.

References

[1] F. de Fouchécour, et al., Biotechnol. Adv. 36 (2018) 1207–1222.
[2] M. Moussa *et al.,* J. Chem. Technol. Biotechnol. 91 (2016) 2276–2285.
[3] G. Burgé *et al.*, J. Chem. Technol. Biotechnol. 91 (2016) 2705–2712.
[4] G. Burgé *et al.*, J. Chem. Technol. Biotechnol. 92 (2017) 2425–2432.
[5] G. Burgé *et al.*, Appl. Biochem. Biotechnol. 177 (2015) 923–939.

ECAB 5
The 5th EUROPEAN CONGRESS OF APPLIED BIOTECHNOLOGY
Florence 15-19 September 2019

Hierarchical and non-hierarchical HZSM5 based catalysts for selective alkylation and hydrogenation of guaiacols in Kraft lignin derived bio-oil.

Ashutosh Agarwal[1], Masud Rana[1], Seong-Jae Park[1], Jeong-Hun Park[1]*

1 Department of Environment and Energy Engineering, Chonnam National University, Gwangju 61186, Republic of Korea

**Corresponding author: parkjeo1@jnu.ac.kr*

Highlights

- Ni and/or Zn impregnated HZSM5 significantly enhanced the formation of alkylated guaiacols
- Hydrogenation was favored over hierarchical catalysts
- Deoxygenation was favored over non-hierarchical catalysts

1. Introduction

Diminishing fossil fuels and increasing energy demand have sparked immense interest in the utilization of biomass as renewable resource for biofuel production [1]. Partly replacing fossil fuels with upgraded bio-oil would be an alternative approach to accomplish reduction in massive consumption of fossil fuels. Lignin is often preferred as renewable feedstock for the production of bio-oil due to its low cost and ease of availability [2]. Among various types of lignin, Kraft lignin is essentially used for the production of bio-oil via thermochemical conversion. Due to low heating value and high instability derived from oxygenated compounds, upgrading of bio-oil becomes inevitable [3].

Bio-oil upgrading normally occurs via three main mechanisms, which involves hydrogenation, hydrodeoxygenation and alkylation. Catalyst employed during bio-oil upgrading chiefly governs the quality and cost of upgraded bio-oil [4]. Noble metal catalysts such as Pd/C, Pt/C and Ru/C which holds high potential for hydrodeoxygenation activates towards bio-oil upgrading remains unpreferred for industrial applications due to high cost and scarcity [5, 6]. Besides this, traditional sulfur based catalysts are also not employed for bio-oil upgrading as they tend to deactivate the catalyst leading to the formation of coke [7]. Non-noble metal catalysts such as Ni and Zn have recently been attracting great attention for hydrodeoxygenation of bio-oil due to their high activity and low cost [8]. Ni metal catalyst activates hydrogen and drastically prohibits the polymerization of unsaturated hydrocarbons while Zn enhances catalytic performance of zeolites during bio-oil upgrading process. Metal catalysts are often incorporated in support material such as zeolite in order to avoid agglomeration of metal catalysts that helps in enhancing their catalytic activity. HZSM5 has been widely used as support material for incorporation of metal catalysts due to its high thermal stability, porous structure, controllable acidity and ability to accomplish hydrodeoxygenation and alkylation [9, 10]. Besides this, HZSM5 zeolite have been known for its ability to convert heavier components of bio-crude into smaller fuel range fractions [11]. Mesoporosity in zeolites enhances production of aromatic compounds enriched biofuel by

promoting easy diffusion of hydrocarbons to acid sites [12]. Further, incorporation of active metal species onto zeolite support improves catalytic activity by promoting hydrogenation of oxygenated compounds [13].

Generally, the size, dimensionality of zeolite channels and its acidity plays vital role in governing the activity and selectivity of HZSM5 for organic reactions. Incorporation of secondary porosity at mesoscale in hierarchical HZSM5 acts as molecular sieves which favors fast mass transport [14]. In this research, we compared the catalytic performances of hierarchical and non-hierarchical Ni and/or Zn/HZSM5 catalyst at different Ni and/or Zn loading ratios for bio-oil upgrading. Several analytical techniques such as FE-SEM, EDS, XPS, ICP-OES, XRD and N_2 adsorption-desorption isotherms were used for catalyst characterization. The catalytic activity of synthesized catalysts was compared with Ru/C catalyst.

ECAB 5
The 5th EUROPEAN CONGRESS OF APPLIED BIOTECHNOLOGY
Florence 15-19 September 2019

Kinetic study of fed-batch production of 3-hydroxypropanoic acid (3-HP) by *Acetobacter aceti* within an integrated process

Florence de Fouchécour[1], Anaïs Lemarchand[1], Claire Saulou-Bérion[1], Henry-Éric Spinnler[1]*

1 UMR 782 GMPA, AgroParisTech, INRA, Université Paris-Saclay, 1 av. Lucien Brétignières 78850 Thiverval-Grignon, France

**Corresponding author: spinnler@agroparistech.fr*

Highlights

- *Acetobacter aceti* is an efficient 3-HP producer from 1,3-propanediol (1,3-PDO)
- 1,3-propanediol is quantitatively converted to 3-HP in a sequential fed-batch process
- *A. aceti*'s growth on glycerol allowed an efficient subsequent bioconversion
- 3-HP production was always accompanied by bacterial growth

1. Introduction

3-hydroxypropanoic acid (3-HP) has been identified by the US Department of Energy as one of the priority chemical targets that can be obtained from biomass, notably due to its variety of applications [1]. 3-HP production is primarily performed using biotechnological processes. However despite ever intensifying research effort on the matter, important hurdles still remain and commercial 3-HP production is not yet achieved [2]. Our work aims at developing an integrated approach for 3-HP production from glycerol. Glycerol is first converted to a mix of 1,3-propanediol (1,3-PDO) and 3-HP by *Lactobacillus reuteri*. Subsequently, 1,3-PDO is selectively oxidized into 3-HP by acetic acid bacterium *Acetobacter aceti*, in order to reach an overall yield from glycerol close to 100 %. To prevent substrate and product inhibition, 3-HP synthesis by *A. aceti* was tested in fed-batch mode in bench-scale bioreactors.

2. Methods

Fed-batch bioconversions of 1,3-PDO to 3-HP by *A. aceti* were carried out using a pH-based feeding strategy: pH was controlled by addition of an equimolar solution of base and 1,3-PDO, so that the substrate (1,3-PDO) was supplied as it was consumed. Both growth-coupled and –uncoupled bioconversion strategies were tested. In the latter case, *A. aceti* was first grown until late exponential phase on glycerol as growth substrate, before initiating the 1,3-PDO feeding. Such growth-uncoupled bioconversions were carried out at different pH: 4.0, 4.5 and 5.0. Bioconversion kinetics were then compared by fitting modified Gompertz to cell and product concentrations. These models could then be used to study the evolution of specific productivities over time.

3. Results and discussion

The pH-based feeding strategy could support simultaneously *A. aceti*'s growth and 1,3-PDO conversion into 3-HP. Yet, cell density remained low, around 0.26 g of cell dry weight (CDW) per

liter. Detrimental accumulation of the intermediary 3-hydroxypropanal (3-HPA) was also observed. In comparison, the sequential fed-batch strategy (*i.e.* growth on glycerol followed by 1,3-PDO feeding) could achieve more efficient 3-HP biosynthesis: maximal specific productivity $q_{3\text{-}HP,max}$, was higher (2.11 vs. 1.90 $g_{3\text{-}HP}$ g_{CDW} h^{-1}), and the final 3-HP titer was increased eight-fold. Moreover, for all tested pH conditions, this sequential strategy prevented *A. aceti* from accumulating 3-HPA: 1,3-PDO was thus quantitatively converted into 3-HP. The bioconversion was found the most efficient for pH = 5.0, in which case dioxygen availability appeared as a limiting factor. Interestingly, a second bacterial growth phase was observed when 1,3-PDO was supplied after a first growth step on glycerol, regardless of the pH at which the bioconversion was performed. Thus the bacterial cell density was further increased, reaching a maximum of 2 g_{CDW} L^{-1}.

4. Conclusions

Acetobacter aceti was found to be a promising biocatalyst for 1,3-PDO conversion into 3-HP. It was found to be the most efficient when first grown on glycerol, prior to 1,3-PDO being supplied to the medium which was controlled at pH = 5.0. Future work will include the implementation of a kinetic model as a tool to better understand the bioconversion and to help integrate this step into the whole integrated process.

References

[1] J. Bozell, G. Petersen, Green Chem. 12 (2010) 539-554

[2] F. de Fouchécour, A.K. Sanchez-Castañeda, C. Saulou-Bérion, H.E. Spinnler, Biotech. Adv. 36 (2018) 1207-1222

Comparison of Lignin Yield from Sugarcane Bagasse Using Liquid Hot Water and Ionic Liquids and Ionic Liquids Only.

Nirmala Deenadayalu[1], Gueh Charles Gnana[1]

1 Department of Chemistry, Durban University of Technology, KwaZulu-Natal, South Africa

**Corresponding author: NirmalaD@dut.ac.za*

Highlights

- Liquid hot water and ionic liquid pretreatment yielded higher yields of lignin (68 m/v %).
- Microwave digestion was effective in isolating the lignin.
- Optimized pretreatment time for only ionic liquids was 20 minutes.
- Ionic liquid 1-ethyl-3-methylimidazolium acetate was more effective than 1-butyl-3-methylimidazolium hydrogen sulphate.

1. Introduction

Globally the high cost and diminishing reserves of crude oil coupled with global warming effects have resulted in research for alternate energy and chemical sources. Lignocellulosic material is one of the largest renewable resources containing hemicellulose, lignin and cellulose. Extraction of the different components of the lignocellulosic material can lead to the valorisation of the biomass and reduce dependence on crude oil.

There are many pretreatment methods for the separation of cellulose, lignin and hemicellulose, namely: acid hydrolysis, base hydrolysis, steam explosion, mechanical and biochemical methods. All of these methods are environmentally harmful due to the release of volatile organic compounds that contribute to global warming effects. A new class of solvents known as ionic liquids are suitable for pretreatment since they have properties such as: low vapour pressure, recyclability, solubility in a range of organic compounds and liquid at room temperature that make them attractive for biomass pretreatment.

Sugarcane bagasse (SCB) is a renewable lignocellulosic resource in South Africa obtained after the sugar milling process. The annual production of SCB is approximately 6 million tons per annum produced by 14 sugar mills that are located on the north coast of KwaZulu-Natal (Paterson – Jones, 1989).

In this work, lignin yields from sugarcane bagasse pellets was investigated using liquid hot water (LHW) and ionic liquids (ILs) and only ionic liquids. The LHW process was applied to sugarcane bagasse pellets at 200 °C, for 30 minutes in a high pressure reactor for removal of hemicelluloses. The complex cellulignin residue was treated with the ILs: 1-ethyl-3-methylimidazolium acetate ([Emim][OAc]) or 1-butyl-3-methylimidazolium hydrogen sulphate ([Bmim][HSO_4]), using microwave digestion at varying time intervals. Direct Ionic liquid treatment was done on sugarcane bagasse pellets with ILs: [Emim][OAc] or [Bmim][HSO_4] using microwave digestion.

2. Methods

The sugarcane bagasse was first ground to 3-5 mm, dried to 10-12 % moisture and pelletized using a pellet mill. 1.0 kg of pelletized bagasse was used for the LHW hydrolysis at a temperature of 200 ^{o}C in a 3.0 L high pressure fixed bed reactor for 30 minutes with a volume flow of 250 ml/min of water. Hemicellulose dissolved in the water and a solid residue (cellulignin) was collected from the reactor. Compositional analysis of the sugarcane bagasse pellets, cellulignin and the complex cellulignin after enzymatic hydrolysis was done using NREL procedures.

For the extraction of lignin, a ratio 1:10 of SBP (0.5 g) and ionic liquid (5 g) was weighed in duplicate and transferred into 65 mL Teflon vessels, transferred to a microwave oven with parameters: power (80 Watt); ramp time (10 minutes); temperature (180 ˚C) and different hold times of 3, 10, 15 and 20 minutes for each run. After each run the extracted lignin was transferred to a 100 mL beaker rinsed thoroughly with 10 mL solution of 1-4 dioxane-water 95:5 (v/v), transferred into a 50 mL volumetric flask and diluted with a mixture of 1-4 dioxane-water 50:50 (v/v) for UV analysis.

3. Results and discussion

The amounts of glucose released in g/L during enzymatic hydrolysis of cellulignin using enzyme Cellic CTec2 or Metaplus/Rapidas was 27.5 g/L and 3.8 g/L after 6 hours of hydrolysis. The effectiveness of the combined enzyme Metaplus/Rapidas was lower than the Cellic ® CTec2 enzyme.

The IL [Emim][OAc] gave the highest lignin yield (68 %) for the LHW and IL method at 10 min. For the sugarcane bagasse pellets the highest yield was 59 98% at a reaction time of 25 min. The IL: [Emim][OAc] was the better of the two ILs used.

4. Conclusions

Liquid hot water and IL extraction of lignin from sugarcane bagasse pellets was successfully used to extract lignin. Although the highest yield was obtained for the LHW and IL method, the preferred method would be IL treatment on the sugarcane bagasse pellets since it eliminates the use of high energy input.

References

[1] J.C. Paterson-Jones, The biological utilization of bagasse, lignocellulosic waste. CSIR: South African National Scientific Programs Report No 149 (1989).

[2] A. Brandt, M.J. Ray, T.Q, To, D.J. Leak, R.J. Murphy, T. Welton, Green Chem. 13 (2011) 2489-2499.

[3] Y.Q. Pu, N. Jiang, A.J. Ragauskas, J. Wood Chem. Technol. 27 (2007) 23-33.

[4] W. Wang, X. Zhuang, Z. Yuan, Q. Yu, W. Qi. Bioresour. Technol. 190 (2015) 7-12.

ECAB 5
The 5th EUROPEAN CONGRESS OF APPLIED BIOTECHNOLOGY
Florence 15-19 September 2019

Non-routine operation management in biorefineries using an operator training simulator with automatic tuning of operating procedures

Joseph Isimite[1], Frank Baganz[2], Volker, C. Hass[*1,2]

[1]Department of Biochemical Engineering, University College London, Gordon Street, London, WC1H 0AH

[2]Furtwangen University of Applied Sciences, Jakob-Kienzle-Straße 17, D-78054 Villingen-Schwenningen, Germany

*Corresponding author: volker.hass@hs-furtwangen.de

Highlights

- Process models incorporating start-up, shut-down and normal operations
- Nelder-Mead algorithm for process optimization and SOP tuning
- OTS with capability to automatically re-parameterize SOPs
- Enables operators to take corrective action to quickly recover from upset events

1. Introduction

The increasing complexities in process configurations, starting raw material options, and the variety of product offerings in modern biorefineries present peculiar challenges for operators and plant process automation systems [1]. Existing operator training simulators (OTS) provide a safe simulated environment for developing the skills of operators, amongst other benefits. In this paper, the usefulness of the traditional OTS is extended by incorporating an algorithm that helps operators effectively manage process upsets and changes in feed properties through automatic tuning and adjustment of standard operating procedures (SOPs).

2. Methods

The C++ based modelling tool C-eStIM [2] was used to develop and parameterize process models for feed pre-treatment, fermentation and distillation. A commercial process control and automation software, WinErs [3], was used to integrate all unit operations into a single functioning biorefinery, with accompanying heat exchangers, pumps, and control valves. Biorefinery standard operating procedures (SOPs) were used to create sequential function charts in GRAFCET [4] for biorefinery operations. Furthermore, a parameterizable SOP for automatic adjustment of enzyme loading in response to fluctuations in inlet feed composition was also implemented using GRAFCET. The Nelder-Mead algorithm [5] for the minimization of multi-dimensional functions was developed for process optimization and automatic tuning of SOPs in response to upsets during fermentation and distillation unit operations.

3. Results and discussion

Modelling results for hydrolysis and fermentation were consistent with published data while the distillation model incorporates a cold start-up, normal batch, semi-batch and continuous

operations, and unit shutdown. The developed OTS can be used to train biorefinery operators for both normal and non-routine operations. Automatic SOP adjustment shows that hydrolysis enzyme dosage is automatically adjusted in response to fluctuations in solids loading concentration (Figure 1).

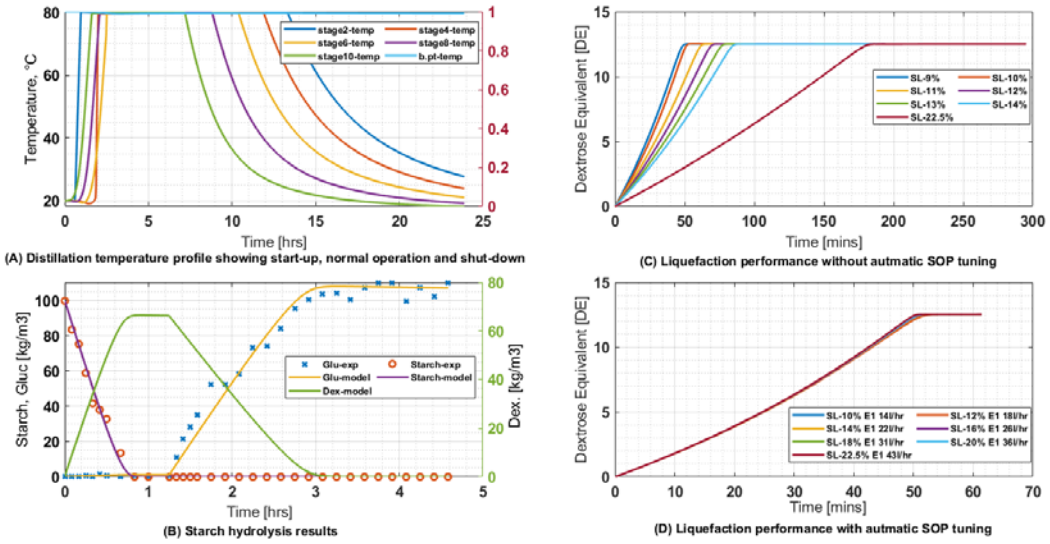

Figure 1. Model results (A & B) and automatic SOP tuning results (C & D)

4. Conclusions

This paper presents the results of the first attempt to incorporate an algorithm for process optimization and automatic tuning of SOPs into an operator training simulator. This extends the usefulness of the traditional OTS beyond operator training to include automatically adjusting production recipe inputs that inform operator corrective action, thereby minimizing material losses and process downtime.

References

[1] Isimite, J.O., Baganz, F. & Volker, C.H. 2018, "Operator training simulators for biorefineries: current position and future directions", *Journal of Chemical Technology & Biotechnology,* vol. 93, no. doi:10.1002/jctb.5583, pp. 1529-1541.

[2] Hass, VC, Kuhnen, F & Schoop, K-M, 2005, "An environment for the development of operator training systems (OTS) from chemical engineering models", Computer Aided Chemical Engineering, vol. 20, pp. 289-293.

[3] Schoop, K-M, 2008, WinErs: Process control and automation system on PC under Windows. Available: http://www.schoop.de/index.php/en/software/winers [2016, Online, Acc. Jan. 2018].

[4] IEC Working Group 3B/WG14 2002, IEC 60848:2013 - GRAFCET specification language for sequential function charts, 2nd [Available online http://snmaicpc.chez.com/pdf_zip/MAI2/cours/norme%20grafcet.pdf] edn, International Electrotechnical Commission, Sweden.

[5] Nelder, J.A., Mead, R. (1965), A Simplex Method for Function Minimization, The Computer Journal 7 (4):308–313, Available online https://doi.org/10.1093/comjnl/7.4.308

ECCE12
The 12th EUROPEAN CONGRESS OF CHEMICAL ENGINEERING
Florence 15-19 September 2019

M³C and scale up&down of lactic acid bacteria fermentations based on pH-gradients and population heterogeneity

Klaus Pellicer Alborch[1], Robert Spann[2], Gürkan Sin[3], Krist V. Gernaey[3], Peter Neubauer[4], Stefan Junne[4]

1 BASF SE, Ludwigshafen am Rhein, Germany; 2 Chr. Hansen A/S, Hørsholm, Denmark; 3 Process and Systems Engineering Center (PROSYS), DTU Chemical Engineering, Department of Chemical and Biochemical Engineering, Technical University of Denmark, Søltofts Plads, Building 227, DK-2800 Kongens Lyngby, Denmark; 4 Chair of Bioprocess Engineering, Institute of Biotechnology, Technical University of Berlin, Ackerstraße 76, ACK24, 13355 Berlin, Germany

**Corresponding author: k.pellicer@pellicerconsultants.com*

Highlights

- Scale up&down of production of lactic acid bacteria starter cultures for dairy industry
- Model-based process monitoring&control with the pH-value as only input variable
- PAT for determination of population heterogeneity under different pH-gradients
- Growth prediction based on single-cell size distribution measurements

1. Introduction

Oscillatory conditions, which usually appear in large scale bioreactors due to limitations in the power input and extended mixing times, can lead to cell stress and increased occurrence of population heterogeneity. Such heterogeneities are regularly observed in industrial production; however, the underlying mechanisms are seldom perceived or considered in bioprocess development. Since the occurrence of subpopulations may have a significant impact on the productivity of industrial cultures, cellular heterogeneity requires quantification with appropriate monitoring tools [1].

In case of lactic acid bacteria production, pH-gradients are the main concern when facing scale-up, since they lead to growth retardation, a loss of productivity and an altered population heterogeneity.

2. Methods

In order to study the impact of these gradients on the population heterogeneity of *Streptococcus thermophilus* cultures, various scale-down approaches were applied. Firstly, compartmentation of different zones was achieved through two- and three-compartment scale-down reactors (Two-CR and Three-CR, respectively), both consisted of a 10 L nitrogen aerated stirred tank reactor (STR) connected to one or two non-aerated plug flow reactors (PFR), respectively [2]. Base addition was performed from the bottom of one PFR, whilst acid was introduced from the bottom of the second PFR in the Three-CR system. Thus, (i) a zone of high pH-value (i.e. the base addition zone in the industrial reactor, simulated in one PFR), (ii) a compartment with low pH environment (i.e. the zone far away from the base addition, mimicked in the other PFR) and (iii) a homogeneous bulk zone

(simulated in the STR) were achieved in lab scale. Secondly, pulse feeding experiments were performed in a one compartment reactor, so that the whole population was subjected to the same pH shifts.

The physiologic heterogeneity of the population was assessed by means of the morphological heterogeneity in cocci chain length formation under optimal and pH-oscillating environments with *at-line* light microscopy analysis and automated cell image recognition. Furthermore, the consequences for cell growth, substrate conversion and product formation were studied in detail.

3. Results and discussion

The authors observed that the chain length of *S. thermophilus* varies as a response to environmental stress. A narrow distribution of short chain lengths during the exponential phase under optimum conditions was revealed, whilst the cell size distribution was broad and shifted to longer chain lengths under pH-gradients, as induced in scale-down fermentations. It could be shown that the appearance of certain cocci chain lengths is directly correlated to a reduced growth activity. Moreover, the different scale-down approaches were compared to the population heterogeneity detected in the production scale to identify the most suitable design.

By coupling of a mechanistic model [3, 4] to predict macroscopic state variables (such as substrate consumption, biomass growth and by-product formation, among others), a population balance model (PBM) was developed. This needs only the actual pH-value in the bioreactor to predict the cocci chain length distribution *on-line*, which gives information about the current biomass quantity as well as quality in the broth (Figure 1). In this manner, a change in the running process (e.g. increase stirring speed to decrease pH-gradients) is still possible in order to ensure the product characteristics at the harvesting point, with the highest yield.

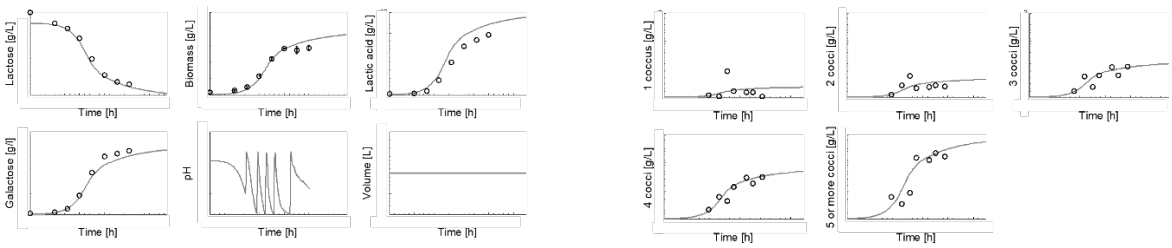

Figure 1. Development of macroscopic variables (left) and of variable chain lengths (right) over fermentation time of a *S. thermophilus* culture under certain pH-gradients. Experimental data (dots) and population balance model (line).

4. Conclusions

The M^3C methodology presented here is able to predict biomass quality (i.e. acidification activity, as a function of the chain length) based solely on the pH-value in the culture broth. Using CFD studies in the industrial scale, pH-gradients and compartmentalization could be easily incorporated into the PBM. This approach, coupled to *in-situ* quantification of the cell size distribution with advanced *on-line* microscopic techniques and image analysis using neural networks (NNs), would enable growth performance prediction in real-time. This would allow for (i) the rapid evaluation of media, (ii) the adjustment of the power input during base addition to keep pH-gradient formation as non-sensitive for process performance, (iii) the determination of a suitable point for harvest under consideration of cell vitality, and (iv) in general the improvement of quality control.

References

[1] K. Pellicer-Alborch, A. Angersbach, P. Neubauer, S. Junne, Front. Bioeng. Biotech. 6, 188 (2018) 1–10.
[2] A. Lemoine, N. M. Martínez-Iturralde, R. Spann, P. Neubauer, S. Junne, Biotech. Bioeng. 112, 6 (2015) 1220-1231.
[3] R. Spann, J. Glibstrup, K. Pellicer-Alborch, S. Junne, P. Neubauer, C. Roca, D. Kold, A. E. Lantz, G. Sin, K. V. Gernaey, U. Krühne, Biotech. Bioeng. (2018) 1-38.
[4] R. Spann, C. Roca, D. Kold, A. E. Lantz, K. V. Gernaey, G. Sin, Biochem. Eng. J. 135 (2018) 49-60.

ECAB 5
The 5th EUROPEAN CONGRESS OF APPLIED BIOTECHNOLOGY
Florence 15-19 September 2019

Relational Database for the Description of Fermentation inside a Simulation Software.

Simoneta Caño de las Heras*, Ulrich Krühne, Seyed Soheil Mansouri
Process and Sytems Engineering Center (PROSYS), Department of Chemical and Biochemical Engineering, Technical University of Denmark, Søltofts Plads, Building 229, 2800 Kgs. Lyngby, Denmark
**Corresponding author: simoca@kt.dtu.dk*

Highlights

- Fermentation simulators could be beneficial to asses the feasibility of different kinetic scenarios.
- A database is developed that incorporates information related to kinetic parameters of fermentation models.
- This database is integrated inside a pedagogical software platform, *FermProc*.

1. Introduction

Simulators are well established tools for instructing, design, and development of bioprocesses with the advantages of its portability, safety, user friendliness, and cost-effectiveness [1]. However, commercially simulators commonly work as a black box and consequently, their mathematical models are not displayed and/or being available for its modification. And therefore, it is not possible to recognize the assumptions made [2], [3] complicating the comprehension of the process. Furthermore, simulators are not generally intended to evaluate the feasibility of the simulated scenarios ergo users require a high previous knowledge of the bioprocess. This is highly relevant in case of fermentation processes as their mathematical models have several complexity layers and involve biological, chemical, physical and mechanical components. Moreover, bioprocess simulators commonly suffer from the lack of an organized database for the differentiation and analysis of the model components as well as the aforementioned limitations [4].

In this work, a prototype database that embeds common limits and values of the parameters of bioprocesses, is presented. This database is integrated inside a software platform called *FermProc*[5]. *FermProc* allows the display, reuse and modification of models and it is being developed at the Department of Chemical and Biochemical Engineering of the Technical University of Denmark as a pedagogical software for teaching of bio-manufacturing processes.

2. Architecture of the system

Figure 1 illustrates the functional system architecture. The architecture is designed with modular capabilities and involves the dynamic simulation of the bioprocess with the automatic solution of the model and its display. To do so, a relational database (in SQL) that collects and reuses interrelated rules, usually associated with characteristic values of the bioprocess is developed. This database uses the parameter, constant or variable as the data value. Therefore, a *"parameter set id"* uniquely identifies the record and associates each of them with specific maximum and minimum values. The *"parameter set id"* is connected with the process conditions such as the microorganism, the limiting substrate or bioreactor that may influence the data.

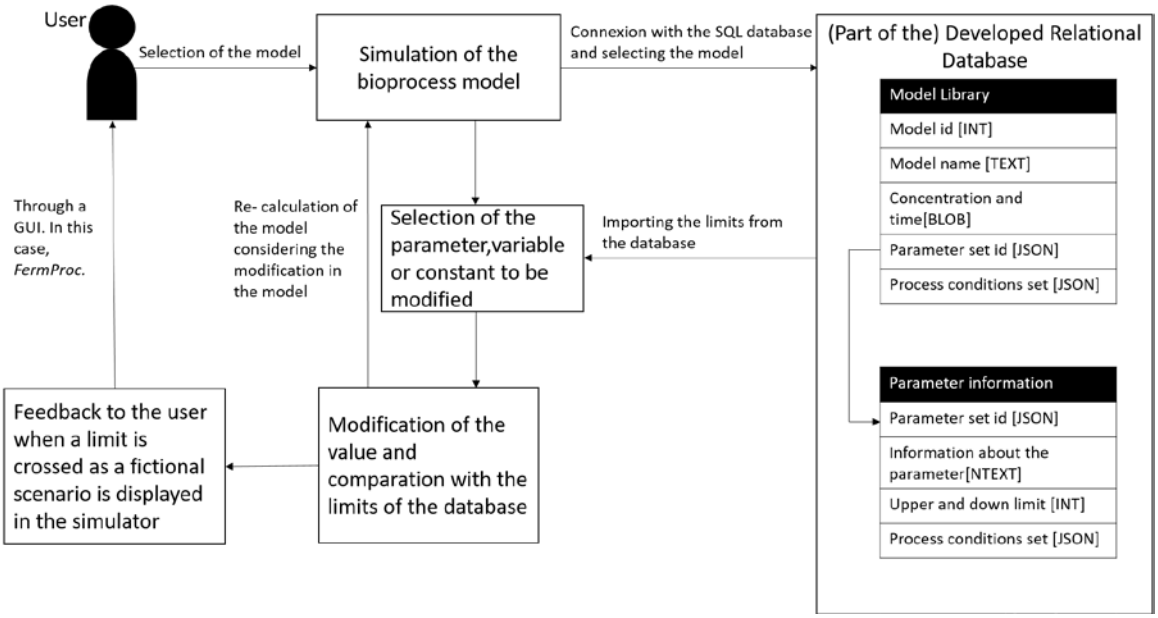

Figure 1. Schematic functional system architecture.

Furthermore, the database includes a theoretical explanation with the source of information so users can trust the database. Finally, an example of the use of the database can be found at https://youtu.be/qhucwjf_i0E. This video shows how a user interacts with a model of the aerobic growth of *Saccharomyces cerevisiae* and how a warming window will pop up when the oxidative yield of the consumption of glucose is modified over the thermodynamic limit [6].

3. Conclusions

Although there are several bioprocess simulators and common values and limits of different parameters involved in fermentation can be found in literature; there is a lack of an integrated system in which this information can be collected and displayed. To fulfill this need, a relational database that stores information about parameters of fermentation processes is developed. Furthermore, the database is implemented in a simulator, called *FermProc,* to facilitate the analysis of fictional scenarios through interactive modifications of the model.

References

[1] H. Shen *et al.*, "Conducting laboratory experiments over the internet," *IEEE Trans. Educ.*, vol. 42, no. 3, pp. 180–185, 1999.

[2] M. G. Rasteiro *et al.*, "LABVIRTUAL-A virtual platform to teach chemical processes," *Educ. Chem. Eng.*, vol. 4, no. 1, pp. 9–19, 2009.

[3] M. Heitzig, G. Sin, P. Glarborg, and R. Gani, "A computer-aided framework for regression and multi-scale modelling needs in innovative product- process engineering," *Comput. Aided Chem. Eng.*, vol. 28, pp. 379–384, 2010.

[4] S. Caño de las Heras, "A Systematic Computer-aided Framework for Development of Pedagogical Process Simulators using Gamification Elements A fermentation case study," Aalborg Universy Copenhagen, 2018.

[5] S. Caño de las Heras, U. Krühne, and S. S. Mansouri, "FermProc : A Pedagogical Simulation Tool for Fermentations," in *Proceedings of the 46th SEFI Annual Conference 2018*, 2018.

[6] P. M. Doran, *Bioprocess Engineering Principles*. 1995.

ECAB 5
The 5th EUROPEAN CONGRESS OF APPLIED BIOTECHNOLOGY
Florence 15-19 September 2019

An Enzymatic Cascade with Integrated Process Intensification for Synthesis of Natural Flavors.

C. Engelmann[1*], N. Ekambaram[1], J. Johannsen[2], T. Waluga[2], G. Fieg[2],

A. Liese[1], P. Bubenheim[1]

[1] *Hamburg University of Technology, Institute of Technical Biocatalysis, Hamburg, Germany;* [2]*Hamburg University of Technology, Institute of Process and Plant Engineering, Hamburg, Germany*

**Corresponding author: Claudia.engelmann@tuhh.de*

Highlights

- Establishment of a 3-enzyme cascade in a two phase system
- Integrated *in situ* cofactor regeneration and *in situ* product extraction
- Process optimization by enzyme immobilization

1. Introduction

Biotechnical processes are a promising alternative to conventional chemical reactions, if they fulfill certain requirements like less byproduct formation, less intermediate separation, environmentally friendly and sustainable reactions. With different methods to improve the productivity, like efficient cofactor regeneration and simplified downstream processing, these enzymatic reactions are of increasing importance for industry.[1,2] In this study a three enzyme cascade in two phases is evaluated, as shown in figure 1. In the aqueous phase an alcohol dehydrogenase (ADH) is reducing the substrate cinnamal to the corresponding alcohol. Since this enzyme is NADH cofactor dependent an *in situ* regeneration is established by formate dehydrogenate (FDH). The product is extracted *in situ* by an organic solvent to realize the esterification by a lipase to the target product cinnamyl cinnamate.

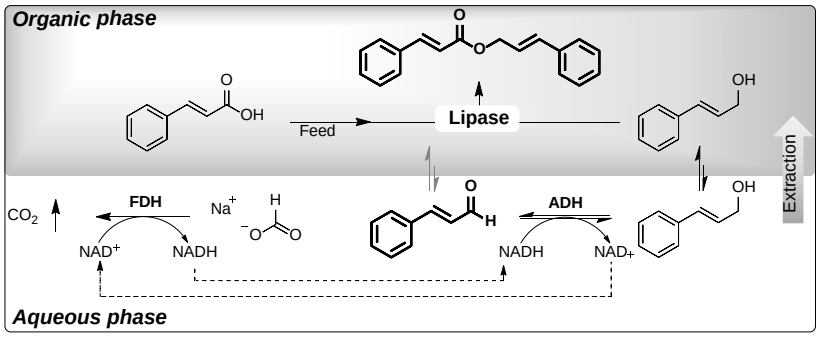

Figure 1. Reaction scheme of the enzyme cascade.

2. Methods

Three different enzymes are investigated, whereby the enzymes used in the aqueous phase are immobilized with different techniques. Characterization of free and immobilized enzymes is performed via activity and kinetic, as well as stability measurements. The whole cascade is carried

out in a reactor concept with an integrated extraction centrifuge and a fixed-bed reactor for the esterification.

3. Results and discussion

A suitable organic solvent has to be identified for the enzymes in the aqueous phase, as well as for the esterification. Buffer saturated with different solvents are screened regarding ADH activity, whereby compounds with high logP values showed the lowest influence on enzyme activity. Xylene is chosen as second phase, due to its high logP value, dissolution of the substrates and good properties regarding process safety. Based on this, the individual enzymes are characterized in xylene saturated buffer and their respective kinetic parameters (Michaelis-Menten) were determined. In addition, the esterification in xylene by an immobilized lipase was carried out and high yields of over 95% for the two reaction steps show the feasibility of this cascade.

To improve the enzyme stability and simplify the downstream processing, immobilization of the biocatalysts in the aqueous phase is investigated in detail, shown in figure 2. Several techniques are screened, whereby cross-linked enzyme crystals (CLEAs) and covalent immobilization on hydrophilic amino-activated supports showed good immobilization yields and the highest residual activities.

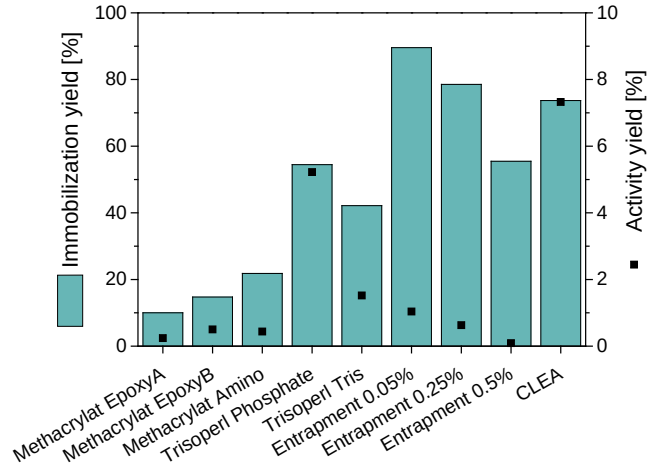

Figure 2. Results of the screened immobilization methods.

4. Conclusions

A multi-enzyme cascade in a two phase system was successfully established and evaluated in detail. Xylene was chosen as suitable organic solvent for the second phase and the enzymes were characterized regarding these reaction conditions. Different immobilization techniques were studied, whereby covalent immobilization on hydrophilic supports showed the most promising results for the ADH. The established system will be further investigated in a larger reactor set-up.

References

[1] K. Goldberg, K. Schroer, S. Lütz, A. Liese, Appl. Microbiol. Biotechnol. 76 (2007) 237–248.
[2] C. Scherkus, S. Schmidt, U.T. Bornscheuer, H. Gröger, S. Kara, A. Liese, ChemCatChem 8 (2016) 3446–3452.

ECCE12
The 12th EUROPEAN CONGRESS OF CHEMICAL ENGINEERING
Florence 15-19 September 2019

Validation of High Lignin Content Biomass Using Supercritical Water Technology.

Tijana Adamovic[1], Celia Martinez[1], María José Cocero[1]

1 High Pressure Processes Group, Department of Chemical Engineering and Environmental Technology, University of Valladolid, 47005 Valladolid, Spain

**Corresponding author: tijanaadamovic@gmail.com*

Highlights

- Selective valorization of high content lignin biomass
- Transformation to lignin-cellulose composites
- Transformation of carbohydrate to sugars with a yield of 88%

1. Introduction

Lignocellulosic biomass is the most abundant and easily grown biomass form. Being composed of three main biopolymers, cellulose, hemicellulose and lignin, it presents a great source of a wide range of chemicals.

SCWH is recognized as a potential hydrolysis technique to decompose lignocellulosic materials due to its properties, low viscosity and high diffusely that facilitate penetration of water into complex biomass matrix, while its low dielectric constant similar to non-polar organic solvents enhances solubility of organic compounds[1]. This technique can be used as a pre-treatment for the selective fractionation of cellulose, hemicellulose and lignin or as a reaction medium to directly hydrolyse the polymers into its constituent[2].

Defatted grape seed is composed of more than 50% of lignin vs 15% of carbohydrates and thus potential feedstock for lignin and aromatic components contained in lignin structure.

2. Methods

Ultra-Fast Supercritical Water Hydrolysis

For biomass fractionation continues pilot plant with a sudden expansion micro reactor was used. The grape seed suspension was pumped up to 26 MPa and instantaneously heated to 385 ^{o}C by mixing it with a SCW stream. The reaction is stopped by depressurizing the product through a high temperature needle valve and therefore instantaneously cooled down. The reaction time was adjusted in the range of 0.16s to 0.65s just by changing the length or the reactor and biomass and water flow.

Analysis

To determine the composition of the raw material and samples Laboratory Analytical Procedure (LAP) from NREL was followed. The analysis used to determine sugar and sugar degradation products is HPLC. The carbon content is determined by Total organic carbon and Elemental Analysis. Gel Permeation Chromatography is used for molecular weight distribution. FTIR and NMR analysis are used to understand the changes in sample structure.

3. Results and discussion

Amount of lignin in solid phase increases with the reaction time (Figure 1.) due to hydrolysis of labile fractions, which is also followed with a decrease of sugars in the solid phase and high yield in the liquid phase (Figure 2.). For reaction time 0.32 s the amount of lignin slightly decreases compared with lower reaction time and this could be the possible time point of lignin hydrolysis. Higher reaction time increase the content of lignin that can be due to lignin repolymerization. This behavior is supported by the sugar yield in the liquid phase. For the reaction time of 0.16 s the yield of sugar in the liquid phase is already high and reach 57%. Further increase in reaction time leads just to a slight increase in sugar yield as the main amount has been already consumed. After 0.32 s the yield of sugar again increases as the new amount of sugars inside the biomass matrix is more available. This is followed by an increase of degradation products during the reaction.

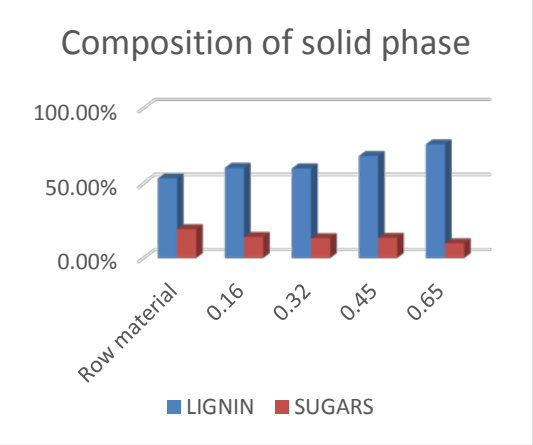

Figure 1. Composition of solid phase

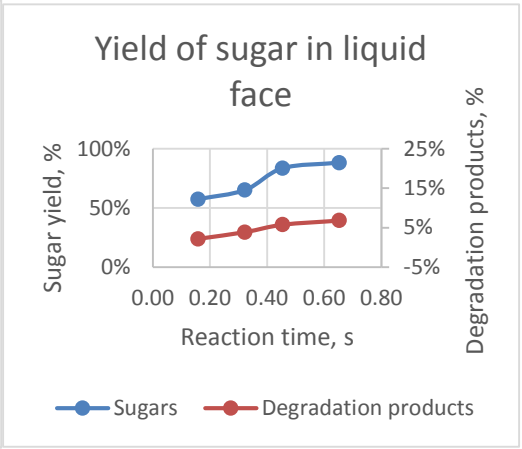

Figure 2. Sugar yield in liquid phase

4. Conclusions

The results of biomass fractionation in SCW show a slight decrease of lignin content in the solid phase at 0.32 s followed with increased sugar yield in the liquid phase that could be due to the lignin hydrolysis and higher availability of sugars at this time. High lignin content in raw material suggests that this biomass could be a great source for aromatic products derived from lignin degradation where more analysis is required in order to determine those products in the liquid phase, while the solid residue could be valorized as lignin-cellulose composites.

References

[1] COCERO, MJ., CABEZA, A., ABAD, N., ADAMOVIC, T., VAQUERIZO, L., MARTÍNEZ CM., PAZO-CEPEDA, MV., Understanding biomass fractionation in subcritical & supercritical water, *J Supercritical Fluids*, 133, Part 2, 2018, 550-565.

[2] Juliana M. Pradoa, Daniel Lachos-Perezb, Tânia Forster-Carneirob, Mauricio A. Rostagnoc, Sub- and supercritical water hydrolysis of agricultural and food industry residues for the production of fermentable sugars, *Food and Bioproducts Processind* Volume 98, April 2016, Pages 95-123

Hydrothermal Liquefaction of Lignocellulosic Ethanol Lignin-Rich Co-Product.

Edoardo Miliotti[1*], Stefano Dell'Orco[1,2], Giulia Lotti[1], Alberto Bini[1], Andrea Maria Rizzo[1], Luca Rosi[1,3], David Chiaramonti[1,2]

1 RE-CORD, Viale Kennedy 182, 50038, Scarperia e San Piero, Florence, Italy; 2 Department of Industrial Engineering, University of Florence, Viale Morgagni 40, 50135, Florence, Italy; 3 Chemistry Department "Ugo Schiff", University of Florence, Via della Lastruccia, 3-13 50019 Sesto Fiorentino, Florence, Italy

**Corresponding author: edoardo.miliotti@re-cord.org*

Highlights

- Temperature is the most significant factor for light and heavy biocrude yield.
- B/W is not a significant factor for light and heavy biocrude yield.
- Good biocrude and low solids yields were achieved without catalysts or capping agents.

1. Introduction

Residual/dedicated lignocellulosic biomass will be the future main feedstock for sustainable biofuel production, now dominated by lipids, which are criticized, since they rely on food and mainly on imported palm oil. The major effort in the EU focuses on developing new industrial energy chains to produce truly sustainable biofuels/bioenergy from lignocellulosic material. The lignocellulosic ethanol route has achieved full industrial scale worldwide and, consequently, a very wet lignin-rich co-product is made available at the production site in considerable amount and affordable costs [1], whose current use is combustion for heat and power generation. However, being lignin the most abundant renewable source of aromatics in nature, its valorization represents a very attractive opportunity for green chemistry. Several studies addressed the economic valorization of lignin-rich streams (LRS) from lignocellulosic ethanol production, highlighting the importance of co-product valorization to achieve commercial competitiveness [2,3]. Hydrothermal liquefaction (HTL) is a thermochemical process, which can convert biomass into a biocrude by using hot compressed water [4,5]. It is a wet process, which does not require feedstock drying, as it is generally required by other technologies like gasification and pyrolysis. As such, HTL is an attractive approach for the conversion of wet biomass into a liquid intermediate for chemicals and biofuels. HTL generates biocrude as main fraction, along with gaseous products, solids, and an aqueous-phase byproduct. Different behavior in pyrolysis of lignin from different origin was demonstrated in an international round-robin [6] and to date, most of the known HTL studies addressed lignin from pulp and paper or high-purity model compounds [7,8], both of them structurally different from lignocellulosic ethanol LRS, which still needs further investigation. The present work aims at partially filling this gap by preliminary assessing the viability of converting this material.

2. Methods

The LRS was characterized and then processed in a custom-made batch test bench. Two solvent extraction methods were investigated and compared for the extraction of a light and a heavy biocrude fraction. A full factorial design of experiment (5 % significance level) was performed, investigating the influence of process parameters on product yields, biocrude elemental composition, molecular weight and carbon balance. Investigated temperature, time and biomass-to-water mass ratio (B/W) were, respectively, 300, 350 and 370 °C, 5 and 10 min, 10 and 20 % w/w. The biocrudes were analyzed in terms of CHN, ash content, GPC and FT-IR.

3. Results and discussion

The feedstock, as received, contained a high amount of moisture (~70 % w/w on wet basis) and nearly 54 % w/w of lignin on dry basis. The total biocrude yields ranged from 39.8 to 65.7 % w/w. Temperature was the main parameter determining a different distribution between the light and heavy fractions: at 300 °C the higher amount of heavy biocrude was recovered, while at 350 and 370 °C the yield of the light fraction increased, reaching 41.7 % w/w at 370 °C. Instead, B/W ratio did not cause a significant effect on light and heavy biocrude yields. A relatively low amount of solid residue was observed (from 11.4 to 19.5 % w/w), even without catalysts or capping agents. Feedstock carbon content was mainly recovered in the biocrude (up to 77.6 % w/w): the distribution between the light and heavy fractions followed the same trend as the yields. The typical aromatic structure of the LRS was also observed in the biocrudes, indicating that mainly hydrolysis depolymerization occurred. The weight-average molecular weight of the total biocrude was strictly related to process temperature, decreasing from 1146 at 300 °C to 565 g mol^{-1} at 370 °C.

4. Conclusions

LRS was converted without catalysts or capping agents in light and heavy biocrude with a relatively low amount of solid residue. Concerning the biocrudes yields, temperature was the most significant parameter. The elemental analysis suggests that the light biocrude was mainly produced by decarboxylation rather than dehydration, which was more evident for heavy biocrude and solids. The aromatic structure typical of lignin was preserved in the biocrudes, indicating the feedstock was mainly subjected to hydrolysis depolymerization. The decreasing values of the molecular weight with temperature indicated that a consistent fractionation occurred.

References

[1] V. Balan, D. Chiaramonti, S. Kumar, Biofuels, Bioprod. Biorefining. 7 (2013) 732–759.
[2] S. Farag, J. Chaouki, Bioresour. Technol. 175 (2015) 254–261.
[3] S. V. Obydenkova, P.D. Kouris, E.J.M. Hensen, H.J. Heeres, M.D. Boot, Bioresour. Technol. 243 (2017) 589–599.
[4] L. Cao, C. Zhang, H. Chen, D.C.W. Tsang, G. Luo, S. Zhang, J. Chen, Bioresour. Technol. 245 (2017) 1184–1193.
[5] D. Castello, T. Pedersen, L. Rosendahl, Energies. 11 (2018) 3165
[6] D.J. Nowakowski, A. V. Bridgwater, D.C. Elliott, D. Meier, J. Anal. Appl. Pyrolysis. 88 (2010) 53–72.
[7] J. Barbier, N. Charon, N. Dupassieux, A. Loppinet-Serani, L. Mahé, J. Ponthus, M. Courtiade, A. Ducrozet, A.A. Quoineaud, F. Cansell, Biomass Bioenergy. 46 (2012) 479–491.
[8] T.D.H. Nguyen, M. Maschietti, L.E. Åmand, L. Vamling, L. Olausson, S.I. Andersson, H. Theliander, Bioresour. Technol. 170 (2014) 196–203.

Hybrid Models: A new generation of predictive models for process design, development and optimisation

Harini Narayanan[1*], Michael Sokolov[1,2], Alessandro Butté[1,2], Massimo Morbidelli[1,2]

1 Institute of Chemical and Bioengineering, Department of Chemistry and Applied Biosciences, ETH Zurich, Zurich, Switzerland; 2 DataHow AG, Zurich, Switzerland

**Corresponding author: nharini@chem.ethz.ch*

Highlights

- Hybrid models have better accuracy in prediction compared to classical PLS models
- Hybrid models have better interpolation and extrapolation capabilities
- Ideal for Experimental Design and process optimization

1. Introduction

Over the last few years, the biopharmaceuticals market has witnessed tremendous growth reaching a value of worth $186,470 million in 2017. Now, the biggest challenge of the industry is to produce high-quality products in a cost–effective manner. To meet the market demands, there is a need for rapid and efficient process development that calls for the use of model-based methods to assist at several stages of process development, monitoring and control. The lack of complete understanding about the metabolic network and reaction pathways observed in the cells, especially mammalian cells hinders the development of First Principle Models (FPMs). Thus, increased efforts have been devoted to the use of statistical models (such as Partial Least Squares – PLS models) using historical, online spectral and sensor data [1]. However, one of the major limitations of statistical models is its invalidity or poor performance outside of the regions not explored in the underlying experiments. As a result, statistical models are not suitable for process design, development and optimization [2]. We propose and quantitatively show the advantages of using Hybrid modeling strategy which explores a synergy between the classical First Principle models and statistical models.

2. Methods

The FPMs provide a mixed system of differential - algebraic equation which often contains specific unknown parameters. The hybrid models establish a synergy by using statistical models to deduce these unknown parameters. Particularly, we pose mass-balance or pseudo mass-balance equations for bioreactor systems and use artificial neural networks to estimate the unknown specific rates. Through different bioprocess case studies, we showcase the added value of hybrid models compared to the state-of-the-art PLS models, in terms of: Predictive accuracy, interpolation and extrapolation capabilities and application in design of experiments for optimization of titer (concentration of monoclonal antibody produced).

3. Results and discussion

Hybrid models have the lowest errors in prediction for the key state variables (Figure 1, Left). Lower prediction errors ensure reliable models that can be used as soft sensors to replace expensive analytics. Secondly, given a fed – batch system with glucose feed from day 3, hybrid models correctly predict a daily continuous decrease in glucose concentration whereas the PLS models are not capable of incorporating the feeding strategies in a physically representative manner. Additionally, Hybrid models is seen to predict process variables accurately outside of the trained or observed operating conditions highlighting its potential application in *in-silico* design of experiments and process optimization (results not shown here).

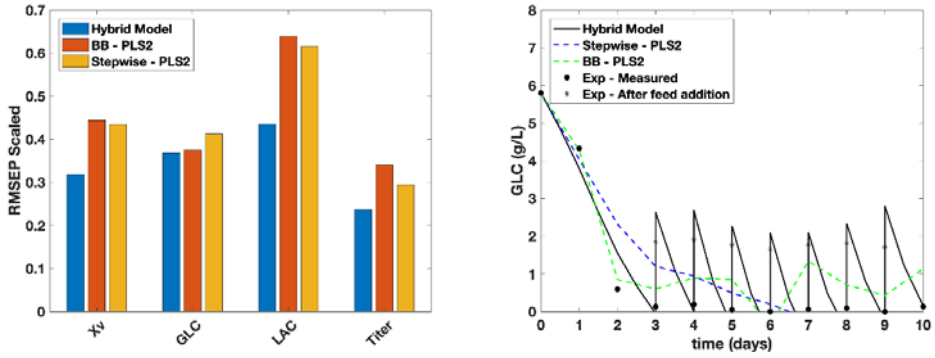

Figure 1. (Left) Comparison of the accuracy of the hybrid model against two statistical models (both based on PLS) in terms of standardized errors in prediction for viable cell density (Xv), Glucose (GLC), Lactate (LAC) and titer. (Right) The concentration of glucose predicted by the three models as a function of time along with the experimental observation.

4. Conclusions

A success in efficient data management and analytics is expected to have a tremendous effect on improving process development strategies and reducing manufacturing costs, thus making these therapies more available to society. We show that a modest modeling effort is sufficient to generate a hybrid model capable of predicting the complete evolution of the process variables and titer solely based on the initial conditions and the process operating conditions. Hybrid modeling also shows good interpolation and extrapolation capabilities in comparison to statistical models, which face intrinsic limitations to predict outside their training process condition space. This extrapolation capability is not only central for model–based process optimization but also for process scale–up, technology transfer and decision-making in process development. Thus, we strongly believe in investing efforts in the direction of hybrid modeling for process optimization and further extend its application to process monitoring and control.

References [Calibri 10]

[1] T. Kourti, “Multivariate dynamic data modeling for analysis and statistical process control of batch processes, start-ups and grade transitions,” J. Chemom., vol. 17, no. 1, pp. 93–109, 2003.

[2] D. Solle et al., “Between the Poles of Data-Driven and Mechanistic Modeling for Process Operation,” Chemie-Ingenieur-Technik, vol. 89, no. 5, pp. 542–561, 2017

ECAB 5
The 5th EUROPEAN CONGRESS OF APPLIED BIOTECHNOLOGY
Florence 15-19 September 2019

Production of lactic acid from the organic fraction of municipal solid wastes using *B. coagulans*.

J. Pablo López-Gómez*, Roland Schneider, Peter Unger, Joachim Venus.

Leibniz Institute for Agricultural Engineering and Bioeconomy

**plopezgomez@atb-potsdam.de*

Highlights

- OFMSW hydrolysate contains more than 50 g/L of fermentable sugars.
- *B. coagulans* was able to grow without the addition of any extra nutrients
- Glucose is completely consumed and LA final concentration reached 60 g/L.
- The conversion yield for the process was 0.79 g_{LA}/g_{sugars}

1. Introduction

Investigations into new substrates for the production of chemicals and energy have become more demanding in recent years; not only looking for renewable sources but also for those that are cheap residues. This study focuses on the valorization of the organic fraction of municipal solid waste (OFMSW) also known as biowaste. On average, 40% of this abundant residue, with an estimated yearly production of 88 million tonnes, is landfilled in the EU. Besides posing an environmental risk, landfilling also disregards the potential of the material for being utilized as the substrate in other processes. The OFMSW, is rich in both carbon and nitrogen sources, which makes it an interesting material for the production of value added chemicals through fermentation. This study evaluates a hydrolysate produced from the OFMSW for the production of l-lactic acid. Besides the numerous applications of this versatile platform chemical, its utilization for polylactic acid (a biodegradable plastic) synthesis has recently raised interest on its production. *B. coagulans* are homofermentative l-lactic acid producers, with low nutritional requirements and the ability of growing at 52°C (reducing risks of contamination) which make them of interest for the valorization of waste streams. A *B. coagulans* isolate was used for the fermentations.

2. Methods

The substrate for the fermentation was a hydrolysate of the OFMSW. It was obtained from IMECAL SA (Valencia, Spain). Chemical compositional analysis of the substrate was performed for the determination of sugars, organic acids, minerals and nitrogen content. *Bacillus coagulans* A160 (Leibniz Institute for Agricultural Engineering and Bioeconomy, Germany) was employed for the fermentation of the OFMSW hydrolysate. The inoculum for the 1 L scale bioreactor was prepared in MRS broth (Merck, Germany) with dolomite EVERZIT Dol 0.5-2.5 mm (Evers, Germany) as buffer, at an orbital shaker set at 100 rpm, 42 °C for 13 h. Following preliminary lab scale fermentations a technical scale fermentation was carried out in a 72 L BIOSTAT UD bioreactor (B-Braun Biotech, Germany) containing 30 L of OFMSW hydrolysate. Fermentation was carried out at 52 °C and pH 6. Stirring occurred at 300 rpm using a double Rushton turbine. Regulation of pH was carried out by adding 20% (w/w) NaOH. The inoculum, 5% (v/v), was

prepared in a 2 L fermentation vessel containing 1 L of OFMSW hydrolysate. Samples were taken regularly for the quantification of sugars and lactic acid.

3. Results and discussion

Results for the compositional analysis of the OFMSW hydrolysate show that, in most cases, the hydrolysate has a concentration of glucose higher than 50 g/L. Results for the variation in concentrations of sugars and lactic acid throughout the fermentation are shown in Figure 1.

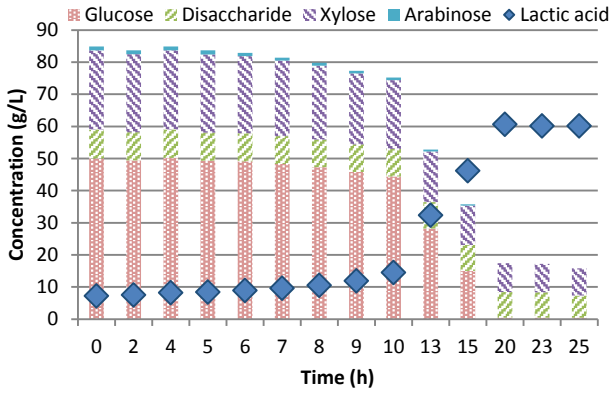

Figure 1. Variation in the concentrations of sugars and lactic acid during a fermentation of OMSW hydrolysate in a technical scale bioreactor (30 L working volumen). The strain used was B coagulans A166 and the fermentation was performed at 52°C and pH was controlled at 6.

LA had a concentration of 7.25 g/L at the start of the fermentation reaching a maximum value of 60.71 g/L by the end of the fermentation. Analysis of enantiomeric purity gave a result of 93.85% for L-LA. As shown in the figure above, the initial concentration of total sugars was around 83 g/L. From that, 50 g/L was glucose, 24.5 g/L xylose, 9 g/L disaccharides and 1.25 g/L arabinose. The fermentation was stopped when the production of LA ceased, by that point the remaining concentration of total sugars was 15.80 g/L. That represents a consumption of approximately 81 % of the initial amount of sugars. The conversion yield for the process was 0.79 g_{LA}/g_{sugars} (79 % conversion).

4. Conclusions

The hydrolysate from OFMSW is a good substrate for the production of lactic acid with a total sugars concentration in the hydrolysate exceeding 70 g/L (50g/L for glucose). Furthermore, the hydrolysate is able to support the growth of the bacteria without the addition of any other nutrients and without any apparent inhibitory effects. After fermentation using *B. coagulans* conversion yield for the process was 0.79 g_{LA}/g_{sugars} and a LA final concentration of 60.71 g/L were achieved.

ECAB 5
The 5th EUROPEAN CONGRESS OF APPLIED BIOTECHNOLOGY
Florence 15-19 September 2019

Startup of a tubular Microbial Electrolysis Cell for biogas upgrading

Lorenzo Cristiani*, Marco Zeppilli, Mauro Majone

Department of Chemistry Sapienza University of Rome, Piazzale Aldo Moro 5 00185 Rome, Italy

**Corresponding author: Lorenzo.cristiani@uniroma1.it*

Highlights

- Biogas Upgrading through bioelectromethanogenesis
- Fluidynamic and polarization curve characterization
- Conversion of electrical current into methane

1. Introduction

Biogas, the main product of the anaerobic digestion (AD) process, is a gas mixture mainly composed by carbon dioxide and methane. To obtain biomethane, with a high percentage of methane (>95%), is necessary a purification to remove the impurities such as NH_3, H_2S, and an upgrade step to remove the CO_2. These last steps are economically expensive and usually the biogas is utilized for the cogeneration of electricity and heat, however, an innovative strategy for biogas upgrading consist in the utilization of a microbial electrolysis cell (MEC) in which the reduction of carbon dioxide to methane is performed by a biocathode. The bioelectromethanogenesis reaction is made by electroactive microorganisms who convert CO_2 into CH_4 (Villano et al., 2010). Here, a fully biological tubular Microbial Electrolysis Cell (MEC) has been developed for the upgrading of biogas produced by a pilot scale two stage AD reactor operated with real agricultural waste from a cattle farm, mainly composed by manure and straw and crops residues. Inside the MEC, the bioreduction reaction occurred in a cathodic chamber converting the CO_2 into CH_4 while the oxidation of the organic matter by an anodic biofilm partially sustained the energy demand of the process. Before the inoculation of the tubular MEC, the fluidynamic of the anodic chamber has been characterized by a tracer test while a polarization curve permitted the description of the potential distribution in the reactor. After the inoculation of the anodic and cathodic chamber the batch startup phase has been conducted by controlling the anodic potential at 0.2V vs. SHE.

2. Methods

The empty volume of the MEC was 12 L; The anodic and cathodic chambers were filled with graphite granules with a concentric configuration, the chambers were separated by a tubular anion exchange membrane (AEM). The synthetic biogas (70-30 % v/v N_2-CO_2) has been fed from the bottom of the biocathode, the graphite granules bed allowed the growing electroactive biofilm on the surface area, available for the mass transfer from gaseous to liquid phase and vice versa. The bioanode was fed with a synthetic mix of organic substrates (glucose, peptone, yeast extract and acetic acid). The MEC polarization was controlled by a three-electrode configuration, in which the anode chamber resulted the working electrode. NH_4^+ was used as tracer for the tracer test analyzed with the Nessler method.

3. Results and discussion

The tracer test permitted to calculate the hydraulic residence time (58 minutes) and the porosity of the graphite granules (0.57), moreover the test showed the complete hydraulic separation of the two chambers. In figure 1 shows the concentration of NH_4^+ during the tracer test.

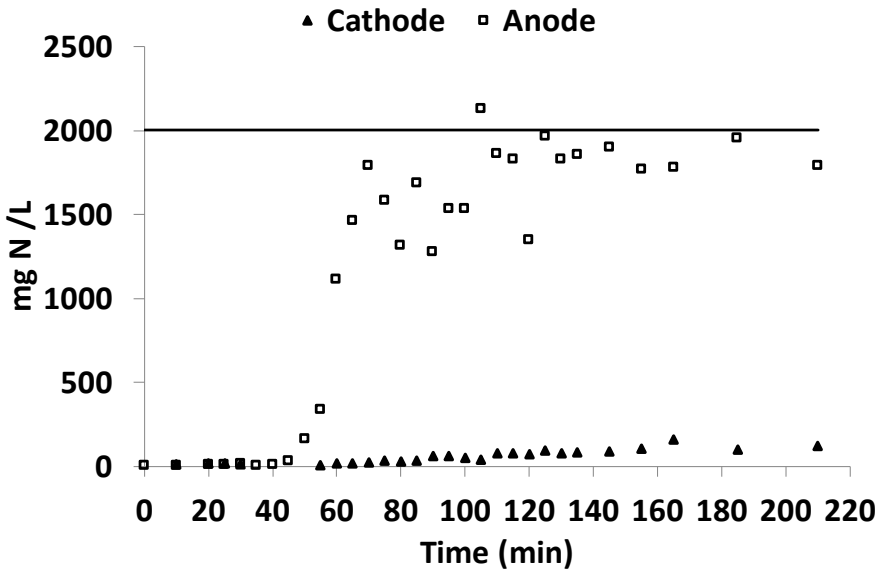

Figure 1. Nitrogen concentration during the tracer test.

The polarization curve of the tubular MEC showed the dependence of the anodic and cathodic electrodic potentials as well as the current flowing in the circuit as a function of the applied potential difference. After the preliminary characterization of the fluidynamic and of the electrodic potentials, the anodic and cathodic chamber have been inoculated with an activated sludge and an anaerobic sludge, respectively. The anodic potential was set at +0.2 V vs SHE and it was fed with the synthetic mix solution with a batch configuration. After nine days from the inoculation of the MEC, the electric current profile showed the production of a current around 100 mA, indicating the capability of the anodic biofilm to consume the organic matter by suing the anode as electron acceptor. The startup process went on for 35 days reaching a maximum of 120 mA, while in the cathodic chamber, the methanogenic biofilm produced 45 mmol/d of methane with an average cathode capture efficiency (i.e. the conversion of the current into methane) around 100 %.

4. Conclusions

The new tubular configuration MEC startup was successfully performed by using synthetic mixture of organic substrates, that permitted the development of electroactive biofilms in the anodic and cathodic chambers to perform the bioelectromethanogenesis reaction, sustained by the COD anaerobic oxidation

References

[1] Villano, M., et al., Bioelectrochemical reduction of CO2 to CH4 via direct and indirect extracellular electron transfer by a hydrogenophilic methanogenic culture. Bioresource Technology, 2010. 101: 3085-3090.

ECAB 5
The 5th EUROPEAN CONGRESS OF APPLIED BIOTECHNOLOGY
Florence 15-19 September 2019

Valorization of distillers dried grains with solubles for the production of enzymes

Jasper Driessen, Solange I. Mussatto

Biomass Conversion and Bioprocess Technology Group,
Novo Nordisk Foundation Center for Biosustainability, Technical University of Denmark
**Corresponding author: jasdri@biosustain.dtu.dk*

Highlights

- Optimization of lignocellulosic biomass pretreatment
- Adaptive laboratory evolution for increased robustness to hydrolysate-associated inhibitors
- Optimization in small-scale fermenters to study scale-up and scale-down effects for increased industrial applicability

1. Introduction

The total production volume of bioethanol reached 96 billion liters in 2015 and economic projections estimating a steady increase until 2020 [1] [2]. A vital part (20%) of the total plant revenue is generated by selling of distillers dried grains with solubles (DDGS) as animal feed. However, since DDGS can only account for 30% of the wildstock feed (dry basis) due to palpability and excessive protein issues, a saturated animal feed market is expected lower DDGS market prices [2]. Bearing these developments in mind, the need of an innovative method to generate value to DDGS grows.

The global industrial enzymes market should reach $7.0 billion by 2023 from $5.5 billion in 2018 at a compound annual growth rate (CAGR) of 4.9% for the period 2018-2023 [3]. Although the industrial production of enzymes is well established, the growing market, high production costs and high level of competition in a changing market have pressed industry to seek new sustainable alternatives for their processes [4] [5]. Next to capital investment (50%), the highest cost factor of industrial enzyme production is associated to raw materials (33%) [6]. Last decades, researchers started to look into using agro-industrial lignocellulosic waste streams as raw material for enzyme production [6].

2. Methods

In this project, we propose an innovative bioprocess for the valorization of DDGS by using it as raw material for enzyme production (Fig.1). First, characterization of feedstock and optimization of biomass pretreatment are required to produce a suitable hydrolysate-based medium. Combining molecular biology tools for strain development and bioreactor design principles for optimized fermentation conditions will ensure that all aspects of enzyme production are covered. In the last phase, the optimized production strain is optimized for different process parameters in small-scale bioreactors. Final experiments in large-scale fermenters are used to validate strain productivity.

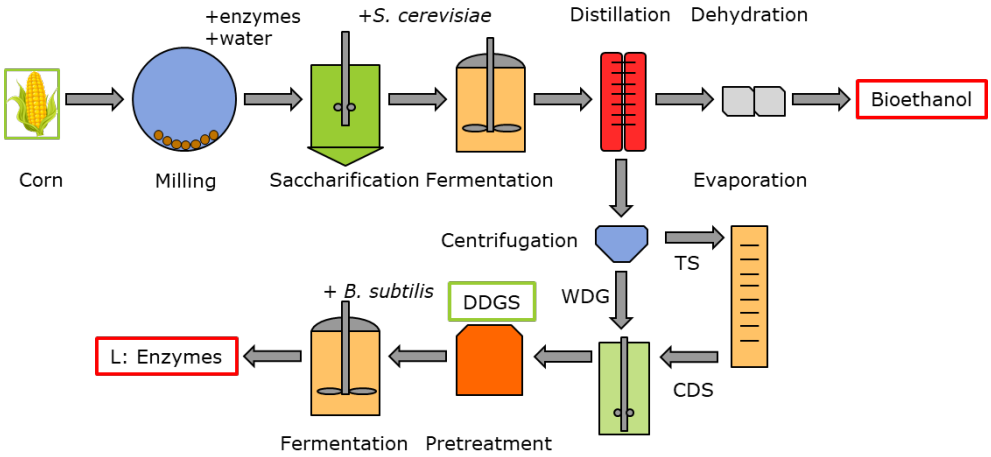

Fig. 1 Valorization of DDGS by enzyme production

3. Results and discussion

DDGS is a highly available material (32.3 kg DDGS /100 kg grains in a dry milling process), rich in nutrients and carbon sources (crude protein 24.9%, cellulose 16%, starch 5.2%, xylan and arabinan 13.5% w/w) [2] [8]. The high amount of sugars released after biomass conversion as well as the crude proteins serve as source of energy, carbon and nitrogen to sustain microbial growth during fermentation. Considering the price and composition of DDGS, valorization via biomass conversion for enzyme production seems to be a promising strategy.

4. Conclusions

The integration of DDGS to a multi-stream process could lead to the generation of different value added products, increasing economic viability and reducing DDGS market saturation associated to the growing bioethanol industry. Insights gained in this project should result in clear and applicable recommendations for the industry.

Acknowledgements: Novo Nordisk Foundation, Denmark, NNF10CC1016517; DuPont Industrial Biosciences.

References

[1] S. I. Mussatto and G. M. Dragone, *Biomass Pretreatment, Biorefineries, and Potential Products for a Bioeconomy Development*. Elsevier Inc., 2016.

[2] A. Chatzifragkou and D. Charalampopoulos, “Distiller’s dried grains with solubles (DDGS) and intermediate products as starting materials in biorefinery strategies,” in *Sustainable Recovery and Reutilization of Cereal Processing By-Products*, 2018.

[3] B. Research, “Global Markets for Enzymes in Industrial Applications,” 2018. https://www.bccresearch.com/market-research/biotechnology/global-markets-for-enzymes-in-industrial-applications.html.

[4] Ling Lin Fu, Zi Rong Xu, Wei Fen Li, Jiang Bing Shuai, Ping Lu, and Chun Xia Hu, “Protein secretion pathways in Bacillus subtilis: Implication for optimization of heterologous protein secretion,” *Biotechnol. Adv.*, vol. 25, no. 1, pp. 1–12, 2007.

[5] A. Sonenshein and R. M. L. , Abraham L., James A Hoch, “Bacillus Subtilis and Other Gram-positive Bacteria : Biochemistry, Physiology, and Molecular Genetics.,” in *Bacillus Subtilis and Other Gram-positive Bacteria : Biochemistry, Physiology, and Molecular Genetics.*, 1993.

[6] R. Ravindran, S. Hassan, G. Williams, and A. Jaiswal, “A Review on Bioconversion of Agro-Industrial Wastes to Industrially Important Enzymes,” *Bioengineering*, vol. 5, no. 4, p. 93, 2018.

[7] M. A. Martin, “First generation biofuels compete,” *N. Biotechnol.*, vol. 27, no. 5, pp. 596–608, 2010.

ECAB 5
The 5th EUROPEAN CONGRESS OF APPLIED BIOTECHNOLOGY
Florence 15-19 September 2019

Development of a high pressure bioreactor system for the production of biomethane from CO2 using an axenic methanogenic culture as biocatalyst

Sébastien Bernacchi[1,*], Arne H. Seifert[1]

Krajete GmbH, Josef Perger-Straße 2, 3031 Pressbaum, Austria

**Corresponding author: sebastien@krajete.com*

Highlights

- Gas to gas (GtoG) converting bioprocess
- CO_2-BMP, an axenic unsterile methanogenic archaea-based process using a fully defined mineral medium for growth
- Gas limitation and liquid limitation in gas converting bioprocesses
- Continuous and intermittent bioprocessing of industrially sampled H_2/CO_2 gas mixtures

1. Introduction

Over recent years the interest in new biofuel generations, based on converting gaseous substrate(s) such as carbon dioxide (CO_2), carbon monoxide (CO) or hydrogen (H_2) to gaseous product(s), arose. An example for such a gas converting bioprocess is the biological methane production process using CO_2 as sole carbon source (CO_2-BMP) [1]. Axenic cultures of *Methanothermobacter marburgensis* grown in a defined mineral medium already proved that high conversion rates of CO_2 and H_2 to methane (CH_4) can be reached [2]. However, this bioprocess was often described in literature as a gas transfer limited bioprocess [3]. Therefore, the kinetic limitation towards an increased methane productivity cannot be overcome solely by the growth of more biomass during continuous operation. More important is the development of a suitable bioreactor system that allows reaching a high mass transfer of the limiting gaseous substrate (H_2) in the liquid phase once an appropriate feeding strategy is applied to maintain sufficient biocatalyst in suspension for converting all the dissolved reactive gases. This work will present development steps [4], [5], methods [6], [7] as well as the applied bioprocess control approach [8] that enabled to construct and operate a custom designed and manufactured high pressure 20 L bioreactor system to overcome the so far existing performance limitations. In this setup, a methane evolution rate (MER) higher than 1.4 $mol_{CH4}\ L_{broth}^{-1}\ h^{-1}$ was reached using an axenic chemostat culture of *Methanothermobacter marburgensis* grown on a defined mineral medium at pressures up to 16 bar while using solely CO_2 as carbon source. The application of this feed forward control strategy enabled to predict and control biomass growth during operation which in return allowed to convert more than 99% of the applied 2.9 vvm [$NL_{gas}\ L_{broth}^{-1}\ min^{-1}$] of H_2-CO_2 into a high purity bio-CH_4 (>95 Vol.% CH_4 in the raw wet gas).

2. Methods

The integrated modular development workflow that will be presented consists of studying the biomethanation process from different angles and using different "levels" of pressurized H_2 and CO_2 gas mixtures to unscramble both, the potential physiologic limitation that could arise on one

side, and the benefits of high pressure on the reaction kinetic on the other side. The following aspects have been investigated: pressure tolerance, media demands, feed strategy development for fermentation and validation runs in continuous culture to reach performances above 20 kg_{CH4} m^{-3} h^{-1} (MER > 1250 $mmol_{CH4}$ L_{broth}^{-1} h^{-1}) in steady state production in order to support process simulation and tecno-economic assessment.

3. Results and discussion

A reference culture of *Methanothermobacter marburgensis* was used to validate the application of the feed forward strategy concept and demonstrate the possibility to control gas transfer limited bioprocesses. This allowed reaching the desired stability for operations as well as predicting media demand when elaborating specific feed strategies for the different operational profiles. An example of a dynamic intermittent operation is shown in **Figure 1**.

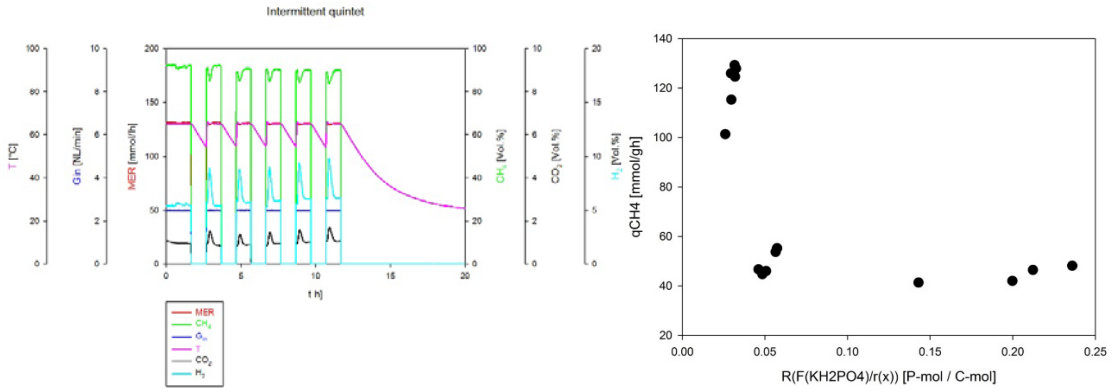

Figure 1. Feed forward strategy application to a CO2-BMP intermittent operation allowed uncoupling biomass growth control from methane production by varying the biocatalyst performances.

The feed strategy used to predict and control operations has been validated in pressure less conditions and further used for designing the cultivation medium for high pressure experiments where pseudo-steady state conditions had to be applied. After that, the know-how on the bioprocess was used for engineering, designing and building a custom-made pressure resistant CSTR that allowed to transfer axenic cultures to an elevated pressure environment (up to 16 barg). The latter allowed reaching unprecedent productivities using solely CO_2 as carbon source.

4. Conclusions

The application of an interdisciplinary modular development approach [9] to the CO2-BMP process allowed on one side assisting the prediction works for tecno-economic analysis [10] and process scale up while on the other hand elaborating a control strategy for the bioprocess suited for a vast range of operational regimes. This resulted in reaching high performances (methane evolution rate (MER) higher than 1.4 mol_{CH4} L_{broth}^{-1} h^{-1}) with sufficient methane (CH_4 > 95 Vol.% for the raw wet gas) that allow to reach most of EU countries gas grid specifications after a final purification step. Greatly acknowledge is the funding from the European Union's Horizon 2020 research and innovation program under grant agreement number 679050 (project: CELBICON).

References

[1] Sébastien Bernacchi and Christoph Herwig, “Challenges and solutions for development of gas limited bioprocesses illustrated by the biological methane production (BMP) process development” Current Biochemical Engineering, Volume 3, Number 3, 2016, pp. 165-176(12).

[2] A. H. Seifert, S. Rittmann, and C. Herwig, “Analysis of process related factors to increase volumetric productivity and quality of biomethane with Methanothermobacter marburgensis,” Appl. Energy, Vol. 132, pp. 155–162, 2014.

[3] N. Schill, W. M. van Gulik, D. Voisard, and U. von Stockar, “Continuous cultures limited by a gaseous substrate: Development of a simple, unstructured mathematical model and experimental verification with Methanobacterium thermoautotrophicum,” Biotechnol. Bioeng., vol. 51, no. 6, pp. 645–658, 1996.

[4] R.-S. Taubner et al., “Biological methane production under putative Enceladus-like conditions,” Nat. Commun., Vol. 9, No. 1, 2018.

[5] S. Bernacchi, S. Rittmann, A. H. Seifert, A. Krajete, C. Herwig, “Experimental methods for screening parameters influencing the growth to product yield (Y(x/CH4)) of a biological methane production (BMP) process performed with Methanothermobacter marburgensis,” AIMS Bioeng., Vol. 1, No. 2, pp. 72–86, 2014.

[6] A. H. Seifert, S. Rittmann, S. Bernacchi, and C. Herwig, “Method for assessing the impact of emission gasses on physiology and productivity in biological methanogenesis,” Bioresour. Technol., Vol. 136, pp. 747–751, 2013.

[7] W. Nischkauer, F. Vanhaecke, S. Bernacchi, C. Herwig, and A. Limbeck, “Radial line-scans as representative sampling strategy in dried-droplet laser ablation of liquid samples deposited on pre-cut filter paper disks,” Spectrochim. Acta Part B At. Spectrosc., Vol. 101, pp. 123–129, 2014.

[8] S. Bernacchi, A. Krajete, C. Herwig “Experimental workflow for developing a feed forward strategy to control biomass growth and exploit maximum specific methane productivity of Methanothermobacter marburgensis in a biological methane production process (BMPP),” AIMS Microbiol., Vol. 2, No. 3, pp. 262–277, 2016.

[9] Christoph Herwig Sebastien Bernacchi, “Application of a modular and interdisciplinary approach to the development of a biological methane production (BMP) process,” 2015.

[10] S. Bernacchi, M. Weissgram, W. Wukovits, C. Herwig; “Process efficiency simulation for key process parameters in biological methanogenesis,” AIMS Bioeng., Vol. 1, No. 1, pp. 53–71, 2014.

Improving CO_2 Bioconversion Processes: Effect of Carbonic Anhydrase and a Fixed Bed Trickle Down System on gas solubilization

Laura Pérez[1], Adrián Marí[1], Annabel Serpico[1], Alba Suárez[1], Edxon Licon[1], Julia García[1]

[1] *LEITAT Technological Center, C/ de la Innovació 2, 08225, Terrassa (Spain)*

**Corresponding author: lperez@leitat.org*

Highlights

- Use of carbonic anhydrase (CA) to enhance CO_2 solubilization.
- Different concentrations of CA tested.
- Use of a fixed bed trickle down system to enhance CO_2 solubilization.
- Comparing the two different strategies and their combination.

1. Introduction

In recent times, CO2 has started to be used as a building block to produce a wide range of chemicals and products *via* biological processes. This has drastically changed the point of view, from seeing it just as a pollutant, to consider it as an economic substrate. This idea totally fits in the idea of circular economy, reducing greenhouse gases (GHG) emissions and converting CO2 into a high value product.

However, one of the major bottlenecks in the conversion of CO_2 into desired molecules *via* industrial biotechnology is the low yield of the target compounds. Among the different factors responsible for this low productivity, issues regarding gas availability should be addressed, like gas-liquid mass transfer and CO_2 solubility.

This study assesses two different strategies and their combination, a fixed bed trickle down system (TBR) [1] and a robust enzyme carbonic anhydrases (CA) [2], [3]. The improvement of gas-liquid mass transfer and CO_2 solubility enhance further 3-hydroxypropionic acid (3-HP) production using the *Cupravidus necator*.

2. Methods

Temperature and pH are two physical conditions that must be defined to promote the solubility of CO_2 and enhance the performance of the selected microorganism or enzyme. In this case, the experiments are performed at 30ºC (optimal temperature for *Cupravidus necator*) and at pH 8 (being the bicarbonate the main chemical species at liquid phase). The solution has a buffer of K^+-PO_4^{3-} and each experiment takes place in 3 hours.

Figure 1 shows the two main strategies for CO_2 solubilisation. On one hand, CO_2 is introduced in a 1 L stirred vessel filled with the buffer solution with and without CA. On the other hand, a TBR filled with Raschig rings (6x6mm) is first optimized in terms of liquid flow and gas flow ratio (in countercurrent) and then the optimized concentration of CA is introduced in the system.

Samples are withdrawn regularly during each experiment to study the kinetics of CO_2 absorption.

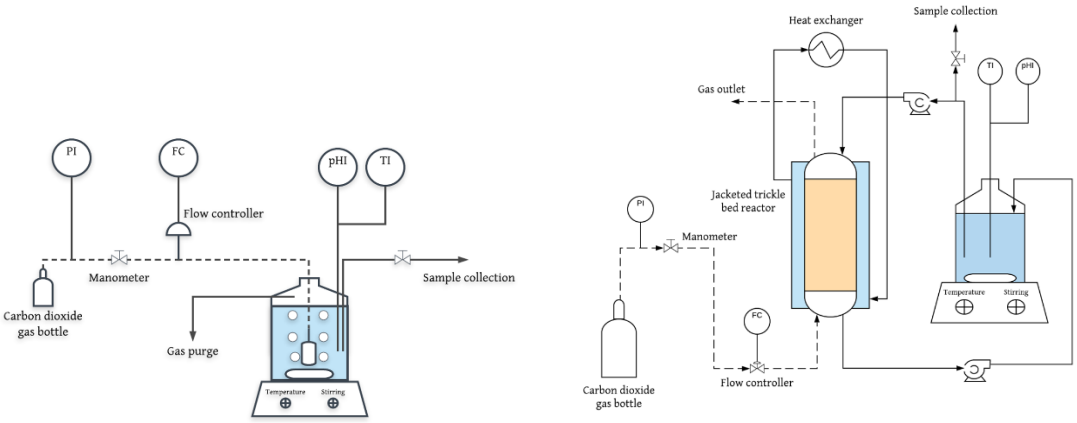

Figure 1. Experimental set-up for solubilization in vessel (left) and in TBR (right).

3. Results and discussion

Table 1 shows the preliminary results of CO_2 absorption in different conditions.

Table 1. Preliminary results on CO_2 absorption.

	Water	Buffer	Buffer + CA	TBR
CO_2 absorbed (%)	6,49	16,34	17,91	39,67

As it can be seen, the use of the buffer increases significantly the amount of CO_2 absorbed as the pH is maintained at 8. The use of CA has a slightly positive effect, but further experiments using higher concentration of CA are needed. Furthermore, the TBR presents the better result in terms of CO_2 adsorption and the use of CA in this system is expected to increase this value even more.

4. Conclusions

The use of CA and TBR has proven to be effective strategies to enhance CO_2 solubility. This will allow the conversion of CO_2 into desired molecules *via* industrial biotechnology to have a higher yield of the target compounds such as 3-HP (as is the case of the project in which this study is framed) and other chemicals and products *via* biological processes.

Acknowledgements

This project has received funding from the European Union's Horizon 2020 research and innovation programme under Grant Agreement no. 761042 (BIOCON-CO2). This output reflects the views only of the author(s), and the European Union cannot be held responsible for any use which may be made of the information contained therein.

References

[1] RANADE, Vivek V.; CHAUDHARI, Raghunath; GUNJAL, Prashant R. Trickle bed reactors: Reactor engineering and applications. Elsevier, 2011.

[2] SAVILE, Christopher K.; LALONDE, James J. Biotechnology for the acceleration of carbon dioxide capture and sequestration. Current opinion in biotechnology, 2011, vol. 22, no 6, p. 818-823.

[3] KANTH, Bashistha Kumar; LEE, Jinwon; PACK, Seung Pil. Carbonic anhydrase: Its biocatalytic mechanisms and functional properties for efficient CO2 capture process development. Engineering in Life Sciences, 2013, vol. 13, no 5, p. 422-431.

Optimizing specific uptake rates of butyric and acetic acid for continuous bioconversion to butanol with *C. saccharoperbutylacetonicum*.

Florian Gattermayr[1, 2], Viktoria Leitner[1], Christoph Herwig[2]

1 Wood K plus – Kompetenzzentrum Holz GmbH, Altenberger Strasse 69, Linz, Austria; 2 Vienna University of Technology, Institute of Chemical Engineering, Getreidemarkt 9/166, Vienna, Austria

**Corresponding author: f.gattermayr@wood-kplus.at*

Highlights

- Continuous conversion of organic acids to solvents
- Minimized loss of glucose in effluent
- Optimized bioprocess for maximum specific uptake rates of organic acids

1. Introduction

Emerging technologies are sought to utilize a multi-feedstock biorefinery process to efficiently convert industrially based lignocellulosic waste streams, such as black liquors or hydrolysates, into high value-added chemicals such as butanol. However, the use of those feedstocks is due to their volatile composition and quality quite challenging.

2. Goal

As initial conversion step of those feedstocks we use the 'carboxylate platform' to produce organic acids which are then supplied to a bioreactor for the production of solvents with solventogenic clostridia. Thereby the ratio and total concentration of those acids as well as the pH are known to significantly affect their uptake rate and thus subsequently the production of solvents [1, 2]. For the prolonged and efficient conversion of waste streams to butanol it is crucial to optimize the bioprocess for high specific uptake rates of organic acids.

3. Methods

The organism *C. saccharoperbutylacetonicum* was grown on a modified Clostridial Growth Medium (CGM). Fermentations are carried out on a parallel bioreactor system (Eppendorf DASGIP) controlled at 30 °C, stirred at 100 rpm and constantly purged with 5 L h^{-1} of sterile N_2 to maintain anaerobic conditions as well as to monitor the production of CO_2 and H_2 with a Micro GC Gas Analyzer (Inficon). Samples are frequently collected from the reactor for HPLC analysis (Shimadzu), determination of the cell dry weight (CDW) and measurement of the optical density (OD).

4. Results and discussion

Previously, we demonstrated the successful uptake of supplied butyric and acetic acid and their conversion to solvents in batch and fed-batch fermentations. We also could confirm that glucose has to be present in the medium for this conversion to function, as it serves both as source of ATP

and electrons for the conversion of butyric acid to butanol as well as carbon source for biomass growth [3]. In this work, we aim to operate a continuous fermentation. As we only want to use glucose, which is necessary for the conversion of acids, the concentration of glucose in the reactor will be kept in a limiting state by applying a pH controlled feeding strategy. With this system, we additionally also minimize the loss of unmetabolized glucose via the effluent stream. Finally, this will ensure an efficient consumption of substrate while maintaining a high uptake rate of fed organic acids for the continuous conversion to solvents.

5. Conclusions

We aim to demonstrate the continuous uptake of butyric and acetic acid and their conversion to solvents. The gained knowledge from this work is a first and important step towards establishing long term stable conversion of volatile lignocellulosic waste streams to butanol for next generation biorefineries.

References

[1] Tashiro, Y., Takeda, K., Kobayashi, G., Sonomoto, K., Ishizaki, A., Yoshino, S.: High butanol production by Clostridium saccharoperbutylacetonicum N1-4 in fed-batch culture with pH-Stat continuous butyric acid and glucose feeding method. Journal of Bioscience and Bioengineering. 98, 263–268 (2004).

[2] Bahl, H., Andersch, W., Braun, K., Gottschalk, G.: Effect of pH and butyrate concentration on the production of acetone and butanol by Clostridium acetobutylicum grown in continuous culture. European journal of applied microbiology and biotechnology. 14, 17–20 (1982).

[3] Richter, H., Qureshi, N., Heger, S., Dien, B., Cotta, M.A., Angenent, L.T.: Prolonged conversion of n-butyrate to n-butanol with Clostridium saccharoperbutylacetonicum in a two-stage continuous culture with in-situ product removal. Biotechnol. Bioeng. 109, 913–921 (2012).

Valorisation of municipal solid waste for succinic acid production via continuous fermentation and value added products through biorefinery

Eleni Stylianou, Dimitrios Ladakis, Chrysanthi Pateraki*, Apostolos Koutinas

1 Agricultural University of Athens, Iera Odos 75, 11855, Athens, Greece;

**Corresponding author: paterakichr@aua.gr*

Highlights

- Organic fraction of municipal solid waste (OFMSW)
- Biorefinery development
- Continuous fermentation
- Technoeconomic evaluation

1. Introduction

Nowadays renewable resources can be used as a potential feedstock for the production of biobased and value-added products. Municipal solid waste (MSW) generation is continuously increasing worldwide. The organic fraction of municipal solid waste (OFMSW) contains high amounts of lipids, protein, pectins and complex polysaccharides. Valorisation of OFMSW though a biorefinery approach could lead to the production of value-added products. Hydrolysis of OFMSW results in the production of a carbon and nutrient rich fermentation supplement. Succinic acid is one of the most important platform chemicals in the bio-economy era. Succinic acid production via continuous fermentation can lead to increased productivities, resulting in an economic feasible process. In this study OFMSW was hydrolysed with commercial enzymes and value-added products (lipids, proteins, pectins) have been subsequently extracted through biorefinery development. OFMSW hydrolysate has been used as the sole fermentation feedstock for the production of succinic acid by *A. succinogenes* via fed-batch and continuous fermentations. Furthermore, technoeconomic evaluation for succinic acid production has been carried out.

2. Methods

The organic fraction of municipal solid waste (OFMSW) was treated with commercial hydrolytic enzymes. Furthermore, through biorefinery development lipids were recovered with hexane and proteins were separated using ultrafiltration with 3 kDa membrane cut-offs. The remaining fraction was treated with acidified water at high temperatures and pectins were recovered with ethanol precipitation. OFMSW hydrolysate was used for continuous fermentations with *Actinobacillus succinogenes* 130Z in a 2L bench top bioreactor. Different dilution rates were evaluated in continuous cultures. The temperature was 37 ◦C, agitation was 100 rpm and continuous sparging of CO_2 at 1 vvm flow rate were contestant throughout the fermentation. C6 and C5 sugars and organic acids were analysed by high-pressure liquid chromatography (HPLC) with refractive index (RI) detector (Shimadzu) and an HPX-87H (7.8 x 300 mm) column (Aminex). The temperature of the

column was 65 °C and the mobile phase was a 10 mM H_2SO_4 aqueous solution with 0.6 mL/min flow rate. A techno-economic analysis of continuous fermentations was developed in order to investigate the commercial viability of biotechnological succinic acid production. The process design of the mass and energy balances was developed in Unisim software.

3. Results and discussion

OFMSW hydrolysate sugar concertation was around 90 g/L. The major carbon source fraction was glucose (84.5 %) followed by xylose (8.4 %), while glycerol, sucrose, galactose, arabinose, mannose and fructose were less than 2.5 %. Free amino nitrogen and inorganic phosphorus concentration was 203.6 mg/L and 100.6 mg/L, respectively. Lipids, proteins and pectins were recovered from the MSW hydrolysate at 90%, 50% and 40% yields, respectively. OFMSW hydrolysate was utilized for succinic acid production in fed-batch and continuous mode. Fed-batch fermentation in OFNSW hydrolysate resulted in more than 35 g/L of succinic acid. Continuous fermentation was carried out at different dilution rates and productivity achieved was higher than 1.5 g/L/h using OFMSW hydrolysate. Technoeconomic evaluation resulted in a minimum celling price of succinic acid below 2.5 $/kg.

4. Conclusions

OFMSW is an ideal raw material for the production of biobased products. Furthermore, various value-added products could be extracted from OFMSW. Succinic acid production was carried out in fed-batch and continuous cultures using OFMSW hydrolysate as the sole carbon source.

Acknowledgments

Received funding by the Bio Based Industries Joint Undertaking under the European Union's Horizon 2020 research and innovation programme, grant agreement No 745828, entitled "Chemical building blocks from versatile MSW biorefinery" (Acronym: PERCAL).

ECAB 5
The 5th EUROPEAN CONGRESS OF APPLIED BIOTECHNOLOGY
Florence 15-19 September 2019

Hydrothermal co-liquefaction of sewage sludge and formic acid

Claudia Prestigiacomo[1], Vito Armando Laudicina[2], Onofrio Scialdone[1], Alessandro Galia[1*]

Dipartimento di Ingegneria, Sezione Chimica Ambientale Biomedica Idraulica e dei Materiali, Università degli Studi di Palermo, Viale delle Scienze, 90128 Palermo, Italy.

[2] Dipartimento di Scienze Agrarie, Alimentari e Forestali, Università degli Studi di Palermo, Viale delle Scienze, 90128 Palermo, Italy.
**alessandro.galia@unipa.it*

Highlights

- Addition of HCOOH allows achievements of higher biocrude yields at higher biomass loadings.
- Addition of HCOOH increases the H/C molar ratio of biocrude.
- Detected production of light hydrocarbons from hydrothermal co-liquefaction of sewage sludge and formic acid.

1. Introduction

The biocrude produced by non-catalytic hydrothermal liquefaction (HTL) has a too high heteroatom content to be used directly as a fuel [1-3]. Several studies found that different H_2 initial pressures during HTL experiments were ineffective in improving the biocrude yield [4-6], nevertheless it was observed that higher initial pressures of H_2 brought an improvement of the concentration of light compounds in the biocrude, decreasing the average molecular weight of biocrude oil. To date H_2 is mainly generated from fossil sources and realization of a possible hydrogen economy from alternative sources presents many challenges. The use of a liquid hydrogen storage media could represent for the HTL process an alternative solution to avoid the mass transport resistance associated to gaseous H_2, furthermore Biller and Ross [7] observed that the addition of selected organic acids had similar effects than the addition of molecular H_2. According to these premises, we studied the influence of formic acid as hydrogen donor on the yield and quality of the biocrude produced by HTL of sewage sludge (SS). Formic acid was selected because it can decompose to hydrogen and carbon dioxide under mild conditions [8] and it can be produced by electrochemical reduction of carbon dioxide, an appealing process to capture atmospheric carbon dioxide under the form of a useful chemical [9].

2. Methods

SS provided by WWTP of Palermo, Italy (A.M.A.P. spa) and formic acid (Alpha Aesar 97 vol%) were used in HTL experiments. $CoMo/Al_2O_3$ (Albemarle, KF1022 cylindrical units) was used as catalyst. Acetone and cyclohexane (Sigma Aldrich, analytical grade) were used to recover the biocrude. A stirred stainless steel reactor with a volume of 30 mL was filled with 10 g of slurry changing the SS loading from 10 to 20 and 30 % w/w, formic acid loading was fixed at 1.8 % w/w. When used catalyst was added with a concentration of 10 %w/w with respect to SS. Set point temperature was reached by a software controlled ceramic heater with a typical heating rate of 13 °C/min and the reaction

time was considered to start when the set-point temperature was reached. The procedures adopted for products separation after HTL tests are the result of the optimization of the methods reported in our previous work [10]. The yields of the products were expressed in dry ash free (daf) form (i.e. referred to the organic content of the feedstock) as reported in the literature [10,11]. All experiments were repeated twice and mean values are reported. Elemental analyses of the biocrudes was performed in a Perkin Elmer 2400 series II elemental analyzer. Biocrude yield was determined after stripping of recovery solvents (daf %vw/w). Light hydrocarbons evaporated during stripping were condensed in a cold trap. Their relative amounts were estimated in term of fractional chromatographic areas (A%) after gas–chromatography analyses of the liquid (GC AutosystemXL Perkin Elmer equipped with a column Zebron ZB-FFAP).

3. Results and discussion

At a SS loading of 30% w/w, the biocrude yield increased from 39±2% w/w to 55±2% w/w when formic acid was added. Furthermore an increase of H/C molar ratio (from 1.54 to 1.96) was observed in the biocrudes produced in the presence of formic acid. The work herein, starting from the observed results found in literature, tried to evaluate the effect of formic acid on the performances of the hydrothermal co-liquefaction process characterizing also the produced light compounds. A technique to recover and to to trap solvent vapours during the stripping process of the biocrude phase was optimized and light hydrocarbons (C10-C18) were effectively detected by gas-chromatography analyses of the trapped phases. By means of this technique cumulative chromatographic area associated to light hydrocarbons increased from 7 to 32% when HCOOH was added at 10% w/w loading of SS.

4. Conclusions

Formic acid, obtainable from electrochemical reduction of carbon dioxide, showed promising result in improving the yield and the quality of biocrude generated from HTL of SS. Furthermore in the presence of formic acid, an increase of produced light hydrocarbons compounds was observed, and a better closure of the mass balance was obtained.

References

[1] T.M. Yeh, J.G. Dickinson, J. Chem. Technol. Biotechnol. 88 (2012) 13-24.
[2] T.C. Ho, Catal. Today 98 (2004) 3-18.
[3] A.Galadima, O. Muraza, Renew. Sustain. Energy Rev. 81 (2018) 1037-1048.
[4] L. Luo, L.Dai, Energy Fuels 29 (2015) 3208-3214.
[5] D.M. Zhang, F.Y. Ye, Catal. Today 234 (2014) 133–138.
[6] X. Liu, S.S. Li, Chin. J. Catal. 36 (2015) 1461–1475.
[7] A.B. Ross, P. Biller, Fuel 89 (2010) 2234-2243.
[8] K. Saito, T. Kakumoto, J. Chem. Physics 80 (1984) 4989-4996
[9] F. Proietto, B. Schiavo, Electrochimica acta 277 (2018) 30-40.
[10] C. Prestigiacomo, P. Costa, The Journal of Supercritical Fluids, 143 (2019) 251-258.
[11] L. Qian, S. Wang, Biores. Technol. 232 (2017) 27-34.

ECAB 5
The 5th EUROPEAN CONGRESS OF APPLIED BIOTECHNOLOGY
Florence 15-19 September 2019

Process development for the bioproduction of L-malic acid with *Aspergillus oryzae* DSM1863

Vanessa Schmitt[1], Katrin Ochsenreither[1]

1 Karlsruhe Institute of Technology (KIT), Institute of Process Engineering in Life Sciences, Section II: Technical Biology, 76131 Karlsruhe, Germany

**Corresponding author: Vanessa.schmitt@kit.edu*

Highlights

- Repeated-Batch cultivations increase the maximal productivity compared to fed-/batch cultivations.
- The highest product titers can be achieved with calcium carbonate as neutralization agent.

1. Introduction

L-Malic acid is a C4-dicarboxylic acid and a potential key building block for a bio based economy. Currently, malic acid is synthesized petrochemically. It is mainly used in the food and beverages industry, in metal cleaning and pharmaceuticals. Due to its bifunctionality, malic acid can also serve as polymerization starter unit and cross linker. A sustainable alternative to petroleum based synthesis is the microbial production of L-malic acid from renewable resources [1]. As CO_2 fixation is involved in biosynthesis, high yields are possible and at the same time greenhouse gases can be reduced. The mould *Aspergillus oryzae* is known for its high production capacity for L-malic acid and has received GRAS status, making it a promising candidate for industrial scale fermentations [2]. The microbial L-malic acid production with *A. oryzae* DSM1863 was evaluated in laboratory scale experiments to gain a better process understanding and to identify obstacles for the transformation into the industrial scale. Different aspects including pH regulation and cultivation strategy were investigated.

2. Methods

Batch, fed-batch and repeated-batch cultivations were performed in in 500 mL shake flasks with baffles and a working volume of 100 mL. A defined medium with glucose as substrate was used. Calcium carbonate was added in advance of the fermentation and as required during the fermentation for pH-regulation. Furthermore, different neutralization agents, including carbonates and hydroxides of calcium, magnesium and sodium, were tested in 2 L bench top fermenters with a working volume of 1.4 L. All fermentations were performed for at least one week and samples were taken daily. Substrate, product and by-product concentrations were measured via HPLC to determine the process characteristics (titre, yield and productivity). Additionally, pictures of the fungi were taken to document macroscopic changes of the morphology.

3. Results and discussion

In repeated-batch cultivations, the productivity was higher and the productive phase was prolonged compared to batch cultivations, in which the L-malic acid concentration reached its maximum after about one week. On the other hand, the productivities in the fed-batch cultivations were lower as in repeated batch cultivations.

The addition of calcium carbonate was proven to be crucial for the L-malic acid production. In reactor experiments with alternative neutralizing agents product titers were significantly lower. Hence, the positive effect of calcium carbonate cannot only be explained by the positive effect of pH-regulation. In addition, the precipitation of L-malic acid as calcium malate plays an important role in the L-malic acid production, as it lowers the acid concentration within the media, thereby preventing product inhibition.

4. Conclusions

In summary, the results obtained from shake flask cultivations proved the suitability of repeated-batch fermentations for the L-malic acid production with *A. oryzae*. The high productivities in repeated-batch fermentations compared to lower productivities in batch and fed-batch cultivations suggest that product inhibition limits the L-malic acid production, while substrate inhibition is of minor importance. The next step would be the upscaling of the repeated-batch fermentation to reactor scale. Furthermore, continuous fermentations with in situ product recovery seem to be an interesting research topic.

Calcium carbonate proved to be the best neutralizing agent for the L-malic acid production with *A. oryzae* DSM1863 in terms of product concentrations by preventing product inhibition. However, by resolving the calcium malate with sulfuric acid in downstream processing, huge amounts of gypsum are produced, generating extra costs for waste disposal. Therefore, liquid neutralizing agents like sodium carbonate or hydroxide should be considered as an alternative, despite the lower product titers observed. Additionally, the issue of product inhibition should be tackled by strain development and/or by applying in situ product removal.

References

[1] S. Dörsam, J. Fesseler, O. Gorte, T. Hahn, S. Zibek, Sustainable carbon sources for fermentative organic acid production with filamentous fungi. Biotechnology for Biofuels 10 (2017) 242.

[2] K. Ochsenreither, C. Fischer, A. Neumann, C. Syldatk, Process characterization and influence of alternative carbon sources and carbon-to-nitrogen ratio on organic acid production by *Aspergillus oryzae* DSM1863. Applied Microbiology and Biotechnology 98 (2014) 5449–5460.

Valorisation of orange peel for bacterial cellulose production via fermentation with simultaneously production of value added products

Dimitrios Ladakis, Harris Papapostolou*, Elina Kopanou, Apostolos Koutinas

Agricultural University of Athens, Iera Odos 75, 11855, Athens, Greece;

**Corresponding author: harris_papapostolou@yahoo.gr*

Highlights

- Orange peel
- Bacterial cellulose
- Biorefinery development

1. Introduction

Citrus residues represent an interesting renewable feedstock because of its wide availability and propensity to yield chemicals and materials. The worldwide citrus production in 2016/17 was 63.3 million tonnes with oranges dominating market share at 80 %. 1 Citrus peel represent the 50% of the total fruit mass and considered as low-value by-product stream from the corresponding processing industries. Orange peels contains bio-active compounds such as D-limonene and pectin as well as important amounts of carbohydrates (potentially more than 80 % of peel weight) 2 that can be used as feedstock for the production of fermentative products such as bacterial cellulose.
Bacterial cellulose (BC), is a highly functional biopolymer that can be find applications in numerous sectors including pharmaceutical, broadcasting, food industry, paper manufacture and mining. Bacterial cellulose (BC) produced mainly via fermentative procedures of Acetobacter species utilizing numerous carbon sources. This study evaluates the potential development of a biorefinery concept focusing on the utilization of orange peels for the production of BC and various value-added co-products.

2. Methods

The valorization of orange peels starts with the recovery of soluble sugars followed by the extraction of bioactive compounds (D-limonene and pectin) while the remaining solid fraction (mainly cellulose) was treated with commercial hydrolytic enzymes. Soluble sugars were removed with water at 60 oC, D-limonene extraction was carried out using the hydro-distillation method and the pectin using acidified water at pH 1.5 with 0.5 M HCl. The remaining solid residue was treated with commercial enzymes for the production of a sugar rich hydrolysate. The hydrolysate mixed with the fraction of the soluble sugars and used as a substrate for bacterial cellulose production via fermentation using the bacterial strain of *Komagataeibacter sucrofermentans* DSM 15973.

3. Results and discussion

The hydrolysate of the orange peel in combination with soluble sugar consist an eventual feedstock for the cultivation of K. sucrofermentans leading to a bacterial cellulose concentration of 6.4 g/L, a yield equal to 0.34 g/L and a productivity of 0.61 g/L/d. D-limonene and pectin extraction reach the values of 3.2 g and 12 g per 100 g of dry orange peel respectively.

4. Conclusions

Orange peel is an attractive raw material for the production of bio-based products. The bacterial strain of Komagataeibacter sucrofermentans DSM 15973 efficient cultivated in low cost feedstock derived from orange peel treatment with adequate production of bacterial cellulose in high yield and productivity values.

References

[1] https://apps.fas.usda.gov/psdonline/circulars/citrus.pdf (accessed in 23th of May, 2018).

[2] L. A. Pfaltzgraff, M. De bruyn, E. C. Cooper, V. Budarin and J. H. Clark. Food waste biomass: a resource for high-value chemicals. Green Chem., 2013, 15, 307-314.

Acknowledgments

We acknowledge support of this work by the project “Research Infrastructure for Waste Valorization and Sustainable Management of Resources, INVALOR” (MIS 5002495) which is implemented under the Action “Reinforcement of the Research and Innovation Infrastructure”, funded by the Operational Programme "Competitiveness, Entrepreneurship and Innovation" (NSRF 2014-2020) and co-financed by Greece and the European Union (European Regional Development Fund).

European Union
European Regional Development Fund
HELLENIC REPUBLIC
MINISTRY OF ECONOMY & DEVELOPMENT
SPECIAL SECRETARY FOR ERDF & CF
EPAnEK 2014-2020
OPERATIONAL PROGRAMME
COMPETITIVENESS
ENTREPRENEURSHIP
INNOVATION
ΕΣΠΑ 2014-2020
Partnership Agreement 2014-2020

Co-financed by Greece and the European Union

ECAB 5
The 5th EUROPEAN CONGRESS OF APPLIED BIOTECHNOLOGY
Florence 15-19 September 2019

Engineering *Yarrowia lipolytica* for high-yield lipid production from lignocellulosic biomass

Sun-Mi Lee[1, 2, 3, *], Sangdo Yook[1], Jiwon Kim[1, 4]

[1] *Clean Energy Research Center, Korea Institute of Science and Technology (KIST), Seoul 02792, Republic of Kore;* [2] *Clean Energy and Chemical Engineering, University of Science and Technology, Daejeon 34113, Republic of Korea;* [3]*Green School (Graduate School of Energy and Environment), Korea University, Seoul 02841, Republic of Korea;* [4]*Department of Biotechnology, Korea University, Seoul 02841, Republic of Korea*

**Corresponding author: smlee@kist.re.kr*

Highlights

- *Yarrowia lipolytica* was engineered to efficiently convert xylose into lipids
- Isomerase-base pathway enabled *Y. lipolytica* high-yield lipid production from xylose
- Isomerase-based pathway supported simultaneous co-fermentation of glucose and xylose

1. Introduction

Lignocellulosic biomass is one of the most attractive renewable resources for fuels and chemicals production. *Yarrowia lipolytica*, non-conventional oleaginous yeast, is a promising host for biodiesel and oleochemical production from lignocellulosic biomass. With advances in metabolic engineering, *Y. lipolytica* efficiently converts glucose into lipids up to 90% of its cell mass [1]. Yet, *Y. lipolytica* hardly utilize xylose, the second most sugar component of lignocellulosic biomass, limiting high-yield lipid production from lignocellulosic biomass.

2. Methods

To efficiently produce lipids from lignocellulosic biomass, we developed an efficient xylose utilizing *Y. lipolytica* harboring isomerase-based pathway. To do so, we first introduced xylose isomerase pathway, and then evolved the rationally engineered strain to better support xylose metabolism. The xylose utilizing performance of the engineered strain was evaluated during xylose fermentation as a sole carbon source, and during the fermentation of lignocellulosic hydrolysates.

3. Results and discussion

The newly developed xylose utilizing *Y. lipolytica* (YSXAK) showed high-yield lipid production from xylose as a sole carbon source. The lipid yield of isomerase-based xylose utilizing strain of YSXAK was five times higher than that of an oxidoreductase-based strain with cofactor imbalance issue [2]. Moreover, YSXAK simultaneously utilized both glucose and xylose to produce lipids suggesting efficient co-fermentation of lignocellulosic biomass. To understand the different genetic background contributed to efficient xylose utilization, comparative whole-genome sequence analysis was conducted identifying beneficial mutations occurred during evolutionary engineering.

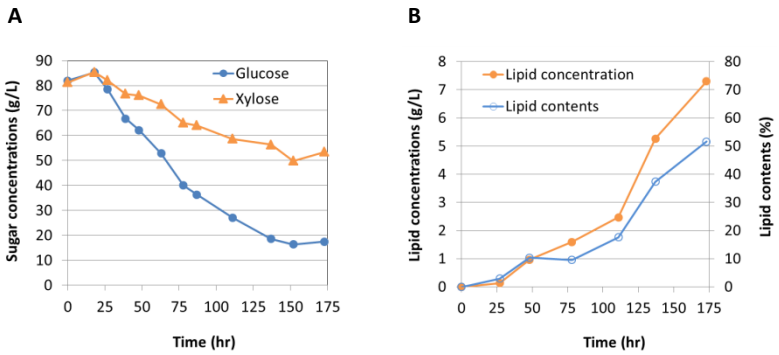

Figure 1. Sugar consumption and lipid production of xylose utilizing *Y. lipolytica* during glucose/xylose co-fermentation

4. Conclusions

Through combinatorial engineering, we developed an efficient isomerase-based xylose utilizing strain of *Y. lipolytica*, and demonstrated high-yield lipid production from xylose and simultaneous co-fermentation of glucose and xylose. This study shows the potential of xylose utilizing *Y. lipolytica* harboring an isomerase pathway for more economical and sustainable biodiesel and oleochemical production from lignocellulosic biomass.

References

[1] J. K. Ko, S. Lee, Curr. Opin. Biotech. 50(2018) 72-80
[2] H. Li, H. Alper, Biotechnol. J. 11 (2016) 1230-1240

ECCE 12
ECAB 5

ECAB 5
The 5th EUROPEAN CONGRESS OF APPLIED BIOTECHNOLOGY
Florence 15-19 September 2019

In line particle and single cell measurements in microbial bioprocesses

Stefan Junne[1], Jörn Emmerich[2], Friedel H. Schwartz[3], Anna-Maria Marbà-Ardébol[1], Klaus Pellicer-Alborch[1], Peter Neubauer[1]

1 TU Berlin, Bioprocess Engineering; Ackerstraße 76 ACK24, D-13355 Berlin; 2 Sopat GmbH, Boyenstraße 41, D-10115 Berlin, S+E Sequip GmbH, Angermunder Str. 22, D-40489 Düsseldorf

**Corresponding author: stefan.junne@tu-berlin.de*

Highlights

- Single cell measurement for intracellular concentration and co-culture monitoring
- *In situ* microscopy identifies budding and non-budding yeast for viability analysis
- Chain length distribution of lactic acid bacteria is related to metabolic activity
- Focus beam backreflection measurement for *on-line* optimization of feedstock pretreatment

1. Introduction

Monitoring tools for the liquid phase of bioprocesses are often restricted to a very few parameters. This might be insufficient if data from the single-cell level is required. While several *off line* tools have been commercialized, not many were adjusted and applied *in line* in bioprocess development and control.

This presentation aims to show the importance of single-cell based measurements and population heterogeneity for scale up and scale down of bioprocesses; recent advances achieved [1]; the potential of such methods to recognize and quantify the impact of unfavorable cultivation conditions in several microbial bioprocesses; and finally several examples of successful application for process optimization, including feedstock pre-treatment and determination of intracellular components on the single-cell level. Examples of long chain fatty acid accumulation in heterotrophic algae, budding in yeast, chain length determination in lactic acid bacteria, optimization of feedstock pretreatment for anaerobic digestion and the application in co-cultures are presented.

2. Methods

Among the techniques that are able to capture the morphological characteristics of cells in real time, automated imaging technologies are promising, because they provide additional information about cellular structures, shape and cell aggregation beyond size. Photo-optical *in situ* microscopy (ISM) and 3-dimensional holographic microscopy (DHM) were used in this study to measure the morphological dynamics in eukaryotic cultures on a single-cell basis, with heterotrophic algae and yeast as examples [2,3]. ISM was used further to monitor the chain length distribution of lactic acid bacteria (LAB). Both, yeast and LAB, were monitored under homogeneous and heterogeneous conditions in a scale down multi-compartment approach. The relation of morphological changes and metabolic activity and growth vitality in relation to scale up effects is assessed for both cases.

A second technique (focus beam backreflection) describes the monitoring of the particle size distribution in culture broth of anaerobic digestion. This method was successfully used to evaluate the efficiency of pre-treatment methods for hydrolysis based on the particle size, while distinguishing between non-living feedstock particles and active cells.

3. Results and discussion

Based on the morphological and optical cell features, the intracellular accumulation of the polyunsaturated fatty acid docosahexaenoic acid (DHA) was monitored in real-time on a single cell level in cultivations of the heterotrophic algae *C. cohnii* [2]. This methods allows to quantify the product yield of a process instead of time consuming *off line* gas chromatography analyses. It further allows to optimize process conditions under consideration of population heterogeneity, as productive cells can be distinguished from weak cells fractions.

Multi-compartment scale-down reactors were used to investigate the influence of gradients, as they occur in large scale, on the morphological heterogeneity in *Saccharomyces cerevisiae* cultures and relate this to process performance [3]. Budding of yeast was monitored *in line* in batch cultivations with ISM [4]. The ratio of budding and total cells was successfully applied to differentiate between the different cultivation stages and to predict growth. Vitality and viability of such cultures can be measured with ISM.

In large-scale lactic acid bacteria production, the main concern is the uneven distribution of the pH value, mainly due to the external addition of base to compensate the acid produced by cells. In order to study the impact of these gradients on the population heterogeneity in various scales, different scale-down approaches were applied, especially multi-compartment systems and pulse-based parallel experiments. A relation was found between gradient formation in large scale cultivations and the development of the chain length formation of *Streptococcus thermophilus*, which allows for an *on line* estimation of the viability. A growth rate prediction based on the cell size distribution was feasible.

The last example shows how feedstock pre-treatment, in particular with ultrasound, can be optimized by particle size measurement with laserlight focus beam back reflection. The same technology allows to distinguish between circular and spiral-shaped organisms, which seems to be a promising feature for the investigation and finally control of co-cultures up to the large scale.

4. Conclusions

The information, which is gained by ISM and laserlight focus beam back reflection can be coupled with population balance models, which enable a model-based prediction of growth and production performance. Coupled with automated image analysis, real-time monitoring and the concept of “population control” [1] becomes possible for a wide range of bioprocesses.

References

[1] F. Delvigne et al. FEMS Microbiol Lett. 365 (2018) 22.
[2] A.M. Marbà-Ardébol et al. Process Biochem. (2017) 52 pp. 223–32.
[3] A.M. Marbà-Ardébol et al. Yeast. (2018) 2 pp. 213–23.
[4] A.M. Marbà-Ardébol et al. Microb. Cell Fact. (2018) 17 (1).

ECAB 5
The 5th EUROPEAN CONGRESS OF APPLIED BIOTECHNOLOGY
Florence 15-19 September 2019

Improvement of Enzymatic Hydrolysis of Cassava Starch to Produce Fermentative 2,3-Butanediol by *Klebsiella Oxytoca* KMS006.

Panwana Khunnonkwao[1], Sirima Suvarnakuta Jantama[2], Kaemwich Jantama[1,*], Claire Joannis-Cassan[3] and Patricia Taillandier[3,*]

[1]School of Biotechnology, Suranaree University of Technology, Nakhon Ratchasima, Thailand
[2] Division of Biopharmacy, Faculty of Pharmaceutical Sciences, Ubon Ratchathani University, Warinchamrap, UbonRatchathani, Thailand, [3]Laboratoire de Génie Chimique, Université de Toulouse, CNRS, INPT, UPS, Toulouse, France

*Corresponding author:Patricia.taillandier@ensiacet.fr, kaemwich@sut.ac.th

Highlights

- *Klebsiella oxytoca* KMS006 produced 2,3-BD from cassava starch with impressive yields.
- 1% (v/v) α-amylase was only used for releasing reducing sugars from cassava starch.
- Cassava starch is a promising feedstock for the economical production of 2,3-BD.
- The fermentation of 2,3-BD was performed in low salt medium to lower production cost.

1. Introduction

2,3-Butanediol (2,3-BD) is one of the building block chemicals which can be used in a variety of industrial applications [1]. Currently, the feasibility of 2,3-BD fermentation on a large scale depends on the use of cheaper renewable resource. The utilization of an inexpensive carbon source such as cassava starch has attracted attentions for the biotechnological production of 2,3-BD from an economic point of view. A metabolically engineered *K. oxytoca* KMS006 was engineered to enhance 2,3-BD production yield by gene deletion and metabolic evolution [2]. However, this strain does not efficiently ferment cassava starch due to low expression of *malS* encoding for *α*-amylase [3]. Thus, an external *α*-amylase enzyme was utilized to release fermentable sugars from cassava starch. The aim of this study was to investigate the optimal condition for enzymatic hydrolysis of cassava starch with α-amylase to obtain fermentable sugars for the production of 2,3-BD by *K. oxytoca* KMS006 in a simple batch fermentation.

2. Methods

Cassava starch (140 g/L or 130 g/L) was gelatinized in 2.5 L bioreactor with 1 L AM1 buffer (pH 6.0) (4) by autoclave at 121 °C for 20 min. A commercial α-amylase was added at concentration of 1% (v/v) into the bioreactor in order to covert cassava starch into sugars with two different conditions: before or after autoclaving. In this last case, the enzymatic hydrolysis step was carried out at 400 rpm during 3h. In both cases, the fermentation was then initiated by inoculation with *K. oxytoca* KMS006 at an initial OD_{550} of 0.1 and carried out at 37 °C, 400 rpm and 0.8 vvm [5,6]. The pH of fermentation broth was maintained at 6.0 by automatic addition of 3 M KOH.

3. Results and discussion

To achieve a high 2,3-BD concentration from cassava starch, α-amylase was utilized to convert cassava starch to fermentable sugars. When the enzyme was added before autoclaving (Fig. 1A), the hydrolysis was not completed, probably due to the inactivation of α-amylase at high temperature. When α-amylase was added after autoclaving, the hydrolysis reaction was carried out for 3 h during temperature dropped from 85 to 45 °C. In this case, a maximum efficiency of starch hydrolysis was obtained as cassava starch concentration (130 g/L) was completely converted to reducing sugar (Fig. 1B). It resulted after fermentation of a final 2,3-BD concentration of 64.8 g/L with a yield of 0.46 g/g and productivity of 1.25 g/L/h at 52 h 8 with few by-product formed (about 3.8 g/L of succinate and acetate).

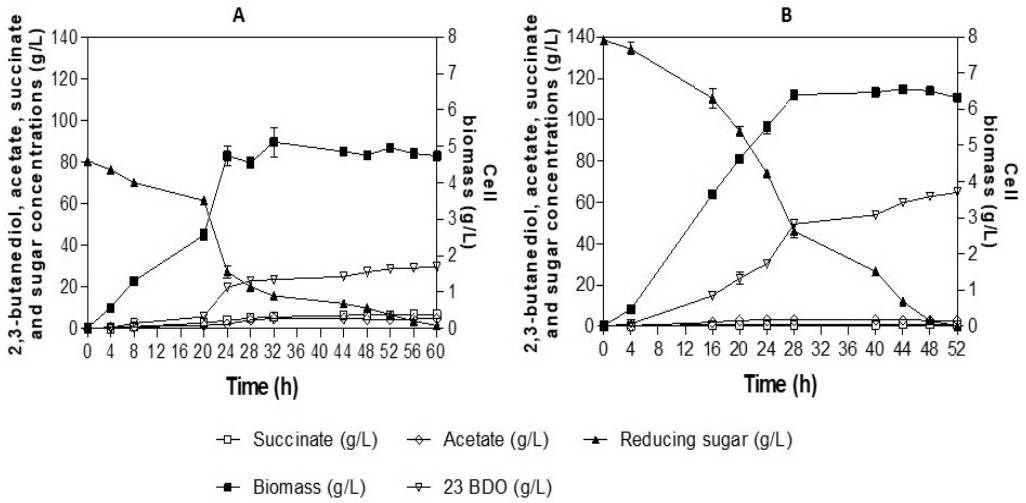

Figure 1. 2,3-BD fermentation from cassava starch using *K. oxytoca* KMS006. **A)** ±-amylase was added into bioreactor before autoclave **B)** ±-amylase was added into bioreactor after autoclave at H85 °C and hydrolysis for 3 h.

4. Conclusions

These results indicated that the fermentable sugars from cassava starch can be obtained by combined heat treatment with autoclave and solely α-amylase. In addition, cassava starch can be considered to be one of the most promising feedstock for cost-effective 2,3-BD production by *K. oxytoca* KMS006.

References

[1] M.J. Syu, Appl Microbiol Biotechnol. 55 (2001) 10-18.

[2] K. Jantama, P. Polyiam, P. Khunnonkwao, S. Chan, M. Sangproo, K. Khor, S.S. Jantama, S. Kanchanatawee, Met Eng. 30 (2015) 16-26.

[3] F. Tsvetanova, P. Petrova, K. Petrov, Appl Microbiol Biotechnol. 98 (2014) 2441-2451.

[4] A. Martinez, T.B. Grabar, K.T. Shanmugam, L.P. Yomano, S.W. York, L.O. Ingram, Biotechnol Lett 29 (2007) 397-404.

[5] S. Chan, S.S. Jantama, S. Kanchanatawee, K. Jantama, Plos one. (2016) 11:e0161503.Doi:10.1371/journal.pone.0161503.

[6] S. Chan, S. Kanchanatawee, S.S. Jantama, K. Jantama, C. Joannis-Cassan, P. Taillandier, J Chem Technol Biotechnol. 93 (2018) 600-608.

In situ on site applicable aptasensor using sandwich-type binding pair of Aptamers

Man Bock Gu*
Department of Biotechnology, Korea University, Seoul, Rep. of Korea
*e-mail: mbgu@korea.ac.kr

Aptamers are single-stranded nucleic acids having molecular recognition properties similar to antibodies, and isolated by *in vitro* selection and amplification process, SELEX. This nucleic acid aptamer is well-known with its stable feature, quick and easy developement, cost-effective production *in vitro*, and so on. To find a most effective atpamer screening method has always been a goal, especially for obtaining a pair of aptamers binding at different sites of a single target. This talk will start with how a pair of aptamers are innovatively screened consecutively, by using a new nano-material, graphene, without the immobilization of targets. A few of successful examples using immobilization-free screening of the pair of aptamers will be presented, which are inevitable for being applied in a stripe-type platform, which could be a reliable platform for commercialization eventually. Finally, a couple of examples for protein biomarkers and pandemic viruses will be presented about how the pair of aptamers were successfully implemented on both lateral flow assay biosensing platform and in situ on site applicable aptasensors by using a mini-potentiostat.

ECCE12
The 12th EUROPEAN CONGRESS OF CHEMICAL ENGINEERING
Florence 15-19 September 2019

KINETICS OF THE CONVERSION OF ETHANOL AND ACETALDEHYDE INTO 1,3-BUTADIENE OVER A TA_2O_5/SBA15 CATALYST.

G.M. Cabello González[1*], M.O. García Sánchez, A. L. Villanueva Perales[1], M. Campoy Naranjo[1], F. Vidal Barrero[1], A. Martínez[2], P. Ollero[1]

[1]*Departamento de Ingeniería Química y Ambiental - Universidad de Sevilla (España)*
[2]*Instituto de Tecnología Química - Universidad Politécnica de Valencia (España)*
**Corresponding author: gcabello3@us.es*

Highlights

- The reaction network including main and by-products was experimentally determined.
- A kinetic model was developed for the second-step of the ethanol to butadiene process.
- The experimental observations were explained through the model parameters.

1. Introduction

1,3-Butadiene is a valuable conjugated diene which is industrially produced as a co-product of naphtha steam cracking. It is used primarily as a chemical intermediate and as a monomer in the manufacture of synthetic rubbers, most of which are destined to the automobile industry. The onset of the US shale gas has impacted the 1,3-butadiene market as the change in feedstock for steam cracking to ethene have resulted in a lower 1,3-butadiene production. Therefore, while the 1,3-butadiene market shrank, the global 1,3-butadiene demand continued to grow. In that context, the conversion of bioethanol to 1,3-butadiene arises as an interesting and environmentally friendly alternative in a highly competitive and unstable marketplace.

In the literature we can find very few kinetic studies of the ethanol to 1,3-butadiene conversion, and none of these studies includes the effect of co-feeding water among with the feedstock. That way, we aim to develop a formal kinetic model describing the main reactions pathway that can predict the catalyst performance in a range of operating conditions close to the optimum.

2. Methods

The catalyst was prepared following the methodology reported in the work of Chae et al. [1]. Catalytic tests were carried out in a continuous flow fixed-bed reactor at 300-350 ºC, 0.22-1.63h^{-1}, 0-7.5% w/w water in the feedstock, ethanol/acetaldehyde mole rate between 1.7 and 2.7, ethanol partial pressure of 0.13 bar and atmospheric pressure. The bed was divided into three sections. The top section was a SiC bed, the middle one comprised a bed of catalyst (0.3-0.5 mm) diluted in the necessary amount of SiC to obtain a bed length of 13 cm, and the bottom section was also a SiC bed. All sections were separated by a glass wool plug. The ethanol was fed with an HPLC-pump

and N_2 was used as carrier gas. The reactor output line was electrically traced and insulated to avoid product condensations before analysis by an Agilent 7890A on-line gas chromatograph (GC) equipped with two flame ionization detectors (FID) and a thermal conductivity detector (TCD).

3. Results and discussion

Making use of the tests carried out in the laboratory-scale reactor, a kinetic model was developed. The reaction scheme considered for the calculation of the balance is a simplification of the most accepted reaction pathway nowadays, lumping some products like olefins and the major lump "others" that includes a huge amount of compounds with little contribution such as acetone, propanal, butanal, methanol, and so on. The differential mole balance equations were solved obtaining an initial guess of the kinetic parameters assuming constant molar flow along the reactor and solving the algebraic system. These rough parameters were used as initial guess values for solving the differential mole balance equations along the reactor.

- Main reaction: $C_2H_5OH + C_2H_4O \rightarrow C_4H_6 + 2H_2O$
- Ethanol dehydration: $2\ C_2H_5OH \rightarrow (C_2H_5)_2O + H_2O$
  $C_2H_5OH \rightarrow C_2H_4 + H_2O$
- Butenes formation: $2\ C_2H_5OH \rightarrow C_4H_8 + 2H_2O$
- Tishenko reaction: $2C_2H_4O \rightarrow CH_3COOC_2H_5$
- Etilacetate to "other compounds" lump (Butanal): $2\ CH_3COOC_2H_5 + C_4H_8O_2 \rightarrow 2C_4H_8O + 2H_2O$
- "Other compounds" lump formation: $C_2H_5OH + C_2H_4O \rightarrow C_4H_8O + H_2O$
- Heavy compounds formation (Diethoxyethane): $3\ C_2H_5OH + 1.5C_2H_4O \rightarrow 1.5C_6H_{14}O_2 + 1.5H_2O$

4. Conclusions

The main products observed while co-feeding ethanol and acetaldehyde over a TA_2O_5/SBA15 catalyst were 1,3-butadiene, ethene, diethyl ether, ethyl-acetate, butenes and heavy compounds. The developed kinetic model may be used to design and optimize an industrial facility. The proposed model fitting concurs with the experimental results.

References

[1] H. Chae, T. Kim, Y. Moon, H. Kim, K. Jeong, C. Kim, S. Jeong, App Catal B, 150-151 (2014) 596-604.

Biorefinery development using spent coffee grounds for the products of bacterial cellulose and value-added products

Sofia Maina, Erminta Tsouko, Apostolis Koutinas*

Department of Food Science and Human Nutrition, Agricultural University of Athens, Iera Odos 75, 11855 Athens, Greece

**Corresponding author: akoutinas@aua.gr*

Highlights

- Phenolic-rich extracts, oil and protein can be extracted from spent coffee grounds
- Hemicellulose hydrolysate has been used for bacterial cellulose production
- Spent coffee grounds is a promising resource for biorefinery development

1. Introduction

The development and implementation of biorefineries dealing with renewable resources strongly depends on the heterogeneity and availability of the feedstock in combination with the profitability of the whole process. Spent coffee grounds (SCGs) are generated as waste streams through the production of instant coffee and coffee brewing and they amount to approximately 6 million t annually [1]. SCGs are rich in polysaccharides and protein [2]. The high carbohydrate content renders SCGs a promising substrate for bioprocesses including carotenoids, poly-(hydroxyalkanoates), enzymes and bioethanol [3]. The recovery of natural antioxidants (mainly caffeine), proteins and lipids contained in SCGs, could enhance the viability and sustainability of a biorefinery development. Under this concept, the main objectives of this study were the fractionation of SCGs for the recovery of value-added products and the production of bacterial cellulose from hemicellulosic hydrolysates derived after diluted acid or enzymatic hydrolysis of hemicellulose.

2. Methods

The fractionation of SCGs included the extraction of phenolic compounds, oil, protein and carbohydrates. Initially, phenolic compounds were extracted and evaluated in terms of total phenolic content (TPC) (via Folin-Ciocalteu method) and antioxidant activity index (AAI) (via 2,2-diphenyl-1-picrylhydrazyl-free radical scavenging method) using ethanol as solvent under different solid to liquid ratios and extraction time. The main phenolic compounds of the extract were identified and quantified employing HPLC-DAD. The phenolic-free solids were subsequently used for oil extraction. The SCGs to solvent ratio and the extraction time were evaluated. The remaining

SCG solids were used for protein recovery. The extraction process included alkaline treatment followed by acidic precipitation at the isoelectric point of the corresponding proteins. At a final step, the remaining lignocellulosic-rich solids were pretreated by mild chemical and enzymatic processes to the respective monomeric sugars. The galactose and mannose rich hydrolysate obtained was utilized for bacterial cellulose production by *Komagataeibacter sucrofermentans* DSM 15973 under batch mode. The physiochemical properties of the produced bacterial cellulose were determined and evaluated.

3. Results and discussion

Phenolic compounds from SCGs were extracted applying an environmental friendly and cost-effective process using aqueous ethanol under mild temperature conditions. SCGs exhibited the highest TPC (15 mg gallic acid equivalents-GAE/ g dry sample) with a liquid-to-solid ratio of 10:1 after 20 minutes of extraction. According to the obtained AAI, extracts were classified as strong antioxidants. Extraction of oil with hexane and n-propanol resulted in high oil recovery (higher than 95%). Protein extraction reached a recovery yield of 92% with high purity.

The hemicellulosic hydrolysate rich in mannose and galactose was utilized as the sole carbon source for bacterial cellulose production with the bacterial strain *K. sucrofermentans*. Bacterial cellulose concentration of 2.4 g/L was achieved after 6 days of fermentation. Properties determination of the produced bacterial cellulose showed enhanced water holding capacity and degree of polymerization. The IR spectrum of bacterial cellulose indicated that the bacterial strain *K. sucrofermentans* synthesizes both Iα and Iβ cellulose types, with Iα cellulose being the dominant type.

4. Conclusions

SCGs were effectively utilized as renewable resource for the development of an integrated bio-refinery leading to extraction and production of high added value products. This approach enables the exploitation of SCGs adding value to this abundant and low-cost feedstock. Further study should focus on practical and novel concepts for potential applications of the obtained products in the food and oleochemical industry.

References

[1] R. Campos-Vega, G. Loarca-Pina, H.A. Vergara-Castañeda, and B.D. Oomah, Trends Food Sci. Technol. 45 (2015) 24-36.
[2] P. S Murthy, & M. M. Naidu, Food and Bioprocess Technology (2012) 5(3), 897-903.
[3] T.M. Mata, A.A. Martins and N.S. Caetano, Bioresour. Technol. (2018) 1077-1084.

ECAB 5
The 5th EUROPEAN CONGRESS OF APPLIED BIOTECHNOLOGY
Florence 15-19 September 2019

Inline microscopy for multidimensional particle characterization in bioprocess monitoring

Jörn Emmerich[1], Sebastian Maaß[2], Peter Neubauer[1], Stefan Junne[1]

1 Technische Universität Berlin, Ackerstr. 76 ACK 24, 13355 Berlin; 2 SOPAT GmbH, Boyenstr. 41, 10115 Berlin

**Corresponding author: joern.emmerich@sopat.de*

Highlights

- High resolution inline microscopy
- Monitoring fatty acid production by microalgae
- Correlation of Budding Index with growth dynamics in yeast fermentations
- Multidimensional and real-time image analysis

1. Introduction

The present work describes the development and methodology to apply a microscopy probe for the measurement of the sizes, shapes, colors and concentrations of particles in biological processes. To date, the direct measurement of these parameters inside the process is a challenge, since the monitoring instrumentation has to be applicable under various process conditions and in different process phases. High particle concentrations, different particles in multiphase systems or changing particle features and velocities are challenging for an inline measurement method. For microscopy in particular, overlapping signals and background can disturb object identification. Nevertheless, recent advances in photo-optics and image processing allow to generate images with a high level of details even under demanding process conditions. This makes it easier to extract individual features from the images. Coupled with image analysis, it allows precise and automated real-time measurements of particle size, shape and concentration.

In this study, an inline microscopy probe was particularly developed for the application in microbial bioprocesses, in which the microbe changes its morphology during the process phases. In a first study, morphological changes in fed-batch cultivations of the heterotrophic algae *Crypthecodinium cohnii* were monitored. It is shown that both size and shape changes relate to the intracellular accumulation of the polyunsaturated fatty acid docosahexaenoic acid (DHA).

In a second study the morphological heterogeneity in yeast fermentations of *Saccharomyces cerevisiae* is investigated by inline microscopy. By means of automatic image analysis, various budding states of the yeasts can be investigated. It is possible to classify budding yeasts with a daughter cell and non-budding yeasts into two different classes. The relation of the two different size and shape distributions resulting from the two classes can be correlated with the growth activity at any point during the process, and thus conclusions on the growth dynamics can be derived.

2. Methods

The general working principle of inline microscopy is bringing the focal plane of the microscopic objective into the sample, which is usually the flow regime inside a process. Therefore, inline microscopes need to be more compact and robust to be integrated into a process. The acquired images are analyzed with an artificial neural network. The employed U-Net is a deep convolutional network for a more advanced segmentation of images. The network learns to segment images in an end to end setting.

3. Results and discussion

In this study, changes in the cell size distribution of the heterotrophic microalgae *C. cohnii* were tracked with an offline holographic microscopy and an inline photo-optical microscopy probe (Figure 1 – a). The accumulation DHA, which is a product of major interest as a dietary supplement for fish production leads to a larger cell diameter (Hillig et al., 2014). On the basis of the cell size and broadness of the size distribution, the applied inline photo-optical measurements enabled to distinguish between cells in the growth phase with little or no intracellular lipid droplet accumulation and production phase with lipid droplet accumulation (Figure 1 – b).

Under conditions of low growth and high fatty acid accumulation, the cell sizes and its distributions were changing accordingly. The correlation between the predicted inline measurements based on the Sauter mean diameter and the measured intracellular DHA content with GC-FID was confirmed and showed a maximum coefficient of determination (R) of 0.983 by regression analysis (Figure 1 – c).

The results obtained by digital holographic and the side scatter values from flow cytometry, which was performed as golden standard method for single cell measurement, were in good agreement with the inline microscopy, which enables this method to photo-optically measure DHA content in real-time (Marbà-Ardébol et al., 2017).

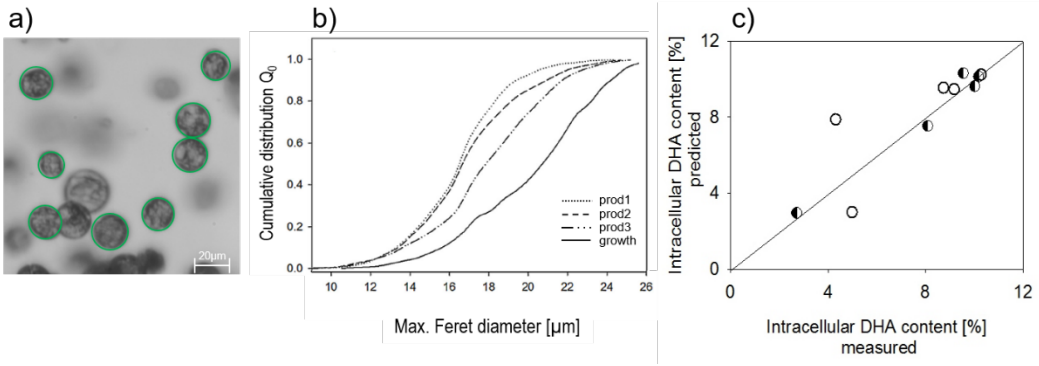

Figure 1: a) Segmented cells, b) Cumulative size distributions in different growth states, c) Second order correlation between DHA content measured offline (GC-FID) and predicted DHA content based on the measured Sauter mean diameter with inline microscopy. Values used for calibration (◐) and for prediction (○).

Yeast is one of the most important species in biotechnology. In this study Baker's yeast *S. cerevisiae* and its morphological changes during fermentation is monitored inline. The morphology of yeast cells is altering during maturation, depending on the growth rate and cultivation conditions. Inline microscopy was used to monitor such morphological changes of individual cells directly in the cell suspension. With automated image analysis it was possible to analyze budding and non-budding cells in parallel based on a trained artificial neural network. Deviations between automated and manual counting were considerably low (Figure 2 – a and b).

The homogeneity among the population during the growth phase increased and at growth retardation, the portion of smaller cells increased due to a reduced bud formation. The maturation state of the yeast cells was determined by the budding index, which Is defined as the ratio between the number of budding cells and the total number of cells. Inline monitoring showed a linear correlation between the budding index (BI) and the growth rate during the batch cultivation (Figure 2 – c and d). An real-time differentiation of growth activity across all process stages of several batch cultivations in complex media became feasible (Marbà-Ardébol et al., 2018b).

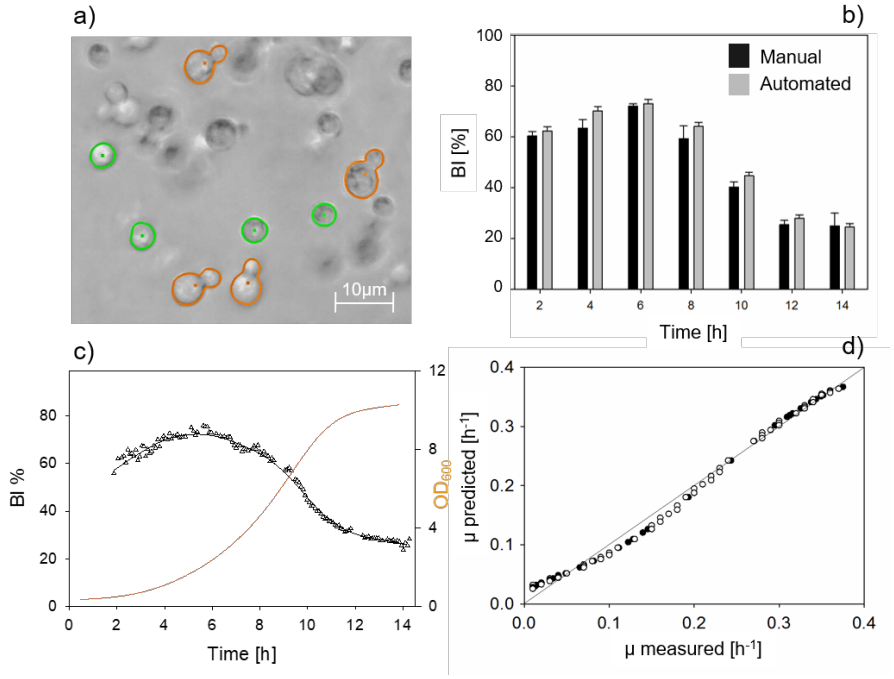

Figure 2: a) segmented and classified cells into budding and non-budding cells, b) Comparison between the budding indices obtained automatically (black bars) and with manual counting (gray bars) resulting in a confidence interval R^2=0,99, c) monitored BI as determined with inline microscopy and OD_{600} of cultures, d) the correlation of predicted and measured growth rates.

4. Conclusions

The presented inline microscope provides accurate automatic particle recognition in highly concentrated disperse systems and provides statistically robust parameters within short calculation times (<5min). The consideration of population heterogeneity based on morphologic features becomes feasible. The method allows both, a deeper understanding of functional relationships in bioprocesses as well as process control - by faster response on process changes.

References

[1] Hillig, F., Porscha, N., Junne, S. and Neubauer, P., Engineering in Life Sciences, 2014, 14(3): 254-263.

[2] Marbà-Ardébol, A.-M., Emmerich, J., Muthig, M., Neubauer, P. and Junne, S., Microbial Cell Factories, 2018, 17(1): 73.

[3] Marbà-Ardébol, A.-M., Emmerich, J., Neubauer, P. and Junne, S., Process Biochemistry, 2017, pp. 223-232.

[4] Ronneberger, O., Fischer, P. and Brox, T., Springer International Publishing, 2015, Cham, pp. 234-241.

ECAB 5
The 5th EUROPEAN CONGRESS OF APPLIED BIOTECHNOLOGY
Florence 15-19 September 2019

Real-time prediction of protein quantity and purity in downstream processing

Michael Melcher[1,2,*], Theresa Scharl-Hirsch[1,2], Dominik Sauer[1,3], Nicole Walch[1,3], Edit Felföldi[1,3], Anna Christler[1,3], Alois Jungbauer[1,3], Astrid Dürauer[1,3] and Friedrich Leisch[1,2]

1 Austrian Centre of Industrial Biotechnology (ACIB), Muthgasse 11, 1190 Vienna, Austria; 2 Institute of Applied Statistics and Computing, University of Natural Resources and Life Sciences Vienna, Peter-Jordan-Straße 82, 1190 Vienna, Austria; 3 Department of Biotechnology, University of Natural Resources and Life Sciences Vienna, Muthgasse 18, 1190 Vienna, Austria

**Corresponding author: michael.melcher@acib.at*

Highlights

- Online-monitoring of capture step of human fibroblast growth factor (FGF) 2
- Multi-analytical approach (Fluorescence, ATR/FTIR, UV, refractive index, …)
- Various statistical learning methods (PLS, Lasso, structured additive regression)
- Prediction errors of approx. 0.5 mg/ml (protein quantity), 200 ppm (host cell protein) and 300 ppm (dsDNA)

1. Introduction

Downstream processing (DSP) describes the purification of biopharmaceuticals with a chromatographic step being the main part. Conventional online sensors such as UV/Vis, pH or conductivity probes are currently used for monitoring this process. Unfortunately, key process parameters such as the concentration of various impurities (e.g. host cell protein HCP or double-stranded DNA, dsDNA) are thereby not accessible requiring time-, labor- and cost-intensive offline measurements of the fractionated eluate [1].

2. Methods

A conventional chromatographic workstation (Äkta Pure 25, GE Healthcare, Sweden) equipped with a multi-wavelength UV/Vis detector (the wavelengths 214, 260 and 280 nm are monitored), a conductivity and a pH probe, was enhanced with a mid-IR spectrometer (MATRIX-FM, Bruker, USA), a fluorescence detector (AvaSpec-ULS-TEC, Avantes, Netherlands), a multi-angle light scattering (MALS) spectrometer (miniDAWN TREOS, Wyatt, USA) as well as with a differential refractive index (RI) detector (Optilab T-rEX, Wyatt, USA). The chromatographic capture step of human fibroblast growth factor 2 (FGF-2) expressed in *E. coli* was monitored. On- and corresponding offline data for protein concentration and purity (HCP and dsDNA) were measured for 16 runs resulting in an extensive data set. Traditional chemometric methods such as partial-least squares (PLS) or principal component regression (PCR) were compared with penalized techniques (ridge and Lasso regression) and structured additive regression (STAR) [2,3]. All computations were performed in the R statistical computing environment [4].

3. Results and discussion

Figure 1 depicts the performance of a quantity model on an independent test run showing good agreement between model predictions and measured values determined for the 15 fractions. On average (over 6 test runs) an accuracy of 0.51 mg/ml (root-mean-squared error) is observed and can be expected for future applications of the model. A reduction of more than 30% in prediction error can be achieved compared by using spectroscopic data compared to models based on UV, conductivity and pH as predictors. Similarly, for HCP and dsDNA errors of approximately 200 and 300 ppm, respectively, are obtained.

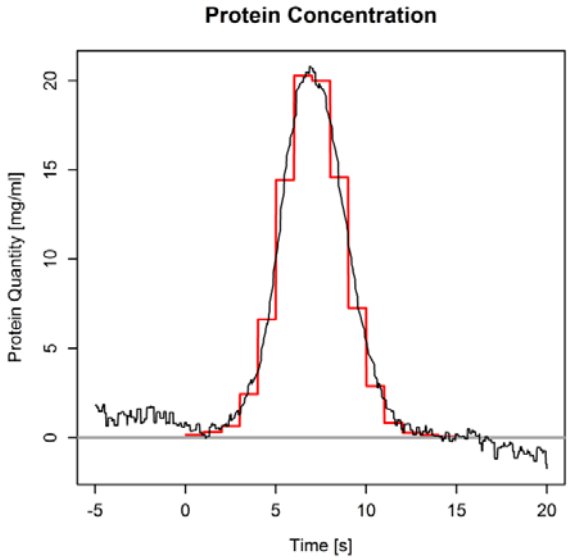

Figure 1. Performance of a structured additive regression (STAR) model for the protein concentration on a new test run – online prediction on a time grid of 1 second (black) and concentration values determined by offline measurements for 15 fractions of 1 ml each (red). Five minutes before and after the elution peak (15 min) are shown.

4. Conclusions

Particularly non-linear STAR models in combination with boosting as a variable selection method allow for a reliable prediction of critical process quantities such as the protein concentration, host cell protein and dsDNA content. While traditional sensors (UV/Vis, pH and conductivity) might be sufficient for the protein concentration, spectroscopic sensor systems are essential for modeling the impurities.

References

[1] D. G. Sauer, M. Mosor, A.-C. Frank, F. Weiß, A. Christler, N. Walch, A. Jungbauer, A. Dürauer, Protein Expr. Purif. 153 (2019) 70-82.
[2] R. Tibshirani, J. Royal Stat. Soc. B 58 (1996) 267-288.
[3] M. Melcher, T. Scharl, M. Luchner, G. Striedner, F. Leisch, Biotechn. Bioeng. 114 (2017) 321-334.
[4] R Core Team, R: A language and environment for statistical computing. R Foundation for Statistical Computing, Vienna, Austria. URL https://www.R-project.org/, 2018.

ECAB 5
The 5th EUROPEAN CONGRESS OF APPLIED BIOTECHNOLOGY
Florence 15-19 September 2019

Valorization of effluents from wood processing industry by removal of bioactive polyphenols and subsequent fermentation

Martin Lindemann[1*], Bernhard Widhalm[1], Cornelia Rieder-Gradinger, Thomas Kuncinger[2], Ewald Srebotnik[3]

1 Competence Centre of Wood Composites and Wood Chemistry, Linz, Austria; 2 Fritz Egger GmbH & Co. OG, Tiroler Straße 16, Unterradlberg, Austria; 3 Institute of Chemical, Environmental and Bioscience Engineering, Technische Universität Wien, Vienna, Austria

**Corresponding author: m.lindemann@wood-kplus.at*

Highlights

- Novel use of effluents from wood processing industry / Circular Economy approach
- Isolation of bioactive polyphenols
- Effluents as cultivation medium for *Pseudomonas sp.*
- VOC reduction by microbial degradation of aldehydes and terpenes

1. Introduction

Large quantities of effluent arise from MDF (Medium Density Fiberboard) production by squeezing out water from steam-pretreated softwood chips, resulting in a high load of TOC (total organic carbon). This process water stream is rich in wood extractives and is mainly composed of various carbohydrates, polyphenols, and organic acids, particularly fatty and resin acids. Process water treatment is laborious and costly, requiring sedimentation, flocculation, biological treatment as well as membrane filtrations and reverse osmosis. In this project, we therefore focus on the utilization of this currently unused process stream by recovering valuable bioactive compounds such as resin acids, lignans, and stilbenes as well as using the remaining carbohydrate rich stream as a carbon source for cultivation of VOC- (volatile organic compound) degrading microorganisms [1]. Since aldehydes and terpenes are among the main sources of VOC in the wood processing industry, these microorganisms may be applied onto woody raw materials as a possible approach to lower VOC emissions of wood products such as fiberboards.

2. Methods

A scalable fixed bed adsorption system for the removal and selective recovery of polyphenols (lignans and stilbenes) from MDF process waters was developed. Before adsorption, fibers and non-colloidal substances were removed from process water by centrifugation, while colloidal fatty and resin acids were removed by filtration through a 30 kDa cut-off membrane. Polyphenols where then isothermally adsorbed on a medium pressure liquid chromatography column packed with a regenerable macroporous, cross-linked pyrrolidone-based (PVPP) resin. Gradient elution of the adsorbed polyphenols from MDF process waters was optimized using a Ø 25 mm adsorber column (5.8 g resin, 15 ml min^{-1}). The carbohydrate rich stream resulting from polyphenol removal was used as a pre-cultivation medium for *Pseudomonas sp.* with terpenes as additional carbon source. The microbial biomass was then applied onto pine wood strands. VOC emissions from

manufactured boards were collected on Tenax TA, desorbed in a thermal desorber and analyzed by means of GC-MS.

3. Results and discussion

Lignans and stilbenes were adsorbed onto PVPP, while highly polar substances such as sugars and sugar alcohols, however, were not retained and remained in the flow-through. Adsorbed lignans were then eluted in successive fractions containing the individual lignans in different proportions, followed by pinosylvin in a separate fraction. (**Figure 1**). The capacity of the PVPP for 7-hydroxymatairesinol (HMR) as a model lignan was determined to be 37.4 mg g^{-1} at 1% breakthrough (data not shown).

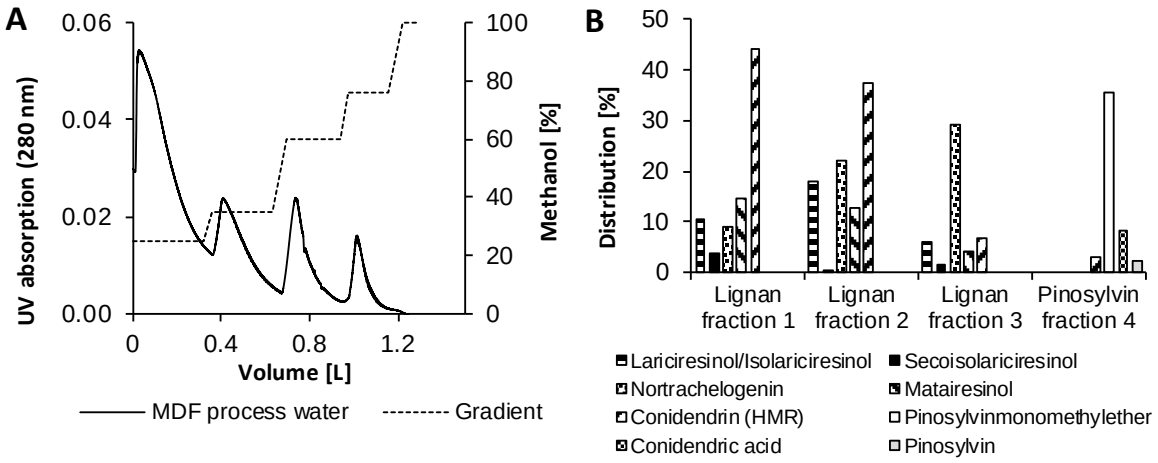

Figure 1 (A) Gradient elution (10 mM H_3PO_4, Methanol) of polyphenols after adsorption monitored at UV 280 nm. (B) Distribution of polyphenols in the collected fractions from gradient elution shown in (a).

Cultivation of *Pseudomonas sp.* in process effluents, after removing polyphenols by adsorption onto PVPP, did prove successful. Microbial pre-treatment of the pinewood strands resulted in a 20% reduction of the TVOC (Total VOC) value within only 6h, increasing to 55% reduction after 48h.

4. Conclusions

PVPP was shown to be particularly suitable for the selective adsorption and subsequent recovery of lignans and stilbenes from complex process effluents. The resulting carbohydrate rich stream after adsorption was successfully used as a cultivation medium for *Pseudomonas sp.* without further adjustments. These results provide a solid basis for technical implementation and, furthermore, the profitable utilization of otherwise valueless industrial process effluents.

References

[1] M. Lindemann, C. Rieder-Gradinger, T. Kuncinger, E. Strebotnik, Holzforschung, (in press) 2019.

ECAB 5
The 5th EUROPEAN CONGRESS OF APPLIED BIOTECHNOLOGY
Florence 15-19 September 2019

Enzymatic hydrolysis of Olive Solid Waste for extraction of polyphenols and reducing sugars using different cellulase enzymes

Carlos Zambra[1*], Susana Nieto[2], Pedro Lozano[2], Julio Romero[3]

1 Departamento de Ingeniería Mecánica, Universidad de Talca, Curicó-Chile; 2 Departamento de Química, Universidad de Murcia, Murcia-España; Departamento de Ingeniería Química, Universidad de Santiago, Santiago-Chile

**Corresponding author: czambra@utalca.cl*

Highlights

- Olive Solid Waste have high concentration of valuable compound.
- Enzymatic hydrolysis would allow increases the polyphenols concentration and reducing sugar.
- The enzymes can be recovered by means filtration.

1. Introduction

The intake of natural antioxidants and waste valorisation are issues of great importance for improving human health and achieve a modern and efficient industry. Powerful natural antioxidants can be found in high concentrations in waste from the olive oil industry [1]. The high concentration of fiber in the Olive Solid Waste (OSW) suggest that enzymatic hydrolysis with cellulase enzymes would allow to obtain an increase of the polyphenols concentration and reducing sugar. In this work the enzymatic hydrolysis of OSW is studied. One of the main drawbacks associated with the use of enzymes are, in many cases, their high production costs. It is for this reason that the recovery of the enzyme from the mixture obtained from the enzymatic hydrolysis is studied.

2. Methods

OSW samples were obtained directly from an olive oil factory located in the Maule Region, Chile. Three types of cellulase enzymes, Celluclast®, Viscozyme L® and Carezyme®, were used in the enzymatic hydrolysis tests. Before being used the enzymes were filtered in a cartridge vivaflow 50 (Sartorious) of 30,000 MWCO (molecular weight cut off). Once filtered, they were refrigerated at 5 ° C until they were used. Samples of 20 grams of OSW and distillate water were mixed with enzymes in volumes of 2.5 ml and 4 ml to obtain a final volume of 182.5 ml in an Erlenmeyer flask. The enzymatic hydrolysis was conducted at 50°C, pH 4.8 and 170 rpm in an incubator and orbital stirring YIHDER (LM-450D). The duration of enzymatic hydrolysis was 120 min. The total polyphenol content and the presence of reducing sugars were determined by colorimetric methods with the Folin-Ciocalteu and the 3,5-dinitrosalicylic acid (DNS) reagent, respectively. A method to recovery the enzyme was tested. The final mixture of the enzymatic hydrolysis was placed in filters Vivaspin Turbo 15 (30,000 MWCO) Sartorious® and these in turn in a Gemmy centrifuge (PLC-0.5) at 2000 rpm for 30 min. The retained liquid is used to carry out a new enzymatic hydrolysis. The cycle is

repeated five times. The recovery of the enzyme is quantified according to the yield in the increase of total polyphenols obtained in each cycle.

3. Results and discussion

Figure 1(a) shows the final concentrations of total polyphenols obtained after 120 minutes of enzymatic hydrolysis with two different volumes of enzyme added (2.5 ml and 4 ml). The total polyphenol content did not exceed 0.01 (g GAE/100 g DM) when hydrolysis was performed without adding enzyme. This value is practically the same to the measured initially (not showed in Fig. 1). All the enzymes tested increase the concentration of total polyphenols. The enzyme Celluclast® achieved the best performance with respect to the increase in total polyphenols (1.01 g GAE/100 g DM for 4ml of added enzyme) while the one with the worst performance was Carezyme® (0.2 g GAE/100 g DM). In figure 1(b) it is observed that the content of reducing sugars has no variation when hydrolysis is performed without adding enzyme (0.45 g glucose / 100 g DM). The enzyme Viscozyme L® showed the best performance to increase the concentration of reducing sugars (19.8 g glucose / 100 g DM for 4 ml of added enzyme). Figure 1 (c) shows the results of total polyphenols after six cycles of enzymatic hydrolysis. The enzyme used in this case was Viscozyme L. Figure 1 (c) shows the results of total polyphenols after six cycles of enzymatic hydrolysis operation. In this study, the increase in the concentration of polyphenols by enzymatic hydrolysis using the liquid retained in the filter, was associated with the quantity of enzyme recovered. Between each one of the cycles of operation the procedure of recovery of the enzyme described in the previous section was carried out. The enzyme used in this case was Viscozyme L. The relative percentage difference of the concentration of total polyphenols reached by the enzymatic hydrolysis decreases up to 68 percent after six cycle of operation

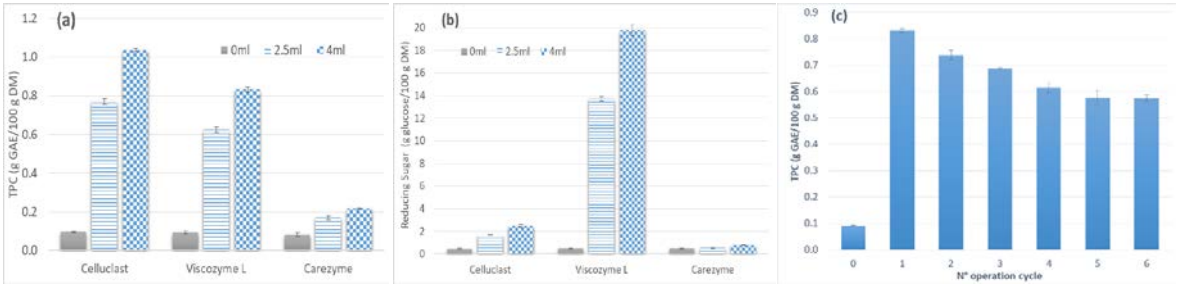

Figure 1. Concentration of total polyphenols (a) and reducing sugars (b) from OSW with three different enzymes and total polyphenols concentration obtained in each operation cycle after the recovery by filtration.

4. Conclusions

In this work was studied the increase in the concentration of total polyphenols content (TPC)) and the reducing sugar (RS) in the OSW using three types of cellulase enzyme. The Celluclast® and Vizcozyme L® shown the best yield for total polyphenol content and reducing sugar increases, respectively.

The physical method studied to recuperate the enzyme shown that its activity to augment the total polyphenols content decrease up to a 68 percent after six operation cycles.

References

[1] D. Makris, G. Boskou, N. Andrikopoulos, J. Food Comp. Anal. 20 (2007) 125-132

Microbial oil production using hemicellulose hydrolysate as feedstock

Erminda Tsouko, Aikaterini Papadaki, Seraphim Papanikolaou, Apostolis Koutinas*

Department of Food Science and Human Nutrition, Agricultural University of Athens,

Iera Odos 75, Athens 11855, Greece

**Corresponding author: akoutinas@aua.gr*

Highlights

- Spent sulphite liquor was used as feedstock for microbial oil production
- Microbial oil derived esters were produced via enzymatic synthesis
- Phospholipids caused inhibition on the transesterification process

1. Introduction

Waste valorization through microbial and enzymatic bioprocesses contributes to the growth of bioeconomy and the elimination of the severe environmental impact caused by the petrochemical industry. Spent sulphite liquor (SSL) is the concentrated liquid stream generated by the pulp and paper industry. Valorisation of SSL through fermentation is challenging due to the high content of inhibitory compounds, such as lignosulphonates (LS), phenolics and organic acids. However, the presence of C5 and C6 sugars create an important feedstock for fermentation processes.

Oleaginous fungi of the phylum *Zygomycota* and yeasts (e.g. *Lipomyces starkeyi*) have been reported to effectively produce lipids, when cultivated on lignocellulosic-derived hydrolysates. *Zygomycetes* can produce γ-linolenic acid (GLA) [1]. Microbial oils rich in GLA can be used in the food industry, nutraceuticals and cosmetics [2]. They have also been used for the production of biodiesel and oleochemicals, such as biolubricants and wax esters [3].

The objective of this study was the valorisation of SSL as fermentation feedstock for microbial oil production using oleaginous yeast and fungal strains aiming to the improving fermentation efficiency through the evaluation of different fermentation conditions (carbon to nitrogen ratio and LS concentration) in batch and fed-batch fermentations. In the case of fungal fermentations, the optimum conditions were identified for the production of GLA-rich microbial oil. GLA-rich lipids from *C. echinulata* were subsequently used as feedstock for the production of bio-based esters via enzymatic synthesis in a solvent-free system. The reaction conditions evaluated were temperature, substrate molar ratio and biocatalyst quantity. Under the optimized conditions, the impact of individual lipid classes to esters yield was assessed.

2. Methods

The yeast *L. starkeyi* DSM 70296 and 2 fungal strains *C. echinulata* ATHUM 4411 and *Mortierella isabellina* ATHUM 2935 were utilized for the production of microbial lipids. Initially, the effect of carbon to nitrogen ratio (calculated and expressed as carbon to free amino nitrogen ratio - C/FAN ratio) was evaluated for all microbial strains using nanofiltrated SSL (30 g/L total sugars and 5 g/L of LS) in shake flask fermentations. The best C/FAN ratio for each microorganism was applied and

the effect of various LS concentrations on lipid production was evaluated using sugar-simulated SSL. Sugar-simulated SSL was prepared using commercial sugars (xylose, glucose, galactose, mannose and arabinose) at the same proportion as in diluted nanofiltrated SSL. Subsequently, *L. starkeyi* and *C. echinulata* were selected for further evaluation in fed-batch fermentations using a bench-top bioreactor. Nanofiltrated SSL was used as fermentation medium. In the case of *L. starkeyi*, experiments were conducted at various C/FAN ratios.

Microbial oil and fractionated lipid classes, including neutral lipids (NL), glycolipids plus sphingolipids (GL+SL) and phospholipids (PL), were used with isopropanol and 2-ethylhexyl alcohol for the enzymatic production of fatty acid esters in a solvent free system catalyzed by Novozyme 435. Transesterifications with microbial oil were studied at various temperatures, substrate molar ratios and enzyme quantity. Transesterifications using NLs were carried out at various molar ratios. The effect of glycolipids plus sphingolipids (GL+SL) and phospholipids (PL) fractions on conversion yield of isopropyl esters was evaluated in mixtures with NL.

3. Results and discussion

In fed-batch fermentation, *L. starkeyi* showed the highest lipid production (40.9 g/L) at a C/FAN ratio of 173. In shake flask fermentations of *M. isabellina*, TDW and microbial oil content were highly inhibited when 10 g/L and 50 g/L of LS were applied. In the case of *C. echinulata*, lipid and GLA contents were positively affected with increasing C/FAN ratios leading to the highest values of 60% and 18.8%, respectively. Removal of phenolic compounds (61%) was also observed by the fungal strain. Fed-batch cultures of *C. echinulata* in bioreactor resulted in total dry weight of 12.2 g/L with a lipid content of 56% in media containing 5 g/L LS. Fed-batch fermentations demonstrated that GLA formation was strongly affected probably due to the applied aeration and agitation.

Transesterification reactions were initially optimised and subsequently transesterifications were conducted using NL, GL+SL and PL. The presence of GL+SL and PL fractions negatively affected enzymatic ester synthesis. Transesterification of the NL fraction with isopropanol and 2-ethylhexanol led to the highest conversion yield of 80.2% and 73.8%, respectively.

4. Conclusions

The present study showed that *L. starkeyi* and *C. echinulata* could tolerate high LS concentrations. Fed-batch bioreactor cultures of *L. starkeyi* under the optimum C/FAN ratio, resulted in high cell density (81.1 g/L) and high lipid content (50%). *C. echinulata* was able to produce PUFAs-rich microbial oil (60%) with simultaneous phenolics removal in batch fermentation.

The efficient enzymatic conversion of GLA-rich microbial oil into esters using Novozyme 435 was demonstrated. Enzymatic synthesis was mainly affected by temperature and substrate molar ratio. Results showed that the different lipid fractions have a key role in enzymatic activity and conversion yield. Specifically, conversion yield was higher when microbial oil was free of PL and GL+SL fractions.

References

[1] B. Kamm, Microorganisms in biorefineries, (Ed.) (2015) Springer 57-70S.
[2] Sergeant, E. Rahbar & F. H. Chilton, European journal of pharmacology 785 (2016) 77-86.
[3] A. Papadaki, K. V. Fernandes, A. Chatzifragkou, E. C. G. Aguieiras, J. A. C. da Silva, R. Fernandez-Lafuente & D. M. G. Freire, 267 Bioresource technology (2018) 311-318.

ECAB 5
The 5th EUROPEAN CONGRESS OF APPLIED BIOTECHNOLOGY
Florence 15-19 September 2019

Innovation of Expanded-Bed Adsorption by Integrating Simulated Moving-Bed Technology.

Trinath Pathapati[1*], Dennis N. Rutze[1], Piet den Boer[1], Menne Zaalberg[1]

1 ProPharma Group (Previously called Xendo B.V.), Schipholweg 73 – 75, P.O. Box 255, 2300 AG Leiden, The Netherlands;

**Corresponding author: Trinath.Pathapati@xendo.com*

Highlights

- Efficient downstream processing of complex biological streams
- Hybrid process by integration of EBA and SMB technologies
- Development of novel equipment for implementation of an EBA-SMB process
- Experimental results prove that the innovation resulted in enhance techno-economic efficiency

1. Introduction

Product stream from a fermentation step is water-based (> 80 wt %) and contains dissolved and suspended impurities. As the choice of technologies define the downstream process efficiency and resulting costs, it is critical to apply innovative and efficient unit operations to achieve people, planet and profit demands [1]. One or more unit operations are employed in each block of downstream processing. An approach to enhance efficiency of such a process is by integrating one or more operating principles into a single unit [2]. The current article emphasizes the integration of expanded-bed adsorption(EBA) and simulated moving-bed (SMB) technologies [3] for selective product capture from unclarified fermentation broth.

2. Methods

An EBA-SMB system with 8 columns, 5 inlets and 5 outlets per column was designed with a bed level detecting mechanism. The recipe consisted of defined zones including adsorption, adsorption wash, elution, elution wash, regeneration and regeneration wash that each EBA column went through during the SMB operation. After validating the system, experiments were performed to purify gamma-amino butyric acid (GABA) from unclarified fermentation broth containing up to 100g GABA/l and 16 g *Escherichia coli* biomass /l. The process conditions studied include,

i. Change in amount of feed fed/ml settled bed resin volume (SBV) to determine the maximum resin binding capacity that can be achieved
ii. NaOH concentration in elution buffer to shows its impact on elution recovery and product titer
iii. Number of columns in series in feed and elution zones for improved separation efficiency and recovery
iv. Entrainment rejection (ER) to prevent yield losses
v. Fractionation of product rich elution stream

3. Results and discussion

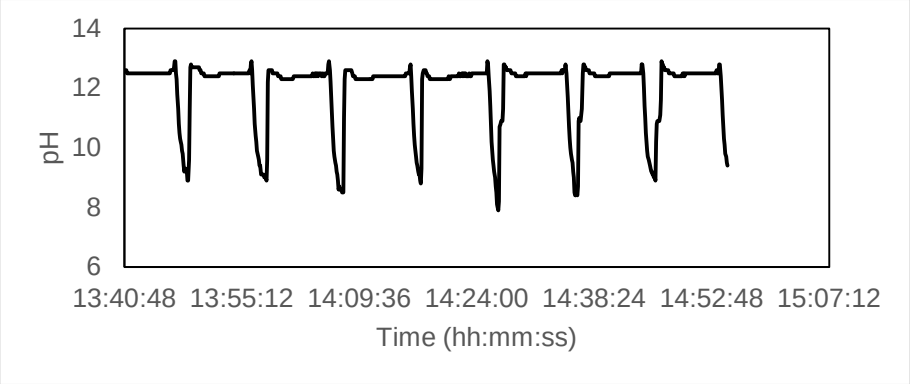

Figure 1. Outlet pH profile while different columns move through the product collection position after 2 cycles

It was observed that decreasing the amount of feed/column and increasing the number of columns in feed zone from 1 to 2 and entrainment rejection had a positive impact. By this approach GABA bound in feed zone increased from about 50 % (EXP001, 002, 003) to about 74 % (EXP004). However, the decrease in BV of feed/column resulted in 39 % reduction of binding capacity. Further, it was identified that due to the 8-column configuration and other critical zones including adsorption wash and elution, the number of columns available for feed zone was limited to 2. Therefore, to achieve further increase in yield and higher binding capacities, it is required to configure more than 2 columns in feed zone. The experiments performed to study the impact of buffer strength proved that by increasing NaOH content from 5 to 8 wt% in elution buffer, GABA recovery increased from about 55 % (EXP001) to about 84 % (EXP003). This, along with fractionation resulted in increase of product titer from 33 g/L to 47 g/L. Further, from the impurity analysis, it was also determined that the one step EBA-SMB purification of unclarified fermentation broth resulted in a product stream containing about 40 g/l GABA with purity >92 % and >98 % removal of biomass.

4. Conclusions

The experimental results proved that the EBA-SMB technology processed complex biological feed streams in one-step by integrating both biomass separation and selective product capture. The desired product purity was achieved. EBA-SMB design was validated by processing feed stream for several SMB cycles. No leakages and pressure buildups were noted. The integration and control strategy not only enabled stable operation, but also provided flexibility for process optimization. Thereby indicating improved techno-economic feasibility for industrial scale implementation. Further, parameters like the number of columns in a zone, feed loaded/SBV and elution buffer strength were identified to be critical to achieve optimal process performance.

References [Calibri 10]

[1] A. Karau, C. Benken, J. Thommes, M. R. Kula, Biotechnology and Bioengineering 1997, 55 (1), 54-64. DOI: 10.1002/(SICI)1097-0290(19970705)55:1<54::AID-BIT7>3.0.CO;2-W

[2] A. Rajendran, G. Paredes, M. Mazzotti, Journal of Chromatography A 2009, 1216 (4), 709-738. DOI: 10.1016/j.chroma.2008.10.075

[3] E. d. Jong, G. Jungmeier, Industrial Biorefineries and White Biotechnology, null. (Eds: A.Pandey, R. Hofer, C. Larroche, M. Taherzadeh and M. Nampoothiri), Elsevier B.V., Amsterdam 2015, Ch. 01.

ECCE12
The 12th EUROPEAN CONGRESS OF CHEMICAL ENGINEERING
Florence 15-19 September 2019

Bio Recovery of Platinum and Palladium From Spent Automotive Catalysts Using the Cyanogenic Bacterium *Chromobacterium Violaceum*.

Salman Karim, Yen-Peng Ting*

Department of Chemical and Biomolecular Engineering, National University of Singapore, Singapore 117585;

**Corresponding author: chetyp@nus.edu.sg*

Highlights

- Development of two-step bioleaching process for Pt and Pd recovery from SAC.
- Pretreatment of catalysts significantly removed the non-target metals.
- Subsequent bioleaching with *C. violaceum* showed recovery of Pt (52%) and Pd (59%).

1. Introduction

Spent automotive catalysts (SAC) are rich in platinum group metals (PGMs: platinum, palladium, and rhodium) [1]. The recovery and recycling of PGMs from SAC is important due to the need for resource conservation and environmental protection [1-3]. Hydrometallurgical and pyrometallurgical processes which are conventionally used for metal recovery are unfortunately highly pollutive. In recent years, there has been increasing interest in the use of bio-hydrometallurgical processes for metal recovery since this approach constitutes a green process [4]. Studies have reported that mesophilic bacteria such as *Chromobacterium violaceum* produce cyanide as a secondary metabolite which may be used in metal extraction due to its ability to form water soluble complexes with many metals. One such study on the recovery of gold from electronic waste by *C violaceum* reported a 23% gold recovery from pretreated electronic waste [5]. In the present study, an environmentally-friendly, sustainable, and an effective process for platinum (Pt) and palladium (Pd) recovery from spent auto catalysts was developed. As a preliminary step, SAC was first pretreated to remove interfering metals at the early stage due to its negative effect on the bio metallurgical processing. Bioleaching was subsequently conducted with *C. violaceum* for enhanced Pt and Pd recovery.

2. Methods

Ultrasonic-assisted nitric acid (US-HNO_3) pretreatment was performed in order to remove interfering (non-target metals Cu, Zn, Fe, and Ti) which otherwise compete with PGMs for the formation of metal-cyanide complexes. Central composite design was used to optimize the factors (US duration, US power, US frequency, HNO_3 conc., and temperature) in the pretreatment process. Using a *C. violaceum*, platinum and palladium were subsequently recovered from the pre-treated SAC in a two-step bioleaching process (where the SAC was added to the bacterial culture after the maximum cyanide concentration has been attained). Various factors affecting the biorecovery (pH, glycine conc., pulp density, additional oxidant H_2O_2, and temperature) were also examined using

central composite design. Multivariate optimization i.e. response surface methodology (RSM) was used to develop the models for optimization of the SAC pretreatment and bioleaching studies.

3. Results and discussion

The interactive effects of various factors were studied in an empirical response surface methodology (RSM) model for process optimization. For SAC pre-treatment study, results showed significant removal of Cu (75%) and Zn (84%) under optimal conditions (US duration 60-90 min, US power 90-108W, US frequency 37kHZ, HNO_3 conc. 7-9M, and temperature 70°C). Subsequent bioleaching of the pre-treated SAC using *C. violaceum* resulted in a recovery of platinum (52%) and palladium (59%) from pre-treated SAC under optimal conditions (pH 9.5, pulp density 0.5 %w/v, glycine conc. 8-10 g/L, H_2O_2 conc., 0.08 %v/v, and temperature 30 °C) over five days [Figure 1].

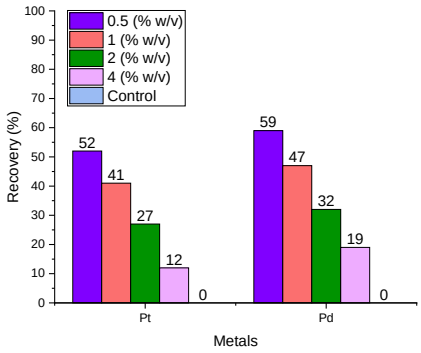

Figure 1. Pt and Pd recovery in two-step bioleaching by *C. violaceum* from SAC (pretreated SAC samples, pH 9.5, glycine conc. 8g/L, H_2O_2 conc., 0.08 %v/v, and temperature 30 °C) at various pulp densities.

4. Conclusions

Overall, this study demonstrates (i) the effect of ultrasonic assisted pretreatment for maximal removal of interfering base metals from SAC and (ii) the potential of cyanogenic bacteria for the recovery of Pt and Pd from SAC under two-step bioleaching process.

References

[1] M. K. Jha, J.-c. Lee, M.-s. Kim, J. Jeong, B.-S. Kim, and V. Kumar, "Hydrometallurgical recovery/recycling of platinum by the leaching of spent catalysts: A review," *Hydrometallurgy*, vol. 133, pp. 23-32, 2013/02/01/ 2013.

[2] A. Fornalczyk and M. Saternus, "Catalytic converters as a source of platinum," *Metalurgija*, vol. 50, no. 4, pp. 261-264, 2011.

[3] G. M. Mudd, "Key trends in the resource sustainability of platinum group elements," *Ore Geology Reviews*, vol. 46, pp. 106-117, 2012.

[4] M. A. Faramarzi, M. Stagars, E. Pensini, W. Krebs, and H. Brandl, "Metal solubilization from metal-containing solid materials by cyanogenic Chromobacterium violaceum," (in eng), *J Biotechnol*, vol. 113, no. 1-3, pp. 321-6, Sep 30 2004.

[5] G. Natarajan and Y. P. Ting, "Pretreatment of e-waste and mutation of alkali-tolerant cyanogenic bacteria promote gold biorecovery," (in eng), *Bioresour Technol*, vol. 152, pp. 80-5, 2014.

ECAB 5
The 5th EUROPEAN CONGRESS OF APPLIED BIOTECHNOLOGY
Florence 15-19 September 2019

Deciphering Alkaloids Bioconversion to High-Added Value Chemicals: the Metabolic Route of Lupanine Degradation in *Pseudomonas Putida* LPK411.

Stella Parmaki[1], Argyro Tsipa[1], Ioannis Vyrides[1], Ana Mota[2], Raquel A. M. Teixeira[3], Frederico C. Ferreira[2], Carlos A.M. Afonso[3], Michalis Koutinas[1,*]

1 Department of Environmental Science & Technology, Cyprus University of Technology, 30 Archbishop Kyprianou Str., 3036, Limassol, Cyprus; 2 Institute for Bioengineering and Biosciences, Department of Bioengineering, Instituto Superior Tecnico, Universidade de Lisboa, Av. Rovisco Pais, 1049-001, Lisbon, Portugal; 3 Research Institute for Medicines (iMed. ULisboa), Faculty of Pharmacy, Universidade de Lisboa, Av. Prof. Gama Pinto, 1649-003, Lisbon, Portugal

**Corresponding author: michail.koutinas@cut.ac.cy*

Highlights

- Systematic biodegradation kinetics of lupanine enantiomers in *P. putida* LPK411.
- A different metabolic pathway for each enantiomer exists.
- Systematic transcriptional kinetics of gene expressing lupanine hydroxylase.
- Systematic transcriptional kinetics of global genes in lupanine biodegradation.

1. Introduction

Lupanine constitutes the main quinolizidine alkaloid contained in *Lupinus albus* seeds. Owing to the useful functionalities of its asymmetric structure, this toxic compound has attracted considerable attention in biotechnological industries and may serve as a starting material for semi-synthesis of a range of novel high added-value compounds [1]. *L. albus* snack manufacturing generates excess of wastewater containing lupanine, while the most common process for lupanine elimination requires exhaustive boiling and leaching of seeds in water [2]. Biodegradation is a promising, greener alternative for detoxification of the wastewater generated. Thus, the objective of this study was to decipher the metabolism of lupanine biodegradation in *Pseudomonas putida* LPK411.

2. Methods

Microbial cultures: Lupanine enantiomers' biodegradation was investigated during fermentation of *P. putida* LPK411 using initial D-(+)-lupanine and L-(-)-lupanine concentration of 0.75 g L^{-1} respectively. The cultures were maintained at 31 ^{o}C, pH 7 and 100 rpm.
Analytical techniques: Culture samples were withdrawn at regular intervals and biomass concentration was determined by absorbance at 600 nm on a UV/VIS spectrophotometer. Lupanine concentration was measured using GC analysis [3].
Molecular biology techniques: Total RNA isolation, cDNA synthesis and Quantitative Real-Time Polymerase Chain Reaction (Q-RT-PCR) was conducted as previously described [4].

3. Results and discussion

Lupanine in nature exists in a racemic mixture of two enantiomers (D-(+)-lupanine and L-(-)-lupanine) [5]. Biodegradation kinetics of D-(+)-lupanine and L-(-)-lupanine was investigated during fermentation of *P. putida* LPK411. Two batch experiments were performed. The results

demonstrated that *P. putida* LPK411 can degrade D-(+)-lupanine, while L-(-)-lupanine concentration was only slightly reduced (Fig. 1). The latter indicates a different metabolic pathway for each enantiomer [6]. Moreover, LPK411 fermentations fed with racemic lupanine clarified that the strain is capable of achieving more than 95% enantiomeric excess of L-(-)-lupanine enabling the fermentative production of enantiopure L-(-)-lupanine, which avoids the application of other costly and laborious chemical methods.

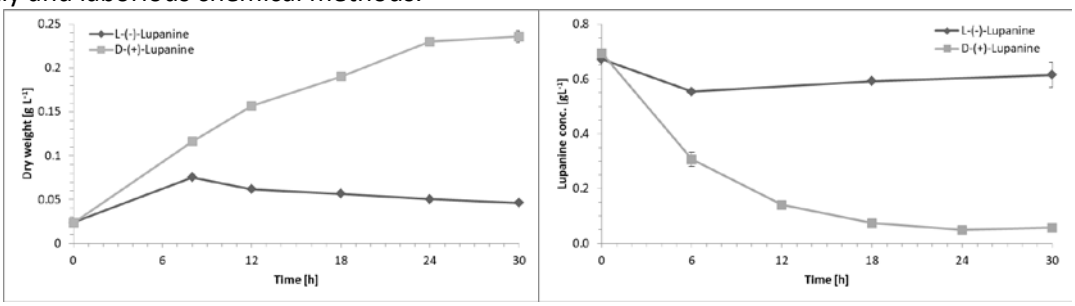

Figure 1. Lupanine enantiomers biodegradation by *P. putida* LPK411. (A) Microbial growth (expressed as dry cell weight), (B) concentration of D-(+)-lupanine and L-(-)-lupanine during fermentation.

Thus far, only a few studies have focused on metabolic mechanisms of quinolizidine alkaloids, such as lupanine. Lupanine hydroxylase catalyses the first reaction of lupanine biodegradation in *P. putida*. The specific enzyme is active only upon D-(+)-lupanine [6] biodegradation. Moreover, we have reported that *P. putida* LPK411 produces three main metabolic products during lupanine fermentation [7]. In this study, we systematically and consistently monitor the transcriptional kinetics of the gene expressing lupanine hydroxylase as well as global genes which may play a critical role during lupanine biodegradation in *P. putida*. We base our hypotheses on the lupanine derivatives' structures previously observed as well as on the selective catabolism of each enantiomer, which could potentially activate carbon catabolite repression (CCR) mechanisms.

4. Conclusions

Deciphering the lupanine biodegradation pathway by a *Pseudomonas* species provides fundamental knowledge of the metabolism during quinolizidine alkaloids biodegradation, which is expected to enhance bioprocess development for the production of high-added value compounds from lupanine wastewater.

5. Acknowledgements

This work was supported by the M-ERA.NET collaborative project Biorg4WasteWaterVal+ co-funded by the Research Promotion Foundation (RPF, Cyprus) and Fundação para a Ciência e a Tecnologia (FCT, Portugal).

References

[1] F. Villalpando-Vargas, L. Medina-Ceja, Seizure 39 (2016) 49-55.
[2] M. Erbas, J. Food Qual. 33 (2010) 742-757.
[3] F.M.C. Santana, A.M. Fialho, I. Sá-Correia, J.M.A. Empis, J. Ind. Microbiol. 17 (1996) 110-115.
[4] M. Koutinas, M. Lam, A. Kiparissides, R. Silva-Rocha, M. Godinho, A.G. Livingston, E.N. Pistikopoulos, V. De Lorenzo, V.A.P. Martins Dos Santos, A. Mantalaris , Environ. Microb. 12 (2010) 1705-1718.
[5] L.A. Nguyen, H. He, C. Pham-Huy, Int. J. Biomed. Sci. 2 (2006) 85-100.
[6] D.J. Hopper, M.A. Kaderbhai, Biochim. Biophys. Acta (BBA)-Proteins Proteomics 1647 (2003) 110-115.
[7] S. Parmaki, I. Vyrides, M.I. Vasquez, V. Hartman, I. Zacharia, I. Hadjiadamou, C.B.M. Barbeitos, F.C. Ferreira, C.A.M. Afonso, C. Drouza, M. Koutinas, Chemosphere 193 (2018) 50-59.

ECAB 5
The 5th EUROPEAN CONGRESS OF APPLIED BIOTECHNOLOGY
Florence 15-19 September 2019

Laccase-catalyzed degradation of micropollutants – Relation between the degradations of bisphenol A and diclofenac when in a mixture

Rosalie Pype[1], Frédéric Debaste[1]

1 Department of Transfers, Interfaces and Processes, Université libre de Bruxelles, Av. F.D. Roosevelt 50, ULB CP165/67, 1050 Brussels, Belgium

**Corresponding author: rosapype@ulb.ac.be*

Highlights

- Bisphenol A radicals enable the degradation of Diclofenac in mixes.
- A kinetic relation can be established between the degradations of BPA and DCF.
- That relation is independent of the initial concentrations and enzymatic activity.

1. Introduction

A micropollutant is a substance that has a negative impact on the organisms of the environment even at very low concentrations (ng/L to µg/L). An important source of micropollutants in surface waters is the release of wastewater treatment plants (WWTPs) effluents [1]. Enzymatic treatments have been studied as a mean to remove micropollutants. One of the most studied enzymes is laccase, an oxidase that oxidizes its substrate to form a reactive radical with the concomitant reduction of molecular oxygen to water. The formed radicals can then undergo non-enzymatic reactions [2]. Several papers highlighted that interactions took place between the compounds when several micropollutants were present in a mix [3,4]. In this study, the mechanisms underlying micropollutants removal were investigated in single-compound reactions and binary mixes, as well as the impacts of the interactions on the degradations kinetics including a relation between the degradations of the two compounds.

2. Methods

Laccase-catalyzed degradations of bisphenol A (BPA) and diclofenac (DCF) were performed at 20°C in phosphate buffer (pH7). The solution Novozym 51003, a commercial laccase preparation from Novozymes, was used as the enzyme source. The laccase activity was determined has described in [5]. The reactions were performed using BPA and DCF in single-compound medium (5 mg/L and 10 mg/L) and mixes (5 mg/L each, 5 mg/L BPA with 10 mg/L DCF and 10 mg/L BPA with 5 mg/L DCF) with either 3000 U/L or 1500 U/L of laccases. Samples were withdrawn at 0h00, 0h30, 1h00, 2h00, 3h00, 4h00, 5h00 and 6h00 of reaction. They were immediately mixed with 30 µL of sodium azide 1M to stop the enzymatic reaction and centrifuged before being analyzed through HPLC-UV. All experiments were performed in triplicate.

Chemical equations and reaction rates were used as a basis to determine the kinetic relation between the degradations of BPA and DCF.

3. Results and discussion

In single-compound reaction, the degradation of BPA at a given time was higher for a higher enzymatic activity (3000 U/L) and for a higher initial concentration (10 mg/L). The augmentation of the degradation when a higher enzymatic activity is used is expected as the laccase catalyze the reaction. The increase of the degradation when a higher concentration of BPA is used can be explained by the reaction of the radicals formed through the laccase-catalyzed oxidation of BPA with BPA molecules.

When in single-compound reaction, DCF was not degraded by laccase. That can be linked to the fact that the laccase contained in Novozym 51003 is a laccase with low redox-potential from *Myceliophthera thermophila*. So, as DCF is more recalcitrant than BPA, its degradation can be impossible for that laccase in the considered conditions.

However, DCF was degraded up to 47% after 6h in presence of BPA. That can be explained by the radicals formed through the laccase-catalyzed oxidation of BPA reacting with DCF. The degradation of DCF (X_{DCF}) was found to be directly linked to the degradation of BPA (X_{BPA}) no matter what the reaction conditions were (see Figure 1). By building a kinetic model, the relation between these two degradations was evaluated by $X_{DCF} = 1 - (1 - X_{BPA})^k$ where k is a constant.

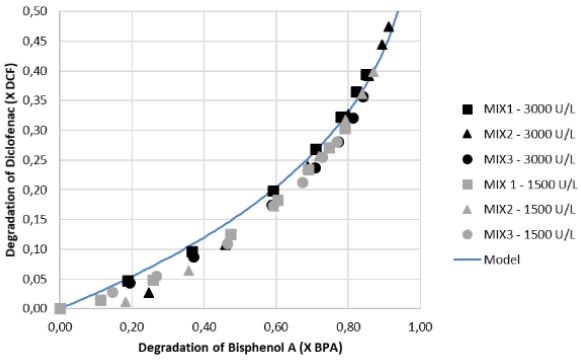

Figure 1. Degradation of DCF in function of the degradation of BPA obtained at the same reaction time. MIX1 = 5 mg/L BPA + 5 mg/L DCF, MIX2 = 10 mg/L BPA + 5 mg/L DCF, MIX3 = 5 mg/L BPA + 10 mg/L DCF. All reactions were performed at pH 7 and 20°C in triplicate (mean values of triplicates plotted). Model is the modelled relation between X_{DCF} and X_{BPA} where the constant k is 0.25.

4. Conclusions

The radicals formed through laccase-catalyzed degradation of BPA can react with other compounds present in the medium. Radicals participate to the degradation of BPA in single-compound medium and enable the degradation of DCF in mixes. A kinetic relation can be established between the degradations of BPA and DCF independently of the initial concentrations and enzymatic activity in the range of the tested conditions.

References

[1] Y. Luo, W. Guo, H. H. Ngo, L. D. Nghiem, F. I. Hai, J. Zhang, S. Liang, X. C. Wang, Sci. Total Environ. 473 (2014) 619-641.
[2] H. Claus, Micron 35 (2004) 93-96.
[3] J. Margot, J. Maillard, L. Rossi, D.A. Barry, C. Holliger, N. Biotechnol. 30 (2013) 803-813.
[4] R. R. Nair, P. Demarche, S. N. Agathos, N. Biotechnol. 30 (2013) 814-823.
[5] C. Hautphenne, F. Debaste, Chem. Eng. Technol. 38 (2015) 1223–1228.

ECAB 5
The 5th EUROPEAN CONGRESS OF APPLIED BIOTECHNOLOGY
Florence 15-19 September 2019

Use of fungi in a Membrane-aerated Biofilm Reactor

Ester Rosa[1], Marcello Pagliero[2], Grazia Cecchi[1], Simone di Piazza[1], Renzo Di Felice[3], Antonio Comite[2], Mirca Zotti[1]

1 Laboratory of mycology, Department of Earth, Environment and Life Sciences, University of Genoa, C.so Europa 26, 16136 Genoa, Italy;

2 Department of Chemistry and Industrial Chemistry, University of Genoa, Via Dodecaneso 31, 16146 Genoa, Italy

3 Department of Civil, Chemical and Environmental Engineering, University of Genoa, Via all'Opera Pia 15, 16145 Genoa, Italy

**Corresponding author: ester.rosa@edu.unige.it*

Highlights

- Membrane aerate biofilm reactor (MABR) is a promising, ecological and economic new technology for biological wastewater treatment.
- The potential role of microfungi in biological wastewater treatment has not received the attention merited, despite their metabolic ability to degrade many organic environmental pollutants.
- Hollow fiber as Accurel PP S6/02 are good for supplying air to fungal biofilm.

1. Introduction

A innovating wastewater treatment is the Membrane Biofilm Reactor (MBfR) based on the transfer of a gas through a membrane to a biofilm. The outer surface of biofilm is in contact with a liquid phase containing the substrates to be metabolized [1].

In a common wastewater treatment using MBfR the biofilm is formed by activated sludge organisms, but in this work it was studied the possibility to develop a biofilm using different fungal strains. [2]

The use of fungi to remove pollutant from environment components is called mycoremediation and is a new eco-friendly technology. Fungi can survive and grow at high concentration of many pollutants and some strains are used in wastewater treatment [3].

In this work a laboratory-scale reactor study was carried out by using commercial hydrophobic hollow fiber membranes, in polypropylene. The aim of work is to verify the capability of different fungi to grow and degrade synthetic or real wastewaters using air through a membrane.

2. Methods

Two common fungal strains usually used for mycoremediation were selected for the biofilm formation on the membrane surface: *Trichoderma harzianum* Rifai group and *Penicillium expansum* Link. The membrane bioreactors were realized starting from commercial fibers Accurel PP S6/2 (3M, Germany).

A small batch MABR consisted of 3 L glass flasks containing a model wastewater and hollow fiber membranes (about 20 cm^2 of the membrane surface area) immersed in the liquid phase and connected to an air feeding line at atmospheric pressure.

Another MABR was built using a hollow fiber membrane module of about 600 cm^2, where the feed was recirculated from a wastewater tank (Fig.1).

Various experiments aimed at evaluating the oxygen transfer rate were carried out at different air and liquid velocities. The biofilm growth was monitored and various operating parameters, as well as temperature, air velocity, and oxygen consumption and demand were studied using model and real wastewaters.

3. Results and discussion

In batch conditions the *Penicillium expansum* showed a better ability than *Trichoderma harzianum* to form a biofilm on the hollow fiber outer surface. In recirculation mode, the oxygen transfer performance of the membrane without biofilm was better by increasing the air and liquid velocity. Adhesion and growth of different fungal strain were tested using the same hollow hydrophobic fibers. The MABR performance where oxygen was supplied directly to the biofilm through the membrane was compared with the one of a suspended aerated biomass reactor based on a conventional sparger.

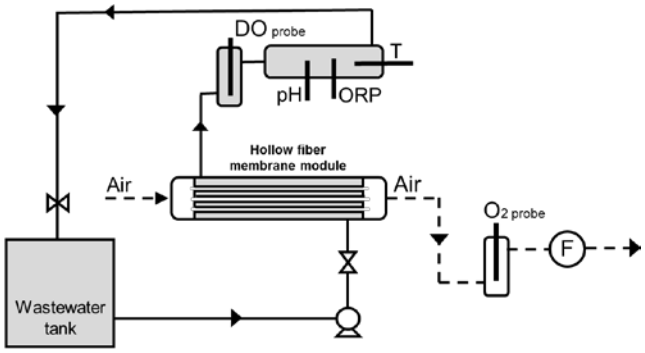

Figure 1. Membrane Areated Biofilm Reactor Plant scheme used for oxygen transfer and fungal growth experiment.

4. Conclusions

Some fungal strains are able to form a stable biofilm on the membranes Accurel PP S6/02. A preliminary screening revealed which strains are able to metabolize simple and more complex organic pollutants. Supplying oxygen directly thought the hollow fiber is an efficient approach to improve the kinetics of the pollutant degradation process. The fungi that have been tested show a different adherence on Accurel PP S6/02 and different capability to degrade the substrate, but it is still research is needed to explore new type of fungi and the substrates tested.

References

[1] A. Basile, Handbook of membrane reactors, first ed., Woodhead Publishing 2, 2013, pp. 763-807.

[2] K.J. Martin, R. Nerenberg, The membrane biofilm reactor (MBfR) for water and wastewater treatment: Principles, applications, and recent developments, Bioresource Technology 122, 2012, pp. 83–94.

[3] G. M. Gadd, Fungi in bioremediation, Cambridge University Press, 2001.

Elucidation of micropollutants biodegradation mechanisms in tertiary MBBR treatment.

S. Mehran Abtahi F[a], Salma Ouali[a] Claire Joannis Cassan[a], Sandra Beaufort[a], Agathe Juppeau Flambard[a] , Sophie Pecastaing[a], Thierry Trotouin[b], Fanny Terrisse[c], Jonathan Gerbore[c], Claire Albasi[a]

a Laboratoire de Génie Chimique, Université de Toulouse, CNRS, INPT, UPS, Toulouse, France.
b Veolia, Centre régional Toulouse Pyrénées, 22 avenue Marcel Dassault, 31506 Toulouse, France.
c Biovitis S.A., Le Bourg, 15400 Saint-Étienne-de-Chomeil, France.
**Corresponding author: claire.albasi@ensiacet.fr*

Highlights

- The potential of tertiary MBBRs was investigated in terms of MPs removal.
- MPs biodegradation by the biofilm was higher than by the suspended biomass.
- The profile of the microbial abundance reveals acclimation of the biofilm biomass.

1. Introduction

Nowadays, the scientific community is faced with the newly-born challenge of micropollutants (MPs) in aquatic resources. Since effluents of wastewater treatment plants have been globally recognized as the main source of these compounds in the aquatic environment, additional steps during wastewater treatment are one of the best options to reduce the release of these compounds into surface waters. To date, identification of technically and economically feasible advanced wastewater treatment options for elimination of MPs from secondary-treated effluent like adsorption processes, advanced oxidation processes and membrane filtrations is gaining importance. Regardless of these options that are recognized costly and laborious, there has been lower attention to innovative and cost-effective moving bed biofilm reactors (MBBRs) so far. High sludge retention time (SRT) obtaining in low hydraulic retention time (HRT) has given a dazzling attitude to MBBR reactors for high-efficient removal of carbon, nutrients and recently MPs. In the present work, we provide further insights into the key parameters involved in the removal of four MPs from secondary-treated municipal wastewater using a pilot-scale MBBR reactor. The biodegradation mechanisms were pointed out as the main removal pathways and the structural behavior of the microbial abundance was followed over the time.

2. Methods

Four identical lab-scale glass MBBR reactors, each with an effective volume of 3.1 L, were operated in a parallel mode under the ambient temperature, fed by a synthetic effluent after seeding with activated sludge. While two of them were used as references, the both others were fed with the MPs (17ß-Estradiol, Diclofenac, Naproxen, et 4n-Nonylphenol). Biofilm development on the surface of Z-MBBR carriers was monitored by microscopic observation (Epifluorescence and SEM).

Samples for MPs measurements were shipped to an indipendant laboratory named La Drome, located in France – to be analyzed under the license of COFRAC by LC-MS-MS measurements). Meanwhile, the biomass profile were characterized by means of DNA extraction and qPCR analysis through the large groups of the microbial [1].

3. Results and discussion

After stepwise establishment of a mature biofilm, abiotic and biotic removals of MPs were studied. Since no MPs reduction was observed by the both photodegradation and volatilization, abiotic removal of MPs was ascribed to the sorption onto the biomass. Target MPs i.e. Naproxen, Diclofenac, 17ß-Estradiol and 4n-Nonylphenol, arranged in the ascending order of hydrophobicity, abiotically declined up to 2.8%, 4%, 9.5% and 15%, respectively. MPs absorption onto the suspended biomass was found around two times more than the biofilm. When comparing abiotic and biotic aspects, we found that biotic removal outperformed its counterpart for all compounds as Diclofenac, Naproxen, 17ß-Estradiol and 4n-Nonylphenol were biodegraded by 72.8, 80.6, 84.7 and 84.4%, respectively. The effect of the changes in organic loading rates (OLRs) was investigated on the pseudo-first order degradation constants (kbiol), revealing the dominant biodegradation mechanism of co-metabolism for the removal of Diclofenac, Naproxen, and 4n-Nonylphenol., while 17ß-Estradiol obeyed the biodegradation mechanism of competitive inhibition. As summarized in figure 1, biotic removals of all MPs were quantified higher in the biofilm compared to the suspended biomass. [1]

The specific monitoring of the microbial community (figure 2) by molecular biology tools allowed us to understand the key role of some microorganisms in the degradation of targeted MPs, to identify those suitable and potentially involved in this degradation. A major presence of *Actinobacteria* was pointed out.

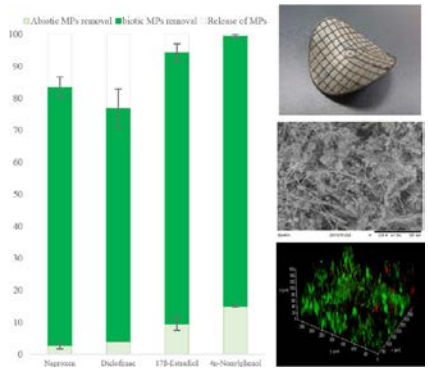

Figure 1. Contribution of micropollutants removal mechanisms

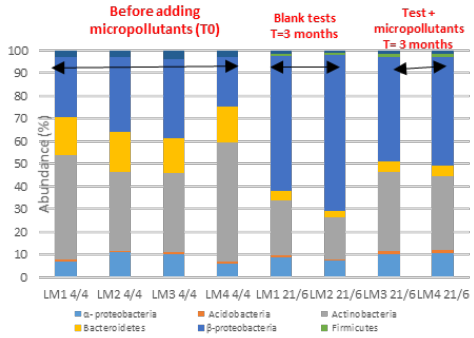

Figure 2 Microbial abundance in the mixed liquor – large groups (same type of data available for biofilm)

4. Conclusions

To draw a conclusion, a quite high removal of recalcitrant MPs is achievable in tertiary MBBRs, thanks to a biomass acclimation with microbial community selection, making them a promising technology that supports both pathways of co-metabolism and competitive inhibition.

References

[1] Stadler et al, 2017. Microbial Biotechnology, 11, 995–1007

[2] **Abtahi, S.M., et al 2018**. Sci. Total Environ. 643, 1464–1480.

Removal of the imidacloprid pesticide from water samples using supported ionic liquids (SILPs) as adsorbents

Sandra C. Bernardo[1]*, Maria João Santos[1], Márcia C. Neves[1], Mara G. Freire[1]

1 CICECO-Aveiro Institute of Materials, Department of Chemistry, University of Aveiro, Aveiro, Portugal.

**Corresponding author: sandrabernardo@ua.pt*

Highlights

- Removal of pesticides from aqueous solutions.
- Supported ionic liquids (SILPs) for solid-phase extraction (SPE).

1. Introduction

Due to the continuous growth of population and related anthropogenic activities, many toxic compounds are released and are reaching the environment [1]. A common type of these pollutants, are pesticides, which include herbicides, fungicides and insecticides. Pesticides comprise a wide group of chemical compounds, ranging from organo-phosphates, carbamates, to pyrethroids [2]. They are widely used to prevent crops destruction and to increase the agriculture productivity, leading to their accumulation in the food chain and to the contamination of air, water and soil [2]. According to the EU Directive on water quality [3], the maximum allowed concentration for pesticides in water is 0.1 µg/L for individual compounds and 0.5 µg/L for total pesticides. In general, pesticides tend to be environmentally persistent, thereby increasing the probability of exposure by non-target organisms [4]. Thus, a particular area of interest is on effective alternatives for environmental treatment of wastewater and groundwater supplies [1]. In recent years, a variety of methods including biodegradation, photodegradation, chemical precipitation, hydrolysis, oxidative degradation, ion exchange, flocculation, neutralization, membrane separation, ultrafiltration, and adsorption strategies have been applied for the treatment of pesticides from wastewaters [5].

Recently, supported ionic liquids (SILPs) have been described as an alternative adsorbent material for solid-phase extraction [6]. Ionic liquids (ILs) are organic salts, which by definition present a melting point below 100°C. Among other interesting features, one of their most relevant characteristics is their tunability. ILs can be designed to present a set of particular characteristics by changing the cation/anion chemical structure – a property that is transferred to SILPs. Based on these advantages, herein we propose the development of a more efficient and economical alternative technique for the removal of pesticides from water using SILPs.

Several supported ionic liquids (SILPs) silica-based materials were synthesized and characterized. Kinetic and equilibrium experimental data were obtained, and models were fitted for imidacloprid, a systemic neural toxic insecticide [4], used here as a model pesticide.

2. Methods

The synthesis of SILPs was previously described [7]. Briefly, commercial silica gel was used as the starting material for SILPs synthesis. In the first step, activated silica particles react with 3-

chloropropyl-methoxysilane, in order to obtain chloropropyl silica (SilprCl). Then, SilprCl material reacts with 1-methylimidazole or other reagents as the source of the cation (see Figure 1). Several techniques were used to characterize these materials. The adsorption kinetics and isotherms of each prepared SILP for imidacloprid were determined at 25°C.

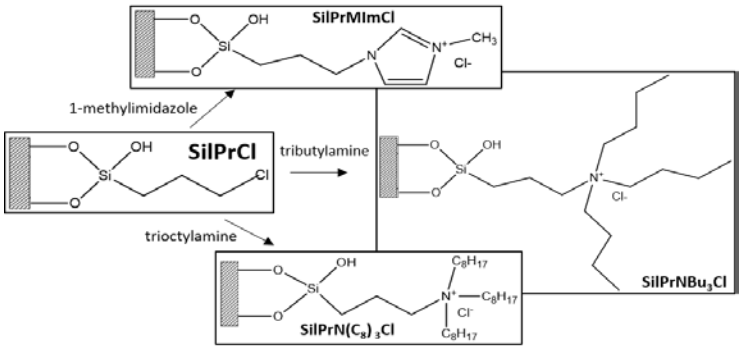

Figure 1. Schematic representation of the prepared SILPs and reagents used as source of the cation.

3. Results and discussion

Adsorption experiments were carried out, including studies of the adsorption kinetics and adsorption isotherms for the prepared materials for imidacloprid. It was found that when using the $SilPrNBu_3Cl$ material the adsorption of imidacloprid is fast (less than 10 min in equilibrium), reaching values of the equilibrium concentration of adsorbate in the solid phase (q_e) of 0.027 $mmol.g^{-1}$.

4. Conclusions

The prepared SILPs show promising results for the removal of imidacloprid from aqueous solutions with high adsorption efficiencies. The best identified SILPs are being tested for the removal of other pesticides from aqueous media, as well as the materials reuse.

Acknowledgments

This work was developed within the scope of the project CICECO-Aveiro Institute of Materials, FCT Ref. UID/CTM/50011/2019, financed by national funds through the FCT/MCTES. This work was developed in the scope of the "Smart Green Homes" Project [POCI-01-0247-FEDER-007678], a co-promotion between Bosch Termotecnologia S.A. and the University of Aveiro. It is financed by Portugal 2020 under the Competitiveness an Internationalization Operational Program, and by the European Regional Development Fund.

References

[1] Hussain, C. M. & Kharisov, B. Advanced Environmental Analysis, Applications of Nanomaterials. 1, (The Royal Society of Chemistry, 2016).

[2] Kaur, R. et al. Synthesis and surface engineering of magnetic nanoparticles for environmental cleanup and pesticide residue analysis: A review. J. Sep. Sci. 2014, 37, 1805–1825 (2014).

[3] European Commission. Directive 2013/39/EU of the European Parliament and of the Council amending Directives 2000/60/EC and 2008/105/EC as regards priority substances in the field of water policy. (2013).

[4] Federoff, N. E., Vaughan, A. & Barrett, M. R. Environmental Fate and Effects Division Problem Formulation for the Registration Review of Imidacloprid. (2008).

[5] Wang, T. et al. Adsorption of agricultural wastewater contaminated with antibiotics, pesticides and toxic metals by functionalized magnetic nanoparticles. J. Environ. Chem. Eng. 6, 6468–6478 (2018).

[6] Fontanals, N., Ronka, S., Borrull, F., Trochimczuk, A. W. & Marcé, R. M. Supported imidazolium ionic liquid phases: A new material for solid-phase extraction. Talanta 80, 250–256 (2009).

[7] Yang, F. et al. Magnetic microsphere confined ionic liquid as a novel sorbent for the determination of chlorophenols in environmental water samples by liquid chromatography. J. Environ. Monit. 13, 440–445 (2011).

ECCE12
The 12th EUROPEAN CONGRESS OF CHEMICAL ENGINEERING
Florence 15-19 September 2019

Role of L-Phenylalanine in 2-Phenylethanol Synthesis by *Kluyveromyces marxianus* ATCC 36907 using *Anacardium occidentale*.

André C. Macedo[1], Fernando K. C. Costa[2], M. Valderez P. Rocha[1], Luciana R. B. Gonçalves[1]

[1]*Departamento de Engenharia Química, Universidade Federal do Ceará, Campus do Pici, CEP: 60455-760. Fortaleza - CE, Brazil.* [2]*Universidade Federal de Santa Catarina, CEP: 88040-970. Florianópolis – SC, Brazil.*

**Corresponding author: acasimiro@gmail.com*

Highlights

- Alternative biotech-process to provide a high-purity 2-PE.
- Possibility and benefits of *CAJB* use as microbial cultivation broth.
- Synergistic effect between sugar concentration and L-Phe/precursor.

1. Introduction

2-Phenylethanol (2-PE) is an aromatic compound with rose-like odours used as a food, cosmetics and perfumery additive. Currently, this aroma is produced from natural rose extracts and chemical synthesis in high-cost processes. Due to this problem, the biotechnological pathway has been described in current literature as a promising alternative process to provide a high-purity 2-PE in an environmentally friendly process (**Etschmann** *et al.* 2002). Significant reports have described the use of *Kluyveromyces marxianus* as the best 2-PE producers. In fact, some yeast strains produce 2-PE by the Ehrlich pathway (**Fabre** *et al.* 1997; **Wittmann** *et al.*, 2002; **Schrader** *et al.* 2004). In this context, a biotech-system has been investigated for the 2-PE production by *K. marxianus* using cashew apple (*Anacardium occidentale L., CAJB*) as a nutritional substrate for microbial cultivation. *CAJB* is a native fruit from Tropical America discarded as an agricultural by-product. Considering the rich composition, CAJB can be used as a low-cost carbon source and other media components, that greatly influence the 2-PE productivity. This study not only explored the possibility and benefits of *CAJB* use, but also describes the role of L-phenylalanine (L-Phe) as a metabolic-key in bioreactions-chain which leads to 2-PE synthesis.

2. Methods

Microorganism: *Kluyveromyces marxianus* ATCC 36907 was used for 2-PE production. **Cultivation Broth**: CAJB (133.4 ± 2.4 g/L total sugar) was used as microbial cultivation broth. Additional L-Phe concentrations (1.0; 3.0; 4.0 and 10.0 g/L) were used in CAJB. All the assays were conducted using a Tec-Bio bioreactor (performed at 35°C, 250 rpm, 2 L/min air, using 750 mL/75 mL of inoculum). **Analytical Methods**: Cell concentration was measured by gravimetric method and 600nm optical density using a spectrophotometer. Sugar concentration measurement were performed using HPLC/RID and Aminex® column (150 mm x 7.8 mm) at 65°C. 1 mmol/L H_2SO_4 was used as eluent at a 0.4 mL/min flow rate. 2-PE concentration was also determined by HPLC/UV (at

254 nm) using Nova-Pak® C18 (5μ, 4.6mm x 150mm) at 35 °C and. Acetonitrile/water (40:60 v/v) was used as eluent at 0.8 mL/min flow rate.

3. Results and discussion

2-PE is synthesized *via* L-Phe transamination to phenylpyruvate, which is decarboxylated to phenylacetaldehyde and finally reduced to 2-PE. This classical Ehrlich pathway (EP) description suggests the important role of L-Phe and thus, it can be predicted that the synthesis of 2-PE is highly influenced by L-Phe in media composition. In fact, the results for cell (X) growth and product (P) accumulation with different concentrations of L-Phe (illustrated by Table 1) confirmed this hypothesis when we evaluated 1.0-3.0 g/L L-Phe, although the similar results for the concentrations of 3.0; 4.0 and 10.0 g/L showed no significant differences in the metabolite production.

Table 1- Description of yield (Y), kinetic (μ) and volumetric productivity (Q_X and Q_P) parameters obtained for *K. marxianus* ATCC 36907 cultivation using CAJB.

Parameter	L-Phe Concentration (g/L)			
	1.0 (g/L)	3.0 (g/L)	4.0 (g/L)	10.0 (g/L)
$Y_{X/S}$ (g/g)	0.115	0.128	0.133	0.135
$Y_{P/S}$ (g/g)	0.004	0.006	0.006	0.006
$Y_{P/X}$ (g/g)	0.035	0.051	0.046	0.049
Q_P (g/L.h)	0.007	0.011	0.011	0.011
Q_x (g/L.h)	0.205	0.244	0.245	0.254
$\mu_{Xmáx}$ (1/h)	0.511	0.342	0.863	0,600

This observation might also reflect the effects of the CAJB complex composition, interfering in the 2-PE bioconversion. Parallel experiments using synthetic broth (10 g/L glucose and 3 g/L L-Phe) pointed 0,028 g/L.h for Q_P. Thus, we can suppose the important metabolic role of L-Phe in 2-PE synthesis when we use nutritionally-poor broths. When we use CAJB the synergistic effect between sugar concentration and L-Phe is more evident. The accelerated cell growth (μ) indicates intensive C-N-energy deviation to the biomass synthesis and limiting EP. EP is still limited by 2-PE inhibition. 2-PE at even low-concentrations could start biological *sensing* mechanisms, limiting EP and 2-PE productivity even when we use appropriate broths or L-Phe high-concentrations.

4. Conclusions

These results suggest that CAJB is an appropriate, unconventional medium for bioproduction of 2-PE by *K. marxianus* ATCC 36907. Also, these results pointed out the synergistic effect between sugar/L-Phe concentration and 2-PE inhibition as an important mechanism for the process optimization.

References

[1] M.M.W. Etschmann, W. Bluemke, D. Sell, J. Schrader, Appl. Microbiol. Biotechnol. 59 (2002) 1–8.
[2] C.E. Fabre, P.J. Blanc, G. Goma, Biotechnol. Tech. 11 (1997) 523–525.
[3] J. Schrader, M.M.W. Etschmann, D. Sell, J.M. Hilmer, J. Rabenhorst, Biotechnol. Lett. 26 (2004) 463–472.
[4] C. Wittmann, M. Hans, W. Bluemke,. Yeast 19 (2002) 1351–1363.

ECCE12
The 12th EUROPEAN CONGRESS OF CHEMICAL ENGINEERING
Florence 15-19 September 2019

Biocompatible electroextraction of proteins from microalgae: protein characterization by mass spectrometry

Vincent BLANCKAERT, Hélène GATEAU, Justine MARCHAND, Benoît SCHOEFS*

Metabolism, Bioengineering of Molecules from Microalgae and Application , Mer Molécules Santé, IUML – FR 3473 CNRS, Le Mans University, Le Mans, France

Corresponding author: benoit.schoefs@univ-lemans.fr

Highlights

- Water-soluble proteins can be electroextracted from green algae
- The electroextraction is biocompatible
- 50% of the proteins originate from the chloroplast

1. Introduction

The increase of human populations and the expansion of cities contribute to an accelerated depletion of agricultural lands and natural resources. To overcome these difficulties, alternative sources of molecules are searched. Among these, microalgae are promising because they produce various molecules with pharmaceutical, nutritional and cosmetic properties (Mimouni et al., 2012). Biotechnological extraction process of these molecules starts with growing biomass, then harvesting microalgae and processing according to a definite downstream program. Vinayak et al. (2015) pointed out disadvantages of these downstream processes i.e. unselective extraction of intracellular compounds, requiring additional purification step(s), waste generation but also energy and time consumption. The need to increase the durability of biotechnological processes requires the development of new extraction methods such as electroextraction. Here, the identification of biocompatibly electroextracted proteins from the green alga *Haematococcus pluvialis* is reported.

2. Methods

Haematococcus pluvialis was grown mixotrophically. Proteins were electroextracted using pulse electric fields (PEF) of 0.5 or 1 kV cm^{-1}. After concentration and filtration, proteins were solubilized and separated by 1DE and 2DE. The resulting material was analysed by mass spectrometry: NanoLC/ESI LTQ-Orbitrap Velos ETD and MS/MS. The raw data were obtained after searching with Mascot Daemon search engine. *Chlamydomonas* was used for comparison because *H. pluvialis* belongs to the same order and it is a model organism (Marchand et al. 2018). Peptides and proteins were confirmed by generating a random peptide Bank "decoy", where the threshold of false positives has been set at 1% for peptides and proteins.

3. Results and discussion

The protein MW ranged from 12.4 to 164.9 kDa confirming that the proteins electroextracted are in a system without proteases. Proteins were identified by microsequencing after 1DE using nanoLC/ESI LTQ-Orbitrap Velos ETD and MS/MS. At maximum 36 proteins could be identified (1

kV cm^{-1}) among which 16 proteins were also electroextracted at 0.5 1 kV cm^{-1}. The localization of the identified proteins indicates that they originate from different cell compartments (Table 1). The comparison of the proteins patterns obtained with PEF of 0.5 kV cm^{-1} (Fig 1A) and 1 kV cm^{-1} (Fig 1B) when analysed by 2DE revealed that 8 spots were present only with PEF at 1 kV cm^{-1}.

Table 1. Identity of the 5 top scoring electroextracted

Uniprot/Protein	MW (kDa)	Peptide matches 0.5/1 kV cm^{-1}	Role and location
Ribulose bisphosphate carboxylase large chain	52.6	0/23	Carboxylation Oxidative fragmentation of the pentose Location: chloroplast
14-3-3 protein	29.3	0/20	Chaperonne Location: subcellular
14-3-3-like protein related	29.5	0/18	Chaperonne Location: subcellular
Tubulin beta chain	49.6	0/17	Constituent of microtubules Location: cytoplasmic
ATP synthase subunit beta	43.8	0/15	ATP synthesis coupled proton transport Location: chloroplast

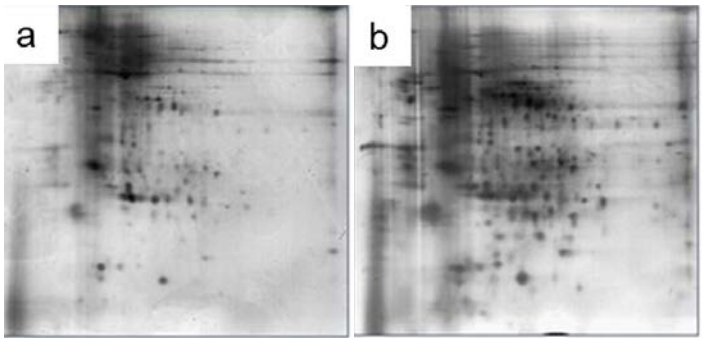

Figure 1. 2-DE of protein electroextracted from *Haematococcus pluvialis* PEF at (a) 0.5 kV cm^{-1} or (b) 1 kV cm^{-1}.

4. Conclusions

PEF of 1 kV cm^{-1} were more efficient in protein electroextraction than 0.5 kV cm^{-1} from the green alga *H pluvialis*. This work confirms the possibility of using PEF technology in blue biotechnology and opens new avenues for the development of biocompatible extraction possibilities.

References [Calibri 10]

[1] Mimouni, V., et al. (2012). "The potential of microalgae for the production of bioactive molecules of pharmaceutical interest. ." Current Pharmaceutical Biotechnology **13**: 2733-2750.

[2] Vinayak, V., et al. (2015). "Diatom milking: a review and new approaches." Marine Drugs **13**(5): 2629.

Microbial cathodes formed from salt marsh sediment may boost the development of microbial fuel cells

Mickaël Rimboud, Alain Bergel, Marie-Line Délia*

Laboratoire de Génie Chimique, Université de Toulouse, CNRS, INP, UPS, Toulouse, France

**Corresponding author: marieline.delia@ensiacet.fr*

Highlights

- Halotolerant O_2-reducing biocathodes were designed using salt marsh sediments
- Maximal current density reached 2.9 A m^{-2} under air saturation at 0.22 V/SCE
- An unusual Gammaproteobacteria was among the dominant bacteria of the biocathodes
- In MFCs the biocathodes led to the highest power density obtained using biotic cathodes

1. Introduction

Microbial fuel cells (MFCs) associate a bioanode, where the catalyst is a microbial biofilm, with a biotic or abiotic cathode. As MFCs consume organic matter as the fuel at the anode, they can produce electrical current by simultaneously abating the organic matter contained in an effluent. MFCs may consequently be promising systems for effluent treatment [1]. Unfortunately, the ionic conductivity of common effluents is far too low to hope an electrochemical process fairly performs. MFC development must therefore be considered in the context of highly saline and hypersaline effluents [2].

Salt marsh sediments have previously demonstrated to be efficient inocula for the design of halotolerant bioanodes working under polarization at +0.1 V/SCE, and saline conditions up to 60 $g.L^{-1}$ NaCl [3,4]. Nevertheless, no efficient cathode exists yet for ensuring O_2 reduction at the neutral pH values, which are required by the bioanodes. No metallic catalyst is known to be efficient for O_2 reduction around neutral pH.

Here, a solution to this issue is proposed by designing O_2-reducing biocathodes from salt marsh sediments. The biocathodes were firstly designed and characterized independently, in electroanalytical conditions. Then, coupled with a bioanode, they led to the highest power density produced so far in highly saline media, using microbial catalysts on both electrodes.

2. Methods

All O_2-reducing biocathodes were designed under polarization at +0.1 V/SCE (chronoamperometry) on graphite felt electrodes. Their electrochemical behaviour was characterized by mean of chronoamperometry and cyclic voltammetry (1 mV s^{-1}). The current produced during operation of MFCs was recorded flowing through a 1200 Ohm resistance. Polarization curves were recorded every 72 hours. Biofilms on electrodes were imaged using epifluorescence microscopy. After extraction, bacterial DNA was sent for 16S-pyrosequencing to RT-Lab Genomics, Lubbock, Texas.

3. Results and discussion

The 8 biocathodes displayed similar electrochemical behaviour. O_2 reduction current started after 3 days of polarization and maximal current density reached 2.0 A m^{-2}, with peaks up 2.9 A m^{-2} during voltammetry recording (1 $mV.s^{-1}$). Current density fluctuated during the 30 days of polarization but was never lower than 0.4 A m^{-2}. Voltammetric recordings evidenced oxygen reduction starting around +0.4 V/SCE. These values are of the same order than the best recorded in the literature for O_2-reducing biocathodes in usual media [5,6].

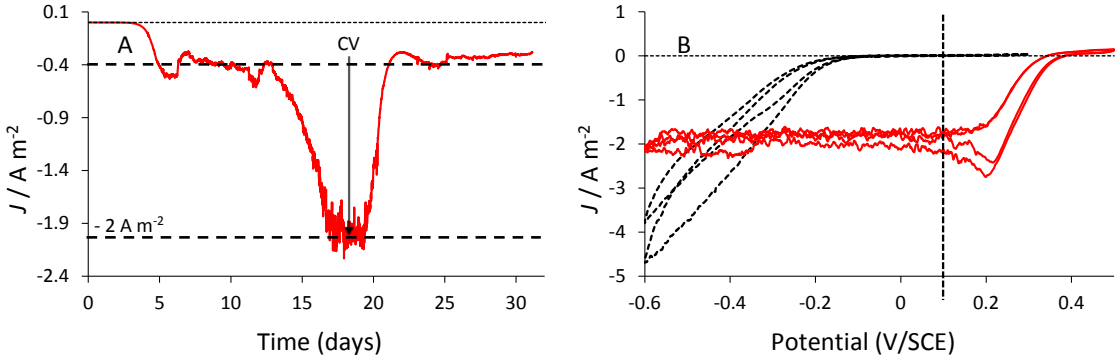

Figure 1. Representative current production recorded with a O_2-reducing biocathode. A: polarization at +0.1 V/SCE; B: Cyclic voltammetry recorded on day 17.5.

Biofilm imaging showed fair colonisation of the felt electrodes. Population analyses of the 8 biocathodes revealed similar microbial populations; their profile were significantly different from previous anodes, notably lacking Deltaproteobacteria. Orders counting potentially autotrophic genera (Rhizobiales and Rhodobacterales) were highly represented, together with an unusual Gammaproteobacteria, phylogenetically closed to *Thioalobacter thiocyanaticus,* a known chemoautotrophic strain. They may play a key role in inorganic carbon fixation and so the sustenance of the whole biofilm [7].

The biocathodes coupled to bioanodes prepared as previously described led to microbial fuel cells that operated for more than 13 days and produced up to 272 mW m^{-2}.

4. Conclusions

The efficient halotolerant O_2-reducing biocathodes designed here, in a reproducible way, should be a key element boosting the actual development of MFCs for the treatment of highly saline and hypersaline effluents.

References

[1] B.E. Logan, K. Rabaey, Science 337 (2012) 686-690.

[2] M. Grattieri, S. Minteer, Bioelectrochemistry 120 (2018) 127-137

[3] R. Rousseau, C. Santaella, W. Achouak, J.J. Godon, A. Bonnafous, A. Bergel, M.-L. Délia, ChemElectroChem. 1 (2014) 1966-1975.

[4] R. Rousseau, C. Santaella, A. Bonnafous, W. Achouak, J.J. Godon, M.-L. Délia, A. Bergel, Bioelectrochemistry 112 (2016) 24-32.

[5] E.M. Milner, D. Popescu, T. Curtis, I.M. Head, K. Scott, E.H. Yu, J. Power Sources 324 (2016) 8-16.

[6] S. Strycharz-Glaven, R.H. Glaven, Z. Wang, J. Zhou, G.J. Vora, L.M. Tender, J. Appl. Environ. Microbiol. 79 (2013) 3933-3942.

[7] T. Ishii, S. Kawaichi, H. Nakagawa, K. Hashimoto, R. Nakamura, Front. Microbiol. 6 (2015) 994-1003

This work was part of the Koropokkuru project (ANR-14-CE05-0004).

Integrated Separation in a Complex 2-Phase Multienzymatic Cascade Reaction System

Jens Johannsen[1*], Claudia Engelmann[2], Andreas Liese[2], Georg Fieg[1], Paul Bubenheim[2], Thomas Waluga[1]

1 Institute of Process and Plant Engineering, Hamburg University of Technology
2 Institute of Technical Biocatalysis, Hamburg University of Technology

**Corresponding author: jens.johannsen@tuhh.de*

Highlights

- A complex 2-phase multienzymatic cascade reaction system is introduced.
- A pilot plant is successfully set up for a continuous process.
- Extractive centrifugation for *in-situ* intermediate recovery is implemented.
- Influence of the extraction temperature on the total production efficiency is evaluated.

1. Introduction

In the field of white biotechnology the sustainable production of flavors and fragrances is increasingly gaining attention [1]. Enzymatic reactions allow for high selectivity and purities under mild reaction conditions, less by-products, and therefore enabling an overall sustainable production process [2]. In this contribution, a novel *in-vitro* multienzymatic cascade reaction system for the continuous and sustainable production of cinnamyl cinnamate from cinnamyl aldehyde in a 2-phase system is introduced. Two co-factor coupled dehydrogenases are used in a water-based buffer system, thus ensuring co-factor regeneration within the reaction pathway. An extractive centrifugation allows for a reaction integrated intermediate separation with an organic phase, consequently enhancing the productivities of the dehydrogenases. In the organic phase, a lipase is used to catalyze an esterification reaction of the intermediates resulting in cinnamyl cinnamate formation. During extractive centrifugation the organic phase is saturated with water, thereby decreasing the lipase activity in the last reaction step. In this contribution, the pilot plant set up, as well as experimental results are presented. Reaction kinetic data of all enzymes were determined. A computer model for the simulation of the cascade reaction is introduced. Experiments in pilot scale were performed, and process parameters were analyzed. Possible solutions to counter the challenge of product saturation in the organic phase are presented and evaluated.

2. Methods

The kinetic data of the two-substrate red-ox reactions catalyzed by the dehydrogenases was determined in the buffer system saturated with the organic solvent. Using ACM© from AspenTech a mathematical model was implemented. Experiments of the co-factor coupled red-ox reactions were performed to validate the model.

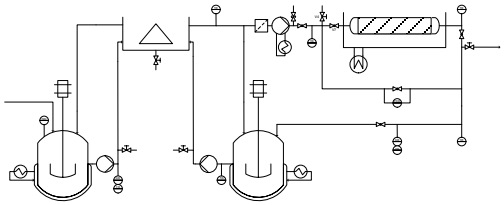

Figure 1. Pilot scale reactor set up with integrated downstream processing.

Experiments of the lipase catalyzed esterification reaction of cinnamyl alcohol and cinnamyl acid to cinnamyl cinnamate were performed in a pilot scale reactor (Figure 1) at the temperature optimum of the lipase (60 °C) to evaluate possible solutions to increase lipase activity. Firstly, the temperature during integrated extraction was varied. Secondly, an integrated adsorption unit operation to dry the organic phase was analyzed.

3. Results and discussion

For the dehydrogenases the maximum activities are 11.3 U/mg and 0.1 U/mg respectively, however, the solubilities of the substrates limit these activities during operation. Exemplary for the results of the pilot scale experiments, Figure 2 shows the lipase activity for extraction temperatures of 15 °C, 30 °C and 60 °C. In all cases, the esterification reaction itself was carried out at a temperature of 60 °C. It can be shown that a temperature decrease of 75 % in the extraction step leads to an activity increase of over 300 %. The activity increase can be explained by analysing the water saturation concentration of the organic phase exiting the centrifuge (Figure 3). A temperature decrease of 75 % during extraction results in a 75 % lower water saturation concentration, thereby decreasing the side product concentration prior to the esterification reaction. These results show that further drying of the organic phase is desirable. Hereby, promising results were achieved using an additional integrated adsorption step.

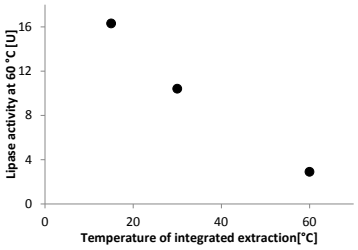

Figure 2. Lipase activity for different extraction temperatures.

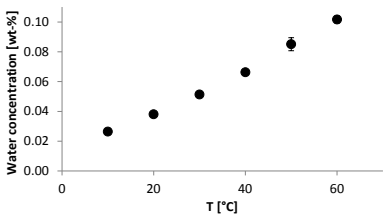

Figure 3. Temperature dependent water solubility in the organic phase.

4. Conclusions

A novel 2-phase multienzymatic cascade reaction system for a continuous and sustainable production of cinnamyl cinnamate is introduced. The kinetic data of the dehydrogenases was determined. A mathematical model was implemented. Additionally, a pilot scale reactor set up for a continuous production of cinnamyl cinnamate is presented. Exemplary for the analyzed process parameters in pilot scale operation the influence of the extraction temperature on the lipase activity was evaluated. Lipase activity was increased by over 300 % by decreasing the extraction temperature from 60 °C to 15 °C. These results can now be compared to an adsorption step prior to the lipase reaction. They are also helpful for a further development of the mathematical model.

References

[1] BMBF (Federal Ministry of Education and Research of the Federal Republic of Germany). 2012. Weiße Biotechnologie – Chancen für eine bio-basierte Wirtschaft.

[2] Abu, R., Woodley, J.M. 2015. Application of Enzyme Coupling Reactions to Shift Thermodynamically Limited Biocatalytic Reactions. ChemCatChem 7, 19, 3094-3105.

ECAB 5
The 5th EUROPEAN CONGRESS OF APPLIED BIOTECHNOLOGY
Florence 15-19 September 2019

Selection of yeast species for hydrocarbons and phenolic compounds degradation

Marlene Lopes[1], Renata Ramôa[1], Sílvia M. Miranda[1], Isabel Belo[1]

1 CEB – Centre of Biological Engineering, University of Minho, Campus de Gualtar, 4710-057 Braga, Portugal

**Corresponding author: marlenelopes@deb.uminho.pt*

Highlights

- *Yarrowia lipolytica* W29 was able to grow on hydrocarbons (hexadecane and hexadecene).
- *Candida tropicalis* demonstrated an extraordinary ability to grow on phenolic compounds.
- Lipase and microbial lipids were produced from hydrocarbons and olive mill wastewater.

1. Introduction

Large amounts of pollutant compounds are present in industrial effluents and, often, they are not totally degraded by physical and/or chemical methods before the discharge into the environment. Hydrocarbons and phenolic compounds are two examples of pollutants present in agro-industrial effluents, respectively in petroleum refinery effluents and olive mill wastewater (OMW). Biodegradation strategies involving microorganisms to simultaneously degrade these wastes and obtain high added-value products become an interesting approach, since the abundance of these compounds ensures the economic viability of bioprocesses while prevents major environmental problems. This work address the study of the ability of yeast species to grow on hydrocarbons and phenolic compounds as sole carbon and energy source. Moreover, the production of valuable compounds from these wastes was also assessed.

2. Methods

96-well microplate experiments were used to evaluate the ability of: (a) 6 yeast species (*Candida tropicalis* ATCC 250, *Candida utilis* CBS 621, *Candida cylindracea* CBS 7869, *Yarrowia lipolytica* CBS 2075, *Yarrowia lipolytica* W29 and *Pichia pastoris* CBS 2612) to grow on 1 $g \cdot L^{-1}$ hydrocarbons (hexadecane) and 1 $g \cdot L^{-1}$ phenolic compounds (catechol, tyrosol and phenol) as sole carbon source; (b) *Yarrowia lipolytica* W29 to grow on different concentrations of hexadecane or hexadecene (1 $g \cdot L^{-1}$ - 10 $g \cdot L^{-1}$); and (c) *Candida tropicalis* to grow on different diluted OMW-based media (5 % - 50 %). Batch experiments in 250-mL Erlenmeyer flasks were carried out to confirm the ability of: (a) *Y. lipolytica* W29 to grow on hexadecane (10 $g \cdot L^{-1}$), hexadecene (7.5 $g \cdot L^{-1}$) and a mixture of both hydrocarbons (5 $g \cdot L^{-1}$ of each hydrocarbon); and (b) *C. tropicalis* to grow on undiluted OMW. The effect of oxygen mass transfer was studied in 500-mL Erlenmeyer flasks, by raising the volume of flask headspace, for both yeast strains. Biomass concentration, lipase activity, microbial lipids content and long chain fatty acids were quantified as described by Lopes et al. [1]. Reducing sugars and total phenols were measured as described by Gonçalves et al. [2].

3. Results and discussion

The first screening carried out in 96-well microplates demonstrated: (a) the extraordinary capacity of *C. tropicalis* to grow in all phenolic compounds tested; and (b) the ability of *Y. lipolytica* W29 to grow on hexadecane. A considerable *Y. lipolytica* W29 growth was obtained in media with 10 $g \cdot L^{-1}$ of hexadecane or hexadecene comparatively to the control (without carbon source). It was also observed that *C. tropicalis* was able to grow on diluted OMW up to 50 % (v/v) medium. In fact, in this condition, a 3-fold improvement on cellular growth was obtained compared to the control (without carbon source). In Erlenmeyer flasks experiments, it was confirmed that *Y. lipolytica* W29 was able to grow on hydrocarbons-based media and using a mixture of hexadecane and hexadecene as carbon source led to an enhancement of final biomass concentration. In these substrates, the yeast had the capability to produce valuable compounds, namely lipase and microbial lipids. The increase of oxygen mass transfer, by raising the volume of Erlenmeyer headspace, had a clearly positive effect on cellular growth, intracellular lipids accumulation and lipase production, especially with hexadecane as carbon source (Table 1).

Table 1. Values of maximum biomass (Xmax), microbial lipids content, microbial lipids concentration and maximum lipase activity obtained from hydrocarbons by *Y. lipolytica* W29 batch cultures in flask experiments.

Flask	Hydrocarbon	Xmax ($g \cdot L^{-1}$)	Microbial lipids (%, w/w)	Lipids concentration ($g \cdot L^{-1}$)	Lipase ($U \cdot L^{-1}$)
250 mL	Hexadecane	3.5 ± 0.02	8.7 ± 0.7	0.3 ± 0.03	1260 ± 125
	Hexadecene	3.0 ± 0.01	9.9 ± 1.4	0.3 ± 0.04	610 ± 112
	Mixture	5.1 ± 0.04	8.5 ± 0.8	0.4 ± 0.003	567 ± 134
500 mL	Hexadecane	4.7 ± 0.03	15.1 ± 0.1	0.7 ± 0.001	2730 ± 304
	Mixture	7.3 ± 0.05	6.6 ± 0.1	0.5 ± 0.01	868 ± 270

Candida tropicalis was able to grow in undiluted OMW and consume almost all of phenolic compounds in Erlenmeyer flask experiments. A considerable amount of microbial lipids was also produced. The increase of oxygen mass transfer led to an improvement on cellular growth and reducing sugars consumption. However, total phenols consumption and intracellular lipids accumulation were not significantly affected by the raise of Erlenmeyer headspace (Table 2).

Table 2. Values of maximum biomass (Xmax), reducing sugars consumption, total phenols consumption, microbial lipids content and microbial lipids concentration obtained from OMW by *C. tropicalis* batch cultures in flask experiments.

Flask	Xmax ($g \cdot L^{-1}$)	Reducing sugars consumption (%)	Total phenols consumption (%)	Microbial lipids (%, w/w)	Lipids concentration ($g \cdot L^{-1}$)
250 mL	16.3 ± 0.03	38.2 ± 1.1	84.2 ± 0.9	18.3 ± 1.5	3.0 ± 0.8
500 mL	32.0 ± 0.4	55.7 ± 1.3	85.2 ± 0.6	19.8 ± 1.9	6.3 ± 0.8

4. Conclusions

This work demonstrated the potential of: (a) *Y. lipolytica* W29 to degrade hydrocarbons-contaminated effluents; and (b) *C. tropicalis* to degrade phenolic-rich effluents. Both yeast strains were able to produce valuable compounds, lipase and microbial lipids, from these pollutants. Microbial lipids, due to its composition (rich in oleic and linoleic acids) can be used to obtain biodiesel, a renewable fuel.

References

[1] M. Lopes, S.M. Miranda, J.M. Alves, A.S. Pereira, I. Belo, Eur. J. Lipid Sci. Technol. 121 (2019) 1800188–1800196.

[2] C. Gonçalves, M. Lopes, J.P. Ferreira, I. Belo, Bioresource Technol 100 (2009) 3759-3763.

Organophosphate pesticide degradation in a continuous biocatalytic membrane reactor

R. Mazzei, G. Vitola, T. Poerio, L. Giorno

Institute on Membrane Technology, National Research Council, ITM-CNR, via P. Bucci, 17/C, I-87030 Rende (Cosenza), Italy

**Corresponding author: r.mazzei@itm.cnr.it*

Highlights

- Continuous biocatalytic membrane reactor development (BMR) to hydrolyse organophosphates
- Significant improvement of immobilized phosphotriesterase stability respect to the free enzyme
- High organophosphate degradation (90%) by the BMR
- Long term stability of the BMR (1 year)

1. Introduction

Organophosphates (OPs) are highly toxic compounds used as pesticides and nerve agents. The devastating effects, reported in different studies, on the environment and human health indicate a serious scenario for both instantaneous and long terms effects. Bio-based strategies for OPs degradation seem the most promising solutions, particularly when extremophiles enzymes are used. These systems permit OPs degradation with high efficiency and specificity under mild conditions. However, as frequently observed, enzymes can easily lose activity in batch systems, so that a strategy to improve biocatalyst stability is highly needed, in order to develop continuous systems. In this work an extremophile enzyme, able to hydrolyze organophosphates, was immobilized on functionalized polymeric membranes to develop a continuous biocatalytic membrane reactor (BMR).

2. Methods

Commercial flat-sheet polymeric membranes of regenerated cellulose (Millipore), PVDF (GVS spa) and PES (GVS spa) were functionalized (Militano et al., 2016, Vitola et al 2016, Vitola et al 2018) in order to covalently bound three different mutants (called SacPox, SsoF and Sso-3M) from Sulfolobus acidocaldarius, Sulfolobus solfataricus (E. Porzio, 2007), kindly supplied by the Institute of Protein Biochemistry of the National Research Council (IBP-CNR). The obtained biocatalytic membranes were characterized by FT-IR, immunoelectron microscopy, enzyme catalytic activity and stability.The activity of the phosphotriesterase towards the pesticide paraoxon at 25 °C was

evaluated measuring the appearance of the reaction product (4-nitrophenol) by a spectrophotometer (405 nm).

3. Results and discussion

Among the different mutants with phosphotriesterase activity tested Sso3M showed the highest specific activity (10.0 ± 0.06 U/mg) in comparison to SsoF (0.65 ± 0.07 U/mg) and SacPox (0.34 ± 0.04 U/mg), respectively.

Sso3M showed the highest specific activity also when immobilized on hydrophilic membranes (PES and RC membranes) respect to hydrophobic (PVDF), giving the highest retained specific activity when immobilized on RC membranes.

The concentration of the immobilized enzyme amount which gives the highest specific activity and the best enzyme distribution on RC membranes (no enzyme aggregation observed by the in situ immunolocalization) is 0.17 (±0.03) mg/cm3. The conversion of the substrate at each passage through the biocatalytic membrane is improved up to 87%, when the residence time up to 0.96 min was increased. The stability of the enzyme in the continuous BMR was monitored for about 10 months and compared to the one of the free enzyme. The immobilized Sso3M showed high stability up to 10 months on the contrary the free enzyme is deactivated within two months

4. Conclusions

A continuous biocatalytic membrane reactor for the degradation of the pesticide paraoxon was developed. Under optimal conditions (residence time 0.96 min, amount of immobilized enzyme: 0.17 mg/cm3), the BMR has shown to detoxify about 90% of paraoxon (1 mM) at each passage through the biocatalytic membrane. Either in batch or in the continuous configuration, the immobilized enzyme showed higher stability than the free form up to 10 months.

References

[1] F. Militano, T. Poerio, R. Mazzei, E. Piacentini, A. Gugliuzza, L. Giorno, Influence of protein bulk properties on membrane surface coverage during immobilization Colloids Surf. B. 143 (2016) 309–317.G.

[2] Vitola, R. Mazzei, E. Fontananova, E. Porzio, G. Manco, S.N. Gaeta, L. Giorno, Polymeric biocatalytic membranes with immobilized thermostable phosphotriesterase, J. Membr. Sci. 516 (2016) 144-151.

[3] Vitola, G. Mazzei, R. Poerio, T. Porzio, E. Manco, G.Perrotta, I.Militano, F. Giorno, L.,Biocatalytic membrane reactor development for organophosphates degradation, Journal of Hazardous Materials 365, 2019, 789-795.

[4] E. Porzio, L. Merone, L. Mandrich, M. Rossi and G. Manco, A new phosphotriesterase from Sulfolobus acidocaldarius and its comparison with the homologue from Sulfolobus solfataricus, Biochimie 89 (2007) 625-636.

Crystal Contact Engineering to Promote Technical Protein Crystallization

Phillip Nowotny*, Johannes Hermann, Dariusch Hekmat, Dirk Weuster-Botz

Technical University of Munich, Institute of Biochemical Engineering, Boltzmannstr. 15, 85748 Garching, Germany

**Corresponding author: p.nowotny@lrz.tum.de*

Highlights

- Crystal contact engineering effects faster crystallization of the enzyme *Lb*ADH
- *Lb*ADH variants crystallize at reduced concentration of crystallization agent PEG
- Both properties result in increased space-time yield and lowered process costs
- Enhanced crystallizability of *Lb*ADH variants can be explained on the atomic level

1. Introduction

Technical protein crystallization is an attractive alternative to preparative chromatography as a main purification step of proteins in biotechnological processes [1]. Recombinant insulin, being the most prominent example, has been industrially crystallized for several decades. However, only a few proteins are sufficiently well crystallizable and molecular processes during protein crystallization are barely understood. Crystal engineering has been investigated since the early 1990s and it has become a common method to optimize crystal size and diffraction quality for crystallographic purpose [2]. Our approach was to transfer and expand the knowledge of crystal engineering towards technical crystallization purposes on the basis of the enzyme *Lactobacillus brevis* alcohol dehydrogenase (*Lb*ADH) [3]. The objectives were to i) enhance its crystallization properties allowing for the use of technical crystallization by engineering the crystal contact patches and ii) to understand the underlying mechanisms on the atomic level.

2. Methods

*Lb*ADH variants were produced with *Escherichia coli* in shaking flasks or stirred-tank bioreactors and purified via affinity chromatography. After dialysis and protein concentration, crystallization was triggered by the addition of a crystallization buffer containing polyethylene glycol (PEG 550). µL-batch crystallization was monitored by automated microscopic imaging, mL-batch crystallization was monitored by measurements of the protein concentration in the supernatant and microscopy of the crystals. In parallel, the enzymatic activity and the purity of all mutants were assessed experimentally. X-ray diffraction was performed for structural analysis of relevant *Lb*ADH mutants.

3. Results and discussion

More than 50 *Lb*ADH variants were designed following deterministic approaches, produced and purified to equal purity grade and protein concentration. Crystallization in microbatch experiments under identical conditions were the foundation for tracing back distinct crystallization properties to single amino acid exchanges. Enzymatically active *Lb*ADH variants were generated with increased crystallization success rate which correlated with a larger amount of crystals, a reduced time till crystallization equilibrium and crystallizability under reduced concentration of crystallization agent PEG 550. X-ray diffraction analysis elucidated enhanced crystallizability of *Lb*ADH variants on the atomic level. Crystallization on a mL scale in stirred tanks revealed increased volumetric productivities and crystallization yield of *Lb*ADH variants (exemplarily shown by WT-*Lb*ADH and variant K32A, Figure 1) [4].

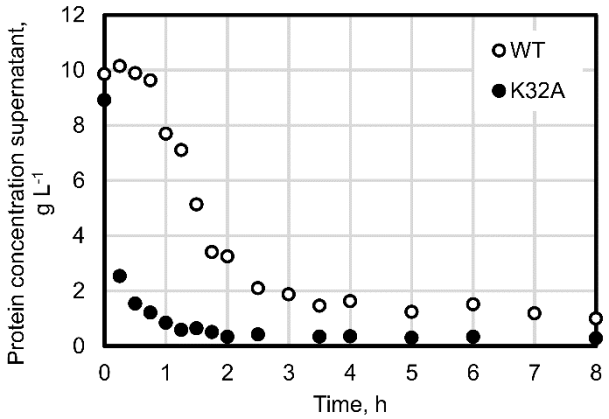

Figure 1. Crystallization kinetics of WT-*Lb*ADH (white) and mutant K32A (black) in a stirred tank crystallizer (V = 5 ml, initial protein concentration = 10 g L^{-1}, T = 20 °C) [4].

4. Conclusions

We have demonstrated for the first time that crystal contact engineering is a powerful tool to improve a protein's crystallizability for the use in technical crystallization. Single amino acid exchanges preserve enzymatic activities of engineered *Lb*ADH variants and lead to significantly enhanced crystallization space-time yields. Moreover, crystallization of *Lb*ADH variants takes place at concentrations of crystallization agent PEG 550 where the WT does not crystallize anymore. Both latter properties reduce process costs of technical large-scale protein crystallization, making it increasingly attractive for its integration into biotechnological downstream processes.

References

[1] D. Hekmat, Bioprocess Biosyst. Eng. 38 (2015), 1209−1231.
[2] Z. S. Derewenda, P. G. Vekilov, Acta Crystallogr., Sect. D: Biol. Crystallogr. 62 (2006), 116−124.
[3] J. Hermann et al., Acta Crystallogr., Sect. F: Struct. Biol. Commun. 74 (2018) 754−764.
[4] P. Nowotny et al., Cryst. Growth Des. 19 (2019) 2380−2387.

ECCE 12
ECAB 5

ECAB 5
The 5th EUROPEAN CONGRESS OF APPLIED BIOTECHNOLOGY
Florence 15-19 September 2019

Evaluation of two-species binding model within anion-exchange membrane chromatography to predict pressure buildup during recovery of a virus

William Kelly[1*], Kelsey O'Donnell[1], Zuyi Huang[1]

Department of Chemical Engineering

Villanova University, 19085 USA

**William.j.kelly@villanova.edu*

Highlights

- Pressure drop across a membrane chromatography unit increases steadily during operation and that this increase is more significant if a higher amount of DNA is present in the feed to the membrane unit.
- A mathematical model was developed that accounts for the competition of DNA and virus for binding sites on the membrane surface, and predicts virus bound per channel length which correlates well with pressure rise.
- The model predicted quite well the experimental breakthrough curves (as well as the amount of virus loaded per membrane channel length) across a range of inlet DNA concentrations from 1 x 10^{-10} to 5 x 10^{-6} g/ml and a range of inlet virus concentration from 1-5 x 10^{-4} g/ml.

1. Introduction

Membrane chromatography is an emerging technology for its effective removal of host cell DNA, proteins, and other small macromolecules throughout downstream purification. Multiple vendors supply this single-use technology in several surface chemistry options. The main feature of chromatographic separations based on membranes is the absence of pore diffusion, which is the main transport resistance in conventional column chromatography. Using porous particles. With the membranes, the molecules move via convection through the pores (1).

2. Methods

The presented findings aim to determine the cause of constant pressure rise observed during the loading phase of a viral recovery process using Sartorius Sartobind Q anion exchange membranes. A mathematical model was developed, based on previous work with expanded bed adsorption of proteins (2). The membrane model accounts for the competition of DNA and virus for binding sites on the membrane surface as they flow convectively through a pores/channel. The adsorption isotherm was modelled as Langmuir-like.

3. Results and discussion

The mathematical model predicted the experimental breakthrough curves (as well as the amount of virus loaded per membrane channel length across a range of inlet DNA concentrations from 1 x 10^{-10} to 5 x 10^{-6} g/ml and a range of inlet virus concentration from 1-5 x 10^{-4} g/ml.

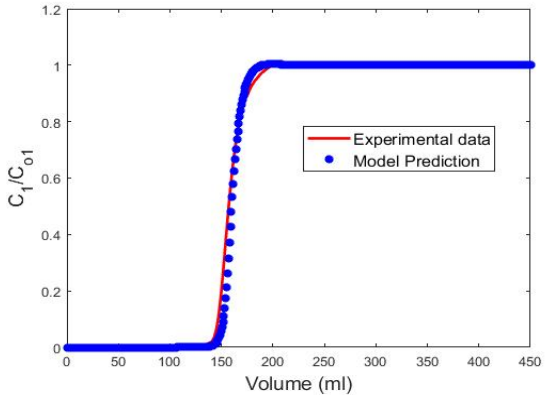

Figure 1. Breakthrough Results – Model versus experimental.

Initial Concentrations: C_{DNA} = 1 x 10^{-8} g/ml and C_{virus} = 3.1 x 10^{-4} g/ml

4. Conclusions

The model predicted quite well the experimental breakthrough curves. The model can be used to predict the time in a batch when the pressure drop across the column reaches a critical maximum limit, which might prompt operators to reduce the pressure drop by reducing flowrate or replacing the membrane.

References

[1] Thoemmes, J. and Kula, M. Membrane chromatography - an integrative concept in the downstream processing of proteins. Biotech. Prog. **1995**; 11(4): 357-367

[2] Kelly, W., Ubiera, A., Kamguia, G., Mullen, P., GÖklen, K., Huang, Z., Jones, G. (2013) "Using a two species competitive binding model to predict expanded bed breakthrough of a recombinant protein expressed in a high cell density fermentation", *Biotechnology and BioProcess Engineering*. Vol.18, No. 3, pp. 546–559. 2013.

ECAB 5
The 5th EUROPEAN CONGRESS OF APPLIED BIOTECHNOLOGY
Florence 15-19 September 2019

Purification of macromolecules combined with a simultaneous BTC analysis on a single Akta system

Rok Ambrožič[1], Petra Modic[1], Gorazd Hribar[2], Aleš Podgornik[1]

1 University of Ljubljana, Faculty of Chemistry and Chemical Technology, Večna pot 113, 1000 Ljubljana, Slovenia

2 Lek d.d., Technical Development Biologics Mengeš, Kolodvorska 27, 1234 Mengeš, Slovenia

**Corresponding author: Rok.Ambrozic@fkkt.uni-lj.si*

Highlights

- Modified chromatographic system with on-line column outflow analysis was designed.
- Robust method enabled breakthrough curve (BTC) detection for different target molecules.
- The limit detection concentration was enhanced by increasing the injected mass.
- Different case studies with different process dynamics were used for validation.

1. Introduction

A preparative high-performance liquid chromatography (pHPLC) remains an extensively used technique for a downstream operation for commercially important bio macromolecules, such as proteins and nucleic acids. Since process time becoming more and more critical for biopharmaceutical manufacturing, fast and effective chromatographic methods are widely required. In this context, target molecule breakthrough point determination should be of a great interest, mainly due to high evaluation of the final product. Therefore, modified chromatographic system with on line examination of preparative column outflow, which enabled detection of target molecule breakthrough point, was developed. Different case study samples, such as i) monoclonal antibodies (mAb), ii) protein aggregates and iii) plasmid DNA (pDNA), were used to validated and verified the system with automotive software method.

2. Methods

All experiments were performed with ÄKTA Explorer (GE Healthcare Life Science, UK) modified HPLC chromatographic system which enabled on-line analysis of preparative column outflow by simultaneously injection outflow from preparative column on separate selective analytical column where target molecule(s) was/were analyzed. Cationic and/or anionic exchangers were used as chromatographic supporters (along with selective protein A membrane), dependent on the investigated case study (feed sample) and its characteristics.

3. Results and discussion

To validate modified system and its method, the sample of pure mAb was loaded on a CEX preparative column and its breakthrough curves were investigated by UV absorbance measurements (Figure 1 left). No noticeable differences between breakthrough profile determined

directly from measurements of UV absorbance from preparative column (blue line) and breakthrough profile determined with on-line detection by protein A analysis (red squares) was detected, meaning system and method were designed correctly. Furthermore, breakthrough curve of unpurified mAb was investigated by the same method (Figure 1 right) to determined breakthrough curve of target molecule (mAb) in heterogeneous mixture (real sample). Although UV absorbance signal directly from preparative column was completely occupied throughout the experiment and as such unusable, on-line detection by protein A membrane enabled clear detection of mAb breakthrough point.

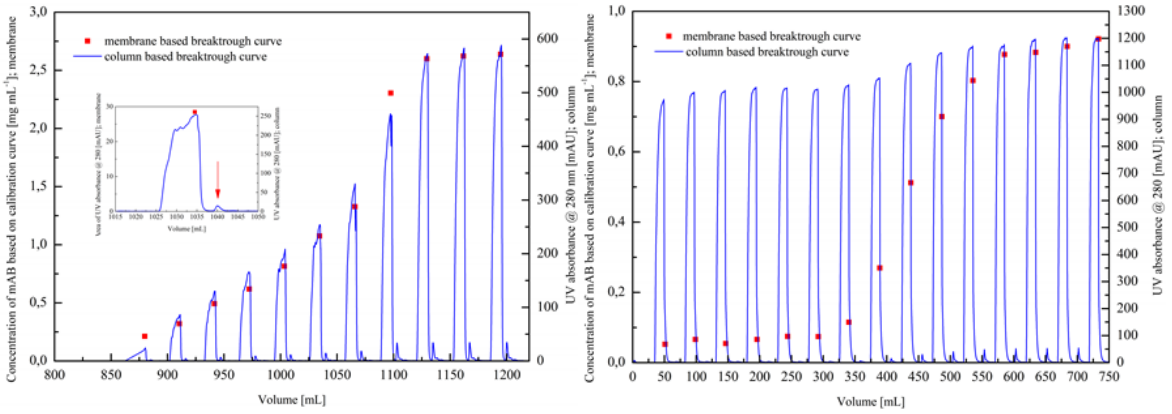

Figure 1. Protein A membrane (red squares) and CEX preparative column (blue line) based breakthrough curve of purified (left) and unpurified (right) mAb.

Additionally, modified HPLC system with the same analytical approach enabled efficient detection of protein aggregate, even below 1 % of total protein concentration. Since protein aggregates present a big concern in protein manufacturing, a fast and an efficient method for its detection should be widely required. Plasmid DNA was selected as a final case study, due to complex pDNA-RNA dynamics. However, excellent results with highly functional analysis for both target types of molecules were obtained without further modification of the system and/or method.

Finally, limit detection concentration was easily reduced by increasing the numbers of injection per each analyze step, what linearly increased injected mass and improved target molecule detection resolution. This simple, but extremely operative, solution was especially useful when target molecule concentration was below detection limit (in the early stages of breakthrough).

4. Conclusions

The modified HPLC system with automatize software method has proved to be very effective in detection of target bio macromolecules in preparative column outflow, even if the target concentration was below 1 % of feed concentration. Furthermore, system and method simple implemented into other pharmaceutical environments and its significant applicative potential should be enormous additional advantage for everyday use.

References

[1] D. Winters, C. Chu, K. Walker, J. Chrom. A 1424 (2015) 51-58.
[2] A. Jungbauer, R. Hahn, J. Chrom. A 1184(1-2) (2008) 62-79.
[3] D. Yoo, J. Provchy, C. Park, C. Schulz, K. Walker, J. Chrom. A 1344 (2014) 23-30.
[4] V. Smrekar, F. Smrekar, A. Strancar, A. Podgornik, J. Chrom. A 1276 (2013) 58-64.

Equilibrium properties of multimodal particle and membrane chromatographic adsorbents

Milan Polakovič*, Jana Adamíková, Monika Antošová, Tomáš Kurák, Tomáš Molnár

Department of Chemical and Biochemical Engineering, Institute of Chemical and Environmental Engineering, Faculty of Chemcial and Food Technology, Slovak University of Technology, Radlinského 9, 81237 Bratislava, Slovakia

**Corresponding author: milan.polakovic@stuba.sk*

Highlights

- Adsorption properties of multimodal particle and membrane adsorbents were investigated.
- Interesting influence of Hofmeister ions on the binding capacity was observed.
- Single- and bi-component adsorption of proteins and DNA was studied.
- Desorption experiments revealed problems with reversibility of binding.

1. Introduction

Multimodal chromatographic adsorbents are novel materials with promising properties for downstream processing of therapeutic glycoproteins. This presentation summarizes the results of our research dealing with the properties of the salt-tolerant chromatographic membrane Sartobind STIC a several particle multimodal adsorbents with both cation- and anion-exchange ligands. The equilibrium properties of these materials were investigated for a number of model proteins and DNA. Moreover, their performance in the purification of recombinant human erythropoietin (rhEPO) from a cultivation broth produced by human embryonic kidney cells was examined.

2. Methods

The investigated adsorbents were MEP HyperCel, HEA HyperCel, and PPA HyperCel from Pall Corporation, Capto MMC, Capto MMC Impress from GE Healthcare, Eshmuno HCX from Merck, and Sartobind STIC from Sartorius Stedim Biotech. The compounds used for adsorption were bovine serum albumin, human serum albumin, ovalbumin, α-lactalbumin, cytoglobin, fetuin, lysozyme, and salmon DNA. rhEPO was produced by cultivation of human embryonic kidney cells 293 (HEK 293) [1]. Static adsorption experiments were carried out either in 96-well plates or in conventional shaken vessels. Flow experiments were carried out using the FPLC system ÄKTA Purifier (GE Healthcare, Uppsala, Sweden). The adsorbents were packed either in small laboratory columns or placed in a membrane module.

3. Results and discussion

One of the investigated aspects was the effect of buffer type on binding on multimodal adsorbents. It was found that no BSA could be bound onto Sartobind STIC from a polyvalent

phosphate buffer at all. On the contrary, salmon DNA binding was not affected by the buffer valency.

The effect of ions of Hofmeister series on the binding capacity was investigated for several adsorbents but most focus was on the performance of the salt-tolerant anion-exchange membrane Sartobind STIC and particle adsorbent with cation-exchange ligands Capto MMC. Eight different salts were examined ranging from strongly kosmotropic ones such as $(NH_4)_2SO_4$ to salts with strongly chaotropic ions such as Mg^{2+} or SCN^-. A typical upper limit of salt concentration was 2.5 M.

Very different behavior was observed. Kosmotropic salts had adverse effect on the adsorption capacity of BSA on Sartobind STIC. The protein was not adsorbed at all at the concentrations of about 0.1 M. On the contrary, the adsorption capacity of several proteins for Capto MMC was essentially unaffected up to the salt concentrations of 1-1.5 M. The binding of DNA on Sartobind STIC had however a different pattern. The binding capacity was more-or-less constant up to 0.6 M kosmotropic salts concentration and then gradually declined to zero at about 1.5 M.

Chaotropic salts had a rather negative effect on the adsorption capacity for Sartobind STIC and Capto MMC. In the case of Mg^{2+} ions, the polyvalent effect of this cation has been manifested. The effect of NaCl concentration was studied most carefully. All adsorbents exhibited salt tolerance when the adsorption capacity often did not change very much if the NaCl concentration was in the range 0–0.5 M. A rather high capacity was observed in many cases at the salt concentrations as high as 2–2.5 M. Differences in the salt concentration effect were observed among individual proteins were observed with respect to pH. This was more emphasized for the multimodal adsorbents with cation-exchange ligands where the electrostatic interactions become dominant for positively charged proteins.

The adsorption capacity of DNA on Sartobind STIC exhibited typically a maximum with the salt concentration. Bi-component binding of DNA and BSA showed that DNA was bound preferentially so the equilibrium adsorbed amounts of BSA were smaller than for single component isotherms. Multicomponent adsorption was studied also for the separation of rhEPO produced by cultivation of human embryonic kidney cells. Cation exchangers, both conventional and salt tolerant, were found to have the best selectivity for this separation which was also verified in column experiments.

4. Conclusions

This work presents the overview of our research activities on the equilibrium and performance properties of multimodal adsorbents.

5. Acknowledgements

This work was supported by the grant from the Slovak Research and Development Agency (Grant number: APVV-16-0111).

References [Calibri 10]

[1] T. Molnár, M. Bartošová, M. Antošová, Ľ. Škultéty, M. Polakovič, Chem. Pap. 73 (2019) 713–718.

ECAB 5
The 5th EUROPEAN CONGRESS OF APPLIED BIOTECHNOLOGY
Florence 15-19 September 2019

Efficient depletion of a fibroblast growth factor 2 variant during polishing using hydrophobic interaction chromatography

Dominik Sauer[1], Magdalena Mosor[1], Alois Jungbauer[1,2], and Astrid Dürauer[1,2*]

1 Austrian Centre of Industrial Biotechnology (ACIB), Muthgasse 11, 1190 Vienna, Austria
2 Department of Biotechnology, University of Natural Resources and Life Sciences Vienna, Muthgasse 18, 1190 Vienna, Austria
**Corresponding author: astrid.duerauer@boku.ac.at*

Highlights

- This two-step purification delivers FGF-2 from *E. coli* with distinctive quality standards
- Polishing by HIC efficiently depletes a N-terminally degraded FGF-2 variant
- The full length product is recovered in the eluate with 100% yield
- HCP and dsDNA are depleted under their limit of quantification

1. Introduction

Fibroblast growth factor 2 (FGF-2) stimulates cell proliferation and differentiation via binding to the tyrosine kinase receptor and is an important therapeutics applied for tissue repair in regenerative medicine and for cancer treatment [1,2]. It is successfully produced by overexpression in the bacterial host *E. coli [3,4]*. During biopharmaceutical production a consistent product quality is of high importance. Typically, during capture the majority of process related impurities are depleted due to their properties which are highly differing from the product ones. In contrast, the polishing step is responsible to remove product variants of high similarity.

2. Methods

In the present study a two-step purification process for FGF-2 from clarified *E. coli* homogenate was developed. As capture step an ion exchange process was applied. The relative amounts of target product, host cell proteins (HCPs), dsDNA, endotoxin, monomer content, and high molecular weight impurities differed along the elution peak [4]. This information on the quality of the eluate is currently only available from time and labor intensive offline measurements. The holding step implemented for this purpose lead to degradation of FGF-2 generating product-related impurities. For robustness and quality assurance a polishing method based on HIC was integrated to assure the depletion of this process-related impurities and the separation of those product variants. The ion exchange eluate was purified using the HIC resin Toyopearl® Hexyl-650C. Its performance was compared to several other HIC resins regarding their impurity depletion.

3. Results and discussion

Toyopearl® Hexyl-650C performed superior compared to the other candidates. The product variants were effectively separated with a step yield of 100%. The HCP and dsDNA content after the HIC step was below the limit of quantification. Endotoxin content was depleted to 0.02 EU/µg FGF-2. The quantification of product variants was performed by an analytical ion exchange HPLC method.

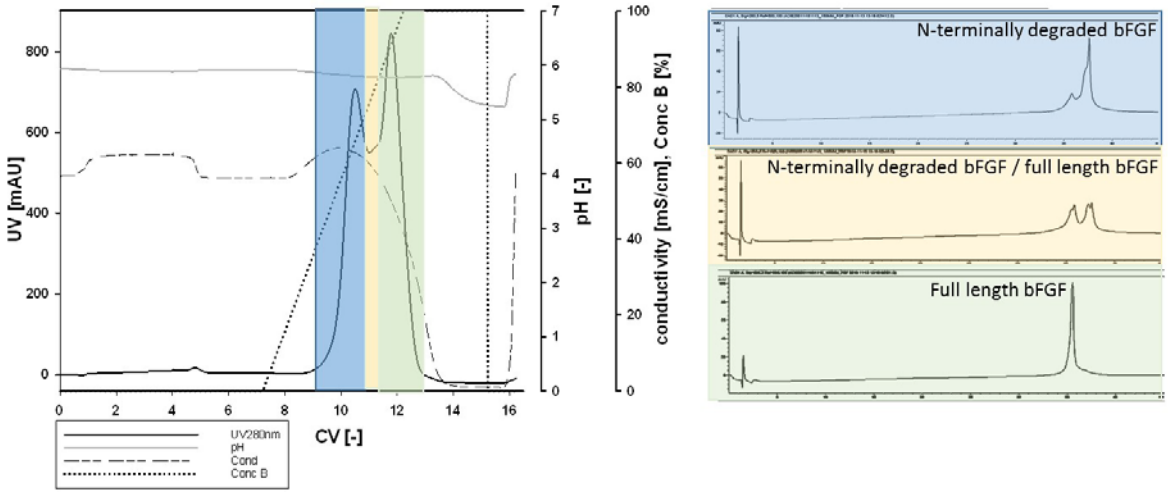

Figure 1. The HIC resin Toyopearl-Hexyl-650C (Tosoh, Japan) enabled the efficient separation of the N-terminally degraded product variant from the full length basic fibroblast growth factor: HIC chromatogram, elution was performed within 5CV with a linear gradient from 0 to 100% buffer B containing 10 mM Na-phosphate (left); Analysis of HIC eluate by IECX HPLC with gradient pH 7 – 10.5 (right)

4. Conclusions

The established polishing method by HIC enables the efficient depletion of the degraded product variant only differing in the loss of eight N terminal amino acids from the full length FGF-2. Toyopearl® Hexyl-650C resin separated the degraded product variant effectively while recovering the full length product with 100% yield. Implementing this polishing step into a two-step purification process started with a CIEX capture step a highly effective separation for FGF-2 was developed which meets distinctive quality standards defined by regulatory bodies. HCP and dsDNA were depleted under their LOQ.

References

1. Burgess, W. H., Maciag, T., The heparin-binding (fibroblast) growth factor family of proteins. Annu Rev Biochem (58) (1989) 575-606.
2. Nunes, Q. M., Li, Y., Sun, C., Kinnunen, T. K., Fernig, D. G., Fibroblast growth factors as tissue repair and regeneration therapeutics. PeerJ (4) (2016) e1535, doi: 10.7717/peerj.1535
3. Soleyman, M.R., Khalili, M., Khansarinejad, B., Baazm, M., High-level expression and purification of active human FGF-2 in Escherichia coli by codon and culture condition optimization, Iranian Red Crescent Medical Journal 18(2) (2016), doi: 10.5812/ircmj.21615
4. Sauer, D.G., Mosor, M., Frank, A.C., Weiss, F., Christler, A., Walch, N., Jungbauer, A., Dürauer, A. A two-step process for capture and purification of human basic fibroblast growth factor from E. coli homogenate: Yield versus endotoxin clearance, Protein Expr Purif (153) (2019) 70-82.

Adhesion of sea-urchin living cells on nano-patterned anodic porous alumina

Carla Falugi[1], Chiara Gambardella[2], Marco Salerno[3], Matteo Neviani[4], Ombretta Paladino[4*]

1 *DISTAV, Università di Genova, Viale Benedetto XV, I-16132 Genova, Italy*
2 CNR-IAS, Via de Marini 6, I-16149 Genova, Italy
3 Materials Characterization Facility, Istituto Italiano di Tecnologia, via Morego 30, I-16163 Genova, Italy
4 DICCA, Università di Genova, Via Opera Pia 15, I-16145 Genova, Italy
**Corresponding author: paladino@unige.it*

Highlights

- Sea-urchin coelomocytes as biosensors for sea water contamination
- Anodic nanoporous alumina as adhesion substrate
- Long-term cultures in polylactic sampling chambers

1. Introduction

In this work we investigated the possibility of using living cells as stress sensing material in biosensors, in the light of the three Rs principle – Replacement, Reduction and Refinement [1]. This approach requires the necessity to cultivate them on biocompatible electrical conducting substrate and to insert the circuit into a culture chamber that must assure both the transport of oxygen and the diffusion of the medium containing the potential stressor to the cells, without modifying their response and the structure of the culture. To this aim we fabricated nano-patterned substrates of anodic porous alumina to be used for enhancing cell adhesion, and culture chambers made in polylactic acid. Sea-urchin cells (coelomocytes) were cultured on these substrates at different times of 1, 3 and 5 days in vitro. Since these cells are progenitors of immune cells in vertebrate systems (blood cells), they carry out similar functions. For this reason, although they can differ considerably from vertebrates, they have been proved to be very promising sentinels of environmental water quality [2], [3].

2. Methods

In order to assess the effect of pore size on the living cell adhesion, pores with different diameter in the range of 10 to 200 nm were prepared on the same substrates [4].

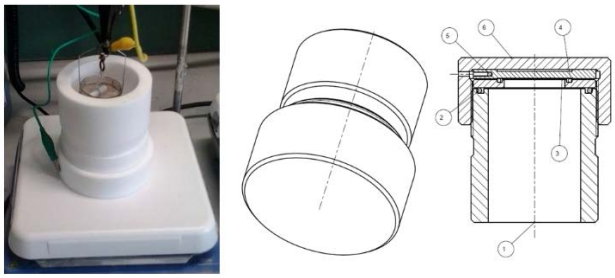

Figure 1. Anodization chamber

In the present version of the patterned substrates the living cell viability were assessed by examining both the presence and the nuclear status of the cells, via DAPI and IP staining, respectively.

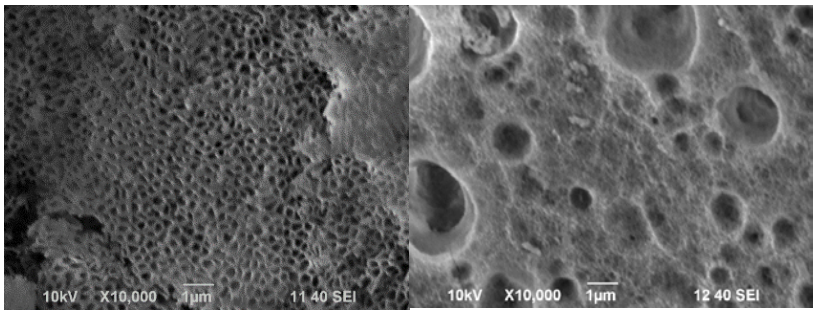

Figure 2. Different APA substrates

3. Results and discussion

All porous surfaces presented a higher number of adhering cells than different smooth controls of glass, polymer, and flat aluminum oxide without cell-adhesion promoting biomolecules. Coelomocytes readily adhered to the APA substrate up to 5 DIV: it can be observed that the nuclei are intact, and are all characterized by the same oval shape and size.

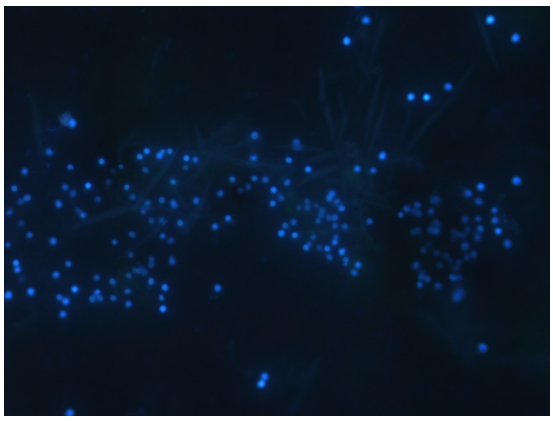

Figure 3. Culture cells on APA at DIV5, after staining with DAPI

4. Conclusions

The different pore size does not seem to have statistically significant effect on cell adhesion and this means that pore dimension can be optimized based on the need to realize an electrical read-out, to be carried out by impedance measurements.

References

[1] T. Hartung, Comparative analysis of the revised Directive 2010/63/EU for the protection of laboratory animals with its predecessor 86/609/EEC – a t4 report. ALTEX 27, 285-303, 2010.

[2] C. Falugi, M.G. Aluigi, M.C. Chiantore, D. Privitera, P. Ramoino, M.A. Gatti, A. Fabrizi, A. Pinsino, V. Matranga, Mar. Environ. Res, 76 (2012) 114-121.

[3] C. Gambardella, S. Ferrando, A. Gatti, E. Cataldi, P. Ramoino, M.G. Aluigi, M. Faimali, A. Diaspro, C. Falugi, Environ. Toxicol. 31 (2016) 1552-1562.

[4] M. Salerno, N. Patra, R. Losso, R. Cingolani, Materials Letters 63 (2009), 1826.

ECAB 5
The 5th EUROPEAN CONGRESS OF APPLIED BIOTECHNOLOGY
Florence 15-19 September 2019

Design of high performance micro-devices for endotoxins removal from biological fluids. Protein-lipid A binding step.

Arantza Basauri[1], Laura Giner[2], Marcos Fallanza[1], Gabriel Moncalián[2], Fernando de la Cruz[2], Inmaculada Ortiz[1]

1 Department of Chemical and Biomolecular Engineering, Universidad de Cantabria, Av. de Los Castros s/n, 39005 Santander, Spain; 2 Institute of Biomedicine and Biotechnology of Cantabria (IBBTEC), Santander, 39011, Spain.

**Corresponding author: ortizi@unican.es*

Highlights

- Microfluidics are applied to the separation of biomolecules
- Protein-lipid A binding interaction is studied
- A recombinant protein has been successfully synthesized and characterized

1. Introduction

The interdisciplinary nature of microfluidics, MFs, as well as its multiple advantages, such as cost and reactants volume reduction, turn out attractive to medical sciences. This novelty has led to the development of bioanalytical devices focusing on different fields like clinical diagnosis, drug discovery or biohazard detection [1]. The favorable characteristics of MFs have paved the way to the design of high performance micro-magnetoforetic devices for the removal of trapped endotoxins from human blood based on the use of functionalized particles [2]. This approach could offer a paramount challenge for prevention, detection and removal of gram-negative bacterial sepsis, as it remains a significant cause of morbidity and mortality in hospitalized patients. Bacterial lipopolysaccharide (LPS) from G(-) is mainly composed of a glycosidic region and a lipidic region or Lipid A, which is the biological active fraction of the molecule. The interaction between Lipid A and different molecules such as antibiotics (PMB), isoenzymes like glucokinase ligand activators, binding proteins (LBP) and peptides as magainine have been subject of study due to the virulence of this kind of endotoxins. In this context, our work is now focalized on the analysis of the endotoxin selective sequestration by a recombinant protein and at the same time, we pursue a kinetic characterization of the lipid-protein interaction in order to contribute to the optimum design of the micro-device.

2. Methods

A separation system is intended to be implemented into a magnetophoretic microfluidic device where a biological fluid is contacted to a saline buffer in order to couple the endotoxin sequestration stage and the LPS-beads removal from the blood stream as depicted in Figure 1.

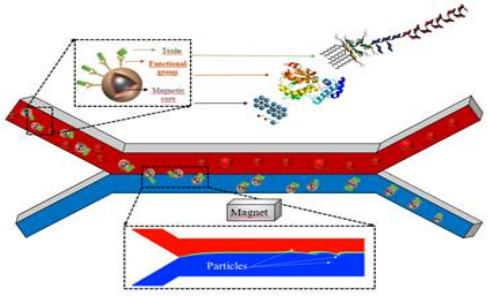

Figure 1. Magnetophoretic system for blood detoxification.

This sequestration stage needs a selective agent able to trap the lipid A. The functional molecule is a recombinant protein, expressed following the main strategies as vector design, host selection, and protein expression and purification [3]. Initially, a plasmid was designed and optimized for Escherichia coli and a histidine tag was added to bind the protein to Niquel carrying micro-beads. After the plasmid assembly, it was transformed into E. coli competent cells for protein overexpression at low temperature. The obtained soluble protein is loaded in 1mL HisTrap column, purified with affinity liquid chromatography techniques and finally concentrated. Then, it is bound to microbeads o/n to assure its complete functionalization. The sample is then centrifuged, the protein excess is removed and its concentration is measured to determine the beads adsorption capacity. Moreover, a fluorescent lipopolysaccharide conjugated with fluorescein isothiocyanate (FITC-LPS) stock solution of 1mg/mL is prepared and contacted to the protein-covered beads in order to analyze the selective binding of endotoxins. The fluorescent characteristic of LPS conjugates facilitates the quantification of the endotoxin removal and its quantification by fluorimetric techniques of samples supernatant.

3. Results and discussion

This work introduces a procedure to obtain a recombinant protein labelled with histidines as a quelating agent as a strategy to assure its binding to the divalent metallic ions of Ni2+ present in the micro-beads and optimizing its adsorption capacity. Preliminary studies have shown that 1mg of the protein binds to 5 µg of LPS, a promising protein activity, taking into account that septic patients show an endotoxin concentration around 300pg/mL. The specific binding takes place between the active site of the protein and the Lipid A of the lipopolysaccharide, but its mechanism needs to be deeply researched and defined with kinetic studies to precisely describe the lipid-protein interaction.

4. Conclusions

Focusing on the design of high performance microfluidic separation of G(-) bacterial lipopolysaccharide from human blood, we have addressed here the analysis of the ~~binding of~~binding of the Lipid A fraction to protein. With this purpose, we have developed a method that provides a soluble recombinant histidine tagged protein avoiding undesirable inclusion bodies. Preliminary studies demonstrate that 1 mg of our functional protein is able to sequestrate 5µg of LPS which constitutes promising results because average endotoxin levels in patients with sepsis are around 300 pg/mL. The encouraging data need further work focusing on the kinetic study of the interaction in order to contribute to biodevices microseparations and endotoxin detection and removal.

References [Calibri 10]

[1] C.J. Thomas CJ, M. Kapoor, S. Sharma, H. Bausinger, U. Zyilan , D.Lipsker, D. Hanau, A Surolia A. FEBS Letters 531 (2002), pp 184-188

[2] J. G-Pastora, J. González-Fernández, E. Real, A. Illes, E. Bringas, I.Ortiz. La bon a chip18 (11), pp 1593-1606.

[3] J.G.Gopal, A. Kumar. The Protein Journal, 32(6), 419–425.

Production of Mannosylerythritol lipids (MEL) from vegetable oils: Exploring lipase application on substrate pretreatment

Petar Keković[1*], Nuno Faria[1], Frederico Ferreira[1]

1 iBB – Institute for Bioengineering and Biosciences, Department of Bioengineering, Instituto Superior Técnico, Avenida Rovisco Pais, 1049-001 Lisboa, Portugal

**Corresponding author: petarkekovic@tecnico.ulisboa.pt*

Highlights

- Free Fatty Acids (FFA) and Esters were used as a feed for production of MEL
- All ester-fed cultures, besides butyl esters, performed better than ones fed with oil
  Cultures fed with FFAs produced resulted in higher productivity and yields of MEL

1. Introduction

Mannosylerythritol lipids (MELs) are a group of extracellular glycolipid biosurfactants, known for their tensioactive versatility. High titers of MELs are obtained using vegetable oils as substrates for *M. antarticus*. However, a significant fraction of the bioproduced MEL is lost during downstream due to difficult separation from triglycerides [1]. Lipases are also produced by *M. antarticus* cultures, which break down the triglycerides that the vegetable oil consists of. Considering these two features of *M. antarticus*, three approaches are explored in this work, with the aim to increase MEL production and enable different downstream routes.: feeding the culture with vegetable oil, using oil partially broken down by lipases produced by *M. antarticus,* or transforming the triglycerides into alcohol esters, and adding them as a carbon source.

2. Methods

Cultures of 50 ml in 250 ml flasks were incubated at 27 °C, 250 rpm for 12 days. Glucose (40 g/l) was used as the initial source of carbon, while soybean oil, pretreated soybean oil and fatty acid alcohol esters (20 g/l) were added on day 4 to some flasks, at the start of the MEL production phase, following the previously established protocol for MEL production by using soybean oil [2]. Oil hydrolysis was performed using lipase-rich supernatant collected from cultures at day 7, and, for proof of concept, esterification was performed with commercially available purified CAL-B, with the addition of methanol, ethanol or butanol. The overview of the experimental plan is presented in Figure 1a.

3. Results and discussion

Lipase-rich supernatant (3 U/ml of activity), was mixed with soybean oil, and maintained at different conditions, with a three level variation of parameters, according to a Box-Behnken experimental design. The best performing conditions reached only 39% hydrolysis efficiency. The addition of 0.5% of emulsifiers, Xanthan and MEL, increased FFA concentrations, with the latter achieving 76% hydrolysis efficiency. Coherently, lipase-rich supernatant performed 15% better

than the commercial enzyme alone (39%), indicating possible positive contribution of the present MEL as an emulsifier, or the possitive effect of ions or cofactors on lipases [3].

The results show that *M. antaricus* was able to metabolize esters. Whether the cell directly uses esters as a carbon source , or they are hydrolyzed extracellularly, with the resulting FFA and alcohol being used as carbon sources, remains unknown. Higher MEL production was achieved with methyl and ethyl ester feeds compared to oil. Some negative effects of alcohol presence in early stages of the fermentation were observed for methanol and butanol, which corresponds to data found in literature on their toxicity to lipase activity [4][5]. The results for the approach where vegetable oil is partially hydrolyzed prior to fermentation are very promising, since availability of FFA in earlier stages of the fermentation seems to stimulate MEL production. MEL profiles indicate that the prehydrolysis step effectively reduced the fermentation period, and enabled reaching higher MEL concentrations compared to feeds with untreated oil. (Figure 1b)

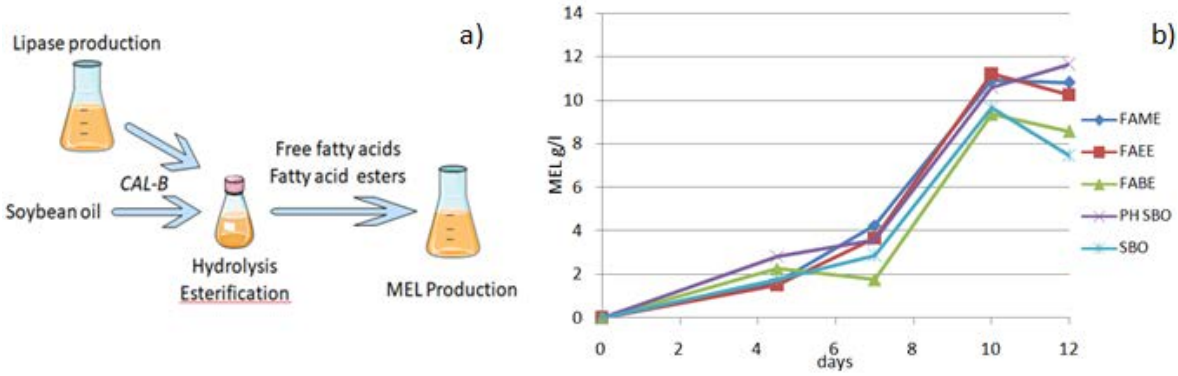

Figure 1. a) Experimental plan overview; b) Preliminary MEL production results. FAME - methyl esters; FAEE - ethyl esters, FABE - butyl esters; SBO - soybean oil; PH SBO - partially hydrolyzed soybean oil.

4. Conclusions

Feeds of prehydrolized and esterified oil increased MEL production efficiency by increasing MEL titres, reducing levels of residual tryglicerides in the broth, with the prospect of shortening the fermentation duration. This approach suggests a more efficient and potentially more sustainable alternative for MEL production when compared with the existing processes.

Acknowledgements

Funding from Fundação para a Ciência and Tecnologia is acknowledged through the projects CRUISE (PTDC/AAG-TEC/0696/2014) and MERO (MIT-EXPL/ISF/0115/2017), the PK scholarship PD/BD/129222/2017(MIT Portugal Program)and iBB(UID/BIO/04565/2013) and from Programa Operacional Regional de Lisboa 2020 (Project N. 007317)

References

[1] A. Shimada, K. Ohashi, Food Sci Technol Res. (2003) 9. 142-147.
[2] D. Kitamoto, T. Ikegami, G.T. Suzuki, A. Sasaki , Y. Takeyama, Y. Idemoto, N. Korua, H Yanagishita, Biotec Lett (2001) 23: 1709.
[3] S.P.M. Ventura, L.D.F. Santos, J.A. Saraiva, J.A.P. Coutinho, B. World J Microbiol Biotechnol. (2012) 28:2303–2310
[4] A.A. Pollardo, H.S. Lee, D. Lee, S. Kim, J. Kim, BMC Biotechnol. (2017) 17(1):70.
[5] S.D. Banik, M. Nordblad, J.M. Woodley, G.H. Peters, ACS Catalysis (2016) 6 (10), 6350-6361

ECAB 5
The 5th EUROPEAN CONGRESS OF APPLIED BIOTECHNOLOGY
Florence 15-19 September 2019

On the enzymatic oxidation of aniline, *p*-aminodiphenylamine (PADPA) or their mixtures by using an industrial laccase and vesicles as templates

Tomoyuki Fujisaki[1], Keita Kashima[1†], Peter Walde[2]

1 Department of Materials Chemistry and Bioengineering, National Institute of Technology, Oyama College, 771 Nakakuki, Oyama, Tochigi, 323-0806, Japan;

2 Department of Materials, ETH Zurich, Vladimir-Prelog-Weg 5, 8093 Zürich, Switzerland

†Corresponding author: keitakashima@oyama-ct.ac.jp

Highlights

- Aniline and PADPA were enzymatically oxidized with a commercial laccase and O_2
- The reaction products resemble the conductive polyaniline emeraldine salt form, PANI-ES
- The products have good stability for at least 28 days if stored at room temperature

1. Introduction

Polyaniline in its conductive emeraldine salt form (PANI-ES) is characterized by a good dispersibility in water phase, and by good thermal and radiation stability.[1] The enzymatic oxidation of aniline or the aniline dimer, *p*-aminodiphenylamine (PADPA), in the presence of dispersed anionic soft-interfaces in slightly acidic aqueous solution is an environmentally friendly process for obtaining PANI-ES. We previously reported about the enzymatic synthesis of PANI-ES-type products from PADPA oxidized with *Trametes versicolor* laccase (TvL)/O_2 as catalyst in aqueous pH = 3.5 solution at room temperature in the presence of anionic vesicles from sodium bis(2-ethylhexyl) sulfosuccinate (AOT) as reaction templates.[2-3] The focus of this previous work was on fundamental aspects of the reaction. For possible industrial applications, two points are important to consider: (i) the use of an industrial laccase which would decreases the production costs, and (ii) enabling the synthesis of PANI-ES from aniline (instead of PADPA), which is cheaper and chemically more stable than PADPA. In this study, the enzymatic oxidation of aniline, PADPA or their mixtures was investigated in the presence of AOT vesicles by using a laccase which is used in food industry. The formation of PANI-ES-type products (with their characteristic absorption bands around 1000 nm) was analyzed by *in situ* UV/visible absorption measurements.

2. Methods

The enzymatic oxidation of aniline, PADPA, or aniline/PADPA mixtures using laccase (Y120, from Amano Enzyme) was investigated. The concentrations of the laccase and the AOT vesicles were fixed at [laccase] = 0.207 µg/mL, [AOT] = 1.5 mM, in a 10 mL reaction volume. The reaction was carried out in 50 mL Schott glass bottles at pH = 3.5 by using an aqueous phosphate solution (0.1 M NaH_2PO_4 + H_3PO_4). The concentrations of the substrates in each reaction mixture were [aniline] = 2.0 mM, [PADPA] = 1.0 mM, or [aniline] = 0.6 mM + [PADPA] = 0.7 mM, respectively. The reaction mixture was withdrawn and poured into a quartz cuvette (l = 0.1 cm, V = 300 µL) at desired times (t = 1 min, 1 h, 4 h, 24 h, 2 days, 3 days, 4 days, 7 days, 14 days, 21 days, 28 days), and the UV/visible absorption spectrum was measured with a UV mini-1240, from SHIMADZU.

3. Results and discussion

Figure 1 shows the time course of the absorbance at λ = 1000 nm (A_{1000}) in each reaction with either aniline, PADPA, or an aniline/PADPA mixture. In the reaction with aniline only, the value of A_{1000} was clearly very low. In the reaction of [PADPA] = 1.0 mM, a major peak developed at λ ≈ 1000 nm which indicates formation of highly conductive PANI-ES. The value of A_{1000} in the reaction with PADPA reached a maximum value after t = 24 h, and then decreased after 7 days. In the reaction of [aniline] = 0.6 mM + [PADPA] = 0.7 mM, the major peak at λ ≈ 1000 nm appeared with almost the same intensity as in the case of the PADPA] = 1.0 mM system. Interestingly, A_{1000} of the reaction with the aniline/PADPA mixture kept a higher value for 28 days than the reaction with PADPA only. In the reactions with PADPA only and with the aniline/PADPA mixture, PANI-ES-type oxidative products were obtained. Especially, the reaction products obtained from the aniline/PADPA mixture showed good stability in aqueous solution.

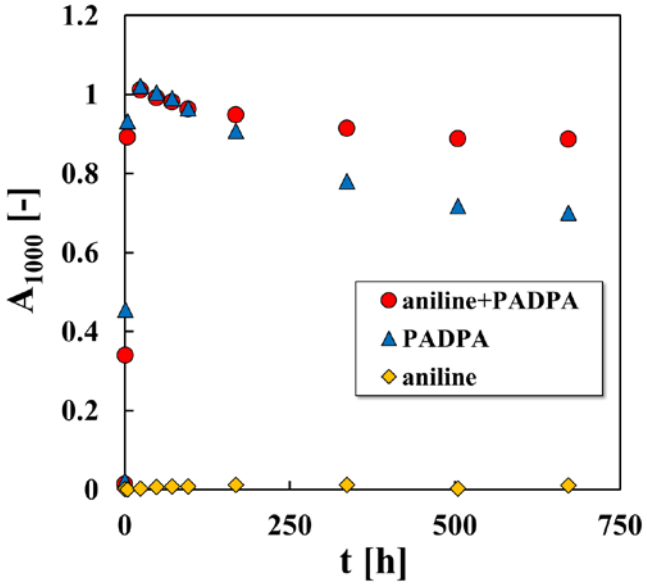

Figure 1. Comparison of the absorbance at λ = 1000 nm (A_{1000}) in three different reaction mixtures, pH = 3.5, [laccase] = 0.207 µg/mL, [AOT] = 1.5 mM. ● [aniline] = 0.6 mM + [PADPA] = 0.7 mM, ▲ [PADPA] = 1.0 mM, ◆ [Aniline] = 2.0 mM.

4. Conclusions

The industrial laccase/O_2-catalyzed oxidation of the investigated aniline/PADPA mixture ([aniline] = 0.6 mM + [PADPA] = 0.7 mM) in the presence of AOT vesicles as templates results in stable conductive PANI-ES-type products. This reaction is promising due to its reduced costs for both, enzyme and substrate, as compared to the previously investigated systems.[2-4]

References

[1] M. Atesa, T. Karazehir, A. Sezai Sarac, *Curr. Phys. Chem.*, 2012, **2**, 224-240.
[2] K. Kashima, T. Fujisaki, S. Serrano-Luginbühl, A. Khaydarov, R. Kissner, A. J. Ležaić, D. Bajuk-Bogdanović, G. Ćirić-Marjanović, L. D. Schuler, P. Walde, *RSC Adv.*, 2018, **8**, 33229-33242.
[3] S. Luginbühl, L. Bertschi, M. Willeke, L. D. Schuler, P. Walde, *Langmuir*, 2016, **32**, 9765-9779.
[4] K. Junker, R. Kissner, B. Rakvin, Z. Guo, M. Willeke, S. Busato, T. Weber, P. Walde, *Enzyme Microb. Technol.*, 2014, **55**, 72-84.

ECAB 5
The 5th EUROPEAN CONGRESS OF APPLIED BIOTECHNOLOGY
Florence 15-19 September 2019

Production, crosslinking and characterization of DexMA/PAA systems

Miriam Cappello[1], Niccoletta Barbani[1], Caterina Cristallini[2], Giovanni Polacco[1] and Sara Filippi[1*]

1 Dipartimento di Ingegneria Civile e Industriale, Università di Pisa, Largo Lucio Lazzarino 2, 56122 Pisa, Italy; 2 CNR, Istituto per i Processi Chimico Fisici, IPCF SS Pisa, c/o Largo Lucio Lazzarino 2, 56122 Pisa Italy

**Corresponding author: sara.filippi@unipi.it*

Highlights

- DexMA/PAA systems were designed for applications in material science and biomedical field
- UV photo-crosslinking and thermal treatment were able to stabilize the systems in water
- FT-IR and DSC analysis showed the presence of chemical interactions between DexMA and PAA

1. Introduction

In the last decades, the use of polysaccharides has undergone a rapid progress in many different areas of material science and engineering including pharmaceuticals, biomedical use, food supplements, and cosmetics. The most widely used polysaccharides as biomaterials are alginate, chitosan, hyaluronan, gellan gum and dextran. Dextran (Dex), a bacterial-derived polysaccharide, consisting essentially of α-1,6 linked D-glucopyranose residues with a low percent of α-1,2-, α-1,3- or α-1,4-linked side chains, has received a great interest for column chromatography application, cell culture technology and drug delivery systems [1]. The elevated hydrophilicity of dextran imparts high resistance to protein adsorption, a fundamental requirement for use in implantable medical devices and drug or protein targeting carriers [2]. Layer-by-layer assembly can be considered a versatile tool for coating of implantable materials based on the use of polyelectrolytes such as polystyrene sulfonate, polyallylamine, chitosan and polyacrylic acid. In this work, the design, preparation and characterization of new materials based on dextran (DexMA) and polyacrylic acid (PAA) was reported in order to obtain a bioartificial material that combines polyelectrolyte properties with high protein surface and anti-fouling characteristics due to polysaccharide moieties.

2. Methods

Dextran derivatized with glycidyl methacrylate (DexMA) was performed according to a literature method [3] and was confirmed by FT-IR analysis. DexMA/PAA systems were prepared by a combination of UV photo-crosslinking and thermal treatment using different DexMA/PAA weight ratio: 100/0, 80/20, 60/40, 40/60, 20/80, 0/100. A morphological (SEM) and physico-chemical characterization (FT-IR, DSC, TGA) was performed on the systems, before and after crosslinking. Swelling and mass loss tests on the samples were also carried out.

3. Results and discussion

SEM images of the DexMA/PAA 60/40 system, before and after crosslinking (Figure 1), show a dense structure for untreated sample and a heterogeneous porosity for crosslinked sample. FT-IR analysis on the same samples (Figure 2) shows a decrease of the band intensity at 1000 cm^{-1}, due to the COC stretching of the pyranose ring, a reduction of bands at 3300 cm^{-1} and 1070 cm^{-1}, both due to hydroxyl groups of dextran, and the appearance of a peak at 1230 cm^{-1}, typical of a C-O ester stretching. These results indicate that the UV photo-crosslinking and thermal treatment lead to the breaking of the pyranose ring and the formation of an ester bond between PAA and DexMA.

DSC analysis, carried out on samples, showed a single glass transition temperature, confirming the presence of chemical interactions between DexMA and PAA.

TGA thermograms show characteristic degradative events of both components, and a mass loss event between 200°C and 300°C that could be ascribed to the breaking of glycosidic bonds caused by thermal treatment.

Stability in water was also tested for all samples. In particular swelling in water, swelling in saturated steam water and mass loss tests were performed. Mass loss tests showed a higher stability in water for DexMA/PAA samples after UV irradiations at 256 nm followed by thermal treatment. Swelling tests confirmed the presence of chemical interactions between the components and the efficacy of crosslinking. Concerning the trend of swelling ratio versus the composition of the DexMA/PAA mixtures, a minimum was observed for the DexMA/PAA 60/40 system.

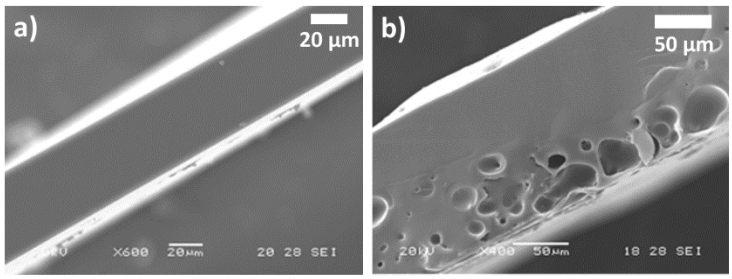

Figure 1. SEM images of untreated DexMA/PAA 60/40 (a) and UV and thermal treated DexMA/PAA 60/40 (b).

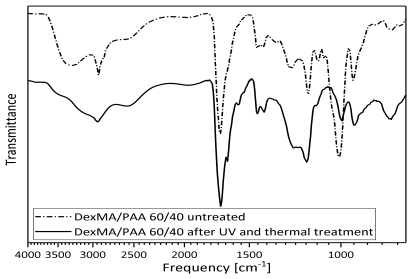

Figure 2. FT-IR of untreated and treated DexMA/PAA 60/40.

4. Conclusions

DexMA/PAA systems were prepared by using an innovative combination of crosslinking treatments thus making these materials attractive for use in many biomedical applications.

References

[1] A. Banerjee, R. Bandopadhyay, International Journal of Biological Macromolecules 87 (2016) 295-301

[2] T. G. Shutava, K.S. Livanovich, A.A. Sharamet , Colloids and Surfaces B: Biointerfaces 173 (2019) 412-420

[3] W.N.E. van Dijk-Wolthuis, J.J. Kettenes-van den Bosch, A. van der Kerk-van Hoof, W.E. Hennink, Macromolecules 30 (1997) 3411-13.

Multilevel Engineering of Microbial Ethyl Acetate Production.

Aleksander Kruis[1], Anna Bohnenkamp[1], Astrid Mars[2], René Wijffels[1],

Servé Kengen[1], Ruud A. Weusthuis[1,]*

1Wageningen University, Wageningen, The Netherlands

2 Wageningen Research, Wageningen, The Netherlands

**Corresponding author: ruud.weusthuis@wur.nl*

Highlights

- Ethyl acetate production by yeasts was elucidated by discovering the "Eat" enzyme family.
- Eat enzymes are located in yeast mitochondria
- Expression of Eat1 in *E. coli* results in ethyl acetate production
- Costs of ethyl acetate production are expected to be lower than those of bioethanol

1. Introduction

This abstract will show our efforts to develop a process for the production of ethyl acetate.
Ethyl acetate is produced from fossil resources at 3.5 million tonnes at a total value of $3.7 billion in 2014. To reduce CO_2 emissions a biobased process is desired. Yeasts are able to produce high amounts of ethyl acetate from sugars and ethanol. The development of an efficient fermentation process was hampered because the key enzyme was unknown.

2. Methods

The Eat1 enzyme was identified by comparing the transcriptome of *Wickerhamomyces anomalus* under producing and non-producing conditions. A fusion protein of Eat1 and Gfp was made to show by light microscopy in which organelle Eat1 was expressed. The mitochondrial targeting sequence was identified using bioinformatics techniques. Eat1 was expressed in E. coli. Ethyl acetate production was optimized by knocking out byproduct formation, optimizing the expression level, removal of the targeting sequence, and in-situ product removal.

3. Results and discussion

We have identified this elusive enzyme. Eat1 is present in all yeasts known to produce ethyl acetate (figure 1, left). It has three activities: alcohol acetyl transferase converting ethanol and acetyl-CoA into ethyl acetate, esterase and thioesterase activity. The latter two activities have a negative effect on ethyl acetate production but were strongly suppressed when ethanol was present (Figure 1, middle)[1]. We have shown that the enzyme is located in the mitochondria, and we have identified the leader sequence responsible for mitochondrial targeting[2].

Expression of Eat1 in *E. coli* resulted in ethyl acetate production (figure 1, right)[1]. We have optimized anaerobic ethyl acetate production in *E. coli* by deleting LdhA and AckA, responsible for lactate and acetate production, respectively. This increased ethyl acetate production but also gave

rise to the accumulation of pyruvate, indicating the Eat1 activity was insufficient. Eat1 activity was improved by optimizing the induction level and by removing the mitochondrial targeting sequence. This reduced production of pyruvate but enhanced the production of acetate and ethanol. This appeared to be caused by the esterase activity of Eat1, hydrolysing ethyl acetate. By stripping the ethyl acetate from the broth, we decreased the time Eat1 could hydrolyse ethyl acetate, resulting in lower acetate and ethanol production. The final ethyl acetate yield obtained was 0.7 mol/mol, or 70% of the maximum pathway yield[3].

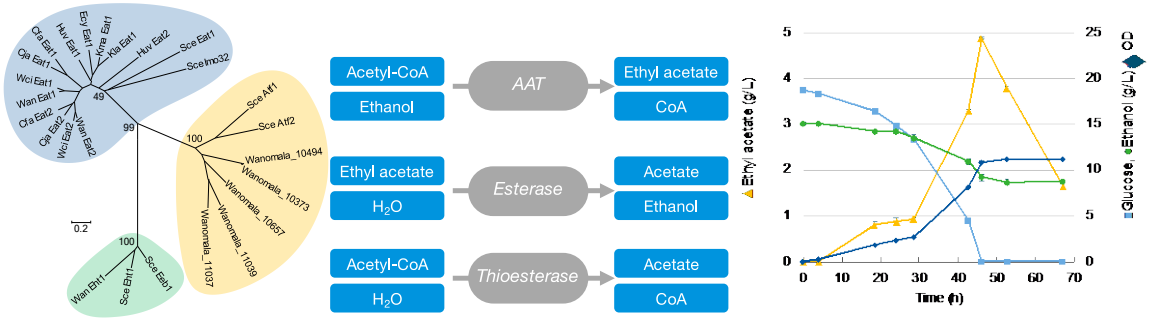

Figure 1. Left. The Eat family is a new alcohol acetyl transferase family, clearly distinct from the Atf and Eeb/Eht families. Middle. Eat1 from *W. anomalus* has three activities. Right. Expression of Eat1 from *W. anomalus* in *E. coli* results in ethyl acetate production.

4. Conclusions

By multilevel engineering – bioprospecting the key enzyme, optimizing its expressing, increasing its activity by protein engineering, knocking out byproduct formation and by applying in situ product recovery - we were able to efficiently produce ethyl acetate in *E. coli*. On paper, the production costs of ethyl acetate are lower than those of bioethanol.

References

[1] Kruis, Alex; Levisson, Mark; Mars, Astrid E.; Ploeg, Max van der; Garcés Daza, Fernando; Ellena, Valeria; Kengen, Servé W.M.; Oost, John van der; Weusthuis, Ruud A. (2017) Ethyl acetate production by the elusive alcohol acetyltransferase from yeast. Metabolic Engineering 41. - p. 92 - 101.

[2] Kruis, A. J., Mars, A. E., Kengen, S. W., Borst, J. W., van der Oost, J., & Weusthuis, R. A. (2018). The alcohol acetyltransferase Eat1 is located in yeast mitochondria. *Applied and Environmental microbiology*, AEM-01640.

[3] Aleksander J. Kruis, Anna Bohnenkamp, Bram Nap, Jochem Nielsen, Pieter Mijnhout, Astrid E. Mars, John van der Oost, Servé W.M. Kengen, René H. Wijffels, Ruud A. Weusthuis. 2019. Enhanced ethyl acetate production in Escherichia coli under anaerobic conditions. In preparation.

Metabolic Engineering of new Streptomyces sp. From Extreme Environments for Novel Antibiotics and Anticancer Drugs

J.A. Asenjo[1], V. Razmilic[1], J.F. Castro[1], D. Lagos[1], A. Rubio[1], S. Jarmusch[2], F. Marchant[1], M. Goodfellow[3], M. Jaspars[2], and B.A. Andrews[1]

[1]*Centre for Biotechnology and Bioengineering, CeBiB, University of Chile Beauchef 851, Santiago, Chile,*
[2]*University of Aberdeen, U.K.,* [3]*Newcastle University, U.K.,*

**Corresponding author: juasenjo@ing.uchile.cl*

Highlights

- Streptomycetes from the Atacama Desert are a good source of bioactive compounds.
- A genome-scale model for *Streptomyces* C34 was developed to study its metabolism.
- This genome-scale model is also used to optimize production.
- Microorganisms from the Atacama Desert inhibit important fungal pathogens.

1. Introduction

Today there is a tremendous need for new antibiotics and novel cytotoxic compounds against cancer cells to develop efficient alternative treatment to chemotherapy. We have searched for highly active Streptomyces strains in the driest desert in the world, the Atacama Desert in northern Chile. We have identified several new strains and found many novel antibiotics and anticancer agents ("Chaxamycins", "Chaxalactins" and "Atacamycins") from *Streptomyces* C34 and C38 [1-3]. With the high-quality genome sequence of *Streptomyces* C34 we identified the biosynthetic gene cluster of Chaxamycins and Chaxalactins showing the genomic potential of this strain to produce bioactive compounds [4,5]. Our aim is to improve the production of these novel compounds through metabolic engineering and to find new interesting bioactive specialised metabolites.

2. Methodology

To find metabolic engineering targets for increasing the production of Chaxamycins and Chaxalactins, we developed a genome-scale model of *Streptomyces leeuwenhoekii* C34 following standard methodology and we performed flux balance analyses. The selected overexpression targets were cloned under a constitutive strong promoter in an integrative plasmid.

The culture collection from the Atacama Desert was subjected to standard bioassays to find bioactive compounds against important fungal pathogens. The selected strains were subjected to chemical fractionation and HPLC-MS/MS analysis.

3. Results and discussion

The genome-scale model, *i*VR1007, has 1726 reactions including 239 for transport, reactions for secondary metabolite biosynthesis, 1463 metabolites and 1007 genes. The model was validated with experimental data of growth on 89, 54 and 23 sole carbon, nitrogen and phosphorous sources, respectively, and showed a high level of accuracy (82.5 %). We have included reactions for desferrioxamines, ectoine, Chaxamycins, Chaxalactins and for the hybrid polyketides/non-ribosomal peptide synthesized by the halogenase cluster. A detailed Metabolic Flux Balance Analysis was carried out in order to study the metabolic pathways of Chaxalactins, Chaxamycins and the product of the halogenase cluster, by recognizing overexpression targets and useful knock-out sites to increase production of these secondary metabolites [6]. Among the metabolic engineering targets found we have successfully overexpressed some of them and found that they indeed improve the production of the antibiotic compounds.

In parallel, we identified several strains belonging to the *Streptomyces* genera, that have antibiotic activity against *Botrytis cinerea, Fusarium oxysporum,* among other fungus of agroindustry importance. The strains that showed higher bioactivities were subjected to HPLC-MS/MS analysis. We are identifying novel compounds that could be responsible for the observed bioactivity.

Our recent results concerning these two topics showing the genomic potential for producing bioactive compounds of the microorganisms of the Atacama Desert and how to improve their compound production will be presented and discussed in this presentation.

4. Conclusions

The development of a genome-scale model for *S. leeuwenhoekii* C34 was useful for the identification of metabolic engineering targets that enhance the production of Chaxamycins and Chaxalactins.

The *Streptomyces* strains isolated from the Atacama Desert have antibiotic activity against important fungal pathogens.

References

[1] Rateb ME, Houssen WE, Arnold M, Abdelrahman MH, Deng H, Harrison WTA, et al. Chaxamycins A - D, bioactive ansamycins from a hyper-arid desert *Streptomyces* sp. J Nat Prod. 2011;74:1491–9.

[2] Rateb ME, Houssen WE, Harrison WTA, Deng H, Okoro CK, Asenjo JA, et al. Diverse Metabolic Profiles of a *Streptomyces* Strain Isolated from a Hyper-arid Environment. J Nat Prod. 2011;74:1965–71.

[3] Nachtigall J, Kulik A, Helaly S, Bull AT, Goodfellow M, Asenjo JA, et al. Atacamycins A–C, 22-membered antitumor macrolactones produced by *Streptomyces* sp. C38*. J Antibiot. 2011;64:775–80.

[4] Gomez-Escribano JP, Castro JF, Razmilic V, Chandra G, Andrews B, Asenjo JA, et al. The *Streptomyces leeuwenhoekii* genome: de novo sequencing and assembly in single contigs of the chromosome, circular plasmid pSLE1 and linear plasmid pSLE2. BMC Genomics. 2015;16:485.

[5] Castro JF, Razmilic V, Gomez-Escribano JP, Andrews B, Asenjo JA, Bibb MJ. Identification and heterologous expression of the chaxamycin biosynthetic gene cluster from *Streptomyces leeuwenhoekii*. Appl Environ Microbiol. 2015;81:AEM.01039-15.

[6] Razmilic V, Castro JF, Andrews B, Asenjo JA. Analysis of metabolic networks of *Streptomyces leeuwenhoekii* C34 by means of a genome scale model: Prediction of modifications that enhance the production of specialized metabolites. Biotechnol Bioeng. 2018;115:1815-1828.

Systems Metabolic Engineering for the Production of Aromatics in Yeast

Nils JH Averesch[1,3] and Jens O Krömer[1,2]
[1] The University of Queensland, Brisbane, QLD 4072, Australia
[2] Department Solar Materials, Helmholtz Centre of Environmental Research - UFZ, Leipzig, Germany
[3] NASA, NASA Ames Research Center, Moffett Field, CA, USA

Aromatics are amongst the most important bulk feedstocks for the chemical industry, however, no viable bioprocess exists today and production is still dependent on petro-chemistry. In order to develop p-hydroxybenzoic acid (PHBA) and p-amino benzoic acid (PABA) production in *Saccharomyces cerevisiae* we employed *in-silico* analysis for the prediction of suitable targets for strain improvement of the shikimate pathway [1]. A key reaction in metabolism was the knockout of pyruvate kinase, which is known to be non-viable on glucose. In addition, the knockout of competing pathways led to very poor growth and auxotrophic strains. To address these problems we have engineered dynamic regulation using a synthetic quorum sensing circuit in *Saccharomyces cerevisiae* [2]. The circuit activates gene expression at a high population density, and is linked with an RNA interference (RNAi) module to enable targeted gene silencing. The circuit was used to control flux through the shikimate pathway for the production of PHBA. Following this, strain and media optimization lead to production in the g/L range [3,4]. This is a starting point for future process development.

1. Averesch, N.J. and Krömer, J.O. Tailoring strain construction strategies for muconic acid production in *S. cerevisiae* and *E. coli*. Metab Eng Comm 2014, 1, 19-28.
2. Williams, T.C.; Averesch, N.J.; Winter, G.; Plan, M.R.; Vickers, C.E.; Nielsen, L.K.; Krömer, J.O. Quorum-sensing linked RNA interference for dynamic metabolic pathway control in *Saccharomyces cerevisiae*. Metab Eng. 2015, 29, 124-134.
3. Averesch, N.J.H., Winter, G., Krömer, J.O. (2016) Production of para-aminobenzoic acid from different carbon sources in engineered *Saccharomyces cerevisiae*. Microb Cell Fact. 15 (1), 89.
4. Averesch, N.J.H., Prima, A., Krömer, J.O. (2017) Enhanced production of pHBA by genetically engineered *Saccharomyces cerevisiae*. Bioproc Biosyst Eng 40 (8), 1283 - 1289.

ECCE12
The 12th EUROPEAN CONGRESS OF CHEMICAL ENGINEERING
Florence 15-19 September 2019

The quest for a cell factory for the production of recombinant proteins: *Pichia pastoris* Vs *Yarrowia lipolytica*.

Marie Vandermies, Chrispian Theron, Patrick Fickers*

Microbial Processes and Interactions, TERRA Teaching and Research Centre, University of Liège - Gembloux AgroBio Tech, Av de la Faculté, 2B. B-5030 Gembloux, Belgium

**Corresponding author: pfickers@uliege.be*

Highlights

- *P. pastoris* and *Y. lipolytica* were compared for the production of recombinant proteins
- Calb lipase was used as a case report
- Protein productivity was higher in *Y. lipolytica* despite a lower gene expression level
- The lower productivity in *P. pastoris* is due to proteasome degradation of CalB

1. Introduction

The production at industrial scale of recombinant proteins (rProt) is of increasing economic importance. Among the different microbial chassis that has been developed for that purpose, yeasts are regarded as the preferred option for the production of recombinant enzymes and therapeutic proteins. The main advantage of yeasts over bacterial systems such as *Escherichia coli* relies on the possibility to obtain posttranslational modified proteins in the culture supernatant at grams per liter. Historically, *Saccharomyces cerevisiae* has been used as the reference eukaryotic chassis, however it suffers several drawbacks such as low protein productivity, overflow metabolism or hyperglycosylation phenomenon. Moreover, it is less metabolically adapted to catabolize raw carbon and nitrogen sources that are nowadays increasingly considered as nutrients in bioprocesses. The non-conventional yeasts *Pichia pastoris* and *Yarrowia lipolytica* are considered as realistic alternatives to *S. cerevisiae* for rProt synthesis. They both combine advantages of growing at high cell density, to produce and secrete rProt at high yield and to have low nutritional requirements, allowing thus to grow them on raw materials or industrial byproducts. Although these two yeasts are well-established cell factories for rProt synthesis in industry, no direct comparison of their performances has been reported so far. Here, we report such a comparison using the CalB lipase from *Candida antartica* as a model protein.

2. Methods

The codon optimized gene sequence of CalB was cloned under the control of strong inducible promoters. For *Y. lipolytica*, the hybrid promoter pEYKA3B inducible by erythritol was used in combination with a EYK1*ko* recipient strain that is unable to metabolize erythritol. For *P. pastoris*, the widely used promoter pAOX1 was used in combination with a MutS recipient strain (methanol low consumption). The resulting strains were then grown in bioreactors in optimized conditions

and parameters such as cell growth, gene expression, carbon uptake rates and extracellular lipase activity were monitored over time.

3. Results and discussion

Y. lipolytica performances were by far superior in terms of cell growth rate and rProt synthesis. Compared to *P. pastoris,* it grew faster, at higher cell density and cells used carbon source more efficiently. The maximal lipase activities were equal respectively to 5540 and 1066 U/mgDCW for *Y. lipolytica* and *P. pastoris*, respectively, representing thus more than a 5-fold increase. Surprisingly, *P. pastoris* showed a significantly higher level (5-fold) of CalB gene expression as demonstrated by qRT-PCR. Several hypotheses has been formulated and tested to explain the reasons behind the observed differences. The lower protein productivity in *P. pastoris* was found related to the intracellular protein degradation by the proteasome complex.

4. Conclusions

From this study, *Y. lipolytica* appears a more efficient cell factory that is in addition not related to the utilization of flammable methanol as inducer.

ECAB 5
The 5th EUROPEAN CONGRESS OF APPLIED BIOTECHNOLOGY
Florence 15-19 September 2019

The Characterization of the Central Carbon Metabolism of Arthrospira Platensis Brings Insights to Its Original Polysaccharides (PS) Composition.

M. Phélippé, G. Thouand, G. Cogne, O.Gonçalves*

GEPEA – UMR CNRS 6144 – U. Nantes, 31 bvd des université – 44600 SAINT NAZAIRE, FRANCE

**Corresponding author: Olivier.goncalves@univ-nantes.fr*

Highlights

- Primary metabolite profiling using routine combined metabolomics approach
- The combined metabolomics approach consisted in using GC-MS and MFA
- *Arthrospira platensis* was cultivated in photobioreactor under various light conditions
- *Arthrospira platensis* EPS and PS fractions were modulated according to the incident light

1. Introduction

Micro-algae are photosynthetic micro-organisms that are able to produce at reduced cost high value products. To control this potential, the understanding of the photosynthetic and energetic metabolism of these micro-organisms at cellular and molecular level is often mandatory. Among the latest available approaches, the characterization and the analysis of the metabolic fluxes distribution is known to contribute accurately to a better understanding of the mobilized metabolic pathways and of the micro-organism behavior in response to environmental changes. For that purpose, metabolomics plays a key role since it enables to characterize these fluxes through high-throughput profiling of tremendous number of metabolites. Among the most cultivated photosynthetic micro-organisms, *Arthrospira platensis* is a cyanobacteria known to produce exopolysaccharides (EPS) and more particularly under light stress. Even though it is worldwide cultivated, only few major articles ([1],[2]) focused on the characterization of its central metabolism since Cogne [3]. Therefore, there is a lack of knowledge to understand the effect of environmental conditions on its energetic regulation metabolism. Knowing these mechanisms, would finally enable more efficient production of the specific PS or EPS.

In this study, the characterization of the carbon central metabolism of Arthrospira platensis cultivated in photobioreactor under growth with different light conditions and regarding EPS and PS production conditions was performed. For that purpose an original combined metabolomics approach was developed. It consisted in a profiling approach [4] allowing to quantifiy in routine the metabolites of the central carbon metabolism of the *Spirulina,* that was combined to a MFA calculation method used to estimate the dynamic of the metabolism thru the estimation of the biochemical reaction rates.

2. Methods

The central carbon metabolism of the *Spirulina* was characterized using the following GCMS analaysis workflow. It was combined to MFA calculation approach constrained by an accurate biochemical profiling approach. The results (absolute quantification and simulated reaction rate) were mapped on a extended central carbon metabolism map in order to check the influence of high light conditions on the PS and EPS fate and composition.

3. Results and discussion

The approach allowed assessing a better understanding of *Spirulina's* behavior facing high light environmental changes impacting more particularly its EPS and PS composition. Indeed, in the tested cultivation conditions (increasing light) it was possible to increase the amount of EPS, but also to modify its composition. The main observed differences concerned the amount of the uronic acids that was found to be drastically inferior to what was previously described [3]. The GCMS profiling of the carbon central metabolism extended to the elementary bricks constitutive of the protein, lipids and polysaccharides suggested more over that an alternative pathways for the uronic acid biosynthesis could be used. The Metabolic Flux Analysis data reinforced the observed hypothesis found using the low resolution metabolomic approach.

4. Conclusions

Finally in this study we were able to demonstrate that using routine low resolution metabolomics profiling approach, it was possible to bring insight to carbon fate regarding more particularly the PS and EPS fractions. Such a routine approach should be used in the next future to bring more informations of the *Spirulina*'s PS and EPS under differents cultivations conditions.

References

[1] Klanchui, A., Khannapho, C., Phodee, A., Cheevadhanarak, S., Meechai, A., 2012. iAK692: A genome-scale metabolic model of Spirulina platensis C1. BMC Syst Biol 6, 1–15. doi:10.1186/1752-0509-6-71

[2] Hasunuma, T., Kikuyama, F., Matsuda, M., Aikawa, S., Izumi, Y., Kondo, A., 2013. Dynamic metabolic profiling of cyanobacterial glycogen biosynthesis under conditions of nitrate depletion. Journal of Experimental Botany 64, 2943–2954. doi:10.1093/jxb/ert134

[3] Cogne, G., Gros, J.-B., Dussap, C.-G., 2003. Identification of a metabolic network structure representative ofarthrospira (spirulina) platensis metabolism. Biotechnology and Bioengineering 84, 667–676. doi:10.1002/bit.10808
doi:10.1186/1475-2859-6-6

[4] Phélippé M., Coat R., Le Bras C., Perrochaud L., Peyretaillade E., Kucma D., Arhaliass A., Thouand G., Cogne G., Gonçalves O.Characterization of an easy-to-use method for the routine analysis of the central metabolism using an affordable low-resolution GC-MS system: Application to Arthrospira platensis. Analytical Bioanalytical Chemistry (2018) 410 : 1341-1361, DOI : 10.1007/s00216-017-0776-x

ECAB 5
The 5th EUROPEAN CONGRESS OF APPLIED BIOTECHNOLOGY
Florence 15-19 September 2019

Improving the accuracy of flux balance analysis through the addition of carbon availability constraints for intracellular reactions

Maximilian Lularevic[1,2], Andy Racher[2], Colin Jaques[2], Alexandros Kiparissides[1]
1 Department of Biochemical Engineering, University College London, WC1E 6BT, UK;
2 Lonza Biologics PLC, 228 Bath Road, Slough SL1 4DX, UK

**Corresponding author: alex.kiparissides@ucl.ac.uk*

Highlights

- A new method to refine the results of Flux Balance Analysis (FBA) is presented.
- Predictions from Carbon-constrained FBA (ccFBA) are in good agreement with ^{13}C data
- ccFBA can improve our ability to predict reaction directionalities compared to FBA.

1. Introduction

Constraint based modelling methods, such as Flux Balance Analysis (FBA), have been extensively used to decipher complex, information rich -omics datasets in order to elicit system-wide behavioral patterns of cellular metabolism. FBA has been successfully used to gain insight in a wide range of applications, such as range of substrate utilization, product yields and to design metabolic engineering strategies to improve bioprocess performance [1]. A well-known challenge associated with large genome-scale metabolic networks (GEMs) is that they result in underdetermined problem formulations. Consequently, rather than single-point solutions, FBA and related methods examine ranges of reaction flux values that are consistent with the studied physiological conditions. The wider the reported flux ranges, the higher the uncertainty in the determination of basic reaction properties, limiting interpretability of and confidence in the results.

2. Methods

Herein we propose a new, computationally efficient approach that refines flux range predictions by introducing an additional set of constraints based on the elemental balance of carbon. Carbon constrained FBA (ccFBA) attempts to refine the feasible solution space, by constraining the permissible flux through intracellular reactions based on the amount of carbon taken up by the cell under the studied physiological conditions While at its core, ccFBA is a set of constraints based on the elemental balance of carbon, several aspects of cellular metabolism need to be taken into account.

3. Results and discussion

We compared carbon constrained FBA (ccFBA) with standard FBA using the latest CHO genome scale metabolic model (iCHO1766) [2] and were able to achieve significantly improved predictions for intracellular reactions. We showed that permissible flux ranges estimated by ccFVA contained the experimentally measured intracellular fluxes in the majority of cases and lead to quantitative predictions in the same order of magnitude as ^{13}C measurements. This can be attributed to ccFVA's ability to mitigate the impact of internal loops or futile cycles by constraining the amount of flux able to pass through any single reaction based on the amount of carbon entering the cell. Finally, when used in combination with random sampling, ccFVA substantially improved our ability to predict reaction directionalities compared to normal FVA.

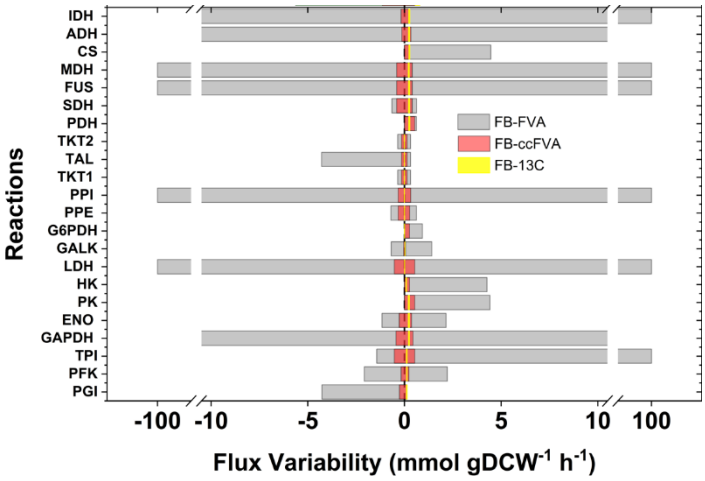

Figure 1. Comparison between FVA (grey bars), ccFVA (pink bars) and intracellular flux measurements (yellow bars) for central carbon metabolism (Glycolysis, TCA, PPP). Data from Templeton et al., 2017 [3]

4. Conclusions

ccFBA is an easy to use and computationally efficient method for reducing flux variability in and improving the accuracy of constrained-based metabolic networks. It can be used as a stand-alone method or as a complimentary tool to most other methods currently available for stoichiometric metabolic network analysis.

References

[1] J. Schellenberger, R. Que, R.M.T. Fleming, I. Thiele, J.D. Orth, A.M. Feist, …, B.Ø. Palsson, Nature Protocols 6(49) (2011), 1290-1307

[2] H. Hefzi, K.S. Ang, M. Hanscho, A. Bordbar, D. Ruckerbauer, M. Lakshmanan, …, N.E. Lewis, Cell Systems 3(5) (2016), 434-443

[3] N. Templeton, S. Xu, D.J. Roush & H. Chen, Met. Eng. 44 (2017), 126-133

ECAB 5
The 5th EUROPEAN CONGRESS OF APPLIED BIOTECHNOLOGY
Florence 15-19 September 2019

Light-induced promoter drives efficient over-expression of alternative nitrogenases in genetically modified *Rhodopseudomonas palustris*

Jan-Pierre du Toit[1], Robert Pott[1] *

1 Department of Process Engineering, Stellenbosch University, South Africa

**Corresponding author:* rpott@sun.ac.za

Highlights

- Volumetric biohydrogen production rate is limited by poor Mo nitrogenase enzyme activity
- V and Fe nitrogenase over-expression by insertion of efficient promoters to override control
- *PucBa* promoter shows promise for high-level, light-induced heterologous gene expression
- Potential of *R. palustris* as photobiological chassis organism is further advanced.

1. Introduction

Biohydrogen has long shown great promise as a clean energy source, produced from organic wastes by metabolically versatile anoxygenic photosynthetic bacteria such as *Rhodopseudomonas palustris*. Despite decades of investigation, feasibility of this potential bio-economy technology at large-scale remains limited by low volumetric hydrogen production rates [1].

The molybdenum (Mo) nitrogenase enzyme, the activity of which yields hydrogen as an obligate by-product, is driven by energy in the form of ATP derived from photosynthesis and electrons from organic substrates according to:

$$N_2 + 8H^+ + 8e^- + 16\ ATP \rightarrow 2NH_3 + H_2 + 16\ ADP$$

This complex, energetically expensive reaction results in a slow catalytic turnover, likely resulting in a bottleneck in the hydrogen production pathway [2]. Previous work on the temperature dependence of H_2 production supports this hypothesis: an increase in production rate was observed up to 40°C under equivalent light intensity, indicating availability of surplus reducing power to drive the reaction under thermodynamic conditions favouring higher enzyme catalysis rates. The energetic cost of nitrogenase activity means expression is tightly-repressed by availability of NH_3, limiting the potential for hydrogen production from organic waste waters containing a ubiquitous nitrogenous substrate [3].

R. palustris possesses two alternative nitrogenases with iron (Fe) and vanadium (V) cofactors, each evolving 3 and 9 H_2 per N_2 reduced respectively [4]. A prime target for addressing poor nitrogenase activity is thus presented, in overexpressing these isozymes via genetic modification.

Here we present the genetic modification of *R. palustris* by insertion of efficient promoters upstream of native nitrogenase gene operons in order to circumvent innate control mechanisms, and the characterisation of gene expression in the resultant strains.

2. Methods

Rhodopseudomonas palustris putative promoter sequences from LH2 protein (*pucBa*: light & anaerobic induced) or citrate synthase (*cisY*: constitutive expression) were inserted upstream of all 3 native nitrogenase gene operons by homologous recombination methods. Nitrogenase gene expression in the six resultant unmarked strains was quantified by RT-qPCR.

3. Results and discussion

Six strains of nitrogenase-overexpressing R. palustris were generated using an optimised protocol. Detailed quantification of transcript levels by RT-qPCR showed efficient upregulation of all genes in nitrogenase operons driven by puc promoter, between 8 to 12 Ct values higher than wild-type (up to ~4000-fold overexpression). Strains under control of cit promoter showed variable success with good upregulation of Vnf but not Anf, suggesting locus-dependent activity.

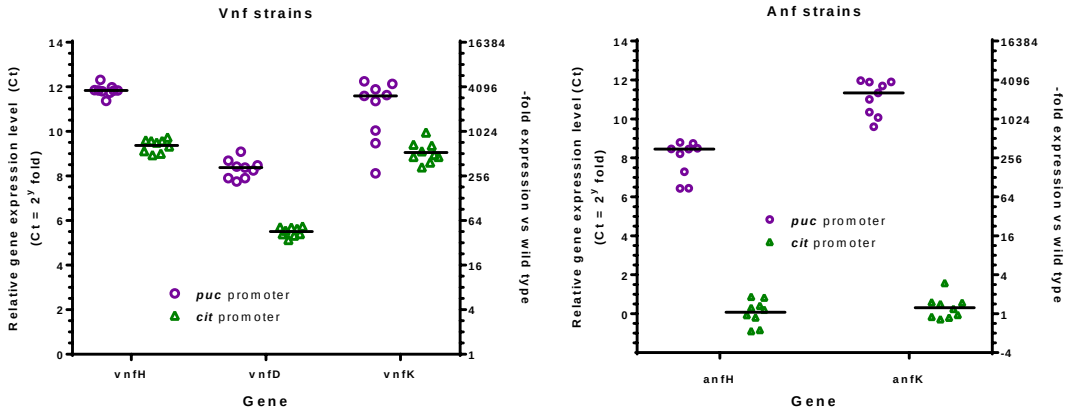

Figure 1. Quantification of gene expression from *R. palustris* vanadium (Vnf) and iron (Anf) nitrogenase operons

4. Conclusions

We present an efficient method for generating strains of *R. palustris* overexpressing complex native, multi subunit genes with a potential for heterologous gene expression. The *pucBa* promoter results in robust, light-induced gene expression useful for bioprocesses which exert high metabolic burden potentially compromising cell viability in absence of photosynthesis-derived energy. The overexpression of alternative nitrogenases will be confirmed by biohydrogen production studies as a direct *in vivo* measure of enzyme activity. In addition to advancing biohydrogen feasibility, the prospect of *R. palustris* as a biotechnological chassis organism is further developed.

References [Calibri 10]

[1] N. Basak, A. K. Jana, D. Das, and D. Saikia, 'Photofermentative molecular biohydrogen production by purple-non-sulfur (PNS) bacteria in various modes: The present progress and future perspective', International Journal of Hydrogen Energy, vol. 39, no. 13, pp. 6853–6871, Apr. 2014.

[2] P. C. Hallenbeck, M. Abo-Hashesh, and D. Ghosh, 'Strategies for improving biological hydrogen production', Bioresource Technology, vol. 110, pp. 1–9, Apr. 2012.

[3] E. K. Heiniger, Y. Oda, S. K. Samanta, and C. S. Harwood, 'How Posttranslational Modification of Nitrogenase Is Circumvented in Rhodopseudomonas palustris Strains That Produce Hydrogen Gas Constitutively', Appl. Environ. Microbiol., vol. 78, no. 4, pp. 1023–1032, Feb. 2012.

[4] J. B. McKinlay, 'Systems Biology of Photobiological Hydrogen Production by Purple Non-sulfur Bacteria', in Microbial BioEnergy: Hydrogen Production, D. Zannoni and R. De Philippis, Eds. Dordrecht: Springer Netherlands, 2014, pp. 155–176.

ECAB 5
The 5th EUROPEAN CONGRESS OF APPLIED BIOTECHNOLOGY
Florence 15-19 September 2019

Textile-Immobilized (Bio-) Catalysts.

Klaus Opwis[1], Katharina Courth[1], Thomas Mayer-Gall[1], Jochen S. Gutmann[1]

[1] *Deutsches Textilforschungszentrum Nord-West gGmbH, Adlerstr. 1, 47798 Krefeld, Germany*

**Corresponding author: opwis@dtnw.de*

Highlights

- Textiles were identified as new and innovative catalyst carrier materials.
- Various permanent immobilization strategies were developed successfully.
- Immobilization products are reusable at least 30 times.
- Results on textile-fixed organic catalysts promise huge economic success.

1. Introduction

The efficiency of most chemical processes is based on the use of catalysts. For many applications the catalysts are embedded in a solid matrix, which allows the recycling of the catalysts and the separation of the products. Such immobilizations offer the multiple or even permanent use. Common carrier materials are from polymeric or mineral nature. But their production and the charging with the catalysts are often complex and high-prized. In contrast, textile carrier materials made of cotton, polyamide or polyester are considerably inexpensive. The flexible construction of fabrics enables reactor constructions of arbitrary geometry and a quick removal of the catalyst without any residues after the reaction. Moreover, their open structure guarantees an optimal substrate turnover and the active surface is easily adjustable by the fiber diameter.

2. Methods

For the catalysts immobilization various fiber-specific wet chemical and photochemical processes were used [1-5]. The methods are summarized schematically in Figure 1. The (bio-) catalytic activity of the immobilized enzymes and organic catalysts were determined by typical enzymatic assays and model reactions.

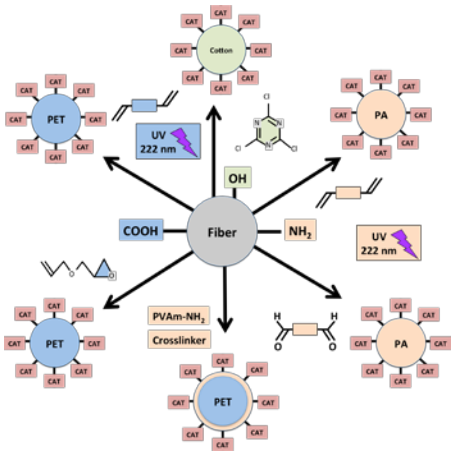

Figure 1. Catalase immobilized on Polyamide Fibers.

3. Results and discussion

We report various successful wet-chemical and photochemical techniques for the immobilization of different types of catalysts (enzymes, organic catalysts) on textile carrier materials. Figure 1 shows a SEM of textile-fixed catalase.

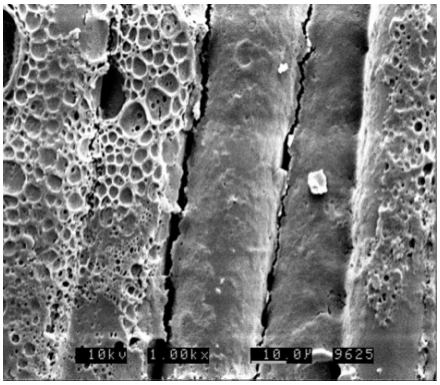

Figure 1. Catalase immobilized on Polyamide Fibers.

Beyond, we provide information on the (bio-) catalytic activity of the immobilized catalysts in repeated use, and explain various relevant applications, e.g., the use of immobilized peroxidases in the bleaching of whey from dairy processes (food industry) and the use of textile-fixed cinchona alkaloids for asymmetric syntheses of pharmaceutical products. For example, the desymmetrization of cyclic anhydrides runs for more than 250 cycles without a significant loss of its catalytic activity and an impressive enantiomeric ratio of 97:3.

4. Conclusions

In summary, we have identified low-cost textiles as alternative carrier materials for catalysts. With a low preparative and economic expense fabrics with a high load, a high catalytic activity and excellent permanence against desorption can be produced. Therefore, our textile-fixed catalysts represent a totally new tool for heterogeneous catalysis with widespread potential applications in pharmaceutics, chemistry and eco-friendly white biotechnology.

References

[1] J.-W. Lee, T. Mayer-Gall, K. Opwis, C.E. Song, J.S. Gutmann, B. List, Organotextile Catalysis, Science 341 (2013) 1225-1229.
[2] K. Kiehl, T. Straube, K. Opwis, J.S. Gutmann, Strategies for the permanent immobilization of enzymes on textile carriers, Engineering in Life Sciences 15 (2015) 622-626.
[3] T. Mayer-Gall, J.-W. Lee, K. Opwis, B. List, J.S. Gutmann, Textile Catalysts - An unconventional approach towards heterogeneous catalysis, ChemCatChem 8 (2016) 1428-1436.
[4] K. Opwis, K. Kiehl, J.S. Gutmann, Immobilization of Peroxidases on Textile Carrier Materials and their Use in Bleaching Processes, Chemical Engineering Transactions 49 (2016) 67-72.
[5] K. Opwis, K. Kiehl, T. Straube, T. Mayer-Gall, J.S. Gutmann, in: Textile Finishing: Recent Developments and Future Trends, K.L. Mittal, T. Bahners (Eds.), Wiley-Scrivener, Beverly, MA, 2017, pp 345-361.

Application of Online Measurement Tools for the Prediction of Residual Substrate Concentration in *Ustilago Maydis* Mixed Cultures on Pectin.

Markus Müller[1], Sarah Stachurski[1], Peter Stoffels[2], Kerstin Schipper[2], Michael Feldbrügge[2], Jochen Büchs[1*]

[1] *Aachener Verfahrenstechnik – Biochemical Engineering, RWTH Aachen University, Forckenbeckstraße. 51, 52074 Aachen, Germany*
[2] *Institute for Microbiology, Heinrich-Heine-University Düsseldorf, Universitätsstraße 1, 40225 Düsseldorf, Germany*

**Corresponding author: jochen.buechs@avt.rwth-aachen.de*

Highlights

- Prediction of residual substrate concentration without offline sampling
- Determination of the pectinolytic activity of *U. maydis* on polygalacturonic acid
- Mixed cultures increase metabolization rate of complex substrates

1. Introduction

The quantification of residual substrate is a major challenge during the microbial conversion of industrial organic waste streams. The pectin fraction of biomasses like sugar beet pulp is robust to acid hydrolysis. Enzymatic hydrolysis during microbial fermentations could thus help to convert complex substrates into fermentable sugars. Galacturonic acid - the main monomeric sugar in pectin - is an unusual carbon source during microbial fermentations. *Ustilago maydis* is well known as expression host for carbon activating enzymes (CAZymes) [1]. It is able to convert galacturonic acid [2]. Therefore, it was chosen as production host for polygalacturonases of intrinsic and heterologous origin.

2. Methods

U. maydis was cultivated in **R**espiration **A**ctivity **MO**nitoring **S**ystem (RAMOS) shake flasks for the online determination of oxygen transfer rate (OTR), carbon dioxide transfer rate (CTR) and respiratory quotient (RQ). The correlation of the consumed overall oxygen with the consumed substrate was demonstrated previously [2]. Production and secretion of endo- and exo-polygalacturonase in different strains was achieved by promoter exchange in the *U. maydis* genome or introduction of heterologous genes. The generated strains were screened for their potential to metabolize polygalacturonic acid, pectin or sugar beet pulp with or without addition of conventional enzyme cocktails.

3. Results and discussion

RAMOS cultivations demonstrated the metabolic activity of an *U. maydis* strain expressing a heterologous exo-polygalacturonase on polygalacturonic acid [2]. However, growth of the culture was limited to the enzymatic activity in the culture supernatant. A screening of three different

U. maydis strains expressing endo-polygalacturonases of intrinsic, bacterial or eukaryotic origin, respectively, was conducted in mixed cultivation with the exo-polygalacturonase expressing strain. Online monitoring of the metabolic activity revealed that the endo-polygalacturonase of eukaryotic origin showed the highest activity on polygalacturonic acid.

This mixed culture was subsequently cultivated on more complex substrates like pectin or sugar beet pulp. The limited metabolic activity demonstrated that additional pectinases are required for efficient conversion of those substrates. As proof of principle, the metabolic activity of *U. maydis* mixed cultures on pectin and sugar beet pulp was increased by addition of conventional enzyme cocktails. Finally, the potential of *U. maydis* to convert the main pectin sugars was demonstrated by cultivation in a minimal medium containing six different carbon sources.

4. Conclusions

A detailed overview of the respiration activity of *U. maydis* during growth on pectic substrates of different complexity was attained. The previously developed methodology for online determination of the residual substrate concentration was applied on a screening of mixed cultures expressing different endo-polygalacturonases. Limitations in the enzyme expression rate were overcome by addition of conventional enzyme cocktails demonstrating the capability of *U. maydis* to convert the main sugars from pectin.

References

[1] E. Geiser, M. Reindl, L.M. Blank, M. Feldbrügge, N. Wierckx, K. Schipper, Appl. Environ. Microbiol. 82:17 (2016) 5174-5185.
[2] M.J. Müller, S. Stachurski, P. Stoffels, K. Schipper, M. Feldbrügge, J. Büchs, J. Biol. Eng. 12:34 (2018).

ECAB 5
The 5th EUROPEAN CONGRESS OF APPLIED BIOTECHNOLOGY
Florence 15-19 September 2019

Improving product specificity of whole-cell alkane oxidation in non-conventional media: A multivariate analysis approach

Frank Baganz[1]*, Johannes F Kolmar[1], Oliver Thum[2]

1 Advanced Centre for Biochemical Engineering, Department of Biochemical Engineering, University College London, Gower Street, London WC1E 6BT, United Kingdom; 2 Evonik Creavis GmbH, Paul-Baumann-Straße 1, 45772 Marl, Germany

**Corresponding author: f.baganz@ucl.ac.uk*

Highlights

- Polarity of co-solvents determines product specificity.
- Accumulation of alcohol over acid using more polar solvents.
- PLS model showed defining factors are solubility parameters

1. Introduction

Two-liquid phase reaction media have long been used in bioconversions to supply or remove hydrophobic organic reaction substrates and products to reduce inhibitory and toxic effects on biocatalysts [1]. In case of the terminal oxyfunctionalisation of linear alkanes by the AlkBGT monooxygenase the excess alkane substrate is often used as a second phase to extract the alcohol, aldehyde and acid products [2]. However, the selection of other carrier phases or surfactants is complex due to the large amount of parameters that are involved, such as: biocompatibility, substrate bioavailability and product extraction selectivity.

This study investigates co-solvents of different polarities and structures as secondary solvents for the whole-cell alkane bio-oxidation by AlkBGT. Initially, the impact of six co-solvents at two concentrations is studied. Particular focus is on the overall product yield and specificity of the bio-oxidation of four linear alkane substrates. In order to efficiently screen this wide range of experimental conditions, a high-throughput microwell platform specifically customised for non-conventional media is used [3]. In a second step experimental data is combined with estimated physicochemical properties of the co-solvents in a multivariate Partial least squares projections to latent structures (PLS) regression analysis. This allows the identification of key properties of co-solvents that specifically affect the AlkBGT reaction in terms of product specificity and yields.

2. Methods

Materials and methods for whole cell bioconversion in customized microwell plates and analysis of the reaction products by gas chromatography has been described in detail in Kolmar et al 2018 [3]. For data analysis physicochemical properties i.e. Hansen and logP parameters were estimated for co-solvents and reaction substrate and products using COMSOquick software. PLS regression analysis was performed (SIMCA 13.0.3, Umetrics) for analysing multiple variables in one model.

3. Results and discussion

Partial least square regression showed that the defining factors for product specificity are the solubility properties of reaction substrate and product in the co-solvent, as measured by Hansen solubility parameters. Thus the polarity of co-solvents determines the accumulation of either alcohol or acid products. Whereas usually the acid product accumulates during the reaction, by choosing a more polar co-solvent the 1-alcohol product can be accumulated. Especially with Tergitol as co-solvent, a 3.2 fold improvement in 1-octanol yield to 2.4 g l^{-1} was achieved relative to the control reaction without co-solvents (Figure 1).

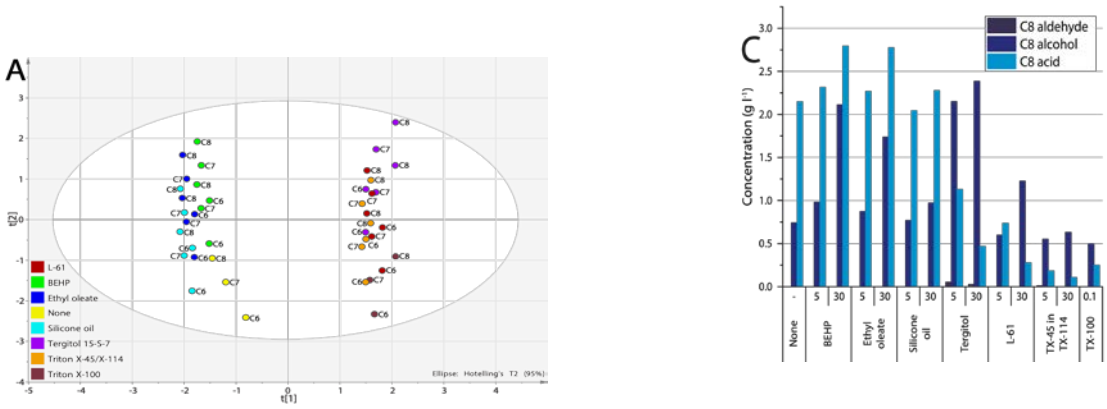

Figure 1. PLS model M2 score scatter plot of response data showing X-scores (t) of the first component along the x-axis and X-scores of the second along the y-axis (A) Co-solvent screening with octane substrate after 24h at 30°C and 250rpm, at varying co-solvent percentages in substrate indicated below x-axis (C).

4. Conclusions

The application of co-solvents is a promising strategy to influence whole-cell alkane oxidations. Further work needs to investigate efficient downstream processing options for the most promising candidates to fully leverage their advantages.

References

[1] P.-Y. Kim, D. J. Pollard, J. M. Woodley, Biotechnology Progress 2007, 23, 74– 82.

[2] C. Grant, J. M. Woodley, F. Baganz, Enzyme and Microbial Technology 2011, 48, 480–486.

[3] J. F. Kolmar, O. Thum, F. Baganz, Microbial Cell Factories 2017, 16, 174.

ECCE 12
ECAB 5

ECAB 5
The 5th EUROPEAN CONGRESS OF APPLIED BIOTECHNOLOGY
Florence 15-19 September 2019

Increasing plasmid copy number of pTRKH3 in *Lactococcus lactis* for biopharmaceutical-grade pDNA production

Sofia Duarte[1], Maria Martins[1], Sílvia Andrade[1], Duarte Prazeres[1,2] and Gabriel Monteiro[1,2*]

1 IBB - Institute for Bioengineering and Biosciences, Instituto Superior Técnico, Universidade de Lisboa, Av. Rovisco Pais, 1049-001 Lisboa, Portugal; 2 Department of Bioengineering, Instituto Superior Técnico, Universidade de Lisboa, Av. Rovisco Pais, 1049-001 Lisboa, Portugal
**Corresponding author: gabmonteiro@tecnico.ulisboa.pt*

Highlights

- pTRKH3-b reached 215 copies in *L. lactis*, a 3.5-fold increase from the wild-type.
- pTRKH3-b had one additional RBS sequence and two additional start codons.
- pTRKH3-b encodes a mRNA secondary structure with the most negative ΔG value.
- pTRKH3-b showed an intermediate amount of transcriptional repressors.

1. Introduction

Pharmaceutical-grade plasmid DNA (pDNA) production in high quantities and in a cost-effective manner is a key point for several biotechnological and pharmaceutical applications, such as the production of DNA vaccines[1] and recombinant proteins and also for the use of food-grade bacteria in live mucosal vaccination.

Traditionally, pDNA is produced in *Escherichia coli*, but the use of this host shows a major drawback because lipopolysaccharides (LPS) may co-purify with pDNA, which raises several safety concerns and increase the manufacture cost[2].

Lactic acid bacteria (LAB), particularly *Lactococcus lactis* are a safer alternative host for pDNA manufacturing since they are naturally LPS-free and have a food-grade and Generally Recognized As Safe status[3]. In order to establish a cost effective *L. lactis*-based pDNA manufacturing platform it is imperative to engineer new high-copy number plasmids, since the highest copy number reported for the commonly used pAMβ1 replicon is around 100 copies, which is much lower than the 500-700 copies reported for *E. coli* pUC vectors[4].

2. Methods

In order to achieve different plasmid copy number (PCNs) in *L. lactis* LMG19460 cells, the RBS sequence of the *repDE* promoter of the pAMβ1 replication origin of the plasmid pTRKH3 was modified by site-directed mutagenesis.

L. lactis LMG19460 cells harbouring the non-modified pTRKH3 and the plasmids with the designed mutations were grown under previously optimized conditions. The PCN per cell was determined by real-time quantitative PCR and the data was analysed using a relative quantification method[5]. The translation initiation rates and consequently the predicted protein expression levels of each designed RBS sequences were evaluated using the RBS Calculator (https://salislab.net/software/, Salis Lab, Penn State University)[6,7]. The mRNA of the *repD* gene, along with the mRNA of its transcriptional repressors (*copF* and *CT-RNA*), were quantified by real-time qPCR, using the same method described above.

3. Results and discussion

The specific growth rates of cells containing the modified plasmids were not significantly ($p<0.05$) affected, suggesting that the modifications in the *repDE* RBS sequence of pTRKH3 do not influence negatively the overall cell metabolism.

With the exception of pTRKH3-a and pTRKH3-e, the average PCN of the modified plasmids at 10.5h of growth (i.e. late exponential/early stationary phase) were statistically higher ($p<0.05$ for pTRKH3-c and $p<0.01$ for pTRKH3-b, pTRKH3-d and pTRKH3-f) than the PCN obtained for the wild-type pTRKH3. The highest average PCN value was obtained for pTRKH3-b (215±38), representing a 3.5 fold increase over the wild-type plasmid (62±5) and much higher than the maximum of ~100 copies obtained for the pAMβ1 replicon in previous studies.

The pTRKH3-b plasmid has neither the most similar RBS to the 16S rRNA sequence nor the strongest RBS predicted by the Anderson library, but instead it was detected an unexpected 77 bp insertion, which led to the creation of an additional RBS sequence and two additional relevant start codons. Without that insertion, the mutant lost the ability to replicate with such a high PCN.

The *in silico* mRNA secondary structures analysis, using RNA folding software tools, predicted the pTRKH3-b mutant as the one having the most negative ΔG value, when compared with the remaining mutants and the parental plasmid, increasing the likelihood that the ribosome will bind to the mRNA and initiate translation of the replication initiation protein, leading ultimately to an increase in the PCN.

A principal component analysis performed with the mRNA quantification results showed that pTRKH3-b had an intermediate amount of CopF and CT-RNA repressors, which seems to allow the perfect balance between transcription initiation and its repression.

4. Conclusions

pTRKH3-b is a very promising high copy number shuttle plasmid that will contribute to bring LAB to the same level as *E. coli* as pDNA producers, with the additional advantage of being endotoxin free, which turns the process more profitable.

The main possible applications for this new plasmid is to use *L. lactis* as efficient producers of pharmaceutical-grade DNA vaccines and recombinant proteins, and as live mucosal vaccination vectors.

Recently, an effort is being made in our research group in order to engineer knockout *L. lactis* strains that could improve even more the quality and quantity of the pDNA produced.

References

[1] E.F. Fynan, S. Lu, H.L. Robinson, *Hum. Gene Ther. 29*(9) (2018) 966–970.
[2] D. Dixon, R. Darveau, *J. Dent. Res. 84*(7) (2005) 584–595.
[3] G. Gram, A. Fomsgaard, M. Thorn, S. Madsen, J. Glenting, *Genet. Vaccines Ther. 5(*3) (2007).
[4] J. Sambrook, E.F. Fritsch, T. Maniatis, Molecular cloning: a laboratory manual, Cold Spring Harbor Laboratory Press, Plainview, NY, 1989.
[5] M. Skulj, V. Okrslar, S. Jalen, S. Jevsevar, et al., *Microb. Cell Fact. 7*(1) (2008) 6.
[6] A.E. Borujeni, A.S. Channarasappa, H.M. Salis, *Nucleic Acids Res. 42*(4) (2013) 2646–2659.
[7] H.M. Salis, E.A. Mirsky, C.A. Voigt, *Nat. Biotechnol. 27*(10) (2009) 946–950.

Coarse Grained Modeling of Ribosome Availability In *E. Coli.*

Ayse Koruyucu[1], Andreas Kremling[1*]

[1] *Systems biotechnology, Technical University of Munich, Garching b München*

**Corresponding author: a.kremling@tum.de*

Highlights

- Kinetic model to describe ribosome abundance for a broad range of growth rates
- Integration of length distribution of individual protein as basis for the determination of active ribosomes
- Estimation of kinetic parameters for protein synthesis in dependence of free available ribosomes

1. Introduction

The set-up of mathematical models is still a challenging task in systems biology. Although experimental data from "omics"-technologies are frequently available, the number of unknown parameters which must be estimated is still high. Therefore, in systems biology, the development of one model type, so called coarse-grained models which have only a minor number of parameters, has attracted attention in last years. This is mainly based on the observation that the relationship between large proteome fractions linearly correlate with the growth rate and allows researchers to set up and validate simple, empirical mathematical models to describe these relationships. In this way, general design principles of cellular resource allocation can be postulated.

2. Methods

A pioneering role plays the group of Terence Hwa, California, U.S.A. which developed a holistic framework for the description of cellular bio-chemical reaction networks [1]. Although simple, these models are used to make predictions for different experimental conditions like additional load in form of foreign protein expression and altered kinetic parameters, for example, for different values of the translation velocity. A general drawback of empirical models is, that they are not based on equations that guarantee mass conservation; this is typically realized by setting up a mass balance equation and deducing equations for intracellular concentrations (typically, units like mol/g dry weight or mol/ l cell are used for components of the network. Kinetic expressions for synthesis and degradation are based on the state variables of the model and therefore contain "lumped" information. In coarse-grained models, the number of state variables is low (smaller than 5) and (in general) they are analytically solvable for quasi steady state: if the dynamic of the system is not in the focus, a set of algebraic equations results from setting time derivatives to zero. Finally, the solution space is analyzed by a variation, for example, of the growth rate and calculation of the steady state values of the state variables.

In the presented study, we focus on the synthesis of the overall proteome of the cell taking into account the availability of ribosomes and neglecting the pure metabolic substrate flux in form of

amino acids. The model takes into account geometric parameters like the length distribution of individual proteins, kinetic parameters for transcription/ translation, and the abundance distribution of proteins measured under different conditions.

3. Results and discussion

For the total protein *P* in the cell, a general differential equation in the form $\dot{P} = r_{syn} - \mu P$ with the total rate of protein synthesis $r_{syn}(n_{Rf})$ and the specific growth rate μ is used. The rate of synthesis depends on the free available ribosomes n_{Rf} in the cell. To count the active ribosome n_{Ra} for a distinct growth rate, we estimate the number of active RNA polymerases and, depending on the position of the RNA polymerase on the DNA strand, the number of ribosomes currently translating the mRNA. For a single transcription unit *j* one get according to [2]: $n_{Rj} = m_j \frac{(n_{Pj}+1)}{2\, d_R}$, with the length m_j of the transcription unit, n_{Pj}, the number of RNA polymerases, and d_R the distance between two ribosomes. This term can be reformulated to take into account the steady state number of the respective protein that depend on the selected growth rate. In this way, integrating over all proteins with individual length and the relationship for the total number of ribosomes, that is, the sum of active and free ribosome ($n_{Rt} = n_{Rf} + n_{Ra}$), we obtain a relationship for the total protein in steady state: $r_{syn}(n_{Rt} - n_{Ra}(P)) = \mu P$. We analyzed several possible kinetic expressions for the rate of synthesis r_{syn} and fit the model to available experimental data for the total number of ribosomes. Figure 1 shows the length distribution for the protein and the final fit for the total number of ribosomes.

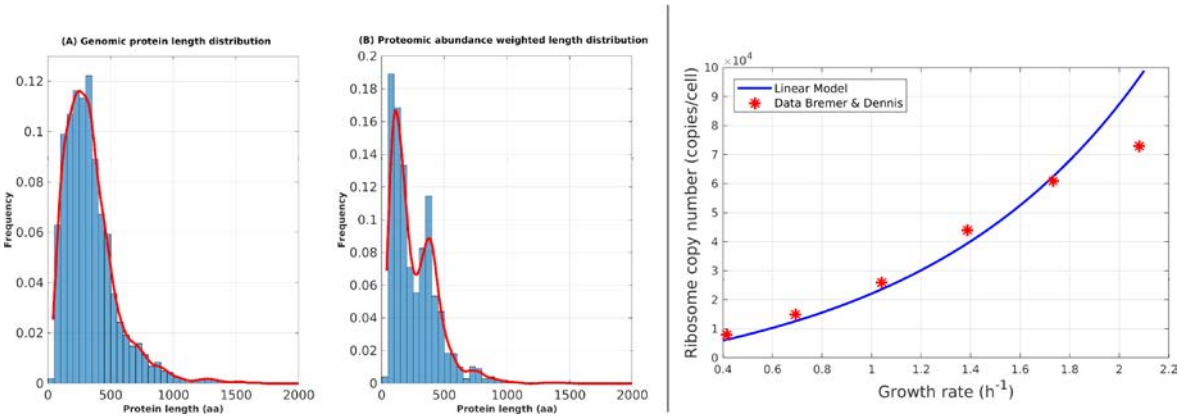

Figure 1. Left: (A) Protein length distribution with data from [3], (B) with steady state data weighted distribution. Right: Experimental data [4] and simulation comparison for the total number of ribosomes.

4. Conclusions

The model successfully describes experimental data for a broad range of the growth rate. Sensitive parameters of the model are the growth rate dependent velocities of the ribosomes and the RNA polymerase, as well as the total number of transcription units in the cell.

References

[1] M. Scott et al., Molecular Systems Biology 10, 2014
[2] A. Kremling, Biotechnology & Bioengineering 96, 2007
[3] A. Schmidt et al., Nature Biotechnology 34, 2016
[4] H. Bremer & P.P. Dennis, EcoSal Plus, 2008

Comparison between carbonic anhydrase biocatalysts for CO_2 capture by enzymatic reactive absorption

Maria Elena Russo[1*], Sara Peirce[2], Sonia Del Prete[3], Clemente Capasso[3], Antonio Marzocchella[2], Piero Salatino[2]

1 Istituto di Ricerche sulla Combustione – Consiglio Nazionale delle Ricerche, P.le V. Tecchio 80, 80125 Napoli, Italy; 2 Dipartimento di Ingegneria Chimica dei Materiali e della Produzione Industriale – Università degli Studi di Napoli Federico II, P.le V. Tecchio 80, 80125 Napoli, Italy, 3 Istituto di Bioscienze e Biorisorse – Consiglio Nazionale delle Ricerche, Via P. Castellino 111, 80131 Napoli, Italy

**Corresponding author: m.russo@irc.cnr.it*

Highlights

- Different immobilization techniques have been applied to carbonic anhydrase.
- Whole cell catalyst bearing carbonic anhydrase has been developed.

1. Introduction

Post-combustion CO_2 capture strategy asks for novel processes avoiding the use of polluting solvents and aimed at CO_2 utilization. CO_2 absorption processes based on the enhancement of capture rate by the enzyme carbonic anhydrase (CA) (EC - 4.2.1.1) have been deeply investigated [1]. CA is able to catalyze the CO_2 hydration reaction and its thermophilic and halophilic forms are active into aqueous alkaline solvents [2]. In addition, the use of carbonate aq solvents and CA allows the exploitation of the bicarbonate enriched solvent for CO_2 utilization processes based on the cultivation of high value microalgae biomass [3, 4]. This contribution reports on recent efforts for the development of three techniques for the production of CA biocatalysts: two different CA immobilization techniques were developed and compared with a whole cell biocatalyst where CA is present on the outer membrane of engineered *Eschierichia coli* cells [5].

2. Methods

Thermostable CA was (Novozymes) and immobilized in the form of Cross Liked Enzyme Aggregates (CLEA) [6] and covalently attached on magnetic nanoparticles (MNP) [7]. Whole cell biocatalyst bearing CA on outer surface of cell membrane were prepared according to Del Prete *et al.* [5]. Kinetic characterization of CA based biocatalyst was performed through CO_2 absorption tests in a stirred cell lab scale bioreactor [6, 7].

3. Results and discussion

Figure 1 shows the immobilization yields (mass of immobilized enzyme/initial mass of enzyme) and the enzyme loadings (mass of enzyme/mass of biocatalyst) after preparation of CA CLEA and MNP with attached CA. CLEA shows remarkable improvement of these characteristics with respect to CA covalently attached on MNP. On the other hand, large CLEA size (low biocatalyst effectiveness) did

not allow kinetic characterization [6]. MNP and free CA apparent kinetics were fully characterized under industrially relevant conditions [7]. Whole cell biocatalyst showed active CA on its membrane [5] and its kinetic characterization is ongoing through CO_2 absorption tests used for CLEA and MNP characterization [6, 7].

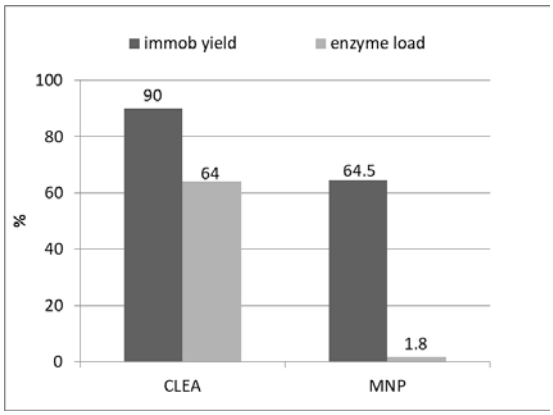

Figure 1. Comparison between CA immobilized on magnetic nanoparticles (MNP)and cross linked enzyme aggregates (CLEA).

4. Conclusions

Three technologies have been developed to produce CA-biocatalysts for the development of CO_2 capture processes oriented through aq phase CO_2 utilization [3, 4]. Table 1 reports pros and cons about each investigated biocatalyst. Among these, MNP biocatalyst is ready to further scale-up tests since assessed kinetic parameters have been used for an absorption column design study [8].

	Free CA/aggregates	CA on MNP	CLEA	Whole cell biocatalyst
Enzyme purification	+	+	+	-
Stability	-	+	+	Ongoing
Biocatalyst effectiveness	+/-	+	-	+
Kinetic parameters	+	+	-	Ongoing

Table 1 Comparison between possible strategies for CA use as promoter of enzymatic reactive absorption for CO_2 capture.

References

[1] M. E. Russo, G. Olivieri, A. Marzocchella, P. Salatino, P. Caramuscio, C. Cavaleiro, Sep Pur Technol, 107 (2013) 331–339.
[2] M. Leimbrink, S. Tlatlik, S. Salmon, A. K. Kunze, T. Limberg, R. Spitzer, A. Gottschalk, A. Górak, M. Skiborowski, Int J Greenhouse Gas Control, 62 (2017) 100–112.
[3] Z. Chi, J. V O'Fallon, S. Chen, Trends Biotechnol. 29 (2011) 537–41.
[4] B. Gris, E. Sforza, L. Vecchiato, A. Bertucco, Ind. Eng. Chem. Res. 53 (2014) 16678–16688.
[5] S. Del Prete, R. Perfetto, M. Rossi, F. A. S. Alasmary, S. M. Osman, Z. AlOthman, C. T. Supuran, C. Capasso, J. Enz Inihib Medicinal Chem, 32 (2017) 1120–1128
[6] S. Peirce, M.E. Russo, R. Isticato, R.F. Lafuente, P. Salatino, A. Marzocchella, Biochem. Eng. J. 127 (2017) 188–195.
[7] S. Peirce, M.E. Russo, R. Perfetto, C. Capasso, M. Rossi, R. Fernandez-Lafuente, P. Salatino, A. Marzocchella, Biochem. Eng. J. 138 (2018) 1–11.
[8] M. E. Russo, P. Bareschino, F. Pepe, A. Marzocchella, P. Salatino, Chem. Eng. Transact. 69 (2018)

ECAB 5
The 5th EUROPEAN CONGRESS OF APPLIED BIOTECHNOLOGY
Florence 15-19 September 2019

Hydrolytic enzymes immobilization on silicate mesoporous materials or carbon nanomaterials: impact on N-acylation performances

C. Bourkaib[1,2], B. Vigolo[3], Y. Guiavarc'h[1,2], S.Delaunay[1,2], A. Desforges[3], C. Humeau[1,2], J-L. Blin[4], I. Chevalot[1,2]

1 CNRS, Laboratoire Réactions et Génie des Procédés, UMR 7274, 2 avenue de la forêt de Haye, TSA 40602, Vandœuvre-lès-Nancy, 54518, France ; 2 Université de Lorraine, LRGP, CNRS UMR 7274, 2 avenue de la forêt de Haye, TSA 40602, Vandœuvre-lès-Nancy, 54518, France ;#B Institut Jean Lamour, IJL, CNRS UMR, 2 allée André Guinier, Campus Artem, BP 50840, 54011 Nancy Cedex; 4 Laboratoire Lorrain de Chimie Moléculaire, L2CM, CNRS UMR 7053, BP 70239, 54506 Vandoeuvre les Nancy cedex.

**Corresponding author: Isabelle.chevalot@univ-lorraine.fr*

Highlights

- Enzymes immobilized on carbon nanotubes and mesoporous silica SBA15 maintained their regioselectivity towards N-acylation of lysine.
- Enzymatic N-acylation performances depended on immobilization materials.
- Functionalization of SBA15 with APTES improved enzyme loading and N-acylation performances

1. Introduction

N-acylation reactions allow the synthesis of amino acids/peptide derivatives, called lipo-amino acids/peptides belonging to the class of surfactants used in food and non-food applications for their good foaming and emulsion stabilization properties. Furthermore, as amino acids and peptides are molecules that may possess biological activities, the acylated derivatives of these molecules may also exhibit these bioactivities, making them detergents of choice in the cosmetic or pharmaceutical formulations. Industrially, the chemical reaction conditions are well known with the Schotten-Baumann reaction, but require the use of fatty acid chlorides in the presence of an organic cosolvent and generate effluents rich in salts. An alternative to this chemical route may be the use of hydrolytic enzymes to catalyse this reaction in aqueous or non-aqueous solvents depending on the enzyme. The use of lipases in non-aqueous media such as organic solvents or ionic liquids have already been reported [1] and aminoacylases in aqueous medium have also been described for the synthesis of acylated amino acids [2]. However to develop enzymatic processes to replace the chemical ones, the immobilization of the biocatalyst is required to improve its stability and allow its recycling. In this context, the aim of this work is to develop immobilization materials and conditions to improve enzymatic performances of both lipase in non-aqueous system or aminoacylases in aqueous medium for the synthesis of acylated amino acids.

2. Methods

The lipase B of *Candida antarctica* and aminoacylases from *Streptomyces ambofaciens* were immobilized either on SBA15 or on carbon nanotubes by physisorption or chemisorption. Preliminary functionalizations of SBA15 with APTES (from 10 up to 50 %) were performed. The synthesis of lauroyl-lysine was carried out with L-lysine (0.12 M) and Lauric acid (0.24 M) in 2 mL of

2-methyl-2-butanol previously dehydrated on 4 Å molecular sieves for CALB and in Tris-HCl 25 mM NaCl 50 mM (pH 8) for aminoacylases. The acylation reaction was performed in an agitated parallel system (Carousel 12 Plus Reaction Station™, Radleys) and is initiated by the addition of lipase B of *C. antarctica* immobilized on carbon nanotubes by physi- or chemisorption or by the addition of aminoacylases immobilized on SBA15. The quantity of supported enzymes was determined depending on the immobilization yield in order to add 1 mg of protein in the reaction medium.

3. Results and discussion

The synthesis of lauroyl-lysine was investigated using the lipase B of *Candida antarctica* immobilized on carbon nanotubes and aminoacylases immobilized on mesoporous silicate SBA15 functionalized with APTES. Both enzymes immobilized on carbon nanotubes or SBA15 maintained their regioselectivity towards N-acylation in α or ε position. By adsorption on SBA15, increased APTES concentration led to an improvement of aminoacylases loading up to 0.07 mg/mg material and increased N-acylation performances (Figure 1).

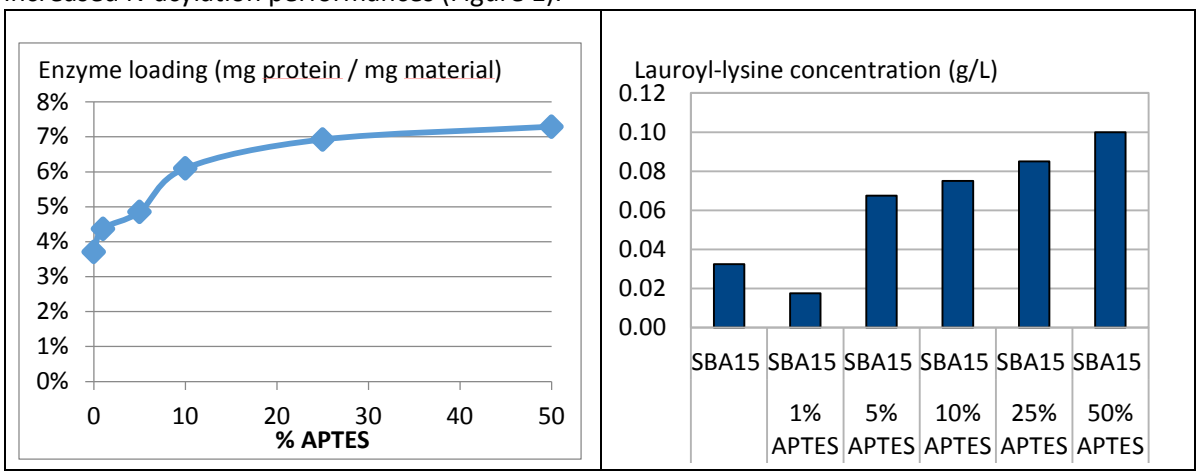

Figure 1. Aminoacylases loading enzyme on SBA15 functionalized with different APTES concentrations and lauroyl-lysine concentration obtained after 48h reaction.

Alternatively, the N-acylation of lysine was carried out with CALB immobilized on carbon nanotubes. Enzyme loading reached 0.16 mg/mg carbon nanotubes by direct adsorption whereas 0.25 mg/mg carbon nanotubes can be achieved by covalent bonding. However, the activity of CALB covalently immobilized on carbon nanotubes was 20 fold less than with Novozyme 435.

4. Conclusions

The regioselectivity of N-acylation was maintained whatever the enzyme and immobilization support. However, the performances of both enzymes depended on immobilization supports by adsorption or covalent bond on SBA15 or carbon nanotubes.

References

[1] Husson E., et al. (2009). Enzymatic *N*-acylation of polar dipeptides: influence of reaction media and molecular environment of functional groups. Process Biochemistry, 44, 428-434

[2] Dettori L., et al. (2018). An aminoacylase activity from Streptomyces ambofaciens catalyzes the acylation of lysine on ±-position and peptides on N-terminal position. Engineering in Life Sciences, 2018, 18, 589–599

ECAB 5
The 5th EUROPEAN CONGRESS OF APPLIED BIOTECHNOLOGY
Florence 15-19 September 2019

Optimization of culture conditions for the production of active inclusion bodies using high-throughput technologies

Robin Lamm[1], Vera D. Jaeger[2], Ramona Kloß[3], Martina Pohl[3], Ulrich Krauß[2], Karl-Erich Jaeger[2,3], Jochen Büchs[1]*

[1] *Aachener Verfahrenstechnik – Chair of Biochemical Engineering, RWTH Aachen University, Forckenbeckstraße 51, 52074 Aachen, Germany*
[2]*Institute of Molecular Enzyme Technology, Heinrich Heine University Düsseldorf, 52425 Jülich, Germany*
[3]*Institute of Bio- and Geosciences (IBG1), Forschungszentrum Jülich GmbH, 52425 Jülich Germany*

**Corresponding author: jochen.buechs@avt.rwth-aachen.de*

Highlights

- Optimization of culture conditions to produce active inclusion bodies
- Application of various high-throughput cultivation technologies
- Investigation of cultivation temperature using a mini reactor-based temperature profiling system

1. Introduction

It is of primary importance to develop new generic methods for simple and cost-efficient production of large amounts of stable enzymes to facilitate industrial applications. Although immobilization methods can improve enzyme stability, the additional processing steps are laborious and thus expensive. In contrast, catalytically active inclusion bodies (CatIBs) are in vivo, carrier-free enzyme aggregates that can be purified in a simple two-step purification process and retain beneficial features of conventional immobilization preparations. CatIBs can be produced in *E. coli* by the fusion of the target enzymes with certain aggregation tags [1, 2].

2. Methods

Active inclusion bodies, consisting of fluorescent reporter proteins or target enzymes, were produced with *E. coli* BL21(DE3) using the pET system. *E. coli* was cultivated in the Respiration Activity MOnitoring System (RAMOS) shake flasks for the online determination of the oxygen transfer rate (OTR). Additionally, different high-throughput online monitoring cultivation devices were used to measure scattered light (biomass, morphology) and fluorescence (product). A mini reactor-based temperature profiling system was used to investigate the impact of the cultivation temperature in a single experimental setup. To prepare IBs for activity determination, *E. coli* cells were lysed and insoluble cell fractions were isolated and washed. The activity of IBs was determined by fluorescence measurements or enzyme activity assays.

3. Results and discussion

First, the cultivation technologies were applied to develop a standard cultivation protocol. A streamlined methodology was developed combing the cultivation protocol, CatIB purification and the activity determination of CatIBs at µL-scale to facilitate process characterization and optimization. Subsequently, the impact of important cultivation parameters like medium composition, oxygen availability, temperature, and induction strength was investigated. Since the expression temperature strongly influenced the CatIB quality, a mini reactor-based high-throughput temperature profiling system was applied to study this effect in-depth. Results show that the cultivation temperature has to be adjusted carefully depending on the target protein and the chosen aggregation tag.

4. Conclusions

Various small-scale high-throughput technologies were applied to study CatIBs in depth. Results show that cultivation conditions have to be carefully adjusted for the production of active IBs. Furthermore, the results underline the great potential for industrial applications, as well as the necessity for further investigations.

References

[1] M. Diener, B. Kopka, M. Pohl, K.-E. Jaeger, U. Krauss, Chem. Cat. Chem. 8(1):142-152 (2016)
[2] U. Krauss, V.D. Jäger, M. Diener, M. Pohl, K.-E. Jaeger, J. Biotechnol. 258:136-147 (2017)

Asymmetric reduction of (R)-carvone by cellular envelopes with an immobilized two enzyme system

Ingmar Polte[1*], Werner Lubitz[2], Dirk Weuster-Botz[1], Kathrin Castiglione[3]

1 Technical University of Munich, Institute of Biochemical Engineering, Garching, Germany; 2 BIRD-C GmbH. Vienna, Austria; 3 Friedrich-Alexander-Universität Erlangen-Nürnberg, Institute of Bioprocess Engineering, Erlangen, Germany

**Corresponding author: i.polte@lrz.tum.de*

Highlights

- Analysis of undesired (2R,5R)-dihydrocarvone isomerization during whole cell-biotransformations
- One-step expression and immobilization of two enzymes in cellular envelopes of *Escherichia coli*
- 66 % reduced (2R,5R)-dihydrocarvone isomerization rates using cellular envelopes compared to whole cells
- The cellular envelope technology can be applied to reduce the effect of undesired side reactions mediated by the host cell metabolism.

1. Introduction

(2R,5R)-dihydrocarvone is a chiral building block which can be obtained by asymmetric reduction of the C-C double bond of (R)-carvone using ene-reductases. A purified ene-reductase from *Nostoc sp.* PCC 7120 (NostocER1) is capable of producing (2R,5R)-dihydrocarvone with a diastereomeric excess (de) ≥ 99 %. However, the application of whole cell biocatalysts expressing the cyanobacterial ene-reductase NostocER1 and a $NADP^+$-accepting formate dehydrogenase (FDH) mutant for internal cofactor regeneration led to a decreased de of 81.7% after 5 h which further dropped to the thermodynamic equilibrium of ~60% after 24 h [1]. The implementation of an *in situ* substrate feeding and product removal (SFPR) system based on polymeric adsorbent resins or ionic liquids could increase the achievable de in biotransformations with the whole cell biocatalysts up to 96.5 % [2], albeit the theoretical limit defined by the pure ene-reductase could not be reached. For different organisms than *Escherichia coli* it is suggested in literature that cytoplasmic components might catalyze the isomerization reaction of (2R,5R)-dihydrocarvone [4,5]. Therefore, in this contribution an inventive procedure for the one-step expression and immobilization of enzymes in cellular envelopes of *Escherichia coli* was applied to the two enzyme system comprising NostocER1 and FDH. The concept of cellular envelopes allows the construction of a biocatalyst lacking undesired catalytic interferences caused by host cell cytoplasmic components while keeping the economically beneficial low production and work-up costs of whole cell biocatalysts.

2. Methods

For the production of cellular envelopes, the two enzymes NostocER1 and FDH were fused on a genetic level to membrane anchorage domains, which allow a post-translational insertion into the

cytoplasmic membrane. In a second step the expression of protein E from phage ΦX174 led to the formation of lysis pores traversing both membranes of *Escherichia coli*. After cross-flow filtration to clean-up the released cytoplasmic components, cellular envelopes with a defined lysis pore and immobilized synthesis enzymes were obtained. Therewith, a biocatalyst with immobilized synthesis enzymes on the one hand but without potentially disturbing soluble host cell components on the other hand could be created.

3. Results and discussion

First it was proven that soluble cytoplasmic components of *Escherichia coli* can catalyze the undesired isomerization of (2R,5R)-dihydrocarvone to (2S,5R)-dihydrocarvone making it reasonable to apply the cellular envelope technology hereafter. Thus, seven different membrane anchorage domains were evaluated for the immobilization of NostocER1 in biotransformations with isolated membrane fractions. The highest activities and maintained stereo specificity were displayed for N- or C-terminal fusions of the hydrophobic transmembrane segment of the Vam3 protein from *S. cerevisiae* (Vam3p') and NostocER1. In these biotransformations FDH was membrane anchored via the C-terminal hydrophobic part of the Ubiquitin-conjugating enzyme 6 (UBC6) from *S. cerevisiae.* Subsequently, both configurations were employed in liter scale fed-batch processes for the production of cellular envelopes with membrane anchored NostocER1 and FDH. For both fusion types of Vam3p' to NostocER1 (N- and C-terminal) cellular envelopes could be prepared with high lysis yields of 99.93 and 97.25% after 27.5 and 29.7 h process time with maximal biomass concentrations of 12.83 and 10.72 g L^{-1}. During five subsequent washing steps of the cellular envelopes the protein concentration in solution as a measure of released cytoplasmic components in general was reduced to less than 4% (~80 µg mL^{-1}) of the starting value. In biotransformations the cellular envelopes displayed both NostocER1 and FDH activity and indeed (2R,5R)-dihydrocarvone isomerization rates were reduced up to 66% in comparison to whole cells.

4. Conclusions

The application of the one-step expression and immobilization procedure to the two enzyme system allowed the production of cellular envelopes with immobilized NostocER1 and FDH activity and high lysis yields. These cellular envelopes showed in biotransformations decreased (2R,5R)-dihydrocarvone isomerization rates compared to whole cell biocatalysts confirming the assumption that at least a part of the isomerization reaction is catalyzed by cytoplasmic compounds and that the cellular envelope technology can be used to reduce undesired side-reactions catalyzed by soluble host cell enzymes. To further investigate the remaining isomerization activity additional experiments regarding the completeness of the workup process should be considered.

References

[1] Fu, Y., Castiglione, K., Weuster-Botz, D., Industrial Biocatalysis (Ed. Grunwald, P.), Pan Stanford Publishing Pte. Ltd., 631-661, 2015.

[2] Castiglione, K., Fu, Y., Polte, I., Leupold, S., Meo, A., Weuster-Botz, D., Biochemical Engineering Journal 117 (2017) 102-111.

[3] Sührer, I., Langemann, T., Lubitz, W., Weuster-Botz, D., Castiglione, K., Microb Cell Fact. 14(2015) 180-189.

[4] Noma, Y., Nonomura, S., Sakai, H., Agricultural and Biological Chemistry, 39 (1975) 437-441.

[5] Van der Werf, M. J., Boot, A. M., Microbiology, 146(2000) 1129-1141.

Application of the sale-down methodology to study the effect of mixing on *Trichoderma reesei* physiology and enzyme production

Tamiris Roque[1], Fadhel Ben Chaabane[1], Frédéric Augier[2], Catherine Béal[3], A. W Nienow[4]

1 IFP Energies nouvelles, 1 et 4 avenue de Bois-Préau, 92852 Rueil-Malmaison, France ; 2 IFP Energies nouvelles, Rond-point de l'échangeur de Solaize, BP3, 69360 Solaize, France ; 2 UMR 782 AgroParisTech INRA, 1 avenue Lucien Brétignières, 78850 Thiverval-Grignon, France ; 3 School of Chemical Engineering, University of Birmingham, Edgbaston, Birmingham B15 2TT, United Kingdom

**Corresponding author: tamiris.goncalves-roque@ifpen.fr*

Highlights

- *Trichoderma reesei* is sensitive to anaerobiosis
- Oxygen gradients in *T. reesei* cultures lead to a complex metabolic response
- Long exposure of *T.reesei* to anaerobiosis decrease the cellulases production

1. Introduction

Techno-economic evaluations of processes for ethanol production from lignocellulosic biomass show that reducing the cost of the cellulases used to hydrolyze the cellulose into glucose is a prerequisite to bring the ethanol cost to values close to the ethanol produced from starch. A very attractive option is to perform the production of enzymes on site in order to substitute expensive and pure carbon sources by lignocellulosic waste generated by the agri-food or forestry activity.

Industrial cellulases are mainly produced by an aerobic filamentous fungus, *Trichoderma reesei*, because of its high secretion capacity. Scaling-up this process is very challenging because of the complex links that exist between the process conditions, the morphology of this fungus and its productivity. Actually, the filamentous morphology induces an increase of the medium viscosity that strongly reduces the oxygen mass transfer rate. To ensure a sufficient rate, the power input has to be increased, which increase the fluid dynamic stresses on the mycelial structures. Carrying out fermentations with these microorganisms is complicated as the fungal morphology impacts process parameters, whereas process conditions affect in return the morphology and possibly the process productivity. Moreover, with increasing scale, the media experiences ever increasing spatial and temporal variations, especially in dissolved oxygen and sugar concentration compared to the bench scale. Scale-down techniques are a way of establishing at the bench scale the large scale behavior and their implications for the economics of the process. The goal of this work is to better understand and evaluate the impact of the upscaling on the physiology of *T. reesei*.

2. Methods

The effect of physical-chemical heterogeneities induced by the scale-up on the behavior of the microorganism are investigated using 2 scale-down approaches : a two-compartment system (2STR) and a single compartment system (1STR). The enzyme production follows a two-steps process: growth and production. The growth step is operated in batch mode in excess of sugar to

reach biomass concentrations of 15g/L. Cultures medium, preculture and operating conditions in growth step are similar to those reported in [1]. The production step is carried out in fed-batch mode. For the 2STR experiment, a 3.5L aerobic bioreactor (2.5L of culture medium) kept at 40% of dissolved oxygen saturation (pO_2) is connected to a 2.0L anaerobic bioreactor (0.5L of culture media) where the pO_2 is kept at 0% by injecting nitrogen. Two peristaltic pumps keep the broth circulating between the two bioreactors throughout the experiment. Two different cycling residence times in the anaerobic zone are tested by changing the volume of the bioreactors. For the 1STR experiment, cycling oscillations in the pO_2 (0-40%) are produced in a single 3.5L bioreactor by injecting a mix of air and nitrogen. For both scale down approaches, the temperature is 27°C and pH is 4.0 for all the experiments. The gas flow rate in the 3.5L bioreactors is constant and equal to 0.25 l/mn. A determination of the secreted proteins concentration is achieved on the medium filtrate by using the DCTM Protein Assay kit (Biorad, Hercules, United States of America) and is based on a range of bovine serum albumin (BSA, 0-1.5 gL-1) [2].

3. Results and discussion

As reported in figure 1.I & II, results indicated a decrease of 20% in the specific production rate and yield for longtime cycling exposures (15min) to anaerobic conditions in the 2STR experiments. This effect is quite low because heterogeneities of 15min are unlikely to occur in full-scale bioreactors. The comparison of the two different scale down approaches (2STR and 1STR) in figure 1.III showed very different results for the same characteristic times (3,4min) in the anaerobic zone. This indicates a) the sensitivity of *T. reesei* to anaerobiosis and b) the fact that the metabolic response is complex and not immediate because it depends on the distribution of the residence times of the microorganisms in the aerated or non-aerated zones.

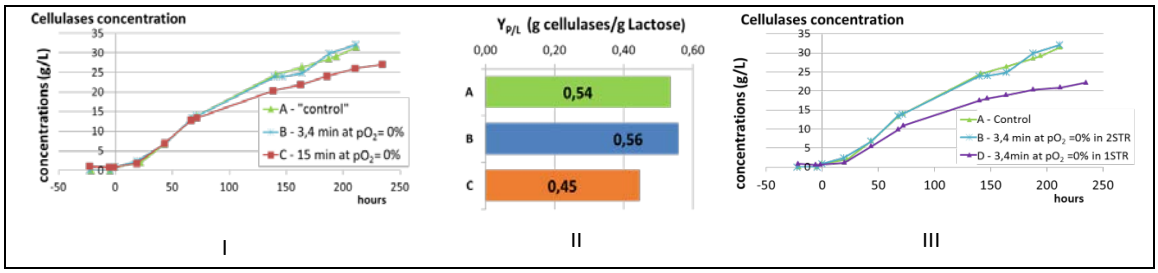

Figure 1. I & II) Comparison of cellulases production and yield (respectively) for three cultures in 2STR *:* A - control (no oxygen oscillations), B - 3,4 min and C - 15 min of cycling exposure to pO_2=0% ; **III)** Comparison of two different scale-down approaches for 3,4 min of cycling exposure to pO_2=0% : B - 2STR and D - 1STR

4. Conclusions

In this study, the effect of oxygen oscillations on enzyme production has been investigated during cultures of *T. reesei*. The possible low sensitivity of the fungus with respect to oxygen heterogeneities in production phase, opens perspectives in terms of technological choice on an industrial scale. However, its complex biological response to oxygen oscillations seems to be correlated with the distribution of the residence time in anaerobic zones inside large bioreactors.

References

[1] Hardy, N., Augier, F., Nienow, A., Béal, C., Ben Chaabane F. (2017), Chem. Eng.Sci., 172: 158-168.
[2] Lowry, O.H., Rosebrough, N.J., Farr, A.L. and Randall, R.J. (1951), J. Biol. Chem., 193: 265–275.

ECAB 5
The 5th EUROPEAN CONGRESS OF APPLIED BIOTECHNOLOGY
Florence 15-19 September 2019

A 5-Regime Kinetic Model for the Study of Heterogeneities in *Bacillus Licheniformis* Aerobic Fed-Batch Fermentation Processes.

Gisela Nadal-Rey[1], Sjef Cornelissen[2], Krist V. Gernaey[1,*]

1 Process and Systems Engineering Center (PROSYS), Department of Chemical and Biochemical Engineering, Technical University of Denmark, Building 229, 2800 Kgs. Lyngby, Denmark; 2 Novozymes A/S, Fermentation Pilot Plant, Krogshoejvej 36, 2880 Bagsvaerd, Denmark

**Corresponding author: kvg@kt.dtu.dk*

Highlights

- A 5-regime kinetic model for *Bacillus licheniformis* has been developed and validated
- Glucose and oxygen variations are considered for a differential cell performance
- The model can be used to assess the impact of gradients on aerobic fed-batch fermentation processes

1. Introduction

The combination of computational fluid dynamics (CFD) and microbial kinetic models is of great interest to investigate the occurrence and magnitude of gradients in process variables [1-3] in industrial-scale reactors, since detailed information of the fermentation environment can be generated. Nevertheless, coupling both models can become rather challenging due to the increased computational effort these types of simulations require. Therefore, it is important that simple, but accurate, kinetic models are developed for the study of heterogeneities.

In this work, a mechanistic model for the industrial workhorse *Bacillus licheniformis* [4] has been developed experimentally and validated. Its large-scale process consists of a high cell density aerobic fed-batch fermentation. Hence, the presence of sugar and oxygen gradients is likely to occur [5]. These gradients lead to the potential occurrence of five different metabolic regimes (acetate limited, fully oxidative, microaerobic and two overflow levels), depending on the concentrations of glucose and dissolved oxygen. With this kinetic model, the already well-established [1-3] CFD models can be extended and glucose and oxygen gradients in *B. licheniformis* fermentation processes can be investigated.

2. Methods

The model considers the different performance of *B. licheniformis* SJ4628 in five metabolic regimes depending on the concentration of glucose and oxygen in the fermentation broth (Figure 1). The switch between regimes is assumed to be instantaneous and based on critical concentrations of oxygen and glucose and on critical specific growth rates. Therefore, fermentations with varied concentrations of oxygen and glucose were performed to investigate the behaviour of *B. licheniformis* under different conditions.

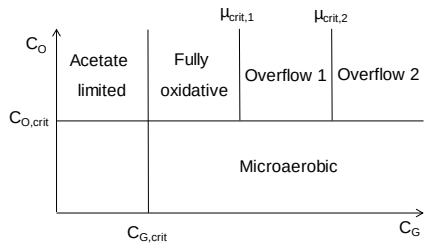

Figure 1. Scheme of the metabolic regimes of the kinetic model and the conditions at which the switch occurs.

The model describes growth with classical Monod kinetics and uses stoichiometric yield and maintenance coefficients to account for glucose, oxygen and acetate uptake and acetate production. More details regarding the equations setup will be given in this contribution.

3. Results and discussion

This work consists of the development and validation of a 5-regime kinetic model for *B. licheniformis* fermentation processes. The model takes into account the glucose and oxygen conditions at which the microorganism is grown, and uses different parameters and equations accordingly. Therefore, it resembles glucose and oxygen uptake in fully oxidative, overflow and microaerobic regimes, acetate re-assimilation under glucose-limiting conditions and acetate production under overflow and microaerobic conditions. Although all these different metabolic behaviors have already been described in literature [6], it is the first time that a 5-regime model with immediate metabolic switches has been experimentally developed and validated. Besides, it is also the first time that the growth, substrate uptake and acetate production kinetics of *B. licheniformis* have been investigated.

In this contribution, besides assessing the model uncertainty, the applications of this model to study glucose and oxygen gradients in fermentation processes will be discussed and exemplified. The implications of such gradients in industrial *B. licheniformis* fermentation processes will also be tackled.

4. Conclusions

With the execution of this work, it has been proven that the behaviour of *B. licheniformis* SJ4628 can be described with an unstructured mechanistic model including five different metabolic regimes. It has also been shown that the model is suitable for the study of glucose and oxygen gradients in industrial fermentation processes.

References

[1] C. Haringa, W. Tang, A. T. Deshmukh, J. Xia, M. Reuss, J. J. Heijnen, R. F. Mudde, H. J. Noorman, Eng. Life Sci. 16(7) (2016) 652-663.

[2] R. Spann, J. Glibstrup, K. Pellicer Alborch, S. Junne, P. Neubauer, C. Roca, D. Kold, A. Eliasson Lantz, G. Sin, K.V. Gernaey, U. Krühne, Biotechnol. Bioeng. (2018) 0-3.

[3] M. Wright, C. Bach, K. V. Gernaey, U. Krühne, Chem. Eng. Sci. 140 (2018) 12-22.

[4] M. W. Rey, P. Ramaiya, B. A. Nelson, S. D. Brody-Karpin, E. J. Zaretsky, M. Tang, A. Lopez de Leon, H. Xiang, V. Gusti, I. G. Clausen, P. B. Olsen, M. D. Rasmussen, J. T. Andersen, P. L. Jørgensen, T. S. Larsen, A. Sorokin, A. Bolotin, A. Lapidus, N. Galleron, S.D. Ehrlich, R. M. Berka, Genome Biol. 5(10) (2004) r77

[5] G. Larsson, M. Törnkvist, E. Ståhl Wernersson, C. Trägårdh, H. Noorman, S.-O. Enfors. 14(6) (1996) 281-289.

[6] A. J. Wolfe, Microbiol. Mol. Biol. Rev. 69(1) (2005) 12-50.

Slow-release based exponential fed-batch for MTP screening platform

Roman Jansen[1]*, Niklas Tenhaef[1], Matthias Moch[1], Wolfgang Wiechert[1], Stephan Noack[1], Macro Oldiges[1]

1 Forschungszentrum Jülich, Institute of Bio- and Geosciences – Biotechnology (IBG-1), Jülich, Germany

**Corresponding author: r.jansen@fz-juelich.de*

Highlights

- High throughput bioprocess development
- Automated exponential fed-batch
- Slow-release system
- Miniaturized cultivation with online signals
- Microtiter plate

1. Introduction

Tremendous developments in the field of metabolic engineering have strongly increased the throughput in the last decade. Through utilization of advanced techniques such as random mutagenesis and highly specific gene editing tools, large strain libraries can be generated in a very short time [1]. To identify the best strain candidates for in depth process characterization, these strains combined with a set of process parameters, have to be tested. Nonetheless, the number of mandatory experiments adds up to be very large [2]. Consequently, systems with increased cultivation throughput are in great demand. Therefore, micro bioreactor systems become a critical tool for accelerated bioprocess development. While most of these systems enable to screen batch cultivation, they lack the means to perform fed-batch processes, which are often the standard in industrial biotechnology. In this study, a novel approach for feedback-driven control of an enzymatic slow-release system is realized by combining a BioLector-based cultivation setup, a liquid handling system and a custom process control system, allowing for 48 parallel fed-batch cultivations in an automated and miniaturized manner.

2. Methods

BioLector cultivations, integrated in a liquid handling system were performed with a tailor made process control system. After an initial batch phase on free glucose as the sole carbon source, fed-batch cultivations were realized through the specific addition of enzyme. The amyloglucosidase is capable of releasing glucose monomers from a dissolved glucose polymer such as dextrin with a constant release rate. Through adaption of the amount of enzyme added, the substrate release rate and consequently the growth rate could be controlled.

3. Results and discussion

Through utilization of the online signals (biomass from backscatter, pH, DO, GFP) provided by the BioLector cultivation, the process can be feedback controlled. The quasi-continuous pH signal allowed for a single sided pH-control, where a small pulse of controlling agent was added to the cultivation well, when the pH dropped below a pre-defined threshold. This pH control was key to

success, since amyloglucosidase activity is very pH sensitive and initial experiments without pH control failed. The backscatter signal of the cultivation was used to calculate the online growth rate as previously described [3]. Once this processed signal fell below another threshold value (growth rate set point μ_{set}) a varying pulse of amyloglucosidase based on the current backscatter signal was added to the medium to increase the glucose release rate again and consequently keep a constant growth rate.

This technology allowed for highly reproducible exponential fed-batch cultivations with *C. glutamicum* in a modified CGXII medium. Four different growth rate set points were tested regarding reproducibility (Figure 1) and protein production with secreted GFP as a model protein. The lowest exponential growth rate set point resulted in an almost doubled GFP production in comparison to a batch process with the same amount of substrate. To test the applicability of this novel technology, exponential fed-batch cultivations with two other industrial relevant microorganisms, *E. coli* and *P. pastoris*, were conducted successfully.

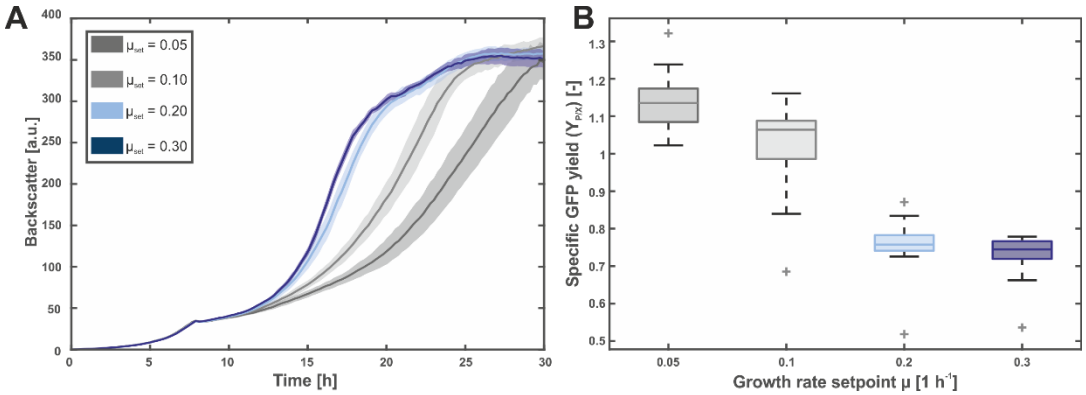

Figure 1. Backscatter curves (A) of *C. glutamicum* BioLector fed-batch cultivation and specific GFP yield (B) at the end of fed-batch cultivation.

4. Conclusions

In this study, a novel technology allowing for 48 parallel micro bioreactor fed-batch cultivation was developed. Via utilization of the online signals provided by the BioLector, a feedback controlled process was established, which showed high reproducibility for a given range of exponential growth range. This platform technology can be easily and cost effectively applied for screening purposes of up to 48 different cultivations.

References

[1] A. V. Shivange, J. Marienhagen, H. Mundhada, A. Schenk, and U. Schwaneberg, “Advances in generating functional diversity for directed protein evolution,” Curr. Opin. Chem. Biol., vol. 13, no. 1, pp. 19–25, Feb. 2009.

[2] Q. Long et al., “The development and application of high throughput cultivation technology in bioprocess development,” J. Biotechnol., vol. 192, pp. 323–338, 2014.

[3] A. Radek et al., “Miniaturized and automated adaptive laboratory evolution: Evolving Corynebacterium glutamicum towards an improved d -xylose utilization,” Bioresour. Technol., vol. 245, pp. 1377–1385, Dec. 2017.

Lipase-Catalyzed Solvent-Free Production of (Meth)Acrylate Monomers.

Wouter Van Hecke, Arjan Heeres, Yamini Satyawali, Karolien Vanbroekhoven

VITO (Flemish Institute for Technological Research) Boeretang 200 2400 Mol (Belgium)

**Corresponding author: wouter.vanhecke@vito.be*

Highlights

- (meth)acrylate esters were obtained at industrially appealing titers;
- nonlinear regression technique was applied to determine reaction rate constants;
- statistical inference was applied to the parameter estimates;
- second order kinetic model fits well with experimental results;

1 Introduction

Specialty or sensitive (meth)acrylate monomers are most often not available in the desired purity and quantity. Therefore, a milder and more sustainable manufacturing process is highly sought after [1]. To this end, lipases are known to catalyze ester synthesis at moderate conditions. Several of these have already been used to catalyse the production of (meth)acrylate esters with different alcohols in the presence of an inert organic solvent [1-3]. However, downstream processing could be simplified in solventless conditions [4, 5]. Hence, the first objective of this study was the solventless lipase catalysed transesterification of (meth)acrylates with various (bio-based) alcohols, enabling a more sustainable process for the production of specialty monomers. The second objective of this manuscript is to develop a generic kinetic model allowing simulation of the entire course of the solventless conversion based on nonlinear regression techniques.

2 Methods

2.1 Enzymes & chemicals

Novozym 435 (Novozymes, Bagsværd, Denmark) was used as catalyst in all tests. All organic alcohols and the methyl(meth)acrylate used for the transesterification had purities above 98% and were purchased from Sigma-Aldrich (Schnelldorf, Germany). A molecular sieve UOP Type 5Å (Sigma-Aldrich, Schnelldorf, Germany) was used to remove methanol.

2.2 Reaction conditions & nonlinear regression procedures

The lightest boiling substrate is added in molar excess to allow close to complete conversion of the highest boiling substrate and to avoid excessive temperatures in the subsequent distillation tower. Therefore, the conversions were only studied in reaction regimes using a molar excess of methyl (meth)acrylate. More detailed information on reaction conditions and the applied nonlinear regression procedures can be found in Heeres et al. [6].

3 Results and discussion

The ping-pong reaction mechanism seems to be the preferred model to describe lipase kinetics. A good fit with high R^2 values resulted from the selection of this mechanism. However, the large confidence intervals suggested overparameterization of the model. The use of a simpler second order rate equation yielded a more accurate model. Table 1 shows the results of the simulations. Higher reaction rate constants were systematically obtained for the transesterification of methyl acrylates, proving this to be a more accepted substrate than methyl methacrylate.

Table 1. The regressed second order reaction rate constants ranked in decreasing order. The lower and upper limit (LL and UL) of the 95% confidence intervals (CI) are also given.

Alcohol	Methyl ester	k_{cat} kg/(mol·h)	CI LL kg/(mol·h)	CI UL kg/(mol·h)
Tetrahydrofurfuryl alcohol	Methyl acrylate	1.69	1.26	1.71
Citronellol	Methyl acrylate	1.31	1.18	1.45
Furfuryl alcohol	Methyl acrylate	0.88	0.67	1.1
2-hexyl-1-decanol	Methyl acrylate	0.69	0.64	0.74
Methoxypropylphenol	Methyl acrylate	No reaction		
Isoeugenol	Methyl acrylate	No reaction		
4-methoxybenzyl alcohol	Methyl methacrylate	0.44	0.40	0.47
Furfuryl alcohol	Methyl methacrylate	0.36	0.25	0.48
Tetrahydrofurfuryl alcohol	Methyl methacrylate	0.35	0.31	0.38
Methoxypropylphenol	Methyl methacrylate	No reaction		
Isoeugenol	Methyl methacrylate	No reaction		

4. Conclusions and perspectives

Industrially appealing conversions and ester concentrations in solventless conditions were reached in this study. Progression curves were simultaneously used as input to estimate second order reaction rates and their confidence intervals based on nonlinear regression techniques. Larger scale production is currently under investigation for production of kg scale quantities.

References

[1] V. Athawale, N. Manjrekar, M. Athawale, Enzymatic synthesis of chiral menthyl methacrylate monomer by *Pseudomonas cepacia* lipase catalysed resolution of (+-)-menthol, J Mol Catal B-Enzym, 16 (2001) 169-173.
[2] V. Athawale, N. Manjrekar, M. Athawale, Lipase-catalyzed synthesis of geranyl methacrylate by transesterification: study of reaction parameters, Tetrahedron Lett, 43 (2002) 4797-4800.
[3] S. Warwel, G. Steinke, M.R. Klaas, An efficient method for lipase-catalysed preparation of acrylic and methacrylic acid esters, Biotechnol Tech, 10 (1996) 283-286.
[4] A.E.V. Petersson, L.M. Gustafsson, M. Nordblad, P. Börjesson, B. Mattiasson, P. Adlercreutz, Wax esters produced by solvent-free energy-efficient enzymatic synthesis and their applicability as wood coatings, Green Chem, 7 (2005) 837-843.
[5] M.B. Ansorge-Schumacher, O. Thum, Immobilised lipases in the cosmetics industry, Chem Soc Rev, 42 (2013) 6475-6490.
[6] A. Heeres, K. Vanbroekhoven, W. Van Hecke, Solvent-Free Lipase-Catalyzed Production of (Meth)acrylate Monomers: Experimental Results and Kinetic Modeling, Biochem Eng J, DOI:10.1016/j.bej.2018.11.011, (2019).

ECCE12
The 12th EUROPEAN CONGRESS OF CHEMICAL ENGINEERING
Florence 15-19 September 2019

Avoiding cross-reactivities in multi-step biocatalysis by light-induced enzyme deactivation

Tim Gerlach[1*], Simone Söltl[1], Thomas Drepper[2], Dörte Rother[1,3]

[1]Institute of Bio- and Geosciences: Biotechnology (IBG-1), Forschungszentrum Jülich GmbH, Jülich, Germany [2]Institute of Molecular Enzyme Technology (IMET), HHU Düsseldorf, Campus Jülich, Germany [3]Aachen Biology and Biotechnology (ABBt), RWTH Aachen University, Aachen, Germany
*Corresponding author: ti.gerlach@fz-juelich.de

Highlights

- The cloning and production of photosensitiser fusion enzymes was successful.
- Enzymes were produced soluble or as catalytically active inclusion bodies.
- The activity of the fusion enzymes was compared to the untagged enzymes.
- Photensitiser fusion enzymes show inactivation after light exposure.

1. Introduction

Cross-reactivity in complex enzyme cascades is a major challenge in the field of multi-step biocatalysis. To eliminate cross-reactivity in one-pot reaction systems, a novel strategy is followed: enzymes prone to side-reactivities are coupled to genetically encoded photosensitisers, which are able to produce reactive oxygen species upon irradiation with a distinct wavelength[1]. The resulting fusion enzymes can be added to the corresponding reaction step enabling the catalyst activity to be switched off after successful transformation. The three-step enzyme cascade starting from 3-hydroxy benzaldehyde and pyruvate to a trisubstituted tetrahydroisoquinoline has been chosen as a test system. This cascade encompasses a carboligation step, a transamination step and a final cyclisation[2]. It is a suitable target as in a one-pot reaction approach cross-reactivity especially of the transaminase occurs and dominant side-products are formed (Fig. 1), which has to be avoided.

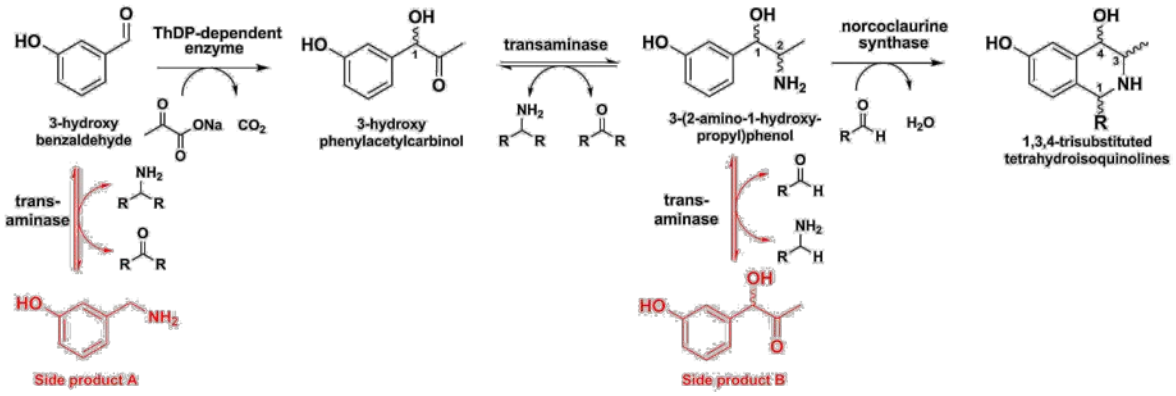

Figure 1. Three-step enzyme cascade starting from 3-hydroxy benzaldehyde and pyruvate to a trisubstituted tetrahydroisoquinoline. Possible side products are implied.

2. Methods

The flavin-binding fluorescent protein from *Bacillus subtilis* was genetically coupled to the pyruvate decarboxylase variant E469G/W543H from *Acetobacter pasteurianus* (Fp-*Ap*PDC-2v) and to the *Chromobacter violaceum* transaminase (Fp-*Cv*2025). The untagged enzymes as well as the fusion enzymes were produced in *Escherichia coli* BL21(DE3). The protein solubility was checked via SDS-PAGE and the proteins were purified using an ÄKTA chromatography system. The activity of the *Cv*2025 variants was measured spectrophotometrically for the reaction from alpha-methylbenzylamine to acetophenone. The activity of the *Ap*PDC-2v variants was determined via HPLC for the reaction from 3-hydroxybenzaldehyde to (S)-3-hydroxyphenylacetylcarbinol.

3. Results and discussion

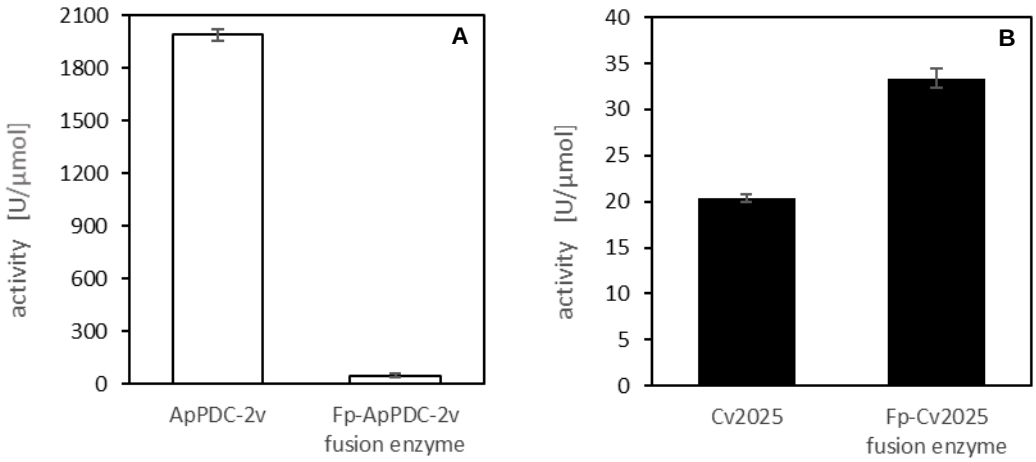

Figure 2. Activities of the photosensitiser fusion variants of *Ap*PDC-2v (A) and *Cv*2025 (B) compared to the respective untagged enzymes.

The Fp-*Ap*PDC-2v shows only 2.5 % of activity compared to the untagged enzyme, while the activity of the Fp-*Cv*2025 is even 30 % higher. The lower activity of Fp-*Ap*PDC-2v is likely to be caused by the structural properties of this enzyme because it is produced as catalytically active inclusion body. Depending on the structure of the untagged enzyme, multimeric photosensitisers seem to mediate the formation of a multi-enzyme network.

Furthermore, a light experiment with Fp-*Cv*2025 revealed, that 10 min of light exposure is sufficient to inactivate the enzyme completely.

4. Conclusions

The characterisation of two photosensitiser fusion enzymes was completed regarding their production and activity. Light experiments have shown that the photosensitiser tags are able to facilitate a fast inactivation of the fusion enzymes. Enzyme inactivation will now be analysed in detail.

References

[1] S. Endres, M. Wingen, J. Torra, R. Ruiz-Gonzáles, T. Polen, G. Bosio, N.L. Bitzenhofer, F. Hilgers, T. Gensch, S. Nonell, K.E. Jaeger, T. Drepper, 2018, Sci. Rep. 8(1), 15021.

[2] V. Erdmann, B.R. Lichman, J. Zhao, R.C. Simon, W. Kroutil, J.M. Ward, H.C. Hailes, D. Rother, 2017, Angew. Chemie - Int. Ed. 56: 12503–12507.

Unique antigenases to enzymatically cleave Tau peptides at C- and N-terminal moieties

Taizo Uda[1], Hiroaki Taguchi[2], Emi Hifumi[3]

1 Research Promotion Institute, Oita University, Oita, 870-1192, Japan; 2 Faculty of Pharmaceuticals Sciences, Suzuka University of Medical Science, Suzuka, Mie 513-8670, Japan; 3 Nano-tech Lab, ISIT, Fukuoka 819-0388 Japan

**Corresponding author: uda@isit.or.jp*

Highlights

- 1. FRET-peptide system was a strong tool for screening catalytic antibodies (antigenases).
- 2. Several antigenases to cleave FRET-Tau peptides were found in this study.
- 3. Each antigenase exhibited a little different feature in the cleavage of the Tau peptide.
- 4. Antigenases against Tau-peptide are involved in human antibody genes.

1. Introduction

Most common cause of dementia among older adults is Alzheimer's disease (AD). In the disease, two kinds of molecules, amyloid β peptide (Aβ) and Tau protein, are considered as the main factors relating with the cause of the disease by the accumulation with neurofibrillary tangles (NFT) or phosphorylated filamentous tau protein, which works as proteinopathies on the brain.

Antigenases (catalytic antibodies) capable of hydrolyzing peptides and proteins (antigenase) are potentially useful agents for therapeutics, through the specific elimination of pathogenic peptides and the essential proteins in microorganisms. Actually, antigenases such as HIV envelope glycoprotein, helicobacter pylori urease, influenza viruses, and amyloid β (Aβ) have been developed in a last few decades.

In this study, Tau protein was targeted in order to make the antigenases capable of enzymatically degrading the protein. For this objective, we designed and synthesized a substrate based on Förster resonance energy transfer (FRET) to efficiently find out the desired antigenases from our protein bank, in which hundreds of human antibody light chains possessing a catalytic triad–like structure are stored as the protein.

2. Methods

The fluorescence-quenched substrates were synthesized by conventional Fmoc SPPS using Rink amide resin. The structure of the substrate was confirmed by ESI-MS after purification by HPLC. After a human antibody light chain gene inserted into pET20b (+), it was transformed into *E. coli* and induced by IPTG. After recovering the soluble fraction of the culture supernatant, it was purified by Ni-NTA chromatography, cation exchange chromatography or size exclusion chromatography. Catalytic activity was measured using synthetic substrates of FRET-Tau (391-408) at C-terminal side and FRET-Tau (19-30) at N-terminal side.

3. Results and discussion

The number of the stored light chains in our protein bank reached to hundreds. Thus, we screened the antigenases capable of cleaving the Tau peptides using the synthesized FRET-Tau peptide substrates. As the results, two antigenases (C1 & C2) to cleave the FRET-Tau (391-408) peptide at C-terminal side were found in 111 light chains examined. On the other hand, one antigenase (N1) to hydrolyze the FRET-Tau (19-30) peptide at N-terminal side was obtained in 96 light chains examined. The C1 antigenase cut the peptide bond between Val399-Ser400 (Fig. 1) and C2 between Gly401-Asp492. The two antigenases showed different enzymatic feature. Regarding the N1 antigenase, the peptide bond between Asp22 and Arg30 was cleaved. It is interesting that there were several antigenases capable of cleaving several sites of Tau protein in the protein bank of antibody light chains, which were prepared from human antibody library. This suggests that the catalytic antibody light chains against Tau molecule can naturally be produced.

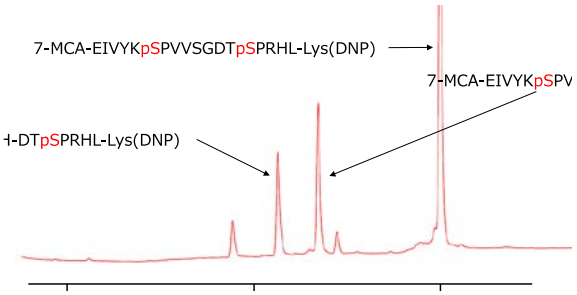

Figure 1. HPLC chromatogram for the products after the reaction of Tau peptide at C-terminal side and C1 antigenase. The peptide bond between Gly401 and Asp402 was digested by C1 antigenase.

4. Conclusions

We found several antigenases capable of cleaving Tau peptides. C1 & C2 antigenases digested the C-terminal (391-408) side peptides. N1 antigenase hydrolyzed the N-terminal side peptide (19-30). These antigenases were present in human antibody genes.

References

[1] E. Hifumi, Y. Mitsuda, K. Ohara, T. Uda, J. Immunol. Methods **269** (2002) 283-298.
[2] E. Hifumi, F. Morihara, K. Hatiuchi, T. Okuda, A. Nishizono, T. Uda, J. Biol. Chem. **283** (2008), 899–907.
[3] E. Hifumi, S. Takao, N. Fujimoto, T. Uda, J. Am. Chem. Soc. **133** (2011), 15015-15024.
[4] E. Hifumi, N. Fujimoto, M. Arakawa, E. Saito, S. Matsumoto, N. Kobayashi, T. Uda, J. Biol. Chem. **288** (2013) 19558-19568.
[5] E. Hifumi, M. Arakawa, S. Matsumoto, T. Yamamoto Y. Katayama, T. Uda, FASEB J. **29** (2015) 2347-2358.
[6] E. Hifumi, S. Matsumoto, H. Nakashima, S. Itonaga, M. Arakawa, Y. Katayama, R. Kato, T. Uda, FASEB J. **30 (**2016) 895-908.

ECAB 5
The 5th EUROPEAN CONGRESS OF APPLIED BIOTECHNOLOGY
Florence 15-19 September 2019

Fouling monitoring in food and bioprocess with MEMS sensor: comparison of local steady and periodic thermal excitation

Yassim Boukazia[1,*], Guillaume Delaplace[2], Mathilde Cadé[3], Frédéric Bellouard[4], Marc Bégué[5], Luc Fillaudeau[1]

1 LISBP (CNRS 5504 - INRA 792 – INSA), Toulouse, FRANCE; 2 PIHM-UMET (INRA 638), Lille, France, 3 IRH Ingénieur Conseil, Ludres, France; 4 Aqualabo, Caudan, France, 5 LMDC, Toulouse, France

**Corresponding author: boukazia@insa-toulouse.fr*

Highlights

- *In-situ* fouling sensor based on MEMS technology and thermal excitation.
- Steady Permanent and Periodic Thermal Regimes are compared.
- Responses are scrutinized versus fouling magnitude and thermal properties.

1. Introduction

In industrial (bio)process, undesirable components impact efficiency [1; 2]. Monitoring and quantification of (bio)fouling through *in-situ* and local sensors constitute scientific and technological challenges. In present work, a prototype fouling sensor based on MicroElectroMechanical System (MEMS) technology and thermal pulse analysis method (INRA patent FR2885694) has been developed and produced by Aqualabo Company (France). Steady permanent Thermal Regime (STR) and Periodic Thermal Regime (PTR) were investigated and compared to theory to extract fouling properties (thickness, thermal conductivity and diffusivity)

2. Methods

Studied sensor is based on hotwire method with powered and regulated Joule effect [1]. Hot wire and fluid temperatures are continuously recorded. According to heat conduction's law, temperature difference ($\Delta\theta$) evolves as linear function with heat flux (φ) and thermal resistance (R_{th}) in STR mode (Eq.1). In PTR mode (Eq.2), sinusoidal excitation is imposed and $\Delta\theta$ evolves as a function of φ and fouling nature [3]. Mean temperature difference, $\overline{\Delta\theta_{PTR}}$, amplitude, A and phase lag, $\Delta\Phi$ enable to determine thermal resistance and diffusivity of deposit. Considering both excitation modes, deposit thermal properties can be extracted and compared with theory.

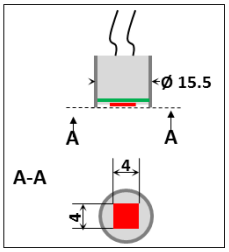

$$\Delta\theta_{STR} = \varphi.\left(\frac{1}{h}+\frac{th_d}{\lambda_d}\right) = \varphi.Rth \qquad \text{Eq.1}$$

$$\Delta\theta_{PTR}(x,t) = \Delta\theta_P(x,t) + \Delta\theta_C(x) = A.cos(\omega t + \Delta\phi) + Rth.\overline{\varphi} \quad \text{Eq.2}$$

$$\text{where } A = Rth.A_{\varphi}.exp\left(-\sqrt{\frac{\omega}{2a}}x\right) \text{ Eq.3, and } \Delta\phi = -\sqrt{\frac{\omega}{2a}}x \text{ Eq.4}$$

$$\text{With } Rth_d = \frac{th_d}{\lambda_d} \text{ Eq.5}$$

Sensor structure includes a plan square MEMS (red line) stuck on a printed circuit board (PCB, *th*=800µm, green wire) and encapsulated in a stainless steel cylinder (grey wires) filled with an electrical insulation resin. MEMS surface is in direct contact with fluid (bulk). Sensor was tested in

a 5L mixing reactor (fluid: water, *Re*=2.2E06 and 20±1°C). Multiple PVC scotch layers (TESA® 53948, *th*=130µm, ρ_d=1300 kg.m^{-3} [4]) were used to generate fouling. Thermal conductivity and heat capacity were measured at λ=0.115 W.m^{-1}.K^{-1} and *Cp*=1025 J.K^{-1}.kg^{-1} (NEOTIM FP2C), thus thermal diffusivity, $a=\lambda/(\rho.Cp)$=8.63E-08 m².s^{-1}. Experiments were performed in clean (reference) and fouled (up to 5 layers) conditions. In STR, five successive heat flux steps were applied (0.2 to 7.5 kW.m^{-2}, 30min/step). In PTR, a mean heat flux, $\overline{\varphi}$=4700W/m² with an amplitude A_φ=4100W/m² was applied. Spectral response was investigated for 8 frequencies (0.001 to 0.2Hz).

3. Results and discussion

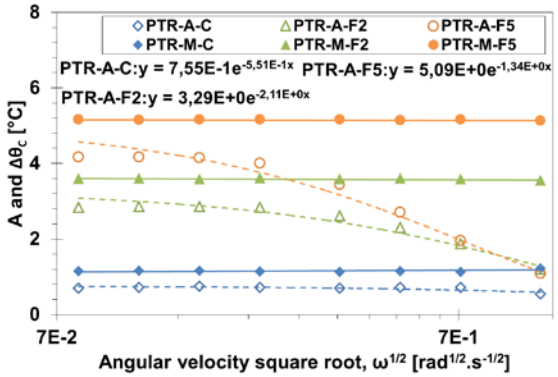

Figure 1 *A* and $\Delta\theta_C$ spectrum in clean (C) and fouled conditions (F2: 2 layers,F5: 5 layers)

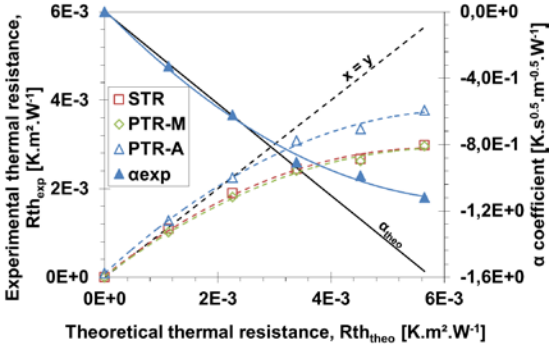

Figure 2 Rth_{exp} (dotted lines) and α coefficient ($-th_d/2.a^{0.5}$) (solids lines) versus Rth_{theo}.

In STR, heat resistances were determined by linearization of thermal responses, $\Delta\theta_{STR}$. In PTR (Figure 1), mean temperature difference (PTR-M) and thermal amplitude (PTR-A) were used to extract heat resistance depending of fouling conditions. Thermal properties were calculated with efficient heat flux identified in STR. Deviation between nominal and efficient flux can be attributed to edge effects due to packaging. Figure 2 compares the evolution of calculated heat resistances (Eq. 1, 2, 3) with theoretical fouling heat resistance (Eq.5). For low thermal resistance, experimental and theoretical values are close. Non-linear evolution of thermal resistances (beyond 3.4 K.m².W^{-1}) indicates the upper sensor limit of detection (LOD). PTR-A response shows better fair values than STR and PTR-M responses. Later inflexion is also noted with α coefficient evolution and confirms the upper LOD observed in STR, PTR-M and PTR-A thermal resistance study. Considering linearity area, thermal diffusivity measured is equal to 9.30E-08 m².s^{-1}.

4. Conclusions

In STR and PTR modes, thermal resistance responses are similar and match with theoretical values. The thermal diffusivity according to literature can be extracted through spectral analysis. Both methods give different upper LOD, at *Rth*=3.6E-03 and 5.5E-03K.m².W^{-1} for STR and PTR respectively. In PTR, LOD is equivalent to a dense biofouling (λ_d=0.6 W.m^{-1}.K^{-1}) of 3.4mm.

References

[1] J. Crattelet, Journal of Food Engineering 119 (2013) 72 – 83.
[2] K. A. Hamilton, Water Research 134 (2018) 261 – 279.
[3] F. Strub, International Journal of Thermal Sciences 44 (2005) 1154 – 1160.
[4] Titow, PVC Technology (1984), p. 857

Aptitude of a microbioreactor as high throughput screening platform for cultivation process development

Mathias Fink[1], Monika Cserjan[1], Johanna Jarmer[2], Gerald Striedner[1]

[1] *Christian Doppler Laboratory for production of next-level biopharmaceuticals in E. coli, University of Natural Resources and Life Sciences Vienna;*

[2] *Boehringer Ingelheim RCV GmbH & Co KG*

**Mathias Fink: mathias.fink@boku.ac.at*

Highlights

- Microbioreactor enables high throughput clone screening
- Microbioreactor enables fermentation process parameter screening
- Fab expression causes lysis after a specific timespan

1. Introduction

We selected Antigen binding fragments (Fabs) as model proteins to evaluate the potential of a microbioreactor system. For this class of molecules a broad range of possible combinations of genetic constructs (host, leader sequence, promoters, mono- or bicistronic constructs, order of heavy and light chain sequences, UTR sequence etc.) is intensively discussed and consequently Fabs are optimally suited to answer this question. Fabs are single monovalent binding arms of IgG molecules, composed of a light and a heavy chain connected by disulphide bonds. As they are distinctive smaller in molecular size than full antibodies, they get producible in *E. coli* which makes it an attractive alternative to mammalian cell culture [1-3].
In the course of this work the main focus was laid on the applicability of a microbioreactor for clone and condition screening and transferability of results to bench top fed batch fermentation processes. The main challenge is to screen a high amount of clones in the shortest possible time, getting significant and reliable data.

2. Methods

We selected four different Fabs (BIBH1, BIWA4, CIM and FabX) with identical constant domains. For translocation to the periplasm a post-translational (ompA) and a co-translational (dsbA) leader sequence were used. *E. coli* BL21(DE3) and *E. coli* HMS174(DE3) were transformed via genome integration resulting in a total number of 16 clones.
For a first screening of the expression systems a microtiter fed batch like cultivation in a BioLector® system was used. After a growth phase of 16 hours we induced the systems with 0.5 mM IPTG and after a 9 hours production phase samples for the determination of intracellular Fab concentration by ELISA were taken.
In a next step we performed fed batch cultivations with all clones in a DASGIP® cultivation system. After a batch phase at 37 °C with a final biomass of approximately 10 gCDM/L a C-limited feed phase

was started with a growth rate of 0.1 h^{-1} at 30 °C. After approximately 0.5 doublings recombinant protein expression was induced for another two doublings. Induction level was kept constant at 2 µmol IPTG/g CDM.

3. Results and discussion

During BioLector ® cultivation Cell growth was not affected by leader/Fab combinations but yield of correctly folded Fab ranged from 0 to 12.5 mg/gCDM. In general K12 clones showed higher specific Fab titers but lower biomass yields than BL21 clones. The microbioreactor fed batch like cultivations with the selected set of host/leader/Fab combinations resulted in a broad range of variations in terms of Fab yields.

During bench top experiments we end up with exactly the same clone ranking in terms of specific Fab yield. However we also observed lower specific yields in the benchtop bioreactor setup which can mainly be assigned to the significantly higher growth rate in the production phase. In addition the production period was longer and approximately 8 hours past induction adverse effects on cell growth were observed. Fab was not only found in the cell fraction but also in the supernatant and DNA quantification in the fermentation supernatant showed that Fab release was caused by lysis which is also highly negatively correlated with the final cell mass that was obtained. The most significant influence on growth was seen for Fabx clones if the Fab was expressed.

4. Conclusions

Summarizing we could show that the microbioreactor system is a well suited HTP tool for clone and condition screening. Results generated in this platform can directly be transferred to benchtop fed batch bioreactor cultivations as long as limitations of the HTP system are adequately included in interpretations.

References

[1] A. de Marco, *Microb Cell Fact.* **2011**, *10*, 44.
[2] O. Spadiut, S. Capone, F. Krainer, A. Glieder, C. Herwig, *Trends in Biotechnology.* **2014**, *32*, 54.
[3] M. Gebauer, A. Skerra, *Curr Opin Chem Biol.* **2009**, *13*, 245.

ECAB 5
The 5th EUROPEAN CONGRESS OF APPLIED BIOTECHNOLOGY
Florence 15-19 September 2019

Efficient synthesis of chiral amino alcohol using 2-step enzyme cascades in repetitive batch mode

Kevin Mack[1,2]*, Vanessa Erdmann[1], Dörte Rother[1,2]

[1] IBG-1: Biotechnology, Forschungszentrum Jülich GmbH; [2] Aachen Biology and Biotechnology, RWTH Aachen University

*Corresponding author: ke.mack@fz-juelich.de

Highlights

- Novel amino alcohol products from cheap bulk chemicals.
- Excellent conversions in combination with excellent *ee* and *de* values.
- Improved specific space-time yield by enzyme immobilization.

1. Introduction

Vicinal amino alcohols can be applied as active pharmaceutical ingredients and key building blocks in industrial applications. Due to their multiple chiral centers, asymmetric synthesis is challenging. Here we present a sequential 2-step enzymatic reaction (**figure 1**) targeting the selective synthesis of three of four stereoisomers of the building block 1-amino-1-phenylpropan-2-ol (APP).

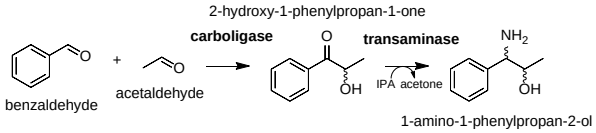

Figure 1: Atom- and step efficient two-step reaction setup for the asymmetric synthesis of all APP isomers.

For the first cascade step, either a benzaldehyde lyase (BAL) or a benzoylformate decarboxylase (BFD) is used.[1,2] This gives access to the intermediate 2-hydroxy-1-phenylpropan-1-one (HPP). The second step to APP is carried out using transaminases. The product APP was produced with excellent sereoselectivity and conversion. For further optimization, the reaction was set up with immobilized enzymes. HaloTag® and EziG™ immobilization methods were chosen and showed similar good results with improved specific space time yields (sSTY).

2. Methods

Conversion of products and intermediates were analyzed by high performance liquid chromatography and a supercritical fluid chromatography. Transaminase activity was determined in a photometer[3]. HaloTag® immobilization was carried out as described [4], the immobilization protocol on EziG™ was developed during this Project.

3. Results and discussion

For the first cascade step of the (*R*)-selective carboligase from *Pseudomonas fluorescens* (*Pf*BAL) or a (*S*)-selective carboligase from *Pseudomonas putida* (*Pp*BFD) is applied.[1,2] This gives access to the intermediate HPP. The second step to APP is carried out with either a transaminase from *Bacillus megaterium* (*Bm*TA) or *Arthrobacter* sp. (*As*TA). The complete cascade was demonstrated in 1 mL scale and scaled up to 30 mL reaction volume. Both scales showed good conversions of 93%-98% and *ee* of 97%-99% as well as *de* of 92%-99% in all three possible cases. To cut on process cost by reusing the catalyst, three different enzyme formulations were compared to each other. The example *Bm*TA showed that HaloTag® immobilization enabled 75% remaining activity while the free enzyme and the EziG™ immobilization had 100% activity. For optimal reaction design and to determine sSTY (free enzyme 0.12 g/(l*h)), the full 2-step reaction to (1*R*,2*S*)-APP was set up with HaloTag®[4] (1.20 g/(l*h)) as well as EziG™[5] (3.77 g/(l*h)) immobilized enzymes in repetitive batch mode and compared.(**figure 2**)

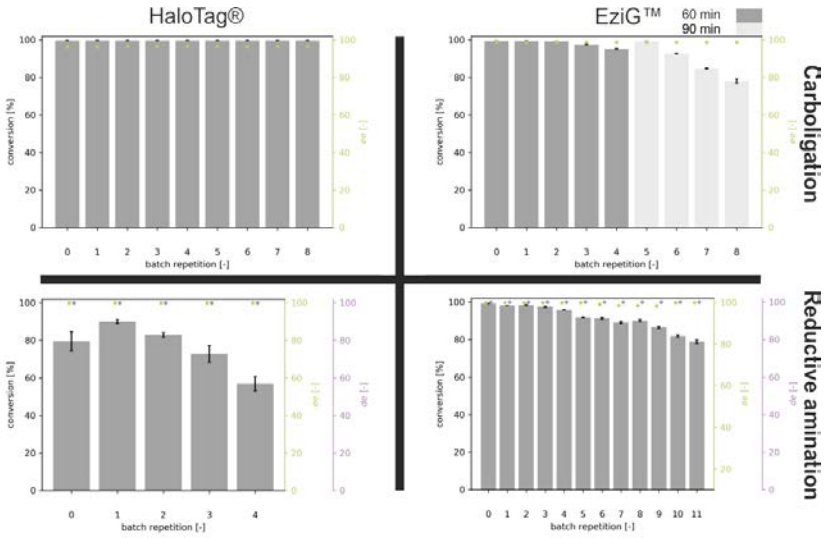

Figure 2: Repetitive batch reaction with HaloTag® and EziG™ towards (1*S*,2*R*)-APP. 60-90 min carboligation with *Pp*BFD var. and 24-72 h Transamination with *Bm*TA

4. Conclusions

The 2-step reaction was displayed with high conversions in combination with excellent *ee* as well as *de* values with purified enzymes. sSTY of the reaction could be improved by immobilizing and reusing the enzyme. In addition to the improved sSTY, the EziG™ carrier was tested for reusability, which could be a crucial step for an ecologic and economic reaction setup and passed the testing with very good results. The concepts presented here will be further expanded to similar products and enzymes to make complex enzymatic and chemo enzymatic cascades feasible with high sSTY in larger scales.

References

[1] Janzen, E. *et al.*; Bioorg. Chem. 34, 345–361 (2006).
[2] Hailes, H. C. *et al.*; FEBS J. 280, 6374–6394 (2013)
[3] Schätzle S. *et al.*; Anal Chem.; 81, 8244-8248 (2009)
[4] Döbber, J. *et al.*; Green Chem. 20, 544-552 (2018)
[5] Cassimhee, K. *et al.*; Chem. Commun. 50, 9134-9137 (2014)

ECAB 5
The 5th EUROPEAN CONGRESS OF APPLIED BIOTECHNOLOGY
Florence 15-19 September 2019

Development of algorisms to introduce a catalytic function into normal antibodies.

Emi HIfumi[1], Yuko Akiyoshi[1], Taizo Uda[2]

1 Research Promotion Institute, Oita University, Oita 870-1192, Japan; 2 Nano-tech Lab, ISIT, Fukuoka 819-0388 Japan

**Corresponding author: e-hifumi@oita-u.ac.jp*

Highlights

- 1. Amino acids of Thr-Arg at 29th and 30th in CDR1 can exhibit a catalytic function.
- 2. Deletion of Pro95 in CDR3 contributes to exhibit a catalytic function.
- 3. Several catalytic antibodies to cleave of Amyloid-beta (Aβ) were found.
- 4. Several algorisms how to make catalytic antibodies from normal antibody are developed.

1. Introduction

Catalytic antibodies capable of hydrolyzing the targeting peptides and proteins are potentially useful agents for therapeutics, through the specific elimination of pathogenic peptides and the essential proteins in microorganisms. Over the course of the last few decades, several groups have reported catalytic antibodies hydrolyzing antigens such as HIV envelop glycoprotein, helicobacter pylori urease, rabies virus, influenza virus and amyloid β peptide (Aβ). However, it is not easy to find out the catalytic antibody from a huge number of normal (non-catalytic) antibodies. It has been desired that the development of an algorism how to easily and effectively introduce a catalytic function into the antibodies. Therefore, for these ten years, the authors have devoted to prepare a protein bank of human antibody light chains having a catalytic triad-like structure. The light chains were cloned from human antibody library and highly purified after the expression in *E. coli* f. The number of the stored light chains has reached to several hundreds. Therefore, in this study, the screening whether or not the stored light chains can possess a catalytic activity for a synthetic substrate, Arg-pNA, and FRET-Amyloid-beta (Aβ), was carried out to obtain important information about the algorism.

2. Methods

The fluorescence-quenched substrates were synthesized by conventional Fmoc SPPS using Rink amide resin. The structure of the substrate was confirmed by ESI-MS after purification by HPLC. After a human antibody light chain gene inserted into pET20b (+), it was transformed into *E. coli* and induced by IPTG. After recovering the soluble fraction of the culture supernatant, it was purified by Ni-NTA chromatography, cation exchange chromatography or size exclusion chromatography. Catalytic activity was measured using synthetic substrates Arg(R)-pNA and FRET-Amyloid-beta (Aβ).

3. Results and discussion

The authors screened the catalytic activity for more than 100 light chains stored in the above protein bank. Out of them, #7wt and #7TR light chains showed interesting results. The former showed the low activity to cleave synthetic substrate Arg-pNA. In contrast, the latter light chain showed the high catalytic activity to cleave the substrate. For FRET-Aβ (26-33) substrate, the former light chain did not decompose at all but the latter did. The difference of both light chains is in the amino acids at 29th and 30th position in CDR1. The former is Gly-Tyr and the latter Thr-Arg. By being replaced with Thr-Arg, the antibody light chain can gain the catalytic function. Interestingly, #7TR light chain could cleave not only FRET-Aβ (26-33) peptide but also Aβ41 of the full size molecule.

In addition, we found other unique human antibody light chains, S35 and S38. The amino acid sequence of both light chains is identical except for Pro95 in CDR3. S35 has the Pro95 residue but S38 deleted the amino acid. The former did not decompose Arg-pNA at all. In contrast, the latter showed high decomposition activity (Fig. 1).

These results are noteworthy, because it enables for us to design a catalytic antibody from the non-catalytic antibody on molecular basis.

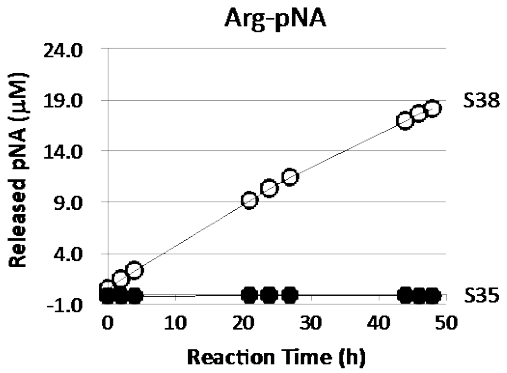

Figure 1. Cleavage reaction of a synthetic substrate, Arg-pNA

4. Conclusions

On molecular basis, several algorisms how to make a catalytic antibody from the general antibody are found.

References

[1] E. Hifumi, H. Taguchi, R. Kato, M. Arakawa, Y. Katayama, T. Uda, Antibody Engineering, Edited by Thomas Boldicke (InTech publishers), 2018, pp231-257

[2] E. Hifumi, M. Arakawa, T. Uda, Frontiers in Clinical Drug Research-Anti Infectives, Bentham Science Publishers, 2017, pp3-35.

[3] E. Hifumi, M. Arakawa, S. Matsumoto, T. Yamamoto Y. Katayama, T. Uda, *FASEB J.*, **29**(2015) 2347-2358.

[4] E. Hifumi, H. Taguchi, E. Toorisaka, T. Uda, FASEB BioAdvances. E-Pub (16 October 2018).

Enhancement of mechanical properties of cross-linked enzyme crystals.

Marta Kubiak[1,], Jennifer Solarczek[2], Karl-Falco Storm, Ingo Kampen[1], Anett Schallmey[2], Carsten Schilde[1]*

1 Braunschweig University of Technology, Institute for Particle Technology, Braunschweig, Germany;
2 Braunschweig University of Technology, Institute for Biochemistry, Braunschweig, Germany
**Corresponding author: marta.kubiak@tu-braunschweig.de*

Highlights

- Investigation of mechanical properties of cross-linked enzyme crystals
- Enhancement of crystal stability due to cross-linking immobilization
- Changing of mechanical properties of protein crystals through protein engineering
- Determination of correlation between crystal structure and cross-linking progress

1. Introduction

Due to their highly selective reactions, safety and sustainability, industrial use of particular biocatalysts, like protein enzyme crystals has been expanded to many manufacturing sectors including the pharmaceutical production. The catalytic activity of those particles correlates with particle size and must maintain as high as possible during enzyme-catalyzed reactions. Hence, the knowledge of mechanical properties is necessary to avoid particles breakage by downstream processing and thereby, changing or loss of the catalytic activity. Mechanical properties of protein enzyme crystals depend on the structure of individual protein molecules, packing density, as well as the conformation within a 3-dimensional structure of protein particles. In recent years, there has been an increasing interest in the improvement of protein performance using immobilization method or due to protein engineering, which aims at the modification of protein sequence, and hence, its structure, in order to create enzymes with improved functional properties.

2. Methods

The purpose of this study was to enhance mechanical stability of protein crystals due to cross-linking immobilization method on the one hand and additional protein engineering for intensified cross-linking on the other hand. For this reason, halohydrin dehalogenase wild type (HheG) was crystallized as model protein, cross-linked using glutaraldehyde and mechanical tested in liquid environment with the aid of an atomic force microscopy (AFM), as described previously[1]. Those measurements allowed investigation of hardness and Young's modulus of prismatic and basal crystal faces of hexagonal crystal's prism depending on the cross-linking duration time. Moreover, a breakage behaviour of cross-linked enzyme crystals, compared to the native crystals is examined using micro-compression tests. In the second step, additional lysine residuals, which can form covalent bonds with the glutaraldehyde-linker, were introduced on the halohydrin dehalogenase wild type (HheG) surface. Then, mutated HheG protein were crystallized, cross-linked and mechanical tested in nanoscale using AFM-based nanoindentation technique again. Due to exchanging of amino acid residuals, increased cross-linking and hence, higher mechanical stability of enzyme crystals was expected.

3. Results and discussion

One of the most significant findings to emerge from this study is that the cross-linking reaction takes place in the first 24-hours. In this time both, hardness as well as Young's modulus increase almost threefold, compared to the reaction time of 4 hours and stay constant at ca. 11.5 MPa (prismatic face) and 500 MPa, respectively. The second major finding was the evaluation of 30%-higher mechanical stability for the basal face. The evidence of this study suggest an anisotropic behavior within the three-dimensional crystal lattice, which was subsequent analyzed using a mathematical model. The applied model enables quantification of theoretical bonds for cross-linking within a supercell and qualitative visualization of potential cross-linking bridges within the crystal structure. The results show that the measured anisotropy might be caused by different direction-dependent amount of bonds on the one hand, and distinct channel orientation within the crystals on the other hand. Interestingly, because of the protein engineering both, hardness and Young's modulus slightly decreased, compared to the mechanical properties of wild type crystals (see Figure 1). However, the statistical consideration of the results showed a significant reduction of the distribution width, indicating an improved crystal packing density with less flaws.

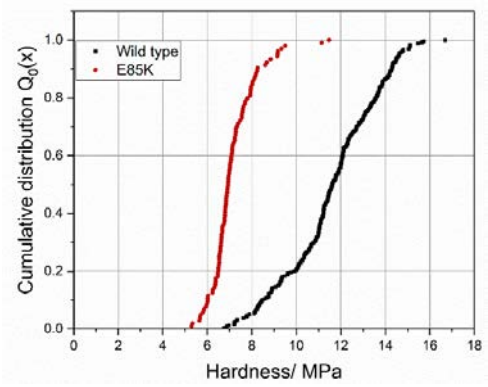

Figure 1. Hardness distribution of HheG wild type and mutant protein crystals. Note that the mean value of mutant HheG crystals decreases by ca. 40%, compared to the wild type crystals.

Additionally, the results of the micro-compression tests show considerable higher mechanical stability against normal forces for cross-linked HheG wild type crystals, compared to the native crystals.

4. Conclusions

The present study was designed to enhance mechanical stability of enzyme crystals due to cross-linking immobilization and protein engineering. Using AFM-nanoindentation technique, we were able to investigate small changes in the mechanical properties, like hardness and Young's modulus on distinct crystal faces dependent on the cross-linking duration time. Due to explanation of measured phenomena using a mathematical model, which bases on the crystal structure, this project provides an important opportunity to advance the understanding of the structure - properties correlation of protein particles and creates fundamentals for future studies on desired formulation of reinforced catalytic active crystalline biocatalysts.

References

[1] Kubiak, M.; Solarczek, J.; Kampen, I.; Schallmey, A.; Kwade, A.; Schilde, C. Micromechanics of Anisotropic Cross-Linked Enzyme Crystals. *Cryst. Growth Des.* **2018**, *18*, 5885–5895.

ECAB 5
The 5th EUROPEAN CONGRESS OF APPLIED BIOTECHNOLOGY
Florence 15-19 September 2019

Activity of extracellular enzymes from *Pleurotus ostreatus* fungi.

Mateja Primožič[1], Katja Vasić[1], Željko Knez[1,2], Maja Leitgeb[1,2,*]

1 University of Maribor, Faculty of Chemistry and Chemical Engineering, Maribor, 2000, Slovenia;
2 University of Maribor, Faculty of Medicine, Maribor, 2000, Slovenia

**Corresponding author: maja.leitgeb@um.si*

Highlights

- Cultivation of *P. ostreatus* on the waste plant biomass for enzymes production.
- The highest enzyme activities were detected after 8th day of fungi cultivation.
- Stabilization of extracellular enzymes from *P. ostreatus* was done using CLEA method.

1. Introduction

Forest and agricultural waste can be a major development and ecological opportunity and can serve as a substrate for medicinal mushrooms cultivation such as *Pleurotus ostreatus*, which can be easily cultivated by everyone. It can successfully grow on a wide range of waste lignocellulosic material [1,2]. *P. ostreatus* is a woody fungus that acts as a saprophyte. It is involved in a process of degradation of hemicellulose, cellulose and lignin. The enzymes laccase and cellulase, which are part of the lignocellulolytic enzyme system, contribute to this degradation. Various substrates affect the activity of the thus obtained enzymes from *P. ostreatus*. The utilization of the waste biomass from forestry and agriculture for the cultivation of *P. ostreatus* mushrooms in order to obtain different enzymes can be integrated to waste management and the development of the bio-economy. Produced enzymes from *P. ostreatus* could be used as nutritional supplements or they can be immobilized as an enzyme cocktail, e.g. laccase and cellulase in the form of cross-linked enzyme aggregates (CLEA) (without a carrier) to improve the enzyme stability. Immobilization of enzymes allows the recycling of these biocatalysts, which is otherwise almost impossible and can improve their stability. In addition, the cost of the biocatalyst could be reduced due to easily separation of biocatalyst from the reaction mixture. Immobilization in the form of CLEA allows the use of so called crude enzymes and therefore, it is not necessary to use a pre-purified enzyme, which reduces processing costs and is interesting for industrial use [3]. The cultivation of *P. ostreatus* fungi on a solid medium (wheat bran) was performed. The activity of laccase and cellulase from fungi extracts after different cultivation time was studied. The optimal time for *P. ostreatus* cultivation to obtain the highest specific activity of laccase and cellulase was determined. The immobilization of extracellular enzymes produced by *P. ostreatus* in the form of CLEA was done and their activity was also studied.

2. Methods

Cultivation of *P. ostreatus*

P. ostreatus was cultivated on wheat bran at 27 °C and at different period of time.

Enzyme extraction from *P. ostreatus*

After defined growing time of *P. ostreatus,* extracellular enzyme extraction with 0.05 M sodium citrate buffer was performed.

Preparation of CLEA

Preparation of CLEA laccase was performed in two steps: precipitation with different solvents (acetone, ethanol etc.) and cross-linking using glutaraldehyde (GA) at different concentrations.

Determination of laccase and cellulase activity

Laccase activity was determined at 420 nm using 2,2-azino-bis(3-etilbenz-tiazolin-6-sulfonat) as a substrate and cellulase activity was defined at 340 nm with a UV-Vis spectrophotometer using the method with Sigmacell solution as a substrate.

3. Results and discussion

After 8th and 14th day of fungi cultivation, enzyme extraction was carried out to determine the activity of the selected enzymes. The optimal incubation time was 8 days, since the activities at that time were the highest. Specific activity of cellulase was 6.3166 U/$mg_{protein}$ and of laccase was 6.7280 U/$mg_{protein}$ (Figure 1). The obtained enzymes extract was used for CLEA preparation. The optimal precipitation reagent was found to be acetone, since highest specific activity of laccase and cellulase was obtained after precipitation in that solvent. With the increase in GA concentration from 1% (v/v) to 8% (v/v) an increase in immobilization efficiency and in specific activity of cellulase and laccase were determined.

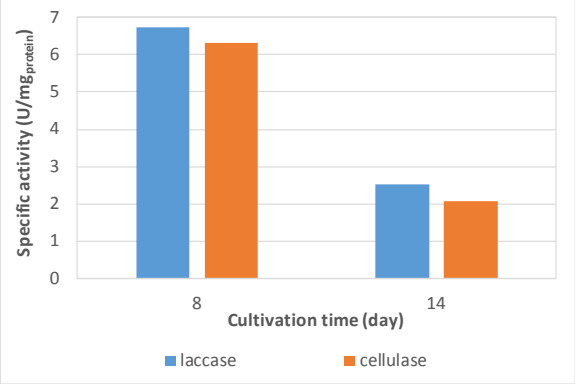

Figure 1. Influence of cultivation time of *P. ostreatus* on laccase and cellulase specific activity.

4. Conclusions

Cultivation of *P. ostreatus* was successfully performed on solid medium using wheat bran as a substrate. The activities of extracellular laccase and cellulase were the highest after 8th day of *P. ostreatus* cultivation. Extracted extracellular enzymes from *P. ostreatus* were immobilized in the form of CLEA for possible application in industrial cascade bioprocesses.

References

[1] S. Ozcirak Ergun, R. Ozturk Urek, Ann. Agrar. Sci., 15 (2017) 273-277.
[2] Z. Tsegaye, G. Tefera, J. Appl. Microb. Res., 1:1 (2017) 01-06.
[3] R.A. Sheldon, Appl. Microbiol. Biotechnol., 92 (2011) 467-477.

ECCE12
The 12th EUROPEAN CONGRESS OF CHEMICAL ENGINEERING
Florence 15-19 September 2019

Kinetic and calorimetric study of an *E. coli* large-oligomer protein

Julia Gallego-Jara[1*], Gema Lozano Terol[1], Manuel Cánovas Díaz[1] and Teresa de Diego Puente[1]

1 Department of Biochemistry and Molecular Biology and Immunology (B), Faculty of Chemistry, University of Murcia, Campus of Espinardo, Regional Campus of International Excellence "Campus Mare Nostrum", Murcia, Spain

**Corresponding author: Julia.gallego@um.es*

Highlights

- Protein aggregation has been recently described as a native and regulated process.
- The *E. coli* sirtuin CobB was purified as a dimer and as a large-oligomer.
- The oligomer showed a higher thermostability than the dimer.
- The dimer and large-oligomer showed similar enzymatic and substrate-binding parameters.

1. Introduction

Escherichia coli (*E. coli*) is a Gram-negative bacterium widely employed in biology and biotechnology as a model microorganism to produce high-value compounds such as proteins or drugs with a great commercial interest (1,2). Recombinant protein overexpression in *E. coli* still is the most used strategy for protein production. However, many difficulties can difficult protein expression and purification, such as low expression, protein toxicity, difficult purification steps or inclusion bodies formation (3). To solve these drawbacks, new purification strategies are being developed (4). Protein inclusion bodies are insoluble protein aggregates which are formed when protein aggregates are large enough. However, proteins can form soluble large-aggregates in response to diverse conditions, such as heat shock, other environmental stress conditions or a fast and high expression of recombinant proteins (5). Moreover, protein aggregation has been recently described as a native and regulated process in bacteria, yeast and mammalian cells (6).

2. Methods

In this study, the overexpression and purification of a soluble large-oligomer *E. coli* CobB protein is presented. Native electrophoresis, HPLC size-exclusion chromatography, enzymatic characterization, Differential Scanning Calorimetry (DSC) and Isothermal Titration Calorimetry (ITC) were carried out to evaluate and compare the two protein conformations.

3. Results and discussion

The results showed that the *E. coli* sirtuin CobB, highly conserved since prokaryotes to humans, was purified in two different conformations: a dimer and a large-oligomer. The two protein conformations were time-stable and an equilibrium between them was not observed. Moreover, the large-oligomer conformation showed an enzymatic activity and a binding constant for Acs

(Acetyl-CoA synthetase) protein similar to the dimer. Finally, the oligomer showed a higher thermostability, with a melting temperature almost 15 degrees higher.

4. Conclusions

The results of this work emphasize the importance of protein large-oligomer conformations for their use in biotechnology as a strategy to carry out processes with extreme conditions (7).

References

1. Becker J, Wittmann C. Systems metabolic engineering of *Escherichia coli* for the heterologous production of high value molecules — a veteran at new shores. Curr Opin Biotechnol. 2016;42:178–88.
2. Mohamed N. Baeshen. Production of biopharmaceuticals in *E. coli*: current scenario and future perspectives. J microbiolgy Biotechnol. 2014;25(7):1–24.
3. Rosano GL, Ceccarelli EA. Recombinant protein expression in Escherichia coli: Advances and challenges. Front Microbiol. 2014;5(APR):1–17.
4. Vargas-Cortez T, Morones-Ramirez JR, Balderas-Renteria I, Zarate X. Production of recombinant proteins in Escherichia coli tagged with the fusion protein CusF3H+. Protein Expr Purif [Internet]. Elsevier Ltd; 2017;132:44–9. Available from: http://dx.doi.org/10.1016/j.pep.2017.01.006
5. Ramón A, Señorale-Pose M, Marín M. Inclusion bodies: Not that bad... Front Microbiol. 2014;5(FEB):2010–5.
6. Tyedmers J, Mogk A, Bukau B. Cellular strategies for controlling protein aggregation. Nat Rev Mol Cell Biol [Internet]. Nature Publishing Group; 2010;11(11):777–88. Available from: http://dx.doi.org/10.1038/nrm2993
7. Parisini E, Redaelli A, Gautieri A, Rigoldi F, Donini S. Review: Engineering of thermostable enzymes for industrial applications. APL Bioeng. 2018;2(1):011501.

ECAB 5
The 5th EUROPEAN CONGRESS OF APPLIED BIOTECHNOLOGY
Florence 15-19 September 2019

Development of an optimal process for the production of a light-coloured and highly soluble sunflower protein isolate

Sara Albe Slabi[1, 2], Christelle Mathé[1], Mélody Basselin[1], Arnaud Aymes[1], Olivier Galet[2] and Romain Kapel[1*]

1 CNRS, LRGP, UMR-7274, University of Lorraine, Nancy, France;
2 Avril Group, 75008 Paris, France
**Corresponding author: romain.kapel@univ-lorraine.fr*

Highlights

- The optimal extraction conditions were found at pH 7.0 and 0.5 mol·L^{-1} NaCl
- Saline ultrafiltration present an original process for sunflower purification that results in highly-purified protein product (around 100 %/dm)
- The established alternative process for sunflower protein production yields in light-coloured and highly soluble isolate (> 75 % at pH 7)

1. Introduction

The growing world population sets a new challenge for food industry because of increased demand for proteins. Sunflower (*Helianthus annuus* L.) is the fourth most important oilseed with production exceeding 47 million tons in 2016 [1]. The solid residue co-produced after oil extraction process (meal) is a valuable source of proteins (30-50 %/dm). Sunflower proteins (helianthinins and SFAs) are considered very promising for human nutrition thanks to many potential nutrition and functional benefits. However, during solid/liquid extraction phenolic complexation to proteins take place resulting in an unsuitable green colour of protein products [2]. Furthermore, a conventional purification of sunflower proteins is carried out by acidic precipitation. This leads to a poor solubility of protein products and an important loss of sunflower albumins [3]. Therefore, the main objective of this work was to propose an optimal process for sunflower protein extraction and an alternative protein purification by ultrafiltration that yields in light-coloured and highly soluble isolate.

2. Methods

In the first part of the work a 3^2 design of experiments was used to investigated the influence of NaCl concertation (0-0.5 mol.L^{-1}) in the range of pH (6-9) on extraction yield, protein composition (helianthinin, SFAs) and phenolic contamination. Then, to select the most appropriated conditions for protein extraction a multi-objective optimization strategy with incorporated constraints in algorithms was applied. Finally, the best scenario for protein purification by ultrafiltration was

established. For this purpose, retention coefficient of target compounds was determined and modelling a protein purity with overall balance of matter was carried out. The solubility of protein isolate obtained using optimized process was characterized.

3. Results and discussion

The response surface revealed a positive, synergic impact of pH and ionic strength on protein extraction yield and helianthinin extractability. Irreversible phenol-protein interactions revealed dramatically increased with extraction pH. Interestingly, a protective effect of NaCl was also shown. Thus, the objective of the multi-objectives optimization was to maximize extraction yield of protein (≥ 45 %) and the content of helianthinins (≥ 65 %) while minimizing phenolic contamination of helianthinins (≤ 8 %) and SFA (≤ 25 %). Based on these results the solid/liquid extraction at pH 7.0 and 0.5 mol·L^{-1} NaCl was found to be the best trade-off between all competing criteria (Fig. 1a). The proteins extracted under optimal conditions were subsequently purified by ultrafiltration using an original protocol with saline diafiltration step (0.5 mol·L^{-1} NaCl). The developed process resulted in excellent separation of sunflower proteins and free phenolic compounds (≥ 95 % after 6 DV) and satisfying purification yield (> 70 %). Consequently, a light-coloured proteins with a high-purity (99.9 %/dm) was obtained (Fig. 1b). Additionally, the solubility of protein isolate (≥ 75 % at pH 7, Fig. 1c) was considerably improved comparing to those purified by acidic precipitation (< 10 % at pH 7) [3].

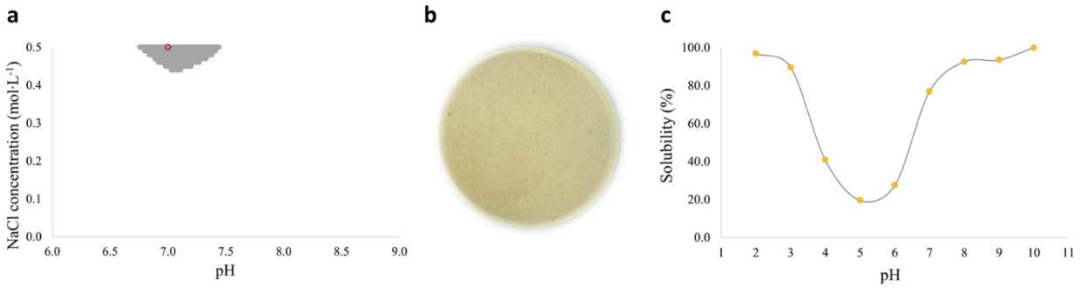

Figure 1. Non-dominated responses (grey points) of multi-objective optimization of protein extraction and the selected optimal condition (red-framed) (**a**). The coulour (**b**) and the solubility of purified proteins as a function of pH (**c**).

4. Conclusions

The obtained response surfaces allowed selecting the optimal extraction conditions found at pH 7.0 and 0.5 mol·L^{-1} NaCl. The further protein purification by ultrafiltration yielded in colour-light and highly soluble protein isolate. Thus, the proposed alternative process for preparation of sunflower proteins could be an answer for sustainable valorization of sunflower meal in food industry.

References

[1] FAOSTAT-Agriculture (2012). FAO Statistics Division. www.fao.org/docrep/016/ap106e/ap106e.pdf
[2] S. R. Wildermuth *et al.*, Compr Rev Food Sci F. 15 (2016) 829-843;
[3] C. Pickardt *et al.*, Food Hydrocolloid. 23 (2009).

ECAB 5
The 5th EUROPEAN CONGRESS OF APPLIED BIOTECHNOLOGY
Florence 15-19 September 2019

Mechanical stress during scale up to membrane aerated stirred bioreactors for rebeccamycin production in filamentous *Lentzea aerocolonigenes*

Kathrin Pommerehne[1,3], Nadine Wurzler[1,3], Marcel Schrader[2,3], Arno Kwade[2,3], Rainer Krull*[1,3]

1 Institute of Biochemical Engineering; 2 Institute for Particle Technology; 3 Center of Pharmaceutical Engineering, TU Braunschweig, Germany

**Corresponding author: r.krull@tu-braunschweig.de*

Highlights

- Filamentous *L. aerocolonigenes* produces the antitumor antibiotic rebeccamycin.
- Particle-induced mechanical stress on *L. aerocolonigenes* increases rebeccamycin titers.
- Simulations can be used to characterize the optimal mechanical stress.
- Membrane aerated bioreactor cultivations result in comparable rebeccamycin titers.

1. Introduction

Filamentous microorganisms represent the majority of natural producers of antibiotics and other active pharmaceutical ingredients (APIs). *Lentzea aerocolonigenes* is a filamentous actinomycete producing the antitumor antibiotic rebeccamycin. The microorganism exhibits a complex morphology ranging from freely dispersed mycelia to dense pellets [1]. The morphology is linked to the product formation and can be controlled by e.g., inoculum concentration and viability, pH, medium composition, hydromechanical stress, addition of inorganic salts or particles [2]. Rebeccamycin formation in *L. aerocolonigenes* was increased by the adjustment of mechanical stress induced by glass particles in shake flask scale [3]. Regarding a scale up from shake flasks to a laboratory scale stirred bioreactor the induced mechanical stress is an important factor.

2. Methods

Cultivations of *L. aerocolonigenes* were conducted in 250 mL shake flasks with 4 baffles and 50 mL filling volume. Glass particles were added for adjustment of the induced mechanical stress. The flasks were incubated on an orbital shaker at 120 min^{-1} (50 mm amplitude) at 28 °C for 10 days.

A scale up to a stirred bioreactor (Applikon, The Netherlands; 6 blade Rushton turbine) with 1.2 L filling volume was performed. Aeration in this bioreactor was conducted via an oxygen permeable silicone membrane (0.2 mm thickness; Reichelt Chemietechnik, Germany). Stirrer speed was set to 400 min^{-1} and pure oxygen was used for aeration (aeration rate 0.2 L min^{-1}).

3. Results and discussion

The influence of mechanical stress on cultivations of *L. aerocolonigenes* in shake flasks was investigated using glass beads in different sizes and concentrations. The highest rebeccamycin concentration of 70 mg L^{-1} after 10 days of cultivation was achieved with 100 g L^{-1} glass beads of

969 µm diameter compared to an unsupplemented control (rebeccamycin concentration after 10 days of cultivation with 5 mg L^{-1}) (**Fig. 1**).

A stirred bioreactor usually generates higher mechanical stress than a shake flask. Therefore this parameter is important to consider during scale up, especially since product formation is influenced. As conventional bubble aeration and agitation induce mechanical stress, a bubble free membrane aeration was chosen to reduce the influencing variables. A first membrane aerated cultivation without glass beads resulted in a rebeccamycin titer of 12 mg L^{-1} after 6 days of cultivation which is comparable to a regular unsupplemented shake flask cultivation (**Fig. 2**).

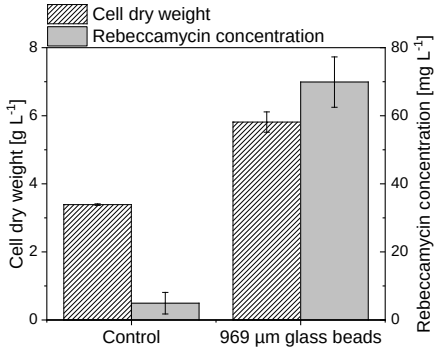

Figure 1. Cell dry weight concentration and rebeccamycin concentration of shake flasks cultivations without and with 100 g L^{-1} glass beads after 10 days of cultivation.

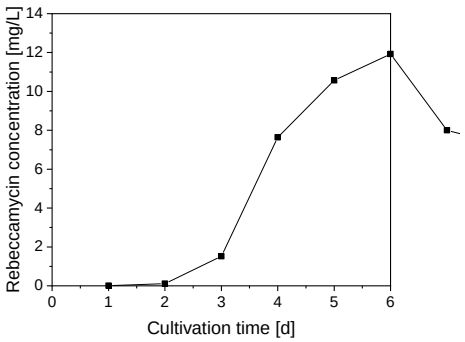

Figure 2. Rebeccamycin concentration of a silicone membrane aerated bioreactor cultivation without glass particles at an agitation rate of 400 min^{-1}.

Coupled CFD-DEM simulations have already been conducted to characterize the induced mechanical stress in shake flasks with glass particles. A similar simulation of the membrane aerated stirred bioreactor will allow a comparison of the induced mechanical stress and thereby an adjustment to the optimal stress found in shake flasks.

4. Conclusions

Rebeccamycin production in *L. aerocolonigenes* is increased by setting an appropriate mechanical stress by glass bead addition in shake flask scale. This knowledge can be used for scale up. A first membrane aerated stirred bioreactor cultivation led to a comparable rebeccamycin titer as in unsupplemented shake flask cultivations. Further adaption of mechanical stress by stirrer speed and geometry as well as the addition of glass beads could lead to even higher rebeccamycin titers.

References

[1] K. Pommerehne, J. Walisko, A., Ebersbach, R. Krull, Appl. Microbiol. Biotechnol. (2019), DOI 10.1007/s00253-019-09741-y.

[2] R. Walisko, J. Mönch-Tegeder, J. Blotenberg, T. Wucherpfennig, R. Krull, Adv. Biochem. Eng. Biotechnol. 149 (2015) 1-27.

[3] J. Walisko, F. Vernen, K. Pommerehne, G. Richter, J. Terfehr, D. Kaden, L. Dähne, D. Holtmann, R. Krull, Process Biochem. 53 (2017) 1-9.

Acknowledgement

The authors gratefully acknowledge financial support from the German Research Foundation (DFG) in the Priority Programme 1934 *DiSPBiotech – Dispersity, structural and phase changes of proteins and biological agglomerates in biotechnological processes*.

ECAB 5
The 5th EUROPEAN CONGRESS OF APPLIED BIOTECHNOLOGY
Florence 15-19 September 2019

Physiological Response of *S. clavuligerus* to shear forces in 2-D Rocking Motion and Stirred Tank Bioreactors

David Gómez-Ríos[1*], Howard Ramírez-Malule[2], Peter Neubauer[3], Stefan Junne[3], Silvia Ochoa [4], Rigoberto Ríos-Estepa[1]

[1] Grupo de Bioprocesos, Departamento de Ingeniería Química, Universidad de Antioquia (UdeA), Calle 70 No. 52-21, Medellín, Colombia; [2] Escuela de Ingeniería Química, Universidad del Valle, A.A. 25360 Cali, Colombia; [3] Chair of Bioprocess Engineering, Department of Biotechnology, Technische Universität Berlin, Ackerstr. 76, ACK 24, 13355 Berlin, Germany; [4] Grupo de investigación en Simulación, Diseño, Control y Optimización de Procesos (SIDCOP), Departamento de Ingeniería Química, Universidad de Antioquia (UdeA), Calle 70 No. 52-21, Medellín, Colombia.

**Corresponding author: dandres.gomez@udea.edu.co*

Highlights

- Low shear forces favor the preservation of macromorphology in *S. clavuligerus.*
- High shear forces promote mycelia thinning and clavulanic acid accumulation.
- Oxygen uptake and clavulanic acid production are affected by mycelia aggregation

1. Introduction

Streptomyces clavuligerus (*S. clavuligerus*) is a Gram-positive filamentous bacterium notable for producing clavulanic acid (CA), which is a potent inhibitor of β-lactamases enzymes that confer resistance to bacteria against β-lactam antibiotics. CA is traditionally produced in stirred tank reactors (STR); nevertheless, the impact of bioreactor geometry on cell performance and CA production has not been completely understood. The present study aims at performing a comparative analysis of the metabolic response of *S. clavuligerus* to low shear stress in 2-D rocking-motion single-use bioreactor and at high mechanical shear stress in STR.

2. Methods

Cultivations of *S. clavuligerus* DSM 41826 in chemically defined media [1] were conducted by duplicate cultivations in a 15 L STR (Techfors S, Infors AG, Bottmingen, Switzerland) and in a 20 L 2-D rocking-motion single-use bioreactor CELL-tainer® (CT) (CELL-tainer Biotech BV, Winterswijk, The Netherlands). Cultivations were operated in batch mode (5 L) during the first 37 h, followed by fed-batch operation (35 mL/h) during 77 h. Cell dry weight (CDW), CA and metabolites quantifications were performed as described by Ramirez-Malule [1]. Mycelia samples were photographed in a Nikon Eclipse Ti2 inverted microscope (Nikon Instruments Inc., Amsterdam, The Netherlands) at 40x and further processed in ImageJ software (U.S. National Institutes of Health, Maryland, USA).

3. Results and discussion

In Figure 1, microscopy images (Figures 1a-1c) and biomass concentration developments of *S. clavuligerus* (Figure 1e) for the STR and CT cultivations are presented. In CT cultivations, the calculated specific growth rate (μ_{max}) and maximum biomass concentration were 0.068 h^{-1} and 10 g/L, respectively. A similar μ_{max} (0.069 h^{-1}), but higher maximum biomass concentration (14.5 g/L) were obtained in STR cultivations. The increase of agitation rate from 300 to 500 rpm in STR caused a decrease in mycelia thickness of 22.5% during the cultivation time (Figure 1e) as consequence of

high shear forces. In contrast, the lower shear forces in CT reactor did not cause hyphal fragmentation leading to more aggregated and thicker mycelia. The mycelial thickness in CT increased 30.6% (Figure 1e) during the same time of cultivation and comparable values of dissolved oxygen in the CT reactor. The higher biomass production observed in STR (Figure 1e) was attributed to the generation of a considerable number of mycelial fragments capable to growth and reproduce [2,3].

CA production is promoted by phosphate limiting conditions [1,4]; although the latter condition was reached in STR and CT reactors, CA release was lower in CT cultivations. The maximum specific CA concentrations were 33.44 mg/g CDW and 14.3 mg/g CDW in the STR and CT cultivations, respectively. In this regard, a reduction in oxygen uptake was observed in CT cultivations due to aggregation and clumping of mycelia. Oxygen uptake has a key role in the secondary metabolism of *S.clavuligerus*, since several oxidation steps reactions require molecular oxygen to occur. Thus, CA accumulation was further enhanced by the high shear stress and hyphal fragmentation that prevent the adhesion of filaments and limitations to oxygen diffusion. These results suggest that environmental conditions in CT reactor promoted a different carbon flux distribution as a consequence of less relative stress conditions, leading to a lower activity of secondary metabolism and hence, lower CA accumulation [4].

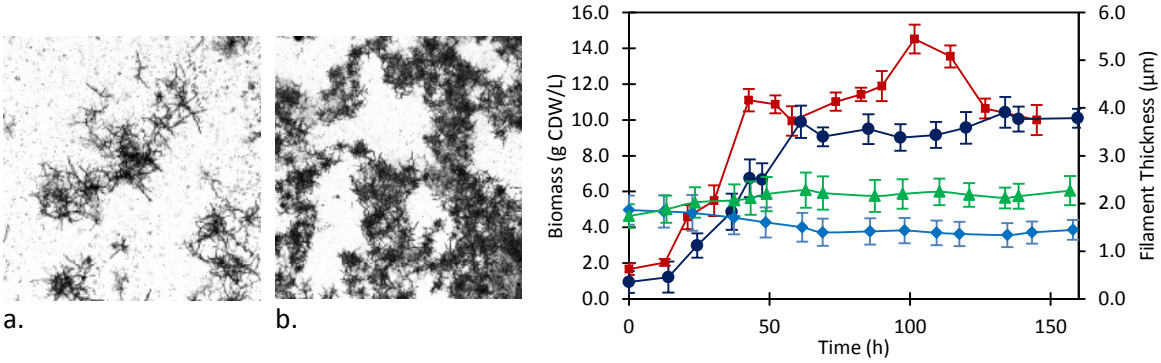

Figure 1. Morphological response of *S. clavuligerus* in STR and CT: a. STR (143 h); b. CT (139 h); e. Time course of biomass in STR (squares) and CT (circles) and mycelia thickness in STR (diamonds) and CT (triangles).

4. Conclusions

Low shear forces did not lead to significant hyphal fragmentation or lysis, on the contrary, it promoted mycelial thickening and branching in *S. clavuligerus*. Hence, the 2-D rocking-wave pattern of agitation favored the preservation of macromorphology in this filamentous organism.

Oxygen plays a key role in enhancing the CA productivity, thus the hyphal fragmentation during the exponential phase and moderate cellular stress seem to be critical for attaining high CA titers.

Acknowledgement: The authors kindly acknowledge the support of Departamento Administrativo de Ciencia, Tecnología e Innovación– COLCENCIAS grant number 111577657246 CT 432-2017.

References

[1] H. Ramirez-malule, S. Junne, M.N. Cruz-bournazou, P. Neubauer, Streptomyces clavuligerus shows a strong association between TCA cycle intermediate accumulation and clavulanic acid biosynthesis, (2018).

[2] E.A. Barka, P. Vatsa, L. Sanchez, N. Gaveau-vaillant, C. Jacquard, H. Klenk, C. Clément, Y. Ouhdouch, P. Van Wezel, Taxonomy , Physiology , and Natural Products of Actinobacteria, Microbiol. Mol. Biol. Rev. 80 (2016) 1–44. doi:10.1128/MMBR.00019-15.Address.

[3] E. Olmos, N. Mehmood, L. Haj Husein, J.L. Goergen, M. Fick, S. Delaunay, Effects of bioreactor hydrodynamics on the physiology of Streptomyces, Bioprocess Biosyst. Eng. 36 (2013) 259–272. doi:10.1007/s00449-012-0794-1.

ECAB 5
The 5th EUROPEAN CONGRESS OF APPLIED BIOTECHNOLOGY
Florence 15-19 September 2019

Evaluating bioreactor performance of a surface-aerated novel horizontal tubular bioreactor with spiral impeller for mammalian cells

Rajesh Sharma[1], Sylva L. Schwager[2], Edward D. Sturrock[2], Susan T. L. Harrison[1], Siew L. Tai[1]

[1]*Centre for Bioprocess Engineering Research (CeBER), Department of Chemical Engineering, University of Cape Town, South Africa*

2Department of Integrative Biomedical Sciences and Institute of Infectious Disease and Molecular Medicine, University of Cape Town, South Africa

**Corresponding author: siew.tai@uct.ac.za*

Highlights

- Spiral impeller enhances mixing and homogeneity due to bidirectional fluid flow
- Spiral impeller improve mass transfer efficiency by increasing surface renewal rate
- Achieved mass-transfer $k_L a$ of 16 hr^{-1} with cell density exceeding 4x10^6 cells/mL
- Achieved high ACE protein expression of 465 mU/mL

1. Introduction

Mammalian cells are often the preferred choice for expressing recombinant proteins because of their superior cellular machinery for post-translational modifications. However, they are very shear-sensitive and prone to hydrodynamic shear as they do not have a cell wall. Increasing demand for the production of large quantities of recombinant protein has driven the development of new bioreactor designs and processes, but small changes in the microenvironment during fermentation can produce heterogeneity in protein structure and varying biological activity [1]. This leads to inter- and intra- batch variation and inconsistent yields and product quality. Liquid shear forces from stirring, bubble formation and direct sparging have drastic effects on the overall cell growth and productivity of the fermentation batch. There is a growing need for a bioreactor design suitable for a wide variety of cell-lines to produce biologics at the lowest cost and with minimum risk. Therefore, a horizontal tubular bioreactor (HTB) with a spiral impeller was designed and fabricated for the propagation of mammalian cells at CeBER. The engineering characterization of the HTB was presented [2] and in continuation of this work, the HTB was further evaluated by growing CHO-K1 cells expressing angiotensin-converting enzyme (ACE) to assess its suitability for the growth of mammalian cells.

2. Methods

The HTB batch was run at 3.0 L capacity which is around 70 % of the total capacity of the bioreactor. Initially, 2.0 L complete serum-free medium (SFM4CHO +4 mM stable glutamine + 0.1 % Poloxamer 188) was charged into the bioreactor for sterility check for 48 h following which the bioreactor was seeded with CHO cells expressing somatic ACE with initial cell density of 0.3 x 10^6 cells/mL. Periodic sampling was done after every 24 h for the determination of cell density, viability percentage and for the spent media analysis. Termination of the batch was carried out when the percentage

viability dropped below 85 %. The bioreactor was operated at a speed of 150 rpm, at the set temperature of 37 °C, pH maintained in the range of 7.0-7.2 during growth phase and reduced to 6.85 - 6.95 after 5th day of protein expression and the air flow rate was kept at 0.2 LPM to maintain the 40 - 50 % of saturation of air. ACE activity was determined by a fluorimetric assay [3]. Spent media was analyzed for glucose consumption and lactate production using HPLC, ammonium ion by a calorimetric method [4] and osmolality with a SLAMED 800 CL Osmometer.

3. Results and discussion

The bioreactor batches were taken at a speed of 150 rpm to avoid hydrodynamic shear to the cells. The cell density achieved was 4.2 x 10^6 cell/mL (Figure 1 a). It is also evident from the cell density and the morphology of the cells that the bioreactor conditions were conducive for cell growth and exerted low shear conditions which result in prolonged longevity of the culture. The ACE maximum ACE activity was 465 mU/mL. The mobility of the proteins on SDS PAGE, using a polyclonal antibody to identify ACE, corresponded to that of purified somatic ACE (Figure 1 b). The glucose concentration decreased over time and the lactate production increased as expected but lactate did not exceed 3.0 g/L. The ammonia concentration and osmolality were 200-250 µg/mL and 300-380 mOsmol/kg respectively, presumably due to the base addition and lactate production during the batch run.

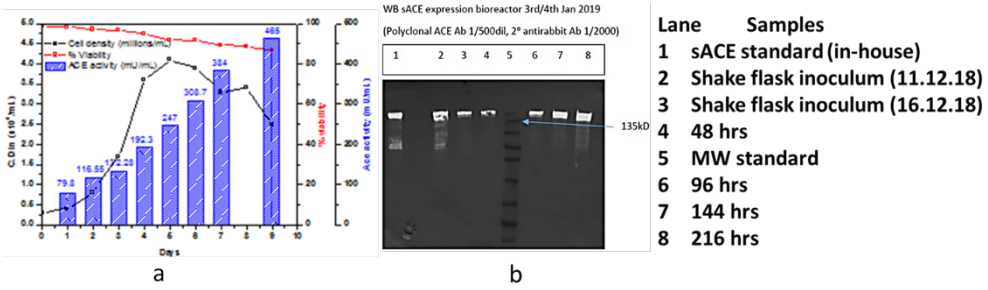

Figure 1. sACE protein expression (a) w.r.t. CHO growth profile in HTB (b) Cell medium was resolved by SDS PAGE and analysed by Western blotting with a sACE polyclonal antibody.

4. Conclusions

Hydrodynamic conditions of the bioreactor are dictated by the aeration-agitation regimen. The horizontal tubular bioreactor with spiral impeller has an edge over traditional STR bioreactor where rising bubbles and high impeller speeds damage the cells while maintaining a high cell density. HTB with spiral impeller is a combination of surface aeration and impeller mixing with enhanced surface renewal rates which resulted in cell density of more than 4 x 10^6 cells/mL with extended longevity. It could be predicted that in fed-batch mode, target cell densities of more than 10 x 10^6 cells/mL is achievable based the obtained ($k_L a$) value of 16 hr^{-1} for this reactor.

References

[1] D. Fernandes, Reducing risk in biopharmaceutical production by controlling glycosylation, Eur. Biopharm. Rev. (2004) 92–97.

[2] R. Sharma, S.T.L. Harrison, S.L. Tai, Evaluating process parameters of surface-aerated horizontal tubular bioreactors for the growth of animal cells, 10th World Congress of Chemical Engineering at Barcelona, Spain (2017).

[3] S.L. Schwager, A.K. Carmona, E.D. Sturrock, A high-throughput fluorimetric assay for angiotensin I-converting enzyme, Nat. Protoc. 1 (2006) 1961–1964.

[4] R. Cramp, M. Gilmour, D.A. Cowan, Novel thermophilic bacteria producing nitrile-degrading enzymes, Microbiology. 143 (1997) 2313–2320.

ECCE12
The 12th EUROPEAN CONGRESS OF CHEMICAL ENGINEERING
Florence 15-19 September 2019

Microstructuring of Bioreactor surfaces with fine Particle Impacts for influencing Biofilm Growth

Paul Breuninger[1*], Daniel Kleine[2], Roland Ulber[2], Sergiy Antonyuk[1]

[1] *Institute of Particle Process Engineering; Technische Universität Kaiserslautern, Kaiserslautern, Germany*

[2] *Institute of Bioprocess Engineering, Technische Universität Kaiserslautern, Kaiserslautern, Germany*

**Corresponding author: Paul.Breuninger@mv.uni-kl.de*

Highlights

- Surface modification of bioreactor substrates by fine particle impacts
- Distinction between elevations and indentations of the surface by adaption of the process parameters
- An Influence on the structure and growth of biofilms was observed
- Results can be used to design certain bioreactor surfaces

1. Introduction

The present study describes a process for microstructuring industrially relevant surfaces of titanium (ASTM grade 2) by fine particle impacts to create a specific micromorphology in the same size of biocells. This influences the cultivation of biocells, for example in bioreactors [1], which affects the composition and productivity of the biofilms formed.

2. Methods

Titanium surfaces have been microstructured by a cold spray setup. The particles dispersed in a nitrogen stream are accelerated to supersonic velocities (up to 900 m/s) and sprayed on a substrate. When the particles exceed a critical impact force, they bond firmly to the surface and create an elevation. If the impact force is less than this limit, the particles rebound and leave a crater. Within this study both phenomena were used to create microstructured surfaces. Titania particles (size between 0.8 and 1.5 µm) were cold sprayed on the titanium surface and created a strong bonding on the surface. This produced a surface with elevations of about 1 µm in size. In addition, titanium surfaces (grade 2) were created with crater structures only. The produces surfaces were cultivated with Lactococcus lactis biofilms in a custom built flow cell. Optical coherence tomography (OCT) was used to observe biofilm formation and morphology.

4. Results and discussion

SEM and Scanning probe microscopy showed a statistical distributed surface morphology, with a roughness of 40% higher than reference substrates (Sq = 200 nm). Renewed roughness measurements after ultrasonic examinations showed a strong adhesion of the particles to the surface, without any change of the roughness. Microscope images of the statistically distributed indentations show depths up to 2 microns and width up to 15 microns. Morphologically different regions of one biofilm were identified by using OCT analysis. These regions consist of either

compact homogeneous biofilm or complex mushroom structures and can be related to the microstructure of the substrate.

4. Conclusions

A statistical distributed microstructure can be applied on the surface of technical substrates by the presented method. By selecting the process parameters it can be distinguished between elevations and indentations of the surface. An influence on the biofilm structure and the growth could be observed. These findings can be used to produce special surfaces for bioreactors.

References

[1] C. Schlegel, J. Chodorski, M. Huster, N. Davoudi, K. Huttenlochner, M. Bohley, I. Reichenbach, S. Buhl, P. Breuninger, C. Müller-Renno, C. Ziegler, J. Aurich, S. Antonyuk, R. Ulber: Analyzing the Influence of Microstructured Surfaces on the Lactic Acid Production of Lactobacillus delbrueckii lactis in a flow-through cell system, Engineering in Life Sciences 8 (2017), 865-873W. Black, E.B. White, The Elements of Science, third ed., MacCluski, New York, 1987.

ECAB 5
The 5th EUROPEAN CONGRESS OF APPLIED BIOTECHNOLOGY
Florence 15-19 September 2019

Obtaining fermented beverages from vegetables and seeds using a commercial lactic culture

Martha Cuenca[1], Milenka Cerda[2], Débora Pizarro[2]

1 Assistant Professor, Program of Chemical Engineering, Unviersidad de Cartagena, Av del Consulado No 48-152, Cartagena, Colombia; 2 External consultants, Escuela de Ingeniería Química, Pontificia Universidad Católica de Valparaíso, Av Brasil 2162, Valparaíso, Chile

**Corresponding author: mcuencaq@unicartagena.edu.co*

Highlights

- Probiotics sources for common people are expensive in Latin America
- Vegetables consumption in Latin America is low
- Seeds and grains can be useful to prepare fermented beverages
- Blends of vegetable purees and seeds extracts can be a cheaper source of probiotics

1. Introduction

Nowadays there is an increasing interest of people to replace consumption of dairy products, not only for health reasons, like lactose intolerance, but also for ethical reasons, as vegans. Vegetable beverages are now a reality, and their studies are focused on beverages from soybean. In case of other legumes, cereals and vegetables, there is not enough information about their products or how the process to obtain them is performed. That is why the use of this engineering is proposed, to obtain fermented beverages through lactic fermentation of vegetable beverages of quinoa and canary seed, considering the addition of carrot and pumpkin puree.

2. Methods

Quinoa (*Chenopodium quinoa*), canary seed (*Phalaris canariensis*), carrots (*Daucus carota*) and pumpkins (*Cucurbita maxima)* were purchased at the local market in Valparaiso, Chile. A Commercial culture Choozit® MY 800 LYO (Dupont), which contains three types of microorganisms: *Streptococcus thermophilus, Lactobacillus delbueckii subsp. lactis* and *Lactobacillus delbueckii subsp. bulgaricus*, was used as fermenting agent. All fermentation tests were done in triplicate, and the culture was added directly to the mixtures according to the manufacturer's dosage instructions.

Preparation of quinoa and canary seed beverages and vegetables purees

It was performed according to methodologies reported by Cuenca and Benavides to obtain soymilk [1,2]

Lactic fermentation of beverages, purees and blends

Lactic culture was added for all cases according to the manufacturer's dosage instructions (0.016 g/kg). 1 kg of beverage, puree or blend was fermented at 42ºC in triplicate using three home yogurt makers (Blanik, model BYM019, 220V, 50-60 Hz, 20W, China) for 5 hours.

Analytical analysis

pH and total acidity measurements, expressed as percentage of lactic acid (% w/v) (methods 981.12 and method 950.15, AOAC, 1998) [3]

Total reducing sugars

Initial and final total reducing sugars were measured by the 3,5 Dinitrosalicyclic Acid Method (DNS) [4]

3. Results and discussion

Table 1 presents different blends evaluated during lactic fermentation, and Figure 1 presents variation of blends F1, F2, F3 and F4 during 5 fermentation hours for pH (a) and Total Acidity (b).

Table 1. Different blends used for evaluating lactic fermentation (% w/w)

Beverages blend	Quinoa beverage	Canary seed beverage	Purees blend	Carrot puree	Pumpkin puree	Formulation	Quinoa beverage	Canary seed beverage	Carrot puree	Pumpkin puree
B1	100%	0%	P1	100%	0%	F1	16%	64%	8%	12%
B2	80%	20%	P2	80%	20%	F2	12%	48%	16%	24%
B3	60%	40%	P3	60%	40%	F3	8%	32%	24%	36%
B4	40%	60%	P4	40%	60%	F4	4%	16%	32%	48%
B5	20%	80%	P5	20%	80%					
B6	0%	100%	P6	0%	100%					

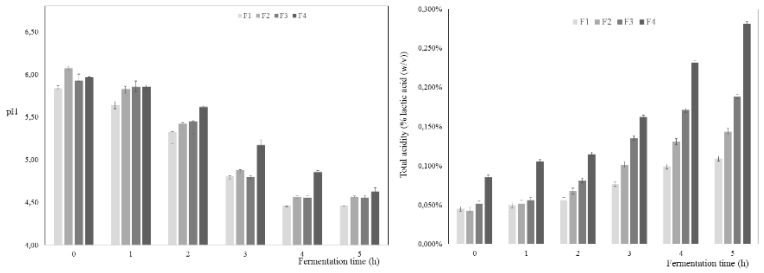

Figure 1. pH (a) and Total Acidity (b) Variation of different blends with quinoa, canary seed, carrot and pumpkin

Through these studies it was determined that despite not being a process as productive as the lactic fermentation of cow's milk, it is possible to carry out the fermentation of the different substrates studied. It was selected F4, which contains an 80% of purees and 20% of vegetable bevereages, presenting values consistently better than other blends, achieving a productivity of 0.563 $g*l^{-1}*h^{-1}$. Final product 1.1 x 10^5 $CFU*ml^{-1}$ of lactic acid bacteria, which is one order of magnitude less than what is required to be named a probiotic, if it has characteristics that would make it an adequate food for consumption.

4. Conclusions

It is possible to obtain vegetable fermented blends that can be a potential source of lactic acid bacteria to people that cannot access to cheap probiotic sources. It remains to study specific parameters of the process, such as its viscosity, and the effect that temperature has on the process. A greater dosage of lactic acid bacteria culture can improve microorganism's count in the final product to be consider a good source of probiotics.

References

[1] M. Cuenca, "Evaluación de la fermentación láctica de una mezcla de bebida de soya y leche de vaca utilizando células inmovilizadas," Universidad Nacional de Colombia sede Bogotá, 2006.

[2] M. A. Benavides, "Evaluación de la fermentación láctica de bebida de soya empleando células inmovilizadas de un cultivo probiótico," Universidad Nacional de Colombia, 2009.

[3] AOAC, *Oficial Metodos of analysis AOAC Internacional*, 16th Editi. Gaithersburg, USA, 1998.

[4] G. L. Miller, "Use of Dinitrosalicylic Acid Reagent for Determination of Reducing Sugar," *Anal. Chem.*, vol. 31, no. 3, pp. 426–428, 1959.

ECAB 5
The 5th EUROPEAN CONGRESS OF APPLIED BIOTECHNOLOGY
Florence 15-19 September 2019

New technological strategies to preserve the pasty-making confectionery food through biological material packaging.

Teresa De Pilli

Department of Science of Agriculture, Food and Environment – University of Foggia

Via Napoli, 25 Foggia (Italy)

**Corresponding author: teresa.depilli@unifg.it*

Highlights

- Edible film slows down the water migration of stored product, decelerating the staling.
- Prevention of growth of mold without use preservative substances like alcohol.
- Low fat content without compromise the sensorial properties of products during shelf life.

1. Introduction

Today the consumption of high amounts of fat is one of the main nutritional problems and it is considered one of the causes of serious health problems such as coronary heart disease and obesity. The foods that mainly contribute to intake of fats, above all in the case of the children, are the confectionary products. Nevertheless, the fats cannot be easily replaced in these kinds of products since they deeply influence their sensorial characteristics. In fact, fat provides to flavour, mouth feel, appearance, palatability, texture and lubricity. Moreover, soft pastries are generally filled with creams with high content of fat rich in saturated fatty acids. A complex set of conditions determines bakery product shelf life, which complicates efforts to extend the "life" of these foods. In fact, when stored at room temperatures, soft bakery product crumb undergoes a progressive deterioration of quality commonly known as staling that involves: hardening and toughening of the crumb; appearance of crumbliness and finally, moisture loss by evaporation. Moreover, during storage of bakery products can occur the development of molds, above all for the products preserved at room temperature and ordinary atmosphere. Ethanol is considered to reduce staling by acting as a plasticizer in the protein network of dough and it is able to inhibit the growth of microorganism. Alcohol give a typical smell when the packet is opened that it is not appreciated by consumers because of aromatic changes of food being in the packaging. In addition, this preservative, although perfectly safe, is more and more criticised above all for food devoted to the children because could be toxic for theirs also at low concentration. A possible solution to these technological drawbacks could be the use an edible biological material packaging applied directly on bakery products that would be able to preserve hygienic and quality characteristics of these kinds of food during shelf life.

The aim of this research was to study an innovative edible film that allows realizing pastry-making confectionery food with low fatty fraction without addition of additive and preservative ingredients, which is able, also, to keep its hygienic and sensorial properties during storage at room temperature and ordinary atmosphere.

2. Methods

Sponge cakes filled with sweet cream, coated with edible coating [1] or not and produced without the addition of preservative and additive substances, were stored at room temperature for 85 days and packaged in plastic bags under ordinary atmosphere. Ten samples were taken every 17 days to evaluate the chemical and mechanical characteristics changes of samples during storage. The

moisture and activity water (a_w) were carried out on crust, crumb and cream while the determination of hardness and the microbiological analyses were evaluated on the whole samples and the apparent viscosity on the filling cream. All analyses were replicated at least three times. The variation of analytical indexes during storage was calculated subtracting the values at the end of storage from the that measured at the start. A positive variation meant an increase of values of analytical index during storage while a negative value meant the decrease one.

3. Results and discussion

The moisture content and a_w values of crust increased during storage while those of crumb and cream decrease for both type of samples even if more moderately for samples with coating. (Table 1). Moreover, samples with edible film did not present mold growth during storage while samples without coating showed a mold concentration like $1.4*10^4$ FCU/g at the end of storage. The hardness of bakery products and apparent viscosity of cream increased during storage, even if samples coated with edible film showed an increase of hardness and viscosity of cream lower than products without coating (Table 2).

		Moisture (%)		aw	
		No coating	*Coating*	*No coating*	*Coating*
Crust	Start storage	8,21	10,47	0,657	0,677
	End storage	19,16	13,05	0,795	0,744
	Variation	***10,95***	***2,58***	***0,138***	***0,067***
Crumb	Start storage	19,05	17,46	0,836	0,76
	End storage	16,46	16,46	0,805	0,748
	Variation	***-2,59***	***-1***	***-0,031***	***-0,012***
Cream	Start storage	50,73	36,8	0,964	0,81
	End storage	18,18	15,9	0,805	0,746
	Variation	***-32,55***	***-20,9***	***-0,159***	***-0,064***

Table 1. Moisture and a_w variation of samples coated or no with edible film during storage.

		Hardness (N)			Viscosity (mPa)	
		No coating	*Coating*		*No coating*	*Coating*
Bakery	Start storage	23,73	35,83	***Cream***	263	388
products	End storage	43,82	48,66		404	416
	Variation	***20,09***	***12,83***		***141***	***28***

Table 2. Hardness and viscosity variation of samples coated or no with edible film during storage.

4. Conclusions

The presence of edible film is able to slow down the water migration inside product and the water evaporation outside food that cause its staling. Moreover, the edible film studied showed a good barrier to water vapor transmission and oxygen transmission. These gas barrier properties prevent the grown of mold without use preservative substances like alcohol, sulphurous anhydride, salts of sorbic acids, etc. The main innovation and advantageous characteristics of this edible film is relating to principal ingredients used to produce it, which are constituted by natural ingredients.

References

[1] T. De Pilli, A. Derossi, M. Prosperi, C. Severini, A. Stasi, Patent number: 0001413327, (2015).

Conservation of the antioxidant activity and nutritional properties of tucumã pulp using vaccum packaging.

Patrícia Albuquerque*, Sthéfanny Azevedo, Sergio Duvoisin Jr.

Amazonas State University, Laboratory of Chemistry Applied to Technology, 1200 Darcy Vargas Ave., Manaus, Amazonas, Brazil, 69050-020.

**Corresponding author: palbuquerque@uea.edu.br*

Highlights

- Tucumã pulp has a high content of β-carotene.
- Vacuum packaging and freezing keeps the tucumã nutritional properties for 30 days.
- Antioxidant activity remained preserved for 2 months in frozen samples of tucumã pulp.

1. Introduction

The Amazon region has different fruits often consumed by local population which present high economic potential [1]. The tucumã, also known as tucumã of the Amazonas, tucumã-açu e jabarana [2] is an example of tropical fruit, derived from the palm tree *Astrocaryum aculeatum* (Arecaceae), which presents significant biotechnological potential. It is characterized as slightly acidic, low sugar, high in β-carotene and high energy fruit [3]. Once the pulp is obtained, it must be consumed within one day at room temperature, or within a week under refrigeration [4]. Since the pulp storage has been performed inappropriately in most of the commercial establishments in Manaus, our objective with this work was to study the conservation of the antioxidant activity and the nutritional properties of tucumã pulp *in natura*, using vacuum packaging.

2. Methods

The tucumã was collected in a rural property located in Rio Preto da Eva, Amazonas (2°37'31.8"S 59°44'52.6"W). The tucumã pulp was obtained according to Flor et al. [5] and stored into polyethylene bags (200 g of pulp per bag) under vacuum. The packs were stored under freezing (18°C) and cooling temperature (5°C). During 150 days, the content of moisture, ash, pH, acidity, ethereal extract, energy, and microbiological growth (coliforms and Salmonella), were verified according to the methodologies describes by the Adolfo Lutz Institute [6]. Antioxidant activity was measured using DPPH• radical scavenging method [7].

3. Results and discussion

It was found that the values of moisture, ash and pH are retained by the use of vacuum packaging, in freezing or cooling temperatures for 5 months; acidity is conserved in vacuum packages only in the freezer for 10 days; the ethereal extract values are maintained for 3 months under freezing temperature and for 1 month when cooled; and the energy value contained in the pulp is kept for 2 months under freezing and for 10 days under cooling. The presence of coliforms and Salmonella

were not detected during 5 months of storage for both frozen and cooled samples; and the antioxidant activity remained preserved for 2 months in frozen samples (Figure 1A), but was not maintained in refrigerated samples (Figure 1B).

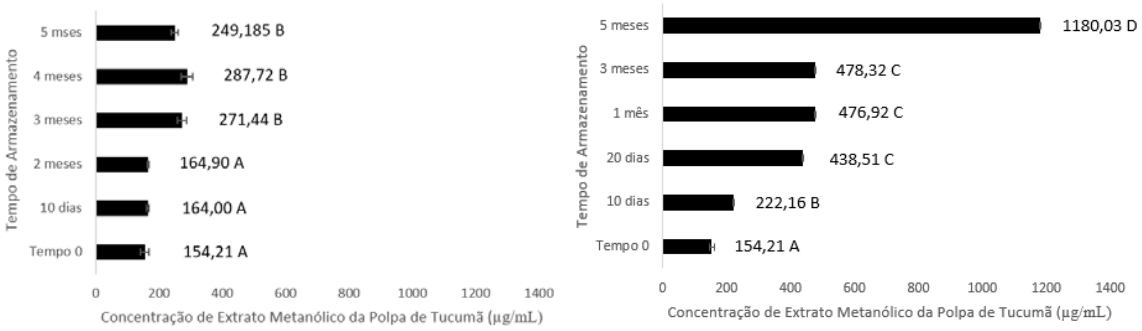

Figure 1. Efficient concentration at 50% (EC_{50}) of tucumã pulp stored in vacuum packaging under cooling (A) and freezing (B) temperature.

The maintenance of antioxidant activity of fruit pulps using freezing temperature was also verified by Freire et al. [8] The authors stored acerola pulp (*Malpighia emarginata*) at -18°C and the antioxidant activity was kept for 3 months. Manach et al. [9] affirmed that the concentration of phenolic compounds that are responsible for the antioxidant activity may be affected by factors such as processing, storage, as well as by environmental factors. It has been observed in the tucumã pulp the presence of different flavonoids, such as rutin and quercetin, as well as tanins, like galic acid, caffeic acid and chlorogenic acid [10].

4. Conclusions

Through this study we found that the use of vacuum packaging, associated with freezing, provides the conservation of the main nutritional properties of tucumã pulp in natura, for 30 days of storage, a simple procedure that can be used by local food suppliers.

References

[1] A. C. Braga, A. E. da Silva, A. C. A. Pelais, C. M. G. Bichara, D. R. Pompeu, Alimentos e Nutrição, 21 (2010) 31-36.
[2] J. R. da Costa, J. van Leeuwen, J. A. Costa, in: P. Shanley, G. Medina (Eds.), Frutíferas e plantas úteis na vida amazônica. CIFOR, Belém, 2005, pp. 209-222.
[3] L. K. O. Yuyama, R. N. Maeda, L. Pantoja, J. P. L. Aguiar, H. A. Marinho, Ciência e Tecnologia de Alimentos, 28 (2008) 408-412.
[4] G. Schroth, M. S. S. Mota, R. Lopes, A. F. de Freitas, Forest Ecology Management, 202 (2004) 161-179.
[5] N. S. Flor, J. S. Andrade, S. A. N. Ferreira, British J Applied Sci Technol, v. 5, n. 4, p. 371-379, 2015.
[6] Instituto Adolfo Lutz, Normas Analíticas do Instituto Adolfo Lutz - Métodos Físico-químicos para análise de alimentos. Instituto Adolfo Lutz, São Paulo, 2008.
[7] J. M. Duarte-Almeida, R. J. dos Santos, M. I. Genovese, F. M. Lajolo, Ciência e Tecnologia de Alimentos, 26 (2006) 446-452.
[8] J. M. Freire, C. M. P. de Abreu, D. A. Rocha, A. D. Corrêa, N. R. Marques, Ciência Rural, 43 (2013).
[9] C. Manach, A. Scalbert, C. Morand, C. Rémésy, L. Jimenez, The American Journal of Clinical Nutrition, 79 (2004) 727-747.
[10] M. R. Sagrillo, J. F. M. Garcia, O. C. de Souza Filho, M. M. M. F. Duarte, E. E. Ribeiro, . C. Cadoná, I. B. M. da Cruz, Food Chemistry 173 (2015) 741-748.

ECAB 5
The 5th EUROPEAN CONGRESS OF APPLIED BIOTECHNOLOGY
Florence 15-19 September 2019

Using Large Data for the Prediction of Quality Attributes of an Antibody Capture Process in Real-Time

Theresa Scharl-Hirsch[1,2,*], Michael Melcher[1,2], Edit Felföldi[1,3], Dominik Sauer[1,3], Nicole Walch[1,3], Alois Jungbauer[1,3], Astrid Dürauer[1,3] and Friedrich Leisch[1,2]

1 Austrian Centre of Industrial Biotechnology (ACIB), Muthgasse 11, 1190 Vienna, Austria; 2 Institute of Applied Statistics and Computing, University of Natural Resources and Life Sciences Vienna, Peter-Jordan-Strasse 82, 1190 Vienna, Austria; 3 Department of Biotechnology, University of Natural Resources and Life Sciences Vienna, Muthgasse 18, 1190 Vienna, Austria

**Corresponding author: theresa.scharl@acib.at*

Highlights

- Online monitoring in downstream processing.
- Real-time prediction of critical quality attributes.
- Machine learning application on large data from biotechnology.
- Pooling algorithm for material collection of an antibody capture process.

1. Introduction

It is state of the art in biopharmaceutical industry to monitor chromatographic processes by standard detectors and probes such as UV/VIS, pH and conductivity. Quality attributes such as product quantity and purity (e.g. dsDNA content, host cell protein concentration and high molecular mass impurities) can only be obtained by collecting and analysing fractions after each unit operation. In our project we have developed an online monitoring system for downstream processes, which is based on an array of online sensors. ATR-FTIR spectrometer, a fluorescence detector as well as a multi angle light scattering detector and a refractive index detector were implemented as additional sensors.

2. Methods

In order to use all available online signals in real time a powerful database environment is needed. Here we use an evon database (https://en.evon-automation.com/xamcontrol/) to store all the data that is measured by the sensors. A quantitative protein A run takes several hours. For the implemented sensors more than 18.000 online signals are measured in a time grid of one second yielding a huge amount of data. For further data usage efficient storage, time alignment and data pre-processing are crucial. In a first step several antibody capture runs were conducted where online signals of all available sensors were measured during the whole run. In addition, fractions were collected where quality attributes were analysed. In the next step all available online and offline data were processed using the statistical computing environment R [1].

3. Results and discussion

Several machine learning methods (e.g., partial least squares, random forests, generalised additive models) were used to find a relation between the measured offline variables such as product concentration or dsDNA content and the available online variables. Structured additive regression models in combination with boosting as a variable selection tool were found to be a useful modelling technique [2]. These prediction models allow online pooling decisions replacing time and labor-intensive laboratory measurements (Figure 1).

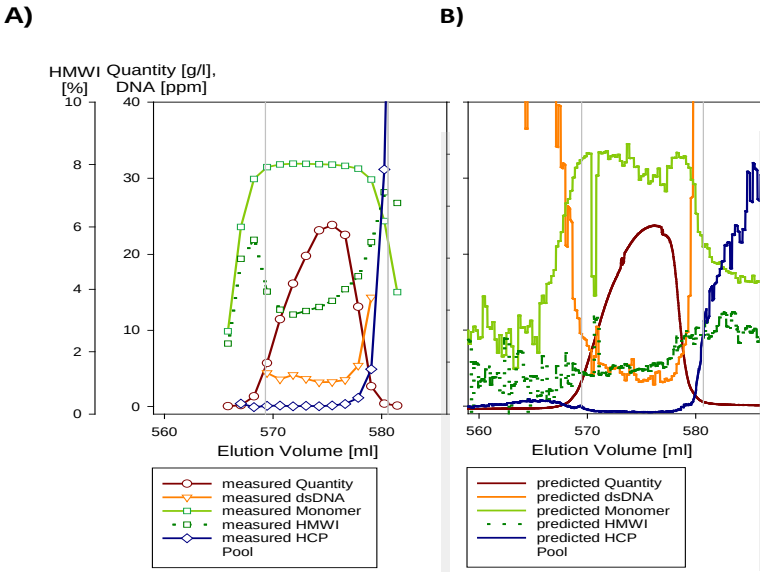

Figure 1. Measured (A) and predicted (B) quality attributes of an antibody capture run.

4. Conclusions

Prediction models solely based on online signals were set up providing real-time predictions. These models can be directly applied in real-time inside the database during a new chromatographic run to predict the quality attributes of a product solely based on the online variables measured. From the quality perspective it is also in accordance with FDA's recommendation. It is requested to include on-line sensors to improve the constant quality of the product.

References

[1] R Core Team, R: A language and environment for statistical computing. R Foundation for Statistical Computing, Vienna, Austria. URL https://www.R-project.org/, 2018.

[2] Melcher, M., Scharl, T., Luchner, M., Striedner, G., Leisch, F., Boosted structured additive regression for Escherichia coli fed-batch fermentation modeling. Biotechnology and Bioengineering, 2017, 114, 321-334.

ECAB 5
The 5th EUROPEAN CONGRESS OF APPLIED BIOTECHNOLOGY
Florence 15-19 September 2019

Adaptive, Model-Based Control of *Saccharomyces cerevisiae* Fed-Batch Cultivations

Christian Appl[1], Christian Fittkau[1], André Moser[1], Volker C. Hass[1,*]

[1]*Furtwangen University, Faculty of Medical and Life Sciences, Villingen-Schwenningen, D-78054, Germany*

**Corresponding author: hass@hs-furtwangen.de*

Highlights

- Adaptive, nonlinear model predictive controller
- Optimization of aerobic *Saccharomyces cerevisiae* cultivations
- Implementation of a NMPC with a commercial process control system

1. Introduction

The Open Loop Feedback Optimal (OLFO) controller belongs to the class of adaptive nonlinear model predictive controllers [1]. The controller consists of a model parameter identification part and an optimization part. Model parameters are estimated frequently on the basis of available online and offline data. The updated model parameters are passed on to the optimization part, where process trajectories like substrate feeding profiles are calculated. Based on the process of yeast cultivation, the controller was tested in virtual and real experiments.

2. Methods

For the implementation of the OLFO controller two communicating WinErs-projects (IB Schoop GmbH) were created and executed simultaneously. Project 1 is a conventional process control project for controlling the bioreactors Biostat B (2 L) and Biostat C (20 L) (B. Braun). Project 2 contains the OLFO controller. The required parameter estimators and process optimizers were realized in WinErs via available packages. In our work the *Saccharomyces cerevisiae* cultivation model was integrated in form of a C-eStIM – WinErs – Interface – *.dll [2]. The basis for model development were several batch and fed-batch cultivations of *S. cerevisiae*. The OLFO project received the required state variables from the current process. These data were used to adapt the parameters and initial states of the deposited yeast culture model. Based on this, the glucose feed rates were calculated to achieve a maximum biomass density in the further course of the process. The calculated feed rates were transferred to the process control system (project 1).

3. Results and discussion

Figure 1 shows the result of a virtual yeast cultivation using the OLFO controller. The controller can adapt the parameterization of the used process model to fit the data of the cultivation process and map the trend.

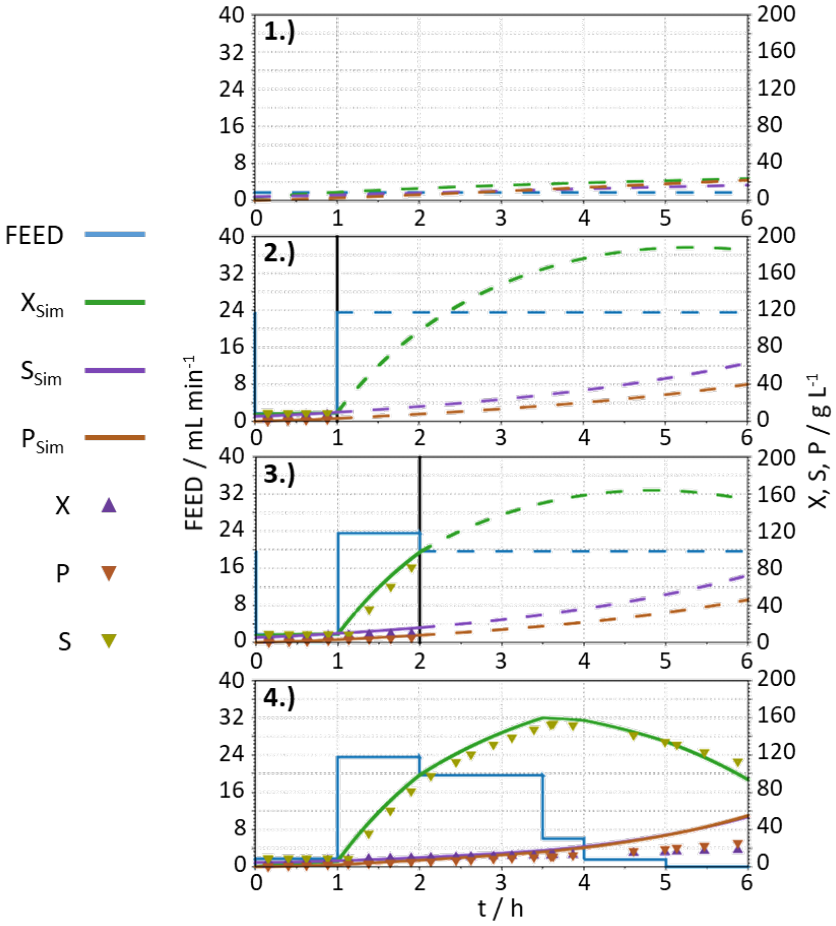

Figure 1. Demonstration of the OLFO controller working principle using a virtual bioreactor [3]. Dashed lines show the predicted trend for feed and concentration of the model utilized by the OLFO Controller.

Furthermore, fed-batch cultivation experiments were carried out in stirred tank reactors (STR). The transfer of the OLFO controller to real experiments was successful. The potential of the OLFO strategy is clearly visible. In subsequent works the OLFO controller will be used to optimize the cultivation process.

4. Conclusions

Our yeast cultivation experiments show, that even fairly simple mathematical models may successfully be used within the OLFO controller and lead to an increase in biomass production. The tool is now available for the systematic optimization of aerobic microbial cultivations.

References

[1] R. Luttmann, et. al., In: Agricultural Feedstock and Waste Treatment and Engineering. Advances in Biochemical Engineering / Biotechnology, Vol. 32, p. 95-205.

[2] F. Kuhnen, Modellierungssystem C-eStIM. Kurzeinführung. Hochschule Bremen, internal communication (2008).

[3] V.C. Hass, R. Pörtner, Praxis der Bioprozesstechnik mit virtuellem Praktikum, 2. Auflage (2011)

ECAB 5
The 5th EUROPEAN CONGRESS OF APPLIED BIOTECHNOLOGY
Florence 15-19 September 2019

Development of an Automated Perfusion Bioreactor 'Ambr® 250 Perfusion'.

Barney Zoro, Asma Ahmad, Alison Rees-Manley,Tom Jeffery

Sartorius Stedim Biotech

**Corresponding author:* barney.zoro@sartorius.com

In recent years a strong trend towards intensified and continuous biopharmaceutical processing has gathered momentum, enabled by key cell culture technologies such as ATF and TFF. However, small-scale application has been limited to traditional benchtop bioreactor formats that are manually intensive, relatively low throughput and costly to operate. Automated high throughput, single-use, mini bioreactor systems with new capabilities to support perfusion culture, including new ambr 15 capability and the novel 'ambr 250 perfusion', can facilitate and significantly accelerate an industry wide transition to intensified and continuous perfusion cell culture processes.

Working in close collaboration with biopharm industry development partners, the design of the 'ambr 250 high throughput' bioreactor system has been modified to include hardware, software and single use components required to operate up to 24 parallel bioreactors with ATF or TFF cell retention modes. Iterative prototype testing with biopharm industry development partners has resulted in a novel ambr 250 system design, shown to be capable of operating for extended culture durations and supporting high cell densities.

Technical description and cell culture results presented for 'ambr 250 perfusion' outline system capability for intensified cell culture applications. Case studies will be presented on the utility of new ambr 15 system features for perfusion mimic applications, together with a range of industry case studies and novel performance data for the new 'ambr 250 perfusion' system. As previously established with ambr 250 for fed-batch processes, 'ambr 250 perfusion' has the potential to provide the biopharm industry with a step change in perfusion process development capacity, enabling implementation of DoE based approaches for perfusion process optimization and characterization.

ECCE12
The 12th EUROPEAN CONGRESS OF CHEMICAL ENGINEERING
Florence 15-19 September 2019

A wind tunnel method to develop products for controlled delivery of volatiles: experimental apparatus and mathematical model.

Fernando Bernardo*, Rita Chim, Mara Braga

CIEPQPF, Department of Chemical Engineering, University of Coimbra
Rua Sílvio Lima, Pólo II, Pinhal de Marrocos, 3030-790 Coimbra-Portugal

**Corresponding author: bernardo@eq.uc.pt*

Highlights

- Method to test/develop products that release volatile active ingredients
- Application to a product releasing an insect attractant compound
- Method semi-validated with first set of assays; further validation is needed
- Useful to assess different product concepts and optimize formulation

1. Introduction

The release of a volatile active ingredient (AI) is a key functionality in a wide range of products, including personal care products, home fragrance products and insecticides. The method here presented was motivated by the development of a product releasing an AI that strongly attracts a particular insect (the beetle Monochamus galloprovincialis), known to be the main vector of the pinewood nematode, which in turn is responsible for the pine wilt disease [1]. The product should be active for several days (or even weeks) and up to a certain distance from the source. Product testing will be done in three stages: lab tests without insects, lab tests with insects and finally field tests (in the pine forest).

The method here described applies to the first stage tests where the goal is to evaluate AI concentration in the surrounding air resulting from a given product formulation, as a function of time and distance from the product. For that purpose, the product is tested in a wind tunnel and AI concentration measured downstream of the product. Complementarily, a mathematical model of AI transport is setup and solved, aiming at producing useful estimates to plan further tests and thus accelerate product optimization. The results from this stage, together with the known threshold concentration (above which attraction effect is significant), will be used to design the second stage tests, where the insect response will be monitored in a larger wind tunnel system.

2. Methods

Figure 1 shows a sketch of the cylindrical wind tunnel. The product is placed on the tunnel axis, 1 meter away from the entrance, where the air fan is located. In the base case here considered, the product is a small porous cylinder composed of an inert polymer (polycaprolactone) loaded with AI (α-pinene). The concentration of AI is measured through adsorption fibres that are first exposed to the flowing air until saturation (which is fast), and then analysed by SPME-GC-MS (details of the procedure and its calibration are not here described). The duration of this analysis only allows the use of four fibres at a time. The four selected positions P, in cylindrical coordinates (z,r), are: P1(0.25,0.085), P1'(0.25,0.035), P2(0.50,0.085) and P3(0.75,0.085) (values in meters; the

product is at the origin (0,0)). The concentration in these four points is measured at different times after the beginning of the assay.

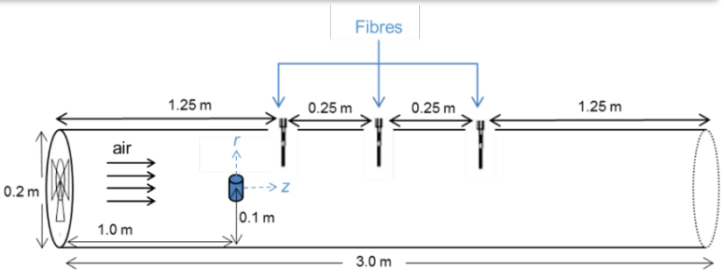

Figure 1. Wind tunnel.

The AI transport model comprises two components: A) release from the cylindrical product (internal diffusion with effective coefficient Di, partitioning at the air/product interface with coef. K, convective transfer to the surrounding air); B) axial and radial dispersion along the tunnel (coefs. Dz and Dr), and axial advection with the cross-section mean velocity (u). Model A has a well-known analytical solution, available in classical textbooks. Model B (with the source at z=0 approximated to a disk) also has analytical solution [2], but we have derived an equivalent one, using simpler methods. The dynamics of transport B is much faster than that of transport A (a few tens of seconds compared with several days). A pseudo-steady-state is then assumed for transport B, resulting in an overall model A+B for which we have derived an analytical solution (and this is a new contribution). The main model parameters are the ones above mentioned (Di, K, Dz, Dr and u). Di was previously determined based on AI release tests under quiescent air, and for the base case here considered is $(0.72\pm0.21)\times10^{-9}$ m^2/s. Initial estimates for the other parameters are: K_0=330 (from AI vapour pressure and Flory-Huggins model), u_0=0.38 m/s (from the fan specifications), Dz_0=0.026 and Dr_0= 0.00017 m2/s (for fully developed turbulent flow in a pipe).

3. Results and conclusions

Figure 2 shows experimental results and the best fit of the model, obtained with $K=23K_0$, $u=1.9u_0$, $Dz=0.12Dz_0$ and $Dr=8.0Dr_0$. The fit is good for points P1 and P1', and not so good for further away points P2 and P3. The model still needs to be improved in order to produce reliable estimates of low concentrations far from the source (e.g., the air flowrate should be directly measured, thus revealing the true value of u). After these improvements, we believe the model may provide valuable guidance in product development (e.g., making predictions for other AIs and for alternative product formulations).

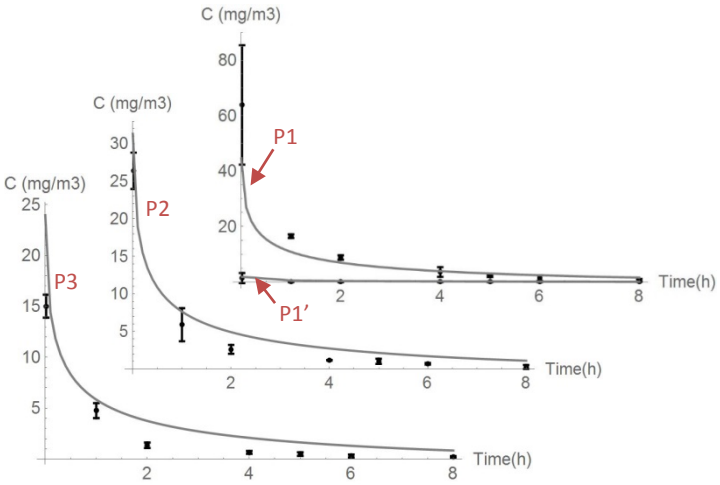

Figure 2. Measured AI concentrations (discrete points) and model predictions (continuous curves).

References

[1] P. N. Calvão et al., Forest Ecology and Management 389 (2017) 105-115.
[2] J-S Chen et al., Journal of Hidrology 405 (2011) 522-531.

Model-Assisted Design of Experiments.

Johannes Möller[1], Kim B. Kuchemüller[1], André Moser[2], Volker C. Hass[2], Tanja Hernández Rodríguez[3], Sahar Deppe[3], Björn Frahm[3], Ralf Pörtner[1,*]

[1]Institute of Bioprocess and Biosystems Engineering, Hamburg University of Technology, Hamburg, D-21073, Germany, [2]Hochschule Furtwangen University, Faculty of Medical and Life Sciences, Villingen-Schwenningen, D-78054, Germany, [3]Biotechnology and Bioprocess Engineering, Ostwestfalen-Lippe University of Applied Sciences, Lemgo, D-32657, Germany,
*Corresponding author: poertner@tuhh.de

Highlights

- Workflow for knowledge-based bioprocess development.
- Combination of mathematical modeling and statistical Design of Experiments.
- Reducing the number of experiments for process design.

1. Introduction

The development of biotechnological processes is still mainly based on one-factor-at-a-time approaches. This increases the time for process development and simultaneously limits the obtained knowledge. As an alternative, Design of Experiments (DoE) tools can be used for the evaluation of multiple variable impacts simultaneously. However, conventional DoE frequently leads to a high number of time-consuming and costly experiments.

In this study, a model-assisted DoE (mDoE) concept is introduced for a knowledge-based process design with a reduced number of experiments. The main part of mDoE is a mathematical process model, which incorporates the prior knowledge and known mechanistic relationships [1]. The combination of the process model with conventional DoE methods enables the knowledge-based reduction of the experimental space. This method is exemplarily shown for the optimization of the initial glucose and glutamine concentration (batch) and the development of a bolus fed-batch strategy (4 parameters) for the cultivation of antibody-producing CHO cells.

2. Methods

For mDoE, data of first cultivations based on literature or prior knowledge (e.g. former studies) is generated. It is used to model biomass growth, metabolic activity and product formation during the process. Models of different complexity may be utilized, describing e.g. phenomenological relationships and effects [2], structured biomass compartments [3], or segregated population dynamics [4]. After process modeling, conventional DoEs are planned and the factor combinations are exported. The planned processes are simulated instead experimentally performed and the DoEs are evaluated using statistical methods. A response-surface model is estimated and a constraint-based optimization of the experimental space is conducted. This loop (see Figure 1) can be repeated several times to reduce the number of experiments further. Finally, a reduced number of cultivations is performed in the optimized experimental space.

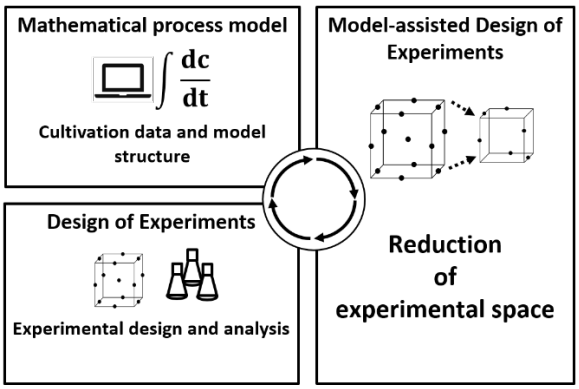

Figure 1. Scheme of the method for mDoE.

3. Results and discussion

The parameters of a mathematical process model [2] were estimated based on data of four first experiments for each application (batch and fed-batch). Conventional DoEs with broadly distributed factor boundary values were planned and the responses were simulated. The experimental spaces were evaluated and the factor boundary values were adapted. Experiments were conducted within the reduced experimental spaces and the results compared to the simulated DoEs. The same optimal conditions were found for both, simulated and experimentally performed cultivations. For the optimization of the initial glucose and glutamine concentration (see Figure 2), the number of experiments could be reduced by 50 % (8 for modeling/validation vs. 16). The number of experiments could be reduced by 72 % (8 for modeling/validation vs. 29) for the development of a bolus fed-batch strategy.

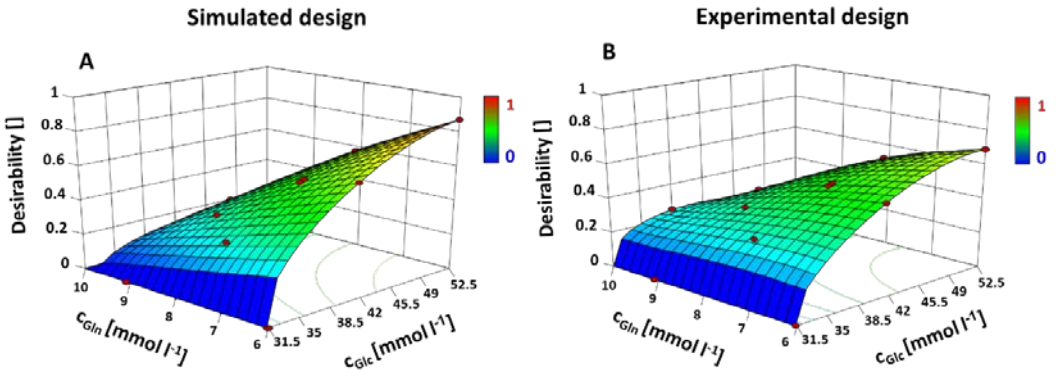

Figure 2. Desirability function for medium optimization, constraints: maximal antibody titer and minimal ammonium concentration. A: simulated responses, B: experimentally determined responses, cultivations as described in [4]

4. Conclusions

mDoE utilizes the currently available process understanding in form of a mathematical process model and significantly reduces the number of experiments.

References

[1] V Abt et al. (2018) Curr Opin Chem Eng, https://doi.org/10.1016/j.coche.2018.11.007
[2] S Kern et al. (2016) Cytotechnology, https://doi.org/10.1007/s10616-015-9858-9
[3] S Brüning et al. (2017) Chem Eng Technol, https://doi.org/ 10.1002/ceat.201600639
[4] J Möller et al. (2018) Biotechnol Bioeng, https://doi.org/10.1002/bit.26828

Multivariate data analysis in gene therapy process development

Joe Emerson[1], Mark J. Willis[1], Jarka Glassey[1]

1 School of Engineering, Newcastle University, Merz Court, Newcastle upon Tyne, NE1 7RU

**Corresponding author: jtemerson@newcastle.ac.uk*

Highlights

- Multivariate techniques were applied to historical process data from vector production and cell processing
- Principal component analysis was used to assess batch-to-batch process variability
- Partial least squares enabled identification of critical process variables and modelled their relationship with critical quality attributes of the product

1. Introduction

Recent developments to vector safety and efficacy have brought about significant renewed interest in gene therapy and evidence of successful clinical trials has been mounting. However, the production processes are at an early stage of development, and process complexity and variability in vector/cell manufacturing processes, combined with the data-lean features of the early development stages in cell-gene therapy are significant contributing delaying factors in the new product development. In this work advanced modelling approaches are applied to process information from vector and cell expansion to bring benefits in process understanding and contribute to more rapid development of new products.

2. Methods

The nature of the data set is typical of bioprocesses, with a high number of inputs (process parameters) and outputs (performance parameters) [1]. In addition, the number of batches is low in many cases due to the treatments being personalized or targeted at rare diseases. The combination of many variables with a low number of repeats is a challenge for modelling practice. In this work, standard techniques were employed though it was necessary to modify the approach to modelling in order to cope with the challenges of the data set. For example, the use of sparse principal component analysis (PCA) was explored as an alternative to standard PCA in order to ease the interpretation of loadings with a high number of variables. Partial least squares (PLS) is an extension of multivariate linear regression, used to model the relationship between a set of independent variables and output variables of interest. PLS models were developed to link process variables to critical quality attributes of the product, critical process parameters were identified, and validation techniques were implemented to assess the predictive capability of the models. The validated models were interpreted to gain valuable process insights.

3. Results and discussion

Demonstrative PCA results are presented here along with a discussion, full results from PCA, sparse PCA and PLS modelling will be presented in the paper. PCA was applied to the production process variables and figure 1 shows the scores for the first three principal components. Figure 1

demonstrates the usefulness of PCA for highlighting and visualizing the differences in operating conditions that occur batch-to-batch. Batches that are close together have similar operating conditions whilst the opposite is true for batches that are further apart. Colouring the batches by the viral titre clearly shows that the operating conditions exhibited in batches 9 to 13 were favourable for a high titre.

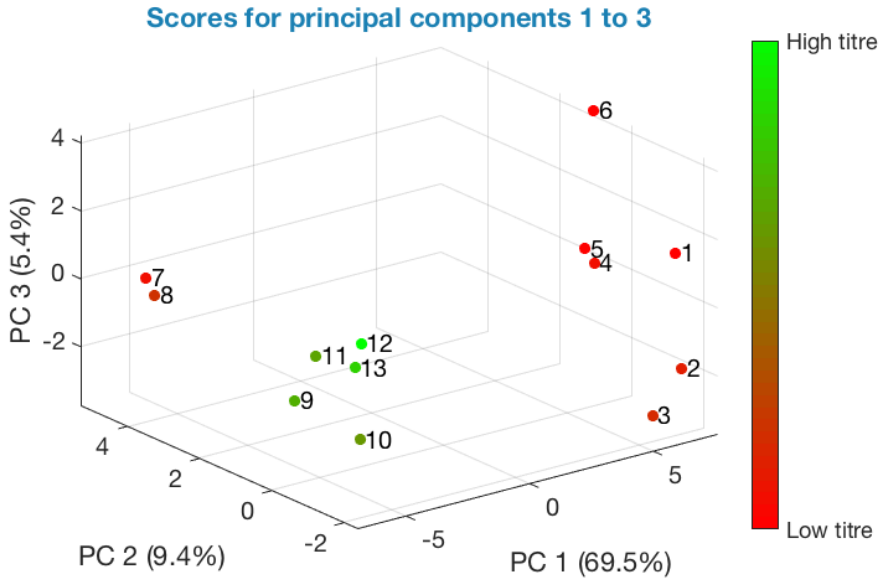

Figure 1. PCA applied to process variables: scores for principal components 1 to 3

To understand the driving forces behind the differences in batch scores, it is necessary to analyse the PCA loadings vector, in this way it is possible to identify variables with high variability and highlight the variables that were changed batch-to-batch and cluster-to-cluster. PLS was used model the relationship between process variables and the viral titre. Using variable selection techniques, it was possible to identify critical process parameters i.e. those influencing the viral titre and responsible for the high titre of batches 9 to 13 on figure 1. The PLS models were cross validated, and models with high predictive capability were selected. The sign on the standardized regression coefficients provided information on whether the variables positively or negatively influenced the viral titre, and the magnitude of coefficients indicated the relative importance of their effect.

4. Conclusions

Multivariate data analysis is a powerful tool for learning from historical process data; which may be particularly useful in cell gene therapy where complex biology and a large number of process parameters interacting, leads to a lack of process understanding. PCA is effective at identifying areas of the process with high variability and characterising the changes that were made during process development. The PLS models developed provided useful insights for process development, including identifying critical process parameters and indicating how these variables may be manipulated to increase the viral titre.

References

[1] A.S. Rathore, S. Mittal, M. Pathak, A. Arora, *Biotechnology Progress*, 2014, *30*(4), pp 967–973.

ECAB 5
The 5th EUROPEAN CONGRESS OF APPLIED BIOTECHNOLOGY
Florence 15-19 September 2019

Investigation of the Mechanical Characteristics of Particle Separation with Dynamic Filtration - Analyzed by Surrogate Particles.

Henrik S. Marke[1*], Martin Peter Breil[2], Manuel Pinelo[1], Ernst Broberg[2], Ulrich Krühne[1]

1) Technical University of Denmark; 2) Novo Nordisk A/S

**Corresponding author: hensmar@kt.dtu.dk*

Highlights

- The mechanics of dynamic filtration has been studied by surrogate particles
- The particle specific pressure was isolated from known pressure components
- A model for the particle resistance was derived from the isolate particle pressure

1. Introduction

Solid separation by membrane filtration promises better separation, with a cleaner permeate fraction compared to centrifugation. Despite those advantages, most cell separations in the bio-chemical industry are still done by centrifugation. The filtration properties of the fermentation broth are too unfavorable for mass embracement of membrane separation for cell recovery [1]. To make membrane filtration of cells from fermentation broth economically variable, novel filtration technologies are needed. One such novel technology is dynamic filtration where filtration is enabled by movement of objects, not movement of liquid. Different methods to inducing such moment have been devised. For instance, by having an impeller rotating above the membrane, or by moving the membrane itself, ether by rotation or by vibration [2]. In this project a system with rotating membranes have been investigated.

The ultimate goal for this project is to describe how different process conditions affect the filtration performance of microorganisms in a rotating filtration system. Due to the complexity of biological

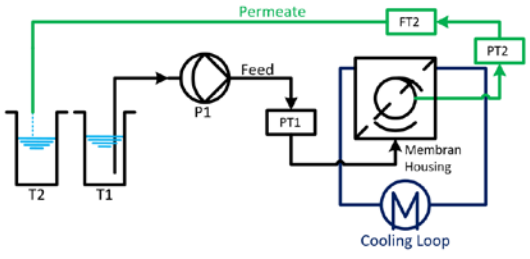

Figure 1: *Schematic of the experimental setup. Particles dilute from T1 are pumped into the membrane house, where they are concentrated. The permeate was collected in T2. The permeate Flow (FT2) and operational pressure (PT1, PT2) was measured*

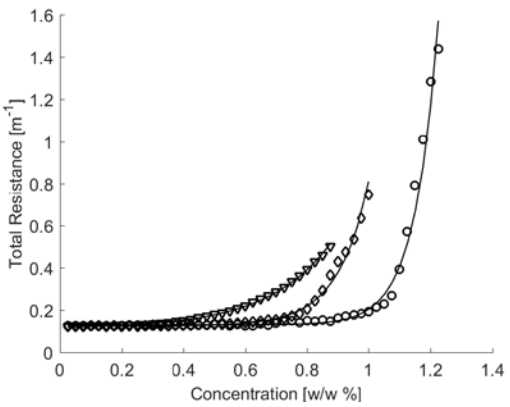

Figure 2: *Total Resistance (R_{tot}) plotted as a function of particle concentration for three different experiments. ◊: High rotation, High Flow. ∇: Low rotation, High Flow. ○: High rotation, low Flow. The solid lines represent the modelled resistance for each experiment.*

feeds, the system was simplified to a more manageable complexity level. The simplified filtration system was made with uniform particles of chalk ($CaCO_3$). The use of a well-defined system ensures experimental reproducibility, which would have been difficult with a biological system.

2. Methods

For the experiments, a dedicated filtration setup was assembled, according to the schematic shown in Figure 1. Operation parameters, such as pump speed and disc rotation were controlled with help of LabVIEW. Pressure and flow measurements were collected likewise. Each experiment consisted of two stages. First, the solvent system was measured, i.e. the membrane resistance was determined without particles. Secondly, the system was investigated with particles in the feed. For each experiment, a dilute solution of chalk particles was prepared. The particles used had a mean size of 2.5 µm, and the solution had a concentration between 1.2 % w/w and 2.7 % w/w. The filtration was performed as a dead-end filtration, meaning particles would accumulate in the house. The particle accumulation leads to an increased operational pressure with time.

3. Results and discussion

For a set of operational conditions, a filtration performance curve was recorded, based on the operational pressure (ΔP). The pressure curve was analyzed by decomposing it into known and unknown pressure components. The known components are related to the solvent system and to the rotation of the membrane. The known parts can be described as:

$$P_{sys} = \underbrace{\mu_s \cdot J \cdot R_m}_{Solvent} + \underbrace{(k_1\omega)^2 \cdot \frac{\rho}{4} \cdot (r_1^2 + r_2^2)}_{Rotation}$$

The unknown components are related to the particles and buildup of cake on the membrane surface. The pressure difference between ΔP and P_{sys} is the pressure resulting from the presents of particles. The difference can be used to find the particle resistance and the total resistance in the system, as presented in Figure 2:

$$R_C = \frac{\Delta P - P_{sys}}{J \cdot \mu_s} \qquad R_{tot} = R_C + R_m$$

Conducting the experiments at different operational conditions, such as different filtration rates, particle concentrations, and membrane rotational speeds, a model for R_C can be derived. With this model, a general performance description of a filtration unit will be derived, facilitating process design.

4. Conclusions

By isolating the particle pressure from the operational pressure, a resistance model can be derived. This model is a starting point for filtration process design.

5. References

[1] S.P. Beier, G. Jonsson, Separation of enzymes and yeast cells with a vibrating hollow fiber membrane module, Sep. Purif. Technol. 53 (2007) 111–118. doi:10.1016/j.seppur.2006.06.019.

[2] M.Y. Jaffrin, Dynamic shear-enhanced membrane filtration: A review of rotating disks, rotating membranes and vibrating systems, J. Memb. Sci. 324 (2008) 7–25. doi:10.1016/j.memsci.2008.06.050.

ECAB 5
The 5th EUROPEAN CONGRESS OF APPLIED BIOTECHNOLOGY
Florence 15-19 September 2019

Continuous Clarification Using an Improved Inclined Plate Settler Concept.

Hannah Engelmaier[1], Nikolaus Hammerschmidt[1] , Christoph Dattenböck[2], Alois Jungbauer[1,3]

1 Austrian centre of industrial biotechnology, acib GmbH, Muthgasse 18, A-1190 Vienna, Austria; 2 Baxalta Innovations GmbH, Industriestraße 131, A-1220 Vienna; 3 University of Natural Resources and Life Sciences, Vienna (BOKU), Gregor-Mendel-Straße 33, A-1190 Vienna

**Corresponding author: hannah.engelmaier@acib.at*

Highlights

- Truly continuous solid-liquid separation
- New concept inclined plate settler
- Stable, high product yield

1. Introduction

With market pressure increasing in the biotechnological and biopharmaceutical industry, the trend is going towards continuous processing [1]. While, continuous chromatography is being readily adopted [2,3], alternative unit operations e.g. flocculation and precipitation are being mostly neglected. These techniques suffer from the fact that there is a lack of efficient continuous solid-liquid separation techniques [4].

2. Methods

We tested our inclined plate settler system with suspensions with different settling behavior. In these tests, operation parameters were optimized to ensure high product yield. The product was simulated to be either, comprised by the solid or by the liquid phase. We also tested the applicability of the optimized conditions during scale-up from one to multiple plates. The solid-liquid separation performance was monitored by online sensors and was verified and complemented by offline measurements.

3. Results and discussion

Using an improved concept for inclined plate settler based solid-liquid separation we were able to demonstrate efficient solid-liquid separation. We have optimized the operation conditions and have obtained high product yield in all operation scenarios. The separation process was highly stable after an initial ramp-up phase.

4. Conclusions

We have developed a new plate settler concept that broadens the application range of inclined plate settlers for solid-liquid separation tasks. Thereby, we provide a possible solution to the bottleneck in continuous processing, being solid-liquid separation.

References

[1] D.J. Karst, F. Steinebach, M. Morbidelli, Continuous integrated manufacturing of therapeutic proteins, Current opinion in biotechnology, 53 (2017) 76-84.
[2] A. Jungbauer, Continuous downstream processing of biopharmaceuticals, Trends in Biotechnology, 31 (2013) 479-492.
[3] O. Kaltenbrunner, L. Diaz, X. Hu, M. Shearer, Continuous bind-and-elute protein A capture chromatography: Optimization under process scale column constraints and comparison to batch operation, Biotechnology Progress, 32 (2016) 938-948.
[4] P. Gagnon, Technology trends in antibody purification, Journal of chromatography. A, 1221 (2012) 57-70.

Development of sustainable nanomaterials for the purification of antileukemic drugs

Mafalda R. Almeida[1*], M. Amélia Barros[2], Mara G. Freire[1], Valéria C. Santos-Ebinuma[3], Cláudia G. Silva[2], Ana P.M. Tavares[1]

1 CICECO-Aveiro Institute of Materials, Department of Chemistry, University of Aveiro, 3810-193 Aveiro, Portugal; 2 Laboratory of Separation and Reaction Engineering-Laboratory of Catalysis and Materials (LSRE–LCM), Faculdade de Engenharia, Universidade do Porto, Rua Dr. Roberto Frias s/n, 4200-465 Porto, Portugal; 3 Department of Bioprocess and Biotechnology, School of Pharmaceutical Sciences, UNESP-University Estadual Paulista, Araraquara, Brazil

**Corresponding author: mafalda.almeida@ua.pt*

Highlights

- Sustainable technologies to purify L-Asparaginase.
- Modified carbon nanomaterials have high affinity for L-Asparaginase.
- The pH and material/biopharmaceutical ratio influence the adsorption performance

1. Introduction

Getting older is the biggest risk factor for most fatal diseases, including cancer, heart diseases and neurological diseases. To overcome such age-related diseases, it is crucial to optimize the production and purification of biopharmaceuticals, such as nucleic-acid-based products, antibodies and recombinant proteins and enzymes. Low cost production combined with high purity levels will allow their routinely use by a widespread population. Amongst the available biopharmaceuticals, continuous progresses have been carried out for the development of recombinant therapeutic enzymes, namely L-asparaginase (LA), which presents antineoplastic properties for the treatment of leukemia, namely Acute Lymphoblastic Leukemia (ALL) [1]. The first-line biologic used to treat ALL, Oncaspar, is currently marketed in the United States, Germany and Poland, accounting with approximately USD $100 million in annual sales [2]. Given their high value, the demand for new biopharmaceuticals and cost-effective production/purification processes play now a priority role [3]. The common strategies for protein purification result in low yields and purity, requiring long processing times, while leading to a consequent increase of the process costs [4]. LA can be produced via fermentation and its purification usually comprises several steps. The methods to purify LA include precipitation, liquid-liquid extraction and chromatography techniques. Among these, ion exchange chromatography, which is often preceded by precipitation with salts as a first pre-chromatographic step, is the most used [4]. This work aims the development of cost-effective technologies to purify LA from the fermentation medium, which is rich in other proteins. Reusable functionalized nanomaterials, namely carbon nanomaterials (CNTs), are investigated as cost-effective purification techniques for the target enzyme, demonstrating to have high affinity for the target biopharmaceutical. The pH, material/biopharmaceutical ratio and contact time effects in the purity and yield of LA were optimized.

2. Methods

The surface chemistry of CNTs was modified by the treatment with nitric acid in liquid phase to introduce oxygen containing surface groups. Different CNTs were obtained and used for the purification of LA. Commercial LA was used for the first tests, in order to understand the behavior of the enzyme in contact with the nanomaterial. Experimental conditions, such as pH, and material/LA ratio, and contact time were studied. LA activity was quantified by Nessler reaction, which quantifies the amount of ammonium released after the enzymatic reaction [5].

3. Results and discussion

The first results reveal a total adsorption of LA by the CNTs. Depending on the CNT functionalization/ treatment, different values of recovered activity of LA were obtained. The pH and material/LA ratio also influence the adsorption of LA on the material surface.

4. Conclusions

The modified CNTs are promising nanomaterials for the purification of LA. The LA was easily attached to CNTs by adsorption under mild conditions. CNTs supports can be considered as a promising alternative for the adsorption and purification of LA.

Acknowledgements

This work was developed within the scope of the project CICECO-Aveiro Institute of Materials, FCT Ref. UID/CTM/50011/2019, financed by national funds through the FCT/MCTES. This work was financially supported by the projects POCI-01-0145-FEDER-006984 – Associate Laboratory LSRE-LCM and POCI-01-0145-FEDER-031268 - funded by FEDER, through COMPETE2020 - Programa Operacional Competitividade e Internacionalização (POCI), and by national funds (OE), through FCT/MCTES. Ana P.M. Tavares and Cláudia G. Silva acknowledge the FCT Investigator Programme (IF/01634/2015 and IF/00514/2014, respectively) with financing from the European Social Fund and the Human Potential Operational Programme. Mara G. Freire acknowledges the European Research Council under the European Union's Seventh Framework Programme (FP7/2007-2013)/ERC Grant 337753.

References

[1] A.M. Lopes, L. de Oliveira-Nascimento, A. Ribeiro, C.A. Tairum Jr., C.A. Breyer, M.A. de Oliveira, G. Monteiro, C.M. de Souza-Motta, P.O. Magalhães, J.G.F. Avendaño, Crit. Rev. Biotechnol. 37(1) (2017) 82-99.

[2] Baxter International Inc, Deerfield, Ill. - May 12, 2015.

[3] S. Gräslund, P. Nordlund, J. Weigelt, B.M. Hallberg, J. Bray, O. Gileadi, S. Knapp, U. Oppermann, C. Arrowsmith, R. Hui, Nat. Methods. 5(2) (2008) 135.

[4] L.L. Tundisi, D.F. Coelho, B. Zanchetta, P. Moriel, A. Pessoa Jr, E.B. Tambourgi, E. Silveira, P.G. Mazzola, Sep. Purif. Rev. 46(1) (2017) 35-43.

[5] A. Magri,M.F. Soler, A.M. Lopes, E.M. Cilli, P.S. Barber, A. Pessoa Jr, J.F.B. Pereira, Anal. Bioanal. Chem. 410(27) (2018) 6985-6990.

Scale up strategy to enhance hydrogen production from wastewater by dark fermentation process

Audrey Soric[1,*], Lucien Duclos[1], Wirginia Tomczak[1], Cassandra Backes[2], Marie-Thérèse Giudici-Orticoni[2]

1 Aix Marseille Univ, Centrale Marseille, CNRS, M2P2, Marseille, France; 2 Aix-Marseille Univ, CNRS, BIP, Marseille, France

**Corresponding author: audrey.soric@centrale-marseille.fr*

Highlights

- Continuous H_2 production in bioreactors inoculated by synthetic consortium or sludge
- Optimization of HRT in both bioreactors gave the same results
- The recirculation ratio has a huge influence on H_2 production and metabolites' concentration profile

1. Introduction

Hydrogen represents a promising clean alternative to fossil fuels, because its combustion produces only energy and water and it is a powerful energy carrier. Among the processes that are commonly used to produce H_2, dark fermentation is considered one of the most attractive, because it employs the ability of anaerobic bacteria to produce H_2 from renewable feedstock such as wastewater. The technical feasibility of H_2 production from wastewater has been largely investigated in upflow anaerobic biofilm reactors (UABR) [1]. Indeed, biofilm provides a good protection to microorganisms against potential changes of operating parameters, thus allowing more flexible operating conditions. However, many studies found low H_2 yields (HY) and instable H_2 production, probably because of the variability of microbial communities and metabolic pathways. The experimental study described here focusses on a multi-scale experimental approach to improve the scale up the process of H_2 production via dark fermentation using wastewater as a substrate. First results from Benomar et al. [2] that have shown stable biofilm formation and improved HY using cocultures of *C. acetobutylicum* and *D. vulgaris* Hildenborough. Based on these results, two continuous UABR were designed, inoculated with the coculture and a natural sludge and operated in different conditions to decipher biological mechanisms of hydrogen production.

2. Methods

A 1L-reactor filled with Kaldnes K1 as biofilm carriers was inoculated with a synthetic consortium of *C. acetobutylicum* and *D. vulgaris* Hildenborough ratio 1:1. In parallel another 1L-UASB was inoculated with a pre-heated sludge from a municipal WWTP. These reactors were operated in continuous for several weeks and fed with a solution of glucose (1 g/L) as the main organic carbon source and micronutrients (ratio of C/N/P was 100/21.4/1.9, which is in the range of typical C/N/P

molar ratios of municipal wastewater) [3,4]. Biogas production was recorded by a Milligas counter (Ritter, Germany) set at the gas outlet of the reactor. H_2 content in biogas was determined using a gas chromatograph Agilent 7820A GC equipped with a 30m column GS-CarbonPLOT (Agilent Technology, USA). Liquid was sampled daily at the outlet of the reactor to follow pH and metabolites concentrations by HPLC system Agilent 1260 Infinity LC (Agilent Technology, USA). After stabilization of bioreactors performances the influence of HRT and inlet/outlet recirculation ratios were studied on hydrogen production rate (HPR) and metabolites' profiles.

3. Results and discussion

First experiments conducted on the consortium showed that the best HRT was 2 hours [3]. These results were confirmed by the experiments conducted with the sludge-inoculated bioreactor (figure 1a).

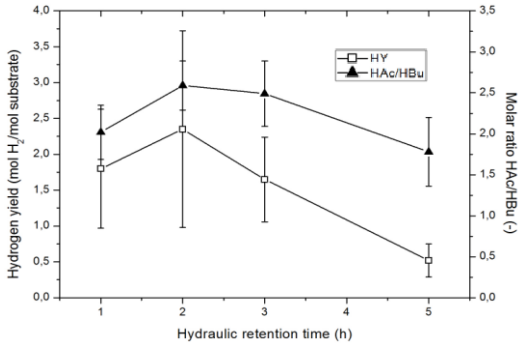

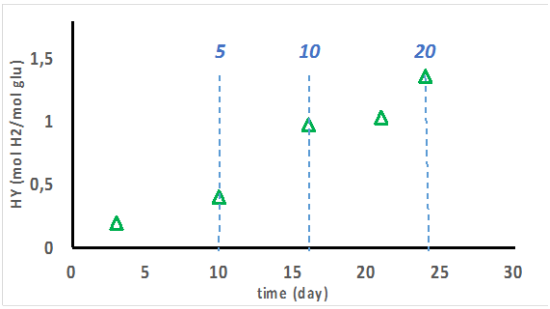

Figure 1a. Influence of HRT on HY and Acetate(HAc)/Butyrate(HBu) ratio [4] –

Figure 1b. Influence of recirculation ratio (in blue) on HY

Experiments conducted on the bioreactor inoculated with the synthetic consortium to determine the best liquid recirculation rate gave interesting results plotted in figure 1b. The recirculation ratio between inlet and outlet of the reactor is an important parameter to optimize HPR. This could be explained by its influence on the profiles of pH and metabolites' (to be shown on the conference).

4. Conclusions

The combination of experiments with a synthetic consortium and WWTP sludge gave interesting results leading to an optimization of hydrogen production via dark fermentation in a labscale reactor. This approach combining synthetic and natural consortium studies is promising for an efficient scale-up of the process.

References

[1] C. Barca, A. Soric, D. Ranava, MT Giudici-Orticoni, JH Ferrasse, Bioresource Technology, 185 (2015) 386-398.

[2] Benomar, S., Ranava, D., Cárdenas, M.L., Trably, E., Rafrafi, Y., Ducret, A., Hamelin, J., Lojou, E., Steyer, J.P., Giudici-Orticoni, M.T., Nat. Commun. 6 (2015) 6283.

[3] C. Barca, D. Ranava, M. Bauzan, JH Ferrasse, MT Giudici-Orticoni, A. Soric, Bioresource Technology, 221 (2016) 526-533.

[4] W Tomczak, J-H Ferrasse, M-T Giudici-Orticoni, A Soric, International Journal of Hydrogen Energy, 43 (41) (2018) 18883-18895.

ECCE12
The 12th EUROPEAN CONGRESS OF CHEMICAL ENGINEERING
Florence 15-19 September 2019

The use of aqueous two-phase separation for the *in situ* production and purification of lipopeptides from *Bacillus amyloliquefaciens*

Robert W.M. Pott[1]

1 Department of Process Engineering, University of Stellenbosch, South Africa, rpott@sun.ac.za

Highlights

- *B. amyloliquefaciens* can be cultivated under two-phase conditions
- Lipopeptides preferentially report to the PEG-rich phase
- Differing PEG molecular weights can selectively partition different lipopeptides

1. Introduction

Significant quantities of fruit and vegetables are lost due to postharvest diseases(1). Disease control using synthetic chemicals are being phased out of use, particularly in the EU. Biomolecules, such as lipopeptides (LPs), that possess antifungal activity, biodegradability and digestibility have attracted interest as potential biocontrol agents as replacements(2). Particular focus has been placed on lipopeptides produced by *Bacillus* spp., as they provide a promising alternative in reducing postharvest spoilage due to fungal phytopathogens. The industrial production of these compounds is a developing field, with some LP products being commercially available(3), while antifungal LPs are not yet produced on an industrial scale. In order to develop a process which can produce these compounds at large scale, significant work in separating and purifying the different homologues of LP is required. In particular, in batch culture, as soon as the bacterial cells enter their stationary growth phase, they begin to metabolize the already produced LPs resulting in reduced product yields(4,5). Current concentration, recovery and purification methods employed such as acid precipitation, solvent extraction and membrane filtration take place after fermentation has been stopped and do not address this problem.

The primary aim of this study was therefore to explore the potential of PEG-salt ATPS as an *in situ* extractive fermentation process to reduce the metabolization of the LPs produced by *Bacillus amyloliquefaciens* DSM 23117. The effect of salt type (tartrate, sulphate, phosphate and citrate) and concentration (Standard media 0.2, 0.4 and 0.8 M) as well as the PEG molecular weight (6000 and 8000) on the growth of the microorganism and LP production were examined and compared against standard growth conditions.

2. Methods

ATPS partitioning in pure component systems was conducted using the appropriate salt, buffer and PEG wt. % determined from binodal curves of ATP systems used for protein purification in literature(6). ATP systems were prepared using known concentrations of salt, PEG, and LP mixtures (surfactin, fengycin). ATP systems were agitated in an incubator at 150 rpm for 15 min at 30°C. After mixing, the systems separated into phases. LP concentrations in top and bottom phases were determined using HPLC (Phenomenex Luna 3 µm C18 column, Dionex Ultimate 3000 Diode-array

detector, trifluoroacetic acid mobile phase). LP homologue partitioning was visualized using thin layer chromatography (as described in (7)). For culture experiments, shake flasks experiments, at 30°C, 100 rpm, in baffled 250ml flasks, were conducted growth rate, substrate utilization and lipopeptide production were determined using cell dry weight and HPLC for the quantification of glucose utilized and lipopeptides produced, respectively.

3. Results and discussion

Some sample results are presented here. Further details will be presented in the full conference presentation.

Surfactin and fengycin were successfully separated into top and bottom phases of several ATPS systems, an example of which is shown below in Figure 1. This is the first instance where comparatively simple separation of lipopeptide homologues has been shown. The implication of this is that fengycin, the compound desired in antifungal applications, is separated from the co-produced but undesired surfactin. Fengycin partitions to the top phase, and can thereafter be precipitated using acid precipitation and used as a purified product. The incidence of product consumption is thus minimized at the same time as purification of the product away from the fermentation broth is enacted.

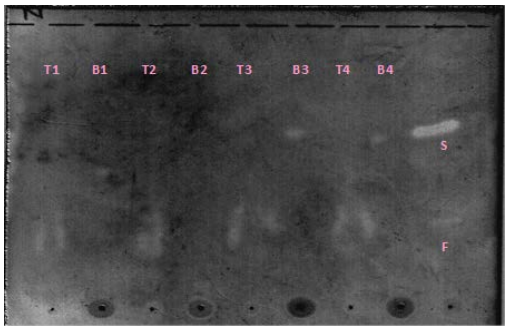

Figure 1. TLC image of lipopeptides in 40% (w/w) PEG 6000 and 49% (w/w) K_2HPO_4. T refers to top (PEG) phase, B refers to the bottom (salt) phase, S refers to the surfactin standard and F refers to the fengycin standard

The organism was found to be able to survive, and even thrive, under increased salt concentrations. This increased salt concentration is a necessary part of operating the culture under *in situ* extraction using ATPS, since 2-phase formation only occurs under sufficient salt concentrations. Following the demonstration of salt tolerance, experiments were conducted using PEG addition to the system. Very similar results were obtained, demonstrating that the organism can viably grow under ATPS conditions. Under the ATPS growth conditions lipopeptide concentration in the top PEG phase was monitored, and found to follow the same trend as standard growth media LP production

4. Conclusions

The production, *in situ* purification and recovery of LPs from *B amyloliquefaciens* was demonstrated using PEG-salt ATPS systems. This work opens the opportunity for the use of ATP systems in the continuous production of LPs, or for a simple purification method to separate LP homologues.

5. Acknowledgements

With thanks to Sebenzile Mazibuko and Dineo Baloyi for their hard work in the laboratory. Generous financial support was provided by Hortgro.

References

1. James A, Zikankuba V. Postharvest management of fruits and vegetable: A potential for reducing poverty, hidden hunger and malnutrition in sub-Sahara Africa. Yildiz F, editor. Cogent Food Agric [Internet]. 2017 Apr 1 [cited 2019 Feb 28];3(1). Available from: https://www.cogentoa.com/article/10.1080/23311932.2017.1312052

2. Pretorius D, van Rooyen J, Clarke KG. Enhanced production of antifungal lipopeptides by Bacillus amyloliquefaciens for biocontrol of postharvest disease. N Biotechnol [Internet]. 2015 Mar 25 [cited 2017 Jun 21];32(2):243–52. Available from: http://www.ncbi.nlm.nih.gov/pubmed/25541516

3. Kaneka. Kaneka surfactin [Internet]. [cited 2019 Feb 28]. Available from: http://www.kaneka.co.jp/en/branch/nb_development/surfactin_catalogue_eng.pdf

4. Mazibuko S. Purification of Bacillus amyloliquefaciens lipopeptides for postharvest disease control. Stellenbosch University; 2018.

5. Rangarajan V, Herbst WJ, Mazibuko S, Clarke KG. Bacillus lipopeptides for a novel postharvest disease control technology. In: 4th international symposium on postharvest pathology. 2017.

6. Asenjo JA, Andrews BA. Aqueous two-phase systems for protein separation: Phase separation and applications. J Chromatogr A [Internet]. Elsevier; 2012 May 18 [cited 2018 Jun 20];1238:1–10. Available from: https://www.sciencedirect.com/science/article/pii/S0021967312004621

7. Dlamini B. Downstream purification of surfactin produced by Bacillus subtilis ATCC 21332. Stellenbosch University; 2017.

ECAB 5
The 5th EUROPEAN CONGRESS OF APPLIED BIOTECHNOLOGY
Florence 15-19 September 2019

Removal of p-coumaric acid and 4-ethylphenol from wine by yeast cell walls.

Elena Bakhos [1,2,4], Alexandre Monnier [1], Nathalie Sieczkowski [2], Roger Lteif [1], Dominique Salameh [3], Cedric Brandam [4]

[1]*Unité de Technologie et Valorisation Alimentaire,* [3]*Unité de recherche Environnement, Génomique et Protéomique, Centre d'Analyses et de Recherche, Université Saint-Joseph de Beyrouth, Faculté des sciences, Campus des Sciences et Technologies, Mar Roukos, Dekwaneh, B.P. 17-5208, Mar Mikhaël, Beirut, 1104 2020, Lebanon*
[2] *Lallemand SAS, 19 rue des Briquetiers, BP 59, 31 702 Blagnac, France*
[4] *Laboratoire de Génie Chimique, Université de Toulouse, CNRS, INPT, UPS, 4 Allée Emile Monso-31029, Toulouse, France*

elena.bakhos@net.usj.edu.lb

Highlights

- The sorption capacity of yeast cell walls changes depending on the type of adsorbate used
- The sorption profile differs between strains issued from the same species of *Saccharomyces cerevisiae*
- The sorption capacity of yeast cell walls changes according to the adsorbate/adsorbent ratio initially added

1. Introduction

During the winemaking process, *Brettanomyces bruxellensis* contaminates the wine by producing volatile phenols such as 4-ethylphenol (4-EP) that is the origin of the unpleasant aroma described as "horse sweat" [1,2]. Several methods were used to prevent wine contamination by these microorganisms such as filtration of wine, the addition of antimicrobial agents, applying high pressures to reduce populations of certain yeasts or the use of PVPP and charcoal to remove the volatile phenols. The latter resulted in the decrease of aromatic compounds concentration and color in red wines [3]. The benefit of using yeast cell walls as biosorbent is mostly driven by the presence of macromolecules such as mannoproteins which are located on the surface of the cell wall and able to retain volatile compounds [4]. The objective was to study the sorption profiles of p-coumaric acid and 4-EP with different specific yeast cell walls of *Saccharomyces cerevisiae*.

2. Methods

Yeast cell walls were produced from biomass that has undergone thermal autolysis and were dried either by lyophilization or spray-drying. The five specific yeast cell walls were provided by Lallemand, Blagnac (France) and were produced from different strains of *Saccharomyces cerevisiae*. Each experiment was conducted in 11 Erlenmeyer flasks containing synthetic wine medium composed of fructose, glucose, yeast extract, $(NH_4)_2SO_4$, citric acid, malic acid, tartaric acid, $MgSO_4$ and KH_2PO_4. The pH of the medium was adjusted at 3.5. Experiments were performed at 30°C in the presence of 3 g/L of yeast cell walls with 10 mg/L of p-coumaric acid or

20, 30, 40 or 50 mg/L of 4-EP and stirred at 250 rpm. Control sample was prepared in the same conditions but without yeast walls. The amount of adsorbate unbound to cell wall was measured by UV spectrophotometry and sorption kinetics for both adsorbates were plotted in order to determine the time required to reach the equilibrium.

3. Results and discussion

Thermodynamic equilibrium time are considered relatively long. This is explained by the microporous structure of the adsorbent, which slows down the diffusion of the liquid since its dimensions are close to the diameter of the molecule. Sorption capacities are really greater with 4-EP than with p-coumaric acid. The maximum percentage of adsorption reached with p-coumaric acid was 20% with the strain named CW1 **(Figure 1)** while the maximum percentage of 4-EP adsorbed by yeast cell walls was between 70 and 80% with the CW5 and CW2 specific cell-walls **(Figure 2)**. A differential mannoprotein content might explain the variation of adsorption capacity by cell wall strains. It is known that the sorption capacity depends on the composition of the cell wall which varies depending on the yeast strain and the culture conditions. Furthermore, *Saccharomyces cerevisiae* adsorb preferentially 4-EP while the *Brettanomyces* adsorb preferentially p-coumaric acid [5]. It is due to the differential cell wall chemical composition between these two genera. In addition, for all specific cell-walls tested, the optimal adsorption concentration of 4-EP is 20 mg/L. The percentage adsorbed decreases inversely proportional with the increased concentration of 4-EP added. This may be explained by the saturation of the yeast wall sorption sites that are specific to 4-EP.

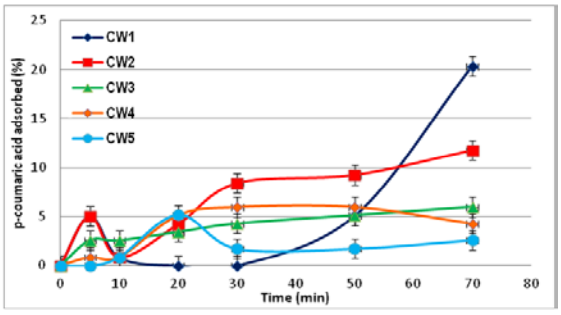

Figure 1. Sorption kinetics of p-coumaric acid

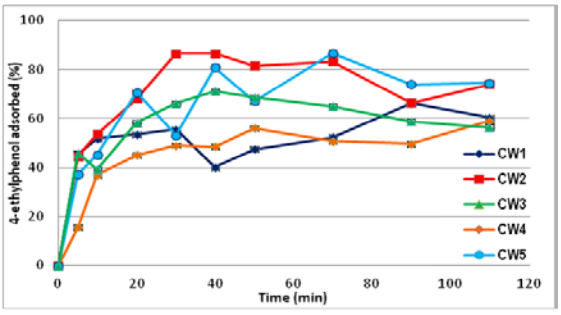

Figure 2. Sorption kinetics of 20 mg/L 4-ethylphenol solution

4. Conclusions

The sorption varies according to the type of adsorbate and the yeast cell wall's type (strain effect). The chemical composition of the yeast cell walls greatly influences the sorption profiles. In the end, this latter is a promising technique for the treatment of wine contaminated by volatile phenols.

References

[1] P. Chatonnet, D. Dubourdieu, J.N. Boidron, Am. J. Enology Vitic. 46 (1995) 463-468
[2] D. Salameh, C. Brandam, W. Medawar, R. Lteif, P. Strehaiano, Food Chem. 107 (2008) 1661-1667
[3] R. Pradelles, H. Alexandre, A. Ortiz-Julien, D. Chassagne, J. Agric. Food. Chem. 56 (2008) 11854-11861
[4] D. Chassagne, M. Guilloux-Benatier, M. Alexandre, A. Voilley, Food Chem. 91 (2005), 39-44
[5] J. Kheir, D. Salameh, P. Strehaiano, C. Brandam, R. Lteif, Eur. Food Res. Technol. 237 (2013) 655-671

ECCE12
The 12th EUROPEAN CONGRESS OF CHEMICAL ENGINEERING
Florence 15-19 September 2019

Conception of a compartmental nitrogen model describing pure cultures of *Saccharomyces cerevisiae* and *Torulaspora delbrueckii* in synthetic media.

Paul Brou[1], Patricia Taillandier[1], Sandra Beaufort[1], Cédric Brandam[1]
1 Université de Toulouse, Laboratoire de Génie Chimique, CNRS, INPT, UPS, Toulouse, FRANCE
** Patricia Taillandier: patricia.taillandier@ensiacet.fr*

Highlights

- A mathematical model was developed to describe pure culture of two oenological yeasts.
- Compartmental nitrogen model enables to accurately describe fermentation kinetics.
- This model was validated in several synthetic media.

1. Introduction

In winemaking the use of mixed cultures combining *Saccharomyces* and non-*Saccharomyces* yeasts is more and more common in order to obtain wines with different organoleptic products. However, the behavior of these yeasts is difficult to control because of the interactions existing between them. In particular, the assimilable nitrogen is often a limiting nutrient in the grape musts and the yeasts are going to be in competition for it [1]. Modeling of the fermentation kinetics taking into account this limiting nutrient could allow to predict the kinetics of mixed culture in a second step.

2. Methods

Two commercial oenological yeasts were used in this study: *Torulaspora delbrueckii* Zymaflore alpha® and *Saccharomyces cerevisiae* QA23® Pure cultures of each yeast were performed in three synthetic media MS170, MS300 and MS300M at 20°C [2]. Each medium contained the same amount of sugars (220 g/L), vitamins and mineral elements but different concentration of nitrogen and/or lipids [1-2]. Growth, substrates and metabolites kinetics were followed during the fermentation.

3. Results and discussion

In all the pure cultures of *S. cerevisiae* and *T. delbrueckii*, it has been observed that yeasts were still growing whereas nitrogen initially present in the medium was completely exhausted (Fig 1). Therefore, after the nitrogen exhaustion the yeasts growth goes on on a nitrogen source located inside the cell. So It is necessary to consider an intracellular nitrogen source to mathematically describe the growth kinetics of the microorganisms studied. We introduce the notions of minimum cellular nitrogen and stored nitrogen to describe population, substrates and metabolites kinetics. This involves the design of a structured model in which the total assimilated nitrogen is divided into two compartments: the constitutive compartment and the storage compartment.

The constitutive compartment contains a quantity of nitrogen equal to the minimum amount of cellular nitrogen (N_{min}). This compartment provides vital minimal functions to keep the cell alive. Like the constitutive compartment, the storage compartment contributes to cell activity. However, only the storage compartment contains the nitrogen reserves available for growth.

The measured molar mass of the yeasts ($CH_xO_yN_z$) varies during fermentation. The molar mass $CH_xO_yN_{z'}$ of a cell containing an empty nitrogen storage compartment was considered constant. The latter molar mass let to propose a stoichiometric growth reaction (r1) for each yeast:

$1\ C_6H_{12}O_6 + g1\ N_S \rightarrow g2\ CH_xO_yN_{z'} + g3\ CO_2 + g4\ H_2O$

The evolution of substrates (sugar (S) and nitrogen (N)) and products (ethanol (E) and glycerol (G)) was described using additional stoichiometric reactions such as fermentation (r2), nitrogen absorption (r3), yeast mortality (r4) and glycerol production (r5):

$$\begin{cases} r1 = X_n.k_\mu.\left(1-\frac{X}{X_{max}}\right).\left(\frac{K_E}{K_E+E}\right).\left(\frac{N_s/X}{N_s/X+K_X}\right) \\ r2 = k_s.X_n.\left(\frac{S}{S+K_S}\right).\left(\frac{K_{ES}}{K_{ES}+E}\right).\left(\frac{N_s/X}{N_s/X+K_{NS}}\right) \\ r3 = k_N.X_n.N \\ r4 = X_n.e^{\left(\frac{E-E_{lim}}{10}\right)} \\ r5 = k_G.X_n.\left(\frac{S}{S+K_{SG}}\right).\left(\frac{K_{EG}}{K_{EG}+E}\right) \end{cases} \quad \begin{cases} \frac{dX}{dt} = (g2*r1-r4) \\ \frac{dS}{dt} = -(r1+r2+r5) \\ \frac{dN}{dt} = -r3 \\ \frac{dN_s}{dt} = (r3-g1*r1) \\ \frac{dE}{dt} = 2*r2 \\ \frac{dG}{dt} = r5 \end{cases}$$

X and X_n represent the living cell expressed respectively in cells/mL and mol/L. The model accurately describes the evolution of the fermentation (Fig 1 and 2). Modification of this model enables to describe precisely effects of lipid supplementation on yeast behavior (data not shown).

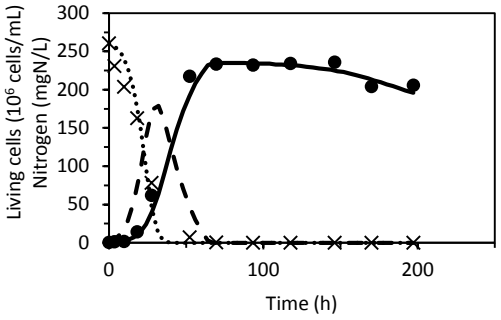

Figure 1. Pure culture of *S. cerevisiae* in MS170.
× Medium nitrogen (exp) ▪▪ Medium nitrogen (model)
● Living cells (exp) ¬ Living cells (model)
¬ ¬ Stored nitrogen (model).

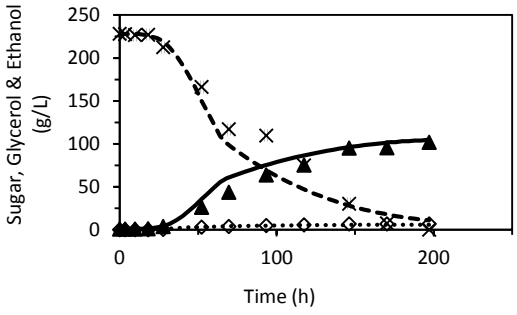

Figure 2. Pure culture of *S. cerevisiae* in MS170.
◊Glycerol (exp) ▪▪ Glycerol (model)
× Sugar (exp) ¬ ¬ Sugar (model)
² Ethanol (exp) ¬ Ethanol (model).

4. Conclusions

The proposed compartmental nitrogen model enables to accurately describe growth, substrates and metabolites kinetics during fermentation. That indicates the pertinence of the hypothesis made and constitutes a first step before modeling mixed culture fermentation.

References

[1] P. Taillandier, Q.P. Lai, A. Julien-Ortiz, C. Brandam. World J Microbiol Biotechnol 30 (2014) 1959–1967.
[2] P. Brou, P. Taillandier, S. Beaufort, C. Brandam. Eur Food Res Technol (2018)

ECAB 5
The 5th EUROPEAN CONGRESS OF APPLIED BIOTECHNOLOGY
Florence 15-19 September 2019

Modelling of Enzymatic Fat Splitting Kinetics in Liquid – Liquid Multiphase System.

Sherly Rusli[1], Julia Lange[1], Janna Grabowski[1], Matthias Kraume[1]

1 Chair of Chemical and Process Engineering, TU Berlin

**Corresponding author: s.rusli@tu-berlin.de*

Highlights

- Modification of Michaelis Menten and Ping Pong Bi Bi Kinetics to accommodate surface area limitation.
- Validation of model by experimental data with in-situ drop size measurement.
- Inclusion of product inhibition in model.

1. Introduction

The enzymatic (trans)esterification process using lipase has attracted attention of both academic and industrial researchers due to its promising applications. This particular enzyme are able to react with two substrates in different phases, water or methanol in aqueous phase, and triglycerides in oil phase. Modelling its kinetics is a challenging task, as the reaction depends on the available surface area, and the surface area is dependent on the emulsification process.

2. Methods

To include the surface area, the Michaelis Menten kinetics was modified into two steps mechanism. The first step is the adsorption of enzyme molecules to the surface area, to create an activated enzyme molecule. The adsorption – desorption constants were fitted from experimental data of enzyme adsorption on single drop. To include the influence of side product Glycerol, the Ping Pong Bi Bi Mechanism is needed. The reaction are then divided into 5 steps, including formation of intermediate products Mono- and Di- Glycerides.

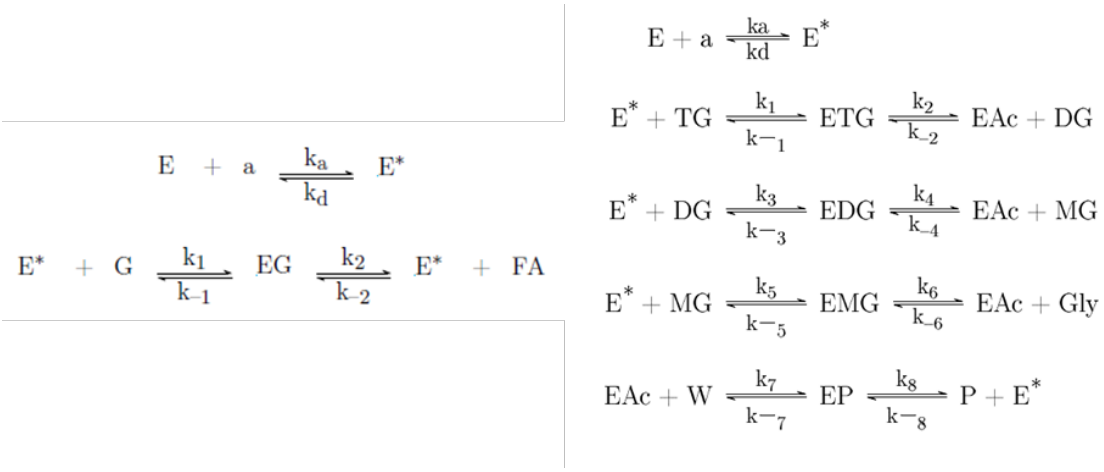

Figure 1. Modified Michaelis Menten (left) and Ping Pong Bi Bi (right) kinetics for inclusion of surface area limitation.

To validate the models, experiments were conducted in a batch stirred tank reactor, equipped with endoscope for measuring the surface area. Increasing the impeller speed decreases the drop sizes. Samples were taken from oil phase and analyzed by HPLC to quantify the amount of substrate and product.

3. Results and discussion

Experimental data shows two different kinetics. The initial reaction rate increases with increasing stirring rate, until all enzyme molecules are adsorbed. Above this point, the kinetics follow conventional enzymatic kinetics without surface area limitation. To make things more complicated, the prediction of drop sizes is dependent on the enzyme concentration, as increasing enzyme concentration decreases the interfacial tension, thus decreasing the drop sizes.

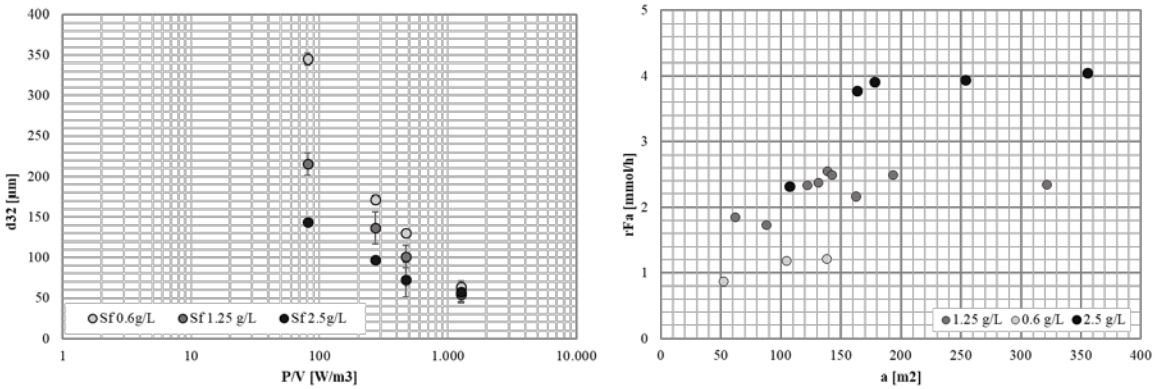

Figure 2. Effect of enzyme on drop sizes (left) and effect of surface area on reaction rate (right).

The two conditions can be predicted by a set of parameters from fitting against experimental data. The inclusion of surface area is imperative in the model, as is predicts the surface limiting mechanism. Without Glycerol inhibition, it is sufficient to model the reaction with the Michaelis Menten Kinetics, as there are no influence of the second substrate (water is in excess). However, when Glycerol is present, Ping Pong Bi Bi Kinetics is needed to predict the shift in reaction equilibrium.

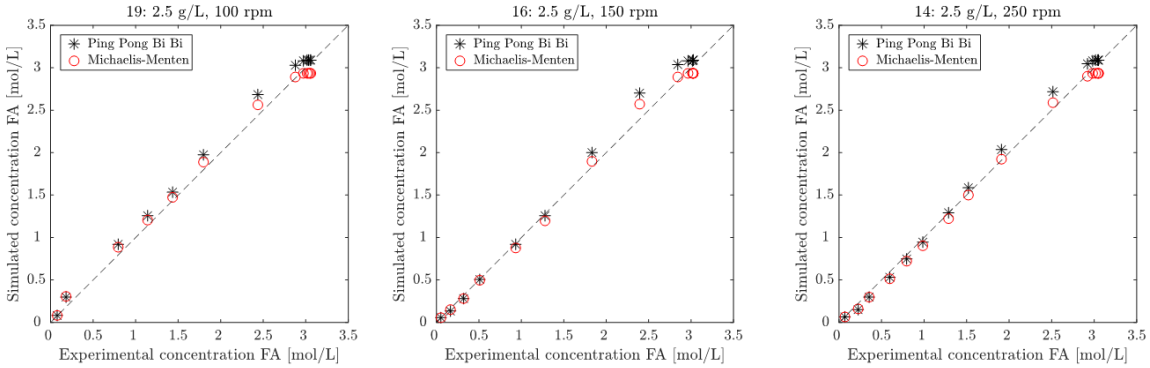

Figure 3. Deviations of experimental data and simulation.

4. Conclusions

To model the enzymatic transesterification, it is imperative to include the surface area and the glycerol concentration in the model.

ECAB 5
The 5th EUROPEAN CONGRESS OF APPLIED BIOTECHNOLOGY
Florence 15-19 September 2019

A two-components model for glucose uptake dynamics of E. coli cells

Vincent QUEDEVILLE[1], Jérôme MORCHAIN*[1], Rodney O. FOX[2], Philippe VILLEDIEU[3]

1 LISBP, Université de Toulouse, CNRS, INRA, INSA, Toulouse, France; 2 IMFT Université de Toulouse, CNRS, INPT, Toulouse, France ; 2 Department of Chemical and Biological Engineering, Iowa State University, Ames, USA; 3 ONERA/DMPE, Université de Toulouse, F-31055 Toulouse, France

**Corresponding author: jerome.morchain@insa-toulouse.fr*

Highlights

- A dynamic model for glucose uptake is proposed
- Two subsystems : PTS and permeases work in parallel
- Batch and continuous culture subject to dilution shifts are simulated
- The overshoots reported in the literature are predicted

1. Introduction

The very specificity of biological systems compared to chemical ones is the ability of cells to modulate the magnitude of the mass transfer between the liquid and biotic phases. A thermodynamic law of equilibrium can be set at the interface between two phases in chemical multiphase systems. However, the situation is much more complex for living systems because cells adapt their uptake capacity dynamically to match their needs. On the top of that, a long series of works from Ferenci proved that multiple transport systems are present [1]. On the long term, a cell regulates its uptake capacity so that the maximum possible growth rate is achieved, but the dynamics toward this steady state situation is far from simple. Little has been made in the modelling community to account for these facts. Our former proposition suffered from many constitutive defaults [2]. In this version, the difference between the actual uptake and the cell needs is used to trigger the regulatory mechanisms that control the cell uptake.

2. Methods

A structured model at the single cell level is formulated and used to write overall mass balance for nutrients and cell number at the reactor scale, resulting in a set of differential equations. Two internal properties are attached to a cell: its maximum potential uptake rate and its maximum elongation rate. The former is expressed as the sum of two contributions by PTS and permeases.

$$q_S = q_{PTS}(S) + q_{perm}(N, A, S)$$

The uptake by permeases implies the product of a number of permeases, N, by a permease activity A. These two quantities evolve in time, increasing when the uptake due to the sole PTS is insufficient to satisfy the cell need for growth (known from the second cell property, its elongation rate) and decreases when sugar uptake overtakes the cell needs. A basic flux metabolic model is used to orient the carbon fluxes toward growth or overflow. Beside the biological properties defining the biological upper limit, the overall uptake rate is obviously upper-bounded by the maximum flux of substrate reaching the cell –liquid interface considering possible external limitation.

3. Results and discussion

Batch and continuous cultures of *E.coli* were simulated. Figure 1 show that PTS dominates at high concentrations at the beginning of the culture. The cell needs are high for the elongation rate is also high. As the sugar concentration decreases, the PTS contribution becomes insufficient and that triggers the activation of the permease system. Interestingly and as reported by Ferenci [3], the induction of permeases occurs well before the sugar concentration has reached the affinity constant of the PTS system (here set to 10 mg/L). This apparent ability of cells to anticipate glucose exhaustion remained unexplained until now, but emerges as a natural consequence of the flux formulation adopted in our model. At the end of the batch, the time lapse before glucose exhaustion is so short that the number of permeases cannot significantly increase.

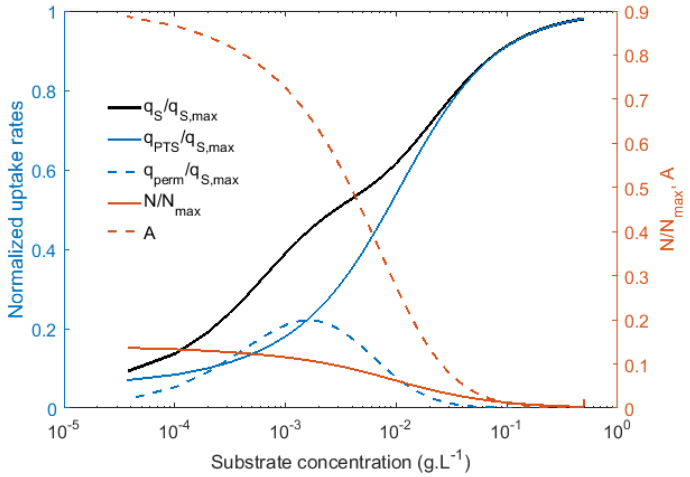

Figure 1. Evolution of PTS and permease contribution to the total uptake rate during the course of a batch culture. Number of permeases and permease activity. Read from right to left to follow the time course of the batch culture

4. Conclusions

A model for the regulation of sugar uptake under transient conditions was formulated and tested under various conditions (setp-up/step-down of the dilution rate, pulse addition). The most striking result is its ability to predict glucose uptake overshoots (far above the maximum value observed in batch) in the following of a pulse addition of substrate, as reported years ago by Neubauer and co-workers [4].

References

[1] T. Ferenci, FEMS Microbiol. Rev. 18 (1996) 301–317. doi:10.1111/j.1574-6976.1996.tb00246.xJ.
[2] V. Quedeville, H. Ouazaite, B. Polizzi, R.O. Fox, P. Villedieu, P. Fede, F. Létisse, J. Morchain, Chem. Eng. Res. Des. 132 (2018) 966–981. doi:10.1016/j.cherd.2018.02.025.
[3] T. Ferenci, Hungry bacteria – definition and properties of a nutritional state, Environ. Microbiol. 3 (2001) 605–611. doi:10.1046/j.1462-2920.2001.00238.x
[4] P. Neubauer, L. Häggström, S.O. Enfors, Biotechnol. Bioeng. 47 (1995) 139–146.

ECAB 5
The 5th EUROPEAN CONGRESS OF APPLIED BIOTECHNOLOGY
Florence 15-19 September 2019

Development, Validation and Comprehensive Sensitivity Analysis of a Fermentation Model Expediting the Process Design of a Biorefinery

Nikolaus I. Vollmer[1], Krist V. Gernaey[1], Solange I. Mussatto[2], Gürkan Sin[1] *

1 PROSYS, Department of Chemical and Biochemical Engineering, Technical University of Denmark;

2 Biomass Conversion and Bioprocess Technology Group, Novo Nordisk Foundation Center for Biosustainability, Technical University of Denmark.

**Corresponding author: gsi@kt.dtu.dk*

Highlights

- Systematic Fermentation Model Development for Biorefinery Process Design.
- Production of Xylitol from Lignocellulosic Biomass.
- Validation and Comprehensive Sensitivity Analysis consolidating the Development Strategy and showing potential for Extended Applications.

1. Introduction

The Sustainable Development Goals of the United Nations (UN-SDG) demand inter alia a transition towards sustainable and responsible economic production patterns [1]. A key approach in achieving these goals is the concept of a biorefinery, in which the processing of lignocellulosic biomass (LB) serves to provide multiple value-adding products [2]. A major drawback though still remains its economic profitability. Therefore, extensive research and development efforts are required to design, analyze and holistically optimize biorefinery concepts in order to enhance their economic feasibility [3]. For these purposes, tools from Process Systems Engineering (PSE) can be employed to give adequate responses to questions from unit level up to the plant-in-market level. The focus of this contribution lies on the production of xylitol by fermentation in a biorefinery. Xylitol can be a highly value-adding product due to its increasing demand in e.g. the health industry [4]. Therefore, a first-principles fermentation model is developed to describe mechanistically the yield of xylitol and the process dynamics. A multi-stage approach is used to develop a customized model which is able to support the process synthesis and design for the biorefinery including performance prediction, sizing and costing analysis. To this end the model accounts for various process phenomena from different scale levels such as biological (e.g. the specific metabolism), chemical (e.g. acid-base equilibria) and physical (e.g. gas-liquid mass transfer) in a fermentation reactor.

2. Methods

The model development incorporates seven subsequent steps, which allow for a gradual implementation: *Step (1)* - Simple Substrate-Product-Biomass correlations, *step (2)* - Oxygen Uptake, *step (3)* - CO_2 production, *step (4)* - Nitrogen Consumption + weak acid-base equilibrium, *step (5)* – Gas-Liquid Mass transfer and Energy Balance, *step (6)* - Internal metabolism reactions and *step (7)* - Additional Products and Substrates. A model framework based upon the matrix formulation of Sin et al [5] is chosen, since it facilitates the desired stepwise implementation.

Exemplary, during *step (1)* an overall mass balance and component mass balances for the substrates, the cell biomass and the products are derived. Conversion rates for all the components are calculated with a stoichiometric matrix of all the components and a process rate vector with all the occurring reactions in the fermentation, which are biomass formation, maintenance and the production of the products [5]. All the further steps aim to add further components and processes to the matrices/vectors and introduce new component or overall mass balances and energy balances. The steps are consecutively validated with data for a specific microorganism employed for xylitol production. Finally, a comprehensive local and global sensitivity analysis is conducted.

3. Results and discussion

The purpose of this approach is to guarantee a sufficient model complexity, while taking into account all necessary mentioned factors avoiding excessive complexity. Hence, *step (1)* is supposed to serve as fundamental model base. Since most microorganisms grow under aerobic conditions, oxygen is integrated into the model in *step (2)* to yield information about the oxygen demand. Since CO_2 is an important end product in the aerobic metabolism, a quantification is important, since it can be sold as by-product. The inclusion of nitrogen in *step (4)* contributes furtherly to the accurate prediction of the biomass growth since the microorganisms require nitrogen to grow. The weak-acid base model is introduced in the same step, because nitrogen sources serve as proton donors and influence the pH value of the liquid directly, which itself influences the concentration of CO_2 in liquid. The consideration of mass transfer refines these phenomena and yield a quantitative response for oxygen and CO_2 concentrations in gas and liquid phase. Considering the evaporation of H_2O is important, since it quantifies its loss and hence equally a necessary compensation to maintain a constant reaction volume. Other contributing factors here a potential heating of the system due to thermophilic conditions or increasing viscosity which influences the mixing effort. The assessment after *step (5)* considers the sufficiency of the prediction qualities of the model. Both *step (6)* and *(7)* denote a trade-off between the model complexity and its final purpose of prediction. Due to the flexibility of the framework this assessment can always be revised, depending on the further needs of the desired application. The validation with data in the chosen case shows a sufficient result in terms of yield prediction for xylitol and the process dynamics after the fifth step, implying to cease the implementation here. The sensitivity analyses show expected results.

4. Conclusions

The presented model structure and in particular its sequential implementation with increasing complexity proves to be a perfectly suitable approach in order to provide a model for this purpose. It ascertains a flexible and easy implementation for all seven steps in case of adaption of the model framework for various microorganisms, products or substrates. Hence, it yields simple yet adequate models for the process design of a biorefinery and thus can support the transition towards more sustainable processes as demanded by the UN-SDG.

References [Calibri 10]

[1] United Nations, Transforming our world: The 2030 agenda for sustainable development, 2015.
[2] F. Cherubini, Energy Conversion and Management 51 (2010) 1412-1421.
[3] S.S. Mansouri et al, in M. Tabatabaei, M, Aghbashlo (Eds.), Biodiesel, Springer, Cham, 2018, pp. 127-148.
[4] S.I. Mussatto, in: S. da Silva, A. Chandel (Eds.), D-Xylitol. Springer, Berlin, Heidelberg, 2012, pp. 309-323.
[5] G. Sin et al, Biotechnology and Bioengineering 101 (2008) 153-171.

ECAB 5
The 5th EUROPEAN CONGRESS OF APPLIED BIOTECHNOLOGY
Florence 15-19 September 2019

The Effect of Co-Solvent and Catalyst Type on the One-Step Supercritical Carbon Dioxide (*Trans*)esterification of *Swietenia Macrophylla* Seed

Juvyneil Cartel[1], Joseph Auresenia[2]

1 Eastern Visayas State University, Tacloban City, Philippines; 2 De la Salle University, Manila, Philippines

**Corresponding author: joseph.auresenia@dlsu.edu.ph*

Highlights

- Utilizing co-solvent gave significant effect to the oil yield where methanol showed to be the best.
- Utilizing base-functionalized MWCNT as catalyst is still more practical rather than using KOH though it exhibited to make the highest yet at par %FAME Yield.
- Cetane number of the biodiesel used showed to be high which can provide short ignition delay in diesel engines when used.

1. Introduction

Mahogany (*Swietenia Macrophylla*) seed, a non-edible seed is not only abundant in most of the localities in the Philippines. It has been found out that the seed has a significant amount of oil of around 39-58% [1, 2]. Moreover, it was proven that Mahogany seed is a potential feedstock for biodiesel production which could meet biodiesel standards, comparable to petroleum-based diesel. However, issues on the presence of a significant amount of impurities like free fatty acid (FFA), moisture, waxes, and gums may arise. To resolve these issues the process may require additional processing steps before this feedstock can be used for biodiesel production using the conventional base-catalyzed process. Otherwise, a process requiring the use of a specific catalyst and /or solvent conditions may be needed to effectively utilize this feedstock. Until now, achieving the supposed potential of seed biofuels remains in the experimental lab scale due to the mundane cost of its production, making them less attractive for long-term operations in the industrial-scale [3].

One-step (*trans*)esterification using supercritical carbon dioxide and two-reactors in series of dried Mahogany seed creates interest and was studied since there is a significant reduction in the process supply chain by combining crucial steps and increasing the residence time which could improve the conversion of triglycerides to FAME. The effect of co-solvent and catalyst type on the relatively novel process was determined and quantified in order to determine their response on oil and FAME yield.

2. Methods

The experimental set-up include: (a) Liquid CO_2 cylinder which provides the carbon dioxide in the process; (b) Micro filter which ensures that no contaminants could enter the system; (c) Chiller which brings down the temperature of the carbon dioxide to 2^{o}C, thus in liquid state; (d) HPLC (High Performance Liquid Chromatography) pump which regulates the flow rate of the carbon dioxide of the system; (e) Oven with installed pre-heater (f) that controls the temperature for the

extraction/(*trans*)esterification; (g) the reactors (approximately 10 and 50-ml capacity) where extraction and (*trans*)esterification are being held; (h) BPR (Back Pressure Regulator) which controls the pressure of the system; (i) Cyclone separator which separates carbon dioxide from the sample; and (j) is the sampler flask. The experiment was divided into two phases. First phase dealt with the effect of co-solvent type on oil yield while the 2nd phase studied on the effect of catalyst type on the FAME yield. All of these were subjected in supercritical carbon dioxide extraction/(*trans*)esterification at a pressure of 30 MPa and temperature of 90°C, and at CO_2 influx of 10 g/min. N-hexane, methanol, mixture of n-hexane and methanol were among the co-solvents used. On the other hand, potassium hydroxide (KOH), acid-functionalized MWCNT (multi-walled carbon nanotubes) and base-functionalized MWCNT were the types of catalyst utilized in this study. One-factor completely randomized design was used as the basis in designing the experiments.

3. Results and discussion

The result has shown that utilizing a co-solvent could give significant effect to the oil yield where methanol showed to be the best. Utilizing n-hexane with methanol as co-solvent could have been a good alternative for it gave a close result to methanol. However, lots of impurities have been observed that 86% have been wasted. Moreover, using more co-solvent types could just make the separation complex. On the other hand, %FAME Yield was highest when OST was run with KOH as catalyst. The result is close to that of the base-functionalized MWCNT catalyst. However, utilizing KOH is cost intensive and will not pose an economic advantage to the process.

The %FAME could have been high enough to meet the European standard of at least 95%, however, optimum conditions for one-step supercritical fluid (trans) esterification could not be met due to the limited capacity of the reactors (e.g. allowable pressure, temperature). In effect of low %FAME important properties of the biodiesel obtained under the supercritical conditions failed to conform to the standards except for Cetane number (CN) which is high. This means that with high CN, the biodiesel produced can provide short ignition delay in diesel engines.

4. Conclusions

In conclusion, it is best to use methanol as co-solvent and base-functionalized MWCNT to obtain the most practical FAME yield. Moreover, the biodiesel produced can give the highest Cetane number which is relative to short ignition delay among the feedstock studied. However, reactors have yet to be upgraded with higher capacity, especially the maximum allowable temperature to possibly obtain higher %FAME and conform to all standards on biodiesel properties.

References

[1] Gumaling, R. P., Joyno, J. R. Q., Pajaron, J. R. P., Joyno, C. Q., Arazo, R. O., Ellacer, N. V. C. R., … Ido, A. L. (2018). Increased bio-oil yield from Swietenia macrophylla seeds through microwave pretreatment and ultrasonic-assisted solvent extraction. Sustainable Environment Research, 28(6), 430–437. https://doi.org/10.1016/j.serj.2018.06.003

[2] Mohan, M. R., Jala, R. C. R., Kaki, S. S., Prasad, R. B. N., & Rao, B. V. S. K. (2016). Swietenia mahagoni seed oil: A new source for biodiesel production. Industrial Crops and Products, 90, 28–31. https://doi.org/10.1016/j.indcrop.2016.06.010

[3] Zahan, K. A., & Kano, M. (2018). Biodiesel production from palm oil, its by-products, and mill effluent: A review. Energies, 11(8), 1–25. https://doi.org/10.3390/en11082132W. Black, E.B. White, The Elements of Science, third ed., MacCluski, New York, 1987.

Mass transfer CFD modeling of biodiesel purification using deep eutectic solvents in a microseparator.

Ana Jurinjak Tušek[1], Davor Valinger[1], Martin Gojun[2], Anita Šalić[2], Bruno Zelić[2*]

[1]University of Zagreb, Faculty of Food Technology and Biotechnology, Pierottijeva 6, HR-10000 Zagreb, Croatia; [2]University of Zagreb, Faculty of Chemical Engineering and Technology, Maruli•ev trg 19, HR-10000 Zagreb, Croatia

*Corresponding author: bzelic@fkit.hr

Highlights

- lipase catalyzed biodiesel transesterification
- biodiesel purification in a microseparator
- analysis of the flow patterns
- CFD simulations of biodiesel and DES flow profiles

1. Introduction

Biodiesel is an alternative fuel, similar to classic fossil fuels that can be used in diesel engines. It is a mixture of alkyl esters of fatty acids that can be produced from vegetable oil, micro algal oil or animal fats [1,2,3]. Biodiesel production is mostly achieved through transesterification, using short-chain alcohols (typically methanol or ethanol). This reaction also produces glycerol, which along with unreacted alcohol and oil, has to be removed from the product before it can be used in commercial application. There are several approaches that can be used for biodiesel purification (sedimentation, decantation, water washing, filtration etc.) but all of them are usually characterized as inefficient, non-ecological, expensive, energy consuming etc. In order to resolve some of this disadvantages microseparators coupled with deep eutectic solvents (DESs) were proposed as solution. Microseparators have been widely used to improve the mass and heat transfer processes between two phases due to the high surface-to volume ratio, higher heat and mass transfer rates and short diffusion distance. To achieve the maximum productivity of the biodiesel purification process in a microseparator it is necessary to take into account nature of the components and the operational conditions, such as temperature, volumetric flow rate, dimensions of the used microchannel. All mentioned parameters significantly influence the flow pattern formation. In this work computational fluid dynamics (CFD) analysis was carried out to illustrate and visualize the interactions between two existing phases in separation systems.

2. Methods

Biodiesel production catalyzed by lipase from *Thermomyces lanuginosus* using edible oil and methanol as the substrates was performed in a batch reactor according to procedure described by Budžaki *et al*. [4]. After biodiesel was produced, it was placed in a separation funnel (traditional approach for glycerol removal) in order to remove glycerol for 24h. After separation of two phases and analysis of biodiesel content separation efficiency was around 90.37%. In order to remove residual glycerol, microseparator (length: width: depth = 332 mm: 500 µm: 50µm; Micronit

Microfluidics B.V. Netherlands) in combination with DES was used. Experimentally obtained data were compared with the CFD simulation results. The CFD simulations of the biodiesel and DES flow profiles in selected microseparator were performed using the finite element software COMSOL Multyphysics v.4.2. A laminar flow model with Lagrangian specification of the field and Ditrich type boundary conditions were used.

3. Results and discussion

In microseparators mass transfer occurs along the interface area between phases so stability of the area is the first necessary condition. The second condition is crucial for phase separation at the exit of microseparator where interface area has to be positioned in the middle of microchannel and flow has to be parallel. Since DES and biodiesel have different physical properties, the input flow rates had to be adjusted so that both phases occupy the same volume in the channel. Therefore, the influence of flow rates on the flow pattern was studied. This was done with the help of a microscope for different flow rates, ranging from 0 to 20 µL min^{-1} for the biodiesel and from 0.02 to 18 µL min^{-1} for DES (Figure 1).

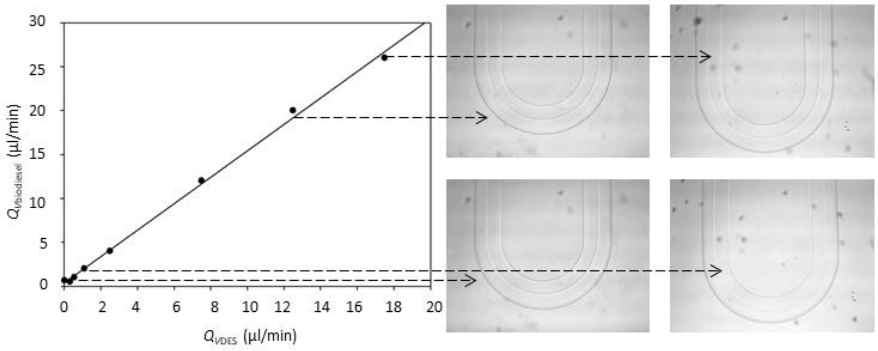

Figure 1. Influence of the velocity on the position of the interphase area

To analyze the hydrodynamics of the selected microseparator system, Re numbers were estimated. The high Re numbers leads to better mixing, and also changes the flow profile. CFD experiments for visualizations of both biodiesel and DES flow profile were carried out by estimating the fluid properties based on assumption of simple mass balance at the beginning and at the end of the microseparator.

4. Conclusions

In this study biodiesel purification using DES in a microseparator was performed. Obtained results indicate that microseparator system is efficient technology for the biodiesel purification. CFD simulations ensure delight insight in the hydrodynamics of biodiesel purification process.

References

[1] T. Issariyakul, A.K. Dalai, Renew. Sust. Energ. Rev. 31 (2014) 446–471.
[2] Z. Yaakob, M. Mohammad, M. Alherbawi, Z. Alam, K. Sopian, Renew. Sust. Energ. Rev. 18 (2013) 184–193.
[3] L. Azocar, G. Ciudad G, H.J. Heipieper, R. Navia, Appl. Microbiol. Biotechnol. 88 (2010) 621–636.
[4] S. Budžaki, A. Šalić, B. Zelić, M. Tišma, Chem. Biochem. Eng. Q. 29 (2015) 329–333.

ECAB 5
The 5th EUROPEAN CONGRESS OF APPLIED BIOTECHNOLOGY
Florence 15-19 September 2019

Novel biosupport material for *A. ferrooxidans* immobilization

Arrate Santaolalla[1*], Naiara Rojo[1], Juncal Gutierrez[1], Gorka Gallastegui[1], Astrid Barona[2]

Department of Chemical and Environmental Engineering; University of the Basque Country UPV/EHU

[1] Faculty of Engineering Vitoria-Gasteiz. Nieves Cano, 18. 01006 VITORIA-GASTEIZ (SPAIN)

[2] Faculty of Engineering of Bilbao. Torres Quevedo, 1. 48013 BILBAO (SPAIN)

**Corresponding author: arrate.santaolalla@ehu.eus*

Highlights

- Bacterial cellulose (BC) is an innovative support for biomass immobilization.
- The active material *A. ferrooxidans*+BC can be used in continuous bioleaching processes.
- The immobilized biomass remains active even at 15 g Cu^{2+}/L.

1. Introduction

Bioleaching is a microorganism-assisted process used to dissolve metals through the action of oxidizing agents. It has been proposed as a sustainable alternative to conventional micromachining and extracting processes for the recovery of valuable metals [1].

Several authors have investigated the immobilization of the bacterium *Acidithiobacillus ferrooxidans* (the most widely studied microorganism for metal bioleaching) on different support materials with a view to increasing microbial density inside the bioreactor and facilitating biomass replacement when required [2,3]. Bacterial cellulose (BC) is a promising candidate to be used as a support material for biomass immobilization due to its peculiar 3D network structure of ribbon-shaped cellulose nanofibrils (2-4 nm in diameter) and its high specific surface [4].

This study's main objective was to assess the response of an innovative active material when used to immobilize *A. ferrooxidans* bacteria. An immobilization methodology was proposed, and the study focused on the influence that the number of attached bacteria and the concentration of dissolved copper had on the time required to recover the oxidant.

2. Methods

Bacterial cellulose (BC) was synthesized following the procedure described by Retegi et al. [5]. Bacteria were immobilized on BC by immersing the biopolymer into an Erlenmeyer flask with a nutrient medium containing 6 g Fe^{2+} L^{-1}. A 5% inoculum of *A. ferrooxidans* in the exponential growth phase was added, and cells were cultivated until the complete oxidation of the Fe^{2+} to Fe^{3+} (Figure 1a). Thus, the active BC was obtained (*A. ferrooxidans*+BC).

The relationship between the number of immobilized bacteria and Fe^{2+} oxidation time was studied by culturing 4, 6 and 8 pieces of the active BC (20x20x7mm) in a fresh medium. In addition, a study was conducted on the effect of copper concentration on the activity of the immobilized bacteria by cultivating active BC pieces in nutrient media containing 0, 5, 10 and 15 g Cu^{2+} L^{-1}.

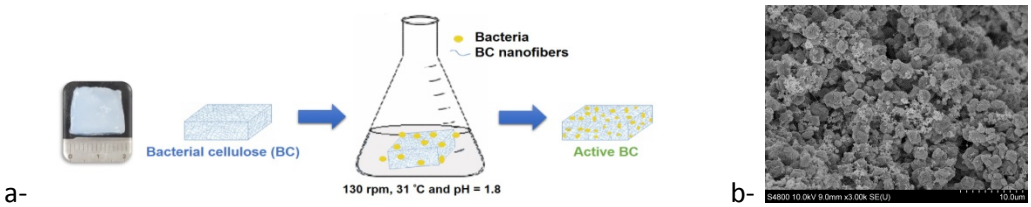

a- b-

Figure 1. a- Preparation of the active BC; b- SEM analysis of A. *ferrooxidans* attached to the BC.

3. Results and discussion

A. ferrooxidans cells successfully colonized the support material, and the time required for the microorganisms to oxidize the Fe^{2+} was not affected by the presence of the BC. It is noteworthy that only one growth cycle was required to obtain the active material (Figure 1b).

The average Fe^{2+} oxidation rate with eight BC pieces was about 25% higher than with four pieces. Regarding the inhibitory effect of dissolved copper on the biological activity of A. *ferrooxidans*, the oxidation time increased linearly with copper content (up to threefold for the highest metal concentration). Nevertheless, when the immobilized bacteria previously exposed to the three concentrations of copper were cultivated in a second cycle, the time needed for the complete conversion of Fe^{2+} was significantly reduced, being similar in all the bioreactors. The most significant difference was recorded in the flask with 15 g Cu^{2+} L^{-1}, where the oxidation time was reduced by 68% compared to that in the first oxidation cycle. These results suggest that the attached bacteria gradually adapted to the presence of Cu^{2+}. Moreover, active BC pieces adapted to 5 and 10 g Cu^{2+} L^{-1} were not inhibited when cultivated in media containing 15 g Cu^{2+} L^{-1} (in a third cycle). These results confirm the successful adaptation of the immobilized bacteria regardless of the initial copper concentration.

4. Conclusions

Bacterial cellulose is an outstanding innovative support material for the immobilization of *A. ferrooxidans,* and therefore a promising carrier for continuous bioleaching processes. Oxidation time was reduced according to the number of active BC pieces, and the immobilized bacteria gradually adapted to the toxicity of high concentrations of dissolved copper, even at 15 g Cu^{2+}/L.

Acknowledgments

The authors wish to acknowledge the financial support received from the State Agency for Research (AEI) of the Spanish Government and the European Regional Development Fund (ERDF) (Project CTM2016-77212-P) and the University of the Basque Country (GIU 15/20).

References

[1] E. Diaz-Tena, A. Barona, G. Gallastegui, A. Rodríguez, et al., Crit. Rev. Biotechnol. 37 (2017) 323-332
[2] A. Giaveno, L. Lavalle, E. Guibal, and E. Donati, J. Microbiol. Methods. 72 (2008) 227–234.
[3] N. Zhu, C. Shi, R. Shang, C. Yang, Z. Xu, and P. Wu. Biotechnol. Appl. Biochem. 64 (2017) 727-734.
[4] M. L. Cacicedo, M. C. Castro, I. Servetas, L. Bosnea, K. et al., Bioresour. Technol. 213 (2016) 172-180.
[5] A. Retegi, N. Gabilondo, C. Peña, R. Zuluaga, C. Castro, et al., Cellulose. 17 (2010) 661-669.

Thermal stability of the inulinase of *Kluyveromyces marxianus* in the presence of organic cosolutos.

(*) Augusto Castillo[1], Angel Castro[2], Roberto Vega[3]

[1]Departamento Académico de Agroindustria, Facultad de Ingeniería Universidad Nacional del Santa, Av. Pacifico 508. Teléfono +5144-312639. Chimbote, Perú; [2]Departamento Académico de Microbiología y Biotecnología, Facultad de Ciencias Universidad Nacional del Santa, Av. Pacifico 508. Teléfono +5144-312639. Chimbote, Perú; [3]Departamento de Bioquímica, Facultad de Farmacia y Bioquímica. Universidad Nacional Mayor de San Marcos, Jr. Puno 1002, Teléfono +5116197000-4831. Lima, Perú.

**Corresponding author: acascal2002@yahoo.es; acastillo@uns.edu.pe*

Highlights

- Exo-inulinase produced by fermentation of *Kluyveromyces marxianus* in yacon extract.
- Checking glycerol, mannitol and sorbitol as stabilizing substances in biocatalysis.
- Improvement of the thermal and kinetic stability of the semi-concentrated inulinase.

.

1. Introduction

The exo-inulinase of Kluyveromyces marxianus NRRL-Y 7571 is an extracellular enzyme that catalyzes the hydrolysis of inulin into practically pure fructose. Also inulinase has been found transfructosilación activities. The biggest problem facing the use of inulinase is its poor kinetic and thermal stability. One way to stabilize an enzyme is to use substances that increase its thermodynamic stability.

2. Methods

A batch culture of K. marxianus was carried out in an automated 2 L fermenter with optimized liquid medium, containing yacon extract, to generate the enzymatic extract, then the separation by centrifugation and semi-concentration of the inulinase by precipitation with ethanol.
The activity and thermal stability data were obtained, incubating 10 mL of the enzyme semi-concentrate containing 5% and 10% of glycerol, mannitol and sorbitol, as corrected, in 0.05 M citrate phosphate buffer, pH 5.0, at 55ºC for different periods, after which the remaining activity was measured. Enzymatic activities were determined by measurements of initial velocity on a standard 20 g / L sucrose solution. The analyzes of reducing sugars and proteins were made by DNS and Bradford.

3. Results and discussion

The results showed that the presence of each of the cosolutos: glycerol, mannitol and sorbitol in their two concentration levels, increased the catalytic activity of inulinase by an average of 15.81%, which shows that each substance had a power-inducing effect catalytic enzyme. Correspondingly, the three cosolutos improved the biocatalytic and thermodynamic stability under non-reactive conditions of the exo-inulinase, with 5% glycerol contributing the best (Fig. 1), reaching the lowest value of the kinetic constant of equal denaturation at 0.0845 h^{-1} and 7.5 times the average life time of the inulinase acting without stabilizer. This is because the substances contributed to maintain the native conformation of the enzyme, deduced that it became more rigid, at least in certain areas of its surface, supported by the mechanism of the exclusion of substances from the surface of the protein, which increases the structured water around that area.

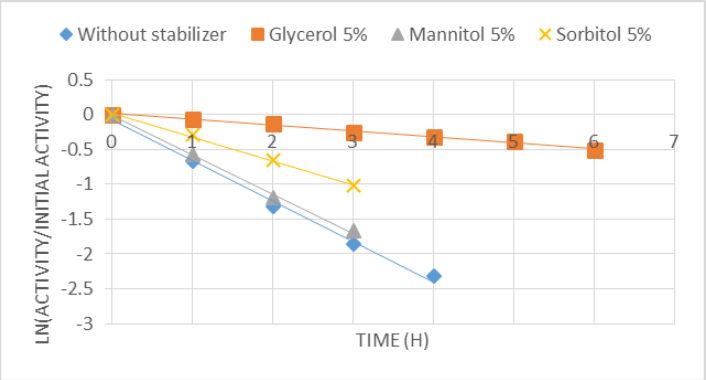

Figure 1. Effect of glycerol, mannitol and 5% sorbitol each on the thermal stability of *K. marxianus* NRRL-Y 7571 inulinase acting on sucrose.

4. Conclusions

The presence of each of the substances: glycerol, mannitol and sorbitol, improved the biocatalytic and thermodynamic stability under non-reactive conditions of the semi-concentrated exo-inulinase of *K. marxianus* NRRL-Y 7571, with glycerol contributing more significantly.

References

[1] S. Belluzo, V. Boeris, B. Farruggia, P. Picó. International Journal of Biological Macromolecules 49 (2011) 936– 941.

[2] J. Diestra, L.Margarito, R. Vega, A. Castillo. Scientia Agropecuaria 6(4) (2015): 303-312.

[3] S. Golunski, V. Astolfi, N. Carniel, D. de Oliveira, M. Di Lucio, M. Mazutti, H. Treichel. Separation and purification technology, 78 (2011): 261-265.

ECAB 5
The 5th EUROPEAN CONGRESS OF APPLIED BIOTECHNOLOGY
Florence 15-19 September 2019

Valorisation of solid waste: Briquettes production from corn-stover

Oluwaseun Oyekola[1], Ongama Soka[1], Felicia Ngubane[1]

1 Department of Chemical Engineering, Cape Peninsula University of Technology, Bellville Campus, Symphony way, Cape Town

**Corresponding author: oyekolas@cput.ac.za*

Highlights

- Effect of temperature, heating rate and hold time on the char HHV from the slow pyrolysis of corn-stover was investigated.
- The optimum conditions for maximal char HHV were found at a temperature of 431°C, 6°C/min heating rate and a hold time of 29 minutes.
- The biochar HHV was 28.64 MJ/kg comparable to that of coal (23.9-26 MJ/kg).
- Briquettes with high density and durability were obtained

1. Introduction

With increasing global population and industrial activities, the world is currently challenged with energy crisis and the associated global warming, and environmental pollution. These issues have been the subjects of intensive research in recent years. Energy shortage is a serious problem in developing countries and the energy sector is looking for alternative sources of energy, which are environmentally friendly and cheaper. South Africa is the largest producer of maize in Africa (10-12 million tonnes per year) (FAO, 2016). Approximately 9 million metric tonnes of corn residues, corncob and corn-stover are produced per annum as agricultural wastes in South Africa (FAO, 2015). Hence, this can be a major pollutant as a solid waste and the disposal thereof can be challenging which can pose as a harmful threat to the environment. Corn-stover is a naturally abundant domestic energy source that is promising to relieve energy scarcity (Morissette et al., 2014). It is sustainably available with no competition for resources with food/feed production and other biomass applications. While there have been comprehensive reports of laboratory-scale studies in South Africa for bioethanol, biochar, bio-oil and gases (Mohlala et al., 2016), there is dearth of literature reporting the use of corn-stover for the generation of briquettes. Briquettes are made from waste materials or partially compressed biomass waste (Morisette et al., 2014). They are eco-friendly alternatives as fuel instead of charcoal, firewood or coal. The purpose of this work is to promote material and energy valorisation of corn-stover. This study investigated the optimisation of the carbonisation of corn-stover. Densification process of biochar resulting in briquette production was carried out.

2. Methods

The corn-stover was collected from a maize farm. The collected samples were dried to 10% and milled to a particle size range of 3.5mm-0.63mm. Biochar was produced via slow pyrolysis using a retort reactor in the absence of oxygen by purging with nitrogen. The ASTM D3175-17 standard methods were used to obtain the ash content of the samples. A central composite design (CCD) of gram scale experiments was used to study the effects of the of temperature, heating rate and hold

time on the char HHV. Design Expert® Software Version 10 (Stat-Ease, Inc., Minneapolis, USA) was used to study the CCD. With regards to the design of experiments (DoE), the selected DoE conditions were 300, 400 and 500°C for temperature, 5, 12.5 and 20°C/min for heating rate and 5, 17.5 and 30 minutes for holding time. Briquettes were produced by adding a starch binder (5 and 10%) to the biochar. Finally, the mixture was compressed using a piston press cylinder to densify the biochar/binder mixture.

3. Results and discussion

The optimum conditions for char production were 453°C, 5°C/min and 29 min. Under these conditions, an average char yield of 34.5% was determined. The final prediction equation obtained from Design Expert® software version 10 for char HHV by temperature (x_1), heating rate (x_2) and hold time (x_3) of a fixed bed reactor is provided by equation 1. The positive quadratic factor coefficients (+1.48 and +0.26) indicate that char HHV tends to increase with a rise in temperature and hold time respectively (Equation 1). While the negative quadratic factor coefficient (-0.5) indicates that an increase in heating rate will result in a reduction in char HHV.

$$\text{Char HHV} = 24.06 + 1.48x_1 - 0.5x_2 + 0.26x_3 - 0.54x_1x_2 - 0.071x_1x_3 - 0.41x_2x_3 - 2.46x_1^2 + 0.15x_2^2 + 0.68x_3^2 \quad \textit{equation 1}$$

The ash content of the untreated corn-stover was 4.96% while the biochar was 13.34%. This indicates its potential to produce smokeless solid fuel. Higher heating value (HHV) of the untreated corn-stover was found to be 18.7 MJ/kg while the biochar HHV was found to be 28.92 MJ/kg comparable to that of coal (23.9-26 MJ/kg) (Morissette et al., 2014). The carbon rich biochar is obtained with higher amounts of fixed carbon of 63.70% and ash content of 13.34%, but lower amounts of volatiles of 20.38% than corn-stover biomass feedstock which means that the biochar produced has improved burning properties because lower volatile matter results in increased burning time and no smoke during burning. The compressive strength obtained from densification was in the range 3.45-6.11 N/mm^2 with increasing binder concentration between 5 and 10%. The density obtained through densification process (20-40MPa) ranges from 420-788 kg/m^3 shows the durability obtained through densification which ranges from 97-100%.

4. Conclusions

Briquettes with high density, durability and fuel properties were obtained. These have potential to substitute or augment reliance on coal.

References

[1] L.M. Mohlala, M.O. Bodunrin, A.A. Awosusi, M.O. Daramola, N.P. Cele and P.A. Olubambi. Alexandria Engineering Journal. 55(2016) 3025-3036.

[2] R. Morissette, P. Savoie, J. Villeneuve. Energies. 4 (2014) 1102-1111.

[3] FAO. Available from: http://www.fao.org/docrep/w2698e/w2698e05.htm#TopOfPage (accessed 22 July 2016)

[4] FAO. Available from: http://www.fao.org/giews/countrybrief/country.jsp?code=ZAF (accessed 11 June 2016).

ECCE12
The 12th EUROPEAN CONGRESS OF CHEMICAL ENGINEERING
Florence 15-19 September 2019

A simulation study to evaluate the potential of semi-transparent solar panels coupled with a closed intensified photobioreactor

Julien Louveau[1], Jeremy Pruvost[1], Mariana Titica[1], Navid Moheimani[2]

1 University of Nantes, Oniris, CNRS, GEPEA, UMR 6144, 44602 Saint-Nazaire Cedex, France

2 Murdoch university WA 6150, Murdoch, Australia

**Corresponding author: Julien.louveau@eut.univ-nantes.fr*

Highlights

- A model coupling semi-transparent solar panels and photobioreactors has been developed
- Synergies and trade-offs between biomass and electricity coproduction were analyzed

1. Introduction

In contrast with open ponds, closed photobioreactor (PBR) technology allows a tight process optimisation which leads to significant productivity enhancement. Nevertheless, when set outdoor (to benefit from natural sunlight), these PBRs are sensitive to climatic fluctuations. Ensuring optimal growth conditions becomes critical. This especially concerns the temperature as enclosed culture volumes tends to overheat [1]. Then, active temperature control could become prohibitive in terms of energy needs.

As microalgae only need a small portion of the solar light (the photosynthetic active range: PAR, [400 – 700] nm), removing the unnecessary light (infra-red: IR and ultra-violet: UV) could reduce the heating of the PBR. To filter the incoming light, the use of semi-transparent solar panels (PV) has been suggested by [2]. Those solar panels are able to capture and convert into electricity some specific radiations depending on their wavelength. Other radiations are transmitted and can be used for biological conversion. Coupling a PBR and a semi-transparent solar panel opens then the perspective to coproduce biomass and electricity while preventing the overheating of the PBR.

In this context, the work presented here has investigated, with a model-based approach, the impact of such coupling on PBR's thermal behaviour, microalgae productivity and electricity production.

2. Methods

The investigation of this study has been done by numerical simulation. Three validated models from the literature were coupled to set a predictive model able to simulate PBR-PV associations. It aims to maximize biomass production while decreasing energy needs. A generic thermal model [1] was used to determine the thermal behaviour of the PBR and the amount of energy required for temperature control. The range of operating temperature was fixed to [15 – 34]°C which is considered suitable for microalgae growth without significant loss in productivity (Todisco et al,. 2019). Second, a microalgae growth model [3] was used to calculate the productivity of the culture in solar radiation conditions, considering light alone limits growth. Finally, an electricity production model [2] was used to compute the production of the solar panel. Different light filters (solar panels) have been tested. Numerical simulations have been performed considering a thin-film solar

photobioreactor: AlgoFilm© *(figure 1)* [1]. The meteorological data used describes the average weather of a year for the city of Nantes. In all simulations, the input light was set in spectral form.

3. Results and discussion

Different simulation scenarios were performed, with a view to analyse synergies and trade-offs between biomass and electricity coproduction. An example of results is presented in Figure 2.

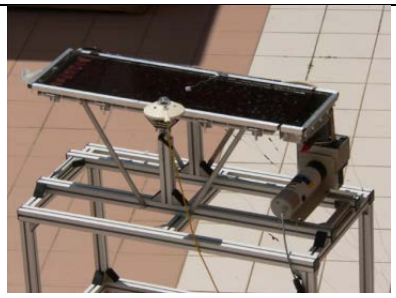

figure 1: The thin-film solar photobioreactor [1]

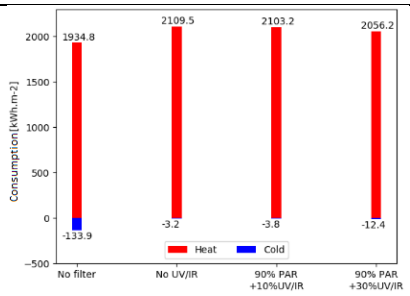

figure 2: Cumulated energy consumption

The simulation study revealed that the use of semi-transparent solar panels allows a significant reduction in PBR's cooling needs. However, it also results in an important raise in heat needs. In winter, with the tested weather, the nights can be as cool as 0°C, thus keeping the reactor at the lower set point requires a large amount of energy *(figure. 2)*. This is particularly true for the considered reactor which has been designed to prevent overheat (large contact area with the ambient air for a small volume). Thus, adding a solar panel was found detrimental for the winter period. Those results points out the necessity to find a compromise. For example, passive cooling and electricity production are increased by reducing the PAR transmitted to the culture. This was found to have a major impact on the reactor heating. It however reduces the biomass productivity (10% to 40% loss). Our model was found useful to obtain input data for a techno-economic analysis which would help to define an association strategy of such a promising hybrid system.

4. Conclusions

An integrated model was developed to simulate PBR-PV association, for the optimal design of a hybrid solar PBR maximizing biomass production while decreasing energy needs. This study showed that the use of semi-transparent solar panels significantly reduced the overheating of our solar PBR. It could however induce negative effects, such as the increase in heating need during the night. Predictions were found useful to determine the best compromise in terms of biomass and electricity production, but also energy saving for thermal regulation. Such a tool also enables to investigate other climates such as Australia where the monthly average temperature reaches 20°C. As the reactor could be warmer even in the night, this may be an interesting passive cooling solution for this location.

References

[1] V. Goetz, F. Le Borgne, J. Pruvost, G. Plantard, et J. Legrand, « A generic temperature model for solar photobioreactors », Chemical Engineering Journal, vol. 175, p. 443‑449, nov. 2011.

[2] D. Parlevliet et N. Moheimani, « Efficient conversion of solar energy to biomass and electricity », Aquatic Biosystems, vol. 10, no 1, p. 4, 2014.

[3] J. Pruvost, F. Le Borgne, A. Artu, J.-F. Cornet, et J. Legrand, « Industrial Photobioreactors and Scale-Up Concepts », in Advances in Chemical Engineering, vol. 48, Elsevier, 2016, p. 257‑310.

ECCE 12
ECAB 5

ECAB 5
The 5th EUROPEAN CONGRESS OF APPLIED BIOTECHNOLOGY
Florence 15-19 September 2019

Biotechnological recycling of platinum group metals and gold from post-consumer products

Yasuhiro Konishi*, Norizoh Saitoh, Toshiyuki Nomura

Department of Chemical Engineering, Osaka Prefecture University

1-1, Gakuen-cho, Naka-ku, Sakai, Osaka 599-8531, Japan

**Corresponding author: yasuhiro@chemeng.osakafu-u.ac.jp*

Highlights

- The use of *Shewanella* bacteria and baker's yeast to recover precious metals.
- Bioreductive deposition of PGMs from the leachate of spent catalysts at pH 6.
- Selective and efficient biosorption of Au from the CPUs leachate at pH 1.
- New biotechnologies to extract PGMs and gold from post-consumer products.

1. Introduction

Many post-consumer products, such as electronic goods and catalytic converters in cars, are important sources of precious and rare metals. Although conventional thermal and chemical techniques remain the best methods for recycling precious and rare metals, these metals have yet to be fully utilized. Therefore, further research and development is needed to fully recycle precious and rare metals from secondary sources. We believe that biological technologies now provide an attractive and eco-friendly alternative strategy. This paper describes our research results from using new biotechnologies to fully recycle platinum group metals (PGMs) from spent automotive catalysts and gold from electronic waste.

2. Results and discussion

We focused on using the metal ion-reducing bacterium, *Shewanella algae*, to recover PGMs from the aqua regia leachate of spent automotive catalysts (Figure 1). The Shewanella bacteria were able to reduce PGMs ions (Pd(II), Pt(IV) and Rh(III)) in the catalyst leachate as metallic nanoparticles on the bacterial cells at room temperature and pH 6 within 60 min, using formate as the electron donor.

We also employed baker's yeast, *Saccharomyces cerevisiae*, as a commercially available biomaterial for collecting gold ions from the aqua regia leachate of spent central processing units (CPUs) from electronic waste (Figure 2). The baker's yeast was able to rapidly and effectively collect only gold ions from the CPUs leachate at pH 1 within 10 min. Importantly, baker's yeast did not react with other heavy metal ions, such as copper, nickel, and iron.

This flow diagram compares the conventional wet chemical process with our new bioprocess for recycling PGMs and gold (Figure 3). Our new bioprocess integrates a complex multistep method into a single-step procedure that separates and concentrates the precious metal from a leaching

solution. Unlike conventional processes, the benefits of this process include a significant reduction in energy consumption and material consumption, and a low environmental impact.

Our highly efficient bioprocess could be introduced at local collection points for post-consumer products and operate as a regionally distributed technology for fully recycling metal resources from post-consumer products, which will lead to the sustainable use of precious metals.

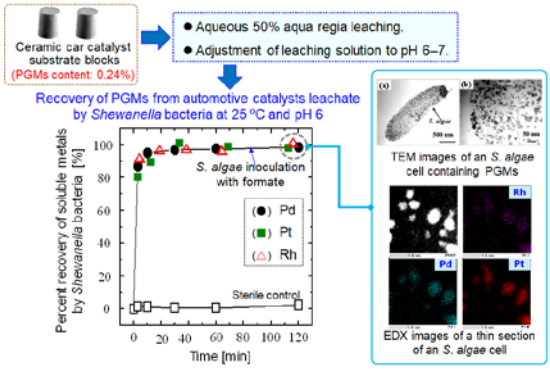

Figure 1. Microbial recovery of platinum group metals (PGMs) from aqua regia leachate of spent automotive catalysts.

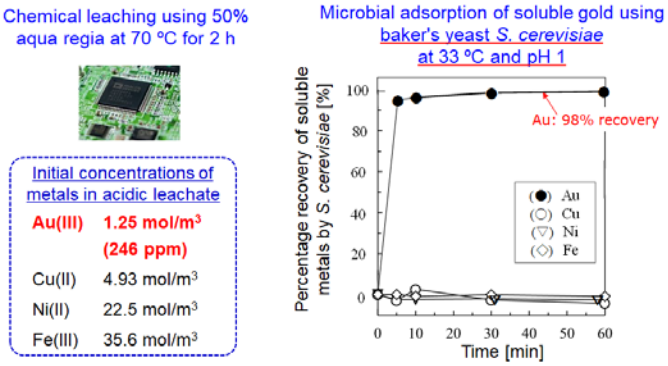

Figure 2. Selective recovery of gold in aqua regia leachate of CPUs at pH 1, 33°C, and 16 kg-dry yeast/m^3.

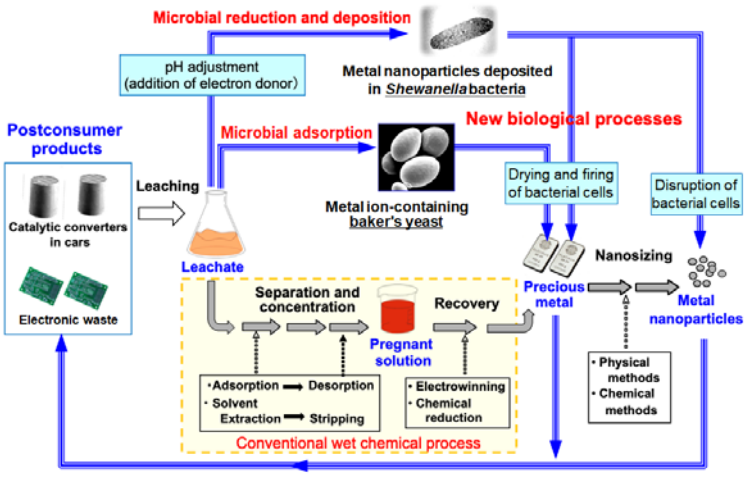

Figure 3. Sustainable use of platinum group metals and gold through biotechnological recycling.

3. Conclusions

We successfully developed new biotechnologies to extract PGMs from spent automotive catalysts and gold from electronic waste.

ECAB 5
The 5th EUROPEAN CONGRESS OF APPLIED BIOTECHNOLOGY
Florence 15-19 September 2019

Fluid dynamics of stirred photobioreactor cuvette

Tomáš Juřena*, Jiří Hájek, Jiří Vondál

[1]*Institute of Process Engineering, Faculty of Mechanical Engineering, Brno University of Technology, Technická 2, 616 69 Brno, Czech Republic*

**Corresponding author: jurena@fme.vutbr.cz*

Highlights

- Modelling approach for bioreactors is described
- Methods of data analysis from CFD models are critically assessed
- Results of fluid dynamics simulation in a mixed, bubbled cuvette are given

1. Introduction

The modeling of bioreactors is a broad sense multi-disciplinary, as it involves fluid dynamics, multiphase flow and mass transfer, radiative energy transfer, and also the growth of the living cells [1]. The complex modelling is however only just emerging [2] and there are many questions that can be answered by simpler models that do not include a complex description of a photobioreactor, only some of the relevant processes [3]. Assessment of parameters connected to mixing and flow pattern can be safely assumed independent of the light intensity and growth dynamics of microalgae.

The modelling of fluid dynamics in a stirred vessel may be performed by any of several approaches, which differ by their inherent assumptions, limitations and answers that they can provide. In the case of a stirred laboratory photobioreactor, its typical structural components include rectangular glass walls, a magnetic stirbar, several sensors (e.g. thermometer, CO_2 probe) and aerator tube. The fluid dynamical system is then composed of three main components, namely the medium, the algae and bubbles. Physical characterization of all the three components is relatively simple.

The purpose of this contribution is comprehensive characterization of the fluid dynamics in a typical laboratory cuvette using computational fluid dynamics (CFD). Model properties, components and numerical performance are critically assessed as well.

2. Methods

The modelling is based on Euler-Lagrange approach, where bubbles and/or algae are tracked in Lagrangian framework, while the medium is described in Eulerian framework as a Newtonian liquid. Governing equations are discretized and solved by the finite volume method.

For all intents and purposes related to fluid dynamics, the medium is water. In this work, we use fresh water, without loss of generality. The cuvette is a standard laboratory equipment, in our case with a volume of about 400mL. The algae exist in a wide variety of species and strains, but for the purpose of fluid dynamics we need to distinguish them only by size and shape. In this

work, we focus on microalgae that are coccoid in shape and their size (diameter) is around 2.5µm. The characterization of bubbles is slightly more difficult, as a bubble may change its shape and even size. The size change is caused either by shedding small bubbles from large ones or by merging (coalescence).

Special care is given to mesh quality and independence of the results on the mesh is documented. The results are reported with focus on choosing the best available parameters that characterize the fluid dynamics meaningfully with respect to the purpose of the photobioreactor. Scalar indicators are sought to provide a global perspective of the system. Local indicators are used sparingly.

3. Results and discussion

The results cover fluid dynamics model development for the specific case of a cuvette equipped with a stirbar, aerator and two probes, as illustrated In Figure 1. Results also include analysis of fluid flow properties in several studied scenarios with different stirbar rotation velocities.

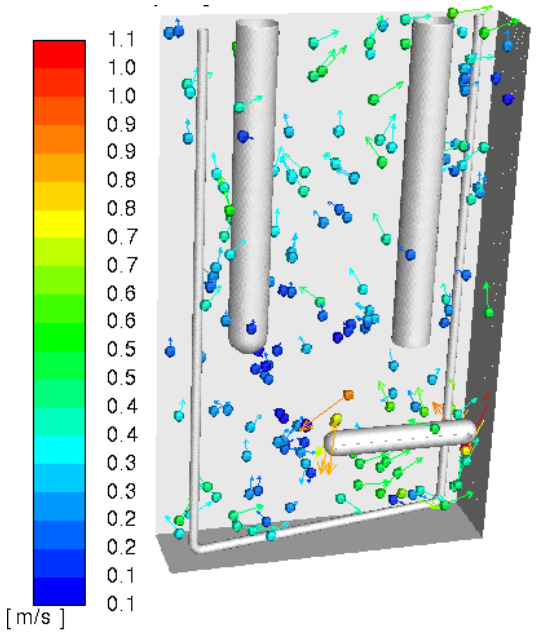

Figure 1. Bubbles colored by their velocity, also shown are their velocity vectors

4. Conclusions

Modelling methodology for fluid dynamics in a photobioreactor including mesh properties has been developed. Suitable indicators and statistics have been defined to characterize the operating conditions.

References

[1] D. Fuente, C. Lizama, J.F. Urchueguía, J.A. Conejero, Journal of Quantitative Spectroscopy and Radiative Transfer 204 (2018) 23–26.
[2] J. Cheng, W. Guo, Y. Song, S. Kumar, K. Ameer Ali, J. Zhou, Bioresource Technology 269 (2018) 1–8.
[3] J.C.M. Pires, M.C.M. Alvim-Ferraz, F.G. Martins, Renewable and Sustainable Energy Reviews 79 (2017) 248–254.

State Substitution: A novel method for parameter identification of large-scale bio-chemical kinetic models

Paulius Rasiukas[1], Chris O'Malley[2], Mark J. Willis[3]
1 School of Engineering Newcastle University, p.rasiukas@ncl.ac.uk; 2 School of Engineering Newcastle University, chris.o'malley@ncl.ac.uk; 3 School of Engineering Newcastle University, mark.willis@ncl.ac.uk

Highlights

- A new method to identify unknown parameters in large scale dynamic models.
- State substitution using a non-parametric model allows decoupled equations to be solved independently.
- A computationally efficient and accurate parameter identification method when compared to alternative techniques.

1.0 Introduction

The ability to identify the parameters of models of complex large-scale (bio) chemical systems is critical in order to develop an understanding of a system as well as to use the model as a basis for process control or process optimization. Established methods of parameter identification normally simultaneously solve the entire set of nonlinear ordinary differential equations (ODEs) that describe the system to determine the model parameters. Generally, the ODEs are numerically integrated and the model parameters obtained using an optimisation algorithm that minimises the difference between the model predictions and the measured process data. However, this is known to be a non-trivial task, often requiring significant solution times and being prone to sub-optimal parameter identification. In this contribution we propose a new method for the identification of unknown parameters of large scale (bio)chemical kinetic models.

2.0 Methods

We decouple the set of ordinary differential equations (ODEs) describing kinetic phenomena into separate sub-systems, whose unknown model parameters can be identified separately. Each ODE is considered a separate sub-system and state substitution is used to replace any coupled model components, i.e. the additional states that would normally be obtained as a result of the numerical integration of the entire system model. The state substitution method we employ relies on the use of measured state variables that are regressed against time using a suitable non-parametric model, e.g. polynomial, spline, neural network. The nonparametric model is then used to replace the states of any of the coupled components of each ODE. This allows numerical integration of each ODE separately and the use of traditional parameter identification techniques to identify any unknown parameters of each sub-model. In a final stage of our method, we then integrate the entire set of ODEs using a global optimisation algorithm using the numerical values of the model parameters obtained from the optimisation of each sub-system as the initial guess. This not only reduces computational time significantly compared to current simultaneous solution methods it ensures statistical optimality of the final parameter values.

To demonstrate the method, it is applied to a biochemical process model described in [1], and compared with a Latin hypercube induced multi-start method, which has been reported to be an efficient method for model calibration in systems biology models [2,3]. The model is shown below where it may be observed that there are 15 unknown kinetic parameters, $p1, \dots, p16$, and each state $x1, \dots, x6$, is assumed measured,

$$\frac{d}{dt}\begin{bmatrix} x1 \\ x2 \\ x3 \\ x4 \\ x5 \\ x6 \end{bmatrix} = \begin{bmatrix} 1 & -1 & 0 & 0 \\ -1/p8 & 0 & -1 & 0 \\ p9/p8 & 0 & p9 & 0 \\ -1/p12 & 0 & 0 & 0 \\ p13/p12 & 0 & 0 & 0 \\ 0 & 0 & 0 & 1 \end{bmatrix} \begin{bmatrix} f1 \\ f2 \\ f3 \\ f4 \end{bmatrix}$$

$$f_i = u_i x1\,, i = 1{,}4$$

$$u_1 = p1\frac{x2}{(p2+x2)}\frac{x4}{(p3+x4)}$$

$$u_2 = p4\frac{1}{(p1-p5x3)}\frac{1}{(p1-p6x5)}\frac{p7}{(p7+x4)}$$

$$u_3 = p10\frac{x2}{(p11+x2)}$$

$$u_4 = p14 + p15\frac{u1}{p16+u1}$$

In the results that follow, the non-parametric model used for state substitution was a cubic spline and each decoupled ODE was integrated using the MATLAB function *ode45*. The optimisation algorithm used to determine the unknown model parameters was the MATLAB function *lsqnonlin* via repeated integration each decoupled sub-component of the overall kinetic model. Simultaneous optimisation of the full kinetic model used MATLAB's genetic algorithm routine.

3.0 Results and discussion

A significant number of comparative studies have been made via adjustment of the number of data measurements assumed available and the level of measurement error (measurement noise). Table 1 indicates a typical scenario comparing the estimated parameter values to the actual (known) model parameters.

Name	$p1$	$p2$	$p3$	$p4$	$p5$	$p6$	$p7$	$p8$	$p9$	$p10$	$p11$	$p12$	$p13$	$p14$	$p15$	$p16$
(1)	1.09	1.1	0.3	0.09	0.01	0.06	0.02	0.11	1.8	1.7	19	0.38	0.85	3.5	25.7	0.02
(2)	1.09	1.06	0.24	0.05	0.03	0	0.40	0.12	1.82	4.07	53.9	0.41	0.86	2.92	26.80	0.02
(3)	1.12	0.91	0.27	0.11	0.01	0	0.50	0.12	1.83	0.79	1.94	0.405	0.82	2.87	25.73	0.01
(4)	4.31	0.01	7.93	4.05	0.10	0.80	286.8	0.34	1.85	18.5	60.1	0.68	0.49	3.86	19.45	0.01

Table 1. Parameter estimates obtained assuming, $x1, \ldots, x6$, are measured every 0.3 h (total number of measurements of each state being 12) with a measurement error of 10% (assumed to be white noise). In the table, (1) Actual values, (2) State – substitution, (3) Multi-start with Latin Hypercube experimental design (4) Simultaneous solution and optimization of the full model.

It may be observed that the parameter estimates obtained using the state-substitution method (2) and the use of a multi-start strategy with Latin Hypercube experimental design to obtain the initial parameter values of each run of the algorithm (3) are of comparable accuracy and are generally significantly superior to that of the simultaneous solution (4). While algorithm run-time will be machine dependent, as an indication of the typical performance of the methods; the state-substitution method (2) took 2371s to find a solution, whereas the multi-start method (3) took 5778s to find a solution while the simultaneous solution (4) ran for 255h and was still not able to converge to reasonable solution.

4.0 Conclusions

A new method for the identification of unknown parameters of large scale (bio)chemical kinetic models was been proposed. For the example given, this provided a fast and reliable parameter estimation procedure. The full paper will present a more detailed assessment of the method using additional bench-mark models [4]. Furthermore, we will use Monte Carlo simulation to provide a statistical perspective on our run-time results and parameter estimates and assess the impact that unmeasured species states have on the identification procedure.

References

[1] Saraiva, I., VandeWouwer, A. and Hantson, A.L. (2015) 'Parameter identification of a dynamic model of CHO cell cultures: an experimental case study', *Bioprocess BiosystEng*, 38(11), pp. 2231-48.

[2] Raue, A., Schilling, M., Bachmann, J., A.L. (2013) 'Lessons learned from quantitative dynamical modeling in systems biology', *PLoS One*, 8(9), p. e74335.

[3] Degasperi, A., Fey, D. and Kholodenko, B.N. (2017) 'Performance of objective functions and optimisation procedures for parameter estimation in system biology models', *NPJ Syst Biol Appl*, 3, p. 20.

[4] Hass, H., Loos, C., Alvarez, E.R., A.L. (2019) 'Benchmark problems for dynamic modeling of Intracellular processes' Bioinformatics.

ECAB 5
The 5th EUROPEAN CONGRESS OF APPLIED BIOTECHNOLOGY
Florence 15-19 September 2019

Influences of environmental factors on *Lactobacillus reuteri* growth and 3-hydroxypropionic acid production in the context of coupling with extraction

Thi-Lan-Phuong Nguyen[1*], Claire Saulou-Bérion[1], Catherine Béal[1]

[1] *UMR 782 GMPA, AgroParisTech, INRA, Université Paris-Saclay, 1 av. Lucien Brétignières 78850 Thiverval-Grignon, France*

**Corresponding author: Thi-Lan-Phuong.Nguyen@inra.fr*

Highlights

- Glycerol bioconversion into 3-hydoxypropionic (3-HP) was performed through a whole-cell biocatalysis strategy with *Lactobacillus reuteri* following bacterial growth.
- Plackett-Burman experimental design was used for screening growth factors influencing bioconversion performances.
- Increased glucose concentration during growth decreased the molar ratio between 3-HP and its coproduct 1,3-propanediol (1,3-PDO).

1. Introduction

In the framework of bioeconomy, 3-HP is gaining interest due to its desirable industrial applications. As a bifunctional molecule, 3-HP can be chemically converted into a variety of added-value chemicals, such as acrylic acid, or biodegradable polyesters. Among non-GMO microorganisms naturally able to produce 3-HP, *L. reuteri* is noticeable thanks to its ability to produce 3-HP from glycerol, a by-product in biodiesel manufacturing industries. This Gram-positive probiotic bacterium is an interesting candidate due to its G.R.A.S. status and ability to synthesize vitamin B12, an essential co-factor for the first enzyme of the bioconversion metabolic pathway. Moreover, *L. reuteri* does not use glycerol as a carbon source, thus avoiding the synthesis of by-products that can hinder conversion yield and further *in situ* extraction. However, the effects of nutritional and environmental factors encountered by cells during growth on their ability to perform bioconversion have not been elucidated yet. The aim of this work is to better understand the effect of these factors on *L. reuteri* growth and bioconversion performances, in order to identify the optimum conditions for 3-HP production.

2. Methods

2.1. A 2-stage process for 3-HP production by *L. reuteri*

L. reuteri DSM 17938 (BioGaia AB, Stockholm, Sweden) was cultivated in batch mode with a controlled 5-L bioreactor until stationary phase of growth. Cells were then harvested by centrifugation (7500 rpm, 10 min, 4°C) before being introduced into a 2-L bioreactor working in fed-batch mode with glycerol addition at 0.5 $g.h^{-1}$. Cell concentration was quantified by flow cytometry (FCM), cellular states were assessed by FCM using carboxyfluorescein diacetate and propidium iodide staining [1], and substrate consumption and metabolite production were measured by liquid chromatography [2].

2.2. Experimental design by Plackett-Burman method

A Plackett-Burman experimental matrix was designed to test the effects of 11 growth factors on the growth phase and bioconversion ability of *L. reuteri* [3]. The tested factors include addition of glucose, yeast extract, phytone peptone, 1,2-propanediol (1,2-PDO), cysteine, betain plus KCl, tween 80, vitamin B12, various pH and base solutions to regulate, various temperature. Models were defined by the general form: $Y_i = k_i + \Sigma a_i \cdot Y_{(+)i}$ (Y_i: response variable; k_i: constant corresponding to the value of Y_i when all 11 variables are at their low levels; a_i: linear coefficient of each variable to express the effect of the high level; $Y_{(+)i}$: value of the plus level of the variable) [3]. Statistical analyses were performed with the software Statgraphic plus, with a 95 % confidence intervals for coefficient estimations.

3. Results and discussion

3.1. Effects of environmental factors on *L. reuteri* growth

As expected, our results showed that increasing glucose concentration during growth led to a higher cell concentration in the stationary phase, together with a higher viable cell concentration. Meanwhile, lower cultivation temperature resulted in less growth and lactic acid production.

3.2. Effects of growth environmental factors on cell ability to perform further bioconversion

By increasing glucose concentration during growth, the molar ratio between 3-HP and its coproduct 1,3-PDO decreased during bioconversion. This can be explained by the fact that the supplemental NADH produced through glycolysis was re-oxidized to NAD^+ preferentially through the glycerol reduction into 1,3-PDO, at the expense of glycerol oxidation into 3-HP. Surprisingly, the addition of vitamin B12 gave a negative impact on 3-HP production. A supplementation of this element during bioconversion instead of during growth may give a better influence. Regarding the duration of 3-HP production, some interesting factors were pointed out, including the addition of betain, 1,2-PDO, and phytone peptone. It seems consistent with previous studies that betain leads to an increased tolerance of *L. plantarum* to osmotic stress [4]. Meanwhile, the presence of 1,2-PDO helps preparing cells to deal with glycerol thanks to the expression of genes encoding the enzymes and structural proteins involved in the bioconversion pathway [5]. Regarding the protein source, phytone peptone was identified as the best for maximizing *L. reuteri* growth [6], so it may be linked to a higher enzymatic ability to synthesize metabolites thereafter.

The experimental design performed in our study allowed identifying a set of growth conditions that lead to a 3-HP production enhanced by 20 % compared to the reference.

4. Conclusions

The present study figured out the influences of growth factors on *L. reuteri* biomass production and ability to produce 3-HP afterwards. The identified factors having positive impacts on the bioconversion performances will be used for growth step. A second experimental design will now be performed in order to optimize the environmental conditions during the bioconversion step.

References

[1] A. Rault, C. Béal, S. Ghorbal, J.C. Ogier, M. Bouix, *Cryobiology*, 55 (2007), pp. 35-43.
[2] G. Burgé, C. Saulou, M. Moussa, F. Allais, V. Athes, H.E. Spinnler, *J. Microbiol.* 53 (2015), pp. 702-710.
[3] R.L. Plackett and J.P. Burman, *Biometrika*, 33 (1946), pp. 305-325.
[4] E. P.W. Kets and J. A.M. de Bont, *FEMS Microbiol. Lett.* 116 (1994), pp. 251-256.
[5] T. Dishisha, S.H. Pyo, R. Hatti-Kaul, *Microb. Cell Fact.* 14 (2015), pp. 200-211.
[6] O. A. Atilola, R. Gyawali, S. O.Aljaloud, S. A. Ibrahim, *Foods,* 04 (2017), pp. 318-327.

ECCE 12
ECAB 5

ECAB 5
The 5th EUROPEAN CONGRESS OF APPLIED BIOTECHNOLOGY
Florence 15-19 September 2019

Temperature Effect in the Production of a Recombinant Antivemon in Fed-Batch Mode.

Susana Alonso Villela[1], Hazar Kraiem[2], Balkiss Bouhaouala[2], Carine Bideaux[1], Cesar Arturo Aceves Lara[1], Luc Fillaudeau[1]

1 LISBP, Université de Toulouse, INSA, INRA, CNRS, Toulouse, France; 2 Laboratoire des Venins et Molécules Thérapeutiques, Institut Pasteur de Tunis, 13 Place Pasteur, BP-74, 1002 Le Belvédère, Tunis, Université Tunis El Manar, Tunisia.

**Corresponding author: alonsovi@insa-toulouse.fr*

Highlights

- Production kinetics was obtained during expression at 28, 30, 33 and 37°C
- Lower expression temperatures yielded higher protein than higher temperatures
- The highest productivity was 0.046 mg/g cdw/h, attained after 10 h at 30°C

1. Introduction

The production of recombinant antibodies in *E. coli* has been widely studied in shake flasks [1], mainly for the study of protein yields under the *lac* promoter expression system. The effect of the inducer (IPTG) concentration during induction has been studied [2-3], but there are no studies on the temperature effect on protein production kinetics. The duo temperature-duration after induction most commonly used is either 37°C-4h or 28°C-12h and only final titers are reported.

In this work the effects of temperature in the production of the chimeric format of bispecific nanobody NbF12-10 against AahI'/AahII toxins of scorpion venom in *E. coli* WK6 were studied at bioreactor scale. The strategy implemented allowed first the production of biomass in fed-batch mode at 37°C, and then the expression of protein under glucose feed and induction temperatures of 28, 30, 33 and 37°C.

2. Methods

Experiments were conducted with *Escherichia coli* K12 / WK6 { Δ(lac-pro), galE, strA, nal; F' lacIq ZΔM15, pro+ } harboring pHEN6 plasmid (derived from pBR322) encoding the bispecific nanobody VHHF12-VHH10 (called NbF12-10) and the chimeric format VHH10-VHHF12 (called CH10-12) retrieved from the combinatorial libraries. Cultures were performed in a 5L bioreactor, Biostat B-DCU (Sartorius) using glucose as carbon source in 1.5 L of defined medium [4]. Batch phase was carried out at 37°C, and at depletion of the 10 g/L of initial glucose, fed-batch mode was applied with an exponential feed imposing a specific growth rate of $\mu = 0.38\ h^{-1}$. Protein expression was induced with 1 mM of IPTG when biomass reached approximately 26 g cdw/L. At induction, glucose feed rate was set to 4.5 g Glc/h (at 300 g Glc/L) imposing a $\mu \leq 0.03\ h^{-1}$. Temperature and duration after induction were set to 28°C-12h, 30°C-10h, 33°C-6h, and 37°C-4h. Cell samples were taken every 2 h for the experiments at 28 and 30°C, and hourly for experiments at 33 and 37°C. After pelleting the cells, the periplasmic proteins were extracted by osmotic shock and purified by

IMAC using His-Select Ni affinity gel (Sigma-Aldrich). After washing with PBS, His-tagged proteins were eluted with imidazole. Biomass was measured by optical density and gravimetric method. Residual glucose and organic acids were quantified by HPLC (Aminex column HPX87H). Quantification of protein was made by a new method of image analysis of electrophoresis gels [5].

3. Results and discussion

The biomass production phase of the four cultures showed high reproducibility, obtaining a μ_{max} of 0.71 h^{-1} in batch mode and the expected μ of 0.38 h^{-1} in exponential feeding fed-batch. During protein expression, a linear growth was maintained, sufficient to satisfy both bacterial and protein production. The protein was produced only after the induction with IPTG. The induction at 37°C was extended and stopped at 6 h. After 5 h of induction, the highest protein yield was 0.015 mg/g cdw at 28 and 30°C, and decreased with the temperature, down to 0.005 mg/g cdw at 37°C. The maximum protein yield achieved was 0.074 mg/g cdw (Figure 1a), after 10 h of induction at 30°C, which is two-fold the yield achieved for the same induction duration at 28°C (0.04 mg/g cdw).

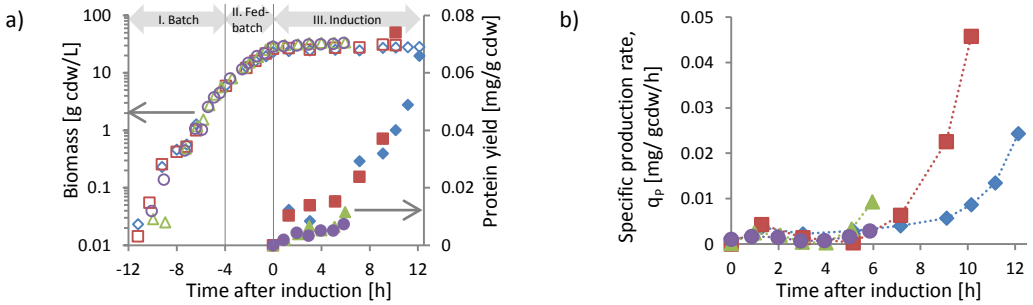

Figure 1. a) Biomass and protein yield evolution in all cultures, and b) Specific production rate of the nanobody produced after IPTG pulse. Symbols: ◊ 28°C, □ 30°C, Δ 33°C, ○ 37°C.

The specific production rate of the protein (Figure 1b) increases after 5 h of induction for all cultures, obtaining the highest productivity of 0.045 mg/g cdw/h at the induction temperature of 30°C. This is more than five-fold the productivity at 28°C at the same production time (10 h), and two-fold the productivity at 28°C at 12 h.

4. Conclusions

The effect of temperature during the induction of a periplasmic-expressed nanobody was tested at bioreactor scale. Culture repeatability was demonstrated, and protein production was achieved during glucose feed. The highest protein titers were obtained at the induction temperature of 30°C. The production of the nanobody at 30°C should be analyzed over a longer period of time to determine the production limits of the strain.

Susana Alonso acknowledges financial doctoral support by the CONACYT (Mexico).

References

[1] S.K. Gupta, P. Shukla, Crit Rev Microbiol. 43 (2017) 31–42.
[2] J. Ruiz, G. González, C. de Mas, J. López-Santín, Biochem Eng J. 55 (2011) 82–91.
[3] D. Calleja, J. Kavanagh, C. de Mas, J. López-Santín, Biotechnol Bioeng. 113 (2016) 772–782.
[4] S. Sunya, F. Delvigne, J.-L. Uribelarrea, C. Molina-Jouve, N. Gorret, Appl Microbiol Biotechnol. 95 (2012) 1021–1034.
[5] S. Alonso Villela, H. Kraiem, B. Bouhaouala, C.A. Aceves Lara, and L. Fillaudeau, [Abstract], Submitted to 5th European Congress of Applied Biotechnology, 2019.

ECAB 5
The 5th EUROPEAN CONGRESS OF APPLIED BIOTECHNOLOGY
Florence 15-19 September 2019

Photon Density Wave spectroscopy for in-line monitoring of biomass in high-density fermentation processes

Thomas Schiewe[1], Lara Santolin[2], Sebastian L. Riedel[2], Roland Hass[1]

1 innoFSPEC, University of Potsdam, Am Mühlenberg 3, 14476 Potsdam, Germany

2 Chair of Bioprocess Engineering, Technische Universität Berlin, Ackerstraße 76, 13355 Berlin, Germany

Corresponding author: tschiewe@uni-potsdam.de

Highlights

- In-line Biomass measurements via Photon Density Wave spectroscopy
- Yeast and bacterial cultivations up to 67 g L^{-1}
- Separate quantification of scattering and absorption properties
- Detection of process deviations

1. Introduction

The ability to monitor and control the formation of biomass during industrial bioprocesses is of high interest as critical factors like maximal biomass production, the physiological state of cells, product formation rate, and product quality are dependent on the specific growth rate [1]. Especially at high cell densities or in very turbid and disperse fermentation media established optical process analytical technologies face signal saturation effects or are prone to probe fouling. In this contribution Photon Density Wave (PDW) spectroscopy will be introduced as an in-line analytical tool for monitoring and control of bacterial and yeast cultivations.
A fully autoclavable and chemically sterilizable, calibration-free process analytical technology suitable to highest concentrations (i.e. > 40 vol%) in stirred or flowing systems is found in Photon Density Wave spectroscopy [2][3]. It allows for the independent quantification of the absorption and scattering properties of disperse materials, i.e. the absorption and the reduced scattering coefficients, respectively. The absorption coefficient exhibits information about concentration changes of light absorbing media components during the investigated process. The reduced scattering coefficient, however is related to the size and concentration of the dispersed particles such as cells.

2. Methods

Fed-batch cultivations of *Escherichia coli* and *Kluyveromyces marxianus* were performed in 3.7 L and 10 L bioreactors respectively using both defined and complex media while focusing on high biomass concentrations. Optical density and cell dry weight (CDW) were obtained by offline sampling. As reference PDW spectroscopy was implemented to track the biomass formation in-line and its performance was compared to other in-line methods, such as turbidity and backscatter measurements.

3. Results and discussion

The reduced scattering coefficient μ_s' obtained by PDW spectroscopy proved to be a reliable indicator for the respective biomass concentration during reactor cultivations. Especially at high turbidities correlation coefficients of $R^2 = 0.99$ between μ_s' and CDW were obtained, while the reference methods showed non-linear responses driven by saturation effects.

More comprehensive understanding of the process could be generated by investigating the simultaneously measured absorption coefficient μ_a in relation to μ_s'. This way process disturbances induced by e.g. inadequate control strategies were detected in-line and early into the cultivations.

4. Conclusions

First investigations show Photon Density Wave spectroscopy to be a promising technique for the monitoring of stirred tank reactor cultivations. It enables the real-time measurement of biomass formation under process conditions without the indication of concentration-induced saturation effects.

References

[1] M.M. Schuler, I.W. Marison, Appl. Microbiol. Biotechnol. 2012, 94:1469
[2] L. Bressel, R. Hass, O. Reich, JQRST 2013, 126:122-129
[3] R. Hass, O. Reich, et al., Anal. Bioanal. Chem. 2015, 407:2791–2802

ECAB 5
The 5th EUROPEAN CONGRESS OF APPLIED BIOTECHNOLOGY
Florence 15-19 September 2019

Fouling sensor based on thermal excitation in bioprocess: investigation of sensor structures on responses and sensitivity.

Yassim Boukazia[1,*], Guillaume Delaplace[2], Mathilde Cadé[3], Frédéric Bellouard[4], Marc Bégué[5], Luc Fillaudeau[1]

1 LISBP (CNRS 5504 - INRA 792 – INSA), Toulouse, FRANCE; 2 PIHM-UMET (INRA 638), Lille, France, 3 IRH Ingénieur Conseil, Ludres, France; 4 Aqualabo, Caudan, France, 5 LMDC, Toulouse, France

**Corresponding author: boukazia@insa-toulouse.fr*

Highlights

- Three thermal fouling sensors (MEMS structures) are compared
- Hot wire method in steady thermal regime and linearized responses were applied
- Metrological limits (accuracy and upper LOD) are reported

1. Introduction

Food and bioprocess efficiency is impacted by (bio)fouling [1, 2]. Monitoring and quantification of deposit through *in-situ* and local sensors constitute technological and scientific challenges. In present work, three fouling sensors based on a thermal excitation (steady thermal regime) with different technology (Macro and MicroElectroMechanical Systems MEMS), geometry (intrusive cylindrical, flush plan) and packaging (nude and encapsulated structure) are compared. Thermal responses are discussed versus heat transfer theory. Performances with model deposit are reported to deduce accuracy to monitor fouling and to determine metrological limitations.

2. Methods

Prototype sensors are based on the hot wire method [1] with powered and regulated Joule effect. Hot wire and fluid temperatures are continuously recorded. According to heat conduction's law in steady thermal regime (equations), the temperature difference ($\Delta\theta$) evolves as a linear function of heat flux (φ) and thermal resistance (R_{th}).

Ref	Temperature difference	Local heat transfer	Deposit thermal resistance
TS1	$\Delta\theta = \theta_{hw} - \theta_b$	$\Delta\theta = \varphi.\left(\frac{1}{h} + \frac{th_p}{\lambda_p} + \frac{th_d}{\lambda_d}\right)$	$Rth_d = \frac{th_d}{\lambda_d}$
TS2			
TS3	$\Delta\theta = \theta_w - \theta_b$	$\Delta\theta = \varphi.\left(\frac{1}{h(r+th_d)} + \frac{r}{\lambda_d} ln\left(\frac{r+th_d}{r}\right)\right)$	$Rth_d = \frac{r}{\lambda_d} ln\left(\frac{r+th_d}{r}\right)$

Three different structures are compared (Figure 1). TS1 is composed of a flat square MEMS structure (red line, 250µm) between a printed circuit board (PCB, green line, 800µm) and a protective packaging (stainless steel and resin layers, grey line, 450µm) in contact with bulk. TS2 is equivalent to TS1 without protective packaging. TS3 is based on a macroscopic cylindrical structure including a central heat wire and a wall temperature measurement (thermocouple). Sensors were tested in a 5L reactor (fluid: water, *Re*=2.6x10^6 and 20±1°C). Multiple layers of PVC scotch (TESA® 53948, *th*=130 µm, and ρ_d=1300 kg.m^{-3} [3]) were used to mitigate fouling. Thermal

conductivity and heat capacity were measured at $\underline{\lambda_d}$=0.115 W.m^{-1}.K^{-1}, Cp_d=1025 J.K^{-1}.kg^{-1} (Neotim FP2C). Experiments were performed in clean (reference) and fouled (up to 5 layers) conditions. Five successive heat flux steps were applied (from 0.2 to 7.5 kW.m^{-2}, 30 min/step). The efficiency was indicated by the evolution of theoretical and experimental thermal resistances.

3. Results and discussion

Considering nominal flux (Figure 2), a non-linear response is observed for all sensors. Strong differences are noticeable and can be attributed to different structures and to heat loss contribution. For plan sensors, TS1 and TS2 inflection inform about the balance between efficient flux and back side and edge heat loss. As expected, the absence of front side packaging improves sensor response (TS2). Initial slope (*Rth*=0) informs about the ratio between efficient and nominal flux equal to 7.8, 29 and 80% for TS1, TS2 and TS3 respectively.

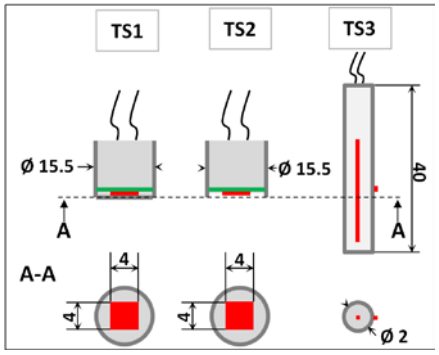

Figure 1: Schemes of TS1, TS2 and TS3 structures

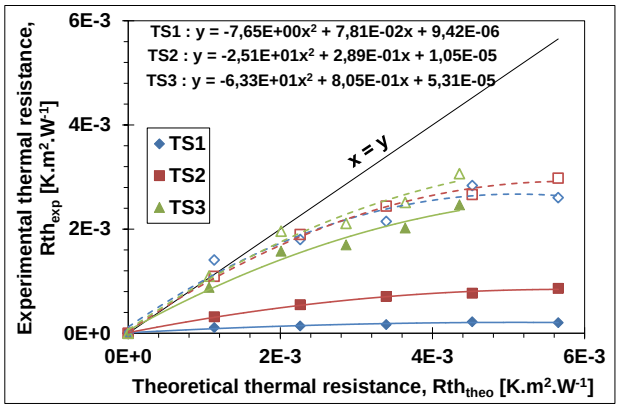

Figure 2: Estimated versus theoretical thermal resistances considering nominal (continuous line) and efficient (dotted line) heat flux.

Considering efficient flux, estimated thermal resistance is consistent with theoretical values even if inflexion is noticeable for all structures with increasing fouling. Under clean condition, heat convection coefficient is highly superior to 1000 W.m^{-2}.K^{-1} and for TS1, thermal resistance of front side packaging (stainless steel and resin layers) is close to 2.8E-03 K.m²/W. For food and bioprocess, it is assumed that a deviation of 30% between estimated and real fouling heat resistance is acceptable to control and regulate the process. In present case, the experimental upper LODs are equal to 3.4, 3.6 and 4.0E-03 K.m²/W for TS1, TS2 and TS3 respectively. Considering a dense biofouling (λ_d=0.6 W.K^{-1}.m^{-1}), it enables to estimate a thickness close to 2mm.

4. Conclusions

Three fouling sensors based on a thermal excitation have been compared and their metrological performances reported. Considering nominal heat flux, intrusive cylindrical structure should be preferred. However, an accurate estimation of efficient flux demonstrates that cylindrical or plan structures exhibit similar performances and upper LOD, which fulfill specifications. Further work will investigate periodic thermal excitation to qualify and quantify deposit.

References

[1] J. Crattelet, Journal of Food Engineering 119 (2013) 72 – 83.
[2] K.A. Hamilton, Water Research 134 (2018) 261 – 279.
[3] Titow, PVC Technology (1984), p. 857

ECAB 5
The 5th EUROPEAN CONGRESS OF APPLIED BIOTECHNOLOGY
Florence 15-19 September 2019

Inhibition Kinetics of a High-Strength Nitrification Batch Reactor

Safae Sali[1], Hamish Robert Mackey[1]*, Guang-hao Chen[2]

1 Division of Sustainable Development, College of Science and Engineering, Hamad bin Khalifa University, Qatar Foundation, Doha, Qatar; 2 Department of Civil and Environmental Engineering, Hong Kong University of Science and Technology, Clear Water Bay, Kowloon, Hong Kong, China.

**Corresponding author: hmackey@hbku.edu.qa*

Highlights

- Urine nitrifying sequencing batch reactor studied for inhibition by FA, FNA and pH
- Large parallel batch testing and 15 inhibition models considered
- Noncompetitive FA, uncompetitive FNA, 2 way Prosser pH model found best
- Ammonia oxidizers insensitive to FA, both nitrifying organisms sensitive to FNA.

1. Introduction

Nitrification is a key biological wastewater treatment process, yet application to high strength wastewaters is challenging due to substrate and product inhibition as well as wide pH variations in poorly buffered systems. Understanding how these inhibitions affect removal kinetics is critical to optimum system design but is confounded by the close relationship between the inhibitors: free ammonia (FA), free nitrous acid (FNA) and pH [1]. Sequencing batch reactors can achieve higher rates of treatment [2], but are also more stressed by these inhibitors compared to more widely studied continuous flow systems [2,3]. Moreover, disagreement remains over the most suitable inhibition models [1,4]. This study undertakes a large set of extended batch tests across a wide range of pH, FA and FNA concentrations and extensive model assessment to determine the most suitable kinetic equations describing high strength nitrification of source separated urine.

2. Methods

A 13.8 L nitrifying SBR was operated with real urine diluted to 30% strength at a loading rate of 380 mg-N.L^{-1}.d^{-1}. Between days 227 and 332 a series of 18 separate 6 h batch experiments were conducted with constant pH using a consistent urine dose and additional spiking of NH_4Cl and $NaNO_2$ to adjust FA and FNA. The tests covered FA concentrations up to 225 mg-N.L^{-1}, FNA concentrations up to 0.20 mg-N.L^{-1} and a pH range of 7 to 9. The nitrifying community was quantified using fluorescent in-situ hybridization and published probe sets. Fifteen separate two-stage nitrification rate expressions were evaluated consisting of different combinations of non-competitive (nc), uncompetitive (uc) and Aiba (A) type inhibition by FA and FNA coupled with either Presser two-way (P2), Cardinal three-way (C3) or Cardinal extended three-way (CE3) pH response models [5]. The system model consisted of a series of ordinary differential equations covering FA volatilization, urea hydrolysis, total ammoniacal nitrogen (TAN) oxidation (FA as substrate) and total nitrite nitrogen (TNN) oxidation with up to 19 parameters for estimation. Parameter estimation used parallel time-series estimation in the COPASI modelling package. Fitted models were validated against an independent batch experiment with uncontrolled pH. Best model selection considered

both the average relative standard deviation (ARSD) of individual parameters across the 18 parallel batch tests and combined absolute error of TAN+TNN+NO_3 predictions for the validation file.

3. Results and discussion

Ammonia oxidizing bacteria (AOB) *Nitrosomonas* (Probe Nso1225) comprised 23.6 ± 0.3 % of the microbial community while *Nitrobacter* was the only nitrite oxidizing bacteria (NOB) detected (probe NIT3) at 1.0 ± 0.1 %. Treatment was stable throughout this period with full conversion of ammonia to nitrate. Evolution strategy was found to be the most successful optimization strategy for the relatively noisy experimental data. nc-FA, nc-FNA inhibition with CE3 pH gave the lowest parameter optimization objective value, while un-FA, nc-FNA with CE3 pH gave the lowest ARSD of 0.22. However, neither showed good fit to the validation data. Rather nc-FA, uc-FNA P2 pH and uc-FA, uc-FNA P2 pH gave the best fits to the experimental data with similar absolute errors across the predictions of TAN, TNN and NO_3 with the former model performing slightly better. Both also showed relatively low parameter optimization objective values and ARSD confirming them as suitable models for high strength nitrification. Both ammonia and nitrite oxidation were relatively insensitive directly to pH. Ammonia oxidation inhibition constants $K_{i,NH3}$ and $K_{i,HNO2}$ were 464 mg-N.L^{-1} and 0.055 mg-N.L^{-1} while for nitrite oxidation they were 9.64 mg-N.L^{-1} and 0.027 mg-N.L^{-1}.This indicates AOB were highly acclimated to high FA concentrations, as expected since the reactor was fed with roughly 2000 mg-TAN/L feed with pH 9.2, while NOB were sensitive to FA in the system. Similar inhibition was experienced by both organisms from FNA.

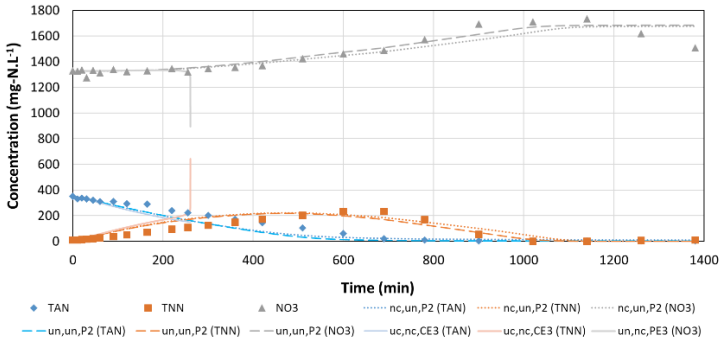

Figure 1. Fit for three models described in text against validation data where X,Y,Z stands for FA,FNA and pH inhibition model. The ODE was unstable for un-FA,nc-FNA,PE3 pH but fit was poor before instability.

4. Conclusions

These results are in contrast to Park and Bae [1] who found un-FA, nc-FNA, and Carerra et al [4] who found Aiba-FA, Haldane-FNA models were best respectively. This highlights the need for large-scale parallel testing and parameter optimization and consideration of pH to unravel interactions between FA, FNA and pH.

References

[1] S. Park, W. Bae, Proc. Biochem. 44 (2009) 631–640.

[2] K.M. Udert, C. Fux, M. Münster, T.A. Larsen, H. Siegrist and W. Gujer, Water Sci. Technol. 48 ,1 (2003) 119-130.

[3] E. Jiménez, J.B. Giménez, A. Seco, J. Ferrer, J. Serralta, Bioresour. Technol. 124 (2012) 478–484.

[4] J. Carrera, I. Jubany, L. Carvallo, R. Chamy, J. Lafuente, Proc. Biochem. 39 (2004) 1159-1164.

[5] R.J.W. Lambert J. Appl. Microbiol. 110, 1 (2011), 61-68.

Efficiency and durability of a bioactive coating in formaldehyde degradation

Cristiana C. Castro[1], Tangi Senechal[2], Julian Viseur[1], Ducoulembier Aline[2], Driss Lahem[2], Anne-Lise Hantson[1]

[1] Chemical and Biochemical Process Engineering Unit, UMONS, Mons, Belgium; [2] Materia Nova, Materials Science Unit, Mons, Belgium

**Cristiana C. Castro: cristianacordeirodecastro@umons.ac.be*

Highlights

- Bacterial cells immobilized in sol-gel coatings were able to degrade formaldehyde.
- Sol-gel coatings containing PEG enhanced the enzymatic degradation of formaldehyde.
- Formaldehyde was efficiently degraded by coatings kept at room temperature during 5 weeks.
- Coatings storage at 37°C decreased formaldehyde degradation ability.

1. Introduction

After the energy crisis of the 90's, new energy conservation measures were adopted in peoples's lifestyles at home and work places. Energy-efficient housing rapidly brought new building materials, interior decoration and consumer products, such as composite wood, foams and plastics, synthetic carpets and households products. These changes have increased the diversity and concentration of pollutants in the indoor air [1], mainly the volatile organic compounds (VOCs) [2]. Formaldehyde is an oxygenated-VOCs, widely used in construction materials, wood processing, furniture, textiles, carpeting, and chemical industries. It is classified as a human carcinogen and it has been given more attention in particular of its adverse effect in health [3], and so, its removal is of widespread interest. The development of bioactive coatings incorporating biomolecules able to capture and degrade this toxic compound is of major interest. It is herein presented the study of the efficiency of hydrophilic sol-gel coatings, easily prepared at low-temperature, incorporating PEG in the formulation to retain a large content of water, and so, improve cells viability and maintain enzymes activities [4]. The conservation of enzymes stability throughout time is of great importance for industrial application of the bioactive coatings.

2. Methods

Hydrophilic sol-gel coatings were prepared using a mixture of 3-glycidoxypropyltrimethoxysilane (GPTMS) and tetraethoxysilane (TEOS) and freeze-dried bacterial cells of *Pseudomonas putida* ATCC 47054. Different ratios of precursors and cells were tested in the presence or absence of the hydrogel polymer polyethylene glycol (PEG) in the coating. Eight coatings formulations were prepared (Table 1). Coatings were applied by spraying to a surface of a thin-layer chromatography (TLC) paper. After 24 h the paper was stored at room temperature and 37°C to evaluate

formaldehyde efficiency throughout storage time. Every week, during 5 weeks, the coated paper was put in contact with the reactional mixture in aqueous solution containing formaldehyde and a co-factor NAD^+. Formaldehyde degradation was quantified by a colorimetric method using the NASH reagent during 48 h.

3. Results and discussion

After 48 h of reaction with the formaldehyde, bacterial cells incorporated in the sol-gel matrices were able to degrade formaldehyde in the surface (Figure 1). Series 1, 2, 7 and 8 obtained the best degradation yields (85, 80, 78 and 85%, respectively) after 24 h of deposition, compared to the others (30%, in average). After 5 weeks of storage at room temperature, formaldehyde degradation yields for the same series were 94, 53, 75 and 45% and the remaining series obtained 13.5% in average. A small decrease was generally verified, except for serie 1 that kept the highest degradation yield. The presence of PEG in serie 1 allowed the retention of large contents of water that improved the activity of formaldehyde-degrading enzymes, which were present in high concentration (40% ($w.w^{-1}$) of cells). After 5 weeks of storage at 37°C, formaldehyde degradation yield was about 10% in average for all the series. Storage temperature decreased the enzymatic activity needed for the transformation of formaldehyde.

Table 1. Sol-gel coatings formulations

	Sol-gel	PEG (g)	Cells conc. (% $w.w^{-1}$)
Serie 1	90-3	8	40
Serie 2	90-3	0	40
Serie 3	90-1	8	30
Serie 4	90-1	0	30
Serie 5	90-3	0	30
Serie 6	90-1	0	40
Serie 7	90-3	8	30
Serie 8	90-1	8	40

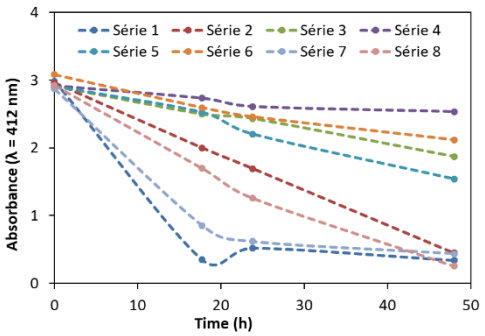

Figure 1. Enzymatic degradation of formaldehyde by coated paper.

4. Conclusions

Bioactive coatings containing freeze-dried bacterial cells were efficient in formaldehyde degradation in solution. The presence of PEG in the sol-gel improves the enzymatic degradation of the pollutant. Formaldehyde degradation efficiency can be kept by storing sol-gel coatings at room temperature.

References

[1] B. Guieysse, C. Hort, V. Platel, R. Munoz, M. Ondarts, S. Revah, Biotechnol. Adv., 26, 2008, 398-410.
[2] T. Salthammer, S. Mentese, R. Marutzky, Chem. Rev., 110(4), 2010, 2536-2572.
[3] A. Roca, J.J. Rodríguez-Herva, E. Duque, J.L. Ramos, Microb. Biotechnol., 1, 2008, 158–169.
[4] V.B. Kandimalla, V.S. Tripathi, H. Ju, Crit Rev Anal Chem., 36, 2006, 73-106.

ECAB 5
The 5th EUROPEAN CONGRESS OF APPLIED BIOTECHNOLOGY
Florence 15-19 September 2019

Simultaneous removal and detoxification of neonicotinoid insecticides by a bacterial degrading consortium at reactor scale

Carlos E. Rodríguez-Rodríguez[1], Gabriel Rodríguez-Castillo[1], Juan Carlos Cambronero-Heinrichs[1], José Pablo Quirós-Fournier[2], Verónica Lizano-Fallas[1], Mario Masís-Mora[1]

1 Centro de Investigación en Contaminación Ambiental (CICA), Universidad de Costa Rica, 2060 San José, Costa Rica; 2 Centro Nacional de Innovaciones Biotecnológicas (CENIBiot), CeNAT-CONARE, 1174-1200 San José, Costa Rica.

**Corresponding author: carlos.rodriguezrodriguez@ucr.ac.cr*

Highlights

- Microbial consortia capable to degrade imidacloprid were isolated
- Cross degradation of other neonicotinoid insecticides was achieved
- Reactor scale treatment (STBR) removed binary and ternary mixtures of neonicotinoids
- The treatment partially detoxified the matrix towards honeybees and other biomarkers

1. Introduction

Neonicotinoid insecticides are widely applied for crop protection, hence their presence in the environment is common, where they exhibit high persistence, particularly in soil. Of particular current concern is the negative effect exerted by neonicotinoid residues on honey bees, causing the decline in their populations [1,2,3], which has led to an European Union decree that banned since the end of 2018 the use of three compounds (clothianidin, thiamethoxam and imidacloprid) on crops pollinated by bees. Biological approaches such as biopurification systems used in the removal of pesticide-containing wastewaters have shown mostly inefficient removal of such compounds, reason why the liquid-phase systems with specialized degrading consortia are explored. This work aimed to isolate and employ degrading-consortia to remove several neonicotinoid insecticides simultaneously at reactor scale, and to monitor the ecotoxicological changes during the treatment.

2. Methods

A selective enrichment approach was employed to isolate microbial degrading consortia with the ability to transform imidacloprid; members of the relevant consortia were identified by sequencing of 16S rRNA or ITS genes. The elimination of imidacloprid and the cross-degrading ability to remove the neonicotinoid insecticides acetamiprid and thiamethoxam was determined at flask scale and monitored by LC-MS/MS. The removal process was scaled-up in a stirred tank bioreactor (STBR) using the consortium exhibiting the best performance to treat mixtures of neonicotinoids. Detoxification in the reactors was monitored by ecotoxicological tests including: seed germination (*Lactuca sativa*), bioluminescence inhibition (Microtox ®) and acute oral test on honeybees.

3. Results and discussion

The selective enrichment using soil pre-exposed to imidacloprid permitted to obtain cometabolic imidacloprid-degrading consortia. The consortia were composed by eight bacterial and one yeast strains, capable of degrading not only this compound, but also thiamethoxam and acetamiprid, as demonstrated in cross-degradation assays. The scaling-up of the process in batch STBR was able to simultaneously remove mixtures of imidacloprid+thiamethoxam or imidacloprid+thiamethoxam+acetamiprid, reaching elimination of 95.8% and 94.4% of total neonicotinoids respectively after 30 d. Removal rates in the bioreactors followed the pattern imidacloprid>acetamiprid>thiamethoxam, including >99% elimination of imidacloprid in 6 d and 17 d (binary and ternary mixtures, respectively). Ecotoxicological evaluation in the STBR revealed partial detoxification of the matrix, with clearer detoxification patterns in the binary mixture compared to the ternary mixture.

4. Conclusions

Considering that the residual ecotoxicity of the synthetic wastewater was partially decreased by the reactor treatment, the liquid-phase approach here described seems a promising strategy to remove the highly toxic and persistent neonicotinoids from agricultural wastewaters. Further research should be focused on optimizing the process to achieve higher detoxification levels, and to adapt it to feasible conditions for farms of different sizes and devoted to the production of diverse crops.

References [Calibri 10]

[1] C.H. Krupke, G.J. Hunt, B.D. Eitzer, G. Andino, K. Given, PLoS One. 7 (2012) 1–8.

[2] E.C. Yang, Y.C. Chuang, Y.L. Chen, L.H. Chang, J. Econ. Entomol. 101 (2008) 1743–1748.

[3] A. Fairbrother, J. Purdy, T. Anderson, R. Fell, Environ. Toxicol. Chem. 33 (2014) 719–731.

ECAB 5
The 5th EUROPEAN CONGRESS OF APPLIED BIOTECHNOLOGY
Florence 15-19 September 2019

From a conventional wastewater sludge to a Photosynthetic Enhanced Biological phosphorus removal system

Virgínia Carvalho[1*], Elisabete Freitas[1], Joana Fradinho[1], Adrian Oehmen[2], Maria Reis[1]

[1]*UCIBIO-REQUIMTE, Department of Chemistry Faculty of Sciences and Technology, Universidade NOVA de Lisboa, 2829-516 Caparica, Portugal*
[2]*Present address: School of Chemical Engineering, University of Queensland, Brisbane, QLD, 4072, Australia.*
**Corresponding author: virginiacfcarvalho@gmail.com*

Highlights

- Phosphorus removal with limited aeration
- Photosynthetic microorganisms as O_2 suppliers
- Phototrophic system for wastewater treatment

1. Introduction

P is an element with vast applications in agriculture and industry but that can negatively impact the environment when released to water streams. One of the options for treatment of P-rich wastewater streams is the enhanced biological phosphorus removal (EBPR) system, that requires intensive aeration and thus increased operational costs [1]. With the aim of reducing the aeration dependence of EBPR processes, a new phototrophic-enhanced biological phosphorus removal (photo-EBPR) process was recently proposed [2]. The photo-EBPR system is composed of a consortium of polyphosphate (poly-P) accumulating organisms (PAOs) and photosynthetic microorganisms (algae, cyanobacteria) operated under dark/light cycles. During the dark anaerobic period, glycogen is hydrolyzed and poly-P is degraded, producing the necessary energy for volatile fatty acids consumption and accumulation as polyhydroxyalkanoates (PHA). During the light phase, photosynthetic microorganisms produce the necessary oxygen and, consequently, PHA is consumed, providing energy and carbon for the regeneration of poly-P and glycogen pools [2].
The first results obtained showed that it is possible to obtain a photo-EBPR system, capable of treating streams with high P concentration (60 mg/L) without need of external aeration, using as inoculum a sludge already enriched in *Candidatus Accumulibacter phosphatis* – well-known organisms for their capacity for high P uptake in conventional EBPR systems [2]. The aim of this study was to determine if it is possible to select a photo-EBPR system using conventional activated sludge from a conventional WWTP as seed sludge and to compare the results to the previous ones.

2. Methods

A sequencing batch reactor was seeded with activated sludge from a wastewater treatment plant in Lisbon and operated in 8 hour cycles (3 h dark, 4 h light and 1 h idle period), with a light intensity of 328 W/m^2 provided by an internal halogen lamp. The sludge retention time was 20 days, hydraulic retention time was 16 hours, with temperature control at 20ºC and pH at 7.5. The reactor was fed with a solution (75%-25%) of acetate and propionate. COD in the feed was adjusted during the experiments, from 60 to 160mg/L, and the P concentration in the feed was 60 mg/L. Air was supplied in the last 2 h of the light phase to ensure that the culture was not limited by O_2. Phylogenetic analysis of the bacterial community was done through Fluorescence in situ hybridization (FISH).

3. Results and discussion

Results show that in the first cycle with 60 mg/L of COD, the culture could not carry out EBPR despite VFAs being totally consumed during the dark phase (Figure 1-A). This suggests that the sludge from the WWTP was not enriched in PAOs and therefore not capable of immediately performing P release/uptake cycles. However, since VFAs were completely consumed in the dark period, COD in the feed was gradually increased along the SBR operation and P uptake in the light phase without aeration increased up to 13 ± 1 mg-P/L (Figure 1-B), a feature that may have resulted from the O_2 availability from algae or direct P uptake by algae. Also, the higher carbon availability in the dark phase enabled more PHA accumulation and with more PHA available, more P can be taken up by PAOs. Although the culture selection process was slower in comparison with cultures already enriched in PAOs (table 1), activated sludge is widely available and a photo-EBPR system can be readily implemented without the need of a seed sludge previously enriched in PAOs.

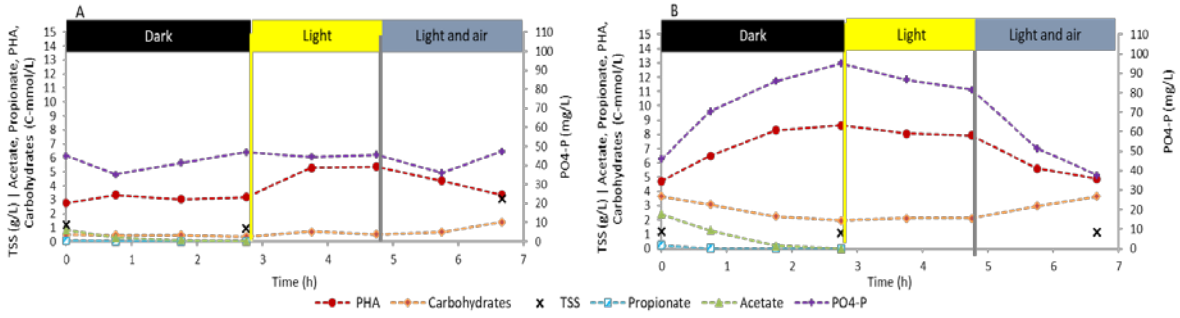

Fig. 1 **-** Profile of P and carbon transformation during SBR operation: A – COD_{feed}= 60 mg/L; B – 160 mg/L

Table 1 - Comparison of the results obtained in the present work with the results obtained in Carvalho et al. (2018).

	P release (mg-P/L)	P uptake (mg-P/L)			Pnet (mg-P/L)	Chlorophyle (mgChlo/gVSS)		FISH		Selection time (days)
	Dark	Light	Light and air	Total		Inicial	Final	PAOmix	CPB_654	
Present work: Seed sludge from a WWTP	47 ± 4	13 ± 1	47 ± 4	60 ± 2	14 ± 7	0.50	7.3	++	++	29
Carvalho et al. (2018) Seed sludge enriched in Accumulibacter phosphatis	34 ± 2	16 ± 6	49 ± 8	65 ± 1	31 ± 0	0.20	4.6	+++	++	14

4. Conclusions

The present study indicates that conventional activated sludge can be enriched in PAOs and photosynthetic organisms capable of performing photosynthetic EBPR. Selecting a photo-EBPR culture directly from activated sludge could simplify the start-up and facilitate the implementation of photo-EBPR systems in wastewater treatment plants. In addition, the implementation of photo-EBPR systems will allow energy savings by eliminating the intensive aeration that increases operation costs in conventional EBPR.

References

[1] Rosso, D., Larson, L.E., Stenstrom, M.K., 2008. Aeration of large-scale municipal wastewater treatment plants : state of the art 973–979. doi:10.2166/wst.2008.

[2] Carvalho, V.C.F., Freitas, E.B., Fradinho, J.C., Reis, M.A.M., Oehmen, A., 2019. The effect of seed sludge on the selection of a photo-EBPR system. N. Biotechnol. 49, 112–119. doi:10.1016/j.nbt.2018.10.003

ECAB 5
The 5th EUROPEAN CONGRESS OF APPLIED BIOTECHNOLOGY
Florence 15-19 September 2019

BIOCOMPATIBLE EXTRACTION OF β-CAROTENE FROM *DUNALIELLA SALINA* – NEW CONTRIBUTION

Guillaume Tanguy*[1,2], Olivier Goncalves[1], Benoît Schoefs[2], Luc Marchal[1]

1 Process engineering, environment and food processing, GEPEA UMR – FR 6144 CNRS, Nantes University, Saint-Nazaire, France

2 Metabolism, bioengIneering of Molecules from Microalgae and Applications, Mer Molécules Santé, IUML - FR 3473 CNRS, Le Mans University, Le Mans, France

**Corresponding author: Guillaume.tanguy1@univ-nantes.fr*

Highlights

- The extraction is biocompatible at the culture level but not at the cell level
- The biocompatibility of the extraction follows a granulo-selective phenomenon
- The extraction kinetics were obtained using Centrifugal Partition Chromatography

1. Introduction

Biotechnological production of carotenoids from the green microalga *Dunaliella salina* involves two steps: (i) biomass growth followed by β-carotene accumulation inside the cell and (ii) carotenoid extraction. Microalgae milking was introduced for the recovery of biomolecules directly from culture broth using long-chain alkanes as solvent [1]. In this condition, photosynthesis was not highly impacted [2] and the fraction of extracted β-carotene from biomass exceeded the fraction of disrupted cells [3]. In a biocompatible extraction or in situ extraction concept, cells remain alive during extraction and the extracted molecules can be re-accumulate [1].

The aim of this study was to determine how the extraction of β-carotene from the green microalga *Dunaliella salina* was biocompatible. The solvent used was *n*-decane and two extraction parameters were investigated: (i) time of contact and (ii) interfacial area between the solvent and the microalgal culture.

2. Methods

Dunaliella salina was grown in a 1L Air-Lift flat panel Photobioreactor (PBR) [4]. To trigger β-carotene accumulation, the green biomass was stressed through a combination of nitrogen limitations and light stress (400 µE/m²/s) or, nitrogen depletion and high light stress (800 µE/m²/s). After carotenoid accumulation, the extraction was run on a Centrifugal Partition Chromatography (CPC), which allowed to control the two liquids phases hydrodynamics with centrifugal acceleration [5]. After extraction the biomass was re-inoculated within the same medium or in the growth medium. The biomass was analyzed before and after extraction and during the re-growth to access the biocompatibility and kinetics of relaxation. Analysis were focused on cell granulometry (density and size), metabolites (pigments and lipids) and dry biomass regarding the extraction parameters.

3. Results and discussion

As a first result, total cell volume decreased as a function of time of contact of the culture media and the solvent (Figure 1). Concerning the cell volume distribution before and after extraction, the biocompatibility is lower for big than for small cells ("granulo-selective" phenomenon) and the median value µ of the distribution decrease ($p < 0.05$). As a consequence, difference between population biocompatibility and individual biocompatibility appeared a key point and a new contribution. These results suggest that carotenoid and lipid extraction yields were correlated with cell destruction.

Finally, a comparison has been made between the two stress applied to the biomass and the scenarii of re-growth to determine the most productive process scheme.

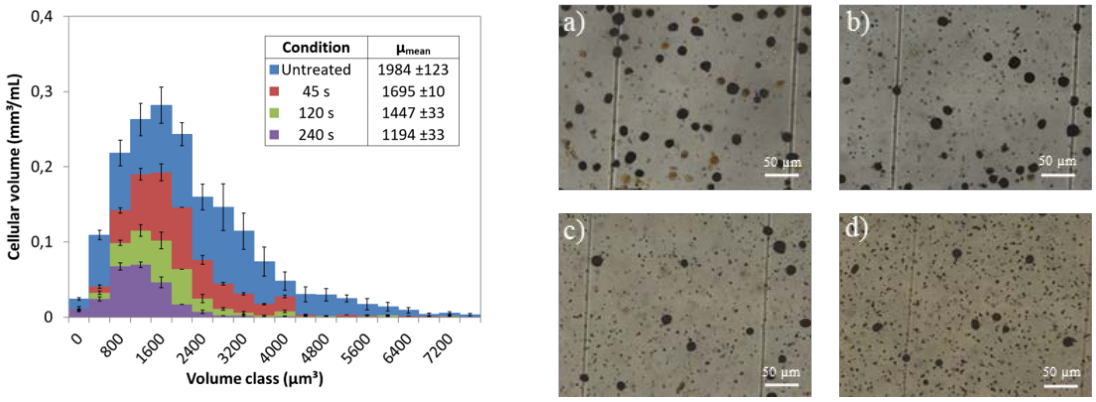

Figure 1. Cell volume distribution (Left) and light microscopy pictures for different extraction time (Right). The larger the extraction time the shorter the mean median value and the fewer cells survive. **a)** Untreated, **b)** 45 s, **c)** 120 s and **d)** 240 s of contact between the solvent and the microalgal culture. Cells were fixed with 1% lugol.

4. Conclusions

Centrifugal Partition Chromatography allowed the decoupling of biomass/metabolites production and the extraction steps giving a better understanding of the mechanism. The granulo-selective effect of the solvent extraction is an original contribution that opens the reflexion for new carotenoid production schemes. The scenarii investigated allowed to choose suitable conditions for the open-loop process with high metabolite productivity and low solvent consumption.

References

[1] Vinayak et al., "Diatom milking: a review and new approaches.", Marine Drugs, 13(5): 2629-2665. (2015)
[2] León et al. ,"Microalgae-mediated photoproduction of β-carotene in aqueous organic two phase systems.", Biomolecular engineering, 20. 177-82, (2003).
[3] Mojaat et al., "Optimal selection of organic solvents for biocompatible extraction of β-carotene from Dunaliella salina.", J. Biotechnol, 133 433-441, (2008).
[4] Taleb et al., "Investigation of lipid production by nitrogen-starved *Parachlorella kessleri* under continuous illumination and day/night cycles for biodiesel application.", Journal of Applied Phycology, 30. 1-12, (2017).
[5] Marchal et al., "Centrifugal partition extraction of β-carotene from *Dunaliella salina* for efficient and biocompatible recovery of metabolites.", Bioresource technology, 134. 10.1016, (2013).

ECAB 5
The 5th EUROPEAN CONGRESS OF APPLIED BIOTECHNOLOGY
Florence 15-19 September 2019

Using machine learning in chemometrics to check validity of existing data driven models for new data

Olivier Paquet-Durand*, Supasuda Assawajaruwan, Bernd Hitzmann

Process analytics and Cereal Science, University of Hohenheim, Garbenstr. 23, 70599 Stuttgart, Germany

**Corresponding author:* o.paquet-durand@uni-hohenheim.de

Highlights

- Online validation of chemometric models
- Evaluation of fluorescence spectra
- Prediction of glucose, ethanol and biomass
- Supervision of cultivation of baker's yeast cells

1. Introduction

A big problem in chemometrics is, that small changes in process setup or equipment or just ageing of compounds might transform existing models useless [1]. Than the chemometric models must be recalibrated. The major catch is, that it is not obvious if a recalibration is necessary or not.

2. Methods

In this contribution we will demonstrate, how machine learning can be used to check existing chemometric models for validity with new data or changing process parameters. To do so, we used an autoencoder [2] which is trained during calibration of chemometric models with the same data and the same number of hidden neurons in the code layer as the chemometric model uses principal components. The basic idea is that when new data point are presented to the chemometric model, the autoencoder error is calculated as well. If this error is significantly higher than during calibration, the used chemometric model is no longer valid and need to be recalibrated. Otherwise a recalibration is not necessary. A 2D fluorescence spectrometer, which was applied in the study, is the BioView fluorescence spectrometer. The device is equipped with 15 different filters for excitation and emission wavelengths. The measurement of one spectrum using the BioView spectrometer has 120 fluorescence intensity variables of excitation and emission wavelength combinations; scattered light is not considered here [3].

3. Results and discussion

The online validation procedure is tested during a cultivation of baker's yeast cells [4]. Here a network with 120 input neurons different hidden layers and 120 output layers are used. The ability of such an autoencoder for a validity check of data driven models will be demonstrated with the evaluation of fluorescence spectra. The data driven models are used for the prediction of glucose, ethanol and biomass. In Figure 1 the autoencoder system used here is present.

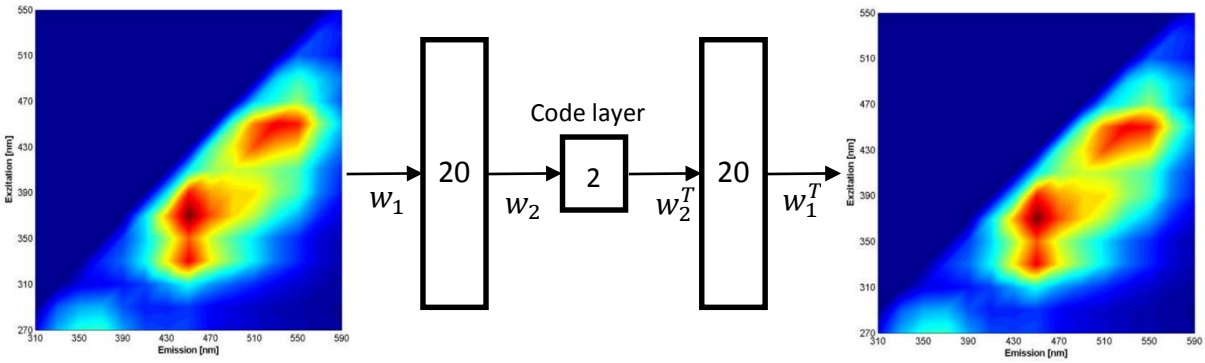

Figure 1. The *autoencoder that is trained to predict the input as output. Within the encode or compression part, the number of neurons per layer progressively decreases. The bottleneck is the code layer with the least number of neurons. Within the decode or decompression part the number neurons progressively increase up to the same dimensions as the input.*

4. Conclusions

The online validation of data driven models is still not satisfactorily resolved [4]. In this contribution autoencoders are used to test the validity of a data driven chemometric model for the prediction of glucose, ethanol and biomass during the cultivation of baker's yeast cells. Although the training of the network takes time, it is very worthwhile to obtain a tool, for the online validity check of the prediction capability of the chemometric model.

References

[1] Dörte Solle, Bernd Hitzmann, Christoph Herwig, Manuel Pereira Remelhe, Sophia Ulonska, Lynn Wuerth, Adrian Prata, Thomas Steckenreiter, Between the poles of data-driven and mechanistic modeling for process operation, *Chemie Ingenieur Technik* 89,5(2017)542-561

[2] Chicco, Davide; Sadowski, Peter; Baldi, Pierre; Deep autoencoder neural networks for gene ontology annotation predictions, *Proceedings of the 5th ACM Conference on Bioinformatics, Computational Biology, and Health Informatics - ACM-BCB 2014*. page 533-540, doi:10.1145/2649387.2649442

[3] Saskia Faassen, Bernd Hitzmann, Fluorescence Spectroscopy and Chemometric Modeling for Bioprocess Monitoring, *Sensors*, 15(2015)10271-10291

[4] Supasuda Assawajaruwan, Philomena Eckard, Bernd Hitzmann, On-line monitoring of relevant fluorophores of yeast cultivations due to glucose addition during the diauxic growth, *Process Biochemistry*, 58(2017)51-59

ECAB 5
The 5th EUROPEAN CONGRESS OF APPLIED BIOTECHNOLOGY
Florence 15-19 September 2019

Improving the calibration of freeze drying models by model-based design of experiments

Riccardo De-Luca[1], Gabriele Bano[1], Emanuele Tomba[2], Fabrizio Bezzo[1], Massimiliano Barolo[1*]

1 CAPE-Lab - Computer-Aided Process Engineering Laboratory, Department of Industrial Engineering, University of Padova, via Marzolo 9, 35131 Padova PD (Italy)
2 GSK, via Fiorentina 1, 53100 Siena SI (Italy)
**Corresponding author: max.barolo@unipd.it*

Highlights

- A lab-scale freeze-drying model is calibrated/validated
- MBDoE is proposed to design the best protocol for model re-calibration for new products
- The optimal recipe for model re-calibration lasts 10 h
- The proposed approach avoids the occurrence of critical operating conditions

1. Introduction

Over the last decades, freeze-drying (lyophilization) process has been extensively used in pharmaceutical manufacturing for the development of heat-sensitive protein-based therapeutic drugs/vaccines. Lyophilization consists in removing a solvent from a frozen solution by sublimation [1], and its characteristic low pressures/temperatures are suitable to guarantee both product stability and easy reconstitution of the dried product before use. Freeze drying is a time consuming process that is carried out through three main steps: freezing, primary drying and secondary drying. Primary drying is the most energy intensive (~36% of the total exergy input [2]) and time consuming step (up to 48h long, corresponding to over 50% of the typical total duration of a drying cycle [3]). Therefore, one way to increase process performance, guarantee product quality and run safe operations is to develop a reliable model to describe the primary drying phase for future optimization. However, once the primary drying model is calibrated for a specific product, new experimental runs are required to identify the model parameters (i.e., model re-calibration is needed) if new formulates are to be processed. In this study, model-based design of experiments (MBDoE) techniques are proposed in order to reduce the time needed for model re-calibration.

2. Methods

In primary drying, the frozen product is processed in vials placed over shelves in a high-vacuum drying chamber linked to a condenser that removes the water vapor generated by ice sublimation. The vials dynamics during the primary-drying phase has been described using a modified version of Fissore *et al*. [4] model. Namely, the original model has been augmented with a dynamic energy balance that takes into account radiation phenomena. The model has been calibrated (and validated) through industrial experimental runs conducted in a VirTis Genesis 25 EL freeze dryer at different chamber pressures and shelf temperatures, using non siliconized vials filled with 0.6 mL

of a 5% w/w sucrose solution. The measured variables are: *(i)* the vial bottom temperature (T_B) for the central zone of the shelves in the freeze-dryer chamber; *(ii)* the chamber pressure obtained using both a Pirani gauge and a capacitance manometer. After validation, the model has been used to optimally design the model identification experiment that is needed when a new formulate needs to be processed in the same freeze-dryer. The MBDoE activity [5] consists on identifying the design vector (initial conditions on measured variables, dynamic profiles of manipulated variables, experiment duration) that maximizes the information related to the mass transfer parameters to be identified.

3. Results and discussion

The optimal experiment designed by MBDoE uses the shelf temperature (T_{shelf}) and chamber pressure (P_c) as manipulated inputs. A piecewise linear profile is designed for the former input, and a piecewise constant for the latter. The maximum experiment length is set to 10 h. As shown in Figure 1a, the optimal profile for the shelf temperature shows an initial ramp lasting ~45 min, to which a stationary phase follows for almost the rest of the experiment; conversely, the optimal chamber pressure profile shows a double pulse about halfway the experiment. As shown in Figure 1b, the final part of the experiment is characterized by short time intervals where the manipulated inputs are slightly adjusted to avoid reaching the formulate collapse temperature (~240 K). By carrying out an experiment according to this schedule, it would be possible to identify all model parameters in a statistically meaningful way.

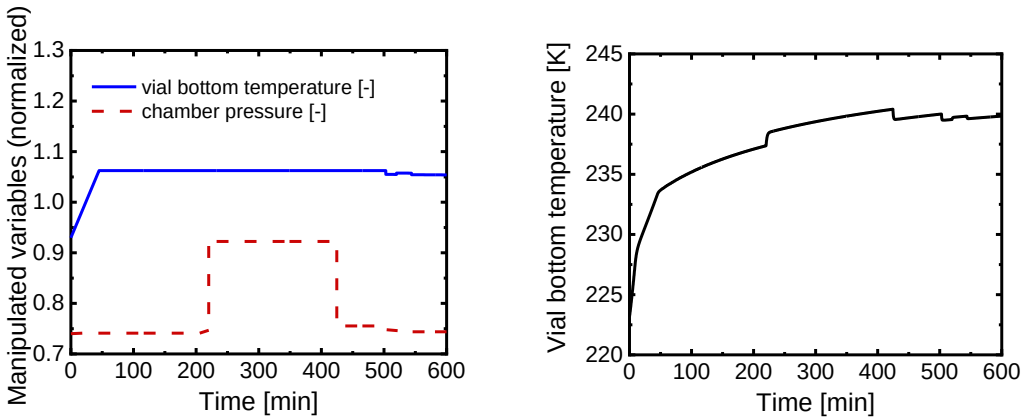

Figure 1. *Time profiles of (a) shelf temperature (blue solid line) and chamber pressure (red dashed line) in the optimally designed experiment; (b) resulting profile of the bottom temperature.*

4. Conclusions

The application of MBDoE techniques showed that one single, optimally designed experiment can be enough to allow a statistically meaningful identification of the mass transfer parameters, while maintaining a reasonable length of the experiment.

References

[1] M. J. Pikal, M. L. Roy, S. Shah, J. Pharm. Sci. 73(9) (1984) 1224–1237.
[2] Y. Liu, Y. Zhao, X. Feng, Appl. Therm. Eng. 28 (2008) 675–690.
[3] M. Bjelošević, K. B. Seljak, U. Trstenjak, M. Logar, B. Brus, Eur. J. Pharm. Sci. 122 (2018) 292-302.
[4] D. Fissore, R. Pisano, A. A. Barresi, in: F. Jameel et al (Eds.), Quality by design for Biopharmaceutical Drug Product Development, AAPS Advances in the Pharmaceutical Sciences Series 18 (2015), pp. 565-593.
[5] G. Franceschini, S. Macchietto, Chem. Eng. J. 63 (2008) 4846-4872

ECAB 5
The 5th EUROPEAN CONGRESS OF APPLIED BIOTECHNOLOGY
Florence 15-19 September 2019

Robust design of experiments for model selection using inverse modeling.

Moritz Schulze[1,2,3], René Schenkendorf[1,2,*]

1 Institute of Energy and Process Systems Engineering (InES), TU Braunschweig, Braunschweig, Germany; Center of Pharmaceutical Engineering (PVZ), TU Braunschweig, Germany; 3 International Max Planck Research School (IMPRS) for Advanced Methods in Process and System Engineering, Magdeburg, Germany

**Corresponding author: r.schenkendorf@tu-braunschweig.de*

Highlights

- One-step model selection under consideration of parameter uncertainties.
- Inverse modeling for an efficient solution of the DoE optimization problem.
- Reliable model identification only when uncertainties are included.

1. Introduction

In terms of quality by design (QbD), the development and production of active pharmaceutical ingredients benefit from a detailed system understanding. To this end, mathematical models might be a useful tool. A crucial task in modeling of (bio)chemical reaction networks is the identification of the most suitable model candidate from a set of various model hypotheses. One possible strategy for model selection is the design of experiments (DoE) approach, where the challenge of model selection is formulated as an optimization problem. An additional consideration of model parameter uncertainties leads to robust predictions of optimal experimental conditions that are expected to provide highly informative data for a reliable model selection.

2. Methods

For an effective solution of the robust model selection problem, we aim at implementing an inverse modeling technique by utilizing the differential flatness concept [2]. With the flatness concept, we avoid simplifying assumptions as linearization and the need for solving differential equations numerically. We consider a biocatalytic step from a carboligation reaction system that forms an essential precursor in the synthesis of natural products and pharmaceuticals [2], see Figure 1.

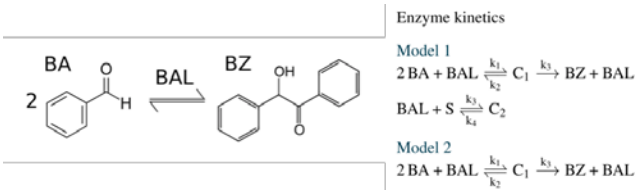

Figure 1. Model candidates of benzaldehyde lyase (BAL)-catalysed reaction network (BA: benzaldehyde, BZ: benzoine).

The two model candidates differ in the following way. Model candidate 1 suffers from a loss reaction where a second substrate (S) is inhibiting. We identify experimental conditions that maximize the differences of the model responses including the uncertain model parameters. The required statistical moments for robustifying the optimization problem are calculated with the Point Estimate Method (PEM) that guarantees low computational cost and sufficient accuracy [3].

3. Results and discussion

In Figure 2, the simulation results of a non-optimized experimental setting are shown on the left. The normalized overlap of the two models' system states is 1.0 and the expected values, i.e., the thick lines in the middle of the confidence intervals indicate that the models are not distinguishable.

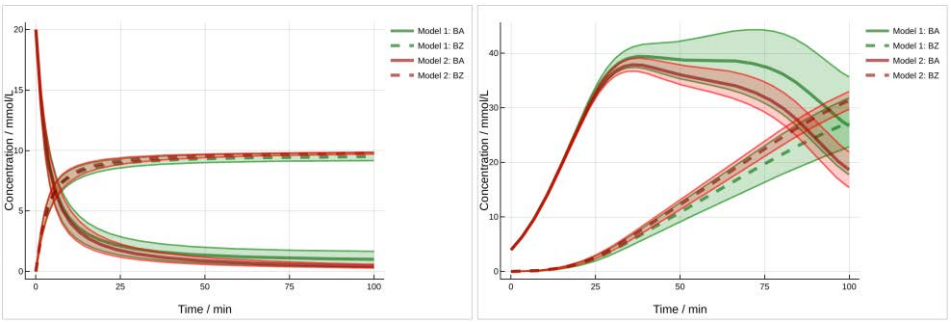

Figure 2. Prior to optimization (left) and after non-robust optimization (right).

First, non-robust optimization was performed to increase the difference in the model responses. The results are shown in Figure 2 on the right-hand side. It is visible that the expected values of the system states are driven apart. However, under consideration of the model parameter uncertainties, the normalized overlap is 1.07 and therefore worse than in the non-optimized case. Reliable identification of a particular model is problematic.

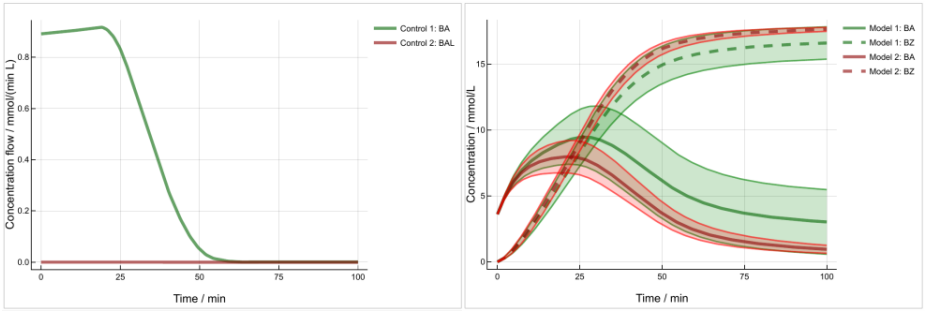

Figure 3. Robust optimized results: controls (left) and measured states (right).

Next, a robust optimization was conducted, where its results are shown in Figure 3. As before, the expected values are driven apart, but additionally, the normalized overlap could be reduced to 0.76. Here, a one-step model selection after running the experiment in the laboratory with the controls shown on the left-hand side in Figure 3 is more likely.

4. Conclusions

We successfully demonstrated how inverse modeling based on flatness could be used for a model selection problem. Furthermore, we showed that the consideration of parameter uncertainties is essential for reliable model identification.

References

[1] M. Fliess, J. Lévine, P. Martin, P. Rouchon, CR Acad Sci Paris (1992), 619–624.
[2] F. Hildebrand et al., Biotechnol. Bioeng. 96 (2007), 835-843.
[3] R. Schenkendorf et al., Processes 6 (2018).

ECAB 5
The 5th EUROPEAN CONGRESS OF APPLIED BIOTECHNOLOGY
Florence 15-19 September 2019

Lipid Production With *Microchloropsis Salina* in Open Thin-Layer Cascade Reactors at Mediterranean Climate Conditions.

Torben Schädler[1,3], Thomas Brück[2,3], Dirk Weuster-Botz[1,3]

1 Technical University of Munich, Institute of Biochemical Engineering, Garching, Germany
2 Technical University of Munich, Werner Siemens-Chair of Synthetic Biotechnology, Garching, Germany
3 Technical University of Munich, AlgaeTec Center, Ottobrunn, Germany

**Corresponding author: t.schaedler@lrz.tum.de*

Highlights

- Batch production of 6 g L^{-1} lipids in open thin-layer cascade reactors
- Accumulation of up to 46 % (w/w) lipids in *M. salina*
- Continuous production of 3.5 g L^{-1} lipids in a reactor cascade

1. Introduction

The utilization of sunlight and carbon dioxide for the production of energy-rich lipids by microalgae offers a possibility to produce renewable liquid fuels. Advances in biomass and lipid productivity are needed to become an economically feasible alternative to fossil fuels. Besides efficient downstream processing and catalysis, high product concentrations are essential to reduce the costs of biomass separation and drying. Because of the increasing light absorption in dense microalgae suspensions, high biomass concentrations can only be achieved in thin fluid layers.

2. Methods

Microalgae growth and lipid production of *Microchloropsis salina* was studied in artificial sea water [1] in open thin-layer cascade photobioreactors at pilot scale (A = 8 m^2). For this purpose, the TUM AlgaeTec Center offers a realistic, dynamic simulation of light and climate conditions to evaluate microalgae processes at potentially suitable large-scale production sites [2]. The target climate of June 15, 2012 in Almería, Spain was physically simulated via an air conditioning system and a combination of natural sunlight and LED-based artificial sunlight. A nutrient limitation was used to induce the accumulation of lipids. Total lipid concentrations were measured via a Sulfo-Phospho-Vanillin assay [3].

3. Results and discussion

Biomass growth and lipid production of *M. salina* were studied in batch processes. At nutrient replete conditions a cell dry weight concentration above 40 g L^{-1} with a lipid content of 16 % was reached. At nutrient limited conditions lipids accumulated up to 46 % of dry weight while simultaneously reducing photosynthetic activity and biomass growth. Lipid concentrations of 6.6 g L^{-1} and an overall volumetric lipid productivity of 0.2 g L^{-1} d^{-1} were achieved after 30 days. Continuous production of lipids was achieved with a two-stage reactor cascade, spatially separating biomass growth and lipid accumulation. The reactor cascade reached a continuous production of up to 3.5 g L^{-1} lipids.

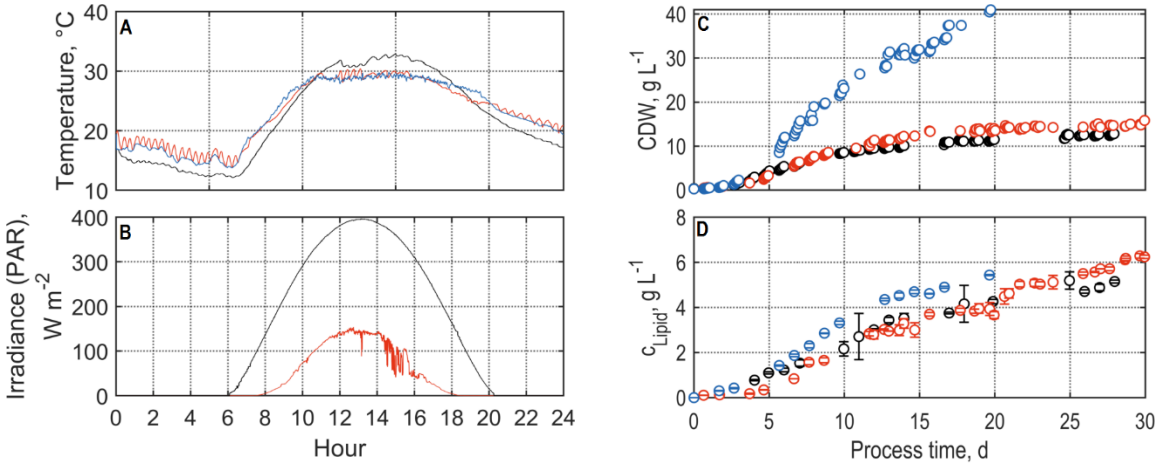

Figure 1. A: Temperature profile of June 15, Almería, Spain (blue), physically simulated temperature in the TUM AlgaeTec Center (red) and water temperature in a thin-layer cascade reactor (black). B: Natural sunlight at TUM AlgaeTec Center on October 19, 2018 (red) and combination of natural and LED-based light (black). C, D: Cell dry weight and lipid concentration in batch processes with *M. salina* in an open thin-layer cascade reactor at physically simulated Mediterranean climate conditions. Blue: Nutrient repletion. Black: Nutrient limitation. Red: Nutrient limitation, doubled initial nutrient concentration

4. Conclusions

As is shown by these results, the continuous production of commodity chemicals and fuels from microalgal biomass remains a promising alternative to fossil resources. Further advances in process engineering as well as strain selection, downstream processing and catalysis are required to compete with petrochemical pathways.

References

[1] Boussiba, S., et al., Lipid and Biomass Production by the Halotolerant Microalga *Nannochloropsis salina*. Biomass, 1987. 12: p. 37-47.

[2] Apel, A.C., et al., Open thin-layer cascade reactors for saline microalgae production evaluated in a physically simulated Mediterranean summer climate. Algal Research, 2017. 25: p. 381-390.

[3] Mishra, S.K., et al., Rapid quantification of microalgal lipids in aqueous medium by a simple colorimetric method. Bioresource Technology, 2014. 155: p. 330-333.

Viability, growth and hydrogen production of green microalgae in novel silica hydrogels

S. V. Homburg[1], O. Kruse[2], A. V. Patel[1*]

1 Bielefeld University of Applied Sciences, Interaktion 1, 33619 Bielefeld, Germany;

2 Bielefeld University, Universitätsstraße 25, 33615 Bielefeld, Germany

**Corresponding author: anant.patel@fh-bielefeld.de*

Highlights

- pH adjustment with Tris resulted in short gelation times and transparent silica hydrogels
- Investigated hydrogels exhibit a 10 times lower stiffness than those in previous reports
- Entrapped microalga *C. reinhardtii* maintained photosynthetic activity and growth
- In silica lenses entrapped cells produced hydrogen with an effectiveness of nearly 70%

1. Introduction

Immobilization of microalgae via entrapment provides protection against shear forces and contaminations. Potential applications are the continuous production of biohydrogen or secreted high-value products with a molecular tool kit [1]. In contrast to biopolymer gels, silica gels show an improved mechanical and chemical stability. Besides, they resist microbial attacks and are optically transparent which is crucial for photosynthetically active cells.

Following up on previous work [2], we developed novel biocompatible entrapment methods for sensitive hydrogen producing *Chlamydomonas reinhardtii* strains, based on three silica precursors, namely tetraethylorthosilicate, sodium silicate and tetra(*n*-propylamino)silane. Therefore, we aimed at improved viability and growth in transparent silica hydrogels by modification of the synthesis through adjustment of the pH with buffers and shortening gelation time. Furthermore, we examined if the entrapped microalgal cells produce hydrogen.

2. Methods

Silica gels and calcium alginate gels were prepared as described in [3]. Briefly, after dilution of precursors tetraethylorthosilicate (TEOS), sodium trisilicate solution and tetra(n-propylamino)silane by-products were removed via evaporation or ion exchanger. For gelation, the pH of the sol was adjusted with KOH, K_2HPO_4 or Tris. Calcium alginate gels as reference were prepared by gelling a 2 wt% sodium alginate solution with 2 wt% $CaCl_2$ solution.

Stiffness was measured from cylindrical blocks via dynamic mechanical analysis collecting the stress-strain curves at room temperature via compression.

Microalgal growth was determined in hydrogel blocks in cuvettes, overlaid with medium. Changes in the optical density at 750 nm were observed daily with a UV/vis-spectrophotometer. Hydrogen production was investigated with cells entrapped in low-sodium silica lenses and compared to free cells and cells entrapped in calcium alginate beads. Therefore, cultivation was conducted in

gas-tight vials at 30 °C and 350 µE in sulfur-depleted medium. Daily, the composition of the gas phase was measured via GC and afterwards flushed with nitrogen.

3. Results and discussion

When KOH was replaced with the buffer substance Tris, gelation times were maintained at 100-150 min for the three sols. Furthermore, absorption at 750 nm decreased by 18-72%. Elevation of precursor concentrations decreased gelation time to 2-3 min.

Stiffness differed between the silica hydrogels, namely 4.23 ± 0.72 kPa for low-ethanol, 0.90 ± 0.19 kPa for low-sodium and 0.04 ± 0.002 kPa for low-propylamine silica hydrogels. In comparison, calcium alginate displayed a stiffness of 0.64 ± 0.17 kPa.

Growth in gel blocks was observed with rates of 0.39 ± 0.02 d^{-1}, 0.25 ± 0.03 d^{-1} and 0.23 ± 0.01 d^{-1} for free cells, cells entrapped in calcium alginate and in all silica hydrogels, respectively (figure 1 A). Increased growth rates in silica gels may be attributed to the low stiffness.

Based on further investigations on growth and photosynthetic activity of cells entrapped in silica lenses (data not shown), the low-sodium gel was selected for examination of hydrogen production. The biocatalyst reached an operative effectiveness factor of 69.20 ± 6.35% when compared to a suspension culture with the same OD of 0.8 (figure 1 B).

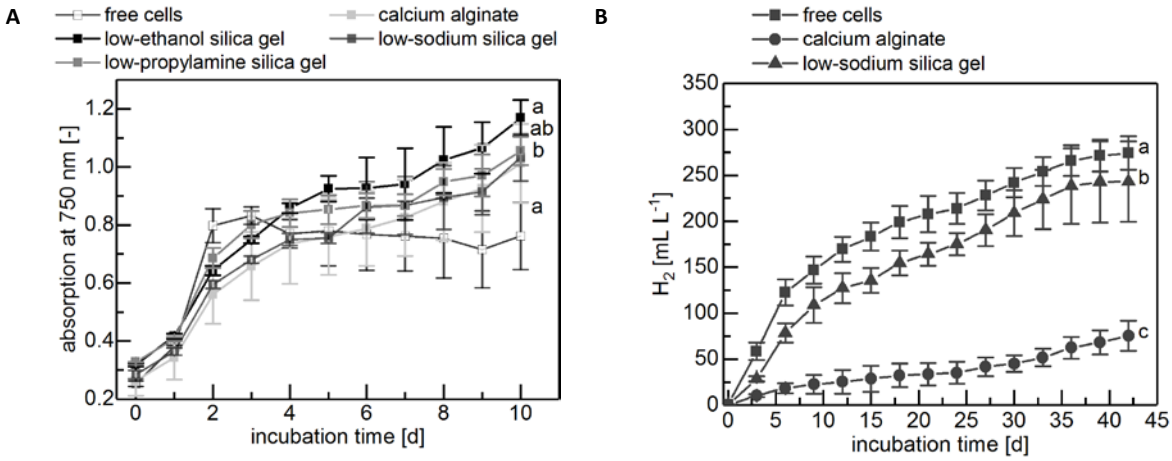

Figure 1. (A) Growth and (B) hydrogen yield of free and entrapped cells (n=5; mean±SD).

4. Conclusions

To the best of our knowledge, this is the first report of entrapment in silica gels that allow cell growth. Furthermore, we reported hydrogen production in lens-shaped particles for the first time. This entrapment method paves the way for transparent silica-gel based biocatalysts that support cell growth and protection against harmful mechanical, biological and/or chemical influences in continuous processes.

References

[1] Lauersen et al, App. Microbiol. Biotechnol., 99 (2015), 3491-3503
[2] Müller et al., Chem. Comm., 49 (2013), 10163-10165
[3] Homburg et al., Colloids Surf. B, 173 (2019), 233-241

ECCE12
The 12th EUROPEAN CONGRESS OF CHEMICAL ENGINEERING
Florence 15-19 September 2019

Mixed-trophies biofilms for high-cell-density cultivation of *Synechocystis* sp. PCC 6803 in capillary reactors for continuous cyclohexane oxidation

Ingeborg Heuschkel, Anna Hoschek, Andreas Schmid, Bruno Bühler, Rohan Karande*, Katja Bühler

Department of Solar Materials, Helmholtz-Centre for Environmental Research, UFZ Permoserstrasse 15, 04318 Leipzig, Germany

**Corresponding author: rohan.karande@ufz.de*

Highlights

- O_2 producing *Synechocystis* was combined with O_2 respiring *Pseudomonas* using proto-cooperation to achieve HCDs of up to 51.8 g_{BDW} L^{-1}.
- This concept was coupled to the challenging C-H oxyfunctionalization of cyclohexane to cyclohexanol with a remarkable conversion of >98% and selectivity of 100 % (KA oil).
- HCD of the photoautotrophic biocatalyst were established and resulted in a productivity of 3.76 $g_{cyclohexanol}$ m^{-2} day^{-1}, which was maintained for at least one month.

1. Introduction

In Nature, almost 385 billion tons of CO_2 are fixed annually by photosynthesis. This power of photosynthesis will be key to make inorganic carbon available for the production of value-added chemicals and fuels and reduce future dependency on fossil resources. Despite photo-biocatalysis developing remarkably and the huge potential of photoautotrophic microorganisms for eco-efficient production scenarios, photo-biotechnology is still in its infancy. The lack of scalable photobioreactors that provide efficient light transmission, CO_2 supply, and O_2 degassing and thus enable high cell densities (HCD), constitutes a key bottleneck, especially if cost-sensitive bulk chemicals are the product of choice. Commercialized tubular photobioreactors with 100 to 600 mm inner diameter offer a surface area to volume ratio (SA/V) of over 100 m^2 m^{-3} enabling the efficient capturing of incident solar radiation.[1] Here we introduce a new generation of photobioreactors based on capillary biofilm reactors. They have a high surface to volume ratio, and thus enhanced light availability, enabling HCDs of photo-autotrophic microorganisms.

2. Methods

For biomass determination mixed-trophies as well as single species *Synechocystis* sp. PCC 6803 biofilms were cultivated for 5 weeks in the biofilm format, either supplied with or without air segments and with or without citrate. Finally dissolved oxygen in the aqueous phase as well as the oxygen content in the gas phase was measured and the biomass removed and quantified.

For the biotransformation the mixed-trophies biofilms were cultivated without citrate and under segmented flow conditions. After 5 weeks of biofilm cultivation the biotransformation was induced and product concentrations as well as oxygen in the gas phase were measured.

3. Results and discussion

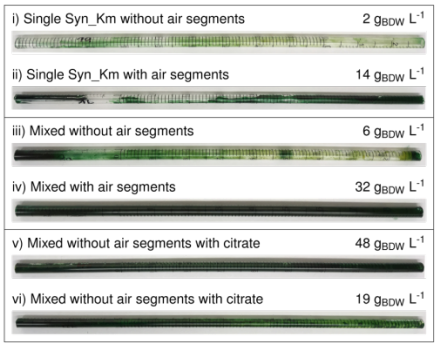

Figure 1. Images of the biofilm capillary reactors 5 weeks after inoculation. i) and ii) Syn_Km: monoseptic biofilm cultures of *Synechocystis* sp. PCC 6803 (pAH032) without and with air segments, respectively. iii) and iv) Dual species biofilm cultures of Syn_Km and *P. taiwanensis* VLB120 (pAH032) operated iii) without and iv) with air segments. v) and vi) correspond to iii) and iv) with citrate in the aqueous medium feed. Final biomass concentrations are given on the right of the respective image. BDW, biomass dry weight.

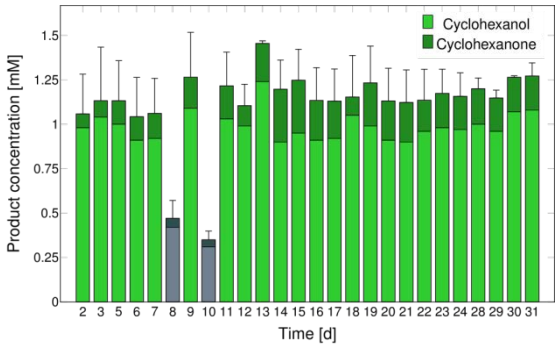

Figure 2. Biocatalytic cyclohexane oxyfunctionalization reaction performed by a dual-species mixed trophies biofilm consisting of recombinant *Synechocystis* sp. PCC 6803 (pAH050) and *P. taiwanensis* VLB120 (pAH050). Biotransformation (started day 0 in Fig.2) was initiated after 5 weeks of biofilm cultivation. The light was switched off for 24 hours during days 8 and 10, respectively. Green and gray bars represent product formation under light and dark conditions, respectively. Light and dark colors refer to the formation of cyclohexanol and cyclohexanone, respectively.

The flow reactor concept for phototrophic biofilm cultivation was coupled to the challenging C-H oxyfunctionalization of cyclohexane to cyclohexanol with a remarkable conversion of >98% and selectivity of 100 % (KA oil). High photoautotrophic biocatalyst concentrations were established and resulted in a productivity of 3.76 gcyclohexanol m^{-2} day^{-1}, which was maintained for at least one month.[3]

4. Conclusions

This work demonstrates prototrophy as a biological strategy for the cultivation of photobiocatalysts in a stable and high cell density format up to 51.8 g_{BDW} L^{-1}, thereby overcoming a key-bottleneck in photo-biotechnology. The crucial problem of O_2 accumulation and thus toxification/inhibition of the photoautotrophic biocatalyst was overcome by utilizing O_2 respiring *P. taiwanensis* VLB120, O_2 extracting air segments and by O_2 dependent biotransformation. Mixed trophies biofilms in capillary reactors were able to produce 3.76 g m^{-2} day^{-1} cyclohexanol for over a month with conversion, and KA oil selectivity values of 98% and 100%, respectively, a milestone in cyclohexane-based chemistry.

References

[1] Posten, C. Eng. In Life Science. (2009) 165-177
[2] Karande R., Hoschek A., Heuschkel I., Bühler K., Schmid A. Patent: PCT/EP2018/074746
[3] Anna Hoschek, Ingeborg Heuschkel, Andreas Schmid, Bruno Bühler, Rohan Karande*, Katja Bühler. Biores. tech. (2019) (submitted)
[4] Karande R., Salamanca D., Engesser K.-H., Buehler K. and Schmid A. Patent. WO/2018/046104

ECAB 5
The 5th EUROPEAN CONGRESS OF APPLIED BIOTECHNOLOGY
Florence 15-19 September 2019

Study of starch accumulation dynamic in nitrogen starved *Chlamydomonas reinhardtii* using controlled torus photobioreactor

Fernando FERREL BALLESTAS[1*], Mariana TITICA[2], Guillaume COGNE[3], Jack LEGRAND[4]

[1,2,3,4]*University of Nantes,* Oniris, CNRS, GEPEA, UMR 6144, 44602 Saint-Nazaire Cedex, France

**Corresponding author: fernando.ferrel-ballestas@univ-nantes.fr*

Highlights

- High starch accumulation by microalgae
- Controlled torus PBR with dissolved oxygen and pH regulation
- Physiological adaptation to nitrogen deficiency

1. Introduction

Chlamydomonas reinhardtii is a green microalgae known to accumulate large amounts of starch in nitrogen-limited conditions, up to 50% of its mass content expressed in dry weight of cells (%DW) that could be used as a feedstock for next generation of biofuels production [1]. In autotrophic nitrogen-starved cultures of *C. reinhardtii*, several physiological changes take place in order to adapt their mass content in pigment content and accumulate starch [2]. Starch accumulation in nitrogen starved cells can be affected by other factors such as anoxic conditions [3], light energy availability [1] and inoculum physiological state. The objective of this work is study of starch accumulation dynamic in nitrogen-starved *C. reinhardtii* in controlled O_2 dissolved (OD), pH and light availability conditions, prior to a modelling study with a view to develop an optimized starch production protocol in nitrogen-limiting conditions.

2. Methods

A wild type strain of *C. reinhardtii* (137H) has been cultivated in autotrophic nitrogen-limited conditions, using Suoeka medium with NH_4Cl concentration of 1,87mM, in a torus-shaped PBR, equipped with a pH-temperature and DO sensor, as well as mass spectrometer for gas analyses. The pH of the microalgae culture was regulated at 7.5 with gaseous CO_2 injection. DO has been regulated with 4.5% O_2 - 95.5% N_2 gas mixture injection flowrate. Limited-growth cultures were performed in batch and at different incident light intensities. Inoculum has been cultivated in 1L air-lift PBR in non-limiting autotropic conditions and pH was regulated by CO_2 injection. The local fluence rate was calculated along batch cultures using the 2-flux model and the radiative properties of culture were determined experimentally using the methodology developed by Pilon *et al*. [4]. Biotic and abiotic phases have been analyzed measuring the dynamic evolution of key nutriments and intermediate metabolites, as well as the analysis of the produced gas .

3. Results and discussion

For nitrogen-limited growth cultures of *C.reinhardtii*, an NH_4Cl initial load of 1.87mM was used to sustain biosynthesis up to 0.25g/L of biomass under standard growth conditions, according to the known stoichiometry. This amount is close to the value obtained during the first 20 hours of culture in concordance with the depletion of NH_4^+ measured (Fig 1A). After that point, an increase in the starch content was observed and a maximum accumulation of 53% was finally obtained after 70 hours of cultivation (Fig. 1A). A stop of cell growth seems to occur at 32 h of culture, once the number of cells remained relatively constant. In contrast, the nitrogen depletion in the medium lead to a remobilization of the total proteins, while reducing their content to 20% (Fig 1A). In the other hand, the pigments content decreased once the NH_4^+ vanished. The total pigments content was stabilized around 1%. This results in a change within the pigment distribution compared to a standard growth culture without any mineral deprivation. The radiative properties were estimated leading to the calculation the energy light profile within the cultivation system during the starch accumulation phase (70h). This assessment showed that light was not a limiting factor since a fluence value was estimated at 21umol/m^2s at the bottom of the PBR (Fig 1B). Throughout the experiment, the dissolved O_2 was regulated to 130% in oxygen saturation in the air, in order to avoid anoxic conditions. Nonetheless, after 63 hours the dissolved oxygen falls as a consequence of low photosynthetic activity (Fig 1C).

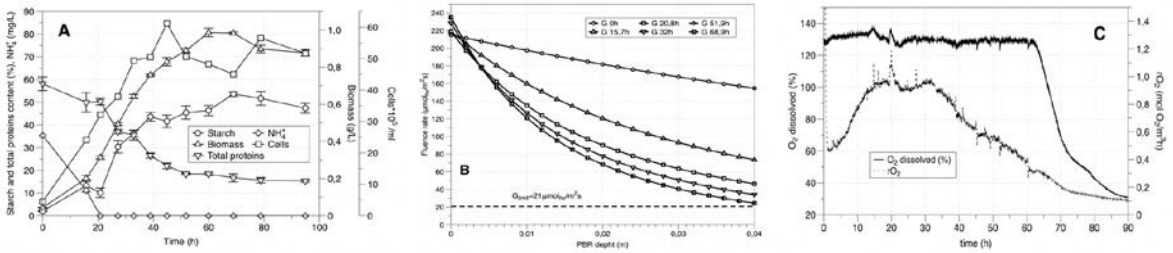

Figure 1. A. physiology response to nitrogen starvation, B. Fluence rate in batch culture q_0= 200umol/m^2s, C. Dissolved oxygen and rO_2 evolution.

4. Conclusions

The use of a controlled torus PBR allowed the study of starch accumulation dynamic after a nitrogen deficiency, where neither light transfer nor dissolved gases (CO_2, DO) influenced the storage of starch. A maximum starch content of 53% was obtained after 70 hours of cultivation. The physiological impact of nitrogen deficiency also led to the remobilization of 30% of the total protein content and to the adaptation in the content and distribution of pigments. This work will lead to the development of a biochemically structured model for starch storage in *C. reinhardtii*.

References [Calibri 10]

[1] Chen C-Y, Zhao X-Q, Yen H-W, Ho S-H, Cheng C-L, Lee D-J, et al. Microalgae-based carbohydrates for biofuel production. Biochemical Engineering Journal 2013;78:1–10. doi:10.1016/j.bej.2013.03.006 .
[2] Antal TK. Microalgal Hydrogen Production: Achievements and Perspectives. Rsc 2018:235–64.
[3] Juergens MT, Deshpande RR, Lucker BF, Park J-J, Wang H, Gargouri M, et al. The Regulation of Photosynthetic Structure and Function during Nitrogen Deprivation in Chlamydomonas reinhardtii. Plant Physiology 2015;167:558–73..
[4] Pilon L, Berbero• lu H, Kandilian R. Radiation transfer in photobiological carbon dioxide fixation and fuel production by microalgae. Journal of Quantitative Spectroscopy and Radiative Transfer 2011;112:2639–60.

ECAB 5
The 5th EUROPEAN CONGRESS OF APPLIED BIOTECHNOLOGY
Florence 15-19 September 2019

Increasing Photoautotrophic Growth and Carotenoid Production with *Dunaliella Salina* .

Lara Wolf*, Dirk Weuster-Botz
Institute of Biochemical Engineering, Technical University of Munich
Boltzmannstraße 15, 85748 Garching, Germany

**Corresponding author: l.wolf@lrz.tum.de*

Highlights:

- Up to sevenfold increase of so far reported maximum biomass concentrations (5 g_{CDW} L^{-1})
- Sixfold increase of β-carotene concentration with nutrient limitation at 18 % salinity (w/v)

1. Introduction

The photoautotrophic production of high-value products from CO_2 with microalgae is of increasing interest. *Dunaliella salina* is a halotolerant microalgae that can survive up to 30 % (w/v) NaCl thereby accumulating increasing amounts of β-carotene in the cells. Thus, *D. salina* is a highly interesting microalgae for outdoor cultivations in open photobioreactors with seawater as the salt content permanently increases due to the continuous evaporation of water. Unfortunately, the final biomass concentrations reported so far with *D. salina* are low compared to other microalgae.

2. Methods

Growth and product formation of *D. salina* was studied in fully-controlled LED illuminated flat-plate gas-lift photobioreactors [1-3] with diurnal light (0 – 1900 µmol m^{-2} s^{-1}) and temperature profiles (15 – 30 °C) according to [4] using CO_2 for pH-control. Additionally, the salt content was increased from 3.5 % (w/v) up to 30 % (w/v) in order to get comparable data to outdoor cultivations with evaporation. Growth and β-carotene formation was studied independently. First, batch processes were performed using a growth medium. Second, *D. salina* was harvested and the cells were resuspended in a medium with reduced nutrient concentration. The salt content in this production phase was kept constant. Optical density, cell dry weight, carotenoid content and transmission were monitored in the batch processes.

3. Results and discussion

Growth of *D. salina* in salt accumulating batch processes was comparable to the growth in batch processes with a constant salt concentration of 7.5 % NaCl. The final cell dry weight of 5 g L^{-1} (40 million cells mL^{-1}) after 7.7 days was increased up to sevenfold compared to so far reported data [5–7]. Neither the variation of pH in a range of pH 7.5 – pH 8.5 nor an increase in temperature from 15 – 30 °C to 20 – 35 °C showed significant changes in biomass formation demonstrating robustness of *D. salina*. A maximum lutein concentration of 8.8 mg L^{-1} (2.0 mg g^{-1} cell dry weight) and a maximum β-carotene concentration of 5 mg L^{-1} (1.1 mg g^{-1} cell dry weight) were measured during growth with increasing salt concentrations. After transferring *D. salina* into a nutrient limited

medium, highest β-carotene concentration could be observed in a batch process with a salinity of 18 % (w/v). The β-carotene concentration was increased sixfold from around 2 mg L^{-1} up to 12 mg L^{-1} (3.2 mg g^{-1} cell dry weight).

4. Conclusion and outlook

The drawback of photoautotrophic processes with *D. salina* (low biomass concentrations) can be solved by changing the cultivation system from shaking flasks, tubular reactors or column reactors to fully-controlled LED illuminated flat-plate gas-lift photobioreactors which resulted in an enhancement of the final dry cell mass concentration by a factor of 7 compared to literature [5–7]. Applying nutrient limitation after growth resulted in an increase of the β-carotene concentration by a factor of 6. Scale-up of microalgae processes from lab-scale flat-plate gas-lift photobioreactors to open thin-layer cascade reactors with physical climate simulation [4] was already shown for several microalgae and will be approved for β-carotene production with *D. salina* in the future.

5. References

[1] Koller AP, Wolf L, Weuster-Botz D (2017): Reaction engineering analysis of *Scenedesmus ovalternus* in a flat-plate gas-lift photobioreactor. Biores Technol 225: 165–174.

[2] Koller A, Loewe H, Schmid V, Mundt S, Weuster-Botz D (2016) Model-supported phototrophic growth studies with *Scenedesmus obtusiusculus* in a flat-plate photobioreactor. Biotechnol Bioeng 114: 308–320.

[3] Pfaffinger CE, Schöne D, Trunz S, Loewe H, Weuster-Botz D (2016): Model-based optimization of microalgae areal productivity in flat-plate gas-lift photobioreactors. Algae Res 20: 153–163.

[4] Apel AC, Pfaffinger CE, Basedahl N, Mittwollen N, Goebel J, Sauter J, Brueck T, Weuster-Botz D (2017): Open thin-layer cascade reactors for saline microalgae production evaluated in a physically simulated Mediterranean summer climate. Algal Research 25: 381–390.

[5] Wu Z, Duangmanee P, Zhao P, Juntawong N, Ma C (2016): The Effects of Light, Temperature, and Nutrition on Growth and Pigment Accumulation of Three *Dunaliella salina* Strains Isolated from Saline Soil, Jundishapur journal of microbiology 9 e26732.

[6] Prieto A, Pedro Cañavate J, García-González M (2011): Assessment of carotenoid production by *Dunaliella salina* in different culture systems and operation regimes. Journal of Biotechnology 151: 180–185.

[7] Morowvat MH, Ghasemi Y (2016): Culture medium optimization for enhanced β-carotene and biomass production by *Dunaliella salina* in mixotrophic culture. Biocatalysis and Agricultural Biotechnology 7: 217–223.

[8] Marín N, Morales F, Lodeiros C, Tamigneaux E (1998): Effect of nitrate concentration on growth and pigment synthesis of *Dunaliella salina* cultivated under low illumination and preadapted to different salinities. Journal of Applied Phycology 10: 405–411.

ECAB 5
The 5th EUROPEAN CONGRESS OF APPLIED BIOTECHNOLOGY
Florence 15-19 September 2019

Scenedesmus Obliquus Growth in Semi-Batch Microphotobioreactor under Non-Limiting CO_2 Supply

Christopher Castaldello[1,2], Eleonora Sforza[2], Fabrizio Bezzo[1,*]

1 CAPE-Lab -- Computer-Aided Process Engineering Laboratory, Department of Industrial Engineering DII, University of Padova, via Marzolo 9, 35131 Padova, Italy
2 PARLab -- Padua Algae Research Laboratory, Department of Industrial Engineering DII, University of Padova, Via Marzolo 9, 35131 Padova, Italy
**Corresponding author: fabrizio.bezzo@unipd.it*

Highlights

- Microalgae growth monitoring assessed with fluorescence measurements.
- Semi-batch microphotobioreactor for non-limiting nutrients condition.
- The system is effective in CO_2 supply.
- It will be possible to assess different light conditions simultaneously.

1. Introduction

Microalgae are nowadays widely used as a source for different chemicals and products of interest. However, the industrial optimization of biomass production is hard to achieve since many factors contribute to their growth, such as nutrients availability and light intensity and many experiments are needed to characterize their impact. A microscale platform would strongly aid with this purpose, allowing the simplification and the parallelization of the reactors [1].

One of the main challenge in micro-photobioreactor (mPBR) technologies is linked to CO2 supply, as it is the main nutrient required for photosynthesis and, even if the mPBR materials are somewhat permeable with gases, the CO_2 concentration in air is far to be non-limiting for microalgal growth. Accordingly, there is the need to provide CO_2 directly into the solution, through an absorption step in a sodium carbonate enriched medium [2].

In this work, a new device with non-limiting CO_2 supply was proposed. Here *Scenedesmus obliquus* was cultivated at constant light intensity by monitoring growth through in vivo chlorophyll fluorescence measurements [3] with the aim to assess the efficiency of CO_2 supply.

2. Methods

The device is made in polydimethylsiloxane (PDMS) which is a polymer with high compatibility with biological application and is transparent to light. The device has been designed to allow up to three different channel, each channel has 8 independent wells (non-mixed photobioreactors). A CFD simulation has been performed in order to ensure homogeneous fluid pattern at the entrance of each well. Since here velocity is almost zero, nutrients enter continuously via molecular diffusion only, avoiding limiting conditions. This device allow up to 24 parallel experiments. A syringe pump is needed to guarantee low and constant flowrates of fresh medium.

To efficiently absorb CO_2 in the liquid phase, the equilibrium of carbonate was exploited [2]. A sensitivity analysis (performed on Aspen Plus using ELECNRTL activity coefficient model), was carried out to select the carbonate concentration needed in order to obtain a suitable pH value in

a liquid which is bubbled whit 100% CO_2. This means that by slightly increasing pH in a buffered solution, is possible to shift equilibrium to increase carbon capture. Enriched medium are loaded into 50 mL syringe that allow to run 5-days long experiments.

S. obliquus was pre-cultured in agitated flask at illumination of 40 µmol photons $m^{-2}s^{-1}$ at 24±1 °C in BG11 medium, cells were then collected in the middle of exponential phase. A correlation line between biomass concentration and F_0 has been set. Measurements were performed with Open FluorCam FC800 (Photon System Instruments, Czech Republic). Microalgae growth has been carried out at ambient temperature with a constant incident light of 40 µmol photons $m^{-2}s^{-1}$. Growth rate was obtained as the slope of logarithmic variation of the concentration over time.

3. Results and discussion

Using a 2.5 g L^{-1} carbonate-enriched BG11, microalgae growth has been evaluated in two cases, with and without CO_2 in Figure 1 (left). The corresponding growth rates, calculated from eight wells replicates each, lead to a µ=0.14±0.12 day^{-1} without CO_2 and µ=0.53±0.03 day^{-1} in the opposite case. These results are statistically different by 1-way ANOVA and a Tukey-Kramer significant difference criterion since p-value<0.05. In the latter case, µ is comparable to traditional cultures where no CO_2 limitation is observed [4].

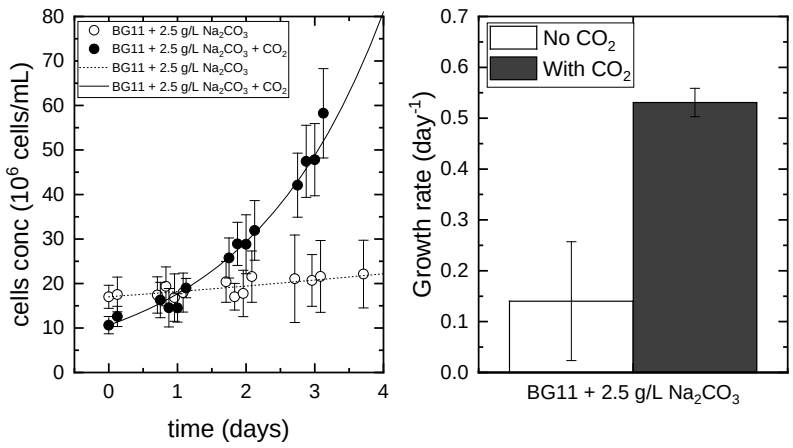

Figure 1. *S. obliquus* growth in mPBR, the lines represent the trend of the exponential phase (left). *S. obliquus* growth rate comparisons (right).

4. Conclusions

A new method to supply CO_2 efficiently in mPBR for photosynthetic organisms was proposed. Microalga *S. obliquus* cultivated in this device showed an increased growth rate of more than three times with respect to air diffusion condition. As the carbon is not limiting, this mPBR can be used in future to assess the effect of other variables such as light intensity.

References

[1] H. S. Kim, T. P. Devarenne, A. Han, Algal Res. 9 (2018) 149-161

[2] B. Gris, E. Sforza, L. Vecchiato, A. Bertucco, Ind. Eng. Chem. Res. 53 (2014) 16678-16688.

[3] G. Perin, E. Cimetta, F. Monetti, T. Morosinotto, F. Bezzo. Algal Res. 19 (2016) 69-76.

[4] B. Gris, T. Morosinotto, G. Giacometti, A. Bertucco, E. Sforza, Appl. Biochem. Biotech. 172.5 (2014) 2377-2389.

ECAB 5
The 5th EUROPEAN CONGRESS OF APPLIED BIOTECHNOLOGY
Florence 15-19 September 2019

Implementation of Moving Bed Bioreactor (MBBR) Technology for Phototrophic Cultivation of Terrestrial Cyanobacteria.

Jakob Walther[1], Michael Stoffel[1], Dorina Strieth[1], Roland Ulber[1]*

1 Institute for Bioprocess Engineering, Kaiserslautern, Germany

**Corresponding author: ulber@mv.uni-kl.de*

Highlights

- Growth of cells without additives on HDPE carriers
- Increase of STY by 34%
- Basis for continuous operation.

1. Introduction

Terrestrial cyanobacteria grow relatively poorly in suspension culture, which is why they have not yet been considered as producers of interesting metabolites such as antibacterial substances. Previous work in our group have shown that surface-associated growth can significantly increase productivity [1]. Moving-bed bioreactor technology, which is already established in wastewater treatment [2], offers a possibility to carry out such growth on a larger scale. The bacteria grow on a solid substrate, which is continuously kept in suspension by gassing or stirring. Integrated cell retention on the substrate allows a continuous process, which can potentially significantly improve the production of secondary metabolites.

2. Methods

The terrestrial cyanobacterium *Trichocoleus sociatus* was investigated, which has shown promising antibacterial properties in previous experiments [1]. The substrate were 1.4x1.4 cm hollow HDPE cylinders with internal fins (Figure 1, right). The initial adhesion of the biomass to the substrate took place for one week in 0.5 L shaking flasks at 100 rpm. For optimization the volume of the culture-media and the amount of substrate was investigated. Then the substrate with the biomass was transferred to a glass cylinder of 9 cm diameter and 30 cm height filled with culture-media which was illuminated from the outside. In these the substrate was either suspended by gassing or operated as a fixed bed by using a pump. Filling degrees of 0.086-0.258 $m^3_{Substrate}/m^3_{Medium}$ and protected surfaces of 0.087-0.259 $m^2_{Substrate}/L_{Medium}$ were investigated as moving beds.

3. Results and discussion

The intial adhesion of cyanobacteria to the substrate directly in the MBBR was not successful. Therefore, an upstream adhesion step was investigated for one week in a shaking flask. The optimal parameters were 30 substrate particles in 50 mL medium at 100 rpm. This immobilized over 90% of the biomass in the substrate, which is considered sufficient. Different cultivations have been carried out in glass cylinders to maximize biomass production.

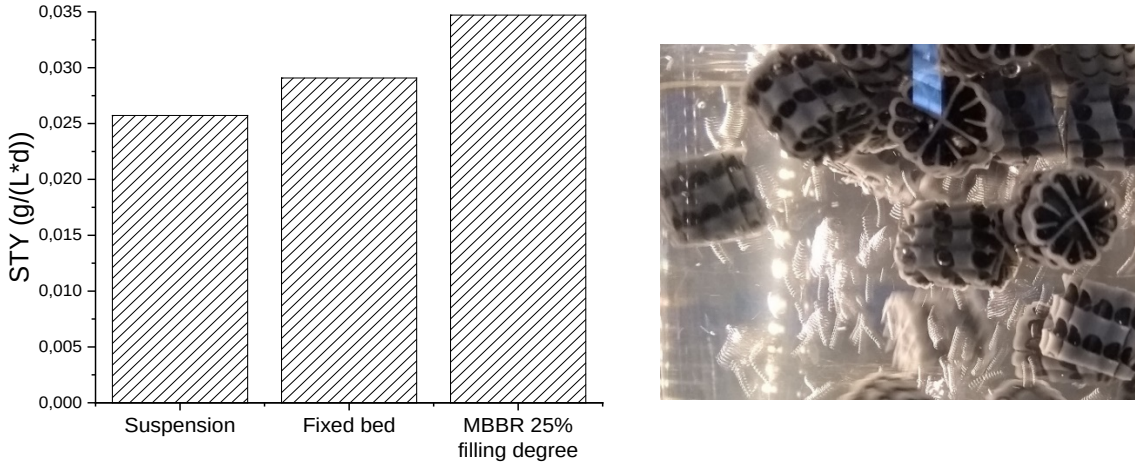

Figure 1. (left) Space-Time-Yield (STY) of different cultivations of *T. sociatus* in a glass cylinder: a.)Moving Bed Bioreactor (MBBR) with 120 substrate particles in one liter medium (corresponds to 25% filling degree); b.) fixed bed with one liter substrate and external circulation with a pump; c.) suspension culture. Cultivation time 25 days, 24°C.(right) *T. sociatus* (dark) on cylindrical growth bodies (white) within a moving bed reactor

In the control without substrate, a space-time yield (STY) of 0.025 $g_{bio\text{-}dry\text{-}mass}$/(L·day) was met. In the fixed bed, a STY of 0.029 g/(L·day) was reached, which corresponds to an increase of 13%. In the MBBR with 25% filling degree even a STY of 0.034 g/(L·day) was achieved, which corresponds to an increase of 34% for control without substrate. Over 92% of the biomass was attached to the substrate. The next step in process development is the implementation of a long-term stable culture for the production of secreted valuable compounds such as antibacterial substances.

According to our knowledge, this is the first time that microalgae have been cultivated on a solid substrate, and not on cloth [3], in a moving bed or fluidized bed. Cyanobacteria have so far only been successfully immobilized in fixed beds on sponges [4] or on cloths [5].

4. Conclusions

A proof of concept for the cultivation of cyanobacteria on a solid substrate within a MBBR was provided. Biomass productivity is significantly higher compared to a suspension culture. Further challenges are the establishment of a long-term stable culture for continuous production and an up-scale, especially with regard to illumination.

The project is financially supported by the DFG (Project number UL 170/16-1)

References

[1] D. Strieth et al., J. of Biotechnology 256 (2017) 6-12.
[2] J.P. Bassin, M. Dezotti, Moving Bed Biofilm Reactor in Advanced Biological processes for wastewater treatment, Springer 2018
[3] Zhuang et al. Bioresource Technology, 153 (2014) 399-402
[4] Chetsumon et al., J. of Appl. Phyc. 6 (1994): 539-543
[5] Fischer et al., J. of Appl. Phyc. 9 (1997) 205-213

ECAB 5
The 5th EUROPEAN CONGRESS OF APPLIED BIOTECHNOLOGY
Florence 15-19 September 2019

Effect of a double stress Light-Salinity, on the polysaccharides compartmentalization of *Porphyridium cruentum*

Antoine Decamp[1], Olivier Gonçalves[2], Dominique Grizeau[3], Jérémy Pruvost[4]

1,2,3,4 University of Nantes, CNRS, Laboratoire GEPEA, UMR 6144, 37 Boulevard de l'Université, CRTT-BP 406, 44602 Saint-Nazaire Cedex, France, https://www.gepea.fr/

*antoine.decamp@univ-nantes.fr

Highlights

- Identification of the critical light stress for polysaccharide accumulation
- Identification of the optimal osmotic/light stress combination for floridoside accumulation
- Optimization of the added value of the biomass of *Porphyridium cruentum*

1. Introduction

Porphyridium cruentum is a photosynthetic micro-organism which could produce many valuable metabolites depending on the growing conditions. In the present work, the effect of the salinity and light on the carbohydrates biosynthesis has been particularly investigated. Floridoside is the major glycoside produced by *Porphyridium* (S. Y. Li *et al.*, 2001). This osmoregulator has been identified as a potential precursor for exopolysaccharide (S. Li & Arad, 2002; S. Y. Li *et al.,* 2001) and it is also an interesting molecule for pharmaceutics and cosmetics application like Antiviral/Antitumoral (Bessie & Magne, 2007), anticomplementary agent focus in therapeutic complement depletion (Courtois, Simon-colin, Boisset, & Berthou, 2008), bone formation promoter (Gyu, 2015) or for other application like biofouling (Taylor et al., 2010). In a previous study, salinity has been identified has the major parameter which interfers in floridoside accumulation and light stress has been identified has the most effective parameter to induce polysaccharide production (bound polysaccharide and released polysaccharides). The aim of this study is to define a treatment post harvesting for polysaccharide and floridoside accumulation.

2. Methods

For that purpose an original approach was developed, combining small scale screening photobioreactors for the testing of the various environmental conditions (EOSS 2), to an original rapid quantification method of the main carbohydrate fractions impacted by the tested cultivation parameters (the starch, the intracellular low weight carbohydrates - LWC, the EPS, BPS, etc…). In this presentation, salt and light stress have been combined, the objective was to accumulate floridoside after an osmotic stress then apply a light stress to produce valuable polysaccharides. Furthermore another protocole has been tried, light stress before the osmotic stress, the objective

was to accumulate both molecule in order to add value to the final biomass. For the first protocol, salinities have been studied from 22, 50 and 72 g $NaCl.L^{-1}$ for two MRPA (Mean Rate of Photon Absorption) respectively 0 and 5,3 µmoles $photon.g^{-1}.s^{-1}$ light stress was applied after 6 hours of osmotic stress for 12 hours. For the second protocol, different MRPA have been applied (from 2 to 25 µmoles $photon.g^{-1}.s^{-1}$) and after 24 hours salinity has been increase to 50 g $NaCl.L^{-1}$ in order to identify the effect of osmotic stress on a starch-rich biomass (Floridoside and starch has a common precursor).

3. Results and discussion

Experimental design identified a relation between light and salinity for floridoside accumulation. Indeed, during the osmotic stress, *Porphyridium* accumulate floridoside for MRPA=0 (from 1,60 mg $Floridoside.10^{-6}$ cells to 2,60 mg $Floridoside.10^{-6}$ cells, so +39% in 3 hours) and more for MRPA= 5,3 (from 1,60 mg $Floridoside.10^{-6}$ cells to 3,41 mg $Floridoside.10^{-6}$ cells so +53% in 3 hours). BPS (bound polysaccharides) accumulation is highly affected by the osmotic stress. Indeed, osmotic pressure block the carbohydrate metabolism. After the light stress, only lower salt concentration cultures have produced a large amount of BPS (+59 % polysaccharide after 14h of light stress). A significant relation appears between salinity concentration and BPS accumulation rate, indeed, BPS accumulation rate is inversely proportional to the salt concentration.

4. Conclusions

These experimentations leads to the determination of the critical light stress (measured by evaluation of the mean rate of photon absorption in µ$mole.g^{-1}.s^{-1}$) and the critical salt concentration for polysaccharides and floridoside accumulation by *Porphyridium cruentum*. *Porphyridium cruentum* has a particular behavior in chemostat and could not produce a large amount of floridoside and bps. This treatment could be applied after harvesting in order to produce floridoside and BPS in the same time which will add value to the final biomass.

Bessie, M., & Magne, C. (2007). Optimization of floridoside production in the red alga Mastocarpus stellatus : Pre-conditioning , extraction and seasonal variations Optimization of floridoside production in the red alga Mastocarpus stellatus : pre-conditioning.
Courtois, A., Simon-colin, C., Boisset, C., & Berthou, C. (2008). Floridoside Extracted from the Red Alga Mastocarpus stellatus Is a Potent Activator of the Classical Complement Pathway, 407–417.
Gyu, D. (2015). Floridoside from Laurencia undulata promotes osteogenic differentiation in murine bone marrow mesenchymal cells. Journal of Functional Foods, 19, 505–511.
Li, S., & Arad, S. M. (2002). FLORIDOSIDE AS A CARBON PRECURSOR FOR THE SYNTHESIS OF CELL-WALL POLYSACCHARIDE IN THE RED MICROALGA PORPHYRIDIUM SP . (RHODOPHYTA), 938, 931–938.
Li, S. Y., Lellouche, J. P., Shabtai, Y., & Arad, S. (2001). Fixed carbon partitioning in the red microalga porphyridium sp. (Rhodophyta). Journal of Phycology, 37(2), 289–297.
Taylor, P., Hellio, C., Simon-colin, C., Clare, A., & Deslandes, E. (2010). Isethionic Acid and Floridoside Isolated from the Red Alga , Grateloupia turuturu , Inhibit Settlement of Balanus amphitrite Cyprid Larvae Biofouling : The Journal of Bioadhesion and Biofilm, (November 2014), 37–41.

ECAB 5
The 5th EUROPEAN CONGRESS OF APPLIED BIOTECHNOLOGY
Florence 15-19 September 2019

Castor Oil a new renewable source of biomass for green diesel production.

Giacomo Rispoli[1]

1 Eni S.p.A. Refining and Marketing, Via Giorgio Ribotta, 51 – 00144 Rome - Italy

**Corresponding author: giacomo.rispoli@eni.com*

Highlights

- The cultivation of castor, in semi-desert or degraded land, is of great interest for the production of more sustainable bio-fuels.
- Eni started an experimental crop of an autochthonous castor genotype in pre-desert lands in North Africa, demonstrating that castor can grow well under harsh climate conditions and with low agronomic inputs.
- The oil extracted from castor seeds of the trial plantation shows a high content of ricinoleic acid and is suitable for processing with Ecofining technology, providing a high quality Green Diesel.

1. Introduction

Castor oil is a vegetable oil obtained from the castor plant (Ricinus communis), widely found in tropical and sub-tropical regions of the planet.

Castor oil is composed of triglycerides of different fatty acids and about 10% of glycerine. It has a high oxidation stability and an excellent lubricating capacity. The high content of ricinoleic acid entails a great versatility of use of the oil. Furthermore, the presence of toxic substances such as ricin and ricinine does not make it suitable for food consumption.

The risk of changing the land use, directly or indirectly, from food crops to energy crops is at the base of the problem concerning the sustainability of biofuel production. This aspect is particularly important, as the EU legislation, through the ILUC and RED II directives, intends to limit the use of unsustainable and in competition with food feedstock.

The cultivation of castor is of great interest for the production of bio-fuels as a promising crop for all the tropical and subtropical climate regions. Thanks to its rusticity, in fact, it is a species able to provide high production yields even in conditions of low agronomic and energy inputs in uncultivated and degraded lands. Furthermore, as a no-edible oil, it is not subject to the caps imposed by EU legislation.

In 2018, Eni started an experimental cultivation of an autochthonous castor genotype in pre-desert lands in North Africa. The project aims to prove the feasibility of the crop under harsh climatic conditions and to collect a series of agronomic data, as well as to demonstrate the sustainability of the feedstock. The extraction of castor oil also generates two important by-products, the extraction panel and the residues of the capsules and racemes, which could be used as a soil improver in the plantation itself and for the production of advanced bio-ethanol.

In a second phase a large-scale cultivation will be started which, given the geographical proximity, will allow to feed the bio-refinery of Gela with a more sustainable short supply chain.

The Ecofining technology, jointly developed by Eni and UOP and implemented in the Eni bio-refineries of Venice and Gela, will allow the processing of castor oil obtaining a high quality Green Diesel compared to standard biodiesel. Castor oil has also proved to be an excellent feedstock for the production of jet fuel, given the outstanding cold characteristics of the oil.

2. Methods

The trial cultivation started in the pre-desert areas of Tunisia in Tatouine and Gafsa in mid-2018. The soils of the experimental crop are characterized by a very high sand content, a very low value of organic matter and high macro-porosity with low water retention. The cultivated area, divided into different plots, amounts to 140 hectares with a plant density of 2000 plants/ha (spaced 2,5 m between lines and 2 m on the line). The irrigation system adopted is a drip system with highly saline water extracted from in-situ drilled wells. The seeds for sowing were selected from an autochthonous genotype. The agricultural works included plowing of the terrains, fertilization and routine irrigation. Plants germinated after 3-5 days. After a couple of months, the plants were approximately 50 cm tall.

3. Results and discussion

After about six months from sowing, it was possible to make a first experimental collection of castor seeds from which the oil was extracted. The characterization of the oil has shown that the content of ricinoleic acid reaches values of 90%. Castor oil proved to be suitable for processing with Ecofining technology, providing a high quality Green Diesel compared to standard biodiesel.

A further objective will be to demonstrate the environmental sustainability of cultivation once in possession of all agronomic data related to the crop, which will reach full maturity after two years. In this case, the cultivation of castor could be scaled-up to obtain a stream of sustainable feedstock for Eni bio-refineries.

4. Conclusions

The results of the present study indicate that castor grows well under semi-arid climate conditions in the pre-desert areas of Tunisia, with irrigation input of high salinity water extracted from in-situ excavated wells, even in the presence of poor soils. The oil extracted from collected seeds proved to be a good feedstock for the Ecofining process providing a high quality Green Diesel.

References

[1] G. Rispoli, A. Amoroso, C. Prati, Venice biorefinery: How refining overcapacity can become an opportunity with an innovative idea, Hydrocarbon Processing, Volume 92 Number 2, 2013.
[2] G. Bellussi, V. Calemma, P. Pollesel, G. Rispoli, Chemical and Fuels from Bio-Based Building Blocks, Eds. F. Cavani, S. Albonetti, F. Basile, A. Albonetti, Wiley-VCH 2016, vol.1, Chapter 5,2016.
[3] G. Rispoli, C. Prati, A. Amoroso, Method for revamping a conventional mineral oil refinery to bio refinery, EP 2 855638 B1, Richiedente ENI SpA, deposito 9/4/2012.
[4] U. Anastasi, O. Sortino, S.L. Cosentino, C. Patanè, Seed yield and oil quality of perennial castor bean in a Mediterranean environment, International Journal of Plant Production 9 (1), 2015.

ECAB 5
The 5th EUROPEAN CONGRESS OF APPLIED BIOTECHNOLOGY
Florence 15-19 September 2019

Controlled release of capsanthin using alginate/κ-carrageenan beads

Tomoya Mizushima[1], Ryoichi Nakayama[1]*, Norikazu Namiki[1], Masanao Imai[2]

1 Applied Chemistry and Chemical Enginnering Program, Graduate School of Engineering,

Kogakuin University, 2665-1 Nakano-machi, Hachioji, Tokyo, 192-0015, JAPAN

2 Course in Bioresource Utilization Sciences, Graduate School of Bioresource Sciences, Nihon University, 1866 Kameino, Fujisawa, Kanagawa, 252-0880, JAPAN

**Corresponding author: bionakayama.ryo@cc.kogakuin.ac.jp*

Highlights

- Biopolymer composite beads were successfully prepared.
- The amount of released capsanthin from alginate/κ-carrageenan composite beads was decreased
- The initial release rate of capsanthin of alginate/κ-carrageenan beads prepared with KCl solution was slow down.

1. Introduction

Biopolymers of marine algae origin are ubiquitous in surface waters and attracted to their potentialities. They present an enormous variety of structures, such as alginate, carrageenan, and chitosan. Sodium alginate is a hydrophilic polysaccharide. It consist of a linear copolymer composed two monomeric units β-D-mannuronic acid and α-L-guluronic acid. It conveniently forms into a gel structure in the presence of divalent cations such as Ca^{2+}. κ-carrageenan is a naturally occurring sulfated polysaccharide extracted from red marine algae. It is a linear polyanionic polysaccharides composed of sulfated galactose and 3,6-anhydrogalactose copolymers, linked by alternating α-1,3 and β-1,4 glycosides. It selects K^+ to stabilize the junction zones within the characteristically firm.

The aim of this study is to develop a biopolymer composite beads for the oral delivery of hydrophobic physiological functions.

2. Methods

2. 1 Preparation of alginate/κ-carrageenan composite beads

Sodium alginate (1g) and κ-carrageenan (1g) was dissolved in DI water (98g) under magnetic stirring at 298K for 12h. Heptane contained capsanthin and Span 85 was added to the sodium alginate/κ-carrageenan solution (20mL), and then it was stirred at 10000 min^{-1} for 5 min. The mixed solution was extruded dropwise through a syringe (inner diameter= 2 mm) into a $CaCl_2$ solution or KCl solution (1mol/L, 200mL) under magnetic string (450 min^{-1}) at 298 K for 10 min.

2. 2 Release of capsanthin from alginate/κ-carrageenan composite beads

The hydrogel beads (thirty units) loaded into an ethanol solution (100mL) under magnetic string (600 min^{-1}) at 298 K. A sample (1mL) was taken from the ethanol solution at desired time. The concentration of capsanthin was measured a spectrophotometer (472 nm).

3. Results and discussion

Fig.1 shows the time course of the concentration of released capsanthin from alginate beads and alginate/κ-carrageenan composite beads. At increasing κ-carrageenan concentration, the amount of released capsanthin from alginate/κ-carrageenan beads was decreased. The improved retention of capsanthin within the alginate/κ-carrageenan composited beads formed at a high concentration of κ-carrageenan.

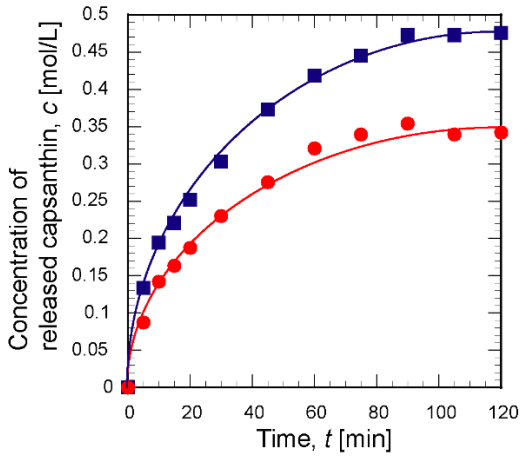

Figure 1. Time course of concentration of capsanthin from alginate beads (■) and alginate/κ-carrageenan composite beads (●) . (1mol/L $CaCl_2$ sol.)

Fig.2 shows the effect of the different cations on the initial release rate from alginate/κ-carrageenan beads. The release rate of capsanthin of alginate/κ-carrageenan beads prepared with Ca^{2+} was 1.7-fold greater than that of the beads prepare with K^+. Alginate/κ-carrageenan composite beads effectively stabilized by slowing down the release of capsanthin by K^+ which cross-linked the κ-carrageenan

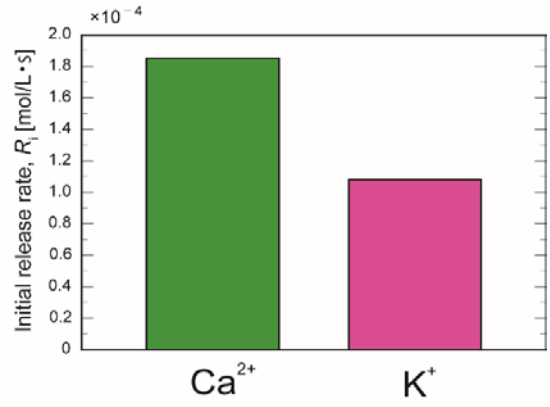

Figure 2. Effect of the different cations on the initial release rate of capsanthin from alginate beads (1mol/L $CaCl_2$ sol., 1mol/L KCl sol.)

4. Conclusions

This work successfully demonstrated that the incorporation of κ-carrageenan in the alginate beads decreased the amount of released capsanthin

ECAB 5
The 5th EUROPEAN CONGRESS OF APPLIED BIOTECHNOLOGY
Florence 15-19 September 2019

Enzymatic Membrane Reactors: a Critical Analysis of Their Interest Through the Coupling of Experiments and Modelling.

Jose Sanchez-Marcano*, Ricardo Abejon, Marie Pierre Belleville.

Institut Européen des Membranes, IEM, UMR-5635, Université de Montpellier, ENSCM, CNRS, Place Eugène Bataillon, 34095 Montpellier, France.

**Corresponding author: jose.sanchez-marcano@umontpellier.fr*

Highlights

- Model of enzymatic membrane reactors (EMRs) analyzing the influence of parameters.
- Reaction kinetics is the most influent parameter on performance of EMRs.
- Model to simulate large-scale EMRs.

1. Introduction

Enzymatic reactors using immobilized enzymes reactors are usually stirred-tank or packed-bed reactors. However in such reactors the yields can be limited by mass transfer phenomena. In enzymatic membrane reactors (EMRs), the biocatalyst can be located on the surface or within the porosity of the membrane; in this last case the reaction takes place during the transfer of substrates through membrane pores using a “flow through membrane reactor concept”. This configuration results in avoiding mass transfer limitations while enhancing the contact between the biocatalyst and the substrates. Indeed, higher yields can be expected [1, 2]. The objective of this work is to carry out a fine analysis of the advantages or drawbacks of EMRs through a multi-scale modelling from the study of local mass transfers coupled with enzymatic kinetics and hydrodynamics up to the optimization of a bundle configuration for two model reactions: the hydrolysis of butyl acetate (HBA) and the degradation of tetracycline (DTC) (as model micro-pollutant) from aqueous solutions with respectively lipase or laccase grafted membranes.

2. Methods

2.1 Experimental. The active membranes (EMs) were prepared according to a method which involves the coating of porous ceramic supports with a gelatin solution, the activation with glutaraldehyde and enzyme grafting [1, 2]. Different ceramic membranes were used (mean pore size from 0.2 µm to 1.4 µm, lengths from 0.13 to 1.1 m and with 1, 7 or 39 channels). The HBA and DTC were used to test respectively EMs prepared with a Lipozyme CALB L from *Candida antarctica* and a Laccase from *Trametes versicolor* in batch reactors or in a pilot unit with a continuous recycling of permeate and retentate.

2.2 Modelling. 3D models were built with COMSOL Multiphysics™ by coupling the experimental reaction kinetics described through the Michaelis-Menten equation together with permeability, Navier-Stokes, Brinkman and continuity equations [2, 3]. The models were validated by comparison of the theoretical and experimental EMRs productivities.

3. Results and discussion.

The experimental results of productivity for HBA with lipase grafted membranes were almost identical (1.2 10^{-4} mol.s^{-1}.m^{-2}) when compared with values obtained by the model (1.1 10^{-4} mol.s^{-1}.m^{-2}), we can then conclude that the model matches well the experimental results. In order to generalize the model to all types of EMRs simulations considering different kinetics and mass transport properties were carried out. As example, in the Figure 1 is shown the evolution of the conversion in function of the membrane permeability (tangential configuration) expressed as permeate (Xperm), retentate (Xret) and global conversions (Xglobal) for (a): a relatively fast reaction kinetics (vMAX = 3.6 10^{-2} mol.s^{-1} m^{-2} and KM = 0.5 mol.m^{-3}) and (b): low reaction kinetics (vMAX = 1.6 10^{-4} mol.s^{-1} m^{-2} and KM = 20 mol.m^{-3}).

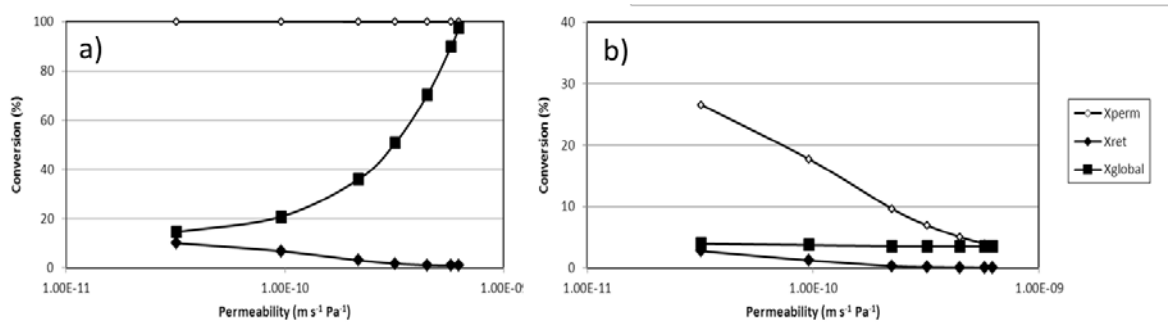

Figure 1. Evolution of the conversion in function of the membrane permeability (tangential configuration) expressed as permeate, retentate and global conversions for (a) fast reaction kinetics (b): low reaction kinetics.

In the case (a), the high reaction rate allows a complete conversion of the permeate stream within the full proposed permeability. Differing to the case of a low reaction rate (b), the global performance of this reactor is strongly influenced by the membrane permeability: while very permeable membranes lead to very high total conversion, less permeable membranes improve the retentate conversion at the expense of the moderate global conversion.

4. Conclusions

An experimentally validated model was developed coupling the measured reaction kinetics with mass transfer. The model allowed the determination of the hydrodynamics and 3D concentration profiles in EMRs. It has been demonstrated that reaction kinetics has the greatest influence among all the analyzed variables. Almost total conversion in the permeate stream can be attained for the fastest reactions, while slow reactions suffer from irrelevant conversions. When the model was applied to the scale-up of EMRs for the DTC it has been demonstrated that EMRs are not really efficient for actual systems presenting relatively low reaction kinetics.

References

[1] M. De Cazes, M. Belleville, M. Mougel, H. Kellner, J. Sanchez-Marcano. J. Membrane Sci. 476 (2015) 476, 384-393.

[2] R. Abejón, C. Gîjiu, M. Belleville, D. Paolucci, J. Sanchez-Marcano. J. Membrane Sci. 473 (2014) 189-200.

[3] S. Ben Ameur, C. Gîjiu, M. Belleville, J. Sanchez, D. Paolucci. J. Membrane Sci. 455 (2014) 330-340.

ECAB 5
The 5th EUROPEAN CONGRESS OF APPLIED BIOTECHNOLOGY
Florence 15-19 September 2019

Co-Culture Fermentation Strategy for Bioethanol Production from Mixed Sugars.

Daniele Farias[1*], Francisco Maugeri Filho[1]

[1]School of Food Engineering, University of Campinas, UNICAMP, Campinas, São Paulo, Brazil

*Corresponding author: danielefarias_@hotmail.com

Highlights

- A mixed sugar composition (C5 and C6) from sugarcane bagasse hydrolysate diluted with molasses was evaluated.
- Hexoses and xylose-fermenting yeast were cultivated together in a single batch fermentation.
- Co-culture strategy was related to upper xylose consumption and bioethanol productivity.
- Maximum productivity was achieved during co-culture with *S. cerevisiae* and *S. passalidarum*.

1. Introduction

Techniques for fermenting mixed sugar in a single process have practical significance since they could improve process economics by shortening fermentation times, and make it possible to improve ethanol yield through complete sugar utilization from sugarcane biomass. In this context, the co-culture strategy could be an alternative process, where *S. cerevisiae* effectively ferments glucose, and the remaining xylose can be fermented by xylose-fermenting species, such as *Scheffersomyces stipitis* and/or *Spathaspora passalidarum* [1,2]. The conceptual idea is the use of first generation (1G) ethanol plants as the host for second generation (2G) ethanol technologies, since these mills have a surplus of electricity, steam, water, bagasse and others facilities. Once proved technically and economically feasible, the proposed fermentation strategy will offer a sustainable and enhanced business opportunity for the sugarcane industry.

2. Methods

2.1. Yeast strains and agro industrial raw materials

Xyloses-fermenting yeasts: *Scheffersomyces stipitis* Y-7124 (SS) and *Spathaspora passalidarum* Y-27907 (SP) were obtained from the ARS Culture Collection. Hexoses-fermenting yeasts: *Saccharomyces cerevisiae* (SA), wild-type, provided by Santa Adélia Sugar Mill, (SP, Brazil) and *Saccharomyces cerevisiae* (acB11) (respiratory-deficient mutant) (SpC), kindly provided by Dr. Mario Barros (State University of São Paulo, São Paulo, Brazil).

Sugarcane molasses ($g.L^{-1}$): 414.31 sucrose (65%), 143.41 glucose (22.5%), and 79.68 fructose (12.5%), corresponding to 637.41 of total reducing sugars (TRS). Sugarcane bagasse (hemicellulosic hydrolysate): obtained after diluted sulfuric acid pretreatment (145 °C, 12 min, 0.5% (v/v) H_2SO_4, 1:10 (w/v)) and evaporation step (to provide partial detoxification and sugar concentration). The

final composition was ($g.L^{-1}$): 94.4 xylose, 12.2 glucose, 8.0 arabinose, regarding reducing sugar; and 5.5 acetic acid, 0.3 formic acid, 0.07 HMF, 0.05 furfural, regarding inhibitors.

2.2. Co-culture fermentation strategy

Co-cultures experiments were performed using hexoses and xyloses-fermenting yeasts in a single process (cell ratio 1:1, 20% of inoculum size). Batch runs were carried out (150 rpm, 28°C, pH 6.0, until sugar exhaustion) using a ratio of mixed sugars of 50:50 (w:w) from each carbon source (hemicellulosic hydrolysate and sugarcane molasses), ranging from 50 to 100 $g.L^{-1}$. The mixture with molasses was proposed in order to improve the medium composition and reduce inhibitors concentrations. Experiments were carried out in duplicate. Periodic monitoring was carried out to assess fermentation performances (cell density by OD; sugar, alcohols and organic acids analyses using HPLC and Dionex apparatus) [3].

3. Results and discussion

The results are shown on Table 1. In all experiments, hexoses content was firstly utilized. Xylose utilization was slower, probably because of O_2 competition and faster ethanol accumulation by *Saccharomyces* species. In order to investigate the O_2 supply, co-cultures with a respiratory-deficient mutant of *S. cerevisiae* (ScP) were performed. During co-culture with SS+ScP, maximum ethanol titer and yield were achieved, even with high acetic acid concentrations (major inhibitor release after bagasse pretreatment). On the other hand, sugar uptake for mutant species were lower compared to wild-types, which led to reduced ethanol productivity.

Table 1. Co-culture fermentation with hexoses and xylose-fermenting yeast using a mixed sugar composition.

Co-culture	$S_{initial}$ ($g.L^{-1}$)	P_{max} ($g.L^{-1}$)	Y_{ps} ($g.g^{-1}$)	Q_{pmax} ($g.L^{-1}.h^{-1}$)	Acetic acid ($g.L^{-1}$)	E (%)
SS + SA	50	24.3	0.486	1.10	1.26	100
	75	27.0	0.411	1.21	1.75	84.7
	100	24.3	0.458	1.37	2.21	94.4
SS + ScP	50	17.8	0.311	1.06	1.42	64.1
	75	31.1	0.391	0.84	2.25	80.6
	100	49.3	0.472	0.60	3.26	97.3
SP + SA	50	24.8	0.491	3.75	1.15	100.0
	75	27.9	0.381	4.05	1.72	78.6
	100	30.2	0.296	4.44	2.26	61.0
SP + ScP	50	16.7	0.338	1.01	1.23	69.7
	75	23.1	0.304	0.94	1.89	62.7
	100	37.2	0.371	0.79	2.26	76.5

4. Conclusions

The co-culture combinations evaluated here were able to consume all reducing sugars. Considering the co-culture strategy (SS+ScP) a significant increase in ethanol concentration (49.2 $g.L^{-1}$) was achieved, obtained when a mutant strain of *S. cerevisiae* (respiratory deficient) and *S. stipitis* were cultivated together. Furthermore, co-culture fermentation using wild-types strains (*S. cerevisiae*, *S. passalidarum*) showed the highest ethanol productivity (Q_p = 4.44 $g.L^{-1}.h^{-1}$), which could be a good strategy to accelerate bioethanol production from lignocellulosic biomass.

References

[1] P. Karagöz, M. Özkan, Bioresour. Technol. 158 (2014):286-293.
[2] S. Ashoor, F. Comitini, M. Ciani, Biotechnol. Lett. 37 (2015):2213-2218.
[3] D. Farias, F. Maugeri, Biochem. Eng. J. 121 (2017):171-180.

ECAB 5
The 5th EUROPEAN CONGRESS OF APPLIED BIOTECHNOLOGY
Florence 15-19 September 2019

Influence in the Mixing Energy and Volumetric O_2 Mass Transfer Coefficient of Exopolysaccharide Production by *Gluconacetobacter Diazotrophicus*.

Sebastián Pineda[1], Carlos Cardona[2], Juan Higuita[3]

[1] spinedap@unal.edu.co; [2]ccardonaal@unal.edu.co; [3] jchiguitav@unal.edu.co

[1 2 3] Universidad Nacional de Colombia sede Manizales

Research group in Chemical, Catalytic and Biotechnological processes.

*Corresponding author: jchiguitav@unal.edu.co

Highlights

- *G. diazotrophicus* is able to produce an exopolysaccharide.
- Exopolysaccharide produced by *G. diazotrophicus changes the properties of medium.*
- Power required for mixing is directly affected by exopolysaccharide production.
- Oxygen transfer decreases in function of exopolysaccharide accumulation.

1. Introduction

Gluconacetobacter diazotrophicus is an endophytic nitrogen fixing bacterium and was the first isolated from sugarcane [1]; genus Gluconacetobacter is able to produce large amounts of exopolysaccharides (EPS) and lipopolysaccharides (LPS) [2]. One of the proposed roles for EPS is the molecular communication between plants and microbes during plant-microbes association [3]. The aim of this article was to grow Gluconacetobacter diazotrophicus using sucrose as carbon source in order to obtain an exopolysaccharide. In addition, the investigation was focused in the production of EPS and its influence in the mixing energy and oxygen consumption.

2. Methods

The strain was grown in a Biorreactor with 14 L of liquid LGI-P fresh medium with sucrose 100gL^{-1} at pH 8. Inoculum was 1.60 liters, which corresponds to 10.25% v/v. Culture was kept at 30°C under constant agitation of 150 rpm for 277 hours. Measurement of G. diazotrophicus growth were performed using the dry weight technique and the EPS was precipitated with cold ethanol (1:1 v/v, -20°C) and recovered by centrifugation at -20°C and 10000 rpm [4]. Quantification was made using a gravimetric analysis.

The Kendall-Monroe equation was used to calculate the blend viscosity as the cubic-root average of the component viscosities. Biomass viscosity can be predicted using the Vand equation and the rest of products have no significant influence on the viscosity. The required mixing power depends on the stirrer speed (N), the impeller shape and size (D_i), the tank geometry, the density (ρ) and viscosity (μ_{mix}) of the fluid [5]. The relationship between these variables is usually expressed using the impeller Reynolds number. Finally, the statistical analysis was performed using descriptive analysis of Microsoft Excel®.

2. Results and discussion

Results show that this microorganism is able to grow in LGI-P medium with sucrose 100gL-1, with a maximum cell concentration of 3.75 +/- 0.13 gL-1 (Figure 1). *G. diazotrophicus* is also able to produce an exopolysaccharide that was quantified by cold precipitation with ethanol with a maximum concentration of 9.20 +/- 0.23 gL-1 (Figure 2).

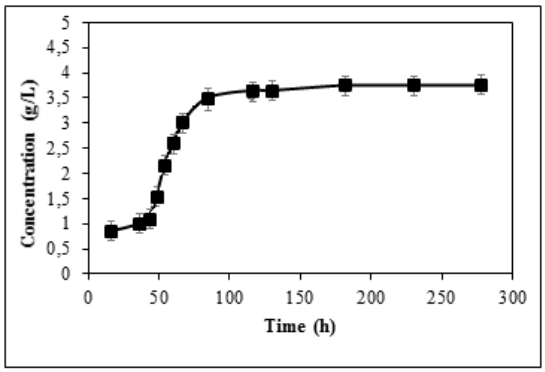

Figure 1. Biomass profile.

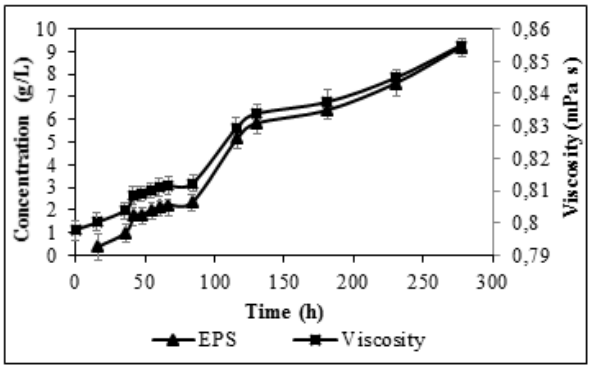

Figure 2. Calculated viscosity in comparison with EPS concentration.

It was also observed that both the mixing energy and the effort of the agitator (torque) were increased. This phenomenon may be due to the fact that exopolysaccharide production changes the rheological properties of the medium since it is a compound with a high viscosity (35 mPa-s). A reduction of 1.32% in $k_L a$ was noticed during fermentation.

3. Conclusions

The results demonstrated that the EPS produced by G. diazotrophicus is a relevant factor in the rheological properties of the medium, which is then related with the increase in power requirement. In addition, this study aims to relate the volumetric oxygen mass transfer coefficient of the microorganism with changes in fluid properties.

References

[1] Cavalcante, V. A., Dobereiner, J., Plant and Soil. 108(1) (1988) 23–31.
[2] Ruka, D. R., Simon, G.P., Dean, K. M. Carbohydrate Polymers. 89 (2) (2012) 613-622.
[3] Braga, R. M., Dourado, M. N., Araújo, W. L. Brazilian Journal of Microbiology, 47 (2016), 86–98.
[4] Serrato, R. V. Frontiers in Cellular and Infection Microbiology. 4 (2014), 119-125.
[5] Doran, P. M. Bioprocess Engineering Principles. Technology (Vol. 9) (2012).

Dynamic Laser Speckle Technique to Monitor Biological Tissues Under Magnetic Field.

Roberto Azevedo[1], Roberto Braga[2], Renato Guimaraes[2], Caio Salgado[3], Leandro Reis[2]

1 IFSULDEMINAS, Campus Machado, Rod. Machado-Paraguaçu km 3, Machado MG, Brazil; 2 UFLA, CP 3037 Lavras MG, Brazil, 3 Klabin, Av. Brasil, 26 Telêmaco Borba PR, Brazil

**Corresponding author: robertobraga@deg.ufla.br, robbraga@gmail.com*

Highlights

- Dynamic laser speckle is sensitive to biological changes in tissues.
- Magnetic field enhance activity in seeds.
- Magnetic field can enhance germination.
- Dynamic laser speckle can identify the increase of activity in seeds after magnetization.

1. Introduction

We live in a permanent magnetic field of low intensity (30 to 60μT), however the increase of the field intensity can influence biological activities. In seeds, the application of a magnetic field around mT can improve their germination [1], while it is also possible to enhance plant growth [2] and some other characteristics in plants [3-7]. Despite the successful results reported, still remains issues about the best level of the magnetic field and its time of application in each biological material. Thus, to test the optimum procedure one needs to validate it using time consuming tests. In order to overcome the time limitations presented by the traditional tests, this work aimed to evaluate a well known optical method dedicated to monitor biological activity named dynamic laser speckle [ ]. This technique could provide faster analysis than the traditional ones as well as provide additional information such as a map of activity.

2. Methods

Seeds of coffee (*Coffea arabica* L.) were submitted to a magnetic field of 28mT during 6 days in a germinator. The field was from a permanent magnet and the seeds were placed inside the magnets associated to create the desired level. The seeds were placed in a germination paper imbibed in water and within the magnets. After 6 days in the germinator, the seeds, divided in control and magnetized, were illuminated by the laser and analyzed using a dynamic laser speckle index, the Absolute Value of the Differences AVD [9], to create a map of activity of the seed.

3. Results and discussion

Figure 2 presents the activity maps of a seed submitted to a magnetic field and another used as a control. In the maps (AVD index) it is possible to observe the higher activity in the embryo region when the 28mT field was applied. In the graphical outcome of the speckle images the pseudo-colors present the level of activity from low activity in blue to high activity in red. The same result was observed with replications. The usage of dynamic laser speckle to access the activity of the coffee's

embryo after 6 days was proved to be reliable if compared to the traditional test that usually demands 30 days in the germinator [8]. With this achievement the dynamic laser speckle can forecast the germination process and reduce significantly the time to test the result of magnetization in seeds with different combinations of time and level of magnetic field.

(a) (b)

Figure 1. Maps of activity of a coffee seed using the dynamic laser speckle index, AVD, where in (a) the embryo presented high activity in red and in (b) the embryo in the bottom left did not presented the same activity in the early protusion

4. Conclusions

The dynamic laser speckle was able to identify the change caused by the magnetization in a coffee seed after 6 days of magnetization and before 24 days of the germination test.

References

[1] P.S. Phirke P.S., M.N. Patil, S.P. Umbarkar, Y.H. Dudhe Seed Sci Technol 24 (1996) 365–373.

[2] K. Namba , A. Sasao , S. Shibusama Acta Hort 399 (1995) 143–145.

[3] A. Aladjadjıyan J. Cent. Eur. Agri. 3 (2002) 89–94.

[4] A. Esitken J. Hort. Sci. Biotechnol. 78(2) (2003) 145–147.

[5] M. Rochalska, A. Orzeszko-Rywka Seed Sci. Technol. 33 (2005) 669–674.

[6] A. Souza, D. Garcia, L. Sueiro, F. Gilart, E. Porras, L. Licea Bioelectromagnetics 27 (2006) 247–257.

[7] E. I. Alemán, A. Mbogholi, Y.F. Yilan Fung Boix, J. González-Olmedo, A. Chalfun-Junior Pol. J. Environ. Stud. 23(1) (2014) 95-101.

[8] P. Vivas, L. Resende, R.A. Braga, R. Guimarães, R. Azevedo, E. Silva, P. Toorop Ann. Appl. Biol. 170 2016) 141-149.

[9] Braga, R. A., Rivera, F. P., Moreira, J. A Practical Guide to Biospeckle Laser Analysis: Theory and Software. (1st ed.). Editora UFLA, Lavras, 2016.

Microwave as Suitable Alternative for Sugar Recovery From Brewer's Spent Grain.

Juan C. López-Linares[1,2], M.Teresa García-Cubero[1,2], Susana Lucas[1,2], Gerardo González-Benito[1,2], Mónica Coca[1,2,*]

1 Institute of Sustainable Processes. University of Valladolid, Spain
2 Department of Chemical Engineering and Environmental Technology, School of Industrial Engineering, University of Valladolid, Dr. Mergelina, s/n, Valladolid, Spain

**Corresponding author: monica@iq.uva.es*

Highlights

- Fractionation of BSG by microwave using water and diluted sulfuric acid as solvents
- Higher sugar recoveries for microwave pretreatment assisted by diluted sulfuric acid
- Hemicellulosic sugar recovery of 71% for microwave assisted sulfuric acid (150 ºC, 10 min)
- Enzymatic hydrolysis yield of 41% for microwave assisted sulfuric acid (150 ºC, 10 min)

1. Introduction

Brewer's spent grain (BSG), which is a low cost lignocellulosic industrial waste obtained from brewing industry, has traditionally been used as cattle feed due to its high content in carbohydrates and proteins. However, the high moisture content of BSG makes it susceptible to fast spoilage. The high content of cellulose and hemicellulose in BSG makes it attractive from the point of view of a biorefinery, being able to produce different products like biofuels, chemicals and high value added compounds [1].

Nevertheless, a pretreatment results essential, as BSG structure must be disrupted in order to fractionate it into its main components (cellulose, hemicellulose and lignin). As a result, the microwave assisted pretreatment has currently gained increasing interest in comparison with conventional heating. The basis of the microwave is the ability to apply an electromagnetic field directly about the heated object. Microwave pretreatment offers a great number of advantages, such as short reaction times, uniform and direct heating, simplicity of the process, higher removal of acetyl groups in hemicellulose and lower generation of inhibitory compounds (such as acetic and formic acids, furfural, 5- hydroxymethylfurfural and phenolic compounds). Moreover, the most important aspect is that microwave assisted pretreatment is an energetically efficient method, which does not cause environmental problems while also having a small capital cost [2,3]. What is more, microwave pretreatment can be assisted by acid catalysts. The use of dilute acid is considered as a powerful and effective pretreatment of lignocellulosic biomass [4]. Nevertheless, it is necessary the use of a corrosion resistant materials, and it is generated a hydrolysate whose pH must be adjusted to a value suitable for enzymatic hydrolysis. Therefore, in this work, a hydrothermal pretreatment is also used, which is less expensive and non-corrosive in comparison with acid or

alkaline catalysts. The objective of this work was to fractionate BSG, removing the hemicellulose present and reaching in this way a cellulose-enriched solid. This study addresses the influence of extraction solvent (water and dilute sulfuric acid) on the recovery of sugars by microwave pretreatment.

2. Methods

Hydrothermal or dilute sulfuric acid pretreatment was performed in a Multiwave PRO SOLV reactor 50 Hz (Anton Paar GmbH, Austria, Europe). The solid concentration was 5% (w/v). Temperature and process time were selected as experimental factors. The temperature was set at 150 ºC and 170 ºC whereas the process time was set at 2.5, 5 and 10 min for each temperature. When dilute sulfuric acid pretreatment was employed, the sulfuric acid concentration was kept at 1% (w/v). Afterwards, the liquid fractions (or prehydrolysates) were separated from pretreated solids by vacuum filtration. Pretreated solids were subjected to enzymatic hydrolysis to compare the influence of extraction solvent. The contents in sugars (glucose, xylose, and arabinose) and potential fermentation inhibitors (acetic acid, formic acid, furfural and hydroxymethylfurfural (HMF) were determined by HPLC [1].

3. Results and discussion

When the hydrothermal pretreatment was used, high oligomeric sugars content (87-95%) was observed in the prehydrolysates whereas moderate hemicellulosic sugar recoveries, between 8 and 31%, were achieved. The maximum hemicellulosic sugar recoveries were observed at the most severe pretreatment conditions tested (170ºC, 10 min), being the influence of temperature more significant. Moreover, a maximum enzymatic hydrolysis yield of 20%, referred to glucose in the raw material (BSG), was reached under these pretreatment conditions.

Nevertheless, for the dilute sulfuric acid pretreatment, oligomeric sugar concentrations in the prehydrolysates were very low (< 3% of total sugars). Hemicellulosic sugar recoveries and enzymatic hydrolysis yields ranged between 62-71% and 35-41%, respectively, reaching the maximum value at 150ºC and 10 min.

4. Conclusions

In comparison with the microwave assisted hydrothermal pretreatment, the microwave assisted dilute sulfuric acid pretreatment is able to obtain higher hemicellulosic sugar recoveries (71 vs 31%) and enzymatic hydrolysis yield (20 vs 41%), referred to glucose in the raw material (BSG) under the experimental conditions analyzed. Further research will be focused on the optimization of pretreatment conditions of microwave assisted diluted sulfuric acid, in order to increase sugar recoveries.

References

[1] P.E. Plaza, L.J. Gallego-Morales, M. Peñuela-Vásquez, S. Lucas, M.T. García-Cubero, M. Coca, Bioresour. Technol. 244 (2017) 166–174.

[2] A. Aguilar-Reynosa, A. Romani, R.M. Rodriguez-Jasso, C.N. Aguilar, G. Garrote, H.A. Ruiz, Energy Convers. Manage. 136 (2017), 50–65.

[3] S.S. Hassan, G.A. Williams, A.K. Jaiswal, Bioresour. Technol. 262 (2018), 310–318.

[4] N. Mosier, C. Wyman, B. Dale, R. Elander, Y.Y. Lee, M. Holtzapple, M. Ladisch, Bioresour. Technol. 96 (2005), 673−686.

Flow Cytometry as a Versatile Tool for Monitoring Biomass Agglomerates.

Lukas Veiter[1,2] and Christoph Herwig*[1,2]

[1]CD Laboratory on Mechanistic and Physiological Methods for Improved Bioprocesses, TU Wien, Gumpendorferstrasse 1a/166, 1060 Vienna, Austria; [2]Research Area Biochemical Engineering, Institute for Chemical, Environmental and Biological Engineering, TU Wien, Gumpendorferstrasse 1a/166, 1060 Vienna, Austria

**Corresponding author: christoph.herwig@tuwien.ac.at*

Highlights

- Fast and reliable method to characterize biomass agglomerates via flow cytometry
- Insights into morphology and viability of biomass agglomerates
- Method successfully tested on filamentous fungi and yeast

1. Introduction

Process performance, process control strategies and productivity in bioprocesses highly depend on morphological elements of the biomass and therefore calls for a segregated view of biomass. This especially concerns filamentous bioreactor cultivations, where the morphology of the fungi is dependent on process conditions and tightly interlinked with productivity. Filamentous fungi show a large variety of morphological forms in submerged cultures, from dispersed hyphae to denser hyphal aggregates, the so-called pellets. Certain characteristics of morphology are favourable and need to be quantified. However, most common methods to characterise morphology are time consuming and mainly involve some form of image analysis based on microscopy.

In my talk, I will introduce an alternative, reliable and fast method based on flow cytometry for at-line and/or future on-line application. New insights into fungal morphology and viability enable at-line use in production environments, where timely assessment of viable biomass characteristics is of prime importance. Finally, I will show that our measurement principles are also applicable to other agglomeration forming organisms such as yeast, making our method a powerful and versatile tool to characterize biomass agglomerates.

2. Methods

This at-line method employs fluorescent staining of biomass and a high-end flow cytometer equipped with an image-in-flow camera feature. So far, *Pichia pastoris* biomass agglomerates and filamentous fungi were extensively characterised.

3. Results and discussion

Distinction between morphological classes is based on Flow Cytometry forward-scatter signals (FWS) and sample length, verifiable via microscopy and an integrated camera.

The use of fluorescent stains enables determination of viability in complex biomass agglomerates. Fluorescein diacetate (FDA) measures enzymatic activity producing green fluorescence. Thereby viable cells are detected. Propidium iodide (PI) is a DNA stain not permeant to live cells, dead cells are detected via red fluorescence. As an example, detailed morphological characterization as well as estimation of viability in yeast agglomerates are depicted in Figure 1.

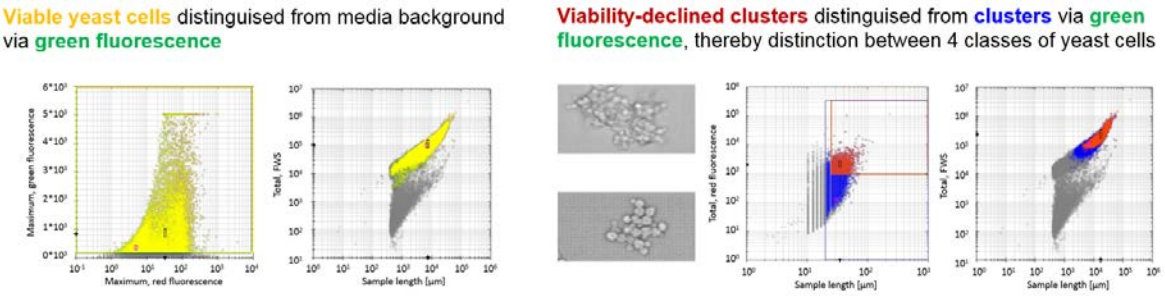

Figure 1. Distinction of yeast cells through employment of fluorescent staining, detection of media background (left) and viability-declined clusters (right)

4. Conclusions

The method's capabilities encompass discrimination of cells in turbid media and further analysis of biomass morphology. Furthermore, viability of various morphological classes can be determined including identification of viable biomass sections within agglomerates.

Analysis of agglomerates in different organisms presently includes agglomerates in glycol-engineered *P. pastoris* strains, viability-declined *P. pastoris* clusters distinguished from viable agglomerates and morphological classification of filamentous fungi.

References

Ehgartner et al. (2017) Morphological analysis of the filamentous fungus Penicillium chrysogenum. Appl Microbiol Biotechnol:1-14 doi:10.1007/s00253-017-8475-2

Pekarsky, Veiter et al. (2018) Production of a recombinant peroxidase in different glyco-engineered Pichia pastoris strains: a morphological and physiological comparison. Microb Cell Fact:17(1) doi:10.1186/s12934-018-1032-6

ECCE12
The 12th EUROPEAN CONGRESS OF CHEMICAL ENGINEERING
Florence 15-19 September 2019

Xylitol Production From Rice Straw Hemicellulosic Hydrolysate Using Cells of *Candida Guilliermondii* Permeabilized With Triton X-100.

Mariana A.G Tiburcio[1] and Inês C. Roberto[1]

[1] *Departamento de Biotecnologia, Escola de Engenharia de Lorena, Universidade de São Paulo, 12602-810 Lorena, SP, Brazil*

**Corresponding author: ines@debiq.eel.usp.br*

Highlights

- The cellular permeabilization medium affects xylitol production in hydrolysate.
- Permeabilized cells increases xylitol productivity by 40 % and yield by 32 %.
- High xylitol productivity (2.0 g/L.h) was obtained with permeabilized cells.
- Permeabilized cells can be reused for at least 4 cycles with preserved viability.

1. Introduction

Xylitol is a five-carbon sugar alcohol with notable applications in the food, medical and pharmaceutical areas. The production of xylitol by biotechnological route is based on the use of whole cells of microorganisms (fermentation process) or by its isolated enzymes (enzymatic technology). The fermentation process has shown significant advances but finds commercial constraints due to low productivities. On the other hand, costs of isolation/purification of enzymes has been pointed as the major barriers to the enzymatic technology. Therefore, it is important to develop an alternative method (biotransformation process) to make the biotechnology route more attractive. In our previous study [1] was demonstrated that under selected process conditions, resting cells of *Candida guilliermondii* permeabilized with Triton X-100 is able to efficiently produce xylitol from a medium composed only by D-xylose, potassium phosphate buffer and $MgCl_2.6H_2O$. In the present study, the potential use of the rice straw hemicellulosic hydrolysate (RSHH) as xylose source to produce xylitol from *C. guilliermondii* permeabilized with Triton X-100 was evaluated. The effects of permeabilization medium (semi-defined medium or hemicellulosic hydrolysate), as well as the addition of potassium phosphate buffer and/or $MgCl_2.6H_2O$ on the RSHH biotransformation was evaluated as an attempt to improve the results of this biotransformation process. The reuse of the biocatalyst in repeated batch was also assessed.

2. Methods

The rice straw hemicellulosic hydrolysate (RSHH) was obtained under conditions previously optimized by our research group. Initially, rice straw was treated with 80 mg NaOH/g of biomass, at 70 °C for 45 min. Then, the solids recovered were hydrolyzed with 85 mgH_2SO_4/g solid, at 150 °C for 10 min. Both treatments were performed in a batch reactor with liquid to solid ratio of 10:1. Cells of *C. guilliermondii* ATCC 201935 were permeabilized by adding Triton X-100 directly to the growth medium at cell to surfactant ratio of 1:0.9 g/g [1]. In this step, two different growth media were assessed: (1) semi-defined medium (SDM), containing in g/L: 30.0 xylose, 1.0 $MgCl_2{\cdot}6H_2O$, 3.0 $(NH_4)_2SO_4$, 0.1 $CaCl_2.2H_2O$, 20 % (v/v) rice bran extract and 0.1 M potassium phosphate buffer (pH 6.5); and (2) rice straw hydrolysate hemicellulosic (RSHH) containing 30 g/L xylose without any supplementation. After defining the best permeabilization medium, assays of biotransformation were carried out. For this, hemicellulosic hydrolysate (56.0 g/L D-xylose, pH 6.8) and permeabilized

cells in MSD (10-12 g/L) were added to a 50-mL Erlenmeyer flask to a final volume of 25 mL. The flasks were incubated in a rotary shaker at 200 rpm, 35°C for 21 h. In this step, the effect of potassium phosphate buffer and $MgCl_2$.$6H_2O$ on biotransformation parameter, as well as the reusability of the permeabilized cells were also assessed. The reusability of the permeabilized cells was evaluated in RSHH without any salt addition. At each 15 h, cells were collected by centrifugation (5600g, 10 °C, 20min), washed twice with 0.1 M potassium phosphate buffer pH 6.5, and then recycled for new reaction medium. Xylose, xylitol and sub-products concentrations were measured using HPLC.

3. Results and discussion

As shown in Table 2, the growth medium used for cellular permeabilization significantly affects the biotransformation parameters of rice straw hemicellulosic hydrolysate (RSHH). The highest Q_P values (2.10 g/L.h) was achieved with permeabilized cells in semi-defined medium (SDM), corresponding to increse of 34.8% in relation to permeabilized cells in RSHH. It can be noted also that the biocatalysts efficiency was not influenced by permeabilization medium showing similar $Y_{P/S}$ values (about 0.57 g/g. These results suggest that affinity of the detergent to the cell wall/membrane was reduced in hemicellulosic hydrolysate.

Table1. Effect of permeabilization medium of *C. guilliermondii* on biotransformation parameters of RSHH, after 15 h.

Biotransformation Parameters	Permeabilization medium	
	MSD	RSHH
Xylitol production (g/L)	30.8±2.05 (21.94±0.60)	23.7±0.11
Xylose utilized (%)	93±1.7 (85±0.5)	75
$Y_{P/S}$ (g/g)	0.57±0.03 (0.43±0.01)	0.56±0.01
Q_P (g.L.h)	2.10±0.13 (1.47±0.04)	1.38±0.01

Values between parentheses correspond to data from non-permeabilized cells.

In this study, was also verified that the addition of potassium phosphate buffer and $MgCl_2.6H_2O$ to the RSHH did not affect the biotransformation parameters, being observed a average production of xylitol of 29 g/L and 92 % of xylose utilized. As compared to the non-permeabilized cells, the impact of using permeabilized cells on xylitol production from RSHH was an increase of 40 and 32 % on Q_P and $Y_{P/S}$, respectively. Besides, permeabilized cells remained viable during 4 cycles of 15 h in repeated batch maintaining its catalytic activity (Q_P~1.93 g/L.h and $Y_{P/S}$~0.59 g/g).

4. Conclusions

The yeast *C. guilliermondii* permeabilized with Triton X-100 proved to be an effective biocatalyst for xylitol production from rice straw hemicellulosic hydrolysate. Moreover, the permeabilized cells may be reused up to 4 consecutive reaction cycles without reducing production rates and yields. This approach may allow the future development of xylitol production from xylose present in lignocellulosic biomass, with additional potential for implementation in biorefinery.

References

[1] D.V. Cortez, S.I. Mussatto, I.C. Roberto, Appl. Biochem. Biotechnol. 180 (2016) 969-979.

Acknowledgments: FAPESP (grant number 15/24813-6); CAPES (Finance Code 001) and CNPq, Brazil.

Lab-Scale Tank and Heap Bioleaching of Light Shred Fractions by *Acidithiobacillus Ferrooxidans.*

Klemens Kremser[1], Stefan Weiss[2], Sophie Thallner[2], Christine Hemmelmair[1], Wolfgang Schnitzhofer[2], Georg M. Gübitz[1,2]

[1] *University of Natural Resources and Life Sciences Vienna BOKU, Dep. of Agrobiotechnology IFA-Tulln, Inst. of Environmental Biotechnology*

[2] *Austrian Centre of Industrial Biotechnology*

Email: klemens.kremser@boku.ac.at

Highlights

- Bioleaching efficiencies up to 80% within 20 days.
- Heap bioleaching shows high potential for Cu and Zn.
- Leaching efficiencies are highly dependent from loading rates.

1. Introduction

Companies in the field of automotive and residual waste usually crush materials in big shredders in order to increase the surface area for further processing. During the shredding process, the so called light shred fraction, containing mainly plastics and other synthetic polymers, is discharged and deposited. However, these fractions still contain reasonable amounts of metals such as Fe, Cu, Ni and Zn, making them an interesting substrate for bioleaching. Within the last six decades, the use of microbes for metal recovery, known as bioleaching, raised the interest of scientists and industry, mainly due to their higher efficiency as well as the milder and environmental friendly process conditions[1]. The extremely acidophilic, metal-sulphide-dissolving bacterium *Acidithiobacillus ferrooxidans* is one of the most prominent and well-studied bioleaching organism which leaches metals either indirect *via* the production of sulfuric acid or direct by enzymatic oxidation[2].

2. Methods

In order to develop a bioleaching process for the metal recovery from shredded fractions, two different approaches including a heap and a continuous-stirred-tank reactor were tested. In stirred tank reactor experiments, a 25 L glass reactor was inoculated with a culture of *A. ferrooxidans* and stirred continuously at 150 rpm. At regular intervals, the concentration of the shredded fraction was increased (up to 100 $g*L^{-1}$) and parameters such as pH and redox potential were measured. In a second approach a heap bioleaching system for metal recovery was

investigated. The system consisted of a 20 L glass reactor with a sieve plate at the bottom, a pump for circulation of the leachate and a sprinkling system at the top. The leachate was inoculated with *A. ferrooxidans* and pumped in a circular way to rinse the substrate from the top of the heap. In both experiments the temperature was kept constant at 30°C and the pH was regulated automatically via dosage of 1 M sulfuric acid. For calculation of the leaching efficiency, the metal concentrations in solid substrate and leachate were measured *via* Inductively Coupled Plasma-Mass Spectrometry (ICP-MS).

3. Results and discussion

Metal recovery from shredded light fractions in the continuous stirred tank bioleaching system showed promising results after 20 days with leaching efficiencies of up to 80% for Cu, Ni and Zn, respectively (Fig.1-A). In the heap reactor, bioleaching with *A. ferrooxidans* resulted in leaching efficiencies of 15–35% after 33 days. By comparing the metal recovery of chemical leaching and bioleaching in the heap reactor, it is clearly visible that Cu and Zn were only leached in the presence of microorganism indicating the high potential of biological leaching (Fig. 1–B).

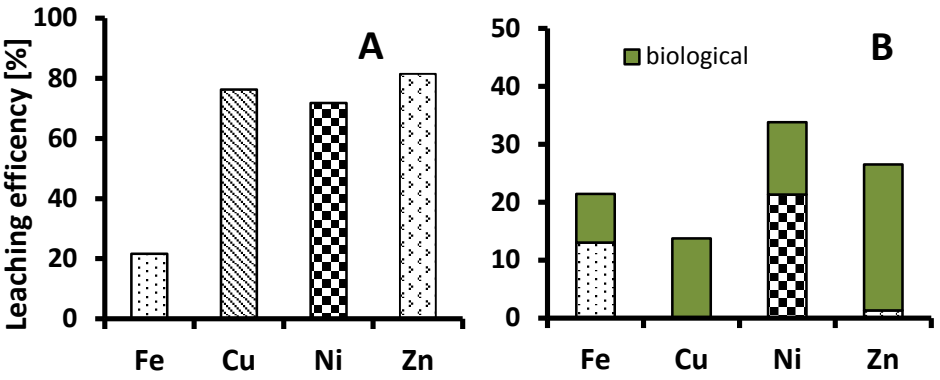

Figure 1. Bioleaching efficiencies of Fe, Cu, Ni and Zn in stirred tank (A) and heap reactor (B). Green bars indicate the biological leaching by *A. ferrooxidans.*

4. Conclusions

Two different bioleaching processes were tested according their ability for metal recovery of Fe, Cu, Ni and Zn from light shred fractions. The stirred tank reactor was operated with loading rates from 10-100 $g*L^{-1}$ showing high leaching efficiencies for all metals. The operation of the heap bioleaching reactor was more difficult but showed high potential in the biological leaching of Cu and Zn. This makes both processes interesting for further investigations and applications in industry and especially metal recovery.

References

1. Lee, J. chun & Pandey, B. D. Bio-processing of solid wastes and secondary resources for metal extraction - A review. *Waste Manag.* **32,** 3–18 (2012).
2. Akinci, G. & Guven, D. E. Bioleaching of heavy metals contaminated sediment by pure and mixed cultures of Acidithiobacillus spp. *Desalination* **268,** 221–226 (2011).

Sericin Obtained from Silkworm As Supplement into Culture Medium for Mammalian Cells.

Satoshi Terada[1]*, Kyohei Kuriyama[1], Ryo Yahagi[1], Kohei Kurebayashi[1],

Jun Takahashi [2] and Masahiro Sasaki [2]

1 Department of Applied Chemistry and Biotechnology, Graduate School of Engineering, University of Fukui; 3-9-1, Bunkyo, Fukui, 910-8507, Japan;

2 R&D Center, SEIREN Co. Ltd.; 2-3-1 Techno Port, Mikuni-cho, Sakai, 913-0038 Japan

**Corresponding author: terada@u-fukui.ac.jp*

Highlights

- Sericin improves the proliferation of the cells in serum-free culture.
- Sericin prevents the cell from apoptosis induced by heating.
- Sericin induced the proliferation of the cells via not only EGF-signaling pathway.
- Sericin induced the proliferation via but also pathway different from EGF-signaling.

1. Introduction

Mammalian cells are extensively cultured for using in tissue engineering and for producing biotherapeutics production. Although mammal-derived factors are supplemented into the culture media, these mammal-derived factors have the risk of zoonotic disease and so must be replaced by non-mammal factors.

Previously, we reported that sericin hydrolysate obtained from cocoon of silkworms successfully induced the proliferation of various cells and significantly improved the cellular survival under stressful conditions.

In this study, we aimed to elucidate the mechanism how sericin promotes the proliferation of mammalian cells. For the purpose, we focused on a human keratinocyte cell line, highly depend on sericin, as well as on EGF. Using this cell line, the proliferation signal pathway from sericin was compared with that of EGF.

2. Methods

Human keratinocyte PHK16-0b cells were sub-cultured in Keratinocyte-SFM medium supplemented with EGF and BPE. One day later, the medium was replaced into that without both EGF and BPE in order to reset the cells. After additional 24 hours for reset, the medium was replaced to fresh one containing EGF or sericin and/or any of signal inhibitors. Then the cells were cultured for three days and the cell number was counted.

The activation or phosphorylation of signal factors including EGF-Receptor and ERK is confirmed by immunoblotting against lysates from the cells treated with sericin or EGF using anti-phosphorylated tyrosine antibodies.

3. Results and discussion

Both EGF-Receptor inhibitor and EGF-Receptor-neutralizing antibody inhibited the proliferation of the cells treated with sericin and EGF, implying that sericin promotes the proliferation through EGF-Receptor as well as EGF.

MAPK pathway inhibitor and JAK/STAT pathway inhibitor inhibited the proliferation of the cells treated with both factors, whereas PI3K pathway inhibitor inhibited the proliferation of the cells treated with sericin only, and failed to inhibited those with EGF; implying that sericin promotes the proliferation of the cells partly through other pathways different from EGF.

Immunoblot analysis found that phosphorylation/activation of EGF-Receptor and ERK in the cells treated with EGF and sericin were suppressed by EGF-Receptor inhibitor and EGF-Receptor-neutralizing antibody.

4. Conclusions

We found that sericin promotes the cell proliferation through EGFR-MAPK and EGFR-JAK/STAT signaling, as well as PI3K signaling independent of EGF.

ECAB 5
The 5th EUROPEAN CONGRESS OF APPLIED BIOTECHNOLOGY
Florence 15-19 September 2019

Characterization of surfactant (polysorbate) inferences in biotherapeutics stability.

Girish H Rajacharya [1,2], Sumit Singh [1], Syed Shams Yazdani [2] and Anurag S Rathore [1]

1 Indian Institute of Technology, New Delhi, India – 110016

2 International centre for genetic engineering and Biotechnology, New Delhi, India

**Corresponding author: asrathore@biotechcmz.com*

Highlights

- Separation of surfactant in drug using ODS Shim Pack MAYI ODS Column
- Characterize the separate surfactant using analytical orthogonal tools (HPLC, HPLC MS and GC MS)
- Observed the major changes in polysorbate structure and identified saturated and unsaturated fatty acids and the estimated levels may cause the stability in the biotherapeutics (mAb) shelf life.
- Identified critical attribute helps to optimize the level of surfactant (polysorbate) in biotherapeutics (mAb) stability.

Introduction

Polysorbates are the most widely used non-ionic surfactants to stabilize protein pharmaceuticals against interface- induced aggregation and surface adsorption. They are effective against various stresses such as agitation (for example, shaking or stirring), freeze/thawing and lyophilization. Nevertheless, some of their characteristics need to be carefully considered and monitored. Commercially avail- able polysorbates (PS) 20 and 80 are chemically diverse mixtures containing mainly sorbitan POE fatty acid esters. Additionally, substantial amounts of POE, sorbitan POE and isosorbide POE fatty acid esters are present. This leads to a significant degree of lot-to-lot variability requiring a close scrutiny of each lot in order to ensure uniform behavior. The presence of residual levels of peroxide in bulk polysorbate is also a concern. There have been reports of a buildup of peroxides in bulk as well as in aqueous solutions of polysorbate, when exposed to ambient oxygen and light. Depending on handling and storage conditions and supplier lot, varying concentrations of peroxides (9 ppm– 250 ppm) were noted among different lots of polysorbates . The buildup of peroxides can be detrimental not only to the stability of polysorbate itself but also to the protein therapeutic, which it stabilizes. Based on this consideration, Harmon et al. have also developed an oxidation stress test relying on peroxides formed in PS80 in the presence of Fe (III). polysorbate or by spiking degradation products resulting from oxidation such as fatty acids and fatty acid esters into protein formulations were investigated.

Methods

1. Surfactant separation using Shim-pack MAYI Column.

Shim-pack MAYI (5 mm L. × 2.0 mm I.D., 50 µm)column in this macromolecular proteins are blocked and cannot enter the pores, smaller molecules infiltrate the chemically modified pores to be retained on the column. By incorporating this column with another column by switching HPLC flow lines, proteins introduced into the pre-treatment (C18 Reverse phase, 100 mm L. × 2.1 mm I.D., 5 µm) column from the autosampler are directly discharged out of the system after passing through the column and using a UV detector (wavelength 280 nm) to monitor an mAb molecule. For details

Table No.1

column	Shim-pack MAYI-ODS (5 mm L. × 2.0 mm I.D., 50 µm)	Zorbax 5u C18 100 Å, (100 mm L. × 2.1 mm I.D., 5 µm)
Mobile phase	A: 10 mmol/L Ammonium Formate in Water B: 2-Propanol	C: 10 mmol/L Ammonium Formate in Water D: 2-Propanol
Time program	Solvent switching, A (0 - 1.5 min) → B (1.5 - 3.5 min) → A (3.5 - 9 min)	D.Conc. 5 % (0 - 1 min) → 100 % (6 - 7 min) → 5 % (7.01 - 9 min)
Flowrate	0.6 mL/min	0.3 mL/min
Extraction time	1 min	-
Injection Vol	10 ul	-
Column Temp	40˚C	40˚C
Detection	UV 280	3200 QTRAP (LC MS), ESI Positive Mode, 50 to 1750 M/Z Scan Mode

Due to the weak UV absorption of polysorbate, a mass spectrometer was used for detection in the analytical flow line. Generally, polysorbate includes a large number of by-products, and because some of these are very strongly retained, 2-propanol was used as the final mobile phase.

2. Analysis of extracted surfactant (polysorbate) using Gas chromatography mass spectrometry (GC MS)

Gas Chromatography Mass spectrometry (GC MS) analysis of extracted (polysorbate) samples were performed using Agilent 7890A series GC system equipped with a Supelco Omega wax column (30m*0.25mm ID, 0.25um thickness, Sigma) coupled with a Agilent 7000 QQQ MS. Omega wax column was used for good separation and for gas chromatography mass spectroscopic detection. Electron ionization system with ionization energy of 70eV was used, 99.99 % pure helium gas was used as a carrier gas at a constant flow rate of 1.1 ml/min. mass transfer line and injector temperature were set at 220˚C and 250˚C respectively, and the oven temperature was programmed, initial temperature was 150 °C for 1 min then 10 °C/min to 240 °C for 15 min with total 25 min run. 1 ul of sample injected in the split mode 10:1. the signals were recorded in full scan mode (m/z 20-600, 250 scan/milli seconds). All components were identified by comparison of theirs mass spectra with those obtained from authentic samples and/or the NIST mass spectral database using AMDIS and mass hunter software.

Results and discussion

Separation of mAb using shim Pack MAYI ODS and C18 Zorbax column.

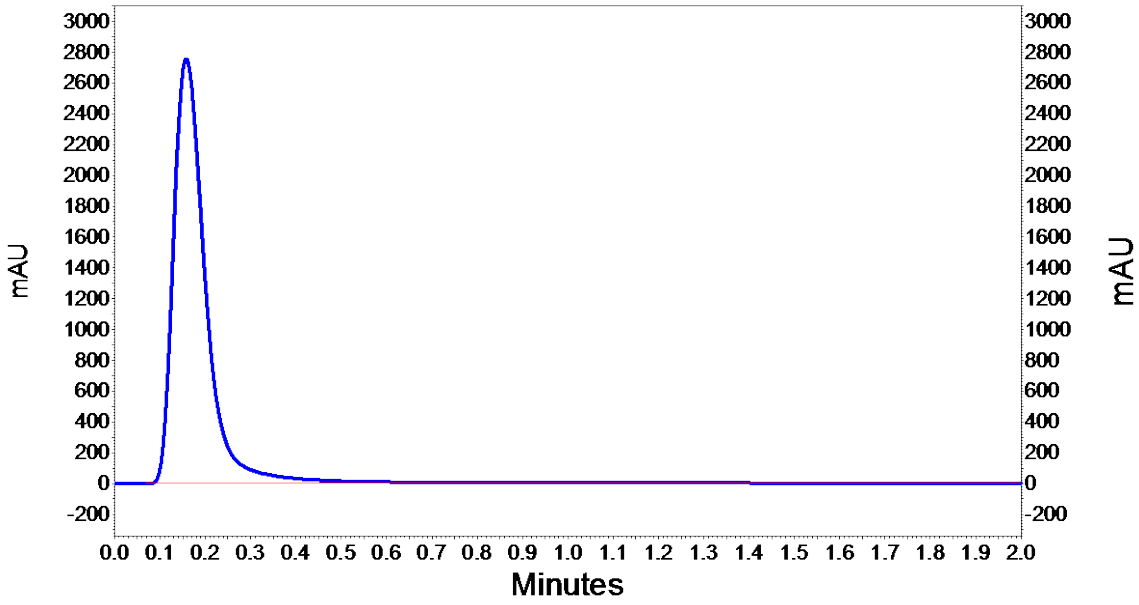

Fig.1 mAb peak separate from surfactant

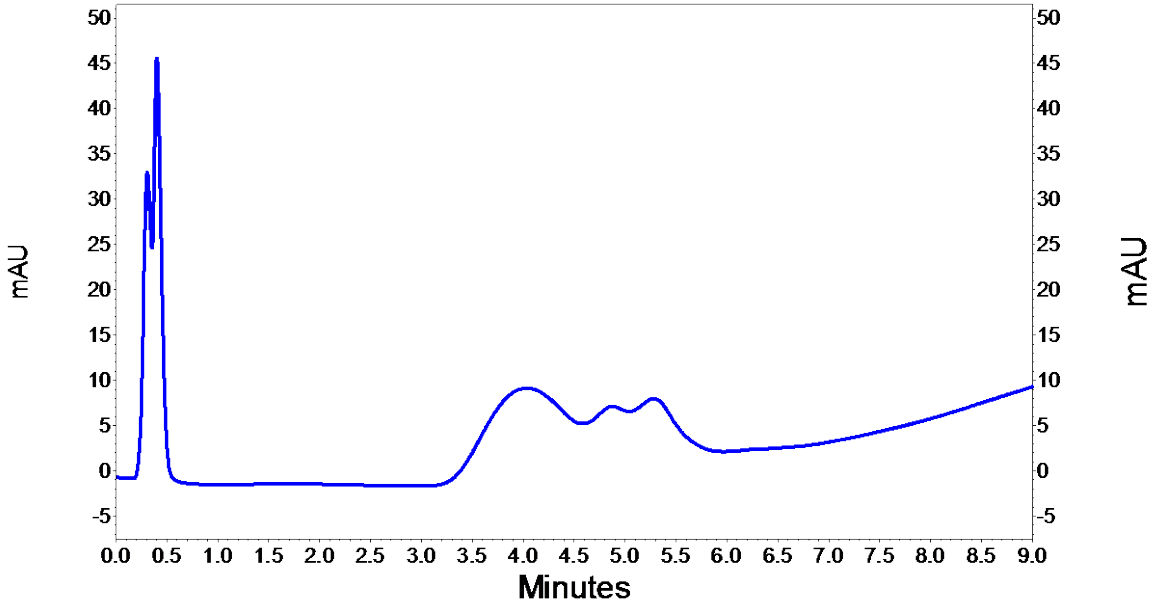

Fig 2. Surfactant peak separated from mAb using Pre-treatment column

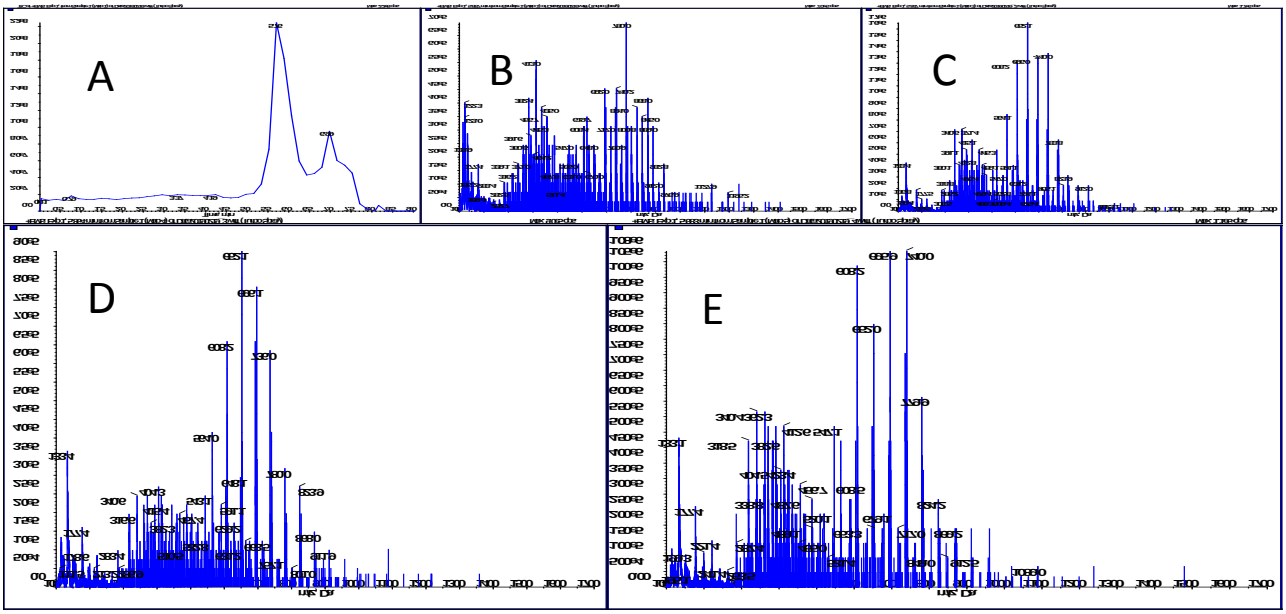

Fig. 3 LC MS data, A. Total ion chromatograph (TIC), B. mAb 1 mass spectrum, C. mAb 2 mass spectrum, D. mAb 3 mass spectrum , E. mAb 4 mass spectrum. The above mass spectrum shows the separation of free fatty acids in polysorbate complex and it is showing doubly and triply charge of free fatty acids.

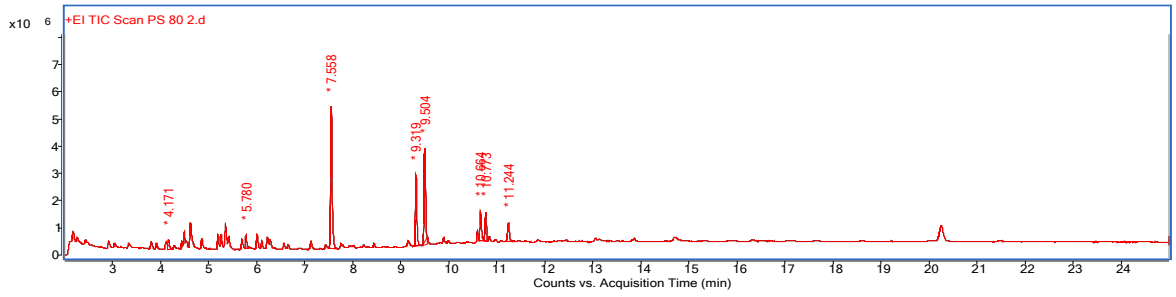

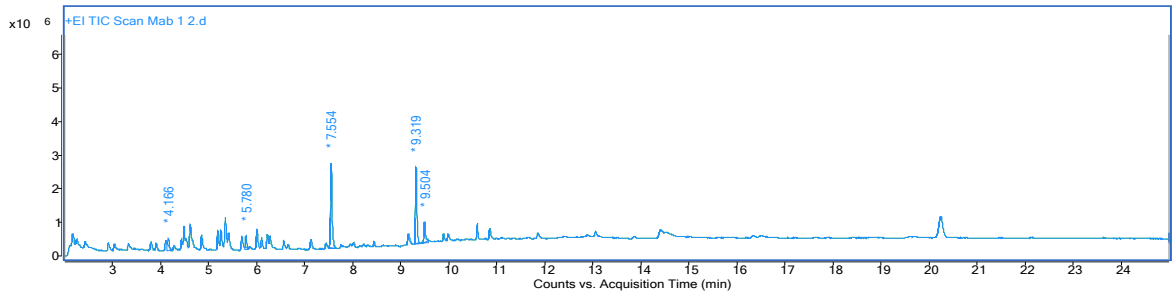

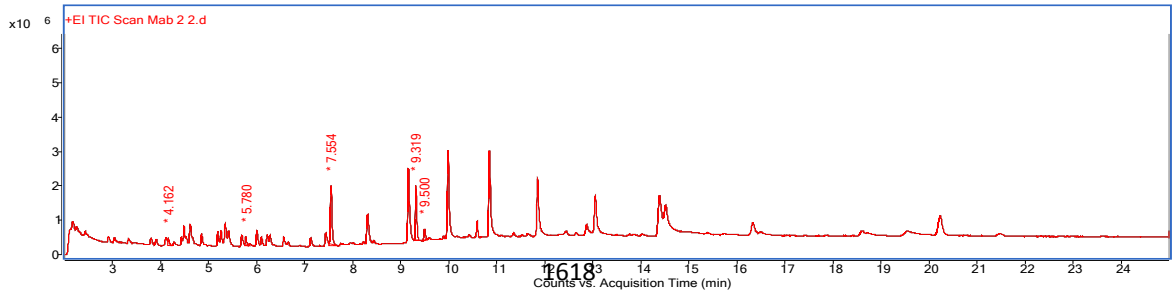

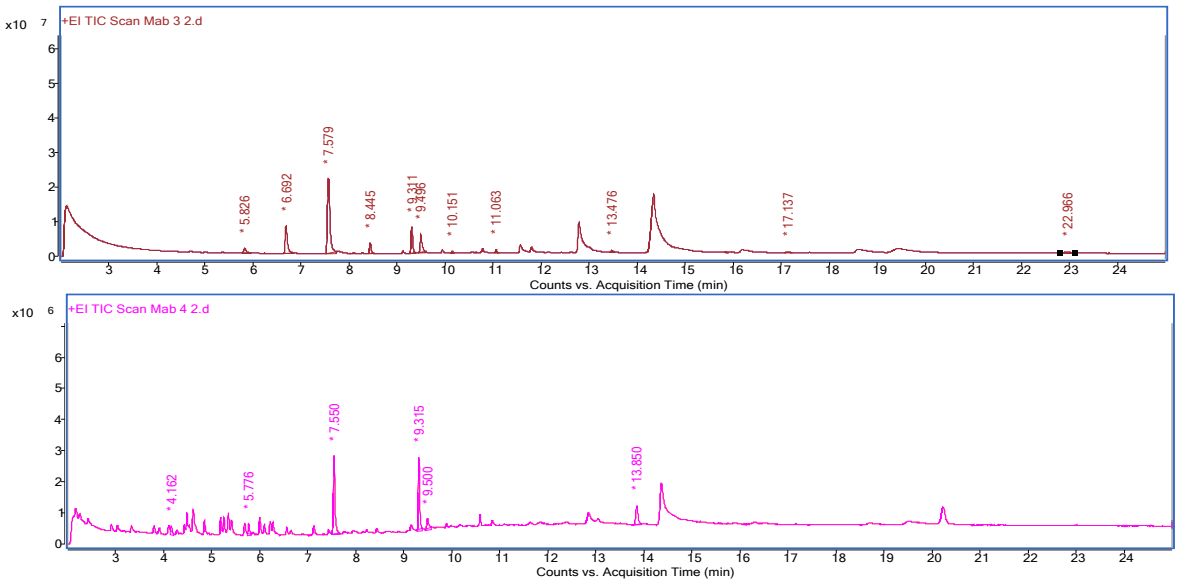

Fig. 4 GC MS data, Gas chromatograph for polysorbate 80 (standard), mAb 1, mAb2, mAb3 and mAb 4 respectively, The above chromatograph shows the separation of free fatty acids which is showing both saturated and unsaturated fatty acid profile.

Table No.2

Saturated fatty acids	Unsaturated fatty acids	RT	PS 80 (Std)	mAb 1	mAb 2	mAb 3	mAb 4
			Level %				
Dodecanoic acid, methyl ester (C12:0)		4.171	2.61	7.00	5.17	3.34	4.37
Tetradecanoic acid, methyl ester (C14:0)		5.78	2.96	5.77	5.95	16.85	5.24
Pentadecanoic acid, methyl ester (C15:0)		6.692				48.65	
Hexadecanoic acid, methyl ester (C16:0)		7.558	36.16	40.82	45.25	4.68	36.87
	9-Hexadecenoic acid, methyl ester, (Z)- (C16:1)	7.789				10.52	
Octadecanoic acid, methyl ester (C18:0)		9.319	16.94	35.65	35.57	10.79	32.02
	9-Octadecenoic acid (Z)-, methyl ester / 9-Octadecenoic acid, methyl ester, (E)- (C18:1)	9.504	22.66	10.76	8.06	0.65	7.68
Nonadecanoic acid, methyl ester (C19:0)		10.151					
	Methyl 9-cis,11-trans-octadecadienoate (C18:2n-7,9 trans,cis)	10.664	6.90				
	Linoleic acid, methyl ester (C18:2)	10.773	6.52			1.15	
Eicosanoic acid, methyl ester (C20:0)		11.101					
	8,11-Octadecadienoic acid, methyl ester (C18:2n-7,10)	11.244	5.26			0.80	
Docosanoic acid, methyl ester (C22:0)		13.518					
	13-Docosenoic acid, methyl ester, (Z)- (C22:1n-9)	13.862				0.90	13.81
Tetracosanoic acid, methyl ester (C24:0)		17.191				1.65	
Hexacosanoic acid, methyl ester (C26:0)		22.966					

Other than stable fatty acids from PS 80 cause reduce the surfactant concentration for stability and it cause the effect on shelf life of the protein and destabilization of protein. saturated fatty acids are less effect to compare to the unsaturated fatty acids levels on stability.

Effect of polyunsaturated fatty acids (PUFA) (C16:1; C18:1; (C18:2n-7,9 trans,cis) ; (C18:2) ; (C18:2n-7,10) ; (C22:1n-9) occurs on mAbs lifetimes and this binding effect on decreasing immunoreactivity with monoclonal antibodies spanning amino acid residues. and this may cause the precipitation and visible particles in PS 80 degradation and this effects instability to the mAb. Interaction propensity of the carboxylate moiety of the fatty acid with the mAb coupled with the low solubility of the fatty acid leading to destabilizing effects. the level of degradant fatty acid reduces the concentration of surfactant and may lead to destabilizing the mAb.

Conclusions

The formulations for biopharmaceuticals invariably comprise of Polysorbates to prevent aggregation and surface adsorption. However, polysorbates consist of trace levels of peroxides as impurities that could catalyze target product degradation via oxidation. In this work, we used HPLC-UV and mass spectrometry to catalogue the polysorbate 80 and its derivatives in commercial biosimilar products. Spiked samples with varying levels of the polysorbate 80 impurities were studied for their impact on the structure and function of the target product. The study reveals that polysorbates in the marketed products vary considerably and the implicate the quality of the product, in several instances. Future work proceeding to Simulations and molecular docking studies provide insights for engineering the product so that the ensuing structural and functional changes are minimized.

References

1. Ariadna Martos et al, Trends on Analytical Characterization of Polysorbates and their Degradation Products in Biopharmaceutical Formulations, Journal of Pharmaceutical Sciences, DOI. 10.1016/j.xphs.2017.03.001
2. Hillgren A, Lindgren J, Alden M. Protection mechanism of Tween 80 during freeze-thawing of a model protein, LDH. Int J Pharm. 2002;237:57–69.
3. Kiese S, Pappenberger A, Friess W, Mahler HC. Shaken, not stirred: mechanical stress testing of an IgG1 antibody. J Pharm Sci. 2008;97:4347–66.
4. Wang W. Protein aggregation and its inhibition in biopharma- ceutics. Int J Pharm. 2005;289:1–30.
5. Mahler HC, Friess W, Grauschopf U, Kiese S. Protein aggrega- tion: pathways, induction factors and analysis. J Pharm Sci. 2009;98:2909–34.
6. Mahler H-C, Mueller R, Friess W, Delille A, Matheus S. Induction and analysis of aggregates in a liquid IgG1-antibody formulation. Eur J Pharm Biopharm. 2005;59:407–17.
7. Cromwell MEM, Hilario E, Jacobson F. Protein aggregation and bioprocessing. Aaps J. 2006;8:E572–9.
8. Carpenter JF, Chang BS, Garzon-Rodriguez W, Randolph TW. Rational design of stable lyophilized protein formulations: theory and practice. Pharm Biotechnol. 2002;13:109–33.
9. Carpenter JF, Pikal MJ, Chang BS, Randolph TW. Rational design of stable lyophilized protein formulations: some practical advice. Pharm Res. 1997;14:969–75.
10. Ayorinde FO, Gelain SV, Johnson Jr JH, Wan LW. Analysis of some commercial polysorbate formulations using matrix-assisted laser desorption/ionization time-of-flight mass spectrometry. Rapid Commun Mass Spectrom. 2000;14:2116–24.
11. Frison-Norrieand S, Sporns P. Investigating the molecular heterogeneity of polysorbate emulsifiers by MALDI-TOF MS. J Agric Food Chem. 2001;49:3335–40.
12. Wasylaschuk WR, Harmon PA, Wagner G, Harman AB, Templeton AC, Xu H, et al. Evaluation of hydroperoxides in common pharmaceutical excipients. J Pharm Sci. 2007;96:106– 16.
13. Ha E, Wang W, Wang YJ. Peroxide formation in polysorbate 80 and protein stability. J Pharm Sci. 2002;91:2252–64.
14. Harmon PA, Kosuda K, Nelson E, Mowery M, Reed RA. A novel peroxy radical based oxidative stressing system for ranking the oxidizability of drug substances. J Pharm Sci. 2006;95:2014– 28.

ECAB 5
The 5th EUROPEAN CONGRESS OF APPLIED BIOTECHNOLOGY
Florence 15-19 September 2019

Influence of Fluid-Dynamic Conditions in STBR on *S.Blattae* (P424ibpso) Cultures for Isobutanol Production.

Miguel G. Acedos, Victoria E. Santos and Felix Garcia-Ochoa*

Chemical and Material Engineering Department, Chemical Sciences Faculty, Universidad Complutense de Madrid (Madrid, Spain)

**Corresponding author: fgochoa@ucm.es*

Highlights

- Hydrodynamic stress was detected for high stirrer speeds in STBR cultures
- Metabolite distribution as function of OTR-OUR variations is shown
- The oxygen conditions have effects over bacterial growth and metabolism

1. Introduction

Nowadays, there are a growing interest in obtaining alternatives for bioethanol as biofuel, among them isobutanol is a good alternative [1]. Isobutanol can be used as additive improving gasoline properties and also as chemical platform, to produce solvents or plasticizers agents [2]. It is well known that the fluid-dynamic conditions could critical in bacteria cultures [3], affecting culture performance. The objective of this work is to study the effect of fluid-dynamic conditions in STBR on *S. blattae* (p424IbPSO) cultures for the production of isobutanol.

2. Methods

Seven STBR cultures of S.blattae (p424IbPSO)[4] strain were carried out under different fluid-dynamic conditions, changing the stirrer speed from 100 to 1200 rpm and remaining constant the air flow (1vvm). The bacteria growth were measured by spectrophotometer analysis and the cell viability evaluated by total viable count technique. The cell morphology was also evaluated by electron microscope observations. During the growth, the time course of glucose, isobutanol and by-products were measured by HPLC analysis. The k_La values were estimated for the seven experiments under different conditions, and OTR, OUR_{max} and qO_2 were also calculated from k_La values and the DO concentration measurements with time. The isobutanol production in resting cells state was also studied employing cells collected from cultures under different fluid-dynamic conditions and growth times.

3. Results and discussion

The biomass growth rate increases in the runs carried out employing stirrer speeds between 100 and 600 rpm, and remain constant in the runs performed from 600 to 1000 rpm. However, the biomass growth rate decreases in the runs using stirrer speeds higher than 1000 rpm. The cell viability decreases for high agitation speeds, in the runs conducted at agitation greater than 800 rpm. Cells aggregates, cell damage and cell elongation were also detected, all these phenomena appearing for high agitation speeds. The increases of stirrer speeds produces an increase in the OTR values, and, depending of the conditions, also in the OUR values. When OTR < OUR maximum

value, the DO concentration quickly falls to zero, and the culture produces more lactic acid, ethanol and isobutanol. On the other hand, when OTR > OUR maximum, the culture produces more acetic acid and biomass. In Figure 1, It can be seen the yield of each compound.

The same carbon flux distribution is maintained when the cultures are performed on resting cells with cells cultured under different oxygen conditions.

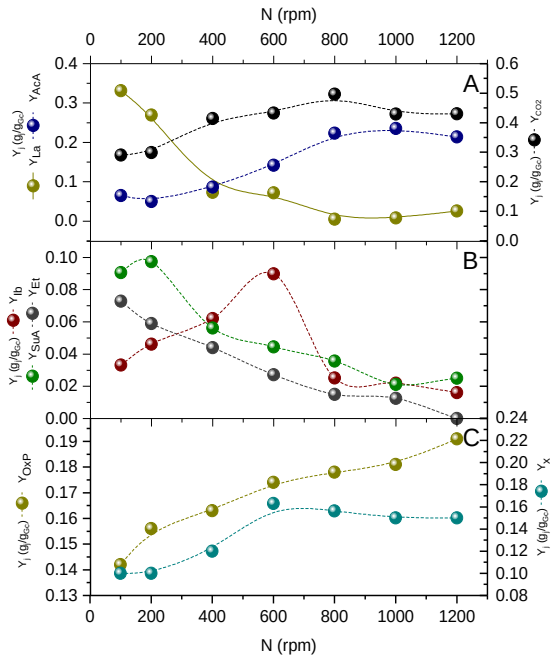

Figure 1. *Yield value on biomass and the main compounds referred to consumed glucose vs stirrer speed in STBR culture. The yield on lactate (La), acetate (Ac) and CO_2 can be seen in graphic A. The yield on isobutanol (Ib), ethanol (Et) and succinate (SuA) for each agitation (N) can be seen in the graphic B. The yield on high oxidation products (OxP) and biomass (X) it can be observed in graphic C.*

4. Conclusions

The hydrodynamic stress appears when high stirrer speeds were employed in STBR. The metabolite distribution is clearly affected by DO concentration, as a consequence of the relative values of OTR and OUR maximum values. It is relevant that these effects are maintained when the culture is carried out in resting cells, in these assays under the same conditions.

References

[1] C. Dellomonaco, F. Fava, R. Gonzalez, The path to next generation biofuels: successes and challenges in the era of synthetic biology, Microb. Cell. Fact., 9 (2010).
[2] L. Tao, E.C.D. Tan, R. McCormick, M. Zhang, A. Aden, X. He, B.T. Zigler, Techno-Economic Analysis and Life-Cycle Assessment of Cellulosic Isobutanol and Comparison with Cellulosic Ethanol and n-Butanol, Biofuels, Bioprod. Biorefin., 8 (2014) 30-48.
[3] F. Garcia-Ochoa, E. Gomez, V.E. Santos, J.C. Merchuk, Oxygen uptake rate in microbial processes: An overview, Biochem. Eng. J., 49 (2010) 289-307.
[4] M.G. Acedos, A. Ramon, S. de la Morena, V.E. Santos, F. Garcia-Ochoa, Isobutanol production by a recombinant biocatalyst *Shimwellia blattae* (p424IbPSO): Study of the operational conditions, Biochem. Eng. J., 133 (2018) 21-27.

ECCE12
The 12th EUROPEAN CONGRESS OF CHEMICAL ENGINEERING
Florence 15-19 September 2019

Production of a fungal fermented product as a meat substitute

Rebecca Gmoser[1]*, Mohammad J. Taherzadeh, Patrik R. Lennartsson

[1]Swedish Centre for Resource Recovery, University of Borås, 50190 Borås. Sweden

*Corresponding author: Rebecca.gmoser@hb.se

Highlights

- Food residues is converted by an edible fungi into a high protein meat replacer.
- The fungal product contain 29 % protein and 0.8 mg/g carotenoids.
- The product showed textural similarities with hamburgers and non-meat products.

1. Introduction

By 2050 world population is set to increase to over 9 billion. In order to feed this larger and wealthier population, food production foresees to rise by 70%. Access to a healthy and sustainable diet will become more important than ever as the planet accommodates for increased population. In this context, the present study presents a way to biotransform food residues into a valuable food product with promising attributes to substitute meat products. The edible filamentous fungi *N. intermedia* was used to create a fungal burger with stale bread and brewers spent grain as substrate. Since more than one billion people worldwide is unable to meet their daily protein requirement [1, 2] and texture is one of the biggest barrier to widespread acceptance for meat alternatives [3], the product was mainly evaluated based on its protein and texture attributes.

2. Methods

Fungal fermentation of the edible food grade filamentous fungi *Neurospora intermedia* CBS 131.92 (Centraalbureau voor Schimmelcultures, The Netherlands) was carried out in sterile petri dishes with bread crumbs alone or addition of brewers spent grain were used as substrate. Total 15 g substrate was inoculated with 1 ml spore suspension of *N. intermedia* separately for each petri dish and initial moisture content was adjusted to 40% (on a dry basis (w/w, db). Solid state fermentation was carried out batch wise for 6 days in a climatic test cabinet (NUVE test cabinet TK 120, Turkey) at 90-95% Rh at 35 °C under light. All the cultivation experiments were conducted in duplicate except for texture analysis where six replicates were made, and the mean values are presented with standard deviations. The textural profile analysis (TPA) of the samples was assessed with a TVT 6700 texture analyser (Perten Instruments, Sweden with software TexCalc version 4.0.2.50). To simulate a bite force through the burgers, a heavy Duty Stand, a knife blade probe with holder and blade set was attached. The maximum force required to break the sample was compared between samples. Instrumental texture measurement of the fermented fungal burgers was investigated after frozen samples for 24 h followed by frying at 100°C in 2 g of canola oil for 10 minutes.

3. Results and discussion

Bite force was measured by shearing with a knife blade to simulate a human bite and ease of chewing through the sample. As expected, the maximum force increased overall with increasing

BSG concentration in the substrate. Texture analysis on *N. intermedia* fungal burgers produced from stale sourdough bread with 0 % addition of BSG revealed a similar bite force response when fried as hamburger whereas addition of 10 % BSG was needed to reach a similar bite force response as a commercial soy burger, Figure 1. The objective textural data contribute to important knowledge about the products quality attributes. The stale bread with 10 % BSG used as substrate was converted into a high protein and nutritional fungal burger where mostly carbohydrates were converted into protein by *N. intermedia*. This fungal burger resulted in a protein increase by 152 % by *N. intermedia*. The increase in protein content is largely explained by a decrease in dry weight content of the fermented material [4]. Moreover, the fungal burger contained 0.95 mg carotenoids/g total material.

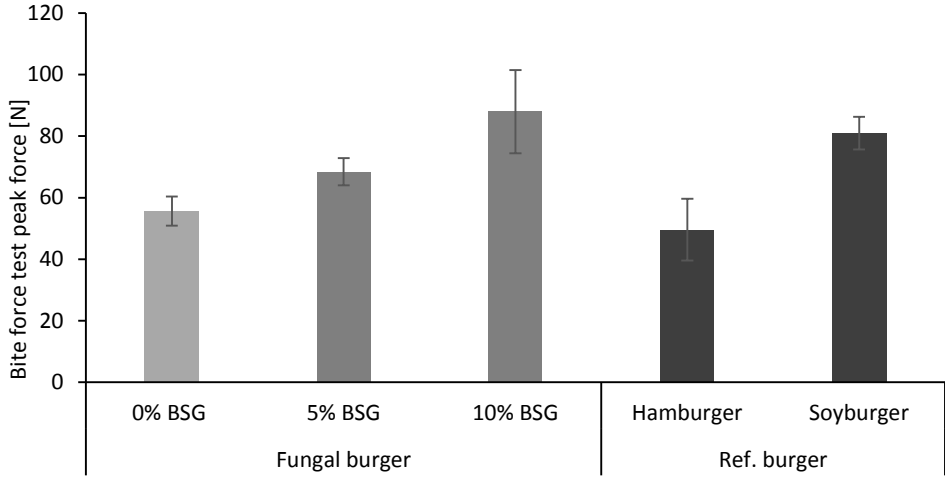

Figure 1. Bite force test of pre-frozen and fried fungal burgers and reference hamburger and soy burger available on the market. Fungal burgers are made from stale sourdough bread + 0, 5 or 10 % brewers spent grain using *N. intermedia* after 6 days solid state fermentation under light at 35 °C, 90 % Rh, and 40 % initial moisture content. Results are expressed as the mean value ± standard deviation.

4. Conclusions

The fermented fungal burger made from stale bread and up to 10 % brewers spent grains present an opportunity for an meat substitute. With up to 36 % protein and similar texture attributes to commercial products on the market, the product present a great addition to a modern diet without over-exploiting natural resources. The additional pigments produced (0.95 mg carotenoids/g total material) in the final product further adds value to the protein-rich fermented product.

References

[1] Godfray, H.C.J.;Beddington, J.R.;Crute, I.R.;Haddad, L.;Lawrence, D.;Muir, J.F.;Pretty, J.;Robinson, S.;Thomas, S.M.;Toulmin, C. Food security: The challenge of feeding 9 billion people. *Science* **2010**, *327*, 812-818.

[2] Hartmann, C.;Siegrist, M. Consumer perception and behaviour regarding sustainable protein consumption: A systematic review. *Trends in Food Science & Technology* **2017**, *61*, 11-25.

[3] Asgar, M.A.;Fazilah, A.;Huda, N.;Bhat, R.;Karim, A.A. Nonmeat protein alternatives as meat extenders and meat analogs. *Comprehensive reviews in food science and food safety* **2010**, *9*, 513-529.

[4] Blakeman, J.P.;McCracken, A.R.;Seaby, D.A. Changes brought about in solid substrates after fermentations of mixtures of cereals and pulses with rhizopus oryzae. *Journal of the Science of Food and Agriculture* **1988**, *45*, 109-118.

ECCE12
The 12th EUROPEAN CONGRESS OF CHEMICAL ENGINEERING
Florence 15-19 September 2019

D-Lactic Acid Fermentation from Orange Peel Waste: Effect of Initial Hydrolysate Concentration.

Isabel de la Torre, Felix Garcia-Ochoa*, Miguel Ladero and Victoria E. Santos

Chemical and Materials Engineering Department, Chemical Sciences Faculty, Universidad Complutense de Madrid (Madrid, Spain)

**Corresponding author: fgochoa@ucm.es*

Highlights

- D-Lactic acid production is carried out from cheaper carbon and nitrogen source
- 83.16 g/L of D-LA are obtained at highest OPW hydrolysate concentration
- 2.35 g/Lh of productivity is attained at the lowest OPW hydrolysate concentration
- A high OPW concentration improves D-LA final titer but worsens its productivity

1. Introduction

D-lactic acid (D-LA) is an organic acid produced mainly by lactic acid bacteria that has gained interest due to its application in the synthesis of poly-lactic acids (PLAs), a biodegradable and environmentally friendly polymer [1, 2]. The main obstacle to produce PLAs is the manufacturing costs caused largely by its monomer production (D-LA). This makes it necessary the use of cheaper carbon source like orange peel waste (OPW) [1]. The OPW is considered an optimum candidate for this applications due to: its high content in free sugars easily extracted (about 10 % in glucose, fructose and sucrose), its high content in polymers (37 % of cellulose and 11 % hemicellulose), which, after hydrolysis, release fermentable carbohydrates, and its low content in lignin (7.5 %), which inhibits enzyme action during hydrolysis and microbial activity in fermentation process. These residues are also notable for its high percentage of humidity [3].

2. Methods

OPW was milled down to 1–2-mm particle size, with a subsequent enzymatic hydrolysis carried out in batch run at 10.1% w/w of dry solid, 50 °C, 300 rpm, and initial pH of 5.2. Fed- batch saccharification was performed with 4 charges (initial + 3) of OPW partially dried by air convection, reducing the humidity from 80 to 60 % and 10.1% w/w of dry solid at initial time, 50 °C, 300 rpm and pH adjusted after added a charge to 5.2. The enzymes employed were Celluclast 1.5L, Novozyme 188 and Pectinex Ultra-SP. The hydrolysate was filtered through 0.2 µm size pore membranes of cellulose acetate for sterilization.

Lactobacillus delbrueckii ssp delbrueckii CECT 286 was employed as the biocatalyst to carry out D-Lactic acid production. Fermentation experiments were performed in 1L stirred tank bioreactor (STBR) BIOSTAT B-Plus with a volume broth of 0.5L and initial biomass concentration of 0.1g/L (5%v/v). The conditions were maintained at 40ºC, 200rpm, pH of 5.8 by adding NaOH 10M and anaerobic atmosphere by bubbling nitrogen before inoculation. The broth employed was OPW hydrolysate supplemented with 37 g/L corn steep liquor (CSL).

3. Results and discussion

D-Lactic acid production was carried out employing cheap carbon (OPW) and nitrogen (CSL) sources. If we pay attention to sugars uptake, glucose is consumed first in all experiments, while fructose and galactose, as observed in figures 1A and 1B, were metabolized later. All sugars were used to produce D-lactic acid, as suggested in those figures. In the figure 1C, results achieved when the hydrolysate concentration is highest are displayed, and it can be observed that the strain is not able to consume all sugars in this condition. If looking at final biomass concentrations, differences are not evident, although the growth rate is slower at higher hydrolysate concentration, as expected with increased inhibition due to either the substrates themselves or polyphenols and other components present in such hydrolysates. This LAB always grows from glucose, but it is not able to grow anymore in the presence of fructose and galactose. The final D-LA concentration improves when the OPW hydrolysate concentration increases, but the productivity decreases.

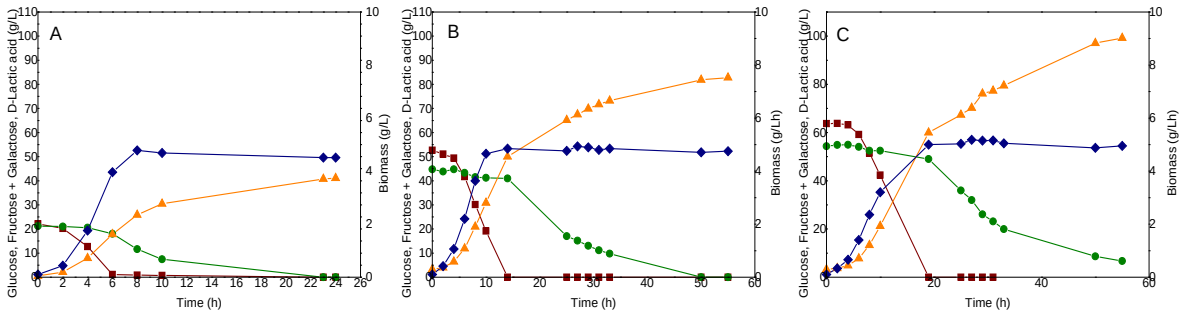

Figure 1.*D-Lactic acid production form OPW hydrolysate.* ***A.*** *Saccharification carried out in batch,* ***B.*** *Saccharification carried out in Fed Batch, hydrolysate diluted 80% and* ***C.*** *Saccharification carried out in Fed Batch, hydrolysate without dilution. Legend: Glucose, squares; fructose and galactose, circles; D-lactic acid, triangles; and biomass, diamonds.*

4. Conclusions

D-Lactic acid production is possible from cheap carbon (OPW) and nitrogen (CLS) sources. An increment in hydrolysate concentration reduces the productivity and growth rate but increases the final D-LA concentration, suggesting that inhibition due to substrates or stress due to phenolics and other chemicals plays a role in D-lactic acid production. At the highest hydrolysate concentration, 83.16 g/L of D-lactic acid were obtained at a productivity of 1.53 g/L·h.

References

[1] Martinez, F.A.C., Balciunas, E.M., Salgado, J.M., González, J.M.D., Converti, A., de Souza Oliveira, R.P., Lactic acid properties, applications and production: a review. Trends in food science & technology, 30(1), (2013) 70-83.

[2] Wang, Y., Tashiro, Y., Sonomoto, K., Fermentative production of lactic acid from renewable materials: Recent achievements, prospects, and limits. Journal of Bioscience and Bioengineering, 119(1), (2015) 10-18.

[3] Satari, B., Karimi, K., Citrus processing wastes: environmental impacts, recent advances, and future perspectives in total valorization. Resources, Conservation and Recycling, 129, (2018) 153-167.

ECAB 5
The 5th EUROPEAN CONGRESS OF APPLIED BIOTECHNOLOGY
Florence 15-19 September 2019

Mitigation of Ammonia Inhibition Through Bioaugmentation in Anaerobic Digestion: Selection of Strains and Reactor Performance Evaluation.

Ziyi Yang[1], Wen Wang[1*], Chao Liu[1], Guangqing Liu[1]

1 Biomass Energy and Environmental Engineering Research Center, Beijing University of Chemical Technology, Beijing 100029, China

**Corresponding author: wangwen@mail.buct.edu.cn, anne_wangwen@163.com*

Highlights

- Bioaugmentation could achieve 71% increased methane production and 85% biodegradability.
- Bioaugmentation with *Syntrophaceticu smithii* + *Methanobrevibacter* spp. was optimum.
- Enhancement of both aceticlastic and hydrogenotrophic methanogenesis was important.
- *Methanobrevibacter* and *Methanosarcina* spp. were non-dominant but important archaea.

1. Introduction

Anaerobic digestion (AD) has gained extreme attention since producing renewable energy [1]. Ammonia is considered as a key parameter affecting AD efficiency [2]. Bioaugmentation could be a potential method to improve AD efficiency [3]. Researchers have attempted to increase methane production (MP) by strengthening the hydrogenotrophic methanogenesis bioaugmentated with certain strains [4]. However, other studies didn't indicate significant improvements [5]. Knowledge of mitigating ammonia inhibition effect with hydrogenotrophic methanogens is lacking. On the other hand, *Methanosaeta* and *Methanosarcina* were found to be dominant archaea [6]. Whether bioaugmentation with aceticlastic methanogens could achieve efficient MP remains unknown. The objectives of the present research are as follows: (1) to compare the bioaugmentation effects of different strains and (2) to develop an ammonia-tolerant environment for MP.

2. Methods

Seven pure strains were selected (Table 1). The total and working volumes were 500 and 350 mL. Glucose and NH_4Cl were applied as carbon and ammonium nitrogen sources. Organic loading rate was 1 g glucose/L/d. Hydraulic retention time was 10 days. The reactors were carried out in a 37 °C continuous stirred shaker. The ammonia level was 4 NH_4^+-N/L. Biogas production, NH_3-N, were determined as publications [7]. Specific methanogenic activity (SMA), stable isotopic analysis (based on α_c values), and 16S rRNA gene sequencing analysis were described in publications [7,8].

Table 1. Abbreviation of different strains used in this study

Pure strain	Abbreviation	Pure strain	Abbreviation
Methanosaeta harundinacea	MSH	*Methanosarcina barkeri*	MSB
Methanobacterium bryantii	MBB	*Syntrophaceticus schinkii*	SS
Methanoculleus bourgensis	MCB	*Tepidanaerobacter acetatoxydans*	TA
Methanobrevibacter smithii	MBS		

3. Results and discussion

Bioaugmentation with SS + MBS was the optimal choice (Figure 1; MP was 71.1% higher than that in Blank), the activity of hydrogenotrophic methanogenesis was greatly heightened according to SMA (Figure 2). And bioaugmentation with MSB alone was also proven efficient (MP was 59.7% higher than that in Blank), both aceticlastic and hydrogenotrophic methanogenesis were enhanced. Further evaluation with carbon isotope fractionations analysis (Figure 3) indicated that balancing the activities of the aceticlastic and hydrogenotrophic methanogenic pathways is of great importance. 16s rRNA gene sequencing results (Figure 4) showed that showed that *Methanobacterium* spp. and *Methanosaeta* spp. were the dominant archaea in all 14 reactors. Nevertheless, bioaugmentation with *Methanosaeta* spp. did not result in a positive effect on MP. On the other hand, *Methanobrevibacter* spp. and *Methanosarcina* spp. were non-dominant archaea (even after bioaugmentation with MBS or MSB, the relative abundances were still poor (< 2%)), but displayed pivotal roles in determining the overall microbial consortium and, in turn, improved the overall performance.

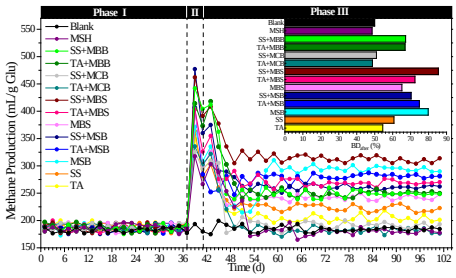

Figure 1. MP and biodegradability of different reactors

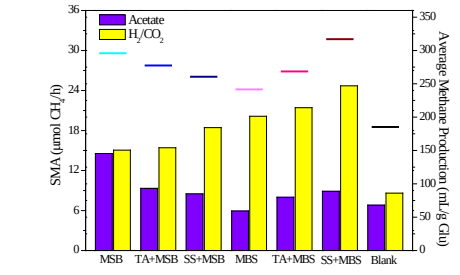

Figure 2. SMA and average MP in different reactors

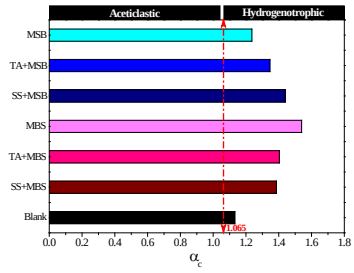

Figure 3. α_c values and pathway in different reactors

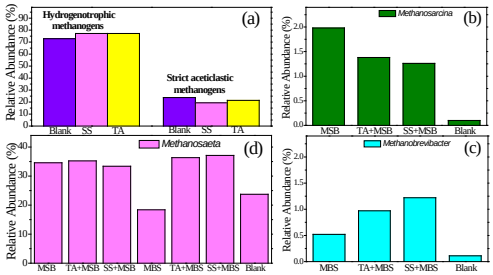

Figure 4. Relative abundance of different methanogens

4. Conclusions

Bioaugmentation could be an efficient way with over 59% increased on MP. aceticlastic and hydrogenotrophic methanogenic pathway should be both taken into account during bioaugmentation and the balance could result in a better reactor performance. Non-dominant archaea might display pivotal roles in improving AD performance.

References

[1] Tampio, E., S. Marttinen, and J. Rintala, J Clean Prod. 125 (2016): 22-32.
[2] Yuan, H.P. and N.W. Zhu, Renew Sust Energ Rev. 58 (2016): 429-438.
[3] Li, Y., Zhang, Y., Sun, Y. M., Wu, S. B., et al., Bioresource Technol. 231 (2017): 94-100.
[4] Fotidis, I.A., Wang, H., Fiedel, N. R., et al. Environ Sci Technol. 48 (2014): 7669-7676.
[5] Westerholm, M., S. Roos, and Schnurer, A., Syst Appl Microbiol. 34 (2011): 260-266.
[6] Westerholm, M., Leven, L., Schnurer, A. Appl Environl Microb. 78 (2012): 7619-7625.
[7] Yang Z.Y., Wang W., He Y.F., Zhang R.H., Liu G.Q., Renew Energ. 125 (2018): 915-925.
[8] Wang, H., I.A. Fotidis, and I. Angelidaki, Bioresource Technol. 209 (2016): 282-289.

ECAB 5
The 5th EUROPEAN CONGRESS OF APPLIED BIOTECHNOLOGY
Florence 15-19 September 2019

Tolerance Improvement of Xylose-Utilizing Yeast Strains on Acetic Acid by Evolutionary Engineering.

Ja Kyong Ko[1], Soo Rin Kim[2], Youngsoon Um[1], Sun-Mi Lee[1,*]

[1] *Clean Energy Research Center, Korea Institute of Science and Technology (KIST), Wharang-ro 14 gil 5, Seongbuk-gu, Seoul 136-91, Republic of Korea;* [2] *School of Food Science and Biotechnology, Kyungpook National University, Daegu, Republic of Korea*

**Corresponding author: smlee@kist.re.kr*

Highlights

- Acetic acid derived from biomass severely inhibits xylose fermentation of yeast.
- Evolutionary engineering strategy was applied to improve acetic acid tolerance.
- Evolved yeasts could serve as platform strains for biofuel production from biomass.

1. Introduction

The presence of inhibitors in the lignocellulosic biomass hydrolysates are inevitable bottlenecks for achieving economic cellulosic ethanol production by *Saccharomyces cerevisiae*. The yeast tolerance toward acetic acid, released during the pretreatment of lignocellulose, needs to be improved for the efficient fermentation of un-detoxified biomass hydrolysates. Specifically, acetic acid stress is more severe on xylose fermentation resulting in decreased cell growth, xylose utilization rate and ethanol yield than glucose fermentation. In this study, an evolutionary engineering strategy was applied to improve fermentation performance of the engineered xylose-utilizing yeasts under acetic acid stress.

2. Methods

We attempted to evolve the two engineered strains harboring xylose isomerase (XUS-E) [1] and oxidoreductase (DY4)-based pathways using serial sub-culturing in synthetic medium with xylose as a sole carbon source in the presence of acetic acid at pH 5. After 13 rounds of exponential phase transfer, the evolved strains, XUS-AE57 and DY4-AE1, were obtained. Transcriptomic characterization of evolved strains through RNA sequencing was performed using tools from Ebiogen, Inc. (Seoul, Republic of Korea).

3. Results and discussion

The evolved strain, XUS-AE57, with xylose isomerase pathway could efficiently convert xylose to ethanol with yields of 0.43-0.47 g ethanol/g xylose even in the presence of 2-5 g/L acetic acid (Figure 1). This strategy not only achieved ~1.7 fold higher level of ethanol yields, but also improved xylose utilization rate by >2 folds. For DY4AE1 harboring an oxidoreductase pathway, the xylose utilization rate was significantly enhanced by ~2.3 fold. To understand the molecular mechanisms underlying the improvement in the acetic acid tolerant phenotypes, the global

transcript profiles of the evolved strains grown under acetic acid stress were analyzed by using RNA sequencing.

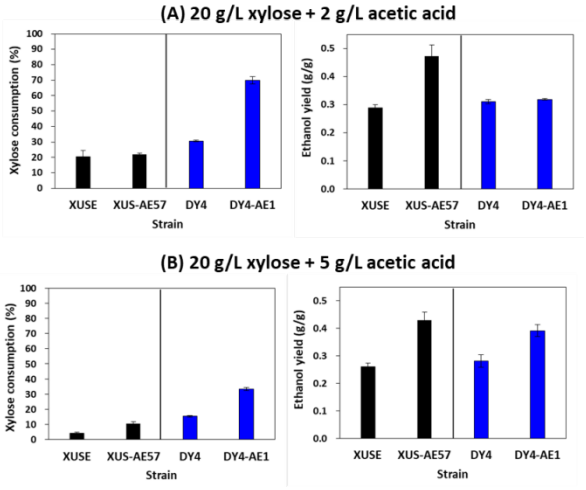

Figure 1. Xylose fermentation performance of the control (XUSE and DY4) and evolved strains (XUSAE57 and DY4AE1) under 2 and 5 g/L acetic acid stress.

4. Conclusions

XUSAE57 and DY41 strains could serve as robust platform strains of *Saccharomyces cerevisiae* for biofuels/biochemicals production from lignocellulosic biomass.

References

[1] J.K. Ko, Y. Um, S-M. Lee, Bioresour. Technol. 222 (2016) 422-430.
[2] P. Tran Nguyen Hoang, J.K. Ko, G. Gong, Y. Um, S-M. Lee, Biotechnol. Biofuels. 11 (2018) 268.

Soybean Protein: a Potential Additive to Improve the Saccharification of Lignocellulosic Biomass in Biorefineries

Mariana G. Brondi[1,2], Roberto C. Giordano[1], Cristiane S. Farinas[1,2*]

[1] *Graduate Program of Chemical Engineering, Federal University of São Carlos, São Carlos, Brazil;*

[2] *Embrapa Instrumentação, São Carlos, Brazil*

**Corresponding author: cristiane.farinas@embrapa.br*

Highlights

- Soybean protein improves biomass saccharification.
- Soybean protein can be used as cost-effective additive.
- Gain of soybean protein is comparable to BSA.

1. Introduction

The conversion of renewable lignocellulosic biomass into biofuels and other bioproducts employing the biochemical route has been considered as a sustainable alternative to implement future biorefineries. However, this process still presents several technological challenges related to the low yield of the enzymatic hydrolysis step and the high cost of the cellulolytic enzymes. Among the strategies to increase the efficiency of the enzymatic hydrolysis reactions of the biomass, the use of additives has shown very positive effects, since they decrease the unproductive adsorption of the cellulases in the lignin, thus reducing the loss of enzymes in the process [1,2,3]. However, there is a clear need to find more cost-effective additives for use in large-scale processes. Here, soybean protein was evaluated as an alternative low-cost additive in the saccharification of pretreated sugarcane bagasse using a commercial enzymatic cocktail.

2. Methods

Liquid hot water pretreated bagasse (LHW) was prepared as described in [3]. Soybean protein (soybean protein isolate with 90% protein content, from Bremil, Brazil) was used at 12% (w/w) per wt of biomass (on a dry basis). The enzymatic hydrolysis experiments were carried out in 5 mL tubes placed in a hybridization incubator operated at an agitation speed of 30 rpm. Solids loadings of 15% (w/v, dry weight basis) of biomass and enzyme loadings of 5, 10, 15 and 20 FPU/g dry biomass were used, at 50 °C, in sodium citrate buffer (50 mM and pH 4.8). Samples were withdrawn every 24, 48 and 72 h for glucose determination using a D-glucose enzymatic assay kit (Labtest, Brazil).

3. Results and discussion

The addition of soybean protein had positive effects on glucose release during the hydrolysis of LHW pretreated sugarcane bagasse, with gains up to 26% when 12% (w/w) soybean protein was used (Figure 1). These improvements were comparable to those obtained using bovine serum albumin (BSA), a much more expensive protein that has been widely reported for such an application [2]. Moreover, addition of soybean protein led to a saving of 48 hours in the hydrolysis reaction time, corresponding to a 66% decrease in the reactor operation time required. In order to achieve the same hydrolysis yield without the soybean additive, the enzyme loading would need to be increased by 50%. Similar gains were also observed when using steam exploded pretreated sugarcane bagasse [2], thus showing the potential of soybean protein for other types of pretreated biomass.

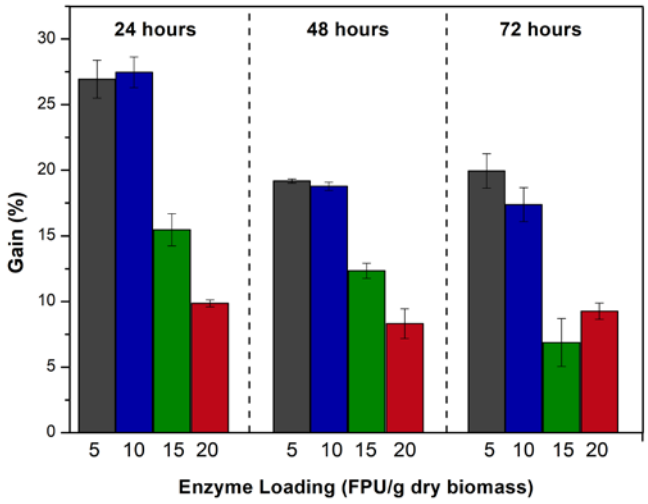

Figure 1. Increase in glucose release after the addition of soybean protein (12% w/w) compared to the bagasse hydrolysis without additive (Gain). The hydrolysis were performed with an enzyme loading of 5, 10, 15 and 20 FPU/g dry biomass, solids loading of 15% (w/v) for 24, 48 and 72 hours.

4. Conclusions

These findings suggest that soybean protein supplementation during enzymatic hydrolysis by commercially available enzymes is an effective strategy for achieving higher saccharification yields from pretreated lignocellulosic biomass, hence improving overall efficiency of future biorefineries.

References

[1] Florencio, C., Badino, A. C. and Farinas, C.S. Bioresour Technol. 221 (2016) 172-180.
[2] Brondi, M. G., Vasconcellos, V. M., Giordano, R. C. and Farinas, C. S. Appl. Biochem. Biotechnol. (2018) https://doi.org/10.1007/s12010-018-2834-z
[3] Florencio, C., Badino, A. C. and Farinas, C.S. BioEnergy Res. (2019) https://doi.org/ 10.1007/s12155-018-9956-6.

ECCE12
The 12th EUROPEAN CONGRESS OF CHEMICAL ENGINEERING
Florence 15-19 September 2019

New Development for Ethanol Production from Lignocellulosic Materials in Fludized Bed Reactor.

Felipe A. F. Antunes[1], Júlia Ribeiro dos Santos[1], Alesson Santos da Silva[1], Anuj K. Chandel[1], Silvio Silvério da Silva[1*]

1 Department of Biotechnology, Engineering School of Lorena - University of São Paulo Area I
Address Estrada Municipal do Campinho, s/nº Postal code: 12.602-810 - Lorena-SP - Brazil

**Corresponding author: silviosilverio@gmail.com*

Highlights

- Sugarcane bagasse is a feasible carbon source for bioprocess
- Fluidized bed reactor can be used for chemical and biochemical process
- Bioprocess conducted in Fed-batch configuration is a potential method

1. Introduction

Due to environmental and political problems regarding the imminent scarcity of fossil fuels, different approaches for biofuels production have been gained great importance in the global scenario. Thus, various agroindustry residues, such as bagasse, bark, grains, straw, among others, are used as raw material for the production of 2G ethanol. Among them, sugarcane bagasse has presented greater advantages due it is available in abundance in countries such as Brazil, India, China and others [1]. Additionally, new studies must be developed in order to produce biomolecules from lignocellulosic materials, since the processes of pretreatment, saccharification and fermentation are still stages that still needs to be optimized, aiming the scale-up and industrial production. Within this context, i.e., the use of fluidized bed reactor (FBR) in chemical and biochemical processes is a potential approach for the conduction of methods applied to scale-up. When compared to the stirred tank reactor, the most commonly used reactor, the fluidized bed reactor has advantages such as: no requirement to use mechanical impellers for agitation, ease control of homogenization by insertion of air or fluid recirculation, and hence, increase of the contact surface between the catalyst and fluid [2]. Taking this into account, we present a new development for ethanol production from lignocellulosic material in fludized bed reactor. Ethanol production was evaluated by conducting saccharification stage in fed-feed process by inserting with alkaline pre-treated sugarcane bagasse, in order to obtain fermentable sugars, followed by and subsequent fermentation, carried out in simultaneous sacharification and fermentation configuration (SSF) in all process conducted in FBR.

2. Methods

Sugarcane bagasse was conducted to alkaline hydrolysis in a fluidized bed reactor (a column reactor from Bioengineering AG - PID Fermenter AWS, Wald, Switzerland- with 540 mm x 55 mm column, with central vertical tube of 9 mm inner diameter) where 30 g of sugarcane bagasse was mixed with 700 mL of 0.5M NaOH alkaline solution at 90 ° C for 120 min in a non-pressurized fluidized bed reactor system, homogenized by insertion of air in 0.3 min^{-1}. After the hydrolysis process, the remaining solid fraction of pre-treated sugar cane bagasse was washed and used in the subsequent

saccharification step. In other similar fluidized bed reactor, homogenized by aeration of 0.3 min^{-1}, sacharification step was conducted at 50ºC by mixing of 700 ml of Citrate buffer (50 mM, pH 4.8), 0.3 ml of twin and 20 FPU of cellulase enzyme complex (Cellulase CP CONC-Dyadic) and 10g of alkaline pretreated sugarcane bagasse, obtained in last step. At every period of hours, 10g of alkaline pre-treated bagasse was added, until the total of 50g was reached. After 48 hours of saccharification, the pH of the medium was adjusted to 5.5 with addition of NaOH solution, and subsequently added 5 g/L of ammonium sulfate, 3 g/L of yeast extract and 3 g/L of extract of malt, according to nutritional medium proposed by Antunes et al. [3]. To the supplemented medium, 0.5 g/L of *Scheffersomyces shehatae* UMFG-HM 52.2 cellular solution was added (wild Brazilian sugars pentose convert yeast). The fermentations were conducted for 72 h in the same fluidized bed reactor, by the aeration of 0.3 min^{-1}, at 30 ° C. Samples were collected periodically for analysis of biomass, fermentable sugars and ethanol.

3. Results and discussion

Figure 1 shows the consumption profile of fermentable sugars (glucose and xylose) obtained by means of enzymatic hydrolysis operated in batch fed alkaline pre-treated sugar cane bagasse and followed used in the conversion of ethanol to a fluidized bed reactor using yeast *Scheffersomyces shehatae* UFMG-HM 52.2.

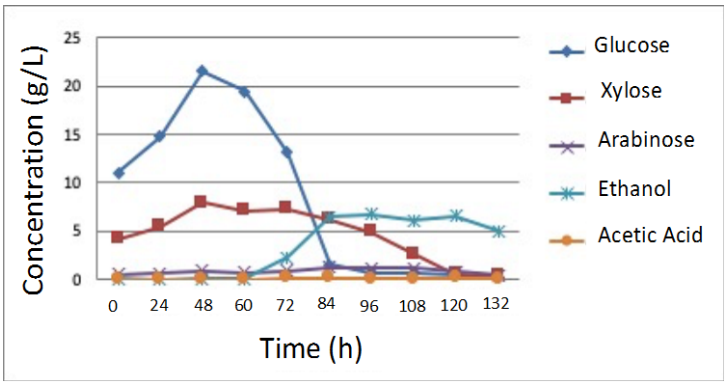

Figure 1. Ethanol production from fermentable sugars of sugarcane bagasse in fluidized by using the yeast *Scheffersomyces shehatae* UFMG-HM 52.2

After conducting 48 h of enzymatic hydrolysis carried out in fed-batch configuration, around 22 g/L and 8 g/L of xylose were observed as available fermentable sugars. From this time, with addition of the microorganism, total consumption of fermentable sugars, with the highest production of ethanol (6.775 g / L) were verified in the followed 48 hours of fermentation (96h of total process), showing ethanol yield ($Y_{P/S}$) of 0.26 g/g and volumetric productivity of 0.14 g/Lh .

4. Conclusions

The potential use of column reactors applied to the stages of pre-treatment of vegetal biomass and fermentation of fermentable sugars was norteworthy, as well as the indication for further of studies of process optimization.

References

[1] A. K. Chandel, F. A. F. Antunes, V. Anjos, et al., Biotech. for Biofuels, (2013) 6:4
[2] F. A.F. Antunes, A. K. Chandel,L. P. Brumano,et al, Renew. Energy, 124, (2018) 189-196
[3] F. A.F. Antunes, A. K. Chandel, T.S.S. Milessi, I. J. Chem. Engin., et al., (2014) ID 180681, 8p

Economic and Environmental Feasibility Assessment of a Mango Kernel Biorefinery

Demetri Petrides[1*], Elpida Sapidou[1], Alexandros Koulouris[2]
[1]Intelligen Inc., Scotch Plains, NJ 07076, USA;
[2]Alexander Technological Education Institute., Thessaloniki, Greece;
Corresponding author: dpetrides@intelligen.com

Process simulators have been used in the petroleum and chemical industries for over four decades to facilitate the development of new processes and optimize the performance of existing ones. Similar benefits can be derived from the use of such tools in the industrial biotechnology arena to aid in the design, feasibility evaluation and environmental impact assessment of biorefinery systems. In this work, we demonstrate such a case for a biorefinery that utilizes mango kernels to produce energy and biochemicals such as oil, proteins and starch.

Enzymatic Recovery of Building Blocks from Textile Blends.

Felice Quartinello[1], Alessandro Pellis[2], Georg M. Gübitz[1]

1 University of Natural Resources and Life Sciences BOKU Vienna, Department of Agrobiotechnology IFA-Tulln,;

2 University of York, Department of Chemistry, Green Chemistry Centre of Excellence,

**felice.quartinello@boku.ac.at*

Highlights

- Circular economy concept
- Textile waste recycling
- Enzymatic separation and degradation of fibres.
- Secondary value-added products

1. Introduction

In the last decades the production of textiles, especially for clothing, is exponentially increasing mostly due to the globalization phenomena [1].In Europe, 80.000 tons of textile waste are generated per year and their end-life is primarily landfilling. Together with soil pollution, this represents also a global warming challenge due the production of greenhouse-gases [2]. For example only 18% of this kind of waste in the last years was used for energy recovery. Furthermore, considering the material composition, the discarded textiles still contains valuable polymers/polymer building blocks that could be reused. In this study we present an enzyme-based strategy for the recovery of valuable building blocks from mixed textile waste and blends as a circular economy concept [3,4].

2. Methods

Textile, waste was sequentially incubated with 1) protease for the extraction of amino-acids from wool components) and 2) cellulases for the recovery of glucose from cotton and rayon constituents. The purity of the remaining poly(ethylene terephthalate) (PET) unaltered by the enzymatic treatments was assessed via Fourier-transformed infrared spectroscopy. Amino acids recovered from wool were characterized via elementary and molecular size analysis, while the glucose resulting from the cotton hydrolysis was successfully converted into ethanol by fermentation with *Saccharomyces cerevisiae*.

3. Results and discussion

The enzymatic hydrolysis of wool- and cellulose- based fibers led to yields of approximately 95% and 85%, respectively. The purity of the resulting poly(ethylene terephthalate) was comparable to the pure PET as demonstrated by FT-IR measurements, allowing recycling. Furthermore, in line with circular economy concepts, the recovered building blocks from wool and cellulose fiber components in blended textiles can be reused. The amino acids and oligopeptides (with molecular weight lower than 10 KDa) obtained from wool degradation can be used as a replacement for carbon and nitrogen sources for germination or phenolic-related compounds for resins according to previous reports. On the other hand, in this paper recovered glucose (around 0.62 g•L^{-1}) was successfully used as carbon source for yeast fermentation to produce ethanol (0.3 g•L^{-1}).

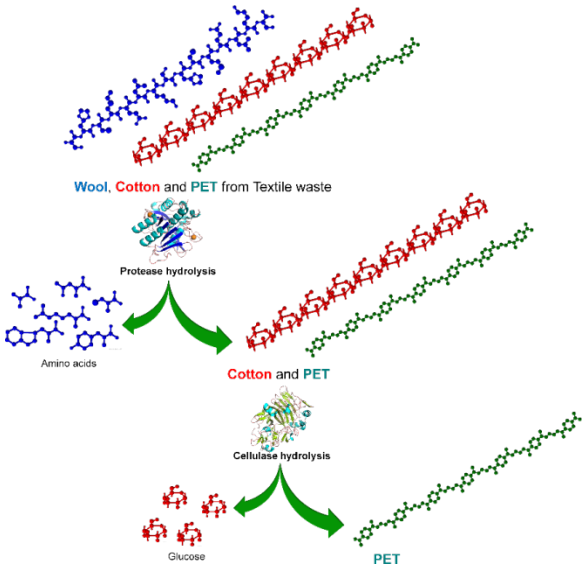

Figure 1. Scheme of enzymatic separation of textile fibers

4. Conclusions

In summary, such step-wise enzymatic process is especially attractive for the recycling of blended materials which are otherwise rather difficult to recycle with other technologies. Furthermore, this work demonstrated that the step-wise application of enzymes can be used for the recovery of pure building blocks and their further reuse, example for fermentative processes (glucose).

References

[1] Zamani, B., Peters, G. & Svasnström, M. Towards Understanding Sustainable Textile Waste Management: Environmental impacts and social indicators. Chem. Biol. Eng. 52 (2014).
[2] European technology Platform. Towards a 4 th Industrial Revolution of Textiles and Clothing.
[3]Pellis, A., Cantone, S., Ebert, C. & Gardossi, L. Evolving biocatalysis to meet bioeconomy challenges and opportunities. N. Biotechnol. 40, 154–169 (2018).
[4]Guebitz, G. M. & Cavaco-Paulo, A. Enzymes go big: surface hydrolysis and functionalisation of synthetic polymers. Trends Biotechnol. 26, 32–38 (2008).

Hybrid Semi-Parametric Modeling of Preparative Protein Chromatography for Online Monitoring and Real-Time Process Control.

Anna Christler[1], Moritz von Stosch[1], Theresa Scharl-Hirsch[1,2], Michael Melcher[1,2], Friedrich Leisch[1,2], Astrid Dürauer[1,3], Alois Jungbauer[1,3]

1 Austrian Centre of Industrial Biotechnology (ACIB), Muthgasse 11, 1190 Vienna, Austria; 2 Institute of Applied Statistics and Computing, University of Natural Resources and Life Sciences (BOKU), Peter-Jordan-Strasse 82, 1190 Vienna, Austria; 3 Department of Biotechnology, University of Natural Resources and Life Sciences (BOKU), Muthgasse 18, 1190 Vienna, Austria

**Corresponding author: anna.christler@acib.at*

Highlights

- A PAT application for preparative protein chromatography was established.
- Non-parametric statistical models were complemented with parametric mechanistic models.
- Hybrid semi-parametric models show enhanced prediction quality of critical quality attributes.

1. Introduction

Regulatory agencies encourage pharmaceutical industry to implement Quality-by-Design approaches into manufacturing processes. We integrated additional online sensors, namely infrared (ATR-FTIR), fluorescence, refractive index and static light scattering detectors, into a conventional chromatography workstation. Obtained online signals were statistically correlated to offline measured parameters of quantity, purity and potency. Thereby, predictive models were generated. Hybrid semi-parametric models combine such statistical correlations with first-principles expert knowledge [1]. Hybrid models are able to balance strengths and weaknesses of different sources of knowledge considering for example extrapolation power and data availability. This has been shown among others for monitoring of bacterial fermentation processes [2]. We applied this approach to optimize loading and elution of chromatographic steps where monitoring is currently mostly done via UV/Vis absorption only.

2. Methods

Multivariate data analysis enables extraction of unknown or unidentified correlations from large amounts of data sets. Online data obtained from implemented spectroscopic sensors were pre-processed to maximize the information content and reduce unspecific noise. Boosting algorithms allowed automated variable selection. CADET was used for efficient computing of mechanistic models [3].

3. Results and discussion

Different combinations of parametric and non-parametric model parts, i.e. parallel and serial hybrid structures, were compared and the best performing identified for monitoring of product attributes. Prediction accuracy and robustness were compared to solely data-based models and differences analyzed. A major advantage of the hybrid models is that predictions can be provided based on the feed composition while non-parametric model estimates are only available retrospectively with a time delay of up to 10 seconds.

4. Conclusions

The generated hybrid models enable controlled loading and peak cutting based on defined quality settings. Time and labor intense offline analytics can therefore be reduced to a minimum for model training and final product release. The developed approach is fundamental for the implementation of real-time batch release and continuous manufacturing in biopharmaceutical industry.

References

[1] M. von Stosch, J. Glassey (Eds.), Hybrid Modeling in Process Industries, CRC Press, Taylor & Francis Group, Boca Raton, Florida, 2018.
[2] M. von Stosch, R. Oliveira, J. Peres, S. Feyo de Azevedo, Comput. Chem. Eng. 60 (2014) 86–101.
[3] S. Leweke, E. von Lieres, Comput. Chem. Eng. 113 (2018) 274–294.

Recovery of lipids from microalgae extracts by membrane processes: Comparison of cross-flow and shear-enhanced filtration performances.

Estelle Couallier[1], Shuli Liu[1], Erika Clavijo [1], Liliana Villafaña Lopéz[1], Matthieu Frappart[1]

[1] *CNRS, GEPEA, CRTT, 37 boulevard de l'université, BP 406*

44602 Saint Nazaire Cedex, France

**Corresponding author: Estelle.couallier@univ-nantes.fr*

Highlights

- Membrane filtration allows the concentration of lipids from disrupted microalgae.
- The rotatin disk filtration with a PAN membrane offers the best performances.
- An optimized coupling between cell disruption and filtration will enhance the biorefining.

1. Introduction

The biorefinery of renewable resources like microalgae offers great opportunities to substitute biomolecules to traditional raw materials in various industry sectors. Such strategies necessitate innovative choices of soft and energy-efficient processes to guarantee the integrity of fragile molecules and develop eco-friendly production. For large-scale production (food, energy or green chemistry), a wet processing of biomass has been proposed, that avoids expensive drying steps and reduces solvent use. However the energetically efficient extraction of biomolecules at low cost and industrial scale is not yet mature. Biomass wet treatment includes 1- the harvesting, 2- the cell disruption step to release the valuable biochemical compounds in the aqueous phase, 3- the fractionation step (extraction, concentration and purification). The integration of membrane processes into the microalgae downstream processing concerns the harvesting and the concentration of microalgae, but membrane filtration is also a promising clean separation process for the fractionation step.

In this work we focus on the recovery of lipids from *Parachlorella kessleri*, cultivated in starving conditions to enhance their lipid production. The lipid recovery from microalgae was mostly performed with supercritical CO_2 on dried matter or solvent extraction. In this study we will focus on the recovery of lipids from aqueous extracts by membrane processes. Clavijo et al. [1] demonstrated that the supernatant after bead milling and centrifugation of *Parachlorella kessleri* contains emulsified lipids in aqueous phase. The membrane separation of those valuable compounds is studied.

2. Methods

In this work a model solution was formulated, based on the analysis of ground *Parachlorella kessleri* [1].Then the performances (retention, flux, fouling, cleanability) of polyacrylonitrile (PAN), polyethersulfone (PES) and polyvinylidene fluoride (PVDF) membranes to concentrate lipids from *Parachlorella kessleri* aqueous extracts were evaluated, using the model solution. The most appropriate material and conditions (TMP) were then selected and validated on real microalgae fractions. Two modules were compared allowing the crossflow (CF) and the rotating disk (RD) filtration.

3. Results and discussion

The PAN 500kDa membrane presented the best performances (flux, lipid retention and cleanability) in crossflow and rotating disk filtrations. It was selected to test the filtration of real aqueous extracts from *Parachlorella kessleri*. The performances of the PAN membrane in CF module with the real products was similar to the one with the model solution despite the composition differences. The lipids are totally retained whereas some of the hydrophilic compounds (polysaccharides and proteins depending on the conditions) could permeate. The use of RD filtration allows reducing the membrane fouling, using a higher transmembrane pressure thus leads to higher fluxes. In the case of real aqueous extracts RD filtration, the water permeability is enhanced by the accumulation of hydrophilic compounds whereas the shear rate limits the membrane clogging by the lipids. The RD filtration using a PAN membrane presents the best performances.

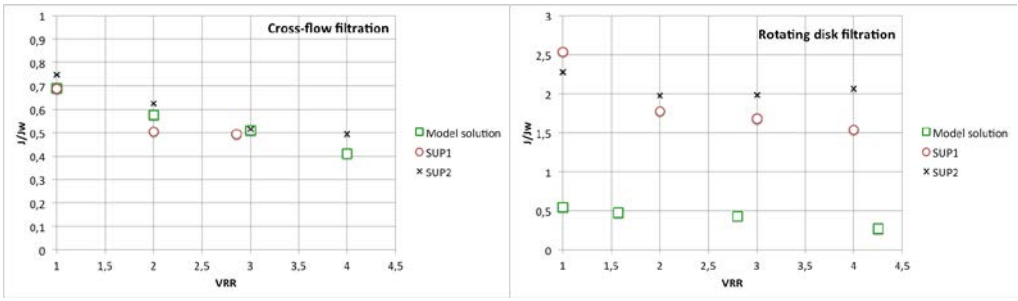

Figure 1. Crossflow and rotating-disk filtrations of an emulsion (model solution of concentrated microalgae aqueous extract) and two real aqueous extracts (SUP1 and SUP2) with a PAN membrane.

4. Conclusions

The membrane filtration is a relevant seperation process to concentrate the lipids, reduce the volume of water to treat for further purification steps and offers interesting opportunities for the fractionation of biomolecules from microalgae. An optimization of the coupling with the upstream operations (culture, cell disruption, clarification) would enhance the separation.

References

[1] E. Clavijo Rivera, V. Montalescot, M. Viau, D. Drouin, P. Bourseau, M. Frappart, C. Monteux, E. Couallier, Bioresource Technology, 256 (2018) 77 - 85

ION EXCHANGE RESINS: AN ALTERNATIVE FOR THE REMOVAL OF PHENOLIC COMPOUNDS FROM BREWER'S SPENT GRAIN

Pedro E. Plaza[1,2], Juan C. López-Linares[1,2], Susana Lucas[1,2], Gerardo González-Benito[1,2], Mónica Coca[1,2], M.Teresa García-Cubero[1,2,*]

1 Institute of Sustainable Processes. University of Valladolid, Spain
2 Department of Chemical Engineering and Environmental Technology, School of Industrial Engineering, University of Valladolid, Dr. Mergelina, s/n, Valladolid, Spain
**Corresponding author: maite@iq.uva.es*

Highlights

- Use of anionic ion exchange resin to remove phenolic compounds
- High efficiencies on the removal of both p-coumaric and ferulic acids in the pretreatment liquid and enzymatic hydrolisates
- Low sugar losses for both the pretreatment liquid and enzymatic hydrolisates

1. Introduction

The use of lignocellulosic biomass as a feedstock for biofuels production is still challenging due to the formation of toxic products in the pretreatment that are inhibitory to fermentation and hence may affect economics. The type and concentration of inhibitors formed depend on the pretreatment technologies, being aliphatic carboxylic acids (e.g. acetic, formic, levulinic acid), phenylic compounds (benzoic acid, phenolic compounds), furans (furfural and hydroxymethylfurfural) and uronic acids (galacturonic and glucuronic acid) the main by-products formed [1]. The presence of inhibitors in the hydrolysates play a vital role in ABE fermentation as they affect negatively fermentation yield and efficiency mainly due to its toxicity to microorganisms. Phenolic compounds including ferulic acid, p-coumaric acid, 4-hydroxybenzoic acid, vanillic acid, and vanillin can cause growth inhibition of *C. beijerinkii* and no butanol production. The presence of phenolic compounds inhibited ABE fermentation at concentrations as low as 0.5 g/L for gallic acid and 0.1 g/L for catechin [2].

To overcome the problem due to the presence of inhibitors, a detoxification step before fermentation is usually carried out. Removal of phenolic compounds involves techniques such as physical methods (evaporation, membrane separations, electrochemical detoxification), chemical methods (neutralization, overliming with calcium hydroxide, addition of reducing agents), liquid-solid extraction (activated carbon treatment, ion exchange resins) and biological detoxification by enzymatic catalysis mainly with the use of laccase and peroxidase [3-5]. The use of ion-exchange resins is also a promising detoxifying technology, due to the selectivity of the resins, which are able to remove practically the totality of the phenolic compounds present with very little losses of monosaccharides

Different anionic exchange resins have been tested and operating conditions were optimized with the objective of removing the inhibitors formed during the pretreatment of brewer´s spent grain before ABE fermentation step with minimum sugar losses.

2. Methods

Model solutions were prepared simulating sugar concentrations of pretreatment liquid obtained during acid diluted pretreatment of brewer´s spent grain (15% dry matter content, 121ºC, 30 min) and enzymatic hydrolysates from pretreated solid (15% solids loadings, 15 FPU/gDM Cellic CTec 2, 48h, pH 4.8). Major phenolic compounds founded in these liquids are p-cumaric acid and ferulic acid and concentrations tested were in the range 0.5-2 g/L. Four different commercial ion-exchange resins (Lewatit Monoplus MP500, Lewatit VPOC, Lewatit S4528 and Lewatit A365) have been tested, operating in batch mode, at solid/liquid ratios of 1%, 2% and 3% w/v. Temperature was maintained at 35ºC, pH of 5.0, 200 rpm and operating time was 24 h for all the experiments. The contents in sugars (glucose, xylose, and arabinose) and phenolics inhibitors were determined by HPLC [6].

3. Results and discussion

A different behavior on the sugar losses and inhibitor´s removal have been found when the pretreatment liquid was detoxified with ion exchange resins. The highest sugar losses (17-21%) were obtained when the resin Lewatit A365 (weak anion exchange resin) was employed and sugar losses increased when resin:liquid ratio increased. On the opposite, the resin Lewatit Monoplus MP500 (strong anion exchange resin) showed the lowest sugar losses (7.8-8.0%) and no influence was observed with resin:liquid ratio. Related with the removal of phenolic compounds, weak anion resins removed almost completely p-cumaric and ferulic acids even at 1% w/v resin:liquid ratio, whereas when strong resins have been tested, it is necessary to work with a 3%w/w resin:liquid ratio to attain phenolic compounds removal higher than 90.0%.

When the enzymatic hydrolysates were detoxified with anion exchange resins, phenolic compounds were completely removed due, mainly due to the lower concentrations founded in these streams. Related with monosaccharides, significantly sugar losses up to 24% have been obtained for both weak and strong resins.

4. Conclusions

Weak anionic resins allow to remove almost completely phenolic compounds from BSG hydrolysates (pretreatment liquid and enzymatic hydrolysates) with relatively high sugar losses. On the contrary, the operation with strong anionic resins lead low sugar losses and phenolic´s removal up to 90%. Further research will be focused on the column operation and optimization of the main parameters (bed volume/h, temperature, time of cycle and regeneration conditions) will be studied.

References

[1] Jönsson and Martín, 2016. Bioresource Technology 199, 103–112.
[2] Bellido et al. 2018. Food and Bioproducts Processing 108, 117-125.
[3] Jönsson et al., 2013. Biotechnology for Biofuels 2013, 6-16.
[4] Lee et al., 2015a. Process Biochemistry 50, 630-635.
[5] Lee et al., 2015b. Bioresource Technolology 187, 228-234
[6] Plaza et al., 2017. Bioresource Technology 244, 166–174

ECAB 5
The 5th EUROPEAN CONGRESS OF APPLIED BIOTECHNOLOGY
Florence 15-19 September 2019

Characterization of a natural isopropanol producer, *Clostridium beijerinckii* DSM 6423, during continuous biofilm fermentation

Maxime Carrie[1], Jean-Christophe Gabelle[1]*, Hélène Velly[2], Fadhel Ben Chabaane[2],

[1] *IFP Energie Nouvelles, Rond-point de l'échangeur de Solaize, BP3, 69360 Solaize*

[2] *IFP Energie Nouvelles, 1 et 4 avenue de Bois préau 92852 Rueil-Malmaison.*

**jean-christophe.gabelle@ifpen.fr*

Highlights

- Enzymatic deconstruction is performed to extract immobilized cells of *Clostridium beijerinckii* from their polymerous matrix.
- Viability analysis is achieved by flow cytometry
- Heterogeneous viability repartition within the biofilm is assessed by confocal microscopy.

1. Introduction

Butanol and isopropanol are commonly used chemicals in the industry as solvent. They can also be employed as fuels and are mainly produced from propylene coming from petrochemistry. To a lesser extent, an alternative bioproduction of Isopropanol and Butanol mixture using solventogenic Clostridium is also currently investigated .

However, this fermentation process is not used at an industrial scale because of low productivity and low solvent yield and titer due to butanol toxicity of classical batch or continuous processes. To overcome this issue, continuous fermentation using immobilized cells on a carrier is currently employed at a laboratory scale. This system allows the continuous removal of butanol, can be operated at high dilution rate without causing cell washout, and gives high productivity (4 $g.L^{-1}.h^{-1}$) [1].

During immobilized cell fermentation, bacteria adhere to the solid and form a structure called biofilm. This biofilm is composed of cells trapped into a gel-like matrix made from a mix of polysaccharides, proteins and extracellular DNA [2]. But the scale-up of an immobilized fermentation system is not easy as bacterial adhesion or biofilm growth and evolution are not well known [3]. This study focuses on cells viability assessment during IBE immobilized fermentation.

Firstly, confocal microscopy is used to show the cells repartition within the biofilm according to their viability. Then a sequential enzymatic lysis of the biofilm matrix coupled to flow cytometry analysis gave us information about physiological state of both sessile and planktonic cells during continuous fermentation.

2. Methods

Four screw scrap bottles, fill with the immobilization carrier, were used as reactors. The system was operated in continuous mode at an useful volume of 80mL. The analysis were performed by scarifying each reactor at different fermentation time.

After staining with a mix of carboxy fluorodesceine diacetate [cFDA] and propidium iodide [PI], the level of viability of the *Clostridium* cells were analysed by flow cytometry (Cyflow Space, Sysmex).

For confocal analysis, the carriers has been removed from the system and gently washed with deionized sterile water to remove planktonic cells attached to the biofilm. Then the carriers were put into staining solution containing propidium iodide and syto 9. After staining the carriers were plonged into PFA solution and then observed under a Zeiss LSM800 confocal laser microscope.

3. Results and discussion

Flow cytometry, showed that enzymatic deconstruction using sequentially Dnase and protease are able to extract cells from the biofilm without altering their viability. Using this method, the percentages of viable planktonic and sessile cells follow similar patterns during fermentation. However the amounts of viable sessile cells on the carriers are less important than the planktonic one. Using confocal microscopy, heterogeneity of viability is observed within the biofilm. Those observations also helped us to describe qualitatively the growth of the biofilm inside the foam during continuous fermentation.

4. Conclusions

In this study, two methods were validated in order to evaluate the physiological state of *C. beijerinckii* cells during continuous fermentation of immobilized cells. Other parameters of cell viability, such as membrane fluidity or polarization, may complement this analysis in the future. In addition, cell viability analysis using confocal microscopy highlight a high heterogeneity within the biofilm but need some improvement in order to better identified solvent producing cells in the biofilm.

References

[1] Bankar, S. B., Survase, S. A., Ojamo, H., and Granström, T., "The two stage immobilized column reactor with an integrated solvent recovery module for enhanced ABE production," *Bioresource Technology*, V. 140, 2013, pp. 269–276.

[2] Pantaléon, V., Bouttier, S., Soavelomandroso, A. P., Janoir, C., and Candela, T., "Biofilms of Clostridium species," *Anaerobe*, V. 30, 2014, pp. 193–198.

[3] Frédéric Habouzit, "Rôle des matériaux-supports sur la mise en place du biofilm : Application au démarrage d'un procédé de méthanisation," Génie des procédés, Université Montpellier II, Science des Procédés-Science des Aliments, Montpellier, 2010, 244 pp.

ECAB 5
The 5th EUROPEAN CONGRESS OF APPLIED BIOTECHNOLOGY
Florence 15-19 September 2019

Alkaline peroxide pretreated sugarcane bagasse as cell immobilization carrier for isopropanol-butanol-ethanol production

Carla Vieira[1*], Mateus Codogno[1], Francisco Maugeri-Filho[2], Rubens Maciel-Filho[1], Adriano P. Mariano[1]

1 School of Chemical Engineering - UNICAMP, Av. Albert Einstein, 500 - Campinas - SP - Brazil
2 School of Food Engineering - UNICAMP, R. Monteiro Lobato, 800 - Campinas - SP - Brazil
**Corresponding author: carlafsvieira90@gmail.com*

Highlights

- The proposed cell immobilization technique was successful in increasing IBE production.
- A more disorganized bagasse structure allowed the adhesion of a greater number of cells.
- Excessive production of biofilm exopolysaccharides affected the IBE yield.

1. Introduction

Cell immobilization techniques have been widely applied to ABE (acetone-butanol-ethanol) [1] and IBE (isopropanol-butanol-ethanol) [2 - 5] fermentation processes to increase productivity and decrease butanol inhibition to Clostridial species. The use of lignocellulosic materials as immobilization carrier can be an economically advantageous alternative due to their low cost and abundance. However, the adhesion of microorganisms cells can be difficult because of the poor permeability of lignocellulosic tissues [6]. Therefore, we evaluated whether the alkaline peroxide pretreatment can improve the efficiency of sugarcane bagasse as a cell immobilization carrier for IBE fermentation.

2. Methods

Sugarcane bagasse was provided by a mill located in São Paulo state, Brazil. The bagasse was pretreated with alkaline peroxide [0.5% (w/v) NaOH, 2% (w/v) H_2O_2, 10% (w/v) biomass loading] for 24 h at 200 rpm and room temperature in dark place [6]. IBE fermentations using *Clostridium beijerinckii* DSM 6423 were conducted in 250-mL flasks (triplicate) containing pretreated bagasse (1:20 liquid to solid ratio) and P2 medium [4] with 60 g/L initial glucose. The flasks were incubated in anaerobic chamber at 35 °C. Experimental controls consisted of fermentations without bagasse and with non-treated bagasse.

3. Results and discussion

Upon pretreatment, we observed a more disorganized morphological structure of the sugarcane bagasse (Figure 1), which allowed the adhesion of a greater number of cells (Figure 2). It had a positive impact on IBE concentration, IBE productivity, and sugar conversion (Table 1). Nevertheless, the decrease in the IBE yield can be attributed to an excessive production of biofilm exopolysaccharides, especially in the fermentation with pretreated bagasse.

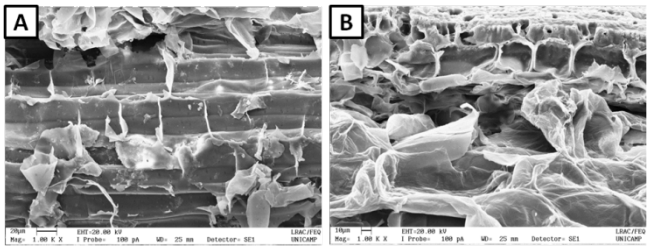

Figure 1 – Morphological structure of the sugarcane bagasse (A) before and (B) after pretreatment with alkaline peroxide.

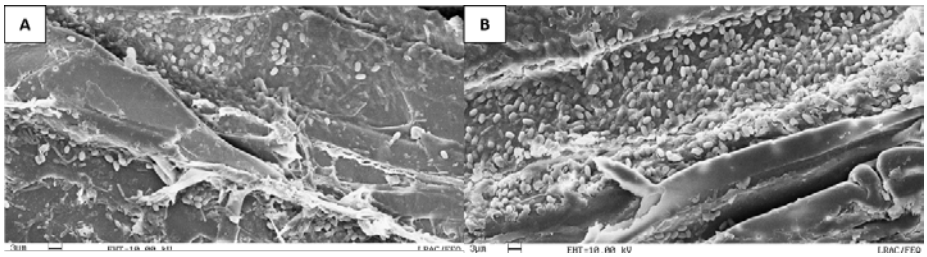

Figure 2 – *C. beijerinckii* DSM 6423 adhered to the sugarcane bagasse after the fermentation process. (A) Non- and (B) pretreated sugarcane bagasse

Table 1 – Performance of the IBE fermentation

	Without immobilization	Non-treated bagasse	Pretreated bagasse
Sugar conversion (%)	32	60	78
Final IBE concentration (g/L)	7.8	12.8	13.9
IBE productivity (g/L.h)	0.19	0.31	0.34
IBE yield (g/g)	0.40	0.34	0.29

4. Conclusions

Sugarcane bagasse as a cell carrier offered remarkable gains (78%) in IBE production. Further gains (8%) can be obtained if the bagasse is pretreated with alkaline peroxide. However, more sugar was used to produce biofilm exopolysaccharides, thereby affecting the IBE yield more intensively. Thus, future studies should focus on attenuating the production of exopolysaccharides by *C. beijerinckii* DSM 6423.

References

[1] M. Kumar, K. Gayen. Appl Energy. 88 (2011) 1999–2012.
[2] S.A. Survase, E. Sklavounos, G. Jurgens, A. Van Heiningen, T. Granstrom. Appl Microbiol Biotechnol 91 (2011) 1305–1313.
[3] S. A. Survase, A. Van Heiningen, T. Grantro. J Ind Microbiol Biotech. 40 (2013) 209–15.
[4] Y. Yang, A. Hoogewind, Y.H. Moon, MOON, D. Day. Bioproc Biosyst Eng. 39 (2013) 421-428.
[5] S. Zhang, C. Qu, X. Huang, Y. Suo, Z. Liao. J. Ind Microbiol Biotechnol. 43 (2016) 915–25.
[6] D. Cai, C. Cheng, Y. Wang, S. Hu, C. Cui, P. Qin, T. Tan. Biores Technol. 220 (2016) 68-75.

ECAB 5
The 5th EUROPEAN CONGRESS OF APPLIED BIOTECHNOLOGY
Florence 15-19 September 2019

Assessing the fate of nitrogen in a novel food waste anaerobic digestion process: Production of digestate with reduced ammonia content.

Panagiota Photiou[1,2], Michalis Kallis[1], Ioannis Vyrides[1], Gloria Fabbri[3], Michele Negre[3], Walter Boero[3], Michalis Koutinas[1,*], Enzo Montoneri[3]

1 Department of Environmental Science & Technology, Cyprus University of Technology, 30 Archbishop Kyprianou Str., 3036, Limassol, Cyprus; 2 Sewerage Board of Limassol – Amathus (SBLA), 76 Franklin Rousvelt, Building A, P.O. Box 50622, 3608 Limassol, Cyprus; 3 Università di Torino, DISAFA, Via Leonardo da Vinci 44, 10095 Grugliasco, Torino, Italy

**Corresponding author: michail.koutinas@cut.ac.cy*

Highlights

- Conversion of food waste to biogas and eco-friendly digestate
- SBO addition enhanced biomethane production reducing the content of NH_3
- Effects of temperature and assessment of nitrogen's fate in the process

1. Introduction

Food waste (FW) is a valuable feedstock utilized as a renewable substrate for obtaining a wide variety of bio-based products [1]. However, the conversion of FW into biogas requires secondary treatment, since the process produces high contents of NH_3 in the digestate, constituting a common inhibitor in bio-waste anaerobic digestion (AD) systems. Excess NH_3 can be reduced through the use of SBO isolated from compost of gardening residues [2]. Many studies have shown promising applications of SBO as chemical auxiliary in the chemical industry and in agriculture. Some existing examples in the relevant literature comprise the use of SBO for textile dyeing [3], detergents manufacturing [3] and hydrocarbons contaminated soil washing [4].

The present study has been carried out within the LIFECAB project funded under the 2016 LIFE program. It aims to evaluate at pilot-scale a novel FW fermentation technology that involves four-steps, including: 1) use of FW as feedstock in two pilot anaerobic digesters, 2) co-composting of the digestate produced with green waste, 3) chemical hydrolysis of the compost generated to produce SBO, and 4) implementation of SBO in AD for enhanced biogas formation and production of digestate with reduced NH_3. The technology will be tested in 3 EU countries (Italy, Greece and Cyprus) through the production of eco-friendly cost-effective biogas and agricultural products. The study will assess the fate of NH_3 removed with the use of SBO in lab-scale experiments and to present preliminary data obtained from the pilot system.

2. Methods

Composting: Green waste was used for composting comprising grass clippings, dry leaves, wood sawdust, tree prunings and soil. The analytical methods applied included monitoring of the organic carbon content, pH, TS, VSS, ash, temperature, phytotoxicity, conductivity and moisture content, water holding capacity, phosphorus content and heavy metals.

AD experiments: Lab-scale experiments were conducted for FW fermentation to produce biogas and digestate with low NH_3 content. SBO was provided from Acea Pinerolese Industriale (Pinerolo, Italy). Four treatments were tested: A) Anaerobic sludge (AS) as control, B) AS with SBO, C) AS with FW, and D) AS with FW and SBO. The amount of SBO used in each treatment was 0.2% (w/w) and the temperatures applied were 30 °C and 55 °C. Gas samples were analysed for CH_4, CO_2, H_2, N_2, O_2 and N_2O using Gas Chromatography. Furthermore, the samples were passed through sorbent tubes (DRAGER tubes) for the determination of NO, NO_2 and NH_3.

3. Results and discussion

Lab-scale experiments were conducted under anaerobic conditions for evaluation of nitrogen's fate in the novel SBO-based process. Four treatments were tested as described above and the gas samples collected were analysed for CH_4, CO_2, H_2, N_2, O_2, N_2O, NO, NO_2 and NH_3. The data obtained from these experiments (Figure 1) demonstrated higher production of biogas and CH_4 in SBO assisted fermentations. Moreover, the GC analysis performed showed a small production of N_2O at the initial stages of experiments and small concentrations of N_2 at the final stages of experiments fed with FW. However, no detection of NO, NO_2 and NH_3 was observed in the gas phase, excluding the formation of the specific molecules due to the addition of SBO. Results from preliminary composting trials in three different countries will be also presented.

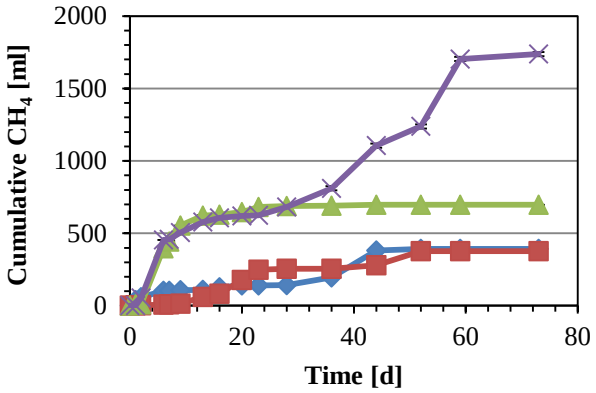

Figure 1. Cumulative volume analysis of CH_4 during lab-scale experiments. Coloured symbols correspond to: (I) control (blue), (II) AS and SBO (red), (III) AS and FW (green), and (IV) AS, FW and SBO (purple).

4. Conclusions

Based on the findings obtained, the fermentation of FW coupled to SBO is capable of significantly reducing the ammonia content of the digestate, producing elevated quantities of methane. Thus, the proposed technology improves both energy efficiency and the environmental footprint of AD.

References

[1] E.U. Kiran, A.P. Trzcinski, W. J. Ng, Y. Liu, Fuel. 134 (2014) 389–399.
[2] E. Montoneri, V. Boffa, P. Savarino, D. Perrone, M. Ghezzo, C. Montoneri, R. Mendichi, Waste. Manage. 31 (2011) 10–17.
[3] P. Savarino, E. Montoneri, S. Bottigliengo, V. Boffa, T. Guizzetti, D.G. Perrone, R. Mendichi, Ind. Eng. Chem. Res. 48 (2009) 3738–3748.
[4] E. Montoneri, V. Boffa, P. Savarino, F. Tambone, F. Adani, L. Micheletti, C. Gianotti, R. Chiono, Waste. Manage. 29 (2009) 383–389.

ECCE 12
ECAB 5

ECAB 5
The 5th EUROPEAN CONGRESS OF APPLIED BIOTECHNOLOGY
Florence 15-19 September 2019

A novel microfluidic device to investigate tumor cell extravasation

Claudia Kühlbach[1, 2], Margareta M. Mueller[1], Frank Baganz[2], and Volker C. Hass[1, 2]*,

1 Furtwangen University, Villingen-Schwenningen, D-78054, Germany; 2 University College London, London, WC1E 6BT,UK

**Corresponding author: volker.hass@hs-furtwangen.de*

Highlights

- Novel microfluidic device for cell extravasation
- Total confluency of functional area for transmigration
- Proof of tumor cell adhesion and transendothelial migration

1. Introduction

The process of metastasis of tumor cells is highly complex and includes the steps of intravasation, tumor cell distribution by blood stream and extravasation into surrounding tissues [1]. The molecular conditions and the mechanism for extravasation are still not fully understood.

To investigate the metastatic cascade, two different microfluidic approaches are frequently pursued. The hydrogel based systems, where the endothelial cells (EC) are embedded in hydrogel take advantage of the capability of the EC to self-assemble into a tubule-like vascular network, however it cannot be subjected to flow [2]. The second approach uses EC in monolayer, cultivated in matrix protein coated microfluidic channels. These devices are often hard to control for EC confluency [3].

Here we introduce a novel microfluidic device to study tumor cell extravasation and proof its functionality, under well-established confluency control as well as the extravasation process under dynamic flow conditions.

2. Methods

Methods used include culturing and seeding of the EC, the introduction of the tumor cells and immune fluorescence staining and are described in detail in Kühlbach et al., 2018 [4].

3. Results and discussion

The microfluidic device consists of three different parts. The upper channel, together with the porous membrane, represents the vessel equivalent (Figure 1A).

The upper channel and the membrane were seeded separately with EC in monolayer. This better represents the in vivo situation, in contrast to devices which work with multilayer EC, embedded in hydrogel [2]. The lower channel acts as reservoir to collect transmigrated tumor cells. In this novel device, the EC monolayer was checked for 100% confluency, before any assembly, as a confluent EC monolayer is essential to assure a tight barrier function. The EC monolayer integrity was verified, showing a regular expression and integration of VE-Cadherin into the EC cell membrane, as described for the in vivo situation in blood capillaries [5].

Additional coating of the microfluidic unit was abandoned, as the used EC secrete collagen IV and therefore establish their own basement membrane, as described before for EC cultures [6].

When adding different flow conditions to the device, the EC changed phenotype and oriented into flow direction, similar as previously described for the in vivo situation [7].
The introduced tumor cells successfully adhere to the endothelial lining under different flow conditions. The number of adherent tumor cells was not influenced when continuous flow was applied. In contrast, when pulsating flow was adopted, the number of adherent tumor cells decreased with increase of flow velocity (Figure 1B).
The successful transendothelial migration of tumor cells under static conditions could be shown.

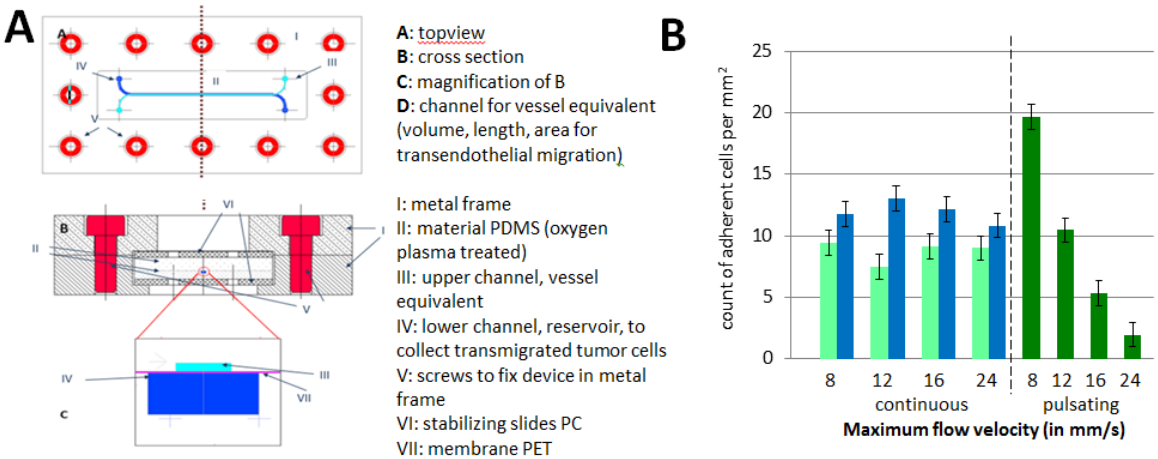

Figure 1: A: Technical drawing and measurements of the novel microfluidic device. Channel sizes: Vessel equivalent: 500 µm x 100 µm x 6.1 cm; Reservoir: 1mm x 500 µm x 6.1 cm; Membrane properties: Pore size 5 µm, pore density $6x10^4$ cm^{-2}, thickness 15 µm. **B:** Count of different tumor cells adherent to the endothelial monolayer within the vessel equivalent [4].

4. Conclusions

With our work, we introduce a novel microfluidic device overcoming problems found with other devices described in the literature. The successful functionality tests indicate that the device can be used for the in vitro research on cell extravasation. By adding adhesion inhibitors or homing factors to the system, the impact of these chemokines onto the adhesion rate and transendothelial migration could be evaluated.

References

[1] S. Ramaswamy, K.N. Ross, E.S. Lander, T.R. Golub, Nat. Genet. 33 (2002) 49–54.
[2] H. Lee, M. Chung, N.L. Jeon, MRS Bull. 39 (2014) 51–59.
[3] X. Cui, W. Guo, Y. Sun, B. Sun, S. Hu, D. Sun, R.H.W. Lam, Biomicrofluidics 11 (2017) 014105.
[4] C. Kühlbach, S. da Luz, F. Baganz, V.C. Hass, M.M. Mueller, Bioengineering 5 (2018) 40.
[5] E. Dejana, Nat. Rev. Mol. Cell Biol. 5 (2004) 261–270.
[6] R.H. Kramer, K.G. Bensch, P.M. Davison, M.A. Karasek, J. Cell Biol. 99 (1984) 692–698.
[7] M.J. Levesque, R.M. Nerem, J. Biomech. Eng. 107 (1985) 341–347.

ECAB 5
The 5th EUROPEAN CONGRESS OF APPLIED BIOTECHNOLOGY
Florence 15-19 September 2019

Production of poly-3-hidroxybutyrate with ultra-high molecular weight by mutant strains of *Azotobacter vinelandii* under microaerophilic conditions.

Elsa Gómez[1], Daniel Segura[2], Alfredo Martínez[1], Carlos Peña[1]

[1] *Departamento de Ingeniería Celular y Biocatálisis,* [2] *Departamento de Microbiología Molecular, Instituto de Biotecnología, Universidad Nacional Autónoma de México, Cuernavaca, Mor. 62210, México.*

**Corresponding author: carlosf@ibt.unam.mx*

Highlights

- The MW of P3HB obtained under oxygen limitation was as high as 25,000 kDa.
- MW of P3HB increased by decreasing the OTR_{max} of the culture.
- *A. vinelandii phbZ*$^-$ strain accumulated up to 93 % of intracellular P3HB.

1. Introduction

Poly-3-hydroxybutyrate (P3HB) is a biopolymer of the polyhydroxyalkanoate family; this bioplastic is produced in the form of intracellular inclusions as a carbon and energy reserve by the bacterium *Azotobacter vinelandii* [1]. P3HB has characteristics similar to those of plastics derived from the petrochemical industry [2]. Its use has been focused on the biomedicine field, because it is also a totally biodegradable and biocompatible polymer [3].

The thermomechanical properties and biodegradability of P3HB are determined by the molecular weight (MW) of the polymer [4]. It has been reported that the synthesis of the polymer is favored when *A. vinelandii* is cultured under oxygen limitation. In recent studies it has been found that, at low percentages of oxygen saturation (1 % DOT), high molecular weight polymers (between 3,500 and 5,500 kDa) are produced [5].

In this study, two mutant strains of *A. vinelandii*, with the ability to produce high molecular weight P3HB were cultured under microaerophilic conditions in bioreactor by using low agitation rates.

2. Methods

Strains of *A. vinelandii* (OP and *phbZ*$^-$) were grown in PY medium, which contains sucrose (20 g L^{-1}), yeast extract (3 g L^{-1}) and peptone (5 g L^{-1}). Batch cultures were carried out in a bioreactor using the OP strain as well as the *phbZ*$^-$ strain with a work volume of 2 L in Applikon 3 L bioreactors. Two agitation conditions were used (300 and 500 rpm) with a 1 vvm aeration, controlling pH to 7.2 and without control of the dissolved oxygen tension.

Recovery of P3HB was performed as described previously [5]. The molecular mass analysis was performed by gel permeation chromatography (GPC) using a Shodex K-800 column in an HPLC system (Waters 2695, USA) coupled with a refractive index detector (Waters 2414, USA). The mobile phase was chloroform at 30°C at a flow rate of 0.7 mL min^{-1}. A calibration curve was constructed with polystyrene standards as described in [5]. Samples were dissolved in chloroform at a concentration of 2-3 mg mL^{-1} and were filtered through a 0.45 µm membranes before being injected into the HPLC.

3. Results and discussion

Results of mean molecular weight (MMW) of P3HB obtained from the cultures performed at 300 and 500 rpm are presented in Figure 1. The MMW of P3HB increased significantly in the cultures carried out at OTR_{max} of 5 mmol L^{-1} h^{-1} (22-25,000 kDa) with both strains, with respect to the MMW reached in the cultures developed at 8 and 11 mmol L^{-1} h^{-1} obtaining a P3HB between 15,000-16,000 kDa (Figure 1).

The initial accumulation of P3HB in the cells was around 50 % with both strains, as the culture evolved, the accumulation of P3HB increased , reaching up to 93 % with respect to dry cell biomass for *phbZ*$^-$ strain and 89 % for the OP strain cultured at high OTR_{max} (8 and 11 mmol L^{-1} h^{-1}).

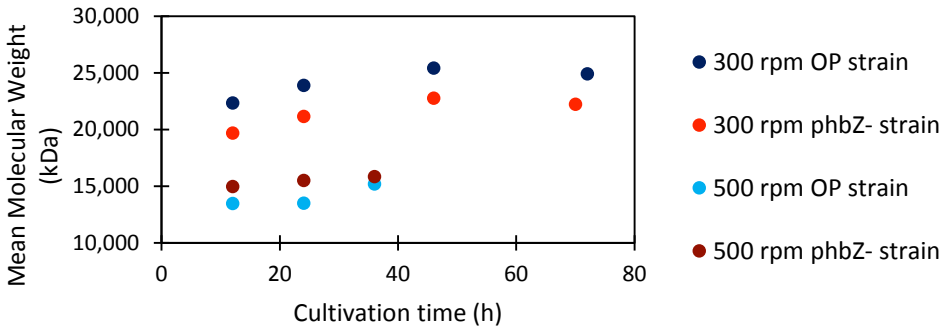

Figure 1. Mean molecular weight of P3HB produced by OP and *phbZ*$^-$ strain at 500 rpm (OTR_{max} of 8- 11 mmol L^{-1} h^{-1}) and 300 rpm (OTR_{max} of 5 mmol L^{-1} h^{-1}).

4. Conclusions

- Microaerophilic conditions promote the production of P3HB with ultra-high molecular weight in bioreactor cultures using *A. vinelandii* strains OP and *phbZ*$^-$.
- There is an inverse relationship between P3HB accumulation and the molecular weight of the polymer, finding that at high OTR_{max} both strains accumulate a high percentage of P3HB (90 %), but with a lower molecular weight (15,000 kDa) than that obtained at low OTR_{max}, where the accumulation was lower, 50 and 70 % respectively with the OP and *phbZ*$^-$ strain; however, the molecular weight reached up to 25,000 kDa with the OP strain and 22,000 kDa with the *phbZ*$^-$ strain.

References

[1] Chen, G. Q., & Wang, Y. (2013). Medical applications of biopolyesters polyhydroxyalkanoates. *Chinese Journal of Polymer Science (English Edition)*, *31*(5), 719–736.

[2] Domínguez-Díaz, M., Meneses-Acosta, A., Romo-Uribe, A., Peña, C., Segura, D., & Espin, G. (2015). Thermo-mechanical properties, microstructure and biocompatibility in poly-b-hydroxybutyrates (PHB) produced by OP and OPN strains *of Azotobacter vinelandii. European Polymer Journal*, *63*, 101–112.

[3] Iwata, T. (2005). Strong fibers and films of microbial polyesters. *Macromolecular Bioscience*, *5*(8), 689–701.

[4] Millán, M., Salazar, M., Segura, D., Castillo, T., Díaz-Barrera, Á., & Peña, C. (2017). Molecular mass of Poly-3-hydroxybutyrate (P3HB) produced by *Azotobacter vinelandii* is influenced by the polymer content in the inoculum. *Journal of Biotechnology*, *259*, 50–55.

[5] Peña, C., Castillo, T., García, A., Millán, M., & Segura, D. (2014). Biotechnological strategies to improve production of microbial poly-(3-hydroxybutyrate): A review of recent research work. *Microbial Biotechnology*, *7*(4), 278–293.

Control-release of polyphenol from biodegradable sericin / chitosan/ glucomannan films

Chutimon Satirapipathkul, Nutyatip Suksawasd
Chemical Engineering Research Unit for Value Adding of Bioresource, Department of Chemical Engineering,Faculty of Engineering, Chulalongkorn University,Phyathai Road, Phatumwan, Bangkok 10330, Thailand

Ab s t r a c t

Biopolymers including chitosan, silk proteins and glucomannan have been the focal point of many research studies reporting their potential use in new biodegradable films. These films exhibit hydrophobic characteristics with controlling water and gas diffusion. They can be used to control and improve bioactive compound releases. In the present study, silk protein /chitosan/ glucomannan films were obtained by solution casting of blends of Silk protein extract (SE) from cocoons of the tropical silkworm *Antheraea mylitta* , glucomannan (GM) and chitosan (CS). Films from a SE/GM/CH blend were characterized by FTIR and SEM. The sorption properties and tensile mechanical of the films were evaluated. The films were also examined to determine the release properties of the polyphenol.

Keyword : silk protein, glucomannan, chitosan, polyphenol

Morphology Analysis of Wild-type *Saccharomyces Cerevisiae* by Using Flow Particle Image Analyzer

Kento Hyodo, Yuto Harada, Tomoyuki Nakagawa, Teppei Imaizumi, Methavee Peanparkdee and Satoshi Iwamoto*

Faculty of Applied Biological Sciences Gifu University
1-1,Yanagido,Gifu 501-1193, Japan

**Corresponding author: isatoshi@gifu-u.ac.jp*

Highlights

- The particle size and circularity of wild-type *Saccharomyces cerevisiae* were calculated.
- *Saccharomyces cerevisiae* could be classified as budding and non-budding by the images.
- The ratio of budding yeast caluculated from the imagies would be a benchmark in culture.

1. Introduction

Fermatation processes in food industries are one of the most important key steps to determine the quality of the food. It has been reqired to set an good parameter to moniter the fermatation processes. The growth of *Saccharomyces cerevisiae*, widely used for fermentation, which affects their shapes and sizes, depends on various conditions such as incubation time, oxygen concentration, pH, and temperature. This study aimed to evaluate the optimum growth conditions of wild-type Saccharomyces cerevisiae by using simple, easy, and rapid technique, namely Flow Particle Image Analyzer (FPIA-3000) which could provide the image of individual particle of wild-yeast in short time. In this study, the effect of incubation time, oxygen concentration and ethanol concentration in culture on the growth pattern of yeast was focused and evaluated by FPIA-3000.

2. Methods

Saccharomyces cerevisiae strain BY 4741 was grown in YPD medium (2% high polypeptone, 1% yeast extract and 2% glucose). In order to evaluate the effect of oxygen concentration on molphology of microorganisms, the wild type yeast was grown in YPD medium and incubated

under 2 different conditions described below.

Condition 1: static culture in a closed vessel with an AnaeroPack (anaerobic).

Condition2: shaking culture in an Erlenmeyer Flasks with baffles(aerobic).

After incubation, a 5.0 ml of sample was applied to FPIA to obtain image parameters of the samples. Gas chromatography was used to determined the ethanol concentration of the sample in culture (aerobic condition).

3. Results and discussion

The total number, particle size and circularity of BY 4741 in culture could be calculated from the obtained images(Figure 1). From these results, BY 4741 grew under anaerobic and aerobic condition at different incubation time showed different total number, particle size and circularity. BY 4741 under aerobic condition had a higher total population than that grown under anaerobic condition. BY 4741 could be classified as budding and non-budding by the degree of circularity calucylated from image data. The budding yeast had a low degree of circularity (< 0.95), whereas the non-budding yeast exhibited a high degree of circularity (> 0.95). The ratio of budding yeast under both conditions increased with increasing incubation time. However, BY 4741 grown under anaerobic condition showed a slower rate of budding than that grown under anaerobic condition. Concentration of ethanol was increasing rapidly just after the total number increasing in the aerobic conditions. The FPIA-3000 is an appropriate technique which can also be applied to monitor the growth pattern of wild-yeast under various growth conditions.

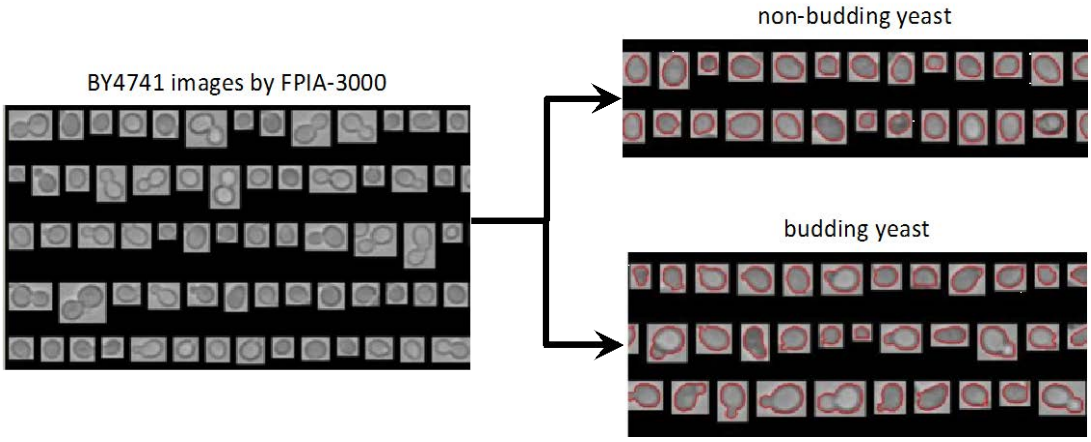

Figure 1. Morphology analysis of *Saccharomyces cerevisiae* strain BY 4741.

4. Conclusions

The particle size and circularity of *Saccharomyces cerevisiae* were calculated. *Saccharomyces cerevisiae* could be classified as budding and non-budding by the images analysis. The ratio of budding yeast caluculated from the imagies would be a benchmark in culture.

References

[1] T. Komabayashi, L. Spångberg, J. Endodontics. 34 (2008) 94-98.

Addition of Sericin, cell-activating factor, together with Carbon Sources into Mammalian Cell Culture for Improving its Biologics Productivity.

Kohei Kurebayashi[1], Ryouma Hirobe[1], Hiroka Maeda[1], Satoshi Terada[1*]

Jun Takahashi [2] and Masahiro Sasaki [2]

1 Department of Applied Chemistry and Biotechnology, Graduate School of Engineering, University of Fukui, 3-9-1, Bunkyo, Fukui, 910-8507, Japan

2 R&D Center, SEIREN Co. Ltd.; 2-3-1 Techno Port, Mikuni-cho, Sakai, 913-0038, Japan

**Corresponding author: terada@u-fukui.ac.jp*

Highlights

- Sericin induces the proliferation of the cells under glucose-limitation condition.
- Sericin improves cell survival under glucose-limitation condition.
- Glucose-limitation increases monoclonal antibody productivity.
- Sericin further increases antibody productivity of the cells under glucose-limitation.

1. Introduction

In recent years, biologics production is increasing. Among the biologics, protein pharmaceuticals such as erythropoietin and antibodies are produced by mammalian cell culture. For the productions, expensive equipment and media are required and so the cost is too expensive.

In this study, we focused on cellular glucose metabolism for reducing the cost of culture medium. Although carbon sources including glucose are pivotal in the cell culture, large part of carbon sources in the medium is not efficiently consumed by the cells. Most of culture media contain abundant amount of glucose and so the cells tend to consume glucose and to produce lactate. But soon glucose concentration decreases and the cells cannot get glucose adequately. Thus, at the first stage of the culture, medium contains excessive amount of glucose that induces cells consume glucose uselessly, and it results in wasteful consumption of glucose and inefficient cell culture.

In this study, to avoid consuming nutrition wastfully, medium was diluted with PBS and at day 2 or day3, condensed medium was added. Or the culture was started with lowered glucose concentration, and then fed with glucose. Further, in order to prevent the starved cells from death and to activate the cells, sericin hydrolysate obtained from silk was added into the diluted or glucose-limiting culture. Sericin hydrolysate is potent culture supplement.

2. Methods

Murine hybridoma cells producing anti-TNP monoclonal antibody were used. Commercially available serum-free medium ASF 104 (Ajinomoto, Japan) was used for dilution culture using by phosphate buffered saline (PBS). For glucose limitation culture, we used RPMI1640 medium (Wako,

Japan). RPMI medium can be purchased with and without glucose, and so we easily prepared medium containing glucose at different concentration.

Silk protein sericin hydrolysate (Wako) and pyruvate was also added to the culture. Proliferation and antibody production of the cells were measured and the culture conditions were evaluated to find optimal condition.

3. Results and discussion

Dilution of ASF104 medium by half largely decreased the maximum cell density, but antibody production was slightly decreased. Antibody concentrations were similar, indicating that the yield of antibody production per medium powder weight was doubled (Figure 1). In addition, sericin improved the viability of the starved cells.

Limitation of glucose in RPMI1640 medium affected both cell proliferation and antibody production. On the other hand, addition of sericin hydrolysate improved glucose-limitation culture. In the presence of sericin hydrolysate, glucose concentration did not affect the cell proliferation (Figure 2).

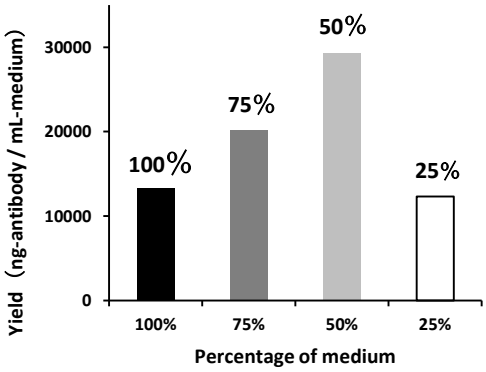

Figure 1. Antibody productivity.

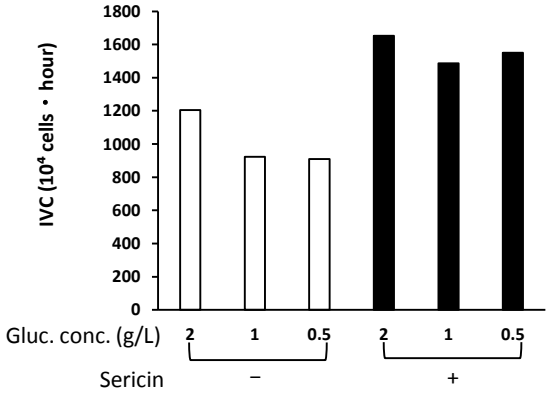

Figure 2. IVC between day 0 - 4.

4. Conclusions

Glucose- or nutrients- limitation culture are useful in cell culture. But the limitation often induce cell death and so decrease the productivity. Addition of sericin hydrolysate activates the starved cells. In this way, culture supplements such as sericin are potent tools for mammalian cell culture.

Synthesis of Cephalexin in Aqueous Two-Phase System.

Lucie Vobecka[1], Linda Ticha[1], Zdenek Slouka[1], Michal Pribyl[1]

1 University of Chemistry and Technology Prague, Technicka 3, 166 28 Prague, Czech Republic

**Corresponding author: lucie.vobecka@vscht.cz*

Highlights

- Optimization of aqueous two-phase systems (ATPS) for the production of cephalexin.
- Optimal conditions for reaction kinetics (temperature, enzyme quantity)
- Extraction of cephalexin and recycling of enzyme on microscale.

1. Introduction

We focus on the possibility of efficient production of cephalexin in microfluidic devices by the enzyme penicillin acylase (E). The following simplified reaction scheme shows the mechanism of the cephalexin (CEX) synthesis:

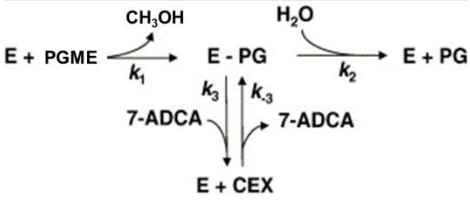

Hydrolysis of substrate phenyl glycine methyl ester (PGME) together with consumption of product by the enzyme take place. To optimize the productivity, it is necessary to separate either the products or the enzyme from the reaction mixture to enable the enzyme recovery and prevent product disintegration. One of the possible solutions is based on the use of aqueous two-phase systems (ATPS), which are widely used in separation and purification applications. Because of high water content in both the immiscible phases, ATPS provide mild environment for proteins or even living cells in downstream processing [1].

Microreactor technologies bring important benefits if compared to classical bioreactor systems such as the reduction of transport resistances, precise control of hydrodynamic conditions, the possibility of integration of several unit operations into one device etc.

2. Methods

The first aim of these studies is to find ATPS with optimal separation efficiency, i.e. ATPS that exhibits a high difference in the partition coefficients of the enzyme and the reaction products [2]. Several ATPS based on polyethylene glycol (PEG)/phosphate are tested. The next aim is to find optimal conditions for reaction kinetics with optimal cephalexin yield, the period with maximal product yield, duration of reaction. The experiments are performed at several temperatures and

with different enzyme concentrations. Further, the extraction of cephalexin and enzyme recovery is studied. The reaction is carried out in the ATPS, then the immiscible phases are separated and the phase with enzyme content is mixed with fresh phase containing reaction substrates. Analysis of substrate and product concentrations are carried out by HPLC analysis using Agilent 1260 Infinity Series device equipped with UV-VIS detector and Waters C18 column (WAT066224). Finally, the whole system is transferred into the microfluidic environment and the process is carried out in a continuous manner with the enzyme recycle.

3. Results and discussion

We found that ATPS consisting of 15 wt % of PEG 4000, 12 wt % of phosphates, 73 wt % of water (pH = 7.0 after dissolution) provides optimal separation of cephalexin which prefers the top PEG phase unlike the free enzyme accumulated in the bottom salty phase [2].

Experiments with reaction kinetics show that higher quantity of enzyme leads to significant increase in the reaction speed but unfortunately decreases stability of synthesized cephalexin. In the same manner, higher temperature increases reaction speed, however, it decreases cephalexin stability. At the end, we found conditions with optimal reaction speed and cephalexin stability.

Figure 1 shows the cephalexin concentration synthesized and extracted to the top phase in each step of enzyme recovery. It is seen that synthesized amount of cephalexin slightly decreases in each step of enzyme recycling, but the enzyme seems to have almost the same activity also after recovery.

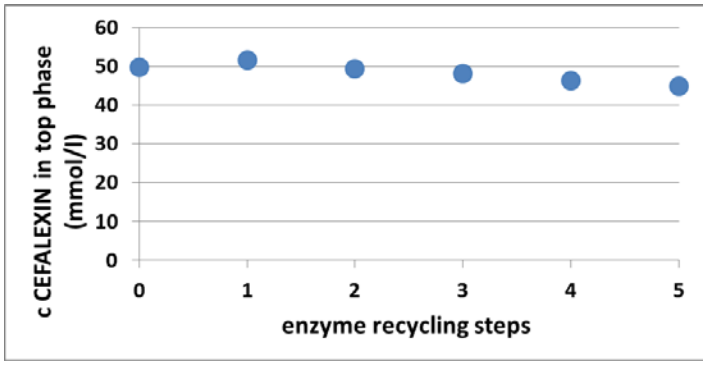

Figure 1. Concentration of Cephalexin in the top phase in the dependence on the number of cycles of the enzyme use.

4. Conclusions

We optimized conditions under which cefalexin is separated from the reaction mixture with the use of aqueous two-phase system. We experimentally determined the composition of the ATPS and also the reaction conditions at which we reach highest cefalexin yield along with reasonable time duration. We further showed that enzyme retains it stability and can be recycled n the given process. This process was adopted to the microfluidic format which allows integration of several processes and very good control of the experimental conditions.

References

[1] S.Raja , V. R. Murty , V. Thivaharan , V. Rajasekar , V. Ramesh, Science and Technology,1,2011, 7-16
[2] L. Vobecká, A. Romanov, Z. Slouka, P. Hasal, M. Pŷbyl, New Biotechnology. 47 (2018) 73-79.

ECCE12
The 12th EUROPEAN CONGRESS OF CHEMICAL ENGINEERING
Florence 15-19 September 2019

Kinetic studies of anaerobic digestion of chicken manure with sawdust and wheat straw after fungal pre-treatmet

Andreja Goršek*, Darja Pečar

University of Maribor, Faculty of Chemistry and Chemical Engineering
Smetanova 17, SI-2000 Maribor, Slovenia

**Corresponding author: andreja.gorsek@um.si*

Highlights

- The pre-treatment was conducted with two white-rot wood decay fungi.
- Anaerobic fermentations of chicken manure with co-substrates were conducted.
- First-order and modified Gompertz kinetic models were employed.
- Kinetic parameters of the fermentation were determined.

1. Introduction

Bioenergy is an alternative, cheap and sustainable source of energy compared to non-renewable energy sources such as fossil fuels [1]. Anaerobic fermentation is one of the most promising renewable energy production processes. However, the feasibility of anaerobic fermentation depends on substrate characteristics, operating conditions and fermenter design.

With increases in poultry breeding, huge amounts of manure are produced. Anaerobic fermentation is the most suitable process to deal with this material [2]. Crops and crop residues which mainly consist of lignin, cellulose and hemicellulose are used as co-substrates in these processes. Lignocellulosic biomass pre-treatment is usually necessary to reduce structural obstacles by breaking the polymer chains of lignin and making cellulose and hemicellulose more accessible for microbial attack. Pre-treatment methods are divided into physical, chemical, and biological. Biological ones are based on fungal, microbial and enzymatic pre-treatment.

Fungal pre-treatment is usually conducted using white-rot, brown-rot and soft-rot fungi. White-rot fungi produce lignolytic enzymes (laccase and peroxidases) and they are known as the most efficient in delignification processes [1].

In this study, for wheat straw pre-treatment white-rot fungi, *Pleurotus ostreatus* (WPO) and *Trametes versicolor* (WTV), were used. Three different mass ratios (80:20, 60:40, 50:50) of chicken manure with saw dust (CMS) to pre-treated (WPO, WTV) and ordinary wheat straw (OWS) were used as substrates in anaerobic fermentations. During the fermentations, the volume of produced biogas and CH_4 concentration were measured. The main goal of our study was to determine the kinetic parameters of CH_4 production during anaerobic fermentation. First-order and modified Gompertz kinetic models were fitted to the experimental data.

2. Methods

The pre-treatment was conducted with white-rot wood decay fungi. All fermentations were carried out in thermostated batch fermenters at different temperatures, ϑ = (35, 40 and 45) ºC. The single experiment was started by loading the reactor with 5 g of pre-treated substrate, 5 g of inoculum (dry mass) and 20 mL of water. Then the fermenters were purged for 2 min with argon to remove all air and to establish anaerobic conditions. The fermenters were thermostated at the desired temperature for 21 d. During the

fermentation, the volume of the biogas produced was measured. It was determined by the water displacement method. The methane concentration was calculated using a Shimadzu GC-2010 gas chromatograph coupled to a thermal conductivity detector TCD. The kinetic data obtained from separate anaerobic digestions were checked for the fitness of first-order kinetics and modified Gompertz equation.

3. Results and discussion

First-order and Gompertz kinetic models were used to simulate anaerobic fermentation of a chicken manure with sawdust with pre-treated and ordinary wheat straw at three mass ratios of used substrates. Activation energies and pre-exponential factors for CH_4 production during the anaerobic fermentation were determined from the reaction rate constants obtained from first-order kinetic model at different temperatures (Table 1).

Table 1. Activation energies and pre-exponential factors for CH_4 production during the anaerobic fermentation.

SUBSTRATE	MASS RATIO	E_a / kJ mol^{-1}	k_0 / d^{-1}
CMS:OWS	80:20	110.8 ± 19.6	$(8.2 \pm 1.5) \cdot 10^{17}$
	60:40	88.3 ± 12.5	$(1.5 \pm 0.2) \cdot 10^{14}$
	50:50	72.1 ± 15.9	$(3.2 \pm 0.7) \cdot 10^{11}$
CMS:WPO	80:20	103.8 ± 38.7	$(5.5 \pm 2.1) \cdot 10^{16}$
	60:40	88.8 ± 19.6	$(1.9 \pm 0.4) \cdot 10^{14}$
	50:50	89.6 ± 14.1	$(2.7 \pm 0.4) \cdot 10^{14}$
CMS:WTV	80:20	109.9 ± 22.9	$(6.9 \pm 1.5) \cdot 10^{17}$
	60:40	79.0 ± 11.6	$(4.7 \pm 0.7) \cdot 10^{12}$
	50:50	65.8 ± 18.7	$(2.8 \pm 0.8) \cdot 10^{10}$

We found out from the results of model accuracies, that both models properly describe the experimental data, but it is more suitable to describe CH_4 production with the first-order kinetic model, rather than with Gompertz kinetic model. The lowest R^2 value for the first-order kinetic model was 0.9780, and for the Gompertz model, 0.9713. The difference can be explained by the instant acceleration of the CH_4 concentration at the very beginning of fermentation. Thus, the profiles of CH_4 concentration are not the typical sigmoidal curves usually described by the Gompertz kinetic model. Generally, maximum CH_4 concentrations determined with Gompertz kinetic model are lower than those determined with the first-order kinetic model.

4. Conclusions

During the fermentation of chicken manure, the amount of biogas produced and the CH_4 concentrations were measured. The volume of biogas produced was slightly lower when ordinary wheat straw was used as co-substrate, compared to the pre-treated wheat straw. The kinetic parameters of CH_4 production during anaerobic fermentation were determined. A comparison between the experimental data and the data calculated by first-order kinetic model and modified Gompertz kinetic model was made. Both models describe the experimental data very well. The kinetic parameters do not significantly differ regarding the substrate; only the activation energies are slightly higher for the pre-treated wheat straw compared to ordinary straw.

References

[1] Rouches, I. Herpoël-Gimbert, J.P. Steyer, H. Carrere, Renew. Sust. Energ. Rev. 59 (2016) 179–198.
[2] C. Li, S. Strömberg, G. Liu, I.A. Nges, J. Liu, Biochemical Eng. J. 118 (2017) 1–10.

Immobilization of *Rhizopus oryzae* lipase in corn cob powder for application in dietetic triglicerydes synthesis

Vinícius Guerso Batista[1], Beatriz Marques da Silva[1], Estela Mesquita[2], Rubens Monti[3], Marcel Otavio Cerri[1], Ariela Veloso de Paula[1]

1 Departament of Bioprocess and Biotecnology, UNESP – Araraquara, Brazil
2 Departament of Organic Chemistry, UNESP – Araraquara, Brazil
3 Departament of Food and Nutrition, UNESP – Araraquara, Brazil

*Corresponding author: ariela.veloso@unesp.br

Highlights

- ID of physical adsorption immobilized derivative was 28.55%.
- ID of covalent binding immobilized derivative was 34.47%.
- Corn cob powder is a successful immobilization carrier for lipase.

1. Introduction

Lipases are glycerol ester hydrolases (EC 3.1.1.3) and are widely employed as biocatalysts in Enzymatic Biotechnology. These enzymes are commonly used for oils and fats modification in the immobilized form. When immobilized, they are easily recovered from the reaction medium. A great variety of methods are used to immobilize enzymes, of which physical adsorption and covalent binding are the most important [1]. Therefore, the objective of this work was to immobilize *Rhizopus oryzae* lipase in corn cob powder in order to apply the immobilized derivative to the synthesis of dietary triglycerides by enzymatic acidolysis of grape seed oil.

2. Methods

2.1 Immobilization of Rhizopus oryzae *lipase*

Immobilization by physical adsorption (PA) was carried out according to Costa (2015) [2]. Immobilization by covalent binding (CB) was carried out according to Bassan et al. (2016) [3].

2.2 Enzymatic acidolysis of grape seed oil

The immobilized derivatives (10% w/w) were used in acidolysis of grape seed oil with capric acid (C10:0) at molar ratio 1:3 in batch reactor (6 x 3 cm) for 24 h (45 °C, 800 rpm). The product was analysed by CG – FID. The incorporation degree (ID, %) was calculated according to equation 1:

$$ID(\%) = \left(\frac{MFA}{TFA}\right) * 100 \quad \text{(Equation 1)}$$

MFA: moles of medium fatty acids (C10:0); TFA: moles of total fatty acids.

3. Results and discussion

The results of ID (%) are presented in Table 1. The ID obtained for the immobilized derivative by PA was 28.55%. Costa et al. (2018) [4] obtained an ID of 34.8%, using a different immobilization carrier

(Eupergit) for olive oil and capric acid acidolysis. The lower ID obtained in this work can be justified by the difference in the carrier material and the substrate used.

Table 1. ID (%) of the fatty acid (C10:0) from *Rhizopus oryzae* lipase immobilized derivative

Fatty acid	Fatty acids (%)		Moles	
	PA	CB	PA	CB
C10:0	19.83	24.52	0.12	0.14
C16:0	8.03	5.68	0.03	0.02
C18:0	2.75	1.95	0.01	0.01
C18:1n9C	20.45	19.95	0.07	0.07
C18:2n6C	45.64	44.63	0.16	0.16
C18:3n3	3.31	3.28	0.01	0.01
Sum	100.00	100.00	0.40	0.41
ID (%)			**28.55**	**34.47**

For the CB immobilized biocatalyst, the ID was 34.47%. Considering that the maximum ID for 1,3 specific lipase dietary triglyceride synthesis is 66.66%, the obtained ID was satisfactory. According to Bassan et al. (2018) [5], who performed the enzymatic acidolysis of grape seed oil using a commercially immobilized lipase (Lipozyme RM IM), the ID was of 34.53%. Our results are similar to that obtained by Bassan et al., which shows the potential of the corn cob powder as a carrier for lipase immobilization.

4. Conclusions

The use of corn cob powder as a carrier for immobilization of lipases presents great potential for the application in dietary triglycerides synthesis.

5. Acknowledgements

The authors gratefully acknowledge the financial support of São Paulo Research Foundation - FAPESP (2017/11482-7; 2018/03932-5; 2018/10194-0).

References

[1] SHELDON, R. A.; PELT, S. Enzyme immobilization in biocatalysis: why, what and how. Chemical Society Reviews, v. 42, n. 15, Mar. 2013.

[2] COSTA, D. M. Sabugo de milho como suporte para imobilização de lipase. 2015.157 f. Tese (Doutorado em Engenharia de Processos) – Universidade Tiradentes, Aracajú/SE, 2015.

[3] BASSAN, C. J.; SOUZA, B. M. T.; PEIXOTO, G.; CRUZ, P. Z. C.; GALÁN, M. P, J.; VAZ, S. B .A.; GARRIDO, S.S.; FILICE, M.; MONTI, R. Immobilization of trypsin in lignocellulosic waste material to produce peptides with bioactive potencial from whey protein. Materials, v. 9, n. 5, 2016.

[4] COSTA, C. M.; OSÓRIO, N. M.; CANET, A.; RIVERA,I.; SANDOVAL, G.; VALERO,F.; FERREIRA-DIAS, S. Prodution of MLM Type Structured Lipids From Grapeseed Oil Catalyzed by Non-Commercial Lipases. European Journal of Lipd Science and Technology, v. 120, 2018.

[5] BASSAN, N. RODRIGUES, R. H.; TECELÃO, C.; MONTI,R.; FERREIRA-DIAS, S.; PAULA, A. V. Enzymatic modification of grape (Vitis vinifera L.) seed oil aimig to obtain dietary triacylglycerols in a batch reactor. LWT - Food Science and Technology, 2018.

Microalgal Triglycerides recovery during Day/Night Cycles: Physiological influence over Downstream

Vladimir Heredia*[1], Marchal Luc[1], Cueff Marie[1], Hervé Laura[1], Gonçalves Olivier[1], Pruvost Jeremy[1]

1 GEPEA-CNRS / 37 Bd de l'Université, 44600, Saint-Nazaire, France;
2 ALGOSOLIS / Chemin des Infirmieres, 44602, Saint-Nazaire, France

**Corresponding author: arturo-vladimir.heredia-marquez@univ-nantes.fr*

Highlights

- Cell destruction is affected by day/night cycles and so TAG availability for downstream
- TAG recovery by wet-extraction was optimized with a Box-Behnken experimental design
- Optimal large scale TAG production relies on a key harvesting time during Day/Night cycles

1. Introduction

Coupling microalgae cultures at photobioreactor with cell destruction and wet-extraction has shown to be energy-efficient for recovering lipids[1]. Also, Nannochloropsis gaditana is capable to produce up to 38% triacylglycerol (TAG) during nitrogen depletion[2]. However, most of these cultures have been done only under continuous light, which means the cells have a constant energy supply for lipid synthesis. Large scale production brings to scene the challenges of maintaining high TAG yields in real day/night cycles (D/N). Notably, not all the produced lipids can be extracted mainly because of losses in downstream.

2. Methods

This approach involves four stages of analysis: I) Tracing the physiological changes and cell destruction during the culture at Subitec Flat panel 200L photobiorectors (One reactor -S2- was filled with ASW+CONWAY(3N3P) medium as a control; the second one –S1- was depleted in nitrogen source to trigger lipid accumulation), II) Bead-milling pre-optimization, III) A Box-Behnken DoE for wet-extraction optimization using a Rousselet centrifugal extractor and IV) Direct Impact of physiological changes on the final TAG recovery. The downstream process optimization has considered bead-milling duration, biomass concentration and solvent consumption.

3. Results and discussion

For a D/N of 15h/9h, it was shown that cell destruction at the end of the night is the most efficient (Figure 1). On the other hand it seems that TAG accumulation reaches its maximal level at the end of the day. Such a result may suggest an optimal harvesting time affecting the entire process which will be discussed. For cells coming from S2 (full media) it was only needed 2 or three destruction

cycles for achieving ~80% destruction while for cells coming from depleted media, it was required 4 cycles. This reveals the influence of "stress by nutrients" over lipid availability.

The Box-Behnken experimental design, also reveals the optimal conditions to get the maximal efficiency for TAG recovery.

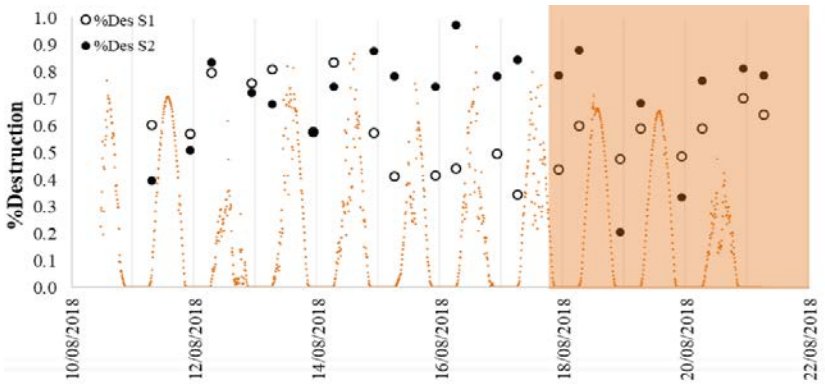

Figure 1. Destruction rate comparison for *Nannochloropsis gaditana* during day/night cycles at two different growth conditions.

4. Conclusions

At the present day, no work had considered the direct effect of the D/N over the final TAG recovery. In the present work, a global approach is proposed to elucidate how D/N affects the cell destruction during nitrogen starvation coupled with the subsequent wet-extraction. Further studies will aim at proposing an optimal coupling between the production and downstream processing stage. This will take into account the dynamic of lipid production/consumption during D/N and changes in cell destruction during nitrogen starvation.

References

[1] Ghasemi Naghdi F, González González LM, Chan W, Schenk PM. Progress on lipid extraction from wet algal biomass for biodiesel production. Microb Biotechnol. 2016;9(6):718-726. doi:10.1111/1751-7915.12360.

[2] Simionato D, Block MA, La Rocca N, et al. The response of Nannochloropsis gaditana to nitrogen starvation includes de novo biosynthesis of triacylglycerols, a decrease of chloroplast galactolipids, and reorganization of the photosynthetic apparatus. Eukaryot Cell. 2013;12(5):665-676. doi:10.1128/EC.00363-12

Enhanced natural attenuation by stimulation of anaerobic microflora in a previously aerobic groundwater

Giovanna Carpani[1], Ilaria Pietrini[1], Luca Serbolisca[1], Camilla Lanari[2], Lucia Poppa[2], Luciano Zaninetta[2]

1 Eni S.p.A., Environmental Technologies (TEAMB); 2 Syndial S.p.A., Research & Technology Innovation

**Corresponding author: giovanna.carpani@eni.com*

Highlights

- Treatment of groundwater contaminated by a mix of chlorinated hydrocarbons
- Isolation of biodegrading aerobic strains
- Trial of treatment of the remaining pollutants under anaerobic conditions
- Monitoring of the treatment

1. Introduction

Halogenated solvent-contaminated sites are a worldwide problem in industrialized countries. Chlorinated ethenes are among the most diffused pollutants in groundwaters; they are prevalently degraded by reductive dechlorination reactions, which take place under anaerobic conditions. In some cases, groundwater conditions does not support anaerobic respiration processes, because of redox conditions and due to the presence of not negligible oxygen concentrations. The present work illustrates a pilot trial of anaerobic treatment in a chlorinated compounds polluted aerobic groundwater, by the use of slow release amendments for the stimulation and growth of the anaerobic microflora after the total consumption of the oxygen present in the water.

2. Methods

Microcosms set up (aerobic conditions). 1L of groundwater was filtered (0,22 μm) and the particulate was used to inoculate a number of aerobic cultures (30 ml each) set up with the same sterilized groundwater additioned of ammonium chloride, potassium phosphate, sodium chloride, oligoelements and vitamins (pH 6,7).

Chemical analysis. 1,2-dichloroethane concentration was followed by Headspace GC analysis on a DB-5 Megabore column. Chemical analysis during monitoring of the pilot test were conducted by a certified laboratory.

qPCR experiments. The DNA extracted from groundwaters was amplified in qPCR experiments using the primers for *Dehalococcoides sp.* (Cocc728f aaggcggttttctaggttgtcac - Cocc944r cttcatgcatgtcaaat) or coding for dehalogenases bvcA, vcrA and tceA (bvc925F aaaagcacttggctatcaaggac – bvc1017R ccaaaagcaccaccaggtc, vcr1022F cgggcggatgcactatttt - vcr1093R cgggcggatgcactatttt, tceA1270F atccagattatgaccctggtgaa – tceA1336R gcggcatatattagggcatctt).

3. Results and discussion

The initial aerobic conditions of the groundwater showed the presence of bacteria able to degrade 1,2-dichloroethane, present in concentrations of 1 - 10 ppm. The degrading species was isolated and identified as *Ancylobacter sp.*; some species, such as *A. dichloromethanicus*, are known to metabolize 1,2-dichloromethane, in addition to other carbon sources (chlorinates alcohols, methanol, formate, succinate and formaldehyde). The species showed a good activity and resistance to 1,2-DCA, up to 800 ppm (*Fig. 2*). After a few years, the analysis of groundwater showed the almost total consumption of this pollutant, while chlorinated ethenes remained non-degraded. The injection of the selected amendment resulted in the change of redox conditions and in the consumption of the oxygen present in almost all the analyzed wells. Monitoring of the chlorinated ethenes showed the initial reduction of concentrations of perchloro- and trichloroethene (PCE – TCE) and the slight start in the increase of 1,2-cis dichloroethene (1,2-cisDCE) as the first product of the metabolic chain a few months after injection (*Fig. 2*). qPCR experiments were set up to identify the presence of species belonging to *Dehalococcoides* group and also for the confirmation of the presence of enzymes involved in PCE – TCE degradation.

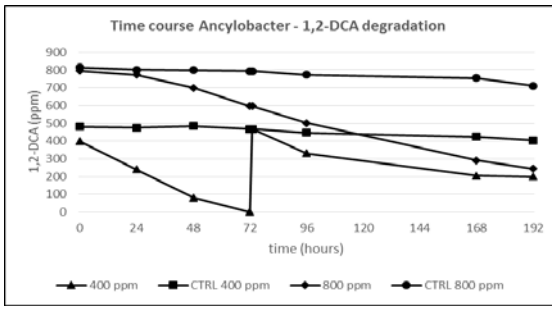

Figure 1. Time course of *Ancylobacter sp*. 1,2-DCA degradation; T=72: 400 ppm spike 1,2-DCA

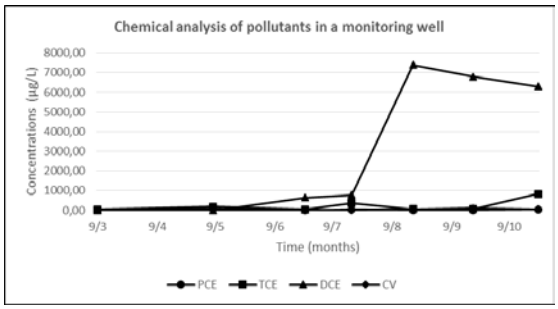

Figure 2. Chemical analysis of the chlorinated hydrocarbons after the injection of the slow-release amendment

4. Conclusions

The preliminary results of this work show the potential, for chlorinated hydrocarbons remediation, to follow natural attenuation in the groundwater conditions if the suitable microbes are present. In a second phase, it is possible to change redox/oxygen conditions shifting to anaerobic conditions and stimulating anaerobic degrading bacteria with appropriate amendments. This protocol is particularly useful in the case of mixed contamination of different chlorinated compounds.

References

[1] A. Tiehm and K.R. Schmidt , Curr. Op. Biotechnol. 22 (2011) 1–7.

ECAB 5
The 5th EUROPEAN CONGRESS OF APPLIED BIOTECHNOLOGY
Florence 15-19 September 2019

Impact of bead collisions on hWJ-MSC culture performances

C.Sion[1,2], C.Loubière[1,2], M. Wlodarczyk-Biegun[3], N.Davoudi[4], C.Müller[4], I.Chevalot[1,2], E. Guedon[1,2], E.Olmos[1,2]

1 CNRS, Laboratoire Réactions et Génie des Procédés, UMR 7274, 2 avenue de la forêt de Haye, TSA 40602, Vandœuvre-lès-Nancy, 54518, France ; 2 Université de Lorraine, LRGP, 2 avenue de la forêt de Haye, TSA 40602, Vandœuvre-lès-Nancy, 54518, France ;#B INM - Leibniz-Institut für Neue Materialien gGmbH,Campus D2 2, 66123 Saarbrücken ; 4 FB Physik und Forschungszentrum OPTIMAS,AG Grenzflächen, Nanomaterialien und Biophysik, Kaiserslautern

**Corresponding author: eric.olmos@univ-lorraine.fr*

Highlights

- Agitation mode and microcarrier distribution within the bioreactor have an important impact on MSC culture.
- Collisions between microcarriers are detrimental to MSC viability

1. Introduction

Mesenchymal stem cells extracted from the Wharton's jelly of human umbilical cords (hWJ-MSC) are of increasing interest for cell therapies due to their reduced immunogenicity, high expansion capabilities, fast growth kinetics and various growth factors synthesis capabilities. To address the problem of cell confluence on microcarriers during their culture in stirred bioreactors, it was previously shown that the addition of fresh microcarriers could maintain the cell growth and could allow reaching higher cell densities than without microcarriers feeding [1]. However, the resulting increase in the bead shocks frequency could also negatively impact cell quantity and quality. Until now, no quantitative study describing the impact of bead interactions on MSC death was reported in the literature. It is crucial to determine the respective influence of microcarrier feed strategy and microcarrier mixing characteristics on cell viability and to propose robust culture conditions of mixing and microcarrier concentrations. The objective of this study was to demonstrate the importance of the agitation mode on the expansion and the ability of cells to migrate to new fresh carriers. It appears that agitation has an important impact on the cell death and more precisely on the cell lysis in microcarrier cell cultures due to the lack of protective cell wall, high cell size and the lack of individual cell mobility [3].

2. Methods

hWJ-MSC were cultivated on Cytodex-1 microcarrier in HPL-supplemented medium, with an initial concentration of 7000 cells/cm^2. Previous studies (Loubière et al. 2018) showed that the best choice of microcarrier for hWJ-MSC adherence and expansion, in dynamic conditions, was Cytodex-1 [2]. Two types of culture systems were evaluated, shaken flaks (orbital agitation) and spinner vessels (mechanical agitation), agitated below or above particle just-suspended agitation rate (N_{js}). Glucose, glutamine, ammonium, lactate and lactate dehydrogenase concentrations were monitored every day. Moreover, cells were counted from the post-processing of DAPI-stained cells

pictures [2]. Using this method, a strategy of microcarrier feeding at an appropriate time during the culture was established to maintain a constant target value of cells per microcarrier [4].

3. Results and discussion

First, it was shown that hWJ-MSC bead-to-bead transfer appeared to be a potential way to avoid or delay cell and microcarrier aggregation, allowing an increase of the maximal total cell number in comparison with a culture with only medium feed addition. This assessment was applied to all culture systems: shaken flasks or spinner vessels. In the meantime, better performance of bead-to-bead transfer could be obtained by controlling N_{js} and the mode of agitation. The results also showed that the addition of fresh microcarriers could have a significant negative impact on cell viability, as revealed by the dead cell staining and the strong increase in LDH concentration in the liquid phase (Figure 1). However, as indicated by LDH concentration measurements, this was particularly the case in orbitally shaken flasks and below N_{js}. For these conditions, a concentration of microcarriers was observed in the lower part of the bioreactor, promoting more frequent collisions.

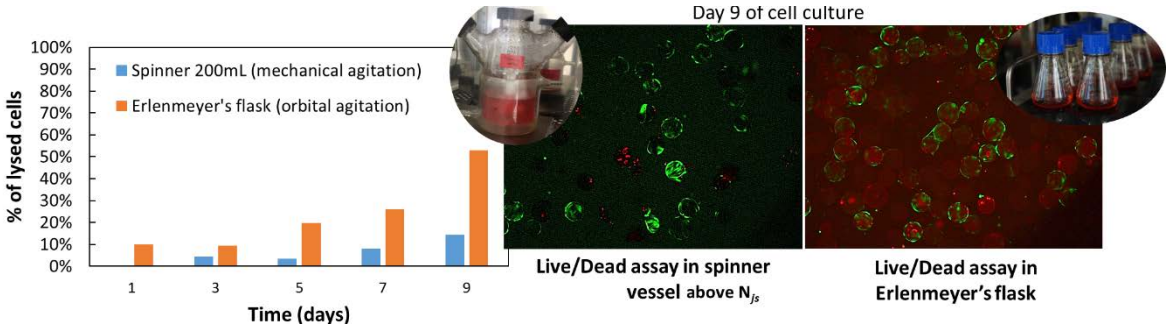

Figure 1. Impact of the cell culture system on viability and cell lysis.

Consequently, these results suggest that the collisional energy dissipation was more detrimental to cell viability than the hydromechanical stress arising from mechanical agitation. Hence, a compromise must be found between a limited concentration in microcarriers and the ability of cells to migrate towards other microcarriers, promoted by contact between them.

4. Conclusions

To conclude, this study underlined the importance of the just-suspended state determination and particle distribution in the bioreactor on the hWJ-MSC performances, notably during the bead-to-bead transfer phenomena.

References

[1] Ferrari, C., et al., (2012). Limiting cell aggregation during mesenchymal stem cell expansion on microcarriers. Biotechnology progress, 28(3), 780-787

[2] Loubière, C., et al., (2018). Impact of the type of microcarrier and agitation modes on the expansion performances of mesenchymal stem cells derived from umbilical cord. Submitted to Biochemical Engineering Journal.

[3] M. S. Croughan, J.-F. Hamel, D. I. Wang, Hydrodynamic effects on animal cells grown in microcarrier cultures, Biotechnology and bioengineering 67 (2000) 841–852.

[4] Sion C., Loubière C., Grandfils C, Sevrin C., Vandeberg R., Guedon E., Chevalot I., Olmos E. Control of microcarrier feed time by quantitative determination of bead-to-bead transfer during hMSC cultures. Conference at the European Society of Biochemical Engineering Science (ESBES), Lisbon, in September 2018

ECAB 5
The 5th EUROPEAN CONGRESS OF APPLIED BIOTECHNOLOGY
Florence 15-19 September 2019

Degradation and valorization of post-consumer textile fiber composite materials

Michael Menden[1], Volker Steidel[2], Volker C. Hass[1,*]

1) Hochschule Furtwangen University, Faculty of Medical and Life Sciences, Villingen-Schwenningen, D-78054, Germany; 2) Lauffenmühle GmbH & Co. KG, Lauchringen, D-79787, Germany

**Corresponding author: hass@hs-furtwangen.de*

Highlights

- Accelerated biological degradation of PET-like textile fibres.
- Anaerobic and aerobic degradation of PET-like fibres.
- Mathematical process models for anaerobic and aerobic degradation.

1. Introduction

Textile polyester wastes are difficult to recycle due to their composition and a large number of different dyes and additives. In 2012 about 1,5 Mio. tons of textile wastes were recycled worldwide, while 4,3 Mio. tons were burned or stored in landfills [1]. Biodegradable synthetic fiber materials can potentially be recycled to generate biogas or be disposed via a composting process. Unfortunately, due to their slow degradation rates, processing them with common biogas- or composting methods would be unprofitable [2].

In this study, the influence of different process parameters on the degradation rate of a PET-like polyester were investigated. Furthermore, enzymatic and hydrothermal pretreatment methods were employed to improve the biodegradability of this polyester. Kinetic process models were developed to systematically plan and evaluate the experiments.

2. Methods

Alkaline and neutral thermal hydrolysis was performed in water or potassium hydroxide solution at different temperatures ranging from 100 to 150 °C in an airtight container. The degree of hydrolysis was determined by measuring the loss of solid material and by measuring the amount of released monomers via HPLC. For the evaluation of anaerobic and aerobic degradation carbon balances were applied to compare different process strategies. For composting, the evolved carbon dioxide was measured gravimetrically in accordance with ISO 14855-2 by absorbing it with soda lime. For anaerobic digestion, methane and carbon dioxide emissions from a miniature biogas plant were measured volumetrically. For future scale up, experiments were performed with composting and fermentation vessels of different volume.

Kinetic models were developed for aerobic and anaerobic degradation as well as neutral hydrolysis. Model parameters and initial states were adapted based on experiments earlier in this study. Based on model behavior process strategies for further experimentation were chosen.

3. Results and discussion

Experiments on aerobic and anaerobic degradation of biodegradable PET-like polyester with different process strategies were performed. The kinetic models have been expanded to reflect the influence of pH and temperature on the degradation process. It has been shown for both the aerobic and anaerobic model, that they can be adapted to reflect the experimental results. For the anaerobic process model-based predictions have been made for different process strategies. The strategy which promised the highest degree of degradation within 31 days was chosen for an additional experiment. As seen in figure 1 the kinetic model could successfully predict an increase of the degree of degradation within 31 days.

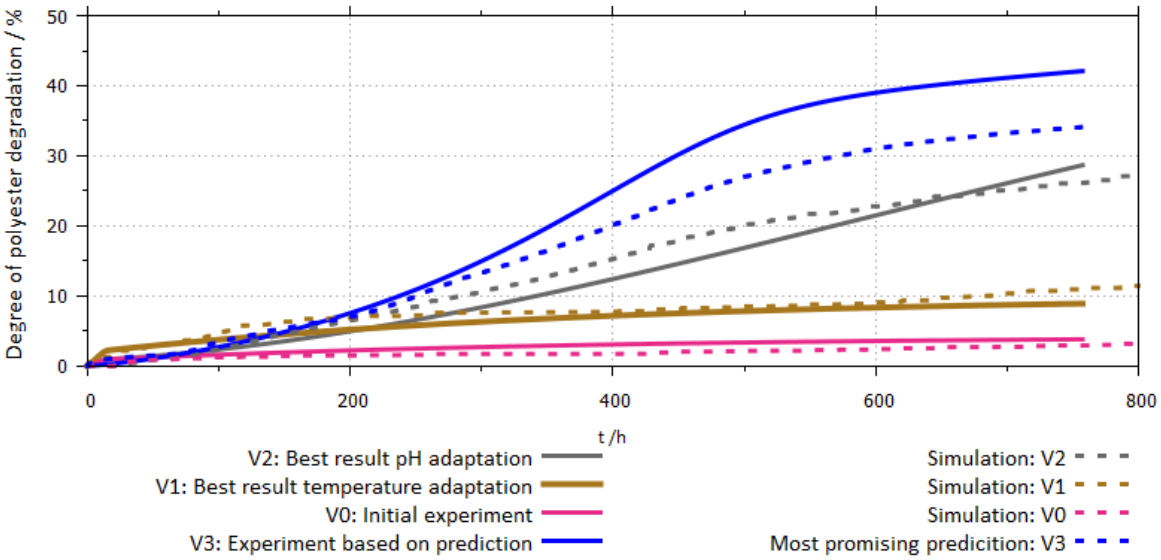

Figure 1. Model based improvement for the anaerobic digestion process of an biodegradable PET-like Polyester. Parameters for the anaerobic digestion model were chosen based on experiments V0, V1 and V2. Different predictions for new process strategies were made via the parametrized model. A new experiment V3 was performed based on the most promising prediction.

For enzymatic and thermal hydrolytic pre-treatment experiments for different pretreatment strategies were performed. The kinetic model for polyester hydrolysis was successfully adapted to reflect the influence of temperature and time on the degree of the resulting hydrolysis.

4. Conclusions

It has been shown, that aerobic and anaerobic degradation of a biodegradable polyester could be accelerated by improved process strategies and enzymatic or thermal hydrolytic pretreatment of the polyester. A kinetic model has been successfully applied to determine an improved strategy for the anaerobic degradation process.

References

[1] Lacasse, K.; Baumann, W. (2012): Textile Chemicals: Environmental Data and Facts. 1 Band. Heidelberg: Springer Science & Business Media.

[2] Soroudi, A.; Jakubowicz, I (2013): Recycling of bioplastics, their blends and biocomposites: A review. In: Eur Polym J 49 (10), S. 2839-2858

[3] G.R. Pangar, L. Liu, in: N.C. Jones, A. Bianchi (Eds.), The Electronic Technology, E-Publishing Inc., New York, 2009, pp. 181–304.

Preparation of water-soluble mercaptocarboxylated silver nanoparticle and its antibacterial properties and Pickering emulsion formation

Yusuke Horiki[1], Momoka Hamano[1], Jun Sawai[2], Kazumitsu Naoe[1*], and Masanao Imai[3]

1 Dept. of Materials Sci. & Chem. Eng.,Faculty of Advanced Eng., National Institute of Technology, Nara College, Yamato-Koriyama, Nara 639-1080, Japan; 2 Dept. of Nutrition & Life Sci., Kanagawa Institute of Technology, Atsugi, Kanagawa, 243-0292, Japan; 3 Graduate School of Bioresource Sci., Nihon University, Fujisawa, Kanagawa 252-0880, Japan

**Corresponding author: naoe@chem.nara-k.ac.jp*

Highlights

- Water-soluble mercaptocarboxylated silver nanoparticles were prepared.
- The silver nanoparticles have antibacterial activity.
- O/W Pickering emulsions using the silver nanoparticles were successfully prepared.

1. Introduction

In recent years, nanomaterials such as metal and semiconductor nanoparticles have been one of the most studied topics in chemistry and physics. Water-soluble nanoparticles have received considerable interest due to the potential environmental and economic benefits of functional "nano" inks and of carrying out catalysis in aqueous systems. Silver is known as an excellent antimicrobial agent and has been well used as disinfectant and microbiocide from old times. Antibacterial activity of silver is enhanced in nano scale and is dependent upon the size of silver particles [1]. Pickering emulsions are emulsions stabilized by solid particles adsorbed at liquid-liquid interface. They are expected as food, pharmaceutical, and cosmetic media because this emulsion system can reduce the use of artificial surfactant. Pickering emulsions stabilized by nanoparticles have been also reported [2]. In this study, preparation of water-soluble silver nanoparticles and their antibacterial properties are investigated. Preparation of Pickering emulsions using the silver nanoparticles is also investigated.

2. Methods

Silver nanoparticles (AgNPs) were prepared by phase transfer method [3]. Using silver nitrate as a model silver salt silver ions were transferred to the organic phase by tetrakis(decyl) ammonium bromide (TDAB) as a phase transfer agent and reduced by sodium borohydride in the presence of 11-mercaptoundecanoic acid (MUA) as a stabilizing agent. The UV-vis spectrum of the prepared AgNPs aqueous solution was measured and the nano-geometry of the AgNPs was characterized by Field Emission (FE)-SEM. Antibacterial activity against *Escherichia coli* (NBRC3301) and *Bacillus subtilis* (NBRC3134) was evaluated. Emulsions were prepared by adding toluene to the AgNPs aqueous phase containing NaCl and stirring them for 2 minutes with a homogenizer.

3. Results and discussion

The prepared AgNPs were well dispersed in aqueous solutions due to the carboxylic group of the stabilizing agent MUA. From UV-vis spectrum measurement the maximum absorption wavelength of the prepared AgNPs was 419 nm (Figure 1). It is known that the maximum absorption wavelength of the UV-vis spectrum of AgNPs exists near 420 nm due to the localized surface plasmon resonance (SPR) of the nanoparticles [4]. FE-SEM measurement showed the diameter of ca. 10 nm of the prepared AgNPs. The AgNPs exhibited excellent antimicrobial activity toward gram-negative *Escherichia coli* and gram-positive *Bacillus subtilis* (Figure 2).

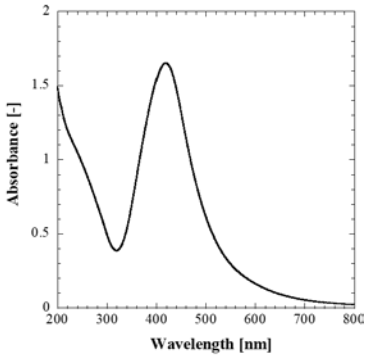

Figure 1. UV spectrum of the mercaptocarboxylated silver nanoparticle aqueous solution.

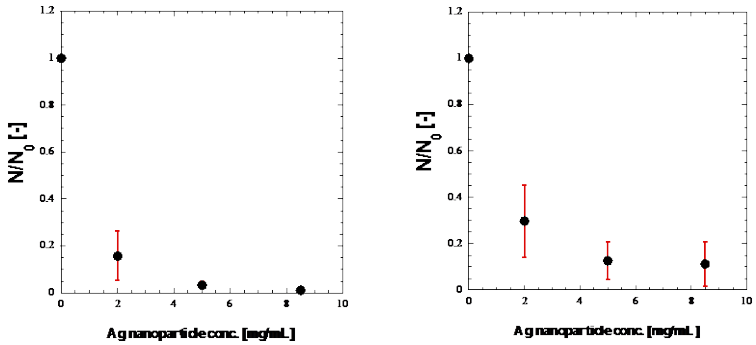

Figure 2. Effect of silver nanoparticle concentration on the growth of target bacteria (a) *E. coli* and (b) *B. subtilis* .

Toluene solution was added to the AgNPs aqueous solution containing NaCl, and mixed by using a homogenizer for 2 min. After mixing the emulsion phase was formed. Emulsions with a diameter of ca. 2 mm were successfully prepared. Fluorescence microscopy of the emulsions with hydrophobic fluorescence dye Nile Red revealed the formation of oil-in-water (O/W) emulsions.

4.Conclusions

Water-soluble AgNPs were prepared by the phase transfer method, and their properties were characterized. The silver nanoparticles have antibacterial activity toward *Escherichia coli* and *Bacillus subtilis.* O/W Pickering emlusions were prepared using the silver nanoparticles.

References

[1] Pancak, A. et al., J. Phys. Chem. B, 110, 16248-16253 (2006)
[2] Yamanaka, K. et al., Colloids Surf. A: Physicochem. Eng. Aspects, 436, 18-25 (2013)
[3] Brust, M. et al., Chem. Commum., 801-802 (1994)
[4] Cliffel, D. E. et al., Langmuir, 16, 9699-9702 (2000)

ECAB 5
The 5th EUROPEAN CONGRESS OF APPLIED BIOTECHNOLOGY
Florence 15-19 September 2019

Cultivation of highly aerobic biomass in an airlift bioreactor with helical flow promoter

Riikka Särkelä[1*], Tero Eerikäinen[1]

1 Aalto University, School of Chemical Engineering, Department of Bioproducts and Biosystems, P.O. Box 16100, 00076 Aalto, Finland

**Corresponding author: riikka.sarkela@aalto.fi*

Highlights

- Airlift reactor with helical flow promoter was studied with aerobic biomass cultivation
- Comparative study was done in similar size stirred tank reactor
- Testing included *e.g.* biomass production rate, final concentration, energy consumption

1. Introduction

Efficient oxygen mass transfer is often a bottleneck factor in aerobic bioprocesses. In addition, poor mixing might cause gradients in the process parameters, such as pH or substrate concentration, which further can cause a stress factor for the cultivated organism. Insufficient oxygen mass transfer and mixing can lead to lower biomass accumulation as well as lower product yield or it can cause the formation of unwanted byproducts. In order to simultaneously improve both, oxygen mass transfer and mixing, with moderate energy consumption, a draft tube sparged airlift bioreactor was occupied with a helical flow promoter in the downcomer zone of the bioreactor (helix-ALR). Besides working as a flow promoter, the helix was used for extra aeration.

2. Methods

The helix-ALR (V=116 L) was tested with aerobic *Pichia pastoris* cultivation to examine its performance with highly aerobic fermentation. Insufficient oxygen supply is unwanted in *P.pastoris* cultivation as it leads to ethanol formation instead of biomass accumulation. The helix in the downcomer zone of the airlift bioreactor was used for the extra aeration in order to improve reactor performance. The aim was to achieve high cell concentration by avoiding high gradients in pH and substrate concentration as well as avoiding oxygen depletion in the bioreactor for the whole cultivation period.

Similar scale conventional stirred tank reactor (V=100 L) was used as a reference for the helix-ALR cultivation. Reactor performances were evaluated in terms of final biomass concentration, biomass yield on carbon source, biomass accumulation rate, glucose consumption rate, total

process time and total energy consumption. Model describing the biomass growth in the helix-ALR was setup.

3. Results and discussion

Previous results with helix-ALR are promising; its energy requirement for volumetric oxygen mass transfer rate of 0.1 s^{-1} was less than 20% of the power requirement of a similar scale conventional stirred tank reactor [1]. In addition, helix-ALR showed good mixing capacity and it was more related to dispersion than to faster liquid circulation, as it is in only draft tube sparged airlift reactor. The mixing at the reactor level was mainly dependent on the sparger aeration rate, but the D-helix aeration had a minor impact on the mixing time as well. Circulation time was mainly dependent on the D-helix aeration rate. Faster circulation time did not mean faster mixing; D-helix aeration extended circulation time, but because of improved dispersion, mixing time was shorter. Based on the results of the previous studies, the reactor performance was enhanced by dividing the aeration with the sparger and the helical flow promoter in the downcomer zone.

4. Conclusions

In an airlift bioreactor with helical flow promoter, mixing and oxygen mass transfer are possible to optimized at the same time, whereas in stirred tank reactors it is difficult [3]. This offered an effective alternative to conventional stirred tank reactor to be used to cultivate highly aerobic organisms, which can reach high cell densities.

References

[1] M. Räsänen, T. Eerikäinen, H, Ojamo, Chem. Eng. and Process: Process Intensif. 108 (2016) 44-57.

[2] R. Särkelä , T. Eerikäinen, J.-P. Pitkänen, S. Bankar, Chem. Eng. and Process: Process Intensif. (submitted)

[3] T. Moucha, V. Linek, E. Prokopova, Gas hold-up, mixing time and gas-liquid volumetric mass transfer coefficient of various multiple-impeller configurations: Rushton turbine, pitched blade and techmix impeller and their combinations, Chem. Eng. Sci. 58 (2003) 1839-1846.

Cell Immobilization on Affordable Inert Supports for Ethanol Production from Cheese Whey Permeate.

Rebeca Díez-Antolínez[1,2], María Hijosa-Valsero[1], Ana Paniagua-García[1,2], Jerson Garita-Cambronero[1], Xiomar Gómez[2]

1 Center of Biofuels and Bioproducts, Instituto Tecnológico Agrario de Castilla y León (ITACyL), Polígono Agoindustrial del Órbigo p. 2-6, E-24358, Villarejo de Órbigo, León, Spain; 2 Chemical and Environmental Bioprocess Engineering Group, Natural Resources Institute (IRENA), University of León, Avda. de Portugal 41, E- 24009, León, Spain

**Corresponding author: dieantre@itacyl.es*

Highlights

- The strain *Kluyveromyces marxianus* DSM 5422 was selected among eight yeast strains.
- Cells were immobilised on alumina beads and Raschig rings of plastic, glass and Tygon.
- Cheese whey permeate (130 g/L lactose) was efficiently fermented yielding 60 g/L ethanol.
- Glass Raschig rings and alumina beads allowed a stable performance during 1,000 h.

1. Introduction

Cheese whey is a liquid by-product of milk coagulation during cheese production. It is characterized by a high organic load with elevated BOD and COD values, which makes this waste a potential source of pollution if it is incorrectly disposed of in water bodies [1].

Cheese whey can be used in ethanol fermentation processes, thanks to its lactose content. However, not all yeast strains are efficient to deal with lactose concentrations above 100 g/L. In addition, it is essential to improve and reduce the costs of fermentation processes, a fact that can be partially achieved by cell immobilization.

2. Methods

The raw material used for fermentations was cheese whey permeate obtained after ultrafiltration of the whey resulting from the production of a mixed cheese of sheep and cow milk, and it was provided by Quesería Entrepinares SAU (Valladolid, Spain). Its lactose content was about 130 g/L with a protein content of 34 g/L.

Eight yeast strains [*Kluyveromyces marxianus* DSM 5418, DSM 5422, DSM 7239 and DSM 70799; *Saccharomyces cerevisiae* CECT 13152, CECT 1383, Ethanol Red and Hércules (Lessafre)] were compared for their ethanol production from cheese whey permeate without nutrient addition. In the case of *S. cerevisae* strains, an enzymatic hydrolysis of lactose before fermentation was necessary. Fermentations were performed in flasks plugged with foam stoppers, at 35°C and 150 rpm. The most efficient strain was selected for further experiments.

Four inorganic materials were employed to immobilize the cells of the selected yeast strain: alumina beads and Raschig rings of plastic, glass and Tygon (5–5.5 mm length). Approximately, 10 g of every support were added to 50 mL of cheese whey permeate and 3.7% (v/v) of the selected yeast cells. Every 48-72 h, fresh whey replaced the exhausted medium.

3. Results and discussion

The strain *K. marxianus* DSM 5422 obtained the best performace, with a production of 60.0 g/L ethanol and 100% lactose consumption in 44 h.

Regarding immobilisation experiments, during the first six fermentation batches, the four inorganic supports had a similar behaviour with final ethanol concentrations about 60 g/L. However, the samples containing Tygon and plastic supports suddenly decreased their ethanol production after that moment. On the contrary, the samples with glass Raschig rings and alumina beads kept a good ethanol production until the 14th batch (total time 1,000 h), with average ethanol concentrations of 58-59 g/L, yields of 0.45 g/g and a lactose consumption of 96-98% [1].

4. Conclusions

Cheese whey permeate with high lactose concentration is an attractive feedstock for ethanol production. The selection of an appropriate yeast strain is essential to avoid nutrient supplementation, enzymatic hydrolysis steps and osmotolerance problems. Moreover, it is possible to immobilise the yeasts on simple inorganic supports, which clearly reduces yeast cultivation costs.

References

[1] R. Díez-Antolínez, M. Hijosa-Valsero, A.I. Paniagua-García, J. Garita-Cambronero, X. Gómez, PLoS ONE 13 (2018) e0210002.

ECAB 5
The 5th EUROPEAN CONGRESS OF APPLIED BIOTECHNOLOGY
Florence 15-19 September 2019

Effect of the treatment of gaseous ammonia emissions from pig farms on greenhouse gas emissions

Éric DUMONT

UMR CNRS 6144 GEPEA, IMT Atlantique, Campus de Nantes, La Chantrerie, 4 rue Alfred Kastler, CS 20722, 44307 Nantes Cedex 3, France
eric.dumont@imt-atlantique.fr

Highlights

- NH_3 treatments of gaseous emissions from pig farms can promote N_2O formation.
- The use of bioscrubbers can increase greenhouse gas (GHG) emissions.
- A denitrification step added to a bioscrubber significantly increases GHG emissions.
- The use of chemical scrubbers has no effect on greenhouse gas emissions.

1. Introduction

Gaseous pollution generated by pig farms can originate from animals and the decomposition of piggery waste manure. Pollutants such as ammonia (NH_3), carbon dioxide (CO_2), methane (CH_4) and nitrous oxide (N_2O) are the most abundant gaseous compounds emitted by pig farms. In order to limit NH_3 emissions, various air cleaning solutions are widely applied, i.e. chemical scrubbers, bioscrubbers and biofilters. However, the biological treatment of NH_3 can itself promote the formation of secondary pollutants such as N_2O. Since N_2O has a large greenhouse warming potential (1 g N_2O emitted is equivalent to 298 g CO_2), it seems relevant to investigate the impact of NH_3 treatment on greenhouse gas (GHG) emissions. The objective of this study is therefore to quantify the impact of air cleaning systems on the overall GHG emissions in pig farms from the literature data. The greenhouse gases emitted at the outlet of three different cleaning systems ("chemical scrubber", "bioscrubber" and "bioscrubber + denitrification step") are quantified and compared with the GHG emissions generated by the exhaust air with "no treatment".

2. Methods

Gaseous emissions from pig farms present significant variations from one farm to another and are related to temperature, ventilation rate, animal activity and the physiological stage of pigs. Consequently, mean values have to be used for pollutant concentrations and ventilation rates. The typical mean concentrations used in the calculations are in agreement with the data reported in the literature [1,2] (i.e. ventilation rate: 35 $m^3\ h^{-1}$ $animal^{-1}$; NH_3: 12 ppmv (9.0 mg m^{-3}); CO_2: 2000 ppmv (3880 mg m^{-3}); CH_4: 40 ppmv (28.2 mg m^{-3}); N_2O: 0.5 ppmv (0.97 mg m^{-3}). From the literature data [2,3], mean NH_3 removal efficiency values of 95% and 70% for "chemical scrubber" and "bioscrubber", respectively, are assumed. NH_3 removal efficiency increases to 85% when a denitrification step is added to a bioscrubber [4]. Moreover, N_2O-N production corresponding to 5% and 25% of the NH_3-N amount removed in bioscrubbers are considered for the cases

"bioscrubber" and "bioscrubber + denitrification step", respectively, on the basis of the literature data [4-5]. Lastly, it is considered that "chemical scrubbers" do not promote N_2O formation [6].

3. Results and discussion

The effect of the three treatments on GHG emissions is shown in Figure 1. According to this figure, GHG emissions are only reduced by the use of a "chemical scrubber" in relation to their ability to remove NH_3 satisfactorily and not promote N_2O generation. Both cases involving a bioscrubber show an increase in GHG emissions. The use of a "bioscrubber" can marginally increase greenhouse gas emissions (+1.9%). Such a finding is due to the large CO_2 footprint, which represents 80% of the total GHG emissions. Therefore, the use of bioscrubbers can be considered an acceptable alternative to chemical scrubbers to treat air from pig farms. However, the addition of a denitrification step to treat the discharge water from a bioscrubber has a significant influence. In this case, yearly GHG emissions move from 1583 to 1800 kg $eqCO_2$ $animal^{-1}$ corresponding to a 13.7% increase in comparison with the case "no treatment".

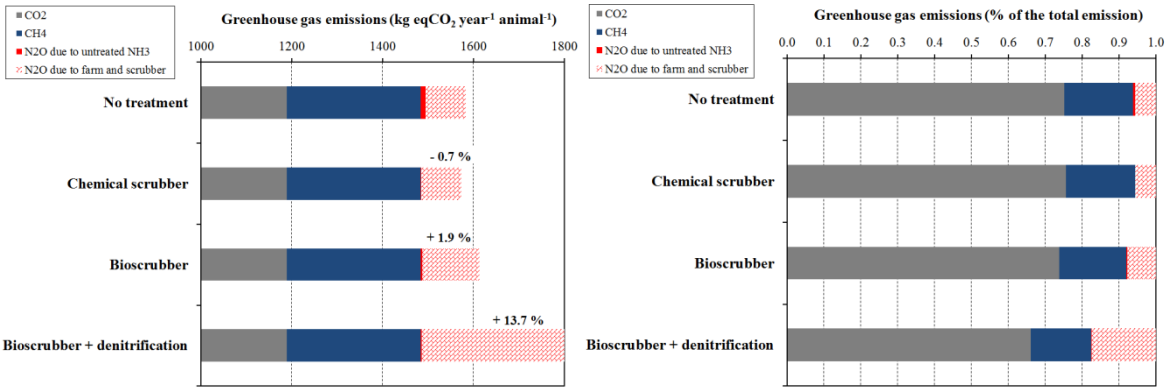

Figure 1. Impact of three NH_3 treatments on GHG emissions.

4. Conclusions

The calculations performed show that a chemical scrubber has no effect whereas biological treatments can increase GHG emissions. The use of bioscrubbers can remain acceptable according to the level of GHG emitted by the pig farm and provided that less than 3 % of the NH_3 entering the apparatus is converted into N_2O. In such a case, a maximum increase of 1.9 % in GHG emissions could be obtained. Conversely, the addition of a denitrification step to the bioscrubber must be avoided. Increases in the overall GHG emissions up to 13.7 % were calculated but more significant increases could occur. With regard to GHG emissions, it is concluded that the use of a chemical scrubber is more suitable than a bioscrubber to treat exhaust air from pig farms.

References

[1] L. Hamon, Y. Andrès, E. Dumont, Environ. Sci. Technol. 46 (2012) 12287–12301.
[2] C. Van der Heyden, P. Demeyer, E.I.P. Volcke, Biosyst Eng. 134 (2015) 74–93.
[3] R. Melse, N. Ogink, Trans ASAE 18 (2005) 2303–2313.
[4] R. Melse, J. Mosquera, Water Sci. Technol. 69 (2014) 994–1003.
[5] R. Melse, J. Ploegaert, N. Ogink, Biosyst. Eng. 113 (2012) 242–252.
[6] C. Van der Heyden C, E. Brusselman, E. Volcke, P. Demeyer, J. Environ. Manage. 181 (2016) 163–171.

ECAB 5
The 5th EUROPEAN CONGRESS OF APPLIED BIOTECHNOLOGY
Florence 15-19 September 2019

A new methodology for the process monitoring of enzymatic proteolysis by size-exclusion chromatography

Sophie Beaubier[1,2], Irina Ioannou[1], Xavier Framboisier[1], Olivier Galet[2], Romain Kapel[1]*

1 *Laboratoire Réactions et Génie des Procédés, Université de Lorraine, CNRS, LRGP, F-54000 Nancy, France*

2 *Avril SCA, 11 rue de Monceau, F-75008 Paris, France*

*Corresponding author: * romain.kapel@univ-lorraine.fr*

Highlights

- A method for monitoring enzymatic proteolysis by SE-HPLC is developed
- The method assesses protein conversion rate, peptide size and DH in a single run
- The approach was tested on various proteins and hydrolysis conditions
- The method is as efficiently as TNBS or pH stat methods for DH quantification

1. Introduction

Enzymatic proteolysis is an industrial process used in a wide range of applications [1]. The extent of the enzymatic proteolysis process is usually quantified as the degree of hydrolysis (DH), which represents the percentage of peptide bonds cleaved compared to the initial number of peptide bonds of the protein [2]. An effective follow-up of the enzymatic proteolysis process requires the quantification of 2 others parameters: the protein conversion rate (Xp) and the mean peptide size released (Naa). These three different parameters are classically determined by three distinct analysis. The DH can be either determined by a method based on a spectrophotometric reaction with amino groups released during hydrolysis or based on a titration of protons released during a peptide bond hydrolysis. To determine Xp, the protein concentration must be specifically quantified by Reversed-Phase High-Performance Liquid Chromatography (RP-HPLC) or Kjeldahl method after protein precipitation with TCA. Molecular weight distribution of peptides is classically achieved by Size-Exclusion High-Performance Liquid Chromatography (SE-HPLC) based on the UV signal at 214 nm. This makes the enzymatic proteolysis process laborious to monitor. In this way, the communication describes an original methodology to quantify simultaneously these three criteria by size-exclusion chromatography (SE-HPLC).

2. Methods

The protein conversion rate is simply deduced from the evolution of the protein peak area in the course of the reaction. With the chosen column (Superdex peptide 10/300 GL column), proteins are eluted in the column dead volume due to the column separation domain (< 7 kDa). For the mean peptide size and DH, the methodology consists in converting peptide UV absorbances of chromatograms into concentrations by applying Beer-Lambert law [4]. To do so, a molar extinction coefficient is assessed for each chromatogram point (Eq. 1). The coefficient depends on the hydrolysate aminoacid compositions and the molar weight corresponding to the considered point (deduced from SE column calibration).

$$\varepsilon_x = \varepsilon_{bond} \times \left(\frac{10^{a \times V_x + b}}{\overline{MM}_{aa}} - 1\right) + \bar{\varepsilon}_{aa}\left(\frac{10^{a \times V_x + b}}{\overline{MM}_{aa}}\right) \quad \text{(Eq. 1)}$$

With ε_{bond}, the molar extinction coefficient of peptide bond and $\overline{MM}$aa, the mean amino acid molar mass of the hydrolysate.

The overall concentration signal is integrated and Naa is calculated with the ratio of the molar quantities of amino acids (determined with Eq. 2) to peptides (determined with Eq. 3) in the hydrolysate. DH is deduced from the ratio of Xp and the mean size of peptide.

$$n_p = Qv \int (Cp_x)\, dt \quad \text{(Eq. 2)} \qquad n_{aa} = Qv \int \left(Cp_x\, \overline{N}aa_x\right) dt \quad \text{(Eq. 3)}$$

with Q_v the elution flow rate and dt a fraction of the elution time.

3. Results and discussion

As a first step, the approach was tested on the hydrolysis of bovine serum albumin (BSA) and rapeseed albumin (RA) by Alcalase 2.4L because of their different origin, structure, isoelectric point and composition. Hydrolysis kinetics were monitored by SE-HPLC (Figure 1A) and the 3 parameters were determined in the course of reaction as described above. Values of DH were also determined by TNBS and pH-stat methods. Most of the hydrolysates obtained showed relative differences <20% with the reference methods (Figure 1B). The method was also adapted to fit the TNBS assay.

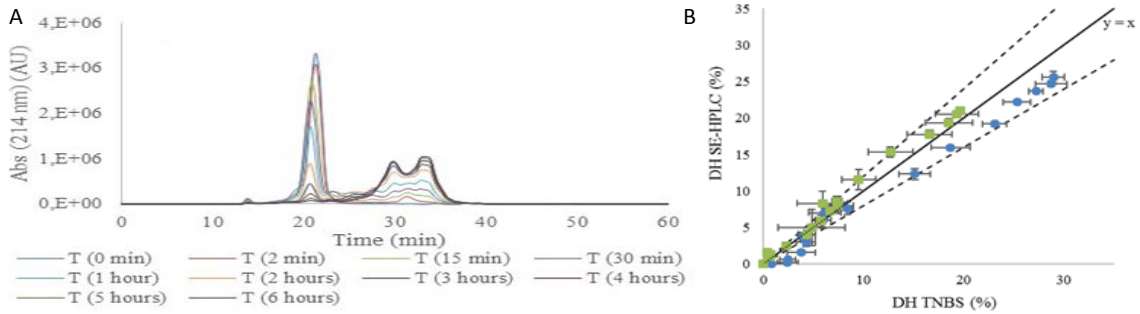

Figure 1. (A) Size exclusion chromatograms obtained for the hydrolysis of 1 % (w/v) RA with Alcalase 2.4 L over 6 h; (B) Comparison of the DH values obtained with the SE-HPLC and TNBS methods for the hydrolysis of 1 % (w/v) BSA (●) and RA (■) with Alcalase 2.4 L. Values are means of triplicate determinations. Error bars show standard deviation.

Then, validation of the methodology was realized through a statistical comparison between the DH values obtained by the method and those obtained with TNBS and pH stat methods for BSA, RA and lysozyme substrates. 39 experimental validation tests were analysed by SE-HPLC, TNBS and pH stat methods. 90% of the validation data show non-significant differences between the DH predicted and the DH measured by TNBS method.

4. Conclusions

The proposed methodology can be efficient for the process monitoring of enzymatic proteolysis while minimizing time and quantity of sample assay required. Moreover, it could be used for functionalities or bioactivities analysis of produced hydrolysates.

References

[1] Tavano, O. L. (2013). Protein hydrolysis using proteases: an important tool for food biotechnology. Journal of Molecular Catalysis B: Enzymatic, 90, 1-11.

[2] Adler-Nissen, J. (1986). Enzymatic Hydrolysis of Food Proteins, Elsevier Applied Science Pub., New York.

[3] Bodin, A., Framboisier, X., Alonso, D., Marc, I., Kapel, R. (2015). Size-exclusion HPLC as a sensitive and calibrationless method for complex peptide mixtures quantification. Journal of Chromatography B, 1006, 71–79.

Lipase production by *Candida tropicalis* in a stirred tank reactor using agro-industrial residues as feedstock

Renata Kelly da Silva[1], Brenda Novais Santos[1], Sueli Rodrigues[1], Luciana Rocha Barros Gonçalves[1*], André Casimiro de Macedo[1]

1 Programa de Pós-Graduação em Engenharia Química, Universidade Federal do Ceará, Campus do Pici, Bloco 709, Fortaleza – CE, Brazil

**Corresponding author: lrg@ufc.br*

Highlights

- Lipase was produced by *Candida tropicalis* URM 7057;
- Enzyme production was conducted using agro-industrial residues: molasses, corn steep liquor and olive mill wastewater (OMW);
- Lipase production was higher when aerated cultivation was conducted.

1. Introduction

Lipases represent around 10% of the global market for enzymes and new processing technologies may boost the interest among researchers to search for new sources of viable lipase stimulating the selection of new strains and the optimization of the production [1].

In this context, this study aimed to evaluate lipase production by *Candida tropicalis* URM 7057 using agro-industrial residues as feedstock in a bench bioreactor. In order to improve enzyme production, some operational strategies were evaluated, such as: effect of aeration and agitation, as well as the effect of feeding pulses of OMW.

2. Methods

The yeast *Candida tropicalis* URM 7057 was isolated from cashew bagasse. The culture was activated in a medium containing 40 g/L of glucose, 10 g/L of peptone in potassium phosphate buffer with PH 7.0 and maintained at 30 °C, 170 rpm for 24 h. To prepare the inoculum, a microbial suspension of cells was transferred to flasks of 500 ml, containing 175 ml of cultivation medium and kept in a rotary sacker at 30 °C and 170 rpm until reaching the concentration of 10^6 UFC/ML.

The cultivation medium contained 5.0 g/L of sugarcane molasses, 6.0 g/L of Corn Steep Liquor (CSL), 0.5% v/v of wastewater from olive plants (OMW), 0.5 g/L of ammonium sulfate and 3.0 g/L of peptone in potassium phosphate buffer, PH 7.0, which was sterilised in autoclave at 110 °c for 15 minutes. The assays were performed in 5L-bench bioreactor (New Brunswick Bioflo Celligen 115, Eppendorf), (HL = 33.00 cm; d = 19.41 cm) with an initial volume of 3.5 L at 30 °C and 300 rpm and pH maintained at 6.5 with NaOH 1, 5m.

The total protein content was determined by the BRADFORD method [2] using bovine serum albumin as the protein standard for the calibration curve. The concentration of reducing sugars was determined by using the DNS reagent [3]. The growth was monitored by counting viable cells in a Neubauer chamber (depth 0.025 mm) performed along the fermentation, using methylene blue

staining technique. *Lipase activity was determined using p-nitrophenyl laurate (pNFL)* as the enzyme substrate [4].

3. Results and discussion

Different agitation speeds and air flows were studied in the production of lipase by *C. tropicalis.* Enzyme production increased with increase in aeration flow rate, figure 1. The production coefficients $Y_{P/S}$ and $Y_{P/x}$ were higher in 0.25 vvm, although the $Y_{P/X}$ for 0.75 vvm was not much different from the value at 0.25 mvv. Table 1 shows the biomass (Y_{XS}) and Product (Y_{PX}, Y_{PS}) yields, as well as lipolity activity and biomass production (titer and productivity).

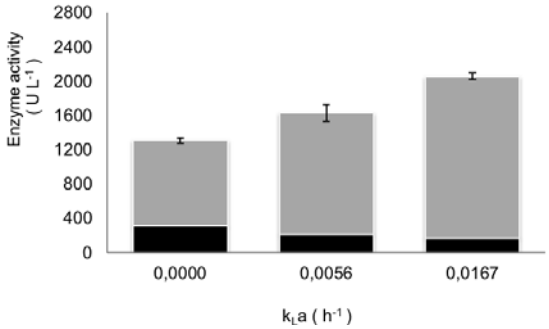

Figure 1. Maximum total enzymatic activity under different aerations: ( ) intracellular activity ( ) Extracellular activity.

Table 1. Kinetic Parameters of batch and batch cultivation fed

Parameter	X_{max} (UFC/ mL)	S_{total} (g/L)	$P_{x,\,max}$ (UFC/mL/L)	$P_{P,max}$ (U/L/h)	Y_{XS} (UFC/gS)	Y_{PX} (U/UFC)	Y_{PS} (U/gS).
Batch	1.9×10^6	4.3	1.8×10^5	24.9	7.6×10^7	0.8×10^{-7}	5.7
Fed-Batch	2.5×10^6	4.7	2.9×10^5	18.1	21.4×10^7	2.3×10^{-7}	50.0

4. Conclusions

In this work, the production of lipase by *C. tropicalis* URM 7057 using agro-industrial residues as feedstock could be optimized in an aerated submerged culture. In addition, batch operation proved to be a good strategy to achieve higher enzyme titer.

References [Calibri 10]

[1] Lai, O.-M., Lee, Y.-Y., Phuah, E.-T., & Akoh, C. C. (2019). Lipase/Esterase: Properties and Industrial Applications. Encyclopedia of Food Chemistry, 158–167. doi:10.1016/B978-0-08-100596-5.21640-5

[2] Bradford, M. M. (1976). A rapid and sensitive method for the quantitation of microgram quantities of protein utilizing the principle of protein-dye binding. Analytical biochemistry, 72, 248–254. doi:10.1016/0003-2697(76)90527-3

[3] Miller, G. L. (1959). Use of Dinitrosalicylic Acid Reagent for Determination of Reducing Sugar. Analytical Chemistry, 31(3), 426–428. doi:10.1021/ac60147a030

[4] Brígida, A. I. S., Amaral, P. F. F., Coelho, M. A. Z., & Gonçalves, L. R. B. (2014). Lipase from Yarrowia lipolytica: Production, characterization and application as an industrial biocatalyst. Journal of Molecular Catalysis B: Enzymatic, 101, 148–158. doi:10.1016/j.molcatb.2013.11.016

ECAB 5
The 5th EUROPEAN CONGRESS OF APPLIED BIOTECHNOLOGY
Florence 15-19 September 2019

Impact of oxygenation and glucose concentration on succinate production by *Corynebacterium glutamicum*

Amani Briki[1,2], Eric Olmos[1,2*], Sabine Bosselaar[1,2], Frantz Fournier[1,2], Stéphane Delaunay[1,2]

*4 CNRS, Laboratoire Réactions et Génie des Procédés, UMR 7274; 2 Université de Lorraine, LRGP, UMR 7274, 2 avenue de la forêt de Haye, TSA 40602, Vandœuvre-lès-Nancy, F-54518, France*1

**Corresponding author: eric.olmos@univ-lorraine.fr*

Highlights

- Sequential production of organic acids according to the oxygen uptake rate
- The succinate re-consumption depends on the glucose concentration
- Kinetic modelling of succinate production/consumption

1. Introduction

Corynebacterium glutamicum is widely used in industry for the production of amino acids and for a few years, it is known that *C. glutamicum* is also capable of producing organic acids under oxygen-limited and anaerobic conditions [1]. Therefore, this work aimed to understand the physiological behavior of *C. glutamicum* in defined and limiting oxygenation conditions and then to give clues concerning the optimal conditions for succinate production.

2. Methods

Batch cultures of *Corynebacterium glutamicum* 2262 were performed in a minimal medium in glass unbaffled shake flasks [1]. For the estimation of the volumetric gas-liquid mass transfer coefficient (k_La), the following correlation was used [2].

$$k_La = 0.024 * N^{1.16} * V^{-0.83} * d_0^{0.38} * d^{1.92} \qquad \text{(eq.1)}$$

with K_La, the volumetric gas-liquid mass transfer coefficient (h^{-1}), N the shaking frequency (s^{-1}), V the filling volume (mL), d_0 the shaking diameter (cm) and d the maximal shake flask diameter (cm).

It was previously demonstrated that the k_La values calculated from eq.1 or determined experimentally were in very good agreement [1]. In the present work, by modifying the shaking frequency, the filling volume and the maximal shake flask diameter, different k_La conditions (5, 11, 15, 20, 31, 44, 77, 90 and 118h^{-1}) could be imposed.

3. Results and discussion

All the cultures were performed in limiting oxygen condition. This one was noticed 2h after the beginning of the culture with k_La values above 77 h^{-1} and after only a few minutes when the k_La values were below 33 h^{-1} [1]. The maximal organic acid concentrations differed according to the oxygenation conditions. Indeed, the succinate maximal concentration (42 mM) was measured for k_La = 5 h^{-1} with a conversion yield of 0.22 mol succinate/mol glucose. The lactate, which was the major fermentation product in all the culture conditions, reached its maximal concentrations

(170mM) for k_La values between 5 and 31 h^{-1}. The highest acetic acid concentration (88 mM) occurred when k_La values were between 31 and 77 h^{-1}. For k_La ≥90 h^{-1}, the biomass concentration (12 g/l) was maximal. A similar impact of oxygenation conditions on the organic acids was previously observed with *C. glutamicum* ATCC13032 (2) and with a mutant strain of *C. glutamicum* 2262 deleted for *ldhA* (1). Interestingly, succinate production occurred in all the culture conditions with a similar specific production rate in the first hours of the cultures. However, the higher the k_La, the earlier the production ceased and the earlier the succinate was consumed (fig. 1).

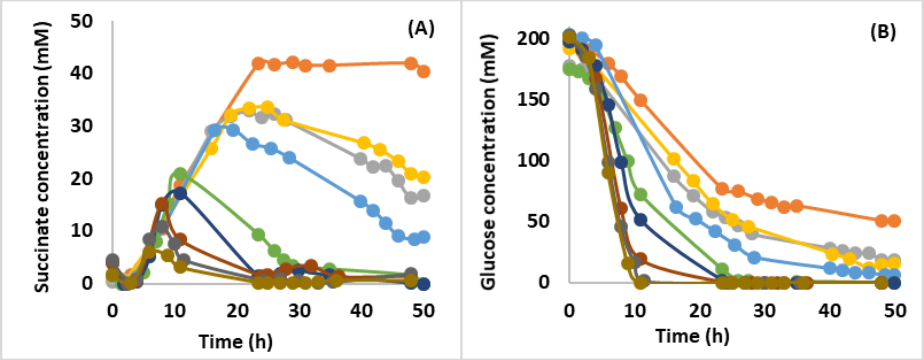

Figure 1. Kinetics of succinate production (A) and glucose consumption (B) by *Corynebacterium glutamicum* 2262 for k_La values of 5 h^{-1} (¬), 11 h^{-1} (¬), 15 h^{-1} (¬), 20 h^{-1} (¬), 31 h^{-1} (¬), 44 h^{-1} (¬), 77 h^{-1} (¬), 90 h^{-1} (¬) and 118 h^{-1} (¬).

The stop in the succinate production was concomitant with a threshold glucose concentration of 50 mM. Glucose and succinate were then both co-consumed until the end of the culture. No growth of *C. glutamicum* was observed with succinate as a unique substrate meaning that the succinate is likely an energy source for this bacterium (complementary data). The specific rates of succinate production were then modeled using Luedeking-Piret equation [3] in which a term modeling the succinate consumption as an energy source was added. The specific rates of succinate production predicted using this model were in accordance with the experimental rates for the different k_La conditions.

4. Conclusions

In oxygen-limited conditions, the specific succinate production by *C. glutamicum* depended on the oxygen uptake rate but its consumption was only observed for concentrations of glucose lower than 50 mM. To identify the metabolic changes responsible for this physiological behavior, the designed kinetic model will be coupled with a FBA simulation using a simplified metabolic model of *C. glutamicum*.

References

[1] A.K. Kaboré, E. Olmos, F. Blanchard, M. Fick, S. Delaunay, Biochem. Eng. J. 101 (2015)237-247.
[2] Y. Shinfuku, N. Sorpitipom, M. Sono, C. Furusawa, T. Hirasawa, U. Shimizu, Microb. Cell Fact (2009)8-43.
[3] R. Luedeking & E.L. Piret, Biotechnol. Bioeng. 67 (2000)636-644.

ECAB 5
The 5th EUROPEAN CONGRESS OF APPLIED BIOTECHNOLOGY
Florence 15-19 September 2019

Influence of working parameters on mixing time values in single-use culture bag rocked in WAVE™ 25 bioreactor

Maciej Pilarek[1], Kamil Wierzchowski[1]

[1]*Warsaw University of Technology, Faculty of Chemical and Process Engineering, Waryńskiego 1, 00-645 Warsaw, Poland*

**Corresponding author: maciej.pilarek@pw.edu.pl*

Highlights

- Mixing time ranged from 3s to 500s characterizes mixing efficiency in WAVE™ bioreactor
- Oscillations angle and frequency robustly impacting on mixing time in WAVE™
- Influence of aqueous phase volume in culture bag is irrelevant to mixing time in WAVE™

1. Introduction

Applications of disposable bioreactors for scaling-up of *in vitro* bioprocesses involving fragile animal cells became common in biopharmaceutical industry. In wave-induced agitation systems, mixing is achieved by horizontal oscillation of a single-use culture bag, which is fixed in a rocker unit. An interfacial area between gas and liquid phases filing the culture bag is continuously renewed, what accomplishes gentle and bubble-free surface aeration of a culture medium [1]. Furthermore, the wave-induced agitation notably limits shear stress effects negatively influencing on shear-sensitive animal cells or aggregates of them. A mixing time is a parameter commonly used to quantify mixing efficiency, and its value represents to the time necessary to reach a defined mixing quality [2]. The mixing time values determined for various types of disposable wave-type agitated bioreactors depended on the volume of culture bag, and presets of working parameters of the rocker.

The aim of the study was to determine influence of working parameters defining wave-induced agitation, on values of the mixing time reached in 2-litre culture bag (i.e. Cellbag™ 2L) oscillatingly rocked in *ReadyToProcess* WAVE™ 25 bioreactor (GE Healthcare, USA). Based on our previously published data, i.e. [3], only the impact of aqueous phase volume inside the culture bag (V_L), and angle of oscillations (α), as well as their frequency (ω), were analysed and their influence on the mixing time values have been quantitatively determined. All the experiments were performed and evaluated according to DoE-standards of statistical data processing.

2. Methods

ReadyToProcess WAVE™25 bioreactor (WAVE 25) equipped with disposable, polymer-based culture bag (Cellbag™ 2L; GE Healthcare, USA) with a total volume of 2 dm^3 has been used as an experimental setup. The following values of the operational parameters established for the mixing time determination have been evaluated: V_L equalled to 0.2 dm^3, 0.6 dm^3 and 1.0 dm^3; α equalled to 2°, 7° and 12°; as well as ω equalled to 2 min^{-1}, 21 min^{-1}, 40 min^{-1}.

The decolourisation iodometry method has been applied for determination of the mixing time in the system [4]. Prior to measurement, 2 cm^3/dm^3 iodine potassium iodide (40 g KI + 20 g I_2/dm^3), and then 5 cm^3/dm^3 starch solution (10 g/dm^3), were added to the constantly waving aqueous phase (37°C) inside the culture bag, to obtain the deep blue coloured aqueous phase. Next, 4 cm^3/dm^3 sodium thiosulfate solution (24.6 g/dm^3) has been pipetted under continuous wave-type agitation, with the immediately started time measurement of the aqueous phase decolourization process. The timing was stopped when the colour change of aqueous phase from deep blue to colourless has been completely achieved.

All experiments were planned and evaluated in STATISTICA® Data Miner 13 (StatSoft Polska, PL) software. The DoE-aided analysis comprising in total 135 experiments (i.e. 27 single experiments repeated in 5 series, three levels of varied factors has been applied to statistical data processing.

3. Results and discussion

The range of experimentally measured values of the mixing time reached for the aqueous phase waving in Cellbag™ 2L, which have been performed in the rocker of WAVE 25 system, i.e. from values of less than 5 s to over two orders of magnitude more (Figure 1), was consistent with previously published literature data on the mixing time determined for other single-use bags variously agitated by the other oscillating devices. Moreover, just α and ω have been identified as the working parameters which relevantly and robustly influencing on the value of the mixing time determined in the studied experimental setup of WAVE 25 bioreactor.

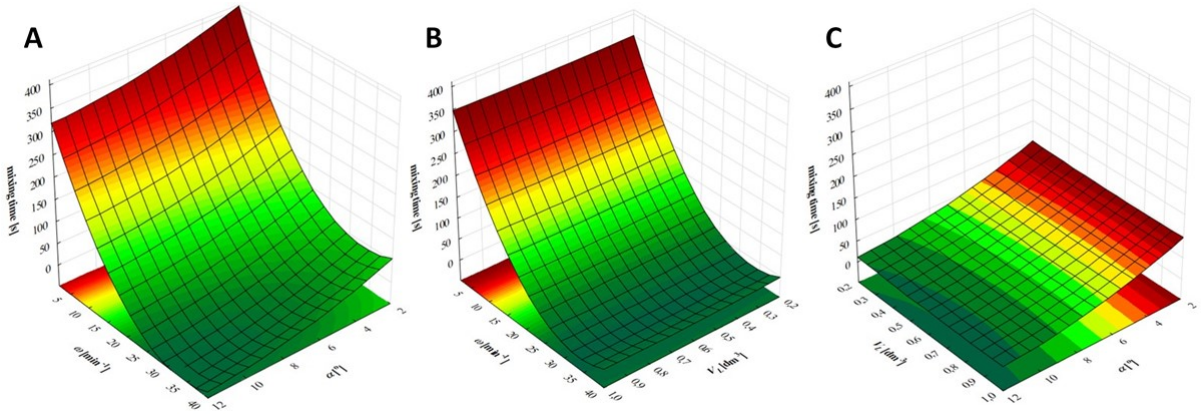

Figure 1. Response surface plots for the mixing time: the influence of α and ω (for V_L = 0.6 dm^3) (**A**), the influence of ω and V_L (for α = 7°) (**B**), and the influence of V_L and α (for ω = 21 min^{-1}) (**C**).

4. Conclusions

The results of the DoE-aided analysis has identified just α and ω as the working parameters which relevantly and robustly influencing on the value of the mixing time determined in the studied experimental setup of WAVE 25 bioreactor. The influence of V_L has been rather minor and may be interpreted as negligible.

References

[1] A.A. Shukla, U. Gottschalk, Trends Biotechnol. 31 (2013) 147-154.
[2] R Eibl, D. Eibl, Single-Use Technology in Biopharmaceutical Manufacture, first ed., Wiley, Hoboken, 2011.
[3] M. Pilarek, P. Sobieszuk, K. Wierzchowski, K. Dąbkowska, Chem. Eng. Res. Des. 136 (2018) 1-10.
[4] W. Meusel, C. Löffelholz, U. Husemann *et al.*, Dechema Biotechnologie, Frankfurt am Mein, 2016.

Autohydrolysis of Wheat Straw for Antioxidants and Cellulosic Fiber Recovery

Andrea Bassani[1,*], Cecilia Fiorentini[1], Vellingiri Vadivel[2], Flavio Manenti[3], Giorgia Spigno[1]

1 Università Cattolica del Sacro Cuore, Department for Sustainable Food Process (DiSTAS), Via Emilia Parmense 84, 29122 Piacenza, Italy; 2 Centre for Advanced Research in Indian System of Medicine (CARISM), SASTRA University, Thanjavur, Tamil Nadu, India; 3 Politecnico di Milano, Department of Chemistry, Materials and Chemical Engineering, Piazza Leonardo da Vinci 32, 20133

**Corresponding author: andrea.bassani@unicatt.it*

Highlights

- Autohydrolysis as suitable process for antioxidants and fibers recovery.
- Antioxidant capacity is more than twice compared to acid hydrolysis.
- Cellulose yield and recovery are 15.88% and 47.01% respectively.

1. Introduction

Wheat straw (WS) is an agricultural residue that presents many interesting characteristics that facilitate its biotechnological upgrade in a bio-refinery framework [1]. Based on the data from FAO, world annual WS production is about 577 million tons in 2016 and is supposed to be higher in the next years. Plant cell walls of wheat straw are formed with a polysaccharide network of which cellulose, hemicelluloses and pectin are the most important components [2]. The antioxidant phenolics and cellulosic fiber were conventionally separated using acid/alkaline hydrolysis [3]. However, from the environmental point of view, it is better to avoid the use of toxic chemicals, like sulfuric acid. For these reason, autohydrolysis process is gaining more attention nowadays and was already tested to recover bound phenols from grape stalks [4]. Hence, in the present study an environmental friendly autohydrolytic process was applied for the recovery of both antioxidants and cellulosic fiber in a single process from wheat straw. The cellulose and antioxidant recovery were compared with the traditional process value.

2. Methods

Acid hydrolysis, alkaline hydrolysis and bleaching steps were described in-deep in our previous work [3]. On the other hand, autohydrolysis was carried out as follow. Wheat straw sample (20 g) was taken with 400 ml of distilled water in a Teflon container and placed inside of high pressure reactor that was operated at 190 ºC and 11 bar for 15 min under agitation. Then, the reactor was slowly cooled down at ambient temperature. The following alkaline hydrolysis and bleaching steps were the same as in the traditional process [3]. The solid recovered was weighed to calculate the cellulose residue yield while the liquid, coming from autohydrolysis reaction, was used for the analysis of antioxidant capacity using ABTS analytical method [3]. Finally, the structural carbohydrates including total reducing sugars, acid soluble and insoluble lignins, glucose, xylose and acetic acid were investigated in the cellulose residue obtained from autohydrolysis [5].

3. Results and discussion

The obtained results are reported in Figure 1. The ABTS inhibition capacity of WS autohydrolyzed liquid is very high when compared to acid hydrolysis liquid, because in the acid hydrolyzed liquid achieved only 40% AOP at 1200 mg GAE/L concentration, whereas WS autohydrolyzed liquid has exhibited 94% AOP at 766 mg GAE/L concentration and thereafter the antioxidant activity attained plateau. The autohydrolysis process yielded slightly lower amount of fiber residue (86%) than the acid hydrolysis process (95%). The cellulose content calculated based on glucose concentration was slightly lower in autohydrolysis process when compared to acid hydrolysis method. However, the cellulose yield (15.88%) and recovery (47.01%) of WS fiber obtained from autohydrolysis is closer to that of acid hydrolysis step. Interestingly, the hemicelluloses, acetic acid, acid soluble and acid insoluble lignins content of autohydrolyzed fiber is lower than acid hydrolyzed sample.

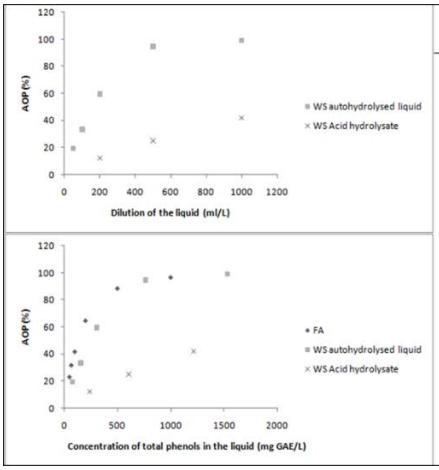

Structural carbohydrates	WS autohydrolysis	WS acid hydrolysis
Total sugars (g / L)	6.22 ± 0.05	6.31 ± 0.04
Glucose content of fiber residue (%)	86.43 ± 0.94	95.54 ± 2.05
Cellulose content of fiber residue (%)	76.06 ± 0.83	84.07 ± 1.80
Cellulose yield from raw material (%)	15.88 ± 0.17	15.10 ± 0.32
Cellulose recovery (%)	47.01 ± 0.51	44.70 ± 0.92
Xylose content of fiber residue (%)	1.14 ± 0.02	2.33 ± 0.13
Hemicellulose content of fiber residue (%)	1.03 ± 0.02	2.10 ± 0.12
Acetic acid content of fiber residue (%)	0.19 ± 0.02	0.59 ± 0.01
Acid soluble lignin (%)	0.90 ± 0.04	1.09 ± 0.03
Acid insoluble lignin (%)	5.47 ± 0.50	12.43 ± 0.24

Figure 1. Comparison of AOP and structural carbohydrates of WS autohydrolysis with acid hydrolysis.

4. Conclusions

Autohydrolysis was found to be highly suitable and environmental friendly process compared to conventional acid/alkali hydrolysis process to obtain the antioxidants and fibers from WS. Future investigation on the use of these antioxidants and cellulosic fibers in the development of active and biodegradable food packaging material is necessary for the utilization of agro-food byproducts towards the enhancement of food industry.

Acknowledgments

This project has received funding from the Bio Based Industries Joint Undertaking under the European Union's Horizon 2020 research and innovation programme under grant agreement No 792261.

References

[1] E. Tomas-Pejo, J. Fermoso, E. Herrador, H. Hernando, S. Jiménez-Sánchez, M. Ballesteros, D. Serrano, Fuel 199 (2017) 403-412.

[2] F. Carvalheiro, T. Silva-Fernandes, L. C. Duarte, F. M. Gírio, Applied biochemistry and biotechnology, 153 (1-3) (2009) 84-93.

[3] V. Vadivel, A. Moncalvo, R. Dordoni, G. Spigno, Waste Management 64 (2017) 305-314.

[4] D. Amendola, D. M. De Faveri, I. Egües, L. Serrano, J. Labidi, G. Spigno, G, Bioresource Technology 107 (2012) 267-274.

[5] A. Sluiter, B. Hames, R. Ruiz, C. Scarlata, J. Sluiter, D. Templeton, D. Crocker, Laboratory analytical procedure, (2010) TP-510-42618

ECAB 5
The 5th EUROPEAN CONGRESS OF APPLIED BIOTECHNOLOGY
Florence 15-19 September 2019

Bacterial alginate production under oxygen transfer rate controlled conditions

Belén Ponce, Alvaro Díaz-Barrera*

Escuela de Ingeniería Bioquímica, Pontificia Universidad Católica de Valparaíso, Av. Brasil 2147 Casilla 4059, Valparaíso, Chile.

** Corresponding author: alvaro.diaz@pucv.cl*

Highlights

- Control of the oxygen transfer rate based on the oxygen in the feed gas
- Alginate production and their molecular weight were affected by oxygen transfer rate control
- Under OTR controlled, alginate molecular weight produced during the stationary phase of growth was constant

1. Introduction

Alginates are polysaccharides composed of (1-4)-β-D-mannuronic acid and its C-5-epimer, α-L-guluronic acid. These polymers are used in the food and pharmaceutical industries as stabilizing, thickening, gel- or film-forming agents [1]. Alginates are produced by brown algae, but they can also be produced by the bacterium *Azotobacter vinelandii*. One strategy to produce alginates with defined molecular weight (MW) is through the manipulation of the culture conditions during fermentation. In our group, we have found evidences that the oxygen transfer rate (OTR) affects the molecular weight of alginate [2]. During the stationary phase of growth, both the OTR and the MW alginate decrease. In order to produce alginates with an MW constant during the fermentation time, it is possible to perform cultures at constant OTR. The aim of this work was to implement a control strategy for maintaining value of OTR constant, manipulating the oxygen in the feed gas. Thus, the alginate production was evaluated under OTR constant.

2. Methods

A. vinelandii ATCC 9046 was used. The bacterium was grown under nitrogen fixation conditions, using sucrose as carbon source. Batch cultures were prepared in a 3-L bioreactor (working volume of 1.5-L). The bioreactor was operated at 500 rpm and 30 °C. Mass flow meters/controllers were used to supply gases, keeping a constant value (1.5 L min^{-1}) by the real-time operation computer control system. The OTR was estimated by online measurements of the oxygen in the exit gas using a gas analyzer (Teledyne Instruments, model 7500). The cultures were conducted under controlled OTR or without controlling OTR. The OTR was controlled by gas blending, using a system based on a proportional-integral control, which automatically adapted the proportions of nitrogen and oxygen in the inflowing gas through mass flow controllers (Brooks Instruments, model SLA5800). Samples of cultures (20 ml) were withdrawn from the bioreactor for analytical measurements. All experiments were conducted in triplicate.

3. Results and discussion

Figure 1 shows the cell growth and OTR evolution under controlled OTR and without controlling OTR. In the cultures without controlling OTR, the maximum biomass (6.7 g L^{-1}) was higher as compared to under OTR control (5.0 g L^{-1}). During the cell growth phase, the cultures performed without OTR control shown an OTR constant, which is indicative of oxygen-limited conditions. After 40 h of cultivation (cells stopped the growing), in the cultures conducted under OTR controlled, the OTR was constant, reaching 20 mmol L^{-1} h^{-1}.

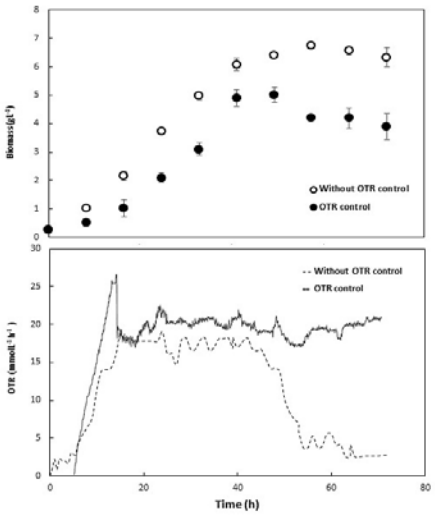

Figure 1. Biomass and OTR evolution in *A. vinelandii* cultures carried out in 3-L bioreactor.

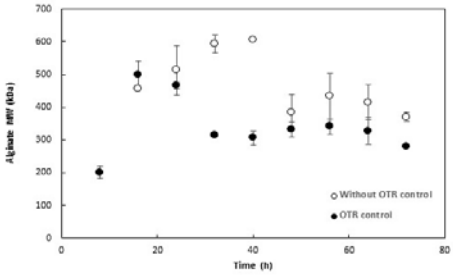

Figure 2. Alginate molecular weight evolution under OTR control and without controlling OTR in 3-L bioreactor.

Table 1. Comparison of specific cell growth rate, biomass yield on sucrose ($Y_{x/s}$), alginate yield on biomass ($Y_{p/x}$), and maximum alginate concentration.

OTR condition	μ (h^{-1})	$Y_{x/s}$ (g g^{-1})	$Y_{Alginate/x}$ (g g^{-1})	Alginate $_{máx}$ (g L^{-1})
Without OTR control	0.12 ±0.01	0.31 ±0.03	0.28 ±0.03	2.88 ±0.10 (56 h)
OTR control	0.17 ±0.02	0.16 ±0.02	1.14 ±0.18	5.34 ±0.13 (64 h)

Figure 2 shows that the OTR control affected the production and the molecular weight of alginate. In the culture with control of the OTR, the alginate MW during the stationary phase of growth was constant (300 kDa). It is possible that changes in genes involved in alginate polymerization and depolymerization could be affected by variation in the OTR during stationary phase. A higher alginate production under OTR controlled was obtained (Table 1).

4. Conclusions

The strategy implemented for controlling the oxygen transfer rate in *A. vinelandii* cultures is useful for maintain constant the molecular weight of alginate during the stationary phase of growth. The OTR control could be used in order to produce alginates with particular characteristics.

References

[1] Hay, I., Rehman, Z., Moradali, MF., Wang, Y., Rehm, BHA. Microbial alginate production, modification and its applications. Microb. Biotechnol. 6 (2013) 637–650.

[2] Díaz-Barrera, A., Gutiérrez, J., Martínez, F., Altamirano, C. Production of alginate by *Azotobacter vinelandii* grown at two bioreactor scales under oxygen-limited conditions. Bioprocess Biosyst. Eng. 37 (2014) 1133–1140.

Biosurfactant production by *Piper hispidum* endophytic fungi using cooking oil residue as substrate.

Segio Duvosin Jr*, Messe da Silva, Patricia Albuquerque

Amazonas State University, Laboratory of Chemistry Applied to Technology, 1200 Darcy Vargas Ave., Manaus, Amazonas, Brazil, 69050-020.

**Corresponding author: sjunior@uea.edu.br*

Highlights

- *Piper hispidum* endophytic fungi are able to produce tensoactive molecules.
- The fungi were able to use the cooking oil residue as substrate.
- The reduction of superficial tension of the cultivation broths was around 40%.

1. Introduction

Fungi found in plant species, called endophytic fungi, present a great potential for the production of new bioactive substances [1]. Among substances of commercial interest are the biosurfactants, amphipathic compounds that present tensoactive properties and are produced by microorganisms [2]. Biosurfactants comprise a wide variety of industrial applications, which include bioremediation, biodegradation, cleaning of oil containers, and have been employed at the food, pharmaceutical, and cosmetic industries. [3] Recently, the use of residues for the production of biosurfactants has gained attention, since it implies in cost reduction [4]. Therefore, this work has evaluated the biosurfactant production on metabolic broths of endophytic fungi isolated from the Amazon species *Piper hispidum* (Piperaceae) using cooking oil residue as substrate.

2. Methods

The endophytes were isolated previously and maintained on BDA tubes, being activated on this media at 28°C during 5 to 10 days. It was produced a spore suspension (1,0 x 10^8 spores/mL), which was inoculated in 125 mL Erlenmeyer flasks containing the liquid media - $MgSO_4$ (0.5 g/L), Na_2HPO_4 (3.0 g/L), KH_2PO_4 (1.0 g/L) and yeast extract (1.3 g/L) [5]. After autoclaving the media, it was added 0.5 g/L of filtered cooking oil residue in order to induce the biosurfactant production. The fungi were cultivated in triplicate during 7 days in a shaker at 28°C and 170 rpm. After the experiment, the cultivated media was filtered and the supernatant was used to evaluate the biosurfactant production. In order to access the biosurfactant production it was determined the emulsification index (E_{24}) [6]. The lowering of superficial tension (ST) was verified with the of a tensiometer [7] in order to verify the efficiency of the biosurfactant.

3. Results and discussion

The endophytic fungi were able to produce tensoactive molecules using the cooking oil residue, since it was observed a lowering of the superficial tension (ST) of the cultivation broths, and the emulsion formation in the presence of kerosene (Table 1). For the fungi PH I 19F, isolated from the

leaf, the ST went from 67.5 to 35.9 Mn/M (46.8% reduction), within 12 days of cultivation in the presence of the residue. The emulsification index (E_{24}) was 30%. For the fungi PH I 12F, also from the *P. hispidum* leaf), the TS reduced from 67.5 to 32.9 mN/m (51.3% reduction) eitihn 8 days, and the E_{24} was 28%.

Table 1. Emulsification index (E_{24}) and superficial tension (ST) of *Piper hispidum* endophytic fungi cultivation broths containing the cooking oil residue.

PH I 12F			**PH I 19F**		
Cultivation Time (days)	E_{24} (%)	ST (mN/m)	Cultivation Time (days)	E_{24} (%)	ST (mN/m)
0	0	67.5	0	0	67.5
4	23	38.7	4	24	34.3
8	27	36.7	8	28	32.9
12	30	35.9	12	22	35.2

According to same authors, biosurfactants that present low molecular weight have the ability to reduce the superficial tension, and those that have higher molecular weights are more likely to promote stable emulsions, acting as a bioemulsifier [8]. Haba et al [9] affirmed that microorganisms that are considered the best biosurfactant producers are capable to reduce the superficial tension to values below 40 mN/m. Therefore, the *P. hispidum* endophytic fungi may be considered as promising biosurfactant producers.

4. Conclusions

It was possible to access *P. hispidum* endophytic fungi that produce biosurfactants which presented promising physical-chemical properties for being used in different industrial areas. The cooking oil residue showed to be a promising substrate for the production of fungi biosurfactant.

References

[1] V. M. Chapla, C. R. Biasetto, A. R. Araujo, Revista Virtual de Química, 5 (2013) 421-437.

[2] C. N. Mulligan, Environmental Pollution 133 (2005) 183-198.

[3] K. Urum, T. Pekdemir, Chemosphere, 5 (2004) 1139-1150.

[4] J. M. Luna, R. D. Rufino, A. M. A. T. Jara, P. P. F. Brasileiro, L. A. Sarubbo, Colloids Surfaces A: Physicochemical Engineering Aspects, 480 (2015) 413-418.

[5] D. F. C. Estudo da influência de biossurfactantes na biorremediação de efluentes oleosos. Masters Thesis, Universidade Estadual de Campinas, 2000.

[6] O. Pornsunthorntawee, P. Wongpanit, S. Chavadej, M. Abe, R. Rujiravanit, Bioresource Technology, 99 (2008) 1589-1595.

[7] J. D. V. HAMME, A. SINGH, O. P. WARD, Biotechnology Advances, 24 (2006) 604-620.

[8] E. HABA, M. J. ESPUNY, M. BUSQUETS, A. MANRESA, Journal of Applied Microbiology, 88 (2000) 379-387.

Integrated micro-system for lipase-catalyzed biodiesel production

Martin Gojun*, Anita Šalić, Bruno Zelić

University of Zagreb, Faculty of Chemical Engineering and Technology, Marulićev trg 19, HR-10000 Zagreb, Croatia

**Corresponding author: mgojun@fkit.hr*

Highlights

- Lipase-catalyzed biodiesel synthesis in microreactors was performed
- Different microreactor systems were investigated
- Integrated system composed of lipase-catalyzed biodiesel production and glycerol separation is proposed

1. Introduction

Due to recent widespread issues concerning the over usage of fossil fuels, alternative sources of energy are developed with fast pace. When it comes to transportation, biofuels such as biodiesel, can become a clean and renewable substitute for petroleum diesel. Biodiesel, a mixture of monoalkyl esters of long-chain fatty acids, provides valuable improvement in comparison with petroleum diesel in terms of biodegradability and renewability, better quality of exhaust gas emission and lower environment harmful effect. [1] Between various production processes of biodiesel, transesterification is most commonly used technique, even though the conventional process has some disadvantages. Microreactor technology, as one possible improvement of conventional processes in terms of mixing, mass transfer and reducing the reaction time, has been thoroughly explored in recent decades. [2] However, enzyme-catalyzed process continues to represent area which need to be more briefly investigated. In this work, lipase from *Thermomyces lanuginosus* was used as catalyst in biodiesel production. Oil, both edible and waste, was used as a substrate. To find out the "ideal system" for biodiesel synthesis, different configurations of microreactors have been used. In addition, some other parameters which affect on biodiesel production have been monitored, such as microchannel size, residence time, reaction temperature and source of catalyst. [3]

2. Methods

Biodiesel production from both edible sunflower oil and waste cook oil using Lipolase 100L was performed in different configurations of microreactors. According to literature data for feeding ratios, microreactor system was set with a goal to find "ideal system". In addition, each configuration was used for a set of different residence times to examine that impact as well. All experiments were performed at 40°C (optimal temperature for enzyme activity) which was secured with a water bath in which microreactor system was placed. While running the process across few

days for each configuration, lipase activity was determined daily, by measuring the change of absorbance at 410 nm with a spectrometer. Feeding inlets in this experiments were edible/waste oil, methanol, enzyme dissolved in buffer and emulsifier. Due to different configurations of microreactors, emulsifier is sometimes needed to prepare stable water:oil or methanol:oil emulsion.

After investigating all different configurations and selecting optimal system, integrated system is introduced. The idea is to connect two microchips in series, so that the first one is used for biodiesel production and the second one is used for simultaneous glycerol separation. [4] The main goal is that glycerol content in biodiesel is below 0.02%, which is limit according to the American standard ASTM D 6571 and the European standard EN 14214.

3. Results and discussion

Different configurations of microreactors with different feeding inlets were used to investigate biodiesel synthesis. Influence of residence time on F.A.M.E. content is shown in Figure 1. for both investigated microreactor systems: a) 2 inlets and 2 outlets, and b) 3 inlets and 2 outlets. Further investigations of different microreactor system configurations and emulsifiers is planned.

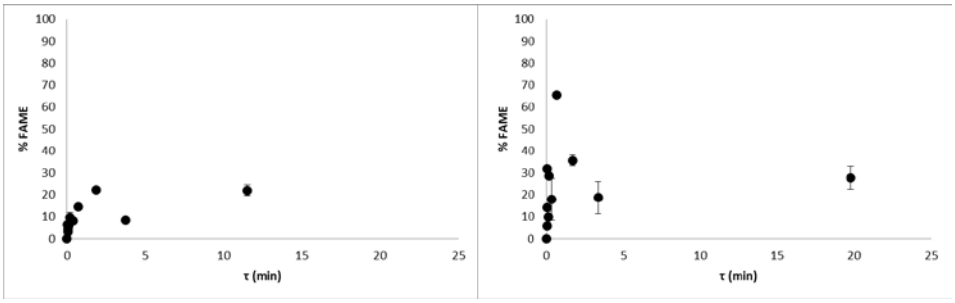

a) b)

Figure 1. Obtained FAME content in a microreactor applzing a) 2/2 microreactor system and b) 3/2 microreactor system.

4. Conclusions

Lipase-catalyzed biodiesel production showed an improvement over conventional transesterification process. Several aspects still need to be investigated. After the biodiesel production, biodiesel purification (removal of glycerol) is required to fulfill American or European standards for biofuels. Thus, integrated system of simultaneous biodiesel production and purification is proposed.

References

[1] A. Mazubert, J. Aubin, S. Elgue, M. Poux, Green Process. Synth. 3 (2014) 419–429.
[2] A. Madhawan, A. Arora, J. Das, A. Kuila, V. Sharma, Biomass Convers. Biorefin. 8 (2018) 485–496.
[3] S. Budžaki, A. Šalić, B. Zelić, M. Tišma, Chem. Biochem. Eng. Q. 29 (2015) 329–333.
[4] A. Šalić, A. Jurinjak Tušek, A. Sander, B. Zelić, New Biotechnol. 47 (2018) 80–88.

ECAB 5
The 5th EUROPEAN CONGRESS OF APPLIED BIOTECHNOLOGY
Florence 15-19 September 2019

CO_2 and SO_2 removal from cement plant flue gases by *Scenedesmus dimorphus* cultivation - Impact on cell growth and biochemical content

Aldo Mirisola[1], Diane Thomas[1], Anne-Lise Hantson[1]

1 Chemical and Biochemical Process Engineering Unit ; UMONS ; Rue de l'épargne, 56 ; 7000 Mons ; Belgium

**aldo.mirisola@umons.ac.be*

Highlights

- Microalgal cultivation is a promising source of bio-based energy
- Industrial flue gases are a propitious source of carbon and sulfur for the cultures
- Sulphites formed by the flue gas dissolution inhibit growth at high concentration
- *S. dimorphus* composition is slightly impacted by the sulfite content of the medium

1. Introduction

Microalgae are considered as a promising source of bio-based energy thanks to their high photosynthetic rates and their rapid growth compared to terrestrial plants, high lipid content, low surface area demand and year-round cultivation. Nevertheless, life-cycle assessment for production of interesting products like biodiesel from microalgae cultivation have shown that the production of biomass needs to be coupled with some other aspects: the valorisation of microalgal high-value-added by-products (antioxidants, protein and/or polysaccharide contents), the CO_2 mitigation and the use of other industrial waste streams[1].

This is why industrial flue gases are a propitious source of carbon and other nutrients for the microorganisms[2,3]. In such an industrial process, some components of the flue gas (mainly CO_2 and SO_2) are transferred into the culture medium and form dissolved CO_2 and SO_2 as well as (hydrogen)-carbonates and (hydrogen)-sulphites. The latter are then oxidised by oxygen to form sulphates. Sulphates and (hydrogen)-carbonates are nutrients for the culture, but some authors have shown that hydrogen sulphites can inhibit microalgal growth[4,5].

The first objective of this work was to determine the composition of *Scenedesmus dimorphus*'s culture medium (3N-BBM medium) at equilibrium with a synthetic cement plant flue gas. According with the equilibrium compositions, three sulphite stresses were performed on *S. dimorphus* cultures in order to evaluate the impact of the sulphite anions on cell growth and biochemical composition (proteins, polysaccharides and lipids).

2. Methods

Absorption equilibrium between the synthetic flue gas and the 3N-BBM culture medium

The 3N-BBM medium is a fresh autotrophic medium[6]. The synthetic flue gas composition is: 300 ppm SO_2, 33 ppm NO_2, 430 ppm NO, 5% O_2, 20% CO_2, balance N_2. The liquid phase was analysed by ionic liquid chromatography associated with a conductivity detector (SO_3^{2-} and SO_4^{2-} contents) and by a total organic carbon analyser (NDIR) for the determination of the carbon species content.

Scenedesmus dimorphus stock culture and stressed cultures

S. dimorphus (CCAP 276/48) stock culture was performed in a 2L sterile bottle placed on an agitated platform, at 25°C, under a 70 µmol PAR photon.m^{-2}.s^{-1} illumination (12h dark/12h light) provided by fluorescent lamps. The culture medium was the 3N-BBM medium at pH 7 (CO_2 supply regulation). Stressed and control cultures were performed in duplicates in 3L airlift flat panel photobioreactors, at 25°C, under a 100 µmol PAR photon.m^{-2}.s^{-1} illumination (12h dark/12h light) provided by fluorescent lamps. The culture medium was the 3N-BBM medium at pH 7 (CO_2 supply regulation). Biomass density was measured by UV-Vis spectrophotometer at 680 nm. Biomass was harvested by centrifugation and freeze-dried. The lipid content was measured by gravimetric method after solvent extraction (methanol, chloroform, water); (poly)saccharides were quantified by the phenol sulphuric method; finally, total proteins were quantified by the BCA test.

3. Results and discussion

The first part of this study showed that the NO/NO_2 are (practically) insoluble in the 3N-BBM culture medium. The S(IV)-containing anions reached a maximal concentration of 250 $mg_{SO_3^{2-}}.L^{-1}$ (figure not shown). The second part of this study investigated the impact of three sulphite concentrations on the microalgal growth and on the biochemical composition of the biomass. Figure 1 shows a growth inhibition at 200 and 600 $mg_{SO_3^{2-}}.L^{-1}$. No inhibition is observed at 50 $mg_{SO_3^{2-}}.L^{-1}$. Both the 50 and 600 ppm stresses did not induce significant changes in the biomass composition in comparison with controls: 20-27% lipids, 30-35% proteins, 30-37% (poly)saccharides. Regarding the 200 ppm stress, a 10% drop and a 7% rise have been found respectively for the protein and the (poly)saccharide contents. These contradictory behaviours can be explained by the variability of the culture duration.

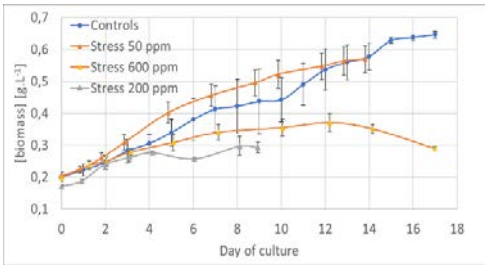

Figure 1. *S. dimorphus* growth under different sulphite stress

4. Conclusions

This study has shown that *S. dimorphus* can grow in a 3N-BBM medium containing 50 ppm of sulphites (related to the solubilization of SO_2) with no significant changes in its biochemical composition. In the future, tests will be done with the *Chlorella vulgaris* and *Cyanidium caldarium* strains. All the cultures will be stopped after 14 days to prevent undesirable differences in the biochemical composition of the biomass due to the culture duration.

References

[1] M.K. Lam, K.T. Lee, A.R. Mohamed, International Journal of Greenhouse Gas Control 10 (2012) 456-469.
[2] J.R. Benemann, Energy Conversion and Management 34 (1993) 999–1004.
[3] D. Hess, K. Napan, B.T. McNeil, E. Torres, T. Guy, J. Mclean, L.C. Quinn², Algal Res. 25 (2017) 68–75.
[4] S. Yang, J. Wang, W. Cong, Z. Cai, F. Ouyang, Enzyme Microb. Technol. 35 (2004) 46–50.
[5] J.A Lara-Gil, M.M. Alvarez, A. Pacheco, J. Appl. Phycol. 26 (2014) 357–368.
[6] CCAP. Bold Basal Medium with 3-fold Nitrogen and Vitamins. at <https://www.ccap.ac.uk/media/documents/3N_BBM_V.pdf>

Algae4Cycle - Exploiting microalgae biotechnology to treat industrial process waters with extremophilic species

Felix Wollmann*[1], Juliane Steingroewer[1], Thomas Walther[1], Felix Krujatz[1]

[1]*Institute for Natural Materials Technology, TU Dresden, Germany, Bergstr. 120, 01069 Dresden*

**Felix.Wollmann@tu-dresden.de*

Highlights

- Industrial wastewater is treatable with microalgae
- Extremophiles exhibits great potential for process water treatment.
- Nitrogen and carbon load can be reduced significantly
- Process heat can be used economically senseful

1. Introduction

Process waters from food and bioenergy industries commonly exhibit a high load of organic (e.g. sugars) and inorganic (e.g. nitrate, phosphate) residues. The disposal of such process waters is a financial burden for the companies due to high disposal fees or the need to build up an own sewage plant.

In this context, microalgae provide an promising option for wastewater treatments due to their metabolic flexibility, i.e. the ability to metabolize a great variety of organic and inorganic compounds at phototrophic, heterotrophic or mixotrophic growth, coupled with the production of valuable metabolites like fatty acids, proteins or natural pigments. Exemplarily work can be found in literature: The treatment of food waste with *Chlorella pyrenoidosa* and *Schizochytrium mangrovei* showed satisfying growth rates and stable nutrient degradation [1]. *Nannochloropsis* sp. was also used to treat industrial wastewater emitted by an oil refinery, which contains environmental challenging components like cyanide, sulphat and ammonium formate [2]. The wastewater coming from an olive mill was used to produce *Scenedesmus* sp. biomass. [3] There are a lot more published processes using microalgae, for piggery wastewater [4], carpet mill effluents [5] or paper industry wastewaters [6]. A problem for all these approaches is to maintain the axenity of the cultures.

The use of extremophilic strains reduces the probability of contaminations with other microorganisms, caused by their very selective growth conditions. Thus, the project Algae4Cycle aims on the design of a modular on-side plant for treating specifically industrial process waters with high sugar contents using mono- or co-cultures of extremophilic microalgal strains.

2. Methods

First, suitable strains were collected focusing on the utilization of carbon and nitrogen in wastewater-relevant concentrations. Therefore, extremophilic species out of Chlorophyta and Rhodophyta are investigated and their degradation capability and growth capacity is quantified. The growth on different carbon and nitrogen sources is investigated in order to create a database of the metabolic properties of the extremophilic strains.

Galdieria sulphuraria naturally exist in hot thermal springs and is capable of handling harsh

conditions like high concentrations of sulfuric acid or temperatures above 50 °C. *G. sulphuraria* is known for its capability to produce phycocyanin, a blue pigments with high economic value. There are already approaches that show promising results by using *G. sulphuraria* treating urban wastewaters in field scale[7].

Pumiliosphaera acidophila is found in mine-impacted environments with high concentrations of transition metals. It grows optimally at pH 2,5 and 30 °C [8] and is therefore a good candidate for acid-containing wastewaters. Another acidophilic candidate is *Clamydomonas acidophila* which grows optimal at pH 2,5 and offers a high content of lutein [9].

In addition to thermophilic strains there are species which shows a psychrophilic behavior. *Koliella antarctica* was found in the Antarctic sea at temperatures of -1,5 °C. Cultured at 10 to 15 °C *K. antarctica* shows a great accumulation of lutein and astaxanthin [10].

Since not all of the aforementioned microalgal strains were studied regarding the metabolization of organic substrates, growth characteristics using typical organic wastewater constituents were analyzed in this study.

3. Results and discussion

In this study we characterize the spectrum of usable energy sources for growth and assess the capacity for degrading substances arising in common industrial processes. We developed an on-site plant concept, for flexible use with different wastewater compositions and characteristics. Produced process-based waste heat is used for reducing the energy costs of the system and cleaned wastewater is recycled for reuse in producing processes. The aim is, to close the energy and material cycle and gain valuable algae-based by-products.

References

[1] Pleissner et al., „Food waste as nutrient source in heterotrophic microalgae cultivation“.W. Black, E.B. White, The Elements of Science, third ed., MacCluski, New York, 1987

[2] Biondi et al., „*Nannochloropsis* sp. F&M-M24: Oil production, effect of mixing on productivity and growth in an industrial wastewater”, Environmental Progress & Sustainable Energy, volume 32 issue 3 p. 846-853, 2013

[3] Di Caprio, Altimari, and Pagnanelli, „Integrated biomass production and biodegradation of olive mill wastewater by cultivation of *Scenedesmus* sp.“, *Algal Research* 9 (Mai 1 2015): 306–11,

[4] Orily Depraetere, Imogen Foubert, und Koenraad Muylaert, „Decolorisation of piggery wastewater to stimulate the production of *Arthrospira platensis*“, *Bioresource Technology* 148 (November 1 2013): 366–72

[5] Senthil Chinnasamy et al., „Microalgae cultivation in a wastewater dominated by carpet mill effluents for biofuel applications“, *Bioresource Technology* 101, Nr. 9 (Mai 1 2010): 3097–3105

[6] Anna Polishchuk et al., „Cultivation of *Nannochloropsis* for eicosapentaenoic acid production in wastewaters of pulp and paper industry“, *Bioresource Technology* 193 (Oktober 1 2015): 469–76

[7] Wolfgang Gross and Claus Schnarrenberger, „Heterotrophic Growth of Two Strains of the Acido-Thermophilic Red Alga *Galdieria Sulphuraria*“, *Plant and Cell Physiology* 36, Nr. 4 (Juni 11995): 633–38

[8] David Barrie Johnson, „Acidophilic Algae Isolated from Mine-Impacted Environments and Their Roles in Sustaining Heterotrophic Acidophiles“, Frontiers in Microbiology 3 (2012)

[9] María Cuaresma et al., „Productivity and Selective Accumulation of Carotenoids of the Novel Extremophile Microalga *Chlamydomonas Acidophila* Grown with Different Carbon Sources in Batch Systems“, *Journal of Industrial Microbiology & Biotechnology* 38, Nr. 1 (Januar 1 2011): 167–77

[10] Vincenzo Fogliano et al., „Functional ingredients produced by culture of *Koliella antarctica*“, *Aquaculture* 299, Nr. 1 (Februar 1 2010): 115–20

ECAB 5
The 5th EUROPEAN CONGRESS OF APPLIED BIOTECHNOLOGY
Florence 15-19 September 2019

Techno-economic analysis of xanthan production from liquid wastes of food processing

Bojana Bajić*, Siniša Dodić, Damjan Vučurović, Vladimir Puškaš, Jelena Dodić

University of Novi Sad, Faculty of Technology Novi Sad, Department of Biotechnology and Pharmaceutical Engineering, Bulevar cara Lazara 1, Novi Sad 21000, Serbia

**Corresponding author: baj@uns.ac.rs*

Highlights

- Xanthan production process and cost model was developed using simulation software
- Results represent a basis for preliminary project design of the suggested bioprocess
- Results can be used for further development of xanthan production bioprocess

1. Introduction

Cleaner production through improved material utilization, reduced energy consumption and lower emission levels represents an effective step towards making any production process sustainable. Utilizing waste streams generated from one production process as raw materials for another is just one option for reaching the aforementioned goal. Since large amounts of waste effluents are generated by the food industry, the biotechnological production of xanthan from these effluents could become a solution for re-using wastewater as well as obtaining a valuable product. By modelling the experimental results through a bioprocess simulation software, additional data can be obtained in order to facilitate further research and lead towards the ultimate goal, which is constructing a plant for xanthan production from liquid wastes of food processing [1-3]. Therefore, the aim of this research was to improve the process and cost model of xanthan production on different wastewaters.

2. Methods

Based on the previously published research [3] and in order to improve the xanthan production process, experiments were designed and carried out under optimized conditions for xanthan production on glucose (G) and three different food processing wastewaters (from the production of: biscuits - W1, ethanol from molasses - W2 and sugar - W3) as a basis of the cultivation medium. Experimental data obtained from these experiments has been incorporated into kinetic models, which have been used to simulate a xanthan production bioprocess by the SuperPro Designer simulation software. Figure 1 represents the simplified process flowsheet for xanthan production.

Economic parameters, such as unit production costs, operating costs, total revenues, have been used to compare and evaluate the simulated xanthan production process with the examined wastewaters.

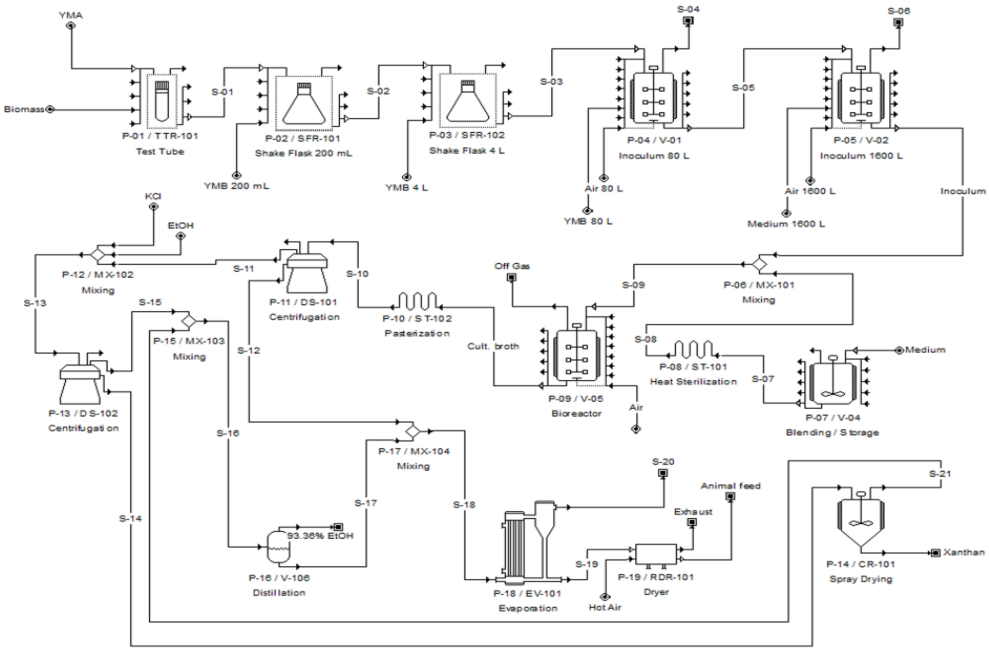

Figure 1. Process flow diagram of xanthan production

3. Results and discussion

As a result of simulated experimental data, table 1 shows the economic analysis of the xanthan production bioprocess model in media based on used wastewaters as well as glucose.

Table 1. Economic analysis of the xanthan production process model

Medium	Working capital [$]	Operating cost [$/year]	Production rate [kg /year]	Unit production cost [$/kg]	Total revenues [$/year]
G	16000	183000	44556.06	4.10	224000
W1	16000	183000	40816.34	4.48	206000
W2	16000	183000	42028.69	4.35	212000
W3	16000	183000	35066.72	5.21	177000

Although xanthan production is the most cost-effective on semi-synthetic glucose based media, the obtained results show that when using different liquid wastes of food processing as a basis of cultivation media, similar values are obtained. Therefore, these wastewaters have great potential to be used as raw materials in this bioprocess.

4. Conclusions

The results obtained through this research showed that the developed process of xanthan production from liquid wastes of food processing is economically and ecologically viable.

Acknowledgement: These results are part of the project TR31002, financed by the Ministry of Education, Science and Technological Development of the Republic of Serbia.

References

[1] M. Golušin, S. Dodić, S. Popov, Sustainable Energy Management, first ed., Academic Press, 2013.
[2] B. Bajić, D. Vučurović, S. Dodić, J. Grahovac, J. Dodić, J Environ Manage. 203 (2017) 999-1004.
[3] B. Bajić, D. Vučurović, S. Dodić, Z. Rončević, J. Grahovac, J. Dodić,, Chem. Ind. Chem. Eng. Q. 24 (2018) 127-137.

ECAB 5
The 5th EUROPEAN CONGRESS OF APPLIED BIOTECHNOLOGY
Florence 15-19 September 2019

Erythritol-inducible promoter efficiently triggers lipase CalB production in bioreactor.

Marie Vandermies[1], Young-Kyoung Park[2], Jean-Marc Nicaud[2], Patrick Fickers[1]*

1 Microbial Processes and Interactions, TERRA Teaching and Research Center, University of Liège - Gembloux Agro-Bio Tech, Av. de la Faculté, 2B. 5030, Gembloux, Belgium
2 Micalis Institute, INRA, AgroParisTech (UMR1319), Université Paris-Saclay, Domaine de Vilvert, Jouy-en Josas 78352, France
**Corresponding author: pfickers@uliege.be*

Highlights

- Three types of erythritol-inducible promoters were compared to *pTEF*.
- *pEYKA3B* and *pHu8EYK* led to 3-fold higher CalB expression than *pTEF*.
- *pEYKA3B* led to 3-fold higher CalB activity than *pTEF*.
- Glycerol 2-L fed-batch enabled consequent *pEYKA3B*-driven CalB production.

1. Introduction

The non-conventional yeast Yarrowia lipolytica is increasingly used as an alternative cell factory for recombinant protein production. Although efficient molecular tools have been developed for this host, there is still a lack of versatile regulated promoters. Such promoters would allow to modulate the detrimental metabolic load inherent to recombinant gene expression [1]. Current regulated promoters respond to hydrophobic inducers, dispersed in the culture medium as an emulsion technically sensitive to maintain, particularly at large scale. Recently, promoters from the erythritol kinase *EYK1* gene [2] and the erythritol dehydrogenase *EYD1* gene [3] have been isolated and shown to be induced by erythritol, a hydrophilic substance. Series of hybrid promoters have been developed from upstream activating sequences (UAS) of *pEYK1*, *pEYD1*, and other promoters, using fluorescent reporter proteins in small-scale cultures [2] [3]. Here we report on the comparison of three types of erythritol-inducible promoters (native, based on *UAS* from *pEYK1*, based on *UAS* from another promoter) and the subsequent selection of the most suitable promoter for proof-of-concept production of the industrial lipase B from Candida antarctica (CalB) in 2-L bioreactor.

2. Methods

CalB expression was driven by promoters *pTEF*, native *pEYD1*, synthetic or *pEYKA3B* (*pEYK1* + 3 *UAS1* of *pEYK1*) and *pHu8EYK* (*pEYK1* + 8 *UAS1* of *pXPR2*). The host strain was optimized for recombinant lipase production, with deletions of alkaline extracellular protease *XPR2*, of extracellular lipases *Lip2*, *Lip7*, *Lip8*, and of *EYK1* gene (to use erythritol as a free inducer, no longer consumed by the cells).

Promoter comparison was based on triplicate 48h cultures in 2Mag mini bioreactors (10 mL working volume). qPCR and lipase activity assays were performed to assess promoter efficiency at gene expression and protein production level, respectively. Proof-of-concept cultures were realized during 72h in duplicate in a 2-L Sartorius bioreactor operated in fed-batch mode, with increasing

glycerol feed values (0.45; 0.9; and 1.35 $g.L^{-1}.h^{-1}$, for 24h each). Lipase activity assays, SDS gel and carbon source HPLC assays were performed on culture supernatants.

The culture medium contained glycerol (10 g/L for 2Mag cultures, 1 g/L initially plus glycerol feed for 2-L cultures) as a main carbon source and erythritol (10 g/L) as an inducer.

3. Results and discussion

Erythritol-inducible promoters *pEYKA3B*, *pHu8EYK*, and *pEYD1* were compared to the strong constitutive promoter *pTEF* for CalB expression and production. At the expression level, *pEYKA3B* and *pHu8EYK* showed a 3-fold higher response than *pTEF*, while *pEYD1* presented the same behavior as *pTEF*. At the production level, *pEYKA3B* delivered a 3-fold higher extracellular CalB activity than *pTEF*, in accordance with qPCR results. *pHu8EYK* and *pEYD1* led to lower CalB activity levels. In consequence, *pEYKA3B* was selected for larger-scale experiments.

In previous studies, the induction levels of *pEYK1*-derived promoters were shown directly correlated with erythritol concentration in the culture medium, and erythritol cellular uptake appeared reduced in the presence of glycerol in the culture medium [2] [4]. Here, reactor cultures were operated in fed-batch mode to allow progressive glycerol feed at 3 increasing concentrations. In these conditions, glycerol accumulation in the culture medium was prevented, while providing sufficient energy for cell growth and CalB synthesis. Hence, during 2-L reactor cultures, CalB was accumulated in the culture medium, reaching a final value of about 900 U/gDCW. SDS gel analysis proved CalB adequate size and integrity in the culture supernatant.

4. Conclusions

Among the three types of erythritol-inducible promoters examined in the present study, the promoter *pEYKA3B* based on 3 UAS_1 from *pEYK1*, stood out with high CalB expression and production levels. Production of lipase CalB in fed-batch bioreactor demonstrated the adequacy of *pEYKA3B* and more generally erythritol-inducible promoters for recombinant protein production.

References

[1] M. Vandermies and P. Fickers, Microorganisms (2019), submitted.
[2] M. Trassaert et al, Microb Cell Fact 16:141 (2017).
[3] Y.-K. Park et al, FEMS Yeast Res 19:1 (2019).
[4] F. Carly et al, Bioresource Technol 247 (2018) 963–969.

ECAB 5
The 5th EUROPEAN CONGRESS OF APPLIED BIOTECHNOLOGY
Florence 15-19 September 2019

RECOVERY AND PURIFICATION OF XYLITOL PRODUCED BY THE BIOTECHNOLOGICAL ROUTE USING HEMICELLULOSIC HYDROLYSIS OF CASHEW APPLE BAGASSE AS FEEDSTOCK

José Edvan Marques Junior[1], André Casimiro de Macedo[1], Maria Valderez Ponte Rocha[1*]

[1]*Department of Chemical Engineering, Universidade Federal do Ceará, Brazil*
**Corresponding author: valderez.rcha@ufc.br*

Highlights

- Cashew apple bagasse can be used as substrate for the production of xylitol;
- The anti-solvent and cooling rate influence the crystallization process;
- High crystallization yield and crystals with high purity were obtained.

1. Introduction

The cashew bagasse, an abundant residue, can be used to produce xylitol (Albuquerque et al., 2015) due to its high content of hemicellulose, and after the hydrolysis it is possible to obtain sugars (i.e glucose and xylose) for the production of bioproducts (Albuquerque *et al*., 2015). These carbohydrates can be metabolized by microorganisms capable of transforming them into bioproducts, among them xylitol. Xylitol is a polyalcohol ($C_5H_{12}O$) with wide applicability, ranging from food industry products, as in sweeteners, and to pharmaceutical industry (Albuquerque *et al*., 2015; Misra et al., 2011).

Xylitol is produced in industrial scale by chemical hydrogenation of xylose, but this process presents high operating costs (Misra et al., 2011). Therefore, many studies have sought alternative routes for its production, such as in processes which microorganisms or their enzymes are involved. After the production of xylitol, the recovery and purification of the product exists. In literature, very little information is available about xylitol recovery and mainly reports are related to the obtainment and treatment of the hemicellulosic hydrolysate, its fermentation and metabolic bioconversion (Wei et al., 2010; Kaialy et al., 2014).

In this context, the biotechnological production of xylitol by yeast *Kluyveromyces marxianus* ATCC36907 using the hemicellulosic hydrolysate from cashew apple bagasse was performed with emphasis in the study of the crystallization process. In this crystallization process, different anti-solvents such as: ethanol, isopropanol and protic ionic liquid 2-(hydroxy)ethylammonium acetate (2-HEAA), percentages of anti-solvents and linear cooling rate were studied.

2. Methods

2.1. PREPARATION OF CASHEW APPLE BAGASSE HYDROLYSATE: Cashew apple (*Anacardium occidentale* L.) bagasse (CAB) was kindly provided by Jandaia Industry of Juice (Ceará, Brazil). The CAB was washed, dried at 60 °C for 24 h and milled to pass through 20-80 meshes. Cashew apple bagasse hydrolysate (CABH) was obtained from the treatment of CAB, with diluted acid sulfuric. The treatment was conducted in autoclave at 121 °C for 15 min, using 0.6 mol L^{-1} H_2SO_4 and a solid

percentage of 20% w v^{-1}. Afterwards, the liquid fraction was collected by vacuum filtration, the pH was adjusted to 6.0 ± 0.2 with $Ca(OH)_2$, and it was filtrated to separate the precipitate. The filtrate, here named CABH, was used as culture media for xylitol production.

2.1 PRODUCTION OF XYLITOL: The biotechnological production of xylitol by *Kluyveromyces marxianus* ATCC36907 was carried out in a shaker using the CABH as fermentative medium. This production occurred at 30 °C, 180 rpm for 96 h using 10% v/v of inoculum.

2.2 SOLUBILITY CURVES AND CRYSTALLIZATION OF XILITOL: Initially, the solubility curves of xylitol in different anti-solvent: water, 50% v/v water-ethanol, 50% v/v water-isopropanol, protic ionic liquid (2% hydroxyethanolamine acetate - 2-HEAA) – water 50% w/v at temperature of 5 °C and 70 °C, were constructed. After, crystallization processes were performed, using xylitol PA and the fermentative medium, evaluating different proportion of anti-solvent (50% and 70%) and the linear cooling rate (0.25 °C/min and 0.5 °C/min).

3. Results and discussion

The xylitol was soluble in the four evaluated anti-solvents (water, ethanol, isopropanol and 2-HEAA) at high temperatures, and the solubility decreases with decreasing temperature. The highest solubility of xylitol was observed in water and the lowest solubility was in 2-HEAA. Due to the shape of the curves one can use crystallization by anti-solvent, or physical precipitation, facilitating the formation of crystals of medium size, and may occur primary or secondary nucleation.

In the experiments of crystallization, the influence of the anti-solvent ratio and the cooling rate (C_r) were evaluated. The three anti-solvents showed close yields in process using xylitol PA, except in the process using ethanol 70% v/v and C_r of 0.25 °C/min, which obtained the highest crystallization yield (93%). C_r influenced the crystallization yield, a higher rate favored crystallization using 70% v/v anti-solvent ratios. However, the low cooling rates favors the formation of crystals at a lower temperature. In some conditions, the produced xylitol was not crystallized using the anti-solvent 2-HEAA and the ethanol at C_r of 0.50 °C/min in both proportions (50% and 70%), and using 70% v/v of isopropanol applying both C_r. One possible reason is the presence of xylose in the fermentative medium. Higher crystal purity 85% and higher crystallization yield 69% were obtained using 50% v/v isopropanol. Similar results were obtained by Wei *et al*. (2010).

4. Conclusions

These results show that the studied microorganism can be applied in promising experiments based on xylitol production from CAB hemicellulosic hydrolysate as carbon sources. Moreover, it was possible to recover xylitol from the fermentation medium through the crystallization process.

References

[1] T. L Albuquerque, S. D. L. Gomes, J. E. M. Junior, I. J. S. Junior, M. V. P. Rocha, Catalysis Today 255 (2015) 33–40.
[2] E. A. Martínez, M. Giulietti, J. B. A. Silva, S. Derenzo, M. G. A. Felipe, J Chem. Technol. Biot. 84 (2009) 376–381.
[3] S. Misra, P. Gupta, S. Raghuwanshi, K. Dutt, R. K. Saxena, Sep. Purif. Technol. 78 (2011) 266-273.
[4] J. Wei, Q. Yuan, T. Wang, L. Wang, Frontiers Chem. Eng. China 4 (2010) 57-64.
[5] W. Kaialy, M. Maniruzzaman, S. Shojaee, A. Nokhodchi, Int. J. Pharm. 477 (2014) 282-293.

Potential effect of crude glycerol components on the lactic acid fermentation by *Lactobacillus sp.*

Laura Castellanos Suárez[1], Luis Javier López Giraldo[1], Viviana Sánchez Torres[1]

1 Grupo de investigación en Ciencia y Tecnología de Alimientos CICTA, Universidad Industrial de Santander. Parque Tecnológico Guatiguará, km 2 vía El Refugio, Universidad Industrial de Santander, Piedecuesta (Santander), 681011, Colombia

**Corresponding author: lauracastellanos9009@gmail.com, ljlopez@uis.edu.co, visantor@uis.edu.co*

Highlights

- Three samples of Colombian crude glycerol were characterized.
- The effect of crude glycerol components on volumetric productivity of lactic acid fermentation was evaluated.

1. Introduction

In recent years, biofuels has been widely used and their production has grown exponentially. Crude glycerol – CG- is the main by-product obtained from the production of biodiesel from vegetable oils, in quantities of 10-40% by weight. In 2017 the production of biodiesel in Colombia was 459,807 tons and it is estimated that by 2020 its production will be six times higher than the market demand. As a consequence, CG has a great potential to be used as a raw material in other processes due to its low commercial price. However, one of the main challenges is the variability of its composition, since it depends on biodiesel production parameters. Despite the importance of CG chemical composition, few references have been found on its characterization [1,2].

On the other hand, our previous work showed that crude glycerol used as a substrate in lactic acid fermentation allows higher productivities than glycerol USP. Therefore, it is vital to understand the effect of CG components on reactions catalyzed by microorganisms [3].

In this sense, this research explains the effect of CG components on the volumetric productivity of lactic acid. To fulfill this scope, the following stages are being developed: a) chemical characterization and identification of CG compounds of three samples, b) design of experiment of mixtures to evaluate the productivity of Lactobacillus sp. in a fermentation medium.

2. Methods

In general, three methods were used for the chemical characterization of CG: the periodic iodometric acid method, liquid chromatography (HPLC), and gas chromatography [1]. The density of CG was determined by measuring volume and weight at room temperature. To determine the pH, CG was measured by a digital pH meter at room temperature. The viscosity of the CG was obtained using a viscometer, and the ash content was determined by a high temperature furnace. The soap and alkalinity content in CG were determined following the methodology recommended in AOCS Cc 17-95. The water content was determined by volumetric Karl Fischer titration. All measurements were made in triplicates [2].

Also, aerobic fermentations were performed with *Lactobacillus* strains (ATCC 7469 and 393) in a medium with CG as a carbon source, which contained nutrients and and trace elements that favored lactic acid production [4].

Fermentations were carried out with each sample of CG, with glycerol USP, and synthetic CG composed of the main CG components. In this way, the influence of the compounds identified as potential substrates in the fermentative production process of lactic acid was evaluated. Considering the CG characterization, different media were formulated. A synthetic glycerol medium was constructed in which three minority components found in the samples were involved, and the fermentation process was developed as described. The simplex network design, Simplex-Centroid Design - DCS, was chosen because it was desired to consider the points inside the region, because in the case of glycerol it is possible to obtain mixtures containing all the components. Finally, the metabolites were identified and quantified by HPLC, each test was done triplicated.

3. Results and discussion

All CG samples showed low FFA contents, it indicates they are derived from the acidification of the soap that existed in it. Also, the soap contents were relatively high. The composition of the samples varied significantly. The strain *Lactobacillus rhamnosus* ATCC 7469 in an axenic culture, achieved a satisfactory assimilation of CG. Reaching conversions up to 90%, after a stage of adaptation. For the evaluated conditions, it was possible to identify that the optimal volumetric productivity is around 10 hours of fermentation.

4. Conclusions

Despite the variation in the proportion of their components, all CG samples were shown to contain glycerol, soap, methanol, FAMEs, water, glycerides, FFAs, and ash. It is necessary to characterize the composition of CG before considering any value-added conversion.

The CG components influence the response variables of the fermentations, which improves or inhibits the growth and the conversion capacity of the microorganism. These effects depend directly on the biodiesel production process and its conditions, the raw materials used and the purification processes.

References

[1] Hu S, Luo X, Wan C, Li Y. Characterization of crude glycerol from biodiesel plants. J Agric Food Chem. 2012. doi:10.1021/jf30086291. Hu S, Luo X, Wan C, Li Y. Characterization of crude glycerol from biodiesel plants. J Agric Food Chem. 2012. doi:10.1021/jf3008629

[2] Thompson JC, He BB. Characterization of crude glycerol from biodiesel production from multiple feedstocks. Appl Eng Agric. 2006. doi:10.13031/2013.20272

[3] Gamboa-Rueda J., Lizcano-González V., Unstructured kinetic model of batch fermentation of usp glycerol for lactic acid production. CT&F-Ciencia, Tecnología y Futuro. Vol. 6. Num 1. Jun 2015

[4] Sumitha V, Christy Mathelin R, Sivanandham M. Effect of major and minor nutrients on lactic acid production using biodiesel waste-derived crude glycerol as a carbon source by Lactobacillus casei NCIM 2125. Energy Sources, Part A Recover Util Environ Eff. 2018;40(11):1322–1331. doi:10.1080/15567036.2018.1475519

Cultivation of phototrophic biofilms in an aerosol-based photobioreactor

Dorina Strieth[1], Judith Stiefelmaier[1], Roland Ulber[1]

1 TU Kaiserslautern, Chair of Bioprocess Engineering, Gottlieb-Daimler Str. 49, 67663 Kaiserslautern

**Corresponding author: strieth@mv.uni-kl.de*

Highlights

- Optimization and characterization of an aerosol-based photobioreactor
- Long-time cultivation and characterization of phototrophic biofilms
- New downstream process for extraction of EPS and pigments

1. Introduction

Cyanobacteria offer a great potential for the production of biotechnological products. They can be divided into two groups: terrestrial and aquatic cyanobacteria. Terrestrial cyanobacteria are living embedded in self-produced extracellular polymeric substances (EPS) and show a pronounced surface-associated or air-exposed growth. They have so far been neglected as potential production organisms due to the lack of cultivation systems (Strieth 2018). And that regardless of the fact, that biofilms can render biotechnological processes simpler and more efficient. Thus, no (harmful to humans) chemicals for an artificial immobilization are necessary because phototrophic biofilms naturally adhere to surfaces. Product purification of secreted substances is facilitated by immobilized cells and higher productivities can be achieved in continuous processes (Strieth 2017) as the growth rate can be decoupled from the dilution rate (Muffler 2014). At the chair of bioprocess engineering an emerse photobioreactor (ePBR) was developed where the medium is given as an aerosol (Kuhne 2014, Strieth 2017). The system imitates natural habitats of terrestrial cyanobacteria in the desert and the rain forest. During the last decade, a few biofilm photobioreactors were developed imitating different natural habitats of terrestrial cyanobacteria. The latest developments are summarized, illustrated and compared in the reviews of Podola 2017 and Strieth 2018. Hitherto, the majority of biofilm photobioreactors are used in lab scale resulting in small amounts of biomass that can be utilized for further analysis. To facilitate the characterization of small amounts of biomass, a combined extraction of EPS and the pigments (i) chlorophyll-a, (ii) carotenoids and (iii) phycobiliproteins has been developed. This is important for a comprehensive characterization of the cells in order to be able to draw conclusions about the state of the cells. For example, EPS are produced as protection against suboptimal culture conditions. Carotenoids are produced, among other things, for cell wall stabilization. Essentially, the pigment composition depends on the available light spectrum, temperature and availability of nutrients.

2. Methods

The most important parameter of the optimized ePBR were characterized like residence time resolution of the aerosol (experimental by using high-speed camera and simulated using OpenFOAM), droplet size, the light and temperature distribution (experimental by using a quantum

sensor and a laser thermometer and simulated using MatLab) and the surface texture (roughness using AFM and hydrophobicity). The terrestrial cyanobacterium *Trichocoleus sociatus* was cultivated on three different substrates (PMMA, borosilicate glass, silicone) in the ePBR at 24 °C and 24 hours of aerosol supply. In addition, the influence of different temperatures (24, 30, 37 °C), amount of aerosol per day (4, 8, 12, 24 h) and the influence of higher amounts of CO_2 (0,03, 2, 5, 10 %) and flue gas were investigated. To characterize the biofilm a new downstream process was developed where the EPS was extracted in a first step using an optimized method and the pigments (phycobilisomes, chlorophyll and c-phycocyanin) in a second step. Optical coherence tomography was used to determine the biofilm thickness over the cultivation time and two-dimensional growth was measured over chlorophyll-a fluorescence using a PAM fluorometer.

3. Results and discussion

Different surfaces showed no influence on the biomass production and the pigment composition, whereas on hydrophilic surfaces more vertical growth and on the hydrophobic surface rather horizontal growth could be observed, which was attributed to the hydrophobicity of *T. sociatus*. In addition, increased EPS production was demonstrated on the hydrophilic surfaces due to the horizontal spread of the biofilm in combination with the hydrophilic properties of the EPS. The layer thickness stagnates in the ePBR at 600 µm, which is presumably caused by the low light availability. Thus, higher layer thicknesses of up to two mm were achieved at higher light intensities. The biofilm thus actively adapts to the availability of light, as shown by the degradation of the pigments but also in the production of EPS. The growth of *T. sociatus* at 24 °C was antiproportional to the amount of aerosol per day and higher EPS yields were achieved at longer dry times. An increase in temperature led to a desiccated biofilm were no growth could be achieved at 37 °C and 8 h aerosol supply. The interaction between aerosol delivery and temperature could be modeled via the black-box system and verified with a further experiment. A developed semi-continuous process led to increased EPS yields with targeted growth and dry phases. In addition, an increased production of an antibacterial substance under extreme conditions was demonstrated. The structure of the substance is currently being investigated. The developed process could be used in industry for the production of EPS or secreted substances. Cultivations with elevated CO_2 concentrations unexpectedly led to growth inhibition. Interestingly, almost identical biomass productivities were achieved using atmospheric CO_2 (380 ppm) and flue gas (10 % CO_2). Thus, CO_2 does not appear to be the reason for growth inhibition at elevated CO_2 concentrations.

4. Conclusions

The cultivation of *T. sociatus* in the optimized ePBR was successful and the influence of temperature and aerosol per day could be modeled. The biomass and EPS productivities in the ePBR are higher than in submerse reactors and can be targeted influenced using different times of dry phases.

References

[1] K. Muffler, L. Lakatos et al. Adv. In biochem. Eng./biotec. vol. 146 (2014), pp. 123-161.
[2] S. Kuhne, D. Strieth, M. Lakatos, K. Muffler, R. ulber, J. Biotechnol. 192 (2014), pp. 28-33.
[3] D. Strieth, R. Ulber, K. Muffler, Bioproc. And Biosy. Eng. 41 (2017), pp. 295-312.
[4] D. Strieth, J. Schwing, S. Kuhne, L. Lakatos, K. Muffler, R. Ulber. J. Biotechnol. 256 (2017), pp. 6-12
[5] B. Podola, T. Li, M. Melkonian. J Chem. Technol. & Biotechnol. (2007), pp. 233-247.

Mild fractionation of hydrophilic and hydrophobic components from *Neochloris oleoabundans* using ionic liquids.

Michel Eppink[1], Corjan van den Berg[1], Rene Wijffels[1,2]

1 Bioprocess Engineering, Wageningen University, 6700 AA, Wageningen, The Netherlands; 2 Nord University, N-8049, Bodø, Norway

**Corresponding author: michel.eppink@wur.nl*

Highlights

- Cyphos 108 is able to permeabilize the cells.
- Lipids are extracted from intact cells.
- Proteins and carbohydrates are recovered after cell disruption
- Hydrophobic and hydrophilic compounds can be efficiently separated.

1. Introduction

Microalgae are promising feedstocks for biofuel production. These photosynthetic microorganism have high lipid productivity and do not compete for arable land when compared to terrestrial oleaginous crops. Microalgae have a very tough cell wall and thus require energy intensive unit operations to break open the cell and release the intracellular content. Apart from lipids, microalgae are also good sources for proteins, carbohydrates and pigments. Utilization of these value added co-products for food, cosmetics, health and chemicals would help in making the process economically feasible.

The primary objective of this article is to fractionate the algal biomass into a hydrophobic fraction (lipids) using mild pre-treatment at low temperature with an aqueous solution of ionic liquid and keep the microalgae intact followed by cell disruption to obtain the hydrophilic fraction (proteins, carbohydrates) in their functional state. [Calibri 11].

2. Methods

N. oleoabundans cells ~10 mg of cells (freeze dried and/or fresh cells) were treated with 1.5 ml of aqueous solution of IL at 45°C for 30 minutes. Fresh and freeze dried cells used in the study were from different batches. The studies were conducted with 2 different ILs BMIM DBP and TBP SO4 (see Table 1). The influence of IL concentrations (40, 80) % w/w on extraction efficiency of lipids was investigated. The amount of lipids extracted in the IL phase was determined by measuring the residual amount of lipids remaining in the cells. [Calibri 11].

Sr. No.	Ionic Liquid Names	Abbreviations
1	Tributylmethylphosphonium methyl sulfate (Cyphos 108) > 95 %	TBP SO4
2	1-Butyl-3-methylimidazolium dibutylphosphate 97 %	BMIM DBP

3. Results and discussion

Two classes of ILs (see Table 1) were studied. Pre-treatment with imidazolium (BMIM DBP) based ionic liquid showed better lipid extraction efficiency and phosphonium (TBP SO4) based ionic liquids showed low extraction efficiency but could have impact on the cell wall and hence selected for further studies. Lipid extraction efficiency of aqueous IL solutions at different concentrations (40, 80) % w/w were studied at temperature of 45°C (see figure 1). In this study, lipids represent the fatty acid methyl ester content that could be converted to biodiesel. As the concentration of IL increases from 40% w/w to 80% w/w at 45°C, the amount of lipid extracted increases from 2.61% to 9.89% per mg of biomass for BMIM DBP and from 1.28% to 3.27% per mg of biomass for TBP SO_4. This increase in extraction capacity could be attributed to the increase in hydrophobicity of the IL solution. IL solutions under mild conditions were able to extract lipids from intact microalgae cells. Based on the results in figure 3, BMIM DBP could permeabilise the cells and extract lipids better than TBP SO4 indicating that the cation and anion influences the extraction efficiency, but to a different degree. Although, TBP SO4 shows low lipid extraction efficiency, it might still have an influence on the cell wall. The hypothesis is that the hydrogen bonding network of the cell wall is disrupted leading to the formation of pores through which lipids can leak-out. ILs are known to solubilize natural polymers such as cellulose and pectin by direct IL interaction. [Calibri 11].

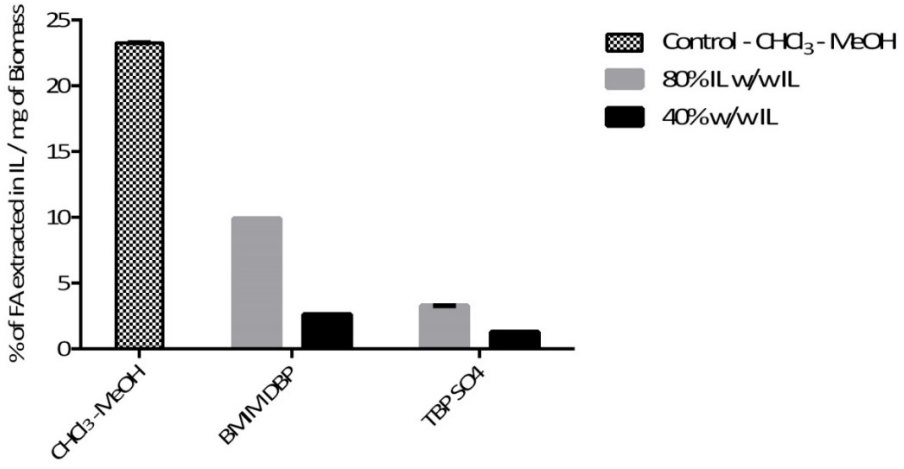

Figure 1. Effect of IL concentration on extraction of lipids at 45°C Caption. [Calibri 9].

4. Conclusions

In this article, pre-treatment of *N. oleoabundans* using ILs and subsequent fractionation into hydrophilic and hydrophobic components was studied for both fresh and freeze dried biomass. Additionally, the lipid extraction efficiency of aqueous IL solution under different concentration conditions were studied. We have demonstrated that aqueous solution of imidazolium and phosphonium based ILs was able to extract lipids from intact microalgae, albeit to a different degree. We have also shown that pre-treatment of microalgae with BMIM DBP and TBP SO4 at low concentration (40% w/w) results in permeabilisation of cells. The biomass can then be fractionated into hydrophilic and hydrophobic components whereby the proteins were recovered without losing their nativity. The recovery of total fatty acids was ~68% and that of proteins and carbohydrates was ~ 80% and 77% respectively of the total amount present in the cells, after pre- treatment of fresh biomass with TBP SO4. [Calibri 11].

References [Calibri 10]

[1] Wijffels, R. H., Barbosa, M. J., An outlook on microalgal biofuels. *Science* 2010, *329*, 796-799.
[2] Wijffels, R. H., Barboas, M. J., Eppink, M. H. M., Microalgae for the production of bulk chemicals and biofuels. *Biofuels, Bioprod. Bioref.,* 2010, 4, 287-295.
[3] Vanthoor-Koopmans, M., Wijffels, R. H., Barbosa, M. J., Eppink, M. H. M., Biorefinery of microalgae for food and fuel. *Bioresource Technology* 2012, *135*, 142-149.
[4] Desai, R. K., Monteillet, H., Li, X., Schuur, B*., et al.*, One-step mild biorefinery of functional biomolecules from microalgae extracts. *Reaction Chemistry & Engineering* 2018, *3*, 182-187.
[5] Desai, R. K., Streefland, M., Wijffels, R. H., Eppink, M. H. M., Novel astaxanthin extraction from Haematococcus pluvialis using cell permeabilising ionic liquids. *Green Chemistry* 2016.
[6] Desai, R. K., Streefland, M., Wijffels, R. H., Eppink, M. H. M., Extraction and stability of selected proteins in ionic liquid based aqueous two phase systems. *Green Chemistry* 2014, *16*, 2670-2679.

ECCE 12
ECAB 5

ECAB 5
The 5th EUROPEAN CONGRESS OF APPLIED BIOTECHNOLOGY
Florence 15-19 September 2019

Recombinant Mut+ *P. pastoris* GS115 hepatitis B virus core-antigen *(HBcAg)* obtainment in methanol PID-controlled fed-batch process

Oskars Grigs[1], Emils Bolmanis[1,2], Vytautas Galvanauskas[3]

1 Latvian State Institute of Wood Chemistry, Dzerbenes str. 27, Riga, LV-1006, LATVIA

2 Latvian Biomedical Research and Study Centre, Ratsupites str. 1, Riga, LV-1067, LATVIA

3 Kaunas University of Technology, Studentu 50-162, Kaunas, LT-51368, LITHUANIA

**Corresponding author: oskars.grigs@edu.rtu.lv*

Highlights

- Methanol feeding rate PID-control
- *P. pastoris* DCW of 100 g/L
- HBcAg yield 3.5 mg (protein)/g (cell wet weight)

1. Introduction

Hepatitis B virus core-antigen (HBcAg)-made capsids are being intensively investigated for various biomedical applications [1]. Industrially-applied recombinant protein expression host of methanotroph *P. pastoris* GS115 is well suitable for obtaining HBcAg. Characteristic methanotroph *P. pastoris* host property is utilization of methanol as a carbon and energy source, while methanol presence in the medium ensures induction of recombinant protein synthesis. Although methanol concentration (MC) influence on recombinant protein synthesis level is well known, this factor is not studied on HBcAg obtainment with *P. pastoris*. If on-line MC measurements are available, PID-control algorithm can be applied for pre-set MC control by manipulating methanol feeding rate to the bioreactor. Screening results of various MC levels of "methanol-limited (≈0 g/L)", 1, 3 and 5 g/L for improved HBcAg obtainment, will be analyzed within the Postdoctoral research project (Project Agreement No. 1.1.1.2/16/I/001, Research Application No. 1.1.1.2/VIAA/1/16/186).

2. Methods

Methanol PID-control algorithm, adapted from Cos O. et al. [2], was programmed in Matlab. Laboratory bioreactor (5 L) communication architecture of DCU-SCADA-(OPC)-Matlab is well described in the previous research [3]. Detailed information on recombinant host and HBcAg downstream processing is available [4]. Cultivation conditions selected regarding Invitrogen co. protocol (Pichia Fermentation Process Guidelines) for Mut+ strains. On-line methanol was measured with BCP-EtOH off-gas analyzer (Bluesens).

3. Results and discussion

Results of methanol 1 g/L set-point control process are shown in Figure 1. Characteristic methanol peak appears at the beginning of methanol feed start phase (peak height around 3 g/L). During culture adaptation to methanol (30-42 h), methanol limited conditions are obtained. Afterwards, automatic methanol feeding for set-point control of 1 g/L was activated. Around 2-hours-long

methanol peak of 2 height g/L appears at the beginning of the automatic methanol control phase. Further methanol control resulted in close process MC to the set-point value, where at the process end phase, due to process disturbance from operator's side and achievement of culture maximum capacity, methanol deviation from set-point occurs. Finally, culture dry weight biomass of 100 g/L was obtained. HBcAg accumulation dynamics was analyzed from "methanol-limited" process: HBcAg yielded in 2.8 mg (protein)/g (wet cell weight) at 48 process h, and 3.5 mg (protein)/g (wet cell weight) at process 75 h. The following identified PID control parameters: Kp=0.05 L*L/g*h (proportional gain) and t_pid=10 min (integral time constant) were used.

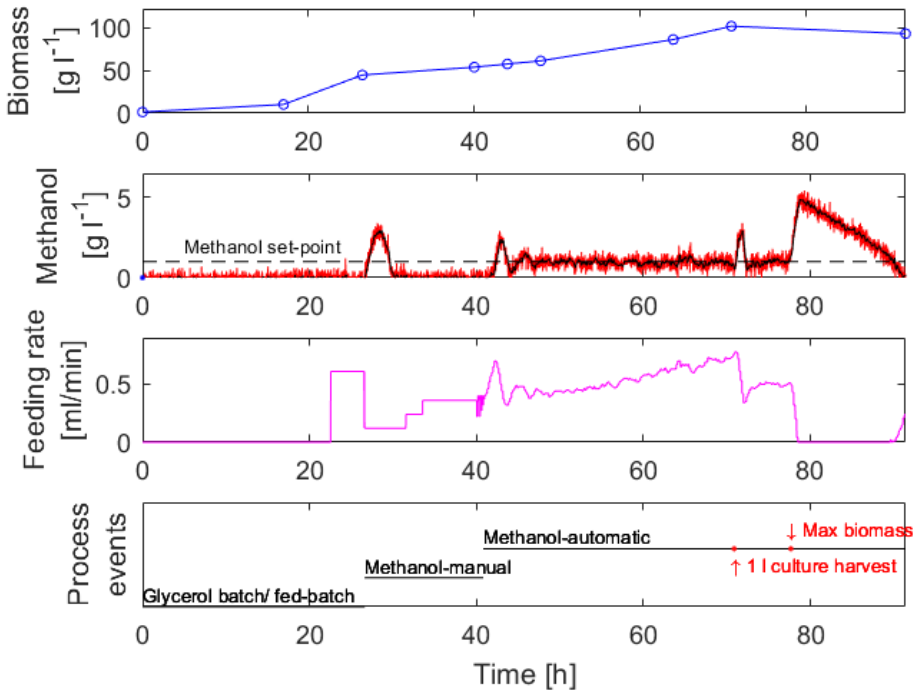

Figure 1. Biomass: off-line dry weight measurements (circles); Methanol: on-line signal (red line), filtered signal (black line), set-point (dashed line); Feeding rate: bioreactor variable; Process events: control, events and observations.

4. Conclusions

Implemented MC PID-control is capable for on-line MC close control to set-point of 1 g/L. Further process optimization with set MC of 3 and 5 g/L should be performed. HBcAg accumulation dynamics in these processes should be analyzed.

References

[1] A. Dishlers, D. Skrastina, R. Renhofa, I. Petrovskis, V. Ose, I. Lieknina, J. Jansons, P. Pumpens, I. Sominskaya. Molecular Biotechnology. 57 (2015) 1038–1049.
[2] O. Cos, R. Ramon, J.L. Montesinos, F. Valero. Biotechnology and Bioengineering. 95 (2006) 145–154.
[3] O. Grigs, V. Galvanauskas, K. Dubencovs, J. Vanags, A. Suleiko, T. Berzins, L. Kunga. Chem. Biochem. Eng. Q. 30 (2016) 47–60.
[4] J. Freivalds, A. Dislers, V. Ose, P. Pumpens, K. Tars, A. Kazaks. Protein Expression and Purification. 75 (2011) 218–224.

Polyhydroxybutyrate (PHB) production by methanotrophic consortia under high methane atmosphere

Elen Aquino Perpetuo[1,3], Letícia Oliveira Bispo Cardoso[2,3], Bruno Karolski[3,4], Louise Hase Gracioso[3,4], Bruna Bacaro Borrego[1,4], Cláudio Augusto Oller do Nascimento[3,4]

1 Department of Marine Sciences, Federal University of São Paulo, Santos, SP, Brazil; 2 The Interunit Graduate Program in Biotechnology, University of São Paulo, São Paulo, SP, Brazil; 3 Environmental Research and Education Center, University of São Paulo, São Paulo, SP, Brazil; 4 Chemical Engineering Department, University of São Paulo, São Paulo, SP, Brazil

**Corresponding author: elen.aquino@unifesp.br*

Highlights

- Selection of four methanotrophic consortia highly resistant to methane.
- Methane consumption confirmed through pMMO activity analyzed by PCR.
- PHB production of 15% (w/w) under 70% methane atmosphere

1. Introduction

Methane gas is abundantly present in the environment due to its both natural and anthropogenic production. However, methane is a harmful gas since it is one of the causes for the greenhouse effect. Its production has been increasing 10 ppb per year [1] and since methane has a greenhouse warming potential (GWP) 28 times higher than carbon dioxide [2], it is necessary to search for alternatives to mitigate it from the atmosphere. The use of methane as substrate for biodegradable plastics production would be an alternative to solve another issue of public awareness: the damage caused by the increasing production of non-biodegradable plastics. Methanotrophic bacteria are ubiquitous in the environment and have the ability of producing polyhydroxybutyrate (PHB) from methane under specific conditions [3]. PHB is a biodegradable plastic that still presents high production costs [4] and using methane as feedstock for biopolymer production could make the price competitive for the commercial market.

2. Methods

Mangrove sediment samples were collected and enriched with methane concentrations in the atmosphere increasing from 20% to 70% (v/v) during 40 days. The enrichment was performed using closed flasks coupled with needles and hoses to perform atmosphere change every seven days. From these samples, four different consortia were selected and analyzed by molecular biology through PCR reaction to confirm the methane monooxygenase (pMMO) activity and methane consumption. These consortia were tested for PHB production with N-free NMS during 30 days

under 28 °C and 180 rpm. By the end of the experiment, PHB was extracted from inside bacterial cells as described in [5], collected and characterized by magnetic nuclear resonance (NMR).

3. Results and discussion

From mangrove samples, four consortia were selected and named MC, MG1 SED, MG2 and MG2 SUB. PCR analysis of the pmoA gene were performed and resulted positively for all the consortia. The gene pmoA is responsible for pMMO enzyme which oxidizes methane to methanol in the first step of methanotrophic metabolic pathway, confirming the methane consumption. PHB production was tested in closed flasks under 70% methane atmosphere in air (v/v). Atmosphere was changed every seven days to ensure the availability of high methane concentration inside the flasks. Results of PHB production reached nearly 15% of PHB (w/w) for all the consortia (Figure 1). Extracted PHB was collected and characterized by RMN to confirm the chemical characterization.

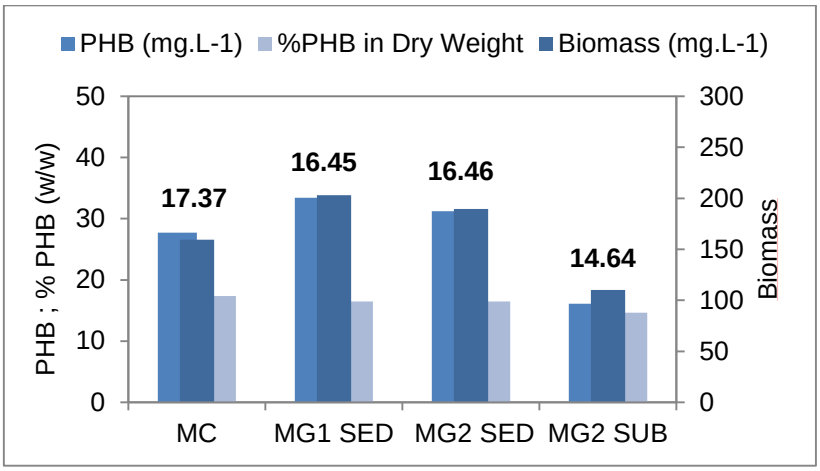

Figure 1. Biomass, PHB production and %PHB (w/w) of the consortia under 70% methane atmosphere after 30 days.

4. Conclusions

Four methanotrophic consortia highly resistant to methane were selected from environmental samples. All of them presented the pmoA gene, ability to consume methane and to produce PHB. PHB production reached 15% (w/w), which is a promising result when considering it has been made using a one-carbon molecule as feedstock.

5.Acknowledgements

The authors gratefully acknowledge support from FAPESP and SHELL Brasil through the 'Research Centre for Gas Innovation – RCGI' (FAPESP Proc. 2014/50279-4), hosted by the University of Sao Paulo, and the support given by ANP (Brazil's National Oil, Natural Gas and Biofuels Agency) through the R&D levy regulation.

References

[1] M Sanois, R B Jackson, P Bousquet, B Poulter, J G Canadell, Environ. Res. Lett. 11 (2016) 1-5.
[2] IPCC, 2014: Climate Change 2014: Synthesis Report. Contribution of Working Groups I, II and III to the Fifth Assessment Report of the Intergovernmental Panel on Climate Change [Core Writing Team, R.K. Pachauri and L.A. Meyer (eds.)]. IPCC, Geneva, Switzerland, 151 pp.
[3] C Zuñiga, M Morales, S Revah, Bioresour. Technol. 129 (2013) 686-689.
[4] J Choi, S Y Lee, Bioprocess Eng. 17 (1997) 335-342.
[5] J H Law, R A Slepecky, J. Bacteriol. 82 (1961) 33-36.

Photohydrogen production from cheese whey by recombinant strains of *Rhodobacter capsulatus*

Patricia Castillo-Moreno[1], Carlos Arturo Martínez[1], Juan Carlos Serrato[1], John Willison[2] and Jean Pierre Magnin[3]

[1]Laboratorio de Ingeniería Química, Universidad Nacional de Colombia, Bogotá, Colombia; [2]Laboratoire de Chimie et Biologie des Métaux, CEA-Grenoble, 38054 Grenoble, France; [3]LEPMI, Grenoble INP- Université de Savoie - Université Grenoble Alpes BP75. 38402 Saint Martin d'Hères Cedex, France

**Corresponding author: pcastillomo@unal.edu.co*

Highlights

- H_2 production from cheese whey was modeled and optimized.
- Recombinant *R. capsulatus* IR3 strain containing the E. coli lacZ gene was used.
- Hydrogen production was obtained with cheese whey concentration of 90%.

1. Introduction

Hydrogen is considered as a clean energetic source [1]. Biological methods are a strong option to produce it because less energy than conventional methods is required, and waste materials or byproducts of the industry can be use as substrate. However, the efficiency of biological methods is low so many researches focus on increase it by optimized conditions and media [2]. Among the industrial effluents that can be use as substrate, cheese whey (CW) was selected due to it's composition [3]. The photofermentation process stands out among the biological methodologies for its rates of substrate conversion. Photosynthetic non-sulfur bacteria catalyze the hydrogen production by the action of the nitrogenase [4,5]. In this study, a photofermentative process was used to produce hydrogen from CW with a recombinant strain of *Rhodobacter capsulatus*. The recombination allows the degradation of the lactose by the action of a plasmid containing β galactosidase gene under dependence of nifH promoter [6].

2. Methods

2.1 Bacterial strain and cheese whey

The bacteria used in this study was *Rhodobacter capsulatus* strain IR3::LacZ originated from a H_2 superproducer strain IR3 [7]. Bacterial pre-culture medium was RCV, under anaerobic conditions. The cheese whey powder used was bought to CIMPA s.a.s a Colombian company. The CWP was solubilized in deionized water (1 kg CWP / 9 L water) and heat-pretreated.

2.2 Batch experiments

Reactors used for the batch experiments were 0.125 L glass square bottles, sealed hermetically with a rubber stopper and with a magnetic stirrer for mixing. The cultures were carried out in an

illuminated incubator (lab-made) with temperature regulation at 30°C. Illumination was provided by a high-pressure Na lamp. Biogas produced volume was measured by water displacement.

2.3 Experimental Design

A Central composite face centered design of experiments was applied using the statistics software Design Expert 8.0 to evaluate the effects of 3 variables: **A.** Cheese whey concentration (%), **B.** Molybdenum concentration (µM), **C.** Light intensity (lx). The response studied was the H_2 specific volumetric production (ml L^{-1}).

3. Results and discussion

A quadratic model was the best fit for the relation between the three continuous parameters and the response (equation 1). The 3 variables studied were significant.

$$\mathbf{Y\ (ml\ L^{-1})} = 5668 + 3118\ A + 1265\ B - 867*C + 1227\ B*C - 2036\ A^2 \quad \text{(Eq1)}$$

The model was statistically validated, and the 3D surface response and the cubic plot were used to describe the behavior of the study's area. Maximum values of H_2 production were observed at superior levels of CW concentration. This is a desirable result because the higher concentration of CW, the lower work volume and that increases the productivity of the process. The equation and plots indicate that the variable that influences the most the H_2 production is the CW concentration. The interaction of Mo concentration and light intensity is also significant to the process.

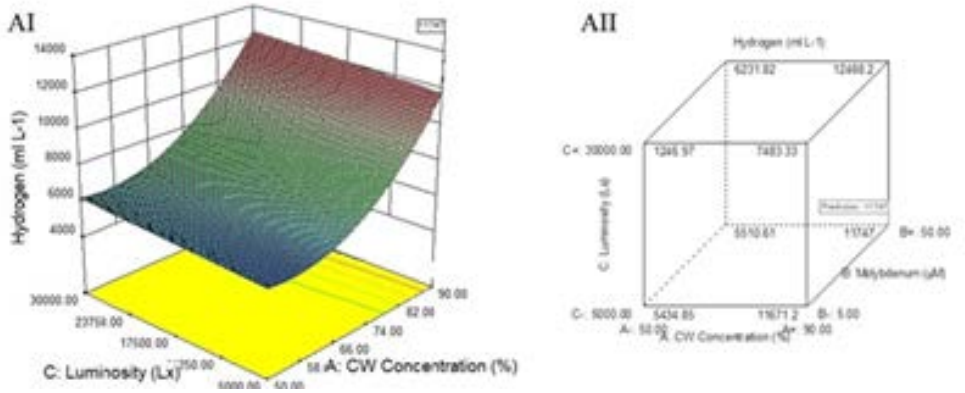

Figure 1 3D and cubic representations of H_2 specific volumetric production

4. Conclusions

The influence of the variables CW and molybdenum concentration and light intensity over the H_2 production by *Rhodobacter capsulatus* IR3::LacZ was successfully determined and optimized with DOE methodology. The study led to improvements in the efficiency and productivity of the process. This methodology proves to be useful both for producing hydrogen and as a treatment for cheese whey. The consumption on lactose, after the bacterial action, can reach 98% reducing the environmental impact of this waste stream.

References

[1] S. Singh, S. Jain, V. Ps, A. K. Tiwari, M. R. Nouni, J. K. Pandey, and S. Goel, "Hydrogen: A sustainable fuel for future of the transport sector," Renew. Sustain. Energy Rev., vol. 51, pp. 623–633, 2015.

[2] G. K. Dinesh, R. Chauhan, and S. Chakma, "Influence and strategies for enhanced biohydrogen production from food waste," Renew. Sustain. Energy Rev., vol. 92, no. May, pp. 807–822, 2018.

[3] A. R. Prazeres, F. Carvalho, and J. Rivas, “Cheese whey management: A review,” J. Environ. Manage., vol. 110, pp. 48–68, 2012.
[4] S. Ghosh, U. K. Dairkee, R. Chowdhury, and P. Bhattacharya, “Hydrogen from food processing wastes via photofermentation using Purple Non-sulfur Bacteria (PNSB) - A review,” Energy Convers. Manag., 2016.
[5] P. Castillo-Moreno, J. C. Serrato, J. C. Willison, and J. P. Magnin, “Photohydrogen production from lactose and lactate by recombinant strains of Rhodobacter capsulatus: Modeling and optimization,” Int. J. Hydrogen Energy, vol. 43, no. 46, pp. 21231–21245, 2018
[6] Colbeau A, Vignais PM. Use of hupS::lacZ gene fusion to study regulation of hydrogenase expression in Rhodobacter capsulatus: Stimulation by H2. Journal of Bacteriology 1992;174:4258–64.
[7] Willison JC, Madern D, Vignais PM. Increased photoproduction of hydrogen by non-autotrophic mutants of *Rhodopseudomonas capsulata*. Biochem J 1984;219:593

Effect of enzymatic pretreatments on sewage sludge anaerobic digestion.

Montserrat Perez[1], Cristina Agabo[1], Juan Parrado[2], Rosario Solera[1]

1. Dept. Environmental Technologies. IVAGRO. University of Cadiz
2. Dept. Biochemistry and Molecular Biology. University of Seville

*montserrat.perez@uca.es

Highlights

- Anaerobic digestion process.
- Enzymatic hydrolysis of sludge.
- Biomethane potential.

1. Introduction

Stabilization of sludge by anaerobic digestion is a crucial step to remove pathogens, solids and bad odours, to increase the ammonia content and to enhance the partial mineralization of organic matter. This operation has an extra value due to the biomethane potential production and hence energy saving. For this purpose, different technologies have been developed in order to increase the biomethane potential in anaerobic digestion processes. These studies are mainly focused on increasing the biodegradability of sludge by physico-chemical and/or biochemical methods, improving hydrolysis step in overall anaerobic digestion process (Yu et al., 2013). In this sense, the application of purified enzymes is recognised as an effective hydrolysis pretreatment in order to increase biodegradability of residues (Zhen et al., 2017).

2. Methods

The inoculum was obtained from 5L single-phase dry-mesophilic AD operating at HRT = 20 d. The sludge as substrate was obtained from the aerobic digester in Experimental WWTP in Center for Water New Technologies (CENTA) in Carrión de los Céspedes (Seville, Spain). The substrates were previously pre-treated by different enzymatic pretreatments Glucanase (G), Cellulase (C) and Protease (P), at concentration 0.3% w/w.

250 ml BMP serum bottles were used in order to determine the methane potential of different pretreated samples. The digesters were initially loaded with a mixture of 40% v/v inoculum and pretreated sludge. Control reactors were also incubated. All the anaerobic digestion experiments were carried out until all the available carbonic content was converted to biogas (23 days). All reactors were run in duplicates. At the beginning and at the end of each experiment the samples were characterized in order to evaluate the biodegradability of the samples. During the experiment volume and composition of biogas produced were registered.

3. Results and discussion.

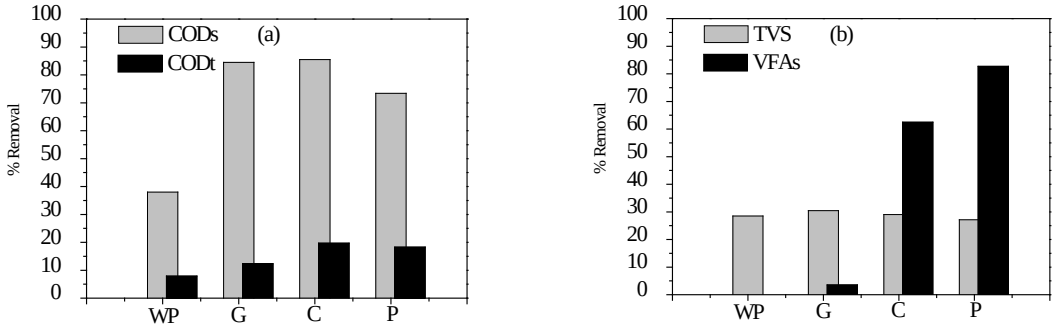

Figure 1. Biodegradability parameters removal. (a) CODs and CODt ; (b) TVS and VFAs.

In general, CODt and TVS removal efficiency is in the range 10-20% and 30% respectively. However, CODs removal percentages are very similar and higher (73.4-85.5%) than control (WP) (38%). In the case of experiments C and P the elimination of VFAs was optimal and in the range of 63-83% typical from sewage anaerobic digestion process. In the case of G pretreatment, the removal of VFA was reduced (about 3.5%) due to the substrate was worse conditioned by using glucanase.

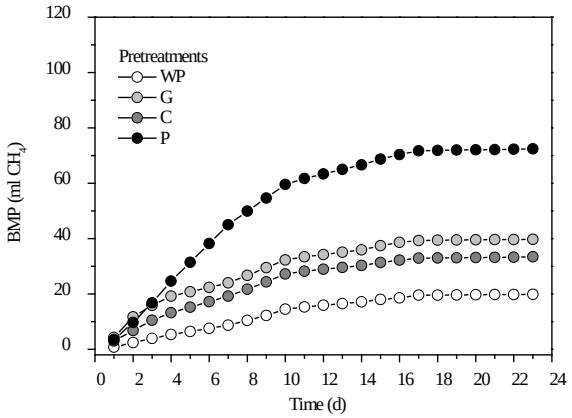

Figure 2. Accumulated biomethane production through the time for different pretreated substrates.

Maximum values of biomethane production (72 mL CH_4) were obtained using substrates pretreated by P treatments. On the other hand, C experiment only produce 33.2 mL CH_4 biogas, probably due to lower values of VFAs removal. Glucanase also increase biomethane production generating values between 30 mLCH_4 in 20 days. Regarding that, control sample (WP) produced only 20 mLCH_4.

4. Conclusions

Any of the tested pretreatments enhance biomethane generation. Pretreatment of protease is the best pretreatment enhancing biodegradability of substrates as well as biomethane production.

References

[1] S. Yu, G. Zhang, J. Li, Z. Zhao, X. Kang, Bioresource Technol. 146 (2013) 758-761.
[2] G. Zhen, X. Lu, H. Kato, Y. Zhao, Y.Y. Li, Renew Sust Energ Rev 69 (2017) 559-577.

Development of a novel biological plant-based protective agent for wood-based materials

Julia Grothkopp*[1], Sibylle Kümmritz[1], Stephanie Stange[2], Hubertus Delenk[2], André Wagenführ[2], Thomas Walther[1], Juliane Steingroewer[1]

[1] *Bioprocess Engineering, TU Dresden, Bergstraße 120, 01069 Dresden, Germany;*
[2] *Wood Technology and Fibre Materials Technology, TU Dresden, Marschnerstraße 32, 01062 Dresden, Germany.*
**Julia.grothkopp@tu-dresden.de*

Highlights

- Plant-based protective agent for wood-based materials
- Biotechnological process with *Salvia* cell suspension cultures
- Combination of sucrose fed-batch and elicitor increase the volumetric triterpene yield

1. Introduction

Wood is one of the most important renewable raw materials. The use of wood preservatives contributes to the protection and increases the resistance of the material against harmful organisms such as mold fungi. Most currently available protective agents for the treatment of wood-based materials are almost completely chemicals that contain substances that are harmful to the environment and hazardous to health. In order to minimize these harmful effects on the environment and humans, manufacturers are searching new bio-active substances as alternative to conventional fungicides for products made of renewable raw materials.

Plant secondary metabolites occur in a wide variety and high structural diversity in all higher plants. They are involved in the defense mechanisms of plants and accumulate in cells when abiotic or biotic stress occurs. Therefore, many secondary metabolites have an antimicrobial, hydrophobic and antifungal effect. *Salvia* species contain a large number of bioactive pharmaceutical ingredients, like flavonoids, terpenes or phenols that exhibit antibacterial, antiviral and antifungal activities. Two of these compounds are oleanolic acid (OA) and ursolic acid (UA). Both are constitutional isomers and belong to the group of pentacyclic triterpenic acids.

Extracts or ingredients of plants are traditional produced from agricultural material. Depending on several influencing factors such as the location and period of production, the obtained extractives differ in quality and quantity. For a continuous, sustainable production of plant ingredients, the use of biotechnological processes based on plant *in vitro* cultures is required. The cultivation of plant cells in a closed bioreactor system ensures the sustainable production of plant secondary metabolites with consistent quality and quantity [1]. To reach reasonable productivities with plant cell suspension cultures, elicitation is a widely used strategy. The systematic use of so-called elicitors in plant cell cultures stimulates the plant defense mechanisms, which can be used to increase the yield of the active substances [2].

The aim of the presented work is to develop a sustainably produced bio-based wood protective agent with plant *in vitro* cultures in a closed bioreactor system. To increase the productivity of the process, an elicitation strategy combining treatment with fungal medium filtrate and sucrose feeding will be applied.

2. Methods

The development process of the production for a protective agent for plant-based wood materials is illustrated in Figure 1.

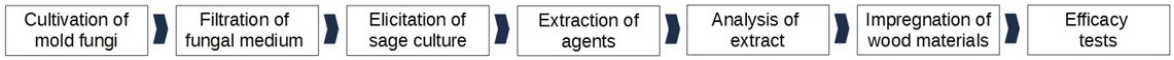

Figure 1. Planned process flow for the production of a bio based protective agent for wood-based materials.

For the fungal medium filtrates, the mold fungi *Aspergillus niger* (DSM 1957) and *Trichoderma virens* (DSM 1963) were each cultivated in 1 l shaking flasks with 500 ml of 1.5 % malt extract medium for 14 days. The mycelium pellets were separated from medium by a three-step filtration [3]. For the plant cell culture, *Salvia fruticosa* was cultivated in Linsmaier and Skoog medium with 30 g l^{-1} sucrose and 0.2 mg l^{-1} 2.4-dichlorophenoxyacetic acid at 26 °C, 110 rpm in darkness and sub-cultivated every 10 days with 20 % inoculum volume. The fed-batch cultivation and the elicitation procedure were performed as described in [3]. The extraction of intracellular triterpenes was carried out with a mortar and ethanol as extraction agent. The analysis of the extracts for OS and US was performed by HPLC [4].

3. Results and discussion

To further increase triterpene productivity of *S. fruticosa* cell suspension, preliminary experiments of nutrient feeding with the application of 30 g l^{-1} sucrose at the end of the cell growth on day 10 successfully led to additional growth and higher levels of triterpene contents, volumetric yield and productivity. With the combination of sucrose fed-batch and elicitation with fungal medium filtrate, this value was further exceeded. Expressed in analytical values, a content of 16.3 mg l^{-1} OA was determined for the pure *S. fruticosa* cell suspension. The yield was increased to 32.6 mg l^{-1} by the addition of *T. virens* fungal medium filtrate. Through the combination of elicitor and sucrose fed-batch the yield could be increased to 112.9 mg l^{-1}, which represents an increase of 500 % in the volumetric triterpene yield. The results with the fungal filtrate of *A. niger* as elicitor showed similar results. For the elicitation, a concentration of 3 % *(v/v)* of each fungal medium filtrate was selected because higher concentrations of 12 % *(v/v)* demonstrated strong growth inhibition of the plant cells. The detailed results of the effects of fungal medium filtrates of *A. niger* and *T. virens* as well as of the sucrose fed-batches on growth and productivity are described in [3].

4. Conclusions

A biotechnological process for the production of triterpenic acids with *S. fruticosa* cell suspension cultures has been developed on a laboratory scale. By an elicitation strategy combining treatment of the cell cultures with fungal medium filtrate and sucrose feeding, the yields of the secondary metabolites could be significantly increased. It was demonstrated that the eliciting effect of the fungal extracts depends on the concentration, the time of addition and the age of the culture. In further studies, the eliciting substances in the plant extracts have to be determined. In addition, the protecting effects of the extracted triterpenic acids for wood-based materials have to be intensively evaluated. Subsequently, the process has to be scaled up into the industrial scale. This work has been financially supported by the Central Innovation Program for SMEs of the Federal Ministry of Economics and Technology (BMWi, grant number KF2049810SA2), German Research Foundation (DFG, Project ID BL345/10-2) and Federal Ministry of Education and Research (BMBF), the project ID is: 031B0691.

References

[1] J. Steingroewer et al., Eng Life Sci, (2013), 26-38.
[2] K. Ramirez-Estrada et al., Molecules 21, (2016), 182.
[3] S. Kümmritz et al., Appl. Microbiol. Biotechnol. 100, (2016), 7071-7082.
[4] S. Kümmritz et al., Nat Prod Commun 9, (2014), 17-20.

ECAB 5
The 5th EUROPEAN CONGRESS OF APPLIED BIOTECHNOLOGY
Florence 15-19 September 2019

Expansion of human mesenchymal stem cells on Corning® Synthemax II™ – coated dissolvable microcarriers in a serum-free cell culture medium

C.Sion[1,2], S. Bailly[3], S. Poncet[3], E. Guedon[1,2], I. Chevalot[1,2], E. Olmos[1,2]

1 CNRS, Laboratoire Réactions et Génie des Procédés, UMR 7274, 2 avenue de la forêt de Haye, TSA 40602, Vandœuvre-lès-Nancy, 54518, France ; 2 Université de Lorraine, LRGP, 2 avenue de la forêt de Haye, TSA 40602, Vandœuvre-lès-Nancy, 54518, France ;#B Corning, Life Sciences, Amsterdam, The Netherlands

**Corresponding author: eric.olmos@univ-lorraine.fr*

Highlights

- Corning dissolvable carriers provided a scalable solution for large-scale harvest of functional hMSC by enabling simplified detachment.
- Complete dissolution of microcarriers was observed during the harvest phase resulting in an efficient hMSC recovery.

1. Introduction

Mesenchymal stem cells extracted from the Wharton's jelly of human umbilical cords (hWJ-MSC) are of increasing interest for cell therapies due to their reduced immunogenicity, high expansion capabilities, fast growth kinetics and various growth factors synthesis capabilities. Development of bioprocesses capable of producing large numbers of hMSC in a robust and safe manner is critical for therapeutic applications. Scalable expansion of hWJ-MSC on Cytodex-1 or other types of microcarriers usually found in cell culture, involved specific cell detachment using trypsin. Trypsin or other cell detachment enzymes could have harmful effects on cells and their viability. Besides, a filtration step is required because carriers remained in the cell culture medium. In this study, the efficiency of novel xeno-free dissolvable microcarriers for the culture and detachment of hWJ-MSC was demonstrated.

2. Methods

hWJ-MSC were cultivated on Corning Synthemax II-coated dissolvable microcarriers (DM) in HPL-supplemented medium, with an initial concentration of 7000 cells/cm^2. Previous studies (Loubière et al. 2018) showed that the best choice of microcarrier for hWJ-MSC adherence and expansion, in dynamic conditions, was Cytodex-1 [1], but cell detachment remained difficult. A culture in 200 mL spinner flasks with DM microcarriers was performed and compared with a culture on Cytodex-1. Glucose, glutamine, ammonium, lactate and lactate dehydrogenase concentrations were monitored every day. Moreover, cells were counted from the post-processing of DAPI-stained cells pictures [1]. At the end of the culture, cells were harvested following the protocol given by Corning. A solution of harvest was prepared using a mix of different enzymes and chemicals: a protease and a pectinase, and a chelating agent (EDTA). This harvest solution was directly used in the culture system and its action was about 20 minutes. After this, cells were directly centrifuged.

3. Results and discussion

The first results showed that the choice of Cytodex-1 or dissolvable carriers from Corning did not influence cell adherence. Cell viability was equivalent and maintained over time in both cultures (Figure 1). Once the attachment and kinetics of cell culture (growth, death, glucose and glutamine consumption, lactate and ammonia production) evaluated, cell detachment was studied. After the treatment with the harvest solution, cells were counted and microcarriers observed under microscope. Results indicated that Corning microcarriers were well digested, and two million of viable cells were collected after centrifugation (95% of viability), against, only 800 000 cells collected from Cytodex-1 using the classical proteolytic harvest treatment (89% of viability). By image analyses, it was shown that with DMC, complete cell detachment and microcarrier dissolution were obtained while cells remained attached on Cytodex-1 microcarriers.

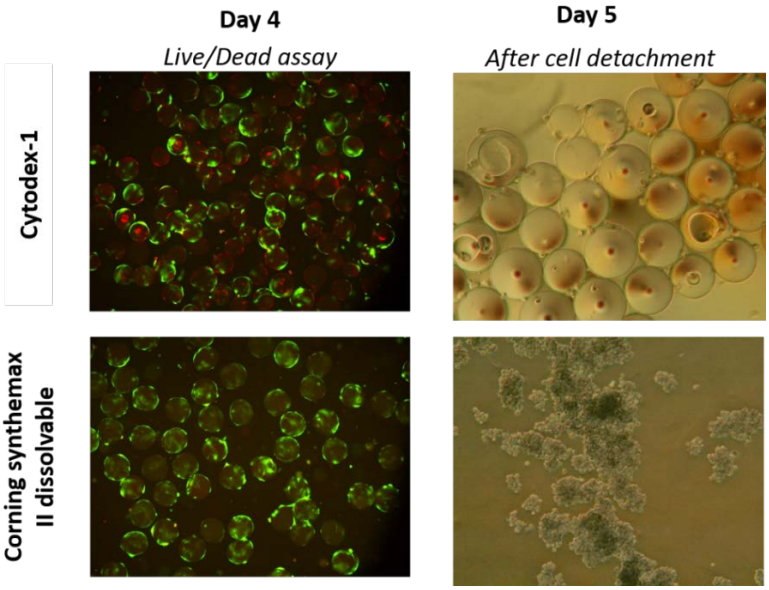

Figure 1. Comparison of cell culture and detachment on dissolvable carriers and Cytodex-1.

4. Conclusions

Recently, Nienow and colleagues developed a method of harvesting cells, which combines more intense agitation speeds, proteolytic enzymes and temperature inside the bioreactor, in order to improve cell detachment and viability. After the cell detachment, most of the applications, especially therapeutics, will require separation of cells from microcarriers, but by using dissolvable carriers this step would be avoided. To conclude, the use of dissolvable microcarriers would be an effective way to do scalable expansion and harvest of hWJ-MSC.

References

[1] Loubière, C., et al., (2018). Impact of the type of microcarrier and agitation modes on the expansion performances of mesenchymal stem cells derived from umbilical cord. Submitted to Biotechnology Progress.

Biological pretreatment of sewage sludge before anaerobic digestion process

Rosario Solera[1], Cristina Agabo[1], Juan Parrado[2], Montserrat Perez[1]

1. Dept. Environmental Technologies. IVAGRO. University of Cadiz - Spain
2. Dept. Biochemistry and Molecular Biology. University of Seville - Spain

*rosario.solera@uca.es

Highlights

- Anaerobic digestion process.
- Biological pretreatment of sludge.
- Biomethane potential.

1. Introduction

The sludge line from conventional wastewater treatment plant (WWTP) generates high amount of sludge after decanting the solids coming from primary (sedimentation) and secondary (biological) treatments. In this sense AEBIOM estimated a potential of 6 billion Nm^3 of biomethane coming from sewage sludge in 2018 (Scarlat et al., 2018). Different biological pretreatments such as temperature phased digestion (TPAD) or fungi treatment are being widely studied to increase the biomethane potential in anaerobic digestion processes. These types of pretreatments are designed in order to improve the hydrolysis step in an eco-friendly way and with no special equipments (Zhen et al., 2017). In this regard, in this work a pretreatment based on fermentation using *B licheniformis* has been carried out with the aim to prepare the sludge for following anaerobic digestion step.

2. Methods

The inoculum was obtained from 5L single-phase dry-mesophilic AD operating at HRT = 20 d. The sludge as substrate was obtained from the aerobic digester from CENTA, in Carrión de los Céspedes (Seville, Spain). The crude and diluted (1:2 and 1:10) sludge was autoclaved (30 min 121 ºc) before fermentation with *B. licheniformis* ATCC 21415. Growing bacteria conditions were: Medium:LB, T =37 ºC, agitation rate =150 rpm, Time = 288 h.

250 ml BMP serum bottles were used in order to determine the methane potential of different pretreated samples. The digesters were initially loaded with a mixture of 40% v/v inoculum and pretreated sludge. Control reactors were also incubated. All the anaerobic digestion experiments were carried out until all the available carbonic content was converted to biogas (23 days). All reactors were run in duplicates. At the beginning and at the end of each experiment the samples were characterized in order to evaluate the biodegradability of the samples. During the experiment volume and composition of biogas produced were registered.

3. Results and discussion

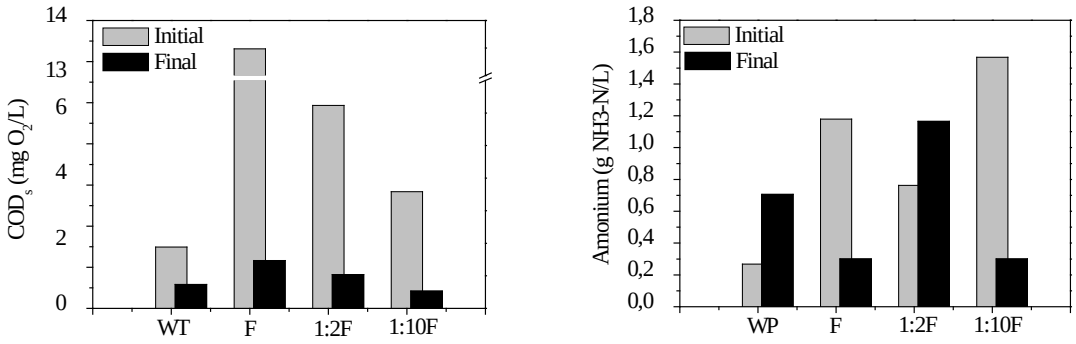

Figure 1. Initial and final CODs and Amonium in BMP experiments.

CODs the removal percentages are very similar and more than twice higher (73.4-82.7%) than control WP (38%). Fermentation pretreatment of crude and diluted substrates obtained high values of ammoniacal nitrogen with values of 0.762, 1.57 and 1.17 g NH3-N/L respectively for pretreatments 1:2F, 1:10F and F. This fact can be explained because protein degradation efficiency during fermentation pretreatments.

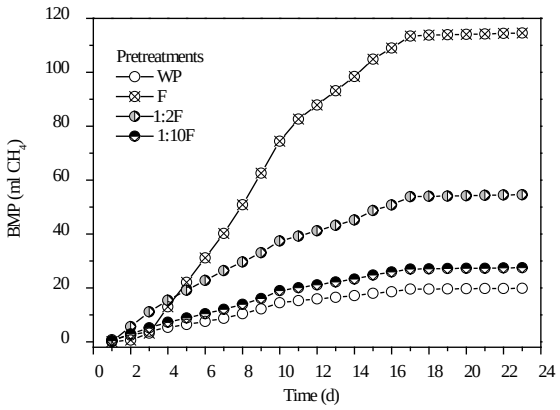

Figure 2. Accumulated biomethane production through the time for different pretreated substrates.

As it can be observed in the Figure 2, F sample need 3 days in order to adapt the inoculum to high ammonium values. In the pretreatment 1:10F there was inhibition by ammonia content because excess of that. This effect could also have happened in the 1:2F pretreated sample but, here, the organic load content was higher, increasing the C/N ratio (and thus the biogas yield).

4. Conclusions

Biochemical treatments tested for sewage sludge result in higher depuration efficiency in terms of CODs. Fermentation increase the biogas volume in 5.77 times respectively compared with control. The selection of optimal pre-treatment must take into account the final C/N ratio.

5. Acknowledgment

This work was funded from the 2020 European Horizont research and innovation programme under Grant Agreement No. 73098, REcovery and REcycling of nutrients TURNing wasteWATER into added-value products for a circular economy in agriculture (Water2REturn).

References

[1] G. Zhen, X. Lu, H. Kato, Y. Zhao, Y.Y. Li, Renew Sust Energ Rev 69 (2017) 559-577.
[2] N. Scarlat, F. Fahl, J.F. Dallemand, F. Monforti, V Motola, Renew Sust Energ Rev 94 (2018) 915-930.

Diversity of the Microbial Populations used to transform Arsenic in natural and industrial situations

M.P. Merino, J.A. Duguet, M. Acuña[1], B.A. Andrews and J.A. Asenjo

Centre for Biotechnology and Bioengineering, CeBiB, University of Chile
Beauchef 851, Santiago, Chile
[1]EcoMetales, Santiago, Chile
**Corresponding author: paz.merino@cebib.cl*

Highlights

- Extreme natural and industrial environments are a source of microorganisms with unique potential.
- An acidophile consortium was isolated from effluents of a mining operation.
- The consortium is capable of oxidizing high arsenic concentrations.
- A metabolic reconstruction of the consortium was developed to study its metabolic capabilities.

1. Introduction

A permanent challenge for the mining industry is the development and application of metal recovery technologies that are efficient, low cost and ecologically friendly, since during the process many contaminating elements are released [1]. Most of the minerals present in the rock represent a rich source of elements of high economic value, but some may contain toxic metals or metalloids, such as arsenic.

Northern Chile has a variety of poly extreme natural and industrial ecosystems, with high rates of solar radiation, low relative humidity, extreme temperature variations and the presence of high concentrations of metals. Microbial life develops under these challenging environmental conditions, which makes it an ideal place to search for extremophile microorganisms with specific physiological and metabolic adaptations.

Our aim is to describe and understand the metabolic capabilities of the microorganisms that are able to resist, reduce or oxidize different metals and metalloids commonly associated with the mining industry, in particular arsenic. In this context, we present a unique opportunity for the discovery and development of technologies that will carry out the transformation of arsenic.

2. Methodology

Microorganisms were isolated from geothermal sites in northern Chile and also from samples of industrial effluents from an arsenic treatment plant. The isolates were identified by Illumina sequencing techniques.

The determination of the diversity of microorganisms present in the samples, allowed the generation of strategies to enhance their growth and oxidative activity, through two approaches:

• Experimentally, optimizing the growth conditions according to the reported nutritional requirements of the microorganisms present.
• Through *in silico* optimization. The consortium's metabolism was reconstructed and modeled, according to the genomic information obtained from the sequencing.

3. Results and discussion

The industrial consortium showed the best oxidation results (about 80% of As(III) oxidized) in solutions with high arsenic and acid content (around 1-3 gpl of As (III) and 20-40 gpl of H_2SO_4). The most likely species in the consortium according to the experimental and metabolic analysis are *Acidithiobacillus, Rhodanobacter, Leptospirillum, Thiobacillus, Terracoccus* and *Acidianus.*

The metabolic model was simplified by depuration and *gap-filling,* and is composed of about 176 reactions representing the consortium. Main pathways of the model are reverse TCA cycle for carbon fixation, energy uptake by iron metabolism and arsenic resistance by detoxifying mechanisms and dissimilatory oxidation of As (III).

We are presently using both the metabolic model and the experimental results necessary for the oxidation of arsenic in order to design a process that takes advantage of the microbial oxidation of arsenic.

4. Conclusions

A consortium was isolated from industrial effluents, which showed high tolerance to mining operation conditions and elevated capacity to oxidize arsenic (III) from acid effluents.

The development of a metabolic model of an industrially isolated consortium was useful to describe and represent the capabilities of these microorganisms to oxidise arsenic in solutions with high acidity and high ion concentrations. This model is being used to simulate growth under different conditions and, in this way, perform mathematical analyzes for optimization.

References

[1] Han FX, Su Y, Monts DL, Plodinec MJ, Banin A, Triplett GE. Assessment of global industrial-age anthropogenic arsenic contamination. Naturwissenschaften. 2003; 90:395-401.

[2] Drewniak L and Sklodowska A. Arsenic-transforming microbes and their role in biomining processes. Environ Sci Pollut Res Int. 2013; 20: 7728–7739.

Removal of pharmaceuticals from artificial and real wastewater matrices using *Trametes versicolor* in fed-batch and trickle-bed bioreactors

Rebeca Tormo-Budowski[1,2], Juan Carlos Cambronero-Heinrichs[2], Esteban Durán-Herrera[1], Mario Masís-Mora[2], José Pablo Quirós-Fournier[3], …, Carlos E. Rodríguez-Rodríguez[2]

1 Escuela de Ingeniería Química, Universidad de Costa Rica, 2060 San José, Costa Rica; 2 Centro de Investigación en Contaminación Ambiental, Universidad de Costa Rica, 2060 San José, Costa Rica; 3 Centro Nacional de Innovaciones Biotecnológicas, CeNAT-CONARE, 1174-1200 San José, Costa Rica.

**Corresponding author: carlos.rodriguezrodriguez@ucr.ac.cr*

Highlights

- The performance of two bioreactor configurations was studied.
- Pharmaceuticals were treated in bioreactors containing *Trametes versicolor*.
- Removals over 95% were achieved for 11 drugs in a fed-batch bioreactor over 14 days.

1. Introduction

The presence of pharmaceuticals in the environment has been a raising concern over the past years. There is lack of information about their effect on ecosystems, making their impact on the environment and public health difficult to predict [1]. Current wastewater treatment plants (WWTP) are not designed to remove these pollutants; consequently, many of them reach surface waters unaltered [2]. In the search for alternatives to minimize their chronicle impact, the use of white-rot fungi as a biological treatment for the removal or transformation of pharmaceuticals has been studied and has been proven to be an environmentally friendly and effective alternative [3]. Specifically, studies using bioaugmentation with *Trametes versicolor* have obtained better pharmaceutical removal values compared to conventional activated sludge (CAS) treatment [4][5]. This work aims to explore the fungal treatment of real wastewater matrices and synthetic wastewater spiked with different pharmaceuticals including psychiatric drugs, anti-inflammatory drugs and antibiotics, in two different bioreactor configurations, a fed-batch stirred tank bioreactor and a trickle bed bioreactor. The fed-batch bioreactor uses molasses, obtained as a secondary product in the production of sugar, as a nutrient source for the employed microorganism. While the trickle-bed bioreactor was designed to be an easy and economically competitive alternative to be used as tertiary treatment in WWTP.

2. Methods

Artificial wastewater was prepared with 16 commercial drugs (1 mg/L each), while real wastewater was obtained from a secondary treatment plant. Two bioreactors containing polluted water, inoculated with *T. versicolor* pellets, were operated in fed-batch mode with intermittent additions of molasses solution as carbon and nitrogen source. Results were verified by triplicate assays in Erlenmeyers, operated under the same conditions. Moreover, three trickle-bed bioreactors were built using a lignin-rich substrate mixed with an artificial substrate for support,

inoculated with *T. versicolor*. In both bioreactor configurations, heat-killed and abiotic control assays were performed in order to determine abiotic losses and sorption to the fungal biomass, as well as ecotoxicological assays with *Daphnia magna* and *Lactuca sativa*. Removal of pharmaceuticals was quantified by LC-MS/MS analysis.

3. Results and discussion

Removals over 95% were achieved for 11 pharmaceuticals during the treatment of synthetic wastewater in the stirred tank bioreactor; in general, individual removal values were above 50% for this system (see Figure 1). The highest removals were found for ceftiofur, lincomycin, acetaminophen and ketoprofen, while the lowest corresponded to azithromycin. Acetaminophen showed the highest removal rate.

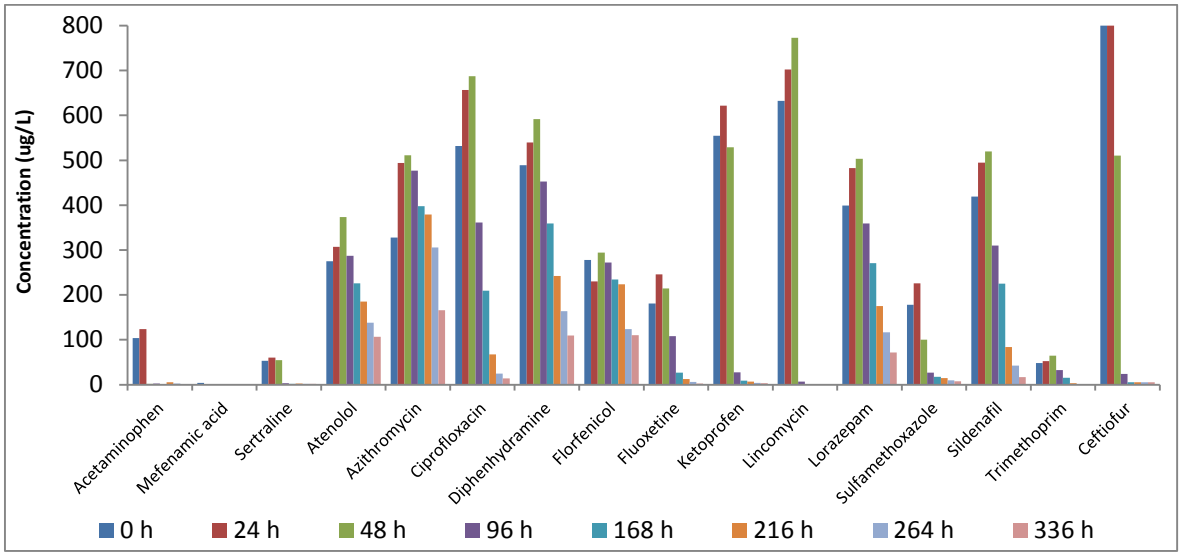

Figure 1. Removal of pharmaceuticals from artificial wastewater in a fed-batch bioreactor with *Trametes versicolor*.

We will further discuss the results obtained for the trickle-bed reactors. Results will include pharmaceutical removal in synthetic and real wastewater matrices, as well as EC_{50} values.

4. Conclusions

The fungal bioreactors studied with *Trametes versicolor* can be used as methods to overcome the lack of specialized treatment given in WWTP. Given the results, a fed-batch stirred tank bioreactor could be used as a removal system for punctual discharge of pharmaceuticals. While on the other hand, the trickle bed bioreactor could be used as a tertiary treatment in farms to treat animal residues, hospital or municipal wastewater, among others.

References

[1] G. Llorens-Blanch, M. Badia-Fabregat, D. Lucas, S. Rodriguez-Mozaz, D. Barceló, T. Pennanen, G. Caminal, P. Blánquez, Environ. Sci-Proc. Imp. 17 (2015) 429–440.

[2] P. Verlicchi, M. Al Aukidy, E. Zambello, Sci. Total Environ. 429 (2012). 123–155.

[3] M.B. Asif, F.I. Hai, L. Singh, W.E. Price, L.D. Nghiem, Current Pollution Reports 3 (2017) 88–103.

[4] D. Lucas, M. Badia-Fabregat, T. Vicent, G. Caminal, S. Rodríguez-Mozaz, J.L. Balcázar, D. Barceló, Chemosphere 152 (2016) 301–308.

[5] C. Cruz-Morató, D. Lucas, M. Llorca, S. Rodriguez-Mozaz, M. Gorga, M. Petrovic, D. Barceló, T. Vincent, M. Sarrà, E. Marco-Urrea, Sci. Total Environ. 493 (2014). 365–376.

ECAB 5
The 5th EUROPEAN CONGRESS OF APPLIED BIOTECHNOLOGY
Florence 15-19 September 2019

Effect of extracellular pH on lactate metabolism in Chinese Hamster Ovary (CHO) cell cultures

Victoria Gkoutzioupa[1], Edward Close[2], Alexandros Kiparissides[1,*]

1 Advanced Centre for Biochemical Engineering, Department of Biochemical Engineering, University College London, London, UK; 2 Process Systems Enterprise Limited, London, UK

**Corresponding author: alex.kiparissides@ucl.ac.uk*

Highlights

- Understanding of the effect of extracellular pH on lactate metabolism, cell viability and product titer
- Improved prediction of lactate concentration including the shift from lactate production to consumption

1. Introduction

In spite of the outstanding research developments in biotechnology, there are still several aspects of cellular metabolism whose impact on bioprocess efficiency and product quality we do not fully comprehend. A notable and industrially relevant example is the interplay between glucose, lactate and amino-acid metabolism and in particular the metabolic switch that occurs in high-density cultures of fast growing mammalian cells from lactate production to lactate consumption (Zhou et al., 1997; deZengotita et al., 2000). Recent studies have shown that supplementing CHO cell cultures with lactic acid or artificially altering extracellular pH can promote the effect resulting in the preferential uptake of lactate even in the presence of excessive amounts of glucose (Li et al., 2012). Surprisingly this transition, from lactate production to consumption, results in higher product yields. The aim of the current study is to develop an in depth, quantitative understanding of lactate metabolism in CHO cells and how it responds to variations in extracellular pH. The experimental data will be subsequently used for the development of a predictive unstructured model.

2. Methods

GS-CHO cells (kindly provided by Lonza Biologics, Slough, UK) were cultured in 500 mL shake flasks (Presens, Germany) with 110 mL working volume. The flasks had integrated pH and oxygen sensors. The cells were incubated at 5% CO_2, 37°C and 180 rpm (d_s=19 mm). Viable cell density, total cell density and average cell diameter were measured with the Vi-CELL XR (Beckman Coulter, USA). Metabolites (glucose, glutamate, glutamine, lactate, ammonia) were quantified with the BioProfile FLEX Analyzer (Nova Biomedical, USA). Monoclonal antibody concentration was determined with the use of High Pressure Liquid Chromatography (HPLC) techniques (Agilent Technologies, USA). pH was maintained in predefined levels with the manual addition of 1M HCl and 1M $NaHCO_3$. pH and oxygen were monitored by using a Presens platform (Presens, Germany).
The gPROMS FormulatedProducts© modelling platform was employed for model development and analysis. The parameters of the model were estimated through minimization of the maximum likelihood objective function, where the experimental data were given as inputs.

3. Results and discussion

ODEs were constructed for the description of the system's dynamic response. Monod-type kinetics were mainly used for the development of the model. So far, equations for viable and total cells, glucose, glutamate, lactate and mAbs have been developed and are given by the following expressions:

$$\frac{d(V\cdot X_V)}{dt} = \mu \cdot X_V \cdot V - \mu_d \cdot X_V \cdot V - F_{out} \cdot X_V \quad (1)$$

$$\frac{d(V\cdot X_T)}{dt} = \mu \cdot X_V \cdot V - F_{out} \cdot X_T \quad (2)$$

$$\mu = \mu_{max} \cdot \frac{[GLC]}{[GLC]+K_{glc}} \cdot \frac{[GLU]}{[GLU]+K_{glu}} \quad (3)$$

$$\mu_d = \mu_{d,max} \cdot \frac{K_{d,glc}}{K_{d,glc}+[GLC]} \cdot \frac{K_{d,glu}}{K_{d,glu}+[GLU]} \cdot \frac{[AMM]^3}{K_{d,amm}{}^3+[AMM]^3} \quad (4)$$

$$\frac{d(V\cdot[GLC])}{dt} = F_{in} \cdot [GLC]_{in} - F_{out} \cdot [GLC] - V \cdot \left(\frac{\mu}{Y_{x,glc}} + m_{glc}\right) \cdot X_V \text{ (Jang \& Barford (2000))} \quad (5)$$

$$\frac{d(V\cdot[GLU])}{dt} = F_{in} \cdot [GLU]_{in} - F_{out} \cdot [GLU] - V \cdot q_{glu,max} \cdot \frac{[GLU]}{[GLU]+K_{glu,2}} \cdot \frac{K_{i,glc}}{K_{i,glc}+[GLC]} \cdot X_V \quad (6)$$

$$\frac{d(V\cdot[LAC])}{dt} = Y_{lac,glc} \cdot V \cdot \left(\frac{\mu}{Y_{x,glc}} + m_{glc}\right) \cdot X_V - V \cdot q_{lac,max} \cdot X_V - F_{out} \cdot [LAC] \quad (7)$$

$$\frac{d(V\cdot[mAbs])}{dt} = V \cdot \left(\frac{\mu}{Y_{x,mab}} + m_{mab}\right) \cdot \frac{[GLC]}{[GLC]+K} \cdot X_V - F_{out} \cdot [mAbs] \quad (8)$$

The values of the parameters differ according to the pH of the media. For pH equal to 7, the parameters that were derived from parameter estimation (PE) are μ_{max} = 0.031 h^{-1}, K_{glc} = 4.098 mM, K_{glu} = 0.045 mM, $\mu_{d,max}$ = 0.016 h^{-1}, $K_{d,amm}$ = 255.711 mM, $K_{d,glc}$ = 21.8 mM, $K_{d,glu}$ = 18.284 mM, $Y_{x,glc}$ = $4.34\cdot10^{8}$ cells·mmol^{-1}, m_{glc} = $2.39\cdot10^{-11}$ mmol·cells^{-1}·h^{-1}, $q_{glu,max}$ = $3.43\cdot10^{-9}$ mmol·cells^{-1}·h^{-1}, $K_{glu,2}$ = 19.11 mM, $K_{i,glc}$ = 0.24 mM, $Y_{x,mab}$ = $3.2\cdot10^{8}$ cells·mg^{-1}, m_{mab} = $2.81\cdot10^{-10}$ mg·cells^{-1}·h^{-1}, K = 0.0375 mM, $Y_{lac,glc}$ = 2.0 mmol·$mmol^{-1}$, $q_{lac,max}$ = $7.0\cdot10^{-11}$ mmol·cells^{-1}·h^{-1}.

The results of the simulation are graphically represented in Figure 1.

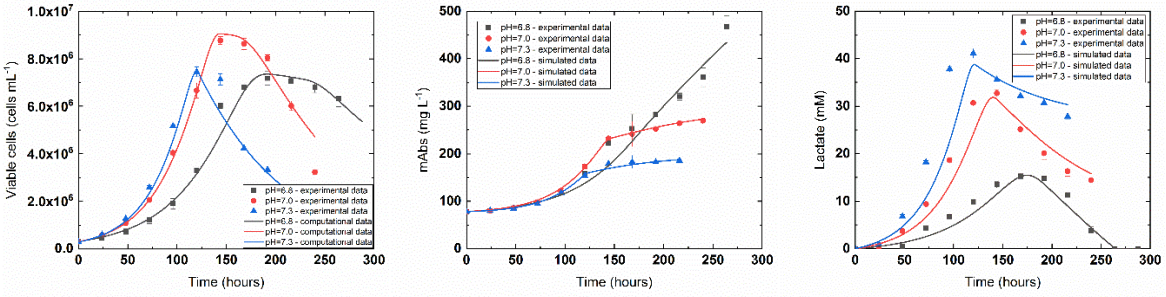

(a) (b) (c)

Figure 1. Simulated and experimental profiles of (a) viable cell, (b) mAb and (c) lactate concentrations for different pH levels in batch cultures.

4. Conclusions

From Figure 1, it is evident that extracellular pH levels affect cell viability and productivity. Specifically, it is observed that lower pH values, in the culture media, result in higher integral viable cell concentration (IVCC) and higher titer. Additionally, extracellular pH levels can control the lactate switch. In higher pHs, more lactate is accumulated in the system (Figure 1c). Regarding the model, the simulated results are in good agreement with the experimental data. We come to the conclusion that Monod and Hill kinetics can adequately describe the dynamics of the system. However, the equations have to be refined with amino acids data.

References

[1] DeZengotita M.V., Miller W.M., Aunins J.G. (2000) Biotech. Bioeng., v. 69, pp: 566-676.
[2] Jang J.D., Barford J.P. (2000) Biochemical Engineering Journal, v. 4, pp: 153–168.
[3] Li J., Wong C.L., Vijayasankaran N., Hudson T., Amanullah A. (2012). Biotechnol. Bioeng., v.109(5), pp: 1173-1186.
[4] Zhou W., Rehm J., Europa A., Hu W.S. (1997) Cytotechnology, v.24(2), pp: 99 – 108.

ECCE12
The 12th EUROPEAN CONGRESS OF CHEMICAL ENGINEERING
Florence 15-19 September 2019

A combined mathematical and experimental investigation of multiphase flow and shear sensitivity in the performance of mammalian cell cultures

Artemis Danae Charalambidou[1*], Martina Micheletti[1], Alexandros Kiparissides[1]

1 University College London, Department of Biochemical Engineering, Torrington Place, London, WC1E 7JE, UK
**Corresponding author: a.charalambidou@ucl.ac.uk*

Highlights

- Conduction of detailed single phase computational fluid dynamics (CFD) simulations in a 250 mL bioreactor.
- Study of the impact of critical simulation parameters on model output and accuracy.
- Experimental validation of CFD simulation output via particle image velocimetry (PIV) measurements.

1. Introduction

The biopharmaceutical industry is in the forefront for the production of innovative drugs from mammalian cell cultures. Baffled or unbaffled stirred tank reactors (STRs) equipped with one or multiple impellers are most commonly used for the production of monoclonal antibodies (MAbs) and recombinant proteins. Their flexibility arises from the ease to control several operating parameters such as impeller speed and aeration techniques, which can improve homogeneity and thus the transport processes in the interior of the vessel (Rodriguez et al., 2013). Nevertheless, the large number of operating parameters makes the selection of an optimal configuration a laborious task and its complexity arises from the lack of detailed understanding of the underlying physics within a stirred vessel (Joshi et al., 2011). Experimental and computational fluid dynamics are widely recognised tools that contribute in the prediction of flow mechanics in STRs and estimation of turbulence associated quantities such as, microeddy formation, energy dissipation rate (EDR) and turbulence kinetic energy (TKE) which might eventually affect cell morphology, viability and productivity (Farzan, Mistry, & Ierapetritou, 2017; Morchain, Gabelle, & Cockx, 2014). However, although many attempts have been made to investigate the flow dynamics in STRs, a well-established and experimentally validated model for the meticulous description of critical hydrodynamic parameters in STRs does not exist. In this study we follow a systematic approach to establish a robust and experimentally validated CFD model based on a 250 mL STR configuration with one Rushton turbine, to assess various turbulent models and mesh structures as well as the effect of each on the estimation of key hydrodynamic parameters which influence mammalian cell cultures.

2. Methods

Commercial CFD software package ANSYS Fluent 19.0 is used to solve the liquid phase hydrodynamics in 3D. The liquid used is water (ρ=998.2 kg m^{-3}, μ=10^{-3} Pa s) and the impeller rotational speed is initially set to 250 rpm, resulting in a Reynolds number of 5,000. Simulations are conducted in both steady state and transient mode via moving reference frame (MRF) and sliding mesh (SM) technique respectively for the simulation of impeller rotation. Convergence criteria were

10^{-5} and 10^{-6} for the continuity and turbulence closure equations respectively. The grid of the rotational zone was formed to be finer than the grid in the outer zone to achieve better accuracy. For mesh independence studies grid densities evaluated varied from 280,638 to 1,728,348 tetrahedral cells.

3. Results and discussion

Figure 1 presents preliminary results of the mesh independence study conducted over a wide range of grid densities. Reynolds Averaged Navier-Stokes equations (RANS) approach coupled with k-epsilon Realizable turbulence model is initially used due to its success to satisfactorily model rotational flows. Global maximum for radial velocity and EDR was located at the impeller plane. Minor differentiations were exhibited among the grid densities for radial velocity profiles (Fig. 1(a)). The consistency of the results was tested via calculating average velocities in dispersed control volumes in the interior of the bioreactor (results not shown). Lower grid density resulted in lower global maximum for EDR (Fig. 1(b)) leading to the conclusion that the corresponding solution is not optimum.

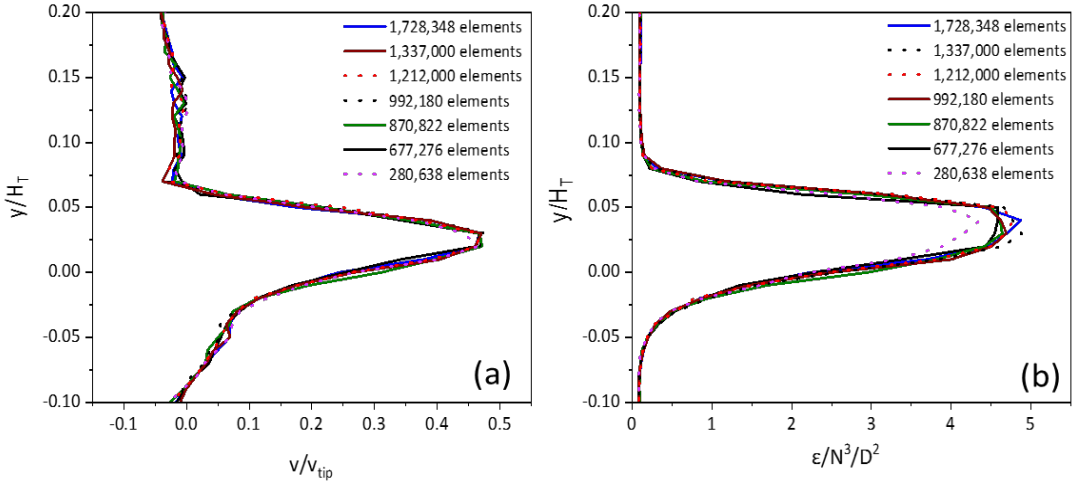

Figure 1. Local effect of grid density in the prediction of selected variables. Axial profiles close to the blade tip (r=T/4) of (a) radial velocity, (b) EDR.

4. Conclusions

A variety of different grid densities gave acceptable approximations for the critical parameters evaluated when RANS approach was used. For both EDR and TKE the results obtained were similar and 11% increase was observed from the coarser to the finer grid density. At the next stage, simulations will be run with structured mesh and different turbulence models to assess results quality and accuracy while experimental validation will mainly contribute in the clarification of the location and intensity of critical hydrodynamic parameters to ultimately quantify potentially destructive effects on mammalian cells.

References

[1] P. Farzan, B. Mistry, M. G. Ierapetritou, *AIChE Journal 63(2)* (2017) 398–408.

[2] J.B. Joshi, N. K. Nere, C.V. Rane, B. N. Murthy, C. S. Mathpati, A. W. Patwardhan, V. V. Ranade, *The Canadian Journal of Chemical Engineering 89*(1) (2011) 23–82.

[3] J. Morchain, J. Gabelle, A. Cockx, *AIChE Journal*, *60*(1) (2014) 27–40.

[4] G. Rodriguez, W. Weheliye, T. Anderlei, M. Micheletti, M. Yianneskis, A. Ducci, *Chemical Engineering Research and Design* 91(11) (2013) 2084–2097.

ECAB 5
The 5th EUROPEAN CONGRESS OF APPLIED BIOTECHNOLOGY
Florence 15-19 September 2019

Surfactin Recovery from *Bacillus subtilis* O9 Cultures by Means of Foam Formation Separation

Joaquín Orejas[1*], María Lucca[2], Marcelo Flores[1]

1 Universidad Nacional de Río Cuarto. Facultad de Ingeniería. Grupo de Ingeniería de las Reacciones (G.I.R.). Ruta Nacional 36 Km 601 CP: X5804BYA. Río Cuarto. Córdoba. ARGENTINA; 2 PROIMI – Universidad Nacional de Tucumán. San Miguel de Tucumán. Tucumán – ARGENTINA

**Corresponding author: jorejas@ing.unrc.edu.ar*

Highlights

- Continuous extraction of foam is an excellent recovery and concentration method for surfactin.
- This technique can be used to reduce costs of extraction and purification of surfactin.
- The proposed method avoids operation problems found in batch bioreactors.

1. Introduction

Surfactin is a very powerful surfactant produced by the bacteria *Bacillus subtilis*, which is able to reduce the interfacial tension of water from 72 to 27 $mN.m^{-1}$. Although it has excellent properties and therefore a large number of potential industrial applications ranging from petrochemistry to pharmacy, the costs involved in its production and purification processes are still restricting its commercialization. A common strategy to reduce these costs is to focus on the optimization and innovation on the purification stages. During the production of surfactin in a stirred tank bioreactor, the continuous change of the physicochemical properties of the culture and the high stirring and aeration requirements are responsible for the formation of a significant amount of foam. Thus, an operation strategy must be used.

In the present study, fractioning with foam was directly applied during the culture of *B. subtillis* in a batch stirred tank bioreactor to concentrate surfactin.

2. Methods

The experiments were performed in a 3 L Applikon® bioreactor provided with a Rushton agitator with 6 paddles, always operating discontinuously and with a working volume of 1.7 L. The diameter of the Rushton turbine is 4.5 cm., while the internal diameter of the bioreactor is 12.9 cm. The exhaustion air outlet was redesigned to continuously collect the formed foam and store it in sterile vessels. Then, the foam was stored at -18 °C to facilitate its collapse. The agitation, air flow, temperature and pH were set and controlled at 200 r.p.m, 1 v.v.m, 30 °C and 7, respectively. Two different chemically defined culture media with slight differences in their elemental traces were used, which had a significant influence on the production of surfactin. During the reaction, the dissolved oxygen concentration was continuously measured. Also, the concentrations of biomass, residual sugar, and surfactin were determined in the bioreactor. Finally, the volume, surfactin and biomass content were analyzed in the obtained foams.

3. Results and discussion

In order to evaluate the efficiency and convenience of the foam separation process coupled to the bioreactor, the variation of foam and remaining culture as a function of time and the surfactin recovery index were analyzed. These results are shown on Figures 1 and 2. The surfactin percentual recovery (SR%) was obtained by means of the following expression:

$$SR\% = \frac{Surfactin\ mass\ in\ the\ foam}{Total\ surfactin\ mass}\ x\ 100$$

This quantity represents the percentage of extracted surfactin in the foam and it is an indicator of the efficiency in the continuous extraction of foam as a fractioning and concentration method for surfactin.

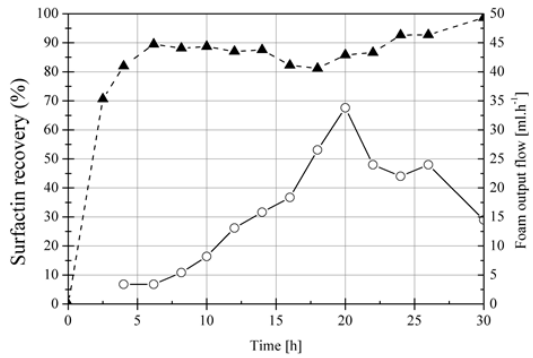

Figure 1. Surfactin recovery % (▲) and foam output flow (○)

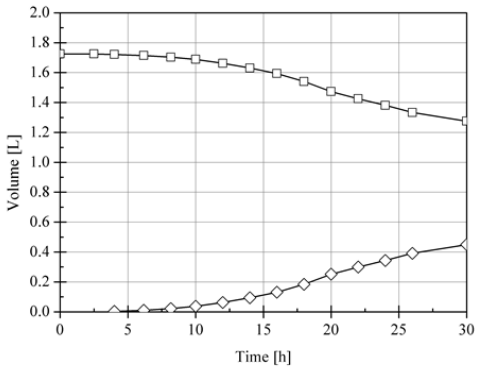

Figure 2. Culture volume in the bioreactor (□) and foam volume (◇)

As shown in Fig. 1, the recovery of surfactin in the foam reaches values over 98% of the total produced surfactin. What is more, by using an agitation of 200 r.p.m. only 26.1 % of the initial liquid volume in the bioreactor is dragged with the foam after 30 hours of operation, as presented in Fig. 2. These results indicate that the production of foam was not significant and didn't complicate the operation of the bioreactor in any way. These results are not in agreement with the ones of Davis et al. [1] where agitation velocities of 204 and 269 r.p.m. generated excessive levels of foam formation and losses of 50% of the culture volume after 36 hours of operation, which consequently led to very low levels of surfactin production. However, the obtained results in the present study agree with Cooper et al. [2].

4. Conclusions

Based on the obtained experimental results, one can conclude that the continuous extraction of foam is an excellent recovery and concentration method for surfactin from a culture medium, with the additional advantage of reducing the extraction and purification costs of the overall process.

References

[1] D.A. Davis, H.C. Lynch, J. Varley, Enzyme and Microbial Technology 28 (2001) 346-354.
[2] D.G. Cooper, C.R. MacDonald, S.J.B. Duff, N. Kosaric.Appl. Environ. Microbiol.42 (1981) 408-412.

ECAB 5
The 5th EUROPEAN CONGRESS OF APPLIED BIOTECHNOLOGY
Florence 15-19 September 2019

Nano-scale enzyme membrane reactors for compartmentalized multienzyme syntheses

Michael Mertz[1], Sarah Poschenrieder[2], Ludwig Klermund[2], Kathrin Castiglione[1*]

1 Institute of Bioprocess Engineering, Friedrich-Alexander-Universität Erlangen-Nürnberg, Paul-Gordan-Straße 3, 91052 Erlangen, Germany; 2 Institute of Biochemical Engineering, Technische Universität München, Boltzmannstraße 15, 85746 Garching, Germany

**Corresponding author: kathrin.castiglione@fau.de*

Highlights

- Vesicles made from amphiphilic block-copolymers were used as reaction compartments.
- Inserting porins into the polymer membrane created nano-scale enzyme membrane reactors.
- Enzymes in the vesicle lumen were spatially separated from inhibitors in the bulk phase.
- New strategies to augment the catalyst loading of the vesicles are under investigation.

1. Introduction

When looking for examples of complex biocatalytic systems, one has not to look far. Already the estimated 3.72*10^13 cells of a human [1] depict a perfect example in which nature designed an astonishing biocatalyst network. In natural cells, a vast array of chemical reactions takes place simultaneously. Two fundamental principles allow these reactions to proceed efficiently: compartmentalization and selective mass transport. By spatial separation of enzymes and control over the reacting compounds, highly productive reaction cascades can be established.

To make use of these principles in bioprocess engineering, nano-compartments made from self-assembling, amphiphilic block-copolymers can be used to mimic these principles of cells and to improve biocatalytic reactions. By entrapping enzymes in vesicles with a selectively permeable membrane, nano-scale enzyme membrane reactors (nano-EMRs) can be created (Figure 1). The spatial separation of incompatible reactions can lead to more efficient one-pot multi-enzyme syntheses by avoiding cross-inhibitions and undesired side-reactions.

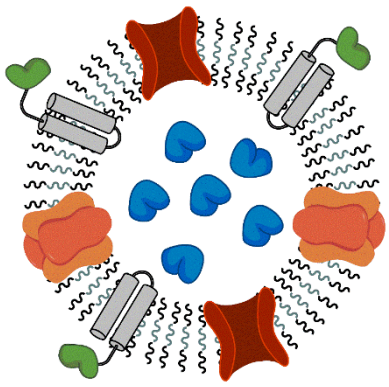

FIGURE 1: Nano-scale enzyme membrane reactor

2. Methods

The triblock-copolymer poly(2-methyloxazoline)$_{15}$-*b*-poly(dimethylsiloxane)$_{68}$-*b*-poly(2-methyl-oxazoline)$_{15}$ (PMOXA-PDMS-PMOXA) is ideally suited for the formation of selectively permeable nano-EMRs because natural (or engineered) channel proteins can be embedded in functional form into this polymer membrane. The polymer vesicles are formed by injecting a 20 % (w/v) polymer solution in ethanol into a stirred tank reactor containing an aqueous phase [2]. Upon vigorous stirring for 1- 3 hours (depending on the composition of the aqueous phase), vesicles with a narrow size distribution (polydispersity index < 0.25) are obtained.

To turn the vesicles into nano-EMRs, enzymes are encapsulated during vesicle formation. Additional enzymes can be immobilized on the surface of pre-formed vesicles by using genetically modified enzymes [3]. By equipping them with membrane anchoring domains, the enzymes of interest can associate with the polymer membrane. In the process of nano-EMR assembly, this is achieved by simply combining the different components. Enzymes with membrane anchoring domains and channel proteins spontaneously integrate into the nano-EMR membrane as the integration minimizes hydrophobic-hydrophilic interactions with the surrounding aqueous phase.

3. Results and discussion

Using the three-step enzymatic synthesis of CMP-*N*-acetylneuraminic acid as an example, it was demonstrated that the nano-EMR technology can be applied to avoid cross-inhibitions mediated by low molecular mass compounds in cascade reactions. This synthesis suffers from a strong inhibition of the first enzyme in the cascade, the *N*-acylglucosamine 2-epimerase (AGE), by CTP, which is a substrate of the third enzyme, the CMP-sialic acid synthetase (CSS). The implementation of a highly specific mass transport over the compartment boundaries was demonstrated by using the engineered channel protein OmpF G119D. This porin was the key element for the spatial separation of two incompatible reactions since it allows for the free diffusion of the substrates of the AGE, but fully excludes the larger substrates of the CSS thereby abolishing their inhibitory effects. It was shown that the compartmentalization of the enzymes enables synthesis of CMP-*N*-acetylneuraminic acid, whereas no product was formed with the free enzymes [4].

One of the major limitations of the nano-EMR technology is the low biocatalyst loading of the vesicles due to the statistical encapsulation of the enzymes during the nano-EMR formation. Thus, several strategies to augment the biocatalyst loading are currently under investigation.

4. Conclusions

The nano-EMRs are new tools to tackle the incompatibility challenge in enzymatic cascade reactions. Further developments of this exciting technology are needed to improve their operational performance, e.g. by increasing the enzyme concentration in the vesicle lumen.

References

[1] E. Bianconi, A. Piovesan, F. Facchin, A. Beraudi,R. Casadei, F. Frabetti, … & S. Perez-Amodio, Annals of human biology, 2013, 40(6), 463-471.
[2] S.T. Poschenrieder, S.G.Wagner, K. Castiglione, Journal of Applied Polymer Sciences, 2016, 133: 43274.
[3] L. Klermund, S.T. Poschenrieder, K. Castiglione, Journal of Nanobiotechnology, 2016, 14:48.
[4] L. Klermund, S.T. Poschenrieder, K. Castiglione, ACS Catalysis, 2017, 7: 3900-3904.

ECAB 5
The 5th EUROPEAN CONGRESS OF APPLIED BIOTECHNOLOGY
Florence 15-19 September 2019

Synthesis of valuable carotenoids in a heterotrophic microalgae fed-batch process – aspects of process modelling and scale-up

Felix Krujatz*[1], Christiane Grasse[2], Felix Wollmann[1], Thomas Walther[1], Juliane Steingroewer[1]

[1]*Institute for Natural Materials Technology, TU Dresden, Germany, Bergstr. 120, 01069 Dresden*

[2]*Li-iL GmbH Arzneimittel und Arzneibäder, Leipziger Straße 300, 01139 Dresden*

**Felix.Krujatz@tu-dresden.de*

- Heterotrophic microalgae bioprocess was scaled-up from shake flask to 50 L stirred tank reactor
- *In-silico* approach allows the design of process strategies
- Heterotrophic fed-batch process yielded dry weight concentrations > 30 g L^{-1}
- Astaxanthin, Canthaxanin and Lutein/Zeaxanthin are the predominant carotenoids.

1. Introduction

Algal biotechnology has gained an increased industrial interest over the last decade. For several years, microalgae served as source for natural-derived antioxidants and coloring carotenoids like ß-carotene or astaxanthin [1]. The photoautotrophic production of algal biomass and products is still state of the art. However, the supply of photosynthetic active radiation (PAR) as sole source of energy in photobioreactors systems remains one of the major challenges for photo-biotechnological processes resulting in low biomass concentrations of 0.5 – 5.0 g L^{-1} dry weight in large scale bioprocesses [2]. Additionally, photoautotrophic production impedes a world-wide production of algae biomass due to the process boundary conditions (e.g. temperature, light). Consequently, a trend is towards the production of high-quality microalgae products (e.g. the production of poly-unsaturated fatty acids by DSM/Evonik) by heterotrophic bioprocesses based on organic carbon and energy sources. This strategy allows the use of established technologies in biotechnology and the avoidance of some bottlenecks using photoproduction. The aim of this study is the development of a heterotrophic bioprocess to produce natural-derived carotenoids (with special focus on Astaxanthin) from microalgae [3].

2. Methods

First, a suitable production strain was identified by screening several *Chlorella* ssp. strains originated from European strain databases (SAG, CCAP, CCALA). The strains were screened on their heterotrophic growth rates µmax [h^{-1}] and yield coefficients $Y_{X/S}$ [g_{dw} g_{Glc}^{-1}] to identify a potential production strain. The chosen strain was characterized regarding the growth kinetics using glucose as sole carbon source (100 mL shake flask scale, modified BM medium) to setup a process model for an in silico process development and scale up (to 3 L and 50 L stirred tank bioreactors).

All modeling approaches were conducted in the free accessible software Berkley Madonna®. Finally, batch and fed-batch processes were performed in 3 L (Labors 5, Infors HT) and 50 L (Applikon Biotechnology) stirred tank bioreactors to validate the scale-up. Process monitoring was performed by glucose and nitrogen analytics, flow cytometry analysis (population dynamics), microscopy, carotenoid extraction and HPLC analysis.

3. Results and discussion

By screening several Chlorella ssp. strains we could identify a suitable natural producer which attained a high yield coefficient $Y_{X/S}$ using glucose as sole carbon source. The kinetic growth parameters µmax, K_S, K_I and $Y_{X/S}$ were determined in shake flask cultivations and implemented into a MONOD based process model. Using the in silico approach a fed-batch feeding strategy was established which was validated in 3 L and 50 L scale-up processes. The heterotrophic bioprocess yielded high dry weight concentrations > 30 g L^{-1}. Astaxanthin, Canthaxanthin and Lutein/Zeaxanthin were identified as the major carotenoid fraction in the cells.

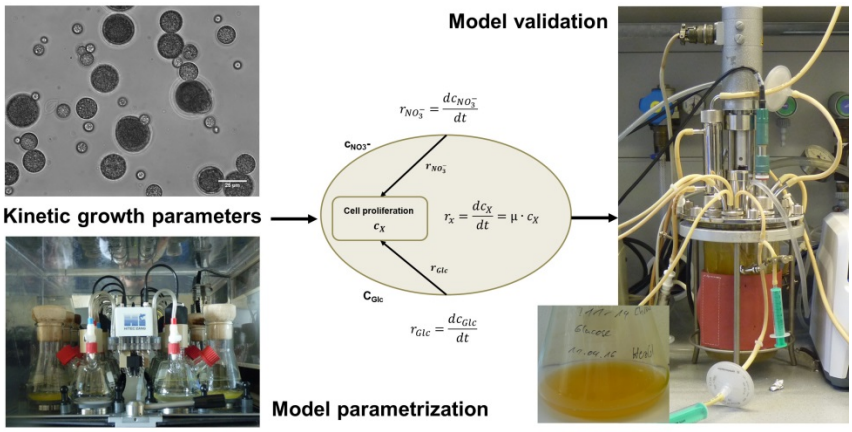

Figure 1. Process development of a heterotrophic *Chlorella* ssp- based bioprocess to produce natural-derived carotenoids.

This process allows the production of high-quality natural carotenoids from microalgae at high cell densities and thus offers an alternative to the complex photoautotrophic production by *Haematococcus pluvialis* which is independent on the production site and their climatic conditions (e.g. temperature, light).

4. Conclusions

Heterotrophic microalgal bioprocesses allow high cell density cultivation and facilitate scaled-up compared to photoautotrophic cultivation. Model validation performed in shake flask experiments and lab-scale bioreactor fermentations indicated robustness of the process model at different scales. Thus, the results provide a foundation for advanced model-based bioprocess development for heterotrophic microalgal processes.

References

[1] L. Gouveia, A. Raymundo, A. P. Batista, I. Sousa, J. Empis,, Eur. Food Res. Technol. 222 (2006) 362–367.
[2] M. Grima E, E.H. Belarbi, F.G. Acién Fernández, A. Robles Medina, Y. Chisti, Biotechnol. Adv. 20 (2003) 491–515.
[3] J. Liu, Z. Sun, H. Gerken, Z. Liu, Y. Jiang, F. Chen, Mar. Drugs, 12 (2014) 3487-3515.

ECAB 5
The 5th EUROPEAN CONGRESS OF APPLIED BIOTECHNOLOGY
Florence 15-19 September 2019

Rapid estimation of fractal dimension of microalgal aggregates

Patricio Lopez-Exposito, Carlos Negro, Angeles Blanco

Universidad Complutense de Madrid
Department of Chemical Engineering and Materials, Avda. Complutense s/n
28040 Madrid
Corresponding author: cengro@ucm.es

Highlights

- A method to estimate the fractal dimension of microalgal aggregates is proposed
- A machine learning model processes laser reflectance data to estimate fractal dimension
- The method is effective to resolve the 3D geometry of microalgal flocs
- The model can be used to control flocculation and produce optimally shaped flocs

1. Introduction

In order to deploy the full potential of microalgae as a source of variety of valuable products, the cultivation and harvesting costs associated to the production of microalgal biomass. The most cost-effective strategy to attain the harvesting of microalgal biomass is considered to consist in the combination of a flocculation stage followed by a concentration step based on settling, filtration or centrifugation. The effectiveness of the concentration step is affected by the size and shape of flocs produced in the flocculation stage. At present, however, no control over these two parameters is carried out at industrial level. The present communication describes a novel approach to estimate the average fractal dimension (D_f) of microalgal flocs suspensions by interpreting chord length distribution spectra acquired through a laser beam reflectance probe. This monitoring method could be applied on-line to control the stirring in flocculation processes so that the average geometry of aggregates is optimal for the subsequent concentration step.

2. Methods

The development of the estimation method involves *in-silico* and experimental steps. First, several families of virtual flocs, each having a consigned fractal dimension were created by means of applying a random growth algorithm. These virtual aggregated were virtually scanned through a computer emulator of the FBRM probe. The data generated were employed to train a machine learning random forest regression model (RFR) to learn the relationship between chord length distribution data and average fractal dimension. The estimation model was validated with real data of microalgal flocs suspensions of known fractal dimension.

3. Results and discussion

- Several families of virtual flocs resembling real ones were generated though a growth algorithm (Fig. 1).
- The virtual flocs were scanned through an FBRM emulator to produce the training data for a random forest regression model (fig. 2a).
- The model was successfully verified with real CLD data of real suspensions of known D_f. (fig. 2a).

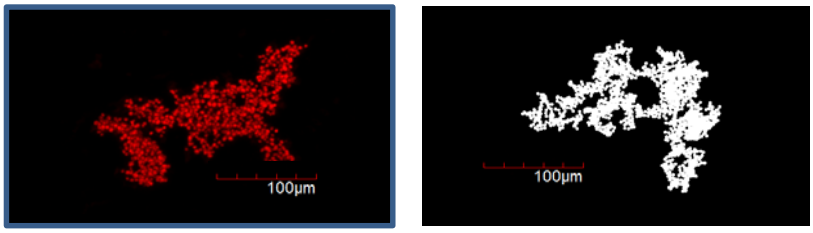

Figure 1. Real (left) and virtual (right) flocs of similar size.

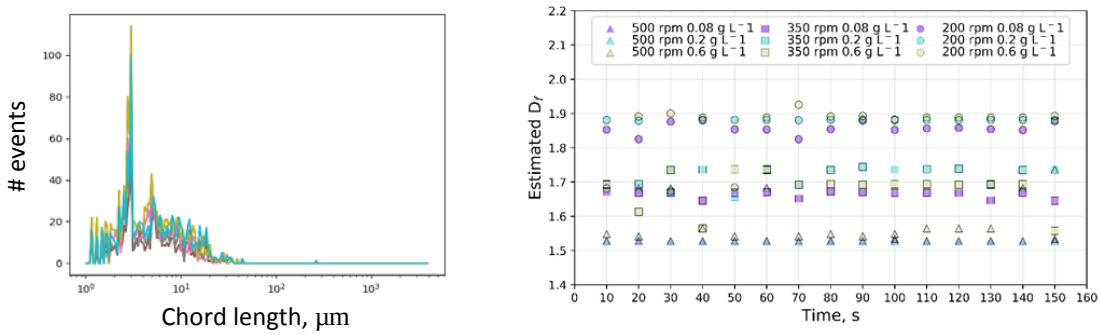

Figure 2. a) CLD of virtual floc and b) estimation of D_f on real data. [Calibri 9].

4. Conclusions

A model to directly estimate the fractal dimension form CLD data was successfully developed and verified with real data. The model can be applied as a means to monitor the flocculation of biomass to tune the stirring conditions so as to produce optimally shaped flocs for the subsequent separation phase. The present method could be adapted to other flocculating systems of organic or inorganic nature involving particles detectable through FBRM.

Acknowledgements

The authors wish to acknowledge the financial support of the Community of Madrid through the RETO-PROSOST-CM Programme (S2013/MAE-2907).

References

Chakraborti, R. K., J. F. Atkinson and J. E. Van Benschoten (2000). "Characterization of alum floc by image analysis." Environmental science & technology **34**(18): 3969-3976.

Gmachowski, L. (2000). "Estimation of the dynamic size of fractal aggregates." Colloids and Surfaces A: Physicochemical and Engineering Aspects **170**(2): 209-216.

Lopez-Exposito, P., Blanco, A., & Negro, C. (2017). Estimating fractal dimension of microalgal flocs through confocal laser scanning microscopy and computer modelling. Algal research, 28, 74-79.Schmid, M., A. Thill,

Vandamme, D., I. Foubert and K. Muylaert (2013). "Flocculation as a low-cost method for harvesting microalgae for bulk biomass production." Trends in biotechnology **31**(4): 233-239.

Wan, C., M. A. Alam, X.-Q. Zhao, X.-Y. Zhang, S.-L. Guo, S.-H. Ho, J.-S. Chang and F.-W. Bai (2015). "Current progress and future prospect of microalgal biomass harvest using various flocculation technologies." Bioresource technology **184**: 251-257.

ECAB 5
The 5th EUROPEAN CONGRESS OF APPLIED BIOTECHNOLOGY
Florence 15-19 September 2019

Effect of the addition of oak wood biochar and hydrochar in anaerobic digestion

Jessica Quintana-Najera[1,*], John Blacker[2], Louise Fletcher[3], Aaron Brown[1], Andrew Ross[1]

1 School of Chemical and Process Engineering, University of Leeds, LS2 9JT Leeds, UK; 2 Institute of Process Research and Development, School of Chemistry, University of Leeds, LS2 9JT Leeds, UK; 3 School of Civil Engineering, University of Leeds, LS2 9JT Leeds, UK

**Corresponding author: pmjqn@leeds.ac.uk*

Highlights

- Anaerobic Digestion
- Hydrothermal Carbonisation
- Pyrolysis

1. Introduction

Anaerobic digestion (AD) is a technology highly used for the sustainable management of a wide variety of waste while producing energy. The main product of AD is biogas, an alternative gaseous biofuel, composed principally of CH_4 [1]. Nevertheless, AD presents a major problem regarding inhibitory compounds from the organic feedstocks or produced during their hydrolysis, which detriment the CH_4 final yields [2]. Among the reported approaches for improving the CH_4 yields is the addition of adsorbent materials. It has been suggested that the addition of carbon materials for their role in the mitigation of the NH_4^+ inhibition, increasing CH_4 metabolism, reducing lag time, and facilitating the syntrophic metabolism between the different microorganisms involved [3].

Therefore, the integration of carbon materials, such as char products from the thermochemical treatment of biomass with AD has a growing interest. The thermochemical products of interest are biochar (BC) and hydrochar (HC). The former is produced by pyrolysis in non-oxidative conditions, whereas the latter is produced by hydrothermal carbonisation (HTC) in water at sub-critical conditions [4]. For the purposes of this work, the term 'char' is used to refer to both BC and HC. Particularly, the interest on the chars is due to certain characteristics, such as inertness, porosity, high surface area, and high surface functionality [5]. Even though there are indications of their positive effect on the stability of the AD process and higher quality of the digestate, their full potential as adsorbent materials in AD has not been properly assessed [2].

2. Methods

Oak wood was employed for the production of the chars. Firstly, the BC450 and BC650 was obtained by pyrolysis in a mono retort reactor at 450 and 650 °C for 1 hour, respectively. Secondly, the HC250 was produced by HTC in a non-stirred 2 L stainless steel batch Parr reactor at 250 °C, for 1 hour at 40 bar. Subsequently, the two biochars (BC450 and BC650) and the hydrochar (HC250) were used for AD. The anaerobic sludge inoculum was collected at Esholt Wastewater Treatment Plant, West Yorkshire, UK. The AD was performed in 500 mL reactors coupled to a Bioprocess™ Automatic Methane Potential Test System (AMPTIIS) system with daily online Biochemical Methane Potential

(BMP) measurement. The reactors were supplemented with inoculum 5 g VS/L, cellulose 5 g/L, and 15 g of the corresponding char, whereas the control contained only the inoculum and the cellulose. At the end of the AD the volatile fatty acids (VFA) content were measured by gas chromatography with an Agilent 7890A GC System, a DB-FFAP column, and a flame ionisation detector (FID).

3. Results and discussion

The effect on the CH_4 production largely differed between the systems with HC and BC (**Fig 1**). Firstly, the addition of HC250 lead to a BMP significantly lower than the control. This inhibitory effect could be related to the VFA accumulation (**Fig 2**) and the acidic nature of hydrochar, since the optimal pH for AD is around neutrality. Secondly, the addition of BC450 lead to a BMP 22% higher than the control. Thirdly, in comparison to the control, the BC650 system presented a similar BMP but a shorter lag phase. The variations on the effect of the chars could also be related to the differences between BC and HC, since their surface functionality and structure are dependent of the pyrolysis and HTC process conditions and the nature of the feedstock employed. For instance, in contrast to the HC, the BC presents a higher porosity and surface area that could promote the immobilisation of cells, and an alkaline nature that could provide a buffering effect. Although while comparing both BCs is worth considering the different temperatures employed for their production, since higher temperatures lead to lower O/H ratios and surface functionality. Thus, the different effect of the chars in AD could be related to their functional and physicochemical properties.

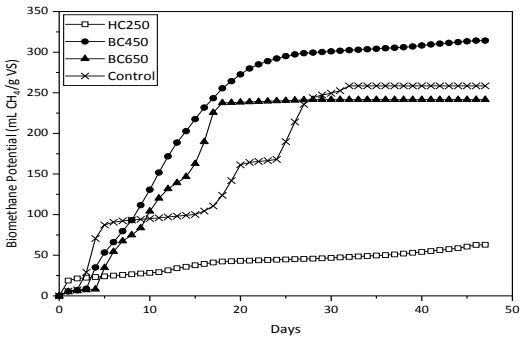

Figure 1. Production of biomethane during AD.

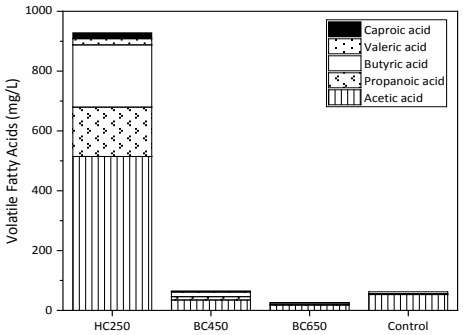

Figure 2. Production of volatile fatty acids during AD.

4. Conclusions

The addition of oak wood BC and HC had a different effect on AD. The HC250 presented an inhibitory effect on the production of CH_4 and a higher accumulation of VFAs. On the other hand, the BCs presented no inhibition on the anaerobic digestion. In consequence, the addition of BC450 improved the BMP and reduced the lag phase, whereas the addition of BC650 presented no significant effect. Therefore, given the BMP values obtained, it could be stated that the oak wood BC could have a beneficial effect on AD, whereas the oak wood HC presented a detrimental effect.

References

[1] J.C. Akunna. Anaerobic Waste-Wastewater Treatment and Biogas Plants: A Practical Handbook. 2018.
[2] M.O. Fagbohungbe, B.M.J. Herbert, L. Hurst, C.N. Ibeto, H. Li, S.Q. Usmani, K.T. Semple. Waste Manage (2017) 61, p. 236-249.
[3] J. Mumme, F. Srocke, K. Heeg, W. Maja. Bioresour Technol (2014) 164, p. 189-197.
[4] J. Zhang, W. Zhao, H. Zhang, Z. Wang, C. Fan, L. Zang. Bioresour Technol (2018) 266, 555-567.
[5] M.E. Gonzalez, M. Cea, N. Sangaletti, A. Gonzalez, C. Toro, M.C. Diez, N. Moreno, X. Querol, R. Navia. Biobased Mater Bio (2013) 7, p. 724-732.

ECAB 5
The 12th EUROPEAN CONGRESS OF CHEMICAL ENGINEERING
Florence 15-19 September 2019

Fed-batch culture of *L. brevis* a probiotic strain that produce lactic acid and other metabolites of biotechnological interest

Alberto Alfano[1], Simona Barbuto Ferraiuolo[1], Vittoria Savio[2], Alessandra Fusco[2], Giovanna Donnarumma[2], Chiara Schiraldi[1]

1 Department of Experimental Medicine, Sect. of Biotechnology Medical Histology and Molecular Biology, University of Campania "Luigi Vanvitelli", via L. De Crecchio n°7, 80138 Napoli Italy*;*

2 Department of Experimental Medicine, Section of Microbiology and Clinical Microbiology, University of Campania "Luigi Vanvitelli", via L. De Crecchio n°7, 80138 Napoli Italy

**Corresponding author: alberto.alfano@unicampania.it; chiara.schiraldi@unicampania.it*

Highlights

Fed-batch experiments increase viable cell density, lactic acid and exopolysaccharides

Lactic acid maybe a valuable side product of the production of probiotic biomasses

Purified exopolysaccharides play a role in inhibiting the growth of pathogen microorganisms

Purification and characterization of exopolysaccharide of potential biomedical interest

1. Introduction

Functional food and nutraceuticals are frequently based on the use of viable probiotic strains. Viable cells at a certain titer are known to be responsible of the beneficial effect on health. However, more recently the specific action of secreted metabolites seems to play a more important role, especially in respect to immonomodlation. Exopolysaccharies in this respect are proposed for use in the food, pharmaceutical and biomedical fields, thanks to their unique properties. We performed a fermentation and downstream process, using *Lactobacillus Brevis*, in order to produce antimicrobial compounds such as lactic acid and exopolysaccharides, that inhibit the growth of pathogens [1]. As a member of the genus Lactobacillus and due to its long-term use in various traditionally fermented food products, *L.brevis* has the GRAS status. Exopolysaccharides and other substances originated *L. Brevis* fermentation such as organic acids (lactic acid), contributed to their antimicrobial properties [2]. EPSs have been used in the production of several fermented foods, thickeners, stabilizers, emulsifiers and gelling or water-binding agents [3]. The possibility to evaluate the potential use of LAB EPS as food supplement or medical device can be explored if they are extensively purified before characterization. The production, partial purification and characterization of exopolysaccharides (EPSs) produced by *Lactobacillus brevis*

was among the target of this paper.In this work, after the centrifugation, membrane processes have been used for the concentration and recovery of products released in the fermentation broth, in order to decrease the number of volume of organic solvent to be used for the precipitation of exopolysaccharides, reducing process costs and above all environmental impact.

2. Methods

The bioreactor used for the batch and fed-batch processes was Biostat CT plus (Sartorius Stedim, Italy) with a total and working volume of 3.2L and 2.4L, respectively. *Lactobacillus brevis* was grown at T= 32°C, pH 6, 100 rpm, 0.75 vvm. Batch experiments were conducted in order to optimize the process parameters, such as gas inlet, pH, stirring, carbon and nitrogen source. Fed-batch experiments start after 12-14h with a predeterminated profile and they were performed in order to increase the viable cell density (CFU/mL), biomass yield and beside, the lactic acid and exopolysaccharide production respect to the batch processes. The antimicrobial activity was evaluated on pathological strains.

3. Results and discussion

In fed-batch processes we obtained a total average CFU/mL of about $9.5x10^9$ CFU/mL, with a final OD600 of 23.4. The lactic acid produced was 63.7 g/L. Comparing the results of fermentation processes it can be seen as the fed-batch processes has increased in terms of cell number and lactic acid production of 2.1 and 2.9, respectively, respect to the batch processes.

4. Conclusions

Using fed-batch processes we doubled the number of live cells compared to the batch process and increased the production of exopolysaccharides and organic acids that were inhibitory for the growth of pathogen microorganisms.

Membrane processes were implemented to recover a High MW fraction in supernatants, with specific interest in the characterization of exopolysaccharides that were determined with specific biochemical and analytical characterization exploiting SEC-TDA chromatographer and light scattering.

References

[1] Schiraldi C., Adducci V., Valli V., Maresca C., Giuliano M., De Rosa M. High cell density cultivation of probiotics and lactic acid production. Biotechnology and Bioengenering. 2003. 82(2), 213-22

[2] Vesterlund S, Paltta J, Lauková A, Karp M, Ouwehand AC. Rapid screening method for the detection of antimicrobial substances. J Microbiol Methods. 2004 Apr;57(1):23-31

[3] Tapan Kumar Singha. *Microbial Extracellular Polymeric Substances: Production, Isolation and Applications.* Department of Microbiology, Maharshi Dayanand University, Rohtak-124001, 2012.

Hempseed protein hydrolysates-antioxidative and anticancer effects

Višnja Gaurina Srček*, Kristina Radošević, Marijan Logarušić, Igor Slivac, Ivana Radojčić Redovniković

University of Zagreb, Faculty of Food Technology and Biotechnology, Laboratory for Cell Technology and Biotransformation, Pierottijeva 6, 10000 Zagreb, Croatia

**Corresponding author: vgaurinasrcek@pbf.hr*

Highlights

- Hempseed protein hydrolysates possess antioxidative activity.
- Hempseed protein hydrolysates showed antiproliferative effects in HeLa cells.
- Protective effects of hydrolysates were observed during H_2O_2 induced oxidative stress.
- Enzyme hydrolysis of hempseed proteins resulted in high value-added products.

1. Introduction

In recent years, many research groups had focused on the production of peptides/hydrolysates with potential application in food and nutraceutical industry. Protein hydrolysates or bioactive peptides derived from food proteins have been reported to exhibit a wide range of bioactivity including immunomodulatory, anticancer, antihypertensive, antioxidant, osteoprotective and antimicrobial effects [1]. Industrial hemp (*Cannabis sativa* L) seed is by-product obtained after utilization of plant fibers and is used as oil and protein source. It contains 20-25% of proteins and its amino acid profile showed similar or even higher level of essential amino acids (except for lysine) in comparison to soy proteins [2]. Recent studies have reported antioxidative properties of hempseed protein hydrolysates obtained by enzyme *Alcalase® 2.4L* on induced oxidative stress in PC12 cells [3]. However, more studies are needed to investigate effects on hempseed protein hydrolysates obtained by other enzymes on different cells. The aim of this study was to prepare hempseed protein hydrolysate (HPH) from hempseed protein isolate (HPI) by three commercial enzymes: *Alcalase® 2.4L, Neutrase and Protamex*. In addition, biological potential of prepared HPHs was measured by ORAC assay as well as their effects on viability and cellular changes of normal and tumor cells.

2. Methods

HPHs were prepared using the commercial enzymes *Alcalase® 2.4L, Neutrase and Protamex* as described by [3]. Antioxidant activity of obtained HPHs was assayed by ORAC method. Effects of HPHs on proliferation of normal (HaCaT) and tumor (HeLa) cells were determined by colorimetric MTS assay while cellular changes were assayed by spectrofluorimeter and MUSE cell analyzer.

3. Results and discussion

Prepared HPHs showed strong antioxidant activity (ORAC values in range 576.52±36.5 - 695.2±6.75 µM TE/g protein) in comparison to 32.6±2.35 µM for HPI, indicating releasing of antioxidant

peptides during hydrolysis process. Tested hydrolysates showed cytotoxic activities toward tumor HeLa cells with no effects on normal HaCaT cells (Figures 1-2). Similar results of concentration-dependent antiproliferative effects of germinated soybean protein hydrolysates on breast and cervical cancer cell lines with minimal effects on normal cells was reported by [4]. Observed antiproliferative effects of HPHs in tumor cells suggested relationship between cytotoxicity and antioxidant activity also indicating their potential as functional food ingredient in anticancer therapy.

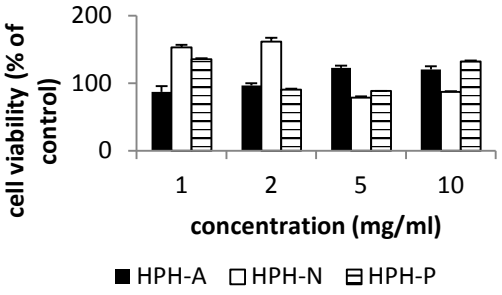

Figure 1. Effects of HPHs on HaCaT cells by MTS assay

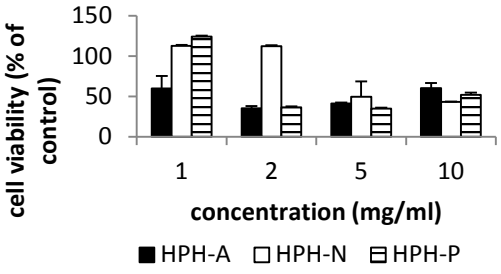

Figure 2. Effects of HPHs on HeLa cells by MTS assay

The ability of HPH-N to protect HaCaT and HeLa cells against oxidative stress induced by H_2O_2 is shown in Figure 3. Pretreatment of cells with HPH-N significantly reduced ROS (+) cells on concentration-dependent manner (29.13-40.5% for HPH-N *vs.* 44.2% for H_2O_2 in HaCaT cells and 27.03 -32.87% for HPH-N *vs.* 54.8% for H_2O_2 in HeLa cells) indicating its protective role against ROS formation.

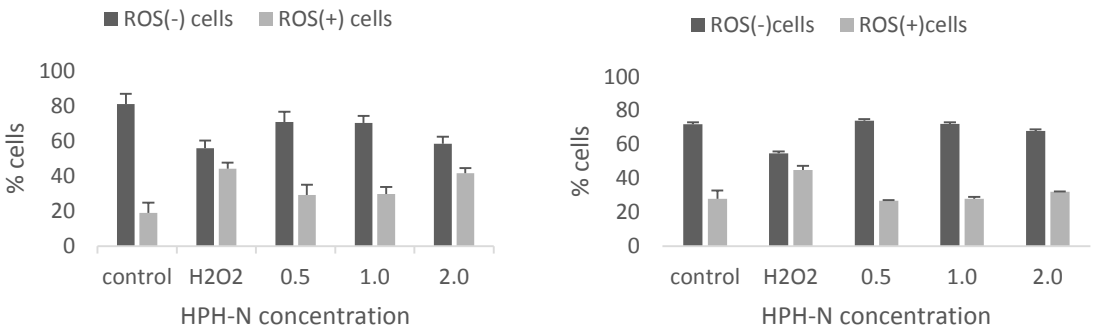

Figure 3. Protective effects of HPH-N on induced oxidative stress in HaCaT (left) and HeLa (right) cells.

4. Conclusions

The results indicate that hempseed protein hydrolisys results in releasing peptides with antioxidative and anticancer activities and might be considered as functional food ingredient.

References

[1] M. Chalamaiah, W. Yu, J. Wu, Food Chem. 245 (2018) 205-222.
[2] J.C. Callaway, Euphytica 140 (2004) 65-72.
[3] C.H. Tang, X.S. Wang, X.Q. Yang, Food Chem. 114 (2009) 1484-1490.
[4] M. González Montoya, E. Ramón-Gallegos, M.C. Robles-Ramírez, R. Mora-Escobedo, Plant Foods Hum. Nutr. 71 (2016) 368-374.

ECAB 5
The 5th EUROPEAN CONGRESS OF APPLIED BIOTECHNOLOGY
Florence 15-19 September 2019

FeedPlatePlus - Fed batch cultivation and protein purification in microtiterplates

Dr. Michael Hofer[1], Dr. Barbara Dittrich[2], Timm Keil[3], Prof. Dr. Jochen Büchs[3], Clemens Lattermann[4]

1 Fraunhofer Institute for Interfacial Engineering and Biotechnology IGB, Schulgasse 11a, 94315 Straubing, Germany, 2 DWI Leibniz-Institut für Interaktive *Materialien e.V., Forckenbergstrasse 50, 52074 Aachen, Germany; 3 AVT – Biochemical Engineering, RWTH Aachen University, Forckenbeckstr. 51, 52074 Aachen, Germany, 4 Kuhner Shaker GmbH, Kaiserstrasse 100, 52134 Herzogenrath, Germany*

**Corresponding author: michael.hofer@igb.fraunhofer.de*

Highlights

- Optical accessible high-throughput fed-batch cultivation in microtiter plates
- High-throughput protein purification in microtiter plates

1. Introduction

For the development of biotechnological processes, a large number of microbial strains or enzyme variants are generated and have to be analyzed by high-throughput technologies. In these small-scale processes, the cultivation conditions are crucial for a successful strain development as well as for high protein productivities. To imitate production conditions already during early process development, the polymer-based Feed Plate® technology enables fed-batch conditions in microtiter plates [1]. Based on this technique, this study develops an upgrade to enable fed-batch feeding, protein purification and optical accessibility in one microtiter plate. This is realized by a 3D shaping of the polymer matrix (so-called feed rings) which are introduced into each well of a microtiter plate. Additionally, the surface of these feed rings is functionalized with Ni-NTA groups, which allows selective binding and thus purification of His-tagged proteins.

2. Methods

Feed Rings were produced by injection molding of a polysiloxane based polymer matrix containing defined amounts of glucose crystals. Surface modification of feed rings was achieved by addition of carboxylated monomers to the polymer matrix and subsequent esterification with suitable Ni-NTA groups.

3. Results and discussion

First prototypes were constructed, realizing the high-throughput fed-batch cultivaton in 96 well plates through the 3D shaped polymer matrix. The matrix is additionally surface modified to allow for targeted protein binding through Ni-NTA groups (figure 1).

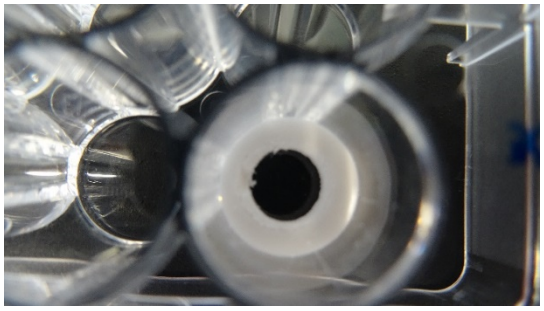

Figure 1. Feed ring in a 96 well plate.

4. Conclusions

Until now, cell culture, digestion, purification and analysis are performed in different microtiter plates. In doing so, almost every step consumes a new plate. Additionally, sterile pipette tips are required for transferring the solutions by means of pipetting. Thus, significant savings in consumables and thus costs can be achieved by the Feed Plate® technology. Another advantage for the scientific work is the reduction of sources of error that occur in particular through frequent pipetting.

References

[1] **EP1879995**

ECAB 5
The 5th EUROPEAN CONGRESS OF APPLIED BIOTECHNOLOGY
Florence 15-19 September 2019

Steps towards continuous cellulose hydrolysis via Oscillatory Flow Bioreactors (OFBs)

Judith Buchmaier[1], Christoph Brunner[1], Anh. N. Phan[2], Adam P. Harvey[2], Rama Krishna Gudiminchi[3], Bernd Nidetzky[3], Bettina Muster[1]

1 AEE - Institute for Sustainable Technologies, Industrial Processes and Energy Systems, Feldgasse 19, 8200 Gleisdorf, Austria
2 Newcastle University, Chemical Engineering and Advanced Materials, Newcastle upon Tyne NE1 7RU, United Kingdom
3 Austrian Center of Industrial Biotechnology, 14 Petersgasse, A- 8010 Graz, Austria

**Corresponding author: j.buchmaier@aee.at*

Highlights

- Oscillatory Flow Bioreactor (OFB) readjusted from batch to continuous mode
- Continuous processing of cellulose slurry with 15% solid loading possible
- 4 continuous hydrolysis procedures for optimized mixing and overcoming product inhibition
- Enhanced conversion rates at low enzyme input

1. Introduction

The extraction of valuable and pure resources from biogenic material such as lignin, hemicellulose and cellulose is of great importance for the economic realization of biorefineries. Lignocellulosic waste (food waste, forest residues, agricultural waste, etc.) is abundant and therefore a source of special interest, when looking at the production of biobased chemicals and commodities. [1]

Within this study a special focus was put on process intensification steps in terms of an innovative reactor design (Oscillatory Flow Bioreactor, OFB) for overcoming some of the main challenges and hurdles occurring in lignocellulosic conversion processes. The OFB was designed addressing the inefficient (mass and heat transfer inefficiencies) and energy consuming mixing of viscous bioslurries which conventionally are handled at low solid loadings in stirred tank reactors and suffer poor process performance due to a rather slow reaction and product inhibition.

2. Methods

A modular setup of the Oscillatory Flow Bioreactor – enabling batch mode as a first step was designed as follows: Reactor length is adjustable by applying 1 to 2 reactors, baffles of various thickness (2 mm and 3 mm) and different shape (helical) can be inserted. Sinusoidal waveform oscillations in ranges of 0-10 Hz frequencies and 0-11 mm amplitudes are imposed. The overall OFB design is based on Oscillatory Baffled Reactor OBR studies in literature [2] such as on experimental studies at the University of Newcastle.

The conversions were conducted with pure α-cellulose in 50 mM sodium citrate buffer (citric acid monohydrate and tri-sodium citrate dehydrate, Merck Millipore) at pH 4.8, at 50 °C. A DMA 35 device (Anton Paar) was used to measure Glucose formation by density assessment with. Conventional Dinitrosalicylic (DNS) assay were used for detailed evaluation. Batch OFB tests were conducted at different angles, frequencies, amplitudes, viscosities, with different media (ligno-cellulosic material), solid loading (mg/ml) and enzyme loadings (FPU).

3. Results and discussion

The specifically designed Oscillating Flow Bioreactor OFB has been successfully developed for high solid loading (SL) biogenic slurries to ultimately switch from batch to continuous enzymatic hydrolysis processes. Enzymatic conversion experiments of 24 h duration showed, that the batch OFB system generated 3,69 % (70,54 mg/ml) more sugar at similar theoretical mixing power density (12% SL, 2,05 Hz) compared to the reference STR system. The treatment of very high SL (15%) revealed sugar formations of up to 6,7 % higher than its reference system. As shown in Table 1 the 3 mm baffle showed a better conversion performance (+5%) than the thinner 2mm type. Notably also, the OFB system demonstrates similar conversion as the STR while using 20% less FPU of enzyme blend at only 4,8 % power density. Summing up the OFB system exhibited high potential for enzymatic conversions.

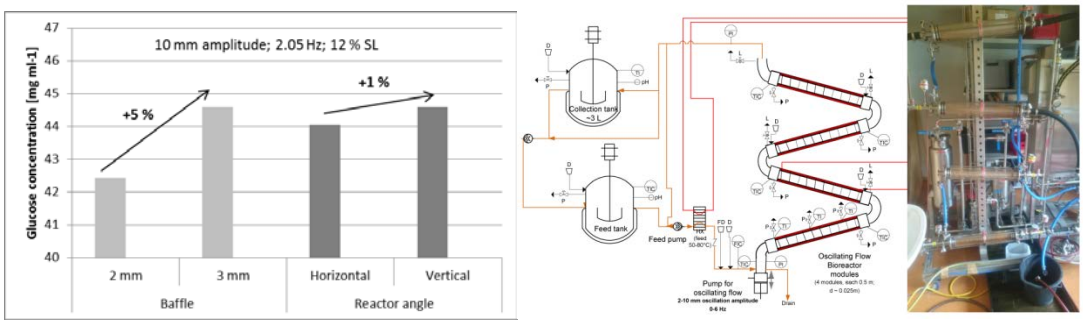

Figure 1. : Steps towards design optimization (left), schematic of OFB plant (right)

The final plant concept is shown in Figure 1 (right side). Conti OFB set-ups consisted of the following configurations ranging from 1-4 OFB reactors in series, Oscillation parameters of 10 mm amplitude, 1-3 Hz and net-flow velocities of up to around 150ml/min.

4. Conclusions

Different steps resulted in best configuration and operating conditions in OFB - Batch mode, these were transferred into OFB - Conti mode. OFB - Batch results gave very satisfying results in terms of glucose production, enzyme input and theoretical energy input, compared to reference STR system. High solid loading of 15% ±-cellulose were reproducibly tested. Various configurations of OFB - Conti tests are tested at the moment. Results will be presented at the conference

References

[1] S. Chundawat, G. Beckham, M. Himmel, B. Dale, Annu Rev Chem Biomol Eng, 2 (2011) 121-145.

[2] M. Abbott, G. V. Perez, A. P. Harvey, M. K. Theodorou, Chem. Eng. Res. Des.92 (2014) 1969.

ECAB 5
The 5th EUROPEAN CONGRESS OF APPLIED BIOTECHNOLOGY
Florence 15-19 September 2019

Maximization of poly(3-hydroxybutyrate) production in fed-batch cultures of *A. vinelandii* based on the variation of the agitation rate

Beatrice Mongili[1], Claudio Alonso Padilla-Córdoba[2], Tonia Tommasi[1], Debora Fino[1], Alvaro Díaz-Barrera*[2]

1 Department of Applied Science and Technology (DISAT), Politecnico di Torino, Corso Duca degli Abruzzi, 24, 10129 Turin, TO, Italy;
2 Escuela de Ingeniería Bioquímica, Pontificia Universidad Católica de Valparaíso, Av. Brasil 2147 Casilla 4059, Valparaíso, Chile.

**Corresponding author: alvaro.diaz@pucv.cl*

Highlights

- Specific growth rate is improved by high k_La
- PHB productivity was affected by the volumetric oxygen transfer coefficient
- Variation of k_La allowed to define maximal PHB productivity

1. Introduction

The poly-hydroxybutyrate (PHB) is a polyethylene-like bioplastic naturally synthetized by several classes of microorganisms, as a source of energy and carbon unit [1]. This material, which is a promising candidate for the replacement of fossil-based plastic, is already present at an industrial scale. However, the maximization of its production process is the goal to achieve in order to reduce production costs. *Azotobacter vinelandii* is strictly aerobic gram-negative soil bacteria, able to produce PHB in a carbon substrate-rich environment and under oxygen-limitation conditions [2]. The production of this polymer is particularly interesting in this species, because it can accumulate up to 85% of its dried biomass as PHB [3]. It is known that agitation rate affects the PHB production by *A. vinelandii* [2]. In this work, the PHB productivity under fed-batch cultivation was evaluated to different volumetric oxygen transfer coefficient (k_La). Thus, it was possible to determine an adequate k_La range for scale-up the production of PHB.

2. Methods

Batch cultures of *Azotobacter vinelandii* OP were performed in a 3 L bioreactor (30 g L^{-1} sucrose as carbon source) at 600 rpm during 30 h. After of this time, the cultures were fed by a single medium feeding pulse of the carbon source and the agitation speed was varied between 400 and 1000 rpm. The biomass evolution and the PHB production were evaluated. The k_La was estimated at different agitation rate using dynamic method.

3. Results and discussion

The maximal accumulation of biomass was 13.3 g L^{-1}, obtained at an agitation speed of 800 rpm (Table 1). A highest agitation speed increased the specific growth rate, reaching a value of 0.069 h^{-1} to 1000 rpm. During fed-batch cultivation, a change in the agitation speed affected the PHB accumulation, obtaining the highest value (79.1 % w w^{-1}) to 600 rpm.

Agitation speed (rpm)	k_La (h^{-1})	μ (h^{-1})	X_{max} (g L^{-1})	PHB (% w w^{-1})
400	30.3	0.011 ± 0.001	9.45 ± 0.14	66.0 ± 2.6
600	65.6	0.021 ± 0.001	11.50 ± 0.24	79.1 ± 1.5
800	103.6	0.062 ± 0.002	13.25 ± 0.49	54.7 ± 3.5
1000	188.0	0.069 ± 0.001	11.80 ± 0.05	46.3 ± 3.0

Table 1: Parameters obtained in the fed-batch cultures of *A. vinelandii*

Figure 1 shows the influence of k_La on the PHB volumetric productivity. A maximal PHB productivity of 0.28 g L^{-1} h^{-1} was obtained at a k_La of 104 h^{-1}. Overcoming the k_La of 104 h^{-1} the PHB productivity decreased until 0.18 g L^{-1} h^{-1}. Under the conditions evaluated, the PHB productivity obtained to 100 h^{-1} was similar to previous studies [2,3].

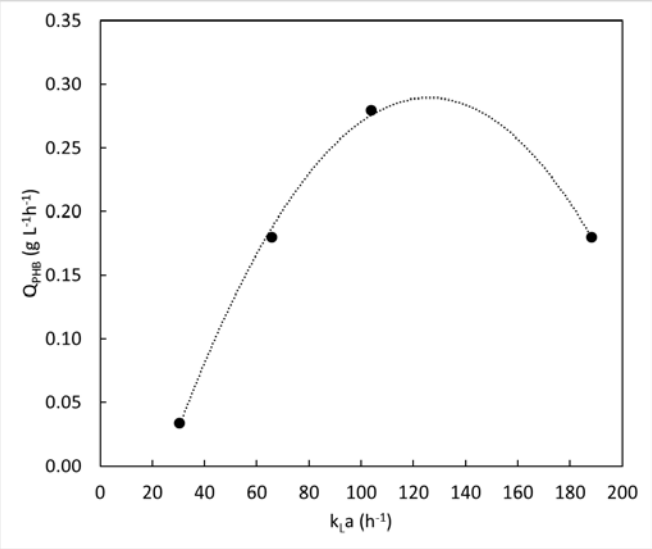

Figure 1. Relationship between the PHB volumetric productivity and k_La values in *Azotobacter vinelandii* OP. The k_La values evaluated correspond to the agitation speed of 400, 600, 800 and 1000 rpm.

4. Conclusions

In fed-batch cultures of *Azotobacter vinelandii*, the PHB productivity was affected by the volumetric oxygen transfer coefficient. The highest PHB productivity was obtained in the cultures performed to 104 h^{-1} (800 rpm). In order to develop a bioprocess to produce PHB, it was possible to identify the optimal oxygen transfer conditions for further bioprocess scale-up.

References

[1] T. G.Y. Amy, C.L. Chen, L. Li, L. Ge, L. Wang, I.M.N. Razaad, Y. Li, L. Zhao, Y. Mo, J.Y. Wang. Polymers (Basel) 6(3) (2014) 706–54.
[2] A. Díaz-Barrera, R. Andler, I. Martinez, C. Peña. J. Chem. Technol. Biotechnol. 91 (2016) 1063-1071.
[3] T. Castillo, C. Flores, D. Segura, E. Guadalupe, J. Sanguino, E. Cabrera, J. Barreto, A. Díaz-Barrera, C. Peña.

J. Chem. Technol. Biotechnol. 92(7) (2017) 1809–16.

ECAB 5
The 5th EUROPEAN CONGRESS OF APPLIED BIOTECHNOLOGY
Florence 15-19 September 2019

Development of an external pH monitoring system for a 10 L bioreactor

Nathalia Peruch[1], Fábio Cavalcante[1], Arnaldo Prata[1*]

[1] *Departament of Biotechnology – Engineering School of Lorena – University of São Paulo*
Estrada Municipal do Campinho, sn - CEP 12602-810, Lorena, São Paulo – Brasil

**Corresponding author: amrprata@usp.br*

Highlights

- External pH monitoring system avoids electrode insertion in the bioreactor cover.
- A nylon cilyndrical device and a peristaltic pump are needed in addition to pHmeter.
- Broth pH can be continuously and accuratelly monitored in simple biorreactors.

1. Introduction

A new bioreactor was designed specifically for culturing shear stress sensitive cells and avoid problems caused by adherent filamentous fungi growth (Domingos et al., 2017). This bioreactor can also be used for other bioprocesses using yeasts and bacteria. It was named *Low Shear Aerated and Agitated Bioreactor* (LSAAB). Once the bioreactor was developed without internal prominent parts to avoid micelial adherence, no electrode or sensor holes were provided in its cover. However, in many cases pH must be monitored and controlled in order to ensure cell growth and product formation during a bioprocess. Domingos et al. (2017) verified that pH increases and it must be controlled during the basidiomycete *Ceriporiopsis subvermispora* culturing in LSAAB for optimizing biomass production. During 2,3-butanediol production by *Klebsiella oxytoca* the pH decreases due to organic acids synthesis and excretion (Tsvetanova, Petrova, Petrov, 2014) and it must be controlled for better enzyme activity. Therefore, in the present work it was proposed a strategy of external broth circulation through a device containing the pH electrode inserted, providing broth pH monitoring in LSAAB. The system was tested with water and during the yeast *Saccharomyces cereviseae* growth.

2. Methods

Electrode holder: The device was first drawn, in order to enable its machining. Nylon was used, an appropriate material for both machining and further sterilizations. A cylindrical configuration was addopted, with a diameter 8 mm larger than that of the pH electrode, for a free broth flow. This device was attached to the bioreactor and the peristaltic pump using silicone hoses.

pH mesuring and liquid circulation: pH was mesured with a Sppencer Scientific SP3611 model pHmeter, with an armored electrode inserted in the holder. Liquids were pumped with a VELP Scientifica SP311 model peristaltic pump.

Tests with water: The system was first tested with water in order to verify pH reading stability as a function of pump flow rate (4.5, 19.0, 39.0, 58.0, 78.0, 92.0 e 112.0 mL/min). Samples were collected and had their pH measured separatelly with the same pHmeter. Following, it was

investigated the time for pH change detection by the electrode after acid (5 mol/L HCl) addition, for each pump flow rate above and under agitation speeds of 140 and 200 rpm. For 200 rpm it was also performed tests with aeration (0.8 vvm). Acid was added at the liquid surface in the bioreactor.

pH monitoring during fermentation: *Saccharomyces cereviseae* was used to carry out the culturing in LSAAB for the external pH monitoring system avaliation. Culturing medium (10 L) consisted of (in g/L): glucose (20.0), $(NH_4)_2SO_4$ (5.0), KH_2PO_4 (3.0), $MgSO_4$ (1.5) and yeast extract (6.0). Initial pH was adjusted to 4.5. Temperature and aeration were 25 ^oC and 0.8 vvm, respectivelly. Substrate and cell concentrations were measured by DNS and optical density methods, respectivelly.

3. Results and discussion

The cylindrical device was attached to the bioreactor and showed to be proper for liquids (water and culturing medium) circulation using flow rates from 4.5 to 112.0 mL/min. Using water, on line pH readings remained constant after 1 minute from the adjusting for flow rates from 19.0 to 112.0 mL/min, indicating an adequate fluid dynamics accross the system. Collected samples and on line pH readings showed a difference from 0.01 to 0.04 pH units, considering all flow rates tested. Considering the simmulation of microrganism actuation, pH readings remained constant after 2.0 minutes from acid addition, for flow rates from 58.0 to 112 mL/min, at 140 rpm agitation. At 200 rpm the time was 1.0 min for flow rates 92.0 and 112.0 mL/min, showing the effect of agitation on the whole broth pH change. Aeration did not affect the time for obtaning on line constant pH readings. This facts indicate that a flow rate about 90 mL/min and an agitation of 200 rpm are sufficient for monitoring and controlling broth pH in LSAAB using the proposed system. It can be considered that a delay of 1.0 minute from acid or alkali addition to pH correction in the whole broth do not compromise the bioprocess.

However, regarding the yeast cultivation, the differences between samples pH and on line pH readings varied from 0.1 to 0.15 pH units. Although higher than those obtained for water, such values represent a maximum of 3.75% of the desired pH value. It should be mentioned that broth samples were cooled and had their pH mesured from 3 to 15 hours after collected. Due to the intense metabolism of the yeast some changes in the broth could have occurred, even during cooling. Therefore, it can be considered that the proposed external pH monitoring system does not interfere in the actual broth pH inside the LSAAB. Further investigations include carrying out fermentations requiring pH adjustment.

4. Conclusions

The external pH monitoring system proposed for LSAAB is adequate for obtaining the actual broth pH value during fermentation processes and its control in simple bench bioreactors, without insertion of an electrode in the bioreactor cover. Best results are obtained with an agitation of 200 rpm and a minimum of 90 mL/min of broth circulation flow rate, considering the geometric characteristics of LSAAB, like liquid height, vessel internal diameter and “L” shaped stirrer.

References

[1] M. Domingos, P. B. Souza-Cruz, A. Ferraz, A. M. R. Prata, Chem. Eng. S. 170 (2017) 670–676.
[2] F. Tsvetanova, P. Petrova, K. Petrov, Biotechological Prod. and Proc. Eng. 98 (2014) 2441-2451.

Use of a filamentous fungus for phosphorus solubilization in iron ore tailings.

José Daniel Gonçalves Vieira*[1], Glalber Luiz da Rocha Ferreira[1], Geraldo Sadoyama[2], Nelson Roberto Antoniosi Filho [3]

[1] *Environmental and Biotechnology Laboratory. Instituto de Patologia Tropical e Saúde Pública. Universidade Federal de Goiás. 74605-050, Goiânia, GO, Brazil*

[2]*Departamento de Biologia, Universidade Federal de Goiás, Campus Catalão*

[3]*Laboratório de Métodos de Extração e Separação. Instituto de Química. Universidade Federal de Goiás*
**Corresponding author: jdgvieira62@gmail.com*, +55 6232096527

Highlights

- Efficiency solubilization of phosphate present in iron ore.
- Iron ores wastes may be used as source of phosphorus when properly treated.
- Biolixiviation using fungus proved to be efficient for reduction of phosphorus in iron ore tailings reducing its environmental pollution.

1. Introduction

In iron and steel production chain, phosphorus element is present in almost all stages, tending to concentrate during the extractive process, due to its ability to pass from the oxidized form to elemental form, being present in metallic iron after reduction mineral (Delvasto et al., 2009). Steel produced at high phosphorus levels will be brittle and can easily break, hence the need for dephosphorization (Chime et al., 2011). As a result, different iron dephosphorization techniques have been developed. These methodologies tend to have high production costs with low productivity (Mendes et al., 2013, Xiao et al., 2015). In view of this problem, it is necessary to develop sustainable and cost-effective processes for the exploitation of minerals containing different levels of phosphorus (Liu et al., 2015). One of the most promising solutions is the use of microorganisms in a process called microbial bioleaching, when compared to other physical-chemical processes (Chime et al., 2011). Its advantage is the use of mild conditions, usually without addition of toxic chemicals. The objective of this work was to test a filamentous fungus isolated from the iron ore tail itself in the solubilization of the phosphorus present in this ore.

2. Methods

Fungus was isolated by enrichment cultivation in NBRIP medium (Nautiyal, 1999), whose phosphate was withdrawn and added 5g of iron ore tailings for the fungus isolation and also as N_2 source. Erlenmeyers containing 50mL of medium were incubated under agitation (130 rpm) at a temperature of 30 ± 2 °C. Every 7 days 1.0 ml aliquot was withdrawn and inoculated into fresh culture medium and incubated for another 7 days. This process was repeated two more times. After last repeat, aliquots were taken, diluted conveniently and inoculated into Petri dishes containing NBRIP medium plus $Ca_5(OH)(PO_4)_3$ as source of phosphorus. Plates were incubated in a BOD oven at 30 ± 2 °C for a period of 7 days. Colonies that had a characteristic halo of phosphorus solubilization were isolated. Following parameters were determined: growth curve, pH evolution, acid phosphatase activity, phosphorus solubilization. Parameters were performed for 168 hours with collection of 24/24 hours. For growth curve, samples were taken at described time, filtered in previously weighed Millipore® type filter (0.22µm). The material was dried in a desiccator with silica gel in an oven at 30 °C for 24 hrs until constant weight and the fungus mass was

deteminated. pH was determined in aliquot of the aliquots after centrifugation using a pHmeter. Phosphatase acid activity was performed using the Labtest® Trade Kit according to the manufacturer's guidelines. Phosphorus solubilization was performed by dosage of the solubilised phosphate using the Spectro Kit of the Alfakit® brand, according to the manufacturer's guidelines.

3. Results and discussion

Results obtained for determination of fungic mass, pH, acid phosphatase activity and phosphate solubilization can be observed in Figure 1.

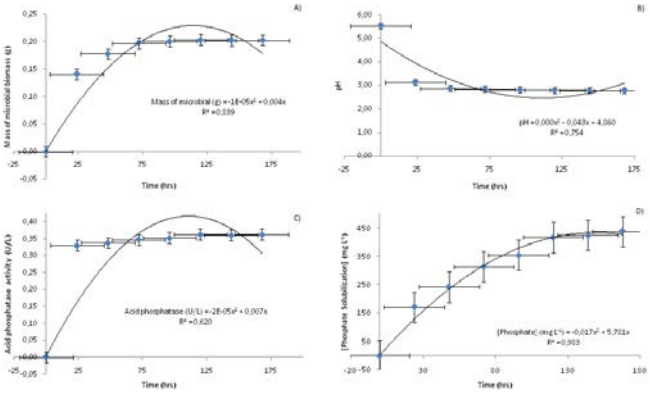

Figure 1. Results obtained for determination of fungal mass (A), pH (B), acid phosphatase activity (C) and phosphate solubilization (D).

According to analyzed parameters, it was observed that, between 144 and 168 hours, its stabilization occurred (Fig. 1). Xiao et al. (2015) testing dephosphorization of iron ore with high concentration of phosphorus by different strains of *Aspergillus niger*, observed similar results of pH reduction, phosphorus solubilization and fungal growth. Phosphate biosolubilization has been shown to be a very efficient process for conversion of insoluble phosphate into phosphorus, corresponding to a solubilization of 43% in 7 days of incubation, ie, equivalent to a mass of 0.1539 g of phosphate in the counterpart of 0.3576 g of iron ore.

4. Conclusions

Using of filamentus fungus for phosphorus solubilization, present in iron ore tailings, proved to be efficient in this study. Researches are underway to make this process feasible on a large scale

References

[1] T.O. Chime, M.C. Menkiti, O.D. Onukwuli, New York Science Journal (2011): 1-6.
[2] Z. Liu, Y.C. Li, S. Zhang, Y. Fu, X. Fan, Appl. Soil Ecol., (2015): 217-224.
[3] G.O. Mendes,. C.S. Dias, I.R. Silva, J.I.R., Júnior, O.L. Pereira, M.D. Costa, World J. Microbiology Biotech. (2013): 29-43.
[4] C.S. Nautiyal, FEMS Microbiol. Lett. (1999): 265-270.
[5] C. Xiao, X. Wu, R. Chi, Appl. Bioch. Biotech. (2015): 518-528.

ECAB 5
The 5th EUROPEAN CONGRESS OF APPLIED BIOTECHNOLOGY
Florence 15-19 September 2019

Structuring and functionalization of magnetic nanoparticles for biotechnological applications

Lennart Kleinfeldt[1,2], Johannes Gädke[2,3], Rebekka Biedendieck[4,5], Rainer Krull[2,3], Georg Garnweitner[1,2,*]

1 Institute for Particle Technology, Technische Universität Braunschweig, Germany; 2 Center of Pharmaceutical Engineering (PVZ), Technische Universität Braunschweig, Germany; 3 Institute of Biochemical Engineering, Technische Universität Braunschweig, Germany; 4 Institute of Microbiology, Technische Universität Braunschweig, Germany; 5 Braunschweig Integrated Centre of Systems Biology (BRICS), Technische Universität Braunschweig, Germany

**Corresponding author: l.kleinfeldt@tu-braunschweig.de*

Highlights

- Synthesis and hierarchical structuring of superparamagnetic iron oxide nanoparticles
- Functionalization with ligand that interacts specifically with recombinant model proteins
- Highly efficient purification and regeneration over multiple cycles
- Modification of nanoparticle structures in terms of magnetization and morphology

1. Introduction

Magnetic nano- and microparticles have become highly promising for diverse areas of biomedicine, including *in vitro* applications in diagnostics and downstream processing due to their highly selective manipulation possible by applying external magnetic fields.[1] For these applications, homogeneous particle properties, e.g. the magnetization, are of crucial importance, allowing a uniform response and defined chemical and physical characteristics. In addition, the surface chemistry must be tailored for the intended application to ensure stability of the particles against agglomeration in the desired medium as well as the targeted interaction with the biological system.

2. Methods

A multi-step synthesis process for biofunctionalized superparamagnetic iron oxide nanoparticles has been established and their application for the purification of recombinant model proteins has been investigated in detail. As-synthesized nanoparticles were structured to hierarchical micron-sized aggregates in a spray drying process to improve the magnetic separation efficiency. The aggregate surface was then modified with a previously established ligand system capable of forming metal complexes with histidine tags that allows for the use in multiple separation cycles.[2] *In situ* purification experiments were performed, separating recombinant proteins with His_6-tags produced by genetically engineered *Bacillus megaterium* in a lab-scale stirred tank bioreactor with an external separation loop using handheld magnets.[3] Additionally, the

modification of the aggregates was studied by varying the magnetization after the partial substitution of the magnetic iron oxide nanoparticles with silica nanoparticles.

3. Results and discussion

Structuring of iron oxide nanoparticles via spray drying of aqueous suspensions leads to micrometer-sized aggregates with a specific magnetization comparable to that of the individual nanoparticles. Modification of the aggregates via addition of silica nanoparticles to the suspension allows for control of the resulting magnetization by adjusting the iron oxide content. Moreover, the morphology of the produced aggregates is gradually shifted from irregular inflated-like shapes in case of pure iron oxide aggregates to spherical structures when bringing the silica-content to only 20 % (see Figure 1).

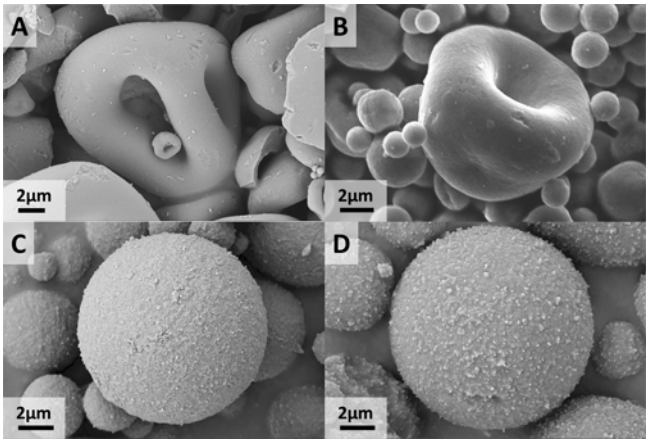

Figure 1. Scanning electron micrographs of spray-dried aggregates with an iron oxide content of (A) 100 %, (B) 90 %, (C) 80 %, and (D) 40 %, respectively.

High efficiency magnetic separation of aggregates with different magnetization is shown. Functionalization of pure iron oxide aggregates with a previously coupled ligand holding an NTA moiety and subsequent loading with Ni^{2+}-ions leads to the ability to bind His_6-tagged target proteins via a chelation complex. The functional recyclability of the particles and the successful application of protein purification in an automated set-up over multiple cycles with a protein purity above 97.5 % will be presented.

4. Conclusions

The successful synthesis of superparamagnetic iron oxide nanoparticles and their structuring in a spray-drying process with subsequent functionalizaton for bioseparation processes will be shown. The highly efficient selective purification of recombinant proteins over mutliple cycles will be demonstrated.

References

[1] J. Gädke, J.-W. Thies, L. Kleinfeldt, T. Schulze, R. Biedendieck, I. Rustenbeck, G. Garnweitner, R. Krull, A. Dietzel, Eur. J. Pharm. Biopharm. 126, (2018), 67-74

[2] J. Gädke, L. Kleinfeldt, C. Schubert, M. Rohde, R. Biedendieck, G. Garnweitner, R. Krull, J. Biotechnol. 242 (2017) 55-63

[3] J. Gädke, J.-W. Thies, L. Kleinfeldt, A. Kalinin, G. Starke, A. Lakowitz, R. Biedendieck, G. Garnweitner, A. Dietzel, R. Krull, Biochem. Eng. J. 126 (2017) 58-67

ECAB 5
The 5th EUROPEAN CONGRESS OF APPLIED BIOTECHNOLOGY
Florence 15-19 September 2019

Synthesis of galacto-oligosaccharides from whey by enzymatic reaction in batch process versus continuous

Poliana C. Tiosso[1], Vanderson C. Fenelon[2], Graciette Matioli[2], Paulo W. Tardioli[3], Flávio F. Moraes[1], Gisella M. Zanin[1*]

1State University of Maringá, Chemical Engineering Department, Maringa – PR, Brazil

2State University of Maringá, Pharmacy Engineering Department

3Federal University of São Carlos, Chemical Engineering Department, São Carlos – SP, Brazil

**giselladeq@gmail.com*

Highlights

- The continuous process allowed double the total GOS yield, compared to batch process.
- The continuous process favors a balance between the transgalactosylation reaction and the hydrolysis reaction.
- The maximum concentration of GOS in the continuous process was 256.72 g mL^{-1} of solution, against 129.90 g mL^{-1} of solution in the batch process.

1. Introduction

Galacto-oligosaccharides (GOS) are nondigestible carboydrates mostly produced from lactose transgalactosylation with β-galactosidases [1]. GOS are synthesized from lactose in a kinetically controlled reaction catalyzed by β-galactosidase (β-D-galactosidase galactohydrolase E.C.3.2.1.23), where the transgalactosylation and hydrolysis reactions occur simultaneously [2]. The high substrate concentration required is one of the main technological challenges in GOS synthesis; because of the relatively low solubility of lactose. Continuous stirred tank reactor has not been so much reported in the literature for the GOS synthesis, being the purpose of this work to evaluate the potentials of this strategy and to compare it with conventional batch synthesis. The present work has been conducted using β-galactosidase immobilized on macro porous silica, implementing a strategy for lactose feeding to the reactor and withdrawal of products; in order to avoid the effects of low lactose solubility, and thus achieve an increase in GOS yield at the end of reaction.

2. Methods

The chemical modification of the controlled porous silica was based on the study of Bernal et al [3]. Silanization was made using GPTMS (3-glycidyloxypropyltrimethoxysilane) solution. The immobilization of β-gal on glyoxyl-silica was done by the covalent method. After the immobilization, the enzyme was cross-linked with glutaraldehyde.

A duplicate experiment of GOS synthesis with *K. lactis* β-galactosidase was conducted in continuous process in order to evaluate its advantages over the batch operation mode. Operational sequence considered three stages at the following conditions: (i) An in initial batch synthesis stage lasting 45 min. (ii) A second stage in which a 40% w/w lactose solution was feed for 16 h at a feed of rate of 0.05 g of solution.$h^{-1}$and withdrawal of products with the same rate. (iii) A final batch stage during the next 48 h. The main product profiles were compared to the ones obtained by batch process. Lactose and products synthesis were done using HPLC system refractive index detector (SHIMADZU, UV-1601PC). The method was adapted from Santos [4].

3. Results and discussion

Figure 1 shows the yields for galacto-oligosaccharides production for batch and continuous process. Analysing this Figure, we can observe that the continuous process allowed double the total GOS yield. This can be explained by the fact that, the concentration of lactose is increased in this process, favouring a balance between the transgalactosylation reaction and the hydrolysis reaction. In the batch process, the GOS production is high only at the beginning, where the lactose concentration is still high, after which only the hydrolysis reaction is favoured.

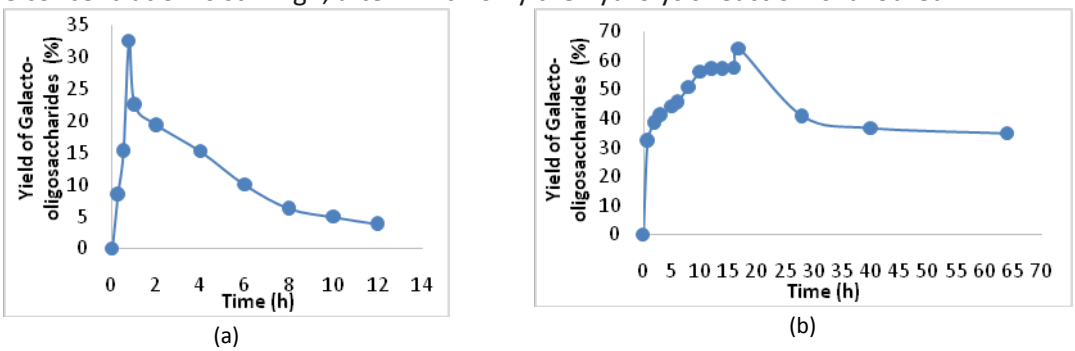

Figure 1. Yields of galacto-oligosaccharides. (a) Batch process, (b) Continuous Process.

4. Conclusions

This work shows that is possible to reach high total concentrations of dissolved sugars (>50% w/w) at moderate reaction temperatures without reduction in GOS yield by considering the synthesis of GOS in continuous process operation. This strategy allowed obtained an optimal final concentration of GOS higher than the one obtained in batch reactor operation.

5. Acknowledgements

The authors thanks CNPq and CAPES for financial support.

References

[1] G. Tzortzis, J. Vulevic, New York: Springer, 2009, 207-244.

[2] A. Gosling, G. W. Stevens, A. R. Barber, S E. Barber, S. E. Kentish, S.L. Gras, Recent Advances in refining galactooigosaccharide production from lactose. Food Chem. 2010; 121:307-318.

[3] C. Bernal, L. Sierra, M. Mesa,Design of β-galactosidase/silica biocatalysts: Impact of the enzyme properties and immobilization pathways on their catalytic performance, Engineering in Life Sciences, 2014, 14: 85-94.

[4] R. Santos, Production of galactooligosaccharide by fungal lactase. Dissertation (Master in Food Science) - State University of Campinas, Campinas - SP, 2006, 54p.

Starter culture development for cocoa bean fermentation using indigenous yeast strains.

David Caballero T.[1], Viviana Sánchez T.[1], Claudia Johana Sandoval[1], Luis Javier López - Giraldo.[1]

1 Grupo de investigación en ciencia y tecnología de alimentos CICTA, Parque Tecnológico Guatiguará, km 2 vía El Refugio, Universidad Industrial de Santander, Piedecuesta (Santander), 681011, Colombia.

**Corresponding author: davidct.ce@gmail.com, ljlopez@uis.edu.co, visantor@uis.edu.co*

Highlights

- The volatile compounds produced by the yeast strains were identified and quantified using SPME-GC-MS.
- Selection of yeast strains with potential to develop starter cultures for cocoa bean fermentation.

1. Introduction

Fermentation is one of the most important steps in the post-harvest process of cocoa, because many of the organoleptic perceptions that will directly impact the quality of the final product are developed in this stage by the action of microorganisms [1]. Among the main microorganisms involved in this process are the yeasts, lactic and acetic bacteria. The yeasts are the microorganism that plays the most important role in the production of volatile organic compounds [2]. The most common metabolites produced are esters which are related to fruit notes, alcohols with floral aromas and aldehydes and ketones with walnuts or almonds [3].

For those reasons is imperative to have more control over the fermentation; and one of the recently proposed alternatives is the use of starter cultures. These starter cultures are made from yeasts isolated from typical cocoa fermentations that have had the effect of producing cocoa paste with fine or flavor characteristics. The use of this approach would not only reduce the fermentation time [4], but also the variability between production lots; ensuring the uniformity of the product in markets that increasingly require more traceability [5]. The main objective of this work is to select yeast isolates that represent potential sources for producing volatile compounds related to desirable perceptions in cocoa beans.

2. Methods

1. The isolation of yeast from fermentation box was done as following: Sampling cocoa beans during fermentation process until cocoa bean was well fermented; once it was

done the sample was diluted serially in order to get single colonies for isolation in Sabouraud media.

2. The growth of yeast and volatile compound production was following by UFC and SPME – GC – MS, respectively. Briefly, the isolated yeast was inoculated in a Sabouraud media and then the growth of yeast was development until reach a 10^6 UFC. After that, the media was placed into a hermetically sealed vial where was developed the solid phase microextraction using the procedure described by Palencia [5]. Then, the identification and quantification of volatile compounds produced by the yeasts was carried out by GC-MS and GC-FID respectively using the HP5 column 30m x 0.25µm x 0.25µm [5].

Finally, the concentration profile obtained was analyzed in order to determine which yeasts have the best potential to produce aroma compounds. Yeast with highest yields in volatile compounds were selected for starter culture development.

3. Results and discussion

Four yeast were selected for the future starter culture development according to aroma profiles produced by each of them identifying and quantifying by using GC. Some volatile compounds produced by selected yeast can be mentioned as follow: alcohols, esters, aldehydes which are related with sensorial perception of floral, fruit, nutty; respectively.

Interestingly, the yeast 111 was be able to produce high concentration of isoamyl ester; this finding would be used for developing cocoa fermentations in order to produce cocoa mass with fruit characteristics, which aren't typically produced in Colombia.

4. Conclusions

In this work there were isolated 90 native yeasts and it was selected 4 of them with potential to use in cocoa fermentations. Remarkably, it was found a yeast with potential to produce high concentration of esters which open the possibility to a development fermentation process to produce Colombian cacao with new sensorial profiles.

References

[1] Kongor J., Hinneha M., Van deWalle D., Afoakwa E., Boeckx P., Dewettinck K. (2016). Factors influencing quality variation in cocoa (Theobroma cacao) vean flavour profile — A review. Food Research International 82, 44–52.W. Black, E.B. White, The Elements of Science, third ed., MacCluski, New York, 1987.

[2] Ho V.T., Zhao J., Fleet G.. Yeasts are essential for cocoa bean fermentation. International Journal of Food Microbiology 174, 72–87. 2014.

[3] Koné M., Guéhi S., Durand N., Ban-Koffi L., Berthiot L., Tachon A., Brou K., Boulanger R., Montet D. (2016). Contribution of predominant yeasts to the occurrence of aroma compounds during cocoa bean fermentation. Food Research International 89, 910–917.

[4] Saltini R., Akkerman R., Frosch S. (2013). Optimizing chocolate production through traceability: A review of the influence of farming practices on cocoa bean quality. Food Control 29, 167-187.

[5] Palencia C., Gualdrón A., Guarín I., Ojeda Y, Villamizar A, Zárate D. López-Giraldo, L.J. Proposition of a semi-quantitative method for determination of volatile compounds in cocoa mass. World Food Science and Technology Congress. 2018.

ECAB 5
The 5th EUROPEAN CONGRESS OF APPLIED BIOTECHNOLOGY
Florence 15-19 September 2019

Thermostable cellulase and xylanase activity from *Sulfolobus shibatae* of potential application in lignocellulosic bioethanol production

Angela Boyce, Gary Walsh*

Department of Chemical Sciences and Bernal Institute, School of Natural Sciences, University of Limerick, Limerick, Ireland.

**Corresponding author: gary.walsh@ul.ie*

Highlights

- In xylan-containing media at 75°C, *S. shibatae* produces cellulase and xylanase.
- The crude enzymes display optimum activity at 100°C and are thermostable.
- The crude enzymes display activity on pretreated straw lignocellulose at 90°C.
- Potential application in hydrolysis of lignocellulose for bioethanol production.

1. Introduction

Enzymes produced by thermophilic microorganisms are of growing interest in industrial applications due to their activity and stability at high temperatures [1]. Amid environmental concerns in relation to the use of fossil fuels, one such industrial application is in the enzymatic hydrolysis of lignocellulosic biomass to produce bioethanol, which can be used as an alternative transportation fuel. The enzymatic hydrolysis of lignocellulose is currently undertaken at 40-50°C and process improvements are necessary to achieve competitive bioethanol production [2]. Increasing the hydrolysis temperature by using thermostable enzymes active at higher temperatures offers several potential advantages including: higher reaction rates, improved hydrolysis performance, decreased hydrolysis times, increased substrate solubility and lower viscosity, reduced risk of contamination and lower cooling costs following thermal pretreatment [2,3]. The identification and characterization of novel thermostable lignocellulose-degrading enzymes suitable for this application is therefore of interest. This study describes the production and initial characterisation of thermostable cellulase and xylanase activities from the archaea *Sulfolobus shibatae* with emphasis on determining potential suitability for lignocellulosic bioethanol production.

2. Methods

Sulfolobus shibatae B12 (DSM 5389) was grown at 75°C in *Sulfolobus* medium [4] containing 0.05% (w/v) yeast extract and 0.1 % (w/v) xylan. After 8 days, the cells were removed by centrifugation and the resulting supernatant (crude enzyme) was concentrated by ultrafiltration using a 10 kDa membrane. Enzyme activity was determined by measuring the amount of reducing sugars released from carboxymethyl cellulose (CMC) or xylan using the dinitrosalicyclic acid method [5].

3. Results and discussion

The thermophilic archaea *Sulfolobus shibatae* was found to produce thermostable cellulase and xylanase activities when grown in xylan-containing media. Upon determination of the effect of

temperature on enzyme activity using CMC as substrate, maximum activity was observed at 100°C with over 70% of maximum activity observed in the temperature range 90-105°C (Figure 1). The crude xylanase activity also had an optimum temperature of 100°C with over 70% of maximum activity observed in the temperature range 85-105°C. Maximum activity on both CMC and xylan was observed at pH 4.

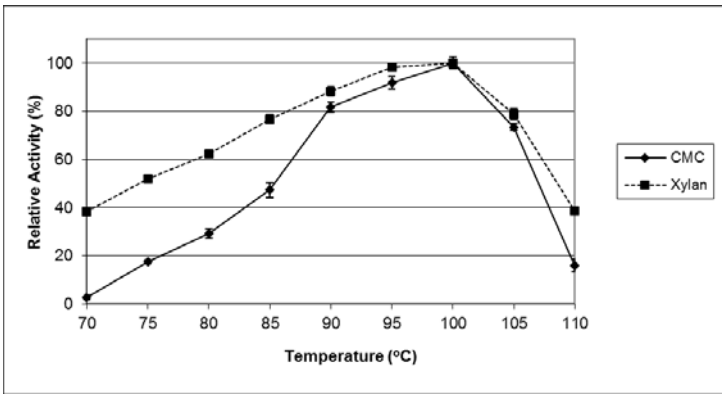

Figure 1. Effect of temperature on the crude enzyme activity from *S. shibatae* on the substrates CMC and xylan. Data expressed as a percentage of maximum activity.

Upon assessment of enzyme thermal stability, 86% of original activity on CMC and 64% of original activity on xylan was detected after incubation of crude enzyme at 80°C for 30 hours. At 95°C, the crude enzyme retained 44% and 23% of original activity on CMC and xylan, respectively, after 24 hours and at 100°C, 63% of original activity on CMC was detected after 30 minutes compared to 41% of original activity on xylan.

The crude enzyme produced by *S. shibatae* was capable of hydrolysing pretreated straw lignocellulose. After 6 hours at 90°C, the amount of reducing sugars released at pH 3.5 was approximately twofold the amount released in the corresponding control samples without enzyme. The crude enzyme also rapidly decreased the viscosity of CMC solution at 90 and 95°C.

4. Conclusions

The properties of the crude cellulase and xylanase activities produced by *S. shibatae*, in particular the high activity and stability observed at high temperatures and ability to hydrolyse straw lignocellulose at high temperature, strongly indicate potential suitability for use in the production of cellulosic bioethanol. While further studies are necessary to confirm industrial applicability, potential uses include the prehydrolysis/liquefaction of pretreated lignocellulose and/or as a component of thermostable enzyme cocktails for hydrolysis of pretreated lignocellulose to fermentable sugars. Moreover, these enzymes may also be of interest in other biotechnological processes undertaken at high temperatures.

References

[1] F. Akram, I.U. Haq, W. Imran, H. Mukhtar, Renewable Energy. 122 (2018) 225-238.
[2] A.K. Patel, R.R. Singhania, S.J. Sim, A. Pandey, Bioresour Technol. 279 (2019) 385-392.
[3] A. Boyce, G. Walsh, Appl Microbiol Biotechnol 99 (2015) 7515-7525.
[4] http://www.dsmz.de/microorganisms/medium/pdf/DSMZ_Medium88.pdf
[5] G.L. Miller, Anal Chem 31 (1959) 426-428.

ECCE12
The 12th EUROPEAN CONGRESS OF CHEMICAL ENGINEERING
Florence 15-19 September 2019

RETRO-TECHNO-ECONOMIC-ENVIRONMENTAL ANALYSIS (RTEEA) APPLIED TO FIRST- AND SECOND-GENERATION ETHANOL PRODUCTION

Andrew M. Elias[1], Felipe F. Furlan[2], Raquel L. C. Giordano[1,2], Roberto C. Giordano[1,2]

[1]*Chemical Engineering Graduate Program, Federal University of São Carlos, PPGEQ/UFSCar*

[2]*Department of Chemical Engineering, Federal University of São Carlos, UFSCar*

Via Washington Luiz, km 235, São Carlos, SP, 13565-905, Brazil

**Corresponding author: roberto@ufscar.br*

Highlights

- Global sensitivity analysis shows that environmental and economic metrics can be divided in two groups.
- Economic metric (NPV) is influenced mainly by the hydrolysis step.
- Environmental metrics are significantly influenced by the pretreatment stage.

1. Introduction

Economic and environmental analysis is an important field in (bio)process engineering, supporting R&D decisions. Process Systems Engineering tools (PSE) allied with techno-economic analysis (TEA) and life-cycle assessment (LCA) can be used to verify process feasibility, to identify possible bottlenecks and optimal operating conditions, among other possibilities.TEA and LCA are usually used to assess the economic and environmental performance of defined process conditions, both structural and operational. RTEA [1] is a novel approach that turns this problem upside down: rather than evaluating the TEA for a predefined processes setup, it provides goals to be pursued by R&D teams, in order to seek feasible operational conditions, based on simulations of the overall process. In this work, RTEA was expanded to RTEEA (Retro-Techno-Economic-Environmental Analysis), incorporating life cycle assessment. RTEEA was applied to the first- and second-generation (1G/2G) ethanol production from sugarcane, using economic and environmental metrics to define feasible regions. Global sensitivity analysis (GSA) was used to identify, with statistical support, critical process variables [2].

2. Methods

RTEEA is constituted by four steps: construction of a base case, incorporation of TEA and LCA analysis into the simulation of the process, selection of key variables through global sensitivity analysis and delimitation feasible spaces. The 1G/2G anhydrous ethanol production from sugarcane industrial process was modelled as described by Longati et al (2018). The energy consumption of the plant was optimized through pinch analysis of the process main stream. In this case study, the Net Present Value (NPV) was chosen as the economic metric. The CML-IA baseline V3.04 (World 2000) method was used to perform the life cycle impact assessment (LCIA). The environmental metrics are derived from LCIA. An initial set of variables was chosen using previous knowledge of the process for the global sensitivity analysis through the Sobol method [2]. The main and total

Sobol indexes were used to select the process variables. To perform the retro-techno-economic-environmental analysis, it is essential that the variables chosen for analysis are process constraints. If this is not the case, other specified variable, correlated with the desire one, must be freed in order to keep null the degree of freedom of the whole-plant model. The TEA and LCA equations that equal the chosen metrics with a threshold value must be solved together with the model equations of the process (energy and mass balances, thermodynamic relations and so on). In this case study, these equations were NPV = 0 and the CML method environmental indicators of the 1G stand-alone process. The chosen process constraints that satisfy those equations are the output of RTEEA.
The platform for the simulations was the software EMSO, which is an equation-oriented simulator.

3. Results and discussion

Among more than twenty-seven thousand process variables are present in the biorefinery model. Therefore, an initial ad-hoc selection of variables, based on previous knowledge, had to be made to obtain a treatable set of variables to be spanned by the global sensitivity analysis. The process variables chosen for this case study are related to the steps of bagasse pretreatment, cellulose enzymatic hydrolysis reactor, and xylose fermentation, in the 2G sector of the plant. These steps are still not industrially consolidated, and the information that RTEEA provides may be useful for R&D teams. The GSA pointed out that there are two distinct groups, that encompass various metrics. The first one, composed of the net present value, global warming potential, and photo-oxidation, is mainly influenced by enzyme load and cellulose conversion in the saccharification reactor. The second group, composed of all other metrics, is mainly influenced by the solid mass fraction in the pretreatment stage, and by the cellulose-to-glucose conversion.

4. Conclusions

In this work, environmental techno-economic analyses were coupled to derive targets for R&D teams, at early stages of the process development. The RTEEA methodology, an extension of RTEA, was able to identify the process variables that show significant influence on economic and environmental performance of the process, to obtain their threshold values, and to make explicit their relations. A case study was used to demonstrate the methodology capabilities: 1G-2G bioethanol production using sugar cane as feedstock. With this methodology, new goals and directions for process development can be quickly defined.

References

[1] Longati, A.A., Lino, A.R.A., Giordano, R.C., Furlan, F.F., Cruz, A.J.G., Bioresour. Technol. (2018) 263, 1–9.
[2] Saltelli, A., Ratto, M., Andres, T., Campolongo, F., Cariboni, J., Gatelli, D., Saisana, M., Tarantola, S., Global Sensitivity Analysis: The Primer, John Wiley & Sons: Chichester, U.K, 2007.

ECCE12
The 12th EUROPEAN CONGRESS OF CHEMICAL ENGINEERING
Florence 15-19 September 2019

EFFECT OF CALCIUM AND XYLOOLIGOSACCHARIDES ON XILOSE ISOMERASE ACTIVITY FOR ISOMERIZATION OF XYLOSE TO XYLULOSE

Felipe A. S. Corradini[1], Thais S. Milessi-Esteves[1], Roberto C. Giordano[1], Raquel L. C. Giordano[1*]

1 Graduate Program of Chemical Engineering, Federal University of São Carlos – UFSCar

**Corresponding author: raquel@ufscar.br*

Highlights

- Kinetic parameters of the enzymatic xylose-to-xylulose isomerization were estimated.
- Ca^{2+} ions are competitive inhibitors of the isomerization enzymatic reaction.
- Xylobiose inhibition is only important at high concentrations.

1. Introduction

Xylose isomerase (XI) catalyzes the reversible isomerization of xylose to xylulose and of glucose to fructose. Its molecular mass is around 173 kDa, formed by four identical subunits of approximately 47 kDa each. Bivalent ions (Mg^{2+}, Mn^{2+} and Co^{2+}) act as important cofactors of the enzyme, some of them being essential components in the reaction medium in order to keep the isomerase activity. XI is one of the enzymes with the highest market demand in the food industry, used for the production of high-fructose corn syrup (HFCS) through the isomerization of glucose to fructose. Due to this industrial application of XI, the kinetics of this reaction was well investigated.

On the other hand, there are few reports in the literature about the enzymatic xylose-xylulose isomerization, most of them between the years 1980-1990, and related to the application of the reaction in the simultaneous isomerization and fermentation of xylose (Simultaneous Isomerization and Fermentation, SIF). These studies aimed at the production of 2G ethanol from hemicellulose, through fermentation of xylulose by *Sacharomyces cerevisiae*, the microorganism conventionally used in the 1G ethanol production. However, the genetic modification of *S. cerevisiae* to allow *in-vivo* isomerization in order to achieve the direct fermentation of xylose was almost the only studied route in the following 20 years. This approach is still not implemented in the industry, so the SIF process study was resumed [1]. Furthermore, XI was also used as a component in a biocatalyst for ethanol production from xylo-oligomers, the Simultaneous Hydrolysis, Isomerization and Fermentation process (SHIF) [2]. In the SHIF process, xylanases hydrolyze xylo-oligomers to xylose, which is then isomerized to xylulose by XI, and xylulose is converted to ethanol by non-modified *S. cerevisiae*. The biocatalyst also contains calcium carbonate in order to control the intra-particle pH. Xylobiose and Ca^{2+} ions are potential inhibitors of the isomerization of xylose to xylulose in the SHIF process. Within this context, the kinetics of this reaction is investigated here.

2. Methods

2.1 Xilose isomerase activity assay: initial velocity of xylulose formation is determined using 5 mL of substrate solution (2 mol.L^{-1} xylose in 50 mmol.L^{-1} tris-maleate buffer pH 7.0 containing 50 mmol.L^{-1} $MgCl_2.6H_2O$ and 2.5 mmol.L^{-1} $CoCl_2.6H_2O$), at 60 °C. Xylulose was quantified using the cysteine-carbazol method [3].

2.2 Preparation of xylobiose rich solution according to [4]. Beechwood xylan solution (50 g.L^{-1} in 50 mM sodium citrate buffer pH 5.5) was hydrolyzed by soluble xylanase NS22036. Xylo-oligosaccharides concentration was determined via HPLC using a SugarPak I column (Waters, Milford, USA).

2.3 Influence of substrate, Ca^{2+} ions and xylobiose (X_2) on the rate of reaction at 35 °C: concentrations were varied, for xylose (15-300 g.L^{-1}), Ca^{2+} ions (0-16 g.L^{-1}) and X_2 (0 - 9.1 g.L^{-1}).

3. Results and discussion

A Michaelis-Menten model with competitive inhibition represented well the influence of Ca^{2+}. The kinetic model describes the competition between Ca^{2+} and Mg^{2+} ions for the metal site within the active site of XI.

Isomerization rates were slightly affected by the presence of X_2 at substrate concentration of 45 g.L^{-1}. Inhibitory effects were better perceived at higher substrate concentrations, keeping the amount of X_2 fixed. A Michaelis-Menten rate expression with uncompetitive inhibition fitted well to the experimental data.

4. Conclusions

This work showed that Ca^{2+} competes with Mg^{2+} for the metal site in the enzyme structure. X_2 is a uncompetitive inhibitor of the reaction, affecting the reaction rates more severely at higher substrate concentrations.

References

1. T.S Milessi, P.M.Aquino, C.R. Silva, G.S. Moraes, T.C. Zangirolami, R.C. Giordano, R.C. R.L.C. Giordano. Biomass and Bioenergy 2018, 119, 277–283.
2. Milessi-Esteves, T.; Corradini, F.; Kopp, W.; Zangirolami, T.; Tardioli, P.; Giordano, R.; Giordano, R. Catalysts 2019, 9, 225.
3. Z. DISCHE, E. BORENFREUND. J. Biol. Chem. 1951, 192, 583–7.
4. T.S.S. Milessi, W. Kopp, M.J. Rojas, A. Manrich, A. Baptista-Neto, P.W. Tardioli, R.C. Giordano, R. Fernandez-Lafuente, J.M. Guisan, R.L.C. Giordano. Catal. Today 2016, 259, 130–139.

Synthesis of graphene oxide - gelatin aerogels and their evaluation as hemostatic agent

Katherina Fernández[1], Jessica Borges[1], Sebastián Guajardo[1], Claudio Aguayo[2]

[1] Biomaterials Laboratory, Department of Chemical Engineering, Faculty of Engineering, University of Concepción, Concepción, Chile.
[2] Department of Pharmacy, Faculty of Pharmacy, University of Concepción, Concepción, Chile.
**Corresponding author: kfernandeze@udec.cl*

Highlights

- GO-G aerogels were synthetized by microwave assited reaction
- The aerogels have a high blood absorption capacity (over 70%)
- The blood cells were retained by aerogels

1. Introduction

Actually, the developing of science and nanotechnology has allowed the synthesis of new materials with biomedical applications. Among them, the graphene and its oxidated forms, such as graphene oxide (GO), have been used in this area for their biological, chemical, physical and mechanical properties [1]. An important application of this material is to be functionalized with biocompatible polymers, as gelatin (G),to obtainGO-G aerogels.These aerogels are materials that present low density, high surface area,and porous structures [2]. Based in this properties, it is possible use them in the biomedical field,as a hemostatic agent, in the control of profuse bleeding generated in wounds. The aim of this study was synthesized GO-G aerogels by microwave assisted reaction, to evaluate their surface properties and hemostatic performance, in order to validate its use as a hemostatic agent.

2. Methods

The GO-G aerogels were developed to different synthesis conditions (pH and GO-G ratio) [1], to analyze the influence of these factors on the physicochemical properties of the biomaterials synthesized. Subsequently, the capacity absorption of the synthesized aerogels on phosphate-buffered saline (PBS) was determined, simulating of pH wound conditions. The internal structure of the synthesized aerogels was evaluated by scanning electron microscope (SEM), to observe the blood cell adhesion to the structure of these materials. Also, a droplet of fresh blood was dropped onto the GO-G aerogels surface at different exposure times (30 to 240 seconds) to evaluate the process of blood absorption. Finally, the blood absorption capacity assays and *in vitro* dynamic whole-blood clotting by absorbance determination were developed [3] using 50 microliters of fresh blood to conditions similar to the previous ones, was carried out to evaluate the hemostatic performance of these aerogels.

3. Results and discussion

Among the developed aerogels, those synthesized at basic conditions and a greater proportion of gelatin had the higher PBS absorption capacity (up to 65%), indicating that these materials could have a better interaction with external media such as blood. Also, the SEM images showed that there was an adhesion of red blood cells in the materials synthesized (see Figure 1) and this phenomenon increased proportional to the content of GO in the aerogels synthesized, as seen in the Figure 1b); regardless of pH conditions used in the synthesis. This phenomenon can explain due the interactions between GO and blood components, favoring the hemostatic performance of these aerogels. Finally, all the synthesized aerogels, had blood absorption capacities higher tan 70%, in a maximum time of 240 seconds, which can favor the control of profuse bleeding and validate that use as possible hemostatic agent.

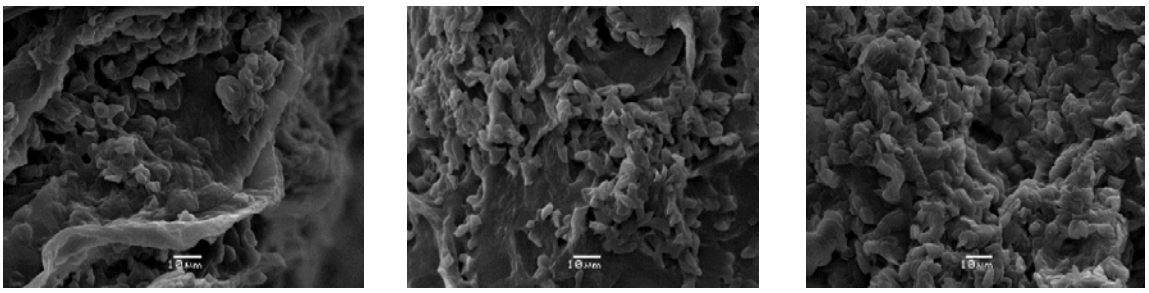

Figure 1 SEM images a) GO-G aerogels at basic pH and 1:15 GO-G ratio, b) GO-G aerogels at acid pH and 1:10 GO-G ratio, c) GO-G aerogels at neutral pH and 2:25 GO-G ratio.

4. Conclusions

The studied showed the possibility of the use of GO-G aerogels as hemostatic agents according to the internal structure and blood absorption capacity reported.

References

[1] Chen, G., Qiao, C., Wang, Y., & Yao, J., *Australian Journal of Chemistry*, 2014, *67*(10), 1532-1537.
[2] Ma, Y & Chen, Y., *Natl Sci Rev*, 2015, 2 (1), 40-53.
[3] Quan, K., Li, G., Yuan, Q & Wang X. *Colloids and Surfaces B: Biointerfaces 132*, 2015, 27-33.

Enzymatic synthesis of tyrosol galactoside: Screening of immobilization resins.

Veronika Hollá[1], Monika Antošová[1], Milan Polakovič[1]

1 Department of Chemical and Biochemical Engineering, Institute of Chemical and Environmental Engineering, Faculty of Chemical and Food Technology, Slovak University of Technology, Bratislava, Slovakia

**Corresponding author: milan.polakovic@stuba.sk*

Highlights

- Screening of six various carriers for immobilization of *β*-galactosidase.
- Tyrosol adsorption on carriers and calculation of Langmuir parameters.
- Synthesis of tyrosol β-galactoside by immobilized biocatalyst.
- Study of operational stability of immobilized biocatalyst on one selected resin.

1. Introduction

Nature produces a vast variety of glycosides with interesting biological properties which could be used in pharmaceutical and cosmetics industry. However, demand for naturally occurring glycosides in reasonable quantities and purity requires their synthesis, either chemical or enzymatic. Enzymatic synthesis represents an effective and direct alternative to the synthesis of glycosides thanks to the stereo- and regioselectivity of enzyme. Enzymatic synthesis of glycosides is carried out using hydrolytic enzymes such as glucosidases, fructosidases and galactosidases. These enzymes possess both hydrolytic and transferase activity, but the ratio of these activities depends on the source of enzyme. Glycosides containing tyrosol or hydroxytyrosol group possess bioactive properties. Tyrosol *β*-galactoside owns many advantageous properties for humans, such as antioxidant, anti-fatigue and anti-hypoxia effects. This study is focused on enzymatic synthesis of tyrosol *β*-galactoside by immobilized *β*-galactosidase from *A. oryzae*. Immobilization was conducted on various commercial resins. All studied resins were used for the enzymatic synthesis of tyrosol *β*-galactoside. Furthermore, adsorption of tyrosol on the resins were measured at two different temperatures and subsequently Langmuir parameters were calculated. Based on the results, one immobilization resin was chosen for study of operation stability in repeated batch experiments.

2. Methods

The investigated resins were Dowex Marathon MSA (Dowex), Lifetech™ ECR1508 (1508), Lifetech™ ECR8309M (Amino C2), Lifetech™ ECR8409M (Amino C6), Lifetech™ ECR8209M (Epoxy) and Lifetech™ ECR8285M (Epoxy Butyl). Before immobilization and adsorption measurement was each resin prepared according to immobilization protocol from supplier. Enzymatic synthesis of tyrosol *β*-galactoside and adsorption of tyrosol on resins were carried out as batch experiments. Samples from adsorption measurements were analyzed by the diode array spectrophotometer HP 8452A (Hewlett Packard, USA) at a wavelength of 275 nm. The HPLC system Agilent 1200 (Agilent Technologies, USA) with diode array detector and a Zorbax Eclipse XDB C-18 column with a guard

column was used to determine the concentrations of tyrosol and tyrosol *β*-galactoside in diluted samples from enzymatic synthesis.

3. Results and discussion

The primary aim of this study was to prepare an immobilized biocatalyst suitable for the synthesis of tyrosol *β*-galactoside. At first, tyrosol adsorption was measured for each studied resin and isotherms at 37°C are illustrated in Figure 1. Carriers 1508 and Dowex are based on non-polar, hydrophobic matrices containing benzene rings, however Amino and Epoxy, Epoxy Butyl carriers are made from more hydrophilic and polar methacrylate resins. Since tyrosol contains a non-polar benzene ring it has a greater binding capacity on non-polar particles. It is clear from the results that Amino C2 and C6 carriers are the most polar particles and therefore they adsorb the least amount of tyrosol which results in the greatest amount of tyrosol available in the reaction solution for synthesis of tyrosol *β*-galactoside.

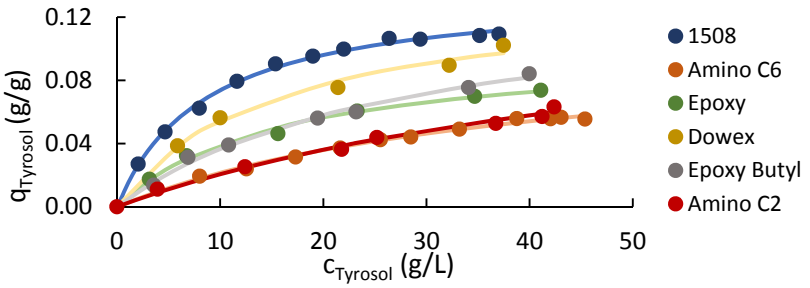

Figure 1. Adsorption isotherms for studied carriers at 37°C. Points represent experimental data, lines represent calculated Langmuir isotherms.

Subsequently, free *β*-galactosidase was immobilized on all studied carriers and was used for synthesis of tyrosol *β*-galactoside from lactose and tyrosol. Experiments were carried out with two different amounts of enzyme. Evident hydrolysis of product was observed for higher amounts of enzyme which is typical for transglucosylation. [1, 2] The highest volumetric productivities and yields were achieved with Amino and Epoxy resins. Epoxy resins were afterwards used for the study of operational stability in fourteen repeated cycles. The formation of tyrosol *β*-galactoside was kept nearly constant during all cycles. The differences among individual runs were within the experimental error. Epoxy resins exhibit covalent binding with enzyme which resulted in high operational stability and no leakage of the enzyme out of the matrix.

4. Conclusions

This work provides the screening of immobilization carriers suitable for enzymatic synthesis of tyrosol *β*-galactoside. Hydrophilic, polar resins and resins with covalent bonding results as the best immobilization carriers for tyrosol galactoside synthesis.

5. Acknowledgements

This work was supported by the grant from the Slovak Research and Development Agency (Grant number: APVV-15-0227).

References [Calibri 10]

[1] E. Potocká, M. Mastihubová, V. Mastihuba, J. Mol. Catal. B Enzym. 113 (2015) 23–28.
[2] V. Hollá, M. Antošová, K. Karkeszová, M. Polakovič, Biotechnol. J., accepted

ECAB 5
The 5th EUROPEAN CONGRESS OF APPLIED BIOTECHNOLOGY
Florence 15-19 September 2019

Bioinformatic approaches reveal the impact of major factors of the environmental metagenome extraction protocol

Ji-Min Park[1], Sung-Min Won[1], In-Gyu Kim[1], Jung-Hoon Yoon[1]*

1 Department of Food Science and Biotechnology, Sungkyunkwan University, Jangan-gu, Suwon, Republic of Korea

**Corresponding author: Jung-Hoon Yoon, jhyoon69@skku.edu*

Highlights

- Protocol on the metagenome extraction for various types of soil was standardized.
- Type and pH of buffer and reaction time were the most statistically significant.
- Quality of DNA extracted from new soil can be calculated from the formula.

1. Introduction

As is well known, the total environmental DNA (=Metagenome) is a key material in the biotechnology field with high added Value. Although many related researches were performed, much remains unclear about the factors affecting the quality of the extracted metagenome. Therefore, optimal methods or major factors for the direct isolation of high-quality DNA from various environments should be developed. So we introduce elaborate statistical techniques and use various bioinformatics tools to improve the extraction protocol and visualize the results. Seven variables from the adjustable parameters present in the protocol were selected, and the most statistically significant factors were the type of buffer, the pH of the buffer, the reaction time and the rate of centrifugation. The process design space and simulation about major factors and profiling was visualized. Our results provide a foundation for future research into clarifying the biodiversity in a specific soil microbial ecosystem, identification and mechanism of active genes and metabolites derived from metagenomes.

2. Methods

Considering some metagenomic DNA extraction protocols of recent related studies, we selected 14 various factors related to chemical reaction, physical force and soil sample. For experimental design, We first used the factorial-complete randomize design, factorial fractional design and taguchi method to check the main effects of some variables on the quality of the extracted DNA and their interaction effects with the samples. Since these statistical models needed some modifications, we customized the analysis design featuring the diversification of attributes and application of quality by design (QbD) and design of experiments (DOE). In data processing, missing values occurred when data collection having some bad influence on the results were dealt with by the 'Multiple imputation' technique. And then we carried out the simple correlation test, cluster analysis, cross tabulation analysis, Logistic regression analysis, conjoint analysis and principle components analysis to get the significant variables and their attributes related to the high quality metagenome. Finally, the simulation, profiling and process design space were performed to find the range of conditions for new soil sample in the future.

3. Results and discussion

Table 1. Summary of the cross tabulation, multiple regression and the cluster analysis related to the optimal group.

Desert				Forest				Marsh			
Variable		Comparative evaluation of attributes		Variable		Comparative evaluation of attributes		Variable		Comparative evaluation of attributes	
		Attribute	Optimized condition			Attribute	Optimized condition			Attribute	Optimized condition
RT (hr)	T (31.6%)	7, 8	4 ~ 8	RT (hr)	T (30.8%)	7 ~ 8	7 ~ 8	RT (hr)	T (75%)	4 ~ 6	6
	S (91%)	>= 4			S (63.2%)	7 ~ 9			S (61.6%)	6 ~ 8	
CFG (rpm)	T (42.1%)	11,000, 12,000	11,000 ~ 12,000	CFG (rpm)	T (53.9%)	5,000 ~ 6,000	5,000 ~ 6,000	CFG (rpm)	T (75%)	5,000 ~ 6,000	5,000 ~ 6,000
	C (55.6%)	11,000			S (79%)	5,000 ~ 10,000			S (53.9%)	5,000 ~ 6,000	
	S (91%)	>= 9,000			.	.			.	.	
pH	T	.	7.0 ~ 7.4	pH	T (53.9%)	7.4 ~ 8.2	7.4 ~ 8.2	pH	T (100%)	7.4 ~ 7.8	7.8
	C (100%)	>= 7.8			S (63.2%)	8.2 ~ 9.0			S (84.7%)	7.8 ~ 9.0	
	S (91%)	<= 7.4			.	.			.	.	
DT (hr)	T (81.8%)	<= 1.5	<= 1					RTemp (°C)	T (50%)	55	55 ~ 60
	C (55.6%)	<= 1							S (61.1%)	60 ~ 75	

The analysis of the size (S), concentration (C), and both (T) of the extracted DNA was conducted. Although the some variable preferred different range of attributes by type of soil, the most of the variables had similar range of attributes. Within the experimental range, when the pH of the buffer is used with 8.0 for 7 hour and the rate of centrifugation was at 6,000rpm, generally high-quality metagenomic DNA was extracted.

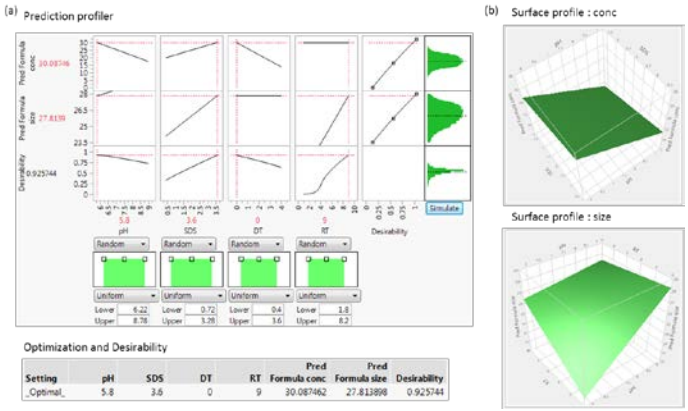

Figure. 1. Optimization and simulation of variables with significant probability (a) The results of the prediction profiler, optimization; (b) The results of the surface profiler: 'conc' variable with pH and SDS, 'size' variable with pH and RT

When the forest soil sample is used, it was predicted that the condition to maximize both the concentration and size of the extracted DNA was to use a buffer (pH 5.8), SDS (3.6%) for 9 hour with no drying time.

4. Conclusions

The metagenome extraction protocol that can be applied to various environments was established through the statistical process based on six selected variables and their attributes. Using three representative types of sample, we present a range of major factors that can be adjusted to extract high-quality metagenomes from new soil samples. The visualization of adjustable range of major variables through the simulation and profiling makes inference of immediate results possible. And the efficiency of extracting high-quality metagenomes from various environments, creating libraries and exploring metagenomes is three times better than those of previous protocol.

References

[1] Bertrand, H., Poly, F., Van, V.T., Lombard, N., Nalin, R., Vogel, T.M., and Simonet, P. (2005). High molecular weight DNA recovery from soils prerequisite for biotechnological metagenomic library construction. J Microbiol Meth 62, 1-11.

[2] Lee, M.H., and Lee, S.W. (2013). Bioprospecting potential of the soil metagenome: novel enzymes and bioactivities. Genomics Inform 11, 114-120.

[3] Nikolski, H.S.M. (2016). Machine learning for metagenomics methods and tools.pdf. 1-19.

ECCE12
The 12th EUROPEAN CONGRESS OF CHEMICAL ENGINEERING
Florence 15-19 September 2019

Biosynthesis performance of phenyllactic acid during fermentation and whole-cell conversion with *Lactobacillus paracasei* strain

Qining Wang, Yixuan fang, Rui Xu, Songhong Zhang, Lingyu Zhu, Junxian Yun

College of Mechanical Engineering, Zhejiang University of Technology, Hangzhou 310032, China

**Corresponding author: yunjx@zjut.edu.cn*

Highlights

- Effective strain of *L*actobacillus *paracasei* for the synthesis of phenyllactic acid
- Cell concentration of 3.2 $g \cdot L^{-1}$ in the fermentation
- Different biocatalytic properties of the cells obtained at different time in the logarithmic phase
- Concentrations of phenyllactic acid of 0.6-0.7 $g \cdot L^{-1}$ with the conversion ratio of 0.3-0.38

1. Introduction

Phenyllactic acid (PLA) is a kind of high-value organic acids with broad-spectrum antibacterial properties and could be used to synthesize the new bio-based materials of poly(phenyllactic acid)s [1-4]. The biosynthesis method for preparing PLA is a more sustainable method than chemical synthesis due to its advantages like more moderate reaction conditions and higher efficiency. In this work, the preparation of PLA by microbial synthesis was achieved via the highly efficient strain screening from Chinese traditional pickles, the microbial fermentation synthesis and whole-cell transformation synthesis process.

2. Methods

L. paracasei 16C3 strain was isolated from Chinese traditional pickles, identified by 16S rRNA gene sequence and deposited as the patent strain at the China Center for Type Culture Collection. The growth performance and fermentation production of PLA of this strain in the MRS medium with the static culture and the biosynthesis of PLA using this strain as the whole-cell biocatalyst and phenylalanine (Phe) as the precursor, were investigated experimentally.

The changing of pH was measured by a pH meter (FE20, Mettler-Toledo Ltd., Switzerland). Concentrations of PLA in the fermentation broth and bioconversion broth were analyzed by high performance liquid chromatography (HPLC) using Agilent 1260 infinity system equipped with DAD detector at the wavelength of 210 nm.

3. Results and discussion

The results showed that the maximum cell concentration of about 3.2 $g \cdot L^{-1}$ in the fermentation broth was achieved, as shown in Figure 1(a). The broth pH decreased with time increasing at the logarithmic phase (3 to 15h), indicating that the Intracellular metabolism was active, and some metabolites such as organic acids were produced into the broth. No significant

decrease was observed in the stable phase (30 to 44h), indicating that the activity of cells and enzymes in the broth at this stage were stable.

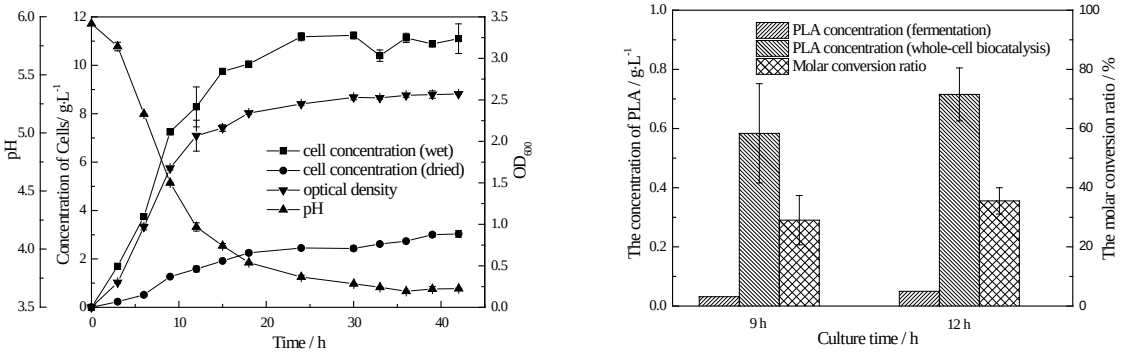

(a) (b)

Figure 1. (a) Cell growth and pH change for *L. paracasei* 16C3 in MRS broth during fermentation process with 30 mL flasks at 35℃. (b) Concentrations of PLA and conversion ratios with cells at different culture time as the whole-cell biocatalysis compared with those obtained at the fermentation. Bioconversion conditions was 2 g• L^{-1} glucose, buffer pH 8.0, 2 g• L^{-1} Phe, 300 g• L^{-1} permeabilized cells and 35°C shaker temperature.

With the cells obtained at different time in the logarithmic phase as the whole-cell biocatalysts, the strain *L. paracasei* 16C3 has different biocatalytic properties, as shown in Figure 1(b). It was found that the bioconversion concentration of PLA was positively correlated with the culture time. The cells cultured about 12 h at the logarithmic phase displayed more effective biocatalytic capacity. The concentration of phenyllactic acid of 0.7 g·L^{-1} with the conversion ratio of 0.38 was achieved, which was high that that with the cells cultured about 9 h, i.e., 0.6 g·L^{-1} with the conversion ratio of 0.3. Moreover, the concentration of PLA with whole-cell biocatalysis from Phe was ten times that produced in the fermentation broth. At the same time, Phe could be the suitable substrates for PLA in bioconversion replaced phenylpyruvate due to the low-cost, stable and water-soluble advantages.

4. Conclusions

L. paracasei 16C3 is an interesting strain for the production of PLA by using Phe as the key substrate by whole-cell bioconversion. The culture time of the cells is one of important parameters influencing the whole-cell biocatalytic properties.

References

[1] J.T. Guan, C.F. Han, Y.X. Guan, S.H. Zhang, J.X. Yun, S.J. Yao, Chin. J. Chem. Eng., 27 (2019) 418−425.
[2] J.T. Guan, Y.X. Guan, J.X. Yun, S.J. Yao, J. Chromatogr. A, 1554 (2018) 92−100.
[3] Y.L. Zhu, J.X. Yun, S.C. Shen, K.J. Yao, J. Chem. Eng. Chin. Univ. 29 (2015) 495−500. (In Chinese)
[4] W.M. Mu, S.H. Yu, L.J. Zhu, T. Zhang, B. Jiang, Appl. Microbiol. Biotechnol. 95 (2012) 1155−1163.

Acknowledgments

The authors gratefully acknowledge the financial supports partially by the National Natural Science Foundation of China (No. 21576240) and the Zhejiang Provincial Natural Science Foundation of China (Nos. LY16B060011, LZ14B060001).

Evaluation of nutrients and oxygen on the production of zeaxanthin by an Anarctic *Flavobacterium*

Eugenia Vila[1], Dámaso Hornero-Méndez[2], Claudia Lareo[1], Verónica Saravia[1]

[1]*Departamento de Bioingeniería, Instituto de Ingeniería Química, Facultad de Ingeniería, Universidad de la República, Montevideo, Uruguay*
[2]*Departamento de Fitoquímica de los Alimentos, Instituto de la Grasa (IG-CSIC), 41013, Seville, Spain*
**Eugenia Vila: mvila@fing.eduuy*

Highlights

- *Flavobacterium frigidarium* is a promising source of zeaxanthin
- Oxygen supply enhanced the zeaxanthin production
- Evaluation of different concentrations of nutrients for the zeaxanthin production

1. Introduction

Carotenoids are the most diverse pigments present in nature. They are used in pharmaceutical, cosmetic and food industry as colorants and antioxidants. Traditional production of carotenoids is by chemical synthesis. However, the increasing negative perception of synthetic additives, demands an alternative such as the biotechnological production of these compounds. Bacterial production of carotenoids is still not competitive compared to chemical synthesis due to the high production cost and lower yields. Flavobacterium species are known as source of carotenoids, being zeaxanthin the principal product [1]. The oxygen supply to the culture is an important factor as oxygen is a precursor in the biochemical pathway for the conversion of β-carotene and β-cryptoxanthin in zeaxanthin. The aim of this work was to optimize the formulation of a media culture to produce zeaxanthin and scale-up the process in a laboratory scale fermenter using an Antarctic *Flavobacterium* sp.

2. Methods

A strain of *Flavobacterium frigidarium* [2] was used as source of carotenoids. The effects of three media components (peptone, yeast extract and NaCl) were studied by a factorial design 2^3 with four central points (Table 1). Media composition was as follows: peptone 2 or 12 g/L, yeast extract 2 or 12 g/L, NaCl 6 or 24 g/L, glucose 6 g/L, $CaCl_2$ 0.3 g/L, $MgSO_4.7H_2O$ 3.4 g/L, urea 0.5 g/L and 400 µL/L of a micronutrient solution. The central point contained: peptone and yeast extract 7 g/L, and NaCl 15 g/L. The strain was cultured in 1-L Erlenmeyer flasks with 300 mL medium in an orbital shaker at 20°C and 200 rpm. The responses studied were zeaxanthin content ($\mu g/g_{biomass}$), zeaxanthin production (g/L), total carotenoid content ($\mu g/g_{biomass}$) and total carotenoid concentration (g/L). Biomass concentration was measured by OD at 600 nm. After 48 hours of growth, cells were harvested by centrifugation. Pellets were washed with distilled water, frozen at

-80°C and lyophilized. Evaluation of dissolved oxygen influence was studied in a bioreactor Biostat A Plus (Sartorius) with 3 L of working volume at 20°C and pH 7. Dissolved oxygen was monitored and maintained above 20% of O_2 saturation of the medium during the bioprocess. Biomass and carotenoid contents were monitored every 12 hours. After 72 hours of growth, cells were harvested and processed as explained previously. Carotenoid quantification was carried out by HPLC-DAD as previously described [2].

3. Results and discussion

The factorial design results are presented in Table 1. The highest zeaxanthin production was achieved in run 5 reaching (256 ± 19) µg/L. However, total carotenoid concentration was maximized in experimental conditions corresponding to the central point.

Run	Factor (g/L)			Content (µg/$g_{biomass}$)		Concentration (µg/L)	
	NaCl	Peptone	Yeast extract	Zeaxanthin	Total carotenoid	Zeaxanthin	Total carotenoid
1	6	2	2	47 ± 3	119 ± 6	112 ± 6	290 ± 13
2	6	2	12	27 ± 1	110 ± 2	111 ± 3	466 ± 6
3	6	12	2	43 ± 2	117 ± 5	132 ± 7	368 ±15
4	6	12	12	14 ± 1	64 ± 1	5 7 ± 1	273 ± 1
5	24	2	2	99 ± 7	172 ± 10	256 ± 19	455 ± 27
6	24	2	12	37 ± 3	109 ± 4	144 ± 10	435 ± 17
7	24	12	2	30 ± 2	92 ± 4	74 ± 6	233 ± 10
8	24	12	12	12 ± 1	56 ± 1	41 ± 1	192 ± 1
9	15	7	7	45 ± 2	121 ± 4	192 ± 9	521 ± 17
10	15	7	7	40 ± 1	110 ± 2	179 ± 2	495 ± 9
11	15	7	7	38 ± 2	111 ± 4	176 ± 9	509 ± 18
12	15	7	7	38 ± 2	107 ± 3	177 ± 7	501 ±12

Table 1. Zeaxanthin and total carotenoid production in shaken flasks

As high levels of oxygen have been widely reported as enhancer of zeaxanthin production, both media were tested in fermenter to study the conversion of β-carotene and β-cryptoxanthin in zeaxanthin. In media 5, zeaxanthin and total carotenoid concentration were similar in shaken flasks and fermenter experiments, reaching in the latest (296 ± 5) µg/L and (443 ± 10) µg/L, respectively. It indicates that in this media, oxygen was not limiting for the production. However, in the central point media culture, total carotenoid production increased to (2358 ± 80) µg/L, with an almost complete conversion to zeaxanthin (2067 ± 70) µg/L. The oxygen supply had an important impact in the carotenoid production as it influences both biomass and zeaxanthin and carotenoid production. Biomass increased from (4.6 ± 0.1) g/L to (5.8 ± 0.1) g/L and zeaxanthin and carotenoid content resulted in (356 ± 12) µg/$g_{biomass}$ and (407 ± 14) µg/ $g_{biomass}$ respectively, 8-fold and 3- fold higher than in shaken flasks.

4. Conclusions

The results showed that the strain could increase the zeaxanthin concentration by 11-fold, showing the dependence of zeaxanthin production with media composition and oxygen supply.

References

[1] R. Carle and R. M. Schweiggert, Handbook on natural pigments in food and beverages: industrial applications, Eds Duxford, UK: Elsevier 2016.

[2] E. Vila, D. Hornero-Méndez, G. Azziz, C. Lareo, V. Saravia, Biotechnol Rep, (2019) e00306.

Purification of recombinant human erythropoietin by multimodal and hydrophobic chromatography

Tomáš Molnár, Monika Antošová, Milan Polakovič*

Department of Chemical and Biochemical Engineering, Institute of Chemical and Environmental Engineering, Faculty of Chemical and Food Technology, Slovak University of Technology, Radlinského 9, 81237 Bratislava, Slovakia

**Corresponding author: milan.polakovic@stuba.sk*

Highlights

- Properties of Capto MMC and Capto Phenyl for rhEPO purification were investigated
- Presence of ionic and hydrophobic interactions at Capto MMC was confirmed
- Non-conventional elution methods must be used
- Strong hydrophobic character of the rhEPO was observed

1. Introduction

Erythropoietin (EPO) is a glycoprotein hormone regulating the production of red blood cells in the organism. EPO is an important and expensive medicinal product. Therefore many purification procedures were developed to obtain pure recombinant human erythropoietin (rhEPO) suitable for clinical use. Conventional methods include the combination of common chromatography purification techniques as ion-exchange, hydrophobic, reverse-phase and size-exclusion chromatography. Some researchers purified EPO by affinity and immunoaffinity chromatography [1, 2, 3]. In this work we compared the properties of a multimodal (Capto MMC) and a strong hydrophobic (Capto Phenyl) chromatography resin during the purification of rhEPO from biological material.

2. Methods

The multimodal adsorbent Capto MMC and the hydrophobic adsorbent Capto Phenyl were obtained from GE Healthcare. rhEPO was produced by human embryonic kidney cell 293 line. The post-culture medium was directly used without any further treatment for the purification experiments. Batch experiments were performed to facilitate the optimization of separation conditions. Flow experiments were carried out using the FPLC system ÄKTA Purifier (GE Healthcare, Uppsala, Sweden). The separation was carried out under the optimized conditions according to batch experiments. The concentration of rhEPO was determined by indirect ELISA assay [4]. The protein concentration was measured according to a standard BCA protein assay protocol [5].

3. Results and discussion

For both tested chromatography resins batch experiments were performed to find the best adsorption and elution conditions. In case of Capto MMC, a larger portion of rhEPO was adsorbed using 50 mM citrate-phosphate buffer with pH 6 supplemented with 300 mM NaCl. Under these

conditions, the binding of contaminant proteins was reduced. Multimodal resins have both ion-exchange and hydrophobic functional groups and this makes the elution of the adsorbed proteins more difficult. Practically no rhEPO was eluted, when the ionic strength of the buffer was increased. 56 % of rhEPO was recovered by simultaneous change of pH and ionic strength of the buffer. The yield of rhEPO was significantly improved by chaotropic agent, arginine. This behavior of the rhEPO confirmed that at multimodal resins, both ionic and hydrophobic interactions can participate in the binding of proteins.

Flow experiments were carried out under the optimized conditions. The adsorption of rhEPO was good, only 3 % of rhEPO was not adsorbed on the resin. The elution was carried out using 50 mM Tris-HCl buffer at pH 7 supplemented with 1 M arginine. During the purification, more than 50 % of contaminating proteins was removed and 80 % of rhEPO was recovered. In a single bind-elute step, the concentration of rhEPO increased nineteenfold compared to that in the feed.

In case of Capto Phenyl, the best rhEPO adsorption was observed at 1.5 M NaCl concentration. The pH of the post-culture medium was adjusted to 6. The adsorption of rhEPO was also enhanced by $(NH_4)_2SO_4$ but due to a possible precipitation of proteins caused by high concentration of $(NH_4)_2SO_4$, the further purification was carried out at the presence of NaCl. Due to the strong hydrophobicity of the resin, commonly used elution procedures during hydrophobic interaction chromatography were not effective. Practically no rhEPO was recovered by reducing the ionic strength of the buffer and only 25 % of the adsorbed rhEPO was eluted by increasing the pH of the elution buffer to 9 and addition of 6 M urea. Good recovery was achieved when organic solvents as ethanol and isopropanol were used.

Flow experiments provided similar results as at Capto MMC. Many of the contaminating proteins left the column during the adsorption and washing phase, while only 5 % of the rhEPO was lost during this stage. Most rhEPO was recovered when 50 % ethanol or 30 % isopropanol in 20 mM Tris-HCl buffer with pH 9 was used for the elution.

4. Conclusions

In this work was investigated the possible application of a multimodal resin Capto MMC and a hydrophobic resin Capto Phenyl for rhEPO purification. In both cases many contaminating proteins were removed in a single bind-elute mode and highly concentrated rhEPO was obtained. According to the results Capto MMC is more suitable for rhEPO purification. Organic solvents, used to recover rhEPO at Capto Phenyl can cause denaturation of the target protein and loss of activity.

5. Acknowledgements

This work was supported by the Slovak Research and Development Agency (Grant number: APVV-16-0111).

References

[1] C.M. Carcagno, M.E. Criscuolo, C.A. Melo, J.A. Vidal, US7012130 (2006).
[2] E.H. Merrifield, EP0358463 (1990).
[3] W. Hinderer, S. Arnold, WO2011035914 (2011).
[4] T. Molnár, M. Bartošová, M. Antošová, Ľ. Škultéty, M. Polakovič, Chem. Pap. 73 (2019) 713–718.
[5] P.K. Smith, R.I. Krohn, G.T. Hermanson, A.K. Mallia, F.H. Gartner, M.D. Provenzano, E.K. Fujimoto, N.M. Goeke, B.J. Olson, D.C. Klenk, Anal. Biochem. 150 (1985) 76-85.

Preparation, isolation and characterization of enzymes for the production of terpenes

Klaudia Karkeszová[1], Viera Illeová, Monika Antošová, Milan Polakovič*

[1] *Department of Chemical and Biochemical Engineering, Institute of Chemical and Environmental Engineering, Faculty of Chemical and Food Technology, Slovak University of Technology, Radlinského 9, 81237 Bratislava, Slovakia*

**Corresponding author: milan.polakovic@stuba.sk*

Highlights

- Adsorption properties of various types of chromatographic adsorbents were tested.
- Good selectivity of a strong multimodal anion exchanger has been achieved.
- Influence of pH and ionic strength on adsorption was studied.

1. Introduction

Monoterpene glycosides play a fundamental role as significant aroma precursors of volatile monoterpenes. They contribute to some of the most important aroma characteristics of wine. These flavor compounds can be released by enzymatic hydrolysis catalyzed by glycosidases to enhance beverage aroma and flavor. The hydrolysis firstly requires the action of a particular enzyme (α-L-arabinosidase, β-D-apiosidase, α-L-rutinosidas, β-D-xylosidase), and secondly the liberated monoglucoside is than hydrolysed by a β-D-glucosidase. Even though one of the most abundant glycosides in fruit juice are apiosylglycosides, there is no pure β-D-apiosidase on the market. This enzyme is often present as a part of commercial enzyme preparations produced by fungi [1].

2. Methods

Static adsorption experiments were performed with six different chromatographic adsorbents. Among the examined adsorbents was one weak anion exchanger (SEPABEDAS-FPDA), three strong anion exchangers (ESHMUNO Q, CAPTO Q, PRAESTO Q), one salt-tolerant anion exchanger (TOYOPEARL NH2-750F) and one strong multimodal anion exchanger (CAPTO Adhere). Column experiments were carried out with the selected adsorbents using the FPLC system ÄKTA Purifier (GE Healthcare, Uppsala, Sweden). Tricorn 5/50 columns were used for the flow experiments.

3. Results and discussion

The purpose of this work was to purify β-apiosidase from an enzyme preparation produced by fungi. The aim of the batch experiments was to observe the behavior of each adsorbent during the adsorption. The effect of pH and salt concentration was examined too. Based on the obtained selectivities, which gave information about the purification of apiosidase from proteins and contaminating glucosidase, three chromatographic adsorbents were selected for flow

experiments. Column experiments were carried out under optimized condition with strong anion exchanger ESHMUNO Q, salt-resistant anion exchanger TOYOPEARL NH2-750F and multimodal anion exchanger CAPTO Adhere. The most promising results were obtained using the multimodal adsorbent CAPTO Adhere. The separation was performed in 25 mM Tris-HCl buffer with pH 9 and 300 mM NaCl and the desorption was conducted by a linear gradient of this solution and a salt-free citrate phosphate buffer with pH 5. Compared to other adsorbents, CAPTO Adhere offered the highest purification factors from proteins (15.6) and glucosidase (5.9).

4. Conclusions

The aim of the work was to study the equilibrium characteristics of adsorbents for chromatographic purification and further characterization of glycoside used in production of terpenes.

5. Acknowledgements

This work was supported by the grant from the Slovak Research and Development Agency (Grant number: APVV-16-0111).

References

[1] V. Mastihuba, E. Karnišová-Potocká, I. Uhliariková, P. Kis, S. Kozmon, M. Mastihubová, Food Chemistry 274 (2019) 543-546

Study of starch accumulation dynamic in nitrogen starved *Chlamydomonas reinhardtii* using controlled torus photobioreactor

Fernando FERREL BALLESTAS[1*], Mariana TITICA[2], Guillaume COGNE[3], Jack LEGRAND[4]

[1,2,3,4]*University of Nantes,* Oniris, CNRS, GEPEA, UMR 6144, 44602 Saint-Nazaire Cedex, France

**Corresponding author: fernando.ferrel-ballestas@univ-nantes.fr*

Highlights

- High starch accumulation by microalgae
- Controlled torus PBR with dissolved oxygen and pH regulation
- Physiological adaptation to nitrogen deficiency

1. Introduction

Chlamydomonas reinhardtii is a green microalgae known to accumulate large amounts of starch in nitrogen-limited conditions, up to 50% of its mass content expressed in dry weight of cells (%DW) that could be used as a feedstock for next generation of biofuels production [1]. In autotrophic nitrogen-starved cultures of *C. reinhardtii*, several physiological changes take place in order to adapt their mass content in pigment content and accumulate starch [2]. Starch accumulation in nitrogen starved cells can be affected by other factors such as anoxic conditions [3], light energy availability [1] and inoculum physiological state. The objective of this work is study of starch accumulation dynamic in nitrogen-starved *C. reinhardtii*, in controlled conditions of O_2 dissolved (OD), pH and light availability, prior to a modelling study with a view to develop an optimized starch production protocol in nitrogen-limiting conditions.

2. Methods

A wild type strain of *C. reinhardtii* (137H) has been cultivated in autotrophic nitrogen-limited conditions, using Suoeka medium with NH_4Cl concentration of 1,87mM, in a torus-shaped PBR, equipped with a pH-temperature and DO sensor, as well as mass spectrometer for gas analyses. The pH of the microalgae culture and inoculum was regulated at 7.5 with gaseous CO_2 injection. DO has been regulated with 4.5% O_2 - 95.5% N_2 gas mixture injection flowrate. Limited-growth cultures were performed in batch and at different incident light intensities. Inoculum has been cultivated in 1L air-lift PBR in non-limiting autotropic conditions. The local fluence rate was calculated along batch cultures using the 2-flux model and the radiative properties of culture were determined experimentally using the methodology developed by Pilon *et al*. [4]. Biotic and abiotic phases have been analyzed measuring the dynamic evolution of key nutriments and intermediate metabolites, as well as the analysis of the produced gases.

3. Results and discussion

For nitrogen-limited growth cultures of *C.reinhardtii*, an NH_4Cl initial load of 1.87mM was used to sustain biosynthesis up to 0.25g/L of biomass under standard growth conditions, according to the known stoichiometry. This amount is close to the value obtained during the first 20 hours of culture in concordance with the depletion of NH_4^+ measured (Fig 1A). After that point, an increase in the starch content was observed and a maximum accumulation of 53% was finally obtained after 70 hours of cultivation (Fig. 1A). A stop of cell growth seems to occur at 32 h of culture, once the number of cells remained relatively constant. In contrast, the nitrogen depletion in the medium lead to a remobilization of the total proteins, while reducing their content to 20% (Fig 1A). In the other hand, the pigments content decreased once the NH_4^+ vanished. The total pigments content was stabilized around 1%. This results in a change within the pigment distribution compared to a standard growth culture without any mineral deprivation. The radiative properties were estimated leading to the calculation the energy light profile within the cultivation system during the starch accumulation phase (70h). This assessment showed that light was not a limiting factor since a fluence value was estimated at 21umol/m^2s at the bottom of the PBR (Fig 1B). Throughout the experiment, the dissolved O_2 was regulated to 130% in oxygen saturation in the air, in order to avoid anoxic conditions. Nonetheless, after 63 hours the dissolved oxygen falls as a consequence of low photosynthetic activity (Fig 1C).

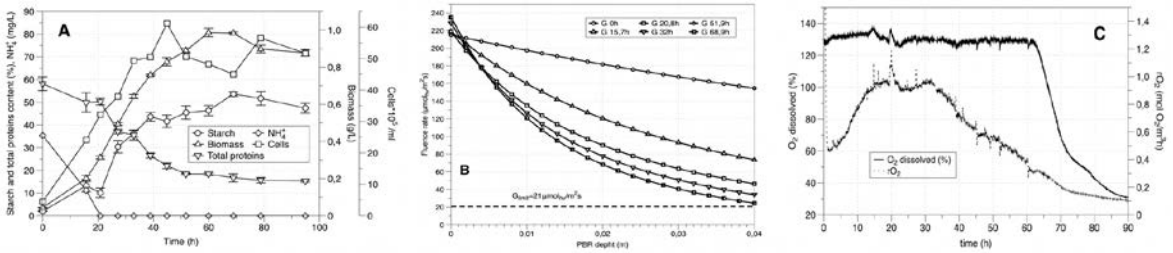

Figure 1. A. physiology response to nitrogen starvation, B. Fluence rate in batch culture q_0= 200umol/m^2s, C. Dissolved oxygen and rO_2 evolution.

4. Conclusions

The use of a controlled torus PBR allowed the study of starch accumulation dynamic after a nitrogen deficiency, where neither light transfer nor dissolved gases (CO_2, DO) influenced the storage of starch. A maximum starch content of 53% was obtained after 70 hours of cultivation. The physiological impact of nitrogen deficiency also led to the remobilization of 30% of the total protein content and to the adaptation in the content and distribution of pigments. This work will lead to the development of a biochemically structured model for starch storage in *C. reinhardtii*.

References [Calibri 10]

[1] Chen C-Y, Zhao X-Q, Yen H-W, Ho S-H, Cheng C-L, Lee D-J, et al. Microalgae-based carbohydrates for biofuel production. Biochemical Engineering Journal 2013;78:1–10. doi:10.1016/j.bej.2013.03.006 .
[2] Antal TK. Microalgal Hydrogen Production: Achievements and Perspectives. Rsc 2018:235–64.
[3] Juergens MT, Deshpande RR, Lucker BF, Park J-J, Wang H, Gargouri M, et al. The Regulation of Photosynthetic Structure and Function during Nitrogen Deprivation in Chlamydomonas reinhardtii. Plant Physiology 2015;167:558–73..
[4] Pilon L, Berbero• lu H, Kandilian R. Radiation transfer in photobiological carbon dioxide fixation and fuel production by microalgae. Journal of Quantitative Spectroscopy and Radiative Transfer 2011;112:2639–60.

Effect of Hofmeister series ions on BSA and DNA adsorption on salt-tolerant interaction chromatography (STIC) membrane

Tomáš Kurák, Milan Polakovič*

Department of Chemical and Biochemical Engineering, Institute of Chemical and Environmental Engineering, Faculty of Chemical and Food Technology, Slovak University of Technology, Radlinského 9, 81237 Bratislava, Slovakia

**Corresponding author: milan.polakovic@stuba.sk*

Highlights

- Single- and bi-component adsorption of BSA and DNA was studied.
- Salt type and concentration has significant effect on binding capacity on salt tolerant membrane
- DNA adsorption on STIC had similar behavior to that of multimodal adsorbents

1. Introduction

Most mAb purification processes include at least one ion exchange chromatography step. Salt tolerant adsorbents are novel materials which are a useful complement to conventional ion exchangers and hydrophobic resins. They maintain binding capacity even in higher salt concentration. This leads to a reduction in the number of operations in downstream separation train. Moreover this opens space for seeking good selectivity in wider salt concentration range.

2. Methods

Model macromolecules used in adsorption experiments were BSA and salmon DNA. Thermodynamics of protein binding was studied for single-component solutions of BSA or DNA and their binary mixture. Experiments were carried out using 96 well plates filled with Sartobind STIC membrane adsorbent. Loading solutions passed through membrane in the well by centrifugal force or a single well was used as a membrane module using the FPLC system ÄKTA (GE Healthcare, Uppsala, Sweden). Four different buffers (phosphate, tris, bis tris, bis tris propane) were chosen to examine effect of pH on protein binding. The influence of salt type and ionic strength was examined for a spectrum of anions (SO42-, HPO42-, Cl-, SCN-,F-) and cations (NH4+, Na+, Mg2+, K+)

3. Results and discussion

Firstly, the influence of pH and buffer type was examined. It was shown that pH affects the binding capacity of both BSA and DNA similarly as in case of conventional anion exchangers. It was however observed that the buffers containing polyvalent salt inhibited strongly binding of BSA but they enhanced adsorption of DNA. Secondly, the influence of salt type and ionic strength on the binding capacity was examined for several anions and cations. The selected ions span the whole Hofmeister series so salts with both chaotropic or kosmotropic effects were investigated here. Chaotropic salts decreased BSA binding capacity with increasing ionic strength but not as rapidly as polyvalent kosmotropic salts (Fig. 1). On the other hand, increasing salt concentration, even of

polyvalent salts, had different effect on DNA adsorption. Binding capacity had a maximum at certain salt concentration. The observed effect can have more general implications for the application of multimodal adsorbents in protein purification. This behaviour can be used to optimize separation conditions (e.g. salt concentration, buffer system and pH).

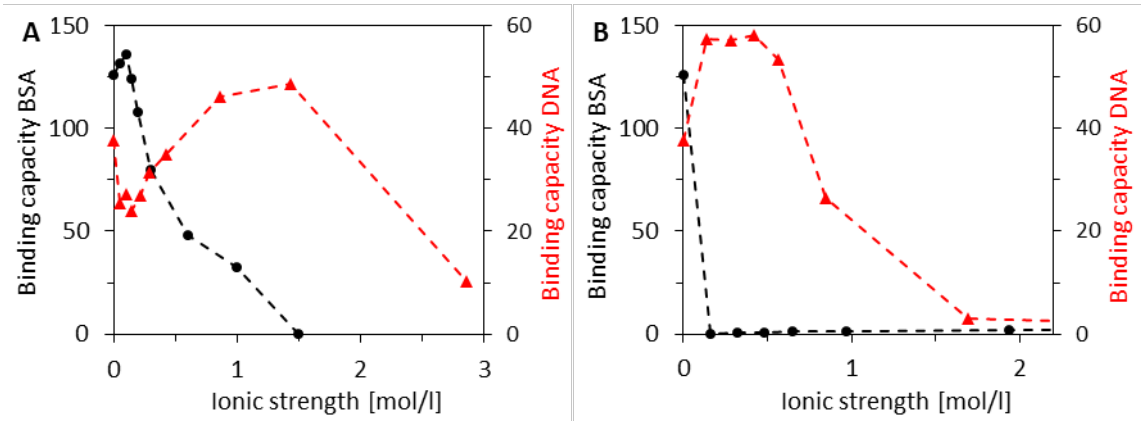

Figure 1. Influence of ionic strength on BSA and DNA binding capacity in the presence of (A) NaCl (B) Na2SO4

4. Conclusions

This work helps to clarify the effect of the composition of the mobile phase on the adsorption of single and bi-component solutions on the salt tolerant membrane adsorbent. The results of the influence of buffer and salt types, pH, and ionic strength on the adsorption equilibrium of BSA and salmon DNA on the Sartobind STIC membrane contribute to understanding of process performance and optimal design of chromatographic separation processes.

5. Acknowledgements

This work was supported by the grant from the Slovak Research and Development Agency (Grant number: APVV-16-0111).

ECCE12
The 12th EUROPEAN CONGRESS OF CHEMICAL ENGINEERING
Florence 15-19 September 2019

Hydrogen production in a pressurized photobioreactor: phototrophic bacterium *Rhodobacter capsulatus*

Jean-Pierre MAGNIN[1,2], Jonathan DESEURE[1,2*],
[1] *Univ. Grenoble Alpes, CNRS, Grenoble INP, LEPMI, 38000 Grenoble, France;*
[2] *Univ. Savoie Mont Blanc, LEPMI, 73000 Chambéry, France*
**Corresponding author: jonathan.deseure@lepmi.grenoble-inp.fr*

Highlights

- Biohydrogen production
- photo-fermentation, *Rhodobacter capsulatus*,
- Wastewater valorization
- Partial changing pathway from growth into survival for Rhodobacter capsulatus

1. Introduction

Energy consumption from fossil feed-stocks increases with human growth and economic growth of emerging countries and lead to the CO_2 formation and consequently to climate changing [1]. Therefore, the large-scale transition from fossil fuel to hydrogen fuel and renewable hydrogen technology can substantially improve air quality and reduce climate change [2]. Biological energy such as photobiohydrogen exhibits a positive global warming potential, low acidification potential, relevant social cost of carbon and a low potential production cost [3]. To make economically possible the use of biohydrogen as energetic vector, high purity of produced hydrogen shall be reached using a pressurized tank process to gas storage. Therefore, the main disadvantage of hydrogen is the difficulty of inexpensive easy storing and dispensing of the hydrogen gas. Direct compression of biohydrogen is a benefit to reach the widespread commercial applications. In the present work, hydrogen production process was achieved on anaerobic photosynthesis using the purple non-sulphur bacterium *Rhodobacter capsulatus*. The bacterial culture was carried out in a photo-bioreactor operated in a closed vessel or opened vessel, using lactate as a carbon source and LED illumination is provided. In previous work [4], we have observed when the gas pressure increases with the bacterial growth (in closed vessel), the pressurized hydrogen production is improved (80%) versus atmospheric hydrogen production.

3. Results and discussion

In present work , we have exhibited the opportunity to obtain pressurized hydrogen close to 1o bar by photofermentation of lactate. We have observed an unexpected enhancement of bio- hydrogen production by the phototrophic bacterium *Rhodobacter capsulatus* in a pressurized photobioreactor: the amount of produced hydrogen from synthetic media (lactate (35 mmol L^{-1}) glutamate (5mmol L^{-1})) under pressurized vessel is multiplied by 1.8 versus atmospheric vessel. Hydrogen purity has overcome 90 % with lactate conversion rate was up to 70 %. It is suspected that the energetic demand of *Rhodobacter capsulatus* increases during culture under pressurized

condition and improves hydrogen production. We have observed that the addition of nitrogen sources can drive the lactate conversion rate. In our cultures, the partial changing pathway is possible from growth to survival; this mechanism could explain the lower growth in the closed vessel than in the open vessel. Therefore, during culture under pressurized conditions, stress appears, and this stress increases the energetic demand and improves hydrogen production. However, we do not know the nature of this stress, and we do not have a hypothesis regarding its origin.

4. Conclusions

The hydrogen production in closed vessel is multiply by 1.8 versus atmospheric opened vessel. Numerous advantages due to the high operating pressure can be itemized:

i) Self-compression of produced hydrogen
ii) Easier control of fed bath or continuous operation
iii) Lower risk of contamination
iv) Easier storage

References

[1] E. L. Miller, DOE hydrogen and fuel cells program: Annual Merit Review Proceedings 2016.
[2] A. F. Ghoniem, Prog. Energ. Combust, 37 (1), 15, 2011.
[3] I. Dincer and C. Acar.. Int. J. Hydrogen Energy 40 (34), 11094. 2015
[4] J. P. Magnin and J Deseure , Applied Energy, 239, 635, 2019

ECAB 5
The 5th EUROPEAN CONGRESS OF APPLIED BIOTECHNOLOGY
Florence 15-19 September 2019

Synergistic interaction of co-encapsulated *Saccharomyces cerevisiae* and *Metarhizium brunneum* used for biological pest control

Katharina Hermann[1,2], Pascal Humbert[1], Anant Patel[1]

1 Bielefeld University of Applied Sciences, WG Fermentation and Formulation of Biologicals and Chemicals, Faculty of Engineering Sciences and Mathematics, Interaktion 1, 33619 Bielefeld, Germany; 2 Bielefeld University, WG Multiscale Bioengineering, Technical faculty, Universitätsstraße 25, 33615 Bielefeld, Germany

**Corresponding author: khermann1@fh-bielefeld.de*

Highlights

- Calcium alginate-based formulation acts as microfermenter for the entomopathogenic fungus *M. brunneum*
- Co-encapsulation of *S. cerevisiae* improves sporulation of *M. brunneum*
- Co-encapsulation of *S. cerevisiae* and *M. brunneum* leads to steep oxygen gradients in alginate beads as revealed by microelectrode measurement

1. Introduction

In the last few years wireworm damage has become an increasing problem in both conventional and organic potato cultivation. Wireworms are polyphagous soil dwelling larvae of click beetles (*Agriotes spp*.) and even low populations lead to severe economic losses since they can live up to five years in soil. Wireworms use CO_2 gradients established in soil by plant roots to locate potential hosts. However, effective plant protection products are currently not available since chemical insecticides have recently been restricted or abandoned. Consequently there is a tremendous need for alternative biological control options. In previous work, a biological bead formulation for wireworm control was developed, based on an attract-and-kill approach that exploits the insect's behavior [1-4]. The calcium alginate beads contain both *Saccharomyces cerevisiae* that produce CO_2 as an attractant and the entomopathogenic fungus *Metarhizium brunneum Cb15 III* acting as the kill component. Additionally, a nutrient supply is added. When the beads are placed in soil, they absorb its moisture, thereby initiating the CO_2 production process as well as the growth of fungus out of the beads. Virulent aerial conidia are formed on the bead's surface. Therefore the co-formulation represents a "microfermenter" [5] that needs to be investigated in more detail. Co-cultivation can alter cell growth [6] and, moreover, lead to morphological and physiological changes possibly resulting in attenuated virulence induced by contact-dependent interaction [7]. Hence, the main objective was to investigate the synergistic interaction of *Saccharomyces cerevisiae* and *Metarhizium brunneum* inside the bead.

2. Methods

M. brunneum was grown in submerged culture for 48 h at 25 °C and 150 rpm in shaking flasks with baffles. Mycelial biomass and blastospores were separated by vacuum filtration.

The encapsulation suspension was prepared by mixing sodium alginate and sterile native corn starch. Then, *S. cerevisiae* and *M. brunneum* biomass were added. For bead formation, the suspension was dripped into a sterile $CaCl_2$ solution. Diameter of beads was 4-5 mm. Subsequently, beads were dried, resulting in a bead diameter of 3 mm.

Formed aerial conidia were rinsed off from the bead surface with a 0,1% Tween 80 solution and conidial concentrations were determined by counting conidia with a Thoma cell counting chamber

Microelectrodes (Unisense, Denmark) with a diameter of 50 µm were used measuring oxygen-, pH- and temperature gradients. For this, beads were fixed, and microelectrodes inserted stepwise (100 µm) into the beads with a manual micromanipulator.

3. Results and discussion

We found that co-encapsulation of *S. cerevisiae* enhanced the sporulation of *M. brunneum* from the beads significantly (Figure 1), probably serving as nitrogen source, since they consist of 80% nitrogen.

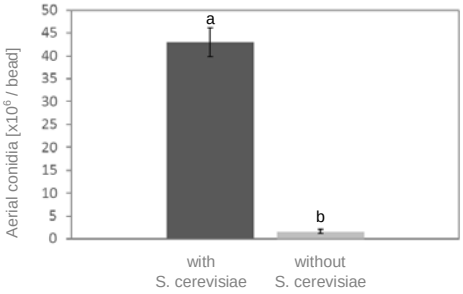

Figure 1: Sporulation of M. brunneum on alginate beads with and without S. cerevisiae. Different letters above bars indicate significant differences based on t-test at p < 0.05 (means ± SD, n = 4).

Further analysis revealed steep oxygen gradients when *S. cerevisiae* is added to the formulation (Figure 2), indicating oxygen limitations in the center. Diffusion limitation in alginate beads can limit cell growth and lead to metabolic changes [8, 9]

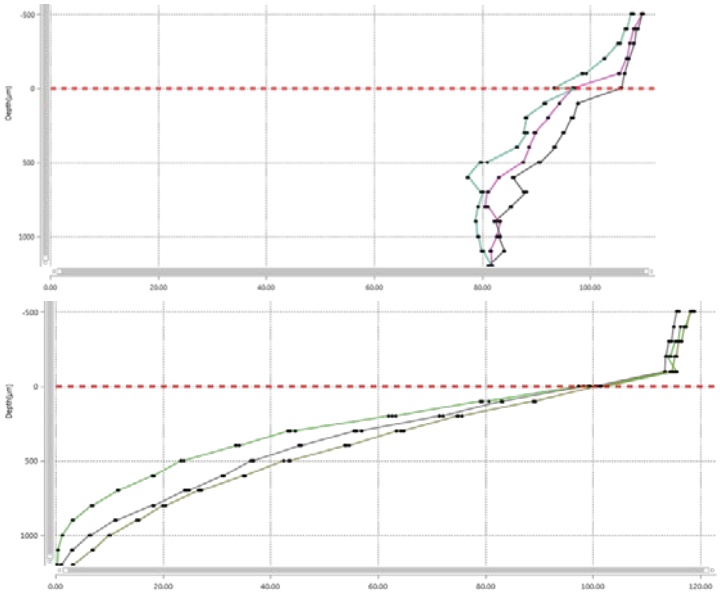

Figure 2: Oxygen gradients in alginate beads loaded with starch and M. brunneum (top) and with starch, M. brunneum and S. cerevisiae (bottom). Abscissa in mV. Red dotted line indicates bead surface.

4. Conclusions

Preliminary results indicate a biological impact of co-encapsulation on fungal development, especially sporulation. A novel method for bead analysis was established in order to examine the physicochemical and biochemical processes. Future work will focus on small-scale submerged co-cultivation (BioLector Pro).
The influence of oxygen limitations will be examined and circumvented by reducing both bead diameter and cell concentration in order to improve efficacy.

References

[1] Humbert, P., Vemmer, M., Giampa, M., Bednarz, H., Niehaus, K., & Patel, A. V. (2017). Co-encapsulation of amyloglucosidase with starch and Saccharomyces cerevisiae as basis for a long-lasting CO 2 release. World Journal of Microbiology and Biotechnology, 33(4), 71.
[2] Humbert, P., Przyklenk, M., Vemmer, M., & Patel, A. V. (2017). Calcium gluconate as cross-linker improves survival and shelf life of encapsulated and dried Metarhizium brunneum and Saccharomyces cerevisiae for the application as biological control agents. Journal of microencapsulation, 34(1), 47-56.
[3] Schumann, M., Patel, A., Vemmer, M., & Vidal, S. (2014). The role of carbon dioxide as an orientation cue for western corn rootworm larvae within the maize root system: implications for an attract-and-kill approach. Pest management science, 70(4), 642-650.
[4] Schumann, M., Patel, A., & Vidal, S. (2013). Evaluation of an attract and kill strategy for western corn rootworm larvae. Applied soil ecology, 64, 178-189.
[5] Przyklenk, M., Vemmer, M., Hanitzsch, M., & Patel, A. (2017). A bioencapsulation and drying method increases shelf life and efficacy of Metarhizium brunneum conidia. Journal of microencapsulation, 34(5), 498-512.
[6] Ström, K., Schnürer, J., & Melin, P. (2005). Co-cultivation of antifungal Lactobacillus plantarum MiLAB 393 and Aspergillus nidulans, evaluation of effects on fungal growth and protein expression. FEMS Microbiology Letters, 246(1), 119-124.
[7] Bor, Batbileg et al. “Morphological and physiological changes induced by contact-dependent interaction between Candida albicans and Fusobacterium nucleatum.” Scientific reports vol. 6 27956. 14 Jun. 2016,
[8] Irrgang, S., Baumgärtl, H., Schlosser, D., Zimelka, W., & Schmauder, H. P. (1993). Investigations of the oxygen supply in Ca-alginate beads and microcapsules loaded with Penicillium raistrickii using a microelectrode. Journal of basic microbiology, 33(5), 311-321.
[9] Ogbonna, J. C., Matsumura, M., & Kataoka, H. (1991). Effective oxygenation of immobilized cells through reduction in bead diameters: a review. Process biochemistry, 26(2), 109-121.

ECAB 5
The 5th EUROPEAN CONGRESS OF APPLIED BIOTECHNOLOGY
Florence 15-19 September 2019

Development of biocatalysts for application in integrated process of lactose hydrolysis and glucose isomerization aiming the production of prebiotics

Carlos A. C. Girão Neto[1], Natan C. G. e Silva[1], Marcele M. S. Vasconcelos[1], Luciana R. B. Gonçalves[1], Maria V. P. Rocha[1]

[1] *Department of Chemical Engineering, Universidade Federal do Ceará, Brazil*

**Corresponding author: valderez.rocha@ufc.br*

Highlights

- The coating of supports with polyethylenimine improves the immobilization parameters.
- The polyethylenimine biocatalysts were very effective in the hydrolysis of lactose.
- High conversion of glucose into fructose was obtained.

1. Introduction

β-galactosidase enzyme (E.C. 3.2.1.23) is widely used in the dairy industry for the hydrolysis of lactose, but over the years it has also increased its use as a catalyst for the synthesis of galactooligosaccharides (GOS) by favoring transgalactosylation reactions, having these GOS a recognized prebiotic function (Urrutia *et al.*, 2018). Besides that, studies have been carried out with the purpose of isomerizing the glucose formed in the hydrolysis reactions to fructose by glucose isomerase enzyme (GI) (E.C. 5.3.1.18) and the obtained fructose can be used as one of the substrates in the transgalactosylation reactions. These enzymes, when immobilized, can be much more effective because some enzymatic characteristics can be improved, such as the stability and activity, specificity or selectivity, and even its purity, besides the possibility of reusing the biocatalysts. The coating of supports has been proposed to extend its useful life, for example, the coating with a multifunctional polymer called polyethylenimine (PEI). This, in turn, involves the enzyme and suits its structure, giving greater stability, especially for multimeric enzymes like β-gal, and also protects from environmental variations, such as temperature, as well as to the aggressive effects of the activating agent (Bolivar *et al.*, 2009; Garcia-Galan, Barbosa and Fernandez-Lafuente, 2013). Therefore, the present work aims initially to evaluate the effects of coating the supports with PEI on the immobilization of β-gal from *Kluyveromyces lactis*, and then to determine the catalytic efficiency of these biocatalysts in the lactose hydrolysis. In parallel, it was evaluated the conversion of the formed glucose into fructose using GI from *Streptomyces murinus*, in order to obtain a product that can be used in the synthesis of prebiotics.

2. Methods

2.1. Immobilization of the [2]-galactosidase: β-gal (E.C. 3.2.1.23) from *Kluyveromyces lactis* was immobilized on chitosan gel (2 % w/v) activated with two different activation agents: glutaraldehyde (0.8 % v/v) according to Albuquerque *et al.* (2018) and glycidol adapted from Guisán (1988), and then the supports were coated with polyethylenimine - PEI (10 % w/v) adapted from Pessela *et al.* (2005). 10 mg of protein per gram of support was used in the immobilization and the process was performed at pH 7.0 and 25 °C in 100 mM potassium phosphate (KH_2PO_4) buffer, containing 0.1 mM $MnCl_2$ and 0.2 mM $MgCl_2$, under gentle agitation on a rotary shaker. The immobilization parameters were determined.

2.2. Catalytic Efficiency of Biocatalysts: The hydrolysis reactions were evaluated for 1.5 hours using a synthetic solution containing 66.7 g/L lactose, under stirring, pH 7.0 and 50 °C. After this process, the [2]-gal enzyme was removed and it was added 0.1 g of immobilized GI (E.C. 5.3.1.18) from *Streptomyces murinus*, 8 mL of KH_2PO_4 buffer, 2 mL of 0.5 mol/L $MgSO_4$, 1 mL of 0.01 mol/L $Co(NO_3)_2$, and the isomerization reactions were evaluated for 4.5 hours under stirring, pH 7.5 and 70 °C. Samples were taken to determine the carbohydrate concentration (lactose, glucose, galactose and fructose) by High Performance Liquid Chromatography (Albuquerque *et al.*, 2018).

3. Results and discussion

The coating of supports with PEI considerably improved the immobilization parameters (Table 1), presenting higher results than those obtained by Albuquerque *et al.* (2018), which used the same immobilization conditions of the present study, but without coating the supports. It was expected since the PEI layer allows a very strong immobilization via multipoint adsorption, besides involving the enzyme and conforming to its structure, avoiding loss of activity due to conformational changes and thus conferring a greater stability to the biocatalyst (Pessela *et al.*, 2005).

Table 1. Immobilization parameters and efficiency of the integrated process of lactose hydrolysis and glucose isomerization by immobilized β-gal and immobilized GI, respectively.

Biocatalyst	Immobilization yield (%)	Activity offered (U/g)	Derivative activity (U/g)	Recovered activity (%)	Conversion of lactose (%)	Conversion of glucose (%)
A	97.45	210.28	95.26	45.30	63.96	36.02
B	92.74	175.36	142.96	81.52	71.72	21.18

β-gal immobilized on: (A) Chitosan activated with glutaraldehyde and coated with PEI; (B) Chitosan activated with glycidol and coated with PEI.

For the hydrolysis of lactose into glucose and galactose, the biocatalyst B showed the closest result at obtained by the soluble enzyme (88 %), after 2 hours of reaction and under the same conditions used (Albuquerque *et al.*, 2018). Biocatalyst B showed the highest conversion of lactose, which was expected since it had a superior enzymatic activity (142.96 U/g). At the end of this process, the reaction media containing the biocatalysts A and B showed concentrations of 44.9 g/L or 50.35 g/L of glucose/galactose and 24.04 g/L or 18.86 g/L of lactose, respectively. For the isomerization reactions, the highest conversion obtained was 36.02 %, an excellent result when compared to that obtained by Yu *et al.* (2011) (45 %), after 16 hours of reaction and using an enzyme dosage of 2 g. However, the reaction medium from biocatalyst B contained higher concentrations of glucose and galactose, and this may have affected the performance of the GI, leading to a lower conversion.

4. Conclusion

The coating of the supports with polyethylenimine improved the immobilization process of β-galactosidases. In addition, these biocatalysts were efficient for the hydrolysis of lactose, and it was possible to convert the obtained glucose into fructose through the isomerization reactions, thus proving that the use of this integrated process is possibly promising to produce prebiotics.

References

[1] Bolivar, J. M. *et al.*, Biomacromolecules. (2009) 742–747.
[2] Garcia-Galan, C., Barbosa, O., Fernandez-Lafuente, R., Enzyme and Microbial Technol. (2013) 211–217.
[3] Guisán, J. M., Enzyme Microbial Technol. 10 (1988) 375–382.
[4] Albuquerque, T.L *et al.,* Process Bioch. 73 (2018) 65–73.
[5] Pessela, B. C. C. *et al.*, Enzyme and Microbial Technol. 37 (2005) 295–299.
[6] Urrutia, P. *et al.*, Biological Macromol. (2018).
[7] Yu, D. *et al.*, Process Bioch. (2011) 599-603.

Carotenoids production in Antarctic *Chryseobacterium marinum*

Florencia Risso[1], Eugenia Vila[1], Verónica Saravia[1]*

1 Departamento de Bioingeniería, Instituto de Ingeniería Química, Facultad de Ingeniería, Universidad de la República, Julio Herrera y Reissig 565, Montevideo, Uruguay.
** Corresponding author: vsaravia@fing.edu.uy*

Highlights

- Psychrotolerant strains from King George Island, Antarctica
- Identification of carotenoids by chromatographic analysis
- *Chryseobacterium marinum* potential source for carotenoids production

1. Introduction

Carotenoids are among the most diverse natural products. They are synthesized de novo by many organisms, mainly plants and microorganisms. They absorb light between 400 to 550 nm, which gives them their yellow-orange color [1]. In fact, as antioxidant compounds, carotenoids have relevant biological functions in quenching of singlet oxygen, light capture and photosynthesis protection. There is currently much interest in biological active compounds derived from natural resources due to the high costs and waste materials associated to the chemical synthesis.
Antarctic microorganisms are exposed to extreme environmental conditions as weather, drastic light changes, nutrient scarcity, and high seasonal ultraviolet radiation incidence increased by the ozone depletion over Antarctica [2, 3, 4]. The isolation and characterization of extreme habitats microorganisms has become more important lately as a mean of identifying adaptations of microorganisms to these extreme conditions, with potential biotechnological application such as carotenoid production. This study involved 20 psychrotolerant strains isolated from sampling events carried out during the Uruguayan Antarctic Expedition (December, 2014) along Fildes Peninsula, King George Island, Antarctica.

2. Methods

Strains characterization and selection: Single colonies that exhibited yellow/orange coloration were subculture in TSA plates. The pigmented colonies were replicated until a pure culture was reached. Strains were conserved at -80°C on glass beads with 20% glycerol in Tryptic Soy Broth. Strains were characterized, influence of temperature on cell growth at 10°C, 25°C and 37°C on TSA. Identification of the strains was done by 16S rRNA analysis [5].

Culture conditions for biomass and pigment production: A factorial experimental design 2^2 was used to evaluate the relative importance of glucose and peptone for biomass production and carotenoids content. Statistica trial version software was used for analysis. Bacterial strains were cultured in 500 mL Erlenmeyer flasks with 150 mL medium in an orbital shaker at 20°C and 200 rpm. The culture media included: yeast extract 2.0 g/L, NaCl 5.0 g/L, K_2HPO_4 2.5 g/L, glucose (15 g/L, 10 g/L or 5 g/L), and peptone (11g/L , 6.5 g/L or 2g/L). For each nutrient variable, a high (+), a low (-) concentration and three center points were tested. After 48 h culture growth, cells were harvested by centrifugation. Cell pellets were stored at -80°C and lyophilized (VirTis BenchTop 2 K Freeze Dryer, SP Industries Inc.).

Pigment extraction and characterization: Approximately 0,05 g of lyophilized biomass was extracted with 4 mL of methanol until bleaching. The extract was dried under a nitrogen stream and dissolved in acetone for chromatographic analysis. Detection was performed at 450 nm.

3. Results and discussion

Phylogenetic analysis sorted the isolated strain as *Chryseobacterium marinum,* a Gram – negative, yellow, rod-shaped aerobic bacterium. The absorption spectrum of the methanol- extracted pigment of *Chryseobacterium marinum* displayed a typical carotenoid spectrum in the visible range with maximum absorbance at 450 nm. Identification of carotenoids was carried out according to the strain producing pigments and the retention time (RT) in the C18 column and was confirmed through coelution with *β*-carotene, *β*-cryptoxanthin and zeaxanthin standards.
Evaluation of nutritional effects in biomass and carotenoids production: Peptone showed either a positive effect in the biomass growth and pigment content. Meanwhile glucose showed a negative effect in the biomass production and in the pigment production. Maximum growth and zeaxanthin concentration were obtained after 48.5h growth at 20° C, pH 7.0, in a medium containing 5 g/L glucose and 11 g/L peptone. Under these conditions, the concentration of total carotenoids from *Chryseobacterium marinum* was 15,1 mg/L. Surfaces responses are showed in Figure 1. Even though, *Chryseobacterium sp.* showed potential as microbial source for producing carotenoids, the carotenoid yield and composition can still be maximized by optimization of the bioprocess.

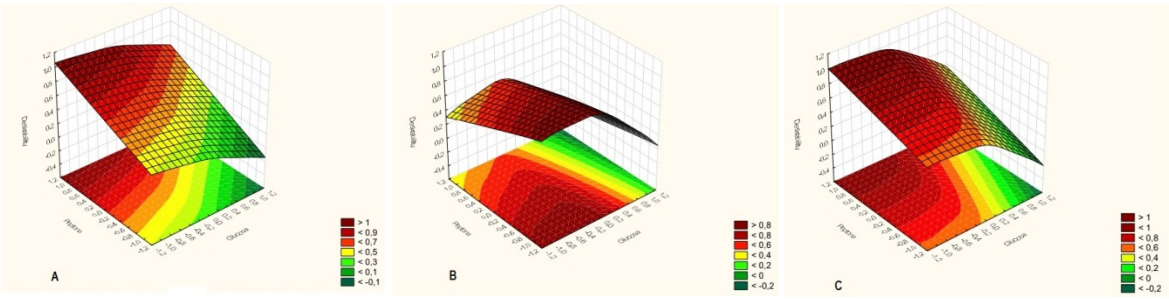

Figure 1. Surface-response graphs generated from the 2^2 statistical factorial design, utilizing peptone and glucose influence on the response factors: (A) Biomass, (B) Carotenoids content and (C) Zeaxanthin production.

4. Conclusions

As reported for the genus *Chryseobacterium: β*-carotene, *β*-cryptoxanthin and zeaxanthin were detected. Carotenoids identified from Antarctic bacteria constitute an alternative for further biotechnological application towards a more sustainable way of pigments production.

References

[1] Britton G. 1995. Structure and properties of carotenoids in relation to function. FASEB J. 9:1551–1558
[2] Margesin R, Miteva V. (2011) Diversity and ecology of psychrophilic microorganisms. Res Microbiol 162:346–361
[3] Margesin R, Schinner F, Marx JC, Gerday C. (2008) Psychrophiles, from Biodiversity to Biotechnology. Springer, Berlin
[4] Uchino O, Bojkov RD, Balis DS, Akagi K, Hayashi M, Kajihara R (1999) Essential characteristics of the Antarctic-spring ozone decline: update to 1998. Geophys Res Lett 26:1377–1380
[5] Vila, E., Hornero- Méndez, D., Azziz, G., Lareo, C., Saravia, V. 2019. Carotenoids from heterotrophic bacteria isolated from Fildes Peninsula, King George Island, Antarctica. Biotechnology Reports 20

Enzymatic activity of commercial enzymes in hydroalcoholic solvents and its effect on bioactive molecules recovery.

Carmen Soto-Maldonado[1*], Paola Poirrier-González; María Elvira Zúñiga-Hansen[2]

1 Centro Regional de Estudios en Alimentos Saludables, Av. Universidad 330, Curauma-Placilla, Valparaíso, Chile; 2 Escuela de Ingeniería Bioquímica, Pontificia Universidad Católica de Valparaíso, Av. Brasil 2085, Valparaíso, Chile.

**Corresponding author: carmensoto@creas.cl*

Highlights

- Antioxidant recovery can be improved by enzymatic treatment
- Enzymes can be inhibited by solvent presence during the extraction process.
- Ethanol 10% allow to maintain enzyme activity almost in a 50%

1. Introduction

Antioxidants are substances that limit the oxidation of several molecules. They are present in fruit and vegetables (pulp, seeds, and skins) (Laroze *et al*. 2010). Extraction of antioxidant compounds depends of several factors. Also, different treatments are used to improve the bioactive compounds extraction, such as the use of plant cell wall degrading enzymes. Few works report enzymatic treatment of vegetable material to improve the antioxidant recovery (Kim *et al.*, 2005; Li *et al.*, 2006; Pinelo *et al.*, 2008; Kapasakalidis *et al.*, 2009; Maier *et al.*, 2008; Laroze *et al*., 2010). In most of them, enzyme incorporation increases the presence of phenolic compounds and its antioxidant activity; however, results depend of several variables, including enzyme inhibition (Kim *et al.,* 2011; Ximenes et al., 2011). Also, authors as Bezerra and Dias (2005) reports that organic solvent as ethanol produce enzyme denaturation. Due to this fact enzyme application during antioxidant compounds extraction with solvents must be not efficient. **The aim** of this work was to evaluate the effect of organic solvent in the enzymatic activity of commercial formulations which are used in the treatment of agro-industrial solid waste to improve the antioxidant compounds extraction.

2. Methods

Enzymes: Commercial enzymes (Grindamyl CA 150 from Danisco; Macer 8 FJ from Biocatalyst; Celluclast 1.5L and Cellubrix L from Novozymes) were characterized about their enzymatic activity.
Enzymatic activity determination: Two types of enzyme activities assays were done. A) Cellulolytic activity was established using carboxymethylcellulose (CMC) as substrate according to Ghose (1987). B) Polygalacturonase activity (pectinase activity), was determined by Ros *et al* (1992) method. The enzymes were dissolved in buffer and then, different amount of solvent was added.
Extraction of phenolic compounds with antioxidant activity: A solid/solvent ratio of 1/10 w/v was used in the extraction of phenolic compounds from Maqui berry pomace, which was used as model raw material because its high antioxidant compound content. Enzymes were dissolved in water, added to the solid, blended, and the solvent was incorporate then. Solid and extracting solvent were put at 50°C during 6 hours under magnetically stirring. Extract was recovery by filtration.

Antioxidant presence: Total polyphenolic compounds (TPC) were determined by Folin-Ciocalteu method, according to Conde *et al.* (2009). **Antioxidant activity** (AA) was determined by two methods (1) The 2,2-diphenyl-1-picrylhydrazyl = 2,2-diphenyl-1-(2,4,6-trinitrophenyl) hydrazyl) (DPPH) radical scavenging capacity was measured according to Laroze *et al.* (2000), and (2) the 2,2'-azino-bis(3-ethylbenzthiazoline-6-sulphonic acid) (ABTS) assay according to Conde *et al.* (2009).

3. Results and discussion

Figure 1 shows the effect of several proportion of ethanol on the enzymatic activity of 4 commercial catalysts. As it is possible to observed in all the cases the presence of ethanol decreases drastically the enzyme activity. Only when 10% of ethanol was used the cellulolytic activity was maintained over 50% of the original value. Then, this solvent (ethanol 10%) was used to probe the enzymatic extraction of phenolic compounds from maqui berry pomace. The Figure 2 shows an increment on the extraction of phenolic compounds from maqui berry pomace and its antioxidant activity when enzymes as Macer 8FJ and Celluclast were used, in comparison to control.

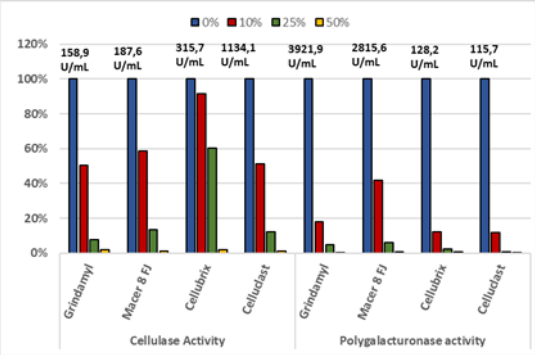

Figure 1. Enzymatic activity of commercial catalyst in ethanol presence.

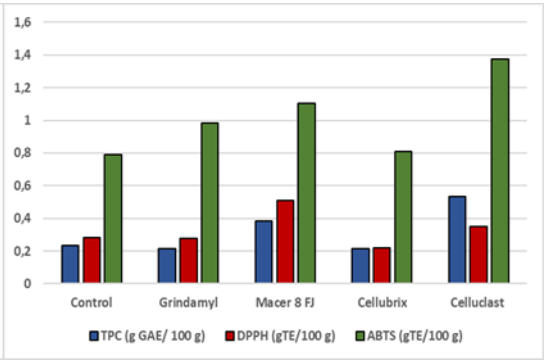

Figure 2: Recovery of phenolic compounds with antioxidant activity using an enzymatic treatment.

4. Conclusions

The extraction of antioxidant compounds is improved when mixtures of organic solvents with water are used, in comparison to only water extraction. In addition, the use of enzymes is an attractive alternative to improve the extraction, but its activity is deeply affected by the presence of organic solvent. Despite that, it is possible to find an amount of solvent that allows the enzymes to act and at the same time improve extraction. Then, catalysts as Celluclast 1.5L and Macer 8FJ allows to increase the efficiency of extraction of phenolic compounds with antioxidant activity from Maqui pomace up to 100%, considering as extraction solvent a 10% of aqueous ethanol.

References

[1] RM.F.Bezerra, A.A.Dias *Appl Biochem Biotech*, 126 (2005) 49-59.
[2] E. Conde, C. Cara, A. Moure, E. Ruiz, E Castro, H.Domínguez, *Food Chem*, 114(2009) 806-812.
[3] T.K. Ghose. Pure & Appl Chem 59(1987) 257-268.
[4] P.G. Kapasakalidis, R.A. Rastall, M.H. Gordon. *J Agr Food Chem*, 57 (2009) 4342-4351.
[5] Y. Kim, E. Ximenes, N. Mosier, M. Ladisch. Enzyme Microb Tech, 48 (2011) 408–415
[6] L. Laroze, C. Soto, M.E. Zúñiga, Electron J Biotechn,13 (2010) 6
[7] B.B Li, B. Smith, M.D.M. Hossain. *Sep Purif Technol*, 48 (2006)189-196.

[8] T. Maier, A. Göppert, D.R. Kammerer, A. Schieber, R. Carle. *Eur Food Res Technol*, 227 (2008) 267-275.
[9] M. Pinelo, B. Zornoza, A.S. Meyer. *Sep Purif Technol*, 63 (2008) 620-627.
[10] J.M. Ros, D. Saura, L. Coll, J. Laencina. Alimentación, Equipos y Tecnología 8(1992)127 –134.
[11] Ximenes, E., Kim, Y., Mosier, N., Dien, B., and Ladisch, M. Enzyme Microb Tech 48 (2011) 54–60.

ECAB 5
The 5th EUROPEAN CONGRESS OF APPLIED BIOTECHNOLOGY
Florence 15-19 September 2019

Effect of metabolite build-up on biofilms of succinic acid producing *Actinobacillus succinogenes*.

Sekgetho Charles Mokwatlo[1*], Hendrik Gideon Brink[1], Willie Nicol[1]

1 University of Pretoria; Department of Chemical Engineering, University of Pretoria, Private Bag X20, Hatfield, 0028, South Africa

**Corresponding author: u11119072@tuks.co.za*

Highlights

- Rapid biofilm formation was observed at low succinic acid concntrations.
- Biofilms were patchy at high succinic acid concentrations and struggled to grow.
- Biofilms developed at high SA concentrations were much less viable in comparison.

1. Introduction

The wild type bacterium *Actinobacillus succinogenes* requires no introduction as a promising biocatalyst for industrial biotechnological production of succinic acid—a reputable platform chemical [1]. Continuous fermentation of *A. succinogenes* unavoidably results in biofilm formation, leading to high cell densities responsible for high succinic acid titers and volumetric productivities reported in literature [2]. This study looked at the impact that acid metabolite build-up in the fermenter has on the overall biofilm development and its viability.

2. Methods

Actinobacillus succinogenes 130Z (DSM No. 22257; ATCC No. 55618) was grown on a glucose substrate in a novel continuous fermenter suitable for sterile and multiple biofilm sampling. Biofilm was cultivated on plastic coupons at both high (16 g L^{-1} succinic acid) and low metabolite (8.6 g L^{-1} succinic acid) build-up conditions by adjusting the fermenter dilution rate. Sampled coupons were stained with Baclight LIVE/DEAD bacterial viability (Thermo Fisher Scientific, USA) stains before acquiring multiple image z-stacks using a Zeiss LSM 880 laser scanning confocal microscope (Zeiss, Germany) at random locations on the coupons. Acquired image z-stacks were analysed using Comstat2 to calculate descriptive biofilm parameters for objective characterisation of the biofilm.

3. Results and discussion

Biofilm formation was rapid when cultivated under low succinic acid (SA) titres, contrary to high SA titre conditions where the biofilm struggled to grow. As such, complete surface coverage was achieved at low SA cultivation whereas a patchy biofilm structure resulted from growth at high SA titre conditions, Figure 1. Furthermore, quantitative analysis showed an average biomass thickness increase from 10 µm on the first day to 30 µm by the third day of sampling for low SA biofilm cultivation in comparison to a 12 µm - 15 µm increase for biofilms cultivated at high SA titres Figure 2b. In addition, elongated bacilli cells were observed at high SA titre biofilm cultivation which may possibly have been a response to stressful conditions, Figure 1b.

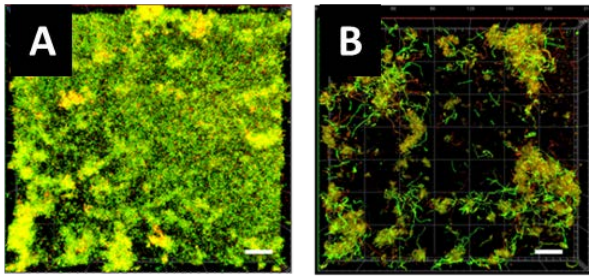

Figure 1. Biofilm images on day 1 of sampling for cultivation at low SA titers (A) and at high succinic acid titers (B). Scale bars indicates 20 µm.

A ratio (viability factor) of the mean intensity of the green fluorescence (for "live" cells) to the mean intensity of the red fluorescence (for "dead" cells) for all the z-stacks collected on a specific day of sampling was computed, which allowed an observation how the overall biofilm viability varied as the biofilm developed, Figure 2a. At low SA titres, the developed biofilm consisted of increasing "live" cells as shown by the increasing viability factor, whereas high SA titre biofilms became increasingly less viable, Figure 2a. The results thus showed that high SA acid titre conditions do not only slow down biofilm development but causes significant loss of biofilm viability.

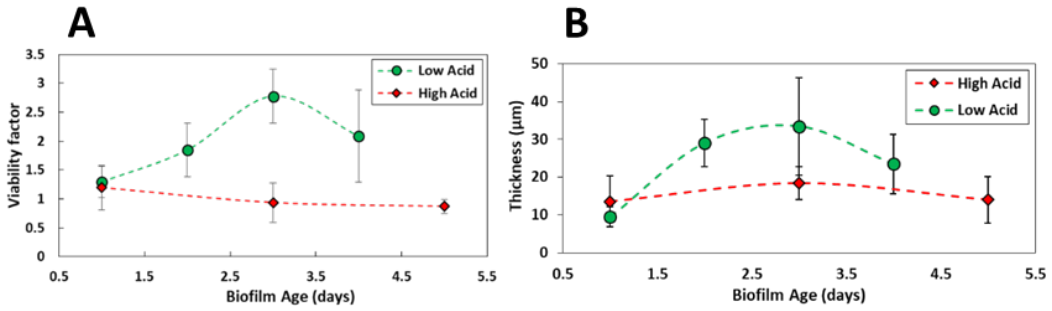

Figure 2. The viability profiles (A) and thickness profiles (B) of biofilms cultivated at both low and high SA acid concentrations.

4. Conclusions

Biofilms developed at both low and high SA titres were compared. High SA acid conditions slowed biofilm growth and resulted in a loss of biofilm viability whereas rapid biofilm growth was experienced at low SA titre conditions with increased biofilm viability.

References

[1] Pateraki C, Patsalou M, Vlysidis A, Kopsahelis N, Webb C, Koutinas AA and Koutinas M (2016) Actinobacillus succinogenes : Advances on succinic acid production and prospects for development of integrated biorefineries, Biochem. Eng. J. Elsevier B.V., 112, pp. 285–303. doi: 10.1016/j.bej.2016.04.005.

[2] Maharaj K, Bradfield MFA and Nicol W (2014) Succinic acid-producing biofilms of *Actinobacillus succinogenes*: Reproducibility, stability and productivity, Appl. Microbiol. Biotechnol., 98(17), pp. 7379–7386. doi: 10.1007/s00253-014-5779-3.

Rich-cheap-raw Inulin shows potential for glutathione production by engineered strain of *Yarrowia lipolytica*.

Diem T. H. Do, Sebastian Steel, Patrick Fickers

TERRA research and teaching center, MiPI, Gembloux Agro-Biotech, Liege University, Belgium

**Corresponding author: hoangdiemdtvn@gmail.com*

Highlights:

- Strong constitutive promoter TEF for overexpression of GSH1 and GSH2 genes.
- Overproduction of glutathione by yeast Yarrowia lipolytica
- Exploitation of alternative subtrates (Inulin)
- Strain can use inulin to produce more yield of glutathione

1. Introduction

The tripeptide glutathione (Gamma-L-Glutamyl-L-Cysteinylglycine) is the most abundant low-molecular-weight intracellular thiol. It plays important roles in cellular redox balance, nutrient metabolism and regulation of cellular mechanism. Glutathione, that could exist as a reduced (GSH) and oxidized (GSSG) state, is synthesised in a two step process. Firstly, glutamate and cysteine are ligated by an gamma-glutamylcysteine synthase (gamma-GCS, EC 6.3.2.2) encoded by GSH1 gene to form a L-gamma-glutamyl-L-cysteine. In a second step a L-gamma-glutamylcysteine-glycine gamma ligase (GS or GSH synthetase, EC 6.3.2.3) encoded by gene GSH2 link a glycin residue on the dipeptide. The yeast *Y. lipolytica*, considered as an emerging industrial chassis was used as a cell factory to produce glutathione from raw material

2. Methods

First, we overexpress GSH1 and GSH2 genes under the control of pTEF, a strong constitutive promoter. The most overexpressing strain was obtained for further manipulation. This yielded to a significant increase (69%) of glutathione production.

In a second step, we genetically adapt the producing strain to different cheap raw sugar-sources, including glycerol, inulin, lactose and starch. Among them, inulin revealed the most suited for glutathione synthesis. The production titre was increased by 61 % as compared to glucose media used as a reference.

3. Results and discussion

In this study, strong constitutive promoter pTEF were used to overexpress genes encoding the two enzymes (L-cysteine gamma-ligase and glutathione synthase) which catalyse the synthesis

of GSH in *Yarrowia lipolytica*. Several strains which can overexpress GSH1 or GSH2 or both of them have been successfully obtained. The newly constructed strains for glutathione overproduction show different comparing to control.

Following the successfulness of GSH-overexpressed genes, after removing leucine and uracil markers, this strain was used as a host for further modifications for exploiting cheap feedstock as main carbon source. We focused on glycerol (overexpression of GUT1 and GUT2 genes), lactose (overexpression of beta-galactosidase gene), starch (overexpression of alpha and gluco-amylase genes) and inulin (overexpression of inulinase encoding gene). Among those feedstocks, inulin yielded to higher amount of glutathione comparing to others.

4. Conclusion

The successful construction of strain that can consume cheap raw materials such as organic waste or by-products from other food processing sectors (cheese making, prebiotic producing, soap making and so on) and produce more glutathione, a higher value compounds have been achieved.

References

1. Anschau A, Santos L O, Alegre RM (2013) A Cost Effective Fermentative Production of Glutathione by Saccharomyces cerevisiae with Cane Molasses and Glycerol. Brazilian Archieves of Biology and Technology Vol.56, n.5: pp. 849-857 ISSN 1516-8913
2. Forman HJ, Zhang H, and Rinna A (2010) Glutathione: Overview of its protective roles, measurement, and biosynthesis. Published in final edited form as: Mol Aspects Med. 2009 ; 30(1-2): 1–12. doi:10.1016/j.mam.2008.08.006
3. Ledesma-Amaro R , Dulermo T, Nicaud JM (2015) Engineering Yarrowia lipolytica to produce biodiesel from raw starch. Biotechnol Biofuels (2015) 8:148, DOI 10.1186/s13068-015-0335-7
4. Liu XY, Chi Z, Liu GL, Wang F, Madzak C, Chi ZM (2010) Inulin hydrolysis and citric acid production from inulin using the surface-engineered Yarrowia lipolytica displaying inulinase. Metabolic Engineering 12 469–476, doi:10.1016/j.ymben.2010.04.004
5. Spagnuolo M, Hussain MS, Gambill L, Blenner M (2018) Alternative Substrate Metabolism in Yarrowia lipolytica. Frontier in Microbiology Volume 9 | Article 1077, doi: 10.3389/fmicb.2018.01077

ECAB 5
The 5th EUROPEAN CONGRESS OF APPLIED BIOTECHNOLOGY
Florence 15-19 September 2019

Modifying Biomaterials as Alternative Antibody Scaffold to Detect Breast Cancer Cells

Samar Damiati [1,2,*], Martin Peacock [3], Rami Mhanna [4], Sindre Søpstad [3,5], Uwe B. Sleytr [6], Bernhard Schuster [1]

1 Institute for Synthetic Bioarchitectures, Department of Nanobiotechnology, University of Natural Resources and Life Sciences (BOKU), Vienna, Austria
2 Department of Biochemistry, Faculty of Science, King Abdulaziz University (KAU), Jeddah, SA
3 Zimmer and Peacock Ltd, Royston SG8 9JL, UK
4 Biomedical Engineering Program, American University of Beirut, Beirut, Lebanon
5 Department of Microsystems, Faculty of Maritime and Natural Sciences, University College of Southeast Norway, Borre, Norway
6 Institute for Biophysics, Department of Nanobiotechnology, University of Natural Resources and Life Sciences (BOKU), Vienna, Austria
**Corresponding author: samar.damiati@gmx.us*

Highlights

- Development of an acoustic sensor to detect breast cancer cells (MCF-7).
- Folate-modified S-layer lattice as antibody-presenting biosensing matrix
- Highly expressed folate receptor on the cell membrane of some cancer cell lines.

1. Introduction

Designing an interface matrix with good biocompatibility for efficient detection of target cancer cells is a critical step in biosensor fabrication[1,2]. Antibody alternatives are attracting more attention to overcome limitations associated with antibody-based bioreceptors, such as high cost and density and orientation of the antibodies on the sensor surface. Exploiting biomaterials capable to present ligand molecules in an optimal density and orientation leads to the fabrication of biosensors with good selectivity and sensitivity. Excellent matrices are monomolecular arrays of protein subunits forming surface layers (S-layers), which are the common structure of the outer cell envelope on almost all archaea and many bacteria[3]. In this study, S-layer proteins were modified with folate to target the overexpressed folate receptors on breast cancer cells (MCF-7). Acoustic detection of MCF-7 was assessed using quartz crystal microbalance with dissipation (QCM-D) monitoring.

2. Methods

Folate was bound to the isolated S-layer protein SbpA from *Lysinibacillus sphaericus* CCM 2177[2]. The QCM-D measurements were run for modified SbpA and MCF-7 cells at 27 and 37 ± 0.02◦C, respectively. To evaluate the efficiency of the developed biosensor, suspensions of MCF-7 cells at different cell densities (1×10^4, 1×10^5, and 5×10^5 cells/mL) were exposed to the folate-modified S-layer lattice.

3. Results and discussion

The fabricated acoustic biosensor showed the efficient recognition of MCF-7 cells in situ and in real-time with a detection limit of 1 × 10^5 cells/mL. The direct recognition of MCF-7 cells on the developed QCM-D sensor was evaluated by monitoring the shifts in the frequency (ΔF) and dissipation (ΔD) (Figure 1). The obtained results revealed a strong shift in ΔF, which is due to the binding of the MCF-7 cells to the sensor surface. Moreover, the recognition of the folate presented on the S-layer lattice by the folate receptors of the MCF-7 cells correlated directly with the MCF-7 cell density. It is known that the cell capture efficiency remarkably increases when the sensing layer has low thickness. Besides the small thickness of the S-layer lattice nanostructure, functionalization with folate instead of adding an extra antibody layer reduces the thickness of the biosensing layer. Moreover, immobilization of antibodies in proper orientation is not a matter because folate was used as an antibody alternative to detect breast cancer cells. However, the nature of the sensor surface has highly affected the interaction between the functionalized sensor and MCF-7 as cell attachment was influenced by the hydrophilicity and wettability of the modified S-layer lattice.

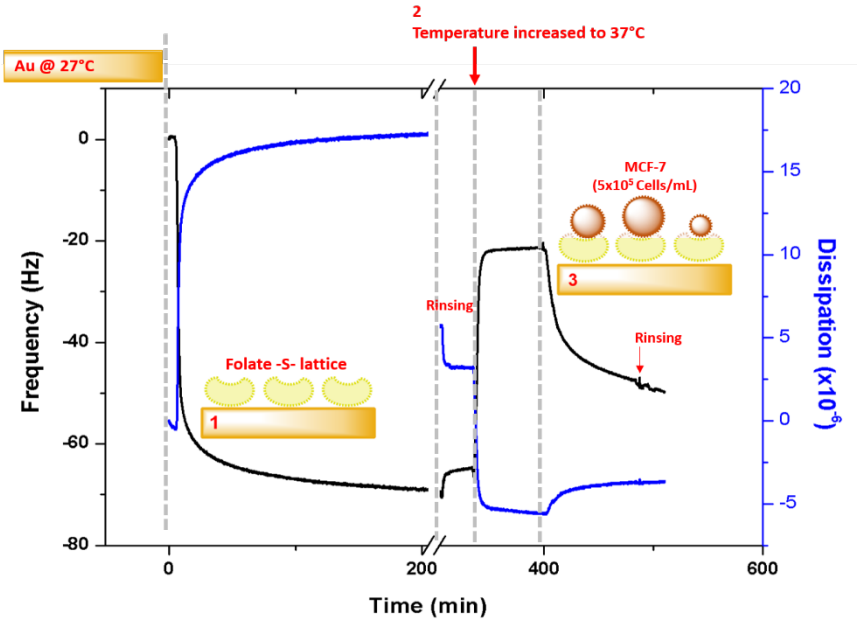

Figure 1. Development of folate-S-lattice platform and the subsequent capturing of MCF-7 cells on MCQ-D sensor.

4. Conclusions

A careful selection of biomaterials that can be assembled together to decorate sensor surfaces can improve the selectivity and sensitivity of diagnostic biosensors. S-layer proteins can be advantageous biomaterials due to their ability to self-assemble to form a nanostructure lattice, which can be easily functionalized with folate to develop functional sensors. The developed biosensor with the folate-modified S-layer lattice as alternative antibody scaffold exhibited well performance for breast cancer detection that can be exploited in future to test the cellular response to chemotherapeutic agents.

References

[1] B. Schuster. Biosensors 8 (2018) 40.
[2] S. Damiati, M. Peacock, R. Mhanna, S. Søpstad, U.B. Sleytr, B. Schuster. Sens. Actuator. B. 267 (2018) 224–230.
[3] U.B. Sleytr, B. Schuster, E. Egelseer, D. Pum. FEMS Microbiol. Rev. 38 (2014) 823–864.

Up-scale fractionation of phenolic compounds using centrifugal partition chromatography

Sónia Ventura[1], João Santos[1], Mafalda Almeida[1], Ana Dias[2], Mara Freire[1], João Coutinho[1]

1 CICECO, Departamento de Química, Universidade de Aveiro, 3810-193 Aveiro, Portugal

2 CESAM – Centre for Environmental and Marine Studies, Department of Environment and Planning, University of Aveiro, 3810-193 Aveiro, Portugal

**Corresponding author: spventura@ua.pt*

Highlights

- Phenolic compounds recognized as relevant building blocks.
- ABS were efficiently applied on their fractionation.
- CPC was efficiently applied on the scale-up of the process.

1. Introduction

Phenolic compounds are ubiquitous biomolecules exhibiting a wide range of physiological properties, with a wide range of different applications. In this work, aqueous biphasic systems (ABS) formed by polyethylene glycol and sodium polyacrylate, and electrolytes (inorganic salts or ionic liquids) were applied for the purification of caffeic, ferulic and protocatechuic acids, vanillin and syringaldehyde. The up-scale of the technology was assessed by successfully applying a centrifugal partition chromatography (CPC).

2. Methods

All materials and methods used are reported in detail in our previous work [1].

3. Results and discussion

Phenolic compounds are relevant biomass building blocks described by their many applications as the most versatile and important industrial organic chemicals. In this sense, these products are considered as economically attractive. In this work, polymer-based ABS (with PEG 8000 + NaPA 8000) using ionic liquids or inorganic salts as electrolytes, were studied in the separation of five model phenolic compounds (caffeic, ferulic and protocatechuic acids, and vanillin and syringaldehyde), all originated from lignocellulosic depolymerisation. The selection of the best ABS and its optimization was performed, followed by its application in CPC to reinforce the technique scale-up. After the development and characterization of the integrated process to fractionate the mixture of phenolic compounds, an environmental evaluation was done considering the carbon footprint as the main output. After the identification of the best ABS platform to separate each phenolic compound (PEG 8000/NaPA 8000/NaCl), its use in CPC followed. After optimizing the CPC operational conditions, it was also proved the success of the scale-up process, since, not only the results defined for the batch system were obtained but also the final process (Figure 1) developed

showed to be simultaneously efficient and of low carbon footprint (36% of carbon footprint reduction for the best scenario explored). In this context, high recovery values were obtained, respectively, 87%, 84% and 65% for caffeic, ferulic and protocatechuic acids, and 82% for the aldehyde-rich fraction (composed of vanillin and syringaldehyde).

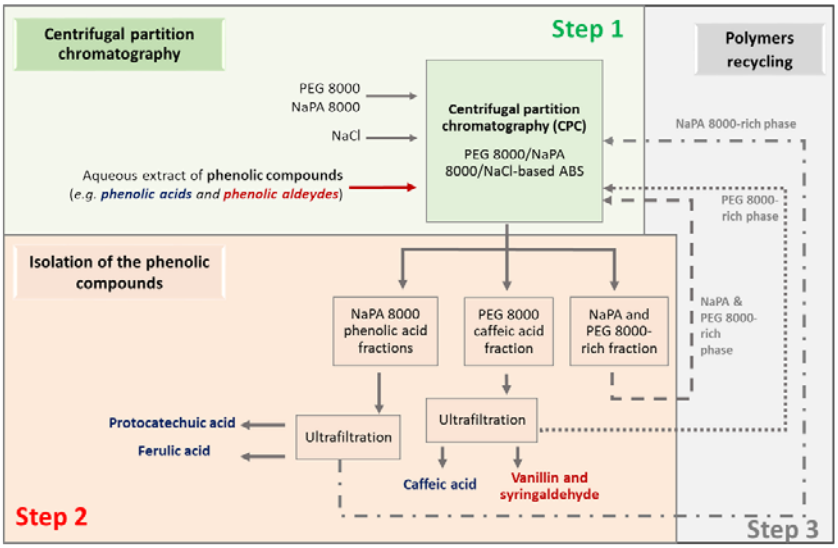

Figure 1. Schematic representation of the process developed. Adapted from [1].

4. Conclusions

An efficient and low carbon footprint up-scale process using CPC was successfully developed to separate phenolic compounds, showing its applicability for the processing of real matrices like agro-forestry and biomass wastes.

Acknowledgements:

This work was developed within the scope of the project CICECO-Aveiro Institute of Materials, FCT Ref. UID/CTM/50011/2019, financed by national funds through the FCT/MCTES. The authors are grateful for the financial support of the FCT for the doctoral grant of SFRH/BD/102915/2014 of J.H.P.M. Santos. S.P.M. Ventura acknowledges for contract IF/00402/2015. M. G. F. acknowledges the European Research Council (ERC) for the grant ERC-2013-StG-337753. The authors acknowledge the FCT funding through the project “Multipurpose strategies for broadband agro-forest and fisheries byproducts valorisation: a step forward for a truly integrated biorefinery (PAC – Programa de atividades Conjuntas) ref: SAICTPAC/0040/2015. A.C.R.V. Dias acknowledges FCT/MCTES for a contract under Investigador FCT 2013 contract number IF/00587/2013, and for the financial support to CESAM (UID/AMB/50017/2019), through national funds, and the cofunding by FEDER, within the PT2020 Partnership Agreement and Compete 2020.

References

[1] J.H.P.M. Santos, M.R. Almeida, C.I.R. Martins, A.C.R.V. Dias, M.G. Freire, J.A.P. Coutinho, S.P.M. Ventura, Green Chem. 20 (2018) 1906-1916.

Study of differential gene expression profile of *E. coli* growing in glucose and acetate.

Gema Lozano Terol[1], Julia Gallego-Jara[1], Ana Écija-Conesa[1], Manuel Cánovas Díaz[1] and Teresa de Diego[1].

1 Department of Biochemistry and Molecular Biology (B) and Immunology, Faculty of Chemistry, University of Murcia, Campus of Espinardo, Regional Campus of International Excellence ''Campus Mare Nostrum'', P.O. Box 4021, Murcia E-30100, Spain

**Corresponding author: gema.lozano@um.es*

Highlights

- The gene expression profile exhibited great differences between both conditions.
- An increment in gene expression under acetate growth was observed.
- EutD and PrcP could be part of the underground metabolism through alternative enzymatic activities.

1. Introduction

Escherichia coli (*E. coli*) metabolism carbon fluxes are an important factor to take into account, since this bacteria is widely employed as a model organism in industrial and biotechnological processes. In this sense, *E. coli* can metabolize diverse carbon sources such as acetate, which is a poor carbon source, or glucose. Under glucose limitation conditions, *E. coli* develops carbon stress responses [1], so this bacteria exhibits an expansion in gene expression [2], the emergence of new pathways and alternative enzymatic activities. Thereby, diverse activities and new pathways could be part of underground reactions which may be connected to the existing network, increasing the potential of employing diverse and new carbon sources [3].

2. Methods

In this work, a gene expression study through a streptavidin-biotin-based microarray assay has been carried out to know the differences between the genetic global expression in *E. coli* K12 MG1655 growing in minimal medium M9 supplemented with glucose or acetate as carbon source. High density arrays "GeneChip E. coli Genome 2.0 Arrays" (P / N 900550, Affymetrix, Incorporated) were used

3. Results and discussion

The transcription profiles of *E. coli* K12 MG1655 growing in acetate supplemented medium exhibited great differences in gene expression respect to the strain growing in glucose supplemented medium. This behavior may be attributable to the increase in the number of genes expressed which allow a large scale carbon-scavenging to metabolize “low quality” carbon source [2]. The adaptation process may involve a refined regulatory response to only activate genes of acetate metabolism (*acs*, *ackA*, *actP*), but we observed an increment in the expression of genes, which belong to other pathways, such as the glyoxylate shunt, methylglyoxylate shunt, TCA cycle,

and gluconeogenic flux, suggesting that these pathways are at least partially controlled at the transcriptional level. Furthermore, *eutD* and *prcP* genes were overexpressed in acetate growing. These two genes belong to the ethanolamine and propionate metabolism, respectively, so in acetate growing EutD and PrcP must present other alternative enzymatic activities and could be part of the underground metabolism reactions.

4. Conclusions

The gene expression change in acetate compared to glucose was used to assess the metabolic flux distribution in key pathways. Furthermore, the results suggest difficulties to identify adaptive mechanisms only through examination of expression changes, since there are other mechanisms that regulate metabolism, such as post-translational regulation, enzyme kinetics and allosteric control.

References [Calibri 10]

[1] Martínez-Gómez, K. *et al.* New insights into *Escherichia coli* metabolism: carbon scavenging, acetate metabolism and carbon recycling responses during growth on glycerol. *Microb. Cell Fact.* **11,** 1–21 (2012).

[2] Blattner, F. R. *et al.* Global Transcriptional Programs Reveal a Carbon Source Foraging Strategy by *Escherichia coli*. *J. Biol. Chem.* **280,** 15921–15927 (2005).

[3] Kintses, B. *et al.* Network-level architecture and the evolutionary potential of underground metabolism. *Proc. Natl. Acad. Sci.* **111,** 11762–11767 (2014).

ECAB 5
The 5th EUROPEAN CONGRESS OF APPLIED BIOTECHNOLOGY
Florence 15-19 September 2019

ANN training with a generative *in silico* model for PAT in the biopharmaceutical DSP.

Matthias Rüdt[1], Jürgen Hubbuch[1,*]

[1] *Karlsruhe Institute of Technology (KIT), Institute of Engineering in Life Sciences, Section IV: Biomolecular Separation Engineering, Fritz-Haber-Weg 2, 76131 Karlsruhe, Germany*

**Corresponding author: juergen.hubbuch@kit.edu*

Highlights

- ANN applied to chromatography in the biopharmaceutical DSP.
- ANN training based on a generative *in silico* model.
- The calibration approach is versatile and scalable.
- RMSEPs compared to a standard PLS could be reduced by 14% to 40%.

1. Introduction

Biopharmaceutics are the fastest growing sector of the modern pharmaceutical industry. Nowadays, seven out of the ten most valuable pharmaceutical products are biopharmaceutics [1]. During the downstream processing (DSP) of biopharmaceuticals, chromatography is the main workhorse. While in production mainly univariate signals are used to monitor chromatographic steps, recently the benefits of multivariate spectroscopic methods for process monitoring have been demonstrated [2]. Data analysis was up to now mostly limited to linear methods such as partial least-squares (PLS) models. Machine learning provides much more powerful methods such as artificial neural networks (ANN). However, ANNs generally need a vast amount of data to be reliably calibrated. In wet lab experiments, this amount of data is difficult to obtain. To circumvent this problem, we developed an approach relying on a generative model to yield artificial process sensor data and the corresponding reference concentrations. Based on this data, the ANN could be successfully trained.

2. Methods

Experimental data from a publication by Brestrich et al. [3] were used in this study. Briefly, preparative chromatography experiments were performed on an Äkta Purifier 10 system (GE Healthcare, Chalfont St. Giles, UK) equipped with a diode array detector (optical pathlength 0.4mm) UltiMate 3000 DAD (Thermo Fisher Scientific, Waltham, US) with a HiTrap 7x25 mm column prepacked with SP Sepharose FF (both GE Healthcare). Experiments were performed for a ternary separation of ribonuclease A, cytochrome c and lysozyme (all Sigma Aldrich, St. Louis, US). Chromatographic separations were modeled with ChromX (GoSilico GmbH, Karlsruhe, Germany).

For generating the *in silico* dataset, first, the mechanistic chromatography model was calibrated based on multiple calibration runs. Simultaneously, a database for spectroscopic data including the relevant reference analytics was established. Next, the design space of the process was randomly sampled yielding 10,000 process chromatograms with simulated concentration traces resulting in

780,000 concentration vectors. For each concentration vector, the database was sampled for the nearest neighbors (Euclidean-distance). Scaled sensor responses were then obtained by multiple linear regression and subsequent matrix multiplication of concentration vectors and spectral matrices. On the obtained dataset, ANNs with different geometries were calibrated with the ANN framework Keras [4]. The regression models were tested on an independent chromatography run.

3. Results and discussion

A workflow was established for calibrating ANNs based on generative approach consisting of a mechanistic chromatography model and a spectral database. The generative approach allows to easily scale the calibration dataset. It thus circumvents some of the issues of using ANNs for process data. Most importantly, overfitting ANNs is reduced. A further benefit of the established workflow is the easy scalability of the spectral database. Thus, the database can easily be extended without significantly complicating calculations. Finally, the workflow captures non-linearities in the sensor response due to the local linear regression.

Based on the generated *in silico* data, two ANNs were calibrated. While a classical (dense) ANN geometry was on par with a reference PLS model, a convolutional ANN surpassed the PLS model in all calculated root mean squared error of calibration (RMSEC) and prediction (RMSEP, see Table 1). The results demonstrate the potential that lies in the application of more complex regression models compared to PLS.

Table 1. Results from the different calibrated models. Best results in each column are underlined.

	Ribonuclease A		Cytochrome c		Lysozyme	
	RMSEC / (g/L)	**RMSEP / (g/L)**	**RMSEC / (g/L)**	**RMSEP / (g/L)**	**RMSEC / (g/L)**	**RMSEP / (g/L)**
PLS	0.0126	0.0149	0.0135	0.0098	0.0132	0.0116
Classical ANN	0.0176	0.0150	0.0122	0.0096	0.0140	0.0108
Convolutional ANN	0.0090	0.0130	0.0065	0.0059	0.0084	0.0073

4. Conclusions

We investigated on a generative *in silico* approach to calibrate ANNs for PAT applications. A workflow was established involving the calibration of a mechanistic model, spectroscopic database establishment, Monte-Carlo-based process sampling, spectra generation, and ANN model calibration. Based on the proposed approach, a convoluational ANN performed 15% to 40% better on an independent chromatography experiment compared to a standard PLS model. The results demonstrate significant potential of the generative approach to ANN calibration.

References

[1] Njardarson JT. Top 200 Pharmaceutical Products by Retail Sales 2018. 2018.

[2] Rüdt M, Briskot T, Hubbuch J. Advances in downstream processing of biologics – Spectroscopy: An emerging process analytical technology. J Chrom A 2017; 1490:2–9.

[3] Brestrich N, Hahn T, Hubbuch J. Application of spectral deconvolution and inverse mechanistic modelling as a tool for root cause investigation in protein chromatography. J Chrom A 2016; 1437:158–67.

[4] Chollet F and others. Keras. 2015. https://keras.io.

Design of a single step chromatographic strategy for the isolation of the cancer-associated antigen STEAP1

Jorge Barroca-Ferreira[1,2], Sandra Rocha[1], Teresa Santos-Silva[2], Cláudio Maia[1], Luís Passarinha[1,2*]

1 CICS-UBI - Health Sciences Research Centre, Faculty of Health Sciences of the University of Beira Interior, Portugal; 2 UCIBIO - Applied Molecular Biosciences Unit, Faculty of Sciences and Technology of the Nova University of Lisbon, Portugal.

**lpassarinha@fcsaude.ubi.pt*

Highlights

- The extraction of STEAP1 was optimized to increase the concentration of total protein.
- A reproducible strategy for STEAP1 isolation and buffers composition were established.
- STEAP1 was isolated by HIC in a single step and co-eluted with residual of contaminants.

1. Introduction

The Six-Transmembrane Epithelial Antigen of the Prostate 1 (STEAP1) is a cell-surface antigen overexpressed in several types of cancer, namely in prostate cancer [1]. In normal cells the levels of STEAP1 are low or absent [1, 2]. Considering its secondary structure and location in the cell membrane, it has been suggested a role in intercellular communication between tumor cells [2, 3]. These features highlight STEAP1 as a promising therapeutic target. The main goal of this work is to express high levels of STEAP1 protein from LNCaP cells and isolate the target protein in a native form by traditional hydrophobic interaction matrices.

2. Methods

LNCaP cells were maintained in a humidified chamber with controlled atmosphere until 90-100% confluence. These cells were lysed onto RIPA buffer or an in-house buffer for nuclear and cytosolic extraction of proteins. This procedure was fully optimized regarding the volume of buffers and the concentration of proteins to further enhance the yield of the isolation process and immunoblot experiments. Total protein samples were loaded onto a butyl sepharose column and the manipulation of ionic strength was used to promote a complete retention of proteins to the matrix and a selective fractionation of impurities. The purification step was monitored by SDS-PAGE and STEAP1 was detected in dot-blot analysis or a single band in western blot with approximately 39 KDa [1]. Mass spectrometry was also used to confirm the identity of the target protein. Lastly, circular dichroism was used to infer if the concentration of ammonium sulphate effectively influences the arrangement of secondary structure of STEAP1 or promote interactions between the target protein and unspecific compounds.

3. Results and discussion

Once STEAP1 is overexpressed in LNCaP, we extracted total protein and also both cytosolic and nuclear fractions. The western blot analysis showed an increased expression of STEAP1 in cytosolic fraction, with similar levels to total protein extracts. These aliquots were applied in the chromatographic studies. The main results demonstrated that STEAP1 was fully captured in butyl sepharose matrix since the concentration of ammonium sulphate in the binding buffer was 1500 mM and 2000 mM. However, the elution profile denoted low selectivity, once STEAP1 was detected at similar levels in distinct steps of the elution salt gradient, namely 10 mM Tris-HCl and H_2O. Likewise, these samples presented a considerable background of impurities that co-elute with the target protein. Interestingly, STEAP1 was not retained at 1000 mM and 1250 mM of salt. This result could be explained considering the presence of a non-ionic detergent in the lysis buffer which condition the exposure of the hydrophobic domains of the predictive six-transmembrane structure of STEAP1. This phenomenon clearly affected the interaction of the target protein with the chromatographic matrix and explains the reason behind the significant retention of several impurities at lower concentrations of ammonium sulphate. Otherwise, as the salt concentration in the binding buffer increases, the interactions between STEAP1 and butyl sepharose are consequently promoted. Nevertheless, these findings were valuable because it was conceivable to isolate STEAP1 in a single chromatographic step with residual amount of interfering biomolecules.

4. Conclusions

This work established for the first time a reproducible chromatographic procedure for the isolation of human STEAP1 with high expression levels and significant grade of purity. These optimized conditions will allow that samples containing the target protein may be further used for a detailed biochemical and structural characterization of STEAP1 and later development of molecules that were able to block its oncogenic functions.

References

[1] R.S. Hubert, I. Vivanco, E. Chen, S. Rastegar, K. Leong, S.C. Mitchell, R. Madraswala, Y. Zhou, J. Kuo, A.B. Raitano. Proc. Natl. Acad. Sci. 96 (1999) 14523-14528.

[2] J. Barroca-Ferreira, J.P. Pais, M.M. Santos, A.M. Gonçalves, I.M. Gomes, I. Sousa, S.M. Rocha, L.A. Passarinha, C.J. Maia. Curr. Cancer Drug Targets. 18 (2018) 222-230.

[3] T. Yamamoto, Y. Tamura, J.I. Kobayashi, K. Kamiguchi, Y. Hirohashi, A. Miyazaki, T. Torigoe, H. Asanuma, H. Hiratsuke, N. Sato. Exp. Cell. Res. 319 (2013) 2617-2626.

The Metagenomics Analysis of Two Waste Mine Ponds from Turkey.

Ahmet Çabuk[1*], Belma Nural Yaman[2], Serap Gedikli[1], Pınar Aytar Çelik[3], Ferhan Korkmaz[1], Mehmet Burçin Mutlu[4]

[1]Department of Biology, Eskişehir Osmangazi University, Turkey; [2]Department of Biomedical Engineering, Eskişehir Osmangazi University, Turkey; [3]Department of Biotechnology and Biosafety, Eskişehir Osmangazi University, Turkey; [4]Department of Biology, Eskişehir Technical University, Turkey

**Corresponding author: ahmetcabuk@gmail.com*

Highlights

- High boron concentrations
- Microbial diversity
- Metagenomics approach
- Bioinformatic analysis
- Environmental biotechnology potential

1. Introduction

Boron can be directly and indirectly involved in different functions and mechanisms in many different organisms. There is some information about this area in literature [1, 2, 3, 4]. Moreover, boron may be toxic to living cell at high concentration [5]. However, some special microorganisms can easily survive in regions with high boron concentrations and these microbes have potential at environmental biotechnology field [6, 7, 8]. Researchers are interested in microorganisms living in high boron content because of their metabolic characteristics. Classical microbiological cultural techniques are not always useful to determinate of microbial species in extreme conditions due to their extreme characteristics and there is no study about specifying microbial diversity by molecular techniques. Therefore, in this study, metagenomics approach as next generation sequencing was used to present of microbial community in area with high concentration boron.

2. Methods

Two different environmental water samples were taken from two places with boron contaminated field in Balıkesir-Bigadiç and Eskişehir-Kırka Works. Metal contents of these samples were determined. The experimental studies were started with the total DNA extraction and metagenomics analysis method was performed. 16S amplicon sequencing in Illumina Miseq Platform was practiced to keep all of microorganisms survive in sampling areas. Metadata of microorganisms was analyzed bioinformatically by QIIME 1.

3. Results and discussion

According to chemical analysis; B, Li, Na, S and Sr contents in Kırka samples were found higher than water samples of Bigadiç. Metagenomics data is shown in Table 1.

Table 1. Dominant genera in sampling areas

Sampling area	Dominant genera
K1 (Kırka boron mine drainage, station 1)	*Rhodobaca, Gloeobacter, Luteolibacter, Fluviicola, Verrumicrobium, Bacteriovorax*
K2 (Kırka boron mine drainage, station 2)	*Rhodobaca, Gloeobacter, Luteolibacter, Verrumicrobium*
B1 (Bigadiç boron mine drainage, station 1)	*Pseudanabaena, Gloeobacter, Hyphomonas, Algoriphagus, Rhodobacter, Anaerospora*
B2 (Bigadiç boron mine drainage, station 2)	*Rhodobacter, Hydrogenophaga, Roseococcus, Anaerospora*

4. Conclusions

This study will provide information about inhabiting microorganisms which are able to tolerate high boron. In future studies, these organisms can be used for environmental biotechnology field.

References

[1] G.R. Anderson and J.V. Jordon, Soil Science. 92 (1961)113-116.
[2] X. Chen, S. Schauder, N. Potier, A. Van Dorsselaer, I. Pelczer, B.L. Bassler, F.M. Hughson. Nature. 415 (2002) 545-549.
[3] V.M. Dembitsky, R. Smoum, A.A. Al-Quntar, H. Abu Ali, I. Pergament, M. Srebnik, Plant Science. 163 (2002) 931-942.
[4] A.C. Negrete-Raymond, B. Weder, Wackett, Appl Environ Microbiol, 69 (2003) 4263-4267.
[5] F. Korkmaz, G. Deniz Sönmez, P. Aytar Çelik, M.B. Mutlu, A. Çabuk, Water and Environment Journal, 32 (2017) 250–258.
[6] I. Ahmed, A. Yokota, T. Fujiwara, Int. J. Syst. Evol. Microbiol., 57 (2007a) 986-992.
[7] I. Ahmed, A. Yokota, T. Fujiwara, Int. J. Syst. Evol. Microbiol., 57 (2007b) 796-802.
[8] H. Miwa and T. Fujiwara, Soil Science and Plant Nutrition, 55 (2009) 643- 646.

Acknowledgments

This study was supported by Eskişehir Osmangazi University Scientific Research Project Committee (Project No: 2018/2262). Belma NURAL YAMAN is supported by TUBITAK-BIDEB 2228-B National Scholarship Programme for PhD Students.

ECAB 5
The 5th EUROPEAN CONGRESS OF APPLIED BIOTECHNOLOGY
Florence 15-19 September 2019

Biological hydrogen production by *Rhodopseudomonas palustris*: comparison of a packed bed and fluidised bed photobioreactor systems.

Brandon Ross[1], Robert Pott[1] *

1 Department of Process Engineering, Stellenbosch University, South Africa

**Corresponding author:* rpott@sun.ac.za

Highlights

- *R. palustris* used in the photobioreactor systems is immobilised in a transparent PVA cryogel
- A packed bed bioreactor and a fluidised bed bioreactor will be compared based on specific hydrogen production
- It is expected that the fluidised bed will outperform the packed bed.

1. Introduction

Biological hydrogen production is a promising replacement for the current modes of hydrogen production seen in industry today. However, key issues with the process still need to be solved before such processes can be scaled up to industrial levels. The use of photosynthetic bacteria such as *Rhodopseudomonas palustris* to produce hydrogen has shown to have a low environmental impact but the required energy input is greater than the energy derived from the hydrogen produced. Therefore, to increase the efficiency of the biohydrogen production process the ratio of energy consumed to energy produced must be improved.

The scalability of processes using photosynthetic bacteria to produce biohydrogen relies on the optimisation of the process parameters, of which the immobilisation of the photosynthetic bacteria in a poly vinyl-alcohol (PVA) based hydrogel by entrapment has been identified as covering several of these key areas. These areas include but are not limited to: i) protection from physio-chemical challenges, ii) cryptic growth, iii) higher biomass concentration than in planktonic systems, iv) reduced number of cell divisions resulting in metabolic energy being focused on product formation [2].

The immobilisation of such bacteria then raises the question, what bioreactor configuration suites photosynthetic biohydrogen production when using immobilised bacteria. Not many configurations have been proposed, let alone investigated, for the use of immobilised photosynthetic bacteria due to most immobilisation matrices being opaque. Thus, two reactor systems were designed to investigate the hydrogen production performance, namely a packed bed photobioreactor (PBPBR) and a fluidised bed photobioreactor (FBPBR).

2. Methods

R. palustris was immobilised in transparent PVA cryogel where the PVA solution was 10% (w/v) PVA dissolved in a 50% (v/v) glycerol-water solution. The PBPBR and FBPBR were designed to allow the synthetic waste stream to pass through the bed of immobilsed bacteria with a 100% recycle stream to operate as a batch system with all hydrogen produced collected off the headspace of the

photobioreactors. The Hydrogen production by immobilised *R. palustris* was compared to planktonic cultures in the same photobioreactor system.

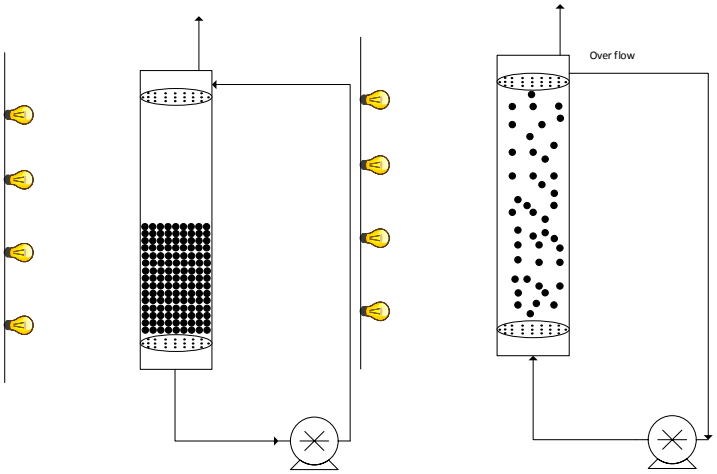

Figure 1. PBPBR and FBPBR experimental setup

3. Results and discussion

It is anticipated that the fluidised bed photobioreactor will outperform the packed bed photobioreactor with respect to the specific hydrogen production (specific in terms of both biomass loading and volume of the reactor). This is due to the motion of the fluidised bed increasing the amount of light that each PVA cryogel bead that contains the immobilised bacteria receives. Full results will be available from the 30th of May 2019.

4. Conclusions

We present a proven design for photobioreactors that can be used in conjunction with transparent immobilised *R. palustris*. Preliminary studies with planktonic media in the photobioreactors proved the viability of the system with regards to production and collection of biohydrogen. Further conclusions with regards to the hydrogen production in the PBPBR and the FBPBR will be drawn once all results have been obtained.

References [Calibri 10]

[1] A. Adessi and R. De Philippis, 'Photobioreactor design and illumination systems for H2 production with anoxygenic photosynthetic bacteria: A review', *International Journal of Hydrogen Energy. Elsevier Ltd*, 39(7), pp. 3127–3141. doi: 10.1016/j.ijhydene.2013.12.084. 2014.

[2] G. A. Dervakos and C. Webb, 'On the merits of viable-cell immobilisation', *Biotechnology Advances*, vol. 9, no. 4, pp. 559–612, Jan. 1991.

X-Ray Tomography evaluation of Microbially Induced Calcite Precipitation (MICP) in mortar cubes

Diana Tamayo-Figueroa[1*], Henry Omar-Meneses[2], Pedro Brandão[3]

1 Doctorado Biotecnología, Instituto de Biotecnología (IBUN), Facultad de Ciencias, Universidad Nacional de Colombia, Bogotá, Colombia; 2 Clínica para Pequeños Animales, Departamento de Salud Animal, Facultad de Medicina, Veterinaria y Zootectnia , Universidad Nacional de Colombia, Bogotá, Colombia; 3 Grupo de Estudios para la Remediación y Mitigación de Impactos Negativos al Ambiente (G.E.R.M.I.N.A.), Laboratorio de Microbiología Ambiental y Aplicada, Departamento de Química, Facultad de Ciencias, Universidad Nacional de Colombia, Bogotá, Colombia.

**Corresponding author: dptamayof@unal.edu.co*

Highlights

- A non-destructive methodology to follow crack repair by MICP is reported.
- MICP treatment showed a higher $CaCO_3$ filling effect when compared to control.
- MICP activity allowed 18-27% of $CaCO_3$ filling of mortar cube holes after 9 weeks.

1. Introduction

Cement based materials are widely used for construction but their durability is affected by cracking, a common phenomenon in this type of materials [1]. The use of microorganisms that induce calcite (calcium carbonate) precipitation (MICP) has been proposed as an alternative crack repair technology [2]. In this process microbial metabolism increases environmental alkalinity that favours $CaCO_3$ precipitation [3]. This phenomenon is an extremely strain-specific (bio)chemical reaction and depends on urease diversity, ion strength, cell density, and medium pH [4]. Current methodologies used to track crack repairs do not provide a clear picture of the system behaviour while the repair occurs, especially in internal cracks, and usually it is necessary to destroy test specimens. This work reports the use of X-ray tomography to evaluate calcium carbonate filling of different size holes in mortar cubes, due to crystals precipitation by *Arthrobacter crystallopoietes* KNUC403, a bacteria previously isolated from a concrete structure [5].

2. Methods

Mortar cubes: For each treatment, a standard mortar mixture was prepared. A ratio of 1:2.75 (cement:sand) was used maintaining a water:cement ratio of 0.52. Curing time was 7 d. Four holes with different diameter sizes (in cm: 0.476, 0.635, 0.794, and 0.952) were made in the mortar cubes. Three replicas were made for each hole size.

Biological treatment of mortar cubes: Two treatments with (B) or without cells (C) were carried out to assess $CaCO_3$ production by *A. crystallopoietes* KNUC403 using X-ray tomography. Treatment B consisted in the addition of bacterial biomass + Urea-$Ca(NO_3)_2$ media to each hole, while control treatment C consisted in the addition of Urea-$Ca(NO_3)_2$ only to each hole. The addition of culture medium, with or without microorganisms, to the mortar cubes was performed every seven days. The mortar cubes were incubated at 30 °C.

X-ray tomography analysis: Mortar cubes holes depth variation was evaluated regularly in a Philips Helical tomograph (Tmoscan AV) by simple cuts with 2 mm thickness, a tube rotation of 2 s, a kilovoltage at 120 Kv, 140 MA, a window level of 3500 and a window width of 1100.

3. Results and discussion

X-ray tomography allowed to monitor the difference in the mortar cubes hole filling processes between treatments, a situation related to the production of $CaCO_3$ by MICP. This technique allowed to measure the change in the holes depth without destroying the sample or altering its mechanical properties (Figure 1), which could be useful to track the repair of material failures. After 9 weeks, the calcium carbonate filling percentage of the different hole sizes evaluated showed differences between the two treatments (Table 1). It is evident that after the experimental time period treatment B showed filling values between 18 and 27% compared to control treatment C with values lower than 8%, reaffirming the feasibility of using X-ray tomography as a strategy to monitor and control crack repair in cement-based materials. The fact that the filling percentage for the different hole sizes is similar for treatment B suggests that microbial behaviour has been affected by the available oxygen, a factor that may influence the amount of precipitated $CaCO_3$. This should be addressed in future studies. Mechanical and permeability tests will be performed to the mortar cubes of both treatments when a filling percentage close to 50% is obtained.

Figure 1. Image obtained by X-ray tomography showing the measurements of width and depth of different holes in mortar cube. Hole diameter sizes: 1 - 0.476 cm; 2 - 0.635 cm; 3 - 0.794 cm; 4 - 0.952 cm.

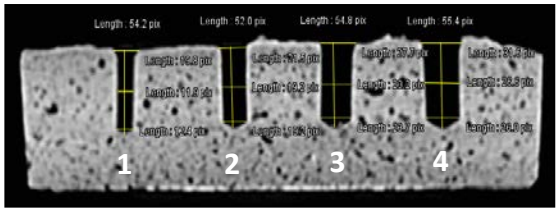

Table 1. Calcium carbonate filling percentage of four different hole sizes in mortar cubes without (C) or with (B) bacterial (*A. crystallopoietes* KNUC403) biomass treatment, after 9 weeks of incubation. Hole diameter sizes: 1 - 0.476 cm; 2 - 0.635 cm; 3 - 0.794 cm; 4 - 0.952 cm.

Hole size	Treatment C [Urea-$Ca(NO_3)_2$ media only]	Treatment B [*A. crystallopoietes KNUC403* + Urea-$Ca(NO_3)_2$ media]
1	2,31%	19,95%
2	3,73%	18,29%
3	2,33%	27,37%
4	7,91%	19,36%

4. Conclusions

X-ray tomography showed a positive effect of using *A. crystallopoietes* KNUC403 on the $CaCO_3$ filling of holes in mortar cubes as compared to control without cells. The technique allows to track the filling of holes in cement-based materials without the need to alter the mechanical properties of the material. This permits to follow-up the repair of superficial and internal cracks on this type of materials using MICP.

References

[1] American Concrete Institute. Control of cracking in concrete: state of the art. Technical document 2006.
[2] W. De Muynck, D. Debrouwer, N. De Belie, W. Verstraete, Cement Concrete Res. 38 (2008) 1005–1014.
[3] W. De Muynck, N. De Belie, W. Verstraete, Ecol. Eng. 36 (2010) 118–136.
[4] F. Hammes, N. Boon, J. de Villiers, W. Verstraete, S.D. Siciliano, Appl. Environ. Microbiol. 69 (2003) 4901–4909.
[5] S.J. Park, Y.M. Park, W.Y. Chun, W.J. Kim, S.Y. Ghim, J. Microbiol. Biotechnol. 20 (2010) 782–788.

ECAB 5
The 5th EUROPEAN CONGRESS OF APPLIED BIOTECHNOLOGY
Florence 15-19 September 2019

Single cell mass spectrometry:

Measuring productivities of microbes, one cell at a time

Christian Dusny[1,*], Martin Schirmer[1] and Andreas Schmid[1]

1 Helmholtz-Centre for Environmental Research, UFZ, Leipzig – Permoserstr. 15, 04318 Leipzig

**Corresponding author: christian.dusny@ufz.de*

Highlights

- Quantitative and label-free analysis of single, living microbial cells via MS
- Determination of uptake and production rates of single cells

1. Introduction

Microbial cells can be used as biocatalysts for complex syntheses of chemicals and energy carriers at physiological conditions and with high efficiency. Although microbial cells have been applied for thousands of years for the production of value-added compounds, there is still little quantitative knowledge about the contribution of the minimal catalytic unit, the single cell, to the macroscopic output of bioprocesses.[1] Up to now, mainly optical analyses have been applied for disclosing a remarkable heterogeneity in cellular features like gene expression, regulatory mechanisms or growth.[2,3] However, absolute numbers on uptake and production rates in single cells are inexistent.[4]

We demonstrate how the label-free quantification of catalytic performance in single cells can be

2. Methods

We applied chip-coupled microfluidics (negative dielectrophoresis cell traps and microdroplets) for analyzing the production of L-lysine by *Corynebacterium glutamicum* via mass spectrometry.

3. Results and discussion

achieved with chip-coupled mass spectrometry.[5] The presented approaches are capable of directly resolving catalytic heterogeneities. This knowledge is key for understanding and improving the efficiency of bioprocesses.

With microfluidic cultivation formats, such as the Envirostat or microdroplets, single cells are isolated and trapped under defined extracellular reaction conditions.[6] By interfacing microfluidic reactor formats with high-sensitivity mass spectrometry, the quantitative analysis of molecules produced by single cells is now possible for the first time. The concept is demonstrated with L-lysine-producing single cells of *Corynebacterium glutamicum*.

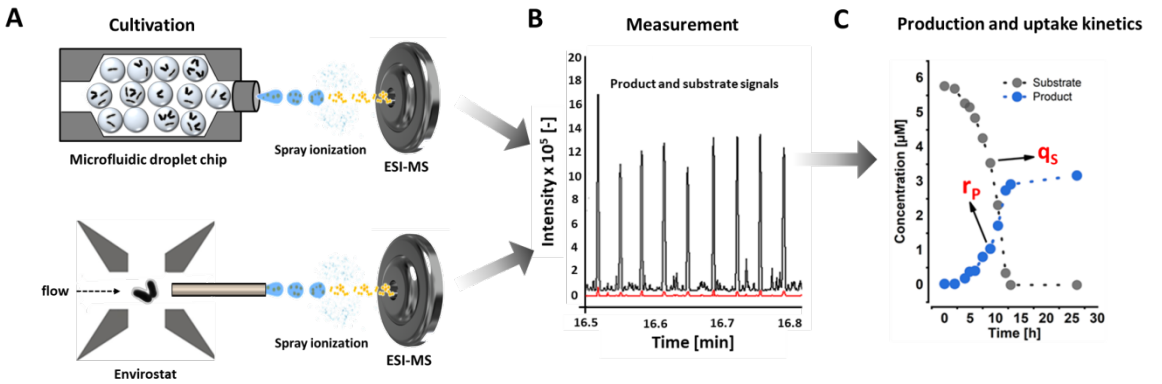

Figure 1. Cultivation and measurement of substrate and product concentrations in microfluidic cultivation setups. A) On-chip cell encapsulation in droplets and deterministic trapping of single cells and small co-cultures with the Envirostat. The analytes in the aqueous medium are ionized via ESI and transferred to the MS. B) Substrate and product concentrations are quantified with isotopically-labelled standards spiked the cultivation media. C) From the uptake and production profiles, production kinetics r_P and uptake kinetics q_S of single cells and small populations are determined.

4. Conclusions

Our approach enables the characterization of the catalytic structure of microbial populations based on single cell activity data and opens the door towards novel approaches for population modeling and improving biocatalytic processes.

References

[1] K. Rosenthal; V. Oehling; C. Dusny; A. Schmid, FEMS Microbiol. Rev. 2017, 41 (6), 751-780.
[2.] F. Delvigne; P. Goffin, Biotechnol. J. 2014, 9 (1), 61-72.
[3] S. Muller; H. Harms; T. Bley, Curr. Opin. Biotechnol. 2010, 21 (1), 100-13.
[4] P. Hammar; S. A. Angermayr; S. L. Sjostrom; J. van der Meer; K. J. Hellingwerf; E. P. Hudson; H. N. Joensson, Biotechnol. Biofuels. 2015, 8, 193.
[5] C. Dusny; M. Lohse; T. Reemtsma; A. Schmid; O. J. Lechtenfeld, Anal. Chem. 2019.
[6] K. Rosenthal; F. Falke; O. Frick; C. Dusny; A. Schmid, Micromachines 2015, 6 (12), 1836-1855.

Development of biorefining schemes for recovery of high-added value products from *Aphanizomenon flos-aquae* biomass

Michail Syrpas[1*], Jolita Bukauskaitė[1], Loreta Bašinskienė[1], Petras Rimantas Venskutonis[1]

[1] *Department of Food Science & Technology, Kaunas University of Technology, Radvilėnų pl. 19, LT-50254 Kaunas, Lithuania*

**Corresponding author: michail.syrpas@ktu.lt*

Highlights

- Supercritical CO_2 extraction can be employed for recovery of lipophilic products
- Residual biomass is rich in antioxidant products
- Phycobiliprotein rich extracts can be obtained by ultrasonic treatments
- A stream of products with various applications can be recovered from this biomass

1. Introduction

Cyanobacteria are ubiquitous photosynthetic bacteria that can have significant effects on the water quality as well as the functioning of aquatic ecosystems [1]. The massive proliferation of cyanobacteria can lead to excessive surface water blooms in heavily eutrophicated systems [2]. During the last decade's appearance of this kind of cyanobacterial blooms has also been verified in the Curonian lagoon [3]. This region, which is listed in UNESCO's world heritage sites, provides many ecosystem services, and thus, it is a crucial area for recreation, tourism, and aquaculture.

Recent reports suggest that removal of wild cyanobacterial blooms from the Curonian lagoon as a management measure, should be considered and prioritized [3]. To turn this threat into gain herein we envisioned the utilization of a wild cyanobacterial bloom as a feedstock within a biorefinery concept. Towards this end, fractionation of this biomass was achieved with high-pressure and or conventional extraction techniques This underutilized biomass could be considered as a source of products with potential biotechnological, food, agrochemical and pharmaceutical applications

2. Methods

For the optimization of SFE-CO extraction, a central composite design (CCD) and response surface methodology (RSM) were used. Fatty acid methyl esters were identified and quantified by means of GC-FID. Tocopherol content was assessed by HPLC with a fluorescence detection. Phycobiliprotein rich extracts were obtained by conventional techniques (freeze-thaw cycles, homogenization, solid-liquid extraction). Ultrasound-assisted extraction in combination with conventional techniques was further optimized with a CCD-RSM for the highest phycocyanin,

allophycocyanin, phycoerythrin and total phycobiliprotein yields. Residual biomass was further treated either with pressurized liquid extraction (PLE) or conventional techniques to obtain antioxidant rich extracts. *In vitro* antioxidant capacity of obtained extracts was evaluated with the Folin-Ciocalteu, DPPH and ABTS assays. Functional properties of obtained extracts were further evaluated for their ability to inhibit catalase, superoxide dismutase and acetylcholinesterase activity. Preliminary phytochemical characterization was achieved by means of UPLC-ESI-TOF-MS.

3. Results and discussion

For the SFE-CO_2 CCD-RSM indicated 42.5 MPa, 55 °C and 120 min of extraction as optimal conditions, under which SFE-CO_2 yielded 4.43 g/100 g DW of non-polar extract characterized by the presence of α-linoleic acid and α-tocopherol [4]. Under optimal extraction conditions, the SFE-CO_2 proved to be faster and more efficient compared to conventional hexane extraction [4]. In a next step, isolation of aqueous phycobiliprotein rich extracts was based on several conventional techniques in combination with optimized ultrasound-assisted extraction. The highest total phycobiliprotein yields were observed for samples, treated with homogenization followed by application of 8.75 min of ultrasounds at 84% amplitude [5]. During the next steps, residual biomass was further treated with increasing polarity solvents either by conventional or pressurized liquid extraction techniques. The acetone, ethanol and water extracts showed a strong antioxidant capacity in various radical scavenging assays. Moreover, the obtained extracts showed inhibitory effects against biologically relevant enzymes. In a last step, preliminary phytochemical composition of obtained extracts as assessed by means of UPLC-ESI-TOF-MS revealed the presence of a number of natural pigments as well as auxins, compounds that could be potentially utilized as biofertilizers.

4. Conclusions

In conclusion, the potential of wild cyanobacteria for recovery of a stream of products within a biorefinery concept were shown. Wildly harvested *Aphanizomenon flos-aquae* biomass could be considered as a feedstock for recovery of products with potential food, nutraceuticals, biotechnological and agricultural applications. Further studies focusing on life-cycle assessment and techno-economic feasibility of the developed biorefinery schemes would be of further interest in this field.

References

[1] W.F. Vincent, Encyclopedia of Inland Waters, Academic press, 2009, 226-232

[2] G.A. Codd, L.F. Morrison, J.S. Metcalf, Toxicol. Appl. Pharmacol. 2005, 203 (3), 264–272.

[3] S. Sulcius, R. Pilkaityte, H. Mazur-Marzec, J. Kasperoviciene, E. Ezhova, A. Blaszczyk, R. Paskauskas, Mar. Pollut. Bull., 99 (2015) 264-270.

[4] M. Syrpas, J. Bukauskaitė, R. Paškauskas, L. Bašinskienė, P.R. Venskutonis, Algal Res. 35 (2018) 10–21.

[5] M. Syrpas, J. Bukauskaitė, K. Ramanauskienė, J. Karosienė, D. Majienė, L. Bašinskienė, P.R. Venskutonis, Manuscript under review

ECCE12
The 12th EUROPEAN CONGRESS OF CHEMICAL ENGINEERING
Florence 15-19 September 2019

Influence of artificial biological aging on physicochemical, biological and ecotoxicological properties of five biochars - a laboratory incubation study

Mónika Molnár[1*], Márta Kőszegi[1], Emese Vaszita[1], Katalin Gruiz[1], Éva Farkas[1]

1 Budapest University of Technology and Economics, Department of Applied Biotechnology and Food Science, H-1111 Budapest, Műegyetem rkp. 3.

**Corresponding author: mmolnar@mail.bme.hu*

Highlights

- Each biochar possessed increased microbial activity after aging
- Increased biological activity was associated with decreased available nutrients
- Initial specific surface area highly affected the aging-mediated changes

1. Introduction

Biochar (BC) is a solid by-product of biomass combustion under oxygen limited conditions, known as pyrolysis [1]. Biochar proved to be useful as soil amendment [2], and considered effective in carbon sequestration and reduction of agricultural greenhouse gas emissions [1,2], contaminant and heavy metal removal, and other applications [1,2]. Biochar effects as soil amendment do not only depend on soil properties, biochar production conditions, but also on a variety of temporal processes in the environment, called "aging", including abiotic and biotic redox reactions, interactions with microbes, organic matter, minerals and solutes in the soil environment [3]. Progressive aging alters biochar quantity and quality [4]. This paper evaluates the effects of simulated conditions of artificial biological aging on the physicochemical, biological, ecotoxicological properties of five biochar types compared to their properties before aging. The aim is to support efficient long-term utilization of biochar in soil focusing also on the potential environmental risks posed to soil biota.

2. Methods

Triplicate samples of five biochar (BC) types were "aged" by placing samples in 750 mL glass containers so that three calcareous sandy soil layers alternated with the biochar layers. The biochar types were the following: grain husk and paper fibre sludge BC (A1), wood screenings BC (B1), woodchips BC (F1), herbal pomace BC (H1), miscanthus BC (M2). The containers were covered with perforated aluminium foil, so that drying could not occur over 11 weeks; microcosms were watered every 3 week with 20 mL microbial inoculant optimized for calcareous soil. Aerobic conditions were provided by glass capillary tubes inserted into the layers. After 11 weeks the biochar and soil layers were carefully separated and removed. The biochars before and after aging were examined by an integrated methodology, including physicochemical (pH, electric conductivity (EC), specific surface area (BET), loss on ignition (LOI), water holding capacity (WHC), permanganate oxidizable carbon (POXC), cation exchange capacity (CEC), organic matter (OM), plant available nutrients (NPK), heavy metals, metalloids, other elements), biological (aerobic heterotrophic cell counts) and ecotoxicological methods (*Sinapis alba* shoot- and root inhibition test, *Folsomia candida* mortality tests*).*

3. Results and discussion

Significant differences between biochars before and after aging were determined by one-way Analysis of Variance (ANOVA) using StatSoft® Statistica 13.1. Table 1 shows the summary of the main effects of biochar aging compared to before aging.

Table 1 Summary of the main effects of biochar aging.

Biochar type	*pH*	*EC*	*LOI*	*WHC*	*BET*	*Pore vol.*	*POXC*	*OM*	*NO_3-N*	*P_2O_5 / K_2O*	*CEC*	*CFU Bacteria*	*Plant growth*
A1	-	-	-	-	-	-	-	-	-	-	-	+	-
B1	-	-	-	-	-	-	-	-	+	-	0	+	+
F1	-	-	-	-	-	-	-	-	+	-	-	+	+
H1	-	-	-	0	0	0	-	-	+	-	-	+	0!
M2	0	-	-	-	-	-	-	-	+	-	-	+	-

– significant decrease | – decrease | + significant increase | + increase | ! ecotoxicity | 0 no effect

Each biochar underwent changes through the aging process, especially regarding nutrients and biological activity. The accelerated biological aging resulted in higher microbial activity in case of all biochars depending on their surface areas (BET). The highest increase (more than two-fold) was found for M2 and F1 biochars with the largest (BET). BET values of biochars correlated with the aerobic heterotrophic cell counts (CFU) of weathered biochars. The total N content of each biochar decreased - except A1 with the highest initial NO_3-N content – while there was an increase in the available nitrate due to the increased bacterial activity. Most of biochars exhibited significant decrease (~40–60%) in the pH, OM and permanganate oxidizable (labile) carbon content (POXC) as well as in available K and P upon aging. These changes were accompanied by decreases in biochar CEC however previous studies reported higher CEC of biochar after aging. We assume that enhanced bacterial activity triggers microbial OM production and sorption of OM, resulting in a range of new organic functional groups affecting CEC.

4. Conclusions

Based on our results the specific surface area of non-aged biochars highly affected the aging-mediated changes. Percentage decrease in available nutrients and labile carbon was the lowest while the decrease in CEC was the highest in the case of M2 biochar with the highest specific surface area suggesting that M2 would be the most efficient and stable charcoal on the long term. Artificial biological aging of biochar represents a promising model for studying weathering effects. Further comparative evaluation of the outcomes of biochar aging in the soil matrix under real field conditions is planned.

References

[1] J. Lehmann, A handful of carbon. Nature 447 (2007) (7141) 143–144.

[2] J. Lehmann, J. Gaunt, M. Rondon, Bio-char sequestration in terrestrial ecosystems – a review. Mitig. Adapt. Strateg. Glob. Change 11 (2006) 403–427.

[3] A. Mukherjee, A.R. Zimmerman, R. Hamdan, W.T. Cooper, Physicochemical changes in pyrogenic organic matter (biochar) after 15 months of field aging. Solid Earth Discuss. 5 (2014) 693–704.

[4] B. Singh, Y. Fang, C.T. Johnston, Fourier-transform infrared study of biochar aging in soils. Soil Sci. Soc. Am. J. 80 (2016) 613–622.

Mass transfer characterization of calcium alginate membrane containing bionanofiber and mechanical strength

Ryoichi Nakayama[1*], Ryotaro Hoshino[1], Norikazu Namiki[1], Masanao Imai[2]

1 Department of Environmental Chemistry & Chemical Engineering, School of Advanced Engineering, Kogakuin University, 2665-1 Nakano-machi, Hachioji, Tokyo, 192-0015, JAPAN

2 Course in Bioresource Utilization Sciences, Graduate School of Bioresource Sciences, Nihon University, 1866 Kameino, Fujisawa, Kanagawa, 252-0880, JAPAN

**Corresponding author: bionakayama.ryo@cc.kogakuin.ac.jp*

Highlights

- Bionanofiber composited membrane was successfully prepared.
- Maximum stress was increased in chitosan nanofiber composited membrane.
- The chitosan nanofiber composted membrane was dramatically decreased compared with alginate-Ca membrane.

1. Introduction

Oceanic bio-polymer have been expected as environmental compatible materials for medical, food and industrial application. Sodium alginate was a typical oceanic bio-polymer and it was sustainably and abundantly produced from kelps. It was widely cultivated in worldwide ocean. Gelling character of sodium alginate by the aid of metal ion exchange was extensively applied to form gel particles and membranes. Molecular size of alginate chain was hardly controlled because of natural bio-products. Biomass nanofiber have been researched for their use in biodegradable packaging due to their renewable, low cost and low density. More recently, this have been reinforced into biopolymers to produced green nanocomposite membrane, with improved thermal, mechanical and oxygen barrier properties.

Membrane separation processes are attractive because of their low energy cost and contaminant-free final product. Interest in using natural materials for the membrane body has increased because of their biocompatibility and environment-friendly disposal.

2. Methods

2.1 Preparation of bio-nanofiber composited membrane

Calcium alginate based composite membrane was cooperated with Chitosan nanofiber (Chi-NF). Aqueous solution of sodium alginate (10 g/L) was prepared by dissolving in pure water. Desirable amount of chitosan nanofiber (Chi-NF) or carboxymethyl cellulose nanofiber (CMC-NF) was added into alginate aqueous solution and mixed magnetic stirrer. The solution was poured into a glass petri dish, and then dried in a thermostat-controlled oven for 12 h at 333 K. Dried sodium alginate with mixed Chi-NF in the petri dish was immersed into the $CaCl_2$ solution (0.1 mol/L) for 20 min. The membrane was washed with pure water to remove excess metal ion.

(a) Alginate-Ca membrane (b) Chi-NF composited membrane (c)CMC-NF composited membrane

Figure 1 Image of alginate-Ca membrane composited nanofiber.

2.2 Mechanical strength

A rheometer was used to measure the mechanical strength of the swollen membranes. The swollen membranes were cut into sample pieces (1 × 4 cm), which were then stretched at a speed of 1 mm/s using the reheometer. The mechanical properties were evaluated in terms of both the maximum stress (δ) when the membrane ruptured.

3. Results and discussion

Figure 2 shows the effect of the maximum stain with the mass fraction of chitosan nanofiber and carboxymethyl cellulose nanofiber in the algnate-Ca membrane. The maximum stress was slightly increased with increasing of mass fraction of chitosan nanofiber until f_{NF}=30%. In contrast, the maximum strain was gradully decreased. The clearance between alginate polymer chains and chitosan nanofiber became narrow with increasing the mass frtion of ChiNF. Chitosan is in higher deacetylation, and has by many amino groups. Deacetlyation contributed to making many hydrogen bonds and prducing stronger mechanical characterics of chiotsan.

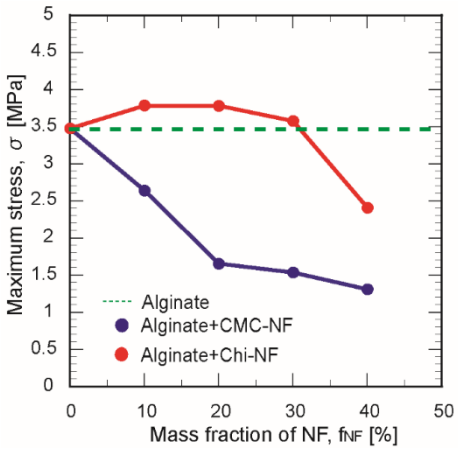

Figure 2 Effect of mass fraction of nanofiber on maximum stress.

4. Conclusions

A stable membrane made of calcium alginate with multiple domains of bio nanofiber was successfully prepared. Maximum stress of membrane a rupture for Chi-NF composited membrane was increased.

ECAB 5
The 5th EUROPEAN CONGRESS OF APPLIED BIOTECHNOLOGY
Florence 15-19 September 2019

Influence of ionic liquids and seawater on the catalytic activity and stability of cellulases from *Penicillium verruculosum*.

Aleksandra Rozhkova[1], Margarita Semenova[1], Ivan Zorov[1,2], Anna Dotsenko[1], Arkady Sinitsyn[1,2]

1 Federal Research Centre «Fundamentals of Biotechnology» of the Russian Academy of Sciences, Moscow 119071, Russia; 2 Department of Chemistry, M.V.Lomonosov Moscow State University, Moscow 119991, Russia

**Corresponding author: amrojkova@mail.ru*

Highlights

- Endoglucanase (EG) possesses higher stability in presence of effectors in compare with cellobiohydrolase (CBH).
- Cellulases stability well correlates with the results of saccharification of aspen wood (AW).

1. Introduction

The main obstacle in the bioconversion of wood is its resistance to enzymatic hydrolysis. Existing pretreatment methods aimed at increasing the reactivity of wood (reducing the degree of crystallinity and lignin content, increasing the available surface area, etc.) remain imperfect in terms of "green chemistry" [1]. The use of ionic liquids (ILs) does not lead to the formation of toxic products; in addition, they are easily regenerated, practically non-volatile, non-combustible, and dissolve many inorganic and organic compounds and gases well [2]. However, the best ILs are extremely expensive for use in industry. In recent years, seawater and its concentrates have been considered an affordable and cheap alternative to ILs [3].

The use of any pretreatment of cellulosic raw materials with its subsequent saccharification should imply the presence of an enzyme complex of cellulases, including cellobiohydrolase (CBH), endoglucanase (EG) and β-glucosidase (BG) that are intact to chemical residue and capable of deep destruction of cellulose. We have previously shown that CBH from the *Tricoderma viride* was more sensitive to the presence of hydrophobic ILs with a long alkyl substituent (1-octyl-3-methylimidazolinium chloride), and EG activity was sensitive to short ([bmim]Cl) while *Aspergillus niger* β-glucosidase was the most stable of the enzymes in the presence of ILs in concentrations of 1, 5 and 10 g/l [4]. In this work, we studied the effect of [Bmim]Br, [Choline]Cl and seawater on the catalytic activity of the cellulase complex from fungus *Penicillium verruculosum*. We simulated the technological process of saccharification of pretreated aspen wood (AW) under conditions of varying degrees of washing from the corresponding reagent.

2. Method

Saccharification of AW (80 g/l in the reaction mixture) was performed under the action of cellulase enzymatic preparation (CEP, 10 mg/g or 0.8 mg/ml of the reaction mixture) with an excess of β-glucosidase activity (0.6 mg/g or 0.048 mg/ml of the reaction mixture) in 2 ml test tubes in a temperature-controlled shaker. The hydrolysis process was carried out in the presence of 0.1 g/l of

ampicillin in 0.1 M Na-acetate buffer pH 5.0 and 40 ° C. To study the effect of effectors, [Bmim] Br, [choline] Cl, (20, 10, 5, 2 and 1% in the reaction mixture) or seawater (200, 100, 50, 20 and 10%) were added to the reaction mixture. During the process, aliquots were taken, in which the glucose concentration was determined.

3. Results and discussion

The presence of 1% [Bmim] Br, 1-2% [Choline] Cl in the reaction mixture did not affect the stability of the EG and CBH. The effect of ILs on cellulases at high concentrations was different: after 48 hours, the EG activity decreased to 75% and 15% in the presence of [Choline]Cl and [Bmim]Br, respectively. The activity of CBH in the presence of [Choline]Cl decreased 2 times, and was not detected after 3 h of incubation in 20% [Bmim]Br. Seawater taken in studied concentartions did not affect the stability of the enzymes (data are not shown). The presence of effectors had little effect on the results of hydrolysis using AW as a substrate (Fig.1). The yield of glucose after 48 hours of hydrolysis in presence of 20% [Bmim] Br or 20% [Choline]Cl was 47 and 67% of the control, with 10% ILs - 72 and 76%, with 5% ILs - 77 and 80%, with 2% ILs - 85 and 91%, with 1% IL - 94 and 100%, respectively. In the presence of 200% seawater, the glucose yield was 74% of the control, at 100% - 87%, in more dilute solutions of seawater, the glucose yield values close to the control were obtained.

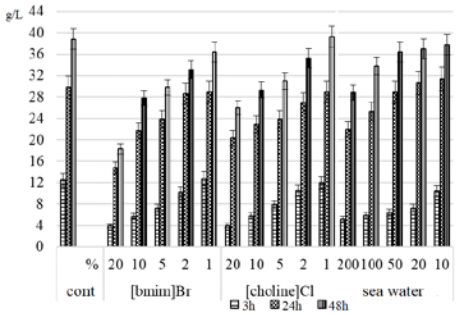

Figure 1. The yield of glucose (g/l) under enzymatic hydrolysis of milled AW (80 g/l) using CEP (10 mg of protein/1 g of substrate) and β-glucosidase (0.6 mg of protein / 1g of substrate) in the presence of ILs and seawater of various concentrations; 50 ° C, 0.1 M Na-acetate buffer with pH 5.0.

4. Conclusions

Pretreatment of aspen wood using ILs or seawater can adversely affect the reactivity and stability of the enzyme complex as a whole or its individual components, therefore the creation of new enzyme preparations that are tolerant to IL exposure is a promising task of industrial biotechnology.

This research was funded by Ministry of Science and High Education (MON) of Russia, project identification number: RFMEFI61617X0081.

References

[1] Conde-Mejiaa C., Jimenez-Gutierreza A., El-Halwagi M. // Process Safety and Environmental Protection.2012. V. 90. P. 189-202.

[2] Heinze T., Schwikal K., Barthel S. // Macromol. Biosci. 2005. V. 5. P. 520-525.

[3] Lechmann C., Sibilla F., Maugeri Z., Streit W. R., de Maria P. D., Martinez R., Schwaneberg U. // Green Chem. 2012. V. 14. P. 2719-2726

[4] Dotsenko A. S., Dotsenko G. S., Senko O. V., Stepanov N. A., Lyagin I. V., Efremenko E. N., Gusakov A. V., Zorov I. N., Rubtsova E. A. // Bioresource Technol. 2018. V. 250. P. 429-438.

Boosting of *Penicillium verruculosum* cellulolytic complex with polysaccharide monooxigenase.

Ivan Zorov[1,2*], Aleksandra Rozhkova[1], Margarita Semenova[1], Vadim Telitsyn[2], Arkady Sinitsyn[1,2]

[1] Federal Research Center «Fundamentals of Biotechnology» of the Russian Academy of Sciences, Moscow 119071, Russia; [2] Department of Chemistry, M.V.Lomonosov Moscow State University, Moscow 119991, Russia

**Corresponding author: inzorov@mail.ru*

Highlights

- Lytic polysaccharide monooxigenase (PMO) significantly boosts the hydrolytic activity of *Penicillium verruculosum* cellulases;
- New strains with optimized ratio of endoglucanases, cellobiohydrolases, β-glucosidases, and PMO were created;

1. Introduction

The use of renewable raw materials, such as agricultural by-products, is becoming increasingly important as a starting material for new biotech products. Agricultural and forestry materials, including (ligno) cellulose or starch, are first converted to sugars, which are later converted to chemicals, bioplastics, biofuels, and pharmaceuticals by fermentation [1]. Cellulose conversion occurs under the action of a complex of cellulolytic enzymes, which include exo-1,4-β-glucanase (CBH), endo-1,4-β-glucanase (EG) and β-glucosidase(BG). Cellobiohydrolases catalyze the degradation of the crystalline sections of cellulose, sequentially, by the processive mechanism, cleaving cellobiose from the ends of the polysaccharide chain. Endoglucanases catalyze the hydrolysis of amorphous sites of cellulose, splitting internal 1,4- β-glucosidic bonds by a disordered mechanism, thereby reducing the degree of substrate polymerization and creating new sites for the action of cellobiohydrolases. β-glucosidases hydrolyze cellobiose and cellooligosaccharides to the final product - glucose [2, 3]. Lytic polysaccharide monooxygenases (LPMO) catalyze oxidative cleavage of cellulose and cello-oligosaccharides. LPMOs are able to oxidise the C–H bond of the glycoside linkage connecting the sugar units in polysaccharides, which ultimately leads to cleavage of the glycoside link and hence boost generation of fermentable sugars. These enzymes are secreted by various fungal strains and are important components of enzyme cocktails used for industrial biomass conversion [4,5]. Improvement of the properties of new enzyme coctails and fine tuning of biocatalytical processes of cellulose-to-biofuels can lead to ecologically friendly and cost-efficient alternatives to fossil-based technologies.

LPMO from *Penicillium verruculosum* was overexpressed in the same fungal strain. The LPMO enzyme preparations with the “basal” cellulolytic enzyme complex, which contains EGs, CBHs, and bG were produced. The yield of fermentable sugars was 45 and 30% higher in microcrystalline cellulose (MCC) and pretreated aspen wood (AW) hydrolysis for some preparations.

2. Methods

LPMO was overexpressed in *Penicillium verruculosum* fungal strain; the number of strains, carrying 5-67% of LPMO were produced. Saccharification of MCC and AW (100 g/l in the reaction mixture) was performed under the action of basal cellulase enzymatic complex (CEC) and CEC+LPMO, normalized by protein to 5 mg/g of substrate or 0.5 mg/ml in the reaction mixture. The reaction conditions: 50mM sodium acetate pH 5.0, 40°C, 5mM of gallic acid was added as an electron donor for LPMO. Samples for reducing sugars and glucose assay were taken after 6, 24, and 48 hours of hydrolysis.

3. Results and discussion

MCC and AW was efficiently hydrolyzed by *Penicillium verruculosum* enzyme preparations with 5-12% of cloned LPMO, while the efficiency decreases dramatically for preparations with higher content of LPMO (Fig. 1). The yield of reducing sugars was ~10% higher in case of AW to compare to MCC. The yield of glucose was also higher with LPMO-enriched enzyme preparations, while the xylose yield remains approximately the same.

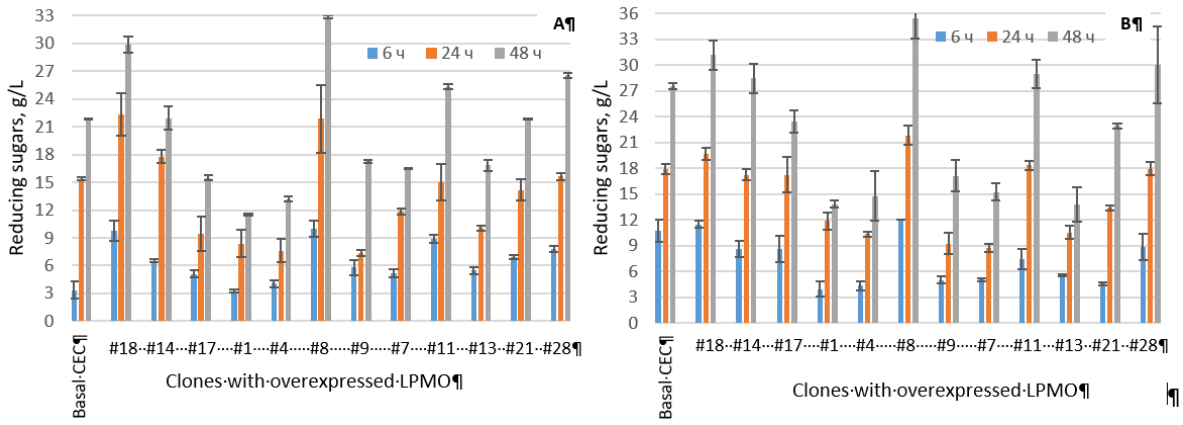

Figure 1. Reducing sugars release after 6, 24, and 48 hours hydrolysis of microcrystalline cellulose (A) and pretreated aspen wood (B) by different LPMO-enriched enzyme preparations. Substrate concentration 100 g/L, protein concentration 5 mg/g of substrate, 40 °C, pH 5,0.

4. Conclusions

New high productive *Penicillium* fungal strains with overexpression of LPMO were developed. The yield of reducing sugars as well as glucose were up to 45% higher for enzyme preparations with 5-12% of LPMO to compare to *Penicillium* basal cellulase enzyme complex. The level of total reducing sugars was approx. 10% higher in case of pretreated aspen wood hydrolysis to compare to microcrystalline cellulose. The content of LPMO does not affect much the level of xylose release in case of aspen wood.

Acknowledgments: the project is supported by Russian Fond of Basic Research, #18-54-80027\18

References

[1] R. Kumar, S.Singh, O.V.Singh, J. Industrial Microbiol.Biotechnol. 35 (2008) 377-391.
[2] S.T.Merino, J.Cherry, Adv. Biochem Eng/Biotechnology 108 (2007) 95-120.
[3] R.E.H. Sims, W.Mabee, J.N.Saddler, M.Taylor, Bioresource Technology 101 (2010) 1570-1580.

[4] M.A.S. Kadowaki, A. Várnai, J-K. Jameson, A.E.T. Leite et al., PLoS ONE 13(2018): e0202148. https://doi.org/10.1371/journal.pone.0202148
[5] E.D. Hedegård, U. Rydea, Chem Sci. (2018) 9(15) 3866–3880.

ECCE12
The 12th EUROPEAN CONGRESS OF CHEMICAL ENGINEERING
Florence 15-19 September 2019

Characterization of liquid-solid adsorption processes in recirculated differential bed (RDB) and spinning basket (SB) set-ups

Simon Crelier[1], Bryan Boisset, Rémy Dufresne, Djano Kandaswamy

[1] *University of Applied Sciences and Arts Western Switzerland, CH-1950 Sion*

**Corresponding author: simon.crelier@hevs.ch*

Highlights

- RDB configuration enables an accurate control of experimental conditions
- Contrary to empirical models, mass transfer-based approaches enable a proper scaling-up of adsorption steps
- RDB configuration has been used successfully with various model systems
- SB configuration enables a more efficient liquid-solid mass transfer than RDB

1. Introduction

Liquid-solid adsorption is at the core of many industrial processes. The phenomenon is relatively easy to investigate at laboratory scale in a stirred vessel, but a proper design and dimensioning requires the acquisition of reliable equilibrium and kinetic data under well-mastered and characterized experimental conditions.

Similarly, the use of empirical rate laws (e.g. pseudo-2nd order, Elovich) to describe the kinetics of adsorption makes a proper scale-up of the adsorption step difficult. This is mainly because these models' parameters are difficult to relate to those commonly used in process engineering such as mass transfer- or diffusion coefficient-related dimensionless numbers.

As a consequence very few of the promising applications that are described in the literature are developed further up to pilot scale operation, not to mention industrial implementation.

We propose here a simple approach that does not require any complex equipment, but nevertheless enables a systematic investigation of the adsorption process and a proper transfer to larger scale. It is based on the use of a recirculated differential bed such as the one described in Figure 1. This set-up allows a precise control of working conditions and an easy determination of process relevant parameters.

This approach has been successfully applied in our laboratory to various model systems. These include the adsorption of Methylene Blue or Allura Red on granulated activated charcoal (GAC), of copper ions on Amberlite IR 120, of 4-nitrophenol or cephalosporin on Amberlite XAD 16, and of BSA or IgG on chromatographic resins.

2. Methods

Measurements were performed at room temperature (20±1 °C). A known volume V_{liq} of a solution of adsorbate with an initial concentration C_0 was contacted with a mass m_{sor} of sorbent.

The residual concentration of adsorbate in the liquid phase, C(t), was determined as a function of contacting time by spectrophotometry, ICP-MS or measurement of a colored complex. The corresponding adsorbed concentrations q(t) were calculated using the mass balance of Eq. 1:

$$q(t) = \frac{V_{liq}}{m_{sor}} \cdot (C_0 - C(t)) \qquad \text{Eq. 1}$$

3. Results and discussion

A short selection of results is shown here. The Recirculated Differential Bed configuration is shown on Figure 1 below. 400 mL of methylene blue solution (C_0=12 mg/L) was pumped at various flow rates Q_{rec} over a shallow fixed bed with 51.2 mg GAC (mean particle diameter 190 µm). The results are shown in Figure 2.

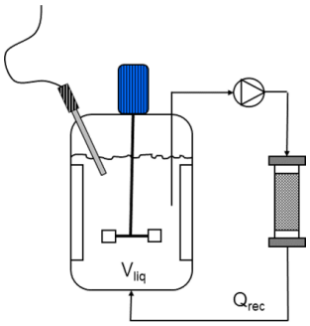

Figure 1. The RDB configuration

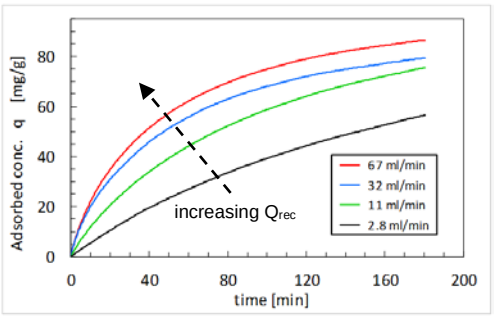

Figure 2. Adsorption kinetics of MB on GAC at various flow rates

External mass transfer coefficient k_l was estimated from the initial slope of the C(t) kinetics curves, as described in [1]. The k_l values ranged from $1.73 \cdot 10^{-5}$ m/s at 2.8 ml/min to $1.18 \cdot 10^{-4}$ m/s at 67 ml/min. This suggests a significant contribution of external mass transfer to the overall adsorption process, as described in [2].

External mass transfer coefficients were also measured with the spinning basket from SpinChem AB (Umeå, Sweden) during the adsorption of methylene blue (12 mg/L) on GAC (mean part. diam. 300 µm). The values of k_l also increased with increasing rotation speed and they varied between $2.71 \cdot 10^{-4}$ m/s at 100 rpm and $7.17 \cdot 10^{-4}$ m/s at 300 rpm.

4. Conclusions

Although the spinning basket contactor enables to reach higher external mass transfer coefficients, the spinning rate is more difficult to relate to hydrodynamic parameters such as Reynolds number, due to a more complex flow pattern. In this respect and although less efficient, the recirculated differential bed gives a better control of operating conditions for characterization and scale-up.

References

[1] Worch, E.: Adsorption technology in water treatment. Fundamentals, processes and modelling. De Gruyter, Berlin (2012)

[2] S. H. Kim et al., Adsorption and Mass Transfer Characteristics of Metsulfuron-Methyl on Activated Carbon. Korean J. Chem. Eng. 18(2), 163-169 (2001)

Characterization of a bioreactor of trays for solid state fermentation under abiotic conditions: Hydrodynamics and heat transfer

Gerardo Gómez-Ramos[1,2*], Carlos Castillo-Araiza[1], Sergio Huerta-Ochoa[2], Moíses Couder-García[1], Lilia Prado-Barragan[2]

1 Laboratory of Reactor Engineering Applied to Chemical and Biological Systems. Chemical Engineering Area. Dept. of IPH. Autonomous Metropolitan University-Iztapalapa, Av. San Rafael Atlixco 186 Vicentina, C.P. 09340, Mexico City; 2 Department of Biotechnology, Autonomous Metropolitan University-Iztapalapa, San Rafael Atlixco 186, Vicentina, C.P. 09340, Mexico City.

**Corresponding author: gagr@xanum.uam.mx*

Highlights

- Solid State Fermentation
- Two-zones model approach.
- Hidrodynamics.
- Heat transfer.

1. Introduction

Solid state fermentation in recent years is booming in the biotechnology industry, due to the potential to produce value-added metabolites in different industries, for example; enzymes, biofuels, food additives, precursor molecules for chemical and pharmaceutical industries, among others [1].But nevertheless; in this type of systems, one of the biggest problems for scaling systems is the heat transfer, Due to the temperature gradients that are generated in the bioreactor, some reports mention gradients of up to 10 ºC [2], this is due to the exotherm of the biological reactions in the fermenter. Several authors have made characterizations of heat transfer; however, we still do not have a reliable methodology to scale the process. This could be due to not considering the effect of hydrodynamics when characterizing the heat transport parameters.

Due to the above, the objective of this work was to characterize the hydrodynamics and the effect it presents in the transport of heat in a tray bioreactor to produce proteases (SSF) under abiotic conditions.

2. Methods

The characterization of the system was carried out in a bioreactor of trays packed with agroindustrial waste (fruit, vegetable and soybean paste).

2.1 Hydrodynamic characterization.

2.1.1 Pressure Drop

To characterize hydrodynamics, pressure drops were determined in the system by varying the aeration flow (VkgM) using two high precision manometers at the inlet and at the bioreactor outlet.

2.1.2 Profile Velocity

To determine the velocity profiles, two hydrodynamic models were used, which are based on the system pressure drop, vacuum fraction, air properties (density, viscosity). The hydrodynamic user models were Navier-Stokes-Darcy-Forchheimer (NSDF) and Two-zones model (developed in the research group). The NSDF model has been proven in previous works that adequately reproduces

the velocity profiles obtained through experimental data, therefore it was used as a basis to compare with the Two-zones model.

2.1 Characterization of heat transfer.

2.1.1. Temperature gradients

The temperature was determined in transient state in different sampling ports along the bioreactor generating wide gradients that allow greater certainty when determining the parameters of heat transport (effective conductivity and the coefficient of heat transfer in the wall). said parameters were estimated by coupling hydrodynamics using Two-zones model.

3. Results and discussion

Figure 1a shows the experimental pressure drops in the system at different aeration flows (VkgM), in figure 1b the velocity profiles (cm s^{-1}) are shown using both hydrodynamic models and figure 1c shows the temperature profile in the bioreactor, this was with constant aeration flow and bath temperature.

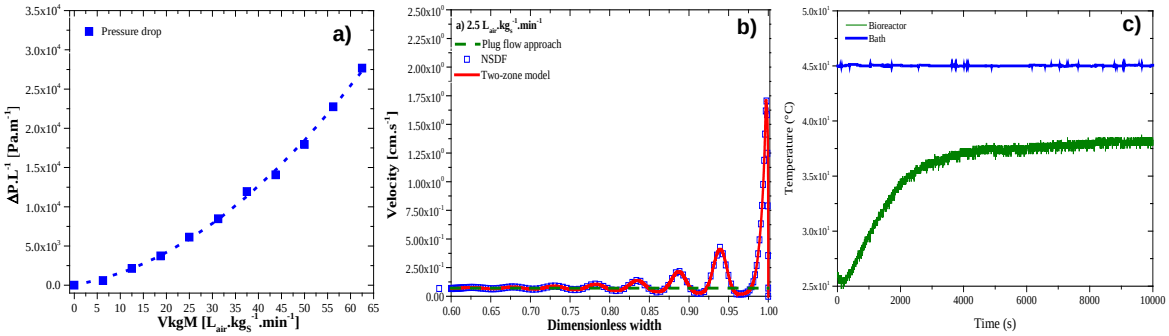

Figure 1. Experimental and theorical results in the system

As shown in Figure 1b, the velocity profiles obtained in the Two-zones model are practically identical to those obtained by means of NSDF (difference less than 3%), which gives us certainty about the results, together with the advantage that under the same computing conditions the processing time is reduced by 3000 times. The hydrodynamics was coupled to the estimation of the heat transfer parameters with the abiotic experimental data. The effective thermal conductivity and wall heat transfer coefficient present a value of ca. $9.49*10^{-3}$ W m^{-1} K^{-1} and $3.68*10^{-1}$ W m^{-2} K^{-1}

4. Conclusions

The Two-zones model allows reliable speed profiles to be obtained, greatly reducing the computation time, on the other hand the coupling of hydrodynamics to the heat transfer model allows to have a greater certainty of the heat transfer parameters and realizes all these analyzes under biotic conditions allow us to determine the effect of the bioreactor in the fermentation.

References

[1] Mitchell, D., Berovix, M., & Krieger, N. (2000). Biochemical Engineering Aspects of Solid State Bioprocessing. Advances in Biochemical Engineering/ Biotechnology, 68, 61-138.W. Black, E.B. White, The Elements of Science, third ed., MacCluski, New York, 1987.

[2] Barrios, A. (2015). Design, start-up and characterization of a bioreactor of trays for solid state fermentation in solid. Master's thesis, Metropolitan Autonomous University- Iztapalapa, Mexico City.

Isolation and characterization of halophiles microorganisms from solar salterns of Trapani, Sicily.

Valeria Villanova[1], Christian Galasso[2], Serena Lima[1], Alberto Brucato[1], Francesca Scargiali[1].

[1] Università degli studi di Palermo, Dipartimento d'Ingegneria, viale delle Scienze, edificio 6, 90128, Palermo (Italy). [2] Stazione Zoologica Anton Dohrn, Villa Comunale, 80121 Naples, Italy.

**Corresponding author: valeria.villanova@unipa.it*

Highlights

- Halophiles microorganisms are very interesting for biotechnological applications.
- These organisms were isolated and characterized from solar salterns in Sicily.
- Tested samples showed potential cosmetic applications.

1. Introduction

Halophiles are those organisms that can grow optimally at high salt concentrations and, hence populate hypersaline environments such solar salterns, salt lakes and Dead sea.
Hypersaline environments are inhabited by various microorganisms belong to all the three domains of living organisms: Archaea (*e.g.* Halophiles), Bacteria (*e.g.* cyanobacteria) and Eukarya (*e.g.* microalgae). The most known and representative microalgae that can be found in high salt concentration are two species of the flagellates green algae *Dunaliella*: *D. viridis* e *D. salina*. The latter is one of the most studied microalgae for their ability to accumulate large amount (up to 14% of dried biomass) of *β*-carotene under extreme environmental [1]. Although *D. viridis* does not accumulate that large amount of *β*-carotene, it can produce oxygenated carotenoids and grow faster than *D. salina* [2]. Similarly to *Dunaliella* species many diatoms, can tolerate high salt concentration and have been found in both solar salterns and very saline and polluted lakes [3]. Moreover, amongst hypersaline bacteria we can find both photosynthetic and heterotrophic bacteria*: i)* the cyanobacteria *Cyanothece* and *ii) Salinibacter rubens*. Several strains of *Cyanothece* group isolated from hypersaline habitats have been characterized for the production of exopolysaccharide (EPS) with biotechnological application [4]. Moreover, halophiles organisms under stress condition such as high salinity and high light intensity accumulated large amount of carotenoids in order to protect the cell against light damage and oxidative stress. Due to the accumulation of these carotenoids, the solar salterns during the summer season are frequently pink-red colored [5]. These carotenoids show beneficial effects for human health, hence the production of halophilic microorganisms' carotenoids is of increasing interest for the blue economy.

2. Methods

The sampling site was the natural area "Saline di Trapani e Paceco", formed by several pans dedicated to the extraction of sea salt in the province of Trapani, city on the west coast of Sicily. Here, the different salt concentration in these pans allows the proliferation of different halophiles microorganisms visible by changing color from white to pink or red. These organisms were isolated with serial dilution methods in both liquid and solid artificial seawater with different salt

concentration (from 20 to 200 g/L of NaCl). The species identification of isolates halophiles were done by Colony PCR using different molecular markers (*i.e.* 16s, ITS, 18S). The cells were grown under different culture conditions in order to stimulate the production of secondary metabolites. High light intensity and salinity (*i.e.* 100 µmol m^{-2} s^{-1} and 200 g/L NaCl) was used as stress condition to stimulate the synthesis of interesting molecules (*e.g.* carotenoids) that can have a beneficial effect on humans. At the end of growth experiment, the cells were collected by centrifugation and the pellet was freeze-dried. Freeze-dried biomass was extracted with an hydroalcoholic solution (Eth/H_2O 3/1, v/v) and the obtained cell extracts were tested in biological assay including antitumor and cell repair activity on human cell.

3. Results and discussion

New strains of microorganisms (bacteria and microalgae) have been isolated from red and pink coloured pan present in the saltworks of "Saline di Trapani e Paceco": *D. viridis*, *Nitzschia dubiiformis, Salinibacter rubens* and *Cyanothece sp.* All the cell extracts did not show any antitumor activity on human cell (*i.e.* HT29 and PC3) at all tested concentration. *D. viridis* extracts from low light and salinity condition showed cytotoxic effects on human epithelial cell BEAS-2 cells increasing with high concentration. The same effect was not showed in the *D. viridis* grown under high light and salinity condition probably for the production of secondary metabolites with beneficial effect. Almost all samples showed a moderate repair activity on human epithelial cell line BEAS 2B, especially at medium and low concentrations (*i.e.* 10 and 1 µg ml^{-1}).

4. Conclusions

This research aims to promote the sustainable production of biomass with high biological value, thanks to the selection of halophiles microorganisms. Here, new strains of hypersaline microorganisms (bacteria and microalgae) were isolated from solar salterns at the natural reserve of "Saline di Trapani e Paceco". Thanks to the use of several molecular markers, it was possible to identify the species of isolated microorganisms. Cell extracts did not show significant cytotoxicity neither on normal nor tumour mammalian cells tested. Almost all samples showed a moderate repair activity showing a potential use of these strains in cosmetics.

References

[1] M. García-González, J. Moreno, J. C. Manzano, F. J. Florencio, Miguel G. Guerrero, Production of *Dunaliella salina* biomass rich in 9-cis-β-carotene and lutein in a closed tubular photobioreactor, Journal of Biotechnology (2005) 115: 81-90.

[2] Moulton, T.P. & Burford, M.A. The mass culture of *Dunaliella viridis* (Volvocales, Chlorophyta) for oxygenated carotenoids: laboratory and pilot plant studies, Hydrobiologia (1990) 204: 401. https://doi.org/10.1007/BF00040263

[3] Sterrenburg, F.A.S., Tiffany, M.A. and Lange, C. Studies on the genera *Gyrosigma* and *Pleurosigma* (Bacillariophyceae). Species from the Salton Sea, California, USA. *Proceedings Academy of Natural Sciences of Philadelphia* (2000) *150: 305-313.*

[4] De Philippis R, Margheri MC, Materassi R, Vincenzini M. Potential of unicellular cyanobacteria from saline environments as exopolysaccharide producers. Appl Environ Microbiol. (1998);64(3):1130–1132.R.

[5] Oren A., Meng F.W., 'Red – the magic color for solar salt production' – but since when?, *FEMS Microbiology Letters*, Volume 366, Issue 5, March 2019, fnz050, https://doi.org/10.1093/femsle/fnz050.

Microalgae bio-products application for nutraceutical sector and cosmetics ingredients

Casella Patrizia [1], Rimauro Juri[1], Iovine Angela[1,2], Mehariya Sanjeet[1,2], Musmarra Dino[2], Molino Antonio[1,*]

1 Italian National Agency for New Technologies, Energy and Sustainable Economic Development (ENEA), Territorial and Production System Sustainability Department, CR Portici Piazzale Enrico Fermi, 1 - 80055, Portici, Italy; 2 Department of Engineering, University of Campania "Luigi Vanvitelli", Via Roma, 29 - 81031 Aversa, Italy

**Corresponding author: antonio.molino@enea.it*

Highlights

- Cosmetics and nutraceutical ingredients as beta-carotene, astaxanthin, methyl linoleate, palmitate, and eicosapantenoic acid are produced from microalgae
- Their extraction by CO_2-SFE was improved to obtain a good standard for nutraceutical and cosmetic application

1. Introduction

Microalgae are promising sources of high value compounds such as carotenoids, beta-carotene, lutein and astaxanthin, and fatty acids, (É3 and É6) that can find application in the growing sectors of nutraceuticals and cosmetics. Nutraceutical sector lies halfway between pharmaceuticals and nutrition, where natural compounds as vitamins, minerals, antioxidants are necessary as ingredients and active principles. Cosmetics industry is a very rich field that has also seen an ever-increasing trend in the demand for natural origin ingredients.

Among microalgae bio-products, beta-carotene is considered an excellent ingredient in nutraceuticals for its pro-vitamin A function, while astaxanthin in the form of oleoresin produced by the microalgae *Haematococcus pluvialis* is currently authorized as a novel food for its antioxidant properties [1]. In addition, the oils produced by the microalgae species *Ulkenia sp.* and *Schizochytrium sp.* have been authorised as novel foods and as sources of omega-3s (EPA and DHA). Lutein, on the other hand, is required as a supplement for its properties against degenerative macular disease. In cosmetic sector, ingredients as beta-carotene and lutein are used as colouring agents and skin conditioning, and polyunsaturated fatty acids (methyl linoleate and palmitate as both skin conditioning and emollient agents.

As part of the European project VALUEMAG (Valuable Products from Algae Using new Magnetic Cultivation and Extraction Techniques), the microalgae *Dunaliella salina*, *Scenedesmus almeriensis*, *Haematococcus pluvialis*, and *Nannochloropsis sp.* were selected for their ability to produce high value compounds such as beta-carotene, lutein and astaxanthin, and polyunsaturated fatty acids (PUFAs). The objective of the this work is to investigate the extraction of these bio-products by supercritical fluid extraction using CO_2 as extraction fluids (CO_2-SFE) and to evaluate the characteristics of extracted compounds compared to the characteristics of the

products currently authorized as novel foods and ingredients in nutraceutical and cosmetic industry.

2. Methods

The complete methodological approach is shown in the figure 1. Microalgae were cultivated testing a six-meter height Soft Magnetic Cone (SOMAC), a magnetic conic photobioreactor. Supercritical fluid extraction (CO_2-SFE) was tested varying temperature (°C), pressure (bar) and CO_2 flow rate (g/min) to extract carotenoids and fatty acids polyunsaturated from *Dunaliella salina*, *Scenedesmus almeriensis*, *Haematococcus pluvialis*, and *Nannochloropsis sp.* freeze dried biomass. The extracts were characterized in term of carotenoids and PUFAs concentration following official methods. The characteristics of extracts were compared with the properties of authorized nutraceutical products. A cost analysis evaluation was finally carried out by a market analysis on the price of authorized products.

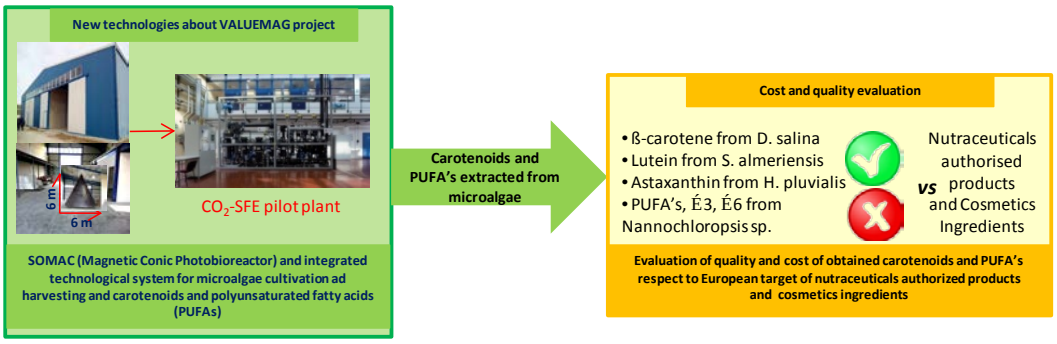

Figure 1. Methodological approach.

3. Results and discussion

Preliminary results have shown that beta-carotene, and astaxanthin can be extracted by CO_2-SFE as the major compounds among carotenoids respectively from *D. salina* and *Haematococcus pluvialis.* The obtained extracts from CO_2-SFE contained also an interesting fatty acids composition regarding compounds as methyl linoleate and palmitate in species such as *D. salina*, *Haematococcus pluvialis* for application as ingredients in cosmetics. In particular, palmitate constituted more than 50% of fatty acids methyl esters extracted from *D. salina* in different conditions.

The extraction was also tested on EPA content by CO_2-SFE from *Nannochloropsis sp.* searching the best operative conditions to improve extraction yield given that EPA content higher than ≥ 10 % is required for nutraceutical EPA rich-oil from *Ulkenia sp.* and and *Schizochytrium sp*. microalgae.

4. Conclusions

Fatty acids and carotenoids composition of extracts obtained from microalgae using CO_2-SFE demonstrated that are promising source for cosmetics and nutraceutical industry.

References

[1] Commission Implementing Regulation (EU) 2017/2470 of 20 December 2017 establishing the Union list of novel foods in accordance with Regulation (EU) 2015/2283 of the European Parliament and of the Council on novel food.

ECAB 5
The 5th EUROPEAN CONGRESS OF APPLIED BIOTECHNOLOGY
Florence 15-19 September 2019

The Role of Simulation and Scheduling Tools in Bioprocess Development and Manufacturing.

Demetri Petrides[1*], Elpida Sapidou[1], Alexandros Koulouris[2]

[1]Intelligen Inc., Scotch Plains, NJ 07076, USA;
[2]Alexander Technological Education Institute., Thessaloniki, Greece;

*Corresponding author: dpetrides@intelligen.com

The successful scale up and commercialization of biopharmaceuticals is a challenging task that requires collaboration of professionals from many disciplines. Process simulators can facilitate this task by assisting scientists and engineers to answer the following and other related questions: What is the impact of product titer increase on the capacity load of the downstream section, the overall throughput of a plant, and the cost of goods? What changes are required in an existing multi-product facility to accommodate the process of a new product? What is the range of variability that a process can accommodate if it operates under a tight cycle time? What is the impact of single-use systems on the demand for utilities, the environment and the cost of goods? Our experience in addressing the above questions will be presented using industrial examples in which we evaluated alternative technologies for producing therapeutic monoclonal antibodies and vaccines.

A microfluidic approach for bioprocess development

Raquel Aires-Barros and Ana Azevedo

iBB – Institute for Bioengineering and Biosciences, Instituto Superior, Lisbon, Portugal
Corresponding author: rabarros@ist.utl.pt

Highlights

- Microfluidic toolbox to expedite the development of downstream processes
- Miniaturization of Aqueous Two-Phase Systems (ATPS
- Chip Chromatography for screening of adsorption/elution conditions

1. Introduction

The number of biotechnology-based pharmaceuticals in the late-stage pipeline has been increasing more than ever in particular monoclonal antibodies (mAbs) representing a quarter of all biopharmaceuticals in clinical trials. As a result, there is an enhanced demand for more efficient and cost-effective processes. Here, the potential of miniaturization as a high-throughput screening tool to speed up process development is explored, considering optimization of antibody extraction conditions with aqueous two-phase systems and chromatographic conditions optimization regarding the capture of an antibody, using a multimodal ligand.

2. Methods

The ATPS-microfluidic setup allowed the screening of a wide range of concentrations inside the microchannel by varying the flow rates of the solutions while using sub-mL volumes for each ATPS-forming system. The partition of molecules between two co-flowing liquid streams confined within a microchannel was demonstrated by the on-line extraction of a fluorescein isothiocyanate (FITC) labeled immunoglobulin G (IgG) from a salt rich flow to a PEG rich flow.

The setup for screening adsorption and elution conditions- Micro- columns on a chip-contains 30 micro-columns in a 15 x 40 mm chip (Resin Volume ~ 35 nL). Fluorescence emission of the packed beads was continuously monitored to obtain the adsorption and elution kinetic profiles.

3. Results and discussion

The ATPS-microfluidic developed setup (Figure 1a) allowed the screening of up to 8 extraction conditions simultaneously, while a second microfluidic structure allows the integration of multi-step extraction steps. The chip chromatography(Figure 1b) microfluidic developed platform allowed the effective screen of multiple adsorption and elution conditions within a few minutes for early stage multimodal chromatography optimization. Both techniques can be used with any target molecule or resin assuming a previous labeling procedure with a proper fluorophore.

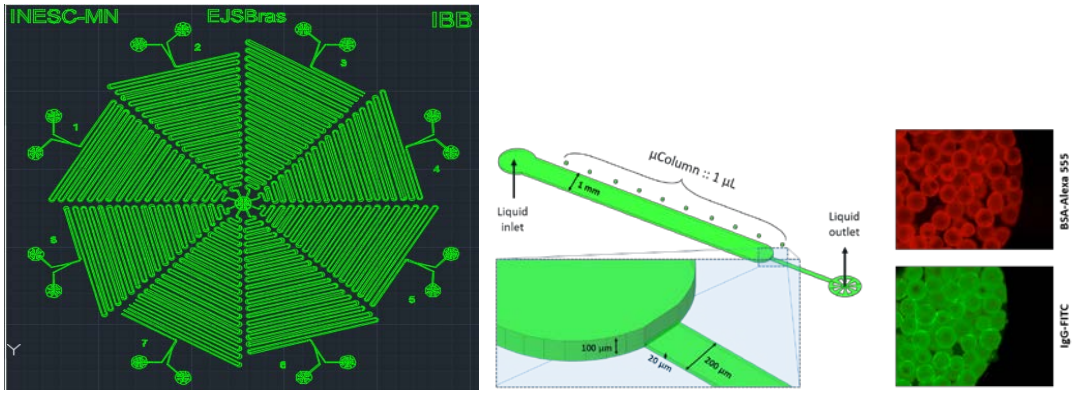

Figure 1. a) Microfluidic-ATPS toolbox; b) Chip chromatography

4. Conclusions

A microfluidic approch was sucessfuly stablished to expedite the development of dsp of biopharmaceuticals using reduced volumes of reagents and shorter experimental times

References

Ruben R. G. Soares, Daniel F. C. Silva, Pedro Fernandes, Ana M. Azevedo, Virginia Chu, João P. Conde and M. Raquel Aires-Barros Biotechnol. J. 2016, 11, 1-15

Ines F. Pinto, Ruben R. G. Soares, Sara A. S. L. Rosa, Maria Raquel Aires-Barros,Virginia Chu, João P. Conde and Ana M. Azevedo Anal. Chem. 2016, 88, 7959−7967

IDENTIFICATION OF HYDROXYLED COMPOUNDS FROM THE BIOCONVERSION OF NARINGENIN BY *Yarrowia lipolytica 2.2ab*

Christian Hernández-Guzmán[1], Angélica Román-Guerrero[2], Lilia Arely Prado-Barragan[3], Miquel Gimeno-Seco[4], Sergio Huerta-Ochoa [5]

1 Departamento de Biotecnología, Universidad Autónoma Metropolitana Unidad Iztapalapa, San Rafael Atlixco 186, Col. Vicentina, Delegación Iztapalapa, CDMX., C.P. 09340, México; 2 Departamento de Alimentos y Biotecnología, Universidad Nacional Autónoma de México, AV. Universidad Nº 3000, C.U., Delegación Coyoacán, CDMX., C.P. 04510, México.
*sho@xanum.uam.mx

Highlights

- We evaluated naringenin bioconversion by whole cells of *Yarrowia lipolytica 2.2ab*
- Some polyhydroxylated flavonoids are first reported by whole cells
- This study allowed selection and operation of the proper bioreactor.

1. Introduction

The flavonoids are plants secondary metabolites that exhibits important antivirals, anti-inflammatory, vasodilators and antioxidant biological activities [1]. Naringenin is classified on the subclass of flavonones and is naturally present in grapes, tomatoes and citric fruits. Due to its positive effects on health, their study has attracted the attention of several research groups [2, 3]. It has been reported that the increase in antioxidant activity in flavonoids is highly related to the degree of hydroxylation and/or methoxylation [4]. *Yarrowia lipolytica* may express the CYP450 enzyme system, which is indispensable to increase the hydroxylation of hydrophobic compounds such as naringenin [5]. Chang et al. [6] reported the bioconversion of naringenin to 8-hydroxynaringenin by *A. oryzae* cells. The hydroxylation of naringenin to eriodictiol by means of the cytochrome P450 monooxygenase enzyme expressed by *P. chrysosporium* was reported by Kasai et al. [7]. The objective of this study was the identification of the compounds obtained from the bioconversion of naringenin by the enzymatic system produced by *Y. lipolytica* 2.2ab (Yl2.2ab).

2. Methods

Bioconversion experiments were prepared in 250 mL Erlenmeyer flasks with 100 mL of Sabouraud culture broth inoculated with $1x10^6$ cells mL^{-1} of Yl2.2ab and 100 mg L^{-1} of naringenin were added. Concentration and identification of residual naringenin and formed products was performed by HPLC, the use of external standard was required [8].

3. Results and discussion

Figure 1 shows the kinetic profile from the bioconversion of naringenin by Yl2.2ab to the polyhydroxylated compounds identified as apigenin, ampelopsin, myricetin, aromadendrin and luoteolin. All the molecules were produced simultaneously throughout the reaction time.

The obtained molecules exhibit higher antioxidant activity related to molecule used as precursor. It has been reported that the increase in antioxidant activity in flavonoids molecules is directly related to the degree of hydroxylation and/or methylation formed in the new formed molecule [4]. The compounds identified in here are of great interest for the pharmaceutic and food industries.

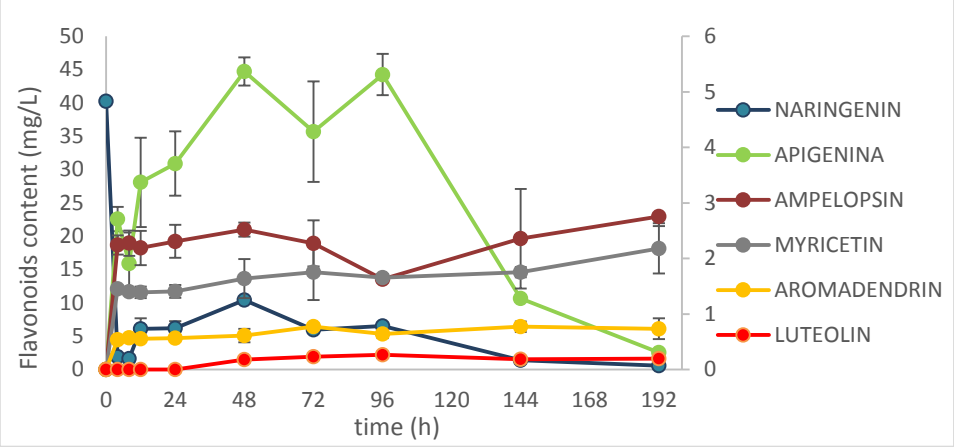

Figure 1. Profile of concentrations during the bioconversion.

4. Conclusions

Five compounds with high valued were obtained during the bioconversion naringenin by Yl2.2ab. The molecules obtained showed higher antioxidant activity than the initial precursor.

References

[1] A. Madej, J. Poplonski, E. Huszcza, Applied Biochemistry and Biotechnology, 173 (2014) 67-73.
[2] E. Álvarez, O. Cambeiro, Offarm, 22 (2003) 130-140.
[3] T.O. Nagy,K. Ledolter, S. Solar, Radiation physics and chemistr,.77 (2008) 728 – 733.
[4] E.N. Prasetyo,G.S. Nyanhongo Guebitz G.M. Process Biochemistry, 46 (2011) 1019-1024.
[5] M.A.Z. Coelho, P.F. Amaral, I.Belo, Applied Microbiology and Microbial Biotechnology, (2010) 930-44.
[6] T-S. Chang, M-Y. Lin, H-J Lin, J. Cosmet. Sci, 61, (2010) 205-210.
[7] N. Kasai, S.I. Ikushiro, S. Hirosue, A. Arisawa, H. Ichinose, H. Wariishi, T. Sakaki, Biochemical and biophysical research communications, 387 (2009) 103-108.
[8] C. Hernández-Guzmán, Master in biotechnology, UAM-I, México, 2015.

Effect of flow behavior in extra-column volumes on the retention pattern of proteins in small columns

Krystian Baran, Wojciech K. Marek*, Izabela Poplewska, Wojciech Piątkowski, Dorota Antos

Department of Chemical and Process Engineering, Powstańców Warszawy Ave. 6, 35-959 Rzeszów, Poland; *wojciech.piatkowski@prz.edu.pl*

Highlights

- Deformation of protein peaks in extra-column volume (ECV) was indicated
- ECV effect stems from radial velocity distribution and slow protein diffusivity
- ECV effect influences on the protein retention on a small column
- Mathematical model was used to predict the extra-column volume effect

1. Introduction

Columns with very small volumes, i.e., maximum 1 mL, are often used in the development stage of protein chromatography to estimate operating parameters for large stale operations at minimal material consumption. Small columns are exploited in high throughput experiments to acquire a huge number of chromatographic elution data that are subjected to statistical analysis to determine the bounds for the process operating window as well as characterize the process dynamics and provide optimum of operating conditions with respect to the process performance. However, reduction in the column size causes an increase in the ratio of the extra-column volume (ECV) in the workstation to the column volume. Therefore, band broadening in ECV can significantly affect the separation efficiency. In this study, the experimental and theoretical analysis of deformation of band profiles in ECV was performed, and its influence on the retention pattern of proteins in a small chromatographic column was quantified [1].

2. Methods

A few model proteins were used for the elution experiments: lysozyme, LYZ; bovine serum albumin, BSA; monoclonal immunoglobulin, IgG4; fibroblast growth factor, FGF2. Additionally, blue dextran as a representative of large macromolecules, and acetone as a representative of small-molecule compounds, were used. The column was packed with a cation exchange resin UNOsphere S (Bio-Rad Laboratories, Hercules, CA, USA, particle diameter 80 μm). The mobile phase was a phosphate buffer pH = 7 free of salt or with 1M NaCl in the solution. Two injection systems were used: a superloop and an injection loop capillary.

3. Results and discussion

The effect of the presence of ECV on shape of band profiles resulted from non-uniform velocity distribution in the radial direction and slow diffusivity of proteins. The phenomenon vanished for a small molecule compound, and it was enhanced with increasing molecular weight of the model compound. The difference in flow behavior of the macromolecule and small-molecule compounds caused them to migrate with different velocities in ECV, which resulted in partial separation of their bands. To describe the elution profiles in ECV and in the column, a mathematical model was used, which accounted for nonideality of the flow pattern. The model reproduced accurately band profiles of macromolecules within a range of relatively low velocities, typical however for protein chromatography.

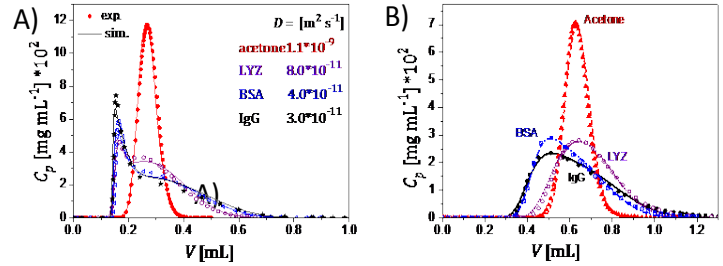

Fig. 1. Experimental band profiles and the corresponding model simulations for small-volume injections for proteins and acetone.
A) in ECV; B) in the column.

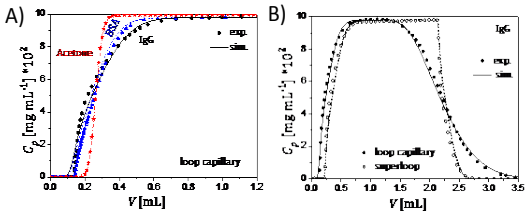

Fig. 2. Band profiles in ECV

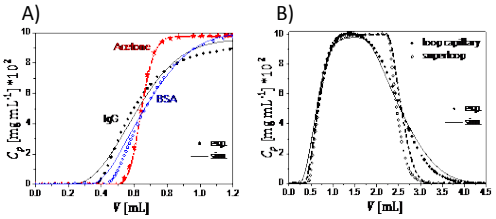

Fig. 3. Band profiles at the column outlet

Experimental band profiles and the corresponding model simulations for large-volume injections. A) Fronts of breakthrough curves for the proteins and acetone injected through the loop capillary; B) comparison of the IgG bands for the injections through the loop capillary and the superloop.

Typical experimental data and the model simulations for small pulse injections recorded in the chromatographic system with and without presence of the column are shown in Figures 1A and 1B respectively. The protein peaks are characterized by deformations which enhance with increase in molecular weight of the protein. Band profiles obtained for large injections are shown in Figs 2 and 3. They exhibit strong asymmetry of the fronts with a slow concentration transition in their upper part. The courses of the concentration decay in the desorption parts of the band profiles obtained by injections using the loop capillary and the superloop differ markedly. In case of the superloop injections, peak tailing is markedly reduced compared to the loop capillary injections. This stems from the differences in the elution pattern of proteins in both injections systems.

4. Conclusions

The ECV effect contributed strongly to the elution behavior of macromolecules in the small column. Peak deformation was observed for small-volume injections and asymmetry of breakthrough curve fronts for large-volume injections. In the latter case, the system performance was higher for the superloop injections compared to the loop capillary injections. Neglecting the EVC effect may result in wrong interpretation of the protein retention mechanism.

References

[1] W. Marek, D. Sauer, A. Dürauer, A. Jungbauer, W. Piątkowski, D. Antos, J. Chromatogr. A, 1566 (2018), 89–101.
[2] K. Baran, W. K. Marek, W. Piątkowski, D. Antos, *Effect of flow behavior in extra-column volumes on the retention pattern of proteins in small columns*, J. Chromatogr. A, submitted.

Financial support of this work by National Science Center Poland (project DEC-2016/22/M/ST8/00193) is gratefully acknowledged.

ECAB 5
The 5th EUROPEAN CONGRESS OF APPLIED BIOTECHNOLOGY
Florence 15-19 September 2019

Doubling humanized L-asparaginase expression by *Pichia pastoris* through DO-stat controlling induction strategy in bench-bioreactor

Leticia Parizotto[1], Adalberto Pessoa Jr[2], Aldo Tonso[1]

1 University of Sao Paulo, Polytechnic School, Dep. of Chem. Eng.
2 University of Sao Paulo, School of Pharmaceutical Sciences, Dep. Bioch. - Pharm. Technology
**Corresponding author: leticia.parizotto@usp.br*

Highlights

- The engineered *Pichia pastoris* expressed humanized L-asparaginase (ASNase)
- Three induction strategies were studied
- DO-stat strategy resulted in, approximately, two-fold more maximum ASNase activity

1. Introduction

During the last ten years, the yeast *Pichia pastoris (Komagataella phaffi)* has been consolidated as a platform for biopharmaceutical production. Moreover, the development of engineered strains capable to perform 'humanized' glycosylation increased the chances to reach the requirements of the regulatory agencies (Jacobs et al, 2009). Facing this potential, a strain of *P. pastoris* Glycoswitch® (Biogrammatics Inc.) was transformed to express the enzyme L-asparaginase (ASNase), which is applied in acute lymphoblastic leukaemia treatment, with 'humanized' glycosylation. The objective of this work is to obtain the highest ASNase activity through studying different induction strategies aiming the scaling up production of this innovative biopharmaceutical.

2. Methods

2.1 Cell strain and expression vector

Pichia pastoris GS115 Glycoswitch® SuperMan$_5$ his$^+$ (Biogrammatics Inc.) transformed by electroporation with the plasmid pJAG_s1 (Biogrammatics Inc.) containing the gene asn*B* (GenScript) of the bacteria *Erwinia chrysanthemi (Dickeya chrysanthemi)* for ASNase expression, the factor αMF for extracellular expression and the gene for G418 resistance for selection (Effer et al, 2019). The plasmid was linearized and integrated to the promoter AOX1.

2.2 Cell storage and reactivation

Cells storage and seeding were performed according to Invitrogen's protocol (Invitrogen, 2002). The pre-inoculum was prepared to inoculate the bioreactor with 1 $g_{drycell}$/L.

2.3 Bioreactor cultures

Bioreactor cultures began with 1 litre of BSM (Basal Salt Medium) and 4.35mL of PTM1 (metal trace *Pichia* solution) formulated according to Invitrogen (2002) in a 2L-BIOSTAT B (Sartorius, Germany). The glycerol batch phase was performed according to the same protocol and equal in the three experiments with dissolved oxygen (DO) kept over 20% air saturation with control cascade of the agitation between 700 and 1000 rpm and aeration kept at 1 litre per minute. Following, there was a period of starving for, approximately, 2 hours and then induction was started. In the experiment

A, the induction was performed with the addition of 10mL-pulses at every 24 hours; in experiment B, methanol was linearly fed with constant rate of approximately 18mL/h and DO was controlled over 20% with pure oxygen feeding; and, in C, methanol was fed to keep DO at 20% in a control mesh (DO-stat).

2.4 Analytic Methods

The dry mass concentration was related to optical density at 600nm measured in a spectrophotometer (Spectra Max®, Molecular Devices); glycerol was evaluated using a colorimetric kit (Triglicerides Liquiform®, Labtest); ASNase activity, modified protocol of Drainas, Kinghorn and Pateman (1977) and protein concentration, BCA method (Bicinchoninic Acid Kit, Sigma®).

3. Results and discussion

The three cultures provided similar performances during the growth phase on glycerol, with a specific maximum growth rate of 0.18±0.02 h^{-1} and cell productivity of 1.1±0.1 $g_{drycell}$/L/h after 24 hours of cultivation. However, during the expression phase, the ASNase production was different according to the induction strategy. The maximum activities were 1674 U/L (100h), 1501 U/L (76h) and 3068 U/L (97h) in A, B and C, respectively. Moreover, the population grew and produced protein significantly only in culture C. Therefore, the induction strategy based on controlling methanol-feeding by O_2 concentration (C) was the most suitable, since the metabolism was permanently stimulated to produce ASNase and consume methanol differently from pulses strategy (A), that was intermittent, and did not achieve toxic levels as in the constant feeding (B). This result agrees with previously reported by Lim et al. (2003) that achieved 40% higher rGuamerin secretion using DO-stat strategy than manual control of methanol-feeding. This strategy avoids methanol accumulation and lack of oxygen, improving cell growth and heterologous protein production (Lim et al, 2003).

4. Conclusions

As described in the literature (Liu et al, 2019), the induction strategy influenced significantly the heterologous protein production. The maximum ASNase activity approximately doubled with methanol-feeding controlled by DO-stat. This strategy kept methanol constant in a range that stimulated ASNase production, but at a level that was not toxic for the cells during the culture. Therefore, the induction strategy that considered aspects of cell metabolism was the most suitable for humanized ASNase production.

References

[1] Jacobs, P. P., Geysens, S., Vervecken, W., Contreras, R., & Callewaert, N, Engineering complex-type N-glycosylation in *Pichia pastoris* using GlycoSwitch technology. Nature Protocols, 4(1) (2009) 58–70.

[2] Effer, B., Lima, G., Cabarca, S., Pessoa, A., Farías, J. G., & Monteiro, G., L-Asparaginase from *E. chrysanthemi* expressed in Glycoswitch®: effect of His-Tag fusion on the extracellular expression. Prep. Bioch. And Biotech, (2019).

[3] Invitrogen, Pichia Fermentation Process Guidelines Overview (2002)., 1–11.

[4] Drainas, C., Kinghorn, J. R., & Pateman, J. A., Aspartic Hydroxamate Resistance and Asparaginase Regulation in the Fungus *Aspergillus nidulans*. Journal of General Microbiology 98 (1977) 493-501.

[5] Lim, H. K., Choi, S. J., Kim, K. Y., & Jung, K. H., Dissolved-oxygen-stat controlling two variables for methanol induction of rGuamerin in *Pichia pastoris* and its application to repeated fed-batch. App. Micro. and Biotech., 62(4) (2003), 342–348.

[6] Liu, W. C., Inwood, S., Gong, T., Sharma, A., Yu, L., & Zhu, P., Fed-batch high-cell-density fermentation strategies for *Pichia pastoris* growth and production. Critical Rev. in Biotech. 39(2) (2019) 258–271.

ECAB 5
The 5th EUROPEAN CONGRESS OF APPLIED BIOTECHNOLOGY
Florence 15-19 September 2019

Antibody variant ion-exchange separation and recovery at varying ligand densities

Greta Jasulaityte[1], Hans Johansson[2], Daniel Bracewell[1*]

1 Department of Biochemical Engineering, University College London, Bernard Katz Building, Gower Street, London WC1E 6BT, United Kingdom; 2 Purolite, Unit D, Llantrisant Business Park, Llantrisant, South Wales CF72 8LF, United Kingdom

**Corresponding author: d.bracewell@ucl.ac.uk*

Highlights

- Ratio between charged variants and main antibody changed with ligand density and pH.
- mAb recovery decreased with increasing ligand density and decreasing pH.
- Analytical studies revealed conformational changes to the mAb.

1. Introduction

Charge variant separation from the main monoclonal antibody is often challenging due to their similarities in charge and size [1]. Numerous separation techniques have been suggested including pH as well as salt gradients, a combination of both, or using different resin types [2,3]. In some cases, these conditions have been linked to a reversible or irreversible two-peak elution profile induced by protein unfolding, aggregation, or presence of specific charge-dependant amino acids [4-6]. In order to understand whether the presence of charge variants can affect the two-peak behaviour, we performed the separation using varying ligand density resins and buffer pH.

2. Methods

Antibody containing high levels of charge variants was run on columns packed with five cation exchange resins containing different ligand densities. The separation was carried out under an increasing salt gradient at three pH conditions. Analytical techniques such as size exclusion chromatography, circular dichroism, isoelectric focusing electrophoresis, and mass spectrometry were used to examine elution peaks.

3. Results and discussion

We found that the two-peak ratio and total protein recovery changed with buffer pH and ligand density. Protein recovery decreased by up to 27% with increasing ligand density, and by up to 51% with decreasing pH. No aggregation or reversible protein association was detected. However, circular dichroism data revealed conformational changes to the antibody structure, whereas isoelectric focusing electrophoresis showed the presence of different charge variants in the two peaks. Further analysis using mass spectrometry was undertaken to understand what caused reduction in protein yield and changes to the two-peak behaviour.

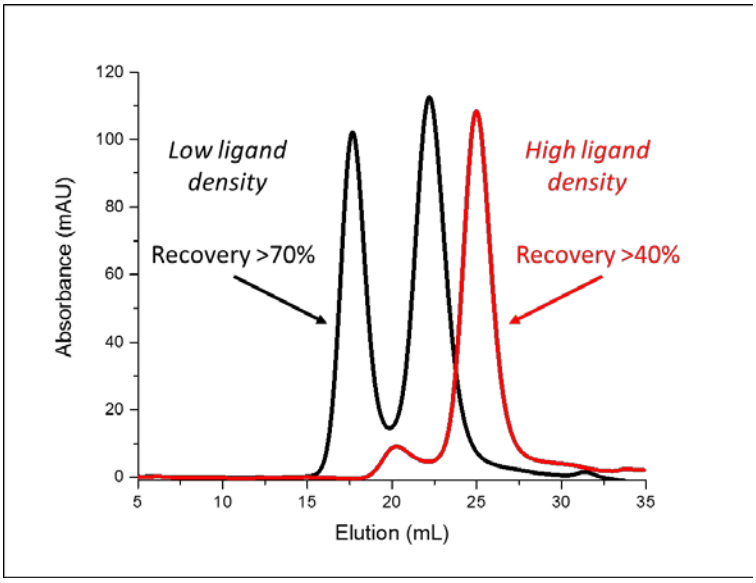

Figure 1. Antibody elution profile and recovery using low and high ligand density resins.

4. Conclusions

The results indicate that ligand density and buffer pH can affect the elution profile and protein recovery. We hypothesize that charge variants become unstable as a result of induced conformational changes.

References

[1] L.A. Khawli, S. Goswami, R. Hutchinson, Z.W. Kwong, J. Yang, X. Wang, et al., MAbs. 2 (2010) 613-624.
[2] T.M. Pabst, G. Carta, N. Ramasubramanyan, A.K. Hunter, P. Mensah, M.E. Gustafson, Biotechnol. Prog. 24 (2008) 1096-1106.
[3] S. Fekete, A. Beck, J. Fekete, D. Guillarme, J. Pharm. Biomed. Anal. 102 (2015) 33-44.
[4] H. Luo, N. Macapagal, K. Newell, A. Man, A. Parupudi, Y. Li, Y. Li, J. Chromatogr. A. 1362 (2014) 186-193.
[5] J. Guo, G. Carta, J. Chromatogr. A. 1388 (2015) 184-194.
[6] H. Luo, M. Cao, K. Newell, C. Afdahl, J. Wang, W.K. Wang, Y. Li, J. Chromatogr. A. 1424 (2015) 92-101.

ECAB 5
The 5th EUROPEAN CONGRESS OF APPLIED BIOTECHNOLOGY
Florence 15-19 September 2019

Creating Renewable Biofuel from Wastewater

Pilar Icaran[1], Maycoll S. Romero[2], Xavier Tomas[2], Victor Monsalvo [3]

1 Aqualia Balmes 36 08007 Barcelona; 2 Aqualia, Camí Sot de Fontanet, 25197 Lleida; 3 Aqualia. Av. Camino Santiago 40, E 28050 Madrid, Spain

**Corresponding author: picaranl@fcc.es*

Highlights

- ABAD Bioenergy© process, developed by Aqualia, for the transformation of biogas into biomethane
- In order to maximize the production of biogas, the pre-treatment of secondary sludge with nitrite and co-digestion have been studied
- Avoiding H_2S contaminant in biogas with micro-aerobic process

1. Introduction

Wastewater treatment plants (WWTPs) use energy intensive processes that consume large amounts of non-renewable energy. In the current context of resources scarcity and environmental protection standards, novel renewable energy sources have become an important issue for the sustainable management of WWTPs. Different approaches have been proposed to enhance sewage sludge digestion, biogas production and exploitation to maximize its value. Aqualia has exerted effort to reduce WWTPs energy dependence and develop new biogas technologies. The present study shows a possible scenario for integrating different technologies in a conventional WWTP (Figure 1). Proposed technologies are focused on i) waste activated sludge (WAS) pre-treatment, ii) low cost biogas up-grading ABAD Bioenergy© and iii) co-digestion with glycerin waters controlling the concentration of hydrogen sulfide with micro-oxygenation technics developed at industrial level.

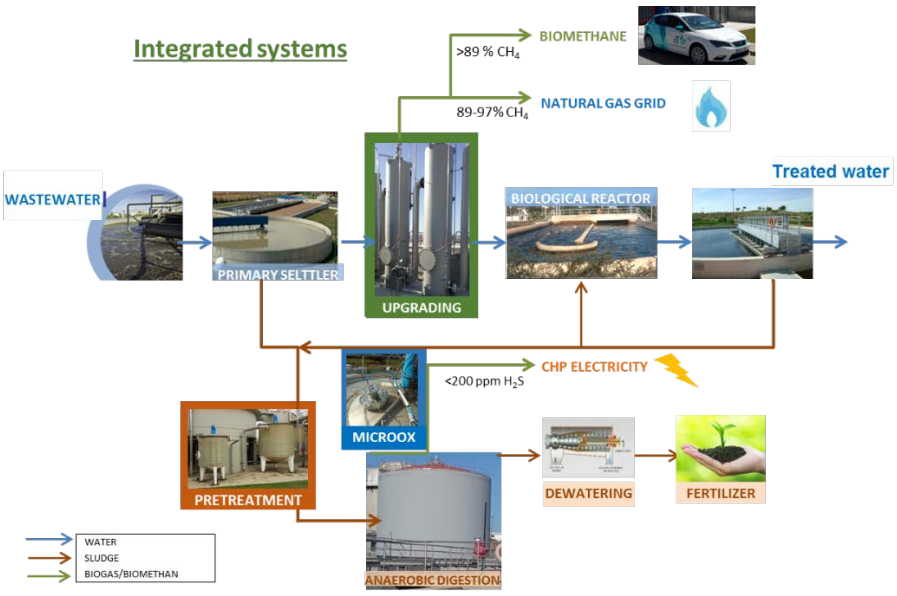

Figure 1. Proposed improvements integrated in a wastewater existing plant

2. Methods

Low cost biogas up-grading. A new up-grading technology (ABAD Bioenergy ©) has been developed by FCC Aqualia (European patent EP 3061515B1, EEUU patent 9901864). This technology is based on a water scrubbing system. Biomethane obtained is H_2S free and contains > 89 % of methane. In contrast with other up-grading technologies, ABAD process presents low energy demand, no need for regeneration of CO_2 absorbent, full integration in the WWTP process, flexibility (operation conditions can be set according to the WWTP regime) and low capital investment.

Pre-treatment. Previous reports have demonstrated that WAS pre-treatment with nitrite (NO_2^-) enhance hydrolysis and acidification processes, stimulating the activities of key enzymes responsible for hydrolysis and acidification [1]. The pre-treatment is achieved through NO_2^- addition (174 mg N-NO_2^-/L) to WAS with a mixing time of 4-5 hours [2]. Batch assays of WAS pre-treatment with NO_2^- have shown that methane production could be enhanced to a range from 12 to 28 % in lab experiments. Also a study was conducted to investigate the influence of nitrite pre-treatments in full-scale continuous anaerobic digesters. Results show the positive effect of nitrite pre-treatments on methane production. An economical assessment was also conducted, showing that pre-treatment benefits, on a full-scale implementation, would be limited to the use of biomethane for electricity generation.

Micro-aerobic process is applied to improve the biogas quality. The supply of O_2 (93 % purity from an O_2 generator) to the headspace of a full-scale digester (2400 m^3) of sewage sludge was studied. The average H_2S concentration in the digester dropped once the microaerobic conditions were applied, the average concentration of H2S in the biogas reach values above 200 ppmv with a removal efficiency of 90-95%. Residual O_2 in the biogas remained below 0.5-1 % during the whole micro-aerobic period and biogas dilution with N_2 was avoided. The energetic content of the biogas was not altered by the oxygen supply, and the CH_4 concentration was 62 % both in anaerobic and micro-aerobic conditions. According to the electric consumption of the generator, operating costs are incredible low compared with iron salts application. Therefore, it is feasible to remove H_2S at full-scale while maintaining the biogas quality and avoiding dilution with N_2 by employing an O_2 generator.

3. Results and discussion

The pilot plant in Guadalete WWTP, located in Jerez de la Frontera (Cádiz, Spain), treats up to 7 Nm3/h biogas. The plant consists on a three stage scrubbing system followed by a polishing process where H_2S, siloxanes and water traces are removed from biomethane. Then, the gas is compressed to 240 bar and stored to refuel car tanks. Two SEAT León have been tested and refueled with the produced biomethane to check its quality.

After 30,000 Km travelling with 100 % autochthonous biomethane produced from wastewater, SEAT will check car components and engines in order to validate this biofuel with all company guaranties.

Biomethane quality. Since November 2016, after the start-up of the pilot plant, biomethane has been produced and stored as compressed natural gas (CNG), used to refuel periodically the two test cars, which were driven intensely. Average gas compositions are shown in Table 1.

	Biogas	Biomethane
CH_4 [%-vol]	65.9 ±2.3	89.2 ±1.1
CO_2 [%-vol]	33.8 ±1.4	4.2 ±1.4
N_2 [%-vol]	2.4 ±1.5	6.6 ±1.1
O_2 [%-vol]	0.5 ±0.5	0.0
H_2S [ppm]	915 ±449	<5
Siloxanes [mg/Nm_3]	10	<1
Water (ppm)	-	<15

Table 1. Gas composition

Biomethane quality meets the legal requirements established by the European Standards [6] with a Wobbe Index close to 45 MJ/Nm^3 and Methane Number of 102.

The pre-treatment system allows to treat 10-20 m^3 of WAS per day, which is the 5-20 % of the total WAS produced and the 10-40% of the WAS feeding the digester. Taking this into account, it could not be possible to observe the effects of nitrite pre-treatment of WAS in full scale implementation. Even so, samples of treated and non-treated WAS were take periodically in order to be characterized by BMP test, solubility (CODs/VS), pH, nitrite (initial / end) and microscopic analysis.

4. Conclusions

A new up-grading technique has been developed by Aqualia to produce biomethane for automotive use from biogas in WWTPs. Its design is focused to be fully integrated in WWTPs with low capital and operating costs. The pilot plant in Guadalete WWTP, as first scale-up, supposes the unique up-grading plant in Spain that produces renewable biofuel from wastewater with a Spanish patent. Biomethane quality meets the legal requirements and real tests in two CNG cars are running.

Operational costs indicate that the patented process ABAD Bioenergy © is competitive with other technics and the investment is the most competitive for a biomethane production from 30 to above 100 m^3/h [3].

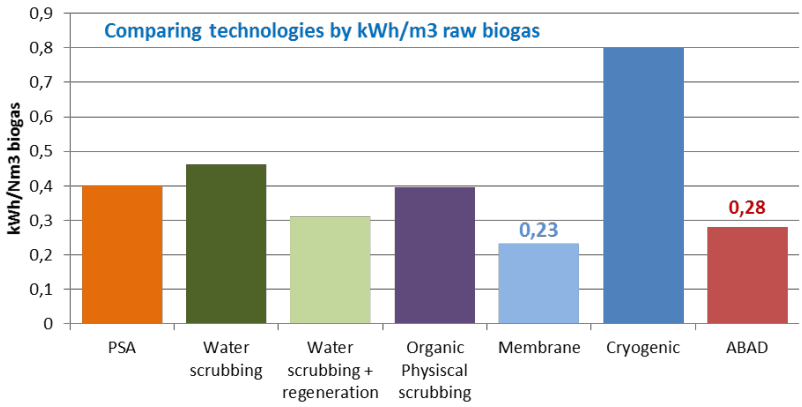

Figure 2. Energy consumption comparison with other upgrading systems

WAS pre-treatment with nitrite was assess in full scale WWTP. Results shows that pre-treatment is highly influenced by temperature, nitrite and VS ratio and WAS evolution in time. Economical assessment shows that nitrite pretreatment presents the highest benefits but those could be seen as limited to engage full-scale implementation when methane is used for electricity generation. Alternative scenario with the use of extra biogas as vehicular fuel could present a better profit.

The micro-oxygenation implanted in various facilities at an industrial level improves the quality of the biogas produced, this being very important for its subsequent valorization as biomethane. It also avoids corrosion problems in the electric cogeneration motors, reducing both preventive and corrective maintenance costs, all of it with a low cost investment and operation.

Acknowledgements

The project SMARTGreengas that supported this work I a CIEN program from CDTI (Centro para el Desarrollo Tecnológico Industrial) and FEDER funds.

References

[1] Zahedi S, Icaran P, Yuan Z, Pijuan M. Assessment of free nitrous acid pre-treatment on a mixture of primary sludge and waste activated sludge. Bioresour Technol 2016;216:870–5.

[2] Zahedi S, Romero-Güiza M, Icaran P, Yuan Z, Pijuan M. Optimization of free nitrous acid pre-treatment on waste activated sludge. Bioresour Technol 2017.

[3] http://publica.fraunhofer.de/eprints/urn_nbn_de_0011-n-948875.pdf

[4] Díaz, I., Pérez, S. I., Ferrero, E. M., Fdz-Polanco, M., Diaz, I., and Perez, S. I. (2011) Effect of oxygen dosing point and mixing on the microaerobic removal of hydrogen sulphide in sludge digesters. Bioresource technology, 102(4), 3768–3775.

[5] Díaz, I., Ramos, I., and Fdz-Polanco, M. (2015) Economic analysis of microaerobic removal of H2S from biogas in full-scale sludge digesters. Bioresource Technology, 192(2015), 280–286.

[6] Natural gas and biomethane for use in transport and biomethane for injection in the natural gas network - Part 2: Automotive fuel specifications. (DRAFT FprEN16723-2) 12-02-2015. European committee for standardization

Determination of maximum specific growth rate of photosynthetic organisms based on steady-state measures in CSTR

Elena Barbera[1], Eleonora Sforza[1], Alessia Grandi[1], Alberto Bertucco[1]

1 Department of Industrial Engineering, University of Padova, via Marzolo 9, 35131 Padova, Italy

**Elena Barbera: elena.barbera@unipd.it*

Highlights

- Diazotrophic cyanobacterium *Anabaena* PCC7122 was cultivated in continuous photobioreactors
- Respirometric tests used to measure kinetic parameters of N, temperature and light
- Maximum specific growth rate was determined from continuous experiments
- Kinetic model was developed and implemented in Aspen Plus process simulator

1. Introduction

Modeling the growth of photosynthetic organisms is challenging, mostly due to the complex role of light, which can be limiting because of self-shading, or photoinhibiting in the case of high intensities. The determination of the maximum specific growth rate is often affected by many variables that, in batch growth systems, may change significantly. On the other hand, in a continuous system, once steady-state is reached, all the process variables remain constant, including the biomass concentration and the specific light supply rate. This allows a quantitative assessment of the effect of this operating variable on the culture performances.

A case of particular interest is represented by nitrogen-fixing cyanobacteria (Anabaena PCC 7122), whose growth is controlled not only by the light intensity, but also by the availability of atmospheric nitrogen, which is related to its liquid solubility. In this work, a new approach, that combines the use of the cultivation in continuous systems and respirometric tests was presented.

2. Methods

Continuous experiments were carried out in vertical flat-panel PBRs with working volume (V_R) of 350 mL and 4 cm thickness, at a temperature T = 24°C. CO_2-enriched air (5% v/v) was sparged from the bottom. Mixing was checked by means of tracer experiments, that allowed to consider the reactor as a completely stirred tank one (CSTR) [1]. Fresh inlet BG11 or $BG11_0$ (with no nitrogen) was continuously fed by means of a tunable peristaltic pump. Continuous artificial white light was provided by a LED lamp.

The equation describing the autotrophic growth rate can be written as a function of biomass concentration (c_x), the maximum specific growth rate (μ_{max}), temperature ($f(T)$), specific light

$(f(I_{sp}))$ and the most limiting nutrient, i.e. nitrogen $(f(N))$. Moreover, the kinetic model takes into account the specific maintenance rate (μ_e) that is a negative term, thus reducing the biomass growth rate (r_x).

$$r_x = c_x \cdot \mu_{max} \cdot f(T) \cdot f(N) \cdot f(I_{sp}) - \mu_e \cdot c_x \quad \text{(Eq. 1)}$$

The kinetic parameters for temperature, nitrogen and light were measured by respirometric tests [2]. The specific maintenance rate (μ_e) was evaluated by elaborating experimental data of continuous cultivation according to the model proposed by Gons and Mur [3]. Finally, the maximum specific growth rate μ_{max} could hence be determined by applying the kinetic model in the material balances of the continuous PBR.

3. Results and discussion

The cyanobacterium was cultivated in continuous photobioreactors with and without supply of nitrates, showing that no nitrogen limitation occurred, and similar productivities were obtained in the two cases. This suggests that the half-saturation constant of the nitrogen is lower than its solubility in water. This was confirmed by the respirometric tests, that resulted in a half-saturation of about 3 mg L^{-1}. In addition, the kinetic parameters for temperature and light were measured by respirometric tests. Afterwards, the experimental results obtained under different incident light intensities were used to evaluate the specific maintenance rate, which was found dependent from the light intensity, ranging between 0.5 and 0.8 d^{-1}. The experimental data were finally elaborated to derive the value of μ_{max} ($8.22 \pm 0.69\ d^{-1}$).

4. Conclusions

In this work, the diazotrophic cyanobacterium *Anabaena* PCC7122 was cultivated in continuous photobioreactors with and without supply of nitrates, to investigate the role of nitrogen, light and residence time on growth kinetics. Based on the results of continuous experiments, the specific maintenance and maximum growth rates were evaluated.

References

[1] Sforza, E., M. Enzo, A. Bertucco. Chem Eng Res Des, 2014. 92: 1153–62.
[2] Sforza, E., Pastore, M., Barbera E., Bertucco A. 2019. Bioprocess Biosyst Eng, 1–12
[3] Gons, H. J., and L. R. Mur. 1980. Arch. Microbiol. 125: 9–17.

ECAB 5
The 5th EUROPEAN CONGRESS OF APPLIED BIOTECHNOLOGY
Florence 15-19 September 2019

High performance and repeated use of immobilized phospholipase A_1 for hydrolysis of phospholipid involved with hydrophobicity of reaction media

Yusuke Hayakawa[1], Ryoichi Nakayama[2*], Norikazu Namiki[2], Masanao Imai[1]

1 Course in Bioresource Utilization Sciences, Graduate School of Bioresource Sciences, Nihon University, 1866 Kameino, Fujisawa, Kanagawa, 252-0880, JAPAN

2 Department of Environmental Chemistry & Chemical Engineering, School of Advanced Engineering, Kogakuin University, 2665-1 Nakano-machi, Hachioji, Tokyo, 192-0015, JAPAN

**Corresponding author: bionakayama.ryo@cc.kogakuin.ac.jp*

Highlights

- Immobilized phospholipase A_1 was successfully prepared.
- Reaction rate increased by glutaraldehyde treatment.
- Repeated use of immobilized phospholipase A_1 was successfully appeared.

1. Introduction

Immobilized enzyme has been expected to industrial applications. Immobilized enzyme effectively enables to separate the enzyme from products, thus facilitating its recovery and repeated use. A hydrophobic material is most favorable to easy diffusion of substrate in inner pore of carrier in order to quick initiation of hydrophobic enzymatic reaction. Recently, hydrophobic materials, primarily a polypropylene porous commercial carrier called Accurel, has been proposed for lipid [1]. In this study, we focused on hydrophobic porous carrier on reactivity of immobilized phospholipase A_1 progressing toward higher reaction rate and high yield in repeated use.

2. Methods

2.1 Phospholipase A_1 immobilization method

Accurel MP 100 (Membrana GmbH, Germany) (Figure 1 and 2) was immersed in ethanol (99.5 v/v%) for 60min. And then, the Accurel carrier was placed into the PLA1 solution and then shaken to adsorbed PLA1 for 24h at 298K.

Next, the dried Accurel carrier with the adsorbed PLA1 was shaken in Glutaraldehyde (GA) solution (1.5~6 v/v%) for 60 min at 298 K. The desorbed amount of PLA1 in the GA solution was the measured. The immobilized PLA1 carrier was briefly washed in distilled water.

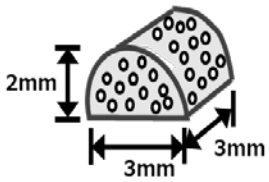

Figure 1. Schematic illustration of Accurel MP100.

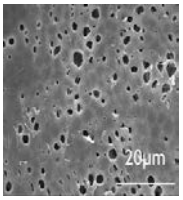

Figure 2. SEM image of Accurel surface.

2.2 Hydrolysis of phospholipid using immobilized PLA1 in Accurel carrier

Phospholipid (from soybean) was dissolved into the organic phase composed of 1-butanol/isooctane. The substrate solution (50mL) was placed in a glass vessel. And then, the substrate solution containing acetate buffer solution (pH5.0) were stirred magnetically for 10min in a water bath (313K). The reaction was initiated when the immobilized PLA1 on Accurel carrier was added to the W/O microemulsion phase. After the reaction was initiated, 0.2 mL of the sample was taken at the desired time in the reaction period. The concentration of produced fatty acid (palmitic acid) was determined by the Lowry-Tinsley colorimetric method [2].

3. Results and discussion

Figure 3 shows the effect of GA treatment on the initial reaction rate (V_i). The V_i increased with increasing GA concentration. Cross-linking of PLA1 by GA was very beneficial for attaining a higher reaction rate.

Figure 4 shows the time course of production of palmitic acid for the repeated use of immobilized PLA1. Repeated use of immobilized PLA1 was successfully appeared without lag time and preserved sufficiently high reaction yield until 2nd run. The activity site of immobilized PLA1 was not damaged after repeated processing.

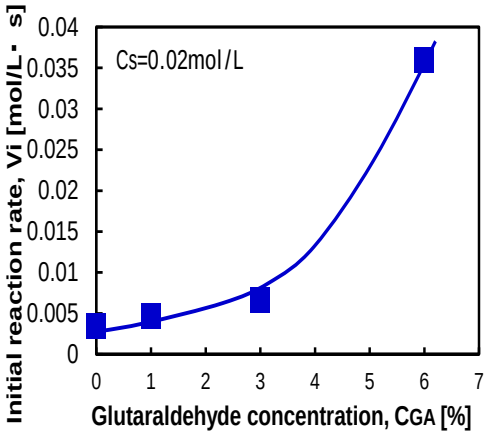

Figure 3. Effect of GA concentration on the V_i.

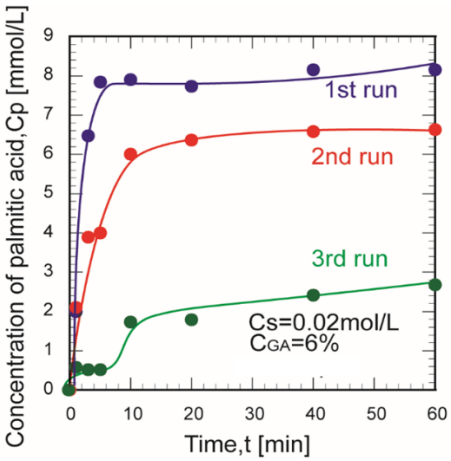

Figure 4. Time course of production for the repeated use of immobilized PLA1.

4. Conclusions

High yield immobilization of phospholipase A_1 and quick initiation of hydrolysis of phospholipid. Immobilized PLA1 was prepared using porous polypropylene carrier (Accurel MP100). Repeated used of immobilized PLA1 was attractively performed and stable. Accurel is expected to hydrophobic friendly phospholipase carrier progressing toward higher reaction rete and high yield in repeated use.

References

[1] M. Naya, M. Imai, Asia-Pac. J. Chem. Eng. 7 (2012) S157-S165.
[2] R.R. Lowry, I.J. Tinsley, J. Am. Oil Chem. Soc. 53 (1976) 470-472.

ECAB 5
The 5th EUROPEAN CONGRESS OF APPLIED BIOTECHNOLOGY
Florence 15-19 September 2019

Economic optimization of ethanol production from corn stover

Victor Grisales[1], Mark J. Willis[2]

1 Universidad Libre Seccional Pereira, Facultad Ciencias de la Salud. Grupo de investigación en Microbiología y Biotecnología MICROBIOTEC, Belmonte Avenida Las Américas; 2 School of Engineering, Newcastle University, NE1 7RU, Newcastle upon Tyne, United Kingdom

**Corresponding author: victorh.grisalesd@unilibre.edu.co*

Highlights

- A kinetic model for ethanol production including acetic acid inhibition is proposed.
- The kinetic model is used to study the economic potential of ethanol production.
- Energy needs in the purification are reduced by 17-23% using de-acetylation.
- The minimum ethanol selling price achieved was 1.83-2.25 USD/gal.

1. Introduction

Ethanol production using corn stover requires physical and/or chemical pretreatment before fermentation. The pretreatment methods that achieve the highest final ethanol concentration (65-90 g/l) have been reported by [1] where, as a precursor to physical pretreatment (mechanical refining), de-acetylation is proposed. As acetic acid is a known inhibitor, its effective removal can increase fermentation performance. After pretreatment, cellulose is partially converted to glucose by enzymatic hydrolysis. Unfortunately, the inhibition of soluble sugars during enzymatic hydrolysis reduces the conversion rate of cellulose to glucose. In addition, it is known that secondary carbon sources (e.g. xylose) are not effectively utilised during fermentation.

The aim of this work is to study the economic potential (EP) of ethanol production from corn stover using a conventional fed-batch reactor with a partial enzymatic hydrolysis step followed by simultaneous fermentation and co-saccharification (SFCS). SFCS offers an interesting means to reduce glucose and xylose inhibition during enzymatic hydrolysis. Two pretreatment strategies are considered; mechanical refining and a de-acetylation step followed by mechanical refining. As ethanol purification is energy intensive, a highly-energy efficient distillation system is also proposed: extractive distillation with vapor compression (ED-VC), as the purification method, as this is known to reduce the energy requirements when compared to a conventional purification system by 55% [2].

2. Methods

A kinetic model describing ethanol production using enzymatic hydrolysis and fermentation under atmospheric conditions is developed. This is based upon previously reported work that considered butanol production [3]. The model is validated using experimental data obtained from batch and continuous fermentations reported by [4,5,6]. The kinetic model includes acetic acid inhibition, preferential consumption of glucose over xylose and xylitol inhibition.

The model is used as the basis for the assessment of the EP of the process where hydrolysis and fermentation operating conditions are optimized in order to achieve the maximum EP. The EP cost

function incudes the capital and expenditure costs of pre-treatment, hydrolysis, fermentation and the distillation systems. A number of optimization scenarios are considered to include all possible ranges of concentrations of non-soluble solids, insoluble solids, glucan, xylan, acetyls, and lignin reported for corn stover by [7]. It is assumed that the corn-stover capacity is 2000 ton/day on a dry basis. The distillation costs and energy requirements are calculated using Aspen Plus V9®.

3. Results and discussion

The proposed kinetic model achieves an average correlation coefficient of 0.995. A typical result is shown in Figure 1a where it may be observed that the model accurately follows the measured experimental data. Through optimisation of the process operating conditions, using the kinetic model as a basis, we have found that the de-acetylation step reduces the energy requirements of ED-VC by 17 - 22.6% (see Figure 1b) which, in turn, reduces the minimum ethanol selling price (MESP) by 10 - 13%.

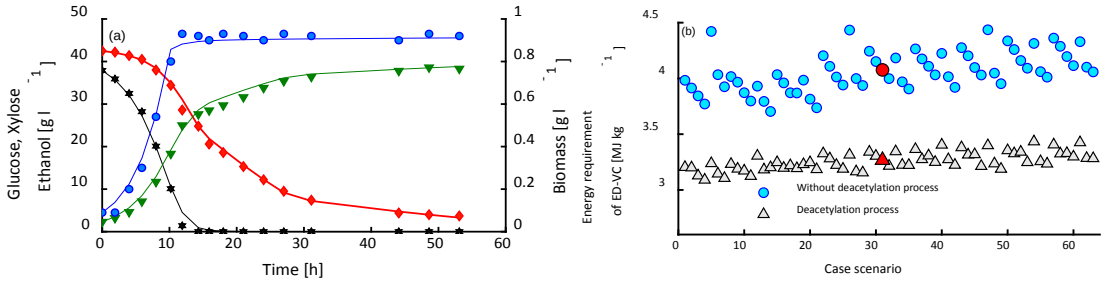

Figure 1. Profiles of the fermentation (initial concentration of acetate of 8 g/l) and energy requirements of ED-VC under optimal conditions. To the left (Figure 1 a) Data points are experimental data: glucose (stars), xylose (diamonds), ethanol (triangle) and biomass (circle). Experimental data was reported by [5]. Continuous lines represent the simulation predictions. To the right (Figure 1b) Fuel requirements of ED-VC. In Figure 1 b the red points represent the base case scenario reported by [7]

4. Conclusions

We have developed a kinetic model that describes ethanol production from corn-stover. The full paper will provide a more detailed account of the kinetic model, however, our results indicate that the inclusion of acetic acid (and the modelling of acetic acid inhibition during fermentation) is required as this significantly affects the EP of the process. Further details of the EP cost function and assumptions made to perform the optimisation will also be provided. In summary, our analysis indicates that the energy needs for ED-VC recovery are between 3.1 and 3.4 MJ fuel/kg ethanol (a reduction of 17 - 22.6% when de-acetylation is not considered) resulting in a minimum ethanol selling price of 1.83-2.25 USD/gal (a reduction of 10 - 13%).

References

[1] X. Chen, E. Kuhn, E.W. Jennings, R. Nelson, L. Tao, M. Zhang, M.P. Tucker, Energy Environ. Sci. 9 (2016)
[2] V.H. Grisales Díaz, G. Olivar Tost, Process Intensif. 108 (2016) 117–124
[3] V.H. Grisales Díaz, M. von Stosch, M.J. Willis, Chem. Eng. Sci. 195 (2019) 707–719
[4] I.S. Kim, K.D. Barrow, P.L. Rogers, Appl. Environ. Microbiol. 66 (2000)
[5] Y.J. Jeon, C.J. Svenson, E.L. Joachimsthal, P.L. Rogers, Biotechnol. Lett. 24 (2002) 819–824
[6] E.L. Joachimsthal, P.L. Rogers, , Appl. Biochem. Biotechnol. 84–86 (2000) 343–56
[7] D. Humbird, R. Davis, L. Tao, C. Kinchin, D. Hsu, A. Aden, P. Schoen, J. Lukas, B. Olthof, M. Worley, D. Sexton, D. Dudgeon, NREL 2011

ECAB 5
The 5th EUROPEAN CONGRESS OF APPLIED BIOTECHNOLOGY
Florence 15-19 September 2019

Crude biofuel for potential off grid remote power generation using waste biomass feedstocks: A feasibility analysis for the case of Botswana.

*Gratitude Charis[1], Gwiranai Danha[1], Edison Muzenda[1,2]

1 Department of Chemical, Materials and Metallurgical Engineering, College of Engineering and Technology, Botswana International University of Science and Technology, Plot 10071, Boseja Ward, Private Bag 16 Palapye, Botswana.;

2 Department of Chemical Engineering in the Faculty of Engineering and Built Environment, University of Johannesburg PO Box 524, Auckland Park, 2006

Johannesburg, South Africa

**Corresponding author: gratitude.charis@studentmail.biust.ac.bw*

Highlights

- There are a number of isolated communities in sparsely populated Botswana with no access to electricity; their connection to main grid deemed very uneconomical.
- Only explored alternative has been solar, meanwhile there is a large resource of waste encroacher biomass which can be used.
- Exploring pyrolysis alternative where the bulky thorny bushes are pyrolysed on site to increase energy density before being transported to a slightly modified sterling engine that can be a stand alone power generator or part of a hybrid system
- Thermochemical characterization for acacia undertaken.

1. Introduction

The case of access to electricity for remote areas has always been topical, especially for developing nations where the energy poverty translates to retarded development for such communities. Botswana is one such nation that has scattered, isolated and sparsely populated settlements where the extension of the main grid is uneconomical. Close to about 43% of rural and 25% of urban households in Botswana have no access to electricity {Formatting Citation}. Most attention has been directed at powering remote off-grid communities using renewable sources like solar, which are accessible everywhere; however, not much attention has been paid on emerging renewable sources like 2nd generation biofuels from lignocellulosic waste. Coincidentally, Botswana is home to notorious woody encroacher species that are costing the government and communities millions of dollars annually through depleting pastures and subsequently livestock productivity [1]–[3]. Some of the money is spent in debushing exercises to restore the aesthetic appeal in cities, towns and villages, since these drought resistant coppices spring up everywhere. Meanwhile nations like Namibia have turned the woody encroacher nuisance into value through very profitable renewable energy ventures like charcoal [4]. This feasibility analysis which is focused on alleviating energy poverty in remote settlements explores all the possible power generation alternatives that could use the encroacher biomass, especially after converting it into a crude biofuel (bio-oil). Relatively simple technologies that can be run within such contexts are explored. Carbonization techniques for raw biomass, pyrolysis and simple upgrading of oil, various power generation alternatives and

hybrid options with prevalent renewable energy initiatives are examined and compared. A preliminary economic feasibility check is done.

2. Methods

Since this is mostly a feasibility analysis, the major avenues of ascertaining facts is being done through desktop studies, interviews of remote community leaders and relevant civil society stakeholders. Economic feasibility is being done by comparing with similar plants and checking prices of equipment from vendors. Thermochemical characterization was done using equipment for elemental analysis, thermogravimetry and calorimetry.

3. Results and discussion

The results so far obtained pertain the properties of the biomass encroacher species, *Acacia Tortillis*, which is one of the major encroacher bushes. These characterization results help to map the conditions and resulting products for thermochemical conversion processes.

Table 1. Results from thermochemical characterization

	Ultimate analysis- average of 2 (Thermo scientific flash 2000 CHNS-O analyser)				Proximate analysis (Dry basis)- averages (Thermogravimetric analyser- Leco TGA 701)				**HHV** (MJ/kg) Bomb CAL2K-2
%	C	H	N	O[a]	Ash	FC	VM	MC	
ACACIA	41.47	5.15	1.23	52.15	3.90	19.59	76.51	3.72	17.267
PINEDUST	45.76	5.54	0.039	48.66	0.83	20.00	79.16	65.41	17.568

The moisture and ash contents are within acceptable limits; while the high volatile matter typical for lignocellulosics shows a high potential for bio-oil generation. The relatively higher ash (compared to Pine) in the feedstock will report to the bio-oil affecting its stability although the margin of effect would still need to be determined.

4. Conclusions

The thin stems of most of the shrub encroachers from debushing exercises are not eligible for charcoal production, the method largely used by Namibia to valorize its large waste encroacher inventory. The larger trees from rangelands can be converted into charcoal; however construction of even mini power plants to use solid fuel for combined heat and power generation will not be very cost effective for smaller populations. An autothermal pyrolysis plant, possibly integrated with solar, can be a quick alternative requiring less sophisticated technology and expertise. A modified sterling engine can be used to generate power from the pyrolysis oil.

References

[1] N. M. Moleele, S. Ringrose, W. Matheson, and C. Vanderpost, “More woody plants? The status of bush encroachment in Botswana’s grazing areas,” *J. Environ. Manage.*, vol. 64, no. 1, pp. 3–11, 2002.

[2] N. Lukomska, “The Economic Value of Real Options in Biodiversity Management - The Case of Bush Encroachment Control in Semi-Arid Rangelands.,” University of Zurich, 2010.

[3] S. Kabajan, K. Kaunda, and K. Matlhaku, “Shoot Production by Acacia tortilis under Different Browsing Regimes in South-East Botswana,” no. January 2011, 2016.

ECAB 5
The 5th EUROPEAN CONGRESS OF APPLIED BIOTECHNOLOGY
Florence 15-19 September 2019

A Kinetic and Metabolic Flux Analysis of the Biphasic Acetone-Butanol Fermentation.

Muven Naidoo[1*], Siew Tai[1], Susan Harrison[1]

1 Centre for Bioprocess Engineering Research (CeBER), Department of Chemical Engineering, University of Cape Town, Rondebosch, 7701, South Africa

**Corresponding author: muven.naidoo@uct.ac.za*

Highlights

- Two-stage kinetic model constrained by the metabolic network of solventogenic *Clostridia*.
- The model accurately represents the acidogenic phase of the fermentation.
- CO_2 and H_2 predicted with consistent material balance without experimental analysis

1. Introduction

The Acetone-Butanol (AB) fermentation can be characterized as a two-phase process via solventogenic *Clostridia.* In the first phase, growth and acidogenesis occur with the production of acetic and butyric acids. In the second phase, a morphological change is observed. Growth ceases and solventogenesis occurs where the acids are re-assimilated by the organism to form solvents. Throughout the fermentation, hydrogen and carbon dioxide gases are released. Previous kinetic and stoichiometric models for the AB fermentation were relatively simple or were not always consistent in terms of the material balance. Further, several models do not account for the biphasic nature of the *Clostridial* biocatalyst. These models are sufficiently accurate for the modeling of batch fermentations without integrated separation. However, when integrated separation is considered in batch, fed-batch or continuous systems, the previous models do not accurately account for the accumulation of intermediary products and productivities are often inaccurately represented. In this work, we introduce a kinetic two-phase model that is constrained by the metabolic network of the *Clostridial* biocatalyst. This model incorporates the morphological change of the biocatalyst and ensures consistency of the material balance.

2. Methods

C. saccharobutylicum P262 was used in this study. A spore suspension of the organism was maintained in deionized water at 4 °C. The seed inoculum was prepared in reinforced clostridial medium (Merck) and the main culture fermented in tryptone-yeast extract-acetate (TYA) medium [1] with 60 g L^{-1} starting glucose concentration. Anaerobic batch cultures were carried out with stirring at 100 rpm at 34 °C in 120 mL serum bottles with an 80 mL working volume. Samples were periodically withdrawn, and fermentations were performed in triplicate.

The metabolic flux analysis (MFA) was based on the metabolic network for *C. acetobutylicum* [2]. The kinetic model was developed using the assumptions listed by [3] except for temperature at 34

°C and pH being uncontrolled. Calculations were carried out on Scilab v. 6.0.1. using the Nelder-Mead simplex method for non-linear regression and the Runge-Kutta method of numerical integration for solving differential equations.

3. Results and discussion

To test the modeling approach without the complexity of the two-phase model, the MFA was coupled to the kinetics of a butyric acid fermentation with *C.* tyrobutyricum ATCC 25755. This is metabolically identical to the acidogenic phase of AB fermentations. Data taken from Song et al [4] were regressed and the results are graphically displayed in Figure 1.

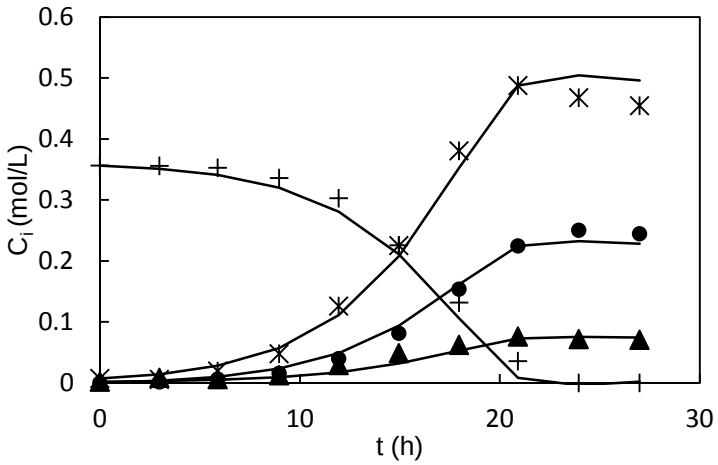

Figure 1. Butyric acid fermentation profile. Raw data taken from Song et al [4]. ✳- biomass (exp), + - glucose (exp), • - butyric acid (exp), ▲- acetic acid (exp). Solids lines indicate predicted concentrations.

By inspection, there is a good fit of the kinetic model to the experimental results. Using MFA, the yields of hydrogen and carbon dioxide were predicted to be 0.02 g $g_{glucose}^{-1}$ and 0.40 g $g_{glucose}^{-1}$ respectively. These results allow for a fundamentally more accurate representation of the fermentation kinetics and material balance.

4. Conclusions

The integration of a kinetic model with the constraint of the metabolic network of solventogenic *Clostridia* has been demonstrated for the acidogenic phase. This allows for a fundamentally more accurate representation of the fermentation profile and ensures consistency for the material balance. Future work will demonstrate the effectiveness of the model including the solventogenic phase.

References

[1] H. Shinto, Y. Tashiro, M. Yamashita, G. Kobayashi, T. Sekiguchi, T. Hanai, Y. Kuriya, M. Okamoto, K. Sonomoto, J. Biotechnol. 131 (2017) 45-56

[2] D. T. Jones, D. R. Woods, Microbiol. Rev. 50 (1986) 484-524

[3] A. Mulchandani, B. Volesky, Can. J. Chem. Eng. (64) 625 – 631

[4] J. Sing, K. Ventura, C. Lee, D. Jahng, Biotechnol. Bioprocess. Eng. 16 (2011) 42 – 49

Phage-free production of artificial ssDNA with *Escherichia coli*

Karl Behler[1]*, Hendrik Dietz[2], Dirk Weuster-Botz[1]

[1]*Technical University of Munich, Institute of Biochemical Engineering*
Boltzmannstraße 15, 85748 Garching, Germany
[2]*Technical University of Munich, Institute of Biomolecular Design*
Am Coulombwall 4a, 85748 Garching, Germany
**Corresponding author: k.behler@lrz.tum.de*

Highlights

- Phage-free ssDNA production
- Custom ssDNA sequence for DNA-origami
- Mass production of ssDNA becomes scalable

1. Introduction

Scaffolded-DNA-Origami is a nanotechnology where, upon hybridization of ssDNA strands, predefined nanostructures can fold in a one-pot self-assembling reaction. For every so produced nano-object one long ssDNA-strand (scaffold) and multiple short ssDNA-strands (staples) are needed. Up to now the staples are chemically synthesized oligonucleotides and the scaffold is a variant of the single-stranded DNA-genome of the M13-phage. [1]

M13-phages can be produced in high cell density cultivations in stirred-tank bioreactors by infecting *E. coli* cells during cultivation [2]. The phages can be obtained from the culture-supernatant and their ssDNA genome can be prepared in a few simple steps. However most of the sequence is set to be the genome of the M13-phage and synthesis of the staples is very costly. Thus it would be interesting to be able to biotechnologically produce a custom ssDNA where most of the sequence is free to choose.

This can actually be done using a phagemid, a phage-plasmid-hybrid, which by default contains only the packaging sequence and the ori of the phage. All additional bases in the phagemid can be chosen freely. Phagemid-ssDNA can be produced by infecting *E. coli* cells carrying one phagemid with a helperphage or by double-transformation of *E. coli* with a phagemid together with a helperplasmid [3, 4] The first technique however will yield a mixture of helperphages and phagemid-particles which then leads to a mixture of ssDNA-species. On top helperphages are virions which might remain in the bioreactor even after sterilization, which makes production by contract manufactures impossible. The second technique gives only very poor yields and cells transferred to fresh medium don't produce at all which makes storing of those cells and scale-up even to the liter-scale more or less impossible.

2. Methods

M13 genome was purchased from New England Biolabs and phagemid vectors (pBluescript) where received from Addgene. For construction of plasmids PCR amplicons (from Plasmid and M13 genome) where assembled using Gibson assembly [5]. For all experiments *E. coli* NEB turbo (New England Biolabs) have been used. All cultivations have been performed in minimal medium [6].

Cultivation in shake flasks was held at 37°C and 250 rpm in a wise cube shaker (Witeg). High-cell density cultivations were performed in a 2.5 liter stirred tank bioreactor KLF2000 (Bioengineering) using a fed-batch operating mode. Execution was adopted from Kick et. al. 2015 [2].

3. Results and discussion

As production of artificial ssDNA using a helperplasmid gives very low yields, decoupling of biomass formation and production had to be achieved. For this purpose *E. coli* carrying a helperplasmid were grown to an optical density OD_{600} of 0.4 and afterwards infected with phagemid-particles. This however yielded no measurable new ssDNA product. The result is most likely to be attributed to the presence of M13 protein pIII which as described before [7, 8] mediates a kind of infection resistance.

To prove the assumption in an experiment, pIII was put under the expression control of a repressible promoter. *E. coli* carrying a plasmid with this gene-III-cassette could be infected with M13 phages when gene-III-expression was not induced but could not be infected, when gene-III-expression was induced. Upon this result we moved gene III from the helperplasmid to the phagemid enabling the infection of *E. coli* cells carrying a helperplasmid without gene III by phagemid-particles.

Using this system biomass formation could be separated from ssDNA production where cells only carrying the helperplasmid could also be stored at -80°C without loss of production capability. Also with this system the yield could be increased two-fold in shake flask cultivations. More importantly though, as production with the conventional method is not scalable, this new method makes biomass production at any scale possible. Using a stirred- tank bioreactor at the liter scale in a fed-batch operation mode, we were able to increase volumetric yields about 30-fold compared to the conventional method.

4. Conclusions

By moving M13 gene III from the helperplasmid to the phagemid a system could be established, where *E. coli* cells carrying only a helperplasmid could be grown without producing any phage-like-particles. Upon infection with phagemid-particles these cells started producing new phagemid-particles. Through this temporal decoupling of biomass formation and phagemid-particle production, *E. coli* cells could (i) be transferred to a bioreactor without losing their ability to produce phage-like-partikles and (ii) *E. coli* cells started producing phagemid-particles upon infection with the latter. This resulted in a 20-fold increase of volumetric ssDNA yield.

References

[1] P. W. K. Rothemund, Nature, vol. 440, no. 7082, pp. 297–302, 2006.
[2] B. Kick, F. Praetorius, H. Dietz, and D. Weuster-Botz, Nano Lett., vol. 15, pp. 4672–4676, 2015.
[3] L. Chasteen, J. Ayriss, P. Pavlik, and A. R. M. Bradbury, Nucleic Acids Res., vol. 34, no. 21, pp. 1–11, 2006.
[4] F. Praetorius, B. Kick, K. L. Behler, M. N. Honemann, D. Weuster-Botz, and H. Dietz, Nature, vol. 552, no. 7683, pp. 84–87, 2017.
[5] D. G. Gibson et al., Nat. Methods, vol. 6, no. 5, pp. 343–5, 2009.
[6] D. Riesenberg et al., J. Biotechnol., vol. 20, no. 1, pp. 17–27, Aug. 1991.
[7] J. D. Boeke, P. Model, and N. D. Zinder, vol. 16, pp. 185–192, 1982.
[8] A. K. Brödel, A. Jaramillo, and M. Isalan, Nat. Commun., vol. 7, p. 13858, 2016.

Use of Genome Scale Models to get New Insights into the Marine Actinomycete genus Salinispora: Metabolic Engineering and its Application in Secondary Metabolite Production

C.A. Contador, V.D. Saucedo, J.A. Asenjo, and B.A. Andrews

Centre for Biotechnology and Bioengineering, CeBiB, University of Chile
Beauchef 851, Santiago, Chile,

**Corresponding author: bandrews@ing.uchile.cl*

Highlights

- Bacteria within the genus *Salinispora* are a well-known source of natural products.
- *Salinispora tropica* is a marine actinomycete that produces diverse secondary metabolites
- The first manually curated genome-scale metabolic model for *Salinispora tropica* was constructed.
- GSMs were constructed for fully sequenced type strains of *S. arenicola*, and *S. pacifica.*

1. Introduction

Bacteria within the order Actinomycetales are a well-known source of natural products such as antibiotics and anticancer agents, and the genus *Salinispora* is no exception. *Salinispora tropica* is a marine actinomycete that produces diverse secondary metabolites, including many that possess pharmaceutical properties such as Salinosporamide A (NPI-0052), a potent anticancer agent, and sporolides, candidates for antiviral compounds. Few manually curated actinomycete reconstructions are currently available despite their important role in drug discovery. Recently, the first manually curated genome-scale metabolic model for *Salinispora tropica* strain CNB-440T was constructed [1]. This model provides a starting point to produce Genome Scale Models (GSMs) of closely related organisms such as other *Salinispora* species. This study is focused on new insights into the metabolism of the three-identified species using constraints-based modeling. GSMs were constructed for fully sequenced type strains of *S. arenicola*, and *S. pacifica*, strains CNH643T and CNR-114T, respectively. We also constructed a Salinispora core model that contains the genes shared by 93 sequenced strains. Functional differences between the developed metabolic networks were identified to have a glimpse into the unique metabolic differences attributable to each *Salinispora* species.

2. Methodology

To create metabolic reconstructions to represent each Salinispora species, the gene sequence from the metabolic model for *Salinispora tropica* CNB-440T was used to identify orthologs. We studied 89 genomes of *Salinispora* strains with high quality draft genomes together with the type

strains. Phylogenetic estimation was carried out using the amino acid sequences of the proteins encoded by the core genes.

3. Results and discussion

The genome-scale metabolic model, *i*CC908 was used to study strain-specific capabilities in defined minimal media and to analize growth capabilities in 41 different minimal growth-supporting environments. These nutrient sources were evaluated experimentally to assess the acuracy of in-silico growth simulations. Here, we update, and expand the scope of the model of *Salinispora tropica* CNB-440T, and GSMs were constructed for two sequenced type strains covering the three-identified species. We also constructed a *Salinispora* core model that contains the genes shared by 93 sequenced strains and a few non-conserved genes associated with essential reactions. The models predicted no auxotrophies for essential amino acids, which was corroborated experimentally using a defined minimal medium (DMM). The Core metabolic content shows that the biosynthesis of specialised metabolites is the less conserved subsystem. Sets of reactions were analyzed to explore the differences between the reconstructions. Unique reactions associated to each GSM were mainly due to genome sequence data except for the ST-CNB440 reconstruction. In this case, additional reactions were added from experimental evidence. This reveals that by reaction content the ST-CNB440 model is different from the other species models. The differences identified in reaction content between models gave rise to different functional predictions of essential nutrient usage by each species in DMM. Furthermore, models were used to evaluate in silico single gene knockouts under DMM and complex medium. Cluster analysis of these results shows that ST-CNB440, and SP-CNR114 models are more similar when considering predicted essential genes.

Also, the GSM of *Salinispora tropica* has been used to define a production medium to improve Salinosporamide A production in a recombinant strain with increases compared to the wild type.

4. Conclusions

This study shows that strain-specific models of *Salinispora* can help to better understand the metabolism of *Salinispora* strains, and gain more knowledge about the physiology of the different species. *Salinispora* models would help researchers to establish links between genetic data and metabolic phenotypes. Additionally, the models developed can be used to systematically analyze the essential growth capabilities of Salinispora metabolism that delineate the adaptation process and enhance the production of specialised metabolites.

References

[1] Contador CA, Rodríguez V, Andrews BA, Asenjo JA. Genome-scale reconstruction of *Salinispora tropica* CNB-440 metabolism to study strain-specific adaptation. Antonie van Leeuwenhoek, Int. J. Gen. Mol. Microbiol. 2015;108:1075–90.

[2] Contador CA, Rodríguez V, Andrews BA, Asenjo JA. Use of Genome Scale Models to get New Insights into the Marine Actinomycete genus Salinispora. 2019; BMC systems Biology, in press.

Biocompatibility of polyurethanes' thin film on smooth muscle cells

María Morales-González[1*], Said Arévalo-Alquichire[1], Luis E. Diaz[2] and Manuel F. Valero[1]

1 Energy, Materials and Environment Group, Faculty of Engineering, Universidad de La Sabana, Colombia; 2 Bioprospecting Research Group, Faculty of Engineering, Universidad de La Sabana, Colombia.

**Corresponding author:mariamorgon@unisabana.edu.co*

Highlights

- Viability of SMC was higher in polyurethanes that have greater PCL content.
- Presence of PCL increased the contact angle of polyurethanes.
- Polyurethanes surfaces showed a hydrophilic behavior.

1. Introduction

Cardiovascular diseases represent the first cause of death worldwide, due to some vascular pathologies such as atherosclerosis, hypertension, thrombosis, angioplasty and restenosis that occur in blood vessels [1]. It is known that those pathologies are related with some disorders in the wall vessel structure like abnormal proliferation of smooth muscle cells (SMC) due to a phenotype change from contractile to synthetic [1,2], that lead a migration and accumulation from the media into the intima [3].

The use of polyurethanes as synthetic materials has gained a lot of attention on the field of tissue engineering, for their production process, versatility and biocompatibility [4], owned by the presence of a segmented chemistry that allow to adjust the mechanical, physical and biological properties by the adjustment of the raw materials [5].

Once the material is immersed in the cellular environment, the processes of adsorption of proteins on the surface of the material allows cell adhesion [6]. The properties of the material surface such as hydrophobicity and chemical composition are important for the biocompatibility of the material and can allow a better performance of the grafts. Thus, the aim of the investigation was to relate the effect of the composition, in terms of the contact angle of polyurethanes and the biocompatibility of smooth muscle cells.

2. Methods

Polyurethanes were synthetized via a two-step polymerization. Polycaprolactone, polyethylene glycol, isophorone diisocyanate and pentaerythritol (crosslinker) were used. Each polyol sample was diluted in 10 mL of DMF at 110 °C, and then IPDI was added at an NCO/OH ratio of 1 and allowed to react for 15 min at 70 °C. PE was added to the prepolymer [7]. Thin films of 150 µm were prepared and cured at 110 °C for 12 h.

Sessile drop method was used to measure contact angle in a MobileDrop (KRÜSS GmbH, Hamburg, Germany) with distilled water at room temperature.

Aortic smooth muscle cells (AoSMCs, Walkersville, Maryland) were cultured and used at passage 6-7. Cell suspension with a density of $1x10^6$ cell/mL were cultured for 12 h. Polyurethane samples

were placed with cells for 24 h (5% CO2 at 37 °C). After, samples were removed and 100 µL of resazurin solution (44 µM) was added and incubated for 4 h. The fluorescent product resorufin was measured with at a wavelength of 590 nm using an excitation wavelength of 560 nm.

3. Results and discussion

Figure 1A shows the results for viability test of SMC in polyurethanes. As it can be seen the viability was higher in polyurethanes that have greater PCL content. PCL is a widely used polymer for biomedical applications as their high biocompatibility [8].

The contact angle values of the surface of PUs are presented in Figure 1B. Contact angels over 90° represent a hydrophobic surface, thereby polyurethanes surfaces showed a hydrophilic behavior, that can be explain by the hydrophilic nature of PEG. The presence of PCL increased the contact angel due to its hydrophobic character [7].

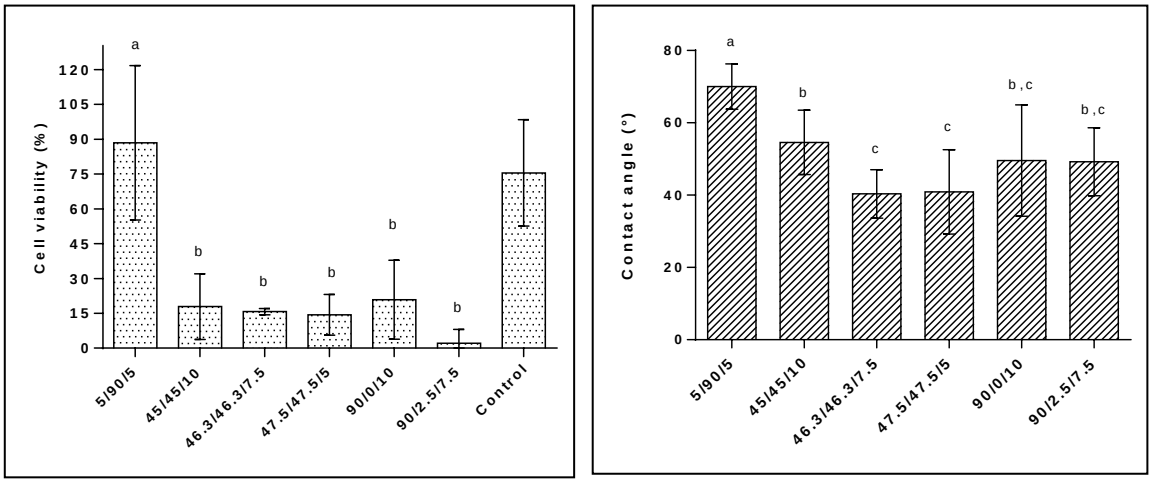

Figure 1. Aortic Smooth Muscle cell viability on polyurethanes (a); Contact angle of polyurethanes surface (b). Polyurethane composition is express as PEG/PCL/PE. Mean (n = 3) ± standard deviation; According to the analyses of variances and Tukey Pairwise Comparisons, means that do not share a letter are significantly different ($p < 0.05$).

4. Conclusions

For AoSMC hydrophobic surfaces allow a better environment for cells. The composition of the material is important for hydrophilicity possibly due to the nature of the polyols (PEG and PCL, hydrophilic and hydrophobic polyols, respectively), which will determine the behavior of the material and subsequently its biocompatibility with smooth muscle cells.

References

[1] F. Wolf, F. Vogt, T. Schmitz-Rode, S. Jockenhoevel, P. Mela, Drug Discov. Today. 21:9 (2016) 1446–1455.
[2] P.H. Blit, K.G. Battiston, M. Yang, J.P. Santerre, K.A. Woodhouse, Acta Biomater. 8:7 (2012) 2493–2503.
[3] H. Chen, G.S. J. Kassab, Biomech. 49:12 (2016) 2548–2559.
[4] F. Montini-ballarin, D. Calvo, P.C. Caracciolo, F. Rojo, P.M. Frontini, G.A.J. Abraham, Mech. Behav. Biomed. Mater. 60 (2016) 220–233.
[5] H.-Y. Mi, X. Jing, B.S. Hagerty, G. Chen, A. Huang, L.-S. Turng, Mater. Des. 127 (2017) 106–114.
[6] H.-I. Chang, Y. Wang, in: Regenerative Medicine and Tissue Engineering - Cells and Biomaterials, 2012, pp. 569–588.
[7] S. Arévalo-Alquichire, M. Morales-Gonzalez, L. Diaz, M. Valero, Molecules. 23:8 (2018) 1942.
[8] J. Horakova, P. Mikes, A. Saman, V. Jencova, A. Klapstova, T. Svarcova, M. Ackermann, V. Novotny, T. Suchy, D. Lukas, Mater. Sci. Eng. C. 92 (2018) 132–142.

ECAB 5
The 5th EUROPEAN CONGRESS OF APPLIED BIOTECHNOLOGY
Florence 15-19 September 2019

Transfer of the TAPPIR®-Technology to a Packed Bed for Separation of Biomolecules

Fabian Görzgen[1], Gerhard Schembecker[1]

1 Laboratory of Plant and Process Design, TU Dortmund University, 44227 Dortmund, Germany

**Corresponding author: gerhard.schembecker@tu-dortmund.de*

Highlights

- Semi continuous aqueous two-phase extraction
- Packed bed application of the TAPPIR®-Technology in a column
- Impregnation stability of porous particles in incident flow

1. Introduction

Since gentle and cost efficient separation techniques for biochemical products are of major interest for the biotech-industry, Aqueous Two-Phase Extraction (ATPE) has been shown to be a promising approach in this regard [1]. This is mainly based on the high biocompatibility of ATPE resulting from the water content of up to 70-90 wt.-%. However, long phase separation times in “conventional” ATPE design (Mixer-Settler-Approach) are the major drawback of this technique, requiring additional equipment and energy to enable faster phase separation [2]. To circumvent this bottleneck, the Tunable Aqueous Polymer Phase Impregnated Resins (TAPPIR®)-Technology is applied. As one phase of the Aqueous Two-Phase System (ATPS) is immobilized in porous particles enabling extraction through dispersion of these particles in the other aqueous phase, a subsequent liquid-liquid separation is no longer necessary. The impregnation stability [3] and competitive mass transfer kinetics of biomolecules within the TAPPIR®-Technology compared to “conventional” ATPE were already proven in batch experiments. In order to implement this technique in an industrial process, in this work the TAPPIR®-Technology is transferred to a column enabling a semi continuous flow-through separation of biomolecules in a packed bed. Consequently, one aqueous phase is used as the mobile phase, whereas the other aqueous phase is stationary impregnated in the particles providing an easy and cost efficient separation process. Within this work, we focused on the impregnation stability of the stationary phase in porous particles in flow through operation as well as the extraction performance in the packed bed.

2. Methods

A polyethylene glycol - tri-sodium citrate (polymer-salt) ATPS was used in this work. If applicable, sodium chloride was utilized as displacement agent. After preparation, the ATPS is equilibrated and transferred to a dropping funnel for settling. Immunoglobulin G serves as a model biomolecule within this work and is introduced into the system using the salt-rich phase of the APTS. Polymer-rich phase impregnated micro porous ceramic particles are packed in a semi-preparative YMC ECOPlus glass column. An ÄKTApurifier from GE Healthcare is used as utility to ensure stable process conditions. The impregnation status can either be determined by adding a dye to the stationary

phase or the retention time of Bovine serum albumin, introduced as a tracer that partitions selectively to the salt-rich phase. An UV detector is used for the analysis of the biomolecule concentrations.

3. Results and discussion

In order to transfer the TAPPIR®-Technology to a semi continuous operation mode in a packed bed column, several factors need to be evaluated: (1) impregnation stability of the stationary phase, (2) uniform flow within the packed bed, (3) extraction performance comprising the kinetics in continuous flow. The impregnation stability in batch experiments of the polymer-rich phase in porous ceramic particles showed negligible leaching as soon as the three-phase contact angle (measured from the polymer-rich phase on solid material in salt-rich phase) showed values < 90 °. However, upon transfer to a column, in which the impregnated particles have to withstand a steady incident flow, several factors influence stability not encountered in batch mode. It is shown that a uniform packing induces slower leaching rates. Also, packed beds formed by larger particles have a higher impregnation stability than those with smaller particles of the same material. Moderate flowrates (e.g. 1 ml/min in a column with a diameter of 1 cm) additionally lower the leaching of the impregnated phase out of the pores. Changing the ATPS composition itself (e.g. using polyethylene glycol with a higher molecular weight), a stable impregnation in steady flow could be achieved for more than 48 hours. This now allows for further characterization of the new setup towards process parameters that enable an optimal extraction efficiency.

4. Conclusions

Within this work, it was shown that the transfer of the TAPPIR®-Technology to a packed bed in a column was possible enabling a semi continuous two-phase extraction. Thereby, additional downstream treatment of the emulsion compared to classical ATPE was avoided. In the packed bed application, factors influencing the impregnation stability of the polymer-rich phase in the porous particles were identified allowing to apply optimal process conditions in semi continuous mode. The extraction performance was competitive to conventional ATPE and can be optimized further by adjusting design and process parameters. It was shown that the TAPPIR®-Technology in a column offers an improved approach for the implementation of ATPE as a separation technique for biomolecules.

References

[1] J. A. Asenjo, B. A. Andrews, J. Chem. Technol. Biotechnol. 83 (2) (2008) 117-120.
[2] U. Gündüz, A. Tolga, J. Chromatogr. B 807 (1) (2008) 13-16.
[3] I. Kaplanow, M. Schmalenberg, I. Borgmann, G. Schembecker, J. Merz, Sep. Purif. Technol. 190 (2018) 1-8.

ECAB 5
The 5th EUROPEAN CONGRESS OF APPLIED BIOTECHNOLOGY
Florence 15-19 September 2019

Study the ability of the rotary evaporator pressure to remove reagent from collagen hydrolyzed fish skin.

Admir Alves[1], Tatiane Balliano[2], João Soletti[3], Venâncio Bezerra[4], Milena Santos[5], Gabriela Carvalho[6], Cristiane Nascimento[7]

1 Programa de pós-graduação em engenharia química-PPGEQ/UFAL;2,6 Institutos de Química e Biotecnologia- IQB/UFAL; 3,4,5 Centros de Tecnologia-CTEC/UFAL.
sendy_ws@hotmail.com
7 Programa de pós-graduação da Rede Nordeste de Biotecnologia- RENORBIO/UFAL

1. Introduction

In order to remove excess acetic acid (HAc) from the reaction product between Nile Tilapia skin and said reagent, a laboratory scale distillation process was carried out by means of a rotary evaporator. Due to the stability of the collagen at low pressures, only the H2O / HAc mixture was evaluated in the distillation process. Given this premise, the Antoine equation was used to know in which pressure the Water and the Acetic Acid would present the vapor state and the operating pressure of the process.

$$\ln P^{sat}(kPa) = A - \frac{B}{T(°C) + C}$$

Where A, B and C are the Antoine parameters which are tabulated and, T the temperature operating in degrees Celsius (ºC).
For plotting the H2O / HAc equilibrium curve, the fundamental equation of Raoult's Law (equation 2.2) was used. For the fractions of the substance and the total pressure of the system (eq. 2.3)

$$y_i P = x_i P^{sat} \quad \text{(eq. 2.2)}$$

$$P = \sum_i x_i P_i^{sat} \quad \text{(eq. 2.3)}$$

Onde:
y_i: vapor fraction of substance *i*;
x_i: Fraction of liquid from the substance*i*;
P: Operating pressure;
P^{sat}: Saturation pressure of substance i

2. Methods

2.2. Collagen Extraction by Acid-Base Method

The extraction were used 100g fish skin, where the methodology was developed from the technique described by Monteiro and Gómez-Guillén. Skin samples were treated using three different solutions, NaCl solution (0.8M) to remove excess water in the skin, and some surface proteins, a solution of NaOH (0.1M) for partial removal of fat in the skin and other impurities, and

finally, a solution of acetic acid (0.05M) for the process of decoupling or breaking of the tissue chain which is also composed of collagen resulting in the hydrolyzed extract.

3. Results and discussion

To determine the operating pressure was used eq. 2.1 for both Water and Acetic Acid (Table 1).

Antoine Parameters				
Acetic Acid		water		Temperature (°C)
A	15,0717	**A**	16,3872	25
B	3580,8	**B**	3885,7	
C	224,65	**C**	230,17	
	kPa	**atm**	**mbar**	
P^{sat}_{H2O}	3,187741617	0,031460564	31,877416175	
P^{sat}_{HAc}	2,071803341	0,020447109	20,718033408	

Table 1: Antoine parameters the HAc e H_2O to determine the saturation pressure in 25ºC
Source: Van Ness, 2007

For better understanding the system pressure, equations 2.2 and 2.3 were used in the range of the molar fractions and the saturation pressures of the substances analyzed in order to plot the liquid vapor equilibrium curves of said reagents (Figure 1).

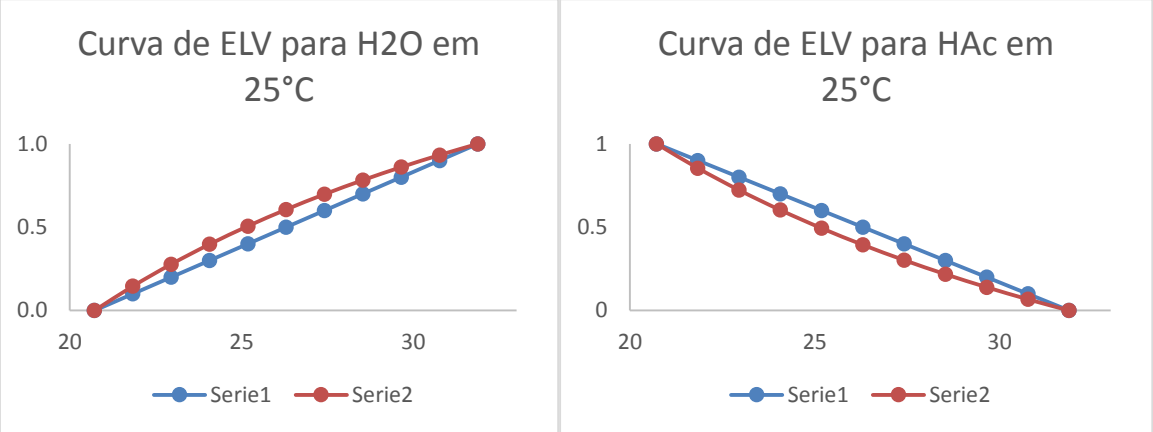

Figure 1: (a) Liquid-Steam Balance for Water at 25ºC (b) Liquid-Steam Balance for Acetic Acid at 25ºC

The region below the blue curve is the region where the water is in the superheated vapor state, while in the region above the orange curve it indicates the state of the subcooling liquid. The region below the blue curve is the region where the Acetic Acid is in the superheated vapor state, while in the region above the orange curve indicates the state of the subcooling liquid.

4. Conclusions

Since the reaction is in equilibrium, the displacement has formed for the reactants, thus generating more associated acetic acid, thus facilitating distillation the hydrolyzate without excess acid.

5. References

[1] GÓMEZ-GUILLÉN, M. C.; GIMÉNEZ, B.; LÓPEZ-CABALLERO, M. E.; MONTERO, M. P. Functional and bioactive properties of collagen and gelatin from alternative sources: A review. FoodHydrocolloids, v. 25, p. 1813-1827, 2011.ISSN 0268-005X.

[2] Smith, J. M., Van Ness, H. C. e Abbott, M. M., Introdução à Termodinâmica da Engenharia Química, 7a Ed., LTC – Livros Técnicos e Científicos Editora, Rio de Janeiro, 2007

Improving the electrochemical production of hydrogen peroxide

R.J.M. Bisselink[1], M. Zijlstra[1], E. Goetheer[2], N.J.M. Kuipers[1]
[1]Wageningen UR Food & Biobased Research
Bornse Weilanden 9, 6708 WG Wageningen, The Netherlands
norbert.kuipers@wur.nl
[2]TNO, department of Sustainable Process and Energy Systems
Leeghwaterstraat 44, 2628 CA Delft, The Netherlands

Hydrogen peroxide (H_2O_2) production is estimated at 4.7 Mton annually by 2017. It is used in various applications such as paper and pulp bleaching, textile bleaching, production of chemicals and environmental applications. Currently, it is industrially produced via the anthraquinone autoxidation process. However, we have shown that with our electrolyser approach (see Figure 1) ~10% H_2O_2 can be produced. This is sufficient for most applications (~75%), except for the production of chemicals which typically requires much higher H_2O_2 concentrations. Electrochemical production of H_2O_2 does not require any chemicals, and allows decentralized in-situ production, which reduces the need for its handling, transport and storage. Our latest research focused on reducing the production costs by increasing space-time yield of hydrogen peroxide and decreasing the electricity usage. Using more concentrated electrolytes, alternative anion exchange membranes, and a better electrolyser design, we were able to decrease the cell voltage considerably (see Figure 2). The electricity consumption could be reduced below 7 kWh/kg H_2O_2 at the industrial relevant current density of 4 kA/m^2.

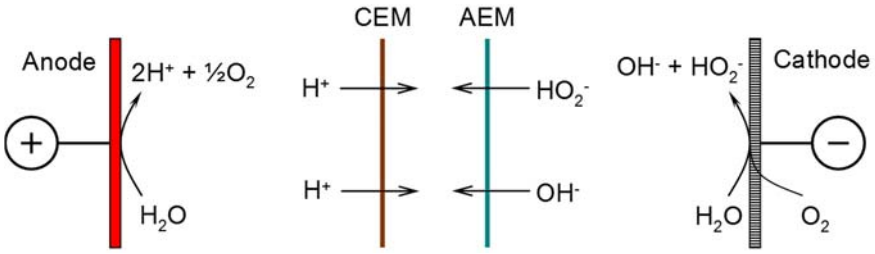

Figure 1: Schematic representation of the H_2O_2 electrolyser configuration.

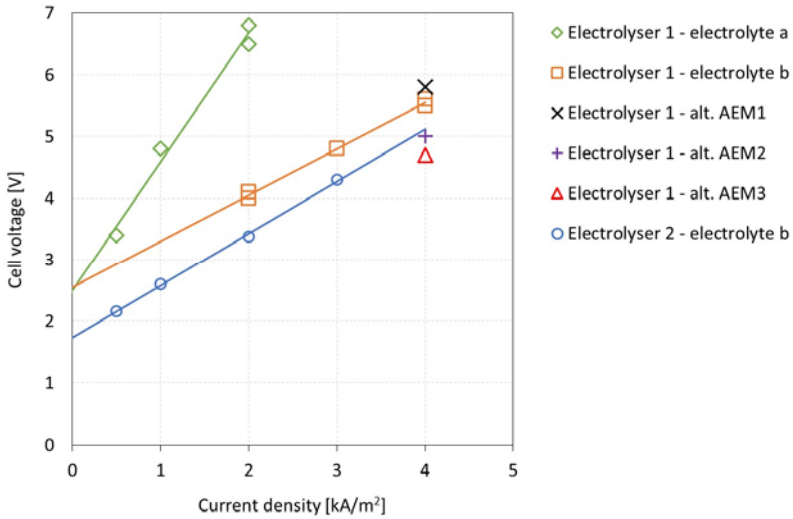

Figure 2: Influence of various parameters on the cell potential.

ECCE12
The 12th EUROPEAN CONGRESS OF CHEMICAL ENGINEERING
Florence 15-19 September 2019

3rd Workshop on Electrochemical Engineering:
Industrial Electrochemistry and Electrocatalysis

Electrochemical Modification of Polymer Chains: Synthesis of Crosslinked Poly(vinylpyrrolidone) Nanogels

Alessandro Galia[1*], Sonia Lanzalaco[2,3], Maria Antonietta Sabatino[1], Clelia Dispenza[1], Onofrio Scialdone[1], Ignasi Sirés[4*]

1 Dipartimento di Ingegneria, Sezione Chimica Ambientale Biomedica Idraulica e dei Materiali, Università degli Studi di Palermo, Viale delle Scienze, 90128 Palermo, Italy.

2 Departament d'Enginyeria Química, EEBE, Universitat Politècnica de Catalunya, C/Eduard Maristany 10-14, Ed. I2, Barcelona, Spain.

3 Barcelona Research Center in Multiscale Science and Engineering, Universitat Politècnica de Catalunya, C/Eduard Maristany 10-14, Ed. I2, Barcelona, Spain.

4 Laboratori d'Electroquímica dels Materials i del Medi Ambient, Departament de Química Física, Facultat de Química, Universitat de Barcelona, Martí i Franquès 1-11, 08028 Barcelona, Spain.

**Corresponding authors: alessandro.galia@unipa.it, i.sires@ub.edu*

Highlights

- Electro-Fenton is a facile, low cost, environmentally-friendly route to crosslink PVP
- Semi-dilute PVP, 0.5-1.0 mmol dm^{-3} Fe^{2+}, low j and short t: R_h < 10 nm (intramolecular crosslinking)
- Longer t and higher PVP and Fe^{2+} contents: M_w increases (intermolecular crosslinking)

1. Introduction

In recent years, increasing attention has been paid to the development of nanogels as nanocarriers for biomedical and bioengineering applications [1], being very useful in key tasks such as anti-cancer treatments [2]. Methods like gamma-ray irradiation or pulse radiolysis, which are based on the generation of free radicals that favour the formation of active centers on the polymer, have been previously investigated to promote the inter and/or intramolecular recombination that causes crosslinking. In a recent investigation, we have reported a certainly promising, innovative and simple electrochemical methodology to generate hydroxyl radicals that trigger the formation of chemically crosslinked nanogels [3]. Poly(vinylpirrolidone) (PVP) is a polymer with high versatility since non-charged PVP shows a high hydrophilicity and biocompatibility, absence of toxicity and adequacy to form interpolymer complexes [4]. In the present work, we have focused the attention on the homogeneous electrogeneration of hydroxyl radicals by electro-Fenton (EF) process in order to modify poly(vinylpyrrolidone) (PVP) in aqueous solutions [3,5].

2. Methods

PVP k-60 (M_r = 1.60×10^5 g mol^{-1}, M_w = 3.95×10^5 g mol^{-1}, 45 wt.% solution) was purchased from Aldrich and used as received. Oxygen (99.999% purity) and nitrogen (99.998% purity) were supplied by Air Liquide. All other chemicals used were from Sigma-Aldrich or Fluka and used as received.

Before each experiment, fresh PVP aqueous solutions were prepared using double-distilled water and stirred overnight, filtered with 0.22 µm nylon filters under vacuum. An undivided thermostated glass cell equipped with a water jacket was used for the electrosynthesis of nanogels. The cell contained 50 cm^3 of PVP solution at a given concentration with 0.05 M Na_2SO_4 in the presence of $FeSO_4$ as catalyst at pH 2.8 under continuous stirring. A carbon-polytetrafluorethylene (PTFE) air-diffusion electrode was used as the cathode to electrogenerate H_2O_2, whereas a Ti/IrO_2–Ta_2O_5 (DSA®) plate was used as anode. The geometric surface area of all electrodes in contact with PVP solution was 3 cm^2. The cathode was fed with pressurized O_2 for H_2O_2 generation. An Amel 2053 potentiostat/galvanostat was employed to operate at constant current.

3. Results and discussion

The main operation parameters such as polymer concentration, reaction time, catalyst (Fe^{2+}) concentration and charge passed (Q) were investigated. The dimensions of the nanogel formed, in terms of hydrodynamic radius (R_h) and weight-average molecular weight (M_w), have been evaluated via dynamic and static light scattering and gel permeation chromatography (GPC) analyses. In all cases, an important reduction of the size of PVP particles was achieved, along with narrower GPC peaks. Chain scission and intra-molecular recombination events were promoted at lower PVP concentration (< 0.50 wt.%) and for the low electrolysis times, leading to a reduction of R_h from 28 to 8-9 nm at catalyst concentration of 0.5-1.0 mM, while intermolecular crosslinking also concurred at longer times. Beside the electrolysis time, catalyst concentration and current density, j, are two other tunable parameters that can shift the balance between chain scission and crosslinking reactions. FT-IR analyses confirmed the functionalization of PVP nanogels, which become suitable for further conjugation reactions with biologically relevant molecules.

4. Conclusions

We found that EF can be adopted to crosslink PVP thus offering a cheap, eco-friendly, simple and fast alternative to current technologies. The adoption of proper balance of operation conditions is crucial for tuning up the main features of the resulting PVP nanogel in terms of particle size, mass and functionalization, which are modulated by the rate of generation of $^{\bullet}OH$ obtained from in situ electrogenerated H_2O_2.

References

[1] A.S. Hoffman, Adv. Drug Deliv. Rev. 64 (2012) 18–23.
[2] C. Dispenza, M.L. Bondì, M.A. Sabatino, M.P. Casaletto, N. Grimaldi, S. Rigogliuso, D. Bulone, G. Adamo, G. Ghersi, Biomacromolecules 13 (2012) 1805–1817.
[3] A. Galia, S. Lanzalaco, M.A. Sabatino, C. Dispenza, O. Scialdone, I. Sirés, Electrochem. Commun. 62 (2016) 64–68.
[4] M. Teodorescu, M. Bercea, Polym. Plast. Technol. Eng. 54 (2015) 923–943.
[5] S. Lanzalaco, I. Sirés, M.A. Sabatino, C. Dispenza, O. Scialdone, A. Galia, Electrochim. Acta 246 (2017) 812–822.

ECCE12
The 12th EUROPEAN CONGRESS OF CHEMICAL ENGINEERING
Florence 15-19 September 2019

3rd Workshop on Electrochemical Engineering:
Industrial Electrochemistry and Electrocatalysis

Electrochemical microfluidic reactors combined with nanofiltration for wastewater treatment – kinetics and modeling studies

Emmanuel Mousset[1*], M. Faidzul Hakim M. Adnan[1], Marta Puce[1], Marie-Noëlle Pons[1]

1 Laboratoire Réactions et Génie des Procédés, Université de Lorraine, CNRS, LRGP, F-54000 Nancy, France

**Corresponding author: emmanuel.mousset@univ-lorraine.fr*

Highlights

- Firs time combination between nanofiltration and micro-reactors for MWWTPs
- Optimal interelectrode gap related to maximal mass transfer
- Non-linear increase of decay rate constants with electrolyte concentration
- Increase of faradic yield with the number of nanofiltration cycles

1. Introduction

The continuous increase of water demand along with the raise of water scarcity due to climate change make water a very precious resource all over the world. To face this issue, it is considered to reuse treated wastewater within the same process or for a secondary purpose such as irrigation and even drinking water. In the aim at succeeding in the water reuse perspective, there are several scientific and technological obstacles to overcome. Numerous studies highlighted the presence of hazardous organic micropollutants (pesticides, pharmaceuticals residues, personal care products,…) in the water bodies at trace levels (from pg/L to µg/L), at the outlet of municipal wastewater treatment plants (MWWTPs). In this context, advanced physico-chemical treatments have been developed. Advanced oxidation technologies produce reactive radicals (e.g. hydroxyl radicals) [1]. Compared to chemical technologies that require the addition of chemicals, emerging electrochemical advanced oxidation processes (EAOPs) implement a clean reagent (e.g. electron) that allows producing *in situ* and continuously the oxidizing species, leading to higher removal yields [2]. Furthermore, the application of microfluidic reactor within the framework of EAOPs has spurred the capability of wastewater treatment. The average ionic conductivity of effluent of MWWTPs (~1 mS cm^{-1}) is apparently too low for conventional macroreactor of EAOPs in–which the distance between electrodes is in the range of 1-4 cm [3]. Hence, supporting electrolyte reagent is very often added to compensate the low value of conductivity as to avoid huge ohmic drop in-between electrodes. In parallel, membrane filtration has been widely applied to produce clean water. It does not require the addition of chemicals and its efficiency has been well established. However, membrane is technically a filter. It is prone to fouling and concentrated effluent containing organics and very likely toxic compounds are separated in the retentate stream that need to be disposed then.

Thus, in this research work, synergy between nanofiltration and EAOPs is investigated. To date, the application of EAOPs to treat the concentrate of membrane separation techniques has already been reported in literature. However, no report has been found on the coupling of nanofiltration with microfluidic reactor moreover to treat the effluent of MWWTPs. As prevalently acknowledged, the

efficiency of degradation of organics by EAOPs depends on various parameters and they behave differently in microfluidic reactors relatively to the macros. Therefore, throughout this study, the influence of different initial concentration of pollutant, inorganic matrix, applied current density, interelectrode distance and flow rate is particularly investigated. Experimental results of degradation and mineralization of representative pharmaceutics are accompanied with mathematical modelling taking into consideration the enhancement of mass transfer of organics, of kinetic of the redox reactions at electrodes and of flow behavior with microfluidic reactor.

2. Methods

A flow-by cell was used in a batch recirculated mode. The cathode was a piece of graphite felt or stainless steel while the anode was in stainless steel or a BDD coated on Niobium. The cathodes and anodes had the same geometric surface area of 50 cm^2. The interelectrode gap was varied using polytetrafluoroethylene (PTFE) spacers of different thicknesses. The current intensity was applied using a power supply. When synthetic solution was used, representative inorganic salts (Ca^{2+}, Mg^{2+}, Na^+, K^+, NH_4^+, NO_3^-, PO_4^{3-}) where added at concentrations similar to those found at outlet of MWWTPs. Real MWWTPs effluent were also used for comparison. The nanofiltration cell was a stainless steel cross-flow filtration unit using polyamide thin film (6.0 × 7.5 cm^2) NF 90 membrane. The applied transmembrane pressure was varied from 3 to 15 bars.

3. Results and discussion

Varying the inter-electrode distance from 50 to 1000 µm highlight the existence of an optimal mass transfer coefficient at 500 µm (Figure 1a). At too short gap, the gas bubbles increase the mass transfer limitation. Interestingly, increasing the electrolyte concentration make increase non-linearly the acetaminophen decay rate constants (Figure 1b).

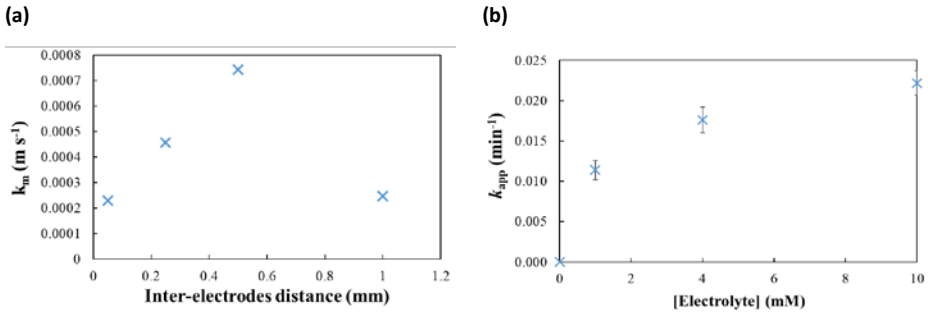

Figure 1. influence of inter-electrode distance on mass transfer (a) and electrolyte concentration on paracetamol decay rate constant (b).

4. Conclusions

The possibility of performing electrolysis at 1 mS cm^{-1} – the average conductivity in municipal WWTP outlets – could be considered in microfluidic reactors. Further results will be presented on the synergy between nanofiltration and electrochemical micro-reactor, i.e. relation between faradic yield and concentration factors.

References

[1] E. Mousset, N. Oturan, M.A. Oturan, Appl. Catal. B Environ. 226 (2018) 135–146.
[2] C.A. Martínez-Huitle, M.A. Rodrigo, I. Sirés, O. Scialdone, Chemical Reviews 115 (2015) 13362-13407.
[3] E. Mousset, S. Pontvianne, M.-N. Pons, Chemosphere 201 (2018) 6-12.

ECCE12
The 12th EUROPEAN CONGRESS OF CHEMICAL ENGINEERING
Florence 15-19 September 2019

Oxidation of 2,4-Dichlorophenoxyacetic acid by Electrogenerated Sulphate Radical Anion

Jingju Cai[1], Minghua Zhou[1], André Savall[2], Karine Groenen Serrano [2*]

1 Key Laboratory of Pollution Process and Environmental Criteria, Ministry of Education, Tianjin Key Laboratory of Urban Ecology Environmental Remediation and Pollution Control, College of Environmental Science and Engineering, Nankai University, Tianjin 300350, China;

2 Laboratoire de Génie Chimique, Université Paul Sabatier, 118 route de Narbonne, 31062 Toulouse Cedex 9, France

**Corresponding author: serrano@chimie.ups-tlse.fr*

Highlights

- 2,4-D can be removed by indirect electrochemical oxidation using persulfate.
- Above 20 °C the decomposition of persulfate occurs during its electrosynthesis.
- The current efficiency decreases from 96 % to 52 % increasing j from 5 to 100 mA cm^{-2}.
- 2,4-D disappearance follows a first-order reaction with a constant rate of 0.22 min^{-1}.

1. Introduction

The use of pesticides and their release into the natural environment constitutes a direct threat for the environment and the living beings especially the human health. Consequently, the development of technics to detoxify the pesticide residues to reduce at least areas and contaminated matrix is needed. Electrochemical oxidation using a boron-doped diamond (BDD) anode allows mineralizing various organics such as pesticides. However, in the case of organochlorides, the reaction with •OH may generate undesired toxic intermediates in the form of organochlorides. Costanza et al. [1] have shown that the reaction of tetrachloroethylene with sodium persulfate at 50°C leads to a complete dechlorination, without production of organochorides.

The approach chosen in this study, in view of treating obsolete pesticides solutions with low concentrations of biorefractory organic species, is to combine the following steps:

(i) the electrochemical production of peroxodisulfates using a BDD anode at low temperature and (ii) peroxodisulfate is injected into the preheated solution containing the target organic compound, the 2,4-Dichlorophenoxyacetic acid (2,4-D), for activation and reaction.

2. Methods

(i) Electrochemical reactor for electrosynthesis: The oxidation of sulfuric acid was performed in a two-compartment electrolytic flow cell under galvanostatic conditions [2]. The electrosynthesis was stopped after reaching a conversion rate of sulphate of 25 % corresponding to a persulfate concentration of 0.2 M.

(ii) Reactor for the coupling processes:

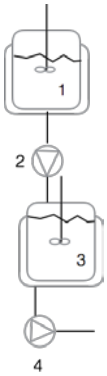

The treated solution containing the target compound, the 2,4-D at 0.45 mM, was stored in a thermostated, stirred tank(1) at 60 °C. The solution was pumped into a continuous thermostated, stirred tank reactor of 100 mL (2) at 60 °C, which initially contained the oxidizing solution, electrosynthesized persulfate. Various flow rates of 2,4-D solution were tested in the range of 1.66-50 mL min^{-1}. The corresponding range of residence time for a 100 mL tank reactor is 2-60 min. A pumping device (4) placed at the outlet of the reactor (3) is used to keep the volume constant in the chemical reactor. The system working as a continuously stirred tank reactor (CSTR) at steady state under isothermal condition.

Fig.1 Set-up used for the disappearance of 2,4-D by reaction with the electrogenerated peroxodisulfate**.** (1) Thermostated, stirred tank containing a 2,4-D solution; (2) pump; (3) Thermostated, stirred tank containing the electrosynthesized persulfate; (4) pump

3. Results and discussion

(i) Electrosynthesis of persulfate:

The electrosynthesis of persulfate was performed under various current densities, from 5 to 100 mA cm^{-2}. It appears that after 180 min of electrolysis the current efficiency ranges from 98% to 48.5% for 5 to 100 mA cm^{-2}. To explain this decreasing faradaic efficiency with the increasing current densities, different hypotheses were established. The most likely explanation is the decomposition of persulfate caused by an increasing temperature.

(ii) Degradation of 2,4-D by electrogenerated radical sulfates:

A first series of experiments were performed to study the effect of the residence time of 2,4-D in the chemical reactor on its disappearance. For a residence time of more than 10 min, the 2,4-D disappearance rate reaches more than 70 %. In parallel, the shape of the TOC disappearance correlates well with that of the target molecule 2,4-D. In addition, one can observe that a disappearance of 84% of 2,4-D corresponds to 54% of TOC removal. Unlike the reaction with hydroxyl radicals, this result shows that the reaction of the target molecule with sulfate radicals leads to the formation of intermediates.

4. Conclusions

Throughout this study, it has been shown that the complete disappearance of 2,4-D is possible by indirect electrochemical oxidation. This process uses the electrosynthesis of persulfate from a 2M sulfuric acid solution. The persulfate is then thermally-activated to produce sulfate radicals, which are strong and selective oxidants. These radicals react with the target molecule. The efficiency of this process depends on both of the following operating conditions:

- When the applied current density is too high, 100 mA cm^{-2} for a 2 M of sulfuric acid, secondary reactions occur.
- The complete disappearance of 2,4-D can be reached if the contact time with sulfate radicals is sufficient; the 2,4-D concentration profile follows a first-order reaction with an estimated constant rate of 0.22 min^{-1} under our operating conditions. The feasibility of the process has been demonstrated.

References

[1] T. Costanza, G. Otano, J. Callaghan, K. D.Pennell, Environ. Sci. Technol. 44 (2010) 9445-9450.

[2] K. Serrano, P.A. Michaud,., C. Comninellis, A. Savall, Electrochim Acta 48 (2002) 431-436.

ECCE12
The 12th EUROPEAN CONGRESS OF CHEMICAL ENGINEERING
Florence 15-19 September 2019

Pilot-scale application of electro-coagulation for treatment of industrial effluents

Pavel Krystynik[1], Petr Kluson[1], Michal Syc[1], Pavel Masin[2], Josef Jadrny[3]

1 Institute of Chemical Process Fundamentals of the CAS, v.v.i., Rozvojova 135/1 Prague 16502 Czech Republic; 2 Dekonta a.s., Dretovice 109, 273 42 Stehlceves, Czech Republic; TERMIZO, a.s., Dr. M. Horákové 571/56, 460 06 Liberec, Czech Republic

**Corresponding author: krystynik@icpf.cas.cz*

Highlights

- The large scale electrocoagulation unit was operated on site - plant for energetic use of wastes.
- The technology showed solution for industrial effluent (removal of Zn, Pb, Cd).
- Removal of contaminants was successful reaching removal efficiencies above 90 %.

1. Introduction

Electrocoagulation is a water treatment method which can be used for removal of a wide range of contaminants, especially dissolved metallic ions via (co)precipitation processes. The method is an alternative method to standard chemical coagulation, which is one of the most common water and wastewater treatment processes. Whilst chemical coagulation is one of the commonly used procedure in industry, where soluble salts of Al or Fe are used (e.g. $Al_2(SO_4)_3$ and $FeCl_3$), in electrocoagulation (EC) precipitating agent (e.g. Al^{3+}, Fe^{3+}) is generated by corrosion of metallic electrodes made of aluminum or steel. The use of electrodes as a source of Fe or Al ions to solution, effectively replaces chemical dosing stations with more compact electrochemical reactors.

2. Methods

The process was tested in pilot-scale unit placed in movable container and operated in continuous regime on site - plant for energetic use of wastes. Two types of process effluent streams were tested:

- Process water at pH 8.4
- Water focused on Zn reduction

3. Results and discussion

Process water at pH 8.4 was tested with different regimes of pretreatment:

- No pH adjustment
- pH adjustment with addition of $Ca(OH)_2$
- pH adjustment with Na_2S

The EC cell was operated with flow rate 350-400 l/h with current input 60 A, providing 150-180 mg/l Fe according to Faraday's law, established voltage oscillated between 1.2 and 3.5 V depending on electrode surface passivation.

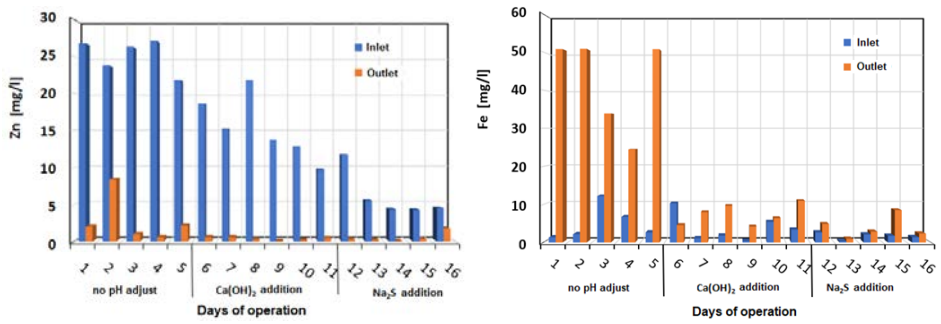

Figure 1. Concentration of Zn (left) and residual Fe (right) during operation with various ways of pretreatment

Figure 1 describes results of Zn concentration before and after treatment by EC with corresponding pretreatment. It is obvious that removal efficiency of Zn in most of the case exceeded 90 % and thus it can be claimed that pH adjustment for Zn removal is not of a significant benefit. Also, other contaminants like Pb or Zn were followed (not plotted). In case of Pb, removal efficiencies were not significantly influenced by pH adjustment while in case of Cd, addition of Na_2S significantly enhanced its removal. That's due to formation of water insoluble CdS. In case of residual Fe, the situation is different. Here, pH adjustment significantly reduces residual concentration of Fe in treated water. The energy consumption during operation was also monitored.

4. Conclusions

The results have shown that the removal efficacies of Zn are satisfactory high and in most of the cases exceeded 90 %. In case of Zn, pH adjustment was not of significant benefit. It is also very reliant on contaminant content in treated effluent. It was verified that electrocoagulation has a great potential in contaminant removal from industrial effluent. The energy consumption was determined to be 0.75-1.1 kWh/m^3 of treated water.

Acknowledgement

Financial support of Technology Agency of the Czech Republic (project No.: TH03030388) is gratefully acknowledged.

ECCE12
The 12th EUROPEAN CONGRESS OF CHEMICAL ENGINEERING
Florence 15-19 September 2019

3rd Workshop on Electrochemical Engineering:
Industrial Electrochemistry and Electrocatalysis

Experimental Characterization and Mathematical Modelling of Miniature Microbial Fuel Cells with Three-dimensional Anodes

Giorgia De Gioannis[1], Mirella Di Lorenzo[2], Marco Isipato[1], Michele Mascia[3*], Aldo Muntoni[1], Daniela Spiga[1]

Dipartimento di Ingegneria Civile, Ambientale e Architettura, Universitá degli Studi di Cagliari, Via Marengo 3, 09123 Cagliari, Italy; 2 Centre for Biosensors, Bioelectronics and Biodevices and Department of Chemical Engineering, University of Bath, Bath, BA2 7AY, United Kingdom; 3 Dipartimento di Ingegneria Meccanica, Chimica e dei Materiali, Universitá degli Studi di Cagliari, Via Marengo 3, 09123 Cagliari, Italy

**Corresponding author: michele.mascia@unica.it*

Highlights

- Three miniature microbial fuel cells with 3D anode are proposed
- The cells are characterized for hydrodynamics and mass transfer
- The performances of the cells for bioelectricity generation are assessed
- A versatile mathematical model of the system has been implemented

1. Introduction

Bioelectrochemical systems, such as MFCs exploit the direct transfer of electrons during oxidation of organic compounds by electroactive microorganisms. Very low values of current density are usually obtained with such devices, so that anodes with high specific surface should be used to increase the electricity generation. Carbon felt, and other carbon-based 3D materials with high surface per unit of volume are largely adopted as anodes in MFCs, although may show significant lack in efficiency due to mass transfer limitations, concentration gradients, velocity distribution and resistivity of the material. [1,2]. Several factors should be then considered in a suitable design of the MFCs with 3D anode.

In this work, the effect of aspect ratio and hydrodynamics on the performance of miniature MFCs with carbon felt anodes was studied. The cells were experimentally characterized for hydrodynamics and mass transfer, as well as for bioelectrochemical activity towards oxidation of acetate.

A mathematical model of the cells was then used to quantify the effect of operative parameters on the bioelectrochemical processes under steady state conditions.

2. Methods

Air-cathode single-cell MFCs were used: the anode compartments have a cross section of 5X5 mm and lengths from 30 to 50 mm. The cells operate in flow-through single-pass mode. Hydrodynamics of the anode compartments was characterized with pulse-response experiments with inert tracer, the mass transfer was characterized by limiting current densities with the standard redox ferricyanide/ferrocyanide couple. The enrichment of electroactive biofilm was performed by

feeding the fuel cells with anaerobic sludge, after enrichment the cells were fed with a synthetic waste water [2].

All the electrochemical tests were performed with a potentiostat-galvanostat (Autolab).

A mathematical model was implemented, which combines fluid flow (Navier-Stokes equations for incompressible fluids in free and porous media), kinetics of electrochemical and bioelectrochemical reactions, chemical equilibria and Ohm's law with conservation of current.

3. Results and discussion

Pulse-response curves show that the system is under non-ideal flow conditions and behave as a plug-flow reactor with axial dispersion.

The steady-state current response with different organic load in the feed stream and inlet flow rates was tested: the curves obtained show a Monod-type behavior, substrate inhibition was also observed, depending on length of the anode and organic load.

Polarisation tests show the presence of significant mass transfer limitations, mainly with low concentration of acetate in the feed.

The model solution provided distribution of velocity, current and potential, and concentration of substrate within the anode chamber. The predicted flow is laminar, as it was expected with the low flow rates used. The concentration profiles show the consumption within the porous anode: depending on organic load in the feed stream, low concentrations of substrate were predicted, which can lead to local starvation. The mass transfer limitations observed from the polarisation studies can be related mainly to concentration gradients in axial direction.

4. Conclusions

The effect of design and operative parameters in the performance of flow-through microbial fuel cells with three-dimensional anodes was investigated. A mathematical model was implemented, which was used to understand and predict the effect of flow rate and organic load of the inlet flow on conversion, potential distribution and electricity production of the cell.

References

[1] J. Chouler, G.A. Padgett, P.J. Cameron, K. Preuss, M.M. Titirici, I. Ieropoulos, M. Di Lorenzo, Electrochim. Acta, 192 (2016) 89-98

[2] S. Mateo, M. Mascia, F. J. Fernandez-Morales, M. A. Rodrigo, M. Di Lorenzo, Electrochim Acta, 297 (2019) 297-306

Acknowledgments

This work is part of a project that has received funding from the European Union's Horizon 2020 research and innovation programme under grant agreement No 826312

ECCE12
The 12th EUROPEAN CONGRESS OF CHEMICAL ENGINEERING
Florence 15-19 September 2019

3rd Workshop on Electrochemical Engineering:
Industrial Electrochemistry and Electrocatalysis

Alkaline water electrolysis stack utilizing polymer electrolyte membrane

Jaromír Hnát[1], Roman Kodým[1], Karel Denk[1], Martin Paidar[1], Jan Žitka[2], Karel Bouzek[1]

1 University of Chemistry and Technology Prague, Technicka 5, 166 28 Prague 6, Czech Republic; 2 Institute of Macromolecular Chemistry, AS CR, Heyrovského Sq. 2, 162 06 Prague 6, Czech Republic,

**Corresponding author: bouzekk@vscht.cz*

Highlights

- Stable alkaline polymer electrolyte developed.
- Design of the laboratory electrolysis stack utilizing polymer electrolyte reported.
- Experimental stack results used to validate mathematical model of the stack.
- Simplified mathematical model of the stack validated.

1. Introduction

Water electrolysis represents a key component of the hydrogen economy concept allowing high capacity and long-term energy storage. It is based on decomposing water molecule into the gaseous hydrogen and oxygen by passing the direct current (DC). Alkaline water electrolysis (AWE) represents most technologically established route of this process. If suitable polymer electrolyte is available (membrane as well as the catalytic layer binder), AWE cell design and operational parameters resembling the PEM water electrolysis can be used. It concerns especially zero gap cell arrangement. At the same time, the advantage of the utilization of the non-PGM catalyst is preserved [1]. This makes alkaline polymer electrolyte water electrolysis (APEWE) highly attractive option. The topic of this study is to report on design of the laboratory APEWE cells stack based on novel alkaline polymer electrolyte developed in our laboratory.

2. Methods

Materials used

Both anodes and cathodes of the stack cells were of identical construction. They were made of nickel foam (INCO Advanced, Technology Materials, (Dalian) Co., Ltd, USA), size 5 × 5 cm^2. Bare, non-activated electrodes were used. Nickel foams served at the same time as a flow field.

Two different anion selective polymer electrolyte membranes were tested as an electrode compartments separator:

- commercial heterogeneous anion selective membrane Ralex® (Mega, Czech Republic)
- experimental polymer electrolyte membrane based on Polystyrene-block-poly(ethylene-ran-butylene)-block-polystyrene (PSEBS) activated by 1,4-diazabicyclo[2.2.2]octane (DABCO) serving as a functional group [2].

Experimental procedures

Stack load curves of the APEWE stack were recorded for the range of current densities up to 390 mA cm^{-2} for operational temperature of 28 °C. Purity of oxygen stream produced during different experiments was determined by means of gas chromatography. Current efficiency was determined in dependence on the concentration of the liquid electrolyte and number of the cells in the stack. It was based on the production of the gases determined using the bubble flow meter.

3. Results and discussion

Distribution of the liquid electrolyte

Sufficient supply of the liquid electrolyte into the electrode compartment represents vital aspect of the alkaline water electrolysis. It was proven, that the proposed geometry of the system ensures homogeneous liquid distribution along the electrodes. This is documented both by load curves, as well as by the flow visualization in the cell.

Influence of the electrolyte feed arrangement

APEWE arrangement allows significant freedom in arrangement of the liquid electrolyte feed into the cell. Both electrode compartments, or just one of them may be supplied by electrolyte [40]. This aspect was found to be of significant importance regarding both, produced gasses purity and cell lifetime. Supplied cathode compartment was found to be preferable regarding the produced gasses purity. But suitable measures have to be introduced to stabilize the electrolyte pH in the range ensuring electrodes stability.

Influence of the electrolyte concentration

Two effects have to be considered in this aspect: (i) due to the improved ionic contact between the electrodes and membrane with increasing KOH concentration current density at given stack voltage increases; (ii) at the same time parasitic current value increases. The second aspect is connected with decreasing resistance of the parasitic current pathways. For the given cell construction KOH concentration of 10 wt.% was chosen as the optimal one.

4. Conclusions

The results obtained within this study prove viability of the water electrolysis stack based on anion selective polymer electrolyte. They allowed to develop necessary cell and system components and to identify bottlenecks in the first version of the cell design. Know how gained allows to continue the development work and to propose new generation of the up scaled alkaline water electrolysis cells stack.

Acknowledgement

The financial support of this research received from the Ministry of Industry and Trade of the Czech Republic under project No. FV10529 is gratefully acknowledged.

References [Calibri 10]

[1] F.M. Sapountzi, J.M. Gracia, C.J. Weststrate, H.O.A. Fredriksson, J.W. Niemantsverdriet, Progress in Energy and Combustion Science, 58 (2017) 1-35.
[2] J. Hnát, M. Plevová, J. Žitka, M. Paidar, K. Bouzek, Electrochimica Acta 248 (2017) 547–555.

ECCE12
The 12th EUROPEAN CONGRESS OF CHEMICAL ENGINEERING
Florence 15-19 September 2019

Operando characterization of products in electrochemical reactions using unique real-time analytics

Peyman Khanipour, Mario Löffler, Andreas M. Reichert, Ricarda Kloth, Iosif Mangoufis-Giasin, Karl J.J. Mayrhofer, Ioannis Katsounaros

Forschungszentrum Jülich GmbH, Helmholtz Institute Erlangen-Nürnberg for Renewable Energy (IEK-11), Egerlandstraße 3, 91058 Erlangen, Germany

**Corresponding author: i.katsounaros@fz-juelich.de*

Highlights

- Electrochemical synthesis can be used to make added-value chemicals of fuels
- Real-time methods are needed to determine selectivity at dynamic conditions
- A novel method to determine products at the time they are formed is presented
- The discovery of new interfaces for selective electrosynthesis will be accelerated

1. Introduction

Electrochemical synthesis is the formation of valuable chemical compounds with the direct use of electricity. The field of electrochemical synthesis is currently growing rapidly because renewable electricity can be harvested to produce highly efficient fuels or fine, added-value chemicals. The classical way to characterize the selectivity of electrochemical reactions involves electrolysis at steady state (constant potential or current) and periodic product determination with GC, GC/MS, HPLC, NMR, IC, etc [1-3]. The advantage of this approach is that quantitation is possible in terms of reaction rates, yields, selectivities or faradaic efficiencies. However, two important limitations exist: First, only one material-electrolyte-potential (or current) combination is addressed at a time, thus looking for selective interfaces for new electrocatalytic processes is time-consuming. Second, the temporal resolution is in the order of minutes so transient, dynamic processes that occur within seconds cannot be captured. To address these points, we developed a new method that allows for the real-time detection of gaseous and liquid electrochemical reaction products.

2. Methods

Electrochemical real-time mass spectrometry (EC-RTMS) is based on coupling an electrochemical cell with two mass spectrometry techniques. It allows for the detection of gaseous products as in previously existing methods (e.g. differential electrochemical mass spectrometry [4]) but also the highly sensitive detection (sub-ppm range) of liquid products independent of their vapor pressure. The achieved acquisition frequency is in the order of 1 Hz, which therefore enables investigations under truly dynamic conditions, e.g. during potential sweep or potential step experiments. In the basic EC-RTMS configuration, the electrochemical reactor is an electrochemical scanning flow cell (SFC) [5], where a channel withdraws the electrolyte at the electrode vicinity for analysis. Gases are extracted from the electrolyte outlet with a hydrophobic membrane and analyzed with electron impact quadrupole mass spectrometry (EI-QMS). The degassed electrolyte is nebulized

and the generated mist is transferred for analysis with direct analysis in real time - time-of-flight mass spectrometry (DART-TOF-MS).

3. Results and discussion

The strength of EC-RTMS in characterizing multiple reaction products in real time will be demonstrated by presenting examples from the reduction of carbon dioxide and the oxidation of C_1-C_3 alcohols. Figure 1 shows the product distribution during the electrochemical oxidation of ethanol on platinum. The potential protocol involved a combination of potential steps at 0 V_{RHE} and sweeps from 0 to +1.2 V_{RHE} (black curve in bottom panel - the oxidation current is also shown in red). Simultaneously, the product formation is followed with EC-RTMS. Gaseous products are CO_2 (m/z = 44 and 22) and CH_4 (m/z = 15), the latter formed from the reduction of adsorbed CHx species at low potential. Liquid products are CH_3CHO (m/z = 45), CH_3COOH (m/z = 61) and ethyl acetate (m/z: 89).

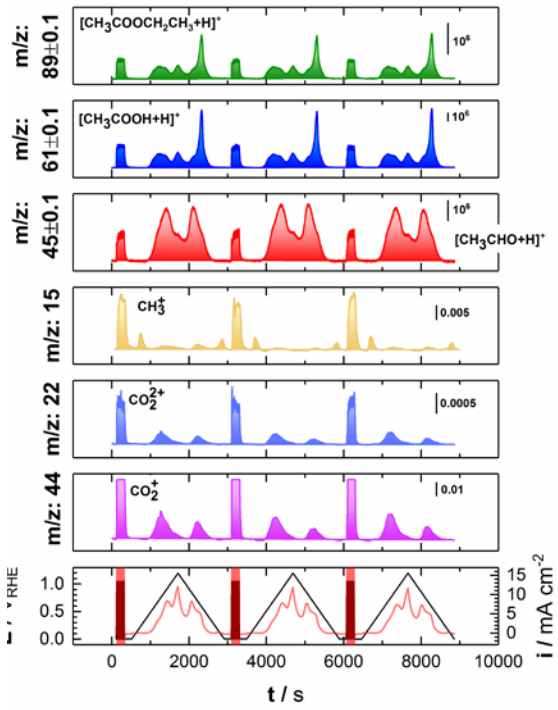

Figure 1. Determination of reaction products with EC-RTMS during the oxidation of 0.2 M ethanol on platinum in 0.1 M $HClO_4$: ethyl acetate (m/z = 89), acetic acid (m/z = 61), acetaldehyde (m/z = 45), methane (m/z = 15), and carbon dioxide (m/z = 22 and 44). The bottom panel shows the electrode potential (black) and the associated current (red).

4. Conclusions

EC-RTMS is a novel method that allows for the simultaneous detection of gaseous and liquid products of electrochemical reactions with excellent temporal and potential resolution. The greatest development is the characterization of liquid products in real time, as it drastically expands the possibilities of complete product determination during an electrochemical reaction independent of analyte vapor pressure or the presence of salts. We anticipate that EC-RTMS will accelerate the design of robust interfaces for highly selective electrochemical processes.

Acknowledgments

This work was funded by the Federal Ministry for Education and Research (BMBF) under the project grants 033RC004C (eEthylen) and 03SFK2Z0 (Power-to-X), and by the Deutsche Forschungsgemeinschaft (DFG, German Research Foundation) under Germany´s Excellence Strategy – Exzellenzcluster 2186 “The Fuel Science Center”.

References

[1] K.P. Kuhl, E.R. Cave, D.N. Abram, T.F. Jaramillo, Energy Environ. Sci. 5 (2012) 7050-7059.
[2] C.W. Li, J. Ciston, M.W. Kanan, Nature 508 (2014) 504-507.
[3] R.S. Sherbo, R.S. Delima, V.A. Chiykowski, B.P. MacLeod, C.P. Berlinguette, Nat. Catal. 1 (2018) 501-507.
[4] H. Baltruschat, J. Am. Chem. Soc. Mass Spectrom. 15 (2004) 1693-1706.
[5] A.K. Schuppert, A.A. Topalov, I. Katsounaros, S.O. Klemm, K.J.J. Mayrhofer, J. Electrochem. Soc. 159 (2012) F670-F675.

ECCE12
The 12th EUROPEAN CONGRESS OF CHEMICAL ENGINEERING
Florence 15-19 September 2019

Electroreduction of CO_2 paired with lactic acid production. Towards an economically feasible system.

Elena Pérez-Gallent[1], Susan Turk[1], Roman Latsuzbaia[1], Rajat Bhardwaj[1], Anca Anastasopol[1], Francesc Sastre-Calabuig[2], Amanda Cristina Garcia[1], Erwin Giling[1], Earl Goetheer[1,3]

1 Department of Sustainable Process and Energy Systems, TNO, Leeghwaterstraat 44, 2628 CA Delft, The Netherlands; 2 Department of Material Solutions, TNO High Tech Campus 25, 5600JW, Eindhoven, The Netherlands; 3 Process and Energy, Delft University of Technology, Leeghwaterstraat 39, 2628 CB Delft, The Netherlands

**Corresponding author: elena.perezgallent@tno.nl*

Highlights

- Co-production of two added value products, carbon monoxide and lactic acid.
- Reduction of 35% in energy consumption.
- 7 fold increase in product value.
- Combined faradaic efficiencies up to 160 %.

1. Introduction

The electrochemical conversion of carbon dioxide presents a significant opportunity to create valuable chemicals or fuels[1]. However, the process is not implemented in the industry due to the high energy needed to overcome the high overpotentials of the reaction[2-3]. The electrochemical reduction of CO_2 can be made economically more interesting by pairing to a compatible reaction where a valuable product is formed. With this approach, two valuable product are formed with the same energy usage. This study proves a paired electrochemical process where carbon dioxide is reduced to carbon monoxide and 1,2-propandiol is oxidized to lactic acid. With this strategy, a reduction of 35% in energy consumption during CO_2 reduction, and a 7 fold increase in product value per unit of energy used was achieved.

2. Methods

The electrochemical measurements were performed in a flow cell with a 200 mL reservoir of anolyte and catholyte which were recirculated at 25 l/h. Different currents (15, 30 50 mA/cm^2) were applied by the use of a potentiostat connected to a 10 cm^2 gold plate cathode and a 10 cm^2 carbon felt anode. A 0.5 M $KHCO_3$ solution where pure CO_2 was bubbled through was used as a catholyte, and a 0.5 M $KHCO_3$/ 0.5 M K_2CO_3 solution which contained 20 mM ACT-TEMPO as a mediator and 20 mM 1,2-propanediol (PDO) as a reactant was used as anolyte. The gaseous products were analyzed by gas chromatography and the liquid products were analyzed by high performance liquid chromatography.

3. Results and discussion

During electrochemical reduction of CO_2 paired with 1,2-propanediol oxidation performed at 15 mA/cm^2 a faradaic efficiency of 80% of carbon monoxide and a faradaic efficiency of 80 % to lactic acid was observed, making a combined 160 % total faradaic efficiency. During the paired reaction, a cell voltage of 2.6 V was measured, while during the non-paired reaction (oxygen formation as counter reaction) a cell voltage of 4 V was measured. The decrease of 1.4 V in the cell voltage lead to an reduction in the cost per ton of CO formed when the reaction is performed in a paired manner. In addition, if the counter reaction is based upon oxygen evolution reaction (non-paired) instead of lactic acid production (paired), only one valuable product is formed. The combined value of carbon monoxide and lactic acid makes the paired reaction economically more beneficial per unit of energy used. Figure 1 shows the value of products formed in € per kWh and the cost in € per ton of CO formed for a) the paired reaction and b) the non-paired reaction.

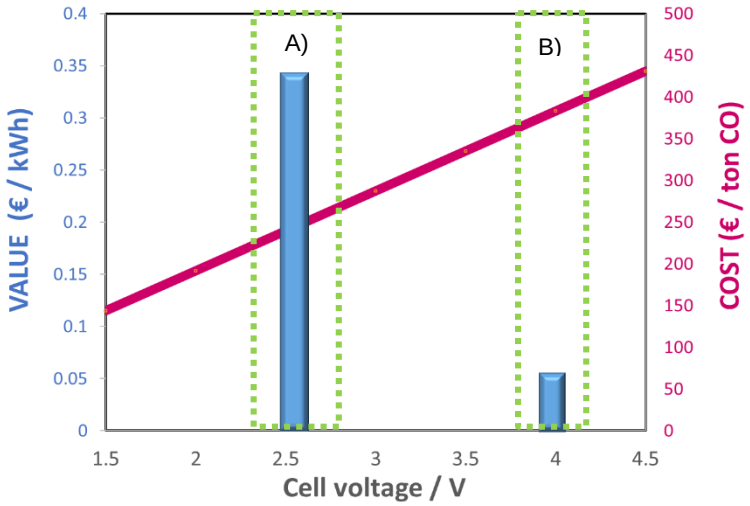

Figure 1. Techno economic comparison of the a) paired and b) non-paired electrolysis in terms of cost per ton of CO formed (pink line) and in terms of the value of the products formed (blue bars). The green boxes indicate the cell potential at which the reactions take place.

4. Conclusions

We have demonstrated that pairing CO_2 reduction to an electrochemical reaction which produce an added value chemical, a significant increase in product value can be achieved. In addition, if the cell potential needed to drive the reactions is reduced, an important decrease in energy usage can be accomplished. This strategy allows to move towards an economically viable electrochemical CO_2 conversion.

References

[1] Hori, Y.; Wakebe, H.; Tsukamoto, T.; Koga, O., *Electrochimica Acta,* 39 (1994) 1833–1839.

[2] Seh, Z. W.; Kibsgaard, J.; Dickens, C. F.; Chorkendorff, I.; Nørskov, J. K.; Jaramillo, T. F., *Science,* 355 (2017) 6321

[3] Durst, J.; Rudnev, A.; Dutta, A.; Fu, Y.; Herranz, J.; Kaliginedi, V.; Kuzume, A.; Permyakova, A. A.; Paratcha, Y.; Broekmann, P.; Schmidt, T. J., *CHIMIA International Journal for Chemistry, 69 (2015) 769-776*

ECCE12
The 12th EUROPEAN CONGRESS OF CHEMICAL ENGINEERING
Florence 15-19 September 2019

Electrocatalytic reduction of CO_2 to solar fuels: Insight into product distribution by varying the current density

Claudio Ampelli[1,*], Chiara Genovese[1], Siglinda Perathoner[1], Gabriele Centi[1]

1 Depts. Of ChiBioFarAm and MIFT (Industrial Chemistry), University of Messina, CASPE/INSTM and ERIC aisbl, Viale F. Stagno d'Alcontres 31, 98166 Messina (Italy)

**Corresponding author: ampellic@unime.it*

Highlights

- The influence of current density on CO_2 reduction product distribution is studied.
- 27.4 % carbon Faradaic efficiency is obtained under industrial relevant conditions.
- CO and formic acid are the main products obtained at high current density.
- Current density directly affects the C-C bond formation.

1. Introduction

The (photo-)electrocatalytic reduction of CO_2 to energy-dense chemicals is an emerging route for storing the intermittent renewable energy produced by sunlight and closing the cycle of CO_2 production/consumption [1]. To achieve higher efficiencies towards hydrocarbons and oxygenates, and limit the side-reaction of water electrolysis, many efforts have been made on designing the electrodes and the related cell [2]. The selective distribution of CO_2 products, in fact, depends not only on the catalytic materials used for assembling the electrodes, but it is strongly influenced by the operational conditions (i.e. electrolyte, pressure, current density, cell configuration). Generally, high current densities are often required for industrial application, in which high space-time yields are mandatory, for reasons related to stoichiometry (the specific rate of an electrode reaction is proportional to the current density by Faraday's law) and economics (to support the capital cost of the electrochemical reactors). Thus, the products may be greatly different by changing the current density and this should be taken into account in scale-up industrial operation.

In this context, the main objective of this contribution is to show the influence of current density on product distribution in CO_2 electroreduction, by testing copper-doped carbon nanotubes deposited on a gas diffusion layer, thus opening the route towards a practical implementation of CO_2 electroreduction process with low-cost and earth abundant materials as electrocatalysts.

2. Methods

Copper nanoparticles (Cu NPs) were deposited on pre-functionalized carbon nanotubes (CNTs) by incipient wetness impregnation. The total amount of Cu loaded onto the CNTs was 5 wt.%. The as-prepared Cu NPs-CNTs were then deposited on a carbon gas diffusion layer (GDL) and finally joined to a proton exchange membrane (Nafion) to form a Membrane Electrode Assembly – MEA (in analogy with fuel cells) [3]. The electrodes were fully characterized by different advanced techniques (such as XRD, SEM, HR-TEM) to study their morphological and structural characteristics, as well as by Linear Sweep and Cyclic Voltammetry to evaluate their electrochemical properties.

Finally, Cu NPs-CNTs/GDL electrodes were tested in the process of CO_2 electroreduction using a homemade compact device working in a three-electrode configuration, by processing pure CO_2 in 0.1 M $KHCO_3$ electrolyte.

3. Results and discussion

The tests were carried out at different applied potentials (from -0.5 to -1.7 V vs. Ag/AgCl), corresponding to different current densities (from 0.1 to 2.3 mA cm^{-2}, respectively). A further test was carried out in amperometric mode applying directly 10 mA cm^{-2}, in order to evaluate the catalytic performance under industrial relevant conditions.

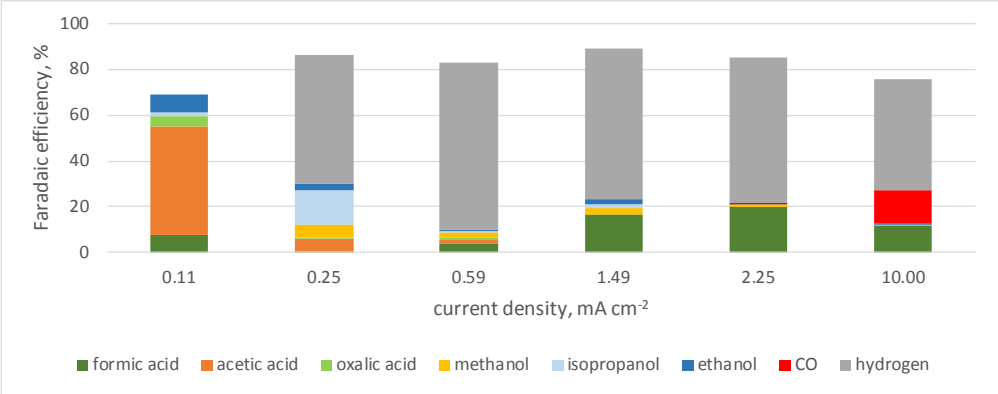

Figure 1. Faradaic efficiency (%) vs. current density.

As shown in Figure 1, the total Faradaic efficiency values are all ranging from 75 to almost 90 %, except when the current density is very low (0.11 mA cm^{-2}). At this current density, no hydrogen was detected, as the applied voltage (-0.5 V vs. Ag/AgCl) was not sufficient to activate water reduction. However, under industrial relevant conditions (10 mA cm^{-2}), the carbon Faradaic selectivity was quite high (27.4 %), indicating Cu NPs-CNTs/GDL as a promising electrocatalyst for CO_2 reduction process. Formic acid was the main carbon product formed, while carbon monoxide started to form at 2.25 mA cm^{-2} and became even higher than formic acid at 10 mA cm^{-2}. At low current density, the product distribution was quite different: methanol, ethanol and isopropanol (especially at 0.25 mA cm^{-2}) were formed, while acetic acid and oxalic acid were produced at -0.5 V vs. Ag/AgCl (0.11 mA cm^{-2}). These are examples of products involving C-C bond formation.

4. Conclusions

These results showed that the current density strongly affects the product distribution. Specifically, acetic acid, ethanol, formic acid, oxalic acid, methanol, and isopropanol are the main products obtained at lower current density, while the production of formic acid, CO and H_2 increased at higher current density, evidencing a direct influence of this parameter on C-C bond formation.

Acknowledgments: *This work was funded by the European Union's Horizon 2020 project A-LEAF (Grant Agreement No. 732840).*

References

[1] B.C. Marepally, C. Ampelli, C. Genovese, E.A. Quadrelli, S. Perathoner, G. Centi, in: S. Albonetti, S. Perathoner, E.A. Quadrelli (Eds.), Stud. Surf. Sci. Catal. 178 (2019) 7–30.
[2] C. Ampelli, F. Tavella, S. Perathoner, G. Centi, Chem. Eng. J. 320 (2017) 352–362.
[3] C. Genovese, C. Ampelli, S. Perathoner, G. Centi, Green Chem. 19 (2017) 2406–2415.

ECCE12
The 12th EUROPEAN CONGRESS OF CHEMICAL ENGINEERING
Florence 15-19 September 2019

Dimensionless approach of a pressurized proton exchange membrane water electrolysis

Maha RHANDI*[1], Farid AUBRAS[2], Amangoua Jean-Jacques KADJO[2], Florence DRUART[1], Brigitte GRONDIN-PEREZ[2], Jonathan DESEURE[1]

1 Univ. Grenoble Alpes, Univ. Savoie Mont Blanc, CNRS, Grenoble INP, LEPMI, 38000 Grenoble, France

2 Univ. De la Réunion, LE2P, 97715 Saint-Denis, France

**Corresponding author: maha.rhandi@lepmi.grenoble-inp.fr*

Highlights

- Proton exchange membrane water electrolysis
- Electrochemical compression/purification
- One dimensional modelling

1. Introduction

The global hydrogen consumption is around 50 Mton per year [1]. However, only a small part is used for energy device as an energy carrier. An energy carrier contains energy, facilitates its transport and storage before it is supplied (and converted) to an end user. Hydrogen fulfils the main characteristics to achieve the performance required for efficient energy carrier, but its low volume density remains a weak point. A very high energy-efficient compression is a necessary step. The main advantage of hydrogen production using water electrolysis is the simplicity of the process: only water and electricity are required. Water electrolysis allows to produce pressurized high purity hydrogen in order to facilitate the storage. Nowadays, mechanical compressors are considered to be the most commonly used in the industry. These systems enable to increase gas pressure by decreasing its volume using a mechanical force (energy). For multistage compression from room pressure to a final pressure of 20 MPa (200 bar), about 8% of the higher heating value (HHV) of the transported gas energy content (here hydrogen) is required [2]. Therefore, direct electrochemical compression is mainly advantageous for hydrogen to become a widespread renewable-energy carrier.

2. Methods

This work focuses on Proton Exchange Membrane Water Electrolysis (PEM-WE) which is considered as the most efficient process. In the literature, the analytical models and dimensionless approaches are essentially used for fuel cells. An interesting aspect of dimensionless study is the panel of dimensionless numbers specific to fuel cells including the Wagner number and the number of Damkholer. According to the author's opinion, the analytical modeling and dimensionless methods are currently underutilized in fuel cell (PEMFC) and electrolysis domain (PEM-WE). The developed analytic approach in this work exhibits an innovative approach to quantify electrochemical performances based on dimensionless methodology.

3. Results and discussion

In the present work, the limiting processes are highlighted using the obtained dimensionless numbers. In the case of PEM-WE, the main phenomena are proton diffusion, electrochemical kinetics at catalytic layers, water transport: diffusion, electro-osmotic and osmotic pressure transport in the membrane [3]. Thanks to this mathematical procedure, it is possible to forecast electrochemical behavior and to grant optimal operating conditions. Equivalent Wagner number and Thiele modulus analogy are presented in this paper. Our dimensionless approach is used to scrutinize the mean values as well as the spatial distributions of current densities, over potential, water contents and membrane resistance. Therefore, it allows to frame the usual differential equations into a dimensionless equation set.

4. Conclusions

Direct electrochemical compression of hydrogen during electrolysis process have been successfully modeled using dimensionless approach. According to the resistive energy losses associated with proton diffusion through the electrochemical cell: doubling the current density, doubles the hydrogen flow, but quadruples the dissipated power. The specific resistance of the membrane is main parameter of electrochemical cell. The overall resistance depends on cell materials as well as operating conditions such as pressure gradient, contact resistance, diffusion profiles, and at the selected current density [4].

References

[1] Evers, AA 2010. The Hydrogen Society: More Than Just a Vision. Oberkraemer, Marwitz, Germany: Hydrogeit Verlag.

[2] W. Vielstich, H. Yokokawa, and H. Gasteiger, Eds., Advances in electrocatalysis, materials, diagnostics and durability; part 2. Chichester: Wiley, 2009.

[3] Aubras et al. International Journal of Hydrogen Energy, 42, 26203, 2017

[4] Peter Bouwman, Chapter 13. Fundamentals of Electrochemical Hydrogen Compression. PEM Electrolysis for Hydrogen Production: Principles and Applications. Edited by Dmitri Bessarabov, Haijiang Wang, Hui Li, Nana Zhao, 2016, eBook ISBN 9781482252323

ECCE12
The 12th EUROPEAN CONGRESS OF CHEMICAL ENGINEERING
Florence 15-19 September 2019

CO_2 crossover in electrochemical CO_2 reduction cells suited for long-time operation at industrially relevant operating conditions

David Reinisch[1], Christian Reller[1], Bernhard Schmid[2], Nemanja Martic[1], Ralf Krause[1], Karl Mayrhofer[3], Günter Schmid[1*]

1 Siemens AG, Günter-Scharowsky-Straße 1, 91058 Erlangen, Germany; 2 Friedrich-Alexander University Erlangen-Nürnberg, Department of Chemistry and Pharmacy, Egerlandstr. 1, 91058 Erlangen, Germany; 3 Helmholtz Institute Erlangen-Nürnberg for Renewable Energy, Egerlandstr. 3, 91058 Erlangen, Germany

**Corresponding author: guenter.schmid@siemens.com*

Highlights

- Electrochemical CO_2 reduction at 300 mA/cm² at Faradaic Efficiencies > 80%
- Stable operation for 7000+ hours
- Reduction of CO_2-crossover by more than 95%

1. Introduction

The electrochemical CO_2 reduction allows to create valuable products from "waste" CO_2 coming from industrial processes, and cheap, renewable energies. Among the different possible electrolysis products, CO is the most promising for industrial application in the near future and thus, has drawn a lot of interest. By now the technology has passed the fundamental catalytical research stage, and different setups have been reported that perform stable, at high faradaic efficiencies for over 1000 hours at industrially relevant current densities [1,2]. In order to keep up with the rapid industrial application plans [3], research is shifting from catalyst design to engineering the electrolysis process and to upscaling of the setups.

2. Methods

The electrochemical experiments were performed in a commercially available flow cell. The different gas streams were quantified, and their composition analyzed via gas chromatography.

3. Results and discussion

Among the stable systems published, the mixed-electrolyte approach detailed in [1] is especially suited for rapid scaling and industrial application, since it does not require expensive ion-selective membranes and is not based on novel, research-level materials. By improving the GDE and the overall system setup, the cell could be operated stably at more than 80% faradaic efficiency for 7000 hours at current densities of 300 mA/cm² (Figure 1).

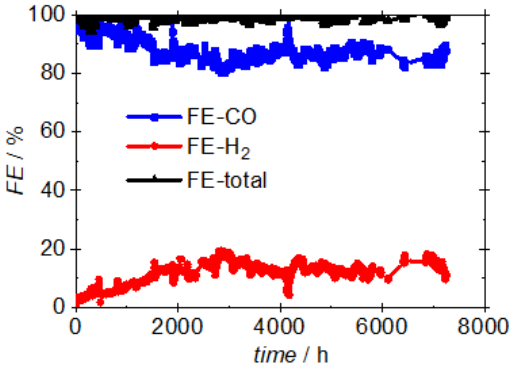

Figure 1. Faradaic efficiencies of a CO_2-electolysis cell operating stably for over 7000 hours

As the technology moves towards industrial application, the transport of CO_2 across the cell becomes an important issue, that has been mostly neglected so far. Due to the formation and neutralization of carbonates, this transport is intrinsic to CO_2 electrolysis and needs to be dealt with [1,2,4]. Here different approaches to minimize the CO_2 transport across the electrolysis cell are introduced, discussed and tested. All methods keep the advantages of a mixed-electrolyte system and work with the previously tested cathodes. By implementing these methods, the CO_2 transport could be reduced by over 95% (Figure 2).

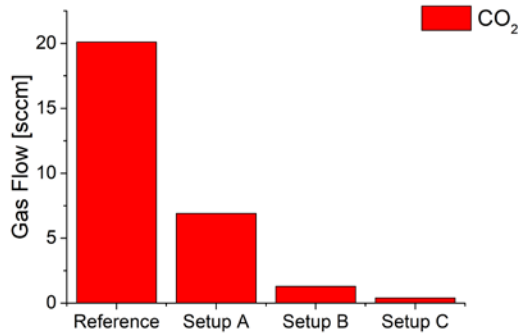

Figure 2. CO_2 content in the anode gas for different setups. Compared to the standard, reference case, the crossover could be reduced by more than 95%.

4. Conclusions

CO_2 electrolysis cells with liquid electrolytes are a viable candidate for near-time industrial application. As in all current approaches, the CO_2 transport across the cell needs to be accounted for and solving this problem is crucial for a successful industrial implementation of this process. The results here show, that an adequate design of the electrolysis setup can achieve this target while maintaining industrially relevant operating conditions without relying on ion-selective membranes.

References

[1] T. Haas, R. Krause, R. Weber, M. Demler, G. Schmid; Nat. Catal. 1 (2018) pp. 32-39
[2] J. Kaczur, H. Yang, Z. Liu, S. Sajjad, R. Masel; Front. Chem. 6 (2018) 263
[3] https://corporate.evonik.com/en/Pages/article.aspx?articleId=106259
[4] A. Pătru, T. Binninger, B. Pribyl, T. Schmidt; J. Electrochem. Soc 166 (2019) F34-F43

ECCE12
The 12th EUROPEAN CONGRESS OF CHEMICAL ENGINEERING
Florence 15-19 September 2019

Low-Temperarue Electrolytes for Aluminium Technology.

Ján Híveš, Emília Kubiňáková, Vladimír Danielik

Slovak Technical University in Bratislava, Faculty of Chemical and Food Technology, Radlinského 9, 812 37 Bratislava, Slovakia

**Corresponding author: jan.hives@stuba.sk*

Highlights

- Aluminium smelter technology
- High-acidic sodium and potassium cryolite melts
- Electrical conductivity
- Tube type cell, electrochemical impedance spectroscopy

1. Introduction

The innovation of aluminium production technology is focused on using the inert electrode materials and low temperature electrolytes. The most significant benefits are energetic, environmental, and economic aspects. The consumable carbon anodes will be replaced by inert, oxygen evolving anodes. Low-melting electrolytes (working temperature 660 °C – 900 °C) are essential due to the oxidation rate of inert electrode materials. The corrosion rate decreases strongly with decreasing temperature. Cryolite-based melts are still the best choice as electrolytes for electrolytic aluminium production, because of its unique capacities as a solvent for electrochemically active compound (alumina). The possibilities for the decreasing of TPC in cryolite-based melts are three: electrolytes based on sodium cryolite with the high excess of AlF_3 (up to 45 mol %), electrolytes based on potassium cryolite, mixture electrolytes with various ratios of sodium and potassium cryolite.

The high addition of AlF_3 into the sodium cryolite systems reduces markedly TPC (up to 700 °C) but also decreases the alumina solubility. The potassium system is more low melting than the sodium system (temperature less than 660 °C). The interest in potassium cryolite melts causes the fact that alumina solubility is higher than in the sodium system at the same conditions. Other properties are less favorable, for instance, the electrical conductivity is considerably lower in the potassium system. The essential physicochemical properties of these low temperature electrolytes, such as solubility of Al_2O_3, density, vapor pressure, viscosity or electrical conductivity were investigated only in less extent. The electrical conductivity is of great importance in the energetic aspects and it also helps with the characterisation of the melts structure. The interest in low temperature electrolytes is growing with the development of inert electrode materials.

2. Methods

Electrochemical impedance spectroscopy is a suitable measurement method for the investigation of electrical conductivity of new types of aluminium electrolytes. Electrical conductivity was measured using a tube-type cell with stationary electrodes applying AC-techniques with a sine wave signal in the high frequency range up to 100 kHz. Electrolytes used in this study contained

high content of aluminium fluoride, up to 45 mol %. Basic binary NaF-AlF_3 melt was studied at different molar ratios MR = (2.0-1.2) in the temperature range from the temperature of primary crystallization to 100 °C overheat. Basic melts KF-AlF_3 and NaF-KF-AlF_3 were studied at molar cryolite ratios MR = (1.5-1.2) in the temperature range defined in the same way as for previous system. The influence of the additions of Al_2O_3, CaF_2, MgF_2 and/or LiF was also investigated.

3. Results and discussion

The electrical conductivity of the NaF AlF3 system as a function of a temperature and composition.

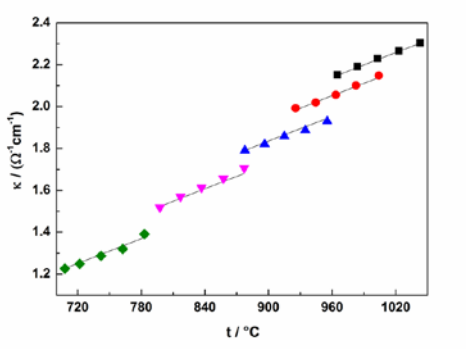

Figure 1. The electrical conductivity of the NaF AlF_3 system as a function of a temperature for compositions: MR = 2.0; ● MR = 1.8; ² MR = 1.6; ¼ MR = 1.4; f MR = 1.2. Symbols represent the experimental data; full lines non-linear regression analysis data.

4. Conclusions

Concentration and temperature dependences of the electrical conductivity for all the studied low-temperature multi-component systems were described by the regression equation. The mutual effect of various combinations of additives on electrical conductivity was similar than the sum of individual allowances. The decrease of electrical conductivity in multicomponent systems for melts with the lowest MR = 1.2 was up to about 13 % when compared to the binary melts. Although LiF improves the value of electrical conductivity, the addition of about 1 wt % of LiF increased the electrical conductivity only by about 1.88 % on average. Temperature and concentration dependencies of the electrical conductivity in studied multicomponent systems were described by regression equations. The summary equation precisely describes the temperature and concentration dependence of electrical conductivity in the whole studied area and can be used for practical purposes.

Acknowledgment

This work was supported by the Slovak Research and Development Agency under the contract APVV 17 0183 and by the Ministry of Education, Science, Research and Sport of the Slovak Republic for project VEGA 1/0343/19.

References

[1] E. Kubiňáková, V. Danielik, J. Híveš, J. Electrochem. Soc. 165 (2018), E793-E797.

ECCE12
The 12th EUROPEAN CONGRESS OF CHEMICAL ENGINEERING
Florence 15-19 September 2019

Electrochemical production of biobased maleic acid.

Roman Latsuzbaia, Richard van Heck, Vinita Lachman, Amanda Garcia, Marc Crockatt, Earl Goetheer[1]

1 TNO, Dept. of Sustainable Process and Energy Systems, Leeghwaterstraat 44, 2628 CA;

**Corresponding author: roman.latsuzbaia@tno.nl*

Highlights

- Furfural oxidation
- Electrochemical maleic acid
- Electro-organic synthesis
- Scale-up

1. Introduction

Lignocellulosic biomass is abundant, cheap, and many platform chemicals can be derived from it. An example of such chemical, furfural is a C5 compound, which is already industrially produced from biomass. Many of value added chemicals can be produced from furfural, for instance, maleic acid. Latter is used in variety processes, such as in production of lubricants, plasticizers, pharmaceuticals [1]. Importantly, maleic anhydride, which is easily made from maleic acid, is used for production of bio-based aromatics [2]. Industrially, produced maleic acid currently is fossil based and is produced by hydrolysis of maleic anhydride, which on the other hand is produced by gas phase thermocatalytic oxidation of butane by oxygen catalyzed by vanadium-based V-P-O catalysts, however the process yields only 50-65 % maleic anhydride, therefore very inefficient. Alternatively, electrochemical oxidation allows selective and less energy demanding conversion at ambient pressures and temperatures using cheap catalysts, such as Pb/PbO_2 [1, 3].

Our research focused on scaling-up of the production of maleic acid to industrially relevant conditions (>5wt %) utilizing a plate-and-frame type electrolyser.

2. Methods

Electrolysis was performed in a divided cell and plate-and-frame type electrolyser (Nafion® membrane) at RT under acidic conditions with anode Pb/PbO_2 and Pt or Pb cathode with anolyte: 0.5 M H_2SO_4 with/without 0.02 M V_2O_5 or 0.02 M $NaMoO_4$ and catholyte 0.5 M H_2SO_4. Potentiostatic and galvanostatic electrolysis modes were used for production of maleic acid.

3. Results and discussion

The electrolysis was investigated directly on Pb/PbO_2 electrode, and the effect of mediators such as V_2O_5 and $NaMoO_4$ was investigated. Optimal potentiostatic operation was performed at 1.5 V vs SCE, whereas the optimal galvanostatic operation was performed at a current density of ~10

mA/cm^2. With starting concentration of 0.05 M furfural, the yield on maleic acid was ~80% with a main side product an oxidation intermediate, formyl acrylic acid. Almost quantitative yields can be achieved if all formylacrylic acid is converted to furfural. Effect of reactant concentration was investigated (0.05- 0.5M furfural). The reaction was tested at temperatures of 25 and 35 ^{0}C, realizing higher reaction rates and yields of maleic acid at elevated temperatures. Permeation of the reactants, products and mediators through membrane was investigated and process optimized. Additionally, downstream processing possibilities of maleic acid have been investigated. Based on the obtained results techno-economic feasibility study has been performed and showed economically favorable production costs.

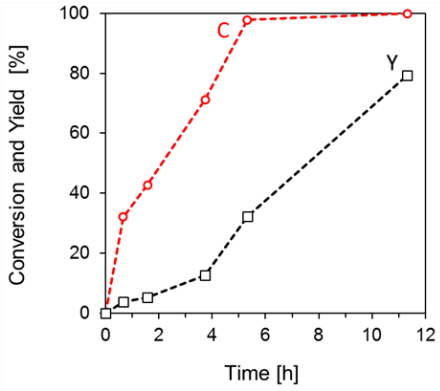

Figure 1. Conversion and yield of electro-oxidation of furfural to maleic acid on PbO_2 electrode in 0.5 M H_2SO_4.

4. Conclusions

Electrochemical production of biobased maleic acid by oxidation of furfural was demonstrated for the first time in a plate-and-frame type electrolyser at industrially relevant conditions. Yields >80% were obtained. Preliminary techno-economic analysis shows that the production process has a high potential to replace fossil based maleic acid production.

References

[1] S.R. Kubota, K.-S, Choi, ACS Sustainable Chem. Eng., 6 (2018), 9596–9600.
[2] Thiyagarajan, et al, Angew. Chem. Int. Ed. 54 (2015)1–5.
[3] V. Mil'man et al., Elektrokhimiya, 14 (1978), 1555-1558.

ECCE12
The 12th EUROPEAN CONGRESS OF CHEMICAL ENGINEERING
Florence 15-19 September 2019

Validation of a novel flexible electrochemical microreactor by its application to electroorganic syntheses

Athanassios Ziogas[1], Christian Hofmann[1], Sebastian Baranyai[1,2], Patrick Löb[1], Gunther Kolb[1]

[1] *Fraunhofer Institute for Microengineering and Microsystems IMM, Mainz, Germany;* [2] *Hochschule Konstanz Technik, Wirtschaft und Gestaltung HTWG, Konstanz, Germany*

**Corresponding author: athanassios.ziogas@imm.fraunhofer.de*

Highlights

- New, modular electrochemical microreactor addressing high pressure operation and production scale.
- Application to electroorganic synthesis.
- Asymmetric Kolbe electrolysis and cation pool / flow method.
- Utilization of additive manufacturing for reactor plates realization.

1. Introduction

Organic electrochemistry is considered as future emerging technology for the environment-friendly production of chemical compounds. The search for "green" synthesis routes, the emergence of novel synthesis strategies and also the ambition for a direct utilization of sustainable (excess) electric energy foster the development in this field.[1] Nevertheless, there are still challenges and problems linked to electrosynthesis and there is also a need for flexible reactor concepts.[2] Electrochemical microreactors - characterized by small electrode distances and great surface-to-volume-ratios - contribute to solve these issues.

2. Design and manufacturing of the novel electrochemical microreactor

Taking into account current user requirements, Fraunhofer IMM developed based on its experience in the field of electrochemical microreactors [3] an innovative reactor concept (Fig. 1) following a plate stack design addressing especially the aspects modularity, flexibility, high pressure operation and accessibility of production scale.

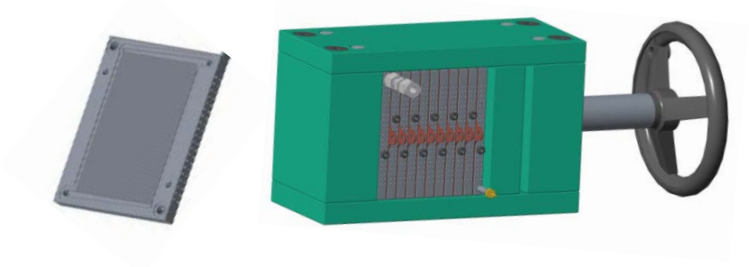

Figure 2.
CAD illustration of single reactor plate with micro-structured electrode and integrated heat exchanger (left). CAD illustration of assembled flexible

electrochemical microreactor with 11 reactor plates (right).

The single reactor plates hosting the structured electrodes typically on both sides and equipped with an integrated heat exchanger have been realized by a sequence of different fabrication steps:

- additive manufacturing to realize the base plates with their complex fluid structures
- surface coating (e.g. with PTFE) of the plates for electric insulation
- milling to create the micro channels on the plates surface
- electroplating to deposit different electrode materials

The basic reactor plates (outer dimension: 100 mm x 118 mm) provide an active electrode surface of 54 cm^2 via 67 micro channels (800 µm x 100 µm x 10 cm) and a channel volume of 0.5 cm^3 per structured plate side. The reactor is designed for operations up to 200 °C and up to 100 bar for electrolyte flow rates up to 200 mL min^{-1}.

3. Results and discussion

The reactor concept allows a multitude of operation possibilities in view of numbers of electrode assembly units in use, functionality (mono or bipolar cell configuration, undivided or divided cell configuration) and operation mode of the stack (parallel, serial or mixed operation). With that also numbering-up and scale-up possibilities are provided. The reactor concept is validated by the use of different reactor assembly configurations for two electroorganic syntheses. Former results regarding the Kolbe electrolysis to produce fuels from fatty acids [4] could be further improved with the new reactor concept. E.g. for the asymmetric continuous Kolbe electrolysis at current densities of 1.7 kA*m^{-2} and residence time of 0.1 s the Faraday efficiency could be increased further to 91% (at quantitative yield and a selectivity towards 97% of n-alkanes). This application example illustrates nicely the precise control over process conditions during the synthesis and the resulting control over product composition (see Figure 2). The Cation Pool / Flow method [5] as modern organic synthesis approach has also been used for the successful reactor concept validation.

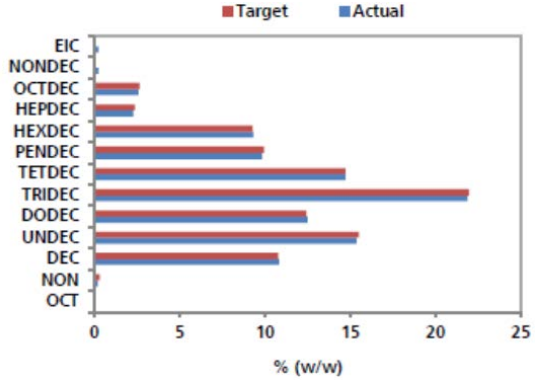

Figure 2. Comparison between target and achieved results of jet oil by Kolbe electroorganic synthesis.

4. Conclusions

Fraunhofer IMM has developed an innovative electrochemical microreactor addressing especially the aspects modularity, flexibility, high pressure operation and accessibility of production scale and validated the reactor concept by applying it in the Kolbe electrolysis and Cation Pool / Flow method.

References

[1] A. Wiebe et al., Angew. Chem. 130 (2018) 2-30.
[2] M. Yan et al., Angew. Chem. Int. Ed. 56 (2017) 2-9.
[3] A. Ziogas et al., J. Appl. Electrochem. 39 (12) (2009) 2297-2313.
[4] A. Ziogas et al., WO 2016/70075 A1.
[5] J. Yoshida et al., Chem. Eur. J. 2002, 8, No.12

ECCE12
The 12th EUROPEAN CONGRESS OF CHEMICAL ENGINEERING
Florence 15-19 September 2019

3rd Workshop on Electrochemical Engineering:
Industrial Electrochemistry and Electrocatalysis

On the role of Au nanoparticles in hybrid TiO_2 structures for photoelectrocatalytic processes

Simonetta Palmas*[1], Michele Mascia[1], Laura Mais[1], Elisabetta M. Usai[1], Annalisa Vacca[1], Roberto Matarrese[2], Isabella Nova[2], Andrea Li Bassi[3], Beatrice R. Bricchi[3], Luca Mascaretti[3], Matteo Ghidelli[3], Valeria Russo[3], Carlo S. Casari[3]

1) Dipartimento di Ingegneria Meccanica Chimica e dei Materiali, Università degli studi di Cagliari, Via Marengo 2 09123 Cagliari; 2) LCCP, Dipartimento di Energia, Politecnico di Milano, via La Masa 34 20156 Milano; 3) NanoLab, Dipartimento di Energia, Politecnico di Milano, via Ponzio 34/3 20133 Milano.

**Corresponding author: simonetta.palmas@dimcm.unica.it*

Highlights

- Photoelectrocatalytic performances of hybrid TiO_2/Au structures are tested
- Different distribution of Au clusters is performed at the TiO2 interface
- The role of Au NP in the working mechanism of the whole structure is investigated

1. Introduction

The paper examines and discusses the behavior of hybrid 3D TiO_2 electrodes, modified with Au nanoparticles (NP), useful as photoanodes for the oxidation of organic compounds from aqueous solution. In such a process H_2 evolution is always the concomitant cathodic reaction, while photogenerated holes are responsible for the oxidation of the organic compound, which may occur either by direct reaction at the active sites of the photoanode, or mediated by OH radicals, generated by the water splitting. In this context, high surface to volume ratios are generally mandatory, being the reactions involved heterogeneous: nano or meso porous structures are commonly used to this aim [1,2]. However, increase of the surface area may not be sufficient to obtain effective catalysts. Actually, the intrinsic characteristics of the semiconductor (SC) cannot be neglected: the structure crystallinity (anatase, rutile or amorphous), as well as the possible presence of defects, which may constitute recombination centers for the photogenerated charges, are of crucial importance to determine the real effectiveness of the SC.

Further considerations are needed when the SC has to be used with solar light. Due to the large band gap, TiO_2 is not suitable in all the wavelength range. In this case, the presence of dopant, or the use of hybrid structures, in combination with another SC with narrow band gap, can allow exploiting the low energetic wavelengths.

Finally, the inclusion of noble metal NPs, such as Ag, Au, Pt, single or alloyed, represents a possible way to enhance the ability of TiO_2 to absorb light in a wider range of wavelength [1, 2] via plasmonic effects, or to favor charge carrier separation to inhibit recombination, directly contributing to the production of long-lived charges, owing to the resulting low Fermi level [3, 4, 5].

In this work the performances of samples of TiO_2 with a hierarchical nanostructure, modified by Au NP, are investigated for the oxidation of bisphenol A, used as model molecule, representative of a class of organic compounds of particular concern for the human health.

2. Methods

Vapor phase Pulsed Laser Deposition (PLD) was used to produce nanostructured TiO_2 photoanode films, while Au NP were produced by PLD or thermal evaporation. By varying the process parameters and exploiting annealing treatments, we tune Au NP size distribution and the hierarchical TiO_2 nanoscale morphology. Optimized Au NPs are coupled with TiO_2, involving deposition of NPs at the bottom or at the top of the TiO_2 as well as co-deposition of integrated TiO_2/Au-NPs assemblies [6]. Photoelectrochemical characterization of the samples was done by direct and alternate current tests: cyclic and linear sweep voltammetry, and photocurrent tests were used in d.c.; electrochemical impedance spectroscopy was used to investigate the response to a.c. signal. A 300 W xenon lamp equipped with air mass (AM) 0 and 1.5 D filters was used to simulate the solar radiation.

3. Results and discussion

The performances of the different samples are investigated, in terms of voltammetric behavior, photocurrent transients, impedance spectroscopy (EIS) responses, in order to understand the working mechanism of the hybrid structures, during electrolysis carried out in supporting electrolyte or in the presence of organic compound, in the dark or under simulated solar light irradiation.

In these conditions the different active centers of the structure play different roles: TiO_2, which always represents the majority component of the hybrid structure, is active for the narrow range of UV light, while Au NP, which constitute the minority component, is fundamental to exploit the Vis range where TiO_2 cannot act. The right combination of the two components is crucial to achieve good performance, in the examined conditions.

4. Conclusions

The results demonstrated that the effectiveness of the samples is connected to both the load and the dispersion of the Au NP with respect to TiO_2. An optimal metal loading has to be individuated in order to guarantee that the Au nanoclusters do not cover all the TiO_2 interface, so that the charge transfer between electrode and electrolyte is not hindered.

Acknowledgments

Research supported by Fondazione di Sardegna, CRP project F71I17000280002 - 2017

References

[1] L. Mais, M. Mascia, S. Palmas, A. Vacca. Sep. and Purif. Technol., 208, (2019) 153-159
[2] S. Palmas, A. Da Pozzo, M. Mascia, A. Vacca, P.C. Ricci. Chem. Eng. J. 211-212, (2012) 285-292
[3] N. Naseri, P. Sangpour and S. H. Mousavi, RSC Adv., 4, (2014), 46697–46703
[4] A. Tanaka, K. Teramura, S. Hosokawa, H. Kominami, T. Tanaka, Chem. Sci. 8 (2017) 2574.
[5] X. Lang, X. Chen, J. Zhao, Chem. Soc. Rev. 43 (2014) 473
[6] B.R. Bricchi, M. Ghidelli, L. Mascaretti, A. Zapelli, V. Russo, C.S. Casari, G. Terraneo, I. Alessandri, C. Ducati, A. Li Bassi, Materials and Design 156 (2018) 311-319.

ECCE12
The 12th EUROPEAN CONGRESS OF CHEMICAL ENGINEERING
Florence 15-19 September 2019

3rd Workshop on Electrochemical Engineering:
Industrial Electrochemistry and Electrocatalysis

A simple model for vanadium precipitation in vanadium redox flow batteries

Killian Poulet-Alligand[1], Florence Druart*[1], Jonathan Deseure[1], Yann Bultel[1]

1 Univ. Grenoble Alpes, Univ. Savoie Mont Blanc, CNRS, Grenoble INP, LEPMI, 38000 Grenoble, France

**Corresponding author: florence.druart@lepmi.grenoble-inp.fr*

Highlights

- Optimization of vanadium redox flow battery
- Impact of precipitation on electrochemical performance
- Half-cell modelling

1. Introduction

The future of the energy grid will require an ever-larger capacity of energy storage. Among all the technological solutions available, the redox flow batteries are ones of the most attractive as they deal a large operation scale, a good efficiency and a large design flexibility [1]. The common and most popular redox flow battery is the all-vanadium redox flow battery, which uses the same element in both cell compartments. This system avoids the contamination risk due to crossover, which occurs with the long-run use. This device leads to ideal sustainability and practical unbounded lifetime.

However, the all liquid vanadium redox flow batteries are limited by the solubility of vanadium in water (from 2 to 4 M of $VOSO_4$ in 2M acid sulfuric [2]). The vanadium ions solubility limits the energy density ca. 15 Wh/kg [1]. This energy density is quite low in contrast with the specific energy of Li-ion batteries (close to 100 Wh/kg [3]). Hence, operating points at high vanadium concentrations are essential to obtain higher energy density. Consequently, high concentration of vanadium results in large risk of precipitation of vanadium salts in the cell.

Numerous models have already been introduced to describe the liquid vanadium redox flow batteries [4–8] but without taking into account the precipitation phenomenon. This work exhibits a 2D transient model which takes into account solubility. In addition an experimental study of flow cells is introduced in order to validate the model.

2. Methods

The model solves usual mass, momentum and energy conservation equations. The Butler-Volmer law describes the electrochemical kinetic of the vanadium. The dissolution/precipitation of the vanadium salts is modelled with first order kinetic law and Fick's equation. We have assumed a pseudo-homogeneous system to solve the equation set.

To validate this model, the oxidation of vanadium (IV) to vanadium (V) is studied in a half-flow-cell made of PMMA, with carbon felt electrodes. The inlet solution of $VOSO_4$ and 3M sulfuric acid could be recycled or the cell could be fed by clean solution. Potentiometric measurement have been performed and compared with the model results. At specific time, the solution of vanadium at the outlet of the flow cell is sampled and the vanadium ions are quantified using UV-visible spectrophotometry for the vanadium (IV) and potentiometric titration with Mohr salt for the vanadium (V).

3. Conclusions

This model allows a better understanding of the impact of the vanadium precipitation on the battery operation at high vanadium concentration and could provide strategies for redox flow battery optimization.

Acknowledgments

This work was supported by the ANR VSL project, grant ANR-17-CE05-0023 of the French Agence Nationale de la Recherche.

References

[1] C. Ponce de León, A. Frías-Ferrer, J. González-García, D. A. Szánto, F. C. Walsh, *Journal of Power Sources* **2006**, *160*, 716.

[2] L. Cao, M. Skyllas-Kazacos, C. Menictas, J. Noack, *Journal of Energy Chemistry* **2018**, *27*, 1269.

[3] M. M. Thackeray, C. Wolverton, E. D. Isaacs, *Energy & Environmental Science* **2012**, *5*, 7854.

[4] M. Li, T. Hikihara, *IEICE Transactions on Fundamentals of Electronics, Communications and Computer Sciences* **2008**, *E91-A*, 1741.

[5] A. A. Shah, M. J. Watt-Smith, F. C. Walsh, *Electrochimica Acta* **2008**, *53*, 8087.

[6] A. A. Shah, R. Tangirala, R. Singh, R. G. A. Wills, F. C. Walsh, *Journal of The Electrochemical Society* **2011**, *158*, A671.

[7] D. You, H. Zhang, J. Chen, *Electrochimica Acta* **2009**, *54*, 6827.

[8] A. Tang, S. Ting, J. Bao, M. Skyllas-Kazacos, *Journal of Power Sources* **2012**, *203*, 165.

ECCE12
The 12th EUROPEAN CONGRESS OF CHEMICAL ENGINEERING
Florence 15-19 September 2019

3rd Workshop on Electrochemical Engineering:
Industrial Electrochemistry and Electrocatalysis

Polyaniline/Metal-based Electrodes: Preparation and use as Anodes in Bioelectrochemical Systems

Laura Mais, Michele Mascia*, Simonetta Palmas, Elisabetta Usai, Annalisa Vacca

Dipartimento di Ingegneria Meccanica Chimica e dei Materiali, Università degli Studi di Cagliari, Via Marengo 3, 09123 Cagliari, Italy
**Corresponding author: michele.mascia@unica.it*

Highlights

- A suitable three-step procedure is tested to coat metal electrodes with polyaniline
- Uniform and stable films of polyaniline can be obtained
- High degree of surface coverage is measured
- The obtained electrodes can be used as bioanodes

1. Introduction

Carbon-based anodes have largely used in bio-electrochemical systems, due to their biocompatibility, chemical and microbial stability. However, carbon has a low electric conductivity, which may decrease the cell voltage and the efficiency of the system. Metals may be a suitable alternative, with high values of electrical conductivity, but few metals are stable in the potential window of bio-electrochemical systems and biocompatible.

Although Copper is known to be a natural antimicrobial material, active biofilms have been obtained on this metal [1]. Coating of metals with conductive and biocompatible polymers such as polyaniline (PANI) may prevent release of toxic ions and promote the biofilm growth. PANI have been proposed for different bioelectrochemical applications, such as electrochemical biosensors [2], cell adhesion [3] and tissue engineering [4].

In the present work, copper and gold substrates have been coated with the conductive polymer polyaniline, and tested for biofilm growth. The coating was obtained with a three-step procedure, proposed in a previous work with gold electrodes: the PANI film showed higher stability if compared with that obtained with simple elctropolymerisation of aniline on bare gold [5].

2. Methods

The experiments were carried out in a flow cell with planar electrodes (0.5 cm^2); gold or copper were used as working electrode, platinum was used as counter electrode.

To obtain a stable and uniform coating of polymer, a three-step approach was followed: nitrophenyl group was grafted to the metal (Cu or Au) surface through electroreduction of nitrobenzendiazonium (NBD) salt in acetonitrile medium; the nitrogroup was then electrochemically reduced to amine in ethanol/water electrolyte; aniline was electropolymerized onto the surface of the amino-phenyl-modified electrodes. After each step, cyclic voltammetry and electrochemical impedance spectroscopy were used to characterize the modified surface.

The cells were then fed with anaerobic sludge and acetate, and the trend with time of the bioelectrocatalytic current of the acetate oxidation under potentiostatic conditions was monitored, as a measure of the biofilm growth onto the PANI/metal surface.

3. Results and discussion

Grafting of nitrophenyl groups onto metal surface was obtained in cyclic voltammetry: well-shaped peaks were observed in the first cathodic and attributed to the electroreduction of nitrobenzendiazonium. The reduction peak disappeared in the other scans, as the active sites of the metal surface were blocked by the organic moieties.

The surface coverage of the NBD modified electrodes was evaluated from the charge transfer resistance to electron transfer of the ferri/ferrocyanide redox probe by electrochemical impedance spectroscopy. Values of coating higher than 98% were obtained with gold electrodes, while lower values were observed with copper electrodes.

During the voltammetric reduction of nitro group to amine a cathodic peak was observed, which decreased with the number of cycles and disappeared after about ten cycles, indicating that all the electroactive grafted groups are reduced.

During electropolymerisation of aniline, well defined oxidation and reduction peaks were observed, indicating that the aminophenyl modified electrodes were effective for the self-catalytic head-to-tail polymerization of PANI. The peaks are less evident with copper electrodes. At the end of the process a uniform, well visible coating of PANI was obtained with both electrodes.

During biofilm cultivation under potentiostatic control with activated sludge and acetate, a growth of current can be observed, with an apparent lag phase.

4. Conclusions

Results show the effectiveness of the three-step procedure used for electrochemical coating of copper and gold with polyaniline. A stable and uniform coating of polyaniline was obtained with both metals.

Preliminary results on the use of PANi/metal electrodes as bioanodes are promising: the presence of PANI made possible to obtain an electrochemically active biofilm with copper electrodes.

References

[1] A. Baudler, I. Schmidt, M. Langner, A. Greiner, U. Schroder, Energy Environ. Sci., 8 (2015) 2048.
[2] A. Morrin, F. Wilbeer, O. Ngamna, A.J. Killard, S.E. Moulton, M.R. Smyth, G.G. Wallace, Electrochem. Commun., 7 (2005) 317
[3] P.R. Bidez, S.X. Li, A.G. MacDiarmid, E.C. Venancio, Y. Wei, P.I. Lelkes, J. Biomater. Sci. Polym. Edn., 17 (2006) 199.
[4] M. Li, Y. Guo, Y. Wei, A.G. MacDiarmid, P.I. Lelkes, Biomaterials, 27 (2006) 2705
[5] A.Vacca, M.Mascia, S.Rizzardini, S.Palmas, L.Mais, Electrochim Acta, 126 (2014) 81

ECCE12
The 12th EUROPEAN CONGRESS OF CHEMICAL ENGINEERING
Florence 15-19 September 2019

3rd Workshop on Electrochemical Engineering:
Industrial Electrochemistry and Electrocatalysis

Thin RuOx films deposited on Ti: Influence of preparation parameters on the electrochemical performances

Giovanni Sotgiu[1*], Monica Orsini[1], Serena De Santis[1], Elisabetta Petrucci[2]

1 Department of Engineering, University of di Roma Tre, Via Vito Volterra, 62 - 00146, Roma ;

2 Department of Chemical Engineering Materials & Environment, Sapienza University of Rome, Rome, Italy, Via Eudossiana, 18 - 00184, Roma

**Corresponding author: giovanni.sotgiu@uniroma3.it*

Highlights

- Ruthenium oxide electrodes have been prepared by spin-coating deposition
- Electrochemical characterization was performed by cyclic voltammetry
- Electrochemical performance was affected mostly by number of cycles and rotation speed

1. Introduction

Metal Oxide electrodes consist of an electrocatalytic thin film of noble metals oxides coating a Platinum or Titanium support. They have been successfully used in the chloro-alkali industry for the last 30 years. In more recent years different compositions (Mixed Metal Oxide MMO), have been extensively used with a view to both fundamental understandings of the processes involved and for treatment of wastewater [1], [2].

Preparation conditions, for instance, the solvent used during preparation, the nature of the oxide precursor and the calcination temperature, affect the physical properties of oxide electrodes [3]. Electrodes were prepared by several techniques: thermal decomposition, sputtering, electrochemical deposition, CVD. The thermal decomposition is the most common technique and the film can be deposited on the substrate by drop-cast, spin-coating, dip coating.

In previous works [4], [5] we have prepared different types of MMO and studied their electrochemical performances. In a standard procedure, the films were obtained by drop-cast. This method is very simple but unfortunately, it is not easy to obtain a uniform and well-controlled film.

In this work, we prepared thin RuOx film by spin-coating, a more accurate and controllable technique. In particular, we studied the influence of different process parameters on the electrochemical performances of electrodes. The investigated parameters were the number of depositions, the speed of spinning, volume, concentration, and aging of precursor solutions.

2. Methods

The cleaning procedure and the precursor solution preparation were described elsewhere [4]. Titanium samples (1.5 cm × 2.0 cm), were coated with the solution containing the precursor by spin coating using Polos SPIN150i / 200i. A variable number of depositions were made and after each of them the sample was dried in an oven at 100°C for 10 min. After the last deposition, a thermal treatment was conducted at 450°C for an hour.

The electrodes obtained were analyzed on the basis of polarization measurements and cyclic voltammetry in aqueous solutions containing Na_2SO_4.The scan rate was fixed at 50 mV/s and the potential range chosen was between -0.2 V and + 1.12 V (*vs* SCE)

3. Results and discussion

The sample prepared are presented in Table 1. As expected and confirmed by a simple visual analysis, a greater number of depositions results in a more uniform and thick film; also a lower rotation speed leads to a more homogeneous film.

Item	Speed [rad/s]	N° deposits	Molarity [mol/L]	Volume [µL]
1	500	3	0.1	10
2	500	3	0.1	20
3	1000	3	0.1	20
4	250	3	0.1	20
5	500	1	0.1	20
6	500	2	0.1	20
7	500	6	0.1	20
8*	500	3	0.1	20
9*	500	3	0.05	20
10*	500	3	0.01	20

Table 1. Prepared samples. * Freshly prepared solution

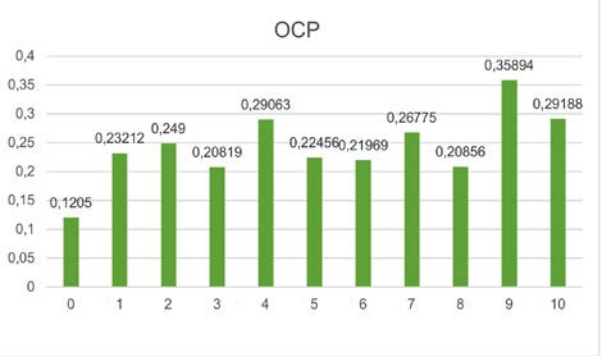

Figure 1. OCP values for the samples

Preliminary results show that all samples have similar and positive values of OCP in the range between 0.2 and 0.35 V. Total charge calculated from voltammograms is reported in Figure 2. The best value is found for sample 7 (greater number of depositions), followed by sample 4 (lower speed of deosition). The worst results are recorded in samples 3 (higher speeds), sample 5 (lower number of depositions) and sample 10 (most diluted solution). The accelerated life tests to evaluate the electrodes durability are still in progress.

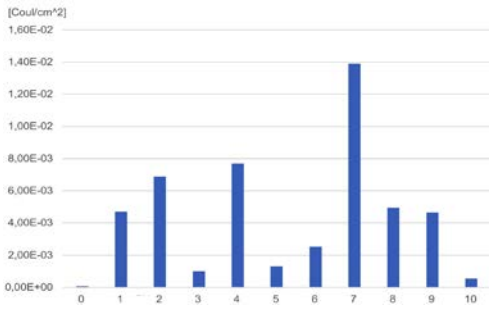

Figure 2. Q* values for the samples

4. Conclusions

We prepared several types of RuOx thin films by spin-coating. Cyclic voltammograms indicate that the total charge (Q*) increases with increasing thickness and homogeneity of the obtained film. Moreover, the electrochemical performances of electrodes obtained from aged solutions are better than the corresponding electrodes obtained with freshly prepared solutions.

References

[1] S. Stucki, R. Kotz, B. Carcer, W. Suter, J. Appl. Electrochem. 21 (1991)
[2] G.R.P. Malpass, R.S. Neves, A.J. Motheo Electrochimica Acta 52 (2006)
[3] S.Trasatti, Electrochemistry of Novel Materials, Frontiers of Electrochemistry, VCH, 1994
[4] E. Petrucci, D. Montanaro, M. Orsini, G. Sotgiu, J. Electroanal. Chem. 808 (2018) 380.
[5] G. Sotgiu, D. Montanaro, M. Orsini, E. Petrucci, Chem. Eng. Trans. 57 (2017) 1639.

ECCE12
The 12th EUROPEAN CONGRESS OF CHEMICAL ENGINEERING
Florence 15-19 September 2019

Structured multiphase reactors for electrocatalytic conversions

J.Ruud van Ommen[1], John Nijenhuis[1], Johan T. Padding[1]

1 Delft University of Technology, TU Delft Process Technology Institute & e-Refinery, Delft, the Netherlands

**Corresponding author: j.r.vanommen@tudelft.nl*

Highlights

- Millichannel reactors are an attractive choice for CO2 conversion.
- Dimensionless numbers show that millichannels have clear advantages over microchannels.
- The channel walls can act as electrodes; the channel flow prevents stagnant bubbles.

1. Introduction

There is a broad consensus that the chemical industry will have to make a transition to renewable feedstocks. An important route will be to use electrochemical processes, driven by electricity from sustainable sources, to produce hydrogen from water, hydrocarbons from CO_2 and water, and ammonia from nitrogen and water. This will require novel reactor designs, with special attention to the structured design of electrodes. Although there is progress in electrochemical flow reactors, scalable macro- and micro-reaction environments need to be developed involving e.g. gas-liquid electrolyte flow [1].

2. Methods

We examine the use of millichannels in designing multiphase reactors for electrocatalytic applications. We give a general analysis based on dimensionless numbers, followed by an illustration of this approach to catalytic packed-bed reactors. Finally, we discuss how such reactors can play an important role of increasing the number of electrocatalytic processes in the chemical industry.

3. Results and discussion

Although the electrocatalysts required for CO_2 reduction receive substantial research interest, the research efforts devoted to the design of electrocatalytic reactors remains behind. Traditionally electrochemical reactors are designed as semi-2D geometries (one dimension much smaller than the other two) because of the use of plate electrodes. However, when gas bubbles are involved (e.g., due to hydrogen formation), the use of small channels might be attractive. Here we study the influence of channel size (hydraulic diameter d_h and length L), possibly filled with particles of diameter d_p, at porosity ε. We consider flow at superficial velocity U of two types of fluids through these reactors, one gas-like and one liquid-like, for which we will use the physical properties of air and water at 20 ^{0}C temperature and 1 atm pressure.

The differential pressure drop necessary to reach significant convective improvement of mixing and heat and mass transfer (typically Re>100) becomes prohibitive for small channels. For example, for an empty structured channel of hydraulic diameter d_h, the pressure drop associated with wall friction can be described by the Darcy-Weisbach equation [2]. Fig. 1 shows $\Delta p/L$ as a function of d_h for liquid-like (black solid line) and gas-like (black dashed line) fluids at Re = 100, assuming f = 64/Re. At this *fixed* Re, U decreases like $1/d_h$, leading to $1/d_h^3$ scaling of the required pressure drop: for d_h = 0.1 mm, the pressure drop to reach Re=100 is already substantial, approximately 10 bar/m, while for d_h = 1 mm the necessary pressure drop is a more manageable: 0.01 bar/m.

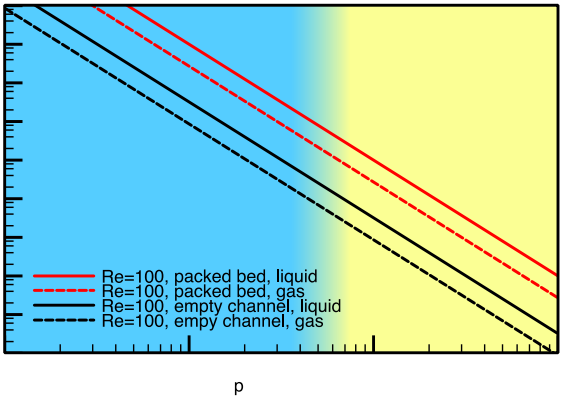

Figure 1. Pressure drop needed to reach Re=100 as a function of hydraulic or particle diameter. Blue: microchannel, yellow: millichannel.

For a channel filled with catalytic particles of diameter d_p, the differential pressure drop can be described by the Ergun equation [3]. Figure 1 shows $\Delta p/L$ as a function of d_p for liquid-like (red solid line) and gas-like (red dashed line) fluids at Re = 100 and ε=0.5. For the Ergun equation, *both* laminar and turbulent terms scale like $1/d_p^3$ at fixed Reynolds number. Under these conditions, for d_p = 0.1 mm, the pressure drop necessary to reach Re=100 is enormous, approximately 1000 bar/m, while for d_p = 1 mm, the necessary pressure drop is much more reasonable, approximately 1 bar/m.

Pressure drop and mass and heat transfer are not the only important consideration. We also need to consider that smaller reactors are also more prone to contaminants and agglomerates getting stuck in corners of the channel or pore space. Moreover, it is important to tune the residence time in the channel to optimize reaction yield or selectivity. The average residence time is $\tau = \varepsilon L/U$. At fixed Re, this leads to $\tau/L = \rho d_h/(\mu \mathrm{Re})$ or $\tau/L = \rho\varepsilon d_p/(\mu \mathrm{Re})$, for the two respective systems. In the regime where inertial flow enhancement becomes relevant (Re>100), reaching sufficiently *long* residence times requires sufficiently wide channels or sufficiently large particles.

4. Conclusions

Millichannels have clear advantages over traditional, non-structured reactors, in electrocatalytic processes. Analysis based on dimensionless numbers shows that the use of millichannels has important advantages over microchannels. The walls can act as electrode, while the channel configuration prevents problems with gas bubbles encountered in other types of electrocatalytic reactors.

References

[1] Walsh, F. C. & Ponce De León, C. 2018, 280, 121-148.
[2] Romeo, E., Royo, C. & Monzón, A. 2002, Chemical Engineering Journal, 86, 369-374.
[3] Ergun, S. 1952, Chem. Eng. Progress., 48, 89-94.

ECCE12
The 12th EUROPEAN CONGRESS OF CHEMICAL ENGINEERING
Florence 15-19 September 2019

Improvements in the treatment of the polluted streams containing non-polar organochlorine pesticides

Alexandra Raschitor, Javier Llanos, Gustavo Santos Acosta, Manuel Andrés Rodrigo, Pablo Cañizares

Department of Chemical Engineering. Faculty of chemical sciences and technologies. University of Castilla-La Mancha. 13071 Ciudad Real. Spain

**Corresponding author: javier.llanos@uclm.es*

Highlights

- The efficiency in the degradation of oxyfluorfen increases with concentration strategies.
- The most efficient process is the combination of electrocoagulation and electroFenton.
- The solid produced in electrocoagulation can be efficiently treated as a solid phase.

1. Introduction

The removal of chlorinated organic compounds from wastewater has become a matter of high interest lately due to their high toxicity, persistency and bioaccumulation.

In order to minimize the mass transfer limitations related to the treatment of low-concentrated streams the development of concentration strategies may be the solution. They can be integrated to the main treatment process or coupled as a pre-treatment step. When choosing a treatment technique, the nature of the pollutant must be considered. According to their physical and chemical proprieties, the organochlorine pesticides can be classified as polar or nonpolar, ionic or nonionic. For the ionic polar pollutants such as 2,4-Dichlorophenoxyacetic acid, electrodialysis combined with electro-oxidation offers a good solution to treat high volumes of wastewater, as demonstrated in our previous work [1].

For the nonpolar nonionic pesticides, the concentration by electrocoagulation was successfully developed in a previous work [2] leading to various treatment options that can be further applied. By applying the electrocoagulation as a pre-concentration step, it can be achieved the transfer of the pollutant from the liquid phase into a smaller volume of solid phase. The solid phase can now be dissolved and treated as a liquid waste or, treated as it is, like a solid or pulp.

This work aims to demonstrate that by concentrating the wastewater applying a cheap and noninvasive concentration technique followed by an aggressive degradation step it is possible to increase the removal efficiency and to reduce the energy consumption. Moreover, different alternatives for the treatment of the concentrated stream are presented and compared.

2. Methods

In this work, 2 types of electrochemical cells and 3 technologies were used. The first cell, a homemade cell equipped with a Fe anode and a BDD cathode it was used for

electrectrocoagulation, EC (j = 50 Am^{-2}). The second cell, a commercial Adamant Cell equipped with BDD electrodes, was used for electrooxidation (EO) and electroFenton, EF (j= 254.67, j= 177.33 and j= 63.6 A/m^2 respectively). In order to dissolve the concentrated phase it was added H_2SO_4.
When the concentrated phase is treated as solid, it must be applied another disturbing agent, ultrasound irradiation in this particular case, (75 khZ and 1MhZ) in order to alter the structure to release the pollutant for its further electrochemical removal step.

The concentration of Oxyfuorfen was measured by means of High Performance Liquid Chromatography (HPLC) equipped with an analytical column Phenomenex Gemini 5 µm C18.

3. Results and discussion

By applying EO to a non-concentrated wastewater, it was possible to achieve a removal of Oxyfluorfen from 100 to 79 mg/l in three hours at j= 254.67 A m^{-2}. When electrocoagulation is previously applied and the concentrated phase is treated as a liquid stream (acidified with H_2SO_4), it is possible to achieve a removal of Oxyfluorfen from 1250 to 776 mg/l with EO, giving a specific power consumption almost 10 times lower than that required when treating the raw diluted solution. When applying EF, the concentration can be reduced from 1340 to 69.3 mg/l F in only three hours at the same current density, thus resulting in the best performance when the concentrated solution is treated as a liquid.
The treatment of the concentrated phase as a solid phase (as it is obtained in the EC process) is still in development but the preliminary results obtained so far show that by applying ultrasonic irradiation to the mixture it is possible to release an important amount of the pollutant that is trapped into the flocs, being the best performance obtained when the lowest ultrasound frequency is applied.

4. Conclusions

This work demonstrates that by previously concentrating a wastewater containing non-polar organochlorine pesticides, it can be significantly increased the removal efficiency, being the combination of EC with EF the process with the better performance.

Moreover, the treatment of the concentrate as a solid phase seems to bring promising results opening a new path for the treatment of this type of contaminants.

Acknowledgements

The financial support from the Spanish Ministry of Economy, Industry and Competitiveness and European Union through project CTM2016-76197-R (AEI/FEDER, UE) is gratefully acknowledged

References

[1] J. Llanos, A. Raschitor, P. Cañizares, M.A. Rodrigo, Exploring the applicability of a combined electrodialysis/electro-oxidation cell for the degradation of 2,4-dichlorophenoxyacetic acid, Electrochimica Acta, 269 (2018) 415-421.
[2] M. Muñoz, J. Llanos, A. Raschitor, P. Cañizares, M.A. Rodrigo, Electrocoagulation as the Key for an Efficient Concentration and Removal of Oxyfluorfen from Liquid Wastes, Industrial and Engineering Chemistry Research, 56 (2017) 3091-3097.

ECCE12
The 12th EUROPEAN CONGRESS OF CHEMICAL ENGINEERING
Florence 15-19 September 2019

Energy and Chemical Engineering

Energy efficiency classification method in processing crude oils using data envelopment analysis tools.

D. Narciso[1], F. G. Martins[1*]

1 LEPABE - Laboratory for Process Engineering, Environment, Biotechnology and Energy, Faculty of Engineering, University of Porto, Rua Dr. Roberto Frias, 4200-465 Porto, Portugal

**Corresponding author: fgm@fe.up.pt*

Highlights

- Topping distillation unit simulation model for a variety of crude oil assays.
- Characterization of the energy efficiency in processing crude oils using data envelopment analysis as a tool.

1. Introduction

Crude oil refining is a very energy intensive industry. Modest increases in performance typically translate into considerable energy savings [1], creating a strong drive in this industry to optimize their operations by focusing on various process options and configurations.

One of the key decisions to be made by refineries' management teams is which crude oils should be selected for attaining the energy consumption target performances. A large number of factors may play a strong role in this selection, including price, estimated product distribution, geo-politics, among others. Given the high impact of energy consumption on refineries, an assessment on crude oil energy efficiency correlates closely with process economics and could be an important and complementary tool for crude oil selection.

2. Methods

The focus of this work is on the impact of the crude oil selection on energy efficiency obtained by simulation approach, using a fixed process set-up and operation objectives, thus enabling a quick scan of many different assays.

A simulation model of a topping distillation unit was implemented in Aspen Plus V9. In this set-up, crude oils are pre-heated through a heat transfer network, and further heated in a furnace before being feed to the distillation unit. The furnace heating power (FP) is the main (heating) energy consumption. The distillation column includes four outlet streams enabling the separation of crude oil components according to their boiling points, obtaining naphtha, kerosene, gasoil and residue as main products. The sum of all heat released is defined as the total cooling power (TCP).

A collection of 10 assays was selected from the Aspen Plus data bank. The distillation system model was simulated using a fixed feed rate for each of the 10 assays.

Data Envelopment Analysis (DEA) is an efficiency-modelling framework [2], where efficiency indexes are expressed as a weighted quotient of (valuable) outputs to (cost) inputs and ranging from 0 (inefficient) to 1 (efficient). The efficiency indexes take the general form:

$$\theta = \frac{\sum_i w_i \times output_i}{\sum_j w_j \times input_j} \quad (1)$$

In the context of crude refining, outputs include one or more product flowrates and inputs include at least one energy consumption. Several output/input configurations were used, each providing complementary information on process energy efficiency. The scenarios considered are presented in Table 1:

Table 1. Scenarios used for energy efficiency ranking.

Scenario	Inputs	Outputs
1	FP	GKN
2	FP, TCP	GKN
3	FP	GKNR
4	FP	NAFHTHA, KEROSENE, GASOIL, RESIDUE

Where GKN is the combined flowrate of gasoil, kerosene and naphtha, and GKNR the total outlet flowrate (GKN and Residue flowrates). For all scenarios, a DEA model was created and energy efficiency indexes were calculated. pyDEA [3] was used as the DEA solver.

3. Results and discussion

The energy efficiency scores obtained for each of the identified scenarios are presented in Table 2:

Table 2. Energy efficiency indicators for each crude oil assay using Scenarios 1 - 4.

Scenario	ARABLT1	ARGYLL	ASHTART	BACHAQUE	OSEBERG	SAHARNBL	DANISH	SKUA	WSTTXINT	BELAYIM
1	0.809	0.822	0.757	0.549	0.865	0.896	0.850	1.000	0.878	0.689
2	0.910	0.910	0.921	0.778	0.942	0.897	0.901	1.000	0.895	0.832
3	0.806	0.778	0.868	1.000	0.785	0.701	0.764	0.698	0.715	0.867
4	1.000	0.985	1.000	1.000	1.000	1.000	1.000	1.000	1.000	1.000

In Scenario 1, the special focus was to obtain more valuable product streams, by excluding the residual stream. SKUA crude oil is the most energy efficient crude oil. Scenario 2 is a slight variation of the Scenario 1, where the furnace heating load and the total cooling are considered as independent inputs, with no significant impacts other than generally increasing the efficiency indicators. In Scenario 3, as the target output was the total production (GKNR), BACHAQUE is considered the most efficient. This crude has a high residue flowrate, which typically requires much less energy consumption. In Scenario 4, all of the outlet flowrates were considered independently, resulting that there are no differences in energy efficiency performance. Increasing the number of independent DEA inputs or outputs typically leads to a loss of resolution. As long as a crude oil yields a high content of any of the refinery's products, its efficiency will be high. In this sense, Scenarios 1 and 3 provide more insightful information on product distribution and energy efficiency.

4. Conclusions

Indicators obtained by DEA have proven to be useful to provide useful information on crude oil energy efficiency. Extensions in the number of assays and benchmarks will provide greater generality.

Acknowledgements: This work was financially supported by: Project "LEPABE-2-ECO-INNOVATION" – NORTE-01-0145-FEDER-000005, funded by Norte Portugal Regional Operational Programme (NORTE 2020), under PORTUGAL 2020 Partnership Agreement, through the European Regional Development Fund (ERDF).

References

[1] http://www.eumerci.eu/sector-technical-analisys/.
[2] W. W. Cooper, L. M. Seiford, K. Tone, Data Envelopment Analysis, second ed., Springer, New York, 2007.
[3] https://pypi.org/project/pyDEA/.

ECCE12
The 12th EUROPEAN CONGRESS OF CHEMICAL ENGINEERING
Florence 15-19 September 2019

Use of Blueprints for Industrial Symbiosis Detection – The Case of Heat Integration Between a Refinery anda District Heating Network.

Hélène Cervo[1, 2, *], Samira Fazlollahi[3], Jean-Henry Ferrasse[1], Greet Van Eetvelde[2, *]

1 Aix Marseille Univ, CNRS, Centrale Marseille, M2P2, Marseille, France;
2 Energy and Cluster Management, Faculty of Engineering and Architecture, Ghent University, Ghent, Belgium; 3 Veolia Recherche et Innovation, 291 Avenue Dreyfous Ducas, 78520 Limay, France

**Corresponding authors: helene.cervo@etu.univ-amu.fr, Greet.VanEetvelde@UGent.be*

Highlights

- Utilisation of blueprints for the detection of industrial symbiosis opportunities
- Heat integration between a refinery and a District Heating Network

1. Introduction

Industrial Symbiosis (IS) is at the heart of the European Union's (EU) strategy to transition towards a lower carbon and more circular economy. It focuses on the cooperation of large and small enterprises in industrial or district clusters for exchanging materials, energy and waste (co-product) [1] as well as services, technologies or even knowledge and information [2], [3]. However, data confidentiality is still a barrier, preventing the discovery of new IS opportunities. The concept of blueprints [4], developed in the framework of the EPOS project [5], is a solution for sharing information across industry sectors. In this abstract, the blueprints' thermal energy profiles of a refinery and a District Heating Network (DHN) are combined in order to find heat integration opportunities between a petrochemical site and a nearby community.

2. Methods

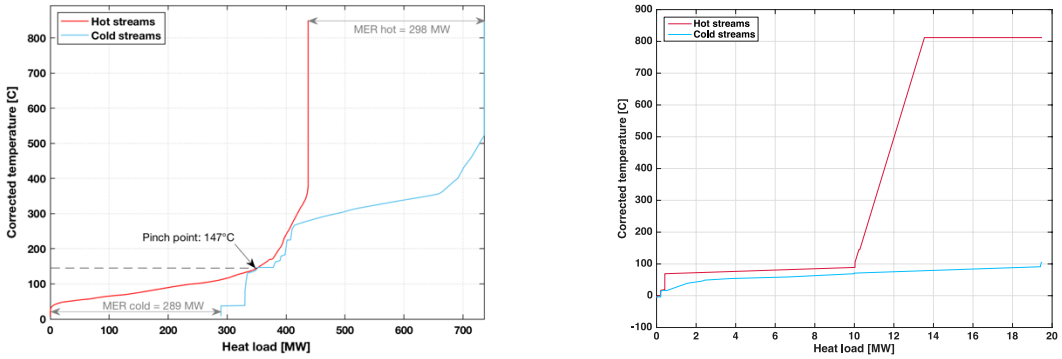

(a) (b)

Figure 1. Refinery (a) and DHN (b) blueprints' thermal profiles

The blueprint's thermal energy profile includes the hot and cold requirements of a given process [4], represented by Pinch Analysis composite curves [6]. The refinery's blueprint consists of 10 interconnected process units comprising: a crude distillation unit, a gas plant, three hydrotreatment units, a catalytic reformer, an isomerisation unit, a vacuum distillation unit, a

visbreaker and a fluid catalytic cracker with a total capacity rate of is 35'000 t_{crude}/d. The DHN blueprint is available for four different climate locations, obtained using the European heating and cooling indices [7]. In this work, the distribution network is located in the Northern Zone (Zone 5) with a population of 10'000 inhabitants. The refinery and DHN thermal profiles are respectively displayed in figure 1.

3. Results and discussion

Table 1 shows the DHN's thermal power consumption before and after heat integration with the refinery. The DHN's energy consumption is decreased by ~50% (-9.57 MW) after the integration with the refinery. It shows that there is an interesting potential for creating a synergy between a refinery and an urban area. Nevertheless, it should be noted that the distance between the refinery and the DHN is not considered (no heat losses and no pressure drop) as well as the related investment costs.

Table 1. DHN thermal power consumptions before and after integration with the refinery

	Power Business as Usual (kW)	Power after integration (kW)
Refrigeration	200	200
Centralised heating	142.2	0
Electrical heating	47.84	0
Heating District Hot Water	2'031	2'031
Space heating	7'446	7'446
Boiler	9'380	0
TOTAL	19'247	9'677

4. Conclusions

The use of blueprints is a powerful tool for overcoming the burden of industrial data confidentiality. The case of heat integration between a refinery and a DHN demonstrates that blueprints can be used for the identification and evaluation of new IS opportunities. When integrated with the refinery, the DHN's energy consumption is reduced by 50%. This case can also be replicated for other geographic zones, different population sizes and for various capacity rates of the refinery. A complete thermos-economic study should also be carried in order to take into account all the costs.

References

[1] M. R. Chertow, 'INDUSTRIAL SYMBIOSIS: Literature and Taxonomy', Annu. Rev. Energy Environ., vol. 25, no. 1, pp. 313–337, Nov. 2000.

[2] G. Van Eetvelde, 'Industrial Symbiosis', in Resource Efficiency of Processing Plants, John Wiley & Sons, Ltd, 2018, pp. 441–469.

[3] D. R. Lombardi and P. Laybourn, 'Redefining Industrial Symbiosis', J. Ind. Ecol., vol. 16, no. 1, pp. 28–37, 2012.

[4] H. Cervo et al., 'Virtual Sector Profiles for Innovation Sharing in Process Industry – Sector 01: Chemicals', in Sustainable Design and Manufacturing 2017, 2017, pp. 569–578.

[5] EPOS, 2018. [Online]. Available: https://www.spire2030.eu/epos.

[6] B. Linnhoff and E. Hindmarsh, 'The pinch design method for heat exchanger networks', Chem. Eng. Sci., vol. 38, no. 5, pp. 745–763, Jan. 1983.

[7] S. Raluca, K. Ivan, B. Hur, G. Luc, and M. Francois, 'Geographically parameterized residential sector energy and service profile', Chem. Eng. Trans., pp. 709–714, 2018008.

ECCE12
The 12th EUROPEAN CONGRESS OF CHEMICAL ENGINEERING
Florence 15-19 September 2019

Optimal Process Design for a Sustainable Methanol Production Using Renewable Energies by Applying the FluxMax Approach.

Dominik Schack[1], Kai Sundmacher[1,2]

1 Max Planck Institute for Dynamics of Complex Technical Systems, Sandtorstr.1, D-39106 Magdeburg, Germany; 2 Otto-von-Guericke-University Magdeburg, Universitätsplatz 2, D-39106 Magdeburg, Germany

**Corresponding author: schack@mpi-magdeburg.mpg.de*

Highlights

- Simultaneous flux optimization and heat integration.
- Decoupling of nonlinearities by discretization of thermodynamic state space.
- Versatility of FluxMax approach demonstrated at different levels of details.
- Powerful tool for identification of novel, non-intuitive, processes.

1. Introduction

In the context of energy transition, one of the major goals of the chemical industry is to replace fossil raw materials with renewable resources by using sustainable process technologies. However, even if in the main focus of interest, not only the substitution of feedstock, but also an increase in energy efficiency will be decisive for a successful transition towards a more sustainable production of chemicals. In order to enhance the overall process efficiency, challenges must be faced at different levels of detail. While at the plant level, more general questions and early stage decisions of chemical production networks are addressed, at the process level and process unit level the detailed optimization of chemical processes and process units is in the focus. We developed the FluxMax approach that enables the simultaneous flux optimization and heat integration by discretization of the thermodynamic state space. As a consequence, process-based nonlinearities are decoupled effectively from the flow optimization problem, which allows the optimization of chemical processes across different length. Heat integration is considered as integrated part of the optimization problem by introducing additional inequality constraints, which results in an outperformance compared to classical, sequential approaches.

2. Methods

The general idea of the FluxMax approach is an effective decoupling of process-based nonlinearities from the subsequent network flux optimization by discretization of the thermodynamic state space. The discretization allows the representation of chemical process across different length scales, which enables the transformation of a nonlinear process optimization problem into a convex flux optimization on a defined network graph. The chemical process is represented as directed graph, where the nodes correspond to thermodynamic substances, elementary processes and heat and work utilities. While each mixture is uniquely determined by thermodynamic coordinates, the elementary processes are uniformly described by stoichiometric equations. The edges, that connect the nodes, correspond to mass- and energy fluxes, and are decision variables of the optimization problem. As a result, the FluxMax approach

can be divided into the three steps: i) discretization of the thermodynamic state space; ii) modeling of elementary processes; and iii) solution of the flux optimization problem.

3. Results and discussion

The methanol synthesis process was selected as example to apply the FluxMax approach to different levels of details. At the plant level [1,2] we systematically analyzed the influence of feedstock and energy sources on the specific methanol production cost and its specific CO_2 emissions. It could be shown that an economically competitive production process can be designed also under the usage of renewable energies (Figure 2 A). As a consequence of the simultaneous consideration of heat integration, the FluxMax approach identified energy-optimal process configurations [3], which outperform configurations identified in a sequential procedure (Figure 2 B). The proof-of-concept for the application at process unit level was provided for the reactor (Figure 2 C) and compressor cascade design of the methanol synthesis [4].

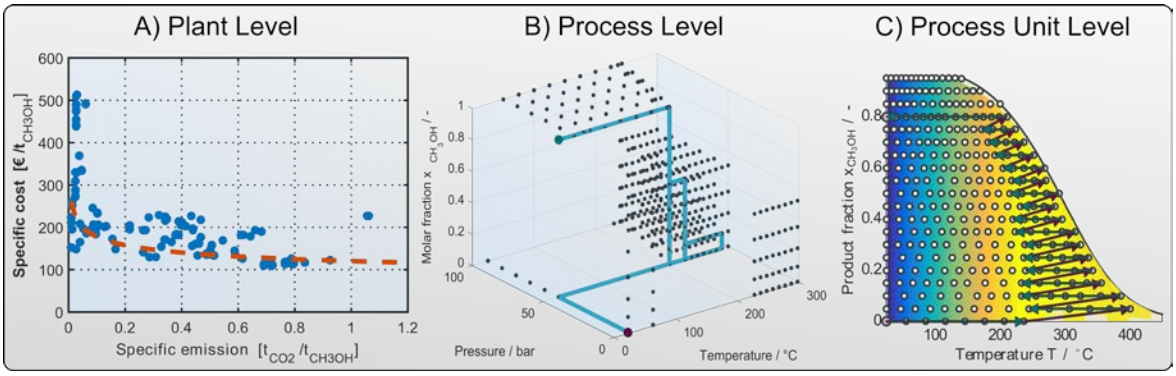

Figure 1. Pareto optimum of competing objectives, specific cost and CO_2 emissions (A), optimal trajectory of methanol synthesis process within discretized thermodynamic state space (B), and kinetic rate optimization of reactor part (C).

4. Conclusions

In this contribution, the FluxMax approach for the optimization of chemical processes across different length scales is presented, which enables the simultaneous flux optimization and heat integration. The introduction of nodes corresponding to mixtures, elementary processes and utilities allows the representation of any chemical process as a directed graph, with the edges corresponding to the mass and energy fluxes to be optimized. As a consequence, the FluxMax approach effectively decouples process based nonlinearities from the optimization problem. The heat integration is considered by additional constraints in the optimization. Using the methanol synthesis process as example, the FluxMax approach was applied to different levels of details. In particular the outperformance compared to classical approaches makes the FluxMax approach a powerful tool for designing chemical processes across different length scales.

References

[1] D. Schack, L. Rihko-Struckmann, K. Sundmacher, Comput.-Aided Chem. Eng. 38 (2016) 1551–1556.
[2] D. Schack, L. Rihko-Struckmann, K. Sundmacher, Ind. Eng. Chem. Res. 57 (2018) 9889–9902.
[3] D. Schack, G. Liesche, K. Sundmacher (submitted).
[4] G. Liesche, D. Schack, K.H.G. Rätze, K. Sundmacher, Comput.-Aided Chem. Eng. 43 (2018) 881–886.

ECCE12
The 12th EUROPEAN CONGRESS OF CHEMICAL ENGINEERING
Florence 15-19 September 2019

Evaluation of Hybrid Electric Steam Generation for a Chemical Plant under Future Energy Market Scenarios

Holger Wiertzema[1], Elin Svensson[2], Simon Harvey[1]

1 Chalmers University of Technology, Division of Energy Technology, 412 96 Göteborg, Sweden;
2 CIT Industriell Energi AB, 412 88 Göteborg, Sweden

**Corresponding author: holgerw@chalmers.se*

Highlights

- Hybrid electric steam generation can be economically feasible already today
- The cost-optimal capacities are very sensitive to future energy market conditions
- Electricity is compared with biomethane as fuel for steam generation

1. Introduction

Industrial processes currently account for 25–35% of the world's total energy demand and related emissions. During recent years, the amount of low-carbon electricity from renewable energy sources (such as wind and solar) has increased continuously while the corresponding electricity generation cost has fallen. This leads to an increasing interest in process electrification to reach long-term goals for reduction of greenhouse gas emissions. One option to reduce CO_2 emissions from the utility system of chemical plants is to implement hybrid electric steam generation concepts in which electric and gas boilers are coupled. It is assumed that the gas boiler can switch freely between natural gas and bio-methane fuels.

The objective of this study was to evaluate hybrid electric steam generation for a specific chemical plant in terms of CO_2 emissions and cost under future energy price and policy conditions.

2. Methods

In the first step, an optimization model was used to identify the optimal boiler capacities to reach the lowest total annualized cost for a hybrid system. The model takes into account the specific characteristics of the steam demand and the steam generation technologies. It was applied to a refence scenario with current Swedish energy market conditions, as well as two sets of future energy market scenarios from the ENPAC model [1]. ENPAC is a tool to generate consistent scenarios for energy prices and marginal CO_2 emissions associated with the use of energy for large-volume industrial customers based on forecasted prices for fossil fuels on the commodity market and costs associated with emitting CO_2. The scenarios used in this work were generated based primarily on output from the "New policies" and "Sustainable development" scenarios from the IEA's World Energy Outlook [2]. For these scenarios, power grid capacity additions are assumed to generate electric power from renewable sources with no CO_2 emissions with wind power as marginal electricity production technology. The scenarios also include data for costs for biomass fuel as well as CO_2 emissions related to increased use of biomass, under the assumption that biomass is a limited resource. In both scenarios, the significant increase over time of the charge for

emitting fossil CO_2 leads to a major increase of the market price of natural gas, but it also leads indirectly to a significant increase of the cost of the biomass feedstock for production of bio-methane.

In this work, steam generation capacities were fixed to values corresponding to the average optimal values resulting from the "New policies" scenarios for the period 2025-2040 in order to simulate an investment decision. The boiler system performance was then evaluated by a what-if analysis in terms of CO_2 emissions and cost for the "New policies" and the "Sustainable Development" scenarios for 2025, 2030 and 2040. Additional runs were performed in which the system was forced to follow an emission reduction path at the lowest cost, allowing the gas boiler to switch from natural gas to biomethane if necessary. The emission reduction was in line with the Swedish target of net zero emission of greenhouse gases by 2045.

3. Results and discussion

Results from the first step show that hybrid steam generation concepts can be economically feasible even under today's energy price conditions. In the "New policies" scenario, the optimal capacity for the electric boiler for the energy market conditions in 2030 and 2040 are only slightly higher than the one in 2025. In contrast, the optimal electric boiler capacity for 2030 and 2040 in the "Sustainable Development" scenario is equal to the maximum steam demand, meaning that there would be no investment in a gas boiler.

The what-if analysis with fixed capacities reveals for the "New policies" scenario that there is only a slight increase in total annualized cost when emission constraints that are in line with the Swedish emission reduction goals need to be respected. Under these conditions, there is a shift of boiler load from the gas to the electric boiler. In 2040, the electric boiler even replaces the gas boiler as baseload technology. For the "Sustainable Development" scenario, there is no change in total annualized cost when adding the emission constraint. This is due to the higher cost associated with natural gas. For both scenarios, the choice of biomethane to reduce CO_2 emissions would be much more expensive than replacing natural gas by electric boiler.

This study takes only yearly values for the electricity price, the natural gas price and cost associated with CO_2 emissions into account. An assessment on an hourly basis would allow a more detailed assessment and would enable a correspondent operational scheduling of the technologies.

4. Conclusions

Electric and hybrid steam generation can reduce emissions of the utility system and can be economically feasible even today. The emission reduction and cost-benefits of the electric steam generation is amplified when taking assumed future energy market conditions into account. From a cost perspective, electricity as fuel to produce steam is more attractive than biomethane.

References

[1] E. Axelsson, S. Harvey, Scenarios for assessing profitability and carbon balances of energy investments in industry, AGS Pathways report 2010:EU1, Göteborg, 2010.
[2] IEA, World Energy Outlook 2018, Paris, 2018.

ECCE12
The 12th EUROPEAN CONGRESS OF CHEMICAL ENGINEERING
Florence 15-19 September 2019

Simulis Pinch: quick and efficient process energy integration in Microsoft® Excel

Olivier Baudouin[1*], Stéphane Déchelotte[1], Philippe Leurent[1], Benjamin Wincure[2]

1 ProSim SA, Immeuble Stratège A, 51 rue Ampère, F-31670 LABEGE, France

2 ProSim, Inc., 325 Chestnut Street, Suite 800, Philadelphia, PA 19106, USA

**Corresponding author: olivier.baudouin@prosim.net*

Highlights

- Process energy integration;
- Pinch technology;
- Microsoft Excel.

Industrial sectors account for one third of global energy consumption. A common feature of industrial processes is reliance on fossil fuels as the primary source of energy, where a large part of the energy consumption is spent on production of utilities. Due to the huge negative impacts of fossil fuel combustion on the environment, the scientific world makes a significant effort to find alternative sources of energy. However, even by the most optimistic assessments, these alternatives are long-term solutions and many projections show that in the near future, fossil fuels will remain the primary sources of energy, in particular for the process industries.

Pinch analysis [1] is a well-known methodology to optimize process energy consumption. It allows the determination of the minimum required process utilities consumption. Simulis Pinch [2], software used directly in Excel, has been developed to perform energy integration calculations with the pinch method, while also systematically considering real-world engineering constraints. Based on a chosen pinch that is acceptable for the whole process, Simulis Pinch calculates the minimum utility requirements and the maximum heat that can be recovered through energy integration. The software also plots the hot and cold composite curves, as well as the grand composite curve. The energy integration concept is used by the software to reach the optimal synthesis of a heat exchanger network that achieves the maximum energy recovery. In Pinch theory, the synthesis of the optimal heat exchanger network is subject to construction rules (for example, the division of the problem into two sub-problems, one below and the other above the pinch temperature). However, the ideal point may not be simple to reach (due to partial exchanges on streams, stream divisions…), and the number of heat exchangers needed may be significant. While optimisation tools can help to determine the optimal structure of the heat exchanger networks using MINLP-type algorithms, these tools often have calculation times that are very long, and their convergence on an industrial scale is not guaranteed. The approach of Simulis Pinch is more pragmatic: the aim is to quickly propose some good solutions with a limited number of heat exchangers. The method is not an “optimal” method in the mathematical sense of the term, as it systematically aims to exchange the maximum power between two streams. If a hot stream and a cold stream can exchange heat, the algorithm searches for the possible couplings that allow the exchange of the

maximal thermal power under certain limitations or “boundary conditions”. The automatic synthesis of a ‘good’ heat exchanger network takes into account the specific constraints on particular exchanges (fluids incompatibility, different units, distance, difficulties…). Between two streams that can exchange heat, the combination of the possible exchanges is limited to a maximum of 3 possible couplings between these streams.

An application example, from an industrial case of an existing bio-refinery, will be presented to illustrate the use of Simulis Pinch. Two heat exchanger networks are proposed, which take into account the on-site constraints. The heat recovered corresponds to more than 80% of the MER (Maximum Energy Recovery).

References

[1] Bodo Linnhoff, PhD thesis “Thermodynamic Analysis in the Design of Process Networks”, Leeds University, 1979

[2] http://www.prosim.net/en/index.php

ECCE12
The 12th EUROPEAN CONGRESS OF CHEMICAL ENGINEERING
Florence 15-19 September 2019

Thermochemical energy storage materials for high-temperature concentrated solar energy

Marco Gigantino[1], Aldo Steinfeld[1*]

[1] *Department of Mechanical and Process Engineering, ETH Zurich, 8092 Zurich, Switzerland*

**Corresponding author: aldo.steinfeld@ethz.ch*

Highlights

- High-temperature heat was stored via the $SrCO_3$/SrO and CuO/Cu_2O cycles.
- MgO and YSZ were selected as support framework to diminish thermal sintering.
- Preparation methods affected the cycling performance.
- Stable energy density was achieved over 100 consecutive cycles.

1. Introduction

Thermochemical energy storage (TCS) employs reversible endothermic/exothermic chemical reactions to store/release heat delivered by concentrated solar energy systems, thus overcoming solar radiation intermittency and enabling round-the clock dispatchability of high-temperature process heat. The TCS approach is considered attractive since it can achieve higher energy densities than sensible and latent energy storage [1]. Several metal oxides which undergo gas-solid reactions are suitable materials for high-temperature TCS systems (>600°C), but very often they exhibit a decreasing extent of conversion (directly related to the energy density) over consecutive charging/discharging cycles due to sintering. Of special interest are the $SrCO_3$/SrO and CuO/Cu_2O cycles that store heat at around 1000°C.

2. Methods

To tackle sintering and maintain cycling stability, sintering-resistant materials MgO and YSZ were incorporated into SrO and CuO, respectively, by means of various mixing methods, namely: dry-mixing, wet-mixing, co-precipitation and sol-gel. The resulting SrO-and CuO-based materials were tested over multiple consecutive charging/discharging cycles in a thermogravimetric analyzer.

3. Results and discussion

The specific thermal energy storage capacity and cyclic stability over multiple carbonation-calcination cycles was systematically investigated by thermogravimetry for different precursors, sintering-resistant additive contents, mixing methods, operating and pre-treatment conditions.

4. Conclusions

Full stability over 100 consecutive charging/discharging cycles was achieved for a MgO-stabilized SrO-based material (40 wt% SrO) and a YSZ-stabilized CuO-based material (65 wt% CuO) with values of gravimetric energy densities of 0.81 MJ/kg and 0.56 MJ/kg, respectively.

References

[1] P. Pardo, A. Deydier, Z. Anxionnaz-Minvielle, S. Rouge, M. Cabassud, P. Cognet,. A review on high temperature thermochemical heat energy storage. Renew. Sustain. Energy Rev., 2014

ECCE12
The 12th EUROPEAN CONGRESS OF CHEMICAL ENGINEERING
Florence 15-19 September 2019

Synthetic inertia provision by fast responsive reversible hydrogen production processes

Jens Baetens[1], Danny Smet[2], Greet Van Eetvelde[1,2] and Lieven Vandevelde[1]

1 Electrical Energy Laboratory (EELAB), Department of Electrical Energy, Metals, Mechanical Constructions & Systems (EEMMeCS), Ghent University, Tech Lane Ghent Science Park – Campus A, Technologiepark-Zwijnaarde 131, 9052 Ghent, Belgium; 2 INEOS Group

**Corresponding author: j.baetens@ugent.be*

Highlights

- Need for synthetic inertia with increasing RES penetration.
- Potential in electrolysis processes and fuel cells.
- Large overall potential in DSM for provision of ancillary services.

1. Introduction

One of the effects of integrating more RES in the electricity grid is the loss of system inertia. Classical thermal power plants have large rotors, all spinning at speeds so to generate power at 50 Hz, hence the term synchronous generators. The total mass of these rotors inherently created a large system inertia, limiting the Rate of Change of Frequency (RoCoF) in case of a disturbance. The RoCoF is a measure for the robustness of the electrical grid and needs to be maintained within certain limits for safe operation.

2. Inertia in the electricity grid

ENTSO-E, the European Network of Transmission System Operators for Electricity, has launched a guidance document for the implementation of Synthetic Inertia (SI) for countries that already see large penetration of RES in their network [1]. ENTSO-E defines SI as a facility provided by a power park or HVDC system to replace the effect of inertia by synchronous generators. While able to be provided by wind or solar power parks [2], also on the demand side possibilities are identified. Already in 2015 a private company made news with the possibility of providing SI with an electrolysis process. The respective system was able to respond within 800 ms and 140 ms for the "turn on" and "turn off" respectively [3]. Indeed, also in the doctoral dissertation of Rezkalla M., Demand Side Management is identified as one of the suitable technologies for inertia support. It is also stated that the capacity of DSM has been underestimated due to the complexity considering monitoring and aggregation [4]. With recent advances on both levels, DSM could withhold a large potential in providing ancillary services, including SI.

While in some EU countries regulation regarding frequency response from large RES power parks are already in place, no real market for inertial frequency response is set-up. This with the exception of Ireland where with the DS3 program system services like synchronous inertial response and fast frequency response are contracted with market parties [5].

3. Link to chemical industry

Building an electrolyser for the sole purpose of supporting the grid by supplying synthetic inertia or Frequency Containment Reserves (FCR) might not be economically viable. For that reason it should be looked at from a different viewpoint. Let's take hydrogen as an example. The large majority of the used hydrogen in chemical industry today is produced by Steam Methane Reforming (SMR) with natural gas, releasing large amounts of CO_2. A hydrogen demanding process could be fed with own – electrolyser produced – hydrogen. Combining intermediate hydrogen or methanol storage with a hydrogen or methanol fuel cell creates ideal storage potential, with the possibility of feeding electricity back into the electricity grid. With respect to the storage, methanol is to prefer over hydrogen for large scale and longer term storage. Drawbacks of hydrogen storage are the diffusivity, high pressures and lower caloric value compared to methanol. Methanol synthesis can be done with CO_2 captured from an own – preferably high CO_2 concentration - process stream, reducing the direct CO_2 emissions.

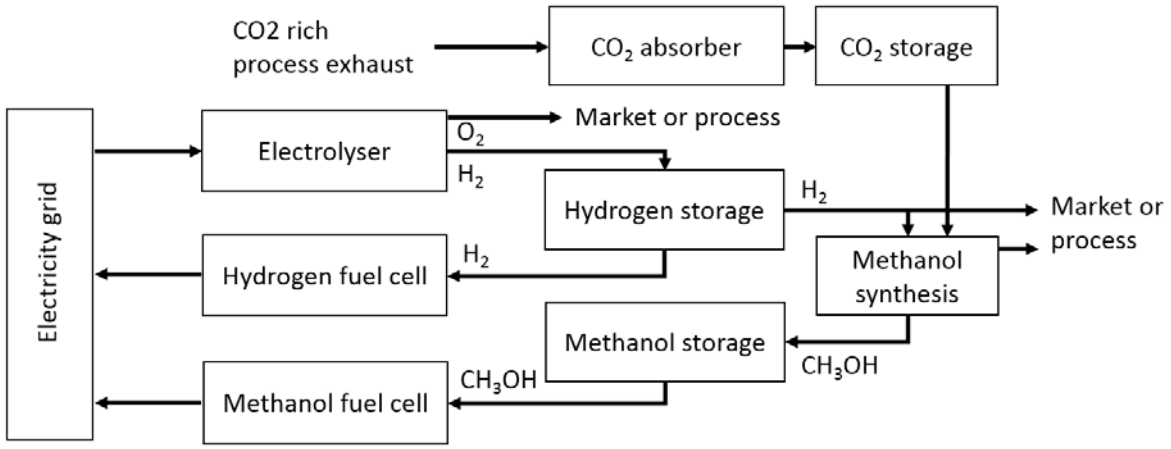

Figure 1: Flow diagram of reversible hydrogen production installation

4. Conclusion

With the increasing penetration of RES in the synchronous grid, caution should be taken to maintain the systems inertia, limiting the ROCOF. In chemical industry, potential is present in the form of electrolysers and fuel cells, which can be controlled to deliver synthetic inertia. The economics of SI provided by dedicated electrolysers might not be viable. Therefore integrated systems could be implemented, in which the provision of SI and ancillary services in general can create extra revenue.

References [Calibri 10]

[1] ENTSO-E, Need for synthetic inertia (SI) for frequency regulation, guidance document, March 2017.
[2] Van de Vyver J., Droop Control as an alternative Inertial Response Strategy for the Synthetic Inertia on Wind Turbines,IEEE Transactions on power systems, March 2016.
[3] ITM Power, Rapid response electrolysis for power-to-gas energy storage, 22 December 2015.
[4] Rezkalla M., Emulated Inertia and Frequency Support from Fast Acting Reserves, doctoral dissertation, 2018.
[5] Eirgrid, Consultation on DS3 System Services Volume Capped Fixed Contracts, DS3 System Services Implementation Project, 25 October 2018
[6] Ikäheimo, J.; Kiviluoma J., On Frequency Stability in the Future Renewable Nordic Power System with Gas Sector Integration, NEOCARBON energy project, 1 August 2018.

ECCE12
The 12th EUROPEAN CONGRESS OF CHEMICAL ENGINEERING
Florence 15-19 September 2019

Usage of Future Energy Market Scenarios for Assessing the Benefits of Residual Heat Recovery From a Chemical Cluster in Western Sweden.

Simon Harvey[1,*], Erik Axelsson[2], Thore Berntsson[3], Johan Holm[2]

1 Energy Technology, Chalmers University of Technology, Göteborg, Sweden;
2 Profu AB, Göteborg, Sweden; 3 CIT Industriell Energi AB, Göteborg, Sweden;
**Corresponding author: simon.harvey@chalmers.se*

Highlights

- 140 MW of residual heat are available at a chemical cluster in Western Sweden
- This heat could be delivered to the city of Göteborg, constituting the largest industrial residual heat recovery project in Sweden
- The costs and climate benefits are analyzed using energy market scenarios

1. Introduction

Over 50% of building heating requirements are covered by district heating in Sweden. Approximately 8% of the heat supply to district heating systems comes from residual heat from industrial processes. Many studies indicate that there is a potential to substantially increase this share, and a number of policies promoting energy efficiency and greenhouse gas emissions reduction are providing incentives to do this. Quantifying the medium and long term economic and climate benefits of such investments is difficult because the background energy system against which new investments should be assessed is also expected to undergo significant change as a result of the afore-mentioned policies. Furthermore, in many cases, the district heating system has already invested or is planning to invest in non-fossil heat sources such as biomass fueled boilers or CHP units. This paper illustrates usage of energy market scenarios for assessing the long term benefits of recovering residual heat from a chemical cluster located approximately 50 km from the city of Göteborg on the West Coast of Sweden and delivering the heat to the city's district heating network which aims to be completely fossil-free by 2030.

2. Methods

Availability and costs for residual heat at the chemical cluster site were investigated in previous work [1] using pinch analysis tools. Piping costs for transporting the residual heat from the chemical cluster to the city's district heating system were estimated from previous studies, as summarized in [2]. The impact of delivery of the residual heat on district heating system production costs and greenhouse gas emissions was performed using the method described in [3]. Energy carrier costs and carbon intensity factors were estimated for future energy market conditions using the ENPAC tool described in [4]. The energy market scenarios include energy prices for years 2030 and 2040 for two different scenarios based on the IEA's World Energy Outlook 2017 [5]: New Policy (NewPol) and Sustainable Development (SustDev). The NewPol scenario reflects implementation of global policy announcements and plans, which is expected to lead to moderately increasing energy prices. The SustDev scenario reflects global commitment to sustainable development, resulting in high carbon dioxide prices, which we have extrapolated to also imply high biomass fuel prices.

3. Results and discussion

140 MW of residual heat are available at the chemical cluster. If recovered and transferred to the district heating in Göteborg, this would be the largest residual heat recovery project in Sweden. The total investment cost to collect 140 MW of residual heat and deliver it to the district heating system is approximately 3 billion SEK. Figure 1 shows the total costs for this investment compared with investment in a biomass-fired CHP plant with the same heat output. The direct climate consequences of using the residual heat are negligible for both the chemical cluster and for the district heating system. However, decreased use of biomass and decreased electricity production will affect the climate impact of the surrounding energy system. Assuming fossil-free grid electricity production in the future, the climate consequences of decreased electricity production in the CHP unit are also close to zero. Hence, decreased firing of biomass in the CHP unit is the main cause of climate consequences of residual heat recovery. Assuming that biomass will be a limited resource in the future, the released biomass can be used to further decrease the use of fossil fuels. In this case, the carbon dioxide decrease is approx. 200 ktonnes per year.

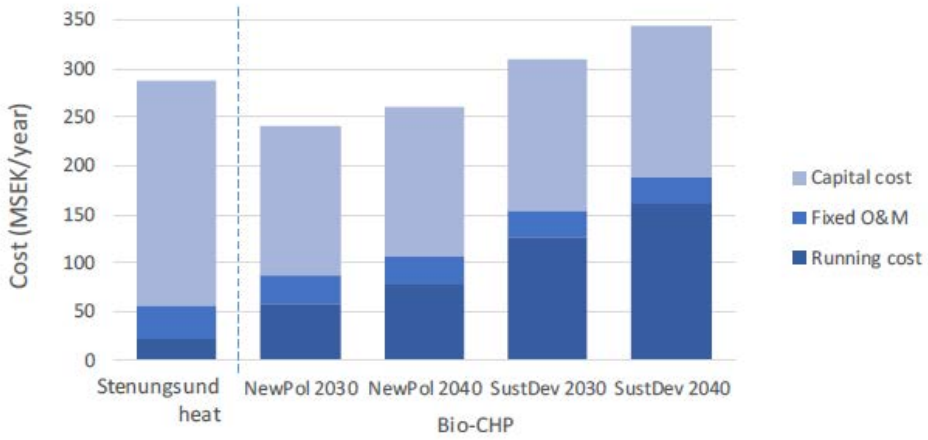

Figure 1. Total cost for residual heat from the Stenungsund chemical cluster and a bio-CHP plant, both delivering 140 MW heat and with about 5000 hours of yearly utilisation time.

4. Conclusions

There are many opportunities to substantially increase recovery of residual heat from industrial processes and clusters. Industry as well as the heating and power sectors are in a period of rapid transition due to ambitious energy efficiency and greenhouse gas emission reduction policy targets. As a result, new methods are necessary to understand the economic and climate consequences of recovering residual heat for use in the heating sector.

References

[1] L. Eriksson, M. Morandin & S. Harvey, Int J Energy Res. 2018;42:1580–1593
[2] E. Axelsson, T. Berntsson, S. Harvey & J. Holm, Nyttjande av industriell restvärme från Stenungsundsindustrierna som fjärrvärme, report, 2018, available at research.chalmers.se
[3] E. Ahlgren & E. Axelsson, The value of excess heat – profitability and CO_2 balances, in System Perspectives on Biorefineries, e-book, 2014, available at research.chalmers.se
[4] E. Axelsson & S. Harvey, Scenarios for assessing profitability and carbon balances of energy investment in industry, AGS Pathways report 2010:EU1, Göteborg, Sweden, 2010
[5] International Energy Agency, World Energy Outlook 2017, Paris, France, 2017

ECCE12
The 12th EUROPEAN CONGRESS OF CHEMICAL ENGINEERING
Florence 15-19 September 2019

Hydrothermal Treatment of Spent Contaminated Ion Exchange Resins in Sub and Supercritical Water.

Antoine Leybros, Jean-Christophe Ruiz, Thibault d'Halluin, Egle Ferreri and Agnès Grandjean

CEA, DEN, Univ. Montpellier, DE2D, SEAD, LPSD, F30207 Bagnols sur Cèze, France;

**Corresponding author: antoine.leybros@cea.fr*

Highlights

- Efficiency of hydrothermal process to degrade Cs; Sr; Co and Eu exchanged IER.
- Leaching yields around 100 % are obtained for Cs; Sr and Eu using batch setup.
- A semi-dynamic process allows an efficient treatment of IERs.

1. Introduction

Some water treatment systems in nuclear industry involve Ion Exchange Resins (IER) to control water chemistry, minimize equipment corrosion and remove radioactive contaminants. Typically, the volume of contaminated IER from a nuclear power plant is around 5-7 m^3 per reactor and per year. The different issues studied for these IER solid waste is either the immobilization in an inert matrix (cement, bitumen, polymer) or the mineralization, so as to obtain inorganic residues before solidification [1]. Among mineralization processes, hydrothermal treatment in sub or supercritical water may be a promising alternative to leach resins and recover radionuclides such as ^{137}Cs, ^{90}Sr, ^{60}Co or transuranic in an aqueous solution. Thus, the secondary waste would be solid waste of lower radioactivity, which may be incinerated or immobilized, and liquid wastewater containing radionuclides, which can be managed simply by the liquid treatment facility. Previous studies carried out using continuous supercritical water oxidation setup allow to reach 99.9% degradation yields on crushed IER [2]. Unfortunately, owing to IER radiolytical and thermal deterioration and high radioactivity, a grinding preprocessing step is not easy to manage. This is the reason why batch and semi-dynamic process have been considered on millimeter size resins. This study deals with the feasibility of leaching IER by hydrolysis and/or oxidation (by H_2O_2) runs carried out with temperature and pressure respectively ranging from 100 and 450°C and from 20 and 300 bar.

2. Methods

Considered IER are strong cationic Amberlite IRN77 and anionic Amberlite IRN78. Contamination of each species of interest (Cs, Sr, Co and Eu) is 10 mg/g IER. The setup used to carry out runs under subcritical and supercritical hydrothermal conditions is described Figure 1. A titanium jacket allows to confine aggressive species and protect reactor outer walls from corrosion. Furthermore, this

jacket is flexible to compensate any difference of pressure with the reactor. During batch experimental runs, {IER/ water or water + H_2O_2 with stoichiometric ratio equal to 1.3} mixture is introduced into the jacket while the reactor is filled with water, with equivalent volume ratios. This ratio has been set to reach targeted autogenous pressure (between 60 and 290 bar) according to operating temperature (300 or 450°C). The duration of runs is about 4h.

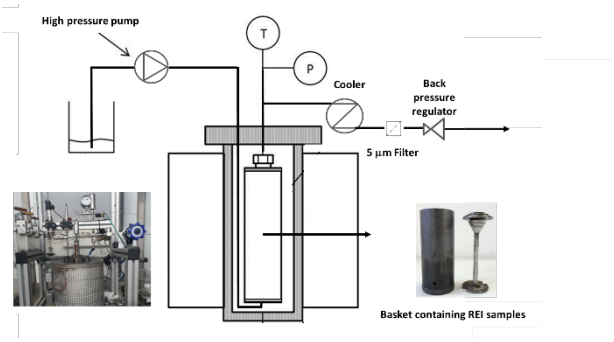

Figure 1. Experimental setup for hydrothermal treatment of IER (semi-dynamic mode)

Then, the experimental setup has been modified to be used in semi-dynamic mode. IER samples are introduced into a basket, inside the reactor, which is then fed continuously with a {water or water + H_2O_2} stream at a 5 mL/min flow rate. The reactor is heated until the working temperature is reached (set between 100 and 290°C). Pressure (from 5 to 50 bar) is controlled by a back pressure regulator. The aqueous effluents are then recovered downstream, in a collector, after cooling and depressurization. The treatment capacity of this setup is 50 g of IER per batch.

Solid residues as well as generated effluents are gravimetrically analyzed. TOC-metry is used to measure carbon degradation yields. ICP-AES and AAS analyzers are used to measure ions release (Sr, Co, Eu and Cs).

3. Results and discussion

Experimental runs in batch mode allow to highlight following trends. Whatever operating conditions, carbon degradation yields higher than 86% are obtained, with especially yield around 99.7% for hydrothermal oxidation of IRN77 IER at 450°C/290 bar. Cs, Sr and Eu leaching yields close to 100% are noticeable not only for supercritical water treatment of IRN77 or {IRN77/IRN78} mixtures but also for subcritical water treatment at 300°C/for 70 bar. On the contrary, Co leaching yield is lower than 10% for each experimental run, because of “CoS type compounds” precipitation. Speciation study in hydrothermal medium is in progress to predict and explain these results.

Semi-dynamic device allows to entirely decontaminate 50g of exchanged IER in 3h with softer operating conditions (200°C/50 bar/oxidation with H_2O_2). Furthermore, significant cobalt extraction capacity, around 460 mg/kg of water, has been obtained. Such results will be considered both for the process scale-up and for the compatibility with the downstream wastewater treatment plant.

References

[1] J. Wang, Z. Wan, Prog. Nucl. Energ. 78 (2015) 47-55.
[2] A. Leybros, A. Roubaud, P. Guichardon, O. Boutin, J. Supercrit. Fluids. 51 (2010) 369-375.

ECCE12
The 12th EUROPEAN CONGRESS OF CHEMICAL ENGINEERING
Florence 15-19 September 2019

The Experiment and Simulation Analysis of the Effect Of CO_2 and Steam On Syngas Composition of Natural Gas Non-Catalyst Partial Oxidation.

Zhenghua Dai*, Guangsuo Yu, Haifeng Lu

Key Laboratory of Coal Gasification and Energy Chemical Engineering of Ministry of Education, East China University of Science and Technology, Shanghai 200237, China

**Corresponding author: chinadai@ecust.edu.cn*

Highlights

- The syngas composition of non-catalyst partial oxidation should be adjusted to satisfy the request of different chemical synthesis.
- CO_2 has bigger adjustment range of H_2/CO ratio than that of steam.
- The multi-reforming by CO_2 or Steam addition is feasible.

1. Introduction

Non-catalyst partial oxidation technology has been widely used to produce syngas by reforming of hydrocarbon, including gas (natural gas, shale gas, refinery gas, coalbed gas, coke oven gas, pyrolysis gas, etc.) and liquid (residual oil, asphalt, deoiled asphalt, biomass oil, etc.). For natural gas non-catalyst partial oxidation, the H_2/CO of syngas is about 1.8, which is agreed well with the request of FT synthesis. But for other process, such as carbonylation and glycol, the H_2/CO should be close to 1 and 2 respectively. So the syngas composition of non-catalyst partial oxidation should be adjusted to satisfy the request of different chemical synthesis. That means a multi-reforming method by CO_2 or Steam addition.

2. Methods

The experimental platform for the non-catalyst partial oxidation of natural gas is shown in Fig.1.

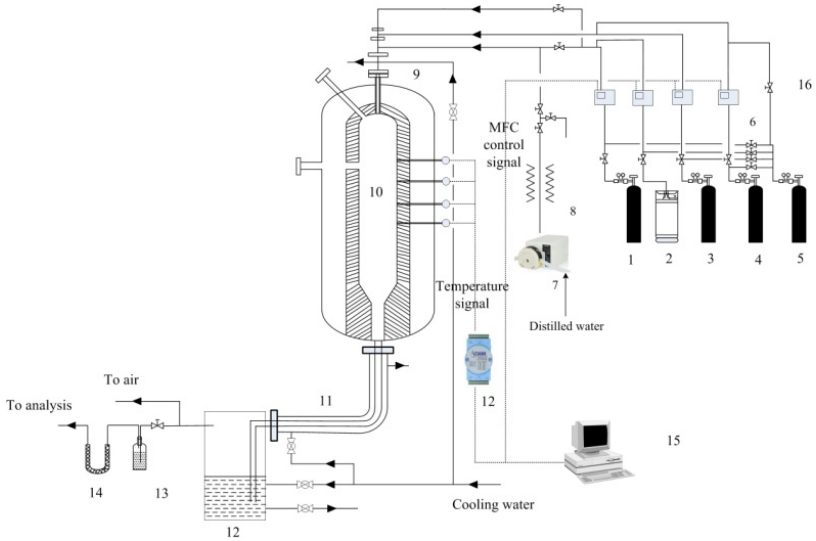

Fig. 1 Diagram of natural gas non-catalyst partial oxidation hot-model experiment platform

The reactor network model of the reformer is shown in Fig. 2.The reactions in the reformer are described by GRI-3.0.

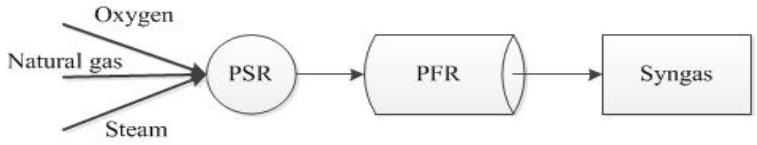

Fig.2 Schematic diagram of reactor network (PSR: 12.758m³; PFR: Length=7.08m, Diameter=1.8m)

3. Results and discussion

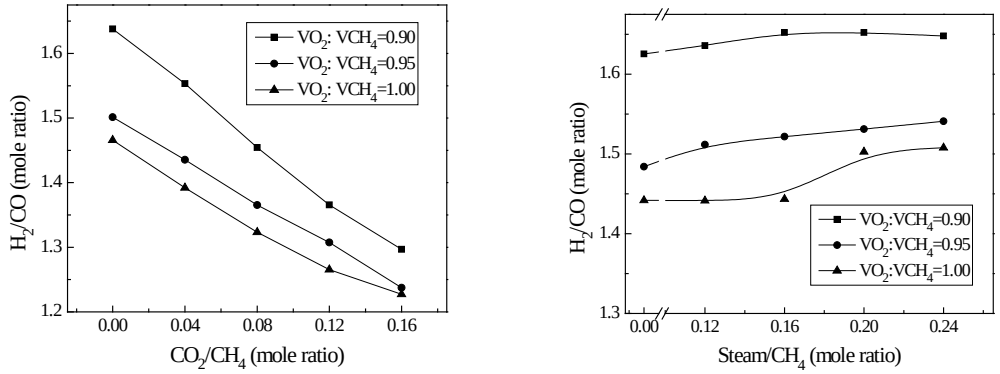

(a) CO2 **(b) Steam**

Fig. 3 Effects of CO2 and Steam addition on the syngas compositions

The experiment results of the Effects of CO_2 and Steam addition on the syngas compositions are shown in Fig.3. For the case of the O_2/CH_4=0.95, the H_2/CO is decreased from 1.5 to 1.24 when the CO_2/CH_4 is increased from 0 to 0.16; However, the H_2/CO ratio is increased slightly from 1.62 to 1.65 When the H_2O/CH_4 ratio is increased from 0 to 0.24.

Table 1 shows the feasibility analysis results of multi-reforming. The greater of required adjustment of H_2/CO ratio, the addition amount of Steam or CO_2 into the reformer is greater. Correspondingly, the oxygen and natural gas consumption per unit effective gas is slightly increased.

Table1 The multi-reforming analysis

	1	2	3	4	5
O_2/NG(v/v)	0.775	0.690	0.657	0.675	0.720
Steam(CO_2)/NG (v/v)	1.80(H2O)	0.48(H2O)	0.107(H2O)	0.15(CO_2)	0.52(CO_2)
H_2(v%)	63.02	63.16	62.83	57.45	45.13
CO(v%)	25.15	31.65	33.87	38.35	44.60
CH(v%)	0.62	0.60	0.76	0.61	0.64
H_2/CO	2.51	2.00	1.86	1.50	1.01
T, K	1522	1562	1578	1570	1533
Oxygen $Nm^3/kNm^3(CO+H_2)$	317	262	247	255	283
Natural gas $Nm^3/kNm^3(CO+H_2)$	409	379	376	378	392

4. Conclusions

CO_2 has bigger adjustment range of H_2/CO than that of steam. This paper presents the feasibility of multi-reforming on the natural gas non-catalyst partial oxidation by CO_2 or H_2O addition.

ECCE12
The 12th EUROPEAN CONGRESS OF CHEMICAL ENGINEERING
Florence 15-19 September 2019

Synthesis and Modification of Water-Stable CPL-2 MOF for Ethylene/Ethane Separation.

Huan Xiang[1], Yilai Jiao[2], Flor R. Sinperstein[1,*], Xiaolei Fan[1,*]

1 School of Chemical Engineering and Analytical Science, The University of Manchester, Manchester M13 9PL, United Kingdom; 2 Shenyang National Laboratory for Materials Science, Institute of Metal Research, Chinese Academy of Sciences, 72 Wenhua Road, Shenyang 110016, China

**Corresponding authors: Flor.Siperstein@manchester.ac.uk; xiaolei.fan@manchester.ac.uk*

Highlights

- CPL-2 MOF exhibits preferential adsorption of ethylene over ethane.
- CPL-2 MOF is relatively hydrophobic and shows excellent water stability under humid conditions.
- Ethylene/ethane adsorption selectivity was enhanced six-fold by silver ions modification.

1. Introduction

Adsorptive separation of ethylene/ethane mixture has growing interest in petrochemical industries compared to the conventional energy-intensive cryogenic distillation.[1] Metal-organic frameworks (MOFs) have attracted considerable attention in gas adsorption and separation due to their combined properties of large surface area, functionalised and adjustable pore structure and surface.[2] However, the open metal sites in MOFs interact strongly with water molecules, resulting in material decomposition and poor water stability,[3] limiting their potential in practical settings. Therefore, development of water-stable materials with high selectivity is of great importance to accomplish the ethylene/ethane separation.

In this work, pillared-layer CPL-2 MOF was selected as the model MOF and synthesised at room temperature for separating binary ethylene/ethane mixture. The water stability of CPL-2 was evaluated under dynamic humid conditions. Ag(I) ions modification of CPL-2 was also conducted to explore the possibility of improving the selectivity of CPL MOFs in ethylene/ethane separation.

2. Methods

Hydrothermal synthesis was used to prepare CPL-2. Silver ions modified CPL-2 MOFs (denoted as Ag/CPL-2) were prepared using the incipient wetness impregnation method. Dynamic water vapour adsorption analyses at 25 °C and 50 °C with relative humidity values ranging from 0% to 90% (10% per step) were measured using a dynamic vapour sorption (DVS 1) equipment. Prior to the water vapour adsorption, all samples were dried at 0% relative humidity for 3 h. Intelligent gravimetric analyser (IGA-001) based on the static gravimetric technique was applied to determine ethylene and ethane adsorption isotherms on developed CPL-2 and Ag/CPL-2 materials at a constant temperature of 25 °C, 35 °C and 50 °C, respectively. The adsorption selectivity was calculated as a ratio of Henry's constants.

3. Results and discussion

CPL-2 can be easily synthesised at room temperature, which was confirmed by XRD and SEM analysis. Characteristic peaks at 2θ = 6.4°, 8.8°, 10.3° and 12.6°, matching the simulated results, were identified in all the synthesised CPL-2 MOFs, confirming the presence of the pillared-layer structure in the crystalline domain. All SEM images show squared slab-shaped crystals aggregated together with sizes ranging from 0.2 µm to 2.5 µm. The synthesised CPL-2 has excellent water stability confirmed by the dynamic water vapour adsorption analysis under 90% relative humidity, showing no significant framework decomposition, even at 50 °C. The calculated selectivity based on gravimetric single-component gas adsorption experiments shows the significantly improved C_2H_4/C_2H_6 selectivity from 1.2 to 6.6 after loading 10% (theoretical) of sliver ions on CPL-2.

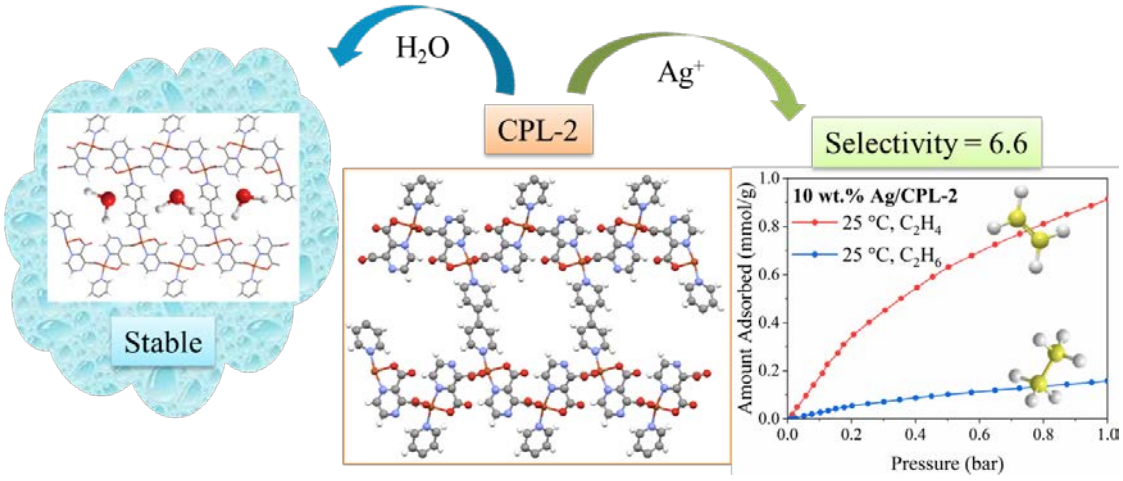

Figure 1. Schematic presentation of CPL-2 framework and its water stability and adsorption performance in C_2H_4/C_2H_6 separation.

4. Conclusions

The synthesis of CPL-2 is facile with fast crystallization, *i.e.* 3 h is sufficient to prepare CPL-2 MOF at room temperature. CPL-2 demonstrated the outstanding water stability under dynamic humid conditions at 25 °C and 50 °C, showing the reversible water vapour adsorption under the conditions used. Gas adsorption study shows that 10 wt.% Ag/CPL-2 by Ag(I) impregnation gave the best adsorption performance considering both capacity and selectivity towards C_2H_4 over C_2H_6. The good selectivity combined with the water stability makes it promising and potentially feasible to use CPL-2 in the separation of ethylene/ethane mixtures, especially under conditions where water vapour exists.

References

[1] L. Li, R.B. Lin, R. Krishna, H. Li, S. Xiang, H. Wu, J. Li, W. Zhou, B. Chen, Ethane/ethylene separation in a metal-organic framework with iron-peroxo sites, Science 362 (2018) 443-446.

[2] Y. He, W. Zhou, R. Krishna, B. Chen, Microporous metal-organic frameworks for storage and separation of small hydrocarbons, Chem. Commun. 48 (2012) 11813-11831.

[3] N. Al-Janabi, P. Hill, L. Torrente-Murciano, A. Garforth, P. Gorgojo, F. Siperstein, X. Fan, Mapping the Cu-BTC metal-organic framework (HKUST-1) stability envelope in the presence of water vapour for CO2 adsorption from flue gases, Chem. Eng. J. 281 (2015) 669-677.

ECCE12
The 12th EUROPEAN CONGRESS OF CHEMICAL ENGINEERING
Florence 15-19 September 2019

Process Integration for Decentralized Power to Fuel Conversion Based on Fischer-Tropsch Synthesis

Hannah Kirsch, Chenghao Sun, Peter Pfeifer, Roland Dittmeyer

Institute of Micro Process Engineering (IMVT), Karlsruhe Institute of Technology (KIT), Hermann-von-Helmholtz-Platz 1, 76344 Eggenstein-Leopoldshafen

**Corresponding author: hannah.kirsch@kit.edu*

Highlights

- Production of liquid fuels by coupling Fischer-Tropsch synthesis and hydrocracking.
- Integration of Fischer-Tropsch synthesis and hydrocracking in a single-stage microstructured reactor.
- Different integration patterns influence the performance of the coupled process.

1. Introduction

Global warming is to be limited to a maximum of 2 °C by 2050 compared with the pre-industrial level [1]. The transport sector's share of anthropogenic greenhouse gas emissions as a percentage of total emissions is almost 20 %, and global demand for mobility will even rise steadily in the future due to the growing world population and rising living standards. Studies show that liquid fuels will continue to play an important role in the transport sector in the future alongside alternative options such as e-mobility and hydrogen, especially for heavy goods vehicles and air traffic. So-called power-to-fuel technology can contribute to the transition of the transport sector from fossil fuels to CO_2-neutral fuels. Renewable energy and carbon dioxide are converted into alternative liquid fuels. These fuels are characterized by negligible aromatics and high volumetric energy density and the drop-in quality makes it possible to use the existing infrastructure [2]. An attractive process route is via Fischer-Tropsch synthesis (FTS) and hydrocracking (HC). Decentralized, compact plants based on process intensification enable dynamic operation in order to meet the challenges of strongly fluctuating and locally distributed renewable energies.

Related to the Kopernikus project Power-to-X and funded by the Peter-und-Luise-Hager Foundation, the process integration of cobalt-catalyzed low temperature Fischer-Tropsch synthesis with the hydrocracking of FT products in one microreactor is investigated in this contribution.

2. Methods

A Co/Re-Al_2O_3 catalyst was selected for the FTS with 20 wt% cobalt and 0.5 wt% rhenium as promoter. It was prepared by an impregnation method with γ-Al_2O_3 (3 µm, 80-120 m^2/g) as support and an aqueous solution of cobalt nitrate and perrhenic acid. The catalyst was tried overnight at 120 °C and then calcined at 400 °C for 2 h. [3]

A Pt-ZSM5 catalyst was chosen for the HC with 0.5 wt% platinum. It was prepared by impregnating H-ZSM5 with an aqueous solution of tetraamineplatinum(II)hydroxide. The catalyst was dried overnight at 120 °C and then calcined at 550 °C for 6 h. [3] Before testing, both catalysts were pelletized, crushed and sieved to obtain a size fraction of 50-100 µm. Moreover, both catalysts were characterized by common methods.

For the study of the single-stage integration of FTS and HC a micro annular fixed-bed reactor was designed (see figure 1). Both catalysts were reduced online in hydrogen atmosphere at ambient pressure and 350 °C for 15 h. Reaction conditions were: 30 bar, 225-260 °C, WHSV 6-12 h^{-1} and H_2/CO ratio 1.9. All products leaving the reactor system were first separated in a wax fraction, liquid product fraction and residual gas by a hot trap (190 °C) and a cold trap (6 °C). The residual gas was directly analyzed by an online GC, whereas the liquid and the wax fractions were sampled and analyzed by an offline GC.

Figure 1. Micro annular fixed-bed reactor for the integration of FTS and HC.

3. Results and discussion

The integration of Fischer-Tropsch synthesis and hydrocracking in a single-stage microstructured reactor for the production of liquid fuels is feasible. The liquid fuel selectivity of the coupled process is higher than for the FTS at the same conditions, indicating that the long-chain hydrocarbons are selectively cracked. Quantitative statements, however, can only be made after the product analyses have been evaluated, but this has not yet been completed. As expected, the conversion increases with rising temperature and decreasing WHSV. Both catalysts showed a reasonable long-term stability during up to 120 h of experiments.

Two different integration patterns were investigated – the sequential bed and the hybrid bed. As anticipated, the catalytic performance of the coupled process is influenced by the integration pattern. As a liquid phase is involved in the process, dilution or bed configuration might effect the wetting of the catalyst particles as well as the flow through the catalyst bed [4]. The observed trends and the reproducibility needs to be further investigated to validate the importance of several possible parameters observed in the present study.

4. Conclusions

The integration of FTS and HC was investigated in a single-stage micro annular reactor for the production of liquid fuels. The coupling of FTS and HC increases the liquid fuel selectivity by selectively cracking the long-chain hydrocarbons. The integration pattern has an influence on the catalytic performance of the combined process. The experiments show that the operation of compact small-scale power-to-liquid plants seems possible.

References

[1] Paris Agreement, United Nations, 2015.
[2] Positionspapier „Fortschrittliche alternative flüssige Brenn- und Kraftstoffe: Für Klimaschutz im globalen Rohstoffwandel“, DECHEMA e.V., 2017.
[3] C. Sun, P. Pfeifer, R. Dittmeyer, Chemical Engineering Journal 326 (2017), pp. 37-46.
[4] G. Hong, Y. Noh, J. Park, etal., Catalysis Today 303 (2018) pp. 136-142.

The model of crude oil oxidation for in-situ combustion technology.

Ushakova Alexandra, Pu Wan-Fen, Zatcepin Vladislav

The models of crude oil oxidation in terms of chain reaction approach have been developed in the recent years. The set of chemical reactions suggested in our work was simplified and solved under certain conditions.

The formation and accumulation of hydroperoxides is a key stage of the oxidation process. First oxygen molecules penetrate into the oil chains and forms free radicals. Radicals are passed from one molecule to another (chain growth), until they form hydroperoxides. Also some products of the reactions are gases CO and CO_2 water, oxidized components, aldehydes, ketones, acids. This stage is widely investigated in experiments and called low temperature oxidation (LTO). The hydroperoxides can decompose into a pair of radicals - this is a branching chain reaction. New radicals initiate the new chains and start the new processes of oxidation. The figure 1 shows the cyclic character of the oxidation through radical appearance and hydroperoxides accumulation. The more hydroperoxides are accumulated the higher is oxidation rate. This process self-accelerates and causes the ignition in crude oil with oxygen. With the temperature growth above 250 °C one can observe non-radical high temperature oxidation where chain mechanism takes place, but it is not the main one.

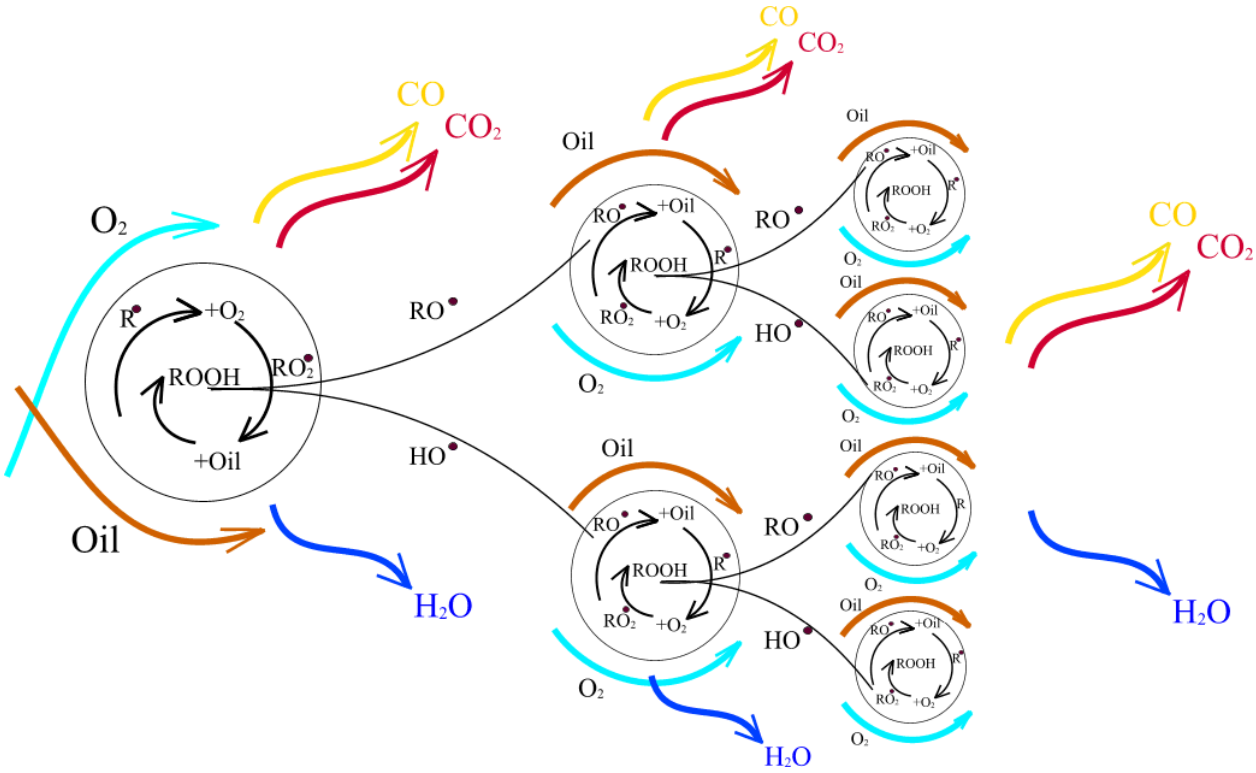

Figure 1. The scheme of chain reaction mechanism of oil oxidation

In the present oxidation scheme we consider active and inactive oil components at the initial oxidation stages. Both of these compounds oxidize simultaneously but they lead to different products. Crude oil separates into the main oxidizing components – alkanes (denoted Sat) and their oxidation inhibitors - aromatic compounds, which then form the fuel (denoted *Inh*). The other components - Resins and Asphaltenes become solid at the early oxidation stages and are out of the investigation here, they just make a gift into the heavy residuals for high temperature combustion.

The time dependence of hydroperoxides concentration strongly depends on the initial reactions rates. We drove out the dependencies for cases of exponential growth of free radical concentration – which lead to self ignition, limited growth – which leads to oxidized compound formation only and intermediate cases which have not been examined before but also exist in experiments of oil oxidation (figure 2).

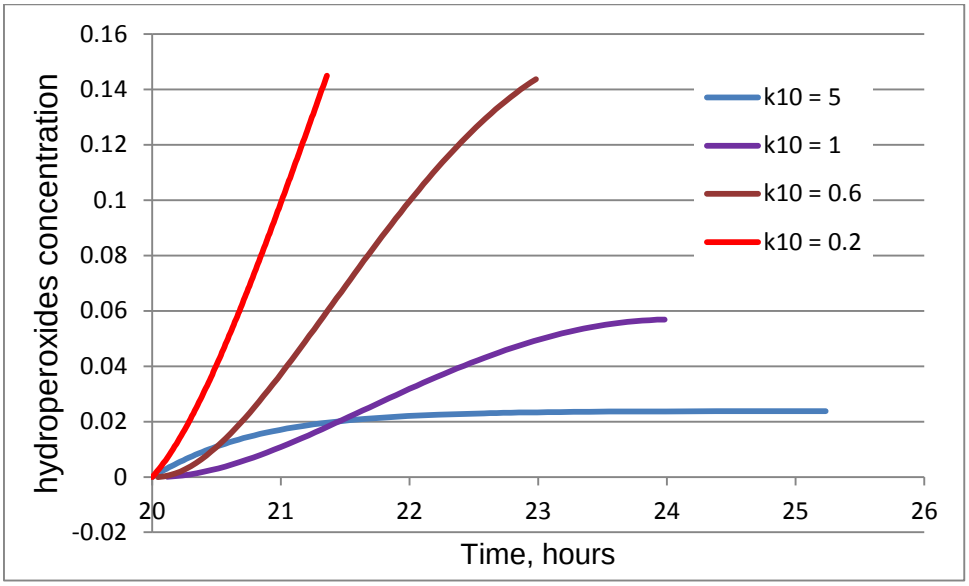

Figure 2. Time dependence of hydroperoxides concentration in oxidation process.

Here we also consider the probability of inhibition on any stage of the reaction scheme – in the chain growth stage, hydroperoxide formation and decomposition stage. In fact different types of inhibitors act at different stages. Here we attempt to solve such system of equation and obtain how the inhibition of different stages governs the whole process. It is needed to mention that oil components are very different and various types of inhibitors exist in crude oils.

We also suppose that catalytic effects of different additives which are explored in many papers cannot be we explained without inhibition scheme consideration. Because lots of catalysts prevent the inhibition reactions, act as inhibitors adsorbents or shift the balance towards slowing down the inhibition processes. All this shows that inhibition consideration is the step preceding any theoretical investigation of catalysts application.

ECCE12
The 12th EUROPEAN CONGRESS OF CHEMICAL ENGINEERING
Florence 15-19 September 2019

A realistic vapour phase heat transfer model for the weathering of LNG stored in large tanks

Felipe Huerta[1*], Velisa Vesovic[1]

1 Department of Earth Science and Engineering, Imperial College London, London SW7 2AZ, United Kingdom

**Corresponding author:* f.huerta-perez17@imperial.ac.uk

Highlights

- A new model to predict the weathering of LNG in storage tanks is developed
- It dispenses with the assumption of vapour being at the same temperature as LNG
- It demonstrates that the vapour to liquid heat transfer is small
- It shows that the initial amount of LNG has a pronounced effect on weathering

1. Introduction

The global energy sector is changing unprecedently as it transitions from its reliance on fossil fuels to renewables. For the transition, natural gas will play an important role because of its competitive cost and lower emissions when compared to other fossil fuels [1]. Natural gas (NG) is predominantly a hydrocarbon mixture consisting mainly of methane and, in general, lower amounts of other *n*-alkanes and small inorganic molecules. It can be distributed to users directly from the source through pressurized pipelines or it can undergo a liquefaction process and then be distributed as liquefied natural gas (LNG), by marine transportation, to large storage facilities. LNG is becoming the preferred way to transport natural gas and it is finding an use as marine and heavy-vehicle fuel.

LNG is industrially stored in highly insulated tanks at cryogenic temperatures below -160°C, that are subject to heat ingress from the surroundings that leads to preferential evaporation of the most volatile components. The vapour produced is denominated boil-off gas (BOG), and it is typically removed to keep the tank pressure constant. The heat ingress and BOG removal produce weathering of the remaining LNG, as the concentration of the heavier components increases over time. This has major industrial implications, as it can induce safety hazards such as rollover and it limits the NG marketability. In this work, a new non-equilibrium model relevant to LNG weathering in large storage tanks has been developed.

2. Methods

The new model treats the heat influx from the surroundings into the vapour and liquid phases separately and allows for heat transfer between the two phases. The main heat transfer mechanisms in the vapour phase are assumed to be advection, due to upward flow of evaporated LNG, and conduction. The vapour heat ingress is included as a source term and the evaporative flow is approximated by an average vertical velocity. The numerical integration is based on adaptive time-steps to capture the strong transient behaviour at the beginning of weathering.

3. Results and discussion

It was observed that the vapour temperature increases monotonically as a function of the height, in agreement with recent experimental results [2] . For three typical LNG mixtures (Light LNG, Heavy

LNG and N_2-rich LNG), we observed very similar temperature profiles and vapour to liquid heat fluxes as we observed for evaporation of pure methane. In all the simulations performed the vapour to liquid heat transfer was small and is estimated to contribute less than 0.3% to BOG rates. A strong transient dynamic was found at the beginning of weathering, until a pseudo-steady state is achieved when the vapour heat ingress is balanced with the vapour to liquid heat transfer and the advective flow. Figure 1 illustrates the BOG as a function of weathering for the LNG studied. For the light and heavy LNG mixtures the model predicts a decreasing BOG rate. In contrast, for the N_2-rich LNG mixture both models predict a local maximum because of the interplay between the decreasing liquid heat ingress and decreasing enthalpy of vaporization. For all mixtures the BOG rates were between 1 and 4 % lower than in previous work [3] because of lower vapour to liquid heat ingresses.

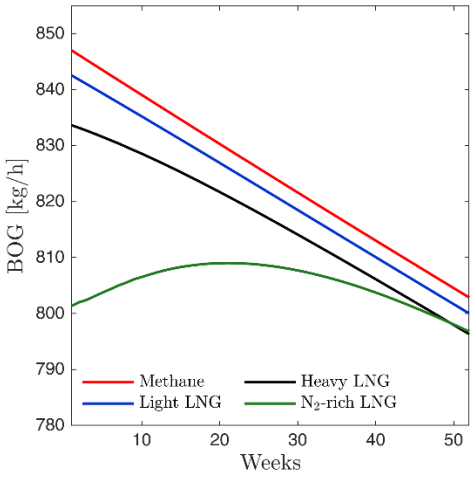

Figure 1. BOG rates as a function of time for three different LNG mixtures

The initial liquid filling has a pronounced effect, leading to a decrease in vapour and boil-off gas temperatures and an increase in boil-off rates. For a storage tank initially filled with 30% of light LNG, using previous non-equilibrium and equilibrium models [3, 4] would overestimate BOG rates by 26% and 100%, respectively. The transient time strongly depends on the initial filling of the LNG tank, with the nearly full tanks taking least time to reach the steady-state.

4. Conclusions

The results of this work indicate that the heat transfer by the advective upward flow dominates the energy transfer within the vapour, while the natural convection, in the body of the vapour, can be neglected. The developed model allows for the optimization of LNG storage tank operations and different scenario planning taking into account the initial liquid filling and nitrogen content.

References

[1] World Energy Outlook 2017. France: International Energy Agency; 2017.

[2] Kang M, Kim J, You H, Chang D. Experimental investigation of thermal stratification in cryogenic tanks. Exp Therm Fluid Sci 2018;96:371-82.

[3] Migliore C, Salehi A, Vesovic V. A non-equilibrium approach to modelling the weathering of stored Liquefied Natural Gas (LNG). Energy 2017;124:684-92.

[4] Migliore C, Tubilleja C, Vesovic V. Weathering prediction model for stored liquefied natural gas (LNG). Journal of Natural Gas Science and Engineering 2015;26:570-80.

ECCE12
The 12th EUROPEAN CONGRESS OF CHEMICAL ENGINEERING
Florence 15-19 September 2019

Ceramic Filter Candle Filled With Catalyst Pellets Inserted in the Freeboard of a Fluidized Bed Gasifier for In-Situ Syngas Conditioning.

Elisa Savuto[1,*], Andrea Di Carlo[2], Katia Gallucci[2], Pier Ugo Foscolo[2], Sergio Rapagnà[1]

1 University of Teramo, Via R. Balzarini 1, 64100 Teramo, Italy; 2 University of L'Aquila, Via Campo di Pile, L'Aquila, Italy

**Corresponding author: elisa.savuto@gmail.com*

Highlights

- A ceramic candle filled with catalyst was inserted in the freeboard of a gasifier
- Two different catalysts (A, B) were tested for tar reforming inside the gasifier
- Catalyst B showed very good performance, reaching 89% of tar conversion
- Catalyst B was more active than catalyst A, even though used at higher GHSV

1. Introduction

Gasification is a very promising conversion process to produce a fuel gas (syngas) from biomass, usable for direct power production or for the synthesis of high quality bio-fuels [1]. However, syngas has to be cleaned before its use, in order to remove main pollutants that may compromise its exploitability: particulate and tar [2]. Fluidized bed gasifiers have several advantages, including the presence of a free space above the bed (freeboard) in which devices for in-situ gas conditioning can be integrated. In this work, a segment of a commercial ceramic filter candle is inserted in the freeboard of a bench scale fluidized bed gasifier for particulate removal, and its internal hollow space is filled with catalyst pellets, in order to perform catalytic reforming of tar in the raw gas. Two different commercial catalysts are tested inside the filter candle and their performance is studied and compared.

2. Methods

Experimental tests were carried out in a bench scale biomass gasification system composed of a cylindrical fluidized bed reactor (ID 0.1 m) heated with an external electric furnace. The bed material is composed by olivine sand and the biomass used is ground almond shells. In the upper part of the reactor a ceramic candle is hosted (L 440 mm, 60 mm OD and 40 mm ID). At the outlet of the gasifier the gas composition (H_2, CO, CO_2, CH_4) is analyzed online and its volume flow is measured; tars are sampled according to the standard CEN/TS 15439 and then analyzed with HPLC. Temperatures and pressures are measured in different points of the reactor. More details on the experimental rig can be found in [3].Tests were carried out with the empty ceramic candle and with the candle filled with two types of Ni based commercial catalysts for steam reforming of methane and naphtha, referred to as A and B, respectively. Catalyst A has the shape of perforated pellets with a high void fraction; catalyst B instead, having the shape of small cylinders, could cause excessive pressure drop. For the tests with catalyst B the cavity of the candle was filled only partially, with an annular bed of catalyst pellets, leaving a cylindrical internal hollow space to reduce the whole pressure drop (see **Figure 1**).

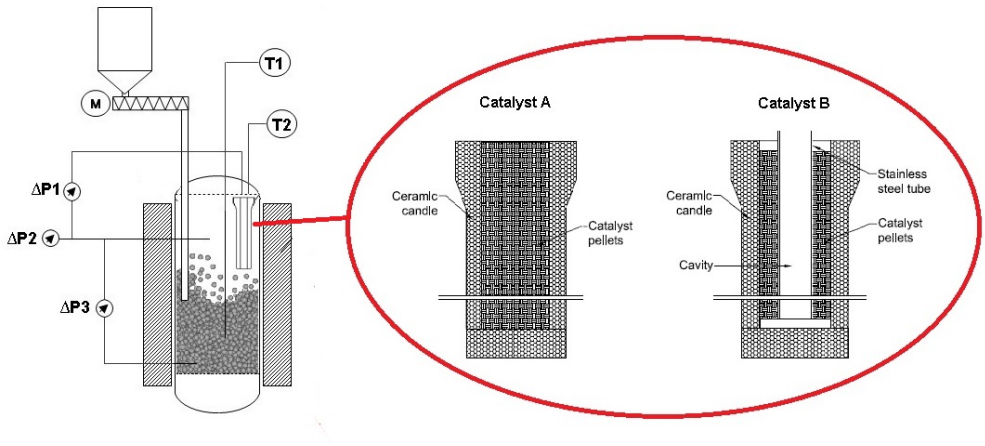

Figure 1. Scheme of gasification reactor and configurations of catalyst filled candle

3. Results and discussion

Table 1. Input conditions and test results

Test	1	2	3
Filter candle	**Empty**	**Catalyst A**	**Catalyst B**
Temperature (°C)	789	770	775
Gas yield (Nm^3 dryN_2free/kg_{bio})	1.13	1.45	1.66
Water conversion (%)	24.25	36.13	53.65
Tar (g/Nm^3 dryN_2free)	3.28	2.75	0.36
GHSV (h^{-1})	-	4211	5729
H_2 (%vol dryN_2free)	40.65	55.34	54.04
CH_4 (%vol dryN_2free)	9.03	2.13	1.20

Results reported in **Table 1** show that both catalysts lead to an upgrading of the gas quality compared to that of the raw syngas. However, catalyst B (even though filling only partially the candle cavity, thus confined in a smaller volume) performed much better than catalyst A, with higher gas yield and water conversion. In fact, with catalyst A, tar is only slightly reduced (16%), while catalyst B brought to almost complete tar conversion (89%) with a final concentration in the gas lower than 0.5 g/Nm^3 dry and N_2 free.

4. Conclusions

The integration of catalyst pellets in the cavity of a ceramic candle placed in the freeboard of a fluidized bed gasifier can be an effective solution for syngas upgrading. In particular catalyst B showed excellent performance in tar reforming, increasing H_2O conversion, gas yield and H_2 content. Even though catalyst B was filling only partially the candle cavity (thus under higher GHSV), better results were obtained compared to those exhibited by catalyst A.

References

[1] Sikarwar VS, Zhao M, Fennell PS, Shah N, Anthony EJ. Progress in biofuel production from gasification. Prog Energy Combust Sci 2017;61:189–248. doi:10.1016/j.pecs.2017.04.001.

[2] Devi L, Ptasinski KJ, Janssen FJJG. A review of the primary measures for tar elimination in biomass gasification processes. Biomass and Bioenergy 2002;24:125–40. doi:10.1016/S0961-9534(02)00102-2.

[3] Rapagnà S, Gallucci K, Foscolo PU. Olivine, dolomite and ceramic filters in one vessel to produce clean gas from biomass. Waste Manag 2017. doi:10.1016/j.wasman.2017.07.038.

ECCE12
The 12th EUROPEAN CONGRESS OF CHEMICAL ENGINEERING
Florence 15-19 September 2019

Photon transport based multi-scale knowledge models for designing efficient photoreactors producing renewable solar photocatalytic hydrogen

Caroline SUPPLIS[1*], Jérémi DAUCHET[1], Victor GATTEPAILLE[1], Fabrice GROS[1], Matthieu ROUDET[1], Jean-François CORNET[1]

1 Université Clermont Auvergne, CNRS, Sigma Clermont, Institut Pascal, F-63000 Clermont-Ferrand, France

**Corresponding author: caroline.supplis@uca.fr*

Highlights

- A solar-from-water photocatalytic H_2 production engineering is presented.
- A predictive model using multi-level light-matter processes description is proposed.
- Validation is done on an accurate experimental bench using an innovative photoreactor.

1. Introduction

Considering the exhaustion of fossil resources and CO_2 emission rise due to their combustion, the use of solar renewable energy is an evidence to cope with the energy demand of Humanity in the future. This resource being naturally fluctuating, it is necessary to convert it into storable energetic vectors. Among solar fuels, one of the first accessible is undoubtedly the H_2, whose production can be carried out in slurry photoreactors [1] making use of photocatalytic water splitting [2]. The challenge is huge as the Humanity needs to develop in the same time efficient and cheap semiconductor photocatalysts and optimized solar photo-reactive processes.

2. Methods

Multi-scale model: From a chemical engineering point of view and considering that photo-reactive processes are limited and controlled by photon transport and conversion, the understanding and optimization of the elementary process of light-matter interaction at different scales and description levels is essential to develop predictive knowledge models. We present such rigorous and generic models with the objective to conceive, size and optimize highly efficient processes for solar-to-hydrogen energy conversion (yield > 15%) by geometric inverse design. Their multi-scale structuration requires first the determination of the spectral optical properties for the photocatalysts which can be found in experimental databases and/or using density functional theory with Kramers-Krönig causality relations. The second step is aimed at determining spectral radiative properties (phase function, absorption and scattering coefficients) of the photocatalyst particle by solving Maxwell's equations using Mie theory (for equivalent sphere approximation), with additional information on shape and size distribution that can be experimentally acquired. The last phase consists in solving the photon transport equation (Boltzmann equation) to determine luminance distribution within the system volume for known boundary condition i.e. the spectral incident photon flux density q_{λ} and its angular distribution. As a result, the (spectrally averaged) Local $\mathcal{A}(\mathbf{x})$ and Mean $\langle\mathcal{A}\rangle$ Volumetric Rates of Radiant Energy Absorbed (LVREA and MVREA) are estimated and linked to local H_2 reaction rate $r_{H_2}(\mathbf{x})$ using mechanistic elementary

thermokinetics coupling laws. The mean H_2 reaction rate $\langle r_{H_2} \rangle$ is then obtained by averaging local kinetics over the entire photoreactor volume.

Experimental set up: First, the radiative properties are experimentally validated thanks to transmittance measurements with an integrating sphere. Then, our knowledge model is validated by carrying out a photocatalytic reaction for H_2 production in a lab-scale photoreactor [3]. H_2 is produced in the gas tight photoreactor illuminated by a LED panel (various spectral distributions) or a solar simulator. Its production rate $\langle r_{H_2} \rangle$ is correlated through a detailed mass balance with the pressure increase in the headspace of the reactor measured with a pressure sensor.

3. Results and discussion

Experimental result will be presented for the pressure time course (with decompression steps) during H_2 production under irradiation of the photoreactor (see figure 1a). It enables to determine the mean H_2 volumetric rate $\langle r_{H_2} \rangle$. Several accurately controlled values of incident photon flux densities q_{n} [4] are tested for a given photocatalyst concentration. For each q_{n} value corresponds a $\langle r_{H_2} \rangle$ value which is plotted as shown in figure 1b. The multi-scale predictive model presented in section 2 is then used to fit the results with the identification of only one lumped parameter.

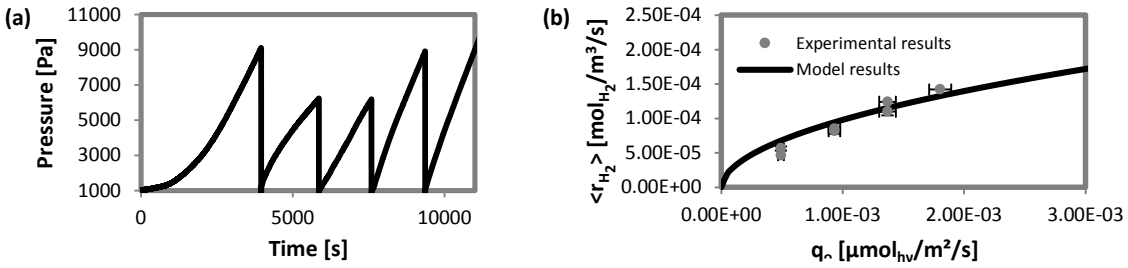

Figure 1. (a) Example of experimental pressure evolution at different photon flux densities q_{n} – (b) Hydrogen mean volumetric rate as a function of incident density photon flux at 0.02 g/L photocatalyst concentration.

New experimental results using costly Pt and cheaper MoS_2 as co-catalysts will be also presented.

4. Conclusions and perspectives

Predictive results obtained by means of our multi scale model accurately fit with our experimental results for $\langle r_{H_2} \rangle$ at different photocatalyst concentrations. The next steps of our study will be: (a) to determine the optical properties of our catalyst by density functional theory; (b) to use other electromagnetic approaches than Mie theory (as T-Matrix and ADDA) to solve Maxwell equations for non-spherical particles of catalysts; (c) to improve the thermokinetics coupling law integrating doping process; and finally (d) test the robustness of our model with natural fluctuating solar light on a new demonstrator under development.

References

[1] Z. Xing et al, *Chemical Engineering Science*, 104 (2013) 125-146.
[2] K. Maeda, *Journal of photochemistry and photobiology C*, 12 (2011) 237-268.
[3] G. Dahi et al, *Chemical Engineering and Processing*, 98 (2015) 174-186.
[4] V. Rochatte et al, *Chemical Engineering Journal*, 308 (2017) 940-953.

ECCE12
The 12th EUROPEAN CONGRESS OF CHEMICAL ENGINEERING
Florence 15-19 September 2019

Gasification of lignocellulosic biomass in a fluidized bed reactor: Catalyst treatment for tar removal and hydrodynamics modelling.

Luis Reyes, Lokmane Abdelouahed, J-C. Buvat, Jundong Wang, Bechara Taouk

1-5-Normandie Univ, INSA Rouen Normandie, UNIROUEN, Laboratoire de Securité des Procédes Chimiques (LSPC EA 4704).

**bechara.taouk@insa-rouen.fr*

Highlights

- Study of the main parameters for the gasification process.
- Use of a green catalyst for the problematic tar removal.
- Usage of Computational fluids dynamics (CFD) to model reactors hydrodynamics.

1. Introduction

In order to minimize the use of conventional fuels, various renewable technologies and alternative energy sources have been studied during past decades, such the gasification of lignocellulosic biomass. Gasification is a thermochemical process of conversion at high temperature (>700°C) of organic matters into synthesis gas such as monoxide of carbon (CO), dihydrogen (H_2), methane (CH_4) and dioxide of carbon (CO_2).However, predicting the behavior of biomass and its products under this particular thermochemical process, especially in a fluidized bed reactor, is not a simple task. Fluidized bed reactors represent a notable advantage for this process because of the fact that the biomass particles interact with inert materials inside the reactor and remain in a fluidized or suspended region, which provides better results in terms of mass and heat transfer. The composition of these products may vary due to the effect of numerous parameters in the gasification process including reactor temperature, residence time of gases, particle size of solids, type of oxidant, oxidant/feed ratio, nature of biomass and type of catalyst used. The latest one is a critical parameter due to the presence of undesirable products in the gasification process known as tar. Tar removal is an important problematic in biomass gasification. Different catalyst such as nickel-based, calcined rocks, alkali metals and others have been tested in order to reduce tar from final products. The use of a green catalyst like biomass biochar is an alternative solution to this problematic, being very effective in tar removal (up to 99% conversion) and considered a sustainable option (El-rub, 2008). Highly accurate techniques to model hydrodynamics, such as Computational Fluid Dynamics (CFD), are used to study gas-solid interactions, reaction kinetics like homogeneous and heterogeneous reactions and reactor hydrodynamics as the parameters used for the latter have proven to influence the final products obtained.

2. Methods

The experimental setup is a fluidized bed reactor in quartz (Fig.1). The biomass is feed at the center of the reactor by a stainless steel tube connected from the top of the reactor. Gases get out from the top to a cyclone in order to collect solids particles trained by the gases. The reactor temperature

varies from 500-1000 °C. Nitrogen (N_2), air and dioxide of carbon (CO_2) were used as carrier gas for gasification reaction. Tar produced was condensed at -13°C temperature and then analyzed in a GC/FID and GC/MS. Product gases are collected in a sample bag and then analyzed in a micro GC/TCD and a GC/FID-TCD according to the system configuration (discontinuous or continuous). For hydrodynamics modelling, a CFD Euler-Lagrange code is used to study the behavior of reactor taking in account the hydrodynamics phenomena.

Figure 1. Fluidized bed reactor dimensions.

3. Results and discussion

The variation of the each operation parameter influence the results of the final composition gases and tar. Gasification oxidant have a strong influence in the results because it favors the main gasification and tar reactions (dry reforming, water gas-shift, etc.). Temperature influencing the thermal cracking and production of light tar and gases. In the case of hydrodynamics parameters, the fluidization velocity strongly influences the behavior of gas and solids inside the reactor. The use of biochar as bed material for gasification reaction showed a high conversion of tars.

4. Conclusions

This work presents an experimental study of the influence of different reactor parameters such as biomass particle size, vapor residence time, reactor temperature, oxidant/biomass ratio, product composition. Tar removal is study using a green and sustainable catalyst (biochar) to show the strong performance of biochar against commercials catalyst. In order to optimize the hydrodynamic of the fluidized bed of biochar, a numerical model has been developed. Additionally, this would help study the shrinkage effects of biomass particles in the process, a phenomenon often neglected in literature.

References

[1] Abu El-Rub. Biomass char as an in-situ catalyst for tar removal in gasification systems. University of Twente, Netherlands (2008).

[2] Al-Rahbi et al. Hydrogen-rich syngas production and tar removal from biomass gasification using sacrificial tyre pyrolysis char. Applied energy, pp. 501-509. Leeds U.K. (2017).

[3] S. Gerber, F. Behrendt, M. OevermannAn Eulerian modeling approach of wood gasification in a bubbling fluidized bed reactor using char as bed material. Fuel, 89 (2010), pp. 2903-2917.

ECCE12
The 12th EUROPEAN CONGRESS OF CHEMICAL ENGINEERING
Florence 15-19 September 2019

Photoreactors design for fuels production

Gianguido Ramis[1], Elnaz Bahadori[1], Antonio Tripodi[2], Ilenia Rossetti[2]

1 Dip. di Ingegneria Civile, Chimica e Ambientale, Università degli Studi di Genova and INSTM Unit Genova, Via all'Opera Pia 15A, 16100, Genova, Italy

2 Chemical Plants and Industrial Chemistry Group, Dip. Chimica, Università degli Studi di Milano, INSTM Unit Milano-Università and CNR-ISTM, via C. Golgi, 19, I-20133 Milano, Italy

**Corresponding author: gianguidoramis@unige.it*

Highlights

- High pressure and high temperature photocatalysis explored
- Productivity boosted by unconventional reaction conditions
- Tunable selectivity to different fuels from renewable or waste materials

1. Introduction

Photocatalysis can be seen as a route for the storage of solar energy by producing "solar fuels", i.e. with artificial photosynthesis. In this work, we dealt with two challenging applications: i) the production of hydrogen through photoreforming of aqueous solutions of organic compounds and ii) the photoreduction of CO_2.

Different carbohydrates (glucose, xylose and arabinose, as well as levulinic and formic acid) were used as renewable substrates for photoreforming, since they may be rather easily obtained from the hydrolysis of biomass. On the other hand, the transformation of CO_2 into regenerated organic compounds, to be used as fuels or chemicals (CH_4, HCOOH, HCHO, CH_3OH) was also studied. Our attention was predominantly focused on the development of innovative photoreactors, operating under unconventional conditions, with the fine tuning of the operation parameters. In particular, we have set up and optimized a new photoreactor operating at pressure up to 20 bar and relatively high temperature (up to 90°C) which allowed to overcome one of the main limitations for the photoreduction of CO_2 in liquid phase, *i.e.* the low CO_2 solubility. The possibility to increase the operating pressure also allowed to explore unconventional reaction conditions, evidencing an unexpected boost of hydrogen productivity when increasing temperature in the case of the photoreforming of carbohydrates.

2. Methods

The selected photocatalysts were based on TiO_2, since the main focus was reactor optimization. The materials were prepared by flame spray pyrolysis as dense nanoparticles, or in mesoporous form through a soft template synthesis, and compared with commercial samples of nanostructured TiO_2 P25 by Evonik. Different metals, such as Cu and Au, Pt, Pd, Ag, Ni, with loading ranging from 0.1 to 1 mol% were added as co-catalysts (mono or bimetallic formulations). The role of the metals was that of electron sinks, to inhibit the electron-hole recombination and they were also selected due to the formation of a plasmon resonance band which improves visible light absorption. The

photocatalytic activity tests have been carried out in batch mode using a high pressure photoreactor (up to 20 bar, 95°C), using a UVA immersion lamp, coaxial with the photoreactor (λ_{max} = 365 nm, ca. 77 W/m^2).

3. Results and discussion

As for the photoproduction of H_2 we have investigated extensively the effect of pressure, temperature, carbohydrate and catalyst concentration, selecting 80°C, 4 bar, 5 g/L of carbohydrate, 0.5 g/L of catalyst and neutral pH as the best operating conditions. The highest productivity was achieved with 0.1 mol%Pt/TiO_2 or 1 mol% Au_6Pt_2/TiO_2, leading to ca. 14 mol/h kg_{cat} of hydrogen.

As for the photoreduction of CO_2, operation at high pressure allowed to boost the conversion to partially reduced compounds (HCOOH, HCHO and CH_3OH), with much more limited conversion to CO and CH_4. The present high pressure photoreactor also showed extremely versatile to drive the reaction towards the desired product among those listed by tuning pressure, temperature, reaction time and pH. The highest productivities reached up to now were obtained with 0.2% Au/TiO_2: 40 mol/h kg_{cat} of HCOOH (7 bar, 80°C, pH=14, 24 h reaction time), 17 mol/h kg_{cat} of HCHO (7 bar, 80°C, pH=14, 6 h reaction time) and 1.7 mol/h kg_{cat} of CH_3OH (7 bar, 80°C, pH=7, 24 h reaction time, 0.2% CuO/TiO_2 as catalyst).

The increase of pressure from 7 to 19 bar almost doubled the amount of HCOOH obtained and, also in this case, the increase of temperature allowed to increase the productivity. This was unexpected, since the increase of temperature is often discussed as negative for photocatalysis due to an increased recombination rate of the photogenerated charges.

The apparent quantum yield (AQY) has been here calculated as follows:

$$AQY\ (\%) = \frac{\text{moles of product(i)}\ per\ second\ \times\ \nu(i)}{Incident\ photons\ per\ second}$$

where ν(i) is the number of electrons consumed to reduce CO_2 to the desired product and is directly calculated from the productivity data here reported. The incident photons flow has been calculated based on the measured intensity of radiation. Considering the productivities here reported we have calculated an AQY much higher than 10% in the best cases.

4. Conclusions

In this work we have investigated the effect of unconventional reaction conditions, i.e high pressure and relatively high temperature, on two of the most challenging photocatalytic processes, such as the photoreduction of CO_2 and the production of H_2 from carbohydrates. The increase of temperature to 80-90°C revealed beneficial for both reactions. The increase of pressure boosted the productivity for CO_2 photoreduction to results presently unrivalled in the literature. For this latter application, the use of this photoreactor also allowed to tune the selectivity towards different compounds by simply changing the reaction conditions.
The main achievement, besides the interesting products yields, is the development of a new concept of photoreactor, which can open new unexplored routes in photocatalysis.

ECCE12
The 12th EUROPEAN CONGRESS OF CHEMICAL ENGINEERING
Florence 15-19 September 2019

Process development of a new green propellant: synthesis, isolation and performances

Valentine Passignat[1], Anne Dhenain[1], Anne-Julie Bougrine[1]

1 Hydrazines and Polynitrogen Energetic Compounds Laboratory – UMR 5278
CNRS/UCBL/CNES/ARIANEGROUP University of Lyon, Claude Bernard Lyon 1 University, France.

**Corresponding author: anne-julie.bougrine@univ-lyon1.fr*

Highlights

- Design of an innovative, efficient and scalable process of synthesis with yields of the useful product higher than those of literature
- Definition and optimization of the unitary operations of extraction by determination of the various solid-liquid-liquid ternary phase diagrams involved
- Characterization of the energetic properties of the propellant of interest
- Very promising substitute for the replacement of highly toxic hydrazines

1. Introduction

Propellants, which are part of the space hydrazines family, are mainly used in the aerospace and defense industries, in storable propellant engines for launchers, in satellite apogee motors as bipropellants, associated with nitrogen peroxide, and as mono-propellants in trajectory correction thrusters. In this paper, we describe the development of a new storable, reducing liquid propellant with prospective use in space launchers. Tetramethyl-2-tetrazene and its derivatives was identified by the French Space Agency (CNES) as interesting candidates[1] to replace highly toxic hydrazines such as monomethylhydrazine (MMH), which is considered a substance of high concern (SHC) and is prone to be banned by the REACH European Union regulation. The molecule of interest in this study is the cyclic tetramethyl-2-tetrazene (1,4,5,6 tetrahydro-1,2,3,4 tetrazine $C_4H_{10}N_4$), which should provide optimum propulsive performances and should not have a significant impact on human health and the environment. The objective of the first stage will be to develop a green synthesis process that is competitive on the international level, in line with sustainable development and which can adapt to market fluctuations.

2. Methods

Cyclic tetramethyltetrazene (c-TMTZ) is obtained by two successive reactions: the first step is the synthesis of the bishydrazine by nitrosation of the amine followed by a reduction[2]. The second reaction is the oxidation of this bishydrazine leading to the formation of c-TMTZ by intramolecular cyclization[3,4]. Due to the low yields described in the literature, a study was carried out in the laboratory to optimize the oxidation conditions of bishydrazine and obtain the highest yields of c-TMTZ. The reaction kinetics were deduced from the in-situ concentrations of c-TMTZ obtained by RMN ^{1}H spectroscopy. The second part of the work focused on the design of the extraction and isolation process of c-TMTZ. In the actual process, the extraction of the bishydrazine (BH) from the complex reaction media is the key and tedious step of the global process, implying numerous

unitary operations of distillation (at various pressures) and filtration, leading to a low yield of extraction. In our new concept, the basic idea would be to benefit from a gap of miscibility at the liquid state in the ternary system BH-H_2O-NaOH. Several isotherms of the solid-liquid-liquid ternary system BH-H_2O-NaOH were thus determined under atmospheric pressure. The demixing binodal curve and limits of each domain were obtained by combination of acidimetric titrations of phases in equilibria and conductimetric measurements. The final part of this work describes some energetic properties of c-TMTZ, essential for spatial applications: temperatures end enthalpies of melting and decomposition (DSC), impact sensitivity (BAM tester) and hypergolicity character.

3. Results and discussion

For the synthesis segment, influence of the nature of the oxidizer, concentration, temperature, solvent and pH was studied for the oxidation reaction of BH, allowing optimal conditions to be identified for c-TMTZ yields higher than 70 %. For the extraction segment, several isotherms of the solid-liquid-liquid ternary system BH-H_2O-NaOH were determined (Figures 1 and 2).

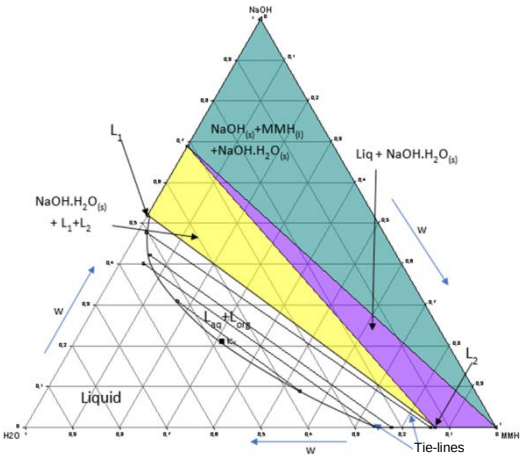

Figure 1. Isothermal 293.15K of the BH-H_2O-NaOH S/L/L ternary system (P_{atm})

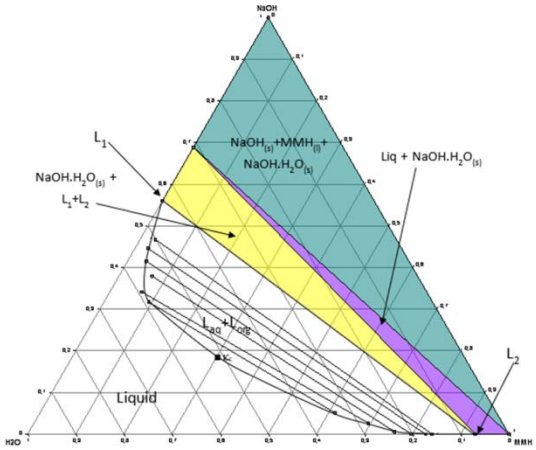

Figure 2. Isothermal 323.15K of the BH-H_2O-NaOH S/L/L ternary system (P_{atm})

These isotherms show the tendency of BH to demixing with NaOH and give the optimal quantities of NaOH to add in order to have the organic species concentrated in a single phase, separated from the salts and with a minimum of water. For the extraction of pure BH, 2 unitary operations are thus required instead of 4. Then, c-TMTZ is recovered by distillation. The characterization of the energetic properties of this propellant reveals a promising substitute: thermal stability on a large range of temperatures, no sensitivity to impact and hypergolic behavior with oxidants.

4. Conclusions

Cyclic tetramethyltetrazene holds great potential to be used as a propellant to replace hydrazines. The global process described in this work is “green” and suitable for large-scale synthesis. Moreover, c-TMTZ can be used to obtain compounds with higher propulsive performances.

References

[1] A. Dhenain, C. Darwich, C.M. Sabaté, D.M. Le, A.J. Bougrine, H. Delalu, E. Lacôte, L. Payen, J. Guitton, E. Labarthe, G. Jacob, Chem. Eur. J. 23 (41) (2017) 9897–9907.
[2] J.N. Hogset, V.E. Matthews, United States Patent: 3365338, January 23, 1968.
[3] S. F. Nelsen, R. Fibiger, J. Am. Chem. Soc. 94 (1972) 8497–8501.
[4] C.J. Michejda, R.S. Koepke, H.D. Campbell, J. Am. Chem. Soc. 100 (1978) 5978–5979.

ECCE12
The 12th EUROPEAN CONGRESS OF CHEMICAL ENGINEERING
Florence 15-19 September 2019

Reaction technology change from semi-continuous to continuous pyrolysis of beech wood

Chetna Mohabeer[1], Antoinette Maarawi[2], Rania Djettene[3], Luis Reyes[4], Lokmane Abdelouahed[5], Bechara Taouk[6*]

1-6 Normandie Univ, INSA Rouen Normandie, UNIROUEN, Laboratoire de Sécurité des Procédés Chimiques, LSPC EA-4704, 76000 Rouen, France

**bechara.taouk@insa-rouen.fr*

Highlights

- Same reaction parameters yielding the maximum bio-oil yield for both reactors.
- Varying pyrolysis temperature impacted significantly on the product distribution while varying gas residence time did not.
- Many non-compliant observations were obtained between the semi-continuous and the continuous setups.

1. Introduction

This study aims to investigate the pyrolysis of the beech wood in a drop tube reactor (DTR) so as to examine the liquid and gas pyrolytic product distributions and also, compare these results with those obtained in a semi-continuous reactor [1].

2. Methods

The pyrolysis runs were done in a semi-continuous quartz tubular set up [1] and in a stainless steel DTR. In the DTR, the biomass was introduced using a screw-fed conveyor. A condenser and a flask, placed inside a cold bath to recover the bio-oils formed from the condensation of pyrolytic vapours were found at the end of the circuit. A sampling bag was used, in which the non-condensable gases were recovered to be later analysed. A flow of 500 mL/min of nitrogen was used as carrier gas. The cold bath and the refrigerant were both kept at a constant temperature of -10 °C. For the purpose of this study, the pyrolysis experiment was conducted in a stainless steel DTR at different temperatures of 500, 550 and 600 °C with varying vapour residence times by changing nitrogen flow rates to 500, 1000 and 2000 mL/min. Gas chromatography-mass spectrometry (GC-MS) and gas chromatography-thermal conductivity detection/flame ionisation detection (GC-TCD/FID) technologies were used to identify and quantify the various components found in the bio-oils recovered and the non-condensable gases collected. Concerning the bio-oils, the components belonging to the same chemical family, that is, possessing the same functional group, were grouped together and their percentage by weight evaluated.

3. Results and discussion

It was firstly seen that the experiment at 500 °C under 500 mL/min N_2 yielded the highest amount of bio-oil (58.8 wt. %). This coincided with the findings from the semi-continuous setup (max. yield of bio-oil: 58.18 wt. % at 500 °C). In contrast to Guizani *et al*. [2], it was seen from this study that the major chemical families present in the collected oils were carboxylic acids (58 mol. %),

phenols (16 mol. %) and alcohols (12 mol. %); this trend was not far from what was found from the semi-continuous setup [1]. However, the percentage for each family differed: the percentage of acids was higher in the DTR (58 mol. % vs. 35 mol. % in the semi-continuous setup). Then, while it was verified that varying the vapour residence times did not impact the product distributions significantly as the reaction regime did not change, varying the DTR temperature did affect the product distributions. It was also observed that both the percentages of carboxylic acids and alcohols tended to decrease with increasing temperature, while phenols demonstrated the opposite trend. This corroborated an inversely-correlated relationship between acids and phenols. This relationship was not observed in the semi-continuous reactor; the inversely-proportional relationship of carbohydrates and acids was more obvious in the latter setup.

Then, it was seen that increasing the reaction temperature favoured the dehydration reaction of the alcohol, carbohydrate and carboxylic acid groups. It was also found that the oxygen content of the bio-oils decreased with mounting DTR temperature. This observation goes along the fact that higher reaction temperatures tend to privilege cracking reactions, and hence, smaller, gas molecules formation. However, the overall oxygen content of the bio-oils remain quite elevated (29-40 mol. %) as compared to that of fossil-derived fuels (~1 %) [3], but also to the oils obtained in the semi-continuous reactor (~33 mol. %). This difference was directly linked to the higher percentage of acids present in the DTR bio-oil samples.

As for the non-condensable gases (NCG) fraction, the species present in majority was CO (58 vol. %), as for the semi-continuous reactor (45 vol. %), but, again comprising a slightly higher percentage. In the DTR, while CO_2 experienced a reduction in its percentage, the CO percentage remained quite stable, contrary to the semi-continuous reactor, where CO increased while CO_2 decreased.

4. Conclusions

It was found that despite not using the same installation, the reaction parameters yielding the maximum bio-oil yield were the same: 500 °C under 500 mL/min N_2 (~58 wt. % in both cases). Also, while varying the temperature impacted significantly on the product distribution (higher temperatures yielded higher gas products and a more acidic oil), varying the gas residence time did not quite alter the product distribution as it was found that the pyrolysis was still taking place within the intermediate regime, and that the reaction was governed by the biomass particle residence time. Finally, many non-compliant observations were obtained between the semi-continuous and the continuous setups. This fact highlighted the heightened error margin present for using results obtained in a semi-continuous or discontinuous setup to globally model pyrolysis as a continuous reaction.

References

[1] C. Mohabeer, L. Abdelouahed, S. Marcotte, and B. Taouk, 'Comparative analysis of pyrolytic liquid products of beech wood, flax shives and woody biomass components', *J. Anal. Appl. Pyrolysis*, vol. 127, pp. 269–277, Sep. 2017.

[2] C. Guizani, S. Valin, J. Billaud, M. Peyrot, and S. Salvador, 'Biomass fast pyrolysis in a drop tube reactor for bio oil production: Experiments and modeling', *Fuel*, vol. 207, pp. 71–84, Nov. 2017.

[3] S. Xiu and A. Shahbazi, 'Bio-oil production and upgrading research: A review', *Renew. Sustain. Energy Rev.*, vol. 16, no. 7, pp. 4406–4414, Sep. 2012.

ECCE12
The 12th EUROPEAN CONGRESS OF CHEMICAL ENGINEERING
Florence 15-19 September 2019

Model development for the gasification of olive mill solid waste.

Janett Ruiz[1,2,*], Gaëlle Ducom[2], Jean-Philippe Tagutchou[3], Jaques Méhu[2,3], Marc Clausse[1]

1 Univ Lyon, CNRS, INSA-Lyon, Université Lyon 1, CETHIL, UMR5008, F-69621 Villeurbanne, France

2 Univ Lyon, INSA-Lyon, DEEP, EA7429, 20 avenue Albert Einstein, F-69621 Villeurbanne, France

3 PROVADEMSE, 66 Boulevard Niels Bohr, F-69100 Villeurbanne, France

**Corresponding author: janett-bianca.ruiz-sanchez@insa-lyon.fr*

Highlights

- Experimental results on olive mill solid waste gasification.
- Development of a 1D steady state stratified model.
- Validation and parametric study performed.

1. Introduction

Gasification is a promising waste-to-energy technique for waste or solid residues from biomass.

In olive-oil producing countries, large amounts of waste material are generated as by-products for which there is no ready use and which may have a negative value because of the cost of disposal. In this case, waste treatment technologies aimed at energy recovery such as gasification represent an interesting option [1].

In the gasification process, the fuel undergoes thermochemical transformations aiming to produce syngas. However, despite major economic, industrial and scientific interests associated with the development of gasification, several technological issues linked to the understanding of the involved mechanisms (chemical reactions, coupled heat and mass transfers, mechanical phenomena, etc.) continue to hinder the development of gasification process [2]. Therefore, a specific model must be developed for each type of fuel.

The objective of this paper is to provide a reliable numerical fixed-bed gasification model for olive mill solid waste, taking into account the thermochemical and fluid flow phenomena that occur during waste gasification process. The model is validated with experimental data of olive mill solid waste gasification.

2. Experiments

Experimental set up consists of a 100 kW downdraft gasifier equipped with temperature, pressure sensors, air flow controllers and syngas analyzer (figure 1).

For this study, an olive mill solid residue was collected from a two-phase extraction process industrial plant located in Spain. The residues were dried on the facility, further extracted with hexane to recover residual oil contents, and then pelletized. The main characteristics of the residue are given in Table 1.

Figure 1. Downdraft gasifier.

Volatile matter (% w/w of DM)	73.5
Fixed carbon (% w/w of DM)	17.6
Ash (% w/w of DM)	8.9
C (% w/w of DM)	48.4
H (% w/w of DM)	6.0
O (% w/w of DM)	34.9
N (% w/w of DM)	1.5
Cl (mg/kg_{DM})	2000
S (mg/kg_{DM})	1250
Higher heating value (MJ/kg_{DM})	19.7
Extractives (% w/w of DM)	47.3
Cellulose (% w/w of DM)	24.8
Hemicellulose (% w/w of DM)	14.5
Lignin (% w/w of DM)	13.4

Table 1. Proximate and ultimate analysis, higher heating value and fiber analysis of olive mill solid waste (taken from [3]), DM = dry matter.

3. Model

A 1D steady state stratified model of the gasifier was developed, assuming local thermal equilibrium. The gasifier was divided into four zones: fuel drying, pyrolysis, oxidation and chemical reduction. The following phenomena were taken into account: chemical reactions with solid/gas, heat and mass transfers. For pressure drop calculation, particle shrinkage was also considered. COMSOL Multiphysics® was used to solve the set of equations.

4. Results and discussion

The model was validated thanks to experimental data. Predictions of the temperature profile, pressure drop and syngas composition are in good accordance with experimental values. The influence of operating conditions (relative fuel air ratio, particle diameter, zone length) on producer gas composition was also investigated. The optimal fuel air ratio was identified.

5. Conclusions

A reliable model for olive mill solid waste gasification was developed and validated. Further improvements will consist in taking into account other mechanical phenomena (e.g. channeling). To achieve this objective, a 2D dynamic approach will be taken.

Acknowledgements

This study is part of the research program ECoGaz, aiming to contribute to the development of waste as an alternative fuel for energy production. The authors wish to thank the Auvergne-Rhône-Alpes Region for the financial support.

References

[1] A.C. Caputo, F. Scacchia, P.M. Pelagagge, Appl. Therm. Eng. 23 (2003) 197–214.
[2] M. La Villetta, M. Costa, N. Massarotti, Renew. Sustain. Energy Rev. 74 (2017) 71–88.
[3] G. Ducom, M. Gautier, M. Pietraccini, J.P. Tagutchou, D. Lebouil, R. Gourdon, Renew. Energy 145 (2020) 180–189.

ECCE12
The 12th EUROPEAN CONGRESS OF CHEMICAL ENGINEERING
Florence 15-19 September 2019

Systematic computer aided methods and tools for lipid process technology

Olivia A. Perederic[1], Bent Sarup[2], John M. Woodley[1], Georgios M. Kontogeorgis[1]

1 Department of Chemical and Biochemical Engineering, Technical University of Denmark, DK-2800 Kgs. Lyngby, Denmark; 2 Vegetable Oil Technology Business Unit, Alfa Laval Copenhagen A/S, DK-2860 Søborg;

**gk@kt.dtu.dk*

Highlights

- State of the art for lipid phase equilibria.
- Systematic identification method for lipid predictive tools improvement.
- Process design and analysis of shea oil fractionation using developed tools.

1. Introduction

Today, chemical engineering methods and tools are widely used for the development and analysis of various processes across different industries. The thermodynamic properties of the involved chemicals, and the models used to describe them, represent the foundation of all the methods and tools used. In recent years, there has been an increasing interest in lipid compounds and their mixtures, which are used in a wide range of applications and industries. A detailed analysis of data and model availability for lipid compounds shows that there is still a need for predictive tools to cover the gaps where experimental data are missing.

The aim of this work is to develop, validate and apply systematic methods and tools for the lipid process technology. Thermodynamic and process aspects of the problem are considered: a systematic method for data analysis and phase equilibria modelling, application of the developed models to lipids processing alongside process modelling, design, analysis and improvement. Particular attention has been given to specialty fats processing using solvent, such as shea oil acetone fractionation. The most important aspects of the process are solvent recovery and product purification of solvent residues.

2. Methods

The detailed analysis of data and models available in the literature for lipid compounds and mixtures was performed and discussed. Further, a systematic method for data analysis and phase equilibria modelling was used for estimate new interaction parameters for lipid compounds. The aim of the method is to improve the quality of phase equilibria prediction for the selected group contribution based methods. The results obtained were used to perform the process modelling, design and analysis for shea oil solvent fractionation process using various tools.

3. Results and discussion

Different models, from EoS to activity and combined models are used to describe lipid phase equilibria. The general trend for increasing deviation of VLE correlation using different activity coefficient models is: NRTL ≈ Wilson < UNIQUAC. The SLE trend for increasing deviation is: UNIQUAC

< Wilson ≈ NRTL. For LLE, NRTL and UNIQUAC prove to have similar performance and both can be used to describe lipid LLE. Although these models provide good predictions, there are a limited number of interaction parameters which cover only a few classes of lipid compounds (e.g: fatty esters, fatty acids). The performance of different UNIFAC variants with their published parameters was tested, and the trend for increasing deviation (ARD%) for VLE description is: Linear UNIFAC < Lyngby UNIFAC< Dortmund UNIFAC < Original UNIFAC. For lipid SLE prediction, the deviation in prediction increase as follows: Original UNIFAC < Dortmund UNIFAC < Linear UNIFAC < Lyngby UNIFAC.

After applying the systematic identification method, the performance of the models using the new lipid-based parameters for describing lipid VLE improves for all the UNIFAC variants, as presented in Figure 1. The extrapolation of the models to SLE prediction using the lipid-based parameters shows little to no improvement compared to the models with the published parameters. Further, Original UNIFAC model with the lipids parameters was used for process modelling, design and analysis of shea oil solvent fractionation.

The shea oil acetone fractionation process consists in three parts: (I) separation by fractional crystallization of shea oil into two products, shea olein and shea stearin; (II) solvent recovery in a series of flash units; and (III) solvent purification and recycling. Improvements of the process (e.g.: heat integration) are performed based on the economic and environmental analysis of the base case scenario.

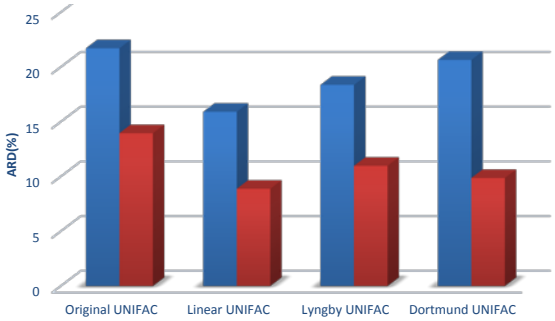

Figure 1. Average relative deviation, ARD(%) for different UNIFAC variants for lipids VLE prediction using published (■) and lipid-based parameters (■).

4. Conclusions

The detailed analysis of available models and data for lipids showed the need of having predictive models to describe lipid systems. By using a systematic identification method, new lipid-based parameters for different UNIFAC variants were estimated and analysed for extrapolation capabilities. Further, the models were used for shea oil acetone fractionation process modelling, design and analysis, and improvements of the process are proposed.

References

[1] D.D. Damaceno, O.A. Perederic, R. Ceriani, G.M. Kontogeorgis, R. Gani, Fluid Phase Equilib. 470 (2018), 249-258.
[2] O.A. Perederic, S. Appel, B. Sarup, J.M. Woodley, G.M. Kontogeorgis, R. Gani, Comput. Aided Chem. Eng. 43 (2018) 737-742.
[3] O.A. Perederic, L.P. Cunico, S. Kalakul, B. Sarup, J.M. Woodley, G.M. Kontogeorgis, R. Gani, J. Chem. Thermodyn. 121 (2018) 153-169.

ECCE12
The 12th EUROPEAN CONGRESS OF CHEMICAL ENGINEERING
Florence 15-19 September 2019

ENHANCED FIXED-BED REACTOR FLEXIBILITY THROUGH OPTIMAL CONTROL AND DESIGN FOR CO2 METHANATION

Jens Bremer[1], Ronny Tobias Zimmermann[2], Kai Sundmacher[1,2]

1 Max-Planck-Institut für Dynamik komplexer technischer Systeme, Sandtorstraße 1, 39106 Magdeburg, Germany

2 Otto-von-Guericke Universität, Universitätsplatz 2, 39106 Magdeburg, Germany;

**Corresponding author: bremerj@mpi-magdeburg.mpg.de*

Highlights

- Detailed model analysis under dynamic conditions with special focus on heat management and catalyst properties.
- Proposing operation strategies to effectively deal with reactor load changes.
- Exploring potentials for advanced control methods (optimal control).

1. Introduction

The current trend towards a more flexible production to react on markets as well as on volatile inputs (e.g., coming from renewable sources), contains many new challenges and requires concepts for dynamic process operation. Thus, the interest in prediction of the process dynamics has become more important than ever before [1-3]. The present work in particular deals with dynamic load changes of fixed-bed reactors for carbon dioxide methanation by use of hydrogen generated via water electrolysis, an important example of Power-to-X (PtX) production processes. Particularly in view of vehicles fueled with compressed natural gas (CNG), synthetic methane (SNG) is a very attractive, easy-to-distribute substitute fuel. Moreover, carbon dioxide methanation is a key reaction in the context of chemical conversion networks for the storage of electrical surplus energy. However, the reaction is strongly exothermic such that distinct hot-spots are formed within the catalytic fixed-bed that can influence the catalyst stability and process safety [4]. On top of that, these reactors are characterized by extraordinary dynamic behaviors (e.g. wrong-way behavior), due to complex interactions between heat and mass transport, reaction, and fluid flow phenomena. Consequently, intelligent dynamic interactions are required to guarantee time-optimal load transitions, while ensuring long-term stable and safe reactor operation.

2. Methods

Detailed dynamic reactor models from first-principals are used to analyze the reactor behavior under dynamic scenarios. One- and two-dimensional, pseudo-homogenous, tubular reactor model including wall and cooling channel are used to get detailed information about the reaction heat propagation and to analyze extraordinary dynamic behaviors. Additionally a heterogeneous model is compared with the homogenous model in order to show the impact of the solid catalytic phase and its corresponding diffusional limitation. Special attention is given to its impact on reactor dynamics, an often stated but rarely illustrated problem under industrially relevant conditions. Furthermore, the reactor models are embedded into frameworks for linear and advanced/optimal control. Thereby, the objective is to keep track of a constant reactor conversion in scenarios of

changing loads (realized via feed velocity and feed pressure changes). All studies are performed in-silico using MATLAB.

3. Results and discussion

Preliminary results for control trajectories performed with and without (closed- and open-loop) well-known PI-controller are illustrated in Figure 1. The changing load influences both the position and the intensity of the reactive zone (hot-spot). Wrong-way behavior occurs within the first minute and lead to a temperature overshoot of up to 100 K. Furthermore, we observed that under certain conditions a load change performed via pressure changes is much less affecting the target conversion, as compared to the velocity-based load change. However, by changing the coolant temperature after disturbing the velocity in a closed-loop set-up with a PI controller, the target conversion is effectively restored after approximately 300 seconds with reduced temperature overshoot. Further results will focus on optimal control trajectories that allow for faster transitions while considering technical restrictions (e.g. maximal catalyst bed temperature).

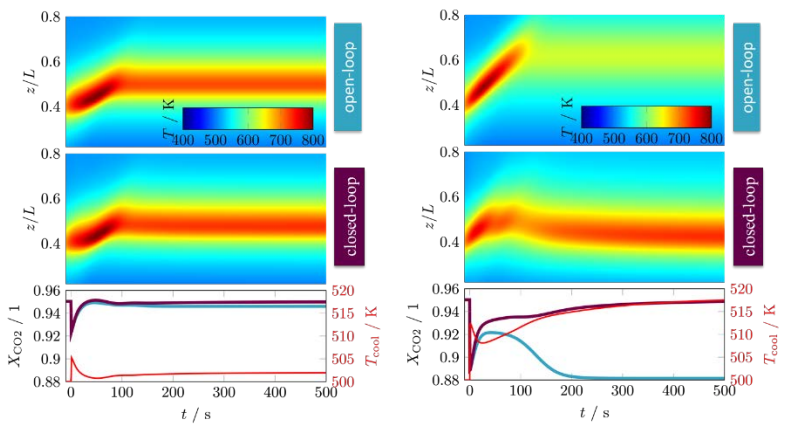

Figure 1. Load change with positive pressure step from 10 to 15 bar (left) and with positive gas flow step from 1 to 1.5 m/s (right). Upper surface plots: space-time behavior at the reactors central axis. Lower plot: control trajectories (red) and CO_2 conversion trajectories in open- (blue) and closed-loop (violet) set-up.

4. Conclusions

Our results comprehensively show how complex the dynamic behavior of the investigated exothermic reactor for methanation is. Powerful computational tools allow for an effective analysis of these behaviors and also reveal to what extent an intervention with suitable controls becomes feasible. With this, we intend to deliver a deeper understanding for dynamic reactor operation and derive new operation strategies that allow for a more flexible and sustainable production within future production concepts. Since our results are mainly related to the heat generated by the reaction, the outcomes of this study are also relevant to other exothermic reactions, e.g. methanol production from CO_2 and green hydrogen.

References

[1] G. Eigenberger, Ullmann's Encyclopedia of Industrial Chemistry, Wiley-VCH, Weinheim, 2003.
[2] G. Eigenberger, H. Schuler, Int. Chem. Eng. 29 (1989) 12 – 25.
[3] O. Kalthoff, D. Vortmeyer, Chem. Eng. Sc. 35 (1980) 1637-1643.
[4] J. Bremer, K.H.G. Rätze, K. Sundmacher, AIChE J. 63 (2017) 23–31.

ECCE12
The 12th EUROPEAN CONGRESS OF CHEMICAL ENGINEERING
Florence 15-19 September 2019

Hydrogenation of CO_2 to methanol in zeolite membrane reactors

Miriam Tovar[1], Raquel Raso[1], Javier Lasobras[1], Javier Herguido[1], Izumi Kumakiri[2], Miguel Menéndez[1]

1 Aragón Institute of Engineering Research, University of Zaragoza, Zaragoza, Spain; 2 Yamaguchi University, 2-16-1, Tokiwadai, Ube, Yamaguchi, 755-8611 Japan

**Corresponding author: jhergui@unizar.es*

Highlights

- Among the tested membranes, zeolite A is the most promising for the purpose.
- The combined traditional + membrane reactor outperforms thermodynamic methanol yields.
- Catalysts less selective to reverse WGS reaction than $CuO/ZnO/Al_2O_3$ are more suitable.

1. Introduction

This work focuses on the hydrogenation of CO_2 to methanol by means of reaction (1), as a way of energy storage that could be applied, for example, to deal with occasional energy overproductions from renewable sources.

$$CO_2 + 3\,H_2 \leftrightarrows CH_3OH + H_2O \qquad (1)$$

Zeolite membrane reactors were proposed [1] to allow lower operating pressure and higher yield in the process. H_2O removal from the reaction environment would ideally increase yields over the equilibrium ones achievable in a conventional reactor.

In this work, we study the separation performance of several zeolite membranes under different operating conditions. Then, the most suitable zeolite is tested for methanol production in membrane reactor using a conventional $CuO/ZnO/Al_2O_3$ catalyst.

2. Methods

Permeation behaviour of zeolite-A and mordenite membranes (prepared at *Yamaguchi University* [2]), as well as of a commercial zeolite-T membrane (provided by *Mitsui Engineering*) were tested by feeding a mixture containing CO_2, H_2, N_2 and H_2O, and using Ar as sweeping gas.

Reaction tests were carried out in both, a traditional fixed bed reactor (FBR) and a combination of it with a zeolite membrane reactor (FBR+ZMR) by feeding a H_2/CO_2 mixture in a 3/1 molar ratio. Temperatures were varied in the range 160-260°C. The non-condensable gases from the reaction were analyzed on-line by gas chromatography and the liquids were analyzed by FTIR.

A $CuO/ZnO/Al_2O_3$ catalyst was loaded in both FBR and ZMR reactors. It was prepared by co-precipitation of the corresponding salts at constant pH, following literature procedures [3].

3. Results and discussion

The separation factor (SF) H_2O/CO_2 obtained with mordenite membranes was quite low (Figure

1), which seems to do with the formation of cracks. Zeolite T provided good SF at 170ºC, but it dropped when was heated up to 240ºC. Moreover, measurements at 170ºC after heating the membrane at 230ºC showed a permanent loss of selectivity which implies that such high temperatures damaged the membrane. Zeolite A provided good separation factors (e.g., SF H_2O/CO_2 higher than 100) although they decreased at high temperatures (240ºC and above).

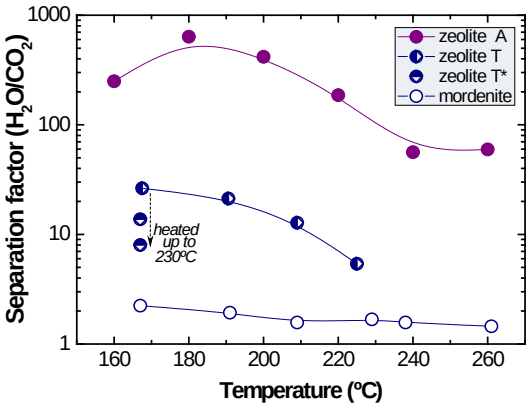

Figure 1. Separation factors for the three tested zeolite membranes

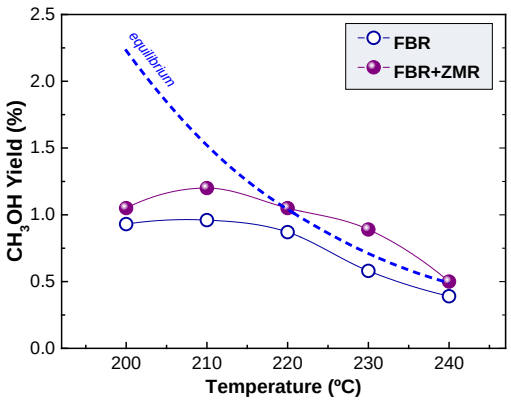

Figure 2. Yield to methanol with the traditional FBR and with the combination FBR+ZMR

An example of comparison of performance using conventional FBR and the configuration FBR+ZMR is shown in Figure 2. The FBR+ZMR combination, using zeolite A as membrane material, outperforms the FBR one in terms of methanol yield. So, yields even over the ones for thermodynamic equilibrium were reached with such a FBR+ZMR configuration.

However, at 240ºC reverse WGS reaction is favored by the removal of water through the membrane and thus the selectivity to methanol is lower with the FBR+ZMR configuration at this temperature, increasing the formation of CO. This strongly suggests that a catalyst with more selectivity to methanol at low pressure than the standard $CuO/ZnO/Al_2O_3$ should be developed, in order to fully profit from the advantage provided by the removal of water through the zeolite membrane.

4. Conclusions

The obtained results open the door for further research, since they show that the zeolite-A membrane reactor can provide higher yields to methanol than the conventional one, allowing operation at lower pressure than the current industrial processes. Further optimization of the full system is necessary to be competitive with the current technology.

References

[1] M. Menéndez, E. Piera, J. Coronas, J. Santamaría, Zeolite membrane reactor for the production of methanol and other alcohols from synthesis gas Spanish Patent ES 2164544B1, (2003).
[2] J. Gorbe, J. Lasobras, E. Francés, J. Herguido, M. Menendez, I. Kumakiri, H. Kita, Sep. Purif. Technol. 200 (2018) 164-168.
[3] Z. Hong, Y. Cao, J. Deng, K. Fan, Catal. Letters, 82 (2002) 37-44.

ECCE12
The 12th EUROPEAN CONGRESS OF CHEMICAL ENGINEERING
Florence 15-19 September 2019

OXIDATIVE COUPLING OF METHANE IN A GAS-SOLID VORTEX REACTOR

Kevin M. Van Geem[*,1]

1 Laboratory for Chemical Technology, Ghent University Technologiepark 125, 9052 Zwijnaarde, Belgium

**Corresponding author: kevin.vangeem@ugent.be*

Highlights

- oxidative coupling of methane in 3D printed reactor
- gas-solid vortex reactor optimization
- reactive simulation using computational fluid dynamics

1. Introduction

Oxidative coupling of methane is considered one of the most promising routes to directly convert methane into more valuable hydrocarbons. The uncertain economics related to the tradeoff between conversion and C2 selectivities is an important reason why OCM is currently not industrially applied.[1] In the last decades, numerous studies have focused on developing a viable catalyst that has the potential to improve the low C2 yields. However, so far, the research on catalyst development has not led to any major breakthrough. One of the reasons is that next to the catalyst aspects, reactor design is of crucial importance for OCM. The lack of an appropriate reactor is one of the primary reasons why OCM has not been commercialized at industrial scale. Previous studies based on bifurcation theory [2] have shown that the key features of an ideal OCM reactor are high thermal backmixing (i.e. high effective thermal conductivity) and low species backmixing (i.e. narrow residence time distributions). Narrow residence time distributions, i.e. plug flow behavior, is necessary to control and maximize the selectivity towards the intermediate products ethane and ethylene. High effective thermal conductivity creates the opportunity to exploit the bifurcation behavior and operate an OCM reactor autothermally, in this way utilizing the reaction heat in the best possible way. Both these characteristics can be obtained in the gas-solid vortex reactor (GSVR) that is studied in this work. In a gas-solid vortex reactor in a static geometry, gas is injected tangentially via a number of inlet slots (see Figure 1). The swirling gas transfers its momentum to the particles in the reactor chamber, which in turn start rotating. A fluidized state is obtained when the drag force exerted by the gas balances the apparent weight of the particles in the centrifugal force field. In contrast to conventional gravitational fluidized beds, higher gas throughput, lower residence times, more uniform beds, higher slip velocities and hence better heat and mass transfer can be achieved in this reactor type. Therefore, the GSVR is an excellent candidate for process intensification. As the reactor can combine short residence times and narrow residence time distributions with optimal heat transfer characteristics, it is a very promising technology for OCM. In this work, the open-source CFD package OpenFOAM is used to simulate an adiabatic gas-solid vortex reactor using an Euler-Euler approach. Detailed microkinetic models are used for different

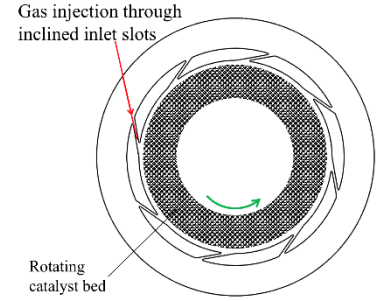

Figure 1. Gas-solid vortex reactor in a static geometry.

types of catalyst (Sn-Li/MgO, Mn/Na2WO4/SiO2, Sr/La2O3). The effect of operating conditions and reactor geometry is evaluated.

2. Methods

The simulated GSVR geometry is adopted from the work of Gonzalez-Quiroga et al. [3] It basically consists of a cylindrical unit positioned along a vertical axis with eight gas injection slots of 1 mm width, equally distributed over the circumferential wall and tangentially inclined at a 10° angle. A reactor diameter of 80 mm and length of 15 mm are defined. The reactive two-phase flow in the GSVR is simulated with an Euler-Euler approach using the open-source CFD package OpenFOAM. A dedicated solver was developed, coupling OpenFOAM and Cantera, the latter being used as mechanism interpreter. This allows to use detailed microkinetic models. In this work, the microkinetic model consists of 39 gas phase reactions and 26 catalytic reactions.[4] The same model can be used for different catalysts (Sn-Li/MgO, Mn/Na2WO4/SiO2, Sr/La2O3), provided the kinetic parameters are adjusted accordingly. The GSVR is simulated as an adiabatic unit.

3. Results and discussion

Non-reactive simulations show that narrow residence times can indeed be obtained in the GSVR. Plug flow behavior for species/mass transport is indicated by the quasi parallel streamlines (see Figure 2) and a simulated Péclet number >> 1. Preliminary reactive simulations also indicate a good thermal mixing in the reactor, without hot spot formation. High C2 selectivities ~75% can be obtained, but in the non-ignited state, methane conversion is limited because of the very small residence times (<5 ms) in the catalyst bed. Employing the effects of ignition/extinction behavior, the methane conversion can be increased while maintaining a high C2 selectivity, and at the same time working at lower inlet temperatures.

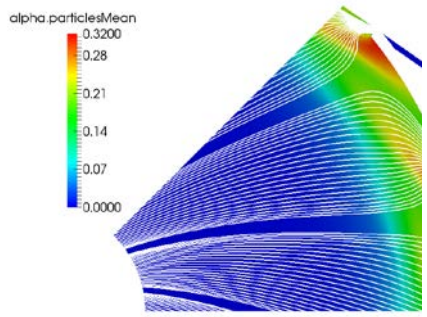

Figure 2. Gas streamlines, shown on top of the catalyst volume fraction field. Simulated conditions: 16-slot GSVR, 75 m/s slot velocity (CH_4:O_2 = 4), 11.2 g catalyst particles (2300 kg/m^3, Ø 500 µm)

4. Conclusions

In this work a new reactor technology is proposed for the oxidative coupling of methane (OCM). A gas-solid vortex reactor (GSVR) combines the two most important features required in an ideal OCM reactor: good heat management and narrow residence time distributions. This allows to utilize the exothermic reaction heat in the best possible way while also maximizing the selectivity towards intermediate C2 products. Computational Fluid Dynamic simulations are used to optimize and design the GSVR specifically for OCM. The CFD simulations show that the narrow residence time distributions and efficient heat management in the GSVR can give rise to C2 yields ~25 %.

References

1. L. A. V. Ismael l Amghizar, Kevin M. Van Geem,Guy B. Marin, *Engineering*, **3**, 0-.
2. L. A. Vandewalle, I. Lengyel, D. H. West, K. M. Van Geem and G. B. Marin, *Chemical Engineering Science*, 2018, DOI: https://doi.org/10.1016/j.ces.2018.08.053.
3. A. Gonzalez-Quiroga, P. A. Reyniers, S. R. Kulkarni, M. M. Torregrosa, P. Perreault, G. J. Heynderickx, K. M. Van Geem and G. B. Marin, *Chemical Engineering Journal*, 2017, **329**, 198-210.
4. P. N. Kechagiopoulos, J. W. Thybaut and G. B. Marin, *Industrial & Engineering Chemistry Research*, 2014, **53**, 1825-1840.

ECCE12
The 12th EUROPEAN CONGRESS OF CHEMICAL ENGINEERING
Florence 15-19 September 2019

Sustainability Dimensions in Hydrogen-Based Distributed Energy Systems

Juan D. Fonseca[1,2*], Mauricio Camargo[1], Jean-Marc Commenge[3], Laurent Falk[3], Iván D. Gil[2]

1 Équipe de Recherche sur les Processus Innovatifs (ERPI), Université de Lorraine, 8 rue Bastien Lepage, Nancy, France ; 2 Grupo de Procesos Químicos y Bioquímicos, Department of Chemical and Environmental Engineering, Universidad Nacional de Colombia, Carrera 30 45-03, Bogotá, Colombia ; 3 Laboratoire Réactions et Génie des Procédés (LRGP), Université de Lorraine, 1 rue Grandville, Nancy, France

**Corresponding author: jdfonsecag@unal.edu.co*

Highlights

- Distributed energy systems including hydrogen as energy carrier were studied
- The design of DES including hydrogen is focused on techno-economic issues
- There is a need of multi-dimensional approaches to evaluate this type of systems

1. Introduction

The constant expansion of world economy and population, as well as the concerns about climate change, represent new challenges for the energy sector [1]. In this line, the emergence of distributed energy systems (DES), and the integration of different energy networks by means of the combination of multiple energy sources, converters and carriers have represented a shift in the energy framework [2]. Among energy carriers, hydrogen has appeared as a promising alternative due to the large range of sources from it can be obtained. Additionally the possibility to use it as raw material, energy storage medium (power-to-gas) or as final energy form emitting only steam and heat in its combustion, make hydrogen a promising energy vector to be integrated in energy systems [3]. However, despite their potential capabilities, introducing hydrogen in the design of distributed energy systems (DES) is a complex problem due to the simultaneous dimensions and constraints that need to be considered, as well as to the high context dependence of this kind of projects [4]. For these reasons, in this work a literature analysis is done with the aim to identify the objectives (technical, economic, environmental and socio/political) and the specific evaluated criteria (profit, NPV, efficiency, emissions, etc) when DES including hydrogen are designed, planned or operated.

2. Methods

The methodology consists on a bibliographic analysis of scientific research papers, by means of a systematic literature review carried out according to the parameters noted in Table 1. Taking into account the great variety of terminology related with DES, the keyword field is composed of a set of terms (e.g. energy hub, microgrid, hybrid energy system), besides to hydrogen and power-to-gas ones.

Table 1. Search strategy parameters.

Field	Option Introduced
Keywords	("energy hub" OR microgrid OR "integrated energy systems" OR "distributed energy system" OR "decentralized energy system" OR "multi energy system" OR "hybrid energy system" OR "polygeneration") AND (hydrogen OR "power to gas")
Search in	Title, abstract, keywords
Period explored	2000 - 2018
Type of documents	Articles and conference papers

3. Results and discussion

Figure 1 shows the distribution of publications according to the evaluated objective. It highlights the prevalence of economic issues, which are involved in almost 80% of studies. Additionally, it appears that around 45% of documents include multi-objective analysis and nine works address economic, technical and environmental goals simultaneously.

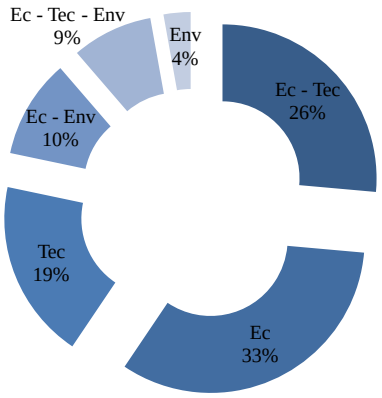

Figure 1. Performance objectives evaluated in DES. (Ec-economic, Tec-technical, Env-environmental)

4. Conclusions

Results indicate that the design and analysis of DES including hydrogen have been predominantly focused on techno-economic issues. Hence, there is an opportunity for future work to include another dimensions (e.g. socio/political), and thus improve the decision-making process for planning this type of energy systems.

References

[1] International Energy Agency (IEA). World Energy Outlook 2017 2017. http://www.iea.org/weo2017/ (accessed April 8, 2018).

[2] Adil AM, Ko Y. Socio-technical evolution of Decentralized Energy Systems: A critical review and implications for urban planning and policy. Renew Sustain Energy Rev 2016;57:1025–37. doi:10.1016/j.rser.2015.12.079.

[3] Dincer I, Acar C. Smart energy solutions with hydrogen options. Int J Hydrogen Energy 2018:1–21. doi:10.1016/j.ijhydene.2018.03.120.

[4] Eriksson ELV, Gray EMA. Optimization and integration of hybrid renewable energy hydrogen fuel cell energy systems – A critical review. Appl Energy 2017; 202: 348–64. doi:10.1016/j.apenergy.2017.03.132.

ECCE12
The 12th EUROPEAN CONGRESS OF CHEMICAL ENGINEERING
Florence 15-19 September 2019

Analysis of Hydrogen Supply Chains for Swiss Mobility

Cristina Antonini[1], Annalisa Guidolin[1], Paolo Gabrielli[1], Marco Mazzotti[1*]

1 Institute of Process Engineering, ETH Zurich, Sonneggstrasse 3, 8092 Zurich, Switzerland
**Corresponding author: marco.mazzotti@ipe.mavt.ethz.ch*

Highlights

- Blue hydrogen production technologies
- Biogas and natural gas reforming with carbon capture
- Swiss blue hydrogen network

1. Introduction

Most recent climate scenarios from integrated assessment models (IAMs) assessed that to reach the 2°C target in 2100 the amount of CO_2 removal required is in the order of several gigatonnes per year (Gt/a) [1][2]. In Switzerland, one third of the carbon dioxide emissions derives from the transport sector, and corresponds to 16.2 Mt_{CO2} in 2016. Considering the abundance of fossil fuels, low-carbon hydrogen production from natural gas and biogas, coupled with carbon capture and storage, seems a promising solution for reducing the emissions of the mobility sector. This type of hydrogen is the so called blue-hydrogen, and it opposes to green-hydrogen from electrolysis.
The design of a blue-hydrogen supply chain in Switzerland requires models that describe the conversion and capture technologies considered. Therefore, the goal of this work is to model the technologies with the required level of details and introduced them in the supply chain model, which should deliver an optimized configuration of a potential hydrogen network in Switzerland. The selected blue hydrogen production processes are reforming of natural gas and biogas. For CO_2 capture, absorption with methyl diethanolamine is considered as reference technology and the novel in house studied adsorption process, vacuum pressure swing adsorption (VPSA), is considered for comparison. As reference, the production of green hydrogen via electrolysis is considered. The Swiss distribution network is optimized for different criteria, where both carbon dioxide emissions and costs are considered.

2. Methods

The hydrogen production as well as the amine carbon capture process are modelled in Aspen Plus®, the adsorption processes are modelled with an in-house simulation tool. The models in Aspen Plus® are built with a step-wise approach; firstly, the key process variables are identified. Secondly, multi parameters sensitivity analysis are performed to better understand the nature of the interaction among the operation variables. Lastly, mathematical optimization is used as a tool to fine-tune the operating conditions of the process. Those models are subsequently simplified and given as input data to the supply chain problem. The geographical region of interest, in this case Switzerland, is spatially discretized and for each node a specific demand for hydrogen is given. The optimizer will define where hydrogen is produced, with which technology and at which scale. Moreover, the

solution of the optimization problem will include the distribution network of hydrogen among the nodes. The Mixed Integer Linear Programming (MILP) model is built in Matlab® and solved with commercial solvers (CPLEX®, GUROBI®).

3. Results and discussion

The technologies have been studied and modelled. The complex process flowsheets have been simplified with linear relationships, easy implementable in the supply chain model. A preliminary version of the supply chain model has been prepared based on previous work done in our group [3]. The spatial discretization has been integrated into the existing model together with the operational specifications of the network. A graphical overview of this procedure is represented in Figure 1.

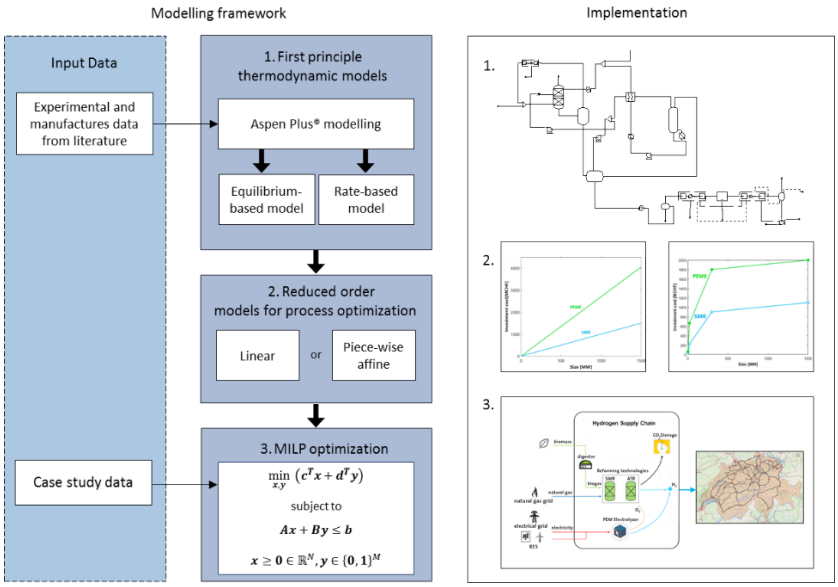

Figure 1. Overview on the modelling framework of this work.

4. Conclusions

This work will focus not only on the construction of a model suitable to shape a Swiss hydrogen network for mobility based on detailed technology descriptions; but it will also focus on the understanding of the trade off deriving from the interactions among the different players. The final goal is to make sure that all the interesting features are considered and adeguately described in the supply chain model.

Acknowledgment

ACT ELEGANCY, Project No 271498, has received funding from DETEC (CH), BMWi (DE), RVO (NL), Gassnova (NO), BEIS (UK), Gassco, Equinor and Total, and is cofunded by the European Commission under the Horizon 2020 programme, ACT Grant Agreement No 691712. This project is supported by the pilot and demonstration programme of the Swiss Federal Office of Energy (SFOE).

References

[1] PCC. (2014). *Fifth Assessment Report.*
[2] Smith, P. D. (2016). Biophysical and economic limits to negative CO2 emissions. *Nature Climate Change*, 42.
[3] Gabrielli, P. G. (2018). Electrochemical conversion technologies for optimal design of decentralized multi-energy systems: Modeling framework and technology assessment. *Applied Energy*, 557-575.

ECCE12
The 12th EUROPEAN CONGRESS OF CHEMICAL ENGINEERING
Florence 15-19 September 2019

Syngas production in the Power-to-Liquid process - Techno-economic assessment of the operating conditions

Sandra Adelung[1], Ralph-Uwe Dietrich[1]

1 German Aerospace Center, Institute of Engineering Thermodynamics, Pfaffenwaldring 38-40, 70569 Stuttgart, Germany

**Corresponding author: Sandra.adelung@dlr.de*

Highlights

- Power-to-Liquid (PtL) process model (Simulation in Aspen Plus®)
- PtL process efficiency for varying process conditions in the syngas unit
- Economic assessment
- Optimum operating conditions of the syngas unit

1. Introduction

In order to decarbonize the transport sector several possible routes and measurements are currently investigated. For the air transport sector, a decarbonization seems not likely in the near future as this is one of the "difficult-to-electrify" sectors. However, a promising approach to incorporate renewable sources in this sector (defossilization) is the production of synthetic fuels from CO_2 and water by using renewable power sources for hydrogen production in an electrolyzer. In this Power-to-Liquid process (see Fig. 1) the CO_2 is activated at high temperature (750-950 °C) and elevated pressure (1-25 bar) via reverse water-gas shift reaction (RWGS). The produced syngas is then converted to hydrocarbons via Fischer-Tropsch synthesis (FTS). Besides the technical challenges to establish an efficient Power-to-Liquid process, the production costs and ways to reduce these costs are of major importance.

Figure 1. Principle scheme of the PtL process.

2. Methods

The process is modelled in Aspen Plus® (see Fig. 2) and the PtL-efficiency is calculated according to:

$$\eta_{PtL} = \frac{\dot{m}_{Product} \cdot LHV_{Product}}{P_{electrical}}$$

Different parameters are varied e.g. temperature and pressure in the RWGS reactor. The evaluation of the optimum process conditions is not trivial. On the one hand, increasing the temperature and decreasing the pressure leads to a higher CO_2 conversion and less CH_4 formation. On the other hand decreasing the pressure leads to an increase in power consumption

due to additional compression work, while higher temperatures require additional high temperature heat. The effect of this variation is assessed and discussed. Further the production costs are calculated using the Inhouse Tool TEPET (Techno-Economic Process Evaluation Tool) [1].

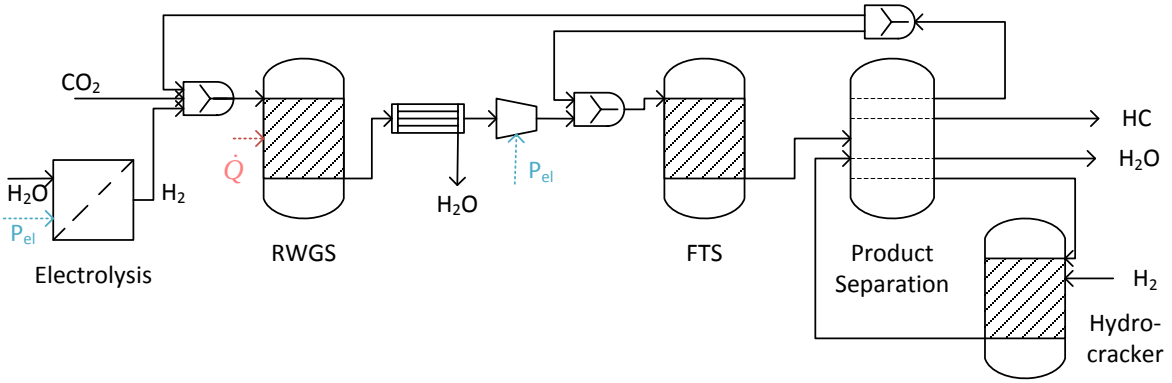

Figure 2. Simplified process scheme of the PtL process.

3. Results and discussion

The assumptions for the process model will be presented. The influence of the parameter variation on the PtL-efficiency will be discussed. Additionally the production costs and the impact of different operating conditions on these costs will be determined.

4. Conclusions

The optimum process conditions regarding the efficiencies and production costs will be presented. Major impacts will be outlined and quantified.

References

[1] F. G. Albrecht, D. H. König, N. Bauck, R.-U. Dietrich, Fuel 194 (2017) 511-526.

ECCE12
The 12th EUROPEAN CONGRESS OF CHEMICAL ENGINEERING
Florence 15-19 September 2019

New insights on the ozone reactive flotation: fundamental study using virgin fibers to model recovered cellulosic fibers

Amina Ghorbel[1]*, Nathalie Marlin[1], Marc Aurousseau[1], Agnès Boyer[1]

[1] Univ. Grenoble Alpes, CNRS, Grenoble INP, LGP2, F-3800 Grenoble, France

*Corresponding author: amina.ghorbel@lgp2.grenoble-inp.fr

Highlights

- Strength properties of fibers are not altered by O_3 and drainability is improved
- O_3 decomposition into water is predominant
- Remaining O_3 mainly reacts with soluble contaminants decreasing the effluent COD

1. Introduction

Nowadays recovered papers and boards constitute the major cellulosic fiber raw material used in papermaking but the utilization rate of recovered paper depends on the paper grade. The production of white graphic papers uses in average a maximum of 10% of recovered paper (CEPI, 2016).To obtain high quality final products, deinking, i.e. ink removal, is required. Flotation process is the most common practice for deinking (Kemper, 1999): it is a physico-chemical unit operation using air bubbles flow to collect and drain ink particles out of the fiber suspension. To improve the efficiency and the sustainability of paper deinking lines, the idea is to add ozone (O_3) as a reactive gas into the gas flow (Marlin et al., 2013). Indeed, O_3 is a well-known oxidant applied for process and urban water treatment (Wei et al., 2016)and also for fiber bleaching in the pulp and paper industry (García et al., 2009). Addition of O_3 in the gas stream during flotation gave promising results with the reduction of COD effluent with 30% and an increase of the fiber yield of 1 point, whereas no effect on ink removal efficiency has been observed (Almeida et al., 2010). However, O_3 may theoretically also depolymerize the cellulosic chains of the fibers (Mishra et al., 2013; Pipon et al., 2007). To investigate more fundamentally the action of O_3 during the flotation process, and especially to examine the reactivity of O_3 with both the contaminants present in solution and the cellulosic fibers, flotation trials have been conducted on model recovered cellulosic fibers free of ink and with tap water or model process water to simulate the presence or not of soluble contaminants.

2. Methods

Recovered cellulosic fibers have been simulated by a mixture of virgin fibers representative of the fiber composition of office waste papers: 90% bleached chemical pulp and 10% mechanical pulp. Before flotation, the pulp models were diluted to 1% consistency (w dry fibers/w suspension) with a conventional alkaline chemistry (Marlin et al., 2013). Flotation trials were performed in a batch pilot flotation cell specially designed to run with corrosive gas such as O_3 (Beneventi et al., 2009), in the following conditions: 2.785 TPN L/min gas flow, 10 minutes flotation time, 40°C, using air or a O_2/O_3 mix as gas flow. In the case of O_2/O_3, O_3 concentration in the gas stream was 160 g/Nm^3, i.e. 4.46 g of O_3 in one trial. Flotation trials have been carried out either with tap water and industrial model water containing contaminants commonly found in process effluent of recovered

paper recycling lines (sodium oleate 0.4 g/L, carboxymethyl cellulose 0.7 g/L and slightly anionic starch 3.15 g/L). Pulp strength properties have been measured on pulp handsheets of 60 g/m^2 prepared according to the standard ISO 5269-3, 2008 method. Tensile strength (Ir) gives the strength of the whole fiber web (ISO 1942-2, 2008) and zero-span strength (Ir_0) measured on wet handsheets, the strength of one isolated fibers (ISO 15361, 2000). The papermaking ability of the pulp was evaluated in terms of pulp drainability via the Schopper-Riegler index °SR (ISO 5267-1, 1999). The global quality of flotation effluents was examined through Chemical Oxygen Demand (COD, mg/L - Hach method). The O_3 consumption (Cons.), expressed in g of O_3 during the trial, has been calculated using the O_3 concentration in the gas phase measured at the inlet and outlet of the flotation cell.

3. Results and discussion

Table 1. Pulp and effluent properties after air and O_2/O_3 based flotation processes

	°SR	Ir (N.m/g)	Ir_0 wet (N.m/g)	COD (mg/L)	pH	Cons. (g)
Air - tap water	40	42 ± 2	50 ± 2	372	9.9	-
O_2/O_3 - tap water	43	48 ± 3	51 ± 3	240	7.6	3.18
Air - model water	55	48 ± 4	50 ± 2	643	9.2	-
O_2/O_3 -model water	44	46 ± 1	48 ± 2	564	7.0	3.76

Inlet pulp properties: pH = 9.6, COD inlet suspension, tap water: 400, air model water: 680, O_2/O_3 model water: 868 (mg/L), °SR=39, Ir: 43±3, Ir_0 wet = 52 ±3 (N/mg)

Before any flotation, it can be observed that the use of model process water reduced the pulp drainability by increasing the °SR from 39 to 55. Air flotation does not modify the pulp drainability (°SR=40) whereas ozone improves it by reducing the °SR from 55 to 44, probably due to the consumption of the soluble contaminants by O_3. This is confirmed by COD and pH results: after air flotation, COD does not change whereas more than 30% COD reduction is obtained after O_2/O_3 flotation (tap or model water); on the same, after air flotation, pH is maintained at 9-10 whereas it decreased to 7-8 when O_3 is used which proves that acidic products are formed. Concerning pulp strength properties, Ir and Ir_0 are conserved showing that neither the fiber web nor the fiber itself is degraded by O_3. Besides, 3.76 g of O_3 is consumed in the trial with model water. As the O_3 consumption into water alone (no fiber, no soluble contaminant) is 3.00 g, O_3 is mainly decomposed by water; contaminants only consumed 0.58 and fibers 0.18 g of O_3.

4. Conclusions

Although O_3 is mainly decomposed into water, the remaining O_3 principally reacts with soluble contaminants thus (1) reducing the COD and (2) preserving the cellulosic fiber from degradation: deinked pulp papermaking ability and strength properties are not altered (Ghorbel et al., 2018).

References

Almeida, F., Marlin, N., Beneventi, D., and Aurousseau, M. (2010). J. Pulp Pap. Sci. 42–48.

Beneventi, D., Almeida, F., Marlin, N., Curtil, D., Salgueiro, L., and Aurousseau, M. (2009). Chem. Eng. Process. Process Intensif. 48, 1517–1526.

CEPI (2016). CEPI's Key Statistics 2016 (CEPI).

García, J.C., López, F., Pérez, A., Pèlach, M.A., Mutjé, P., and Colodette, J.L. (2009).Holzforschung 64, 1–6.

Ghorbel, A., Marlin, N., Boyer, A., and Aurousseau, M. (2018). 6th International Congress on Green Process Engineering, Toulouse (France), p. 172 (4 pages).

Kemper, M. (1999).Int. J. Miner. Process. 56, 317–333.

Marlin, N., Almeida, F., Aurousseau, M., Herisson, A., and Beneventi, D. (2013). Ozone Sci. Eng. 35, 381–389.

Mishra, S.P., Lachenal, D., and Chirat, C. (2013). Tappi J. 12, 39.

Pipon, G., Chirat, C., and Lachenal, D. (2007).Holzforschung 61.

Wei, C., Zhang, F., Hu, Y., Feng, C., and Wu, H. (2016).Rev. Chem. Eng. 33, 49–89

ECCE12
The 12th EUROPEAN CONGRESS OF CHEMICAL ENGINEERING
Florence 15-19 September 2019

MINERVE an innovative Power-to-Gas pilot unit in Nantes, France: presentation and energy performances.

Freddy Durán-Martínez[1,2*], Mylène Marin-Gallego[1], Khaled Loubar[1], Mohand Tazerout[1], Bernard Lemoult[1,2]

1 GEPEA-CNRS UMR 6144, IMT Atlantique, Nantes, 44300. France; 2 AFUL Chantrerie, IMT Atlantique, Nantes, 44300

**Corresponding author: freddy-libardo.duran-martinez@imt-atlantique.fr*

Highlights

- An experimental Power-to-gas pilot unit has been built in Nantes, France
- PEM electrolyzer is used to produce H_2, methanation is processed in 2 fixed bed reactors
- Renewable synthetic natural gas (SNG) is produced to provide fuel at a Green-gas station

1. Introduction

Storing renewable electricity surplus in a natural gas grid is an attractive concept. Hydrogen storage via chemical conversion with carbon dioxide into methane (also referred as CO_2 methanation or *Power-to-Gas* (PtG), see equation (1)) allows the storage, distribution and reconversion to power, benefitting from the readily available natural gas infrastructure [1-3].

$$CO_2 + 4\,H_2 \text{ ” } CH_4 + 2\,H_2O \quad (1) \qquad \Delta H_R° = -165 \text{ kJ mol}^{-1}$$

Up to now, a reduced number of PtG “demo plants” have been appeared in an effort to scale up lab pilots. MINERVE project aims to show the PtG process feasibility via the first French Methanation demo plant. Experiments are carried out to understand the impact of operating parameters such as reactants volumetric flow rate, H_2:CO_2 ratio, pressure or temperature among others and to find out the optimal condition operation.

2. Material and Methods

This study focused in two main parts of the PtG pilot unit (see figure 1). In one hand, the hydrogen production is carried out by a 20kW PEM electrolysis reactor capable of generating up to 2.4 Nm^3/h of hydrogen and in the other hand, the catalytic reaction section which converts hydrogen into methane using 2 fixed bed reactors (FBR) functioning in series and a commercial Ni/Al_2O_3 catalyst. In order to determine reaction performance, an online infrared methane sensor BCP-CH4 is used as well as an on-line multi-component (CH_4, CO_2, CO, H_2 and O_2) analyzer. Gas samples are also taken at each reactor outlet and analyzed with an Agilent Technologies 3000A Micro GC.

3. Results and discussion

Methanation experiments were carried out at different pressure, temperature, H_2 excess and flow rate, and CO_2 ratio between the reactors FBR1 and FBR2 (see table 1).

Pressure (bar)	Temperature (°C)	Excess of CO_2 in FBR1 and FBR2 (%)	H_2 flow rate (NL/min)	CO_2 ratio between FBR1 and FBR2 (%)
[1-10]	[280-380]	[0-100]	[10-30]	[0-100]

Table 1. Methanation operating conditions.

Figure 2 illustrates a typical monitoring of methanation. Four steps are identified in the reactor:

- Step 1: Rise of temperature. In this step, the temperature in the reactors reaches the set point. A constant value of H_2 flow rate is imposed.
- Step 2: Rise of H_2 flow rate. The H_2 flow rate reaches the set point with a constant slot equal to 36 (NL/min). The production of methane starts and the temperature increases. The temperature is maintained as constant as possible by playing with the CO_2 ratio between both reactors.
- Step 3: Steady State. The H_2 flow rate is constant and the production of methane is stable.
- Step 4: End of the reaction.

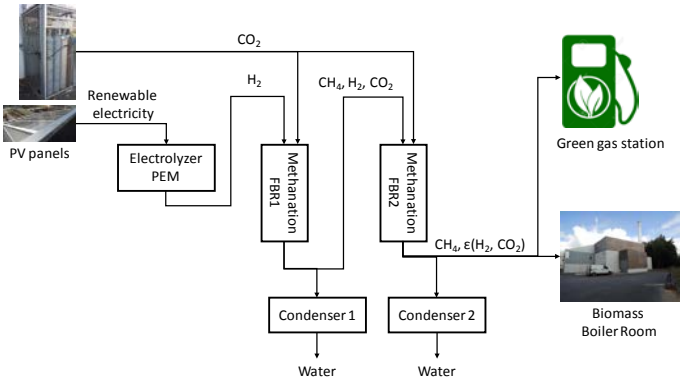

Figure 1. Schematic representation of MINERVE PtG pilot unit installed at AFUL Chantrerie, Nantes (France).

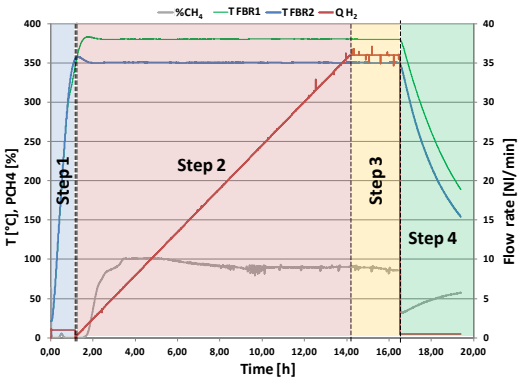

Figure 2. Methanation monitoring: Q_{H_2} = 36 (NL/min), P = 5 bar, T_{R1} = 350°C, T_{R2} = 380°C, stoichiometric conditions, CO_2 ratio = 60%.

4. Conclusions and perspectives.

A CO_2 conversion of 90% and a purity of methane equal to 86%vol were achieved in the current conditions. A parametrical study of the pilot unit is in progress to optimize it. The challenging part of the monitoring of the reactor is the control of the exothermicity of the reaction.

References [Calibri 10]

[1] M. Bailera, P. Lisbona, L.M. Romeo, S. Espatolero, Renew. Sustain. Energy Rev. 69 (2017) 292–312.

[2] M. Lehner, R. Tichler, H. Steinmüller, M. Koppe, Power-to-Gas: Technology and Business Models 93 (2014).

[3] M. Götz, J. Lefebvre, F. Mörs, A. McDaniel Koch, F. Graf, S. Bajohr, et al., Renew. Energy 85 (2016) 1371–1390.

ECCE12
The 12th EUROPEAN CONGRESS OF CHEMICAL ENGINEERING
Florence 15-19 September 2019

Plan B: Taking the Carbon out of Fossil Fuels with Catalytic Reactive Separation

Eric Mcfarland, Horia Metiu, Clarke Palmer, Jiren Zeng, Nazanin Rahimi, Dohyung Kang

There is no evidence that significant reductions in the carbon dioxide emissions associated with power generation will be cost effectively achieved using current commercial alternatives to abundant and inexpensive fossil fuels. Clean burning hydrogen has long been considered the fuel of the future, however, cost-effective production methods have not been proven. Technoeconomic comparisons of electrolysis, steam methane reforming, and pyrolysis shows that the lowest cost process for producing hydrogen and/or dispatchable electricity without CO_2 emissions can utilize pyrolysis of abundant, natural gas. The challenge is to achieve high methane reaction rates and high conversion to molecular hydrogen in a reaction environment where solid carbon can be continuously separated. Reactive separation using high temperature (~1000 ^oC) catalytic complex liquids has been investigated in several multiphase reaction systems and high rates (>1 mole/m^3-s) of methane decomposition and high selectivity for molecular hydrogen observed. When the physical properties of the liquids are selected optimally, conveniently separable solid carbon is produced from methane dehydrogenation in bubble column reactors. Solid catalysts in specific melts may also be continuously reactivated as the high temperature liquid serves as a solvent to remove carbonaceous surface deposits prior to the irreversible formation of deactivating coke. Single pass methane conversion of over 95% to molecular H_2 at over 98% selectivity is demonstrated in complex melt systems. Process designs for solid carbon synthesis with zero carbon hydrogen and/or electricity production together with relative technoeconomics will be presented.

ECCE12
The 12th EUROPEAN CONGRESS OF CHEMICAL ENGINEERING
Florence 15-19 September 2019

Pyrazole derivatives as a potential liquid organic hydrogen carriers: evaluation of thermochemical data

Sergey Verevkin[1], Andrey Pimerzin[2]

1 Department of Physical Chemistry, University of Rostock, 18059, Rostock, Germany

2 Chemical Department, Samara State Technical University, 443100, Samara, Russia

**Corresponding author: sergey.verevkin@uni-rostock.de*

Highlights

- Vapor pressures of alkyl pyrazoles measured by transpiration method.
- Vaporization enthalpies were derived and compared with the literature.
- Combustion experiments were performed on 1-methylpyrazole.
- Energetics of de(hydrogenation) reactions was discussed.

1. Introduction

Because of significant fluctuations in the daily power production and consumption of by the conventional and renewable energies, the development of new storage technologies for energy is necessary. Hydrogen is a very interesting option to overcome the drawbacks of other established storage options like *e.g*. storage under high pressures and very low temperatures. The reversible hydrogenation of liquid organic hydrogen carriers (LOHCs) is a new concept for a long-term storage of hydrogen. LOHCs can be efficiently used as an energy-carrying materials for mobile or stationary energy storage [1]. Generally, all unsaturated compounds could serve as hydrogen carriers. The hydrogenation of the LOHC is thermodynamically favorable [2-5]. An ideal LOHC is expected to possess the hydrogenation enthalpy at the level not higher than 40 kJ·mol-1/H_2 [6]. This paper presents studies of thermochemical properties (enthalpies of formation and enthalpies of vaporization) for pyrazole derivatives that can be potentially used for hydrogen storage. A comparative thermodynamic analysis of the hydrogenation/dehydrogenation reactions was performed.

2. Methods

Combustion calorimetry: Standard molar energies of combustion of 2-methyl pyrazole was measured with a self-made high-precision isoperibolic calorimeter with a static bomb and a stirred water bath. The samples were placed (under an inert atmosphere in a glove-box) in polythene capsules and burned in oxygen at 3.04 MPa pressure.

Transpiration method: vapor pressure measurements. Vapor pressures of furfuryl alcohol and tetrahydrofurfuryl alcohol were measured using the transpiration method. About 0.5 g of the sample was mixed with small glass beads and placed in the thermostatted U-shaped saturator. A nitrogen stream with well-defined flow rate was passed through the saturator at a constant temperature (± 0.1 K), and the transported material was collected in a cold trap. The amount of condensed sample was determined by GC analysis using the n-undecane as an external standard.

The absolute vapor pressure p_i at each temperature T_i was calculated from the amount of the product, collected within a definite period.

Computational details. Quantum-chemical calculations have been performed with the Gaussian 09 series of programs. Energies E_0 and enthalpies H_{298} of most stable conformers were calculated by using the composite G4-method.

3. Results and discussion

Experimental results are compiled in the tables below.

Thermochemical data at T = 298.15 K ($p°$ = 0.1 MPa) for pyrazole derivatives (in kJ·mol^{-1})

Compound	$\Delta_f H^o_m$(liq/cr)	$\Delta^g_{l,cr} H^o_m$	$\Delta_f H^o_m(g)_{exp}$	$\Delta_f H^o_m(g)_{G4}$
1-methyl-pyrazole (liq)	121.8±1.5	44.3±0.4	166.1±1.6	163.2±4.5
1-ethyl-pyrazole (liq)	79.3±2.2	49.2±0.8	128.5±2.3	132.4±4.5
3-methyl-*1H*-pyrazole (liq)	74.2±1.7	65.8±1.0	140.0±2.0	139.7±4.5
3,5-dimethyl-*1H*-pyrazole (cr)	18.9±1.7	83.3±0.4	102.2±1.8	102.0±4.5
1,3,5-trimethyl-pyrazole (cr)	19.9±2.0	73.1±1.3	93.0±2.4	86.5±4.5
1-benzyl-pyrazole (liq)	202.8±2.1	72.0±0.8	274.8±2.3	270.2±4.5

Results from G4 calculations of thermodynamics of hydrogenation of pyrazole derivatives, at T = 298.15 K ($p°$ = 0.1 MPa) in kJ·mol^{-1}.

Compounds [a]		$\Delta_f H^o_m$(g)	$\Delta_f H^o_m$(g)[c]	$\Delta_r H^o_m$(g)	$\Delta_r S^o_m$(g)	$\Delta_r G^o_m$(g)	Kp(g)
1-methyl-pyrazole		163.2	110.2	-47.9/24.0	-254	27.8	1□10^{-5}
1-phenyl-pyrazole	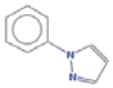	289.6	40.8	-239.3/47.8	-608	-57.8	1□10^{10}

4. Conclusions

It has turned out that according to the calculated $\Delta_r G^o_m$(g, 298.15 K), that the hydrogenation of 1-methyl-pyrazole is thermodynamically not favourable, but in contrast the hydrogenation of 1-phenyl-pyrazole is very promising for the hydrogen storage with the large gas-phase equilibrium constant K_p(g) = 1□10^{10}.

Authors gratefully acknowledge financial support from the Government of Russian Federation (decree №220 of 9 April 2010), agreement №14.Z50.31.0038.

References

[1] D.J. Durbin, C. Malardier-Jugroot, Int. J. of Hydrogen Energy 38 (2013) 14595-14617.
[2] S.P. Verevkin, V.N. Emel'yanenko, A. Heintz, K. Stark, W. Arlt, Ind. Eng. Chem. Res. 51 (2012) 12150–12153.
[3] K. Stark, V.N. Emel'yanenko, A.A. Zhabina, M.A. Varfolomeev, S.P. Verevkin, K. Müller, W. Arlt, Ind. Eng. Chem. Res. 54 (2015) 7953–7966.
[4] V.N. Emel'yanenko, M.A. Varfolomeev, S.P. Verevkin, K. Stark, K. Müller, M. Müller, A. Bösmann, P. Wasserscheid, W. Arlt, J. Phys. Chem. C. 119 (2015) 26381–26389.
[5] K. Müller, K. Stark, V.N. Emel´yanenko, M.A. Varfolomeev, D.H. Zaitsau, E. Shoifet, C. Schick, S.P. Verevkin, W. Arlt, Ind. Eng. Chem. Res. 54 (2015) 7967–7976.
[6] E. Clot, O. Eisenstein, R.H. Crabtree, Chem. Commun. 22 (2007) 2231–2233.

ECCE12
The 12th EUROPEAN CONGRESS OF CHEMICAL ENGINEERING
Florence 15-19 September 2019

Integration of hydrothermal liquefaction in wastewater treatment plants: Biogas vs Bio-crude

Rafael Castro-Amoedo[1*], Theodoros Damartzis[1], François Maréchal[1]

[1]*Industrial Process and Energy Systems Engineering (IPESE), École Polytechnique Fédérale de Lausanne, Rue de l'Industrie, 17, 1950, Sion, Switzerland*

**Corresponding author: rafael.amoedo@epfl.ch*

Highlights

- Bio-crude is a viable option for sludge treatment, competing with current biogas.
- WWTP is particularly suitable for HTL treatment.
- Primary sludge filtration increases HTL economic feasibility.

1. Introduction

The concept of wastewater has seen in recent years a major change; rather than a mere waste that is expensive and tedious to treat, new approaches are regarding it a valuable source of energy and resources. Furthermore, given the current energy paradigm they cannot be ignored.

Typical wastewater treatment plants (WWTP) comprise a pre- and primary treatment, followed by an aerobic and secondary treatments. Besides the treated effluent, a mixed sludge (which is in reality the combination of several stages' sludges) comes as a by-product. Typically, the sludge is anaerobically digested (producing biogas), followed by dewatering and final disposal, like landfill, incineration or eventually used as a fertilizer.

A major drawback to this conversion path is the carbon potential wasted, with 70 to 75% of the original carbon content being converted, and released as CO_2. Only the remaining 25 to 30% is converted to methane. This requires the use of more efficient processes that are able to capture the intrinsic quality of wastewater. In a recent publication [1], the use of biomass as a filtration media for sludge treatment has shown the potential to increase the solid content of sludge, which in turn increases hydrothermal liquefaction performance and subsequent bio-crude yield. At the same time, it reduces the amount of biological oxygen demand (BOD) to be treated in the aeration step, dramatically reducing the electricity need of this step which is responsible for a substantial share of the total electricity consumption.

The focus of this work is, given a wastewater composition and flow, finding the optimal set of solutions that for a certain investment, minimize operating costs and implicitly, the environmental impact. For the sake of simplicity, the choice is given between biogas or bio-crude production.

The sludge used in hydrothermal liquefaction (HTL) was considered to have between 20 and 25% total solids, mainly due to the filtration step. Bio-crude is sold after HTL step and no upgrade was considered inside the WWTP facility.

2. Methods

Based on [2], a MILP formulation was applied for optimal utility selection. The main objective is to minimize the operational costs, while constraining investment values (ε-constraints), subject to a set of constraints for the mass and energy balances (heat cascade included). Furthermore, binary variables are considered for the units' use and continuous variables are associated with their size.

3. Results and discussion

The optimization procedure is able to choose, considering the mathematical formulation, the combination of units that minimize the operating cost. Figure 1 shows the flowsheet implemented.

A reference scenario considering the conventional wastewater destination for biogas production was considered. The extended model including the HTL unit allows operational savings between 10 and 30% variations are due to different scenarios assumptions, in particular the bio-crude market value and sludge water content.

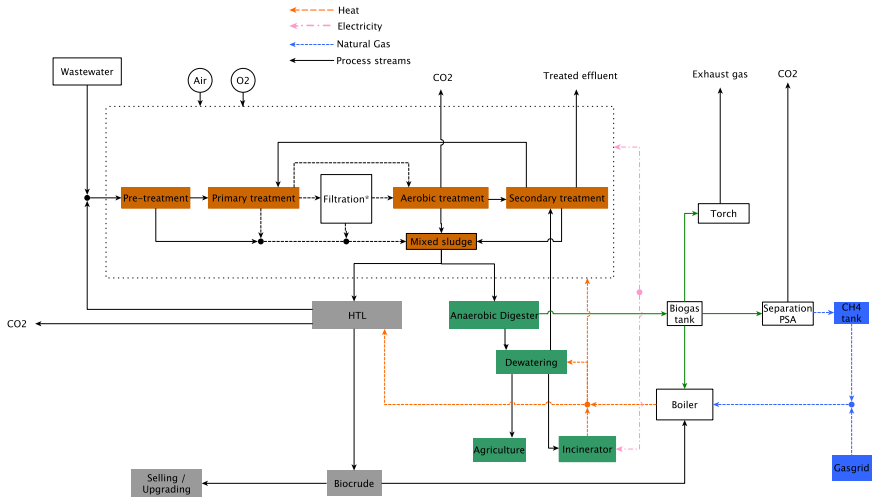

Figure 1. WWTP with HTL unit including mass and energy connections.

4. Conclusions

Hydrothermal liquefaction inserted in a wastewater facility in combination with a biomass-aided filtration is a promising solution for the increasing amounts of sewage sludge. Bio-crude can be directly sold to an upgrading facility or used as fuel for internal consumption, reducing the overall costs in a WWTP. The integration in a WWTP is especially suitable, as HTL water phase can be used as wastewater input. Furthermore, HTL is flexible enough to handle different inlet sludge compositions, even tolerating the presence of components (like plastics) that are inadmissible when anaerobic digestion is considered.

As identified in the flowsheet, a huge potential for CO_2 capture and utilization is available, in particular by making use of renewable power, especially in periods of excessive production.

References

[1] Biller, P., Johannsen, I., dos Passos, J. S. & Ottosen, L. D. M. Primary sewage sludge filtration using biomass filter aids and subsequent hydrothermal co-liquefaction. *Water Research* **130**, 58–68 (2018).

[2] Marechal, F. & Kalitventzeff, B. Targeting the integration of multi-period utility systems for site scale process integration. *Applied Thermal Engineering* **23**, 1763–1784 (2003).

ECCE12
The 12th EUROPEAN CONGRESS OF CHEMICAL ENGINEERING
Florence 15-19 September 2019

Single Cell and System Modeling of Tubular Proton Conducting Solid Oxide Steam Electrolyzers for Intermittent Operation

Stefan Fogel*, Holger Kryk, Uwe Hampel

Helmholtz-Zentrum Dresden-Rossendorf e.V., Bautzner Landstraße 400, 01328 Dresden, Germany

**Corresponding author: s.fogel@hzdr.de*

Highlights

- Transient FEM simulations of a single tubular SOEC using a 2D model.
- Examination of the cell behavior for different load variation speeds & flow configurations
- Development of a quasi-2D system model of a tubular stack & system behavior simulations
- Use of different load switching speeds is proven to be insufficient for cell control

1. Introduction

Due to the constantly growing utilization of wind and solar energy, the demand for technologies for temporal and spatial decoupling of energy provision and consumption is steadily increasing [1]. The application of proton-conducting solid oxide electrolysis cells (H-SOEC) has been a main concern in recent research activities since they offer an environmentally friendly and efficient technique for the conversion of excess energy into hydrogen [2]. As renewables occur intermittently, SOEC designs and all employed materials have to be capable of withstanding large electrical transients and therefore harsh operating conditions [3]. Tubular cell designs of SOEC received increased attention in recent years due to their inherent advantages. They offer rapid startup capabilities as well as high resistance to heat, thermal cycling, thermal stresses and high-pressure application capabilities [4, 5]. Since the knowledge of the dynamic behavior of SOECs is key to their future application, this work aims to study the transient behavior of a single, proton conducting SOEC during rapid load variations and of multi-tubular stacks on a system scale under high-pressure operation. The use of different load variation speeds is discussed with respect to cell control.

2. Methods

A 2D, dynamic and axisymmetric model of a tubular, proton conducting SOEC has been developed using the commercial software package COMSOL Multiphysics® 5.3a. The cell performance characteristics during rapid, short-period load variations are simulated. The model can be divided into four sub-models: the electrochemical sub-model, the heat transport sub-model, the hydrodynamics as well as the mass transfer sub-model. The simulations are used to identify limiting operating conditions as well as beneficial process parameter combinations for an improved cell operation. Furthermore, a dynamic, system scale and quasi-2D model of a tubular H-SOEC stack has been developed within the framework of MATLAB® Simulink® including first peripheral system components.

3. Results and discussion

The cell current in each simulated case is increased from 0 A to 30 A starting at the time of 10 s. Five different load gradients are studied, for which the full-load operation of the SOEC is reached within 0.1 s, 0.3 s, 2 s, 20 s and 200 s. Figure 1 (left) shows the cell potential as a function of time for the transient analysis. Due to the abrupt current changes, the cell potential shows different electrical transients with an increase from the initial open cell voltage of 0.95 V.

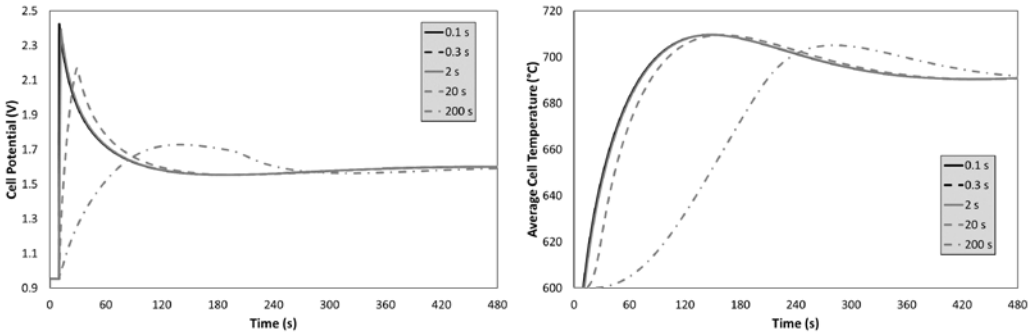

Figure 1. Cell potential (left) and temperature (right) as a function of time after different changes of the cell current from 0 A to 30 A (current changes of 0.1 s and 0.3 s show identical progressions).

For 0.1 s and 0.3 s, the time evolutions of the cell potential are nearly identical and are characterized by a large overshoot within the first seconds after the current change. The cell voltage increases to 2.42 V and decreases towards the stationary cell voltage of 1.60 V. However, the current changes within 2 s and 20 s show different potential progressions. The overshoot decreases with increasing switching time with maximum voltage values of 2.39 V and 2.17 V for the current change of 2 s and 20 s, respectively. In contrast, the cell potential progression for 200 s exhibits a noticeably reduced overshoot up to a cell voltage of 1.73 V. After applying the current changes, the average cell temperature increases from its initial value of 600 °C due to Joule heating and electrochemical heat sinks or sources as shown in Figure 1 (right). The thermal dynamics of the cell for the simulated current changes generally reveal a similar behavior with noticeable differences with respect to the apparent maximum temperature and the time needed to reach the steady state temperature. With longer current change duration, the cell needs more time to reach the steady state temperature.

4. Conclusions

The simulations show that different load switching speeds cannot be used as a sufficient operational strategy to prevent or generate specific temporal temperature progressions. Besides a distinct overshoot of the cell potential, there are no major differences in the electrical behavior of the cell, especially for fast load steps. No limiting operational states were identified.

This work is supported by the Sächsische Aufbaubank (SAB) and the European Union (EFRE) within the research project DELTA (Grant No. 100258734).

References

[1] I. Ridjan, B. V. Mathiesen, D. Connolly, D. Duic, Energy 57 (2013) 76–84
[2] M. Ni, M. K. H. Leung, K. Sumathy, D. Y. C. Leung, Int. J. Hydrog. Energy 31 (2006) 1401–1412
[3] J. Udagawa, P. Aguiar, N. P. Brandon, J. Power Sources 180 (2008) 354–364
[4] S. Hashimoto, Y. Liu, M. Mori, Y. Funahashi, Y. Fujishiro, Int. J. Hydrog. Energy 34 (2009) 1159–1165
[5] W. Winkler, J. Krüger, J. Power Sources 71 (1998) 244–248

ECCE12
The 12th EUROPEAN CONGRESS OF CHEMICAL ENGINEERING
Florence 15-19 September 2019

Energy and Chemical Engineering

Evaluation of acid doped PBI membranes for the SO_2 depolarized electrolysis at high temperature

Manuel A. Rodrigo*, Sergio Díaz Abad, Mireya Carvela, María Millán and Justo Lobato
Chemical Engineering Department, University of Castilla-La Mancha, Enrique Costa Novella Building, Av. Camilo José Cela nº 12, Ciudad Real, Spain.

**Corresponding author: manuel.rodrigo@uclm.es*

Highlights

- Electrochemical comparison of a commercial and a composite TiO_2 PBI based membrane.
- Novel gas phase SO_2 depolarized electrolysis.
- Study of the effect different operation conditions on the electrolysis process.
- SO_2 depolarized electrolysis at temperatures higher than 100°C

Renewable energies are the alternative for a sustainable energy production future. Due to the weather dependence of these energies there is a need for its storage. For example, solar energy has a production peak during the day, however the production is zero at night. This production excess can be used to produce hydrogen, which can be transported and stored for later use.
Hydrogen has a strong potential to become one of the leadings energy carriers in all energy sectors such as fuel for electric vehicles, in combined heat and power plants or fuel cell applications. However, one of the main technical hurdles to overcome to make hydrogen economy [1] a real alternative is relative to hydrogen production. It is mainly produced from fossil fuels by steam reforming of natural gas or high energy consumption processes, which are not environmentally friendly [2]. Thus, new routes for hydrogen production are to be developed for a sustainable energy generation in the "hydrogen economy". By using renewable energy sources, a "Green Hydrogen" can be produced, being water the ideal raw material. Hydrogen could be produced from water by a single thermal dissociation step, however, due to the considerably high energy consumption this process is not the best candidate [3]. Nevertheless, other routes combine a chemical step and a thermal step which are the most promising technologies for hydrogen production [4].
One of the leading thermochemical cycles to produce hydrogen with a high sustainability is the hybrid Sulphur cycle, also known as Westinghouse cycle. It is a hybrid electrochemical-thermochemical cycle. It was originally proposed in 1975 [5] and developed by Westinghouse electric corporation. The process is labelled "hybrid" because of the substitution of one thermochemical reaction by the electrochemical oxidation of SO_2 with water to yield sulphuric acid and hydrogen [3]. The SO_2 is electrochemically oxidized at the anode to form sulphuric acid, protons and electrons (E^0 = 0.158 V vs SHE). The protons are conducted across a proton exchange membrane (PEM) that acts as a separator to the cathode where they recombine with the electrons to form hydrogen according to equations 1 and 2 [3].

$$SO_2(aq) + 2\ H_2O \rightarrow H_2SO_4(aq) + 2H^+ + 2\ e^- \quad (1)$$
$$2H^+ + 2\ e^- \rightarrow H_2(g) \quad (2)$$

The typical PEM used in the electrolysis cell is a Nafion membrane. However, Nafion based membranes show several limitations, including the inability to operate at elevated temperatures and the decreased performance observed when exposed to high acid concentrations [6].

This work is focused on the study of the SO_2 depolarized electrolysis at high temperature (100-200°C) using acid doped PBI membranes as PEM. Two different membranes will be studied for the electrolysis, a commercial PBI membrane and a composite membrane modified with TiO_2, this method is explained elsewhere [7], as inorganic filler with the aim to enhance the electrolyte conductivity, hence reducing the membrane resistance, by improving the acid uptake and retention. The tests are performed in a 25 cm^2 SO_2 depolarized electrolysis cell. A novel operation process consisting on working with SO_2 in the gas phase and generating steam which will be mixed with the SO_2 flow, with a determined molar ratio, before entering the electrolyzer will be tested. A platinum loading of 0.9 mg Pt/cm^2 was employed on both electrodes (anode and cathode) using 40% Pt/Vulcan carbon XC72 as catalyst by spraying a catalytic ink on the electrode surface. Different operation conditions are evaluated such as temperature, SO_2 flow and the SO_2/H_2O molar ratio. The acid uptake and the acid retention will be measured as well as the ion conductivity of the studied membranes. Polarization curves and impedance spectroscopy analysis are carried out to evaluate the performance of the cell and the ohmic and charge transfer resistances. A preliminary stability test will be performed to assess the stability of the different components of the cell (membrane and electrodes).

References

[1] Winter, C.J.; Nitsch, J. Hydrogen as an Energy Carrier: Technologies, Systems, Economy; Springer Berlin Heidelberg, 2012.
[2] R. M. Navarro, M. A. Peña and J. L. G. Fierro, Chem. Rev. 107 (2007) 3952–3991.
[3] Sattler, C.; Roeb, M.; Agrafiotis, C.; Thomey, Sol. Energy 156 (2017) 30–47.
[4] Gorensek, M.B.; Edwards, T.B., Ind. Eng. Chem. Res. 48 (2009) 7232–7245.
[5] Brecher, L.E.; Wu, C.K. (Westinghouse Electric Corporation, Pittsburg, PA, United States). Pers. Commun. 1975.
[6] Staser, J.A.; Gorensek, M.B.; Weidner, J.W., J. Electrochem. Soc. 157 (2010) 952–958.
[7] J. Lobato, P. Cañizares, M.A. Rodrigo, D. Úbeda, F.J. Pinar, Journal of Membrane Science 369 (2011) 105-111

Acknowledgements

Financial support from the Junta de Comunidades de Castilla-La Mancha and the FEDER –EU Program, Project ASEPHAM. Grant number “SBPLY/17/180501/000330” is gratefully acknowledged.

ECCE12
The 12th EUROPEAN CONGRESS OF CHEMICAL ENGINEERING
Florence 15-19 September 2019

3D-printed magnetically induced fluidized-bed reactor for electrochemical applications

André Tschöpe[1], Matthias Franzreb[1]

1 Karlsruhe Institute of Technology, Institute of Functional Interfaces, Karlsruhe, Germany

andre.tschoepe@kit.edu

Highlights

- Fully 3D-printed novel reaction system
- Solution of the contacting problem of a fluidized-bed electrode
- Improvement of electrochemical conversion by up to 100 percent with this system

1. Introduction

Electrochemical reactions are an interesting and versatile tool in modern bioengineering. On the one hand, they can be used for e.g. waste water treatment of pharmaceutical plants. On the other hand, electrochemical synthesis offers a way to transfer small organic building blocks originating from fermentations into higher value compounds.

Electrochemical processes proceed at the boundary between the electrode and the surrounding solution. In order to achieve high conversion rates, the ratio of electrode surface area to solution volume must therefore be maximized. Due to their high specific surface area, fluidized-bed electrodes are particularly suitable for this purpose. However, in practice they are rarely used because the controlled fluidization as well as the electrical contacting of these fluidized-beds are major challenges and so far only partially solved. One approach for better contacting of the conductive particle electrodes is the magnetically induced fluidized-bed reactor. Here, the fluidized bed is intended to be under the influence of a magnetic field and at the same time serve as an electrode for the electrochemical reaction.

2. Methods

To meet these challenges a scalable magnetically induced fluidized-bed reactor was designed and afterwards fabricated by 3D-printing. The fluidized-bed reactor consists of four elements and can be closed by means of two clamps. The reactor offers standard connectors, which allow e.g. the connection of analytical equipment like flow-through spectrometer, redox-electrode or pH-electrode. For the characterisation of the novel reactor design, suitable fluidized-bed particles and a model reaction for the electrochemical conversion were chosen. A composite material consisting of activated carbon and magnetite was used as fluidized-bed electrode with a particle size distribution between 100 µm and 300 µm. Before the electrochemical experiments, the percentage of the fluidized-bed expansion was measured at different flow rates. As model reaction, the reduction of potassium ferricyanide $[K^+]_3[Fe(CN)_6^{3-}]$ to potassium ferrocyanido $[K^+]_4[Fe(CN)_6^{4-}]$ was chosen. The electrochemical conversion in the fluidized-bed reactor was compared between the magnetically influenced system and the system without any magnetic influence.

3. Results and discussion

To improve the contact between the magnetic electrode particles, an external magnetic field was generated outside the reactor. **Figure 1 left** shows the expansion behavior of the fluidized bed electrode in relation to the different flow rates. Here the expansion of the fluidized bed electrode with and without magnetic field influence rises with increasing flow rate. Under the influence of a magnetic field, however, a reduced expansion behavior can be demonstrated, so that the assumption can be made that an improved electrode particle contact exists and an improved electrochemical conversion can be achieved. **Figure 1 right** shows the influence of the magnetic field on the electrochemical conversion. First, the achievable current can be increased by the addition of magnetic electrode particles only, meaning without the additional application of a magnetic field, simply because of the increased electrode area. However, if a magnetic field is applied an additional strong increase of the achievable current and therefore of the intensity of the corresponding electrochemical reaction can be observed. At an applied potential of -0.8V this increase achieves 100 percent from -2.2 A to -4.5 A.

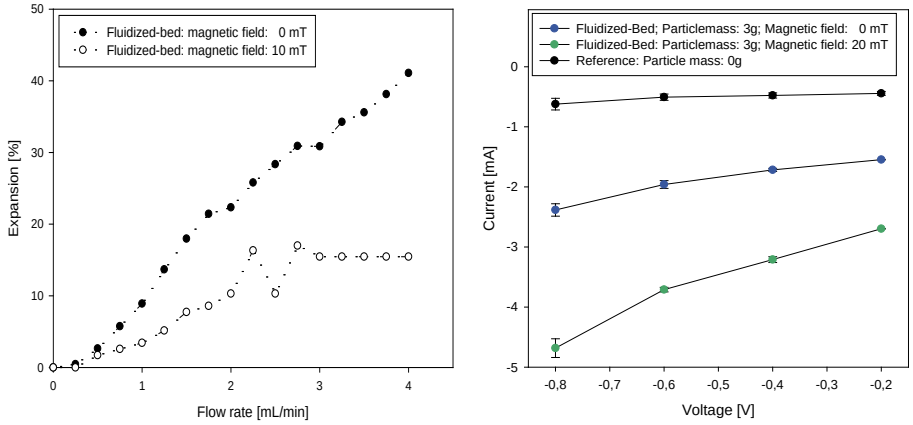

Figure 1. left: Expansion in percent of the fluidized bed plotted against the flow rate in mL/min: Comparison with and without magnetic field at 10 mT; **right**: Current of the electrochemical model reaction: reduction of a 3 mM potassium ferricyanide solution in a magnetically induced fluidized-bed reactor

4. Conclusions

With the developed magnetically influenced electrochemical reaction system, the efficiency of fluidized particle electrodes can be strongly improved. This offers new potential applications of electrochemical reactions within solutions with suspended solids, which would quickly plug conventional particle or wire mesh electrodes.

References

[1] Franzreb M, Hausmann R, Hoffmann C, Höll W (2001) Liquid-phase mass transfer of magnetic ionexchangers in magnetically influenced fluidized beds I. DC fields. Reactive & Functional Polymers

[2] Hausmann R, Reichert C, Franzreb M, Höll W (2004) Liquid-Phase Mass Transfer of Magnetic Ion Exchangers in Magnetically Influenced Fluidized Beds. II. AC Fields. Reactive & Functional Polymers

ECCE12
The 12th EUROPEAN CONGRESS OF CHEMICAL ENGINEERING
Florence 15-19 September 2019

Economic analysis of oxy-combustion technology with carbon capture

Thang Toan Vu[1], Young-Il Lim[1*], Daesung Song[2], Tai-Young Mun[3], Young-Cheol Park[3], Jai-Goo Lee[3]

[1]*Department of Chemical Engineering, Hankyong National University, Gyeonggi-do, Anseong-si, Jungang-ro 327, 17579 Korea*

[2]*Department of Safety Engineering, Hankyong National University, Gyeonggi-do, Anseong-si, Jungang-ro 327, 17579 Korea*

[3]*Korea Institute of Energy Research, Daejeon, Yuseong-gu, Gajeong-ro 152, 34129 Korea*

**Corresponding author: limyi@hknu.ac.kr*

Highlights

- Process simulation for 500 MW_e air and oxy-coal power plants with CO_2 capture
- Amine absorber unit (AAU) and CO_2 processing unit (CPU) for CO_2 capture
- Oxy-combustion with CPU was more efficient than air-combustion with AAU

1. Introduction

Carbon dioxide (CO_2) has been considered as a major greenhouse gas (GHG), and the fossil fuel combustion produced about 41% of global GHG in 2010 [1]. The CO_2 capture and storage (CCS) is important for the coal-fired power plant to meet future targets on reduction of GHG emissions [2]. The amine absorber unit (AAU) is typically used in the air-coal combustion power plant for CCS [3.4]. The CO_2 processing unit (CPU) with a cold box is applied to the oxy-coal power plant due to high CO_2 content in flue gas [2]. However, few researchers have addressed the energy and economic analyses under the same operating parameters of the two plants with CCS. There remains a need for a comparison between the two plants to identify the economic feasibility. This study aims to develop the process flow diagram (PFD) of the two plants with and without CCS, and to evaluate economic values such as the total capital investment (TCI), total production cost (TPC), capital investment cost (CIC), carbon capture cost (CCC), and levelized-cost of electricity (LCOE).

2. Methods

The PFDs of the two power plants were simulated by a commercial code (ASPEN Plus) to calculate the mass and energy balances. The PFD of the air-coal power plant consisted of five main areas: A100 (coal pretreatment), A200 (circulating fluidized-bed combustion-CFBC), A300 (electricity generation), A400 (flue gas desulfurization-FGD), and A500 (AAU). In the oxy-coal power plant, A400 was replaced by a flue gas conditioning (FGC), A600 (air separation unit-ASU) was added, and A500 was substituted with A700 (CO_2 processing unit-CPU).

The operating parameters applied equally to the two plants included: (1) The coal feed rate is fixed at 3080 t/d, (2) The CFBC is operated at 875°C and 1 atm, (3) The heat loss of CFBC is 5 % of LHV during coal combustion, (4) The equivalence mass ratio (O_2 to fuel) is 2.5, (5) Ultra super-critical (USC) steam (600°C and 300 bar) is generated, (6) 90% SO_2 is removed inside the combustor by CaO

(limestone), (7) The CFBC includes SCR with aqueous NH_3 for NOx removal, and electrostatic precipitator (ESP) for dust removal, (8) The produced CO_2 over 95 % purity and over 90% recovery in the gas phase aims to be sequestrated under the ground, (9) The produced CO_2 at 8 bar and 20 °C contains water under 250 ppm, and (10) The total amount of CO_2 captured are the same. Three cases were considered to compare the energy and economic analyses: Case 1 (air-coal power plant without carbon capture), Case 2 (air-coal power plant with AAU), and Case 3 (oxy-coal power plant with CPU). The energy and economic analyses included the net thermal efficiency, heat penalty, TCI, CIC, CCC, LCOE.

3. Results and discussion

The process performance of the three cases is shown in Table 1. Case 1 has the highest net electricity and net thermal efficiency because of no carbon capture. The heat penalty of Case 2 (air-coal power plant with AAU) is higher than that of Case 3 due to high amine regeneration heat in AAU. As mentioned earlier, the CO_2 captured is the same for Cases 2 and 3. The TCI of Cases 2 and 3 is higher by 66.42 and 91.3 M$, respectively, than that of Case 1. The LCOE increases by 39.4 and 25.6 $/MWh for Cases 2 and 3, respectively, because of CO_2 capture. The CIC and CCC of Case 2 are higher than those of Case 3 and higher the CO_2 price (26.3 $/t) was reported by Moioli *et al*. (2017) [5]. Therefore, Case 3 (oxy-coal power plant with CPU) shows the better energy and economic performances than Case 2.

Table 1. Process performance of air- and oxy-coal power plants.

Performance indicators	Case 1	Case 2	Case 3
Net electricity (MW_e)	502	403	420
Net thermal efficiency ($\%_{HHV}$)	45	36.1	37.6
Heat penalty (%, based on Case 1)	–	20.5	16.8
CO_2 captured (t/d)	–	7278.7	7282.4
TCI (M$)	361.2	427.6	452.5
LCOE ($/MWh)	78.5	117.9	104.1
CIC ($/kWh.y)	132.9	307.0	280.2
CCC ($/t)	-	28.08	25.50

4. Conclusion

The CO_2 capture is important for the coal-fired power plant to reduce the CO_2 emission. The energy and economic performance was evaluated for the 500 MW_e air-coal and oxy-coal power plants with CO_2 capture under the same operating parameters. It was found that the oxy-coal power plant with CPU was more efficient than the air-coal power plant with AAU in terms of LCOE, CIC and CCC. It would be better to design effectively heat networks.

Acknowledgements

This research was financially supported by KIER (Korea Institute of Energy Research).

References

[1] E. Agbor, A. O. Oyedun, X. Zhang, A. Kumar, Appl. Eng. 169 (2016) 433-449.
[2] H. Hagi, Y. L. Moullec, M. Nemer ,C. Bouallou, Energy 69 (2014) 272-284
[3] J. Davison, Energy. 32(7) (2007) 1163-1176.
[4] E. S. Rubin, C. Chen, A. B. Rao, Eng. Policy 35(9) (2007) 4444-4454.
[5] A. Pettinau, F. Ferrara, V. Tola, G. Cau, Appl. Eng. 193 (2017) 426-439.

ECCE12
The 12th EUROPEAN CONGRESS OF CHEMICAL ENGINEERING
Florence 15-19 September 2019

Bio-ethanol a building block of the future.

Elio Santacesaria*[1], Riccardo Tesser[2], Martino Di Serio[2]

1 Eurochem Engineering srl, Milano, Italy; 2 Dipartimento di Scienze Chimiche Università di Napoli, Italy

**Corresponding author: info@eurochemengineering.com,www.eurochemengineering.com*

1. Introduction

Bio-ethanol production is growing in different countries for the convenience of using it as biofuel. It is well known that an intensive use of a raw material, as a vector of energy, promotes the use of the same material for the production of chemicals as occurred in the past for coal and petroleum originating respectively carbochemistry and petrochemistry. Ethanol can easily be transformed in other useful molecules such as, for example: ethylene by dehydration, acetic acid by oxidation, ethyl acetate or acetaldehyde by dehydrogenation. Bio-ethanol could become, therefore, a building block allowing the production of acetic acid derivatives with simple processes occurring in mild conditions. The mentioned processes require the improvement or development of opportune catalysts able to increase the yields of the desired products.

2. Methods

The kinetic runs have been carried out in a packed bed tubular reactor, alternatively filled with 2 or 50 g of catalyst, approximately isothermal, by feeding pure ethanol together with a mixture of nitrogen and hydrogen as carrier gas. Kinetic runs have been made by changing the temperature, in the range of 200-260°C, the pressure between 10 and 30 bars and the space time from 1 to 100 ($g.h.mol^{-1}$). We have verified, at first, that inter-phase and intra-phase mass transfer limitations were negligible in the adopted conditions.

3. Results and discussion

Catalysts promoting ethanol dehydration to ethylene and ethanol oxidation to acetic acid will be reviewed together with the operative conditions and related performances. A particular attention will be devoted to the reaction of ethanol dehydrogenation to obtain ethyl acetate [1], in one step reaction in the presence of the commercial catalyst: $CuO/Cu/CuCr_2O_4/Al_2O_3/BaCrO_4$ pre-reduced catalyst (BASF Cu-1234-1/16-3F). The mentioned catalyst has been reduced with hydrogen before the use and tested in a fixed bed laboratory reactor by feeding ethanol in a stream of H_2 diluted in N_2 (H_2/N_2=6/94 mol/mol), by exploring a temperature range of 200-260°C and a pressure range of 10-30 bars. This catalyst has shown high activity, selectivity and thermal stability. The best results have been obtained by operating at 220-240°C, 20 bars and 98 (grams hour/mol) of ethanol contact time, corresponding to 65% of conversion and 98-99 % of selectivity to ethyl acetate. The conversion is the maximum obtainable at the equilibrium and the selectivity is the highest value obtained until now for this reaction. Therefore, this catalyst is a good candidate for developing a new process to produce ethyl acetate. It is important to point out that the same catalyst allows to obtain also acetaldehyde in a good yield just reducing the pressure in

the reactor [2]. At last, it is worth of mention that this process has the advantage to produce pure hydrogen (exempt of CO) as by-product useful to be employed in the fuel cells [2]. A detailed kinetic [3] approach for this catalytic process has been made giving interesting suggestions about the reaction scheme and mechanism:

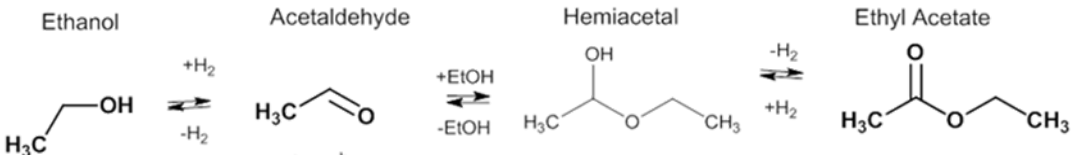

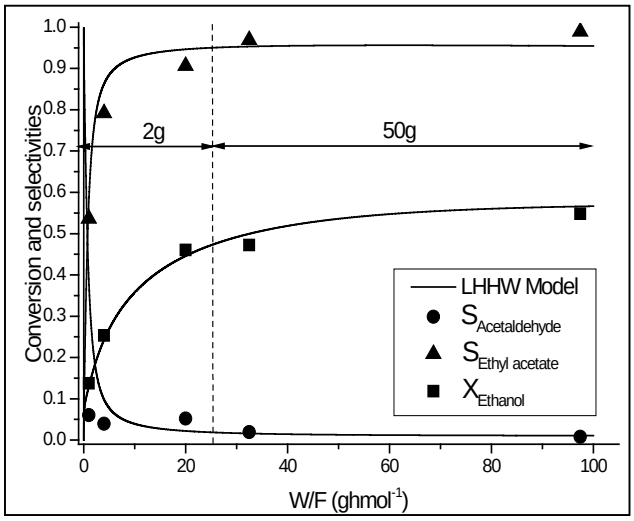

A Langmuir-Hinshelwood-Hougen-Watson kinetic model has been used for interpreting all the experimental data collected. This model corresponds to a mechanism in which the first step is the dissociative adsorption of ethanol on the surface, giving an adsorbed ethoxy group. Then, two other consecutive steps give place to respectively acetaldehyde as intermediate and ethyl acetate. This kinetic model allows a satisfactory fitting of all the performed experimental runs with a standard error below 15% for the runs performed with 2g of catalyst and less than 12% for the runs made with 50 g of catalyst.

4. Conclusions

Ethanol can give place to different interesting reactions and become a building block for producing some different commodities provided that its cost as fuel decreases at a competitive level. Clearly catalysis plays a fundamental role in promoting new innovative processes like the ones described in this presentation

References

[1] E. Santacesaria , G. Carotenuto, R. Tesser, M. Di Serio; Ethanol Dehydrogenation to Ethyl Acetate by Using Copper and Copper Chromite Catalysts; Chemical Engineering Journal ; 179 (2012) 209-220.
[2] G. Carotenuto, R. Tesser, M. Di Serio, E. Santacesaria; Bioethanol as feedstock for chemicals such as acetaldehyde, ethyl acetate and pure hydrogen; Biomass Conversion and Biorefinery (2013) 3, 55-67
[3] G. Carotenuto, R. Tesser, M. Di Serio, E. Santacesaria; Kinetic study of ethanol dehydrogenation to ethyl acetate promoted by copper/copper-chromite based catalysts; Catalysis Today 203(2013)202-210.

ECCE12
The 12th EUROPEAN CONGRESS OF CHEMICAL ENGINEERING
Florence 15-19 September 2019

Experimental study of a novel finned and tube phase change material storage for low-temperature applications

Giorgio Besagni[1], Lorenzo Croci[1]

1 Ricerca sul Sistema Energetico - RSE S.p.A., Power System Development Department, via Rubattino 54, 20134 Milano (Italy)

**Corresponding author: giorgio.besagni@rse-web.it*

Highlights

- A pilot-scale phase change material storage is build and tested.
- The effect of operating parameters have been evaluated.
- The energy stored is 80% higher compared with a water storage.

1. Introduction

Thermal energy storage (*TES*) is a matter of intense research and discussion, to decouple the "*demand-side*" and the "*supply-side*". This field of study is of paramount importance interesting in the residential sector, to support the large-scale deployment of renewable energy-based technologies to support the decarbonistaion pathways. A promising solution to reduce the primary energy consumption at the household scale regards solar-assisted systems (i.e., solar assisted heat pumps, *SAHPs*). In this perspective, this paper contributes to the existing discussion by developing a "*pilot-scale*" finned and tube phase change material storage for low-temperature applications (viz., storage temperatures in the range of 20 - 30 °C, accordingly with the experimental outcomes of Besagni et al. [1])

2. Methods

A novel "*pilot-scale*" phase change materials storage is proposed, designed and tested. To this end, a laboratory test facility has been designed and build; it aims testing the influence of a variation in the boundary conditions (flow rate, temperature, heating load) on the global and local performances and charging/discharging times (Figure 1, see Table 1 for the details of the instrumentation). Following the discussion of Palomba et al. [2], a fin-and-tube heat exchanger is selected (see Table 1). The phase change material used is paraffin *RT26* [3].

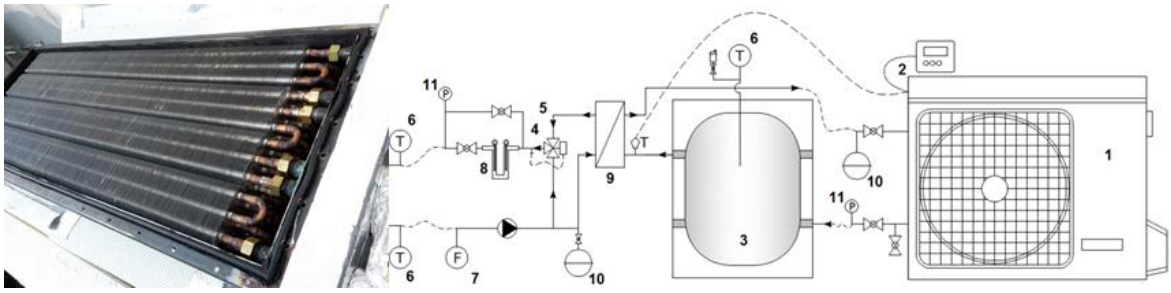

Figure 1. Test facility (details of the experimental system is Table 1).

Table 1. Details of the experimental system.

Code name (Figure 1)	Equipment and details
1	Reversibile heat pump (MAXA, i-HWAK//V4 06, R410A)
2	Remote control system for the reversible heat pump
3	Buffer storage tanks for heat pumps; 51l, water storage
4	Deviation valve
5	Variable speed circulation pump
6	Temperature probe - RTD Pt100 (1/5DIN)
7	Electromagnetic flow meter
8	Two electrical resistances (1500 W each)
9	Plate heat exchanger
10	8dm^3 expansion tank
11	Pressure Transducer

3. Results and discussion

The heat exchanger was tested in two different configurations (viz. series and parallel), to investigate the influence of the non-uniformity of heat exchange on the global (energy storage) and local (local temperature inside the storage). For example, Figure 2a shows the energy storage inside the storage unit for given inlet (T_{in}) and outlet (T_{out}) temperatures. Conversely, (the locations of T_1, T_2 and T_3 are displayed in Figure 2b. It was found that the exchanger in the parallel configuration was able to achieve better performances, stored approximately 80% higher compared with a water storage (temperatures in the range of 15 ° C - 40 ° C). This increase is higher than that the one previously shown in the previous literature [2].

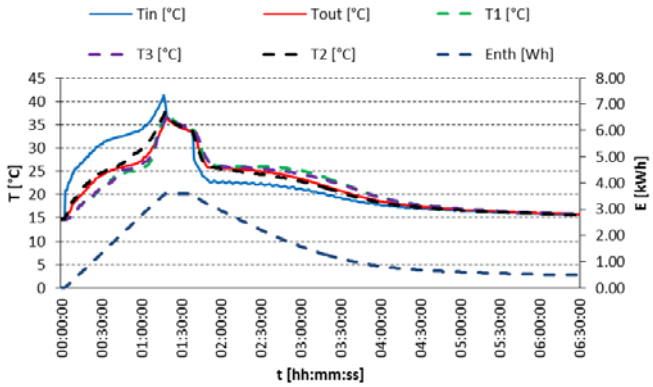

(a) heating load 2.8 kW, parallel configuration

(b) location of internal probes

Figure 2. Test Experimental results.

4. Conclusions

A "*pilot-scale*" finned and tube phase change material storage for low-temperature applications was built and tested, showing promising performances (i.e., energy stored is 80% higher compared with a water storage). In future studies, the obtained data can also be used to calibrate and validate a numerical model.

References

[1] G. Besagni, L. Croci, R. Nesa, L. Molinaroli, Renewable energy 132 (2019): 1185-1215.
[2] V. Palomba, V. Brancato, A. Frazzica, Applied energy 199 (2017): 347-358.
[3] Rubitherm GmbH, «RT 26,». Available: www.rubitherm.eu/en/index.php/productcategory/organische-pcm-rt.

ECCE12
The 12th EUROPEAN CONGRESS OF CHEMICAL ENGINEERING
Florence 15-19 September 2019

Energy and Chemical Engineering

Advanced fixed-bed Ca-Cu looping process for the CO_2 capture in steel mills

José Ramón Fernández[1]*, Vincenzo Spallina[2], Juan Carlos Abanades[1]

[1]Spanish Research Council, INCAR-CSIC, Francisco Pintado Fe, 26 (33011) Oviedo, Spain, tel.+34 985 11 90 90

[2] Department of Chemical Engineering and Analytical Science, University of Manchester, Sckville street, M13 9PL, Manchester, United Kingdom, tel. +44 161 30 69339

*Corresponding author: jramon@incar.csic.es

Highlights

- A novel process for H_2 production by the SEWGS of blast furnace gas is proposed
- A Cu/CuO chemical loop supplies the energy required for the regeneration of the sorbent
- A process design has determined the operating windows for each stage of the system
- Results show theoretical viability of the process and potential for further development

1. Introduction

Steelmaking is the main energy-consuming industry in the world, accounting for 27 % of the total CO_2 emissions from industrial processes [1]. CO_2 Capture and Storage (CCS) is the only alternative that can lead to a drastic reduction in CO_2 emissions far beyond that currently achievable in the steelmaking industry and achieve the climate change mitigation targets set as long term objectives after COP21 [2]. The implementation of pre-combustion capture systems on the blast furnace gas (BFG) appears to be an attractive option to achieve higher carbon capture rates in the steelmaking process [3], since BFG contains 60-80% of the total carbon entering the steel mill in the form of CO and CO_2. The Sorption Enhanced Water Gas Shift (SEWGS) can be particularly suitable to decarbonize the BFG and produce a H_2-enriched fuel gas that can be easily integrated throughout the steel mill [4]. In the SEWGS, a high-temperature sorbent (typically a hydrotalcite-like or a CaO-based material) removes the CO_2 from the gaseous phase as soon as it is produced [5]. The WGS equilibrium is then shifted towards a higher production of H_2 according to the Le Chatelier's principle. As a result, the almost total conversion of CO can be achieved. CaO-based materials exhibit very high theoretical energy recovery and also have higher CO_2 carrying capacities: up to 45% wt. in newly developed CaO materials compared to 8% for hydrotalcites. The main challenge for the scaling-up of the SEWGS is the need to find an efficient and low-priced method for the regeneration of the CO_2 sorbent. The Ca-Cu chemical looping process, patented by CSIC in 2009 [6], is based on the "unmixed reforming" concept [7], but with the key difference that the heat needed for $CaCO_3$ calcination is supplied in situ by the exothermic reduction of CuO to Cu with a gaseous fuel. Significant progress in reactor modelling, thermal integration and materials durability have been made over the last years in the Ca-Cu looping process [8]. This concept has also been experimentally validated in fixed beds at TRL4 [9]. In recent works [10], the Ca-Cu process has been proposed to decarbonize the off-gases of steel mills using an arrangement of interconnected fluidized-bed reactors operating at atmospheric pressure. In this work, an

advanced configuration based on several fixed-bed reactors operating in parallel is proposed to integrate the Ca-Cu looping process in a steel mill. This configuration facilitates the performance at high pressure, which allows higher energy efficiencies to be achieved and avoids the need for downstream solid-gas separation devices.

2. Process description

The proposed Ca-Cu looping process follows a sequence of at least three reaction steps. A H_2-rich gas is first obtained through a sorption enhanced water gas shift (SEWGS) process of BFG at 600-650ºC and 20 bar, while CO_2 reacts with CaO to form $CaCO_3$. In a second stage, Cu oxidation takes place at 20 bar with diluted air (about 3% of O_2) by recirculating part of the N_2 obtained as product to limit the temperature of the bed material below 880ºC, thereby minimizing the calcination of the CO_2 sorbent (i.e., the CO_2 slip during this stage). In the third stage, the necessary heat to calcine $CaCO_3$ is directly supplied by the exothermic reduction of CuO-based solid with a gaseous fuel (that can be coke oven gas or external natural gas), thereby producing a highly concentrated stream of CO_2 and H_2O(v). An appropriate $CuO/CaCO_3$ ensures that the heat generated during the CuO reduction is sufficient to decompose completely the calcium carbonate.

3. Results and discussion

Balances of a steel mill integrated with the Ca-Cu process are solved and compared with those obtained for a reference steelworks plant with post-combustion CO_2 capture through amine absorption. Using exclusively the coke oven gas (COG) available in the steel mill as reducing gas in the reduction/calcination stage around 30% of the BFG can be decarbonized in the SEWGS reactor. An overall CO_2 capture efficiency in the steel plant higher than 90% can be achieved if additional natural gas is used as fuel in the reduction/calcination reactor together with the COG. The proposed Ca-Cu looping process offers great CO_2 capture rates with moderate energy consumption. A specific primary energy consumption for CO_2 avoided (SPECCA) in the Ca-Cu looping process of 2.3 MJ/kg CO_2 has been calculated, which is much lower than the energy consumed in the reference plant with CO_2 capture using amine absorption (i.e. 4.3 MJ/kg CO_2).

References

[1] IEA, 2017. CO2 Emissions from Fuel Combustion. OECD/IEA, Paris.

[2] IPCC, 2018: Global warming of 1.5°C. V. Masson-Delmotte, P. Zhai, H. O. Pörtner, D. Roberts, J. Skea, P.R. Shukla, A. Pirani, W. Moufouma-Okia, C. Péan, et al. Switzerland, 2018.

[3] Santos S. Overview of the current state and development of CO2 capture technologies in the ironmaking process. Cheltenham, UK: IEA Publications; 2013.

[4] M. Gazzani, M.C. Romano, G. Manzolini, Int. J. Greenh. Gas Contr. 41 (2015) 249-267.

[5] E.R. van Selow, P.D. Cobden, P.A. Verbraeken, J.R. Hufton, R.W. van den Brink, Ind. Eng. Chem. Res. 48 (2009) 4184-4193.

[6] J.C Abanades, R. Murillo, Method of capturing CO_2 by means of CaO and the exothermic reduction of a solid, US8506915 B2. Priority date Sept 16, 2009.

[7] R.V. Kumar, R.K., Lyon, J.A. Cole, Unmixed reforming: a novel authotermal cycling steam reforming process. In Advances in Hydrogen Energy; Gregoire Pedro, C. E., Laurent, F. W., Eds; Kluwer Academic Publishers: Higham, MA, USA, p 31, 2000.

[8] J.R. Fernández, J.C Abanades, Curr. Opin. Chem. Eng. 17 (2017) 1-8.

[9] J.R. Fernández, J.C Abanades, Chem. Eng. Sci. 193 (2019) 120-132

[10] J.R. Fernández, I. Martinez, J.C Abanades, M.C. Romano, Int. J. Hydrog. Energ. 42 (2017) 11023-11037.

ECCE12
The 12th EUROPEAN CONGRESS OF CHEMICAL ENGINEERING
Florence 15-19 September 2019

Oil-Water Biphase Chaotic Mixing Enhanced by Elastic Combination Impeller in Mixer-Settler.

Zuohua Liu[1], Chuang Wang[1], Deyin Gu[1], Facheng Qiu[1], Changyuan Tao[1], Yundong Wang[2]

1 School of Chemistry and Chemical Engineering, Chongqing University,Chongqing400044,China; 2 State Key Laboratory of Chemical Engineering, Department of Chemical Engineering, Tsinghua University, Beijing 100084,China

**Corresponding author: Prof. LIU Zuohua, liuzuohua@cqu.edu.cn*

Highlights

- The spring of the elastic impeller is easy to stretch and bend, which can change the way of impeller disturbing the flow field structure.
- The elastic combined impeller strengthens the energy dissipation mode of the flow field through the deformation and energy storage of the spring, and improves the chaotic mixing degree of the liquid and liquid biphases.

1. Introduction

The problem of low energy consumption and high efficiency exists in the traditional liquid-liquid biphase extraction in the mixer-settler. By means of Lab View software, pressure pulsation signals in the mixed fluid in the disturbing and clarifying tank of the rigid impeller, rigid -flexible combined impeller and elastic combined impeller are respectively collected. And then get the largest Lyapunov exponent (LLE) and multiscale entropy (MSE) which are reflects the degree of chaos in the fluid. At the same time, the fluid field's visualization technology was adopted to observe fluid mixing performance, the influence of the length, diameter and outer diameter of the spring on the chaotic characteristics of the flow field is also investigated. The results indicated that compared with the rigid impeller and the rigid-flexible combined impeller, the elastic combined impeller strengthens the energy dissipation mode of the flow field through the deformation and energy storage of the spring, and improves the chaotic mixing degree of the liquid and liquid biphases. The LLE was over zero, testifying the fluid mixing system in chaotic state. In the elastic combination impeller system, not only are the values of LLE and MSE significantly higher, but also the time of complete decolorization is the shortest in the visualization experiment.

2. Methods

Experiments are conducted in the mixer settler and control room temperature 24 ℃ - 27 ℃, water and kerosene as experiment medium oil-water and two chaotic mixing experiment, the experimental process control the volume flow of water and kerosene ratio of 1:1. The pressure pulsation signal is collected on the mixed indoor wall of the mixing clarifying tank. After that, the pressure sensor, data acquisition card and data acquisition system composed of workstation are converted and processed on the Lab View working platform and then output. The output data are programmed and calculated by Matlab software. Where, each group of experiments was sampled

for 15 min with a sampling frequency of 65 Hz. The mixer-settler and impellers used in the experiment are shown in Fig. 1 and Fig. 2 respectively.

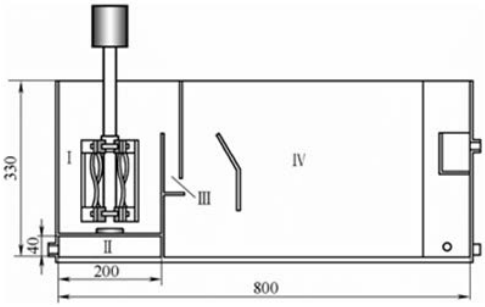

Figure 1. Structure of mixer-settler

Ⅰ-mixing chamber; Ⅱ-submersible mixing chamber;

Ⅲ-overflow area; Ⅳ-clarification chamber

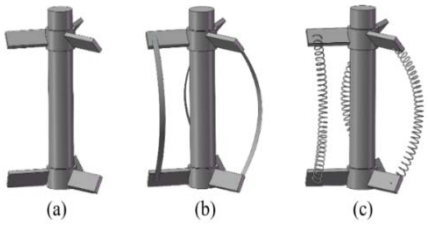

Figure2. Impellers used in experiment

(a)rigid combination impeller (b)rigid-flexible combination impeller (c)elastic combination impeller

3. Results and discussion

The LLE is an important parameter to measure the dynamic characteristics of the system. It reflects the average exponential rate of convergence or divergence between adjacent orbits in the phase space system [1]. Multi-scale entropy (MSE) is to calculate the sample entropy of time series at multiple scales, which reflects the irregularity of time series at different scales. It has good anti-noise and anti-interference ability, and the analysis of time series is more systematic. The experimental results are shown in figure 3 and 4.

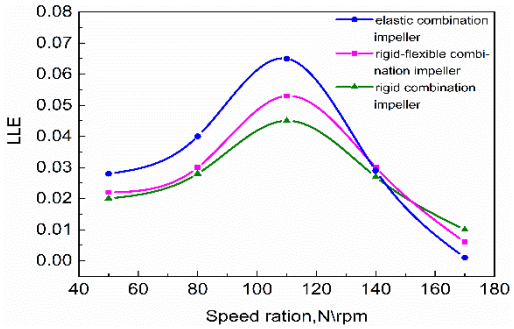

Figure 3. Effect of impeller type on LLE

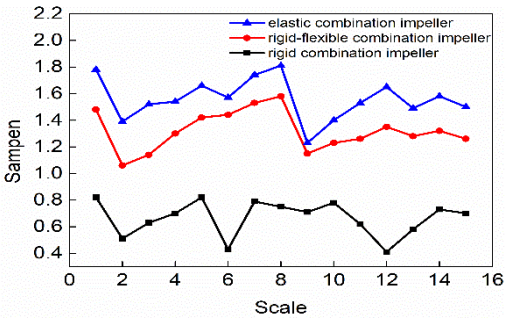

Figure4. Effect of impeller type on MSE

4. Conclusions

Due to the spring's characteristics of being easy to stretch and bend, the elastic combination impeller can effectively destroy the stability of the flow field structure near education and regulate the flow field, thus strengthening the chaotic mixing of the flow field. The mixing effect is obviously better than that of the rigid-flexible combination impeller and rigid combination impeller.

References

[1] LIU Z H, ZHENG X P, LIU D, et al. Enhancement of liquid-liquid mixing in a mixer-settler by a double rigid-flexible combination impeller [J].Chemical Engineering and Processing: Process Intensification, 2014, 86: 69-77. A. Bianchi, N.C. Jones, Chem. Eng. J. 157 (2019) 326–337.

ECCE12
The 12th EUROPEAN CONGRESS OF CHEMICAL ENGINEERING
Florence 15-19 September 2019

Effect of Surfactant on Velocity and Oxygen Mass Transfer of a Single Bubble Rising in a Liquid.

Gaëlle Lebrun[1,*],Feishi Xu[1],Gilles Hébrard[1] and Nicolas Dietrich[1]

LISBP, Université de Toulouse, CNRS, INRA, INSA, Toulouse, France
**Corresponding author: Gaelle.Lebrun@insa-toulouse.fr*

Highlights

- Effect of contaminant on hydrodynamic of a bubble rising in a liquid.
- Combined effects of polymer and surfactant on oxygen mass transfer.

1. Introduction

Dispersion of bubbles in liquid for oxygen transfer found applications in a wide range of fields such as medicine (oxygenation of blood) or environment (wastewater treatment). It is known that presence of surface-active agent in liquid lead to an inhibition of gas-liquid mass transfer [1]. Indeed, they can affect the oxygen mass transfer from a bubble via the modification of the hydrodynamic of the bubble such as its velocity, shape and diameter, but also by affecting directly the diffusion coefficient of oxygen [2]. Although researches about this subject increased, interfacial phenomenon that occurs during the mass transfer is not clearly understood. Surface contamination by surfactant of a bubble rising in a liquid is a time dependent parameter. Indeed, the kinetic of adsorption depends on the diffusion coefficient of the surfactant which is linked to the nature of both surfactant and bulk [3], improvement of the knowledge about contamination kinetic could be useful for a better understanding of interfacial phenomena.

The aim of this study is to highlight the effect of surfactants in different bulks on the bubble hydrodynamic and mass transfer. For that purpose, we studied hydrodynamic of bubbles in different liquids compositions and compared with pure water. In addition, to link this phenomenon with mass transfer, the same solutions has been used and mass transfer of oxygen has been determined by Planar Laser Induced Fluorescence Inhibition (PLIF-I) method [4]. This method has already been used in literature to identify an important decrease of mass transfer when polymer [5] and surfactant [1] are added to water; here the combined effect of each has been investigated.

2. Methods

The column where oxygen transfer occurred was filled with the different compositions: pure water, surfactant (SDS and Triton X-100), polymer (polyacrylamide and polyalkylene glycol) and surfactant mixed. Surfactants were characterized by their composition, density, static and dynamic surface tensions. The liquid has been deoxygenized with nitrogen before each experiment. A single bubble was generated with a syringe pump and injected through a stainless steel needle into the column. To excite fluorescence, horizontal laser sheet was generated by a laser (Nd:YAG laser: DANTEC Dynamics Dualpower 200-15, 15Hz, 2×200 mJ) . The image of fluorescence in the wake of the bubble were recorded by a Charged Coupled Device camera (CCD camera: DANTEC Dynamics

flowsense CM, 12 bits, 15 fps, 2048×2048 pixels) located at the bottom of the column and focused on the laser sheet. In order to avoid recording the light provided by the laser sheet, a 570 nm high pass filter was placed in front of the lens. The fluorophore used was ruthenium complex ($C_{36}H_{24}Cl_2N_6Ru;xH_2O$, Sigma-Aldrich) at a concentration of 70 mg/L. The hydrodynamics properties of bubbles in the column where obtained from the sequences of images recorded by a high speed camera (Photon SA3, 8 bits, 2000 fps, 1024×1024 pixels), and images recorded gave access to the velocity, the shape and the diameter of bubble along the column.

3. Results and discussion

For each solution prepared, the diameter, the shape, contamination have been determined, along with adimensional numbers (Reynolds, Schmidt, Scherwood). In these last solutions, results obtained from the PLIF-I method allow to quantify the flux of oxygen in the wake of the bubble and thus the diffusion coefficient. The results showed a drastic change in the hydrodynamic parameters of solutions, accompanied by a decrease of amount of oxygen transferred when surfactant are present in the solution. We calculated a division by 20 of the mass transfer coefficient when triton X-100 is added to water at a concentration lower than the CMC. This effect was even more marked when polymer and surfactant were both added to water.

4. Conclusions

Our experimental set up allowed us to visualize in the same times changes in hydrodynamics conditions of bubbles rising in liquids and oxygen mass transfer. The effect of both polymer and surfactant have been studied and showed a drastic decrease of the amount of oxygen transferred. This can be explained by changes in hydrodynamic conditions, but others effects can play a role in this diminution. Results highlighted the importance of improving our knowledge about the interface and organization of surfactant in this area for a better understanding of gas-liquid mass transfer phenomenon.

Acknowledgment

This work benefited from the support of the project MAMOTHS ANR-17-CE06-0001 of the French National Research Agency (ANR).

References

[1] M. Jimenez, Etude du transfert de matière gaz/liquide en milieux complexes: quantification du transfert de l'oxygène par techniques optiques, INSA, 2013.
[2] G. Hebrard, J. Zeng, K. Loubiere, Chem. Eng. J. 148 (2009) 132-138.
[3] B. Zhmud, F. Tiberg, Advances in Colloid and Interface Science 113 (2005) 21-42.
[4] J. François, N. Dietrich, P. Guiraud, A. Cockx, Chem. Eng. S. 66 (2011) 3328-3338.
[5] F. Xu, A. Cockx, G. Hebrard, N. Dietrich, Ind. Eng. Chem. Res. 57 (2018) 15181-15194.

ECCE12
The 12th EUROPEAN CONGRESS OF CHEMICAL ENGINEERING
Florence 15-19 September 2019

Geothermal Energy – An Imperishable Source Of Energy an All Aspects of Life

Anjani Mamidala [1], Akanksh Mamidala [2], Aashrith Thatipalli [3], Pentapati Naga Prapurna [4]

1. *Sem VI, Chemical Engineering, Chaitanya Bharathi Institute of Technology, Hyderabad, India – 500075;*
2. *Sem IV, Chemical Engineering, Chaitanya Bharathi Institute of Technology, Hyderabad, India – 500075;*
3. *Sem IV, Chemical Engineering, Chaitanya Bharathi Institute of Technology, Hyderabad, India – 500075;*
4. *Associate Professor, Department of Chemical Engineering, Chaitanya Bharathi Institute of Technology, Hyderabad, India – 500075*

** Corresponding author: naga.prapurna@gmail.com*

Highlights

- This paper presents information on how geothermal energy is trapped, transported and also about the recent methods applied for geothermal systems.
- Production of geothermal energy as an alternative source of fuel is possible.
- Selection of materials used for the transportation of geothermal energy.
- Geothermal energy in mining developments.

1. Introduction

Renewable energy is energy that is collected from renewable sources, which are naturally replenished on a human time scale, such as sunlight, wind, tides, waves and geothermal heat. Geothermal energy is thermal energy generated and stored in the earth. The geothermal energy of the earth's crust originates from the original formation of the planet and from radioactive decay of materials. The heat present inside the earth's crust can never be perishable and it is simply power. It is present from the shallow ground to deep down beneath the surface of the earth to the extremely hot molten rock called magma. The process of heat production from the earth's core is similar to that of petroleum production which involves drilling, and complete wells and produce fluids from wells present in the marked formations beneath the surface. The ultimate goal in the extraction of geothermal energy is the heat and not the fluid as in case of petroleum production. The energy required for the total world population is 2.2 terra watts and the energy produced from geothermal source is 44 terra watts which is more than sufficient for the world population. By trapping some parts of this source, we can reduce the usage of non-renewable sources which will deplete on further use. There is a lot of risk involved in the production of heat from the geothermal mines due to its high temperature and also requires high initial cost for the setting up of the plant. Trapping of hot steam from the earth's crust is the basic instinct during the usage of geothermal energy. For the process of trapping of steam, selection of materials is very essential. Materials that are heat resistant and which have high melting points can be used as the temperature of steam coming from the earth's crust is nearly 1300^0C for the transport of the energy. The first major hydrothermal developments were located in areas with high tectonic activity marked by volcanoes, geysers, hot springs and large hot water reservoirs. These resources are relatively shallow and often flow to the surface naturally.

2. Methods

Today, engineers and geophysicist are bringing techniques for enhanced geothermal systems (EGS) to high temperature dry reservoirs at a depth of 3-10 kms. At these depths, the rock is hot enough to convert water to superheated steam. The hot dry rock system recovers the earth's heat from hot but dry regions through the closed loop circulation of pressurized fluid. This fluid, injected form the surface under high pressure,

open spree existing joints in the basement rock, creating a man-made reservoir. The fluid injected into the reservoir absorbs thermal energy from the high temperature rock surface and then serves as the conveyor for transporting the heat to the surface for practical use.

There are 3 types of power plants for the extraction of geothermal power.

- Dry steam power plants are the most basic style of geothermal power plants. Steam piped from a hydro thermal reservoir directly enters turbine to generate electricity. As the steam cools and condenses, the water is gathered and injected back into the reservoir.
- Flash steam plants use hot water that is below the boiling point while at reservoir pressure but that flashes to steam at lower surface pressure.
- Binary power plants use a closed system to exploit even cooler reservoirs whose water temperatures are less than 150^0C. Water flows or is pumped to the surface and enters a heat exchanger where it brings a second fluid, to its boiling point, which must be below that of water. This fluid maybe circulated and this powers electricity generating turbines.

Geothermal energy can be extracted without burning of fossil fuel such as coal, gas or oil. Geothermal fields produce only about 1/6th of carbon dioxide that a relatively clean natural gas-fueled power plant produces. Though geothermal energy involves many risks, they can be transported through pipelines which are made up of heat resistant materials as the natural gas transportation is done in the recent times. Carbon nanotubes can be used for transportation of geothermal energy for its applications in many aspects. They are very economical and can withstand high temperatures up to 3400K. The multi walled carbon nanotubes do not burn at all, an intriguing property of carbon nanotube is their ability to harbor heat. Mining and geothermal production also share a dependence to the concepts of accessibility and extractability. Mineral deposits must have sufficient economic value to be mined at a profit. In geothermal production, it is the fluid's heat content, accessibility and extractability that determines whether a geothermal resource is economically valuable and warrants production.

3. Results and discussion

The geothermal energy trapped and transported using the above methods can be used in the production of electricity, as a fuel, as an alternative for fossil fuels. The low temperature geothermal energy can be used for fishing, household purposes. Balneotherapy is the treatment of diseases by spa which requires hot springs and geysers produced from a geothermal power plant is pumped over a lava bed rich in Sulphur and silica content. These elements react with the hot water from the power plant and imbibe healing properties. Geothermal energy also shows high efficiency of about 86-95% which is very high compared to other renewable energy sources and whose supply is continuous and reliable.

4. Conclusion

Geothermal energy is an alternative and a considerable energy source in the present era as we are becoming deficit of non-renewable energy sources. Due to the use of geothermal energy, emission of greenhouse gases can also be minimized which in turn could reduce global warming.

References

1. Craig beasley, Rio de Janeiro, Brazil, Oilfield Review Winter, 21, no.4, 2009.
2. Sadiq J Zarrouk, Department of Engineering Science, University of Auckland, Auckland, New Zealand, Proceedings World Geothermal Congress, 2015.
3. Paul L Younger, University of Glasgow, Transactions of the Institute of Mining and Metallurgy, Section A: Mining Technology 123(2): 107-118, 2014.
4. Mukul Bora, Dibrugarh University, National Seminar on Renewable Energy Technologies: Issues & Prospects, At NE-RIST, DOI: 10.13140/2.1.2508.8969, 2010.
5. R R Shah, A.D. Patel Institute of Technology, Int. Journal of Engineering Research and Applications, ISSN: 2248-9622, Vol. 4, Issue 4(Version 5), pp. 63-68, 2014.
6. Anthony Bryant, Senior Project, Alaska Pacific University, Proceedings Geothermal Power Production, 2010.
7. Paul L Younger, University of Glasgow, Energies 8(10): 11737-11754, 2015.

ECCE12
The 12th EUROPEAN CONGRESS OF CHEMICAL ENGINEERING
Florence 15-19 September 2019

To the Calculation of the Average Value of the Volume Fraction of the Key Bulk Component at The Intermediate Stage of Mixing with an Inclined Bump.

Anna Kapranova[1], Ivan Verloka[1], Daria Bahaeva[1], Mikhail Tarshis[1], Sergey Cherpitsky[1]

1 Yaroslavl State Technical University, Moskovsky Prospect, 88, Yaroslavl, 150023, Russia

**Corresponding author: kapranova_anna@mail.ru*

Highlights

- The calculation of the increment angles of reflection of rarefied flows is proposed.
- Distribution functions over the states of the macrosystems are taken into account.
- The basis is the results of stochastic modeling of mixing of flowing media with brushes.
- The effectiveness of the intermediate stage of mixing with the bump is analyzed.

1. Introduction

The urgency of the problem of mixing loose components is explained by the diversity of the purpose of the mixtures obtained for the needs of various industries and the agro-industrial complex. The development of methods for mixing loose components in a regulated ratio of 1:10 or more requires the designers of the respective equipment to perform a system-structural analysis of this process. The basis of this analysis is a theoretical prediction of the efficiency of the mixing process at each stage. The gravitational method for obtaining a free-flowing mixture with the specified ratio of components in the finished product proposed in [1] implies the presence of three mixing stages on trays with two steps in each. In this case, the first step involves the use of additional mixing elements in the form of brushes, and the second - fender surfaces.

2. Methods

The aim of the work is to develop a method for calculating the average value for the volume fraction of the key bulk component at the intermediate stage of gravity mixing using an inclined - bump stop surface. This characteristic of the mixing process is necessary in assessing the quality of the mixture with a regulatory ratio of 1:10 components, as an indicator of the effectiveness of the intermediate stage of the process under study. The proposed expression for the desired characteristic of the key component was obtained on the basis of the stochastic approach [2, 3], taking into account the results of modeling the formation of rarefied streams of solid dispersed materials. In this case, at the first step for the stage of intermediate mixing, the use of brush elements on a rotating drum is supposed [4-6]. At the second step, an impact surface is used [7–9] for shock interaction with rarefied streams of mixed materials formed after scattering with brushes. The specified expression uses the function for the volume fraction of the key component depending on the angles of reflection of each of the two bulk materials from the bump stop surface [8]. In addition, the latter function takes into account the method proposed earlier by the authors for calculating the volume fractions [10, 11] for the mixed portions of the components, which correspond to the intermediate

stage of this process. Note that a convenient in this case, the criterion for assessing the quality of the mixture is its coefficient of heterogeneity, which is determined in the traditional way [10, 11].

3. Results and discussion

The calculation of the maximum values for the reflection angles of each of the bulk components from the bump stop surface at the studied intermediate stage of their mixing is performed taking into account their increments. These increments are calculated depending on the scattering angles of the particles of the components in their rarefied flows, formed after scattering with brush elements. An expression for the nonequilibrium differential distribution function of each component in the scattering angle from brushes was used [4-6]. This function is obtained taking into account the design and operational parameters of the mixer unit "drum-brush elements". When describing the relationship between the scattering angle from the brushes and the angle of reflection from the bump stop [7, 8], the recovery factor is used, which characterizes the directions of the average velocities of the sparse fluxes of each component when striking the bump stop and when they are reflected from it. Modeling the desired average value for the volume fraction of the key bulk component at the intermediate stage of gravitational mixing using an inclined impact surface allows you to calculate the corresponding coefficient of heterogeneity.

4. Conclusions

Using the example of model mixing of two non-humidified components, comparable in size and density (sand and semolina), the heterogeneity coefficient of the resulting mixture for the intermediate stage was calculated. For this stage, mixing is assumed in equal proportions between the resulting mixture after the initial stage and the new portion of the key component (sand). The results of the work can be used in the formation of an engineering method for calculating a new gravity mixer of non-humidified bulk components in predetermined ratios of 1:10 or more with additional mixing elements (brushes and bump stops).

References

[1] A.I. Zaitzev, A.E. Lebedev, A.B. Kapranova, I.I. Verloka. Patent 2586126 Russian Federation, IPC B01F3/18. Gravity-type bulk solids mixer. June 2016.

[2] Y.L. Klimontovich, Turbulent Motion and Chaos Structure: A New Approach to the Statistical Theory of Open Systems, LENAND, Moscow, 2014.

[3] A.B. Kapranova, I.I. Verloka, A.E. Lebedev, A.I. Zaitzev, Czas. Tech. Mech. 113 (2, 2016) 145-150.

[4] A.B. Kapranova, M.N. Bakin, I.I. Verloka, A.I. Zaitzev, Vestn. TGTY Her TGTY. 58 (11, 2015) 296-304. doi:10.17277/vestnik.2015.02.pp.296-304.

[5] A.B. Kapranova, I.I. Verloka, Theor. Found. of Chem. Eng. 52 (6, 2018) 1004-1018. doi:10.1134/S0040579518050330.

[6] A.B. Kapranova, M.N. Bakin, I.I. Verloka, Chem. and Petrol. Eng. 54 (5-6, 2018) 287-297. doi:10.1007/s10556-018-0477-0. Suppl. 54 (7-8, 2018) 618. doi:10.1007/s10556-018-0524-x.

[7] A.B. Kapranova, I.I. Verloka, Vestn. IGEY Her IGEY. 3 (2016) 78-83. doi:10.17588/2072-2672.2016.3.078-083.

[8] I. Verloka, A. Kapranova, M. Tarshis, S. Cherpitsky, Int. J. Mech. Eng. Technol. 9 (2, 2018) 438-444.

[9] A.B. Kapranova, I.I. Verloka, J. Chem. Eng. Process Technol. 8 (5 (Suppl), 2017) 59. doi:10.4172/2157-7048-C1-009.

[10] A.B. Kapranova, I.I. Verloka, J. Chem. Eng. Process Technol. 9 (2018) 53. doi:10.4172/2157-7048-C3-018.

[11] A.B. Kapranova, I.I. Verloka, P.A. Yakovlev, D.D. Bahaeva, Rossiyskiy khimicheskiy zhurnal (Zhurnal khimicheskogo obshchestva im. D.I. Mendeleyeva) 62 (4, 2018) 48-50.

ECCE12
The 12th EUROPEAN CONGRESS OF CHEMICAL ENGINEERING
Florence 15-19 September 2019

A Study on the Efficiency Improvement of Vanadium Electrolyte Solution.

Seon Gyun Rho[1], Ung il Kang[1] Choon-Hyoung Kang[2]

1 Department of Fire Service Administration, Honam University, 417, Eodeung-daero, Gwasan-gu Gwangju, 62399, Korea, 2 School of Applied Chemical Engineering, Chonnam National University, Gwangju 61186, Korea

**Corresponding author: skno@honam.ac.kr*

Highlights

- Manufacture of electrolytic solution using glycerol as reducing agent.
- After the electrolytic solution was prepared from a low-concentration sulfuric acid-supported electrolyte, a sulfuric acid solution was added.

1. Introduction

One of the safest of large-capacity energy storage system is the vanadium redox flow battery.

In the vanadium redox flow Battery, the electrochemical reaction of oxidation and reduction takes place in the stack, and the energy storage is stored in an electrolyte stored in a separate electrolyte tank. The electrolytic solution accounts for about half of the cost of the vanadium redox flow battery. For this reason, the development of efficient electrolytes is essential. In this study, we have experimented to manufacture electrolytes to improve the efficiency of vanadium electrolytes[1].

The reaction formula of the anode and the cathode of the vanadium redox flow cell is as follows.

Positive electrode reaction: $$VO^{2+} + H_2O \underset{Discharge}{\overset{Charge}{\rightleftharpoons}} VO_2^{+} + 2H^{+} + e^{-} \quad E^0 = 1.0\ V$$

Negative electrode reaction : $$V^{3+} + e^{-} \underset{Discharge}{\overset{Charge}{\rightleftharpoons}} V^{2+} \qquad E^0 = -0.26\ V$$

2. Methods

The preparation of the electrolyte solution was carried out in the following order.

First, V(IV) solution was prepared by using VOSO4 in a low aqueous sulfuric acid solution. Second, V (III) solution and V (V) solution were prepared from V (IV) solution using charge/discharge cell. Third, the V(V) solution is reduced to V(IV) using a glycerol reducing agent and then mixed with the

V (III) solution to prepare a 3.5-valence electrolyte solution. Finally, sulfuric acid was added to the 3.5 valence electrolyte solution to prepare

3. Results and discussion

Figure 1 shows the electrical properties of the prepared electrolyte solution by Cyclic Votammetry(CV). Both curves show the electrical characteristic curves of a typical vanadium electrolyte. Figure 2 shows the results of charge/discharge test of the completed vanadium electrolyte solution for 50 times by adding 2M H_2SO_4 to the supporting electrolyte 1M H_2SO_4. Figure 3 shows the results of charge/discharge test of the completed vanadium electrolyte solution for 50 times by adding 1M H_2SO_4 to the supporting electrolyte 2M H_2SO_4. In the case of energy efficiency and voltage efficiency, better efficiency was obtained when the initial H_2SO_4 concentration was 1M.

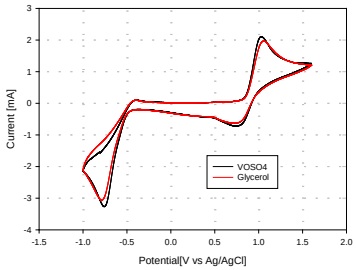

Figure.1 CV curve of V (IV) electrolyte solution prepared with $VOSO_4$ and V (IV) electrolyte solution reduced with glycerol reducing agent.

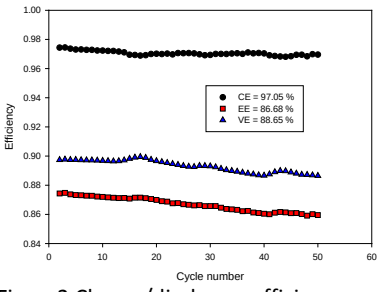

Figure2 Charge/discharge efficiency curve for 50 cycles (1M H_2SO_4 electrolyte solution + 2M H_2SO_4 addition).

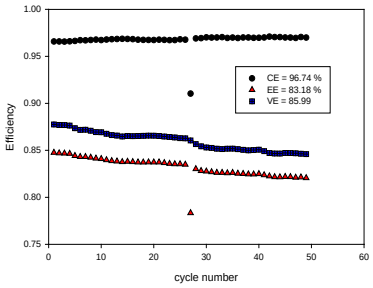

Figure 3 Figure2 Charge/discharge efficiency curve for 50 cycles (2M H_2SO_4 electrolyte solution + 1M H_2SO_4 addition).

4. Conclusions

Energy efficiency increased from 83.18% to 86.68%, and voltage efficiency increased from 85.99% to 88.65%. It was confirmed that the completion of the vanadium electrolyte using a low concentration of the supporting electrolyte in the preparation of the electrolyte solution, and then the addition of the concentration of H_2SO_4 to the final completion of the electrolyte solution can be improved in the improvement of the energy efficiency and the voltage efficiency.

References

[1] S. Roe, C. Menictas, and M. S. Kazacosa, Journal of the Electrochemical society 163.1(2016) A5023–A5028.

ECCE12
The 12th EUROPEAN CONGRESS OF CHEMICAL ENGINEERING
Florence 15-19 September 2019

High performance dual-electrolyte aluminum-air flow battery

Pemika Teabnamang[1], Soorathep Kheawhom[1,2,*]

1 Department of Chemical Engineering, Faculty of Engineering, Chulalongkorn University, Bangkok, Thailand; 2 Research Unit of Advanced Materials for Energy Storage, Chulalongkorn University, Bangkok, Thailand

**Corresponding author: soorathep.k@chula.ac.th*

Highlights

- Dual-electrolyte cell using methanol anolyte suppresses anode corrosion.
- Flowing anolyte prevents passivation of aluminum anode.
- Higher water content improves discharge current density.
- Higher water content increases self-corrosion.

1. Introduction

Recently, climate change has become increasingly significant putting considerable pressure on various aspects of our environment. To address this problem, a sustainable solution for energy generation and storage are actively investigated. Electrical energy storage (EES) systems are essential for the effective utilization and integration of renewable energy sources to the power grid. EES systems offer many benefits including improving the way energy is delivered, consumed and generated. Rechargeable batteries are the most common energy storage system.

Rechargeable aluminum-air batteries are a promising EES system. Aluminum-air batteries have a high specific capacity of 2.98 Ah/g. Furthermore, the aluminum anode is an inexpensive, abundant and environmentally friendly metal with high recyclability. Nonetheless, corrosion of the aluminum anode is a critical issue for traditional aluminum-air batteries. The anodic corrosion results in the accumulation of hydrogen gas in the cell and increases the hydrogen explosion possibility. Besides, it causes unacceptably high energy losses. Various works have attempted to inhibit aluminum self-corrosion by alloying aluminum with other elements or modifying the electrolyte using certain additives. Nevertheless, these efforts have shown limited success and have often increased the complexity of the battery system. To address this issue, aluminum oxidation should take place in a non-aqueous environment with high aluminum anode activity while suppressing the corrosion rate. Methanol (CH_3OH) used as the electrolyte was found to provide a high capacity under a dual-electrolyte system in an aluminum-air battery whereby a non-aqueous electrolyte was used for the anolyte and an aqueous electrolyte was used for the catholyte. Hence, this work proposes a dual-electrolyte aluminum-air flow battery with a structure of an aluminum anode | methanol electrolyte || gel polymer electrolyte | air cathode.

2. Methods

The corrosion behavior of the aluminum anode in methanol with varying the amount of deionized water (0%, 5%, 10% and 20%) and 3 M KOH-methanol mixed solution was examined by measuring the volume of evolved hydrogen gas as a function of time. Also, the half-cell test was carried out

using a three-electrode cell was used to study the electrochemical measurement and characterization. The battery cell structure consisting of aluminum anode | anolyte | anion exchange membrane | catholyte | air cathode was fabricated as shown in Fig. 1. The anolyte is 3 M KOH in methanol containing different percentages of deionized water. The catholyte is a gel polymer electrolyte based on Carbopol 940. Performances of the batteries were then examined.

3. Results and discussion

The volume of hydrogen evolved can speculate how much aluminum consumed without discharging. The results showed that hydrogen evolution is higher when the percentage of water is raised. The highest weight loss of aluminum occurred in the condition of 20% water; this condition contained the highest deionized water percentage. The results of electrochemical impedance spectroscopy showed that water in the anolyte had various effects such as decreasing aluminum double-layer, increasing mass transfer owing to the decrease in electrolyte viscosity and enhancing conductivity. Thus, increasing of deionized water leads to higher anodic corrosion.

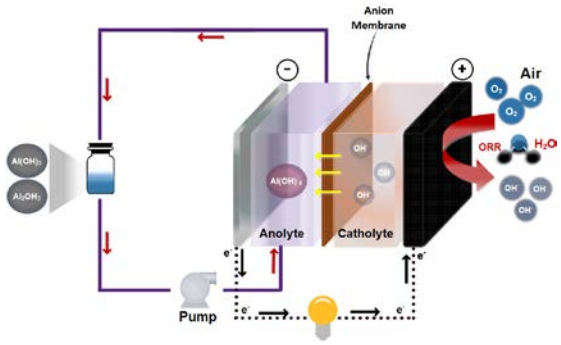

Figure 1. Schematic diagram of a dual electrolyte aluminum-air battery.

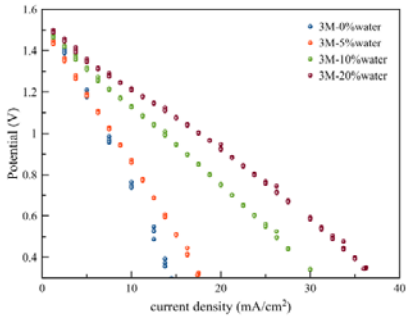

Figure 2. Polarization characteristics of the aluminum-air flow battery using different anolytes.

Figure 2 shows the polarization characteristics of the aluminum-air battery. The limiting current density for each condition slightly increased as follows: 14.97 mA/cm^2, 17.50 mA/cm^2, 30 mA/cm^2 and 36.3 mA/cm^2 at 0, 5, 10 and 20% water, respectively.

The anhydrous methanol anolyte achieved a specific capacity of 2,328 mAh/g for around 40 hrs. When the deionized water increased, the specific capacity decreased consecutively: from 1,700 mAh/g, 1,130 mAh/g and 465 mAh/g at the condition of 5, 10, and 20% water, respectively. Simultaneously, when the deionized water was increased, discharge voltage also increased, but the aluminum utilization percentage decreased. In the anhydrous methanol anolyte, the corrosion of aluminum is significantly inhibited, but the corrosion substantially increased when the amount of water increased.

4. Conclusions

The dual-electrolyte system using methanol-KOH anolyte completely suppressed the anodic corrosion and provided the highest specific capacity of 2,328 mAh/g discharging at 10 mA/cm^2. The aluminum consumption had more than 75%. In addition, the discharge voltage of the battery increased when the electrolyte contained water. However, the presence of water in the anolyte decreased the specific capacity as the corrosion increased. Trade-off between discharge performance and corrosion can be done adjusting the water content in the methanol-KOH anolyte.

ECCE12
The 12th EUROPEAN CONGRESS OF CHEMICAL ENGINEERING
Florence 15-19 September 2019

Power-to-Syngas Processes by Reactor-Separator Superstructure Optimization

Andrea Maggi[1]*, Marcus Wenzel[1], Kai Sundmacher[1, 2]

1 Max-Planck-Institute for Dynamics of Complex Technical Systems, Sandtorstr. 1, 39106 Magdeburg, Germany; 2 Otto-von-Guericke-University Magdeburg, Universitätsplatz 2, 39106 Magdeburg, Germany

**Corresponding author: maggi@mpi-magdeburg.mpg.de*

Highlights

- Power-to-Syngas process superstructure for different syngas compositions introduced.
- Optimal energy pathways to syngas from renewables identified via LP.

1. Introduction

The transition from fossil (coal, oil, gas) to renewable feedstock and energy carriers (solar, wind, water, biomass) has become a matter of uttermost importance in the chemical industries. Moreover, the current large CO_2 emissions represent both a threat for the climate and an opportunity for an alternative carbon source. Schack et al. [1] showed how the shift towards sustainable production scenarios could be accomplished by identifying well-suited target products. In this regard, syngas is an ideal candidate: as reported by Wenzel et al. [2], it bridges the inputs from renewables and state-of-the-art downstream processes to fuels and chemicals by adjustment of the H_2/CO ratio. Reactor-separator processes are the tool allowing for such bridging. Different process alternatives available in this context suggest the deployment of a superstructural representation wherein different technologies can be embedded. Categories of available separation methods to purify and adjust the syngas to the requirements of the desired downstream processes include membrane separation, pressure swing adsorption, scrubbing and cryogenic operations.

2. Methods

In our superstructure approach, different types of catalytic conversion steps and separation methods are combined. The superstructure is the basis for the formulation of a Linear Program (LP) used for process optimization. The complexity of the system is reduced by assuming Gibbs reactors and sharp-split separation tasks. As shown in Figure 1, the feedstocks considered are water and biomass. The most promising reactor technologies considered are reverse water gas shift (RWGS) and steam reforming of methane (SR).

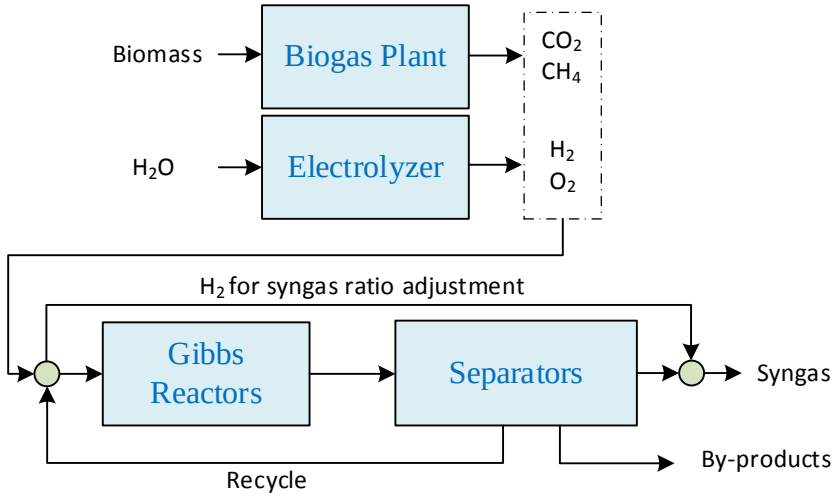

Figure 1 Schematic representation of a syngas plant. Biomass and water are converted into the reactants required for the generation of the final product.

The first objective to be minimized is the total energy requirement. Furthermore, pseudo prices are applied to the variables in the objective function to allow for the differentiation between day and night plant operations, therefore accounting for the intermittency of the renewable power sources. The solutions depend on the hydrogen to carbon monoxide ratio which the syngas must fulfil to meet the product specification.

3. Results and discussion

Preliminary results indicate that, for RWGS, the optimal syngas production route consists of water removal followed by a sequence of pressure swing adsorption steps for the adjustment of the hydrogen to carbon monoxide ratio. This approach is extended to scenarios where SR is included in the same optimization problem. Water electrolysis proves to be a bottleneck for the syngas production, possibly mitigated by the synergy between SR, yielding a high H_2/CO ratio, and RWGS.

4. Conclusions

The derivation of the method presented in this work is motivated by the need for an effective screening tool to identify the most energy efficient process within a large number of alternatives. The energy efficiency is of foremost importance in the context of Power-to-Chemical conversion systems, where the energy and raw chemicals are to be supplied from renewable sources. Nevertheless, this approach does not contrast with economic based optimizations but it offers a complementary standpoint.

References

[1] D. Schack, L. Rihko-Struckmann, K. Sundmacher, Ind. Eng. Chem. Res. 57 (2018) 9889–9902.
[2] M. Wenzel, L. Rihko-Struckmann, K. Sundmacher, AIChE Journal, 63 (2017) 15-22.

ECCE12
The 12th EUROPEAN CONGRESS OF CHEMICAL ENGINEERING
Florence 15-19 September 2019

Study on the deactivation of the CaO containing catalysts used in transesterification of sunflower oil with methanol

Ivana Lukić[1*], Željka Kesić[1], Miodrag Zdujić[2], Dejan Skala[1]

1 University of Belgrade, Faculty of Technology and Metallurgy, Karnegijeva 4, 11000 Belgrade, Serbia;

2 Institute of Technical Sciences of SASA, Knez Mihailova 35, 11000 Belgrade, Serbia.

**Corresponding author:ivanal888@yahoo.co.uk*

Highlights

- CaO based catalysts were prepared by mechanochemical treatment.
- $3CaO{\cdot}SiO_2$ mixed oxide showed better stability than CaO·ZnO.
- Deactivation was caused mainly by adsorbed organic compounds on active sites.

1. Introduction

The synthesis of biodiesel, a mixture of fatty acid methyl esters (FAME), applying heterogeneous catalytic process could solve most of the economic and environmental drawbacks of the conventional homogeneous process. Solid catalyst can be easily separated from the reaction mixture, regenerated and reused, what make the biodiesel synthesis cost-effective and also enables the continuous process development [1]. However, one of the main problems associated with solid catalysts is their deactivation, caused by poisoning of active sites, leaching of active component into the reaction mixture, or structural change of the catalyst.

CaO based catalysts, CaO·ZnO and $3CaO{\cdot}SiO_2$ mixed oxide prepared by mechanochemical treatment and subsequent calcination exhibited excellent activity in transesterification of sunflower oil at 60 °C [3-5]. In this work, stability and deactivation of these CaO based catalysts was studied and compared to the activity and deactivation of pure CaO. The possibility to reuse the catalysts in consecutive runs was examined, as well as the leaching of the active component of the catalyst in the reaction mixture. The characterization of catalysts after reaction was performed in order to find out the cause of deactivation.

2. Methods

The fresh and reused catalysts were characterized by XRD, TGA/DSC, FTIR, SEM/EDX and base strength using Hammett indicator method. The details on the preparation of catalysts and the used instruments for their characterization are described elsewhere [2-4]. The methanolysis of sunflower oil was carried out in a 250 ml three-necked glass flask with a condenser and magnetic stirrer at 60 °C, methanol to oil molar ratio of 10:1 and 2 wt% of catalyst based on oil weight.

3. Results and discussion

The results showed that CaO·ZnO catalyst could be reused only 2 times without losing its activity, while already in the third cycle the FAME yield declined to 47%, and in fourth cycle the catalyst was practically not active (Figure 1). $3CaO{\cdot}SiO_2$ showed better stability, maintaining very good activity and high FAME yield, above 97%, for 4 cycles. For comparison, the activity of pure CaO

decreased in four consecutive runs [5]. To evaluate leaching of the active component, the catalyst sample was placed in contact with methanol under reaction conditions. After the catalyst was removed by filtration, methanol was mixed with the fresh sunflower oil. When CaO·ZnO was used, FAME yield was 0.21%, revealing negligible leaching of active component, while for $3CaO·SiO_2$ FAME were not detected. This finding confirmed the stabilization of CaO by the presence of another phase, since CaO, when used as pure compound, is partially dissolved in methanol [1].

The FTIR spectra of fresh and 4-times used $3CaO·SiO_2$ catalysts are very similar, indicating the stability of the catalyst during its use in transesterification of sunflower oil, and only negligible adsorption of organic compounds on the catalyst surface (Figure 2). XRD patterns of reused CaO·ZnO revealed only peaks assigned to ZnO, while peaks corresponding to CaO were not observed, indicating that they were blocked by products or intermediates. FTIR analysis confirmed the presence of organic compounds on the surface of CaO·ZnO catalyst.

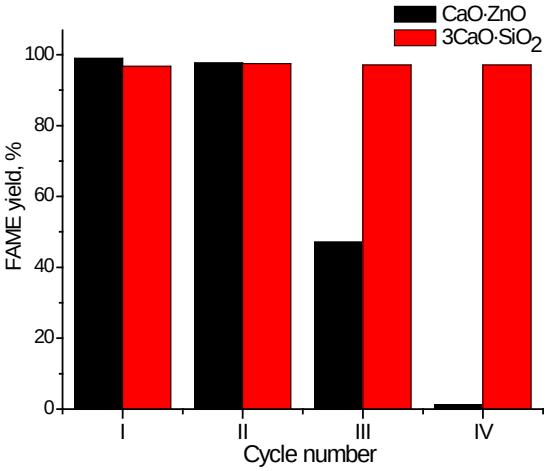

Figure 1. Number of repeated use.

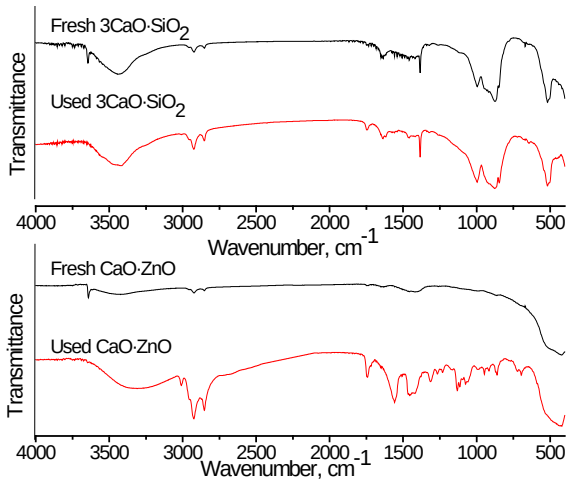

Figure 2. FTIR spectra of fresh and used catalysts.

4. Conclusions

$3CaO·SiO_2$ catalyst showed good stability in transesterification of sunflower oil, while drop of activity occurred already in the third reuse cycle when CaO·ZnO catalyst was used. The observed catalyst deactivation was probably the result of active site blockage by adsorbed organic compounds from the reaction mixture.

Acknowledgement

This work was financially supported by the Ministry of Education, Science and Technological Development of the Republic of Serbia (Project No III 45001).

References

[1] M. López Granados, D. Martín Alonso, I. Sadaba, R. Mariscal, P. Ocon, Appl. Catal., B 89 (2009) 265–272.

[2] Ž. Kesić, I. Lukić, D. Brkić, J. Rogan, M. Zdujić, H. Liu, D. Skala, Appl. Catal., A 427–428 (2012) 58–65.

[3] I. Lukić, Ž. Kesić, S. Maksimović, M. Zdujić, H. Liu, J. Krstić, D. Skala, Fuel 113 (2013) 367–378

[4] M. Zdujić, I. Lukić, Ž. Kesić, I. Janković-Častvan, Č. Jovalekić, D. Skala, Adv. Powder Technol. Submitted for publication

[5] M. Kouzu, S. Yamanaka, J. Hidaka, M. Tsunomori, Appl. Catal., A 355 (2009) 94–99.

ECCE12
The 12th EUROPEAN CONGRESS OF CHEMICAL ENGINEERING
Florence 15-19 September 2019

"Egg-Yolk" Catalyst Particle Design for Improved Flexibility of Industrial Scale Fixed-Bed Reactor used for CO_2 Methanation

Ronny Tobias Zimmermann[1], Jens Bremer[2], Kai Sundmacher[1,2]

1 Otto-von-Guericke Universität, Universitätsplatz 2, 39106 Magdeburg, Germany;

2 Max-Planck-Institut für Dynamik komplexer technischer Systeme, Sandtorstraße 1, 39106 Magdeburg, Germany

**Corresponding author: ronny.zimmermann@mpi-magdeburg.mpg.de*

Highlights

- Combined catalyst particle and reactor optimization.
- Dynamic and flexible fixed-bed reactor operation.
- Reduced parametric sensitivity of reactors filled with "egg-yolk" particles.

1. Introduction

Surplus electrical energy harvested from renewable energy sources can be efficiently stored by generation of hydrogen via electrolysis of water. Due to the missing hydrogen infrastructure, it is favorable to convert hydrogen together with carbon dioxide into synthetic methane. Methane can be readily distributed in existing pipeline networks and is a key substance of the chemical industry. However, the high exothermicity of the methanation reaction imposes a challenge for the operation of the typically employed fixed-bed reactors. Due to catalyst deactivation, safety constraints and the thermodynamic equilibrium of the reaction, the temperature of the fixed-bed has to be limited [1]. For dynamic operation of these reactors, according to the availability of surplus energy, high parametric sensitivity and wrong-way behavior further amplify this aspect [2]. Much research has been done to keep the fixed-bed temperature in defined bounds, mostly focusing on the manipulation of variables on the reactor scale [3]. However, the knowledge about the influence of the catalyst particle design on the reactor behavior is rather limited. Therefore, in this contribution, the influence of the catalyst particle design on the reactor behavior has been investigated.

2. Methods

The influences of the catalyst particle activity, permeability and heat conductivity on the performance of the reactor have been examined by employing a dynamic heterogeneous reactor model. Homogeneously active particles and particles with multiple zones, focusing on particles with an "egg-yolk" configuration, were compared. Subsequently, the carbon dioxide conversion of the reactor was optimized subject to these degrees of freedom for the different particle concepts without surpassing the catalyst particle deactivation temperature. The optimized concepts were further compared by sensitivity analyzes regarding coolant temperature, reactor inlet flow rate and reactor pressure as well as by dynamic simulation studies.

3. Results and discussion

The sensitivity analysis regarding the coolant temperature reveals a reduced temperature increase on the ignition curve of the reactor filled with optimized "egg-yolk" catalyst particles in comparison

to the reactor filled with optimized homogeneously active catalyst particles as shown in Figure 1. This allows for the operation of the fixed-bed reactor at high carbon dioxide conversions without surpassing the critical catalyst particle deactivation temperature in a broad range of coolant temperatures. The same is not possible with homogeneously active particles.

Similar results were obtained from the sensitivity analyzes of the inlet flow rate and the reactor pressure. The carbon dioxide conversion and the maximum particle temperature of reactor filled with homogeneously active particles show a large sensitivity with regard to these parameters. In contrast, the carbon dioxide conversion and the maximum particle temperature are almost constant in the reactor filled with “egg-yolk” particles in the investigated parameter range.

Furthermore, the dynamic simulation studies show a fast transition between the operation points of the reactor filled with “egg-yolk” particles. The transition of the operation points of the reactor filled with homogeneously active particles takes much longer and can exhibit significant wrong-way behavior.

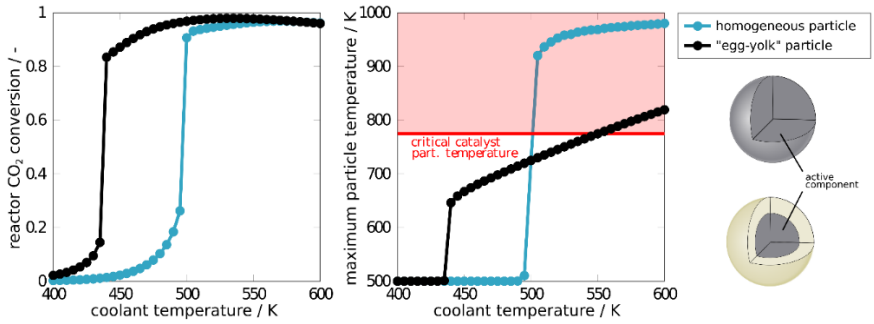

Figure 1. Comparison of the ignition curves of a catalytic fixed-bed tubular reactor filled with optimized homogeneously active particles and optimized “egg-yolk” particles fed by a stoichiometric and undiluted mixture of CO_2 and H_2.

4. Conclusions

The high exothermicity of the methanation reaction imposes a challenge for fixed-bed methanation reactors during steady state and dynamic operation, as the fixed-bed temperature has to be limited, mainly due to catalyst deactivation. Therefore, the carbon dioxide conversion of an industrial scale fixed-bed methanation reactor has been optimized by variation of degrees of freedom on the particle scale without surpassing the critical catalyst deactivation temperature for different particle concepts. Subsequent sensitivity analyzes and dynamic simulation studies revealed beneficial behavior of reactors with “egg-yolk” particles in comparison to the typically used homogenously active catalyst particles. Reactors filled with “egg-yolk” particles show a much broader range of operation points with high carbon dioxide conversion without surpassing the critical catalyst deactivation temperature and faster transition between operation points.

Acknowledgement

This research work was conducted within the Priority Program SPP 2080 “Catalysts and reactors under dynamic operating conditions for the storage and conversion of renewable energy”. The financial support from the German Research Foundation (DFG) is gratefully acknowledged.

References

[1] S. Rönsch, J. Schneider, S. Matthischke, M. Schlüter, M. Götz, J. Lefebvre, P. Prabhakaran, S. Bajohr, Fuel 166 (2016) 276-296.
[2] D. Schlereth, O. Hinrichsen, Chem. Eng. Res. & Des. 92 (2014) 702-712.
[3] J. Bremer, K. H. G. Rätze, K. Sundmacher, AIChE J. 63 (2017) 23-31.

ECCE12
The 12th EUROPEAN CONGRESS OF CHEMICAL ENGINEERING
Florence 15-19 September 2019

Conceptual and Basic Design of an Innovative Catalytic Reactor for Dehydrogenation of Liquid Organic Hydrogen Carriers

S. Ehsan Emamjomeh[1]*, Arian Shoshi[1], Yongdan Cen, Eberhard Schlücker[1]

1 Institute of Process Machinery and Systems Engineering, University of Erlangen-Nuremberg, Germany

**Corresponding author: ehsan.emamjomeh@fau.de*

Highlights

- Most of existing LOHC dehydrogenation models suffer from a low reaction yield.
- Followed concept promises an efficiency enhancement, modularity & scalability.
- The optimized basic design is achieved by series of analyses & simulations.

1. Introduction

The greatest hurdles in terms of traditional energy storage are the improvement of efficiency and the minimization of final costs, whereby sustainable resources are both seasonal and daylight-dependent. The storage of energy in the form of liquid organic hydrogen carriers, the so-called LOHC, is a new, progressive trend. LOHC are hetero- or homocyclic aromatic hydrocarbons and because of their unsaturated chemical structure, they are able to store additional hydrogens (as energy carrier) in a chemically bonded form. In addition, these energy-carrying materials will not be consumed during their utilization, but instead will be recycled for further loading and unloading cycles. A whole storage system includes a water-electrolyze unit, a water reservoir, a hydrogenation reactor, two LOHC tanks, a dehydrogenation reactor and a hydrogen-burning unit. The division into sector steps is a significant benefit of this new system, e.g. the division into hydrogenation unit and dehydrogenation unit. The dehydrogenation side is highly endothermic (70 kJ/mol H_2) and its thermal efficiency is very crucial in the energy aspects of the overall system. We have developed a concept, which is positively remarked in the evaluations. This concept is inspired by helical heat exchangers, which benefit from a high thermal efficiency and relatively lower pumping energy [1].

2. Conceptual design

The existing reactor models are based on horizontal shell-and-tube heat exchangers in which the bottom halves of the tubes are filled with catalyst pellets. The loaded LOHC is pumping through the reaction tubes, which are heating to the reaction temperature and after passing the residence time, the hydrogen will release on the surface of the catalyst and can leave the reaction zone via empty top halves of the tubes [2]. The heat transfer values are in the expected range. Nevertheless, the overall performance of the reactor is not satisfactory. This is probably due to the large volume of hydrogen released (9 mol H_2/mol LOHC), which pushes the LOHC out of the reactor, reducing the residence time.

Our new concept solves the problems of the large volume increase during the reaction and poor heat transfer. The Figure 1 shows the general structure of this concept. The idea here is to run the hydrogenated LOHC (loaded form) on an open plate, where a semi-helical heat exchanger provides the necessary temperature and heat flux for the dehydrogenation reaction. The hydrogen releases by bringing the reactants in contact with the heating coils along an open coiled channel filled by catalyst pellets or granules, which are small enough to cover all the empty spaces.

Being modular and scalable in this particular concept is very advantageous. The basic components of reaction plate are designed for a simple modification or extension. This makes the concept unique and it eases to reconstruct the reactor plate on different capacities or stack-on more parallel plates in a pressure vessel for any demanded purposes and power-outputs.

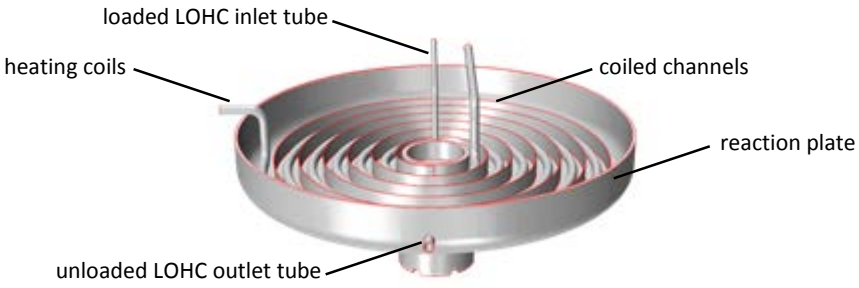

Figure 1. General schematics of a single internal plate of the reactor

3. Basic design

In the next step, mathematical & theoretical analyses, simulations and experimental investigations are concerned. The reaction kinetics of perhydro-dibenzyltoluene are studied and verified [2]. Maintaining the residence time and heat of reaction are the key parameters, which are followed as the functionality basics of any concepts, and in addition to developing a reasonable and functional dehydrogenation reactor, finding the essential influencing parameters on thermal efficiency and reaction progress are mainly in focus. Optimization of the thermal efficiency addresses mainly the reaction zone inside the plate and channel geometries. Here the channel size and paired heating-coil measures must be optimized. Regarding plate's outside, the inlet temperatures, flow directions, vessel's pressure must be studied and optimized. In case of stacked-on plates, the plates' gaps and similarity for the even heat and flow regulations are particularly important. As an example, the temperature profiles by three different channel widths are shown in Figure 2.

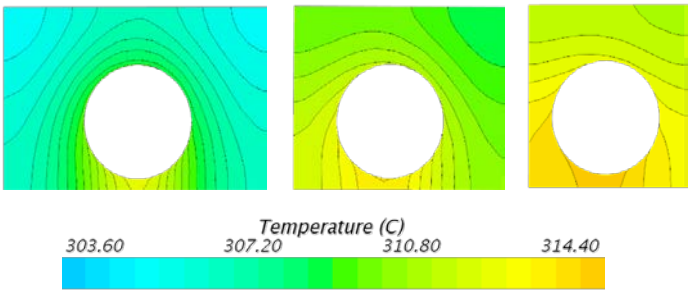

Figure 2. Temperature profiles in cross section of channel with 3 widths

4. Conclusions

Currently, the semi-helical structure reports to be known as the most promising concept for dehydrogenation of LOHC. Very less limitation concerning released amount of hydrogen gas makes this concept already attractive in the conceptual design step, in addition to notable improvements on heat transfer and residence time in the optimized basic design. After experimental verification of optimized parameters in series of empirical studies, the detailed engineering step follows.

References

[1] S.E. Emamjomeh, E. Schlücker, Book of Abstracts: 10th World Congress of Chem. Eng. (2017) p. 469.
[2] P.K.E. Preuster, Development of a reactor for the dehydrogenation of chemical hydrogen carriers as part of a decentralized, stationary energy storage system, Doctoral Thesis, Erlangen 2017.

ECCE12
The 12th EUROPEAN CONGRESS OF CHEMICAL ENGINEERING
Florence 15-19 September 2019

Experimental study and CFD simulation of thermal energy storage (TES) in a pilot scale packed-bed

Philippe Béard[1], Ludovic Noël[1], Pierre Balz[1], Sofiane Bekhti[1], Guillaume Vinay[2], David Teixeira[2]

1 IFP Energies nouvelles, Etablissement de Lyon, BP 3, 69360 Solaize, France

2 IFP Energies nouvelles, 1 & 4 avenue de Bois-Préau, 92852 Rueil-Malmaison cedex, France

**Corresponding author: philippe.beard@ifpen.fr*

Highlights

- Experiments and transient CFD modelling of TES during a full cycle.
- Influence of physical properties variations with temperature.
- Good agreement between experimental and numerical results.

1. Introduction

Compressed air energy storage exists since 1978 in the form of improved gas power-plant with an energy efficiency of only 50 %. In these older Compressed Air Energy System (CAES), heat produced by the compression is lost. A more advanced concept, AA-CAES (Advanced Adiabatic CAES), has the advantage of storing the heat of compression and achieving a much higher efficiency. IFPEN proposes a system (Figure 1) based partly on already existing components such as compressors and turbines but also on new components such as Thermal Energy Storage (TES) systems. The load is achieved by air compression and heat storage. Electricity production is realized through a turbine in which the compressed air is expanded after being reheated in TES.

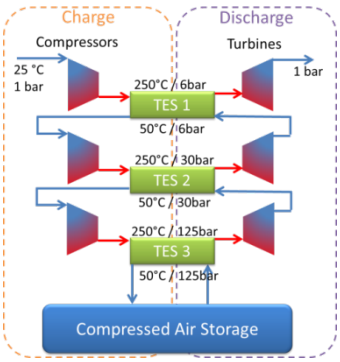

Figure 1. AA-CAES principle.

In recent years, due to the development of AA-CAES and of Concentrated Solar Power (CSP) in particular, sensible heat storage in packed beds has received much interest [1,2].

2. Methods

Complete TES cycles were studied in an insulated glass tank (diameter 0.3 m) filled with uniform 10 mm concrete beads (Figure 2) and equipped with 26 thermocouples to map the temperature.

Figure 2. Experimental TES test rig with and w/o insulation.

CFD (Computational Fluid Dynamics) calculations were performed with ANSYS® Fluent® using a non-equilibrium thermal model in the porous bed zone. The sensitivity to physical properties was investigated as few data are available for concrete at high temperatures [3]. The beads specific heat was measured within the considered temperature range (15-250 °C).

3. Results and discussion

The temporal evolution of the temperature in the bed during the different phases of the cycle is well predicted, in particular along the axis (Figure 3). It was shown that the most influencing property is the specific heat and that an accurate description of the insulation is required.

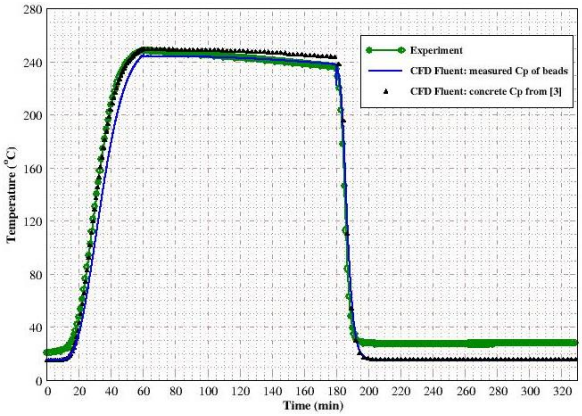

Figure 3. Comparison between experimental and numerical results on the bed axis during a full cycle.

4. Conclusions

The agreement between measured and numerical results during a full TES cycle is quite good. Those results will be assessed in a larger experimental set-up in the near future prior to be able to design industrial systems.

References

[1] G. Zanganeh, A. Pedretti, S. Zavattoni, M. Barbato, A. Steinfeld, Solar Energy 86 (2012) 3084-3098.
[2] M. Cascetta, G. Cau, P. Puddu, F. Serra, Aplied Thermal Engineering 98 (2016) 1263–1272.
[3] J. Pan, R. Zou, F. Jin, Energies 10, 33 (2017).

ECCE12
The 12th EUROPEAN CONGRESS OF CHEMICAL ENGINEERING
Florence 15-19 September 2019

Biogas to Methanol: comparison between CHP and different CHCP plant configuration

Daniele Previtali[1], Giulia Bozzano[1], Carlo Pirola[2], Flavio Manenti[1]

[1] Politecnico di Milano, Dipartimento di Chimica, Materiali ed Ingegneria Chimica "Giulio Natta", Piazza Leonardo da Vinci 32, 20133 Milano, Italy; 2 Università degli Studi di Milano, Dipartimento di Chimica, Via Golgi 19, 20133 Milano, Italy

*Corresponding author: flavio.manenti@polimi.it

Highlights

- Biogas is used in CHP plant for electricity production causing net CO_2 emissions.
- CHCP plant can use Biogas for bio-methanol production avoiding CO_2 emissions.
- CHCP plant is economically feasible considering actual incentives.

1. Introduction

Biogas is a mixture of methane (CH_4) and carbon dioxide (CO_2), produced by anaerobic digestion of organic matter (sewage, manure, organic/agricultural waste, etc.). It is currently considered an important resource by the European Union, since many claims that it allows production of heat and electric energy at zero carbon emissions [1]. Therefore, biogas is usually converted into heat and/or electricity as is, using a Combined Heat & Power (CHP) plant, and/or upgraded to bio-methane, via removal of CO_2 and other impurities, and then injected into the natural gas distribution grid. Although these two techniques for energy production (thermal and/or electrical) may be considered greener than those currently in use, they still have a non-zero carbon footprint. The latter is comprised of the CO_2 emissions of all the processing steps needed to produce the feedstocks, synthesize biogas and use it. Thus, it is important to consider alternative uses of biogas, associated with no carbon emissions, e.g. the novel concept of Combined Heat, Power and Chemical (CHCP) plant. A CHCP plant converts biogas into bio-methanol (MeOH) such that part of the carbon of the biogas feedstock is not released back into the atmosphere as CO_2 (bio-methanol is a solvent and a building-block that can be utilized to produce other chemicals, e.g. dimethyl ether, acetic acid and formaldehyde). This chemical conversion process takes place in two principal unit operations, namely a reformer and a methanol synthesis reactor, of which the first converts biogas into syngas while the second transforms syngas into methanol [2]. Compared to most conventional biogas conversion processes, CHCP plants offer a lower environmental impact and generate valuable chemicals. CHCP plant was studied analyzing 2 different configurations for syngas production: steam reforming (SRtoM) and tri-reforming (TRtoM) [3]. The aim of this work was the comparison between CHP and different CHCP configurations.

2. Methods

We hypothesized three different biogas composition (30%, 40% and 50% of CO_2) and three different flowrates (100, 200, and 500 kg/h). In CHP plant all biogas is burnt to maximize the electricity production, instead of CHCP process, where biogas is partially used for the methanol

synthesis and partially burn to supply the duty necessary to reforming section. Only in this way the CHCP process can be considered energetically self-sustainable. Operative conditions of reformer and methanol synthesis reactor were optimized in order to maximize the methanol productivity. Profits depend on electricity production in case of CHP plant, and on methanol production in case of CHCP. Methanol and electricity prices have been studied evaluating the importance of government incentives. The different processes were simulated using PRO/II® 10.0, a steady-state simulation software. The economic evaluation was performed using the model costing technique [4].

3. Results and discussion

SRtoM and TRtoM process are both technically feasible. The latter can produce more syngas but nitrogen, added as air, acts as inert increasing the dimension of the methanol synthesis section. The economic profitability of CHP and CHCP processes is strictly related to CO_2 content and process configuration. Generally, higher the scale (500 kg/h of biogas) lower is the payback time and higher is the methane content lower is the profitability. Biogas with a high CO_2 content (50%) increases the payback time at over 10 years and makes CHPC process economically unfeasible while CHP could be interesting since the payback time is slightly lower, 7 years. In all the simulation and considering incentives, the lower payback time is obtained with SRtoM process due to the high value of methanol. TRtoM is less competitive than SRtoM since the methanol synthesis section is bigger, and so more expensive.

4. Conclusions

The aim of the work was the comparison of different process for biogas use. Results show that government incentives and CO_2 content are the main limits for economic feasibility. With actual government incentives the CHCP process has the lower payback time. CHP can be considered a better option with high CO_2 concentration. Considering also the lower carbon emissions CHPC plant could be an interesting alternative to CHP.

References [Calibri 10]

[1] EurObserv'ER Report, 2016, The State of Renewable Energies in Europe.
[2] Manenti, Processo di conversione del biogas, 2015, patent: "102017000073797, 2017".
[3] Vita A., Italiano C., Previtali D., Fabiano C., Palella A., Freni F., Bozzano G., Pino L., Manenti F., Renewable Energy (2018), 673-684
[4] Turton R.C., Bailie R.C., Whiting W.B., Shaeiwitz J.A., Bhattacharyya D., (2012), Analysis synthesis, and design of chemical processes fourth ed.

ECCE12
The 12th EUROPEAN CONGRESS OF CHEMICAL ENGINEERING
Florence 15-19 September 2019

Feasibility studies on biomass waste utilization for alternate energy generation

Hammad Siddiqi[1*], B. C. Meikap[1,2]

1 Department of Chemical Engineering, Indian Institute of Technology (IIT) Kharagpur, West Bengal-721302, India

2 Department of Chemical Engineering, School of Engineering, Howard College, University of Kwazulu-Natal, Durban, 4041 South Africa

**Corresponding author: hsiddiqi@iitkgp.ac.in*

Highlights

- Alternate energy from biomass waste.
- Thermo-kinetic studies to access its feasibility.
- Prediction of reaction model using master plots.

1. Introduction

Rising energy consumption and the acute energy crisis lead to a long-term cleaner and renewable alternative that is abundantly available, easily accessible and also have positive footprints on the environment along with its economic feasibility. Another major challenge that is also associated with population rise is waste management. Therefore, utilization of this waste for energy production will be most viable solution to these two problems. Present work focuses on generation of alternate energy from a biomass waste, a detailed thermo-kinetic analysis to evaluate its energy potential. The effect of various physiochemical properties will be investigated to correlate its effect on final product distribution via thermochemical conversion

2. Methods

Physiochemical characterization include proximate and ultimate analysis which was carried out using ASTM standards. Also the components of cell wall consisting of hemicellulose, cellulose and lignin have been determined using chemical process. Thermo-gravimetric analysis at different heating rates for non-isothermal heating have been performed to determine the kinetic factors and further the reaction model.

3. Results and discussion

The activation energy of the sample was determined using different differential and integral isoconversional models and the average value is calculated as 109.90 kJ/mol. Also the physiochemical analysis indicate the energy potential in the feedstock. Further the pre-exponential factor was evaluated along with the reaction model which indicate a two stage process. The values of change in enthalpy, entropy and free energy suggests spontaneity of the process and its thermodynamic feasibility.

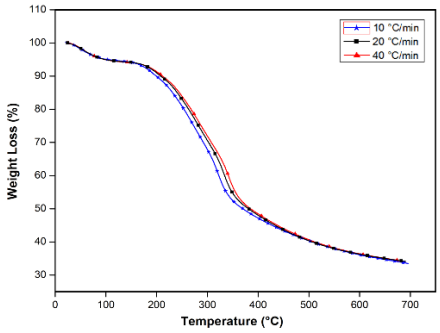

Figure 1. Weight loss curve at different heating rate.

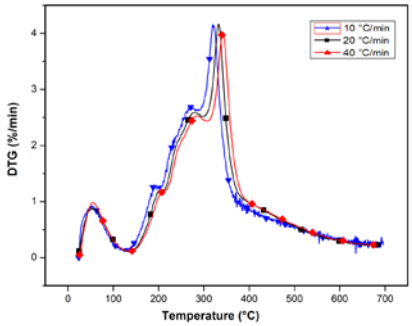

Figure 2. DTG curve at different heating rate.

4. Conclusions

Detailed physiochemical characterization of feedstock clearly indicates that energy can be extracted from it and it can be utilized as an alternate source of energy giving various liquid, gaseous and solid products. The various kinetic parameters indicates the mechanism taking place for the thermochemical conversion of this biomass. It indicates system is very reactive at the beginning and its reactivity decreases with extent of reaction. Further these studies will be significant in design of reactors, mass and energy balance and process optimization.

References

[1] I. Ali, H. Bahaitham, R. Naebulharam, A comprehensive kinetics study of coconut shell waste pyrolysis, Bioresouce Technol. 235 (2017) 1–11.

[2] R. K. Mishra, K. Mohanty, Pyrolysis kinetics and thermal behavior of waste sawdust biomass using thermogravimetric analysis, Bioresouce Technol. 251 (2018) 63–74.

[3] P. McKendry, Energy production from biomass (part 1): overview of biomass, Bioresouce Technol. 83 (2002) 37–46.

[4] M. J. Starink, The determination of activation energy from linear heating rate experiments: a comparison of the accuracy of isoconversion methods, Thermochim. Acta 404 (2003) 163–176.

[5] V. Dhyani, J. Kumar, T. Bhaskar, Thermal decomposition kinetics of sorghum straw via thermogravimetric analysis, Bioresouce Technol. 245 (2017) 1122–1129.

[6] P. S. Jimenez, L. P. Maqueda, A. Perejon, J.M. Criado, Generalized master plots as a straightforward approach for determining the kinetic model: the case of cellulose pyrolysis. Thermochim. Acta 552 (2013) 54–59.

[7] F. J. Gotor, J. M. Criado, J. Malak, N. Koga, Kinetic analysis of solid-state reactions: the universality of master plots for analyzing isothermal and nonisothermal experiments. J. Phys. Chem. A 104 (2000) 10777–10782.

[8] S. R. Naqvi, R. Tariq, Z. Hameed, I. Ali, M. Naqvi, W. H. Chen, S. Ceylan, H. Rashid, J. Ahmad, S. A. Taqvi, M. Shahbaz, Pyrolysis of high ash sewage sludge: Kinetics and thermodynamic analysis using Coats-Redfern method, Renew. Energ. 131 (2019) 854-860.

ECCE12
The 12th EUROPEAN CONGRESS OF CHEMICAL ENGINEERING
Florence 15-19 September 2019

Comparison of CuO-ZnO-X catalysts (X = Al_2O_3, MnO, ZrO_2) for the reverse water gas shift reaction at low pressure

A. Portillo*, A. Ateka, J. Ereña, A.T. Aguayo, J. Bilbao

Dep. Chemical Engineering, Univ. of the Basque Country UPV/EHU, P.O. Box 644, 48080 Bilbao, Spain;
*tel. +34 946015361, e-mail: *Corresponding author: ander.portillo@ehu.eus*

Highlights

- The r-WGS reaction at low pressure allows obtaining high CO yields from CO_2.
- r-WGS is interesting as a preliminary stage of the synthesis of hydrocarbons from CO_2.
- The CuO-ZnO-ZrO_2 catalyst is the most suitable for the r-WGS reaction.

1. Introduction

CO_2 valorization to fuels and chemicals plays a key role in the current commitment for reducing the consequences of global warming. In this regard, the direct synthesis of hydrocarbons (Fischer Tropsch, FTS) and the indirect synthesis through methanol (MeOH) as intermediate receive great attention. In both routes the r-WGS reaction plays a relevant role, since CO is more reactive than CO_2 [1]. Nowadays, the indirect synthesis is receiving more attention, since in this process catalyst deactivation and methane formation are lower.

Therefore, the aim of this work is to compare the activity of different CuO-ZnO based catalyst, doped with Al_2O_3, MnO or ZrO_2 (named CZA, CZMn and CZZr, respectively) for the r-WGS reaction at low pressure. The activity and stability of these catalysts for the synthesis of MeOH has already been established [2] and the low pressure study conducted here will allow to: i) identify CO yield avoiding its conversion to MeOH, and, ii) evaluate future prospects of these catalysts for the r-WGS reaction at low pressure as a previous stage in the hydrocarbons synthesis processes, given the advantages over CO_2 valorization, thus, greater reactivity of CO and lower water concentration in the medium (which attenuates reaction and favors catalyst deactivation)

2. Methods

CuO-ZnO-XO (CZX) metallic functions have been prepared by precipitation of the aqueous nitrate solution (1M) with the desired Cu/Zn/X ratio of 2/1/1.5 (being X= Al, Mn, Zr) with Na_2CO_3 (1M) at pH=7 and 70°C. The following stages consist of aging the precipitate at 70°C for 1 h, filtering and washing the precipitate to remove the remaining Na^+ ions, drying and calcination (300°C, 10h).

The runs have been conducted in a fixed bed reactor (Microactivity-Reference, PID Eng. Tech.) connected on-line to a Varian CP4900 micro gas-chromatograph for the continuous analysis of the products. Reaction conditions are as follows: H_2/CO_2 molar ratio in the feed, 3; temperature, 200-300 °C; pressure, 1.6-6 bar; space time, 5-13.5 $g_{cat}h(mol_C)^{-1}$; time on stream, up to 24 h.

3. Results and discussion

As an example, Figure 1a and 1b show the effect of pressure and temperature on the yield of the CO_2 hydrogenation reaction products (CO and MeOH) and CO/MeOH molar ratio, with CZMn catalyst and 13.5 $g_{cat}h(mol_C)^{-1}$. In light of the results in Fig. 1a, as predicted thermodynamically, higher pressures lead to higher MeOH production, while CO yield is lightly affected. However, increasing temperature (Fig. 1b) gives way to higher CO yield, as WGS equilibrium is highly dependent on temperature. Furthermore, MeOH production shows a maximum at 225ºC, justified both by the improvement of the kinetics at higher temperature, and to the thermodynamic limitations of exothermic reactions, as it is the case.

Fig 1c shows the catalytic behavior of the three studied catalysts. For CZZr catalyst, a remarkably higher CO yield is achieved at 3 bar and 350 ºC, which is the pursued goal for the selection of the most suitable catalyst to be used in the CO_2 valorization processes.

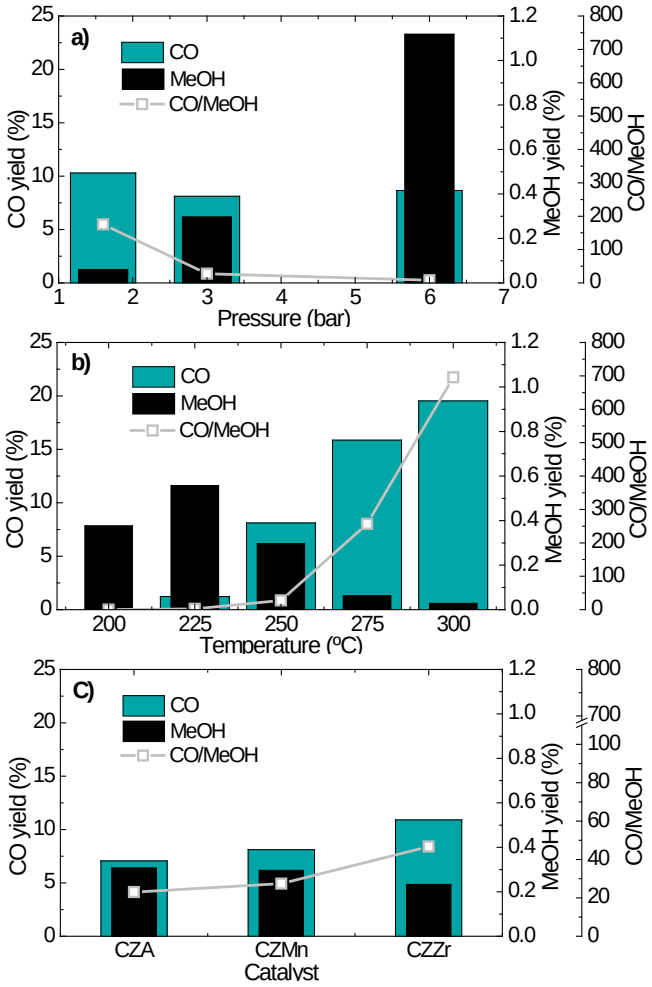

Figure 1. CO and MeOH yields and CO/MeOH ratio for CZMn at 13.5 g_{cat} h mol_C^{-1} and 250 ºC; 3 bar (b); and at 250 ºC and 3 bar for CZA, CZZr and CZMn.

4. Conclusions

Low pressure experiments have allowed ascertaining the activity for the r-WGS reaction of catalysts commonly used for the synthesis of MeOH, among which the activity of CZZr stands out. These results are interesting to contemplate the installation of a low pressure r-WGS unit (of moderate costs) as a previous stage to the synthesis hydrocarbons (at high pressure), with the advantages of the higher reactivity of CO and the presence of water in the feed, which would be separated at the outlet of the r-WGS unit).

Acknowledgements

This work has been carried out with the financial support of the Ministry of Economy and Competitiveness of the Spanish Government (CTQ2016-77812-R), the ERDF funds and the Basque Government (Project IT748-13). Ander Portillo is grateful for the Ph.D. grant from the Ministry of Science, Innovation and Universities of the Spanish Government (BES-2017-081135).

References

[1] E. Catizzone, G. Bonura, M. Migliori, F. Frusteri, G. Giordano. Molecules, 2018. *23,* 31

[2] A. Ateka, I. Sierra, J. Ereña, J. Bilbao, A.T. Aguayo. Fuel Proc. Tech. 2016. *152*, 34-45.

ECCE12
The 12th EUROPEAN CONGRESS OF CHEMICAL ENGINEERING
Florence 15-19 September 2019

Catalytic thermal decomposition of methane using solar energy

SungEun Kim[1], HakJoo Kim[2,*], JongKyu Kim[2], SangNam Lee[2]

1 Korea University, 5 Anam-ro Seoul Republic of Korea;

2 Korea Institute of Energy Research, 152 Gajeong-ro Daejeon Republic of Korea

**Corresponding author: hakjukim@kier.re.kr*

Highlights

- Methane was catalytically decomposed to hydrogen and carbon black.
- Various carbon-based catalysts were tested.
- Pore size and content of disordered carbon affected the catalytic activity and stability.
- Carbon black catalysts were active and stable for long operation time.

1. Introduction

Biogas produced from municipal waste typically contains methane and carbon dioxide as main products. Since methane concentration in the biogas is generally around 50%, it is combusted as a fuel for heating or cooking. Combined with the removal process of CO_2, methane can also be used in a gas engine to convert its energy into electricity and heat or compressed as CNG to power motor vehicles. Since methane is combusted in the gas or motor engines, production of CO_2 is inevitable. The thermal decomposition of methane (TDM) to hydrogen and carbon black using renewable energy is considered as a promising route to use efficiently the energy of methane without emitting greenhouse gas CO_2. The carbonaceous solid product can be either sequestered without CO_2 release or used as a valuable material commodity in different applications. It can also be applied as reducing agent in metallurgical industry. The generated H_2-rich gas mixture can be directly used as fuel for internal combustion engines or further processed to high purity H_2 for being used in fuel cells [1]. TDM (non-catalytic) typically requires temperatures higher than 1,300 ^oC in order to achieve reasonable reaction rates. Consequently, the use of catalysts (either metallic or carbonaceous catalysts) was investigated in order to operate at lower temperature and improve the process kinetics [2].

2. Methods

In this work, carbonaceous catalysts were prepared by pelletizing commercial carbon black with chemical binders and iso-propyl alcohol and thermal aging process. The prepared catalysts were characterized by SEM, XRD, BET, TGA, FT-IR. The activity of the catalysts toward methane decomposition was evaluated in a conventional fixed bed reactor. The catalysts, under a stream of CH_4/N_2 (50%vol CH_4/ N_2 at a total flow of 100mLmin^{-1}), were heated from RT up to 1,000 ^oC at 10 ^oC min^{-1} and kept constant at 1,000 ^oC for 4h.

3. Results and discussion

Four type of carbon-based catalysts, activated carbon(AC) derived from palm trees, commercial carbon blacks(CB) in bead and pellet form and mesoporous carbon were tested. From the analysis of N_2 adsorption isotherms, CB bead and mesoporous carbon showed an isotherm pattern having mesoporous pore structure. The methane decomposition was carried out at 1,000°C with the residence time of 1.02s. Among the catalysts tested, CB catalyst in bead form showed the best activity and stability with 200 minutes of reaction time. All other catalysts showed an incremental deactivation or poor initial activity. The catalyst activity is summarized by comparing the values of maximum and stabilized conversion level. The physical properties of the used catalysts were found to dramatically change with the reaction. A deep loss of BET SA was observed with all the tested catalysts, especially with those having mainly micro pore structures like the AC and CB pellet form catalysts. Pore re-construction was thought to be present due to the deposition of carbon within the pore structure of the catalysts. Average pore diameters tended to increase after the reaction. Graphitic mesoporous carbon had poor activity towards methane decomposition. Among the tested catalysts, CB bead form catalyst retained its mesoporous structure within after exposure to the high temperature reaction temperature, carbon nano-tubes were found to be formed with the pores of the catalysts. Initial turbostratic carbon and mesoporous pore structure present in the CB bead catalyst was found to be resistant for the pore re-construction and blockage leading to catalyst deactivation.

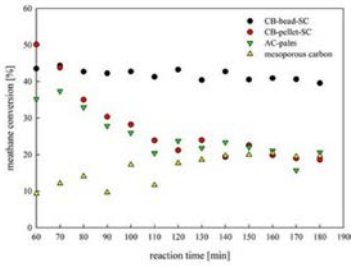

Figure 1. Catalyst activity.

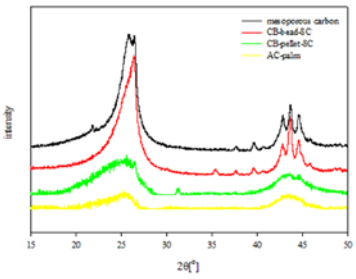

Figure 2. XRD patterns

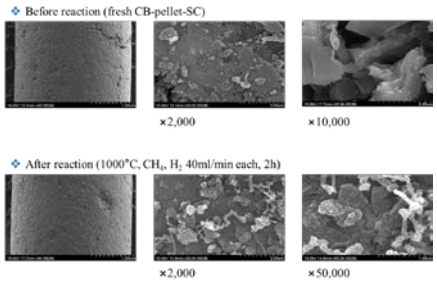

Figure 3. SEM images of CB pellet catalyst

4. Conclusions

Pore re-construction has undergone during methane decomposition. Filamenteous carbon growth blocked the mouth of micro-pores, which decreased severely the BET SA and developed new meso-pores. Catalytic activity of methane decomposition catalysts was related to the nature of carbon present on the surface in the order of amorphous > turbostratic > graphitic.

References

[1] S. Abanades, H. Kimura, H. Otsuka, Fuel Proces. Tech. 122 (2014) 153-162.

[2] R. Guil-Lopez, J.A. Botas, J.L.G. Fierro, D.P. Serrano, Appl. Catal. A Gen. 396 (2011) 40-51.

ECCE12
The 12th EUROPEAN CONGRESS OF CHEMICAL ENGINEERING
Florence 15-19 September 2019

CFD simulation of steam distribution in vertical tube bundle at high pressures.

Arijit Ganguli[1]

1 School of Engineering and Applied Sciences, Ahmedabad University, Ahmedabad, Gujarat, 380009

**Corresponding author: arijit.ganguli@ahduni.edu.in*

Highlights

- CFD simulations in header and tube assembly to quantify extent of non-uniformity.
- Mal-distribution at high pressures
- Attempt to design innovative distributor to reduce mal distribution

1. Introduction

The distribution of a fluid stream into a number of parallel substreams by means of the channels is accompanied by fluid pressure changes owing to the change of fluid momentum in the conduits, while the effect of wall friction in the conduits is negligibly small compared with that in the channels (Bassiouny and Martin, 1984). Such arrangements are found in industrial equipments (heat exchangers) where the flow is distributed from a main header to a number of tubes. Ample amount of research has been done on this problem by researchers over the past (Acrivos et al., 1959; Bassiouny and Martin, 1984). In such cases, the sudden changes in flow direction make the pressure rise in the top header and fall in the bottom header (Gandhi et al. 2011). Gandhi et al. (2011) have carried out simulations at high pressures and eliminated the middle tube for achievement of uniform flow distribution. However, in some situations where the geometry is such that the middle tube is exactly beneath the feed pipe then the use of internals may help in achieving better distribution. CFD studies for pressures around 60-70 atm is difficult and is rarely found in the literature

2. Methods

A three dimensional grid has been considered in the study. A non-uniform hexahedral mesh has been created for each configuration. For the geometry the mesh size is 18,634 hexahedral cells with fine cells inside the tubes and walls and uniform mesh at the headers. The grid independency for the geometry was carried out with three different grids namely 128,000, 186,000 and 232,000 and the centerline axial velocity was checked. Since the difference between the magnitude of centerline axial velocity was 1% for the 186000 and 232000 grids, 186000 grids was selected for investigation. The basic governing equations of continuity and momentum in Cartesian co-ordinates have been used. The k-ω turbulence model has been used for modeling the turbulence. The commercial software Ansys FLUENT 18 has been used. In case of k-ω model, Quadratic upstream interpolation for convective kinetics (QUICK) discretization scheme was used for the

turbulence parameters. For final sweep over each segment, upwinding has been performed using the QUICK with a second order pressure scheme. The QUICK formulation has a third order accuracy and which helps to mitigate the unfavorable effect of artificial diffusion that can occur when using low order upwinding schemes. All the discretized equations were solved in a segregated manner with the PISO (Pressure Implicit with Splitting of Operators) algorithm. In the present work, steady simulations were performed. All the solutions were considered to be fully converged when the sum of residuals was below 10^{-5}.

3. Results and discussion

The pressure drop is calculated as: Pressure Drop $(\Delta P) = \sum_{x/L=0}^{1} \left(P_{(x/L)_T} - P_{(x/L)_B} \right)$.

The pressure drop profile is shown quantitatively in Figure 1A. Further, the velocity distribution has also been shown in Figure 3B. The dimensionless velocities at the top and the bottom headers show high velocities at the inlet. This indicates that all the fluid passes from the center of the tubes as shown in Figure 1B.

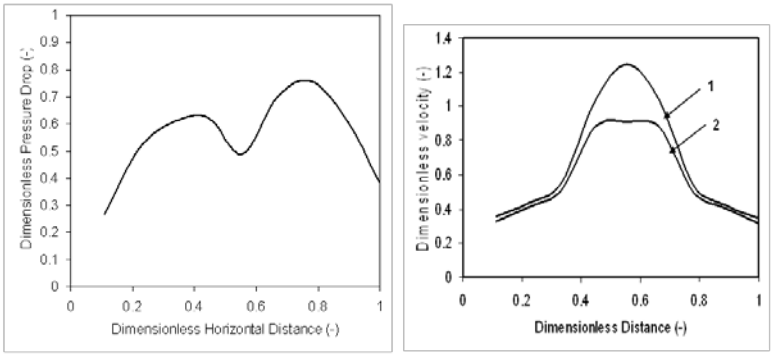

Figure 1. (A) Effect of dimensionless pressure drop with dimensionless horizontal distance (B) Effect of non-dimensional velocity on non-dimensional horizontal distance (1) At the inlet of the central tube (2) At the outlet of central tube.

4. Conclusions

CFD simulations have been carried out for header tube geometry where inlet and outlet are at the middle of the top and bottom headers. It is seen that at low pressures the extent of non uniformity increases with an increase in pressure when conventional geometry is considered. For very high pressures upto 70 bars the mal-distribution is significantly lower than the parent one

References [Calibri 10]

[1] Acrivos A., Babcock B.D., Pigford R.L., Chem. Eng. Sci. 10, (1959) 112-124.
[2] Bassiouny M.K., Martin H., Chem. 858 Eng. Sci. 39, (1984) 693–700..
[3] Gandhi M.S., Ganguli A.A., Joshi J.B., Vijayan P.K., Chem. Eng. Res. Des. 2011.

ECCE12
The 12th EUROPEAN CONGRESS OF CHEMICAL ENGINEERING
Florence 15-19 September 2019

Energy and Chemical Engineering

The development of an exergoeconomic indicator to define the optimum blending fraction in processing crude oils

P. S. O. Silva[1], F. G. Martins[1*]

1 LEPABE - Laboratory for Process Engineering, Environment, Biotechnology and Energy, Faculty of Engineering, University of Porto, Rua Dr. Roberto Frias, 4200-465 Porto, Portugal]

**Corresponding author: fgm@fe.up.pt*

Highlights

- Heavy crude oils have a better exergy efficiency.
- Conventional crude oils are more profitable.
- An indicator is proposed to achieve a compromise between sustainability and profitability.

1. Introduction

The reserves of typical crude oils (CO) are scarce, although the society still heavily depends on them. The society is consuming this resource in a non-sustainable way which will make it collapse. 70% of the CO resources are available as heavy CO, oil sands and bitumens, which are less attractive to refineries. Refining these types of CO is more expensive due to their high viscosity and high sulfur content but they are very cheap. Refineries must often blend different types of CO to achieve the desired products specifications. An objective of blending is using heavy CO without compromising the quality of products while increasing the profitability and sustainability of the refining processes.

2. Methods

In this work, it is evaluated the impact of the blend composition on the performance of the topping distillation unit. The blend considers the CO: Sahara Blend and Tia Juana Heavy. The mass fraction of each CO is the manipulated variable while the other operatory conditions are kept constant.

Energy analysis is performed to quantity heating and cooling requirements. This is combined with an exergy analysis to identify how energy quality is conserved during the process. Exergy is strongly related to sustainability because it allows reducing the degradation of energy quality.

Exergy is divided into physical and chemical exergy. Chemical exergy is difficult to quantify, especially in petroleum cuts. Each of these cuts is defined as a pseudo-component because its chemical composition cannot be specified. In order to obtain this value, a set of correlations has to be used [1].

Feed composition affects the products obtained in the distillation unit. Heavy CO yield higher percentages of residues which have a lower economic interest. An economic analysis has also performed to identify which compositions are more profitable.

Analyses, where the economic and exergetic perspectives are combined, have been proposed in some literature and are called exergoeconomics analysis [2]. In this work, a new exergoenomic indicator is proposed because improving the exergy efficiency may incur in additional costs and it may not be attractive for a company to implement the proposed optimization.

3. Results and discussion

Heating and cooling duties vary during this analysis because a lighter blend requires more heating due to a higher content of light-ends to be distilled (Figure 1).

Exergy efficiency decreases with the amount of typical CO (Figure 2). Heavy CO yield a greater amount of fractions with high boiling points and, according to the definition of exergy, a stream with higher temperature has more energy quality.

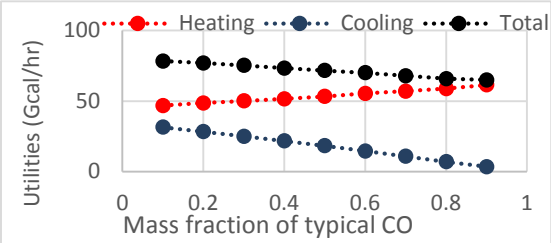

Figure 1 – Effect of the feed composition on the utilities consumption.

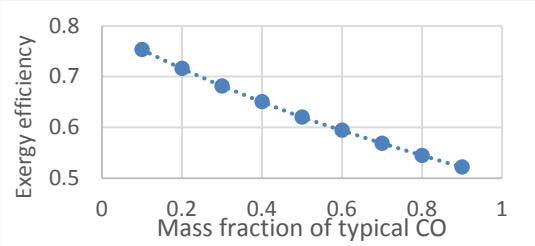

Figure 2 – Effect of the feed composition on the exergy efficiency.

Economically, conventional CO increase the profitability of the process because the fractions obtained have higher economic interest (Figure 3). This indicator measures the added value to the production. Since exergy and economic indicators have contrasting results, a new indicator was proposed to evaluate both aspects simultaneously. This indicator is a compromise between the profitability and sustainability of the process and is obtained through the multiplication of the previous indicators (Figure 4).

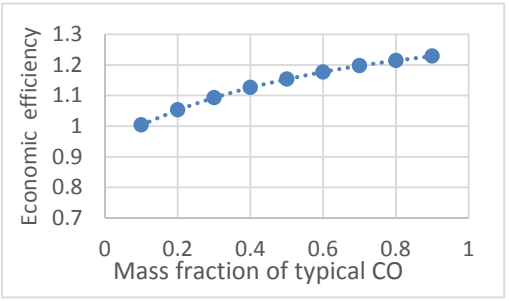

Figure 3 – Effect of the feed composition on the economic efficiency.

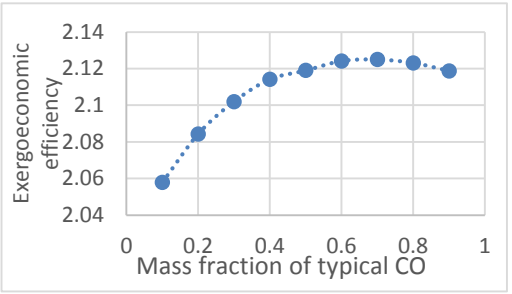

Figure 4 – Proposed exergoeconomic indicator.

4. Conclusions

In this work, it was evaluated the effect of crude oil composition on the overall performance of the topping distillation unit. Energy, exergy and economic analyses were performed. Heavy CO have higher exergy efficiencies while conventional CO are more profitable. A new indicator was proposed to achieve a compromise between profitability and sustainability indicating the optimum blend fraction.

Acknowledgements: This work was financially supported by: Project "LEPABE-2-ECO-INNOVATION" – NORTE-01-0145-FEDER-000005, funded by Norte Portugal Regional Operational Programme (NORTE 2020), under PORTUGAL 2020 Partnership Agreement, through the European Regional Development Fund (ERDF).

References

[1] Coker, A.K., Petroleum Refining Design and Applications Handbook. 2018: John Wiley & Sons.
[2] Tsatsaronis, G., Definitions and nomenclature in exergy analysis and exergoeconomics. Energy, 2007. 32(4): p. 249-253.

ECCE12
The 12th EUROPEAN CONGRESS OF CHEMICAL ENGINEERING
Florence 15-19 September 2019

Electrochemical system for wastewater treatment and low voltage water electrolysis decoupling hydrogen production using bioelectrochemical system

Jonathan DESEURE[1,2*], Pierre BELLEVILLE[1,2], Gérard MERLIN[1,2,3]
[1] *Univ. Grenoble Alpes, CNRS, Grenoble INP, LEPMI, 38000 Grenoble, France;*

[2] *Univ. Savoie Mont Blanc, LEPMI, 73000 Chambéry, France*

[3]*Laboratoire d'Optimisation et Conception d'Ingénierie Environnementale (LOCIE), UMR CNRS 5271 Université de Savoie Mont-Blanc, Le Bourget du Lac, FRANCE*

**Corresponding author: jonathan.deseure@lepmi.grenoble-inp.fr*

Highlights

- Hydrogen generation coupling Electrolyser with MFC device
- Hydrogen production with only 1 V of cell voltage
- Wastewater valorization

1. Introduction

Wastewater is a huge reservoir of biomass energy already collected but still generating more costs than added-value products. Microbial electrochemistry technology development is a real opportunity to take advantage of this energy source. Freshly we have validated the proof of concept of an innovative device associating a bioelectrochemical system and a decoupled water electrolysis in order to produce hydrogen [1]. This architecture consists of two reactors running separately linked through a redox mediator cycle : i) a Microbial Fuel Cell (MFC) cascade system which oxidates wastewater while reducing potassium hexacyanoferrite ii) an electrolysis cell using a semipermeable separator which produces H_2 while regenerating the mediator.

,2. Methods

Microbial fuel cell (MFC) is a spontaneous electrochemical process that allows current recovery between two reactions: acetate oxidation at the anode and HCF(III) reduction at the cathode.

$$C_2H_3O_2^- + 4H_2O \rightarrow 2HCO_3^- + 9H^+ + 8e^- \quad (1)$$

$$[Fe(CN)_6]^{3-} + e^- \rightarrow [Fe(CN)_6]^{4-} \quad (2)$$

In the electrolyser, two reactions occur at anode electrode, the HCF(II) oxidation and the water reduction in the catholyte solution. The anolyte pH must be maintained to high values (alkaline) to avoid an acidic reaction on HCF (II). In addition, NaH2PO4 buffer solution is employed and K2SO4 salt is added to increase ionic conductivity. Therefore, catholyte had the similar pH value and similar buffer composition.

[Fe(CN)6]4- → [Fe(CN)6]3- + e- (3)

According to De Silva Munoz et al. [2] two steps of electrochemical reduction are possible in phosphate buffer:

$$H_2PO_4^- + e^- \rightarrow H_{ad} + \mathrm{H}PO_4^{2-} \quad (4)$$

$$e^- + H_{ad} + H_2PO_4^- \rightarrow H_2 + \mathrm{H}PO_4^{2-} \quad (5)$$

And the acid-base equilibrium:

$$\mathrm{H}PO_4^{2-} + H_2O \rightarrow H_2PO_4^- + OH^- \quad (6)$$

With the acid-base equilibrium leads to water reduction as follow:

$$2H_2O + 2e^- \rightarrow H_2 + 2OH^- \quad (7)$$

3. Results and discussion

On one hand, organics acid oxidation is coupled to HCF(III) reduction. On the other hand, oxidation of HCF(II) is coupled to water splitting. HCF couple appears to be an interesting opportunity as a mediator in electrolyser for several reasons : i) a low overpotential at low current density which will overcome MFC system limitation using oxygen reduction reaction; ii) a low thermodynamic redox potential which reduces energy costs for water splitting (vs anodic water oxidation); iii) a high reversibility and stability which justifies its wide use in electrochemical system. The aim of this work is to validate the feasibility of such coupled systems as a proof of concept. Using a simple architecture, our MFC cascade system fed with glucose produces a current density up to 1.9 $A.m^{-2}$ (with a COD removal rate of 30 mol.m-2.d^{-1} and a HCF(III) reduction rate of 8.9 $mol.m^{-2}.d^{-1}$).

4. Conclusions

The apparatus can lead to hydrogen production by water electrolysis at cell potential below 1V with a current density up to 30 $mA.cm^{-2}$. This technology offers new perspectives for microbial electrochemistry technology development while limiting several bottleneck of direct energy recovery using microbial electroactivity. Decoupling hydrogen production and biocatalyzed biowaste oxidation permits to i) avoid oxygen reduction reaction limitations in both units, ii) produce energy vector in low cost reactor ant to yield high rate hydrogen in usual electrolyzer. In order to propose low cost system, we have developed mediator electrolyser using carbon and stainless steel electrodes.

References

[1] Belleville et al. International Journal of Hydrogen Energy, 43, 14867, 2018

[2] De Silva Munoz et al. International Journal of Hydrogen Energy, 35,8561, 20 0

ECCE12
The 12th EUROPEAN CONGRESS OF CHEMICAL ENGINEERING
Florence 15-19 September 2019

Carbon flows in macro energy planning: The case of the Swiss energy system

Xiang Li[1], Theodoros Damartzis[1], Zoe Stadler[2], Stefano Moret[1], Boris Meier[2], Markus Friedl[2], François Maréchal[1]

[1]*Industrial Process and Energy Systems Engineering (IPESE), Ecole Polytechnique Fedérale de Lausanne (EPFL) Valais, 1951, Sion, Switzerland;* [2]*Hochschule für Technik Rapperswil, Oberseestrasse 10, Rapperswil, Switzerland*

**Corresponding author: xiang.li@epfl.ch*

Highlights

- Macro energy systems planning by prospective optimization modeling based upon Energyscope.
- Complete carbon flow chain from *cradle to grave* in different scenarios.
- Exploration of the role of CCUS (carbon capture, utilization and sequestration) and a broad set of Power-to-X technologies in energy transition.
- Analysis on the quasi-neutrality of carbon emission.

1. Introduction

Decarbonation as one of the core objectives delivered by Paris Agreement [1] in 2015, is expected to be approached by: 1) massive introduction of renewable energy sources; 2) deployment of CCUS technologies. Some prospective energy models declare that the anthropogenic carbon emissions in Switzerland in 2050 could be optimized to below 5-10 Mt/year, which is however difficult to get further mitigated taking into consideration the emissions during construction periods in the perspective of a Life Cycle Analysis (LCA).

Compared to intermittent renewables, the emission of biomass technologies in construction period is trivial, despite relatively important emissions during the operational periods, which is yet possible to be recovered by applying carbon capture technologies. The captured GHG (Green House Gases) could be either sequestrated directly underground, or take the role as a storage medium for intermittent electricity from renewables, e.g. by participating in electrolysis and methanation processes known as Power-to-Gas. Up to now, merely 4% [2] of fossil carbon is used in non-energy use to make products in Switzerland. Therefore, it is promising to produce chemical products such as plastics, commodity chemicals and energy carriers free from fossil CO_2 by carbon reutilization technologies. This article aims at estimating the possible carbon demand for different usage in long terms, and exploring the optimal configuration of carbon flows by linking the carbon sources and carbon sinks in techno-economic and ecologic perspectives.

2. Methods

The methodology of the research is categorized into 3 steps: first the carbon sources and carbon sinks in Switzerland are identified, including the demand for carbon-related chemical products; then a broad set of conversional technologies are modelled and integrated based upon existing

technologies and newly added biomass and CCUS technologies in Swiss Energyscope (SES) [3], an open-source MILP (Mix Integer Linear Programming) optimization tool for energy system developed by EPFL. The model takes a “snapshot” of the optimized Swiss energy system in 2050, with the objective of minimizing the total cost subjected to various constraints [4] such as supply-demand, availability of resources, as well as the potential of conversional technologies. CCUS technologies are categorized into CC (carbon capture), CCS (carbon storage) and CCU (carbon utilization) in order to precisely depict the carbon flows. Each technology within its corresponding category is associated with a specific cost and an energy penalty coefficient. In this model, the carbon sources are divided into two branches: carbon-intensive energy industries, such as fossil-based power plants, cements etc., and carbon from the atmosphere. It is assumed that only the DAC (Direct Air Capture) technology could be applied to atmospheric carbon capture. The total Global Warming Potential (GWP) is then expressed as a trade-off between the carbon emissions and the reduction by deploying CCUS, which is subjected to an ε-constraint limiting the upper bound of GHG emissions. The third step lies in scenario generation for understanding the impact of different pathways of carbon flows into the energy system.

3. Results and discussion

The energy system will become inevitably more expensive by increasing carbon mitigation. Carbon flows Sankey diagrams illustrate the carbon sources and sinks and the corresponding conversional technologies. In a low carbon scenario with high penetration of renewables, more biomass technologies are used to produce bio-diesel or synthetic natural gas for satisfying in principle the mobility demands. The CCUS technologies do not appear until the total emission threshold reaches 5 - 10 Mt/year, where amine gas treating becomes dominant among carbon capture technologies. Carbon sequestration is less competent compared to carbon utilization contributing to reduce the total cost by decreasing chemical products import expenses.

4. Conclusions

The study sheds light on the optimized configuration of carbon flows in the horizon of 2050 for Switzerland, displaying the importance of biomass in the future energy system as the dominant carbon source in operation. CCUS implementation is obligatory in order to realize quasi-neutrality of carbon emission: the results demonstrate that the total GWP emission in the point of LCA could be controlled within 4 - 6 Mt and 0 - 3 Mt respectively in the absence and presence of CCUS technologies, respectively.

References

[1] J. Rogelj et al., Paris Agreement climate proposals need a boost to keep warming well below 2 °C, Nature, vol. 534, no. 7609, pp. 631–639, 2016.

[2] International Energy Agency. 2017. Statistics. Available at: https://www.iea.org/statistics/?country=SWITLAND&year=2015&category=Energy%20supply&indicator=OilProd&mode=table&dataTable=OIL

[3] S. Moret, V. Codina Gironès, F. Maréchal and D. Favrat, Swiss-energyscope.ch: a plat- form to widely spread energy literacy and aid decision-making, 17th Conference on Process Integration, Modelling and Optimisation for Energy Saving and Pollution Reduction, Czech Republic, 2014.

[4] V. Codina Gironès, S. Moret, F. Maréchal, and D. Favrat, Strategic energy planning for large-scale energy systems: A modelling framework to aid decision-making, Energy, vol. 90, pp. 173–186, 2015.

ECCE12
The 12th EUROPEAN CONGRESS OF CHEMICAL ENGINEERING
Florence 15-19 September 2019

Hydrogen Storage in LOHC and the Chances for Energy Supply, Mobility and Society

Eberhard Schluecker[1]

1 University of Erlangen-Nuremberg, Germany, Cauerstr. 4, D-91058 Erlangen

**Corresponding author: sl@ipat.uni-erlangen.de*

Highlights

- Hydrogen Storage in LOHC; 2,1 KWh/Kg.
- Examples for the developed and used Equipment.
- Decentral energy supply, effects on society, chances for mobility
- Examples for energy efficiency due energy networks

1. Introduction

Due to the ongoing observed developments and trends of our climate, it can no longer be denied that human impact on global cycles cause our planet great, perhaps even irreparable damage that future generations will have to bear. We therefore need to think about regenerative energy technology goals and decentral energy supply, for the preservation of mankind and the planet.
This presentation will therefore focus exclusively on the Hydrogen LOHC storage method for the use as energy supply of the future, but also the chances for mobility and society.
When we think about our future, we have to live independent from fossil resources. Therefore, hydrogen is the most favourable for a certain basic energy supply. Hydrogen is available in water but at the same time, we do not want to consume it, rather to put it into a cycle. Hydrogen as a basis for chemical processes is very energy-rich at 33 - 39.41 KWh/Kg calorific value, but it also has some disadvantages in energy storage. It has the lowest density of all gases and difficult to store. The classical storage method, to achieve the necessary density, therefore used are the compression up to 70 MPa or the cryogenic state (liquid hydrogen). Unfortunately, the high pressure and/or the extreme cooling requirements are problematic and cost-intensive. Last, but not least, there are still safety considerations regarding to compressed hydrogen and also to free hydrogen.

2. Methods

The new method of hydrogen storage technology – presented - eliminates all these problems and concerns by storing the hydrogen in chemically bound form on a LOHC (Liquid-Organic-Hydrogen-Carrier). Of necessity, this chemical must be chemically very stable so that the thermally driven separation of the hydrogen (recovery) does not destroy the molecules. At the same time, the molecules should not produce any toxins (i.e. no nitrogen, chlorine, etc.) if they should be burned as residues and only the pure aromatics remain. To prevent the toxicity di-benzene-toluene was chosen. Here 18 atoms hydrogen can dock and also “REACH” documentation (safety documents) exist for this chemical. The energy that can be stored in it is 2.1 KWh/litre, which is roughly

equivalent to the amount of hydrogen in 70 MPa containers. Another advantage is, the liquid is absolutely safe against ignitions.
The presentation shows the whole system but also some special apparatuses and further equipment used.

3. Results and discussion

With this energy storage technology, with an exothermal reaction process (250°C, waste heat), you now have a liquid that fits exactly into our heating oil and petrol infrastructure. The LOHC is oil-like and therefore readily pumped. The disadvantage that needed to be overcome was the relatively high temperature (300°C) necessary for dehydration. This was the focus of recent research which showed it was possible to reduce the required temperature to approx. 130°C using a clever combination of parameters (patent pending). This means that LOHC technology can now be used in many different ways as dehydrogenation can now be carried out with the waste heat from a fuel cell, which we use to convert hydrogen into electricity. But in addition, sunlight or other waste heat sources can be used.
One example of this is in sewage treatment plants. Here the oxygen can be used for the purification process of the sewage and the waste heat for drying sludge, while the hydrogen is stored and used for energy consumption elsewhere (equipment run with hydrogen, hydrogen filling station, etc.). It quickly becomes clear that other business models are also possible and, for example, a sewage treatment plant can become an energy seller.
There are also possibilities in urban or industrial environments always in combination with hydrogen storage:

1. Oxygen for efficient combustion processes or for steel mills
2. Waste heat for local and distributed heating supply but also for cooling devices in summer
3. Waste heat utilisation for seawater desalination, for thermal production processes (extraction, rectification, reaction) and for cooling or for greenhouses in winter
4. Boosting the geothermal capacity with LOHC waste heat: Build the reactor into the upflow of geothermal energy. The Carnot efficiency could thus be increased from 16 - 20% to approx. 50%. And the remaining residual heat could still be used in heat networks.

4. Conclusions

The described new energy storage method allows to store huge amounts of energy just in tanks and is a big chance for decentral energy supply but also can be used for mobile applications like ships, trucks, or cars. Furthermore the shown LOHC-System can be a basis for high efficient energy networks and may be a basis for the change of the society (participation or identification)

References

[1] https://www.fz-juelich.de/SharedDocs/Pressemitteilungen/UK/DE/2018/2018-04-19-lohc-zug.html .
[2] Milella, V.O.; Koelpin, A.; Schluecker, E.: Automation of the Storing-In Part of a Hydrogen-Storage System using Liquid Organic Hydrogen Carriers (2017), https://doi.org/10.1002/ente.201700519
[3] Reuß M.; Grube T.; Robinius A.; Preuster P.: Wasserscheid, P.; Stolten. D.: Seasonal storage and alternative carriers: A flexible hydrogen supply chain model, Applied Energy, 0306-2619/© 2016 Published by Elsevier Ltd. http://dx.doi.org/10.1016/j.apenergy.2017.05.050,
[4] Brückner, N.; Obesser, K.; Bösmann, A.; Teichmann, D.; Arlt W.; Dungs, J.; Wasserscheid, P.: Evaluation of Industrially Applied Heat-Transfer Fluids as Liquid Organic Hydrogen Carrier Systems
(2013), CHEMSUSCHEM, https://doi.org/10.1002/cssc.201300426

ECCE12
The 12th EUROPEAN CONGRESS OF CHEMICAL ENGINEERING
Florence 15-19 September 2019

Explosion Parameters of Hydrocarbons from Fischer-Tropsch Synthesis

Jan Skřínský

Energy Research Center, VŠB-TU of Ostrava, 17. listopadu 2172/15, 708 00 Ostrava, Czech Republic

**Corresponding author: jan.skrinsky@vsb.cz*

Highlights

- Explosion parameters of HCs from F-T synthesis for the first time.
- Preliminary investigation in the 20-L vessel before being scaled-up to 1.00 m^3.
- Comparison with pure HCs.

1. Introduction

Nowadays there is a worldwide demand to develop energy efficient and economical processes for sustainable production of alternative chemical compounds and fuels as a substitute for those emerging from petroleum [1]. Small-scale characterisation in the liquid phase towards understanding explosion deflagration over a range of fuel concentrations, temperatures and pressures has been published limitedly [2-6]. In comparison with the pure liquid-fuels for the more complex mixtures, no studies are available. The present paper describes a series of preliminary experiments performed to study the explosion parameters of complex hydrocarbons (HCs) fuel produced from micro-scale Fischer-Tropsch Synthesis (FTS). Such metodology allows rigorous insightful chemical interpretation of well-defined sample and deeper experimental view into a chemical explosion problem. The results could be in the future used to evaluate mass burning rate and flame development duration and combustion duration.

2. Methods

A micro-scale FT plant with fixed bed reactor was designed and used at ERC, VŠB-TU of Ostrava to study the production of liquid hydrocarbons over Co-based FT catalysts. A simulated N_2-rich syngas (containing: H_2, CO and N_2) was used to feed into the reactor inlet for the production of synthetic liquid hydrocarbon fuels. The liquid hydrocarbon products were analyzed off-line using a DB1 column combined with a gas chromatography-mass spectrometry (GC–MS) PerkinElmer. These products include light hydrocarbons (C1 and C2), olefins, LPG (C3-C4), naphtha (C5-C11), diesel (C12-C20) and wax (>C20) fractions. Explosion parameters values of the pure liquids and the mixtures were determined experimentally according to the EN 15967:2011. The 0.02 m^3 oil-heated spherical vessel setup was used to record pressure-time curves. The 0.02 m^3 apparatus incorporated a digitally adjustable external control device Presto A30 (SN: 10291377, JULABO GmbH, Seelbach, Germany). The dynamic pressure in the vessel was measured by a pair of quartz pressure sensors (SN: 4512821 and SN: 4512822, model 701A, Kistler, Winterthur, Switzerland) and recorded with a charge amplifier (Kistler, model 5041E0). Programmable logic controller (model 5073A211 in 0.02 m^3, Siemens, Munich, Germany) connected to a PC was used with the interface (PROMOTIC system, MICROSYS, spol. s.r.o., Ostrava, Czech Republic) to automatically control the whole testing procedure.

3. Results and discussion

Figure 1 plot examples of the normalized explosion pressure, p_{max}/p_0, versus the concentration for FT–air mixtures. The normalized explosion pressures were obtained at initial temperature (78 °C). The maximum value of explosion pressure and the deflagration index were found at the concentration close to 12 vol. %. The shape of the explosion pressure versus concentration show a reasonable agreement with the previous studies [2-6] with the exception for the explosion pressure difference between the lower/upper explosion limit and its subsequent concentration. As compared with the published experimental results, the presented values sharply drop to zero from 4.8 bar and 5.8 bar, respectively. Such a behaviour involves the lower ignitability in comparison with the pure liquid-fuels. The described behaviour needs more rigorous experimental investigation from the chemical point of view to elucidate the possible mechanisms of action behind the presented experiments.

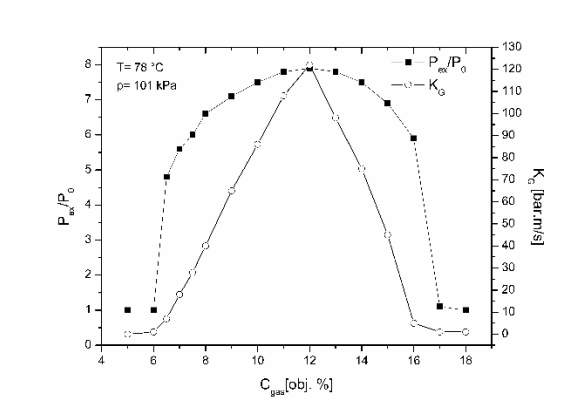

Figure 1. The explosion pressure and the deflagration index at different concentrations.

4. Conclusions

The explosion pressure p_{exp} and and the deflagration index K_G, were examined on the basis of combustion pressure history and compared with the pure liquid-fuels.

1. Explosion pressure and deflagration index of the F-T mixture reach maximum values at the stoichiometric concentration C = 12.0 vol. % within the studied range from 5.0 to 18.0 vol. % at representative initial temperature of 78 °C and initial pressure of 101 kPa.
2. The maximum explosion pressure, p_{max}, was determined as the highest p_{ex} found for the mixture compositions investigated and is equal to 7.9 ± 0.2 bar.
3. The deflagration index was calculated from the experimentally determined $(dp/dt)_{max}$ value and is equal to 122 ± 10 bar.m/s.

References

[1] Q. Li; Y. Cheng; Z. Huang *J. Loss Prev. Proc.* **2015**, *37*, 91–100.
[2] Q. Li; Y. Cheng; W. Jin; Z. Huang *Fuel* **2015**, *161*, 78–86.
[3] M. Mitu; E. Brandes *Fuel* **2015**, *158*, 217–223.
[4] M. Mitu; E. Brandes *Fuel* **2017**, *203*, 460–468.
[5] M. Mitu; E. Brandes; W. Hirsch *Process Saf. Environ. Prot.* **2018**, *117*, 190–199.
[6] J. Skrinsky ; T. Ochodek, *Energies* **2019**, *12*(8), 1574.

ECCE12
The 12th EUROPEAN CONGRESS OF CHEMICAL ENGINEERING
Florence 15-19 September 2019

Hydrothermal carbon materials for energy and biomass conversion

Natalia Rey-Raap[1], Lucília S. Ribeiro[1], Rafael G. Morais[1], José J.M. Órfão[1], José L. Figueiredo[1], M. Fernando R. Pereira[1]*

[1] *Laboratory of Separation and Reaction Engineering - Laboratory of Catalysis and Materials (LSRE-LCM), Department of Chemical Engineering, Faculty of Engineering of the University of Porto, Rua Dr. Roberto Frias s/n, 4200-465 Porto, Portugal*

** Corresponding author: fpereira@fe.up.pt*

Highlights

- The properties of hydrothermal carbons can be easily controlled.
- Well-developed microporosity results in materials with higher electrocatalytic activity.
- Total conversion of cellulose and a sorbitol yield of 59 % is attained after 3 h.

1. Introduction

Energy and biomass conversion are two of the most important issues to achieve a sustainable society. Fuel cells are one of the most efficient technologies for energy conversion. The performance of a fuel cell is mainly controlled by the oxygen reduction reaction (ORR) that takes place at the cathode. The most efficient electrocatalysts for ORR are based on platinum (Pt/C), which is costly and scarce, and hence, replacing platinum by materials with lower cost and broader availability has become a major challenge. A sustainable society is also focused on the direct conversion of biomass into valuable chemicals, being sorbitol one of the most promising platform molecules. Ruthenium catalysts supported on carbon materials have shown to be very effective supports for the direct conversion of cellulose to sorbitol. However, the best results to date are obtained using long reaction times, high metal loadings or expensive carbon supports. Thus, further research needs to be carried out in an attempt to match or surpass the results obtained to date by using cheaper carbon supports. In this context, the perspective of processing waste biomass into valuable carbonaceous materials has gained an increasing interest in the field of materials science. Carbon-based materials are highly promising catalysts for several applications, due to their high catalytic activity, cost-effectiveness, and durability. The optimization of the catalytic activity of carbon-based catalysts lies in the appropriate design of the materials' properties. To this end, it is essential to understand the influence of the textural and chemical properties on the performance of carbon-based catalysts. Accordingly, this work aims to prepare glucose-derived carbons with tailored textural properties via hydrothermal carbonization and subsequent physical activation, in order to study the effect of porosity and chemical composition on the performance of the catalysts in two different applications related to energy and biomass conversion.

2. Methods

Glucose-based carbon materials were prepared by hydrothermal carbonization (HTC). The solid/water ratio (w/v) was fixed at 1:5 and the HTC process was performed at 180 ºC for 12 h. The

materials were then carbonized at 700 ºC under N_2 for 2 h (CG) or physically activated at 900 ºC under CO_2 atmosphere for 4 and 6 h (AG_{4h} and AG_{6h}). The prepared materials were then directly used for the ORR testes, which were performed in a three-electrode cell by cyclic and linear sweep voltammetry measurements. For the biomass conversion, ruthenium catalysts were prepared by incipient wetness impregnation of Ru (0.4 wt.%) on the prepared carbon supports and the one-pot hydrolytic hydrogenation of cellulose into sorbitol was performed in a reactor at 205 ºC for 5 h. All materials were characterized by nitrogen adsorption, microscopy (SEM and TEM), elemental analysis, TGA, TPD, XRD, XPS and ICP.

3. Results and discussion

All the prepared materials display a type I isotherm, which is characteristic of microporous solids. In addition, the microporosity increases due to the rise in the temperature and time of activation applied. The electrochemical results show two main differences: i) the onset potential shifts to more positive values by increasing the time of activation, which can be related to the more graphitic structure that is generated during activation; and ii) the value of the limiting current density increases with microporosity, which can be related to the more developed porous structure [1]. On the other hand, the prepared Ru catalysts were highly efficient for the one-pot reaction, yielding 100 % cellulose conversion after just 3 h. The conversion rate seemed to increase for the materials with the most developed porous structure. Moreover, the production of sorbitol increases with the surface area (Table 1), probably due to the faster access to the metal, favoring the hydrogenation of glucose into sorbitol [2].

Table 1. Textural properties and catalytic results

Sample	Supports			Ru catalysts	
	S_{BET} ($m^2\ g^{-1}$)	V_{DR} ($cm^3\ g^{-1}$)	E_{onset} (V)	Yield of sorbitol (%, 3 h)	Conversion (%, 3 h)
CG	573	0.22	0.683	33	100
AG_{4h}	936	0.38	0.751	53	100
AG_{6h}	1984	0.85	0.782	59	100

4. Conclusions

The appropriate combination of activation conditions during the polymerization of glucose led to the most efficient catalyst for both the oxygen reduction reaction (onset potential 100 mV higher) and the production of sorbitol (59 % of sorbitol was achieved after just 3 h of reaction).

Acknowledgments

Financed by projects: "UniRCell", with the reference POCI-01-0145-FEDER-016422; NORTE-01-0145-FEDER-000006 - funded by NORTE2020 through PT2020 and ERDF; Associate Laboratory LSRE-LCM - UID/EQU/50020/2019 - funded by national funds through FCT/MCTES (PIDDAC).

References

[1] R.G. Morais, N. Rey-Raap, J.L. Figueiredo, M.F.R. Pereira, Beilstein J. Nanotech. 10 (2019) 1089-1102.
[2] N. Rey-Raap, L.S. Ribeiro, J.J.M. Órfão, J.L. Figueiredo, M.F.R. Pereira, Appl. Catal. B 256 (2019).

ECCE12
The 12th EUROPEAN CONGRESS OF CHEMICAL ENGINEERING
Florence 15-19 September 2019

Fouling Detection in Industrial Heat Exchanger

Using Neural Network Models

Željka Ujević Andrijić[1*], Nenad Bolf[1], Adriana Brzović[1], Hrvoje Dorić[1]

1 University of Zagreb, Faculty of Chemical Engineering and Technology, Zagreb, Croatia

**Corresponding author: zujevic@fkit.hr*

Highlights

- There is a need for continuous detection of fouling formation on heat exchangers
- NN models are developed for predicting heat exchanger outlet temperatures.
- By applying models on-site more stable operation and significant savings are expected.

1. Introduction

Companies are more than ever aware of the potential that lies in machine learning for improving predictive maintenance in order to increase process efficiency and address concrete process issues.

One of the major problems in operation of a refinery plant is the heat exchanger fouling build-up, so there is a need for continuous detection of fouling formation on heat exchangers in order to optimize servicing within preventive maintenance programme.

Traditional diagnostics of the fouling formation methods have a number of limitations, with some requiring stationarity of the process. In more than a few instances fundamental models are difficult to develop. On the other hand data-driven models can be developed using identification methods.

In our research an online monitoring system is developed for a shell and tube heat exchanger at hydrocracking plant. Neural network models are developed using inferential variables (temperature and flow rates of hot and cold stream) for predicting heat exchanger outlet temperatures. The deviation between predicted and actual values indicates performance degradation due to fouling. The developed models are designed to establish an on-line monitoring system for maintaining operating efficiency of refinery plants.

2. Methods

The first step was choosing the data representative for the overall dynamical process and selecting data from the period when fouling does not yet appear (right after cleaning). The model inputs for predicting outlet temperatures of hot and cold streams are: the inlet cold stream temperature ($T_{C,i}$), the inlet hot stream temperature ($T_{H,i}$), the hydrogen mass flow rate ($\dot{m}$). The neural networks models were developed using R software. Data preprocessing included detection and removing outliers. Heat transfer coefficient for clean and dirty heat exchanger is calculated using (1) and (2):

$$U_{\text{fouling}} = \frac{\dot{m} * c_{\text{p}} * \left(T_{\text{H,i}} - T_{\text{H,o}}\right)}{A * F * \frac{\left(T_{\text{H,i}} - T_{\text{C,o}}\right) - \left(T_{\text{H,o}} - T_{\text{C,i}}\right)}{\ln\left(\left(T_{\text{H,i}} - T_{\text{C,o}}\right) / \left(T_{\text{H,o}} - T_{\text{C,i}}\right)\right)}} \quad (1)$$

$$U_{\text{clean}} = \frac{\dot{m} * c_{\text{p}} * \left(T_{\text{H,i}} - T_{\text{H,o,model}}\right)}{A * F * \frac{\left(T_{\text{H,i}} - T_{\text{C,o,model}}\right) - \left(T_{\text{H,o,model}} - T_{\text{C,i}}\right)}{\ln\left(\left(T_{\text{H,i}} - T_{\text{C,o,model}}\right) / \left(T_{\text{H,o,model}} - T_{\text{C,i}}\right)\right)}} \quad (2)$$

U_{fouling} is calculated based on the measured outlet temperatures, while U_{clean} is calculated based on the predicted outlet temperatures. The heat exchanger performance is then assessed by comparing results of clean and fouled systems. Any trend observed at the model residual indicates that the performance is decreased due to fouling. The fouling factor is calculated according to the (3).

$$R_f = \frac{1}{U_{\text{fouling}}} - \frac{1}{U_{\text{clean}}} \quad (3)$$

3. Results and discussion

Good matching between actual outlet temperature and the model prediction right after the cleaning is observed. Over the longer period the deviation constantly increases as a result of emergence fouling. From Fig.1 it can be seen that initially, the fouling factor fluctuates close to zero indicating no fouling is occurring. After a while the fouling factor begins to rise indicating deposition. Calculated value of fouling factor is similar to the design fouling value of this heat exchanger.

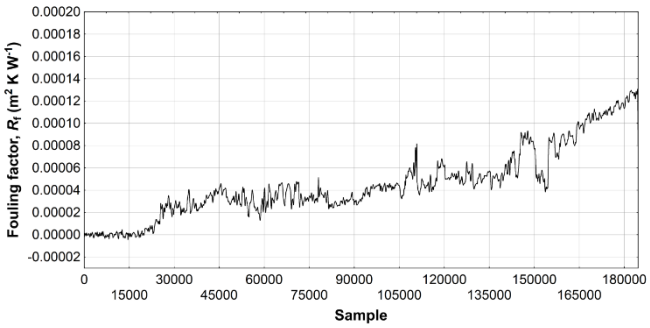

Fig. 1. Fouling factor

4. Conclusions

The performance criteria of developed models together with residual monitoring indicate that the neural networks effectively detect fouling formation. By applying developed models on-site more stable plant operation and significant savings could be expected.

References

[1] C. Ahilan, J. Edwin Raja Dhas, K. Somasundaram and N. Sivakumaran, "Performance assessment of heat exchanger using intelligent decision making tools", Applied Soft Computing, vol. 26, pp. 474-482, 2015.
[2] S. Lalot and H. Pálsson, "Detection of fouling in a cross-flow heat exchanger using a neural network based technique", International Journal of Thermal Sciences, vol. 49, no. 4, pp. 675-679, 2010.
[3] M. Navvab Kashani, J. Aminian, S. Shahhosseini and M. Farrokhi, "Dynamic crude oil fouling prediction in industrial preheaters using optimized ANN based moving window technique", Chemical Engineering Research and Design, vol. 90, no. 7, pp. 938-949, 2012.

ECCE12
The 12th EUROPEAN CONGRESS OF CHEMICAL ENGINEERING
Florence 15-19 September 2019

Energy and Chemical Engineering

Techno-economic analysis of the conversion process of SRF derived syngas to methanol with CO_2 capture.

Diego Barletta[1*], Aristide Giuliano[1], Massimo Poletto[1],
Gaetano Iaquaniello[2,3], Annarita Salladini[3]

[1] Dept of Industrial Engineering, University of Salerno, Via Giovanni Paolo II, 132, Fisciano (SA), 84084, Italy
[2] KT – Kinetics Technology SpA, Viale Castello Della Magliana 27, Roma, 00148, Italy
[3] Processi Innovativi Srl, Via di Vannina 88/94, Roma, 00156, Italy
*Corresponding author: dbarletta@unisa.it

Highlights

- Complete process flowsheet for SRF derived syngas to methanol.
- Alternative CO_2 capture technologies for syngas are assessed.
- Methanol synthesis loop is optimized
- Positive profitability indices are obtained.

1. Introduction

Waste production is constantly growing in the developing countries, while in the developed areas, techniques for the exploitation of waste have been gradually introduced. Wastes are used in order to obtain raw materials (separate collection) or to produce energy by thermal treatments (waste-to-energy, gasification). Solid recovered Fuel (SRF) is a type of fuel derived from the processing of non-hazardous solid urban waste. The aim of producing a fuel derived from waste is the creation of an energy carrier with standard features allowing exploitation in energy production processes [1].

A possibility to valorize waste material consists in gasification to produce syngas and subsequently high-added value products, as methanol [2]. Challenges arise to reach the specific features from the obtained raw syngas, in terms of gas pollutant concentration to avoid catalysts deactivation and of H_2/CO ratio. Alternative solutions to purify and to condition the syngas were proposed in the literature [2]. These analyses indicate that the purification and conditioning processes require significant additional capital costs, in particular for the CO_2 capture units. Improvement of process integration of these two plant sections is necessary to obtain convenient economic indices.

In this work, the process design and the preliminary cost assessment of purification and conditioning section of syngas obtained from a gasification plant of RDF and of the methanol synthesis section are proposed.

2. Methods

Process flowsheet was simulated by means of Aspen Plus© V8.8 in order to perform mass and energy balance and to carry out the optimal design of main process units. For this purpose, rigorous models taking into account kinetics were employed to design reactors and rigorous stage by stage methods were used for separation columns accounting non ideal vapor liquid equilibria and mass transfer resistance. Process heat integration was addressed and heat exchanger network was

designed by means of Aspen Energy Analyzer V8.8. Cost analysis was carried out with the help of Aspen Process Economic Analyzer V8.8.

3. Results and discussion

Main results of the simulation work concern the conditioning section of syngas obtained by gasification of SRF was carried out. Syngas was purified from Sulphur organic compounds (mainly COS and CS2) and from HCN by a hydrolysis reactor with Al_2O_3-TiO_2 catalyst which was properly sized to obtaining conversion larger than 99%. H_2S was converted to elemental Sulphur by means of Lo-Cat® technology and remaining traces were further removed by PURASPEC™ adsorption technology. Next, the hydrogen content in the clean syngas was increased from 16% to 31% by a high temperature Water Gas Shift stage (Fe_3O_4/Cr_2O_3 catalyst), which was sized to obtain 87% CO conversion. Subsequently the CO_2 capture was addressed by two alternative absorption processes: Selexol® process and MEA absorption process. For both cases, a CO_2 recovery equal to 95% and a CO_2 purity equal to 99% were fixed as process specifications. An economic comparison between the two CO_2 capture processes was carried out. Comparable operating costs resulted for both processes, while in term of investment costs the Selexol® process appeared more convenient than absorption by MEA.

The Methanol synthesis loop was designed to feed the methanol reactor with a stream with an optimal molar ratio (H_2-CO_2)/(CO+CO_2) by mixing the fresh syngas with the recycled reactants and pure hydrogen separated by PSA. The multitubular fixed bed reactor with heat exchange was designed to attain an optimal temperature profile to minimize the catalyst bed weight for methanol conversion of about 40%. Methanol separation and purification was obtained by a distillation train.

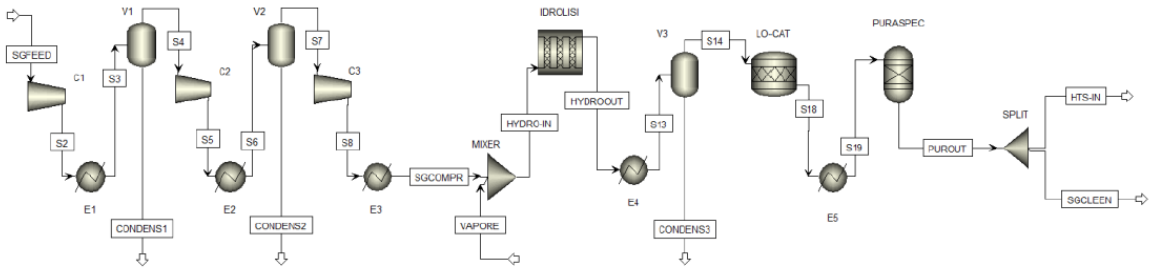

Figure 1. Simulation flowsheet of the syngas cleaning section.

4. Conclusions

A complete flowsheet for the production of methanol from SRF derived syngas was simulated. CO_2 capture was also addressed. Selexol® process resulted the optimal solution in terms of costs. Methanol synthesis loop was optimized to maximize the methanol production. Process heat integration was performed to limit the utilities cost. Final economic analysis provides positive net present value and satisfactory rate of return of the investment confirming the profitability estimated in a previous approximate analysis [2].

References [Calibri 10]

[1] G. Iaquaniello, G. Centi, A. Salladini, E. Palo, S. Perathoner, Chemistry 24 (2018) 11831-11839.
[2] G. Iaquaniello, G. Centi, A. Salladini, E. Palo, S. Perathoner, L. Spadaccini, Biores. Technol. 243 (2017) 611-619.
[3] G. Bozzano, F. Manenti, Prog. Energy Combust. Sci. 56 (2016) 71–105.

Study of the correlation between the production of radicals •OH and the radiative field in a photocatalytic reactor

Ana Gómez Llanos[1], Richard Ruiz Martínez[1], Ariadna Morales Pérez[1], Carlos Castillo Araiza[1]

1 Laboratory of Reactor Engineering Applied to Chemical and Biological Systems. Chemical Engineering Area. Dept. of IPH. Autonomous Metropolitan University-Iztapalapa, Av. San Rafael Atlixco 186 Vicentina, C.P. 09340, Mexico City; 2 Affiliation and address

**Corresponding author: alexisgomez@xanum.uam.mx*

Highlights

- Energy radiative balance.
- Production of hydroxyl radicals.
- photocatalytic efficiency.
- photocatalytic activity with different sources.

1. Introduction

It has been demonstrated that photocatalysis is efficient in the degradation of a wide range of organic pollutants present in water [1]. Although the potential advantages of using photocatalytic reactors in the degradation of refractory contaminants, there are still problems to face. One of the main problems is the lack of adequate radiation models, as well as kinetic models and design procedures to scale up photocatalytic reactors [2], [3]. The main deficiencies in heterogeneous photocatalysis are: i) that there are no studies describing kinetics and radiation adequately, ii) no in-depth study has been carried out on the production of hydroxyl radicals and their correlation with the radiative, iii) it is not known if the rate of formation of hydroxyl radicals depends on the wavelength with which the photocatalyst is activated, and d) there is no model that describes with certainty the process of production of hydroxyl radicals, and thus perform a scale up reactor. A lot of research still needs to be done about those topics, as the research that is done till now resulted in kinetics and optical parameters that included several phenomena such as hydrodynamics, mass transfer and radiation. In addition, no comparison between the use of different light sources and the obtained specific extinction coefficients has been made and no intrinsic kinetic study about the production rate of the •OH using titanium dioxide (TiO_2) as a catalyst was done.

2. Methods

A tubular photoreactor 10 cm length, 2.2 cm diameter where the suspended photocatalyst flows was used to get the experimental data

2.1 Radiative characterization

2.1.1 Calculation of the extinction coefficient

For the optical parameter, extinction coefficient of the catalyst, experiments were carried out irradiating with an external source (one LED in front of the reactor) to the reactor using the approximation of Beer-Lambert Law and the energy balance was calculated.

2.1.2 Isoactinic conditions

To achieve that the radiative energy was constant at different positions of the reactor, a strip of LEDs was placed around it, thus allowing to reach isoactinic conditions and avoid the change of the production of hydroxyl radicals at different positions inside the reactor.

2.2 Production of hydroxyl radicals

•OH radicals have a low stability and consequently a high reactivity. For this research, terephthalic acid was used to react with the formed •OH. This reactant reacts with •OH to form a highly fluorescent product 2-hydroxyterephtalic acid (2-HdA), fluorimetry is used to detect 2-HdA.

3. Results and discussion

the extinction coefficient can give an initial idea about the activation of photocatalysts, as the first result it was expected to be able to calculate the coefficient of intrinsic form (independent of the concentration of the catalyst) which was achieved when it is irradiated with wavelengths inside of the absorption spectrum of the material Figure 1a, on the other hand this parameter, since it does not depend on other phenomena.

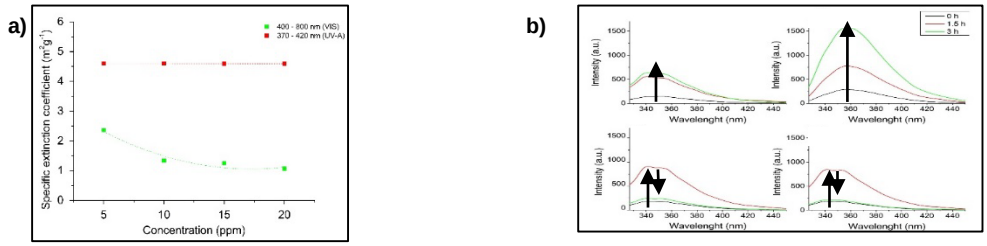

Figure 1. a) Specific extinction coefficients of 400-800 nm and 370-420 nm in front of the reactor, b) Production of 2-HdA after reaction (3 hours) between •OH and terephthalic acid with different TiO_2 concentrations.

The measured intensities of the 2-HdA are shown in function of the wavelength and corresponds to the formed amount of •OH. At 5 and 10 ppm of TiO2, the intensity of the formed 2-HdA increases over time and consequently also the produced •OH. when the solution passes for a longer time through the reactor, more catalyst particles are activated by the radiation source and the production increases Figure 1b.

4. Conclusions

Higher intrinsic specific extinction coefficient (4.6 $m^2 g^{-1}$) with purple LED, more absorption by TiO_2 whit the same LED, production of •OH is influenced by the catalyst concentration.

References

[1] M. Chong, B. J. (2010). Recent developments in photocatalytic water treatment technology: a review. *Water research*, 2997-3027.

[2] Li Puma, G. &. (2007). Dimenssionless analysis of slurry photocatalytic reactors using two flux and six flux radiation absorption scattering models. *Catalysis Today*, 78-90.

[3] Valades Pelayo P.J., J. M. (2014). Boundary conditions and phase functions in a photo-CREC Water-II reactor radiation field. *Chemical Engineering Science*, 123-136.

ECCE12
The 12th EUROPEAN CONGRESS OF CHEMICAL ENGINEERING
Florence 15-19 September 2019

CO_2 Reduction Using Glucose in Hydrothermal Media in a Continuous Plant

María Andérez-Fernández,[1]* Joao P.S. Queiroz[2], Eduardo Pérez,[1] Ángel Martín,[1] M. Dolores Bermejo[1]

[1]*BioEcoUVa. Research Institute on Bioeconomy. High Pressure Processes Group. Department of Chemical Engineering and Environmental technology. Universidad de Valladolid, Valladolid, 47011, Spain*
[2] *Department of Chemical Engineering, University of São Carlos, Brazil*
**Corresponding author: mariaanderezfernandez@gmail.com*

Highlights

- For the first time, hydrothermal reduction of $NaHCO_3$ using glucose has been performed in a continuous pilot plant.
- Yields to formic acid up to 63% were achieved after 10min at 300ºC in batch reactions.
- This work is a starting point to use residual biomass as reductant.

1. Introduction

Several alternatives have been proposed in order to mitigate the potential irreversible damages that can cause the increasing levels of CO_2 in atmosphere. Hydrothermal reduction is one of the most promising procedures for CO_2 conversion into chemicals, such as formic acid, by means of water at high temperature and pressure (high temperature water, HTW), which owns outstanding properties compared to those of water at room temperature, being able of acting in the reaction as solvent, catalyst or reactant. Furthermore, due to the depletion of fossil fuels, lignocellulosic biomass has been envisioned as a plausible substitute for obtaining chemicals and fuels, and HTW has been intensively studied during the past years as an excellent method for its liquefaction and conversion into useful products.

Previous works showed the possibility of combining both CO_2 reduction using several biomass derivatives, from isopropanol to lignocellulosic derivatives[1,2]. However, these studies have been performed at laboratory scale. In this study, the hydrothermal reduction of sodium bicarbonate ($NaHCO_3$, as source of CO_2) and glucose conversion was carried out in a continuous pilot plant, showing the possibility to implement the process in CO_2 production focus.

2. Methods

Reactions were performed by two different procedures: batch mode and continuous mode. Batch reactions were previously described[2]. Continuous mode reactions were carried out in a pilot plant, in which a solution of $NaHCO_3$ and glucose (1.0M and 0.1M, respectively) was pumped up to operational pressure and mixed with a preheated water stream, achieving an instantaneous heating of reactants. Reaction temperature (300ºC) and pressure (200 bar) were kept through the reactor, placed in an oven, and reaction was stopped by a decompression valve and cooling down the outlet. Liquid samples were analyzed using HPLC techniques. Experiments were repeated at least twice to ensure reproducibility, achieving less than 15% of deviation.

3. Results and discussion

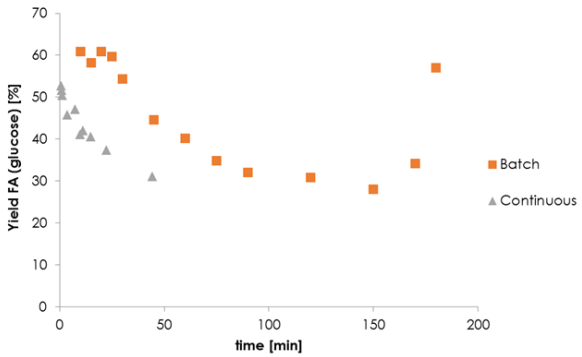

Figure 1. Yield to formic acid (referred to the initial amount of glucose) as a function of reaction time in batch and continuous reactions

As shown in Figure 1, despite the difference in the yield to formic acid achieved at the same reaction time in both reaction methods, there is a clear similitude in the trend that yield follows with reaction time. In batch reactions, yield to formic acid was higher at shorter reaction times, achieving up to 63% after 10 min in batch reactions. However, yield to formic acid decreased when reaction time, probably due to the decomposition of formic acid into CO_2 at high temperatures, achieving the minimum yield at 150 min. After this time, the yield to formic acid increased again, indicating a different mechanism for formic acid production. The same trend is addressed for results obtained in the continuous pilot plant. However, in the continuous facility it is possible to work with residence times as low as 1 minute where maximum yields in continuous are observed.

Higher yields in batch reactions can be explained by the different heating profiles in both reaction systems. While in the continuous systems the heating time for reaching 300ºC could take around 30 min, in the continuous system the heating till 300ºC is instantaneous. In both cases, byproducts obtained from glucose conversion in hydrothermal processes were acetic acid, lactic acid, glycolaldehyde and glyceraldehyde.

4. Conclusions

In this work, the hydrothermal reduction of $NaHCO_3$ using glucose (lignocellulosic derivative) as reductant achieved a yield to formic acid up to 63% after 10 min of reaction at 300ºC in a batch reactor. In continuous maximum yields are obtained at with residence times of 1 min, decreasing afterwards. Despite a lower yield to formic acid achieved in the continuous pilot plant, it opens the opportunity of implementing the process in those focus of CO_2 production.

Acknowledgments

This project has been funded by Junta de Castilla y León through project VA248P18. MAF acknowledges Junta de Castilla y Leon for predoctoral position (Orden EDU/520/2017). MDB thanks MINECO for Ramon y Cajal position.

References

[1] Z. Shen, Y. Zhang, F. Jin, RSC Adv. 2 (2012) 797-801

[2] M. Andérez-Fernández, E. Pérez, A. Martín, M.D. Bermejo, J. Supercrit. Fluids 133 (2018) 658-664

ECCE12
The 12th EUROPEAN CONGRESS OF CHEMICAL ENGINEERING
Florence 15-19 September 2019

Catalytic pyrolysis of biogas digestate

Mihaela Bombos[1], Dorin Bombos[2], Sanda Velea[1], Gabriel Vasilievici[1], Cristina-Emanuela Enascuta[1], Catalina Calin[2], Elena-Emilia Oprescu[2*]

[1] *National Research and Development Institute for Chemistry and Petrochemistry ICECHIM, 202 Splaiul Independentei St., 060021, Bucharest, Romania*

[2] *Petroleum-Gas University of Ploiesti, 39 Bucharest Blv., 100680 Ploiesti, Romania*

**oprescuemilia@gmail.com*

Highlights

- Catalytic pyrolysis of biogas digestate.
- Optimization of operating parameters.
- The composition of pyrolysis oil is influence by catalysts presence.

1. Introduction

Biogas production by anaerobic fermentation is a promising method of producing an energy carrier from renewable resources [1].The digestate resulted from biogas production is widely used as a fertiliser in farm land[2,3]. However, there is a concern about land spreading of digestate due to the possible heavy metals and pathogen content if not controlled properly. Alternative uses of digestate such as incineration, pyrolysis and gasification of the biogas digestate have been investigated by several researchers[3]. The objective of this study was to investigate catalytic pyrolysis of biogas digestate in order to obtain liquid fractions with potential as fuels components.

2. Methods

The pyrolysis of the digestate was carried out in a continuous system, using a quartz tubular reactor positioned in the central area of a vertical furnace provided with temperature control system. To perform pyrolysis tests, the digestate was conditioned. The preliminary pyrolysis experimental program was performed at the following operating parameter values: I) atmospheric pressure; II) temperature in the isothermal reaction zone: 420°-550° C; III) bulk velocity: 0.1-1 h^{-1}.

3. Results and discussion

The tests of biogas digestate pyrolysis were carried out in presence or absence of catalysts, at different operating parameters. The catalytic pyrolysis was done over nanostructured metal catalysts, prepared by precipitation of copper and iron precursors in presence of various anti-agglomeration additives. The analysis of bio-oil resulted from catalytic pyrolysis of biogas digestate indicates a composition suitable as fuel components. The main compounds identified were linear and branched aliphatic hydrocarbon components, unsaturated compounds, alcohols, carbonyl compounds.

4. Conclusions

The results indicated superior performance for the pyrolysis process in the presence of nanostructured metal catalysts compared with the non-catalytic process.

Acknowledgement: The authors gratefully acknowledge the financial support of the UEFISCDI, Romania, in the framework of PN-III-P1-1.2-PCCDI-2017, financing contract no. 32 PCCDI/2018

References

[1] T. Rehl, J. Mülle, Conservation and Recycling (2011) 56 92–104.
[2] G. Kocar, Energy Educ Sci Technol Part A: Energy Sci Res. (2012) 30(1) 545–552.
[3] A.K. Hossain, C. Serrano, J.B. Brammer, A. Omran, F. Ahmed, D.I. Smith, P.A. Davies, Fuel (2016) 171 18–28.

ECCE12
The 12th EUROPEAN CONGRESS OF CHEMICAL ENGINEERING
Florence 15-19 September 2019

Continuous In Situ Extraction of Volatile Fatty Acids in an Anaerobic Digestive System.

Gerard James[1], Robert Pott[1]

1 Department of Chemical Engineering, Stellenbosch University, Western Province, South Africa

**Corresponding author: rpott@sun.ac.za*

Highlights

- Liquid-liquid equilibrium studies were conducted using TOA and TBP in canola oil.
- Extraction efficiencies of VFAs differ between synthetic and AD solutions.
- Continuous extraction of VFAs allow for a pH control setup.

1. Introduction

The global demand for sustainable renewable energy has increased exponentially over the past decade. One of the approaches for renewable energy has been anaerobic digestion (AD) for the production of biogas [1]. However, AD is susceptible to acidification, which can cause the anaerobic digester to fail. Acidification is caused when there is an excessive accumulation of volatile fatty acids (VFAs) in the broth. This accumulation of VFAs reduces the pH of the broth, which can cause further methanogenic consortia decay [2]. Therefore, a more sustainable/preferred approach to AD would be to co-produce VFAs and biogas, which could be achieved by continuous *in situ* extraction of the VFAs from the AD process using liquid-liquid extraction (LLE). Laboratory-scaled experiments indicate a strong correlation between the degree of VFAs extracted and the pH of the solution. This implies that LLE can be applied to an AD system to control the pH of the system to prevent the accumulation of VFAs [3]. The successful implementation of an *in situ* pH control process can be used for the continuous removal of VFAs from an AD bioreactor. This energy efficient processing method will increase the productivity of AD and will bring additional revenue to the AD industry, through the sale of VFAs in addition to biogas.

2. Methods

LLE experiments were conducted in batch, using either a synthetic solution of VFAs or AD effluent obtained from a previous student's work. Equal volume of solvent (organic phase) was added to the aqueous phase and vortexed for 5 minutes. The samples were kept in a shaker incubator at 37°C and 150 rpm, and left for 24 hours to ensure equilibrium was reached. The samples were centrifuged and allowed to settle for 1 hour before determining the VFA concentration in the aqueous phase by HPLC. The VFA concentration for the organic phase was calculated by mass balance. The solvent consisted of 20 vol% of the extractant (either TBP or TOA) and canola oil (diluent). The synthetic aqueous solution contained approximately 14 g/l of VFAs in distilled water. The individual concentration for acetic acid, propionic acid, butyric acid and valeric acid are given as 65%, 15%, 14%, and 6% respectively. Experiments were done in triplicate at the centre point.

3. Results and discussion

Laboratory-scaled experiments suggest that there is a significant difference between the degree of extraction in the synthetic solution and the AD effluent (Figure 1A). This could be due to certain ions present in the AD effluent [4]. A strong correlation can also be seen (from Figure 1A) between the extractive efficiency of the solvent and the pH of the solution. This is largely due to the ability of the solvent to extract VFAs below their pKa value [5]. This suggests that there is a trade-off between the amount of VFAs that can be extracted and the amount of methane production. However, an alternative solution would be to design an *in situ* LLE unit to control the pH of the digester to prevent acidification, shown in Figure 1B. This would be achieved by continuously removing VFAs to prevent excessive accumulation. Therefore, the digester would be able to co-produce methane and VFAs, which could bring additional income to the AD system. Similar LLE results were achieved using TOA/TBP in lamp oil and oleyl alcohol.

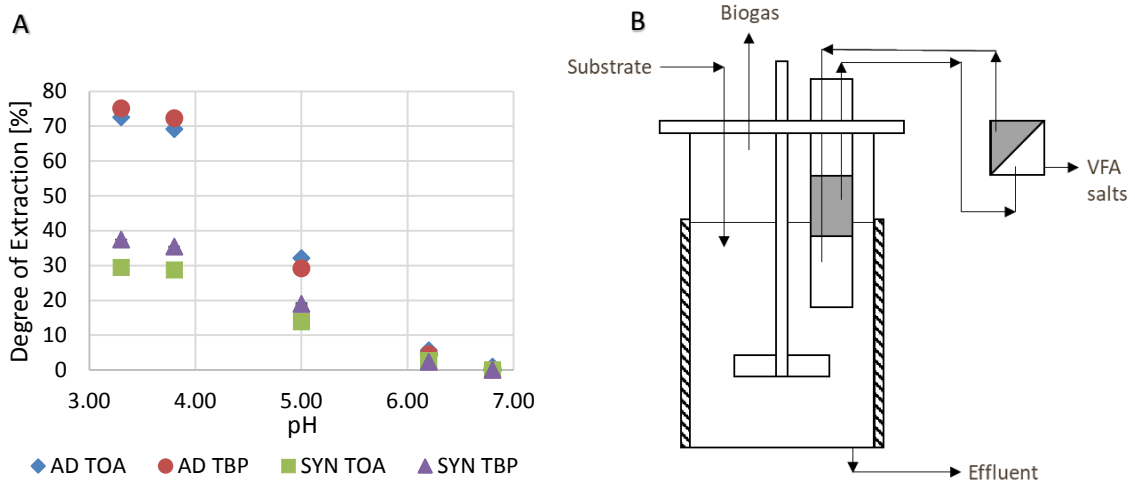

Figure 1: Liquid-liquid extraction of volatile fatty acids using 20% TOA/TBP in canola oil at various pH: (A) A degree of extraction comparison of synthetic solution and AD effluent, (B) Design of a continuous *in situ* extraction anaerobic digester to control pH with a back-extraction unit for solvent recovery.

4. Conclusions

Liquid-Liquid experiments were conducted using TOA/TBP in canola oil, at various pHs, to extract VFAs from a synthetic solution and AD effluent. These experiments indicate a difference between the extractability of the solvent in the synthetic solution and the AD effluent. However, this could be explained by certain ions present in the effluent. The results also indicates a strong correlation between the extractability of the solvent and the pH of the solution. As a result, a more sustainable approach would be to implement a continuous *in situ* extraction of VFAs using LLE to prevent product inhibition of the methanogens.

References

[1] N. A. Mostafa, 'Production and recovery of volatile fatty acids from fermentation broth', *Energy Convers. Manag.*, vol. 40, pp. 1543–1553, 1999.

[2] T. Hori *et al.*, 'Involvement of a novel fermentative bacterium in acidification in a thermophilic anaerobic digester', *FEMS Microbiol. Lett.*, vol. 361, no. 1, pp. 62–67, 2014.

[3] V. . Yabannavar and D. I. . Wang, 'Extractive Fermentation for Lactic Acid Production', *Biotechnol. Bioeng.*, vol. 37, pp. 1095–1100, 1990.

[4] E. Reyhanitash, B. Zaalberg, S. R. A. Kersten, and B. Schuur, 'Extraction of volatile fatty acids from fermented wastewater', *Sep. Purif. Technol.*, vol. 161, pp. 61–68, 2016.

[5] E. Alkaya, S. Kaptan, L. Ozkan, S. Uludag-Demirer, and G. N. Demirer, 'Recovery of acids from anaerobic acidification broth by liquid-liquid extraction', *Chemosphere*, vol. 77, no. 8, pp. 1137–1142, 2009.

ECCE12
The 12th EUROPEAN CONGRESS OF CHEMICAL ENGINEERING
Florence 15-19 September 2019

GASOLINE BLENDING and DISTRIBUTION SCHEDULING

Feleke Bayu, Debashish Panda, Munawar Shaik, Manojkumar Ramteke

Department of Chemical Engineering,

Indian Institute of Technology Delhi, India

E-mail: ramtekemanoj@gmail.com, mcramteke@chemical.iitd.ac.in

Tel No.: (91)-1126591026 (Office); Fax No: +91-1126581120

Highlights

- Graphical GA is used to minimize gasoline blending and distribution operating cost
- The efficacy of the proposed model is checked by solving an industrial problem
- It gives about 1.1-million-euro cost reduction compared to the benchmark reference

1. Introduction

Scheduling of gasoline blending and distribution scheduling (SGBD) is a process of allocating resources in the way the cost is minimized without compromising the quality and the demand of the products. Gasoline accounts about 43% of the total crude oil products. According to the 'International Energy Agency's (IEA) New Policies Scenario' [1] estimates, the total crude oil demand will increase from 95 Mb/d to 115 Mb/d between the year 2016 and 2040. Although the usage of renewable energy sources is significantly increasing, for the next two decades, Crude oil will remain the main energy source, particularly for transportation. Therefore, optimizing gasoline blending process enables to boost the profitability and productivity of crude oil refinery plants which intern reduces the environmental load.

Gasoline blending involves combining the refining intermediate products in a way that gasoline yield becomes maximized since gasoline has a high-profit margin compared to the other products. In the meantime, maintaining gasoline property indices such as octane number (ON), Reid vapour pressure (RVP), anti-nocking and stability specifications, sulphur content, ASTM distillation point and flash point come together.

2. Methods

A graphical genetic algorithm (GGA) which has a sparse representation compared to the conventional GA (CGA) is used to optimize gasoline blending and distribution process. GGA uses a graphical representation where the material flow is represented by the arrow (edge) and processing units or orders by the box. Here, a discrete time-based (period-wise) model is developed. For each period, unlike CGA, in the chromosome structure, GGA considers only the feasible edges which

leads to a tremendous chromosome size reduction. Moreover, it executes genetic operation (crossover and mutation) using a graphical method. During decoding as well as after a genetic operation, the correction will be performed whenever there is constraint violation. Other than the aforementioned differences it follows the same procedure with the conventional NSGA_II.

3. Results and discussion

Using the proposed model, an industrial problem is solved. The result is shown in the table 1. As shown in the table, compared to the CGA there is a significant variable and constraint size reduction for GGA which will enable it to solve complex industrial problems. At the same time, it has around 5 % of production cost reduction compared to the benchmark reference which is a mathematical programming-based model.

Table 1: Model statistics

Number of Variables	Number of			Costs (k€)	
% Reduction over CGA	Constraints for CGA	Penalty function for GGA	% Reduction	Cerda et al [2]	Proposed GGA
87	11541	309	97	18517.24	17413.85

4. Conclusions

The proposed model is more compact and has a better computational efficiency compared to the CGA and it also gives a better economic benefit relative to the benchmark reference[2].

[1] E. W. Rocha, P. Huet, and G. M. Mohatarem, The 2040 Economy: Long-term growth determinants, in *Global Economics & Country Risk Conference*, 2014.

[2] J. Cerd, P. C. Pautasso, D. C. Cafaro, and I. U. N. L. Conicet, A Cost-effective model for the gasoline blend optimization problem, *AIChE J.*, vol. 62, no. 9, 2016.

ECCE12
The 12th EUROPEAN CONGRESS OF CHEMICAL ENGINEERING
Florence 15-19 September 2019

Crosslinked Carboxymethyl Cellulose–Polyethylene Glycol Binder for the Improved Cycle Performance of Silicon Anodes in Li–Ion Batteries

Dongsoo Lee[1], Kangchun Lee[1], Seho Sun[1], Jeongheon Kim[1], Bonggu Kim[2], Junseong Kim[2], Yeongil Jung[2], and Ungyu Paik[1*]

[1]*Department of Energy Engineering, Hanyang University, Seoul, Republic of Korea, 133-791*

[2] *School of Materials Science and Engineering, Changwon National University, Changwon, Gyeongnam 641-773, Korea*

**Corresponding author: upaik@hanyang.ac.kr*

Highlights

- A facile in situ crosslinked binder system is proposed by a convenient, environmental-friendly and low-cost methodology for the practical use.
- The silicon anode prepared with the CMC-PEG binder shows stable cycling performances as lithium-ion batteries.

1. Introduction

Silicon has been widely studied due to its relative abundance and high theoretical specific capacity (~3572 mAh g^{-1}) as an anode material for lithium ion batteries (LIBs). However, the drastic volume changes up to 300% associated with Li still hinder the practical implementation of Si. Herein, we report an in situ cross-linked carboxymethyl cellulose-polyethylene glycol (CMC-PEG) binder and its application to the silicon anode for the long-term cycle life of LIBs. potential to be used for Si and other active materials experiencing volume expansion for LIBs.

2. Methods

For slurry preparation of the reference electrode with CMC, silicon , conducting carbon, CMC, and SBR were placed into deionized water in a weight ratio of 85 : 5 : 8 : 2. For slurry preparation of the electrode prepared with the crosslinked CMC-PEG binder, silicon, conducting carbon, CMC, PEGDE, and SBR were placed into deionized water in a weight ratio of 85 : 5 : 6.4 : 1.6 : 2.

3. Results and discussion

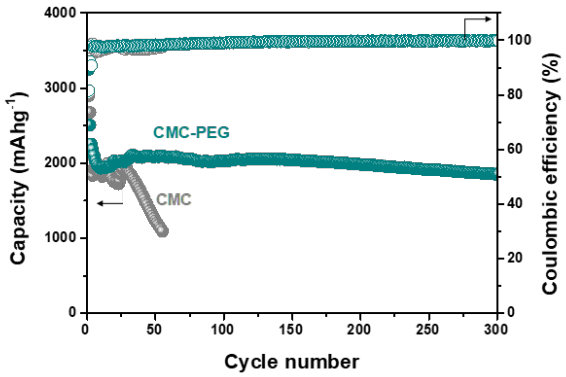

Figure 1. Cycling performance of the silicon electrodes prepared with CMC and crosslinked CMC-PEG binders at 0.5 C rate.

The crosslinked CMC-PEG binder is simply prepared during the electrode drying process without an additional process. In particular, the crosslinked CMC-PEG binder enables the improved and adhesion between active materials and a current collector, and cohesion between active materials. The silicon anode prepared with the crosslinked CMC-PEG binder exhibits stable cycling performance with a capacity of ~2000 mAh g−1 over 300 cycles.

4. Conclusions

Crosslinked CMC-PEG binder was prepared by a facile and low-cost approach. The silicon electrode prepared with the CMC-PEG binder exhibited outstanding cycle performance over 300 cycles at 0.5 C. In terms of the simplicity, in situ crosslinked CMC-PEG binder has a potential to be applied to the silicon anodes for stable cycle performance of LIBs.

ECCE12
The 12th EUROPEAN CONGRESS OF CHEMICAL ENGINEERING
Florence 15-19 September 2019

Quantitative analysis of gasification of Botswana coal using a 5kg/h auger reactor

Mmoloki Makoba[1*], Paul Agachi[1]

1Department of Chemical, Materials and Metallurgical Engineering, Faculty of Engineering and Technology, Botswana International University of Science and Technology, Private Bag 0016, Palapye, Botswana

**Corresponding author: makobam@biust.ac.bw*

Highlights

- To perform gasification of three different coals in Botswana
- Comparison of the product gas in terms of the amount of gas produced.
- To determine which coal field produces most product gas

1. Introduction

Botswana has approximately 212 Billion tons of coal of which less than a quarter of a billion tons is mined annually forming a part of the Karoo supergroup. It is in the region of what is called the Karoo Supergroup which is the most widespread stratigraphic area in Africa south of the Sahara Desert [1]. These reserves have been found to have high ash, medium calorific value, and low-medium quality bituminous coal [2]. Despite these coal riches, Botswana has only one power plant that generates and supplies electricity to the whole country being able to meet only 30% of the demand in the country. Botswana is developing at a high rate with a lot of infrastructure being erected which calls for more power supply that can be done through the process of coal gasification.

Gasification is the thermochemical conversion of carbonaceous material into valuable synthetic gas. The process takes place in the presence of steam and oxygen. An auger type reactor is a mechanically forced reactor with a screw driven by a motor to control its residence time. This feature allows for agitation which allows for contact with metallic surface and therefore more efficient heat transfer rate.

The auger reactor housed in BIUST is specifically 400 mm long with capabilities of up to 1050 °C temperature, up to 5 kg/h feed rate and residence time of at least 5s.

2. Methods

The samples were first taken through a TGA to determine physical properties. The feeder was then set to run at the required feed rate and the reactor to the required residence time. Heater duty was put to 10 kW. Main parameters for this process were oxygen and steam at 1 atm pressure and temperatures up to 1323 K. All parameters and measurements were recorded during the test. The results were then analyzed and concluded.

3. Results and discussion

Minergy coal shows to be the highest quality coal with lowest ash content and highest volatile matter and fixed carbon as shown by Table 1 and Figure 1. This coal field also produced more gas due to the highest percentage of volatiles.

Coal Fields (Composites)	Characteristics of Composite Coal				Quantitative analysis (per kg)
	Moisture	Volatile Dry	Ash Dry	FC Dry	
Mabesekwa	7.55	23.91	43.66	32.43	115 litres
Minergy	8.49	27.34	33.34	39.32	135 litres
Morupule	8.78	19.2	52.94	28.23	95 litres

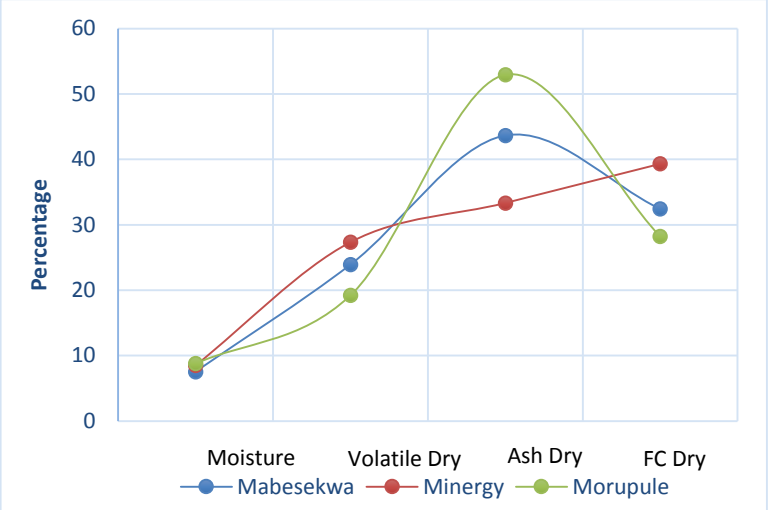

Figure 1. Proximate analysis of three coal fields in Botswana

4. Conclusions

Comparing coals from three different mines across the country, Minergy coal field shows to have the most valuable coal followed by Mabesekwa coal field and then Morupule coal field according to the amount of product gas collected compared under the similar conditions. Coal in Botswana differs across the belt.

References

[1] M. R. Johnson, C. J. Van Vuuren, W. F. Hegenberger, R. Key, and U. Shoko, "Stratigraphy of the Karoo Supergroup in southern Africa: An overview," *Journal of African Earth Sciences*. 1996.

[2] R. Grynberg, *Coal Exports and the Diversification of Botswana ' s The Coal Export Industry Diversification of Botswana ' s Economy*. 2012.

ECCE12
The 12th EUROPEAN CONGRESS OF CHEMICAL ENGINEERING
Florence 15-19 September 2019

Using the PC – SAFT model to estimate the speed of sound in synthetic and natural oil and gas mixtures

Samarov A.A.[1], Toikka A.M.[1], Prikhodko I.V.[1], Golikova A.D[1], Zvereva I.A.[1], Farzaneh-Gord M.[2]

1 Saint Petersburg State University, St. Petersburg, 199034 Russia; 2 Ferdowsi University of Mashhad, Mashhad, 9177948974 Iran

**Corresponding author: samarov@yandex.ru*

Highlights

- Thermodynamic properties
- Sound speed
- PC – SAFT
- Natural gas

1. Introduction

The speed of sound is an important thermophysical quantity, which is used for practical purposes to assess the density of formation fluids in wells in a wide range of external conditions. Along with temperature and pressure, the speed of sound is one of the parameters easily determined in the experiment that can be used to find the molecular weight and density of the gas mixture, as well as to estimate the magnitude of natural gas consumption at gas distribution stations.

Among modern equations of state that are tested by different researchers to improve the quantitative description of the speed of sound in pure and mixed fluids of different nature, the equations of the SAFT (Statistical Associating Fluid Theory) family are distinguished [1]. One of such state equations, the state equation based on the statistical theory of an associated fluid with a perturbed chain (Perturbed Chain – SAFT), was proposed by Gross and Sadowski [2].

In this paper, we applied the version of the PC – SAFT model to estimate and predict the speed of sound for a number of multicomponent systems containing oil and gas fluids. The model calculations performed give good results, sufficient for practical assessments and control of the sound speed (and densities) in the fluid mixtures under consideration.

2. Results and discussion

In this paper, we used the CP – PC – SAFT state equation (Critical Point-based Perturbed Chain – Statistical Association Fluid Theory) and tested the performance of the proposed Polishuk and co-authors method [3] in estimating the sound speed for multicomponent systems containing components of natural gas with different methane content (74–97 mol%). For the calculations, synthetic gas mixtures and natural gas mixtures from different fields were selected, with known experimental sound speeds in a wide range of pressures for a range of temperatures. The average absolute error of the obtained sound speed values in all considered systems does not exceed 2.0%, which indicates high accuracy characterizing the properties of the studied gas mixtures.

According to literature data, the results of predicting the speed of sound and density for a synthetic gas mixture using the CP – PC – SAFT model are somewhat inferior in accuracy given by the GERG-2008 multiparameter correlation equation of state (0.1%), which is recommended and widely used in engineering calculations for oil and gas industry.

3. Conclusions

The results of sound speed and density determination in systems formed by oil and gas components indicate the promise of further use of the PC – SAFT model for evaluating the thermodynamic and thermophysical properties of natural gas for applied purposes.

References [Calibri 10]

[1] W.G. Chapman, K.E. Gubbins, G. Jackson, M. Radosz, Ind. Eng. Chem. Res. 29 (1990) 1709–1721.
[2] J. Gross, G. Sadowski, Ind. Eng. Chem. Res. 40 (2001) 1244–1260.
[3] I. Polishuk, Ind. Eng. Chem. Res. 53 (2014) 14127–14141.

ECCE12
The 12th EUROPEAN CONGRESS OF CHEMICAL ENGINEERING
Florence 15-19 September 2019

The Contribution Of CO_2 Utilisation to GHG Emission Reduction: Some Results BasedoOn A European Supply Chain Optimisation.

Federico d'Amore, Victor Baldo, Fabrizio Bezzo*

CAPE-Lab - Computer-Aided Process Engineering Laboratory, Department of Industrial Engineering, University of Padova, via Marzolo 9, 35131 Padova PD (Italy).

**Corresponding author: fabrizio.bezzo@unipd.it*

Highlights

- Optimisation of a carbon capture, transport, storage and utilisation network.
- <0.6% of European CO_2 from coal/gas plants can be removed through utilisation.
- 5.5% cost reduction achievable thanks to revenues deriving from utilisation.

1. Introduction

In the last 50 years, CO_2 constituted nearly the 80% of overall anthropogenic greenhouse gases (GHGs) emissions; global actions are therefore needed to tackle the increase of carbon concentration in the atmosphere [1]. Carbon capture and storage (CCS) has been highlighted as one of the most promising options. Recently, also carbon utilisation pathways have been highlighted as potential options to reduce the costs that derive from the installation and operation of a more general CCS and utilisation (CCUS) infrastructure. Nevertheless, there is debate on the actual effectiveness of the chemical conversion of CO_2, indicating that only minor environmental benefits could be obtained [2]. In this work, the aim is to evaluate the effects of CCUS from an economic perspective and to assess what contribution may derive from CO_2 utilisation for conversion into chemical products at a European level.

2. Methods

This contribution proposes a static mixed integer linear programming model for the economic optimisation of European CCUS supply chains (SCs). Building up from [3], the European territory is discretised by aim of set *g* of 124 squared cells and the SC takes into account the location of large stationary sources of CO_2, the techno-economic description of set *k* for carbon capture options, of set *l* of transport means, the location and size of storage basins, and the techno-economic features of the CO_2 utilisation stage via set *c* of chemical outputs. Given the numerous reaction mechanisms for CO_2 conversion [4], a restricted number of processes was selected according to the following principles: (*i*) minimum production threshold according to market demand (>1Mt/year of converted CO_2); (*ii*) techno-economic data availability (productivity and costs); (*iii*) environmentally promising (CO_2 emissions lower than consumption); (*iv*) current technology economically promising (the conversion process must generate a profit). As a result, set *c* = {PPP, MeOH}.

3. Results and discussion

The CCUS model was optimised using the GAMS CPLEX solver on a 16GB RAM pc in 27h (optimality gap <1%). As reference case, results from [3] of the optimal CCS network are reported (Scenario 0).

The CCUS system (Scenario A) is optimised according to the selection of a reduction target of 43% of European CO_2 emissions from large stationary sources (consistent with [5]), and imposing to satisfy the current European production of PPP and MeOH. As a result, the SC entails a total cost *TC* for installing and operating the CCUS network that is reduced by 5.5% with respect to Scenario 0, because the introduction of chemical conversion brings in some revenues (with a profit equal to 1.57€/t). Conversely, the chemical conversion of CO_2 allows just a slight reduction of 0.7% of total capture costs *TCC*, which decrease from 30.93€/t (Scenario 0) down to 30.72€/t (Scenario A). The total transport cost *TTC* slightly varies from 1.96€/t (Scenario 0) to 1.90€/t (Scenario A). Despite a small decrease in the exploitation of geological storage (i.e., -1.44%), total sequestration costs *TSC* are unchanged between Scenario 0 and Scenario A (0.47€/t and 0.46€/t, respectively). In terms of CO_2 emission reduction, the net impact of utilisation amounts to 0.58% of the overall captured amount (comparable with [2]). It can be observed that the SC configuration is nearly identical between Scenario 0 and A (Figure 1). Including utilisation, capture points do not change and the main driver to establish the transport system is still the location of the sequestration sites.

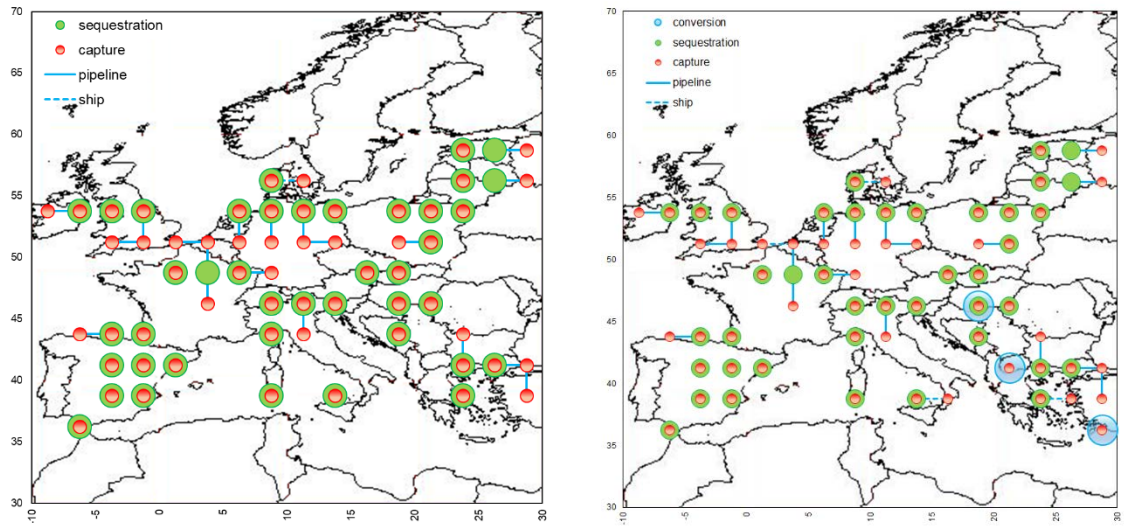

(a) (b)

Figure 1. Final SC configurations for (a) Scenario 0 and (b) Scenario A.

4. Conclusions

This work has assessed the potential impact of a European CCUS SC. Results show that the environmental impact of CO_2 utilisation is likely to be a minor one (<0.6% reduction in GHG emissions for the chemicals considered in this study). The main benefit is the reduction of the overall costs (decreasing by 5.5%), since conversion would provide for new revenues (differently from sequestration).

References

[1] IPCC, Climate Change-Synthesis Report, Geneva, 2014.
[2] N. Mac Dowell, P.S. Fennell, N. Shah, G.C. Maitland, Nat. Clim. Chang. 7 (2017) 243-249.
[3] F. d'Amore, F. Bezzo, Int. J. Greenh. Gas Control 65 (2017) 99-116.
[4] M. Aresta, A. Di Benedetto, A. Angelini, J. CO_2 Util. 3-4 (2013) 65-73.
[5] EC, Implementation of Directive 2009/31/EC, Brussels, 2017

ECCE12
The 12th EUROPEAN CONGRESS OF CHEMICAL ENGINEERING
Florence 15-19 September 2019

Investigation of Mass Transport and Crystallization Processes of Acoustically Levitated Droplets under Elevated Pressures

Danijel Boroša

BOROSA Acoustic Levitation GmbH, Universitätsstr. 142, Technologie-Zentrum Ruhr,

44799 Bochum/Germany, www.borosa.de, info@borosa.de

Highlights

- Acoustic Levitation
- Wall-Contact-Free Crystallization
- Gas Hydrates
- Physical Properties & Mass Transport

1. Introduction

Mass transport and crystallization experiments are among the most challenging measurements in the field of process engineering and chemistry. The results of these studies provide an important basis for many chemical engineering processes and other technical systems. Mass transport studies of liquids in the presence of dense gases are usually performed with the aid of the pendant-drop-method. Especially, in case of phase-conversion processes, which cause a solidification of the hanging droplet, the disadvantage is the contact between the droplet and the capillary, which is influencing the solidification process. Therefore, a non-contact method would be desirable to observe the mass transport and crystallization processes, e. g. hydrate formation. The acoustic levitation represents a possibility to examine samples without contact to any wall [1] [2].

The modification of a high-pressure-view-cell led to a successful implementation of an acoustic levitator into a pressure- and temperature resistant housing (pressure maximum = 20 MPa, temperature maximum = 453 K). The new measurement device allows the investigation of gas hydrate formation at a contact-free acoustically levitated droplet under elevated pressures.

In preliminary investigations it was possible to show the formation and controlled decomposition of carbon dioxide hydrates. The formation of carbon dioxide hydrates was observed for the first time at acoustically levitated water droplets.

2. Methods

The experiments were carried out with a high-pressure view-cell including an integrated acoustic levitation device. The compact laboratory device L800 is well-suited for accurate measurements of mass-transport mechanisms of small samples. The specifically developed software detects the acoustically levitated sample automatically and analyzes the contour of the droplet. With this information the volume of the rotationally symmetric sample can be measured and documented.

3. Results and discussion

Previous experiences according to gas hydrate formation measurements show that the exact determination of the transition time of larger test samples cannot be simply done. As a result, it is easier to observe one droplet in order to measure its phase change behaviour and the corresponding test parameters. Furthermore, the small sample has got an almost uniform temperature distribution during the measurement. The images illustrate an example of an experiment regarding the formation of a CO_2-hydrate (Fig. 1).

The continuous phase is CO_2 with a constant pressure of 2.9 MPa. The temperature of the continuous phase is about 281 K. Shortly after the injection of the water droplet, the cooling of the continuous phase is started. When a temperature of about 279 K is reached the bottom of the droplet begins to solidify. Then the crystal growth covers the entire droplet. The whole process from a liquid droplet to a gas hydrate was in this case about 8 minutes long. The diagram (Fig. 1) contains the measurement results compared with literature data. Each measurement point is a result of the arithmetic average of three measurement points.

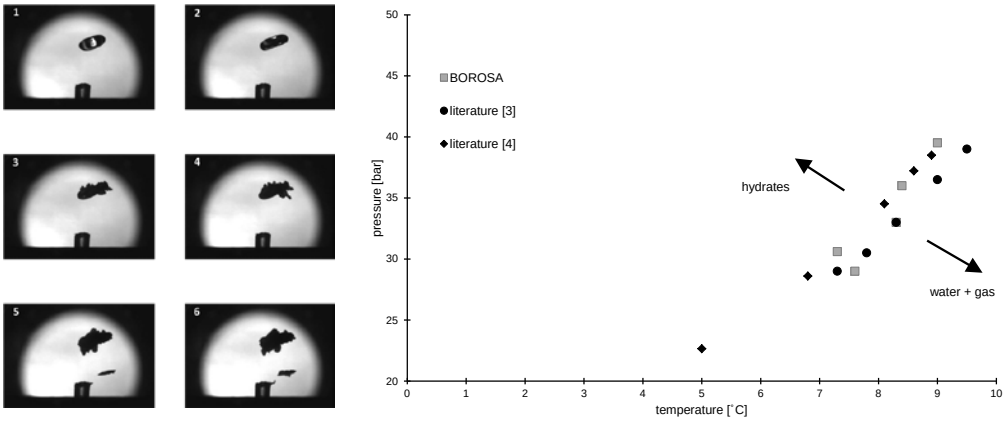

Figure 1: Contact-free CO2-hydrate formation, p= 2.9 MPa / T = ca. 281 K (start) – 279 K (end) [1] / pT-diagram [3] [4]

4. Conclusions

Through the successful combination of a high-pressure measurement cell and an acoustic levitator it was possible for the first time to observe the formation of CO_2 gas hydrates contact-free. It was necessary to develop a method for injecting liquid water droplets in the pressurized view-cell without an unwanted crystallization in the pipes. Finally, it was possible to acoustically levitate a water droplet and to observe its phase change from liquid to solid state. The acquired measurement data were compared with literature data. A good agreement with literature data can be confirmed. Consequently, the new apparatus L800 is suitable to measure gas hydrate formation regarding sample volume, composition and morphology at the same time.

References

[1] D. Borosa, Entwicklung und Aufbau eines akustischen Levitators zur Untersuchung von Stofftransport-Partikelbildungsmechanismen von Proben unter hohen Drücken, Dissertation, 2013.

[2] E. G. Lierke, Akustische Positionierung – ein umfassender Überblick über Grundlagen und Anwendungen, Acustica, 82, 220-237, 1996.

[3] W. J. North, V. R. Blackwell, J. J. Morgan, Studies of CO2 Hydrate Formation and Dissolution, Environ. Sci. Technol., 32, 676-681, 1998.

[4] M. Wendland, H. Hasse, G. Maurer, Experimental Pressure-Temperature Data on three - and four - Phase Equilibria of Fluid, Hydrate, and Ice Phases in the System Carbon Dioxide-Water, J. Chem. Eng. Data, 44 (5), 901-906, 1999.

ECCE12
The 12th EUROPEAN CONGRESS OF CHEMICAL ENGINEERING
Florence 15-19 September 2019

Assessing different modelling approaches for secondary nucleation

Luca Bosetti, Marco Mazzotti*

Institute of Process Engineering, ETH Zurich, 8092 Zurich, Switzerland

**bosettil@ethz.ch*

Highlights

- Attrition considered as a breakage phenomenon and as the source of secondary nucleation
- Physical expression of breakage rate, daughter distribution and secondary nucleation rate
- Comparison of secondary nucleation and breakage by attrition
- Combination of numerical methods: finite volume, fixed pivot, fractional step

1. Introduction

The production of active pharmaceutical compounds relies upon continuous crystallisation, during which the crystals produced are formed via secondary nucleation. A precise physical and mathematical description of the phenomena occurring during secondary nucleation has been neither fully understood, nor fully described yet. One of the possible mechanisms for the formation of nuclei is attrition[1], which is a purely mechanical process that generates fragments that are removed from the crystal surface and then grow or dissolve in the bulk solution. In this study, the formation of secondary nuclei is considered to be a consequence of the detachment of small fragments from a mother crystal, because of impact with the stirrer, which is the most common phenomenon[1].

2. Methods

The scope of this work is to compare two approaches to include secondary nucleation in a mono-dimensional population balance equation model (PBE). The first approach is the one usually used in the literature [1], where a semi-empirical expression for secondary nucleation is included as a boundary condition of the PBE model, in analogy with primary nucleation. Such an expression is usually dependent on the energy input, e.g. stirring intensity, supersaturation and an integral property of the crystals' population, e.g. the total area or the total mass [2,3]. The second approach consists in considering secondary nucleation as a pure attrition mechanism, thus accounting for it through a source term in the PBE, namely an integral term.

In order to model attrition as a source term, we have defined a daughter distribution of fragments [2] and an attrition frequency to quantify the size distribution and occurrence of the attrition events, respectively. Moreover, not all the particles produced through attrition evolve in the same way. In fact, a particle will grow depending on its size according to a size-dependent growth expression. The entire process has been modelled at isothermal conditions, in a batch crystallizer.

The phenomena considered are growth, dissolution, breakage and secondary nucleation. The numerical methods used are hybrids between finite volume[4] for growth, dissolution, and secondary nucleation and fixed pivot[5] for breakage. In presence of source terms, a fractional-step method has been applied[4].

3. Results and discussion

The phenomenon of formation of nuclei (or fragments) has been successfully described by the two modelling approaches, even though they are conceptually very different, since one is active only in the presence of supersaturation, i.e. secondary nucleation, and the other is always active. The results show that we can achieve similar results regarding the production of fines, but the effect of supersaturation is obviously different. Thanks to this result, we are able to have an insight into the two phenomena, starting from physical properties of the system, and physical operative conditions. The study has been conducted in a fully parametric way, which make the model very flexible to change in operating conditions and in changes of the material to crystallize.

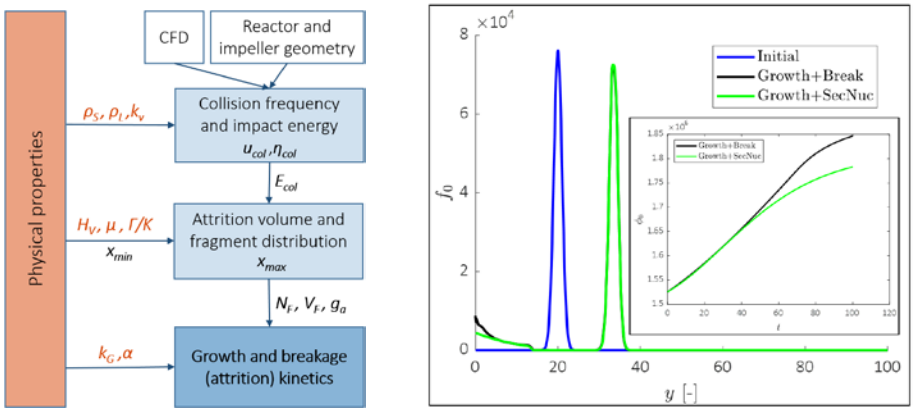

Figure 1. (a) Schema for the physical determination of the breakage rate and of the daughter distribution. (b) Comparison of the final populations obtained with the model with growth and breakage (black) and with the one with growth and secondary nucleation (green).

4. Conclusions

In this work, it has been shown how the two modelling approaches lead to similar conclusions, when the expressions for secondary nucleation and that for breakage by attrition have been derived from the physical properties of the system and its operative conditions. Experimental validation of the model will allow to clarify which approach is more suitable to describe continuous crystallization.

References

[1] Agrawal, S. G., & Paterson, A. H. J. (2015). Chemical Engineering Communications, 202(5), 698–706.
[2] Mersmann, A. (Ed.). (2001). Crystallization technology handbook. CRC Press.
[3] Gahn, C., & Mersmann, A. (1999). Chemical Engineering Science, 54(9), 1273–1282.
[4] Leveque, R. J. (2002). Finite volume methods for hyperbolic problems (Vol. M).
[5] Iggland, M., & Mazzotti, M. (2011). Crystal Growth and Design, 11(10), 4611–4622.

This project has received funding from the European Research Council (ERC) under the European Union's Horizon 2020 research and innovation programme under grant agreement No 2-73959-18.

ECCE12
The 12th EUROPEAN CONGRESS OF CHEMICAL ENGINEERING
Florence 15-19 September 2019

Crystallization fundamentals and industrial processes

Kinetic Assessment for Continuous Crystallization Process of Early Development Compound

Gladys Kate Pascual[1], Marko Ukrainczyk[1]*, Gary Morris[1], Brian Glennon[1], Alain Collas[2], Ronny Vanierschot[2]

1 APC Ltd, Cherrywood Business Park, Loughlinstown, Co. Dublin, D18 DH 50, Ireland; 2 Crystallization Technology Unit (CTU), Janssen Pharmaceutical Companies of Johnson & Johnson, Beerse, Belgium

**Corresponding author: marko.ukrainczyk@approcess.com*

Highlights

- Kinetic assessment for continuous crystallization developed
- Population balance kinetic model (PBM) built for two solvent systems to evaluate solvent dependency
- MSMPR process parameters optimized and validated through PBM

1. Introduction

In the pharmaceutical industry, crystallization is a key unit operation utilised to produce particles with desired properties, such as the particle size distribution, as this has an influence on downstream processes such as filtration and drying. The acquisition of reliable kinetic correlations that describe how rates of nucleation and growth vary over the crystallization design space is necessary for enabling robust prediction of crystallizer performance. The aim of this study was to generate a standardised workflow approach for the generation of crystallization kinetics data using population balance modelling (PBM), and to assess the batch crystallization process for feasibility of continuous processing for an early development compound.

2. Methods

Initially, the crystallization growth kinetics were estimated by means of seeded isothermal desupersaturation experiments in a batch reactor. PAT tools such as Attenuated Total Reflectance-Fourier Infrared (ATR-FTIR) spectroscopy and Focused Beam Reflectance Measurement (FBRM) were utilised for *in situ* to track the desupersaturation profile and the progression of the seed distribution, respectively. The initial crystal size distributions (CSDs) and desupersaturation profiles were used to estimate the growth kinetics as a function of temperature and supersaturation. Two solvent systems were tested to extract growth kinetics and were used for comparison. Furthermore, activity coefficients as a function of temperature and composition were considered in the kinetic model, which enabled to directly evaluate the solvent dependency effect. Following satisfactory validation of crystal growth kinetics, a continuously operated single-stage mixed suspension mixed product removal (MSMPR) crystallizer was used to extract the secondary nucleation kinetics.

3. Results and discussion

Three seeded isothermal desupersaturation experiments were performed to estimate the crystal growth kinetics, which are outlined in Table 1. A conservative approach of using a high seed loading of 50% allowed for the estimation of growth kinetics in the absence of nucleation. Furthermore, the temperature and initial relative supersaturation range covered in the parameter estimation was between 0 to 30°C and 0.226 to 0.670, which ensured that the entire phase diagram was covered and that the estimated parameters could describe the growth over a wide range of operating conditions. One experiment (exp 4) was performed to validate whether the growth is size dependent or independent by using a larger seed fraction.

Table 1. Experimental conditions for parameter estimation for solvent system 1

Experiment	Temperature (°C)	Relative S0 (-)	Seed Loading (%)
1	0	0.670	50
2	15	0.474	50
3	30	0.226	50
4	30	0.226	50

During the continuous crystallization study, a recycling system was employed to significantly reduce the waste of raw materials during the MSMPR study prior to the onset of steady state, which can be very useful during the early stages of process development where limited amount of product is available. Furthermore, problems such as blocking of transfer line and feed inlet were eliminated, by applying a rapid intermittent withdrawal of slurry via dipped pipe[1], and by using a tube-in-tube configuration to insulate the feed inlet line. Finally, a novel 3D printed jacketed nozzle was attached at the end of the feed inlet line to avoid the saturated solution from crystallizing which can lead to blockage. Based on PBM and utilisation of the kinetic data[2], CSD was simulated and residence time distribution, operating temperature and productivity of the MSMPR were optimised and finally experimentally verified. Overall, a standardised workflow was developed for the kinetic assessment of an early development compound for continuous crystallization.

References

[1] G. Hou, G. Power, M. Barrett, B. Glennon, G. Morris, Y. Zhao, Cryst Growth Des. 14 (2014) 1782-1793
[2] G. Power, G. Hou, V. K. Kamaraju, G. Morris, Y. Zhao, B. Glennon, Chem. Eng. Sci. 133(2015) 125-139

ECCE12
The 12th EUROPEAN CONGRESS OF CHEMICAL ENGINEERING
Florence 15-19 September 2019

Crystallization fundamentals and industrial processes

Precipitation and characterization of vanadium V(II), V(III) and V(V) sulfate compounds in Vanadium Redox Flow Battery electrolyte

Waldemir M. Carvalho Jr.*, Laurent Cassayre, Theodore Tzedakis, Fabien Chauvet, Ranine El-Hage, Béatrice Biscans.

Laboratoire de Génie Chimique, Université de Toulouse, CNRS, INP, UPS, Toulouse, France

**Corresponding author: waldemir.mouradecarvalho@ensiacet.fr*

Highlights

- V(II), V(III) and V(V) supersaturated solutions were prepared by electrolytic dissolutions of commercial vanadium salt in sulphuric acid solutions.
- Pure crystals of hydrated V(II), V(III) and V(V) sulfates ($VSO_4 \cdot 7H_2O$, $V_2(SO_4)_3 \cdot 10H_2O$ and $V_2O_5 \cdot 1.5H_2O$) were isolated and identified as precipitating phases, in different conditions.

1. Introduction

The vanadium redox flow battery (VRFB) has been receiving considerable attention in recent years, as one of the most viable energy storage technologies for large-scale application. It eliminates the cross-contamination present in flow battery, enables long cycle life (>10000 cycles), high-energy efficiencies and relatively low-cost structure for large storage capacities [1]. As the concentration of vanadium species in the H_2O-H_2SO_4 electrolyte determines the VRFB energy density, high concentrations are required. Meanwhile, major precipitation of vanadium compounds must be avoided [2]. Despite current researches aiming at understanding the vanadium salts precipitation in a VRFB, very little has been done to identify the phases precipitated in the vanadium acidic solution used as VRFB electrolyte. This study has thus focused on (i) preparing V(II), V(III) and V(V) supersaturated solutions (ii) identifying the precipitation products in VRFB operating conditions, with an aim of improving the understanding of vanadate chemistry in a high concentrated sulphuric acid solution.

2. Methods

The vanadium supersaturated solutions are prepared by dissolution of commercial $VOSO_4$ powder suspension, and subsequent electrochemical oxidation (for V(V) preparation) or reduction (for V(II) and V(III) preparation) in one of the compartment of a two-compartment electrolytic cell separated by a Nafion cationic membrane. Thick carbon felts (5mm) were used as anode and cathode. Based on the solubility curves of the vanadium salts available in the literature [2], 60.63 grams of $VOSO_4$ powder (corresponding to 5 mol L^{-1}) were added in 50 mL of a 5 mol L^{-1} H_2SO_4 solution, and placed either into the negative half-cell to prepare V(II) and V(III) supersaturated sulfate solution, or into the positive half-cell to prepare V(V) sulfate solution. The galvanostatic electrolyzes were run at a constant current density (1 A) with a DC power supply. The vanadium species concentration was followed by UV-vis spectroscopy for V(II) and V(III) solution and by titration for V(V) solution. When the required vanadium conversion was achieved , the supersaturated solution was transferred to another vessel where they were aged at constant temperature (30 °C for V(II) or V(III) and 60 °C for

V(V)) and at constant agitation (400 rpm), while the vanadium species concentrations were monitored until precipitation occurred. The precipitated products were then filtrated, washed with ethanol, dried at 60 °C for 4 hours, and analyzed by X-ray diffraction (XRD), thermogravimetric analysis (TGA) and UV-Vis spectroscopy.

3. Results and discussion

The initial vanadium concentrations were measured before the aging process as 3.2, 3.5 and 4.0 mol L^{-1} for V(II), V(III) and V(V) solutions, respectively. Significant amounts of precipitated solids were obtained in V(II) and V(III) solutions, after 12 h (purple precipitate for V(II) and green precipitate for V(III)). For the V(V) solution, 11 days were required to produce enough solid (orange/brown precipitate) for further characterization. The obtained precipitated powders were then diluted in a sulphuric acid solution and analyzed by UV-Vis spectroscopy. They all showed their own specific absorption profile, confirming that each of the precipitates corresponds to a specific oxidation state, depending on the initial solution. Powder XRD analysis of each of the dried precipitates was performed (Figure 1). The precipitate obtained from the V(II) solution perfectly match the $VSO_4 \cdot 7H_2O$ phase, and the solid produced from V(III) and V(V) solutions fairly match $V_2(SO_4)_3 \cdot 10H_2O$ and $V_2O_5 \cdot 1.5H_2O$ phases, respectively. These phases were similar for different aging/precipitation durations. To confirm the V(III) and V(V) precipitates identification, the powders were heat-treated at 200 °C in air and analyzed again by XRD. This temperature (200 °C) was determined by TGA. It enables a complete removal of the water from the hydrates without any decomposition (to SO_3 for example) nor any phase transition (due to oxidation for instance). After the heat treatment, the V(III) and V(V) precipitates perfectly match the $V_2(SO_4)_3$ and V_2O_5 pattern respectively.

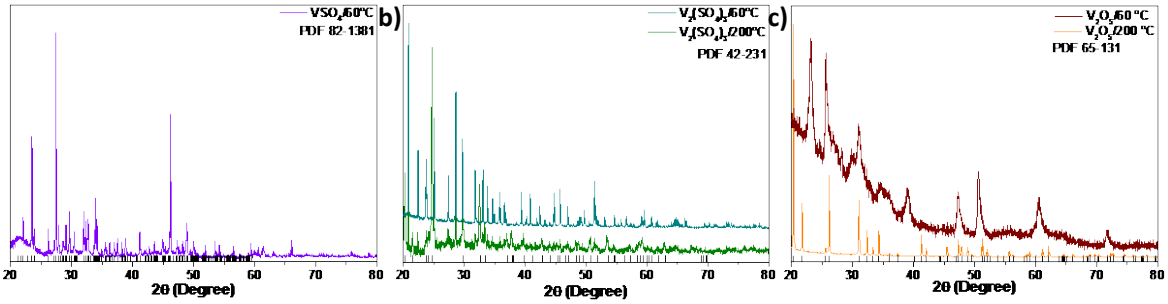

Figure 1. X-ray diffraction pattern of the precipitation product of the (a) V(II), (b) V(III) and (c) V(V) solution after aging.

4. Conclusions

In summary, we report a method to prepare V(II), V(III) and V(V) supersaturated solutions in an H_2SO_4-H_2O electrolyte, from the only vanadium sulfate compound commercially available ($VOSO_4$). We also identify the precipitation products which may form in a VRFB operated with such supersaturated solutions. The results showed that V(II), V(III) and V(V) sulfate solutions precipitate as VSO_4, $V_2(SO_4)_3$ and V_2O_5 hydrates and not in their anhydrous form. Taking into account this hydration degree might change the vanadium concentration limits of a VRFB and the occurrence of precipitation which are currently calculated in the literature with the anhydrous form [1].

References

[1] L. Cao, M. Skyllas-Kazacos, C. Menictas, J. Noack, J. Energy Chem. 27 (2018) 1269–1291.

[2] F. Rahman, M. Skyllas-Kazacos, J. Power Sources. 189 (2009) 1212–1219.

ECCE12
The 12th EUROPEAN CONGRESS OF CHEMICAL ENGINEERING
Florence 15-19 September 2019

Isothermal cold crystallization kinetics and properties of thermoformed poly(lactic acid) composite films

Anongnat Somwangthanaroj[1,2,*], Chutimar Deetuam[1], Chavakorn Samthong[1], Suphattra Choksriwichit[1]

1 Department of Chemical Engineering, Faculty of Engineering, Chulalongkorn University, Bangkok 10330, Thailand; 2 Special Task Force of Activating Research (STAR) in Novel Technology for Food Packaging and Control of Shelf Life, Chulalongkorn University, Bangkok 10330, Thailand
**Corresponding author: anongnat.s@chula.ac.th*

Highlights

- Effects of fillers and silane surface functionalization were investigated.
- Faster cold crystallization of PLA with the presence of fillers was observed.
- Talc is the most effective nucleating agent for PLA.

1. Introduction

Biodegradable polymers have gained great attention as eco-friendly alternatives to conventional plastics derived from fossil fuels. Poly(lactic acid) (PLA) is the most well-known biodegradable thermoplastic that has been extensively used for diverse applications, such as household appliances, automobile interiors, tissue engineering, drug delivery, and food packaging materials [1, 2] because of its unique properties including biodegradability, biocompatibility, high transparency, and high tensile strength (75 MPa) and modulus (3.2 GPa) [3, 4]. Nevertheless, PLA has some weaknesses including brittleness with elongation at break less than 4%, poor melt strength, poor thermal stability, and low gas barrier properties. Further, PLA is also known as a slow crystallizing polymer; this leads to a very long injection moulding cycle time during the cooling step, and the end-use products have low crystallinity, which strongly affects its optical, thermal, and mechanical properties [5]. Accordingly, slow crystallization behaviour of PLA should be improved for potentially being used in the industrial applications as it deserves. In this work, the effect of the addition of talc, $CaCO_3$, and cassava starch at various contents on the morphology, mechanical and thermal properties, and isothermal cold crystallization kinetics of PLA composites is examined.

2. Methods

The isothermal cold crystallization kinetics is investigated by fitting the experimental data from differential scanning calorimetry (DSC) with a theoretical Avrami model. The study on annealing effect under cold crystallization on the thermal and tensile properties is performed by comparing cast films with thermoforming films. Eventually, surface treatment of talc with vinyltriethoxysilane (VTES) and 3–aminopropyltriethoxysilane (APTES) is also performed to examine the silanization effect on the properties of PLA composites in comparison with the untreated system. Tensile properties including tensile strength, elongation at break, Young's modulus, and tensile toughness of cast films and thermoforming films of neat PLA and PLA composites were measured at room temperature using a universal testing machine (Intron model 5567, USA) in accordance with ASTM D882.

3. Results and discussion

The Avrami model was employed to study the isothermal cold crystallization kinetics by DSC. Dynamic DSC results revealed that incorporation of filler can facilitate the cold crystallization of PLA. The highest isothermal cold crystallization rate constant *k* and the shortest crystallization half time $t_{1/2}$ were achieved for the PLA/talc composites under isothermal temperature of 100 °C, implying that talc was the most effective nucleating agent for PLA in this study. After annealing the cast films under isothermal cold crystallization condition to induce the orientation of PLA chains, the thermoforming films had higher degree of crystallinity as well as improved tensile strength and Young's modulus. The successful grafting of silane coupling agent onto the talc surface was confirmed by FTIR measurement and it was noticed that films with the silanization of talc surface with APTES showed the fastest cold crystallization rate. Therefore, the strong interfacial adhesion in the PLA composites containing APTES treated talc resulted in less debonded talc particles from the cryofractured surfaces and an enhancement of tensile properties.

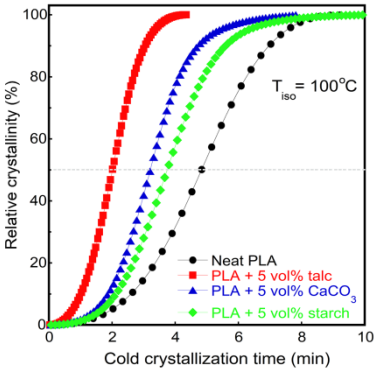

Figure 1. Relative degree of crystallinity X_c of neat PLA and its composite cast films containing 5 vol% untreated fillers at T_{iso} = 100 °C. Inserted horizontal line is X_c = 50%.

4. Conclusions

The effects of three different fillers and silane surface functionalization on morphology, thermal and tensile properties of the poly(lactic acid) (PLA) composites were comparatively examined. The surface functionalization of talc particles by silanization reveals higher tensile strength as well as faster cold crystallization rate, which is attributed to the enhanced interfacial interaction between PLA chains and talc particles. Therefore, it can be summarized from our work that cold crystallization behaviour of the polymer composites depends not only on inherent nucleating ability of filler, but also the surface functionality of the filler particles.

References

[1] Arrieta, M. P.; López, J.; Hernández, A.; Rayón, E. *Eur. Polym. J.* **2014,** *50*, 255.
[2] Samthong, C.; Seemork, P.; Nobukawa, S.; Yamaguchi, M.; Praserthdam, P.; Somwangthanaroj, A. *J. Appl. Polym. Sci.* **2015,** *132*, 41415.
[3] Huang, T.; Yamaguchi, M. *J. Appl. Polym. Sci.* **2017,** *134*, 44960.
[4] Deetuam, C.; Samthong, C.; Pratumpol, P.; Somwangthanaroj, A. *Iran. Polym. J.* **2017,** *26*, 615.
[5] Auras, R.; Lim, L. T.; Selke, S. E. M.; Tsuji, H. In Poly(lactic acid): Synthesis, Structures, Properties, Processing, and Applications; John Wiley & Sons Inc.: New Jersey, **2011**.

ECCE12
The 12th EUROPEAN CONGRESS OF CHEMICAL ENGINEERING
Florence 15-19 September 2019

Crystallization fundamentals and industrial processes

Ternary solvent system for crystallizing the desired solid form of indomethacin with increased productivity

Iben Ostergaard[1*], Chandrakant Malwade[1], Heidi Lopez de Diego[2], Haiyan Qu[1]

1 Department of Chemical Engineering, Biotechnology, and Environmental Technology, University of Southern Denmark, Campusvej 55, 5230 Odense, Denmark; 2 Process Chemistry, H. Lundbeck A/S, Ottiliavej 9, 2500 Copenhagen, Denmark

** ibo@kbm.sdu.dk*

Highlights

- Novel antisolvent crystallization process for Indomethacin
- Increased productivity obtained from ternary solvent system
- Desired polymorph obtained via seeding

1. Introduction

Development of crystallization processes for manufacturing of active pharmaceutical ingredients (APIs) with the desired purity, solid form, particulate properties, as well as sufficiently high process yield is very crucial for pharmaceutical industry. Polymorphism, particle size distribution and crystal shape of APIs are a complex function of crystallization process parameters, whereas the productivity of a batch crystallization process strongly depends on the difference between the API concentration at the initial operating conditions and the final condition of the batch. A high process yield requires a solvent system that provides high API solubility at the initial batch conditions and a remarkable change of the API solubility with the changing operation parameter, i.e., decreasing of temperature and/or addition of antisolvent [1]. In this work, we show that the use of binary solvent mixture compared to the pure solvent can provide increased solubility leading to the increased productivity of APIs during crystallization. We also show that the altered solute-solvent interactions favoring the formation of desired polymorph can be obtained by using solvent mixtures instead of pure solvents. Indomethacin (IMC), a nonsteroidal anti-inflammatory drug, is used as the model compound. It has been reported that IMC can form five polymorphs and several solvates [2]. However, metastable α-IMC having needle like crystal shape and thermodynamically most stable γ-IMC having plate like crystal shape are most commonly observed. In this work, antisolvent crystallization of IMC from acetone-methanol-water system has been carried out with acetone-methanol (66.5-33.5 Wt%) as solvent and water as an antisolvent.

2. Methods

Binary solvent mixture acetone-methanol was selected based on the solubility of γ-IMC in single and binary solvent mixtures (Fig. 1) reported earlier [3,4]. Firstly, the solubility of γ-IMC in acetone-methanol-water with varying composition of water was measured at 25 °C. Based on the determined solubility data, seeded and unseeded antisolvent crystallization experiments of IMC from acetone-methanol-water were performed at 25 °C. The procedure included dissolution of IMC in 30 g of acetone-methanol solvent contained in a 100 ml reactor followed by stepwise addition of

water as an antisolvent. Each experiment was performed at two different initial concentrations of IMC as shown in Fig. 2. In experiments with high (C_i^1) and low (C_i^2) initial concentrations, 9 and 12 g water was added, respectively to obtain the respective solvent composition of 23 and 28.5 wt% water as shown in Fig. 2. In case of seeded experiments, seed load (γ-IMC, 71-125 µm) of 0.75, 1.5, 3, and 4% of Δ*C* were used. The experiments were monitored with ATR-FTIR probe and characterization of IMC crystals was carried out with XRPD, SEM and particle size analyzer.

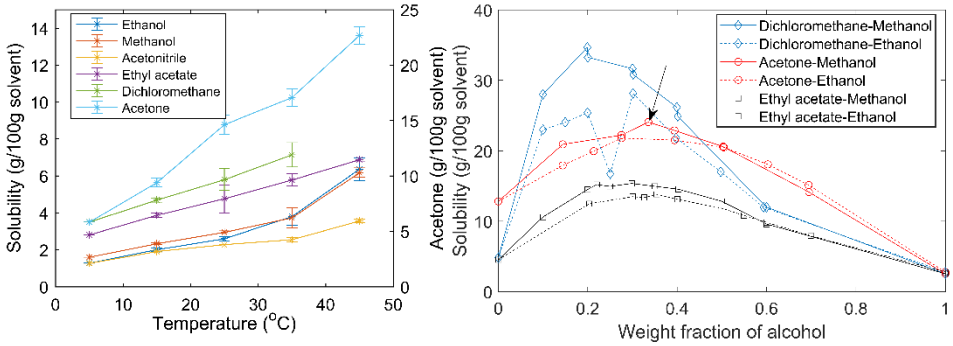

Figure 1. Solubility of γ-IMC in pure organic solvents (left) [4] and in binary solvent mixtures at 25 °C (right) [3].

3. Results and discussion

In comparison to the seeded cooling crystallization of IMC from ethanol reported earlier [4], significantly high productivity was obtained during antisolvent crystallization of IMC from acetone-methanol-water (Table 1). Increased crystal yield was obtained mainly due to the extended thermodynamic boundaries allowing much higher initial concentration of IMC in acetone-methanol binary mixture [5].

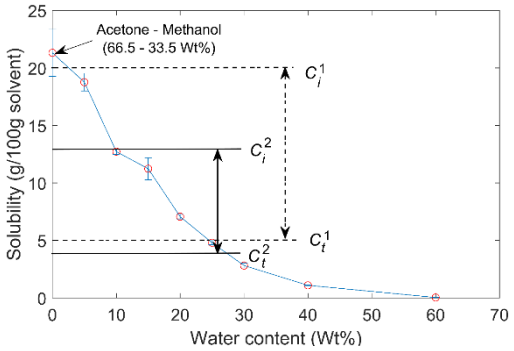

Figure 2. Measured solubility of γ-IMC in acetone-methanol-water at 25 °C.

Table 1. Results from antisolvent crystallization of IMC from acetone-methanol-water at 25 °C.

Properties	Unseeded		Seeded	
	C_i^1	C_i^2	C_i^1	C_i^2
Solid form	Solvate	Solvate	γ-IMC	γ-IMC
Productivity (mg/g/min)	-	-	0.75	0.38
			0.015*	

*Maximum productivity of IMC obtained during cooling crystallization from ethanol [4]. Productivity values for current work are for highest seed load.

4. Conclusions

In this work, we have shown that the desired γ-IMC can be produced consistently through seeded antisolvent crystallization from acetone-methanol-water with improved productivity.

References

[1] J.W. Mullin, Crystallization, fourth ed., Butterworth-Heinemann, 2001.
[2] B. Nicolaï, R. Céolin, I.B. Rietveld, J. Therm. Anal. Calorim. 102 (2010) 211–216.
[3] S. Hellstén, H, Qu, M. Louhi-Kultanen, Chem. Eng. Technol. 34 (2011) 1667-1674.
[4] C.R. Malwade, H. Qu, Org. Process Res. Dev. 22 (2018) 697-706.
[5] C.R. Malwade, H. Qu, Org. Process Res. Dev. 23 (2019) 968-976.

ECCE12
The 12th EUROPEAN CONGRESS OF CHEMICAL ENGINEERING
Florence 15-19 September 2019

Crystallization fundamentals and industrial processes

Determining particle size distributions from chord length measurements for different particle morphologies

Jochen Schoell[1]*, Roberto Irizarry[2], Eric Sirota[3], Cameron Mengel[3], Lorenzo Codan[1], and Aaron Cote[3]

1 Process Research &Development, MSD Werthenstein BioPharma, 6105 Schachen, Switzerland
2 Data Science and Applied Mathematics, Merck & Co., Inc., West Point, PA 19486 USA
3 Process Research & Development, Merck & Co., Inc., Rahway, NJ 07065 USA.
**Corresponding author: jochen.schoell@merck.com*

Highlights

- Data-driven model for CLD-to-PSD prediction
- Model required limited data and showed good generalization properties
- Applicable to different crystal morphologies (rod, compact, platelets)
- Comparison with model variations using PCA and geometric models

1. Introduction

In pharmaceutical crystallization, Focused Beam Reflectance Measurement (FBRM) has become a standard tool for in situ particle monitoring due to its ease of process implementation and ability to operate at high solids concentrations. However, a major limitation of this technique is that its measurement signal, i.e., the chord length distribution (CLD), differs fundamentally from particle size distribution (PSD) data due to the FBRM measurement principle described in literature [1,2]. Thus, the measured CLD is not only a function of particle number and size, but is generally also affected by particle morphology and various process parameters, e.g., probe positioning, particle concentration, and optical effects of the continuous and dispersed phase. The combination of these factors produces the actual measurement signal, which differs from a theoretically calculated CLD. Thus, a data-driven modeling approach has been proposed recently which allowed the quantitative determination of 1D and 2D PSDs from measured CLDs, suggesting an effective solution to the above-mentioned limitations of the FBRM [1]

2. Methods

The data-driven model architecture is based on three sequential steps:

1. CLD data is compressed into a small set of CLD descriptors (low order moments).
2. The CLD descriptors are mapped into a small number of PSD moments using a regression model.
3. Finally, the PSD moments are expanded into a full particle size distribution using a 2-layer network model.

Fundamental for the final step are parameterized functions (herein called generating functions) which reduce the number of model parameters. It is noteworthy that this model architecture has undetermined parameters in step 2 and step 3 which need to be estimated using a training data set to fit these parameters for the system being monitored. The model training was performed with three compounds featuring different particle morphology as shown in Fig. 1.

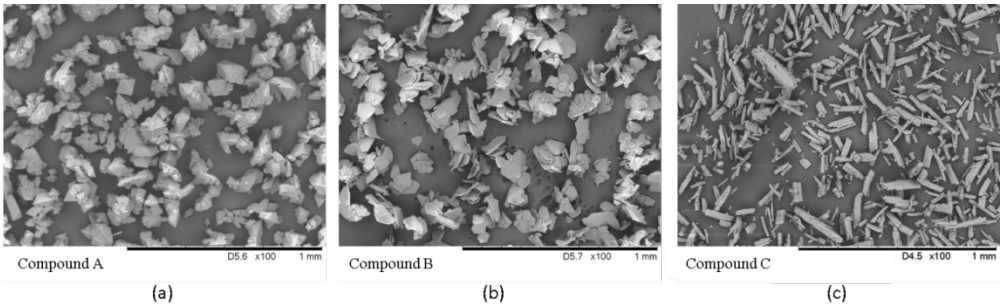

Figure 1. Three compounds featuring different crystal morphologies modeled with the data-driven model: (a) compact, (b) platelet, and (c) rod morphology.

3. Results and discussion

A limited training set of four different PSDs each at four different solid concentrations proved to be sufficient for all three morphologies. Fig. 2 shows as example the comparison of the measured PSD and the PSD estimated from CLD and solids concentration data for the platelet compound:

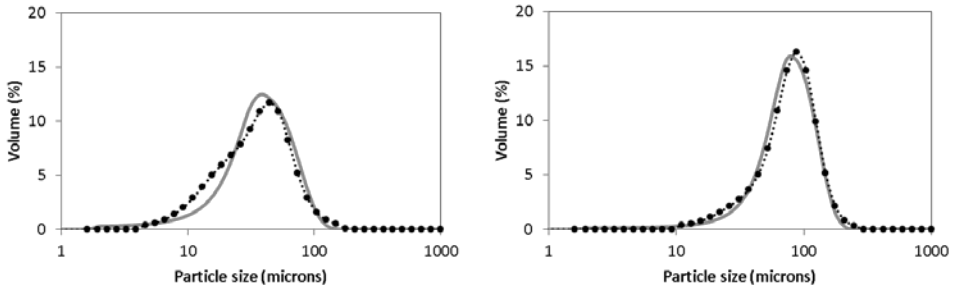

Figure 2. Experimental laser diffraction PSDs for the platelet morphology shown as dots (dotted lines are a guide for the eye) together with corresponding PSD predictions from CLD and solid concentration data.

Model accuracy was assessed using the root mean square deviation between measured and simulated PSDs. The RMSD values were similar not only for all three compounds but also for development batches monitored years before compiling the training data, indicating robust generalization.

4. Conclusions

A data-driven CLD-to-PSD model was applied to compounds with different morphologies at slurry concentrations typical for industrial crystallization processes. In all cases, a limited experimental data set which can be generated in less than two days was sufficient to obtain a model which is able to accurately predict particle size distributions from CLD and solids concentration measurements. While the approach has thus far only been tested on three systems, the breadth of morphologies which yielded positive results suggests that this framework has the potential to have a broad application.

References

[1] R. Irizarry, A. Chen, R. Crawford, L. Codan, J. Schoell. Chem Eng Sci. 164 (2017) 202-218.
[2] N. Kail, H. Briesen, W. Marquardt. Part Part Syst Charact. 24 (2007) 184–192.

ECCE12
The 12th EUROPEAN CONGRESS OF CHEMICAL ENGINEERING
Florence 15-19 September 2019

Crystallization fundamentals and industrial processes

Deracemisation via temperature cycles: the effect of the initial and operating conditions

F. Breveglieri*, B. Bodák, and M. Mazzotti

Institute of Process Engineering, ETH Zurich, 8092 Zurich, Switzerland

**Corresponding author: fbrevegl@ethz.ch*

Highlights

- Effect of the initial and operating conditions on the deracemisation process.
- Qualitative comparison between experiments and PBE model.
- Experimental variability due to small variations of the experimental conditions.

1. Introduction

Solid-state deracemisation via temperature cycles is among the techniques used to attain chiral purity. By applying periodic temperature variations to a suspension of a conglomerate forming compound in the presence of a racemisation reaction occurring in solution, only one pure enantiomer is obtained[1].

Previous contributions have shown that by starting the process with asymmetric initial conditions, i.e. an excess of one enantiomer, this one will be isolated at the end of the process[1]. However, a thorough investigation of the conditions affecting the deracemisation outcome has been performed only for a similar isothermal deracemisation process[2]. In this work, we combine results obtained by performing experiments and by running simulations to investigate the effect of the initial and operating conditions on the process outcome. Particularly, we analyse how the initial enantiomeric excess (ee_0), the parameters describing the initial particle size distribution (PSD), and their combination affect the attained handedness and the deracemisation time, when performing temperature cycles. We also evaluate some additional parameters, such as the suspension density, to better explain the variability of the outcome observed in some deracemisation experiments.

Finally, we vary several operating conditions, especially the temperature profile, to investigate their effect on the process in terms of time and productivity.

2. Methods

The simulations of the process are performed with a PBE-based model, previously presented[3]. The experiments are carried out using chiral model compounds and a base as racemising agent. The temperature profile is monitored with thermocouples and the evolution of the enantiomeric excess over time with chiral HPLC[4].

3. Results and discussion

In the case of experiments as well as of simulations, when the process started with the same PSD for both enantiomers and an initial excess of the desired one, the deracemisation proceeded towards this handedness (Fig. 1) [4,3]. In the absence of ee_0, the asymmetry in the initial conditions

can be introduced by differentiating the PSD of the two enantiomeric populations. These differences would determine the outcome of the deracemisation process.

We also combined the parameters describing the PSD and the ee_0, looking at how they compete for the initial asymmetry. For example, when the process started with an excess of the D-enantiomer, we obtained the L-enantiomer, if the mean size of its population was large enough to counterbalance the ee_0.

The described sensitivity to the initial conditions, is used to better analyse the variations among experiments repeated at the same nominal conditions. Taken an experimental parameter, we exploited the process model to test the variation of the deracemisation outcome as a function of small realistic deviations from the nominal value of this parameter. We, hence, qualitatively compared experimental and simulation results and we verified the agreement among the trends, when small variations are introduced.

By investigating different operating conditions, i.e. the cooling rate and the temperature range, we have verified how the process time shortens when the cooling rate increases. Thanks to the combination of experimental and simulation results, we could verify the presence of optimal conditions.

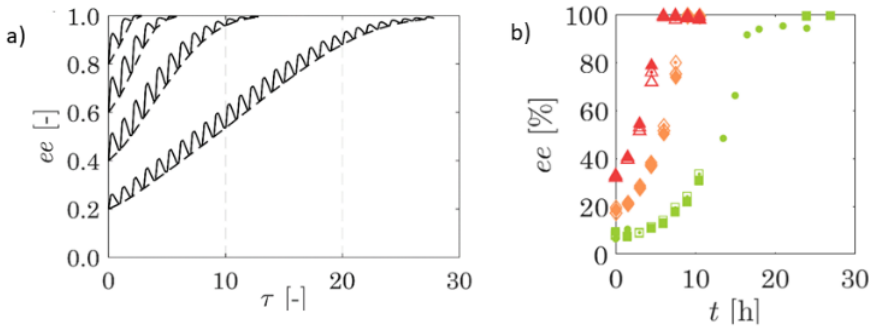

Figure 1. Effect of the initial enantiomeric excess. Evolution of the enantiomeric excess over time, obtained by running simulations at ee_0 = 0.2, 0.4, 0.6, 0.8 (a) and experiments at ee_0 = 7, 18, 32 % (b).

4. Conclusions

We have shown, experimentally and by running simulations, that the outcome of the deracemisation via temperature cycles is strongly influenced by the initial conditions, i.e. enantiomeric excess and particle size distribution. By further analysing the initial conditions, we have shown how the high sensitivity of the process to these parameters explains the variability observed during experiments. Finally, we investigated several operating conditions, and we identified the ones favourable for the process.

References

[1] W.W. Li, L. Spix, S.C.A. de Reus, H. Meekes, H.J.M. Kramer, E. Vlieg, J.H ter Horst, Cryst Growth Des. 16 (2016) 5563-5570.
[2] M. Iggland, R. Müller, M. Mazzotti, Cryst Growth Des. 14 (2014) 2488-2493.
[3] B. Bodák, G.M. Maggioni, M. Mazzotti, Cryst Growth Des. 18 (2018) 7122-7131.
[4] F. Breveglieri, G.M. Maggioni, M. Mazzotti, Cryst Growth Des. 18 (2018) 1873-1881.

This research has received funding as part of the CORE project (October 2016 – September 2020) from the European Union's Horizon 2020 research and innovation programme under the Marie Sklodowska-Curie grant agreement No 722456 CORE ITN

ECCE12
The 12th EUROPEAN CONGRESS OF CHEMICAL ENGINEERING
Florence 15-19 September 2019

Modeling Batch Preferential Crystallization for Conglomerates Forming Systems using Shortcut Models

S. Bhandari[2*], T. Carneiro[1], E. Temmel[1], H. Lorenz[1,2], A. Seidel-Morgenstern[1,2]

1. Max Planck institute for Dynamics of complex technical Systems, Magdeburg, Germany
2. Otto von Guericke University, Chair of Chemical Process Engineering, Magdeburg, Germany

bhandari@mpi-magdeburg.mpg.de

Highlights

- Shortcut models are formulated and introduced for Preferential Crystallization
- Enantiomers of Monohydrate and anhydrate systems are studied
- Key performance indicators are evaluated

1. Introduction

Evaluating various kinetic mechanisms, Population Balance Models (PBMs) are a powerful tool to describe crystallization processes. Due to the consideration of many details, the resulting set of equations is difficult to solve and expensive in applying it for simulation and optimization. Preferential crystallization (PC) is a strong technique capable to resolve mixtures of enantiomers [1, 2]. In this study a shortcut model based on assuming uniform particles sizes and only one lumped kinetic mechanism is introduced. Correspondingly model parameters are calculated using the experimental data for batch preferential crystallization of conglomerate forming chiral systems. The analysis is based on the enantiomers of DL-threonine in water and DL-asparagine (DL-Asn) in water. The latter system forms a monohydrate. An evaluation of Key Performance Indicators (KPI) of the process (i.e. productivity and purity) is performed for the two systems using the shortcut models. The predictions are compared with the experimental results. A possible extension of the shortcut models to simulate preferential crystallization in racemic compound forming systems will be also shortly discussed.

2. Methods

The shortcut models are developed to describe batch preferential crystallization (PC) exploit the principle of “total mass transfer” that causes mass depletion of the liquid phase and mass build-up of the solid phase during the process. The following assumptions are made to derive the shortcut model for PC:

- Nucleation and growth rate are lumped and connected with a constant k_{GB}^{eff}. The two mechanism jointly cause liquid phase mass depletion and solid phase mass build up
- All crystals of one enantiomer are spheres of the same increasing size (no size distribution)
- A certain number of very small “crystals” of the counter-enantiomer are assumed to be initially present along with the seeds of the preferred enantiomer
- A production time t_{prod} is introduced as a function of supersaturation, which is the time at which the crystals of counter enantiomer is activated
- Driving forces respect metastable solubility limits in the 3-phase regions
- No aggregation or breakage occurs.

The basic equations of the model are:

Liquid phase mass balance:

$$\frac{dm_i}{dt} = -k_{GB}^{eff} 4\pi N_i R_i^2 (S_i - 1)^{n^{eff}} \quad i \in \{1,2\} \tag{1}$$

Solid phase mass balance:

$$\frac{dR_i}{dt} = \frac{k_{i,GB}^{eff}}{\rho_{Sol}} (S_i - 1)^{n_i^{eff}} \quad i \in \{1,2\} \tag{2}$$

3. Results and discussion

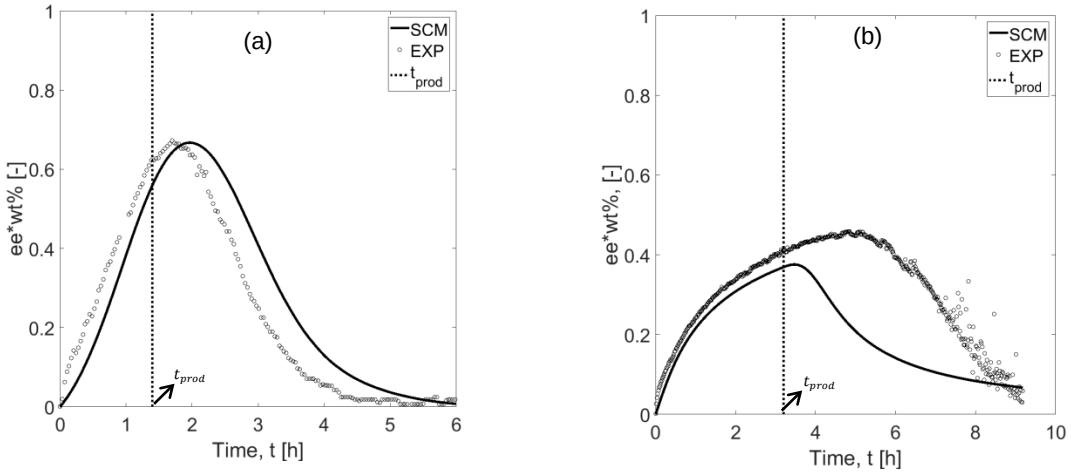

Figure 1. Comparison between shortcut model and experimental data of batch isothermal PC. Enantiomeric excess profiles of case (a) DL-threonine in water and (b) DL-asparagine monohydrate in water

Experimental results of case (a) threonine [3] and case (b) asparagine monohydrate were used to evaluate the potential of the shortcut model. As shown in Figure 1, both cases differ significantly in the initial rates and the process trajectories. The shortcut model is capable to capture these differences by using different effective order of crystallization kinetics (n^{eff} = 1 and n^{eff} = 6.6) respectively. The other two parameters required in shortcut model for PC is effective crystallization rate constant k_{GB}^{eff} and stop time t_{stop}. The parameter estimation in both the cases is performed using least square fitting method. Figure 1 clearly shows the performance of the model within the production time is satisfactory as compared with the experimental results.

4. Conclusions

The above results show that shortcut models can describe essential features of the PC process. The experimental results regarding enantiomeric excess compare well with predictions of the shortcut model. It is seen as a useful tool for preliminary estimations of KPI as productivity, yield, purity and identifying optimal operating parameters. Clear limitation of the shortcut model is the fact that it cannot predict the crystal size distribution and higher moments are not conserved.

References

[1] J. Jacques (1994): Enantiomers, Racemates and Resolutions. Krieger Publishing Company Malabar, FL.
[2] G. Coquerel (2007): Preferential Crystallization. Top Curr Chem 269, 1-51
[3] M. Eicke (2016): Process Strategies for Batch Preferential Crystallization (Doctoral dissertation). Retrieved from Otto-von-Guericke University, Magdeburg Bibliography Database.

This research has received funding as part of the CORE project (October 2016 – September 2020) from the European Union's Horizon 2020 research and innovation programme under the Marie Sklodowska-Curie grant agreement No 722456 CORE ITN

ECCE12
The 12th EUROPEAN CONGRESS OF CHEMICAL ENGINEERING
Florence 15-19 September 2019

Efficient assessment of combined crystallization, milling, and dissolution cycles for crystal size and shape manipulation

Pietro Binel[1]*, Fabio Salvatori[1], and Marco Mazzotti[1]

[1] Institute of Process Engineering, ETH Zurich, 8092 Zurich, Switzerland

*Corresponding author: binel@ipe.mavt.ethz.ch

Highlights

- Crystallization, dissolution, and milling selectively manipulate crystal shape
- The simulations identify general trends used for process characterization
- The interplay of critical operating variables and system parameters is elucidated

1. Introduction

The size and shape of crystals in a powder are important properties that significantly contribute to determining the quality of the final commercialized product and that affect several steps in the downstream process [1]. Different approaches have been proposed to modify the morphology of crystalline products. Here, we assess the effectiveness of a 3-stage process [2] consisting of cycles of crystallization, milling, and dissolution for products with different features, aiming at a robust and quick process design [3].

2. Methods

The 3-stage process is investigated through simulations and experimental work. A lab-scale setup is used to perform crystallization, wet milling, and dissolution while monitoring the solute concentration with the ATR-FTIR technology. The number of cycles performed and the rotor speed of the wet mill device are chosen as process variables. To measure the particle size and shape distribution (PSSD) of the population after each step of the process, the optical imaging device µDISCO [4] is employed. The simulations are based on two-dimensional morphological PBEs tailored to best describe every step of the process.

3. Results and discussion

Two model compounds featuring a needle-like crystal habit, namely β L-Glutamic acid and γ D-Mannitol, are used to map the design space spanned by the process variables onto the space plane, i.e. the plane where average length L_1 and width L_2 of the crystal population are plotted. For this purpose, a factorial design approach is adopted to minimize the experimental effort. It is observed that, although with β L-Glutamic acid a broad range of sizes and aspect ratios can be reached, γ D-Mannitol exhibits a very narrow attainable region for the same combination of operating variables. Simulations allow us to demonstrate that the different behavior or β L-Glutamic acid and γ D-Mannitol, which affects the shape of the attainable region (Fig. 1), is due to a major difference in the kinetics of growth and dissolution, then validated through direct experimental measurements or by comparison with values reported in literature.

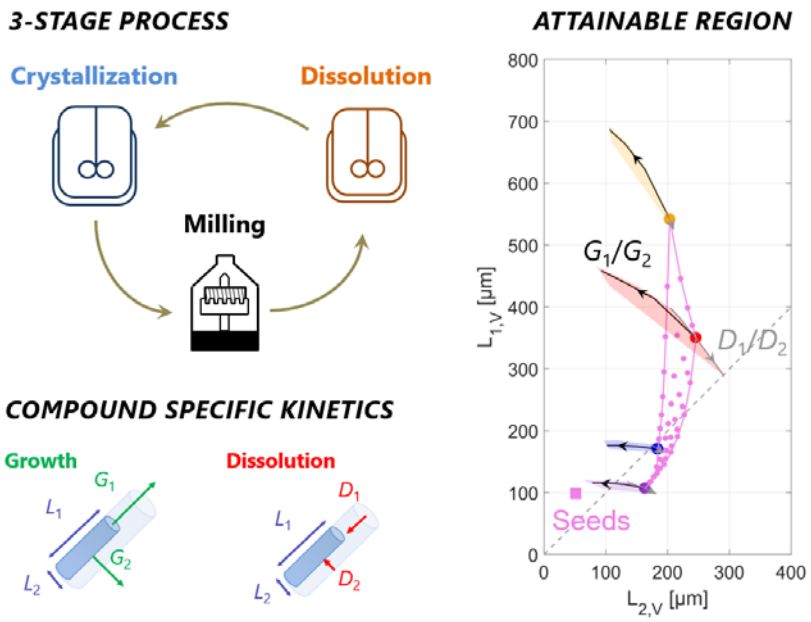

Figure 1. The 3-stage process consists of cycles of crystallization, milling, and dissolution. The attainable region in shape and size of the final population heavily depends on the kinetics of growth and dissolution of the product.

4. Conclusions

The outcome of the 3-stage process and its effectiveness in manipulating the shape and size of the crystals are related to both operating variables and system parameters, namely the growth and dissolution rate ratios. Simulations allowed determining generally valid compound-dependent features which relate the type of attainable region to the magnitude of the aforementioned ratios. The observation resulting from the in-silico work is demonstrated by running an experimental campaign.

References

[1] M. A. Lovette, A. Robben Browning, D. W. Griffin, J. P. Sizemore, R. C. Snyder, M. F. Doherty Ind. Eng. Chem. Res. 47 (2008) 9812– 9833.
[2] F. Salvatori, M. Mazzotti, Ind. Eng. Chem. Res. 56 (2017) 9188–9201.
[3] F. Salvatori, P. Binel, M. Mazzotti, Chem. Eng. Sci. X, in press, DOI 10.1016/j.cesx.2018.100004
[4] A. K. Rajagopalan, J. Schneeberger, F. Salvatori, S. Bötschi, D. R. Ochsenbein, M. R. Oswald, M. Pollefeys, M. Mazzotti, Powder Technol. 321 (2017) 479–493.

ECCE12
The 12th EUROPEAN CONGRESS OF CHEMICAL ENGINEERING
Florence 15-19 September 2019

A new combined theoretical and experimental approach for graphene driven membrane crystallization

Elena Tocci[1]*, M. L. Perrotta[1], L. Giorno[1], F. Macedonio[1], E. Drioli[1], A. Gugliuzza[1]

1 Istituto per la Tecnologia delle Membrane (CNR-ITM), via P. Bucci 17/C 87036 Rende (CS), Italy

**Corresponding author: e.tocci@itm.cnr.it*

Highlights

- Crystal nucleation and growth of NaCl in membrane-assisted crystallization were investigated
- PVDF with graphene speeded up crystal nucleation *in comparison to.* pristine PVDF

1. Introduction

Membrane-assisted crystallization is an emerging membrane process with the capability to extract simultaneously fresh water and valuable components from various streams: crystal nucleation and growth are carried out in a well-controlled pathway by using a porous hydrophobic membrane. Successful application of crystallization for produced water treatment, seawater desalination and salt recovery has been demonstrated [1–2]. Nano-composite membranes enriched with two-dimensional (2D) materials are becoming promising in membrane technology because they can assist mass transfer through membranes under specific conditions [3]. The understanding of crystal nucleation is far from complete [4]. This is because the molecular details of the process appear in a very small length scale of the order of nanometers, and they are, by definition, unstable and therefore form only transiently, so they are quite challenging to probe even in real time. However, today, with state-of-the-art measurements, nucleation has also been observed at the molecular scale [5]. Computational modelling and in particular molecular dynamics (MD) provide exciting insights into the mechanisms of such phenomena and enable kinetic and thermodynamic quantities to be estimated [6]. Here, we present the results from molecular dynamics simulations of the crystal nucleation and growth of a sodium chloride solution in contact with hydrophobic polymer surfaces of polyvinylidene fluoride (PVDF) containing also graphene at 5% wt and at 10% wt. In parallel, membrane crystallization experiments were performed utilizing the same kind of polymeric membranes in order to compare the experimental findings with the computational data.

2. Methods

Unbiased molecular dynamics simulations using all atom were performed for the investigation of the feasibility of growing NaCl crystals. The initial amorphous PVDF model (density of 1.9 g/cc) was constructed using the amorphous cell module in the commercial software, Material Studio package (version 7.0) of BIOVIA Dassault Systemes [7] and the COMPASS force field [8]. All MD simulations were then performed using the GROMACS software package, version 5.1.4 [9]. After equilibration, production runs of 200 ns were carried out.

3. Results and discussion

Crystals obtained from crystallization experiments and simulations showed the characteristic cubic block-like form in accordance with the expected geometry of the NaCl crystals.

Lower nucleation time and crystal growth rate were observed for PVDF with Graphene at 5% and 10% wt systems in comparison with the pristine PVDF indicating that the aggregation of Na^+ and Cl^- in crystals was faster for membrane systems containing Graphene that native PVDF (Figure 1).

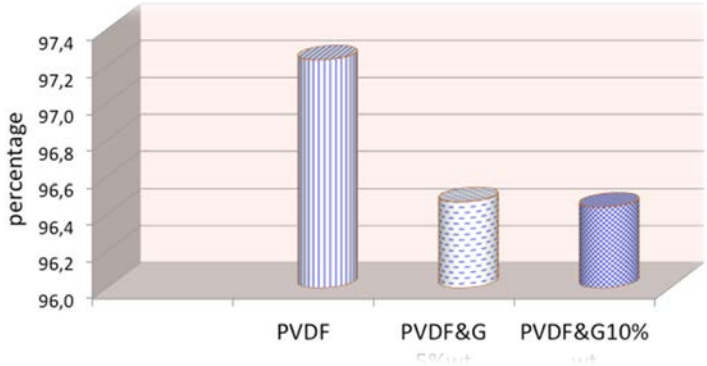

Figure 1. Percentages of ion in crystals after 200 ns of simulations.

4. Conclusions

Both experimental tests and MD simulations demonstrate that the chemical composition of the membrane surface affect the crystallization of salts in nucleation grow rate, crystal size and shape: the nanomaterials influence kinetics of crystal formation, reducing the nucleation times.

Aknowledgment: The Great Relevance International Project Italy (MAECI)-China (NSFC) 2018-2020 - New Materials, with particular reference to Two-dimensional systems and Graphene (Prot.MAE0088962) funded by Ministero degli Affari Esteri e della Cooperazione Internazionale, Direzione Generale per la Promozione del Sistema Paese is gratefully acknowledged.

References

[1] E. Curcio, A. Criscuoli, E. Drioli, Ind. Eng. Chem. Res. 40 (2001) 2679–2684.
[2] C.A. Quist-Jensen, F. Macedonio, E. Drioli, Crystals 6 (2016) 36-49.
[3] F. Macedonio, A. Politano, E. Drioli, A. Gugliuzza, Mater. Horiz. 5 (2018) 912–919.
[4] P.G. Vekilov, Nanoscale 2 (2010) 2346–2357.
[5] A.E.S. Van Driessche, N. Van Gerven, P.H.H. Bomans, R.R.M. Joosten, H. Friedrich, D. Gil-Carton; N.A.J.M. Sommerdijk, M. Sleutel, Nature 556 (2018) 89–94.
[6] J.-H. Tsai, M.L. Perrotta, A. Gugliuzza, F. Macedonio, L. Giorno, E. Drioli, K.-L. Tung, E. Tocci, Appl. Sci. 8(11) (2018) 2145-2161
[7] Materials Studio 7.0; Dassault Systèmes BIOVIA: San Diego, CA, USA, 2013.
[8] H. Sun, J. Phys. Chem. B 102 (1998) 7338–7364.
[9] B. Hess, C. Kutzner, D. Van der Spoel, E. Lindahl, J. Chem. Theory Comput. 4 (2008) 435–447.

ECCE12
The 12th EUROPEAN CONGRESS OF CHEMICAL ENGINEERING
Florence 15-19 September 2019

Crystallization fundamentals and industrial processes

An *In Silico* Tool for a Pharmaceutical Crystallization Process Development: Comprehensive Sensitivity Analysis for Process Risk Assessment

Merve Öner[1], Stuart M. Stocks[2], Jens Abildskov[1], Gürkan Sin[1]*

1 Process and Systems Engineering Center (PROSYS), Department of Chemical and Biochemical Engineering, Technical University of Denmark, DK-2800 Kgs. Lyngby, Denmark;

2 LEO Pharma A/S, Industriparken 55, DK-2750 Ballerup, Denmark

**Corresponding author: gsi@kt.dtu.dk*

Highlights

- An *in silico* tool was developed for a pharmaceutical crystallization process.
- Developed tool was used for process risk assessment.
- A comprehensive uncertainty and sensitivity analyses were performed to explore operation design space.

1. Introduction

Crystallization is still predominant separation and purification method during the recovery of solids from solutions especially in pharmaceutical industries [1]. The operating condition of a crystallization process is of critical importance because properties of a crystal product such as purity, size, shape distribution and polymorphic form depend strongly on the condition under which the crystallizer is operated [2, 3]. Moreover, these product properties affect the performance of the following downstream operations such as filtration and drying, and eventually efficacy of the product formulation. Traditionally, crystallization processes have been operated recipe-based in the pharmaceutical manufacture and the quality of the product has been determined by testing at the end of the process. Quality-by-testing (QbT) has often resulted in failed batches, which in return led to loss of profit, while the pressure of producing faster, cheaper and more efficiently has been increasing day by day [2, 4]. Process systems engineering methods and tools possess significant advantages over traditional methods; improving process understanding, speeding up process development and providing better control over process variables. Additionally, the FDA has promoted the usage of quality-by-design (QbD) approaches, integration of process analytical technology (PAT) tools into the process design and manufacturing as well as identification of uncertainties and quantification of process risk assessment [5, 6]. Therefore, the objective of this work is to develop an *in silico* tool for a pharmaceutical crystallization process to support design, optimization, control and uncertainty/sensitivity analysis for process risk assessment. The developed tool was used to explore an operational design space in order to guide the design using comprehensive sensitivity and uncertainty analysis. Additionally, we performed experiments to verify predicted results.

2. Methods

An *in silico* tool was developed for a batch cooling crystallization system. Crystallization of paracetamol from ethanol was chosen as a case study. The solubility and crystallization kinetic data

of the mentioned solute-solvent system were taken from the literature [7, 8]. Related mass, energy and population balance equations are implemented and solved in MATLAB/Simulink environment. Several sources of uncertainties in process are identified and the effect of uncertain process parameters on the process output variability are quantified through uncertainty analysis. Sensitivity analysis is performed to investigate the design space of initial concentration, seed specification (mass, mean, sigma), cooling time and cooling profile. Additionally, experimental data are used to verify model predictions in terms of solute concentration and final crystal size distribution.

3. Results and discussion

A risk based approach requires understanding of how process factors affect the quality and performance of the product/process, which process variabilities have critical importance to achieve consistent product within desired quality requirements and therefore to quantify the risk of producing poor quality product. To this end, several uncertainties in the crystallization design space were identified. Using the developed tool, a study on the quantification of process risks was performed. The effect of the initial concentration, seed specification, cooling time and cooling profile on the process output in terms of process yield and nucleation was investigated though sensitivity analysis. Simulation results showed that cooling time, seed mass and cooling rate were the most significant factors that affected strongly the product yield and nucleation. Therefore, more effort should be given to optimize these parameters to get higher yield and avoid nucleation. Additionally, after performing experiments to compare simulation outcomes, we observed that model predictions were in good agreement with the experimental data.

4. Conclusions

In this study, we presented an *in silico* tool for a pharmaceutical crystallization process. We used uncertainty and sensitivity analysis to identify process variables and to quantify their effect on the process outcome for process risk assessment. As a case study, an application on the exploration of the operational design space was shown. We compared also experimental data with model predictions. In conclusion, *in silico* tools provide an effective and cost-efficient platform to develop processes, investigate design spaces, to explore feasibility of different operation and control strategies and to quantify the process risks. Pharmaceutical industries can benefit from model based approaches through reduction of process failures, consistent batch-to-batch products and gaining acceleration to compete with challenging market driving forces.

References

[1] Z. Gao, S. Rohani, J. Gond, J. Wang, *Engineering* 3 (2017) 343-353.
[2] Z.Q. Yu, J.W. Chew, P.S. Chow and R.B.H. Tan, *Chem. Eng. Res. and Des.* 85(A7) (2007) 893-905.
[3] J. Chen, B. Sarma, J.M. Evans, A.S. Myerson. *Crystal Growth & Design* 11 (2011) 887-895.
[4] F.C.C. Montes, K. Gernaey, G. Sin, *Ind. Eng. Chem. Res.* 57 (2018) 10026-10037.
[5] FDA, Pharmaceutical CGMPs, 2004.
[6] K.V. Gernaey, A.E. Cervera-Padrell, J.M. Woodley, *Comp. and Chem. Eng.* 42 (2012) 15-29.
[7] C. Fernandes, 14th International Symposium on Industrial Crystallization (1999).
[8] N.A. Mitchell, PhD Thesis, University of Limerick (2012).

ECCE12
The 12th EUROPEAN CONGRESS OF CHEMICAL ENGINEERING
Florence 15-19 September 2019

Crystallization fundamentals and industrial processes

PET Recycling – Contributions Of Crystallization to Sustainability.

Claudia Pudack[1], Manfred Stepanski[1]

1 Sulzer Chemtech Ltd, Neuwiesenstrasse 15, 8401 Winterthur, Switzerland

**Corresponding author: Claudia.Pudack@sulzer.com*

Highlights

- Chemical PET recycling allows to upcycle all types of waste PET plastic.
- The de-polymerization process breaks down the waste PET into its monomers, MEG and DMT.
- The monomers can be purified and re-polymerized into high purity, food-grade PET.
- Solvent-free melt crystallization of DMT removes all coloring and critical impurities.

1. Introduction

Polyethylene terephthalate (PET) is the most common thermoplastic polymer of the polyester family. It is a naturally transparent and semi-crystalline plastic widely used as a fiber for clothing, as an effective moisture barrier with wide applicability in bottling and packaging, and as an engineering plastic when it is combined with other materials. Some of the most important characteristics of PET include its resistance to water, its high strength to weight ratio, and its wide availability as an economic and recyclable plastic. PET was first polymerized in the 1940s by DuPont chemists looking to develop polymer materials for use as textile fibers. It is produced from the synthesis of mono ethylene glycol (MEG) and dimethyl terephthalate (DMT) or purified terephthalic acid (PTA). The former is a transesterification reaction that produces methanol as a by-product, whereas the latter is an esterification reaction that releases water.

Once the polymer is formed, it is very difficult to purify and for this reason, the purity of the starting materials is of high importance. Vacuum distillation processes are used to purify ethylene glycol, whilst DMT and terephthalic acid are conventionally purified by suspension crystallization. For DMT, the suspension crystallization plant and associated solvent recovery section typically account for 45% of the total investment costs [1]. Therefore, an improved DMT process has been developed, which replaces the suspension crystallization with solvent-free melt crystallization technology. This reduces both, investment and operating costs, and improves the operability and flexibility of the process. The resulting high-purity DMT has an excellent quality and color stability and is suitable for the manufacture of high molecular weight PET.

According to some reports, the current global polyester production is around 56 million tons, mainly for synthetic fibers (more than 60%). However, the demand for PET in the bottling and packaging industry, particularly for food and beverages, is growing and already accounts for roughly 30% [2]. In general, polymers are increasingly used in a variety of applications and have become a major concern in the marine environment because of their persistence at sea. Scientists estimate that more than eight million tons of plastic are being washed into the oceans every year [3]. Moreover,

the cumulative quantity of plastic waste available to enter the ocean from land is predicted to increase even further. Finding solutions for the plastic debris problem is complex and requires a combination of recycling, closing the source and cleaning up what has already accumulated in the oceans. The current study will focus on the recycling routes of PET, with special emphasis on the chemical recycling of PET bottles by means of methanolysis.

This chemical recycling process degrades PET into two main reaction products, DMT and MEG, the starting materials for the transesterification process. The main advantage of this method is that the methanolysis can be installed in the existing polymer production line, since the DMT obtained has a product quality identical to virgin DMT [4]. In addition, MEG and methanol can be easily recovered and recycled. Moreover, purification of the DMT by melt crystallization will reliably remove critical impurities (e.g., water, glycols, alcohols and phthalate derivatives) that will have a negative impact on its conversion rate to PTA.

References

[1] E. Schäfer, M. Stepanski, K. Fiedler, Hydrocarbon Engineering, 2002, pp. 64-68.
[2] X. Wang, B. Xu, Q. Xiao, Applied Mechanics and Materials, 312 (2013), pp. 406-410.
[3] R. Jambeck, R. Geyer, C. Wilcox, T. R. Siegler, M. Perryman, A. Andrady, R. Narayan, K. L. Law, Science, 347 (2015), pp. 76-77.
[4] V. K. Sinha, J. V. Patel, M. R. Patel, Journal of Polymers and the Environment, 18 (2010), pp. 8-25.

ECCE12
The 12th EUROPEAN CONGRESS OF CHEMICAL ENGINEERING
Florence 15-19 September 2019

Selective Sequential Crystallization of Racemic and Enantiopure Mandelic Acid at The Solution Eutectic.

Johannes Hoffmann[1], Raghunath Venkatramanan [1], H. Lorenz[2], A. Seidel-Morgenstern[2], Joop H. ter Horst[1]

1. EPSRC Centre for Innovative Manufacturing in Continuous Manufacturing and Crystallisation (CMAC), Strathclyde Institute of Pharmacy and Biomedical Sciences (SIPBS), Technology and Innovation Centre, University of Strathclyde, UK; [2]Max-Plack Institute for dynamic of complex technical systems Magdeburg, Germany

**Corresponding author: johannes.hoffmann@starth.ac.uk*

Highlights

- Chiral Separation at the eutectic using serial crystallization works resulting in high enantiopurity
- In situ monitoring of the enantiomeric excess with Raman is possible.

1. Introduction

As the majority of new pharmaceutical substances are chiral, pharmaceutical industry seeks access to a broad range of chiral resolution methods to separate enantiomers of such chiral compounds. While new resolution methods such as attrition enhanced deracemization are developed, preferential crystallization (PC) has been proven to be an efficient and selective method to separate enantiomers in a conglomerate system. Interestingly, if the crystallization feed is sufficiently enriched using another separation technology, PC of the preferred enantiomer can also be applied to racemic compound forming systems [1]. Here we present a simple PC process to efficiently and robustly produce enantiopure crystals, starting with a suspension of both enantiopure and racemic compound crystals in a solution of eutectic composition.

2. Methods

In the feed vessel, an enriched suspension with both racemic and enantiopure mandelic acid crystals in water was equilibrated at temperature T_1 so that the feed solution composition was equal to that of the eutectic point at the same temperature (Figure 1). A filtered solution was continuously pumped from the feed vessel into the first crystallizer (racemic compound DL crystallizer) and from that into the second crystallizer (enantiopure product D crystallizer), continuing as a recycle for the feed vessel. The crystallizer suspensions were held at a slightly lower temperature $T_2<T_1$ and were monitored by in situ Raman spectroscopy. The crystallizers initially contain solution at the eutectic composition and respectively racemic and enantiopure seed crystals.

3. Results and discussion

Due to the small temperature difference between feed flow and crystallizer suspension a small supersaturation is created which induces the seed crystals to grow while preventing nucleation. Therefore, DL-Mandelic acid is crystallized in the first DL crystallizer while D-Mandelic acid is

crystallized in the second D crystallizer increasing suspension densities in both crystallizers. The differences in the pure D- and DL-mandelic acid solid Raman spectra allow to monitor in situ the solid composition while the intensity changes of these differences allow to estimate their suspension density changes. This thus enables detection of contamination of the undesired DL mandelic acid in the D crystallizer due to primary nucleation events.

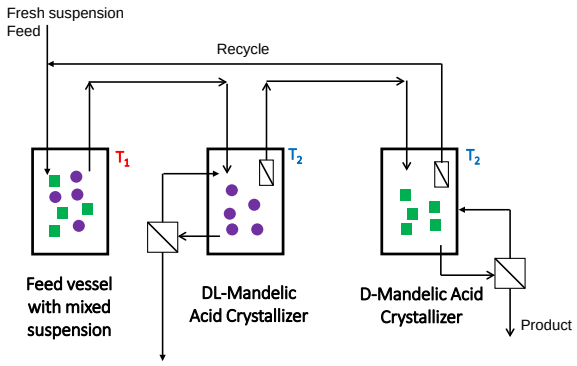

Figure 1. Sequential Cascade Crystallizer set up for the separation of conglomerate and racemic compound forming systems at eutectic composition.

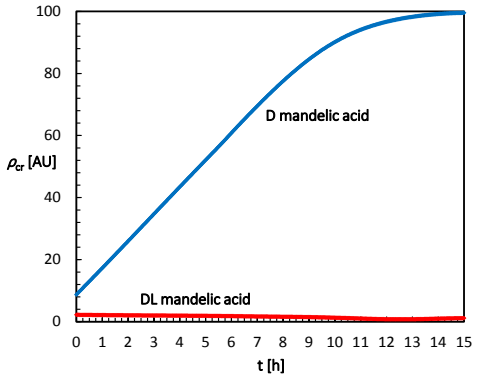

Figure 2. Estimated suspension densities ρ_{cr}(D) and ρ_{cr}(DL) (in arbitrary units) of D and DL mandelic acid in the D-Mandelic acid crystallizer during the separation process determined from in situ Raman spectroscopy.

Typical results in figure 2 show an increase in the suspension density of D-Mandelic acid (blue line figure 2). The presence of DL-mandelic acid crystals was not detected in the D crystallizer throughout the entire experiment (red line figure 2) indicating that the supersaturation towards this compound in the D acid crystallizer was sufficiently lowered by the crystallization of DL-Mandelic acid in the DL crystallizer. Eventually, nucleation of D-Mandelic acid in the DL crystallizer occurred and the D concentration in the Feed to the D crystallizer decreased, lowering the increase of the D-Mandelic acid suspension density in the D crystallizer.

4. Conclusions

The sequential crystallization of DL- and D-Mandelic acid allows for a robust process that results in a fast and stable chiral separation of mandelic acid at the eutectic. In addition, we show that Raman spectroscopy can be used to monitor the purity and suspension densities of the desired and undesired products. This process will also be applied to conglomerate forming systems with and without racemizing agents.

References

[1] Gou, L., et al., *A hybrid process for chiral separation of compound-forming systems.* Chirality, 2011. **23**(2): p. 118-27.

This research has received funding as part of the CORE project (October 2016 – September 2020) from the European Union's Horizon 2020 research and innovation programme under the Marie Sklodowska-Curie grant agreement No 722456 CORE ITN

ECCE12
The 12th EUROPEAN CONGRESS OF CHEMICAL ENGINEERING
Florence 15-19 September 2019

Crystallization fundamentals and industrial processes

Precipitation of lithium carbonate by homogeneous carbonate reactions and heterogeneous CO_2 reactions

Bing Han[1], Marjatta Louhi-Kultanen[1]

1 School of Chemical Engineering, Aalto University, P.O. Box 16100, FI-00076 Aalto, Finland

**Corresponding author: marjatta.louhi-kultanen@aalto.fi*

Highlights

- Precipitation processes to separate lithium as carbonate were investigated
- Temperature and mixing intensity affected mainly precipitation
- lithium will be a key element for modern electric vehicles and devices
- Efficient recovery of lithium from secondary materials will be crucial in future

1. Introduction

The demand of lithium is expected to increase significantly within next ten years mainly due to the need to increase battery production capacities for electric vehicles. It is reported that batteries consume 39 % of total lithium [1]. This is because lithium is the lightest metal and the most energy dense of battery materials [2]. It is essential to recover and recycle lithium more efficiently from different sources to avoid the shortage of this critical metal. Xu et al [3] investigated the usage of saline lake waters as feedstock for lithium recovery. The review published by Swain [4] introduced the lithium recovery processes from brines. In our previous work, Han et al. [5], we investigated the recovery of lithium carbonate by precipitation from aqueous multicomponent solution simulating battery waste leachate. Precipitation results of lithium carbonate (Li_2CO_3) via homogeneous reactions with sodium carbonate as the reactant are reported by [5-7]. A few studies [8, 9] reported the application of CO_2 to precipitate Li_2CO_3. However, there has not been a study to compare the homogeneous reaction and heterogeneous reaction for the Li_2CO_3 precipitation. The aim of the present work was to compare precipitation and reaction kinetics of lithium with reactant of Na_2CO_3 solution and reactant CO_2 gas in alkaline solution at various operational conditions in terms of residence time, mixing intensity and precipitation temperature.

2. Methods

In the present work semi-batch precipitation of lithium carbonate was investigated by homogeneous and heterogeneous reactions in a stirred jacketed crystallizer. For homogeneous reaction study, sodium carbonate was used as the reactant. Na_2CO_3 solution was pumped to Li_2SO_4 solution to precipitate Li_2CO_3. In heterogeneous reaction study, CO_2 gas was used as a carbonate source to feed into the Li_2SO_4 solution to precipitate Li_2CO_3. NaOH solution was added to adjust the solution pH at the beginning. Different variables including temperature, stirring rate and feeding rate (residence time) were studied. Conductivity and pH was monitored with a Consort Multi-parameter analyzer (C3050). A thermostat (Lauda ECO RE630) with an external temperature sensor that immersed into the solution was used to control the temperature of the solution. An inline probe (Particle track G400, Mettler Toledo) was placed into the reactor and used to monitor the whole precipitation process in order to obtain kinetics data. After precipitation, the solid sample was separated by vacuum filtration with a Büchner funnel. The crystals were characterized by X-ray powder diffraction (XRD, X'Pert PRO), and Raman spectroscopy (PicoRaman, Timegate Instrument

Oy) to determine crystal composition and crystal morphology. The crystal yield was determined with the mass of precipitates.

3. Results and discussion

Generally, high temperature can accelerate reaction, and enhance the nucleation and crystal growth. Figure 1 shows conductivity and pH changes in heterogeneous reaction with temperature of 25 and 50 °C. It can be clearly seen that the pH reduced slightly at the beginning, then dropped suddenly at some point, and kept decreasing gently for both temperatures. The conductivity reduced gently for a certain period and then kept constant at the end for both cases. The clear differences within two studied temperatures can be found: residence time is shorter at higher temperature. This means that the chemical reactions and precipitation are faster at higher temperature. The crystal yield obtained from precipitation process at 50 °C was even doubled at higher temperature. Another reason is also due to the lower solubility of Li_2CO_3 at higher temperature [10]. Stirring rate enhanced the reaction, which can accelerate the occurrence of precipitation.

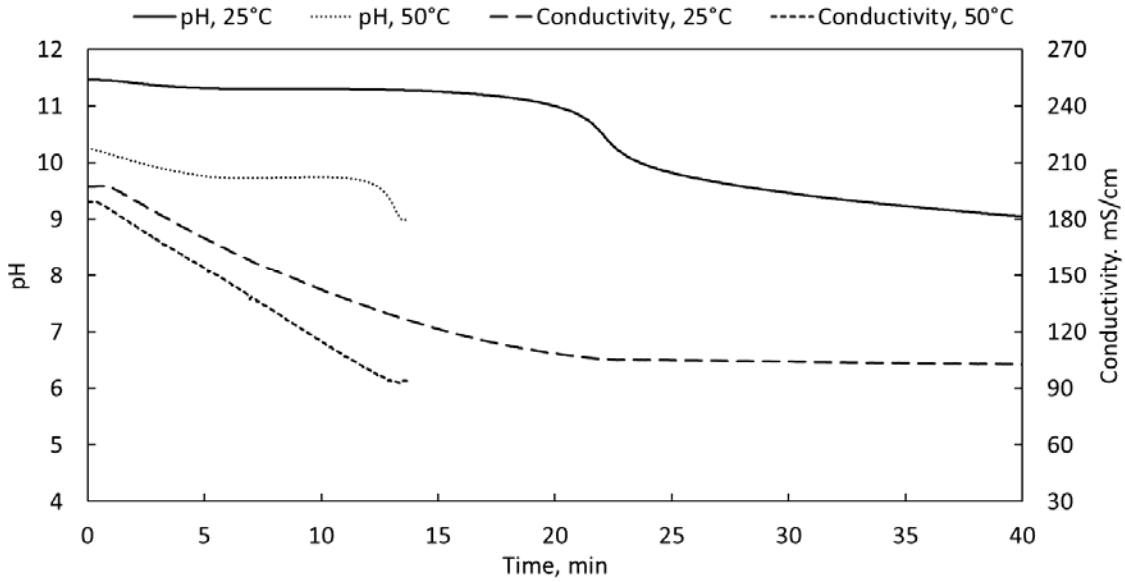

Figure 1. Trends of pH and conductivity changes at 25 and 50 °C in heterogeneous reaction.

4. Conclusions

The precipitation of Lithium carbonate from homogeneous and heterogeneous reactions were compared. Higher crystal yield can be obtained at higher temperature. Precipitation was enhanced by the increase of stirring rate.

References

[1] Discover what is hype and reality, and what counts most, in: BU-308: Availability of Lithium, Isidor Buchmann 2016.
[2] M. S Whittingham, Chem. Rev. 104, (2004), 4271−4301.
[3] Z. Xu, H. Zhang, R. Wang, W. Gui, G. Liu, Y. Yang, Ind. Eng. Chem. Res. 53, (2014), 16502-16507.
[4] B. Swain, Separation and Purification Technology 172 (2017), 388-403.
[5] B. Han, A. Porvali, M. Lundström, M. Louhi-Kultanen, Chem. Eng. Technol. 41(6), (2018), 1205-1210.
[6] P. W. Zhang, T. Yokoyama, O. Itabashi, T. M. Suzuki, K. Inoue, Hydrometallurgy 47, (1998), 259–271.
[7] A. A. Nayl, R. A. Elkhashab, S. M. Badawy, M. A. El-khateeb, Arabian J. Chem. 10, (2017), S3632–S3639.
[8] M. Matsumoto, Y. Morita, M. Yoshinaga, S. Hirose, K. Onoe, JCEG 42, (2009), s242-s248.
[9] Z. Zhou, F. Liang, W. Qin, W. Fei. AIChE 60, (2014), 282-288.
[10] J.W. Mullin, Crystallization, 4th ed., Butterworth Heinemann, Oxford, 2001, p. 485.

ECCE12
The 12th EUROPEAN CONGRESS OF CHEMICAL ENGINEERING
Florence 15-19 September 2019

Reactive crystallization of dolomite by CO_2 fine bubble injection from concentrated brine and conversion to inorganic phosphor

Taichi Kimura[1], Yoshinari Wada[1], Shinnosuke Kamei[1], Koji Masaoka[1, 2], Toshihiko Hiaki[1], Masakazu Matsumoto[1*]

1 College of Industrial Technology, Nihon University, 1-2-1 Izumi-cho Narashino, Japan;
2 Research Institute of Salt and Sea Water Science, The salt Industry Center, 4-13-20 Sakawa, Odawara, Japan

**Corresponding author: matsumoto.masakazu@nihon-u.ac.jp*

Highlights

- Minimizing bubble size increased produced weight and Mg/Ca ratio of $CaMg(CO_3)_2$.
- Mg/Ca ratio of $CaMg(CO_3)_2$ increased with an increase in crystallization time.
- Emission intensity of $CaMg(CO_3)_2$ phosphor increased with increasing the immerse time.

1. Introduction During the salt manufacturing process in Japan, NaCl is manufactured by evaporative crystallization after concentrating seawater through electric dialysis membranes, and the concentrated brine which contains ions such as K^+, Ca^{2+} and Mg^{2+} with high concentration is discharged. To build a utilization system for seawater resources based on the salt production process, a recovery and upgrading method for Ca^{2+} and Mg^{2+} from the concentrated brine is demanded. From the viewpoint of solubility of salts, the synthesis of carbonate by reactive crystallization between the dissolved Ca^{2+} and Mg^{2+} in the concentrated brine and CO_2 can be considered an effective separation/recovery method, as the solubility of carbonate of Ca^{2+} and Mg^{2+} is lower than the solubility of hydroxide in the solution at a pH range below 8.0. In particular, dolomite ($CaMg(CO_3)_2$), which is the double salt derived from the structure of calcite by the ordered replacement of Ca^{2+} and Mg^{2+}, is used in various industrial fields. To improve the functionality of $CaMg(CO_3)$, it is essential to gain access to the Mg/Ca ratio of 1.0. Generally, high concentrations of Ca^{2+}, Mg^{2+} and CO_3^{2-} are necessary for synthesis of $CaMg(CO_3)_2$ with a high Mg/Ca ratio [1]. In this study, the fine bubble formation technique that enables the generation of regions with a higher ion concentration near the gas-liquid interfaces was applied to the reactive crystallization of $CaMg(CO_3)_2$ from the concentrated brine. Furthermore, $CaMg(CO_3)_2$ with a high Mg/Ca ratio can be converted to phosphor which is superior to emission intensity and quantum efficiency, because Mg^{2+} ions in crystal structure of $CaMg(CO_3)_2$ are arrayed more regularly than solid solution. In this paper, we report the effects of CO_2 fine bubble injection on the produced weight of $CaMg(CO_3)_2$ ($W_{dolomite}$) and the Mg/Ca ratio during reactive crystallization of $CaMg(CO_3)_2$ from concentrated brine, and the effects of immerse time on emission intensity of phosphor converted from the obtained $CaMg(CO_3)_2$.

2. Experimental

2.1 Reactive crystallization of $CaMg(CO_3)_2$ from the concentrated brine by fine bubble injection

The concentrated brine that is removed K^+ by cooling crystallization of KCl after NaCl production in salt manufacturing process was used. The major components of the concentrated brine are $MgCl_2$, NaCl and $CaCl_2$ which have the concentrations of 2.1, 0.8 and 0.7 mol/L, respectively. Fine bubbles with an average bubble diameter (d_{bbl}) of 40 µm were generated using a self-supporting bubble generator by shear of impeller and a negative pressure owing to high-rotation, with the rotation rate maintained at 1500 min^{-1} and the CO_2 flow rate controlled at 11.9 mmol/(L·min). For comparison, the bubbles with d_{bbl} of 2000 µm were obtained using a dispersing-type generator. At 298 K, CO_2 bubbles were continuously supplied to 300 mL of concentrated brine, and $CaMg(CO_3)_2$ was crystallized within a crystallization time (t_c) of 60 min. The solution pH during crystallization was maintained constant at 6.8 by adding 8.0 mol/L-NaOH aqueous solution. The Mg/Ca ratio of $CaMg(CO_3)_2$ was estimated from the amount of peak shift from calcite $CaCO_3$ to $CaMg(CO_3)_2$ [2].

2.2 Conversion to phosphor from the $CaMg(CO_3)_2$ obtained by CO_2 fine bubble injection

10.0 g/L of the obtained $CaMg(CO_3)_2$ at t_c of 60 min were immersed into mixed solution of 0.1 mol/L $TbCl_3$ and 0.1 mol/L $CeCl_3$ at 298 K. The immerse time (t_i) is controlled in the range of 0 – 24 h. Fluorescence spectra of the $CaMg(CO_3)_2$ phosphor were measured by fluorescence spectrometer.

3. Results and discussion

3.1 Effects of CO_2 fine bubble formation on the reactive crystallization of $CaMg(CO_3)_2$

The reactive crystallization of $CaMg(CO_3)_2$ from the concentrated brine was performed at d_{bbl} of 40 or 2000 µm. $W_{dolomite}$ and the Mg/Ca ratio at d_{bbl} of 40 µm was obviously higher than the 2000 µm at all values of t_c, and the Mg/Ca ratio at d_{bbl} of 40 µm reached 0.86 with 60 min crystallization. The results indicate that generation high concentration of Ca^{2+}, Mg^{2+} and CO_3^{2-} probably because of the acceleration of CO_2 absorption and the electrification of the fine bubble surface caused by minimization of the bubble diameter.

3.2 Conversion to phosphor from obtained $CaMg(CO_3)_2$

The obtained $CaMg(CO_3)_2$ with a Mg/Ca ratio of 0.86 crystallized by fine bubble injection at d_{bbl} of 40 µm was converted to phosphor. The fluorescence spectra of the $CaMg(CO_2)_3$ phosphor are shown in **Figure 1**. Under light irradiation at wavelength of 254 nm, the green emission was observed in visual at all t_i values and the emission peak intensities at 489, 544, 548 and 621 nm increased with an increase in t_i. This is caused that the replacement of Mg^{2+} in $CaMg(CO_3)_2$ to Tb^{3+} acting as an emission center and Ce^{3+} acting as a sensitizer proceeded with increasing t_i.

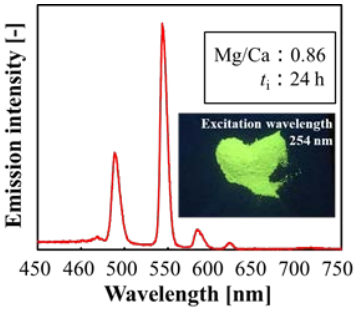

Figure 1. Fluorescence spectra of phosphor

4. Conclusions Using the CO_2 bubbles with different d_{bbl} values, the reactive crystallization of $CaMg(CO_3)_2$ from the concentrated brine was carried out. The results indicate that the minimization of d_{bbl} led to the increase in $W_{dolomite}$ and Mg/Ca ratio. Additionally, when the obtained $CaMg(CO_3)_2$ with Mg/Ca ratio of 0.86 converted to phosphor by immersing into 0.1 mol/L $TbCl_3$ and $CeCl_3$ solution, the emission intensity of $CaMg(CO_3)_2$ phosphor increased with increasing t_i.

Acknowledgements This work was financially supported by the Salt Science Research Foundation (No. 17A3), Japan. We also acknowledge the Naikai Salt Industry Co., Ltd for provision of Bittern.

References

[1] T. Oomori, K. Kaneshima, T. Taira, Y. Kitano, Geochem. J. 17 (1983) 327-336.
[2] H. Mitsusio, H. Nishizawa, K. Matsuoka, Res. Res. Kochi Univ. Nat. Sci. 32 (1983) 327-334.

ECCE 12
ECAB 5

ECAB 5
The 5th EUROPEAN CONGRESS OF APPLIED BIOTECHNOLOGY
Florence 15-19 September 2019

Kinetics of Crystallization in Solid Solution Forming Systems

Maksymilian Olbrycht[1*], Maciej Balawejder[2], Heike Lorenz[3], Andreas Seidel-Morgenstern[3,4], Wojciech Piątkowski[1], Dorota Antos[1]

1- Department of Chemical and Process Engineering, Rzeszow University of Technology, 35-959 Rzeszow/PL; 2- Chair of Chemistry and Food Toxicology, University of Rzeszow, 35-601 Rzeszow/PL; 3- Max Planck Institute for Dynamics of Complex Technical Systems, 39106 Magdeburg/DE; 4-Faculty of Process and Systems Engineering, Otto von Guericke University Magdeburg, 39106 Magdeburg/DE

**m.olbrycht@prz.edu.pl*

Highlights

- Separation of stereoisomers by crystallization.
- SLE for two selected solid solution forming systems.
- Crystallization kinetics for the two systems.

1. Introduction

A significant number of the drugs currently in use contain chiral substances as active pharmaceutical ingredients (API). Therefore, a considerable interest has arisen in pharmaceutical companies in chiral separations in order to eliminate the unwanted isomer. The most frequently used method for chiral separations is the so-called classical resolution method, which involves formation of diastereoisomeric salts. The diastereoisomers are then separated by conventional crystallization. The efficiency of the operation is determined by the solid phase behavior of chiral systems. The separation is the most challenging when solid solutions are formed, which occurs for components with miscibility in the solid phase.[1]

2. Methods

Two different model systems were analysed, which consisted of pharmaceutically active stereoisomers that showed miscibility in the solid phase: System I, which was a mixture of diastereoisomeric salts of citalopram with (+)-O,O'-di-p-toluoyl-D-tartaric acid, ((+)DTT)), and System II, which was a mixture of stereoisomeric salts of nafronyl with oxalic acid. The nafronyl molecule possesses two stereogenic centers.

3. Results and discussion

The solid-liquid equilibrium (SLE) data acquired for System I are presented in Fig. 1A. It is evident that the solubility of S-citalopram·(+)DTT is higher compared to R-citalopram·(+)DTT, therefore, the former can be enriched in the mother liquor. The SLE data indicate the formation of solid solutions in the crystalline phase. The equilibrium relationship for the mixture of nafronyl oxalate stereoisomers in System II is much more complex (Fig. 1B), particularly in case of the dependency $x^{L}_{eq,1,3} = f_p(x^{S}_{2,4})$, for which the equilibrium curve consists of the upward and downward sloping parts. The composition region, in which the same liquid concentration can be matched with more than one equilibrium concentration in the solid phase indicates the possibility of establishing multiple equilibrium states.[2]

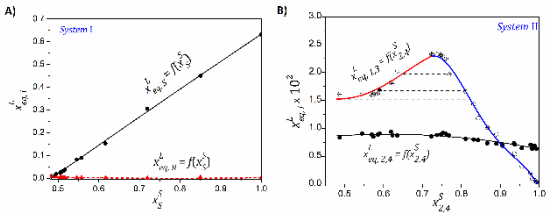

Figure 1. Characterization of SLE for *System* I (A), *System* II (B). Symbols – exp. data, lines - polynomial approx.

This phenomenon can be most probably attributed to polymorphic behaviour of one component showing also miscibility at the solid state.

The crystallization kinetics for System I were measured for different compositions diastereoisomeric mixtures of S- and R-citalopram·(+)DTT. The experiments were performed for the seeded and unseeded solutions. From Fig. 2. A it can be observed that the process can be accelerated by seeding the solutions. In case of the seeded crystallization, the concentration drop in the mother liquor is almost instantaneous, while it is delayed for the unseeded one. This indicates that nucleation is the rate limiting step of the operation.

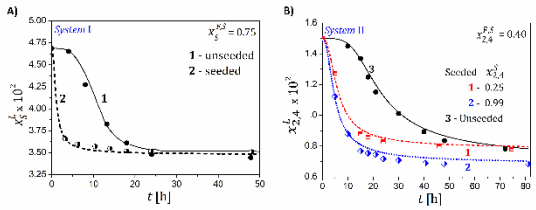

Figure 2. Course of the crystallization for seeded and unseeded solutions in: A) *System* I, B) *System* II [3]

The crystallization kinetics for System II were measured for the mixtures of two racemates 2,4 and 1,3. To determine the impact of seeding on both the process kinetics and the phase behavior, the seeded and unseeded crystallizations were performed in parallel for solid mixtures with the feed composition in the range corresponding to the occurrence of dual equilibrium states (hatched area in Fig. 1B). The seeded crystallization was markedly faster than the unseeded one (Fig. 2B), and the composition of seeds determined the course of the process and the equilibrium state (curves 1,2,3 in Fig. 2B), therefore, the course of the crystallization and the occurrence of the desired state could be imposed by addition of seeds with appropriate composition. When no seeds were added, the equilibrium states corresponding to the left-hand side or right hand-side of the equilibrium curve for racemate 1,3 (Fig. 1B) were established randomly (Fig. 2B). This behavior could be attributed to the co-existence of different polymorphs, which both formed solid solutions but with different solid phase compositions.

To describe the crystallization kinetics, a mathematical model was developed based on the moment method. The model accounted for cooperative nucleation and crystal growth in the solid solution forming system. The model was efficient in reproducing the kinetic profiles in the seeded as well as unseeded crystallization in both systems. Typical results of the model simulations are compared to the experimental data in Fig. 2.

4. Conclusions

Both Systems I and II differed in phase behavior; in the former the target compound was enriched in the mother liquor, whereas in the latter one in the crystalline phase. In System I the equilibrium states were established reproducibly regardless of the composition of the mixture, whereas in System II multiple equilibrium states were established, which most probably was caused by the formation of polymorphs. The mathematical model developed can potentially be used for description of crystallization kinetics in other solid solution forming systems.

References

[1] H. Lorenz, A. Seidel-Morgenstern, Angew. Chem., Int. Ed. **53** (2014) 1218 – 1250.
[2] Balawejder M., Mossety-Leszczak B., Poplewska I., Lorenz H., Seidel-Morgenstern A., Piątkowski W., Antos D., Fluid Phase Eq., **346** (2013), 8–19.
[3] M. Olbrycht, D. Kiwala, M. Balawejder, A. Seidel-Morgenstern, W. Piątkowski, D. Antos, Cryst. Growth Des. **16** (2016) 5049−5058.
[4] M. Olbrycht, M. Balawejder, I. Poplewska, H. Lorenz, A. Seidel-Morgenstern, W. Piątkowski, D. Antos, Cryst. Growth Des., just accepted, 10 January (2019), DOI: 10.1021/acs.cgd.8b01768.

Financial support of this work by National Science Center (project UMO2013/08/M/ST8/00982) is gratefully acknowledged.

ECCE12
The 12th EUROPEAN CONGRESS OF CHEMICAL ENGINEERING
Florence 15-19 September 2019

Bulk Density Control in the Cooling Crystallization of L-Methionine with pH Control

Wang-Soo Kim, Kee-Kahb Koo

Department of Chemical and Biomolecular Engineering, Sogang University, Seoul 04107, Korea

**Corresponding author: koo@sogang.ac.kr*

Highlights

- Explosive primary nucleation of L-methionine (L-Met) was induced by pH control.
- Agglomeration was observed with particle counts measured by FBRM.
- Larger and thicker L-Met agglomerates with high bulk density could be obtained by cooling L-methionine slurry made by pH increase.

1. Introduction

L-Methionine (L-Met), which is one of hydrophobic amino acids, has been used for a dietary source due to the role as a donor of an active methyl group [1]. Generally, it is difficult to obtain single crystals of L-Met due to strong tendency for agglomeration and final L-Met agglomerates obtained by cooling from aqueous solution has very low bulk density due to their hollow structures [2]. In the present work, to improve the bulk density, L-Met was crystallized by pH increase with one-pot injection of an electrolyte aqueous solution into saturated acidic solution of L-Met and then large-sized agglomerates with high bulk density could be obtained by slow cooling the suspension made by the one-pot injection.

2. Methods

L-Met was crystallized with pH increase of acidic L-Met solution (saturated state of 60 °C from 300 g water with addition of 2 wt % sulfuric acid) by the injection of sodium acetate aqueous solution (1 mole dissolved in 20 g water). After the injection was completed, the slurry was stirred for about 2 h to agglomerate L-Met crystals and then cooled to 30 °C with a slow cooling rate of -6 °C/h. During crystallization by pH increase, particle counts were in-situ monitored by focused beam reflectance measurement (FBRM) and hydrogen ion concentration was observed with real time by measuring pH values using the relation, $pH = -\log[H^+]$. Size and morphology of L-Met agglomerates were confirmed by images of scanning electron microscopy (SEM).

3. Results and discussion

Figure 1 shows the history of particle counts and pH values when sodium acetate aqueous solution was injected with one-pot using a syringe. As soon as the injection was carried out, the pH increased instantaneously from 2.6 to 4.0 and particle counts were observed to drastically rise. Thereafter, the pH remained constant, but the particle counts began to decrease monotonically. This result indicates that the great number of tiny L-Met crystals generated by explosive primary nucleation tend to agglomerate continuously. The total number of particle counts measured by FBRM (Figure 1a) is the sum of the number of chord length (Figure 1b; the range of 1 – 1000 μm) that is the

distance of laser light from FBRM probe traveling over each particle surface [3]. When the suspension in which agglomeration occurs is monitored by FBRM, particle counts are generally decreased due to high possibility of measuring the largest chords of agglomerates. Therefore, it can be expected that the decreases in both particle counts and chord length distribution area are caused by agglomeration.

Figures 2a and 2b show that L-Met agglomerates obtained by pH increase were found to be denser and thicker than those by just cooling. As shown in Figure 2c, much larger and denser L-Met agglomerates was found to be obtained with crystallization by pH increase followed by the cooling process. It can be concluded that supersaturation generated by cooling was predominantly consumed to enlarge L-Met agglomerates.

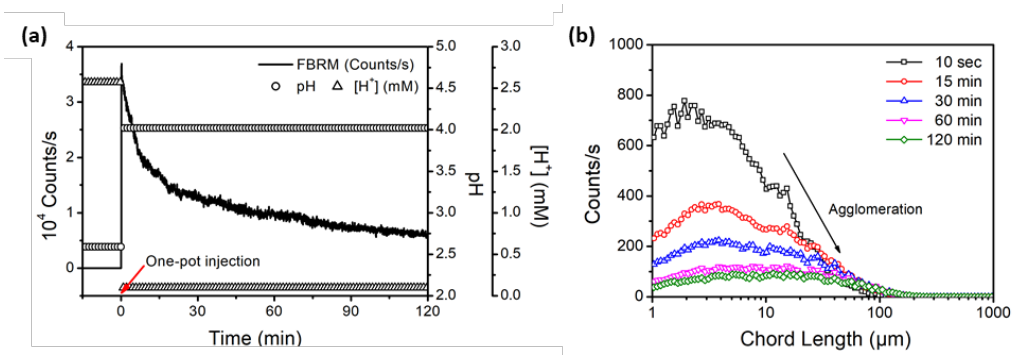

Figure 1. (a) Total counts and pH values in case of one-pot injection, (b) chord length distribution varying with time.

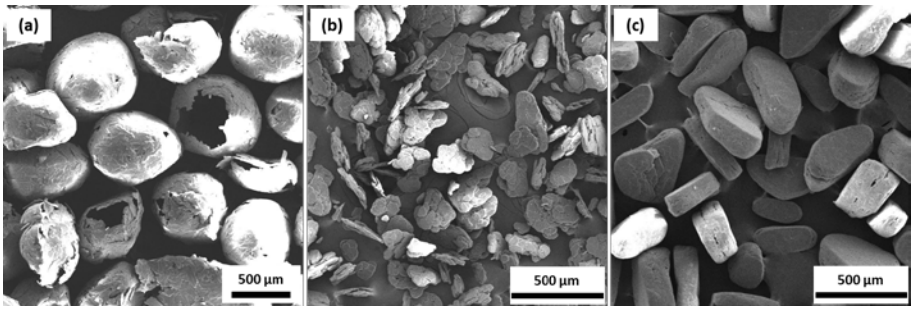

Figure 2. SEM images of L-Met agglomerates obtained by (a) cooling from 60 to 30 °C, (b) pH increase from 2.6 to 4.0, (c) pH increase followed by cooling.

4. Conclusions

Explosive nucleation was generated by instantaneous pH increase, resulting in production of L-Met agglomerates with the bulk density of 500 g/L. Furthermore, as a result of additional cooling, large and dense agglomerates with 760 g/L could be successfully obtained. On the other hand, the bulk density of L-Met agglomerates with the hollow structure obtained from just cooling was 200 g/L.

References

[1] S. Roje, Phytochemistry, 67 (2006) 1686-1698.
[2] H. Steckel, H.G. Brandes, Int. J. Pharm., 278 (2004) 187-195.
[3] M.R. Abu Bakar, Z.K. Nagy, A.N. Saleemi, C.D. Rielly, Cryst. Growth Des., 9 (2009) 1378-1384.

ECCE12
The 12th EUROPEAN CONGRESS OF CHEMICAL ENGINEERING
Florence 15-19 September 2019

Multiphase CFD Simulation of Small-Scale Crystallization Reactors

Ramona Achermann[1], Pawel M. Orlewski[1], Marco Mazzotti[1*]

1 ETH Zurich, Institute of Process Engineering, Sonneggstrasse 3, CH-8092 Zurich, Switzerland;

**Corresponding author: marco.mazzotti@ipe.mavt.ethz.ch*

Highlights

- Multiphase CFD simulation of small-scale crystallization reactors
- Qualitative and quantitative information on flow and mixing behavior
- Better design of high-throughput crystallization experiments

1. Introduction

Crystallization is a widely used purification step in the fine chemical and the pharmaceutical industry. Reducing the reactor volume to study crystallization processes is especially beneficial at an early stage of research since it saves valuable compounds, reduces costs and allows for high-throughput screening[1]. Thus, in recent years small-scale crystallization reactors have gained increasing popularity within the crystallization community[1,2]. However, compared to large-scale crystallizers, different hydrodynamic properties of these miniaturized reactors have not yet been thoroughly studied. Therefore, to close the gap, by performing a multi-phase modelling using CFD (Computational Fluid Dynamics), a better understanding of the effect of operating conditions on the flow properties in such small reactors could be obtained. In this work, two commercially available micro reactors using different stirrers, namely the overhead stirrer and the stirrer bar, have been modelled with and without the addition of solid particles. Knowing the hydrodynamics of such small stirred vials will improve the overall understanding of the occurring crystallization phenomena such as nucleation, growth or breakage since shear forces or mixing can have a significant influence on them[3,4].

2. Methods

The commercial CFD code ANSYS Fluent 18.2 was used to conduct the simulations. To model the turbulence, the Reynold's stress model (RSM) was applied and standard multiphase models were used to model the effects of solids on the flow field. An enhanced wall treatment model was added to better capture the behavior near the wall and the grid was refined until mesh-independent results were obtained. For both stirrers, a single reference frame (SRF) was used and the simulations were run at steady state.

3. Results and discussion

A complete qualitative and quantitative comparison of the two investigated stirrers was performed with and without solids for a wide range of operating conditions. This gave information on the

distributions in the reactor of the velocity, of the turbulent energy dissipation rate, as well as of the solids together with their exposure to shear forces and the homogeneity of the system. Figure 1 shows the velocity distribution for the two configurations investigated.

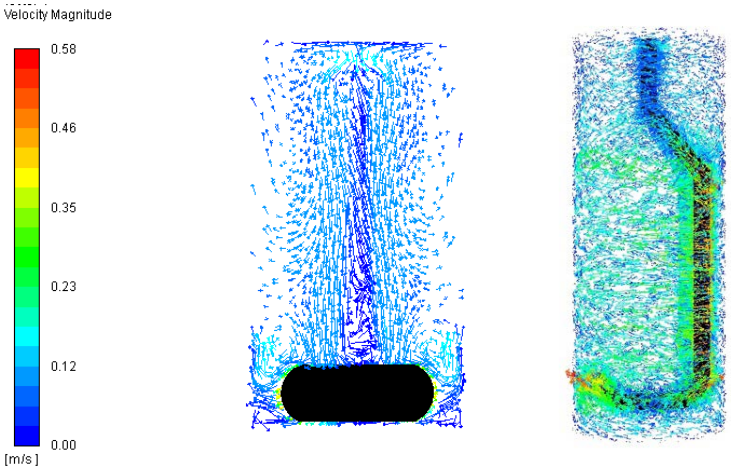

Figure 1. Comparison of the velocity distribution in the stirrer bar (left) and overhead stirrer (right).

4. Conclusions

In this work, the mixing and flow behavior of the overhead stirrer as well as the stirrer bar used in commercially available micro reactors were studied with and without solid addition using CFD modelling. Obtained results allowed for a better understanding of the hydrodynamics in the system and of their dependence on the operating conditions, which could then allow for an improved overall understanding of the phenomena occurring in the crystallization processes studied in those systems.

References

[1] E. Simone, J. McVeigh, N. M. Reis, and Z. K. Nagy. A high-throughput multi-microfluidic crystal generator (mmicrocrygen) platform for facile screening of polymorphism and crystal morphology for pharmaceutical compounds. Lab Chip, 18:2235–2245, 2018.

[2] Giovanni M. Maggioni, Luca Bosetti, Elena Dos Santos, and Marco Mazzotti. Statistical analysis of series of detection time measurements for the estimation of nucleation rates. Crystal Growth and Design, 17(10):5488-5498, 2017.

[3] Christian Lindenberg, Jochen Schöll, Lars Vicum, Marco Mazzotti, and Jörg Brozio. L-Glutamic Acid Precipitation: Agglomeration Effects. Crystal Growth & Design, 8(1):224-237, 2008.

[4] Pawel M. Orlewski, Yan Wang, Mercedeh Sadat Hosseinalipour, David Kryscio, Martin Iggland, and Marco Mazzotti. Characterization of a vibromixer: Experimental and modelling study of mixing in a batch reactor. Chemical Engineering Research and Design, 137:534–543, 2018.

Acknowledgement

This project has received funding from the European Research Council (ERC) under the European Union's Horizon 2020 research and innovation programme under grant agreement No 2-73959-18.

ECCE12
The 12th EUROPEAN CONGRESS OF CHEMICAL ENGINEERING
Florence 15-19 September 2019

Crystallization fundamentals and industrial processes

High-throughput droplet-based platform for studying nucleation

Elena C. dos Santos, Giovanni M. Maggioni and Marco Mazzotti
Institute of Process Engineering, ETH Zurich, 8092 Zurich, Switzerland
edossantos@ipe.mavt.ethz.ch

Highlights

- Droplet-based microfluidics
- Stochasticity of primary nucleation
- Effect of shear rate on nucleation
- Nucleation rates estimation and uncertainty propagation.

1. Introduction

Nucleation, the very early stage of crystallization processes, is of fundamental importance on defining crystal properties such as purity, size distribution and polymorphism [1]. It is well established that nucleation is a stochastic phenomenon [2-3], which imposes challenges to obtaining reproducible experimental data. Thus, numerous identical experiments are essential to correctly estimating primary nucleation kinetics. In this context, droplet-based microfluidics offers, not only good control of transport phenomena (enhanced mass and heat transfer), little or no gravity effect, and few impurities, but also, the ability of generating thousands of nanodroplets in a nearly monodisperse fashion. Such a high-throughput technique enables to probe a considerable number of identical discrete crystallizers, necessary to build representative statistics. Nevertheless, the error committed by not sampling the entire population (finite sampling) will invariably exist. The magnitude of this stochastic uncertainty depends solely on the number of samples and on the chosen confidence interval. Such an uncertainty needs to be quantified, firstly, as a criterium for guaranteeing randomness of the process and secondly to be properly propagated to the parameters to be estimated, e.g., nucleation rate. The nucleation rate is the number of nuclei formed per unit time and volume at a given supersaturation. The latter can be regarded as the difference in chemical potential between the supersaturated and equilibrium states of the compound in solution, i.e., the driving force of the nucleation process. However recently, a few studies have discussed that shear promotes the aggregation of meso-scale clusters into stable clusters, so that nucleation proceeds via a two-step mechanism [4-5]. Despite the number of studies, the exact mechanism controlling nucleation under fluid dynamic conditions is still unclear.

2. Methods

We used PEEK T-junctions followed by translucent FEP tubes to study crystallization in droplets under flow conditions at different droplet velocities. The experimental set-up consists of three main parts. Firstly, in the generation zone (GZ), immiscible fluids were fed with syringe pumps into a PEEK T-junction, where droplets were formed. These components were placed inside a temperature-controlled incubator to maintain solutions at the desired dissolved state. After been formed, droplets flow to the crystallization zone (CZ), which consists of a certain length of FEP tube placed in a cold-water bath. Due to the supersaturation created by reducing the system temperature, a number of droplets crystallizes while travelling along the tube depending on the tube length, which

was varied in order to probe different nucleation residence times. Finally, droplets moved to the observation zone (OZ), where the FEP tube was placed under a light microscope, to monitor through image acquisition whether droplets have crystallized, thus enabling building nucleation statistics.

3. Results and discussion

For each single experiment, we have assessed its internal consistency via statistical analysis based on slicing the population of droplets, e.g., comprising of about 3000 droplets, in smaller subgroups. In Fig. 1, we show this procedure and plot both the experimental probability values as a function of the number of droplets, and the uncertainty band. The spread in probability values towards lower number of droplets shows repeatedly strong consistency, and hence, this variability is entirely due to stochasticity. In Fig. 2, values of nucleation rates estimated via the linearized form of the cumulative exponential distribution function are plotted with their corresponding confidence intervals obtained through the propagation of the uncertainties in nucleation probability. In this figure, we observe an increase in nucleation rate of about 3 orders of magnitude in respect to the stagnant situation. Such a high difference can be associated with the recirculation flow patterns, generated inside the droplets at flowing conditions. The latter may favor nucleation via aggregation of pre-clusters by enhancing particle collision, but at the same time may hinder nucleation by reducing contact and bridging time.

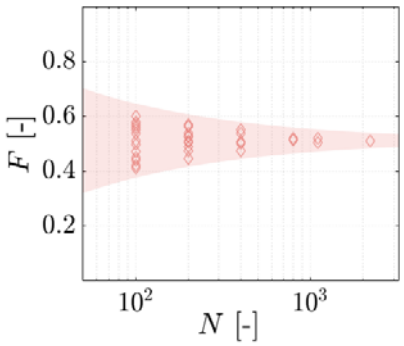

Figure 1. Probability points of single experiments sliced in smaller number of droplets.

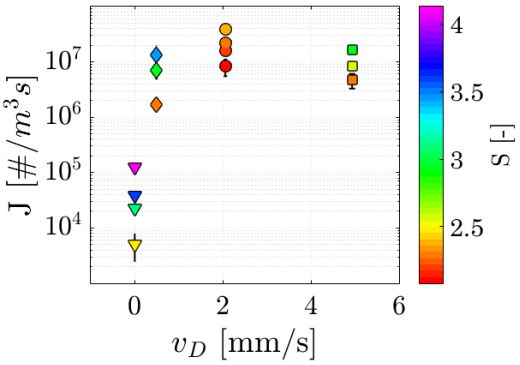

Figure 2. Probability points of single experiments sliced in smaller number of droplets.

4. Conclusions

We estimated primary nucleation kinetics from large number of nanodroplets in varying fluid dynamic conditions. Making use of statistical tools, we were able to assess the statistical representability of the experimental data and to estimate their inherent uncertainty. Finally, we showed that nucleation rates increase non-monotonically with droplet velocity, possibly because there exists an interplay among the effects of energy dissipation due to mixing on clusters' agglomeration.

Acknowledgements: This project has received funding from the European Research Council (ERC) under the European Union's Horizon 2020 research and innovation programme under grant agreement No 2-73959-18.

References

[1] H. H. Tung, Org. Process Res. Dev. 17 (2013) 445-454.
[2] G. Capellades, et. al, Cryst. Growth Des. 17 (2017) 3287-3294.
[3] G. M. Maggioni, L. Bosetti, E. C. dos Santos, M. Mazzotti, Cryst. Growth Des. 17 (2017) 2852-2863.
[4] A. Jawor Baczynska, J. Sefcik, B. D. Moore, Cryst. Growth Des. 13 (2012) 470-478.
[5] J. Liu, A. C. Rasmuson, Cryst. Growth Des. 13 (2013) 4385-4394.

ECCE12
The 12th EUROPEAN CONGRESS OF CHEMICAL ENGINEERING
Florence 15-19 September 2019

Protein Crystallization Kinetics – Determination by a Through-flow Small-Angle X-ray Scattering Method

Izabela Poplewska[1,*], Andrzej Łyskowski[2], Michał Kołodziej[1], Piotr Szałański[3], Wojciech Piątkowski[1], Dorota Antos[1]

[1] *Department of Chemical and Process Engineering, Rzeszów University of Technology,*
[2] *Department of Biotechnology and Bioinformatics, Rzeszów University of Technology*
[3] *Faculty of Chemistry, Rzeszów University of Technology*
Powstańców Warszawy Ave. 6, 35-959 Rzeszów, Poland]
** ipoplewska@prz.edu.pl*

Highlights

- Protein crystallization kinetics was determined using a modified SAXS technique.
- Results obtained were comparable to those measured in a seeded tank crystallizer.
- The modified SAXS setup can support development stage of bulk crystallization.

1. Introduction

Determination of the process kinetics and development of adequate kinetic rate equations for design of bulk crystallization is based on measurements of time-dependent concentration profiles. Typical experimental setups for acquisition of kinetic data consist of a small-volume tank, in which the supersaturated solution is stirred. Samples of the solution are collected at different time intervals and subjected to the concentration analysis. This procedure is laborious and consumes a large amount of often valuable protein solution. Therefore, in this work we propose another approach for the characterization of crystallization kinetics of proteins in situ, which is based on a modification of small-angle X-ray scattering (SAXS) technique. The kinetic data acquired in the SAXS setup were compared to those taken from a stirred-tank crystallizer (STC) setup, in which unseeded (uSTC) and seeded (sSTC) crystallization was analyzed [1].

2. Methods

The model protein for the study was lysozyme (LYZ), which was crystallized from supersaturated aqueous solutions of ammonium sulfate. The kinetic measurements were performed in SAXS, uSTC and sSTC for the supersaturated protein solutions with the same compositions.

In the SAXS system a small amount of the protein solution (1.5 mL) was forced to recirculate within the setup. The SAXS intensity curves were measured at different time intervals and converted into kinetic profiles using a calibration factor. The diffraction images of the sample taken at the end of the kinetic experiments were recorded to confirm the presence of the crystalline phase (Fig. 1).

In the STC setup the crystallization kinetics of LYZ was measured in a 10 mL tank. In the uSTC setup the protein solutions were stirred with a magnetic stirrer at 400 rpm. In the sSTC setup, the experiments were repeated under the same conditions, but the solutions were seeded with 1.6 mg of the seed crystals.

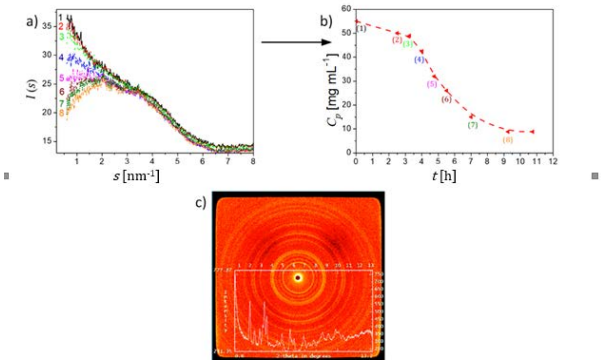

Figure 1. Course of the crystallization in SAXS. (a) Time evolution of the scattering intensity curves plotted against the modulus of the momentum transfer, *s*; (b) the corresponding kinetic curve; dashed line - guide to the eye; (c) typical diffraction image recorded at the end of the experiment

3. Results and discussion

The analysis of the experimental data indicated that the kinetic rate accelerates with increasing the supersaturation degree, and decelerates with increasing ammonium sulfate concentration (C_{salt}) in both systems (Figs 2a, 2b). The seeded crystallization is accomplished significantly faster than the unseeded one (Fig. 2a). Moreover, the hydrodynamic conditions in the SAXS setup could be adjusted for which a quantitative agreement between the kinetic data acquired from both systems was achieved (Fig. 2b).

To predict the time evolution of concentration profiles of the protein in the liquid phase and quantify the crystallization kinetics, a population balance model was used, which consisted of kinetic rate equations of nucleation and crystal growth [1]. The same kinetic equations could be used to describe the course of crystallization in both systems. The results of the measurements and numerical simulations were compared (Figs 2a, 2b).

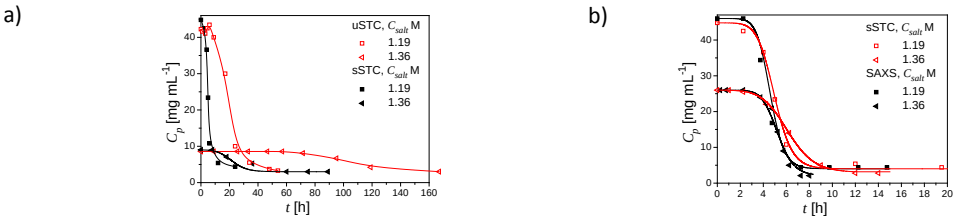

Figure 2. Comparison of the kinetic curves measured in the (a) sSTC and uSTC; (b) sSTC and SAXS setups

4. Conclusions

The modified SAXS setup can be applied to support kinetic measurements for bulk crystallization. The implementation of flow motion in the SAXS setup enhances the rate of crystallization kinetics and reduces the time of measurements. The method allows online monitoring the presence of the crystalline phase as well as acquiring kinetic profiles using very small volumes of valuable protein solutions.

References

[1] I. Poplewska, A. Łyskowski, M. Kołodziej, P. Szałański, W. Piątkowski, D. Antos, Chem. Eng. Res. Des. (2019), 141, 580-591

ECCE12
The 12th EUROPEAN CONGRESS OF CHEMICAL ENGINEERING
Florence 15-19 September 2019

Crystallization fundamentals and industrial processes

Determination of nucleation kinetics from metastable zone width and induction time data for sonocrystallization of pyrazinamide.

Abhishek Maharana[1], Debasis Sarkar[2]

[1,2] Dept of Chemical Engg, IIT Kharagpur, West Bengal, India

*Corresponding author: abhi.mrana@gmail.com

Highlights

- Nucleation kinetics is estimated from MSZW and induction time data.
- Sangwal's nucleation theory is used for estimating nucleation parameters.
- Induction time showed a sharp decrease with increase in ultrasound amplitude.

1. Introduction

Crystallization is an important separation and purification technique in many chemical and pharmaceutical industries. Most industries use simple batch crystallization for generating crystals of definite crystal size distribution (CSD) and purity. However, it is very difficult to control primary nucleation to obtain crystals of definite properties because it occurs in a thermodynamically unstable region [1]. Primary nucleation requires very high levels of supersaturation which brings difficulty in controlling the crystallization process. To overcome this situation sonocrystallization can be used. Cavitation induced during ultrasound can create high supersaturation even at a lower superstation ratio which can induce nucleation to achieve target CSD and create nuclei of desired polymorph [2]. MSZW denotes region between solubility curve and onset of nucleation. Information about MSZW helps in avoiding excessive nucleation, ensures required CSD and also helps in determining nucleation kinetics. Induction time is the measure of ability of a supersaturated solution to remain in state of metastability. It has been related to size of nuclei and thus it is important for evaluation of nucleation kinetics.

Pyrazinamide is an important API drug for treatment of *Mycobacterium tuberculosis.* The effect of continuous sonication with different amplitude on nucleation kinetics for cooling crystallization of pyrazinamide from its solution in acetone is studied. Nucleation parameters are calculated from metastable zone width (MSZW) and induction time experimental data. To the best our knowledge, a study on effect of continuous sonication on nucleation kinetics of pyrazinamide has not been reported in open literature.

2. Methods

Solubility of pyrazinamide in acetone is computed gravimetrically in the temperature range of 283.15 K to 323.15 K. A 500 ml jacketed crystallizer with a temperature controller having a precision of ±0.05 K is used. Probe sonicator is installed to introduce ultrasound of different amplitude. The ultrasound probe is dipped 1 cm from the solution surface. The onset of nucleation is observed by visual inspection. Polythermal method is used to determine MSZW and isothermal method is used to determine induction time. Next classical nucleation theory is used to estimate the nucleation rate:

$$J = A\exp\left[-\frac{B}{\ln S_{\max}^2}\right], \text{ where } B = \frac{16\pi}{3}\left(\frac{\gamma\Omega^{\frac{2}{3}}}{T_{nuc}k_B}\right)$$

3. Results and discussion

Figure 1 represents MSZW in presence and absence of ultrasound. It is evident from the figure that in presence of ultrasound, the MSZW decreases significantly. The Sangwal's classical three dimensional nucleation theory approach is used for estimation of nucleation parameters as follows:

$$\left(\frac{T_0}{\Delta T_{\max}}\right)^2 = F - F_1 \ln R, \text{ where } F = F_1\left(X + \ln T_0\right),\ F_1 = \frac{1}{B}\left(\frac{\Delta H_g}{RT_{nuc}}\right)^2,\ X = \ln\left(\frac{A}{f}\frac{RT_{nuc}}{\Delta H_g}\right)$$

The value of $\Delta H_g/R$ can be obtained from the plot of mole fraction of solubility versus $1/T_0$. The value of f is inverse of molecular volume of pyrazinamide. The parameters A and B is estimated from the plot of $(T_0/\Delta T_{max})^2$ versus lnR. Figure 2 represents effect of supersaturation on induction time. The decrease in induction time with increase in ultrasound amplitude is shown in Figure 3.

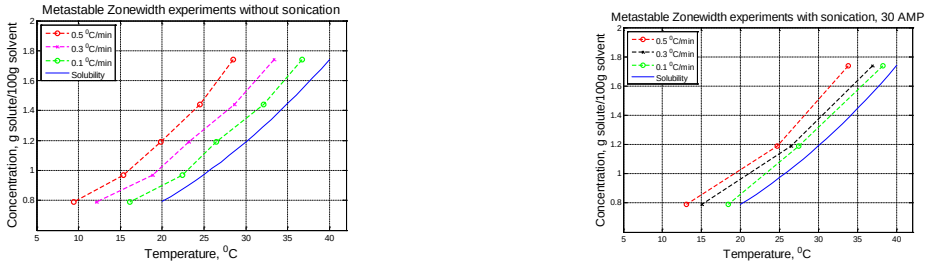

Figure 1. MSZW experiments in presence and absence of ultrasound.

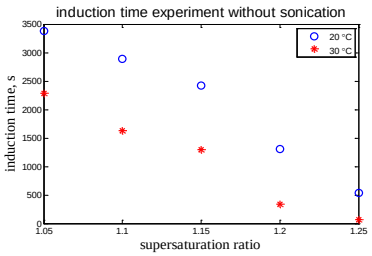

Figure 2. Plot of induction time vs. supersaturation

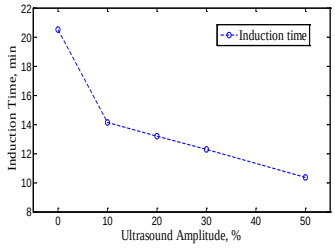

Figure 3. Induction time at different ultrasound amplitude

4. Conclusions

The metastable zone width was measured for different cooling rates and different ultrasound amplitudes. It was observed that the MSZW increases with increase in cooling rate and decreases with increase in ultrasound amplitudes. The nucleation parameters (A and B) were calculated from Sangwal's classical three dimensional approach. Induction time decreases with increase in supersaturation ratio. It also showed a sharp decrease with increase in ultrasound amplitude at constant supersaturation.

References

[1] Z. Guo, A.G. Jones, N. Li, Chemical Engineering Science, Volume 61, Issue 5, 2006, 1617-1626.
[2] C. Virone, H.J.M. Kramer, G.M. van Rosmalen, A.H. Stoop, T.W. Bakker, Journal of Crystal Growth, Volume 294, Issue 1, 2006, 9-15.

ECCE12
The 12th EUROPEAN CONGRESS OF CHEMICAL ENGINEERING
Florence 15-19 September 2019

Reactive crystallization of Ca and Mg carbonates by CO_2 fine bubble injection into concentrated brine −Effects of solution pH and temperature–

Yoshinari Wada[1], Koji Masaoka[1,2], Yukikazu Takashima[1], Toshihiko Hiaki[1],
Masakazu Matsumoto[1*]

1 College of Industrial Technology, Nihon Universiry, 1-2-1 Izumi-cho Narashino, Japan

2 Research Institute of Salt and Sea Water Science, The salt Industry Center, 4-13-20 Sakawa, Odawara, Japan

**Corresponding author: matsumoto.masakazu@nihon-u.ac.jp*

Highlights

- Dolomite is selectively crystallized at pH of 5.3–6.8 and temperature of 273–298 K.
- Aragonite with high selectivity is obtained in range over 333 K at pH of 5.3 and 6.0.
- $Mg(OH)_2$ as by-product is produced besides carbonates in pH range over 7.8 at 298 K.

1. Introduction

So as to build up a utilization system of seawater resources based on the salt production process, a recovery and upgrading method for calcium (Ca) and magnesium (Mg) from the discharge concentrated brine of salt manufactory in Japan was studied. From the viewpoint of solubility of salts, the synthesis of carbonate by reactive crystallization between the dissolved Ca^{2+} and Mg^{2+} in concentrated brine and CO_2 can be considered as an effective separation/recovery method. In this study, the production regions of Ca and Mg carbonates from the concentrated brine were classified for operational parameters during the reactive crystallization using the minute gas-liquid interfaces around CO_2 fine bubbles as novel reaction fields where the crystal nucleation proceeds predominantly. In the regions near the gas-liquid interfaces of CO_2 fine bubbles, the local increase in the concentrations of Ca^{2+}, Mg^{2+}, and CO_3^{2-} caused by the electric charge on fine bubble surface and the acceleration of CO_2 mass transfer owing to minimizing the bubble diameter [1]. In this paper, we report that the effects of the solution pH and reaction temperature (T_r) on the selectivity of Ca and Mg carbonates during reactive crystallization from the concentrated brine with CO_2 fine bubble injection.

2. Experimental

2.1 Concentrated brine The concentrated brine discharged from salt manufacture was used. In Japan, NaCl is manufactured by evaporative crystallization after concentrating seawater through an electric dialysis membrane, and the concentrated brine that removed K^+ by cooling crystallization is obtained concurrently with KCl. The major components of the above concentrated brine are $MgCl_2$, NaCl and $CaCl_2$, which have the concentrations of 2.1, 0.8, and 0.7 mol/L, respectively.

2.2 Experimental apparatus CO_2 fine bubbles were continuously supplied to 300 mL of the concentrated brine, and $CaMg(CO_3)_2$ was crystallized in a crystallization vessel. CO_2 fine bubbles

with an average bubble diameter (d_{bbl}) of 40 μm were generated using a self-supporting bubble generator by increasing the impeller shear rate under reduced pressure [1], with the rotation rate maintained at 1500 min^{-1} and the CO_2 flow rate controlled at 11.9 mmol/(*l*·min).

2.3 Experimental procedure The initial solution pH in concentrated brine was adjusted at a specified value of 4.3–8.3 by adding 4.0 mol/*l*–NaOH or 1.0 mol/*l*–HCl solution, and the solution pH during reactive crystallization was maintained constant at a set value by adding 4.0 mol/*l*–NaOH solution. T_r varied in the range between 278 and 348 K using a thermostat bath, and the reaction time (t_r) was controlled within 60 min. After the crystallization progressed for a specified length of time, the suspension was filtered and the reaction products were washed with deionized water and then dried at 373 K in a dryer. The selectivity of solid products was identified by the peak area ratio from X-ray diffraction.

3. Results and discussion

The selectivity of solid products at a t_r of 60 min plotted against solution pH and T_S is shown in **Figure 1**. At a pH of 5.3–6.8 and T_S of 278–298 K, the dolomite ($CaMg(CO_3)_2$) crystallization proceeded dominantly. When T_S increased to 333 K at pH of 5.3 and 6.0, aragonite $CaCO_3$ as the dominant product was obtained. At a constant T_S of 298 K, aragonite $CaCO_3$, $CaMg(CO_3)_2$, and $Mg(OH)_2$ were simultaneously obtained in the pH range over 7.8, and the selectivity of $Mg(OH)_2$ became high at a pH of 8.3.

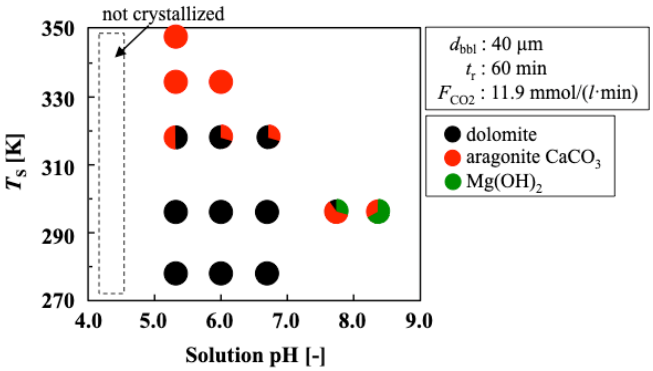

Figure 1. Effects of solution pH and T_S on the selectivity of solid products.

4. Conclusions

The production regions of Ca and Mg carbonates from the concentrated brine by fine bubble injection were classified by the solution pH and T_S. Consequently, the production of $CaMg(CO_3)_2$ with high selectivity was confirmed at a pH of 5.3–6.8 and T_S of 278–298 K. The aragonite $CaCO_3$ was preferentially produced in the T_S range over 333 K at pH of 5.3 and 6.0. When the solution pH was greater than 7.8 at a constant T_S of 298 K, not only $CaMg(CO_3)_2$ and aragonite $CaCO_3$ but also $Mg(OH)_2$ as a by-product was precipitated.

Acknowledgments

This work was financially supported by the Salt Science Research Foundation (Nos. 17A3, 18A3), Japan. We also acknowledge the Naikai Salt Industry Co., Ltd. for provision of Bittern.

References

[1] M. Matsumoto, T. Fukunaga, K. Onoe, Chem. Eng. Res. Des. 88 (2010) 1624–1630.

ECCE12
The 12th EUROPEAN CONGRESS OF CHEMICAL ENGINEERING
Florence 15-19 September 2019

ADREM: Benchmarking new modular reactor technologies

Emmanouela Korkakaki[1], Koos Overwater[1], Marco van Goethem[1], Stéphane Walspurger[1]

1 TechnipFMC B.V., Afrikaweg 30, 2700 AB, Zoetermeer, the Netherlands

**Corresponding author: emma.korkakaki@technipfmc.com*

Highlights

- Methane conversion to liquid chemicals in one-step process has been benchmarked.
- Microwave technology replaces thermal methods for benzene with energy savings of 40%.
- C2 mixtures are produced with plasma technology with the minimum environmental impact. (a significant decrease of GHG emissions)
- OCM in gas solid vortex reactor is scalable and outperforms fixed bed reactors.

1. Introduction

The aim of the ADREM project is to develop new modular and flexible reactor technologies, that can accommodate different methane-rich sources, such as flared gas, associated gas from oil extraction, or biogas, and valorize it directly to chemicals. Some examples of key candidates that could be used on that concept are flared gas (which for 2017 was approximately 141 bcm), and the biogas that has reached 50 bcm in 2017. The impact of the flared gas to the environment is huge, since only for 2017, approximately 140 bcm were flared, equivalent to approximately 400Mt CO_2 and enough to provide the annual gas consumption of Germany and France.

In this work we focused on the integration of new reactor concepts, developed during the ADREM project, in the overall process design and on the evaluation of the feasibility for the technology upscale from an engineering point of view. The aim was modular, flexible units, that can be easily transported to remote locations, or to methane sources with small gas production.

2. Methods

Lab-scale results from the ADREM partners were used for the reactor performance evaluation, while for the pretreatment and downstream of the products state-of-the-art was used. Two cases of throughput were considered for the process design: i) associated gas and, ii) biogas. Liquid products (e.g. mixture or low purity products) that are easily transportable to a centralized purification unit were defined as process output. For each chemistry a flow scheme was developed, based on the product and on the reactor's requirements. The mini-methanol plant (commercially available) was used as a benchmark. The ADREM novel reactor concepts that were evaluated were: i) microwave assisted non-oxidative methane coupling, ii) plasma non-oxidative methane coupling, iii) oxidative coupling of methane (OCM) in gas solid vortex reactor with and, iv) plasma dry reforming. The performance indicators of each concept were the productivity, the total energy consumption and the specific energy consumption of each scenario, the CO_2 emissions and the

carbon formation rates. Based on these numbers, the two “most promising” reactor concepts were selected for TRL5 demonstration.

3. Results and discussion

The process design revealed interesting results for the four different reactor concepts, when considering that electricity is decarbonized. The microwave non-oxidative methane coupling for benzene production showed low energy consumption. Compared to the benchmark case, the energy demand decreased by 40% in the case of associated gas. With respect to the CO_2 emissions, there is up to 50% reduction compared to flaring, depending on the throughput. Plasma coupling of methane to C2 mixtures showed operational flexibility, reducing significantly the CO_2 emissions. However, the energy requirements when the plasma technology was implemented, were increased two-fold in the best-case scenario (with associated gas as the feedstock) compared to the benchmark case. This reactor concept resulted in a decrease of CO_2 emissions by 50-80% compared to direct flaring. Plasma technology in the dry reforming for syngas (and subsequently methanol) production had a similar performance; the energy requirements of the plasma technology were on the high side, with a four-fold increase compared to the benchmark case, while the CO_2 emissions had a tremendous reduction of 70%. Finally, the gas solid vortex reactor had quite a unique setup, easily scalable, compact and yet able to handle large throughput, with relatively low energy consumption. In this concept, the energy requirements of the entire process were comparable to the benchmark case, with a 10% energy savings when associated gas was used. In this reactor concept, CO_2 emissions were reduced between 20-40% compared to direct flaring. Based on the comparison of the performance indicators, the microwave assisted methane coupling and the plasma coupling were selected for TRL5 demonstration.

4. Conclusions

The present work shows the potential of the ADREM new reactor technologies on the integrated overall process scheme. This work gives more insights on the modular and flexible reactor technology that can accommodate methane-rich sources and convert them to a liquid product. For all the evaluated reactor technologies, the CO_2 emission profile was low compared to flaring, while some of them showed competitive energy requirements compared to the conventional thermal methods.

This project has received funding from the European Union’s Horizon 2020 research and innovation programme under grant agreement No 636820.

ECCE12
The 12th EUROPEAN CONGRESS OF CHEMICAL ENGINEERING
Florence 15-19 September 2019

Modelling of reverse water-gas shift on copper-based catalysts using a convection-diffusion packed bed microkinetic model

Damjan Lašič Jurković[1], Anže Prašnikar[1], Andrej Pohar[1], Blaž Likozar[1]

1 Department of Catalysis and Chemical Reaction Engineering National Institute of Chemistry, Hajdrihova 19, 1000 Ljubljana, Slovenia

**Corresponding author: damjan.lasic@ki.si*

Highlights

- RWGS was performed with 4 different catalysts (10% Cu / Al_2O_3, TiO_2, SiO_2, ZrO_2)
- Data was compared with modelling results for different reactor types – CSTR, PFR and PB
- Bulk-gas diffusion plays an important mass-transfer role at our operating conditions
- DFT-derived RWGS kinetic model from literature was improved for higher predictive power

1. Introduction

Over the last decades, there is an increasing need to capture and convert CO_2 to help reduce the effect of global warming. One of such routes is to convert CO_2 to syngas via reverse water-gas shift reaction (RWGS), and then further synthesize useful products such as liquid fuels and chemicals.[1] In order to produce efficient catalysts for this process, a thorough understanding of the surface reaction mechanisms is needed. Microkinetic modelling, with the help of experimental data and reaction parameters obtained by ab-initio methods such as DFT,[2] is a useful tool that can be used both for understanding the process and process optimization. In this work, different reactor models are developed and used with experimental data from activity[3] and analytics to fine-tune the reaction parameters and obtain good model predictive power.

2. Methods

For the experimental part, four different copper-based catalysts (10 wt. % Cu on Al_2O_3, TiO_2, SiO_2 and ZrO_2) were synthesized using the deposition-precipitation method. The synthesized catalysts were analyzed with different experimental techniques, such as XRD, BET, SEM, EDX and various chemisorption techniques such as H_2 TPR, H_2 and CO TPD and pulsed N_2O oxidation. The latter was used to determine the concentration of surface active sites that was later used as an input to the model and varied with the supporting material used.

A one-dimensional packed bed reactor model was developed for system simulation. The model accounted for both convective and diffusive mass transport, as well as the full microkinetic chemistry consisting of surface reactions, and adsorption/desorption processes obtained from [2]. The model was solved using the CVODE solver written in C,[4] and the numerical regression with

the experimental data using the model was performed using the COBYLA method from the SciPy library written in Python.[5]

3. Results and discussion

The microkinetic model from the literature was used to calculate the conversions and product selectivity at the experimental conditions used, and compared to experimental data. The type of the reactor used in the model (CSTR, PFR or PB) was given additional attention.

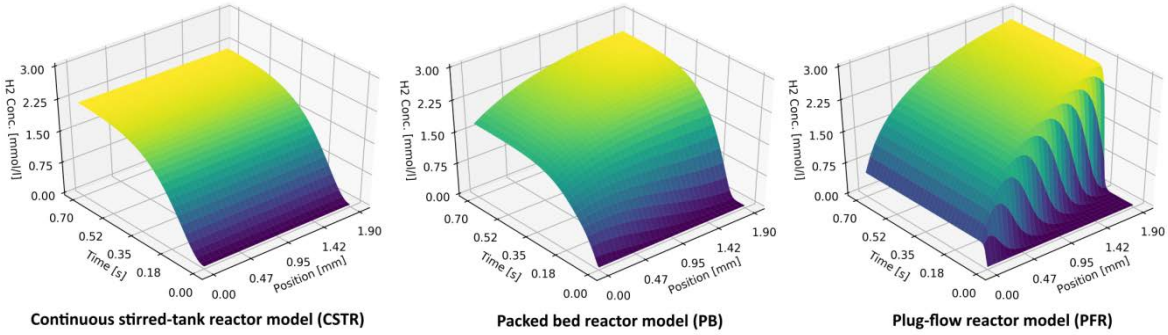

Figure 1. Comparison of different reactor models for the microkinetic RWGS reaction system. Depicted is the dependence of hydrogen concentration on the position of the reactor and the time in the simulation.

As seen in Figure 1, significant differences can be obtained when different models are used at the conditions in this study. This is due to the diffusion playing and important role at the gas flows and packed bed heights used. It can be seen that the packed bed reactor falls between the CSTR and PFR approaches with the degree of the reaction.

All of the models were used in numerical regression and the PB model gave the best fit to the experimental data. It was shown that with the improved model, it is possible to correctly predict the activity of copper based supported catalysts only from N_2O oxidation data, regardless of the supporting material used.

4. Conclusions

In this work, we show that for most experimental setups, gas diffusion plays an important role in mass transfer and has to be taken into account when modelling such systems. In addition, using the data obtained by experiments performed on different copper based catalysts, we explored various DFT-derived RWGS models from the literature and adjusted the best-fitting one to further improve its predictive power. It was shown that using N_2O oxidation data and our updated model, it's possible to correctly predict RWGS experimental activity of copper catalysts using different supporting materials.

References

[1] E. Schwab, A. Milanov, S. A. Schunk, A. Behrens, N. Schödel, Chemie Ing. Tech. 87 (2015) 347–353

[2] I. Fishtik, R. Datta, Surface Science 512 (2002) 229–254
[3] D. L. Jurković, A. Pohar, V. D. B. C. Dasireddy, B. Likozar, Chem. Eng. Technol. 40 (2017) 973–980
[4] Cohen S. D., Hindmarsh A. C.: Computers in Physics, 1996, 10(2), 138-143
[5] Powell M J D.: Acta Numerica, 1998, 7, 287-336

ECCE12
The 12th EUROPEAN CONGRESS OF CHEMICAL ENGINEERING
Florence 15-19 September 2019

Methane conversion to ethylene in nanosecond-pulsed discharge reactors

Evangelos Delikonstantis, Marco Scapinello, Georgios D. Stefanidis*

Process Engineering for Sustainable Systems, Department of Chemical Engineering, KU Leuven, Belgium

**Corresponding author: georgios.stefanidis@kuleuven.be*

Highlights

- Methane can be directly converted to ethylene at 20% yield and 2020 kJ/mol$_{C2H4}$ energy consumption in nanosecond pulse discharges at >3 bar without use of catalyst.
- 25.7% ethylene yield at 1642 kJ/mol$_{C2H4}$ can be attained from a two-step non-oxidative methane coupling process in a hybrid plasma-catalytic reactor.

1. Introduction

Ethylene, one of the most important commodity chemicals, is mainly produced by thermal cracking of long hydrocarbons but can also be formed from methane via non-oxidative coupling (NOMC). In view of crude oil depletion and abundant reach-in-methane gas reservoirs discovery, NOMC becomes an appealing route for ethylene formation. Processes, other than thermocatalytic ones, operating at lower temperatures and utilizing low-CO_2 electricity instead of heat are currently investigated for methane-to-ethylene conversion. Among them, non-thermal plasma can activate methane coupling reactions at lower temperatures, overcoming thermal losses in gas heating, while green electricity can be utilized for plasma ignition thereby avoiding fuel burning [1]. However, plasma is usually (i.e., at most common operating conditions) not very selective to ethylene since the energetic thresholds of the electron impact reactions of CH_3, CH_2 and CH (precursors of C_2H_6, C_2H_4 and C_2H_2, respectively) are comparable.

The present work focuses on ethylene production via NOMC in a nanosecond pulsed spark discharge. In this context, two process alternatives are developed and optimized: 1) a single-step selective conversion of methane to ethylene in plasma without use of catalyst; 2) a two-step process in which mainly acetylene is produced in the plasma zone and, subsequently, undergoes selective hydrogenation to ethylene in a catalyst zone downstream of the discharge, in a single reactor volume, using heat and H_2 produced in the discharge itself.

2. Methods

Plasma-assisted NOMC experiments were carried out in a tubular reactor comprising an inner, axial (2.2 mm diameter) copper-made wire (high voltage electrode) and an outer, co-axial (7 and 10 mm internal and external diameter, respectively) stainless-steel tube (ground electrode). The discharge gap was 2.4 mm wide while the coaxial plasma reactor length was 25 cm. The plasma reactor was powered by a nanosecond pulsed power supply (NPG-24/3000, Megaimpulse Ltd.,) triggered by a

waveform generator (33220A, Keysight Technology) at 3 kHz pulse frequency. A commercial Pd-based catalyst supplied by Johnson Matthey was used in the two-step process.

3. Results and discussion

High ethylene yield in a single step without catalyst use is attained in the discharge. At moderately elevated pressures (5 bar) and H_2 cofeeding (CH_4:H_2=1:1), acetylene formation is suppressed, and ethylene is produced at ~20% yield [2] per pass (Figure 1-left), consuming 2020 kJ/mol$_{C2H4}$. A reaction mechanism that explains the C_2 product distribution in this case has been suggested in Ref. [3]. Ethylene production at lower energy cost can be attained in a hybrid plasma-catalytic reactor system in which methane is first converted to acetylene in a nanosecond pulsed spark discharge, reaching up to 23.5% yield per pass, and, subsequently, acetylene is hydrogenated to ethylene by a Pd-based catalyst, which is placed in the post-plasma zone. Overall, ethylene is formed as major product at 25.7% yield per pass (Figure 1-right), consuming 1642 kJ/mol$_{C2H4}$. The two-step process is carried out in a single reactor volume that aside from the discharge energy does not require any additional heat or H_2 input since both are provided by methane cracking in the plasma zone itself.

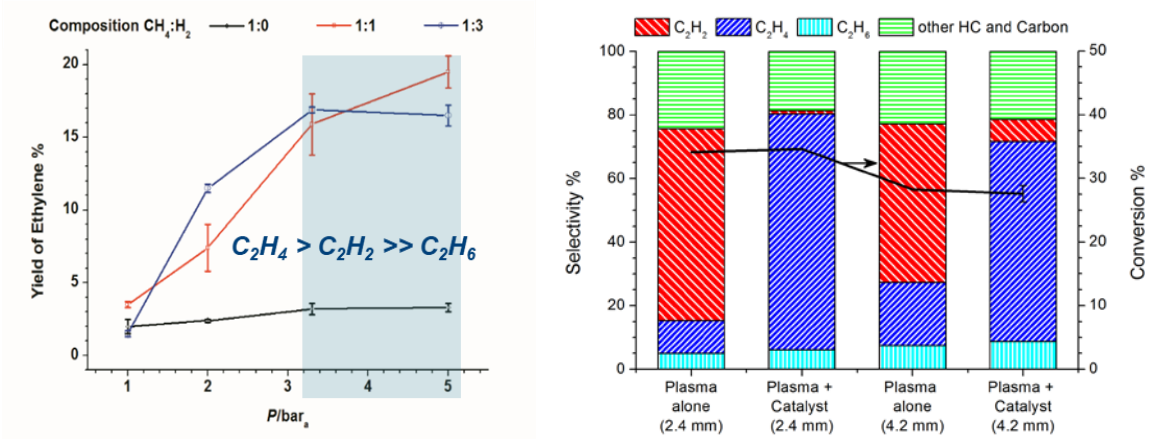

Figure 1. Ethylene formation as major product from methane in nanosecond pulsed discharges: *left*: single-step process operating at overpressure; *right*: two-step process operating at atmospheric pressure.

4. Conclusions

Ethylene can be produced as major product in nanosecond pulsed spark discharges via NOMC either in a single-step process at elevated pressures (>3 bar) without using catalyst, or in a two-step plasma-catalytic process operated at ambient pressure. 25.7% ethylene yield was attained in the two-step process at an energy consumption of 1642 kJ/mol$_{C2H4}$. This performance is relatively close to the recently published state-of-the-art using conventional thermal catalysis (23.4% ethylene yield at 1363 K) [4]. Compared to the latter work though, the advantages of the plasma process reported herein are that the exit bulk gas temperature is relatively low (650–750 K) and the technology is directly compatible with the emerging concept of powering chemical reactors with renewable electricity.

References

[1] E. Delikonstantis, M. Scapinello, G.D. Stefanidis, Processes. 7 (2019) 68.
[2] M. Scapinello, E. Delikonstantis, G.D. Stefanidis, Fuel. 222 (2018) 705–710.
[3] M. Scapinello, E. Delikonstantis, G.D. Stefanidis, Chem. Eng. J. 360 (2019) 64–74.

[4] X. Guo et al. Science. 344 (2014) 616–620.

ECCE12
The 12th EUROPEAN CONGRESS OF CHEMICAL ENGINEERING
Florence 15-19 September 2019

Traveling Microwave Reactor

Alberto Martínez González, Farnaz Eghbal Sarabi, Andrzej Stankiewicz, Hakan Nigar*

Process & Energy Department, Delft University of Technology, Leegwaterstraat 39, 2628CB, Delft, The Netherlands

**Corresponding author: H.Nigar@tudelft.nl*

Highlights

- Traveling Microwave Reactor (TMR) enables the process scale-up.
- Traveling-wave concept prevents the formation of a standing wave.
- It is suitable for high-energy demanding reactions, e.g., catalytic methane coupling
- TMR enables the temperature homogenization along the reactor.

1. Introduction

With the growing influence of renewable electricity as a primary energy source on Earth, the significance of the electricity-based technologies in process industries is likewise expected to increase. Microwave (MW) heating is a well-established electricity-based industrial technology employed on the commercial scale in various operations, such as drying, thawing, pasteurization, sintering, and ceramic processing. MW-assisted chemical reactions have been investigated for more than three decades, starting with liquid-phase homogenous systems then also in the heterogeneous solid gas-phase catalytic processes. Although there are many encouraging results of various laboratory-scale studies, commercial implementations of MWs in heterogeneous catalysis are non-existent. This is essentially due to the complexity of the interaction between MWs and solid catalysts, as well as to several important design factors influencing the performance of a continuously operated MW-assisted flow reactor [1]. The current study examines the above interactions and factors in a novel reactor concept, the so-called Traveling Microwave Reactor (TMR) [2]. The TMR concept will be validated on a high-energy demanding process, i.e., non-oxidative methane coupling.

2. Methods

The TMR has been designed based on the coaxial cable configuration. To do this, a three-dimensional finite element model, which couples electromagnetic waves and heat transfer, has been developed using the COMSOL MULTIPHYSICS® simulation environment. Figure 1 shows a cross-sectional schematic view of the modeled TMR along the axial direction. The TMR has been constructed with the stainless-steel inner and outer conductors, which form the coaxial structure having a reaction zone in between, see Figure 1. The reaction zone is an annular space between two concentric quartz cylinders. The heating tests have been conducted with different geometry (e.g., foams and extrudes) of silicon carbide (SiC) material in the packed-bed configuration. The temperature measurement has been performed with four thermocouples introduced inside the reactor through a hole in the inner conductor.

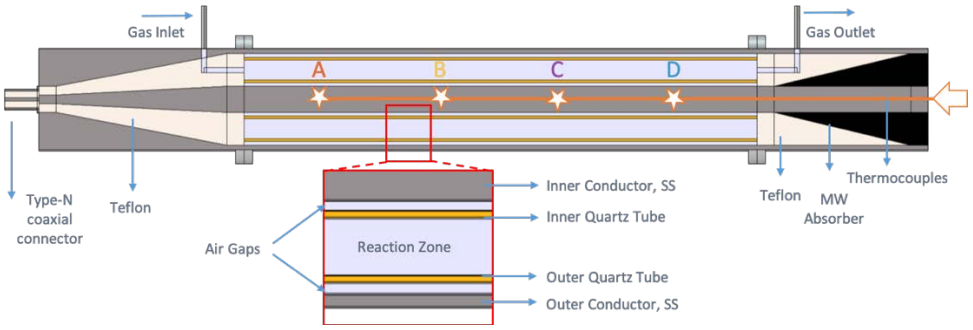

Figure 1. A cross-sectional schematic view of the TMR.

3. Results and discussion

Simulation results show that the MW energy is transported in the fundamental transverse electric and magnetic (TEM) mode, where the electric field lines run radially, while the magnetic field lines run in circles around the inner conductor. The good matching of spectral response and impedance characteristics shows that the behavior of the microwave model agrees well with the experimental setup which allows the validation of the model from the electromagnetic point of view. The transient temperature profile in the TMR fully loaded with a SiC packing is presented in Figure 2. The results reveal that the front part of the reactor has a temperature range 475-550ºC (thermocouples A, B, and C) and the final part has a range of 250-300ºC (thermocouple D). Since SiC is a good MW absorbent, most of the MW energy has been consumed in the front part of the reactor. Different packed-bed length and diameter are going to be further studied to improve the homogenous temperature distribution.

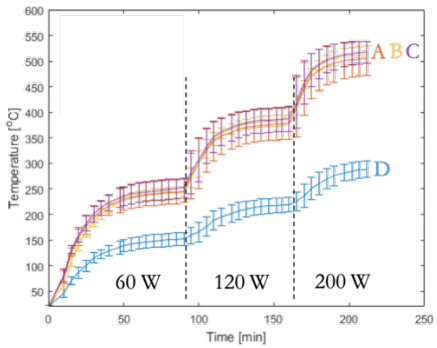

Figure 2. Transient temperature profiles with different MW power input.

4. Conclusions

A novel coaxial traveling microwave reactor is proposed to optimize the heat generation by avoiding the resonance. Simulation results prove that standing wave is not formed along the reactor and microwave energy travels ahead. Consequently, the heating uniformity in the TMR is expected to improve. To validate that expectation, heating characteristic of different catalysts in the designed reactor are under investigation. It is envisaged that this particular reactor concept may enable process scale-up beyond the intrinsic restrictions of cavity systems.

References

[1] A. Stankiewicz, F.E. Sarabi, A. Baubaid, P. Yan, H. Nigar, Chemical Record, 19 (2019) 40-50.
[2] G.S.J. Sturm, A. Stankiewicz, G.D. Stefanidis, RSC Green Chemistry (2016) 93-125.

ECCE12
The 12th EUROPEAN CONGRESS OF CHEMICAL ENGINEERING
Florence 15-19 September 2019

Development of a catalyst for oxidative coupling of methane in a gas-solid vortex reactor

Saashwath Swaminathan Tharakaraman[1], Guy B. Marin[1], Mark Saeys[1*]

1 Laboratory for Chemical Technology, Ghent University, Technologiepark 125, 9052 Gent, Belgium;

**Corresponding author: Mark.Saeys@ugent.be*

Highlights

- Synthesis of a thermally and mechanically stable catalyst for OCM in a GSVR.
- First demonstration of oxidative coupling of methane in GSVR.
- Process intensification of OCM

1. Introduction

Oxidative coupling of methane (OCM) is a promising pathway for the direct synthesis of C_2 hydrocarbons from methane according to the following global chemical reactions.[1]

$$2CH_4 + O_2 \rightarrow C_2H_4 + 2H_2O \qquad \Delta H_r^0 = -282 \text{ kJ mol}^{-1} \qquad (1)$$

$$2CH_4 + 0.5O_2 \rightarrow C_2H_6 + H_2O \qquad \Delta H_r^0 = -177 \text{ kJ mol}^{-1} \qquad (2)$$

The presence of oxygen and the high reaction temperature can facilitate the overoxidation of reactants and products to CO and CO_2, typically limiting the C_2 hydrocarbon yields to below 30%.[2]

$$CH_4 + 2O_2 \rightarrow CO_2 + 2H_2O \qquad \Delta H_r^0 = -801 \text{ kJ mol}^{-1} \qquad (3)$$

The high reaction exothermicity moreover dictates the need for a suitable heat management strategy.

In a gas-solid vortex reactor (GSVR), a rotating fluidized bed of solids is obtained by the tangential injection of gas at high velocities (Figure 1). [3] In the bed, the centrifugal forces on the catalyst particles balance the drag forces, leading to a dense and uniform bed. The very high gas-solid slip velocities intensify interfacial transfer of mass, energy and momentum, allowing a reduction in gas phase residence time. Using extensive computational fluid dynamics (CFD) simulations, a gas-solid vortex reactor has been designed and commissioned at Ghent University[3]. The diameter of the reaction chamber is 80 mm, containing 8 inlet slots with a width of 1 mm (Figure 1).[3]

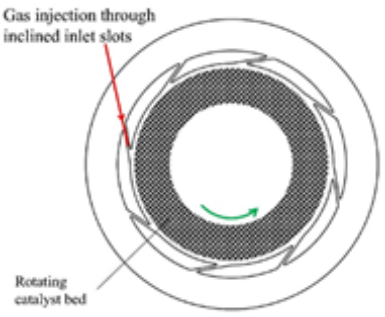

Figure 1 . Top view and operation of a gas solid vortex reactor in static geometry

Using bifurcation analysis incorporating detailed microkinetic models, Vandewalle et al. [4] showed that the good thermal back mixing combined with limited species back mixing in the GSVR can potentially improve C_2 yields when the reactor is operated on an ignited branch close to the extinction state. [5]

The high reaction temperature, the high solid velocities, and the low space times in the GSVR at those conditions require the development of a novel catalyst with high attrition resistance, high thermal stability, high activity, and proper size distribution. In this presentation, we report the

development of such a supported catalyst, and compare its performance in a fixed bed reactor with that in the GSVR.

2. Results and Discussion

Cold flow experiments were performed in the GSVR with inlet gas flow rates in the range of 15-30 $Nm^3\ hr^{-1}$, and slot velocities exceeding 100 m s^{-1} to test the stability of the catalyst bed and its attrition resistance. Under these conditions, a stable bed of 10 g of catalyst material with a thickness of about 10 mm could be retained in the GSVR at room temperature for a duration of 1 hour (Figure 2a). Over the 1 hour experiment, less than 1% of the material was entrained. Similar experiments with conventional Sr/La_2O_3 OCM catalyst pellets and with inert α-Al_2O_3 pellets resulted in rapid attrition and entrainment of the pulverised pellets with the gas stream. The gas flow rates and the catalyst material holdup in the GSVR correspond to very low space times of 0.1 $kg_{cat}\ s\ mol^{-1}_{CH4,0}$. For these space times, the synthesized catalyst material was tested in a quasi-isothermal fixed bed reactor at 800 °C and for a O_2:CH_4 inlet ratio of 4. A reasonable C_2 selectivity of 40-50% and a CH_4 conversion of 5-10 % were obtained for this high activity catalyst (Figure 2b). Typical OCM catalysts like Li/MgO and $NaMnWO_4/SiO_2$ show essentially no CH_4 conversion for space times below 5.0 $kg_{cat}\ s\ mol^{-1}_{CH4,0}$. [6] Next, the synthesized catalyst will be tested under reactive conditions in the GSVR. Based on detailed microkinetic simulations based on the fixed-bed experiments, a methane conversion of 4% and a C_2 selectivity of 45% are expected.

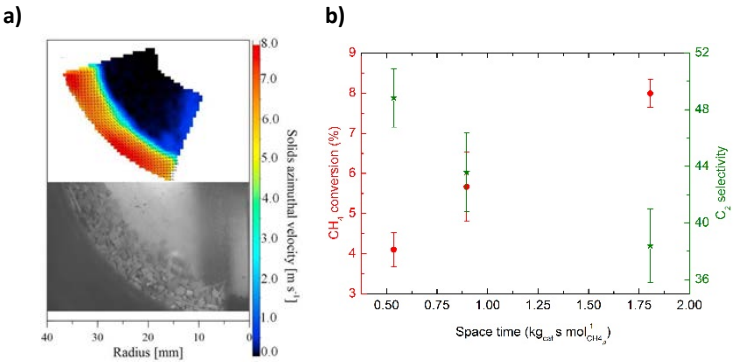

Figure 2 a) Azimuthal velocity of solids in the GSVR [3] and b) CH_4 conversion and C_2 selectivity vs. space time for synthesized catalyst at 800 °C

3. Conclusions

A thermally and mechanically stable OCM catalyst material was synthesized, which forms a stable catalyst bed under the harsh conditions in the GSVR reactor. At the conditions and at low space times, the synthesized catalyst material displayed a methane conversion between 5 and 10 % and a C_2 selectivity around 50%. Detailed simulations indicate that a similar performance can be expected in the GSVR. These proof-of-concept experiments are currently scheduled and will be reported at the conference.

References

[1] G. Keller, M. Bhasin. J. Cat. 73 (1982). 9-19.
[2] U. Zavyalova, M. Holena, R. Schlögl,M. Baerns. ChemCatChem 3 (2011). 1935-1947.
[3] A. Gonzalez-Quiroga, P.A. Reyniers, S.R. Kulkarni, M.M. Torregrosa, P. Perreault, G.J. Heynderickx, K.M. Van Geem,G.B. Marin. Chem. Eng. J .329 (2017). 198-210
[4] L.A. Vandewalle, I. Lengyel, D.H. West, K.M. Van Geem, G.B. Marin. Chem. Eng. Sci. (2018).
[5] S. Sarsani, D. West, W. Liang,V. Balakotaiah. Chem. Eng. J.328 (2017). 484-496
[6] V. Alexiadis, M. Chaar, A. van Veen, M. Muhler, J. Thybaut, G.B. Marin. App. Cat. B: Environmental 199 (2016). 252-259

ECCE12
The 12th EUROPEAN CONGRESS OF CHEMICAL ENGINEERING
Florence 15-19 September 2019

Enhancement of methane non-oxidative coupling performance: from metal incorporation strategies to selective catalyst heating via MW irradiation

Ignacio Julian[1,2,3], Jose L. Hueso[1,2,3,4], Scott Mitchell[3], Reyes Mallada[1,2,3,4], Jesus Santamaria[1,2,3,4]

[1] *Department of Chemical and Environmental Engineering, University of Zaragoza, Zaragoza (Spain)*

[2] *Institute of Nanoscience of Aragon (INA), University of Zaragoza (Spain)*

[3] *Institute of Materials Science of Aragon (ICMA), CSIC-University of Zaragoza (Spain)*

[4] *Networking Research Centre CIBER-BBN, 28029, Madrid (Spain)*

**Corresponding author: jlhueso@unizar.es*

Highlights

- Supercritical-solvothermal Mo/ZSM-5 synthesis boosts Mo dispersion and MDA stability
- The use of small polyoxometalates as Mo precursors of Mo/MCM-22 improves MDA performance
- Selective MW-assisted catalyst heating inhibits undesired gas-phase MDA reactions

1. Introduction

Non-oxidative methane coupling (MNOC) is a promising route to directly convert natural gas into more valuable hydrocarbons in one-step catalytic process. However, its industrial implementation is still hindered due to the relative low methane conversion and selectivity towards the products of interest as well as due to the low process stability derived from catalyst coking.

In the frame of the H2020 European Project ADREM (Adaptable Reactors for Resource- and Energy-efficient Methane Valorization), this works reports a multipurpose approach to enhance MNOC performance on the basis of the development of more stable and active catalysts and on the use of alternative heating sources to provide energy-efficient selective heating of the catalysts. The following topics were covered: 1) the development of a novel supercritical solvothermal synthesis for the benchmarking catalyst Mo/ZSM-5 in order to enhance metal dispersion and boost catalyst stability along the time on stream; 2) the use of small polyoxometalates as Mo precursors for the synthesis of Mo/MCM-22 in order to reduce the size of the initial Mo clusters and enhance metal dispersion in comparison to that obtained using the conventional Mo salts; 3) the use of microwave-assisted heating to improve the energy efficiency of the MNOC process while inhibiting the formation of heavy polyaromatics (i.e. hard coke precursors) as it is described by Julian et al. [1].

2. Methods

The supercritical solvothermal synthesis (SC-STS) of 5%Mo/ZSM-5, Si/Al = 23, was carried out using a self-built reactor set-up described elsewhere [2] in which a cold precursor solution

containing Mo with added support material (H-ZSM-5) is mixed with a hot solvent inside the reactor. Upon mixing at supercritical conditions, a super-fast precipitation of atomized metal precursor occurs within the zeolite pores.

A selection of polyoxomolybdate anions were employed as Mo precursors of Mo/MCM-22 catalysts under the assumption that the different structural arrangement of their Mo atoms within the polyoxometalate molecules would help to generate repulsion between discrete Mo centres, thereby avoiding the formation of Mo agglomerates on the zeolite surface and enhancing metal dispersion. MCM-22 (Si/Al = 20) was synthesized following the procedure of Corma et al. [3] and employed as support whereas the polyoxometallates were incorporated via incipient wetness impregnation.

All catalytic tests under conventional heating were carried out under benchmarking operational conditions: 700°C, 1500 mL/g_{cat}h, CH_4:N_2 = 80:20 and fixed bed configuration. Experiments performed under MW-heating were carried out at the same catalyst temperature and methane concentration but different space velocity (3000 mL/g_{cat}h).

3. Results and discussion

Comparing TEM micrographs (Figure 1.a) and MNOC catalytic performance of 5%Mo/ZSM-5 samples prepared by SC-STS and impregnation (Figure 1.b), it is found that both metal dispersion and hydrocarbon productivity are drastically improved using the proposed SC-STS method.

The Mo/MCM-22 catalysts prepared with the precursor $[(n\text{-}C_4H_9)_4N]_2[Mo_6O_{19}]$, especially the 5% Mo6/MCM-22 (Si/Al = 20), showed an excellent stability along 22 hours on stream keeping a nearly constant 5.8% benzene yield (>80% selectivity) without apparent catalyst deactivation, which is among the best reported long-term yields in literature for the MNOC process.

The use of MW-heating allowed inhibiting MNOC gas-phase reactions, i.e. polyaromatics production from the pool of methyl radicals and benzene molecules, thus, reducing hard coke deposition on the catalyst and enhancing catalyst stability.

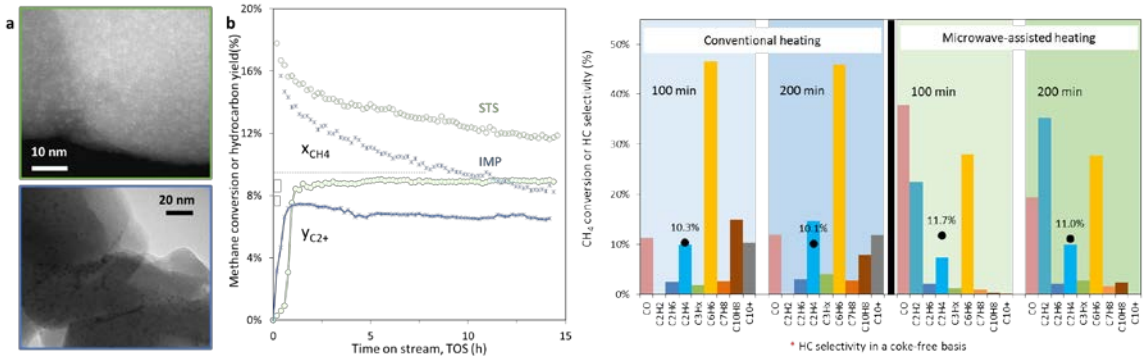

Figure 1. a) TEM micrographs illustrating metal dispersion provided by SC-STS and impregnation methods, b) experimental MNOC performance of 5%Mo/ZSM-5 catalysts prepared by SC-STS and IMP working at 700°C, 1500 mL/g_{cat}h and 0.5 g_{cat}, c) methane conversion and hydrocarbon products selectivity (coke-free basis) after 100 and 200 min on stream for MNOC on 4%Mo/ZSM-5@SiC operating at 700°C and 6000 mL/g_{cat}h under CH and MW heating

4. Conclusions

The three proposed approaches helped to enhance both catalyst stability and C_{2+} productivity with respect to conventional procedures, i.e. electrical heating and catalyst synthesis based on impregnation.

References

[1] I. Julian, H. Ramirez, J.L. Hueso, R. Mallada, J. Santamaria, Chem. Eng. J. (2018). *In press*.
[2] C. Kallesøe, H.F. Clausen, L.H. Christensen, EP Patent App. EP 3092067 A1 (2016).
[3] A. Corma, C. Corell, J. Pérez-Pariente, Zeolites 15 (1995) pp.2-8

ECCE12
The 12th EUROPEAN CONGRESS OF CHEMICAL ENGINEERING
Florence 15-19 September 2019

Optimal Scheduling and Operation of a Food Industrial Plant.

Georgios P. Georgiadis[1,2], Chrysovalantou Ziogou[2], Borja Mariño Pampín[3], Daniel Cabo[4], Miguel Lopez[4], Carlos G. Palacín[5], Cesar de Prada[5,6], Carlos Vilas[7], Antonio A. Alonso[7], Michael C. Georgiadis[1,2,*]

1 Department of Chemical Engineering, Aristotle University of Thessaloniki, Thessaloniki 54124, Greece; 2 Chemical Process and Energy Resources Institute (CPERI), Centre for Research and Technology Hellas (CERTH), PO Box 60361, 57001, Thessaloniki, Greece; 3 Frinsa del Noroeste S.A., Avenida Ramiro Carregal Rey – Parcela 29, Ribeira, La Coruña, Spain; 4 ASM Soft S.L., Crta de Bembrive 109, Vigo, Spain; 5 Dpt. Of Systems Engineering and Automatic Control, University of Valladolid, c/ Real de Burgos s/n, EII, 47011, Valladolid, Spain; 6 Institute of Sustainable Processes (IPS), University of Valladolid, C/Real de Burgos, s/n, Valladolid 47011, Spain;7 (Bio)Process Engineering Group, Instituto de Investigaciones Marinas (CSIC), C/ Eduardo Cabello,6 36208, Vigo, Spain

**Corresponding author: mgeorg@cperi.certh.gr*

Highlights

- Optimal short-term scheduling of a real-life food industrial facility

1. Introduction

Current market trends and business globalization have steered industries towards large production volumes, complex alternative recipes and a larger product portfolio, thus leading to processes of increased complexity. Optimal production scheduling has a direct impact on the overall efficiency of processing facilities and can lead to increased productivity and minimal costs. Although a plethora of works study the optimal production scheduling problem [1], academic developments have been mostly tested on generic but small problem instances. This is mainly due to the computational complexity of real industrial problems, which easily become intractable. This gap between theory and industrial practice has been identified by the scientific community [2] and some recent works have successfully investigated medium to large problem instances [3]. In this work different solution strategies are proposed for a large real-life food industry.

2. Methods

The case of a canned fish production facility for a large-scale Spanish industry (Frinsa del Noroeste, S.A.) is considered. The first main goal is to develop an optimized weekly schedule, in order to minimize an objective metric (makespan, total production costs). Since no clear production bottlenecks exist, all three processing stages (filling and sealing, sterilization, packaging) of the facility need to be considered. The proposed methodology consists of three main pillars: a) a batching algorithm which translates the incoming product-orders to batches and lot-sizes; b) an MILP-model based on the general precedence framework; and c) a two-step (temporal and order-based) decomposition strategy. In order to extract a valid schedule, the MILP-model, which constitutes the core of the suggested solution strategy, consists of all the necessary timing, sequencing and allocation constraints. Additionally, plant-specific operational constraints are imposed by adding tight integer cuts in the model.

Furthermore, mathematical models are derived in order to describe the specific features of the sterilization process including product quality and safety, energy consumption and processing times. Quality is related to the surface colour of the canned tuna after the sterilization whereas safety refers to thermal destruction of harmful microorganisms. Such models are used in an optimal schedule of the sterilization processes based on the feasible scheduling solution obtained on the first step. Consumption of shared resources is also considered in order to prevent an overlapping in the demands that, for example, could make the previous solution unfeasible in the real implementations. This new optimization problem can focus on the features previously calculated with the realistic models, such as minimizing colour lost if the plant requires a special production, or increasing production by minimizing the sterilization process duration keeping the microorganism lethality over the security limit. The optimization focus on providing a real-time tool that helps the operator, which makes the horizon required to solve short, but increase the resolution speed requirements.

3. Results and discussion

The MILP model was implemented in GAMS 25.1 and solved using CPLEX 12.0. Optimality is reached for all iterations of the suggested solution strategy. Moreover, the problem is solved in a time acceptable by the company (1 hour). Compared to the real weekly schedule proposed by Frinsa, no overtime production during weekends was required.

Mathematical models for the sterilization process were developed. Order reduction techniques were implemented to increase simulation efficiency.

The sterilization optimal schedule is solved in a few minutes, which makes the solution suitable for launching the resolution each half an hour and obtaining a two hours prediction.

4. Conclusions

This work presents the optimization-based production scheduling and operation of a real-life food industry of high complexity. It was shown that the proposed strategy can schedule the plant under study and eliminate unnecessary overtime production.

Acknowledgements

The work leading to this publication has received funding from the European Union's Horizon 2020 research and innovation program under grant agreement No 723575 (Project CoPro) in the framework of the SPIRE PPP.

References

[1] Méndez, C.A., Cerdá, J., Grossmann, I.E., Harjunkoski, I., Fahl, M., 2006. State-of-the-art review of optimization methods for short-term scheduling of batch processes. Comput. Chem. Eng. 30, 913–946.

[2] Harjunkoski, I., Maravelias, C.T., Bongers, P., Castro, P.M., Engell, S., Grossmann, I.E., Hooker, J., Méndez, C., Sand, G., Wassick, J., 2014. Scope for industrial applications of production scheduling models and solution methods. Comput. Chem. Eng. 62, 161–193.

[3] Kopanos, G.M., Puigjaner, L., Georgiadis, M.C., 2010. Optimal Production Scheduling and Lot-Sizing in Dairy Plants : The Yogurt Production Line. Ind. Eng. Chem. Res. 49, 701–718.

ECCE12
The 12th EUROPEAN CONGRESS OF CHEMICAL ENGINEERING
Florence 15-19 September 2019

Optimal Site-Wide Planning of A NH_3 Network – A Study on Uncertain Logistic Constraints –

Simon Wenzel[1,*], Yannik-Noel Misz[1], Keivan Rahimi-Adli[1,2], Benedikt Beisheim[1,2], and Sebastian Engell[1]

1 TU Dortmund University, Biochemical and Chemical Engineering, Process Dynamics and Operations Group, Emil-Figge-Straße 70, 44227 Dortmund, Germany;
2 INEOS Manufacturing Deutschland GmbH, Alte Straße 201, 50769 Köln, Germany

**Corresponding author: simon.wenzel@tu-dortmund.de*

Highlights

- Optimal scheduling for physically coupled production plants.
- Application to an NH_3 network at an integrated petrochemical production site.
- Investigation of uncertain logistics in the supply chain on the optimal schedule.

1. Introduction

Many companies in the process industries operate in a highly competitive market environment and are thus obliged to improve continuously their production in terms of energy and material efficiency and to become greener [1]. In general, the value chain of chemical production consists of several, sometimes many production steps and complex interactions between these production steps exist, which lead to highly integrated and physically coupled systems of systems [2]. In large (petro-) chemical production sites, complex networks of flows of material and carriers of energy link the production plants. For an optimal operation of the overall system, mathematical modeling of the constituent systems and a joint optimization has to be employed to find site-wide optimal and feasible operating conditions according to different objectives such as material efficiency, reduction of carbon footprint, or economic performance indicators. The scope of such an optimization can, however, not be limited to the units and buffers of the production site, but it also has to consider exogenous influences such as fluctuating market prices for energy and raw materials and the logistics of their provision and distribution. Recently, there has been an increased interest in expanding the domain of optimization and thus enlarging the scope of the formulated optimization problems to include these aspects [3].

2. Method and case study

In [4], a mixed-integer linear program (MILP) optimization model with an expanded scope that includes demand side management (DSM), network optimization, plant optimization, and logistic constraints has been proposed for site-wide scheduling of integrated petrochemical production sites. It has been parametrized to generate a one month optimal schedule for the NH_3 network of INEOS in Köln, a large petrochemical production site in Germany. The logistic constraints cover the

deliveries to and the shipping of raw materials and base chemicals from the site via barges on the river Rhine and via train vessels. The nature of the solution of MILP is that the resulting schedule operates at the bounds, e. g., a tank is emptied just before a barge arrives. In practice, however, many exogenous influences and thus also the logistic constraints are not known precisely ahead of time. For instance, in Germany in the summer of 2018, the river Rhine was at such a low water levels that barges could only carry a fraction of their usual load or were even not able to deliver at all. Many chemical companies that are dependent on barge deliveries had to reduce their capacities or even had to shut down complete plants or production complexes.

3. Investigated scenario

In this contribution, we investigate the sensitivity of the optimal schedule for the operation of the INEOS in Köln production site with respect to this kind of events. We analyze the situation of a delayed barge, which is a common situation in daily operation. With the help of the formulated optimization model, we identify which measures should be taken in a critical situation. We investigate which process or plant has to reduce its load first or which production capacities can be shifted in order to ensure a seamless operation of the coupled production plants.

4. Conclusions

The analysis of the sensitivity of the optimal schedule for the operation of the NH_3 network at INEOS in Köln reveals important insights into where the site runs into critical limitations in a situation of unforeseen uncertain events such as delayed ships. The analysis is applicable to answer similar what-if scenarios for structurally related questions such as unforeseen equipment failures or plants shutdowns. The proposed optimization model offers a powerful tool to guide the planners' decisions at large (petro-) chemical production sites in the process industries.

Acknowledgement

The project leading to this publication has received funding from the European Union's Horizon 2020 research and innovation programme under grant agreement No 723575 (CoPro) in the framework of the SPIRE PPP.

References

[1] R. Baños, F. Manzano-Agugliaro, F. G. Montoya, C. Gil, A. Alcayde, and J. Gómez, "Optimization methods applied to renewable and sustainable energy: A review," Renew. Sustain. Energy Rev., vol. 15, no. 4, pp. 1753–1766, May 2011.

[2] S. Engell and C. Sonntag, Eds., Proposal of a European Research and Innovation Agenda on Cyber-physical Systems of Systems, 2016-2025. CPSoS EU Project, 2016.

[3] P. M. Castro, I. E. Grossmann, and Q. Zhang, "Expanding scope and computational challenges in process scheduling," Comput. Chem. Eng., vol. 114, pp. 14–42, Jun. 2018.

[4] S. Wenzel, Y.-N. Misz, K. Rahimi-Adli, B. Beisheim, R. Gesthuisen, and S. Engell, "An optimization model for site-wide scheduling of coupled production plants with an application to the ammonia network of a petrochemical site," Optimization and Engineering, pp. 1-31, Mar. 2019.

ECCE12
The 12th EUROPEAN CONGRESS OF CHEMICAL ENGINEERING
Florence 15-19 September 2019

Optimal Production Scheduling in the Packaged Consumer Goods Industry

Apostolos P. Elekidis[1,2], Vassilios Yfantis[3], Francesc Corominas[4], Michael C. Georgiadis[1,2*], Sebastian Engell[3*]

1 Department of Chemical Engineering, Aristotle University of Thessaloniki, Thessaloniki 54124, Greece; 2 Chemical Process and Energy Resources Institute (CPERI), Centre for Research and Technology Hellas (CERTH), PO Box 60361, 57001, Thessaloniki, Greece; 3 Process Dynamics and Operations Group, Department of Biochemical and Chemical Engineering, TU Dortmund University, Emil-Figge-Str. 70, 44227 Dortmund, Germany; 4 Procter & Gamble, Temselaan 100, 1853 Strombeek-Bever, Belgium

**Corresponding authors:* mgeorg@cperi.certh.gr, sebastian.engell@tu-dortmund.de

Highlights

- Real-life large-scale consumer goods industrial case study
- MILP-based decomposition algorithm
- Plant reconfiguration
- Flexible production layout

1. Introduction

The ever-increasing competitiveness of large-scale industries necessitates the increase of productivity and minimization of production costs. Production scheduling has a direct impact on the overall efficiency of industrial facilities by minimizing, among others, changeover times which cause production downtimes, waste and energy consumption/use of resources. Potential plant reconfigurations also provide significant room for improvements of the overall productivity. Although production scheduling problems have received significant attention [1], the majority of the work is focused on relatively small to medium size problem instances. A few recent contributions have studied the application of scheduling techniques in medium- and large-scale industries [3]. In this work two MILP-based approaches are proposed for the optimization-based scheduling of a real-life large-scale consumer goods production plant. The first approach focuses on the optimal scheduling of the current plant layout while the second one is applied to a reconfigured flexible layout allowing the decoupling of the formulation and packing stages.

2. Methods

2.1 Current Layout

An MILP-based decomposition algorithm is proposed for the optimal production scheduling of the current plant layout focusing on the packing stage. The proposed MILP model optimizes the production sequence while considering constraints related to the allocation of the final products as well as the timing of processing steps [2]. Products' due dates, as well as appropriate constraints referring to the production/formulation stage of the plant, are taken into account to ensure near-optimal production schedules. The algorithm operates on an iterative fashion and a subset of the involved product orders is scheduled at each iteration.

2.2 Reconfigured flexible layout

In order to avoid varying bottlenecks in the process due to the product dependent maximum production rate of the formulation and the packing stage, the two stages can be decoupled. In the current layout the stages are closely coupled in each line, whereas the flexible layout relaxes these connections and includes an additional shared buffer between the two stages. The solution approach is again based on an MILP model and a decomposition algorithm, the main difference being the inclusion of material balances due to the limited capacity of the buffer.

3. Results and discussion

3.1 Current layout

A number of different case studies with varying numbers of products have been examined using the aforementioned scheduling algorithm and detailed near-optimal production schedules have been generated. Results indicate that a significant reduction in the changeover time can be achieved even for problems with more than 120 products.

3.2 Reconfigured flexible layout

A number of different case studies were examined for the flexible layout as well, again employing an optimization-based decomposition scheduling algorithm. The results demonstrate potential improvements, should this layout be adopted. Good schedules were obtain within very short computation time, which poses a major benefit, as computational efficiency is a key priority in an industrial setting.

4. Conclusions

In this work two mathematical frameworks, relying on MILP-based decomposition algorithms, were proposed for the optimization-based production scheduling of a packaged consumer-goods plant. The first approach considers the plant in its current layout, while the second examines a potential flexible layout. A case study with real-life data is used to illustrate the applicability and efficiency of the proposed approaches leading to a noticeable reduction of the changeover times.

5. Acknowledgements

The work leading to this publication has received funding from the European Union's Horizon 2020 research and innovation program under grant agreement No 723575 (Project CoPro) in the framework of the SPIRE PPP.

References

[1] Méndez, C.A., Cerdá, J., Grossmann, I.E., Harjunkoski, I., Fahl, M., 2006. State-of-the-art review of optimization methods for short-term scheduling of batch processes. Comput. Chem. Eng. 30, 913–946.
[2] Kopanos G.M., Méndez C.A., Puigjaner L., 2010, MIP-based decomposition strategies for large-scale scheduling problems in multiproduct multistage batch plants: A benchmark scheduling problem of the pharmaceutical industry, *European Journal of Operational Research*, 207, 2, 718-735
[3] Kopanos, G.M., Puigjaner, L., Georgiadis, M.C., 2010. Optimal Production Scheduling and Lot-Sizing in Dairy Plants : The Yogurt Production Line. Ind. Eng. Chem. Res. 49, 701–718.

ECCE12
The 12th EUROPEAN CONGRESS OF CHEMICAL ENGINEERING
Florence 15-19 September 2019

Energy-efficient Operation of a Multi-unit Recovery Cycle in EU's largest Viscose Fiber Plant.

José Luis Pitarch[1], Christian Jasch[2], Marc Kalliski[3], Yannik-Noel Misz[3], María P. Marcos[1,4], César de Prada[1,4], Gerhard Seyfriedsberger[2], Sebastian Engell[3]

1 *Systems Engineering and Automatic Control department, Universidad de Valladolid. C/Real de Burgos S/N, 47011, Valladolid, Spain;* ***2*** *Lenzing AG. Werkstraße 2, 4860, Lenzing, Austria;* ***3*** *Department of Biochemical and Chemical Engineering, Technische Universität Dortmund, Emil-Figge-Str. 70, 44221, Dortmund, Germany;* ***4*** *Institute of Sustainable Processes, Universidad de Valladolid. C/Real de Burgos S/N, 47011, Valladolid, Spain.*

**Corresponding author: jose.pitarch@autom.uva.es*

Highlights

- Improved control and real-time process optimization leads to substantial savings.
- Monitoring and modelling the performance degradation in equipment is key.
- Integrating control, optimization and maintenance scheduling is the future path.

1. Introduction

Lenzing AG in Austria is the world's largest viscose fiber production plant. Lenzing's fibers are made from wood: They are botanic products derived from renewable sources and processed with resource conserving technologies. The production of these high-quality viscose fibers is a multi-step chemical technological process. The key role in terms of resource efficiency within the viscose-fiber production belongs to the spinbath recovery cycle. The recovery cycle itself (see Figure 1) is a sequence of basic operations carried out in several multi-unit networks. Due to its high-energy demand, the LENZING use case within the SPIRE project CoPro is particularly focused on the evaporation stage and the heat-recovery network.

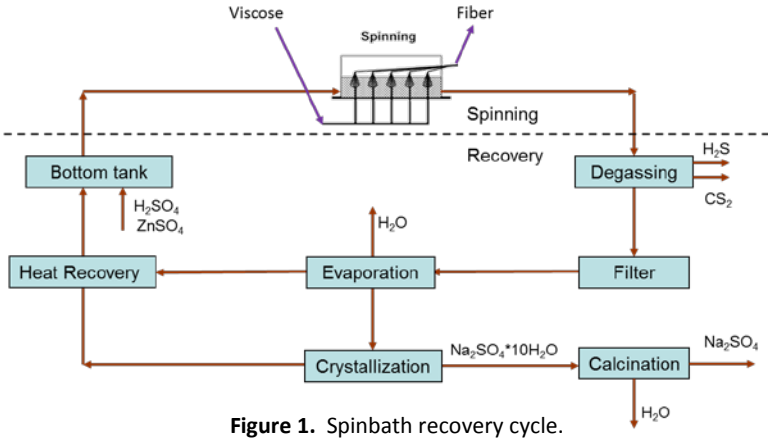

Figure 1. Spinbath recovery cycle.

2. Challenges

The first challenge concerns with the evaporation stage, where about 30 plants of different capacities and performances need to be allocated to recover the spinbath of around 10 lines of fibers production. Furthermore, in addition to fulfill continuous production demands, operational constraints such as possibility of physical connection or plants temporal availability need to be enforced. And, of course, this load allocation from spinbaths to plants needs to be done in the most energy-efficient way, i.e. with minimum specific-steam consumption (SSC).

Additionally to the above allocation problem, the evaporation plants suffer from performance degradation due to fouling inside the heat exchangers. Various cleaning operations can be chosen to

get rid of the fouling effects, but the personnel for maintenance is limited, so only a single plant can be cleaned per day. Hence, a *feasible* (must) and *optimal* (desired) scheduling of the maintenance operations over time is to be found. However, this is not independent from load allocation, and it is also affected by uncertainty in future predictions of production demands and weather. Therefore, an integral real-time scheduling optimization is a desirable outcome of the CoPro project.
Some of the plants are equipped with surface condensers as cooling systems. These condensers are fed with river water and the issue is: the more water is directed to the condensers, the more efficient the plants are. However, water is shared in a network with other parts of the factory, and its usage is subject to environmental regulation. Thus, an additional problem is to find the optimal water distribution to the evaporation network. But, this task is coupled with the plants allocation, as varying performance of the cooling systems may enable different decisions in the load allocation. Therefore, a tradeoff between plants efficiency and water usage is to be set up for optimization.

3. Results so far and outlook

In order to address the above challenges, a physics-based grey-box model for an evaporator was initially built to find the optimal control policy (lowest SSC) and to study the fouling effects [1]. Then, based on this work, simplified surrogate models for each plant operating with the new control were built. These models (updated periodically) serve in a mixed-integer quadratic optimization which suggests the best plant allocation to spinbaths in near-real time [2]. Savings of around 250 k€/year (1.8% more efficient operation) were gathered with the new decision support system (DSS). In parallel to this, models to predict the performance loss over time due to fouling were identified from experimental tests so that, by balancing the operation and cleaning costs, nonlinear optimization problems predict the best future day for cleaning in each plant, as well as the optimal cleaning task [1],[2]. Preliminary tests onsite with 5 plants show a potential benefit of 25 k€/year. The implementation to the whole evaporation network and heat-recovery one as well is ongoing.
Regression models for the surface condensers have been also identified from experiments, measuring the SSC variations at different water flows and temperatures. With these, a nonlinear optimization suggests the best water distribution to plants by balancing the savings in SSC with the water costs (subject to usage constraints) [3]. This setup can be integrated with the load-allocation optimization in a centralized fashion, and solved in near-real time using BONMIN. Tests in simulation show additional savings about 200 k€/year, but these may be too optimistic, as the effects of limiting the water usage in other parts of the factory is not considered yet in the optimization.
Finally, the integration of the plants load allocation and maintenance scheduling is already set up and tested in simulation with reasonable computational demands [4]. However, including uncertainty via scenarios in a two-stage optimization approach increases considerably the problem complexity (hence, resolution time) so alternatives for problem decomposition are under study.

References

[1] J.L. Pitarch, C.G. Palacín, C. De Prada, B. Voglauer, G. Seyfriedsberger. Optimisation of the resource efficiency in an industrial evaporation system. Journal of Process Control, 56, 2017, pp. 1–12.
[2] M. Kalliski, J.L. Pitarch, C. Jasch, C. de Prada. Support to Decision-Making in a Network of Industrial Evaporators. Revista Iberoamericana de Automática e Informática Industrial, 16(1), 2019, pp. 26-35.
[3] M.P. Marcos, J.L. Pitarch, C. de Prada, C. Jasch. Modelling and real-time optimisation of an industrial cooling-water network. 22nd Inter. Conf. on System Theory, Control and Computing, 2018, pp. 591-596.
[4] C.G. Palacín, J.L. Pitarch, C. Jasch, C.A. Méndez, C. de Prada. Robust Integrated Production-Maintenance Scheduling for an Evaporation Network. Computers & Chemical Engineering, 110, 2018, pp. 140-151.

ECCE12
The 12th EUROPEAN CONGRESS OF CHEMICAL ENGINEERING
Florence 15-19 September 2019

Workshop on Crystallization Science and Engineering

Continuous crystallization to separate enantiomers exploiting two coupled fluidized bed crystallizers

Andreas Seidel-Morgenstern
Max-Planck-Institut für Dynamik komplexer technischer Systeme, Magdeburg, Germany

**Corresponding author:* seidel-morgenstern@mpi-magdeburg,mpg.de

Crystallization is one of the most effective ways to separate mixtures of enantiomers. Preferential Crystallization (PC) has proven to be applicable to provide selectively pure enantiomers from racemic mixtures of conglomerate forming systems [1]. Primarily batch processes are used so far. However, there are intensive efforts to develop continuous enantioselective crystallization processes [e.g. 2,3].
This contribution presents results of applying a fluidized bed crystallizer configuration for the continuous provision of enantiomers from a racemic feed solution. Objective is the supply of pure crystals with a defined narrow size distribution. To crystallize both enantiomers simultaneously two tubular fluidized bed crystallizers are coupled via their liquid phases. Saturated racemic solution is supplied at the bottom of the double jacketed crystallizers. To initiate the separation process seed crystals of both enantiomers are added. The growth of these crystals reduces the supersaturation of the processed liquid phases. The depleted mother liquors of both crystallizers are recycled via heated tubes into the feed tank. Thus, a racemic composition of the feed solution is maintained. A special feature of the process is the fact that the lower sections of both crystallizers are conical to offer the opportunity of classified product removal at certain heights [4]. This allows adjusting the mean product crystal sizes via the feed flowrate and provides narrow size distributions [5]. To ensure that the process operates continuously, larger particles and formed agglomerates are crushed in a mill. The fragments are returned as continuous seed streams. Undesired nuclei of the counter enantiomer and small particles leave the crystallizers with the fluid phases and are dissolved on the way back to the feed reservoir.

We will describe results of an interdisciplinary project devoted to solve three tasks. At first, the impact of important operating conditions (e.g. crystallization temperature and the various flowrates) is studied experimentally for two chiral systems. Secondly, the hydrodynamics of the two-phase flow are evaluated using Computational Fluid Dynamics (CFD) and the Discrete Element Method (DEM) [6, 7]. Further, in order to be able to optimize the crystallizer geometry and the operating conditions, a reduced process model based on population balances is developed exploiting Proper Orthogonal Decomposition (POD) [8,9].

Acknowledgment:

The financial support of Deutsche Forschungsgemeinschaft (DFG, Priority Program SPP 1679 "Dynamic simulation of interconnected solids processes") is gratefully acknowledged.

References

1. Lorenz H., Seidel-Morgenstern A., Process to separate enantiomers, Angew. Chem. Int. Ed. 53, 2014, 1218-1250.
2. Galan K., Eicke M.J., Elsner M.P., Lorenz H., Seidel-Morgenstern A., Continuous Preferential Crystallization of Chiral Molecules in Single and Coupled Mixed-Suspension Mixed-Product-Removal Crystallizers, Cryst. Growth Des., 15, 2015, 1808-1818.
3. Köllges, T., Vetter, T., Design and Performance Assessment of Continuous Crystallization Processes Resolving Racemic Conglomerates, Cryst. Growth Des., 18, 2018, 1686-1696.
4. Tung H.-H., Paul E.L., Midler M., McCauley J.A., Crystallization of Organic Compounds: An Industrial Perspective, Wiley, Hoboken, New Jersey, 2009.
5. Binev D., Seidel-Morgenstern A., Lorenz H., Continuous separation of isomers in fluidized bed crystallizers, Cryst. Growth Des., 16, 2016, 1409-1419.
6. Kerst, K., Medeiros de Souza, L., Bartz, A., Seidel-Morgenstern, A., Janiga, G., CFD-DEM simulation of a fluidized bed crystallization reactor, Comput. Aided Chem. Eng., 37, 2015, 263-268.
7. Kerst K., Roloff C., Medeiros de Souza L.G., Bartz A., Seidel-Morgenstern A., Thévenin D., Janiga G., CFD-DEM simulations of a fluidized bed crystallizer, Chem. Eng. Sci. 165, 2017, 1–13.
8. Mangold M., Khlopov D., Palis S., Feng L., Benner P., Binev D., Seidel-Morgenstern A., Nonlinear model reduction of a continuous fluidized bed crystallizer, J. Comput. Appl. Math., 289, 2015, 253-266.
9. Mangold M., Khlopov D., Temmel E., Lorenz H., Seidel-Morgenstern A., Model based analysis of a continuous fluidized bed crystallizer for separation of enantiomers, Chem. Eng. Sci., 160, 2017, 281-290.

ECCE12
The 12th EUROPEAN CONGRESS OF CHEMICAL ENGINEERING
Florence 15-19 September 2019

Workshop on Crystallization Science and Engineering

Model-based analysis of continuous crystallization-milling processes with respect to productivity, particle size and polymorphic purity

Thomas Vetter

Department of Chemical Engineering and Analytical Science, University of Manchester, Oxford Road, M13 9 PL, Manchester, United Kingdom

thomas.vetter@manchester.ac.uk

Highlights

- Continuous crystallization processes of varying complexity are analyzed using population balance equation models.
- Attainable regions of particle sizes are identified for various continuous crystallization processes.
- For polymorphic systems, regions where phase pure material can be generated are identified and rationalized in terms of the required operating conditions.

Manufacturing pure material at a reasonable productivity and with good robustness is the goal of any industrial crystallization process. In this contribution, a few case studies will be presented where continuous crystallization processes have been analyzed using population balance equation models. The case studies will include works that elucidate the envelope of feasible product particle sizes from a given continuous crystallization process[1,2], as well as works where innovative milling/crystallization processes coupled with ancillary unit operations have been used to generate polymorphically[3,4] pure products. Across both sets of works, feasible operating conditions were identified and the process performance (with respect to yield, mean particle size, and phase purity) within this feasible region was investigated. While using the devised models quantitatively for this purpose relies on suitable kinetic parameters, it will be shown that even the qualitative (and quite general!) trends obtained from the models are of great use from a process design perspective.

References

[1] T. Vetter, C.L. Burcham, M.F. Doherty, Chem. Eng. Sci. 106 (2014) 167-180.
[2] T. Vetter, C.L. Burcham, M.F. Doherty, Ind. Eng. Chem. Res. 54 (2015) 10350-10363.
[3] T. Köllges, T. Vetter, Org. Process Res. Dev. 23 (2019) 361-374.
[4] Y. Li, S. O'Shea, Q. Yin, T. Vetter, Cryst. Growth Des. 19 (2019) 2259-2271.

ECCE12
The 12th EUROPEAN CONGRESS OF CHEMICAL ENGINEERING
Florence 15-19 September 2019

Workshop on Crystallization Science and Engineering

Process Analytical Tools for Monitoring, Design and Model-free Control of Crystallization Systems

Zoltan K Nagy[1, 2, *]

[1] Department of Chemical Engineering, Loughborough University, Loughborough, LE11 3TU, United Kingdom;

[2] Davidson School of Chemical Engineering, Purdue University, West Lafayette, IN, 47907, United States

*Corresponding author: z.k.nagy@lboro.ac.uk

Highlights

- Process analytical tools for crystallization will be reviewed
- Application of model-free feedback control will be presented
- Monitoring and control of batch and continuous crystallization systems

1. Introduction

In the absence of a dedicated monitoring and control system, industrial crystallizers often perform sub-optimally, which is mostly reflected in a low-quality product with a wide or multimodal size distribution, undesirable mean crystal size, a sub optimal crystal shape or an unwanted crystal structure. Recent developments in in situ monitoring, modeling as well as in both model-free and model-based control strategies, however enable new opportunities in the design and application of control strategies for practical applications (Nagy and Braatz, 2012; Nagy et al., 2013). **2.**

2. Results and discussion

This lecture provides an overview of the state-of-the-art in the monitoring and model-free control of industrial crystallization processes and through a series of case studies illustrates how these recent developments can contribute to better product quality and improved performance of industrial crystallization systems. The advantages of using integrated in situ and in line monitoring systems as a composite sensor array in conjunction with a crystallization process informatics system will be illustrated, which enables robust data reconciliation, automated calibration and sensor fault detection as well as an intelligent, rapid design and of robust crystallization processes with precise control of critical quality attributes (Fig. 1). The key process analytical tools (PATs) that can be used for in situ monitoring of crystal size, shape, polymorphic form and purity will be described. Model-free control approaches, such as supersaturation control (SSC) and direct nucleation control (DNC) will be described and illustrated with industrial case studies. The control of batch, continuous stirred tank and tubular crystallization systems will be corroborated. The final part of the lecture will introduce the application of monitoring and control systems for novel integrated systems to achieve high degree of control of various crystal properties, including integrated crystallization and wet mill process and continuous plug flow crystallization platforms with spatially distributed control strategy and controlled spherical crystallization that enable the simultaneous control of the trade-off between bioavailability and manufacturability of the final product.

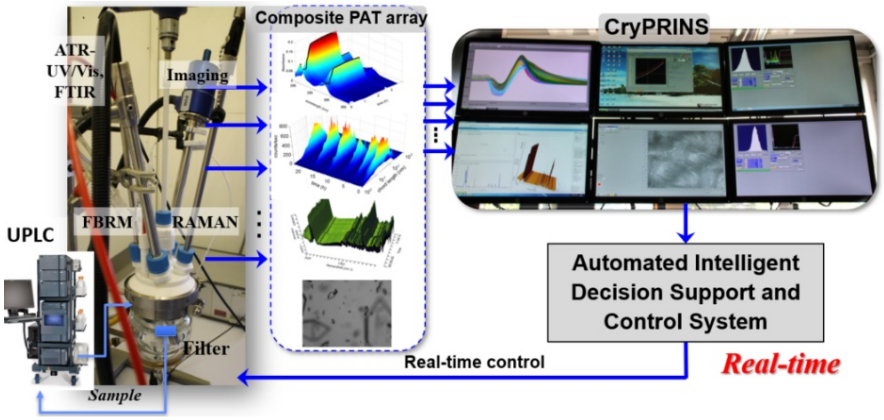

Figure 1. Fully automated batch/continuous reactor/crystallization platform with array of in situ and in line PAT.

References

[1] Nagy, Z. K., Braatz, R. D. (2012). Advances and new directions in crystallization control, Annu. Rev. Chem. Biomol. Eng., 3, 55-75.

[2] Nagy, Z.K., Fevotte, G., H., Kramer, Simon, L.L. (2013). Recent advances in the monitoring, modelling and control of crystallization systems, Chem. Eng. Res. Des., 91 (10), 1903-1922.

ECCE12
The 12th EUROPEAN CONGRESS OF CHEMICAL ENGINEERING
Florence 15-19 September 2019

Workshop on Crystallization Science and Engineering

Applications of Crystallization Science and Engineering to Industrial Processes

Brian Glennon

APC Ltd, Cherrywood Business Park, Loughlinstown Co. Dublin, Ireland

**Corresponding author: brian.glennon@apprcess.com*

Highlights

- Thermodynamics and kinetics
- Diastereomeric and enantiomeric separations
- PAT applications

1. Introduction

A challenge in the translation of academic research into industrial applications is achieving alignment between the requirements for academic rigor and originality and the industrial demands for minimizing cost and time while maximizing quality.

In this presentation, examples of efforts to streamline the implementation of complex crystallization methods in addressing industrial crystallization challenges will be presented.

ECCE12
The 12th EUROPEAN CONGRESS OF CHEMICAL ENGINEERING
Florence 15-19 September 2019

Particle generation process by crystallization : a multiscale approach.

Béatrice Biscans

Laboratoire de Génie Chimique CNRS/INP/UPS

Toulouse FRANCE

**Corresponding author: beatrice.biscans@ensiacet.fr*

Crystallization science and engineering workshop organized by EFCE Working Party on Crystallization

Crystallization is a separation and purification process used in the production of a wide range of materials. Many aspects of industrial crystallization have been developed in the past years and have a good scientific basis. Recent developments are in progress such as isolation of polymorphs and resolution of enantiomeric systems, molecular modelling, effect of added impurities on the crystal growth process, use of computed aided fluid dynamic modelling or new methods for crystal characterization. However, new challenges arise from new industrial needs. These developments create research on complicated substances such as drugs or proteins in complicated or new solvents or multi-phase systems and lead to consider what is called “complex media”.

This presentation gives some examples of crystallization in complex media. Different reactor scales are used as generic tools studying crystal nucleation and growth.

Scale 1: an original microfluidic device was developed for investigating nucleation rate, growth kinetics, and phase transition of organic crystals in organic solvents (1,2) . This set-up allows to store up to 2000 small crystallization containers (20 to 100nL) and to control precisely their temperature and supersaturation. The case of eflucimibe showing two polymorphs and ibuprofen,in different organic solvents are studied. We believe that this microfluidic system gives new opportunies to study nucleation and phase transition of complex materials.

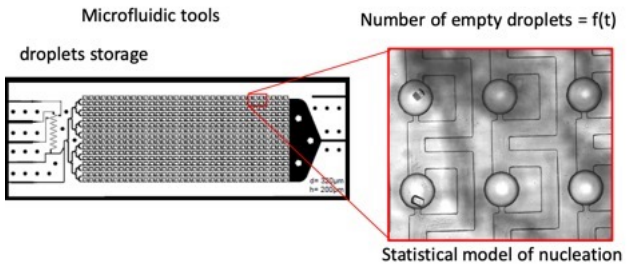

Scale 2: in a batch reactor the effect of additives on crystal growth is difficult to study because of the supersaturation evolution. We propose to adapt the constant composition (constant supersaturation) method in a semi-batch reactor, to compare the effect of several additives (3).

This study provides insights on the mechanisms governing the inhibition $CaCO_3$ crystallization at local scale, and enable to benchmark several additives.

Scale 3: transposition of the kinetics laws obtained are made at industrial scale with respect to changes in operating conditions. Observations at lab-scale allows to propose laws for governing mechanisms and explains the trends observed at pilot-plant scale.

References

(1) VITRY Y., TEYCHENE S, CHARTRON S., LAMADIE F., BISCANS B.
Investigation of a microfluidic approach to study very high nucleation rates involved in precipitation processes. Chem. Eng. Science, 2015, vol.133, pp. 54-61.

(2) BOURGEOIS F., TEYCHENE S., BISCANS B.
Applicability of probabilistic nucleation modelling for analysis of microfluidics data
KONA Powder and Particle Journal, 2018, n°35, pp. 258-272

(3) CHHIM N., KHARBACHI C., NEVEUX T., BOUTELEUX C., TEYCHENE S., BISCANS B.;
Inhibition of calcium carbonate crystal growth by organic additives using the constant composition method. Journal of Crystal Growth, 2017, Vol. 472, pp. 35-45

ECCE12
The 12th EUROPEAN CONGRESS OF CHEMICAL ENGINEERING
Florence 15-19 September 2019

Workshop on Crystallization Science and Engineering

Application of multiscale modelling and deep learning tools for flash nanoprecipitation and reactive crystallization

Daniele Marchisio[1], Antonio Buffo[1], Gianluca Boccardo[1], Alessio Lavino[1], Maria Laura Para[1], Matthew Riella[1]

1 Department of Applied Science and Technology, Institute of Chemical Engineering, Politecnico di Torino, C.so Duca degli Abruzzi 24, 10129 Torino

**Corresponding author: daniele.marchisio@polito.it*

Highlights

- Multiscale modelling is applied to the simulation of crystallization processes
- Multiscale modelling is augmented by artificial intelligence and deep learning tools
- Experimental data is used for model validation
- Two examples are discussed: flash nanoprecipitation and reactive crystallization

1. Introduction

Crystallization and precipitation are very important in chemical engineering as numerous particulate products are manufactured by relying on these processes. Examples span from the pharmaceutical industry to the materials industry, including catalysis and batteries. The final products properties are characterized in terms of distributions, notably the size distribution. In turn the particle size distribution (PSD), or crystal size distribution (CSD), is strongly affected by the operating conditions under which the process is carried out and in order to design, scale up and down and optimize the process, computational models are extremely useful. In fact, they can answer the complex question: under what operating conditions a specific PSD or CSD can be obtained? In this contribution the main computational modelling techniques are presented and discussed.

2. Methods

As the main emphasis is on the prediction of the PSD/CSD the most popular computational models are based on the solution of the population balance equations (PBE), that dictates the evolution of the PSD/CSD. However, since the PBE is strongly connected with the fluid dynamics of the crystallizer, very often the PBE is tightly coupled with a computational fluid dynamics (CFD) model. The coupling is often realized with quadrature-based moments methods (QBMM) such as the quadrature method of moments (QMOM) or the conditional quadrature method of moments (CQMOM) [1].

Moreover, as the rates with which particles and crystals are formed are governed by molecular processes, very often these models are coupled also with atomistic and molecular models. Among

the different modelling choices full atom molecular dynamics (MD) and coarse-grained molecular dynamics (CGMD) are mostly employed.

A plethora of codes is used to run these simulations, to couple the different models and to orchestrate the workflows, ranging from Ansys Fluent, OpenFOAM, code_saturne, LAMMPS, GROMACS, Salome, etc.

All the above-mentioned models, being based on first principles and physical laws are labelled as physics-based models. However, recently the simulation of these processes also relies on the use of artificial intelligence and deep learning tools to build data-driven models, which is contrast to the previous ones, are not based on first principles. An interesting idea is that since very often the amount of experimental data is often not enough to build a data-driven model, validated physics-based models can be used to augment and enrich a limited experimental data set and to build the data-driven model, following the digital twin concept.

3. Results and discussion

Two examples will be discussed in this presentation. The first one focuses on flash-nanoprecipitation via solvent-displacement for the production of amorphous polymer nanoparticles for controlled drug delivery applications, whereas the second focuses on the precipitation of inorganic crystals via reactive crystallization or precipitation. In the first example it will be shown how multiscale modelling can be used to simulate the polymer particle formation process, starting from molecules up to the actual crystallizer and to successfully predict the effect of the choice of the good solvent, of paramount important in these processes [2,3]. In the second example the use of these computational tools will be discussed for a different application process involving inorganic crystals.

References

[1] Marchisio D.L., Fox R.O. Computational models for polydisperse multiphase and particulate flows (2013) Cambridge University Press, Cambridge, UK.

[2] Lavino, A.D., Banetta, L., Carbone, P., Marchisio, D.L. Extended Charge-On-Particle Optimized Potentials for Liquid Simulation Acetone Model: The Case of Acetone-Water Mixtures (2018) Journal of Physical Chemistry B, 122 (20), pp. 5234-5241.

[3] Lavino, A.D., Di Pasquale, N., Carbone, P., Marchisio, D.L. A novel multiscale model for the simulation of polymer flash nano-precipitation (2017) Chemical Engineering Science, 171, pp. 485-494.

ECCE12
The 12th EUROPEAN CONGRESS OF CHEMICAL ENGINEERING
Florence 15-19 September 2019

Workshop on Crystallization Science and Engineering

Synthesis and assembly of nanostructures in flow.

Klavs Jensen[1]

1 MIT, Department of Chemical Engineering,

**Corresponding author: kfjensen@mit.edu*

Highlights

- Continuous flow synthesis of nanocrystalline materials.
- Effect of reaction conditions on growth and crystal structure.
- Sequential growth of core-shell and modified nanoparticles.

Abstract

Continuous flow systems are shown to have advantages in synthesis and assembly of nanomaterials, including faceted metal nanoparticles, quantum dots, and nanodendrites. Synthesis in flow leads to sharper size distribution and faster growth than typically achieved in batch processes. The choice of reactor configuration, solvents, reagents, and exposure environment has significant impact on the resulting nanostructures. Chaining multiple flow systems provides control of nucleation, growth, ageing, and over-coating of core-shell nanoparticles, as exemplified with the synthesis of InP quantum dots. Sequential flow synthesis steps also enable synthesis of hierarchically structured nano and meso scale structures.

ECCE12
The 12th EUROPEAN CONGRESS OF CHEMICAL ENGINEERING
Florence 15-19 September 2019

Workshop on Crystallization Science and Engineering

Crystallization in Complex Multicomponent Chiral Systems

Joop H. ter Horst

EPSRC Centre for Innovative Manufacturing in Continuous Manufacturing and Crystallisation (CMAC), Strathclyde Institute of Pharmacy and Biomedical Sciences (SIPBS), Technology & Innovation Centre (TIC), University of Strathclyde, Glasgow, G1 1XQ, United Kingdom

Joop.terHorst@strath.ac.uk

Highlights

- Resolution Control in a Continuous Preferential Crystallization Process
- Continuous Antisolvent Deracemization
- Semi-continuous Deracemization via Racemic Crystal Transformation monitored by in-situ Raman Spectroscopy

The biological activity of a chiral compound often depends on its handedness. However, the physical properties of left- and right handed molecules are the same. The manufacture of just one of the two chiral forms, therefore, is a challenge. Crystallization is an extremely powerful technology to enable the manufacture of enantiopure crystalline products: Enantiopure crystals are highly selective towards incorporation of enantiomer solutes with the same handedness. Therefore, chiral separation of the enantiomers through crystallization can lead to high enantiopurities, for instance through preferential crystallization. The extension of the crystallization process with a racemization reaction in the solution (deracemization) has additional benefits for yield as well as process stability: the counter enantiomer is racemized towards the preferred one (higher yield) so that the supersaturation for the counter enantiomer remains low (no crystal nucleation of the counter enantiomer crystals). In addition, for continuous manufacturing of enantiopure compounds these crystallization processes can be beneficial due to steady state operation and continuous control opportunities.

I will discuss a number of process configurations in which controlled crystallization is used to obtain an enantiopure product from complex multicomponent racemic systems.

Acknowledgements

This research received funding as part of the CORE project (October 2016−September 2020) from the European Union's Horizon 2020 research and innovation programme under the Marie Sklodowska-Curie grant agreement No. 722456 CORE ITN (www.coreitn.eu) and as part of the EPSRC Centre for Innovative Manufacturing in Continuous Manufacturing and Crystallization (www.cmac.ac.uk) (EPSRC funding under Grant Reference: EP/I033459/1).